# Laboratory Directed Research and Development

Los Alamos National Laboratory

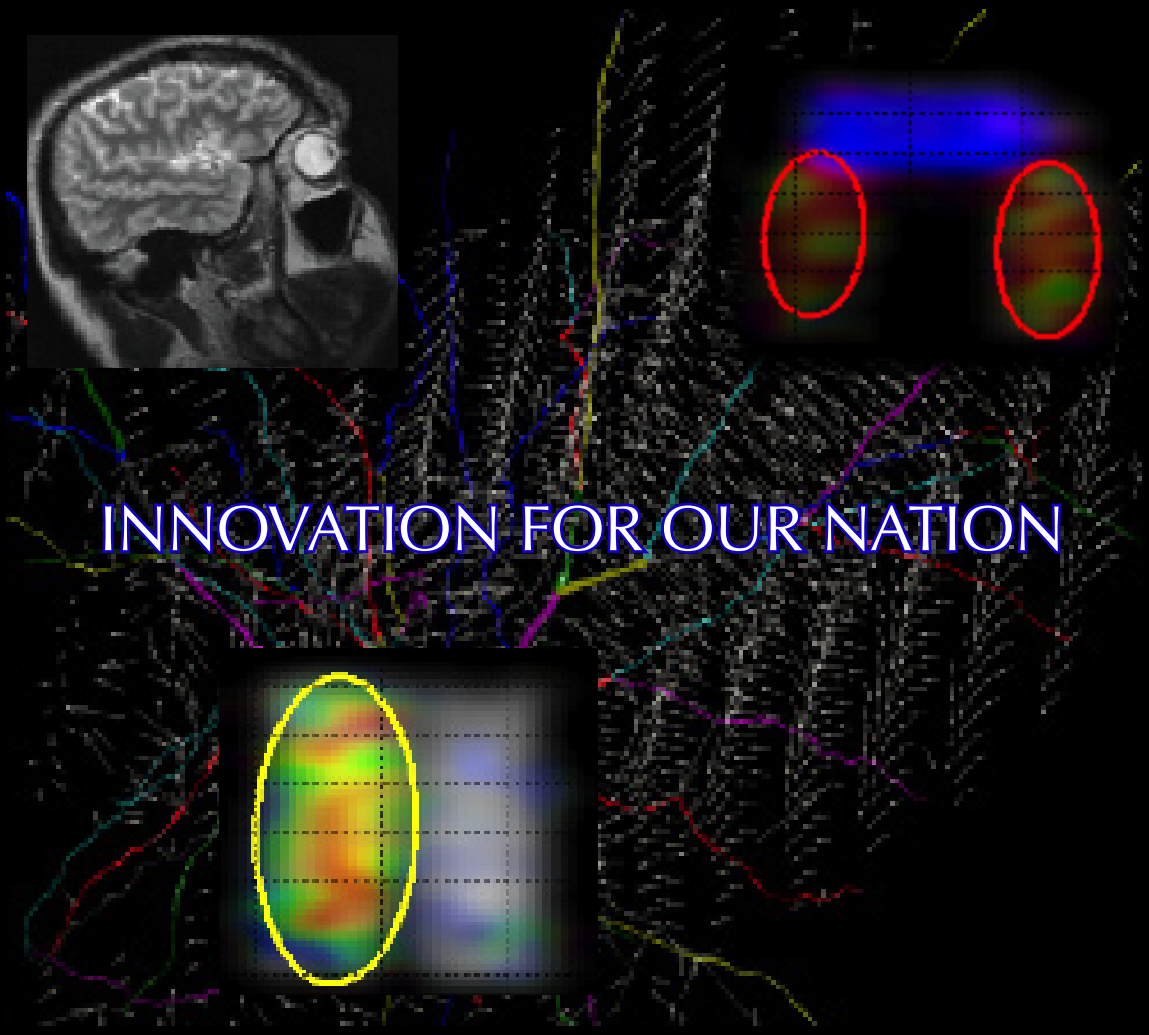


## FY09 Annual Progress Report

LA-UR 10-00925

This page was intentionally left blank.

## About the Cover

Ultra-low-field Magnetic Resonance Imaging (ULF-MRI) technology developed with funding from LDRD is now being used in MagViz – a revolutionary scanning machine that distinguishes potential-threat liquids from harmless shampoos and sodas screened at airport baggage checkpoints. Screeners using the MagViz system will be able to differentiate and identify many materials that may be packaged together or separately. The physics that underlies how MRIs differentiate between the tissue types in the brain (i.e. white and gray matter) is the same as that used by MagViz to tell the difference between safe liquids and threat substances. This effort has successfully completed a proof of concept of an extremely sensitive screening technology that scans magnetic changes of individual materials at the molecular level.

The goal for the airport screening technology is reliable, high-throughput detection of liquids, in a form that is non-contact, non-invasive, requires no radiation, produces no residue, and uses the existing airport security portal. The long-range goal for MagViz is to develop the capability to screen carry-on bags without requiring the "3-1-1" bag system. While such a goal is several years in the future, a more near-term goal for MagViz is to screen materials in the presence of or through virtually any packaging, including leather, cardboard, wood, clothing, and even metallic containers.

The Los Alamos MagViz Team garnered a 2009 R&D 100 Award for this work. The ULF-MRI technology is being applied to MagViz though a large grant from the U.S. Department of Homeland Security.

Los Alamos
NATIONAL LABORATORY
EST. 1943

## Disclaimer

The Los Alamos National Laboratory strongly supports academic freedom and a researcher's right to publish; therefore, the Laboratory as an institution does not endorse the viewpoint of a publication or guarantee its technical correctness. With respect to documents available from this server, neither the United States Government nor the Los Alamos National Security, LLC., nor any of their employees, makes any warranty, express or implied, including the warranties of merchantability and fitness for a particular purpose, or assumes any legal liability or responsibility for the accuracy, completeness, or usefulness of any information, apparatus, product, or process disclosed, or represents that its use would not infringe privately owned rights. Reference herein to any specific commercial products, process, or service by trade name, trademark, manufacturer, or otherwise, does not necessarily constitute or imply its endorsement, recommendation, or favoring by the United States Government or the Los Alamos National Security, LLC. The views and opinions of authors expressed herein do not necessarily state or reflect those of the United States Government or the Los Alamos National Security, LLC., and shall not be used for advertising or product endorsement purposes. Unless otherwise indicated, this information has been authored by an employee or employees of the Los Alamos National Security, LLC. (LANS), operator of the Los Alamos National Laboratory under Contract No. DE-AC52-06NA25396 with the U.S. Department of Energy. The U.S. Government has rights to use, reproduce, and distribute this information. The public may copy and use this information without charge, provided that this Notice and any statement of authorship are reproduced on all copies. Neither the Government nor LANS makes any warranty, express or implied, or assumes any liability or responsibility for the use of this information.

Issued March 2009

LA-UR 10-00925

## Structure of this Report

In accordance with U.S. Department of Energy Order (DOE) 413.2B, the Laboratory Directed Research and Development (LDRD) annual report for fiscal year 2009 (FY09) provides summaries of each LDRD-funded project for the fiscal year, as well as full final reports on completed projects. The report is organized as follows:

Overview: An introduction to the LDRD Program at Los Alamos National Laboratory (LANL), the program's structure and strategic value, the LDRD portfolio management process, and highlights of outstanding accomplishments by LDRD researchers.

Project Summaries: The project summaries are organized first by science and technology categories: Physics, Chemistry and Material Sciences, Environmental and Biological Sciences, Information Science and Technology, and Technology. Within each category, summaries are organized by LDRD component: Directed Research (DR) projects first, Exploratory Research (ER) second, and Postdoctoral Research and Development (PRD) projects last. Full final reports are included at the end of each section.

Projects are listed in numerical order according to their project identification number, which consists of three parts. The first is the fiscal year in which the project began; the second is a unique numerical identifier; and the third identifies the project component.


## Acknowledgements

**Technical Review**
William Priedhorsky
Robert Kraus Jr.

**Publication Editor and Designer**
Andrea Maestas

**Team Contributors**
Lennett Rendon
Stephen Schultz
Debbie Martinez
Ronnie Quintana
Susan Whittington
Douglas Wokoun
Benjamin Brown

# Table of Contents


15 Overview

## Chemistry and Material Sciences

30 **Hot Spot Physics and Chemistry in Energetic Materials Initiation**
*Dana M. Dattelbaum*

34 **Design, Synthesis, and Theory of Molecular Scintillators**
*Rico E. Del Sesto*

37 **Ultrafast Nanoscale XUV Photoelectron Spectroscopy**
*George Rodriguez*

41 **Advanced Fuel Forms with Microstructures Tailored to Naturally Induce Fission Product Separation During Service**
*Kurt E. Sickafus*

44 **Predictive Design of Noble Metal Nanoclusters**
*Jennifer Martinez*

48 **Understanding Anisotropy to Develop Superconductors by Design**
*Filip Ronning*

52 **Spatial-temporal Frontiers of Atomistic Simulations in the Petaflop Computational World**
*Timothy C. Germann*

56 **Enhance Radiation Damage Resistance via Manipulation of the Properties of Nanoscale Materials**
*Michael A. Nastasi*

59 **Seaborg Institute Fellows**
*Albert Migliori*

62 **Strongly Correlated Electrons: Duality and Implications**
*Cristian D. Batista*

69 **Novel Inclusion Compounds for Hydrogen Storage**
*Yusheng Zhao*

75 **Correlations and Control of Properties of Metallic U and Pu**
*Jeremy N. Mitchell*

83 **Metamaterials for Threat Reduction Applications: Imaging, Signal Processing, and Cloaking**
*Antoinette J. Taylor*

89 **Coexistence of Magnetic and Superconducting Electrons in Strongly Correlated Matter**
*Joe D. Thompson*

96 **Physics of Helium Retention in Palladium/Tritum Systems**
*Douglas J. Safarik*

102 **Quantum Control in Condensed Media for Studies of Direct Optical Initiation of Explosives**
*David S. Moore*

106 **Biomimetic Hydrogen Production by Photoinitiated Transition Metal Catalysis**
*Reginaldo C. Rocha*

114 **Detection of Respiratory Infection by Scent**
*Jurgen G. Schmidt*

117 **Spins in Organic Semiconductors**
*Brian K. Crone*

120 **Strain-induced Novel Physical Phenomena in Epitaxial Ferroic Nanocomposites**
*Quanxi Jia*

123 **Genetically Engineered Polymer Libraries**
*Jennifer Martinez*

124 **Probing Unconventional Superconductivity in Heavy Fermion Thin Films**
*Vladimir Matias*

127 **Photocatalytic Materials Based on Quantum Confined Semiconductor Nanocrystals**
*Milan Sykora*

130 **Molecular Scale Shock Response of Explosives**
*Shawn D. Mcgrane*

132 **Multifunctional Materials**
*James E. Gubernatis*

135 **Photodynamics and Photochemistry of Carbon Nanotube Materials**
*Sergei Tretiak*

138 **Compositionally Graded InGaN-based High Efficiency Photovoltaic Devices**
*Mark A. Hoffbauer*

140 **Plasmonic Bandgap Materials: Fusion of Interparticle and Particle-Photon Interactions at the Nanoscale**
*Stephen K. Doorn*

143 **Probing the Origin and Consequences of Quantum Critical Fluctuations**
*Tuson Park*

146 **Linear Scaling Quantum-Based Interatomic Potentials for Energetic Materials**
*Marc J. Cawkwell*

149 **Transparent Organic Solar Cells**
*Ian H. Campbell*

151 **Uranium Imido Complexes as Catalysts for the Reduction of Carbon Dioxide**
*James M. Boncella*

153 **Improved Length Scaling in Accelerated Molecular Dynamics Methods**
*Arthur F. Voter*

158 **Coulomb Mechanisms for Ion Damage in Insulators in the Electronic Stopping Regime**
*Cynthia J. Reichhardt*

163 **Synthesis of Nanowire Heterostructures for Strain-Controlled Bandgap Engineering**
*Samuel T. Picraux*

169 **Synthetic Decoys for Biothreat Agents**
*Rashi S. Iyer*

173 **Magnetic Resonance Force Microscopy Studies of Ferromagnets on a Nanometer Scale**
*Roman Movshovich*

178 **Controlling Oxidation-States in Actinide-Oxides through Crystal Lattice Pinning**
*Quanxi Jia*

182 **Tunable Infra-Red Chromophores through N-Type Doping of Wide-Gap Semiconductor Nanocrystals**
*Sergei A. Ivanov*

187 **Non-Precious Metal Nanocomposites for Fuel Cell Catalysis**
*Piotr Zelenay*

194 **Novel Materials for Gamma-Ray Detection based on Nano-Engineered Semiconductor Nanocrystals**
*Richard D. Schaller*

197 **Parallel-Replica Dynamics Study of Tip-Surface and Tip-Tip Interactions in Atomic Force MicrosCopy and the Formation and Mechanical Properties of Metallic Nanowires**
*Arthur F. Voter*

202 **Chemical Chronometers for Nuclear Forensics Applications**
*David L. Clark*

205 **Superconducting Nanowire Single Photon Detector Development**
*Michael W. Rabin*

210 **High-Nitrogen Polydentate Ligands for Lanthanide/Actinide Separations**
*Jacqueline M. Veauthier*

214 **Advanced Measurements in Designed Nanostructures to Establish Measurement Techniques for Electrosynthetic Production of Fuels**
*Albert Migliori*

217 **Molecular Level Investigation of Tunable Energetic Mixtures**
*David S. Moore*

219 **First-Principles-Based Equations of State Including Multi-Phase Chemical Equilibrium**
*Milton S. Shaw*

222 **Study of Hybrid Semiconductor/Molecular Systems for Photo-production of Hydrogen**
*Andrew P. Shreve*

224 **Synthesis and Characterization of Novel Metal-Organic Frameworks for Hydrogen Storage**
*Toti E. Larson*

227 **Bio-Directed Assembly of Multicolored One-Dimensional Quantum Dot Light-Emitting Devices**
*Gabriel A. Montano*

230 **Semiconductor Nanowire Heterostructures**
*Samuel T. Picraux*

234 **Local Atomic Arrangements in Phase Change Materials**
*Thomas E. Proffen*

237 **Effect of Charging on Carrier Relaxation Dynamics in Quantum Confined Semiconductor Nanocrystals**
*Milan Sykora*

240 **The Kondo Lattice Problem**
*Joe D. Thompson*

242 **Classical/quantum Mechanical Simulations of Electronic Nanomaterials**
*Sergei Tretiak*

244 **Energy Transfer Processes in Type-Specific Single-Walled Carbon Nanotubes**
*Stephen K. Doorn*

246 **Vanadium Catalyzed Aerobic Oxidations**
*John C. Gordon*

248 **In situ X-ray Microdiffraction Study of Nanomechanical Behavior**
*Amit Misra*

250 **Novel Fabrication of Metal-Semiconductor Heterostructured Nanowires**
*Jennifer A. Hollingsworth*

253 **Nanogenerators Driven by Both Magnetic and Mechanical Waves**
*Quanxi Jia*

255 **New Generation of Fluorescent Probes for In-Vivo Imaging**
*Jennifer Martinez*

257 **Lifting the Quantum Critical Conundrum**
*Joe D. Thompson*

261 **Synthesis of Molecular Actinide Nitrides**
*David L. Clark*

265 **Accelerated Molecular Dynamics at Complex Interfaces**
*Arthur F. Voter*

270 **A Chemical Route to Integrate Carbon Nanotubes into Microelectromechanical Systems**
*Quanxi Jia*

273 **Molecular Actinide Alkylidene Complexes**
*Jaqueline L. Kiplinger*

278 **Superconductivity in Non-Centrosymmetric Materials**
*John Singleton*

282 **Multifunctional Copper-Carbon Nanotube Nanocomposites**
*Amit Misra*

285 **Multiscale Simulations for Cascade Overlap in Irradiated Materials**
*Arthur F. Voter*

290 **Ultrafast Non-equilibrium Physics of the Fractional Quantum Hall System**
*Antoinette J. Taylor*

295 **Time-Dependent Density Functional Theory for Ultrafast Optical Phenomena in Strongly Correlated Electron Materials**
*Jian-Xin Zhu*

298 **Sensitization of Lanthanide Ion Fluorescence Using Nanocrystal Quantum Dots**
*Jennifer A. Hollingsworth*

303 **Chemically Synthesized Germanium Nanocrystals for Applications in Solar-Energy Conversion**
*Victor I. Klimov*

306 **Synthesis, Chemistry and Theoretical Studies of 5f-Element Hydride Complexes**
*Jaqueline L. Kiplinger*

312 **Structure-Property Relationship for Strained One Dimensional Ferroelectric Nanostructures**
*Quanxi Jia*

## Environmental and Biological Sciences

315 **One-step Biomass Conversion: Looking to Nature for Solutions to Energy**
*Paul Langan*

319 **Flash Before the Storm: Predicting Hurricane Intensification using LANL Lightning Data**
*Christopher Jeffery*

322 **Genomes to Behavior: Predicting Bacterial Response by Constrained Netork Interpolation**
*John M. Dunbar*

325 **Complex Biological and Bio-Inspired Systems**
*Robert Ecke*

329 **Undertanding Drug Resistance and Co-inefectivity in HIV and TB Infections**
*Bette T. Korber*

332 **Distributed Metabolic Regulation: The Key to Symthetic Biology for Carbon Nutral Fuels**
*Pat J. Unkefer*

335 **High-Resolution Physically-Based Model of Semi-Arid River Basin Hydrology**
*Everett P. Springer*

340 **Rapid Iterative Detection Using Smart Pathogen Signatures**
*John M. Dunbar*

345 **A Systematic Strategy for Gene Function Discovery**
*Clifford J. Unkefer*

351 **Host-Pathogen Interactions (Pathomics) in Avian Influenza**
*Ruy M. Ribeiro*

357 **Identifying High Risk Species Critical for the Emergence of Pandemic Influenza**
*Jeanne M. Fair*

360 **The Effect of Acoustical Waves on Stick-Slip Behavior in Sheared Granular Media: Implications for Earthquake Recurrence and Triggering**
*Paul A. Johnson*

363 **Developing a Remote Sensing of the Solar Surface**
*Joseph E. Borovsky*

366 **A New Approach to Unravel Complex Microbial Community Processes**
*Cheryl R. Kuske*

369 **Nonequilibrium Mechanics of Geomaterials**
*James A. Tencate*

371 **Evolution and Function of Microbial Signatures**
*Murray A. Wolinsky*

375 **Coupling of Genetics and Metabolism and the Orgin of Life**
*Hans J. Ziock*

378 **Using Small Molecules to Control RNA Conformations**
*Kevin Y. Sanbonmatsu*

381 **Functional Gene Discovery Using RNAi-based Gene Silencing**
*Elizabeth Hong-Geller*

384 **A Visionary New Approach to Assess Regional Climate Impacts on Vegetation Survival and Mortality**
*Nathan G. Mcdowell*

386 **Membrane Micro-chromatography: A Novel Approach to Preparative Nucleic Acid Sample Processing**
*Goutam Gupta*

390 **Isotopic Tracer for Climate Relevant Secondary Organic Aerosol**
*Thomas A. Rahn*

393 **Evolving a Thermostable Cellulase by Internal Destabilization and Evolution**
*Andrew M. Bradbury*

395 **Functional Proteomics Studies of Bacillus Anthracis**
*Ryszard Michalczyk*

400 **Drug Binding and Catayltic Mechanism in DHFR**
*Paul A. Langan*

405 **Substrates for the Detection and Differentiation of Influenza Viridae**
*David B. Kimball*

410 **Magnetic Turbulence and Kinetic Dissipation in Solar Wind and Solar Corona Plasmas**
*Hui Li*

413 **Understanding a Killer: A Predictive Model of Tumor Development**
*Yi Jiang*

418 **An Experimental and Theoretical Framework for Reactive Micromixing**
*Amr I. Abdel-Fattah*

424 **Subsurface Transport Parameter Estimation with Multiscale, Multiobjective Optimization**
*Andrew V. Wolfsberg*

429 **New Frontiers in Viral Phylogenetics**
*Tanmoy Bhattacharya*

432 **Cellulosomes in Action: Peta-Scale Atomistic Bioenergy Simulations**
*Kevin Y. Sanbonmatsu*

436 **The Dynamics of Change in Global Energy Systems**
*Rajan Gupta*

439 **Transformative Capability for Bioassessment of Engineered Nanomaterials**
*Rashi S. Iyer*

443 **Inferring Functional Determinants of Microbe Pathogenicity by Computational Pathogen Characterization**
*H H. Cui*

448 **Large-Scale, Carbon-Sequestration Flows—Laboratory Measurement and Simulation**
*Scott N. Backhaus*

452 **Feasibility of GHG Monitoring from Space: Verification of Los Angeles Emissions**
*Manvendra K. Dubey*

455 **Simulating Vegetation Impacts on River Basin Water Balance**
*Everett P. Springer*

460 **Creating a Mathematical Foundation for High-Dimensional Search and Optimization Algorithms to Solve Complex Nonlinear Models**
*Bruce A. Robinson*

464 **The Role of NS1 in Disrupting Immune Responses During Influenza Infection: A Modeling and Experimental Approach**
*Alan S. Perelson*

466 **Pore-Scale Modeling of Multiphase Flow and Reaction in Charged Porous Media**
*Qinjun Kang*

468 **Modeling Fast Basal Sliding of Ice Sheets for Climate and Sea Level Prediction**
*William H. Lipscomb*

471 **Spectroscopic Studies and Photonic Applications of "Giant" Nanocrystal Quantum Dots**
*Victor I. Klimov*

474 **Modeling Control of Viruses by Immune Responses**
*Alan S. Perelson*

478 **Multi-scale Analysis of Multi-physical Transport Processes of Electroosmosis in Porous Media**
*Qinjun Kang*

481 **Fluvial Geomorphic Response to Permafrost Thawing: Implications for the Global Carbon Budget and Arctic Hydrology**
*Cathy J. Wilson*

483 **Determinaing the Mechanisms of Enzymes Xylose Isomerase and HIV Protease using Neutron Crystallography**
*Paul A. Langan*

485 **Analysis of Protein Structure-Function Relations in Antibiotic Biosynthesis and Signal Transducing Receptors**
*Louis A. Silks III*

488 **Carbon and Oxygen Isotopic Variability in Succulent Plants and Their Spines: A New Tool for Climate and Ecosystem Studies in Desert Regions**
*Claudia Mora*

490 **Probing Molecular Physics of Biological Nano-channels: from Viruses to Biosensors**
*Benjamin H. Mcmahon*

493 **Photodegradation of Leaf Litter in Water-Limited Ecosystems**
*Thomas A. Rahn*

498 **Modeling the Immune Response to Pathogens**
*Alan S. Perelson*

503 **3-Dimensional Tracking of Single Quantum Dots: The Case for 2-Photon Excitation**
*James H. Werner*

## Information Science and Technology

506 **Automated Change Detection in Remote Sensing Imagery**
*James P. Theiler*

512 **Information Science and Technology: Metagenomics**
*Nicolas W. Hengartner*

516 **Statistical Physics of Networks, Information and Complex Systems**
*Robert E. Ecke*

521 **Information Science and Technology: Streaming Data**
*Sarah E. Michalak*

524 **Synthetic Cognition through Peta-Scale Models of the Primate Visual Cortex**
*Luis Bettencourt*

528 **RADIUS: Rapid Automated Decomposition of Images for Ubiquitous Sensing**
*Lakshman Prasad*

530 **The Physics of Algorithms**
*Michael Chertkov*

535 **Nonconvex Compressed Sensing**
*Rick Chartrand*

537 **Foundations for Practical Pattern Recognition Systems**
*Reid B. Porter*

540 **Multilevel Adaptive Sampling for Multiscale Inverse Problems**
*John D. Moulton*

543 **Adaptive Algorithms for Inverse Problems in Imaging**
*Brendt E. Wohlberg*

546 **Designing Communication Methods for Bottom-Up Self-Assembled Nanowire Networks of Emerging Computer Architectures**
*Hsing-Lin Wang*

549 **Stochastic Transport on Networks: Efficient Modeling And Applications to Epidemiology**
*Nicolas W. Hengartner*

551 **Critical and Crossover Behaviors at Jamming Transitions**
*Charles Reichhardt*

554 **Time-reversible Born-Oppenheimer Molecular Dynamics**
*Anders M. Niklasson*

558 **Developing Adaptive High-Order Divergence-Free Methods for Magneto-Hydrodynamics Turbulence Simulations**
*Shengtai Li*

561 **Efficient Interdiction**
*Feng Pan*

564 **A Hybrid Transport-Diffusion Method for Radiation Hydrodynamics**
*Jeffery D. Densmore*

566 **Robust 3D Moving Mesh Adaptation Based on Monge-Kantorovich Optimization**
*John M. Finn*

569 **New Approach to Bayesian Inference Under Modeling Uncertainty**
*Nicolas W. Hengartner*

574 **Sharp Characterization of Minimizers (typically) Involving Interfaces in Images**
*Pieter J. Swart*

577 **Instabilities Driven Turbulence and Mixing in Convergent Geometries**
*Daniel Livescu*

584 **Moment-Based Interface Tracking for Multi-Material Flows**
*Rao V. Garimella*

589 **Hyperbolic Polynomials Approach to Approximate Counting and Lower/Upper Bounds in Combinatorics, Statistical Physics and Computational Geometry**
*Leonid Gurvits*

592 **Excited States and Optical Response of Nanosized Molecules at Linear Scaling Numerical Cost**
*Sergei Tretiak*

596 **Agent-Based Modeling and Simulation of Cellular Signaling Systems**
*William S. Hlavacek*

600 **Fast Approximation Algorithms for Systems of Linear Inequalities**
*Donald R. Hush*

603 **Minimal Description of Complex Shapes with Applications to Experiments and Validation of Large-Scale Codes**
*Mark B. Mineev*

607 **A New Architecture Revolution for Supercomputing**
*Zachary K. Baker*

611 **Towards Human Level Artificial Intelligence: A Cortically Inspired Semantic Network Approach to Information Processing and Storage**
*Luis Bettencourt*

613 **Finite State Projection for Accurate Solution of the Master Equation**
*Michael E. Wall*

615 **Statistical Physics of Optimization**
*Michael Chertkov*

618 **Multiscale Variational Approaches to Markov Random Fields**
*Michael Chertkov*

621 **Quantum Information Processing: Capabilities and Limitations**
*Robert E. Ecke*

623 **Self-Organizing Wireless Ad-Hoc and Sensor Networks with Functional Guarantees**
*Stephan J. Eidenbenz*

## Physics


626 **Development of a Magnetically Driven Target for Thermo-Nuclear Burn Studies (*U)**
*Robert G. Watt*

629 **Prompt and Radiochemical NTS Diagnostics and New Measurements (U)**
*David J. Vieira*

631 **Global Monitoring of the Sky with Thinking Telescopes: Finding and Interrogating Cosmic Explosions**
*W T. Vestrand*

634 **Carrier Multiplication in Nanoscale Semiconductors for High-Efficiency, Generation-III Photovoltaics**
*Victor I. Klimov*

637 **Probing Physics Beyond the Standard Model through Neutron Beta Decay**
*Alexander Saunders*

640 **Cosmic Explosions Probing the Extreme: X-Ray Bursts, Superbursts, and Giant Flares on Neutron Stars**
*Sanjay Reddy*

644 **Novel Signatures of Beyond the Standard Model at the Large Hadron Collider**
*Rajan Gupta*

648 **High-Precision Spectroscopic Search for Variation of the Fine-Structure Constant**
*Justin R. Torgerson*

651 **Double Beta Decay**
*Steven R. Elliott*

654 **Turbulence By Design**
*Malcolm J. Andrews*

658 **New and Enhanced Capabilities in Quantum Information Processing**
*Malcolm G. Boshier*

661 **Revolutionary Science at the Intersection of Extreme and Transient Events, Natural Hazards, and National Security**
*Gerald L. Geernaert*

665 **Beyond the Neutrino Matrix**
*Andrew Hime*

670 **Dark Energy and the Cosmic Web**
*Katrin Heitmann*

676 **High-Current, High-Energy, Laser-Driven Ion Accelerators: An Enabling and Revolutionary Scientific Research Tool**
*Juan C. Fernandez*

685 **Cold Atom Surface Imaging**
*Eddy M. Timmermans*

691 **Multiscale Modeling of Strongly Interacting Systems**
*Robert E. Ecke*

701 **Understanding Dynamical Diversity of Extrasolar Planets**
*Hui Li*

703 **Precision Cosmology and the Neutrino Sector**
*Salman Habib*

705 **Finding the First Cosmic Explosions**
*Daniel Holz*

708 **Materials and Device Optimization towards Room Temperature Spin-Transport through Single-Walled Carbon Nanotubes**
*Stephen K. Doorn*

711 **The First Precise Determination of Quark Energy Loss in Nuclei**
*Ivan M. Vitev*

715 **Entanglement in Quantum Ground States**
*Michael Chertkov*

718 **CP-violating Moments of Atoms and Nuclei**
*Anna C. Hayes-Sterbenz*

720 **Ultrafast Nanoplasmonics for Photonics and Quantum Control at the Nanoscale**
*Anatoly V. Efimov*

723 **Probing physics beyond the Standard Model with supernovae**
*Alexander Friedland*

727 **Understanding the Feedback of Active Galaxies in Galaxy Clusters**
*Hui Li*

729 **The First Characterization of Large Interstellar Dust**
*Sigrid Close*

732 **Soild Helium-4: A Supersolid or Quantum Glass?**
*Matthias J. Graf*

735 **A Novel Millimeter-Wave Traveling-Wave Tube Based on an Omniguide Structure**
*Evgenya I. Smirnova*

737 **Development of a Muon to Electron Conversion Experiment at LANSCE/MaRIE: Search for Physics beyond the Standard Model**
*Takeyasu Ito*

739 **Unconventional Methods for Quantum-enhanced Metrology**
*Malcolm G. Boshier*

741 **First Unambiguous Measurement of Jet Fragmentation and Energy Loss in the Quark Gluon Plasma**
*Gerd J. Kunde*

744 **Breakthroughs in Magnetic Reconnection Enabled by Petaflop Scale Computing**
*Lin Yin*

747 **Disentangling Quantum Entaglement**
*Wojciech H. Zurek*

750 **Backward Stimulated Raman and Brillouin Scattering of Laser in the Collisional Regime**
*Lin Yin*

753 **Transport in Magnetized Dense Plasmas for Magneto-Inertial Fusion**
*Xianzhu Tang*

755 **Novel Cone Targets for Efficient Energetic Ion Acceleration for Light Ion-Driven Fast Ignition Fusion**
*Kirk A. Flippo*

759 **General Relativity as a Probe of Cosmology**
*Daniel Holz*

762 **Experimental Study of Driven Magnetic Relaxation in a Laboratory Plasma**
*Scott C. Hsu*

765 **Beta Decay of Polarized Radioactive Atoms in an Optical Tweezer**
*Xinxin Zhao*

768 **Nano-Engineered Casimir Forces**
*Diego A. Dalvit*

772 **Probing Correlated Electron Behavior via Direct Uranium-235 Nuclear Magnetic Resonance**
*Eric D. Bauer*

777 **Cold Atom Quantum Liquid Mixtures**
*Eddy M. Timmermans*

782 **Investigation of Energetic Ion Generation and Transport in Ultra-Intense Laser-Matter Interaction**
*Brian J. Albright*

786 **New States of Matter in Stars, Nuclei and Cold Atoms**
*Sanjay Reddy*

791 **Ultra-Low Field Resonant Absorption Magnetic Resonance Imaging of Neural Activity**
*Petr L. Volegov*

796 **Unique Observations of Nature's Largest Explosions**
*W T. Vestrand*

801 **Electron-Neutrino Correlation in Neutron Beta Decay**
*Wesley S. Wilburn*

804 **Experimental and Computational Studies of Magnetic Bubble Expansion as a Model for Extra-galactic Radio Lobes**
*Scott C. Hsu*

807 **Three-Dimensional Dynamics of Magnetic Reconnection in Space and Laboratory Plasmas**
*William S. Daughton*

812 **The Roadrunner Universe**
*Salman Habib*

815 **Implicit Monte Carlo Calculations of Supernova Light-Curves**
*Aimee L. Hungerford*

818 **Instabilities Driven Reacting Compressible Turbulence**
*Daniel Livescu*

822 **Saturation of Backward Stimulated Scattering of Laser In The Collisional Regime**
*Lin Yin*

827 **Lagrangian Approach to Capturing Interactions Between Wind-Energy Turbines and Atmosphere**
*Rodman R. Linn*

**830** **High Altitude Water Cherenkov Observatory**
*Brenda L. Dingus*

**833** **Gamma-Ray Bursts and Gravitational Waves from Compact Mergers**
*Christopher L. Fryer*

**835** **Detecting Dark Matter with Cryogenic Liquids**
*Andrew Hime*

**837** **Dynamics of Quantum First Order Phase Transitions**
*Dima V. Mozyrsky*

**840** **Nonequilibrium Quantum Phase Transitions**
*Eli Ben-Naim*

**842** **Dissipation and Decoherence in Complex Many-Body Systems**
*Wojciech H. Zurek*

**844** **Strongly Coupled Fermion Systems: From Atomic Gases to Dark Matter**
*Sanjay Reddy*

**847** **Matter and Light**
*Katrin Heitmann*

**849** **Unconventional Superconductivity in Heavy Fermion Materials**
*Cristian D. Batista*

**851** **Disorder in Frustrated Systems**
*Avadh B. Saxena*

**853** **Measurement of Transverse Single-Spin Asymmetries of Neutral Pion and Eta Meson Production in Polarized p+p Collisions Using the PHENIX Detector at RHIC**
*Melynda L. Brooks*

**855** **Exploring the Expanding Universe and the Nature of Dark Energy**
*Katrin Heitmann*

**858** **Neutrino Physics and Its Applications**
*Joseph A. Carlson*

**860** **Non-equilibrium Phenomena in Physics, Biology and Computer Science**
*Michael Chertkov*

**862** **Theoretical/Computational Research on Particle Acceleration by Intense Laser Pulse**
*Brian J. Albright*

**864** **Single-Nanocrystal Photon-Correlation Studies of Carrier Multiplication**
*Victor I. Klimov*

**867** **Ultrafast Phenomena: Short-Pulse laser Interactions with Atoms and Molecules**
*Lee A. Collins*

**871** **Theoretical and Experimental Investigation of Relaxation Mechanisms in Ultra-low Field NMR for Magnetic Resonance Imaging**
*Michelle A. Espy*

**874** **Noise in Biochemical Networks: Rigorous Analysis with Field-Theoretic Tools**
*Ilya M. Nemenman*

**877** **Entanglement and Correlations in Complex Physical Systems**
*Wojciech H. Zurek*

**879** **Detecting the Highest Energy Gamma-Rays and Neutrinos to Determine the Origin of Cosmic Rays**
*Brenda L. Dingus*

**882** **Anti-Neutrino Oscillation and Cross Section Measurements at MiniBooNE**
*Geoffrey B. Mills*

**884** **Phase Transitions in Quantum Systems and Quantum Information**
*Wojciech H. Zurek*

**888** **The Dynamics of Dark Energy**
*Katrin Heitmann*

**891** **Strong Dynamics in Physics Beyond the Standard Model**
*Rajan Gupta*

**893** **Richtmyer-Meshkov Instability Studies**
*Katherine P. Prestridge*

## Technology

**895** **Construction and Use of Superluminal Emission Technology Demonstrators with Applications in Radar, Astrophysics, and Secure Communications**
*John Singleton*

**900** **Image Reconstruction with Time-Reversal Mirrors**
*Paul A. Johnson*

**905** **Terahertz Generation Harnessing the Two-Stream Instability**
*Kip A. Bishofberger*

910 **Efficient Structures for Low-Energy Acceleration of Light Ions**
*Sergey S. Kurennoy*

914 **Compact Millimeter Wave Spectrometer Based on a Channel Drop Filter**
*Lawrence M. Earley*

917 **Novel High Performance Terahertz Metamaterial Photonic Devices**
*John F. O'Hara*

920 **Efficient and Selective Photon Detection**
*Michael D. Di Rosa*

923 **Compact Solid State Tunable THz Source**
*Nathan A. Moody*

926 **Cerium-Doped Glass Scintillators**
*Markus P. Hehlen*

931 **Nano-Structured Foams for Hydrogen Storage**
*Erik P. Luther*

936 **Nano-Composite Scintillator for Neutron Capture Measurements**
*Ernst I. Esch*

940 **From Novel Principles to Novel Device Structures for High-Efficiency Generation of Solar Electricity**
*Victor I. Klimov*

945 **X, Gamma, Alpha : Ultra-High Resolution Spectroscopy**
*Michael W. Rabin*

951 **A Novel Approach to Manufacturing Ultra-Tall Carbon Nanotube Forests**
*Quanxi Jia*

955 **Optical, Electronic, and Magnetic Doping of ENABLE Grown Semiconducting Films**
*Mark A. Hoffbauer*

960 **Accuracy of Laser-Induced Breakdown Spectroscopy for Trace Detection**
*Roger C. Wiens; Geoffrey D. Reeves*

968 **Designing Intelligence into the Next Generation Wind Turbine**
*Francois M. Hemez*

972 **Chiral Metamaterials for Terahertz Frequencies**
*John F. O'Hara*

# Los Alamos National Laboratory: Science that Matters

by William Priedhorsky, LDRD Program Manager

A large fraction of taxpayer resources is dedicated to national security in its many forms. This is appropriate; as John Foster Dulles articulated (1957), "of all the tasks of government the most basic is to protect its citizens against violence." Only a secure nation can travel its sometimes-painful path towards a society based on liberty and justice.

A modest but critical component of the national security mission is research and development. Indeed, science and technology are arguably the nation's best option for advantage against our adversaries. As the National Science Board points out, "The scientific and technological advances that have led to our Nation's remarkable ability to create new industries and jobs, improve the standard of living for people, and provide sophisticated technology that ensures our national security can be traced back to the outcomes of basic research."

Los Alamos is proud of its history as the senior national laboratory in the U.S. Department of Energy (DOE) complex. At Los Alamos, we develop and apply science and technology to:

- Ensure the safety and reliability of U.S. nuclear deterrent,
- Reduce the threat of weapons of mass destruction, proliferation, and terrorism, and
- Solve national problems in defense, energy, environment, and infrastructure.

These missions inspire us to *anticipate, innovate, and deliver* to meet a broad range of national security challenges – ones with no previous solution, where new discoveries can lead to dramatic breakthroughs in both national security and drive the frontiers of science, technology, and engineering.

Our missions require both breadth and depth in science and technology. The complexity of our programs demands a span of excellence that crosses nearly every discipline in science. However, each of the DOE national security science laboratories has distinct areas of emphasis. Los Alamos, at the top level, emphasizes three areas of "Science that Matters" – science thrusts that are critical to solving current or future national security concerns:

- Information science and technology enabling predictive science,
- Experimental science focused on materials for the future, and
- The science of signatures of nuclear, biological, and chemical threats.

These interdependent thrusts support program focus areas that are as diverse as performance prediction within the weapons program, sustainable nuclear energy, and cybersecurity, space situational awareness, and persistent surveillance within Global Security. Our thrusts guide investments of resources, including institutional support, program development, strategic recruitment, and particularly laboratory-directed research and development.

With the support of Laboratory Directed Research and Development (LDRD) program, Los Alamos contributes towards its vision: to be the National Security Science Laboratory of choice, ready to take on whatever complex issue that the nation asks of us.

# Laboratory Directed Research and Development

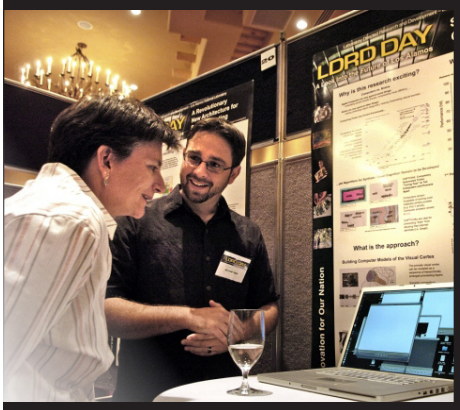

"...the Los Alamos LDRD program creates a free market for ideas that draws upon the bottom-up creativity of the Laboratory's best and brightest researchers."

The LDRD program is the most prestigious source of research and development funding at the Laboratory. The LDRD program follows a strategic guidance derived from the missions of DOE, the National Nuclear Security Administration, and the Laboratory. To execute that strategy, the Los Alamos LDRD program creates a free market for ideas that draws upon the bottom-up creativity of the Laboratory's best and brightest researchers. The combination of strategic guidance and free-market competition provides a continual stream of capabilities that position the Laboratory to accomplish its missions.

The LDRD program provides the Laboratory Director with the opportunity to strategically invest in forward-thinking, potentially high-payoff research that strengthens the Laboratory's capabilities for national problems. Funded with approximately 6.5% of the Laboratory's overall budget, the LDRD program makes it possible for the best and brightest researchers to pursue cutting-edge research and development. This in turn enables the Laboratory, to anticipate, innovate, and deliver world-class science, technology, and engineering.

## Program Structure

The LDRD program is organized into three program components with distinct institutional objectives: Directed Research (DR), flagship investments in mission solutions; Exploratory Research (ER), smaller projects that invest in people and skills; and Postdoctoral Research and Development (PRD), recruiting bright, qualified, early-career scientists and engineers. In FY09, the LDRD program funded 267 projects with a total budget of $127.5 million. These projects were selected through a rigorous and highly competitive peer-review process and are reviewed formally and informally throughout the fiscal year.

### Directed Research

The DR component makes long-range investments in multidisciplinary scientific projects in key competency or technology-development areas vital to LDRD's long-term ability to execute Laboratory missions. In FY09, LDRD funded 53 DR projects, which represents approximately 58% of the program's research funds. Directed Research projects are typically funded up to a maximum of $1.7M per year for three years.

The DR component is guided by the LDRD Strategic Investment Plan, which is in turn guided by eight Grand Challenges that define the advances in science and technology that are needed to address the Los Alamos mission. These challenges were originally set out in the Los Alamos National Security contract and refined in a Laboratory-wide workshops. In the 30 months since the Grand Challenges were first established, the world changed both in science and technology opportunities and missions.

To revitalize the Grand Challenges, the LDRD Program Director, Associate Directors and Principal Associate Director for Science, Technology and Engineering collaborated to develop a broad outline of the revised

Grand Challenges for FY10. Figure 1 shows how the new Grand Challenges align with the Laboratory's three "Science that Matters" thrusts.

## Exploratory Research

The ER component is focused on developing and maintaining technical staff competencies in key strategic disciplines that form the foundation of the Laboratory's readiness for future national missions. Largely focused on a single discipline, ER projects explore highly innovative ideas that underpin Laboratory programs. In FY09, LDRD funded 136 ER projects, which represents approximately 35% of the program's research funds. Exploratory Research projects are typically funded up to a maximum of $375K per year for three years.

Unlike DR proposals, division endorsements are not required for ER proposals; instead, this component of the LDRD program is operated as an open and competitive path for every staff member to pursue funding for his/her great idea. The ER component is a critical channel for purely bottom-up creativity at the Laboratory. Nonetheless, it is strongly driven by mission research and development needs via the definition of the ten research categories, and the assignment of investment between them. FY09 saw the start of a top-to-bottom reframing of the ER categories that will guide investment in FY11 and beyond.

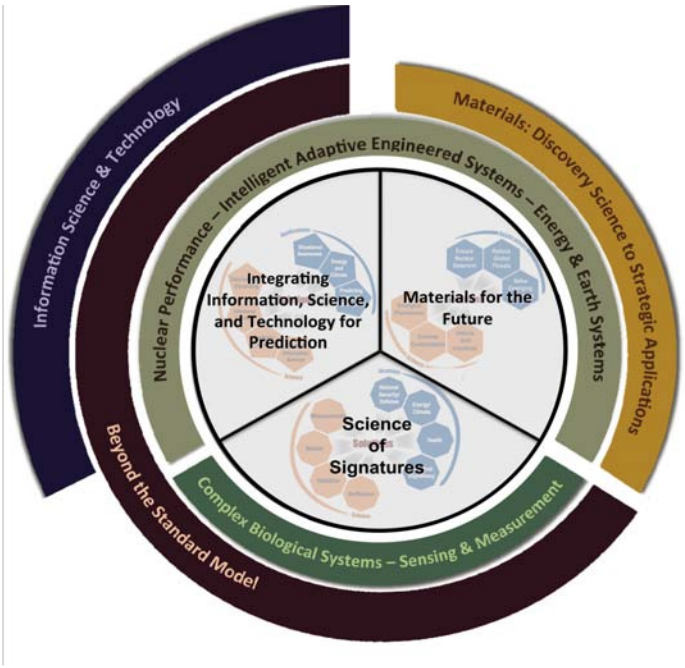


*Figure 1: The science and technology Grand Challenges that guide the LDRD program's investment in Directed Research are aligned with the Laboratory's three "Science that Matters" thrusts.*

| Directed Research Grand Challenges | Mission Impact |
|---|---|
| Beyond the Standard Model | Sensitive instrumentation and tools to manipulate massive data volumes, in support of national security missions |
| Materials: Discovery Science to Strategic Applications | Energy sources, efficiency and storage; sensing for threat reduction; materials underpinnings of stockpile security |
| Complex Biological Systems | Energy, national security, health and the environment |
| Information Science and Technology | Overarching capability supporting all Laboratory missions |
| Earth and Energy Systems | Energy and climate security |
| Nuclear Performance | Stockpile safety, surety and reliability |
| Sensing and Measurement Science for Global Security | Nuclear weapons of mass destruction, space situational awareness, global environmental treaty monitoring and emerging threats |
| Intelligent, Adaptive Engineered Systems | Systems-level solutions for all missions |

| Exploratory Research Technical Categories | Laboratory Capability |
|---|---|
| Nuclear Physics, Particle Physics, Astrophysics and Cosmology | Nuclear physics, astrophysics and cosmology |
| Materials Science | Materials |
| Earth and Environmental Sciences and Space Physics | Earth and space sciences |
| Chemistry and Chemical Sciences | Chemical sciences |
| Engineering and Engineering Sciences | Weapons science and engineering, advanced manufacturing, sensors, remote sensing and sensor systems |
| Computational, Information and Knowledge Sciences | Information and knowledge sciences, computer and computational sciences |
| High-Energy Density, Plasma and Fluid Physics | High-energy density plasmas and fluids |
| Biological Science, Biosecurity and Cognitive Sciences | Biosciences |
| Atomic, Optical and Quantum Physics | Chemical sciences |
| Energy Sciences, Technology and Engineering | Energy sciences, technology and engineering |

## FY09 LDRD Funding to DOE Missions

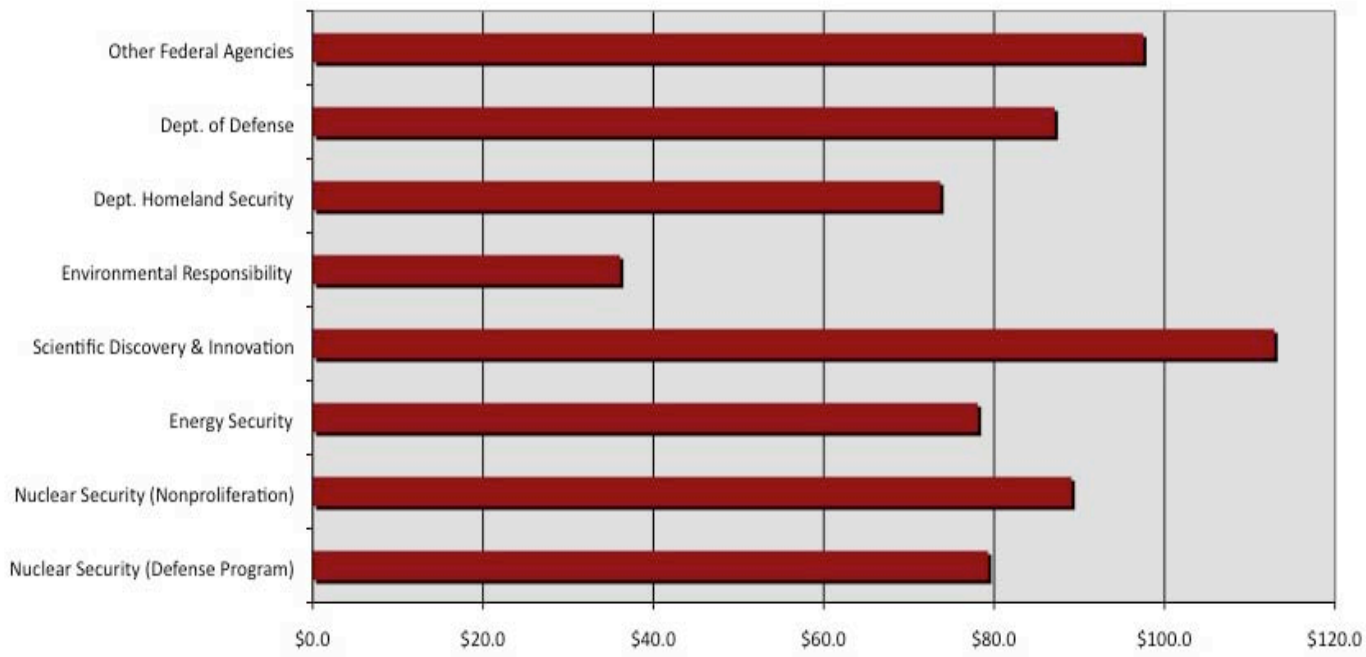

## Postdoctoral Research and Development

The PRD component of the program ensures the vitality of the Laboratory by recruiting early-career researchers. Through this investment, the LDRD program funds postdoctoral fellows to work for two years under the mentorship of PIs on highly innovative projects. The primary criterion for selection of LDRD-supported postdocs is the raw scientific and technical talent and performance of the candidate, with the exact specialty of the candidate a secondary factor. In FY09, LDRD funded 78 PRD projects, which represents 7% of the program's research funds. Postdoctoral Research and Development researchers are supported full-time for two years.

As the principal pipeline for new technical staff, the health of the postdoctoral program is of vital interest to the Laboratory. There is strong evidence that the postdoctoral program is excelling:

- Acceptance rate for Laboratory offers of postdoc appointments remains high, at 89%.
- Retention rate of postdocs who are converted to technical staff is high. Over the last ten years, these ex-post docs have shown an annual retention rate of 96.1%. The loss rate of 3.9% is extraordinary considering the mobility of their generation, and the challenges (fire, shutdown, security challenges, management transition) that the Laboratory has faced in that decade.
- Most Los Alamos postdocs successfully move to their next career step, whether inside or outside the Lab, at the end of their appointments. Only 4% leave their position without arranging another position, and many of these find an appointment within a few weeks.

Even more LDRD-funded postdocs are hired through DR and ER projects than directly through PRD appointments. Counting both avenues, the LDRD program supports about one-third of the Laboratory's 335 postdocs. Among the DOE labs, the LANL postdoc population is exceeded only by Lawrence Berkeley National Laboratory, which has a special relationship with the neighboring University of California campus. The Los Alamos population is 83% greater than the next DOE National Lab (Argonne), and more than twice as large as the next NNSA Laboratory (Sandia).

In addition to approximately 50 "Director's Postdocs," the LDRD program supports up to six distinguished postdoctoral fellows at a higher salary and for a three-year term. Distinguished postdoctoral fellow candidates typically show evidence of solving a major problem or providing a new approach or insight to a major problem; in other words, they show evidence of having a major impact in their research field. To recognize their role as future science and technology leaders, these appointments are named after some of the greatest leaders of the Laboratory's past. The distinguished postdoc positions were founded in the mid-1970's. Since that date, alumni of this program have gone on to become:

- Laboratory Fellows (11)
- Member of the National Academy
- Astronaut
- Los Alamos Center Director
- Department Chair (2)
- University dean
- University provost

**Chris Graves**, a current Seaborg Postdoc Fellow in the Condensed Matter and Thermal Physics Group in the Materials Physics and Applications Division is the 2009 winner of the Los Alamos Postdoctoral Publication Prize in Experimental Sciences.

Graves, nominated by his mentor, Jackie Kiplinger, was recognized for his major contribution to the manuscript "Organometallic Uranium (V)-Imido Halide Complexes: From Synthesis to Electronic Structure and Bonding," published in the **Journal of the American Chemical Society**.

This work has already made a significant impact. As of the date of submission of the nomination in March of 2009, the paper had already been cited a number of times, many that were from research groups outside the United States. The international impact of the contribution was further highlighted by Dr. Marinella Mazzanti (Director, Inorganic-*f*-Element Chemistry Group, CEA-Grenoble), who stated that Chris' contribution represented "a milestone in the history of organometallic actinide chemistry." Dr. David Clark (Director, G.T. Seaborg Institute, LANL), sums up the significance of the work in his supporting letter, citing the work as "truly ground-breaking."

## Program Reserve

Most LDRD investments are selected in a rigorous, multi-step peer-review process during the nine months preceding the new fiscal year. However, in a fast-changing world, there are needs that cannot wait until the next cycle of competition. The LDRD Program Office holds a reserve each year for these needs. This reserve is small on a program basis, but allowed the opportunity to make modest investments that address new opportunities. In FY09, the reserve budget was $3M.

The top priority for the reserve is feasibility studies: short projects aimed at a key proof-of-principle, which open the door to either external or more substantial LDRD funding in the out years. Reserve is held foremost to exploit opportunity, rather than fix problems, and the expectation is that reserve projects will be the first step in a chain that leads to bigger things.

Reserve decisions are guided by strategic priorities articulated by Division Leaders, Associate Directors, and more senior management. They are also informed by the just-concluded competitive cycle, in which selection panels sometimes identify ideas that are exciting but just not mature enough for a full-scale investment.

Past reserve projects have had a significant impact. In FY08, we initiated a set of projects that made possible the initial scientific exploitation of Roadrunner, still the world's faster computer. In FY09, reserve opened the door for a new set of initiatives in energy security and allowed an accelerated start for the new Intelligent Adaptive Engineered Systems Grand Challenge. These feasibility studies have been successful in moving immature ideas to the competitive level.

### Roadrunner: The World's Fastest Computer

On May 26, 2008, the Roadrunner supercomputer achieved more than a thousand trillion operations per second, or one sustained petaFLOPS, becoming number one on the TOP500 list of supercomputers. Built by IBM with funding from the NNSA for Los Alamos National Laboratory, Roadrunner is a "hybrid supercomputer," integrating a new Cell-based processor designed and built by IBM with a traditional microprocessor supplied by Advanced Micro Devices. Coupled with programs designed to utilize its unprecedented performance, Roadrunner will foster scientific discovery in many fields, ranging from physical sciences to biology and medicine, and it will provide a petaFLOPS-scale scientific computing capability for the nation's weapons program.

LDRD projects have played a major role in the initial exploitation of Roadrunner. For example, a 2008 Reserve project titled "Saturation of Backward Stimulated Scattering of Laser in The Collisional Regime," supported the migration of the VPIC particle-in-cell simulation code, a best-in-class plasma kinetic modeling code, to the Cell chip used by Roadrunner. (VPIC is a state-of-the-art, fully relativistic, explicit, charge-conserving, electromagnetic, particle-in-cell kinetic plasma modeling code developed at LANL.) Extensive testing and analysis was done on Roadrunner during the stabilization/open science phase and this work led to advances in the stability and usability of the platform for applications beyond the laser-plasma interaction (LIP) project.

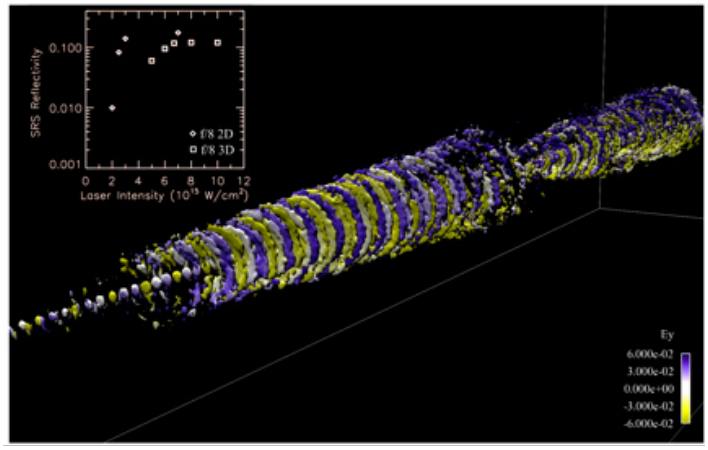


*3D VPIC simulations of stimulated Raman scattering in a laser speckle.*

In a 2009 ER project titled "Breakthroughs in Magnetic Reconnection Enabled by Petaflop Scale Computing," Yin is studying 3D VPIC simulations of magnetic reconnection performed on Roadrunner. From two-dimensional

## Project Selections

The Los Alamos LDRD program operates as a free market for ideas driven by Laboratory strategy: Senior Laboratory leadership set science and technology priorities, then open an LDRD competition for ideas across the breadth of the Laboratory. Proposals are rigorously reviewed by panels drawn from Laboratory's intellectual leaders. Conflict of interest is carefully regulated. Evaluation criteria include innovation and creativity, potential scientific impact, viability of the research approach, qualifications of the team and leadership, and potential impact on strategically important issues for the Laboratory. The selection processes are modeled on best practices established by the National Science Foundation (NSF) and National Institutes of Health (NIH).

To guarantee fairness and transparency, and to ensure that the strongest proposals are funded, the selection panels include line managers and technical staff drawn from the full range of technical divisions.

## Annual Project Appraisals

In FY09, the LDRD Program Office conducted an appraisal of every ongoing project it intended to fund in the next fiscal year. The primary objective is to assess progress and provide peer input to help PIs maintain the highest quality of work. The appraisals also help the LDRD Program Office monitor and manage the program portfolio. In addition to formal project appraisals, which are conducted annually, the LDRD Program Director and Deputy Program Director meets informally with PIs in their labs at least once a year to discuss their projects. The purpose of these one-on-one meetings is to give PIs individualized assistance and to determine what the LDRD Program Office can do to positively impact the success of the project. Each DR project is also assigned a Program Development Mentor to assist the transition of LDRD successes to mission.

Continuing DR projects are appraised every year of the life of the project, beginning with a short review the first year, followed by an intense appraisal midway though year two and ending with a follow-up review with program development mentors in the third year. The second-year review is open to all Laboratory staff and leaders. Four project appraisers – two internal and two external – are nominated by the PI and approved by the LDRD Program Director.

Written appraisals, held in the LDRD archives, address: (1) Brief summary of accomplishments; (2) Assessment of quality of science and technology, relevance to Laboratory and national missions and the degree to which the project may establish or sustain a position of scientific leadership for the Laboratory; and (3) Recommendations by the committee for changes in the scope or approach of the project. The criteria for the most important point – number (2) above – are derived from criteria developed by the National Academy of Science to assess all federally sponsored research.

Continuing ER projects are appraised in their first and second years. The LDRD Deputy Program Director collaborates with the technical divisions to conduct project appraisals. PIs are now required to submit self-assessment to the LDRD Program Office addressing the following points: introduction to the problem and goals of the project; background and significance of the work in terms of impact of the work; methods developed during the course of the project; results and accomplishments; and future work for the upcoming year and/or efforts to develop new funding.

Once the PI appraisal inputs are complete, the LDRD Program Office forwards the presentations to the respective division leadership for a formal appraisal. The projects are appraised according to the Federal criteria of quality, performance, leadership, and relevance.

### FY09 DR Project Appraisal Highlights

**Carrier Multiplication in Nanoscale Semiconductors for High-Efficiency, Generation-III Photovoltaics**

**PI: Victor Klimov, Chemistry Division**

**Objective:** Study the basic science of the formation of multiple nanosized semiconductor particles and to determine the feasibility of exploitation of this effect in photovoltaic (PV) devices.

*"It is the unanimous opinion of the members of the review committee that this is a high-quality research team whose research productivity and impact has been outstanding and promises to continue at this level for the remainder of the LDRD/DR project. Because of their sustained level of high-quality research, the researchers involved in this project are currently recognized among the world as leaders in semiconductor nanocrystal research."*

**Review Committee:**
Daniel Gamelin, University of Washington
Anvar Zakhidov, University of Texas, Dallas
Tom Picraux, Los Alamos National Laboratory
Darryl Smith, Los Alamos National Laboratory

**Ultrafast Nanoscale XUV Photoelectron Spectroscopy**

**PI: George Rodriguez, Center for Integrated Nanotechnologies**

**Objective:** Establish a transformational capability combining angle-resolved photoemission spectoscopy (ARPES) with high time and spatial resolution to explore the electronic structure, emergent properties and dynamics of complex materials such as *f*-electron systems, unconventional superconductors or nanostructures.

*"Given the short time of the project, great technical progress has been achieved in this LDRD with the construction of a unique ultrafast photoemission setup and first measured experiment traces. If full energy and momentum resolution is demonstrated soon, this setup will constitute the most technically advanced setup for ultrafast ARPES worldwide. The team should be commended for their ambitions approach...which places them at the leading edge in a quickly evolving field of research."*

**Review Committee:**
Robert Kaindl, Lawrence Berkeley National Laboratory
Tom Miller, University of Illinois Urbana-Champaign
Jonathan Workman, Los Alamos National Laboratory
Richard Martin, Los Alamos National Laboratory

## FY09 ER Project Appraisal Highlight

**High Altitude Water Cherenkov Observatory**

**PI: Brenda Dingus, Physics Division**

**Objective:** Los Alamos researchers have developed a new technology to view large portions of the overhead sky for emission from very-high-energy gamma rays. The next step in this development is to build the High Altitude Water Cherenkov (HAWC) observatory, which is based on the design of the Milagro observatory located at Los Alamos National Laboratory. The project aims to develop the scientific case for the HAWC observatory through analysis of the Milagro data as well as data from NASA's GLAST gamma-ray observatory. The work impacts the sensng and measurement missions of the Laboratory.

*"This last year, as a result of this LDRD, Brenda Dingus produced three highly recognized peer reviewed publications and was an invited speaker at five conferences around the world. The work included analysis of Milagro data, leading to the detection of TeV gamma rays where the Fermi Observatory sees GeV Pulsars. The source of TeV gamma-rays is different from GeV: Fermi sees pulsars, Milagro sees Pulsar Wind Nebulae; HAWC will measure the (TeV) morphology and spectra. As US co-spokesperson and project manager for HAWC, Brenda Dingus has helped form a strong international collaboration for HAWC.*

*This LDRD maintains LANL's leadership by applying new knowledge from Milagro TeV and Fermi GeV observatories to justify next generation observatories , e.g. HAWC, and optimizing the analysis of Milagro, the predecessor to HAWC, to demonstrate the capabilities of HAWC."*

This project appraisal was conducted by David Schmidt, Deputy Group Leader of the Applied Modern Physics Group.

## Mission Relevance

The LDRD Program Office treats mission relevance as one of the most important criteria in the evaluation of a potential LDRD project. Mission impact is considered carefully in project selection. Later, the mission impact of funded projects is tracked annually through the data sheet process. Because of the basic science and engineering nature of most LDRD projects, the work often proves to be relevant to numerous missions and agencies. In the chart below, the sum of the total LDRD investment in DOE missions is significantly greater than the annual LDRD budget because LDRD investment in a single project may be counted as relevant to more than one mission area.

Our turbulence studies provide compelling examples of research that has broad-reaching relevance across many mission areas and sponsor interests. Turbulence is a major component of missions that range from renewable energy to nuclear weapons. For example, turbulence is a critical component of understanding how wind interacts with turbine blades, both individually and in groups, supporting towers, and the surrounding topography. Turbulence is also important for understanding how ocean currents mix and interact with landmasses, crucial aspects of studying climate and climate change. Understanding turbulence and how to computationally model turbulence is central for understanding vortexes that form around airframes, how oil trapping salt domes form, and how plasmas behave in fusion reactors, nuclear weapons, and supernovae.

### Turbulence by Design

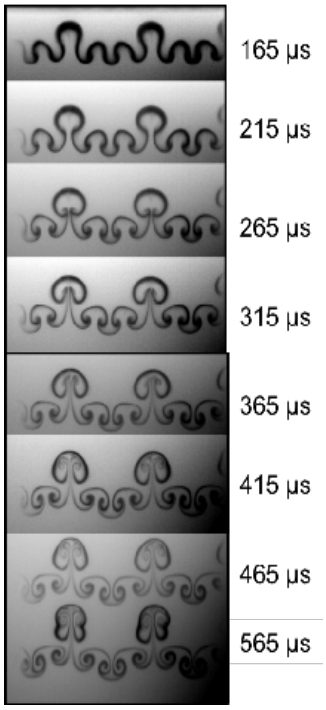


Malcolm Andrews leads a DR project to determine the extent to which certain starting conditions can be used to predict and design turbulent transport/material mixing. The broad impact of this research includes the ability to design ICF targets for net energy gain, determination of early-time astrophysical processes and a better understanding of climate and ocean flow dynamics.

The figure at left shows the results of a computational model that was run on the LANL Roadrunner supercomputer, in which flow instabilities lead to the formation of complex eddies. Such models provide predictive capabilities for missions from climate modeling to high-energy plasmas.

## Mission Impact

**LD**RD delivers capabilities and explores mission solutions for all Los Alamos missions: Nuclear Security, Global Security, Energy Security, and Scientific Discovery. In some cases these lead to clearly identified follow-on projects. In part, this can be attributed to the program development mentors who help transition these projects from LDRD to external funding.

Putting a quantitative metric on mission impact is difficult. The obvious metric –follow-on funding – omits qualitative benefits such as new ideas and approaches that feed into ongoing work. Counting dollars is also imperfect because, although LDRD is part of what enables new mission solutions, the Laboratory brings other assets to bear, including facilities, ideas, and personnel from a range of programs.

Nonetheless, if we look at admittedly rough numbers, we find that the LDRD projects that concluded in FY09 played an important part on the path to $100M of externally funded R&D. Even this is not the end of the story, because follow-on projects often do not begin immediately upon the conclusion of the LDRD. A study carried out in FY08 showed that follow-on projects over a five-year period totaled approximately twice the original LDRD investment. The path from the LDRD program to mission impact is clearly demonstrated by follow-on projects from sponsors that range, inside DOE, from the nuclear weapons program to nonproliferation programs, applied energy programs, and the Office of Science, and more broadly, across a range of sponsors that include DoD (DARPA, ONR, and DTRA), DHS and DNDO, NIH and CDC, classified agencies, and a range of industrial partners. The capabilities sustained by these external sponsors feed back once again to enable the Laboratory's execution of NNSA missions.

It is impossible to list every successful LDRD transition to external funding, so we highlight just a few:

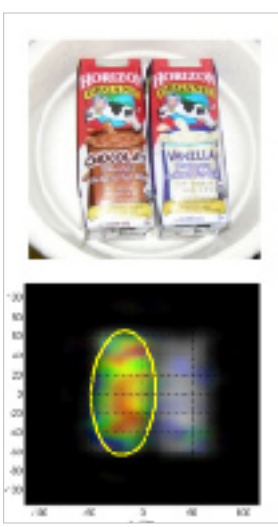

The project "*Ultra-Low Field Resonant Absorption Magnetic Resonance Imaging* of Neural Activity" investigated new techniques for imaging the brain and its activity. The same techniques can be used to discriminate benign liquids from liquid explosives, which could make all of our lives simpler at the airport. The Department of Homeland Security has invested $9M so far to further develop this R&D 100 –winning technology.

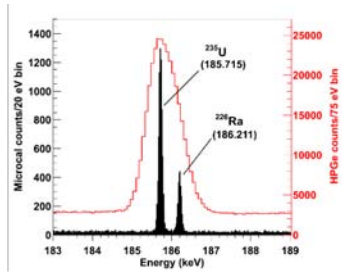


*Microcalorimeter spectrometry:* Investment in superconducting microcalorimeters led to a new generation of gamma-ray spectrometers with unprecedented resolving power. A spectrum from our LDRD-supported instrument (black in the graphic above) clearly resolves the signature peak of highly enriched uranium from the common background material Ra-226. The previous gold standard for gamma-ray detection, high-purity germanium (red), cannot distinguish the nuclear threat from the common background. Our technology has been adopted for further development by DHS/ Domestic Nuclear Detection Office and NNSA/NA-22.

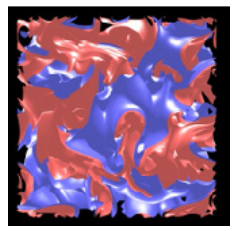

Investment in "*Rapid Iterative Detection Using Smart Pathogen Signatures*" allowed us drive forward a palette of technologies required for smart, autonomous biothreat detection, including biochemical assays, microfluidics for chemical processing, and miniaturized optical sensors to read out the biochemistry. Success in these areas led to more than $10M of follow-on from DHS, DTRA, and bioenergy funding sources.

An ER project focused on *fluid turbulence* in violently accelerated environments, with a view towards supernova explosions. The figure shows the turbulent environment, in which a heavy fluid mixes with a light one. An accompanying reserve project helped move the codes onto the Roadrunner supercomputer. Because of the benefit of these tools to stockpile stewardship, follow-on work has been supported by Campaign 4.

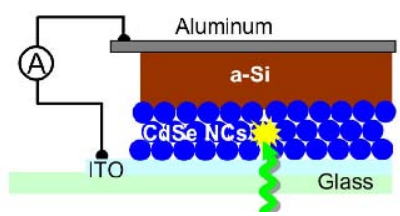


*Nanoparticle carrier multiplication for solar energy*: We invested ER and DR in the fundamental physics of carrier multiplication – that is, moving towards more efficient solar cells by exploiting the propensity of certain tiny particles to produce more than one electron when struck by a solar photon. Besides great scientific success, these projects led to a DOE Energy Frontier Research Center at Los Alamos for Advanced Solar Photophysics, and industrial support for this technology from Sharp Corporation. This was one of two EFRCs at Los Alamos, both of which were made possible by LDRD support.

## LDRD Program Impacts

The LDRD program is a key resource for addressing the long-term science and technology goals of the Laboratory, as well as for enhancing the scientific capabilities of Laboratory staff. Through careful investment of LDRD funds, the Laboratory attracts programmatic resources, recruits and retains excellent scientists and engineers, and prepares to meet evolving national needs. The impacts of the LDRD program are particularly evident in the number of publications, patents, and disclosures resulting from LDRD-funded research; the number of postdoctoral candidates supported by the program; and the number of awards received by LDRD researchers.

### Publications

LDRD produces a large volume of high-quality scientific contributions relative to its portion of the Laboratory's budget. The numerous publications made possible with funding from LDRD program help the Laboratory maintain a strong presence and scientific reputation in the broader scientific community. In calendar year 2009, LDRD researchers generated 427 peer-reviewed publications, accounting for 24% of the Laboratory's total.

### Patents and Disclosures

A strong indication of the cutting-edge nature of the research funded by LDRD is the contribution the program makes to the intellectual property of the Laboratory. LDRD projects consistently generate at least one quarter of the patents awarded to the Laboratory. In FY09, LDRD-supported research resulted in 14 patents, accounting for 23% of the Laboratory's patents, and 41 disclosures, which accounted for 38% of all Laboratory's disclosures.

### Postdoctoral Support

In an increasingly competitive job market, the Laboratory must foster an environment that attracts the best talent so that it may be applied to solving national security problems. LDRD remains an important vehicle for recruiting the brightest researchers to the Laboratory, where they become innovators and scientific leaders. In FY09, LDRD supported 305 postdocs (in-full or in-part), accounting for 64% of the Laboratory's postdocs. In FY09, the Laboratory converted 37 postdocs converted to full-time technical staff members; LDRD funded 43% of those conversions.

### Collaborations

External collaborations are often critical to a successful LDRD project. Formal collaborations between LDRD PIs and researchers at other national laboratories, academia, and industry enable to access world-leading facilities and knowledge. Such collaborations also enable LDRD PIs to be active and prominent members of the broad scientific and technical communities. Some of the best LDRD research teams are involve external collaborations that complement Los Alamos' capabilities and expertise. In addition, LDRD collaborations create strong relationships that are valuable for the Laboratory's pipeline for recruiting scientific and engineering personnel.

| Calendar Year 2009 Publications | | |
|---|---|---|
| LANL refereed publications | LDRD-supported refereed publications | % due to LDRD |
| 1780 | 427 | 24% |

| FY09 Patents and Disclosures | | |
|---|---|---|
| LANL patents | LDRD-supported patents | % due to LDRD |
| 57 | 14 | 23% |
| LANL disclosures | LDRD-supported disclosures | % due to LDRD |
| 107 | 41 | 38% |

| FY09 Postdoctoral Support | | |
|---|---|---|
| LANL postdocs | LDRD-supported postdocs | % due to LDRD |
| 477 | 305 | 64% |
| LANL postdoc conversions | LDRD-supported conversions | % due to LDRD |
| 37 | 16 | 43% |

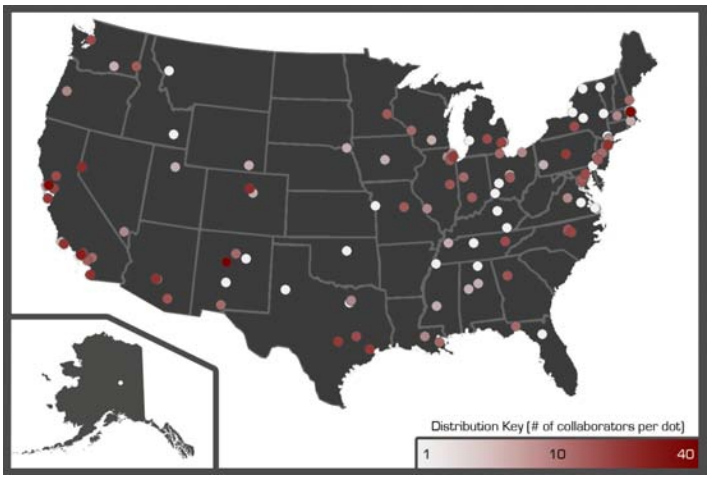


*LDRD researchers establish external collaborations with national laboratories, academia and industry across the U.S. and beyond. Darker dots indicate a higher concentration of collaborations.*

## Program Highlights

America is currently facing energy, security and environmental challenges that, in their scope and complexity, are perhaps unparalleled in the nation's history. In that context, the national laboratories are being called on to provide the scientific breakthroughs that will be needed to develop long-term solutions. At Los Alamos, those breakthroughs are often recognized as the result of early LDRD investment. With support from the LDRD program, Los Alamos researchers are pursuing high-risk, big-payoff ideas that win the attention of the broader scientific community; this is most strongly evidenced by the many awards, journal covers and media attention garnered by LDRD researchers annually.

### R&D 100 Awards - Work Rooted in LDRD

**Gentle MRI may help void airline liquids restrictions**

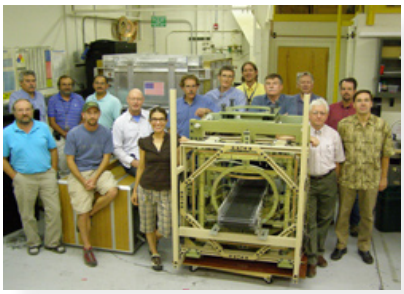

*Los Alamos MagViz Team*

Sometimes, solutions occur as the result of intersecting technologies. MagViz, a 2009 R&D 100 Award winner from Los Alamos, scans liquid items such as those travelers wish to carry on aircraft and assesses them for threat materials. It operates in much the same way as a conventional x-ray conveyor belt in the airport security line. Unlike conventional MRI, however, low-power magnetic fields are used to measure the relaxation times of protons exposed to the field. It can gain useful information because the detectors have been re-designed from the ground up using technology developed by experts in superconducting technology. These detectors, called superconducting quantum interference devices, or SQUIDS, can glean chemical information from comparatively low-power signals. While the technology may soon free airline travelers from carry-on restrictions, it also frees useful MRI from bulky magnets, and potentially opening up new materials science and imaging applications.

**Process pulls $CO_2$ from fossil fuel plants**

*SIMTECHE $CO_2$ Capture Process*

Fossil fuels supply 85% of the energy used in the U.S. and roughly 90% of the greenhouse gases. Facing pressure to reduce carbon dioxide emissions, power utilities and energy companies seek systems for $CO_2$ control. The SIMTECHE $CO_2$ Capture Process from Los Alamos, and SIMTECHE, Redding, Calif., provides low-cost $CO_2$ separation and compression capable of removing 65% to 90% or more of the $CO_2$ emitted by fossil fuel power plants and other operations.

Based on a reversible reaction of $CO_2$ and cold water, the process captures $CO_2$, regenerates it at elevated pressures, and delivers it at pipeline pressures for commercial use or sequestration. The process pulls $CO_2$ out of a flowing mixture of gases and traps individual $CO_2$ molecules within tiny molecular cages made of water. The resulting ice-like compound is a crystalline solid called $CO_2$ hydrate. Once separated from the gas stream, the $CO_2$ hydrate crystals can be decomposed to regenerate $CO_2$ gas at elevated pressures for sequestration or sale on the emerging $CO_2$ market.

**Artificial retina: Restoring sight to the blind**

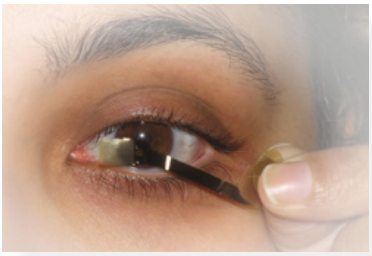

*Los Alamos LDRD PIs took part in collaborative research to develop a retinal prosthesis.*

Researchers at five national laboratories, four universities, and an industrial partner have developed the Artificial Retina, a retinal prosthesis that can be used to treat age-related macular degeneration and inherited retinal disorders such as retinitis pigmentosa. The device uses application-specific integrated circuits to transform digital images from a camera into electrical signals in the eye that the brain uses to create a visual image. The system features a video camera and transmitter mounted in sunglasses, a visual processing unit, and a battery pack to power the device that is worn on the belt. The retinal implant receives a signal via wireless transmission, encodes it into specific patterns of stimulation pulses that are conducted through a cable to the electrode array that stimulates the retina. The brain perceives the patterns of light spots corresponding to the stimulated electrodes. In clinical trials, patients with vision loss were able to identify objects, increase mobility and detect movement.

The role of the Los Alamos team has been to develop and apply techniques for functional imaging of retinal activation using fast intrinsic optical signals and microelectrode arrays, to characterize information encoding and processing by the retina, and to validate the efficacy of electrical stimulation. The Los Alamos team also develops advanced concepts for device design, manufacturing, and stimulation protocols for prosthetic systems.

**Computer chips in 3-D**

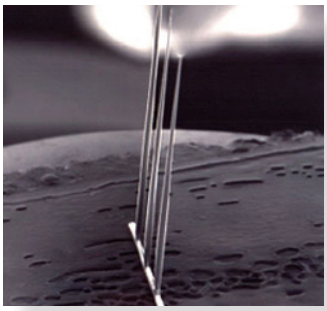

*LASONIX promises to revolutionize electronics fabrication.*

Historically, semiconductors have been fabricated using photolithographic and related technologies, which are predominantly oriented to two dimensions. Lasonix, a new technology from Los Alamos, can be used to grow and fabricate semiconductor, metallic, and insulating structures in three dimensions while controlling their composition, doping levels, and crystal structure. The concept is based on a Laser-Weave in which inorganic fibers and textile are synthesized by focusing lasers onto a target in a chamber in the presence of certain gases. An adjustable nozzle sends in gases, or precursors—such as silicon, gallium arsenide, and silicon carbide—into the chamber either one at a time or in combination. The gases decompose at the laser-heated spots to produce solid fiber deposits. When the focused laser spots are drawn backward, the fibers follow, and long fibers are grown. Through the addition of trace quantities of other materials, the fibers can be doped to produce diodes, transistors, and conductive wires. By changing the gas composition, different materials can be grown on top of each other, forming heterojunctions between semiconductor layers.

The technology, which also reduces the potential for heat by creating conductive features within 3-D fibers of silicon or other semiconductors, should help enable the creation of high-density electronic packages and other complex 3-D structures.

## Early Career Awards

**Office of Science Early Career Research Program**

Five Los Alamos scientists were awarded five-year research grants under the American Reinvestment and Recovery Act through the U.S. Department of Energy's prestigious Office of Science Early Career Research Program. Two of the award recipients are LDRD researchers. The award-winning LDRD projects are:

**Nathan G. McDowell -** *An Integrated Theory on the Mechanisms of Vegetation Survival and Mortality During Drought*

McDowell's goal is to develop and test a unified theory of vegetation mortality and survival during drought. He came to Los Alamos as a Director's Postdoctoral Fellow in 2003 and became a staff scientist in 2004. McDowell serves on advisory committees for the National Science Foundation, DOE, and the Laboratory. He is an associate editor for two international journals and has testified before Congress regarding DOE's climate change research.

**Evgenya Smirnova -** *Advancing Our Understanding of Photonic Band Gap Structures for Accelerators*

Smirnova's objective is to advance Photonic Band Gap (PBG) accelerator technology for use in the next generation of particle accelerators for high-energy physics. Superconducting PBG accelerator technology could also deliver extremely intense, short-wavelength laser radiation needed for free-electron lasers. Smirnova came to Los Alamos from the Massachusetts Institute of Technology as a visiting student in 2003. In 2005 she joined the High-Power Electrodynamics Group as a Director's Postdoctoral Fellow and later became a Laboratory staff member in 2007. Smirnova received the American Physical Society's Outstanding Doctoral Thesis in Beam Physics Award and is a recipient of several Laboratory awards.

**2009 Presidential Early Career Award**

Los Alamos physicist Ivan Vitev received a prestigious Presidential Early Career Award for Scientists and Engineers (PECASE). The honor is the highest bestowed by the U.S. government to outstanding scientists early in their careers. Vitev joined the Laboratory in 2004 as a J. Robert Oppenheimer Postdoctoral Fellow, the most distinguished postdoctoral appointment at the laboratory. Vitev is widely recognized for his expertise in quantum chromodynamics, the theory of strong interactions, and in energy loss of high-energy particles in hot, dense matter. His scientific work has been used to determine properties of the quark-gluon plasma, a new state of matter discovered in 2000 that is similar to what many scientists believe conditions of the universe were like immediately after the Big Bang. Vitev's research was funded by LDRD and DOE's Office of Science. As a PECASE recipient, he will receive up to five years' funding from the Office of Science to advance his research.

## Journal Cover Highlights

**Malcolm Boshier** and colleagues developed a new experimental technique for manipulating atomic Bose-Einstein condensates (BECs). A BEC is a gas of around 1 million atoms cooled to a temperature of less than 1 microKelvin above absolute zero, at which point it can behave as a single quantum object. BECs are a promising technology for making new types of sensors, measuring instruments, and quantum computers. They are also important for studying fundamental physical phenomena such as quantum phase transitions, which is one objective of the research.

Boshier is considering two possible applications of this technique. The first is painting waveguide circuits for matter waves that could be used to fabricate interferometric sensors. The second is creating controllable disordered potentials for quantum emulation, exploiting the existing ability to control the shape, depth, and position of the wells in a potential landscape, load a BEC into its ground state, and then change the potential with time in any way chosen. The research is featured in a research highlight in the May 14 issue of ***Nature***. The Los Alamos LDRD program funded Boshier's work.

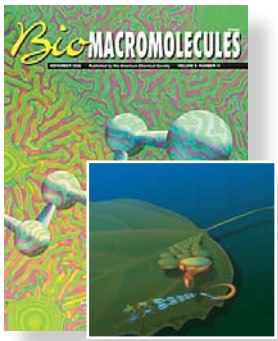


**Paul Langan** and colleagues are studying Lignocellulosic biomass - an inedible fibrous material derived from plant cell walls. Its main cellulose component is an abundant potential source of natural sugars that could be used for producing biofuels, such as ethanol and butanol. However, energy-efficient and cost-effective processes for breaking up the plant cell wall and releasing these sugars are needed. To address this problem, Langan is focusing on understanding the interactions between atoms that hold cellulose together. His work published in the November 2008 edition of ***Biomacromolecules*** was supported by the Los Alamos LDRD program.

## Book Highlights

**Paul Johnson** has an invited entry in the annual, **McGraw Hill Yearbook of Science and Technology**, 10th edition. The Yearbook is an encyclopedia of current research topics worldwide that are deemed significant. The entry describes application of time reversal to imaging and acoustic/seismic source complexity in solids and in Earth. The idea is to focus sound from sound sources located on a sample surface, in a 3-dimensional solid using time reversal, point by point, and look for wave scatterers (e.g., a crack). Scattered wave data are collected on the sample surface, time reversed and run backwards through a numerical model with the same mechanical properties as the sample. The Los Alamos LDRD program supported Johnson's research.

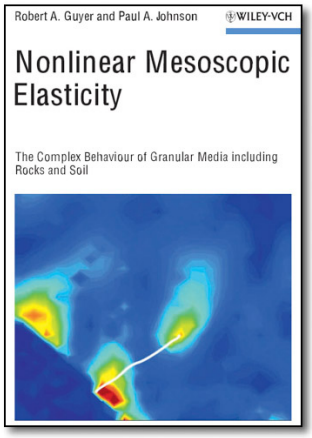


Johnson also co-authored a book titled **Nonlinear Mesoscopic Elasticity**. The book describes nonlinear behavior primarily in Earth materials—rock and unconsolidated materials such as sand. The book also includes some industrial materials that show how universal the nonlinear behaviors of granular media are. Johnson and coauthor Robert Guyer (University of Massachusetts - Amherst) discuss topical, practical uses for an improved understanding of the complex behavior of rocks and other materials. The book, which is a culmination of many years of research in this field by Johnson and Guyer, presents new tools and models in a systematic and thorough way. The DOE Office of Basic Energy Sciences and LDRD program also supported Johnson's work.

## LDRD Day 2009 - A Look Into the Future of Los Alamos

The Los Alamos LDRD Program Office hosted its first-ever LDRD Day in September 2009 in Santa Fe, NM. With 41 poster presentations and more than 200 attendees, the event was a huge success.

Members of the public--students, venture capitalists, business owners, and curious citizens--purused the posters and then voted on the ones they enjoyed the most. With subject matter ranging from technologies to improve

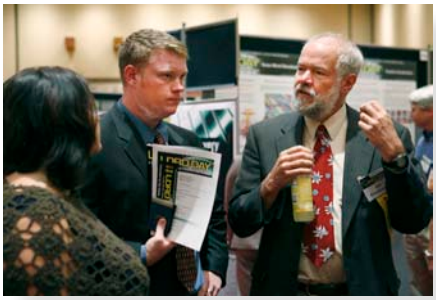

solar panels to the use of lasers for accelerating hydrogen atoms to speeds high enough to zap brain tumors, viewers had a lot of material from which to choose. In the end, Malcolm Andrews of Computer, Computational and Statistical Sciences and colleagues won the Best Poster Award for his poster describing how a clearer understanding of turbulence can help explain climate change or lead to the creation of better engines.

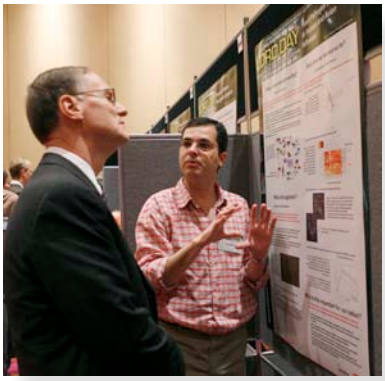

In reference to the LDRD PIs who presented posters, a reporter from the Santa Fe New Mexican wrote, “They were some of the Los Alamos National Laboratory scientists at the cutting edge of new discoveries that could change our world.”

# Chemistry & Material Sciences

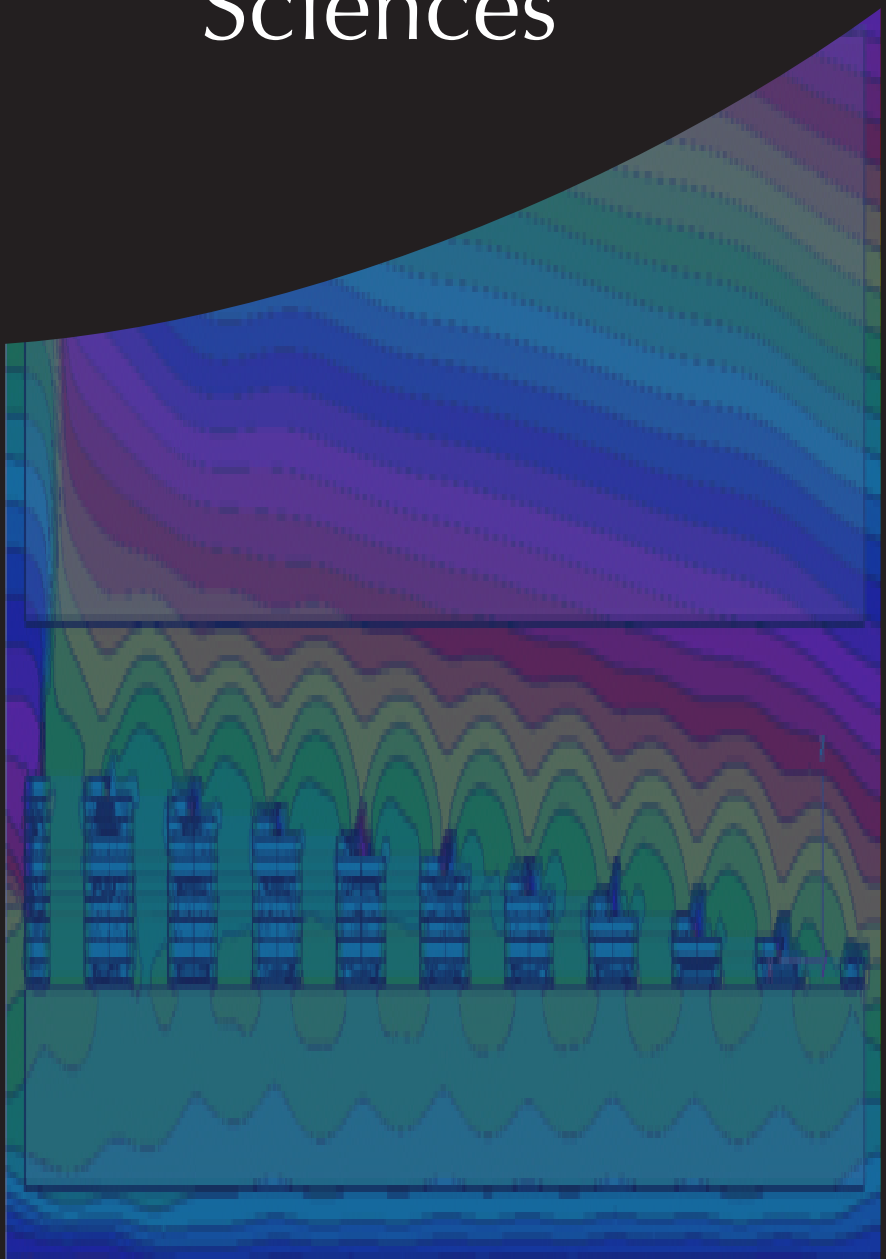

LABORATORY DIRECTED RESEARCH AND DEVELOPMENT

# Hot Spot Physics and Chemistry in Energetic Materials Initiation

*Dana M. Dattelbaum*
20080015DR

## Introduction

The overwhelming consensus in the high explosive community is that the generation of hot spots (localized regions of high temperature and pressure from which ignition occurs) is essential to the initiation and detonation properties of most condensed phase high explosives, whether conventional (e.g. plastic bonded explosive (PBX) 9501), insensitive (e.g. PBX 9502) or non-ideal (e.g. ammonium nitrate fuel oil - ANFO). The potential origins of hot spots are numerous, and include dynamic pore collapse, plastic shear band formation, or reflections from other *in-situ* interfaces. Despite many decades of research into the physics of high explosives, at present we only have a very basic understanding of the broad mechanisms underlying shock-induced hot spot generation and ignition, hot spot interaction and reaction wave spread leading to HE initiation and detonation. Consequently, all current high explosive models treat hot-spot physics empirically; these models have poor predictive capabilities, requiring substantial model calibration to experimental results to account for material or geometry variability. A new generation of predictive reactive flow models for all types of HE can only come from a fundamental understanding of mesoscale hot-spot physics. The methodology used in this project is to obtain an understanding of hot spot phenomena through the study of prototypical energetic materials – nitromethane, PETN, AN, RDX etc. - seeded with defect sources that are well controlled and tractable, towards understanding their influence on *initiation* (mechanisms, thresholds, etc.), Figure 1.

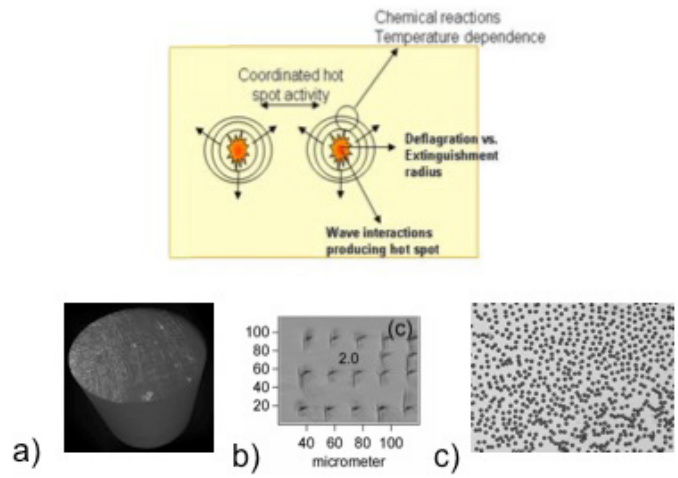


*Figure 1. Schematic illustration of two interacting hot spots in a shocked energetic material; We are starting with defect free homogeneous explosives (RDX in a), and introducing controlled heterogeneities by laser.*

## Benefit to National Security Missions

The goal of the work is to advance our understanding of hot spots to a level that will translate into the ability to design explosives with improved reproducibility, performance, and surety, as well as provide a credibly predictive set of tools for simulating explosives behavior. The research described supports National and Laboratory missions in stockpile stewardship, DOE-DoD partnerships, and emerging thrusts in threat reduction and homeland security.

## Progress

Fabrication of Hot Spots: Fabrication and characterization of controlled heterogeneities in explosive samples are essential to interpreting hot spot effects on initiation. Hot spots have been introduced into homogeneous (defect-free) energetic materials in two ways: a) controlled placement of voids in explosive crystals, and b) random placement of well-defined

particles into gelled liquid explosives. Controlled Hot Spots: A femtosecond laser micromachining apparatus has been developed and used to successfully machine void features *internally* (100 micron depth, Figure 1) on the nanometer and micron length scale into single crystals of the explosives HMX, PETN, and RDX - a major advancement considering the inherent fragility of the molecular crystals. [1] The relevant parameters of laser power, pulse length, and repetition rate have been determined, and the team is currently perfecting the capability to produce line features exceeding 1 mm, Figure 2, complementing micro-scale mechanical machining techniques developed in parallel. Random Hot Spots: Randomly-seeded hot spots offer insights into hot spot conditions more readily observed in real explosive formations. Gelled nitromethane samples with glass (silica) beads have been prepared using guar gum in the range 1.5-2.0 wt%. 1.75 wt% Guar was selected for gelling nitromethane explosive samples containing 6 wt% solid silica beads of discrete diameters ~ 1-4, 40, and 100 microns. Optical and scanning electron microscopy methods, as well as x-ray radiography, have been used to characterize bead diameters and agglomeration in gelled solutions.

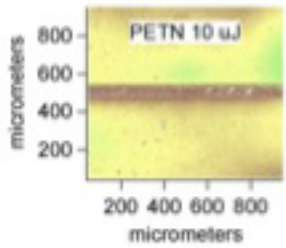


*Figure 2. Large-scale channel feature machined into PETN using fs-laser pulses at 10µJ. Void features are shown in Figure 1.*

**Atomistic to Molecular (Å to nm)**
*Molecular Modeling*

Simulations have been performed on a shocked RDX crystal with the shock propagating along the [100] direction (*up* = 1 km/s; P= 9.7 GPa). Nanoscale shear bands nucleate homogeneously due to the crystal anisotropy, and give rise to high local temperatures behind the shock front [2]. Temperatures associated with the nucleated shear bands at 5 nm and 140 nm behind the front have been statistically extracted, with temperatures reaching 700-800K along shear bands. Additional simulations on RDX at this length scale have examined dynamic pore collapse. In the pore collapse simulations, a nominally-50 nm pore is introduced into the RDX crystal. Stress localization is observable at the pore boundary as the pore collapses and jets. Even on the molecular scale, the salient features of hot spot formation from pore collapse are consistent with meso- and large-scale experimental observables.

**Molecular to Multi-molecular (10's to 100's of nm)**
*Molecular Dynamics and Atomistic Shock-Induced Hot-spot Modeling*

Non-reactive Molecular Dynamics (on RDX) and reactive atomistic (using AB model kinetics 2AB → A2+B2) simulations on prototypical energetic materials have been performed to examine the effects of single and multiple shock induced void collapse on shock hydrodynamics, temperature generation and reaction. In the MD simulations (collapsing void in RDX, above), high temperatures are generated by void jetting. Intense plastic deformation in the vicinity of the void also gives rise to non-trivial local heating. In the reactive atomistic modeling, similar phenomena were observed, although less plastic heating was observed because of the low melting point of the model material. The larger length scale accessible to the model reactive materials allowed us to study how two voids seeded into a sea of AB molecules could interact. For the case where two voids are in close proximity (~3 diameters), the curvature in the shock front resulting from the first void collapse could result in accelerated burning at the second void, depending on the geometric arrangement. At larger separations (~10 diameters), such features dissipated.

*Laser-Driven Shock Wave Experiments and µm-scale Temperature Diagnostics*

Laser-driven shock wave experiments have been conducted at our laser shock facility on liquid and gelled NM, without and with hot spots. Laser shock generation and dynamic ellipsometry (UDE) on (neat) liquid nitromethane samples have been conducted to provide a baseline comparison to gas-gun data (unreacted Hugoniot, and reaction on-set). UDE of shocked neat NM reveals that shocks below 7.9 GPa result in unreacted Hugoniot loci in good agreement with gas gun data. Above 7.9 GPa, changes in the UDE spectra may be indicative of reaction onset. Femtosecond stimulated Raman Scattering (FSRS), femtosecond coherent anti-Stokes and Stokes Raman scattering (CARS/CSRS) and related methods have been tested for sensitivity in single shot Stokes/anti-Stokes configurations. The attainment of temperature diagnostics is important for diagnosing hot spot formation, and could provide insights into deflagration (burn) front velocities under shock conditions.

**Interfacial/Meso-scale (1-100s of microns)**
*Gas gun-driven Shock Initiation of HE Crystals with Engineered Voids*

Gas gun driven shock experiments on PETN crystals have shown that the short run-distance initiation threshold for

homogeneous-PETN exceeds 18 GPa. The next step is to determine the initiation threshold in the absence of voids, then introduce a void channel, resolving the wave velocities concomitant with its collapse. 100 micron diameter half-pipe-shaped channels have been introduced into PETN for the upcoming experiments.

*Gas gun-driven Shock Initiation of Heterogenous-NM*

Gas gun-driven plate impact experiments have been performed on gelled nitromethane with 6 wt% size-selected silica beads. Pop-plots (run distance to detonation vs. input shock pressure, Figure 3) for gelled-NM containing two discrete silica particle sizes, and rough silica have been determined. The data reveal that in all cases, the addition of silica has a sensitizing effect (e.g. lowering initiation thresholds); however, different behaviors are observed for small (1-4 µm) vs. large (40 µm) beads at 6 wt% loading. Through the use of embedded particle velocity gauges, a transition from homogeneous initiation behavior, characteristic of neat liquid explosives, to a heterogeneous-like initiation behavior commonly observed in plastic-bonded explosives was observed in the same 40 µm bead materials depending on shock input pressure. The large diameters and interbead spacing on the order of ~100 µm may reveal an upper limit on critical hot spot size relative to necessary hot spot interaction time scales under shock loading.

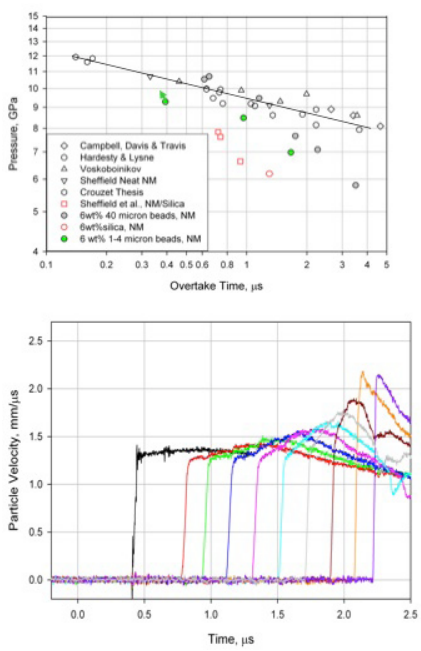


*Figure 3. (top) Pop-plots derived from gas gun-drive initiation experiments on heterogeneous-NM materials. (btm) Example wave profiles of initiation of gelled-NM containing 1-4 µm beads shocked at 7 GPa.*

*Meso-scale Multi-Material Hot-Spot Simulation: Initiation and detonation*

A mathematical framework to capture the physics of hot spot criticality (ignition vs. quenching) is being developed based on energy deposited into a condensed phase explosive via hot-spots. Cases being examined currently include spatial and temporal length scales of the power deposition such that hot spots evolve according to a balance between compressible and chemical interactions or a balance between thermal conduction and chemical interactions. Further, simulations of hot-spot induced shock initiation and detonation are conducted through the state-of-the-art, multi-material, parallel, adaptive mesh refinement computational simulation capability MultiMat in AMRITA. Preliminary calculations on quasi-2D experiments using simplified Tait equations of state and pressure dependent reaction rates have been conducted to evaluate the computational approach. Simulations of heterogenous-NM rate-sticks experiments, where the detonation failure diameter is observed to be a sensitive function of the diameter and spacing of glass beads have also been conducted. High-resolution simulations of shock-induced hot-spot generation and evolution are also being conducted with the LANL code NOBEL. For a 10 GPa shock in NM, the bulk temperature was determined to be ~ 1000K with hot spot temperatures reaching 1500K, as a result of interacting shock waves between the silica beads.

## Future Work

The overarching goal of the remainder of the LDRD project is to bring to fruition the convergence of theoretical developments, simulation insights, and experimental observables from plate-impact, chemiluminescence and laser-shock experiments, and refine theoretical approaches using experimental insights on the smaller length scales (e.g. improved EOS, temperatures measured under hot spot generation on micron length scale, resolved wave velocities near hot spots).

## Conclusion

The successful accomplishment of this project will significantly advance us toward a robust, rapid-response predictive capability for multi-agency national security needs relating to energetic materials, including developing quantitative understanding of the safety and initiation of stockpile explosive materials, assisting DoD in the development of combat safe munitions, and predicting the threat characteristics of improvised and exotic energetic materials.

## References


1. McGrane, S. D., A. Grieco, K. J. Ramos, D. E. Hooks, and D. S. Moore. Femtosecond micromachining of internal voids in high explosive crystals for studies of hot spot initiation. 2009. Journal of Applied Physics. 105 (7): 073505.

2. Cawkwell, M. J., K. J. Ramos, T. D. Sewell, and D. E. Hooks. Homogeneous Dislocation Nucleation and Anomalous Hardening in Cyclotrimethylene Trinitramine. To appear in Physical Review B.

3. Perry, W. L., T. D. Sewell, B. B. Glover, and D. M. Dattelbaum. Electromagnetically-induced localized ignition in secondary high explosives. 2008. Journal of Applied Physics. 104: 094906.


## Publications


Cawkwell, M. J., T. D. Sewell, L. Zheng, and D. L. Thompson. Shock-induced shear bands in an energetic molecular crystal: Application of shock-front absorbing boundary conditions to molecular dynamics simulations. 2008. Physical Review B. 78 (1): 014107.

Menikoff, R., and M. Shaw. Review of the Forest Fire Model for High Explosives," Combustion Theory and Modelling. 2008. Combustion Theory and Modelling. 12 (3): 569.
Perry, W. L., T. D. Sewell, B. B. Glover, and D. M. Dattelbaum. Electromagnetically-induced localized ignition in secondary high explosives. 2008. Journal of Applied Physics. 104: 094906.

Stevens, L. L., N. Velisavljevic, D. E. Hooks, and D. M. Dattelbaum. Hydrostatic compression curve for triamino-trinitrobenzene (TATB) determined to 13.0 GPa with powder X-ray diffraction. 2008. Pyrotechics, Explosives, and Propellants. 33 (4): 286.

Stevens, L. L., N. Velisavljevic, D. E. Hooks, and D. M. Dattelbaum. The high pressure phase behavior and compressibility of 2,4,6-trinitrotoluene (TNT). 2008. Applied Physics Letters. 93: 081912.

# Design, Synthesis, and Theory of Molecular Scintillators

*Rico E. Del Sesto*
20080037DR

## Introduction

This project involves the development of new scintillator materials for large-scale, high resolution, real time radiation detection. These materials will be hybrid organic-inorganic materials in order to achieve the performance of the individual components used in scintillators today. Studies on existing materials over the last several decades have provided some understanding of the process of scintillation, but there are still some missing pieces which are much less well understood. Using what we know now about the interaction with incident radiation with a material, we can design materials using synthetic chemistry to incorporate functional units which optimize the known processes of scintillation. Designing these functional units, along with characterizing the resulting materials and theoretical predictions of the response of a material to radiation, will allow us to gain an in-depth understanding of the entire process including the missing pieces. From the knowledge gained in this project, we can continue to optimize the materials for their response to radiation. Additionally, with the materials being organic in nature, they can be processed and scaled up as typical plastic scintillators are now, but with the added inorganic components which provide the energy resolution necessary for efficient isotope identification.

## Benefit to National Security Missions

This project will support the DOE mission of Threat of Weapons of Mass Destruction through enhancement of current capabilities for detecting nuclear threats. Existing scintillators lack characteristics to fully address radiation detector needs. Specifically, it is necessary to have large-volume, low-cost, high-performance materials to satisfy radiation detector requirements.

## Progress

The synthesis of molecular scintillators focuses on the development of high-Z clusters with either organic dyes or lanthanide (Ln) centers incorporated as the luminescent centers. Previously synthesized Ln-doped polyoxotungstate clusters has yielded liquid and polymeric materials which respond to x-ray ionizing radiation, and exhibit light output within an order of magnitude relative to plastic scintillator, primarily as Eu(III) and Tb(III)-based materials. Since all of the lanthanides except for Ce(III) and Eu(II) exhibit lifetimes on the order of milliseconds, these clusters are not practical in terms of detector materials. The Ce(III) and Eu(II) analogs could not be made due to their incompatibility with the polyoxotungstates, yielding non-luminescent Ce(IV)- or long-lifetime Eu(III)-clusters. The polyoxotungstate clusters therefore tend to be incompatible with Ce(III), Eu(II), and many other desired luminescent organic dyes. Therefore, the development of these materials are no longer being pursued, but simply result in demonstrating our proof-of concept that energy transfer can occur in molecular scintillator materials following ionizing irradiation of high-Z clusters, resulting in visible light output. In terms of pursuing materials that can be practical as detectors, we are developing other high-Z materials including bismuth oxide clusters, in which both Ce(III) or organic dyes can be incorporated. We have successfully synthesized bismuth clusters as mixed oxide-organic ligand compounds, with both Ce(III) and Eu(III) incorporated into the cluster. Under x-ray ionizing radiation, they exhibit a response at about 10% of plastic scintillator, Figure 1. However, these materials as-synthesized are typically insoluble in organic solvents, resulting in lower-than-expected light outputs due to scattering. Due to the organic and inorganic nature of these compounds, the ligands attached to the clusters can be readily modified to dramatically improve solubility in both organic solvents and plastics. Additionally, these materials are inherently difficult to characterize structurally (single crystal diffractometry), and thus the exact structure and incorporation of lanthanides into the bismuth clusters is not entirely clear. Therefore, we are currently modifying synthetic conditions to improve crystallinity, which will allow us to obtain structural information critical to

understanding the optical and scintillation mechanisms in these materials. Additionally, as the clusters are ligated by organic groups, we will also attempt to add organic luminescent dyes to the clusters as an alternative to the Ce(III) incorporation. Other new materials are also being pursued which contain other metal oxide clusters, including tungsten and lanthanides, with coordinated organic dyes. Recent work suggests that hydrothermal synthesis can encourage these framework structures, which will yield high-Z clusters in ordered networks with organic dyes providing the luminescence for detection.

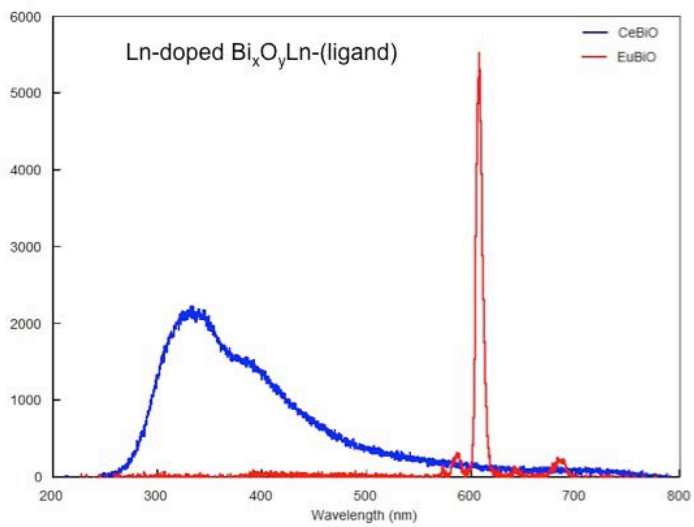


*Figure 1. Radioluminescence of [BixOyL]n- clusters doped with $Eu_3$+ (red) and $Ce_3$+ (blue).*

Electron energy loss measurements using an electron microscope to study the energy deposition mechanism have been performed on some of the materials. Initial results on the polyoxotungstate clusters synthesized at LANL and measured at ASU indicate that a major component of the energy loss is via coupling to a plasmon or plasmon-like resonance. This indicates that the coupling to the excitation mechanism is responsible for a significant fraction of the energy loss. This supports the underlying case for high-Z molecular scintillators for gamma-ray spectroscopy. We are currently performing energy loss measurements as a function of cluster size and as compared to analogous molecular species to determine at which size regimes this mechanism emerges, in order to help guide future materials development.

Time Dependent Density Functional Theory (TDDFT) calculations of the electronic structure of several dyes and a number of W and Mo based POMs have been calculated. The predicted optical absorption and emission properties are in good agreement with our experimental observations. Additionally, the vibrational spectra are also in good agreement with experimental data, suggesting that we now have a good handle on predicting properties of some of the desired materials, as demonstrated with the Ce(IV)-polyoxometalate infrared and raman spectra shown in Figure 2. However, as we move towards more complex systems which are not closed-shell systems, e.g. those that have unpaired f-electrons as with many Ln(III) materials, predictions will be more difficult, and we are currently improving on existing models to handle this. We have also developed effective dielectric models for calculation of excitation transition rates and energy loss functions, and rate equations for the calculation of TSL (thermally stimulated luminescence), and PL (photo-luminescence) characteristics in the scintillators, and using the results from the first principles TDDFT calculations to describe the dielectric response of specific scintillator materials. We have calculated random phase approximation (RPA) dielectric function results based on the Penn model of semiconductors to investigate the effect of an energy gap in the scintillator electronic excitation spectra and calculated RPA dielectric function results based on a finite cluster tight-binding model to investigate the effect of the discrete scintillator electronic excitation spectra. Results show that as the energy gap is increased, the plasmon broadens and moves to higher energy. Our phenomenological model of rate equations for energy transfer, specifically developed for luminescence properties, goes beyond standard approximations of nearest-neighbor excitation transfer only. In particular, it incorporates the important back transfer from traps to acceptors, which naturally accounts for afterglow. This model is being benchmarked against experiments on the time evolution of photoluminescence ranging from the nanoseconds to microseconds. Recently we have measured energy transfer from a simple high-Z compound, $CeBr_3$(ligand)4, to an organic coumarin dye, and the effect on the luminescence lifetimes as a result of the energy transfer. This represents the simplest example of the high-Z cluster/dye composite materials that are of interest for this project. The models are being optimized to understand this energy transfer and luminescence decay, and will then be applied to more complex systems.

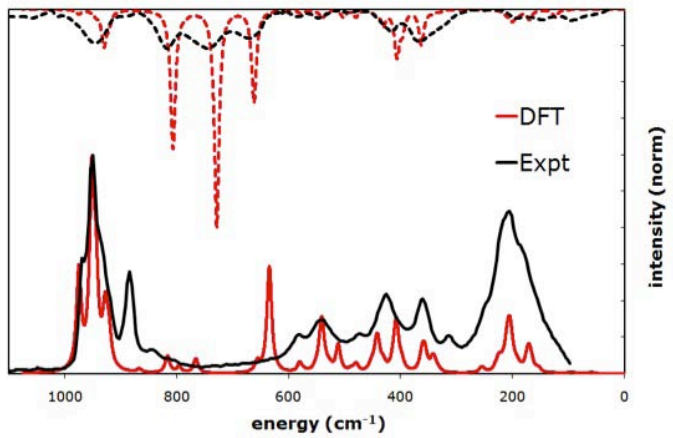


*Figure 2. Experimental (black) vs. calculated (red) spectra for $Na_8$[Ce(W5O18)2] and [Ce(W5O18)2]8-, respectively, in Infrared (top) and Raman (bottom).*

## Future Work

The development of new materials for radiation detection is the focus of this project. Therefore, we will continue to synthesize new materials that allow us to experimentally study the properties of materials under ionizing radiation. The relationship of this scintillation mechanism as a function of the structural features of the material will provide the critical information to advance materials with high scintillation efficiency. Additionally, understanding these mechanisms through theoretical models will continue to advance our understanding of materials in response to radiation across many time and length scales. The materials development will continue along the path of high-Z bismuth clusters with incorporated Ce(III) and organic luminescent sites. Modifications to these structures will be performed to yield new compounds that are more facile to characterize structurally, and allow us to readily modify the clusters to render them soluble in organic solvents and polymers/plastics. We will also continue to explore new materials via alternative synthetic methods, such as under hydrothermal conditions. We will continue the detailed study and modeling of the charge thermalization process of a high-energy charged particle in a scintillator, and transport of ionization and excitations within the scintillator. The integration of the theoretical models with the experimental characterization will continue to develop in order to understand the scintillator functions, as a result of the structural and materials properties of these new molecular scintillators.

## Conclusion

The design of new materials using a functionally compartmentalized approach has provided us with a unique set of materials with which to study and model the electronic and optical properties when exposed to both non-ionizing and ionizing radiation. As the models and experimental data allow us to understand the contributions of these components to the overall scintillation mechanisms in a material, we will be able to begin optimization of the processes involved in scintillation through further component design, as well as materials design specific for various applications. The project will continue along the path of utilizing high-Z cluster materials with both organic and Ce(III) luminescent sites, which we are becoming more familiar with, and which will provide the critical information buried in the scintillation process of conversion of high-energy charged particles to a number of photons in the visible region for detection. This program is a result of a laboratory-wide collaboration of synthetic, theoretical and physical chemists, condensed matter theorists, and nuclear physicists. The fundamental understanding of these materials will allow us to expand our capabilities from developing new radiation detection materials to the design of application specific materials for numerous applications.

## Publications

Ortiz-Acosta, D., R. Del Sesto, A. Gaunt, M. Lucero, G. Purdy, B. Bennett, C. Macomber, B. Scott, R. Muenchausen, T. McCleskey, R. Martin, R. Gilbertson , and E. McKigney . Ionic Liquid Polyoxometalates as Light Emitting Materials. Presented at 214th Electrochemical Society Meeting: Molten Salts XVI. (Honolulu, HI, 12-17 Oct 2008).

# Ultrafast Nanoscale XUV Photoelectron Spectroscopy

*George Rodriguez*
20080097DR

## Introduction

This project exploits the coherent properties of short wavelength light and ultrafast short pulse laser technology to convert femtosecond (10-15 sec) visible light pulses to the extreme ultraviolet (XUV) soft x-ray portion of the electromagnetic spectrum. Previously only accessible at large synchrotron light facilities, a scaled-down table-top version is now possible through advances in the physics of short pulse laser light-matter interaction for light conversion into the XUV regime. Armed with such a light source, the extremely short wavelength and coherence properties of the light allows imaging and time resolutions that approach the intrinsic spatial and time scales of matter, nanometer (10-9 m) scale in space and femtosecond scale in time. We use this unique light source to probe material core level electronic structure and dynamics using a technique called angle-resolved photoelectron spectroscopy (ARPES). In XUV ARPES, extreme ultraviolet light is used to force electrons to be ejected from the material that are subsequently analyzed for their kinetic energy content and angular spatial distribution, providing a detailed signature of material bulk electronic structure and dynamics. Insight into quantum effects and collective particle behavior are thereby provided for complex materials and nanotechnology engineered devices whose emergent properties are critical for understanding function. This project is applying these methods to materials relevant to Laboratory science in actinides, superconductivity, energy conversion, nuclear waste, and sensor technologies.

## Benefit to National Security Missions

The primary scientific motivation underpinning this project is a desire to advance our understanding of the electronic structure and dynamics of complex emergent materials at the nanoscale. The proposed cross-disciplinary studies will contribute to multiple DOE and NNSA missions including Energy Security, Weapons Physics, Threat Reduction and Nanotechnology.

## Progress

In FY09, major instrumentation achievements include: (a) Demonstration of XUV harmonic generation in Ar gas with an estimated total flux of greater than 1010 photons per sec. Harmonics with photon energies out to 50 eV have been observed. The beam is spatially and temporally coherent with a beam spatial divergence of less than 0.5 mrad, an individual pulse width less than 10 fs, and a pulse repetition rate of 10 kHz; (b) Construction and testing of the angle-resolved ultra high vacuum system and for electron photoemission experiments in time-domain was also completed. The spectra of correlated compounds have been measured, including $UO_2$ with monochromatized light from the harmonic generator. (c) In addition, design, purchase and mounting of the closed-cycle Helium refrigerator with appropriate sample holders for temperature-dependent experiments is also complete; (d) finally, the construction of the quick load sample transport system to accommodate temperature-dependent studies and enlarge sample throughput was installed.

Experiments in FY09 consisted of testing major instrument components after system integration using several surrogate materials that included metals (Pt and Cu), a semiconductor (GaAs), and the correlated f-electron material $UO_2$. The photoelectron spectrum of $UO_2$ (exhibiting a sharp 5-f electron peak close to the Fermi level) was taken with the full polychromatic beam, Figure 1, revealing harmonic orders in our XUV beam up to 42 eV, spaced by 3.1 eV, with a bandwidth of approximately 1 eV per harmonic. Upon installation of the monochromator, selection of a single harmonic (monochromatized beam) was then used to make angle-integrated measurements of freshly cleaved $UO_2$ sample using the 21st harmonic (32.5 eV). Figure 2 shows the results of those measurements compared with similar data obtained at 34 eV from a synchrotron source (Figure 2 inset) indicating that the laser harmonic-based XUV beam can be successfully used

to map out electronic band structure similar to that obtained at synchrotron, but with the added benefit and capability of femtosecond time-resolved dynamic s in electronic structure dynamics. These early results in $UO_2$ are promising, as this correlated 5f electron system is of particular interest to our program. $UO_2$ is a Mott insulator with possible exotic states expected to be found in the gap at low temperatures. Also, the exact gap size in this system is of interest for both theory/modeling and experiments. However, all previous attempts to measure the electronic structure below a temperature of 150K have failed because of material charging effects caused by creation of positively charged carriers in the sample when studied with synchrotron based XUV sources. Thus far, our laser based XUV harmonic system does not seem to cause the $UO_2$ sample to suffer the same consequence (possibly due to the extremely short pulse nature of our source), thereby permitting first time measurements on $UO_2$ band structure near the Fermi edge at temperatures across the transition (30K) where the material is expected to go to anti-ferromagnetic phase state.

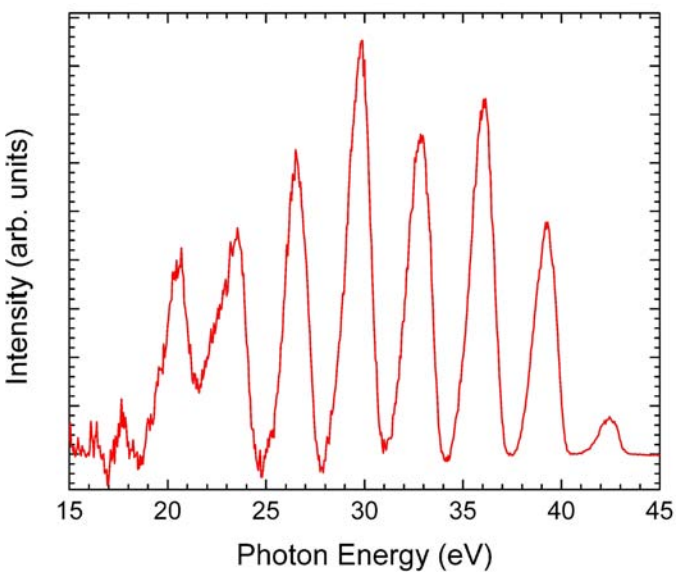


*Figure 1. Output photoelectron spectrum produced from uranium dioxide ($UO_2$) surface after illumination of the sample using the beam from table-top ultrafast laser based coherent XUV light source. The XUV beam is produced by nonlinear high harmonic generation in Ar gas that is ionized by an energetic ultrafast optical pulse in the near-infrared at 1.5 eV (800 nm). The plot shows that harmonic generated XUV photons out to at least 42 eV are generated. XUV light beyond 100 eV is expected for similar condition using He gas instead of Ar.*

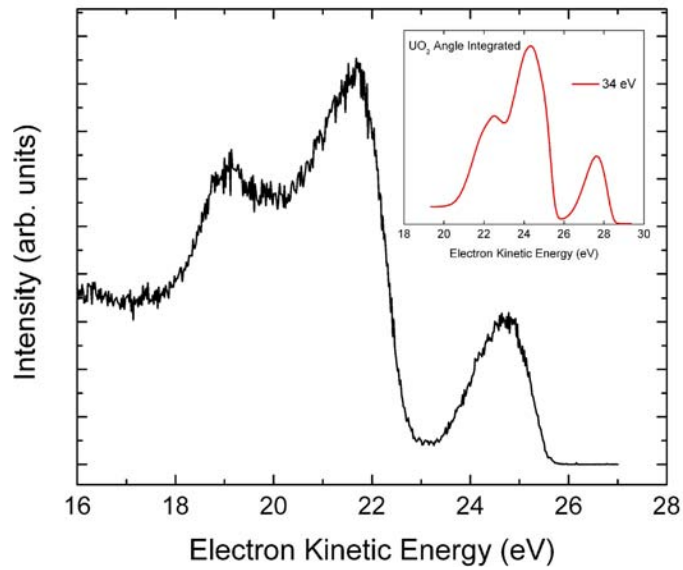


*Figure 2. Graph demonstrating the comparable performance of the table-top laser based XUV light source (black line) to synchrotron based data (red line in inset) on a sample of uranium oxide ($UO_2$). Photoelectron kinetic energy spectrum of $UO_2$ at room temperature was recorded using a single wavelength selected harmonic with an energy of 32 eV. For comparison, the inset shows the same spectrum of $UO_2$ recorded using a synchrotron source at 34 eV.*

In order to exploit the unique ultrafast time resolution capability of our XUV ARPES station, a femtosecond optical-pump XUV-probe beam line experimental configuration was assembled. In Figure 3 a diagram our experimental layout is displayed showing the various components in our facility along with the pump-probe beam lines. The pump is an ultrafast visible laser pulse that is used to excite and perturb the electronic states of the sample, and then with the time-delayed XUV probe pulse, the sample is interrogated using ARPES. The energy exchange dynamics of the ensemble of populated and unpopulated are then extracted by varying the delay between pump and probe while monitoring the ARPES signal. Time domain optical-pump XUV-probe ARPES should allow us to pump/populate the 5f states above Fermi level in $UO_2$ , measure the gap directly, and the electronic carrier recombination dynamics in the system. These experiments are in progress and are the first of their kind to be performed on any f-electron based material. In addition to optical-pump XUV-probe time-resolved ARPES experiments, the project is also supporting complementary ultrafast time resolved optical pump-terahertz (THz) probe and optical pump-probe experiments across the transition temperature in $UO_2$ to study photoexcited carrier conductivity (THz probe) and relaxation (optical probe) dynamics. These experiments aid in understanding the nature of carrier conduction in various phases and coupling mechanisms that may play

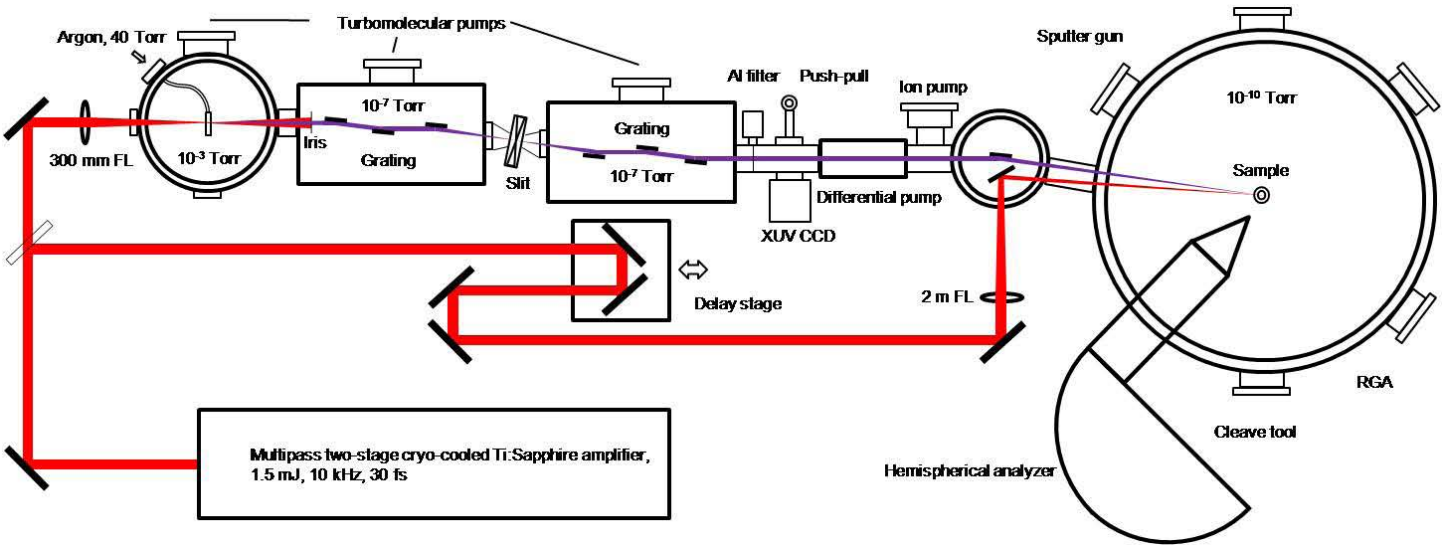


*Figure 3. Experimental layout showing the major components of the table-top ultrafast laser based coherent XUV light source and photoelectron (ARPES) spectrometer. The ultrafast coherent XUV beam is produced by nonlinear high harmonic generation in an Ar gas cell that is subsequently tuned using a pulse time preserving monochromator before injection into the sample chamber. The figure also shows a second visible pump beam line in air that is used for our optical-pump XUV-probe ultrafast ARPES experiments.*

an important role in determining localized versus itinerant carrier behavior.

For the theory effort, calculations relating the electronic spectral function A(k,w) to the ARPES measurements are in progress. Full description of the time-dependent behavior must include excitation and relaxation processes under a nonequilibrium many-body theory, which is a scientific challenge for complex materials with strong correlation and strong coupling. However, when the time scale to release the energy from one subsystem (e.g., electron) to another (e.g., phonon) is much longer than the kinetics within each individual subsystem, one can effectively model the electron properties with a two-temperature model. In this simplification, the time dependence is encoded in the temperature relaxation between these two subsystems. We thus transform the challenge to the one of calculating the effective electronic temperature dependence of the spectral function A(k,w,Te). Within the two temperature model, we have considered two examples (i) the evolution of spectral function in high-Tc superconductors due to electron-boson coupling, which tracks the change of dip-hump structure; (ii) the evolution of spectral density in the delta-Pu within the local density approximation and many-body approach, the dynamical mean-field theory (LDA+DMFT), which shows the "incoherent" atomic states of 5f electrons. Application of this approach to the UO2 experiments is next.

## Future Work

Future work under this project will focus on obtaining time resolved ARPES measurements on the f-electron system $UO_2$ at room temperature and across the anti-ferromagnetic phase transition (30K). Carrier dynamics across the 5f electron band gap will be probed for discovery of possibly new excited sates and their relaxation channels back to ground state. After $UO_2$, there are number of proposed material systems for time-resolved ARPES studies that include heavy fermion systems such as unconventional superconductors ($CeIn_3$), polaron dynamics in multiferroics and manganites, or even 1-D nanostructures such as semiconductor based Ge nanowires where quantum confinement effects alter Fermi edge band structure.

The set of experiments under consideration are aimed demonstrating the novel capability for ultrafast and ultrasmall scale metrology. Ultrafast techniques provide the means to investigate dynamic non-equilibrium phenomena approaching the fundamental timescales of electronic and atomic motion, offering a unique snap-shot into the properties of cooperative condensed matter and material systems. The high photon energy of the ultrafast XUV beam provides access to states (i.e, f-electron systems) that were previously only accessible with synchrotron light and without time resolution. Coupling the light source to a photoelectron spectrometer allows one to study photoexcited carrier relaxation dynamics with energy and momentum resolution probing electrons of deeply bound, or from previously unfilled orbitals, and from many body interactions that affect their transport or determine band structure.

## Conclusion

This project will aid us in understanding detailed nano-scale quantum properties of materials establishing a basis from which emergent functional materials may designed. The DOE Basic Energy Science (BES) or Defense Homeland Security (DHS) Programs could directly benefit from these studies as interest for nanowire-based sensors and devices have applications ranging from ultra-sensitive drug detection chemistry to gas sensing of chemical bio-warfare agents and solar energy conversion. Other mission-centric actinide materials science questions will also benefit, enabling a rational design basis for materials that can enhance the US energy security portfolio in superconductivity, nuclear energy, and nuclear waste.

## Publications

Dakovski, G. L., Y. Li, T. Durakiewicz, and G. Rodriguez. High-harmonic XUV source for time- and angle-resolved photoemission spectroscopy. Presented at Ultrafast Optics (UFO VII) and High Field Short Wavelength (HFSW XIII) Conference 2009. (Arcachon, France, 31 Aug. - 4 Sep. 2009).
Durakiewicz, T.. Quest for band renormalization and self-energy in correlated f-electron systems. Presented at Meeting of the Polish Synchrotron Society. (Podlesice, Poland, 24-26 Sept, 2009).

Kim, K. Y., A. J. Taylor, J. H. Glownia, and G. Rodriguez. Coherent control of THz supercontinuum generation in ultrafast laser-gas interactions. 2008. Nature Photonics. 2 (10): 605.

Prasankumar, R. P., S. G. Choi, G. T. Wang, S. T. Picraux, and A. J. Taylor. Ultrafast carrier dynamics in semiconductor nanowires. 2009. In Proceedings of the 16th International Conference on Ultrafast Phenomena. (Stresa, Italy, 9-13 Jun. 2008). , p. 271. New York: Springer.

Prasankumar, R. P., S. G. Choi, G. T. Wang, S. T. Picraux, and A. J. Taylor. Ultrafast carrier dynamics in semiconductor nanowires. Invited presentation at Conference on Lasers and Electro-Optics. (San Jose, CA, USA, 4-9 May 2008).
Prasankumar, R. P., S. G. Choi, S. A. Trugman, S. T. Picraux, and A. J. Taylor. Ultrafast electron and hole dynamics in Germanium nanowires. 2008. Nano Letters. 8 (6): 1619.
Rodriguez, G., and K. Y. Kim. THz supercontinuum generation in gas filaments: 'current ' perspective and applications. Invited presentation at Second International Symposium on Filamentation. (Paris, France, 22-25 Sep. 2008).
Trugman, S. A.. Quasiparticles, dynamics, and coupled nanowires. Presented at XXXIII International Workshop on Condensed Matter Theories. (Quito, Ecuador, 16-22 Aug. 2009).

# Advanced Fuel Forms with Microstructures Tailored to Naturally Induce Fission Product Separation During Service

*Kurt E. Sickafus*
20080114DR

## Introduction

Our objective is to investigate key scientific and technological issues underpinning the design of a revolutionary nuclear fuel form possessing desirable attributes of conventional nuclear fuel ($UO_2$ or mixed oxide (MOX) fuel), but with a tailored microstructure that radically eases separation of fission products, drastically reduces separation costs, and substantially mitigates proliferation risks of the separated material. Our advanced nuclear fuel design is based on a dispersion (two-phase composite) nuclear fuel (so-called "dispersion fuel") concept. Our goal is to develop the underpinning science to facilitate more rapid evaluation and acceptance of new fuel forms and to demonstrate a LANL institutional capability to deliver innovative approaches to solving complex national problems. This supports DOE's overarching mission: "to advance the national, economic, and energy security of the United States and to promote scientific and technological innovation in support of this mission."

## Benefit to National Security Missions

This project supports the DOE mission for Energy Security, especially the DOE overarching mission: "to advance the national, economic, and energy security of the Unites States and to promote scientific and technological innovation in support of this mission."

## Progress

Our advanced nuclear fuel design is based on a composite microstructure wherein small fissile material domains (spherical particles or layers) are dispersed in a non-burnable host matrix. Fission products with high kinetic energies form during irradiation and travel about 5-10 microns before stopping in the host matrix. Thus, a natural partitioning evolves between fuel actinides and fission products as this fuel burns. Or goal is to: 1) fabricate prototype fuel structures; 2) irradiate these structures to simulate their behavior in a reactor and characterize the evolution of key properties such as microstructural changes and solubility; and 3) use theory and atomistic models to optimize fuel chemistry / microstructures.

Initially, our studies focused on $MgO/HfO_2$ composites, wherein MgO represents a chemically-separable host matrix phase, while $HfO_2$ is a surrogate for a fissile, $UO_2$ minority phase. Collectively, these composites have the common feature that both the majority and minority phases are oxides, i.e., ceramic phases. Such composites are often referred to as *cercer* composites. Our accomplishments on this project are divided into three principal tasks:

**Synthesis & Fabrication**

Here, we fabricated model composite samples using thin film growth. The thin films are multilayers with structures given by, e.g., $HfO_2/MgO/HfO_2/Si$.

**Irradiation & Characterization**

Here, we irradiated samples with heavy ions (Au) at high energies (10 MeV) at room temperature, to test microstructural stability under extreme environment conditions. We characterized the radiation damage response of our composites using a variety of experimental techniques, including transmission electron microscopy (TEM), and X-ray diffraction (XRD). We find that our composite samples are quite durable under high-energy, heavy ion irradiation, especially as demonstrated by their resistance to radiation-induced amorphization. However, we have recently discovered that our composites are susceptible to void formation at interfaces, which is not a desirable characteristic for nuclear fuel applications.

Figure 1 shows cross-sectional TEM images obtained from a pristine tri-layer sample and tri-layer samples irradiated with 10 MeV Au ions to fluences of $5x10^{14}$, $5.1x10^{15}$ and $3.7x10^{16}$ Au/cm$^2$. The pristine sample (Figure 1a) consists of three polycrystalline layers.

After irradiation to a fluence of $5x10^{14}$ Au/cm$^2$ (Figure 1b), the tri-layer structure did not change. A tenfold increase in ion fluence (to $5.1x10^{15}$ Au/cm$^2$; Figure 1c) did not produce any significant changes in the tri-layer structure.

At the highest fluence of $3.7x10^{16}$ Au/cm$^2$ (Figure 1d), both $HfO_2$ layers were significantly modified. For instance, both $HfO_2$ layers exhibited non-uniform thicknesses following irradiation. But the most significant change was found in the lower $HfO_2$ layer, where the TEM image revealed voids at the $HfO_2$/MgO interface.

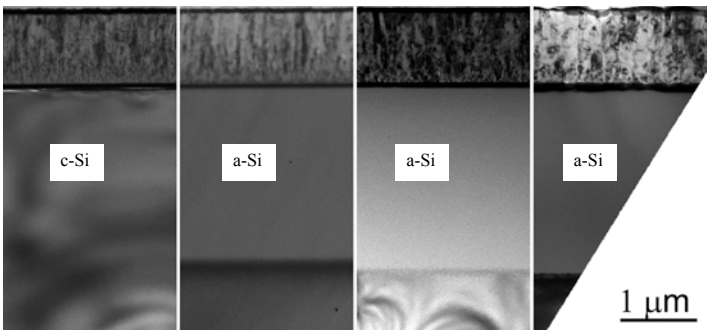


*Figure 1. Cross-sectional TEM images obtained from the following thin-film $HfO_2$/MgO/$HfO_2$ tri-layer samples (deposited on a Si substrate): (a) pristine, unirradiated tri-layer sample; (b, c, d) tri-layer samples irradiated at room temperature with 10 MeV Au ions to fluences of 5x1014, 5.1x1015 and 3.7x1016 Au/cm2, respectively. A narrow dark band on the top of each image is the upper $HfO_2$ layer. The wide band of light contrast in each image is the middle MgO layer. Beneath the MgO, the dark band is the lower $HfO_2$ layer. The region below this is the Si substrate. Amorphous and crystalline regions in the Si substrate are labeled a Si and c Si, respectively.*

Figure 2 shows STEM images obtained from the tri-layer sample irradiated to ion fluence of $3.7x10^{16}$ Au/cm$^2$. The voids observed at the lower MgO/$HfO_2$ interface are indicated by circles in both Figures 2a,b.

The observation of voids at the lower MgO/$HfO_2$ interface is interesting because, to our knowledge, void-type defects do not form in either bulk MgO or bulk $HfO_2$ subjected to ion irradiation. Thus, even though void formation is not characteristic to the individual components, the tri-layer structure is conducive to void nucleation and growth, at least at the bulk interface. This effect is undesirable, since void formation will result in poor mechanical properties of such a composite structure, due to weak bonding along the interfaces.

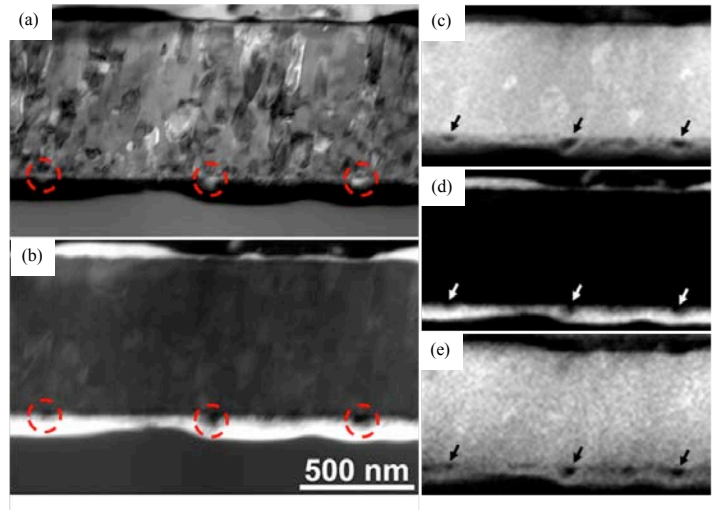


*Figure 2. Cross-sectional scanning transmission electron microscopy (STEM) bright-field (BF) image (a) and corresponding STEM high-angle annular dark-field (HAADF) image (b), obtained from a tri-layer sample irradiated at room temperature with 10 MeV Au ions to a fluence of 3.7x1016 Au/cm2. Circles in (a,b) indicate voids formed at the interface between the MgO layer and the lower HfO2 layer. (c, d, e) STEM-energy-dispersive X-ray spectroscopy (EDXS) maps for Mg, Hf, and O, respectively, obtained from the same sample area as shown in (a,b). Arrows in the STEM-EDXS maps indicate the locations of microstructural voids induced by ion irradiation.*

**Modeling & Simulation**

We performed atomistic simulations using first-principles calculations (specifically using density-functional theory or DFT) to determine the solution energies of prominent fission products, namely xenon (Xe), cesium (Cs) and strontium (Sr), in the two composite fuel phases, i.e., $UO_{2\pm x}$ and MgO. In so doing, we are able to compare and contrast the relative stabilities of fission products (FPs) in each phase of a model *cercer*, $UO_2$/MgO composite nuclear fuel. Using the incorporation energies of Xe, Cs, and Sr in UO2, the solution energies in both $UO_{2\pm x}$ and MgO at 1700 K were obtained. These results are plotted in Figure 3. Overall, the solution energies of fission products in MgO are substantially higher than those in $UO_2$, except for the case of Sr in hypostoichiometric $UO_{2-x}$, where Sr prefers the inert material over the fissile material. Since $UO_2$ is more likely to be hyperstoichiometric ($UO_{2+x}$) in fuel applications, our calculations suggest that, thermodynamically, the fission products Xe, Cs, and Sr should prefer to reside in the fissile phase ($UO_2$) instead of in the MgO inert phase.

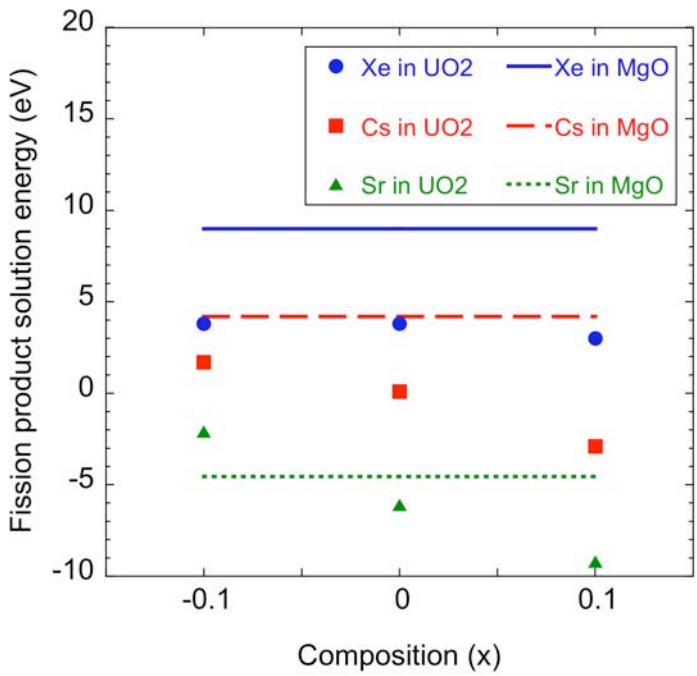


*Figure 3. Calculated solution energies of Xe, Cs, and Sr in $UO_{2\pm x}$, in comparison with calculated values in MgO.*

## Future Work

In the last year of this project, we have chosen to work on the following composite system: $UO_2$-$ZrO_2$. We will use *depleted uranium* (DU) for these studies.

**Synthesis & Fabrication**

We will use hot-isostatic pressing (HIPing) to produce $UO_2$ & $ZrO_2$ monolithic samples, and a variety of compositions of $UO_2$-$ZrO_2$ *cercer* composite samples.

**Irradiation & Characterization**

A. We will perform *high-temperature* ion implantations using 10 MeV strontium (Sr) ions (Tandem accelerator in the IBML) into $UO_2$ & $ZrO_2$ control samples, and into $UO_2$-$ZrO_2$ *cercer* composites, in order to examine: (1) the behavior of Sr (intended to represent the FP $^{90}$Sr) in pure $UO_2$ and $ZrO_2$; and (2) the propensity for segregation of Sr to either the $UO_2$ or $ZrO_2$ phases (this may change as a function of *m*, *t*, or *c*-$ZrO_2$). Implanted samples will be characterized using cross-sectional transmission electron microscopy (XTEM).

B. We will perform ion implantations using 400-600 keV xenon (Xe) ions into $UO_2$ & $ZrO_2$ control samples, and into $UO_2$-$ZrO_2$ *cercer* composites, in order to examine: (1) the behavior of Xe in pure $UO_2$ and $ZrO_2$; and (2) the propensity for segregation of Xe to either the $UO_2$ or $ZrO_2$ phases (this may change as a function of *m*, *t*, or *c*-$ZrO_2$) and to observe the nucleation and growth of fission gas bubbles in these ceramics.

**Separation of $UO_2$ from $UO_2$-$ZrO_2$ via Heat Treatment & Selective Dissolution**

A. We will heat-treat $UO_2$-$ZrO_2$ *cercer* composite samples at high temperature in air or flowing oxygen, in order to convert (oxidize) the $UO_2$ to $U_3O_8$. This transformation will be accompanied by a significant volume change. This should break up the *cercer* pellets. The $ZrO_2$ should be unaffected by the heat treatment.

B. We will selectively dissolve the $U_3O_8$ phase in the $U_3O_8$-$ZrO_2$ composites using a nitric acid ($HNO_3$) solution. The $ZrO_2$ phase should be unaffected by this dissolution process.

**Modeling & Simulation**

We will perform first-principles calculations to predict the thermodynamic stability of various FPs in $UO_2$ and $ZrO_2$, as well as the propensity for segregation of these FPs to either the $UO_2$ or $ZrO_2$ phases in a $UO_2$-$ZrO_2$ *cercer* composite (this may change as a function of *m*, *t*, or *c*-$ZrO_2$).

## Conclusions

We expect to determine whether or not we can create a two-part, *cercer* nuclear fuel that eases the complexities associated with spent fuel chemical separations processes. This fuel form must not only be easy to separate chemically, but during service as an energy source, it must exhibit both robust and predictable behavior. We will test our advanced fuel materials to ensure that they possess the necessary physical and chemical stabilities. The natural, in-service chemical separations strategy associated with our novel approach will greatly reduce both technological challenges and costs compared to conventional reprocessing.

## Publications

Liu, X. Y., B. P. Uberuaga, and K. E. Sickafus. First-principles study of fission product (Xe, Cs, Sr) incorporation and segregation in alkaline earth metal oxides, HfO2, and the MgO-HfO2 interface. 2009. *Journal Of Physics: Condensed Matter.* **21**: 45403.

Usov, I. O.. Irradiation effects in an HfO2/MgO/HfO2 tri-layer structure induced by 10 MeV Au ions. 2009. *Nuclear Instruments and Methods B.* **267**: 1918.

# Predictive Design of Noble Metal Nanoclusters

*Jennifer Martinez*
20090017DR

## Introduction

The next revolution in materials science will be the first principles design and "atom-by-atom" assembly of nanoarchitectures having specific emergent properties. Biological systems have evolved efficient mechanisms for the atom-by-atom assembly of materials with precise control of both structure and function. In nature, the design and function of materials are genetically encoded. From this genetic blueprint, protein and peptide templates are produced that precisely control the assembly and orientation of inorganic atoms, leading to materials with controlled structure and emergent properties that span length scales from the molecular to the mesoscopic.

Our goals are to mimic and exploit biology to develop noble metal nanoclusters from soluble precursors with exquisite precision. Fluorescent metal nanoclusters are collections of small numbers of gold or silver atoms (4-30 atoms, ≤ 1 nm) with intriguing photophysical properties, including strong size-dependent emission. These clusters have good quantum yields and are stable at physiological pH and room temperature (> 1 year). While these clusters are intriguing, current approaches still do not allow the precise control of cluster size necessary to produce highly fluorescent materials and to accurately understand and predict how size and structure affect photophysical properties. Our major goals are: **1)** to gain synthetic control over the size and structure of nanoclusters; **2)** to develop predictive models of the electronic structure and photophysical properties; and **3)** to incorporate nanoclusters into biological structures for imaging and sensing applications.

## Benefit to National Security Missions

This project will support the DOE mission in Threat Reduction by enhancing our understanding of the design and synthesis of materials with defined properties for application in chem/biothreat reduction, imaging, and the biosciences missions of the DOE Office of Science.

## Progress

Within the first year of this proposal we have made exciting progress on production of nanoclusters. We have shown that small molecule ligands can be used to make clusters of defined fluorescence. Through a series of investigations we have begun to understand the functionality that is important for not only gold coordination, but also templation of the cluster. Through photophysical characterization we have defined the size of the fluorophore and determined fluorescence lifetime and brightness (quantum yield etc). Together with the synthetic work we find these clusters to be easily produced and as fluorescent as many organic dyes. Further, we have begun to template clusters in DNA for their easy conjugation to proteins, leading to cellular labeling, and we have made cationic clusters of defined size that can be investigated for the charge induced property of fluorescence. Through structural and electronic studies we have begun to understand ligand effects on structure and fluorescence properties. A few of these exciting results are presented below.

### Small Molecule Ligands

Toward the goal of making small and biologically attachable fluorescent probes, we have investigated the production of fluorescent gold nanoclusters using Good's buffers. Good's buffers, such as MES and HEPES, are common pH buffers with morpholine or piperazine backbones and have previously been shown to be good Au(I) ligands with reduction potentials sufficient to produce gold nanoparticles. In a typical experiment, Au nanoclusters were synthesized by mixing a gold chloride aqueous solution with a Good's buffer at room temperature, with subsequent incubated shaking. This simple procedure typically generated clear solutions with gold nanoparticle precipitates on the bottom of the tubes. In contrast to the precipitates, over a matter of days the supernatant of this reaction becomes fluorescent (Figure 1). We tested a variety of Good's buffers and other similar small molecules for their ability to template gold nanoparticles and clusters. Some small molecules produced single fluorescent species and others produced mixtures of fluorescent species. Single species exhibit a single emission

peak when excited at different wavelengths, while multiple species exhibit different emission peaks when excited at different wavelengths. As we have reported here, in the process of metal cluster synthesis, gold nanoparticles are formed first and only after many days, as these nanoparticles partially dissolve in the reaction medium, are the fluorescent clusters formed. Our detailed experimental investigation suggests that the Good's buffer stabilized clusters are produced from an etching process of Good's-protected nanoparticles.

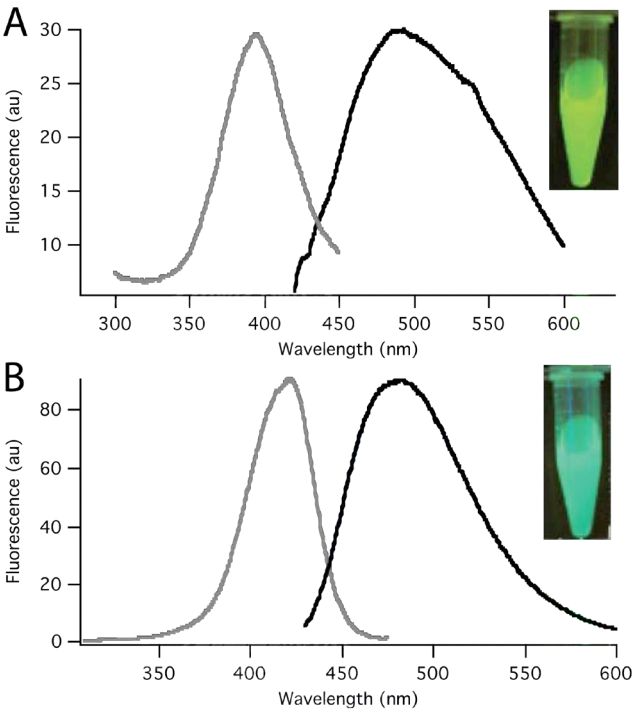


*Figure 1. Fluorescence excitation (gray) and emission (black) spectra of small molecule stabilized Au nanoclusters: (a) HEPES and (b) MES. Insert photography was taken by illuminating the solution with a mercury arc lamp through a bandpass filter centered at 405±20 nm.*

Ultimately, our objective is to compare experimentally observed and theoretically predicted photophysical transitions for each complex, so that we may tailor the chemical synthesis to produce highly stable fluorescent nanoclusters with predicted photophysical properties. Toward this goal, we have characterized the nanoclusters by bulk fluorescence measurements, fluorescence correlation spectroscopy (FCS), and time correlated single photon counting (TCSPC). FCS was used to measure the emission rate per cluster, hydrodynamic radius, and to estimate the concentration of the fluorescent clusters synthesized. We found, through measurement of photon detection rates, that MES (5.7 kHz) and HEPES (1.7 kHz) stabilized clusters were comparable in fluorescence to the maximum photon detection rate of norharmane (~2 kHz), a UV dye with similar excitation spectra and a large quantum yield (Q.Y. = 58%), suggesting that our synthesized clusters are as bright, or brighter than commercial dyes. Further, from the measured diffusion coefficients, determined by FCS, we infer that the fluorescent species is substantially larger than a complex between a single gold atom and a single MES or HEPES molecule, but with approximate diameters of 7.4±0.7 Å (for MES-templated clusters) and 9.0±4.4 Å (for HEPES-templated clusters).

In summary, we have produced a new method for preparing fluorescent and water-soluble Au nanoclusters using small molecules as reducing agents and stabilizing ligands. The reaction proceeds by first forming irregularly shaped nanoparticles, which are subsequently etched by excess ligands to produce fluorescent nanoclusters. These reaction mixtures yield fluorescent species with sizes consistent with gold cores of a few atoms, and have large effective quantum yields with nanosecond fluorescence lifetimes. Although the detailed mechanisms of Au-ligand nanocluster coordination need further studies, the findings of the current work hold promise for designing capping ligands for the synthesis of fluorescent Au nanoclusters that can be directly linked to biological molecules. This study also provides a starting point toward understanding the formation and stabilization of small size nanoclusters and may represent an inexpensive method to produce fluorescence species from bulk colloidal gold. This work has been submitted for review and publication to *Journal of Physical Chemistry C*.

Additionally, we have synthesized specific sized cationic gold clusters using traditional inorganic methods. Our goal was to understand the effect ligand type had on fluorescence properties and the change in geometry, and effective change on photophysics, with ligand exchange. We find that the as -ynthesized phosphine protected clusters are nonfluorescent. Yet, when ligand exchanged with a series of amine ligands, the protected gold clusters are highly emissive. These results are highly intriguing as traditionally soft metals, such as gold, bind more strongly to soft ligands such as phosphines. However, only when a hard ligand, such as an amine, is bound they become fluorescent. The nature of this quandary and ligand binding strength is being investigated using density functional theory calculations.

**Nanoclusters in biological structures**

Efforts are being made to tune the emission wavelength of metallic nanoclusters to make them useful for multiplex assays both for *in-vivo* and *in-vitro* studies. Most multiplex assays for biological molecules are performed under one buffer condition and usually at physiological pH. Prior to our work no one had yet synthesised nanoclusters emitting at different wavelengths without changing the surrounding

conditions *i.e.* pH, buffer, temperature. We have developed procedures for the synthesis of Ag-nanoclusters fluorescing at different wavelengths that depend upon the sequence and length of the DNA strands, and that are synthesized with the same salt and pH-conditions (Figure 2). In one of these constructs the silver cluster was templated by an aptamer that recognizes the protein thrombin. We find that our silver nanocluster-aptamer can be used to detect nM quantities of thrombin, without competing reactions with other proteins (Figure 3). Thus, not only are we able to form clusters in biological molecules, we are able to use them for biological detection. These clusters are also being used to study the energy transfer between clusters, organic dyes and nanoparticles. These experimental results will be compared to resently developed theoretical approaches by our team for understanding energy transfer of gold and silver nanoclusters. Two papers are in progress for submission detailing the results described above.

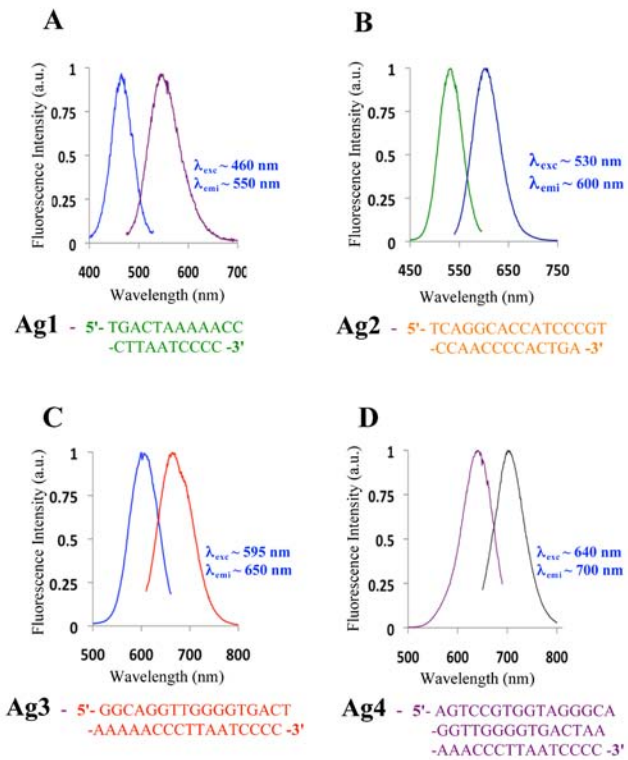


*Figure 2. Excitation and emission spectra of Ag-nanoclusters encapsulated by different DNA strands. (A) Green nanoclusters. (B) Orange nanoclusters. (C) Red nanoclusters (D) Far-red region nanoclusters. (Also the DNA strands encapsulating each nanoclusters along with the emissive solutions of nanoclusters are shown).*

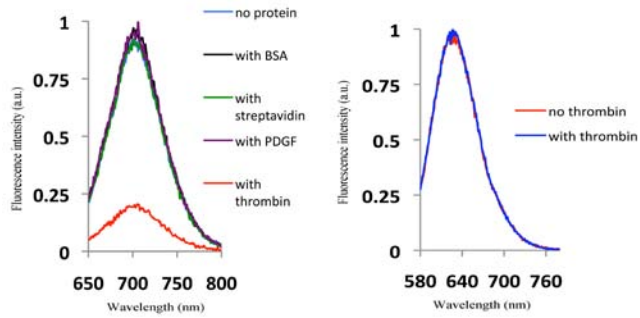


*Figure 3. Our silver nanocluster aptamer can detect tiny (nM) quantities of the protein thrombin, and is not confused by other proteins. Fluorescence emission of Ag-nanoclusters after addition of different proteins. (a) The effect of different proteins on the fluorescence emission of thrombin aptamer templated silver nanoclusters (b) the effect of thrombin protein on random DNA sequence templated silver nanoclusters (i.e. control).*

## Future Work

We will: **A)** explore bio-inspired and traditional methods of cluster synthesis [tasks: A1) design MBP and protein scaffolds for nanocluster synthesis; A2) conduct phage display panning to find peptides that template nanoclusters; A3) clone peptides into proteins; A4) develop and understand small molecule templates for cluster synthesis; A5) synthesize clusters in DNA scaffolds], **B)** characterize cluster morphology and photophysical properties [tasks: B1) characterize morphology of clusters by Raman, TEM, and FCS; B2) determine cluster number by mass spectrometry; B3) characterize photophysical properties], **C)** correlate these experimental measurements with electronic structure and dynamics calculations to improve fundamental understanding of cluster properties [tasks: C1) use first principles based calculations to model electronic structure and photoexcited state dynamics of clusters; C2) better understand the mechanisms for fluorescence; C3) better understand the transition to nanoparticles], and **D)** demonstrate the utility of the clusters for applications in biological imaging and sensing.

## Conclusion

We have shown that small molecule ligands can be used to make clusters of defined fluorescence. Through a series of modeling and synthetic investigations we have begun to understand the functionality that is important for not only gold coordination, but also templation of the cluster. Through photophysical characterization we have defined the size of the fluorophore and determined fluorescence lifetime and brightness (quantum yield etc).

## Publications

Bao, Y., H. Yeh, C. Zhong, S. Ivanov, J. Sharma, D. Vu, A. Shreve, R. Dyer, J. Werner, and J. Martinez. Formation and stabilization of fluorescent gold nanoclusters using small molecules. *Journal of Physical Chemistry C.*

Yeh, H., J. Sharma, Y. Bao, J. Martinez, and J. Werner. Photophysical characterization of fluorescent metal nanoclusters synthesized using oligonucleotides, proteins, and small reagent molecules. Presented at *2010 BiOS SPIE Photonics West.* (San Francisco, January 23-28, 2010).

# Understanding Anisotropy to Develop Superconductors by Design

*Filip Ronning*
20090022DR

## Introduction

Condensed matter physics is entering an exciting age where our emerging ability to control materials properties holds tremendous promise for addressing the world's most basic needs. Superconductivity, the perfect flow of electricity resulting from quantum mechanics on a macroscopic scale, will be critical for meeting the energy demands of the future. Unconventional superconductors, with their inherent strong electronic correlations that allow the flow of current without loss at temperatures nearly half that of room temperature, provide the best opportunity for meeting these energy needs. To date, the inability to design superconducting materials from basic principles has plagued the international scientific community and represents one of its greatest challenges. Recent experimental discoveries reveal materials-specific anisotropic characteristics of these complex electronic oxides and metals that enhance their superconducting properties, but their microscopic origins are completely unknown. Our scientific objective utilizes a novel approach to discover the fundamental atomic-scale, structure-property materials' characteristics that generate this unconventional superconductivity, by employing a comprehensive suite of experimental probes and state-of-the-art theoretical tools. Success will take condensed matter to a whole new level of understanding in superconductivity and materials research.

## Benefit to National Security Missions

This project will support the DOE mission in nuclear weapons by enhancing our understanding of actinide materials in general. In addition, we will directly support the DOE mission in energy security by enhancing our understanding of superconductors.

## Progress

Much of the work in the first year has focused on optimizing and testing experimental and theoretical techniques. We will apply these techniques in years 2 and 3. After receiving electro-refined Uranium (which is ultra high purity) from Ames in February, we have synthesized several known heavy fermion superconductors. These include Uranium-Cobalt-Germanium and Uranium-Palladium-Aluminum. We are also finished refurbishing a zone refinement setup and are building our own electrorefining setup which can remove strain and magnetic impurities from crystals, respectively. Our goal is higher quality crystals which will result in much better signal to noise ratios in our measurements. This will allow us to observe the physics that is responsible for superconductivity.

Various measurements, including angle-resolved photoemission spectroscopy (ARPES), quantum oscillation, specific heat, tunneling, nuclear magnetic resonance (NMR), and neutron scattering have been initiated on the crystals we have grown as well as on Plutonium-Cobalt-Gallium. These measurements allow us to study the charge, spin, and superconducting gap anisotropy. A uniaxial pressure setup for measuring the charge degrees of freedom with quantum oscillation studies of unconventional superconductors has been constructed. We have also investigated the pressure dependence of Uranium-Nickel-Silicide, a 90 K ferromagnet. High pressure (6GPa) completely suppressed the ferromagnetic transition, but there was no evidence for superconductivity [7]. Perhaps cleaner crystals are required. We refurbished a dilution refrigerator in order to acquire better NMR data. With these data, we will study the spin degrees of freedom on superconductors in zero magnetic field. Our measurements are in progress.

Our theoretical team has implemented a Numerical Renormalization Group (NRG) solver to perform single-site Dynamical Mean Field (DMFT) calculations. DMFT is a powerful new theoretical technique to study strongly correlated materials, but one must choose a particular solver depending on the energy scales of interest. The NRG solver will permit accurate calculations at the low energies of interest for superconductivity. We performed calculations on Plutonium-Cobalt-Gallium, specifically to compare with the experimental results from the ARPES work. We have developed a large-N equation-of-motion impurity solver [5], and are also developing and debugging the NRG algorithm for two-impurity models. This is an important step for trying to understand the Coulomb interaction between two different f-element atoms. Specifically, this will permit our calculations to explicitly look

for effects due to magnetism and be able to predict superconducting transition temperatures.

In addition, the recently discovered "pnictides" represent a new class of superconductors, which appear to be highly tunable, and thus relevant to our approach. We have established that the Nickel-based systems are likely to be conventional superconductors [4]. Surprisingly, the superconducting transition temperature scales in the Nickel compounds in a similar way to the Iron compounds which suggests that coupling to the lattice is more important than originally thought for producing the relatively high transition temperatures [6]. We have also performed dHvA [3] and theoretical modeling work [2] to understand the interplay of magnetism with the anisotropic pairing potential which generates superconductivity. NMR measurements have shown that the magnetism coexists microscopically with the superconductivity [1]. As promised, we have also synthesized new systems with actinides and the iron-arsenide compounds, discovering a new Uranium-Iron-Arsenide material. This material is magnetic. As in other iron arsenide compounds, it may require pressure or doping to generate superconductivity.

To further understand the role of structure and bonding in generating the strong correlations which are favorable for superconductivity, we have synthesized 12 new cerium, ytterbium, and uranium compounds. Many compounds had structural aspects in common with other known superconductors. Of these compounds we found that a cerium-platinum-indium compound displays superconductivity under applied pressure [8]. This compound is more layered than other known cerium based magnetic superconductors, yet the transition temperature of 2 K is the same as other known cerium based superconductors. Theoretical analysis allows us to speculate that the reason for the lack of increase in transition temperature is due to a reduction in the spin fluctuations.

## Future Work

Understanding the strong electronic correlations that give rise to the anisotropies beneficial to unconventional superconductivity is the most direct path to move beyond serendipity into designing improved superconductors. The entwined spin, charge, and lattice degrees of freedom in strongly correlated systems require closely coupled experimental and theoretical efforts combined within a non-trivial (but direct) approach. To be successful in this endeavor, we must:

1. experimentally identify and subsequently decouple the momentum-dependent spin and charge anisotropies and energy scales relevant for unconventional superconductivity
2. theoretically determine the microscopic aspects of the underlying crystal structure/chemistry that lead to these correlation-driven anisotropies
3. integrate these experimental and theoretical thrusts to produce a microscopic understanding of the interactions that enable prediction and synthesis of new enhanced unconventional superconductors

We will achieve this by using pressure, magnetic field, and chemical tuning to vary superconducting behavior, and observe with a set of spin, charge, and lattice probes to identify which responses are correlated with superconductivity. On the theoretical side, we will use band structure and dynamical mean-field theory to identify which aspects of a crystal structure are responsible for those responses. Finally, we will combine theory and experiment to identify new crystal structures promising for superconductivity, and ways to improve existing materials.

## Conclusion

We expect to develop a playbook to design new superconducting materials. We will achieve this by learning how tuning a material's structure drives specific material properties which we can correlate with superconducting properties. Los Alamos is uniquely poised to capitalize on this new understanding for designing the next generation of improved correlated electron superconductors, through an integrated experimental and theoretical approach performed by its assembled team of world-class experts in superconductivity that will test and expand the limits of research at high magnetic fields and pressure, materials synthesis, and of theory and simulation. We now possess the capability of synthesizing the cleanest samples possible, which will allow us to detect what are the key factors for generating superconductivity, and we will be able to address the observation of why layered superconductors with increased spin fluctuations appear to be favorable for superconductivity.

## References


1. Baek, S.-H., H. Lee, S. E. Brown, N. J. Curro, E. D. Bauer, F. Ronning, T. Park, and J. D. Thompson. NMR Investigation of Superconductivity and Antiferromagnetism in CaFe[sub 2]As[sub 2] under Pressure. 2009. *Physical Review Letters.* **102** (22): 227601.
2. Dai, J. H., Q. M. Si, J. X. Zhu, and E. Abrahams. Iron pnictides as a new setting for quantum criticality. 2009. *Proceedings of the National Academy of Sciences of the United States of America.* **106** (11): 4118.
3. Harrison, N., R. D. McDonald, C. H. Mielke, E. D. Bauer, F. Ronning, and J. D. Thompson. Quantum oscillations in antiferromagnetic CaFe/sub 2/As/sub 2/ on the brink of superconductivity. 2009. *Journal of Physics: Condensed Matter.* **21** (32): 322202 (4 pp.).
4. Kurita, N., F. Ronning, Y. Tokiwa, E. D. Bauer, A. Subedi, D. J. Singh, J. D. Thompson, and R. Movshovich. Low-

Temperature Magnetothermal Transport Investigation of a Ni-Based Superconductor BaNi[sub 2]As[sub 2]: Evidence for Fully Gapped Superconductivity. 2009. *Physical Review Letters.* **102** (14): 147004.

5. Qi, Y. N., J. X. Zhu, and C. S. Ting. Validity of the equation-of-motion approach to the Kondo problem in the large-N limit. 2009. *Physical Review B.* **79** (20).
6. Ronning, F., E. D. Bauer, T. Park, S.-H. Baek, H. Sakai, and J. D. Thompson. Superconductivity and the effects of pressure and structure in single-crystalline SrNi[sub 2]P[sub 2]. 2009. *Physical Review B (Condensed Matter and Materials Physics).* **79** (13): 134507.
7. Sakai, H., S.-H. Baek, E. D. Bauer, F. Ronning, and J. D. Thompson. 29Si-NMR study of magnetic anisotropy and hyperfine interactions in the uranium-based ferromagnet UNiSi2. 2009.
8. Bauer, E. D., V. A. Sidorov, H. Lee, N. Kurita, F. Ronning, R. Movshovich, and J. D. Thompson. Coexistence of Antiferromagnetism and Superconductivity in CePt2In7.. 2009.

## Publications

Baek, S.-H., H. Lee, S. E. Brown, N. J. Curro, E. D. Bauer, F. Ronning, T. Park, and J. D. Thompson. NMR Investigation of Superconductivity and Antiferromagnetism in CaFe[sub 2]As[sub 2] under Pressure. 2009. *Physical Review Letters.* **102** (22): 227601.

Bauer, E. D., V. A. Sidorov, H. Lee, N. Kurita, F. Ronning, R. Movshovich, and J. D. Thompson. Coexistence of Antiferromagnetism and Superconductivity in CePt2In7.. 2009.

Bobev, S., S. Q. Xia, E. D. Bauer, F. Ronning, J. D. Thompson, and J. L. Sarrao. Nickel deficiency in RENi2-xP2 (RE = La, Ce, Pr). Combined crystallographic and physical property studies. 2009. *Journal of Solid State Chemistry.* **182** (6): 1473.

Dai, J. H., J. X. Zhu, and Q. M. Si. f-spin physics of rare-earth iron pnictides: Influence of d-electron antiferromagnetic order on the heavy-fermion phase diagram. 2009. *Physical Review B.* **80** (2).

Dai, J. H., Q. M. Si, J. X. Zhu, and E. Abrahams. Iron pnictides as a new setting for quantum criticality. 2009. *Proceedings of the National Academy of Sciences of the United States of America.* **106** (11): 4118.

Harrison, N., R. D. McDonald, C. H. Mielke, E. D. Bauer, F. Ronning, and J. D. Thompson. Quantum oscillations in antiferromagnetic CaFe/sub 2/As/sub 2/ on the brink of superconductivity. 2009. *Journal of Physics: Condensed Matter.* **21** (32): 322202 (4 pp.).

Hu, X., C. S. Ting, and J. X. Zhu. Vortex core states in a minimal two-band model for iron-based superconductors. 2009. *Physical Review B.* **80** (1).

Klimczuk, T., T. M. McQueen, A. J. Williams, Q. Huang, F. Ronning, E. D. Bauer, J. D. Thompson, M. A. Green, and R. J. Cava. Superconductivity at 2.2 K in the layered oxypnictide La[sub 3]Ni[sub 4]P[sub 4]O[sub 2]. 2009. *Physical Review B (Condensed Matter and Materials Physics).* **79** (1): 012505.

Kurita, N., F. Ronning, C. F. Miclea, E. D. Bauer, J. D. Thompson, A. S. Sefat, M. A. McGuire, B. C. Sales, D. Mandrus, and R. Movshovich. Low-temperature thermal conductivity of BaFe[sub 2]As[sub 2]: A parent compound of iron arsenide superconductors. 2009. *Physical Review B (Condensed Matter and Materials Physics).* **79** (21): 214439.

Kurita, N., F. Ronning, Y. Tokiwa, E. D. Bauer, A. Subedi, D. J. Singh, J. D. Thompson, and R. Movshovich. Low-Temperature Magnetothermal Transport Investigation of a Ni-Based Superconductor BaNi[sub 2]As[sub 2]: Evidence for Fully Gapped Superconductivity. 2009. *Physical Review Letters.* **102** (14): 147004.

Qi, Y. N., J. X. Zhu, and C. S. Ting. Validity of the equation-of-motion approach to the Kondo problem in the large-N limit. 2009. *Physical Review B.* **79** (20).

Ronning, F., E. D. Bauer, T. Park, N. Kurita, T. Klimczuk, R. Movshovich, A. S. Sefat, D. Mandrus, and J. D. Thompson. Ni2X2 (X = pnictide, chalcogenide, or B) based superconductors. 2009. *Physica C-Superconductivity and Its Applications.* **469** (9-12): 396.

Ronning, F., E. D. Bauer, T. Park, S.-H. Baek, H. Sakai, and J. D. Thompson. Superconductivity and the effects of pressure and structure in single-crystalline SrNi[sub 2]P[sub 2]. 2009. *Physical Review B (Condensed Matter and Materials Physics).* **79** (13): 134507.

Sakai, H., S.-H. Baek, E. D. Bauer, F. Ronning, and J. D. Thompson. 29Si-NMR study of magnetic anisotropy and hyperfine interactions in the uranium-based ferromagnet UNiSi2. 2009.

Sefat, A. S., D. J. Singh, R. Y. Jin, M. A. McGuire, B. C. Sales, F. Ronning, and D. Mandrus. BaT2As2 single crystals (T = Fe, Co, Ni) and superconductivity upon Co-doping. 2009. *Physica C-Superconductivity and Its Applications.* **469** (9-12): 350.

Sefat, Athena S., Michael A. McGuire, . , Brian C. Sales, . , . , E. D. Bauer, and . . Structure and anisotropic properties of BaFe[sub 2 - x]Ni[sub x]As[sub 2] (x = 0, 1, and 2) single crystals. 2009. *Physical Review B (Condensed Matter and Materials Physics).* **79** (9): 094508.

Si, Q. M., E. Abrahams, J. H. Dai, and J. X. Zhu. Correlation effects in the iron pnictides. 2009. *New Journal of Physics.* **11**.

Vorontsov, A. B., I. Vekhter, and M. J. Graf. Pauli-limited upper critical field in dirty d-wave superconductors. 2008. *Physical Review B (Condensed Matter and Materials Physics).* **78** (18): 180505 (5 pp.).

# Spatial-temporal Frontiers of Atomistic Simulations in the Petaflop Computational World

*Timothy C. Germann*
20090035DR

## Introduction

In recent years the field of atomistic-scale simulations has seen two exciting developments. First, the continuing advances in high-performance computing, in particular the maturation of massively parallel supercomputers consisting of hundreds, to hundreds of thousands, of processors working in concert, have enabled the study of complex phenomena in fluids and solids by the direct atom-by-atom ("molecular dynamics" (MD)) modeling of systems containing millions to billions of atoms. Secondly, "accelerated MD" algorithms, developed at Los Alamos over the past decade, are enabling the modeling of thermally activated, rare event processes that take place on timescales of seconds or longer, far beyond the nanoseconds (billionths of a second) that traditional MD simulations have been able to reach. However, such accelerated simulations have thus far been limited to several hundred to a few thousand atoms at most. The goal of this project is to develop and validate techniques for combining the accelerated and large-scale MD techniques, enabling for the first time atomistic simulations with both large size and long time scales, that will in certain cases directly overlap those of ultrafast, high-resolution experimental measurements. We are pursuing two distinct approaches for achieving this integration, and focusing on two specific scientific materials science problems for study: (1) the nucleation, growth, and coalescence of voids leading to failure in metals; and (2) the interaction of a dislocation pileup forced against a grain boundary (GB), a fundamental issue controlling material strength. These phenomena are representative of a large class of problems that have until now been tantalizingly just out-of-reach of current simulation techniques: requiring timescales of microseconds to milliseconds that have eluded direct MD, and sample dimensions as large as a micrometer that accelerated MD techniques have not been able to reach.

## Benefit to National Security Missions

Atomistic-scale simulations are playing an increasing role in fundamental and applied materials science. Los Alamos has two distinct internationally recognized capabilities in this area: large-scale molecular dynamics (MD) simulations, specifically the SPaSM (*Scalable Parallel Short-range Molecular dynamics*) code supported primarily by the weapons program (ASC), and accelerated molecular dynamics algorithm development and implementation under the auspices of LDRD and Basic Energy Sciences (BES). The goal of this project is to develop and demonstrate the coupling of these two capabilities to address heretofore inaccessible problems in materials science. The resulting transformational capability is expected to have immediate benefits to DOE missions in the Office of Science and Nuclear Weapons (NNSA Advanced Simulation and Computing) programs, by providing new computational tools and enhancing our understanding of the fundamental dynamics of materials, in particular under extreme loading conditions that are difficult to probe experimentally. The methods demonstrated here should have applications beyond these initial materials science issues that we will focus on, for instance in studying the resistance of materials to other extreme conditions including radiation and corrosive environments; similarly, the materials science questions addressed here have impacts in nuclear and non-nuclear energy (e.g. turbine blade design), DOD programs (e.g. armor/anti-armor), and beyond.

## Progress

As shown in Figure 1, two different routes are being pursued to couple large-scale and accelerated MD: (1) for situations where likely "active sites" of interest can be identified (e.g. locations where cracks are forming, voids are opening up, or more generally there is a high concentration of defects such as voids, interstitial atoms, or dislocations), SPaSM will provide the long-range stress boundary conditions for these active sites, using a subset of the available processors on a parallel supercomputer such as Roadrunner. At the same time, the remaining processors will be used to carry out accelerated molecular dynamics simulations of the active sites using the parallel replica dynamics ("ParRep") technique, which is particularly well-suited to the hybrid architecture of Roadrunner. Alternatively, (2) a recently developed "local-bias hyperdynamics" method offers a way to simultaneously accelerate dynamics across a large

system, without the need to identify active sites ahead of time. This approach adds a local, rather than global, bias potential to the potential energy surface on which the system evolves.

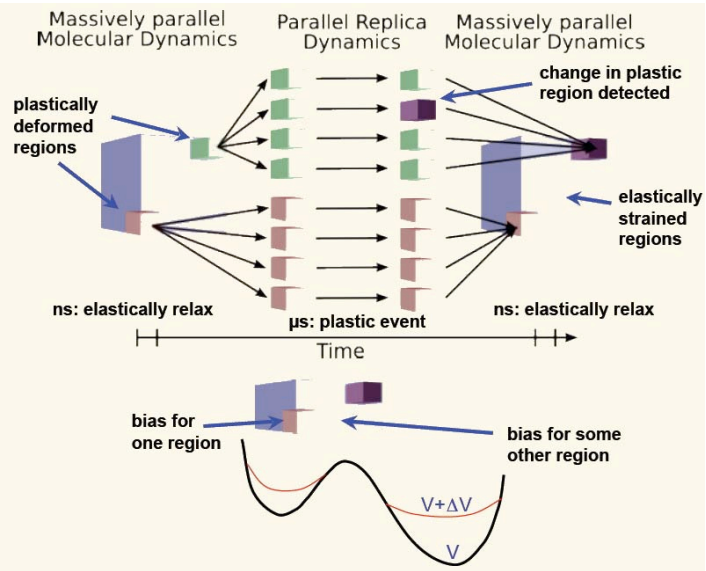


*Figure 1. Schematic of the two hybrid accelerated/large-scale molecular dynamics algorithms which are being developed under this project. (Top) Concurrent approach in which large-scale MD provides the elastic strain boundary conditions for smaller regions in which rare events are expected to occur. These smaller regions are followed with the parallel replica dynamics approach until such a rare event is detected, typically resulting in plastic deformation which may alter the long-range elastic strain field, provided by large-scale MD. (Bottom) Local-bias hyperdynamics, in which the force field in each region is systematically modified to accelerate local events, but with a system-wide synchronization so that events in different regions occur in the proper sequence.*

The concurrent SPaSM-ParRep algorithm has undergone initial "proof-of-concept" testing of its two separate phases: first, carving an active site out of a larger simulation model, and then distributing it among a number of parallel replicas to accelerate transition events. This testing is being done for the dislocation-GB problem, with promising initial results as described below. We have also modified the SPaSM code to partition the available processors between the large-scale simulation model and a single ParRep model of an active site; this assumption of a single active site is appropriate for the dislocation-GB problem which we are studying first, and will be straightforward to generalize to the arbitrary number of active sites that may be required for other problems. We have also tested the local-bias hyperdynamics approach on a model system with a wide range of transition rates. As desired, a uniform boost factor (acceleration) is seen for the entire set of transitions, giving confidence in our approach. We are optimizing the calculation of the local bias potential and tuning the parameters involved before implementing it in SPaSM (including the Roadrunner version).

On the materials science side, we are studying two problems: (1) the interaction of a dislocation pileup forced against a GB (Figure 2), a fundamental mechanism which often determines the strength of materials, and (2) the nucleation, growth, and coalescence of voids under tension, which can lead to "spall" failure of ductile metals following shock impact. Work in the first year has been focused on preparing for the integrated large scale/accelerated molecular dynamics (MD) simulations that will be carried out in FY10. To do so, we have been utilizing separate large scale and accelerated MD studies to probe different aspects of these two phenomena. Direct large-scale studies of spall failure of copper single crystals and bicrystals, as well as copper-zirconium bulk metallic glasses, have resulted in one paper in the *Journal of Applied Physics*, and several others in press. This work, which included several production simulations on Roadrunner during its "Open Science" period, has provided insight about how voids nucleate (primarily at dislocation intersections or GBs), grow (once they reach a critical void size), and coalesce. Of particular note, we have demonstrated a competition between heterogeneous nucleation of voids at GBs, which leads to spall failure along such boundaries at slower strain rates, and the homogeneous void nucleation inside crystalline grains at higher strain rates (Figure 3). This latter process has also been studied by accelerated MD simulations (temperature accelerated dynamics, or TAD), revealing some basic unit processes which produce Frenkel pairs (a lattice atom moving into an interstitital position, leaving behind a vacancy), dislocation loops, or other defects under uniaxial tension. We have discovered a remarkable property of such simulations due to their high degree of symmetry that enables us to make conclusions about the spontaneous defect formation timescales in macroscopic samples.

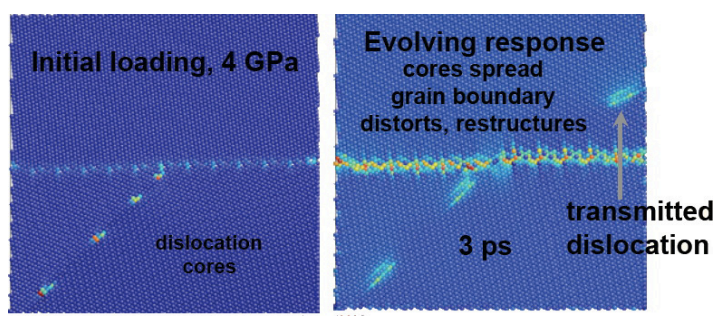


*Figure 2. Conventional MD simulation of a dislocation pile-up at an aluminum grain boundary. Atoms are colored according to their local potential energy. (Left) Initial unrelaxed configuration consisting of a four-dislocation pileup against an asymmetric grain boundary, with an applied shear stress of 4 GPa. (Right) Configuration after 3 ps at room temperature. The leading two dislocations have entered the grain boundary, and one has already been transmitted into the top grain.*

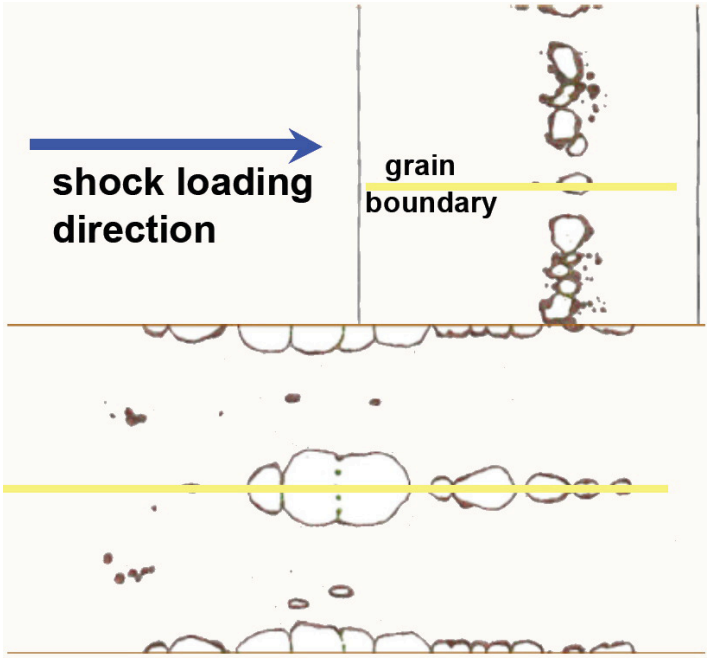


*Figure 3. Incipient spall failure in a copper bicrystal, showing how different failure mechanisms can occur at different strain rates. Only atoms at the surface of a void are shown, after the initial nucleation and growth stage when nearby voids have begun to coalesce. Two simulations are shown, both with a bicrystal 225 nm tall (i.e. each grain is 112.5 nm tall) with one grain boundary as indicated and a second at the periodic (top/bottom) boundary. The samples are 20 nm thick, and shocked with a 400 m/s impact velocity. (Top) Sample length 205 nm, which results in a very high tensile strain rate and homogeneous nucleation within the grains, leading to a vertical spall plane. (Bottom) Sample length 1025 nm, which results in a lower tensile strain rate and a longer time for heterogeneous nucleation of voids along the grain boundaries. These simulations were performed on Roadrunner, and include 54 and 270 million atoms, respectively.*

For the dislocation pileup problem, we have chosen a "typical" asymmetric GB in aluminum, applying dislocation pileup theory to introduce the leading few (3-5) dislocations which are atomistically represented, and the elastic strain field due to the remaining, more distant, dislocations in the pileup. An alternate method in which dislocations are introduced one at a time, allowing the system to relax at each step, has also been developed and will enable us to study scenarios in which the loading is gradually increased at a constant strain rate. The configuration created by either technique is then imported into SPaSM, which applies the appropriate shear boundary conditions as implemented on both the Roadrunner and conventional code versions. We have studied a variety of GBs, using conventional MD simulations at high applied stresses so that dislocation absorption, reflection, and/or transmission occur at the ps-to-ns timescales accessible without acceleration. This have given insight into the processes that may occur, including GB geometries with several competing mechanisms whose balance will likely change at more realistic strain rates (timescales of μs to ms) that we will be able to access with the hybrid techniques we are developing. We have also carved out a small active site near the GB, both before and after introducing the dislocation pileup, to accelerate using ParRep. These tests suggest that one of our main concerns, that a GB could rapidly hop between a very large number of detailed atomistic configurations and limit the potential boost (acceleration), is not the potential roadblock that we feared. Indeed, even after introducing the dislocation pileup (and more disorder) near the GB, only a few dozen distinguishable states have been found.

## Future Work

In the remaining two years of this project, we are planning to complete the development and testing of both algorithms, resulting in computer codes that effectively utilize Roadrunner. Through applying these techniques to the spall and dislocation pileup problems, we will gain a firm understanding of the strengths and weaknesses of each approach for these model problems. Finally, we expect that both these novel algorithms, and the insight they will provide into these two fundamental materials science phenomena, will be published in top-notch peer-reviewed scientific journals.

## Conclusion

This project is expected to lead to one or more algorithms and practical computer codes that will effectively utilize DOE supercomputer platforms - in particular LANL's Roadrunner - to study microscopic phenomena underlying the mechanical behavior and strength of materials at an atom-by-atom level, for size and time scales that are both larger and longer than currently possible. We will then utilize this unique capability to investigate fundamental materials science questions that have eluded direct study for a half-century or longer. Through this effort, we will help maintain America's leadership role in advanced high-performance computing, materials science, and nanotechnology.

## Publications

Arman, B., S. N. Luo, T. C. Germann, and T. Cagin. Dynamic response of Cu46Zr54 metallic glass to high strain rate shock loading: plasticity, spall and atomic-level structure. *Physical Review B.*

Germann, T. C.. Large-scale classical molecular dynamics simulations of shock-induced plasticity in bcc niobium. To appear in *16th American Physical Society Topical Conference on Shock Compression of Condensed Matter.* (Nashville, TN, 28 June - 3 July 2009).

Germann, T. C., and K. Kadau. Large-scale molecular dynamics simulations of the fcc-fcc volume collapse transition in shocked cesium. To appear in *16th American Physical Society Topical Conference on Shock Compression of Condensed Matter.* (Nashville, TN, 28 June - 3 July 2009).

Han, L. B., Q. An, S. N. Luo, and T. C. Germann. The effects of defects on melting of copper. To appear in *16th American Physical Society Topical Conference on Shock Compression of Condensed Matter.* (Nashville, TN, 28 June - 3 July 2009).

Luo, S. N., Q. An, T. C. Germann, and L. B. Han. Shock-induced spall in solid and liquid Cu at extreme strain rates. 2009. *Journal of Applied Physics.* **106** (1): 013502.

Luo, S. N., T. C. Germann, Q. An, and L. B. Han. Shock-induced spall in copper: the effects of anisotropy, temperature, defects, and loading pulse. To appear in *16th American Physical Society Topical Conference on Shock Compression of Condensed Matter.* (Nashville, TN, 28 June - 3 July 2009).

Luo, S. N., T. C. Germann, and D. L. Tonks. Spall damage of copper under supported and decaying shock loading. To appear in *Journal of Applied Physics.*

Pozzi, C., T. C. Germann, and R. G. Hoagland. Molecular dynamics simulations of dislocation emission from shocked aluminum grain boundaries. To appear in *16th American Physical Society Topical Conference on Shock Compression of Condensed Matter.* (Nashville, TN, 28 June - 3 July 2009).

Ravelo, R., B. L. Holian, and T. C. Germann. High strain rate effects in quasi-isentropic compression of solids. To appear in *16th American Physical Society Topical Conference on Shock Compression of Condensed Matter.* (Nashville, TN, 28 June - 3 July 2009).

# Enhance Radiation Damage Resistance via Manipulation of the Properties of Nanoscale Materials

*Michael A. Nastasi*
20090061DR

## Introduction

We are working to enhance the radiation resistance of materials by manipulating their properties at the nanoscale to directly affect the evolution of damage cascades. The design of future nuclear power reactors, including advanced fuel cycles, Gen IV and fusion reactors places high demands on reactor cladding and structural materials. These extreme operating conditions include extremely high irradiation doses, corrosive liquid metal environments, and higher operating temperatures with minimal change in mechanical properties. At present, the best engineered materials for high dose nuclear applications reach their structural limit at relatively low irradiation dose. Their mechanical integrity at elevated temperatures degrades at even lower irradiation doses. Thus, transformative research in materials development is required to meet the needs of future nuclear reactors.

The reason why materials fail under irradiation can be traced at the most fundamental level to the accumulation of the defects produced during the irradiation process. Left unbridled such processes lead to swelling and chemical changes that compromise the material's mechanical and corrosion resistant properties. Therefore, the principal challenge in the development of materials with radically extended performance limits in extreme radiation environments is to increase the recovery efficiency of radiation-induced defects.

Our approach in addressing this problem will be to develop materials that will contain special internal features, i.e., interfaces, that can be designed at the atomic-scale to attract, absorb and annihilate radiation-induced defects, thereby allowing design of nanostructured materials for radiation damage tolerance. This will build on recent scientific breakthroughs at LANL that presents a new paradigm in designing materials with the specific property of radiation damage tolerance. The central idea of this proposal is atomic-scale design of stable internal interfaces that impart radiation tolerance to materials by attracting, absorbing, and annihilating point defects.

## Benefit to National Security Missions

This work will support the mission of the DOE Office of Science, explicitly the BES-stated Basic Research Needs for Advanced Nuclear Energy Systems, included a priority research direction on Nanoscale Design of Materials and Interfaces that Radically Extend Performance Limits in Extreme Radiation Environments.

## Progress

### Experimental

For copper-niobium multilayers, we have completed experiments on the irradiation response, studying the helium solubility at interfaces. The helium-ion irradiated samples were examined in a transmission electron microscope (Figure 1) to determine the depth range over which helium bubbles were detected. The helium concentration profile was measured accurately with ion beam method: nuclear reaction analysis. These experiments show that helium solubility increases from below 0.1 atomic% in pure copper, to 2 atomic% in 5 nm copper-niobium layers, to 4 atomic% in 2.5 nm layers. These experiments validate the atomistic model predictions of high helium solubility at interfaces due to the atomic structure of the interface. To compare different interfaces, similar experiments are now in progress in vanadium-silver multilayers.

Focused-ion-beam machined micropillar specimens were used to obtain compressive stress-strain curves for Cu/Nb multilayers before and after ion irradiation. For these mechanical tests, a series of helium (He) ion irradiations with different energies and doses were performed at room temperature to produce a near constant He concentration of 6 ± 1 at% over a depth of 1__m in Cu-Nb multilayers with individual layer thicknesses ranging from 2.5 nm to 50 nm. Transmission electron microscopy shows He bubbles, approximately 1 nm in diameter, throughout the multilayered films, but the average helium bubble density, swelling and lattice expansion reduce with decreasing bilayer period. Consistent with the reduction in damage with reducing layer thickness, the magnitude of radiation hardening decreases significantly

with decreasing layer thickness, without any measurable loss in deformability.

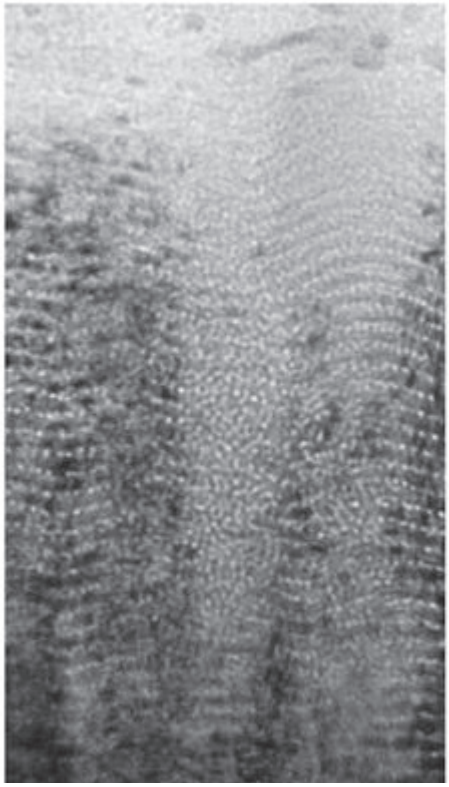

*Figure 1. Under-focused bright field transmission electron microscope (TEM) micrograph showing helium bubbles "white dots" in a 2.5 nm Cu/2.5 nm Nb ion irradiated multilayer. Comparison of this image with measured helium concentration as a function of depth gives a measure of the minimum helium concentration above which bubbles are resolved.*

**Modeling**

The Boltzmann form $n_v = e^{-\Delta E_f / k_B T}$ for vacancy concentrations states that the thermal equilibrium number of vacancies decreases to zero as the temperature is lowered to zero. We found, however, that interfaces present in Cu-Nb multilayer composites contain a non-zero concentration of ground state or "constitutional" vacancies, which are present even at zero temperature. These vacancies form due to the unusual lowest-energy structure of Cu-Nb interfaces, shown in Figure 2. Here blue atoms are Nb, yellow atoms are Cu in perfect crystal sites, and red atoms are Cu situated in areas of high free volume. Because these high volume sites provide preferential trapping locations for misfitting interstitial solutes, this structure accounts for the high solubility at Cu-Nb interfaces of He, a deleterious element that gets implanted in materials operating in some extreme irradiation environments like the interiors of magnetic confinement fusion devices. This finding is described in a manuscript currently under review in Physical Review B—Rapid Communications.

To better understand how He becomes trapped at high free volume sites, how it diffuses between them, as well as the conditions under which it begins to precipitate out in the form of nanoscale bubbles, we are constructing an Embedded Atom Method (EAM) potential to describe Cu-Nb-He system. To this end, we are carrying out density function theory (DFT) calculations to study the behavior of interstitial and substitutional He in FCC Cu and BCC Nb. This potential will also allow us to investigate the dependence of interface mechanical properties (for example the shear and tensile strength) as a function of the concentration of He trapped at the interface. By providing insight into the connections between interface structure and He solubility, our work is laying the foundation for tailoring nanocomposites to survive exposure to radiation environments with high implanted He/dpa (dpa: displacement per atom) ratios, such as those found in fusion reactors.

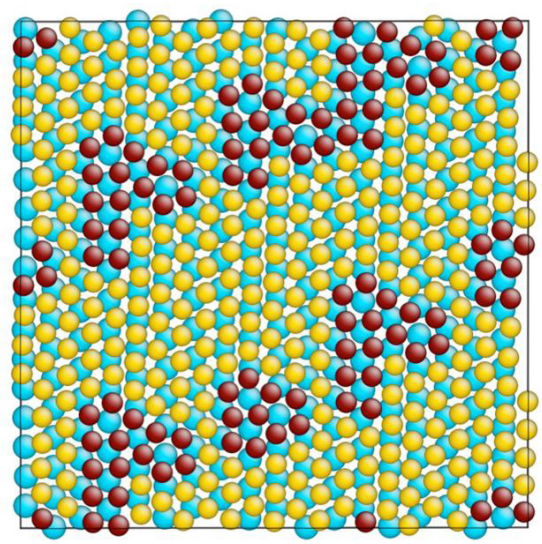

*Figure 2. Ground state Cu-Nb interface configuration. Blue atoms are Nb and yellow atoms are Cu with 6 nearest neighbors in the interface Cu (111) plane. Red atoms have less than 6 nearest neighbors in the interface Cu (111) plane and have a higher free volume than the rest of the Cu-Nb interface.*

We have also examined the role that grain boundaries play in the radiation tolerance of nanostructured materials, using a tilt grain boundary in Cu as a model system (Figure 3). We focused on two time-scale regimes: the ps time scale over which damage (primarily interstitials and vacancies) is created by collision cascades (using molecular dynamics) and the longer time scales over which those defects annihilate and aggregate (using accelerated molecular dynamics). We found the efficiency of grain boundaries to absorb defects depends on the distance the collision cascade occurs from the boundary. In most cases, more defects remain after the cascade in materials with boundaries than without, suggesting poorer radiation tolerance. However, when long-time behavior is accounted for, we find that grain boundaries exhibit an enhanced self-healing capability and that inter-

stitials absorbed at the boundary during the cascade can be reemitted to annihilate with vacancies in the bulk. This "interstitial emission" mechanism occurs with a very small barrier of 0.17 eV (compared to 0.7 eV for bulk vacancy migration) and can annihilate defects that are separated by 4-5 nearest neighbor distances. This mechanism leads to superior radiation tolerance at temperatures where vacancies are essentially immobile. These results explain experimental observations of radiation damage effects in nanocrystalline gold, which show worse tolerance than large-grained counterparts at low temperature but enhanced recovery at intermediate temperatures.

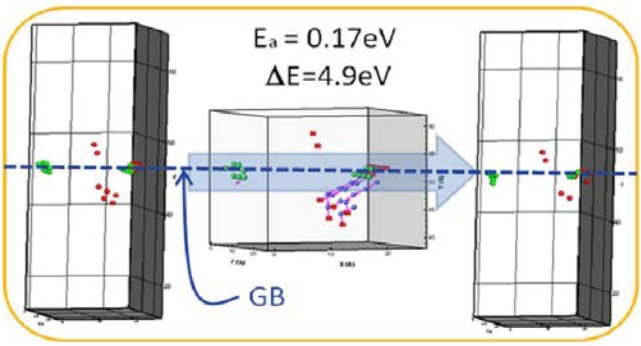


*Figure 3. Mechanism of interstitial emission as observed in the dynamical evolution of cascade damage near a sigma 11 symmetric tilt boundary in Cu via temperature accelerated dynamics. One event with a barrier of 0.17 eV leads to the annihilation of 3 vacancies in the bulk region by the emission of 3 interstitials loaded into the boundary. This mechanism occurs much faster than vacancy diffusion (0.7 eV barrier). Further studies show that the loading of the boundary with radiation-induced interstitials is crucial for this mechanism to occur.*

## Future Work

Following our discovery of "super sink" interfaces we have a truly unique opportunity to develop highly radiation tolerant nanocomposite materials. We have shown that such interfaces stabilize material microstructure and efficiently heal radiation damage by attracting, absorbing, and catalyzing the annihilation of radiation-induced point defects. Our objectives in this work will be: 1) develop a generalized description, applicable to any interface in any material, of the properties that make an interface a "super sink" for radiation-induced defects; 2) explore the irradiation stability of nano-composites over a broad spectrum of extreme environments (high irradiation dose, long time, high temperature, and corrosion to simulate real reactor environments conditions); and 3) explore the effect of irradiation (particularly at high doses) on mechanical properties such as strength and ductility. Our approach integrates theory, modeling, and experiments to formulate, validate, and test the limits of strategies for enhancing radiation damage resistance of materials by maximizing their content of super sink interfaces. Our findings will lay the scientific foundations for intelligently designing radiation tolerant materials for future nuclear reactors.

## Conclusion

We have 3 objectives in this research that we believe will lead to the development of materials with high radiation tolerance. First, to develop a generalized description, applicable to any interface in any material, of the properties that make an interface a "super sink" for radiation-induced defects. Second, explore the irradiation stability of nanocomposites over a broad spectrum of extreme conditions (high irradiation dose, long time, high temperature, and corrosion). Third, explore the effect of irradiation (particularly at high doses) on mechanical properties such as strength and ductility.

## Publications

Demkowicz,D.Bhattacharyya,et.al., M. J.. High helium solubility at Cu-Nb interfaces due to ground state vacancies. *Physical Review B - Rapid Communications.*

# Seaborg Institute Fellows

*Albert Migliori*
20090475DR

## Introduction

This project is directed toward development of new actinide science capabilities to respond to the future national security mission environment, nuclear energy, weapons complex transformation, and the evolution of actinide science and technology that will be applicable to national security. We will address fundamental science that will enhance stockpile stewardship, reduce global nuclear threats, and lead to sustainable nuclear energy. Los Alamos strengths in actinide chemistry, material synthesis, condensed matter physics, complex systems, emergent phenomena, and theory and modeling provides a world-class foundation from which to develop these capabilities, and help transform the Laboratory mission over the next five years.

## Benefit to National Security Missions

Knowledge and expertise in actinide science is central to the mission of DOE and the NNSA, including national defense, threat reduction, nuclear forensics, fundamental science, energy security, environmental restoration, and radioactive waste management.

## Progress

We describe here highlights of progress made in FY 2009 by the (at present) 12 Seaborg postdocs.

### Exploring New Ligand Archetypes for *f*-Element Catalyzed Organic Transformations

Over the last decade, well-defined lanthanide (Ln) and actinide (An) precatalysts have been increasingly utilized to promote organic transformations including olefin polymerization, alkyne oligomerization, hydrosilylation, and hydroamination to render *f*-element complexes more tolerant of functionalized substrates than their transition metal congeners. Progress has been made in developing several tripodal ligand precursors. In this project so far, attempts have yet to yield tractable products, currently being investigated for lanthanide complexation. It is envisioned that addition of a ligand diiodide salt to a $Ln^0$ precursor could result in the preparation of neutral lanthanide hydride complexes. This work is ongoing.

### Grain boundary structures and influence on segregation properties in oxide nuclear fuels

Uranium dioxide ($UO_2$) is the standard nuclear fuel in pressurized water reactors. Fission gases such as xenon (Xe) migrate to regions between grains called grain boundaries and cause swelling of the fuel. This phenomenon ultimately threatens the mechanical integrity of the fuel. This task has concentrated on how Xe segregates to grain boundaries in $UO_2$ using empirical potentials and density functional theory. Our calculations predict the energy of segregation to be very sensitive to the local atomic environment of the solute atom in the host and that there is a substantial difference in the overall segregation propensity to the four boundaries of a grain. Future work would include utilization of the atomistic segregation data for informing higher scale models to predict the fuel performance within the reactor environment and to extend this study for mixed oxide fuels.

### Spectroscopic Analysis of Actinyl Systems

Actinyl cations are ubiquitous in higher oxidation state actinides and are relevant to environmental remediation, nuclear waste management and nuclear fuel separation technologies. The goal of this task is to increase our understanding of the electronic structure and bonding properties of the actinyls by focusing on probing the actinyls through polyoxometalate (POM) coordination. Our luminescence studies have revealed mechanisms to enhance coordination in aqueous solutions. Subtle changes in the uranyl coordination environment have resulted in significant changes in spectral signatures and luminescence lifetimes. Our studies have been extended to $5f^1$ transuranic neptunyl(VI) systems. We have also studied palladium hydrides with an in-situ hydrogenation apparatus for synchrotron diffraction and x-ray absorption. This system was tested at the SLAC National Accelerator Laboratory and has led directly to a follow-on project studying uranium and plutonium hydrides.

**Mechanisms and applications of natural U-series fractionations**

Precise measurements of $^{238}U/^{235}U$ ratio by multiple-collector inductively coupled plasma mass spectrometry (MC-ICPMS) have revealed that natural fractionation of U can take place in low temperature environments. The potential applications of low temperature $^{238}U/^{235}U$ fractionations include studying the formation of U ore deposits, monitoring U remediation, understanding biogeochemical cycling of U and quantifying paleo-weathering environments. By measuring low temperature fractionation, reaction pathways can be determined. We are currently setting up analytical methods for ICP-MS.

**Capturing a Terminal Uranium Nitride**

As we face a global energy crisis and anthropomorphic global warming, we need to look to nuclear energy sources, among others. Uranium nitride $[UºN]_x$ has arisen as a promising alternative to the ubiquitous mixed oxide fuels (MOX), with advantages including a higher melting point and thermal conductivity. Very little is known about the UºN linkage and its chemical behavior and reactivity. In this task, the safe generation of uranium azide complexes ($U\text{-}N_3$) was established by developing a new synthetic methodology that didn't involve $NaN_3$. This new oxidative functionalization protocol uses gold (I) complexes that oxidize uranium (III) complexes to uranium (IV) complexes, accompanied by ligand transfer from gold to uranium photolyzed with UV light. The mechanism of this reaction was studied computationally and found to proceed through a highly reactive terminal uranium nitride complex. These results have important implications for the use of the alternate nuclear fuel $[UºN]_x$ and have shown that photochemistry may be a useful tool for inducing a variety of redox processes on the actinides.

**Electronic Structure of Neptunium**

A critical problem in actinide physics is to understand the effect of electron-electron correlation effects on *5f* actinide orbitals. Two methods have been often used to explore the actinides: first-principles electronic band-structure or local-density-functional (LDA) methods and dynamical mean-field theory (DMFT). This task will the gap between these two methodologies by using quasi-particle GW (QSGW) theory, a rigorously based first-principles perturbative correction to band-structure theory that can handle weak to moderate correlation strengths. We used QSGW theory to examine what happens in the strongly correlated limit to delta-Pu. Our results showed that the single-particle band structure obtained with the QSGW method differs from the LDA in two significant ways: (1) The 5f electron energy dispersion is flatter and (2) the crystal field splitting between 5f states is significantly smaller. We have now done similar calculations on Np, which show similar effects but with smaller intensity.

**Synthesizing new uranium(VI) bis(imido) compounds**

This project focuses on synthesizing new uranium(VI) bis(imido) compounds and one- and two-electron reductions aimed toward uranium (IV and V) bis(imido) complexes. This chemistry has resulted in the isolation of several new uranium(VI) bis(imido) species, containing both *tert*-butyl and phenyl imido ligands. Examples include $[U(N\mathit{t}Bu)_2(\text{triglyme})I]I_3$, $U(NPh)_2(\mathit{t}Bu_3\text{terpy})Cl_2$, and $[U(NPh)_2I(THF)_4]I_3$. To date, attempted reductions with sodium naphthalene, sodium bipyridine, potassium hydride, sodium borohydride, and decamethylcobaltocene have not yet yielded tractable products.

**Ultrasonic Measurements of Actinides**

Measurements of the temperature dependence of the elastic moduli of alpha, beta, gamma, and delta plutonium are essential for both engineering and for calibration of theories of Pu properties. The moduli, Figure 1, show extreme softening on warming by an order of magnitude more than expected for ordinary metals with similar Debye temperatures. In this project measurements were analyzed to produce new values for beta and gamma Pu. The shear modulus is surprisingly continuous between beta and gamma phases. The project has produced so far numerical values for elastic moduli that are extremely accurate, and of archival quality on well characterized material. Future work will include measurements from 5 K to 700 K using the RUS (Resonant Ultrasound Spectroscopy) on pure delta Pu.

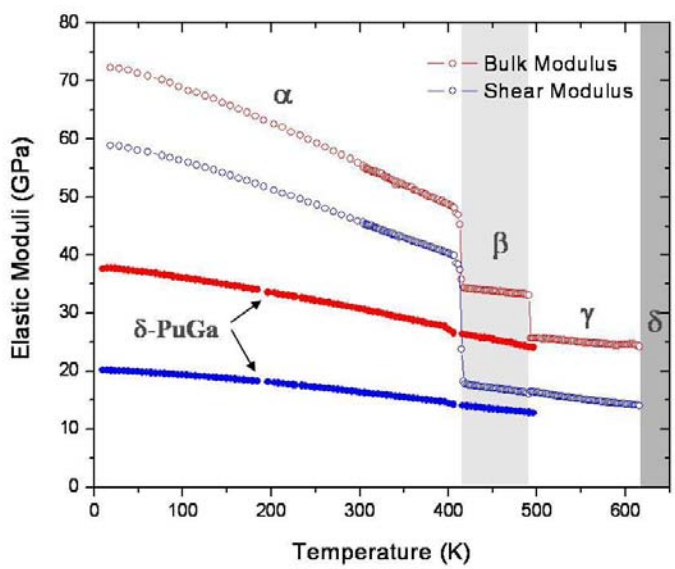


*Figure 1. Evolution with temperature of the elastic moduli of pure Plutonium (open symbols) and Gallium-stabilized delta-Plutonium (closed symbols). Bulk modulus is shown by red symbols and shear modulus by blue symbols.*

**Synthesizing single-crystal of heavy fermion intermetallics**

$UIr_4Al_{15}$ was recently discovered and was isolated from Al flux reactions using the corresponding elements. The observed physical properties exhibited by the compound shows promise that further more elaborate studies will be

completed in the near future and currently attempts to synthesize analogues to it are currently underway. $UCu_4Al_8$ is another tetragonal system synthesized in this project. On-going studies are attempting to grow large single-crystals of the compound. Structurally, the compound is of interest because of the relation with the well known heavy fermion superconductor $UPt_3$. $UIrSi_3$ and $UNiGa_3$ have both been prepared.

**Uranium(VI) Chemistry: Bis(imido) Uranium(V)/(VI) Complexes**

For the past 150 years, studies of uranium(VI) have been generally directed towards understanding the chemical behavior and unique bonding in the uranyl ion ($UO_2^{2+}$). We have reported the syntheses of isoelectronic bis(imido) $[U(NR)_2]^{2+}$ and oxo-imido $[U(NR)(O)]^{2+}$ ions, which possess many of the bonding features, found in $[UO_2]^{2+}$. Given their unprecedented nature, this task is focused on exploring their reactivity, structure, and bonding with a goal to explore the differences between the uranium centers in isoelectronic $[U(NR)_2]^{2+}$ and $[UO_2]^{2+}$ ions. Striking differences in reactivity were observed. This task has also probed U-Cl bond of $[UO_2Cl_4]^{2-}$ and $[U(N^tBu)_2Cl_4]^{2-}$ ions. XAS studies suggest there are increased covalent interactions in the U-Cl bond. While the reasons for this discrepancy remain unclear, we are currently examining these observations with other spectroscopic and theoretical measurements. During the course of studies on $(C_5Me_5)_2U(N^tBu)_2$ we found that the a dimeric uranium(V) bis(imido) complex could be synthesized. This discovery represents a rare and important finding in actinide science that demonstrates f-electron communication can be achieved between actinide metal centers.

## Future Work

This R&D project is executed under the technical leadership of the G.T Seaborg Institute for Actinide Science (Seaborg Institute). While it must meet the same standards for excellence as other LDRD projects, it is strongly related to the broader mission of the Seaborg Institute which is, briefly, to advance actinide chemistry, actinide materials science, and actinide simulation and modeling in order to position LANL for excellence in an area that is an important provence of LANL, important to LANL long-term science excellence in missions of energy security and nuclear weapons.

## Conclusion

The tasks in this LDRD project are dedicated to addressing important gaps in our current level of understanding of actinides, promoting a creative and expert core actinide workforce, and to scientific excellence in the many important scientific problems in the field. LDRD resources are used to build capabilities, address outstanding scientific problems, advance new scientific concepts via initial support to seed research elements of feasibility studies, and cutting-edge scientific research that addresses critical scientific questions.

## Publications


Chantis, A. N., R. C. Albers, A. Svane, and N. E. Christensen. GW correlation effects on plutonium quasiparticle energies: changes in crystal-field splitting. 2009. *Philosophical Magazine.* **89**: 1801.

Chantis, A. N., R. C. Albers, M. D. Jones, M. van Schilfgaarde, and T. Kotani. Many-body electronic structure for metallic uranium. 2008. *Physical Review B (Rapid Communications.* **78**: 811101.

Spencer, L. P., E. J. Schelter, P. Yang, R. L. Gdula, B. L. Scott, J. D. Thompson, J. L. Kiplinger, E. R. Batista, and J. M. Boncella. Cation-cation interactions, magnetic communication, and reactivity of the pentavalent uranium Ion [U(NtBu)2]+. 2009. *Angewandte Chemie International Edition.* **48** (21): 3795.

Spencer, L. P., P. Yang, B. L. Scott, E. R. Batista, and J. M. Boncella. Uranium(VI) bis(imido) chalcogenate complexes: synthesis and density functional theory analysis. 2009. *Inorganic Chemistry.* **48** (6): 2693.

Spencer, L. P., P. Yang, B. L. Scott, E. R. Batista, and J. M. Boncella. Oxidative addition to U(V)-U(V) dimers: facile routes to uranium(VI) bis(imido) complexes. To appear in *Inorganic Chemistry.*

Spencer, L. P., R. L. Gdula, T. W. Hayton, B. L. Scott, and J. M Boncella. Synthesis and reactivity of bis(imido) uranium(VI) cyclopentadienyl complexes. 2008. *ChemComm.* : 4986.
Thomson, R. K., C. R. Graves, B. L. Scott, and J. L. Kiplinger. Noble reactions for the actinides: safe gold-based access to organouranium and azido complexes. 2009. *European Journal of Inorganic Chemistry.* **2009** (11): 1451.

# Strongly Correlated Electrons: Duality and Implications

*Cristian D. Batista*
20060043DR

## Abstract

Actinide and Lanthanide elements are among the most complex materials from the point of view of their electronic structure. This complex behavior is one of the paradigms of modern condensed matter due to the diversity of quantum states of matter that emerge from it. The goal of the current project was to model heavy elements such as actinide and lanthanide based compounds in order to reconcile several experimental observations that seemed to be contradictory. In particular, we explained the origin of the "dual nature" of f-electrons (electrons seem to be localized or itinerant depending on the experimental probe) and found novel forms of "normal" states that are precursors of the unconventional superconductors. One of the high potentials of these new findings is the comprehensive understanding of different classes of seemingly unrelated materials through the identification of universal low-energy models. In this way, our results will have an important impact not only in f-electron materials, but also in other systems such as the high-temperature cuprate superconductors.

## Background and Research Objectives

The combination of our experimental and theoretical efforts was crucial for understanding electron duality in different f-electron materials. We focused on families of actinide and lanthanide based compounds that exhibit localized or itinerant behaviors depending on the property that is measured. By applying a very broad spectrum of experimental techniques, we managed to build a very complete picture of the metallic phase of these strongly correlated systems. By modeling these experimental results we discovered novel f-electron states that were not contemplated in the traditional paradigm based on the known behavior of dilute systems (compounds containing a low concentration of magnetic impurities). This discovery allowed us to find commonalities between the normal phase of f-electron compounds that exhibit unconventional superconductivity at low temperatures, and other families of unconventional superconductors.

The concept of duality was extended to pure elements such as metallic Pu. We found a low energy model for delta-Pu that reproduced the photoemission measurements done at LANL and revealed some key aspects that distinguishes Pu from the rest of the actinides. Moreover, we demonstrated that the physics of metallic delta-Pu is closer to the physics of some Lanthanides, such as Ce or mixed valent Sm, than to the physics of the other 5f elements. Interestingly, all of these elements exhibit large volume collapses as a function of temperature. Our studies suggest that the volume collapse has a common root on the similar electronic properties.

We also extended the notions of duality to insulators, i.e., materials that cannot conduct electric currents because their valence electrons are localized near the corresponding ions. By studying the potential effects of partial delocalization in Mott insulators, i.e., materials in which the electrons are localized by the strong Coulomb repulsion, we discovered that it is possible to have orbital electronic currents in these materials. This new state of matter was never discussed before. An important aspect of this discovery is that these states exhibit novel functionalities associated with electronically driven magneto-electric effects. This is the ability of inducing electric polarization by applying magnetic fields or magnetization by applying electric fields. The concepts discovered in this area set the basis for a new line of experimental and theoretical research that will be pursued at LANL in the near future.

## Scientific Approach and Accomplishments

The dual nature of electrons was probed experimentally in 4f (Ce and Yb)- and 5f (U)-based strongly correlated compounds by a wide range of techniques, including thermodynamic, electrical transport, neutron diffraction,

nuclear magnetic resonance (NMR), deHaas-van Alphen, muon spin resonance, angle-resolved photoemission (ARPES), and Andreev reflection spectroscopy measurements. Each of these techniques was chosen to reveal particular signatures of duality, for example, in electronic structure and excitations, spin structures and dynamics, electronic scattering and magnetic entropy. Applying these techniques to a single material is insufficient to establish the generality of electronic duality and conditions under which it determines physical properties, and, consequently, we explored materials whose ground states are superconducting, magnetically ordered, paramagnetic, near or far from a quantum-phase transition and that form in several different crystal structures.

In spite of the breath of ground states and crystal structures, two interactions dominate in these systems: 1) a Kondo-like interaction between the f-electron spin and the spin of itinerant electrons, which tends to form a non-magnetic ground state and 2) a long-range Rudermann-Kittel-Kasuya-Yosida (RKKY) interaction between f-electrons, which is mediated by itinerant electrons and promotes magnetic order. Nearly forty years ago, Doniach proposed a theoretical model based on the competition between these two interactions. This model has been used widely in the intervening years to interpret physical properties of electronically correlated 4f- and 5f-electron systems, but it did not consider the possibility of electronic duality. We have shown that electronic duality can be viewed as a consequence of Kondo and RKKY interactions and that the new conceptual framework of electronic duality collapses strongly correlated 4f- and 5f-electron systems onto a universal phase diagram, something impossible without duality.

Consistent with all our measurements, f-electrons are essentially localized at 'high' temperatures, typically above 100-200 K, and interact weakly with itinerant electrons through the Kondo interaction. From our measurements and those of others, we identified in these materials a characteristic low-temperature scale T* at which there are changes in physical properties. For a given material, T* was independent of the type of identifying measurement, whether from thermodynamic and transport, NMR, μSR or Andreev reflection. For temperatures T<< T*, these measurements were consistent with a substantial itinerant nature of the f-electrons, and therefore, we associated the scale T* with the crossover from localized to the onset of itinerant character of the f-electrons. With this association, T* denotes the temperature or equivalently the energy scale $E^*=k_BT^*$ on which electronic duality starts to become significant, and this scale arises because of the RKKY interaction between f-electrons. Independently, we also determined the energy scale $T_K$ for the Kondo interaction from experiments that probed this interaction when the f-ion was a dilute impurity in a non-magnetic counterpart host. For example, if we were studying duality in $CeRhIn_5$, we determined $T_K$ from measurements of very dilute Ce in the host $LaRhIn_5$. Because this dilute limit is well understood theoretically and there is no electronic duality, we could extract straightforwardly the magnetic exchange parameter *J* upon which $T_K$ depends exponentially. The RKKY interaction increases as $J^2$, and consequently, we expected $J\rho = -1/\ln[T_K\rho)] = [c^{-1}T^*\rho)]^{1/2}$, where ρ is the experimentally determined electronic density of states of the non-magnetic, uncorrelated counterpart compound. The validity of this simple relationship is shown in Figure 1 where we plot $(T^*\rho)^{1/2}$ as a function of $-[\ln(T_K\rho)]^{-1}$ for several different strongly correlated 4f- and 5f-electron materials that we have studied.

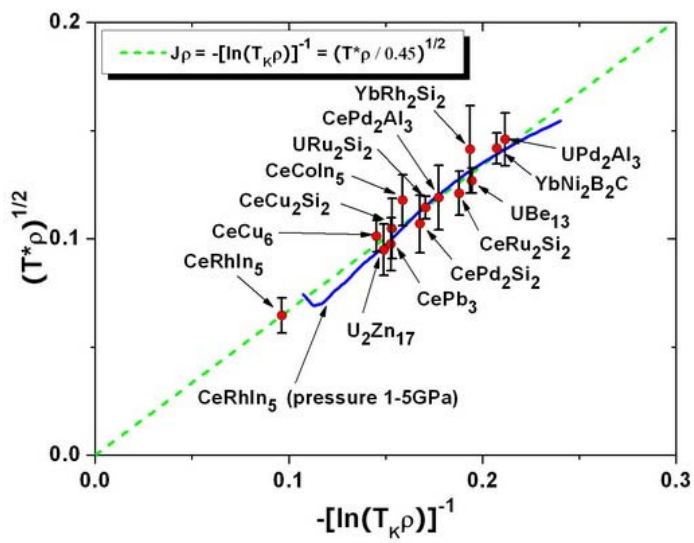


*Figure 1. (T*ρ)1/2 as a function of –[ln(TKρ)]-1 for strongly correlated 4f- and 5f-electron materials with different ground states and different crystal structures. Unexpectedly, all of these materials have a common, materials- independent linear relationship.*

Unexpectedly, this figure shows that these quantities are related by a materials-independent constant c=0.45 and, most surprisingly, that the development of electronic duality, i.e. T*, depends only on simple, measureable quantities. This remarkable correlation establishes for the first time that electronic duality evolves as a function of temperature; however, it does not predict the ultimate, zero-temperature state that a particular material will have if its exchange parameter *J* is known. Nevertheless, empirically it does appear that superconducting materials cluster around $(T^*\rho)^{1/2} \approx 0.1$ and materials with magnetic ground states tend to have smaller values of $(T^*\rho)^{1/2}$. This is borne out in our study of the pressure dependence

of $CeRhIn_5$, which is a strongly correlated magnet at low pressure and becomes an unconventional superconductor at higher pressures. Pressure tunes the magnitude of *J* and, hence, the evolution of $(T^*\rho)^{1/2}$ and $-1/\ln[T_K\rho)]$ that is plotted by the blue curve in Figure 1. The lower end of this curve corresponds to lower pressures.

The physical picture that has emerged from these studies is that electronic duality can be viewed as the quantum mechanical collective entanglement of f-electrons with surrounding itinerant electrons. The language used in this description, however, is specific to the starting point from which we derived the relationships discussed above. At a more microscopic level, the essential parameter *J* is proportional to the square of the hybridization strength between f- and itinerant electrons, i.e., $J \propto V_{kf}^2$. It is, then, hybridization that determines the extent of electronic duality and the scale T*. We have established this clearly in several different ways, one being through our discovery and study of a new family of strongly correlated 5f-compounds, ($UM_2Zn_{20}$, where M= Co and Rh). In these crystals, the U atom is structurally surrounded by a cage of electronically inert Zn atoms, which minimizes hybridization of the 5f-electrons with itinerant electrons of the transition metals Co or Rh. As a result, the physical properties of these compounds can be described almost completely by well-known theoretical models in which strong electronic correlations derive only from local, Kondo-like spin-hybridization effects; that is, the 5f-electrons do not exhibit any pronounced duality, at least for any U-based correlated system.

Resonant photoemission measurements provide a probe of the energetic distribution of f-electrons and were applied to the strongly correlated series $CeRh_{1-x}Ir_xIn_5$ to explore the interpretation of duality from hybridization. As mentioned, the x=0 end member of this series is an antiferromagnet with small $J\rho$. In contrast, the x=1 end member is an unconventional superconductor with larger $J\rho$, i.e., T*, and for intermediate values of x, the ground state evolves systematically from magnetic to superconducting. Figure 2 shows the progression in the 4f-electron derived photoelectron intensity as this series is crossed at temperatures less than T*. For x=0.25, there is more intensity at lower kinetic energy (more localized-like 4f electrons) but more intensity near the Fermi energy (more itinerant-like 4f electrons) for larger x. Significantly, even with this progression from more localized to more itinerant-like behaviors of the 4f electron, which is a hallmark of increasing f-electron hybridization, there is intensity indicative of simultaneous localized and itinerant character in the 4f electron of cerium for all values of x. Though clearly establishing the transfer of 4f-electron spectral weight from more localized to more itinerant natures with increasing hybridization, these particular experiments are insensitive to the possibility of anisotropic hybridization. Indeed, angle-resolved photoemission studies of the x=1 compound have established that hybridization is anisotropic and further, that the resulting 4f electronic density of states has a temperature dependence predicted by our model that led to Figure 1. One of the consequences of electronic duality in $CeIrIn_5$ is a new electronic state discovered as part of our investigation of duality. This unexpected state emerges just above the onset of superconductivity and completely surrounds the field-dependent evolution of superconductivity. In several respects, this new state appears analogous to the 'pseudogap' state that precedes the onset of high temperature superconductivity in the strongly correlated copper-oxide materials. The detailed relationship among duality, the new state in $CeIrIn_5$ and the cuprate pseudogap are being pursued by collaborators.

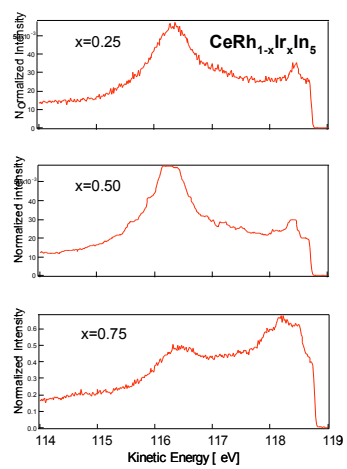


F*igure 2. Resonant photoemission exhibiting the two characteristic contributions from the 4f electron of Ce, localized character at a binding energy near 116 eV and itinerant character at the Fermi energy near 119eV.*

Numerous phenomenological parallels have been drawn between f- and d- electron systems in an attempt to understand their display of unconventional superconductivity. The microscopics of how electrons evolve from participation in large moment antiferromagnetism to superconductivity in these systems, however, has remained a mystery. Knowing the origin of Cooper paired electrons in momentum space is a crucial prerequisite for understanding the pairing mechanism. Of especial interest are pressure-induced superconductors $CeIn_3$ and $CeRhIn_5$ in which disparate magnetic and superconducting orders apparently coexist – arising from within the same f-electron degrees of freedom. We made ambient pressure quantum oscillation measurements on

$CeIn_3$ that crucially identified the electronic structure – potentially similar to high temperature superconductors. Heavy pockets of f-character were revealed in $CeIn_3$ (Figure 3), undergoing an unexpected effective mass divergence well before the antiferromagnetic critical field (Figure 4). We thus uncovered the softening of a branch of quasiparticle excitations located away from the traditional spin-fluctuation dominated antiferromagnetic quantum critical point. The observed Fermi surface of dispersive f-electrons in CeIn3 could potentially explain the emergence of Cooper pairs from within a strong moment antiferromagnet.

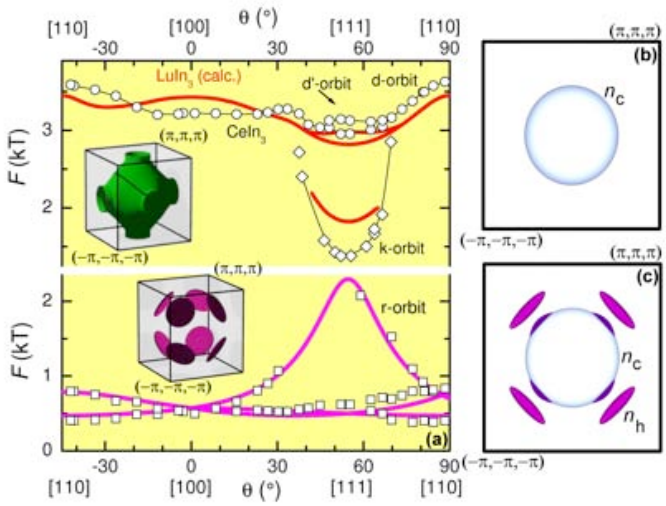


*Figure 3. Measured Fermi surfaces of $CeIn_3$. (a) measured d, k- and r- orbit quantum oscillation frequencies F related to the Fermi surface (FS) cross-sectional area Ak , versus the orientation of H. Electrons undergoing cyclotron motion in real-space circumnavigate the FS in momentum space k. Measured d- and k- band frequencies are similar to those in nonmagnetic LuIn3 (red lines) calculated by an augmented plane wave method, whereas r-orbit frequencies, found only in $CeIn_3$, correspond to simulations (purple lines) of the 8 ellipsoidal pockets depicted in the lower inset. The upper inset shows a less than half filled f-electron Fermi surface sheet from LDA calculations in the paramagnetic phase of $CeIn_3$. (b) Schematic representation of the conduction electron Fermi surface (d-sheet) expected within the strong moment Kondo lattice model. In this picture, any mass enhancement would occur due to conduction-f electron hybridization over the entire conduction electron Fermi surface. (c) Schematic for unconventional participation of f-electrons in Fermi surface indicated in $CeIn_3$. A distinct heavy surface of principally f-electron character appears, causing an enhancement of the conduction electron density of states only in the regions of conduction-f electron band proximity.*

Our deHaas-vanAlphen measurements were modeled and explained by solving a single band Hubbard model for the f-electrons. Figures 3 and 4 show comparisons between the deHass-vanAlphen measurements and the theoretical results. Our model fully accounted for these observations and also predicted specific signatures in angle-resolved photoemission. Though these signatures could not be observed fully in our ARPES experiments because of insufficient energy resolution (>70meV), experimental results were consistent with trends expected from our predictions. An important conclusion of this work is the potential for finding Mott physics (the properties of a doped Mott insulator) in 4f electron compounds. This state of matter that is the precursor of the unconventional superconductivity in the cuprate high-temperature superconductors was never considered to be present in 4f-eletron compounds. Our discovery in $CeIn_3$ suggests that the same deHass-vanAlphen measurements should be done in $CeRhIn_5$ under pressure to find out if similar f-electron pockets appear above the critical pressure necessary for inducing coexistence of superconductivity and antiferromagnetism.

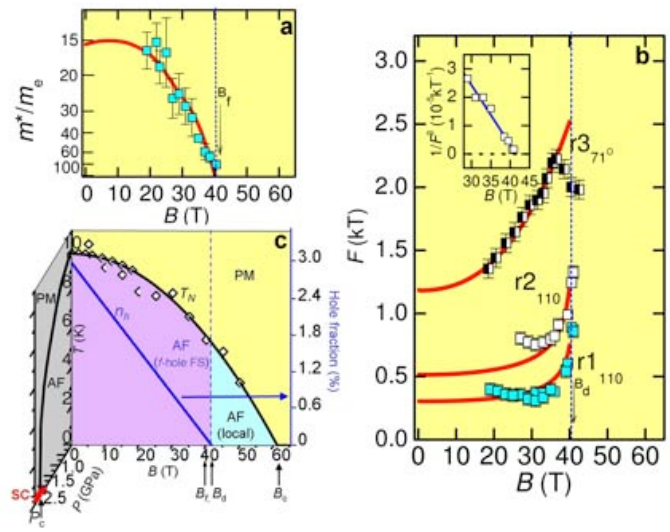


*Figure 4. Intermediate transition field from experiment and theory. (a) Inverse effective mass of itinerant charges 1/m* (cyan squares), in agreement with theoretical prediction (red lines), vanishes at Bf ≈ 0.7Bc - suggesting m* divergence within the antiferromagnetic phase (b) Measured deHaas-vanAlphen frequencies (squares) compared with theoretical simulations (red lines) for an f-hole Fermi volume of V = 0.375 × (1-B/Bd)% per ellipsoid (Brillouin zone percentage). (c) Experimentally and theoretically determined field-pressure phase diagram for $CeIn_3$.*

## Impact on National Missions

Strong electronic correlations define every major problem at the forefront of condensed matter physics. Traditional electronic band structure calculations and minimal many-body models are inadequate to reproduce macroscopic electronic, metallurgical and crystallographic properties of strongly correlated materials and the rich spectrum of complex states found in them. These deficiencies have exposed critical gaps in our understanding of condensed matter that cannot be ignored. By providing an essential

new understanding and interpretative frameworks for f-electron compounds we have closed some of these gaps. The relevance of these achievements extends beyond the exciting challenges for condensed matter physics. Many of the Laboratory's special, materials-dependent mission needs depend critically on strong electronic correlations, whether it is the equation of state and metallurgy of actinides, control of quantum excitations for new sensor technologies or emergent functionality in nano-structured materials. To ensure that its long-term core missions can be met, Los Alamos cannot afford to lose its leadership position in the synthesis, characterization and modeling of strongly correlated electron materials and phenomena. Substantial and internationally-recognized successes of team members in the study of strong correlations have come from close integration of experiment and theory, in a deliberate strategy built around a set of well-defined scientific problems. The challenge of discovering and understanding the physical manifestations of f-duality and their implications for new states of matter has stretched limits of the Laboratory's experimental and predictive capabilities that underpin the science and technology needs of the Lab and addresses an exceptional problem of immediate interest to the international condensed matter community. The involvement of team members in the study of Pu in this project has ensured the cross-fertilization of insights and capabilities needed to improve our predictive understanding of the complex electronic and metallurgical properties of plutonium's solid state.

In summary, by exposing and understanding the dual nature of f-electrons in strongly correlated materials we have underpinned our ability to predict the consequences of strong electronic correlations that are responsible for complex states of worldwide interest and that control solid state properties of mission-relevant materials.

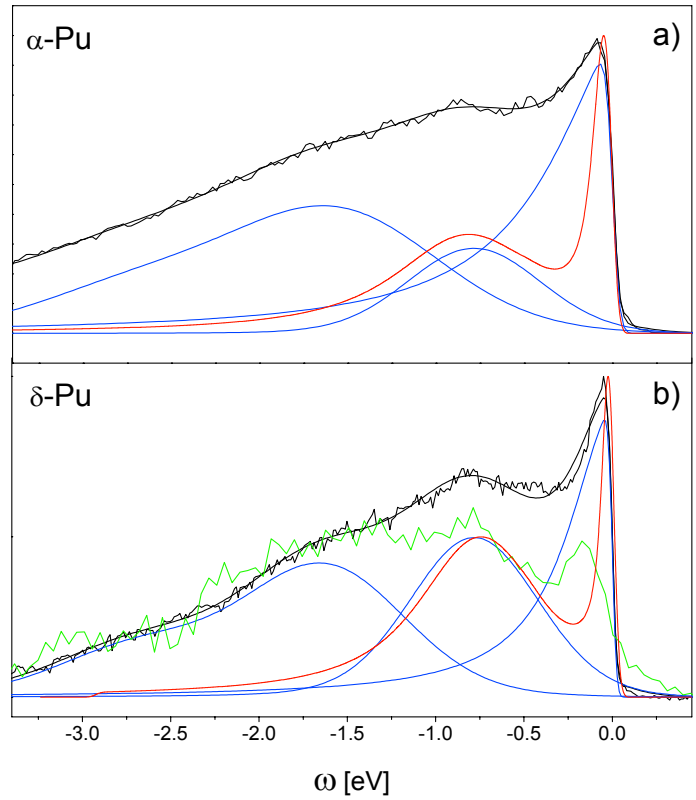


*Figure 5. Measured angle-integrated photoemission spectrum for alpha-Pu (a) and delta-Pu (b). Experimental data and fit are shown in black lines. The different peak components obtained from the fit are shown as blue lines, while the measured curve convoluted with the experimental conditions is shown in red. Panel (b) also shows the 115eV resonance scan for delta-Pu as a green line.*

## Publications


P.Julien, J., J. -X. Zhu, and R. C. Albers. Coulomb correlation in presence of spin-orbit coupling: application to plutonium. 2008. *Physical Review B 77, 195123 (2008)* . **77** (-): 195123.

X.Zhu, J., A. K. McMahan, M. D. Jones, T. Durakiewicz, J. J. Joyce, J. M. Wills, and R. C. Albers. Spectral Properties of delta-Plutonium: Sensitivity to 5f Occupancy. 2007. *Physical Review B* . **76** (245118): 245118.

Albers, R. C., and J. -X. Zhu. Vacillating Valence. 2007. *Nature.* **446**: 504.

Batista, C. D.. Effective Hamiltonian for metallic Plutonium. 2009. *Journal of Nuclear Materials.* **385** (-): 60.

Batista, C. D., J. E. Gubernatis, T. Durakiewicz, and J. J. Joyce. Strong coupling approach to actinide metals. 2008. *Physical Review Letters.* **101**: 016403.

Bauer, E. D., C. Wang, V. R. Fanneli, J. M. Lawrence, E. A. Goremychkin, N. R. de Souza, F. Ronning, J. D. Thompson, A. V. Silhanek, V. Vildosola, A. M. Lobos, A. A. Aligia, S.

Bobev, and J. L. Sarrao. Simplifying strong electronic correlations in uranium: localized uranium heavy fermion UM2Zn20 (M=Co,Rh) compounds. 2008. *Physical Review B.* **78**: 115120.

Bauer, E. D., J. D. Thompson, J. L. Sarrao, and M. F. Hundley. Ferromagnetism and crystalline electric field effects in cubic UX2Zn20 (X=Co, Rh, Ir). 2007. *Journal of Magnetism and Magnetic Materials.* **310**: e449.

Durakiewicz, T., C. G. Olson, K. S. Graham, D. P. Moore, J. J. Joyce, and L. A. Morales. Localized and itinerant states in actinide materials. 2007. *Materials Research Society Symposium Proceedings.* **986**: 35.

Durakiewicz, T., J. J. Joyce, J. M. Wills, and C. D. Batista. Notes on the dual nature of 5f-electrons. 2006. *Journal of the Physical Society of Japan.* **75**: 39.

Goodrich, R. G., N. Harrison, and Z. Fisk. Fermi surface changes across the Neel phase boundary of NdB6. 2006. *Physical Review Letters.* **97** (-): 146404.

Gout, D., O. Gourdon, E. D. Bauer, F. Ronning, J. D. Thompson, and T. Proffen. An experimental and theoretical study of the variation of the 4f hybridization across La1-xCexIn3. 2008. *Inorganic Chemistry.* **47**: 2569.

Harrison, N., S. E. Sebastian, C. H. Mielke, A. Paris, M. J. Gordon, C. A. Swenson, D. G. Rickel, M. D. Pacheco, P. F. Ruminer, J. B. Schillig, J. R. Sims, A. H. Lacerda, M. -T. Suzuki, H. Harima, and T. Ebihara. Fermi Surface of CeIn3 above the Neel Critical Field. 2007. *Phys. Rev. Lett. .* **99**: 056401.

Heffner, R. H., D. E. MacLaughlin, J. E. Sonier, M. F. Hundley, and J. D. Thompson. Two-fluid model of heavy fermion formation and muon spin resonance Knight shift measurements in UBe13. 2007. *Journal of Magnetism and Magnetic Materials.* **310**: e6.

Joyce, J. J., J. Wills, T. Durakiewicz, M. T. Butterfield, E. Guziewicz, D. P. Moore, J. L. Sarrao, L. A. Morales, A. J. Arko, O. Eriksson, A. Delin, and P. H. Anderson. Dual nature of the 5f electons in plutonium materials. 2006. *Physica B.* **378-380**: 920.

Julien, J., J. Zhu, and R. C. Albers. Coulomb correlation in presence of spin-orbit coupling: application to plutonium. 2008. *Physical Review B.* **77**: 195123.

M.Chia, E. E., H. J. Lee, N. Hur, E. D. Bauer, T. Durakiewicz, R. D. Averitt, J. L. Sarrao, and A. J. Taylor. Quasiparticle relaxation across the spin gap on the itinerant antiferromagnet UNiGa5. 2006. *Physical Review B.* **74**: 140409.

M.Chia, E. E., J. -X. Zhu, D. Talbayev, R. D. Averitt, K. -H. Oh, I. -S. Jo, S. -I. Lee, and A. J. Taylor. Observation of competing order in a high-Tc superconductor with femtosecond optical pulses. 2007. *Phys. Rev. Lett. .* **99**: 147008.

Nair, S., S. Wirth, M. Nicklas, A. Glaudun, J. L. Sarrao, J. D. Thompson, and F. Steglich. A precursor state to superconductivity in CeIrIn5. 2008. *Physical Review Letters.* **100**: 137003.

Oh, Y. S., K. H. Kim, P. A. Sharma, N. Harrison, H. Amitsuka, and J. A. Mydosh. Interplay between Fermi Surface Topology and Ordering in URu2Si2 Revealed through Abrupt Hall Coefficient Changes in Strong Magnetic Fields. 2007. *Phys. Rev. Lett. .* **98**: 016401.

Ohishi, K., R. H. Heffner, G. D. Morris, E. D. Bauer, M. J. Graf, J. -X. Zhu, L. A. Morales, J. L. Sarrao, M. F. Fluss, D. E. MacLaughlin, L. Shu, W. Higemoto, and T. U. Ito. Muon spin rotation measurements of the superfluid density in fresh and aged superconducting PuCoGa5. 2007. *Phys. Rev. B .* **76**: 064504.

Park, W. K., H. Salzer, J. L. Sarrao, J. D. Thompson, L. D. Pham, Z. Fisk, J. Federick, P. C. Canfield, and L. H. Greene. Point-contact Andreev spectroscopy of heavy-fermion/superconductor junctions. 2008. *Physica B.* **403**: 818.

Park, W. K., J. L. Sarrao, J. D. Thompson, L. D. Pham, Z. Fisk, and H. L. Greene. Andreev reflection spectroscopy of the pure and Cd-doped heavy-fermin superconductor CeCoIn5: detecting order parameter symmetry and competing phases. 2008. *Physica B.* **403**: 731.

Park, W. K., J. L. Sarrao, J. D. Thompson, and L. H. Greene. Andreev reflection study of the heavy-fermon superconductor CeCoIn5: Detecting order parameter symmetry. 2008. *Physical Review Letters.* **100**: 177001.

Park, W. K., L. H. Greene, J. L. Sarrao, and J. D. Thompson. Andreev reflection spectroscopy of the heavy-fermion superconductor CeCoIn5 along different crystallographic directions. 2007. *Physica C.* **460-462**: 206.

Qi, Y., J. Zhu, S. Zhang, and C. S. Ting. Kondo resonance in the presence of spin polarized currents. 2008. *Physical Review B.* **78**: 045305.

Sabastian, S., N. Harrison, P. Sengupta, C. D. Batista, S. Francoual, E. Palm, T. Murphy, N. Marcano, H. A. Dabkowska, and B. D. Gaullin. Fractalization drives crystalline states in a frustrated spin system. 2008.

*Proceedings of the National Academy of Sciences.* **105** (51): 20157.

Sebastian, S. E., N. Harrison, C. D. Batista, S. A. Trugman, V. Fanelli, M. Jaime, T. P. Murphy, E. C. Palm, H. Harima, and T. Ebihara. Heavy holes precursor to superconductivity in antiferromagnetic CeIn3. 2009. *Proceedings of the National Academy of Sciences.* **106** (19): 7741.

Sharma, P. A., N. Harrison, M. Jaime, Y. S. Oh, C. D. Batista, J. A. Mydosh, and H. Amitsuka. Phonon thermal transport of URu2Si2: Broken translational symmetry and strong-coupling of the Hidden Order to the lattice.. 2006. *Physical Review Letters.* **97** (15): 156401/1.

Yang, Y., H. O. Lee, Z. Fisk, J. D. Thompson, and D. Pines. Scaling the Kondo lattice. 2008. *Nature.* **454**: 611.

Zhu, J., I. Martin, and A. R. Bishop. Kondo stripes in an Anderson-Heisenberg model of heavy fermions. 2008. *Physical Review Letters.* **100**: 236403.

Zhu, J., S. Kirschner, R. Bula, and Q. Si. Zero-Temperature Magnetic Transition in an Easy-Axis Kondo Lattice Model. 2007. *Physical Review Letters.* **99**: 227204.

# Novel Inclusion Compounds for Hydrogen Storage

*Yusheng Zhao*
20070008DR

## Abstract

Hydrogen storage is the top technological challenge for the future of the hydrogen economy, requiring revolutionary R&D improvements and breakthroughs. We have conducted a fundamental study of hydrogen clustering in nanoscale cavities, guest-host interactions, and the stability of the host frameworks. A crystal design approach was used to synthesize novel inclusion compounds with cage-/channel-topology and hydrogen-/intermolecular-bonding chosen to facilitate hydrogen storage. We addressed effective gas separation and encapsulation, $H_2$ storage capacity and phase stability, and controlled kinetics of formation and degassing. We applied shape-, size-, and bonding-selectivity rules to maximize storage efficiency. In particular, we have synthesized and characterized tens of new metal-organic frameworks (MOFs), several of which have exceptional gas adsorption capabilities, high thermal stability and/or favorable uptake/release kinetics. Our integrated experimental approaches using neutron diffraction, synthetic chemistry, thermal analysis, quartz crystal microbalance (QCM) measurements and chemical engineering analysis , coupled with theoretical modeling, have enabled innovative molecular design, thermochemical control, and an assessment of process scale-up. Technological improvements have thus been made in materials design, sorption reversibility, reaction kinetics and feasible *P-T* conditions towards practical applications.

## Background and Research Objectives

Ever-increasing fossil energy consumption and associated global environmental concerns have provoked intensive searches for alternative energy resources. Hydrogen in the form of $H_2$, the most abundant gas in the universe, is considered to be one of the most promising alternatives to fossil energy [1]. The energy content of hydrogen (142 MJ $kg^{-1}$) is at least three times more than that of any other chemical fuel (e.g., the equivalent value for hydrocarbons is 47 MJ $kg^{-1}$). Hydrogen is also the cleanest combustion fuel, where the only exhaust is water vapor. Developing prototype cars powered by hydrogen, together with the advantages of fuel cells, is a promising concept for transportation. However, incorporation of large amounts of hydrogen into a material that ensures both safe storage and ease of release for energy conversion is one of the most daunting challenges to the realization of the hydrogen economy. The U.S. Department of Energy set targets for hydrogen storage of 9.0 wt% and/or 2.7 kWh/liter by 2015. Hydrogen storage is highlighted not only as an important techno-scientific problem but also as an urgent socio-economic issue. Meeting the hydrogen storage challenge requires revolutionary improvements and breakthroughs in science and technology.

An ideal hydrogen storage technique should capture a high hydrogen mass with a low volume fraction, be safe and inexpensive, and have fast kinetics for absorbing and releasing $H_2$ reversibly in a controllable fashion. Conventionally, hydrogen has been stored as compressed gas or cryogenic liquid. However, compressed gas stores relatively low contents of hydrogen (about 1 wt% at 200–300 bars), and cryogenic liquid requires significant energy (i.e., high cost) to maintain cryogenic conditions. In addition, both methods have safety issues and are not yet practical for mobile applications. Solid-state storage has also been considered as a possible safe and effective way of routinely handling hydrogen, e.g., in the form of metal hydrides (such as LiBH4) and via carbon nanotube absorption. Solid-state forms have different properties in terms of balancing high energy density with easy reversibility of adsorption/desorption. For instance, the hydrogen content of $LiBH_4$ is high (18 wt%), but it can only release hydrogen at high temperatures (as high as 900 K) [2]. As an alternative, we focus on 3-dimensional frameworks of inclusion compounds with cages/cavities that can host and release hydrogen molecules under milder conditions. Novel inclusion

compounds with hydrogen-/intermolecular-bonding and cage-/channel-framework topologies have great potentials to host large quantities of gas molecules. Because of their vast variety of possible structures and their differences in pressure/temperature stability and in framework-molecule interaction mechanisms, these compounds may be suitable for various gas storage/separation applications. Separation applications were focused on during the latter phases of this project.

The discovery of hydrogen clathrate presents a new methodology for hydrogen storage using hydrate polyhedral cages to host substantial amounts of molecular hydrogen [3-5]. Strong intermolecular interactions result in multiple hydrogen molecules occupying a single nanoscale clathrate cage, yielding $H_2$ content of about 5 wt% at P = 100 MPa and T = 180 K. The local $H_2$ density within the polyhedral cage is even higher than that in solid/metallic hydrogen due to quantum intermolecular bonding.
High energy content, fast kinetics, easy reversibility, and excellent recharge ability are ultimate materials objectives for hydrogen storage.

We have extended the studies of hydrate clathrates to those of metal-organic frameworks (MOFs). We have conducted fundamental studies of hydrogen clustering in nanoscale cavities, guest-host intermolecular interactions, and framework stability. A crystal engineering approach was used to design and synthesize novel MOFs with cage-/channel-topology and hydrogen-/intermolecular-bonding tailored for hydrogen storage. We addressed effective gas separation and encapsulation, $H_2$ storage capacity and phase stability, and controlled kinetics of formation and degassing. We applied shape-, size-, and bonding-selectivity rules to maximize storage/separation efficiency. Our integrated experimental approaches of neutron diffraction, thermodynamic and kinetic analysis, synthetic chemistry, and chemical engineering enable innovative molecular design, thermochemical control, and ultimately process scale-up. Theoretical modeling was integrated with the experiments relevant to gas separation/storage applications.

## Scientific Approach and Accomplishments

### Materials Design and Synthesis

To develop desired materials for storage/separation of gases, especially hydrogen, we have designed and synthesized a number of new metal-organic frameworks (MOFs) using hydrothermal/solvothermal methods. Particularly, we used the following design strategies to tune gas storage and separation capacities of porous MOFs: 1) creating open metal sites, 2) varying pore sizes, 3) functionalizing pore walls, and 4) producing framework interpenetration.

Some of the new MOFs that we have synthesized include:

- $Y(BTC)(H_2O).4.3\ H_2O$ (H3BTC = 1,3,5-benzenetricarboxylate acid) (Figure 1) [6];
- $[Co_2(OH)(3,4\text{-}PBC)_3]_n$ (3,4-PBC = 3-pyrid-4-ylbenzoic acid) [7];
- $[Zn_3Na_2O(BTB)_2(DMF)_2](DMF)(H_2O)$ (Figure 2);
- $[Zn_2K_3(BTB)_2(HCOO)(DMF)_3](DMF)_3(H_2O)_2$;
- $[Zn_2(OH)(3,4\text{-}PBC)_3]_n$ (3,4-HPBC = 3,4-pyridylbenzenecarboxylate acid);
- $[Zn(3,3\text{-}PBC)_2.\ H_2O]n$ (3,3-HPBC = 3,3-pyridylbenzenecarboxylate acid);
- $[Cu(4\text{-}TYMP)_2]_n$ (4-HTYMP = 4-(1h-1,2,4-triazol-1-ylmethyl) benzoic acid);
- $[Cd(4\text{-}TYMP)2]_n$;
- Zn(II)-4-tetrazole-pyridine;
- Cu(II)-4-tetrazole-benzonic acid framework;
- $ZnNa(BTC)(DMF)(H_2O)_{0.5}$ (BTC = 1,3,5-benzenetricarboxylate); and
- $[Zn_4O(BTB)(H_2O)_2](H_2O)_{3.5}$ (BTB = benzene-1,3,5-tribenzoate) (Figure 3).

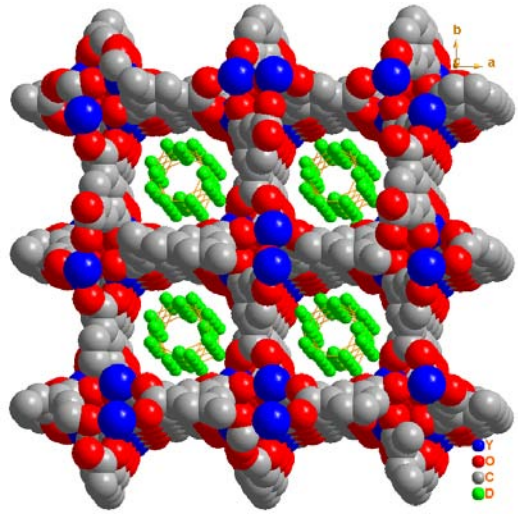


*Figure 1. The structure of Y(BTC) MOF with hydrogen clusters (green) formed inside its cages.*

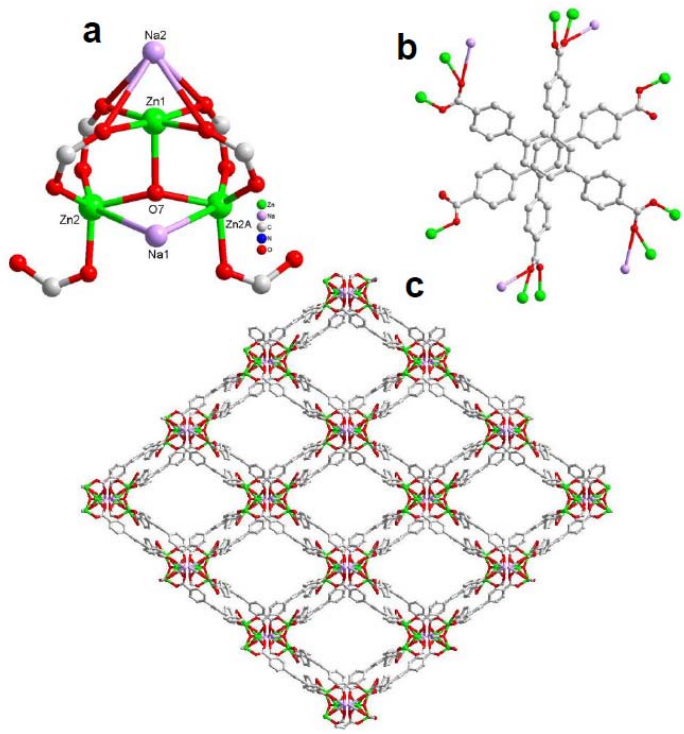


*Figure 2. Crystallography of $[Zn_3Na_2O(BTB)_2(DMF)_2](DMF)(H_2O)$: (a) local coordination environment of $Zn_3Na_2(\mu_4\text{-}O)$ MBB (symmetric codes: A = x, -y + 2.5, z), (b) coordination modes of staggered BTB ligand pairs, and (c) three-dimensional sodium-bridged two-fold interpenetrated network with open channels.*

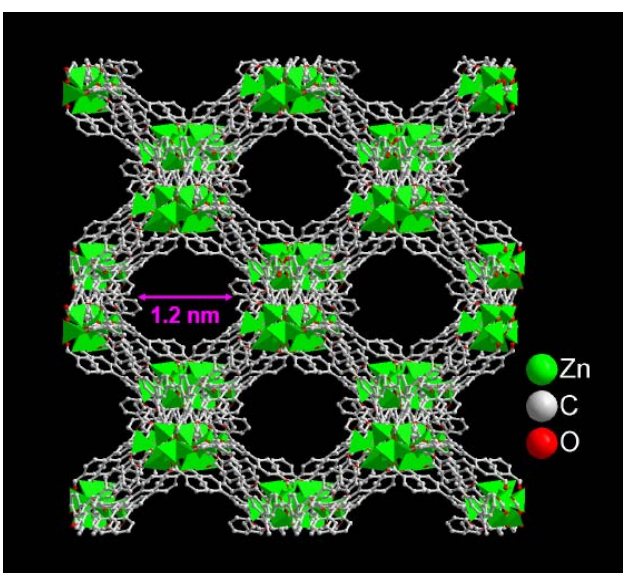


*Figure 3. Structure of $[Zn_4O(BTB)(H_2O)2](H_2O)_{3.5}$.*

High-quality crystals of these compounds were grown, and their structures were solved with single-crystal X-ray diffraction. The samples were also characterized by IR spectrometry, thermogravimetry, powder X-ray diffraction and gas adsorption measurements. In addition, we have explored the methodology of using GC-MS to study gas separation capabilities of MOFs. This technique also has the advantages of determining their thermal stability and activation conditions and has proved very useful in MOF research.

The new MOFs exhibit novel framework structures, high gas adsorption capabilities, high thermal stability and/or favorable uptake/release kinetics. For example, $[Zn_3Na_2O(BTB)_2(DMF)_2](DMF)(H_2O)$ and $[Zn_2K_3(BTB)_2(HCOO)(DMF)_3](DMF)_3(H_2O)_2$ adopt similar alkali-bridged two-fold interpenetrated, (3,6)-connected nets with the rtl-c topology, though they consist of different molecular building blocks, $Zn_3Na_2(\mu_4\text{-}O)$ and $Zn_2K_2(HCOO)$ clusters, respectively. The samples were prepared via solvothermal reactions of $Zn(NO_3)_2.6H_2O$ and NaCl or KCl with the trigonal-planar ligand, benzene-1,3,5-tribenzoic acid ($H_3BTB$). The alkali-bridged interpenetration reduces the flexibility of their interpenetrated nets, leading to their permanent porosity and high thermal stability. These two MOFs also exhibit high capacities of hydrogen uptake and strong solid fluorescent emissions. Another example is $Y(BTC)(H_2O).4.3\ H_2O$, which was synthesized from reaction of $Y(NO_3)\cdot 6H_2O$ and H3BTC. The resulted MOF has a pore size of 5.8 angstrom and is thermally highly stable (up to 475 C). Gas adsorption measurements show that it is highly selective for hydrogen over nitrogen and can take up hydrogen of about 2.1 wt% at 77 K and 10 bar. This compound is rather unusual inasmuch as it is the first MOF containing a rare-earth cation (yttrium), rather than transition metal cations as in most of the previously reported MOFs [6]. We anticipate several additional publications and reports related to these new MOF compounds.

We have also developed a new type of porous materials, named “metal-organic aerogels (MOAs)”, that have high surface areas (> 1000 $m^2/g$) and good solvent/chemical stability. This represents a structurally expansion of aerogel materials from traditional main group element-to-element interaction systems, such as oxides, carbons, and chalcogenide clusters, to metal-ligand coordination based systems. By replacing oxygen atoms with organic ligands and replacing silicon atoms with metals (or metal clusters) in conventional aerogels, we produce a new class of metal-organic aerogels. These MOAs have unique hierarchical architectures classified from atomic- (*primary*) to micro- (*secondary*) to macro- (*tertiary*) length scales. This work provides a new perspective on utilizing the growing knowledge base in coordination chemistry, including the concepts of secondary building units in metal-organic frameworks and hard-soft acid-base theory, to facilitate the design and fabrication of aerogel materials for a wide range of scientific and technological applications.

Another effort was devoted to studies of conducting

polymers for hydrogen storage. In particular, we have studied interaction of polyaniline (PANi) with $H_2$ to form "quasi-chemical" bonding that has significant effects on its electrical conductivity [8]. The hydrogen storage potential of PANi was explored via PANi morphology control and synthesis of MOF/PANi composites. Our results show that reaction conditions affect the polymerization kinetics and thus the morphology of the final polymeric product. The formation of a distinct reaction intermediate under low proton concentrations is found to relate to polyaniline nanotube formation. By controlling the formation and aggregation rate of the intermediate, rectangular polyaniline nanotubes are synthesized with high yields.

**Neutron Diffraction**

We performed neutron diffraction experiments of Prussian blue analogue $Cu_3[Co(CN)_6]_2$ [5] and Y(BTC) [6] at various $H_2$ gas loading, temperature and pressure conditions. Rietveld analysis of the diffraction data allowed determination of lattice parameters, atomic positions and atomic displacement parameters. Since the scattering power of neutrons does not vary with the number of electrons in an element (as for X-rays), neutron scattering is much more sensitive to the positions of light elements (especially hydrogen and its isotopes) and is thus a powerful technique for studying hydrogen-bearing materials. For example, in Y(BTC), difference Fourier analysis of neutron powder diffraction data revealed four distinct $D_2$ sites that are progressively filled within the nanoporous framework. Interestingly, the strongest adsorption sites identified are associated with the aromatic organic linkers rather than the open metal sites, as occurred in previously reported MOFs. Our results provide for the first time direct structural evidence demonstrating that optimal pore size (around 6 angstrom, twice the kinetic diameter of hydrogen) strengthens the interactions between $H_2$ molecules and pore walls and increases the heat of adsorption, thereby allowing for enhanced hydrogen adsorption through the interaction between hydrogen molecules with the pore walls rather than with the normally stronger adsorption sites - the open metal sites. At high $H_2$ loadings (5.5 $H_2$ molecules (3.7 wt%) per Y(BTC) formula), $H_2$ molecules form highly symmetric novel nanoclusters with H2-H2 distances even shorter than that in solid $H_2$. These observations are important and hold the key to optimizing this new class of rare metal-organic framework (RMOF) materials for practical hydrogen storage applications.

**QCM Measurements**

To determine the kinetics of $H_2$ sorption/desorption process, we conducted quartz crystal microbalance (QCM) measurements of $Cu_3[Co(CN)_6]_2$ as a function of particle size, film thickness and temperature. The $H_2$ uptake capacity of $Cu_3[Co(CN)_6]_2$ film with a thickness of a few micron can be as high as 4.6 wt% at ambient conditions. However, as the film thickness increases, the $H_2$ uptake decreases, suggesting that gas diffusion dominates its $H_2$ soption/desorption process. In addition to hydrogen, we studied gas adsorption of He, $N_2$, and $CO_2$ in $Cu_3[Co(CN)_6]_2$. This compound shows strong interaction with $H_2$ and $CO_2$ and can thus be used for separation of $H_2$ and $CO_2$ from their $N_2$ mixtures.

**Theoretical Modeling**

We focused our theoretical effort on the Cu Prussian Blue analogue system to understand hydrogen sorption properties. First-principles quantum chemical calculations have been performed on both cluster and periodic representations of the crystal structure. At the periodic level, it has been determined that currently available density functionals provided in plane wave codes are inadequate to correctly represent the weak interactions present involving hydrogen molecules interacting with both the isocyanide and metal centres. At the cluster level, wavefunction methods such as Hartree Fock with $MP_2$ corrections appear to account for the interactions correctly. We predict binding energies ranging from 4-8 $kJmol^{-1}$ at the free Cu(II) binding sites, which are considerably less than for molecular nitrogen and carbon dioxide at the same site. This result correlates well with our QCM measurements.

We have performed simulations of hydrogen molecule binding on the Zn-TBC MOF structure using periodic density functional theory as implemented in the cp2k software [9]. Three binding sites were predicted. The most favorable site is located between two benzene rings at an average distance of 2.3 A from the carbon atoms (Figure 4). The predicted binding energy is 7.4 kJ/mol. The other two binding sites are located in the vicinity of the Zn tetrahedral framework site and close to the tetrazole ring, respectively.

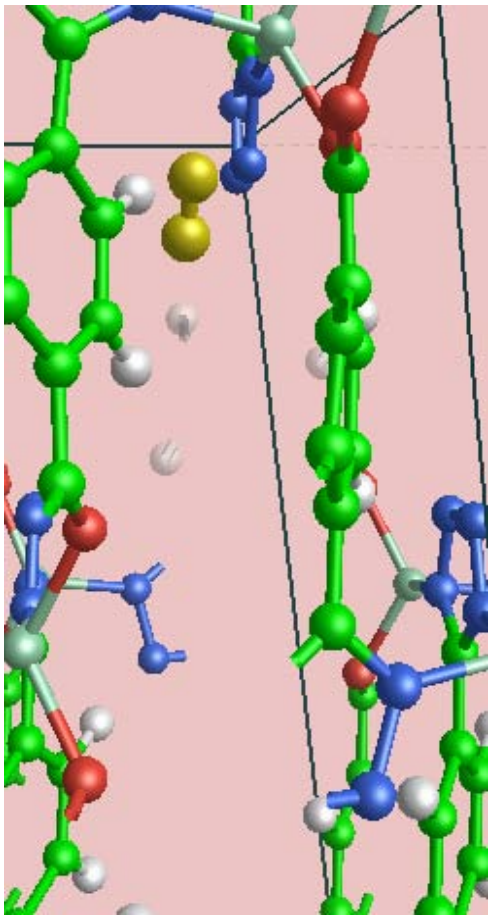

*Figure 4. The most favorable calculated binding site for hydrogen in Zn-BTC MOF (hydrogen in yellow)*

**Chemical Engineering**

A new concept for electric field enhancement of gas adsorption was developed that includes design of highly polarizable centers within porous adsorbants. We have conducted an initial experimental demonstration of electric field modulated gas storage centered on $CO_2$ capture. We realized that the strong quadrupole found in $CO_2$ was a "handle" that, if properly exploited, could facilitate separation. A series of proof-of-concept experiments were performed in a small Metal-Insulator-Metal capacitor bank. Thin copper sheets were used as the capacitor plates while MOF-5 was used as the insulator material. Once loaded, the capacitor bank was inserted into a pressure vessel equipped with electrical leads. The gas used was a mixture of $CO_2$, $O_2$, and $N_2$. These experiments showed that $CO_2$ was selectively pulled into MOF-5 upon application of an electrical potential. This system was found to be reversible; upon discharging the capacitor the $CO_2$ was released back into the gas phase. Quantification of $CO_2$ uptake showed that the $CO_2$ held within the energized capacitor cell was in fact enhanced over the concentration found in the absence of the electric field. This effort has resulted in an externally-funded (DOE-EERE) project on hydrogen storage.

**Summary**

Novel inclusion compounds for hydrogen storage must be workable over readily accessible temperatures and pressures, in order to be economically feasible. Within the R&D scope of the project, we have: (1) provided novel engineering materials that can potentially be used for hydrogen and byproduct gases separation and storage in energy application and environmental protection; and (2) developed new unique experimental capabilities and innovative theoretical modeling methods for the Laboratory that may be applicable to tritium problems relevant to the national security and (3) identified methods to enhance performance of the adsorbent materials (e.g. by applying external electric fields).

## Impact on National Missions

We address vital research issues on energy security and environmental remediation, providing underpinning S&T to address materials science focusing on hydrogen storage. The project integrates approaches of molecular design, thermochemical control, and high-pressure neutron diffraction. Efficient separation and storage of gaseous phases are crucial bottlenecks in the future hydrogen economy of the Nation and for many other energy applications. The novel (patented) materials developed in this project are currently being marketed to a wide range of external customers (DOD, DHS, etc.). New projects related to MOFs have been funded by Chevron and DOE-EERE.

## References


1. Schlapbach, L., and A. Zuttel. Hydrogen-storage materials for mobile applications. 2001. *Nature.* **414**: 353.

2. Grochala, W., and P. P. Edwards. Thermal decomposition of the non-interstitial hydrides for the storage and production of hydrogen. 2004. *Chemical Reviews.* **104**: 1283.

3. Mao, W. L., and H. K. Mao. Hydrogen storage in molecular compounds. 2004. *Proceedings of the National Academy of Sciences.* **101**: 708.

4. Lokshin, K. A., Y. Zhao, D. He, W. L. Mao, H. K. Mao, R. J. Hemley, M. V. Lobanov, and M. Greenblatt. Structure and dynamics of hydrogen molecules in the novel clathrate hydrate by high pressure neutron diffraction. 2004. *Physical Review Letters.* **93**: 125503.

5. Zhao, Y., H. Xu, L. L. Daemen, K. Lokshin , K. T. Tait , W. L. Mao , J. Luo , R. P. Currier , and D. D. Hickmott . High-

pressure/low-temperature neutron scattering of gas inclusion compounds: Progress and prospects. 2007. *Proceedings of the National Academy of Sciences.* **104**: 5727.

6. Luo, J., H. Xu, Y. Liu, Y. Zhao, L. L. Daemen, C. Brown, T. V. Timofeeva , S. Ma , and H. C. Zhou. Hydrogen adsorption in a highly stable porous rare-earth metal-organic framework: Sorption properties and neutron diffraction studies. 2008. *Journal of the American Chemical Society.* **130** (30): 9626.

7. Luo, J., Y. Zhao, H. Xu, T. L. Kinnibrugh, D. Yang, T. V. Timofeeva, L. L. Daemen, J. Zhang, W. Bao, J. D. Thompson, and R. P. Currier. A novel helical double-layered cobalt(II)-organic framework with tetranuclear [Co4( 3-OH)2] clusters linked by an unsymmetrical pyridylbenzoate ligand. 2007. *Inorganic Chemistry (Communication).* **46** (22): 9021.

8. Ding, Z., D. Yang, R. Currier, S. Obrey, and Y. Zhao. Self-assembled polyaniline nanotubes with rectangular cross sections. 2009. *Macromolecular Physics and Chemistry.* : DOI: 10.1002/macp.200900250.

9. Mundy, C. J., F. Mohamed, F. Schiffman, G. Tabacchi, H. Forbert, W. Kuo, J. Hutter, M. Krack, M. Iannuzzi, M. McGrath, M. Guidon, T. D. Kuehne, T. Laino, J. VandeVondele, and V. Weber. CP2K. 2009. *http://cp2k.berlios.de.*

## Publications

Ding, Z., D. Yang, R. Currier, S. Obrey, and Y. Zhao. Self-assembled polyaniline nanotubes with rectangular cross sections. 2009. *Macromolecular Physics and Chemistry.* : DOI: 10.1002/macp.200900250.

Ding, Z., D. Yang, S. Obrey, R. Currier, and Y. Zhao. Reaction mechanism to morphology control of polyaniline nanomaterials. 2009. *Polymer Preprints.* **50** (1): 350.

Luo, J., H. Xu, Y. Liu, Y. Zhao, L. L. Daemen, C. Brown, T. V. Timofeeva , S. Ma , and H. C. Zhou. Hydrogen adsorption in a highly stable porous rare-earth metal-organic framework: Sorption properties and neutron diffraction studies. 2008. *Journal of the American Chemical Society.* **130** (30): 9626.

Luo, J., Y. Zhao, H. Xu, T. L. Kinnibrugh, D. Yang, T. V. Timofeeva, L. L. Daemen, J. Zhang, W. Bao, J. D. Thompson, and R. P. Currier. A novel helical double-layered cobalt(II)-organic framework with tetranuclear [Co4( 3-OH)2] clusters linked by an unsymmetrical pyridylbenzoate ligand. 2007. *Inorganic Chemistry (Communication).* **46** (22): 9021.

Mao, W. L., C. A. Koh, and E. D. Sloan. Clathrate, hydrates under pressure. 2007. *Physics Today.* **60** (10): 42.

Yang, D., and B. R. Mattes. Investigation of interaction among polyaniline, organic acid, and water. 2008. *Synthetic Metals.* **158**: 654.

Zhao, Y., H. Xu, L. L. Daemen, K. Lokshin , K. T. Tait , W. L. Mao , J. Luo , R. P. Currier , and D. D. Hickmott . High-pressure/low-temperature neutron scattering of gas inclusion compounds: Progress and prospects. 2007. *Proceedings of the National Academy of Sciences.* **104**: 5727.

# Correlations and Control of Properties of Metallic U and Pu

*Jeremy N. Mitchell*
20070013DR

## Abstract

The mechanical and physical properties of U and Pu are unusual when compared to other well-understood materials. This unusual behavior is attributed to the presence and interactions of 5*f* electrons and their transitional behavior between acting as unpaired electrons, also known as localized, and participating in bonding, also known as itinerant. The electron-electron interactions, or correlations, are the central theme of this research. In this project, we developed new experimental and theoretical tools to help understand the behavior of electrons in actinides and the role that this behavior plays in determining their properties. Experimental tools focused on direct electronic structure measurements using high-magnetic fields, photoemission spectroscopy, and neutron scattering. Simultaneously, we developed theoretical methods that provide a better understanding of electron correlation physics. The application of variably sophisticated theoretical tools allowed us to gradually increase correlation effects and validate with experiment. The new state-of-the-art experimental and theoretical tools have produced unique data sets that are driving the future of actinide condensed matter science.

## Background and Research Objectives

When compared to metals such as copper, the mechanical and physical properties of plutonium and uranium are very unusual. The distinctive behavior of these actinide metals is attributed to the presence of 5*f* electrons. Some theoretical models have successfully predicted the experimentally-observed atomic volumes of the various phases of Pu. In such schemes, the transitions between the phases are associated with rearrangements of the *f* electrons; in particular, changes of some or all of the *f*-electrons from localized (unpaired) to itinerant (participating in bonding). A key problem for such calculations is that localization of *f* electrons should result in the ions acquiring observable magnetic moments, and even magnetic order. However, there is no experimental evidence for localized magnetic moments in Pu. It is possible that a large rapidly-fluctuating moment could have gone undetected, but the negative result remains a problem for most of the theoretical approaches. It is almost certain that strong correlations – interactions between the electrons themselves – are responsible for this difference between theory and experiment. In metals such as copper, the role of correlations is small, and conventional theories are able to predict almost all properties rather well; by contrast, the *f* electrons in Pu and U are thought to be very prone to such interactions, leading to the observed complex, unpredictable behavior.

This project took advantage of recent advances in condensed matter theoretical and experimental techniques to make a fresh attempt to sort out and understand the physics of electron correlations in actinides. We measured a variety of properties within varying magnetic fields and temperatures where appropriate. We applied the most advanced theoretical physics tools to understand correlations and how they affect the properties of actinides. Uranium has weaker electronic correlations than Pu and working on both simultaneously, as well as understanding the difference between the two, provided important clues as to how correlations control the properties of these materials.

## Scientific Approach and Accomplishments

### Synthesis, Characterization, & Properties

*Synthesis*

The key to a strong experimental effort on the properties of actinides is the production of high-quality samples. Moreover, due to the accumulation of radiation damage and the affect of this damage on properties, it is paramount to able to harvest, prepare, mount, and ship samples as quickly as possible, preferably within hours. Our ability to succeed in these areas was challenged when the sole actinide crystal growth and small-scale alloy

synthesis laboratories in Wing 2 of the CMR Building were closed in February 2007. After 9 months of activity approval, we resumed making Pu samples in Wing 5 in March 2008.

*Transport Measurements*

The materials we selected and produced all had specific or predicted qualities that lend themselves towards studying correlations. For example, to study correlations at the dilute limit we made single crystals of compounds such as $Lu_{1-x}Pu_xCoGa_5$ (x = 0.005, 0.01, 0.02). We measured their electric resistivity and found no evidence for the development of a characteristic (Kondo) energy scale for Pu in these systems. We did discover a new family of $UM_2Zn_{20}$ (M=Co, Rh), in which the U atoms weakly interact with a shell of Zn atoms, and therefore behave as local-moments embedded in a metallic host. Our measurements reveal that these materials have a characteristic energy scale (Kondo temperature) of order $T_K$=20 K. Thus, these $UM_2Zn_{20}$ materials are model systems to investigate a particularly simple limit that incorporates strong electronic correlations.

In our search for strongly correlated Pu-based compounds, we synthesized a new material $Pu_2Ni_3Si_5$. This material has the same crystal structure as the unconventional and strongly-correlated superconductor $Ce_2Ni_3Ge_5$. Magnetization measurements reveal a complex magnetic structure involving ferromagnetism at $T_C$=70 K and subsequent antiferromagnetic transition at $T_N$=35 K (Figure 1). Thus, this compound appears to be on the localized side of the localized/itinerant boundary that is so prevalent in the actinides.

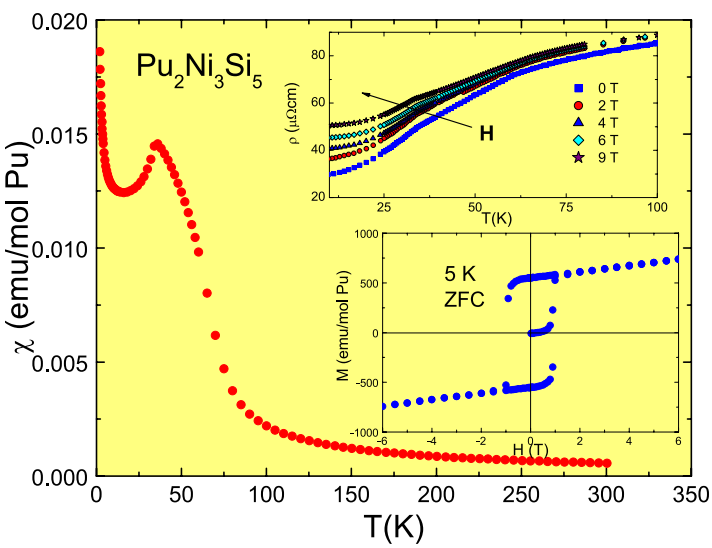


*Figure 1. Magnetic susceptibility vs temperature of $Pu_2Ni_3Si_5$ showing a ferromagnetic transition at 70 K, followed by an antiferromagnetic transition at 35 K. Top inset: electrical resistivity vs temperature showing the two magnetic transitions. Bottom inset: Magnetization vs magnetic field at T=5 K also providing evidence for the two magnetic transitions.*

*Radiation Effects*

Aging effects are of particular concern for performance of the nuclear stockpile and they may have important consequences for the electronic structure of δ-Pu and its relation to strongly correlated behavior. We used x-ray absorption fine-structure (XAFS) spectroscopy and muon-spin relaxation measurements to examine the effects of self-radiation damage on superconducting $PuCoGa_5$, which has a very similar electronic structure to that of δ-Pu. The XAFS measurements indicate that the local crystal structure is disordered much more strongly than anticipated. The results suggest that strong distortions around radiation-induced defects create disorder throughout the damage cascade region. These experiments help to refine standard damage models and suggest the need to accurately account for the changes in electronic structure in the damaged regions. In a tour de force muon spin relaxation experiment, we have set a very stringent limit on any size of the static magnetic moment of Pu of less than 0.001 Bohr magnetons—a very small value, indeed.

*Elastic Constants*

Resonant ultrasound spectroscopy (RUS) provides the highest absolute accuracy of any routine elastic modulus technique. Elastic moduli are the first measurable properties that can be computed from theoretical electronic structure models, so we applied RUS to pure Pu with the goal of providing accurate elastic moduli from cryogenic temperatures to well above room temperature. We measured the bulk and shear moduli for the entire temperature range of existence for α-, β-, and γ-Pu. The shear modulus change between β and γ phases is unexpectedly small.

*Angle-Resolved Photoemission Spectroscopy*

Angle-resolved photoemission spectroscopy (ARPES) provides key experimental evidence for the nature of 5*f* electrons. Figure 2 shows the first ever ARPES results from a Pu material and shows that the 5*f* electrons in $PuSb_2$ near the Fermi energy are well described by a quasiparticle peak which moves through the Fermi energy near the center of the Brillouin zone. These data provide an anchor point for modeling the electronic structure of $PuSb_2$. Whatever computational framework or model is used to describe the electronic structure of $PuSb_2$, it should account for a narrow, dispersive quasiparticle peak, of substantial 5*f* character, crossing the Fermi energy. These data show a similarity to the narrow electronic structure feature in $USb_2$, which provided the first evidence of kink physics in *f*-electron materials. The kink physics identifies an energy scale for enhanced electron correlation, which

provides insight into the electronic structure generally beyond the scope of density functional theory.

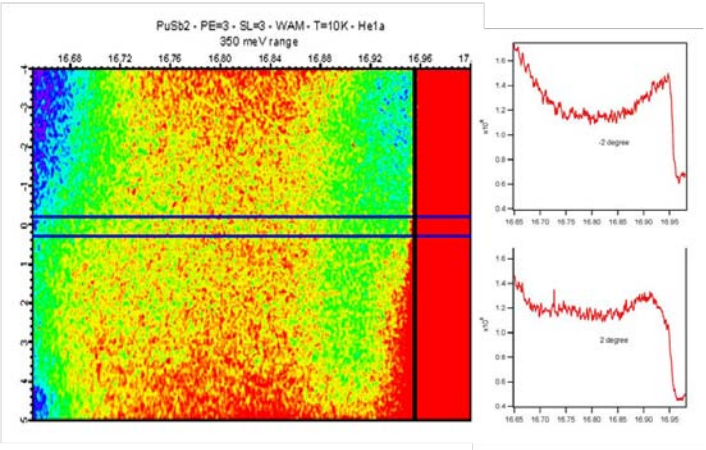


*Figure 2. The two dimensional energy vs. crystal momentum mapping for $PuSb_2$. The black vertical line is the Fermi energy at 16.955 eV, the blue horizontal lines show the angular acceptance of the energy distribution curves shown on the right of the figure. Red is low spectral intensity, blue is high.*

**Neutron Scattering Studies**

Unpaired electrons play a role in the electronic structure of Pu and its compounds, so any magnetic properties would shed light on the electronic structure of the material. Neutron scattering is often used to characterize the magnetic structure and dynamics of materials at the atomic level. The lack of a magnetic signal from unpaired electrons in δ-Pu is interpreted to be a consequence of the delocalization of the unpaired valence electrons on the Pu atoms amongst all of the atoms rather than being localized on a single atom. This leaves open the question of whether an applied external magnetic field on a sample of δ-Pu could cause the electrons to localize resulting in a measurable signature of magnetic structure by using neutron diffraction. Low temperatures also encourage less disorder and distinct magnetic structures. We therefore carried out a detailed search for the signature of a magnetic structure of δ-Pu using magnetic fields in the range of 0-7 Tesla and the temperature range of 1.5 – 300 K. Within the sensitivity of the neutron technique we did not observe any signature of a coherent magnetic structure in d-Pu. This demonstrates that neither a 7 Tesla field nor low temperatures are sufficient to force localization of unpaired electrons in δ-Pu.

Another approach to understanding the role of the electrons in δ-Pu is to probe the range of non-magnetic atomic structures observed for plutonium compounds. We focused on a search for the structural signal from α'-Pu which is observed upon cooling Ga-stabilized δ-Pu to sub-ambient temperatures. The onset and characteristics of this transformation are dependent on the cooling rate and the composition of the alloy, indicating a subtle signature of a change in electronic and atomic structure. Experiments were done on samples of $^{242}$δ-Pu that were expected to transform upon cooling. No unequivocal structural signal could be observed using neutron scattering, suggesting that the transformation is subtle in origin and more detailed work is needed to further elucidate the origin of the bulk signature of α'.

**High-Magnetic Field Measurements**

*Infrared Measurements in High Magnetic Fields*

We used the cyclotron resonance effect to study electronic structure and the evolution of correlation effects. A material's band structure will evolve as a result of chemical substitution or some external parameter change. Correlation effects in the 5*f* elements are especially important to track as one of these parameters is changed since the role of these carriers have the potential to cause a substantial change in the response of the material to external perturbations. We developed a cyclotron resonance measurement capability at ultra-high magnetic fields and then applied the technique to actinides. Experiments on $^{238}$U-doped Si showed a dramatic hysteretic transition in the infrared transmission to fields of 156 T. We are still developing this technique for Pu.

*Upper Critical Phase Diagram of $PuCoGa_5$*

Superconducting $PuCoGa_5$ piqued the interest of the condensed matter physics community several years ago upon its discovery at LANL. The anisotropy of the upper critical field has only been studied to ~0.9 $T_c$ since the $dH_{c2}/dT$ slope is so large. This puts the theoretical understanding of the pairing anisotropy at a severe disadvantage when compared to many other contemporary superconductors. The reason for the lack of data are the safety challenges associated with magnetic field generating systems such as pulsed magnets. We addressed these challenges by designing and building a pulsed magnet that is highly reliable and has a conservative 50 T range of maximum field. Next, we refined a method for measuring the superconducting anisotropy and tested it on a non-actinide sample. The new method called, the proximity detector oscillator (PDO), was then applied to $PuCoGa_5$ to map out the upper critical field anisotropy. Figure 3 shows the preliminary data for $PuCoGa_5$ measured in pulsed magnetic fields to 45 Tesla.

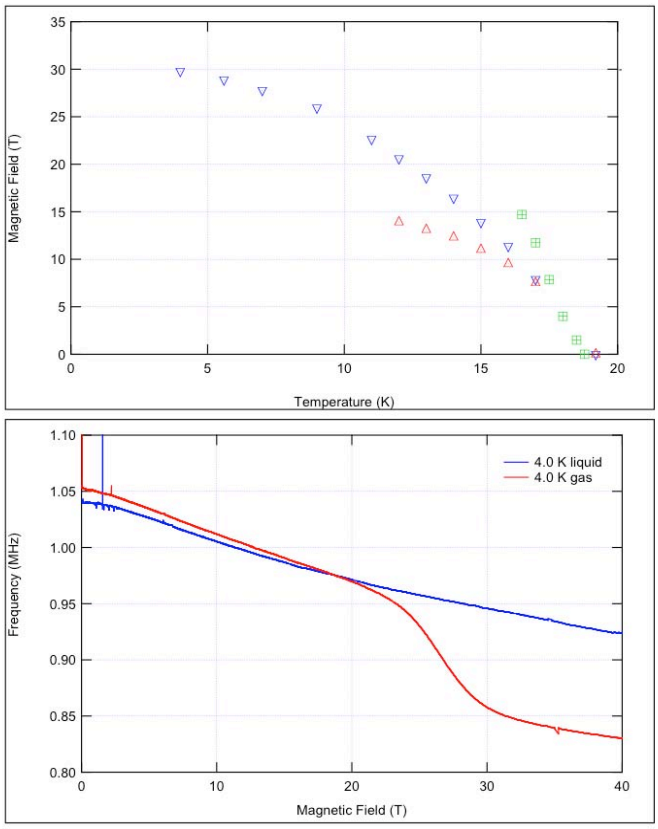


*Figure 3. (Top) The upper critical field of $PuCoGa_5$ measured in pulsed magnetic fields. Although the blue triangles look like a convincing H-T curve, the deviation from the DC field points (green checkers) indicate that the transient nature of the pulsed magnetic field is causing heating. (Bottom) Two different pulses with the sample in He-4 gas (red curve) and He-4 liquid (blue curve). The added heat capacity of the liquid He-4 prohibits the sample from heating during the pulse proving that the H-T plot is indeed inconclusive.*

*Magnetic Quantum Oscillations*

$USb_2$ has been studied in high magnetic fields to reveal the Fermi surface via magnetic quantum oscillations. We have revisited the material in much higher magnetic fields using the improved PDO method. We also studied $PuSb_2$ to investigate the effect of narrow bandwidths associated with Pu. Surprisingly, no magnetic quantum oscillations were measured in $PuSb_2$ (Figure 4) despite the significant effort to get the sample measured within 8 hours from the time that it was removed from the furnace. It is likely that substitution of Pu for U has significantly increased the effective mass of the electrons in the metal; an enhanced mass will make magnetic quantum oscillations much harder to detect.

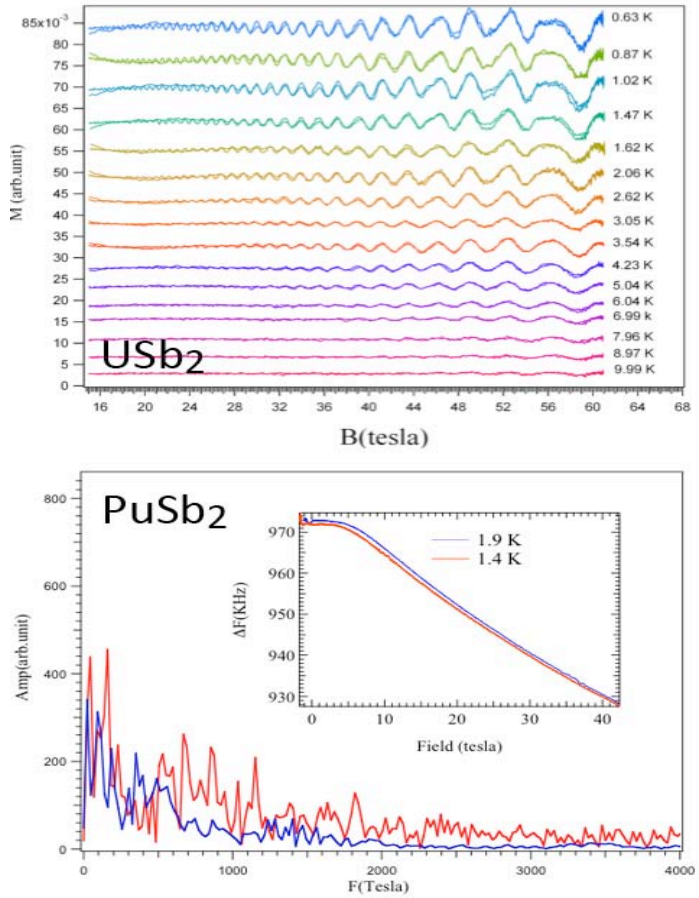


*Figure 4. (Top) Clear magnetic quantum oscillations in $USb_2$ measured with the PDO method in pulsed magnetic fields. (Bottom) The results of the PDO method applied to $PuSb_2$ measured in pulsed magnetic fields. No clear quantum oscillations are detected.*

**Theory**

Our theoretical efforts applied methods at three different levels of sophistication: (1) conventional first-principles band-structure theory that contain only minimal electronic correlation; (2) the first-principles GW method, which includes the lowest-order electronic correlation beyond band structure methods; and (3) including many body effects by using such methods as density functional theory (DFT), dynamical mean-field theory (DMFT), and Gutzwiller.

*Band Structure*

We performed band-structure calculations on pure actinide elements and several compounds to provide the necessary input for the more sophisticated approaches. For magnetic compounds, however, these methods are sufficiently accurate in themselves to provide new insights. We achieved particular success in showing how orbital order can enhance the net magnetic moment dramatically. Agreement between band structure calculations and experimental data has now improved significantly.

*GW Method*
We successfully used the GW method to explain why electronic correlation in pure U appears surprisingly weak. Correlation is actually significant in this material, but only shows up strongly in the unoccupied electron states and hence the occupied electrons are still described well by conventional band structure. We have also used the GW method to show that non-local exchange effects change the k-dependence of the band structure and that electronic correlations modify the crystal field splitting as well as the effective dispersion of the actinide band structures.

*DFT*
Density functional theory (DFT) codes describe with excellent accuracy the simple metals, and have done so for some time. Efforts to further develop the DFT codes to more accurately calculate the electrons' behavior in the heavy fermions, on the other hand, form a very active field of research. The results from these calculations provide researchers with maps of the electron density in real space, showing where the electrons prefer to sit. However, the electrons' behavior has much more to do with their momentum than their position, and so much more information can be found in maps of the electrons' momentum, i.e., in reciprocal space.

Experimentalists benefit from reciprocal-space maps of the electrons that respond to their experimental probing with electric or magnetic fields. The reciprocal-space map of these electrons forms the so-called Fermi surface. Figure 5 shows the Fermi surface calculated for $USb_2$, where the tubular nature of the Fermi surface in reciprocal space reflects the layered structure of the crystal in real space. This 2D character is likely a key component of this materials' superconductivity. Experiments cannot directly plot the Fermi surface itself, but they can quantify its character with de Haas-van Alphen (dHvA) measurements.

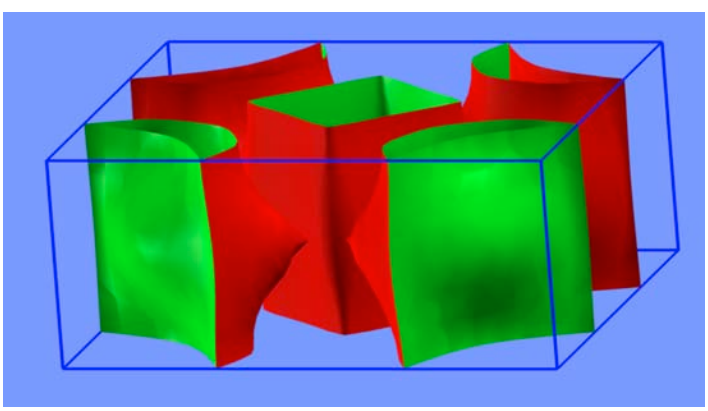

*Figure 5. Two calculated sheets of the Fermi surface of $USb_2$.*

*DMFT and Gutwiller methods*
Our use of many-body Gutzwiller and DMFT methods has shown the sensitivity of the spectral function to the 5*f* electron occupancy in δ-Pu; our results compare better with the photoemission data than that achieved by any other calculation. We have also developed better methods for handling the spin-orbit interaction for the Coulomb effects as well as improvements for the DMFT method.

## Impact on National Missions
This project supported one graduate student and four postdocs, one of which was converted to staff. We generated state-of-the-art experimental and theoretical tools and unique data on Pu and U. These results have enhanced our understanding of electron correlations and these new tools continue to push the frontiers of actinide science. Application of these tools beyond this project can enable predictions on the effect of extreme perturbations on relevant nuclear weapons systems and their evolution over time.

## Publications

Albers, R. C., N. E. Christensen, and A. Svane. Hubbard-U band structure methods. 2009. *Journal of Physics: Condensed Matter.* **21** (36): 343201.

Albers, R. C., and J. X. Zhu. Vacillating valence. 2007. *Nature.* **446**: 504.

Altarawneh, M. M., C. H. Mielke, and J. S. Brooks. Proximity detector circuits: an alternative to tunnel diode oscillators for contactless measurements in pulsed magnetic field environments. 2009. *Review of Scientific Instruments.* **80** (6): 066104.

Altarawneh, M. M., K. Collar , C. H. Mielke, N. Ni, S. L. Bud'ko, and P. C. Canfield. Determination of anisotropic Hc2 up to 60 T in Ba0.55K0.45Fe2As2 single crystals. 2008. *Physical Review B Rapid Communication.* **78** (22): 220505.

Balatsky, A., A. N. Chantis, H. P. Dahal, D. Parker, and J. X. Zhu. Incommensurate spin resonance in URu2Si2. 2009. *Physical Review B.* **79**: 214413.

Batista, C. D.. Effective Hamiltonian for metallic Pu. 2009. *Journal of Nuclear Materials.* **385** (1): 60.

Batista, C. D., J. E. Gubernatis, T. Durakiewicz, and J. Joyce. Strongly correlated approach to actinides. 2008. *Physical Review Letters.* **101** (1): 016403.

Bauer, E. D., C. Wang, V. R. Fanelli, J. M. Lawrence, E. A. Goremychkin, N. R. de Souza, F. Ronning, J. D. Thompson, A. V. Silhanek, V. Vildosola, A. M. Lobos, A. A. Aligia, S. Bobev, and J. L. Sarrao. Simplifying strong electronic correlations in uranium: localized uranium heavy fermion UM2Zn20 (M = Co, Rh) compounds . 2008. *Physical Review*

*B.* **78** (11): 115120.

Bauer, E. D., F. Ronning, T. Park, J. N. Mitchell, C. H. Mielke, R. D. McDonald, J. D. Thompson, and J. L. Sarrao. Superconductivity in U- and Pu-based heavy fermion materials. Presented at *Actinides 2009.* (San Francisco, CA, 12-17 July 2009).

Bauer, E. D., J. N. Mitchell, D. S. Schwartz, J. D. Thompson, and J. L. Sarrao. From delta-Pu to PuCoGa5: Kondo effect investigations of strong electronic correlations in Pu. Presented at *American Physical Society March Meeting.* (Denver, CO, 5-9 March 2007).

Bauer, E. D., J. N. Mitchell, D. S. Schwartz, J. D. Thompson, and J. L. Sarrao. Kondo effect investigation of strong electronic correlations in Pu. Presented at *Plutonium Futures - The Science.* (Dijon, France, July 2008).

Bauer, E. D., T. Park, R. D. McDonald, M. J. Graf, L. N. Boulaevskii, J. N. Mitchell, J. D. Thompson, and J. L. Sarrao. Possible two-band superconductivity in PuRhGa5 and CeRhIn5. To appear in *Journal of Alloys and Compounds.*

Booth, C. H., E. D. Bauer, M. Daniel, R. E. Wilson, J. N. Mitchell, L. A. Morales, J. L. Sarrao, and P. G. Allen. Quanitfying structural damage from self-irradiation in a plutonium superconductor. 2007. *Physical Review B.* **76**: 064530.

Booth, C. H., E. D. Bauer, and J. N. Mitchell. A moving target: responding to magnetic and structural disorder in lanthanide- and actinide-based superconductors. *Materials Science and Engineering .*

Booth, C. H., M. Daniel, R. E. Wilson, E. D. Bauer, J. N. Mitchell, N. O. Moreno, L. A. Morales, J. L. Sarrao, and P. G. Allen. Self-irradiation damage and 5f localization in PuCoGa5. 2007. *Journal of Alloys and Compounds.* **444-445**: 119.

Bouchet, J., R. C. Albers, and G. Jomard. GGA and LDA+U calculations of Pu phases. 2007. *Journal of Alloys and Compounds.* **444**: 246.

Chantis, A. N., R. C. Albers, M. D. Jones, M. van Schilfgaarde, and T. Kotani. Many-body electronic structure of metallic alpha-uranium. 2008. *Physical Review B.* **78** (8): 081101.

Chantis, A. N., R. C. Albers, M. van Schilfgaarde , and T. Kotani . GW Study of Actinides: alpha-uranium and delta-plutonium. Presented at *American Physical Society March Meeting.* (New Orleans, LA, March 2008).

Chantis, A. N., R. C. Albers, N. E. Christensen, and A. Savane. GW correlation effects on plutonium quasiparticle energies: changes in crystal-field splitting. 2009. *Philosophical Magazine.* **89** (22-24): 1801.

Cox, S., E. Rosten, R. D. McDonald, and J. Singleton. Comment on 'Pinning frequencies of the collective modes in alpha-uranium'. 2007. *Physical Review Letters.* **98**: 249701.

Dai, J., J. X. Zhu, and Q. Si. f-spin physics of rare-earth iron pnictides: Influence of d-electron antiferromagnetic order on the heavy-fermion phase diagram. 2009. *Physical Review B.* **80**: 020505.

Durakiewicz, T., P. S. Riseborough, C. G. Olson, J. J. Joyce, E. D. Bauer, J. L. Sarrao, S. Elgazzar, P. M. Oppeneer, E. Guziewicz, D. P. Moore, M. T. Butterfield, and K. S. Graham. Observation of a kink in the dispersion of f-electrons. 2008. *Europhysics Letters.* **84**: 37003.

Heffner, R. H., K. Ohishi, M. J. Fluss, G. D. Morris, D. E. MacLaughlin, L. Shu, B. W. Chung, S. K. McCall, E. D. Bauer, J. L. Sarrao, T. U. Ito, and W. Higemoto. The search for magnetic order in delta-Pu metal using muon spin relaxation. 2007. *Journal of Alloys and Compounds.* **444**: 80.

Hu, S. Y., M. E. Baskes, M. Stan, and J. N. Mitchell. Phase-field modeling of coring structure evolution in Pu-Ga alloys. 2007. *Acta Materialia.* **55**: 3641.

Hu, S. Y., M. L. Baskes, M. Stan, J. N. Mitchell, J. X. Zhang, and L. Q. Chen. Effect of elastic anisotropy and inhomogeneity on coring structure evolution in Pu-Ga alloys - phase field modeling. 2007. *Journal of Computer-Aided Materials Design.* **145**: 389.

Jones, M. D., and R. C. Albers. Spin-orbit coupling in an f-electron tight binding model: electronic properties of Th, U, and Pu. 2009. *Physical Review B.* **79** (4): 045107.

Joyce, J. J., T. Durakiewicz, K. S. Graham, D. P. Moore, E. D. Bauer, J. N. Mitchell, J. M. Wills, and J. X. Zhu. Electronic structure of Pu materials from angle-resolved photoemission. *Actinides 2009.* (San Francisco, CA, 12-17 July 2009).

Julien, J. P., J. X. Zhu, and R. C. Albers. Coulomb correlation in presence of spin-orbit coupling: application to plutonium. 2008. *Physical Review B.* **77** (19): 195123.

Julien, J. P., R. C. Albers, and J. Bouchet. Effect of spin-orbit coupling on an ab initio Gutzwiller approach for Pu. 2007. *Journal of Alloys and Compounds.* **444-445**: 285.

Lookman, T., A. Saxena, and R. C. Albers. Phonon

mechanisms and transformation paths in Pu. 2008. *Physical Review Letters.* **100** (14): 145504.

Manley, M. E., A. Said, M. J. Fluss, M. Wall, J. C. Lashley, A. Alatas, and K. T. Moore. Phonon density of states of alpha- and delta-plutonium by inelastic x-ray scattering . 2009. *Physical Review B.* **79** (5): 052301.

Mielke, C. H., and R. D. McDonald. Single turn multi-megagauss system at the NHMFL-Los Alamos to study plutonium. 2007. In *Megagauss Magnetic Fields and High Energy Liner Technology.* (Santa Fe, NM, USA, 4-8 November 2006). , p. 227. New York, NY: IEEE.

Mielke, C. H., and R. D. McDonald. Single turn multi-megagauss system at the NHMFL-Los Alamos to study plutonium. 2008. In *Proceedings of the 2006 International Conference on Megagauss Magnetic Field Generation and Related Topics.* (London, UK, 8 - 14 September, 2006). , p. 227. Piscataway, New Jersey: IEEE.

Migliori, A., C. Pantea, H. Ledbetter, I. Stroe, J. B. Betts, J. N. Mitchell, M. Ramos, F. Freibert, D. Dooley, S. Harrington, and C. H. Mielke. Alpha-plutonium's polycrystalline elastic moduli over its full temperature range. 2007. *Journal of the Accoustical Society of America.* **122** (4): 1994.

Migliori, A., I. Mihut, J. B. Betts, M. Ramos, C. Mielke, C. Pantea, and D. Miller. Temperature and time-dependence of the elastic moduli of Pu and Pu-Ga alloys. 2007. *Journal of Alloys and Compounds.* **444-445**: 133.

Migliori, A., I. Stroe-Mihut, J. B. Betts, and J. N. Mitchell. Temperature as a driver for localization in plutonium. Presented at *American Physical Society March Meeting.* (New Orleans, LA, March 2008).

Mitchell, J. N., C. J. Boehlert, and F. J. Freibert. Microstructural influence on the delta to alpha prime transformation in Pu-Ga alloys. Presented at *Actinides 2009.* (San Francisco, CA, 12-17 July 2009).

Mitchell, J. N., F. J. Freibert, M. E. Bange, and D. S. Schwartz. Unconventional delta-phase stabilization in Pu-Ga alloys. 2009. *Journal of Nuclear Materials.* **385** (1): 95.

NChantis, A., R. C. Albers, A. Svane, N. E. Christensen, M. van Schilfgaarde, and T. Kotani . 'GW correlation effects on the quasiparticle energies of Np and Pu. Presented at *American Physical Society March Meeting.* (Pittsburg, PA, 16-20 March 2009).

Ohishi, K., R. H. Heffner, G. D. Morris, E. D. Bauer, M. J. Graf, J. X. Zhu, L. A. Morales, J. L. Sarrao, M. F. Fluss, D. E. MacLaughlin, L. Shu, W. Higemoto, and T. U. Ito. Muon spin rotation measurements of the superfluid density in fresh and aged superconducting PuCoGa5. 2007. *Physical Review B.* **76** (6): 064504.

Ohishi, K., R. H. Heffner, G. D. Morris, E. D. Bauer, M. J. Graf, J. X. Zhu, L. A. Morales, J. L. Sarrao, M. J. Fluss, D. E. MacLaughlin, L. Shu, W. Higemoto, and T. U. Ito. Influence of self irradiation on the magnitude of superfluid density in PuCoGa5 probed by muon spin rotation. 2008. *Physica B.* **403** (5-9): 1013.

Park, T., V. A. Sidorov, F. Ronning, J. X. Zhu, Y. Tokiwa, H. Lee, E. D. Bauer, R. Movshovich, J. L. Sarrao, and J. D. Thompson. Isotropic quantum scattering and unconventional superconductivity. 2008. *Nature.* **456** (7220): 366.

Qi, Y., J. X. Zhu, S. Zhang, and C. S. Ting. Kondo resonance in the presence of spin-polarized currents . 2008. *Physical Review B.* **78** (4): 045305.

Qi, Y., J. X. Zhu, and C. S. Ting. Validity of the equation-of-motion approach to the Kondo problem in the large-N limit. 2009. *Physical Review B.* **79** (20): 205110.

Sarrao, J. L., and J. D. Thompson. Superconductivity in cerium- and plutonium-based 115 materials. 2007. *Journal of the Physical Society of Japan.* **76**: 051013.

Schwartz, D. S., J. N. Mitchell, and R. A. Pereyra. Detection and quantification of residual alpha-phase in delta-stabilized plutonium. *Materials Science and Engineering.*

Stroe, I., J. B. Betts, A. Trugman, C. H. Mielke, J. N. Mitchell, M. Ramos, F. J. Freibert, H. Ledbetter, and A. Migliori. Polycrystalline gamma-plutonium's elastic moduli versus temperature. To appear in *Journal of the Acoustical Society of America.*

Talbayev, D., K. S. Burch, E. E. M. Chia, S. A. Trugman, J. X. Zhu, E. D. Bauer, J. N. Mitchell, J. D. Thompson, J. L. Sarrao, and A. J. Taylor. Hybrization and superconducting gaps in heavy-fermion superconductor PuCoGa5 probed via the dynamics of photoinduced quasiparticles. *Physical Review Letters.*

Thompson, J. D.. Actinide superconductivity: PuCoGa5 and related materials. Invited presentation at *Materials Research Society Symposium Proceedings.* (Boston, Nov. 2006).

Thompson, J. D., N. J. Curro, T. Park, E. D. Bauer, and J. L. Sarrao. PuCoGa5 and related materials. 2007. *Journal of Alloys and Compounds.* **444-445**: 19.

Trouw, F., J. J. Rhyne, and J. N. Mitchell. Pu neutron

scattering studies - magnetism and structure. 2009. *Journal of Nuclear Materials.* **385** (1): 35.

Wang, C. H., A. D. Christianson, J. M. Lawrence, E. D. Bauer, E. A. Goremychkin, A. I. Kolesnikov, F. Trouw, F. Ronning, J. D. Thompson, M. D. Lumsden, and P. C. Canfield. Neutron scattering and scaling behavior in URu2Zn20 and YbFe2Zn20. *Physical Review B.*

Yang, X., P. S. Riseborough, T. Durakiewicz, C. G. Olson, J. J. Joyce, E. D. Bauer, J. L. Sarrao, D. P. Moore, K. S. Graham, S. Elgazaar, P. Oppeneer, E. Guziewicz, and M. T. Butterfield. Unusual quasiparticle renormalizations from angle resolved photoemission on USb2. 2009. *Philosophical Magazine.* **89**: 1893.

Zhu, J. X.. Spectral properties of elemental plutonium. Presented at *International Conference on Strongly Correlated Electron Systems.* (Houston, 13-18 May, 2007).

Zhu, J. X., A. K. McMahan, M. D. Jones, T. Durakiewicz, J. J. Joyce, J. M. Wills, and R. C. Albers. Spectral properties of delta-plutonium: sensitivity to 5f occupancy. 2007. *Physical Review B.* **76** (24): 245118.

Zhu, J. X., A. K. McMahan, M. D. Jones, T. Durakiewicz, J. J. Joyce, J. M. Wills, and R. C. Albers. Spectral properties of elemental plutonium. Presented at *American Physical Society March Meeting.* (Denver, CO, 5-9 March 2007).

Zhu, J. X., A. K. McMahan, M. D. Jones, T. Durakiewicz, J. J. Joyce, J. M. Wills, and R. C. Albers. Theoretical studies of spectral properties of plutonium. 2008. In *Materials Research Society Symposium Proceedings.* (San Francisco, 25-28 March 2008). Vol. 1104, p. 59. Warrendale, PA: MRS.

Zhu, J. X., I. Martin, and A. R. Bishop. Kondo stripes in an Anderson-Heisenberg model of heavy fermion systems. 2008. *Physical Review Letters.* **100** (23): 236403.

# Metamaterials for Threat Reduction Applications: Imaging, Signal Processing, and Cloaking

*Antoinette J. Taylor*
20070060DR

## Abstract

Improving our ability to detect, modulate, and direct electromagnetic radiation is crucial for threat reduction missions. Metamaterials research enables a predictive approach to the realization of materials with tailored electromagnetic properties since subwavelength elements can be designed that respond resonantly to the electric or magnetic field of the incident radiation. The added flexibility this provides in creating composite electromagnetic materials is a revolutionary conceptual advance with practical implications. Indeed, negative refractive index materials, perfect near-field imaging, and compact lightweight lenses have all been realized during the past decade using such composite metamaterials. The objective of this project was to advance the understanding of metamaterial properties with a view towards utilizing such structures to create functional electromagnetic materials for threat reduction applications.

## Background and Research Objectives

The field of metamaterials (MM) has blossomed with the realization that it is possible to create "artificial" electromagnetic composites that combine tailored magnetic and electric response. This has led to the demonstration of unique functional behavior such as a negative index of refraction, which is not attainable with naturally occurring materials. Such novel electromagnetic properties, coupled with the scalability of the metamaterial response from radio-frequency to near optical frequencies, have resulted in a flurry of research activity with a view towards both fundamental understanding and practical applications. In short, *metamaterials provide a new scale-invariant design paradigm to create functional materials that revolutionize our ability to manipulate, control, and detect electromagnetic radiation.* Our objective is to advance the understanding of metamaterial properties with a view towards utilizing such structures to create functional electromagnetic materials and devices for threat reduction applications at terahertz (THz) frequencies. Specifically, we will design, fabricate, and characterize the following THz metamaterial devices: (i) *Active metamaterial switches:* we will develop metamaterial modulators for high-bit-rate signal processing and covert communication. (ii) *Metamaterials enhanced thermal detector:* we will develop bimaterial cantilever detectors where the absorption of electromagnetic radiation is enhanced through the incorporation of resonant metamaterials. (iii) *Electromagnetic cloaking:* recent results reveal the ability of electric and magnetic metamaterials to hide objects from electromagnetic radiation. Our major goal is to advance our ability to model, fabricate, and characterize non-planar three dimensional metamaterial structures for cloaking at THz frequencies.

## Scientific Approach and Accomplishments

### Active metamaterial switches

Although the metamaterial resonant response is mainly determined by the geometry and dimensions of the metamaterial elements, we found that incorporation of additional materials, e.g. semiconductors, as the substrate or as an integral part of the metamaterial particles, can enable dynamical control over the metamaterial resonances through external stimuli to achieve novel functionalities. We fabricated split ring resonator (SRR) arrays on high resistivity GaAs semiconductor substrates that reveal very strong resonances. Under near-infrared photoexcitation, we demonstrated that the generated photocarriers on the substrate surface make it conducting and short-circuit the split gaps, therefore dynamically switching the resonances and tuning the values of the effective permittivity and/or permeability. Consequently, the transmission of the THz radiation was also switched over a narrow frequency range centered at the resonance. Such an all-optical dynamic switching (modulation)

of THz radiation could be very fast if the lifetime of the photocarriers can be reduced. We demonstrated an ultrafast switching (~20 ps) of THz transmission using GaAs:ErAs nanoisland superlattice substrate where the carrier lifetime can be engineered from sub-picosecond to tens of picoseconds. As a device, this dynamical switching of THz transmission through metamaterials exhibits very high switching efficiency and ultrafast switching speed and requires very low photoexcitation fluence.

The resonant nature of metamaterials results in high frequency dispersion and narrow bandwidth where the center frequency is fixed by the geometry and dimensions of SRR elements comprising the metamaterial composite. The creation of frequency agile metamaterials would extend the spectral range over which devices function and further, enable the manufacture of new devices such as dynamically tunable notch filters. Figure 1 reveals such frequency-agile THz metamaterials accomplished through incorporation of semiconductors in critical regions of metallic SRRs. Through photoexcitation of the semiconductor regions, we have experimentally demonstrated over 20% tuning of the resonance frequency, in excellent agreement with numerical simulations.

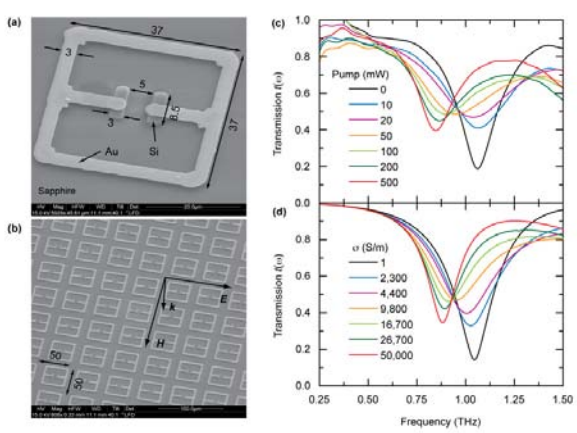


*Figure 1. Scanning electron microscopy images of the frequency-agile planar metamaterial, (a) an individual unit cell, and (b) a periodically patterned square array. (c) The experimental THz electric field transmission amplitude under various photoexcitation fluences, and (d) results of numerical simulations by varying the silicon conductivity.*

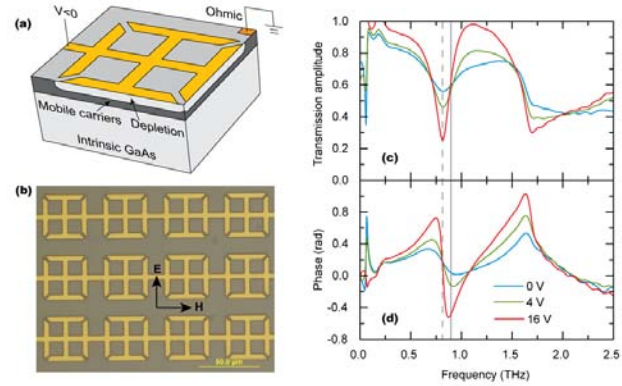


*Figure 2. (a) Schematic of a unit cell for the active THz metamaterial. (b) Optical microscopy image of the active THz metamaterial. (c) THz transmission amplitude and (d) phase spectra under various voltage biases.*

An electrical approach to control the metamaterial resonances is often desirable. We have accomplished electrically switchable metamaterials by fabricating gold SRR array on a thin *n*-doped GaAs layer on an intrinsic GaAs substrate. The interface of metal SRRs and the substrate forms a Schottky diode structure, where a reverse voltage bias actively depletes free electrons from the split gaps, modifying the resonant response. The effective permittivity can then be conveniently tuned between positive and negative values, alleviating the strict design requirements. We have demonstrated that the electrical approach of THz modulation is capable of a modulation depth as high as 80% at a designed resonance frequency of 0.8 THz, and a modulation speed up to 2 MHz, limited only by the stray capacitance. Our metamaterial modulator exhibits a twenty-fold improvement in modulation depth over previous electrically-driven THz-modulators based on semiconductor quantum-well structures while operating at room temperature.

We further demonstrated that, at the resonance wing (0.89 THz) where the THz transmission intensity remains constant, the THz transmission phase had a linear dependence on the applied voltage bias, and a maximum change of $\pi/6$ was achieved for such a single layer metamaterial under relative low voltage bias (16 volts), making it an excellent solid state THz phase modulator. Larger values of phase modulation could be easily achievable by stacking multi-layered metamaterial structures. Although both the intensity and the phase modulation are narrowband, their correlation enables broadband modulation when applying an AC control voltage. The band roughly covering the frequencies

between the two metamaterial resonances, which can be engineered to span the whole THz regime. We also fabricated a metamaterial device with independently controllable pixels, demonstrating a spatial light modulator for THz imaging applications.

**Metamaterial-enhanced thermal detector**

We have explored the use of bimaterial cantilever detectors where the absorption of electromagnetic radiation is enhanced through the incorporation of resonant metamaterials. This approach is based on metamaterials, which provide for the synthesis of design-specific electromagnetic resonances coupled with MEMS (MicroElecroMechanical Systems) cantilever technology. Fabrication of strongly absorbing metamterials elements on a MEMS cantilever will lead to a deflection of the cantilever when terahertz radiation is incident. The principle of operation is that cantilevers are fabricated from two materials with different coefficients of thermal expansion. In these bimaterial cantilevers the absorption-induced deflection can be measured using optical readout. The possibility of incorporating metamterials into the detector is of crucial importance at THz frequencies where it is difficult to find highly absorbing materials at this wavelength range that, further, are compatible with MEMS processing. A crucial aspect of any thermally-based detection radiation detector is to have a low thermal mass to obtain the greatest possible temperature change for a given incident flux. Free standing cantilevers meet this requirement. Additional advantages include the potential for straightforward fabrication of a focal plane array. A thermal analysis of these detectors suggests that it should be possible to achieve a noise equivalent temperature difference of ~10mK, a very competitive technology for the detection of THz radiation.

We have focused on interfacing metamaterials with various MEMS technologies to create new composites and devices that operate at terahertz frequencies. This includes non-planar flexible composites and micromechanically active structures where the orientation of the electromagnetically resonant elements can be precisely controlled with respect to the incident field. We have fabricated arrays of gold split ring resonators on 400-nm-thick silicon nitride films where each individual unit cell is a free-standing cantilever. Through temperature tuning, the orientation of the SRRs can be precisely controlled. This, in turn, provides direct control of the electromagnetic response enabling independent access and tuning of the electric and magnetic properties. These structures provide an important approach towards creating a thermally active metamaterial-based detector that is amenable to focal plane integration.

We have fabricated a split ring resonator (SRR) on bimaterial cantilevers using silicon nitride and gold. With SRRs fabricated on top of the cantilever, this allows for a thermally responsive reorientation of the SRRs with respect to the incident terahertz radiation field resulting in dramatic changes in the resonant electromagnetic response [6]. Figure 3(a) shows the basic idea where each unit cell consists of a SRR on a free-standing 400 nm thick layer of silicon nitride which is connected to a supporting substrate by the bimaterial cantilever arms. With the incident field orientation as depicted in the figure, there will not be a resonant response when the SRRs lie in the plane of the substrate. However, if the temperature is increased, the cantilevers will bend upwards leading to a penetration of the magnetic field through the SRRs which will then drive the magnetic resonance. Figure 3(b) shows fabricated bimaterial cantilever metamaterials lying in-plane and bent upwards out of the plane of the substrate. The corresponding electromagnetic response for the two configurations is shown in Figure 3(c). A strong magnetic resonance is evident for the out-of-plane SRRs. These results highlight the possibility of creating reconfigurable metamaterials potentially leading to dynamically reversible refractive index structures and/or thermal detectors.

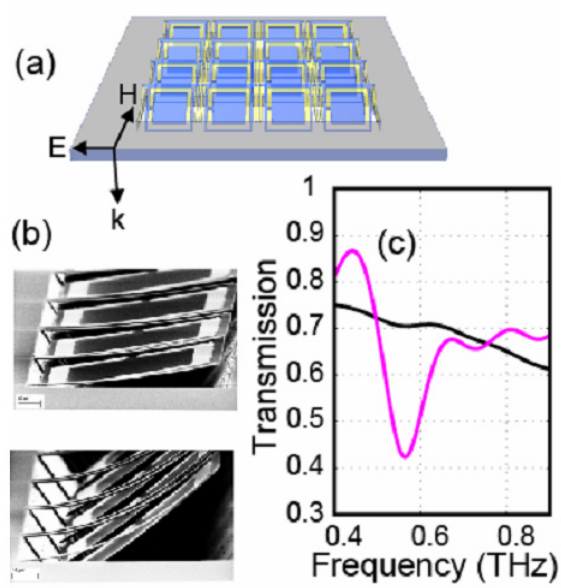


*Figure 3. (a) Schematic of "pop-up" MM and field orientation for measurements. (b) Scanning electron microscopy pictures of split ring resonators (SRRs) for in-plane and out-of-plane configuration. (c) THz-transmiision spectra – a magnetic resonance appears when the MM are bent out-of-plane and couple to the THz magnetic field.*

An issue which determines, in part, how well a metamaterial enhanced thermal detector works is how much of the incident radiation is absorbed. Our design consists of a bilayer unit cell which allows for maximization

of the absorption through independent tuning of the electrical permittivity and magnetic permeability. We have now demonstrated several improved metamaterial absorber designs operating at THz frequencies. These absorbers have experimentally achieved absorption values of 95%. Studies, both computational and experimental, have investigated the impact of off- normal absorption for both S and P-polarizations. Absorption coefficients of $\alpha$=2000cm$^{-1}$ have been shown, thus indicating the great potential for metamaterial absorbers to perform as bolometric pixels in focal plane arrays for THz imaging.

**Electromagnetic cloaking**

The concept of cloaking an object from electromagnetic radiation using metamaterials was based on ideas related to sculpting the path of electromagnetic radiation using coordinate transformations [1]. The design and implementation of a cloak is technically challenging in terms of fabrication and design. Thus, during the project, we did not expect to produce a THz cloak, rather to advance simulation and fabrication for creating non-planar metamterial composites required for cloaking.

Therefore, we worked to develop a metamaterial device that demonstrates the tools that serve as the foundation for a THz cloak. This device is a negative-index metamaterial (NIM) prism, which demonstrates three essential components of a THz cloaking: 1) beam steering in a defined manner, 2) simultaneous tuning of both the permittivity and permeability, 3) three-dimensional THz metamaterial fabrication. The following describes the design, simulation, and fabrication processes that have resulted from our studies.

The design parameters of a bulk THz cloak require comparatively thick interlayer spacing (10-20 µm) comprised of dielectric. Such layers are hard to fabricate by traditional deposition techniques of well known dielectrics ($SiO_2$, SiN, etc). We have thus designed our THz NIM based on a stacked metallic "fishnet" structures with interlayer spacing provided by 18 µm thick Kapton. We are fabricating the sample in collaboration with Oklahoma State University (OSU). The metallic fishnet layers are deposited using standard photolithography. To form the dielectric spacing layers we used liquid polyimide (Kapton is cured polyimide). Following metal deposition of the fishnet structure on each layer we spin coat a thick layer of polyimide and follow a prescribed curing process that we perfected with OSU. The process repeats 10 times until we have built up a bulk 3D THz metamaterial. Using selective etching techniques we can then remove the thick layers of polyimide from inside the holes of the fishnet structure as well as remove excess material to sculpt the prism profile. This fabrication process took several months to develop and is nearing the final stages presently.

We have thoroughly characterized our design by using the measured properties of cured polyimide as well as detailed electromagnetic simulations. The prism simulation set up is shown in Figure 4(a). A plane wave incident on the flat surface of the prism from the bottom undergoes negative refraction at 0.8 THz as shown in Figure 4(b). We have also simulated the propagation of 1.3 THz through the same structure and have clearly observed a positive refraction. The only remaining task is to measure the electromagnetic response of this NIM prism. We do not foresee any complications and intend to complete this high-impact measurement.

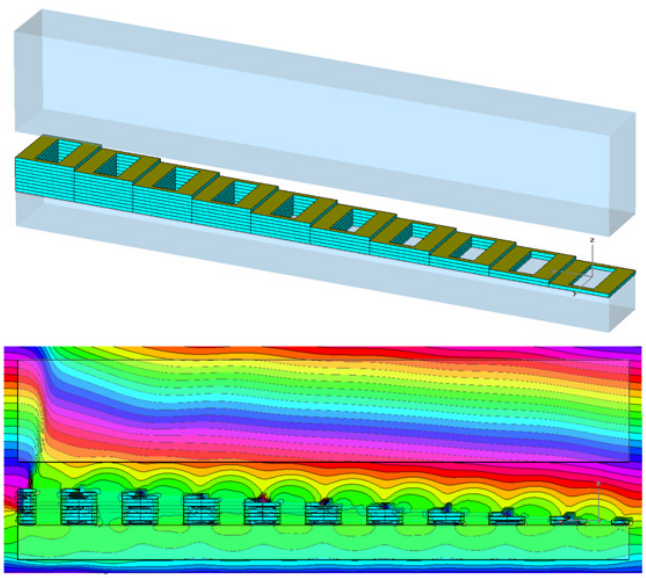

*Figure 4. (a) Geometry of the prism simulation. (b) The resulting electromagnetic wave simulation reveals the negative refraction of the THz wave after propagating through the prism. A prism with normal (positive) index of refraction would bend the wavefront in the opposite direction relative to the normal to the prism.*

## Impact on National Missions

This project is of strategic importance to the Laboratory since it is advancing the science and technology of artificially engineered electromagnetic metamaterials for threat reduction applications. The ability to (i) covertly transmit data at high bit-rates at difficult to intercept wavelengths, (ii) to image objects at far-infrared frequencies, or (iii) to cloak an object from interrogating radiation are highly desirable goals for threat reduction. Thus, such electromagnetic MM devices offer considerable potential as transformational components of an overall system architecture designed to mitigate or detect a potential threat. This project has enhanced the Laboratory Grand Challenges in Materials and Sensing and was timely

given the keen international interest in metamaterials.

Further, R&D in metamaterials represents a strategic growth opportunity for the Laboratory in the threat reduction arena, providing an avenue for applying LANL's forefront materials fabrication, design, and characterization capabilities in partnership with its detection and sensor expertise. This project has enabled the funding of several external projects from sponsors from the threat reduction arena, including a highly competitive project from DARPA on "Engineering the Casimir Force with Metamaterials." Further, the particular emphasis in this project is the development of metamaterials for sensors and detectors in the THz frequency range. The Laboratory is interested in developing such THz technology for nonproliferation and defense transformation applications because it is the shortest wavelength electromagnetic radiation that can be used in all weather conditions, day or night, in the W-band water vapor window. This project will underpin future endeavors in the MaRIE's signature facility at LANL controlling materials functionality for global security applications.

This project has enabled this team to ensure a continuing leadership role for the Laboratory in the emerging technology of metamaterials, as demonstrated by the large number of publications in peer reviewed journals and the many plenary and invited talks at international conferences given by team members. This project also hosted two International Workshops on Electromagnetic Metamaterials which were heavily attended by leaders of international metamaterials community. The topic of metamaterials is highlighted in BESAC's report *Directing Matter and Energy: Five Challenges for Science and the Imagination* [2], where it is stated that "artificially engineered structures have properties not found in nature and not observed in their constituent materials." As this report describes future directions for DOE-BES, this project has provided the foundational science for growth from that basic science sponsor, as well.

## References


1. Pendry, J. B., D. Schurig, and D. R. Smith. Controlling electromagnetic fields. 2006. *Science.* **312**: 1780.

2. Hemminger, J., G. Fleming, and M. Ratner. Directing Matter and Energy: Five Challenges for Science and the Imagination. 2007. *US Department of Energy.*


## Publications


Acuna, G. P., S. F Heucke, F. Kuchler, H. T. Chen, A. J. Taylor, and R. Kersting. Surface plasmons in terahertz metamaterials . 2008. *Optics Express.* **16**: 18745.

Azad, A. K., A. J. Taylor, E. Smirnova, and J. F. O'Hara. Characterization and analysis of terahertz metamaterials based on rectangular split-ring resonators. 2008. *Applied Physics Letters.* **92**: 011119.

Azad, A. K., H. T. Chen, A. J. Taylor, E. Akhadov, N. R. Weisse-Bernstein, and J. F. O'Hara. Flexible quasi-three-dimensional terahertz electric metamaterials. 2009. *Terahertz Science and Technology.* **2**: 15.

Azad, A. K., H. T. Chen, S. R. Karsala, A. J. Taylor, J. F. O'Hara, Z. Tian, X. Lu, W. Zhang, and A. C. Gossard. Ultrafast optical control of terahertz surface plasmons in subwavelength hole-arrays at room temperature. 2009. *Applied Physics Letters.* **95**: 011105.

Chan, W. L., H. T. Chen, A. J. Taylor, I. Brener, M. J. Cich, and D. M. Mittleman. A spatial light modulator for terahertz beams. 2009. *Applied Physics Letters.* **94**: 213511.

Chen, H. T., H. Lu, A. K. Azad, R. D. Averitt, A. C. Gossard, J. F. O'Hara, S. A. Trugman, and A. J. Taylor. Electronically switchable terahertz surface plasmon resonance. 2008. *Optics Express.* **16**: 7641.

Chen, H. T., J. F. O'Hara, A. J. Taylor, R. D. Averitt, C. Highstrete, M. Lee, and W. J. Padilla. Complementary planar, terahertz materials. 2007. *Optics Express.* **15**: 1084.

Chen, H. T., J. F. O'Hara, A. K. Azad, A. J. Taylor, R. D. Averitt, D. B. Shrekenhamer, and W. J. Padilla. Experimental demonstration of frequency agile terahertz metamaterials. 2008. *Nature Photonics.* **2**: 295.

Chen, H. T., S. Palit, T. Tyler, C. M. Bingham, J. M. O. Zide, J. F. O'Hara, D. R. Smith, A. C. Gossard, R. D. Averitt, W. J. Padilla, N. M. Jokerst, and A. J. Taylor. Hybrid metamaterials enable fast electrical modulation of freely propagating terahertz waves. 2008. *Applied Physics Letters.* **93**: 091117.

Chen, H. T., W. J. Padilla, J. M. O. Zide, A. C. Gossard, A. J. Taylor,, and R. D. Averitt. All Solid-State Metamaterial Devices. 2006. *Nature.* **444**: 597.

Chen, H. T., W. J. Padilla, J. M. O. Zide, S. R. Bank, A. C. Gossard, A. J. Taylor, and R. D. Averitt. Ultrafast optical switching of terahertz metamaterials fabricated on ErAs/GaAs nanoisland superlattices. 2007. *Optics Letters.* **32**: 1620.

Chen, H. T., W. J. Padilla, M. J. Cich, A. K. Azad, R. D. Averitt, and A. J. Taylor. A metamaterial solid-state terahertz phase modulator. 2009. *Nature Photonics.* **3**: 148.

Chen, H. T., W. J. Padilla, R. D. Averitt, A. C. Gossard,

C. Highstrete, M. Lee, J. F. O'Hara, and A. J. Taylor. Electromagnetic metamaterials for terahertz applications. 2008. *Terahertz Science and Technology* . **1**: 42.

Landy, N. I., S. Sajuyigbe, J. J. Mock, D. R. Smith, and W. J. Padilla. Perfect Metamaterial Absorber. 2008. *Physical Review Letters.* **100**: 207402.

O'Hara, J. F., A. K. Azad, H. T. Chen, A. J. Taylor, and E. Smirnova. Effects of microstructure variations on macroscopic terahertz metafilm properties. 2007. *Active and Passive Electronic Components* . **2007**: 49691.

O'Hara, J. F., E. Smirnova, H. T. Chen, A. J. Taylor, R. D. Averitt, C. Highstrete, M. Lee, and W. J. Padilla. Properties of Planar electric metamaterials for novel terahertz applications. 2007. *Journal of Nanoelectronics and Optoelectronics* . **2**: 90.

O'Hara, J. F., R. Singh, I. Brener, E. Smirnova, J. Han, A. J. Taylor, and W. Zhang. Thin film sensing with planar metamaterials: sensitivity and limitations. 2008. *Optics Express.* **16**: 1786.

Padilla,, W. J., M. T. Aronsson, C. Highstrete, M. Lee, A. J. Taylor, and R. D. Averitt. Novel electrically resonant terahertz metamaterials: Theoretical and experimental investigations. 2007. *Physical Review B.* **75**: 041102R.

Peralta, X. G., E. Smironova, A. K. Azad, H. T. Chen, A. J. Taylor, I. Brener, and J. F. O'Hara. Metamaterials for THz polarimetric devices. 2009. *Optics Express.* **17**: 773.

Singh, R., A. K. Abul, J. F. O'Hara, A. J. Taylor, and W. Zhang. Effect of metal permittivity on resonant properties of terahertz metamaterials. 2008. *Optics Letters.* **33**: 1506.

Singh, R., E. Smirnova, A. J. Taylor, J. F. O'Hara, and W. Zhang. Optically thin terahertz metamaterials. 2008. *Optics Express.* **16**: 6537.

Tao, H., A. C. Strikwerda, K. Fan, C. M. Bingham, W. J. Padilla, and R. D. Averitt. Terahertz metamaterials on free-standing highly-flexible polyimide substrates. 2008. *Journal of Physics D: Applied Physics.* **41**: 232004.

Tao, H., A. C. Strikwerda, K. Fan, W. J. Padilla, X. Zhang, and R. D. Averitt. Reconfigurable terahertz metamaterials. To appear in *Physical Review Letters.*

Tao, H., C. M. Bingham, A. C. Strikwerda, D. Pilon, D. Shrekenhamer, N. Landy, K. Fan, X. Zhang, W. J. Padilla, and R. D. Averitt. Highly-flexible wide angle of incidence terahertz metamaterial absorber. 2008. *Physical Review B.* **78**: 241103R.

Tao, H., N. I. Landy, C. Bingham, X. Zhang, R. D. Averitt, and W. J. Padilla. A metamaterial absorber for the terahertz regime: design, fabrication and characterization . 2008. *Optics Express.* **16**: 7181.

Wong, R., and H. T. Chen. Taming the terahertz. 2008. *Nature Photonics.* **2**: 324.

# Coexistence of Magnetic and Superconducting Electrons in Strongly Correlated Matter

*Joe D. Thompson*
20070064DR

## Abstract

Revealing and understanding the relationship between magnetism and superconductivity was a centerpiece of physics for nearly half the 20th century. This relationship, which is critical for the design of today's superconducting technologies, is now well understood in conventional superconductors in which magnetism and superconductivity develop from distinctly unrelated electrons. In contrast, recent discoveries have suggested that unconventional superconductivity and magnetism in classes of strongly correlated electron materials, ranging from oxides to f-electron metals, might arise from the same electrons. One family of 4f-electron unconventional superconductors discovered by us has emerged as the prototype for understanding how the same electrons can produce simultaneously magnetism and superconductivity. Our project has focused on this family in which we have found experimentally that unconventional superconductivity and magnetism not only coexist microscopically and arise from the same electrons but indeed they require each other. We have shown theoretically how this can happen and have established commonalities between these 4f-electron and the oxide unconventional superconductors. Insights, acquired from in-depth studies of high quality crystals, also have been applied to understand the low transition temperatures in a new family of superconductors we have discovered. Accomplishments in this project represent significant progress on the challenge to 'master the control of energy-relevant complex systems that exhibit collective, cooperative and/or adaptive behaviors' and to 'use the complexity of matter as an asset rather than an obstacle by 'tuning' the properties of matter with small changes in composition or with the application of pressures or a magnetic field.'

## Background and Research Objectives

There are thousands of materials that, at sufficiently low temperatures, become superconducting. The physics of their conventional superconductivity is very well understood theoretically, and this theory also predicts that the electrons participating in superconductivity cannot be magnetic, a conclusion supported by many experiments. Unexpected discoveries during the past decade have shown, however, that some materials become superconducting only when magnetism is present or 'nearby' and when complex electron-electron correlations are very strong. These unconventional superconductors cannot be explained by any theory, yet they hold substantial promise for future energy-saving technologies. The problem posed by coexisting unconventional superconductivity and magnetism is a declared Grand Challenge. Our goal has been to establish experimentally and theoretically how the same electrons allow magnetism and unconventional superconductivity to coexist and the consequences of their coexistence.

The copper oxides, with superconducting transition temperatures exceeding 100K, hold most promise for technological applications, but they are very complex structurally and electronically, which has made if very difficult to unravel the relationship between magnetism and their unconventional superconductivity--an essential step toward developing a theory of unconventional superconductivity. A family of f-electron materials of the form CeMIn5 (where M=Rh, Co, Ir), discovered at Los Alamos, also supports unconventional superconductivity, and, unlike the oxides, they crystallize as exceptionally pure single crystals. We have shown that there are remarkable similarities between essential physical properties of the oxides and CeMIn5 members: unconventional superconductivity in both develops in proximity to antiferromagnetic order, the symmetry of the superconducting electrons is the same in both cases, and both have the same unusual characteristics of their normal state. Though most worldwide attention has focused on studies of the copper oxides, the $CeMIn_5$ materials offer a number of advantages, especially

the ability to tune these materials easily by chemical substitutions, pressure and magnetic field. This tunabilty has allowed insights not possible in the copper oxides, but they should be applicable to the oxides as well as to other electronically correlated systems. As discussed below, these insights now set the stage for a microscopic theory of unconventional superconductivity.

## Scientific Approach and Accomplishments

Departing from traditional approaches that attempt to understand the strongly correlated magnetic or nearly magnetic normal state and its consequences for unconventional superconductivity, we have used the unconventional superconductivity itself as a primary diagnostic of the relationship between magnetic and superconducting electrons. Both approaches are complementary, and in the course of this project, we have had to understand experimentally and theoretically the normal state as well but in the context of what we have learned from the superconducting electrons. Experimentally, a wide range of techniques have been applied to the problem, including electrical transport and thermodynamic measurements that provide a macroscopic perspective as well as neutron scattering, nuclear magnetic resonance, photoemission and point contact spectroscopies that probe electrons on a microscopic level. Many of these measurements were made at extremes of very low temperatures, high pressures and high magnetic fields. Theoretically, Ginzburg-Landau models have been used to capture macroscopic consequences of coupled magnetic and superconducting electrons; whereas, analytical and numerical solutions to low-energy effective theories provided interpretations of microscopic mechanisms. In the following, we briefly summarize a few of the many important discoveries that have come from this project.

Our earlier thermodynamic studies of CeCoIn5 revealed the emergence of a new phase transition, labeled T2 in Figure 1, in its superconducting state at low-temperatures and high magnetic fields. An analysis of these observations suggested that the new phase could be the long-sought inhomogeneous superconducting state predicted 40 years ago by Fulde, Ferrell, Larkin and Ovchinnikov (FFLO). Nuclear magnetic resonance (NMR) should exhibit characteristics that would prove this suggestion. Instead, our NMR measurements found evidence for antiferromagnetic order in the T2-phase [1]. To confirm this, we used neutron diffraction to establish unambiguously that long range magnetic order develops in the low-temperature, high-field superconducting state of $CeCoIn_5$, and most significantly that magnetism exists *only* inside the superconducting state. This exciting result, published in Science [2], confirmed our earlier conclusion from NMR that superconductivity is, in fact, necessary for magnetic order, *a totally new and unexpected state of matter that derives from the coupling of magnetic and superconducting electrons.* These experiments, however, left open the question of whether magnetic or superconducting electrons drove this new state. From specific heat measurements on $CeCoIn_5$ with very slight (0.05% or less) substitutions of Hg for In, we concluded that unconventional superconductivity underlies the origin and that field-induced magnetic order is detrimental to the possible FFLO state [3]. The coupling between magnetic and superconducting electrons also should influence the nature of quantized units of magnetic flux that result from applying a magnetic field to any superconductor. Again, using neutron diffraction techniques, we discovered that quantized units of magnetic flux assume an unusual distribution in the superconducting state of $CeCoIn_5$ and, most significantly, that the flux units became more well-defined with increasing field. This result, never seen before and also published in Science [4], is a direct result the proximity of CeCoIn5 to magnetic order.

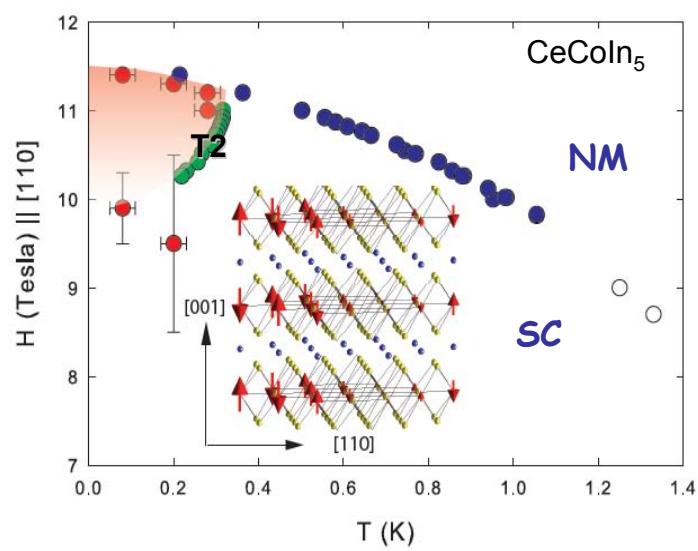


*Figure 1. Low-temperature, high-magnetic field portion of the superconducting phase diagram of $CeCoIn_5$. The solid blue symbols denote a first-order transition from the superconducting (SC) to non-magnetic (NM) normal phase; whereas, the green symbols define a line of second-order phase transitions, labeled T2, into a possible FFLO phase. The solid red symbols are results of neutron diffraction experiments that signify the observation of magnetic order which exists only in the shaded area of the T2 phase. The structure of the magnetic order also is shown by red arrows.*

Besides a magnetic field, replacing larger amounts of In with either Cd or Hg induces long-ranged antiferromagnetic order, determined by neutron diffraction and NMR, that coexists with superconductivity [5]. By

several techniques, we found that Cd and Hg substitutions have nearly identical effects, and because Cd and Hg have qualitatively different atomic size but the same electronic charge, this implies an electronic origin for the response to these substitutions. Detailed NMR experiments on Cd-substituted samples showed that magnetism nucleates initially around the substituted atoms and then spreads to microscopically coexist with superconductivity throughout the sample [6]. Results of neutron diffraction [7] on a sample with Cd-induced coexisting magnetic and superconducting order are summarized in Figure 2 where we see magnetic scattering intensity growing below the magnetic transition at 3 K, but the growth is arrested abruptly with the onset of superconductivity at 1.2 K. Like neutron measurements in pure CeCoIn5 at high fields, these experiments show that there is a direct coupling between magnetic and superconducting electrons, a far stronger statement about their relationship than previously possible. This conclusion also was supported by point contact spectroscopy studies that revealed the development of a change in electronic response at the magnetic transition and that superconductivity emerged from this new electronic state [8].

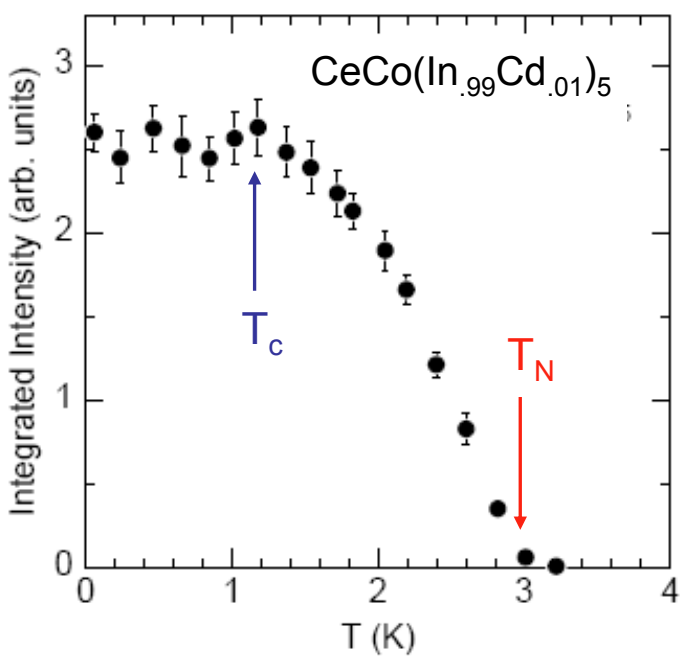


*igure 2. Magnetic scattering intensity as a function of temperature for $CeCoIn_5$ in which 1% of the In atoms have been replaced by Cd. As expected, magnetic intensity grows in below the onset of antiferromagnetic order at TN, but at lower temperature, this growth is arrested abruptly with the onset of bulk unconventional superconductivity at Tc. These results indicate a direct coupling between magnetic and superconducting electrons.*

$CeRhIn_5$ offered an example where we could study coexisting magnetic order and superconductivity in the absence of an applied field or chemical substitution. In this case, the 'clean' variable pressure allowed access to the coexistence. In a very productive collaboration, we used specific heat measurements under pressure to establish that pressure-induced superconductivity in $CeRhIn_5$ is unconventional when it coexists with antiferromagnetic order and that the unconventional nature does not change when magnetism is suppressed at higher pressures. Indeed, this higher-pressure limit of CeRhIn5 appears very analogous to pure $CeCoIn_5$ at atmospheric pressure in which there is no long-range magnetic order in zero field. These experiments on $CeRhIn_5$ were essential in establishing the generality of conclusions deduced from $CeCoIn_5$.

Of the $CeMIn_5$ materials, $CeIrIn_5$ has been the most difficult to understand. In contrast to $CeCoIn_5$ and $CeRhIn_5$ under pressure, the superconducting transition temperature of $CeIrIn_5$ is much lower, but there had been no obvious reason why this should be. From very careful study of the response of $CeIrIn_5$ to magnetic field, we discovered a new electronic state that develops on the same temperature scale as superconductivity in the related family members. [9] This new state has magnetic character that is revealed explicitly in our neutron scattering experiments on samples with small amounts of Hg. Interestingly, the Hg-induced magnetic order is slightly different from that found in $CeRhIn_5$ or in substituted $CeCoIn_5$ materials, and further, the new electronic state in pure CeIrIn5 appears analogous to the so-called pseudogap state in the copper-oxide superconductors. Our experiments strongly suggest that the new electronic state in $CeIrIn_5$ competes for electrons that eventually become superconducting at lower temperatures, a conclusion that remains very controversial in the copper oxides.

All of these studies consistently find that magnetic and superconducting electrons are intimately coupled and that the 4f electron of Ce is critical to both magnetism and superconductivity. Because superconductivity develops among itinerant electrons and the 4f electron has strongly localized character, we were faced with the question of how this can happen. Several experiments, but especially photoemission spectroscopy that directly probes the electronic structure, shed light on this question. These measurements found that the 4f electron is localized close to the ionic core for a broad temperature range below room temperature, but at temperatures below about 20 K, the 4f electron begins to take on itinerant character due to its interaction with itinerant s, p, and d electrons [10]. Alternatively stated, a strongly

interacting band of quantum mechanically entangled 4f and itinerant electrons emerges below 20 K, and it is this entangled electronic state that gives both magnetism and unconventional superconductivity or either magnetism or superconductivity depending on pressure, magnetic field and chemical substitution. (We return to this point in the discussion of theory.) Further, our high-resolution photoemission measurements that probe the momentum dependence of the strongly interacting band showed that electronic structure developed a 'kink' as the band dispersed toward the Fermi energy below which all electronic states are occupied. This is not unique to the $CeMIn_5$ materials, as we found the same 'kink' in strongly correlated but non-superconducting USb2 [11] and it also had been found earlier in the copper oxide superconductors.

In the last year of this project, groups in Asia reported superconductivity at temperatures above 50 K in two families of Fe-based magnetic materials, the first example of such high transitions in materials without Cu. Besides being the first to discover that applying pressure to one of the magnetic parent compounds $CaFe_2As_2$ induced superconductivity, we also discovered superconductivity in new Ni-based analogs $BaNi_2AS_2$, SrNi2$As_2$ and $SrNi_2P_2$ [12,13,14] of the Fe systems. Unlike the Fe-based materials, there is no evidence of magnetism in these Ni-materials and their transition temperatures are an order of magnitude lower than in the Fe-systems. These discoveries have been important because they suggest that magnetism plays a role in enhancing the transition temperature of the Fe-based systems.

Experimental discoveries have been placed in context by theory. Ginzburg-Landau models of coupled magnetic and superconducting order can account for several observations, but we have gone beyond these models to develop microscopic understanding. To understand the nature of the localized-delocalized transition for f-electrons and the interplay with the magnetic properties, we derived for the first time a low-energy effective Anderson model that is valid right at the transition between the two different regimes (C. D. Batista, unpublished). An important precondition for the validity of this derivation is that the f-d hybridization must cancel at the Fermi level. This effective model has two important characteristics that lead to a rather surprising conclusion: the localized-delocalized f-electron transition becomes a selective Mott transition when the hybridization cancels at the Fermi level. One of the consequences of our conclusion is that the localized-delocalized f transition does not coincide with the suppression of the magnetic ordering that is present in the localized regime. In other words, there is a region of coexistence of magnetic ordering and f-electron delocalization. This conclusion has been important to understand how the f-electrons simultaneously provide magnetic ordering and superconductivity.

We also constructed a model that incorporates local spin correlations in a magnetically disordered system with strong electronic correlations and have shown that this model leads to novel inhomogeneous states that are characterized by non-harmonic charge modulation and spatially dependent interactions among correlated electrons. The existence of these 'Kondo stripes' opens the possibility of coexisting superconductivity or magnetism. [15] In parallel and complementing this work, we used a low-dimensional limit of the infinitely strongly interacting variant of the Anderson model to prove that such a model contains an unconventional mechanism for superconductivity when the localized electrons have a long enough antiferromagnetic correlation length. The superconducting pairing in this case is due to a confining interaction between topological defects (solitons) attached to each carrier. We showed that a robust pairing mechanism emerges under these condition and leads to dominant superconducting fluctuations. Further, we showed that the mechanism survives in dimensions higher than one [16].

In the context of our work on Fe- and Ni-based superconductors, we determined the criteria for thermodynamic stability of 'odd-frequency' superconductivity wherein superconducting electrons form a state without a gap in the electronic excitation spectrum. [17] This work demonstrated the fundamental possibility of odd-frequency superconductivity, a subject of long-standing controversy, and significantly that this exotic type of superconductivity accounted in a consistent way for photoemission and NMR observations on the Fe-based superconductors.

## Impact on National Missions

The discovery nearly 20 years ago of high temperature superconductivity in complex copper oxide materials held great promise for revolutionizing electrical power transmission and storage technologies, but this promise has not been realized, in part because of the absence of understanding how strongly interacting electrons produce unconventional superconductivity. Using 4f-electron materials as prototypes of the physics, we have uncovered game-changing insights into this problem and have laid a solid foundation for a microscopic theory of unconventional superconductivity. Our accomplishments represent significant advances toward meeting the Grand Challenge posed by the Department of Energy and the

Laboratory to understand how remarkable properties of matter emerge from complex correlations of atomic and electronic constituents.

## References


1. Young, B. L., R. R. Urbano, N. J. Curro, J. D. Thompson, J. L. Sarrao, A. B. Voronstov, and M. Graf. Microscopic evidence for field-induced magnetism in CeCoIn5. 2007. *Physical Review Letters.* **98**: 036402.

2. Kenzelmann, M., T. Strassle, C. Niedermayer, M. Sigrist, B. Padmanabhan, M. Zolliker, A. D. Bianchi, R. Movshovich, E. D. Bauer, J. L. Sarrao, and J. D. Thompson. Coupled superconducting and magnetic order in CeCoIn5. 2008. *Science.* **321**: 1652.

3. Tokiwa, Y., R. Movshovich, F. Ronning, E. D. Bauer, P. Papin, J. F. Rauscher, S. M. Kauzlarich, and Z. Fisk. Anistropic effect of Cd and Hg doping on the Pauli limmited superconductor CeCoIn5. 2008. *Physical Review Letters.* **101**: 037001.

4. Bianchi, A. D., M. Kenzelmann, L. DeBeer-Schmitt, J. S. White, E. M. Forgan, J. Mesot, M. Zolliker, J. Kohlbrecher, R. Movshovich, E. D. Bauer, J. L. Sarrao, Z. Fisk, C. Petrovic, and M. R. Eskildsen. Superconducting vortices in CeCoIn5: toward the Pauli limiting field. 2008. *Science.* **319**: 177.

5. Booth, C. H., E. D. Bauer, A. D. Bianchi, F. Ronning, J. D. Thompson, J. L. Sarrao, and Z. Fisk. Local structure and site occupancy of Cd and Hg in CeTIn5 (T=Co,Rh, Ir). 2009. *Physical Review B.* **79**: 144519.

6. Urbano, R. R., B. L. Young, N. J. Curro, J. D. Thompson, L. Pham, and Z. Fisk. Antiferromagnetism and superconductivity in a hole doped Kondo lattice. 2007. *Physical Review Letters.* **99**: 146402.

7. Nicklas, M., O. Stockert, T. Park, K. Habichy, L. D. Pham, J. D. Thompson, Z. Fisk, and F. Steglich. Magnetic structure of Cd-doped CeCoIn5. 2007. *Physical Review B.* **76**: 052401.

8. Park, W. K., J. L. Sarrao, J. D. Thompson, and L. H. Greene. Andreev reflection in heavy-fermion superconductors and order parameter symmetry in CeCoIn5. 2008. *Physical Review Letters.* **100**: 177001.

9. Nair, S., S. Wirth, M. Nicklas, J. L. Sarrao, J. D. Thompson, Z. Fisk, and F. Steglich. A precursor state to unconventional superconductivity in CeIrIn5. 2008. *Physical Review Letters.* **100**: 137003.

10. Koitzch, A., I. Opahle, S. Elgazzar, S. V. Borisenko, J. Geck, V. B. Zabolotonyy, D. Inosov, H. Shiozawa, M. Richter, M. Knupfer, J. Fink, E. D. Bauer, J. L. Sarrao, and R. Follath. Electronic structure of CeCoIn5 from angle-resolved photoemission spectroscopy. 2009. *Physical Review B.* **79**: 075104.

11. Durakiewicz, T., P. S. Riseborough, C. G. Olson, J. J. Joyce, E. D. Bauer, J. L. Sarrao, S. Elgazzar, P. M. Oppeneer, D. P. Moore, M. T. Butterfield, and K. S. Graham. Observation of a kink in the dispersion of f-electrons. 2008. *Europhysics Letters.* **84**: 37003.

12. Ronning, F., N. Kurita, E. D. Bauer, B. L. Scott, T. Park, T. Klimczuk, R. Movshovich, and J. D. Thompson. First order transition and superconductivity in BaNi2As2 single crystals. 2008. *Journal of Physics: Condensed Matter .* **20**: 342203.

13. Bauer, E. D., F. Ronning, B. L. Scott, and J. D. Thompson. Superconductivity in SrNi2As2 single crystals. 2008. *Physical Review B.* **78**: 172504.

14. Ronning, F., E. D. Bauer, T. Park, S. H. Baek, H. Sakai, and J. D. Thompson. Superconductivity and the effects of pressure and structure in single-crystalline SrNi2P2. 2009. *Physical Review B.* **79**: 134507.

15. Zhu, J. X., I. Martin, and A. R. Bishop. Kondo stripes in an Anderson-Heisenberg model of heavy fermion systems. 2008. *Physical Review Letters.* **100**: 236403.

16. Al-Hassanieh, K. A., C. D. Batista, P. Sengupta, and A. E. Feiguin. Topological confinement and superconductivity. 2009. *Physical Review B.* **80**: 115116.

17. Solenov, D., I. Martin, and D. Mozyrsky. Thermodynamic stability of odd-frequency superconducting state. 2009. *Physical Review B.* **79**: 132502.


## Publications

Local structure and site occupancy of Cd and Hg in CeTIn5 (T=Co,Rh, Ir). 2009. *Physical Review B.* **79**: 144519.

Al-Hassanieh, K. A., C. D. Batista, P. Sengupta, and A. E. Feiguin. Topological confinement and superconductivity. 2009. *Physical Review B.* **80**: 115116.

Baek, S. H., N. J. Curro, T. Klimzcuk, E. D. Bauer, F. Ronning, and J. D. Thompson. First First order magnetic transition in single crystal BaFe2As2 detected by 75As NMR . 2009. *Physical Review B.* **79**: 052504.

Baek, S. H., T. Klimczuk, F. Ronning, E. D. Bauer, N. J. Curro,

and J. D. Thompson. Microscopic 75As NMR study of the effect of impurities on the first0order spin-density wave transition in BaFe2As2. 2008. *Physical Review B.* **78**: 212509.

Bao, W., Y. C. Gasparovic, J. W. Lynn, F. Ronning, E. D. Bauer, and J. D. Thompson. Commensurate magnetic structure of CeRh4.85Hg0.15. 2009. *Physical Review B.* **79**: 024519.

Bao, W., Y. Chen, K. Yamada, A. Savic, P. Russo, J. E. Lorenzo, and J. H. Chung. Fincher-Burke spin excitations and omega/T scaling in insualting La.195Sr.05CuO4. 2007. *Physical Review B (Rapid Commun.).* **76**: 247203.

Bauer, E. D., F. Ronning, B. L. Scott, and J. D. Thompson. Superconductivity in SrNi2As2 single crystals. 2008. *Physical Review B.* **78**: 172504.

Bauer, E. D., F. Ronning, S. Marquilon, L. D. Pham, J. D. Thompson, and Z. Fisk. Occurrence of magnetism in CeMIn5-xHgx (M=Rh, Ir). 2008. *Physica B.* **403**: 1135.

Bianchi, A. D., M. Kenzelmann, L. DeBeer-Schmitt, J. S. White, E. M. Forgan, J. Mesot, M. Zolliker, J. Kohlbrecher, R. Movshovich, E. D. Bauer, J. L. Sarrao, Z. Fisk, C. Petrovic, and M. R. Eskildsen. Superconducting vortices in CeCoIn5: toward the Pauli limiting field. 2008. *Science.* **319**: 177.

Booth, C. H., E. D. Bauer, A. D. Bianchi, F. Ronning, J. D. Thompson, J. L. Sarrao, and Z. Fisk. Local structure and site occupancy of Cd and Hg in CeTIn5 (T=Co,Rh, Ir). 2009. *Physical Review B.* **79**: 144519.

Bulaevskii, L. N., and E. M. Chudnovsky. Electromagnetic radiation from vortex flow in type-II superconductors. 2006. *Physical Review Letters.* **97**: 197002.

Donath, J. G., F. Steglich, E. D. Bauer, F. Ronning, J. L. Sarrao, and P. Geggenwart. Influence of lattice anisotropy and disorder on quantum critical behavior. To appear in *European Physics Letters.*

Durakiewicz, T., P. S. Riseborough, C. G. Olson, J. J. Joyce, E. D. Bauer, J. L. Sarrao, S. Elgazzar, P. M. Oppeneer, D. P. Moore, M. T. Butterfield, and K. S. Graham. Observation of a kink in the dispersion of f-electrons. 2008. *Europhysics Letters.* **84**: 37003.

Hruvska, M., and L. N. Bulaevskii. Effects of magnetic excitations on the I-V characteristics of magnetic superconductors. 2006. *Comptes Rendus Physique.* **7**: 42.

Kaneshita, E., I. Martin, and A. R. Bishop. Commensurate-incommensurate transition and coolective modes in the stripe phase of cuprates near 1/8 hole-doping. 2007. *Physical Review B.* **76**: 054507.

Kenzelmann, M., T. Strassle, C. Niedermayer, M. Sigrist, B. Padmanabhan, M. Zolliker, A. D. Bianchi, R. Movshovich, E. D. Bauer, J. L. Sarrao, and J. D. Thompson. Coupled superconducting and magnetic order in CeCoIn5. 2008. *Science.* **321**: 1652.

Koitzch, A., I. Opahle, S. Elgazzar, S. V. Borisenko, J. Geck, V. B. Zabolotonyy, D. Inosov, H. Shiozawa, M. Richter, M. Knupfer, J. Fink, E. D. Bauer, J. L. Sarrao, and R. Follath. Electronic structure of CeCoIn5 from angle-resolved photoemission spectroscopy. 2009. *Physical Review B.* **79**: 075104.

Koitzch, A., S. V. Borisenko, J. Geck, V. B. Zabolotonyy, H. Shinozawa, M. Knupfer, J. Fink, B. Buchner, E. D. Bauer, J. L. Sarrao, and R. Follath. Hybridization effects in CeCoIn5 observed by angle-resolved photoemission. 2008. *Physical Review B.* **77**: 155128.

MendoncaFierreira, L., T. Park, V. A. Sidorov, M. Nicklas, E. M. Bittar, R. Lora-Serrano, E. N. Hering, S. M. Ramos, M. B. Fontes, E. Baggio-Saitovich, H. O. Lee, J. L. Sarrao, J. D. Thompson, and P. G. Pagliuso. Tuning the pressure-induced superconducting phase in doped CeRhIn5. 2008. *Physical Review Letters.* **101**: 0175005.

Movshovich, R., Y. Tokiwa, F. Ronning, A. Bianchi, C. Capan, B. L. Young, R. R. Urbano, N. J. Curro, T. Park, J. D. Thompson, E. D. Bauer, and J. L. Sarrao. Interplay of Magnetism and Superconductivity in CeCoIn5. 2009. In *Electron transport in nanosystems, NATO science for peace and security series B: physics and biophysics.* , p. 127. Netherlands: Springer.

Movshovich, R., Y. Tokiwa, N. Kurita, F. Ronning, E. D. Bauer, A. Bianchi, P. Papin, and Z. Fisk. Possible Fulde-Ferrell-Larkin-Ovchinnikov inhomogeneous superconducting sate in CeCoIn5. 2009. *Journal of Superconductivity and Novel Magnetism.* **22**: 291.

Nair, S., M. Nicklas, F. Steglich, J. L. Sarrao, J. D. Thompson, A. J. Schofield, and S. Wirth. precursor state to superconductivity in CeIrIn5: unusual scaling of magnetotransport. 2009. *Physical Review B.* **79**: 094501.

Nair, S., S. Wirth, M. Nicklas, J. L. Sarrao, J. D. Thompson, Z. Fisk, and F. Steglich. A precursor state to unconventional superconductivity in CeIrIn5. 2008. *Physical Review Letters.* **100**: 137003.

Nicklas, M., C. F. Miclea, J. L. Sarrao, J. D. Thompson, G. Sparn, and F. Steglich. Antiferromagnetic fluctuations and the Fulde-Ferrell-Larkin-Ovchinnikov state in CeCoIn5. 2007. *Journal of the Physical Society of Japan.* **76**: 128.

Nicklas, M., C. F. Miclea, J. L. Sarrao, J. D. Thompson, G. Sparn, and F. Steglich. Influence of antiferromagnetic fluctuations on the Fulde-Ferrell-Larkin-Ovchiinikov state in CeCoIn5. 2007. *Journal of Low Temperature Physics.* **146**: 669.

Nicklas, M., O. Stockert, T. Park, K. Habichy, L. D. Pham, J. D. Thompson, Z. Fisk, and F. Steglich. Magnetic structure of Cd-doped CeCoIn5. 2007. *Physical Review B.* **76**: 052401.

Park, T., E. D. Bauer, and J. D. Thompson. Probing the nodal gap in the pressure-induced heavy-fermion superconductor CeRhIn5. 2008. *Physical Review Letters.* **101**: 177002.

Park, T., J. L. Sarrao, and J. D. Thompson. New quantum state in the heavy fermion superconductor CeRhIn5. 2007. *Physica C.* **460-462**: 137.

Park, T., J. L. Sarrao, and J. D. Thompson. Upper critical field (Hc2) scaling near a quantum critical point in the heavy fermion compound CeRhIn5. 2007. *Journal of Magnetism and Magnetic Materials.* **310**: 712.

Park, T., M. J. Graf, L. Bulaevskii, J. L. Sarrao, and J. D. Thompson. Electronic duality instrongly correlated matter. 2008. *Proceedings of the National Academy of Science.* **105**: 6825.

Park, T., V. A. Sidorov, F. Ronning, J. X. Zhu, Y. Tokiwa, H. O. Lee, E. D. Bauer, R. Movshovich, J. L. Sarrao, and J. D. Thompson. Isotropic quantum scattering and unconventional superconductivity. 2008. *Nature.* **456**: 366.

Park, W. K., J. L. Sarrao, J. D. Thompson, and L. H. Greene. Andreev reflection in heavy-fermion superconductors and order parameter symmetry in CeCoIn5. 2008. *Physical Review Letters.* **100**: 177001.

Ronning, F., E. D. Bauer, T. Park, S. H. Baek, H. Sakai, and J. D. Thompson. Superconductivity and the effects of pressure and structure in single-crystalline SrNi2P2. 2009. *Physical Review B.* **79**: 134507.

Ronning, F., N. Kurita, E. D. Bauer, B. L. Scott, T. Park, T. Klimczuk, R. Movshovich, and J. D. Thompson. First order transition and superconductivity in BaNi2As2 single crystals. 2008. *Journal of Physics: Condensed Matter .* **20**: 342203.

Ronning, F., T. Klimczuk, E. D. Bauer, H. Volz, and J. D. Thompson. Synthesis and properties of CaFe2As2 single crystals. 2008. *Journal of Physics: Condensed Matter.* **20**: 322201.

Rusz, J., P. M. Oppeneer, N. J. Curro, R. R. Urbano, B. L. Young, S. Lebegue, P. G. Pagliuso, L. D. Pham, E. D. Bauer, J. L. Sarrao, and Z. Fisk. Probing the electronic structure of pure and doped CeMIn5 (M=Co,Rh,Ir) crystals with nuclear quadrupolar resonance. 2008. *Physical Review B.* **77**: 245124.

Solenov, D., I. Martin, and D. Mozyrsky. Thermodynamic stability of odd-frequency superconducting state. 2009. *Physical Review B.* **79**: 132502.

Spehling, J., R. H. Heffner, J. E. Sonier, N. Curro, B. Hitti, G. Morris, E. D. Bauer, F. J. Litterst, and H. H. Klaus. Field-induced magnetism in the vortex state of the heavy-fermion superconductor CeCoIn5. *Physical Review Letters.*

Tokiwa, Y., F. Ronning, J. D. Thompson, R. Movshovich, L. D. Pham, and Z. Fisk. Effect of Cd doping on superconductivity in CeCoIn5. 2008. *Physica B.* **403**: 879.

Tokiwa, Y., R. Movshovich, F. Ronning, E. D. Bauer, P. Papin, J. F. Rauscher, S. M. Kauzlarich, and Z. Fisk. Anistropic effect of Cd and Hg doping on the Pauli limmited superconductor CeCoIn5. 2008. *Physical Review Letters.* **101**: 037001.

Urbano, R. R., B. L. Young, N. J. Curro, J. D. Thompson, L. D. Pham, and Z. Fisk. Coexistence of antiferromagnetism and superconductivity in a hole doped Kondo lattice. 2008. *Physica B.* **403**: 1056.

Urbano, R. R., B. L. Young, N. J. Curro, J. D. Thompson, L. Pham, and Z. Fisk. Antiferromagnetism and superconductivity in a hole doped Kondo lattice. 2007. *Physical Review Letters.* **99**: 146402.

Voronstov, A. B., I. Vekhter, and M. J. Graf. Pauli-limited upper critical field in dirty d-wave superconductors. 2008. *Physical Review B-Rapid Communications.* **78**: 180505.

Vorontsov, Anton B., and Matthias J. Graf. Fermi-liquid effects in the Fulde-Ferrell-Larkin-Ovchinnikov state of two-dimensional d-wave superconductors. 2006. *Phys. Rev. B .* **74**: 172504.

Yang, X., P. S. Riseborough, T. Durakiewicz, C. G. Olson, J. J. Joyce, E. D. Bauer, J. L. Sarrao, D. P. Moore, K. S. Graham, S. Elgazzar, P. M. Oppener, E. Guziewicz, and M. T. Butterfield. Unusual quasiparticle renormalizations from angle resolved photoemissin on USb2. 2009. *Philosophical Magazine.* **89**: 1893.

Young, B. L., R. R. Urbano, N. J. Curro, J. D. Thompson, J. L. Sarrao, A. B. Voronstov, and M. Graf. Microscopic evidence for field-induced magnetism in CeCoIn5. 2007. *Physical Review Letters.* **98**: 036402.

Zhu, J. X., I. Martin, and A. R. Bishop. Kondo stripes in an Anderson-Heisenberg model of heavy fermion systems. 2008. *Physical Review Letters.* **100**: 236403.

# Physics of Helium Retention in Palladium/Tritum Systems

*Douglas J. Safarik*
20070074DR

## Abstract

The objective of this LDRD-DR project was to develop an atomic-level understanding of "aging" of palladium (Pd) tritide. "Aging" refers to the decreased capacity of the Pd host to store the radioactive gas tritium (T), and to retain helium-3 ($^3$He) generated by radioactive decay of the tritium, with time. We had proposed to study the aging phenomenon using a *"science-based"* approach, integrating experimental measurements, theory, and computer modeling. Unfortunately, we were unable to complete all facets of the proposed research. The main reason was that we could not obtain tritium gas, which was essential for our research. Indeed, for 30 of the 36 months of this project, the Laboratory's WETF tritium facility was out of commission for renovations, safety assessments, changes in operational procedures, etc., etc. We named this "the WETF debacle", and we comment on it later in this report. In addition to the WETF debacle, we lost several critical personnel during the project, including two Laboratory Fellows who retired as part of the Laboratory's voluntary separation plan in January 2008. In response to these unforeseen changes, we redefined the scope of the project. Specifically, we limited its scope to understanding the interaction of Pd with the two other (non-radioactive) isotopes hydrogen, protium and deuterium. We made several important advancements during this project, among them a clearer picture of how dislocations affect H-absorption/desorption hysteresis, a new understanding of the phase diagram of Pd-hydride (and metal-hydrides in general), an atomistic computer model that accurately predicts the Pd-H phase diagram, and an understanding of hydrogen motion and short-range ordering in Pd-H. We also constructed three experimental apparatuses, two of which are specifically designed for use with radioactive tritium gas. This research has already generated 5 published (or in-press) papers, with 4 more manuscripts submitted and another 4 manuscripts planned.

## Background and Research Objectives

Tritium (T), and its non-radioactive isotopes hydrogen (H) and deuterium (D), is easily absorbed into Pd metal, where it occupies interstitial sites of the type (½, 0, 0). Inside the Pd-tritide, $^3$He atoms are continuously born by the radioactive decay of tritium (half-life of 12.3 years). It is usually assumed that newly born $^3$He atoms reside in the same (½, 0, 0)-type lattice position occupied by the parent tritium atom, although this has never been verified by experiment. Initially, each $^3$He atom is isolated from its neighbors. However, as more $^3$He is generated, the $^3$He atoms coalesce into dimers, trimers, and higher-order aggregates. The physics of this coalescence process is not understood. When a $^3$He aggregate reaches a critical size, it transforms into a bubble, where the $^3$He atoms are no longer in registry with the Pd lattice. Over time, more $^3$He is incorporated into a bubble, causing it to grow in size via the emission of dislocation loops. Eventually, all of the $^3$He contained in the bubbles is released, presumably by fracture in the Pd-tritide host. This completes the aging process.

There are two main differences between the research approach taken in this project and that taken in previous efforts to understand aging in Pd-tritide: (1) We employed a science-based approach, integrating experiment, theory, and computer-modeling, to gain *atomic-level* insight. In contrast, previous efforts focused only on modeling, or only on experiment, and failed to generate an atomistic picture. (2) We focused on the *early* stages of aging, when the $^3$He atoms are initially formed and first agglomerate. In contrast, previous studies focused on the bubble characteristics (such as morphology and internal $^3$He pressure) and their growth mechanism [1-5].

In this project, we accomplished all objectives that were associated with the non-radioactive isotopes, H and D. However, we accomplished none of the objectives requiring the use of radioactive tritium gas. *The*

*main reason is that the WETF tritium facility was out of commission, and unable to deliver tritium gas, for 30 of the 36-month length of the project*. In addition to this "WETF debacle", we also lost several key personnel, including the original PI and co-PI of the project. Despite these difficult circumstances, we made several new discoveries that contribute to our understanding of the thermodynamic and elastic properties of Pd-H and Pd-D, and of metal-hydrides in general. The same fundamental physics that we discovered for Pd-H(D) should apply to Pd-T as well.

## Scientific Approach and Accomplishments

**Thermodynamics of the Pd-H(D, T) System**

Although the Pd-H system has been extensively studied, many of its thermodynamic properties (e.g., the phase diagram) are only partially known, or are poorly understood. Furthermore, the literature contains scarcely little thermodynamic data for the Pd-T system. To understand the aging process, we must first characterize and understand the phase diagram of Pd-H isotope systems. We therefore built two Sieverts' machines for measuring the equilibrium phase diagram of Pd-H isotope systems. One machine, located at MST-8, was used to characterize Pd-H and Pd-D systems. The other machine, located at the WETF tritium facility, was supposed to be used to study Pd-T and Pd-T-$^3$He systems.

In the literature, the equilibrium Pd-H phase diagram, plotted on a pressure-composition diagram, shows a single miscibility region where the alpha and beta phases coexist. On studying the properties of coexisting alpha and beta phases, one finds that properties such as resistance, lattice parameter, and in particular, equilibrium hydrogen chemical potential, have different values depending on whether the measurements are done during absorption or desorption of hydrogen. Several theories have been developed to explain the hysteresis. Because the presence of hysteresis in reversible transformations cannot be explained by conventional thermodynamics, it has been attributed to dissipative phenomena such as the generation and annihilation of dislocations. However, a dislocation-based explanation is contrary to what one infers from TEM observations [6] and from theories for work hardening. Schwarz and Khachaturyan (SK) proposed [7] that the hysteresis is due to elastic strains that exist between the alpha and beta phases when these phases are coherent. The coherency strain generates a macroscopic elastic energy barrier that must be overcome both during the forward alpha to_beta transformation (monotonic increase in H content) and the reverse beta to alpha transformation (monotonic decrease in H content).

An important prediction of the SK model is that the palladium-hydrogen phase diagram has *two*-miscibility curves (rather than one, as appears in the literature): one for the *coherent* decomposition, and another for the *incoherent* decomposition, as illustrated in Figure 1. During H loading, the Pd-H system follows curve A-H-B-E-F-D, whereas during the removal of hydrogen, the system follows curve D-F-C-G-H-A.

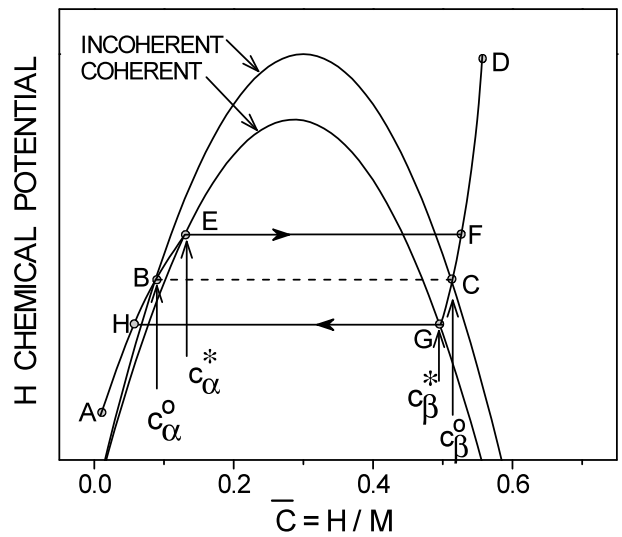


*Figure 1. Coherent and Incoherent phase diagram for the palladium-hydrogen system according to the work of Schwarz and Khachaturyan [7].*

Figure 2 shows, as an example, our data for Pd-deuterium at 140.1 C. In this plot, the ordinate is the molecular deuterium gas pressure that is in thermodynamic equilibrium with the Pd sample. The logarithm of this pressure is proportional to the chemical potential in Figure 1. Curves similar to those in Figure 2 were measured at various temperatures and the data was used to delineate the correct phase diagram for the Pd-deuterium system, which is shown in Figure 3. This diagram represents a great improvement over the earlier published diagrams for the Pd-hydrogen system and demonstrates the importance that the coherency strains have on the transformation.

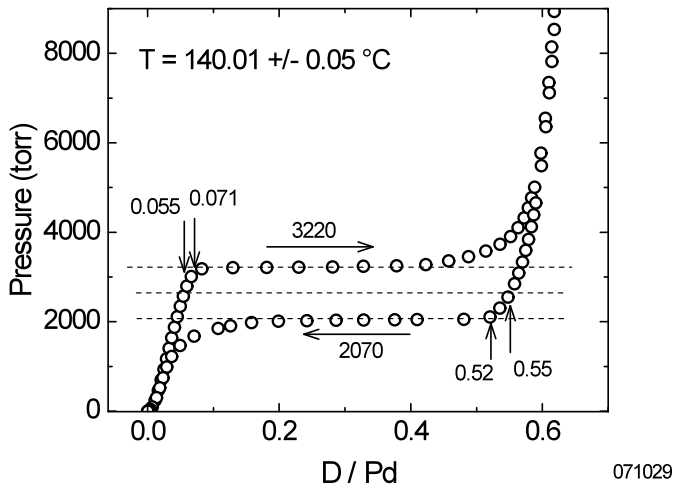


*Figure 2. Our measurement of the pressure-composition equilibrium curves for the palladium-deuterium system at 140.1 C.*

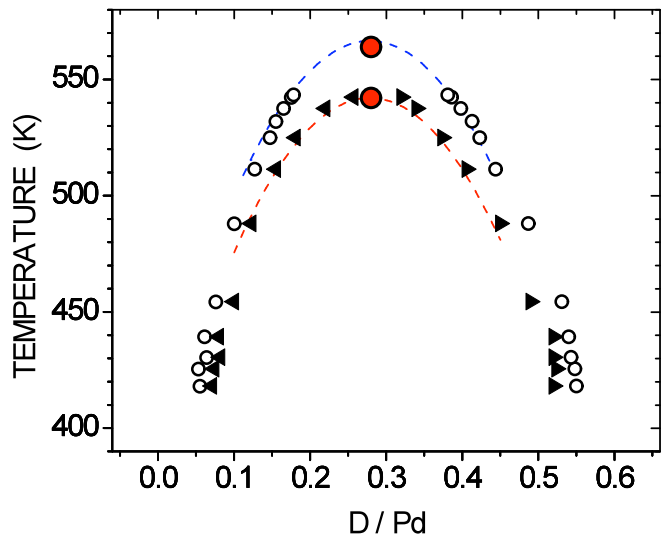


*Figure 3. Our experimentally determined coherent (solid symbols) and incoherent (open symbols) phase diagram for the Pd-deuterium system. The large red circles on top of the dashed curves are the critical points for the coherent and incoherent phase diagrams. These points were independently determined from an analysis of the data in terms of the Landau-type model we developed to explain the decomposition.*

As seen in Figure 2, the coherent and incoherent phase diagrams terminate at tri-critical points located at the top of the parabolic-shape curves. The SK model predicts that hysteresis vanishes at the critical point of the *coherent* phase diagram. To analyze the behavior of the Pd-deuterium system near the critical points we developed a model based on Landau's theory for second-order phase transitions. The critical points deduced from this analysis are shown as solid circles in Figure 3.

**Atomistic simulations of the Pd-H system**

One goal of this project was to provide an atom-level description for the behavior of $^3$He atoms in a beta-phase Pd-tritide host. To achieve this goal, we started by developing an atomistic model for the Pd-H system. All previous efforts to model this system had failed to reproduce its equilibrium phase diagram mainly because they relied on too-simple interatomic potentials. Because Pd is a transition metal that has a partially filled d-band, its atomistic interactions must be treated by a model such as the Modified Embedded Atom Method (MEAM) that explicitly accounts for the directionality of the bonding. We developed MEAM potentials that represent, in a more realistic manner, the Pd-Pd, Pd-H, and H-H interactions present in a Pd-hydrogen alloy.

We calculated the phase diagram of Pd-H using our MEAM interatomic potentials described above and chemical potentials obtained through the Grand Canonical Monte Carlo method. Figure 4 compares our calculated equilibrium phase diagram for the Pd-H system with that measured by various authors, and evaluated by Manchester [8]. The symbols are literature data and the solid curves are the results of our GCMC calculations. The heavy horizontal lines give the chemical potential within the coexistence two-phase region.

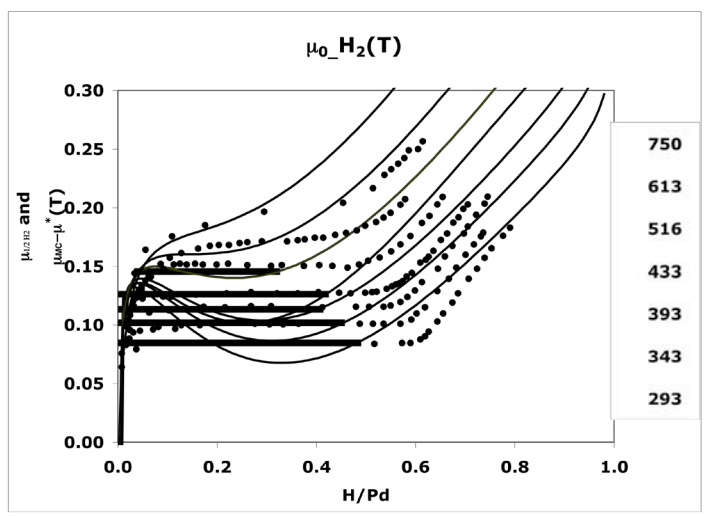


*Figure 4. Comparison of our calculated phase diagram for the Pd-H system (solid curves) and the data compiled in the review of Manchester et al. The abscissa gives the chemical potential for a H atom in the Pd-H alloy.*

As shown in Figure 4, the agreement between our Monte Carlo simulations and the measured phase diagram for the Pd-H system is quite good. The plateau chemical potentials denoting the co-existence of the dilute alpha-phase Pd(H) solid solution, as well as the concentrated beta-phase Pd-hydride, are well-reproduced at all temperatures.

**Elastic properties of $PdH_x$**

In beta-phase Pd-H(D,T), the hydrogen atoms are not randomly distributed on the octahedral interstitial sites of the Pd host. Indeed, ultrasonic [9] and neutron diffraction [10] measurements suggest the presence of short-range ordering (SRO) of the hydrogen atoms. This implies that there are regions within the Pd-tritide lattice that are devoid of tritium atoms, and hence $^3$He atoms cannot be born.

We studied the H-atom SRO in single-phase beta-$PdH_x$ single crystals ($0.62 < x < 0.71$) by measuring the shear moduli $C_{prime} = (C_{11}-C_{12})/2$ and $C_{44}$ between 1.4 and 296 K. For $C_{prime}$, we observe an anomaly at ≈50 K during warming, and a hysteresis between cooling and warming, whereas for $C_{44}$ we observe no anomaly or hysteresis. Based on these data, we proposed that the H-atom SRO becomes *kinetically* "frozen" as the Pd-H alloy is cooled to low temperatures, and then "thaws" as it is warmed. Furthermore, the presence of the hysteresis in $C_{prime}$ but its absence in $C_{44}$ strongly suggests preferential crystallographic orientation of the SRO. Our data are inconsistent with a low-temperature thermodynamic phase transition, as is claimed in the literature.

For two-phase (alpha+beta)-$PdH_x$ ($0.01<x<0.62$), the alpha and beta phases are coherent. Here, we find that the composition dependence of both $C_{44}$ and $C_{prime}$ deviate negatively from a Vegard-type volume average for all temperatures in the range $1.4<T<296$ K. Data for the composition dependence of $C_{prime}$ is shown in Figure 5. We attribute the deviation from Vegards law to two effects: (1) the partly in-series arrangement of the precipitate and matrix phases, relative to the externally applied stress, and (2) thermally activated anelastic relaxations involving the rapid motion of H interstitial atoms, leading to slight changes in the shape of *coherent* precipitates. The first effect is present for both $C_{prime}$ and $C_{44}$ and is temperature independent, whereas the second is present only for $C_{prime}$ and is strongly temperature dependent.

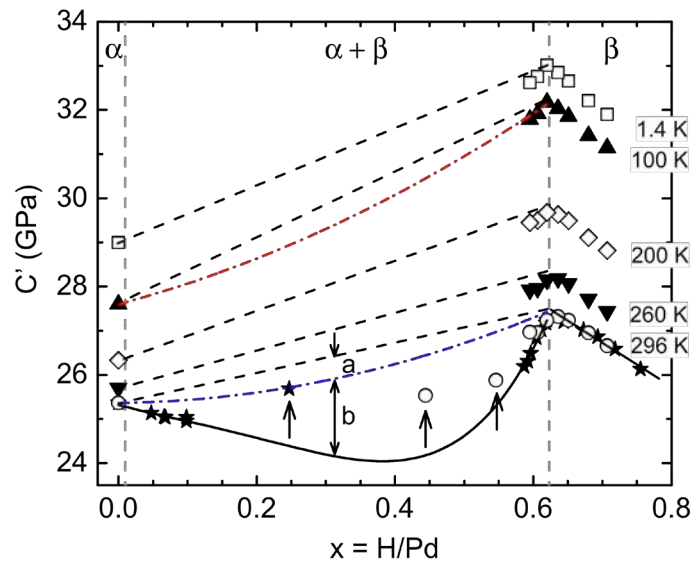


*Figure 5. Composition dependence of $C_{prime}$ = (C11-C12)/2 for beta- and (alpha+beta)-phase PdHx, in the range 1.4 < T < 296 K. The alpha-, (alpha+beta)-, and beta-PdHx phase fields are indicated in the figure, with the phase boundaries denoted by vertical dashed lines. The diagonal dashed lines show the composition dependences of Cprime in the two-phase region, assuming a Vegard-type volume average. The up-pointing arrows denote compositions where many of the precipitates were at least partially incoherent with the matrix. In the β phase region, Cprime decreases linearly with increasing x. In the (alpha+beta)-phase region, C follows a polynomial dependence on x, as demonstrated by the solid curve and the dash-dotted curves (red and blue). The distance (a) denotes the temperature-independent contribution to the deviation from Vegard's law, and (b) denotes the temperature-dependent contribution to the deviation, both for 296 K.*

**Ion channeling/nuclear reaction analysis studies of the position of $^3$He in Pd**

To understand aging, we must know where a newly born $^3$He atom resides within the Pd-tritide lattice. Because the recoil energy of the $^3$He atom is only a few electron volts, it is usually assumed that a newly born $^3$He atom resides in the same octahedral interstitial site occupied by the parent tritium atom. This assumption, however, has never been verified by experiment.

We performed ion channeling/nuclear reaction analysis experiments on single crystals of $PdD_{0.02}$, using 750 keV $^3He^+$ ions. Our measurements confirmed that deuterium atoms indeed occupy only the octahedral interstitial sites of the Pd lattice. The next step was to determine the lattice position of the $^3$He atoms formed by radioactive decay of tritium atoms in Pd-T. Although we prepared a Pd-$^3$He single crystal for these measurements, the management at TA-16 has not yet allowed us to remove the sample from the WETF tritium facility, due to the ongoing facility shutdown.

**The WETF tritium facility debacle**

Our report would be incomplete without a brief discussion of the WETF tritium facility debacle. Here we use the word "debacle" to describe the inability of WETF administration to keep the facility operational while renovations, self-assessments, and changes in operational procedures were done at the facility. Indeed, WETF was not operational, and thus unable to deliver tritium gas, from October 2006 to May 2007 (due to reconstruction of the ventilation system), from approximately November 1, 2007 to March 15 2008 (due to concerns about the facility's overpressure release systems), and from June 1, 2008 to September 30, 2009 (due to a broken compressor, to implementation of new conduct of engineering and conduct of operations guidelines, and due to pressure safety issues). Thus, WETF delivered tritium only for ~6 of the 36 months of this project, and these months were mainly at the start of the project when we were still constructing our tritium-capable Sieverts's apparatus [discussed in (1)] and our tritium-capable, liquid-helium cooled Resonant Ultrasound Spectroscopy system. Several times we investigated the possibility of performing the tritium work at another facility, such as Savannah River National Laboratory or the European Union facility at Karlsruhe, Germany. Ultimately we did not pursue this route because (1) we would have to "start over" and construct again our specially designed tritium-capable equipment, (2) it would have been an embarrassing admission of LANL's inability to perform tritium work, (3) we were repeatedly told by management that WETF would deliver tritium "soon", or by a particular date. Time and again, however, tritium gas was not delivered. Eventually it became clear to us that accomplishing the goals of this LDRD project, and of other laboratory programs, was **not** a priority to the WETF management.

## Impact on National Missions

Understanding the properties of the Pd-T-$^3$He system, and how they change with aging, are important to the national security mission of the Laboratory. Obviously, then, we were disappointed that the WETF facility could not supply the tritium necessary for the proposed research. Nonetheless, we made several important contributions to understanding the properties of metal hydrides, and these contributions are also relevant to Pd-tritide. We also constructed three new experimental apparatuses, namely a tritium-capable Sieverts' machine for measuring the equilibrium phase diagram of metal tritides, a protium- and deuterium-capable Sieverts' machine, and a tritium-capable, helium-cooled Resonant Ultrasound Spectroscopy system, for measuring the elastic properties of tritided materials. With these experimental capabilities already established, this research could resume (under the auspices of Laboratory programs) if and when the WETF facility reopens.

## References


1. Thomas, G., and J. Mintz. Journal of Nuclear Materials. 1983. . **116**: 336.
2. Wolfer, W. G.. Philosophical Magazine A. 1989. . **59**: 87.
3. Thiebaut, S.. Journal of Nuclear Materials. 2000. . **277**: 217.
4. Abell, G., and D. Cowgill. Physical Review B. 1991. . **44**: 4178.
5. Wolfer, W. G.. Philosophical Magazine A. 1988. . **58**: 285.
6. Ho, E., H. A. Goldberg, G. C. Weatherly, and F. D. Manchester. Acta Metallurgica . 1979. . **27**: 841.
7. Schwarz, R. B., and A. G. Khachaturyan. Acta Materialia. 2006. . **54**: 313.
8. Manchester, F. D.. Phase Diagrams of Binary Hydrogen Alloys. 2000. *American Society of Metals Handbook of Binary Phase Diagrams.*
9. Leisure, R. G., T. Kanashiro, P. C. Riedi, and D. K. Hsu. Physical Review B. 1983. . **27**: 4872.
10. Blaschko, O., R. Klemencic, and P. Weinzeirl. Acta Crystallographica. 1980. . **A36**: 605.


## Publications


Klimczuk, T., D. J. Safarik, and D. D. Byler. Physical properties of Al-rich V-Al binary compounds. *Solid State Communications.*

Safarik, D. J., R. B. Schwarz, S. N. Paglieri, R. L. Quintana, D. G. Tuggle, and D. D. Byler. Composition dependence of the elastic constants of beta-phase and (alpha + beta)-phase PdHx. To appear in *Ultrasonics.*

Safarik, D. J., T. Klimczuk, and D. D. Byler. Rattling and tunneling in the cage compound VAl10. *Physical Review B.*

Safarik, D. J., and R. B. Schwarz. The 50 K Anomaly in the Shear Modulus of β-PdH0.71. 2008. *Proceedings of TMS (The Minerals, Metals, and Materials Society) 2008 Meeting: Materials Processing and Properties.* **1**: 601.

Safarik, D. J., and R. B. Schwarz. Ultrasonic Study of Short-Range Hydrogen Ordering in Pd-Hydride. 2008. *International Journal for Materials Reserach.* **99**: 535.

Safarik, D. J., and R. B. Schwarz. Elastic Constants of Amorphous and Single Crystal Pd40Cu40P20. 2007. *Acta Materialia* . **55**: 5736.

Safarik, D. J., and R. B. Schwarz. Evidence for highly anharmonic, low frequency vibrational modes in bulk amorphous Pd40Cu40P20. 2009. *Physical Review B.* **80**: 094109.

Schwarz, R. B., A. G. Khachaturyan, and D. J. Safarik. A model for the critical point in the Pd H system. *Acta Materialia.*

Schwarz, R. B., and A. G. Khachaturyan. Coherent Decomposition in a Metal Hydrogen System: Influence of Elastic Anisotropy on the Hysteresis. *Physical Review B.*

# Quantum Control in Condensed Media for Studies of Direct Optical Initiation of Explosives

*David S. Moore*
20070077DR

## Abstract

The detonator is the weak safety link in explosive systems. Detonators can use environmentally hazardous materials (lead and mercury), or be accidentally set off by electrostatic discharge or illicit means. These drawbacks can be avoided using less sensitive materials, but with the consequent need for larger energy because explosives are very difficult to directly initiate using lasers; low-density pressings and large laser energies are required, if initiation can be achieved at all. This project developed a new laser method – coherent control using shaped laser pulses tailored specifically to each energetic material – to initiate detonation in low sensitivity energetic materials, increasing the safety of detonators. The technique uses adaptive pulse-shaping techniques to drive the desired chemical reaction. An additional layer of safety is achieved because the pulse shape is like a "key" in the detonation "lock". A model system (photochemical branching in stilbene) was used to optimize laser sources and develop and test control algorithms. Those results were extended to direct quantum-controlled initiation of explosives. Large scale modeling was performed to guide the control feedback experiments, and also to achieve inversion of the optimal control waveform into real molecular coordinate space on the potential energy surfaces, giving insight into the fundamental reaction dynamics and perhaps promoting a discovery path towards new potential (and better) detonator materials.

## Background and Research Objectives

The current generation of exploding bridge wire (EBW) detonators has the inherent potential for accidental initiation via electrostatic discharge (ESD) events, which has driven the development of direct optical initiation (DOI) schemes. Current DOI schemes are essentially an "optical" EBW. Recent advances in ultrafast laser technology were extended in this project to achieve direct quantum controlled initiation (QCI) of explosives. In QCI, a laser pulse is temporally shaped to achieve initiation, an iterative process using adaptive genetic algorithms. The use of shaped laser pulses tailored specifically to each energetic material offers a new approach for efficient initiation at much lower energies than used in DOI. At these low laser energies, only the shaped pulse can achieve initiation, leading to safer, and perhaps encryptable, systems.

More fundamentally, experimental quantum control of molecular dynamics in condensed phases is an emerging field with widespread application in controlling and understanding mechanisms of chemical and physical reactions.

The research objectives were as follows. Use adaptive pulse shaping to control both the cis/trans isomerization ratio and cyclization quantum yield in stilbene solutions and solid mixtures, using UV/visible absorption as feedback. Perform accurate dynamics simulations on stilbene's well-characterized potential energy surfaces; compare to experiment. Extend the stilbene results to explosives. Manufacture several HE (e.g., PETN, HMX, RDX, HNS) single crystals and polycrystalline thin films; measure vibrational dephasing times (when not known). Perform control algorithm feedback experiments on thin single crystal HE samples using UV/visible absorption, Raman, and infrared absorption feedback (UV/visible absorption is the easiest experimentally). Extend feedback experiments to polycrystalline samples. Compare molecular modeling to experimental results; use modeling to guide feedback experiments. Develop theory and modeling necessary to invert the optimal control algorithm onto molecular coordinates. Finally, devise methods to transfer optimal pulse shapes to photonics engineered devices.

## Scientific Approach and Accomplishments

We achieved coherent control of photoisomerization branching in our model system - stilbene. The laser source, ultrafast pulse shapers, control algorithms,

and closed-loop optimization from those studies were applied to carefully manufactured explosives samples. The feedback that indicates successful initiation was obtained using one of several spectroscopic or thermal diagnostics. Large-scale modeling was performed to guide experiments and gain insight into the fundamental reaction dynamics, with perhaps clues towards new potential detonator materials with strong quantum key safeguards.

We designed a simple scheme for efficient, global (coarse-grained) parameter space optimization for the stilbene ground and excited state potential energy surface (PES) dynamics. The scheme included the means for efficient calculation of the ground and excited state PES and the inclusion of the shaped electric field into the quantum molecular dynamics simulations. We generated a program that can simulate the numerically exact quantum wavepacket dynamics for a single degree of freedom interacting with an electric field of arbitrary form. The electric field was also added to a more approximate quantum MD code that is capable of treating the dynamics of molecules with many degrees of freedom. The latter code was tested successfully against the numerically exact code for an ultra-short electric field pulse.

To study the vibrational energy transport, which is a vital component of chemical reaction dynamics in energetic materials, we developed a first principles computational package (integrating commercially available packages, i.e. VASP and a suit of home made parallel codes and scripts) for determining the vibrational band structure and anharmonic couplings between phonon modes in polyatomic materials with periodic structure. This approach utilizes a state of the art generalized super cell method. The code was applied to model vibrational structure in PETN materials in order to calculate the density of states and phonon dispersion relations. Further application of the methodology resulted in the calculations of anharmonic model couplings and determination of the IR line shape function and vibrational energy transfer rates.

Understanding photoexcited reaction dynamics in energetic materials and further development of the strategies for their optical control requires simulations of the vibrational wavepacket dynamics in the vicinity of the level crossing and in particular near the conical intersections (unavoided level crossings). We developed a generalized time-dependent (dynamical) variational approach, which accounts for the degenerate or almost degenerate ground state structure (conical intersection). In combination with semiclassical wave packet propagation techniques (semiclassical molecular dynamics), the developed approach can be used for accurate calculations of electronic spectra in the vicinity of conical intersections.

We calculated the reaction chemistry of high explosives (HMX and TATB) at high temperature and pressure, in preparation for modeling the control of HE reaction chemistry, with classical MD using the ReaxFF reactive force field from Caltech. We made significant headway in understanding the reaction kinetics of HMX decomposition and the difference in carbon condensation for the two explosives. We developed a first principles computational package for determining the anharmonic couplings between vibrational normal modes (phonons and vibrons) in molecular crystals and in particular in energetic materials, including efficient parallel code to handle the extended super cell geometry.

Using high-level quantum chemistry methods, we studied the excited electronic states of several high explosives that are candidates for experimental quantum control studies. Our aim was to map out the potential energy surfaces for excited states that are accessible via photo-excitation with 400 nm light. We investigated the absorption spectrum in the 400 nm region, the excited state reaction pathways and the mechanisms for radiative (fluorescence or phosphorescence) and non-radiative decay of the excited molecules. Overall, we have developed a deeper understanding of the excited electronic states and their interplay in many important high explosives. This theoretical work provides useful information for ongoing experimental efforts toward spectroscopic and photochemical control of these compounds.

The results from our generalized time dependent variational approach for calculations of electronic spectra during transit near and through a conical intersection guided our experiments by indicating the optimal spectroscopic probes. We determined some of the critical initiation diameters of HE of interest using a flexible test bed for initiation spot size testing. We utilized single crystal HE samples to understand basic HE material phenomena such as defect concentration, quasistatic compression, isothermal compression, isentropic compression, and THz spectroscopy. We utilized 2D-IR spectroscopy to measure vibrational dynamics in thin PETN polycrystalline films. The 2D-IR results include the homogeneous line width, inhomogeneous line width, dephasing times (from 1.8 to 3.5 ps) and intra-vibrational mode couplings.

We developed a state of the art optimal quantum control capability including pulse shaping, measurement of fitness or result, and closed-loop computer controlled optimization of the pulse shape to maximize or minimize the fitness. We developed this capability in the visible (800 nm) as well as UV (both 400 and 266 nm - the latter a world's first). We then used this capability to demonstrate control of the photoisomerization branching ratio in

stilbene, enhancing or suppressing the cis and trans yields at will. We produced some well-controlled HE samples needed to extend this optimal quantum control capability into the realm of HE initiation control. Because the control bandwidth was deemed inadequate to achieve initiation in real HE samples, we constructed and tested pulse spectral broadening in a gas cell to allow greater control bandwidth and have achieved more than a factor of four increase. Greater bandwidth allows a larger span of molecular vibronic features in the control space. We demonstrated vibrational spectroscopic control of nitromethane in various solvents, achieving several orders of magnitude greater control than with the narrower band commercial laser system. We developed and optimized a spectrally resolved electronic transient absorption spectrometer that can measure small changes in spectra across the range 320-750 nm in a single laser shot. We used this capability to measure the transient absorption spectral characteristics of several explosives to aid determination of the optimal feedback mechanism and to benchmark the modeling efforts. All of these experimental efforts will continue using follow-on funding (from DHS, ONR, and DOE).

We formulated a nanogold / PETN detonator powder and performed DOI experiments to demonstrate plasmonic resonance enhancement. The gold nanoparticle size was chosen to maximize coupling to the 1064 nm drive laser wavelength. The DOI data indicated a level of performance equal to or better than the present vapor-plated Ti film based DOI system, and pointed the way towards another factor of two or more improvement, which will be pursued using follow-on funding.

Finally, we investigated the properties of the control pulse shape needed to achieve a quantum key. The idea of "quantum key" hinges on the assumptions that these pulse shapes are 1) relatively rare due to the complexity of the system, and 2) hard to obtain. Due to the complex nature of the chemical control landscape, we tend to think that both these assumptions are probably valid.

## Impact on National Missions

The QCI approach may provide resilience not only against accidental initiation through the use of less sensitive explosives, but also against illicit initiation through a "quantum key" concept, which benefits both nuclear weapons (NW) and threat reduction (TR) NNSA missions by improving the safety and security of the stockpile.

## Publications


Cawkwell, M. J., K. J. Ramos, T. D. Sewell, and D. E. Hooks. Homogeneous dislocation nucleation and anomalous hardening in cyclotrimethylene trinitramine (RDX). *Physical Review.*

Greenfield, M., S. D. McGrane, and D. S. Moore. Control of cis-stilbene photochemistry using shaped ultraviolet pulse. 2009. *Journal of Physical Chemistry A.* **113**: 2333.

Hooks, D. E., and K. J. Ramos. Measurement of the dynamic elastic limit in cyclotrimethylene trinitramine: Wave profiles from 1.0 GPa shocks including the effects of voids and cracks. *Propellants, Explosives, and Pyrotechnics.*

Lee, H. J., J. Workman, J. S. Wark, R. D. Averitt, A. J. Taylor, J. Roberts, Q. McCulloch, D. E. Hof, N. Hur, S. W. Cheong, and D. J. Funk. Optically induced lattice dynamics probed with ultrafast x-ray diffraction. 2008. *Physical Review B.* **77**: 132301.

McGrane, S. D., M. Greenfield, and D. S. Moore. Construction and characterization of ultraviolet acousto-optic modulator based femtosecond pulse shapers. *Review of Scientific Instruments.*

McGrane, S. D., R. J. Scharff, M. Greenfield, and D. S. Moore. Coherent control of multiple vibrational excitations for optimal detection. To appear in *New Journal of Physics.*

Moore, D. S.. Optimal coherent control of sensitivity and selectivity in spectrochemical analysis. 2009. *Analytical and Bioanalytical Chemistry.* **393**: 51.

Moore, D. S.. Unraveling shock-induced chemistry using ultrafast lasers. To appear in *Shock Compression of Condensed Matter - 2009.* (Nashville, TN, 29 June - 3 July, 2009).

Moore, D. S., A. A. Akinci, A. M. Giambra, and S. A. Clarke. Plasmonic enhancement of direct optical initiation of explosives. To appear in *Shock Compression of Condensed Matter - 2009.* (Nashville, TN, 29 June-3 July, 2009).

Piryatinski, A., S. Tretiak, and V. Chernyak. Dynamical variational approach to non-adiabatic electronic structure. 2008. *Chemical Physics.* **347**: 25.

Quenneville, J., T. C. Germann, A. P. Thompson, and E. M. Kober. Molecular dynamics studies of thermal induced chemistry in TATB. 2007. In *Shock Compression of Condensed Matter 2007.* (Kailua-Kona, 24-29 June 2007). Vol. 955, p. 451. Melville, NY: AIP.

Quenneville, J., and D. S. Moore. Theoretical studies on the reaction pathways of electronically excited DAAF. To appear in *Shock Compression of Condensed Matter - 2009.* (Nashville, TN, 29 June-July 3, 2009).

Stevens, L. L., D. E. Hooks, and D. M. Dattelbaum. Hydrostatic Compression Curve for Triamino-trinitrobenzene (TATB) Determined to 14.0 GPa with Powder X-ray Diffraction. 2008. *Propellants, Explosives and Pyrotechnics.* **33** (4): 286.

Stevens, L. L., D. M. Dattelbaum, and D. E. Hooks. The high-pressure phase behavior and compressibility of 2,4,6-trinitrotoluene (TNT). 2008. *Applied Physics Letters.* **93**: 081912.

Velizhanin, K. A., S. Kilina, T. D. Sewell, and A. Piryatinski. First-principles calculations of vibrational normal modes in polyatomic materials with translational symmetry: application to PETN molecular crystal. 2008. *Journal of Physical Chemistry B.* **112**: 13252.

Velizhanin, K. A., T. D. Sewell, and A. Piryatinski. First-principles based calculations of vibrational mode couplings and IR line shape in PETN molecular crystal. *Journal of Physical Chemistry A.*

Whitley, V. H., D. E. Hooks, K. J. Ramos, J. F. O'Hara, and A.. K. Azad. Polarization orientation dependence of the far infrared spectra of oriented single crystals of 1,3,5-trinitro-S-triazine (RDX) using terahertz time-domain spectroscopy. 2009. *Analytical and Bioanalytical Chemistry.* **395** (2): 315.

Yellampalle, B., E. E. M. Chia, K. Kim, A. J. Taylor, and R. Averitt. Three pulse envelope approach for ultrashort pulse characterization in a pump-probe experiment. 2008. *Applied Physics Letters.* **92**: 061111.

Yellampalle, B., K. Y. Kim, and A. J. Taylor. Amplitude ambiguities in second harmonic generation frequency resolved optical gating. 2007. *Optics Letters.* **32**: 3558.

# Biomimetic Hydrogen Production by Photoinitiated Transition Metal Catalysis

*Reginaldo C. Rocha*
20070096DR

## Abstract

Energy security is a dominant national security issue and has posed urgent socioeconomic, political, and scientific challenges. The goal of this project was to enhance our national energy security by developing a new approach to the production of hydrogen fuel from renewable sources: water and solar energy. The potential capacity for solar energy is extremely large, sufficient to meet the rapidly increasing demands for the foreseeable future. Nature solved the problem of efficient capture, transport and storage of solar energy billions of years ago, through the development of photosynthetic systems. By adopting a bio-inspired approach in this project, we proposed to combine experiment and theory into the design and development of efficient light-driven molecular catalysts for $O_2$ and $H_2$ production from water splitting. In analogy to the biological modular systems, the oxidation and reduction half-reactions were conceptualized as separate $O_2$ and $H_2$ modules which, upon detailed understanding and individual optimization, can be photoelectrochemically coupled into an integrated assembly toward the clean, renewable production of hydrogen energy using only water and sunlight as the energy source.

## Background and Research Objectives

Our overall objective was to develop a new, biomimetic approach to the production of hydrogen fuel from solar water splitting. Natural photosynthesis converts solar energy into high-energy chemical bonds by splitting water to form ATP, NADPH (analogous to $H_2$), and $O_2$. Photosynthetic water oxidation is catalyzed by the oxygen-evolving complex of photosystem II. Hydrogenases from various microorganisms catalyze the production of $H_2$ from protons and electrons at extraordinarily high rates (up to $10^4$ turnovers/sec) using nonprecious metals such as iron. Despite decades of efforts, scientists have not yet come close to mimicking these natural systems. Two major scientific barriers persist: developing efficient molecular catalysts for splitting into $O_2$ and $H_2$, and coupling these reactions to a photochemical energy source. In order to tackle the photochemical water splitting, which involves extremely challenging multi-electron/proton coupled reactions, we aimed at using the natural systems to guide the design of synthetic, transition-metal inorganic catalysts and their assembly. One of the primary lessons from biology about efficient water splitting is the use of separate functional modules for light harvesting, water oxidation, electron/proton transfer, and production of $H_2$ equivalents. As detailed in the following sections, our research followed the lead of Nature in order to develop functional modules for independent optimization and further assembly into a complete scheme to photochemically drive the oxidative and reductive catalytic cycles toward the renewable production of solar fuels.

## Scientific Approach and Accomplishments

Our approach to photocatalytic water splitting was to subdivide this complex problem into tractable pieces. The key elements are synthetic "modules" involving molecular chemistry that can be established independently and then assembled pairwise to test photochemical behavior. Therefore, *our focus was on the molecular catalysis related to $H_2$ and $O_2$ production*, which sets our approach apart from existing schemes because most deficiencies of solid-state materials relate to difficulties in carrying out the required multi-step, proton-coupled electron-transfer reactions to completion, yielding incompletely oxidized/reduced intermediates that are highly reactive and deleterious. In our biomimetic design, we chose transition-metal molecular complexes with properties and functions inspired by the principles operating in hydrogenases and photosystem II. In this modular concept, the protons and electrons needed to produce $H_2$ at the cathodic phase are furnished by the oxidation of water or organic substrates at the photoanodic module. To this end, our team combined experimental and theoretical expertise

and capabilities in synthetic chemistry, spectroscopy, electrochemistry and photochemistry, photosynthesis, and nanoscience. Although our progress is organized below by modules, each of these comprises a highly interactive effort among the subteams on synthesis, measurement, and theory.

## $O_2$ Module – Oxidation Catalysis

*Experiment*

A major challenge in molecular photocatalysis for water oxidation has been the realization of multi-component assemblies that can meet the required kinetics and thermodynamics while integrating (i) charge-transfer photoexcitation and accompanying stepwise transfer of a single electron to an acceptor at the chromophoric end with (ii) proton-coupled, multi-electron redox buildup and chemical reactivity at the catalytic unit. Toward this goal, we designed and synthesized a family of molecularly bridged dyad assemblies of ruthenium-polypyridyl complexes containing a sensitizing unit for visible photoexcitation and a catalytic unit with capability for multi-electron/multi-proton reactivity (Figure 1). To prepare such chromophore-catalyst systems, we developed a synthetic methodology for coupling chromophore and catalyst using various types of bridging ligands [1,2]. The bimetallic dyads and corresponding monometallic components were characterized structurally and electronically by a variety of spectroscopic techniques and electrochemistry, including spectroelectrochemical approaches for the study of multiple proton-coupled redox processes in situ (e.g. $H_2O$-$Ru^{II}$/HO-$Ru^{III}$/O=$Ru^{IV}$) [1-3]. The chemically relevant metal-to-ligand charge-transfer states of the photoexcited dyads were identified and investigated using time-resolved fluorescence spectroscopy and transient absorption pump-probe measurements [4]. Essential to photophysical studies were the analytical comparisons between the absorption/emission properties of the dyad systems and their building blocks [4,5].

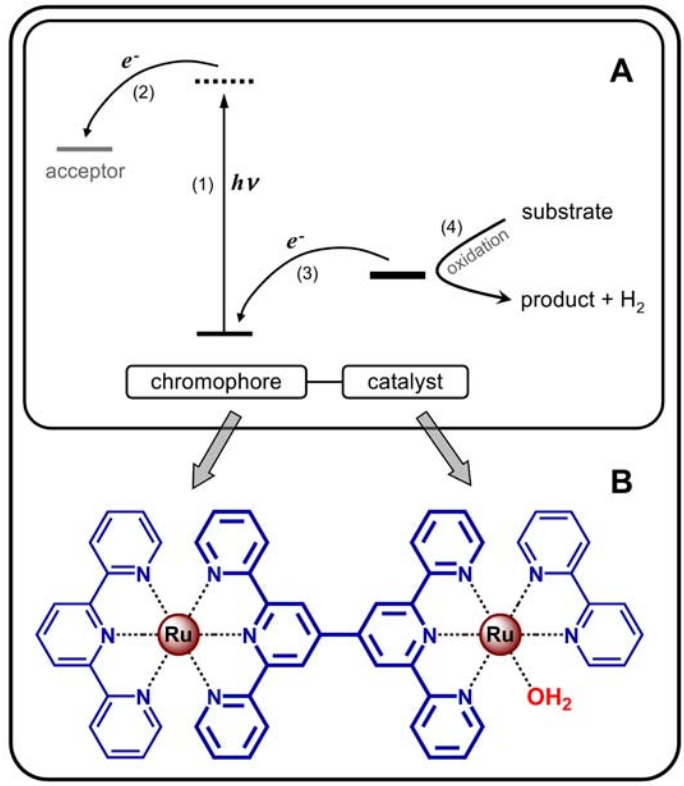


*Figure 1. (A) Schematic of the main steps involved in the oxidation of organics or water (step 4) upon photoactivation of the catalyst following sequential repetition of the photoexcitation and electron transfer processes (steps 1-3); acceptor = sacrificial electron-accepting molecule or nanoparticulate $TiO_2$. (B) Representative structure of one of the dyads of ruthenium-polypyridyl complexes. Other structurally related assemblies were also prepared by varying the bridging ligand (boldfaced fragment).*

Among our key accomplishments was the successful demonstration that, under simulated solar irradiation and in the presence of sacrificial electron acceptors, the chromophore-catalyst assemblies in water, at ambient conditions can (i) undergo activation by photoinitiated stepwise electron transfer and charge separation, and (ii) perform the visible light-driven catalytic oxidation of organics (including the 2-electron/2-proton photoconversion of a series of aliphatic and benzyl alcohols into the corresponding aldehyde or ketone products) with very high selectivity (≈100%) and tens of turnover cycles per hour in some cases [1], as probed by NMR spectroscopy and gas chromatography. We also initiated kinetic and mechanistic studies of water oxidation with $O_2$ evolution for monometallic catalysts to be optimized and incorporated into new dyads with capability for the 4-electron/4-proton photooxidation of water.

*Theory*

The monometallic catalyst/chromophore components

in Figure 1 were used here for the optimization of a catalyst-chromophore-semiconductor assembly in which the catalyst-chromophore dyad was attached onto nanostructured $TiO_2$ by phosphonate anchoring groups at the terminal ligands of the chromophore (Figure 2). Upon excitation with visible light, this assembly should be capable of electron injection into the $TiO_2$ semiconductor and subsequent proton-coupled electron transfer, with concurrent regeneration of the hole on the chromophore and first oxidation of the water ligand at the catalytic center. Our theoretical efforts focused on understanding (i) the electronic structure and excited state properties of the molecular components alone as well as the overall assembly, and (ii) the electron injection into the $TiO_2$ nanoparticles.

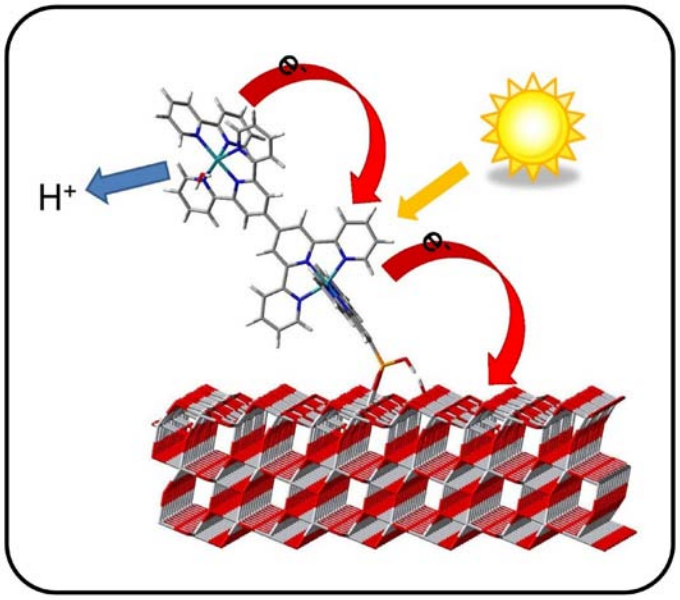


*Figure 2. Calculated structure of a catalyst-chromophore-$TiO_2$(nanoparticle) assembly constructed by attachment of the molecular photocatalyst (in Figure 1) onto the semiconductor surface via phosphonate anchoring groups. Photoexcitation of the chromophore with visible light is followed by electron injection into the conduction band of $TiO_2$. The hole created at the chromophoric unit is then filled by a secondary proton-coupled electron transfer from the catalytic unit. Red arrows denote the movement of electrons (e-) and blue arrow the movement of the proton (H+).*

First, we characterized the ground- and excited-state structures of the individual monomers and found that these complexes undergo metal-to-ligand charge transfer (MLCT) photoexcitation following visible-light absorption. The resulting triplet potential-energy surfaces are complicated, with several metal-centered ($^3$MC) and $^3$MLCT states very close in energy. Furthermore, the energy gap between the lowest $^3$MC and $^3$MLCT states is strongly influenced by the solvent environment and decreases (the $^3$MLCT state is stabilized) with the increasing solvent polarity [5]. Next, we studied interfacial electron transfer (IET) processes in chromophore-semiconductor and catalyst-chromophore-semiconductor assemblies [6]. For the chromophore-$TiO_2$ assembly, we found that IET takes 1–10 ps, a time comparable to the lifetime of the excited electronic state of the chromophore. The calculated IET in the catalyst-chromophore-$TiO_2$ assembly was slower due to localization of the electronic excitation into the bridge between catalyst and chromophore, which is weakly coupled to the electronic states of the conduction band of $TiO_2$. By modifying the ligands of the original assembly, we designed new derivatives where the electronic excitation is shifted toward the terminal ligand, which has a stronger coupling with the $TiO_2$ conduction band and should promote more efficient electron injection into the semiconductor.

## $H_2$ Module – Reduction Catalysis

*Experiment*

The goal here was to synthesize functional mimics of iron-hydrogenases from mononuclear iron(II) complexes to function as inexpensive catalysts for $H_2$ production. Complexes containing at least one carbonyl ligand and one or more protonatable ligands are desired to aid heterolysis of $H_2$ and its reverse formation from protons and electrons. Starting from simple carbonyl precursors or chloride salts of iron(II), several synthetic routes to possible catalysts were devised. Various ligand systems were also explored to assess the importance of soft (sulfur) vs hard (nitrogen) donor groups in assisting the conversion of protons and electrons into $H_2$ at the Fe center. An important question to address from these studies was the actual function of the ubiquitous thiolate in natural hydrogenases. Therefore, we specifically focused on models containing $Fe^{II}$ centers supported by thioamine, diphosphine and carbonyl or isocyanide ligands [7]. Typical examples that we targeted as synthons for potential hydride/dihydrogen binding are shown in Figure 3. Following the spectroscopic (infrared and NMR) and electrochemical characterization of their structure and complex redox properties, these systems are now being tested for their ability to bind/cleave $H_2$ as well as for their chemical linkage to photoreceptor sites to provide a direct pathway for transfer of electrons.

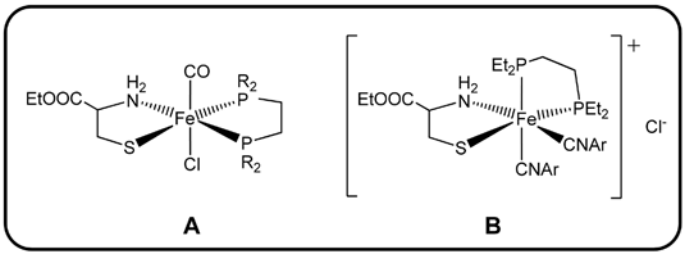


*Figure 3. Structural formulas of representative mononuclear iron(II) complexes prepared as precursors to $H_2$-producing catalysts (R = various alkyl groups; Ar = 2,6-dimethylphenyl).*

Another front of investigation was the potential use of $Pd^{II}$-Trost* complexes (Figure 4) to catalytically produce $H_2$ via cyclic interconversion between $Pd^0$ and $Pd^{II}$. We focused on the two possible mechanistic pathways shown in Figure 4. First, we examined the likelihood of pathway (a) in dichloromethane, but $^{31}P$ and $^1H$ NMR spectroscopy indicated only the presence of unreacted $[Pd^{II}\text{-Trost*}]^0$, with no formation of the $[Pd^0\text{-Trost*}]^{2-}$ dianion. By using strong reductants and heating toluene solutions to 50 °C, the starting complex was reduced but not to the diamagnetic $Pd^0$ species, as suggested by the paramagnetism in $^{31}P$ NMR spectra. EPR spectra displayed an inorganic signal assigned to the open-shell ($d^9$) $Pd^I$ center. Therefore, pathway (a) does not appear to operate in the observed $H_2$ production. Turning to mechanism (b), addition of two equivalents of a strong acid to the $Pd^{II}$-Trost* complex resulted in quantitative formation of the doubly protonated $[Pd^{II}\text{-Trost*}(H)_2]^{2+}$ species, while addition of less than one equivalent afforded a mixture of $[Pd^{II}\text{-Trost*}(H)]^+$ and $[Pd^{II}\text{-Trost*}(H)_2]^{2+}$. Then, treatment of $[Pd^{II}\text{-Trost*}(H)_2]^{2+}$ in dichloromethane with the reductant resulted, again, in a paramagnetic species (likely $Pd^I$) with no regeneration of the starting material. Given that pathway (b) offered the most promising route in facilitating $H_2$ production, we explored its potential for electrocatalysis via cyclic voltammetry, which displayed a quasi-reversible reduction process at -1.95 V vs ferrocene for the catalyst in dichloromethane. Upon addition of acid, an electrocatalytic response was observed, with the reduction potential shifted to about 0 V. This result suggests that the $Pd^{II}$-Trost* system is capable of catalytic $H_2$ production, and further experiments should elucidate the kinetic and mechanistic details.

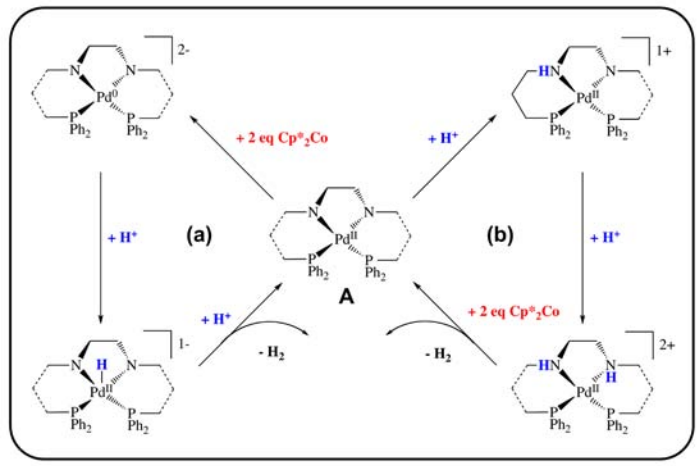


*Figure 4. Possible mechanistic pathways for H2 production by the Pd-Trost* catalyst (structure A): reduction first then protonation [(a), left] and protonation first then reduction [(b), right]; Cp*2Co = reductant.*

*Theory*

Our initial efforts focused on the calculation of one-electron redox potentials for dinuclear $Fe^IFe^I$ model complexes mimicking the active sites of iron-hydrogenases. By using density functional theory (DFT) with the appropriate functionals (GGA), we achieved excellent agreement with experiment [8,9]. Also, the redox potentials directly correlate to the spectrochemical series of the ligands and can be justified by the electron density donated by the ligand onto the iron centers. We also extended this analysis to other transition-metal complexes with varying oxidation states, and a natural starting point was ferrocene. From this example, we showed that solvation free energies alone are not an appropriate quantity when referencing calculated potentials to standard hydrogen electrode. Moreover, if results are referenced to a *calculated* standard such as ferrocene, one can effectively cancel out all additional thermodynamic assumptions necessary for modeling experiment.

We also contributed to the theory-driven $H_2$ catalyst design using mononuclear Fe complexes [10]. Using DFT methods and based on several known experimental results in the literature, we proposed a complex (with carbonyl, cyanide, and pyridine thiolate ligands) as a plausible catalyst for $H_2$ production (Figure 5). Upon reduction, our system forms a five-coordinate species with the open site *trans* to the carbonyl ligand. However, double reduction is necessary to facilitate the formation of a $Fe^{II}$-H species. Once the hydride intermediate is formed, a second proton should readily coordinate to the hydride to give a Fe-$H_2$ complex and $H_2$ will dissociate in the presence of a strongly coordinating solvent. Our results will aid experimentalists in the rational design of these types of Fe systems.

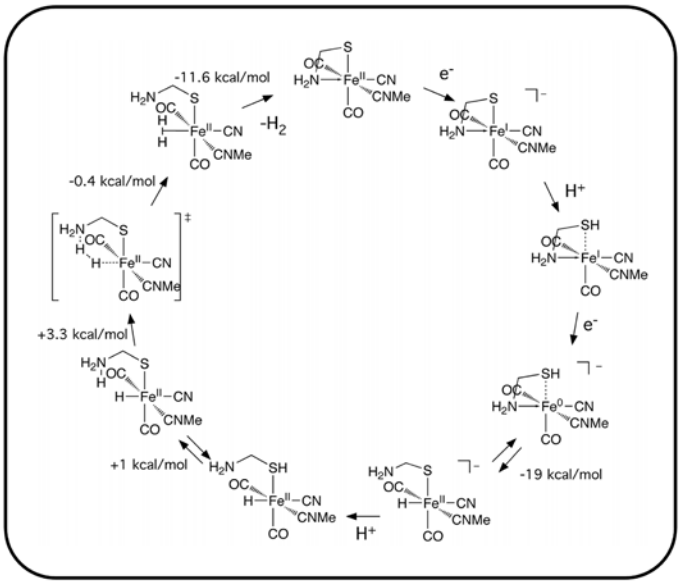


*Figure 5. Calculated catalytic cycle for $H_2$ production by mononuclear iron(II) complexes.*

Another aspect of our work relates to the stability of molecular platinum catalysts. Recently, several groups reported that $Pd^{II}$ or $Pt^{II}$ diimine complexes can act as efficient $H_2$-evolving catalysts. However, other reports suggest that such molecular catalysts photodecompose to colloidal Pd or Pt, which are presumably the true $H_2$-generating catalysts. We performed DFT and time-dependent DFT calculations on two $Pt^{II}$ diimine systems and found that, while these compounds are stable upon reduction, photoexcitation of the reduced species leads to dissociation of the ligand set. The decomposition sequence occurs upon formation of an unstable $Pt^{I}$ or $Pt^{0}$ species by occupying a strongly $\sigma$ antibonding $Pt(d_{x^2-y^2})$ orbital with the surrounding ligands [11]. In a different approach to Pd chemistry, our team explored $H_2$ catalysts based on Pd-Trost complexes (see above), for which we worked closely with our experimentalists to elucidate the possible operating mechanisms [12].

**Technique Development**

New instrumentation was required to interrogate the complex mechanisms and fast kinetics of photophysical/photochemical processes in our systems. In one activity, for instance, a step-scan Fourier transform infrared instrument for time-resolved vibrational spectroscopy was designed, developed, and applied to our studies [13]. The unparalleled performance of this new instrument was confirmed through the characterization of our challenging molecular assemblies. As another example, we developed a spectrally tunable Raman spectrometer that was also used in our investigations. Combined, these new capabilities will provide us with important, unprecedented information regarding strategies to optimize charge- and energy-transfer processes in molecular-based, solar-energy devices.

**System Integration**

Following our studies of oxidation photocatalysis by the chromophore-catalyst systems in homogeneous conditions (Figure 1), we prepared and characterized heterogenized "triad" assemblies from attachment of the molecular dyads onto a metal-oxide semiconductor/acceptor (nanoparticulate $TiO_2$) via functionalization of the chromophore unit with a suitable surface-anchoring group (e.g. phosphonate). The interfacial electron injection upon photoexcitation and resulting photooxidation catalysis at these heterogeneous systems in aqueous environment was also demonstrated [14]. This scheme for organic transformations is of relevance to hydrogen-based energy technologies because the liberation of protons and electrons at the photoanode can be coupled with recombination on a cathodic terminal for $H_2$ fuel production in an integrated photoelectrochemical synthesis cell. Motivated by these remarkable results, we used the same principles of this proof-of-concept into promising steps toward a complete scheme for water-oxidation photocatalysis integrated with the $H_2$ module.

In addition to $TiO_2$, we explored other nanomaterials as semiconductor components for integration of modules in our devised photoelectrochemical scheme. For instance, we developed a sol-gel method for constructing thin films of nanocrystalline $WO_3$, which was incorporated into a tandem cell for successful demonstration of solar water splitting [15]. Although platinum was initially used as a catalyst for $H_2$ production in our proof-of-principle, it will be replaced with the catalysts developed in our project and optimized for efficient production of solar fuel.

## Impact on National Missions

This research supports the DOE missions and addresses our primary LANL institutional goals in *national energy security* by providing significant advancements toward *carbon-neutral renewable energy technologies* and by enhancing the *fundamental understanding of materials*.

## References

1. Chen, W., F. N. Rein, and R. C. Rocha. Homogeneous photocatalytic oxidation of alcohols by a chromophore-catalyst dyad of ruthenium complexes. To appear in *Angewandte Chemie.*

2. Chen, W., F. N. Rein, B. L. Scott, and R. C. Rocha. Preparation, structural characterization and proton-coupled oxidation chemistry of a family of ligand-bridged unsymmetrical dyads of ruthenium-polypyridyl complexes. *Journal of the American Chemical Society.*

3. Chen, W., F. N. Rein, and R. C. Rocha. Proton-coupled electron transfer: redox leveling at Ru(II)-quo/Ru(III)-hydroxo/Ru(IV)=oxo catalytic sites. *Inorganic Chemistry.*

4. Dattelbaum, D. M., W. Chen, and R. C. Rocha. Systematic photophysical studies of a series of molecular dyad assemblies by time-resolved fluorescence and transient-absorption spectroscopies. *Journal of Physical Chemistry.*

5. Jakubikova, E., W. Chen, D. M. Dattelbaum, F. N. Rein, R. C. Rocha, R. L. Martin, and E. R. Batista. Electronic structure and spectroscopy of [Ru(tpy)2]2+, [Ru(tpy)(bpy)(H2O)]2+, and [Ru(tpy)(bpy)(Cl)]+. To appear in *Inorganic Chemistry.*

6. Jakubikova, E., R. C. I. Snoeberger, V. S. Batista, R. L. Martin, and E. R. Batista. Interfacial electron transfer in TiO2 surfaces sensitized with Ru(II)-polypyridine complexes. To appear in *Journal of Physical Chemistry A.*

7. Baker, R. T., J. C. Gordon, G. J. Kubas, T. Li, B. L. Scott, and A. D. Sutton. Biomimetic hydrogenase models: synthesis, structure and properties of iron(II) complexes containing thioamine, diphosphine, and carbonyl/isocyanide ligands. *Journal of the American Chemical Society.*

8. Roy, L. E., E. Jakubikova, M. G. Guthrie, and E. R. Batista. Calculation of one-electron redox potentials revisited. Is it possible to calculate accurate potentials with density functional methods?. 2009. *Journal of Physical Chemistry A.* **113**: 6745.

9. Roy, L. E., E. R. Batista, and P. J. Hay. Theoretical studies of reduction potentials of mono-iron complex models of hydrogenases. 2008. *Inorganic Chemistry.* **47**: 9228.

10. Roy, L. E., E. R. Batista, and P. J. Hay. Theory-driven catalyst design for hydrogen production: will only one Fe work?. *Journal of the American Chemical Society.*

11. Roy, L. E., G. Scalmani, R. Kobayashi, and E. R. Batista. Theoretical studies on the stability of molecular platinum catalysts for hydrogen production. 2009. *Dalton Transactions.* : 6719.

12. Roy, L. E., and E. R. Batista. Theoretical analysis of Pd Trost complexes: studies into possible H2 catalytic activity. *Inorganic Chemistry.*

13. Magana, D., R. B. Dyer, and A. P. Shreve. Implementation of time-resolved step-scan FTIR using a kHz repetition rate pump laser. *Applied Spectroscopy.*

14. Chen, W., F. N. Rein, and R. C. Rocha. A family of chromophore-catalyst assemblies attached to nanostructured TiO2 for visible light-driven oxidation catalysis. *Angewandte Chemie.*

15. Angiuli, F., C. A. Bignozzi, and R. B. Dyer. Mesoporous WO3 thin film development for photochemical hydrogen production. *Journal of the American Chemical Society.*

## Publications

Angiuli, F., C. A. Bignozzi, and R. B. Dyer. Mesoporous WO3 thin film development for photochemical hydrogen production. *Journal of the American Chemical Society.*

Baker, R. T., J. C. Gordon, G. J. Kubas, T. Li, B. L. Scott, and A. D. Sutton. Biomimetic hydrogenase models: synthesis, structure and properties of iron(II) complexes containing thioamine, diphosphine, and carbonyl/isocyanide ligands. *Journal of the American Chemical Society.*

Batista, E. R., and R. L. Martin. Electron localization in the ground state of the ruthenium blue dimer. 2007. *Journal of the American Chemical Society.* **129**: 7224.

Beck, D., J. Brewer, J. Lee, D. McGraw, B. A.. DeGraff, and J. N. Demas. Localizing molecular probes: Inclusion of Re(I) complexes in cyclodextrin. 2007. *Coordination Chemistry Reviews.* **251**: 546.

Carlson, C. N., J. M. Veauthier, K. D. John, and D. E. Morris. Electronic and magnetic properties of bimetallic ytterbocene complexes: the impact of bridging ligand geometry. 2008. *Chemistry - European Journal.* **14**: 422.

Carlson, C. N., W. Chen, K. D. John, R. C. Rocha, and D. E. Morris. A comparitive electrochemical and spectroscopic study of metal-metal coupling in terpyridyl-based bridged Ru(II) bimetallic complexes. *Inorganic Chemistry.*

Chen, W., F. N. Rein, B. L. Scott, and R. C. Rocha. Preparation, structural characterization and proton-coupled oxidation chemistry of a family of ligand-bridged unsymmetrical dyads of ruthenium-polypyridyl complexes. *Journal of the American Chemical Society.*

Chen, W., F. N. Rein, and R. C. Rocha. Homogeneous photocatalytic oxidation of alcohols by a chromophore-catalyst dyad of ruthenium complexes. To appear in *Angewandte Chemie.*

Chen, W., F. N. Rein, and R. C. Rocha. Proton-coupled electron transfer: redox leveling at aquo-Ru(II)/hydroxo-

Ru(III)/oxo=Ru(IV) catalytic sites. *Inorganic Chemistry.*

Chen, W., F. N. Rein, and R. C. Rocha. A family of chromophore-catalyst assemblies attached to nanostructured TiO2 for visible light-driven oxidation catalysis. *Angewandte Chemie.*

Concepcion, J. J., D. M. Dattelbaum, T. J. Meyer, and R. C. Rocha. Probing the localized-to-delocalized transition. 2008. *Philosophical Transactions of the Royal Society A.* **366**: 163.

Dattelbaum, D. M., J. B. Butler, J. R. Schoonover, M. W. George, and T. J. Meyer. Application of Transient Infrared and Near-infrared Spectroscopy to Excited States in Transition Metal Complexes. 2007. *Coordination Chemistry Reviews.* **251**: 492.

Dattelbaum, D. M., W. Chen, and R. C. Rocha. Systematic photophysical studies of a series of molecular dyad assemblies by time-resolved fluorescence and transient-absorption spectroscopies. *Journal of Physical Chemistry.*

Demadis, K. D., D. M. Dattelbaum, J. D. Paul, J. Conception, T. J. Meyer, and P. S. White. Vibrational mapping of molecular and electronic structures in [Os(pp)3]n+ (pp = 2,2'-bipyridine, 1,10-phenanthroline, n = 2+, 3+). 2007. *Inorganica Chimica Acta .* **360**: 1143.

Dyer, R. B., and W. H. Woodruff. Vibrational spectroscopy. 2007. In *Applications of physical methods to inorganic and bioinorganic chemistry.* Edited by Scott, R. A., and C. M. Lukehart. , p. 489. Chichester, UK: John Wiley & Sons.

Fleming, C. N., D. M. Dattelbaum, D. W. Thompson, A. Y. Ershov, and T. J. Meyer. Excited state intervalence transfer in a rigid polymeric film. 2007. *Journal of the American Chemical Society.* **129**: 9622.

Hornstein, B. J., D. M. Dattelbaum, J. R. Schoonover, and T. J. Meyer. The reactivity of a bound Ru(VI)-oxo complex: oxidation of benzyl alcohol. 2007. *Inorganic Chemistry.* **46**: 8139.

Jakubikova, E., R. C. I. Snoeberger, V. S. Batista, R. L. Martin, and E. R. Batista. Interfacial electron transfer in TiO2 surfaces sensitized with Ru(II)-polypyridine complexes. To appear in *Journal of Physical Chemistry A.*

Jakubikova, E., W. Chen, D. M. Dattelbaum, F. N. Rein, R. C. Rocha, R. L. Martin, and E. R. Batista. Electronic structure and spectroscopy of [Ru(tpy)2]2+, [Ru(tpy)(bpy)(H2O)]2+, and [Ru(tpy)(bpy)(Cl)]+. To appear in *Inorganic Chemistry.*

Jude, H., F. N. Rein, P. S. White, D. M. Dattelbaum, and R. C. Rocha. Synthesis, structure, and electronic properties of a dimer of Ru(bpy)2 doubly bridged by methoxide and pyrazolate. 2008. *Inorganic Chemistry.* **47**: 7695.

Jude, H., F. N. Rein, W. Chen, B. L. Scott, D. M. Dattelbaum, and R. C. Rocha. Pyrazole and pyrazolyl complexes of cis-bis(2,2'-bipyridine)chlororuthenium(II): synthesis, structural and electronic characterization, and acid-base chemistry. 2009. *European Journal of Inorganic Chemistry.* : 683.

Jude, H., P. S. White, D. M. Dattelbaum, and R. C. Rocha. Trans-diaquabis(2,2'-bipyridine)ruthenium(II) bis(trifluoromethanesulfonate). 2008. *Acta Crystallographica.* **E64**: m1388.

Kubas, G. J.. Breaking the H2 marriage and reuniting the couple. 2006. *Science.* **314**: 1096.

Kubas, G. J.. Metal-dihydrogen complexes. Prototypes for the coordination chemistry of saturated molecules. 2007. *Proceedings of the National Academy of Sciences USA.* **104**: 6901.

Kubas, G. J.. Fundamentals of H2 binding and reactivity on transition metals underlying hydrogenase function and H2 production and storage. 2007. *Chemical Reviews.* **107**: 4152.

Kubas, G. J.. Dihydrogen and other sigma bond complexes. 2006. In *Comprehensive Organometallic Chemistry III.* Edited by Crabtree, R. H., and D. M. P. Mingos. Vol. 1, p. 671. Oxford: Elsevier.

Kubas, G. J.. The extraordinary dynamic behavior and reactivity of dihydrogen and hydride in the coordination sphere of transition metals. 2006. In *Handbook of hydrogen transfer.* Edited by Schowen, R. L.. Vol. 1, p. 603. Weinheim: Wiley-VCH.

Kubas, G. J.. H2 binding and reactivity on transition metals underlying biomimetic H2 production and new materials for H2 storage. 2009. In *Materials issues in a hydrogen economy.* Edited by Jena, P., A. Kandalam, and Q. Sun. , p. 83. New Jersey: World Scientific Publishing.

Kubas, G. J.. Hydrogen activation on organometallic complexes and H2 production, utilization, and storage for future energy. 2009. *Journal of Organometallic Chemistry.* **694**: 2648.

Kubas, G. J., and D. M. Heinekey. Dihydrogen complexes. To appear in *Physical inorganic chemistry.* Edited by Bakac, A..

Magana, D., R. B. Dyer, and A. P. Shreve. Implementation of time-resolved step-scan FTIR using a kHz repetition rate pump laser. *Applied Spectroscopy.*

Muckerman, J. T., E. Fujita, C. D. Hoff, and G. J. Kubas. Theoretical investigation of the binding of small molecules and the intramolecular agostic interaction at tungsten centers with carbonyl and phosphine ligands. 2007. *Journal of Physical Chemistry B.* **111**: 6815.

Rocha, R. C., F. N. Rein, H. Jude, A. P. Shreve, J. J. Concepcion, and T. J. Meyer. Observation of three intervalence transfer bands for a class II-III mixed-valence complex of ruthenium. 2008. *Angewandte Chemie - International Edition.* **47**: 503.

Roy, L. E., E. Jakubikova, M. G. Guthrie, and E. R. Batista. Calculation of one-electron redox potentials revisited. Is it possible to calculate accurate potentials with density functional methods?. 2009. *Journal of Physical Chemistry A.* **113**: 6745.

Roy, L. E., E. R. Batista, and P. J. Hay. Theoretical studies of reduction potentials of mono-iron complex models of hydrogenases. 2008. *Inorganic Chemistry.* **47**: 9228.

Roy, L. E., E. R. Batista, and P. J. Hay. Theory-driven catalyst design for hydrogen production: will only one Fe work?. *Journal of the American Chemical Society.*

Roy, L. E., G. Scalmani, R. Kobayashi, and E. R. Batista. Theoretical studies on the stability of molecular platinum catalysts for hydrogen production. 2009. *Dalton Transactions.* : 6719.

Roy, L. E., P. J. Hay, and R. L. Martin. Revised basis sets for transition metal atoms using the LANL effective core potentials. 2008. *Journal of Chemical Theory and Computation.* **4**: 1029.

Roy, L. E., and E. R. Batista. Theoretical analysis of Pd Trost complexes: studies into possible H2 catalytic activity. *Inorganic Chemistry.*

# Detection of Respiratory Infection by Scent

*Jurgen G. Schmidt*
20080317ER

## Introduction

The recent spread of H1N1 " Swine Flu" to become a pandemic threat shows the limited ability and resources to detect and respond rapidly to challenges from natural emerging pathogens. The early detection of epidemic pathogens requires simple, robust and easily deployed assays. While current detection methods rely on rather sophisticated RNA, protein – antibody and laboratory based methods, simpler detection schemes that do not require instrumentation are currently overlooked. Human preference for visual sensory input biases current detection technologies towards optical read-out of a recognition event, equally discriminatory senses such as olfaction are underutilized in their potential to afford pathogen detection, which is surprising as respiratory infections are located in one of the most ubiquitous sensors available to humans – the nose! A rapid detection of the presence of influenza by scent would allow instrumentation free self diagnostics of an infection.

Influenza viridae carry multiple copies of an enzyme - neuraminidase - that cleaves cell surface sialic acids, thus liberating the viral progeny from cell debris. Our project explores the synthesis and biological function of chimeric substrates of sialic acids and odorants. Such substrates will be cleaved by the innate enzymatic activity of the virus and the released odorant stimulates the olfactory receptors to alert the host (Figure 1 illustrates this concept).

This detection scheme substitutes instrumentation with the exquisite ability of humans to discriminate and recognize smells for truly field-able diagnostics. The presence of multiple copies of the enzyme on any viral particle, enzymatic turnover of multiple substrates all combined with the olfactory system amplification may allow detection of viral respiratory infection before a patient becomes aware of symptoms. Our final goal is to screen a library of such chimeric odorant substrates, optimize the assay and select for molecules that are cleaved differently by viral and bacterial neuraminidases. A discriminatory assay with two easily recognized scents that distinguish bacterial from viral infections can guide the early deployment of medical countermeasures and select the appropriate drugs at an early and most beneficial stage for the patient.

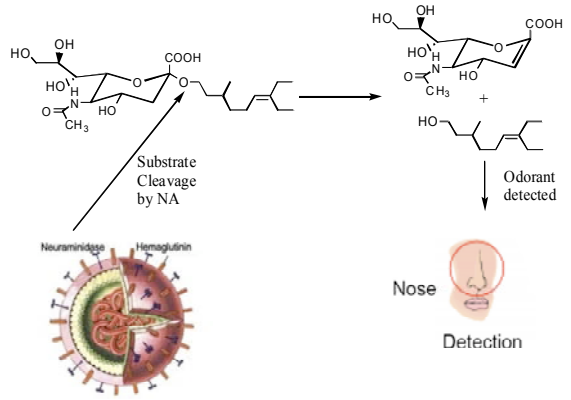


*Figure 1. Schematic representation of influenza detection by scent*

## Benefit to National Security Missions

The recent emergence of a novel influenza strain H1N1 (Swine Flu) made the news headlines. Novel detection methods to indicate the presence of influenza to monitor global outbreaks of influenza will become essential tools to mitigate and counter the spread of influenza infections. This research will enable dire needed novel detection techniques for this emerging health threat. The basic research supports the DOE mission of National Security. In addition this project will further lead to enhanced capabilities for the DHS and the HHS in the detection of emerging biothreats.

## Progress

The detection of influenza by a release of an odorant from synthetic substrates will provide a new instrumen-

tation free and rapid detection for influenza infections. The scent is detected and amplified by the receptors in the nose and will likely allow a pre-symptomatic screen. The syntheses of chimeric products of odorants attached to sialic acids, such as Neuraminic acids (NA), are among the most challenging synthetic problems in glycoside chemistry as the anomeric attachment site provides multiple options for side reactions.

Among multiple investigated options, reported in the literature for sugar coupling, only methods using phosphonic acid activations of the anomeric center proved successful in generating the odorant alcohol NA chimera. We have designed, executed and repeated the diethylphosphonate coupling to multiple odorants with highly diverse structures. These reactions yield between 30 and 50% of the product after purification and have now been optimized for combinatorial exploration of structural and "scent" diverse libraries of targets. All compounds were purified and their structure confirmed by 1H, 13C – NMR (Nuclear Magnetic Resonance) and mass spectrometry.

The direct attachment of the more volatile aldehyde and ketone odorants to NA was less successful, producing only traces of the product, we, however, believe that switching from highly basic conditions to more mild reaction conditions will overcome this problem.

While initial experiments on the neuraminidase cleavage of the substrates were conducted with commercial purified enzyme, the goal of this project is to show the release of the odorant with influenza samples. In the biology section of this project influenza virons have been expressed and UV inactivated. The PCR amplification of potential remaining viral genes and attempts to culture the virus showed no residual viral infectivity after carefully optimizing the inactivation procedure. Commercial neuraminidase activity assays proved that the enzymatic reactivity is retained. These samples are now BSL-1 level and have been released to work within our mass spectrometry facility. The current focus in this area optimizes reaction conditions and buffer systems to retain the enzyme activity while using volatile salts, suited for mass spectrometry, in the buffers.

While at the beginning of this project combinatorial and parallel syntheses seemed cost prohibitive, we have now access to free odorant samples. A Tecan liquid handling robot is currently adapted to combinatorial chemistry. This robotic station will allow the syntheses of 96 products in parallel under controlled temperature and inert atmosphere to explore the chemistry and provide hundreds of samples for the enzyme studies. This will expedite the availability of the assay for emerging and potentially pandemic influenza outbreak preparedness.

During FY 09 we have filed an invention disclosure on the methods and our work on substrates. We have trained one summer student in chemical methods of carbohydrate chemistry, who joined the University of New Mexico and gave a favorable received talk on his work. The postdoctoral associate funded and mentored under this project has now joined Astra Zeneca in permanent staff position.

## Future Work

We develop methods to use influenza specific neuraminidase catalyzed reactions on man made substrates, which releases an odorant on the primary location of respiratory infections, and, therefore, detect their presence directly in the nose. We design and synthesize a panel of substrates and test their enzymatic turnover monitoring the odorant release by mass spectrometry. Specific cleavage over non specific hydrolysis will be optimized by judicious choice of the connection chemistry in the substrates. Substrates are developed further into a selective and discriminatory detection that distinguishes among the most common causative agents of respiratory infection. Our detection approach will combine 4 distinct amplification steps – the presence of multiple neuraminidase copies on a pathogen, the catalytic substrate cleavage, the direct release of the trigger on the sensor and the biological cascade of smell, with a unique pathogen specific event and the exquisite selectivity of olfactory sensing to provide a sensitive, instrumentation free and potentially pre-symptomatic detection scheme.

This research will provide odorant substrates for neuraminidase and we expect to reach the following milestones: The chemistry of attaching odorants to sialic acids will be developed. Synthetic protocols for the incorporation of a wide range of linkages will be established. Substrates will be tested by mass spectrometry with neuraminidase for the odorant release. We will find critical contacts to the enzyme by Nuclear Magnetic Resonance spectroscopy and modeling. Modeling guides the rational optimization of substrates. Chemistry for odorant attachment to branched scaffolds and stereoselective attachment chemistry will be developed to enable discriminatory detection among respiratory causative agents, even in the presence of complex interfering matrices.

## Conclusion

An assay will be developed that specifically detects respiratory infections. We expect to develop chemical entities that are converted by an influenza specific event to release odorants. This triggers the smell receptors in the nose to allow a "patient" to be alerted of the presence of a patho-

gen. The exquisite sensitivity and selectivity of olfactory sensing not only provides the means to encode multiple pathogens with different smell, but such an assay will likely allow presymptomatic detection before the onset of other signs of infection.

## References


1. Kale, R. R., H. Mukundan, D. N. Price, J. F. Harris, D. M. Lewallen, B. I. Swanson, and J. G. Schmidt. Development of a "carboassay". Detection of Influenza virus using capture and reporter biotinylated biantennary S-sialosides. . 2008. *Journal of the American Chemical Society.* **130**: 8169.
2. Schmidt, J. G., D. Kimball, R. R. Kale, and S. S. Iyer. Detection of Intact Influenza. To appear in *Carbohydrate Biosensor session at the American Chemical Society National Meeting in Salt Lake City 237th ACS National Meeting and Exposition.* (Salt Lake City, 22-26 March, 2009).


## Publications


Kale, R. R., H. Mukundan, D. N. Price, J. F. Harris, D. M. Lewallen, B. I. Swanson, J. G. Schmidt, and S. S. Iyer. Development of a "carboassay". Detection of Influenza virus using capture and reporter biotinylated biantennary S-sialosides. 2008. *Journal of the American Chemical Society.* **130**: 8169.

# Spins in Organic Semiconductors

*Brian K. Crone*
20080323ER

## Introduction

Today's electronics are based on the electron charge. Using electron spin to compliment electronic charge for information storage and transmission in electronics is the basis for a major international research activity called "spintronics." An ideal spintronic device consists of a magnetic contact to inject spin polarized current into the device, an active layer to manipulate the spin polarization, and a magnetic contact to detect the final spin polarization. Organic semiconductors are attractive candidates for the active layer in spintronic devices because they have much longer spin lifetimes than inorganic semiconductors due to their weak spin-orbit interaction, which is the principal spin de-phasing mechanism in these materials. However, the spin-orbit interaction is also responsible for selection rules that allow optical generation/detection of polarized electron spin distributions. Optical injection and detection was important in the development of electrical spin injection in inorganic semiconductors, but now both electrical spin injection and detection has been clearly demonstrated in these materials. The purpose of this work is to develop both optical and electrical methods to inject and detect spins in organic semiconductors and demonstrate the advantages of these materials for spintronic applications. We initially focused on optical spin injection/detection, using organic materials containing a heavy metal atom to increase spin orbit coupling. In parallel, we are exploring the use of ferromagnetic contacts to electrically inject and detect spins in organic materials. This parallel approach of optical and electrical methods of spin injection improves our chances of success in this important area of study. During the course of this work we have demonstrated that spin noise spectroscopy is very promising approach for the study of spin dynamics in semiconductors and we are continuing to develop this new method.

## Benefit to National Security Missions

This project will support DOE missions in basic science and threat reduction by providing the fundamental understanding of spin-based processes in organic materials needed to enable new technologies including quantum information processing and computing. These technologies will support our national security by providing powerful tools for data encryption and decryption.

## Progress

Our research into spins in organics has taken a multi-pronged approach. We have investigated: 1) methods to electrically inject spin polarized electrons into organic semiconductors, 2) device theory of spin injection and transport in organics semiconductors, 3) ab initio quantum chemical modeling of magnetic semiconductors for use as spin injectors, and 4) new methods to measure spin polarizations in semiconductors. We will address these topics in order. 1) Investigated the use of the magnetic semiconductor europium sulfide (EuS) as a possible spin injector for organic semiconductors. It has been previously shown (by D. Smith, an investigator on this project) that the conductivity mismatch between a magnetic metal and a semiconductor prevents injection of a spin polarized current unless some barrier is inserted between the two. We are pursuing using a magnetic semiconductor as a spin injector, thereby circumventing the conductivity mismatch problem. We have shown electron injection from EuS into the organic semiconductor Alq. We made devices ITO/PEDOT/Alq/Au, where ITO/PEDOT is a hole injecting contact, and Au (gold) is also a hole injecting contact. These devices are hole only devices and emitted no light. By incorporating a EuS layer between the Alq and Au, we increased the current and got light emission due to electron injection. 2) Investigated spin injection from ferromagnetic metals into organic semiconductors. This work has shown that one can't inject a spin polarized current from a magnetic metal directly into a semiconductor. This is easily explained by the concept of thermal equilibrium. If a magnetic metal is in equilibrium with a non-magnetic semiconductor, then currents will flow to maintain this equilibrium. This means the spin polarization in the semiconductor will remain zero. To enable spin polarization in the semiconductor one needs to pull the interface out of equilibrium, either by inserting a barrier between the

metal and semiconductor as has been demonstrated in inorganic semiconductors, or by replacing the metal with a semiconductor which can be drawn out of equilibrium by current flow. 3) We used screened hybrid DFT to compute the electronic properties of EuS. This material is a strongly correlated insulator, and conventional density functional theory predicts it to be metallic. The screened hybrid approach utilized here does yield an insulator, with a computed gap of the order of 1eV, which is reasonable, but appears somewhat low compared with experiment. The Eu site contains nearly exactly 7 unpaired electrons in the f orbitals, coupled to a high-spin S=7/2 moment. There is a very slight negative spin polarization on the surrounding sulfur atoms. 4) Typical spin injection and detection schemes rely on tunneling to avoid the conductivity mismatch problem. However, tunneling introduces a strong applied voltage bias dependence to the polarization. Using a combination of magneto-optical and electronic transport techniques, we investigated the process of spin detection in lateral spin transport devices. Our results show that spin detection sensitivities do not simply follow trivially from the spin-polarized conductivities of the contacts, but rather can be enhanced or suppressed due to the electric fields that exist in real semiconductor channels. We have used experiments and theory to show that the bias dependence of the spin polarized tunneling current in combination with field dependence of the spin transport can be used to control, in a predictable way, the sensitivity of spin detection in lateral ferromagnet/semiconductor structures. Thus, not only can spin polarized electrons be made to induce both positive or negative voltages at spin detection electrodes, but also some detector sensitivities can be enhanced over ten-fold with applied bias. Part of our effort has focused on alternative, noise-based schemes to measure the dynamical properties of electron spins in semiconductors. Whereas most traditional studies of dynamics employ pump-probe methods to perturb and then measure the recovery of a spin system (such as ultrafast spectroscopy, or pulsed ESR), the Fluctuation Dissipation Theorem guarantees that the same dynamical information is available if one can “listen” to the intrinsic fluctuations of the spins while in thermal equilibrium. We have recently demonstrated that such noise-based approaches can actually work, using n-type GaAs as a canonical solid-state spin system. We used sensitive optical magnetometry based on off-resonant Faraday rotation to measure the frequency spectra of stochastic electron spin noise as a function of electron density, temperature, and interaction volume. Even more recently, we have applied these techniques to study the spin fluctuations of electrons and holes that are quantum-mechanically confined in zero-dimensional semiconductor quantum dots. Future work is aimed at exploiting this technique to ascertain the true spin coherence time of holes in these quantum dots, which preliminary work suggests is far longer than originally expected.

## Future Work

Work in the third year of this project will include three interrelated tasks: 1) modeling the behavior of organic semiconductor devices in which electrical injection is spin polarized, 2) modeling ferromagnetic metal/organic semiconductor interfaces that are used to achieve spin polarized electrical injection, and 3) measurements of spin noise spectroscopy used to characterize spin polarization in semiconductors. In Task 1), we will model electrical injection of spin polarized electrons and holes from ferromagnetic contacts into conjugated organic semiconductors. Transport in the semiconductor will be treated by the spin dependent continuity equations coupled with Poisson’s equation. The boundary conditions used to solve the continuity equations will be given by specifying the spin polarized particle currents at the boundaries. Injected spin currents are related to the charge currents via the transport parameters of the ferromagnetic contacts. In Task 2), we will study the interface between a ferromagnetic metal (Fe) and an organic semiconductor (pentacene). We will focus on structural questions and develop an appropriate force field and perform molecular dynamics simulations of the deposition of the organic onto the metal surface. We will be particularly interested in learning the nature of the interactions which lead to specific structural motifs and in methods to characterize the nature of the disorder at the interface. As our understanding of the possible interfacial arrangements grows, we will investigate these structures with electronic structure calculations examining the specifics of charge injection and band matching at the interface. In Task 3), we will measure the dynamical properties of electron spins in semiconductors. Progress in our laboratories over the last two years, has shown that spin noise spectroscopy is a viable alternative to more conventional pump-probe techniques. Together with our efforts to develop 100% efficient digital noise spectrometers, we will attempt two main experiments: a) spin noise measurements on a single electron confined in a single semiconductor quantum dot, and b) measurement of the very long intrinsic hole spin relaxation time in quantum dot ensembles. The former will be facilitated by modifications to our existing setup to include a high-numerical aperture microscope objectives for sub-micron focusing of the probe beam, while the latter will exploit the passive nature of noise spectroscopy to reveal the unperturbed hole lifetime.

## Conclusion

The goal of this work is to explore optical and electrical generation and detection of spin polarized electron distributions in organic semiconductors, and to use these techniques to study organic semiconductor devices based on electron spin dynamics. We have established spin noise spectroscopy as a very promising technique for the study of electron spin dynamics in semiconductors. These results will enable organic semiconductor based spintronic

devices which are promising candidates for quantum information processing and computing.

## Publications

Chantis, A. N., D. L. Smith, J. Fransson, and A. V. Balatsky. Scanning tunneling microscopy detection of spin polarized resonant surface bands: The example of Fe(001). 2009. *Physical Review B.* **79** (16): 165423.

Chantis, A. N., and D. L. Smith. Theory of electrical spin-detection at a ferromagnet/semiconductor interface. 2008. *Physical Review B.* **78** (23): 235317.

Crooker, S. A., E. S. Garlid, A. N. Chantis, D. L. Smith, K. S. M. Reddy, Q. O. Hu, T. Kondo, C. J. Palmstrom, and P. A. Crowell. Bias-controlled sensitivity of ferromagnet-semiconductor electrical spin detectors. 2009. *Physical Review B.* **80** (4): 041305(R).

Crooker, S. A., J. Brandt, C. Sandfort, A. Greilich, D. R. Yakovlev, D. Reuter, A. D. Wieck, and M. Bayer. Spin noise of electrons and holes in self-assembled quantum dots. *Physical Review Letters.*

Crooker, S. A., L. Cheng, and D. L. Smith. Spin noise of conduction electrons in n-type bulk GaAs. 2009. *Physical Review B.* **79** (3): 035208.

Pershin, Yu. V., N. A. Sinitsyn, A. Kogan, A. Saxena , and D. L. Smith. Spin polarization control by electric steering: proposal for a new spintronic device. 2009. *Applied Physics Letters.* **95** (2): 022114.

Ruden, P. P., and D. L. Smith. Modeling spin injection and transport in organic semiconductor structures. To appear in *Organic Spintronics.* By Vardeny, Z. V..

Yunus, M., P. P. Ruden, and D. L. Smith. Spin injection effects on exciton formation in conjugated organic semiconductors. 2008. *Applied Physics Letters.* **93** (12): 123312.

Yunus, M., P. P. Ruden, and D. L. Smith. Macroscopic modeling of spin injection and spin transport in organic semiconductors. To appear in *Synthetic Metals.*

# Strain-induced Novel Physical Phenomena in Epitaxial Ferroic Nanocomposites

*Quanxi Jia*
20080394ER

## Introduction

The vast range of structures and properties of ferroics (i.e. ferroelectric and/or ferromagnetic materials) provides an excellent case platform to investigate novel device functionalities. By combining efforts from both theoretical prediction and experimental verification, we have developed a theoretical model for investigating and predicting the magnetoelectric coupling effects on ferroelectric/ferromagnetic films. We have also grown ferroelectric/ferromagnetic nanocomposite (which is composed of two or more constituents differing in form and/or composition in the nanoscales) films with desired functionalities. By integrating properties of individual ferroics, we can overcome the problem that single phase multiferroic (i.e. showing both ferroelectric and ferromagnetic properties) materials are rare and only display a very weak magnetoelectric coupling effect at room temperature. Also, our research work holds great promise for enhancing various fundamental and applied studies of functional metal-oxides. This research ensures LANL's continued leadership in nanotechnology and functional materials. LANL's thrusts in functional materials, nanotechnology, and sensors can all benefit from this project.

## Benefit to National Security Missions

This research ties to the mission of DOE Office of Science for fundamental understanding of materials. LANL's thrusts in functional materials, nanotechnology, and sensors will directly benefit from this project.

## Progress

As outlined in our last progress report, we have made tremendous progress in the preparation and characterization of nanocomposite ferroic films using both pulsed laser deposition and polymer-assisted deposition. Specifically, we have modeled ferroelectric domain structures of single-crystal like $BiFeO_3$ thin films using a theoretical approach. We have experimentally demonstrated nanocomposite $BiFeO_3$ (BFO):$Sm_2O_3$ (SmO) films, and observed that there is a reduction in the dielectric loss for the BFO/SmO nanocomposite, compared to the pure films of the two phases.

Since the last review report, we have systematically studied the effect of chemical composition and processing parameters on the structural and physical properties of two-phase vertically aligned nanocomposite (VAN) $(BiFeO_3)_x$:$(Sm_2O_3)_{1-x}$ thin films. We showed that the VAN thin films exhibited a highly ordered vertical columnar structure with high structural quality. We demonstrated the strains of the two phases in both out-of-plane and in-plane directions could be tuned by the deposition parameters during growth, e.g. deposition frequency and film composition of the nanocomposite. The strain tunability was found to be directly related to film composition and the systematic variation of the column widths in the nanocomposite. Our experimental results for the first time suggest a promising avenue in achieving tunable strain in functional oxide thin films by using VAN structures.

Specifically, we processed single-crystal like $(BFO)_x$:$(SmO)_{1-x}$ VAN thin films with various compositions and deposition frequencies on $SrTiO_3$ substrates, and observed that the out-of-plane lattice parameter/strain is sensitive to the composition x and deposition frequency (as shown in Figure 1). The overall trend is that, as the deposition frequency decreases and the BFO content increases, the out-of-plane lattice parameter of BFO increases and the strain switches from compressive strain (x=0.5 and 0.6) to slightly tensile strain (x=0.75). On the other hand, the out-of-plane lattice parameter of SmO decreases and the strain switches from tensile (x=0.5 and 0.6) to slightly compressive (x=0.75). This suggests that both film composition and deposition frequency play a very important role in the overall strain control. When the film composition in the neighborhood of x=0.5, the VAN films show obvious vertical strain control rather than the substrate strain control. However when the composition reaches a certain limit (e.g., x=0.75), the VAN structure lost its vertical strain control and the substrate strain control dominates the overall film strain. We believe that the systematic variations in the BFO out-of-plane strain is most likely related to the size variation. This can be understood through the thin film growth kinetics. Lower deposition frequency results

in longer resting time in between laser pulses and thus longer atomic diffusion path and larger column width. This observation can also explain the systematic variation in BFO's out-of-plane compressive strain. As the frequency reduces, the BFO column width increases and the total amount of the vertical column boundaries reduces. These will cause the reduction in the vertical strain control in between BFO and SmO columns and therefore the out-of-plane compressive strain of BFO reduces.

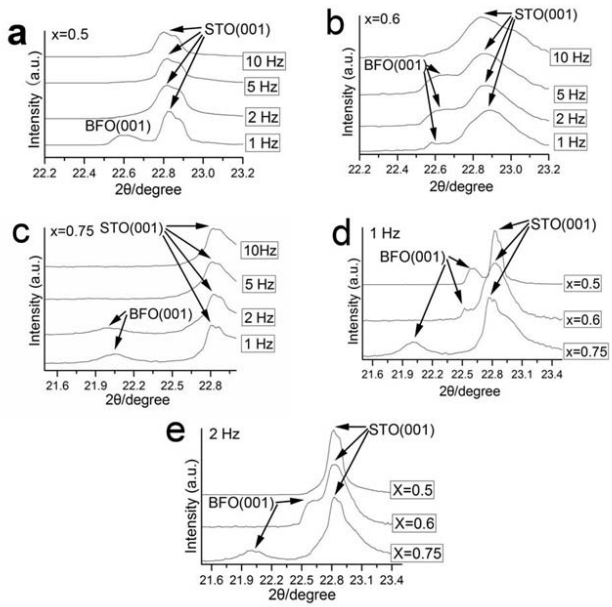


*Figure 1. Local XRD theta~2theta scans of BFO(001) peak as a function of deposition frequency for films with a) x = 0.5; b) x = 0.6; c) x = 0.75; and as a function of film composition for films deposited at frequency of d) 1Hz; e) 2Hz.*

Theoretically, we investigated the effect of anisotropic strains on the phase transitions and structures of ferroelectric thin films using different approaches. The misfit strain - misfit strain domain stability diagrams, i.e. the graphical representations of stable ferroelectric phases and domain structures as a function of strains, were predicted.

Furthermore, we explored the interplay of elastic interactions on functionality such as electronic, magnetic and polarization. To this end, we have demonstrated analytically and numerically boundaries between transformable regions that is surrounded by a parent non-transformable domain. Our approach allows us to explore the fundamental question of how the transition temperature and microstructure crucially depend on the size of the transformed region.

## Future Work

We will use our theoretical modeling tool to guide our experiments. Three different forms of nanocomposites deposited by either pulsed laser deposition (PLD) or polymer-assisted deposition (PAD) will be investigated. We will also fabricate proof-of-principle dual-tuning microwave devices by utilizing the multifunctional properties of materials.

- Investigation of the strain effect on the properties of ferroics using the phase-field method: The phase-field method, which describes the microstructure using a set of conserved and non-conserved field variables that are continuous across interfacial regions, has recently emerged as a powerful computational approach to modeling and predicting mesoscale (in the range of nanometers to microns) morphological and microstructural evolutions in materials. We will use this approach to simulate the effect of the lattice strain on the properties of nanocomposite ferroics films.

- Growth and characterization of epitaxial nanocomposites: We will investigate three particular epitaxial ferroic nanocomposite architectures: the vertically aligned nanocomposite, the layered laminar-like nanocomposite, and the particulate nanocomposite. We will use pulsed laser deposition to grow the first two architectures whereas polymer-assisted deposition will be used to construct the particulate nanocomposite.

- Fabrication of proof-of-principle dual-tuning microwave devices: A microwave device can be tuned by changing the microwave propagation factor through physical, electrical, or magnetic means. We will design and fabricate proof-of-principle dual-tuning microwave devices to evaluate the desired functionality of nanocomposites.

## Conclusion

We systematically investigated novel strain-induced physical phenomena in ferroic nanocomposite films. Instead of fitting experimental data using a given physical model to explain the experimental results, we used our theoretical modeling tool to guide our experiments. We explored the interplay of elastic interactions on functionality such as electronic, magnetic and polarization. Experimentally, we studied the effect of chemical composition and processing parameters on the structural and physical properties of epitaxial two-phase vertically aligned nanocomposite (VAN) $(BiFeO_3)_x$:$(Sm_2O_3)_{1-x}$ thin films.

## Publications


Beaud, P., S. L. Johnson, E. Vorobeva, U. Staub, C. J. Milne, Q. X. Jia, and G. Ingold. An Ultrafast Structural Phase Transition Driven by Photo-Induced Melting of Charge and Orbital Order. 2009. *Phys. Rev. Lett..* **103**: 155702.

Bi, Z., J. W. Lee, H. Wang, H. Yang, Q. X. Jia, and J. L. MacManus-Driscoll. Tunable Lattice Strain in Vertically Aligned Nanocomposite (BiFeO3)x(Sm2O3)1-x Thin Films.

To appear in *J. Appl. Phys..*

Choudhury, S., J. X. Zhang, Y. L. Li, L. Q. Chen, Q. X. Jia, and S. V. Kalinin. Effect of Ferroelastic Twin Walls on Local Polarization Switching: Phase-Field Modeling. 2008. *Appl. Phys. Lett..* **93**: 162901.

Choudhury, S., Y. L. Li, L. Q. Chen, and Q. X. Jia. Strain Effect on Coercive Field of Epitaxial Barium Titanate Thin Films. 2008. *Appl. Phys. Lett.* **92**: 142907.

Fouchet, A., H. Wang, H. Yang, J. Yoon, Q. X. Jia, and J. L. MacManus-Driscoll. Spontaneous Ordering, Strain Control and Multifunctionality in Vertical Nanocomposite Heteroepitaxial Films. 2009. *IEEE Trans. Ultrasonics, Ferroelectrics, and Frequency Control .* **56**: 1534.

Li, Y. L., S. Y. Hu, S. Choudhury, M. I. Baskes, A. Saxena, T. Lookman, Q. X. Jia, D. G. Schlom, and L. Q. Chen. Influence of Interfacial Dislocations on Hysteresis Loops of Ferroelectric Films. 2008. *J. Appl. Phys..* **104**: 104110.

MacManus-Driscoll, J. L., P. Zerrer, H. Wang, H. Yang, J. Yoon, S. R. Foltyn, M. G. Blamire, and Q. X. Jia. Spontaneous Ordering, Strain Control and Manipulation in Vertical Nanocomposite Heteroepitaxial Films. 2008. *Nat. Mater .* **7**: 314.

Sheng, G., J. X. Zhang, Y. L. Li, S. Choudhury, Q. X. Jia, Z. K. Liu, and L. Q. Chen. Domain Stability of PbTiO3 Thin Films Under Anisotropic Misfit Strains: Phase-Field Simulations. 2008. *J. Appl. Phys.* **104**: 054105.

Sheng, G., J. X. Zhang, Y. L. Li, S. Choudhury, Q. X. Jia, Z. K. Liu, and L. Q. Chen. Misfit Strain – Misfit Strain Diagram of Epitaxial BaTiO3 Thin Films: Thermodynamic Calculations and Phase-Field Simulations. 2008. *Appl. Phys. Lett..* **93**: 232904.

Soukiassian, A., W. Tian, V. Vaithyanathan, J. H. Haeni, L. Q. Chen, X. X. Xi, D. G. Schlom, D. A. Tenne, H. P. Sun, X. Q. Pan, K. J. Choi, C. B. Eom, Y. L. Li, Q. X. Jia, C. Constantin, R. M. Feenstra, M. Bernhagen, P. Reiche, and R. Uecker. Growth of Nanoscale BaTiO3/SrTiO3 Superlattices by Molecular-Beam Epitaxy. 2008. *J. Mater. Res.* **23**: 1417.

Yang, H., H. M. Luo, H. Wang, I. O. Usov, N. A. Suvorova, M. Jain, D. M. Feldmann, P. C. Dowden, R. F. DePaula, and Q. X. Jia. Rectifying Current-Voltage Characteristics of BiFeO3/Nb-doped SrTiO3 Heterojunction. 2008. *Appl. Phys. Lett.* **92**: 102113.

Yang, H., H. Wang, G. F. Zou, M. Jain, N. A. Suvorova, D. M. Feldmann, P. C. Dowden, R. F. DePaula, J. L. MacManus-Driscoll, A. J. Taylor, and Q. X. Jia. Leakage Mechanisms of Self-assembled (BiFeO3)0.5:(Sm2O3)0.5 nanocomposite Films. 2008. *Appl. Phys. Lett.* **93**: 142904.

Yang, H., H. Wang, J. Yoon, Y. Q. Wang, M. Jain, D. M. Feldmann, P. C. Dowden, J. L. MacManus-Driscoll, and Q. X. Jia. Vertical Interface Effect on the Physical Properties of Self-assembled Nanocomposite Epitaxial Films. 2009. *Adv. Mater..* **21**: 3794.

Zhang, J. X., Y. L. Li, S. Choudhury, L. Q. Chen, Y. H. Chu, F. Zavaliche, M. P. Cruz, R. Ramesh, and Q. X. Jia. Computer Simulation of Ferroelectric Domain Structures in epitaxial BiFeO3 thin films. 2008. *J. Appl . Phys.* **103**: 094111.

# Genetically Engineered Polymer Libraries

*Jennifer Martinez*
20080395ER

*This report contains proprietary information and cannot be released at this time. For more information about this project, contact the Los Alamos LDRD Program Office at ldrd@lanl.gov.*

# Probing Unconventional Superconductivity in Heavy Fermion Thin Films

*Vladimir Matias*
20080519ER

## Introduction

Superconductivity occurs when a material loses all resistance to electric current below a certain transition temperature. There are many classes of superconductors among which are the high temperature superconductors that contain copper oxide with a superconducting transition temperature around 100 K (or about -300°F). Superconducting materials could dramatically increase efficiency of electrical energy distribution and revolutionize electricity use. We are exploring the physical nature of superconductivity in a class of compounds known as 'heavy fermion' or heavy-electron materials. These materials contain rare earth or actinide elements, such as cerium, and exhibit unusual superconductivity whose mechanism is still under scientific debate. Although the heavy fermion superconductors have low transition temperatures their mechanism is believed to be related to the high temperature superconductors. LANL discovered a plutonium-containing compound in this class of superconductors with a critical temperature of 18 K and the search is still on for even higher transition temperatures [1]. Our project aims to make thin layers of these superconductors for scientific study of their unusual superconductivity. The project combines LANL's advanced thin film technology currently used for high temperature superconductors with the LANL-established expertise in 'heavy fermion' materials to access new physical measurements and shed new light on unconventional superconductivity. We study thin films of the 'heavy-fermion' compound CeCoIn5. We intend to use the thin films for model studies of electrical transport across grains within the material. A particular result of this work will be to test the symmetry of superconductivity in these materials, which is presumed to be not spherically symmetric. Furthermore, thin films offer the unique possibility to control the dimensionality of the samples, which will lead to further insight into the spatially inhomogeneous superconducting phases that have been discovered for larger samples of this material [2]. Insights from this work should lead researchers to better understand the limits of superconductivity and how to increase the superconducting transition temperature.

## Benefit to National Security Missions

This project will support the DOE mission in Office of Science by enhancing our understanding of unconventional superconductivity and through the search for new superconducting materials. Superconductivity is potentially a key technology for national energy security.

## Progress

For the deposition of heavy-fermion thin films we are attempting two approaches. One approach is pulsed laser deposition (PLD) from a number of different targets and the second is by co-evaporation of individual elements. We modified our vacuum chambers to the needs for growing these heavy fermion intermetallic films. Figure 1 shows the schematic of our PLD approach. We use a novel target method, for which we submitted a patent disclosure. The target consists of concentric-ring elemental sections. This target, illustrated in Figure 1a, allows one to adjust the composition continuously by moving the laser across the different rings. Using this method we can do experiments with a varying composition range at an atomic mixing level. We are also using a linear combinatorial approach to sample synthesis to increase our sample fabrication throughput [3]. Substrates for deposition are placed on a linear 'conveyor belt' of samples, as is illustrated in Figure 1b. In this manner many samples can be prepared in one pump-down of the vacuum chamber. We are making use of the user facility at the Center for Integrated Nanotechnologies (CINT) at LANL to help us with characterization of our films. The phase formation in the films is analyzed by x-ray diffraction, the stoichiometry by inductively coupled plasma spectroscopy and energy dispersive x-ray spectroscopy (EDX), for spatially resolved analysis. The electrical properties of selected samples were measured in a four point measurement

geometry in a Quantum Design PPMS $He_3$ low temperature measurement system.

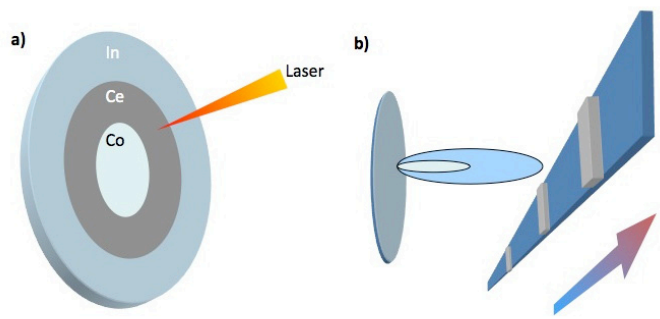


*Figure 1. Schematic of the pulsed laser deposition method from a concentric-ring target, shown on the left, (a), and the conveyor belt sample transport using metal tape as a carrier of single crystals, shown on the right, (b).*

With the PLD approach we have succeeded in making films of $CeIn_3$ and $CeCoIn_5$. The crystallites of $CeCoIn_5$ in the film are epitaxial with the substrate, but the sample is not phase homogeneous. Electrical transport has been measured to low temperatures and we observe a superconducting transition temperature of 1.95 K [4]. Figure 2 shows the dependence of the transition temperature on the magnetic field. The transition temperature of the film is slightly depressed compared to that of bulk crystals whose transition temperature is 2.3 K. We are trying to ascertain whether this is an intrinsic low-dimensional effect or due to some weaker superconducting regions in the film sample.

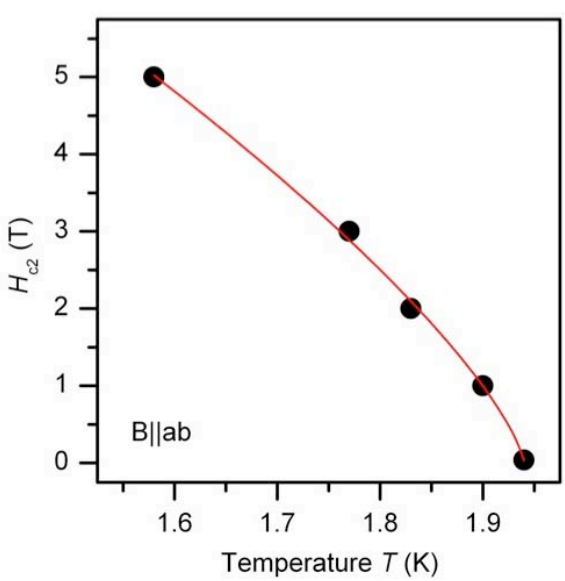


*Figure 2. Temperature dependence of the upper critical field of the $CeCoIn_5$ phase from the PLD film.*

Our best samples to date by PLD were made with In-rich targets and at temperatures of 400 – 500°C. The main obstacle to obtaining single phase film growth appears to be that indium does not wet the insulating substrates and tends to form islands, which are In-rich. SEM images together with EDX analysis show the formation of these large In-rich particles. The main substrates that we use are MgO and $MgF_2$; the latter one itself has an excellent lattice match to $CeCoIn_5$. To improve the wetting we are attempting to deposit buffer layers before deposition of Ce-In compounds. Thus far we were able to get excellent epitaxial films of chromium and tungsten on MgO, however indium wetting appears still to be an issue. In depositing films by co-evaporation we are focusing more on utilizing *in situ* reflection high-energy electron diffraction (RHEED) to observe epitaxy and atomic layer smoothness in real time. We are also utilizing time-of-flight ion scattering spectroscopy for *in situ* analysis of our thin film samples. We believe that the *in situ* monitoring approach is necessary in the end to successfully make these films with atomic-level control. We found that the growth conditions for epitaxy by co-evaporation seem to require low indium content and low deposition temperatures. This is in contrast to our best PLD films that were made at somewhat higher temperatures with higher indium content. However, this is in agreement with recent results by a Japanese group that reported first films of $CeCoIn_5$, although not yet epitaxial films [5].

We used the experience that we gained in this project to put together a mid-scale instrumentation proposal to the DOE BES office for an MBE (molecular beam epitaxy) System that would be dedicated to synthesis of intermetallic thin films. Although our present deposition systems can be used for synthesis of these intermetallics, the vacuum level in our current chambers is still not high enough as is needed for this work. Furthermore, the current systems are used for a number of different projects, which makes it difficult to conduct this research on a continuous basis.

## Future Work

The objective of the proposed work is to gain a more thorough understanding of the unconventional superconductivity in heavy fermion superconductors. We propose to do this by studying state-of-the-art epitaxial thin films. Specific goals of this research will be to produce epitaxial films, optimize and understand their growth, and understand the differences and commonalities with single crystals. The films will then be used to understand transport across model grain boundaries and to test the order parameter symmetry.

**Sample Fabrication**
We will continue to grow the heavy fermion thin films by pulsed laser deposition and co-evaporation. We will be exploring the growth condition parameter space by studying growth of the parent compound CeIn3. Various epitaxial buffer layers, such as chromium and tungsten, are explored for the best film growth. The goal is to make high-quality epitaxial films of the superconductor $CeCoIn_5$.

**Structural and transport measurements**
In parallel with the sample fabrication, we will continuously characterize the samples with respect to their structural and superconducting properties. High-quality samples will be selected for further transport studies including transport and susceptibility measurements in a dilution refrigerator down to 20 mK and in a field up to 14 T. We will also work on the theoretical understanding of the electrical transport in these materials.

## Conclusion
We are studying the fabrication of a class of superconductors represented by the compound CeCoIn5 in the form of thin films. By studying film growth we hope to gain insights into how to tailor the materials synthesis for new superconductors. We also intend to use the thin films for model studies of electrical transport. A result of that will be to test the symmetry of superconductivity in these materials, which are presumed not to be spherically symmetric. This has important implications for determining the physical mechanism that is responsible for superconductivity and how to raise the superconducting transition temperature.

## References

1. Sarrao, J. L., L. A. Morales, J. D. Thompson, B. L. Scott, G. R. Stewart, F. Wastin, J. Rebizant, P. Boulet, E. Colineau, and G. H. Lander. Plutonium-based superconductivity with a transition temperature above 18 K. 2002. *Nature.* **420**: 297.

2. Bianchi, A., R. Movshovich, C. Capan, P. G. Pagliuso, and J. L. Sarrao. Possible Fulde-Ferrell-Larkin-Ochinnikov Superconducting State in CeCoIn5. 2003. *Physical Review Letters.* **91** (18): 187004.

3. Matias, V., and B. J. Gibbons. Linear combinatorial approach to thin film research. 2007. *Review of Scientific Instruments.* **78** (7): 072206.

4. Haenisch, J., F. Ronning, R. Movshovich, and V. Matias. Pulsed laser deposition of CeCoIn5 thin films. To appear in *Physica C.*

5. Izaki, M., H. Shishido, T. Kato, T. Shibauchi, Y. Matsuda, and T. Terashima. Superconducting thin films of heavy-fermion compound CeCoIn5 prepared by molecular beam epitaxy. 2007. *Applied Physics Letters.* **91**: 122507.


## Publications

Haenisch, J., F. Ronning, R. Movshovich, and V. Matias. Pulsed laser deposition of CeCoIn5 thin films. To appear in *Physica C.*

# Photocatalytic Materials Based on Quantum Confined Semiconductor Nanocrystals

*Milan Sykora*
20080523ER

## Introduction

The objective of the research is to develop a new class of nanoscale photocatalytic materials, which upon solar irradiation can produce molecular hydrogen via photochemical decomposition of organic substrates or water (Figure 1). The approach is based on exploiting unique properties of semiconductor nanocrystaline quantum dots (NQDs) in assemblies where they are coupled to established molecular catalysts. In the photocatalytic assembly NQD functions as a light harvester and a charge generator, which activates a molecular catalyst via charge transfer (CT). The assemblies take advantage of unique properties of NQDs, such as high light harvesting efficiency, size-tunable absorption spectra and the ability to convert photon energy to charge with higher than 100% efficiency via the process of carrier multiplication (CM). While the construction of an NQD-based device for solar hydrogen production is beyond the scope of the project the goal of the research is to address fundamental problems that are necessary first steps towards its development. Specifically: (1) Development of new nanoscale fabrication methods for chemical coupling of NQDs to molecular catalysts and nanocrystaline metal oxides and new approaches to characterization of these structures. (2) Identification of factors that dictate the efficiency of heretofore virtually unstudied interfacial charge transfer at NQD-semiconductor and NQD-molecule interfaces. (3) Fabrication of a photocatalytic assembly with the ability to efficiently harvest the solar radiation, convert it into charge show catalytic activity towards organic substrates or water. This assembly is a key component of the photoanode of the potential device. In addition to the obvious potential practical benefit, the pursuit of the above objectives is expected to provide important insights into some of the most intensely studied problems in chemistry.

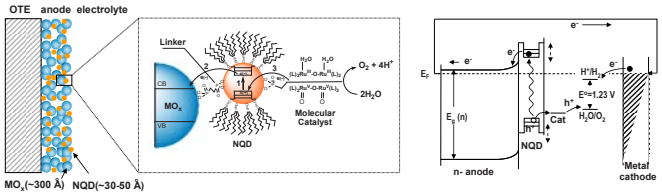


*Figure 1. Left: Schematic diagram of the nanoscale photocatalytic assembly based on coupling of semiconductor NQDs and molecular catalysts. Irradiation of the NQD with visible light leads to generation of one or more electron-hole pairs (1), followed by rapid photoinjection of an electron into the conduction band (CB) of the metal oxide (MOx) (2). This electron is relayed through the external circuit to a metal counter electrode, where it reduces protons to molecular hydrogen. The hole in the valence band (VB) of the NQD is quenched by electron transfer from a molecular catalyst (3). When oxidized (activated) to its active form the molecular catalyst can oxidize the substrate (i.e., organic material or water) generating protons as a byproduct. Although multiple cycles are typically required to oxidize the catalyst to its active form, the number of photons required can be reduced through CM, thus increasing the overall efficiency of the energy conversion process. Right: Energy diagram of the photoelectrolytic cell in which the composite material could be used as a photoanode (Cat is the molecular catalyst). Hydrogen production occurs at a metal (e.g., Pt) cathode. Development of the actual device is not the objective of the current project.*

## Benefit to National Security Missions

This project will support the drive toward national energy security, a key DOE mission. In particular, the work will enhance our understanding of how nanoscale materials can be utilized to improve the efficiencies of the solar energy conversion technologies.

## Progress

During the second year of the project we have made progress in following areas.

### Synthesis of materials

Synthesis of materials for the photocatalytic assemblies remained an important component of our effort. In the

second year our focus was on optimization of synthesis of the CdSe and CdS NQDs, which showed to be the most promising sensitizers for the activation of Ru-based molecular catalysts. We have also improved the synthetic procedure for preparation of $TiO_2$ to yield more monodisperse nanocrystals with significantly improved optical properties. A significant portion of our synthetic effort was dedicated to the synthesis of new molecular catalysts. Following recent report by T. J. Meyer and co-workers that mononuclear Ru-polypyridine complexes can effectively oxidize water we have synthesized following series of Ru-polypyridine water oxidation catalysts: $[Ru(tpy)(bpm)(OH_2)](OTf)_2$, $[Ru(tpy)(bpz)(OH_2)](ClO_4)_2$, $[Ru(tpy)((PO_3H_2)_2(bpy)(OH_2)](ClO_4)_2$, $[Ru(tpy)(bpm)(OH_2)](PF_6)_2$. These new water oxidation molecular catalysts will be tested as components of the photocatalytic assemblies.

**Development of fabrication methods for construction of nanoassemblies**

*Fabrication of NQD/catalyst assemblies*

We have made important progress in our understanding of the mechanism of the NQD/catalyst chemical coupling (see summary shown in Figure 2). Using steady-state and time-resolved photoluminescence spectroscopies we have determined that the coupling of the catalyst to the NQD surface is associated with a rapid (few seconds) deprotonation of the anchoring carboxylic acid functionality to carboxylate. Using a novel experimental method based on Attenuated Total Reflectance Fourier Transform Infrared (ATR-FTIR ) Spectroscopy we were able to monitor in real time the substitution of the protective organic layer on the surface of NQDs with a catalyst and study the mode of catalyst-NQD attachment. To be able to better interpret our experimental results we have initiated collaboration with a theory group of Dr. Sergei Tretiak at the Center for Integrated Nanotechnology (CINT) at LANL. By modeling the process of catalyst-NQD assembly formation using Density Functional Theory we have shown that the binding energy of the carboxylate functionality exceeds that of the carboxylic acid by ~1eV, which explains the experimentally observed deprotonation associated with the catalyst-NQD coupling. Theory also suggests that the binding mode of the carboxylate group is bidentate with the catalyst bound exclusively to the metal sites of the NQD and that binding of the catalyst leads to a significant increase in the electron density in the NQD at the catalyst binding site. These results provided important insights necessary for us to understand not only how the catalysts bind to the NQDs, but also how the redistribution of electron densities associated with the coupling may affect the efficiency of the photoinduced charge transfer in the resulting assemblies.

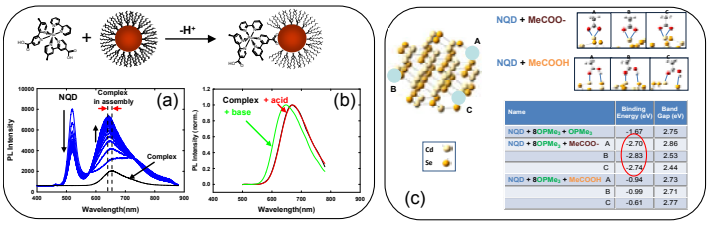


| Name | | Binding Energy (eV) | Band Gap (eV) |
|---|---|---|---|
| NQD + 8OPMe$_2$ + OPMe$_2$ | | -1.67 | 2.75 |
| NQD + 8OPMe$_2$ + MeCOO- | A | -2.70 | 2.86 |
| | B | -2.83 | 2.53 |
| | C | -2.74 | 2.44 |
| NQD + 8OPMe$_2$ + MeCOOH | A | -0.54 | 2.73 |
| | B | -0.99 | 2.71 |
| | C | -0.61 | 2.77 |

*Figure 2. Experimental and theoretical studies of coupling of Ru catalysts to NQDs. (a) Evolution of the PL spectra of the NQD/catalyst mixture following the addition of a catalyst over period of 10 seconds. The red arrows indicate magnitude of the blue shift in the PL band of the catalyst induced by the coupling to the NQD. (b) Similar shift in PL is observed in an independent experiment where catalyst is deprotonated by addition of a strong base, such as NaOH. (c) The theoretical studies show that there three nonequivalent sites on the surface of the NQD, which can serve as binding sites for the catalyst. As indicated by more negative binding energies the binding of the catalyst to all three sites is more favorable if the anchoring group of the catalyst is deprotonated. The most thermodynamically favorable mode of binding is bidentate structure where both oxygen atoms of the anchoring group are bound to a single cadmium atom of an NQD.*

*Fabrication of NQD/MOx assemblies*

We made important improvements in the process for fabrication of $TiO_2$ mesoporous films by switching from "doctor-blading" to screen-printing approach. The physical and optical properties (e.g., thickness, porosity, optical transparency) of films prepared by the later method are much more reproducible. This new approach allowed us to optimize the method for infiltration of the $TiO_2$ films with NQDs. Using Light Harvesting Efficiency (LHE) of the composite films as a figure of merit we found that the reduction in the thickness of the organic passivating layer on NQD surfaces leads to significant improvement in the ability of the composites to absorb visible light. We have also found that upon air exposure the NQDs infiltrated in the $TiO_2$ films undergo rapid photo-induced oxidation when irradiated with simulated solar light. While under aerobic conditions the oxidation leads to gradual decomposition of the NQDs, the NQDs are stable under argon or nitrogen atmospheres. Following this observation we have developed new procedures for fabrication of the composites under fully anaerobic conditions.

**Studies of interfacial processes in NQD/catalyst assemblies**

*Energy and charge transfer at the NQD/catalyst interface*

During the first year of the project we showed using the steady state photoluminescence spectroscopy that the mechanism of interaction (energy transfer (ET) or CT) in the NQD/catalyst assemblies depends on the NQD size. During the second year we focused on studies of the dynamics of the ET and the CT. We found that in assemblies

where ET is the dominant process the ET occurs on time scale ~1 ns. In the assemblies where the dominant process is CT our studies of relaxation dynamics suggests that the CT is much faster, with corresponding time constant <10 ps (Figure 3). An apparent difference in the dynamics of the ultrafast photoluminescence and transient absorption suggests that the charge transferred from the NQD to the complex is a hole rather than an electron. This is an encouraging result as the NQD→complex hole transfer is the process required for conversion of the catalyst to its active form. Ultrafast spectroscopy studies of the catalyst spectral signatures are currently in progress to confirm the CT mechanism.

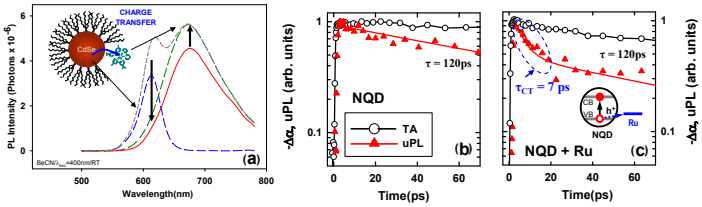


*Figure 3. Results of steady state and time-resolved photoluminescence (PL) and transient-absorption (TA) studies of NQD-catalyst electronic interactions. a) In assemblies consisting of large (>4 nm diameter) NQDs the reduction of PL of the NQD is paralleled by a decrease in the PL of the catalyst, which indicates NQD-to-catalyst charge transfer. The differences in PL and TA relaxation dynamics of the NQDs in the absence (b) and presence (c) suggest that photoexcitation of NQD is followed by a rapid (~ 7ps) transfer of a hole from NQD to the surface adsorbed complex, which is an optimal mechanism of CT for utilization of NQD-catalyst assemblies in practical applications.*

*Photoinduced charge transfer (CT) at the NQD/$TiO_2$ interface*

Improvement in the fabrication methods allowed us to more accurately study the interfacial CT in the NQD/$TiO_2$ assemblies. We have found that, contrary to our preliminary results and reports available in literature, efficient charge transfer across the NQD/$TiO_2$ interface is not contingent upon the use of organic linkers to provide electronic coupling between NQD and $TiO_2$ . Using measurements of External Quantum Efficiency (EQE) of the $TiO_2$/NQD-based photoelectrochemical devices we found that in the assemblies where the NQDs are adsorbed onto $TiO_2$ surface without the use of a linker, the charge transfer efficiency can exceed 50%. We also found that the thickness of the organic passivating layer significantly impacts the efficiency of CT and that in the best NQD/$TiO_2$ assemblies the efficiency of interfacial CT exceeds 80%.

## Future Work

Based on our progress during the second year, in third year we will focus on following studies:

Fabrication of NQD/catalyst assemblies: Complete the studies of chemical coupling between NQDs and catalysts. Evaluate the feasibility of NQD-catalyst coupling with functional groups other than carboxylic acid (e.g, phosphonic acid, bipyridyl amine) and construct assemblies with the series of oxidation catalyst synthesized in year two.

Interfacial CT: Complete studies of single exciton studies of CT at the NQD/catalyst interface to determine the CT mechanism. Extend studies of interfacial CT at NQD/catalyst and NQD/$MO_x$ to multiexciton regime. The objective is to determine the potential of utilizing the CM effect in the assemblies.

Building on our nanoscale fabrication know-how developed in first two years of the project we will attempt to construct $MO_x$/NQD/catalyst assemblies where all the components of the assembly are electronically coupled. We will study the photoinduced CT in these assemblies with the goal to demonstrate efficient charge separation between the $TiO_2$ and the catalyst mediated by the NQD. We will then investigate the photocatalytic activity of these assemblies with respect to organic substrates and/or water.

Conclusion

In terms of basic science the main objective of the proposed research is improvement of our understanding of how nanoscale materials can be utilized to enhance the efficiencies of the solar energy conversion technologies. The practical objective is a development of a new class of nanoscale materials with potential to produce molecular hydrogen from organic substrates or water upon solar irradiation. These objectives are aligned with DOE's energy security mission as they have potential to reduce our energy dependence on oil and other fossil fuels.

# Molecular Scale Shock Response of Explosives

*Shawn D. Mcgrane*
20090186ER

## Introduction

The initial events that occur upon shock loading explosives are crucial in determining the sensitivity of the material. Various theories have been proposed regarding the reaction mechanisms, but there are few experiments to test them. This project develops experiments sensitive to the time and length scales needed to observe chemical kinetics in shocked explosives.

Our measurement look into a shocked explosive at time scales of a millionth of a millionth of a second and length scales 100 times smaller than a human hair. By making direct measurements of the energy flow at the molecular level, mechanistic insights can be obtained that will impact modeling and optimization of explosive safety and performance.

The state of the art experimental developments required have many other scientific applications. These techniques are expected to impact fields such as energy sciences (photovoltaics) and matter under extreme conditions (such as material testing of power plant alloys).

## Benefit to National Security Missions

This project supports the Department of Energy (DOE) mission in Nuclear Weapons by enhancing our knowledge of explosive issues important to the aging stockpile. This project supports  Department of Defense (DoD) missions that require better predictions and optimization of explosive behavior. DOE Office of Science missions are supported through development of new ultrafast laser methods.

## Progress

### Overview

We have developed new experimental measurement tools and coupled them to existing shock experiments. This involved significant time building, testing and optimizing experimental designs. Transient absorption experiments are producing useful data on shocked explosive crystals. We have begun testing transient measurements of temperature and chemistry.

We have performed transient absorption measurements in shocked explosive crystals and thin films. We observe the effects of the shock wave, and under some conditions evidence of ionic or electronic excitations that are predicted by some models. Figure 1 shows an explosive crystal that exhibits increased absorption under shock loading. These results are beginning to test the assumptions underlying common modeling approaches. However, we need to continue experiments under stronger shock loading, where the reaction mechanism may change.

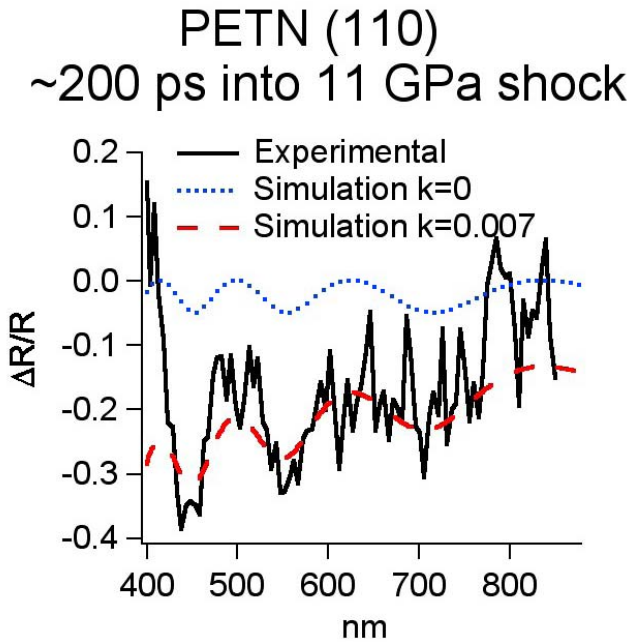


*Figure 1. A crystalline explosive, PETN, shock loaded for 200 ps shows increased absorption (k>0) indicating reaction.*

Several new methods of measuring temperature and chemistry are being developed that work on timescales of a millionth of a millionth of a second. This is required to observe energy flow in a shocked explosive, on the molecular time scale. These methods are entirely new, and we are working out many of the details necessary for their use in single shot dynamic experiments.

**Presentations and publications**
This work has been presented at the American Physical Society Shock Compression of Condensed Matter conference (June 2009) and as part of a Defense Threat Reduction Agency (DTRA) Basic Science Program Review (Oct. 2009).

A conference proceedings paper has been accepted and an Optics Letter is in preparation.

**Collaborations**
This ER project has led to a new collaboration with the French atomic energy agency, Drs. Viviane Bouyer and Phillipe Herbert.

**Student support**
An undergraduate summer student worked on programming and data analysis in support of this project.

**Follow on funding**
DTRA is funding a project to apply the experimental methods developed in this project to the study of a DoD explosive, funded at $150K/yr for three years.

**Outlook**
These experiments are very high risk (many aspects have never been attempted before), but offer the ability to directly measure several previously inaccessible quantities. These measurements are necessary for explosive modeling of interest to DOE, DoD, the Department of Homeland Security (DHS) and other government agency customers. We are actively achieving the objectives and have contingency plans for successful development of the highest risk aspects of the project.

## Future Work
The goals of this project are to experimentally address fundamental underpinnings of explosive initiation and detonation physics. Achieving these goals involves advancement of experimental measurement and analysis beyond the current state of the art. These advances are expected to have broad scientific applicability- the development of which is a corollary goal of the project.

## Conclusion
Explosives are composed of molecular crystals that undergo extremely fast reaction once stimulated by shock or heat. Understanding how explosives react to stimuli that may set off their destructive power is crucial for modeling explosive safety and performance.

The data provided in this project seeks to experimentally measure molecular scale mechanisms of reactivity in shocked explosives. These data are necessary to answer even qualitative questions regarding explosive initiation. These questions must be answered to identify the correct theoretical framework to understand, predict, and simulate explosive initiation.

## Publications
McGrane, S. D., D. S. Moore, V. H. Whitley, C. A. Bolme, and D. E. Eakins. Molecular shock response of explosives: electronic absorption spectroscopy. To appear in *AIP Proceedings of the Shock Compression of Condensed Matter Conference.* (Nashville, TN USA, June 28-July 3, 2009).

# Multifunctional Materials

*James E. Gubernatis*
20090187ER

## Introduction

An outstanding challenge in materials science is "bridging the gaps." Materials science typically is studied at three different length scales: the macroscopic (what we see unaided), the mesocopic (what we see with conventional microscopy); and the microscopic (what we can see with sophisticated microscopy). Our understanding of materials must be consistent among the scales. Establishing this consistency however has been difficult. For a particular class of materials, the multifunctionals, we are proposing to achieve consistency in a novel way by placing the mesoscale Landau phenomenological theory for the free energy at the center of our analysis. Then we will fix as many of its unspecified parameters as possible by deriving them from microscopic theory and by measuring them experimentally. The question to be answered is: With the phenomenology parameterized better than ever, can we predict the many phase transitions exhibited by multifunctional materials and also predict the evolution of their mesoscale structure? The answer to this question is important for the quest of the predictive design of such devices as switches, sensors, and actuators.

Multifunctional materials are those that have cross-field responses between two (or more) applied fields. For example, in a piezoelectric material, a stress field produces an electric polarization and an electric field produces strain. Normally, strain is the response to a stress field and polarization is the response to an electric field. It is these types of novel responses that makes the multifunctional materials interesting scientifically and important technologically. Currently, a Landau phenomenology has not been developed to study such responses. Our objective in co-generating a Landau theory on the mesoscopic and microscopic scales is assuring the "uploading" of maximal information from the microscopic to the mesoscopic scale. Such information will include these responses.

Experiment will play a special role in our research. We recently developed unique capabilities for measuring an important class of cross-field responses, that is, magneto-electric responses. These measurements will enable benchmarking the theory in a way never before possible.

## Benefit to National Security Missions

This project will support the Department of Energy's Office of Science missions by enhancing our understanding of multifunctional materials and establishing a theoretical paradigm for addressing their properties. In particular, it supports the Basic Energy Science program office mission for fundamental materials science research for energy independence.

## Progress

We began by studying the properties of a family of compounds fabricated with elements from the fourth and sixth columns of the periodic table. These materials are insulators (poor conductors of electricity) in contrast to metals (good conductors). Many in this family show a paraelectric to ferroelectric transition (the electrical analog of a non-magnetic to magnetic transition), which is accompanied by a change in their length and shape. At high temperatures, most exist in the same very simple crystal structure as table salt. On the addition of a very small number of magnetic atoms to their composition, a number of them become magnets. Additionally, the properties of all are very sensitive to the density of electrons participating in their electrical conduction. Thus, this family sports crystallographically simple representations of a system having multiple simultaneous phases, that is, states of matter with specific symmetries and different physical properties. Further, their properties are potentially tunable by modest modifications of their electron densities. These types of materials are the central theme of our research. In particular, we focused on tin-tellurium, a low temperature ferroelectric.

From the viewpoint of individual atoms, the temperature dependent mechanism for the structural transition associated with the length and shape changes is generally viewed as either being a change in the motion of the electrons, the vibration frequency of the atoms in the crystal, or the interaction between these two dynamical effects. We judged that the structural transitions re-

quired at least a combination of the last two mechanisms to capture published measurements. Accordingly, we adopted a microscopic (atomistic) model for these materials proposed by Sakai [1] that does this synthesis. From this model, a Landau phenomenological theory is relatively easy to derive. We did this and got the needed parameters in terms of the parameters in the microscopic model. In the process, we accomplished one objective of our project.

Benchmarking the results of theory required repeating and then extending of several specific measurements of the properties of our focus material. To our surprise, we found that these measurements exhibited not two but three phases with the lowest temperature phase not being ferroelectric (insulating) but metallic. These unexpected findings, challenging sixty years of published literature, forced us to execute a series of other measurements to confirm our results. Completed were an extensive series of angular-resolved photoemission measurements. This technique directly produces the electron energies in a cross-sectional plane of their possible values. A typical measurement is shown in Figure 1 for the highest and lowest temperature phases. First, we see few differences between the two pictures, suggesting that the electronic structure is unmodified by the phase changes. Next, we see in both figures that the pattern is periodic, attesting to good atomic ordering in both phases. Most importantly, we note that the bright lines represent allowable electronic states. This particular figure in fact unambiguously establishes the material as a metal. We are in the process of analyzing it and similar data to understand why it is a metal. We also need to determine the crystal structures of the three phases as their identities affect the details of the modeling. These structural measurements will be performed soon. We believe the reason why our results are so different from those of the past lies in better materials preparation and instrumentation.

Using group theory, the mathematics of symmetries and their relationships, we verified the Landau phenomenology generated microscopically is correct for the crystal structures, the length changes, and the shape changes traditionally asserted. To study phase transitions in materials that couple electrical and magnetic orderings, it is important to incorporate the symmetries of magnetism into group theory by augmenting the crystallographic groups with time-reversal symmetry, which leads to what are called color (or black and white) groups. We enumerated the color groups in quasi-one-dimensional and quasi-two-dimensional cases and studied a representative phase transition. We also suggested possible chemical compositions of quasi-one-dimensional materials with coupled magnetic and electric orders and quasi-two-dimensional materials coupling electric, magnetic, and structural orders. In addition, we enumerated all classes of chemical species consistent with two-dimensional magnetic groups.

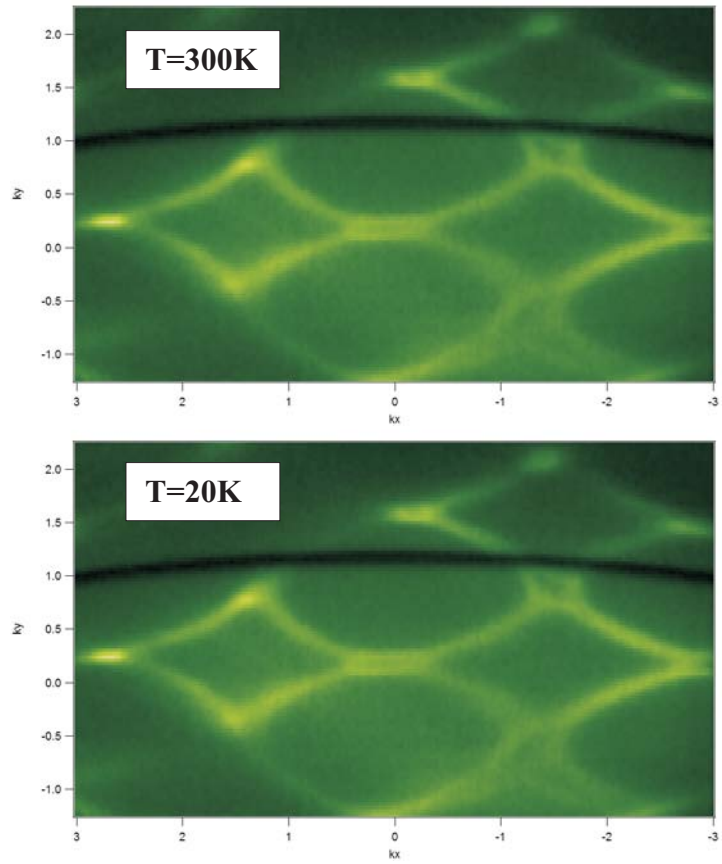


*Figure 1. A two-dimensional representation of the electron energy in tin-tellurium measured by photoemission spectroscopy at two different temperatures. The bright lines indicate the existence of some electron energies. This particular plot is sufficient to establish the material is a metal. By more quantitative analysis of this and similar data, we will understand why it is a metal (The black line was caused by an interruption in the data transfer during the measurement.)*

Overall, the proposal is about investigating symmetry changes in materials possessing two or more simultaneously ordered phases. Of particular interest is the interplay between the parameters describing the phases. To this end, we experimentally studied other materials [2] in addition to the column four-six compounds. Consequently, we prepared and characterized materials with cross-coupled order parameters, for example, coupled magnetic and electrical orders. We successfully measured four cross-coupling constants. Our successful measurements of three of these couplings accomplished one of the major experimental objectives of our proposal.

## Future Work

After reformulating the microscopic model, we are confident that the use of the Landau phenomenology for microstructure growth prediction will permit us "to bridge the micron gap" between microscopic and mesoscopic length scales. To this end we will co-generate a mesoscopic and microscopic-based Landau free energy, fix the phenomenological parameters in the theory, evolve granular, mag-

netic domain, and polar domain structures predicatively, and then compare the results with experiment. Typically, a Landau free energy phenomenology lacks the cross-field responses distinguishing a multifunctional material, for example, missing information reflective of symmetries broken microscopically but not macroscopically.

At the mesoscopic level, our Landau free energy will include multiple multi-component order parameters. Novel will be our introduction of an order parameter for orbital ordering whose symmetry is the same as it is in our microscopic models. Orbital orbiting is the atom-by-atom cooperative arrangement of local spatial patterns of electron densities. We will answer the question, "How much do the predictions of magnetization, polarization, and structural distortion change when their order parameters are constrained by the symmetries of this additional order?" At the microscopic level, we will derive a Landau free energy expansion for the orders present in several multi-orbital many electron models. Macroscopically, we will exploit new unique capabilities that enable the measurement of magneto-electric responses, perhaps the most important of the cross-field responses. This information has been missing for benchmarking microscopic and mesoscopic theories.

## Conclusion

We believe we can successfully produce a Landau free energy phenomenology for the targeted materials. Available experimental data is likely insufficient for fitting the theory over large ranges of parameters. We will thus be less interested in a quantitative agreement with experiment but will be more interested in answering such questions as: Are we capturing the right phase transitions?, Are they located in the right places?, Are our predictions of microstructure, magnetic domains, and electric domains reasonable?, and What does their interplay of these mesoscale structural features suggest about multifunctionality? In short, have we bridged the gaps?

## References


1. Sakai, K.. Vibronic theory of a structural phase transition and a tricritical point in IV-VI compounds. 1986. *Physical Review B* . **34**: 8019.

2. Lashley, J. C., S. M. Shapiro, B. L. Winn, C. P. Opeil, M. E. Manley, A. Alatas, W. Ratcliff, T. Park, R. A. Fisher, B. Mihaila, E. K. H. Salje, and J. L. Smith. Observation of a continuous phase transition in a shape-memory alloy. 2008. *Physical Review Letters* . **101**: 135703.


## Publications


Lashley, J. C., S. M. Shapiro, B. L. Winn, C. P. Opeil, M. E. Manley, A. Alatas, W. Ratcliff, T. Park, R. A. Fisher, B. Mihaila, P. Riseborough, E. K. H. Salje, and J. L. Smith. Observation of a continuous phase transition in a shape-memory alloy. 2008. *Physical Review Letters.* **101**: 135703.

Saxena, A., and G. Aeppli. Phase transitions at the nanoscale in functional materials. 2009. *Los Alamos National Laboratory Technical Report LA-UR-09-05010.*

Yang, X. D., P. S. Riseborough, K. A. Modic, R. A. Fisher, C. P. Opeil, T. R. Finlayson, J. C. Cooley, J. L. Smith, P. A. Goddard, A. V. Silhanek, and J. C. Lashley. Influence of magnetic fields on structural martensitic transitions . 2009. *Philosophical Magazine.* **89**: 2083–2091.

# Photodynamics and Photochemistry of Carbon Nanotube Materials

*Sergei Tretiak*
20090253ER

## Introduction

Carbon nanotubes constitute a class of the most promising technological materials for high-strength materials with desirable - and tunable - electrical properties. Our progress in understanding and manipulating nanotube's fundamental electronic properties, and subsequent practical applications has been slow due to difficulties in synthesizing sample materials. A lack of the experimental knowledge of electronic processes in carbon nanotubes has impeded advances in theory and simulations. We have still not achieved a quantitative understanding and prediction of nanotube materials properties, however, several challenges in nanotube science are expected to be overcome in the near future. Carbon nanotube and graphene based electronics are rapidly becoming today's reality given the huge R&D effort in the industry. This creates a need for modeling and simulation effort to predict physical phenomena and deliver comprehensive theoretical framework of electronic structure and dynamics in carbon nanotubes. Such theory should provide guidance and a platform for future experimental studies, and impact technology. We will conduct systematic theoretical investigation of electronic structure and excited state dynamics in carbon nanotube materials. Our modeling will use LANL-developed quantum chemical tools, which outperform similar techniques world-wide. Time dependent semiempirical and density functional theory will be used as the basic quantitative framework for computing electronic structure and photoexcited trajectories and dynamics. Our research program involving the necessary expertise in quantum chemistry, condensed matter, spectroscopy, synthesis, and optical physics, will provide detailed understanding of fundamental physical processes, which in particular, govern the operation of nanotube-based electronic devices.

We expect to answer many outstanding questions in nanotube science. Namely, an interplay between excitonic and vibrational effects in photochemistry, the role of dark excitons and chemical defects in luminescence, formation of polarons and triplet states, transport, intertube and solvent interactions, nonlinear dynamics and localization effects will be investigated in detail.

## Benefit to National Security Missions

This project will make a significant contribution to our basic understanding of materials, a LANL Grand Challenge. Carbon nanotube technology is widely expected to impact many areas including energy security, threat reduction, ubiquitous sensing, among others. These are major mission areas within DOE, DHS, DOD, and other government agencies.

## Progress

During the first year of the project our effort focused on two areas. First of all, we have used STM setup built at CINT to successfully demonstrate binding geometry of single strand DNA to carbon nanotube. STM images revealed that ssDNA prefers to wrap around CNTs of particular (6,5) chirality with a coiling period of 3.3 nm, which agreed very well with our theoretical predictions [1,2]. This allow us for the further elucidation of self-assembling and structure-property predictions of CNTs functionalized by DNA – a topic of general interest due to the recent focus on bio-applications of such hybrid systems, including drag delivery, cancer diagnostics and therapy. The next step in these studies would involve electronic characterization of DNA-CNT hybrids with various CNT chiralities and DNA sequences. Ultimately, we will try to reveal the dependence of electronic properties of hybrids on their internal structure, which will provide valuable guidance for developing new methods for CNT dispersion and metal-semiconductor CNT separation using ssDNA. Another paper summarizing the theoretical results is currently in being drafted. In another area we have explored theoretically subtleties of electronic states and structure of the lowest excitonic states in carbon nanotubes in the presence of environment, which is essential to tuning photophysical properties and

enhancing behavior for nanotube separations and sensing applications. This work has been done in collaboration with experimental group of Stephen Doorn. Experimental studies have been done in two areas. i) Saturation of Surfactant Structure: We demonstrate that surfactant structure can be modulated at the nanotube surface by varying charge-screening effects through addition of electrolyte, or by adjusting surfactant concentrations. Density-based separations of metallic nanotubes from semiconducting species show that above a certain threshold level of surfactant or electrolyte, metallic densities can no longer be altered, while semiconducting densities can be further lowered. We also note that the ability to use electrolyte additions to increase PL intensities in the semiconducting nanotubes can be tuned by adjusting surfactant concentrations and species. The results suggest that a saturation density of surfactant at the nanotube surface will arise under certain solution conditions. This is significant for its impact it can have on generating nanotubes with stable PL properties and has implications for generating surface structures that are optimal for sensing and separations applications [3]. ii) Raman Spectroscopy of Structurally Pure Nanotube Samples. Probing the G-band (carbon-carbon deformations at frequencies of ~1600 cm-1) behavior of nanotubes with Raman spectroscopy can provide information on electronic structure unavailable with investigation of lower frequency phonons. To do so, however, requires working with samples consisting of a single nanotube structure or chirality. We have performed G-band Raman excitation profiling of a set of 12 different pure chiralities to test several models for the nanotube Raman response. Typical excitation profiles for such a high frequency mode will show two resolved bands for resonances with the excitation and scattered photons of the Raman process. Surprisingly, we find that the scattered resonance is significantly weaker than the excitation resonance. This is a general result for all chiralities and classes of structure. The results may be modeled in a 4-level molecular picture of the scattering process. Future work is aimed at understanding the result in terms of non-Condon behavior of the electronic transitions. Using the time dependent density functional theory (TD-DFT), we were able to analyze the energy splitting, relative ordering, electron-hole binding, and localization properties of the optically active and forbidden excitations in nanotubes. This detailed analysis provides an explanation for the low luminescence efficiency of these materials. Our research has been finalized in the perspective feature article [4] and has been selected to represent the issue of this journal by highlighting graphical summary of our paper on the journal's cover (Figure 1). Finally we investigated theoretically the electronic couplings and interactions in the carbon nanotube ensembles to understand properties of bulk materials [5]. In general, our research establishes a systematic and insightful understanding of photoinduced electronic dynamics in nanotube based materials, which will guide the design of new experimental probes, and potentially lead to new nanotechnological applications.

*Figure 1. Light excites multiple excitonic states of carbon nanotubes.*

## Future Work

Our team has pioneered applications of methodologies we previously developed for molecular materials to carbon nanotubes. We applied our experience and theoretical methodologies well characterizing molecular systems such as conjugated polymers, to nanotubes. This resulted in a number of studies addressing virtually every aspect of photophysics of an isolated tube from the very different perspective with respect to what has been published before. In this proposal we consider real nanotube materials. We apply 'molecular-type' approach, which assumes analysis of finite-size systems. This method is ideally suited to study inhomogeneous structures (from amorphous materials to perfect periodic systems), various disorders, local defects, chemical functionalizations, intertube interactions, etc. Molecular modeling software we are using and developing, can routinely compute excited state structure and follow the ultrafast dynamics on femto- to picosecond timescales in large molecular systems of thousands of atoms in size (tens of nm length-scale).

Using our theoretical modeling, we intend to reach detailed understanding of electro- and photo-dynamics in carbon nanotubes and related hybrid materials, which govern the operation of molecular electronic devices. This includes charge transport and energy transfer in the presence of defects, functional groups, and intertube interactions. For example, the interplay between ballistic,

polaronic, and incoherent hopping charge transfer regimes is critical for transistor electronics based on nanotubes. We further pose a question: how could we engineer nanotube materials to gain specific functionalities (i.e. materials by design)? For example, nanotubes are weakly luminescent materials, by knowing all the 'bells and whistles' of their electronic structure, can we suggest specific chemical functionalizations to enhance dramatically their luminescent efficiency? Our theoretical results will be immediately tested and verified by experiment (synthesis, spectroscopy and STM) at LANL. The experimental component of the project is greatly enhanced by our well established experimental collaborations world-wide.

## Conclusion

Our proposal will achieve a quantitative description and a fundamental understanding of electronic processes in nanotube materials, provide novel material design strategies, and suggest practical nanotube applications.
We expect to develop synthetically viable strategies in order to improve dramatically photoluminescence and electroluminescence of carbon nanotubes. Development of novel hybrid materials such as nanotubes wrapped with polymers/DNA and tubes with intercalated dyes opens new and exciting functionalities.
The results will be immediately implemented synthetically and experimentally tested using spectroscopic and STM facilities at LANL. This will provide guidance to world-wide efforts in development of new functional nanotube-based electronic materials and devices.

## References


1. Yarotski, D., A. Balatsky, S. Kilina, A. Talin, J. X. Zhu, S. Tretiak, and A. Taylor. Scanning Tunneling Microscopy of DNA-Carbon Nanotube Hybrids. 2009. *Nano Letters .* **9**: 12.

2. Structure of DNA-wrapped carbon nanotubes revealed. 2009. *PADSTE HIGHLIGHTS .*

3. Niyogi, S., C. G. Densmore, and S. K. Doorn . Electrolyte Tuning of Surfactant Interfacial Behavior for Enhanced Density-Based Separations of Single-Walled Carbon Nanotubes. 2009. *Journal of the American Chemical Society.* **131**: 1144.

4. Kilina, S., E. Badaeva, A. Piryatinski, S. Tretiak, A. Saxena, and A. Bishop. Bright and Dark Excitons in Semiconductor Carbon Nanotubes. 2009. *Physical Chemistry Chemical Physics.* **11**: 4113.

5. Wong, C. Y., C. Curutchet, S. Tretiak, and G. D. Scholes. Ideal dipole approximation fails to predict electronic coupling between semiconducting single wall carbon nanotubes. 2009. *Journal of Chemical Physics.* **130**: 081104.


## Publications


Structure of DNA-wrapped carbon nanotubes revealed. 2009. *PADSTE HIGHLIGHTS .*

Kilina, S., E. Badaeva, A. Piryatinski, S. Tretiak, A. Saxena, and A. Bishop. Bright and Dark Excitons in Semiconductor Carbon Nanotubes. 2009. *Physical Chemistry Chemical Physics.* **11**: 4113.

Niyogi, S., C. G. Densmore, and S. K. Doorn . Electrolyte Tuning of Surfactant Interfacial Behavior for Enhanced Density-Based Separations of Single-Walled Carbon Nanotubes. 2009. *Journal of the American Chemical Society.* **131**: 1144.

Wong, C. Y., C. Curutchet, S. Tretiak, and G. D. Scholes. Ideal dipole approximation fails to predict electronic coupling between semiconducting single wall carbon nanotubes. 2009. *Journal of Chemical Physics.* **130**: 081104.

Yarotski, D., A. Balatsky, S. Kilina, A. Talin, J. X. Zhu, S. Tretiak, and A. Taylor. Scanning Tunneling Microscopy of DNA-Carbon Nanotube Hybrids. 2009. *Nano Letters .* **9**: 12.

# Compositionally Graded InGaN-based High Efficiency Photovoltaic Devices

*Mark A. Hoffbauer*
20090260ER

## Introduction

PV technology will significantly impact our nation's energy portfolio only when the costs are significantly reduced. Three materials systems are being aggressively explored for use in single p-n junction PV devices: Si, CdTe, and CIGS (Cu-In-Ga-Se). PV devices are made from either expensive single crystalline Si (efficiency ~24.7%) or from relatively inexpensive polycrystalline Si, CdTe, or CIGS based devices (all presently limited to about 10% efficiency). Clearly, breakthroughs in the cost and efficiency of PVs are needed for widespread deployment.

This project seeks to create efficient, inexpensive, single-junction photovoltaic (PV) devices based on compositionally graded InGaN thin film materials offering unprecedented overall efficiencies approaching 30% for solar energy conversion. The InGaN materials are grown using a new technology for creating compositionally graded materials for PV devices combining the advantages of high-efficiency single crystalline Si-based PV devices with the low cost and simplicity of thin film-based PV devices. These devices will combine the advantages of the high efficiency of single crystalline Si PV devices with the low cost and simplicity of CdTe and CIGS based devices. Our device architectures are based on p-i-n semiconductor structures functioning like a single junction PV device but made from compositionally-graded, device-quality InGaN films using a unique LANL technology called ENABLE. This project's success will have important consequences for our Nation's energy security.

In nearly all conventional PV devices, the material's bandgap is fixed at a single value (e.g. Si = 1.1eV), limiting device efficiency because of two basic issues. Photon energies below a material's band gap are not absorbed, and the extra photon energy above of the band gap is generally converted into heat without producing charge carriers (electricity). The ideal PV device would encompass two demonstrated methods for improving efficiency. Fabrication from a single material system having tunable (multiple) band gaps tailored to match the full solar spectrum, and the use of PV films with high mobility charge carriers. Because the bandgap of InGaN system can be tuned from the infrared to the ultraviolet by varying the In and Ga concentrations (0.7eV for InN to 3.4eV for GaN), the PV materials and device architectures can be optimized to maximize efficiency. For widespread use, PVs must also be manufactured inexpensively from stable and non-toxic materials. Graded InGaN-based PV devices offer several advantages: absorption of photons over a wide spectral range directly creates charge carriers; the polar material generates an electric field enhancing carrier transport; and the high bandgap active layer increases output power. The potential of the InGaN materials system offers a real opportunity for realizing low-cost, high-efficiency PV devices. This project is poised to realize these breakthroughs, and substantial progress has been achieved in our first year of effort.

## Benefit to National Security Missions

The development of new electronic and photonic materials directly supports the national energy security and threat reduction missions of LANL and DOE. This research directly supports DOE's core mission by developing an entirely new material system for PV applications offering unprecedented efficiency and lower costs that are key elements in several DOE programs including the Solar America Initiative. The results of this project will position us to compete for follow-on funding from DOE (e.g. DOE/BES, ARPA-E, and EERE initiatives) to expand this effort into a much larger program. There is also growing DOD and DARPA program interests in efficient PVs for satellite power, battlefield systems, etc. Given the potential of the InGaN materials system, the results of this project should be valuable in realizing the full potential of the InGaN materials system for making practical, high-efficiency PVs widely available with important consequences for our Nation's energy security and our environment.

## Progress

Significant progress towards our project goals has already been achieved in the first year of this project. The developments are summarized as follows:

- Isothermal growth of GaN, InN and high-In-content InGaN has been routinely achieved, with the films

showing excellent crystallinity and optical properties (Figure 1). These results are critical for this project, since creating graded structures over a significant composition range requires isothermal growth. We have demonstrated growth of graded composition films covering the range from pure GaN to high-In-content InGaN to pure InN, and are investigating methods for forming the uniform gradients in InGaN composition that are necessary for the proposed PV devices. We are also exploring the rate at which we can change the graded composition as a function of film thickness, which will determine the thickness of the graded layers.

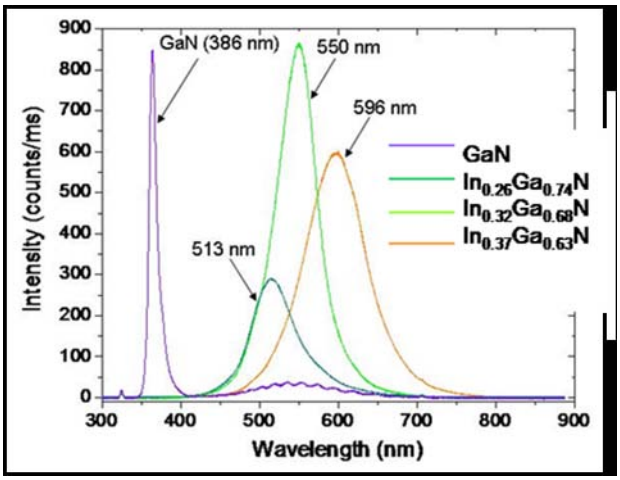


*Figure 1. Photoluminescence (PL) intensity vs. wavelength for three InGaN films with the indicated compositions grown using ENABLE at 750 oC. The absolute PL intensities are plotted along with PL from ENABLE grown GaN. The films were all ~800 nm thick. The range of peak PL wavelengths and peak widths are indicative of tuning the bandgap of the InGaN semiconducting material.*

- By carefully controlling impurities and other sources of contamination in our source gas streams, we have significantly lowered (a >100X reduction) the background carrier concentration in the semiconducting GaN-related films being grown. Typical levels are now routinely in the low-$10^{17}/cm^3$ range. This result has also led to improvements in carrier mobility and other electrical properties of InGaN films that are needed for making working PV devices.

- We have solid preliminary evidence indicating successful p-type doping of high-In-content InGaN films. Spectrally resolved electroluminescence measurements (EL) indicate that Mg can be doped into InGaN at In contents up to ~50% yielding bright, tunable band edge EL. Our next step is to grow a p/n junction in films of the same materials, verify EL, and characterize the transport properties. These steps are critical for creating actual PV devices and measuring their efficiencies, particularly since the bottom n- and p-type films needed for our proposed device structure will be doped In-rich InGaN.

- The ENABLE system has been modified to routinely grow GaN-related thin films over larger substrate areas. We have transitioned our substrates from one square cm areas to 5 cm diameter substrate wafers, the standard size for research grade devices. The larger substrate sizes will facilitate the fabrication of prototype PV devices.

- The growth of high-quality GaN on silicon and glass substrates has been demonstrated. These experiments yielded highly-crystalline GaN films (~100% c-axis orientation) even on amorphous glass substrates. Once optimized, the ability to grow GaN-related thin film materials on inexpensive substrates will significantly reduce the costs of PV devices.

## Future Work

Preliminary results show a clear path to making device quality InGaN materials. Some improvements in further reductions in the carrier mobilities are still needed. Our next task will be to optimize p-type doping of fixed-composition, high-In content InGaN films needed for devices. N-type doping of InGaN films should be relatively straightforward with some minor modifications to the ENABLE system. Creating high quality compositionally graded InGaN over well-defined, relatively narrow composition ranges for optimal performance in single junction PV devices will be a primary focus in the second year of this project. These optimized InGaN films will serve as the basis for our last task of fabricating prototype PV devices and measuring their performance. Our ultimate goal is to achieve ~30% PV efficiency for these graded composition devices and explore fabricating these devices on inexpensive glass substrates.

## Conclusion

A new type of PV device based on compositionally graded InGaN thin film material is being investigated. These single-junction PV devices will be alternatives to current thin film single-junction PV devices that are being aggressively researched by others. Compositionally graded InGaN devices have the potential to achieve record efficiencies of ~30%, allowing them to produce electricity at $0.05/kWh (cost competitive with fossil fuel generated electricity). A unique LANL technology is the only one shown to be capable of growing high-quality compositionally graded InGaN over the full composition range, allowing the successful development of this important PV technology.

# Plasmonic Bandgap Materials: Fusion of Interparticle and Particle-Photon Interactions at the Nanoscale

*Stephen K. Doorn*
20090325ER

## Introduction

Optical excitation of surface electrons (plasmons) within multiple interacting metal nanoparticles can result in huge amplification of associated surface enhanced Raman (SERS) responses from adsorbed molecules, providing single-molecule sensitivity. Gaining a fundamental understanding of these interparticle plasmonic interactions is essential for future exploitation of this phenomenon for next-generation sensing needs. Engineering such plasmonic nanoparticles into ordered arrays that also exhibit tunable photonic bandgap properties (with well-defined optical resonances) will present a novel system for exploring optical behaviors that will provide new modes for sensing opportunity. Our broad goal is to probe, understand, and manipulate the interparticle and particle-photon interactions required to realize a functional plasmonic/photonic-bandgap material hybrid.

To do so, we will pursue a fundamental understanding of the interparticle plasmonic interactions responsible for SERS signal amplification through probing controlled 2-Dimensional and 3-Dimensional assemblies of SERS-active particle aggregates. We will also generate a new class of nanoparticles that combine magnetic and plasmonic properties. These hybrids will allow self-assembly of interacting nanoparticles with long-range 3-Dimensional order. The result will be a tunable dynamic photonic bandgap material that displays SERS activity. Finally, we will incorporate functional elements into this dynamic plasmonic/photonic lattice to impart a chemoresponsive route to manipulation of its optical properties.

Our efforts represent the development of novel fabrication and self-assembly routes for producing 2- and 3-D plasmonic and plasmonic/photonic-bandgap hybrid nanoparticle assemblies. These new materials will be a powerful testbed for understanding the fundamental properties of coupled photonic/plasmonic metamaterials and will lead to novel sensing approaches not previously explored. We anticipate this novel approach will generate more sensitive and more tunable sensing platforms than are currently available.

## Benefit to National Security Missions

We address DOE's goal of developing advanced functional nanomaterials. DOE is also interested in materials that function at the nano-bio interface. Our plasmonic bandgap materials will ultimately be functionalized to interact with bioanalytes at the nanoscale. These materials also have applications relevant to threat reduction missions.

## Progress

The overall goal of this proposal is to develop novel approaches to nanoparticle aggregate formation using SERS activity as a metric for successful particle geometries. Along these lines, this work utilizes several parallel approaches for particle synthesis and manipulation that have each moved forward on their respective scientific fronts.

From an instrumentation standpoint, our surface patterned, 2-d particle assemblies have been limited by e-beam lithography difficulties requiring extensive instrument overhaul. After multiple repair iterations with the manufacturer, the instrument is now fully operational. A first generation of patterned surfaces has been completed. Illustrations of the 2-D particle assembly approach and our first generation of patterned surfaces are shown in Figure 1. Our proposed approach to extending these concepts to 3-d particle geometries involves the use of a laser trapping system that is currently being built with collaborators in B-Division. The principal component of this system, the spatial light modulator (SLM), was selected, ordered and delivered at the end of the current fiscal year.

Realization of the self-assembled plasmonic photonic lattices will require synthesis of multilayered, multifunctional particles with complex surface chemistry. The synthetic aspect of this work therefore involves development of techniques for generating magnetic and plasmonic nanoparticles. These must be integrated in a core-shell geometry. Methods for generation of complex particle geometries and surface functionalization are also necessary.

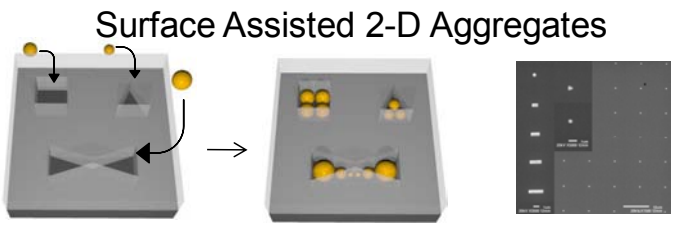


*Figure 1. Illustration of approach to generating well-defined interaction geometries for plasmonic nanoparticles. Patterned wells on the size scale of 100s of nanometers with different geometries are generated on a silicon substrate (left). Nanoparticles of different size and compostion are drawn into the wells using surface-tension effects (center). A micrograph of a first-generation set of wells is shown on the right.*

We have developed synthetic approaches for generating simple colloidal particle systems, and also the development of new particle structures that have promise in SERS applications. We have demonstrated the synthesis of solid noble metal (Au and Ag) colloidal systems as well as core-shell nanoshell geometries as effective SERS active materials. These particles are being examined for multiplexing capabilities and single particle spectroscopy using the flow cytometry resourses in B-division. Additionally, they will be the primary particles of interest in the 2-D and 3-D aggregate assembly experiments that will be performed when the aforementioned instruments are operational.

As an extension on this initial particle work, we have been developing several synthetic routes to magnetic plasmonically active particle architectures. In this area, significant work has gone into developing colloidal $Fe_3O_4$ particle systems with overall diameters on the order of 100nm. Attempts at these particles have been marginally successful, in that we have been able to generate F $e_3O_4$ materials that are magnetically active; however, the particle sizes and morphologies are highly heterogeneous and require further refinement before plasmonic-photonic materials are realized. Current work seeks to improve on this synthetic route to yield homogeneous magnetic materials. Additionally, in parallel, we have successfully developed several alternate routes to similar superparamagnetic materials using different synthetic approaches. We have been successful in creating silica core particles that have been decorated with small (~10nm) iron oxide particles that act as nucleation points for subsequent metallization (Figure 2). We are also pursuing use of larger iron oxide particles (~18nm), which serve as the central core of an oxide-metal, core-shell particle system. These particles have been extensively characterized for overall homogeneity in size and morphology. They are currently being investigated for magnetic properties at the NHMFL. In both approaches, our capability for generating core-shell materials is essential.

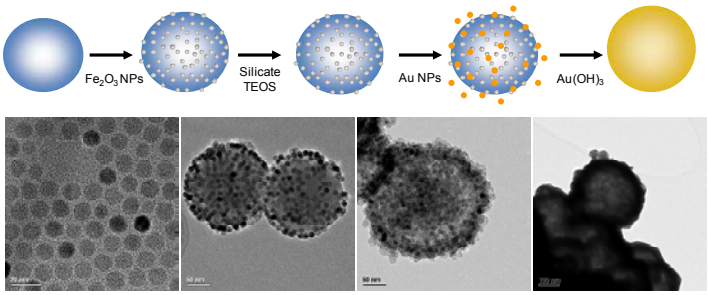


*Figure 2. Process for generating core-shell nanoparticles with a magnetic core paired with a gold plasmonic shell. The top demonstrates the process for synthesis. A 100 nm core silica particle is functionalized with 10 nm superparamagnetic particles. The assembly is coated with a thin silica shell and then functionalized with 5 nm gold seed particles. A final gold shell is then generated. At bottom are transmission electron micrographs illustrating the appearance of actual particles produced at each step of the synthesis strategy.*

As part of our efforts to generate complex multifunctional particle geometries with tailored surface functionalization, we have also demonstrated the ability to combine multiple particle types into a larger assembly on support bead structures (Figure 3) [1]. The goal in this case was to increase the range of spectral responses available with SERS-active nanoparticle spectral tags (SERS-tags). Individual tags were generated by adding a Raman-active dye label to the surface of a plasmonic nanoparticle. The tag is coated with a silica shell, which was then functionalized with a bioreceptor molecule. Three different types of tags were generated. We demonstrated the ability to generate more complex spectral signatures through controlled assembly of different ratios of the three tags at the surface of a support bead. The self-assembly was driven by strong bioreceptor interactions available with appropriate functionalization of the bead and tag surfaces.

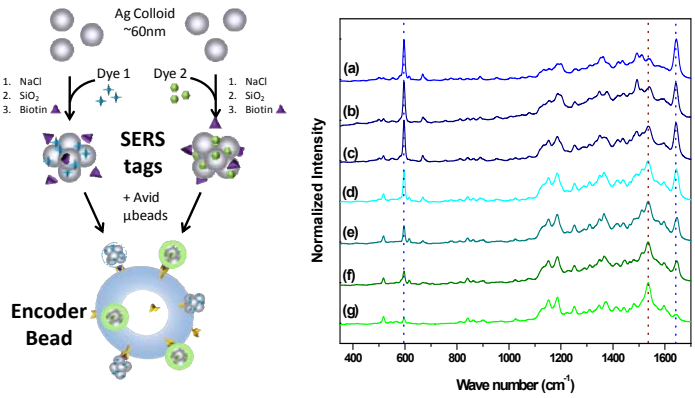


*Figure 3. Illustration of the process for building up complex surface enhance Raman (SERS) spectral signatures at a micron-sized support bead surface (left). Examples of the seven spectral signatures that can be generated from an initial library of three unique SERS tags are shown at right.*

## Future Work

In the area of studying well-defined 2-D nanoparticle interactions, we will begin by demonstrating the ability to fill our patterned nanowells with a range of plasmonic nanoparticles. Initially we will be using simple one component colloidal systems, which will then be extended to higher order particle architectures (core-shells). Additionally, the successful synthesis of homogeneous magnetic particles that are incorporated into plasmonic (metallic) particle architectures will be an ongoing research thrust.

We will pursue self-assembly of 3-D photonic lattices whose optical properties are coupled to plasmonic behavior of its constituent SERS-active particles. Noble metal nanoparticles, when induced to interact can be used as highly effective SERS substrates, serving as easily accessible starting points for SERS-active metamaterials. However, control of these particle aggregates is difficult, with few fundamental studies having investigated the ideal aggregate size and geometry for maximum SERS excitation. Using new concepts in surface-based particle patterning techniques, we will introduce a combinatorial approach to assembling simple metallic particle aggregates in an effort to deduce ideal aggregate structures for efficient intra-particle SERS hot spot generation.

These particle architectures will then be extended to 3-D through the assembly of particle aggregates via optical trapping as well as magnetic assembly. By manipulating the aggregates into 3-D architectures, we hope to generate readily observed intense SERS hot spots within the core of the particle aggregate. The results will have broad reaching impacts on the understanding of the underlying mechanisms responsible for SERS. By assembling the plasmonic aggregates into arrays with long range order, we will leverage the high sensitivity aspect of SERS based substrates with the unique optical properties of a fully 3-D photonic crystal.

Our assemblies will represent the first tunable photonic/plasmonic hybrid metamaterials, providing a route to probing unexplored behaviors of these emerging novel materials. Optimized geometries for the hybrid material with the most efficient coupling between these two optical phenomena will be isolated by immobilizing the aggregate array in a hydrogel matrix that is preloaded with analyte receptor sites. This novel nanocomposite will yield a multimodal approach to sensing via analyte modulation of the photonic lattice properties and inter-particle plasmon field overlap which will result in greatly improved SERS-based analyte detection.

## Conclusion

Ultimately, this project will produce a better understanding of the critical parameters associated with surface enhanced Raman (SERS) responses that yield single-molecule sensitivity. This is critical to the realization of new sensing materials capable of the stringent sensitivity and confidence requirements of the threat reduction community. Our efforts will also produce a totally new class of materials that combine SERS-active "plasmonic" properties with ordered "bandgap materials" that provide highly tunable optical properties. This fusion of properties opens up novel sensing approaches that will be explored.

## Publications

Brady, C. I., N. H. Mack, L. O. Brown, and S. K. Doorn. Self-assembly approach to multiplexed SERS encoder beads. 2009. *Analytical Chemistry.* **81**: 7181.

# Probing the Origin and Consequences of Quantum Critical Fluctuations

*Tuson Park*
20090335ER

## Introduction

Electronic technology has advanced in step with our increased understanding of how electrons behave in materials. In recent years, however, we have witnessed a crisis in our fundamental knowledge of the way electrons behave in certain materials in which the electrons interact strongly with each other. Our historical understanding of the electron cannot be applied to these correlated electron metals and requires a new paradigm. Studies of strongly correlated electron materials have revealed that quantum effects, usually only significant at very low temperatures, dominate the character of electrons even at finite temperature and may be responsible for producing new forms of unconventional superconductivity at unexpectedly high temperatures. The goal of this project is to create a proper understanding of the new quantum phenomena and with this knowledge to transform the modern crisis into an opportunity that will advance our scientific understanding as well as create new technology.

In our research, we propose to identify the spectrum of electronic fluctuations that results from the quantum effects and that can be tuned by applied magnetic field and pressure. Anisotropic electrical resistivity and momentum-dependent superconducting properties depend on the nature of the quantum fluctuations, and these are precisely the properties that we will measure to explore the origin and consequences of quantum fluctuations. A triple axis vector magnet, which has three sets of independent magnets, will enable us to probe these anisotropic properties at any arbitrary magnetic field direction when a single crystal is subjected simultaneously to high pressure, a unique capability that is needed to guide a theoretical description of these phenomena.

## Benefit to National Security Missions

This project directly supports the DOE mission in Energy Security by enhancing our fundamental understanding of materials with high superconducting temperatures, which hold promise for efficient transmission and storage of electricity.

## Progress

During the first year of this project, research has been devoted to probing the connection between unconventional superconductivity and quantum critical fluctuations that arise from a zero-temperature magnetic to non-magnetic transition. For our initial study, we performed field-orientation specific heat studies of the pressure-induced superconductor cerium-rhodium-indium (CeRhIn5), in which a maximum in the superconducting transition temperature occurs right at the pressure where fluctuations associated with an antiferromagnetic quantum critical point are most pronounced. These experiments provided the momentum-dependent superconducting gap function for the first time in any pressure-induced superconductor. In the lower pressure coexisting phase of superconductivity and antiferromagnetism, field rotation within the ab-plane of the tetragonal structure revealed fourfold modulation in the density of states, which favors a d-wave superconducting order parameter. This same fourfold modulation was found at the optimal pressure where quantum fluctuations dominate physical properties, and there is no long range magnetic order for small applied magnetic fields. Thus, we have demonstrated that our unique vector-magnet experimental apparatus is a powerful tool to understand the nature of superconductivity in pressure-induced superconductors and further that the nature of the superconducting gap function is independent of the presence or not of magnetic order, contrary to some theoretical predictions. The confirmation of d-wave superconductivity indicates that these materials are similar to other classes of superconductors, notably the high-Tc cuprates and the plutonium superconductors. To further explore the nature of antiferromagnetic quantum fluctuations on unconventional superconductivity, we have begun measurements of the temperature- and pressure-dependent anisotropy of the electrical resistivity of a related material superconductor cerium-cobalt-indium (CeCoIn5), in which d-wave superconductivity emerges from a quantum critical state at atmospheric pressure. A preliminary analysis of these data indicates that the nature of the quantum critical fluctuations is different from that found in the rhodium compound (CeRhIn5) under pressure.

Thus, it appears that the same type of unconventional superconductivity can be produced by quantum fluctuations of different natures, a new and unexpected result.

We also have performed preliminary studies on the strongly correlated superconductor cerium-iridium-indium (CeIrIn5). Though this material does not order magnetically, several different experiments have indicated that a zero-temperature antiferromagnetic transition and its associated critical fluctuations may be close by. To understand the relation between superconductivity and possible quantum criticality in more detail, we have measured its specific heat under pressure and have found a broad maximum in specific heat just above the superconducting transition at a pressure of 15 kbar. This broad feature quite likely reflects a precursor to long-range magnetic order that coexists with superconductivity and that is a minimum condition for quantum criticality. These results indicate that, again, magnetic fluctuations may provide the glue that binds the superconducting electrons together in these strongly correlated electron materials. Preliminary field-angle specific heat measurements under pressure on CeIrIn5 suggest a d-wave superconducting order parameter, and on-going measurements and analysis are expected to resolve a current controversy over the particular structure of the superconducting gap in this material.

In another class of materials, the recently discovered iron-pnictides, we have shown that applying pressure tunes the magnetic transition in calcium-iron-arsenic (CaFe2As2) from 170 K at atmospheric pressure toward zero temperature at pressures less than 10 kbar. It would be reasonable to expect strong quantum fluctuations and associated enhanced scattering of electrons in the vicinity of this pressure where the magnetic transition approaches zero temperature and superconductivity appears. Indeed, we found enhanced scattering in this pressure range, but this material also exhibits complex structural changes as a function of pressure. Our interpretation of these results is that pressure-induced superconductivity appears because of structural inhomogeneities and affiliated magnetic fluctuations, possibly of a quantum critical type. Our experiments, however, are unable to establish definitively that quantum fluctuations drive the appearance of superconductivity in this weakly correlated electron material. In this context, we also measured the pressure dependence of the superconducting transition temperature of a related material barium-nickel-arsenic (BaNi2As2) and found that its structural phase transition, from a tetragonal to orthorhombic structure, was suppressed with increasing pressure up to 27 kbar and that its superconducting transition temperature increased from 2 K to 3 K at this high pressure. This compound, unlike the calcium compound (CaFe2As2), is not magnetic, and, consequently, our experiments on the barium compound (BaNi2As2) show that structural changes cannot be ignored in interpreting properties of this class of materials.

## Future Work

A quantum critical point (QCP) is an instability between ordered and disordered magnetic states at T=0K, with the transition between them driven by Heisenberg's uncertainty principle. Strongly correlated f-electron materials have been a prime testing ground to explore the consequences of such an instability. Among many anomalous properties associated with the QCP, two consequences stand out: a strange metallic state that persists from very low to high temperatures and the emergence of unconventional superconductivity nearby the QCP. A microscopic understanding of these phenomena poses a fundamental challenge in the condensed matter community.

Identification of the relevant fluctuation spectrum is needed to guide a theoretical description of these phenomena. Compared to chemical substitution that induces chemical disorder and modifies the fluctuations, applying pressure is an ideal knob to tune compounds to a QCP without additional complication. Though microscopic measurements, such as neutron scattering, are well-suited to characterize the fluctuation spectrum, they are impossible to perform with sufficient resolution under high pressure conditions. Instead, relatively simple anisotropic transport and thermodynamic measurements under pressure place strong constraints on the fluctuation spectrum and their origin. Field-angle-dependent transport and thermodynamic measurements complimented with point contact spectroscopy will be exploited to determine the order parameter symmetry of pressure-induced or pressure-tuned superconducting states, which will allow us to critically determine the relationship between quantum fluctuations and unconventional superconductivity.

We will study representative correlated f-electron systems, including antiferromagnetic cerium-rhodium-indium (CeRhIn5) and related material and ferromagnetic uranium-germanium (UGe2), which can be tuned by pressure to quantum critical and superconducting states. The high purity of these stoichiometric compounds with energy scales amenable to detailed study makes them ideal test systems. The generality of understanding gleaned from the f-electron compounds will be tested by complementary experiments on electron doped cuprates, iron-pnictide and charge-density-wave superconductors.

## Conclusion

The unique combination of the vector magnet and high pressures will allow us to probe the nature of electrons in correlated materials in ways never before possible. Specifically, we expect to: (i) determine the origin of quantum fluctuations that are responsible for a strange metallic state in correlated f-electron compounds, and (ii) to make the first determination of the superconducting order parameter for any pressure-induced superconductor. Knowledge obtained through this study will be applied to d-electron high-temperature superconductors, providing fundamental information to superconducting technology

that will help to ensure the Nation's energy security.

## Publications

Lee, H. O., E. Park, T. Park, V. A. Sidorov, F. Ronning, E. D. Bauer, and J. D. Thompson. Pressure-Induced Superconducting State of Antiferromagnetic CaFe2As2. 2009. *Physical Review B.* **80**: 024519.

Park, T., H. Lee, E. D. Bauer, J. D. Thompson, and F. Ronning. Pressure Dependence of BaNi2As2. To appear in *Journal of Physics.*

Park, T., and J. D. Thompson. Magnetism and Superconductivity in Strongly Correlated CeRhIn5. 2009. *New Journal of Physics.* **11**: 055062.

# Linear Scaling Quantum-Based Interatomic Potentials for Energetic Materials

*Marc J. Cawkwell*
20090369ER

## Introduction

The fundamental mechanical and chemical events that lead to the detonation of explosives are so rapid that they are extremely difficult to study experimentally. Furthermore, the postmortem analysis of samples is usually impossible. For these reasons, computational modeling of atomic level events in explosive crystals using molecular dynamics simulations is one of the few tools available to study the phenomena leading to detonation. However, the reliability of the predictions provided by such calculations is almost entirely dependent on the mathematical description of interatomic bonding employed. Current descriptions of interatomic bonding in explosives are either accurate but computationally challenging or computationally efficient but with dubious accuracy.

We have developed a method and supporting code that enables quantum mechanical simulations of energetic materials at a computational cost comparable to those of empirical potentials. Unlike the popular empirical models currently in use, our scheme is applicable equally to all organic energetic materials and detonation products without the requirement for costly refitting to experimental or calculated data. Hence, our code 'LATTE' (Los Alamos Transferable Tight-binding for Energetics) can provide accurate theoretical analysis of even hypothetical energetic materials, as well as those of interest to the DOE, DOD and DHS.

## Benefit to National Security Missions

This project supports the DOE/NNSA mission in Nuclear Weapons by enhancing our understanding of the initial mechanical and chemical events that lead to the detonation of conventional explosives. Furthermore, the predictive capabilities the project will provide will enhance DOD and DHS programs on energetic materials. The deliverables of this project will see applications to basic research on the physical properties of several classes of complex materials. Hence, mission relevance extends to all areas where a fundamental understanding of materials is required.

## Progress

Molecular dynamics simulations require a rapid and accurate calculation of the forces acting on atoms from a physics-based, mathematical representation of interatomic interactions. Our primary aim over the first year of the project was the development of a molecular dynamics code with interatomic forces provided by the self-consistent charge transfer tight-binding method (SCC-TB) [1, 2]. The SCC-TB formalism is the simplest quantum mechanical method that captures the key chemical concepts of the formation of covalent bonds, the transfer of charge between species of differing electronegativity, and their interplay and environmental dependencies. We have extended our formalism such that long-range, van der Waals interactions are also captured, allowing us to model all of the most important interactions in organic molecular materials.

Our SCC-TB model is framed explicitly on the concept of the bond-order since this leads to a physically transparent representation of electronic structure and, more importantly, permits the use modern of linear scaling computational methods during the calculation of energies and forces. At the start of the project, we anticipated that our code would be based around purification methods for the calculation of the bond-order, but we have successfully expanded the scope and flexibility of the code to include diagonalization, purification [3], and recursive expansions of the Fermi operator [4]. The latter two methods are most significant for this project since they offer a route toward linear scaling computational cost and parallelization even on non-standard computational architectures such as LANL's Roadrunner and the under-utilized commodity GPUs (graphics processing units) that sit in all desktop computers. In Figure 1 we present a comparison of the scaling with system size of each method in sparse and dense form.

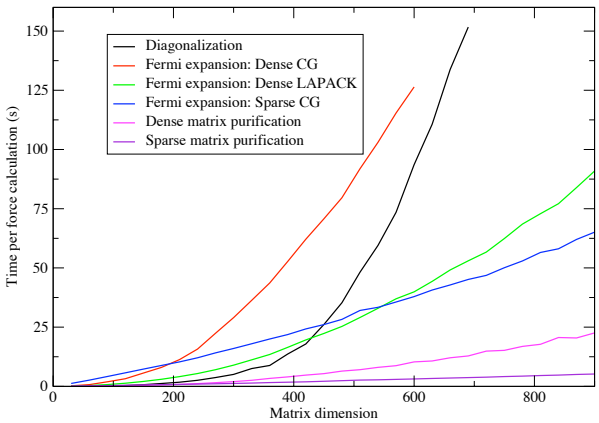


*Figure 1. Comparison of computational time per molecular dynamics time step as a function of the dimension of the Hamiltonian matrix for the methods employed in LATTE for the calculation of the bond-order matrix.*

The analysis of the performance of LATTE highlighted two bottlenecks to performance when using purification and Fermi expansion methods. First, during the calculation of forces at each time step a large number of matrix–matrix multiplications are required. These multiplications scale as the cube of the matrix dimension and limit the performance of the code during large-scale simulations. We are actively pursuing two routes to improve the performance of our matrix-matrix multiplier. The first involves taking full advantage of the sparsity of the matrices to eliminate redundant work. Our second avenue involves porting several LATTE subroutines to Roadrunner to enlist the exceptional floating-point performance of the Cell processors. Preliminary results are presented in Figure 2 that indicate that this approach will be essential for large systems with dense bond-order matrices.

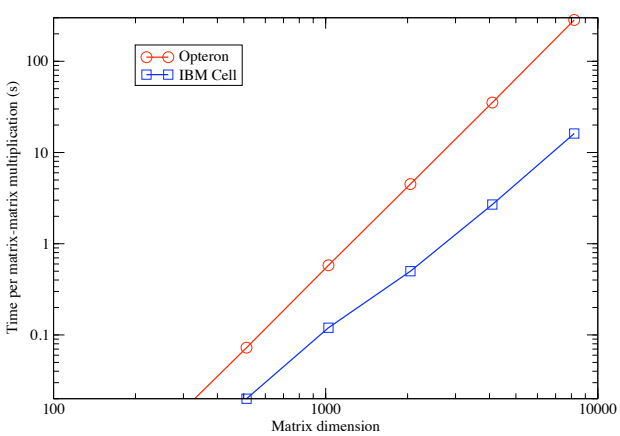


*Figure 2. Computational time for dense matrix-matrix multiplication on Opteron and Cell processors on Roadrunner.*

The second performance bottleneck to running molecular dynamics simulations with LATTE is the number of self-consistent field (SCF) calculations required which calculating forces at each time step. By implementing in LATTE Niklasson's extended Lagrangian Born-Oppenheimer (XBO) molecular dynamics formalism [5], we have reduced the number of SCF cycles by more than an order of magnitude to just one. In Figure 3 we show how total energy is not conserved during standard, non-XBO, simulations, the dependence of these simulations on the number of SCF cycles, and the precise energy conservation obtained when XBO-methods are employed with just 1 SCF cycle per time step. It should be noted that LATTE is the only code based on the TB approximation to offer this functionality.

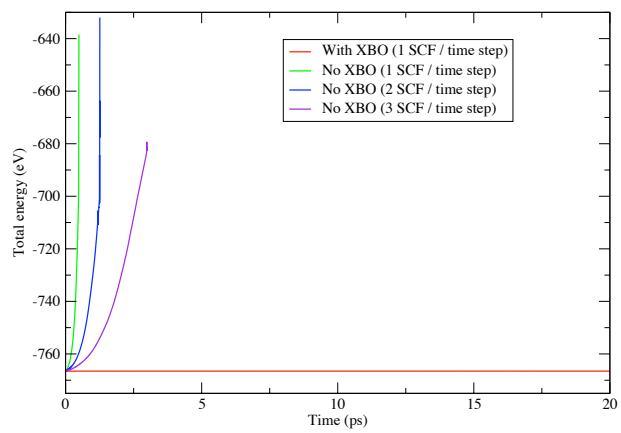


*Figure 3. Energy conservation in LATTE molecular dynamics simulations using XBO and non-XBO propagation of quantities. The energy conservation as a function of the number of SCF cycles per time step in non-XBO simulations is also presented.*

A set of charge-dependent TB interatomic potentials that include long-range van der Waals interactions have been constructed for hydrocarbons by the parameterization of the models to the results of first principles, quantum chemistry calculations. Our quantum chemistry calculations employ the Theoretical Division-developed code 'FreeON'. While we can reproduce much of this highly accurate data by fitting the adjustable parameters via analytic conditions, we are at the same time pursuing automated, machine-based optimization schemes. We believe that methods such as simulated annealing will allow quantify the quality, accuracy, and transferability of our potentials. The use and importance of such automated fitting methods will increase as new chemical elements are added to LATTE's capabilities.

We did not anticipate applying our code and methods to 'real world' situations until the third year of our project. However, owing to our early success in the development of LATTE, we have already begun a collaboration with colleagues in LANL's Dynamic and Energetic Materials Division. We have focused our code on the simulation of chemical events in various complex hydrocarbons under shock compression. While we cannot yet simulate explicitly the propagation of a shock wave though these materials, we can probe on-Hugoniot conditions and monitor bond

making and breaking events. These simulations are allowing us identify those shock-induced chemical events that previously could only be implied from complex experimental data sets.

## Future Work

Earlier LANL work on molecular dynamics simulations of detonation using empirical reactive interatomic potentials demonstrated that there is a minimum system size that must be reached before predictions for relative quantities of detonation products become independent of further increases system size. In order for us to reach this 'minimum limit', we must increase the performance of LATTE by a factor of about 100 (note that the performance of non-linear scaling codes must be increased by a factor of about $10^6$). Over the course of the next year we will continue to pursue the applied mathematics and algorithms that will yield true sparse matrix multiplication and storage. This work is of general interest to this field, and others, and advances in this area will have a very high impact. We will also parallelize those LATTE subroutines that are bottlenecks to performance as well as reprogramming LATTE to port certain algorithms to the IBM Cell processors in Roadrunner and GPUs. All of these research areas developed a very sound foundation during year 1 of this project. The speed of the serial version of LATTE can be increased by a factor of at least 10 by porting certain subroutines to Cells and GPUs, and parallelizing LATTE to run on several hundred processors is not a particularly complex undertaking. Hence, a speed up by a factor of 1000 over the current version of the code is not an overly optimistic aim.

Work toward the completion of our interatomic potentials for CHNO-containing molecules will continue in parallel with work on LATTE itself. In particular, we will complete the population of our database of quantum chemistry-calculated energies and continue the development of algorithms that facilitate the automated optimization of LATTE potentials to our database. We will also work toward putting the SCC-TB framework on a more rigorous theoretical basis by developing a fully quantum mechanical, many-body treatment for the van der Waals interactions and short-range repulsion between atoms rather than making the usual approximation that these interactions are only pair-wise in nature.

The collaboration we have started with experimental programs in DE-9 will be pursued both to provide these efforts with theoretical input and to highlight where LATTE and its associated interatomic potentials can be improved. We will also pursue a collaboration with the group of Professor Michael Pravica at the University of Nevada-Las Vegas on structural phase transformations in organic materials induced by static high pressures (see, for example, [6]).

Once work on the construction of a set interatomic potentials for C, H, N, and O is complete, we will simulate the chemical and mechanical events that lead to detonation in energetic materials of interest to the NNSE, DoD, and DHS, etc. We will also determine our capabilities for predicting the structure and properties of experimental and hypothetical compounds with LATTE.

## Conclusion

Computer modeling and molecular dynamics simulations are one of the few tools available for the study of the initial mechanical and chemical events at the atomic scale that lead to detonation in energetic materials. This project is working toward the delivery of a new class of interatomic potentials for energetic materials that will for the first time facilitate large-scale simulations with quantum-mechanical accuracy and unprecedented transferability. Our supporting code, LATTE, already demonstrates class-leading performance. These interatomic potentials and code will revolutionize our understanding of detonation chemistry in existing, experimental, and even hypothetical explosive materials.

## References


1. Elstner, M., D. Porezag, G. Jungnickel, J. Elstner, M. Haugk, T. Frauenheim, S. Suhai, and G. Seifert. Self-consistent-charge density-functional tight-binding method for simulations of complex materials properties. 1998. *Physical Review B.* **58** (11): 7260.

2. Finnis, M. W.. Interatomic Forces in Condensed Matter. 2003.

3. Niklasson, A. M.. Implicit purification for temperature-dependent density matrices . 2003. *Physical Review B.* **68** (23): 233104.

4. Niklasson, A. M.. A note on the Pulay force at finite electronic temperatures . 2008. *Journal of Chemical Physics.* **129** (24): 244107.

5. Niklasson, A. M.. Extended Born-Oppenheimer molecular dynamics . 2008. *Physical Review Letters.* **100** (12): 123004.

6. Tkachev, S. N., E. Kim, E. Romano, P. F. Weck, and M. Pravica. High-pressure studies of 1,3,5,7-cyclooctatetraene: experiment and theory . 2008. *Journal of Physical Chemistry A.* **112** (45): 11501.

# Transparent Organic Solar Cells

*Ian H. Campbell*
20090393ER

## Introduction

The ideal solar cell would convert every bit of energy in photons originating from the sun into usable energy. We propose a completely novel approach, which would "milk" a small amount of energy from solar photons in a most unobtrusive fashion. We propose to develop a new class of truly transparent solar cells using organic semiconductors. A transparent solar cell is designed to have > ~85% transmission in the visible region of the solar spectrum. Although transparency necessarily decreases the maximum possible efficiency of the cell, it enables two specialty applications: windows and stealth. A transparent solar cell for windows is designed to use window glass as the substrate for the solar cell and thus reduce costs associated with fabrication and installation. Many of the materials required for transparent solar cells are already used in high performance windows and transparent solar cells can be designed to also function as low-e window coatings. Transparent solar cells for stealth applications are designed to provide power in applications where the solar cell should be difficult to detect, for example, it can be added to an existing surface to provide power for surreptitious electronic devices.

## Benefit to National Security Missions

This work will contribute to enhancing the national energy security, a key DOE mission area. The ability to incorporate solar cells into conventional windows, using many of the materials and coatings already used in high performance windows, could provide an economic method to deploy solar cells.

## Progress

We are using a closely coupled fabrication/measurement/theory approach to demonstrate and optimize transparent organic solar cells. We are fabricating specialized material test structures and prototype solar cells to understand the semiconductor and device parameters that control the cell performance. Simultaneously, the electronic structure and optical properties of the organic semiconductors are being calculated and the results used to interpret the test structure and device performance and, most importantly, to guide materials design modifications needed to maximize device performance. We are using our established relationships with semiconductor companies to obtain new, specialized organic semiconductors. The project naturally divides into work focusing on two tasks: 1) understanding the relevant properties of the organic semiconductors and 2) designing and fabricating solar cells made from these materials.

The organic semiconductors we are working with are naphthalocyanine compounds that are transparent in the visible spectrum and absorb strongly in the infrared. We are exploring two major types of naphtalocyanine compounds: those that can be solution processed and those that can be thermally evaporated in vacuum. Solution processing is a very low cost method of producing thin films and electronic devices but the chemical purity of the materials can be difficult to control. Thermal evaporation in vacuum is also a low cost technique for device fabrication and it has the advantage that the materials used may be purified by a variety of sublimation techniques. The solution processed materials are part of the family of octabutoxy naphthalocyanines (OctNc), as shown in Figure 1. We are making chemical substitutions to the base OctNc molecule by adding a central metal atom or varying the ligands attached to the naphthalocyanine core to control the molecule's absorption in the infrared. The vacuum processed materials are part of the family of naphthalocyanines (Nc) where we are again making chemical substitutions to control the molecular optical properties. These two classes of molecules are very similar as they share the naphthalocyanine core. In addition to their processing and purity differences, the two molecular families have very different intermolecular interactions in the solid state. In the solid state, the absorption of the smaller, vacuum evaporated molecules can shift by ~ 100 nm, significantly improving their infrared response. In contrast, the absorption properties of the solution processed molecules are essentially unchanged in the solid state. We are performing theoretical calculations of the electronic structure of these molecules to understand them and design new molecules with improved properties.

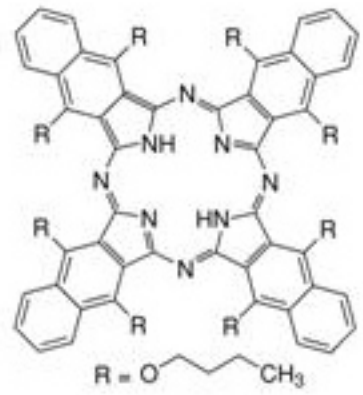


*Figure 1. Chemical structure of octabutoxy naphthalocyanine.*

We are fabricating and testing transparent, organic solar cells using these naphthalocyanine compounds as the critical, infrared absorbing layer. Indium tin oxide (ITO) is used as a transparent electrode. When combined with special surface layers, ITO can function as either an electron or hole injecting material. This is critical to retain the high transparency required in these devices. We are using very thin layers of C60 to dissociate excitons produced in the Nc layer and we have also explored large energy gap organic semiconductors such as bathocuproine to serve as an exciton blocking layer. The initial device results are very encouraging. We have made structures that are > 80% transparent throughout the visible spectrum and have strong absorption in the infrared. These devices have near ideal IR quantum efficiency, i.e. every photon absorbed produces one electron of photocurrent. We are now trying to design improved molecules and alternate solar cell device architectures that increase the IR absorption while maintaining visible transparency. We are currently assembling this work into two journal publications: one on the fundamental organic semiconductor properties and one on transparent solar cell performance.

## Future Work

The goals of this work are to demonstrate, for the first time, a truly transparent solar cell by exploiting the unique electronic structure of organic semiconductors, and to understand and optimize the electronic structure of these materials for this application. Technologically, organic semiconductors are of increasing importance for large area low cost applications such as displays, solid state lighting, large area electronics, and solar cells. From a scientific perspective, organic semiconductors offer a model system for studying multiscale physics involving, for example, the properties of individual molecules and their solid state intermolecular interactions.

Solar cell performance is controlled by exciton processes (transport and dissociation), charge carrier transport, and device open circuit voltage. Electronic processes in organic semiconductors are poorly understood: exciton processes are difficult to calculate and they have been reliably measured in few materials; charge carrier transport can be measured reliably but predicting the carrier mobility of solid films from molecular properties is problematic; and the open circuit voltage is determined by organic material/electrode interactions which only follow general relationships such as approximate scaling with electrode work function. Because organic semiconductors are condensed phases of organic molecules or polymers there is an essentially unlimited variety of organic semiconductors that can be created. Fundamental understanding is required in order to provide insight to develop new materials with properties tailored for this application.

We will continue to use a closely coupled fabrication/measurement/theory approach to demonstrate and optimize transparent organic solar cells. We will fabricate specialized material test structures and prototype solar cells to understand the semiconductor and device parameters that control the cell performance. Simultaneously, the electronic structure and optical properties of semiconductors will be calculated and the results used to interpret the test structure and device performance and, most importantly, to guide materials design modifications needed to maximize device performance.

## Conclusion

We propose to create a new class of truly transparent solar cells. A transparent solar cell is designed to use window glass as the substrate for the solar cell and thus reduce costs associated with fabrication and installation. Simply replacing the glass on office buildings could generate a large fraction of the building's electric power requirements. This would help the U.S. become energy independent in a cost effective manner.

# Uranium Imido Complexes as Catalysts for the Reduction of Carbon Dioxide

*James M. Boncella*
20090397ER

## Introduction

This project will attempt to use the unique chemical properties of uranium compounds as the foundation for a method for the conversion of carbon dioxide into fuel. It will also attempt to utilize this unusual chemistry for the conversion of acid to hydrogen, a fuel that generates only water as a byproduct when used to produce energy. By generating gaseous products from uranium, the project attempts to mitigate the concerns related to the use of radioactive materials to do catalytic chemistry to make useful products because the separation of the products from the radioactive uranium will occur with absolutely no uranium contamination and thus no potential for contamination of the products or environment. This work is cutting edge science because it will develop chemistry of uranium that is completely unique and apply it to develop a practical solution to an important problem in the field of energy production. Even if the project does not result in the development of a practical system for carbon dioxide conversion, the lessons learned will undoubtedly be useful to anyone working in this general area of chemical research. Thus, this project if successful, will enable progress toward a carbon neutral fuel cycle and will reduce the production of greenhouse gases.

## Benefit to National Security Missions

This project directly supports the U.S. drive for energy security and to maintain a safe nuclear stockpile by enhancing our understanding of actinide coordination and organometallic chemistry. The work supports DOE energy security and nuclear weapons missions.

## Progress

During the first year of the project we have been able to synthesize and characterize a series of new uranium bis (imido) complexes whose reactivities we are investigating. The successful synthesis of the series of U(V)-U(V) dimer complexes (Figure 1) will allow us to investigate their reactivity with carbon dioxide and hydrogen as a function of ligand. During this work, computational analysis of these dimers suggested that the single f electron on each U metal should interact with one another via a spin pairing interaction (antiferromagnetic coupling). This was demonstrated experimentally and is only the second molecular actinide complex that shows such electronic interactions and resulted in a publication in *Angew. Chem. Int. Edn.* The synthesis of the series of derivatives including Iodide, Bromide, Chloride and aryl sufide compounds will allow us to learn how the nature of the ligands affect the ability of the U atoms in these compounds to undergo electronic communication. These derivatives will be useful in studying how the oxidation reactions of the U compounds are controlled by the ligand environment which surrounds the U metal center.

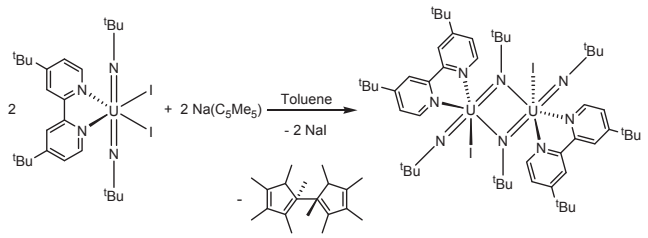


*Figure 1. Synthesis of a bis(imido) U(V) complex*

We have also been investigating the reactivity of the U(V)-U(V) dimers with respect to their ability to be oxidized to U(VI) complexes. These compounds react with weak oxidants such as silver salts and elemental sulfur and selenium. The products are generally not accessible via other synthetic techniques and include the first examples of U(VI) atoms that are bridged by sulfur or selenium atoms. Controlling the stoichiometry of the reactions determines whether single atom of multi atom bridges are formed. The reactions with silver and gold reagents proceed via oxidative group transfer from the silver or gold compound U with formation of U(VI). These reactions have produced the first example of a simple U(VI)-carbon bond in the U(VI) methyl complex that is formed when MeAu(PPh3) is allowed to react with the U(V)-U(V) dimer.

The reaction chemistry with reagents such as isocyanates (RNCO), a carbon dioxide surrogate, have produced new compounds that are clearly the result of oxi-

dation of the metal to U(VI) because they are diamagnetic. However, their complete characterization has not yet been achieved and awaits the judicious choice of R group to generate tractable materials. The reaction with molecular hydrogen also occurs rapidly, giving U(VI) products, but these materials have proven difficult to identify unequivocally.

We have also begun to investigate the use of polydentate mono- or di- anionic ligands with the bis(imido)U(VI) metal framework. The intention is to design a ligand set which facilitates the reduction of U(VI) to mononuclear U(V) or U(IV) complexes whose reactivity with hydrogen or carbon dioxide will then be investigated. Electrochemical studies have not demonstrated reversible reduction of the U(VI) halide complexes, though reduction obviously occurs. Furthermore, reaction of the halide compounds with chemical reductants results in the formation of the dimers or intractable, reduced materials. By generating reduced, mononuclear, uranium bis(imido) complexes, we will be in the position to better understand and control the oxidation of these novel molecules.

## Future Work

The ultimate goal of this research is to develop the redox chemistry of a series of unique uranium complexes and apply it to the conversion of substrate molecules to useful products. The electron rich uranium complexes that are the focus of this proposal have the potential to function as electrocatalysts for the reduction of carbon dioxide generating products that can be used as fuels. They also have the potential to generate hydrogen from protons, a fundamental process that is vital to the function of light driven water splitting reactions, and is carried out in biology by hydrogenase enzymes. Understanding these kinds of thermodynamically uphill chemical transformations will be central to solving some of the most vexing and important energy problems that our society currently faces. This research will be the first example of using 5f electron species to perform these types of reactions and it is enabled by our ability to access a new class of bis(imido) uranium complexes.

The successful electrocatalytic reduction of carbon dioxide or the conversion of protons to hydrogen will demonstrate that it is possible for actinide complexes to be used for such purposes and could make the practical application of actinide catalysis a real possibility. It is unlikely that the complexes that are now in hand will be the best catalysts that we will develop. The search for better catalysts through modification of the ligands that comprise the coordination sphere of the uranium atom will undoubtedly answer the question of whether it is possible dictate the chemistry of a 5f element through changes in the electronic properties of its ligands. Such tuning would represent a giant advance in actinide chemistry of the type that would be fitting for an institution with LANL's tradition in actinide chemistry.

## Conclusion

We have demonstrated that the reduction of U(VI) complexes to stable U(V) products are possible. The conversion of the U(V) compounds back to U(VI) complexes through their reactions with organic substrates has also been demonstrated. This cycling of the oxidation states between U(V) and U(VI) is the first step in utilizing this class of U compounds for catalytic transformations such as the reduction of carbon dioxide to give organic products or the reduction of protons for the production of hydrogen.

## References


1. Spencer, L., P. Yang, B. Scott, E. Batista, and J. Boncella. Uranium(VI) Bis(imido) Chalcogenate Complexes: Synthesis and Density Functional Theory Analysis. 2009. *INORGANIC CHEMISTRY.* **48** (6): 2693.

2. Spencer, L., E. Schelter, P. Yang, R. Gdula, B. Scott, J. Thompson, J. Kiplinger, E. Batista, and J. Boncella. Cation-Cation Interactions, Magnetic Communication, and Reactivity of the Pentavalent Uranium Ion [U(NtBu)(2)](+). 2009. *ANGEWANDTE CHEMIE-INTERNATIONAL EDITION.* **48** (21): 3795.

3. Spencer, L., R. Gdula, T. Hayton, B. Scott, and J. Boncella. Synthesis and reactivity of bis(imido) uranium(VI) cyclopentadienyl complexes. 2008. *CHEMICAL COMMUNICATIONS.* (40): 4986.

4. Spencer, L. P., P. Yang, E. R. Batista, B. L. Scott, and J. M. Boncella. Oxidative addition to U(V)-U(V) dimers: facile routes to uranium(VI) bis(imido) complexes. To appear in *Inorganic Chemistry.*


## Publications


Spencer, L., E. Schelter, P. Yang, R. Gdula, B. Scott, J. Thompson, J. Kiplinger, E. Batista, and J. Boncella. Cation-Cation Interactions, Magnetic Communication, and Reactivity of the Pentavalent Uranium Ion [U(NtBu)(2)](+). 2009. *ANGEWANDTE CHEMIE-INTERNATIONAL EDITION.* **48** (21): 3795.

Spencer, L., P. Yang, B. Scott, E. Batista, and J. Boncella. Uranium(VI) Bis(imido) Chalcogenate Complexes: Synthesis and Density Functional Theory Analysis. 2009. *INORGANIC CHEMISTRY.* **48** (6): 2693.

Spencer, L., R. Gdula, T. Hayton, B. Scott, and J. Boncella. Synthesis and reactivity of bis(imido) uranium(VI) cyclopentadienyl complexes. 2008. *CHEMICAL COMMUNICATIONS.* (40): 4986.

# Improved Length Scaling in Accelerated Molecular Dynamics Methods

*Arthur F. Voter*
20061423ER

## Abstract

The molecular dynamics (MD) method, in which the classical equations of motion are evolved for a system of atoms, is a powerful and commonly used simulation method in physics, materials science, and many other fields. A limitation of MD, however, is that the accessible time scale is limited to roughly one microsecond. Accelerated molecular dynamics (AMD) methods developed at Los Alamos can be used to achieve much longer simulation times than are possible with MD for systems that exhibit infrequent event behavior, such as the occasional jump of a defect in the system. However, these AMD methods are limited to systems no larger than a few thousand atoms. In this project, we developed modifications and extensions to this AMD approach to allow the treatment of much larger systems so that they can be applied to a wider range of important problems. We developed a spatially parallel version of the temperature accelerated dynamics method that can treat much larger systems. We applied this method to simulate the growth of a copper surface at very low temperatures, allowing a reinterpretation of an experimental observation for that system. We also developed a modification of the hyperdynamics method, in which the bias force is defined locally instead of globally, so that the computational speedup is not diminished as the system size increases, but instead remains constant. Simulation tests of this method against exact MD results show that it is very accurate. It should be possible to implement this local hyperdynamics method on massively parallel computers to accelerate the dynamics of systems with billions of atoms.

## Background and Research Objectives

The molecular dynamics method is an extremely powerful tool for studying problems in chemistry, biology, physics, and materials science. Starting only with an interatomic potential describing the forces between atoms, a system is propagated forward in time using Newton's laws, and the true dynamical behavior of the system emerges. This approach is now commonly used to study processes such as fast fracture of a solid, structural fluctuations in a protein, liquid diffusion, fast chemical reactions in solution, and sputtering of a solid surface. A major limitation, however, is that because the equations of motion must be integrated with time steps on the order of femtoseconds (one femtosecond is a millionth of a millionth of a second), the longest time a simulation can run on current computers is typically less than one microsecond. This precludes direct simulation of a vast number of interesting and technologically relevant processes, such as surface diffusion and surface growth, deformation of a surface during manipulation with an atomic probe, thermally activated annealing processes after a radiation damage event or ion implantation, protein folding, grain boundary diffusion, etc. Because we cannot access these longer time scales directly, we typically resort to more approximate models that do not properly incorporate the full complexity of the atom-by-atom interactions and motions, and we have no real error control on the predictions from these higher-level models.

For many systems, the long-time dynamical evolution consists of infrequent events; the system is caught in a single energy basin, wandering around for millions or billions of vibration periods before finding an escape path (e.g., the hop of a surface adatom) that takes it over a barrier to a new energy basin, where it begins vibrating again. Over the last ten years at Los Alamos, we have been developing a new simulation approach that exploits the characteristics of this infrequent-event behavior to reach much longer time scales than one can access using direct molecular dynamics. The key concept in this "accelerated molecular dynamics" (AMD) class of methods [1] is to let the trajectory find an appropriate way to escape from each basin, but to trick it into doing so more quickly, perhaps at the expense of losing information about the vibrational motion. The result is

that the system passes from state to state in a dynamically correct way reaching times of milliseconds, and sometimes even seconds and beyond, with full atomistic fidelity.

We have developed three methods in this AMD class. The first is *hyperdynamics* [2], in which the potential energy surface of the system is modified adding a bias potential to make the escape from each energy basin occur more quickly. This bias potential must meet specific requirements for the state-to-state evolution to remain valid. The second is *parallel replica dynamics* [3], in which the entire system is replicated on each of a number of processors. The first escape event occurring on any processor can be shown to be the correct event to take the system to a new state, and the simulation waiting time (aside from some overhead) is sped up by the number of processors. The third method is *temperature accelerated dynamics* [4], in which the system temperature is increased, causing escape attempts out of the current basin to happen more frequently. From these first few attempted escapes, we have derived a way to determine, with a desired confidence, which one would have been the first escape at the lower, proper temperature.

Over the past decade or so, we have applied these methods to a number of different systems to demonstrate their power as well as to address real materials science problems (e.g., see [5], and references therein). In some cases the computational speedup has been in the millions and billions, providing a view of dynamics on time scales we have never before achieved (and may never be achieved with direct molecular dynamics, since computer speeds will ultimately stop improving). Interestingly, the transitions the system makes are often much different than we would have expected from our intuition. A remaining problem with these AMD methods, however, is that they are limited to small systems, no larger than a few thousand atoms, and this project is aimed at improving on this.

The objective in this project has been to develop new procedures and algorithms to extend the accessible size scale of these AMD methods so that a much wider range of phenomena can be treated. We have approached (and achieved) this objective through two complimentary paths. First, we have developed a way to spatially parallelize the temperature accelerated dynamics method [6]. This work was done in collaboration with Professor Jacques Amar at University of Toledo. Our second path involved a reformulation of the hyperdynamics method, so that the bias force is introduced in a local, instead of global, fashion, so that the computational boost factor does not decay as the system becomes larger. Our first applications of these new methods have been to the growth of metal films, although the methodology is general, and not limited to a particular type of material system.

## Scientific Approach and Accomplishments

In the basic TAD method [4], acceleration is achieved by raising the temperature of the dynamics, but confining the system to a single state (potential energy basin). In this way, attempted escape events are rapidly discovered, each associated with a particular time. Each of these high-T events can mapped (after finding the saddle point energy for the transition) onto a corresponding time at which the same event that would happen at the desired low temperature. It is possible to show that after a certain amount of high-temperature simulation time, we know with a desired confidence that one of the observed escape attempts would have been the *first* escape event at the lower temperature. This event is then accepted, the system is moved to the corresponding state, and the procedure is begun again. This TAD procedure can give huge boost factors (e.g., thousands, millions, or billions) compared to regular MD when the barriers are high relative to the temperature of the system, but the method has a strong computational scaling with system size, limiting TAD to systems of a few thousand atoms. Recently, Shim and Amar [7] developed a spatial parallelization procedure for kinetic Monte Carlo that we realized could be adapted to achieve spatial parallelization of the TAD method. In this approach, each single TAD simulation is performed on a small system that is embedded in the larger system. The key to this method is to subdivide the full system into patches, one for each processor, and then further subdivide the system into a sublattice of smaller patches. For a two dimensional system, appropriate for studying surface diffusion or growth, a square lattice is employed, and the sublattice becomes a 2x2 set of 4 subpatches for each processor, as shown in Figure 1. The simulation proceeds by running TAD on one sublattice patch for each processor, while the other three sublattice patches remain dormant. These dormant areas between the dynamically active areas guarantee that there are no “collisions” (interacting events) between processors at the boundaries. By cycling through the four subpatches, running for a short “cycle time” on each subpatch, accurate TAD dynamics for the system is achieved. The additional approximation relative to regular TAD is that this ParTAD procedure inhibits reactive events involving a large number of atoms. Multi-atom events can (and do) occur, but they cannot be any larger than the size of a subpatch. In exchange for this additional approximation, a much better scaling with system size is achieved, as shown in Figure 2.

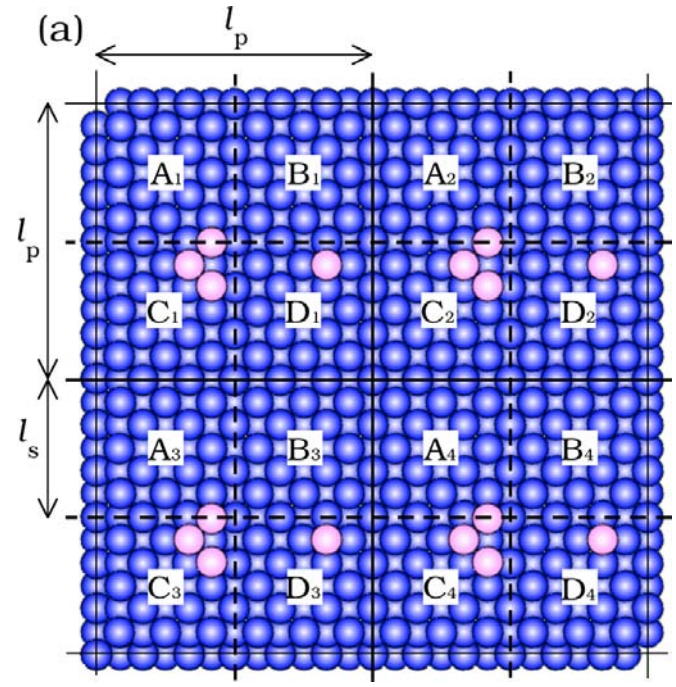


*Figure 1. The processor patches and sublattice patches employed in the ParTAD method. TAD dynamics are evolved on one subpatch at a time on each processor. Cycling through the sublattice patches advances the dynamics of the whole system in a way that is accurate for short cycle times, and avoids event collisions at the boundaries between processor patches. In this case, there are four processors (1-4) and four subpatches per processor patch (A-D).*

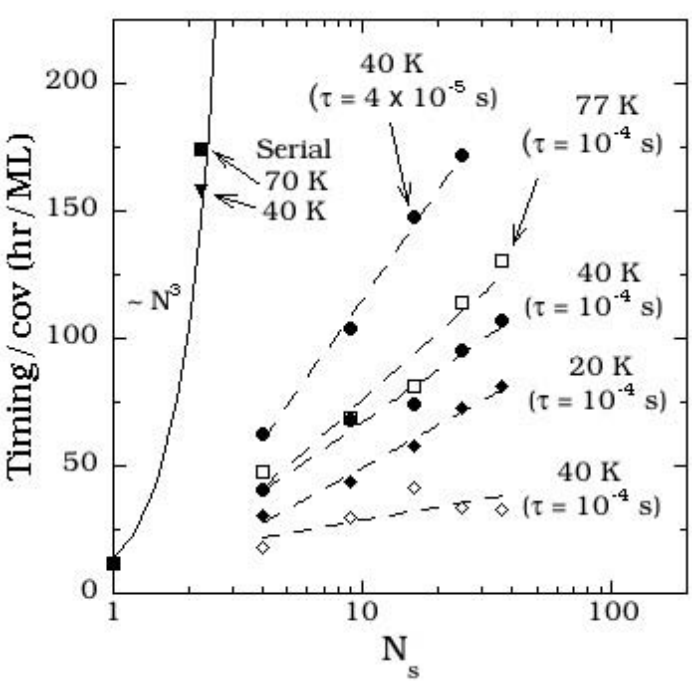


*Figure 2. Size scaling of ParTAD compared to regular TAD, tested on a copper surface system during simulated vapor deposition under various conditions of temperature and deposition rate.*

We have applied the ParTAD method to study the growth of a copper surface from vapor deposition at low temperature [8]. X-ray diffraction experiments performed by Miceli's group [9] over the last few years have indicated that for growth below T=~100K, there is a significant strain in the film, which they interpreted as arising from a significant number of bulk vacancies (~2%) incorporated into the growing film. Combining molecular dynamics deposition simulations (lasting a few picoseconds per deposition) with ParTAD simulations to evolve the system for the much longer time between deposition events, we have been able come much closer to the true experimental deposition conditions than have been possible before now. We employed a much larger system than we could have with regular TAD, and this larger system was necessary to fully understand the morphology of the growing surface. We achieved a deposition rate of 5000 monolayers per second, which is much faster than in the experiment, but is roughly 5 orders of magnitude slower than is possible with a direct molecular dynamics (MD) study, allowing us to study the effect of thermally activated events.

From the films grown using MD+ParTAD, we have simulated the X-ray diffraction patterns for comparison with the experiment, as shown in Figure 3. Using direct MD simulations, in which no thermal events have time to occur between successive depositions, we find reflectance oscillations that are in near-quantitative agreement with the experimental pattern (see Figure 3b) when we use a deposition angle of 55 degrees (where zero degrees would be normal deposition). The experimental deposition angle is thought to be close to this value. Comparing the MD simulations with ParTAD simulations, we find that the effect of thermal events, up to a temperature of T=77K, is to slightly soften the reflectance oscillations in the X-ray diffraction spectrum, but the shape is largely unchanged (as shown in Figure 3c).

Perhaps most significantly, as shown in Figure 4, we see an interesting nano-scale roughness in the grown surface, even after just a few (e.g., 7) monolayers, with surprising [100] oriented vertical cliffs (Figure 4d). It appears that this roughness, rather than the incorporation of vacancies into the film, is responsible for the experimentally observed strain in the film. In contrast to the experimental claim of 2% vacancy concentration, we observe a much lower concentration of incorporated vacancies (less than 0.1%). Moreover, we find that if these vacancies are filled in before modeling the X-ray spectrum, the spectrum is essentially unchanged, indicating fairly conclusively that the peaks in the X-ray diffraction spectrum are not due to vacancies.

Most recently, we have begun applying the ParTAD method

to the study of radiation damage annealing in metallic solids, a problem notorious for requiring longer time scales than MD can reach, as well as requiring larger systems than TAD can handle once the impact energy is high.

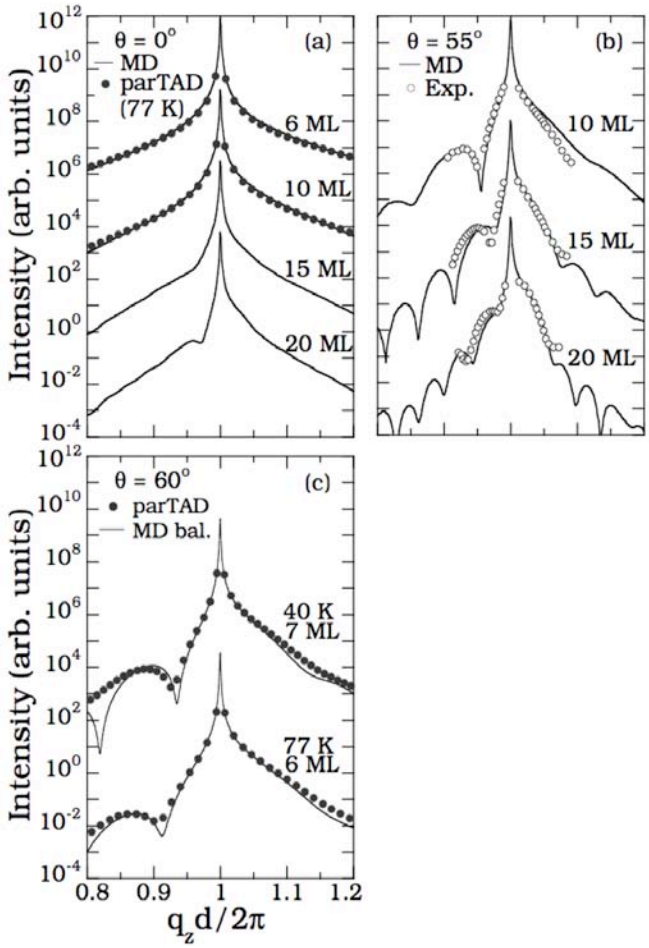


*Figure 3. Xray diffraction patterns, experimental and simulated, for the few-monolayer copper system grown with vapor deposition, as discussed in text.*

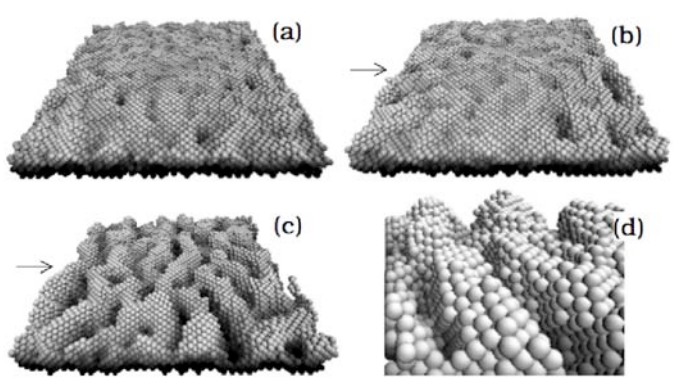


*Figure 4. Simulated copper films grown using direct MD for the deposition events and ParTAD for the much longer time between events. Three different angles of deposition are shown: (a) normal to the surface, (b) 30 degrees off normal, and (c) 60 degrees off normal. The arrows indicate the off-normal direction. Panel (d) is a close-up of the 60-degree film in (c), showing the surprisingly vertical [100] cliffs that form during this growth.*

On our second project path, we developed a generalized version of hyperdynamics in which the bias potential is defined locally, thereby allowing arbitrarily large systems to be propagated forward in time. In normal hyperdynamics, if the system comes near to making a transition anywhere in the system, the bias potential is shut down for the entire system. This requirement on the bias potential ensures the dynamical evolution is accurate, but it also guarantees that for a large enough system, the computational speedup will become vanishingly small. We have developed an algorithmic procedure for this new local hyperdynamics and we have implemented it for both model systems and for more realistic embedded atom method (EAM) systems. We have developed an efficient on-the-fly approach for fitting the coefficients that define the bias potential; this refitting needs to be performed each time the system enters a new state. For the three different model systems, we have shown that this local hyperdynamics approach gives very accurate results. One of these model-system tests is shown and described in Figure 5. In our most demanding and precise test, the method gives rate constants that agree with the exact results (from direct MD) to within 5% or better for boost factors up to 100. Presumably the method works well for even larger boosts, but it becomes prohibitively expensive to compute the exact MD results to compare with. We have not yet been able to provide a mathematical proof that the method is valid, but we have a heuristic derivation and we believe the method can be shown to be exact in some limits. A particularly exciting feature of this local hyperdynamics is that it should be easy to implement in the context of large-scale molecular dynamics simulations. For example, on the new Los Alamos Roadrunner system, this could allow us to reach an unprecedented size and time scale of billions of atoms for microseconds.

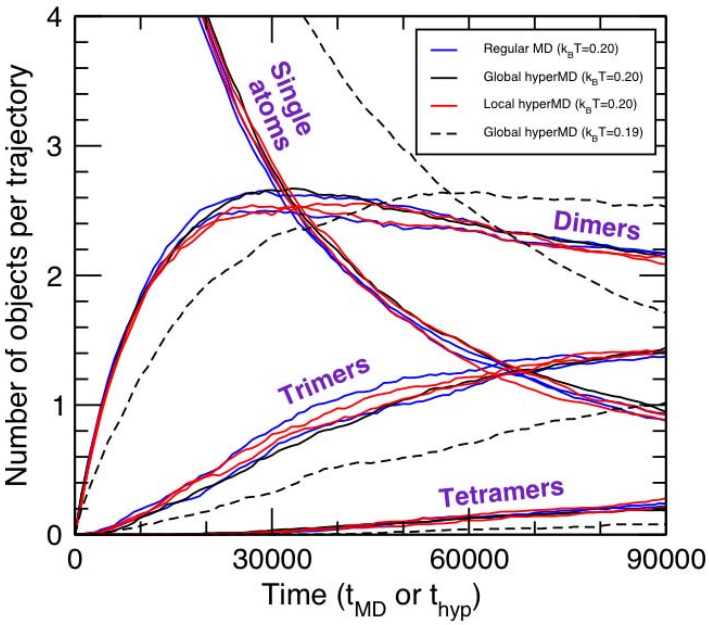


*Figure 5. Results from a test of the local hyperdynamics method on a prototype two-dimensional (1+1) surface diffusion system. Beginning from a particular initial configuration with no nearest-neighbor adatoms, the adatoms make diffusive hops in one dimension as time evolves, passing through many kinds of states. The observable property that we compare against methods known to be accurate or exact (normal hyperdynamics and regular MD, respectively) is the concentration of clusters of a certain size. The dashed lines are the correct (hyperdynamics) results for a system at a 5% lower temperature (T=0.19 instead of T=0.20). This is shown to indicate how much even a small change in the system parameters perturbs these results, to give a sense of how accurately the local hyperdynamics is reproducing the correct results at T=0.2.*

## Impact on National Missions

This work advances the state of the art for simulation of processes such as radiation damage in nuclear fuels and nuclear waste, dislocation motion in structural materials, surface growth processing, and fracture. Problems in these areas for which direct molecular dynamics simply cannot reach the relevant time scales are extremely common. These methods offer ways to probe the behavior on these longer time scales, and to test and validate more approximate models that are often employed. This work thus contributes to the DOE missions in Energy Security, Nuclear Security, Environmental Responsibility, and Scientific Discovery and Innovation. The local hyperdynamics methodology developed in this program was part of the motivation for, and is being further developed under, the new LDRD-DR program entitled "Spatio-Temporal Frontiers of Atomistic Simulations in the Petaflop Simulation World," Tim Germann, PI.

## Publications


Perez, D., B. P. Uberuaga, Y. Shim, J. G. Amar, and A. F. Voter. Accelerated molecular dynamics methods: Introduction and recent developments. 2009. *Annual Reports in Computational Chemistry.* **5**: 79.

Shim, Y., J. G. Amar, B. P. Uberuaga, and A. F. Voter. Reaching extended length scales and time scales in atomistic simulations via spatially parallel temperature-accelerated dynamics. 2007. *Physical Review B.* **76**: 205439.

Shim, Y., V. Borovikov, B. P. Uberuaga, A. F. Voter, and J. G. Amar. Vacancy formation and strain in low-temperature Cu/Cu(100) growth. 2008. *Physical Review Letters.* **101**: 116101.

# Coulomb Mechanisms for Ion Damage in Insulators in the Electronic Stopping Regime

*Cynthia J. Reichhardt*
20070156ER

## Abstract

Currently, there is no understanding of the microscopic formation of damage tracks by fission fragments in the electronic stopping regime. This process is important for ceramic fuel materials which can provide an alternative energy source to fossil fuels. We use a combination of theory, simulation, and experiment to construct and study a detailed microscopic mechanism of damage in the electronic stopping regime based on Coulomb explosion processes which result from intense electric fields generated in the ion tracks. We have developed the Screened Ion Spike model as a highly viable microscopic mechanism, and have tested aspects of the model through large scale simulations and a series of heavy ion irradiation studies.

## Background and Research Objectives

Ion damage processes are important in a range of technological applications and have recently attracted attention due to their role in the stability of nuclear fuel material. Fission fragments generated within a fuel lose energy as they travel through the bulk material and can in some cases produce latent damage tracks, which are cylindrical regions along the path of the fragment in which the material is either amorphized, crystallized in a different form, or damaged in some way. Existing models for ion damage processes in the electronic stopping regime, which accounts for most of the energy loss of fission fragments, are inadequate to provide reliable predictive power over all relevant energies, and it is not yet possible to predict what materials will suffer damage and how much damage will occur. Controversy persists over the microscopic damage mechanism and recent work has been focused on two main areas. In the thermal spike model [1,2], which is widely applied, the energy deposited by the fission fragment in the electronic degrees of freedom is converted to lattice phonons that locally melt the lattice over long time scales. Although this is a strongly nonequilibrium process, the models are typically formulated using equilibrium thermodynamic concepts. In ion spike or Coulomb explosion models [3], the fission fragment ionizes atoms along its trajectory and the target ions recoil under their mutual Coulomb repulsion, resulting in damage. Ion spike mechanisms have been relatively neglected due to the expectation that the charge of the ion track will be neutralized on a time scale that is too short for significant target ion motion to occur; however, this has never been tested in detail. Experimental observations of track formation suggest that there is a nontrivial connection between track formation and the conductivity properties of the sample, which would be consistent with an ion spike but not necessarily with a thermal spike mechanism. Inspired by these and related results, in this project, we revisit the ion spike concept and find evidence that highly nonequilibrium short time scale processes could result in the formation of latent damage tracks of the type observed experimentally. We have developed the Screened Ion Spike model as a result of this study.

## Scientific Approach and Accomplishments

We use a combination of theory, simulation, and experiment to explore processes related to damage formation in ion spikes. Advances in the theoretical model occurred throughout the lifetime of the project and as a result it was not possible to test all aspects of the model in our simulations and experiments. Simulations were performed using highly efficient parallel large-scale molecular dynamics code. Experimental tests of track formation in a series of insulating materials were performed using high energy ion irradiation.

The Screened Ion Spike model contains several components that were not considered in the original ion spike mechanisms. The first is a more careful consideration of the effects of ionization on the target atoms. When the fission fragment directly strikes a

target atom in the electronic stopping regime, it ionizes the atom and ejects one or more electrons. In the standard Coulomb explosion model, the target ions attempt to move apart under Coulomb repulsion; however, this motion is ineffective at generating damage due to a lack of free volume into which the ions can move [4]. A similar problem arises in thermal spike models. In our model, the ionization of the target ions causes their effective Pauling radii to decrease, meaning that each ion effectively becomes smaller. The increase in available free volume dramatically increases the mobility of the target ions [5], greatly facilitating the possibility of the creation of damage.

The second aspect of the Screened Ion Spike model is a concept which we term Nonequilibrium Coulomb Explosion (NCE). In the standard Coulomb explosion model, the target ions are assumed to start at rest, and all the motion of the target ions within the fission fragment track is a result of their acceleration by repulsive Coulomb forces. There are two problems with this picture. The first is that the time required to accelerate a target ion to the point where it is able to be displaced over distances as large as a lattice constant is prohibitively long; it is likely that the charge of the fission track will be neutralized before then (track charge is addressed in more detail below). Additionally, light atoms should be accelerated faster than heavy atoms, and there is no good evidence for this. The second problem is that the radial acceleration of the target ions away from the fission track tends to produce a coherent radial motion of the target ions. The coherence inhibits the types of plastic or incoherent motions required to form defect sites that can persist after the track charge has been neutralized. In our NCE model, we eliminate the false hypothesis that the target ions start at rest within the track. In an actual sample, the target atoms are undergoing thermal vibrations in random directions. At the moment that the target atoms are ionized by the fission fragment, the bonding between neighboring atoms is effectively destroyed, and rather than continuing to vibrate thermally, each of the target ions moves ballistically at whatever thermal velocity it had at that moment. Two important effects result from the NCE model. First, it is no longer necessary to wait for Coulomb repulsion to accelerate the target ions; they move immediately with their thermal velocities, and there is no longer a bias toward the easier motion of lighter atoms. Second, there is no longer a radial pulse of displacements. Instead, the displacements are randomly directed, giving a much better chance of the type of incoherent motion required to create a defect site in the lattice. Note that the NCE model no longer contains a true Coulomb explosion; the important effect achieved by removing electrons from the fission fragment track is to eliminate the binding between target ions rather than to accelerate those ions away from each other.

The final new aspect of the Screened Ion Spike model, and that which gives the model its name, is the concept of temporary electronic defect formation in a halo region surrounding the fission fragment track, as illustrated in Figure 1. The problem with all ion spike models is that even in insulating materials, thermally excited conduction electrons should very quickly move into the depleted fission track and neutralize its charge. In order for an ion spike to produce damage, there must be a mechanism that can slow the charge neutralization process. Our Screened Ion Spike concept provides a mechanism that has never been previously considered, to the best of our knowledge. During the formation of the charged fission track, electrons ejected from the track pass ballistically into the material surrounding the track where they eventually lose their energy through inelastic collisions. The range of these ejected electrons depends strongly on the energy of the fission fragment and on the electronic properties of the target. In other models the ejected electrons are ignored, but in our model we consider the fact that the existence of these electrons implies that a cylindrical region around the track experiences a temporary increase in the density of electronic scattering centers in the form of atoms that are either ionized or excited by the ejected electrons. Electrons in the bulk of the target that are attempting to travel to the depleted fission track must pass through this region and will experience higher than normal scattering. The apparent mean free path of the material is decreased around the fission track and it takes the electrons longer than normal to traverse it. As a result, the lifetime of the fission track charge can be extended, and in some materials and for high enough fission fragment energies, the track lifetime becomes long enough for the damage processes described above to occur. Since the increase in scattering centers is only temporary, this halo region around the actual latent damage track is normally not observable, although in materials such as LiF where electronic excitations can be trapped as color centers, a large “infratrack” region around the latent damage track has been observed [6].

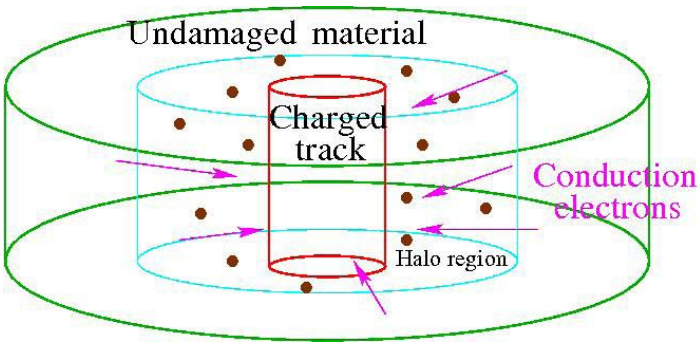


*Figure 1. Schematic of Screened Ion Spike model. Conduction electrons rushing toward the positively charged track of a fission fragment are slowed in an electronically damaged halo region. Brown circles represent target atoms that have been ionized or excited by electrons ejected from the charged track.*

In our simulations, we are able to access the nanosecond timescale on a size scale of 10,000 to 1 million atoms. We performed comparative simulations of three damage processes: standard Coulomb explosion with ionization effect, nonequilibrium Coulomb explosion, and thermal spike. In the standard Coulomb explosion with ionization effect, we mimic the decrease in effective ionic radius predicted to occur due to loss of outer electrons by changing the parameters of the atomic interaction potentials on the fly so that the effective interaction between ions is of shorter range than that between undisturbed target atoms. Acceleration due to Coulomb repulsion of the ions is modeled by giving the ions a momentum distribution directed radially away from the path of the fission fragment. After an adjustable period of time representing the lifetime of the charged track, we restore the effective ionic radii to their original values. For the nonequilibrium Coulomb explosion, we also reduce the range of the effective interaction between ions during the charged track lifetime, but the ions are given an isotropic thermal momentum distribution at the temperature of the sample. Finally, for comparison we perform a thermal spike simulation in which the interaction range is unchanged but all target atoms within a cylindrical region are given a thermal velocity distribution representing a very high temperature. In each case we monitor the number of defects present in the sample as a function of time. We find evidence that the nonequilibrium Coulomb explosion process produces an increased number of persistent defects in the lattice structure of the target compared to the other two processes. Figure 2 illustrates the damage process in spinel samples under the thermal spike mechanism at two different temperatures. More damage occurs in the higher temperature sample, but much of the damage anneals out over time, demonstrating that equilibrium thermal processes are insufficient for damage formation and that additional physics, such as that in the Screened Ion Spike model, is required.

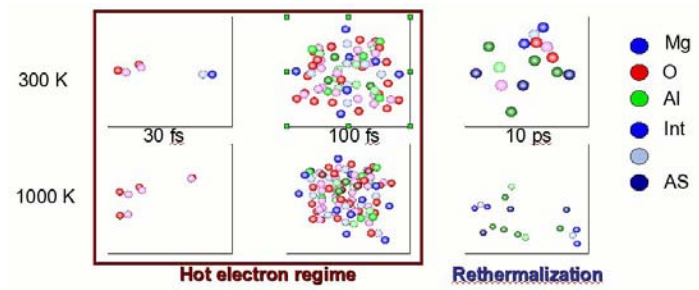


*Figure 2. Results from a large scale atomistic simulation of a thermal spike damage process in a spinel. Only defect atoms are shown; the pristine crystal is not shown. Defects can be created on short (femtosecond) time scales but almost completely recombine within 10 picoseconds.*

In experiment, we performed heavy ion irradiations and damage characterizations of sets of samples that had the same lattice structure but varying atomic number. These studies were designed to test the effect of changes in the number of electrons ejected from the heavy ion track on subsequent damage formation, and we found a correlation between increase in atomic number and increase in damage for sample sets which had similar electronic properties. Polycrystalline samples of $Lu_2O_3$ and $Sc_2O_3$ were fabricated with conventional ceramic processing procedures and irradiated with 2.3 GeV Pb ions at Gesellschaft fur Schwerionenforschung (GSI) in Darmstadt, Germany. We observed evidence of a phase transformation in damage tracks which formed in $Lu_2O_3$ , indicating a significant amount of lattice displacement. Figure 3 shows a transmission electron microscope image of a $Lu_2O_3$ damage track. In addition to studies of $Gd_2Ti_2O_7$ and $Gd_2Hf_2O_7$, we also performed measurements on the delta-phase oxides $Sc_4Zr_3O_{12}$ and $Lu_4Zr_3O_{12}$. These compounds are of particular interest since they are structurally related to fluorite compounds which have potential application as host materials for nuclear waste or as advanced nuclear fuel forms for the transmutation of minor actinides. We irradiated the sintered polycrystalline sample pellets with 185 MeV Au ions at the Heavy-Ion Accelerator Facility of the Australian National University, Canberra, Australia, in order to simulate radiation damage effects similar to those induced by fission products in nuclear fuel. X-ray diffraction and transmission electron microscopy measurements reveal that although both compounds are resistant to swift heavy ion irradiation-induced amorphization, an order-disorder transformation occurs from the original ordered delta-phase structure to a disordered cubic fluorite structure within the ion tracks. Damage occurs more readily in the compound with higher atomic number. We also find evidence of volume change within the tracks, suggesting that the ionization effects

in the Screened Ion Spike model could play a part in the damage formation.

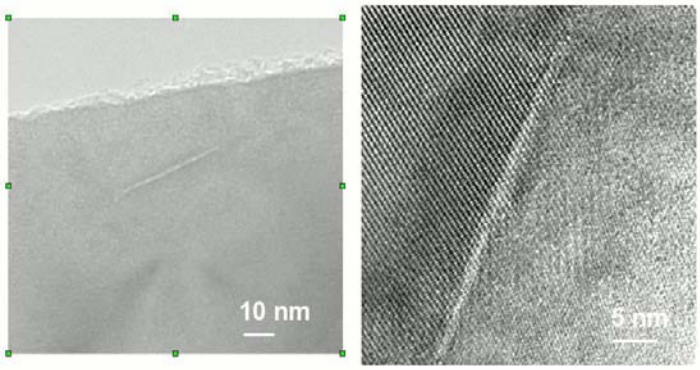


*Figure 3. Transmission electron microscope images of a damage track in $Lu_2O_3$.*

## Impact on National Missions

This project supports the DOE mission in Energy Security and the Office of Science mission in Nuclear Energy by enhancing our understanding of the microscopic mechanism of fission fragment damage in ceramic nuclear fuel materials. To reduce the nation's dependence on foreign oil, it is important to develop alternative energy resources such as nuclear energy. This project addresses aging and damage processes that affect ceramic nuclear fuel materials. A better understanding of the damage process will improve our predictive power for the properties of nuclear fuels and could lead to the development of better, more damage resistant fuel materials in the future.

## References

1. Toulemonde, M., C. Dufour, and E. Paumier. Transient thermal process after a high-energy heavy-ion irradiation of amorphous metals and semiconductors. 1992. *Physical Review B.* **46** (22): 14362.

2. Szenes, G.. General features of latent track formation in magnetic insulators irradiated with swift heavy ions. 1995. *Physical Review B.* **51** (13): 8026.

3. Fleischer, R. L., P. B. Price, and R. M. Walker. Ion explosion spike mechanism for formation of charged-particle tracks in solids. 1965. *Journal of Applied Physics.* **36** (11): 3645.

4. Bringa, E. M.. Molecular dynamics simulations of Coulomb explosion. 2003. *Nuclear Instruments and Methods in Physics Research B.* **209**: 1.

5. Drocco, J. A., M. B. Hastings, C. J. Olson Reichhardt, and C. Reichhardt. Multiscaling at point J: Jamming is a critical phenomenon. 2005. *Physical Review Letters.* **95** (8): 088001.

6. Schwartz, K., C. Trautmann, T. Steckenreiter, O. Geiss, and M. Kraemer. Damage and track morphology in LiF crystals irradiated with GeV ions. 1998. *Physical Review B.* **58** (17): 11232.

## Publications

Blair, M. W., M. R. Levy, R. W. Grimes, B. P. Uberuaga, C. Jiang, J. A. Valdez, J. J. Williams, M. Tang, C. R. Stanek, and K. E. Sickafus. Charge compensation in an irradiation-induced phase of delta-Sc4Zr3O12. 2009. *Journal of Materials Science.* **44** (17): 4754.

Drocco, J. A., C. J. Olson Reichhardt, and C. Reichhardt. Fluctuation theorem in dynamical systems with quenched disorder. *Physical Review Letters.*

Ishimaru, M., Y. Hirotsu, M. Tang, J. A. Valdez, and K. E. Sickafus. Ion-beam-induced phase transformations in delta-Sc4Zr3O12. 2007. *Journal of Applied Physics.* **102**: 063532/1.

Libal, A., C. Reichhardt, and C. J. Olson Reichhardt. Point-defect dynamics in two-dimensional colloidal crystals. 2007. *Physical Review E.* **75** (1): 011403.

Libal, A., C. Reichhardt, and C. J. Olson Reichhardt. Enhancing mixing and diffusion with plastic flow. 2008. *Physical Review E.* **78** (3): 031401.

OlsonReichhardt, C. J., and C. Reichhardt. Viscous decoupling transitions for individually dragged particles in systems with quenched disorder. 2008. *Physical Review E.* **78** (1): 011402.

Reichhardt, C., and C. J. Olson Reichhardt. Disordering transitions and peak effect in polydisperse particle systems. 2008. *Physical Review E.* **77** (4): 041401.

Reichhardt, C., and C. J. Olson Reichhardt. Nonequilibrium phases for driven particle systems with effective orientational degrees of freedom. 2009. *Physical Review E.* **79**: 061403.

Reichhardt, C., and C. J. Olson Reichhardt. Random organization and plastic depinning. To appear in *Physical Review Letters.*

Reichhardt, C., and C.J. O. Reichhardt. Defect fluctuations and lifetimes in disordered Yukawa systems. 2007. *Physical Review E.* **75**: 051407/1.

Reichhardt, C.J. O., C. Reichhardt, and A. R. Bishop. Structure and fragmentation in colloidal artificial molecules and nuclei. 2007. *European Physical Journal E.* **22**: 11.

Rushton, M.J. D., C. R. Stanek, A. R. Cleave, B. P. Uberuaga, K. E. Sickafus, and R. W. Grimes. Simulation of defects and defect processes in fluorite and fluorite related oxides: Implications for radiation tolerance. 2007. *Nuclear Instruments and Methods in Physics Research B.* **255**: 151.

Shen, T. D., S. Feng, M. Tang, J. A. Valdez, Y. Wang, and K. E. Sickafus. Enhanced radiation tolerance in nanocrystalline MgGa2O4. 2007. *Applied Physics Letters.* **90**: 263115/1.

Sickafus, K. E.. Introduction to mathematical models for irradiation-induced phase transformations. 2007. *NATO Science Series, Series II: Mathematics, Physics and Chemistry.* **235**: 321.

Sickafus, K. E., R. W. Grimes, J. A. Valdez, A. Cleave, M. Tang, M. Ishimaru, S. M. Corish, C. R. Stanek, and B. P. Uberuaga. Radiation-induced amorphization resistance and radiation tolerance in structurally related oxides. 2007. *Nature Materials.* **6**: 217.

Tang, M., J. A. Valdez, B. P. Uberuaga, and K. E. Sickafus. Irradiation-induced amorphization and order-disorder transformation in the tungsten delta-phase oxides Yb6W1O12 and Y6W1O12. 2009. *American Institute of Physics Conference Proceedings..* **1099** (1): 973.

Tang, M., J. A. Valdez, K. E. Sickafus, and P. Lu. Order-disorder phase transformation in ion-irradiated rare earth sesquioxides. 2007. *Applied Physics Letters.* **90**: 151907/1.

Tang, M., J. A. Valdez, K. E. Sickafus, and P. Lu. Irradiation-induced order-to-disorder phase transformation at different temperatures in Dy2O3. 2007. *JOM.* **59** (4): 36.

Tang, M., J. A. Valdez, and K. E. Sickafus. Ion irradiation damage effects in delta-phase Y6W1O12. 2008. *Journal of Nuclear Materials.* **376** (2): 247.

Tang, M., K. S. Holliday, J. A. Valdez, B. P. Uberuaga, P. O. Dickerson, R. M. Dickerson, Y. Wang, K. R. Czerwinski, and K. E. Sickafus. Radiation damage effects in the uranium-bearing delta-phase oxide Y6U1O12. 2009. *Journal of Nuclear Materials.* **389** (3): 497.

Tang, M., P. Kluth, J. Zhang, M. K. Patel, B. Uberuaga, C. Reichhardt, and K. E. Sickafus. Swift heavy ion irradiation-induced microstructure modification of two delta-phase oxides: Sc4Zr3O12 and Lu4Zr3O12. *Nuclear Instruments and Methods in Physics Research B.*

Tang, M., P. Lu, J. A. Valdez, C. R. Stanek, and K. E. Sickafus. The order-disorder phase transformation in ion-irradiated rare earth sesquioxide Dy2O3. 2007. *Physica Status Solidi C.* **4** (3): 1171.

Uberuaga, B. P., A. F. Voter, K. E. Sickafus, A. Cleave, R. W. Grimes, and R. Smith. Structure and mobility of radiation-induced defects in MgO. 2007. *Journal of Computer-Aided Materials Design.* **14** (SUPPL 1): 183.

Usov, I. O., J. A. Valdez, J. Won, M. Hawley, D. J. Devlin, R. M. Dickerson, B. P. Uberuaga, Y. Q. Wang, C. J. Reichhardt, G. D. Jarvinen, and K. E. Sickafus. Irradiation effects in an HfO2/MgO/HfO2 tri-layer structure induced by 10 MeV Au ions. 2009. *Nuclear Instruments and Methods in Physics Research B.* **267** (11): 1918.

Valdez, J. A., Z. Chi, and K. E. Sickafus. Light ion irradiation-induced phase transformation in the monoclinic polymorph of zirconia. 2008. *Journal of Nuclear Materials.* **381** (3): 259.

Xu, P., M. Tang, and J. C. Nino. In situ studies of ion irradiated inverse spinel compound magnesium stannate (Mg2SnO4). 2009. *Journal of Nuclear Materials.* **389** (3): 410.

# Synthesis of Nanowire Heterostructures for Strain-Controlled Bandgap Engineering

*Samuel T. Picraux*
20070204ER

## Abstract

In this project we have systematically explored silicon-germanium nanowire heterostructures through novel growth strategies, nanowire structure and property characterization, atomistic simulations, and theoretical modeling. Key deliverables have included: 1) established the synthesis of axial and radial silicon-germanium nanowire heterostructures; 2) experimentally measurement and theoretically predicted the degree of sharpness of interfaces; 3) developed atomistic simulations of nanowire heterostructure strain distributions and predicted strain localization effects; 4) predicted the limits of defect free growth of nanowire strained heterostructures achievable in unconstrained nanowire heterostructures; and 5) determined the strain-dependent change in germanium and silicon band gaps for highly strained heterostructures. The fundamental knowledge gained from these studies will enable rational design of defect-free, 3D nanoscale heterostructures with materials combinations, interfaces, and strain-induced electronic effects not previously accessible.

## Background and Research Objectives

The goal of this project has been to gain a fundamental understanding of the *synthesis of epitaxial nanowire heterostructures*. These quasi one-dimensional (1D) nanomaterials have received widespread attention because of their potential for achieving new electrical, optical, and thermal properties not achievable in bulk materials[1]. The long term objective of our work is to exploit nanowire heteroepitaxy to create new nanomaterials with properties not possible previously. This research contributes to both fundamental solid state sciences as well as to emerging nanotechnologies. The heteroepitaxy can be along the length of the nanowire or in concentric core-shell structures around the nanowire (Figure 1). Results from these studies provide quantitative insight into the role of dimensionality and strain in physical properties of low dimensional structures compared with their 3D bulk counterparts, We believe the new results obtained here for silicon (Si) and germanium (Ge) semiconductor nanowire materials will have high impact for: 1) energy applications through new low cost solar cells and high efficiency thermoelectric devices, 2) next generation electronics through 3D architectures with high performance, and 3) threat reduction applications through new low power chemical/biomolecular sensing approaches.

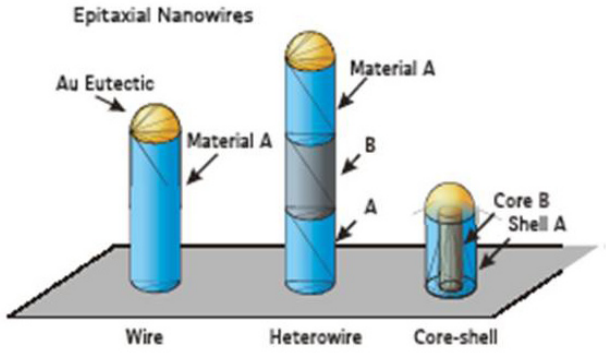


*Figure 1. Schematic of epitaxial nanowire (NW) axial and core-shell heterostructures.*

Epitaxy is a process to grow high quality crystalline materials in a layer-by-layer process. It is particularly important for electronic and photonic materials where defects degrade and limit materials performance. Heterostructures are structures which combine two or more materials together. The epitaxial growth of one material on another is referred to as heteroepitaxy. Combining the properties of two or more materials in a single structure is a way to achieve multifunctionality in materials (i.e., materials which combine different desirable characteristics to optimize its overall property). If the materials combined by heteroepitaxial growth have slightly different lattice constants, then strain is introduced into the structure. This strain alters the

bandstructure of the materials to produce new electronic properties and the effect is referred to as strain-controlled band gap engineering. Because of their small dimensions nanowires offer new, previously unexplored opportunities for band gap engineering.

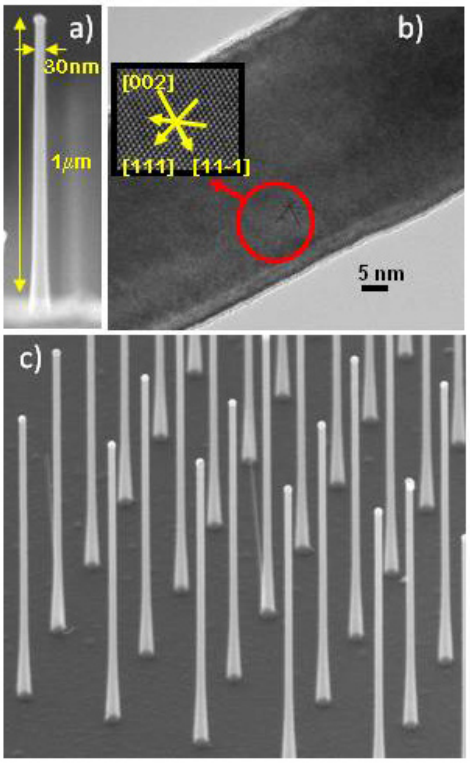


*Figure 2. a) and b) SEM and TEM of Si0.1Ge0.9 alloy NW. c) Ge NW array.*

In the past semiconductor heterostructures have been grown epitaxially on thick substrates, so that their strain is controlled by the substrate. In the 1980s this synthesis approach resulted in great progress in quantum well, superlattice, and strained layer physics and in subsequent device applications. In the 1990s these concepts were extended to higher temperature growth to form and study quantum dots where the strain was again determined by the substrate. Using the vapor-liquid-solid (VLS) technique, low temperature epitaxial growth of nanowires offers a whole new approach to strain engineering due to their small diameter (~10 to 50nm) and thus lack of lateral confinement. For example we predict strain relaxation to occur within a distance a fraction of the nanowire diameters from the heteroepitaxy interface (~5 to 50nm) without defects, in contrast to the 1000 to 10,000nm required for strained layer structures where a high density of detrimental threading dislocations are also present. Lack of lateral constraint also means strain partitioning occurs between the core/shell or between the two sides of an axial nanowire. Thus far larger lattice mismatches can be introduced without requiring strain relaxing defects or surface roughening (typically only 3 to 4 atomic layers are possible for Ge layers on Si substrates, whereas Si/Ge nanowire heterostructures without any dislocations should be attainable). As a result it is possible to introduce large strains with their associated bandstructure changes near interfaces for nanowires. Further the strain can be shifted into the chosen layer by adjusting the 3D design through shell and disc thicknesses—the strain is concentrated in the thinner layer. This flexibility and tolerance to high strains allows new materials combinations to be considered and offers a new approach to strain-controlled bandgap engineering based on heavily strained nanowire architectures. Such materials are anticipated to open the way to new applications in solar cells, thermoelectrics, and low power electronic sensing devices [2-4].

The research objective of these studies has been to exploit the unique combination of a new electrically doped Si/Ge nanowire growth capability with nanoscale characterization tools and theoretical simulations with the aim of:

- understanding the *principles of the synthesis of atomically sharp nanowire heterostructures* by VLS epitaxy, and
- designing, growing and understanding the properties of the resulting new highly strained *nanoscale heteroepitaxial materials*.

The ultimate goal is to design and synthesize novel axial and core-shell nanowire heterostructures demonstrating strain-controlled carrier separation, confinement, and novel electronic and thermal transport validated by measurement and bandstructure calculation.

## Scientific Approach and Accomplishments

Our approach is based on our chemical vapor deposition system which has been specifically designed for the catalytic growth of electrically doped semiconducting nanowires and nanowire heterostructures. The small size and high strain of these three-dimensional nanostructures provide a new approach for the rational design of multifunctional materials exhibiting properties not previously attainable. Our studies exploit the unique combination of a new electrically doped Si and Ge nanowire growth capability, nanoscale characterization tools, and the new nanowire computational simulation capability developed in this project.

The nanowires are synthesized by the vapor-liquid-solid (VLS) growth mechanism in a new cold wall, low-pressure chemical vapor deposition (LPCVD) reactor at Los Alamos National Laboratory. This computer-controlled system is

specially designed for the simultaneous use of silane and germane and doubly diluted diborane and phosphine for n and p electrical doping with fast switching between all gas species for sharp interfaces. This VLS approach has been well established for single-crystal nanowire growth from vapor sources by us and many others, but has seen only very limited investigation for heterostructure nanowire growth. The mechanism is based on a catalyst such as gold (Au) which forms a liquid nanoscale droplet, for example a Au-based eutectic melt with Si and Ge. This catalyst floats on top of the growing nanowire, induces liquid phase epitaxial growth, and defines the nanowire diameter. The Au nanodots are formed by thermal self-assembly from a deposited Au film on a hydrogen-terminated Si surface. For monodispersed arrays of Au nanodots Au colloids or e-beam patterning of deposited Au is used. During VLS growth the silane (germane) decomposes at the Au surface and Si (Ge) is transported through the liquid Au droplet to epitaxially grow at the liquid-solid Si (Ge) interface. VLS epitaxy enables the controlled growth of axial heterostructures at low temperatures (e.g. 400-600C) for sharp interfaces. The strategy for shell growth is to first form the nanowire core by VLS synthesis and then use more reactive vapor phase conditions (for example, lower pressures and higher temperatures) for 'blanket' growth of surfaces to form the nanowire shell. The challenge is combining these longitudinal and coaxial growth conditions for defect free heterostructure growth, and synthesizing novel 3D nanowire heterostructures.

Previous work has demonstrated nanowire heterostructure growth in only limited cases for Si and Ge [5, 6}. Prior to this work the maximum change in composition for axial heterostructures has been less than 20%, whereas we have achieved 100% composition changes from pure Ge to pure Si axial nanowires. For core-shell nanowire heterostructures we have demonstrated an all in situ single crystal Si/Ge heteroepitaxial growth process for the first time (Figure 3). We have also demonstrated independent electrical doping control for these Si/Ge heterostructures. We have also been the first to achieve 3D atomistic simulations of the strain in nanowire heterostructures which we have used these to determine localized strain, electronic band structure, and stability limits for nanowire heterostructures. Highlights of our accomplishment are described below.

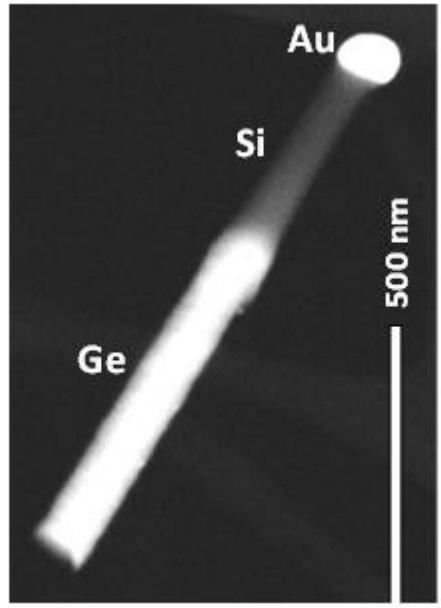


*Figure 3. Electron microscope image of axial Si-Ge NW heterostructure.*

We first established the conditions for the vertical epitaxial growth of silicon, germanium, and silicon-germanium alloy nanowires with uniform sidewalls by the vapor-liquid-solid technique using the new LANL cold wall, low pressure chemical vapor deposition system (Figure 2). Uniform growth with smooth sidewalls is critical in achieving axial heterostructures where the composition of the nanowire is changed from one material (e.g. Si) to the other material (e.g. Ge). The temperature, pressure, and pre-anneal conditions for nanowire growth have been determined and qualitatively understood using scanning and transmission electron microscopy characterization. In addition the conditions for the growth of n- and p-type electrically active Si and Ge nanowires using phosphine and diborane, respectively, as the doping precursor have been established. Four point electrical transport characterization was used to infer the doping concentrations. Ultrafast optical pump-probe techniques have been used to explore the carrier dynamics in Ge nanowires for the first time and the excited state carrier lifetimes are shown to increase with nanowire diameter.

Diffusion of Au along the nanowire surface to form tiny Au nanodots was discovered to occur when silane or germane precursor gases are pumped out at elevated temperatures. This discovery is critical to proper process control at the end of nanowire growth and during gas switching in heterostructure growth. If Au nanodots are present on the sides of the nanowires during shell growth rough sidewalls will result. For electronic or solar cell devices such Au contamination will lead to detrimental carrier recombination. In contrast, for thermoelectric devices this

effect allows controlled roughening of the nanowire sides for enhanced phonon scattering to further reduce thermal transport and enhance thermoelectric efficiency.

Methods to synthesize axial and radial silicon/germanium nanowire heterostructures with sharp interfaces have been investigated in detail. Maintaining uniform growth upon switch-over of the precursor gases at the heterostructure interface has been the most challenging issue of the project. The change in growth temperature and chemical potentials upon switching between the Si and Ge precursor gases creates instabilities in the liquid metal seed at the end of the nanowire. This effect can cause unstable growth morphology and kinking of the wires and is believed to be the reason Si/Ge axial heterostructures with large compositional changes have not achieved previously. We have made significant progress in establishing growth conditions to minimize or eliminate these instabilities. This control has enabled the growth of axial heterostructures of pure germanium to pure silicon nanowires for the first time (see Figure 3), as well as between the pure elemental and silicon-germanium alloy nanowires of fixed composition. Using transmission and scanning electron microscopy techniques we determined the composition profile across the heterostructure interface. A new theoretical model to describe the interface sharpness of axial heterostructures was developed and shown to correctly predict the experimentally observed profiles (see Figure 4). This new model allows us to predict the dependence of the interface sharpness on experimental parameters with no free parameters. The results indicate that the interface sharpness scales with nanowire diameter and can be significantly increased by reducing the nanowire diameter and lowering the growth temperature. For radial heterostructures atomically abrupt interfaces are obtained due to the vapor-solid growth in this case. Careful control of the growth parameters have allowed us to demonstrate core/shell heterostructures in a single growth process sequence, without external processing or annealing for the first time. We have also achieved axial and radial electrical doping of these structures for p-n junction formation.

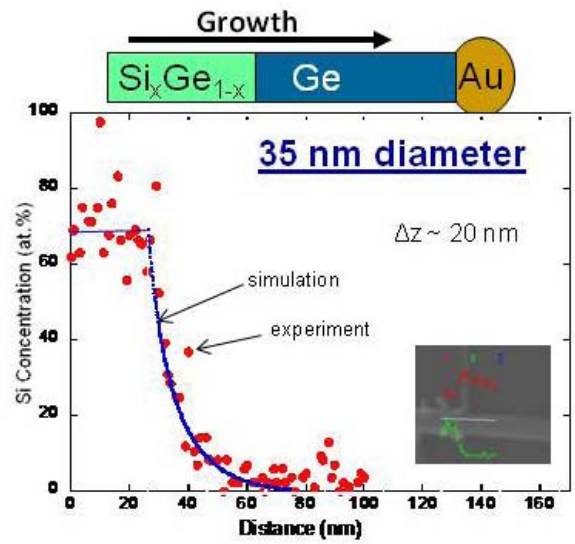


*Figure 4. Experimental concentration profile compared to theoretical prediction for Si concentration profile at a Ge/$Si_{0.7}Ge_{0.3}$ axial NW heterostructure interface.*

A molecular dynamics atomistic simulation code was developed for the first time to predict the strain distributions and stability of nanowire heterostructures. The code is based on the Modified Embedded Atom Method (MEAM). A MEAM silicon-germanium interatomic potential has been developed and verified based on known materials properties of silicon-germanium alloys as well as those of elemental silicon and germanium crystals. These atomistic simulations were applied to silicon/germanium axial and radial heterostructures and the strain distributions determined (Figure 5). It was discovered that localized regions of strain confinement occur at the interface even in uniform nanowires with an abrupt composition transition and unanticipated diameter-dependent deformations of the interface atoms are present. Deformation potential theory was used to show that large changes in the band gap (up to 50% reduction for Ge) can be achieved due to the large strains in these nanostructured materials. Also the strain localization near the interface is shown to scale with nanowire diameter. Such molecular dynamics modeling of realistic-sized nanowire heterostructures has not been carried out previously and many of these results could not have been predicted from previously used continuum modeling approaches.

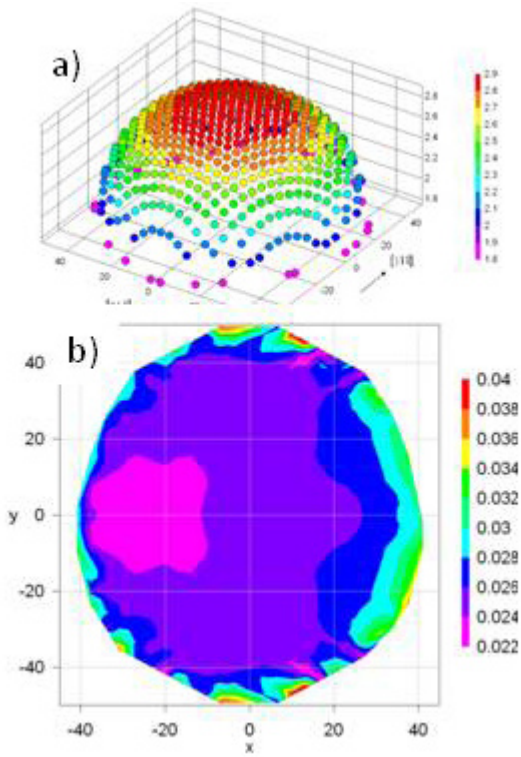


*Figure 5. Atomistic simulation of a) the Ge interface atom height and b) the εxx strain map across the interface for a Si/Ge axial NW heterostructure.*

These simulations also allowed us to predict the limits of defect free nanowire growth at large diameters for the heterostructured nanowires. For a pure silicon to pure germanium interface, which corresponds to a 4.1 % lattice mismatch, the axial heterostructure results show the interface to be stable against misfit dislocation formation for nanowire diameters below 70 nm regardless of the nanowire length. This limit falls well within the10 to 50nm diameter region of desired nanowire design and is qualitatively consistent with experiments. This stability results from strain sharing and a lack of lateral confinement. Nanowire heterostructures are thus found to have much greater stability than 2D silicon-germanium layered heterostructures, where dislocation introduction occurs at approximately 1.4 nm layer thicknesses. As a result much greater strains and resulting band gap modifications are possible in nanowire heterostructures than in conventional layered structures, supporting a key premise of this LDRD project.

## Impact on National Missions

These new 1D nanomaterials are of great interest for applications in low power electronics, third generation solar cells, chemical/biomolecular sensing, high efficiency thermoelectrics, and next generation 3D electronics. Low power nanowire sensors have the potential to impact threat reduction missions. We are currently developing nanowire crossbar sensor arrays with this objective based on the results obtained here; the work is funded by the National Nanotechnology Enterprise Development Center. Energy missions are also anticipated to be impacted. An Integration Focus Area on Nanowires for Energy Applications has been established by the Center for Integrated Nanotechnologies to pursue enabling science for thermoelectric and photovoltaic energy harvesting. In addition, S.T. Picraux has just received an EERE contract (3 year $1,000,000) in collaboration with Sharp Laboratory of America to assess the underlying issues for implementing radial p-n junction Si nanowires as a new high efficiency, low cost approach for solar cells.

## References

1. Xiaetal., Y.. One-dimensional nanostructures: synthesis, characterization, and applications. 2003. *Adv. Mater.*. **15**: 353.

2. Kayesetal., B. M.. Comparison of the device physics principles of planar and radial p-n junction nanorod solar cells. 2005. *J. Appl. Phys, .* **97**: 114302.

3. Chenetal., G.. Recent developments in thermoelectric materials. 2003. *Inter. Mater. Rev.*. **48**: 45.

4. Zhengetal., G.. Multiplexed electrical detection of cancer markers with nanowire sensor arrays. 2005. *Nature Biotech. .* **23**: 1294.

5. Clarketal., T. E.. Diameter dependent growth rate and interfacial abruptness in vapor-liquid-solid Si/SiGe heterostructure nanowires. 2008. *Nano Lett. .* **8**: 1246.

6. Lauhonetal., . J.. Epitaxial core-shell and core-multishell nanowire heterostructures. 2002. *Nature .* **420**: 57.

## Publications

Choi, S. G., P. Manandhar, J. Y. Huang, and S. T. Picraux. Vapor-liquid-solid epitaxy of vertically oriented Si1-xGex alloy nanowires . *J. Appl. Phys..*

Ingole, S., P. Aella, P. Manandhar, S. B. Chikkannanvar, E. A. Akhadov, D. J. Smith, and S. T. Picraux. Ex-situ doping of silicon nanowires with boron. 2008. *J. Appl. Phys..* **103**: 104302.

Ingole, S., P. Manandhar, J. A. Wright, E. Nazaretski, J. D. Thompson, and S. T. Picraux. Assembly and magnetic properties of nickel nanoparticles on silicon nanowires. 2009. *Appl. Phys. Lett..* **94**: 223118.

Ingole, S., P. Manandhar, S. B. Chikkannanavar, E. A. Akhadov, and S. T. Picraux. Charge transport characteristics

in boron doped silicon nanowires. 2008. *IEEE Trans. on Elect. Devices.* **55**: 2931.

Leonard, F., A. A. Talin, B. S. Swartzentruber, and S. T. Picraux. Diameter-dependent electronic transport of Au-catalyst/Ge-nanowire Schottky diodes. 2009. *Phys. Rev. Lett..* **102**: 106805.

Pransankumar, R. P., S. Choi, S. A. Trugman, S. T. Picraux, and A. J. Taylor. Ultrafast electron and hole dynamics in germanium nanowires. 2008. *Nano Lett..* **8**: 1619.

Sierra-Sastre, Y., S. A. Dayeh, S. T. Picraux, and C. A. Batt. Epitaxy of Ge nanowires from biotemplated Au nanoparticle catalysts. *ACS Nano.*

Sierra-Sastre, Y., S. Choi, S. T. Picraux, and C. A. Batt. Vertical growth of Ge nanowires from biotemplated Au nanoparticle catalysts. 2008. *J. of the Amer. Chem. Soc..* **130**: 10488.

Swadener, J. G., and S. T. Picraux. Strain distributions and electronic property modifications in Si/Ge axial nanowire heterostructures. 200. *J. Appl. Phys..* **105**: 44310.

Swadener, J. G., and S. T. Picraux. Coherent interface limits at high misfit strain in Si/Ge axial nanowire heterostructures. *Nano Lett..*

# Synthetic Decoys for Biothreat Agents

*Rashi S. Iyer*
20070270ER

## Abstract

As widespread resistance to conventional antibacterial agents continues to pose a major threat, the demand for novel therapeutic approaches to the treatment of infection is increasing. The ability to inhibit bacterial cell-to-cell communication and ensuing virulent gene expression offers a novel treatment strategy. Most microbes require a 'quorate population' to manifest an infection in its target host. Quorum sensing (QS) is triggered by highly specialized molecules synthesized by individual bacteria and is critical for cell-to-cell communication. Many human pathogens, including the Bacillus (anthracis), Pseudomonas, Burkholderia, Salmonella, Staphyloccoci and Yersinia species, regulate expression of virulence factors required for pathogenicity via QS. Given the central role of QS systems in successful bacterial pathogenesis and possibly host cell defense mechanisms, these bacterial-derived chemicals and their molecular targets present an excellent therapeutic opportunity. The overall goal of this project was to design, synthesize and use chemical analogs of QS molecules (mimics) as a therapeutic strategy in microbial infections. In the current study we determined the pathogenic response of the bacteria to these novel synthetic analogs and investigated the efficacy of the synthetic decoys to inhibit bacterial growth and biofilm formation, as well as, attenuate bacterial infection in target host cells.

## Background and Research Objectives

### QS disruptors as therapeutics

QS regulation is often used by bacteria to facilitate their competition with, and exploitation of, other bacterial, fungal, plant and animal species. Thus competitors and hosts alike have evolved diverse mechanisms to circumvent this process. For example, several plants have evolved strategies to interfere with the bacteria's AHL (N-acyl-L-homoserine lactone) signaling system preventing them from initiating a pathogenic attack. Such interference includes the production of signal mimics, signal blockers or degrading enzymes, or the production of compounds that block the activity of the AHL-producing enzymes. Examples of compounds with signal inhibiting properties are known and there is evidence for the production of AHL inhibitory molecules by bacteria, algae and plants. In the simplest case, an AHL produced by one bacterial species may be antagonistic to the activity of an AHL used by a second species as seen in the case of *Chromobacterium violaceum*. More complex blocking molecules are produced by the marine alga, *Delisea pulchra* which produces halogenated furanones with some structural similarity to AHLs. These AHL blockers are used to inhibit bacterial cell swarming and attachment responses, preventing the build-up of bacterial biofilms. There is some precedence for this overall strategy as seen with synthetic agonists and antagonists of QS molecules, known as autoinducers which can potentially be used to disrupt or 'deceive' bacterial QS networks thus interrupting the infection process. Of particular relevance to this proposal is the demonstration that disruption of the QS response system can effectively reduce expression of bacterial pathogenic genes, making QS molecules a novel therapeutic target. Hentzer *et. al*. used these natural antagonists as a starting point for antagonist design and demonstrated that the synthetic furanone compound 4bromo-5-(bromomethylene)-2(5H)-furanone specifically targeted quorum-sensing systems and inhibited virulence factor expression in *P. aeruginosa*. To date, several small molecules have been identified as quorum-sensing inhibitors and have been shown to inhibit QS-regulated planktonic growth and virulence factor production in *P. aeruginosa*. Still, the accepted clinical intervention strategy in bacterial infections is treatment with antibiotics. However, currently prescribed small molecule antibiotics have limitations, especially in advanced infectious states when systemic application cannot provide the required local dose of antibiotics necessary for effective bactericidal action due to compromised half-life of the drug. The efficacy of the antibiotic depends on factors such as selective toxicity, bioavailability of the drug and penetration into the target bacteria. Some very effective antibacterial compounds

are unacceptable for human use as they are toxic at their prescribed doses, chiefly due to the fact that current delivery regimens are systemic, thus requiring a whole body dosage to achieve necessary local concentrations. Each of these factors can be suitably addressed by either perturbation or inhibition of critical survival mechanisms, as may be the case with QS-utilizing pathogens, or precise delivery of an antibiotic to its target (Figure 1). Since bacteria utilize AHL molecules for their survival, they can be used to deliver antibiotics using a Trojan horse approach.

*Specific Aim 1: (year 1 and 2)*

- design and synthesis of QS analogs (QSA) libraries
- rate of hydrolysis using stable isotopes labels

↓

*Specific Aim 2: (year 2 and 3)*

Efficacy of QSA in disrupting bacterial functions

- growth
- swarming-motility
- biofilm formation
- virulence protein expression

↓

- Selection of QSA with bacterial pathogenic inhibitory functions
- Correlation of synthetic analog to specific bacterial response affected

↓

*Specific Aim 3: (year 1, 2 and 3)*

- Prevention of bacterial infection in target host cell by selected QSA
- Differential host cellular responses to synthetic QS molecules and QS analogs

*Figure 1. Research objectives and timeline.*

Our specific goal is to perturb bacterial communication and signaling using synthetic QS analogs, thus providing targeted therapeutic intervention (Figure 2). Towards this goal, we propose to: *1. design and synthesize QS analogs that can act as decoys 2. determine the pathogenic response of the bacteria to these synthetic analogs and 3. investigate the efficacy of the synthetic decoys in attenuating bacterial infection in target host cells.*

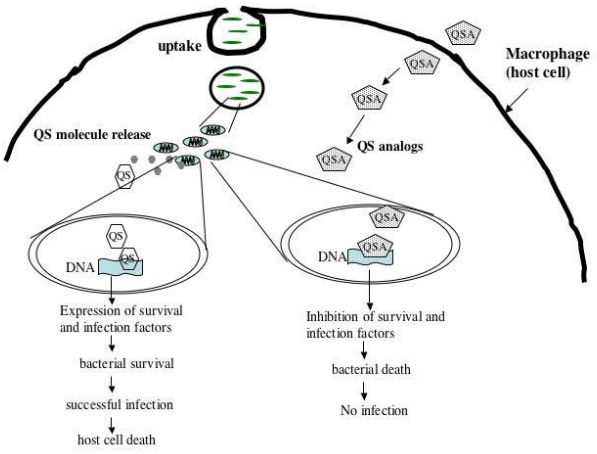


*Figure 2. Using QS decoys to prevent host cell infection.*

## Scientific Approach and Accomplishments

Specific Aim 1: We have successfully synthesized several analogs of AHL molecules that we have determined to be effective in perturbing inter-bacterial QS communication. The bacteria thus far studied to be responsive to our synthetic analogs are, Pseudomonas aeruginosa (PA), Yersinia pestis (YP), Yersinia enetrocolitica (YE) and Burkholderia cepecia (BC).

We synthesized and screened two new AHL-2 ($C_4$HSL) analogs (Figure 3), QS1207 and QS0108 (US Patent number 12/551,994), with 'agonistic' properties that could potentially be used for enhanced penetration of the biofilm and consequently the targeted delivery of antimicrobial agents. In addition, an antagonistic QS analog QS0208 significantly inhibited biofilm formation in BC and Yersinia spp. QS0208 inhibits growth of YP, YE and Y. pseudomonas in biofilm but not in planktonic growth. Our data indicates that the QS0208 analog may effectively inhibit virulence of all three tested strains of Yersinia, Y. pestis, Y. enterocolitica and Y. pseudomonas (Figure 4).

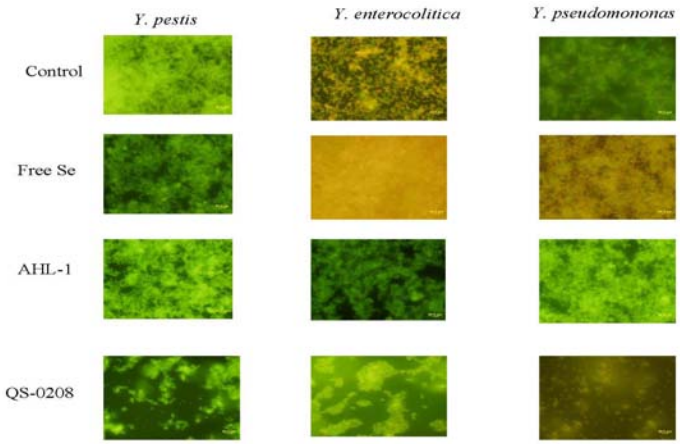


*Figure 3. Attenuation of biofilm formation by QS-0208 in the different Yersinia strains.*

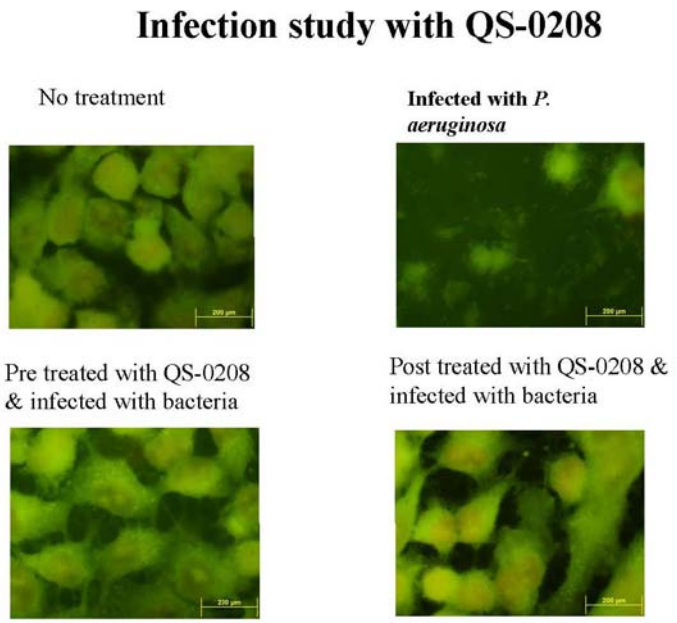


*Figure 4. Inhibition of host infection by P. aeruginosa on treatment with QS-0208*

Specific Aim 2: Using the analogs QS1207 and QS0108 we examined several virulence and pathogenic responses of PA, YP, YE and BC. We screened the different analogs for effectiveness in shutting down virulent bacterial proteins and correlated the type of virulent response affected by a specific synthetic analog. The following key parameters were evaluated; growth characteristics of bacterial cultures, flagellar and twitching-motility and biofilm formation (critical in the infection process), production of pyocyanin (required for pathogenecity) a key virulence factor and protease activity. In this study we included P. aeruginosa PAO-1 (wild type) and its three mutants JP-1 (-/- C12HSL), PDO-100 (-/- C4HSL) and JP-2 (-/- C12HSL and C4HSL) to observe change in biofilms formation in presence of QS-S analog [1].

Results indicate that both the QS analogs AHL-S1207 and QS0108 may potentially enhance virulence of PA, this is probably due to increased uptake of the QS Analogs at below threshold concentrations. This function of the QS analogs can be exploited in two ways, 1. QS Analog AHL-S1207 and QS0108 can potentially be used to 'deceive' bacterial cells to express early virulent genes and pathogenic behavior, thus 'revealing' themselves to host immune cells before they reach a quorate population or result in a biofilm-protected colony, and 2. The QS Analog AHL-S1207 and QS0108 can be conjugated to a relevant antibiotic resulting in not only targeted delivery but also enhanced uptake of the antibiotic by PA, increasing efficacy of antibiotics that are currently being used to combat biofilm producing pathogens.

Specific Aim 3: We investigated the ability of the selected synthetic AHL analogs to prevent host infections caused by QS using pathogens. Since, QS0208 effectively inhibited biofilm production and the expression of other virulence factors in PA we set out to determine if QS0208 was effective in preventing *P. aeruoginosa* infection in target host lung epithelial cells. In these experiments cells were either treated with the QS0208 alone, PA alone, and QS0208 pre and post-infection with PA. As expected, significant cell infection and death was observed in the PA-infected cells. In contrast, cells that were exposed to PA and either pre-treated or post-treated with QS0208 did not demonstrate any significant cytotoxicity or growth of bacteria. These results clearly indicate that QS0208 can potentially protect target host cells from infection by PA (Figure 5).

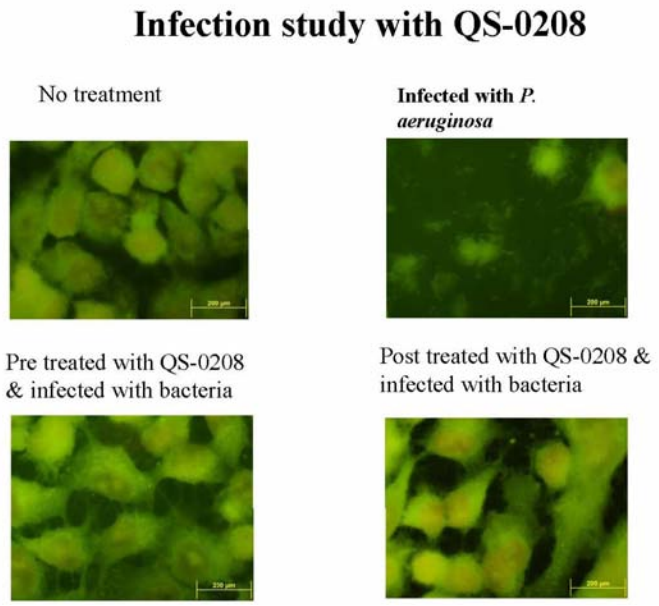


*Figure 5. Infections studies using QS-0208*

Additional objectives:

Use of QS analogs as delivery vehicles for the targeted delivery of conventional antibiotics.
Since extensive biological investigation of the QS1207 and QS0108 analogs suggested a growth promoting activity for these analogs in *Pseudomonas* controlling biofilm production and exo-protease secretion, we hypothesized that these thiolactone analogs could be potentially utilized as potent drug delivery vehicles against biofilm-producing pathogens. As a proof of principle we conjugated the single sulfur analog QS0108 with the broad-spectrum antibiotic, ciprofloxacin (QS0108-Cip). The QS analog-antibiotic conjugate was significantly more effective at disrupting both the nascent and mature biofilms of *P. aeruginosa* than the free antibiotic. In addition we evaluated the response of Yesrinia and Burkholderia strains to this Cip-conjugated analog. QS0108-Cip was highly effective in preventing the

growth and biofilm generation of these bacteria compared to treatment by the antibiotic alone [1].

## Impact on National Missions

The synthesis of intelligent QS inhibitors will have a significant impact on both, clinical and agricultural strategies to combat infections. Results from this project provided targets for drug development. Development of novel therapeutics will have a significant impact on national security and public health. This project could tremendously improve our ability to develop an entirely new treatment paradigm for bacterial infection. Improved treatments against bacterial infection directly support biothreat reduction and improving human health, missions particularly relevant to DOE, DHS, NIH, and other government agencies. Using the data obtained from this study we have submitted a grant proposal to DTRA for further funding to progress to Phase 2 studies using animal models. The post-doc who worked on this project is being considered as a new staff hire and the process has been initiated.

## References


1. deKievit, T., and B. Iglewski. Bacterial quorum sensing in pathogenic relationships. 2000. *Infection and Immunity.* **68** (9): 4839.

2. Suga, H., and k. Smith. Molecular mechanisms of bacterial quorum sensing as a new drug target. 2003. *Current Opinion of Chemical Biology.* **7** (5): 586.

3. Habeck, M.. Stop talking at the back. 2003. *Drug Discovery Today.* **8** (7): 279.

4. Hentzer, M.. Inhibition of quorum sensing in Pseudomonas aeruginosa biofilm bacteria by a halogenated furanone compound. 2002. *Microbiology* . **148** (Pt 1): 87.


## Publications

Ganguly, K., M. Ollivault-Shiflett, R. Wu, L. Silks III, and R. Iyer. Design, synthesis and a novel application of quorum sensing agonists as potential drug-delivery vehicles . *Journal of Clinical Investigation.*

Ganguly, K., M. Shiflet, P. Silks, S. Iyer, and R. Iyer. Strategies for targeting therapeutics to infectious agents. Invited presentation at *6th International Nanomedicine and Drug Delivery Symposium (NanoDDS'08) .* (Toronto, Canada, 17-20 Oct, 2008).

# Magnetic Resonance Force Microscopy Studies of Ferromagnets on a Nanometer Scale

*Roman Movshovich*
20070330ER

## Abstract

Information storage technology experienced tremendous growth over the past few decades. Currently, information is stored with density of 150 Gbit/inch$^2$ (conventional hard drives) and there are projections envisioning 250 Gbit/cm$^2$ density in the near future. An ever-present push towards the increase in the information storage density demands development of both tools to study magnetic phenomena at the nanometer scale (nanoscale) as well as deeper understanding of the properties of magnetic materials that emerge at the nanoscale. We have developed a dual capability instrument to study magnetic phenomena on the nanoscale: Magnetic Resonance Force Microscope (MRFM) / Magnetic Force Microscope (MFM), capable of temperature controlled operation between 1.9 K and 250 K. We used the MRFM option of this unique apparatus to study bulk and local properties of ferromagnetic films and structures, for the first time creating and resolving local resonant modes induced by the rapidly varying in space magnetic field produced by the ferromagnetic tip of the MRFM cantilever. MFM mode of operation allowed us to study superconducting vortices on the scale down to few tens of nanometers, and to extract with high degree of accuracy the magnetic penetration depth in a superconducting niobium film.

## Background and Research Objectives

When the size of a ferromagnetic particle is sufficiently reduced, its magnetization can behave as a single large spin that is thermally fluctuating in time between various local ground states (directions of the magnetization). This phenomenon determines the limiting small size of the magnetic particle that can be used in information storage devices, and is called superparamagnetism, where a large particle behaves as a giant magnetic top that can flip the axis of its spinning. The energy barriers between these states depend on several fundamental interactions within a single particle(i.e. electron-electron, electron-lattice, spin-orbit) via the sample's shape and crystallographic or surface anisotropy. We used magnetic resonance force microscopy (MRFM) to study the effect of these properties on the superparamagnetic behavior of individual particles.

Ferromagnetic phenomena studied until now were those exhibited by the entire macroscopic sample, i.e. bulk ferromagnetic resonant modes. With the advent of the MRFM, with magnetic tip that produces spatially localized sharply varying magnetic field, the opportunity exists to excite and detect a dynamic local ferromagnetic mode on a scale determined by the field profile produced by the magnetic tip, which in turn varies on the scale of the size of the tip itself, on the order of few microns. Such local ferromagnetic resonant modes in a continuous film were predicted by Michael Cross and collaborators at Caltech, but have not been produced/ detected before this project. The search for this novel behavior constituted a major part of this proposal.

In addition, we have implemented the Magnetic Force Microscopy (MFM) mode of operation of our low temperature scanning magnetic probe apparatus, in order to enhance the spatial resolution of magnetic imaging. We built a modular cantilever stage that allows for an easy replacement of the cantilevers. We substituted a commercial MFM cantilever for our home-made MRFM cantilever, and optimized data acquisition software for MFM mode of operation of the apparatus. In addition, we implemented a scanning probe controller , SPM100 from RHK Technology, to use as a part of a dual Magnetic Resonance Force Microscope / Magnetic Force Microscope (MRFM/ MFM) apparatus, and used this apparatus to produce MFM images of the patterned micron-sized squares of ferromagnetic film, and for the first time in our lab, to superconducting vortices in a niobium film. An overview of this dual

apparatus and its performance are described in an article published in the Review of Scientific Instruments [1], and featured in September 14, 2009 issue of Virtual Journal of Nanoscale Science & Technology. The dual MRFM/MFM low temperature capability is unique, and enhances LANL's suite of the magnetic scanning probes into the nanometer range. The advantage of MFM is a much higher spatial resolution, compared to MRFM, which was used for detailed investigation of the magnetic phenomena (ferromagnetism, vortex matter in superconductors) on the scale down to few tens of nanometers. There is a number of exciting avenues of research that are open with low temperature MFM. The two that we focused on are vortex lattice imaging and determination of the magnetic penetration length in superconducting compounds.
The impetus for this choice was two-fold. Firstly, a number of unconventional superconductors display a complicated phase diagram of the Flux Line Lattice (FLL). The superconducting vortex (also called a flux line) has a single quantum flux on magnetic field penetrating superconductor at the core of the vortex, and this field is screened from the rest of the bulk of the superconducting sample by supercurrents that are circulating around the core, hence the name vortex. Most of the vortex structures and their rearrangements are determined via Small Angle Neutron Scattering (SANS) technique. MFM allows for direct vortex visualization, and thereby straightforward determination of the FLL domains, and potentially the vortex pinning mechanism in a particular compound.

## Scientific Approach and Accomplishments

Significant progress was made on a number of fronts, using both MRFM and MFM modes of operation of our apparatus.

MRFM investigations of ferromagnetic films have yielded a number of important results. Investigation of the samples fabricated with optical lithographic techniques, where different ferromagnetic films were separated by a distance of a few micrometers demonstrated (i) submicron resolution of the MRFM apparatus; (ii) that MRFM can differentiate the material under the tip, i.e. it is material-sensitive. The results of this work were published in References [2,3].

The field profile of a magnetic tip in MRFM has always presented a practical problem: many tips were fabricated by ion beam milling of a larger magnetic particle attached to a micro-mechanical cantilever. As a result of a possible ion beam bombardment damage to the ferromagnetic material of the remaining material, and an irregular shape of the remaining magnetic particle, the field profile, crucial to the analysis of the data and model simulations, was not known. We have approached this problem from two directions. Firstly, the utilization of a regular few-micron size spherical particle of ferromagneitc NdFeB, allowed us to model the field of the cantilever as that of a perfect dipole. However, even in that case, uncertainty might exist as to the direction of the magnetic field created by the magnetic tip due to possible micro-domain structure, direction of the field due to the crystalline and surface anisotropy. We have developed the experimental approach to characterize spatial distribution of the magnetic field produced by cantilever tip of an arbitrary shape by performing MRFM measurements on a well characterized diphenyl-picrylhydrazyl (DPPH) film. Thereby we were able to map the 3D field profile produced by a Nd2Fe14B probe tip by using the "leading edge" of the MRFM spectra obtained as the sharp edge of the DPPH is approached at different distances from the edge. This method was described in Reference [4]. MRFM mode of operation of our apparatus was then used to image permalloy and cobalt magnetic films separated by few microns (see Figure 1), demonstrating both high resolution of the apparatus and ability to identify the nature of the ferromagnetic film under the tip.

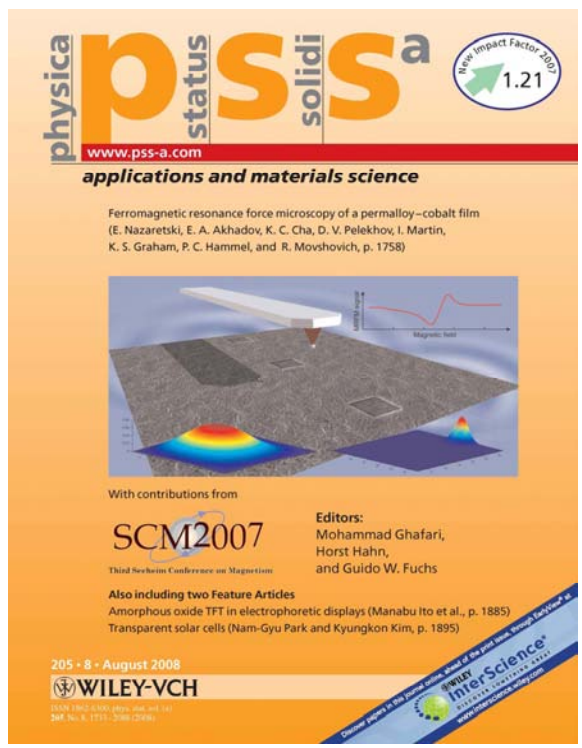


*Figure 1. Schematics of the MRFM experiment where the field tilted with respect to the perpendicular direction to the sample surface.*

Our collaboration with the Ohio State University group of Pr. C. Hammel resulted in a demonstration of the direct imaging of the array of the micron-size ferromagnetic particles with Magnetic Resonance Force Microscopy [5]. This work revealed the mechanism for high spatial resolution in FMRFM imaging: the strongly inhomogeneous local magnetic field of the cantilever mounted micromagnetic probe magnet used in FMRFM enables selective, local excitation of ferromagnetic resonance (FMR). This approach, demonstrated in individual permalloy disks, is straightforwardly extended to excitation of localized FMR modes, and hence imaging in extended films. This work was also was featured in May 26, 2008 issue of Virtual Journal of Nanoscale Science & Technology.

As a continuation of this work, we have performed magnetic resonance force microscopy of a 50 nm thick permalloy film as a function of the probe-sample distance and the angle between the film plane and the direction of the externally applied magnetic field. At larger angles the multiple resonance modes were observed at small probe-sample distance. Micromagnetic simulations, which include the inhomogeneous magnetic field of the probe tip, reveal the localized nature of the excited resonance modes [6]. Observation of the localized modes is the first step on the way to spatially resolved ferromagnetic resonance measurements in a continuous ferromagnetic media. This article [6] was featured in April 13, 2009 issue of Virtual Journal of Nanoscale Science & Technology.

The development of the complimentary to MRFM low temperature MFM capability allowed us to study electromagnetic phenomena on the scale down to few tens of nanometers. In particular, we have directly imaged collection of vortex-antivortex front propagating in the niobium field upon the reversal of the applied magnetic field. Observation of the process of the vortex-antivortex pair annihilation will be s significant next step in the studies of vortex pinning and dynamics. MFM tip is capable of vortex manipulation via the field produced by the magnetic tip. Depending on the direction of the applied magnetic field (or polarity of a vortex) with respect to the field produced by the MFM tip, the interaction between the vortex and the tip can be repulsive of attractive, allowing the tip to respectively pull or push the vortex. Such interaction will therefore allow us to study vortex pinning – its strength and mechanism.

We have extended the vortex studies to precise imaging of the field profile of a single isolated vortex (in the very weak applied magnetic field). The imaging of the magnetic field outside of the sample of the superconducting material allowed us to model the field expected to be generated by a single vortex, with the magnetic penetration depth $\lambda$ being the only adjustable parameter. We used MFM to image a single vortex in superconducting Nb film in these investigations (see Figure 2), and we developed a method for quantitative extraction of the penetration depth from single-parameter simultaneous fits to the lateral and height profiles of the MFM signal, and demonstrate that the obtained value is in excellent agreement with that obtained from the bulk magnetization measurements. The simulations of field profile above a single vortex are shown in Figure 3, where both experimental data three different distances between the cantilever and the substrate are shown, together with the model curves for three different values of the magnetic penetration length for each of the experimental conditions. High degree of agreement is obtained for $\lambda$ = 106 nm. We expect that this approach will be used for determination of the penetration depth in a variety of novel superconductors and will open new avenues for the application of MFM in the *quantitative* studies of materials. These results are reported in an article submitted to the Applied Physics Letters [7].

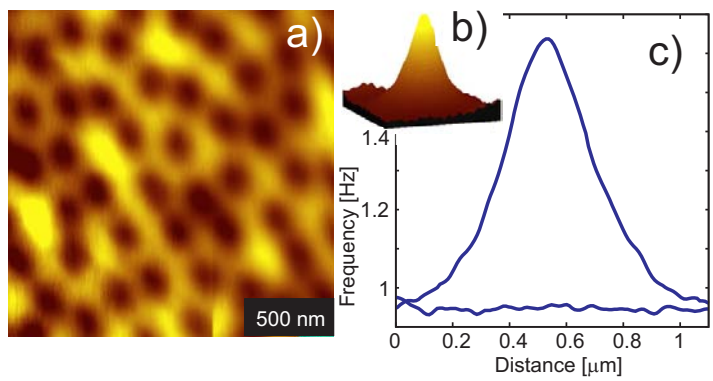


*Figure 2. a) 1.9x1.9 sq. microns scan of a Nb film at 4.3 K. The field of view contains 53 vortices, and the vortex density agrees well with the expected value in 30 mT field. b) image of an individual vortex acquired in the external field of 1 mT, the color scale corresponds to 0.7 Hz cantilever resonance frequency change. c) cross section of the vortex and the background noise.*

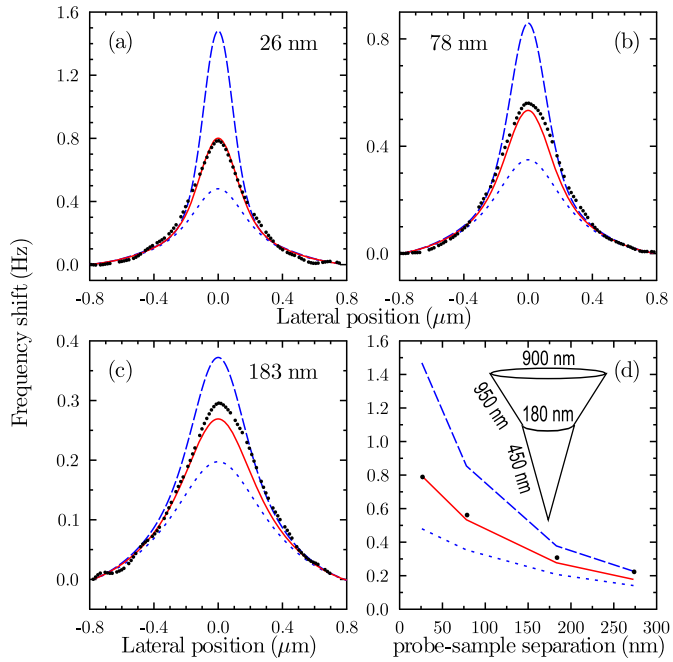


*Figure 3. Comparison of the model to the experimental data (dots) for lateral scans, a)-c), and the probe-sample separation (vertical) scans, d). magnetic penetration length of 60; 109; 160 nm correspond to dotted, solid, and the dashed lines respectively. The probe-sample distance is indicated in each panel.*

## Impact on National Missions

Nanotechnology is a rapidly growing field that impacts much of modern technology. Developing the tools to study nanomaterial properties is crucial for continued advancement of this field. A dual capability surface scanning probe - Magnetic Resonance Force Microscope (MRFM) and a Magnetic Force Microscope (MFM) in a single instrument allows investigations of dynamic and static properties of a variety of materials. This unique instrument expanded the suite of the surface scanning probes at LANL, already in use at the Center for Integrated Nano Technologies (CINT) and other laboratories throughout LANL. One of the specific foci of this work is on information storage and retrieval that impacts numerous missions in DOE, DHS, and other government agencies. The MFM capability can be readily applied to studies of superconducting films and bulk samples, as well as to study electromagnetic phenomena on the scale of few tens of nanometers in general. This capability will find an important applications in the field on energy transport and security.

## References


1. Nazaretski, E., K. S. Graham, J. D. Thompson, J. A. Wright, P. C. Hammel, and R. Movshovich. Design of a variable temperature scanning force microscope. 2009. *Review of Scientific Instruments.* **80**: 083704.

2. Nazaretski, E., E. A. Akhadov, K. C. Cha, D. V. Pelekhov, I. Martin, P. C. Hammel, and R. Movshovich. Ferromagnetic resonance force microscopy studies of a continuous permalloy-cobalt film. 2008. *Physica Status Solidi A.* **1-4** (205): 1758.

3. Nazaretski, E., D. V. Pelekhov, I. Martin, K. C. Cha, E. A. Akhadov, P. C. Hammel, and R. Movshovich. Localized ferromagnetic resonance force microscopy of permalloy-cobalt films. 2009. *Journal of Applied Physics.* **106**: 046103.

4. Nazaretski, E., E. A. Akhadov, I. Martin, D. V. Pelekhov, P. C. Hammel, and R. Movshovich. Spatial characterization of the magnetic field profile of a probe tip used in magnetic resonance force microscopy. 2008. *Applied Physics Letters.* **92**: 214104.

5. Obukhov, Y., D. V. Pelekhov, J. Kim, I. Martin, E. Nazaretski, R. Movshovich, P. Banerjee, S. An, T. J. Gramila, S. Batra, and P. C. Hammel. Local Ferromagnetic Resonance Imaging with Magnetic Resonance Force Microscopy. 2008. *Physical Review Letters.* **100**: 197601.

6. Nazaretski, E., D. V. Pelekhov, I. Martin, M. Zalalutdinov, D. V. Ponarin, A. Smirnov, P. C. Hammel, and R. Movshovich. Observation of localized ferromagnetic resonance in a continuous thin film via magnetic resonance force microscopy . 2009. *Physical Review B.* **79**: 132401.

7. Nazaretski, E., J. P. Thibodaux, L. Civale, J. D. Thompson, I. Vekhter, and R. Movshovich. Direct measurements of the penetration depth in a superconducting film using magnetic force microscopy. *Applied Physics Letters.*


## Publications


Ingole, S., P. Manandhar, J. A. Wright, E. Nazaretski, J. D. Thompson, and S. T. Picraux. Assembly and magnetic properties of nickel nanoparticles on silicon nanowires . 2009. *Applied Physics Letters.* **94**: 223118 .

Mewes, T., C. K. Mewes, E. Nazaretski , and P. C. Hammel. Detection of higher order modulation harmonics in magnetic resonance force microscopy . 2007. *Journal of Applied Physics .* **102**: 033911.

Nazaretski, E., D. V. Pelekhov, I. Martin , K. C. Cha, E. A. Akhadov, P. C. Hammel, and R. Movshovich. Localized ferromagnetic resonance force microscopy of permalloy-cobalt films . 2009. *Journal of Applied Physics.* **106** : 046103 .

Nazaretski, E., D. V. Pelekhov, I. Martin, M. Zalalutdinov, D. V. Ponarin, A. Smirnov, P. C. Hammel, and R. Movshovich. Observation of localized ferromagnetic resonance in

a continuous thin film via magnetic resonance force microscopy . 2009. *Physical Review B.* **79**: 132401.

Nazaretski, E., E. A. Akhadov, K. C. Cha, K. Graham, I. Martin, and R. Movshovich. 6. Ferromagnetic resonance force microscopy studies of a continuous permalloy-cobalt film. 2008. *Physica Status Solidi A.* **205**: 1758.

Nazaretski, E., E. Akhadov, I. Martin, R. Movshovich, D. V. Pelekhov , and P. C. Hammel. 9. Spatial characterization of the magnetic field profile of a probe tip used in magnetic resonance force microscopy . 2008. **92**: 214104.

Nazaretski, E., I. Martin, and R. Movshovich. Ferromagnetic Resonance Force microscopy on a thin permalloy film. 2007. *Applied Physics Letters.* **90**: 234105.

Nazaretski, E., J. D. Thompson, and R. Movshovich. Magnetic resonance force microscopy studies in a thin permalloy film. 2007. *Journal of Magnetism and Magnetic Materials .* **310**: e941.

Nazaretski, E., J. D. Thompson, and R. Movshovich. Temperature-dependent Magnetic Resonance Force Microscopy studies of a thin Permalloy film. 2007. *Journal of Applied Physics.* **101**: 074905.

Nazaretski, E., J. P. Thibodaux, L. Civale, J. D. Thompson, I. Vekhter, and R. Movshovich. Direct measurements of the penetration depth in a superconducting film using magnetic force microscopy. *Applied Physics Letters.*

Nazaretski, E., K. S. Graham, J. A. Wright, P. C. Hammel, and R. Movshovich. Design of a variable temperature scanning force microscope. 2009. *Review of Scientific Instruments.* **80**: 083704.

Obukhov, Y., D. V. Pelekhov, E. Nazaretski, R. Movshovich, and P. C. Hammel. Effect of the probe magnetic field on the uniform ferromagnetic resonance mode in a thin film . 2009. *Applied Physics Letters.* **94**: 172508 .

Obukhov, Y., D. V. Pelekhov, J. Kim, P. Banerjee, S. An, T. J. Gramila, P. C. Hammel, I. Martin, E. Nazaretski, R. Movshovich, and S. Batra. 8. Local Ferromagnetic Resonance Imaging with Magnetic Resonance Force Microscopy. 2008. *Physical Review Letters .* **100**: 197601.

# Controlling Oxidation-States in Actinide-Oxides through Crystal Lattice Pinning

*Quanxi Jia*
20070380ER

## Abstract

The study of oxidation-states of the actinide-oxides, such as uranium-oxides, is of great interest to the U.S. Department of Energy as it addresses the issues of national nuclear security, the safety of the environment, and the safe handling and storage of waste generated by energy and nuclear weapons production. Scientifically, many important aspects of the oxidation kinetics of the materials have not been fully understood. Technologically, actinide materials' long-term storage properties are an area of key importance to the future of nuclear energy and require a good understanding of the chemical interaction between such materials with the environment. Historically, sintered *polycrystalline actinide oxides* (where the grain boundaries and/or crystallographic imperfections can have a profound effect on the experimental results) have almost always been used *exclusively* for modeling and understanding such materials. This has been primarily due to limited capabilities to prepare single-crystals with controlled oxidation-states. In this project, we have prepared *single-crystal like epitaxial uranium-oxides with desired oxidation-states through pinning the crystal lattice*. This is the first such attempt in this area of study.

## Background and Research Objectives

Actinides such as U and Pu are used for nuclear power plants and nuclear weapons. The long-term storage properties of spent nuclear fuels or wastes are main concerns of the U.S. Department of Energy. This is understandable considering that the U.S. has currently an inventory of over $10^9$ pounds of depleted uranium waste materials resulting from the manufacture of nuclear weapons and the nuclear power industry. Therefore, the study of oxidation-states of actinide-oxides such as uranium-oxides is of great interest. For example, the formation of $U_3O_8$ has been studied for the last 40 years because the oxidation of $UO_2$ forms powder-like $U_3O_8$ that can lead to the splitting of the reactor sheath [1]. The formation of the powder-like phase can essentially complicate the subsequent handling and storage of the fuel. In addition, we need to have a better control of the surface chemistry and the phases ($UO_2$, $U_3O_7$, $U_3O_8$, and $UO_3$) of oxides if we want to make new potential applications of depleted uranium possible.

To model and understand the oxidation-states and surface chemistry of actinide-oxides such as uranium-oxides, sintered *polycrystalline materials* have almost always been used *exclusively* mainly due to limited capabilities to prepare single crystal actinide-oxides with controlled oxidation-states. The use of polycrystalline materials in experiments can create tremendous ambiguity to extract intrinsic properties of the materials. For instance, experimental results indicate that the kinetic rate of $U_3O_7$ formation on $UO_2$ changes with the forms of materials such as powders, polycrystalline pellets, and crystals [2]. It has also been shown that intra-granular oxidation proceeds more slowly than oxidation along the grain boundaries [3]. This can probably be anticipated considering that the grain boundaries and/or crystallographic imperfections can have a profound effect on experimental results. Neglecting the impact of the preferential diffusion of oxygen along grain boundaries can eventually lead to an inappropriate interpretation of the surface chemistry of the materials. It is crucial then that high quality single-crystal-like actinide-oxides be prepared for a better understanding of the *intrinsic physical properties* of actinides as these are fundamental physics and materials issues of great scientific interest. Technologically, the use of depleted uranium-oxides for electronic devices needs high quality well-oriented films because such films have fewer structural and chemical imperfections. Ideal performances are best achieved by minimizing crystallographic imperfections (e.g. grain boundaries) and chemical non-uniformity (e.g. variations in the stoichiometry of a material). Nevertheless, no epitaxial uranium-oxides, according to our knowledge, have ever been grown with any thin film deposition techniques, though a few studies have been reported to

have grown polycrystalline $UO_2$ films through sputtering and sol-gel processes.

This project has successfully addressed this challenge by combining the ideas of locking-in or clamping lattice in heteroepitaxy and controlling the oxidation-states in actinide-oxides through pinning the crystal lattice. The detailed research objectives include i) growth of epitaxial uranium-oxide films to control the phases of oxides since different oxidation-states coexist; ii) growth of polymorphic uranium-oxides to control the crystal structure since, for example, both orthorhombic and hexagonal structures co-exist in $U_3O_8$; iii) Investigation of the physical and structural properties of epitaxial uranium-oxide films with different oxidation-states; and iv) growth of other actinide-oxide films using our chemical solution deposition technique.

## Scientific Approach and Accomplishments

We have predicted that one should be able to clamp or lock-in the lattice of actinide-oxides through pinning the crystal lattice in epitaxy if one uses the right substrate or epitaxial template (Figure 1). Epitaxial films, whose crystallographic order is mainly controlled by that of the substrate, have often been adopted as a substitute for single crystals and have been extensively used in the semiconductor industry. For example, epitaxial materials are routinely utilized as active layers to build high performance devices because they exhibit much better physical properties than polycrystaline substrates. The simplest form of epitaxy is homoepitaxy on which the same material is grown on top of a crystalline source. Heteroepitaxy, on the other hand, is the growth of a given material upon a different substrate. The crystal structure of the substrate can greatly influence the film's preferred crystallographic orientation and structure.

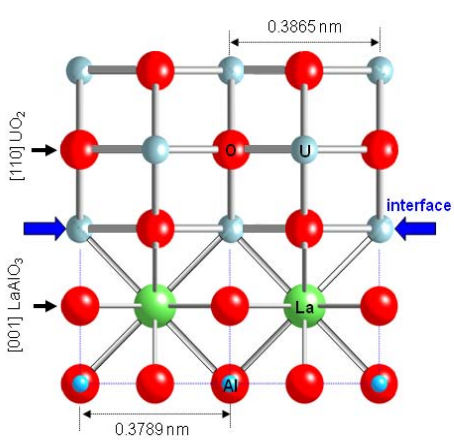


*Figure 1. Schematic drawing of $UO_2$ epitaxially grown on $LaAlO_3$. Epitaxial $UO_2$ can be easily achieved by pinning the crystal lattice because of the strong bonding across the interface between the substrate and the film. In this representative case, the lattice mismatch along [110] $UO_2$ and [001] $LaAlO_3$ is only about 2%.*

To grow uranium oxides with controlled oxidation states, we used a polymer-assisted deposition (PAD), LANL patented process [4]. The PAD technique offers significant advantages over other techniques in the preparation of uranium oxide films, as it neither necessitates an expensive vacuum technique, nor requires reactive organometallic actinide precursors like other solution techniques. More importantly, the bottom-up route for heteroepitaxy by PAD, in contrast to a top-down growth model commonly used in the *in-situ* physical vapor deposition, makes it possible for the substrate to pin the crystal lattice of the epitaxial layer. In our experiments, the precursor for the deposition of epitaxial films, which was a simple aqueous solution of $UO_2(OAc)_2 \cdot 2H_2O$, was added to a polyethylenimine (PEI) polymer to form an aqueous solution with an adjusted pH of 8.0. This solution was spun coated onto the desired substrates such as $LaAlO_3$ (LAO) or *c*-plane or *R*-plane $\alpha$-$Al_2O_3$, which were then annealed at 1000 °C under the atmosphere of either $O_2$ or air.

High quality epitaxial $UO_2$ films were successfully grown through this project. Figure 2 shows the x-ray diffraction patterns of (a) $\theta$-$2\theta$ scans and (b) $\phi$-scans from (220) $UO_2$ and (101) LAO. As shown in Figure 2(a), only the (*h00*) peaks of $UO_2$ and LAO are observed, suggesting that the $UO_2$ film has a single phase with a preferential *a*-axis orientation. The calculated lattice parameter of the $UO_2$ film based on the diffraction pattern is 0.5472 nm, which is almost the same as the 0.5466 nm of the bulk cubic $UO_2$. The four peaks from the reflections of the (220) $UO_2$, shifted 45_degree with respect to (101) LAO, show that the $UO_2$ is epitaxy when rotated 45_degree with respect to the LAO lattice. The epitaixal relationship between the $UO_2$ and LAO can be described as $(100)_{UO2}||(100)_{LAO}$ and $<110>_{UO2}||<001>_{LAO}$. Considering the lattice parameters of $UO_2$ (see Figure 1) and LAO (pseudocubic, $a$ = 0.3789 nm), this epitaxial relationship is favorable since the lattice mismatch along <110> $UO_2$ and <001> LAO is only about 2%. A cross-sectional transmission electron microscopy (TEM) analysis on the film further confirms the successful epitaxial growth of high quality $UO_2$ on the LAO substrate. As shown in Figure 3 (a), there is a sharp interface (marked with two wedges) between the $UO_2$ and the LAO without any indication of interfacial reactions. Selected-area-diffraction (SAD) patterns, presented in Figure 3 (b), show the same epitaxial relationship with an x-ray analysis. Surface infrared (IR) spectroscopy shows no absorption peaks in the range for U=O stretches (700 – 950 $cm^{-1}$), confirming the absence of higher oxides in the film.

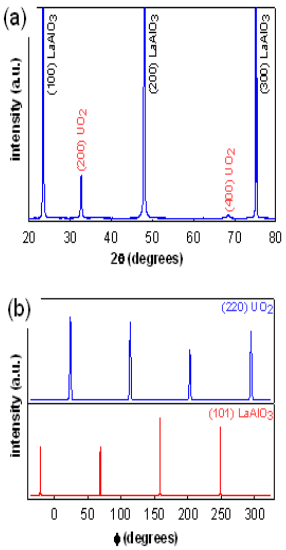


*Figure 2. X-ray diffraction spectra. a) theta–2theta scans of $UO_2$ films deposited on a single crystal (100) $LaAlO_3$ substrate; b) phi-scans of the (220) epitaxial $UO_2$ films and the (101) $LaAlO_3$ substrate. a.u. = arbitrary units. The epitaxial relationships between the $UO_2$ and the $LaAlO_3$ (LAO) substrate are (100) $UO_2 || (100)_{LAO}$ and $<110>_{UO2} || <010>_{LAO}$.*

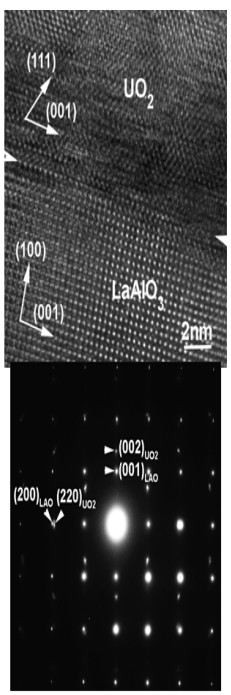


*Figure 3. Epitaxial (100) $UO_2$ films deposited on a single crystal (100) $LaAlO_3$. top) a cross-sectional high-resolution electron microscopy (HRTEM) image taken along the [100] $LaAlO_3$ zone axis; bottom) the selected-area electron diffraction pattern. The HRTEM image shows a very sharp interface between the $UO_2$ film and the $LaAlO_3$ substrate. There are no detectable second phases and no voids in the film. The well-defined and sharp diffraction dots on the diffraction patterns further confirm that the $UO_2$ film is of high quality epitaxy.*

We have been able to grow polymorphic hexagonal and orthorhombic $U_3O_8$ films using different substrates with appropriate in-plane lattice parameters even though uranium oxides have different oxidation states with different crystal structures. Figure 4 shows θ–2θ scans for films on both the *c*-plane and the *R*-plane α-$Al_2O_3$ substrates ($a$ = 0.4759 nm, $c$ = 1.2992 nm). As can be seen from Figure 4, films on α-$Al_2O_3$ substrates exhibit completely different x-ray diffraction patterns than films on LAO do, even though they have been coated with the same solution and treated under the same conditions. From both the x-ray diffrrcation and the cross-sectional TEM image, we confirmed that the epitaxial $U_3O_8$ on the *c*-plane α-$Al_2O_3$ has a hexagonal structure with lattice parameters of $a$ = 0.6815 nm and $c$ = 0.4144 nm. On the other hand, $U_3O_8$ on the *R*-plane α-$Al_2O_3$ substrate has an orthorhombic structure. The formation of $U_3O_8$ on both the *c*-plane and the *R*-plane α-$Al_2O_3$ substrates has also been confirmed by the IR absorption. Absorption peaks have been observed at 733 $cm^{-1}$ and 760 $cm^{-1}$ for films on the *c*-plane and the *R*-plane α-$Al_2O_3$ substrates, respectively.

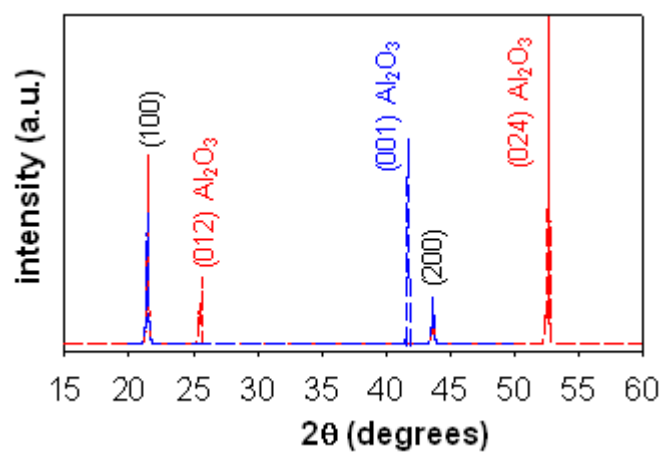


*Figure 4. X-ray diffraction spectra. blue) a theta–2theta scan of the $U_3O_8$ film deposited on a single crystal (001) $Al_2O_3$ substrate; red) a theta–2theat scan of the $U_3O_8$ film deposited on a single crystal (012) $Al_2O_3$ substrate. The preferential orientation of $U_3O_8$ along (100) is obvious regardless of the orientation of the $Al_2O_3$ substrate.*

Photoemission was used to characterize surface quality and resistance to atmospheric conditions, as well as crystallinity of samples. For electronic structure comparisons, we have also used very high quality macroscopic single crystal $UO_2$ as a reference. In comparison, our epitaxial $UO_2$ film on LAO shows the same electronic structure features such as band dispersions and binding energies as single-crystal $UO_2$.

We have observed that the epitaxial $UO_2$ and $U_3O_8$ films are extremely stable in air. Our x-ray diffraction measurements

do not show any noticeable degradation after the films have been exposed to air at room temperature for more than 400 days. This lack of sensitivity to atmospheric conditions may be expected, since the films were formed at 1000 C in an atmosphere of either $O_2$ or air. The extraordinary stability of $UO_2$ films down to a few top-most crystal layers is further confirmed by the lack of significant changes in the valence band structure between the as-deposited and the sputter-etched surfaces.

Other important accomplishments include i) the deposition of other actinide-oxides films based on this concept. For example, we have demonstrated epitaxial growth of $ThO_2$ film on $UO_2$; ii) the growth of $NpO_2$ films using a chemical solution deposition technique; iii) the delivery of our actinide-oxides to LLNL for further structural study and to other research group in LANL for irradiation damage investigation; iv) the preliminary demonstration of uranium-nitride films based on polymer-assisted deposition.

## Impact on National Missions

This project supports the DOE mission in nuclear security, safety of the environment, and the safe handling and storage of waste generated by energy and DOE's nuclear weapons production. The knowledge gained through this project has a tremendous impact on both actinide materials science and nuclear physics since high quality single-crystal-like epitaxial actinide-oxides with different oxidation-states become available. Our capability to make epitaxial actinide-oxides easily accessible has placed LANL in the forefront of understanding the intrinsic physical properties of actinides. LANL's strategic goals in materials science, energy security, and nuclear weapons benefit from this project.

## References


1. Boase, D. B., and T. T. Vandergraaf. Canadian spent fuel storage canister - some materials aspects. 1977. *Nuclear Technology.* **32** (1): 60.

2. McEachern, R. J.. A review of kinetic data on the rate of U3O7 formation on UO2 . 1997. *J. Nucl. Mater..* **245** (2): 238.

3. McEachern, R. J., J. W. Choi, M. Kolar, W. Long, and P. Taylor. Determination of the activation energy for the formation of U3O8 on UO2 . 1997. *J. Nucl. Mater..* **249** (1): 58.

4. Jia, Q. X., T. M. McCleskey, A. K. Burrell, Y. Lin, G. Collis, H. Wang, A. D. Q. Li, and S. R. Foltyn. Polymer-assisted deposition of metal-oxide films. 2004. *Nature Mater..* **3**: 529.


## Publications


Burrell, A. K., T. M. McCleskey, P. Shukla, H. Wang, T. Durakiewicz, D. P. Moore, C. G. Olson, J. J. Joyce, and Q. X. Jia. Controlling oxidation states in uranium oxides through epitaxial stabilization. 2007. *Adv. Mater..* **19**: 3559.

Burrell, A. K., T. M. McCleskey, and Q. X. Jia. Polymer assisted deposition. 2008. *Chem. Comm.* (11): 1271.

Durakiewicz, T., Q. X. Jia, L. E. Roy, R. L. Martin, J. J. Joyce, A. K. Burrell, and T. M. McCleskey. 5f band dispersion in epitaxial films of UO2. To appear in *Vacuum.*

Jia, Q. X., M. Jain, A. K. Burrell, T. M. McCleskey, and Y. Lin. Epitaxial growth of metal-oxide films by a polymer-assisted deposition. *MRS International Materials Research Conference.* (Chongqing, China, June 9 - 12, 2008).

Luo, H. M., A. H. Mueller, T. M. McCleskey, A. K. Burrell, E. Bauer, and Q. X. Jia. Structural and Photoelectrochemical Properties of BiVO4 Thin Films. 2008. *J. Phys. Chem. C.* **112**: 6099.

Luo, H. M., Y. Lin, S. A. Baily, H. Wang, M. E. Hawley, T. M. McCleskey, A. K. Burrell, E. Bauer, L. Civale, and Q. X. Jia. Silica Nanoparticles-Oxide Composite Epitaxial Thin Films. 2008. *Angew. Chem. Int. Ed.* **47**: 5768.

McCleskey, T. M., E. Bauer, A. K. Burell, M. Jain, Q. X. Jia, and H. Luo. Polymer assisted deposition of thin films. *MRS Spring Meeting.* (San Francisco, CA, , March 24 - 28, 2008).

# Tunable Infra-Red Chromophores through N-Type Doping of Wide-Gap Semiconductor Nanocrystals

*Sergei A. Ivanov*
20070445ER

## Abstracts

*Colloidal semiconductor quantum dots* (QDs) of II-VI materials are 2-6 nm spherical particles composed of Zn, Cd, or Hg metal atoms bound with non-metallic S, Se, or Te. Unlike bulk form of the same material, one of the striking properties of these QDs is their ability to efficiently emit photons in the visible part of spectrum upon being illuminated with UV light. This UV light promotes electrons from occupied levels to the empty levels of higher energy. The energy difference between the occupied and the empty levels, $E_g$, determines the color of the material's luminescence. Synthetic methods for such high-quality QDs have been well reported. However, QDs of these materials emit only visible light and are restricted to visible-light applications only (laser medium, biolabeling, tagging). To use these QDs in such important applications as tunable *infrared* (IR) sensors, tunable low-threshold lasers and photovoltaics, one needs QDs with smaller $E_g$. The goal of this project was to convert conventional QDs into IR-active material via their *n*-doping. *n*-Doping is an introduction of extra electrons onto initially empty electron levels of QDs by exchanging $Cd^{2+}$ ions with formally $In^{2+}$ or $Ga^{2+}$ ones in the QD lattice. Two synthetic pathways to n-doped materials were utilized: a *Single-Source Precursor* (*SSP*) approach and the QD *Seed-Based* approach. Multiple *SSP*s were synthesized and tested under the first approach, resulting in partially successful doping of CdS QDs with $In^{3+}$. The second approach has been shown to be unsuccessful due to dopant desorption from QD surface. Despite the success of doping of CdS with $In^{3+}$, reduction of this system with extra electron to convert it into *n*-doped CdS QDs so far has proven to be still unsuccessful.

## Background and Research Objectives

*Colloidal semiconductor quantum dots* are small, 2-6 nm in diameter, spherical particles of crystalline material. They are also coated with certain type of organic molecules (ligands) to protect these particles from sticking together, to make them dispersible in solvents, and to inactivate (passivate) their surface from further reactions. *Binary II-VI semiconductor* particles are composed of Zn, Cd, or Hg metal atoms bound with non-metallic S, Se, or Te. In these materials, each atom in the lattice forms four bonds to the nearest neighbors in pyramidal fashion with alternating metal and non-metal atoms. Unlike bulk form of the same material, one of the striking properties of ligand-passivated QDs is their ability to efficiently emit photons in the visible part of spectrum upon being illuminated with UV light (luminescence).

Initially, the electronic structure of the QDs is presented by electron levels from lower to higher energy ones. Several lower-energy levels are occupied by electrons, while the rest are empty. The UV light promotes (excites) electrons from occupied levels to the empty (unoccupied) levels higher in energy (Figure 1). The difference in energies between the highest occupied and the lowest unoccupied levels is called the *energy gap*, $E_g$, of the material and determines the color of the material's luminescence together with other optical properties of this material (Figure 1). In turn, the energy gap of QDs is determined by the size of the particle and the *larger* the particle, the *smaller* the $E_g$; eventually, as the semiconductor particle grows in size, its $E_g$ comes down to the value for the energy gap in bulk material. As such, the change in the particle size leads to the change of $E_g$ value within some energy interval, and thus to tuning of the emission color of the QD. Noteworthy, that the energy separation between two unoccupied levels gets smaller as one moves up the energy scale (Figure 1).

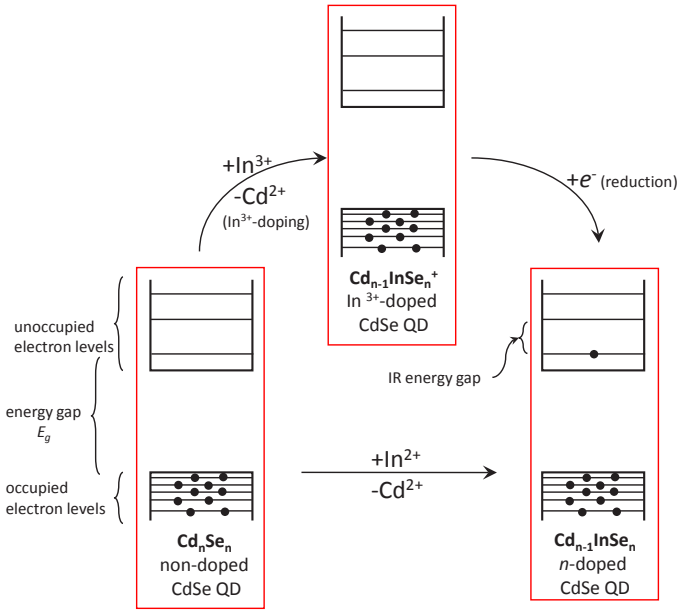


*Figure 1. Electronic structures of non-doped CdSe QDs (A), In(III)-doped CdSe QDs (B), and n-doped CdSe QDs (C). Processes leading from one structure to another are designated with arrows.*

Synthetic methods for such high-quality QDs of II-VI materials with high uniformity in size and soluble in many solvents have been well reported [1]. However, since energy gaps in many II-VI bulk materials are large, QDs of these materials emit only visible light and are restricted to visible-light applications only (e.g., biolabeling, tagging). As such, our ability to tune their optical properties by adjusting the particle size is limited. To use QDs in important applications such as tunable *infrared* (IR) sensors, tunable low-threshold lasers and photovoltaics, one needs QDs with smaller $E_g$. One of the ways to circumvent the limitation on the $E_g$ tuning would be the *n- doping* of the II-VI material. Each atom in the lattice of a material brings certain number of electrons into material's electronic structure. The *doping* of the material is called the replacement of few original atoms in the crystal lattice with atoms of other kind that bring *more or less* number of electrons with them. If new atoms bring *more* electrons with them, extra electrons will take previously empty electron levels (*n*- doping) (Figure 1). If new atoms bring fewer electrons, then previously occupied higher-energy levels will become empty (*p*-doping). As we mentioned, the energy separation between two originally empty electron levels gets smaller up the energy scale. As such, the positioning of electrons on previously empty levels will effectively lower Eg, producing *IR energy gap* (Figure 1). Then, this *n*-doping procedure would "convert" II-VI "visible" QDs into IR-active material (material that interact with IR light).

Although QD research has flourished over last 20 years, ways to dope QDs are limited to doping with isovalent transition metal (TM) atoms [2]. The large number of surface atoms in a typical QD compared to the total number of atoms in the QD translates into a large portion of dopant atoms are being present at or near the surface layers, causing the diffusion of dopant atoms out of the growing QD ("self-purification" process). Traditional high-heat (lyothermal) syntheses of QDs involve the injection of QD reagents into hot coordinating solvent. Then, high concentrations of QD precursors induce the formation of critical nuclei (very small clusters of the material around which the rest of the QD particle grows) followed by the QD growth at lower precursor concentrations [1]. Inclusion of a dopant into the critical nucleus increases the energy required for the nucleation (e.g., makes the nucleus less stable). Therefore, in a lyothermal doping, the nucleation of doped crystals might not be competitive with nucleation of pure (non-doped) ones. As such, the successful doping procedures must employ techniques for QD growth that do not involve critical nuclei. To this end, we proposed to explore two synthetic pathways meeting these requirements: a *Single-Source Precursor* approach [3,4] (Path A) and the QD *Seed-Based* approach [5,6] (Path B) (Figure 2).

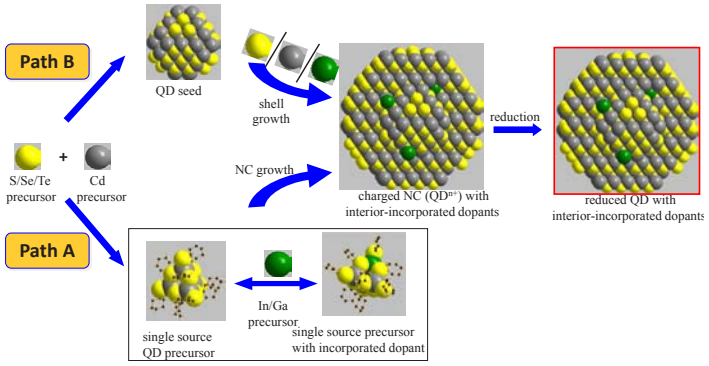


*Figure 2. Proposed two approaches (Path A and Path B) to synthesize the n-doped II-VI QDs. Path A leads through the initial synthesis of the Single Source Precursor, followed by QD growth and reduction, whereas the Path B leads through the generation of QD seed first, followed by the dopant absorption, QD growth and reduction.*

## Scientific Approach and Accomplishments

In our approach, we have tested two paths to the *n*-doped QD material. Path A first involved the preparation of a reagent, the contents of which would include both the components of QD material and the doping atoms (*SSP*). Controlled thermal breakdown of *SSP* would lead to the formation of QD critical nucleus with dopant atom in it and subsequent QD growth. The path B first involved the nucleation of small non-doped QD nucleus. After nucleation, the nucleus was treated with dopant-containing reagent to affix the dopant on the QD surface

(dopant adsorption). After the adsorption, the QD was grown further in the attempt to incorporate the dopant into the QD interior. Once doped QD was grown, the correct number of electrons was tried to be adjusted by the QD reduction (addition of one more electron per QD).

It was identified [7] that CdS, CdSe, CdTe, or ZnSe with $In^{2+}$ or $Ga^{2+}$ would be good systems to study *n*-type doping in II-VI materials. Since $In^{2+}$ or $Ga^{2+}$ are relatively unstable oxidation states, it was decided to dope the II-VI material with $In^{3+}$ or $Ga^{3+}$ and then reduce the doped QDs thereby inducing *n*-doping of the final product. Out of four common II-VI materials, CdS, CdSe, CdTe, and ZnSe that were acceptable for *n*-doping [7], two systems, CdS and CdSe were identified as primary for future work. ZnSe is less desirable as fewer *SSPs* are available and CdTe is prone to oxidation and its *SSPs* are unstable. Since $In^{3+}$ ionic radius is the closest to that of cadmium among elements of the 13th group of Periodic Table, and relatively stable low oxidation states of indium are accessible in indium compounds, we have identified this element as the most suitable for CdS and CdSe doping.

We have synthesized multiple Cd-In-S and Cd-In-Se *SSPs* together with several In-S and In-Se complexes, and numerous reaction conditions were tested to incorporate indium into CdS or CdSe QDs via *SSP* route (Figure 2, Path A). We were able to isolate small Cd-S and Cd-Se nuclei from different reactions that lead to the formation of final QD product, but these nuclei did not contain dopant indium atoms. It has been a conventional wisdom that under lyothermal conditions, the dopants would not incorporate into the QD interior as such process is thermodynamically unfavorable. However, we undertook quantum-mechanical study of this phenomenon, using small Cd-S clusters as models for real size critical nuclei, and results indicated that both processes, the exchange of $Cd^{2+}$ with $In^{3+}$ on the QD surface and the subsequent reduction (addition of an electron), are likely energy *preferred* processes (Figure 3) in small QDs.

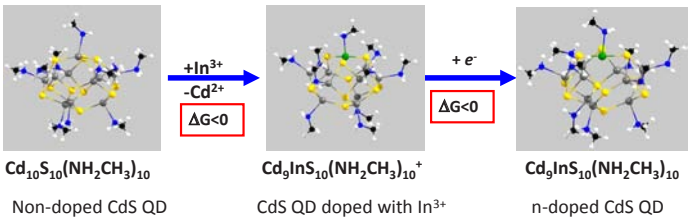


*Figure 3. Theoretical analysis of $Cd_{10}S_{10}(CH_3NH_2)_{10}$ - a model of CdS QD. Step A - replacement of $Cd^{(2+)}$ with $In^{(3+)}$. The process is preferred since the Gibbs energy (delta G) of the process is negative. Step B - reduction of the system with extra electron, thereby converting it to n-doped CdS QDs. The process' delta G is also negative.*

Finally, one of the reaction conditions was proven to be successful to include $In^{3+}$ ion(s) into CdS QD (Figure 4) in agreement with our calculations. However, the amount of $In^{3+}$ ions in CdS QDs could not be easily and predictably controlled. Most of the doping reactions resulted in phase-separation of indium and cadmium products, when instead of incorporation into CdS or CdSe QDs, indium would form $In_xS_y$ or $In_xSe_y$ and separate from the dopant-free CdS or CdSe QDs.

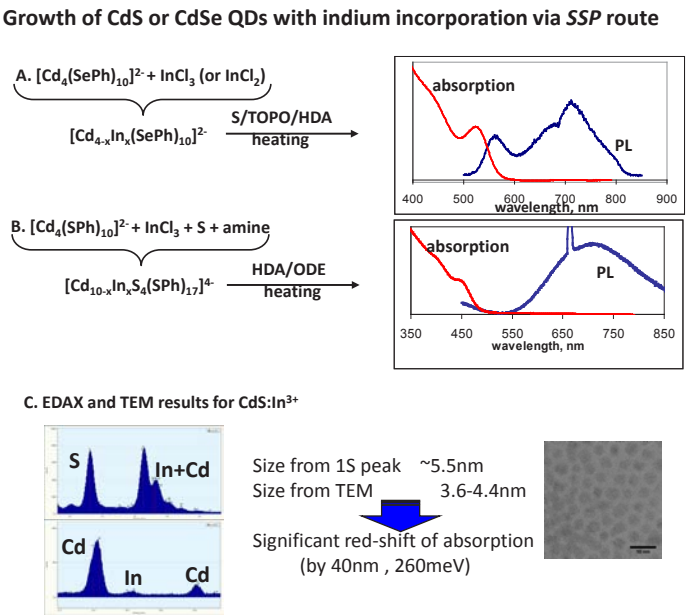


*Figure 4. Synthetic schemes (panels A and B) showing the route to the successful inclusion of In into CdS or CdSe QDs. PL - photoluminescence; HDA - long-chain amine, hexadecylamine; ODE - long-chain hydrocarbon, 1-octadecene. In the panel C, the results of elemental (EDAX) analysis and the Transmission Electron Microscopy (TEM) of In-doped CdS QDs are presented. EDAX data show the presence of In in CdS QDs. TEM data reveal that size of CdS QDs is significantly smaller than would be expected for non-doped CdS QDs with the same absorption spectrum as in panel B. This leads to the positive conclusion on In incorporation into interior of CdS QDs.*

Together with lyothermal synthesis above, we have conducted experiments with microwave synthesis of doped QDs, since it requires lower temperatures [8,9] that might facilitate dopant inclusion and deliver the energy directly to the reactants without significant heating. Results of elemental analysis and powder X-ray diffraction indicate that $In^{3+}$ can be put into the crystal lattice of CdS QDs, although the amount of dopant in the system is significantly less than targeted and still poorly controlled.

We have tested multiple conditions of the path B approach to adsorb indium dopant on a surface of small nanocrystal seeds followed by further seed growth. Elemental analysis of best In-doped CdS and CdSe QD samples showed $In^{3+}$

content less than 0.2%. This indicates that desirable concentration of the dopant inside of QDs has not been achieved via path B route. The main obstacle is the stabilization of adsorbed dopant on the surface of the QD seed long enough to overcoat it with a shell of the same semiconductor material.

Despite the initial theoretical results, it appears that the main challenge in QD doping is still the heat-induced removal of dopant of the nanocrystal during the growth stage due to the close proximity of the QD surface. If it is true, the doping of *semiconductor nanowires* (SNWs) has to be easier. Indeed, since SNWs are thicker than QDs, their surface is not as close to the center of SNW along two dimensions and even further away along the third, SNW-growth dimension. We have successfully doped ZnSe SNWs with such a conventional dopant as $Mn^{2+}$, confirming that the surface proximity does play an important role in the doping efficiency of nanomaterials.

Since our overarching goal for this project was to "convert" visible QDs into IR-active ones, we even tested two alternative ways to obtain IR-active QDs. In the first way, we attempted to dope QDs with lanthanide (Ln) ions. It was expected that via an energy transfer process, the QDs would cause the IR emission from the Ln dopant. We explored the doping of $In_2O_3$ and InP QDs with IR-emitting Ln ions: Er (emission at 1540 nm), Yb (emission 980 nm). Since $In^{3+}$ and the Ln ions are isovalent (favoring doping) and that energy gap of $In_2O_3$ is 380nm, while that of InP is 600nm, the inclusion of Er and Yb could potentially lead to IR emission from wide-gap QDs of $In_2O_3$ and InP. Each of these systems was attempted. However, the desired IR emission was not observed. It is still likely that doping was limited to surface regions, where Ln quenching and removal is likely. Elemental analysis was unable to confirm the presence of the Ln ions, despite high Ln content in the initial reaction mixture.

In the second alternative approach, to gain an insight into the doping mechanism, we undertook a study of a reverse system, where $Cd^{2+}$ ions were put into the lattice of InAs. Preliminary results again point to the incorporation of the dopant, but optimal conditions for efficient incorporation have not been achieved.

Although we have successfully doped CdS and CdSe with $In^{3+}$, the reduction of the doped system to obtain *n*-doped material was not achieved. We have attempted to reduce the system chemically and electrochemically, but it did not result in any appearance of *n*-doped QD properties. No decrease in the energy gap absorption in UV-Vis spectra of doped QDs was observed. Also, no appearance of IR absorption and/or luminescence were recorded. It is likely, that the promotion of an extra electron into the empty electron levels for n-doping requires large potential barrier for the electron so it could avoid escaping the QD.

One of the impediments to efficient $In^{3+}$ doping of CdS or CdSe NCs with further reduction can be the charge imbalance as one replaces $Cd^{2+}$ with $In^{3+}$. To address it, $M^{+}$-$M'^{3+}$ charge balance scheme is still in the process of been tried. In this approach, $In^{3+}$ dopant ions are used with $Cu^{+}$ cations in 1:1 ratio. As $In^{3+}$ and $Cu^{+}$ get included into the lattice by replacing two $Cd^{2+}$ ions, the overall charge of the system does not change (Figure 5). Also, two-step process (doping and reduction) is again reduced to more efficient one-step in the charge balance approach.

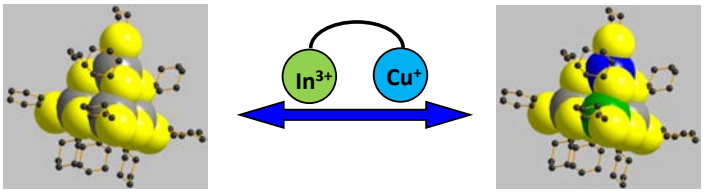


$Cd_n(SR)_m^{q-}$ $Cd_{n-2}InCu(SR)_m^{q-}$

**$In^{3+}$ with $Cu^{+}$ give average charge of 2+ per metal ion (approach is analogous to known $Al^{3+}$-$Cu^{+}$ systems)**

*Figure 5. Scheme demonstrates the concept of charge balance in preparation of a Single-Source Precursor. Replacement of two cadmium +2 ions with one indium +3 ion and one copper +1 ion won't change the charge of the system, but will introduce an extra electron for n-doping of CdS QD. R - alkyl or aryl organic substituent.*

## Impact on National Missions

Our goal was to develop IR-active materials out of semiconductor QDs that would provide critical technology for major advances in both basic and applied energy sciences, such as a) tunable IR sensor systems, b) high-efficiency photovoltaics, c) tunable low-threshold lasers. Robust optical media for use in sensor systems would support the missions of the DOE and DHS in reducing the threat of WMD and terrorism. Further, an optimized *n*-doped QD medium would comprise a new technology for next generation photovoltaics supporting the DOE's Energy Security mission.

Solution of the key issue – stable population of higher electronic levels of a QD – would allow doped QDs to make substantial contributions to fundamental nanochemical/physical studies. The solution also would enable cutting-edge sensor and energy-capture technologies, providing an important alternative to traditional applications.

Partial success of the project together with analysis of reasons for unsuccessful n-doping results allows us to reevaluate the approach to *n*-doping of QDs. In light of

conducted experiments, it is imperative to focus on the prevention of electron from escaping the higher electron levels in further studies on *n*-doping of QDs.

## References


1. Semiconductor and Metal Nanocrystals. 2004.

2. Erwin, S. C., L. Zu, A. L. Efros, T. A. Kennedy, and D. J. Norris. Doping semiconductor nanocrystals. 2005. *Nature.* **436** (7): 91.

3. Cumberland, S. L., K. M. Hanif, A. Javier, G. A. Khitrov, G. F. Strouse, S. M. Woessner, and C. S. Yun. Inorganic clusters as single-source precursors for preparation of CdSe, ZnSe, and CdSe/ZnS nanomaterials . 2002. *Chemistry of Materials.* **14**: 1576.

4. Lover, T., W. Henderson, G. Bowmaker, J. M. Seakins, and R. P. Cooney. Electrospray mass spectrometry of thiophenolate-capped clusters of CdS, CdSe, and ZnS and of cadmium and zinc thiophenolate complexes: Observation of fragmentation and metal, chalcogenide, and ligand exchange processes . 1997. *Inorganic Chemistry.* **36**: 3711.

5. Peng, Z. A., and X. G. Peng. Formation of high-quality CdTe, CdSe, and CdS nanocrystals using CdO as precursor . 2001. *Journal of the American Chemical Society.* **123**: 183.

6. Hines, M. A., and P. Guyot-Sionnest. Bright UV-blue luminescent colloidal ZnSe nanocrystals . 1998. *Journal of Physical Chemistry.* **102**: 3655.

7. Desnica, U. V.. Doping limits in II-VI compounds - challenges, problems and solutions . 1998. *Progress in Crystal Growth and Characterization of Materials.* **36** (4): 291.

8. Rao, K. J., B. Vaidhyanathan, M. Ganguli, and P. A. Ramakrishnan. Synthesis of inorganic solids using microwaves. 1999. *Chemistry of Materials.* **11**: 882.

9. Thostenson, E. T., and T. W. Chou. Microwave processing: fundamentals and applications . 1999. *Composites Part A-Applied Science And Manufacturing.* **30**: 1055.

# Non-Precious Metal Nanocomposites for Fuel Cell Catalysis

*Piotr Zelenay*
20070451ER

## Abstract

The project focused on the development of inexpensive oxygen reduction reaction (ORR) catalysts for polymer electrolyte fuel cells (PEFCs). Two novel approaches to ORR catalysis were employed. The first approach involved incorporation of transition metals in matrices of heteroatomic polymers, such as polypyrrole. The second approach relied on the modification of electronic and surface properties of carbon-based materials to create surface sites with significant oxygen reduction activity. These materials were obtained by pyrolysis of heteroatomic polymers, e.g., polyaniline doped with transition metals or mixtures of cyanamide with transition metal salts. Among the non-pyrolyzed catalysts, Co/polypyrrole/carbon composite exhibited highest activity and durability. Its activity can be tied to Co centers coordinated by pyrrolic nitrogen and hydroxyl anions that may transitionally form during ORR. Remarkably better activity and durability was achieved for the second group of ORR catalysts. The catalysts obtained by pyrolysis of cyanamide and iron precursors exhibited the highest ORR activity. The catalysts synthesized through thermolysis of polyaniline doped with Fe, Co and their mixtures offered the most favorable combination of activity and durability. The active site in the heat-treated catalysts could not be unambiguously determined. It is possible that the active site may be different for various heat-treated catalysts. The research demonstrated that developing practical non-precious catalysts for PEFCs is within reach.

## Background and Research Objectives

The process of electrochemical combustion of a fuel in PEFCs occurs by means of two separate electrochemical reactions, fuel oxidation and oxygen reduction, at the fuel cell anode and cathode, respectively. Such a direct conversion of chemical energy into electrical energy results in higher conversion efficiency than in a thermal process. The combination of this characteristic together with the small size and fast start-up make PEFCs an excellent candidate for the use in mobile power applications. However, in spite of the significant progress made to date, the technology has not yet reached the point of commercial viability. This is mostly because of the limited resources and extremely high cost of platinum, which is currently the most powerful catalyst of oxygen reduction reaction known.

The search for alternative ORR catalysts started many years ago and has greatly intensified during the last decade [1]. The catalytic activity in ORR has been reported for several materials including transition metal macrocycles, pyrolyzed carbons, conductive polymers, metal chalcogenides, heteropoly acids, and metal carbonyls [1], to name just a few. Among these materials, pyrolyzed macrocycles and pyrolyzed complexes of transition metals with non-macrocyclic ligands containing nitrogen [1] make best non-precious ORR catalysts. The ORR overpotential on some heat-treated catalysts differs by less than 100 mV from those typical for Pt [1]. In spite of the attractiveness of these materials, relatively little is known about their structure. Even the origin of their catalytic activity has remained controversial [1-9]. An agreement seems to exist that the presence of transition metals is necessary to induce the catalytic activity, but the catalytic site itself is attributed to either a surface metal [1-5] or surface nitrogen species [1,6-8]. Irrespective of that controversy, the catalyst synthesis is very frequently aimed at reproducing the $N_4$-coordination of the transition metal, which exists in some simple ORR-active compounds, e.g., metal porphyrins.

The objective of the project was to develop novel ORR catalysts that could effectively compete with platinum in PEFCs. For this research study, the class of ORR catalysts containing transition metals and nitrogen was selected, as these materials seemed to offer the highest catalytic activities among non-precious metal catalysts. Our approach was more methodical than in the majority of

competing work. A strong emphasis was placed on both fundamental aspect of catalyst synthesis and on extensive materials characterization. Our systematic approach resulted in a number of catalysts with ORR activity that matches or exceeds the best non-precious ORR catalysts [1]. We also significantly improved the catalyst durability in fuel cell operation, which has been a major drawback of virtually all non-precious metal ORR catalysts developed so far. As a result, we were able to develop ORR catalysts with the best combination of ORR activity and performance durability reported to date.

## Scientific Approach and Accomplishments

Our approach to ORR catalysis was based on the notion that both nitrogen and transition metal play a role in creating ORR active sites in catalyst synthesis, but do not necessarily have to be a part of those active sites. Consequently, as opposed to a significant number of previous research studies, we did not attempt to deliberately produce the $N_4$-coordination of the transition metal in our catalysts. Instead, we focused on increasing the surface density of metal-nitrogen bonds and thus possibly also catalytic sites. In order to accomplish that, we polymerized simple nitrogen-containing ligands, e.g., pyrrole and aniline. The resulting polymers with high nitrogen content were further doped with transition metal precursors to create the desired metal-nitrogen bonds. This new approach was applied to synthesize two different classes of ORR catalysts. Our initial intention, realized in the first phase of the project, was to create active ORR sites without any thermal treatment. In the later phase, transition metal-doped polymers were also used as substrates for synthesis of heat-treated catalysts. Both synthetic approaches resulted in materials with high catalytic activity and durability.

The catalysts obtained without a thermal treatment included three transition metal/polypyrrole/carbon composites containing cobalt, iron and copper, as well as a bimetallic Co/Fe/polypyrrole/carbon compound. The Co/polypyrrole/carbon composite exhibited highest catalytic activity, but the remaining catalysts were only slightly less active. At the time, a superior catalytic activity in PEFCs was reported for some heat-treated ORR catalysts. However, their durability was very limited, whereas the non-heat-treated composites developed in this study were much more durable. The discovery of the metal/polymer/carbon composites was published in *Nature* [10]. To date, the article was cited more than 100 times in scientific literature.

Further research on this class of ORR catalysts predominantly focused on the determination of active ORR sites. This has been a formidable task, as these composites are inherently difficult to characterize. Several material characterization methods were used, including rotating ring disk electrode (RRDE) voltammetry, X-ray photoelectron spectroscopy (XPS), electron paramagnetic resonance spectroscopy (EPR) as well as *ex situ* and *in situ* X-ray absorption spectroscopy (XAS). The latter technique included X-ray absorption near edge structure (XANES) and extended X-ray absorption fine structure (EXAFS) at the K-edge of cobalt as well as XANES at nitrogen K-edge. The possible catalyst structure and the mechanism of ORR were also examined using semi-empirical molecular modeling at the PM3 (parameterized model 3) level.

The picture that emerges from the combined electrochemical, spectroscopic and molecular modeling data is rather complex. As indicated by *ex situ* XAS data, the major cobalt species in active catalysts is mononuclear, i.e., isolated from other Co atoms. The single cobalt center has approximately six nearest nitrogen and/or oxygen neighbors. The average bond length (2.04 - 2.08 Å) between Co and its neighbors is compatible with +2 oxidation state of cobalt. However, no isolated Co atoms in +2 oxidation state with the expected $d^7$ electronic configuration could be detected by EPR. The unpaired electron spin density in active catalysts is highly delocalized. This suggests that Co(+2) donates one of its d-electrons to the polypyrrole backbone and thus becomes low spin diamagnetic Co(+3) with $d^6$ configuration. Similar conclusion was reached from the PM3 computations. The modeling also revealed that isolated Co centers cannot be effective catalytic sites for complete 4-electron ORR. The 4-electron process can occur effectively on Co centers bridged by $OH^-$ ligands (Figure 1). In presence of highly acidic polymer electrolyte, such bridges may transitionally form as the product of ORR. The expected short lifetime of the OH-bridges can explain why they were not detected by XAS.

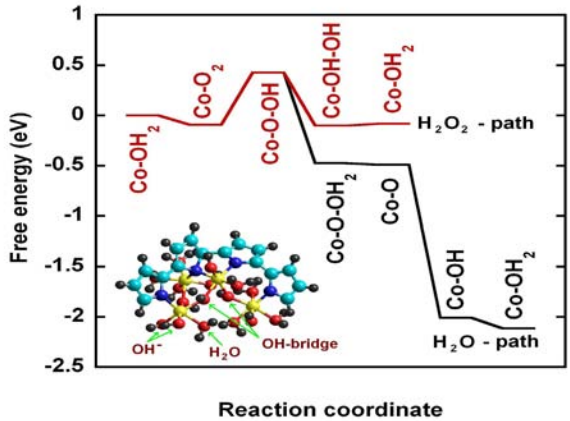


*Figure 1. Free energy changes at 0.7 V associated with ORR catalyzed by the molecule depicted in the bottom left corner of the graph. The molecule was derived from tetrapyrrole, two Co(III) and two Co(II) centers in a series of spontaneous chemical reactions and subsequent oxidation under fuel cell conditions. Before reduction, $O_2$ molecule substitutes $H_2O$ molecule coordinating the leftmost Co center. Note OH-bridges that spontaneously formed between Co centers. Element color: Co - yellow, C - cyan, N - blue, O - red, H - black.*

In addition to the publication in *Nature* [10], the research on non-heat-treated transition metal/polypyrrole/carbon composites was presented in more than ten presentations at international and national meetings. In preparation, there is a paper that will summarize the characterization and ORR mechanistic data for the composites. Together with the National Research Council in Canada, we are also preparing a paper on the molecular modeling of the composites. Our partners from Canada are contributing their accurate density functional theory computations for a number of model Co-oligopyrrole molecules.

The discovery of the durable transition metal/polypyrrole/carbon composites [10] was a breakthrough in non-precious ORR catalysis. Unfortunately, the maximum catalyst activity of the composites was still insufficient for practical PEFC application. Consequently, we explored the viability of using such composites as precursors for heat-treated catalysts. The underlying idea of that approach was that high concentrations of both transition metal and nitrogen in these materials could help generate highly active ORR catalysts. We also tried an alternative way of supplying high concentration of carbon-bound nitrogen in catalyst synthesis by using cyanamide (CM) as nitrogen precursor. Both methods resulted in very promising catalysts and reassured us that developing practical non-precious catalysts for PEFCs is within reach.

The heat-treated cyanamide-based catalysts exhibit the highest initial activity we have observed so far. In RRDE testing, the half-wave potential for ORR on some of the Fe/CM/C catalysts is only 70 mV less positive than that measured for platinum (Figure 2). This exceptional result has been already presented at two electrocatalysis workshops in Tokyo, Japan in August 2009 and at the Electrochemical Society Meeting in Vienna, in October 2009. The catalyst is also highly selective for complete (four-electron) oxygen reduction to water, with the hydrogen peroxide generation rate on the order of only 1%. The high activity and selectivity of the CM-based catalysts confirm the feasibility of our approach to catalyst synthesis. Unfortunately, the durability of these materials is insufficient, inferior to that of polyaniline-derived catalysts described below.

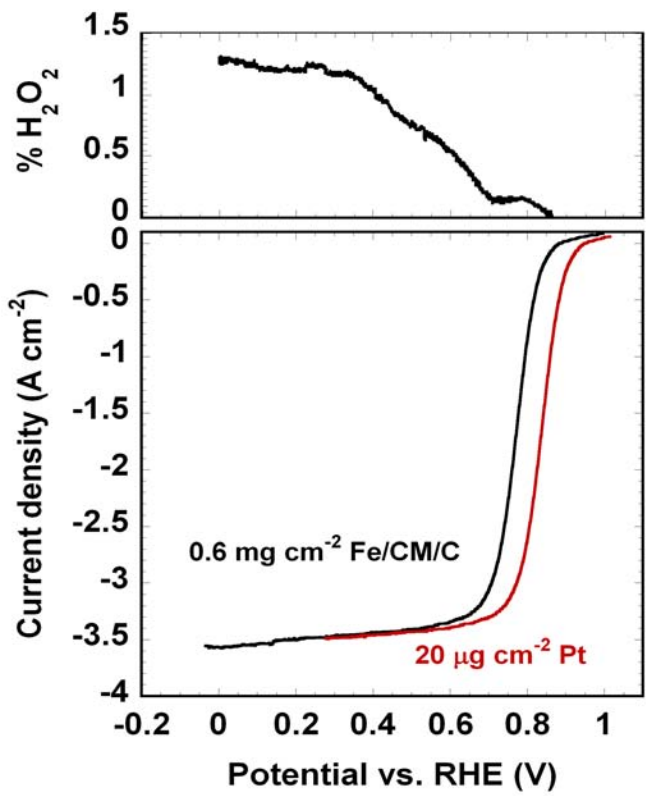


*Figure 2. Lower plot: RRDE voltammetry of oxygen in 0.1 mol dm 3 $HClO_4$ on heat-treated Fe/CM/C catalyst (black curve) and on Pt (red curve). Upper plot: Peroxide generation efficiency for heat-treated Fe/CM/C . Temperature: 25°C. Scan rate: 5 mV s 1. Electrode rotation rate: 900 rpm.*

Two polymeric matrices, polypyrrole (PPy) and polyaniline (PANI), were used in the second method of catalyst synthesis. The metals incorporated in these matrices were those frequently used in other ORR catalysts, i.e., cobalt, iron and their mixtures. We found that the heat-treatment of PANI-based precursors at 900°C results in materials with the highest catalytic activity. The catalytic activity also depends on the metal. In RRDE studies, the Fe-based catalysts are most active among the PANI-derived materials. The Co-based composites are the least active, whereas the activity of mixed-metal (Fe+Co) catalysts

lies in between. The catalyst selectivity changes in the same direction, i.e., the amount of hydrogen peroxide ORR is the lowest on the Fe/PANI catalysts (<1%) and the highest on the Co/PANI catalysts highest (>5%). However, the fuel cell performance does not follow the trend, with the best performance measured for catalysts containing both metals. The mixed Fe+Co/PANI catalysts are also more durable in fuel cell testing. The best performing catalyst contains Fe and Co in 3:1 molar ratio. As of today, the Fe+Co/PANI catalyst has been tested at the fuel cell cathode at 0.4 V for nearly 600 hours, with only minor performance degradation (Figure 3). To our knowledge, this is the most durable heat-treated ORR catalyst reported to date. This result has been recently presented at the 216th Meeting of the Electrochemical Society in Vienna.

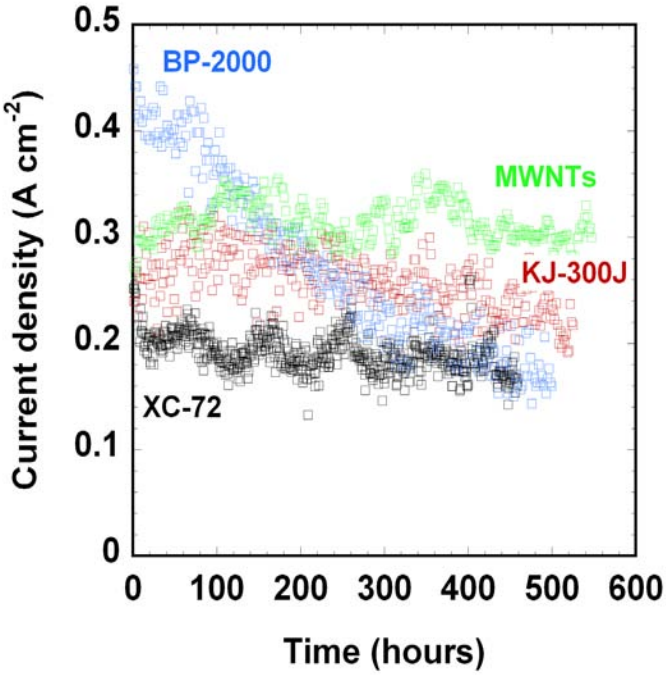


*Figure 3. Fuel cell durability of heat-treated Fe/PANI/C catalysts with various carbon supports. Carbon support: BP-2000 - blue; KJ-300J - green; XC-72 - black; multi-wall nanotubes (MWNTs) - red. Anode: 0.25 mg cm 2 Pt (E-TEK), 2.8 bar H2. Cathode: 4.0 mg cm 2 PANI-derived, 2.8 bar air. Membrane: Nafion® 1135. Cell temperature: 80°C. Cell voltage: 0.4 V.*

While not as durable as the PANI-based materials, the polypyrrole-derived catalysts perform better during initial hours of fuel cell operation, e.g., the Fe/PPy/C catalyst outperforms its PANI analogue during the initial 50 hours at 0.4 V. The differences in performance and durability can be correlated with a different state of the metal in both catalysts, as demonstrated by the XAS spectra of the catalysts at iron L-edge (Figure 3). The total electron yield (TEY) spectra for the PANI-based catalyst have well defined L3 and L2 features, whereas no respective peaks are observed for the PPy-based material. On the contrary, the L3 and L2 peaks are clearly visible in the fluorescence spectra of both materials. These results demonstrate that there is no detectable iron on the surface of the Fe/PPy/C catalyst. Due to the low energy of X-rays corresponding to the iron L-edge, only electrons ejected from Fe atoms present on the surface have sufficient energy to escape from the sample and contribute to the spectrum. As there is no such limitation for photons, iron present in the bulk of both catalysts is clearly visible in their fluorescence spectra (Figure 4).

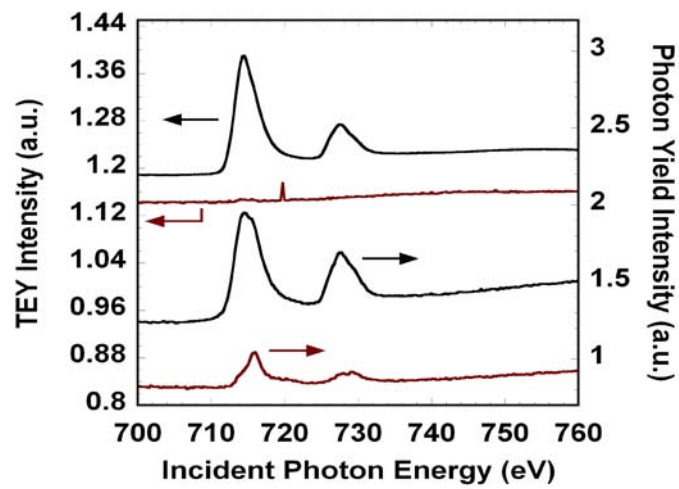


*Figure 4. XANES spectra of heat-treated Fe/PPy/C (red) and Fe/PANI/C (black) catalysts at the iron L-edge in TEY and photon yield (fluorescence) modes.*

Despite the correlation between the surface content of iron and the catalyst activity and durability, other surface components may also be responsible, perhaps even exclusively, for these catalyst properties. This concept is supported by XAS spectra at the nitrogen K-edge of fresh and fuel-cell tested membrane electrode assemblies with Fe/PANI/C catalysts (Figure 5). The spectra in Figure 5 reveal that the coordination of surface nitrogen in both fresh and fuel cell tested electrodes is significantly different than that in model coordination compounds of iron. Roughly estimating, no more than 5% of surface nitrogen may form coordination bonds with the metal. This finding reduces probability of iron being involved in catalysis. Moreover, the electron density on nitrogen significantly decreases as the result of fuel cell operation. This can be inferred from the corresponding shift of the nitrogen pre-edge features below 407 eV to higher X-ray energies. The changes are consistent with aromatic nitrogen that has a neighboring atom which becomes oxidized. Such atoms, e.g., in aliphatic functional groups might be the actual active sites. The aromatic nitrogen may play a double role

in such a mechanism. It may facilitate the oxidation of the aliphatic group and, if protonated, act as the proton donor in the immediate vicinity of the reaction site.

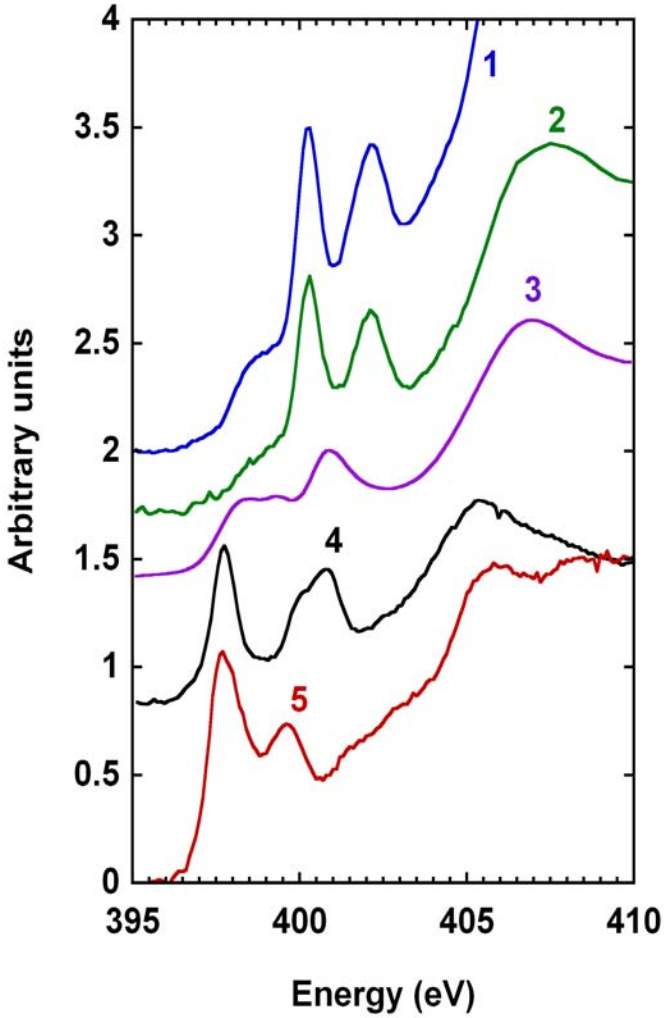


*Figure 5. Nitrogen K-edge XANES spectra of fuel cell cathodes (membrane electrode assemblies, i.e., MEAs) utilizing heat-treated Fe-PANI catalysts compared with the spectra of model iron coordination compounds. 1 - MEA after fuel cell operation at 0.6 V; 2 - MEA after fuel cell operation at 0.4 V; 3 - fresh MEA; 4 - Fe porphine; 5 - Fe phthalocyanine.*

Interestingly, no correlation has been found between the quantity of total or pyridinic nitrogen on and near the surface and catalytic activity of the CM-based catalysts. As determined by XPS, the content of both total and pyridinic nitrogen decreases with the heat-treatment temperature (850°C - 1050°C). At the same time, the catalyst thermally treated at 1000°C is less active than those heat-treated at lower (900°C) and higher (1050°C) temperatures, adding to the difficulty in active site determination. The question of the ORR active site on heat-treated catalysts still remains unanswered. As of today, one cannot even exclude the possibility that there is no common active site for all seemingly similar heat-treated ORR catalysts.

## Impact on National Missions

The project addressed one of the few remaining barriers to commercialization of polymer electrolyte fuel cells. It directly enhanced LANL's expertise in oxygen reduction catalysis, which is of particular importance for fuel cells. In this way, it supported the DOE mission to protect national and economic security by promoting a diverse supply and delivery of reliable, affordable, and environmentally-sound energy, providing world-class scientific research capacity, and advancing scientific knowledge.

The MPA-11 Group has been involved, although under many different names, in fuel cell research for over 30 years. During that time, platinum, due to its favorable properties, has been an ORR catalyst of choice for fuel cells. The research performed during this project demonstrated the high potential of non-precious ORR catalysts and helped create a new promising direction in our effort to make the fuel cell technology economically viable. The project attracted a number of postdoctoral fellows and visiting researchers. Two of them were converted to staff.

## References


1. Matter, P. H., E. J. Biddinger, and U. S. Ozkan. Non-precious metal oxygen reduction catalysts for PEM Fuel Cells. 2007. *Catalysis.* **20**: 338.

2. Joyner, R. W., J. A. Robert van Veen , and W. M. H. Sachtler. Extended X-ray absorption fine structure (EXAFS) study of cobalt-porphyrin catalysts supported on active carbon. 1982. *Journal of the Chemical Society, Faraday Transactions 1.* **78**: 1021.

3. Lefevre, M., J. P. Dodelet , and P. Bertrand. Molecular oxygen reduction in PEM fuel cells: evidence for the simultaneous presence of two active sites in Fe-based catalysts. 2002. *Journal of Physical Chemistry B.* **106**: 8705.

4. Gouerec, P., A. Biloul, O. Contamin, G. Scarbeck, M. Savy, J. Riga, L. T. Weng , and P. Bertrand. Oxygen reduction in acid media catalysed by heat treated cobalt tetraazaannulene supported on an active charcoal: correlations between the performances after longevity tests and the active site configuration as seen by XPS and ToF-SIMS. 1997. *Journal of Electroanalytical Chemistry.* **422**: 61.

5. Faubert, G., R. Côté, J. P. Dodelet, M. Lefèvre , and P. Bertrand. Oxygen reduction catalysts for polymer electrolyte fuel cells from the pyrolysis of Fe-II acetate adsorbed 3,4,9,10-perylenetetracarboxylic dianhydride. 1999. *Electrochimica Acta.* **44**: 2589.

6. Strelko, V. V., N. T. Kartel, I. N. Dukhno, V. S. Kuts, R. B. Clarkson , and B. M. Odintsov. Mechanism of reductive oxygen adsorption on active carbons with various surface chemistry. 2004. *Surface Science.* **548**: 281.

7. Sidik, R. A., A. B. Anderson, N. P. Subramanian, S. P. Kumaraguru , and B. N. Popov. O2 reduction on graphite and nitrogen-doped graphite: Experiment and theory. 2006. *Journal of Physical Chemistry B.* **110**: 1787.

8. Maldonado, S., and K. J. Stevenson. Influence of nitrogen doping on oxygen reduction electrocatalysis at carbon nanofiber electrodes. 2005. *Journal of Physical Chemistry B.* **109**: 4707.

9. Matter, P. H., E. Wang, M. Arias, E. J. Biddinger , and U. S. Ozkan. Oxygen reduction reaction catalysts prepared from acetonitrile pyrolysis over alumina-supported metal particles. 2006. *Journal of Physical Chemistry B.* **110**: 18374.

10. Bashyam, R., and P. Zelenay. A class of non-precious metal composite catalysts for fuel cells. 2006. *Nature.* **443**: 63.

## Publications

Bashyam, R., C. M. Johnston, S. D. Conradson, and P. Zelenay. Oxygen reduction electrocatalysis on non-precious metal nanocomposites. Invited presentation at *233rd American Chemical Society National Meeting.* (Chicago, Illinois, March 25-27, 2007).

Bashyam, R., C. M. Johnston, S. D. Conradson, and P. Zelenay. Non-precious metal nanocomposite ORR catalysts: RRDE and single fuel cell studies. Presented at *212th Meeting of The Electrochemical Society.* (Washington, DC, 7-12 October 2007).

Bashyam, R., S. Conradson, F. Garzon, J. Chlistunoff, and P. Zelenay. PEFC cathodes based on Co- and Fe-polypyrrole composites. Presented at *9th Gordon Research Conference on Fuel Cells.* (Smithfield, Rhode Island, July 22-27, 2007).

Borup, R., J. Myers, B. Pivovar, Y. S. Kim, N. Garland, D. Myers, R. Mukundan, M. Wilson, F. Garzon, D. Wood, P. Zelenay, K. More, T. Zawodzinski, J. Boncella, J. E. McGrath, M. Inaba, K. Miyatake, M. Hori, K. Ota, Z. Ogumi, S. Miyata, A. Nishikata, Z. Siroma, Y. Uchimoto, and K. Yasuda. Scientific aspects of polymer electrolyte fuel cell durability and degradation. 2007. *Chemical reviews.* **107**: 3904.

Chen, Z., C. Johnston, Y. Yan, and P. Zelenay. Polypyrrole-carbon based non-precious metal nanocomposite electrocatalysts for oxygen reduction reaction at PEFC cathode. Presented at *213th Meeting of The Electrochemical Society.* (Phoenix, AZ, 18-22 May, 2008).

Chlistunoff, J.. Oxygen reduction at transition metal/ heteratomic polymer catalysts. Presented at *2008 Mesilla Chemistry Workshop: New Frontiers of Electrocatalysis.* (Mesilla, NM, 9-13 Feb. 2008).

Chlistunoff, J.. Oxygen reduction at transition metal/ heteroatomic polymer catalysts. Invited presentation at *Purdue School of Engineering and Technology, Mechanical Engineering, Indiana University-Purdue University Indianapolis (IUPUI).* (Indianapolis, IN, 3 March, 2008).

Chlistunoff, J., and P. Zelenay. Semi-empirical modeling of Co-polypyrrole composites: oxygen reduction catalysis. Presented at *213th Meeting of The Electrochemical Society.* (Phoenix, AZ, 18-22 May, 2008).

Chung, H., C. Johnston, F. Garzon, and P. Zelenay. A non-precious electrocatalyst for oxygen reduction based on simple heat-treated precursors. 2008. In *214th Meeting of the Electrochemical Society.* (Honolulu, HI, 12-17 Oct. 2008). Vol. 16(2), p. 385. Electrochemical Society Transactions: the Electrochemical Society.

Chung, H., C. Johnston, F. Garzon, and P. Zelenay. A non-precious electrocatalyst for oxygen reduction based on simple heat-treated precursors. Presented at *214th Meeting of the Electrochemical Society.* (Honolulu, HI, 12-17 Oct. 2008).

Chung, H., C. Johnston, J. Chlistunoff, and P. Zelenay. Synthesis and evaluation of heat-treated cyanamide-derived non-precious catalysts for oxygen reduction. Presented at *216th Meeting of the Electrochemical Society.* (Vienna, Austria, 4-9 Oct. 2009).

Ferrandon, M., D. Myers, A. Kropf, G. Wu, and P. Zelenay. X-Ray absorption characterization of polyaniline-derived polymer electrolyte fuel cell cathode electrocatalysts . Presented at *216th Meeting of the Electrochemical Society.* (Vienna, Austria, 4-9 Oct. 2009).

Kropf, A. J., D. Myers, M. C. Smith, J. Chlistunoff, G. Wu, and P. Zelenay. In situ XAFS analysis of cobalt-containing fuel cell cathode electrocatalysts. Presented at *237th Meeting of American Chemical Society.* (Salt Lake City, UT, 22-26 March 2009).

Myers, D., M. Smith, A. J. Kropf, J. Chlistunoff, C. M. Johnston, S. D. Conradson, and P. Zelenay. In situ X-ray absorption and scattering studies of cathode electrocatalysts. Presented at *Progress MEA 2008, First CARISMA International Conference.* (La Grande Motte,

France, 21-24 Sept, 2008).

Smith, M., J. Kropf, D. Myers, J. Chlistunoff, C. Johnston, S. Conradson, and P. Zelenay. Non-precious metal nano-composite oxygen reduction electrocatalysts: in situ X-ray absorption spectroscopy studies. Presented at *213th Meeting of The Electrochemical Society.* (Phoenix, AZ, 18-22 May, 2008).

Wu, G., C. Hoon, Z. Lin, K. Artyushkova, F. Garzon, and P. Zelenay. New non-precious catalysts with high ORR performance. Presented at *3rd LANL-AIST-NEDO Workshop on Fuel Cells and Hydrogen Storage.* (San Diego, CA, 8-11 Sept, 2008).

Wu, G., L. Xie, T. Zhang, Y. Yan, and P. Zelenay. Carbon nanotubes as support for heteroatomic polymer-derived non-precious metal oxygen reduction catalysts . Presented at *216th Meeting of the Electrochemical Society.* (Vienna, Austria, 4-9 Oct. 2009).

Wu, G., M. Ferrandon, J. Kropf, K. Artyushkova, C. Johnston, D. Myers, and P. Zelenay. Performance durability of heteroatomic polymer-derived non-precious cathode catalysts. Presented at *216th Meeting of the Electrochemical Society.* (Vienna, Austria, 4-9 Oct. 2009).

Wu, G., Z. Chen, K. Artyushkova, F. Garzon, and P. Zelenay. Polyaniline-derived non-precious catalyst for the polymer electrolyte fuel cell cathode. 2008. In *214th Meeting of the Electrochemical Society.* (Honolulu, HI, 12-17 Oct, 2008). Vol. 16 (2), p. 159. Electrochemical Society Transactions: The Electrochemical Society.

Wu, G., and P. Zelenay. Polyaniline-derived non-precious catalyst for the polymer electrolyte fuel cell cathode. Presented at *214th Meeting of the Electrochemical Society.* (Honolulu, HI, 12-17 Oct. 2008).

Wu, G., and P. Zelenay. Progress in the development of non-precious fuel cell cathode-catalysts at Los Alamos National Laboratory. Presented at *Canada-USA Polymer Electrolyte Membrane Network Research Workshop.* (Vancouver, Canada, 16-17 Feb. 2009).

Wu, G., and P. Zelenay. Performance durability of polyaniline-derived nonprecious cathode catalysts. Presented at *216th Meeting of the Electrochemical Society.* (Vienna, Austria, 4-9 Oct. 2009).

Zelenay, P.. Alternative catalysts for PEM fuel cells. Invited presentation at *Europacat VIII.* (Turku/Abo, Finland, August 26-31, 2007).

Zelenay, P.. The grand challenge of fuel cell catalysis. Invited presentation at *Lujan Seminar Series on Energy Storage and Energy Materials.* (LANL, July 31, 2007).

Zelenay, P.. Cathode Electrocatalysis: A Great Challenge of Polymer Electrolyte Fuel Cells. Invited presentation at *National Research Council of Canada, Institute for Fuel Cell Innovation.* (Vancouver, Canada, April 7, 2007).

Zelenay, P.. Alternative Oxygen Reduction Catalysts for Polymer Electrolyte Fuel Cells. Invited presentation at *University of Yamanashi (departmental seminar).* (Kofu, Japan, February 5, 2007).

Zelenay, P.. Alternative catalysts for oxygen reduction reaction at the PEFC cathode. Invited presentation at *Los Alamos National Laboratory - NEDO - AIST Workshop.* (Tokyo, Japan, 29 Oct. - 1 Nov. 2007).

Zelenay, P.. Alternative catalysts for oxygen reduction in polymer electrolyte fuel cells. Invited presentation at *Department of Chemistry, University of Tokyo,.* (Tokyo, Japan, 2 Nov. 2007).

Zelenay, P.. Alternative oxygen reduction catalysts for polymer electrolyte fuel cells. Invited presentation at *US-Canada fuel cell workshop.* (Vancouver, Canada, 17-18 March, 2008).

Zelenay, P.. Advances in direct methanol fuel cells at Los Alamos National Laboratory:The formidable challenge of cathode and anode electrocatalysis in DMFCs.. Invited presentation at *Center for Emerging Energy Technologies (CEET) Workshop on 'Spectroscopic methods in structure-to-property correlation for catalysts and electrocatalysts'.* (Santa Fe, NM, 25-26 Sept, 2008).

Zelenay, P., B. Rajesh, J. H. Choi, S. Conradson, and A. Wieckowski. Pt-free electrocatalysts for polymer electrolyte fuel cells. 2006. In *2006 Fuel Cell Seminar Abstracts.* (Honolulu, Hawaii, November 13-17, 2006). Vol. n/a, p. n/a. Fuel Cell Seminar Abstracts: Fuel Cell Seminar.

Zelenay, P., G. Wu, and H. Chung. New non-precious oxygen reduction catalysts for polymer electrolyte fuel cells. Presented at *The 7th Spring Meeting of the International Society of Electrochemistry.* (Szczyrk, Poland, 22-25 March 2009).

# Novel Materials for Gamma-Ray Detection based on Nano-Engineered Semiconductor Nanocrystals

*Richard D. Schaller*
20080660ER

## Abstract

Improvements in the performance of fieldable gamma-ray detectors that operate at room-temperature (non-cryogenic) are critically needed to augment national security as well as to enhance nonproliferation capabilities. Plastic scintillators and thallium-doped NaI crystals are of interest for use in portal monitoring, but both perform less than ideally in terms of a key scintillator figure of merit: energy resolution [1], which is principally related to the number of photons emitted for a given gamma-ray energy. Energy resolution is crucial because it provides the capability to identify specific radioisotopes so that false-positive rates can be reduced. Colloidally prepared nanocrystals (NCs) of semiconductor materials are promising candidates for scintillator applications and are actively under study at LANL, LLNL, and ORNL. NCs are of interest due to their near-unity photoluminescence quantum yields at room temperature (unlike their bulk counterparts), tunable z through choice of material composition (CdSe vs. CdTe vs. HgTe), facile material processibility, and potential for low-cost. While demonstrations of NCs as gamma-ray scintillators exist and their potential for performance is superb, measured gamma-ray photon yields (and, thus, energy resolution) to date are lower than expected [2].

We have made progress in the development of the capability to experimentally simulate gamma-ray excitation of NC ensemble samples with 1-ps electron pulses of tunable energy (0.5-50keV) and detect the emitted photons with a high time-resolution streak camera (<2ps). This transient cathodoluminescence method, with extraordinary and critically needed temporal- and spectral-resolution will allow us to directly measure the low-energy material excitations that result from interactions with energetic electrons. Because it is a transient method, short-lived trions and multiexcitons will be observable and quantifiable due to known spectral and temporal signatures. We have also performed studies of energy transfer in mixed nanocrystal systems as a means to introduce a larger Stokes shift of emission than is typical of NCs.

## Background and Research Objectives

Gamma-ray photons cannot be controllably pulsed. However, they do interact with matter to produce energetic secondary electrons (keV-MeV). The secondary electrons produce cascades of lower-energy electrons that eventually generate relatively low-energy material excitations such as proximal electron-hole pairs ("excitons") which can recombine radiatively [1]. However, in addition to exciton formation, electrons can ionize NCs and may also produce multiple excitons within individual NCs. Ionized NCs (containing an uncompensated electron or a hole) cannot emit. A NC that contains both an exciton and an additional charge (a so-called trion) will emit with greatly reduced-efficiency due to unfavorable competition with ultrafast (~5-300ps) non-radiative Auger recombination. Multiple excitons produced within a NC will also emit with reduced efficiency due to Auger recombination (Figure 1). To date, no one has been able to directly measure the branching ratios of material excitations from electron interactions. This transient cathodoluminescence method, once it is fully operational, will allow us to directly measure the low-energy material excitations that result from interactions with energetic electrons. Because it is a transient method, short-lived trions and multiexcitons will be observable and quantifiable due to known spectral and temporal signatures. We will also quantify normally non-emissive, singly-charged NCs by photoexcitation of the sample prior to the arrival of the electron pulse such that transiently emissive trions, in place of ionized NCs, are formed. Direct knowledge of the branching ratios from a survey of several NC samples would allow for feedback into the synthetic design of the NCs. If ionization is the dominant problem, one could attempt to minimize it via the growth of thick, low-z material shells on high-z NC cores. If we find multiexciton formation to be the main problem,

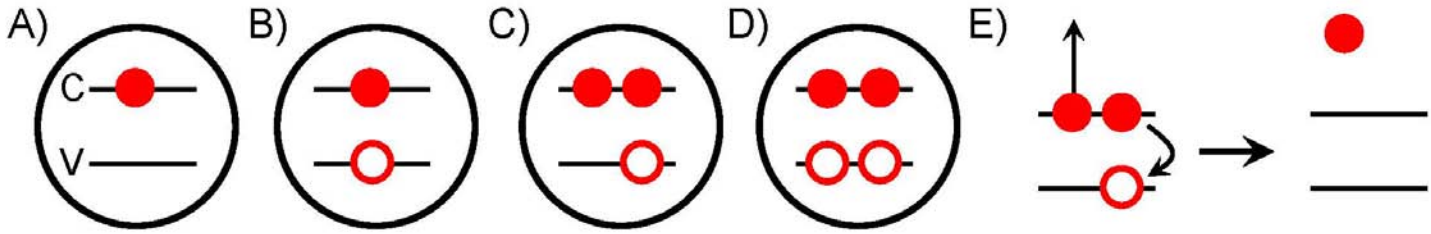


*Figure 1. Excitations in semiconductor nanocrystals. Red circles are electrons (filled) and holes (unfilled). "c" and "v" are conduction and valence energy levels, respectively. A) A singly charged NC is non-emissive. B) A single electron-hole pair or "exciton" is highly emissive with a lifetime of ~20ns or greater depending upon the material (desired). C) An exciton plus an additional charge or "trion" is transiently emissive with a significantly red-shifted emission relative to single excitons (200meV). D) Multiple excitons within a single NC also emit transiently with a 10meV spectral shift. E) Auger recombination is a non-radiative process wherein an exciton recombines and the energy is transferred to a third particle. Excitations C & D can undergo Auger.*

one could reduce NC size to reduce the energy deposited per NC (electron energy deposition is understood to be a function of path, ~6eV/nm for CdTe, so smaller NCs may equal fewer multiexcitons) such that single excitons are principally formed.

In this work, we target semiconductor nanocrystals (NCs) for use as gamma ray detector materials. Nanocrystals are nanometer sized crystals of various semiconductors that have a bandgap which differs from the bulk material due to its small size [3]. NCs have many properties that are desirable for gamma-ray detection including large Z for strong interaction with gamma rays, high photoluminescence quantum yields (up to 90%), emission wavelength tunability from the ultraviolet to the infrared, and solution processibility. However, some properties of typical NCs are not advantageous for scintillator applications such as a relatively small Stokes shift of the emission (typically ~60 meV or ~20 nm in the visible wavelength range), which causes significant reabsorption of emitted photons in thick solid films.

## Scientific Approach and Accomplishments

In the course of this project, we have conducted two types of work. One involves the construction and testing of a pulsed electron gun that will enable exploration of the behavior of semiconductor nanocrystals in conditions that mimic gamma ray excitation. Specifically, a picosecond cathodoluminescence capability would allow for determinations of excitation branching ratios. The other involves energy transfer studies between nanocrystals of two different compositions to determine rates of energy transfer and efficiency.

Regarding the ultrafast cathodoluminescence capability, to date, we have completed construction of the electron gun itself, the vacuum chamber needed for its operation, and have photoexcited the photocathode to produce pulsed electron current. Photos of the electron gun and chamber are shown in Figure 2. The electron gun construction follows that which was exploited by Zewail an coworkers for ultrafast electron diffraction [4], which makes use of a highly biased, semitransparent gold photocathode, extraction electrode and an Einzel lens. The photoelectrons are generated via the photoelectric affect, which requires an ultraviolet photon source in the instance of gold. Thus, we frequency triple a 50fs titanium sapphire laser from 800nm to 266nm and focus this light onto the photocathode. Light induced photocurrent has been measured using a Keithley picoammeter that is connected to the ground cap of the electron gun. Recently, our research team acquired a picosecond-time resolution streak camera that soon will be incorporated into this apparatus as the photodetector.

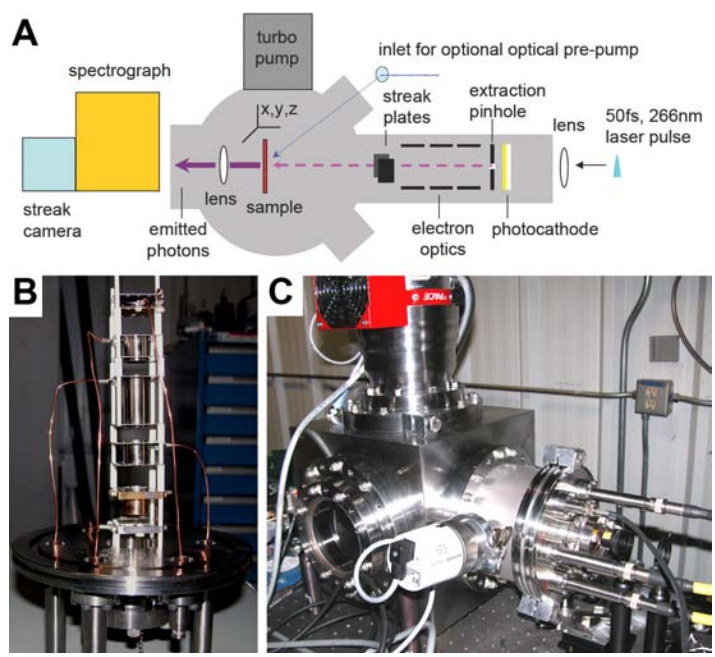


*Figure 2. Ultrafast cathodoluminescence. A) 266nm, 50 fs pulses are focused onto a 20-nm thick gold photocathode that is highly biased. Ejected photoelectrons (dashed pink line) are extracted toward a pinhole, collimated with electron optics, and directed*

*into a sample that is rastered. Photons produced by the sample are collected and directed into an existing spectrograph & streak camera for spectral and temporal recording. Streak plates in the electron gun are used to characterize electron pulse width. B) Operable electron gun. C) Electron gun in 10¬-7 Torr vacuum, optical access chamber. We have drawn electron current but have not yet coupled to the streak camera.*

Also, we have been performing energy transfer studies of mixed NC films in order to determine the feasibility of this approach for increased Stokes shift such that photoemission may be detected from thick films. Mainly we have been studying CdSe-PbSe films that emit in the near-infrared. We observe fast (<200ps) and efficient energy transfer, though this system is not ideal for scintillation-based detection due to the inefficiency of near-infrared photodetectors in comparison to visible ones.

## Impact on National Missions

Radiation detection is a key capability in detecting nuclear materials. This work directly supports nuclear threat reduction and nonproliferation activities that are key mission areas in DOE, DHS, and other government agencies. Semiconductor nanocrystals are good candidates for gamma-ray detectors that are efficient, scalable, operate at room temperature, and are low-cost.

## References


1. Knoll, G. F.. Radiation Detection and Measurement. 2000.

2. Letant, S. E., and T. F. Wang. Semiconductor quantum dot scintillation under gamma-ray irradiation. 2006. Nano Letters. **6**: 2877.

3. Alivisatos, A. P.. Semiconductor clusters, nanocrystals, and quantum dots. 1996. Science. **271**: 933.

4. Ihee, H., V. A. Lobastov, U. M. Gomez, B. M. Goodson, R. Srinivasan, C. Y. Ruan, and A. H. Zewail. Direct imaging of transient molecular structures with ultrafast diffraction. 2001. Science. **291**: 458.

# Parallel-Replica Dynamics Study of Tip-Surface and Tip-Tip Interactions in Atomic Force MicrosCopy and the Formation and Mechanical Properties of Metallic Nanowires

*Arthur F. Voter*
20080759ER

## Abstract

Metallic nanowires, with diameters of a few atoms down to even a single atom, will play an important role in future-generation nanodevices, such as electrical conductors, electrical and perhaps even mechanical switches. Enabling this technological paradigm shift will require a deep understanding of the unique formation mechanisms and mechanical properties of such nanoscale structures. Up to now, atomistic simulations aimed at understanding these processes have been necessarily limited to time scales that are short of the experimental reality by a factor $10^3$ to $10^7$. By porting our Parallel Replica Dynamics (Par-Rep) code to Roadrunner (RR), we made possible the first-ever atomistic simulations of the deformation of metallic nanowires of silver on experimentally accessible time scales of milliseconds. The Par-Rep method, an accelerated molecular dynamics methods developed at LANL, gives exact long-time evolution of an infrequent-event system. The ported version of the Par-Rep code takes unique advantage of the RR architecture, attaining unprecedented atomistic simulation speeds. We demonstrate that Par-Rep on RR can achieve around 0.1 ms of simulation time per wall-clock hour for a 1000-atom system, a ten-thousand-fold improvement over the fastest existing conventional MD capability.

## Background and Research Objectives

The invention of surface scanning probes, like scanning-tunneling microscopes (STM) and atomic force microscopes (AFM), marked the beginning of the age of nanotechnology. These powerful tools, with which one can image, manipulate, and even fabricate structures at scales all the way down to individual atoms, remain at the forefront in this revolution. One mode of operation of an STM or AFM is to allow the tip to come into complete contact with the surface. In the case of a metal tip contacting a metal surface or another tip, a bonded contact forms, and if the tip is then lifted away from the surface, surface reorganization and diffusion often creates a nano-wire of metal that maintains a connection between the tip and surface. This process, as captured by high-resolution transmission electron microscopy (HRTEM), is shown in Figure 1. This kind of manipulation can be exploited for the intentional creation and study of nanowires, whose width can sometimes be reduced all the way down to a single atomic chain by continuing the retraction process. These nanowires are an ideal probe of the nanoscale behavior of materials, be it mechanical [2], or electrical [3], and hence are of interest both for fundamental studies and because of their expected importance in various nanotechnology applications such as electrical conductors, and electrical or mechanical switches. For example, it has been proposed that on-the-fly formation and annihilation of Ag nanowires could act as atomic-scale electric switches [4]. However, a deeper understanding of the fundamental nanoscale behavior of materials is required before these applications can become widespread. Indeed, experiments at the nanoscale are hard to control and usually lack the time resolution necessary to fully understand how the systems behave. For example, metallic nanowires are often seen to completely disappear from one frame to another, leaving one completely in the dark about the basic mechanisms leading to their failure. Further, the act of imaging itself leads to an uncontrolled increase of the temperature of the wire, making it very difficult to perform these experiments in controlled and reproducible conditions.

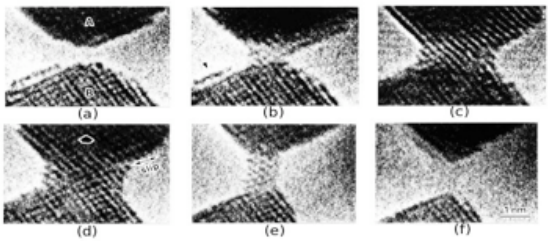


*Figure 1. Series of high resolution transmission electron microscope (HRTEM) images showing the contact formation - retraction - and rupture processes of two Au tips. (a)-(c): contact formation process with (a) corresponding to t=0 sec, (b) t=110/30 sec, (c) t=129/30 sec; (d)-(f) retraction and rupture processes: (d) t=0 sec, (e)t=2 sec, (f) t=3 sec. Figures taken from reference [1].*

There is thus a pressing need for atomistic numerical simulations to complement such experiments and help interpret and understand them. The most powerful tool to perform this kind of simulations is molecular dynamics (MD), whereby one integrates the equations of motion of all the atoms in the system, advancing the positions and velocities of the atoms by repeatedly taking small steps forward in time. In this way, one learns about the evolution of the system with full atomistic detail. However, for many systems and processes we would like to study, there is a serious problem with the mismatch in time scale. The nanowire-stretching process discussed above is a perfect example of this problem. These experiments usually take place over seconds or, at the very fastest, milliseconds. In contrast, conventional MD simulations are limited to a time scale of about one microsecond, even on the fastest parallel computer. Thus, the tip motion in the simulated version of this process is $10^3$ to $10^7$ times faster than the experimental reality. Because of this extremely large gap, physical arguments suggest that current simulations do not adequately represent reality.

Over the last 10 years, we have been developing accelerated molecular dynamics (AMD) methods [5,6,7] aimed at this MD time scale problem. These methods shorten the time between thermally activated rare events that take the system from conformation to conformation (or, equivalently, from state to state), without making prior assumptions about what those events will be. One of these AMD methods, Parallel-Replica Dynamics (Par-Rep) [6] is the main methodological tool of our study. The Par-Rep method relies on the fact that, if the state-to-state (or configuration-to-configuration) dynamics of a system is thermally activated (which is almost always the case for solids around room temperature), the probability of escaping from a given state during an infinitesimal time interval is constant. Using this fact, one can show that the time taken by a single instance of the system to find an exit from a state is statistically identical to the total time accumulated by N independent replicas of the system before any one of them finds an exit path. Thus, the process of escaping from a state can be efficiently parallelized in time (in contrast with the usual spatial approach of large-scale MD) with a theoretical speedup of up to N. The method is schematically illustrated in Figure 2. Par-Rep is the ideal method for this study for two reasons: first, it is the most accurate of the AMD methods and, in fact, produces the *exact* state-to-state dynamics of the system if implemented correctly; second, we have shown that the method is still valid when treating *driven* systems, in which the boundary conditions are changing in time [8].

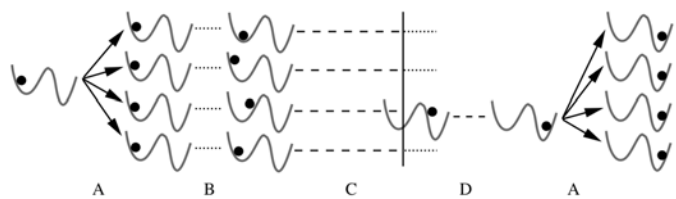


*Figure 2. Illustration of the Parallel Replica Dynamics procedure: the sample to study is replicated on all available processors (A). Independent copies are then prepared (B) and propagated in time using molecular dynamics (C) until a structural transition occurs on one of them (D). Correlated dynamical events are allowed to occur (D). The time accumulated by all copies is summed and the process repeated. Careful implementation gives exact long-time dynamics.*

In parallel with these methodological advances, a revolution in the way super-computers are designed is in progress. Indeed, starting with Roadrunner, it is expected that most world-class computers will rely on so-called hybrid architectures (see below for details). This fundamental change in the way computers are built offers a whole new set of possibilities and challenges to scientific developers who will have to learn to harness the power of these machines in new and imaginative ways if their immense potential is to be realized.The objective of this project is to adapt the Par-Rep method so that it can make optimal use of RR's hybrid architecture. Using this new capability, we demonstrate that it is possible to simulate the evolution of nano-systems like nanowires on an experimentally accessible millisecond timescale. This has not been possible until now, and cannot be achieved on any machine we know of other than Roadrunner.

## Scientific Approach and Accomplishments

Due to its hybrid architecture, RR is a prime example of the new generation of super-computers. Indeed, most of RR's processing power is not provided by conventional general-purpose CPUs but by "accelerators" which provide very high performance by using specialized hardware at the cost of very stringent constraint on how they operate.

In RR's case, the general purpose processors are Opterons while acceleration is provided by IBM's Cell Broadband Engine or Cell, as illustrated in Figure 3. A Cell is composed of a general purpose element (the PPE) to which are connected eight vector processing elements (the SPEs). Taking full advantage of the SPEs can theoretically deliver an impressive 204 GFlop/s (i.e., 204 billion operations per second) in single precision or 102 GFlop/s in double precision (check). While this level of performance is enticing, this new architecture poses serious challenges to scientific programmers. Indeed, performance gains can only be realized at the price of major redesigns of existing codes. High-performance applications will now need to manage fine-grained, parallelization over a heterogeneous collection of processing units (the Opteron, the PPE and the SPEs) on top of the usual coarser-grained parallelization between Opterons, the former now becoming increasingly performance-critical. New strategies are thus needed if the promise of next-generation supercomputers like RR are to be realized. Specifically, the challenge here is to adapt the Par-Rep method to this novel architecture in order to push the timescale horizon even further.

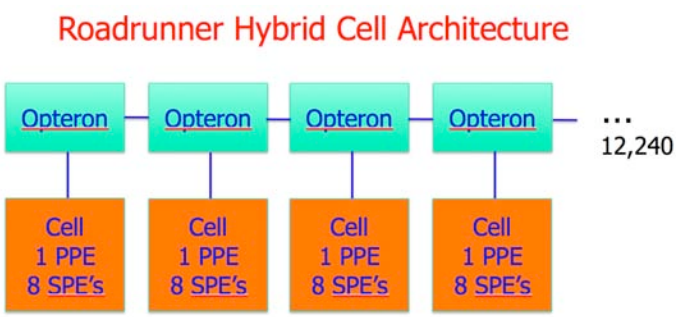


*Figure 3. Illustration of the Roadrunner hybrid Cell architecture. The backbone consists of 12,240 Opteron processors connected by fast communication lines. Each Opteron has direct access to a much faster Cell, within which there is one general purpose element (the PPE) and 8 vector processing elements (SPEs). Each SPE is very fast, but has very limited memory, and its speed can only be fully exploited with very specialized code. The parallel-replica dynamics (Par-Rep) algorithm takes unique advantage of the hybrid architecture for high parallel efficiency. The entire atomistic system, which is small (e.g., 1000 atoms), can fit into the memory on each SPE. The Cell, using all 8 SPEs, performs hundreds of molecular dynamics steps on the 1000-atom system before it needs to send any information back up to the Opteron. The Opterons only need to communicate with each other when a transition is detected in the atomistic system. The overhead cost of transferring information between the Cell and the Opteron, and the communication between Opterons, is thus extremely low.*

It turns out that RR is ideally suited to the requirement of Par-Rep [9]. Indeed, the overall efficiency of simulations on RR strongly depends on the efficient use of the SPEs. The challenge is formidable since the local memory on the SPEs [the so-called Local Store (LS)] is very small: at most a few thousand atoms can be stored in the LS, the rest remaining in the Cell's main memory. This implies that if the system assigned to each Cell is larger than this, atoms will need to be repetitively copied in and out the LS to keep the SPEs continuously busy. Further, some of the bookkeeping information that is kept around in most MD codes will not be reusable and will instead have to be recomputed each time, leading to degraded performance. In contrast with conventional space-wise parallelization schemes of MD, Par-Rep performs best when simulating nano-scale systems containing a thousand atoms or so, because the small size limits the rate at which transitions can occur. Furthermore, there is a cost associated with moving data back and forth from the Opteron processor to the Cells. In Par-Rep, this overhead is minimized because blocks of many MD steps can be carried out independently on the Cells before the results are to be transmitted to the Opteron, and eventually to other replicas. Finally, the overhead cost of the method is proportional to the number of replica used. By efficiently using 10 computing elements (1 Opteron core, 1 PPE and 8 SPEs) for each replica, we keep this number much lower than on conventional platforms. These factors all contribute to making RR the ideal machine to extend the timescale available to direct MD simulations by many orders of magnitude.In order to demonstrate this approach, we ported our in-house Par-Rep code --- AMDF --- to RR. To benefit from the hybrid architecture, we rewrote the most time-consuming sections of the code (the computation of the forces acting on each atom and the integration of their equations of motion) and offloaded them to the Cell processor. Using our implementation, we determined that the time it takes to compute the force on a single atom is around 1microsecond (µs) on the Cell, while it is close to 10 µs on the Opteron alone. RR thus provides us with a ten-fold acceleration per replica compared to a standard architecture. Note that, for the reasons discussed above, this is almost five times faster than implementations where the system as a whole does not fit into Local Store.

Beyond this impressive single replica performance, RR enables us to run Par-Rep simulations with up to 12,240 replicas at the same time. We demonstrated that our code still performs at a parallel efficiency of 70-90% on the whole machine when transitions are rare enough. This means that we can simulate a 1000-atom system interacting through an empirical potential at the rate of more than one microsecond of simulated time per wall-clock minute, or about 0.1 millisecond/wall-clock hour.

To put this into perspective, a standard MD simulation on a fast workstation requires roughly a *month* to simulate one microsecond. Roadrunner thus provides us with an unrivaled capability to reach extremely long timescales while maintaining full atomistic accuracy, enabling a direct correspondence between simulations and experiments.

The main deliverable for this LDRD program is the RR implementation of the Par-Rep code, and the resulting material simulation capability. To demonstrate the power of this approach, we now briefly discuss some simulations on metallic nanowires we have performed since the completion of the port. Specifically, we wish to understand how these wires react to external mechanical perturbations, like strain, and how this reaction depends on critical factors like strain rate (the velocity at which the wire is deformed), temperature and size. As mentioned earlier, the answer to these questions is extremely valuable to interpret experiments where the environment is difficult to control. In contrast, in simulations, we have a total control on the conditions and we have access to all physical quantities fully resolved in both time and space.

During the open-science period ending in September 2009, we simulated the stretching of three different sizes and shapes of silver nanowires under different conditions of temperature and strain-rate, reaching more than one millisecond of simulation time in a few instances, more than a thousand times longer than conventional techniques would have allowed. Overall, we were able to study the change of behavior of these wires while varying the strain rate by more than 4 orders of magnitudes, a feat that was unthinkable before the advent of RR.While the analysis of the results is still ongoing, a picture of the evolution of these systems is emerging. The basic plastic reaction of the system when subjected to strain is to create stacking faults along (111) planes. These stacking faults are highlighted in red in Figure 4. The formation of a zig-zag network of such stacking faults causes the release of internal stresses while leading to the elongation and narrowing of the wire. Interestingly, almost all wires, almost independently of temperature or strain rate initially behave this way. However, the subsequent evolution of the wire is exquisitely sensitive. As shown in Figure 5, these stacking faults are stable on MD timescales (at a strain rate of $10^{-1}$ m/s) and they act as nucleation points for more defects that ultimately accumulate and lead to the necking and failure of the wire after being stretched by about 25%. In contrast, at Par-Rep-accessible strain rates of $10^{-5}$ m/s, these stacking faults have time to annihilate, leaving behind a defect-free wire that is uniformly thinned down relative to the initial configuration (see bottom part of Figure 5). This process then repeats, postponing failure to around 50% stretch or more. While the analysis of the exact mechanisms leading to failure at lower strain rates is not completed, we have already established that their nature is completely different on experimental timescales than on MD timescales, clearly demonstrating the need for tools like Par-Rep on RR if connection to experiments is sought.

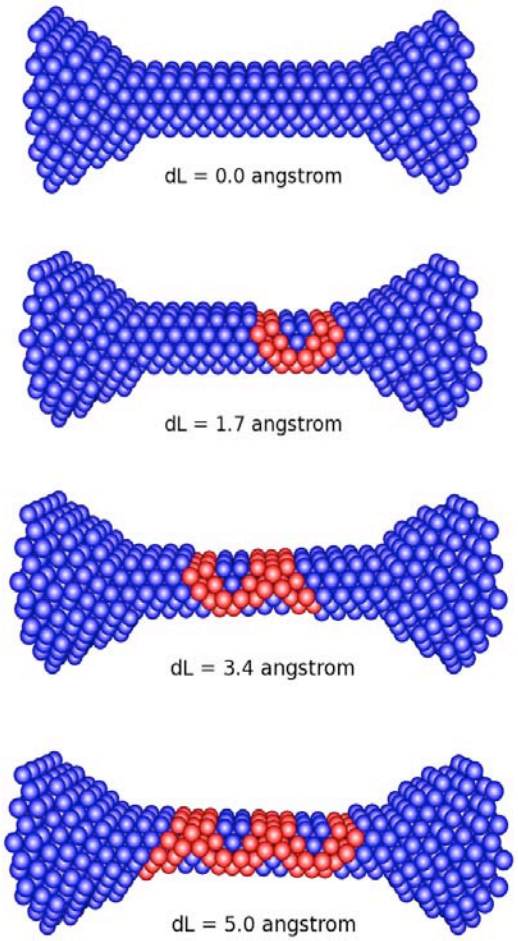


*Figure 4. Silver nanowire at different amounts of stretching (dL) with stretching velocity 10-6 m/s from our Roadrunner simulation. Atoms colored in red highlight stacking faults.*

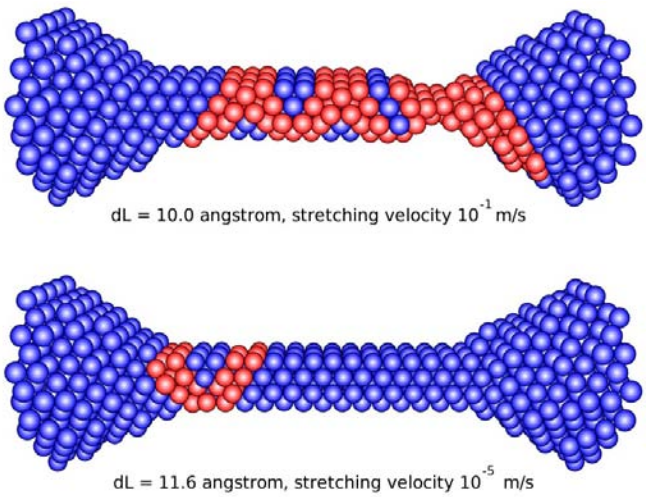


*Figure 5. Snapshots of two silver nanowires stretched at 10-1 m/s and 10-5 m/s, respectively. Note the necking and imminent failure in the fast-strained wire (top). Atoms colored in red highlight stacking faults and other defects.*

## Impact on National Missions

The main impact of the project is to add a unique extremely-long-timescale atomistic simulation capability to the laboratory's portfolio. Such a capability can be leveraged to benefit many of the ongoing efforts related to the understanding of materials, ranging from radiation-damage annealing to stress-corrosion cracking, to nanoscale friction. This work thus contributes to the DOE missions in Energy Security, Nuclear Security, Environmental Responsibility, and Scientific Discovery and Innovation. We are already using this new capability in our core BES program on accelerated molecular dynamics methods, and soon will be using it in our SciDAC program on stress-corrosion cracking [10] and in the recently funded EFRC program on controlling radiation damage through interface design.

## References

1. Kizuka, T.. Atomic process of point contact in gold studied by time-resolved high-resolution transmission electron microscopy. 1998. *Physical Review Letters.* **81**: 4448.

2. Liang, W., M. Zhou, and F. Ke. Shape memory effect in Cu nanowires. 2005. *Nano Letters.* **5**: 2039.

3. Pascualetal, J. I.. Properties of metallic nanowires: From conductance quantization to localization. 1995. *Science.* **267**: 1793.

4. Terabeetal, K.. Quantized conductance atomic switch . 2005. *Nature.* **433**: 03190.

5. Voter, A. F.. A method for accelerating the molecular dynamics simulation of infrequent events. 1997. *Journal of Chemical Physics.* **106**: 4665.

6. Voter, A. F.. Parallel replica method for dynamics of infrequent events. 1998. *Physical Review B.* **57**: 13985.

7. Sorensen, M. R., and A. F. Voter. Temperature-accelerated dynamics for simulation of infrequent events. 2000. *Journal of Chemical Physics.* **112**: 9599.

8. Uberuaga, B. P., S. J. Stuart, and A. F. Voter. Parallel replica dynamics for driven systems: Derivation and application to strained nanotubes. 2007. *Physical Review B.* **75**: 014301.

9. Perez, D., A. F. Voter, and S. Swaminarayan. Exploiting the Cell BE architecture on Roadrunner for long-time atomistic dynamics. 2008. *ADTSC Highlights.*

10. Vashishtaetal, P.. Hierarchical petascale simulation framework for stress corrosion cracking. 2007. *Journal of Physics: Conference Series.* **78**: 012036.

# Chemical Chronometers for Nuclear Forensics Applications

*David L. Clark*
20090482ER

## Abstract

In this project we explored the different rates of oxidation of gallium and plutonium in gallium stabilized delta phase plutonium alloys, and whether these differences could be used to develop a new chemical chronometer for use in nuclear forensics science. The fundamental premise was that differences in electronegativity between plutonium and the alloying element impart different rates of chemical oxidation which can be used as a chemical chronometer. We utilized X-ray Absorption Fine Structure (XAFS) spectroscopy to study both the gallium and the plutonium oxidation of a series of artificially-corroded samples of plutonium-gallium alloys. We found that the delta phase plutonium corroded rapidly, while alpha-prime oxidized more slowly, with both plutonium phases oxidizing much faster than the gallium. The different ratios of oxidized:metallic material for the separate Pu and Ga environments as measured by XAFS therefore constitute a potential chronometer that can determine the time since it was exposed to the environment. The system proved more complex than anticipated, and the relationship between concentration and time that defines the working of the clock itself was not determined during the short (less than one year) duration of this project, but the work led to two new funded projects in nuclear forensics.

## Background and Research Objectives

Our research objective was to demonstrate proof of principle of a new chemical chronometer for use in nuclear forensics applications. Traditional long-lived actinide ***nuclear chronometers*** based on $^{241}Am/^{241}Pu$ ratio are currently used in nuclear forensics to date the time since the last chemical separation of plutonium. While heavily relied upon in nuclear forensics due to their high precision, they provide no information about chemical composition (speciation) that can provide additional information on sample history, source, and intended use. In the case of plutonium alloys used in nuclear devices, we proposed development of a new ***chemical chronometer*** based on fundamental differences in electronegativity of plutonium and alloying elements. These differences in electronegativity impart different rates of chemical oxidation which can be used as a chemical chronometer. By combining nuclear and chemical chronometers, a much greater level of understanding can be achieved to better characterize the history, origin, and intended use of nuclear material.

To understand the relevance of a chemical chronometer to national security, consider the *Denver scenario*, where a terrorist group is building a nuclear or radiological device in the Denver Metropolitan area. A sample is detected and determined to contain plutonium. Isotopic analysis (nuclear chronometer) reveals that the plutonium was last separated 40 years ago. For national security response, we must be able to determine if this plutonium is 40 year old legacy contamination from the decommissioned Rocky Flats site, or whether 40 year old material was *recently* in metallic form in the past few weeks or months, and therefore an indication of a terrorist threat. For this, we need to identify the chemical form of the different elements, and then work backwards to assess its chemical aging history. Determining this connection through differences in oxidation rates between Pu and Ga within an alloy forms the basis for a ***chemical chronometer***, and represents the underlying science of this proposal.

The critical issue in this scenario is not when the plutonium was originally produced and separated, but how recently it may have been metallic or in another chemical form indicative of an end use of immediate or future concern to the U.S. intelligence and security communities. In contrast to production or separation date, *there is currently no method or suite of measurements in the forensics field that can provide this*

*historical information on chemical form that is essential in assigning a degree of threat and formulating the appropriate response*. This work offers the initial proof of principle for an approach that will fill this gap.

## Scientific Approach and Accomplishments

The most common form for metallic Pu, established during the Manhattan Project, is the alloy with around one weight-percent Ga to retain it in the malleable δ phase. For this study, several coupons of δ-stabilized PuGa of around 1 wt-% Ga were prepared. They were polished in sequence, and immediately placed in a chamber with controlled temperature and humidity. Unlike a powder, oxidation will be limited by diffusion as the oxide layer on the surface becomes thicker. Corrosion times were 0, 7, 14, 30 and 60 days. At the end of this time all of the coupons were moved together into an inert atmosphere that should terminate the oxidation process, loaded into XAFS sample holders taking care not to remove the surface oxide, and shipped to the Stanford Synchrotron Radiation Laboratory where Pu $L_3$- and Ga K-edge XAFS measurements were performed at 80 K. The extent of oxidation was determined by comparison with the same alloy sample that has not been exposed to air and water vapor as both the loss of the metallic species –in terms of the reduction in amplitude of both the first and the third nearest neighbor shells of the metal structure – and the direct observation of neighbor shells that are uniquely assigned to oxide.

Because of the element specificity of X-ray Absorption Fine Structure (XAFS), we were able to observe that the average Ga environment underwent significantly less chemical oxidation than the Pu (Figure 1). In other words, the Ga XAFS was very similar to metallic Ga in unoxidized alloy samples whereas the Pu XAFS showed a mixture of Pu metal and oxide. It suggests a differential rate of corrosion of Pu and Ga within the alloy. The differential rates of corrosion apply to the local environments of the Pu and Ga atoms even when they are intimately mixed on the atomic scale in Pu-Ga alloys. In the sample that was measured (Figure 1, bottom), Pu atoms that are not in proximity to Ga atoms readily react with air to form $PuO_2$-like environments. In contrast, Pu atoms in proximity to Ga are inhibited so that the Ga environments remain very similar to what they are in the original metallic form (Figure 1, top). Differential corrosion rates are consistent with our current understanding of plutonium behavior, and we currently employ differences in oxidation chemistry within the ARIES process to preferentially extract Pu from other metals in composite assemblies . In the Ga-stabilized Pu alloys, the nanoscale Ga-centered domains will eventually oxidize to $Ga_2O_3$ – as we have observed in our studies of $PuO_{2+x}$ – but at a much slower rate than the oxidation of Pu. The different ratios of oxidized:metallic material for the separate Pu and Ga environments as measured by XAFS therefore constitute a potential chemical chronometer for δ Pu(Ga) that will determine the time since it was exposed to the environment in its original pure alloyed metal form.

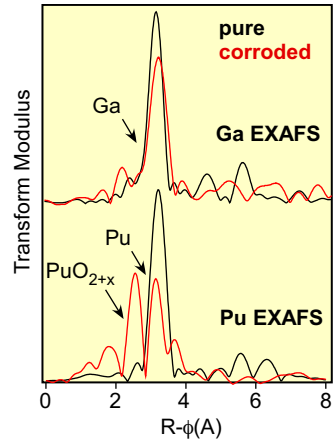


*Figure 1. Ga (top) and Pu (bottom) XAFS spectra of a pure δ-Pu 1.4 wt% Ga sample shown in black. Shown in red are the Ga (top) and Pu (bottom) XAFS of a corroded sample showing the retention of Ga metal and oxidation of Pu to $PuO_{2+x}$.*

Bulk XAFS results on a series of samples show that upon corrosion of metallic Pu with water vapor, the fraction of Pu in ordered metallic form was found to decrease, but by a mechanism much more complex than has been previously described. The α′ component in the mixtures was completely retained over the entire duration of the exposure. All of the losses of metallic Pu therefore occurred in the δ component, and this included the Ga. The lost δ Pu that was presumably oxidized was shown to form $PuO_{2+x}$ with an average, 2.5 Å Pu-O bond length that does not occur in any of the $PuO_2$-like materials that we have previously measured. This work demonstrated that differences in chemical corrosion rate between Pu and Ga are observed. More work is needed to work out details for development of an actual chemical chronometer.

## Impact on National Missions

The need to employ new nuclear forensics techniques is vital to sponsors and decision-makers for source attribution. A revolutionary approach to nuclear forensic analysis has direct benefit to three difficult to address national security issues; 1) identifying materials associated with illicit material handling and trafficking; 2) locating clandestine facilities producing, processing, and weaponizing nuclear material; and 3) detecting undeclared operations within nuclear facilities under IAEA safeguards. The improved ability to distinguish samples with differing processing and environmental exposure histories, as described in the Denver scenario, are key to

all of these applications. For example, the IAEA collects environmental swipe samples for particle analysis under the Additional Protocol inspection regime. Occasionally, a particle analysis yields isotopic data that is not consistent with declared operations. It is often difficult to assess these incidents, as a particle could be legacy material from before the facility came under safeguards, or even brought in on equipment or personnel from another facility. If particle weathering and aging could be assessed through chemical speciation then it would be immediately obvious if the particle in question were from a recent operation or was legacy material or even from another site.

Work performed under this proposal laid important groundwork for FY10 funding. Portions of that concept that employed traditional forensics analysis (morphology of uranium oxides) are now funded in FY10 by the Domestic Nuclear Detection Office at that Department of Homeland Security (DNDO/DHS), and portions utilizing XAFS spectroscopy are now funded by the FBI.

# Superconducting Nanowire Single Photon Detector Development

*Michael W. Rabin*
20090483ER

## Abstract

Photon detection lies at the heart of numerous applications in national security and fundamental science. Space surveillance [1], nuclear threat detection [2], quantum science, and biomolecular imaging all have a compelling need for broadband, high efficiency, low noise, fast single photon detectors. Conventional technologies fall short in at least one of these areas, forcing application-specific compromises. A new class of cryogenic detector, the superconducting nanowire single photon detector (SNSPD, Figure 1), has the potential to revolutionize the field of single photon detection through a combination of unsurpassed performance in all critical parameters (scalability, broadband efficiency, dark count rate, speed). Current development of these detectors is limited by materials difficulties that affect yield and performance, making it impossible to study the underlying physics and determine the fundamental limits of detector operation. To overcome these problems, we are using two complementary thin-film growth techniques that are unique to Los Alamos National Laboratory: Energetic Neutral Atom Beam Lithography & Epitaxy (ENABLE) [3] and Polymer Assisted Deposition (PAD) [4]. We are now applying these capabilities to systematically tune materials properties, correlate device performance with materials characterization (Figure 2), and develop the needed theory for dissipation in nanoscale superconductors. One of our major goals is to transform the SNSPD field from one based on empirical device designs (i.e. irreproducible recipes) to a quantitative, systematic discovery of device physics (predictive science with control). We have already made progress, as demonstrated by three crucial results from our team in the past year:

- **Film growth**— *Both methods proven to make the high quality films needed (Figure 2).*
- **Materials control**— *Transition temperature adjustable by growth parameters.*
- **Theory**— *A new paradigm for dark counts in nanoscale superconducting detectors.*

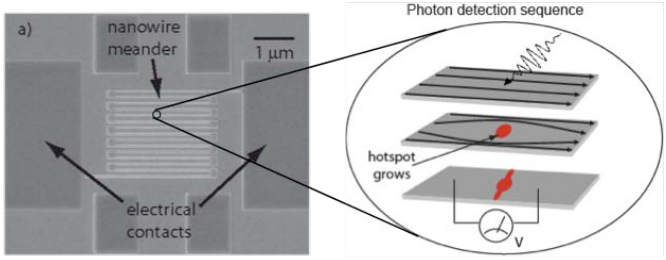


*Figure 1. Scanning-electron micrograph of a superconducting nanowire single photon detector (SNSPD) consisting of a serpentine-shaped niobium nitride nanowire (courtesy MIT). Schematic diagram of photon absorption, hotspot formation, and creation of fully-normal section of the nanowire.*

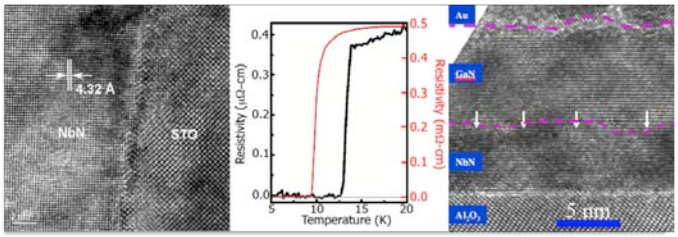


*Figure 2. Microstructure and superconducting transition of high-quality LANL-grown NbN thin films. Left Panel: High-resolution transmission-electron micrograph (HRTEM) of PAD-grown epitaxial NbN (18 nm thin) on $SrTiO_3$. HRTEM shows excellent crystallinity and sharp interface with substrate. Center Panel: ρ(T) around Tc for films shown in left panel (black) and right panel (red). Tc=14K for film in left panel; Tc=10K for film in right panel; difference in Tc due to thickness. Right Panel: HRTEM of ENABLE-grown epitaxial NbN (5 nm thin) on $Al_2O_3$ with GaN cap layer (8 nm). HRTEM shows excellent crystallinity, sharp interface with substrate, ~0.3 nm rms roughness at NbN-GaN interface, and ~5 nm grain size. Grain boundaries are indicated by arrows.*

## Background and Research Objectives

The fundamental technical advantage of cryogenic sensors is ultra-low noise due to their low operating temperatures that can be exploited to achieve extraordinary signal-to-noise ratio (SNR) for photon detection. Cryogenic detectors are becoming practical alternatives to conventional detectors due to two advances that overcome previous technical challenges. First, advanced refrigerators are now commercially available, delivering low (T<4K) temperatures with no liquid helium [5]. Second, new techniques have been developed for fabrication and readout of large focal-plane arrays (e.g. >1200 pixels per chip for submillimeter astronomy, >60 pixels per chip for gamma-ray spectroscopy) [6]. Furthermore, there has recently been intense creativity in this field resulting in the invention of new classes of cryogenic detectors including the voltage-biased transition-edge-sensor (TES), kinetic inductance bolometers, superconducting serpentine delay-lines, and SNSPDs [7,8]. Even though a few groups have succeeded in making NbN films of sufficient quality to make SNSPDs, major issues impede their development and widespread use. First, the best detectors are made from films deposited by reactive sputtering at high temperatures, precluding the fabrication of monolithic devices integrated with readout and biasing electronics or a full optical cavity that can be used to increase the detectors' efficiency to a value close to unity. Process yield, film uniformity, and reproducibility are far too low to allow either the fabrication of large-scale SNSPD arrays or the creation of sufficiently large active areas suitable for efficient coupling to an external light source. Finally, most importantly, the rather crude sputter deposition methods used thus far to make SNSPDs offer few opportunities for systematically varying film properties, such as crystallinity and grain size, in a controllable fashion. Published work also lacks thorough studies correlating specific, controllable materials parameters (e.g. grain size or crystal phase) with device performance—a critical step for improving SNSPDs.

An SNSPD is a long (~1000 µm), narrow (~100 nm), and thin (~4 nm) superconducting wire in a serpentine pattern (typically 10 µm x 10 µm) biased close to the critical superconducting current ($I_c$), the current at which the nanowire becomes resistive (i.e. normal conducting). As depicted in Figure 1, absorption of a photon in the wire creates a "hotspot" of high-resistance material in the normal state. The superconducting current diverts around the hotspot, increasing the current density in the "sidewalks" of the device. If the current density in the sidewalks exceeds the critical current density ($J>J_c$), then both the sidewalks and hotspot become normal, a small section of the wire is no longer superconducting (red stripe across the nanowire in Figure 1), and a voltage is produced. Joule heating causes electrothermal runaway, and more of the nanowire becomes normal conducting. Consequently voltage increases to measureable levels (~mV) and the current decreases (depending on circuit). Hence, the device recovers. The entire process of hotspot formation and recovery can take less than a nanosecond, giving GHz count rates and timing resolutions of tens of picoseconds.

## Scientific Approach and Accomplishments

Our two complementary growth techniques provide us with an exceptional opportunity to develop a theoretical framework that can be validated by controlled experimental studies. Initial films have been characterized, and the results are being used to grow films with specific physical properties. In parallel, a theoretical model is being developed for predicting the relationships between material characteristics (crystallinity, grain size, dynamic response) and basic superconducting properties (critical temperature $T_c$, coherence length $\xi$, and penetration depth $\lambda$). Film characterization results and device performance are being used to test theoretical models. In this manner, theory and experiment are coupled for predictive science, rather than trial and error, to optimize detector design and performance.

(1) In combination with film characterization, theory is addressing the key questions of the degree of structural, electrical, and superconducting granularity of the nanowire. Generally, granularity limits the SNSPD operation due to a distribution of weak *inter-grain* links, making it difficult to bias the detector close to the *intra-grain* critical supercurrent. Hence, photon detection efficiency of a detector with grain size D of the order $\xi$ is expected to be suppressed, as it will be dominated by the weakest link with small photon absorption cross-section. To extract the relevant *superconducting* granularity, we used microscopic structural measurements (TEM, AFM) and electric transport measurements at temperatures above and below the superconducting transition $T_c$. From measurements of resistivity, critical current, and the width of $T_c$, theory can identify if the film is uniform or granular and guide detector development accordingly. This is crucial for optimizing growth conditions for both ENABLE and PAD.

(2) Understanding and controlling dark counts is essential for designing high-efficiency detectors with high signal to noise ratios. Dark counts are induced by thermal fluctuations of the superconducting condensate, and thus are unavoidable, especially at high bias currents. In this project, we have made significant progress in identifying the microscopic mechanism for dark counts. In thin uniform films of thickness d, where the Pearl length $\Lambda=2\lambda^2/d$ is much larger than the magnetic penetration depth $\lambda$ or the width

*w* of the wire ($\Lambda \gg w \gg \xi$), we have proposed that dark counts are caused by single vortices (topological defects in the superconducting wave function) crossing the wire. This scenario breaks with the widely held belief that vortex-antivortex pair unbinding is responsible for dark counts [9], which has been unsuccessful in describing measured I-V (current-voltage) characteristics of thin films.

Our newly developed theory goes beyond the mean-field theories for thin films [10], which can qualitatively explain the three observed regimes in the I-V characteristics (ohmic, power-law, and exponential regimes (see Figure 3) depending on the bias current). However, mean-field theories neglect thermal fluctuations. They fail to quantitatively describe the I-V characteristics by several orders of magnitude. In the past, thermal fluctuations have only been considered for the case of one-dimensional wires [11]. We have, for the first time, devised a numerical technique for determining the effect of thermal fluctuations in *two*-dimensional nanowires such as SNSPDs. Similar to the work by McCumber and Langer [11], our theory is based on rate equations for transitions between metastable states of a film with decaying supercurrent, where a single crossing vortex induces a transition between metastable states [12]. Hence, we can calculate numerically the potential barriers for vortex entry, as well as crossing rates as a function of applied bias current, temperature, film width and thickness.

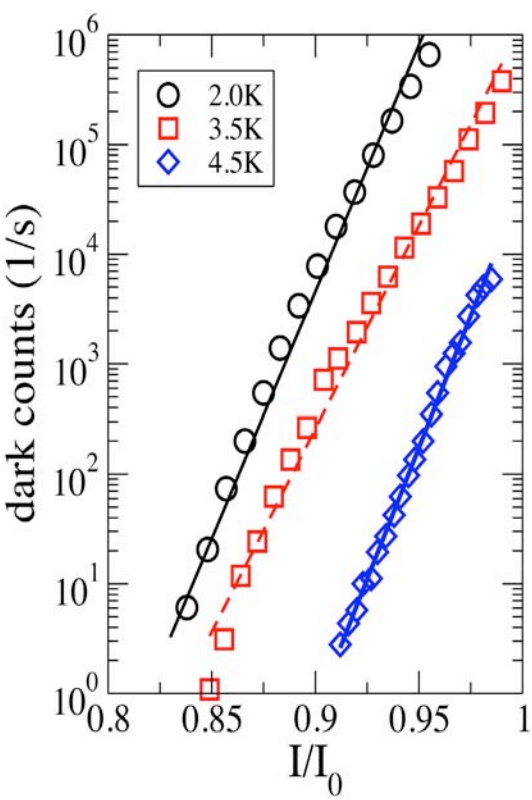


*Figure 3. First attempt to compare theory with data in exponential I-V regime; dark counts are proportional to voltage.*

We can test the validity of our theory by comparing our predictions (based on the parameters extracted in step (1) above) with observed dark count rates and I-V characteristics. Experimentally, dark counts have the same voltage pulse shape V(t) as counts arising from photon absorption, a clear indication of hotspot formation and electrothermal runaway. In the case of dark counts, the deposited energy is not due to a photon, but rather is generated by the dissipative motion of a vortex crossing the wire. Another prediction of our theory is the existence of "cold" dark counts, which correspond to vortex crossings that do not induce a hotspot, and thus may not be visible within our electrical bandwidth. However, they generate a background DC voltage in the SNSPD that can be extracted to estimate their occurrence rate. We are the first to predict the magnitude and duration of V(t) with time-integrated value $\int V(t)dt=\Phi_0$, with flux quantum $\Phi_0$.

Polymer-assisted deposition (PAD) is a chemical solution deposition technique invented at LANL/MPA [13] used to grow epitaxial complex metal oxide and nitride thin films. In this process, the soluble polymer plays a significant role in preparing high quality compound films by controlling the desired viscosity for the process and binding the metal ions to prevent premature precipitation and formation of metal oligomers. The result is a homogeneous distribution of the metal precursors in the solution and the formation of uniform metal oxide or nitride films. PAD can be used to grow epitaxial films even when a large lattice mismatch exists, which has been shown to be helpful for SNSPD operation [14]. PAD has recently been used to grow thin (18 nm) epitaxial NbN films on a $SrTiO_3$ (STO) substrate (12.6% lattice mismatch), with high superconducting critical temperature of 14 K and excellent interface quality (Figure 2). PAD-grown NbN has impressive materials properties: using X-ray diffraction and electron micrcoscopy, we find these films are highly crystalline ($\Delta\theta$=1.5°), well aligned in plane, smooth, dense, uniform, and relaxed (low stress). Consistent with these materials characteristics, the superconducting properties are also outstanding: metallic conduction from room temperature to $T_c$, a sharp transition (Figure 2, center panel), large critical current density (~5MA/cm$^2$), and (to the best of our knowledge) the largest residual resistivity ratio (RRR) yet measured for thin film NbN (RRR=98.4) [4]. We are currently growing thinner NbN films (4-10 nm) for characterization.

Energetic Neutral Atom Beam Lithography & Epitaxy (ENABLE) can be used to controllably grow extremely high-quality epitaxial, highly crystalline thin films at low temperatures. ENABLE utilizes a collimated beam of neutral reactive nitrogen (N) atoms with kinetic energies of

a few electron volts (1 to 5 eV) to activate surface chemical reactions. The kinetic energy and high reactivity of neutral N atoms allow low-temperature growth of nitride thin film materials by simultaneously exposing substrates to energetic N atoms and an evaporated metal flux [15]. This capability for low-temperature growth is in contrast with other methods (including PAD whose NbN process uses a 950°C annealing step) for making epitaxial nitride films (e.g. InGaN, NbN). Since the kinetic energy range covers most chemical bond energies but is too low to induce damage, it is ideal for synthesizing a wide range of high-purity thin film materials with few intrinsic defects. Unlike reactive sputtering, the destructive method used by other groups to grow SNSPDs, the ENABLE process allows fine control over material parameters (e.g. composition, granularity, phase, etc.). As shown in Figure 2, ENABLE has grown superconducting NbN *in our target thickness range* (4-10 nm), with excellent materials characteristics. Films are highly crystalline (δ-fcc phase, Δθ=0.3°), smooth (rms roughness approx. lattice spacing), and continuous; from HRTEM images, we see the sharp interface with the sapphire substrate and a grain size of ~5nm. The superconducting transition occurs at $T_c$=10 K and is slightly rounded ($\Delta T_c$=0.5 K), consistent with our expectations for grain size comparable to the coherence length. By comparing $T_c$ and thickness (d) of several ENABLE-grown films with the expected $T_c$ suppression ($T_{c,bulk}$-$T_c$1/d) and literature values, we conclude that these films are on par with the best films for a given thickness.

Demonstrated tunability of ENABLE film growth: Importantly, we have also demonstrated that we have access to parameters (other than growth and annealing temperature), for adjusting film properties. Figure 4 shows that increasing the N atom flux increases the transition temperature $T_c$. This increase in $T_c$ is also strongly correlated with a crossover from two dimensional, layer-by-layer growth to three-dimensional, island growth, as determined from *in-situ* electron diffraction (RHEED) patterns. Based on the high N atom flux and similarity to other nitride systems [3,15], our expectation is that the ENABLE-grown NbN is stoichiometric and increasing N atom flux principally changes morphology, not composition. Under these conditions, ENABLE offers direct tunability between growth modes and associated film characteristics. Additionally, there are several parameters we have not yet explored: N atom energy (currently ~1.8 eV), overall growth rate (known to be crucial for epitaxy of other nitrides and oxides), substrate materials, nucleation layers, and substrate pretreatment.

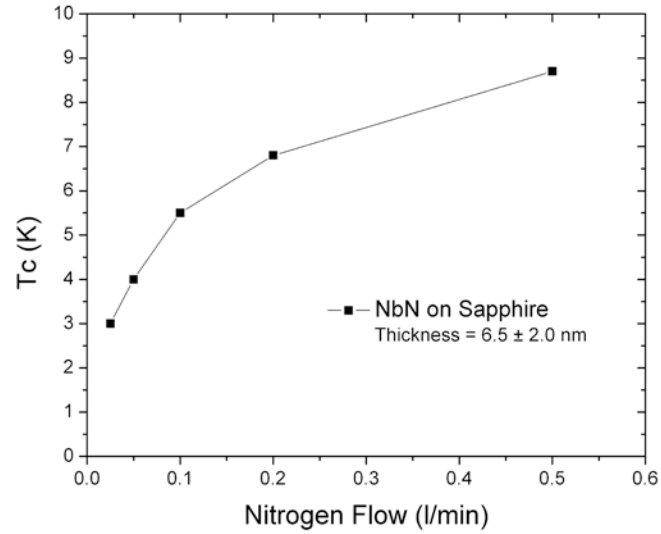


*Figure 4. Tunability of ENABLE films. The superconducting critical temperature increases with the flow of nitrogen, as discussed in the text.*

## Impact on National Missions

A major goal of our work is to establish the scientific foundation in nanoscale superconductivity (theory, materials & device physics) necessary to develop SNSPDs into a technology that will deliver a broadband, high-efficiency, high-speed, low-noise single photon camera—a truly revolutionary technology. This project for developing SNSPDs should be viewed in the context of developing a larger LANL program for applying cryogenic detectors to national security problems. The success reported above is based on one year of LDRD "reserve funding" and has provided the necessary catalyst for an expanded LDRD-DR FY10-12 project. In particular, it led to the conversion of T. Williamson from postdoctoral researcher to staff.

As indicated by a DARPA workshop, DOE-sponsored conferences, and DHS proposal calls, several government agencies recognize the need for advanced detector technologies. In the long term, we foresee instruments based on SNSPD focal-plane arrays replacing existing technology in three major LANL mission areas demanding maximum sensitivity: low-light imaging (RULLI/NCAM), SSA, and IR hyperspectral imaging. Each of these mission areas relies on LANL science capability and has strong programmatic backing.

## References

1. Siegmundetal, O.. Advanced Photon Counting Imaging Detectors with 100ps timing for Astronomical and Space Sensing Applications. 2006. In *Advanced Maui Optical and Space Surveillance Technologies Confererence.* (Maui, 15-22 Sep 2006). , p. 1. Maui: AMOS.

2. deHaas, J. T., and P. Dorenbos. Advances in yield calibration of scintillators . 2008. *IEEE Transactions in Nuclear Science .* **55**: 1086.

3. Williamsonetal, T.. Highly luminescent In{sub x}Ga{sub 1-x}N thin films grown over the entire composition range by energetic neutral atom beam lithography and epitaxy (ENABLE) . To appear in *Physica Status Solidi.*

4. Zou, G.. Ultrathin epitaxial superconducting niobium nitride films grown by a chemical solution technique. 2008. *Chem Commun.* **2008** (45): 6022.

5. http://www.hpd-online.com; operating at T=65mK routinely at LANL/TA35/2/C150. 2009. *http://www.hpd-online.com; operating at T=65mK routinely at LANL/TA35/2/C150..*

6. Dorieseetal, W. B.. A 14-pixel, multiplexed array of gamma-ray micro-calorimeters with 47 eV energy resolution at 103 keV. 2008. *Applied Physics Letters.* **151**: 191910.

7. Irwin, K. D.. Seeing with superconductors. 2006. *Scientific American.* **295** (5): 86.

8. Topics in applied physics cryogenic particle detection. 2005.

9. Kitaygorsky, J.. Dark counts in nanostructured NbN superconducting single-photon detectors and bridges. 2007. *IEEE Transactions on Applied Superconductivity.* **17**: 275.

10. Tafurietal, F.. Dissipation in ultra-thin current-carrying superconducting bridges; evidence for quantum tunneling of Pearl vortices. 2006. *Europhysics Letters.* **73**: 948.

11. Langer, J. S.. Theory of nucleation rates. 1968. *Physical Review Letters.* **21**: 973.

12. Boulaevskii, L. N., M. J. Graf, and V. G. Kogan. Entropy protected superconducting current in rings made of thin wires or thin films. To appear in *TBD.*

13. McCleskeyetal, T. M.. Polymer-assisted deposition of films. 2008. *U. S. Patent Office, U. S. Patent No. 7,365,118, issued April 29, 2008..*

14. deLamaestreetal, R. E.. Microstructure of NbN epitaxial ultrathin films grown on A-, M-, and R-plane sapphire . 2007. *Applied Physics Letters.* **91**: 232501.

15. Muelleretal, A. H.. Low-temperature growth of crystalline GaN films using energetic neutral atomic-beam lithography/epitaxy . 2006. *Applied Physics Letters.* **88**: 041907.

# High-Nitrogen Polydentate Ligands for Lanthanide/Actinide Separations

*Jacqueline M. Veauthier*
20090490ER

## Abstract

We have examined a new class of ligands for advanced lanthanide/actinide separations chemistry. These ligands referred to as bitetrazole amine are polydentate high-nitrogen content ligands that are water soluble and are relatively inexpensive and simple to prepare on large scales. To date, we have prepared and characterized several new lanthanide complexes of bitetrazole derived ligands and examined their separations properties by electronic structure theory calculations and liquid-liquid extraction studies using radioactive tracers. We have shown that these ligands form stable complexes with lanthanides and actinides and have good evidence to suggest that these new cost effective ligands separate lanthanides from actinides at pH values between 2.0 and 3.0.

## Background and Research Objectives

There has been a resurgent interest in actinide chemistry to support nuclear energy production [1]. If the U.S. nuclear energy footprint is to increase, as present trends indicate, improved methods for the treatment of spent nuclear fuel (SNF) will have to be developed. Indeed, the 2006 report by the US DOE Office of Basic Energy Sciences on *Basic Research Needs for Advanced Nuclear Energy Systems* identified the grand challenge of "*Understanding and Designing New Molecular Systems to Gain Unprecedented Control of Chemical Selectivity during Processing",* and explicitly calls for advanced separations chemistries to be developed that utilize new and novel chemistry agents [2]. The Separations Campaign of the AFCI has recently established a Sigma Team to undertake high-risk research on advanced nuclear fuel reprocessing methods. The current "Grand Challenge" of this team is to develop a more robust one-step actinide/lanthanide separation process.

The primary commercial process used to treat spent nuclear fuel, PUREX, recovers Pu and U from spent nuclear fuel (SNF). The AFCI has developed a series of liquid-liquid extraction processes called UREX+ to further partition SNF to allow complete actinide recycle and more efficient disposition of the fission products. Although UREX+ has been an outstanding achievement, the *separation of trivalent minor actinide (Am, Cm) from the lanthanides (Ln) is a key step that is currently accomplished with a complex series of processes that would be costly to implement in a commercial facility*. Although the TRUEX-TALSPEAK processes (Figure 1) can be used to achieve this separation, the required conditions are not ideal. For example, the extraction works only for solutions of low acidity (i.e., pH ~ 3.0) although typical feed solutions are > 1.0 M nitric acid and feed adjustment to accommodate TALSPEAK adds substantially to the cost. Additionally, the TALSPEAK process contains diluents and extractants that do not follow the CHON principle. The CHON principle requires molecules to consist of only carbon, hydrogen, nitrogen, and oxygen such that they are completely incinerable and secondary waste is minimized. This principle is extremely important to European methods of nuclear fuel reprocessing. Research over the last decade involving polydentate soft donor ligands has evolved to produce new extractants that could revolutionize lanathanide/actinide separations science [3, 4]. The ligands that have shown the most promise are polydentate high-nitrogen content ligands such as bis-triazinyl pyridine (BTP), shown in Figure 2. The use of BTP-type ligands has been shown to dramatically improve separations of transplutonium elements (Am and Cm) from lanthanides with separation factors ($SF_{Am/Eu}$) ≥ 100 [4]. Although these ligands could serve as strong extractants for actinides over lanthanides the disadvantages to their use include the high cost of synthesis and inadequate radiation stability. Still, the progress with this new approach suggests that other high-nitrogen content polydentate ligands might display similar or even greater separations efficiency with lower cost and potentially greater stability. For example, bitetrazole amine (Figure 2) has been shown

to form N-bonded polydentate complexes with a variety of transition metals, including Fe, Cu, Ni, and Co [5]. There are several potential advantages to the use of BTA type ligands relative to BTP such as the low cost and relatively simple large-scale preparation of the neutral ligand, the ability to form a highly charged species in solution (Figure 2, deprotonated form), and water solubility which in turn could improve the kinetics of metal complexation.

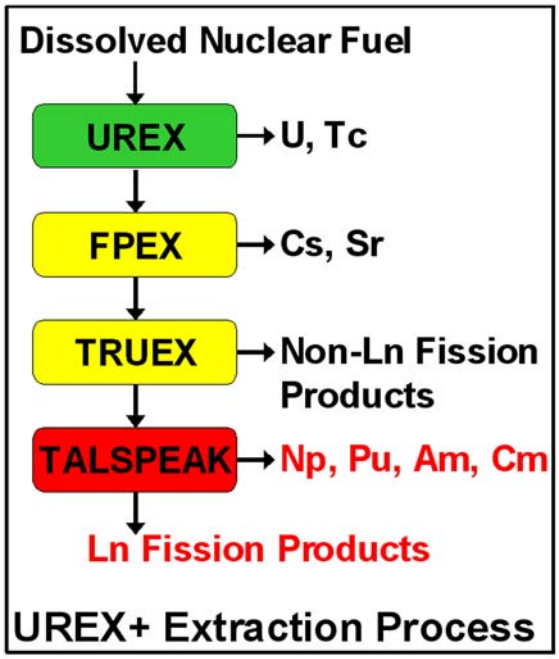


*Figure 1. Urex+ extraction Process*

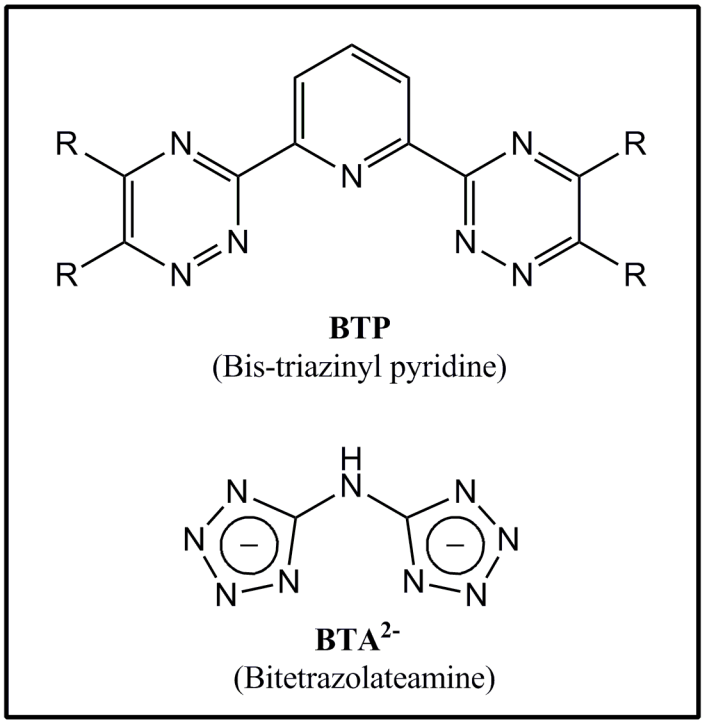


*Figure 2. High Nitrogen Polydentate Ligands*

Fundamental studies by our team have revealed that f-element complexes of BTA can be prepared and lanthanide complexes have been isolated in high yield and have been fully characterized. Theoretical calculations predict that actinide complexes of BTA should be stable and preferred over lanthanide complexes. Specifically, calculations show that actinide complexation is favored over lanthanide extraction by 18-56 KJ/mol. To date, extraction studies with BTA, a co-extractant (HDEHP) and radioisotopes americium-241 and europium-152 suggest that separation is favorable above pH 2.

## Scientific Approach and Accomplishments

We have examined the fundamental chemistry of the high nitrogen ligands BTA with several lanthanides. We have found that these ligands coordinate lanthanide cations well. Indeed, $La^{3+}$, $Ce^{3+}$, $Pr^{3+}$, $Eu^{3+}$ and $Nd^{3+}$ all form stable complexes with BTA in aqueous solutions under ambient conditions with high yield and purity. These new complexes have been characterized by X-ray crystal diffraction (Figure 3), elemental analysis, FT-IR spectroscopy, and NMR spectroscopy. Additionally, we measured the equilibrium constants of BTA by titrating acidic solutions of diammonium BTA and lanthanum BTA with a standard sodium hydroxide (NaOH) solution. The results are shown in Figure 4. All new lanthanide complexes were safety tested and do not show any energetic sensitivity towards thermal stress (DSC differential scanning calorimetry) drop weight impact, friction, or spark. Preliminary studies suggest that BTA does bind to uranium(VI) in neutral aqueous solutions but isolation of this new compounds and definitive characterization by X-ray crystallography has not been confirmed.

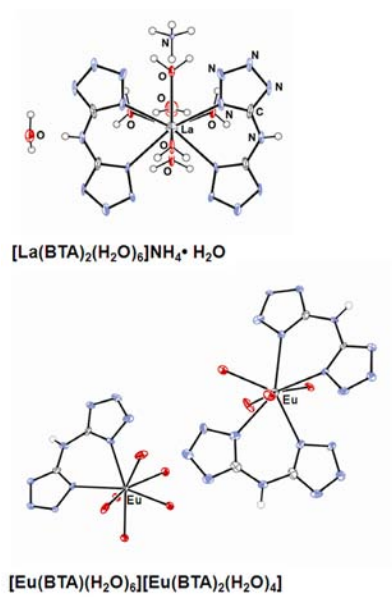


*Figure 3. X-ray Crystal Structure of La-BTA and Eu-BTA*

| Equilibrium Equation | Equilibrium Constant Conditional ($I_M$ = 0.1 M $NaNO_3$) |
|---|---|
| $BTA^{2-} + H^+ ?\ BTAH^-$ | Log $\beta_{101} = 5.71 \pm 0.01$ |
| $BTA^{2-} + 2H^+ ?\ BTAH_2(aq)$ | Log $\beta_{102} = 8.88 \pm 0.02$ |
| $BTA^{2-} + La^{3+} ?\ \{BTA\text{-}La\}^+$ | Log $\beta_{110} = 2.5 \pm 0.1$ |
| $2BTA^{2-} + La^{3+} ?\ \{2BTA\text{-}La\}^-$ | Log $\beta_{201} = 5.6 \pm 0.1$ |

*Figure 4. Equilibrium Constants for BTA at 20C with $HNO_3$ and NaOH*

Density functional theory (DFT) calculations in collaboration with Neil Henson and Rich Martin (T-1) to investigate the electronic structure theory of BTA ligands with lanthanide and actinides were performed. The optimized geometries for Ln(III) complexes are in good agreement with our crystallographic data suggesting that the DFT models are good and crystal packing has little effect on the preferred structure. The DFT calculations further predict that it is thermodynamically possible to add more than two BTA ligands to an f-element (i.e., actinide or lanthanide) and that the average binding energy for the BT/BTA ligands to the metal is 5-8 times greater than for a water molecule. These calculations also predict that these high nitrogen ligands should effectively separate actinides from lanthanides. More specifically, actinide extraction by BTA is favored over lanthanide extraction by 18-56 KJ/mol [6].

To evaluate, further, the potential for BTA-type ligands to separate lanthanides from actinide separations in spent nuclear fuel, we performed liquid-liquid extraction studies using radioactive tracers (gamma emitters Am-241 and Eu-152). More specifically, we measured the distribution coefficients ($D_{org/aq}$) of either Am-241 or Eu-152 in organic and aqueous phases of solutions containing the BTA ligand, a co-extractant di-2-ethylhexylphosphoric acid (HDEHP), nitric acid ($HNO_3$), and hydrochloric acid (HCl) between pH values of 0 and 3. The results of these extractions are shown in Figure 5. Although these values are preliminary and further studies are needed to confirm these results, the data suggest that separation begins to occur near pH 2.0 but is much stronger at pH 3.0. The data are consistent with the results of theoretical calculations such that the actinide (Am-241) binds more strongly to BTA and remains in the aqueous phase in the presence of HDEHP while the lanthanide (Eu-152) is more easily extracted into the organic phase by HDEHP.

| pH | BTA, HDEHP | Isotope | $D_{Organic/Aqueous}$ | $SF_{Am/Eu}$ | $SF_{Eu/Am}$ |
|---|---|---|---|---|---|
| 0.0 | 0.01 M, 0.01M | Am-241 | 0.1 | No Separation | No Separation |
| | 0.01 M, 0.01M | Eu-152 | 0 | | |
| 1.0 | 0.01 M, 0.01M | Am-241 | 0.1 | No Separation | No Separation |
| | 0.01 M, 0.01M | Eu-152 | 0 | | |
| 2.2 | 0.01 M, 0.01M | Am-241 | 0.2 | 0.034 | 30 |
| | 0.01 M, 0.01M | Eu-152 | 5.9 | | |
| 2.7 | 0.01 M, 0.01M | Am-241 | 0.1 | 0.0012 | 800 |
| | 0.01 M, 0.01M | Eu-152 | 84 | | |

*Figure 5. Separations Data for Liqui-Liquid Extractions with Am-241 and Eu-152*

In summary, we have prepared and characterized several new lanthanide complexes of the high nitrogen ligand BTA. Electronic structure theory calculations suggest that BTA should favor actinide binding over lanthanide binding and could serve as potential extractants for spent nuclear fuel. Preliminary separations studies using radioactive tracers confirm these calculations but more experiments are necessary to determine if BTA could be used to develop a more robust lanthanide-actinide separations process. However, the results of this work have also led to new studies to prepare organic soluble BTA ligands which could have potential as a one-step lanthanide-actinide single liquid-liquid extractant.

## Impact on National Missions

Revolutionary separation processes to partition actinides from lanthanides and other fission products could result from the fundamental knowledge developed through this work. They would lead to improved safety, economics, and proliferation resistance of future plants for partitioning spent nuclear fuel. This includes separation processes for the spent fuel produced by the fast reactor systems that are designed to fission the actinide inventory more effectively than the light water reactors. The increased control of f-element coordination chemistry would also be expected to provide new synthetic approaches to prepare more challenging fuel types, such as the transmutation fuels for fast reactors.

## References


1. Statistics from the Nuclear Energy Institute, Washington, DC, http://www.nei.org. 2007. *Washington, DC.*

2. Report of the Basic Energy Sciences Workshop on Basic Needs for Adbvanced Nuclear Energy Systems. 2006. *Department of Energy, ANES.*

3. Ekberg, C., A. Fermvik, T. Retegan, G. Skarnemark, M. Foreman, M. Hudson, S. Englund, and M. Nilsson. An overview and historical look back at the solvent extraction using nitrogen donor ligands to extract and separate An(III) from Ln(III). 2008. *Radiochimica Acta.* : 225.

4. Kolarik, Z.. Complexation and Separation of Lanthanides(III) and Actinides(III) by Heterocyclic N-Donors in Solutions. 2008. *Chemical Reviews.* : 4208.

5. Tappan, B., M. Huynh, M. Hiskey, D. Chavez, E. Luther, J. Mang, and S. Son. Energetic decomposition of high-nitrogen metal complexes and the formation of low-density nano-structured metal monoliths. 2006. *Journal of the American Chemical Society.* : 15.

6. Veauthier, J., and D. Clark. Report for Project 20080717ER. 2008. *LANL LDRD Office.*

# Advanced Measurements in Designed Nanostructures to Establish Measurement Techniques for Electrosynthetic Production of Fuels

*Albert Migliori*
20090517ER

## Abstract

LANL has established that one central aspect of the Laboratory's now-publicly-stated initiatives in energy will be distributed electrical energy storage. Noting that of the many approaches to energy storage worldwide, only a few, among them electrosynthetic production of fuels and electrochemical capacitors require *fundamental* science. There is also a synergy in any process involving electrodes and electrolytes (such as hydrogen electrolysis, ammonia synthesis, charging and discharging batteries, ultracapacitors, fuel cells and more) because there is a region of operation where no current flows and no chemistry occurs, and another region where current flows and chemistry does occur. Expanding upward in voltage the zero-current region increases the energy density of ultracapacitor-like devices, while expanding downward in voltage the current-flow region improves the efficiency of electrosynthetic-like processes. However, at the most fundamental science level, it is clear that these processes are simply limits of one science driver. The goal of this work was to begin laying groundwork for *"Understanding energy storage via electron-matter interactions at nano interfaces far from equilibrium, under extremes of electric field and at pH and temperature levels outside the biological envelope."*

## Background and Research Objectives

In this LDRD reserve project, it is important to realize that only a very small but crucial part of this overall research plan could be executed. Thus in an attempt to focus on a challenge that is achievable, sets the stage for more comprehensive research, and provides validation of measurement, fabrication, and analysis capabilities that we are just now bringing to bear on the problem, we proposed to use electyrode-electrolyte geometry to explore the efficacy of electrodynamic and optical probes of the active region of an electrochemical cell that can act as both capacitor and electrolysis system.

## Scientific Approach and Accomplishments

We describe advances in theory, catalyst support structures in the form of carbon nanotubes that can be modified later to carry many types of catalyst, measurements of supercapacitors in water-based electrolytes, and preliminary work on the interaction of catalysts and magnetic fields.

### Producing carbon nanotubes with a narrow size distribution

In any attempt to improve the signal to noise ratio of a measurement, a common approach is to signal average. Signal averaging is commonly achieved by time averaging a measurement. However, it is also possible to ensemble average. That is, make a single measurement in a short time on many identical systems, thus multiplying the weak, noisy signal from, say, one carbon nano tube by the total number of nano tubes in the measurement array. To do this requires multiple identical nano tubes. To obtain enrichment of a single type of nanotube with the goal of narrow diameter distributions, we used a salt-enhanced density gradient separation method on metallic and semiconducting single-wall nano tubes (SWNT) fractions. In Figure 1 it is clear to the eye that excellent separation has occurred in these chiral SWNTs, confirmed by optical absorption studies (not shown).

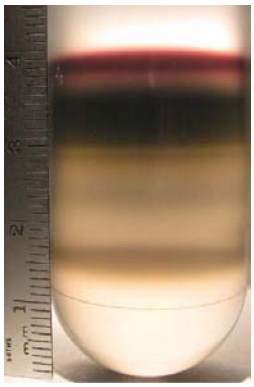

*Figure 1. Demonstrated enrichment of (6,5) small diameter semiconducting SWNT fraction.*

**Carbon-nanotube-based supercapacitors in aqueous electrolytes**

Carbon nanotube arrays are promising as electrodes for electrochemical systems because they provide a large surface area and a very straight current path to the base. Such systems can produce specific capacitances of order 100 F/g, and the direct current path is expected to yield a lower series resistance, a primary energy loss mechanism. The carbon nanotube arrays used for this work were assembled by first growing a forest at standard conditions, where the tubes are multi-walled and nearly parallel. The growth substrate is not conducting, a fact that greatly complicates their use as electrodes. Electrical contact is made to the array by depositing a 0.5 micron gold layer which forms a sheet connecting the ends of the thousands of nanotubes. The freestanding array is placed in an electrochemical cell where the capacitance is measured (Figure 2). The mass will be determined later, but arrays of that size typically weigh 1 mg. Then, the specific capacitance is at least approximately 10 F/g. Similar results were obtained with other samples, probably because the electrolyte is most likely not wetting the full surface area of the nanotubes. The arrays were treated with a number of wetting agents, but only immersion in methanol resulted in a small improvement (~12 %) of the electrode capacitance. An appropriate approach in the future is to adjust the process parameters to vary the spacing between the nanotubes to increase the electrolyte penetration and electroactive surface area.

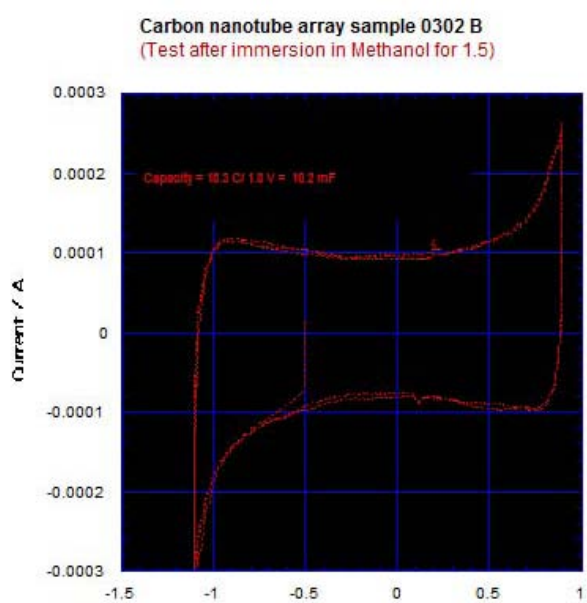


*Figure 2. Cyclic voltammmogram of a carbon nanotube electrode in a 0.1 M electrolyte at 25 ºC. The electrode capacitance was calculated from the charge of the anodic scan between -1.0 and 0.8 V.*

**Oxygen Reduction Reaction (ORR) in High Magnetic Fields**

A strong fundamental understanding of oxygen electrocatalysis on metal surfaces is of vital importance in improved engineering of the electrocatalyst layers in fuel cells and electrosynthesis. Diatomic oxygen molecules dissociate when they adsorb onto some metal surfaces promoting the charge transfer processes. The role of element/alloy composition on oxygen reduction has been studied primarily for Pt group metal (PGM) catalysts and their alloys. Density functional theory calculations predict an increase in oxygen reduction activity by weakening the adsorption of strongly bound oxygen containing surface intermediates via d-band center shifting [1]. The primary method of testing and refining DFT theory of electrocatalysis is through measurements of oxygen reduction activity on a series of PGM alloys. While alloying does shift the d band centers, the alloying elements tend to surface segregate and change surface composition and thus change intermediate adsorbate interactions. It is preferable to shift the d-band center at a given electrochemical potential without changing the composition of the surface or particle size or shape. This may be accomplished through the use of a high magnetic field. The interaction of the d-band electrons with the applied magnetic field may provide a powerful clean probe of the role of d-band position on oxygen reduction kinetics.

We constructed a probe to measure the effects of a high magnetic field on the oxygen reduction reaction kinetics at the electrolyte-Pt interface using Pt microelectrodes. Because of the enhanced planar diffusion provided by microelectrode Pt disks, quiescent systems can be examined over a large current density range before reaching mass transport limitations [1]. Figure 3 shows typical voltammograms obtained at a Pt-perflouro-ionomer (Nafion ™) interface. These sigmoidal i-V curves make it possible to determine ORR kinetic parameters over the range 0.7 to 0.95 volts. Very high magnetic fields may lead to significant changes in the electronic structure of the Pt catalyst, which would affect the ORR at the metal-electrolyte interface. ORR kinetics studies are of paramount relevance for fuel cells (FC), because even with the best catalyst (Pt) the rate of this reaction supports high currents only at large overpotentials, a significant energy loss mechanism.

**Modeling of overpotentials**

We have performed molecular dynamics simulations with a molecular mechanics forcefield on a supercapacitor model consisting of a carbon nanotube electrode (radius 5A) in an ionic liquid (tetraethylammonium, TEA, boron tetrafluoride, $BF_4$, with a acetonitrile, ACN, dielectric) at varying electrode charge densities. The goal is to compute

where the electrical charges come to rest. Calculated radial electrical charge distribution functions show the formation of the electrical double layer within 10ns. Figure 4 shows the calculated radial distribution for the centres of mass of the three electrolyte components with a positively charged electrode. The negatively charged $BF_4$- ions are located primarily at the wall of the nanotube, whereas the positively charged TEA ions are slightly further out. The calculated capacitances are in the range of those measured experimentally for similar compositions. We are currently working on extending this test system to the potassium sulphate electrolyte system for which we have experimental data.

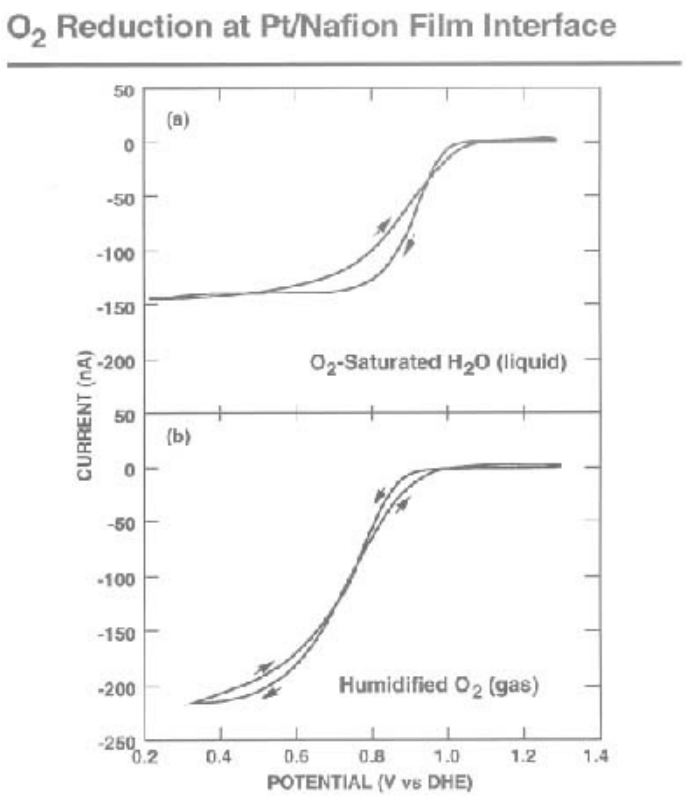


*Figure 3. Current-voltage characteristics of $O_2$ reduction at a Pt microdisk (100 µm diam) covered with a ca. 10 µm-thick recast Nafion film. Scan rate: 5 mV/s; Temperature: 22 ºC (a) Electrode immersed in $O_2$-saturated deionized water; (b) Humidified gaseous $O_2$ atmosphere.*

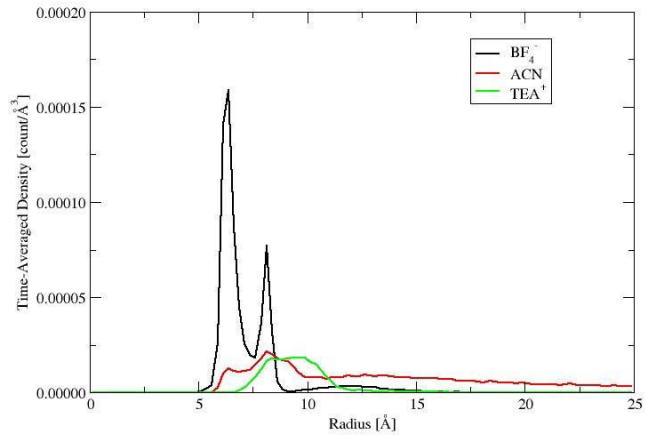


*Figure 4. The calculated radial distribution for the centres of mass of the three electrolyte components with a positively charged electrode.*

## Impact on National Missions

This directly supports expansion of the use of renewable electrical energy.

## References


1. Yang, L., B. H. Fishbine, A. Migliori, and L. R. Pratt. Molecular simulation of electric double-layer capacitors based on carbon nanotube forests . 2009. *Journal of the American Chemical Society* . **1311** (34): 12373.


## Publications

Yang, L., B. Fishbine, A. Migliori, and L. Pratt. Molecular simulation of electric double-layer capacitors based on carbon nanotube forests. 2009. *Journal of the American Chemical Society.* **131** (34): 12373.

# Molecular Level Investigation of Tunable Energetic Mixtures

*David S. Moore*
20070766PRD4

## Introduction

Explosive materials (e.g., HMX, PBX) generate rapidly expanding gases, which can cause unnecessary collateral damage. A safer alternative is in intermetallic- forming reactive mixtures, which can undergo ultra-fast shock-induced reactions, releasing significant heat during the formation of solid products, and thereby provide for the controlled defeat of targets. The challenge associated with reactive mixtures has been to determine the molecular-level mechanisms that govern the initiation and kinetics of shock-induced reactions. We are studying the shock-induced initiation of intermetallic reactions through combined laser-driven shock-compression experiments and computer modeling, performed on a range of binary reactive systems, in order to determine the influence of heterogeneity on the molecular-level processes responsible for reaction. Multi-component reactive films (e.g., V/Si, Mo/Si, Al/PTFE) up to 2 µm in thickness are deposited onto transparent substrates using e-beam deposition and/or spin casting. A novel dynamic masking technique, in which a mask is translated between the source and substrate during deposition, is employed to construct films with a predefined thickness gradient. This method, performed in forward and reverse mask mode with reactive complements, is used to fabricate bi-layer films with an internal interface, inclined to the substrate normal by a specified angle. Measures of the total film thickness, roughness, and interface angle, necessary for proper interpretation of results, are characterized through SEM, AFM, and profilometry. A Ti:sapphire laser system, focused at the substrate/film interface to a spot size of 75 µm, is then used to drive an ultra-fast, supported shock wave (10-20 ps rise-time, >200 ps shocked duration) through the bi-layer. Spatially flat shocks (1-D) can be produced using a field-flattener. Ultra-fast dynamic ellipsometry is employed at the film/air interface to obtain time- and spatially-resolved surface displacements in a single given experiment, and detect short timescale phase shifts corresponding to the onset of molecular-level reactions. Varying the film species (metals, metalloids, polymers), interface angle during deposition (gradient and non-gradient), and laser-drive energy, provides great flexibility in further studying the role of heterogeneity in the kinetics of shock-induced reactions at the molecular-level. This experimental work is complemented by multi-scale numerical simulations, used to develop and validate new predictive models for the controlled, ultra-fast initiation of intermetallic reactions.

## Benefit to National Security Missions

The results from this study are directly applicable to threat reduction mission needs, enabling the design of a new class of application-based energetic materials for controlled defeat of targets.

## Progress

We completed addition of the dynamic masking system to our bell jar vapor deposition system necessary to produce multi-component films with a predefined thickness gradient. We successfully deposited a series of amorphous Si films with a thickness gradient, and characterized their uniformity using SEM.

We found a complex ultrafast dynamic ellipsometry (UDE) time response after shocking these films using our ultrafast laser shock system. We realized this complex time response could be due to changes in particle velocity due to reaction or phase transformation, or to changes in the shocked material index of refraction. The initial films cleverly used silicon both as a window and as one of the reaction components, but we discovered that the shock response of amorphous silicon was not very well understood. However, we also discovered a large body of work on the shock response of single crystal silicon. We then devised a method to produce thin film samples of single crystal silicon, and located a photolithography/MEMS vendor willing and able to manufacture the required array of supported thin film samples from a single crystal silicon blank. We have since used these samples to acquire an extraordinary set of UDE results on the ultrafast time response of shocked single crystal silicon. We implemented two approaches to analyze the time dependent UDE data. One involves

a time dependent change in the index of refraction of the shocked material with either sigmoidal or logarithmic approach to a new constant value. The other involves a first order reaction with progress variable, and calculates the time dependent index of refraction. To implement, the UDE ellipsometric data are fit using four variables instead of three, with the fourth describing the time dependent index of refraction.

However, the similar UDE contributions from changes in shocked material index of refraction and the shock velocity necessitated an additional diagnostic. We are presently implementing a scheme to independently measure the shock velocity (using both 800 nm – transparent to silicon – and 400 nm – reflects from silicon – probes), which will allow us to pin down one of the fitting variables in our UDE methodology and thereby extract the remaining variables (particle velocity and index of refraction) with greater confidence and accuracy.

We have also produced Mo/Si and V/Si binary films with a sharp (near vertical) step between the two layers. The spatially resolved UDE data are being obtained and will be analyzed using similar tools to those developed for the non-gradient films. Continuum-level simulations of this configuration have been performed using the multi-material Eulerian shock code, CTH, to estimate the magnitude of particle-velocity mismatch at such an interface.

## Future Work

We will complete the single crystal Si UDE work, and publish the results. We also intend to look for chemical reaction products using the technique of femtosecond stimulated Raman spectroscopy (FSRS). While UDE can supply the details of interface migration and refractive index changes, FSRS can be used to reveal the elimination and formation of vibrational modes associated with the presence of reactants and products, respectively, and their related timescales. Additionally, probing both the Stokes and anti-Stokes Raman transitions can be used to measure temperature, and more completely survey the thermodynamics of ultrafast chemical reactions.

## Conclusion

The study will provide the first insight into the critical molecular-level processes responsible for ultra-fast shock induced reactions in multi-component energetic mixtures, and their dependence on system heterogeneity. The results will have a broad impact on conventional reactive material systems, supply the fundamentals to directly manipulate and optimize chemical behavior. This understanding will enable the design of a new class of application-based energetic materials, demonstrating tunable sensitivity, reaction kinetics, and energy yield.

## Publications

Eakins, D. E., and N. N. Thadhani. Mesoscale simulation of the configuration-dependent shock-compression response of Ni+Al powder mixtures. 2008. *Acta Materialia.* **56** (7): 1496.

Eakins, D. E., and N. N. Thadhani. Shock compression of reactive powder mixtures. 2009. *International Materials Reviews.* **54** (4): 181.

# First-Principles-Based Equations of State Including Multi-Phase Chemical Equilibrium

*Milton S. Shaw*
20080695PRD1

## Introduction

The goal of the proposed work is to refine and extend computational methods for building an equation of state for chemical explosive detonation products. The principal vehicle for achieving this is the development of a Monte Carlo simulation method specially designed to capture the complexities of chemistry under extreme conditions of temperature and pressure. A very efficient procedure will be implemented for evaluating equilibrium averages with electronic structure-based (quantum chemistry) energies in place of approximate functional forms, whereby many steps in a reference system (characterized by a computationally inexpensive "model" potential) are used to generate a single electronic structure configuration. This effectively reduces by up to three orders of magnitude the number of electronic structure calculations required to build ensemble averages. We will also introduce efficient means for accurately describing chemistry at the surfaces of carbon nanoclusters that are known to exist in detonation product fluids.

Replacement of approximate potentials with highly accurate ab initio energy evaluation, especially in the context of Monte Carlo in a reactive ensemble, promises considerable improvement in accuracy over that of previous work. Namely, it permits evaluation of statistical properties accounting for rare events (in this case, chemical reactions among fluid components) on a highly accurate and reactive potential energy surface, but without actually having to sample those regions of the potential most sensitive to error (i.e., the chemical reaction barrier tops). In addition to enhancing the predictive capability of the Laboratory's continuum detonation models, these developments should be of broad interest to computational scientists in government, industrial, and academic contexts.

## Benefit to National Security Missions

This project will support the DOE/NNSA mission in Nuclear Weapons (and e.g. Homeland Security and Office of Science) by enhancing our understanding of the extreme pressure and temperature environment occurring in the detonation of chemical high explosives including near-first-principles prediction capability.

## Progress

Over the course of the last year we have made considerable progress in our efforts to improve the accuracy and efficiency of atomistic Monte Carlo simulation. Our focus in particular has been description of molecular fluids subjected to extreme temperatures and pressures, approximating thermodynamic conditions that follow detonation of high explosive compounds.

We formulated a new Monte Carlo method for efficiently sampling accurate ab initio and density functional theory (DFT) energies in lieu of approximate model potentials. Our method uses Boltzmann sampling of a pair potential to statistically decorrelate successive evaluations of a much more accurate and computationally expensive DFT potential. A sequence of single-particle steps made in the reference system (described by the pair potential) is combined to yield a composite step made in the full system (described by DFT). Through a slight modification of the acceptance probability, one recovers Boltzmann sampling of the full system. By statistically decorrelating samples of the DFT potential, fewer evaluations of it are required to obtain ensemble averages having low variance. The efficiency of this decorrelation process is significantly enhanced by maximizing the overlap of the distribution of reference system states with that of full system states. This, in turn, is achieved by variation of the full system temperature and pressure such that an a priori estimate of the acceptance probability for composite steps is maximal. Monte Carlo simulation at the new, optimal conditions can then be performed; we have dubbed this procedure the optimized-Nested Markov Chain Monte Carlo (o-N(MC)$^2$) method. We published a largely methodological discussion [1] in the Journal of Chemical Physics as well as presenting a talk at the 2009 APS Shock Compression of Condensed Matter Conference and the associated conference proceedings [2] to be published.

After laying the theoretical groundwork, we applied our technique to the description of compressed nitrogen fluid as described by the Perdew-Burke-Ernzerhof exchange-correlation functional and a 6-31G* basis set. The required simulations took ~6 months and represented the most accurate potential applied to the largest simulation performed to date on this system. The Monte Carlo simulation results were then reworked to yield the nitrogen Hugoniot, the locus of states accessible upon shock loading of an initial state. Our Hugoniot results reflected precision levels of ~2% were in quantitative agreement with experiments. This implementation was published in the Journal of Chemical Physics [3]. This work was also presented at a talk at the 2009 APS Shock Compression of Condensed Matter Conference and will appear in the conference proceedings [4].

In the process of improving the thermodynamic description of molecular fluids at high pressure and temperature, we discovered that elements of our methodology could be applied to modeling spectroscopic signals recorded for such systems. Using a rapidly-evaluatable reference potential as in our thermodynamic work, we collected statistics on dense fluid nitrogen using Monte Carlo sampling of an accurate density functional theory potential and its forces. Introduction of a novel methodology then enabled us to convert the DFT forces into Raman line shifts as a function of pressure (density). The results were in quantitative agreement with experiments previously performed at LANL, and reported in Chemical Physics Letters [5].

We have developed a method combining the best features of the optimized Nested Markov Chain Monte Carlo with Hybrid Monte Carlo. In essence, this allows the use of molecular dynamics, with all of its advantages, as the trial move within the optimized method. The implementation is currently being tested.

## Future Work

The scientific issue addressed will be a highly accurate fundamental theoretical description of the complex fluid mixture at the extreme temperature and pressure that results from detonation of high explosives. The system is a multiphase, chemically reacting mixture of dense molecular fluids and nano-clusters of carbon consisting of about 1000 atoms with an equally reactive surface coupled to the surrounding fluid. Given the limitations of experimental measurements at these extreme conditions, this theoretical approach gives the best opportunity of understanding the underlying physics and chemistry.

The specific tasks are basically the evaluation of potential energy hypersurfaces corresponding to at least 100 molecules, and the evaluation of thermodynamics including equilibrium composition by accurate simulation methods with sufficient speed to be tractable. State-of-the-art density functional electronic structure methods will be used for the energies of fluid configurations as well as for representative segments of carbon nano-cluster surfaces including incorporation of H, N, and O. The thermodynamics simulations will be based on a very efficient implementation of the Monte Carlo method that allows large steps through configuration space that requires only a small number of uncorrelated configuration energies evaluated by the very expensive (due to the large number of atoms) quantum chemistry methods. Of particular importance is the extension of the simulation methods to incorporate the chemical equilibrium composition

Specific goals are: Build on the already successful progress to refine the thermodynamic simulation methods required to efficiently sample the equation of state as well as thermodynamic equilibrium of the systems described above. Apply these methods to specific simulations that showcase the fundamental chemistry and physics of this complex system and reproduce available experimental benchmarks.

## Conclusion

We will develop improved methods for predicting the pressures, temperatures, and chemical composition of high explosive products of detonation. These are required as input to models of explosive performance and behavior with a wide variety of applications ranging from military defense (NNSA/DoD) to homeland security (DHS). The fundamental methodology, which we will develop, involves intelligently (optimally) combining Monte Carlo simulation techniques with quantum chemistry, and will be of general use in many situations involving chemically reactive mixtures involving multiple phases, for instance formation of nanocarbon clusters from a reactive fluid.

## References


1. Coe, J. D., T. D. Sewell, and M. S. Shaw. Optimal sampling efficiency in Monte Carlo simulation with an approximate potential. 2009. *Journal of Chemical Physics.* **130** (16): 164104.

2. Coe, J. D., T. D. Sewell, and M. S. Shaw. Optimized nested Markov chain Monte Carlo sampling: theory. (Nashville, TN, 28 June - 3 July 2009).

3. Coe, J. D., T. D. Sewell, and M. S. Shaw. Nested Markov chain Monte Carlo sampling of a density functional theory potential: equilibrium thermodynamics of dense fluid nitrogen. 2009. *Journal of Chemical Physics.* **131** (7): 074105.

4. Shaw, M. S., J. D. Coe, and T. D. Sewell. Optimized nested Markov chain Monte Carlo sampling: application to the liquid nitrogen Hugoniot using density functional theory. (Nashville, TN, 28 June - 3 July 2009).

5. Coe, J. D., T. D. Sewell, M. S. Shaw, and E. M. Kober. A quantum chemical method for calculating vibrational line shifts in diatomic fluids. 2008. *Chemical Physics Letters.* **464** (4-6): 265.

## Publications

Coe, J. D., T. D. Sewell, M. S. Shaw, and E. M. Kober. A quantum chemical method for calculating vibrational line shifts in diatomic fluids. 2008. *Chemical Physics Letters.* **464** (4-6): 265.

Coe, J. D., T. D. Sewell, and M. S. Shaw. Optimal sampling efficiency in Monte Carlo simulation with an approximate potential. 2009. *Journal of Chemical Physics.* **130** (16): 164104.

Coe, J. D., T. D. Sewell, and M. S. Shaw. Nested Markov chain Monte Carlo sampling of a density functional theory potential: equilibrium thermodynamics of dense fluid nitrogen. 2009. *Journal of Chemical Physics.* **131** (7): 074105.

Coe, J. D., T. D. Sewell, and M. S. Shaw. Optimized nested Markov chain Monte Carlo sampling: theory. To appear in *2009 American Physical Society Shock Compression of Condensed Matter Conference.* (Nashville, TN, 28 June - 3 July 2009).

Shaw, M. S., J. D. Coe, and T. D. Sewell. Optimized nested Markov chain Monte Carlo sampling: application to the liquid nitrogen Hugoniot using density functional theory. To appear in *2009 American Physical Society Shock Compression of Condensed Matter Conference.* (Nashville, TN, 28 June - 3 July 2009).

# Study of Hybrid Semiconductor/Molecular Systems for Photo-production of Hydrogen

*Andrew P. Shreve*
20080700PRD1

## Introduction

Charge transfer is one of the basic steps required for solar energy conversion to electricity or chemical fuels where the charge transfer occurs to a conduction band (producing electricity) or to other molecules (chemical processes). The mechanisms and kinetics of charge transfer within semiconductor, molecular and catalytic systems will be studied using static and time-resolved spectroscopies. The studies to be performed here will provide new fundamental knowledge regarding the rates of these processes and will also address how structural changes in the materials can mediate the efficiency of charge transfer in various systems. Ultimately, such information will contribute to optimization strategies for systems that use photo-induced catalytic splitting of water for solar production of hydrogen fuel.

## Benefit to National Security Missions

This project supports the DOE mission in Energy Security and the Office of Science by improving fundamental understanding of photo-induced charge separation processes relevant to solar energy applications. In addition, the technology developed here can also be applied to biophysical studies of protein structure, dynamics and function, and to the investigation of chemical reactivity in more general areas outside of energy-related studies.

## Progress

We have continued development of step-scan Fourier Transform infrared spectroscopic instrumentation that allows the study of the structure and dynamics of photo-excited molecules. The instrumentation is based on using a kHz repetition rate excitation laser synchronized with the stepping of a spectroscopic interferometer in such a manner as to allow averaging over many excitation pulses at each interferometer position. Previous implementations of this type of spectroscopic instrumentation have been limited to acquisition of results from a single excitation pulse at each interferometer step. With this instrument we have demonstrated that the photo-excited states of catalytically active molecules can be studied with much greater precision than ever before. For example, in Figure 1 we show the excited state infrared spectrum for a ruthenium complex whose excited state is characterized by a transfer of an electron from the metal ion to a bipyridine ligand. The excited state of this compound is active for charge injection processes on semiconductor surfaces and for mediation of photocatalytic reactions. The spectrum shown in Figure 1 is, by far, the highest signal-to-noise infrared spectrum that has ever been obtained for this transient species, which lives for only a few hundred nanoseconds. Analysis of the infrared absorption features and further analysis of the temporal dynamics of this species, especially in combination with semiconductor nanoparticles or catalytic molecules, is work in progress and will lead to improved understanding of the nature of photo-induced chemical reactivity relevant to energy production processes. We are also exploring the combination of photo-active mediator molecules, such as the complex just mentioned, with hydrogenase proteins. Ultimately such hybrid systems could allow the photo-induced production of hydrogen using efficient biological catalysis. Currently we are using time-resolved spectroscopies to understand the kinetics of charge transfer between the photo-excited molecules and reactive centers in the proteins. One paper that will describe the instrumentation we have developed is in the final stages of submission to Applied Spectroscopy, and two follow up manuscripts are in the initial stages of preparation for scientific journals.

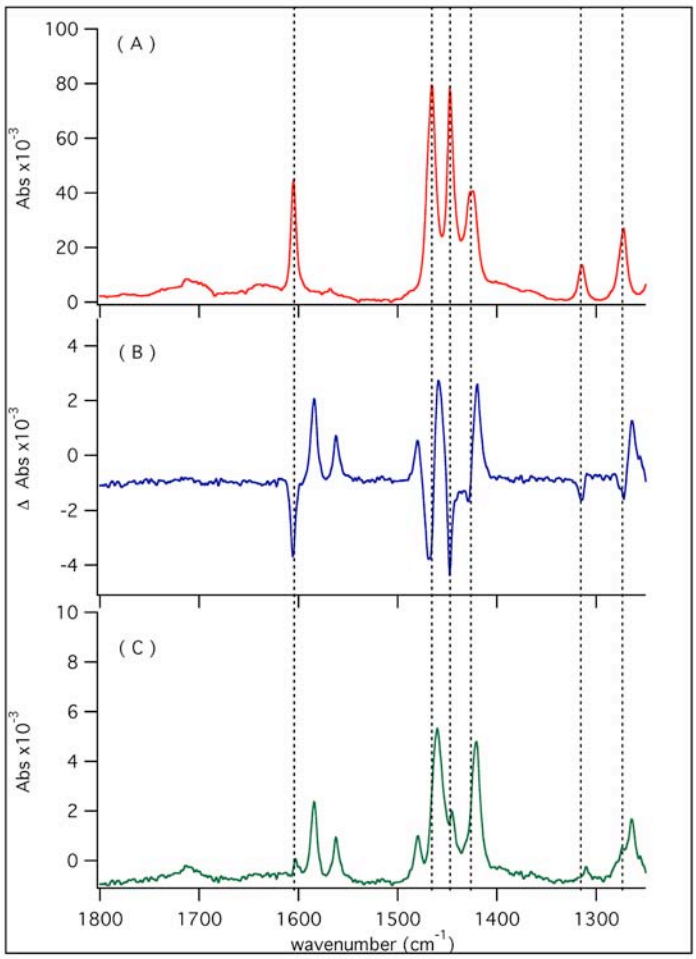


*Figure 1. A ruthenium bipyridine complex was photo-excited using a near-ultraviolet pulsed laser. The solution containing the compound was interrogated using a Fourier-Transform infrared (FTIR) spectrometer operating in step-scan mode. The FTIR was operated at 100 Hz collecting 10 spectra while averaging 30 pulses per step. A) Ground state absorption spectrum of the ruthenium complex. B) Difference spectrum reflecting the change in absorbance associated with photoexcitation. C) Excited state spectrum obtained by adding a fractional amount of the ground-state spectrum into the difference spectrum.*

## Future Work

Continuation of the studies outlined above will lead to an increased understanding of the fundamental charge transfer process that allow the production of chemical fuels through photoexcitation processes. A number of chemical compounds that have both photoexcitable metal centers and catalytically active metal centers are available for study, with the goal of elucidating the kinetics of photo-induced charge transfer and the structural rearrangements that mediate charge-transfer efficiency. Both of these topics are critical to understand in order to be able to optimize solar energy conversion processes. In addition, hybrid systems that involve the interface of molecular compounds with either semiconductor particles or proteins will be explored. The former is important for the solar production of fuels such as hydrogen through chemical catalysis, while the latter provides a biological or enzymatic pathway to solar fuel production. In both cases, significant questions remain about the nature of charge transfer between dissimilar materials, and the time-resolved structural studies we are now able to perform will be used to examine the mechanisms and kinetics of these reactions.

## Conclusion

To produce hydrogen from water in a process driven by light, one must have material components that absorb light and components that catalyze the chemical transformations involved. Since the chemical transformation require the addition or removal of electrons on the catalysts, the transfer of electrons between the light absorbers and the catalysts must be efficient. We will attempt to better understand the relevant photo-induced electron transfer process by applying static and time-resolved optical spectroscopies to study composite materials in which light absorbers and catalysts are assembled together. Ultimately, such studies will help optimize methods for the solar production of hydrogen.

# Synthesis and Characterization of Novel Metal-Organic Frameworks for Hydrogen Storage

*Toti E. Larson*
20080780PRD2

## Introduction

There are many challenges in the implementation of the new energy economy. The least recognized but most critical is the need for storage of high purity hydrogen. For example, the development of hydrogen-fueled vehicles requires new materials that can store large amounts of hydrogen molecules at accessible pressure/temperature conditions and are capable of storing and releasing hydrogen efficiently. This research aims to design, synthesize and test novel Metal-organic frameworks (MOFs) for hydrogen storage/separation as well as exploring their application to environmental, energy and national security problems. Since the discovery of the first MOF compound, hundreds of different MOFs have been developed and reported. MOFs are generally synthesized by self-assembly of metal ions/clusters as coordination centers and organic ligands as linkers. They possess intriguing chemical and physical properties and are structurally tunable, thermally stable and mechanically sound. MOFs are increasingly proving to be a superior class of materials for state-of-the-art applications in crystal engineering, chemistry, and materials science.

## Benefit to National Security Missions

This project supports the DOE mission in Energy Security and Environmental stewardship by developing novel metal organic frameworks (MOFs) for hydrogen storage and purity as well as their applications in other fields. The impact of this project will be significant if the concept is successfully utilized for storage/separation science. For example, we are currently pursuing the application of MOFs for novel filtration and sensing of Chemical Threat Agents and capture of carbon dioxide. These two additional applications are considerably important to the LANL's Global Security mission of Sensing and Measurement Science, Monitoring, and treaty Verification.

## Progress

Since July 7, 2008 I completed the required training and work authorizations for safety and security. I have synthesized and characterized structurally a series of novel MOFs for tailored applications, such as hydrogen storage, $CO_2$ capture, and sampling of chemicals. I investigated the reticular design of their functionalized pore wall structures, and demonstrated some of their novel applications. I designed and assembled two instruments for gas separation and variable-pressure gas-loading cells in conjunction with neutron scattering instruments, allowing *in-situ* and real-time examination of guest uptake/release processes in MOF compounds at the molecular site-specific level. I am now working with Toti Larson to develop MOFs for applications in High-efficiency sampling, preservation, and sensing of chemical threat agents. The following research tasks were accomplished during the past year:

**Design and syntheses of tailored MOFs for hydrogen storage**

I have synthesized a series of MOF compounds from reactions of different functionalized ligands with metal salts under various reaction conditions. These MOFs have different pore sizes and polar pore walls and exhibit excellent gas adsorption and separation capacities. Specifically, they can be categorized into three types.

- MOFs with unsaturated metal coordinated sites on the walls of channels, which enhance the framework-guest interaction and thus increase the chemical threat agent adsorption capacity. Three kinds of MOFs with different open metal sites were synthesized and characterized (Figure 1). Reactions of benzene-1,3,5-carboxylic acid ($H_3BTC$) with metal nitrate ($Cu^{II}$ or $Zn^{II}$) created two novel MOFs with similar molecular structures: $Cu_3(BTC)_2(H_2O)_3$ and $Zn_3(BTC)_2(H_2O)_3$ (Figure 1a,1b). Both MOFs contain paddle wheel $M_2(CO_2)_4$ molecular building block units (MBBs). The open metal sites are originally occupied by water molecules, which are easily removed via (150 ºC for 4h) without decomposition of host frameworks. By replacing the metal cations with the same ligand, another two kinds of MOFs, $Ln(BTC)(H_2O)$ (Ln = La - Yb) and $Zn_2Ca(BTC)_2(H_2O)_2$ were also solvothermally synthesized (Figure 1c,d). Their coordinated water molecules are easily

removed to offer open metal sites. These MOFs with open metal sites exhibit excellent hydrogen adsorption capacities (Figure 1). Results show that MOFs with open metal sites strength the enthalpies of hydrogen adsorption and improve the hydrogen uptake capacities.

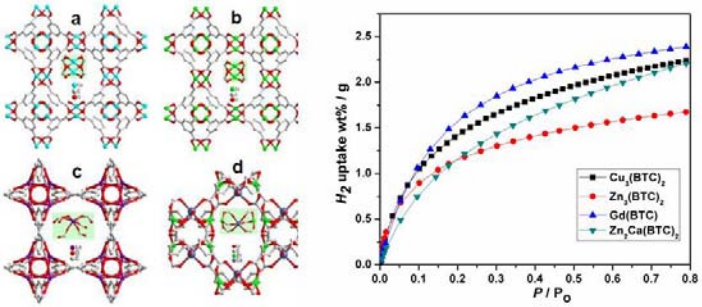


*Figure 1. Hydrogen uptakes in four MOFs with open metal sites at 77K: $Cu_3(BTC)_2$, $Zn_2(BTC)_2$, Gd(BTC), and $Zn_2Ca(BTC)_2$. BTC = benzene-1,3,5-tricarboxylate.. Insert: molecular building block units with open metal sites.*

- MOFs containing functionalized organic ligands with active -$NH_2$, -Br, and -$NO_2$ groups, which offer strong polar sites on the pore walls. These results will serve as a baseline for our development of new MOFs tailored for sampling or sensing chemical threat agents. For example, we primarily synthesized and characterized four MOFs with the similar structures of $Zn_2(TPT\text{-}X)_2$(Dzbo), (TPT-X = terephthalate, 2-aminoterephthalate, 2-nitroterephthalate, or 2-bromoterephthalate; dzbo = 1,4-diazabicyclo[2.2.2] octane) (Figure 2). These functionalized organic linkers will strengthen the framework-guest interaction, respectively. We will identify how these MOF materials selectively respond to the compound of interest and preserve an irreversible effect when exposed. These MOFs with functionalized organic linkers exhibit various hydrogen adsorption capacities. The result shows that MOFs with functionalized organic linkers enhance the hydrogen uptake capacities via intermolecular hydrogen bonding interactions.

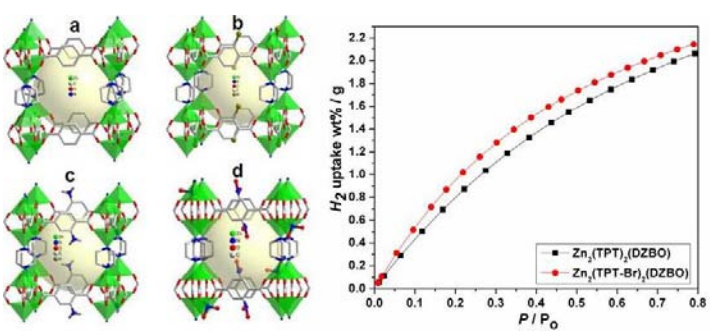


*Figure 2. Hydrogen uptakes in the predesigned MOFs with functionalized organic linkers at 77K: $Cu_3(BTC)_2$, $Zn_2(BTC)_2$, Gd(BTC), and $Zn_2Ca(BTC)_2$. BTC = benzene-1,3,5-tricarboxylate.*

- MOFs exhibiting a wide range of pore sizes, which can be used for adsorption and separation of hydrogen (For example, the sizes of pores of several MOFs are between the van der Waals kinetic diameters of $H_2$ and $N_2$, and thus are suitable for $H_2/N_2$ separation). As shown in Figure 3, I designed and synthesized four novel MOFs with various pore or window sizes with different metal and ligand. Their pore sizes can range form 0.3 to 3.2 nm. I investigated how the pore sizes of these MOF materials can influence their hydrogen adsorption/separation capacities. The primary result indicates MOFs with 0.4 ~ 0.8 nm pore sizes are most suitable for hydrogen storage.

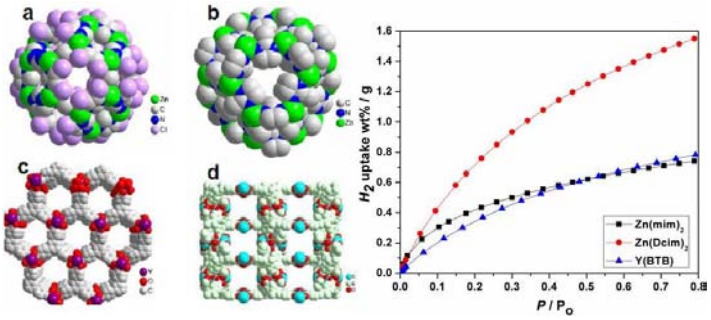


*Figure 3. Hydrogen uptakes in tailored MOFs with various pore sites at 77K: Zn $(Mim)_2$, $Zn(Dcim)_2$, Y(BTB), and $Ce_2(BTB)_3(NO_3)_3$. Mim= 2-metylimidazolate, Dcim = 4,5-dichloroimidazolate, and H3BTB = 1,3,5-tribenzoic acid.*

**Design and assembly of special devices for gas storage and separation-catalysis**

I designed and assembled two special devices for gas storage and separation-catalysis. The *in-situ* neutron diffraction gas-sorption evaluation cell can monitor complex compositional and exact gas sorption sites inside pores of MOFs at various pressure and temperature conditions. As the lightest element, the hydrogen atom contains only one electron and thus has the weakest X-ray scattering cross-section of all of the elements. In contrast, the scattering power of neutrons does not vary with the number of electrons in an element, and neutron diffraction is much more sensitive to the positions of hydrogen (or its isotopes such as deuterium) and other light elements, making neutron scattering well suited for studying hydrogen-containing or other gas-containing materials. In addition, as neutrons are more penetrating than X-rays, one can probe samples inside high-pressure vessels, within refrigerators and furnaces, or measure deeply buried local structures within a bulk host material. Hence, the home-made gas cell was designed and assembled for *in-situ* neutron scattering analysis. To support these experiments, a gas separation-catalysis evaluation apparatus was assembled for various applications of MOFs including hydrogen purification, gas separation, as well as catalysis.

**Chemical threat agent adsorption investigation**

Recently, I began collaborating with Toti Larson to develop MOFs for applications in High-efficiency

sampling, preservation, and sensing of chemical threat agents. I designed and synthesized a new MOF $Zn_2Ca(BTC)_2$ (BTC = benzene-1,3,5-tricarboxylate) for adsorption of chemical threat agents. This MOF has been structurally characterized by single-crystal X-ray diffraction demonstrating that the title compound self-assembles a three-dimensional porous framework with open metal sites on the channel walls. Therefore, the open metal sites can act as valid active sites for chemical threat agent adsorption. I started to investigate their adsorption capacity for one of hydrolytic products (methylphosphonic acid) of nerve agents. It is not possible to work actual chemical threat agents at LANL, so we are conducting a flexible simulation for actual agents from our methylphosphonic acid results. The results demonstrate that open metal nodes in MOFs are valid bonding sites for the adsorption of methylphosphonic acid. Further investigation will be carried out to identify the selectivity of adsorption using other surrogates for chemical threat agents.

To summarize, I synthesized and characterized structurally a series of new MOFs. Two special devices have been assembled for in-situ time-resolved neutron scattering analysis and gas separation-catalysis evaluation. Hydrogen adsorption measurement toward several new MOFs has been carried out, and the corresponding result will be published. A highlight article has been accepted for publication in CrystEngComm journal. Additional papers were submitted and prepared during my first year at LANL.

## Future Work

I will design, synthesize and characterize a series of novel MOFs tailored for hydrogen storage/separation and other applications in relation to energy utilization and environmental remediation. During my second year at LANL I will experiment with hydrogen storage capacities under various conditions (such as temperature and pressure). Secondly, some new MOFs with various ligands will be designed and prepared. The structures, chemical bonding and gas absorption properties of these compounds will be characterized by a variety of techniques including diffraction, spectroscopy and gas absorption surface-area measurements. Hydrogen binding sites and energies will be determined using in-situ high-pressure/low-temperature neutron scattering at Los Alamos Neutron Science Center (LANSCE). Efforts will also be made to integrate neutron diffraction with calorimetry, which will be particularly useful for characterization of MOFs. Valuable information from the theoretical calculations will be used to further optimize the hydrogen storage and sorption/desorption performance of the resulting MOFs. In addition, I will develop MOFs for high-efficiency sampling, preservation, and sensing of chemical threat agents will be further developed.

## Conclusion

A series of novel MOFs have been synthesized and structurally characterized. Their hydrogen storage capacities have been investigated. New MOFs will be designed and prepared to optimize the hydrogen storage performance. Through exploring new chemistry and synthetic approaches, the proposed research will produce novel materials that can store large amounts of hydrogen. We expect to contribute significantly to the utilization of hydrogen in future transport/mobile applications. The results of this research will also provide basis for utilizing similar techniques in environmental and threat-reduction applications. Example of other applications includes fast and reversible detection of trace amounts of high explosives and chemical threat agents via MOF's various physical and chemical properties of organic pore walls or metal clusters in MOFs.

## Publications

Zou, R., A. Abdel-Fattah, H. Xu, A. Burrell, T. Larson, T. McCleskey, Q. Wei, M. Janicke, D. Hickmott, T. Timofeeva, and Y. Zhao. Porous metal-organic frameworks containing alkali-bridged two-fold interpenetration: Synthesis, gas adsorption, and fluorescence Property. *Crystal Growth & Design.*

Zou, R., A. Abdel-Fattah, H. Xu, Y. Zhao, and D. Hickmott. Storage and separation application of nanoporous metal-organic frameworks. To appear in *CrystEngComm .*

# Bio-Directed Assembly of Multicolored One-Dimensional Quantum Dot Light-Emitting Devices

*Gabriel A. Montano*
20080784PRD3

## Introduction

The goal of the proposed work is to use organizational properties of biological systems to create efficient and inexpensive platforms usable for various nanotechnology applications. For example, we are in the process of using active biological molecules to drive assembly of multicolored quantum dots into ordered structures for Light Emitting Devices (LED). Technology developed in this research project is also being utilized to develop nanoplasmonic platforms as well as for light-harvesting and energy transfer systems. Further, bio-templating architectures are also being utilized as platforms for investigating fundamental physical and biophysical properties of nanomaterials. Our approach is interdisciplinary, incorporating aspects of molecular biology, chemistry and engineering, and spanning the fields of nanoelectronics, nanophotonics and nanoscale assembly. By combining the merits of biology-enabled self-assembly, the proposed research and technology eliminates complicated and costly microfabrication processes. Project success would enable manufacturing of integrated nanoscale devices for a vast array of electronic and photonic applications.

## Benefit to National Security Missions

The proposed research directly ties into the area of Energy Security. The ability to generate inexpensive efficient photonic and electronic devices is of the utmost importance to both the US and the world. Further, this research relates directly to projects outlined in BES for nanoscience initiatives, specifically emergent properties at the nanoscale.

## Progress

This project is focused on bio-assembly strategies for development of nano-optical and nano-electronic architectures and devices. Significant progress has been made in characterizing our assembly system and planning modifications to enhance controlled assembly strategies. We have primarily focused on enhancing control of one- and two-dimensional architectures formed by microtubule structures. While the long-term goal of our work is to create ordered assemblies for practical applications, the research being performed is focused on development of strategies for dynamic assembly and directed organization. Thus, we have initially focused our efforts on characterization of spontaneous formation of microtubule circles upon addition of various nanoparticles (Figure 1a). For example, this has been accomplished by tethering streptavidin coated gold nanoparticles to the biotinylated microtubules (MT's) and monitoring via a variety of techniques, including dark field imaging, atomic force microscopy and electron microscopy. Research thus far has shown the ability to create ring structures of various sizes, with high-resolution AFM and TEM indicating rings are due to a serpentine pattern formed by the translational and rotational movement of the microtubules. Architectures are currently being investigated for controlled plasmonic response. A dark field image of gold nanoparticle (AuNP) decorated MT ring structure is shown in Figure 1b demonstrating the microscopic microtubule ring organization with incorporation of the AuNP. In these assemblies, AuNP are being used to monitor any changes in potential plasmonic responses.

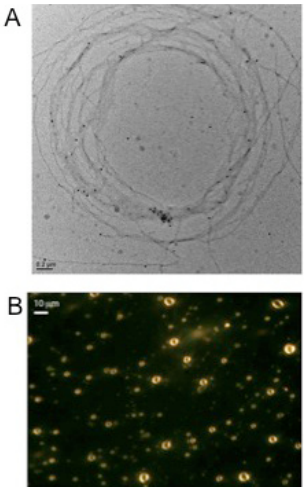


*Figure 1. AuNP-decorated microtubule ring structures. (a) TEM image exhibiting supercoiled organization of microtubules with addition of streptavidin-coated AuNP. (b) Dark field microscopy image of Au-decorated microtubules with microscopic ring architectures of various size.*

Quantum dots (QD's) have the potential to be used as light-harvesters in solar cell devices. However, there still exist many fundamental questions as to understanding the photophysics of energy transfer within QD-light harvesting systems as well as a potential need to develop dynamic and highly organized QD-photophysical platforms. Figure 2a shows an example of energy transfer occurring in a microtubule- QD ring organization. In this assembly, two types of QD's are used with photoluminescence emission at 525 nm and 585 nm, respectively. With UV excitation that excites both QD species, fluorescence is observed almost completely from only the long-wavelength species, indicating efficient energy transfer from the 525 nm to the 585 nm QD. TEM images show close packing of the QD's in the MT ring structures that enables the efficient energy transfer (Figure 2b). These MT-QD arrangements thus allow not only for development of ordered architectures but potential for studying fundamental physical processes that will be discussed in the future work.

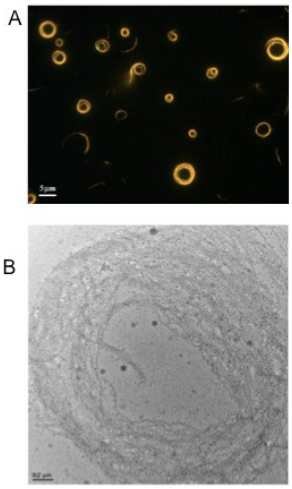


*Figure 2. QD- MT ring assemblies. (a) Fluorescene microscopy image of microtubules decorated with 2 QD's- 525 & 585 nm species. Yellow fluorescence of 585 nm QD observed with little 525 nm emission due to energy transfer to long wavelength QD. (b) TEM showing densely decorated QD's on MT's allowing for efficient energy transfer.*

Lastly, Dr. Liu has shown the ability to organize segments of microtubules decorated with QD's of one wavelength into one-dimensional multi-colored arrays as shown in Figure 3. Boxes are drawn around two multi-colored 1D structures of significant length, however, the image is decorated with many examples. These structures represent the necessary first step toward high-ordered arrays for use in LED and other photonic applications. Currently, we have exhibited the ability of synthesizing such structures, however controlled assembly into specifically desired segments and order has yet to be demonstrated. This will be the focus of this aspect of research.

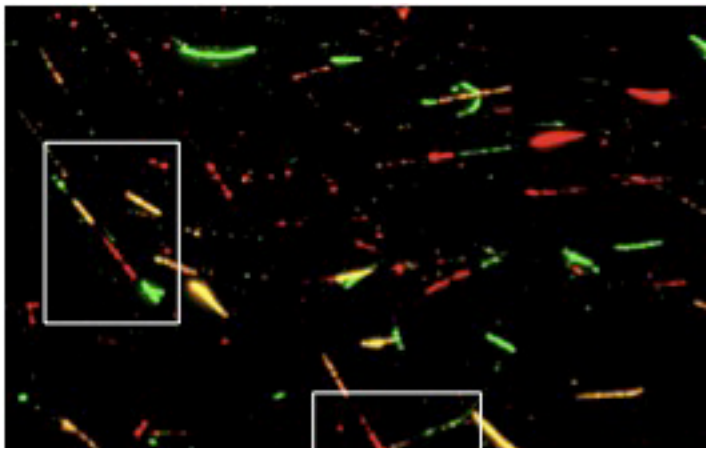

*Figure 3. One-dimensional multicolored QD-MT arrays.*

## Future Work

We have made significant progress toward development of nanophotonic and nanoelectronic assemblies. As described above, Dr. Liu has exhibited the ability to synthesize one dimensional- multi-colored arrays of QD's and well as exhibit controlled ring assembly of various nanoparticles. Current and future work in this area is focused on developing strategies to allow for a controllable system for more complex two-dimensional assemblies. Specific goals are to exhibit controlled ordering in one-dimension and use biological and chemical recognition strategies to develop two-dimensional architectures. We are currently investigating common bio-recognition strategies such as biotin-streptavadin conjugation as well as more advanced strategies such as phage-display technology and chemical recognition.

We are also using the ring architectures described earlier to investigate fundamental physical properties of light-harvesting and energy transfer in QD systems by controlling the density and arrangement of QD's in these systems. We will use time-resolved fluorescence spectroscopy to investigate energy transfer processes in a two-QD-MT system. Further, we will be receiving a new scanning confocal microscope with fluorescence lifetime imaging (FLIM) capabilities that will allow us to resolve multiple energy transfer processes occurring on a single ring structure. By controlling density of QD's and their arrangement in ring architectures we will be able to obtain more understanding on the light-harvesting and energy transfer processes that occur in these semiconductor systems. We have also developed an ongoing collaboration with Dr. Igal Brennar of Sandia National Laboratory to continue development of the MT system for plasmonic architectures. Similar to the QD systems, we will both continue development of useful architectures for technology applications as well as use the architectures to investigate fundamental physics of plasmonic effects.

Lastly, we have begun a new collaboration with Dr. Vamsi Yadavalli at Virginia Commonwealth University

to investigate mechanical properties of MT systems. Particularly, we will investigate aspects of conformation strain in ordered assemblies as well as load bearing potential of the MT system.

## Conclusion

This research project has developed beyond our initial proposed development of QD-LED devices. While one of the goals of this proposal is to develop QD-LED architectures, the focus has shifted to our ability to control the bio-templating strategies and use of such architectures to develop other photonic and electronic nano-scaled assemblies, as well as use the architectures as a framework to investigate fundamental physics of nanomaterials. We will continue to focus our efforts on development of the bio-templating strategies while utilizing the expertise of our collaborators in development of nano-device architectures.

# Semiconductor Nanowire Heterostructures

*Samuel T. Picraux*

20080785PRD3

## Introduction

Advances in the synthesis of semiconductor nanowires (NWs) have prompted intensive debate about the science of their growth and the technological applications they promise. The diversity in synthesized materials and synthesis techniques lead to improvised revisions to previously accepted models in some cases, and contradicting them in others. In FY09, we have performed studies that shed light on different aspects of the nucleation and growth of semiconductor nanowires and their heterostructures. We provide in this report a brief overview of some of our most significant results including: (i) First experimental verification of the Gibbs-Thomson effect in semiconductor nanowires. (ii) Elimination of the post-growth gold (Au) diffusion on the NW sidewalls for radial Germanium-Germanium and Germanium-Silicon heterostructure nanowires for high current, low power and high speed transistors and for high quantum efficiency infrared detectors and solar cells. (iii) Realization of 100 % compositionally modulated axial heterostructure nanowires which are relevant to future concepts on low-off current and high-on current tunnel transistors.

## Benefit to National Security Missions

This project supports the DOE missions in threat reduction, energy independence, and nuclear weapons by advancing our fundamental understanding of nanoscale electronic materials for new materials synthesis, chemical and biological sensing, thermoelectric energy conversion, and electronics systems for future low power, miniaturized applications. We already see a number of new device and system concepts emerging that are anticipated to be important to these areas.

## Progress

### Gibbs-Thomson Effect in Semiconductor Nanowires:

Semiconductor nanowires (NWs) are one-dimensional structures with typical diameters of 5 – 100 nm, and typical lengths of 1 – 100 µm. Most NWs with high aspect ratio and decent control over their morphology are grown using the vapor-liquid-solid (VLS) growth mechanism. For instance, Ge NW growth is catalyzed by Au nanoparticles. At a growth temperature greater than the Au-Ge eutectic temperature, the Au-Ge alloy melts and further input of germane precursor supersaturates this alloy and leads to layer-by-layer precipitation of solid Ge at the Au-Ge/substrate (liquid/solid) interface resulting in Ge NW growth.

The size of the nucleating Au particles is an important parameter that controls the NW diameter and its electrical and optical properties. Understanding key processes relevant to size-dependent NW growth is of great scientific and technological interest. As the size of the Au nanoparticle decreases, the surface energy of the NW facets have great impact on the thermodynamic properties of the nanoparticle itself. The vapor pressure of the nanoparticle increases and the solubility of Ge increases as the nanoparticle diameter decreases, a phenomenon known as the Gibbs-Thomson effect. An increase in the equilibrium solubility means reduced supersaturations during the NW growth. We have controlled the diameter and and spacing of Au nanoparticles using e-beam lithography and performed studies of their growth behavior with and without doping impurities. Figure 1 a shows a scanning electron microscope (SEM) image of an ordered array of Ge NWs of constant diameter and Figure 1 b shows an SEM image of row of NWs grown with 500 nm spacing and with diameters ranging from 37 nm to 76 nm. It is evident from Figure 1 b that the growth rate decreases as the NW diameter increases due to the Gibbs-Thomson effect. We have further performed in-situ transmission electron studies to measure the solubility fraction of Ge in the Au nanoparticles as function of diameter. We found that the smaller diameters have higher solubility and therefore lower supersaturations ,which correlates well with the diameter-dependent growth behavior. The experimental observations and accompanied analysis provide new insights into the thermodynamics of nanoscale materials [1].

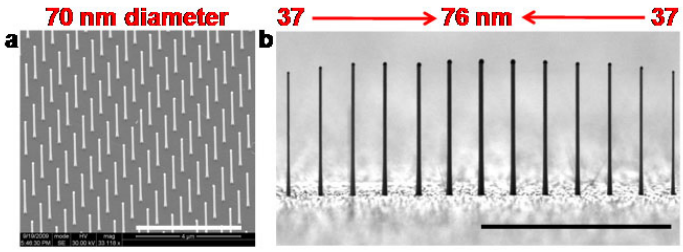


*Figure 1. SEM images of Ge NW arrays. a) An array of 1 µm inter-spaced 70 nm-diameter Ge NWs. scale bar is 4 µm. b) A row of different diameter Ge NWs inter-spaced by 500 nm. Scale bar is 3 µm.*

**Elimination of Au Diffusion in Ge Core-Shell NWs:**

Much of our efforts concentrate on modulation of composition and doping in radial NW heterostructures as these allow the realization of devices that have several advantages compared to bulk semiconductor materials. For example, a radial NW p-i-n junction has potential for high efficiency solar cells at much lower costs when compared to high quality planar materials because light can be absorbed in the longitudinal direction of the wire and carriers can be separated and collected efficiently in the radial direction of the NW. Another example is utilizing radial doping in surround gate field-effect transistors which allow optimal control over the channel electrostatics to better modulate the current and achieve high on/off current ratios. To grow radially on a semiconductor NW, one has to minimize the axial elongation and promote side-wall deposition on the NW circumference, which can only be achieved at high temperatures. Such temperatures however reduce the stability of the Au particle on the NW tip leading to Au diffusion on the NW sidewall.

To overcome the Au diffusion problem, we devised a growth approach in which we deposit a thin Si interfacial layer between the Ge NW and the Au catalyst at low temperature. Silane, the silicon precursor, can decompose at temperatures in excess of 500 °C; the presence of the Au nanoparticle however catalyzes locally the decomposition of silane such that some Si is incorporated into the Au nanoparticle and precipitate as a barrier layer between the Au nanoparticle and the Ge nanowire. The interfacial Si layer has higher surface energy than Ge which favors the particle energetically to remain atop the NW rather than at its surface. Figure 2 a shows a TEM image of the tip of 30 nm diameter NW; the dark contrast region is the Au nanoparticle. Figure 2 b shows the tip of a similar NW that have undergone temperature ramp to 410 °C; dark spots represent few monolayers of Au that have diffused on the sidewalls. The whole volume of the Au nanoparticle started to diffuse downward on the NW sidewalls. Figure 2 c shows the tip of a similar NW that have undergone heating to 410 °C but with a Si barrier interfacial layer. No Au diffusion is observed in this case. Au diffusion can cause unwanted surface roughening in the case of core-shell growths – which are essential to achieve the device architectures discussed above – and also act as recombination centers for charge carriers. Growth of a shell on the Ge NW that had Au diffusion leads to a rough surface morphology as shown in Figure 2 d. For the same growth conditions but with a Si barrier layer at the NW tip, growth of a shell on such a NW leads to very smooth morphology as demonstrated in Figure 2 e. Further, this technique allows us to deposit single crystalline Si shells on Ge NWs. Figure 2 f shows a high-resolution TEM image of a single crystalline Ge NW, where atomic planes can be clearly resolved and Figure 2 g shows a high-resolution TEM image of a Ge core – Si shell with single crystal quality. Such control over the NW core-shell growth is uniquely achieved at LANL [2].

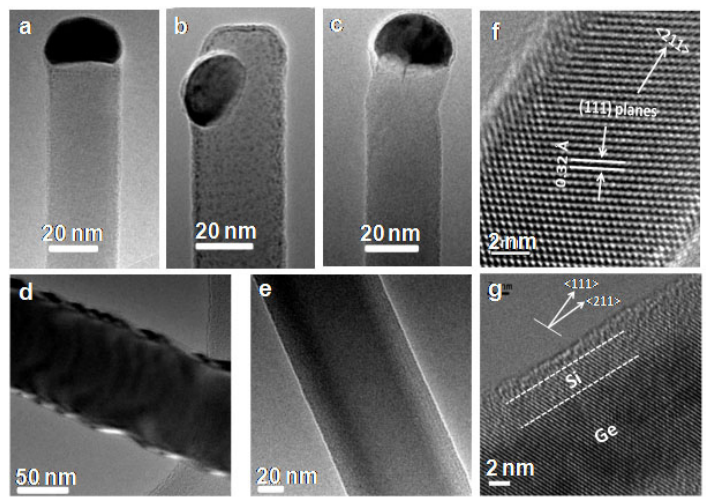


*Figure 2. TEM images of Ge NWs. a) Tip of a 30 nm diameter NW as grown. b) Same as (a) but with temperature ramp to 410 °C showing dark spots due to Au diffusion. (c) Same as (a) but with a thin Si layer between the Au and the Ge NW which stabilizes Au atop the NW. d) same as (b) but with a Ge shell growth which causes a rough surface. e) same as (c) but with Ge shell growth which results in a smooth interface. f) Single crystal Ge NW with 10 nm diameter. g) similar to (a) but with a 2 nm thick single crystal Si shell.*

## Future Work

**Realization of Ge-Si axial NW Heterostructures:**

In the VLS growth of semiconductor NWs, we have the advantage of changing the doping and composition in the axial direction which allows us to engineer the energy band-gap edge in the direction of transport of charge carriers, i.e. the axial direction of the NW, which is not possible in current technologies of thin-film growth where charge carriers move in the planar direction perpendicular to the growth direction. Such ability further advances the possibility of realizing novel devices with exceptional performance, such as the tunnel field-effect transistor (T-FET) as an example, a new generation of infrared and other radiation detectors, and a new

approach to dual layer solar cells with high efficiency. To give one specific example in this report, the T-FET relies on electron tunneling from a highly doped source to an intrinsic channel whose potential is modulated by a gate electrode to turn the device on and off, with electrons being collected (drained) at the drain side. Since most T-FET devices use homo-interfaces such as Ge or Si, when the device is biased in the off regime electrons can back-tunnel to the channel and exhibit a large leakage current which causes increased power dissipation in the off-state. With the axial heterostructures that we grew, the source can be Ge material (allowing efficient tunneling through the small Ge bandgap of 0.64 eV) and the drain can be Si material (preventing tunneling through the larger Si bandgap of 1.12 eV). To grow such structures, one has also to overcome Au diffusion and prevent kinking. While prior reports in the literature have grown Ge-SiGe heterostructure NWs with only 12-16 % modulation in alloy composition, we are able to grow 100 % modulated Ge-Si axial heterostructures [3]. Device fabrication of the T-FET is currently initiated with some preliminary growth results are summarized in Figure 3.

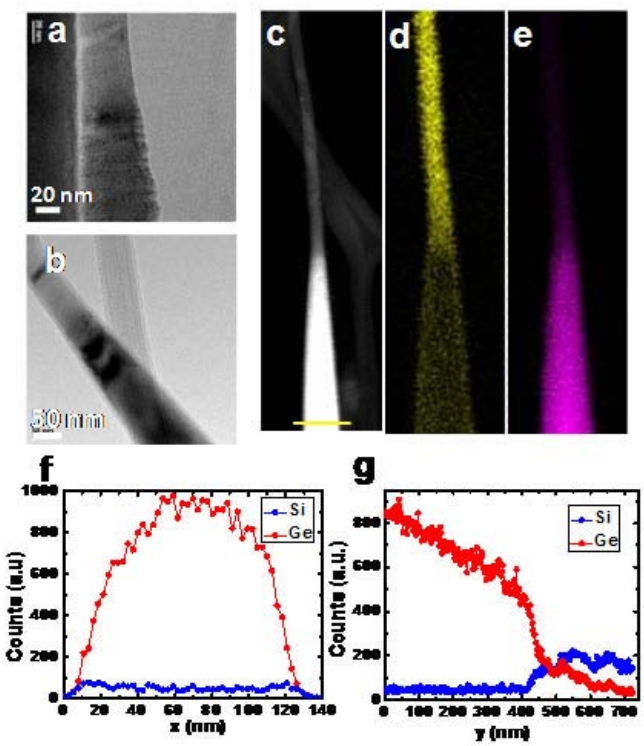


*Figure 3. a) TEM image at the junction of a 40 nm diameter Ge-Si heterostructure NW with black dots at the junction indicating Au diffusion. b) same as (a) with new growth procedure which eliminate Au diffusion. c) Scanning TEM image of a Ge-Si axial NW heterostructure and false color maps of (d) Si and (e) Ge indicating Si segment growth at the end of the tapered Ge region. f) line scan along the diameter of the Ge segment showing no Si shell deposition but only Si axial growth. G) Line scan along the axial direction of the NW showing a Ge signal in the Si segment that decays to the background level in a distance of ~ 250 nm.*

## Conclusion

We will establish synthesis methods for silicon/germanium/III-V nanowires and their combinations in integrated device structures. By understanding how to control surface properties through radial heterostructures, how to overcome the limits of contact resistance, and how to integrate nanowires into functional nanosystems we will obtain new properties and performance not previously possible. These novel materials are of great interest for applications in energy areas such as a new generation of solar cells, new high performance thermoelectric materials for energy harvesting from heat sources, and new electronic device concepts with performance not previously achievable.

## References


1. Dayeh, S. A., E. Sutter, and S. T. Picraux. Direct observation and analysis of the Gibbs-Thomson effect in germanium nanowires. 2009. *in prep for Nature Materials.*

2. Dayeh, S. A., and S. T. Picraux. Eliminating Au diffusion in core-shell nanowire growth for high performance majority and minority carrier devices". 2009. *in prep for Nature.*

3. Dayeh, S. A., and S. T. Picraux. A p+-i-n Ge-Si heterostructure tunnel FET: uniqueness of the VLS growth mechanism. 2009. *in prep. for Science.*


## Publications


Dayeh, S. A.. Electron transport studies in InAs nanowires. To appear in *Semiconductor Science and Technology.*

Dayeh, S. A., C. Soci, X. Bao, and D. Wang. Advances in the synthesis of InAs and GaAs nanowires for electronic applications. 2009. *Nano Today.* **4**: 347.

Dayeh, S. A., D. Susac, K. L. Kavanagh, E. T. Yu, and D. Wang. Structural and electrical properties of zincblende and wurtzite InAs nanowires. 2009. *Advanced Functional Materials.* **19**: 2102.

Dayeh, S. A., E. T. Yu, and D. Wang. Surface diffusion and substrate – nanowire adatom exchange in InAs nanowire growth. 2009. *Nano Letters.* **9**: 1967.

Dayeh, S. A., E. T. Yu, and D. Wang. Diameter dependent transport properties in InAs nanowire field effect transistors. 2009. *Small.* **5**: 77.

Law, J., S. A. Dayeh, D. Wang, and E. T. Yu. Scanning capacitance characterization of potential screening in InAs nanowires. 2009. *Journal of Applied Physics.* **105**: 014306.

Raychaudhuri, S., S. A. Dayeh, D. Wang, and E. T. Yu. Pre-

cise semiconductor nanowire placement through dielectrophoresis. 2009. *Nano Letters.* **9**: 2260.

Sierra-Sastre, Y., S. A. Dayeh, S. T. Picraux, and C. A. Batt. Epitaxy of Ge nanowires from biotemplated Au nanoparticle catalysts. *ACS Nano*

# Local Atomic Arrangements in Phase Change Materials

*Thomas E. Proffen*
20080791PRD4

## Introduction

Optical storage devices have revolutionized our lives in the past decade. The basis of optical and electronic memory device technology is relatively simple, but surprisingly, improvements in the underlying phase-change materials (PCM) to date have largely been made through a trial and error process. We are usomg state-of-the-art local structure studies, using neutron and synchrotron X-ray total scattering techniques, to address these deficiencies and provide a better understanding of the crystal chemistry, local structure, bonding, and properties in well-established and novel phase-change materials. Along the way, we are advancing scattering capabilities necessary for their understanding.

## Benefit to National Security Missions

This project will support the missions of the Office of Science by enhancing our understanding of complex disordered materials on the atomic level. This project also supports DOE missions by enhancing experimental techniques to study complex materials. Specifically, we are developing data reduction and refinement programs that will aid in bridging to tools for investigating amorphous to crystalline transitions in solids. These advances will broadly impact government agencies and programs.

## Progress

We have made significant progress in the last ten months towards our studies of local atomic arrangements in phase-change materials. We have prepared bulk crystalline GeTe samples and made considerable advancements in tuning reaction conditions for quenching amorphous $GeTe_4$, $Ge_7Te_{33}$, and $Ge_3Te_{17}$, which fall in the glassy region of the Ge-Te phase diagram. We are making these samples by melt-quenching in evacuated quartz tubes in the Lujan Center chemistry laboratory. This spring we were granted user project status at LANL's Center for Integrated Nanotechnology (CINT) for preparation of phase change thin films by sputtering. To this point we have prepared 100 nm, 200 nm, 300 nm, 400 nm, 500 nm, 600 nm, 700 nm, 800 nm, 900 nm, 1 um, and 10 um $GeSb_2Te4$ thin film samples on both glass and Si substrates. We have confirmed the samples are amorphous as deposited and can be converted to the metastable disordered rocksalt crystalline phase with heat treatment. The amorphous and metastable forms are those required for the functionality of phase change technology, and therefore provide a prototype for our local structure investigation. We have also partnered with university and industry collaborators in Japan who have provided a large quantity of 1 um film samples of the canonical $Ge_2Sb_2Te_5$ phase-change material for our studies.

We have begun to study in detail the lattice distortions, chemical short range order, and local bonding arrangements in these materials by total scattering methods. The pair distribution function (PDF) formalism offers the advantage of providing directly both local structure correlations at low real-space dimensions, and intermediate range order at higher ranges, a distinct advantage for following the relevant phase transition in PCM. We acquired beamtime at both the Advanced Photon Source (Argonne National Laboratory) and at the Lujan Center (Los Alamos National Laboratory) for X-ray and neutron total scattering experiments on the bulk and thin film phase change materials.

During our synchrotron beamtime we explored the sample and measurement conditions that provided high quality pair distribution function (PDF) data for thin film study of this materials family. These experiments are challenging and we investigated materials deposited on various substrates, at various thicknesses, and situated in several orientations for measurements. The best data were collected for films that were deposited on amorphous glass, and measured at 60 keV in transmission mode. Room temperature experimental PDFs for as-deposited and heat treated 1000 nm films are given in Figure 1 over a large range in atom-atom distances. In (a) data are shown for the deposited material, (b) shows data for the same sample annealed for several hours at 150°C, and (c) displays data for the sample annealed for several hours at 220°C. The increase in crystalline correlation length

with furnace annealing is apparent. Our analysis supports a transition from an amorphous phase to the metastable rocksalt phase, and then to a second, higher temperature crystalline phase at 220°C. These results are currently written up.

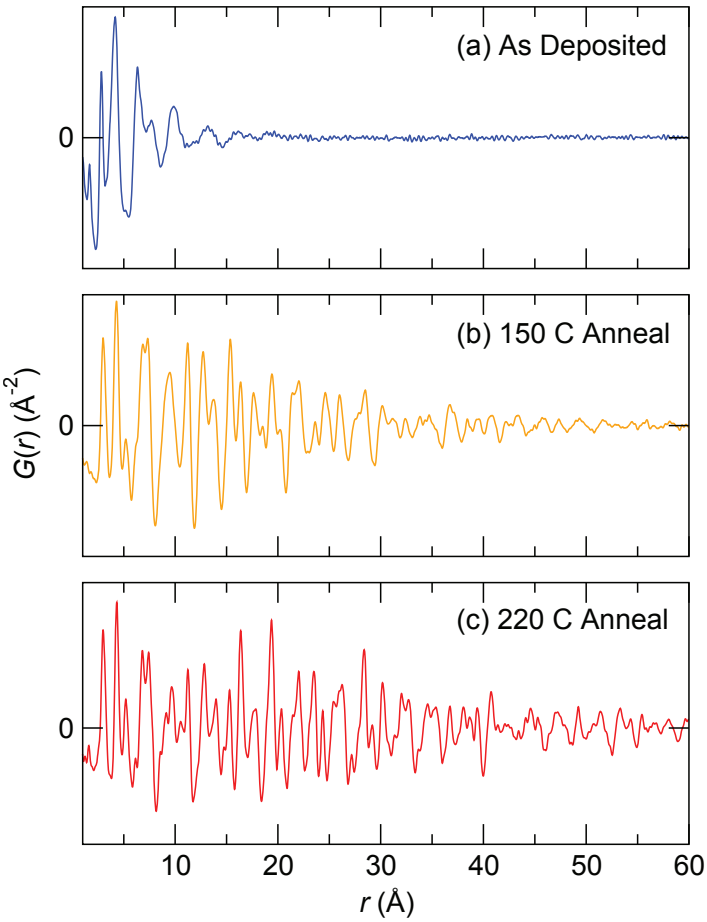


*Figure 1. Experimental atomic Pair Distribution Functions (PDF) extracted from X-ray total scattering experiments at 11-ID-B for 1000 nm $GeSb_2Te_4$ thin films deposited on amorphous glass and measured at 60 keV at room temperature. (a) Shows the PDF for the deposited material, (b) shows the PDF for the same sample, annealed for several hours at 150 °C, and (c) displays the PDF for the sample annealed for several hours at 220 °C. The increase in crystalline correlation length with annealing is apparent.*

A main component of our efforts involve advancing scattering capabilities for thin film materials and for characterization of amorphous-crystalline phase transitions in solids. To this end we have worked in recent months on developing capabilities for differential pair distribution function extraction using respective X-ray and neutron data sets as well as incoherent scattering corrections for neutron total scattering experiments. The ability to distinguish separate peak contributions to pair correlation functions in highly disordered or amorphous compounds is often limited. For example, various types of local order have been reported for amorphous $Ge_xTe_{1-x}$ phases, including both random mixtures and discrete structural units, and both 4-fold and 6-fold coordination around Ge.

With our neutron total scattering beamtime we completed initial measurements of amorphous and crystalline GeTe samples and some data for methods development. We have developed capabilities for extracting and refining differential pair distribution function data sets using our neutron and x-ray total scattering data. Differential PDFs for amorphous $GeTe_4$ were extracted from combined synchrotron X-ray (11-ID-B, APS) and neutron (NPDF, Lujan Center) total scattering experiments (Figure 2). The nearest neighbor distances in the amorphous glass are made up of Ge-Te atom-atom pairs and slightly longer Te-Te atom-atom pairs. The second neighbor distances are all Te-Te pairs. The data also shows that correlations beyond the nearest neighbor are due to the Te network. We will be able to test results of Reverse Monte Carlo modeling of this system against these observations. The amorphous and metastable $Ge_xTe_{1-x}$ series of data will allow for a direct comparison of materials properties (crystallization temperatures, optical contrast between phases, and phase change speed, etc.) with observed local structure across the series. This information is expected to be of great utility in studying more complicated materials systems, including the thin film alloys we are studying concurrently.

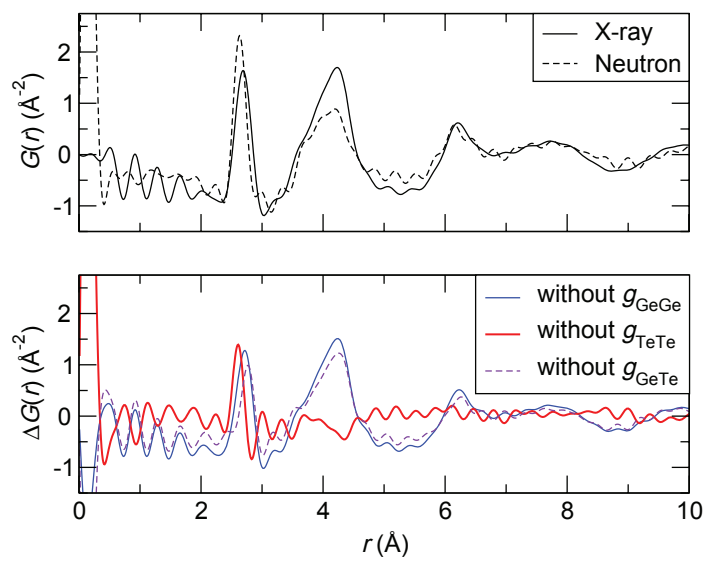


*Figure 2. (Top) X-ray and neutron GeTe4 Pair Distribution Functions (PDF) obtained from 11-ID-B (Advanced Photon Source) and the Neutron Powder Diffractometer (Lujan Neutron Scattering Center) for an amorphous sample. (Bottom) The corresponding extracted differential PDFs from the combined synchrotron and neutron data.*

## Future Work

The basis of optical and electronic memory device technology is simple: a deposited crystalline phase is liquefied with a laser and solidified with quenching to form an amorphous one. Low intensity light or an electrical pulse ´reads' the distinct reflectivity or resistivity in the amorphized region while a longer and more intense

source can render it crystalline once again, enabling re-writable media. Surprisingly, improvements in phase-change materials to date have largely been made through a trial and error process; very little is known about the precise mechanisms of phase-change and the local atomic arrangements that give rise to the distinct properties of the crystalline and amorphous states. We will continue our work with state-of-the-art local structure studies, using neutron and synchrotron X-ray total scattering techniques, to address these deficiencies. The merit of the proposed work lies in the promise of better understanding of the crystal chemistry, local structure, bonding, and properties in well-established and novel phase-change materials, and the advancement of scattering capabilities necessary for their understanding.

Current phase-change materials are group 15 and 16 alloys with octahedral-like atomic arrangements in the crystalline state. Successful candidates have large optical or electrical contrast between phases, thermal and chemical stability, fast switching speed for the phase change, and scalability. We will study the local bonding arrangements that promote amorphous-crystalline cyclability and lead to optical and electronic contrast in traditional and new phase-change materials we prepare.

Our most significant areas of progress have been in preparing thin films of the canonical phase change material $GeSb_2Te_4$ and establishing the methods we will use to characterize the local atomic structure of materials in the phase change material family. Our next steps will be to study in situ the annealing behavior of thin film materials based on a pseudobinary $GeTe$-$Sb_2Te_3$ (GST) composition ($GeSb_2Te_4$), where crystallization is thought to be nucleation controlled, and materials based on the $Sb_{70}Te_{30}$ eutectic ($Sb_2Te$), where crystallization is believed to be growth controlled. We will monitor how chemical short-range order and local bonding environments vary in the transformation from the amorphous to metastable to crystalline states. Amorphous films of these compositions will be prepared at various thicknesses by sputtering from stoichiometric targets in our laboratories. Some of the films will be crystallized with thermal or laser annealing and the properties of both as-deposited and crystalline films will be characterized through X-ray florescence measurements, spectroscopic ellipsometry, electron microscopy, X-ray diffraction, and differential scanning calorimetry. These approaches will allow us to investigate how lattice distortions, vacancy concentrations, dopant metals, chemical short-range order, crystalline length scale, and local bonding environments vary in amorphous and crystalline states of phase change materials, and may allow us to track these effects through melting and crystallization cycles.

## Conclusion

This project is aimed at understanding the interplay between structure and property in the remarkable class of existing phase-change materials and expanding the number and types of compounds available for future data storage technology. This work will complement LANL strengths in theory and engineering, bringing the much anticipated non-volatile universal memory closer to reality. In the broadest sense, this work will advance the methods of characterization available for amorphous-crystalline phase transitions in solids, bridging an important gap in solid state characterization as it is pursued today.

## Publications

Im, W. B., K. Page, S. P. DenBaars, and R. Seshadri. Probing local structure in the yellow phosphor LaSr2AlO5:Ce3+, by the maximum entropy method and pair distribution function analysis. To appear in *Journal of Materials Chemistry.*

Melot, B. C., K. Page, R. Seshadri, E. M. Stoudenmire, L. Balents, D. L. Bergman, and T. Proffen. Magnetic frustration on the diamond lattice of the A-site magnetic spinels CoAl2-xGaxO4: The role of lattice expansion and site disorder. 2009. *Physical Review B.* **80**: 104420.

Page, K., and T. Proffen. Nanoparticle structure from neutron total scattering: the pair distribution function approach. *Neutrons and Nanoscience.* Edited by Hurd, A. J., and S. Sinha.

# Effect of Charging on Carrier Relaxation Dynamics in Quantum Confined Semiconductor Nanocrystals

*Milan Sykora*
20080793PRD4

## Introduction

Due to the projected increase in the global demand for energy there has been a growing interest in harnessing solar energy in an efficient and cost-effective manner. Nanomaterials and more specifically quantum confined semiconductor nanocrystals (NCs) or nanocrystal quantum dots (NQDs) have potential to play an important role in the next generation of lasers and light-emitting diodes (LEDs) as well as technologies for conversion of solar energy into electricity (photovoltaics, PV). Their appealing properties include size-tunability of their luminescence and absorption spectra, and the ability to generate multiple excited electron–hole pairs, or excitons, from a single photon via the process of carrier multiplication (CM). While a great deal of progress has been made on the photophysics of neutral NQDs, little is known about charged NQDs. This deficiency is crucial to remedy as the operation of practical LED or PV devices is likely to lead to the formation of significant populations of charged NQDs (Figure 1), which can dominate the carrier relaxation and recombination processes and thus dictate the device performance. In this project we study the fundamental physics of charged NQDs with the goal to determine the potential impact of charging on the performance of LED and PV devices based on NQDs.

## Benefit to National Security Missions

This project will primarily support the drive toward national energy security. In particular, the work will enhance our understanding of how nanoscale materials can be utilized to improve the efficiencies of solid lighting and solar energy conversion technologies.

## Progress

One of the challenges in studies of charged nanocrystal quantum dots (NQDs) is achieving a high level of control over the number of carriers introduced into the NQD. As was shown previously, an accurate control over the degree of charging is possible through combination of electrochemical and optical methods. Our initial focus on the project was on development of relevant

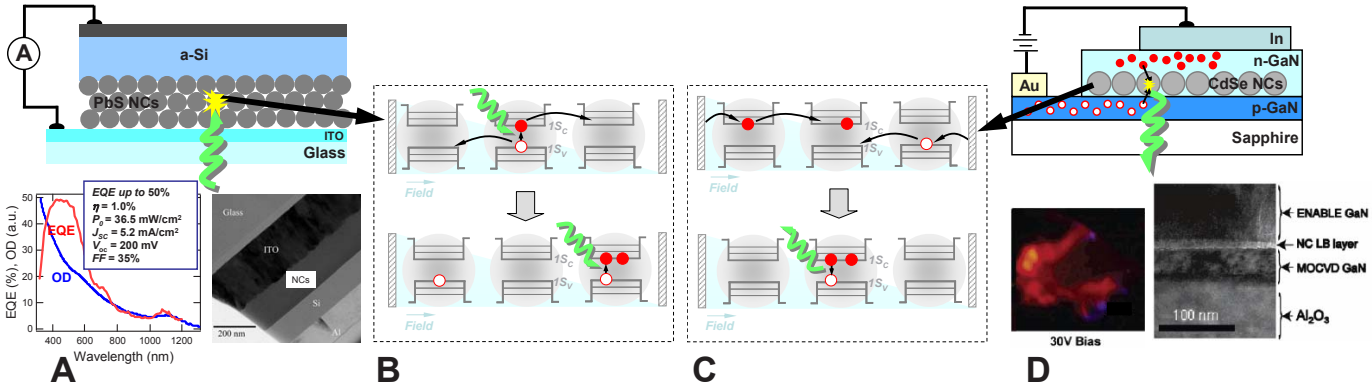


*Figure 1. Formation of excitons in charged NCs in PV devices and light-emitting diodes (LEDs). (A) Schematic diagram, performance characteristics and a transmission electron microscopy (TEM) cross-section of an example PV device based on PbS NCs. (B) Scheme showing formation of excitons in charged NCs during operation of a PV device. Top: Following photon absorption the carriers are separated by NC-to-NC carrier hopping driven by the internal field (in principle, multiple charges can be present in each NC as a result of carrier hopping). Bottom: Following absorption of a second photon an exciton is formed in a charged NC. The effects of an excess charge on exciton relaxation are currently virtually unknown. (C) Scheme showing formation of excitons in charged NCs during operation of an LED. (D) Schematic diagram of an example LED based on CdSe NCs, red electroluminescence observed during the device operation and a TEM cross-section of the device.*

instrumental and experimental capabilities.

In our initial experimental tests we found that the most convenient way to simultaneously monitor the electrochemical and optical properties of the NQDs is in an arrangement where NQDs are deposited onto the transparent conductive electrode (e.g., tin doped indium oxide, ITO) in form of thin film. We have performed a series of experiments to determine the conditions under which the film, immersed in electrolyte solution, would display robust electrochemical performance. We found that efficient charging of NQDs is achieved only after timed soaking of the film in electrolyte solution prior to use, so that supporting electrolyte may efficiently permeate the film. We have also found that reversible charging and discharging of the NQDs requires strict exclusion of oxygen from the film's environment. Following this observation we have designed a special type of air-free optical cell, which allows simultaneous monitoring of optical and electrochemical properties of the NC film under air-free conditions.

As was shown in previous studies the extent of NQD charging can be most reliably determined by linear absorption spectroscopy, whereby the extent of the loss (bleach) of the absorption band associated with the band-edge optical transition in NQDs is directly proportional to the extent of charging. To be able to monitor the extent of NQD charging optically we have designed and developed a new optical setup (Figure 2) that allows simultaneous monitoring of current-voltage characteristics of NQD films, their linear absorption and photoluminescence (PL). In addition, our experimental setup also allows for monitoring time-resolved PL with very high temporal resolution ~15 ps.

Our initial experimental studies of NQD films show several interesting insights.

1. We found that when the external potential is applied onto the electrode with the NC films, the injection of carriers into the NQD cores is preceded by deposition of carriers onto the NQD surface (Figure 2A). The deposition of carriers onto the NQD surface typically leads to enhancement of the steady-state PL, while the injection of the carrier into the NQD core leads to PL quenching. The latter is consistent with the expected triggering of the multi-carrrier Auger relaxation process.

2. We have compared the electron injection potentials for CdSe NQDs and the same NQDs overcoated with thin shells of ZnS. Because of their enhanced PL properties CdSe/ZnS structures are often used as components of light emitting devices. We have found that introduction of even the thinnest (1-2 monolayers) ZnS shell leads to a significant (~1 V) increase in the charging potential. Thus, our findings indicate that introduction of protective shells, while enhancing the PL properties of the NQDs, may actually hinder the overall performance of an electrically-driven device such as an LED.

3. We have found that exciton relaxation dynamics in NQDs is significantly altered by the NC charging (Figure 2C). Our analysis shows that charging of NQDs induces two competing effects: a) enhancement of radiative decay manifested as enhancement in PL at short delays b) enhancement of nonradiative relaxation via Auger decay manifested as a drop in PL intensity at long delays. We have initiated an effort to more quantitatively analyze these effects.

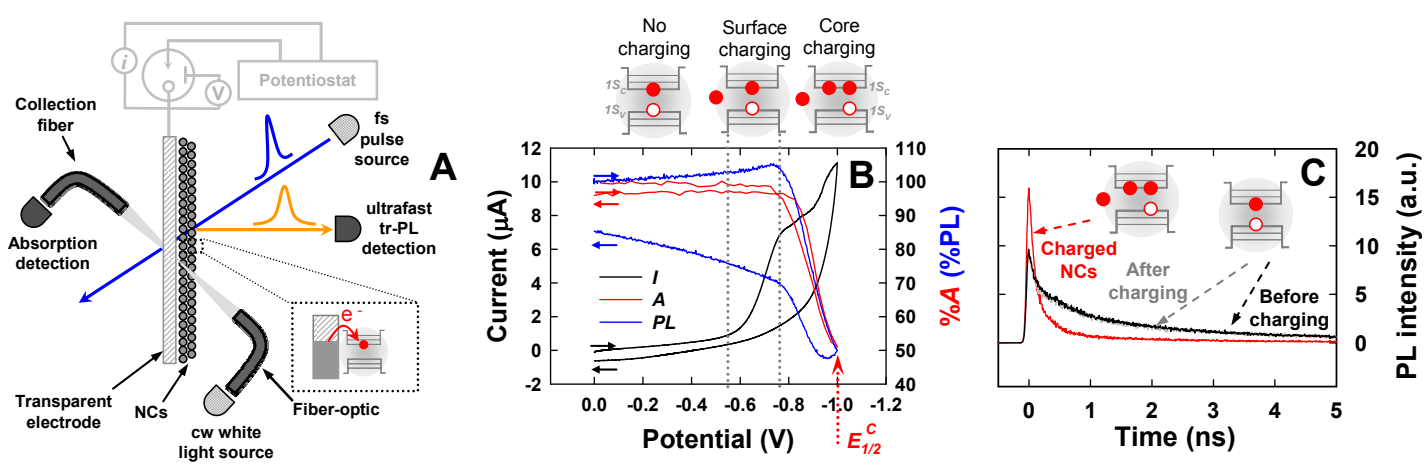


*Figure 2. (A) Schematic diagram of the experimental setup for studies of optical properties of charged NCs. (B) Preliminary results showing changes in current (I), absorbance bleach (A) and photoluminescence intensity (PL) as a function of applied potential. Combination of electrochemical and optical methods allows determination of the potential needed for deposition of charges onto the NC surface and injection into the NC core. The potential at which 50% of the band edge absorption is bleached defines the absolute energy of the conduction band offset (E1/2C). (C) Results of preliminary studies of the effect of charging on the carrier relaxation dynamics. The exciton relaxation is significantly faster in charged NCs and the changes in the dynamics are reversible upon removal of excess charge.*

## Future Work

The objective of the ongoing work is to study carrier relaxation dynamics in charged nanocrystal quantum dots (NQDs) using ultrafast laser spectroscopy. Central to this work will be determining the variations in the rates of both radiative and nonradiative relaxation processes as a function of the excess charge introduced to the NQDs. There are three different tasks that will be addressed.

**Radiative recombination in charged NQDs**

In charged NQDs the photoexcitation should lead to a population of different electronic states than in "neutral" NQDs. This should lead to a significant decrease in the observed radiative lifetime of the charged NQDs compared to the neutral NQDs. To determine if charging in fact affects the rate of radiative recombination and to quantify the magnitude of the effect, ultrafast photoluminescence studies of NQDs will be performed with various degrees of charging.

**Auger recombination dynamics in charged NQDs**

Carrier relaxation in multiply excited semiconductor NQDs is typically dominated by the Auger process. While the Auger recombination process is also expected to be efficient in singly excited charged NQDs this has not yet been studied experimentally. To quantitatively understand the effect of charging on nonradiative relaxation in NQDs the Auger recombination dynamics in charged NQDs and its relationship to the multiexciton Auger dynamics in neutral NQDs will be investigated.

**Carrier Multiplication (generation of multiple excitons following absorption of single photon) in charged NQDs**

Building on understanding of the carrier recombination dynamics in charged NQDs in the presence of a single exciton, studies will be extended to the multiexciton regime. Here, the main interest is in developing an understanding of how the efficiency of CM varies with the extent of NQD charging. This understanding may be of critical importance for exploitation of the CM effect in solar energy conversion applications.

The use of films in electrochemical control of NQD charging complicates the study of carrier dynamics. Removal of a portion of the organic molecules on the NQD surface, necessary for formation of uniform films, leads to regions where carriers may become trapped. Energy transfer within the film also influences the observed dynamics. To overcome this limitation we are developing an air-free thin-layer electrochemical cell containing a platinum mesh electrode. This light-transmitting electrode allows charged NQDs to be formed and studied optically directly in electrolyte solution.

## Conclusion

In terms of basic science the main objective is to develop understanding of physics of charged NQDs. The practical objective is to determine how charging of individual nanocomponents of a LED or a PV device during its operation affects its performance and how the potential losses in the performance can be minimized. By reaching the project goals we will be able to more accurately assess how nanoscale materials can be utilized to enhance the efficiencies of the solid state lighting and solar energy conversion technologies. These objectives are aligned with DOE's energy security mission as they have potential to reduce our energy dependence on oil and other fossil fuels.

# The Kondo Lattice Problem

*Joe D. Thompson*
20080794PRD4

## Introduction

Strong interactions among electrons force a correlated, collective response to their physical and chemical environments. Experimental and theoretical work over the past three decades to understand these correlated responses have failed to provide a microscopic or even firmly based phenomenological understanding of the complex underlying physics of such systems. A recent conceptual breakthrough from our examination of one large class of electronically correlated materials, so-called Kondo-lattice materials, provides an entirely new phenomenological description of the complex physics. This project has the goals of exploring the predictive consequences of this phenomenology, especially regarding the possible emergence of unconventional superconductivity from this model. Additionally, we will explore whether a more basic microscopic understanding of this phenomenology can be developed.

## Benefit to National Security Missions

Complex correlations among electrons control the physical properties of unconventional superconductors and actinide materials that are important for DOE missions for energy security and understanding materials. This work attacks the unsolved problem of complex correlations from a completely new perspective, with the goal of understanding how they control physical properties.

## Progress

Progress has been made in five directions:

1. Experimental point-contact spectroscopy studies of Kondo-lattice compounds observe a voltage asymmetry in spectra that emerges below in a material-dependent temperature scale T*. Until now there has been no understanding of the origin of this asymmetry. Within the framework of our new phenomenology, we have developed a semi-microscopic interpretation based on the quantum interference between 'light' and 'heavy' electrons that accounts for these experimental observations. This work has been published as a Rapid Communication in the journal Physical Review B [1].

2. We have applied our phenomenology of the Kondo-liquid to provide a natural explanation for the evolution of the experimentally determined spin susceptibility (Knight shift) in the superconducting state of the Kondo-lattice material $CeCoIn_5$. A principal conclusion from this theoretical modeling is that unconventional superconductivity in $CeCoIn_5$ originates from the condensation of electronic excitations intrinsic to a Kondo liquid that displays quantum critical fluctuations below T*. Because the characteristic temperature scale T* of the Kondo liquid is given by the magnetic interaction between the magnetic f-electrons of Ce ions in this material, our analysis further concludes that the superconducting transition temperature is actually controlled by this single microscopic interaction, the magnetic exchange interaction. This conclusion points to a possible direction for pursuing new superconductors with higher transition temperatures. This work has been accepted for publication in the journal Physical Review Letters [2]. An extension of the above method to the Kondo-lattice antiferromagnet $CeRhIn_5$ also reveals that antiferromagnetism originates from the heavy electron Kondo liquid. This work is still in progress.

3. The fundamental difference between our new phenomenology and the conventional scenario is the emergence of heavy electron coherence with a characteristic energy scale T*. In our scenario, this coherence emerges primarily from the exchange correlation between magnetic ions that is controlled by the energy scale T*, while the conventional scenario proposes a lattice extension of single impurity Kondo screening due to the conduction electrons. A possible way to resolve this issue is to measure the microscopic development of the f-electron spectra by angle-resolved photoemission experiments. This work is still in progress and a paper on this proposal has been submitted to Acta

Physica Polonica A [3].

4. The recent experimental observation of specific structure in the electronic spectrum of the Kondo-lattice antiferromagnet $CeIn_3$ has led to the proposal of a selective Mott ('insulator' to metal, localized to itinerant) transition in the antiferromagnetic state, analogous the physics of high Tc cuprate superconductors. We have carried out analytical and numerical calculations that confirm such a similarity under certain circumstances, in contrast to the conventional scenario, which predicts a transition from an antiferromagnetic state to a nonmagnetic metallic Kondo state. With itinerant heavy electrons in the antiferromagnetic phase, our interpretation also provides a possible explanation for the microscopic coexistence of antiferromagnetism and superconductivity found in some Kondo-lattice materials. The fundamental energy scale for the itinerant electrons is set by the magnetic exchange interaction, consistent with our previous prediction of T*. A paper on this work is in preparation.

5. In Kondo-lattice superconductors, nonmagnetic impurities break up superconducting electron pairs and reduce the superconducting transition temperature. This impurity effect has been understood to originate from excited electronic states that appear in certain momentum directions where the superconducting energy gap goes to zero, that is, nodal points of the superconducting gap. We have examined specific heat data of some Kondo-lattice superconductors that allow us to determine the fraction of heavy electrons that participate in superconductivity. Our results suggest an inhomogeneous picture, with all unpaired heavy electrons accumulated around the impurities in the real space, in contrast to previous understanding. A paper on this work is in preparation.

## Future Work

Solution to the problem of a single localized f-electron interacting with a sea of $10^{23}$ conduction electrons, the Kondo-impurity problem, was a major breakthrough in condensed matter theory in the 1960s. Despite enormous effort in the intervening decades, the problem of $10^{23}$ interacting Kondo impurities, the Kondo-lattice/heavy-electron problem, remains one of the most important open challenges to theory. Recently, we have identified a dominant temperature scale T* below which universal behavior of the Kondo lattice emerges as a new quantum state of matter (the Kondo liquid) that differs distinctly from the individual response of $10^{23}$ non-interacting Kondo impurities. This observation provides an entirely new framework for understanding the fundamental physics of heavy-electron materials. The central task now becomes that of using this new framework to understand how the Kondo liquid gives rise to the rich physical behaviors, such as quantum criticality and unconventional superconductivity, observed in many heavy-electron materials. In concert with experiment, this theoretical investigation has the goal of providing a much more complete and realistic microscopic understanding of heavy-electron physics.

## Conclusion

Future technologies that save energy and advance our standard of living may ultimately be based on materials whose functional properties result from the correlated and collective responses of electrons. Though some of these responses are known through observation, as yet, we are unable to predict them. Hence, we are unable to predict material behavior and potentially revolutionary responses must await serendipitous discovery. Research pursued in this project has the goal of understanding how electrons become highly correlated and how their collective response can be controlled for useful functions.

## References


1. Yang, Y. F.. The Fano effect in the point-contact spectroscopy of heavy electron materials. 2009. *Physical Review B.* **79**: 241107(R).

2. Yang, Y. F., R. Urbano, N. J. Curro, D. Pines, and E. D. Bauer. Magnetic excitations in Kondo liquid: Superconductivity and hidden magnetic quantum critical fluctuations. To appear in *Physical Review Letters.*

3. Durakiewicz, T., P. S. Riseborough, C. D. Batista, Y. F. Yang, P. M. Oppeneer, J. Joyce, and E. D. Bauer. Quest for band renormalization and self-energy in correlated f-electron systems. *Acta Physica Polonica A.*


## Publications


Durakiewicz, T., P. S. Riseborough, C. D. Batista, Y. F. Yang, P. M. Oppeneer, J. Joyce, and E. D. Bauer. Quest for band renormalization and self-energy in correlated f-electron systems. *Acta Physica Polonica A.*

Yang, Y. F.. The Fano effect in the point-contact spectroscopy of heavy electron materials. 2009. *Physical Review B.* **79**: 241107(R).

Yang, Y. F., R. Urbano, N. J. Curro, D. Pines, and E. D. Bauer. Magnetic excitations in Kondo liquid: Superconductivity and hidden magnetic quantum critical fluctuations. To appear in *Physical Review Letters.*

# Classical/quantum Mechanical Simulations of Electronic Nanomaterials

*Sergei Tretiak*
20080795PRD4

## Introduction

The idea of harnessing molecular building blocks to assemble nanometer-scale devices promises many fascinating applications in fields ranging from electronic to medical. Unfortunately, our fundamental understanding of the underlying physics and chemistry of such complex structures lag the experimental observations; the major reason being the computationally unmanageable number of atoms in such systems. Our goal is to be able to compute the optical and transport properties of these complex molecular composites. This project will combine two approaches: ab initio methods (giving an accurate electronic structure of a system) and force field (FF) methods (providing reasonably fast geometries, packing, and dynamics for large molecules). We propose to: i) construct new FF potentials using quantum mechanical calculations (e.g., Density Functional Theory, DFT) to be performed on a set of representative units; ii) conduct FF simulations of the dynamics of the entire system at specific temperature, pressure, etc; iii) DFT and time-dependent DFT calculations of electronic structure of ground and excited states using selected resulting geometries (snapshots); iv) modify a Gaussian computational package to allow non-adiabatic photoinduced dynamics based on correlated excited states in time-dependent DFT method. Using this approach, the ultimate goal is to predict and to explain experimental results on several nanoscale molecular composites/hybrids.

## Benefit to National Security Missions

This project directly addresses LANL institutional goals in basic understanding of materials, energy security, and threat reduction. Furthermore, the project strongly connects to thrusts of the DOE-funded Center for Integrated Nano-Technology (CINT) by impacting priorities in nanotechnology, multi-scale material modeling, and sensing.

## Progress

We use a combination of ab initio techniques, such as density functional theory (giving an accurate electronic structure of a system), with classical force field calculations (providing reasonably fast geometries, packing and dynamics for large molecules) to predict and to explain experimental results on dynamics, transport, and optical properties of several hybrid composites and nano-scaled materials. During the past year we have investigated optical response and phonon induced dynamics in the pure CdSe quantum dots (QD) and QDs functionalized by different organic molecules [1,2]. Currently, our main focus is on organic ligands that cover the QD surface. The role of ligands is expected to be crucial in the carrier multiplication processes experimentally observed in these systems and promising for the harvesting of solar energy. Surface ligands also impact phonon-assisted carrier dynamics that competes with carrier multiplication. In contrast to the common point of view, we found that ligands strongly impact charge relaxation in QDs for high-energy excitations. No molecular orbitals of ligands appear as trap states inside or near the band gap of the QD. We found that the surface ligands introduce new electronic states which are strongly delocalized over the ligands and the dot surface and open new relaxation paths for the nonradiative charge relaxation increasing relaxation rates [3]. These results were first obtained for small Cd33Se33 clusters passivated by different organic molecules. Now we extend our investigations to the larger systems (Cd111Se111) which are comparable to the common QDs used in experiments. These investigations have resulted in several articles published [1-3] and other papers are expected to be submitted soon. Our results were also presented in several conferences. We also investigate optical and transport properties in dye-functionalized metallic clusters self-assembled on the DNA template. Some of our results have been already published [4]. All these composites hold great promise in the areas of bio-inspired self-assembly of electronic circuits.

Finally, our results on excitonic and electron-phonon couplings in semiconductor carbon nanotubes (CNTs) and quantum dots were also summarized in the book [5,6] that was published by World Scientific/ Pan Stanford (a science publishing company of high

reputation) this summer (Figure 1). This project is now extended by studies of photocurrent and its dependence on the photoexcitation energies in CNTs.

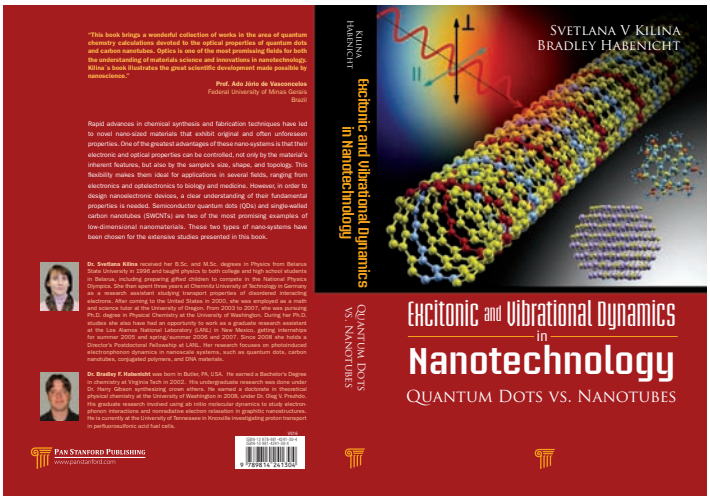


*Figure 1. This book brings collection of works in the area of quantum chemistry calculations devoted to the optical properties of quantum dots and carbon nanotubes.*

## Future Work

Developed methodology will be applied to: i) Adsorbed DNA strands or other bio-molecules on metallic surfaces. Here the unique STM spectra of bases promise resolution of the structure and fast sequencing of DNA. To interpret experimental results, the Postdoc will simulate tunneling spectra and identify the underlying electronic features; ii) Semiconductor quantum dots to clarify the role of soft ligand layer and surface roughness on electron-electron and electron-phonon coupling important in experimentally observed efficient carrier multiplication processes. These systems are promising for harvesting of solar energy; iii) Molecular-functionalized carbon nanotubes to investigate computationally photoinduced structural relaxation and uncaging. This has a potential to make carbon nanotubes into highly luminescent materials.

## Conclusion

We will apply our new methodologies to a variety of materials, which are promising for optoelectronics and sensing, and several bio-applications such as drug delivery, cancer diagnostics and therapy. Many other applications are envisioned and broad dissemination of these methods is expected. Besides providing fundamental theoretical understanding of transport, and photoexcited properties of complex molecular composites, this research is envisioned for developing a fast and accurate "virtual computational nano-scale laboratory" to be used in a variety of projects with significant LANL, DOE, and NIH investments, and will support a number of experimental efforts currently carried out at LANL/CINT.

## References


1. Isborn, C., S. Kilina, X. Li, and O. Prezhdo. Generation of Multiple Excitons in PbSe and CdSe Quantum Dots by Direct Photoexcitation: First-Principles Calculations. 2008. *Journal of Physical Chemistry C.* **112**: 18291–18294.

2. Kilina, S., and O. Prezhdo. Breaking the Phonon Bottleneck in PbSe and CdSe Quantum Dots: Time-Domain Density Functional Theory of Charge Carrier Relaxa. 2009. *ACS Nano.* **3**: 93.

3. Kilina, S., S. Ivanov, and S. Tretiak . Effect of Surface Ligands on Optical and Electronic Spectra of Semiconductor Nanoclusters. 2009. *Journal of the American Chemical Society .* **131**: 7717–7726.

4. Kilin, D., K. Tsemekhman, S. Kilina, A. Balatsky, and O. Prezhdo . Photoinduced Conductivity of a Porphyrin-Gold Composite Nanowire. 2009. *Journal of Physical Chemistry C.* **113**: 4549.

5. Habenight, B., and S. Kilina . Excitonic and Vibrational Dynamics in Nanotechnology: Quantum Dots vs Carbon Nanotubes. 2009.

6. Svetlana Kilina coauthors book on nanotechnology. 2009. *PADSTE HIGHLIGHTS .*


## Publications


Svetlana Kilina coauthors book on nanotechnology. 2009. *PADSTE HIGHLIGHTS .*

Habenight, B., and S. Kilina . Excitonic and Vibrational Dynamics in Nanotechnology: Quantum Dots vs Carbon Nanotubes. 2009.

Isborn, C., S. Kilina, X. Li, and O. Prezhdo. Generation of Multiple Excitons in PbSe and CdSe Quantum Dots by Direct Photoexcitation: First-Principles Calculations. 2008. *Journal of Physical Chemistry C.* **112**: 18291–18294.

Kilin, D., K. Tsemekhman, S. Kilina, A. Balatsky, and O. Prezhdo . Photoinduced Conductivity of a Porphyrin-Gold Composite Nanowire. 2009. *Journal of Physical Chemistry C.* **113**: 4549.

Kilina, S., S. Ivanov, and S. Tretiak . Effect of Surface Ligands on Optical and Electronic Spectra of Semiconductor Nanoclusters. 2009. *Journal of the American Chemical Society .* **131**: 7717–7726.

Kilina, S., and O. Prezhdo. Breaking the Phonon Bottleneck in PbSe and CdSe Quantum Dots: Time-Domain Density Functional Theory of Charge Carrier Relaxa. 2009. *ACS Nano.* **3**: 93.

# Energy Transfer Processes in Type-Specific Single-Walled Carbon Nanotubes

*Stephen K. Doorn*
20080797PRD4

## Introduction

Single-Walled Carbon Nanotubes (SWNTs) have remarkable optical and electrical properties. The photophysical properties are heavily dependent on the sidewall pristinety, diameter and chirality (a property of the geometry) of the tube. This heterogeneity offers many opportunities in sensing and electronic applications. However, full utilization of these properties requires the development of well defined materials. This includes controlling the energy transfer (ET) that occurs between distinct tube types and between the tube and environment. Control of ET is important because it can enhance and/or quench the detectable photophysical properties of the tubes, and allows tunability of their absorption range. Current research on bulk samples is lacking because the heterogeneity inherently limits the sensitivity and reproducibility of the measurements. However, new separation techniques allow access to chirality-enriched samples. This offers the possibility of engineering samples with specific bandgap and reactivity properties. We will utilize enriched chirality samples to engineer and enhance ET reactions between specific tube types and between SWNTs and molecules in ensemble systems and at the single molecular level.

## Benefit to National Security Missions

This project supports the development of advanced functional nanomaterials that support threat reduction, energy security, human health, and basic science missions in DOE and other government agencies.

## Progress

This project began on January 25th, 2009--start date for Juan Duque. Since then Juan has devoted his time to several aspects of the effort. These include developing an understanding of surfactant interactions at the nanotube surface to further our separations methods. Additionally, he has performed Raman spectroscopic studies aimed at further defining the role of tube structure in determining solubility. In addition to generating a number of publishable results, these projects have helped him become familiar with the different instrumentation and experimental setups here at LANL; despite his short time here, several major accomplishments have been made.

First, Juan was able to reproduce previous results from our lab on the correlation between surfactant organization and the optical properties of single-walled carbon nanotubes (SWNTs) via salt titration. Moreover, he has expanded our current understanding of the interfacial interaction between surfactants and SWNTs to other anionic surfactants. His results have shown that the structure, packing density, and concentration of surfactant around the SWNTs are the major components that affect the optical properties of SWNT suspensions. This work is directly relevant to our efforts in the separation of different SWNT chiralities via ultracentrifugation, and has helped us further understand and corroborate a LANL-developed model for SWNT separation. As a result, we are nearing submission of a manuscript explaining the effects of surfactants on the optical properties of SWNTs and their correlation to packing density. Some of the techniques employed by Juan to obtain these results include Ultraviolet-Visible-near-Infrared Absorbance and fluorescence spectroscopy.

Second, Resonant Raman scattering experiments using excitation wavelengths in the visible and near infrared regions were performed with SWNTs. This work is in collaboration with Juan's former university (Rice University, Houston TX) and aims to establish some factors that contribute to the solubility and optical properties of SWNTs in suspensions for optoelectronic and nanophotonics applications. His resonant Raman results showed that different SWNT batches can have different diameter distributions for all chiralities of tubes present in the suspension, and that the solubility of SWNTs in superacids and surfactants is diameter dependent. The outcome of these results is part of a manuscript, which will be submitted to the Journal of the American Chemical Society (JACS) within the coming weeks. Furthermore, this experience helped to familiarize him with the extensive Raman facilities here at LANL, and currently he has begun work on probing

the fundamental electronic structures of separated SWNTs using excitation wavelengths in the ultraviolet (UV) region. This type of work is the first of its kind in the SWNT community and aims to answer fundamental questions on the exciton-phonon coupling of SWNTs and their transition energies. This work is being conducted in collaboration with a group from DuPont led by Ming Zheng.

Juan has also been involved in developing new matrix materials in which to integrate nanotubes. The goal is to generate new nanotube environments that will maintain their luminescence properties. The new matrices are anticipated to enable Juan to perform ET experiments over a broad temperature range. This effort is in collaboration with Andrew Dattelbaum and Gautam Gupta of CINT. To date Juan has developed an approach to efficiently incorporate nanotubes into a sol-gel matrix. By varying the composition of the initial nanotube surfactant suspensions, Juan is able to generate highly luminescent materials. We also anticipate the new matrices can be extended to encompass aerogels. Beyond enabling new ET measurements, these matrices will be interesting as new sensing platforms as well.

## Future Work

SWNT suspensions with tailored bandgap and narrow electronic properties will be developed. This will allow engineering of suspensions in which the intertube interactions between select types will be studied. Optical and electronic enhancement will be investigated between specific diameter semiconductors, allowing the identification of the most efficient ET pathway for photophysical processes and energy harvesting. Metallic-semiconductor interactions will give insight to the electronic and optical quenching pathways SWNTs undergo. These parameters will be studied as a function of the difference in bandgap energies and relative chirality overlaps. The energy transfer between SWNTs and photoactive organic and inorganic molecules, or dopants, will also be studied. This will provide further knowledge of energy processes that specific SWNTs undergo by offering a point of reference to evaluate the efficiency and ET yield of each tube type. Examples include squarylium dye which does not overlap with SWNT absorbance and quantum dots which have easily manipulated absorbance and emission profiles. Engineering of the surfactant structure around the SWNTs will also be important to control the bandgap and Fermi level which then allows tunability of the degree, type and rate of interactions between tube types and tube-dopant. Photoluminescence excitation (PLE) maps and Raman spectroscopy will be the primary analysis tools for these studies because they provide information on the specific interactions that affect the electronic and optical structure of SWNTs. Therefore, we will analyze the energy flow in the system and the electronic properties of the tubes as a function of the photoluminescence, surfactant and relative SWNT side-wall structure. We can also extract information on the tube energy levels and the most energy-favorable path for ET processes between tube-tube and tube-dopants by selecting and adjusting the desired bandgap and Fermi level via surfactant selection, thus allowing control over the ET rates.

## Conclusion

In summary, the goal of Juan's work here at LANL is to conduct fundamental studies of the spectroscopic energy transfer and photophysical processes between SWNTs and their surroundings both in bulk and at the single molecular level for energy harvesting applications. His early experiments are helping us understand the optical and electronic structures of SWNTs, and consequently will help us engineer and design new experiments involving single-molecule spectroscopy for energy transfer and chemistry at the single tube level.

This project will be the first of its kind to correlate the ET of various tube-tube and tube-molecule interactions both in ensembles and at the single molecular level. It aims to define the electronic transitions that occur in a variety of SWNT systems to improve the control and predictability of the electronic and optical properties of SWNTs. The results of this project will answer fundamental questions on intertube and tube-molecule ET so that SWNT suspensions can be engineered with predictable photophysical properties, and thus have an impact on optoelectronic, sensing, and energy harvesting applications.

# Vanadium Catalyzed Aerobic Oxidations

*John C. Gordon*
20090492PRD1

## Introduction

The development of alternatives to petroleum-based fuels and chemicals is becoming increasingly urgent due to concerns over climate change, growing world energy demand, and energy security issues. Biomass is the only renewable carbon feedstock available, and thus much recent effort has focused on developing technologies that convert biomass into chemicals and fuels. The majority of non food-derived biomass is in the form of lignocellulose, which is often not fully utilized due to difficulties associated with breaking down both lignin and cellulose. Cellulose is composed of strands of glucose monomers connected by β-1,4-glycosidic linkages, which are cross-linked together through an extensive hydrogen bonding network. Because it is so difficult to break apart the carbon-carbon and carbon-oxygen linkages, lignin is resistant to chemical degradation, playing an important role in nature in protecting plants from attack by microorganisms.

## Benefit to National Security Missions

Using non-food derived biomass to produce renewable feedstocks for chemicals and fuels is a particularly attractive possibility. However, the majority of biomass is in the form of lignocellulose, which is often not fully utilized due to difficulties associated with breaking down both lignin and cellulose. This kind of fundamental research will provide valuable information towards addressing one of the biggest current technological challenges – *sustainable use of the Earth's carbon resource*s. The discovery of new efficient chemical pathways to convert biomass-derived polymers into useful feedstocks and fuels in line with the Energy and Earth Systems Grand Challenge and its sub-components. The Department of Defense, the largest consumer of petroleum in the world, has significant interest in the development of domestically sourced biologically-derived fuels.

## Progress

The goal of this project was to explore a new strategy of using an earth-abundant transition metal (vanadium) catalyst to break apart lignin and cellulose. This could lead to selective methods to transform lignin and cellulose into more useful chemicals and fuels. We selected vanadium for investigation because in oxidation reactions, vanadium complexes are known to break carbon-carbon and carbon-hydrogen bonds. Vanadium is also an ideal candidate for oxidation of lignin and cellulose because it has a high oxidation potential in oxidation state +5, but can still be regenerated by air. Using air as the terminal oxidant is ideal from both economic and environmental perspectives, as it is inexpensive and water is the only by-product of oxidation.

We have synthesized and characterized several vanadium complexes that could potentially catalyze the oxidation of lignin and cellulose. Due to the inherent chemical complexity of both cellulose and lignin, it is difficult to analyze chemical reactions of these polymers, both in terms of determining the extent of conversion and the products formed. For this reason, we began by studying the reactivity of smaller organic compounds that mimic the structural frameworks of lignin and cellulose. The pertinent linkages in lignin were modeled using compounds with 1,2-alcohol ether substituents, such as pinacol monomethyl ether, 2-phenoxyethanol, 1-phenyl-2-phenoxyethanol, and 1,2-diphenylethanol (Figure 1, 2).

One of the main candidates tested as a catalyst for the oxidation reactions was the complex (dipic)V(O)OiPr (1) (dipic = dipicolinic acid, OiPr = isopropoxide). The dipicolinic acid was used as a ligand for the vanadium, because it was hypothesized that this class of ligand would facilitate re-oxidation of the low-valent vanadium by air. We tested the reactivity of this compound with the lignin and cellulose model complexes. The oxidation

of the cellulose models pinacol and 1,2-diphenylethanediol was carried out. Experiments carried out show that the vanadium center plays a key role in the oxidation reaction. Prior to these discoveries, only a few examples of the aerobic oxidation of diols using homogeneous vanadium catalysts had previously been reported. The successful oxidative carbon-carbon bond cleavage of diols under mild conditions using air suggests the potential of the catalyst 1 to break carbon-carbon bonds in cellulose. Future experiments will focus on studying the reactivity of vanadium complexes with the carbohydrates glucose, cellobiose, and cellulose.

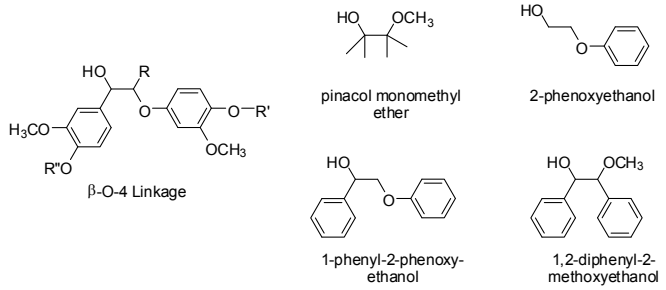


*Figure 1. β-O,4-linkage and organic compounds used as models for initial reactivity studies.*

The catalytic oxidation of several other lignin model complexes using compound 1 and air was explored (Figure 3). It was found that the compounds with phenyl substituents (1-phenyl-2-phenoxyethanol and 1,2-diphenyl-2-methoxyethanol) were oxidized much faster than the substrate with no phenyl groups (2-phenoxyethanol). When the oxidation of the lignin model 1-phenyl-2-phenoxyethanol was carried out using complex 1 in DMSO (dimethylsulfoxide) solvent, both products of both carbon-carbon bond cleavage (formic acid, benzoic acid, phenol), and carbon-hydrogen bond cleavage (2-phenoxyacetophenone) were observed (Figure 3). Both carbon-carbon and carbon-hydrogen bond breaking reactions were also observed in the oxidation of 1,2-diphenyl-2-methoxyethanol. Several control experiments demonstrated that air is the oxidant in this reaction, and the vanadium plays a key role as a catalyst (no reaction occurs in the absence of the vanadium complex). Potential intermediates in the catalytic reactions were identified in attempt to elucidate how the oxidation reaction occurs. A manuscript describing the details of the catalytic oxidations discussed above has been submitted for publication. Overall, using the vanadium catalyst and air as the oxidant is a completely new method for breaking carbon-carbon bonds in these lignin model complexes (this is the first example of catalytic aerobic oxidative C-C bond cleavage of 1,2-hydroxyether complexes). This approach affords aromatic monomers from the lignin model complexes under mild conditions. The results described above suggest the potential utility of dipicolinate vanadium complexes to produce valuable chemicals from lignin.

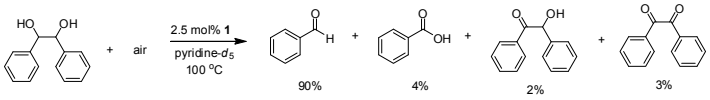


*Figure 2. Catalytic oxidation of 1,2-diphenylethanediol, a cellulose model. The carbon-carbon bond is broken in the oxidation reaction.*

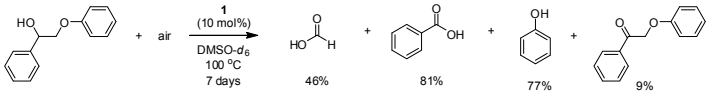


*Figure 3. Catalytic oxidation of 1-phenyl-2-phenoxyethanol. Products where both carbon-carbon and carbon-hydrogen bonds are broken were observed.*

## Future Work

The results described above suggest the potential utility of dipicolinate vanadium complexes to produce valuable chemicals from lignin. Furthermore, the homogeneous nature of the catalyst provides new opportunities for ligand design to optimize activity and selectivity in these reactions. Experiments to develop more active catalysts are currently underway.

## Conclusion

Overall, using these vanadium catalysts and air as the oxidant is a completely new method for breaking carbon-carbon bonds in these lignin model complexes (this is the first example of catalytic aerobic oxidative C-C bond cleavage of 1,2-hydroxyether complexes). This approach affords aromatic monomers from the lignin model complexes under mild conditions. The results described above suggest the potential utility of dipicolinate vanadium complexes to produce valuable chemical feedstocks from lignin.

# In situ X-ray Microdiffraction Study of Nanomechanical Behavior

*Amit Misra*
20090513PRD1

## Introduction

Investigations into the role of plasticity in the mechanical behavior of materials have great importance to the field of materials science, especially in today's nano-age where submicron and nanoscale devices are built near the size of their microstructural features. The creation of such small components requires a thorough understanding of the mechanical properties of materials at these small length scales. Integration of nanoscale materials into bulk composite materials systems such as nanolayered copper-niobium developed at LANL opens the opportunity to develop bulk materials with ultra-high strengths. Recent DOE, BES workshop reports on Materials under Extreme Environments and Advanced Nuclear Energy Systems have called for structural materials that are tolerant to damage under extreme mechanical and radiation environments. The evolution of damage in nanocomposite materials remains an open question. In this work, x-ray diffraction techniques, including synchrotron white-beam x-rays, will be utilized to evaluate the defect densities in deformed and ion irradiated nanolayered composites. Especially, an in situ x-ray microdiffraction observation of a nanolayered sample, while it is being deformed, will provide insights into the dislocation hardening mechanisms that have been not possible from post mortem studies that show minimal retained defects. This study will provide the fundamental understanding crucial to the design of nanomaterials that are ultra-high strength and possess high radiation damage tolerance.

## Benefit to National Security Missions

This project supports the missions of DOE and other agencies in areas of defense, nuclear energy, and other mission spaces by providing fundamental understanding of damage tolerance of ultra-high strength nanolayered composite materials. In particular, it provides the scientific underpinning of damage tolerant nanolayered composites for materials under extreme environments for defense, nuclear energy and transportation applications.

## Progress

The key accomplishments since the initiation of the project in late March 2009 are summarized as follows. First, single crystal multilayers of copper-niobium were grown on heated sapphire substrates using electron beam evaporation via control of deposition rate and substrate temperature. This is a significant achievement since the earlier work at LANL only produced polycrystalline copper-niobium multilayers via magnetron sputtering. The synthesis of high quality single crystal nanolayers is crucial for Laue microdiffraction experiments to be performed at Advanced Light Source at Berkeley. Second, the single crystal multilayers of copper-niobium were characterized at LANL using x-ray diffraction and transmission electron microscopy. These multilayers were found to be high quality single crystals with no grain boundaries in the layers. For samples deposited at the highest temperature (750 °C), some layer pinch-off was observed, as shown in Figure 1. To ensure continuity of layers, after seed layer deposition at 750 °C, subsequent layers were deposited at lower temperatures ranging from 250 °C to 600 °C. The individual copper and niobium layers in the multilayers ranged in thickness from 5 to 50 nm. Third, focused-ion-beam milling was used to machine pillar samples for compression tests, with approximate diameter of 2 micrometers and height of 6 micrometers. The micropillars were compressed using a flat punch tip in a nanoindenter to measure the compressive flow stress-strain response. Fourth, undeformed and compressed pillars of single crystal multilayers of copper-niobium were examined using Laue micro-diffraction at Advanced Light Source at Berkeley during the two days of beam time available in the first week of June. The data from the synchrotron beamline experiments are being analyzed, and preliminary analysis indicates limited broadening of the diffraction spots. Future experiments include *in situ* compression of pillars in a synchrotron beamline at Paul Scherer Institute (Switzerland) during Spring 2010 beam times. Samples for proof-of-principle test of *in situ* compression of micro-pillars in a synchrotron beamline have been sent to Paul Scherer Institute.

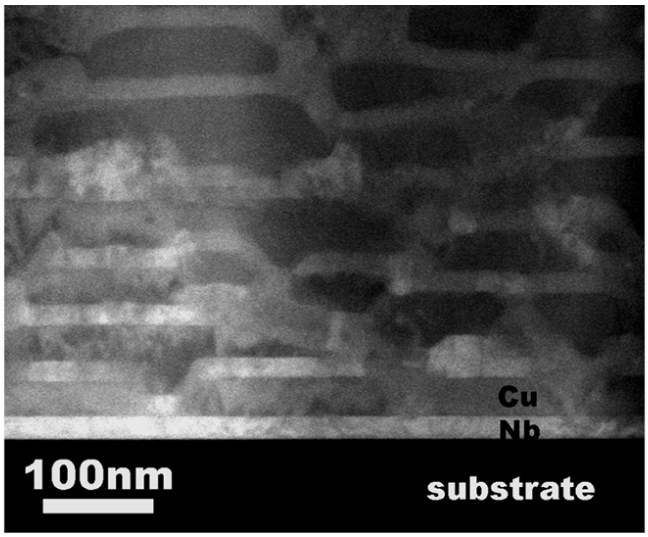


*Figure 1. Transmission electron micrograph of a copper-niobium multilayer deposited at 750 °C on sapphire substrate. The individual layers are single crystalline, although some layer pinch-off is noted.*

## Future Work

Future work includes *in situ* compression of pillars in a synchrotron beamline at Paul Scherer Institute. These pillars will be of copper-niobium multilayers of varying individual layer thickness from 5 to 50 nm. At LANL the diffraction peaks will be computed for copper-niobium multilayers for different layer thickness. The calculations will use atom positions at interfaces from atomistic modeling. Thus, the effect of the defects at interfaces on peak broadening will be computed directly and matched with experiments. To compare different interfaces, nanomechanical testing on other systems such as Aluminium-Niobium will be conducted.

## Conclusion

This research will provide fundamental insights into the damage tolerance of nanolayered metallic composites subjected to large strain plastic deformation. Specifically, it will elucidate the nature of interfaces in composite materials and nanostructuring length scales that are ideal for designing damage tolerant nanocomposites that may have applications as super-strong, light-weight engineering materials and structural components in nuclear energy reactors.

# Novel Fabrication of Metal-Semiconductor Heterostructured Nanowires

*Jennifer A. Hollingsworth*
20090514PRD1

## Introduction

Semiconductor nanowires (SC-NWs) have tremendous potential as building blocks in the assembly of nanoscale devices and nanocircuits for optoelectronics and electronics applications. For these applications, however, electrical contacts must be made to the SC-NWs. To date, electron-beam lithography is the common approach employed to define contacts for constructing, for example, single-SC-NW devices. The contacts created via this approach are considerably larger than the SC-NWs themselves, limiting many advantages of nanoscale systems. To address this problem, fabrication of integrated nanoscale contacts have been proposed, but only a few demonstrated: (1) the localized electroless deposition of gold (Au) on the tips of cadmium selenide (CdSe) nanorods [1], (2) the lithographic patterning of metallic nickel (Ni) on silicon (Si) NWs to form NiSi/Si/NiSi metal/SC/metal NWs [2], and (3) the electrodepositions of Au/cadmium sulfide/Au NWs [3]. These techniques are limited by choice of metal, inadequate size control, and/or the low quality of the electrodeposited SCs. Therefore, a new and more versatile approach for fabrication of functional nanoscale metal-SC-NW interfaces is required to facilitate SC-NW device applications. Here, we will employ a novel technique that couples two solution-phase growth methods—electrochemical metal NW growth and Solution-Liquid-Solid (SLS) semiconductor NW growth (Figure 1)—to allow controlled synthesis of nanoscale semiconductor-metal contacts for vastly improved integration into optoelectronic and electronic devices. In the SLS method, low-melting metal catalysts [e.g., indium (In), bismuth (Bi), and tin (Sn)] support the growth of high-quality semiconductor-nanowires—upon supersaturation of chemical precursors in the molten catalyst, the semiconductor-nanowire nucleates and then grows with high crystallinity. The template-directed synthesis is ideal for metal growth, and it is a facile method for fabricating multi-segmented metal nanowires via sequential reductions of metal ions into a nanopore template. The unique combination of these techniques will enable fabrication of heterostructured metal-semiconductor nanowires integrated at the nanoscale.

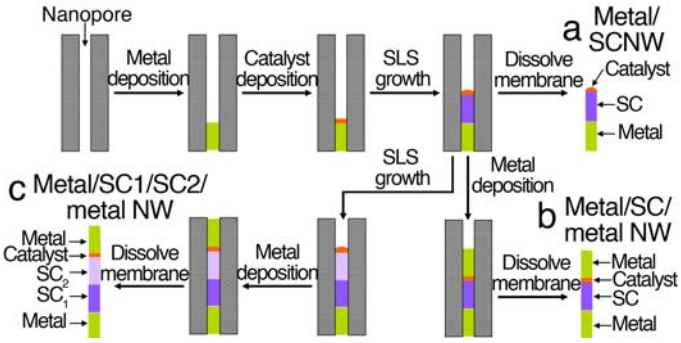


*Figure 1. Schematic of our approach to fabricating high-quality hybrid metal-semiconductor nanowires that combines electrochemical metal nanowire growth with Solution-Liquid-Solid semiconductor nanowire growth.*

## Benefit to National Security Missions

This project will support the DOE missions in Energy Security and Threat Reduction by providing critical supporting technologies that will enable the further miniaturization of functional devices with enhanced efficiencies. For example, the materials fabrication strategies developed will be applicable to photovoltaics and sensor technologies.

## Progress

### Capability Development

Three new electrochemical systems were established in the CINT nanomaterials synthesis laboratory: (1) an electrochemical work station for general electrochemical measurements, as well as electrochemical synthesis, especially of metal nanowires and, uniquely, low-melting metal-catalyst "slugs" (e.g., Bi), (2) an anodization process for in-house controlled fabrication of alumina ($Al_2O_3$) and titania ($TiO_2$) porous-membrane templates, and (3) an electrophoresis system for separation of nanomaterials.

More specifically, setup (1) consists of a potentiostat and an electrochemical deposition cell that was custom-made to support membrane electrode assemblies.

Commercially available membranes with pore diameters of 200 nm were successfully used as templates to synthesize single- and multi-segmented metal nanowires, i.e. Au, Au/Bi, silver (Ag)/Au/Bi (first example of this heterostructure). Most challengingly, electrodeposition conditions, such as the composition of the plating solution, the deposition potential and the potential waveform, were optimized to synthesize Bi segments with controlled lengths and diameters, where the Bi is a low-melting metal that is molten at the reaction temperatures used for subsequent *non*-electrochemical growth of semiconductor nanowires, i.e., the Bi serves as a catalyst for solution-liquid-solid (SLS) growth of semiconductor nanowires.

Setup (2) consists of a DC voltage power supply and an anodization cell that is designed to house an anode and a cathode for anodization of metal (e.g., aluminum and titanium). This setup gives us the ability to prepare in-house $Al_2O_3$ and $TiO_2$ porous-membranes, possessing controlled thicknesses and pore diamters. This will facilitate our overall goal of growing hybrid metal-semiconductor nanowires of controlled lengths, diameters, and metal-semiconductor interfacing. Specifically, the width of the membrane-templated Au or Au/Ag nanowires determines the diameter of the Bi plugs grown on them. Further, the diameter of the Bi plug determines the diameter of the semiconductor nanowires that are subsequently grown from them via SLS. To this end, we are working with Kevin Baldwin (MPA-CINT) and Aaron Gin (SNL-CINT) to fabricate silicon substrates coated with aluminum or titanium layers as our starting materials.

For Setup (3) we are designing a microfluidic chip that will be used for separating nanowires by electrophoresis. This approach will allow us to select nanowires of specific size (lengths and or diameters) in the case of nanowires grown without a template, as well as to separate other nanomaterials such as quantum dots. Through separation, we should be able to optimize nanomaterials properties as size and shape, for example, can correlate with properties.

**Research Results**

In addition to establishing new capabilities in the areas of electrochemical characterizations, synthesis, and separations, the Director's Funded Postdoc has acquired the enabling skills from our existing capabilities to permit her to realize the hybridization of electrochemical and colloidal synthesis approaches for the targeted fabrication of high-quality metal-semiconductor nanoscale structures. She has learned quantum dot synthesis, shell growth by Successive Ionic Layer Adsorption and Reaction (SILAR), Solution-Liquid-Solid (SLS) nanowire synthesis, and our novel flow-SLS nanowire synthesis technique.

Specifically, using setup (1): A 2 µm length of Au segment was electroplated into an alumina membrane with pore diameters of 200 nm. An approximately 200 nm thick Bi layer was subsequently deposited. These membranes were suspended in solution for SLS growth of CdSe nanowires. We have successfully prepared Au-CdSe nanowires in this way; however, the commercial membranes are very long (~60 microns), inhibiting penetration of semiconductor nanowire precursor compounds into the membrane. Thus, semiconductor nanowire growth using the commercial alumina membranes is less uniform and controlled than is desired. Nevertheless, we were able to improve the synthesis (e.g., adjusting size of precursor molecules to facilitate penetration into the deep membranes, etching of membranes to thin them, filling membranes with long Ag segments) to the point that we are able to clearly grow metal-semiconductor heterostructured nanowires, where these are of high crystalline quality and the first to be synthesized using combined electrochemical synthesis and SLS.

To achieve greater control over membrane depth and pore diameters, we utilized setup (2) to fabricate ultra-thin porous anodic alumina membranes – both substrate-bound and free-standing. In the former case, an aluminum metal layer was evaporated onto a thin layer of Au that had been sputtered onto a single-crystalline silicon substrate (an intermediate titanium layer was also deposited to increase adhesion of the aluminum layer to the Au layer). In the latter case, an aluminum metal foil was used as the aluminum starting material, and Au was sputtered onto one side to create the required metal contact. In both instances, ultrathin—from 250 nm to 6 micron—porous alumina membranes were created by anodization (electrochemical oxidation) of the aluminum metal (Figure 2). Au nanowire was subsequently electrochemically grown, establishing the metal nanowire component of our desired structure (Figure 1), followed by electrochemical deposition of a thin layer of Bi onto the Au. Using this Bi metal catalyst, the SLS semiconductor nanowire growth method was then used to synthesize high-quality, single-crystalline CdSe off of the gold wires, with the bismuth forming a droplet-shaped tip at the end of the semiconductor (Figure 3). With minimal additional optimization, we will submit our work for publication, establishing our novel approach to fabrication of high-quality hybrid metal-semiconductor, and more complex, nanowires.

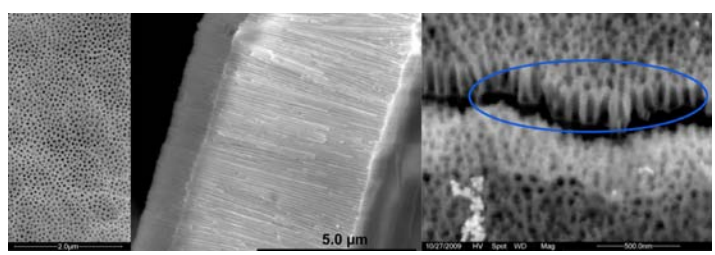


*Figure 2. Scanning electron microscopy images of ultra-thin porous alumina membranes. Left: Top-view. Middle: Side-view of free-standing membrane. Right: Side-view of substrate-bound membrane.*

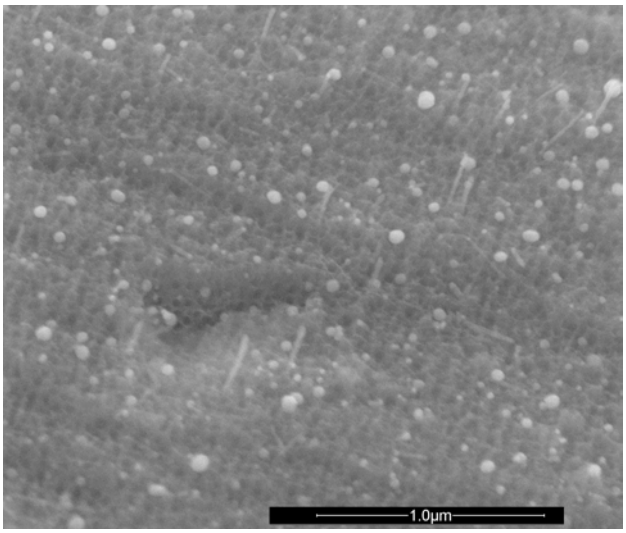


*Figure 3. Scanning electron microscopy image of Bi-tipped CdSe nanowires grown off of Au nanowires protruding from an alumina membrane. Bright spheres (small and larger) are Bi tips.*

## Future Work

With the need for a more versatile approach for the fabrication of functional nanoscale metal-semiconductor nanowire interfaces evident to facilitate semiconductor-nanowire device applications, we proposed a novel technique that couples two solution-phase growth methods: Solution-Liquid-Solid (SLS) semiconductor-nanowire growth with template-based metal electrodeposition. As a 'proof-of-concept' experiment, we create a bi-segmented metal-semiconductor nanowire by first electrodepositing a metal segment (Au) into a membrane template, followed by deposition of an SLS metal catalyst (Bi) and subsequent semiconductor-nanowire growth (CdSe). More complex metal/semiconductor/ metal nanowires will also be demonstrated via an additional step of metal electrodeposition. To date, the resulting nanowires have been imaged using scanning electron microscopy, but in the future will be crystallographically characterized using transmission electron microscopy and their electrical properties will be investigated using a gate-dependent I-V measurement. More intricate architectures—metal/ multi-segmented-semiconductor/metal nanowires (Figure 1)—will be produced by incorporating a new technique recently developed in the LANL Center for Integrated Nanotechnologies, namely, 'flow-SLS'. This technique involves the sequential feeding of precursors into a microflow reactor for controlled multi-segmented SLS SC growth (e.g., to create Type-II heterojunctions that promote beneficial electron-hole charge separation). Finally, in addition to the primary aim of creating nanoscale electrical contacts, we will attempt to integrate additional functionality by including, for example, magnetic segments that would facilitate post-growth magnetic manipulation and assembly of the nanowires.

## Conclusion

The primary aim is to develop a novel method for creating nanoscale electrical contacts. Successful coupling of the now distinct metal and semiconductor nanowire growth techniques will allow us to establish a general route to new, hybrid nanoscale structures, including technologically important (but currently impractical) high-density, vertically addressable nanowire assemblies, enhancing LANL's reputation in the growing field of nanomaterials design and integration. Simply put, the new class of metal-semiconductor nanowires will expedite the revolution of nanoscale electronic devices and circuitry.

## References

1. Mokari, T., E. Rothenberg, I. Popov, R. Costi, and U. Banin. Selective growth of metal tips onto semiconductor quantum rods and tetrapods . 2004. *Science.* **304** (5678): 1787.

2. Wu, Y., C. Yang, W. Lu, and C. Lieber. Single-crystal metallic nanowires and metal/semiconductor nanowire heterostructures . 2004. *Nature.* **430** (6995): 61.

3. Pena, D., J. Mbindyo, A. Carado, T. Mallouk, C. Keating, B. Razavi, and T. Mayer. Template growth of photoconductive metal-CdSe-metal nanowires . 2002. *Journal of Physical Chemistry B.* **106** (30): 7458.

# Nanogenerators Driven by Both Magnetic and Mechanical Waves

*Quanxi Jia*
20090519PRD2

## Introduction

Wireless devices are promising in real-time biomedical monitoring and operation, but their practical applications are limited by the short lifetime of present power sources. In order to work in a long-term of period and avoid the cost of battery replacement, these devices should be self-powered or powered by the energy from non-contact sources such as mechanical or magnetic waves. Nowadays, the development of nanotechnology dramatically reduces the size of the devices into nano-scales. It is indispensable that nanogenerators are developed so that they can be used to power these devices. Recently, piezoelectric nanogenerators, which could transform vibrational or mechanical energy directly to electricity to power nano devices, were reported. However, when the wireless devices are embedded into a substance, the body may absorb and decrease the applied vibration energy. We propose to develop a nanogenerator that can be driven by both magnetic and mechanical waves. Compared to mechanical source, a magnetic source is easier to be controlled by adjusting the frequency and intensity of the magnetic field. Therefore, the nanogenerators may not only be an efficient power source, but also enable the wide application of nano wireless devices.

## Benefit to National Security Missions

This research ties to the mission of DOE Office of Science for fundamental understanding of materials. LANL's thrusts in functional materials, nanotechnology, and sensors will directly benefit from this project.

## Progress

Dr. Junyi Zhai, the Director Funded Postodc fellow, was officially hired on April 20, 2009. He has gone through all of the necessary trainings, a lengthy process for any experimental work.

Even for such a short period of time, Junyi has been trained on the pulsed laser deposition of variety of different ferroelectric and ferromagnetic thin films. He has been further trained on the electrical and structural characterization of electronic materials. For example, he has been using x-ray diffraction to evaluate the crystal structure and crystallinity of the metal-oxide films. He has been also mastered the electrical characterization of ferroelectric thin films using necessary electrical testing tools. The following is a list of experiments we have done.

- Ferroelectric $BaTiO_3$ films were successfully deposited by pulsed laser deposition. Their ferroelectric properties were also characterized by transport measurements.
- We, for the first time tested the $BaTiO_3$:$Sm_2O_3$ nanocomposite films by pulsed laser deposition with very interesting structural and dielectric properties.

## Future Work

We propose to develop a nanogenerator that can be driven by both magnetic and mechanical waves. Compared to mechanical source, a magnetic source is easier to be controlled by adjusting the frequency and intensity of the magnetic field. Therefore, the nanogenerators may not only be an efficient power source, but also enable the wide application of nano wireless devices.

To develop nanogenerators, our tasks and approaches are composed of patterned carbon nanotube arrays and BaTiO3/Ni-ferrite thin films, by using both piezoelectric effect (converting mechanical energy to electrical energy) and magnetoelectric effect (converting magnetic energy to electrical energy). First, carbon nanotube arrays with well-controlled patterns will be fabricated on silicon or other ceramic substrates. The nanotube array changes the 2D substrate to a 3D template, which facilitates the fabrication of complex composite structures. Following that, piezoelectric BaTiO3 (BTO) and magnetic NiFe2O4 (NFO) films will be subsequently coated on the carbon nanotube arrays. A large magnetoelectric coupling from BTO/NFO composite is expected due to the strain transition at the interface. We will investigate the magnetoelectric coupling in the nano-scaled BTO/NFO composites (in comparison with

the composites in the bulk format). To fabricate these materials, we will use pulsed laser deposition (PLD) and polymer assistant deposition methods, both are available at LANL, to deposit BTO and NFO on nanotube array templates. The microstructure of the nanocomposites will be characterized by XRD and TEM. The structure-property relationship of this composite is expected to be established through such systematic investigation. The output voltage as a function of both mechanical and magnetic signals will be investigated thereafter.

Our goals are to (i) develop a new pattern design method in nanostructured materials by using carbon nanotube arrays; (ii) investigate the magnetoelectric coupling of nanoscaled BTO/NFO composites; and (iii) develop nanogenerators driven by both mechanical and magnetic waves.

## Conclusion

We expect to accomplish the following through this project: (i) to develop a new pattern design method in nanostructured materials by using carbon nanotube arrays; (ii) to investigate the magnetoelectric coupling of nanoscaled composites; and (iii) to develop nanogenerators driven by both mechanical and magnetic waves.

# New Generation of Fluorescent Probes for In-Vivo Imaging

*Jennifer Martinez*
20090534PRD3

## Introduction

Selection of suitable probes for in-vivo imaging has been a challenge for decades. A plethora of organic dyes are available for these studies, but they can suffer from poor photostability and low probe brightness. Quantum dots have recently been introduced as new probes for in-vivo and in-vitro studies. Although quantum dots have greater photostability and brightness, their utility is limited by their intermittent blinking, large size, and toxicity. Noble metal nanoclusters (made of 4-30 atoms, ≤ 1nm) may bypass these problems, since they possess unique size-dependent fluorescence properties. Noble metal nanoclusters were originally made in the gas phase, followed by synthesis of monolayer-protected nanoclusters with limited solubility in water and with low quantum yield (10^-3 to 10^-4). Recently, Martinez and colleagues developed strategies to synthesize water-soluble nanoparticle-free nanoclusters. Although these results are exciting, they still do not allow the precise control of nanocluster size in order to tune their fluorescent properties. Moreover, development of templating strategies and exploitation of biomimetic approaches to nanocluster synthesis remain as challenges. We will create nanoclusters of defined size/fluorescence, using biological molecules as templates to guide their formation. DNA, proteins, and peptides will be used to create clusters as part of a molecular recognition unit. The nanocluster tag will thus let us detect the molecular recognition target, opening new possibilities for ultrasensitive biochemical assay. A multifunctional molecule will be created (i.e. in DNA) that has both regions to template nanoclusters of defined size and a molecular recognition unit for direct use in biological assays. Conversely, peptides will be rationally designed and combinatorialy selected to template the formation of clusters. These peptides will then be engineered into larger protein structures, with nanoclusters just where we want them.

## Benefit to National Security Missions

This project is largely focused on threat reduction and health science as applicable for NIH and DoD/DHS agencies

## Progress

This project started approximately one month prior to the end of the fiscal year. We look forward to a productive next year. However, the postdoc has started to learn phage display procedures and theory. He has also synthesized and purified four peptides, and begun use for detection.

## Future Work

The goal of our work is to produce stable, biocompatible nanoclusters with complete control over their sizes in order to tune their fluorescent properties. To achieve this goal a) we will explore bio-inspired and traditional methods of synthesis, b) characterize their morphology and photophysical properties, and c) demonstrate the utility of these nanoclusters in biological imaging and sensing. In addition to exploiting existing synthetic (dendrimers, polymers) and biological (peptides, proteins) templates to generate size-controlled nanoclusters, our major efforts will be focused on developing genetically engineered biological templates, so that we can ultimately create peptide sequences that can give any protein the ability to template fluorescence nanoclusters. Cyclic or encapsulating linear peptides will be rationally designed (different backbones and side chains will be tested), and combinatorial biology will be used to create Au or Ag nanocluster templating sequences. State-of-the-art facilities available at LANL will be employed to characterize the newly developed nanoclusters. Nanocluster size and morphology will be determined by electron microscopy, mass spectrometry and scattering techniques. Raman, single-molecule, and time-resolved laser spectroscopies will be employed to characterize their photophysical properties in collaboration with Drs. Jim Werner and Andy Shreve.

## Conclusion

To synthesize nanoclusters with specific photophysical properties is a great intellectual challenge with profound implications. In general, biological sensors require stable and small-sized probes with wide-ranging fluorescence, which we propose to develop here. By developing nanoclusters that span a wide range of

fluorescence frequencies and are much smaller than the biological molecules (proteins etc), we can understand the dynamic changes in different proteins, simultaneously, without disrupting their structures and movements. Our nanoclusters can be used for a variety of other purposes including catalysis, light harvesting, biological sensing and fluorescence imaging.

# Lifting the Quantum Critical Conundrum

*Joe D. Thompson*
20061383PRD1

## Abstract

The quantum-critical conundrum, simply stated, is the problem posed by our inability to understand the nature and consequences of a phase transition at absolute zero temperature. One of the most promising candidates for resolving this conundrum is an antiferromagnet whose transition temperature is tuned to zero temperature by adjusting some non-thermal variable, such as pressure or magnetic field. Relatively huge pressures or fields are needed to achieve this in conventional antiferromagnetic materials, such as gadolinium metal. On the other hand, antiferromagnetic order in strongly correlated compounds is tuned easily to zero temperature. This work has used strongly correlated $CeRhIn_5$ as a prototype for exploring the quantum-critical conundrum. With applied pressure, its antiferromagnetic order can be tuned to coexist with superconductivity and at somewhat higher pressures to a zero-temperature transition, a magnetic quantum-critical point. Our detailed anisotropic resistivity studies as a function of pressure, field and temperature have revealed a new form of 'local' quantum criticality and that the consequences of fluctuations associated with this criticality is the emergence of superconductivity. In addition, we have developed and applied the entirely new technique of specific heat measurements under pressure in which a magnetic field can be rotated around any crystal axis of the sample. With this technique, we have probed the momentum-dependent electronic structure of $CeRhIn_5$ in its superconducting state and have shown that the pressure-induced coexisting superconductivity is unconventional. Building on these capabilities, we have explored related systems in which antiferromagnetic order also has been tuned by pressure or chemical substitutions to zero temperature, resulting in unexpected consequences. These accomplishments represent major advances in resolving the quantum-critical conundrum.

## Background and Research Objectives

All materials undergo some form of phase transition that is induced by a change in temperature. A well-known example is the solid-liquid transition from ice to water. These classical, thermally-driven phase transitions are well understood, but there is another class of phase transitions that occur at absolute zero temperature and that are not driven by a change in temperature but instead arise because of purely quantum mechanical effects. A zero-temperature magnetic to non-magnetic phase transition induced by a non-thermal variable is an example of this class of quantum-phase transitions. Unlike classical transitions, quantum transitions are not understood nor are the new states of matter that emerge from them. This is the quantum critical conundrum, a fundamental, unsolved problem at the forefront of materials physics. Unlike a thermally induced transition, which changes properties of a material over a narrow temperature interval around the transition, a quantum transition extends its influence over a wide temperature range above absolute zero to create quantum mechanically entangled states of electrons that give materials entirely new functions. Resolving the quantum conundrum is, thus, both a significant scientific and technologically relevant problem.

A commonly used theory of quantum criticality, the so-called standard model developed by Hertz, Millis and Moriya, considers the consequences of tuning a magnetic transition to absolute zero temperature. The applicability of this theory, however, rests on the nature of the magnetic transition, which is taken to be one that arises from a magnetic instability of itinerant electrons. Though there are a few examples where this theory appears to be consistent with some experiments, there are many counter examples where it is unable to account for observations. To account for these discrepancies, a very different theory of magnetic criticality has been proposed in which the magnetic

transition is assumed to develop among electrons that are localized. Unfortunately, this theory is very difficult and has not been able to calculate many physical properties of materials. Despite this problem, a few basic consequences of this so-called local or Kondo-breakdown type of magnetic criticality are known, and they are quite distinct from the commonly assumed form of criticality. In particular, a local quantum-phase transition is more 'violent,' creating a change in the number of electronic states that contribute to electrical conduction. This change is not allowed in the more traditional theory. Because of its violent nature, it has been assumed that local quantum criticality would not lead to a spectrum of magnetic and electronic fluctuations that would be favorable for creating superconductivity. Among other accomplishments discussed below, we have shown for the first time that this assumption is not valid.

## Scientific Approach and Accomplishments

Our approach has been two pronged. Most attention focused on the strongly correlated antiferromagnet $CeRhIn_5$ whose earlier study at Los Alamos had shown that its magnetic ordering temperature could be tuned toward zero temperature with modest pressures, of order 1 GPa. As a complement to this system, we also studied the isostructural compound $CeCoIn_5$, also discovered at Los Alamos and known to be a superconductor in which superconductivity developed out of an anomalous normal state apparently describable by the Hertz-Millis-Moriya theory. However, until our work, there was no evidence for a magnetic origin of this strange normal state. In both cases, high quality single crystals were studied by a variety of techniques at very low temperatures as a function of pressure and applied magnetic field.

The temperature-pressure phase diagram of $CeRhIn_5$ determined by our specific heat measurements is plotted in Figure 1. At atmospheric pressure, antiferromagnetic order develops among localized 4f electron on the cerium ion. As seen in Figure 1, applying pressure to $CeRhIn_5$ induces a phase of coexisting magnetism and superconductivity below a critical pressure P1. At P1, the antiferromagnetic transition temperature becomes equal to the pressure-induced superconducting transition temperature, and above P1, all evidence for magnetic order disappears. An extrapolation of the antiferromagnetic ordering temperature at pressures above P1 suggests that, if it existed, the magnetic transition would reach zero temperature at the pressure P2. Though absent in zero magnetic field, antiferromagnetic order reappears inside the superconducting state at pressures above P1 by applying a magnetic field, and the field-induce magnetic transition goes to zero at quantum-critical point P2 [1]. From an analysis of specific heat measurements as functions of temperature, pressure and magnetic field, we have established that superconductivity coexists with localized, magnetic 4f electrons below P1, and that at P1 there is pronounced change in the topology and nature of electronic states that is a continuation of field-induced quantum phase transition at P2. These discoveries were published in the Proceedings of the National Academy of Science [2].

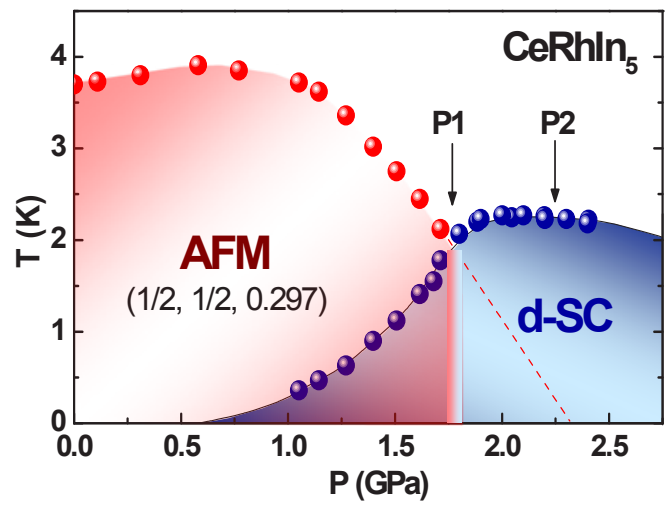


*Figure 1. Temperature versus pressure phase diagram of $CeRhIn_5$ determined from specific heat measurements. Below the pressure P1, antiferromagnetic order (AFM) and unconventional superconductivity (d-SC) coexist. For pressure above P1, evidence for magnetic order disappears but reappears with an applied magnetic field. The field-induced magnetic transition goes to zero temperature at the quantum-critical point P2.*

Though important, this study was unable to show definitely the nature of the criticality at P2 and its relationship to pressure-induced superconductivity. From a detailed investigation of the anisotropic electrical resistivity of $CeRhIn_5$ to pressures of 5 GPa and in magnetic field to 14 T, we discovered strong evidence that the criticality at P2 is of the local type and that fluctuations associated with local quantum criticality are responsible for superconductivity. [3] These results are summarized in Figure 2. The upper panel is a color representation of the resistivity anisotropy where we see that anisotropy intrinsic to high temperatures remains unchanged on cooling for a cone of pressures centered on P2. If the quantum criticality at P2 were of the conventional type, we would expect new anisotropies to develop because of stronger electron scattering along certain directions induced by quantum-critical fluctuations. Our observations are in direct contrast to expectations of the conventional model but can be understood if scattering by quantum fluctuations are local in character. Not only is the scattering above

P2 isotropic, it also produces a very unusual sub-linear temperature dependence to the resistivity, which also is in direct contrast to predictions of the standard model where a power law between 1 and 1.5 is expected. We have shown that this sub-linear dependence is consistent with a local, Kondo-breakdown type of quantum-phase transition. Further, the bottom panel of Figure 2 is a color plot of the magnitude of the resistivity as a function of temperature and pressure. The dark red region centered on P2 indicates the highest normalized resistivity, that is, strongest electronic scattering. The absolute value of the resistivity in this region exceeds the value found in $CeCoIn_5$ when it is disordered sufficiently to completely suppress its superconductivity. Pressure does not induce disorder, but instead this very strong scattering at P2, where the superconducting transition temperature of $CeRhIn_5$ is a maximum, arises from quantum-critical fluctuations. These observations strongly suggest that fluctuations from the local-type of quantum criticality are responsible not only for the high scattering at P2 but also provide the mechanism for superconductivity. This work represents a major step in lifting the quantum critical conundrum and sets new directions for scientific inquiry.

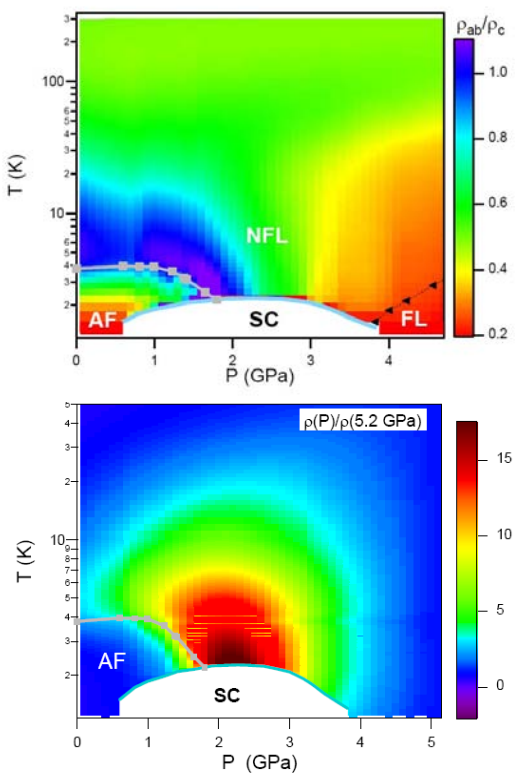


*Figure 2. Upper panel: a color plot of anisotropy in the electrical resistivity of $CeRhIn_5$ as a function of temperature and pressure and its relationship to antiferromagnetic order (AFM) and superconductivity (SC). The anisotropy is measured by the ratio of in-plane to out-of-plane resistivity in this tetragonal compound. Note that anisotropy remains the same from high to very low temperature in a cone of pressures centered on P2 at 2.3 GPa, indicative of local quantum criticality (NFL). Bottom panel: a color plot of the resistivity magnitude, normalized by its value at 5.2 GPa far away from the quantum-critical region. The highest resistivity is centered on the quantum-critical point at P2 where the superconducting transition temperature also is the highest. This correlation suggests that local quantum-critical fluctuations produce superconductivity.*

To understand the relationship between coexisting antiferromagnetism and superconductivity in $CeRhIn_5$, we developed a unique capability of field-angle dependent specific heat measurements under pressure and with it discovered a four-fold modulation in the specific heat in the superconducting state of $CeRhIn_5$. [4] This discovery is a direct indication that the superconductivity is unconventional.

In several respects, the ambient-pressure superconductor $CeCoIn_5$ appears to be a high-pressure analog of $CeRhIn_5$, but to establish this relation, it would be useful to apply a negative pressure to induce magnetic order. Because this is not possible, we attempted to induce a negative chemical pressure by substituting a small amount of In by Cd. Indeed, replacing only 1 or 2% of In atoms with Cd induced a temperature-substitution phase diagram that is the mirror image of Figure 1. In this case, we start from a superconductor $CeCoIn_5$, which itself is quantum critical, and induce a phase of coexisting superconductivity and antiferromagnetic order that evolves with increasing Cd concentration to a solely magnetic phase. Applying pressure to these Cd-doped $CeCoIn_5$ materials accurately reversed the effect of Cd substitution, and we could map the resulting temperature-doping-pressure phase diagram onto that of $CeRhIn_5$ by assuming that Cd acts as a negative chemical pressure. [5] However, there is no detectable change in the crystal volume, that is, no negative pressure. This suggests that the primary role of Cd substitution is to produce very slight changes in electronic density because Cd has one less electron than In. This conclusion is quite reasonable because we know that a slight decrease in the electronic density provided by Cd substitution should favor magnetic order. As a corollary, applying pressure to either $CeCoIn_5$ or $CeRhIn_5$ should increase the electronic density, accounting for our observations. However, this result does not account for why the quantum criticality in $CeCoIn_5$ can be described reasonably well by the standard model, but a local, Kondo-break down criticality describes $CeRhIn_5$. We believe this is a further clue to solving the quantum conundrum, namely that subtle details of electronic structure, determined in large part by electronic correlations, may be a deciding factor in the nature of the quantum criticality.

In the course of this research, the scientific community was surprised by reports of superconductivity near 50 K in two new families of materials, each of which contains layers of FeAs. Like the high-temperature superconductors based on CuO structural units, superconductivity in these new materials is induced by electronic doping that suppresses a magnetic transition, which is accompanied by a structural transition as well. By applying pressure to a new member of these families $CaFe_2As_2$, we have shown for the first time that superconductivity can be induced without electronic doping. This discovery [6] suggests that these new superconductors may be more like $CeRhIn_5$ than the CuO superconductors in which only electronic doping induces superconductivity. Under pressure, this material is structurally and magnetically more complex that $CeRhIn_5$ or $CeCoIn_5$, which has left open the question of the existence and consequences of quantum-critical fluctuations.

## Impact on National Missions

Discovering and understanding new states of matter, such as high temperature superconductivity, offers the potential for previously unimagined new energy and sensor technologies relevant to DOE missions. Research in this project has had the goal of uncovering the quantum nature of these new states, which is key to realizing new technologies, and directly supports the Laboratory's strategic goal to provide a fundamental understanding of materials, especially f-electron systems with strong electronic correlations. To achieve our goals, we have developed an ability to make specific heat measurements under pressure and simultaneously in a rotating magnetic field. This very powerful capability presently unique to Los Alamos, has formed the basis for new projects at the Laboratory and is being duplicated by others around the world.

## Publications


Jelbert, G., T. Sasagawa, J. D. Fletcher, T. Park, J. D. Thompson, and C. Panagopoulos. Measurement of low energy charge correlations in underdoped spin-glass La-based cuprates using impedance spectroscopy. 2008. *Physical Review B.* **78**: 132513.

Lee, H. O., E. Park, T. Park, F. Ronning, E. D. Bauer, and J. D. Thompson. Magnetism, structure and superconductivity in CaFe2As2. 2009. *Physical Review B.* **80**: 024519.

MenoncaFerreira, L., T. Park, V. A. Sidorov, M. Nicklas, E. M. Bittar, R. Lora-Serrano, E. N. Hering, S. M. Ramos, M. B. Fontes, E. Baggio-Saitovich, H. O. Lee, J. L. Sarrao, J. D. Thompson, and P. G. Pagliuso. Tuning the pressure-induced superconducting phase in doped CeRhIn5. 2008. *Physical Review Letters.* **101**: 0175005.

Nicklas, M., O. Stockert, T. Park, K. Habicht, K. Kiefer, L. D. Pham, J. D. Thompson, Z. Fisk, and F. Steglich. Magnetic structure of Cd-doped CeCoIn5. 2007. *Physical Review B.* **76** (5): 052401.

Park, T., E. D. Bauer, and J. D. Thompson. Probing the nodal gap in the pressure-induced superconductor CeRhIn5. 2008. *Physical Review Letters.* **101**: 177002.

Park, T., E. Park, H. O. Lee, T. Klimczuk, E. D. Bauer, F. Ronning, and J. D. Thompson. Pressure-induced superconductivity in CaFe2As2. 2008. *Journal of Physics: Condensed Matter.* **20**: 322204.

Park, T., F. Ronning, H. Yuan, M. B. Salamon, R. Movshovich, J. L. Sarrao, and J. D. Thompson. Hidden magnetism and quantum criticality in the heavy fermion superconductor CeRhIn5. 2006. *Nature.* **440**: 65.

Park, T., J. L. Sarrao, and J. D. Thompson. New quantum phase in the heavy-fermion superconductor CeRhIn5. 2007. *Physica C.* **460**: 137.

Park, T., J. L. Sarrao, and J. D. Thompson. Upper critical field scaling near a quantum critical point in the heavy-fermion compound CeRhIn5. 2007. *Journal of Magnetism and Magnetic Materials.* **310**: 712.

Park, T., M. J. Graf, L. Boulaevskii, J. L. Sarrao, and J. D. Thompson. Electronic duality in strongly correlated matter. 2008. *Proceedings of the National Academy of Sciences.* **105**: 6825.

Park, T., V. A. Sidorov, F. Ronning, J. X. Zhu, Y. Tokiwa, H. O. Lee, E. D. Bauer, R. Movshovich, J. L. Sarrao, and J. D. Thompson. Isotropic quantum scattering and unconventional superconductivity. 2008. *Nature.* **456**: 366.

Park, T., Y. Tokiwa, E. D. Bauer, F. Ronning, R. Movshovich, J. L. Sarrao, and J. D. Thompson. Normal state properties at a field-tuned quantum-critical point in the heavy-fermion superconductor CeRhIn5. 2008. *Physica B.* **403**: 934.

Pham, L. D., T. Park, S. Marquilon, J. D. Thompson, and Z. Fisk. Reversible tuning of the heavy-fermion ground state in CeCoIn5. 2006. *Phys. Rev. Lett..* **97**: 056404.

# Synthesis of Molecular Actinide Nitrides

*David L. Clark*
20061395PRD1

## Abstract

Many of the important properties that make actinide nitrides and oxides desirable as nuclear fuels are related to their electronic structure, which has been particularly difficult to determine experimentally. In this work, we focused our efforts on recent developments in electronic structure theory and x-ray spectroscopy to probe how the relative roles of atomic orbitals manifest themselves in the chemical bonding between actinide centers with light atoms such as oxygen and nitrogen. To accomplish this we developed two synchrotron x-ray experimental capabilities for actinides: ligand K-edge x-ray absorption spectroscopy (XAS) and non-resonant inelastic x-ray scattering (NRIXS). By combining the intensity data from NRIXS with the energy resolution of XAS, we can determine the roles of 5*f* and 6*d* orbitals in metal-ligand bonding, and how they interact with light atoms such as nitrogen and oxygen to make up metal-ligand bonds. Changes in the metal-ligand bonding result in changes in properties of materials. Electronic structure calculations are used as a guide to develop peak assignments in comparison to the experiments. The combination of these techniques to study light atoms and covalency in actinide materials is unique worldwide. The project developed this capability for Laboratory missions, provided new insights into actinide chemical bonding, and facilitated the conversion of the project's research lead - a Reines Postdoctoral Fellow - into a Los Alamos Technical Staff member.

## Background and Research Objectives

Many of the chemical properties of actinide nitrides and oxides that make them useful as nuclear fuels are governed by hybridization and covalency between the atomic orbitals that make up the metal-ligand bonds within the materials. The original scope of the project was to combine synthesis and electronic structure studies on metal nitrides, but recent experimental developments in synchrotron radiation studies led to a more focused study on electronic structure. Many of the important properties that make actinide materials such as nitrides and oxides desirable as fuels are related to their electronic structure, which has been particularly difficult to determine experimentally. In this work, we employed recent developments in electronic structure theory and x-ray spectroscopy to probe how the relative roles of atomic orbitals manifest themselves in the chemical bonding of these fascinating materials. To accomplish this we focused on the development of two synchrotron x-ray experiments: ligand K-edge x-ray absorption spectroscopy (XAS) and non-resonant inelastic x-ray scattering (NRIXS). In ligand K-edge XAS, one can examine bound state transitions in the x-ray absorption spectrum of ligand atoms (N, O, C, etc.) that arise due to covalent mixing between the metal and ligand atom (N, O, etc.). The intensity of the transition provides a direct measure of the relative contributions of 5*f* and 6*d* atomic orbitals in actinide metal-ligand bonding. At the extremely low energies of the first row atoms (N, O), XAS suffers from x-ray self-absorption effects. Another way to obtain the same information is through non-resonant inelastic x-ray scattering (NRIXS). The x-ray scattering is not subject to self-absorption, but does suffer from lower resolution and longer data acquisition time. By combining the intensity data from NRIXS with the energy resolution of XAS, we can determine the roles of 5*f* and 6*d* orbitals in metal-ligand bonding, and how they interact with light atoms to make up metal-ligand bonds. Changes in the covalency will result in changes in properties of materials. Electronic structure calculations are used as a guide to develop peak assignments in comparison to the experiments.

## Scientific Approach and Accomplishments

As part of our effort to understand fundamental electronic structure of nitrogen-containing materials, we developed a unique capability to measure core-electron transitions from light elements (nitrogen, oxygen) to empty 5*f* and 6*d* orbitals on actinide metal centers (Th, U, Np, Pu). Light atom x-ray spectroscopy turned out to

be far more complicated than originally envisioned, and therefore we also evaluated non-Resonant Inelastic X-ray Scattering (NRIXS). In both techniques, one can examine bound state transitions between 1*s* core electrons on the nitrogen or oxygen and virtual metal-based orbitals that arise due to covalent mixing between the metal and ligand atom (N, O, etc.). The intensity of the transition provides a direct measure of the relative contributions of 5*f* and 6*d* atomic orbitals in actinide metal-ligand bonding.

In order to work out the experimental details we turned to a discrete molecular system with a well understood electronic structure. Due to a paucity of discrete molecular metal nitrides we turned our attention to metal oxide anions as proof of principle. We performed a comparison of O K-edge XAS and NRIXS measurements conducted on symmetrical molecular $ReO_4^-$ anion. For the $ReO_4^-$ ion, electronic transitions from O 1*s* core electrons into the e and $t_2$ 5*d* molecular orbitals under $T_d$ symmetry, give rise to two pre-edge peaks in all four spectra. These assignments were confirmed by DFT calculations that simulate the spectra and provide oscillator strengths and energies for the transitions. The comparison of experimental FY data, curve fits of intensity, and time-dependent Density Functional Theory (TDDFT) simulation, are shown in Figure 1. Curve fitting reveals that peak areas from NRIXS and FY only differ by 0.6% while the other approaches differ by up to 30%. The large differences have been traced to physisorbed oxygen and sample pathlength. The NRIXS measurement, with higher penetration depth is not heavily influenced by physisorbed oxygen and surface contamination. Ground state electronic structure calculations indicate that total covalency for $ReO_4^-$ is 22%. At present, there is no experimental standard available for quantitative studies of covalency in O K-edge XAS. Therefore, we measured the FY O K-edge XAS of $MoO_4^{2-}$ and $WO_4^{2-}$, and used the O K-edge peak intensity of $ReO_4^-$ as a standard with 22% covalency. This gave experimental covalency values of 16% and 15% for $MoO_4^{2-}$ and $WO_4^{2-}$, respectively, which compare favorably to the values of 19% and 16% determined for these systems from DFT calculations. While clearly more developmental work is necessary, we believe that $ReO_4^-$ may serve as a useful intensity standard for O K-edge XAS, and allow us to evaluate covalency in metal-oxo bonds in actinide systems.

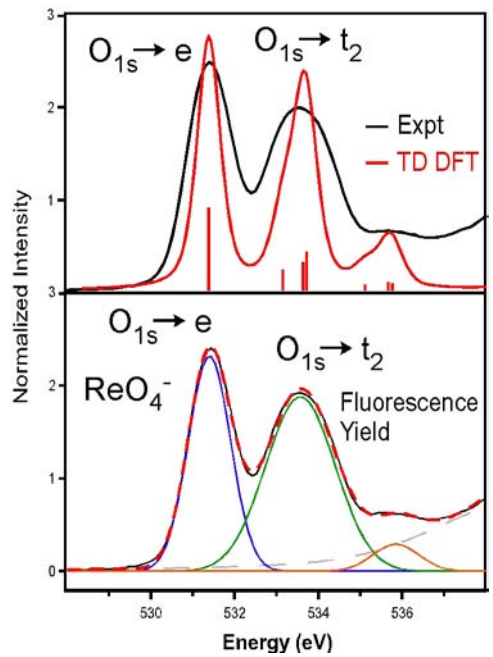


*Figure 1. Bottom – Data and fits to the pre-edge features of the O K-edge XAS of $NaReO_4$. Top – data (black) and simulated (red) pre-edge features for $NaReO_4$.*

For actinide systems, we turned to the class of actinyl oxo ions $AnO_2^{2+}$ (An = U, Np, Pu, and Am) that form a unique series of positively charged linear dioxo cations. These cations are remarkably stable, showing a high degree of covalency and chemical inertness with respect to the axial An=O bonds, which has a profound influence on their chemistry. Many studies in both theory and spectroscopy have helped to elucidate the nature of the chemical bond in this structural motif.[1] The metal orbitals have $6d_\sigma$, $6d_\pi$, $5f_\sigma$, and $5f_\pi$ symmetry giving an overall $\sigma^2_g\pi^4_g\sigma_u^2\pi_u^4$ electronic configuration, and a formal An□O triple bond. The use of 5*f* orbitals in π bonding may only take place at the very short bond distances seen in An=O bonds which span 1.74 – 1.80Å. Therefore, the actinyl ions are of great importance in order to truly assess the relative roles of 6*d* and 5*f* orbitals in chemical bonding, and the approach to An 5*f* – O 2*p* degeneracy within a common structural unit. For UHV studies of O K-edges of actinide systems, we developed an encapsulation of $Cs_2UO_2Cl_4$ in polystyrene with 12 Å of vapor-deposited graphite on the surface as an alpha-particle barrier within the UHV chamber. The O K-edge XAS spectrum from FY detection is shown in Figure 2 along with pre-edge peak fits. The FY spectrum is also compared to the single crystal spectrum reported by Denning and coworkers in 2002 that is the only other published example of O K-edge XAS on actinide molecular systems.[2] Our spectra give identical peak positions to Denning *et al.*, but do not suffer from x-ray self-absorption that is apparent as dramatic differences in pre-edge peak intensity between the two studies. The three pre-edge

peaks are assigned as O 1*s* core electron transitions into the virtual $5f_{\pi*}$, $5f_{\sigma*}$, and $6d_{\pi*}$ orbitals of the uranyl O□U□O unit. Curve fits give intensity data that compare extremely well with ground state electronic structure calculations when using $ReO_4^-$ as the intensity standard.

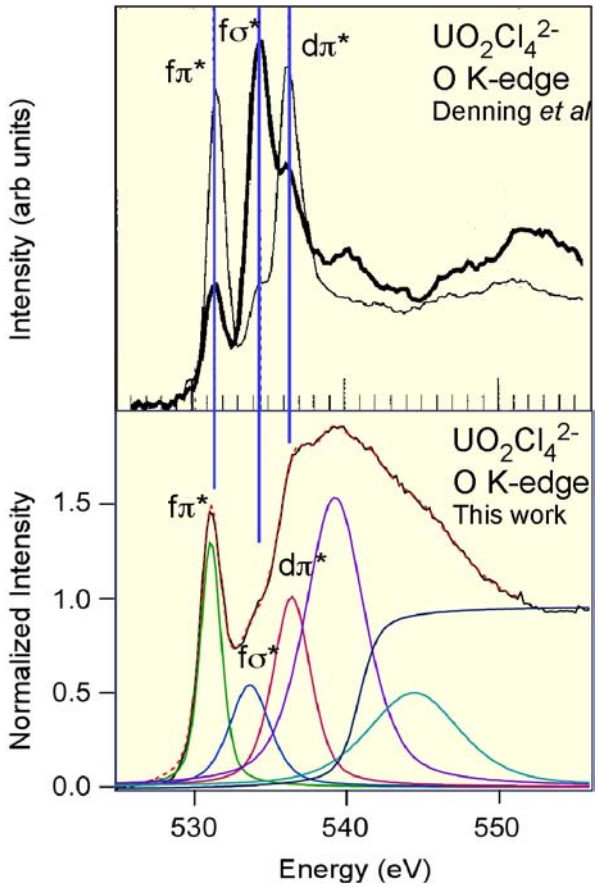


*Figure 2. Top – Single crystal O K-edge XAS Data for $Cs_2UO_2Cl_4$ showing perpendicular and parallel x-ray polarization, from Denning et al. Bottom – data (black) and fit (red) of the pre-edge features $Cs_2UO_2Cl_4$ obtained from FY detection. Individual curve fits are shown below the spectrum.*

## Impact on National Missions

The project goal was to develop new understanding of electronic structure in actinide materials with applications in advanced nuclear fuel and separations materials. This work established the principles for quantitative light atom x-ray studies for covalency determination. This application is unique worldwide and has given Los Alamos Leadership in this area. New understanding from such studies should make these materials more accessible for reactor and accelerator based systems, for long-term storage, and for efficient separations. Finally, this project served to provide a Reines Fellow with new experiences that led to his conversion to a Los Alamos staff member.

## References


1. Denning, R. G.. . 1992. *Structure and Bonding (Berlin, Germany).* **79**: 215.

2. Denning, R. G., J. C. Green, T. E. Hutchings, C. Dallera, A. Tagliaferri, K. Giarda, N. B. Brookes, and L. Braicovich. . 2002. *Journal of Chemical Physics.* **117** (17): 8008.


## Publications


Batista, E. R., P. Yang, R. L. Martin, S. A. Kozimor, S. D. Conradson, and D. L. Clark. Quantification of covalent interaction in actinide-ligand bonds. 2009. *Abstract of Papers, 238th ACS National Meeting, Washington, DC, United States, August 16-20, 2009.* : NUCL.

Clark, D. L., E. R. Batista, J. A. Bradley, K. S. Boland, C. J. Burns, S. D. Conradson, S. A. Kozimor, R. L. Martin, G. T. Seidler, M. P. Wilkerson, L. E. Wolfsberg, and P. Yang. Covalency in actinide metal-ligand bonds: New insights from synchrotron X-ray techniques and quantum chemical simulations. 2009. *Abstract of Papers, 238th ACS National Meeting, Washington, DC, United States, August 16-20, 2009.* : NUCL.

Clark, D. L., E. R. Batista, K. S. Boland, C. J. Burns, S. D. Conradson, S. A. Kozimor, P. J. Hay, R. L. Martin, D. E. Schwarz, M. P. Wilkerson, L. E. Wolfsberg, and P. Yang. Applications of X-ray absorption spectroscopy to the electronic structure of actinide ions. 2008. *Abstracts of Papers, 235th ACS National Meeting, New Orleans, LA, United States, April 6-10..* : NUCL.

Clark, D. L., E. R. Batista, K. S. Boland, C. J. Burns, S. D. Conradson, S. A. Kozimor, R. L. Martin, D. E. Schwarz, M. P. Wilkerson, L. E. Wolfsberg, and P. Yang. On the relative roles of 5f and 6d orbitals in uranium metal-ligand bonds. 2008. *Abstracts of Papers, 235th ACS National Meeting, New Orleans, LA, United States, April 6-10..* : INOR.

Clark, D. L., S. A. Kozimor, E. R. Batista, K. S. Boland, C. J. Burns, S. D. Conradson, R. L. Martin, M. P. Wilkerson, and L. E. Wolfsberg. Trends in covalency for d- and f-element metallocene dichlorides: Insights on theory and experiment from P. Jeffrey Hay. 2009. *Abstract of Papers, 238th ACS National Meeting, Washington, DC, United States, August 16-20, 2009.* : NUCL.

Conradson, S. D., A. Andersson, K. Boland, D. L. Clark, S. Kozimor, and X. J. Espinosa-Faller. Addressing the structural chemistry of UO2+x and PuO2+x with laboratory and computer experiments. 2008. *Abstracts of Papers, 235th ACS National Meeting, New Orleans, LA, United States, April 6-10..* : NUCL.

Graves, C. R., P. Yang, S. A. Kozimor, A. E. Vaughn, D. L. Clark, S. D. Conradson, E. J. Schelter, B. L. Scott, J. D. Thompson, P. J. Hay, D. E. Morris, and J. L. Kiplinger. Organometallic uranium(V)-imido halide complexes: from synthesis to electronic structure and bonding. 2008. *Journal of the American Chemical Society.* **130** (15): 5272.

Kozimor, S. A., E. R. Batista, K. S. Boland, C. J. Burns, C. N. Christensen, D. L. Clark, S. D. Conradson, P. J. Hay, R. L. Martin, D. E. Schwarz, M. P. Wilkerson, and P. Yang. Covalency trends in metallocene dichlorides (M = Ti, Zr, Hf, Th, U). A chlorine K-edge XAS study. 2008. *Abstracts of Papers, 235th ACS National Meeting, New Orleans, LA, United States, April 6-10..* : INOR.

Kozimor, S. A., E. R. Batista, K. S. Boland, J. M. Boncella, C. J. Burns, D. L. Clark, S. D. Conradson, R. L. Gdula, C. R. Graves, P. J. Hay, J. L. Kiplinger, L. P. Spencer, L. R. Martin, M. P. Wilkerson, L. P. Wolfsberg, and P. Yang. Utilizing oxygen k-edge X-ray absorption spectroscopy to compare covalency for d- and f-block metals. 2008. *Abstracts of Papers, 235th ACS National Meeting, New Orleans, LA, United States, April 6-10..* : NUCL.

Kozimor, S. A., P. Yang, E. R. Batista, K. S. Boland, C. J. Burns, C. N. Christensen, D. L. Clark, S. D. Conradson, P. J. Hay, J. S. Lezama, R. L. Martin, D. E. Schwarz, M. P. Wilkerson, and L. E. Wolfsberg. Covalency Trends in Group IV Metallocene Dichlorides. Chlorine K-Edge X-Ray Absorption Spectroscopy and Time Dependent-Density Functional Theory. 2008. *Inorganic Chemistry.* **47** (12): 5365.

Kozimor, S. A., P. Yang, E. R. Batista, K. S. Boland, C. J. Burns, D. L. Clark, S. D. Conradson, R. L. Martin, M. P. Wilkerson, and L. E. Wolfsberg. Trends in Covalency for d- and f-Element Metallocene Dichlorides Identified Using Chlorine K-Edge X-ray Absorption Spectroscopy and Time-Dependent Density Functional Theory. 2009. *J. Am. Chem. Soc..* **131** (34): 12125.

Wilkerson, M. P., J. M. Berg, D. L. Clark, S. D. Conradson, D. E. Hobart, and S. A. Kozimor. Electronic structure measurements of Cs2Np(VI)O2Cl4 using fluorescence emission and ligand k-edge X-ray absorption spectroscopies. 2008. *Abstracts of Papers, 235th ACS National Meeting, New Orleans, LA, United States, April 6-10..* : NUCL.

Yang, P., E. R. Batista, P. J. Hay, R. L. Martin, C. N. Carlson, D. L. Clark, S. D. Conradson, S. A. Kozimor, D. E. Schwarz, and M. P. Wilkerson. Quantification of covalency in An-Cl bonds. 2007. *Abstracts of Papers, 234th ACS National Meeting, Boston, MA, United States, August 19-23..* : NUCL.

# Accelerated Molecular Dynamics at Complex Interfaces

*Arthur F. Voter*
20061524PRD3

## Abstract

Simulating materials atom-by-atom with molecular dynamics (MD) is essential to understand their behavior. However, the timescale horizon of the standard simulation techniques is so restrictive that connection with relevant experiments is often extremely difficult. With conventional methods, one can run out of computer time before anything really happens in the (simulated) life of the material. While accelerated molecular dynamics (AMD) methods can alleviate this limitation in some cases, many complex, multi-timescale systems like complex interfaces are still out of reach. In this project, we develop new computational tools and generalize AMD methods --- like the super-state parallel replica dynamics (Par-Rep) and the self-learning hyperdynamics --- so that we are better equipped to tackle some of these challenging problems and provide previously unavailable information on the long timescale behavior of these systems. Applications of these new tools to solid-solid heteroepitaxial interfaces and to defect diffusion on free surfaces are presented.

## Background and Research Objectives

It has long been understood that many of the properties of materials ultimately stem from their atomic-scale structure and dynamics. For example, the band-gap of semi-conductors depends sensitively on the amount of dopants that are embedded within the system, but also on their precise organization, e.g., as isolated interstitials or as clusters. In order to be able to predict the behavior of novel materials or to optimize some of their desirable properties, we must thus be able to simulate their statics and dynamics directly at the atomic scale. The method of choice to do so is to simply integrate the equations of motions of the atoms, i.e., to perform MD. However, a downside of this approach is its significant computational cost that limits one to relatively small systems over short timescales (<1 microsecond). In many cases, this is too short to observe even a few topology changes (i.e., hops of a dopant). While massively parallel computers are routinely used to extend the spatial reach of MD up to trillions of atoms, novel methodological approaches are required to extend the timescales that can be reached by direct MD simulations.

In the last decade, we have developed powerful AMD methods [1,2,3] in order to address this issue. By capitalizing on large separations of timescales between the vibration of the system around a local minimum of the potential energy surface and the transition to basins of attraction of other minima (which are also called states), accelerations ranging from ten-fold to million-fold have been demonstrated on a wide variety of solid-state systems [4].

The various AMD methods however suffer from a common limitation: if the separation of timescales between vibration and topology change is small, then the possible computational gains become modest. This means that for many systems, our understanding is still limited to times below the microsecond wall of MD. A particularly problematic example occurs when an interface between two “phases” with very different kinetic properties is present. For example, corrosion can proceed as slow reactions occurring at the interface between a solid substrate and a liquid solution. In this case, vibrational motion of the atoms occurs on a picosecond timescale, topological transition in the liquid occurs on only slightly longer times (ten ps or so), while topological changes of the solid phase require anywhere between microseconds and seconds. Since the gap between vibrations and transitions is completely closed by the frequent topological changes in the liquid, conventional AMD method are inapplicable.

The main objective of this project was to generalize AMD methods so that they become applicable to systems where the gap between vibrations and transitions is too small for the conventional approaches to be efficient. As the project progressed, this objective was widened to include cases where such a gap usually exists but where

it varies considerably during the course of a simulation, so that adaptative methods are required to insure that both performance and accuracy are maintained. Significant effort also has been dedicated to the implementing these novel ideas in a new computational tool that is now the basis of many of the group's efforts.

## Scientific Approach and Accomplishments

In the first part of the project, we focused on the acceleration of complex interfaces where one fast "phase" exhibits very rapid kinetics compared to another "slow" phase. As stated above, conventional AMD methods rely on a large separation of time scales between vibrations of atoms within a state and escape from the state. However, this separation is not present in liquids where vibration and diffusion occur on similar time scales. A naive application of the AMD methods would thus be overwhelmed by the incessant change of state of the liquid, and wouldn't provide acceleration of the dynamics of the solid atoms, which is the quantity of interest. One way to solve this problem is to generalize the definition of a state such that a separation of timescale between intra-state and inter-state characteristic timescales is restored. If such a definition is possible, it then becomes straightforward to generalize the AMD methods.

A simple strategy to reach this goal is to define "super-states" based on the configuration of the slow degrees of freedom (DOF) in the system, i.e., every "micro-"state in which the slow DOF share the same configuration belong to the same super-state, notwithstanding the state of the fast DOF. If the typical time scale over which the fast DOF evolve is much faster than that of the slow DOF, the validity of the statistical framework upon which the AMD methods are based will be insured and their efficiency restored.

For typical solid/liquid interfaces --- for example, a metal in contact with water at room temperature --- this segregation of DOF into fast and slow subsets can be defined as follows: coordinates of the liquid atoms form the fast subset while coordinates of the solid atoms form the slow subset. Since topological transitions in liquids typically occur thousands of times faster than rearrangements of the solid atoms, this definition should be adequate. In the first year of the project, we demonstrated that this super-state definition is indeed appropriate for solid-liquid interfaces. However, this avenue was not pursued further in this LDRD project, as it became vital to an ongoing SciDAC effort on stress corrosion cracking in which we are involved [5]. Instead, we applied these ideas to an even more challenging problem, namely the simulation of complex solid-solid interfaces.

Indeed, while most liquids cleanly decouple from the slow kinetics at a wetted solid surface, other complex interfaces do not permit such a simple definition of super-states. For example, in the case of heteroepitaxial deposition of a solid onto another solid, a lattice mismatch at the interface can induce a multitude of very shallow potential energy basins. One such case is observed during the deposition of silver on a copper substrate. Since the lattice constant of silver is larger than that of copper, the two materials cannot share the same crystal structure: the core of the silver island instead tends to hover above the substrate, switching from one possible conformation to the next every few picoseconds, only a few times slower than typical vibration periods of the system. However, when the island relaxes to its equilibrium hexagonal shape (see Figure 1), two of its edges become pinned to the substrate. We showed that the dynamics of vacancy diffusion along these edges is the key factor controlling the long time behavior. This fact suggests that we can define super-states based on the conformation of the edges alone, the cores of the island being effectively "slaved" to those slow variables, a hypothesis that we then validated.

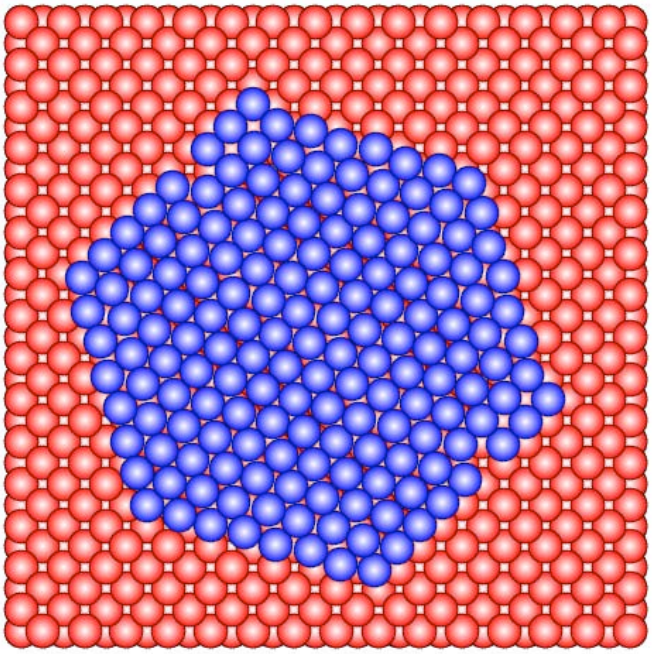

*Figure 1. Hexagonal island of silver (blue) on a copper substrate (red). Notice the presence of vacancies along two of the edges of the island.*

Our study showed that this complex interface system exhibits an extremely unusual behavior [6]. Indeed, it is commonly assumed that only isolated atoms or small islands (<10 atoms) move on surfaces. However, in this case, islands containing up to 217 atoms were seen to

diffuse as coherent units on timescales much shorter than that of a single atom hopping. By carrying out super-state Par-Rep at low temperature, we were able to identify the mechanism by which these islands are able to diffuse. We were also able to show that they exhibit a so-called magic-size behavior whereby small (<127 atoms) and large (>271 atoms) islands are essentially fixed while intermediate sizes diffuse very rapidly. This study was made possible because the super-state Par-Rep approach enabled significant speedup of the simulations despite the complexity of the system. In fact, we demonstrated that these simulations could scale up to 256 processors, making practical what would have taken years to achieve using standard MD, or even using standard AMD. This work demonstrates that super-state AMD methods considerably expand the applicability of AMD methods to complex systems by enabling the exploitation of any sufficiently large separation of timescales.

In the second part of the project, we tackled another problem that limits the application of AMD methods to complex systems. Many systems possess a very wide spectrum of transition timescales that varies strongly from state to state. For example, individual adatoms deposited on a silver (100) surface usually diffuse rather slowly because hopping is associated with a large (~0.5eV) activation barrier. However, if an adatom meets with two others and that they form a trimer, new transition with very low barriers (~0.2 eV) become available, thereby increasing the overall transition rate by a factor of a thousand or more. This kind of wildly varying characteristic timescales make the proper tuning of the AMD method very difficult.

For example, in hyperdynamics, one needs to design a bias potential that turns off in the vicinity of transition states (the top of the energy barriers that separate the different states) [2]. Since the speedup depends exponentially on the strength of this bias potential, it is imperative to make it as large as possible. However, if not carefully constructed, high bias regions can act as barriers that effectively isolate parts of the basin (and their associated transition pathways) from one-another. As a rule-of-thumb, if these bias-induced barriers are anywhere close to the height of some "real" transition barriers, then the dynamics will be corrupted. Coming back to the original problem, this mean that an aggressive bias potential will corrupt the kinetics out of states with low-barriers for escape. However, a potential tuned to handle the shallowest state will perform poorly on states surrounded by high barriers.

The solution to this problem involves the design of self-tuning or self-learning algorithms that automatically adapt themselves to the instantaneous characteristics of the system. Following this idea, we designed and implemented a self-learning hyperdynamics algorithm [4,7] that provides optimal accuracy and performance by constantly adapting to the system's behavior. Our algorithm relies on the efficient computation of the potential of mean force (PMF --- the averaged effective potential that a subset of the systems DOFs experiences) along the coordinates that are affected by the bias potential. By gradually ramping up the bias potential, hyperdynamics can be used to considerably speed up the calculation of the PMF and hence the optimal parameterization of the bias potential. The evolution of the hyper-time (the effective accelerated time) as a function of the MD time (the computational effort invested in the simulation) is shown in Figure 2 for two distinct states: a single monomer or a trimer sitting on a silver (100) surface. The results show that after a few ps of MD simulations, the self-learning algorithm starts to provide acceleration and that it reaches optimal performances in a few hundred ps. However, in the case of the fast state (the trimer) the speedup (the boost-factor, see inset) saturates at around 80 while it reaches almost 1000 for the slow one. This demonstrates that it is possible to efficiently reparametrize the bias potential for each new state that the system visits, thereby eliminating the need to provide a "one-size-fits-all" bias that would be severely sub-optimal in most complex systems where different states of the system possess very different kinetic characteristics. This method was also used during scoping runs for our Par-Rep simulations of nanowire stretching on Roadrunner (under LDRD 20080759ER). In this context, the method is very useful because the kinetic behavior of the wire is extremely sensitive to the imposed strain. As shown in Figure 3, the method naturally decreases the acceleration factor (the slope of the curve) when the system is trapped in shallow states, and ramps it back up once it stabilizes, insuring optimal performance and accuracy without external intervention.

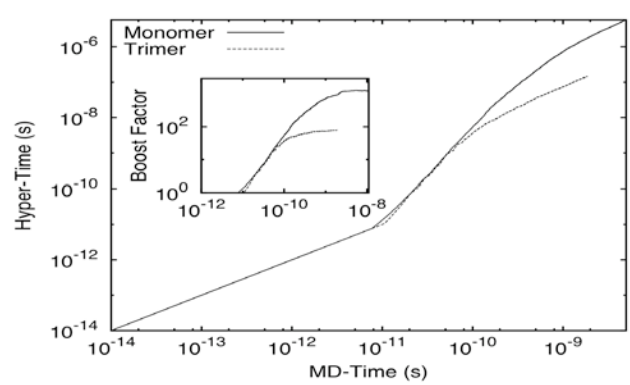


*Figure 2. Evolution of the hyper-time as a function of MD-time for a monomer and a trimer on a silver (100) surface at T=300K using self-learning hyperdynamics. Inset: Evolution of the corresponding boost (acceleration) factors as a function of MD-time.*

We also modified the Par-Rep method to make it more efficient in cases where repetitive fast transitions limit the efficiency and parallel scaling of the method. Indeed, the computational overhead of Par-Rep is controlled by the frequency of transitions since extra work is necessary to prepare independent replicas each time a new state is visited. The main improvement in this respect was the design of a state recognition algorithm that can determine if a given state (or a state equivalent under symmetry operations) has been visited before. If so, previously saved information can be recycled, hence amortizing the overhead cost and increasing the efficiency. Using this trick it becomes possible to increase the number of processors put to work and hence significantly decrease the time-to-solution.

Finally, significant effort has been dedicated to the implementation of a new computational tool that implements all the methodological improvements described above. This new code, called amdf, is now able to carry out MD, Par-Rep, super-state Par-Rep, driven Par-Rep, hyperdynamics, self-learning hyperdynamics, and even to combine these methods, e.g., Par-Rep hyperdynamics. It was used to carry out all of the simulations discussed above and it constitutes the basic framework that was ported to Roadrunner. This tool is now shared with internal and external collaborators. For example, it is the main computational tool used in a project lead by Ashlie Martini at Purdue University where we are studying interfacial friction at the nanoscale [8] using a flavor of Par-Rep appropriate for driven systems (i.e., systems subjected to time-dependent constraints) [9].

## Impact on National Missions

The main contribution of this project is to significantly extend the range of systems that are amenable to direct atomistic simulations over long timescales to include those which exhibit complex, multi-timescale kinetics, like complex interfaces. This enables us to tackle some pressing challenges facing the nation. For example, we have begun preliminary work in collaboration with the group of Michel Dupuis at PNNL on the possible application of self-learning hyperdynamics to the study of various water reactions on $TiO_2$ surfaces. These simulations could provide very important insights on how to optimize the production of hydrogen from water hydrolysis; a very promising way to address the pressing need for clean and renewable energy sources. This work thus contributed to the DOE missions in Energy Security, Nuclear Security, Environmental Responsibility, and Scientific Discovery and Innovation.

Another important contribution of this project is the development of amdf, a computational framework that provides a wide range of state-of-the-art AMD capabilities to LANL. This software demonstrated that it is able to exploit computers ranging from desktops to super-computers like Roadrunner to provide long-time information about the behavior of materials, information that is totally inaccessible through other means.

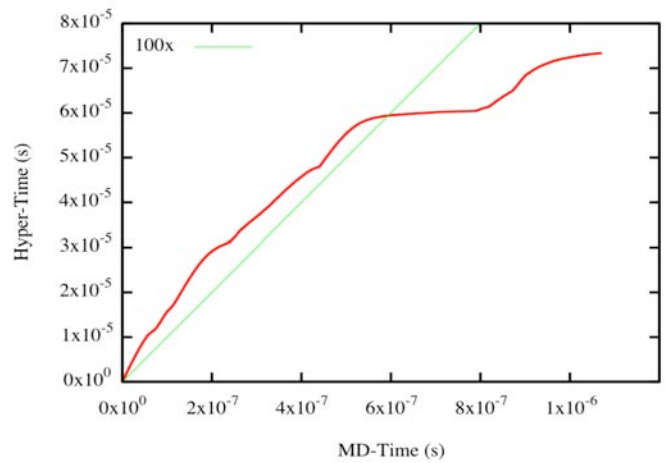


*Figure 3. Evolution of the hyper-time as a function of MD-time for a silver nanowire in the process of being stretched. The changes in the acceleration factor (the slope of the curve) reflect unsupervised adaptation by the self-learning algorithm. The green line represents a constant 100-fold acceleration.*

## References


1. Sorensen, M. R., and A. F. Voter. Temperature-accelerated dynamics for simulation of infrequent events . 2000. *Journal of Chemical Physics.* **112**: 9599.

2. Voter, A. F.. A method for accelerating the molecular dynamics simulation of infrequent events . 1997. *Journal of Chemical Physics.* **106**: 4665.

3. Voter, A. F.. Parallel replica method for dynamics of infrequent events. 1998. *Physical Review B* . **57**: 13985.

4. Perez, D., B. P. Uberuaga, Y. Shim, J. G. Amar, and A. F. Voter. Accelerated molecular dynamics methods: introduction and recent developments. 2009. In *Annual reports in computational chemistry.* By Wheeler, R. A.. Vol. 5, p. 79. The Netherlands: Elsevier.

5. Vashista, P., R. K. Kalia, A. Nakano, E. Kaxiras, A. Grama, G. Lu, S. Eidenbenz, A. F. Voter, R. Q. Hood, J. A. Moriarty, and L. H. Yang. Hierarchical petascale simulation framework for stress corrosion cracking. 2007. *Journal of Physics: Conference Series* . **78**: 012036 .

6. Uche, O. U., D. Perez, A. F. Voter, and J. C. Hamilton. Rapid diffusion of magic-size islands by combined glide

and vacancy mechanism. 2009. *Physical Review Letters.* **103**: 046101.

7. Perez, D., and A. F. Voter. Accelerating atomistic simulations through self-learning bond-boost hyperdynamics. *Journal of Chemical Physics.*

8. Martini, A., Y. Dong, D. Perez, and A. F. Voter. Low-speed atomistic simulation of stick-slip friction using parallel replica dynamics. 2009. *Tribology Letters.* **36**: 63.

9. Uberuaga, B. P., S. J. Stuart, and A. F. Voter. Parallel replica dynamics for driven systems: derivation and application to strained nanotubes. 2007. *Physical Review B .* **75**: 014301.

## Publications

Martini, A., Y. Dong, D. Perez, and A. F. Voter. Low-speed atomistic simulation of stick-slip friction using parallel replica dynamics. 2009. *Tribology Letters.* **36**: 63.

Perez, D., B. P. Uberuaga, Y. Shim, J. G. Amar, and A. F. Voter. Accelerated molecular dynamics methods: Introduction and recent developments. 2009. In *Annual reports in computational chemistry.* Edited by Wheeler, R. A.. Vol. 5, p. 79. The Netherlands: Elsevier.

Perez, D., and A. F. Voter. Accelerating atomistic simulations through self-learning bond-boost hyperdynamics. *Journal of Chemical Physics.*

Uche, O. U., D. Perez, A. F. Voter, and J. C. Hamilton. Rapid diffusion of magic-size islands by combined glide and vacancy mechanism. 2009. *Physical Review Letters.* **103**: 046101.

# A Chemical Route to Integrate Carbon Nanotubes into Microelectromechanical Systems

*Quanxi Jia*
20061615PRD4

## Abstract

As mechanical elements, carbon nanotubes (CNTs) are amongst the strongest known fibers. CNTs can undergo large nonlinear deformations or even buckling without permanent damage to the atomic structure, and have demonstrated exceptionally high thermal conductivity. These unique properties allow for many potential applications. To study the mechanical and electrical properties of CNTs, our first step was to optimize the growth parameters for CNTs with desired properties. We have successfully synthesized CNTs using chemical vapor deposition. We for the first time used a chemical route to connect CNTs to Si surface based on hydrogen bonds and electrostatic interactions at room temperature. We also used polymer/carbon nanotubes (CNTs) composite films to enhance both the mechanical and electrical properties. Due to the exceptional length of these high-quality CNTs and the ease of loading them into polymer polyethyleneimine (PEI), the PEI/CNTs composite films exhibit good conductivity.

## Background and Research Objectives

There is currently great interest in the controlled synthesis of CNTs with unique structures [1]. The functionality of CNTs can be significantly tailored by control of their diameter, length, alignment and areal density. CNT arrays, in which CNTs are nearly parallel to each other and perpendicular to the substrate, have been widely investigated for many promising applications, such as field emission devices, energy storage, gas sensors, and structural composites. Controlling the morphology of CNT array is an essential step towards these applications. Furthermore, CNT fibers have attracted great efforts. The extremely high strength and low density of CNTs make them very promising candidates for ultra-strong and light-weight fibers. Pioneer works have reported CNT fibers prepared by gas-state spinning from reaction furnace and wet-spinning from CNT solutions, but the performance was highly limited by CNT dispersion, alignment, and length. To achieve real applications in the industry, both the performance and synthesis method of CNT fiber need to be improved. A breakthrough has been made when continuous CNT yarns were directly drawn from a vertically aligned CNT array, which leaded to dry-spun CNT fiber and CNT sheet with more interesting applications.

It should be noted that CNTs are amongst the strongest known fibers [2]. Carbon nanotubes can undergo large nonlinear deformations or even buckling without permanent damage to the atomic structure, and have demonstrated exceptionally high thermal conductivity. These unique properties allow for many potential nanosystem functions such as large non-linear deflections in nanotube supported structures and resonant sensors with molecular level mass sensitivity. However, the electromechanical traits of CNTs have typically been characterized using atomic force microscope. In this project, our objective is to use more economical microsystem technology as a flexible platform to study the mechanical and electrical properties of CNTs. To accomplish this goal, our first step is to investigate the growth parameters for CNTs and their composite, and the electrical properties of CNTs.

## Scientific Approach and Accomplishments

We used chemical vapor deposition (CVD) to grow CNTs. The CVD process was performed in a 1 inch (2.54 cm) diameter quartz tube furnace. A film of Fe(1.0 nm)/$Al_2O_3$(10 nm), which was deposited on Si wafers with 1 µm $SiO_2$ layer, were used as catalyst. Forming gas (Ar with 6% $H_2$) was used as carrier gas, and ethylene served as carbon source. CNT growth was carried out at 750°C with 140 sccm forming gas and 30 sccm ethylene for 10 min. Thin and clean CNT fibers (see Figure 1) were spun from arrays of well-aligned, millimeter-long CNTs.

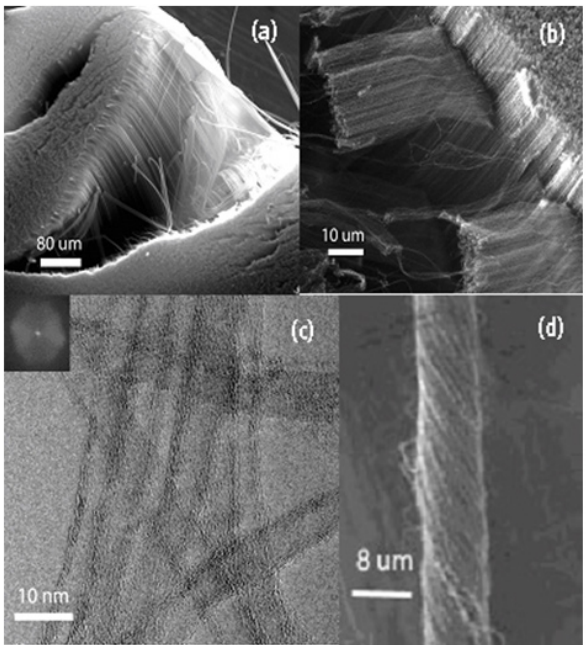


*Figure 1. Field-emission scanning electron microscopy (SEM) images of carbon-nanotube arrays from different angles: (a) and (b); high resolution transmission electron microscopy image of carbon nanotubes: (c); te field-emission SEM image of a carbon nanotube fiber: (d).*

We have used a chemical route to connect CNTs to Si surface based on hydrogen bonds and electrostatic interactions at room temperature. In other words, molecular interaction in chemistry provides a simple and flexible route to the integration of CNTs with Si. We have used polyethylenimine (PEI) as a reagent. It is well known that there are many nitrogen atoms in cationic polymers. The positive nitrogen charges facilitate the hydrogen bonding and electrostatic interactions between molecules. Furthermore, PEI is a soluble reagent under physiological conditions. Therefore, this technology can be potentially applied to nano-biomedical therapeutic devices.

The connection between CNTs and Si has been verified by scanning electron microscopy (SEM) as shown in Figure 2. SEM shows an intact CNT fiber, which is 8.2 μm in diameter and 5 cm in length. The CNT fiber appears compact. Dispersed oxidized tips of CNT fiber shows more contacting area between the CNTs and the Si. It should be noted that it is easy to join PEI-terminated Si and CNT via electrostatic interactions. SEM clearly shows that many carbon nanotubes around the fiber tip are in good contact with the Si. Furthermore, the CNT fibers keep their pristine structure and shape. It is known that the functionalized surface-bound CNTs lose some of their electric and optical properties since it takes a change of only about 1 in 100 carbons along CNTs to cause a loss of the sensitive UV van Hove singularities. In addition, the active central parts of CNTs cannot remain unperturbed when the CNTs' surface structure is modified. Therefore, this Si-PEI-CNT junction could supply the basis for directing CNTs to precise links in electronic, optical, and sensor arrays.

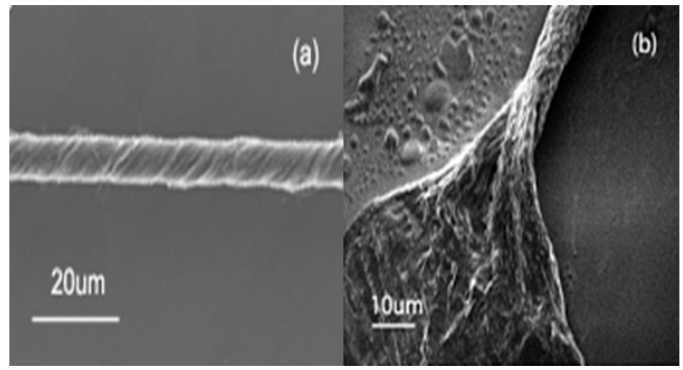


*Figure 2. (a) SEM images of a single CNT fiber; connection of a CNT fiber's tip to Si (b).*

We have also prepared CNT - polymer polyethyleneimine (PEI) composite films by a spin-coated process. This solution is composed of homogeneous long CNTs in water-soluble PEI. Figure 3 shows the surface morphologies of the PEI/CNT composite film. As can be seen from Figure 3a, the composite film is very uniform. The enlarged image in Figure 3b exhibits the high loading of CNTs in the composite films. And the CNTs tightly combine with each other with the assistance of PEI. The high density of CNTs is very helpful to improve the conductivity of the PEI/CNT composite film. Due to long length CNTs and their easy loading in PEI, the CNT/PEI composite films exhibit enhanced conductivity. The conductivity of the composite films is steadily improved as the concentration of CNTs increases. Figure 4 shows conductivity of composite films as a function of loading concentrations of CNTs. It is found that the concentration of CNTs has a significant effect on the conductivity of the composite films. The conductivities are 0.01, 0.21, 31.12, and 43.73 S/cm when the concentration of CNTs is 0.05, 0.5, 1, and 3 wt%, respectively. Although PEI shows insulating characteristic, the conductivity of the composite films increases rapidly to 0.01 S/cm with a small amount of CNT inclusion (~ 0.05 wt%). In comparison with the conductivities of other composite films with low loading of CNTs, the present composite films show even higher conductivities. We believe that the large aspect ratio and the nanoscale dimension of nanotubes play very important roles in enhancing the electrical conductivity of the PEI/CNT composite films with low loading of CNTs. In the PEI/CNT composites with low loading concentration of CNTs, Bai et al reported orders of magnitude enhancement of conductivity when the CNTs' length was increased from 1 to 50 μm [3]. In our case, the length of CNTs, in average, is about 5 mm. In addition, well-dispersed nanotubes

have higher effective aspect ratio than that of nanotube aggregates. Both the large aspect ratio of long CNTs and good dispersion of CNTs in polymer have key effects on the conductivity of composites with low concentration of CNTs.

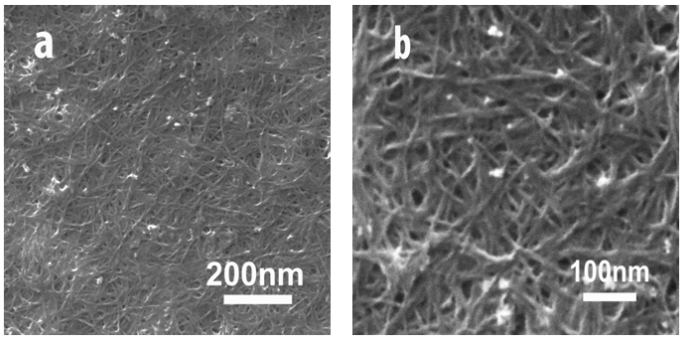


*Figure 3. Scanning electron microscopy images of PEI/CNT composite films with different magnifications.*

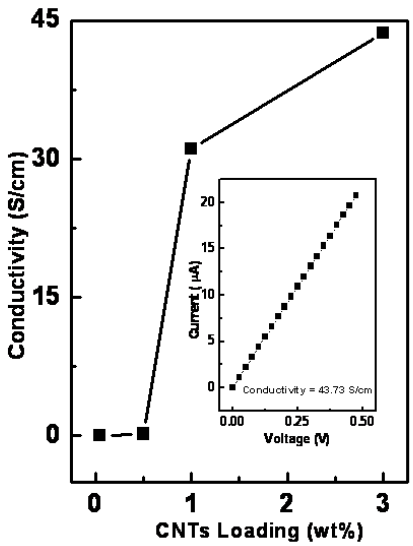


*Figure 4. The conductivity of composite films as a function of loading concentrations of CNTs; Inset presents the current vs voltage characteristic of composite film with 3 wt% CNTs loading.*

## Impact on National Missions

This project supports DOE's missions in nanotechnology, energy security, and sensors for threat reduction applications. This work opens the way to the electromechanical characterization of CNTs. It also provides a better understanding of the fundamental physics of novel materials.

## References


1. Demczyk, B. G., Y. M. Wang, J. Cumings, M. Hetman, W. Han, A. Settl, and R. O. Ritchie. Direct mechanical measurement of the tensile strength and elastic modulus of multiwalled carbon nanotubes . 2002. *Mater. Sci. Eng..* **334** (1-2): 173.
2. Hata, K., D. N. Futaba, K. Mizuno, T. Namai, M. Yumura, and S. Iijima. Water-assisted highly efficient synthesis of impurity-free single-waited carbon nanotubes. 2004. *Science.* **306** (5700): 1362.
3. Bai, J. B., and A. Allaoui. Effect of the length and the aggregate size of MWNTs on the improvement efficiency of the mechanical and electrical properties of nanocomposites - experimental investigation . 2003. *Composites Part A.* **34** (8): 689.


## Publications


Zhang, Y. Y., G. Zou, S. K. Doorn, H. Htoon, L. Stan, M. E. Hawley, C. J. Sheehan, Y. T. Zhu, and Q. X. Jia. Tailoring the morphology of carbon nanotube arrays: from spinnable forests to undulating foams . 2009. *ACS Nano.* **3**: 2157.

Zou, G., H. Luo, E. Bauer, T. M. McCleskey, A. K. Burrell, and Q. X. Jia. General chemical solution route to epitaxial carbide films . *the 238th ACS National Meeting & Exposition.* (Washington DC, 2009).

Zou, G., H. Luo, F. Ronning, B. Sun, T. M. McCleskey, A. K. Burrell, and Q. X. Jia. A facile chemical solution deposition to high mobility epitaxial Ge films on Si. *Angewandte Chemie International Edition .*

Zou, G., H. yang, M. Jain, H. H. Zhou, D. Williams, M. Zhou, A. K. Burrell, T. M. McCleskey, and Q. X. Jia. Vertical connection of carbon nanotubes to silicon at room temperature using a chemical route. 2009. *Carbon.* **47**: 933.

Zou, G., M. Jain, H. H. Zhou, H. M. Luo, S. A. Baily, L. Civale, E. Bauer, T. M. McCleskey, A. K. Burrell, and Q. X. Jia. Ultrathin Epitaxial Superconducting Niobium Nitride Films Grown by a Chemical Solution Technique. 2008. *Chem. Commun..* **45**: 6022.

Zou, G., M. Jain, H. Yang, Y. Y. Zhang, D. Williams, and Q. X. Jia. Recycling and electrically conducting carbon nanotube composite films. *Nanoscale.*

Zou, G., M. Jian, H. Luo, T. M. McCleskey, A. K. Burrell, and Q. X. Jia. NbN films by chemical solution deposition. Presented at *APS March meeting.* (New Orleans, 10-14 March, 2008).

Zou, G., T. McCleskey, A. Burrell, and Q. X. Jia. Connection of carbon nanotubes to silicon using chemical route atroom temperature. *236th ACS National Meeting & Exposition.* (Philadelphia, Pennsylvania, 2008).

# Molecular Actinide Alkylidene Complexes

*Jaqueline L. Kiplinger*
20070525PRD1

## Abstract

This is the final report of a two-year Director's Funded Postdoctoral project at Los Alamos National Laboratory. The project started in December 2006 and ended at the beginning of December 2008. As indicated by the title, the original objective of this project was to prepare uranium alkylidene complexes, which are compounds containing U=C bonds. However, a game-changing discovery during the early stages of this project uncovered a general and versatile route for the synthesis of pentavalent uranium complexes by the 1-electron oxidation of tetravalent uranium complexes with copper(I) salts. This is remarkable because it has long been held that uranium in the pentavalent oxidation state, U(V), is unstable in solution and prone to redox disproportionation to generate the more stable oxidation states U(IV) and U(VI). The copper oxidation protocol systematically overturned this established dogma by enabling the preparation of an entirely new class of molecular complex containing stable U(V) in nonaqueous solution. A milestone in the history of actinide chemistry, this disclosure quickly catalyzed an explosion of activity in the field as evidenced by follow-up papers on pentavalent uranium. Finally, the copper(I)-based oxidation chemistry was also found to provide easy chemical control over uranium in oxidation states ranging from U(III) to U(VI). The large range of accessible oxidation states using a single non-toxic reagent is unprecedented and has substantial implications for actinide separations schemes and longer-term impact for advanced nuclear fuel cycles.

## Background and Research Objectives

The original objective of this project was to prepare uranium alkylidene complexes, which are compounds containing U=C bonds. However, a game-changing discovery during the early stages of this project uncovered a general and versatile route for the synthesis of pentavalent uranium complexes by the 1-electron oxidation of tetravalent uranium complexes with copper(I) salts. The new research objectives for this project became to collect a large amount of previously unavailable information on the chemistry and electronic structure of this rare uranium oxidation state, which as discussed below represents a very important step-forward in our understanding of chemistry, properties and bonding in the actinides.

Although uranium has various oxidation states (III, IV, V, VI) in both solution and the solid-state, the trivalent, tetravalent and hexavalent complexes have dominated the landscape of uranium chemistry, with the corresponding pentavalent systems remaining comparatively rare. Historically, this deficit has been attributed to the instability of pentavalent uranium toward redox disproportionation in aqueous solution to produce the more stable oxidation states U(IV) and U(VI). This instability also reflects the extreme air and water sensitivity of pentavalent uranium and its easy conversion/oxidation to hexavalent uranium in the presence of trace amounts of oxygen or water. Generally speaking, until the discoveries made during the course of this project, rational synthetic schemes were simply unknown and the few reported molecular U(V) systems came from serendipitous discoveries that were not reproducible. As a consequence, very little was known about pentavalent uranium.

In recent years, techniques for handling and characterizing air- and water-sensitive materials have vastly improved, enabling a variety of new approaches for synthesizing pentavalent uranium compounds. In fact, in what can only be described as a renaissance in research activity in the field over the past few years, uranium(V) has been shown to be far more stable than previously thought, and its chemistry is important in understanding the behavior of actinides in the environment, corrosion, waste, the nuclear fuel cycle and long-term storage of spent nuclear fuel. For

example, this once discounted uranium oxidation state has been implicated in the low–temperature chemistry of uranium in reducing, heterogeneous aqueous systems, the biogeochemical reduction of uranium in the environment, and the immobilization of actinides in the environment.

These single-electron systems provide fertile ground for not only advancing theoretical capabilities but also our fundamental understanding of actinide electronic structure, reactivity and bonding. For example, because electron repulsion is absent and at most six transitions are allowed in the optical spectrum, the $f^1$ electronic configuration facilitates the interpretation of spectroscopic and magnetic data. Additionally, convergence difficulties in Density Functional Theory (DFT) calculations can occur for actinide complexes with multiple unpaired electrons; however, the $f^1$ electronic configuration in U(V) minimizes these problems compared to systems in lower oxidation states (i.e. $f^2$, $f^3$). Combined, these techniques provide important insight into 5f element electronic structure and how it manifests itself physically in molecular solution and solid-state structure, as well as chemically through its influence on spectroscopic and thermodynamic properties. Ultimately, this knowledge will enhance our overall ability to reliably predict the chemical behavior of f-element compounds in applications such as stockpile stewardship, environmental remediation, and waste management within the DOE complex.

## Scientific Approach and Accomplishments

**Pentavalent Uranium Chemistry – From Synthesis to Electronic Structure and Bonding**

During our efforts to prepare uranium alkylidene complexes ($U{=}CR_2$) we discovered a general and versatile route for the synthesis of organometallic pentavalent uranium-imido halide complexes by the 1-electron oxidation of tetravalent uranium-imido complexes with copper(I) salts (Figure 1). Although examples of tetravalent and hexavalent uranium compounds are prevalent in the literature, the corresponding U(V) systems are scarce with little accompanying characterization data. As such this discovery was quite exciting as it enabled a complete study of the electronic structure and bonding in pentavalent uranium systems. From a heuristic perspective, the U(V) oxidation state with its simple $5f^1$ valence electronic configuration remains a highly attractive target. Over the course of this project, a whole suite of U(V) complexes $(C_5Me_5)_2U(=N\text{-}Ar)(X/Y)$ (where X=F, Cl, Br, I; Y=OTf, SPh, SePh, TePh, $NPh_2$, OPh, Me, Ph, C≡CPh, $N{=}CPh_2$) were prepared. This series includes the first examples of pentavalent uranium with anionic sp, $sp^2$, and $sp^3$ carbon moieties other than carbocyclic ($C_5R_5$, $C_7H_7$, $C_8H_8$) ligands as well as the first selenate and tellurate systems. That a wide range of substituents can be supported within the wedge of these U(V)-imido complexes refutes prior assertions that pentavalent uranium complexes are inherently unstable.

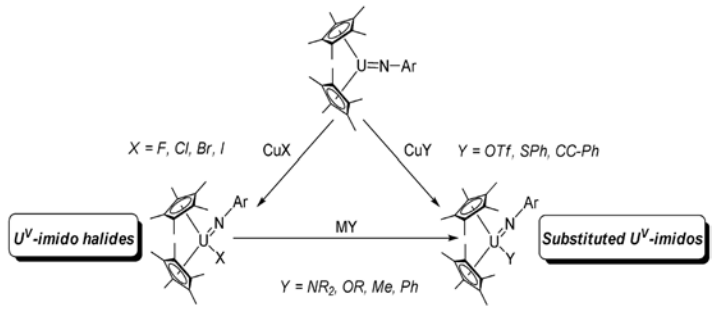


*Figure 1. Synthesis of substituted U(V) complexes.*

The series of $(C_5Me_5)_2U(=N\text{-}Ar)(X/Y)$ (where X=F, Cl, Br, I; Y=OTf, SPh, SePh, TePh, $NPh_2$, OPh, Me, Ph, C≡CPh, $N{=}CPh_2$) complexes with electronically diverse X/Y ligands and studied using a combination of cyclic voltammetry, UV-visible-NIR absorption spectroscopy, and variable-temperature magnetic susceptibility, which provide a coherent description of the electronic structure of these pentavalent systems and indicate that both the U-X/Y and U=N bonds exhibit covalency. All of the pentavalent uranium compounds exhibit U(VI)/U(V) and U(V)/U(VI) redox couples by voltammetry. The potential separation between these metal-based couples remaining essentially constant at ~1.50 V, but both processes shift in tandem in potential by ~700mV across the series of X/Y ligands. Temperature dependent magnetic susceptibilities are reported for all complexes with $\mu_{eff}$ values ranging from 2.22-2.53 μB. The onset of quenching of orbital angular momentum by ligand fields is observed to occur ~40 K in all cases. There are no significant differences between $\mu_{eff}$ values or temperature dependencies in the magnetic susceptibility based on the identity of the ancillary X/Y ligand. However, an excellent linear correlation was observed between the chemical shift values of the $C_5Me_5$ ligand protons in the $^1H$ NMR spectra and the oxidation potentials of $(C_5Me_5)_2U(=N\text{-}Ar)(X/Y)$, suggesting that there is a common origin – overall σ-/π-donation from the ancillary X/Y ligand to the metal, contributing to both observables. As illustrated in Figure 2, combined, these data confer the following trend in increasing σ/π-donating ability of the X/Y ligand to the U(V) metal center: OTf < I < Br < Cl < SPh < C≡CPh < F < [OPh ~ Me ~ Ph] << $NPh_2$ < $N{=}CPh_2$.

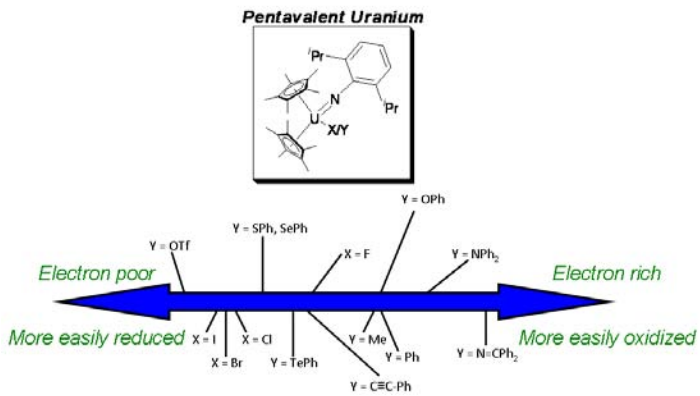


*Figure 2. Showing the effect of ligand substitution (X/Y) on the electronics of the $(C_5Me_5)2U(=N\text{-}2,6\text{-}iPr_2\text{-}C_6H_3)(X/Y)$ complexes.*

The electronic spectra are comprised of π-π* and π→$nb_{5f}$ transitions involving electrons in the metal-imido bond, and metal-centered f-f bands illustrative of the $5f^1$ valence electron configuration. Two distinct sets of bands have been attributed to transitions derived from this $5f^1$ configuration, and the intensities in these bands are increased dramatically over those found in spectra of classical $5f^1$ actinide coordination complexes. Density functional theory (DFT) results for the model complexes $(C_5Me_5)_2U(=N\text{-}Ph)(F)$ and $(C_5Me_5)_2U(=N\text{-}Ph)(I)$ show good agreement with experimental structural and electrochemical data and provide a basis for assignment of spectroscopic bands. The bonding analysis describes multiple bonding between the uranium metal center and imido nitrogen which is comprised of one σ- and two π-interactions with variable participation of 5f and 6d orbitals from the uranium center. When considered in the broader context of other recent results for organouranium complexes, the results obtained for the U(V)-imido complexes $(C_5Me_5)_2U(=N\text{-}Ar)(X/Y)$ provide an important bridge between those for U(VI)-bis(imido) systems (e.g., $(C_5Me_5)_2U(=N\text{-}Ar)_2$) that have long been regarded as possessing substantial covalency in the metal-ligand multiple bonds and the more recent data for U(IV)-ketimide systems (e.g., $(C_5Me_5)_2U(\text{-}N{=}C\text{-}Ar_2)_2$) that possess metal-ligand bonding intermediate between single and double bonds based on structural data. All three systems, $(C_5Me_5)_2U(=N\text{-}Ar)_2$, $(C_5Me_5)_2U(=N\text{-}Ar)(X/Y)$, and $(C_5Me_5)_2U(\text{-}N{=}CAr_2)_2$, exhibit similar experimental hallmarks for covalent metal-ligand bonding. While it is not possible to make quantitative comparisons regarding the degree of covalency from the existing data, the emerging picture is that all three uranium oxidation states are able to support covalent bonding in these organometallic complexes.

**Trivalent Uranium Oxidation Chemistry**

Finally, during this project we also found that the copper(I)-based oxidative functionalization protocol provides a simple and mild method for synthesizing the corresponding U(IV) complexes in good yield (Figure 3). Reaction of the trivalent uranium complexes $(C_5Me_5)_2UI(THF)$, $(C_5Me_5)_2U[N(SiMe_3)_2]$, $(C_5Me_5)_2U(NPh_2)(THF)$ and $(C_5Me_5)_2U(\text{-}O\text{-}2,6\text{-}{}^iPr_2\text{-}C_6H_3)(THF)$ with copper(I) iodide affords the corresponding tetravalent uranium diiodide, amide-iodide, and aryloxide-iodide complexes $(C_5Me_5)_2UI_2$, $(C_5Me_5)_2U[N(SiMe_3)_2](I)$, $(C_5Me_5)_2U(NPh_2)(I)$ and $(C_5Me_5)_2U(\text{-}O\text{-}2,6\text{-}{}^iPr_2\text{-}C_6H_3)(I)$, respectively. This protocol was also extended to the synthesis of the alkyl-iodide complex $(C_5Me_5)_2U(CHPh_2)(I)$. The isolation of this complex from the *in situ*-generated trivalent uranium alkyl complex $(C_5Me_5)_2U(CHPh_2)(THF)$ illustrates the synthetic value of this oxidation procedure in those situations where the U(III) metallocene complex cannot be isolated or is unstable. Over-oxidation and ligand redistribution are not observed with this Cu-based U(III)→U(IV) oxidation procedure, making it an attractive synthetic alternative to the existing routes for the preparation of mixed-ligand metallocene complexes of the type $(C_5Me_5)_2U(X)(Y)$ (where X = halogen; Y = alkyl, amide, aryloxide, etc.).

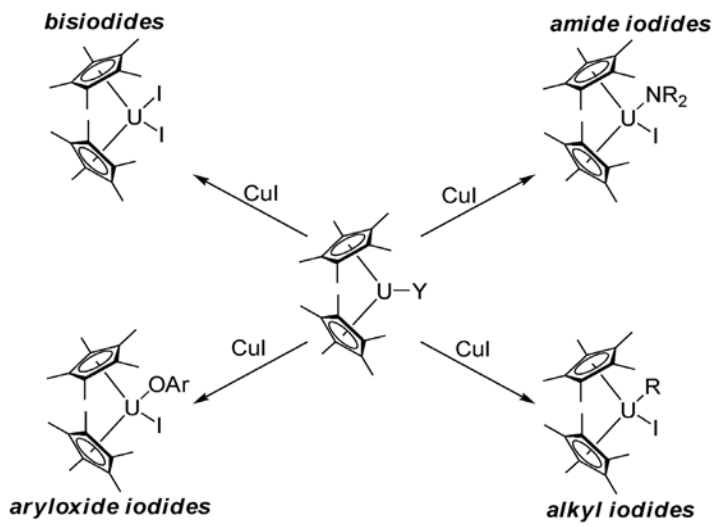


*Figure 3. Synthetic procedure for the 1-electron oxidation of organometallic U(III) complexes to their U(IV) counterparts with copper(I) iodide.*

**Notable Accomplishments/Impact**

The efforts funded by this project have already resulted in 12 publications in print, with 3 more publications currently in preparation, and 11 invited presentations at conferences, universities, companies, and national laboratories. Based chiefly on these accomplishments the research produced during the course of this project has received international acclaim through no less than 3 journal covers as shown in Figure 4. Before our work, the last review on pentavalent uranium chemistry was published in 1969. The impact of the LANL pentavalent chemistry studies has been evidenced by the large number

of papers that have appeared on pentavalent uranium complexes following our initial disclosure. It is now a hot field and accordingly we were invited to write a review on this body of work. This review appeared this year in *Chemical Communications* (**2009**, 3813-3968) as a Feature Article entitled "*Pentavalent Uranium Chemistry – Synthetic Pursuit of a Rare Oxidation State*." Additionally, the postdoctoral research associate working on this project was recognized for his scientific contributions by a LANL Award for Outstanding Achievement and Dedication (2007), the LANL Postdoctoral Distinguished Performance Award (2008), the Postdoctoral Publication Prize in Experimental Sciences, Los Alamos National Laboratory (2009), and a LANL Glenn T. Seaborg Postdoctoral Fellowship (2008-2009).

*Figure 4. Representative journal covers that the work in this project has garnered.*

## Impact on National Missions

The chemistry of the actinide elements is critical to DOE nuclear weapons mission areas (stockpile stewardship, environmental remediation, waste management). The synthesis of new actinide compounds not only provides important information about metal-ligand bonding but also improves our ability to reliably predict chemical behavior in a variety of environments. As evidenced by this project, the DOE complex and LANL clearly benefits from simple exploratory research. Although silver salts have been successfully utilized as chemical oxidants, these were the first examples demonstrating the oxidation and functionalization of organometallic species using $Cu^{I}$ salts. This copper route also avoids the use of silver and thallium salts (RCRA-listed), thereby greatly diminishing the generation of mixed radioactive hazardous waste and potential exposure to highly toxic thallium reagents. As such, the copper(I)-based oxidation chemistry provides easy chemical control over uranium in oxidation states ranging from U(III) to U(VI). The large range of accessible oxidation states using a single non-toxic reagent is unprecedented and has substantial implications for actinide separations schemes and longer-term impact for advanced nuclear fuel cycles. Outside of our group, the value of this protocol is being noticed by other groups throughout the chemistry community and has been successfully extended to other uranium chemistry. Finally, this new copper-based oxidation protocol avoids the generation of mixed low-level radioactive hazardous waste and reduces labor hours and money spent in management of this waste stream. Notably, research from this project lay the foundation for a *2009 LANL Pollution Prevention Award* in recognition of the numerous attractive features this chemistry (including a ~50-fold decrease in waste treatment and disposal costs) offers LANL and the DOE complex (Figure 5).

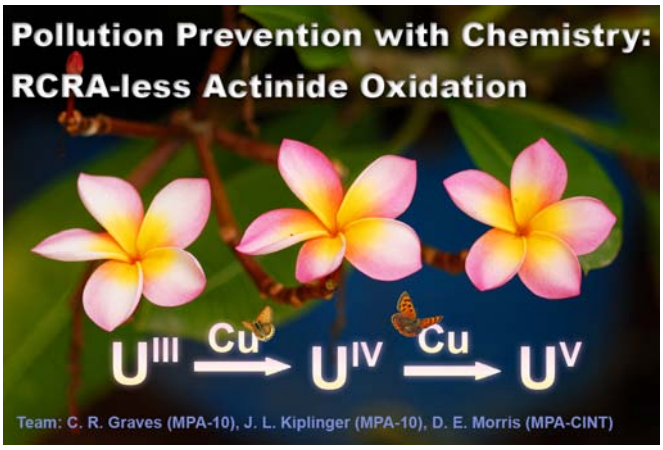


*Figure 5. Graphic highlighting the copper-based actinide oxidation chemistry which was awarded a 2009 Pollution Prevention Award sponsored by the Environmental Protection Division Risk Reduction Office at LANL.*

## Publications

Cantat, T., C. R. Graves, B. L. Scott, and J. L. Kiplinger. Challenging the Metallocene Dominance in Actinide Chemistry with a Soft PNP Pincer Ligand: New Uranium Structures and Reactivity Patterns. 2009. *Angewandte Chemie, International Edition.* **48**: 3681.

Cantat, T., C. R. Graves, K. C. Jantunen, C. J. Burns, B. L. Scott, P. J. Hay, D. E. Morris, and J. L. Kiplinger. Evidence for the Involvement of 5f-Orbitals in the Bonding and Reactivity of Organometallic Actinide Compounds: Thorium(IV) and Uranium(IV) Bis(hydrazonato) Complexes. 2008. *Journal of the American Chemical Society.* **130**: 17537.

Graves, C. R., A. E. Vaughn, E. J. Schelter, B. L. Scott, J. D. Thompson, D. E. Morris, and J. L. Kiplinger. Uranium(V)-Imido Complexes - Probing the Electronic Structure and Redox Energetics in Pentavalent Organoactinide Complexes. 2008. *Inorganic Chemistry.* **47**: 11879.

Graves, C. R., B. L. Scott, D. E. Morris, and J. L. Kiplinger. Tetravalent and Pentavalent Uranium Acetylide Complexes

Prepared by Oxidative Functionalization with Cu-C□C-Ph.. 2008. *Organometallics.* **27**: 3335.

Graves, C. R., B. L. Scott, D. E. Morris, and J. L. Kiplinger. Selenate and Tellurate Complexes of Pentavalent Uranium. 2009. *Chemical Communications.* : 776.

Graves, C. R., D. E. Morris, B. L. Scott, and J. L. Kiplinger. Facile Access to Pentavalent Uranium Organometallics: One Electron Oxidation of Uranium(IV) Imido Complexes with Copper(I) Salts. 2007. *Journal of the American Chemical Society.* **129**: 11914.

Graves, C. R., D. E. Morris, and J. L. Kiplinger. Pentavalent Uranium-Imido Complexes. To appear in *Inorganic Syntheses.*

Graves, C. R., E. J. Schelter, T. Cantat, B. L. Scott, and J. L. Kiplinger. A Mild Protocol to Generate Uranium(IV) Mixed-Ligand Metallocene Complexes Using Copper(I) Iodide.. 2008. *Organometallics.* **27**: 5371.

Graves, C. R., P. Yang, S. A. Kozimor, A. E. Vaughn, D. L. Clark, S. D. Conradson, E. J. Schelter, B. L. Scott, J. D. Thompson, P. J. Hay, D. E. Morris, and J. L. Kiplinger. Organometallic Uranium(V)-Imido Halide Complexes: From Synthesis to Electronic Structure and Bonding.. 2008. *Journal of the American Chemical Society.* **130**: 5272.

Graves, C. R., and J. L. Kiplinger. Pentavalent Uranium Chemistry – Synthetic Pursuit of a Rare Oxidation State. 2009. *Chemical Communications.* : 3813.

Schelter, E. J., J. M. Veauthier, C. R. Graves, K. D. John, B. L. Scott, J. D. Thompson, D. E. Morris, and J. L. Kiplinger. 1,4-Dicyanobenzene as a Scaffold for the Preparation of Covalently Linked Bimetallic Actinide Complexes Exhibiting Metal-Metal Communication. 2008. *Chemistry – A European Journal .* **14**: 7782.

Thomson, R. K., C. R. Graves, B. L. Scott, and J. L. Kiplinger. Noble Reactions for the Actinides: Safe Gold-Based Access to Organouranium and Azide Complexes. 2009. *European Journal of Inorganic Chemistry .* : 1451.

# Superconductivity in Non-Centrosymmetric Materials

*John Singleton*
20070541PRD1

## Abstract

Dr Yuan performed experiments on unusual superconductors using the high-magnetic-field facilities at MPA-NHMFL. Perhaps his most influential result was to find that the iron-arsenic-based superconductors are markedly different from all previously-known layered superconductors (e.g. the cuprates and the crystalline organic metals). He suggested that this is attributable to the distinctive electronic structure of the iron-arsenide compounds, also the subject of current high-field measurements at MPA-NHMFL. Most importantly, his results show that, in contrast to the assumptions based on the cuprates, reduced dimensionality is not a prerequisite for "high-temperature" superconductivity [1,2].

## Background and Research Objectives

This project investigated materials that show new and unusual types of superconductivity. By using the very high magnetic fields and very low temperatures that are available at the Materials Physics and Applications Division's National High Magnetic Field Laboratory (MPA-NHMFL), superconductivity was switched on and off in a controllable manner. This enabled the microscopic properties of the underlying electrons to be uncovered using unique experimental tools designed by Dr Yuan. In this way, important progress has been made in understanding the mechanism for superconductivity. This is a useful step along the route to enable superconductors with desirable properties (e.g. zero resistance at relatively high temperatures, resistance to high magnetic fields) to be designed from scratch. Eventually, such materials will have an important impact on technologies such as electrical power distribution and transport, and on applications of electromagnets such as MRI; the application of "designer superconductors" could yield greatly increased efficiency, reduced power consumption (important for energy security) and protection against large-scale power outages caused by grid failures.

## Scientific Approach and Accomplishments

Dr Yuan performed a number of influential experiments on exotic superconductors and correlated-electron systems and wrote several papers. He also spoke by invitation at a number of international conferences and at overseas universities. As a result he was appointed professor at Zhejiang University on returning to China.

The most important results are described below. It is gratifying to note that Dr Yuan's stay in Los Alamos has greatly strengthened collaborations with leading Chinese universities and government research laboratories. Consequently, further experiments are in progress (Professor Yuan is now an external MPA-NHMFL user) and samples of new materials continue to arrive from his network of international collaborators.

- Furious scientific activity, measureable as hundreds of papers posted at xxx.lanl.gov, has been generated by discovery of superconductivity in two families of iron-arsenic-based compounds (the "iron pnictides") early in 2008. Superconducting transition temperatures Tc as high as 55 K have been observed, naturally provoking comparisons with the well-known "High Tc" cuprate superconductors, plus renewed speculations about imminent magnetically-levitated trains and dissipation-free powerlines! In addition to high superconducting temperatures, the cuprates and the iron-arsenide superconductors both possess layered crystal structures.

  In the early days of High Tc, the layered crystal structure of the cuprates led to the widely-held belief that reduced dimensionality (i.e. being more like a two-dimensional system than three) is a necessary prerequisite for superconductivity at temperatures above about 30 K. Indeed, many theoretical models still treat the cuprates as a purely two-dimensional system, neglecting the interactions between the layers of the crystals. At first sight,

the iron-arsenic compounds, which (as mentioned above) also possess layered structures, give additional credence to this idea.

Dr Yuan obtained (RE,La)(O,F)FeAs superconductor samples in early 2008 and began to investigate their properties using the high-field facilities at MPA-NHMFL [1]. However, his most important achievement was to show that the layered iron-arsenide-based superconductor (Ba,K)$Fe_2As_2$ is in fact far from two-dimensional [2], in contrast to the above expectations. By applying pulsed magnetic fields of up to 60 T to single crystals of the superconductor, Dr Yuan was able to measure the upper critical field (the field at which superconductivity is destroyed) down to low temperatures (Figure 1). He found that the low-temperature critical field was virtually the same irrespective of the direction in which the magnetic field was applied (Figure 2). This suggests that the electronic properties of the iron-arsenic-based superconductor are in fact three dimensional, rather than two dimensional, contrary to early expectations.

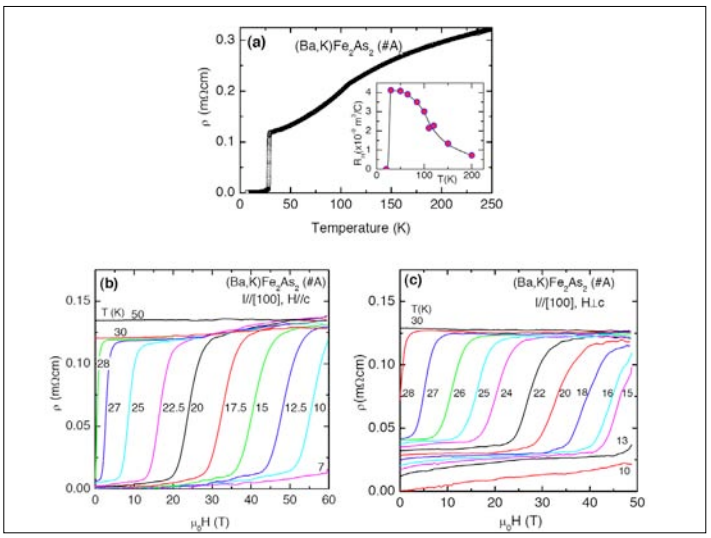


*Figure 1. In-plane electrical resistivity of single crystals of the superconductor (Ba,K)$Fe_2As_2$ measured in pulsed high magnetic fields. (a): The temperature dependence of the resistivity rho(T) at zero magnetic field. Note that there is a weak kink around 108 K in rho(T) which may correspond to a spin-density-wave or structural transition. The inset shows the temperature dependence of the Hall coefficient RH obtained in pulsed magnetic fields of up to 60T. The field dependence of the resistivity rho(B) at various temperatures is shown in (a) and (b) for field parallel and perpendicular to the c-axis, respectively.*

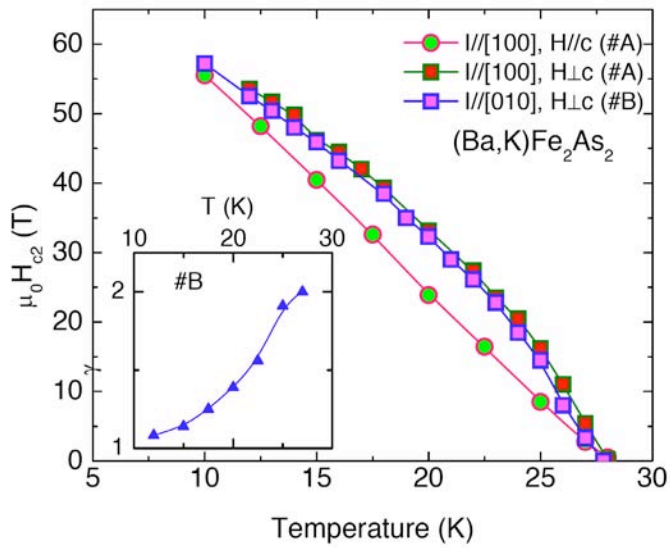


*Figure 2. The upper critical field $H_{c2}$(T) of single crystals of the superconductor (Ba,K)$Fe_2As_2$. The main figure shows $H_{c2}$ versus temperature for magnetic field parallel to the c-axis (circles) and perpendicular to the c-axis (squares), in which the critical fields $H_{c2}$(T) are determined from the midpoint of the sharp resistive superconducting transitions. Remarkably, the two samples (#A and #B) behave nearly identically in spite of different purities. The inset shows the anisotropy parameter gamma plotted as a function of temperature. The parameter gamma is about 2 near Tc, a value close to what other groups derived in low-field measurements, but decreases with decreasing temperature and approaches to 1 as T tends to zero, indicating isotropic superconductivity. This is a most surprising finding in a layered material.*

Yuan's Nature Letter demonstrates [2] that in their three-dimensionality the iron-arsenic-based superconductors are markedly different from all previously-known layered superconductors (e.g. the cuprates and the crystalline organic metals). Yuan suggests that this is attributable to the distinctive electronic structure of the iron-arsenide compounds, also the subject of current high-field measurements at MPA-NHMFL. Most importantly, Yuan's results show that, in contrast to the assumptions based on the cuprates, reduced dimensionality is not a prerequisite for "high-temperature" superconductivity [2]. Further studies of different FeAs-based superconductors by Dr Yuan have confirmed this idea and will be published in the near future.

- Dr Yuan observed a field-induced Fermi-surface topology change in $CeRhIn_5$ for the first time. This is important evidence about the nature of the field-induced quantum critical behavior in this compound. The result was reported at two APS March meetings and is being prepared for publication.

- The unusual layered compound $Na_xCoO_2.H_2O$ was

investigated using heat-capacity measurements to reveal the superfluid density and the existence of two separate superconducting states for the first time [3].

- The triple-layered ruthenate $Sr_4Ru_3O_{10}$ was investigated. Only one ferromagnetic phase was found, and the data meant that it was possible to rule out several previously-proposed antiferromagnetic phase transitions. A magnetic domain model was proposed to account for previously-observed magnetotransport and metamagnetic behavior [4].

- The superconducting order parameter in the non-centrosymmetric superconductors $Li_2(Pd,Pt)_2B$ was studied using magnetic penetration-depth measurements. The data suggest that an unusual spin-triplet state develops with increasing Pt content due to the broken inversion symmetry [5]. Similar techniques were applied to a number of heavy-fermion superconductors [6].

- The metallic states close to the quantum phase transition in cubic FeGe were investigated using very high pressures and electrical resistivity. It was found that the long-wavelength helical order was suppressed by a pressure of 19 GPa, and the observed strong deviations from Fermi-liquid behavior disagree with the standard vision of a quantum critical phase transition [7].

In summary, Dr Yuan was a very energetic and enthusiastic experimentalist. He developed several collaborations with some of the best sample growers in the world, so that he had access to high-quality samples of the "hottest" materials. Consequently, his work did much to raise the international profile of MPA-NHMFL.

## Impact on National Missions

This project supported the LANL's Grand Challenge to enhance the nation's fundamental scientific capabilities by improving our understanding of superconductivity. This helps design better practical superconductors, supporting DOE's mission to improve the nation's energy security (i.e. by reducing electrical power consumption). Finally it helps in understanding complex substances such as plutonium, an important part of LANL's stockpile stewardship mission.

## References


1. Chen, G. F., Z. Li, G. Li, J. Zhou, D. Wu, J. Dong, W. Z. Hu, P. Zheng, Z. J. Chen, H. Q. Yuan, J. Singleton, J. L. Luo, and N. L. Wang. Superconducting properties of the Fe-based Layered Superconductor LaFeAsO0.9F0.1-delta. 2008. *Phys. Rev. Lett..* **101**: 057007 1.

2. Yuan, H. Q., J. Singleton, S. Baily, F. F. Balakirev, G. F. Chen, and J. L. Luo. Nearly Isotropic Superconductivity in (Ba,K)Fe2As2. 2009. *Nature.* **475**: 565.

3. Mochizuki, M., H. Q. Yuan, and M. Ogata. Specific heat and superfluid density for possible two different superconducting states in NaxCoO2 H2O. 2007. *Journal of the Physical Society of Japan.* **76**: 023702.

4. Qu, Z., L. Spinu, H. Q. Yuan, V. Dobrosavljevic, W. Bao, J. W. Lynn, M. Niklas, J. Peng, T. Liu, D. Forbes, E. Flesch, and Z. Q. Mao. Unusual heavy-mass nearly ferromagnetic state with a surprisingly large Wilson ration in the double-layered ruthenates (Sr(1-x) Cax)3Ru2O7. 2008. *Physical Review B.* **78**: 180407.

5. Yuan, H. Q., M. B. Salamon, P. Badica, and K. Togano. A penetration depth study on the non-centrosymmetric superconductors Li2(Pd(1-x)Ptx)3B. To appear in *Physical Review B.*

6. Steglich, F., C. Geibel, F. M. Grosche, M. Loewenhaupt, O. Stockert, S. Wirth, and H. Q. Yuan. Experimental evidence for unconventional BCS states in heavy-fermion metals. 2008. *Physica B.* **403**: 968.

7. Pedrazzini, P., H. Wilhelm, D. Jaccard, T. Jarlborg, M. Schmidt, M. Hanfland, L. Akselrud, H. Q. Yuan, U. Schwarz, Y. Grin, and F. Steglich. Metallic state in cubic FeGe beyond its quantum phase transition. 2007. *Physical Review Letters.* **98**: 047204.


## Publications


Chen, G. F., Z. Li, G. Li, J. Zhou, D. Wu, J. Dong, W. Z. Hu, P. Zheng, Z. J. Chen, H. Q. Yuan, J. Singleton, J. L. Luo, and N. L. Wang. Superconducting properties of the Fe-based layered superconductor LaFeAsO0.9F0.1-delta. 2008. *Physical Review Letters.* **101**: 057007 1.

Mochizuki, M., H. Q. Yuan, and M. Ogata. Specific heat and superfluid density ofr possible two different superconducting states in NaxCoO2.H2O. 2007. *Journal of the Physical Society of Japan.* **76**: 023702.

Pedrazzini, P., H. Wilhelm, D. Jaccard, T. Jarlborg, M. Schmidt, M. Hanfland, L. Akselrud, H. Q. Yuan, U. Schwarz, Y. Grin, and F. Steglich. Metallic state in cubic FeGe beyond its quantum phase transition. 2007. *Physical Review Letters.* **98**: 047204 1.

Qu, Z., L. Spinu, H. Q. Yuan, V. Dobrosavljevic, W. Bao, J. W. Lynn, M. Nicklas, J. Peng, T. Liu, D. Forbes, and E. Flesch. Unusual heavy-mass nearly ferromagnetic state with a surprisingly large Wilson ratio in the double layered ruthenates (Sr$_{1-x}$Ca$_{x}$)$_{3}$Ru$_{2}$O$_{7}$. 2008. *Physical Review B.* **78**: 180407.

Steglich, F. C., F. M. Geibel, F. M. Grosche, M. Loewenhaupt, O. Stockert, S. Wirth, and H. Q. Yuan. Experimental evidence for unconventional BCS states in heavy-fermion metals. 2008. *Physica B.* **403** (5-9): 968.

Yuan, H. Q., J. Singleton, S. Baily, F. F. Balakirev, J. L. Luo, and N. L. Wang. Nearly isotropic superconductivity in (Ba,K)Fe2As2. 2009. *Nature.* **475**: 565.

Yuan, H. Q., M. B. Salamon, P. Badica, and K. Togano. A penetration depth study on the non-centrosymmetric superconductors Li2(Pd1-xPtx)3B. 2008. *Physica B.* **403**: 1138.

# Multifunctional Copper-Carbon Nanotube Nanocomposites

*Amit Misra*
20070585PRD2

## Abstract

Carbon nanotubes (CNTs) possess unusually high stiffness and strength and can be electrically conducting. However, it has been a challenge to integrate CNTs in bulk structures to exploit their extraordinary mechanical properties. Here, we have used a synthesis approach that combines ball milling and high-pressure torsion to produce bulk composites of Cu reinforced with CNTs. These novel Cu-CNT composites exhibit significant improvement in strength, without loss of ductility, compared to nano-structured single-phase Cu and other CNT-reinforced composites reported earlier. This ultra-high strength, lightweight bulk nanocomposites have potential applications in energy, transportation and defense industries.

## Background and Research Objectives

Carbon nanotubes (CNTs) have a unique structure, possess extraordinary mechanical properties of super-high elastic modulus and strength, and also own a novel set of attributes: lightweight, high aspect ratio, high electrical conductivity for a non-metal, and excellent chemical stability [1]. On the other hand, efforts to strengthen pure metals such as Cu typically result in a loss in ductility and electrical conductivity. CNTs could be the ideal nanoscale reinforcement to design multifunctional Cu-CNT composites with superior performance.

Synthesis methods of CNTs-reinforced metallic composites that require heating typically result in chemical reactions between the CNT and the metal matrix and significantly increased grain size resulting in modest or insignificant improvement in strength and often decreased ductility compared to their monolithic counterparts. For advanced structural applications, strong and ductile composites are desired. However, nano-grained metal-CNT composites with both high strength and good plasticity have not been reported so far. The aim of present study is to develop nanostructured CNT-reinforced Cu matrix composites that exhibit high strength and ductility.

## Scientific Approach and Accomplishments

To fabricate high quality nanostructured Cu-CNT composites with excellent mechanical performance, there are two primary challenges. The first one is to distribute CNTs homogeneously in Cu matrix because CNTs have a strong tendency to form bundles, which degrade the strength and ductility of composites. To overcome this challenge, high-energy ball milling was applied to mix Cu powders (particle sizes: 0.5-1.5µm) and 1wt.% CNTs (length: 10-30µm; inner diameter: 2-5nm; outer diameter: <10nm) for 5 hrs in an inert argon gas environment. For comparison, Cu powders without CNTs were also made at the same conditions. Scanning electron microscopy (SEM) analysis demonstrated that after ball milling, CNTs have been incorporated into Cu powders. Distribution of CNTs will be detailed later. The second challenge is to obtain dense small-grained microstructures. In earlier studies, heating was used to make dense metal-CNT composites. However, these composites are usually coarse-grained and have low strength. Here, high-pressure torsion (HPT) was chosen because it has a two-fold advantage. One is to make samples fully dense, and the other is to refine the internal grain size of the structure to nanometer scale by severe plastic deformation while preserving the bulk dimensions of the sample. The ball-milled powders were first compacted into 10mm diameter discs, which were then consolidated via HPT at 5GPa for 5 revolutions. Both were performed at room temperature. In the course of HPT, subgrain boundaries first form via dislocation accumulation and rearrangements under severe shear strain, and then develop into high-angle grain boundaries, resulting in grain refinement. At the same time, dynamic recovery and recrystallization reduce the dislocation density and may increase the grain size. The balance of these two opposite processes determines the final grain size.

Figure 1 presents dark-field transmission electron microscopy (TEM) images of the HPT-processed samples with 1 wt.% and 0 wt.% CNTs. Clearly, both samples have a nanocrystalline structure. The average grain size is about 22nm and 29nm for Cu-CNT composite and Cu, respectively. The grain size distribution of Cu-CNT composite is apparently narrower than that of Cu. According to the principle of HPT stated above, with the incorporated CNTs, dislocation motion could be blocked at CNT-Cu interfaces. Thus the dislocation accumulation becomes enhanced. As a result, the presence of CNTs leads to a decrease in grain size. Figure 2 shows CNTs embedded in the Cu matrix. In Figure 2(a), some CNTs penetrate the Cu grains, while in Figure 2(b), some CNTs appear to surround the Cu grains with CNTs confined at grain boundaries. The distribution of CNTs was characterized using both microscopic and macroscopic approaches. First, TEM observations did not find CNT clusters, suggesting a good dispersion of CNTs into Cu matrix. Second, microhardness of Cu-CNT composite was measured. The independence of microhardness on measurement location also suggests that the distribution of CNTs in Cu matrix is homogeneous since the strength of metal-CNT composites is sensitive to the CNT contents.

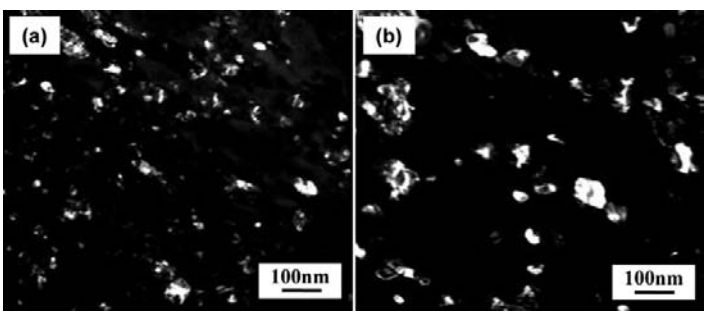


*Figure 1. Dark-field TEM micrographs of nanostructured (a) Cu-CNT composite and (b) pure Cu.*

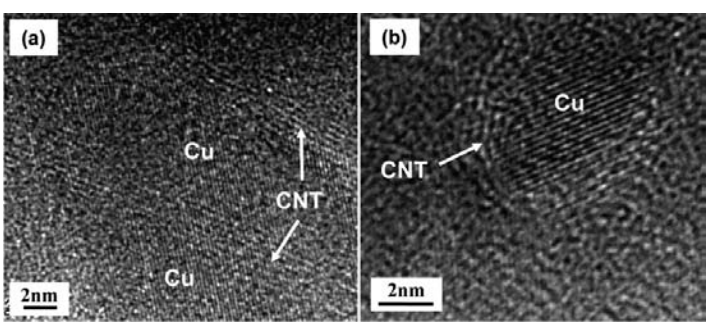


*Figure 2. High-resolution TEM micrographs showing (a) intra-grain and (b) intergranular dispersion of CNTs in Cu matrix.*

Mechanical properties of nanostructured Cu and Cu-CNT composite were investigated by pillar compression tests at a strain rate of $1\times10^{-3}$ $s^{-1}$. Figure 3(a) presents a cylindrical pillar machined from the Cu-CNT nanocomposite. The diameter and length of all the pillars are about 5µm and 11µm, respectively, leading to an aspect ratio of 1:2. The pillar compression technique has been used to measure the effect of sample size on the strength of metallic single crystals. In the case of nanolayered and nanostructured metals, when the pillar dimension is much larger than the crystallite size, the pillar compression test can be used to study the effect of crystallite size on the strength, as opposed to the sample size. Figure 3(b) illustrates a failed sample of Cu-CNT composite, which exhibits shear instability, a typical failure mode in compression testing. Compressive results showed that both samples have high strength. Furthermore, the yield strength (0.5% plastic strain offset) increased from 847±62 MPa to 1273±27 MPa with an addition of only 1wt.% CNTs. The grain size of current Cu-CNT composite is on the order of 20 nm. At such small grain sizes, grain interiors are usually devoid of dislocation sources and, therefore, dislocations nucleate at grain boundaries or CNT-matrix boundaries. Figure 2 has shown that CNTs can be distributed intra- as well as inter-granularly. In both cases, they may be able to inhibit dislocation nucleation and motion, thereby leading to an increase in the yield strength.

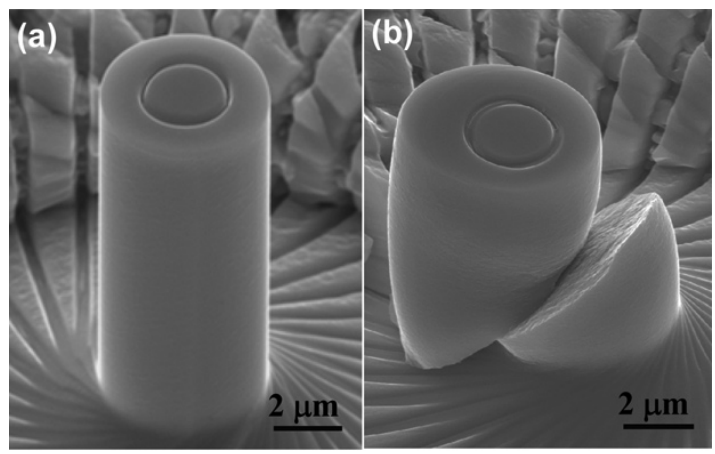


*Figure 3. SEM images of (a) as-processed and (b) compressed to fracture micro-pillar of Cu-CNT composite.*

In other investigations of CNT-reinforced metallic composites, the plastic strain to failure of composites was observed to be lower than the monolithic metals. In the current study, incorporating CNTs into Cu matrix results in a great gain in strength without notable sacrifice in ductility. For example, plastic strains are 28.4±1.9% and 30.7±0.9% for nanostructured Cu-CNT composite and Cu, respectively. In addition, nanoindentation measurement discloses that the presence of CNTs also increased the stiffness. Moreover, the area underneath stress-strain curves, an indicator of toughness, is about 10% larger for Cu-CNT composite than for Cu. Figure 4 summarizes the reported and current compression data, where red

and blue points denote maximum and yield stress data, respectively. For a comprehensive comparison, tensile results for Al-, AlSi-, 2024Al-, Cu-, Mg-, Ni-, and AZ91D-CNT composites are also included [2]. Like nanocrystalline metals, CNT-reinforced metallic composites also show a feature of strength-ductility tradeoff in that increasing strength is usually accompanied with decreasing ductility. However, nanostructured Cu-CNT composite fabricated in this study are clearly distinguished from the general trend and show the best combination of strength and ductility.

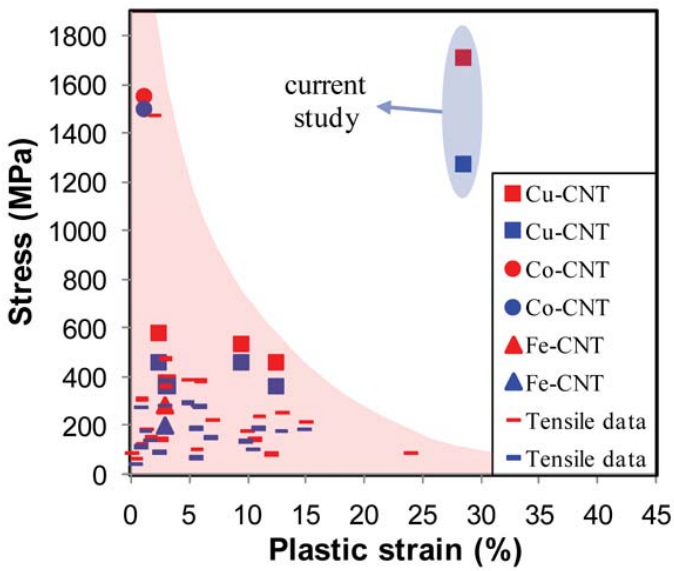


*Figure 4. A summary of strength and plastic strain to failure of several metal-matrix composites reinforced with CNTs.*

In summary, Cu-CNT composite with a grain size of about 22nm has been successfully produced. An addition of 1wt.% CNTs can cause grain refinement and narrower grain size distribution. In the Cu matrix, CNTs are distributed either at grain boundaries or in grain interiors. First, compared with its counterpart without CNTs, nanostructured Cu-CNT composite possesses improved strength, stiffness and toughness without a loss in ductility. Second, compared with metal-CNT composites reported earlier, the present Cu-CNT nanocomposites exhibit a significantly improved combination of strength and ductility.

## Impact on National Missions

This project is closely related to the lab's missions in the field of materials science: i) developing new materials essential to assessing energy materials performance; ii) understanding fundamental materials physics in nanostructured materials. The multifunctional Cu-CNT nanocomposites developed here are expected to have a combination of high strength, good ductility, lightweight as well as good electrical conductivity. These novel material systems with unprecedented levels of strength and ductility will impact a diverse range of DOE missions in energy security, transportation and national defense.

## References


1. Ajayan, P. M.. Nanotubes from carbon. 1999. *Chemical Reviews.* **99** (7): 1787.

2. Li, H., A. Misra, Z. Horita, C. C. Koch, N. A. Mara, P. O. Dickerson, and Y. T. Zhu. Strong and Ductile Nanostructured Cu-Carbon Nanotube Composite. To appear in *Applied Physics Letters.*


## Publications


Li, H., A. Misra, Y. T. Zhu, Z. Horita, C. C. Koch, and T. G. Holesinger. Processing and Characterization of Nanostructured Cu-Carbon Nanotube Composites. To appear in *Materials Science and Engineering A.*

Li, H., A. Misra, Z. Horita, C. C. Koch, N. A. Mara, P. O. Dickerson, and Y. T. Zhu. Strong and Ductile Nanostructured Cu-Carbon Nanotube Composite. To appear in *Applied Physics Letters.*

# Multiscale Simulations for Cascade Overlap in Irradiated Materials

*Arthur F. Voter*
20070640PRD2

## Abstract

Defect formation and propagation in materials is a complex phenomenon that spans atomic length and time scales (nm and ps, respectively) to macroscopic scales at the microstructure level (mm and min, respectively). Large concentrations of defects in a material crystalline structure are created during irradiation of materials. Depending on the defect source and the material, different defect shape and size distributions are observed, which ultimately determine the physical, chemical and mechanical properties of the material. Unfortunately, currently we do not have computational methods that are accurate yet computationally efficient so that we can study and predict such complex phenomena. In this work, we have developed four computational methods that address some of the challenges that are involved.

## Background and Research Objectives

Study of dynamics of thermally activated phenomena in solid-state materials at experimental laboratory length and time scales is essential for designing materials with desirable characteristics. In these materials, atomic processes that govern macroscopic phenomena often occur over a broad range of time scales. However, it well understood that in many situations current materials modeling techniques cannot simultaneously access large length and time scales without making severe approximations that typically corrupt the dynamical evolution. These shortcomings severely impede our ability to employ current modeling techniques as predictive tools for materials design.

Over the last dozen years, a suite of accelerated molecular dynamics methods has been developed at LANL that can reach reasonably long time scales [1]. In particular, the temperature accelerated dynamics (TAD) method [2] is a powerful computational tool for studying thermally activated phenomena in solid-state materials over large time scales, such as seconds. In the TAD method, transitions from state to state are made to occur more rapidly by raising the temperature of the system. Although the wrong event sometimes occurs first at higher temperature, the TAD algorithm corrects for this, only allowing the correct events (with a desired confidence) to be accepted. Despite the advantages of TAD, the method cannot be applied to large systems due to the poor scaling one obtains with TAD in terms of number of atoms present in the system.

Such a situation is encountered in defect cascade overlap due to radiation damage in materials. Much like a cascade of collisions resulting from a car colliding with stationary cars in front of it, a displacement cascade is generated when a highly energetic impinging atom locally displaces the material atoms. Interaction of two or more of such cascades, termed as cascade overlap, cannot be modeled using existing modeling tools. While continuum models are too approximate to capture the complex interactions, molecular models, including TAD, are computationally too expensive to model the large number of atoms that are present in the system.

The underlying goal of this project was to overcome some of these challenges by developing variations of existing materials modeling methods, namely temperature accelerated dynamics and kinetic Monte Carlo methods, in a way that retains the accuracy of these methods yet provide computational speed-up of several orders of magnitude. The important challenges that we identified at the beginning of this project included developing the capability to accurately identify the complicated atomic processes in these materials and to develop computationally efficient strategies that will enable us to simultaneously reach the large length and time scales. These attempts are among the first in the context of accelerated molecular dynamics and entailed non-trivial extensions of methods developed by Voter and co-workers at LANL, as well as developing completely new computational techniques.

Due to the large computational cost associated with

performing simulations for cascade overlap in radiation damage, we focused on much simpler testbed systems for method development, such as thin film growth, which has applications in electronic, magnetic, and catalytic applications. As a result of our efforts, we were able to develop four new techniques, namely, process catalog TAD method, the TAD-KMC method, accelerated superbasin KMC (AS-KMC) method and the local AS-KMC method. These developments lay important stepping stones which would enable efficient studies of radiation damage in the future.

## Scientific Approach and Accomplishments

Research performed during the last two years resulted in the development of four new methods. Below we provide a brief description of these methods and highlight their importance.

*p-TAD method*

Based on this philosophy of the TAD method (see introduction), we have developed a new formulation of the TAD method called the process list-TAD method, or simply p-TAD [3]. The p-TAD method is used for systematically generating a kinetic Monte Carlo (KMC) process list for a given material system. A process list is a list of reaction mechanisms, and associated rate constants, for escape from the present state of the system. The method guarantees that all relevant processes at a particular temperature have been detected with a user-specified confidence over large time scales. This solves the long-standing problem of how to find a complete (or complete enough with desired confidence) list of KMC rate processes for a given system in a given state. Generation of such accurate KMC process lists, with error control, is not possible with any other currently available technique. Though the p-TAD algorithm resembles the original TAD algorithm in many ways, the p-TAD method introduces significant improvements to the existing TAD method. For example, it offers a more direct way to parallelize the dynamics for small (or large) systems, and it can be made more accurate event by event if desired, because the accurate rate constant is computed at low temperature directly. It also offers the possibility of including quantum dynamical (e.g., tunneling and zero-point) effects. A manuscript describing the p-TAD method will be submitted for publication to the Journal of Chemical Physics shortly.

The p-TAD method was employed to study diffusion processes in the copper-silver alloy system. An example of the performance for this case is shown in Figure 1. Material simulations of such metal alloys are common, and typically are performed with the assumption that only simple single atom processes are present. The major finding from this study was that a complex range of many-atom processes can occur in this system. Many of these processes cannot be guessed intuitively. Some of these processes are shown in Figure 2. The p-TAD calculations were able to reach long time scales up to a few seconds, which is not possible with the standard molecular dynamics (MD) methods, resulting in several orders of magnitude speed-up over MD. These observations were extremely promising since it can be expected that several complicated many-atom processes will be present in radiation damaged materials.

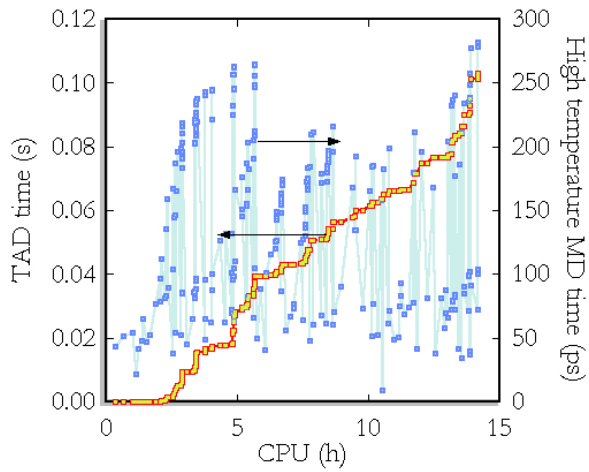


*Figure 1. Accelerated time accessed during a 14-hour p-TAD simulation of silver deposited on the copper (100) surface. The high temperature molecular dynamics time is also plotted.*

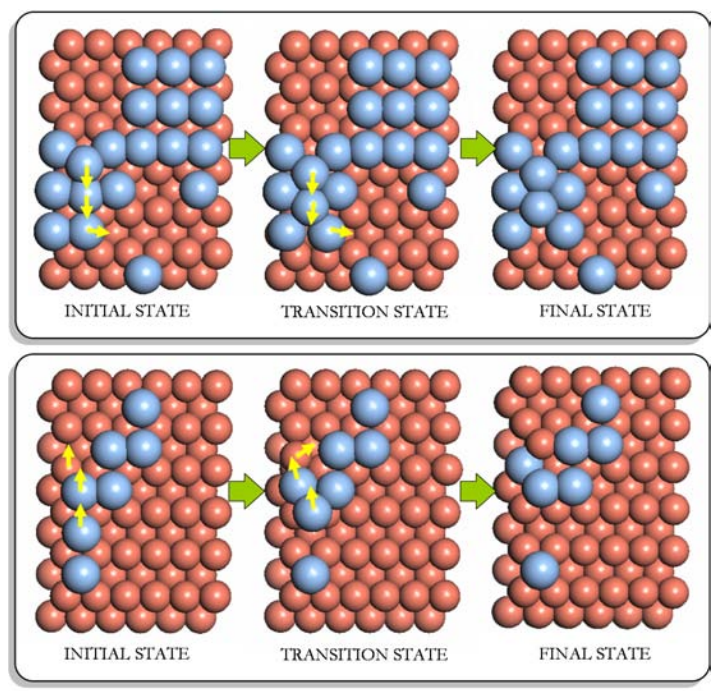


*Figure 2. Initial state, transition state, and final state of two 3-atom processes discovered during a p-TAD simulation of the diffusion of silver atoms on a copper (110) surface. The silver atoms are blue and the copper atoms are brown.*

**TAD-based KMC method**

The TAD-based KMC method (TADKMC) [4] is a powerful method developed to simultaneously overcome the length and time scale problem. The method identifies unique local environments, i.e., relative atomic arrangements around each atom, in the material system using a sophisticated pattern recognition algorithm. A list of relevant KMC processes is continuously generated with a user-specified confidence for the unique local environments using the p-TAD method described above. Parallel p-TAD calculations are straightforward using multiple processors. KMC process lists from local environments are compiled to generate an on-the-fly master KMC process catalog. Processes are selected using the efficient n-fold KMC method. Once a KMC catalog is generated, it can be reused for other calculations with the same material at conditions different from ones the catalog was originally generated for. An exciting aspect is that the TADKMC scales sublinearly with the number of atoms in the material system, which contributes to its high computational efficiency. Other important features of the working code developed for this method include, but are not limited to: a) performing p-TAD based on-lattice or off-lattice KMC simulations, as well as their combinations in a spatially adaptive fashion, b) overcoming time scale separation resulting from fast and slow processes, c) compiling KMC catalogs generated from different KMC process list generation methods, d) database management system for efficient storage and retrieval of information, and e) adaptive methods for maximum exploitation of available processors. The code has enabled us to study dynamics of a 50,000-atom metal system over milliseconds with a few hours of computational time using four processors. The modeling of larger systems, e.g. million atoms or more, should be possible with relatively modest computational overhead. This method is more approximate than a full TAD or p-TAD simulation, due to the environment localization, but it is substantially more accurate than the standard KMC approach that it is meant to compete with, and offers error control for the first time in any KMC method.

We have employed the TADKMC method for deposition of copper on copper substrates. Figure 3 shows an example of such a simulation where roughly one monolayer of copper atoms was deposited on an initially clean copper (100) surface containing 25,920 atoms. The total computational time required with TADKMC was 3 days, which is much smaller than the time required if the p-TAD method were to be used for the entire copper system. The underlying p-TAD calculations determined process catalogs for more than 15,000 local environments. This is a far greater number of environments than are considered in a typical KMC simulation. A publication of the TADKMC method is under preparation.

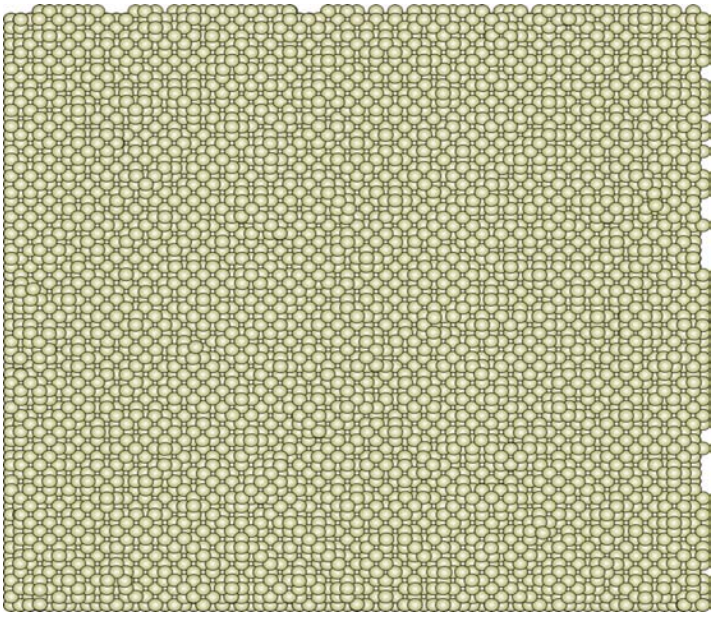

*Figure 3. Copper deposited on a copper (100) surface using the TADKMC method.*

**Accelerated-superbasin kinetic Monte Carlo method**

The kinetic Monte Carlo (KMC) method [5-7] is often the method of choice in a broad range of materials applications, such as surface adsorption, diffusion and crystal growth, catalysis, separations, electronics, nuclear science, and even in biology. KMC can be used to study evolution of material structure more efficiently than molecular dynamics and *ab initio* methods without significant loss in accuracy simply by using an accurate list of processes obtained from the aforementioned p-TAD method. These traits make the KMC method a powerful materials modeling tool. However, KMC is known to become computationally inefficient than more approximate techniques when the phenomenon of interest involves rare-events at longer time scales. Here rare-events refer to processes that occur less often than frequent processes in the system. This represents a major challenge in KMC modeling, since rare-event phenomena are ubiquitous in nature.

In this work, we introduced a novel method, namely the accelerated superbasin-KMC (AS-KMC) method [8], to efficiently study rare-event dynamics. The AS-KMC method provides substantial speed-up over KMC when rare events are present, while requiring CPU resources comparable to that of KMC when that is not the case; this property makes AS-KMC an ideal tool for a wide range of applications. AS-KMC relies on building a database of processes and counting the number of times each process is observed. The number of sightings for a process is used as an indication of the presence of rare events. When certain processes are seen more frequently than others,

these frequent processes are selected less often in the future during an AS-KMC calculation. Over time the rare processes have a higher probability of being selected in AS-KMC than in KMC. The strength of the AS-KMC method lies in the large computational speed-up obtained and its general applicability to any arbitrarily complex material. It does not require any sophisticated algorithms for identifying the frequent and rare processes or require complicated matrix manipulations prior to selecting a rare process, which are often used in other methods to study rare-event phenomena. The overall accuracy of the AS-KMC method can be controlled using a user-specified error measure.

We have assessed the performance of the AS-KMC method for various simple as well as complex systems. An example of a complex system we studied is shown in Figure 4. Here the evolution of a nanowire to a more compact, thermodynamically favorable structure was studied. It was found that the computational speed-up of a factor of 200 over KMC can be achieved with the AS-KMC method without any significant loss in accuracy. The inset in Figure 4 shows that the aspect ratio of the nanostructure plotted against of time, as obtained from AS-KMC and KMC methods, are in good agreement. Figure 5 shows an example of the connectivity of states within one of the superbasin encountered in this system. After careful testing, we have found the method is both accurate and computationally efficient even when rare-events were missing. The AS-KMC method solves the long-standing problem of providing a general procedure for providing accurate accelerated dynamics when rare-event phenomena are present. We are in the process of submitting a manuscript on the AS-KMC method for publication in the Journal of Chemical Physics.

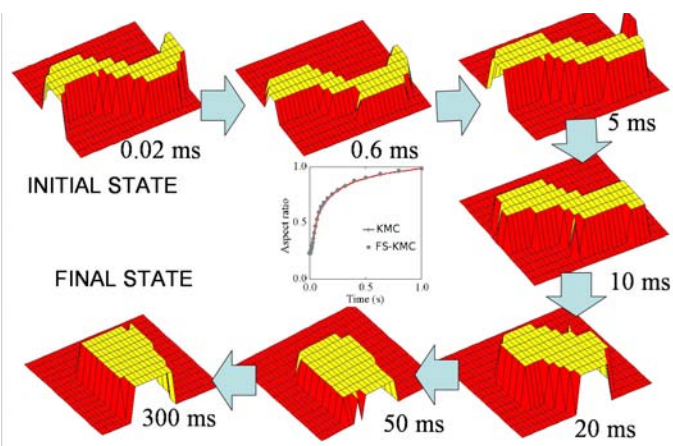


*Figure 4. Transformation of a submonolayer nanowire structure studied using AS-KMC. The inset in the center shows the excellent agreement between AS-KMC and the more accurate KMC method (using the same process catalog) for the time-dependent aspect ratio of the nanowire.*

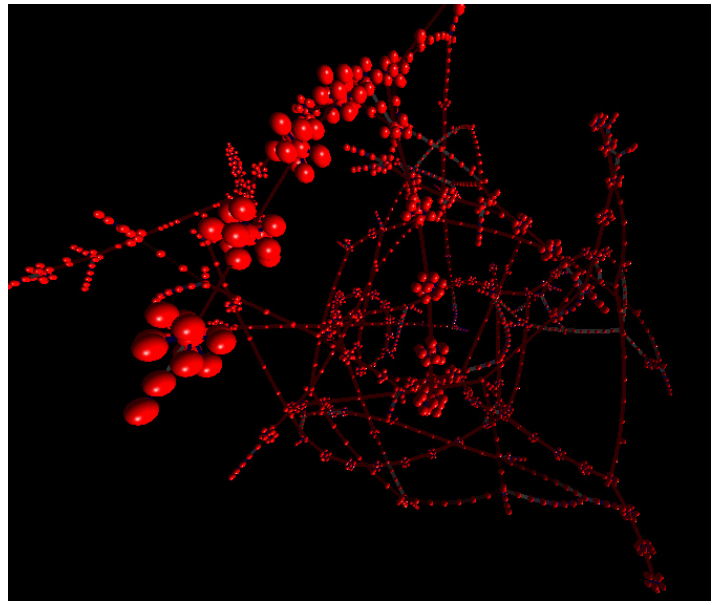

*Figure 5. Connectivity map for the fast processes (lines) connecting 1941 states (spheres) in the example studied in Figure 4. The AS-KMC drastically lowers the computational cost for simulating large numbers of fast processes.*

Recently, we have developed other variations of the AS-KMC which are even computationally more efficient. An example of such a technique is the fuzzy superbasin KMC (FS-KMC) method which is found to be 10 times faster than the AS-KMC method.

**Local accelerated-superbasin kinetic Monte Carlo method**
The accelerated superbasin KMC method requires frequent comparison of states stored in the memory. As the number of atoms in the system increases typically the number of states increases in a combinatorial manner. Memory issues can be avoided by storing states defined over a smaller patch of the system, and then reconstructing the entire state of the system using the "local" states. Computational speed-up larger than AS-KMC are obtained when the system can be decomposed into small domains such each domain evolves independently of the other, a situation that is commonly found in nature. In this manner, each domain can be advanced in time independently, which reduces the overall computational and memory costs for the method.

Preliminary LAS-KMC calculations for Ostwald ripening of a nanoparticle are promising. However, addition progress needs to be made in the development of this method.

## Impact on National Missions

This project will improve our understanding of the complex microstructural behavior of materials under irradiation, which is important to DOE's missions, especially regarding next-generation nuclear energy. This understanding is

needed for designing improved nuclear fuels, longer-lasting structural materials, and radiation-resistant matrix materials for long-term waste storage. The computational tools developed in this project will be used in the recently funded Energy Frontiers Research Center (EFRC) that is focused on understanding the role of interfaces (e.g., grain boundaries) in irradiated materials.

## References


1. Voter, A. F., F. Montalenti, and T. C. Germann. Extending the Time Scale in Atomistic Simulation of Materials. 2002. *Annual Reviews of Materials Research.* **32**: 321.

2. Sorensen, M. R., and A. F. Voter. Temperature-accelerated dynamics for simulation of infrequent events. 2000. *Journal of Chemical Physics.* **112**: 9599.

3. Chatterjee, A., and A. F. Voter. Process-based Temperature Accelerated Dynamics. 2009. *in preparation.*

4. Chatterjee, A., and A. F. Voter. Temperature accelerated dynamics with process list generation and local environments - the TAD-KMC method. *in preparation.*

5. Bortz, A., M. Kalos, and J. Lebowitz. A new algorithm for Monte Carlo simulation of Ising spin systems. 1975. *Journal of Computational Physics.* **17**: 10.

6. Voter, A. F.. Introduction to the Kinetic Monte Carlo Method. 2006. In *Radiation Effects in Solids.* Edited by Sickafus, K. E., E. A. Kotomin, and B. P. Uberuaga. , p. 1. Netherlands: Springer, NATO Publishing Unit.

7. Gillespie, D. T.. A general method for numerically simulating the stochastic time evolution of coupled chemical reactions. 1976. *Journal of Computational Physics.* **22**: 403.

8. Chatterjee, A., and A. F. Voter. Accurate acceleration of kinetic Monte Carlo simulations through the modification of rate constants. *in preparation.*

# Ultrafast Non-equilibrium Physics of the Fractional Quantum Hall System

*Antoinette J. Taylor*
20070654PRD2

## Abstract

Recent years have seen significant advances in materials' science and technology, leading to the emergence of exotic phenomena like high temperature superconductivity[1], multiferroics and metamaterials[2]– nano-engineered materials with unprecedented optical properties like negative index of refraction. The unusual electronic and magnetic properties exhibited by these materials are naturally of tremendous technological importance. Materials with negative index of refraction allow for the possibility of cloaking macroscopic objects or imaging objects with super resolution. Further advances in high-temperature superconductors would lead to significant gains in energy efficient electronics. The exotic properties of these materials are typically determined by the complex interaction and dynamics of the charge-carriers in the material. For example, one of the key open questions in high temperature superconductivity is the nature of the interaction between electrons and how their interaction is mediated by other particles such as phonons or magnons. Similarly, the lifetime of photoexcited carriers in the constituent layers of a metamaterial and our ability to manipulate these carriers allows the control its optical properties. Ultrafast optical techniques enable the elucidation and control of the complex dynamics of charge carriers in complex materials.

The work done under this project has two major thrusts: a) *Active Metamaterials:* We have fabricated a metamaterial device at telecommunication wavelengths that modulates light within a picosecond – 100 times faster than current technology. The device is nanoscale in size, tunable over the near-IR spectrum and energy efficient. b) *Non-linear Infrared Spectroscopy of Strongly Correlated Materials:* we have developed new instrumentation that allows us to excite low-energy states and collective modes in strongly correlated systems. We then directly probe how these excitations influence material properties. With this instrumentation, we will investigate the role of phonons in high-temperature superconductors. These two thrusts directly impact our understanding and control over next generation materials and devices, ranging from semiconductors to nanostructures.

## Background and Research Objectives

Ultrafast optical spectroscopy is a powerful technique to study femtosecond dynamics in various systems with very high temporal resolution. In particular, tools like all optical pump-probe spectroscopy and four-wave mixing have contributed greatly to our understanding of electron-electron scattering, electron-phonon interactions, etc. in semiconductors [3], conventional metals and correlated electron materials [4]. Other tools like Terahertz-Time Domain Spectroscopy allow us to directly measure the complex conductivity in correlated electron materials like high-temperature superconductors. Ultrafast optical spectroscopy has allowed us to actively control various photonic devices with unprecedented speeds.

### Active Metamaterials

Metamaterials [2] are a new class of nanostructured materials that offer novel optical properties such as a negative index of refraction. To date, much effort has been devoted to the fabrication of these materials, the characterization of their linear optical properties, and the extension of their wavelength range to the near-infrared (NIR) and visible. However, only limited results have been presented on the modulation of these properties in the THz (~ 20 ps response) and NIR (~ 60 ps response) spectral regions. The metamaterial includes metal and semiconductor components nano-engineered to yield the required optical properties. By optically injecting carriers into the semiconductor portion of the metamaterial, one can dynamically affect the optical behavior. In our work[5,6], by utilizing a previously unused regime in α-Silicon dynamics – the semiconductor in our device, we achieve a modulation time of only 0.6 picoseconds. This is two orders of magnitude faster than previous experiments in the NIR. The sub-ps response has the

potential for all-optical ultrafast communication, important for continuing advances in information technology. Further, due to the enhanced non-linearities in metamaterials, our device is only 116nm thick, unlike other all-optical modulators that are centimeters in length. The nanoscale size results in a compact, efficient device easily integrated with other photonic devices. In addition, by scaling metamaterial dimensions we can tune the device response over the entire near-IR spectrum.

**Non-linear Infrared Spectroscopy of Strongly Correlated System**

Standard band theory has been tremendously successful in describing the behavior of most solid state materials. However, in certain materials, the presence of strong Coulomb interactions between charge carriers results in anomalous effects that classical band theory fails to explain. These include high-temperature superconductors, colossal magneto-resistance materials, and heavy fermions, such as Pu. An understanding of the unusual electronic and magnetic properties of these materials is of tremendous technological interest.

Linear optical spectroscopy of these systems has yielded critical information on the elementary, low-energy excitations and the collective modes in these systems. Non-linear optical spectroscopy has elucidated the dynamics of the quasiparticles[4]. For example, Optical Pump Terahertz (THz) Probe (OPTP) experiments on high-temperature superconductors provide information on the dynamics of quasiparticles and Cooper pairs simultaneously with picosecond resolution, as the system evolves following optical excitation. However, in OPTP experiments, the pump energy is in the visible range (1-3eV), while the typical low-energy modes responsible for strong correlations fall in the mid-far IR (1-100meV) range. By exciting the system in the visible, one generates a slew of high energy excitations, making it difficult to isolate specific low-energy modes.

In this thrust, we have succeeded in building a Mid-IR pump THz Probe system that is capable of selectively pumping low-energy excitations in a material and probing the resultant dynamics in the far-IR with picosecond resolution. For example, we can now exclusively pump the low energy phonon modes in a high-temperature superconductor and observe the resultant dynamics of quasiparticles and Cooper pairs. This will elucidate the role of phonons in the electron-electron interaction. We have demonstrated the functionality of the setup by studying the dynamics of carriers in InSb – a semiconductor with a low energy bandgap.

## Scientific Approach and Accomplishments

To further our understanding of these advanced materials, we employ the following pump-probe technique: we use extremely short pulses of light (less than 100 femtoseconds in duration) to excite specific states of the material. The excitation is followed by another short pulse of light to probe the changes resulting from the previous excitation. By delaying the arrival of the probe pulse over time, we can track the temporal evolution of the change in material properties with picosecond resolution. This technique is able to then provide the timescale on which we manipulate material properties. It can also identify the various interactions in the material, which come into play on differing timescales. Thus we get new information regarding collective, complex behavior in these materials.

*Active Metamaterials:* We first fabricated a fishnet structure metamaterial to get a negative index resonance in the near-IR. This structure is composed of two 28 nm thick silver films separated by a 60 nm thick $\alpha$-Si film for a total thickness of 116 nm. A two-dimensional square periodic array of elliptical holes penetrates all three layers. Figure 1 shows the schematic of the design as well as a SEM image of the fabricated structure. In our work, light is polarized with the *E*-field parallel to the thinnest metal lines and the propagation direction (*k*) is across the film thicknesses. The device exhibits two negative index resonances. The longer wavelength negative-index resonance, previously reported in similar structures, is at ~1.68 $\mu$m. There is a second, shorter wavelength negative-*n* resonance at ~ 1.13 $\mu$m. The wavelength ratio of the two resonances, ~$2^{0.5}$, suggests that the long wavelength resonance is associated with the periodicity of the holes ($p$ = 340 nm) while the shorter one is associated with the periodicity along the diagonals (~$p/2^{0.5}$~ 240 nm). This identification is confirmed by electromagnetic modeling. These two resonances allows us to tune (by adjusting structural dimensions) the functionality of the device over the entire near-IR range – the fundamental resonance over the 1.5-2.0 µm range and the secondary resonance over the 1.0-1.5 µm range.

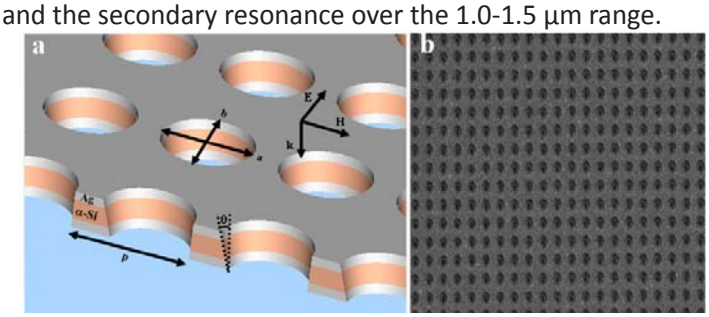


*Figure 1. The fishnet structure metamaterial. a) Schematic b) SEM image of fabricated device. The fishnet structure metamaterial is composed of three layers of Ag/α-Si/Ag of thickness 28/60/28 nm thickness. The three layers are perforated by elliptical holes (a, b = 227, 164 nm) with a sidewall angle ϑ=8°.*

The optical properties of the metamaterial are modulated by photoexciting carriers into the semiconductor layer, i.e. the α-Si layer. By flooding the α-Si with photoexcited electrons and holes, it behaves temporarily like a conductor. Thereby, the basic metamaterial structure behaves temporarily like a metal-metal-metal stack rather than the designed metal-semiconductor-metal stack. This changes its basic optical properties on the timescale that the carriers survive in the α-Si. Here, we use a sub-100 femtosecond, visible pump pulse to photoexcite carriers above the α -Si bandgap (~731 nm). We measure the transmission of a near-IR probe pulse through the device with and without photoexcitation. By delaying the probe pulse with respect to the pump pulse, we obtain the time-resolved change in transmission on a scale of picoseconds. The visible pump and near-IR probe pulses were obtained by using a 100 kHz, sub-60 fs, 800 nm regenerative amplifier to simultaneously seed visible and NIR optical parametric amplifiers (OPA).

Due to the elliptical holes in the metamaterial, there is a strong negative index resonance only for one polarization. Correspondingly, a strong pump-probe signal is observed only for that probe polarization. In Figure 2, the change in transmission of the near-IR probe pulse ($\Delta T/T$) versus pump-probe delay at three different pump fluences is plotted. Here, the pump (probe) is at 550 nm (1180 nm). The dashed lines show a numerical fit to the data. We see a fast 600 fs component, an intermediate few-picosecond component, and a slow nanosecond component. The inset shows the total modulation and the relative contributions of each of these components as a function of pump pulse power. Over 80% of the signal amplitude is due to the fast 600 fs component, which increases rapidly with pump fluence. A $\Delta T/T$ of ~ 20% was obtained at the highest available 550 nm pump fluence of 1.35 mJ/cm$^2$. This translates to a mere 3nJ of energy to modulate a single bit in our demonstration. One can scale the energy requirements of the device into the pJ/bit range by easily reducing the probe spot size.

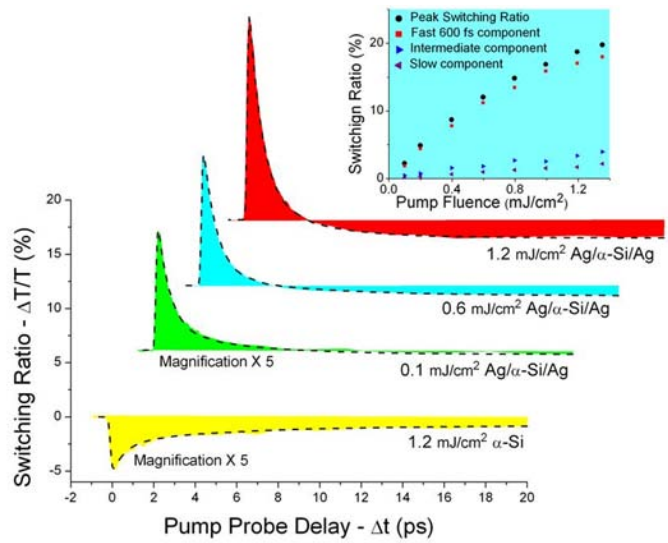


*Figure 2. The time-resolved change in transmission through Metamaterial device. We see that the significant modulation takes place within a picosecond. For the highest pump power available, we obtain ~20% modulation.*

In conclusion, we have demonstrated a nanometer scale, sub-picosecond metamaterial device capable of over Tb/s all-optical communication in the near-IR. We achieve a 600 fs device response by utilizing a regime of sub-ps carrier dynamics in α-Si and 20% modulation in a path length of only 116 nm by exploiting the strong nonlinearities in metamaterials. We introduce a new, shorter wavelength, higher-order negative-index resonance in fishnet metamaterial structures, thereby allowing us to extend device functionality from 1.0 – 2.0 µm via structural tuning. This device opens the door to other compact, tunable, ultrafast photonic devices and applications.

*Non-linear Infrared Spectroscopy of Strongly Correlated Systems:* In order to study quasiparticle interactions in strongly correlated systems, it is important to create low-energy excitations and then probe the dynamics in the far-IR. It is also convenient for the instrumentation to be able to create high energy excitation when desired, allowing for easy comparison to previous studies in strongly correlated materials. We have successfully designed, built and tested such a system.

Figure 3 shows the basic design of our optical system. We start with a commercial 3W pulsed laser, with pulses of 800 nm wavelength, 60 fs pulse durations and a repetition rate of 1-kHz. Approximately 1.5 W of energy from this amplified laser are directed towards an Optical Parametric Amplifier (TOPAS) that generates light from 1.2 - 25 µm, depending on the adjustable configurations of the TOPAS. Of the remaining 1.5 W of energy, 1 W is used to provide high-intensity, high-energy 800 nm pump pulses, if required. These pulses can also be frequency doubled to

produce 400 nm or 266 nm pulses. The remaining 0.5W of laser energy is used to generate and detect few-cycle THz pulses using ZnTe crystals as emitters and detectors.

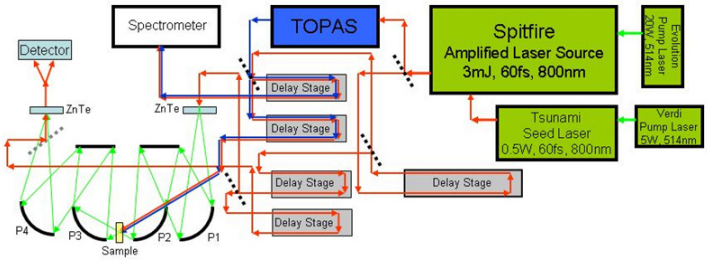


*Figure 3. Layout of the Pump-Probe system capable of exciting with high-energy (3.0eV) to low energy (48meV) excitations while probing optical conductivity dynamics with picosecond THz pulses.*

This instrumentation thereby allows us to compare the dynamics of strongly correlated systems when excited by high energy optical pulses (e.g. 400nm or 3eV pulses) as well as when the system is excited by very low energy excitation of 25 µm wavelength (48meV). Such a comparison will be a powerful tool, allowing us to gain new understanding regarding low-energy excitations and will add significant depth to previous studies using high-energy excitations. In order to compare these results effectively, it is important that the system allow for easy transitions from the high-energy pulses to the low-energy pulses generated by the TOPAS. Great care has been taken in the design and building of the optical system, such that minimal effort is required to switch (~5min) and other experimental parameters (e.g. pulse timing, power, etc.) can be effectively compared.

In addition, it is important to be able to focus the low energy mid-IR pulses as tightly as possible, since we require large intensities for the experiments and the energy output of the TOPAS falls dramatically as we get to the long wavelengths or low energy outputs. Small pump spot sizes require small THz spot sizes, since the THz probe spot must probe only that area on the sample that has been photoexcited. Using 4” diameter parabolic mirrors and the right combination of focal lengths of the THz optical system (P1=P4=12.8”, P2=P3=6” in Figure 3), we obtain THz spot sizes of 900 µm in diameter. This is very close to the diffraction limit of THz pulses, since radiation at 1 THz has a wavelength of 300 µm.

In order to test our system, we performed initial experiments at 10K on a low-energy bandgap semiconductor – InSb, as indicated in Figure 4. After photoexciting carriers above the InSb bandgap (5.2 microns or 230meV at 0K), we measure the conductivity of the photoexcited carriers with THz probe pulses. Thereby we access the dynamics of the photoexcited carriers in the semiconductor. As we decrease the energy of our pump pulse below the InSb bandgap, we see a rapid decrease in the signal. In this case, since the photoexcitation pump energies are below the bandgap, no carriers are generated and the THz pulses pass through the semiconductor unaffected.

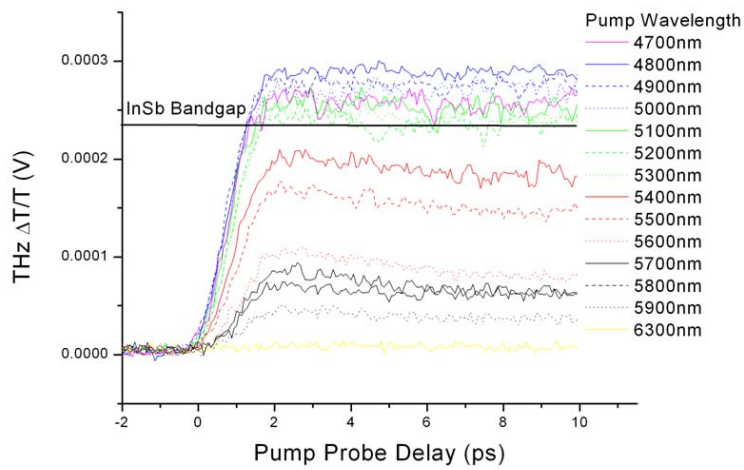


*Figure 4. THz conductivity dynamics resulting from low-energy bandgap excitation of InSb. We see a strong THz conductivity response only when pumping above the InSb bandgap (230meV or 5.2 µm). Excitations below the bandgap show a rapidly decreasing signal while also exhibiting a different temporal profile. The change in temporal profile is indicative of a change in interaction dynamic.*

Besides confirming our ability to excite low-energy modes, this data already reveals some interesting carrier dynamics. When exciting above the bandgap, the decay of photoexcited carriers remains relatively flat over the short time period of measurement (~10 ps).However, as we excite below the bandgap, in addition to the decrease in signal strength, we also see a short peak start to develop close to zero pump-probe delay. This is an indication of another mechanism or dynamic coming into play as the photoexcited carriers decay. In this way, ultrafast spectroscopy can separate out the complex interactions that come into play in strongly correlated systems – different interactions occur on different timescales allowing us to separate their mechanism and relative importance in a time-resolved measurement.

## Impact on National Missions

This project on the ultrafast spectroscopy of complex materials has a direct impact on next generation materials and devices, ranging from high-temperature superconductors to semiconductors to nanostructures, all of which are important to DOE missions in national

security. Our new device not only promises to contribute significantly to high-speed communication – essential for national security in today's data driven world, but will also lead to significant advances in the next generation of ultrafast, energy efficient photonic devices. The instrumentation to study non-linear infrared spectroscopy of strongly correlated systems will open new avenues in the understanding of these complex materials and their interactions. This will provide critical information for both basic science and materials technology.

## References


1. Ginzburg, V. L.. High-temperature superconductivity . 1991. *Soviet Physics Usp.* **34**: 283.

2. Sarychev, A. K., and V. M. Shalaev. Electrodynamics of metamaterials. 2007.

3. Chemla, D. S., and J. Shah. Many-body and correlation effects in semiconductors. 2001. *Nature.* **411**: 549.

4. Averitt, R. D., and A. J. Taylor. Ultrafast optical and far-infrared quasiparticle dynamics in correlated electron materials. 2002. *Journal of Physics of Condensed Matter.* **14**: R1357.

5. Dani, K. M., Z. Ku, P. Upadhya, R. Prasankumar, S. R. J. Brueck, and A. J. Taylor. Subpicosecond optical switching with a negative index metamaterial. . To appear in *Nano Letters.*

6. Ku, Z., K. M. Dani, P. C. Upadhya, and S. R. J. Brueck. Bianisotropic negative-index metamaterial embedded in a symmetric medium. 2009. *Journal of the Optical Society B.* **26**: B35.


## Publications


Dani, K. M., I. A. Cotoros, J. Wang, J. Tignon, D. S. Chemla, E. G. Kavousanaki, and I. A. Perakis. Observation of an inter-Landau level quantum coherence in semiconductor quantum wells. 2008. *Physical Review B.* **78**: 041301R.

Dani, K. M., Z. Ku, P. C. Upadhya, R. Prasankumar, S. R. J. Brueck, and A. J. Taylor. Subpicosecond optical switching with a negative index metamaterial Dani, K. M., Z. Ku, P. C. Upadhya, R. P. Prasankumar, S. R. J. Brueck, and A. J. Taylor. Sub-picosecond optical switching with a negative index metamaterial . To appear in *Nano Letters.*

Ku, Z., K. M. Dani, P. C. Upadhya, and S. R. J Brueck. Bianisotropic negative index metamaterial embedded in a symmetric medium. 2009. *Journal of the Optical Society B.* **26** (12): B34.

# Time-Dependent Density Functional Theory for Ultrafast Optical Phenomena in Strongly Correlated Electron Materials

*Jian-Xin Zhu*
20070690PRD3

## Abstract

Electronic properties control the functionality of electronic devices. From this aspect, the understanding of electronic low-lying excitations becomes extremely important. Time-resolved techniques such as ultrafast optical spectroscopy are making strides. In this project, we (i) apply existing first-principle techniques based on time-dependent density functional theory to study these electronic excitations in atoms, single molecules, and polymers; and (ii) develop a fully microscopic theory to investigate the time-resolved electronic excitation process and the response of resultant nonequilibrium strongly correlated systems such as unconventional superconductors. The developed theory will be used to interpret the measurements by the Los Alamos Ultrafast Optical Spectroscopy team of transition-metal, lanthanide and actinide systems.

## Background and Research Objectives

Theoretical understanding of electronic structures of molecules and solids plays a crucial role in the design, synthesis, and improvement of materials. The most efficient way to calculate the properties of materials is density functional theory (DFT), in which the energy of the system can be expressed as a functional of the electron density. Because the DFT is a fast method capable of treating large systems and no other methods can achieve comparable accuracy at the same computational cost, development of DFT has provided alternative to conventional wavefunction methods. With the rapid development of reliable density functionals, this theory has become the most popular method in electronic structure calculations, and has made a notable impact on condensed matter physics, chemistry, and molecular biology. Since the DFT is only suitable to describe the ground-state properties, it cannot properly describe the time-dependent or excited-state processes. Time-dependent (TD) DFT is the most important extension of the ground-state DFT and in recent years it has become a powerful tool in the calculation of dynamical properties of materials.

With the dramatic improvement of short-time pulse experimental techniques, many important advances in femtosecond optics have been achieved in recent years. In order to fundamentally understand the physics behind these optical phenomena, in particular the significance of quantum many-body effects, it is necessary to perform a detailed theoretical analysis on these time-dependent processes. This analysis can also serve as a guide in the design of materials with desired properties and in the application of this technology to fabrication and optimization of fast-switching devices. The technique becomes significantly important in the area of strongly correlated electron materials, for which the conventional density functional theory fails.

## Scientific Approach and Accomplishments

We carried out the project by using two complementary approaches. The first one is based on the first principle electronic structure calculations with the DFT method. This approach is conventional and the results correspond to the experimental measurement in the linear response regime, that is, under the condition that the external field does not disturb the system away from its equilibrium. The second one is based on quantum mechanics theory for nonequilibrium systems. In this setting, one first disturbs the system out of its equilibrium state and then measures the system response.

In the development and application of DFT, we have completed the following work:

(i) We have tested a nonempirical density functional on jellium, which is a simple model of metals and a standard testing ground for density functionals, both for bulk and for surface properties. We have calculated the surface properties of jellium in the presence of magnetic fields. The results [1] agree well with those of the highly-accurate but computationally-demanding

Quantum Monte Carlo method; (ii) Atomic shell structure, electron pair domains, π-electron subsystems, etc., are common concepts in descriptive chemistry and play a significant role in modern electronic structure theory. These concepts help us to visualize the bonding between atoms in terms of small groups of localized electrons (e.g. two electrons of opposite spin in a simple covalent bond) and therefore play an important role in predicting new molecular structures and in describing structural changes due to chemical reactions. Recently we have constructed a physically-motivated electron localization function [2] in terms of the quantum stress, which can be easily calculated from DFT; (iii) We have found a way to construct [3.4,5] more accurate energy functionals. These high-level energy functionals may solve the problems that commonly-used density functionals have encountered; (iv) Successful prediction of lattice constants plays a crucial role in the design and fabrication of the electronic devices. It is well known that van der Waals interaction affects the properties of materials. We proposed a simple way [6] to evaluate the effect of the van der Waals interaction upon the DFT lattice constants of the alkali metals.

Excitation energy is an important quantity in chemistry and biology. Successful prediction of this quantity plays a significant role in the study of chemical reaction mechanism, biological process, and light-emitting materials. Recently we have proposed a theoretical way [7] to calculate excitation energies. This method is exact for one-electron systems and for many-electron systems at sufficiently high frequency. We have also tested [8] commonly-used time-dependent (TD) DFT methods on the excitation energies of prototype small molecules, for which accurate experimental values are available for comparison. We have found that TDDFT can give an excellent description of excitation energies of molecules. Encouraged by this result, we applied TDDFT to the calculation of absorption spectra of light-emitting organic materials. These organic electroluminescence materials have been used to develop high-performance organic light-emitting diodes and can be employed to fabricate high-resolution, full-color, and flat-panel displays. Our calculations [9,10] show that the calculated TDDFT excitation energies agree well with experiment for molecular materials. However, the TDDFT excitation energies [11] of conjugated polymers agree with experiment only when the dihedral angles obtained from the ground-state DFT calculation are close to experimental measurements. This investigation provides a detailed interpretation of experiments and relevant guide for experimentalists to search for luminescence materials with desirable multifunctional properties.

In the study of quasiparticle relaxation of superconductors and optical conductivity, we formulated a microscopic theory in time domain to calculate the dynamics of quasiparticles in metals and superconductors exposed in a time-dependent laser field. The theory is illustrated with superconductors of both *d*-wave and *s*-wave pairing symmetry.

## Impact on National Missions

Los Alamos National Laboratory is one of world leaders in the experimental study of optical properties in functional materials, ranging from the nanoscale semiconductors, biological molecules, all the way to the complex materials including transitional-metal oxides, lanthanides, and actinides. In these latter materials, the kinetic energy and Coulomb interactions among electrons are competing with each other. As such the electrons have the dilemma to decide their fate as to whether they should be itinerant or localized in space. The strong correlation gives rise to many anomalous phenomena, which are challenging modern condensed matter physicists. The ultra-fast optical spectroscopy can characterize the competing energy scales. Conventionally, these optical phenomena are understood within some phenomenological model. This project goes beyond an effective model and develops a full microscopic model to treat the pump and probe field on the same footing. The developed technique will provide a theoretical underpinning of the optical phenomena. It will support experimental effort in this important area.

## References


1. Tao, J., J. P. Perdew, L. M. Almeida, C. Fiolhais, and S. Kummel. Nonempirical density functionals investigated for jellium: spin-polarized surfaces, spherical clusters, and bulk linear response. 2008. *Physical Review B.* **77**: 2454107.

2. Tao, J., G. Vignale, and I. V. Tokatly. Quantum stress focusing in descriptive chemistry. 2008. *Physical Review Letters.* **100**: 206405.

3. Tao, J., V. N. Staroverov, G. E. Scuseria, and J. P. Perdew. Exact-exchange energy density in the gauge of a semilocal density functional approximation . 2008. *Physical Review A.* **77**: 012509.

4. Perdew, J. P., V. N. Staroverov, J. Tao, and G. E. Scuseria. Density functional with full exact exchange: balanced nonlocality of correlation, and constraint satisfaction. 2008. *Physical Review A.* **78**: 052513.

5. Perdew, J. P., and J. Tao. When does static correlation scale to the high-density limit as exchange does?. *Journal of Molecular Structure: (THEOCHEM).*

6. Tao, J., J. P. Perdew, and A. Ruzsinszky. Long-range van der Waals attraction and alkali-metal lattice constants. *Physical Review Letters.*

7. Tao, J., X. Gao, G. Vignale, and I. V. Tokatly. Linear continuum mechanics for quantum many-body systems. 2009. *Physical Review Letters.* **103**: 086401.

8. Tao, J., S. Tretiak, and J. X. Zhu. Absorption spectra of blue-light emitting oligoquinolines from time-dependent density functional theory. 2008. *Journal of Physical Chemistry B.* **112**: 13701.

9. Tao, J., S. Tretiak, and J. X. Zhu. Excitation energies from a time-dependent nonempirical density functional. 2008. *Journal of Chemical Physics.* **128**: 084110.

10. Tao, J., and S. Tretiak. Absorption spectra of new blue-light emitting oligoquinolines bearing pyrenyl and triphenyl endgroups from time-dependent density functional theory. 2009. *Journal of Chemical Theory and Computation.* **5**: 866.

11. Tao, J., S. Tretiak, and J. X. Zhu. Can time-dependent density functional theory predict the excitation energies of conjugated polymers?. *Physical Review B.*

## Publications

Perdew, J. P., V. N. Staroverov, J. Tao, and G. E. Scuseria. Density functional with full exact ex- change: balanced nonlocality of correlation, and constraint satisfaction. 2008. *Physical Review A.* **78**: 052513.

Tao, J.. Van der Waals-corrected density functional theory. Presented at *Workshop on mathematical and algorithmic challenges in electronic structure theory.* (Minnesota, Sept. 29-Oct. 3, 2008).

Tao, J., G. Vignale, and I. V. Tokatly. Quantum stress focusing in descriptive chemistry. 2008. *Physical Review Letters.* **100**: 206405.

Tao, J., I. V. Tokatly, and G. Vignale. Quantum stress focusing in descriptive chemistry. 2008. In *American Physical Society March Meeting.* (New Orleans, March 10-14, 2008). Vol. 53, p. 275. College Park, MD: American Physical Society.

Tao, J., J. P. Perdew, L. M. Almeida, C. Fiolhais, and S. Kummel. Nonempirical density functionals investigated for jellium: spin-polarized surfaces, spherical clusters, and bulk linear response. 2008. *Physical Review B.* **77**: 2454107.

Tao, J., S. Tretiak, and J. X. Zhu. Excitation energies from a time-dependent nonempirical density functional. 2008. *Journal of Chemical Physics.* **128**: 084110.

Tao, J., S. Tretiak, and J. X. Zhu. Absorption spectra of blue-light emitting oligoquinolines from time-dependent density functional theory. 2008. *Journal of Physical Chemistry.* **128**: 084110.

Tao, J., S. Tretiak, and J. X. Zhu. Can time-dependent density functional theory predict the excitation energies of conjugated polymers?. *Physical Review B.*

Tao, J., V. N. Staroverov, G. E. Scuseria, and J. P. Perdew. Exact-exchange energy density in the gauge of a semilocal density functional approximation . 2008. *Physical Review A.* **77**: 012509.

Tao, J., X. Gao, G. Vignale, and I. V. Tokatly. Linear continuum mechanics for quantum many-body systems. 2009. *Physical Review Letters.* **103**: 086401.

Tao, J., and J. X. Zhu. Optical conductivity in strongly correlated electron materials. 2008. In *American Physical Society March Meeting.* (New Orleans, March 10-14, 2008). Vol. 53, p. 391. College Park, MD: American Physical Society.

Tao, J., and J. X. Zhu. Real-time photoinduced quasi-particle excitation of superconductors. 2009. In *American Physical Society March Meeting.* (Pittsburgh, 15-20 March). , p. Q33.00008. Pittsburgh: American Physical Society.

# Sensitization of Lanthanide Ion Fluorescence Using Nanocrystal Quantum Dots

*Jennifer A. Hollingsworth*
20070722PRD3

## Abstract

Once excited, lanthanide (Ln) ions emit light for long (millisecond) lifetimes. Depending on which Ln photoemitter is chosen, light emission can be obtained in the visible and/or the infrared (IR), and it is ultra-narrowband. These characteristics, and especially the long luminescence lifetimes, make Ln's ideal candidates for applications in 1) imaging biological molecules and clinical diagnostics, 2) optical amplification and lasing, and 3) photon up-conversion (lower energy excitation yields higher energy emission). However, Ln's absorb light only weakly, which leads to reduced brightness and has prevented their full exploitation in these areas. Further, Ln emission can be "deactivated" (vibrationally quenched) in the presence of common chemicals, especially protic solvents (O-H and N-H bonds). Our work focused on semiconductor nanocrystal quantum dots (NQDs) as novel sensitizing agents to enhance Ln absorption and protect Ln emission.

## Background and Research Objectives

Lanthanides (Ln's) are stable, narrow-band photoemitters with long millisecond life-times. Depending on the Ln, emission can be obtained in the visible and/or the infrared (IR). These characteristics, and especially the long luminescence lifetimes, make Ln's ideal candidates for applications in (1) *bio-imaging and clinical diagnostics*, where the long lifetimes allow for facile discrimination between background autofluorescence from biological material, characterized by short lifetimes, and the Ln optical tag signal using simple time-gating techniques, (2) *optical amplification and lasing*, where long lifetimes support the creation of the required excited-state/ground-state population inver-sions, and (3) *photon up-conversion (lower energy excitation → higher energy emission)*, where the long lifetimes support the required excited-state absorption processes. However, Ln's have small absorption coefficients, which has prevented their full exploitation in these areas.

For this reason, much research is currently focused on enhancing Ln absorption through sensitization. The approaches explored most commonly suffer from limited absorptivities and/or tunability of the employed sensitizers. We sought to make use of an alternative class of sensitizers, namely, semiconductor nanocrystal quantum dots (NQDs). NQDs are characterized by large absorption cross sections over a wide spectral range and tunable color responses, and thus were predicted to serve as effective "light antenna" in an NQD-Ln coupled system. Furthermore, it was anticipated that these NQD antenna would then transfer their collected energy to their Ln partners. It has been demonstrated previously that NQDs serve as efficient energy transfer (ET) partners for a variety of materials systems—from other NQDs to dye molecules to transition metal luminescent ions. By optimizing the chemical coupling strategies for creating Ln-NQD ET pairs, we sought to facilitate excitation of efficient Ln ion emission and, thereby, contribute to the establishment of a new class of functional, hybrid fluorophores with utility in key applications from bio-imaging to solid-state lighting.

## Scientific Approach and Accomplishments

We proposed a novel approach to sensitizing Ln emitters, namely, the use of NQDs as efficient absorbers and ET agents for (1) Ln's doped directly into an NQD matrix and (2) Ln nanophosphors (*e.g.*, $LaPO_4$:Ln) associated with or chemically attached to NQDs. NQDs constitute extremely efficient and broadband absorbers (absorption coefficients up to several orders of magnitude greater than organic dyes). Further, NQDs can efficiently transfer excitation energy to an ET couple, as has been demonstrated extensively for NQD-NQD ET systems, as well as NQD-organic dye ET systems. We anticipated that the NQD sensitizer would enable direct Ln fluorescence via single-photon excitation, as well as Ln up-conversion fluorescence via

population of higher Ln excited states through sequential ET of multiple photons. We focused on indium phosphide (InP) and indium oxide ($In_2O_3$) as the NQD component of the NQD-Ln ET couple, though CdSe NQDs were also employed. The In-based compositions comprise non-toxic and environmentally friendly alternatives to the more traditional heavy-metal based materials (e.g., cadmium and lead selenide). Furthermore, indium-based NQDs were considered reasonable matrices for doping of $Ln^{3+}$ ions based on comparable ionic radii and equivalent charge (e.g., ytterbium, $Yb^{3+}$: 101 pm vs. $In^{3+}$: 94 pm) for improved NQD dopant compatibility – important criteria as NQDs may extrude defects (such as dopant ions) to the NQD surface. It was determined to be critical that the Ln ions would be well segregated to the core of the NQD (or the inert matrix, *e.g.*, $LaPO_4$) to prevent significant interaction of the Ln with surface-associated solvent molecules that, through vibrational quenching, would otherwise defeat the emission processes. Finally, through particle size control, the InP NQD emission (semiconductor bandgap) energy could be tuned from the blue-visible to the very near-IR (~850 nm), while $In_2O_3$ provided access to ultraviolet energies. By controllably altering NQD emission energies, we intended to optimize NQD-Ln couples for sensitization and, ultimately, Ln emission efficiencies.

During the first third of the project, we utilized $In_2O_3$, a $III_2VI_3$ NQD, as an active matrix for protecting *and* sensitizing $Eu^{3+}$ emission. We achieved sensitized $Ln^{3+}$ emission with significantly improved quantum yields (QYs) compared to literature values, and we conclusively showed simultaneous protection of the $Ln^{3+}$ emission. Finally, we demonstrated a simple and effective chemical extraction procedure for providing definitive chemical evidence for $Ln^{3+}$ incorporation that is generalizable to other NQD:Ln systems. [See Performance Data Publications.]

Specifically, $In_2O_3$:Eu NQDs were prepared from n-decanol, $Eu(NO_3)_3$, $In(OAc)_3$, and myristic acid in octadecene. After 7-70 m growth at 290 °C, the Ln-"doped" NQDs were purified by precipitation with acetone-methanol (3:1 v/v). Examination of $In_2O_3$:Eu NQDs in hexane by steady-state PL spectroscopy (*cw*-PL) showed a broad $In_2O_3$ NQD emission centered at 390 nm and sharp peaks typical of Eu3+-based luminescence at 588 nm ($^5D_0$ to $^7F_1$), 614 nm ($^5D_0$ to $^7F_2$), and 698 nm ($^5D_0$ to $^7F_4$) (fwhm = 7-18 nm) (Figure 1). PL QYs ranged from 1-6% for $In_2O_3$ and 0.1-0.6% for sensitized $Eu^{3+}$ emission ($l_{exc}$ = 330 nm, avoiding possible direct excitation of $Eu^{3+}$). The latter is ~1000-fold higher than that previously reported for $Tb^{3+}$ in CdSe NQDs [2] and ~10-fold higher than that previously reported for $Eu^{3+}$ in $TiO_2$ NQDs [3]. QYs showed some variation based on Eu content and NQD growth times.

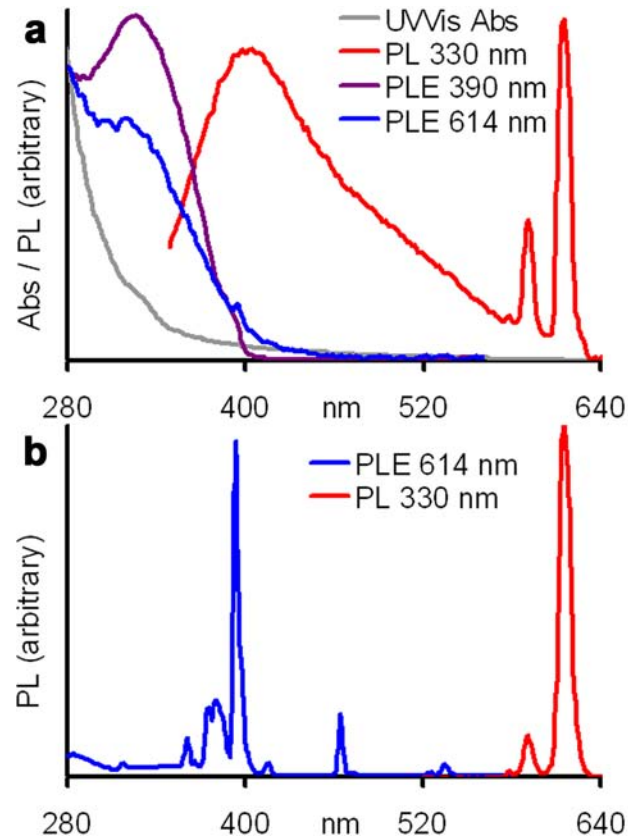


*Figure 1. (a) Absorption (Abs), PL and PLE spectra of $In_2O_3$:Eu NQDs, (b) PL and PLE of $Eu(NO_3)_3$/TOP.*

To confirm $Eu^{3+}$ sensitization through the NQD host, photoluminescence excitation (PLE) spectra were obtained for $In_2O_3$:Eu NQDs at the main Eu emission wavelength (614 nm) (Figure 1). To confirm $Eu^{3+}$ protection resulting from incorporation into the $In_2O_3$matrix, we performed time-resolved PL spectroscopy and monitored the time decay in Eu3+ emission intensity ($\lambda_{em}$ = 614 nm) for $In_2O_3$:Eu NQDs and different $Eu^{3+}$ control samples in various solution environments (Figure 2). The $In_2O_3$:Eu NQD time constant was used to estimate the *intrinsic* QY of the $Eu^{3+}$ ions. Assuming a radiative lifetime for $Eu^{3+}$ of 9.0 ms (taking into account the dielectric interface effect between $In_2O_3$ and hexane), we obtained QYs of 6%. The significant difference between the intrinsic QY and the sensitized QY implied that $In_2O_3$ NQD emission remains favored over energy transfer to $Eu^{3+}$. Nevertheless, absorption and PLE results indicated that sensitization is important — direct $Eu^{3+}$ excitation was not evident in absorption spectra (clearly dominated by $In_2O_3$), nor, in general, in PLE. The PLE in Figure 1 is an exception (395 nm $Eu^{3+}$ peak is visible). Even here, the sensitization factor (sensitized $Eu^{3+}$ PLE intensity/direct $Eu^{3+}$ PLE intensity) was found to be 3.3 at 395 nm, while that at excitation wavelengths for which there is no strong $Eu^{3+}$ peak is even higher (12 at 350 nm; 18 at 330 nm). We were thus able to conclude that the $In_2O_3$ matrix provides for facile excitation at wavelengths inaccessible by direct

$Eu^{3+}$ excitation. Finally, the $In_2O_3$:Eu NQDs were structurally characterized by X-ray diffraction (XRD) and transmission electron microscopy (TEM) (Figure 3).

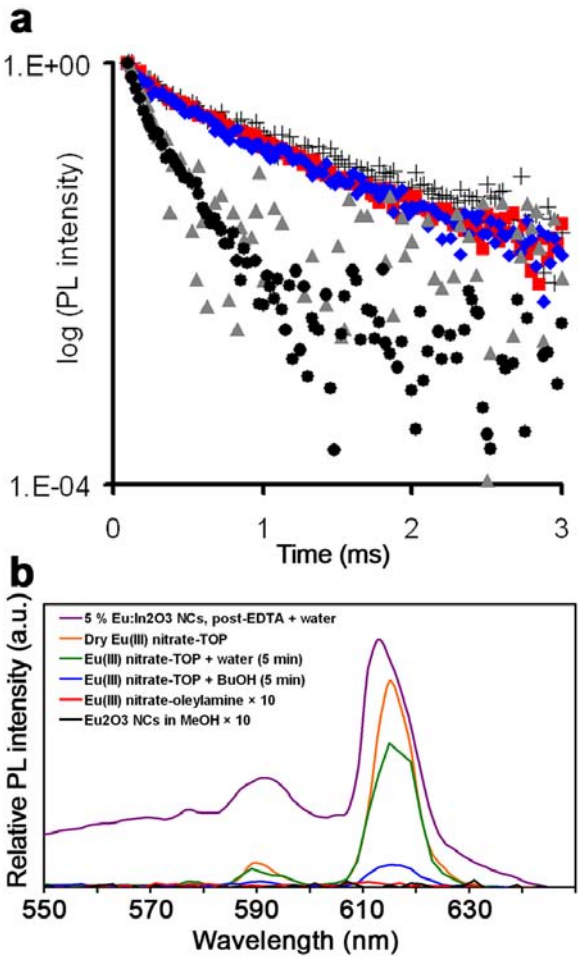


*Figure 2. a. PL time-decay (emission wavelength = 614 nm, excitation wavelength = 355 nm) for 50% (red square) and 5% Eu (blue diamond) $In_2O_3$:Eu NQDs, $Eu(NO_3)_3$/TOP (+), $Eu(NO_3)_3$/ oleylamine (black circle), and $Eu_2O_3$ NCs/MeOH (gray triangle). b. Photoluminescence spectra for the controls and the $In_2O_3$:Eu NQDs, revealing that addition of water or other protic reagents quenches control emissions but does not affect emission from the $In_2O_3$:Eu NQDs.*

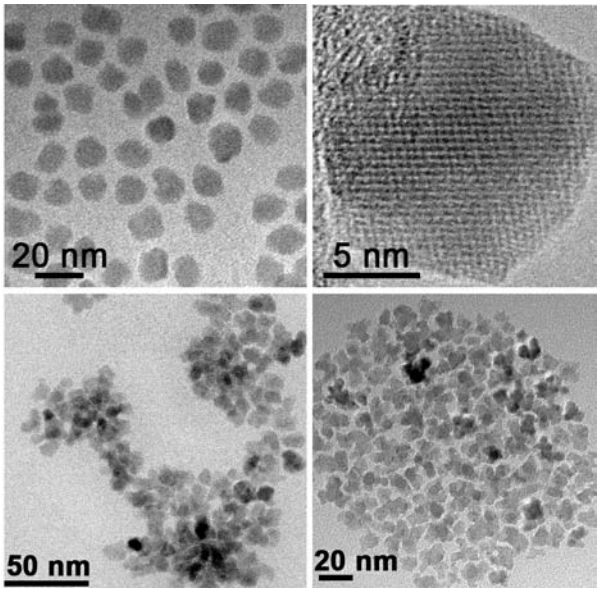


*Figure 3. Low (left) and high-resolution (right) TEM images of $In_2O_3$:Eu NQDs (5% Eu).*

During the second third of the project and working from the successes of our Eu-doped $In_2O_3$ effort, we attempted to prepare additional NQD-Ln couples by way of NQD doping but using (1) alternative Ln ions and (2) alternative NQD compositions. We developed synthetic procedures for the preparation of several new Ln-doped NQDs – $In_2O_3$:Er, $In_2O_3$:Yb, and $In_2O_3$:Yb/Er. For these, the goal was to obtain near-infrared emission by way of ultraviolet light excitation of the $In_2O_3$ matrix. To date, we have not been able to detect the anticipated infrared emission (i.e., 1540 nm from Er-doped $In_2O_3$ and 980 nm emission from Yb-doped $In_2O_3$). Attempts to characterize these systems using energy dispersive X-ray spectroscopy (EDX) have been inconclusive, implying that doping levels are lower than anticipated based on the reaction chemistries employed. Energetically, the Yb-doped systems were not ideal, as Yb has a unique transition at ~960 nm considerably red-shifted from the $In_2O_3$ emission. However, Er ions can be excited at 380 nm providing for excellent overlap with $In_2O_3$ emission. In addition to $In_2O_3$ as an NQD matrix, we attempted an InP matrix.

Synthetic procedures were also developed for InP:Er, InP:Yb, and InP:Yb,Er Ln-doped NQDs. Similar to the new $In_2O_3$ systems, infrared emission was not apparent for the InP-based materials, and EDX was equally inconclusive. Up to this point, we had based our choice of NQD largely on whether or not its semiconductor bandgap energy (effectively emission energy) matched an absorbing transition in the Ln. However, given the poor performance of our more recently attempted NQD-Ln systems, we became concerned that NQD semiconductor bandgap energies were perhaps not the primary factor

in determining whether an NQD could efficiently transfer absorbed energy to a Ln dopant. Depending on the mechanism of ET—Forster-like (coulombic interaction) or Dexter-like (electron-exchange interaction)—the bandgap energy overlap may be less important than absolute energy-level overlap, especially of the NQD conduction band energy with the Ln redox potential energy, respectively. We, therefore, compiled the available data for NQDs and Ln's and determined that if electron-exchange interactions dominated NQD-Ln interactions, then neither $In_2O_3$ nor InP NQDs were ideal candidates for ET-pair systems. Rather, ZnSe was found to be a more ideal matrix, at least for Yb and Eu, and neglecting bandgap overlap with Ln excitation energies. We therefore prepared ZnSe:Eu and ZnSe:Yb. The Eu version provided the anticipated emission in the red-visible, while the Yb version remained optically silent in the near-infrared. These systems require further optimization, however, by adjusting the Ln content and perhaps incorporating Er, rather than Yb.

We have also initiated work toward our second proposed coupling strategy – interacting NQDs with Ln nanophosphors. To this end, we synthesized $YVO_4$:Ln nanophosphors. These were: $Nd_{0.01}Y_{0.99}VO_4$, $Ho_{0.04}Y_{0.96}VO_4$, $Eu_{0.05}Y_{0.95}VO_4$, and $Er_{0.02}Yb_{0.20}Y_{0.78}VO_4$, where the former three were based on literature preparations and the latter represented new chemistry. In all cases, we were able to obtain spectra of the Ln emissions, ranging from the red-visible to the near-infrared depending upon the specific Ln. These nanophosphors were then mixed with NQDs and formed into solid-state films in order to obtain sensitization-enhanced Ln emission. The process of thin-film formation entailed mixing the two types of nanomaterials in a concentrated solution, dropcasting a droplet of the solution, and evaporating the solvent to leave a solid film. Here, it was necessary to co-solvate the nanomaterials, which entailed rendering the NQDs water-soluble (negatively charged surfaces). To date, we have prepared thin solid films from mixtures of the Ln nanophosphors ($YVO_4$:Nd and $YVO_4$:Eu) and NQDs (CdSe with emission energies of 586 nm and 520 nm, respectively). The films were subsequently analyzed by spectroscopic techniques, including an investigation of the impact of the relative concentrations of the two species—Ln nanoparticle and NQD—on the efficiency of sensitization.

Here, we provide spectral data for a representative system – $YVO_4$:Nd and 586 nm-emitting CdSe NQDs (Figure 4). The presence of CdSe NQDs provides for enhanced emission at all excitation energies, and it provides for excitation at energies at which the Nd does not possess a transition. Together, these results suggest that we can sensitize Ln-containing nanoparticles, both in terms of increasing the Ln's effective absorption cross section and in expanding the spectral window for excitation. However, photo-luminescence excitation spectroscopy (PLE) revealed that these effects of the NQDs are not a result of NQD-Ln energy transfer, but, instead, Ln re-absorption of NQD emission (Figure 5). This result suggested to us that we have likely not achieved intimate mixing of the two nanomaterials systems *at the nanoscale* in the thin solid films as currently prepared. Instead, the $YVO_4$:Nd and CdSe nanomaterials are more likely spatially segregated within the films, preventing efficient CdSe- $YVO_4$:Nd energy transfer, as energy transfer is a highly distance-dependent process. Finally, in addition to attempting to enhance Ln emission from Ln nanophosphors by coupling them to NQDs, we also sought to do so through higher Ln doping concentrations. We successfully modified the literature-reported synthesis [4] to increase doping levels from 1% to 5% and 10% in the $YVO_4$:Nd system. We observed an ~10-fold increase in emission in increasing the doping level to 5%. In contrast, at 10% loading, Nd-Nd quenching may have been active, as significant additional enhancement was not observed. Thus, a loading of between 5 and 10% may represent an upper loading limit for maximizing infrared emission signal from this system.

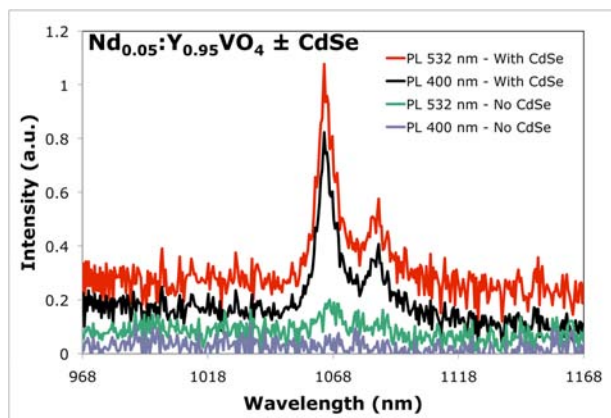


*Figure 4. Photoluminescence (PL) spectra obtained using a Horiba Jobin Yvon NanoLog Spectrofluorometer equipped with an InGaAs array infrared detector; excitation provided by a xenon lamp. Spectra show PL from Nd:$YVO_4$ nanophosphors co-deposited with CdSe nanocrystal quantum dots (NQDs) under 532 nm excitation (red trace) and 400 nm excitation (black trace), as well as PL from Nd:$YVO_4$ nanophosphors in the absence of CdSe NQDs under 532 nm excitation (green trace) and 400 nm excitation (purple trace).*

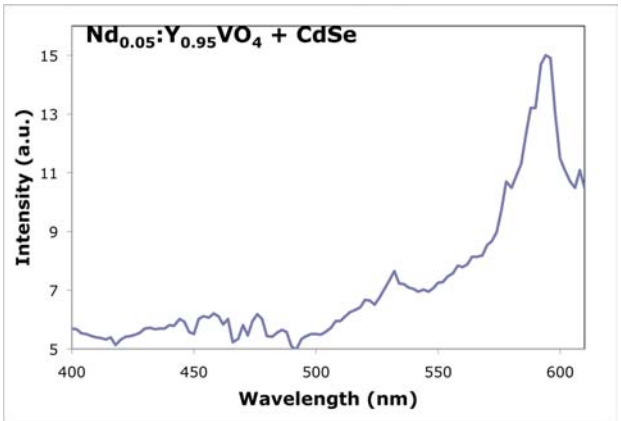


*Figure 5. Photoluminescence excitation spectrum (PLE) for 1066 nm emission from Nd:$YVO_4$ nanophosphors co-deposited with CdSe NQDs revealing excitation through Nd absorption, rather than through CdSe-Nd energy transfer.*

In the final third of the project, we attempted to achieve truly intimate—at the nanoscale—mixing of our Ln nanophosphors and NQDs. Our approach here was to provide the NQDs with positively charged surfaces. In this way, they were water soluble and able to electrostatically couple with our negatively charged $YVO_4$:Nd particles, providing a means for *direct chemical coupling* of these systems. We developed two approaches to assembling thin films comprising intimately mixed CdSe and $YVO_4$:Nd. First, we mixed the respective solutions, which resulted in immediate precipitation of electrostatically coupled aggregates that were collected by centrifugation, spread onto a glass slide, and pressed between the slide and a glass coverslip. Secondly, we used a dip-coating method to sequentially deposit monolayers of CdSe NQDs and $YVO_4$:Nd nanoparticles. In this case, up to ten monolayers of each material were deposited. Thin films obtained from both approaches were analyzed by PL and PLE, where infrared emission was detected upon excitation at 350 nm (a wavelength that does not produce Nd emission in the absence of CdSe) and where PLE suggested excitation was through the CdSe, rather than directly through the $YVO_4$:Nd. The results were promising, but require further investigation to be conclusive.

One of the goals in combining NQDs with Ln's is to synthesize a fluorophore that does not exhibit fluorescence intermittency, or "blinking." Given this aim, the Director's Funded Postdoc also became very active in our studies of blinking behavior in NQDs. He learned how to measure and analyze blinking in single-NQDs and made significant contributions to the publications in this area [see Performance Data Publications]. He also contributed significantly to our understanding of the effect of NQD growth conditions and crystal structure on blinking suppression.

## Impact on National Missions

This project supported the missions of the DOE Office of Science in advancing fundamental science in support of the national, economic, and energy security of the United States. The resulting scientific understanding will ultimately support technology advances in telecommunications, efficient lighting/lasing, secure printing, optical tags, bioimaging, and radiation detection.

## References

1. Bünzli, J. C., and C. Piguet. Taking advantage of luminescent lanthanide ions. 2005. *Chemical Society Reviews.* **34** (12): 1048.

2. Chengelis, D. A., A. M. Yingling, P. D. Badger, C. M. Shade, and S. Petoud. Incorporating lanthanide cations with cadmium selenide nanocrystals: A strategy to sensitize and protect Tb(III) . 2005. *Journal of the American Chemical Society.* **127** (48): 16752.

3. Stouwdam, J. W., and F. C. J. M. van Veggel. Sensitized emission in Ln(3+)-doped TiO2 semiconductor nanoparticles. 2004. *ChemPhysChem.* **5** (5): 743.

4. Buissette, V., A. Huignard, T. Gacoin, J. P. Boilot, P. Aschehoug, and B. Viana. Luminescence properties of YVO4:Ln (Ln = Nd, Yb, and Yb-Er) nanoparticles. 2003. *Surface Science.* **532-535**: 444.

## Publications

Chen, Y., J. Vela, H. Htoon, J. L. Casson, D. J. Werder, D. A. Bussian, V. I. Klimov, and J. A. Hollingsworth. "Giant" multishell CdSe nanocrystal quantum dots with suppressed blinking . 2008. *Journal of the American Chemical Society.* **130** (15): 5026.

Hollingsworth, J. A., J. Vela, Y. Chen, H. Htoon, V. I. Klimov, and A. R. Casson. Giant multishell CdSe nanocrystal quantum dots with suppressed blinking: novel fluorescent probes for real-time detection of single-molecule events. 2009. *Proceedings SPIE.* **7189**: 718904.

Vela, J., B. S. Prall, P. Rastogi, D. J. Werder, J. L. Casson, D. J. Williams, V. I. Klimov, and J. A. Hollingsworth. Sensitization and protection of lanthanide ion emission in In2O3:Eu nanocrystal quantum dots. 2008. *The Journal of Physical Chemistry - C.* **112** (51): 20246.

Vela, J., and J. A. Hollingsworth. Semiconductor nanocrystals: Doped compositions. 2008. In *Nanomaterials: Inorganic and bioinorganic perspectives.* Edited by Lukehart, C. M., and R. Scott. , p. 705. Chichester, UK: John Wiley & Sons, Inc..

# Chemically Synthesized Germanium Nanocrystals for Applications in Solar-Energy Conversion

*Victor I. Klimov*
20070723PRD3

## Abstract

Photovoltaic technologies will not be competitive with fossil fuels in the larger energy market until substantial reductions in the cost/efficiency ratio are achieved. One approach to accomplishing this is the development of more advanced solar cell designs capable of higher efficiencies, such as multi-junction "tandem" architectures or those capable of exploiting multiple exciton generation (carrier multiplication). Such cells require materials with narrow energy gaps, including non-toxic and relatively common germanium. The usefulness of germanium in its traditional "bulk" form in PV technologies, however, is limited by its indirect band gap (which results in poor light absorbance) and its instability towards oxidation. The goal of this research is to synthesize germanium nanocrystals by low-cost, scalable colloidal methods to overcome these shortcomings inherent in the bulk form. By careful choice of reactants and conditions, we were able to synthesize a series of germanium nanocrystals varying in size from 3 - 6 nm in diameter which show clear signs of partial direct-gap character in the infrared, including size-dependent fluorescence with unprecedented efficiencies up to 8%. We further demonstrate that oxidation can be suppressed by use of alkenes as terminating ligands, such that the resulting nanocrystals are stable for months under ambient conditions. These results have enabled follow-on research projects of fundamental importance to the science of quantum confinement, including advanced spectroscopic studies of carrier dynamics to confirm the origin of the fluorescence and probe the effect of confinement on Ge electronic properties. At the same time, the new Ge NCs have tremendous potential for immediate exploitation in advanced solar cell design and fabrication, including within our new DOE-funded Energy Frontier Research Center, the *Center for Advanced Solar Photophysics*. Because of both its significant fundamental and technological potential in advancing solar energy research, this work is vitally important to the DOE missions in Energy Security.

## Background and Research Objectives

With increasing concerns regarding elevated levels of carbon dioxide emission, solar radiation is widely considered the most attractive, sustainable, carbon-free energy source. However, current photovoltaic (PV) technologies encounter cost and scalability issues, and suffer from efficiencies that are significantly below the limits calculated based on thermodynamic considerations. Currently the PV industry is dominated by silicon. This material has an energy gap of ~ 1 eV, which is well suited for simple, single-junction devices. However, more advanced designs capable of higher efficiencies, such as multi-junction "tandem" architectures or those capable of exploiting multiple exciton generation (carrier multiplication), require materials with a narrower energy gap. One such promising material is germanium (Ge), which has a band gap of ~0.7 eV. The usefulness of Ge in its traditional "bulk" form in PV technologies, however, is limited because of the indirect character of its energy gap, which leads to poor light absorbance. Further, "chemical" factors such as formation of unstable oxides also complicate applications of Ge.

The purpose of this project was to develop a new synthesis of nanoscale colloidal Ge nanocrystals (NCs) with enhanced potential for applications in solar cells. Because of quantum-confinement effects unique to the nanoscale, Ge NCs should exhibit significant direct-gap character, including enhanced absorption compared to the bulk and, potentially, efficient fluorescence. While weak infrared fluorescence has been observed in Ge NCs fabricated by physical methods these methods are expensive, unscalable, and produce matrix- or substrate-bound NCs with limited potential for application. Colloidal synthesis, on the other hand is a cheap yet powerful method for producing high-quality NCs of a range of materials. Moreover, colloidal methods allow

unmatched control over surface termination, which not only can effect fluorescence efficiency, but also the stability of the NCs toward, e.g., oxidation. Previous to our work, however, efforts toward colloidal synthesis of Ge NCs had been largely unsuccessful, as control over size and crystallinity remained elusive, and infrared fluorescence had never been observed.

We found that Ge NCs of controlled size and high crystallinity could be made by a novel, controlled reduction pathway. We also discovered that alkene termination resulted in both good air-stability and previously unobserved infrared fluorescence. Finally, in conjunction with our synthesis work, other members of our team collaborated on studies of the electronic and optical properties of these new engineered nanostructures, with a focus on the role of quantum confinement in determining their electronic structure and behavior.

## Scientific Approach and Accomplishments

Our basic approach focused on employing reduction of germanium halides, such as $GeI_2$, by controlled methods in the presence of carefully chosen surfactant "ligands" that would give us the desired surface termination. This required careful examination of the desired reaction, and consideration of ideal reactant properties. For a high-melting element like Ge, highly crystalline NCs requires the use of relatively high reaction temperature. At the same time, it is also important to keep all reactants soluble, so that the reaction proceeds predictably. Hexadecylamine was chosen as the reaction solvent, because it proved to be particularly effective at dissolving $GeI_2$ and amenable to reaction temperatures at or above 300 °C. Likewise, highly-soluble n-butyllithium was chosen over more established but poorly-soluble reducing agents like alkali metals or metal hydrides. Finally, based on chemistry known for silicon, which is very similar to Ge, we used the long-chain alkene 1-octadecene (ODE) as a terminating surfactant ligand.

By slight variations of reaction concentrations and time, we were able to synthesize Ge NCs ranging in diameter from 3.2 ± 0.4 nm to 6.4 ± 1.9 nm. Most excitingly, these nanocrystals showed fluorescence with efficiencies of up to 8%, with a size-dependent peak wavelength ranging from 900-1400 nm (Figure 1B). In fact, the observed size-dependence trend was similar to that predicted for quantum-confined particles by a simple particle-in-a-box model, with exact values similar to those predicted by more sophisticated tight-binding calculations, highly suggesting that the infrared emission comes from a band-edge transition. These NCs were found to be highly crystalline cubic Ge by a combination of powder X-ray diffraction, energy dispersive X-ray spectroscopy, and high-resolution TEM (Figure 1A inset), with no evidence of Ge oxides.

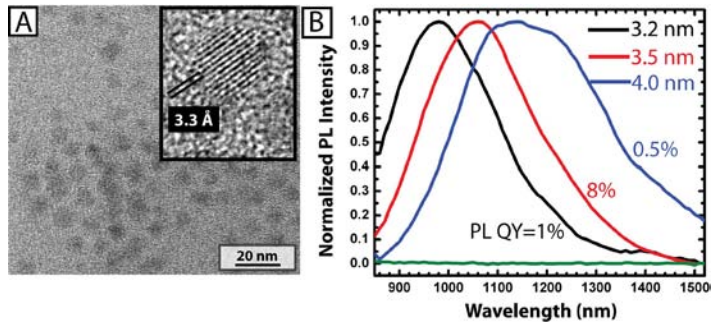


*Figure 1. A) Transmission electron microscope (TEM) image of colloidal Ge NCs. Inset features a high-resolution image demonstrating the high crystallinity. B) Size-dependent fluorescence [or photoluminescence (PL)] for three Ge NCs of three diameters. Green trace shows trioctylphosphine-terminated NCs, which are non-emissive.*

Ge NCs synthesized using ODE are not only emissive, but also demonstrably more stable towards oxidation than NCs made with other ligands, such as trioctylphosphine (TOP). This is demonstrated starkly in Figure 2A, in which hexane solutions of TOP-terminated (or "capped") and ODE-capped NCs were stirred in the presence of equal amounts of water. The ODE-capped sample remains distinctly brown, indicating the presence of Ge NCs, for at least several weeks, whereas, the TOP-capped solution loses all color within 72 hours, indicating that the NCs were oxidized into water-soluble germanium oxides. The enhanced qualities of ODE-capped Ge NCs are likely due to strong, covalent Ge-C bonds formed at the NC surfaces, evidence of which can be found in the Fourier transform infrared (FT-IR) spectra (Figure 2B). The lack of characteristic 1-alkene peaks (at ~900, ~1000, ~1620 and immediately higher than 3000 $cm^{-1}$) and the appearance of a sharp Ge-C stretch peak at 700 $cm^{-1}$ are indicative of the reaction of ODE with Ge NC surfaces. Further evidence of the effectiveness of this passivation in Ge NCs can also be found in Figure 2B. After 5 months under ambient conditions, spectra of TOP-capped NCs feature a strong, broad band at 840 $cm^{-1}$ not found for ODE-capped NCs, which can be attributed to Ge-O bonds. This implies that Ge-C bond formation enhances the resistance of Ge NCs towards oxidation.

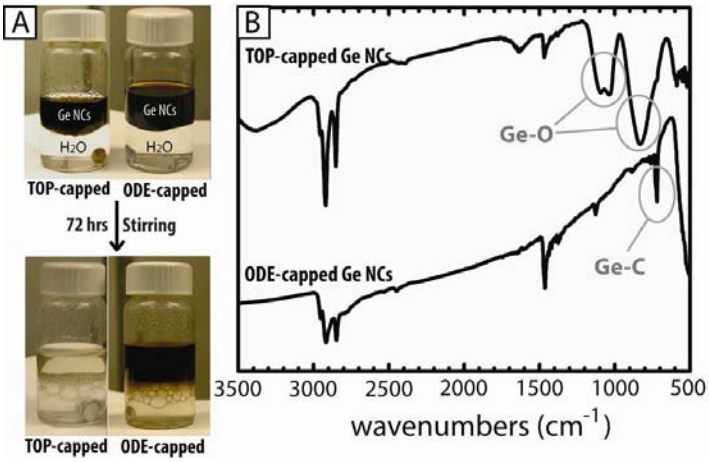


*Figure 2. A) Solutions of TOP-capped (left) and ODE-capped (right) Ge NCs, before (top) and after (bottom) rapid stirring with water for 72 hrs. While TOP-capped NCs are completely oxidized and dissolved, ODE-capped NCs remain. B) FT-IR spectra of TOP-capped and ODE-capped Ge NCs. ODE-capped NCs give signatures of strong Ge-C bond formation, while TOP-capped NCs give evidence of surface oxidation.*

This work produced the first colloidal Ge NCs with infrared fluorescence, which we attribute to a band edge transition. This is a key first step in demonstrating the relevance of Ge NCs in so-called Generation III photovoltaic devices, in which advanced physical concepts and low-cost fabrication methods are combined to produce solar cells with efficiencies at or above the thermodynamic limits of single-junction cells. Because of its importance to a general audience, this work was published in the *Journal of the American Chemical Society*, flagship journal of the world's largest scientific society [Lee, et al., *J. Am Chem. Soc.* **131**, 3436 (2009)].

Synthetic work conducted in this project has enabled a series of follow-up spectroscopic studies dealing with the effects of quantum confinement on electronic and optical properties of indirect-gap semiconductors. As one specific example, in a collaboration with other Softmatter Team members, the nature of the lowest-energy emitting states have been investigated using ultra-fast time-resolved fluorescence measurements as a function of temperature (1.7-300 K) and magnetic field (0-15 T). The dependence of fluorescence lifetime on these parameters can give insight into the role of carrier spin and momentum in the emitting transition, which will help elucidate whether quantum confinement is responsible for the enhanced properties of Ge NCs. These studies have shown that as temperature decreases, lifetime increases strongly. Taken together with a weaker but still meaningful dependence on magnetic field strength, these results indicate the presence of a non-emissive "optically dark" lowest excited state, which is separated from the optically bright state by only ~1 meV. Thus, at room temperature, mixing between these states allows the observed, efficient fluorescence. These and further details will appear in a forthcoming submission to *Physical Review Letters,* perhaps the most respected journal dedicated to physics research.

## Impact on National Missions

In this project, we develop novel inexpensive wet-chemistry techniques for the fabrication of Ge nanocrystals. It has enabled follow-on research projects of fundamental importance to the science of quantum confinement, including advanced spectroscopic studies of carrier dynamics to confirm the origin of the fluorescence and probe the effect of confinement on Ge electronic properties. At the same time, these novel Ge NCs have tremendous potential for immediate exploitation in advanced solar cell design and fabrication. In fact, the methods developed in this project are in current use for exploration of Ge-based solar cells within our new DOE-funded Energy Frontier Research Center, the *Center for Advanced Solar Photophysics*. Because of both its significant fundamental and technological potential in advancing solar energy research, this work is vitally important to the DOE missions in Energy Security.

## Publications

Lee, D., I. Robel, J. M. Pietryga, R. D. Schaller, D. Werder, and V. I. Klimov. Solution-phase synthesis of infra-red emitting germanium nanocrystals. 2009. *Journal of American Chemical Society.* **131** (10): 3436.

# Synthesis, Chemistry and Theoretical Studies of 5f-Element Hydride Complexes

*Jaqueline L. Kiplinger*
20070768PRD4

## Abstract

This is the final report of a two-year Director's Funded Postdoctoral project at Los Alamos National Laboratory. The project started in October 2007 and ended in October 2009. As indicated by the title, the original objective of this project was to prepare and study uranium hydride complexes, which are compounds containing U-H bonds. Inspired by the ability of ligands that combine both hard and soft coordination environments to stabilize highly reactive functional groups on transition metals and lanthanides, we extended this strategy to the actinides using the PNP ligand, which is a monoanionic pincer ligand that combines a hard central donor atom (N=amide) with two soft ancillary soft donors (P=phosphine). Soft donor ligands have been largely ignored as supporting ligands for early actinide chemistry, with the exception of coordination complexes featuring phosphorus and chalcogenide ligands prepared to investigate actinide/lanthanide separation technologies and questions about covalency in "hard-soft" interactions. Given that soft donor ligands provide an excellent opportunity to promote the low-valent chemistry of uranium, we initiated a program to develop the coordination chemistry of the PNP ligand towards uranium and thorium. This work represents the first time that the PNP ligand has been used to support actinide chemistry. The PNP ligand was shown to provide a more sterically congested environment and greater electronic density at the metal center compared to the classic metallocene ligand framework. Synthetic studies not only demonstrated that "dead-ends" encountered in actinide metallocene chemistry can be avoided using the soft PNP ligand, but also showed that the PNP ligand framework supports novel structures and promotes new reactivity patterns for the actinide series. This ultimately has important implications for actinide catalysis and separations based upon soft donor ligands.

## Background and Research Objectives

One of the key missions throughout the DOE Complex as well as the Chemistry, Materials, and Theoretical Divisions at LANL concerns research on the light actinides (Th-Am) to predict f-element behavior in a variety of applications such as materials disposition, selective chemical separations, and actinide materials compatibility. Though a key corrosion phenomenon of actinide metals, reaction with hydrogen (hydriding), is a major problem, f-element hydrides surprisingly remain a relatively unexplored.

One objective of this project was to fill this technology gap by developing methods for the preparation of well-defined uranium hydride complexes, studying these systems theoretically using DFT calculations, and exploring their reactivity towards small molecules. In fact, recent studies have shown that actinide hydride complexes can promote remarkable transformations on small molecules and engage in multi-electron chemistry. This work will advance our understanding of the chemical and physical properties of uranium hydrides in addition to providing critical information regarding the interaction of hydrogen with actinide metals. These species are promising materials to access new actinide-based functional groups and materials and provide important information regarding hydriding at the molecular level.

## Scientific Approach and Accomplishments

### The 5*f* Element Difference: Trivalent and Tetravalent Uranium Halide Complexes Supported by One and Two PNP Ligands

Cyclopentadienyl-based ligand sets, and in particular the bis(pentamethylcyclopentadienyl) platform, have been enormously successful as frameworks for supporting actinide chemistry and no alternative to these metallocene systems has proven as fruitful

to date. However, the bis($C_5Me_5$) framework suffers from severe drawbacks such as the chronic release of $(C_5Me_5)_2$ dimer upon oxidation of $(C_5Me_5)_2U$ complexes. Inspired by the ability of ligands that combine both hard and soft coordination environments to stabilize highly reactive functional groups on transition metals and lanthanides, we extended this strategy to the actinides using the mono-anionic bis[2-(diisopropylphosphino)-4-methylphenyl]amido (PNP) ligand. The PNP ligand is a monoanionic pincer ligand that combines a hard central donor atom (N=amide) with two soft ancillary soft donors (P=phosphine) (Figure 1). Soft donor ligands have been largely ignored as supporting ligands for early actinide chemistry, with the exception of coordination complexes featuring phosphorus and chalcogenide ligands prepared to investigate actinide/lanthanide separation technologies and questions about covalency in "hard-soft" interactions. Given that soft donor ligands provide an excellent opportunity to promote the low valent chemistry of uranium, we initiated a program to develop the coordination chemistry of the robust mono-anionic bis[2-(diisopropylphosphino)-4-methylphenyl]amido or PNP ligand towards the uranium halide complexes, $UCl_4$ and $UI_3(THF)_4$. This work represents the first time that the PNP ligand has been used to support actinide chemistry.

Over the course of this project, several trivalent and tetravalent uranium PNP halide complexes were prepared as potential starting materials for accessing the targeted hydride complex. As depicted in Figure 1, the reaction between (PNP)K (**2**) and one equivalent of $UI_3(THF)_4$ in the presence of 4-tert-butylpyridine afforded the trivalent halide complex (PNP)$UI_2$(4-$^t$Bu-pyridine)$_2$ (**3**). The same reaction carried out with $UCl_4$ and no donor ligand gave $[(PNP)UCl_3]_2$ (**4**), in which the uranium coordination sphere in the (PNP)$UCl_3$ unit is completed by a bridging chloride ligand. When $UCl_4$ is reacted with one equivalent (PNP)K (**2**) in the presence of THF, trimethylphosphine oxide (TMPO) or triphenylphosphineoxide (TPPO), the tetravalent halide complexes (PNP)$UCl_3$(THF) (**5**), (PNP) $UCl_3(TMPO)_2$ (**6**) and (PNP)$UCl_3$(TPPO) (**7**), respectively, are formed in excellent yields.

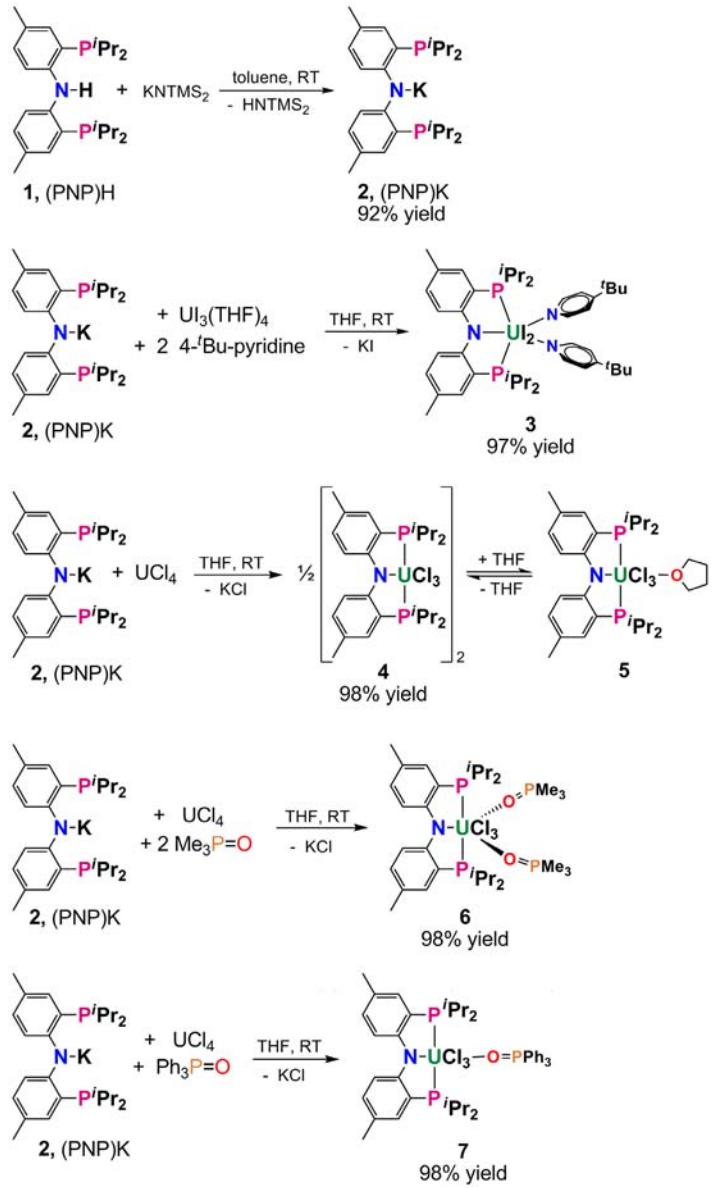


*Figure 1. Synthesis of trivalent and tetravalent uranium mono(PNP) halide complexes.*

The bis(PNP) complexes of uranium(III), $(PNP)_2UI$ (**8**), and uranium(IV), $(PNP)_2UCl_2$ (**9**), were easily isolated from the analogous reactions between two equivalents of (PNP)K (**2**) and $UI_3(THF)_4$ or $UCl_4$, respectively (Figure 2). Complexes **8** and **9** represent the first examples of complexes featuring two PNP ligands coordinated to a single metal center. The new complexes **3**-**9** were fully characterized using a combination of multinuclear ($^1$H, $^{31}$P) NMR spectroscopy, elemental analysis and X-ray diffraction analysis. Presumably to the large size of uranium, these complexes show unprecedented binding modes for the PNP ligand set. The PNP ligand can adopt both *pseudo*-meridional and *pseudo*-facial geometries when it is $\kappa^3$-(*P*,*N*,*P*) coordinated, depending on the steric demand at the uranium metal center. Additionally, its hemi-labile character was demonstrated with an unusual

$\kappa^2$-(*P*,*N*) coordination mode that is maintained in both the solid-state and in solution. This is in marked contrast to transition metal PNP complexes, where this ligand is rigorously tridentate $\kappa^3$-(*P*,*N*,*P*) (bound through the one nitrogen atom and the two phosphorus atoms), but for the uranium complex **9** we observe the PNP ligand coordinated to the metal in a bidentate $\kappa^2$-(*P*,*N*) , with one dangling phosphorus. Finally, comparison of the structures of the mono(PNP) and bis(PNP) complexes **3**, **5**, **7**-**9** with their respective $C_5Me_5$ analogues revealed that a more sterically congested environment is provided by the PNP ligand.

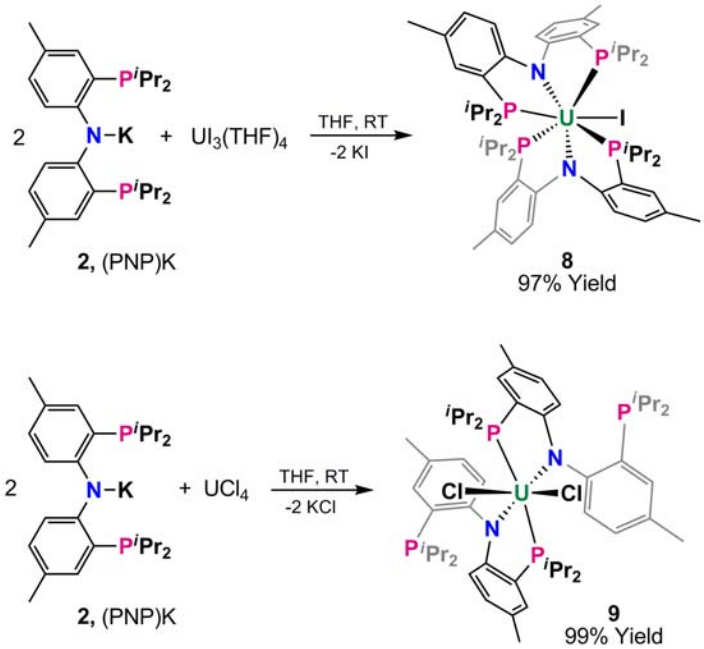


*Figure 2. Synthesis of trivalent and tetravalent uranium bis(PNP) halide complexes.*

The electronic influence of replacing the $C_5Me_5$ ligands with PNP was investigated using electronic absorption spectroscopy and electrochemistry. For **8** and **9**, a chemically reversible wave corresponding to the $U^{IV}$/$U^{III}$ redox transformation comparable to that for the known $(C_5Me_5)_2U(THF)(I)$ and $(C_5Me_5)_2UCl_2$ was observed. However a ~350 mV shift of this couple to more negative potentials was observed on substitution of the bis($C_5Me_5$) by the bis(PNP) framework, therefore pointing to a greater electronic density at the metal center in the PNP complexes. The UV-visible region of the electronic spectra for the mono(PNP) and bis(PNP) complexes appear to be dominated by PNP ligand-based transitions that are shifted to higher energy in the uranium complexes than in the simple ligand anion (**6**) spectrum, for both the $U^{VI}$ and $U^{III}$ oxidation states. The near IR region in complexes **3**, **5**, **7**-**9** and their $C_5Me_5$ analogues is dominated by f-f transitions derived from the $5f^3$ and $5f^2$ valence electronic configuration of the metal center. Though complexes of both ligand sets exhibit similar intensities in their f-f bands, a somewhat larger ligand-field splitting was observed for the PNP system, consistent with its higher electron donating ability.

**Challenging the Metallocene Dominance in Actinide Chemistry with a Soft PNP Pincer Ligand: New Uranium Structures and Reactivity Patterns**

Exhaustive studies over the course of this project have showed that none of the uranium PNP complexes form stable U-C bonds, which are necessary precursors to a hydride linkage. Nevertheless, this ligand framework was shown to open up new reactivity patterns for the actinides. As discussed above, actinide chemistry is largely founded on carbon-based metallocene complexes such as "$(C_5Me_5)_2U$" but many of these compounds are unstable because the cyclopentadienyl ligands fall off the metal and form $(C_5Me_5)_2$ dimer during oxidation reactions. However, during this project it was discovered that this problem can be circumvented by using the combined 'soft' and 'hard' coordination environments provided by the PNP ligand.

A classic uranium(II) synthetic equivalent, trivalent $(C_5Me_5)_2UI(THF)$ (**10**) in the presence of Na/Hg amalgam or $KC_8$, is known to provide up to four reducing equivalents in its chemistry. As such, initial studies with $(PNP)_2UI$ (**8**) were targeted at establishing the capacity of the bis(PNP) platform to support low-valent uranium chemistry (Figure 3). Treating a cold (-35˚C) toluene solution of $(PNP)_2UI$ (**8**) and $KC_8$ with hexachloroethane ($C_2Cl_6$) resulted in an immediate color change from deep green to bright red and formation of the known uranium(IV) $(PNP)_2UCl_2$ complex (**9**) in 96% isolated yield following workup. These observations clearly demonstrate that the PNP ligand can indeed support low-valent uranium with the $(PNP)_2UI$ (**8**)/ $KC_8$ system able to function as a new uranium(II) synthon.

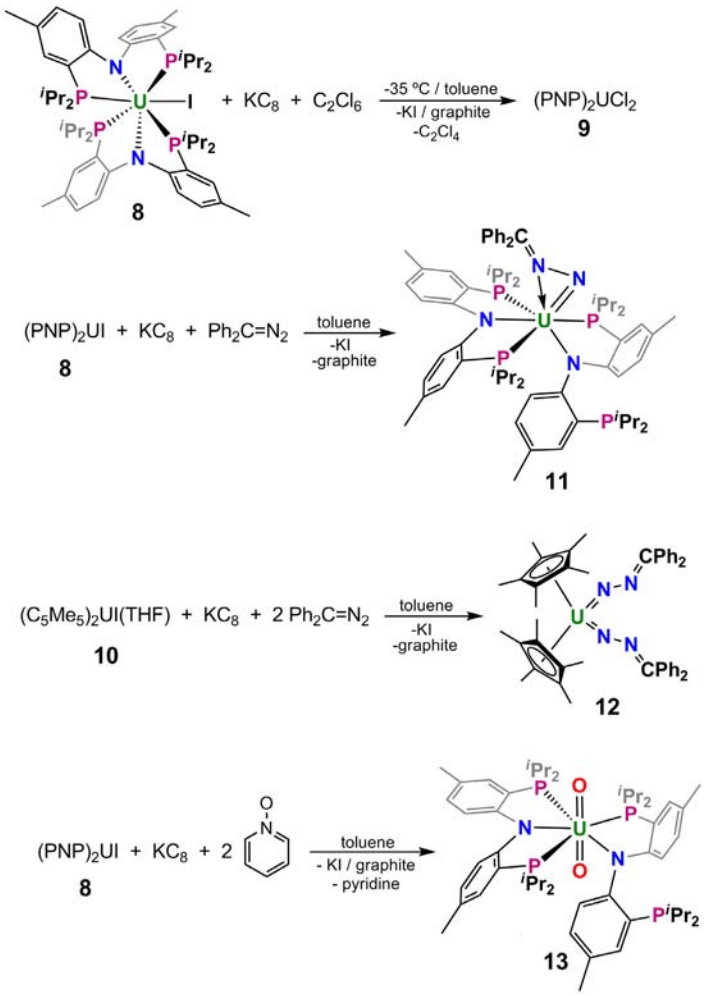


*Figure 3. Reaction chemistry displayed by low-valent PNP-uranium complex $(PNP)_2UI$ (8).*

The reducing ability of "$(PNP)_2U$" was explored towards a variety of different substrates and, significantly, every single reaction showed chemistry distinct from that of the metallocene complement, leading to structures unknown for the actinides or the transition-metals. For example, whereas reaction chemistry of $(PNP)_2UI$ (**8**) with $Ph_2CN_2$ gave the first actinide hydrazonido complex, $(PNP)_2U[\eta^2\text{-}(N,N')\text{=N-N=CPh}_2]$ (**11**), $(C_5Me_5)_2UI(THF)$ (**10**) is oxidized to a uranium(VI) bis(imido) complex (**12**) under the same conditions. Importantly, the hydrazonido complex, $(PNP)_2U[\eta^2\text{-}(N,N')\text{=N-N=CPh}_2]$ (**11**) will be quite attractive as a precursor to uranium nitrides by N-N bond cleavage. This clearly shows that the bis-PNP framework enables new reactivity patterns and supports new structures for the actinides and it ultimately validates our strategy.

The reaction chemistry of $(PNP)_2UI$ (**8**) is not limited to the formation of uranium(IV) complexes and reaction with pyridine *N*-oxide yields the first uranyl complex of a phosphine, $(PNP)_2UO_2$ (**13**). This transformation also has never been observed and provides an important missing link between non-aqueous and aqueous actinide chemistry. Under the same conditions, $(C_5Me_5)_2UI(THF)$ (**10**) is decomposed to the $(C_5Me_5)_2$ organic dimer. Not only does this work demonstrate how "dead-ends" encountered in actinide metallocene chemistry can be avoided using the soft PNP ligand, but also has important implications for actinide catalysis and separations based upon soft donor ligands. This landmark study appeared as a communication in *Angewandte Chemie International Edition* (**2009**, *48*, 3681-3684) and was chosen by the editor to be featured as a journal cover (Figure 4). The high impact of this work is further evident in that it was subsequently highlighted in *Nature Chemistry* (February 27, **2009** issue; doi:10.1038/nchem.163) and was the subject of a 2-page focus article "Highlight" that recently appeared in *Angew. Chem. Int. Ed.* (**2009**, *48*, 4898-4899).

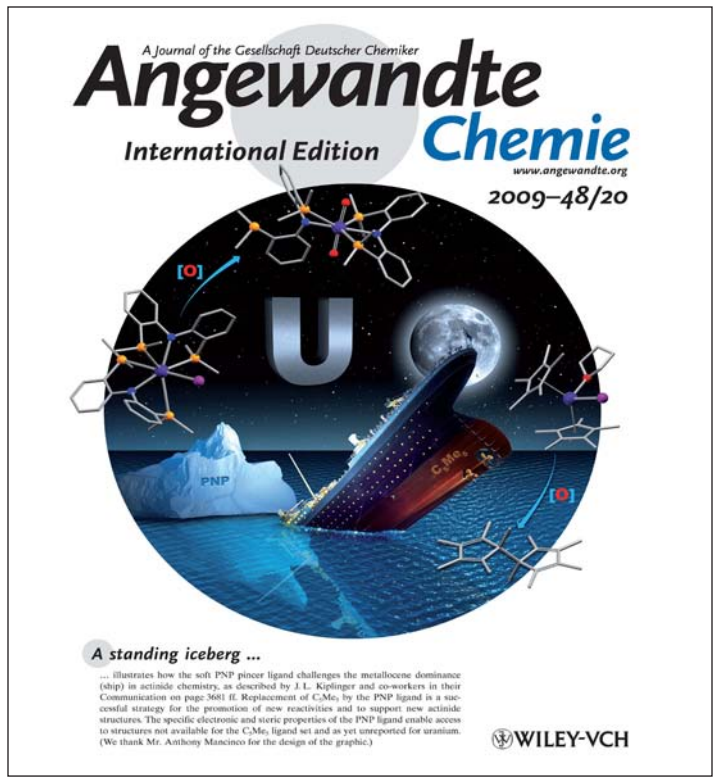


*Figure 4. Editor's choice for journal cover art that the work in this project has garnered.*

**Towards Uranium-Hydride Complexes: Unprecedented Phosphorus-Carbon Bond Cleavage and Phosphinidene Group Migration**

Under reducing conditions without added substrate, the PNP ligand framework is susceptible to reaction chemistry with the low-valent uranium metal center, which oxidatively inserts into one of the P-C bonds of the PNP ligand generating a uranium(IV) aryl phosphide complex, $[\kappa^3\text{-}(P,N,P')][\kappa^3\text{-}(P,N,C_{Ar})]U(P^iPr_2)$ (**15**) (Figure 5). This intramolecular oxidative addition has never been seen before and represents a new chapter in actinide chemistry. Interestingly, the aryl phosphide complex **15** is

merely a kinetic product and undergoes an unprecedented phosphinidene group ($P^iPr$) migration in which the "=$P^iPr$" group transfers from an $sp^3$ $C_{iPr}$ and inserts into a U-$C_{Ar}$ bond to give the uranium(IV) alkyl phosphide complex, [κ³-(*P*,*N*,*P'*)][κ³-(*P*,*N*,*P'*$_{iPr}$)]U($^iPr$) (**16**). This isopropyl complex is unstable and instantly rearranges to the uranium(IV) hydride complex, [κ³-(*P*,*N*,*P'*)][κ³-(*P*,*N*,*P'*$_{iPr}$)]U(H) (**17**) with loss of propene. Support of this mechanism is not only provided by x-ray crystallography (structures obtained for complexes **15** and **17**), but also by the observation of propene by $^1$H NMR spectroscopy when the reaction is performed in a sealed NMR tube. This is the first time a phosphinidene has been implicated in chemistry for any part of the periodic table and represents a new chapter in not only actinide chemistry but also main group chemistry. Subsequent calculations have suggested that the energy for this migration is quite low and can be exploited for organophosphorus group-transfer processes and other C–P bond-forming reactions.

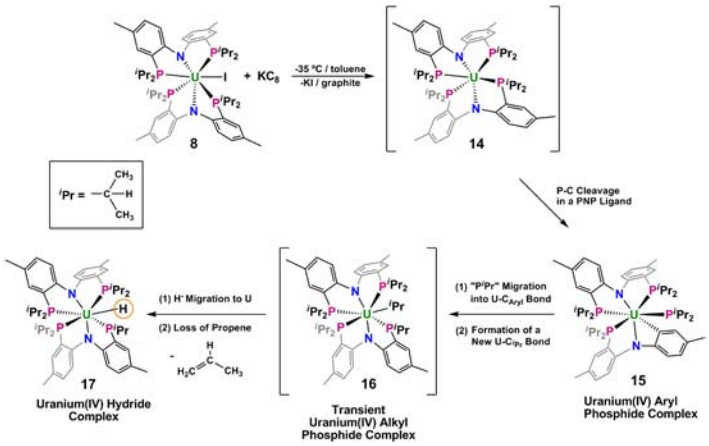


*Figure 5. Without a small molecule to react with, the PNP ligand undergoes chemistry with the low-valent uranium metal center: first, the uranium metal inserts into a P-C bond of one of the PNP ligands. This is followed by an unprecedented migration of a "PIPr" group (also known as a phosphinidene) mediated by uranium. Ultimately, a uranium(IV) hydride complex is formed.*

**A New Era for Thorium Chemistry: Access to Anhydrous Thorium Tetrachloride Complexes using Commercially Available and Inexpensive Starting Materials**

A final objective of this PNP chemistry was to extend it to thorium. However, access to anhydrous thorium starting materials has been limited because of the lack of available thorium metal. The other options have been limited by reproducibility of existing literature preps using toxic/pollutant chemicals or those requiring expensive inert atmosphere furnace setups to perform unsafe high-temperature chemistry between thoria ($ThO_2$) and $CCl_4$. In the final months of this project, this issue was overcome and a multi-gram scale synthesis of anhydrous $ThCl_4(DME)_2$ was developed using commercially available, stable and inexpensive starting materials. This breakthrough will open up new frontiers in the development of thorium chemistry and the thorium fuel-cycle. Put succinctly, we anticipate that our route to $ThCl_4(DME)_2$ will have the same impact on the field of thorium chemistry as $UI_3(THF)_4$ did for uranium.

**Notable Accomplishments/Impact**

The efforts funded by this project have already resulted in 4 publications in print, 2 submitted and under review, with 4 more publications currently in preparation, and 8 invited presentations at conferences, universities, companies, national and international laboratories. Based chiefly on these accomplishments the research produced during the course of this project has received international acclaim through no less than 1 journal cover (Figure 5), a highlight article in *Nature-Chemistry* (February 27, **2009** issue; doi:10.1038/nchem.163) and a special highlight article in *Angewandte Chemie, International Edition* (**2009**, Volume 48; Issue 27; pp 4898-4899). Additionally, the postdoctoral research associate working on this project was recognized for his scientific contributions by the 2008 Best Thesis Award of the École Polytechnique (Palaiseau, France) in Chemistry as well as the highly coveted ParisTech Best Thesis Award.

## Impact on National Missions

The chemistry of the actinide elements is critical to DOE nuclear weapons mission areas (stockpile stewardship, environmental remediation, waste management). The synthesis of new actinide compounds not only provides important information about metal-ligand bonding but also improves our ability to reliably predict chemical behavior in a variety of environments. As evidenced by this project, the DOE complex and LANL clearly benefits from simple exploratory research. The first actinide complexes supported by one and two bis[2-(diisopropylphosphino)-4-methylphenyl]amido ligand (PNP) ligands have been synthesized in high yields and fully characterized. The complexes demonstrate that new coordination modes are available for the PNP ligand. The PNP ligand was shown to provide a more sterically congested environment and greater electronic density at the metal center compared to the classic metallocene ligand framework. Synthetic studies not only demonstrated that "dead-ends" encountered in actinide metallocene chemistry can be avoided using the soft PNP ligand, but also showed that the PNP ligand framework supports novel structures and promotes new reactivity patterns for the actinide series. This ultimately has important implications for actinide catalysis and separations based upon soft donor ligands.

## Publications

Cantat, T., B. L. Scott, D. E. Morris, and J. L. Kiplinger. What a Difference a 5f Element Makes: Trivalent and Tetravalent Uranium Halide Complexes Supported by One and Two PNP Ligands. 2009. *Inorganic Chemistry.* **48**: 2114.

Cantat, T., B. L. Scott, and J. L. Kiplinger. Convenient Access to the Anhydrous Thorium Tetrachloride Complexes ThCl4(DME)2, ThCl4(1,4-dioxane)2 and ThCl4(THF)3.5 using Commercially Available and Inexpensive Starting Materials. *Chemical Communications.*

Cantat, T., C. R. Graves, B. L. Scott, and J. L. Kiplinger. Challenging the Metallocene Dominance in Actinide Chemistry with a Soft PNP Pincer Ligand: New Uranium Structures and Reactivity Patterns. 2009. *Angewandte Chemie, International Edition.* **48**: 3681.

Cantat, T., C. R. Graves, K. C. Jantunen, B. L. Scott, E. J. Schelter, C. J. Burns, P. J. Hay, D. E. Morris, and J. L. Kiplinger. Evidence for the Involvement of 5f-Orbitals in the Bonding and Reactivity of Organometallic Actinide Compounds: Thorium(IV) and Uranium(IV) Bis(hydrazonato) Complexes. 2008. *Journal of the American Chemical Society.* **130**: 17537.

Graves, C. R., E. J. Schelter, T. Cantat, B. L. Scott, and J. L. Kiplinger. A Mild Protocol to Generate Mixed-Ligand Uranium(IV) Metallocene Complexes Using Copper(I) Iodide.. 2008. *Organometallics.* **27**: 5371.

# Structure-Property Relationship for Strained One Dimensional Ferroelectric Nanostructures

*Quanxi Jia*
20080705PRD1

## Abstract

In general, the fabrication of one-dimensional nanostructures involves either bottom-up chemical synthesis or top-down micro/nano-fabrication approaches. We have utilized unique LANL facilities for the growth of nanostructured materials with desired structural and physical properties. In particular, we have concentrated on nanolayered ferroelectric films. The resulting layered films were characterized with various advanced facilities at LANL such as scanning electron microscopy, atomic force microscopy, and x-ray diffraction. We also studied the ferroelectric properties of the materials at different temperature and frequencies.

## Background and Research Objectives

Nanostructured ferroelectric oxide thin films with perovskite (i.e. $ABO_3$) structure have been of great technological interest due to their excellent properties for applications in dynamic random access memories (DRAMs), electromechanical transducers, tunable devices, multifunctional devices, etc. Pure $BaTiO_3$ is ferroelectric at room temperature and shows three-phase transitions with $T_c$ ~ 400K. In general, it has been observed that a film with similar composition, thickness, and substrate derived using different techniques may still show dissimilar properties. In addition, experimental results have shown that the ferroelectric property is a strong function of film thickness, in particular, when the film thickness was reduced to nanoscales. It should be noted that $BaTiO_3$ with magnetostrictve materials in nanocomposites (i.e. composed of two or more constituents differing in form and/or composition), such as BTO-$CoFe_2O_4$, BTO-$NiFe_2O_4$, etc. have also been studied for the magnetoelectric devices [1].

In this project, we targeted the structural and physical properties of $BaTiO_3$ films when the $BaTiO_3$ was reduced to nanoscale thickness. We have utilized unique LANL facilities for the growth of high quality ferroelectric films. The resulting nanostructured films were characterized with various advanced facilities at LANL such as scanning electron microscopy (SEM), atomic force microscopy (AFM), and x-ray diffraction (XRD).

## Scientific Approach and Accomplishments

Both pulsed laser deposition (PLD) and polymer-assisted deposition (PAD) were used to deposit nanostructured ferroelectric (such as $BaTiO_3$) films. One of the main advantages of PLD for ferroelectric films is good chemical composition preservation. On the other hand, PAD, LANL patented process [2], which is based on a chemical solution deposition to grow metal-oxide thin films, has the advantage of low cost, easy setup, and coating large area substrates. The major distinction for PAD compared to the other chemical solution lies in the soluble polymer, which plays a significant role in preparing high quality metal-oxide films. In other words, the polymer not only controls the desired viscosity for the process, but also binds the metal ions to prevent premature precipitation and formation of metal-oxide oligomers. The results are a homogeneous distribution of the metal precursors in the solution and the formation of uniform metal organic films.

To grow 10 nm thick epitaxial $BaTiO_3$ films MgO substrates based on PLD, we used a sintered stoichiometric ceramic target. To avoid the influence of deposition variables on the film properties, we kept the same processing conditions for the growth of the films: a deposition temperature of 750 °C and an oxygen pressure of 200 mTorr. These conditions were chosen because high performance $Ba_{1-x}Sr_xTiO_3$ $SrTiO_3$ film on MgO was routinely obtained under these processing parameters [3]. It should be noted that the films, following the deposition, were cooled to room temperature in an oxygen pressure of 300 Torr without any further thermal treatment. To grow 10 nm thick epitaxial $BaTiO_3$ films by PAD, we used a process that is similar to the process described in our earlier publication [4].

Figure 1 presents the hysteresis loops (or the remanent polarization vs. electric field characteristics) calculated based on our theoretical model for four representative strains within the range, namely, 0.1%, -0.13%, -0.165%, and -0.3%, where polarization represents the displacement which is inherent to the crystal structure of the ferroelectric material and does not disappear in the absence of the electric field. It is seen that the remanent polarization increases monotonically as the substrate strain changes from tensile to compressive, and the highest remanent polarization is obtained at strain -0.3%. It is interesting to observe that unlike the remanent polarization, the coercive field (i.e. in a single domain crystal, the coercive field can be interpreted as the field at which the polarization switches from one state to another) does not change monotonically as the strain is varied from tensile to compressive. Although the coercive field is the minimum at the tensile substrate strain of 0.1%, the coercive field at the compressive substrate strain of -0.13% is about 1.4 times higher than that at -0.165%. The highest coercive field is observed for strain -0.3%. Experimentally, our 10 nm thick $BaTiO_3$ film made by PLD showed the similar property as the film having a thickness great than 100 nm. This implies that the ferroelectric property of the $BaTiO_3$ at this length scale has nothing to do with strain. In other words, the strain does not play a critical role in determining the ferroelectric properties if the film thickness is thicker than 10 nm.

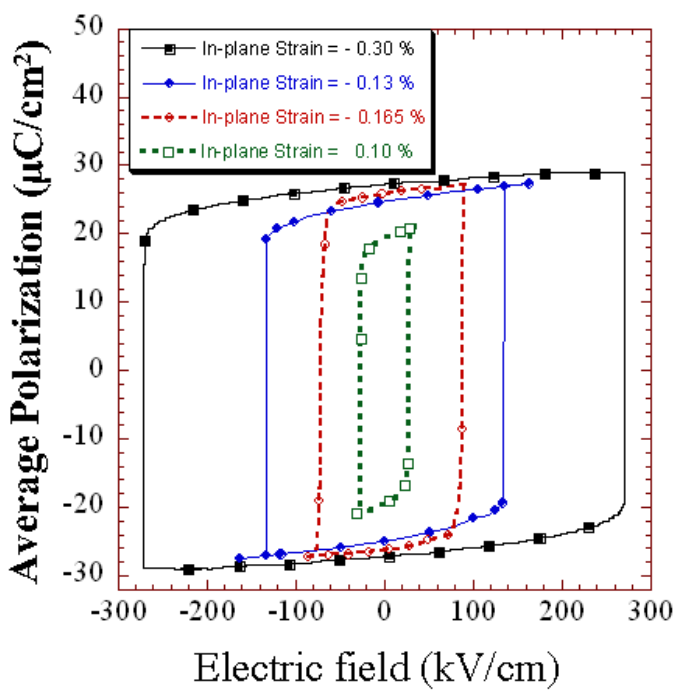


*Figure 1. Hysteresis loops for epitaxial $BiTaO_3$ thin films at 273 K with four representative in-plane strains*

The $BaTiO_3$ films prepared by PAD were fully characterized by XRD. We only observed preferentially oriented diffraction peaks of the film and the substrate ($LaAlO_3$) in the normal scans, suggesting that the $BaTiO_3$ film is single phase. The full width at half maximum (FWHMs) of rocking curves from the reflections of $BaTiO_3$ film is around 0.5°, suggesting good cystallization of the film. The in-plane scan was measured on $BaTiO_3$ and $LaAlO_3$ to check the epitaxial properties of the samples. Four peaks from $BaTiO_3$ with an average value of FWHM of 0.7°, comparing to the average value of 0.5° for the substrate, showed the films to be of good epitaxial quality.

## Impact on National Missions

This project supports DOE's mission in Energy Security by exploring energy transfer in nanomaterials. It also support the mission of Office of Science in fundamental science by enhancing our understanding of multifunctionality and ferroelectricity in nanostructured materials. This project will further support Laboratory's thrusts in fundamental understanding of materials.

## References


1. Nan, C. W., M. I. Bichurin, D. Viehland, and G. Srinivasan. Multiferroic magnetoelectric composites: Historical perspective, status, and future directions. 2008. *J. Appl. Phys.*. **103**: 031101.

2. Jia, Q. X., T. M. McCleskey, A. K. Burrell, Y. Lin, G. Collis, H. Wang, A. D. Q. Li, and S. R. Foltyn. Polymer-assisted deposition of metal-oxide films. 2004. *Nature Mater.*. **3**: 529.

3. Park, B. H., Y. Fan, Y. Gim, and Q. X. Jia. High nonlinearity of Ba0.6Sr0.4TiO3 films hetero-epitaxially grown on MgO substrates. 2000. *Appl. Phys. Lett.*. **77**: 2587.

4. Lin, Y., J. S. Lee, H. Wang, Y. Li, S. R. Foltyn, Q. X. Jia, G. Collis, A. K. Burrell, and T. M. McCleskey. Structural and dielectricproperties of epitaxial Ba1-xSrxTiO3 films grown on LaAlO3 substrates by polymer-assisted deposition. 2004. *Appl. Phys. Lett.*. **85**: 5007.


## Publications


Choudhury, S., Y. L. Li, L. Q. Chen, and Q. X. Jia. Strain effect on coercive field of epitaxial barium titanate thin films. 2008. *Appl. Phys. Lett.*. **92**: 142907.

# Environmental & Biological Sciences

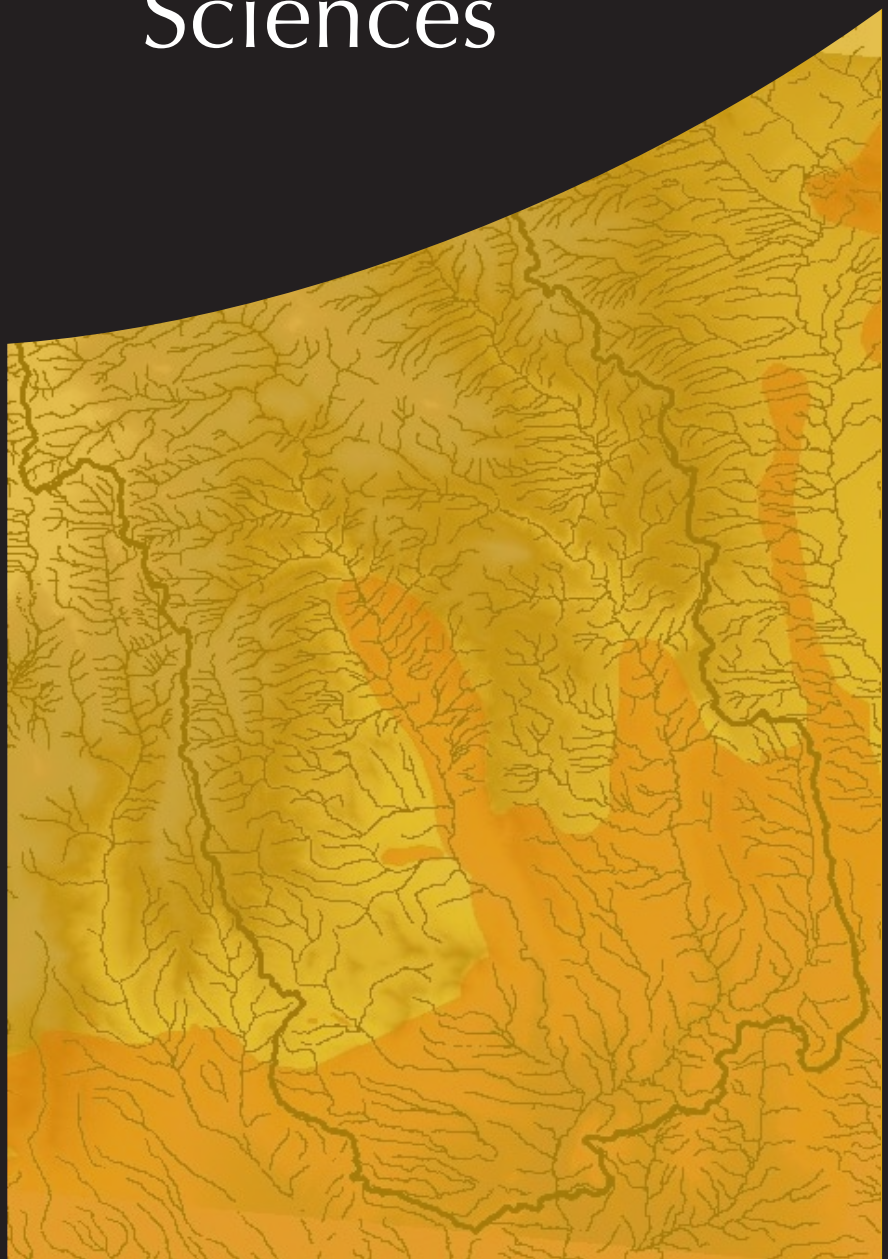

LABORATORY DIRECTED RESEARCH AND DEVELOPMENT

# One-Step Biomass Conversion: Looking to Nature for Solutions to Energy Security

*Paul A. Langan*
20080001DR

## Introduction

Biofuels are an alternative to conventional energy sources that increase our Nation's energy security by reducing dependence on imported oil. Our growing biofuels industry is largely based on the use of starch in grains such as corn to produce ethanol. However, there are advantages in using cellulosic biomass as an alternative feed stock, and in producing more advanced biofuels than ethanol. The development of cellulosic biofuels has attracted considerable commercial and government investment. Early results from these efforts indicate that many factors are important at different points in the life cycle of a biofuels program, and contribute towards its overall cost-competitiveness. However, it remains clear that converting biomass into sugars is the main cost-burden. *The aim of this project is to develop innovative science and technology to cost-effectively convert biomass into sugars.*

Several approaches are used to produce cellulosic ethanol at refineries. Most include energy intensive pretreatments and then enzymatic depolymerization. Alternative pretreatments with ionic liquids and ammonia are being developed. There are widespread efforts to reduce the cost of producing enzymes and to increase their performance. We collaborate with several groups, and have our own initiatives, in these areas. However, the main goal of this project is not incremental improvement, but a revolution in cost-efficiency through a scientific breakthrough that results in a completely new process.

We look for this breakthrough in nature. Although many fungi degrade parts of the cell wall, white rot fungi are unique in their ability to degrade it completely. We are identifying the key lignin degradation mechanisms of *P. chrysosporium* and then combining them with depolymerizing enzymes in a consolidated biomass conversion process.

## Benefit to National Security Missions

This project supports DOE missions in energy security by reducing our dependence on imported oil and bringing us closer to a carbon neutral fuel cycle.

## Progress

Our research plan is organized into three goal-oriented sections that address the following major objectives.

1. Define the key cofactors, mediators, and enzymes in the fungal degradation of lignin.
2. Characterize the structure of biomass and how it is degraded by interaction with these cofactors, mediators, and enzymes.
3. Combine key cofactors, mediators, and enzymes with cellulases and hemicellulases in a consolidated biomass conversion process.

This plan is executed through several technical thrusts each with a leader, and coordinated by the PI through regular team meetings. The use of multidisciplinary thrusts together with our innovative objectives, positions us in a complementary but competitive way to larger biofuels projects. Our organization into thrusts has allowed us to be responsive to diverse opportunities, and we have been able to submit proposals for several spin-off projects and collaborations.

The project was successfully reviewed in May 2009 by a committee consisting of two external and two internal experts. The external experts were Paul Adams and Steve Decker, from the DOE BER funded Bioenergy Research Centers JBEI and BESC, respectively. At the out-brief session the committee noted the excellent progress made and had no significant recommendations for changing course. The quality of the science and technology being produced is internationally recognized, as reflected in 19 publications in international journals, numerous talks and posters at scientific meetings, the award of several tens of million of dollars worth of beam time at central X-ray and neutron facilities throughout

the world, and are teaming with established research groups in this field. A website has been constructed with information about our capabilities: http://biofuels.lanl.gov. We were also directly involved in the organization of a conference "Energy for the 21st Century" Santa Fe May 2009, and a special session "Renewable Energy and the Environment" at the "International Conference on Neutrons in Biology" Santa Fe, October 2009, which highlighted work from this project.

Some highlights from our technical thrusts are given below.

**Theory**
Novel computational studies have been performed at both atomistic and coarse-grain scales to investigate the stability of cellulose under different conditions and also to investigate to what extent this stability is controlled by hydrogen bonding. The combination of theoretic studies with experimental results from our crystallographic thrust is a major scientific success story and has been highlighted in LANL and USDA news releases, several publications (including a front cover of the Biophysics Journal) and reported by news agencies worldwide. These studies involved developing and applying for the first time statistical mechanical methods and Replica Exchange Molecular Dynamics simulations to oligosaccharides.

**Multiplatform Microscopy**
Several different microscopy techniques have been applied to study biomass and its response to fungal, chemical and biochemical pretreatments, including scanning electron microscopy for high resolution and elemental mapping, confocal fluorescence microscopy for fluorescence and 3D mapping, Raman microscopy for chemical imaging and visible microscopy for time lapse microscopic movies of dynamic samples. An unexpected, but very exciting development is a novel technique that we have developed for incorporating gold and silver nanoparticles into biomass by first swelling the biomass in ionic liquid. This development allows nanosensors to be placed at the cell wall in order to report the chemical environment during fungal or biochemical pretreatments. The relative strength of Raman signals near the incorporated nanoparticles is enhanced by several orders of magnitude.

**Protein Science**
Fungal cultures were established to provide the capability to provide experimental samples for analysis by the degradomics thrust. The objective is to track the production of enzymes, which are the major players in the penetration of the lignin wall, and to harvest them for use as catalyst in reactors. In parallel we have pursued in vitro studies of an enzyme that is known as a key player in lignin wall dedgradation. The mechanism by which the ligin wall is enzymatically degraded is not presently understood. Our goal is to is to identify the enzyme catalyst that might be most effectively used in lignin degradation.

**University of New Mexico**
Lignin presents a "chain-linked fence" to enzymes produced by of *P. chrysosporium* A series of model lignin compounds has been synthesized and the mechanism of their depolymerization studied using a number of techniques. The results clearly indicate that particular bonds are preferentially broken in lignin. This work is being followed by similar studies on the enzymatic degradation of the same synthetic lignins, and the initial results suggest that the lignin peroxidase enzymes might be playing a more direct role than expected. If confirmed, this result will have a major impact on our understanding of the mode of action of lignin degrading enzymes, and their possible incorporation into cocktails for biomass conversion.

**Proteomics**
In conjunction with the Protein Science Thrust, we have launched a liquid fungal culturing system and experimented with various types of growth conditions, in order to produce ligninolytic and non-ligninolytic conditions. Time courses have been conducted, and conditions for concentrating and preparing the samples for mass spectrometry have been established. Furthermore, we have demonstrated that secreted proteins show high signal and excellent resolution on the MALDI. We are now working on separating the protein fragments in a way that aids in identification, as well as focusing on methods for quantifying differential expression between samples.

**USDA Forest Product Lab**
Research focused on the production of metabolites that fungi secrete into their surroundings to deconstruct lignocellulosic biomass. Of particular interest are metabolites that may have a role in lignin degradation, a key step in making cellulose available for biotechnological applications. So far the experiments have shown that one fungus secretes a previously unknown metabolite. This metabolite is aromatic, as shown by the finding that it becomes radiolabeled when $^{14}C$-labeled phenylalanine is supplied to the wood cultures. In associated work, we have identified a transporter protein, located in the cell membrane of *P. chrysosporium*, which is up-regulated during ligninolytic metabolism and thus may have a role in the secretion of biodegradative metabolites. Also identified during this study was a ligninolytically up-regulated, membrane-associated alcohol oxidase which likely has a role in production of the hydrogen peroxide needed to support the action of lignin-degrading peroxidases during wood deconstruction by *P. chrysosporium*.

**Degradomics**
Using mass spectrometry, several compounds have been identified whose concentration changes during fungal culture of biomass, and which may prove to be targets for incorporation into enzyme cocktails for biomass conversion. The key technical challenges that remain are

in data analysis and compound identification, which is now proceeding rapidly.

**Crystallography**
A unique capability is our neutron Protein Crystallography Station that is being used to elucidate the mechanisms of enzymes involved in the production of biofuels including xylanases and xylose isomerase. In addition, other central X-ray and neutron facilities are being used. A success of this thrust has been its contribution in creating an X-ray scanning microprobe community at BioCAT at the Advanced Photon Source (APS) of Argonne National Laboratory, the first of its kind in the USA. Our work in using this technique to understand biomass is being reported as a scientific highlight in the 2009 annual report of the APS and was reported in an invited talk at the APS. Results from this thrust are closely integrated with those from the theory and microscopy thrusts.

## Future Work
We propose to reverse-engineer the key degradation mechanisms of white rot fungi and optimize them for industrial application in biomass conversion to sugar. In particular this will involve investigating how metabolites and metabolite-enzyme interactions are used in the initial lignin degradation strategies of fungi and combine them, for the first time, with industrial cellulases to create an accelerated, consolidated biomass conversion process.

## Conclusion
This project, which has been reviewed this year and is progressing well, is focused on bringing about the revolution in cost and efficiency of biomass conversion needed to make biofules from biomass an economic reality, benefiting our security and our environment.

## Publications

Hammel, K., and D. Cullen. Role of fungal peroxidases in biological lignolysis. 2008. *Curr. Opin. Plant. Biol..* **11**: 349.

Kinne, M., M. Poraj-Kobielska, E. Aranda, R. Ullrich, and K. Hammel. Regioselective preparation of 5-hydroxypropranolol and 4 '-hydroxydiclofenac with a fungal peroxygenase . 2009. *Bioorganic & Medicinal Chemistry Letters .* **19**: 3085.

Kinne, M., M. Poraj-Kobielska, S. Ralph, M. Hofrichter, and K. Hammel. Oxidative ether cleavage by an extracellular fungal peroxugenase. 2009. *J. Biol. Chem..* **284**: 29343.

Kinne, M., R. Ullrich, K. Hammel, K. Scheibner, and M. Hofrichter. Regioselective preparation of (R)-2-(4-hydroxyphenoxy)propionic acid with a fungal peroxygenase. 2008. *Tetrahedron Letters .* **49**: 5950.

Kovalevsky, A., A. Katz, H. Carrell, L. Hanson, M. Mustyakimov, S. Fisher, L. Coates, B. Schoenborn, G. Bunick, J. Glusker, and P. Langan. Hydrogen location in stages of an enzyme catalyzed reaction: time of flight neutron structure of D-xylose isomerase with bound D-xylulose. 2008. *Biochemistry.* **47**: 7595.

Kovalevsky, A., L. Hanson, S. Fisher, M. Mustyakimov, S. Mason, T. Forsyth, M. Blakeley, D. Keen, G. Wagner, H. Carrell, A. Katz, J. Glusker, and P. Langan. Metal roles and possible hydrogen movement during the reaction catalyzed by D-xylose isomerase. *Structure.*

Martinez, D., J. Challacombe, I. Morgenstern, and E. Tal. Genome transcriptome and secretome analysis of wood decay fungus Postia placenta supports unique mechanisms of lignocellulosic conversion. 2009. *Proc. Nat. Acad. Sci. USA .* **106**: 1954.

Nishiyama, Y., G. Johnson, A. French, T. Forsyth, and P. Langan. Neutron crystallography, molecular dynamics, and quantum mechanics studies of the nature of hydrogen bonding in cellulose Ib. 2008. *Biomacromolecules.* **9**: 3133.

Nowak-Lovato, K., and K. Rector. SERS Nanosensors for whole cell pH imagery. 2009. *Applied Spectroscopy .* **63**: 389.

Nowak-Lovato, K., and K. Rector. Use of targeted SERS Nanosensors in whole cell pH analysis. To appear in *Microscopy and microanalysis proceedings.*

Shary, S., A. Kapich, E. Panisko, J. Magnuson, D. Cullen, and K. Hammel. Differential expression in Phanerochaete chrysosporium of membrane-associated proteins relevant to lignin degradation. 2008. *Applied and Environmental Microbiology.* **23**: 7252.

Shen, T., P. Langan, A. French, G. Johnson, and S. Gnanakaran. Conformational flexibility of soluble cellulose oligomers: chain length and temperature dependance. 2009. *Journal of the American Chemical Society.* **131**: 14786.

Shen, T., P. Langan, S. Gnanakaran, A. French, and G. Johnson. Shift in conformational flexibility of soluble cellulose oligomers with increasing chain length. 2008. In *Journal of the American Chemical Society.* (Salt Lake City, 22-26 March 2009). , p. 2008. Salt Lake City: Journal of the American Chem Soc..

Shen, T., and G. Gnanakaran. The stability of cellulose: A perspective from the statistical mechanics of hydrogen bond networks. 2009. *Biophysical Journal.* **96**: 3032.

Wada, M., L. Heux, Y. Nishiyama, and P. Langan. X-ray

crystallographic, scanning microprobe X-ray diffraction, and cross-polarized/magic angle spinning 13C nuclear magnetic resonance studies of the structure of cellulose III(II). 2009. *Biomacromolecules.* **10**: 302.

Wada, M., L. Heux, Y. Nishiyama, and P. Langan. The structure of the complex of cellulose I and ethylenediamine by X-ray crystallography and cross-polarization/magic angle spinning 13C nuclear magnetic resonance. To appear in *Cellulose.*

Wada, M., Y. Nishiyama, H. Chanzy, T. Forsyth, and P. Langan. The structures of cellulose. 2008. *Powder diffraction.* **23** (2): 92.

Wada, M., Y. Nishiyama, H. Chanzy, T. Forsyth, and P. Langan. The structures of celluloses. 2008. *Advances in X-ray Analysis.* **51**: 138.

Yelle, D., K. Hammel, J. Ralph, and F. Lu. Evidence for cleavage of lignin by a brown rot basidiomycete. 2008. *Environ. Biol. .* **10**: 1844.

# Flash Before the Storm: Predicting Hurricane Intensification using LANL Lightning Data

*Christopher A. Jeffery*
20080126DR

## Introduction

In the wake of the devastating 2005 hurricane season, government agencies, scientific boards and advisory panels have unanimously called for urgent increases in hurricane research and improvements in hurricane forecast accuracy. In coordination with this national agenda, our LDRD project has the following high-profile science & technology objectives:

- Instrument oil platforms in the northern Gulf of Mexico with LANL's unique 3D total lightning mapping system, capable of remotely probing the violent and opaque hurricane eye-wall.
- Discover and quantify the dynamics and convective structure of the hurricane eye-wall region as revealed for the first time in the 3D spatial structure, intensity and evolution of the lightning data.
- Develop a new hurricane model that assimilates this real-time knowledge of eye-wall convective strength, and demonstrate a 50% improvement in 48-hour intensity (wind speed) forecast errors.

The relevance and timeliness of these objectives is central to the potential impact and high-potential science of this project; our project aligns not only with LANL's "predicting emerging environmental threats" Grand Challenge and energy security priorities, but also with (i) a recent National Science Board report calling for a new national hurricane research initiative; (ii) a recent NOAA science advisory board report advocating "novel methods for data assimilation founded on improved observations of the hurricane". Additionally, the new dual VLF-VHF lightning mapping array that we are building in the Gulf of Mexico will be of great technological value to the US space-based nuclear denotation monitoring system (USNDS).

## Benefit to National Security Missions

This project supports DOE's threat reduction mission by enhancing our understanding of the strength and organization of eyewall convective processes that trigger rapid hurricane intensification, and by developing a new hurricane model to improve forecast accuracy. We contribute to energy security with new tools to anticipate threats to the oil infrastructure. Our project leverages investment in nuclear security to solve problems of national importance. This summer we were interviewed by the Associated Press and by the Weather Channel; this publicity highlighted our new application of nuclear non-proliferation technology to the problem of hurricane intensity forecasting.

## Progress

Our project has three key components:

1. Development of a new dual VLF-VHF "total lightning mapping" array technology, and establishment of a new RF lightning array in the Gulf of Mexico.
2. Development of the first-ever hurricane forecast model that includes cloud electrification and lightning prediction;
3. Development of a new data assimilation scheme to ingest lightning data into our unique hurricane forecast model.

During year two of this project, we focused on all three tasks.

**New Gulf Lightning Array**

We have continued to build and extent our new dual VLF-VHF lightning mapping technology and array. This sensor combines LANL's unique VLF technology, which records and transmits over the internet the VLF waveform, with a new VHF mapping capability. Ten sensor units were built in FY08; an additional four sensor units were built this year. During year one, we established a new sensor array in the New Orleans area. The array represents a new collaborative effort between LANL, Chevron, Nicholls State University, Louisiana State University, the Port Fourchon Authorities, the Associated Branch Pilots, and the Louisiana Universities Marine Consortium (LUMCON). During year two, we have added five new partners that host LANL lightning sensors: Louisiana Department of Wildlife and Fisheries, Town of

Jean Lafitte, Rotorcraft Leasing Co., LLC, U.S. Coast Guard, and the U.S. Fish & Wildlife Service. During year 1 of our project we had several sensors destroyed by Hurricane Gustav; increasing station redundancy has been a key priority for this year.

**New Hurricane Model with Electrification**

During year one, we developed the world's first high-resolution hurricane forecast model with cloud electrification and lightning prediction. This model builds on and extents the cloud electrification parameterizations developed at Oklahoma University (our collaborator) for extra-tropical thunderstorms. We are excited to report that our hurricane model demonstrates the following important physical processes and validates a key scientific hypothesis of our project. We have used our new hurricane model with electrification to compare and contrast the intensification and lightning produced by a sudden burst of intense vertical convection in the eyewall of a simulated hurricane. Comparing the intensification and lightning produces by these eyewall "hot towers" of varying strength, we find that weak hot towers--which produce little intensification--produce negligible lightning, while strong hot towers produce rapid hurricane intensification and trigger a sudden burst of eyewall lightning. This exciting result validates a central scientific hypothesis of our project that a sudden burst of eyewall lightning activity is associated with rapid hurricane intensification. During year two, we have focused on studying the evolution of two Hurricanes--Rita and Katrina--by developing a new weather-forecast capability that implements accurate model boundary-conditions supplied from the National Weather Service database. We are pleased to report that our model produces lightning rates that are consistent with our observations. A particularly fascinating, and unexpected, outcome of this work, is that we have discovered that rainband location and information--retrieved from our unique LANL lightning data--can be incorporated as initial model conditions and improves forecast accuracy.

**New Lightning Data Assimilation Scheme**

We have made good progress this year, in developing the foundations of a new lightning data assimilation scheme. One of the difficult challenges of lightning data assimilation is that lighting is not, in itself, a dynamical relevant variable. Rather, it is a surrogate for the intense convection, which we would like to assimilate into our model. As a first step in developing a lightning data assimilation scheme, we have focused on an important lightning surrogate: latent heating. We have taken an extremely high-resolution data source--the EDOP air-borne dual-Doppler system that provides 2D wind fields--and processed this data into 3D latent heating fields. We then assimilated this latent heating data into our hurricane model, and discovered that it greatly improves forecast accuracy. The next step in this work is to develop a statistical relationship between lightning flash rate and latent heating, and then use this relationship to assimilate the lightning data.

## Future Work

This project is motivated by our remarkable observations of abundant lightning activity in the eyewall of Hurricanes Katrina, Rita and Wilma that coincided with rapid intensification and that were observed by LANL RF sensors sparsely located over the Great Plains and Florida. Intense vortical convective towers in the hurricane eyewall are believed to trigger intensification; the new lightning channel mapping array that we will deploy on oil platforms in the Gulf of Mexico will provide a continuous eyewall monitoring capability that will reveal the formation, merger and decay of these vortical structures as seen in the evolution of their three-dimensional charge structure. We will build a new LANL hurricane model that assimilates our real-time lightning observations and lead the field in achieving success in the national challenge posed by NOAA:

"to demonstrate a 50% improvement in 48 hour hurricane intensity (wind speed) forecast errors using "advanced numerical models, novel methods of data assimilation, and improved observations."

In summary our three major goals are:

1. Develop a new observational array of lightning sensors along the Gulf of Mexico coast and on offshore oil platforms.

2. (Using this unique data source, develop a new understanding of the vortical hot towers in the hurricane eye wall and the role of these towers in triggering intensification.

3. Demonstrate that assimilation of our unique lightning data into a hurricane forecast model can produce a 50% improvement in 48 hour hurricane intensity forecast errors.

## Conclusion

Our project will perform the first-ever real-time 3D mapping of convective events in the hurricane eyewall using a new lightning remote-sensing capability developed by LANL. We will use this new understanding and remote sensing capability to demonstrate that rapid hurricane intensification, the sudden large-scale transition of violent weather, can be accurately forecast using a novel model that assimilates real-time knowledge of critical small-scale processes--specifically, observations of violent eyewall convection provided by a hurricane lightning imaging system. This new predictive capability of hurricane intensification will save lives and protect infrastructure

along the energy critical Gulf coast.

## Publications

Chylek, P., and G. Lesins. Multi-decadal variability of Atlantic hurricane activity: 1851-2007. 2008. *Journal of Geophysical Research.* **113**: 22106.

Fierro, A., X. M. Shao, J. Reisner, J. Harlin, and T. Hamlin. Evolution of eyewall convective events as indicated by lightning during hurricane intensification. *Nature Geoscience.*

Harlin, J., X. Shao, T. Hamlin, N. O'Connor, T. Lavezzi, and C. Jeffery. LASA Observations of lightning in hurricanes. Presented at *American Geophysical Union Fall Meeting.* (San Francisco, 15-19 Dec., 2008).

Henderson, B., D. Suszcnysky, K. Wiens, T. Hamlin, C. Jeffery, and R. Orville. Lightning and radar observations of hurricane rita landfall. *Monthly Weather Review.*

Jeffery, C., and N. Jeffery. Theory and computation of wavenumber-2 Vortex Rossby Wave instabilities in hurricane-like vortices. Presented at *Geophysical Turbulence Phenomena.* (Boulder, 27-29 Feb., 2008).

Reisner, J., and C. Jeffery. A smooth cloud model. 2009. *Monthly Weather Review.* **137**: 1825.

Shao, X., J. Harlin, D. Suszcynsky, and C. Jeffery. Hurricane lightning: a new campaign to investigate hurricane intensification by using lightning observations. Presented at *American Meteorological Society 88th Annual Meeting.* (New Orleans, 20-24, Jan., 2008).

Shao, X., and A. Jacobson. Model simulation of VLF/LF lightning signal propagation over intermediate ranges. 2009. *Transactions on Electromagnetic Compatibility.* **51**: 519.

Williams, B., J. Kao, M. Hubbard, and D. Higdon. Uncertainty quantification with data constraints using a Bayesian approach. To appear in *Defense Research Review.*

# Genomes to Behavior: Predicting Bacterial Response by Constrained Network Interpolation

*John M. Dunbar*
20080138DR

## Introduction

The DOE Office of Science envisions direct prediction of microbe behavior (response to stimuli) from a genome sequence, but is stymied by a lack of methods. Consequently, the DOE, DHS, NIH, and IC rely on slow, expensive empirical methods to determine the response of new strains and species to particular stimuli and to identify the genetics underpinning response. For example, knowledge of strain virulence is needed in biothreat risk assessment, but can only be estimated at present through slow, expensive animal studies. Similar hurdles occur in bioenergy and waste remediation. This creates an increasingly severe bottleneck as the accumulation of genome sequences (already >1000 partial or complete) greatly outstrips the capacity for experimental analysis.

To alleviate this bottleneck, we are developing a framework to predict bacterial response to stimuli by constrained extrapolation from experimentally well-characterized model organisms. This project exploits high throughput experimental biology and computation at LANL. As a test system, we are focusing on the genus Burkholderia. This genus contains species that impact biothreat, bioremediation, bioenergy, and public health missions of interest to DOE, NIH, and the IC.

The impact of our work will be similar to the impact of protein-structure homology modeling, which enables rapid functional analysis and redesign of proteins. The project will lay the foundation for a new kind of homology modeling in which the response networks of model bacteria are experimentally characterized at key intervals across the bacterial domain and are used to interpolate responses from other genome sequences.

## Benefit to National Security Missions

This project supports DOE missions in biothreat reduction, bioenergy, carbon management, and bioremediation by profoundly improving the capacity to decode and harness the capabilities encoded in microbial genomes. This project targets a fundamental bottleneck identified by DOE Office of Science within the Life Sciences.

## Progress

We are achieving our two major aims, namely 1) characterization of stimulus-response circuits in a model organism and 2) prediction of conservation of these circuits in increasingly distant organisms. We have developed a rich resource of data, capabilities, new tools that support the general research community, and are beginning to uncover a series of significant research findings. We are integrating all of these into a transition plan to expand LANL's contributions to external programs benefiting public health and national security.

We are making excellent progress in our first objective: characterizing gene regulatory circuits in a model organism. We acquired 90% of the experimental data expected for this task and are on track to exceed our data acquisition targets. We acquired 160 gene expression profiles from our model organism grown under 20-40 growth conditions. This provides approximately a 15-fold increase in data publically available and relevant to development of countermeasures for the biothreat agent Burkholderia pseudomallei and the public health threat, Burkhoderia cepacia. In response to suggestions from an external review committee, we augmented our gene expression data by acquiring sets of time series measurements of gene expression and acquiring snapshots of gene expression via cutting-edge sequencing technology.

We are currently mining our rich resource of gene expression data to reconstruct the major elements and architecture underlying regulatory networks in cells. For example, we have found that the gene expression data enables validation of 1) predicted locations of the "on/off switches" (i.e. promoters) controlling gene expression, and 2) predicted operons (i.e. contiguous genes jointly controlled by one promoter). With these architectural components, we are integrating data from a new capability established at LANL through this project—a technology to identify the specific DNA sequences recognized by bacterial regulatory proteins to modify gene expression. With this technique, we discovered DNA binding sites for 8, thus far, of 20 major

regulatory proteins. We are using the measured binding sites to predict sets of co-regulated genes and using the gene expression data for validation and refinement. Towards this end, we developed a stand-alone software tool that can process tens of thousands of predicted binding sites for a particular regulatory protein in a genome and identify the short list of genes most likely to be controlled by the regulatory protein. With the entire compendium of information, we are making good progress reverse engineering a regulatory network for our model bacterium, Burkholderia thailandensis. We have already made unexpected findings, such as linking type III secretion systems in our model organism (a system that exports virulence factors into host cells) with sets of proteins that were previously unknown to play a role in pathogenesis. With such findings, we are proceeding to our second objective: predicting conservation of behavior in closely related pathogen genomes.

We solved a fundamental problem essential to extending regulatory networks to genomes from closely related species. The current state-of-the-art for extension of regulatory networks between genomes is a simple comparison of gene inventories. We have already completed a comparison of the gene inventory of our model organism with 20 genomes representing closely related species and will soon filter these results through our reverse-engineered regulatory network model (above). To move substantially beyond current state-of-the-art, we sought to add genome-wide comparisons of cis-acting DNA regulatory regions that control gene expression. These regulatory regions typically lie between genes (hence, "intergenic" regions). We found that genome-wide comparisons of conservation of intergenic regions are routinely precluded because the predicted boundaries of the intergenic regions are wildly inconsistent between genomes. In other words, the input data are lousy.

We solved this fundamental problem by developing an algorithm to improve the consistency of gene boundaries among closely related genomes. Using this algorithm, we improved consistency of gene boundaries among our test set of 21 genomes from 45% to 98% consistent. We further developed this algorithm as a stand-alone software tool that can be broadly exploited by the external research community. This achievement has enabled us to proceed to our major objective: facile, genome-wide comparison of intergenic regions to predict cellular behavior based on conservation of gene regulation. This major step is already indicated limits on the phylogenetic distance over which we can extrapolate behavior. Although we are just beginning to exploit this advance, it clearly opens to the door to demonstrating the fundamental concept of this LDRD-DR project.

## Future Work

Cellular behavior is determined by gene inventory and gene regulation. Gene inventory defines a cell's potential capabilities. Gene regulation determines which capabilities are actually used in various conditions. Recent advances enable reverse-engineering of gene regulatory networks for a single genome. The next logical progression is to translate regulatory networks from one genome to another. To date, the translation of networks between genomes has focused exclusively on comparisons of gene inventory. The goal of this project is to develop a capability to predict regulatory networks in new genomes based on conservation of gene inventory as well as gene regulatory elements from a model system.

We are rapidly achieving our two primary aims:

1. Provide a detailed experimental characterization and systems-level model of the response of a reference organism to a variety of external stimuli. This is a low risk objective. In this aim, we will obtain a regulatory network model for a bacterium that is relevant to biothreat reduction.

2. Extend a regulatory network model to infer the response networks of organisms with similar genomes. This is an innovative component of the project, and builds on our combined expertise in experimental microbial physiology, network reconstruction, structural modeling, and bioinformatics methods. Extending (and validating) pathways from our model system to closely related genomes is a moderate risk objective. As a higher risk objective, we will define the phylogenetic "radius of convergence"—the evolutionary distance over which a response network can be extended.

Our immediate tactical goal is to exploit our accumulated data to describe one or several stimulus-response circuits in the model organism, then predict conservation across multiple genomes as a proof-of-principle demonstration of our acquired capability.

Our near-term strategic goals are to use the accumulated data to acquire external funding that expands our scope and deliver our rich trove of scientific findings and products to the external community to expand LANL's contributions to public health and national security programs.

## Conclusion

This project aims to create a fundamental capability that could transform comparative genomics and reduce the need for experimentation 10 to 100-fold, profoundly cutting costs and accelerating solutions to central problems in biosecurity, bioenergy, carbon management, and bioremediation.

## Publications

Chen, G., B. H. McMahon, and C. S. Tung. Molecular dynamics simulations of phosphorylation-induced

conformational transitions in the Mycobacterium tuberculosis response regulator PrrA. 2009. *Los Alamos National Laboratory, LAUR 08-05233.*

Dreisigmeyer, D. W., J. Stajic, I. Nemenman, W. S. Hlavacek, and M. E. Wall. Determinants of bistability in induction of the Escherichia coli lac operon. 2008. *IET Systems Biology.* **5**: 293.

Edwards, J. S., J. R. Faeder, W. S. Hlavacek, Y. Jiang, I. Nemenman, and M. E. Wall. q-bio 2007: a watershed moment in modern biology. 2007. *Molecular Systems Biology.* **3**: 148.

Frauenfelder, H., G. Chen, J. Berendzen, P. W. Fenimore, H. Jansson, B. H. McMahon, I. R. Stroe, J. Swenson, and R. D. Young. A unified model of protein dynamics. 2009. *Proceedings of the National Academy of Science.* **106**: 5125.

Martin, R. G., E. S. Bartlett, J. L Rosner, and M. E. Wall. Activation of the Escherichia coli marA/soxS/rob regulon in response to transcriptional activator concentration. 2008. *Journal of Molecular Biology.* **380**: 278.

Nemenman, I., W. S. Hlavacek, Y. Jiang, and M. E. Wall. Editorial: Selected papers from the Second q-bio Conference on Cellular Information Processing. 2009. *IET Systems Biology.* **3** (5): 297.

Wall, M. E., D. A. Markowitz, J. L. Rosner, and R. G. Martin. Model of transcriptional activation by MarA in Escherichia coli. To appear in *PLoS Computational Biology.*

# Complex Biological and Bio-Inspired Systems

*Robert E. Ecke*
20080673DR

## Introduction

The understanding and characterization of the fundamental processes of the function of biological systems underpins many of the important challenges facing American society, from the pathology of infectious disease and the efficacy of vaccines, to the development of materials that mimic biological functionality and deliver exceptional and novel structural and dynamic properties. These problems are fundamentally complex, involving many interacting components and poorly understood bio-chemical kinetics. We use the basic science of statistical physics, kinetic theory, cellular bio-chemistry, soft-matter physics, and information science to develop cell level models and characterize material properties of bio-mimetic materials. Specific objectives are to determine how cell level processes such as response to mechanical stresses, chemical constituents and related gradients, and other cell signaling mechanisms. These efforts may lead to the development of bio-sensors to detect hazards from pathomic viruses to chemical contaminants. Other potential applications include the development of efficient bio-fuel alternative-energy processes and the exploration of novel materials for energy usages. Finally, we use the notions of "coarse-graining," which is a method for averaging over less important degrees of freedom, to develop computational models to predict cell function and systems-level response to disease, chemical stress, or biological pathomic agents.

## Benefit to National Security Missions

This project supports Energy Security, Threat Reduction, and the missions of the DOE Office of Science through its far reaching efforts to accurately model biological systems at the molecular and cellular level with applications to biofuels, to novel sensors and to materials with broad use for energy or threat reduction.

## Progress

Agent-based models were employed to describe numerous processes in immunology. Simulations based on these types of models have been used to enhance our understanding of immunology and disease pathology. We reviewed various agent-based models relevant to host-pathogen systems and discuss their contributions to our understanding of biological processes. We also described in the journal *Information Sciences* some limitations and challenges of agent-based models and encouraged efforts towards reproducibility and model validation.

We developed a theory of photon emissions from a single molecule driven by laser excitation. The frequencies of the fluoresced photons are explicitly considered. Calculations were performed for the case of a two-level dye molecule, showing that measured photon statistics will display a strong and non-intuitive dependence on detector bandwidth. Moreover, it is demonstrated that the anti-bunching phenomenon results from correlations between photons with well-separated frequencies. This work was published in *Physical Review Letters*.

Biochemical processes typically involve huge numbers of individual steps, each with its own rate constants. For example, kinetic proofreading processes rely upon numerous sequential reactions in order to guarantee the precise construction of specific macromolecules. In work submitted to *Physical Biology*, we study the transient properties of such systems and fully characterize their completion distributions. In particular, we provide expressions for the mean and the variance of the completion time. We find that, for a wide range of parameters, as the system size grows, the completion time behavior simplifies: it becomes either deterministic or exponentially distributed, with a very narrow transition between the two regimes. These findings suggest that one may not be able to understand individual elementary reactions from macroscopic observations, but that such understanding may be unnecessary.

Structures, dynamics, and stabilities of different sized cellulosic oligomers need to be considered when designing enzymatic cocktails for the conversion of

biomass to biofuels since they can be both productive substrates and inhibitors of the overall process. In work published in the *Journal of the American Chemical Society*, the conformational variability, hydrogen bonding, and mechanical properties of short, soluble cellulose chains, an example of which is shown in Figure 1, are investigated as a function of chain length. As the chain length is increased, the conformations of the oligomers become more rigid and likely to form intra-chain hydrogen bonds, like those found in crystals.

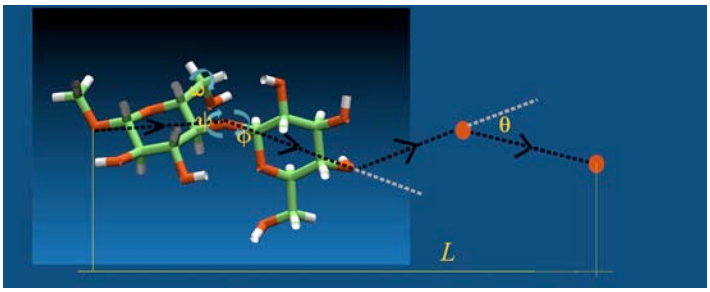


*Figure 1. Structure of a cellulosic oligomer that needs to be considered when designing enzymatic cocktails for the conversion of biomass to biofuels since they can be both productive substrates and inhibitors of the overall process.*

No simple model can accurately describe the melting behavior and breathing dynamics of double-stranded DNA as a function of nucleotide sequence. This is especially true for homogenous and periodic DNA sequences, which exhibit large deviations in melting temperature from predictions made by additive thermodynamic contributions. We previously extended the nonlinear Peyrard-Bishop-Dauxois (PBD) model of DNA to include a sequence-dependent stacking term, resulting in a model that can accurately describe the melting behavior of homogenous and periodic sequences. Using comparison between experiments and our numerical simulations we showed that our extended PBD model will facilitate thermodynamic and dynamic simulations of important genomic regions and disease-related repeats. We also assessed the role of DNA breathing dynamics as a determinant of promoter strength and the transcription start sites (TSS). We designed a DNA promoter-modification which experimentally demonstrated that: DNA dynamic activity at the TSS can be suppressed by a few long-range mutations that do not affect transcription factor binding-DNA contacts but repress the transcription. We used this effect to establish the separate contributions of transcription factor binding and DNA dynamics to transcriptional activity. Our results, accepted for publication in *Nucleic Acid Research*, argue against a purely "transcription factor-centric" view of transcription initiation, and suggest that transcription factor binding and breathing dynamic activity are both necessary for cellular gene transcription and are interdependent.
Nuclear pore complexes (NPCs) act as effective and robust gateways between the nucleus and the cytoplasm, selecting for the passage of particular macromolecules across the nuclear envelope. NPCs comprise an elaborate scaffold that defines a ~30 nm diameter passageway connecting the nucleus and the cytoplasm. To test whether a simple passageway and a lining of selective binding sites are sufficient for selective transport, we designed a functionalized membrane that incorporates just these two elements. We demonstrated that this membrane functions as a nano-selective filter, efficiently passing the complexes that bind selectively at the pore binding sites, while significantly inhibiting the passage of proteins that do not bind. This inhibition is greatly enhanced when transport factor is present. We showed that this artificial system faithfully reproduces key features of trafficking through the NPC, including the transfer of important transport factors. Our theory has been compared extensively with experimental data (via collaborators at Rockefeller Univ.). Of particular note is work published in *Physical Review Letters* on how the interaction of species within the channel can causing "jamming" and effect transport times.

We showed in work published in *Molecular Systems Biology* that the random fluctuations of cellular constituents (mRNAs Proteins, etc.) carry within them valuable information about the underlying genetic network. This ever-present cellular noise acts as a rich source of excitation that, when processed through a gene network, carries a distinctive fingerprint that encodes a wealth of information about that network. We demonstrate that in some cases the analysis of these random fluctuations enables the full identification of network parameters, including those that may otherwise be difficult to measure. This establishes a potentially powerful approach for the identification of gene networks and offers a new window into the workings of these networks.

Phylogenetics is the study of the relationships among groups of organisms that are obtained by analyzing molecular sequencing data. By using statistical methods, shown schematically in Figure 2, one can estimate the degree to which different organisms are related to each other in an evolutionary sense. This has particular importance in on-going epidemics where the ability of, for example, viruses to evolve can determine the efficacy of treatments or vaccines. In one study completed this year, we have been able to reconstruct specific events associated with an epidemic using the phylogenetic analysis of viral sequences.

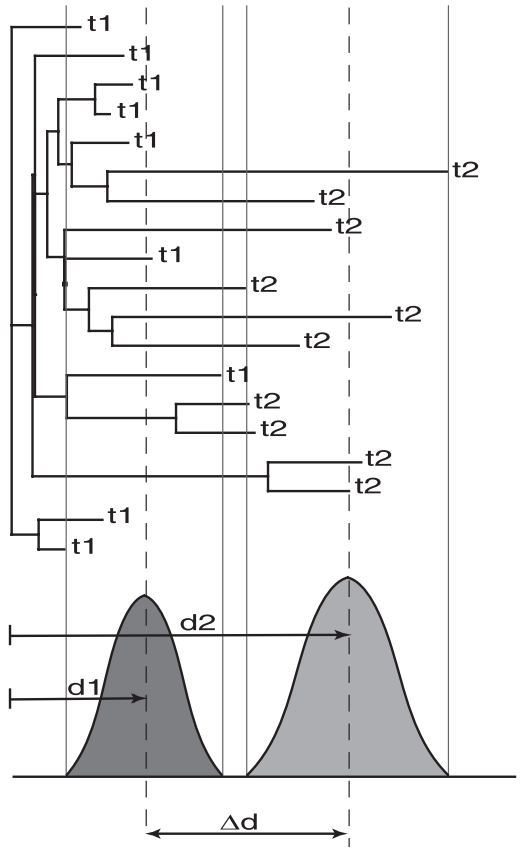


*Figure 2. Schematic illustration of the statistical construction of a phylogenetic tree from genetic sequence data.*

Demographic models built from genetic data play important roles in illuminating prehistorical events. We introduce, in a paper submitted to *PLoS Genetics*, an inference method based on the spectrum of genetic variations within and between populations. For candidate models we numerically compute the expected spectrum using a diffusion approximation. As applications, we model human expansion out of Africa and the settlement of the New World, using non-coding DNA resequenced in 68 individuals from 4 populations.

## Future Work

We will characterize complex biological and soft materials and to study complex biological systems through theoretical and computational approaches with the following specific objectives:

1. Study the mechanisms of adaptive immune responses to infection or vaccinations at the molecular level by modeling the responses triggered by cell-surface receptors, such as antigen-recognition receptors, and study the molecular mechanisms of virulence factors that interfere in immune response.

2. Explore artificial thin-film materials for purposes such as biosensor design, characterization of membrane-protein interactions, and constructing spatial arrays of proteins and other materials with desired patterns.

3. Develop comprehensive models of cellular systems, such as genome-scale metabolic and genetic regulatory networks in bacteria, for the purposes of metabolic engineering or design of synthetic cellular regulatory systems that yield cells with desired behavioral properties.

4. Pursue studies, particularly of cellular information processing, that take advantage of large datasets and account for stochastic and spatial effects.

5. Develop multi-scale, tissue-level models based on cell dynamics, cell-cell interactions, and cell-microenvironment interactions, e.g., study bio-film formation, tissue response to viral and bacterial infections, tissue permeability to biological and chemical agents.

## Conclusion

By building accurate models of how molecular processes interact within a cell to create cell specificity and function, scientists can begin to manipulate those functions for new applications. A specific example is designing an efficient biological biomass conversion process that could help address energy sustainability issues. Other implications of our work include better predictability of the spread of contagious disease and the design of effective vaccines for such diseases. Using these biological systems and their models as a basis, we can design new materials that mimic the function of membranes, vesicles, and muscle.

## Publications

Adamczyk, Z., P. Weronski, and J. Barbasz. Formation of multilayered structures in the layer by layer deposition of colloid particles. 2008. *JOURNAL OF COLLOID AND INTERFACE SCIENCE.* **317** (1): 1.

Alexandrov, B., V. Gelev, S. W. Yoo, L. Alexandrov, A. Bishop, K. Rasmussen, and A. Usheva. DNA Dynamics Play a Role as a Basal Transcription Factor in the Positioning and Regulation of Gene Transcription Initiation. To appear in *Nucleic Acid Research.*

An, G., J. Faeder, and Y. Vodovotz. Translational systems biology: Introduction of an engineering approach to the pathophysiology of the burn patient. 2008. *JOURNAL OF BURN CARE & RESEARCH.* **29** (2): 277.

Bauer, A. L., C. A. Beauchemin, and A. S. Perelson. Agent-based modeling of host-pathogen systems: The successes and challenges. 2009. *Information Sciences.* **179** (10): 1379.

Beauchemin, C. A., J. J. McSharry, G. L. Drusano, J. T. Nguyen, G. T. Went, R. M. Ribeiro, and A. S. Perelson. Modeling amantadine treatment of influenza A virus in

vitro. 2008. *JOURNAL OF THEORETICAL BIOLOGY.* **254** (2): 439.

Bel, G., B. Munsky, and I. Nemenman. Common complex biochemical processes exhibit simple completion time distributions . *Physical Biology.*

Bel, G., and I. Nemenman. Ergodic and non-ergodic anomalous diffusion in coupled stochastic processes. 2009. *New Journal of Physics.* **11**: 083009.

Benoit, J., and A. Saxena. Spherical vesicles distorted by a grafted latex bead: An exact solution. 2007. *PHYSICAL REVIEW E.* **76** (4): 041912.

Dreisigmeyer, D. W., J. Stajic, I. Nemenman, W. S. Hlavacek, and M. E. Wall. Determinants of bistability in induction of the Escherichia coli lac operon. 2008. *IET Systems Biology.* **2** (5): 293.

Edwards, J. S., J. R. Faeder, W. S. Hlavacek, Y. Jiang, I. Nemenman, and M. E. Wall. q-bio 2007: a watershed moment in modern biology. 2007. *MOLECULAR SYSTEMS BIOLOGY.* **3**: 148.

Gutenkunst, R. N.. Proteins with greater influence on network dynamics evolve more slowly but are not more essential. *Molecular Biology and Evolution.*

Gutenkunst, R. N., R. D. Hernandez, S. H. Williamson, and C. D. Bustamante. Inferring the joint demographic history of multiple populations from multidimensional SNP data. To appear in *PLoS Genetics.*

Lipniacki, T., B. Hat, J. R. Faeder, and W. S. Hlavacek. Stochastic effects and bistability in T cell receptor signaling. 2008. *JOURNAL OF THEORETICAL BIOLOGY.* **254** (1): 110.

MaljkovicBerry, I., T. Wallstrom, C. Franzen, J. Albert, A. Veglio, H. Skar, K. Aperia, and T. Leitner. Reconstruction of epidemiological events by phylogenetic analyses of viral sequences. *Epidemics.*

Motter, A. E., N. Gulbahce, E. Almaas, and A. Barabasi. Predicting synthetic rescues in metabolic networks. 2008. *Molecular Systems Biology.* **4**: 168.

Munsky, B., B. Trinh, and M. Khammash. Listening to the noise: Random fluctuations reveal gene network parameters. 2009. *Molecular Systems Biology.* **5**: 318.

Nemenman, I., W. S. Hlavacek, Y. Jiang, and M. E. Wall. Selected papers from the Second q-bio Conference on Cellular Information Processing. 2009. *IET Systems Biology.* **3** (5): 297.

Ramachandran, S., H. Tang, R. N. Gutenkunst, and C. D. Bustamante. Human population genetics and genomic. To appear in *Human Genetics: Problems and Approaches, 4th Addition, Springer Verlag by Vogel and Motulsky.*

Shen, T., P. Langan, A. D. French, G. P. Johnson, and S. Gnanakaran. Conformational flexibility of soluble cellulose oligomers: Chain Length and temperature dependence. 2009. *Journal of American Chemical Society.* **131**: 14786.

Shen, T., and D. Hamelberg. A statistical analysis of the precision of reweighting-based simulations. 2008. JOURNAL OF CHEMICAL PHYSICS. **129** (3): 034103.

Shen, T., and S. Gnanakaran. The stability of cellulose: A statistical perspective from a coarse-grained model of hydrogen bond network. 2009. *Biophysical Journal.* **96**: 3032.

Weronski, P., and M. Elimelech. Novel numerical method for calculating initial flux of colloid particle adsorption through an energy barrier. 2008. *JOURNAL OF COLLOID AND INTERFACE SCIENCE.* **319** (2): 406.

Yang, J., M. I. Monine, J. R. Faeder, and W. S. Hlavacek. Kinetic Monte Carlo method for rule-based modeling of biochemical networks. 2008. *Physical Review E.* **78** (3): 031910.

Zilman, A., J. Pearson, and G. Bel. Effects of Jamming on Nonequilibrium Transport Times in Nanochannels. 2009. *Physical Review Letters.* **103** (12): 128103.

# Understanding Drug Resistance and Co-infectivity in HIV and TB Infections

*Bette T. Korber*
20090098DR

## Introduction

Mycobacterium tuberculosis, which causes tuberculosis (TB), has ravaged mankind for several thousand years and claims over 4000 lives worldwide every day. TB infections are increasing, particularly in Africa and Eastern Europe, and the World Health Organization estimates that ~2 billion people are infected. HIV/AIDS is estimated to infect 33 million people. Despite therapies, more than 2 million people die of AIDS each year. While the characteristic patterns of mutations that confer resistance to specific classes of HIV drugs are known, those associated with TB drug resistance are still being mapped. There is no information about the genetic diversity of primary TB infections, evolutionary processes leading to acquired multiple drug resistance are poorly characterized, and the impact of HIV co-infection on genetic diversity is unknown. Further, key virulence factors are not well known and for those that are known, research tools (e.g., antibodies) do not exist to characterize them. In this study, we have begun characterizing the genetic diversity in initial HIV infections. We hope to track the evolution of both HIV and TB as a function of treatment using new pyrosequencing methods that allow rapid and extensive sequencing. We will better understand the acquisition of genetic markers of drug resistance, and facilitate the development of new diagnostic approaches. These approaches will permit early diagnosis and help track virulence factors to guide drug treatment. Ultimately, we will apply the diagnostic and genetic analysis tools developed in the initial phases of the project for each pathogen separately, to better understand HIV-TB co-infections.

## Benefit to National Security Missions

We are developing new methodologies for diagnostics and genomics applied to both a rapidly evolving virus and a bacterial genome. These could be readily transitioned to apply to a broad spectrum of other pathogens, addressing Threat Reduction, human health, and basic science missions relevant to DOE, DHS, and other government agencies. LANL has a strong foundation in the analysis of HIV pathogen genetic diversity, and the development of detection assays for TB and other agents. We are building on this foundation to develop new detection methods for drug resistance and pathogenesis and disease progression, and improve our understanding of the associated biological and evolutionary processes.

## Progress

We have developed an assay for a TB biomarker called LAM, and have shown that its presence in patient urine is directly correlated with disease. During the course of these studies we discovered a new assay approach for measuring LAM as well as other biomarkers for TB. This new approach relies on partitioning of the biomarker into supported lipid bilayers, followed by detection using a reporter ligand that binds to an exposed region of the biomarker and signals its presence. This new approach provides an ultrasensitive assay for LAM and ESAT-6, two virulence factors for TB, and also works for many other biomarkers for human bacterial infections and cancer. The results obtained to date have resulted in two provisional patent applications. We have also received patient samples (serum and urine) that can be used to follow the evolution of biomarker concentrations as a function of the disease progression as well as therapeutic intervention. These patient samples are from the Masan TB hospital in South Korea and they represent samples from patients with drug sensitive and drug resistant TB but with no co-infection from HIV. Analysis of these patient samples will provide the basis needed for future studies of samples from co-infected patients.

Many of the biomarkers we have studied in the context of TB are shared by Mycobacterium bovis, the causative agent of tuberculosis in cattle, an important national and international problem. Preliminary results show that our new membrane-based assay can be extended to bovine TB, resulting in initiation of New Mexico Small Business Assurance and State of New Mexico funded research projects. We are currently preparing manuscripts on this work and a patent disclosure has been filed.

We are making progress with the mass spectroscopic

characterization of TB biomarkers, hoping to extend our marker discovery and validation work with these methods. Also, we have had some success with the development of antibodies to identify one TB biomarker, Antigen 85. This is extremely important because Antigen 85 is a virulence factor for which good recognition ligands are currently unavailable, limiting its application to diagnostic and therapeutic strategies.

LANL has historically been the leading edge of efforts to sequence the human genome and complete bacterial genomes. Here we are working to extend LANL's capabilities to the study of highly variable and rapidly evolving pathogens, (in contrast to single bacterial genomes), using high-throughput sequencing technology. Our first DR project in this area was to develop analysis methods to study the evolutionary trajectory of the emergence of drug resistance within HIV-infected individuals. We initially focused on the drug vicriviroc, that blocks HIV entry (Tsibris, PLoS One, May 2009 4:e5683). The new methodology allowed an unprecedented view of within-patient HIV diversity, with between 25,000–140,000 sequences obtained per sample. We developed a strategy to contend with experimental error, and observed extraordinary within-patient diversity in chronic infection prior to therapy. Extreme and rapid shifts in viral populations were observed, with unexpected increases in diversity over the first weeks of therapy.

In this second study, our experimental group in B-division developed the capability to conduct the 454 ultra-deep sequencing, while the T-division group improved computational methods for data cleanup and analyses. While further developing the methodology, we studied another critical biological scenario, the emergence of immune escape during acute HIV infection. HIV was sequenced from three newly infected individuals over time to study the earliest evolution of the virus in regions targeted by the human T-cell immune response. While the overall rate of sequencing errors using 454 technology is comparable to the natural substitution rate, the predominant errors are of a different nature. This allowed us to identify and resolve most of the experimental errors. Once the data was cleaned up, complex patterns of selection were observed, and dozens of different immune escape forms were found to be co-circulating in the infected individual. In some samples, this diversity collapsed later with the outgrowth of one of these forms. We currently have a manuscript in preparation describing this work, and a new suite of tools for analyses of ultradeep sequences have been developed. We have also now shown, base on up to 40,000 HIV sequences from a single sample, that HIV infection indeed appears to be established by a single transmitted virus.

The enormous amount of sequence data from early homogeneous samples also allowed us to model the substitution rates per generation in vivo directly. Since standard coalescent programs have not been designed to handle this quantity of data, we have developed the required statistical techniques for analysis. We have found that the substitution rates in vivo varies among subjects, and may be larger than the mutation rate estimates used by HIV scientists for the last decade.

We have also completed 454 ultradeep sequencing of simian immune deficiency virus (SIV) in macaques in an analogous study to the HIV acute infection study. The SIV macaque model allows more comprehensive and controlled data acquisition to inform our understanding of early infection. We also have in the pipeline a data set that will enable us to explore the acquisition of drug resistance to tenofovir, an antiretroviral drug that is being tested in a South Africa to see if it can prevent sexual transmission of HIV when applied in a gel.

## Future Work

We will continue to characterize diversity in primary HIV and TB infections and track and model evolution as a function of treatment to gain understanding regarding the acquisition of genetic markers of drug resistance and the underlying biology. This will facilitate the development of new diagnostic approaches to permit early diagnosis and also help track virulence factors to guide drug treatment and to better understand HIV-TB co-infections. High throughput sequencing studies will also be performed on longitudinally collected samples of infected TB patient samples (~ 8), allowing us to model the evolution of TB and resolve the basic parameters that impact the acquisition of drug resistance. To this end, we are currently negotiating a possible collaboration with scientists at Harvard, and in Durban, South Africa. Through the study of HIV and TB, we will help shape the cutting edge of this new technology, while working on pathogens of the utmost importance with respect to public health. Urine from infected TB patients will be analyzed for the presence of known and likely TB-specific biomarkers using mass spectrometry. Furthermore we will develop ligands that bind to these biomarkers for assay development. Sensitive and specific immunoassays and oligonucleotide probes for the simultaneous detection of multiple markers will be developed using both the waveguide-based optical biosensor and a nanotechnology biobarcode-based amplification diagnostic method. We will apply what we learn to better understand how HIV co-infection impacts TB's evolutionary trajectory with regard to rapid emergence of drug resistance and death.

## Conclusion

The WHO designates TB and HIV/AIDS as 2 of the 3 most deadly diseases confronting mankind. These pathogens, each deadly in its own right, operate synergistically, and HIV-induced suppression of the immune system allows activation of latent TB, leading to progressive, contagious, and drug resistant TB. The biology underlying

the interaction between these two pathogens is not understood. We are applying and developing new technologies that enable identification of markers of disease progression for TB, designing diagnostics for HIV and TB drug resistance and progression, and studying the evolution of these two pathogens in infected and co-infected individuals.

## Publications

Lynch, R. M., T. Shen, R. Rong, B. Li, W. Honnen, S. Allen, S. Zolla-Pazner, A. Pinter, S. Gnanakaran, and C. A. Derdeyn. Subtype-specific conservation of Isoleucine 309 in the Env V3 domain is linked to immune evasion in subtype C HIV-1 infection. *Journal of Virology.*

Mukundan, H., H. Xie, D. Price, J. Kubicek-Sutherland, W. Grace, A. Anderson, J. Martinez, N. Hartman, and B. I. Swanson. Quantitative multiplex detection of pathogen biomarkers on multichannel waveguides. To appear in *Analytical Chemistry.*

Neher, R., and T. Leitner. Recombination rate and selection strength in HIV intra-patient evolution. *PLoS Computational Biology.*

Rebecca, M., T. Shen, S. Gnanakaran, and C. Derdeyn. Appreciating HIV-1 diversity: subtypic differences in Env. 2009. *AIDS Research and Human Retroviruses.* **25**: 237.

Tsibris, A. M., B. Korber, R. Arnaout, C. Russ, C. C. Lo, T. Leitner, B. Gaschen, J. Theiler, R. Paredes, Z. Su, M. D. Huges, R. M. Gulick, W. Greaves, E. Coakley, C. Flexner, C. Nusbaum, and D. R. Kuritzkes. Quantitative deep sequencing reveals dynamic HIV-1 escape and large population shifts during CCR5 antagonist therapy in vivo. 2009. *PLoS One.* **4** (5): 5683.

# Distributed Metabolic Regulation: The Key to Synthetic Biology for Carbon Neutral Fuels

*Pat J. Unkefer*
20090117DR

## Introduction

DOE's goal of harnessing biological systems for renewable energy production and carbon sequestration is frustrated by our limited understanding of cellular-level metabolic regulation. Decades of reductionist scientific approaches failed to provide solutions; it is now clear that cells are complex systems with diverse metabolic control mechanisms and these control mechanisms must be understood to develop biological solutions to these problems. Measurements of cellular constituents (transcriptome, proteome, metabolome, etc.) and advances in network modeling have revealed a higher level of regulatory complexity than previously appreciated. Control is exerted at all functional levels, including DNA methylation, transcription, translation, post-translational modification and protein activity. Control of these functions is carried out by diverse classes of molecules, such as DNA, RNA, proteins, and metabolites.

To understand and ultimately to harness living systems for renewable energy production, carbon sequestration and environmental remediation, we must a) know the functions of cell parts, b) assess the roles that the cell parts play in operational networks (i.e., RNA, protein, and metabolite networks), and c) decipher how control processes are integrated within and between these operational networks. Much progress has been made on characterizing the functions of cell parts and their operational networks. However, we do not yet understand how their networks are integrated. Proof of this lack of knowledge is our failure over the past two decades to *optimize* cells for over-production of any chemical. This problem will be particularly acute in engineering organisms to produce massive amounts of biofuels or to maximize carbon sequestration.

One of the least understood but critical integrating functions in the cell is the transcription factor (TF)-mediated regulation of gene expression. TF-mediated regulation allows cells to respond to environmental changes and yet control cellular metabolism to maintain their homeostasis and to survive. It is this ability of cells to over-ride the disruption caused by environmental challenges that confounds our ability to truly optimize/engineer organisms for industrial/practical purposes (e.g., production of biofuels, carbon sequestration, chemical or drug synthesis). TFs regulate the expression of sets of genes, called regulons, which are composed of sub-groups of genes termed operons. TFs bind to specific DNA sequences upstream of the regulated gene(s) and either induce or repress gene expression. TF recognition and binding to a particular DNA sequence is modulated by the binding of a small-molecule effector to the TF.

The binding of an effector by the TF alters the TF's conformation. The conformational change alters the affinity of the TF-effector complex for the DNA sequence. This mechanism, termed allostery, is widely used by biological systems to modulate protein function; it is especially valuable in sensing/response systems because it allows a few components to respond appropriately to numerous signals. The conventional view of TF-effector complexes has been that they are simple "On/Off" switches. We believe that their activity is far more complex, but experimental difficulties have thus far hindered progress in characterizing their regulatory activity. Only a few effector molecules have been identified and little quantitative information is available about their binding with TFs.

More importantly, the complexity and sophistication of effector-TF interactions has been overlooked. Our work suggests that TFs can act as sophisticated signal processors, not merely as "On /Off' switches because they can bind multiple effector molecules. Multiple effectors with similar binding affinities for a TF interact with the TF and potentially generate a complex set of effector-TF complexes. These various complexes, with their respective, complex conformational changes likely have complex influences on gene/operon expression. For example, the different effectors could induce TF conformational changes that fundamentally change the recognition specificity and affinity, allowing the TF to bind to different DNA sequences. The literature on expression repeatedly observes "regulatory noisy." Our

proposed model of TF-effector activity is a very plausible explanation for this "noise."

The major objectives of the project are to identify DNA recognition motifs and small molecule effectors for as many transcription factors (TFs) as possible from a list of 125 TFs that are common to the Burkholderia genus. We are on track to achieve our milestones.

## Benefit to National Security Missions

Our progress formed the basis for a preproposal submission to DTRA this fall on the potential for transcriptional regulators to become targets for a next generation of antimicrobial drugs; the need for these new drug targets has been identified as a critical need by the US Department of Defense. The work also directly supported and strengthened LANL's submission for an Algal Biofuels Center for DOE Energy Efficiency and Renewable Energy.

## Progress

The first steps in achieving these objectives are TF gene cloning and TF protein purification. We completed the laborious, multistep process of cloning the first 30 of 125 transcription factor genes from the bacterium, *Burkholderia xenovorans*, into a protein expression vector in *E. coli.* We amplified the remaining 95 TF genes and purified the amplified DNA in preparation for cloning. We began protein purification of the first 30 cloned TFs for effector binding assays and DNA binding assays. We will are continuing to clone the remaining 95 transcription factors.

Another major step is the development of TF-binding microarray optimized for microbial TFs. We have designed such a TF-binding microarray; it includes all (6-mer half-site – gap – repeat) sequences, where the gap is from 0-26 bp, and the repeat is either the direct or palindromic 6-mer half-site. The design has been printed on arrays that have been received by the Bulyk lab; these arrays will be tested using protein provided by LANL.

To compliment and extend the value of the microarray we are developing a computational method for predicting TF binding sites that incorporates not only chemical binding information but also structural information. To evaluate our method, we designed metrics for benchmarking our method against other commonly used methods. Using experimental data for Fis binding to DNA, we find that our method correctly predicts Fis TF binding sites with an accuracy that exceeds that of the other methods with significantly fewer false positives. We are designing experiments to validate selected TF binding site predictions obtained with our computational method.

Discovering the small molecule effector is experimentally difficult if it is done without any insight into its structure. To aid this process, we have created a prototype web-based tool to allow us to capitalize upon conservation of genome structure or organization that can be revealed by examining the genomic context of the target TF gene across several hundreds of microbial genomic sequences. This tool finds clusters of structural genes located in close proximity to the TF; these clusters are thought to be functionally associated with the TF and thus can potentially offer insights into the regulon controlled by the TF. For example, this tool places the unknown TF, yafC , within a cluster of proteins involved in the detoxification of methylglyoxal by the glyoxylase system. The enzymes methylglyoxal reductase (EC. 1.1.1.78) and hydroxyacylglutathione hydrolase (EC 3.1.2.6) and several acyl-carrier-proteins are found in the genomic neighborhood of TF yafC in a set of bacteria. Thus we provisionally assigned TF yafC as regulating the metabolism of methylglyoxyl and thus we can now test methylglyoxyl and other pathway intermediates as potential effectors this TF.

## Future Work

We will characterize additional TFs and identify their effectors. We will identify the DNA binding sites for characterized TFs. When practical, we will associate the TF with the metabolic pathway(s) it is regulating.

## Conclusion

To realize the Department of Energy goal of utilizing biological organisms for renewable energy and carbon sequestration, we must know the functions of the operational cellular networks and how control is integrated within and between networks. We do not understand how these networks are integrated to regulate metabolism. This project focuses on the critical but poorly understood roles transcription factors play in regulating and coordinating gene expression with the cells metabolic status. The major objectives of the project are to identify DNA recognition motifs and small molecule effectors for as many transcription factors (TFs) as possible from a list of 125 TFs that are common to the Burkholderia genus. We are on track to achieve our milestones. We have cloned the first 30 of our 125 target TFs and established purification methods for TFs. We have developed and refined the necessary high throughput assay to discover and characterize the small molecule metabolite effectors of each of the TFs and begun screening for effectors. We created a web-based tool to examine the genomic context of the target TF gene across hundreds of organisms to assist discovery of the effectors; using this tool we provisionally assigned TF yafC as regulating the metabolism of methylglyoxyl. Finding the pathway regulated by the TF was an unexpected benefit of the work. We have improved prediction of TF DNA binding sites by utilizing chemical and structural information.

## Publications

Bauer, A., W. Hlavacek, and F. Mu. Using sequence-specific chemical and structural properties of DNA to predict transcription factor binding sites. Presented at *q-Bioconference.* (Santa Fe, June 26-28. 2009).

Mu, F., A. Bauer, J. Faeder, and W. Hlavecek. Using systems biology techiques to determine metabolic fluxes and metabolic pool sizes. To appear in *Handbook of Chemoinformatics Algorithms.* Edited by Faulon, J., and A. Bender.

# High-Resolution Physically-Based Model of Semi-Arid River Basin Hydrology

*Everett P. Springer*
20061493DR

## Abstract

Computer simulation models allow a water resource manager to test "what if" type of questions and examine the response of water resources to environmental changes. Los Alamos National Laboratory (LANL) used the watershed model, triangular integrated network Real-time Integrated Basin Simulator (tRIBS), in collaboration with New Mexico Tech University to simulate river basin response. LANL's brings its capabilities in high performance computing to the problem of simulating river basin water resources providing faster solutions. The tRIBS code was adapted to the LANL parallel computing machines, and results found that speed increased by five times for 32 processors over a single processor. The Rio Ojo Caliente was designated as the test basin for this project. The Rio Ojo Caliente had a die-off of pine trees in the early 2000's that provided an opportunity to examine the effects of this environmental change on the basin water resources. The simulation required data on weather for the period, soil properties and vegetation data. Collaborative work with Texas A&M University developed a novel approach to estimate tRIBS soil parameters using available properties. Vegetation was estimated using remote sensing data for the period from 1989 – 2007 to include the time when the vegetation die-off occurred. The LANL Ponderosa Pine site provides high quality data on surface runoff and subsurface water balance components to test tRIBS performance in these environments increasing our confidence in its application. LANL collaborated with the National Science Foundation Science and Technology Center for Sustainability in semi-Arid Hydrology and Riparian Areas (SAHRA) on application of models to water resources problems, and found that framing the question is a critical requirement for successful resolution. This project supports LANL's mission in Energy Security focusing on the environmental impacts of climate change.

## Background and Research Objectives

Environmental decision makers require tools to understand the responses of human and natural systems along with the feedback between these two systems. Computer simulation models provide information that allows decision makers to forecast and understand how the environment behaves. The other alternative to computer modeling is data collection, but it is very difficult to collect the necessary measurements to evaluate the system behavior in space and time. The hydrologic or water component is critical to solve environmental problems because geologic material and chemicals are transported by water.

Loague and VanderKwaak [1] have provided a brief review of watershed simulation models, and two basic types, empirical and conceptual, emerge. Empirical models are useful and work when the same conditions occur as when the model parameters were estimated. The concern is that both the representation of hydrologic processes and associated parameter values lose their physical meaning in empirical models because of these models depend on the collected data to estimate parameters. Conceptual models use basic knowledge of physical processes to derive the functional forms for the hydrologic processes. Parameters for these functions are based on knowledge of the physics of the system being simulated and the range that these parameter values can take in nature. This knowledge represents an advantage over the empirical models, but other issues arise with conceptual models especially measuring of the spatial variabilities of these parameters over the landscape.

The goal of this project was to apply LANL's high performance computing capability to simulate the water cycle in semi-arid river basins using a conceptual watershed model. Other efforts are ongoing to address these water resources issues, but the uniqueness of this research over these ongoing efforts was the increased spatial and temporal resolution that was made possible by LANL's computing resources.

The triangular integrated network Real-time Integrated Basin Simulator (tRIBS) is the watershed model that was used in this project [2]. LANL developed a version of tRIBS that ran on parallel computers. Data were developed from existing sources to apply this computer model to the Rio Ojo Caliente Basin in New Mexico. We were unable to complete the simulation, but we did

make significant strides in terms of developing the model and data for this simulation.

## Scientific Approach and Accomplishments

The modification of the tRIBS code to run on LANL's parallel computers is a necessary step to attain the computer speeds needed so that results are provided in a timely manner. Using a test problem from the original tRIBS development because we knew the correct answers, the time to complete the simulation on different numbers of computer processors is shown in Figure 1. The results in Figure 1 indicate that a five times increase in computational speed can be obtained using parallel computers for these problems. It is noted that the example problem in Figure 1 was small in terms of the number of computational nodes, and the increase in speed may be even higher for problems on larger watersheds.

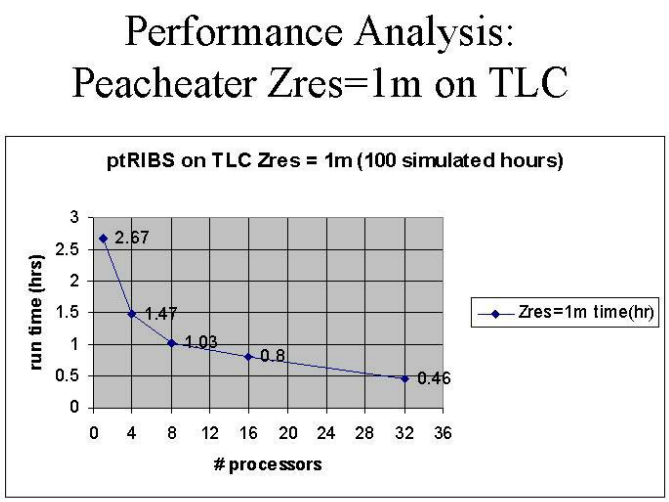


*Figure 1. Performance of tRIBS for different processors on test case.*

The basin for application of tRIBS is the Rio Ojo Caliente in northern New Mexico (Figure2). The basin is broken into elements, nodes and triangles for tRIBS. In Figure 2, the tRIBS description of the Rio Ojo Caliente is described by 261,956 triangles and 132,051 nodes for the selected resolution. The Rio Ojo Caliente was subject to rapid vegetation change in the lower part of the basin during the drought that occurred in the early 2000's and shown as the orange area in Figure 3. This vegetation change event presents an opportunity to determine the effects of these types of changes on water resources in the basin. The lower 30 percent of the basin was impacted by the loss of pine trees during this drought period. Our goal was to evaluate the impact on water balance components such as soil water, groundwater, and snow accumulation and melt after this vegetation change occurred. Therefore, we collected from available sources the required data to simulate the 1995 – 2004 period.

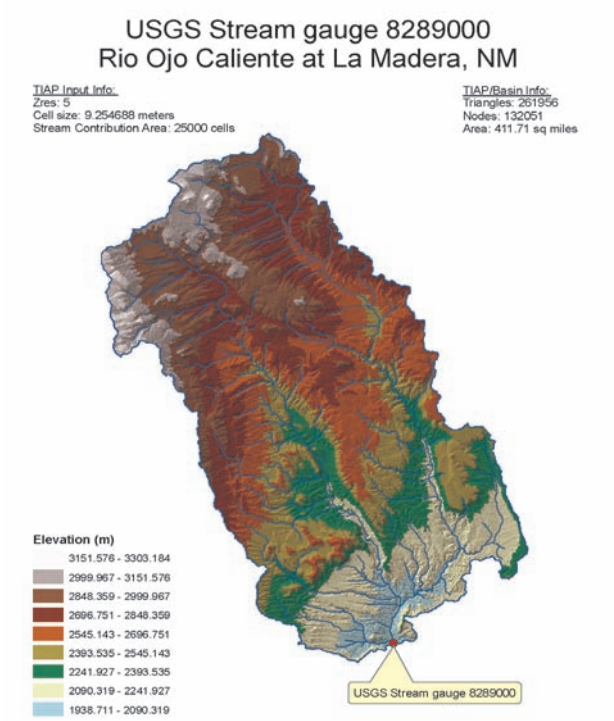


*Figure 2. The Rio Ojo Caliente Basin in New Mexico with information for application of tRIBS.*

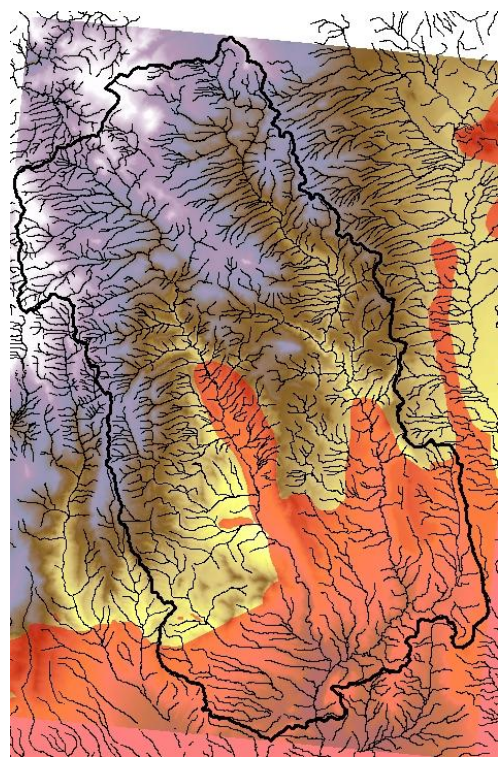

*Figure 3. The loss of trees in the Rio Ojo Caliente Basin represented by the orange shaded area provides an opportunity to examine the impacts on the water balance in the basin.*

A critical data set is the weather variables that drive the tRIBS code. The University of California at Irvine has

generated a set of weather data for the southwestern U. S. on a 4 x 4 km grid [3]. We extracted for the Rio Ojo Caliente the weather data extracted for the 1995 – 2004 period overlapping the period when the vegetation change occurred on the Rio Ojo Caliente Basin.

In addition to the weather variables, parameters are needed for soils and vegetation for each tRIBS node. The Pedo-Transfer Functions (PTFs) approach to estimating soil parameters uses available or easily measured soil properties such as soil texture or percentage of sand, silt and clay particles in the soil to provide required soil parameters for the model. Most previous PTF studies, however, derive these soil properties and parameters at the same scale or size as the sample was obtained for the input data. This presents a problem in model applications because the area represented by a tRIBS node may be much on the order of meters to 100s of meters while the sample is collected 10 centimeters. To address this mismatch, a collaborative effort between Texas A&M University and LANL developed a Bayesian framework to estimate key soil properties and parameters including a measure of the error at the local scale using PTFs trained with coarser scale United States Department of Agriculture Soil Survey Geographic (SSURGO) Database soil data [4,5]. The Bayesian method allows available information to be included in the parameter estimate. A PTF tool with training and confirmation data collected in two different regions in USA was developed. The two study areas are the Las Cruces Trench site in the Rio Grande basin of New Mexico [6], and the Southern Great Plains 1997 hydrology experimental region in Oklahoma [7]. The PTF for each of the two locations was trained using soil texture and bulk density data from the SSURGO database (scale 1:24,000). Then the PTFs predicted the soil water contents at selected values of soil water pressure using data collected at the two experimental sites previously listed. The resulting outputs were corrected for errors using either a linear or nonlinear correction technique. The results revealed good agreement between the soil water content values measured at the point scale, and those predicted by the Bayesian-based PTFs for both the study sites [4,5].

Remote sensing is the most practical method to assess vegetation change and to provide vegetation parameters for tRIBS. The remote sensing measurement that we used to identify vegetation for this study was the normalized vegetation difference (NDVI) defined by ratios of bands from the Advanced Very High Resolution Radiometer (AVHRR), which is on a satellite. The NDVI is a measure of the photosynthetic capacity, which is related to the amount of green vegetation within the remote sensing image. Scenes from AVHRR are available approximately every two weeks, and the quality of the images depends on the atmospheric conditions such as clouds. Available, bi-weekly images beginning in 1989 were analyzed for the Rio Ojo Caliente, and the NDVI trend is presented in Figure 4. The red area in the center of Figure 2 along with the downward trending mean NDVI line indicates the major drought period. The post-drought period indicates a rapid response in vegetation, but this is herbaceous vegetation such as forbs or grasses that come into the area after the trees have died.

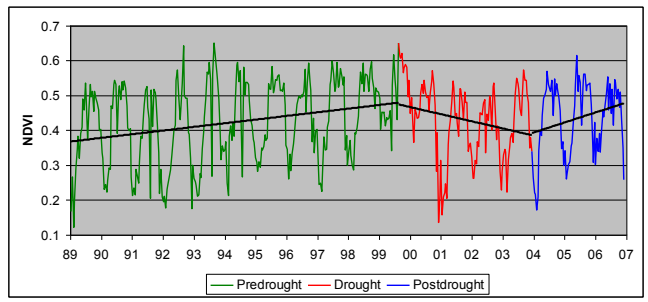


*Figure 4. Mean NDVI trend for the Rio Ojo Caliente watershed for the period 1989 to 2007 indicating the period of Pinyon mortality in early 2000s.*

The vegetation change on the Rio Ojo Caliente can be seen in Figure 3. The heavy black line is the outline of the basin, and the colors represent elevation with white being the highest areas. The orange shading over the lower part of the basin was derived from remotely sensed images and indicates the area that experienced a decrease in NDVI, which is assumed to be Pinyon mortality. It is key to note that the mortality is located in the lower elevation zones, consistent with Pinyon and Juniper woodlands. Data were developed using the NDVI to track the changes in vegetation over the simulation, and these data were put into tRIBS.

Model testing is critical to demonstrate that the model responds correctly or at least within bounds that have been identified in advance and provide confidence for the model application. The term validation is used to describe this activity, but there has been considerable controversy about whether models of earth systems can be validated so the term model testing is applied here. In the past watershed models have been tested against streamflow usually at a point and perhaps a number of groundwater wells. The limitation is that with distributed models and only a single test point that integrates many processes such as streamflow there is sufficient flexibility in the model that a number of fits to the data can be obtained. It has been shown by Beven [8] that many different parameter sets can provide an equally good representation of the test data. This result does not generate any

confidence in simulations. The goal here is to provide some spatial data to help in fitting the model so that the solutions are more reliable.

Mean daily streamflow from the U.S. Geological Survey (USGS) gauge located at La Madera, New Mexico ( ), which has been in operation since 1932 was available for this study.

Distributed models need spatial data for model testing much as time dependent models need a time series. Model testing data sets are being developed by studies in the Rio Grande Basin, which are part of the National Science Foundation Science and Technology Center for Sustainability in semi-Arid Hydrology and Riparian Areas (SAHRA). Information on SAHRA is available at (). SAHRA has established a transect that consist of atmospheric flux towers, soil moisture measurements stations, groundwater monitoring arrays and stream gauging on the East Fork of the Jemez River in the Valles Caldera. Data are collected in space and time so this provides a unique opportunity for model testing on a smaller spatial domain than the Rio Grande Basin, and these unique datasets will allow simultaneous checking of multiple processes such as evapotranspiration, streamflow, groundwater, and soil moisture providing added checks on the model parameters.

The Ponderosa Pine Hillslope site at LANL is another site to test the tRIBS code through a detailed surface/subsurface data. In particular, significant differences in snow accumulation and melt conditions at the Ponderosa site during the 1990s generated flow in two different ways, namely dominant surface runoff during years with low snow accumulation, and significant lateral subsurface flow in years with high snow pack. In addition, the site is well characterized with soil samples, infiltration rates, soil water content and runoff data [9,10]. Using the soil and surface elevation data from the Ponderosa site [9], we built a solid earth model that honored the layered stratigraphy. In collaboration with LANL, New Mexico Tech University collaborators began to develop a Ponderosa site specification for tRIBS. Using the subsurface soil layers, surface elevation data, vegetation maps, and weather data they conducted preliminary simulations of surface runoff.

In conjunction with SAHRA investigators, the use of models in decision-making was considered. The SAHRA Integrated Modeling project area adopted a multi-resolution modeling strategy to examine water resource issues within the Rio Grande Basin in Mew Mexico [11]. The three resolutions used were a coarse or basin scale model, a medium resolution on the order of 5 – 10 km grid cells, and fine resolution with grid cells on the order of 10 – 100 m. Application of the appropriate model resolution rapidly becomes an issue of the question being asked. For example, if the questions concerns flow out of an area, then the coarse resolution model may be appropriate. Another questions may deal with the source of a pollutant, and the medium or fine resolution model will be needed to provide the location of the pollutant in the basin. The paper by Liu et al. [11] was selected the best paper Integrated Modeling paper for 2008 by the Editors and Board members of the Environmental Modeling and Software Journal.

## Impact on National Missions

This project supports the LANL mission in energy security through understanding the environmental impacts of energy use and climate change. This project supported the water-energy nexus program development activity. The application of LANL's high performance computing capabilities to environmental assessments will allow more rapid decisions. This project addressed the philosophy of applying models to environmental problems.

This project supported a post-doctoral candidate at LANL and a student at Texas A&M University.

## References

1. Loague, K., and J. E. VanderKwaak. Physics-based hydrologic response simulation: platinum bridge, 1958 Edsel, or useful toot . 2004. *Hydrological Processes.* **18** (15): 2949 .

2. Ivanov, V. Y., E. R. Vivoni, R. L. Bras, and D. Entekhabi. Preserving high-resolution surface and rainfall data in operational-scale basin hydrology: a fully-distributed, physically-based approach. 2004. *Journal of Hydrology.* **298**: 80.

3. Li, J., X. Gao, and S. Sorooshian. Modeling and analysis of the variability of the water cycle in the upper Rio Grand basin at high resolution. 2007. *Journal of Hydrometeorology.* **8**: 805.

4. Jana, R. B., B. P. Mohanty, and E. P. Springer. Multiscale pedotransfer functions for soil water retention. 2007. *Vadose Zone Journal.* **6** (4): 868.

5. Jana, R. B., B. P. Mohanty, and E. P. Springer. Bayesian neural networks for multi-scale soil hydraulic parameter estimation. 2008. *Water Resources Research.* **44** (8): 1.

6. Wierenga, P. J., R. G. Hills, and D. B. Hudson. The Las Cruces trench site: Characterization, experimental results, and one-dimensional flow predictions. 1991. *Water Resources Research.* **27** (10): 2695 .

7. Mohanty, B. P., T. H. Skaggs, and J. S. Famiglietti. Analysis and mapping of field-scale soil moisture variability using high-resolution, ground-based data during the Southern Great Plains 1997 (SGP97) Hydrology Experiment . 2000. *Water Resources Research.* **36** (4): 1023 .

8. Beven, K.. Changing ideas in hydrology - the case of physically-based models. 1989. *Journal of Hydrology.* **105**: 157 .

9. Wilcox, B. P., B. D. Newman, D. Brandes, D. W. Davenport, and K. Reid. Runoff from a semiarid ponderosa pine hillslope in New Mexico. 1997. *Water Resources Research.* **33** (10): 2301.

10. Newman, B. D., A. R. Campbell, and B. P. Wilcox. Tracer-based studies of soil water movement in semi-arid forests of New Mexico. 1997. *Journal of Hydrology.* **196** (1-4): 251.

11. Liu, Y., H. Gupta, E. Springer, and T. Wagener. Linking science with environmental decision making: experiences from an integrated modeling approach to supporting sustainable water resources management, . 2008. *Environmental Modelling and Software.* **23** (7): 846.

## Publications

Dickinson, J. E., S. C. James, S. W. Mehl, M. C. Hill, S. A. Leake, G. A. Zyvoloski, and A. A. Eddebbarh. A new ghost-node method for linking different models and initial investigations of heterogeneity and nonmatching grids. 2007. *Advances in Water Resources.* **30** (8): 1722.

He, K., L. Zheng, S. Dong, L. Tang, J. Wu, and C. Zheng. PGO: A parallel computing platform for global optimization based on genetic algorithm. 2007. *Computers and Geosciences* . **33**: 357.

Jana, R. B., B. P. Mohanty, and E. P. Springer. Multiscale pedotransfer functions for soil water retention. 2007. *Vadose Zone Journal.* **6** (4): 868.

Jana, R. B., B. P. Mohanty, and E. P. Springer. Bayesian neural networks for multi-scale soil hydraulic parameter estimation. 2008. *Water Resources Research.* **44** (8): 1.

Keating, E., and G. Zyvoloski. A stable and efficient numerical algorithm for unconfined aquifer analysis. 2009. *Ground Water.* **47** (4): 569.

Liu, Y., H. Gupta, E. Springer, and T. Wagener. Linking science with environmental decision making: experiences from an integrated modeling approach to supporting sustainable water resources management, . 2008. *Environmental Modelling and Software.* **23** (7): 846.

Luo, Y., Z. Lei, L. Zheng, S. Yang, Z. Ouyang, and Q. Zhao. A stochastic model of soil water regime in the crop root zone. 2007. *Journal of Hydrology* . **335**: 89.

Sviercoski, R. F., and B. J. Travis. Analytical effective coefficient for flow equations in porous media by homogenization theory. 2007. In *III International Conference in Multi-scale Materials Modeling.* (Freiburg, Germany, 18-22 Sep. 2006). , p. 885. Stuttgart: Fraunhofer-IRB-Verlag .

Tartakovsky, D. M., A. Guadagnini, and B. Wohlberg. Machine learning methods for inverse modeling. 2008. In *VI International Conference on Geostatistics for Environmental Applications (geoENV 2006).* (Rhodes, Greece, Oct. 25 - 27,2006). Vol. 14, p. 117 . DORDRECHT, NETHERLANDS: Springer.

# Rapid Iterative Detection Using Smart Pathogen Signatures

*John M. Dunbar*
20070010DR

## Abstract

The dissemination of pathogens, either intentionally or through natural outbreaks, is an ongoing threat to human health, agriculture, and economics. Rapid pathogen detection can mitigate this threat. Current devices for autonomous biosurveillance perform poorly. A third generation of biosensors with improved technology is needed.

We aimed to create a prototype of a new biosensor platform with significantly higher efficiency, detection speed, and lower operational cost. Our approach exploited physical field-based manipulation for sample preparation, fabrication of customized microfluidic components, sample interrogation with a novel assay format, and data acquisition with a cutting edge miniature flow cytometer.

We successfully developed key components and integrated subsystems for the biosensor platform. Our acoustic-based sample preparation was superior to conventional methods. Our microfluidic fabrication approach was faster, easier, and cheaper than conventional methods. We delivered a suite of optimized microfluidic devices and force-field parameters for 1) cell trapping and mixing, 2) cell lysis, and 3) trapping and purification of cellular components (e.g. DNA and proteins). We demonstrated a novel type of multiplex assay for detection of 6 pathogens causing flu-like symptoms, including the biothreat pathogens for anthrax, plague, and tularemia. We also developed the flow cytometry platform for sample interrogation and the software/hardware control system for the integrated biosensor. However, our microfluidic DNA amplification device, required for the pathogen detection assays, failed. We observed similar limitations with a device from a leading commercial provider, and are currently testing a potential solution. Additional funding will be required to integrate a functioning DNA amplification device and achieve a fully integrated, autonomous biosensor.

This project provided vital capability development in force field-based sample manipulation and biosurveillance. This enabled team members to acquire $ 11.4M of funding (Oct. 2007-present) from DHS, DTRA, DOE, and private industry, expanding Los Alamos National Laboratory contributions to national security programs (biosurveillance and bioenergy).

## Background and Research Objectives

Widespread dissemination of pathogens, either intentionally or through natural outbreaks, is an enduring threat to human health, agriculture, and economics. Rapid pathogen detection can mitigate this threat. Although attempts to develop autonomous sensor platforms for environmental surveillance are widespread, only a few devices have been deployed and these devices perform poorly. In particular, sample preparation relies on bulky, inefficient devices, and sample interrogation lacks the flexibility needed for affordable and efficient surveillance. A third generation of biosensors with improved technology is needed.

To fill this gap, we aimed to create a new sensor platform. We envisioned a prototype with significantly higher performance efficiency, detection speed (about 5-10 minutes), and lower operational cost.

Our original strategy for a prototype biosensor was to use force-field manipulation for sample preparation and exploit *iterative* sample interrogation. This approach would eliminate complex microfluidics and parallel assays that fail due to cross reactivity of reagents and cost. We aimed to use computationally designed 'smart signatures' to perform hierarchical sample interrogation, in which feedback from sample analysis is used to guide further interrogation. However, approximately four months after project initiation, the iterative strategy was largely abandoned for two reasons. First, it became

clear that little cost saving could be achieved from an iterative approach owing to the complexity of microbial diversity in biosurveillance samples (e.g. aerosols and clinical samples like throat or nasal swabs). Second, we devised an innovative assay format with the potential to overcome the cross-reactivity and cost problems encountered with conventional assay formats.

In our revised strategy, we continued developing sample preparation via force-field manipulation in microfluidic devices, but focused on sample interrogation with our novel assay format. Our approach to sample manipulation allowed us to design a flexible biosensor, able to accommodate different interrogation strategies (including iterative schemes) and different types of assays, depending on the deployment scenario.

## Scientific Approach and Accomplishments

To guide prototype development, we focused on detection of seven priority viral and bacterial pathogens in aerosol or clinical samples able to cause flu-like systems. The target pathogens were *Staphylococcus aureus*, *Streptococcus pyogenes*, and *Streptococcus pneumoniae*, the biothreat agents *Bacillus anthracis*, *Yersinia pestis*, and *Francisella tularensis,* and Influenza virus. Exploiting a mix of engineering, molecular biology, and computational biology, we developed eight vital components for the prototype biosensor (Figure 1) as follows:

- microfluidic chip for cell trapping and mixing.
- microfluidic chip for cell lysis
- microfluidic chip for trapping and segregation (purification) of cellular macromolecules (DNA/RNA, proteins)
- thermal cycling chip for DNA amplification assays
- miniature flow cytometer
- software/hardware control system to run the integrated components
- novel assays to detect flu, anthrax, plague, and tularemia pathogens
- integrated subsystem for cell lysis and DNA trapping

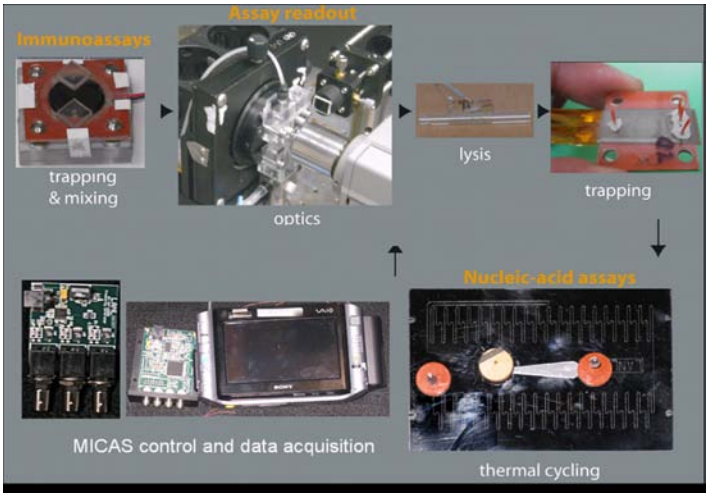


*Figure 1. Component devices developed for the prototype biosensor.*

Our thermal cycling component failed, despite many iterative design and fabrication improvements and hundreds of optimization and trouble-shooting experiments. We observed similar limitations with a thermal cycling chip from a leading commercial provider. We isolated a possible design feature that might cause the failure. We implemented the design change and fabricated a new device to test the solution, but have not yet completed testing. Lacking a fully functional thermal cycling component, we were unable to demonstrate an integrated, autonomous sensor prototype.

We made outstanding achievements in two principle areas: 1) sample preparation with custom fabricated microfluidic devices and 2) development of novel pathogen detection assays. For sample preparation we had several outstanding accomplishments.

First, for sample processing we developed a physical field-based approach that is adaptable to microfluidics and can achieve all the necessary steps in sample processing. This is a major advance for biosurveillance sample processing. Our approach can 1) trap and wash cells, spores, and viruses, 2) lyse them 3) segregate liberated proteins from DNA/RNA, and 4) trap and purify the liberated DNA/RNA. For each sample-processing step, we evaluated almost all possible field manipulation techniques in isolated devices (Figure 2). This allowed us to down-select the best fields and devices for use in our prototype biosensor. For example, we used dielectrophoresis (DEP) only for DNA trapping because substantial performance and device improvements were required for practical use in other steps. Conversely, acoustic manipulation was suitable for many steps. Using several benchmarks, we showed that our acoustic lysis procedure and devices were as effective as or significantly better than standard methods

for lysis of bacterial cells, spores, and viral particles (Figure 3). Also, we demonstrated three important phenomena. 1) Our procedure generates minimal passive heat and therefore proteins remain intact, enabling use of biosurveillance assays targeting proteins. 2) There are specific radio frequencies, which we mapped, suitable for robust trapping of DNA in a DEP field. 3) We can tune the frequencies to specifically trap DNA fragments of particular length or range of base composition. The simplicity and effectiveness of our approach is a major advance enabling faster, more efficient sample processing for autonomous biosensors. This work is described in 4 papers, currently being revised for publication.

| | Deflect | Lysis | Transport | Positioning | Trapping | Mixing |
|---|---|---|---|---|---|---|
| Optical | | | | | | |
| Acoustic | | | | | | |
| Magnetic | | | | | | |
| DEP | | | | | | |

| | |
|---|---|
| | Not applicable |
| | Fair Results |
| | Chips in hand |
| | Possible under specific conditions |
| | Not tested |

*Figure 2. Evaluation of physical fields for sample manipulation in microfluidic devices.*

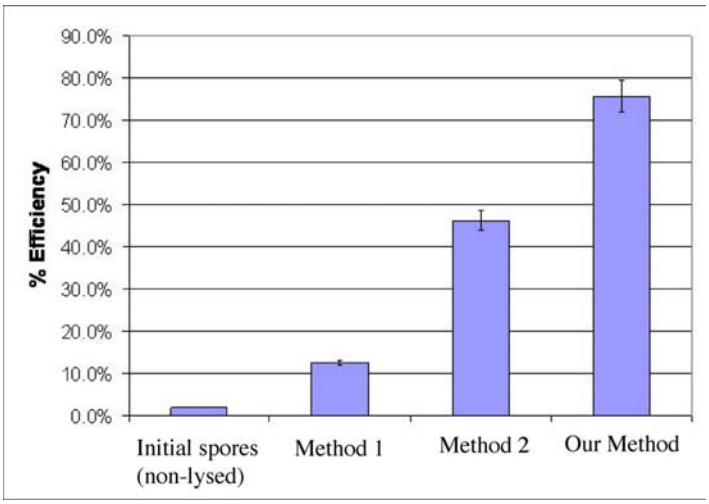


*Figure 3. Efficiency of acoustic lysis of Bacillus spores. Method 1 is the conventional gold-standard—physical disruption of cells by bead beating. Method 2 exploits acoustic waves through a planar surface for cell lysis. Our novel method exploits acoustic waves through a hemispherical surface for cell lysis. We used our method in all subsequent microfluidic flow-through devices for acoustic lysis. Lysis efficiency was the amount of liberated DNA relative the original total calculated in non-lysed spores. Error bars are the standard deviation of three trials.*

Second, we demonstrated an approach for microfabrication that is faster, easier, and cheaper for prototyping than conventional methods. Rapid prototyping of microfluidic devices is often impeded by the materials costs, need for sophisticated facilities, and fabrication time. We used off-the-self materials (e.g. acrylic sheets, flexible circuits, piezo-disks) and a $CO_2$ laser engraver to fabricate a suite of devices for automated biological sample preparation and analysis. Finished prototypes were readily fabricated in less than 30 minutes without need for clean-room facilities. Using this approach, we were able to fabricate and test many iterative design changes. As a result we successfully developed and validated all of the necessary prototype microfluidic components for our biosensor, as follows: 1) cell trapping and mixing chambers, 2) lysis chambers, 3) DNA trapping and purification chambers, 4) thermal-cycling chambers. This work is described in two papers, currently being revised for publication.

Third, we significantly extended technology recently developed at Los Alamos and awarded an R&D 100 prize. The cutting edge technology was a miniature flow cytometer. The long transit times and high event rates given by acoustic focusing enable higher sensitivity measurements. We extended this technology to create a four parameter, two laser instrument capable of multiplexed bioassays on intensity-coded microspheres. We further developed and validated a square-channel acoustic focusing cell. This development makes the detector compatible with microfabricated systems, thus greatly expanding the range of potential applications and commercial viability. In particular, it enables the use of acoustic positioning in a microfluidic format for data acquisition in an autonomous biosensor. This work is described in one paper, currently being revised for publication.

Fourth, we moved beyond single devices and developed an integrated, automated subsystem, demonstrating our capacity for integration and automation. We assembled an integrated subsystem containing a cell lysis device, a DNA trapping device, a microfluidic pump, and a software/hardware control system that automated fluid flow and generation of physical fields. We showed that the net efficiency of this system in providing a purified sample of DNA from *Bacillus* spores for surveillance assays was 60% (Figure 4), at least a 2 to 10-fold improvement over the efficiency expected with other commonly used systems. This exceptionally high performance level was achieved by independently optimizing the performance of the lysis and DNA trapping devices. Maximizing performance levels is significant because it improves the detection sensitivity of biosurveillance devices.

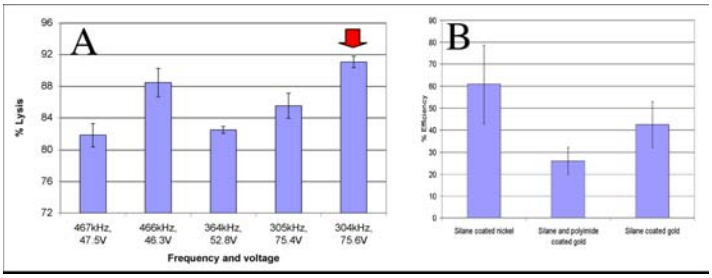


*Figure 4. Subsystem performance. The subsystem included two microfabricated devices for cell lysis and DNA trapping, a microfluidic pump, and a control system automating the flow and force-field generation. Panel A shows strong dependence of lysis efficacy on the acoustic frequency. The red arrow indicates conditions used to assess net performance of the integrated lysis and trapping subsystem (Panel B). Performance was assessed by comparing the free DNA concentration to the total concentration calculated in the original Bacillus spores prior to lysis. Error bars are the standard deviation from three trials.*

For pathogen detection, we focused on developing technology to improve protein-based (immunological) assays as well as RNA and DNA-based assays for viruses and bacteria. Our major accomplishment was development and validation of a new DNA assay format, called Multiplex Oligonucleotide Ligation Polymerase Chain Reaction (MOL-PCR). This assay format, invented at LANL and patented in 2006, offers the ability to perform large multiplexes with relative ease compared to current state-of-the-art technologies such as Multiplex PCR or Taqman assays. This format can detect different types of variation in DNA, such as unique sequences and also single nucleotide differences in DNA segments that are present in multiple strains or species. The ability to perform multiple tests, or queries, in a single assay reduces costs. The capacity to perform multiple queries also provides higher diagnostic confidence when positive results are obtained and can provide additional information about a pathogen, such as its antibiotic resistance, thereby facilitating attribution and clinical treatment. Using the MOL-PCR format, we developed a 26-plex assay for the detection of six respiratory bacterial pathogens and evaluated its performance on DNA extracted from complex matrices (blood, pus, liver tissue, pleural fluid). We also developed a protocol for efficient conversion of RNA into DNA, enabling extension of MOL-PCR to detection of viral targets such as influenza.

The accomplishments above as well as other achievements are being described in a total of 19 publications, 7 of which are already in print.

## Impact on National Missions

The project had impacts in education, capability development, and has fostered collaborations enabling program growth. The project supported eight students and two postdocs. It supported retention of a technician and a staff member, as well as conversion of a Masters student to a technician. It fostered a productive collaboration with the New Mexico Department of Health. Several new collaborations arose within and between divisions at LANL that continue to bring new work from external agencies to the laboratory. It significantly expanded expertise in microfabrication and microfluidics at Los Alamos National Laboratory, creating a strong capability for program growth. Results, capabilities, and collaborations that arose from the project have directly contributed to expansion of LANL's contributions to national security and energy programs as follows: Approximately $9M of new work from DHS and DTRA in biosurveillance was acquired from 2007 to present. This includes a 5.2M/yr DHS program that is starting now and will endure for several years. Additionally, $1.4M was acquired for energy work and an additional $637K of bioenergy work from industry and government sources. Approximately $7.3M of follow-on biosurveillance and bioenergy work from NIAID, DOE, and ARPA-E is pending proposal review.

## Publications

Deshpande, A., J. Gans, S. W. Graves, L. Green, L. Taylor, H. B. Kim, Y. A. Kunde, P. M. Leonard, J. Mark, M. Vuyisich, and P. S. White. A Rapid Multiplex Assay for Nucleic Acid-Based Diagnostics. To appear in *Journal of Microbiological Methods.*

Gans, J. D., and M. Wolinsky. Genomorama: genome visualization and analysis. 2007. *BMC Bioinformatics.* **8**: 204.

Gans, J. D., and M. Wolinsky. Improved assay-dependent searching of nucleic acid sequence databases. 2008. *Nucleic Acids Research.* **36**: e74.

Habbersett, R. C., M. A. Naivar, T. A. Woods, G. R. Goddard, and S. W. Graves. Evaluation of a green laser pointer for flow cytometry. 2007. *Cytometry Part A.* **71A**: 809.

Mark, J. A., L. D. Green, A. Deshpande, and P. S. White. System integration and development for biological warfare agent surveillance. 2007. *Proceedings of the SPIE.* **6540**: 6540D1.

Naivar, M. A., J. D. Parson, M. E. Wilder, R. C. Habbersett, B. S. Edwards, L. Sklar, J. P. Nolan, S. W. Graves, J. C. Martin, J. H. Jett, and J. P. Freyer. Open, reconfigurable cytometric acquisition system: ORCAS . 2007. *Cytometry Part A.* **71A**: 915.

Rich, R. L., G. A. Papalia, P. J. Glynn, J. Furneisen, J. Quinn, J. S. Klein, P. S. Katsamba, M. B. Waddell, M. Scott, J. Thompson, J. Berlier, S. Corry, M. Baltzinger, G. Zeder-Lutz, A. Schoenemann, A. Clabbers, S. Wieckowski, M. M. Murphy, P. Page, T. E. Ryan, J. Duffner, T. Ganguly, J. Corbin, S. Gautam, G. Anderluh, A. Bavdek, D. Re-

ichmann, S. P. Yadav, E. Hommema, E. Pol, A. Drake, S. Klakamp, T. Chapman, D. Kernaghan, K. Miller, J. Schuman, K. Linkquist, K. Herlihy, M. B. Murphy, R. Bohnsack, B. Andrien, P. Brandani, D. Terwey, R. Millican, R. J. Darling, L. Wang, Q. Carter, J. Dotzlaf, J. Lopez-Sagaseta, I. Campbell, P. Torreri, S. Hoos, P. England, Y. Liu, Y. Abdiche, D. Malashock, A. Pinkerton, M. Wong, E. Lafer, C. Hinck, K. Thompson, C. D. Primo, A. Joyce, J. Brooks, F. Torta, A. B. Bagge Hagel, J. Krarup, J. Pass, M. Ferreira, S. Shikov, M. Mikolajczyk, Y. Abe, G. Barbato, A. M. Giannetti, G. Krishnamoorthy, B. Beusink, D. Satpaev, T. Tsang, E. Fang, J. Partridge, S. Brohawn, J. Horn, O. Pritsch, G. Obal, S. Nilapwar, B. Busby, G. Gutierrez-Sanchez, R. D. Gupta, S. Canepa, K. Witte, Z. Nikolovska-Coleska, Y. H. Cho, R. D'Agata, K. Schlick, R. Calvert, E. M. Munoz, M. J. Hernaiz, T. Bravman, M. Dines, M. H. Yang, A. Puskas, E. Boni, J. Li, M. Wear, A. Grinberg, J. Baardsnes, O. Dolezal, M. Gainey, H. Anderson, J. Peng, M. Lewis, P. Spies, Q. Trinh, S. Bibikov, J. raymond, M. Yousef, V. Chandrasekaran, Y. Feng, A. Emerick, S. Mundodo, R. Guimaraes, K. McGirr, Y. J. Li, H. Hughes, H. Mantz, R. Skrabana, M. Witmer, J. Ballard, L. Martin, P. Skladal, G. Korza, I. Laird-Offringa, C. S. Lee, A. Khadir, F. Podlaski, P. Neuner, J. Rothacker, A. rafique, N. Dankbar, P. Kainz, E. Gedig, M. Vuyisich, C. Boozer, N. Ly, M. Toews, A. Uren, O. Kalyuzhniy, K. Lewis, E. Chomey, B. J. Pak, and D. G. Myszka. A global benchmark study using affinity-based biosensors. 2009. *Annals of Biochemistry.* **386**: 194.

# A Systematic Strategy for Gene Function Discovery

*Clifford J. Unkefer*
20070029DR

## Abstract

The large-scale genome sequencing effort of the last decade revealed that we know essentially nothing about the function of a very large fraction (20-40%) of the genes in the sequenced genomes. The most widely used function discovery method is to determine if the target gene has a homologous sequence to a gene of known function, with sequence similarity implying a similar of function. However, many genes belong to homology groups for which no functional information exists.
The goal of this project was to develop an effective, systematic approach to discovering gene function based on a combination of experimental analysis and advanced computational methods. Our approach capitalizes on the functional significance of transcription regulator effector molecules and the functional relationships that exist within groups of coordinately regulated genes, thus enabling the discovery of the function of *groups* of genes. We developed the key tools necessary: a high-throughput screen to discover the metabolite effectors of transcriptional regulators that allow us to define their function; experimental and data analysis techniques for stable isotope-enhanced functional metabolomics to identify metabolites related to the transcriptional regulators by known biochemical transformations and much better biochemical reaction prediction software. These advances will allow us to postulate new testable metabolic pathways and biochemical functions associated with specific transcriptional regulators.

## Background and Research Objectives

### Functional annotation of genes

DNA sequencing has yielded over 850 complete genome sequences of microorganisms. Bioinformatic techniques, which are used to identify hypothetical genes or open reading frames (ORFs) encoding proteins, have predicted a total of 5.4 million proteins. Discovering the function of these proteins is the next critical step in achieving a complete understanding of cellular function. In all sequenced bacteria, the group of homologous ORFs with no assigned function comprises a large fraction (25-45%) of the genomes. The importance of these ORFs is demonstrated by the fact that sequence homologs are frequently identified in hundreds of other genomes. By focusing on homologous groups of genes with no assigned function but that are conserved across multiple organisms, we can make a significant impact on solving the enormous function assignment problem. In addition to identifying homologous groups of genes, BLAST comparisons can provide some functional insight about this class of ORFs. As examples, sequence analysis can frequently identify potential cofactor or metal ion binding sites, which allow general assignment of classes of enzymes or redox proteins. Sequence analysis also allows identification of the DNA-binding domain of transcriptional regulators (TRs), a class of proteins that regulate the expression of groups of genes in a regulon. In all sequenced bacteria, there are a few hundred identified TRs and each TR has homologs in hundreds of other bacteria. *As discussed in detail below, our systematic approach to function discovery starts with assignment of function to TRs, which yields information pertinent to the function of all of the genes in their corresponding regulons.*

### A New Strategy is Essential

Historically, to discover function, scientists addressed a larger metabolic function, at the level of metabolic pathways, and such as how would a specific metabolite be synthesized? or how could an organism grow on a specific substrate? This approach provided functional context for investigating the pathway. In this context, specific biochemical transformations could be more readily postulated to assemble a “testable” pathway. Then assays developed for each metabolic transformation were used to isolate the proteins based on their function. Genetic approaches validated the function *in vivo.* In this way information about one

member of the pathway provided insight into the entire pathway.

Now, we face a different problem of discovering the function of a very large number of genes about which we have very little functional insight. Current efforts are largely focused on one gene/one protein at a time approaches that capitalize on insights gained by sequence homology to gene of known function, where they exist. Large-scale function discovery clearly demands a new systematic approach. The keys to successful gene function discovery are to find broad functional insight and capitalize upon sequence derived information.

Our strategy takes advantage of the higher-level functional context inherent in the regulation of gene expression; genes for specific metabolic pathways are grouped into and controlled as regulons. A specific TR-effector pair controls the expression of the genes in a regulon. The effectors are usually a metabolite or product of the pathway and its structure provides key metabolic insights into the chemistry carried out by the pathway. Thus the insights gained by identifying the TR effector can be used to replace the old pathway level hypothesis by providing insight into the function of genes in the entire regulon.

**Our New Systematic Strategy for Gene Discovery**

*In contrast to previous efforts that focused on single genes or proteins, we propose a systematic approach to function discovery that utilizes the functional relatedness inherent in the regulation and operation of biochemical pathways*. We propose a systematic approach to function discovery that capitalizes upon integrating the information gained by exploiting several fundamental biochemical concepts. First, the synthesis of most enzymes involved in biochemical pathways is regulated by transcriptional regulators that coordinately activate or repress the expression of groups of proteins involved in specific metabolic pathways. For example, the principles of regulation by the transcriptional regulator MetJ in the methione biosynthesis pathway are illustrated in Figure 1A. Gene transcription, the first step in protein expression, is catalyzed by RNA polymerase and regulated by the binding of the transcriptional regulator MetJ. When MetJ is bound to DNA upstream of the protein-coding region, RNA polymerase is blocked from moving along the DNA and transcribing the gene. The binding of MetJ to the DNA is determined by the concentration of an effector molecule, which is often a product of the biochemical pathway, in this case, the molecule S-adenosyl-methionine (SAM). When the concentration of SAM is high, the SAM•MetJ-binary complex predominates in solution; the binary complex has high affinity for a specific DNA sequence upstream of the transcribed genes and binding of the binary complex to DNA blocks transcription. In this example, MetJ acts as a repressor of transcription; in other cases, transcriptional regulators are activators. Because they can be identified by their characteristic sequences and because they function by binding effector molecules that are part of the regulated biochemical pathway, transcriptional regulators are a springboard for systematic discovery of the function of all members of a regulon. As described below, we have expressed transcriptional regulators and developed mass spectrometry-based binding assays to rapidly screen for effector molecules. In the MetJ example, our assay identified SAM, methylthioadenosine, and adenine as binding to MetJ and as potential effectors. Because the binding of a metabolite from a pathway is the signal that controls the transcriptional regulator, the identification of the effector molecule yields information about the function of the proteins encoded in the regulon.

A.

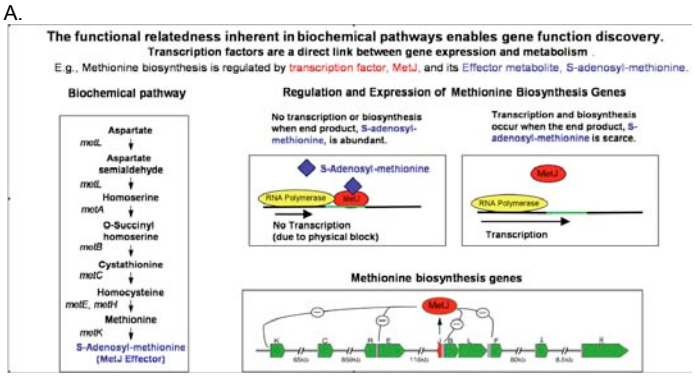


B.

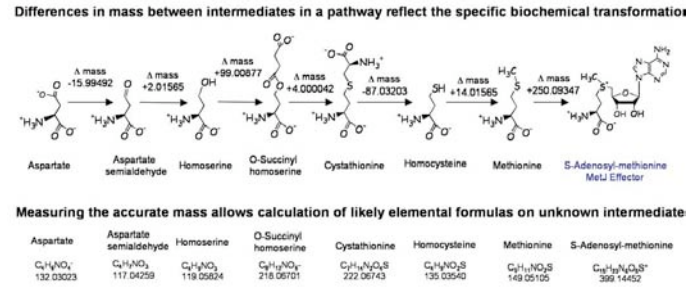


*Figure 1. (A)Transcriptional regulation of the pathway for methionine biosynthesis. MetJ, the transcriptional regulator, blocks transcription when bound to the product of the S-adenosyl-methionine pathway. (B) Intermediates of the methionine biosynthesis pathway. Classes of biochemical reactions can be classified by their characteristic Δmass and the chemical formulas can be derived from accurate mass determination.*

**Pathway Prediction**

Identifying the genes in the regulon, and hence the encoded/regulated pathway, provides information on the length of the pathway and, based on homology, provides insights into the functions of the enzyme (or transporter, etc) that each gene encodes. Because the TR effectors

are usually products or intermediates in the pathway, their identification is extremely valuable to postulating the metabolic pathway. Another functional relationship exploited in our strategy is that coordinately regulated genes encode functionally related proteins. One simple functional relationship is that the product of one enzymatic step is the substrate for the next enzyme in a metabolic pathway. The methionine biosynthetic pathway in our example (Figure 1B) is initiated by the aspartate kinase catalyzed reduction of aspartic acid to yield aspartate semialdehyde, which serves as a substrate for the next step in the pathway. Most biochemical transformations involve changes in mass between substrates and products, and the mass differences between substrates and products for large classes of enzyme-catalyzed reactions are characteristic of the reaction types. For example, dehydrogenation (±2.01565), decarboxylation (-43.98983), dehydration (±18.01057), phosphorylation (±75.95177), adenylation (±250.09347) and transamination (±2.03946) yield predictable mass changes. These mass differences are a powerful tool for tracing metabolic pathways. By examining metabolite profiles to find metabolites that are related by a standard biochemical transformation to the TR effector molecule, we will be able to discover pathway intermediates. With these data and our knowledge of biochemical transformations, we will be able to postulate the biochemical pathways encoded in the regulons.

Project Objectives: Our strategy for gene function discovery examines genes in functional groups called regulons using TR and their effectors as a handle. The goal of this project was to develop the basic tools necessary to accomplish this strategy. These included a mass spectrometry-based high-throughput assay to identify TR effectors and pathway prediction and analysis and improved reaction prediction software,

## Scientific Approach and Accomplishments

**High throughput TR effector assay**

We have developed a high-throughput binding assay for TR effectors using frontal affinity chromatography-mass spectrometry (FAC-MS). In FAC-MS, a target protein, in our case a TR, is immobilized on a suitable support for liquid chromatography and packed into a column. A mixture of potential ligands (metabolites) is continuously infused through the column and into the mass spectrometer. Metabolites that do not bind to the immobilized protein will immediately elute from the column. The metabolite effectors will bind to the immobilized protein until the column capacity is reached, at which point their concentrations in the effluent will increase to their infusion concentrations. The breakthrough volume of bound ligands is related to the protein/ligand binding affinity with tighter binding ligands eluting at larger breakthrough volumes (longer times). Because detection is by mass spectrometry, we can detect ligands at concentration ranges necessary to characterize TR effector binding and obtain structural information on the retained ligands by predicting the molecular formulas of unknown bound ligands to facilitate their identification.

**Expression of TR-fusion proteins**

We overexpress TRs in *E. coli* and purify using IMAC affinity chromatography; this requires a C- or N-terminal $his_{6-10}$ affinity tag. The FAC-MS experiments also require immobilization of the TR, which we accomplished by adding a commercial AviTag peptide (GLNDIFEAQKIEWHE), which is biotinylated *in vitro*. We immobilize the biotinylated TRs using the irreversible binding of biotin to commercial avidin-coated beads ($K_d$~$10^{-15}$).

*MetJ FAC-MS experiments*

In FAC-MS, the dissociation constant, $K_d$, is related to the experimental parameters via equation 1, where $[A]_0$ is the infusion concentration of the ligand, $B_t$ is the number of moles of immobilized protein binding sites, and $V-V_0$ is the breakthrough volume:

$$V-V_o = B_t/([A]_0-K_d). \qquad \text{(Eq. 1)}$$

The biotinylated MetJ has a monomer molecular mass of approximately of 17,000 kDa. Based on a our column which retains 0.36 µmol of the TR, Table 1 shows the ligand breakthrough volume as a function of $K_d$ when the ligand is infused at a concentration of $10^{-6}$ or $10^{-7}$ M, which we can easily detect using our mass spectrometer. While the breakthrough volume is most sensitive when the ligand infusion concentration ($[V]_0$) is equal to the dissociation constant ($K_d$), we are able to resolve ligands with dissociation constants as high as $10^{-5}$.

**Table 1.** FAC-MS breakthrough volume.

| | $V/V_o$ | |
|---|---|---|
| $K_d$ | $[A]_o = 10^{-6}$ M | $[A]_o = 10^{-7}$ M |
| $10^{-4}$ | 1.00 | 1.00 |
| $10^{-5}$ | 1.04 | 1.04 |
| $10^{-6}$ | 1.18 | 1.33 |
| $10^{-7}$ | 1.33 | 2.79 |

The FAC-MS analysis of ligand binding to MetJ is shown Figure 2. In this case, ten structurally related ligands were infused through a column containing immobilized $H_2N$-MetJ-AviTag-$His_{10}$-COOH fusion. The experiment is initiated when the column input is switched to buffer containing all 10 ligands. Mass spectra are obtained as a function of

time. Initially, the ligand concentration is zero and peaks attributable to the ligands are not observed. Panel A shows a typical mass spectrum at a later time when all of the ligands are detected at their infusion concentration. Panel B shows the normalized ion intensity as a function of time. The last ligand to elute is S-adenosyl methionine (SAM), which is a known effector of MetJ. Because of their large breakthrough volume, we demonstrated that MetJ also has significant affinity for adenine and methylthio adenosine, structural analogues of SAM. Experiments with pairs of ligands, SAM and adenine, SAM and methylthio adenosine, and adenine and methylthio adenosine, show that these three ligands compete for the same binding site. AMP elutes at the void volume and the slight differences in elution time for $NAD^+$, CoA, cAMP, etc. represent non-specific binding likely due to ionic interactions.

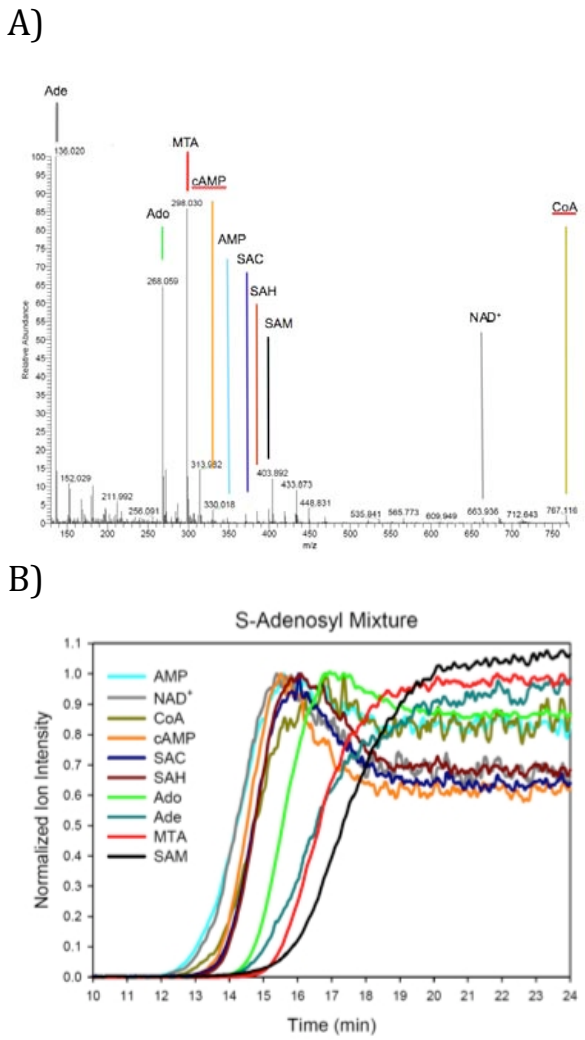


*Figure 2. FAC-MS analysis of effectors binding to MetJ. A) A mixture of ligands each at 10 µM in ammonium formate buffer (20 mM, pH 7.2) was infused through a column containing immobilized MetJ using a syringe pump (85 µl/m). The effluent of the column was mixed with an equal volume of methanol containing formic acid (0.2 M) and pumped into the electrospray ion source of a Thermo Finnigan LTQ-FT mass spectrometer. Mass spectra were obtained in positive ion mode. Compounds were detected at as M+ or MH+ ions at the following m/z values: AMP, 348.07036; NAD+, 163.10857; CoA, 767.11466; cAMP, 130.05980; SAC, 371.11322; SAH, 385.12887; Ado, 268.10403; Ade, 136.06178; MTA, 298.09684; SAM, 399.14451. B) Traces normalized ion intensity as a function of time. The relative affinity of the ligands is obtained from the elution time with the highest affinity ligands eluting last.*

By varying the ligand infusion concentration, this FAC-MS experiment can be used to determine the dissociation constant for a ligand that binds. Figure 3 shows the elution of methylthio adenosine and six infusion concentrations and the determination of the $K_d$ using equation 1.

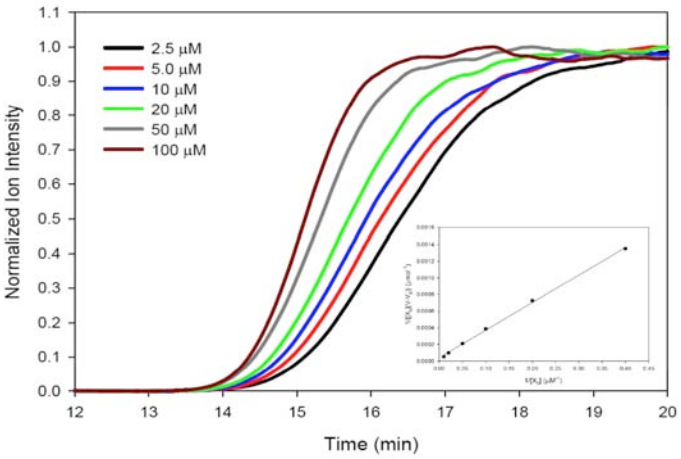


*Figure 3. FAC-MS determination of the dissociation constant for methylthio adenosine binding to MetJ. Normalized intensity of the peak at M/z = 298.09684 was obtained in separate experiments infusing methylthio adensine at 2.5, 5.0, 10, 20, 50, and 100 µM. Using equation 1, Kd determined from the slope of a plot of 1/[A]0 · (V-V0) vs 1/[V]0 (inset, Eq 1) is 80.5 µM for methylthio adenosine (r2 = .9988).*

**Pathway Analysis**

As discussed in the Approach section of this proposal, the exact difference in mass between metabolites can be used to predict known metabolic transformations. During this project we developed a significant metabolomic capability and used it to analyze the *E. coli* metabolome. We obtained *E. coli* metabolite profiles using LC/Electrospray/High resolution MS in both positive and negative ion modes (Figure 4) and using our nominal mass GC/GC/TOF. We used these methods to obtain metabolite profiles of cells cultured on unlabeled and uniformly $^{13}C$-labeled growth substrates. The development of these methods allows us to effectively use mass spectrometry in combination with $^{13}C$-isotope labeling to track specific carbons into and through a metabolic pathway, an advance that greatly enhances discovery of metabolic pathways. Our approach was sufficiently

effective to allow real time metabolic flux analysis. As we expected, the high-resolution mass spectrometer data yields elemental formulas and its MS/MS fragmentation is valuable in identifying metabolites of unknown function. For example uniform $^{13}C$- or $^{15}N$-labeling allows us to count the number of carbons or nitrogens in the molecule and thus to confirm or to refine the chemical formulas. During the last year of this project, we realized that we needed to be able to take advantage of signal averaging to obtain better spectra, minimize artifacts from ion suppression and obtain MS/MS data on all metabolites to facilitate structural assignment of the E. coli metabolome. We purchased a nanospray ion source that allowed the split sample to be fractionated and archived. MS/MS analysis is obtained on all metabolites in each of the fractions. In the last few months of our project we were able to obtain extensive data on the E. coli metabolome, which is in the process of analysis.

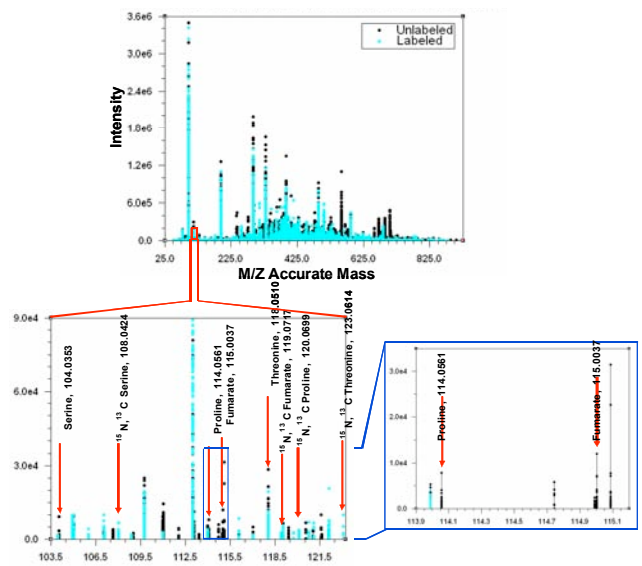


*Figure 4. Tracking of complex mixtures with isotopes. The top panel shows the full mass spectrum for labeled vs. unlabeled E. coli metabolites. The bottom left panel shows a small section of the mass spectrum (~ 2% of total mass range), with selected compounds and their labeled isotopomers identified. The bottom right panel zooms in still further to show the resolvability of regions that appear overlapped in the bottom left panel. Taken together, these figures illustrate that high-resolution data are critical for label tracking in complex mixtures, and that tools for single-compound analysis will quickly be overwhelmed. Abstract (used to extract the data in the figure) is specifically designed to perform whole system and isotopomer analyses. This figure also shows the power of isotope labels for structural assignment. Uniform 13C- and 15N-labeling shifts the mass of furmarate with four carbons from 115.0037 to 119.0171 while proline with five carbons and a nitrogen shifts from 114.0561 to 120.0699 exactly as predicited. By comparing data from labeled and unlabeled samples, we can easily identify peaks that are not metabolites because they appear at the same mass in both experiments. Peaks that are not isotopically shifted are not cellular metabolites.*

**Reaction prediction software**

We developed an accurate (>80%) chemical principles-based reaction prediction tool for the largest class of biochemical reactions, the dehydrogenases. To overcome the false positives problem, we extended rule-based prediction methodology to incorporate machine learning. Binary classifiers were trained to distinguish true reactants from false ones on the basis of readily calculated properties of atoms in a potential reaction center.

## Impact on National Missions

Understanding the function and integrated control of the genes and proteins of bacteria is central to essential to harnessing bacterial systems for DOE's biotechnology missions including environmental remediation, carbon sequestration and energy production. The large fraction of genes of unknown function in what is actually a small number of bacteria (850) among the millions that exist present a very significant barrier to successfully using microbial systems (energy production or remediation) or predicting (carbon sequestration or climate change) the magnitude of microbial impacts on global cycles.

## Publications

Fox, D. T., K. Hotta, C. C. Browder, C. Kim, P. J. Unkefer, C. J. Unkefer, and A. T. Koppisch. Biosynthesis of the 3,4-Dihydroxybenzoate Moieties of Petrobactin by Bacillus Anthracis. 2008. : NWRM.

Koppisch, A. T., K. Hotta, D. T. Fox, C. E. Ruggiero, C. Kim, T. Sanchez, S. Iyer, C. C. Browder, P. J. Unkefer, and C. J. Unkefer. Biosynthesis of the 3,4-dihydroxybenzoate moieties of petrobactin by Bacillus anthracis. 2008. **73** (15): 5759.

Marti-Arbona, R., H. Teshima, P. Anderson, P. J. Unkefer, and C. J. Unkefer. FAC-MS Uncovers New Effectors for Old Transcriptional Regulators, Discovery of Novel Transcription Factor Effectors for MetJ. 2009. In *American Society of Mass Spectrometry.* (Denver, 29May 3 June, 2009). Vol. Abstracts, p. 2161. Journal of Mass Spectrometry : American Society of Mass Spectrometry .

Marti-Arbona, R., H. Teshima, P. Anderson, P. J. Unkefer, and C. J. Unkefer. Discovery of novel transcription factor effectors for MetJ. 2009. In *238th ACS National Meeting.* (Washington, August 16-20 2009). Vol. , Edition, p. BIOL. Abstracts of Papers: American Chemical Society.

Mu, F., R. F. Williams, C. J. Unkefer, P. J. Unkefer, J.

R. Faeder, and W. S. Hlavacek. Carbon-fate maps for metabolic reactions. 2007. **23** (23): 3193.

Velappan, N., H. Fisher, E. Pesavento, L. Chasteen, S. D'Angelo, C. Kiss, M. Longmire, P. Pavlik, and A. Bradbury. A comprehensive analysis of filamentous phage display vectors for cytoplasmic proteins: an analysis with different fluorescent proteins. To appear in *Nucleaic Acids Research.*

# Host-Pathogen Interactions (Pathomics) in Avian Influenza

*Ruy M. Ribeiro*
20070099DR

## Abstract

A better understanding of influenza's potential for human-to-human transmission and severity of disease is crucial. Such knowledge will allow better preparation and deployment of countermeasures during epidemics or pandemics. Unfortunately, the knowledge to make these predictions based on robust experimental assays does not exist. We addressed this deficiency by innovatively combining experimental analyses of molecular markers with new computational tools. Our objective was to ascertain the differences in virulence among diverse types of influenza ("strains").

We developed a full program of study of influenza infection, comparing the host (human) response to infection with many different strains. We used both seasonal and high pathogenic avian influenza strains. We found that there are important differences in the response against these diverse strains. These responses should allow the prediction of differences in pathogenesis. We developed both experiments and theoretical analyses with the objective of extracting a small set of robust features that will allow the development of an assay for virulence prediction. This research was possible through the collaborative work of a multidisciplinary team of scientists. This novel approach also afforded important biological insights into influenza virulence and evolution.

This project implemented the capabilities for a new area of study at the Laboratory, in the field of viral respiratory infections. These new capabilities open the doors for opportunities of external funding. The investment made was also crucial in attracting new funding for the Laboratory and one of the project's postdoctoral researchers was converted to technical staff member. LANL now has a team of interdisciplinary scientists committed to influenza research.

## Background and Research Objectives

As the recent outbreak of novel H1N1 influenza has shown, we are not well prepared to quickly identify and characterize new influenza viruses that enter the population. In addition, there are still ongoing cases of avian (H5N1) influenza with high mortality. Thus, we need to understand influenza's potential for human-to-human transmission and severity of disease [1]. Unfortunately, the knowledge to make these predictions based on robust experimental assays does not exist. We address this gap by innovatively combining experimental analyses of molecular markers with new computational tools ("the functional profile"). Our objective is to ascertain the basis of differences in virulence among diverse influenza strains.

Many research groups are trying to address similar issues by focusing on individual virulence factors or animal experiments with limited numbers of strains [2, 3]. Our approach, studying multiple influenza strains, is innovative because we are combining theoretical and experimental tools to the problem of predicting, in a complex system, the outcome of infection. We have worked on an in vitro assay to identify predictive host responses. The potential to develop the knowledge and tools necessary to predict the pandemic potential of any influenza virus is a crucial scientific objective. Moreover, our results have significant implications for understanding genomic-virulence relationships [2].

## Scientific Approach and Accomplishments

Our objective was to find out what differentiates highly pathogenic strains (those that cause severe disease in humans) from less pathogenic ones (typically, strains responsible for yearly seasonal influenza epidemics). We used select avian H5N1 strains as prototypes of highly pathogenic strains, and select H3N2 and H1N1 seasonal strains as prototypes of less pathogenic strains. We also availed ourselves of a specific H5N1 avian strain with demonstrated low virulence in humans. We then

infected in vitro normal human lung epithelial (NHBE) cells or a lung epithelial cell line (A459 cells) with those strains. We measured the response of the cells to infection using two methodologies. 1) Full genome microarrays, i.e., we measured qualitatively the response to infection of every gene in the human genome. And 2) quantitative real-time polymerase chain reaction (qRT-PCR), i.e., we measured quantitatively the gene expression of a select number of genes during response to infection. The objective was to analyze by computational tools the massive amounts of data generated to distinguish the responses to high and low pathogenic infection. The assay thus developed could be used to analyze and characterize future outbreaks of influenza with unknown strains. Thus, in the last 2 months of the project, we started characterizing the novel H1N1 flu strain, responsible for the current pandemic [4].

The experimental plan involved preparing >400 flu-treated airway cell samples for real-time and microarray analyses, at LANL. These samples encompass airway cell lines (A549) treated with four different low- and medium-virulence influenza strains at eight different time points, with two different multiplicities of infection and three controls. The response to infection has been analyzed by real-time PCR of 28 different genes. This produced >33,000 data points for analysis of cellular response to different strains. In addition, H5N1 infections were done by our collaborators at Lovelace Respiratory Research Institute, under bio-safety level 3 conditions. These experiments generated an additional 160 flu-treated airway cell samples. These samples encompass airway cell lines treated with three different high and low H5N1 strains at eight different time points, with two different multiplicities of infection and three controls. We then extracted and prepared the RNA for real-time PCR and microarray analyses, at LANL. This produced >13,000 data points for analysis of cellular response to H5N1. On the other hand, from the microarray measurements in NHBE cells, we obtained 54 sets of full human genome expression data. These experiments measure the level of "activation" of each of the >30,000 human genes at 0, 8h and 24h post-infection. Thus, in this project we generated massive amounts of data, detailing the human cellular response to flu infection.

Representation and analysis of such large datasets are a challenge. How to distill the data into important results that can be understood and further analyzed? Instead of approaching this as an arbitrary clustering problem, we sought to take advantage of the time course aspect of the data. We did this by applying techniques of molecular phylogeny (a.k.a. evolutionary trees) reconstruction under an appropriate model. Since the dimensionality of the space is large (30,000+) and noise and random changes are significant, trajectories in time can be described as a diffusion process. Dimensions (*i.e.*, genes) dominated by biological processes, rather than random drift or noise, are expected to reveal their relationships in the tree. Figure 1 shows a tree generated from the expression data for virus infected and mock infected cells. There are several features of Figure 1 that should be noted: most replicates (e.g., 1-3) of the same experiment are grouped; 24-hour experiments appear to diverge from the 8 hour experiments, particularly for seasonal strains (Sydney and Beijing samples); seasonal flu and the associated mock infections cluster separately from H5N1 strains.

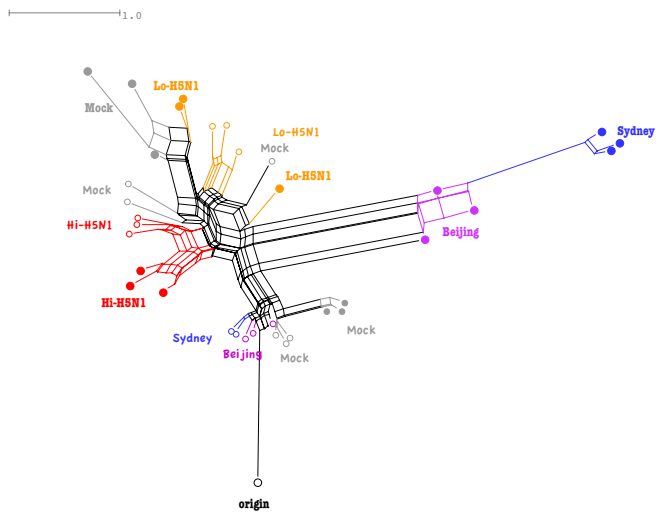


*Figure 1. Visualization of gene expression experiments post influenza infection. In this figure each experiment (with its >30,000 genes analyzed) is represented by a circle, with open and closed circles indicating 8h and 24h post-infection, respectively.*

We can now focus the analysis on specific branches in the tree. Experiments in the neighborhood of branches of interest can be averaged. Subtracting those averages reveals the major changes between the branches. The genes are then sorted based on magnitude of change relative to noise. Complete lists of genes significantly up or down regulated as determined by these analyses are available on the internal wiki website set-up for this project. As a summary, we can indicate that this and other analyses suggest the following genes as putative markers for early and high pathogenic H5N1-specific infection: genes induced by interferons, which are molecules involved in the immune response (e.g., IFI, G1P, MX, OAS); chemokine genes (e.g., CXCL, CCL); inflammatory cytokines (e.g., IL1$\alpha/\beta$, IL6); and anti-viral serum amyloid proteins (e.g., SAA1-4). To better understand the biology of high pathogenic infection, we mapped the cellular pathways involving genes identified by our analyses. For example,

Figure 2 shows a comparison of the activation of the interferon pathway 24h after infection. Dissecting the steps in the cellular response where the differences are most pronounced will improve the reliability of our markers and also lead to better understanding of this response.

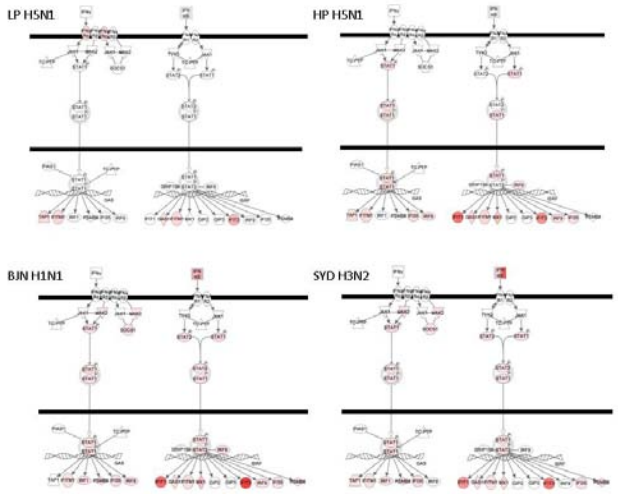


*Figure 2. Comparison of the activation of the interferon pathway 24h after infection with different influenza strains. For each gene indicated, the darker the red coloring the higher the expression level as measured in our experiments. Four strains are compared: low-pathogenic avian influenza (LP H5N1); highly-pathogenic avian influenza (HP H5N1); and two seasonal influenza strains BJN H1N1 and SYD H3N2.*

We have also taken a complementary approach to identify and validate markers of virulence. Gene expression measured using RT-PCR was performed for different flu strains infecting a robust cell line (A549). The analysis goals were to (*i*) identify clusters in the data, i.e. similarly responding genes and similar viruses as seen by changes in gene expression, and (*ii*) seek gene expression characteristics that distinguish low and high virulence strains. Gene expression data were collected at multiple time points post-infection. An initial clustering analysis shows that the gene expression at all time points of the highly pathogenic strain clusters with the early time points of the low virulence strains (Figure 3). Does a signal exists in the gene expression data that discriminates low pathogenic from high pathogenic strains? We are employing a "decision tree" methodology to address this issue. Preliminary analyses found that decisions based on the genes FasR, IL-18 and IL-8 predicted virulence with some statistical support. FasR is involved in the apoptosis pathway, while IL-18 and IL-8 are involved in the inflammation pathway.

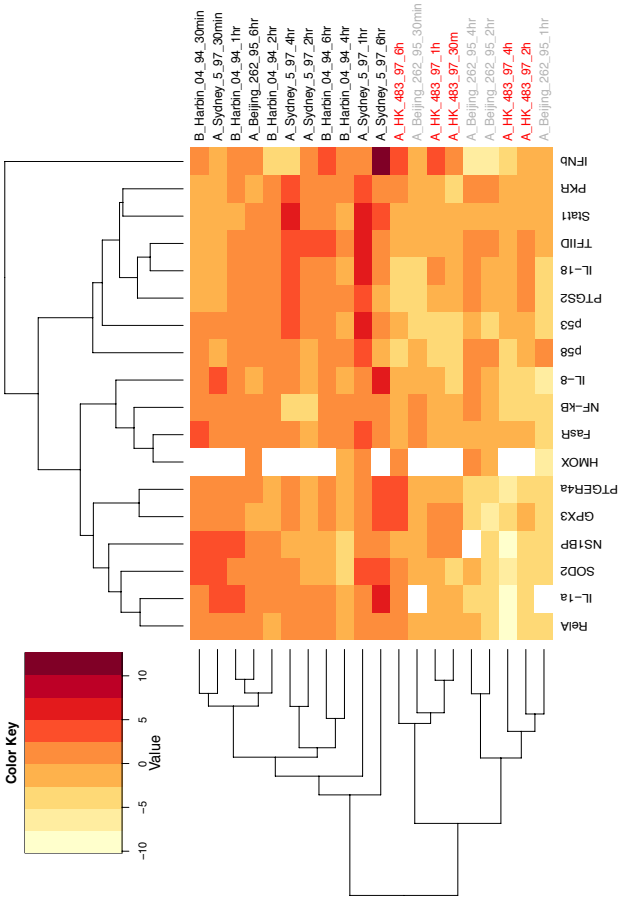


*Figure 3. Visualization of similarity across gene expression patterns. Two rows grouped together (tree at left) indicate similar patterns of gene expression (across all genes) for the influenza conditions shown on the right. Likewise, two columns that are grouped together indicate a similar pattern of gene expression (for the gene at the bottom) across all influenza conditions.*

We are interested in developing an assay that will predict virulence. Thus, we also need to understand the function of identified proteins and to look for proteins with similar function. We, therefore, developed a collection of software tools and database resources, called BIOGRAM (BIOlogical GRaph Metrics). BIOGRAM uses the mathematical structure underlying the Gene Ontology (GO) to measure protein/gene similarity based upon annotations assigned to nodes of the GO [5]. The method is "fuzzy" in nature, accounting for near misses and more distant relationships within the ontology. In addition to generating hierarchical comparison metrics for the annotation sets of pairs of proteins, BIOGRAM produces a detailed "explanation" of the similarities and differences between them. BIOGRAM has been designed as a tool to help guide the expert in an exploration of functional similarity.

Most of our work was focused on understanding the host (*i.e.*, human) response to infection. However, we also developed research to understand viral properties

responsible for virulence. In this area, we developed several successful studies:

- We expanded earlier bioinformatics methods to study the evolution of highly pathogenic avian influenza A virus (HPAIV). Thus, we analyzed the evolution of HPAIV by the dual processes of re-assortment and point mutation [6]. Re-assortment allows the HPAIV to make long jumps in sequence space creating discontinuous evolution. Point mutation operates on a finer scale, occurs more frequently, and leads to relatively smooth evolution. Surprisingly, we found that the early evolution of HPAIV was dominated by re-assortment, while more recent evolution has been largely in the absence of re-assortment. We also found that recent HPAIV have diverged into three different sub-lineages by point mutation and selection. Analyzing evolution on these two different scales allowed the identification of specific molecular signatures of the three sub-lineages. Some changes are extremely rare in the viral population as a whole, and yet are maintained within the respective HPAIV sub-lineages. By evaluating the prevalence of each signature change, we have identified 5 amino acid changes that we hypothesize are essential for the fitness of the virus. These will be tested experimentally by collaborators at the University of Wisconsin (since they have animal laboratories with the appropriate bio-safety level).

- We also studied the humanization of a well-characterized mouse antibody. This antibody recognizes domains of the viral M2 protein. M2 is a conserved protein crucial in the viral lifecycle. The antibody has shown protective activity in mouse models of influenza infection. Antibody humanization involved making the antibody sequence more human, an approach that has been used before. For therapeutics this is important as human antibodies elicit immune responses far weaker than mouse antibodies, making them far less effective. Our humanized antibody showed the same reactivity profile as the original antibody. And it was also able to reduce viral spread in an *in vitro* model [7]. The antibody recognized different forms of M2. Further work has been funded recently by the NIH.

- We studied the viral NS1 protein, which is crucial for viral replication and for preventing the host antiviral responses. Thus, NS1 is considered an important virulence factor for influenza. We developed models of this protein's structure and interactions with host molecules. Among others, as an example, we show in Figure 4 our predictions for the way NS1 may activate the human protein PI3K. This human protein is involved in regulating signaling cascades that control diverse cellular processes: cell survival, metabolism, proliferation, and inflammation/ immunity. Models of the interactions between NS1 and PI3K can lead to a better understanding of virulence (*i.e.*, how virus can defeat host immunity).

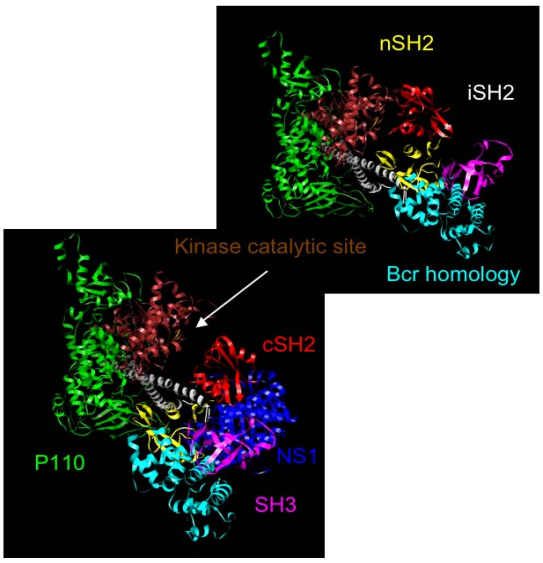


*Figure 4. Structural model of activation of a human protein by docking of the NS1 viral protein. Models of the human protein PI3K with and without NS1 are shown. Upon binding of NS1 protein (blue), the domain shown in red is pulled away from the catalytic site, activating the protein.*

- One of our objectives was to develop mathematical models of infection, which help in analyzing the results and in biological prediction. We worked on models [8] describing both the *in vitro* and *in vivo* (with mouse model data from our collaborators at St. Jude's Children's Hospital) progression of infection (Figure 5). These models allowed us to estimate critical parameters of infection, such as viral clearance and infected cell loss rates. We also used these models to analyze *in vitro* drug treatment data. In the future, they should help evaluate the effect of different therapies.

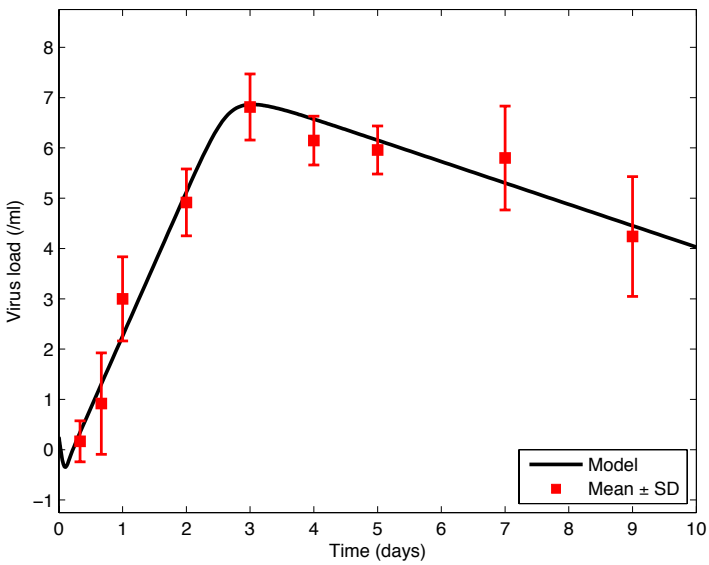


*Figure 5. Fit of our model to the in vivo viral dynamics of influenza (mouse model). Some parameters, such as infected cell death rate, depend on the virulence of the infecting strain. These models will help tailor appropriate therapies for different strains of virus.*

The project already generated 15 (published or about to be submitted) papers with four more in preparation and lead to nine external collaborations. Our work was instrumental in successful competition for >$3,900,000 in external funding from spin-off projects. Team members have also made presentations (>10) of the results at international meetings and at invited talk at multiple institutions (USA, Austria, Canada, Australia). Finally, to engage the community, the principal investigator has given several lectures for the public.

## Impact on National Missions

From a general perspective, this project supports the DOE mission in Threat Reduction and also the mission of Harnessing the Power of the Living World, by defining and predicting what makes (influenza) viruses pathogenic. In terms of actual near-term impact, with important strategic implications for the Laboratory, we created new experimental and theoretical capabilities in influenza research. At the start of this project, there were no scientists or laboratories at LANL capable of studying viral respiratory infections. We developed the necessary institutional bio-safety board authorizations, experimental protocols, and technical skills to carry this influenza work. These new capabilities open novel opportunities of external funding from many sponsoring agencies in important national security missions. The investment made was also crucial in attracting new funding for the Laboratory. Importantly, one of the project's postdoctoral researchers was converted to technical staff member. LANL now has a team of interdisciplinary scientists committed to influenza research from multiple, complementary approaches.

## References


1. Zimmer, S. M., and D. S. Burke. Historical perspective - Emergence of influenza A (H1N1) viruses. 2009. *New England Journal of Medicine.* **361**: 279.

2. Allen, J. E., S. N. Gardner, E. A. Vitalis, and T. R. Slezak. Conserved amino acid markers from past influenza pandemic strains. 2009. *BMC Microbiology.* **9**: 77.

3. Zambon, M. C.. The pathogenesis of influenza in humans. 2001. *Review of Medical Virology.* **11**: 227.

4. Dawood, F. S., S. Jain, L. Finelli, M. W. Shaw, S. Lindstrom, R. J. Garten, L. V. Gubareva, X. Xu, C. B. Bridges, and T. M. Uyeki. Emergence of a novel swine-origin influenza A (H1N1) virus in humans. 2009. *New England Journal of Medicine.* **360**: 2605.

5. Ashburner, M., C. A. Ball, J. A. Blake, D. Botstein, H. Butler, J. M. Cherry, A. P. Davis, K. Dolinski, S. S. Dwight, J. T. Eppig, M. A. Harris, D. P. Hill, L. Issel-Tarver, A. Kasarskis, S. Lewis, J. C. Matese, J. E. Richardson, M. Ringwald, G. M. Rubin, and G. Sherlock. Gene ontology: tool for the unification of biology. The Gene Ontology Consortium. 2000. *Nature Genetics.* **25**: 25.

6. Smith, D. J., A. S. Lapedes, J. C. de Jong, T. M. Bestbroer, G. F. Rimmelzwaan, A. D. Osterhaus, and R. A. Fouchier. Mapping the antigenic and genetic evolution of influenza virus. 2004. *Science.* **305**: 371.

7. Gabbard, J., N. Velappan, R. Di Niro, J. Schmidt, C. A. Jones, S. M. Tompkins, and A. R. Bradbury. A humanized anti-M2 scFv shows protective in vitro activity against influenza. 2009. *Protein Eng Des Sel.* **22** (3): 189.

8. Beauchemin, C. A., J. J. McSharry, G. L. Drusano, J. T. Nguyen, G. T. Went, R. M. Ribeiro, and A. S. Perelson. Modeling amantadine treatment of influenza A virus in vitro. 2008. *J Theor Biol.* **254** (2): 439.


## Publications

Mathematical and Statistical Estimation Approaches to Epidemiology. 2009.

Beauchemin, C. A., J. J. McSharry, G. L. Drusano, J. T. Nguyen, G. T. Went, R. M. Ribeiro, and A. S. Perelson. Modeling amantadine treatment of influenza A virus in vitro. 2008. *J Theor Biol.* **254** (2): 439.

Bettencourt, L. M., R. M. Ribeiro, G. Chowell, T. Lant, and C. Castillo-Chavez. Towards real time epidemiology: data assimilation, modeling and anomaly detection of health surveillance data streams. 2007. In *2nd NSF Workshop, Biosurveillance, 2007.* (New Brunswick, NJ, 22 May 2007). Vol. 4506, p. 79. Heidelberg: Springer-Verlag Berlin.

Bettencourt, L. M., and R. M. Ribeiro. Real time bayesian estimation of the epidemic potential of emerging infectious diseases. 2008. *PLoS ONE.* **3** (5): e2185.

Chowell, G., H. Nishiura, and L. M. Bettencourt. Comparative estimation of the reproduction number for pandemic influenza from daily case notification data. 2007. *J R Soc Interface.* **4** (12): 155.

Chowell, G., L. M. Bettencourt, N. Johnson, W. J. Alonso, and C. Viboud. The 1918-1919 influenza pandemic in England and Wales: spatial patterns in transmissibility and mortality impact. 2008. *Proc Biol Sci.* **275** (1634): 501.

Davenport, M. P., G. T. Belz, and R. M. Ribeiro. The race between infection and immunity: how do pathogens set the pace?. 2009. *Trends Immunol.* **30** (2): 61.

Gabbard, J., N. Velappan, R. Di Niro, J. Schmidt, C. A. Jones, S. M. Tompkins, and A. R. Bradbury. A humanized anti-M2 scFv shows protective in vitro activity against influenza. 2009. *Protein Eng Des Sel.* **22** (3): 189.

Lay, M. D., L. Zhang, R. M. Ribeiro, S. N. Mueller, G. T. Belz, and M. P. Davenport. Kinetics of major histocompatibility class I antigen presentation in acute infection. 2009. *J Immunol.* **182** (2): 902.

Macken, C.. Evolution of highly pathogenic avian H5N1 influenza viruses. 2009. *Los Alamos Unclassified Report 09-06579.*

Smith, A. M., F. R. Adler, J. L. McAuley, R. M. Ribeiro, J. A. McCullers, and A. S. Perelson. Effect of 1918 PB1-F2 expression on influenza A virus infection kinetics. 2009. *Los Alamos Unclassified Report 09 - 06271.*

Smith, A. M., and R. M. Ribeiro. Modeling the viral dynamics of influenza A infection. To appear in *Critical Reviews in Immunology.*

Song, J., J. Gans, M. Wolinsky, P. Li, E. Curd, C. Detter, and H. Cai. Algorithms for designing the minimal set of multiplexed degenerate universal tagged primers for RNA virus detection. 2008. In *International Conference on Bioinformatics & Computational Biology (BIOCOMP'08).* (Las Vegas, NV, 14-17 July 2008). Vol. 1, p. 198. Las Vegas: CSREA Press.

Tatebe, K., A. Zeytun, R. M. Ribeiro, G. Gupta, R. Hoffmann, K. S. Harrod, and C. V. Forst. Response network analysis of differential gene expression in human epithelial lung cells during avian influenza infections. To appear in *BMC Bioinformatics.*

Zeytun, A., J. C. van Velkinburgh, P. E. Pardington, R. R. Cary, and G. Gupta. Pathogen-specific innate immune response. 2007. *Advances in Experimental Medicine and Biology.* **598**: 342.

# Identifying High Risk Species Critical for the Emergence of Pandemic Influenza

*Jeanne M. Fair*
20080230ER

## Introduction

Management and detection of highly pathogenic influenzas in animal populations requires a better understanding of the determinants of host range. The major host range determinant for influenza is the binding site for the virus, sialic acids (Sia) that varies between mammalian and avian cell membranes [1]. The specific hypothesis behind the proposed research is that the characterization of Sia in each Family in the Class Aves can be used as a phylogenetic guide map to the host range for influenza and that data can then be used along with species distribution information to guide surveillance efforts for strains of public health concern. To begin to understand this interaction we first set out to characterize sialic acid species in the respiratory, digestive tracts, and on erythrocytes between five peridomestic and phylogenetically different bird species. We will then investigate for correlations between these three physiological landscapes in order to conduct a sialic acid survey in a wide range of bird species using the simplest tissue(s) to acquire yet still describe an animal's sialome. Sialic acid characterization in birds is being measured using a new method that makes use of stable isotope labeled substrates (neuraminyllactose) for binding to both neuraminidase and hemagglutinin present on the surface of the virus, resulting in a risk assessment for priority species. In a similar comparison and to gain a deeper understanding of differences in host susceptibility, we will measure and compare immune function parameters to inactivated H5N1 virus using the assay platforms of single cell, high sensitivity technologies in the Bioscience Division.

The data collected from this research effort will identify the key species that we need to be concerned about for potential increase in the probability for reassortment of the influenza virus due to similarities in sialic acid with humans. In short, we will enhance our Nation's ability to find "mixing vessels". Mixing vessels are those species that can be infected by both human and avian adapted viruses and thus might transmit novel resorted (mixed) viruses to humans. The end results of this project will be a much needed phylogenetic guide map created by overlaying Sia quantification and linkage data with species distribution information that will result in a prioritization of avian species that may asymptomatically carry influenza viruses of public health concern. This project is building a science foundation for the challenge of avian influenza surveillance around the world.

## Benefit to National Security Missions

This project supports the biothreat reduction missions within DOE, DHS, and other government agencies by enhancing the understanding of emerging diseases in non-human populations, focusing on avian and pandemic influenza. This project also supports our ability to improve world-wide human health.

## Progress

In order to successfully complete the scope of work for our project of completing a phylogenetic analysis of the key receptor protein, sialic acid (Sia) in birds, we needed to: (1) obtain blood samples from numerous avian species, (2) develop a novel database, and finally, (3) isolate and quantify Sia using cutting-edge stable isotope technology at Los Alamos National Laboratory (LANL). We gratefully collaborated with a multitude of researchers in the field and with zoological parks across North America. During the first two years of this project we have obtained over 800 blood samples from a majority of the 23 Orders needed for the comparative analysis. Blood samples from the over 800 birds were collected in 2009 from numerous collaborators that include the Saint Louis Zoo, Brookfield Zoo, Monterey Bay Aquarium, the Albuquerque Zoo, and researchers within the United States Geological Survey and National Wildlife Research Center. In addition, waterfowl (a key host for influenza) that died at the Bosque Del

Apache National Wildlife Refuge were collected as part of an ongoing collaboration and dissections of 40 birds have been completed and used for tissue Sia method development and Sia quantification. Unused samples have been stored for future work over the winter months. To investigate variation in Sia's that may be due to infection or age and sex, we collected tissue and blood samples from mallards that were part of an influenza infection study at the National Wildlife Research Center in Fort Collins, CO, as well as a cohort of breeding American kestrels of different ages and sexes in Colorado.

The relational database has been completed and work is nearly completed on the production of a web interface that can be accessed by multiple Divisions and collaborators.. The database will be capable of tracking Sia levels in gut and respiratory tissues by location and will interact with a geographic information system in order to accommodate spatial analyses. It also is a informational database for collection and identification of all samples collected in the field. We are working with Koranne Ostic-Randow, software developer with SAE-3 who is using Microsoft SQL Server 2008 for this project. Data are currently entered into the preliminary database on the project's Sorceforge internet site maintained by LANL. Protocols for total Sia quantitation in chickens, pigeons, and bluebirds were successfully developed in fiscal year 2009. We believe these protocols can be used on myriad species' samples. Analyses of mass spectrometer (MS) results were performed using Center for Disease Control standards and preliminary results in pigeons have been validated by the Glycotechnology Core Resource at UC San Diego demonstrating a working assay. Bovine fetuin that is used as a control protein for Sia was analyzed and also showed a strongly consistent standard curves (Figure 1). Between-assay runs showed reproducible results in the MS. Amounts of a common type of Sia (Neu5Ac) in chickens varied from 14.99 to 22.48 µg Neu5Ac/ml of red blood cells (RBC) (n = 4), higher than both pigeons and western bluebirds (Figure 2). We have detected Sia concentrations as low as 0.5 µg/ml in RBC using our current MS protocols and have discovered the presence of a form of Sia (*N*-glycolylneuraminic acid, Neu5Gc) on pigeon RBC membranes thought to be rare in birds (Figure 3). The time of this assay is 30 minutes per sample and the lowest volume being currently used is 50 µl RBCs. This volume size will allow for analysis of blood samples from small birds (e.g. Order Passeriformes) and the time will allow for multiple samples to be run overnight by the mass spectrometer. We are working toward lower detection thresholds of Sia via fluorescent marker labeling. Also, we are further reducing sample preparation time, and are investigating the histology of Sia is under way via a new collaboration with UC San Diego Glyobiology Research and Training Center.

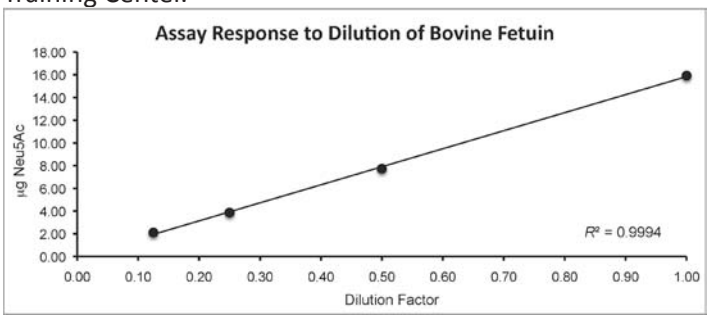


*Figure 1. Our newly developed assay shows a consistent response across sample dilutions for the common form of Sia, N-acetylneuraminic acid (Neu5Ac) for bovine protein (fetulin) standard.*

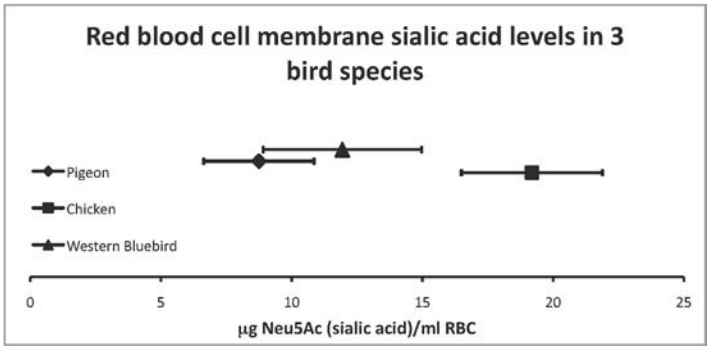


*Figure 2. Using our validated assay, we determined that the Sia content present on chicken red blood cell membranes is greater tha on rock pigeon and western bluebird red cell membranes (mean +/- 95% confidence interval).*

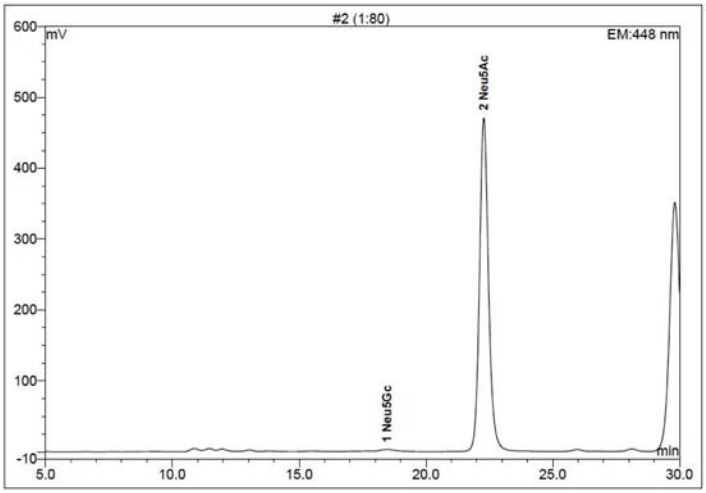


*Figure 3. In collaboration with UC-San Diego, we dicovered a form of Sia (N-glycolylneuraminic acid) in pigeon red blood cell sample that is thought to be rare in birds.*

## Future Work

The next year of this project will focus on completing the sialic acid characterization across the avian landscape (tissues) in order to provide detailed guidance for the

surveillance of species critical for transmission and reassortment of influenzas. Sia quantities and linkage types will be compared between erythrocyte and tissues with comprehensive validation by way of virus binding assays and sophisticated microscopy. We hope to prove that the Sia makeup in blood samples mimic tissue samples, thereby making surveillance testing easier. The end results of this project will be a much needed phylogenetic guide map created by overlaying Sia quantification and linkage data with species distribution information that will result in a prioritization of avian species that may asymptomatically carry influenza viruses of public health concern.

## Conclusion

The proposed study addresses a potentially catastrophic public health problem — the increased possibility of a pandemic influenza strain due to current circulation of H5N1 in both wild and domestic birds, in other mammals hosts, and in humans. Attempts to eradicate or control H5N1 have been unsuccessful, and between April 2005 and April of 2006 the number of countries with positive H5N1 infections in birds increased from five to fifty-five countries. The scientific gains of this research include a better understanding of the potential host range of birds in order to have effective, focused, and meaningful surveillance of influenza in host populations. This work will fill extensive knowledge gaps in the types and quantities of sialic acid birds that will lead to an increased knowledge of influenza viral evolution by default. So far sample acquisition and total Sia quantity methodology have been successfully developed and measured for avian species. Methodology for stable isotope Sia measurement in birds have been developed which allows for high throughput analysis with increased sensitivity thresholds. Also a relational database is now available to track samples and study the geospatial relationship of Sia types in tissue samples. The end result of this work will be a phylogenetic analysis tool that incorporates sialic acid differences in taxons that can be utilized into perpetuity.

## References

1. Suzuki, I. T., T. Suzuki, and T. Holland. Sialic acid species as a determinant of host range of influenza a viruses. 2000. *Journal of Virology.* **74**: 11825.

## Publications

Fair, J., K. McCabe, Y. Shou, and B. Marrone. Immunophenotyping of Chicken Peripheral Blood Lymphocyte Subpopulations: Individual Variability and Repeatability. . 2008. *Veterinary Immunology and Immunopathology.* **In Press**: In Press.

# The Effect of Acoustical Waves on Stick-Slip Behavior in Sheared Granular Media: Implications for Earthquake Recurrence and Triggering

*Paul A. Johnson*
20080268ER

## Introduction

Dynamic earthquake triggering remains a compelling mystery: how do transient seismic waves with micrometer displacements trigger earthquakes, often with failure occurring long after the waves have passed? How can triggering take place at distances of hundreds of kilometers, from the earthquake generating the seismic waves? We are addressing how triggering takes place; however the work will also lead to a new understanding of the importance of seismic energy on earthquake physics and more generally, there will be broad impact on unexpected material failure induced by moderate-amplitude sound. To address our goals and simultaneously test a model we recently developed (1), we are conducting laboratory studies of stick—slip in granular media and its response to applied acoustic waves. In preliminary studies, we used glass beads to simulate granular fault zone wear material (gouge), sheared under constant normal stress while subject to acoustic waves. We observed evidence for triggered "earthquakes" when applied sound-wave amplitudes exceeded several microstrain. We were surprised to also observe significantly delayed "earthquakes" relative to those observed without wave perturbation (increased recurrence), as well as strain memory of the sound perturbation in the granular material. These phenomena persisted despite the severe material reset that takes place during a large "earthquake". We will determine how and why these phenomena occur and place them in the context of real earthquakes, as well as other failure scenarios including avalanches, landslide and failure of incipient damage in the presence of moderate amplitude sound.

## Benefit to National Security Missions

There is a large class of diverse applications of this work that include predicting unexpected breakdown behavior. This project will support the DOE missions in Science by enhancing our understanding of earthquake prediction, and Nuclear Weapons by enhancing our understanding of small amplitude vibration on incipient damage in components.

## Progress

In addition to very small amplitude wave displacements that cause triggering, earthquake nucleation depths are of order 10-20 km, and thus static overburden might be expected to prohibit triggering by seismic wave stress perturbations (~100000 Pa). To better understand the physics of dynamic triggering, we are conducting laboratory studies of stick—slip in granular media with and without applied acoustic waves. Laboratory studies of granular friction have emerged as a powerful tool for investigating tectonic fault zone processes and earthquake phenomena including post-seismic slip, interseismic frictional restrengthening, and earthquake nucleation. In this work, we explore experimentally the effects of dynamic loading on stick—slip behavior and speculate how our results impact understanding of earthquake processes, in particular, dynamic earthquake triggering and stick—slip recurrence. Dynamic earthquake triggering involves seismic waves from one earthquake promoting or inhibiting failure on faults they disturb. Dynamic triggering has been clearly documented in a few cases far from an earthquake source, at distances much greater than the fault radius of the triggering source (outside the traditional 'aftershock zone'), and mounting evidence suggests it commonly occurs near the earthquake source.

In our 3-D experiments, glass beads are used to simulate granular fault zone wear material, sheared in a double-direct configuration under constant normal stress, while subject to transient or continuous perturbations by acoustic waves. In past work we observed dynamic laboratory 'earthquake' triggering as well as strong effects on laboratory earthquake recurrence (2). This past year we observed that the horizontal stress applied plays a crucial role in the response of the glass beads to applied waves. Under relatively small normal stress, and subject to modest wave amplitudes typical of seismic waves 100-1000 km from a medium sized earthquake, we observe induced slow (silent) slip. Triggered silent slip is a phenomenon observed in the earth as well, and these are the first laboratory experiments that we are aware of that show such behavior. Under slightly larger

normal stress observe both instantaneous and delayed 'earthquake' triggering. Waves also cause significant disruption in the laboratory earthquake recurrence rate. The effects of waves are observed for many major-event cycles after wave excitation ceases, indicating a strain memory of waves in the granular material. Again, similar effects are observed in the earth. Under slightly larger horizontal stress, we observe instantaneous earthquake triggering followed by *slow dynamics*—meaning the shear modulus recovers linearly with the-logarithm-of-time back to equilibrium over hundreds of seconds, something we have observed in experiments in granular media and rock when no shearing takes place (e.g., (3,4). Slow dynamics is a classical elastic nonlinear (anelastic) behavior observed in acoustical experiments with rock samples in the lab as well as in Earth.

Wave-induced disruption of periodic stick—slip is linked to failure of granular force chains. In 2-D experiments we are applying photoelastic discs in stick—slip measurements in order to visualize the evolution of the force chain network (Figure 1). Photoelastic measurements provide insight into failure, and in particular small adjustments in the force chains network that presage failure. A phenomenological model similar to a well known model originally developed by Knopoff-Burridge shows the same general behaviors. Our results should lead to a new understanding of the importance of seismic energy on earthquake physics and more generally, we anticipate that it will have broad impact on unexpected material failure induced by moderate-amplitude elastic waves, including avalanches, landslide and failure of incipient damage in solids.

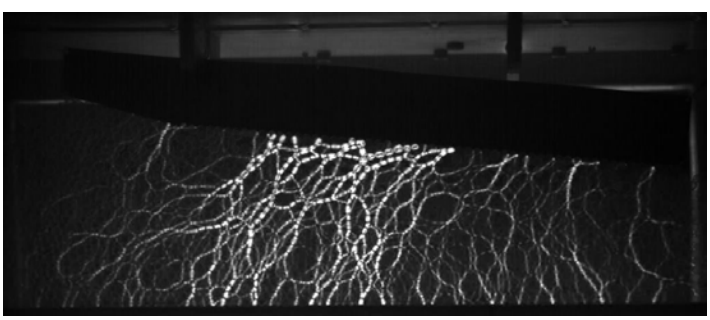

*Figure 1. Two dimensional experiment of stick slip in laboratory experiments using beads that illustrates "force chains". Force chains in granular material carry the material strength-- they are the most stressed portion of the two-dimensional bead pack. An effect known as birefringence allows one to see the force chains. The gray regions also contain beads, but they carry no force and so they cannot be easily seen. A sand pile has force chains, as does fault gouge in the earth. The black object above the chains is a mass that is pulled across the top of the beads. It is the mass that induces the force chains. We study stick-slip behavior of the mass to help understand processes in three dimensional experiments where no visualization can be made, and to infer fault processes in the earth (photo courtesy of B. Behringer).*

The origin of dynamic earthquake triggering by transient seismic waves is a complex problem. Our results show that granular-friction processes are consistent with four of as yet unexplained observations in earthquake seismology: 1) small amplitude waves can trigger failure both immediately and delayed failure relative to the strain transient, 2) earthquake recurrence patterns are complex; 3) small amplitude waves can trigger slow, silent-slip; 4) small amplitude waves can induce long term recovery processes similar to slow dynamics. Understanding the role of vibration-induced disruption of earthquake recurrence could have significant implications for seismic hazard assessment and reliable forecasting of earthquakes.

## Future Work

Our goal is to unravel how dynamic earthquake triggering takes place, by employing laboratory studies of stick-slip and observational studies of earthquakes. The work will have direct impact on other avalanche –type behavior (see below).

Our hypotheses are,

(a) that dynamic waves trigger earthquakes due to nonlinear softening-to-weakening, both in the laboratory and in the Earth, due to the nonlinear response of the fault gouge, given certain conditions (critical state, shear weakness and/or low effective pressure, elevated strain); toward that goal we are working on the nonlinear elastic response of granular media, and have recently published a paper on this topic (3,4).

(b) that slow silent slip is induced by the same processes but only when in situ stresses are very small;

(c) that strain memory is responsible for delayed triggering in the lab and in the Earth, and for disrupted recurrence in the lab, and potentially in the Earth;

(d) that the origin of behaviors is explained by the micromechanics of the medium—the force chains—and that these processes may be widespread (sound induced crack failure, landslides, avalanche).

Our tasks are to, (i) test the hypotheses in laboratory and model stick-slip studies, and (ii) inspect seismic data for observations that may support or refute the hypotheses. Whether or not the processes are nonlinear in origin, our ultimate objective is to understand the role of dynamic waves on earthquake processes, and apply what we learn to a scope of problems that are related to catastrophic breakdown due to moderate amplitude sound. Without such tools we have no hope of predicting earthquakes (a very hard problem in any case) or understanding when cracks in a component may breakaway due to the presence of sound. Each task will be considered met with a series of peer-reviewed journal publications submitted. In addition, we add the task of looking for applications of interest to DOE, in particular, to issues related incipient damage

where components may be in the presence of moderate amplitude sound.

## Conclusion

Triggering is an intriguing scientific question that confounds, and we find that the effects of acoustics on faulting in the laboratory create many other questions as well. Our work will tell us what effect seismic waves generated by one earthquake have on a fault located nearby or far away. We already have evidence that the effects could be significant, and that seismic waves may strongly effect time-dependent earthquake forecasting, a primary goal of seismologists. Ultimately, predictive models used in earthquake prediction will surely have to include earthquake triggering and wave effects on fault recurrence and memory.

## References


1. Johnson, P., and X. Jia. Nonlinear dynamics, granular media and dynamic earthquake triggering. 2005. *Nature.* : 871.

2. Johnson, P., H. Savage, M. Knuth, J. Gomberg, and C. Marone. The effect of acoustic waves on stick-slip behavior in sheared granular media: implications for earthquake recurrence and triggering . 2008. *Nature.* **451**: 57.

3. Brunet, T., X. Jia, and P. Johnson. Transitional, elastic-nonlinear behavior in dense granular media. 2008. *Geophysical Research Letters.* **35**: L19308.

4. Guyer, R., and P. Johnson. . 2009. In *Nonlinear Mesoscopic Elasticity: The complex behaviour of granular media Including rocks and soil.* , First Edition, p. 410. Berlin: Wiley-VCH.


## Publications


Brunet, T., X. Jia, and P. A. Johnson. Transitional, elastic-nonlinear behaviour in dense granular media. 2008. *Geophysical Research Letters.* **35**: L19308.

Guyer, R. A., and P. Johnson. . 2009. In *Nonlinear Mesoscopic Elasticity: the complex behaviour of granular media including rocks and soil.* By Guyer, R., and P. A. Johnson. , First Edition, p. 410. Berlin: Wiley-VCH.

Johnson, P. A., H. Savage, M. Knuth, J. Gomberg, and C. Marone. The effect of acoustic waves on stick-slip behavior in sheared granular media: implications for earthquake recurrence and triggering. 2008. *Nature.* **451**: 57.

Johnson, P., P. Bodin, J. Gomberg, F. Pearce, Z. Lawrence, and F. Menq. Inducing in situ, nonlinear soil response applying an active source. 2009. *Journal of Geophysical Research.* **114**: B05304.

# Developing a Remote Sensing of the Solar Surface

*Joseph E. Borovsky*
20080321ER

## Introduction

Understanding the electromagnetic medium that impinges upon and surrounds the earth is crucial to virtually every aspect of space flight, from spacecraft and sensor design to safety considerations in manned space flight. Furthermore, the ionic medium surrounding the earth impacts all manner of communications and sensing systems. The ultimate goal of this LDRD/ER Project is to develop a new research area connecting the physics of the solar surface with the physics of the solar wind (consisting of a variety of particles originating from the sun), thereby advancing the understanding of both.

This LDRD/ER Project has three research objectives. (1) To survey the properties of the solar wind that emanates from different features on the sun. This will provide a large body of information about the sources of the solar wind. (2) To map the magnetic flux tubes measured by the ACE spacecraft to their specific regions of origin on the solar surface. This will provide a large body of information about the origin of structure in the solar wind, about the predictability of patterns in the solar wind, and about the properties of important magnetic-flux concentrations that escape from the sun. (3) To develop a technique to use existing solar-wind instruments to make remote measurements of the time-dependent dynamics of the magnetic flux concentrations as they escape from the sun.

## Benefit to National Security Missions

This project will enhance our understanding of the solar wind and its impact on the space environment, which affects space-based platforms and sensors. This project will support the missions in Threat Reduction and treaty verification important to DOE, DHS, and other government agencies.

## Progress

In the second year of this LDRD/ER project the major progress concerned six topics.

1. Using ULYSSES satellite measurements, it was demonstrated that the flux tubes of the solar wind become flat as they are carried out beyond the orbit of Earth. This finding helps to settle the issue of whether the flux tubes are fossil structure from the Sun (which would become flat beyond Earth) or structure constantly regenerated by solar-wind turbulence (which would not become flat).

2. Using ACE satellite measurements, the shape of the flux tubes was examined in one-dimensional compression zones of the solar wind near Earth. It was found that the flux tubes flatten when slowly compressed, supporting the fossil-flux-tube model. This examination was submitted for publication [1].

3. In mapping the measured magnetic field of the solar wind back to the Sun along the Parker spiral, our flux-tube model was used to map the fluctuations of the magnetic field back to the Sun. This flux-tube mapping predicts a dual population of fluctuations near the Sun: a large population of small fluctuations and a small isotropic population. The majority of the fluctuations are smaller than the fluctuations predicted with turbulence models. This mapping investigation was submitted for publication [1].

4. A theory for the coefficient of fluid viscosity for the solar wind was developed which does not rely on particle collisions. In this new picture the viscosity comes about from electromagnetic processes acting on shear flows. For a hot plasma such as the solar wind, the new viscosity is orders of magnitude larger than previous estimates. This theory has appeared in print [2,3].

5. For the solar-wind turbulence that is confined to the flux tubes, a theory was developed that carries an anisotropy parameter into calculations of turbulence parameters such as turbulent heating rates, Reynolds numbers, and dissipation scales. Owing to the confinement in flux tubes, the turbulence of the solar wind is forced to be anisotropic. This theory has appeared in print [3].

6. By changing the manner in which spacecraft data is analyzed, more-accurate estimates of the properties of the turbulence in the solar wind were obtained, and turbulence parameters such as Reynolds numbers and heating rates were recalculated. The new estimates of the amplitudes were obtained by eliminating the large signals from the fossil structure of the solar wind. The methodology for this analysis has been submitted for publication [4] and the utilization of the results have appeared in print [3].

An depiction of the structure of the solar-wind plasma filling the inner solar system (submitted for publication [1]) appears in Figure 1. The figure depicts the flux-tube texture and the radially increasing braiding angles of flux tubes about the Parker-spiral direction. Here, individual solar-wind flux tubes are drawn in various colors. The depiction of is approximately to scale utilizing the measurements of tube diameters and angles at Earth's orbit: the diameters and braiding angles of the flux tubes at Earth reflect the statistics of ACE measurements. In going around the circumference of the orbit of the Earth, about 1000 flux tubes are encountered.

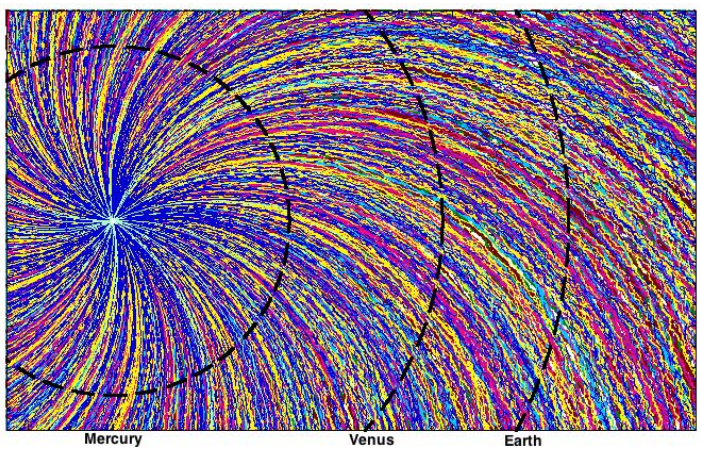


*Figure 1. A depiction of the flux-tube structure of the solar wind. The viewer is looking down on the ecliptic plane. The diameters of the orbits, the radius of the Sun, and the diameters and braiding angles of the flux tubes at 1 AU are approximately to scale. The pattern of flux tubes convects radially outward with the solar-wind speed and the tubes undergo transverse Alfvenic motions. The braiding angles of the flux tubes is envisioned to give rise to the angular spread in magnetic-field directions about the Parker spiral.*

In support of this project the investigators have organized a session entitled "Merging Different Views of Structure" at the SHINE Workshop in August 2009 and the principal investigator was co-organizer of a "Workshop on Thin Current Sheets" in September 2009.

## Future Work

This project has three research objectives.

1. To survey the properties of the solar wind that emanates from different features on the sun. In particular the central portions of off-equatorial and equatorial coronal holes and coronal-hole edges will be compared. This will involve coordination of the ACE spacecraft data with models of where the solar wind originates from the solar surface. The goal will be to obtain a large data base of coordinated solar-wind properties and solar source locations. This objective will provide a large body of information about the sources of the solar wind.

2. To map the magnetic flux tubes measured by the ACE spacecraft to their specific regions of origin on the solar surface. This will also involve coordination of the ACE spacecraft data with models of where the solar wind originates from the solar surface. The goal will be to obtain a large data base of solar-wind flux-tube properties and their solar source locations. This objective will provide a large body of information about the origin of structure in the solar wind, about the predictability of patterns in the solar wind, and about the properties of important magnetic-flux concentrations that escape from the sun.

3. To develop a technique to use existing solar-wind instruments to make remote measurements of the time-dependent dynamics of the magnetic flux concentrations as they escape from the Sun. This will involve detailed and statistical comparisons of the locations of solar-wind discontinuities seen in the magnetic-field measurements, in the plasma measurements, and in the energetic-electron measurements. Displacements of the various discontinuities represents the amount of magnetic-field reconnection near the sun. The goal will be a statistical picture of the reconnection rate in chromospheric structures.

## Conclusion

We expect that this project will provide bodies of information about the sources of the solar wind and about the origin of structure in the solar wind, about the predictability of patterns, and about the properties of important magnetic-flux concentrations that escape from the sun.

We expect to develop a technique to use solar-wind instruments to make remote measurements of the dynamics of the flux concentrations as they escape from the sun.

The ultimate goal of this project is to develop a research area connecting the physics of the solar surface with the physics of the solar wind.

## References


1. Borovsky, J. E.. On the variations of the solar-wind magnetic field about the Parker-spiral direction. *Journal of Geophysical Research.*

2. Gary, S. P., and J. E. Borovsky. Damping of long-wavelength kinetic Alfven fluctuations: Linear theory. 2008. *Journal of Geophysical Research.* **113**: A12104.

3. Borovsky, J. E., and S. P. Gary. On shear viscosity and the Reynolds number of MHD turbulence in collisionless magnetized plasmas: Coulomb collisions, Landau damping, and Bohm diffusion. 2009. *Physics of Plasmas.* **16**: 082307.

4. Borovsky, J. E., and M. H. Denton. Solar-wind turbulence and shear: A superposed-epoch analysis of corotating interaction regions at 1 AU. *Journal of Geophysical Research.*


## Publications


Borovsky, J. E.. Flux tube texture of the solar wind: Strands of the magnetic carpet at 1 AU?. 2008. *Journal of Geophysical Research.* **113**: A08110.

Borovsky, J. E.. On the variations of the solar-wind magnetic field about the Parker-spiral direction. *Journal of Geophysical Research.*

Borovsky, J. E., and Michael H. Denton. Solar-wind turbulence and shear: A superposed-epoch analysis of corotating interaction regions at 1 AU. *Journal of Geophysical Research.*

Borovsky, J. E., and S. P. Gary. On viscosity and the Reynolds number of MHD turbulence in collisionless plasmas: Coulomb collisions, Landau damping, and Bohm diffusion. 2009. *Physics of Plasmas.* **16**: 082307.

Gary, S. P., and J. E. Borovsky. Damping of long-wavelength kinetic Alfven fluctuations: Linear theory. 2008. *Journal of Geophysical Research.* **113**: A12104.

Tessein, J. A., C. W. Smith, B. T. MacBride, W. H. Matthaeus, M. A. Forman, and J. E. Borovsky. Spectral indices for multi-dimensional interplanetary turbulence at 1 AU. 2009. *Astrophysical Journal.* **692**: A12104.

# A New Approach to Unravel Complex Microbial Community Processes

*Cheryl R. Kuske*
20080464ER

## Introduction

Soil organic matter is the largest pool of terrestrial carbon on Earth. Soil microbiota (bacteria, fungi, microfauna) are responsible for stabilization and release of this pool via complex processes such as decomposition. Although key to carbon flux in terrestrial ecosystems, microbial decomposition is one of the major unknowns for prediction of carbon sequestration, ecosystem responses to climate change, and contaminant mitigation. Our project aims to provide an *in situ* assessment of microbial decomposition rates and energy sources using a unique Tunable Diode Laser Spectroscopy (TDL) system in parallel to identification of the active microbial participants using stable isotope probing and metagenomic analysis. This combination of new techniques is being applied to soil microcosms of field soil samples from LANL's woodland observatory and other ecosystems, to provide an understanding of soil biota that control degradation of plant carbon and their rates of activity under different conditions. Scientific contributions from this project will include 1) demonstration of a suite of novel approaches to identify connections between soil microbial community composition, activity and metabolic processes, 2) determination of the active soil microbial populations that are capable of degrading complex plant biomass across multiple soils, and 3) assessment of the effects of moisture pulses on soil decomposition rates and associated microbial community structure.

## Benefit to National Security Missions

This project endeavors to synthesize two, novel technologies from different scientific disciplines in order to better understand and characterize carbon cycling in soils, specifically complex carbon decomposition. Soil carbon among the largest sources of $CO_2$ input to global atmospheric $CO_2$, and decomposition processes influence the movement of organic pollutants and toxic metals, supporting missions in DOE/SC, and other government agencies.

## Progress

Progress in year two of the project included the following:

1. Established stable isotope probing (SIP) procedures for use with soil microcosms to isolate soil microbial community DNA representing the active populations.

2. Developed and tested a coupled soil-mesocosm-tunable diode laser system for monitoring the isotopic composition ($\delta^{13}C$ and $\delta^{18}O$) of $CO_2$ decomposed by soil microbes. An experiment to evaluate the effects of pulsed water addition on soil community respiration, in soils that differ in carbon content and composition, is in progress.

3. Conducted replicated time course series experiments on the degradation of $^{13}C$-cellulose by soil microorganisms from three soils that represented different carbon-use scenarios. Measurements included metagenomic identification of the active bacterial and fungal populations in each soil, $CO_2$ flux, and $\delta^{13}C$ and $\delta^{18}O$ of respired $CO_2$.

4. Developed a metagenomic analysis pipeline for analysis of soil microcosms. In doing so, identified dominant soil bacterial and fungal populations that responded to cellulose, some of which were consistent populations among different soils.

**Detailed results this year.**

A stable isotope probing (SIP) procedure was developed and calibrated for sealed soil microcosms. The procedure was not informative for simple carbon substrates (e.g. glucose and acetate) due to the broad range of microorganisms capable of utilizing these simple carbon sources as well as the natural range in G+C content of the microbial community interfered with selection of $^{13}C$-labeled DNA in gradient ultracentrifugation. The method worked exceptionally well with more complex carbon sources and is being used in experiments with $^{13}C$- cellulose. Figure 1 illustrates the separation of 'heavy' $^{13}C$-enriched DNA from the total pool of soil DNA.

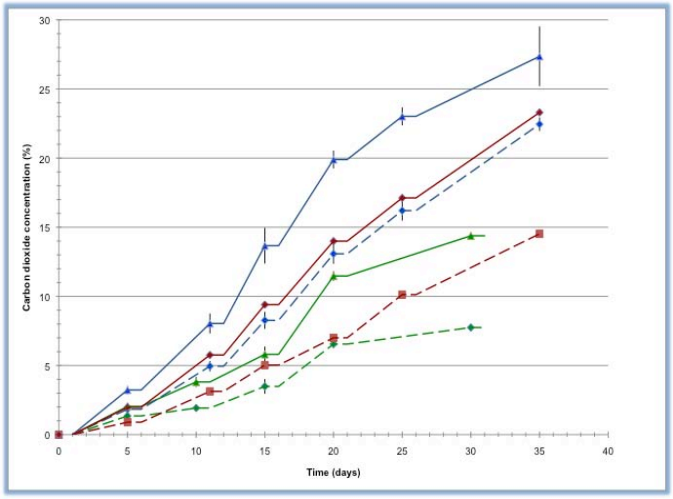


*Figure 1. Carbon dioxide concentrations over time for soil microcosms containing root zone soil of dead pinyon (blue), live pinyon (red) and a Midwestern grassland soil (green). Each point represents the $CO_2$ concentration averaged over three replicate microcosms (with standard deviation as bars). Solid lines represent soil microcosms to which 13C-cellulose was added to track the active microbial communities. Dashed lines represent native control soils.*

Time course experiments to determine the bacterial and fungal populations capable of $^{13}C$-maize cellulose decomposition were completed for three different soils. Results showed that, in soils from living pinyon root zones, which contains a very low amount of plant biomass carbon, a variety of microbes in the microbial community responded to added $^{13}C$ -cellulose. In contrast, in soils from beetle-killed dead pinyon, which contain high levels of complex plant-derived organic matter, a select group of bacterial and fungal species became dominant after cellulose addition and degraded cellulose at higher rates than in the live pinyon root zone. This demonstrates that microbial populations, and their functions in decomposition and release of soil carbon, is expected to differ in ecosystems that have extensive mortality such as throughout Southwestern USA. In a Midwest soil with lower pH and higher organic matter, the composition of dominant bacteria and fungi responding to $^{13}C$- cellulose was different than the pinyon soils, even though initial soil microbial compositions were similar between the soils (at the Order level). The soil respiration rate was higher in the pinyon soils (both $^{13}C$-maize cellulose amended and unamended soils) than the Midwest soil (Figure 2). These results suggest that the either the Midwestern soil is more efficient at complex carbon incorporation into biomass or exhibits slower decomposition rates, since less was released as carbon dioxide.

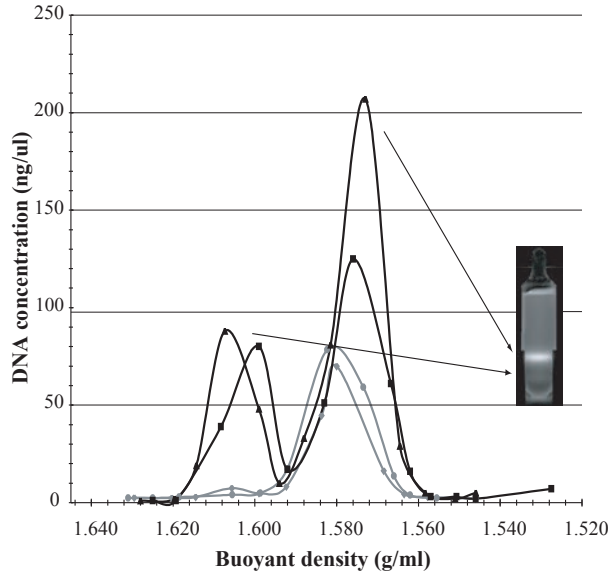


*Figure 2. Figure represents an example of cesium chloride fraction collection, DNA concentration (ng/ul) verses the buoyant density (g/ml). Picture (inlet) represents a typical cesium chloride gradient. Replicate control microcosms (no added carbon, 5 grams of soil) are depicted with gray data points & lines, whereas the replicate 13C cellulose microcosms (0.05g 13C cellulose/5 grams of soil) are depicted with black data points & lines.*

Time course measurements of the isotopic composition of $CO_2$ respired from soils demonstrates the importance of water in regulating microbial decomposition of carbon in soils (Figure 3). The spikes in all three panels of Figure 3 are due to the weekly addition of water. Our goal was to keep water content of soils constant across treatments because microbial metabolism is dependent on water content and we wanted to exclude that as a factor in the experiment, allowing us to determine the role of soil type (collected beneath live or dead trees) and cellulose addition. All of the jars had similar respiration rates and isotopic composition at the beginning of the experiment, validating that the soils had similar initial carbon and that any changes are due to the addition of cellulose. The respiration rate, which is equivalent to the amount of $CO_2$ released through decomposition, became higher for soils with cellulose added (Figure 3A). The $\delta^{13}C$ composition of respiration showed a consistent result, with the cellulose added soils shifting their signature towards that of the added cellulose (denoted by the dashed line), verifying that the microbial populations were decomposing the added cellulose. Notably, the consistent difference between live and dead control soils (no added cellulose) indicates that the carbon sources differ in the soils beneath live and dead soils. Lastly, the $\delta^{18}O$ signature of respiration carries the signature of added water, and thus it should be the same for all soils because we added the same amount and type of water to each jar. Thus monitoring the $\delta^{18}O$ provides a inter-jar test of comparability. The consistency of the $\delta^{18}O$ patterns across treatments provides confidence in our carbon results.

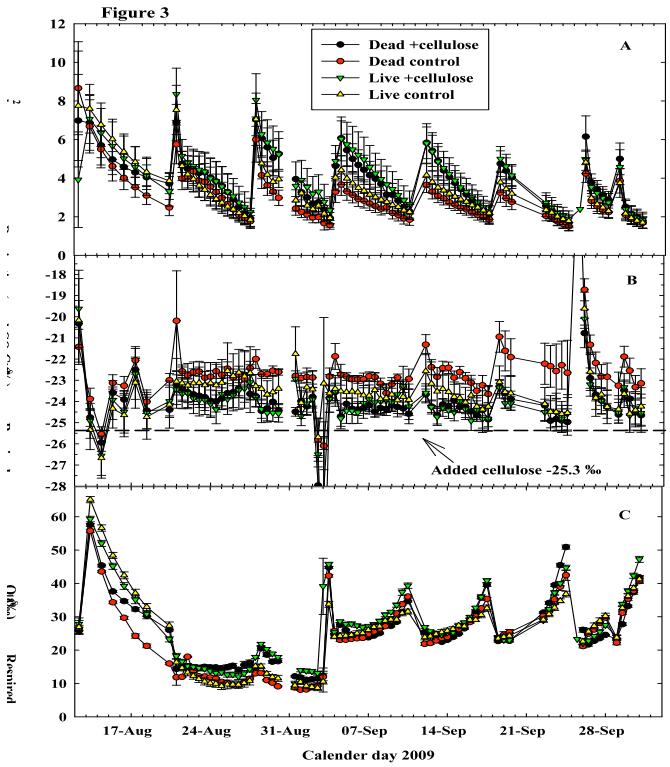


*Figure 3. A summary of results from our most recent soil-mesocosm experiment. Weekly spikes are associated with watering, which was done equally to each jar in each treatment. (3A): Soil respiration rates for the four treatments (see legend caption in figure for treatment symbols). Respiration was higher in cellulose-added jars. (3B): The carbon isotope composition of soil respiration for the four treatments. The cellulose-added jars shifted their isotopic signature towards that of the added cellulose, indicating increased use of the added cellulose. (3C): The oxygen isotope composition of soil respiration for the four treatments. The lack of difference between treatments provides confidence that our experimental infrastructure is operating properly, without biases between jars or treatments.*

## Future Work

Our studies to date have determined that (a) soil type (pH, organic matter content, parental material and other geochemical factors) greatly affect the composition of dominant soil microbes capable of degrading plant cellulose, (b) the input of large amounts of complex plant-derived carbon into a single soil type (by tree death) also dramatically effects the composition of microbial species capable of degrading that substrate, and (c) the metabolism of the microbial population responds through utilization of the added carbon.

In year three of the project, we will expand our determination of the dominant microbial communities capable of $^{13}$C-cellulose decomposition, across a broader range of soils that differ in parent material, pH, nature and content of soil carbon, and dominant vegetation to identify the cellulose-degrading soil microorganisms and link these populations to readily measured soil geochemical parameters. This information will be useful in gauging the relative contributions of soil fungi and bacteria in plant carbon decomposition, toward developing predictive models for major processes in carbon cycling across different soils. Molecular tools to track the bacterial and fungal species identified in our year two experiments will be developed to allow us to monitor their activities in further microcosm experiments that use the tunable diode laser to monitor $CO_2$ flux. Our follow on microcosm studies will include temperature treatments to investigate the impact of global warming on microbial processes in soils.

## Conclusion

Assessing the relative contribution of different soil microorganisms to decomposition in parallel with undisturbed metabolism measurements has been a major goal of soil science for over five decades. We are refining parallel measures of the process (using a novel tunable diode laser) and active microorganisms (metagenomics).

## Publications

Powers, H., J. Hunt, P. Hanson, and N. McDowell. A dynamic soil chamber system coupled with a tunable diode laser for online measurements of delta13C and delta18O of soil respired CO2. . To appear in *Rapid Communications in Mass Spectrometry.*

# Nonequilibrium Mechanics of Geomaterials

*James A. Tencate*
20080603ER

## Introduction

Work by Los Alamos researchers during the past decade has pioneered a new direction in the study of nonlinear-elastic, dynamic behavior in materials. Certain materials display surprisingly large nonlinearities. Both conditioning and memory effects appear at wave strains smaller than parts per million. These are disturbances equivalent to seismic waves far from an earthquake epicenter. The materials relax in a very peculiar way over very long durations after the wave disturbance. This is a nonequilibrium phenomenon termed "slow dynamics." The uniformity of these behaviors over a wide variety of complex materials promises a new era in understanding and characterizing their behavior. Geomaterials are prototypes for these (apparently) unrelated solids. These include granular materials, sintered and damaged metals, some ceramics, and even high explosives. Though there are some clues as to the processes leading to the bulk behavior, the microphysics of the nonequilibrium behavior remains unknown. We plan a new generation of experiments that we expect will redefine the field. We are pursuing a joint experimental and theoretical effort to develop an overarching description valid for these common yet unusual materials. Our framework employs a mesoscale description of a free-energy landscape (i.e., fluctuating potential barriers) of the dynamical behavior. Such a predictive capability will have a major impact on diagnostics of materials, and on earthquake mechanics, and seismic wave propagation.

## Benefit to National Security Missions

This project will primarily support the DOE/NNSA mission in Science by greatly enhancing our understanding and ability to model consolidated, cemented materials. These range from geomaterials to explosives. The project will also support the missions of science for Nuclear Weapons (explosives) and Energy Security. Understanding oil- gas-bearing reservoir rocks and $CO_2$ sequestration are examples of the latter.

## Progress

Classical thermodynamics is all about state variables and the related equations of state and, while vast amounts of research has been done and is known about the equilibrium and nonequilibrium behavior of gases and liquids, very little is known for solids. The nonequilibrium thermodynamics of the specific solids we are interested in, i.e., poorly-cemented sandstones or limestones typical of an oil/gas or $CO_2$ sequestration reservoir, have some very unique behaviors (e.g., slow dynamics) and have been just barely studied, the main focus of this research. We summarize our progress below, both theoretical and experimental.

At low strains, geomaterials display a frequency softening that follows non-equilibrium thermodynamics (Landau theory). However, nonlinear coefficients are large and these large values are currently not derivable from an underlying physical cause. Because the nonlinearities are so large, they are hard to untangle from the non-equilibrium relaxation process (slow dynamics) seen in experiments. A theoretical framework that can incorporate both of these features has now been constructed using Landau-Ginzburg theory. It has been generalized for nonlinear losses. In addition, the origins of the loss mechanisms in geomaterials are complex and not well understood. The large dynamic nonlinear coefficients mentioned above make it likely that the loss mechanisms are also nonlinear. Any connection between the losses and the dynamical nonlinearities will contain hints of the underlying physical processes. Thus they are important to investigate. Fortunately the values of some of the coefficients arising in the Landau-Ginzburg theory can be fixed from experimental results at low strains. Others can be fitted with current slow dynamics experiments. The experimental work is needed to feed the theoretical and modeling effort. To this end, the theoretical work has progressed to the point of having a paper in preparation on the previous year's experimental results.

There are three different kinds of experiments we perform. All experiments are done by varying a single state variable to drive the rock out of equilibrium, and then measuring its return. These will define the regimes for the description of the dynamics of the non-

equilibrium behavior of rocks. Most of the previous years' work consisted of applying a static stress with a load frame and measuring the creep and recovery rates. Additional experiments where the stress was cycled constantly while strain was measured were also done. Creep and recovery are, however, dc-load experiments. Initial slow dynamics experiments used an ac (acoustic) source to drive a sample away from equilibrium. All these and implications are presently of great interest to seismologists and thus will be the subject of an invited talk at the American Geophysical Union's Fall meeting (December 2009).

Exploring higher strain regimes with a cyclic loading brings out hysteresis in a rock. We have shown that if the rate of the experiment is slow enough however, the hysteretic effects vanish. For certain rates it is possible to keep the sample in a metastable thermodynamic equilibrium for the whole experiment. A significant result (published 2009) is that historically experiments were done too quickly. Simply, these have been shown to be "contaminated" with non-equilibrium effects. We also have demonstrated the necessary temperature stability for the concluding set of measurements this year.

New experimental work has also continued along a parallel path. These are experiments where we drive a rock away from equilibrium with a small ac drive instead of a pressure/stress. In fact, this is slow dynamics as defined by TenCate and Shankland in the mid-1990s. The recovery of these samples to equilibrium has been carefully studied. However, the behavior of the sample during the early initial application and removal of the drive has not been measured until this past year, both by us and by colleagues at the University of Illinois (Weaver and Lobkis[1]). Lobkis and Weaver did a different experiment than us, they dropped a small wooden ball on a sample instead of applying an AC driving force. While the topic of their paper was not slow dynamics but monitoring small changes in material properties, they were able to resolve (in a cement sample) log(*time*) behavior starting from 22 ms after the drop. Our investigations with an AC drive on a sandstone show log(*time*) from about 1 s to well beyond (Figure 1). Remarkable results, to see log(*time*) behavior *over a range which spans 6 orders of magnitude*!

## Future Work

Our final experiments are to explore the very long tails of this recovery. The log(*time*) recovery cannot continue forever and where exactly it changes to something else is of great interest. To date there is only one data point (on a Lavoux limestone) and it was likely contaminated by temperature effects. Our present measurements should have no such problems and we look forward to getting these results on a wide variety of rock samples. The theoretical framework being built employs a mesoscale description of a free-energy landscape (i.e., fluctuating potential barriers) of the behavior. Describing the nonlinearity with nonequilibrium dynamics via effective field theories is a key goal. Predictions will be compared to experimental observations.

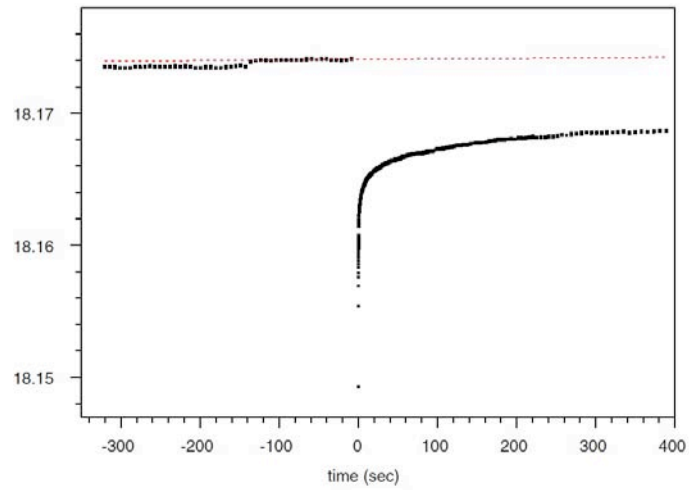


*Figure 1. Slow dynamics recovery as a function of time immediately before and after a small inpulse is applied to a cement sample. Frequency is on the left hand axis, time along. log(time) begins at about 22 ms. From [1] courtesy of the authors.*

## Conclusion

This work will lead to an increased understanding of how materials like oil- gas-bearing rocks and explosives react to wave excitation. Slow dynamics occur as a result of the way these materials are cemented together. Current models for these materials are not unique. Every rock requires its own tailor-made model. Non-equilibrium statistical mechanics has never been used to describe these materials. It will provide a robust description and model of the dynamics. Understanding these will help predict porosity and permeability in reservoir rocks ($CO_2$ sequestration) and crack density (for explosives) and yield improved models of wave propagation for earthquake and man-made explosion forensics.

## References

1. Lobkis, O., and R. Weaver. On the Larsen effect to monitor small fast changes in materials. 2009. *Journal of the Acoustical Society of America.* **125**: 1894.

## Publications

Claytor, K. E., J. R. Koby, and J. A. TenCate. Limitations of Preisach theory: Elastic aftereffect, congruence and end point memory. 2009. *Geophysical Research Letters.* **36** (L06304): L06304, 1.

# Evolution and Function of Microbial Signatures

*Murray A. Wolinsky*
20080618ER

## Introduction

The primary goal of this proposal is to develop the science underlying microbial signatures. For us, signatures are relatively short nucleic acid sequences that can be used to identify bacteria or viruses of interest. Signatures are of great practical importance in medical diagnostics, biodefense, microbial forensics and related disciplines, but they also pose fundamental scientific questions pertaining to evolution, functional organization, microbial diversity and speciation, which have been inadequately addressed.

Currently the most successful techniques for identifying useful nucleic acid detection or diagnostic signatures rely on an computational comparison of the sequences for target groups of interest with the sequences for all background organisms. Any differences which appear between the target sequences and the background sequences represent potentially useful signatures.

This work aims at trying to understand the biological significance of these signature elements "after the fact": knowing that these signatures distinguish target groups of interest from background groups, what can we learn about their roles and distribution?

This work has the potential to shed light on the definition of microbial species and to develop new methods for predicting sequence function.

## Benefit to National Security Missions

Better understanding of microbial signatures supports biothreat reduction and basic bioscience missions in DOE, DHS, and other government agencies. The work will develop a scientific basis for understanding how the evolution of pathogens may impact our techniques for their detection.

## Progress

Some of our major findings were recently published in BMC Genomics (BMC Genomics 2009, 10:501). Table 1 is taken from that paper and shows the identity of some of the targets we identified. Figure 1 shows the location of these targets in a "pathogenicity space." The identified targets appear in yellow and green.

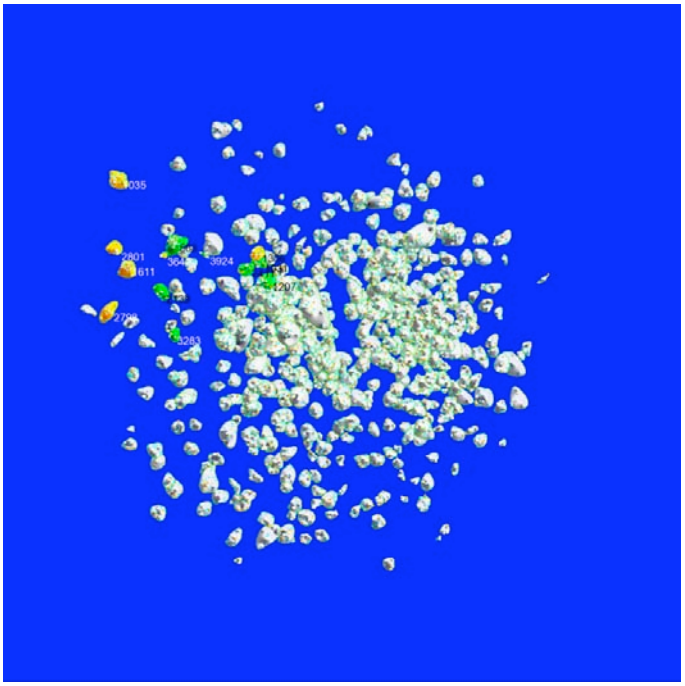

*Figure 1. Visualization of potential broad-spectrum targets (signatures) in a "pathogenicity space." Targets shown in yellow and green were predicted to be good candidates for countermeasure development. Targets shown in yellow have been experimentally verified to be involved in pathogenicity.*

We entered into a small work-for-others agreement with a company called Genetic Chemistry, Inc. based on the signature work undertaken here. This work is exciting because the goal of that effort is to use some of our early results as targets for treatments (drugs) for a disease (melioidosis, caused by the pathogen *Burkholderia pseudomallei*). If this work is successful, our effort will directly contribute to the development of a new therapeutic treatment.

We are entering collaboration with a Canadian national defense laboratory (PI Dr. Jonathan Wong) to better

| CI | YPTB Locus | Definition | 50-90 Cluster | Total non-pathogens | Total pathogens | Pathogen strains |
|---|---|---|---|---|---|---|
| **0.01** | 2410 | Magnesium transport ATPase mgtB | 1035 | 3 | 8 | Bme, Bma, Bp |
| **0.03** | 2913 | Deoxyribopyrimidine photolyase phrB | 2801 | 0 | 6 | Vc |
| **0.06** | 2705 | Putative manganese transport protein | 1611 | 3 | 8 | Ba, Bma, Bp |
| **0.12** | 3827 | Outer membrane biogenesis protein | 2798 | 0 | 5 | - |
| **0.13** | 0181 | Putative protohaeme IX biogenesis | 3642 | 0 | 5 | - |
| **0.16** | 0756 | Superoxide dismutase C sodC | 1306 | 0 | 9 | Bme, Cb, Ft, |
| 0.39 | 1340 | Lysine specific permease cadR | 563 | 2 | 9 | Ba, Bma, Bp, |
| 0.42 | 0242 | Glycerophosphoryl diester | 2411 | 0 | 7 | Bma, Bp |
| 0.45 | 2699 | Hypothetical protein | 3924 | 0 | 7 | Bma, Bp |
| 0.76 | 1424 | Hypothetical protein | 1031 | 3 | 9 | Bma, Bp, Ft, |
| 0.87 | 3166 | Thiol:disulphide interchange protein dscB | 3283 | 0 | 5 | - |
| 2.38 | 0188 | Frataxin-like protein cyaY | 2139 | 2 | 6 | Vc |
| 3.15 | 3505 | Stringent starvation protein sspB | 1207 | 3 | 7 | Cb, Vc |
| ND | 1167 | Phosphate starvation protein | 3911 | 0 | 6 | - |
| ND | 1251 | Ecotin | 3380 | 0 | 6 | - |
| ND | 2026 | MviN-like protein | 1296 | 3 | 9 | Bma, Bp, Cb |
| ND | 2995 | Putative surface antigen | 2296 | 2 | 7 | Vc |

*Table 1. Selected targets. Virulence-associated genes identified by computational methods and selected for experimental screening. These targets have been ranked by their competitive index (CI) value in Y. pseudotuberculosis. The CI value shown is the mean of the CI calculated from 3 spleens individually plated in triplicate. The top six candidates are deemed virulence-related by our experimental criteria. Hits to pathogens include all five members of the Enterobacteriaceae (Ec, Se, Sf, St, Yp) plus some additional strains.*

understand regulatory functions. His lab will be able to perform experimental investigations based on what we learn computationally.

This work has directly contributed to obtaining DHS funding for a spin-off forensics effort ($500K for a 1 year effort and an additional $500K for a second year) as well as a larger bioassay effort headed by Karen Hill (approximately $2.5 million total, of which about $550K represents work that is related, though distinct, to the work being performed on the LDRD).

We have applied for National Institutes of Health (NIH) funding to advance some of this work. In the course of preparing that proposal, we developed some new approaches to identification of signatures that remove some of the limitations of our existing methods. See Figure 3 for a description of aspects of this new approach.

We have largely have completed the first year's major goal: the main goal of that effort was to obtain empirical distributions for bacterial signatures over the nodes of an authoritative phylogenetic tree.

The work on modeling that distribution is still in progress. The amount of effort needed to obtain the needed phylogenetic tree was seriously underestimated in our original proposal -- resulting in some delay to our current status -- Ben McMahon has updated some of the work done in building the phylogenetic tree and is preparing this work for publication. See Figure 2 for part of this tree.

We have begun some of the Year 3 effort -- which is out of phase with our original plans but turns out to be somewhat independent of many of these tasks. In particular, we have made progress on improving signature robustness. Recently we have developed collaboration with U. Alabama at Birmingham (Dr. Elliot Lefkowitz) to help with some of that work.

*Figure 2. Part of a new bacterial phylogeny developed as part of this project. This project required the development of a new bacterial phylogenetic tree which is [a] comprehensive (in that it contains as many taxa as possible) and [b] has accurate branch lengths. Ben McMahon in T-10 developed this tree and is in thr process of preparing a publication on the methods used to develop it.*

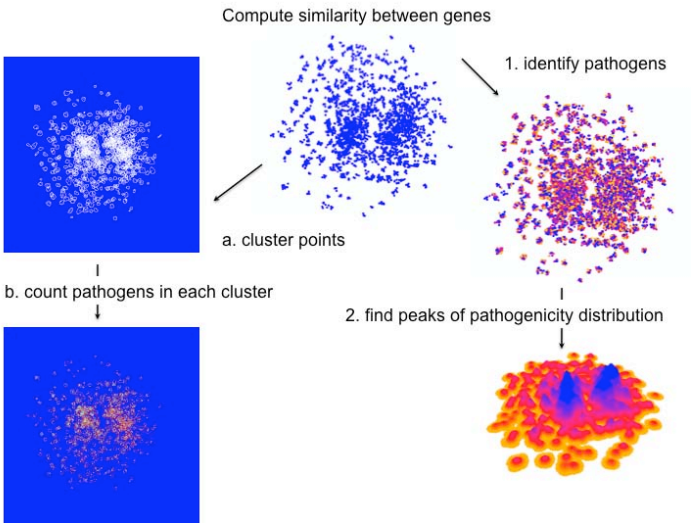


*Figure 3. A new approach to target identification -- how one can find targets which favor pathogens without clustering. Start with similarity comparisons between individual gene (or domain or k-mer) sequences. This similarity matrix can be visualized as a spatial distribution of points (each point representing, e.g., a gene sequence in a particular organism). This distribution is shown in the upper center of the figure. Originally we first created clusters (a, on upper left) using heuristically-chosen thresholds. These clusters were ranked according to their content of pathogens (b, lower right). Clusters containing high pathogen excesses were chosen as targets. The proposed methodology does not require thresholds. Rather, we can directly attribute pathogenicity to each sequence based on the organism it belongs to (1, on upper right) and directly choose points that correspond to pathogen excesses (2, visualized as peaks of a "pathogenicity distribution.")*

## Future Work

We intend to answer the following questions:

- Can the distributions of microbial signatures (short nucleic acid sequences) be predicted?
- Do signatures support a coherent definition of microbial species? What are the implications of signature distribution for microbial diversity?
- How are signatures related to regulation and function?
- Can robustness of signatures be predicted?

We will develop computational tools that:

- Identify functional signatures.
- Produce more robust signatures.

A major task will be to develop mathematical models that predict number of signatures and compare with computational "measurements" on microbial populations.

Specifically, by choosing a broad class of microbes (e.g., Proteobacteria) and counting signatures, and then progressing to smaller sub-groupings and counting signatures, we will get empirical signature distributions that can be compared to theoretical models. If we get good fits, we will obtain values for microbial evolutionary speciation rates and for total microbial population sizes. Thus our methods may furnish independent ways of estimating microbial biodiversity.

We will also study how these distributions are affected by signature lengths. Do the features of the distributions of signature counts remain fixed or are there signature lengths for which these distributions show marked changes? Answering this question will shed light on whether microbial species constitute a meaningful and discrete level of biodiversity.

Year 1: Understand the distribution of microbial signatures

- Model signature evolution and compare with distributions of number of signatures
- Determine the expected distribution of signatures as a function of signature size and correlate with the size scales of functional elements
- Analyze implications of results on definitions of microbial species.

Year 2: Characterize our empirical signatures as to function using literature and bioinformatics methods.

Year 3: Develop methods to predict robust signatures

- Identify methods to predict lateral gene transfer and study effects on signature robustness.
- Develop methods to predict signature robustness and thereby acquire the ability to prioritize signatures.

## Conclusion

The results of this research are expected to have practical benefits in terms of improved signatures for public health and biodefense use. This work will lead to better and more reliable detection of threat agents and thereby help limit their potential damage. It will also lead to improved scientific models of microbial speciation (and its interpretation) and an improved characterization of microbial diversity. This increased scientific knowledge can be expected to enhance our understanding of, and abilities to coexist with and benefit from our biological environment.

## Publications

Stubben, C., M. Duffield, J. Song, J. Gans, and M. Wolinsky. Steps toward broad-spectrum therapeutics: discovering virulence-associated genes present in diverse human pathogens. 2009. *BMC Genomics.* **10**: 501.

# Coupling of Genetics and Metabolism and the Orgin of Life

*Hans J. Ziock*
20080716ER

## Introduction

The goal of this project is to demonstrate in an artificial process the most important capability of any living system, namely the use of external energy and resources to replicate its information system (in our case, a nucleic acid polymer, i.e. DNA). This is a problem that Nature must have solved in order to have life emerge and remains an underlying fundamental property of life today. To address this problem, the project seeks to modify and adapt an experimentally proven light-driven information-metabolic process that we previously developed. The modification consists of adapting the existing photo-chemically driven process to one capable of reproducing a DNA chain by activating short DNA fragments which base-pair with the original chain. The activation allows the activated fragments to bind to each other to form a continuous chain, which is a complimentary copy of the original information containing double stranded DNA. Such a reproduction of the information-metabolic complex is a hallmark of life. The process we are pursuing is far simpler than any such process in modern life and unique from any other being pursued by others in the scientific community.

On the science side, the assembly and demonstration of such an information reproduction system would represent a significant advance in the study of the emergence of life. On the application side, the demonstration of a simple non-enzymatic direct and switchable light-driven DNA ligation [polymerization of short DNA single strands (oligomers) or nucleotides resulting in DNA replication and possible activation] would potentially have an extraordinary impact in biochemistry and therapeutics.

We are also investigating the entire concept of information and its ties to life.

## Benefit to National Security Missions

This project supports the DOE/NNSA mission of supporting US leadership in science and technology. Developing and gaining insights into what information is has universal applications. By the end of the project we will have developed a technique for using light to drive and control DNA replication (a critical step in developing light controlled therapeutics and self-healing organic nanomaterials), learned about systemic issues related to the origin of life, and developed a more universal definition of information while understanding its relation to life.

## Progress

Progress in FY 2009 has been along several parallel fronts. We developed a new analytical tool for quantitative analysis of the metabolic reactions of a protocell that we are attempting to integrate into a protocell. We have demonstrated that we are able to get the needed strong association between all the elements of the protocell we are attempting to build, and that the underlying metabolic reaction mechanism we are trying to develop remains functional and is actually enhanced when the components are associated with each other. We have continued to work on the theoretical and experimental development of the proposed ligation (bonding) method of two short pieces of DNA on a DNA template to allow the duplication of the DNA and hence information component of the protocell. We have acquired additional diagnostic hardware that will enable us to implement and do the quantifying experimental measurements.

We have also been working on obtaining a better and more complete understanding of the general concept of information, which not only provides a new robust definition of information, but also establishes how information could have first originated, while simultaneously developing a strong linkage between life and the concept of information itself. This work is reported in one of the new papers.

Our work has resulted in a strong new collaboration with the University of Southern Denmark, and Hans Ziock has received the Hans Christian Anderson Fellowship there. The project has also resulted the recruitment of a new postdoc and the extended tenure and transfer of a second postdoc. Our work has also spun off two new projects, one sponsored by NASA and titled Prebiotic Formation of Membranes and the Role of Membranes in Energy Uptake: An Essential Step in the Origin of Protocellular Life, and one supported by the intelligence community and which is using the same underlying metabolic chemistry developed by the LDRD project and whose goal is to detect ionizing radiation via generation of an odorant.

Finally, the project represents the type of basic science that is critical to the continued recruitment of first class personnel to the Laboratory. We have successfully recruited a new highly qualified postdoc. who made the alternate list for the prestigious Director's postdoc award at the Laboratory.

To date the project has resulted in the publication of 6 papers listed in the reference section as well as the contribution of several chapters and assistance in the review/publication of the book Protocells, Bridging Nonliving and Living Matter, Ed. Rasmussen, S., Bedau, M.A., Chen, L., Deamer, D., Krakauer, D.C., Packard, N.H., Stadler, P.F., The MIT Press, Nov. 2008.

We have had an additional paper accepted for publication in Astrobiology: S. E. Maurer, D. W. Deamer, J. M. Boncella, P.-A. Monnard; Chemical Evolution of Amphiphiles: Glycerol monoacyl derivatives stabilize plausible prebiotic membranes; and have revised and updated another paper which is now ready for submission: S. A. Colgate, H. Ziock; A New Definition of Information and its Relationship to Life.

Finally, we are currently writing an invited review paper for Reports on Progress in Physics on protocells: Monnard, P-A., Fellermann, H., Goranovic ,G., Hanczyc, M.M., Ziock, H.-J., Boncella, J.M., Rasmussen, S.; Assembly of minimal living systems: Towards self-replicating nanomaterials; and are preparing a paper on the reaction kinetics associated with our protocellular chemical system.

## Future Work

Our goal is to experimentally demonstrate the key remaining missing feature in the production of an artificial protocell: The use of an information mediated metabolic process capable of harvesting external resources and energy to direct the replication of an information molecule (DNA). To achieve this, several steps are required. First, the various components of the protocell must be collocated. We have already added "tails" to our metabolic/information molecules that allow them to "stick" to our protocell. To optimize our system, we will continue to determine the range of conditions that preserve the functionality of metabolic/information molecules.

Currently our metabolic/information molecule is a ruthenium tris-bipyridine derivatized with a single nucleobase. In the proposed effort, this single nucleobase will be replaced by a DNA strand to meet the more standard definition of an information molecule. Attaching the DNA strand will be achieved by standard bioconjugate chemistry. By varying the DNA sequence, we will prove the specificity of the information content for metabolic reactions. That is, some strands yield a functional metabolic complex and others don't.

Next is information replication using the well-known complementarity of DNA bases. A short DNA template and 2 oligomers (even shorter DNA single-stands), which are complementary to the different halves of the DNA template, will be provided. One oligomer will be chemically activated, while the other has a protecting group attached. The oligomers can base-pair with the template, but must still be bonded end-to-end to form a continuous complementary strand. Our metabolic/information molecule will be used to link the two oligomers, thus replicating the template information. This molecule absorbs light energy and uses that energy to cleave the protecting group, allowing that oligomer to react with the activating group of the other oligomer yielding a continuous strand. Showing this light driven/controlled replication of the DNA is our final task. The needed preliminary work here is complete and we are now starting the actual chemical implementation.

## Conclusion

Learning and understanding how nature was first able to replicate information is fundamental to understanding life's origins and life's march to ever increasing complexity/capability. This is something that science has tried to discover throughout the ages. On the applied side, the demonstration of a method allowing one to artificially harvest light energy and applying it to reproducing the information system itself is the first step in the development of truly capable self-repairing materials and light switchable and controlled therapeutics. Imagine a nano-treatment system that could be switched on in specific locations or that's able to reproduce itself when needed.

## Publications

Protocells, bridging nonliving and living matter. 2008.

DeClue, M. S., P. - A. Monnard, J. A. Bailey, S. E. Maurer, G. E. Collis, H. - J. Ziock, S. Rasmussen, and J. M. Boncella. Nucleobase mediated, photocatalytic vesicle formation from ester precursor . 2009. *Journal of the American Chemical Society.* **131**: 931.

Fuchslin, R. M., H. Fellermann, A. Eriksson, and H. - J. Ziock. Coarse-graining and scaling in dissipative particle dynamics. 2009. *The Journal of Chemical Physics.* **130**: 214102.

Monnard, P. A., M. S. DeClue, and H. Ziock. Amphiphile nanostructures as model for artificial cell-like entities. 2008. *Current Nanoscience.* **4**: 71.

Rasmussen, S., J. A. Bailey, J. M. Boncella, L. Chen, G. Collis, S. Colgate, M. S. DeClue, H. Fellermann, G. Goranovic, Y. Jiang, C. Knutson, P. - A. Monnard, F. Mouffouk, P. Nielsen, A. Sen, A. Shreve, A. Tamulis, B. Travis, P. Weronski, J. Zhang, X. Zhou, H. Ziock, and W. H. Woodruff. Assembly of a minimal protocell. 2008. In *Protocells: Bridging Nonliving and Living Matter.* Edited by Rasmussen, S., M. A. Bedau, L. Chen, D. Deamer, D. C. Krakauer, N. H. Packard, and P. F. Stadler. , p. 125. Cambridge, Massechusetts: MIT Press.

Tamulis, A., V. Tamulis, H. Ziock, and S. Rasmussen. Influence of water and fatty acid molecules on quantum photo-induced electron tunneling in self-assembled photosynthetic centers of minimal protocells. 2008. In *Multiscale Simulation Methods for Nanomaterials.* Edited by Ross, R. B., and S. Mohanty. , First Edition, p. 9. Hoboken, N.J: Wiley.

Zhou, X., Y. Jiang, S. Rasmussen, and H. Ziock. A method to bridge different-level coarse-grained models by estimating free energies of high-dimensional conformations: jump-in-sample simulations. 2008. *The Journal of Chemical Physics.* **128** (17): 174107.

# Using Small Molecules to Control RNA Conformations

*Kevin Y. Sanbonmatsu*
20090163ER

## Introduction

A riboswitch is a molecule inside a bacterium that turns genes on or turns genes off. The riboswitch is controlled by small molecules present inside the cell, such as vitamins, amino acids, and metabolites. They are exciting because they represent a new form of gene control that was only recently discovered. They have applications in the development of new antibiotics. How they work is not understood in atomic detail. If we can understand how they work, then we can design better ones. Upon binding of small molecules, molecular switches called riboswitches are able to control genes. Riboswitches can easily discriminate between similar small molecules. Considering that a prototype riboswitch-based biosensor chip has been constructed, riboswitches are excellent candidates for next generation biosensors. The sensitivity to minute differences between ligands also makes the riboswitch a promising target for antibacterial drug design. Drugs that target riboswitches have the potential to affect only the process controlled by the riboswitch without producing harmful side-effects.

Our goal is to understand how these switches switch. We will address the following three questions,

1. How does the small molecule bind?
2. How does binding result in switching? and
3. How tunable is the switch?

In particular, we will investigate the hypotheses:

- Stabilization of a compact binding domain upon ligand recognition occurs through a series of intermediate states.
- Switching occurs by morphing between the two riboswitch states through a series energetically favorable intermediates, as opposed to unfolding and refolding.

## Benefit to National Security Missions

The project is directly related to the “Biological Sensor Systems” of the “Ubiquitous Sensing” grand challenge and the sensing component of the “Biology of Infectious Agents” key capability. The project is also related to the “Biology of Infectious Agents” by its applications to antibiotic design.

## Progress

In this year, we completed every objective that was stated in our proposal for year one. We also made significant headway on one objective for year twour results were featured on the cover of Biophysical Journal in January 2009. Below we outline our results.

- Performed extensive chemical protection experiments on the SAM riboswitch and determined that long range interactions affect SAM binding. To study the conformational change of the S-adenosylmethionine (SAM) riboswitch that occurs upon SAM binding, we performed a large suite of chemical protection experiments that yield information on the change in structure. We also performed nucleotide analog interference modification (NAIM) studies to determine the effect of long-ranged interactions on SAM binding. We found that the riboswitch undergoes an open-to-closed transition during binding and we found that long-range interactions are critical.

- Performed Go-model calculations on the folding of the SAM riboswitch. Our model is an all-atom structure-based model and is the first of its kind for RNA. Our simulations were published in Biophysical Journal and reveal the order of helix formation. They also show the range of conformation that the riboswitch undergoes and were used to design single molecule experiments. In particular, Our results suggest that folding of the P1 (non-local) helix is rate limiting in aptamer domain formation. S-Adenosylmethionine (SAM) binds to a preformed P3 helix and assists folding of P1 by reducing the associated free energy barrier. These finding are consistent with the correlated P1 folding/binding event being the functional “switch”.

- Performed explicit solvent simulations of the SAM riboswitch using replica exchange molecular dynamics. Here, we simulated the inner core of the SAM aptamer domain, using 48 replicas. The total sampling was ~ 1.8 microseconds. These simulations show that the binding region undergoes a base-flipping transition consistent with our experiments. The simulations are also consistent with the x-ray all atom crystallography structures of Batey, who determined the structure in the presence and absence of SAM.

- Performed single molecular fluorescence experiments of SAM binding. Our experiments show the various fluorescence energy resonance transfer (FRET) states taken by the SAM riboswitch in the bound and unbound states. Our single molecule experiments use surface immobilization and have been done in collaboration with Scott Blanchard at Cornell University.

- Finally, we have constructed a new experimental assay to study the switching of the riboswitch. This two-piece system monitors switching in a controlled environment, competing the aptamer domain against the anti-terminator. We have studied the effect of SAM on switching and the effect of various mutants. Our chemical protection studies were used to discover the optimal mutants to study the mechanism of switching. We mutated an important interaction region called the pseudo-knot. The mutations in the pseudo knot had a profound effect on switching. This has set up and laid the foundation for a very extensive study of switching, both via simulation and experiment. Our results constitute the first study of switching in a controlled environment. We study the effect of key tertiary contacts and how or if they can control changes in the secondary structure of the SAM switch.

## Future Work

We will investigate small molecule signal detection by controlling the conformations of RNA-based molecular switches called riboswitches. Upon binding of small molecules, riboswitches are able to precisely control gene expression. A riboswitch may take on one of two folds, depending on the presence or absence of this small molecule. Because riboswitches are highly specific, they can easily discriminate between similar small molecules. Our goal is to understand how these switches switch. We will address the following questions:

- How does the small molecule bind?

- How does binding result in switching?

- How tunable is the switch?

These hypotheses will be tested using an approach that integrates experiment and simulation. High performance computing simulations based on basic physics principles will be used to design and interpret single molecule fluorescence experiments. Single molecule experiments will be performed to isolate intermediate states and to provide constraints for simulations. The study will be the first single molecule and first computational investigation of the switching mechanism. Our results on the molecular mechanism will shed light on the more general problem of gene regulation by non-coding RNAs.

## Conclusion

We will use computers to figure out how to do the single molecule experiments, specifically, where to place fluorescent labels on the biomolecule. We will also use biochemical experiments to help with this. We will use single molecule experiments to study movement of the riboswitch. Our goal is to learn more about the process of switching and the process of small molecule binding to the switch.

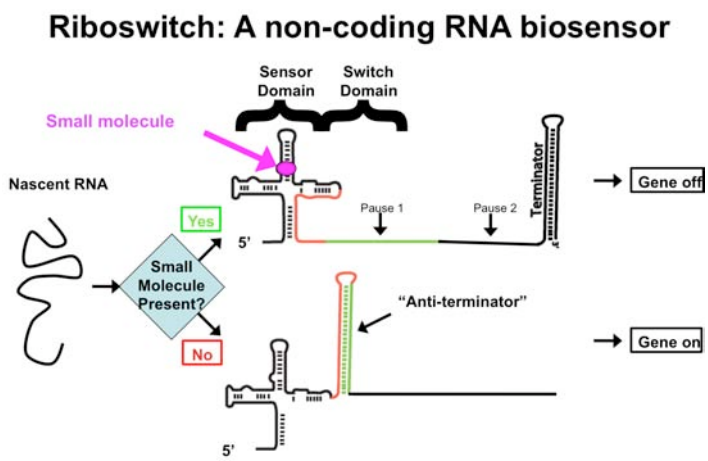


*Figure 1. Schematic of a specific type of biosensor called a riboswitch. After nascent RNA of the riboswitch is transcribed, it folds into one of two shapes depending on the presence of a small molecule (in this case S-adenosylmethionine, or SAM). If the shape containing the terminator helix is formed , then the gene expression is terminated. Otherwise, the gene expression occurs and the corresponding protein is synthesized.*

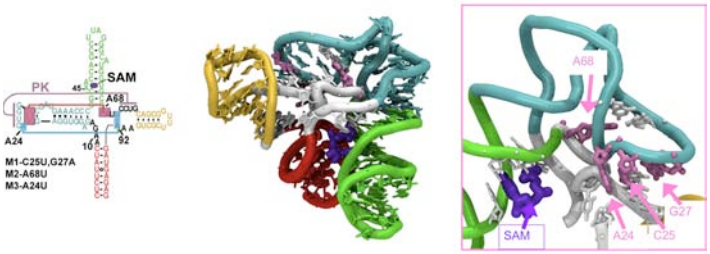


*Figure 2. 3-D structure of riboswitch sensor domain (structure determined by Batey and co-workers, Nature 2006). The small molecule controlling the switch is SAM. Left, 2-D representation. Middle, 3-D structure. Right, 3-D interactions that are changed by mutations to test the effect of 3-D interactions. Colors, different parts of the riboswitch.*

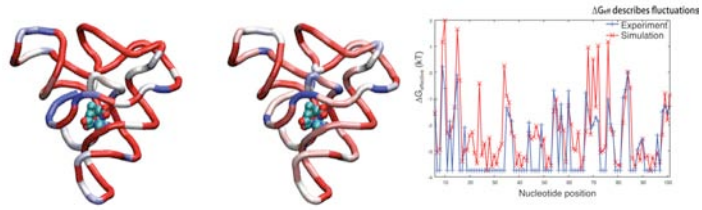


*Figure 3. Comparison between simulation and experiment. Left: fluctuations in experiments. Middle, fluctuations in simulations. Right, free energy estimates for each position in riboswitch for experiment (blue) and simulation (red).*

## Publications

Whitford, P. C., A. Schug, J. Saunders, S. P. Hennelly, J. N. Onuchic, and K. Y. Sanbonmatsu. Nonlocal helix formation is key to understanding S-adenosylmethionine-1 riboswitch function. 2009. *Biophysical Journal.* **92** (2): L7.

Whitford, P. C., J. K. Noel, S. Gosavi, A. Schug, K. Y. Sanbonmatsu, and J. N. Onuchic. An all-atom structure-based potential for proteins: bridging minimal models with all-atom empirical forcefields. 2009. *Proteins: Structure, Function, and Genetics.* **75** (2): 430.

# Functional Gene Discovery Using RNAi-based Gene Silencing

*Elizabeth Hong-Geller*
20090202ER

## Introduction

Human pathogens have evolved sophisticated mechanisms by which to attack the host immune system. *Yersinia pestis*, the causative agent of plague, is a CDC Category A pathogen with bioweapon potential, and thus represents a high-value target for the development of novel therapeutic strategies [1]. *Y. pestis* employs multiple virulence strategies during host infection, including the type III secretion system (TTSS), a "syringe-like" needle complex that injects virulence proteins, or Yop effectors, into the host cell. (Figure 1A) In the proposed study, we will identify host proteins that are targeted by *Y. pestis* during infection using RNA interference (RNAi), a powerful tool for analyzing gene function by silencing, or inactivating, target genes through the specific destruction of their mRNAs. (Figure 1B) Small interfering RNAs (siRNAs) are short RNA sequences that can silence the gene to which its sequence is complementary [2]. We will perform high-throughput genome-wide screens and more directed automated confocal microscopy studies to select for genes, that when silenced, lead to inhibition of *Y. pestis* infection. From these functional genomics studies, we will identify host proteins targeted by *Y. pestis* and thus, be able to exploit their associated mechanisms of pathogenicity to develop therapeutic countermeasures against *Y. pestis* infection.

## Benefit to National Security Missions

This project will support the DOE/NNSA mission in Threat Reduction by enhancing our understanding of host-pathogen interactions and biodefense capabilities. It is important to the support of other missions of the Laboratory as well (e.g., Homeland Security), but not to the exclusion of the DOE/NNSA missions. We have already secured funding from DTRA to use our methodology to investigate host genes targeted by *Burkholderia pseudomallei*.

## Progress

The specific research objective of this proposal is to identify and validate host proteins that are targeted by *Y. pestis* during infection. At the beginning of FY09, we hired an excellent post-doc, Sofiya Micheva-Viteva, to perform many of the molecular and cellular experiments in the project.

### Construction of in-house siRNA library by enzymatic engineering of cDNA libraries

For the construction of the human siRNA library, we had purchased two cDNA libraries derived from human RNA, MegaMan Human Transcriptome Library (Stratagene) and Human Peripheral Blood Library (Open Biosystems), in order to ensure complete coverage of genes from the immune system. We performed a set of complex molecular cloning steps that encompassed PCR amplification of the human genes, digestion of the PCR products with select restriction enzymes to produce blunt ends, cloning of PCR fragments into a Y-linker, generation of mature 18-20 nt siRNAs, and final cloning into the retroviral vector pPRIME-CMV-GFP-FF3. To validate the siRNA library construction, we selected 192 different constructs, isolated the plasmid DNA, sequenced the siRNA inserts, and aligned the library sequences with human genome databases using BLASTN. We obtained about 35 positive clones that were complementary to human genes, which will nucleate our planned siRNA library. Currently, we are optimizing steps in our cloning strategy to increase the cloning efficiency of the library construction.

### Establishing infection model between *Yersinia* and human cells expressing siRNAs

We are testing a variety of host immune responses to *Yersinia* infection to develop an assay that can be used in our high-throughput screening, including cell viability/death, actin cytoskeletal changes, transcription factor activation, and cytokine release. (Figure 2) Since *Yersinia spp* are not obligatory intracellular pathogens, we cannot use a simple intracellular growth assay to measure *Yersinia* amplification. We need to look for morphological or biochemical changes in the host cell as a response to bacterial infection. Currently we are using the pathogenic *Yersinia enterocolitica* WA0:8 strain to assay activation of apoptosis and cell death in the HeLa epithelial cell model. *Yersinia spp* infection of HeLa cells induces a

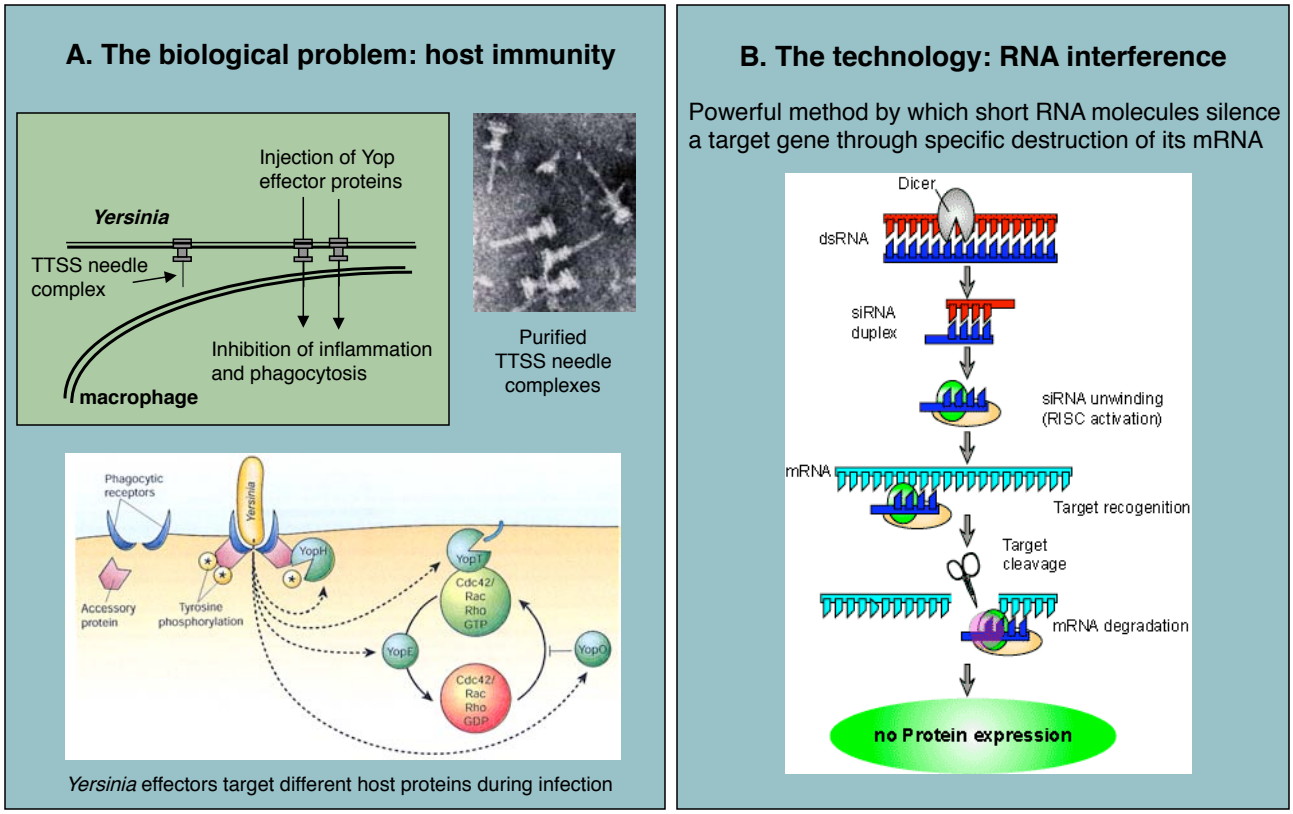


*Figure 1. Yersinia pestis Type III secretion system and siRNA methodology*

similar physiological response found in natural target cells of monocytic or lymphoid origin, and HeLa cells can be transfected at a 100-fold higher rate to increase the overall efficiency of the HTS screen.

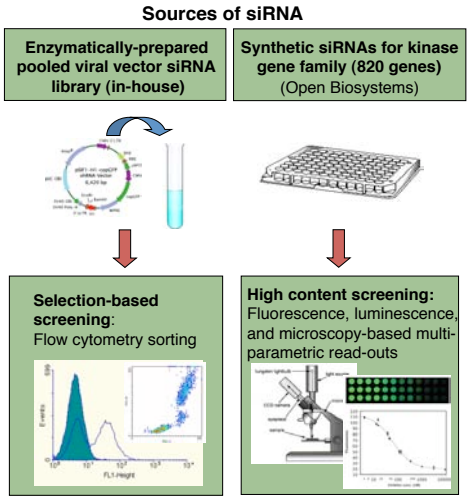


*Figure 2. High-throughput genome scale loss-of-function screens using siRNA libraries*

Surprisingly, the *Y. enterocolitica* WA0:8 strain induced close to 100% host cell death at MOI 100 after 20 hrs of infection, compared to ~40% cell death by pathogenic strains of *Y. pestis* (KIM, CO92). This difference can be attributed to the poor transfer of the *Yersinia* YopP/J effector virulence protein into the host during infection in *Y. pestis* compared to *Y. enterocolitica* [3]. Given its strong cell death phenotype, we have decided to use *Y.enterocolitica WA0:8* for the initial HTS assay to identify siRNAs that inhibit *Yersinia* pathogenicity. A secondary screen will then be performed to identify host genes targeted by *Y. pestis* by expressing the *Y. pestis* YopP/J gene directly in host cells, instead of using the whole *Y. pestis* bacteria, to more strongly stimulate a host immune response.

**Performing genomic screen using shRNA libraries**

To complement our genomic screens, we have obtained two sub-family short hairpin (shRNA) libraries for Kinase genes (~760 genes, ~2000 constructs) and Druggable target genes (~7000 genes, ~20,500 constructs) cloned into a lentiviral vector pGIPZ from Open Biosystems. These libraries will be used in HTS screens using fluorescent, luminescent and automated confocal microscopy assays to identify host genes targeted by *Yersinia* during infection. (Figure 2) These shRNA libraries come as bacterial stocks, so we are in the process of generating high quality plasmid DNA from the bacterial stocks for host cell transfection experiments. We have generated purified DNA from the entire shRNA kinase library and have started DNA plasmid isolation from the druggable target library.

We have spent a lot of effort to optimize the experimental

conditions for the HTS assays, including equal transfection levels of shRNA plasmid DNA into HeLa cells in a 96 well format, GFP and biomarker analysis of transfected cells in a HTS flow cytometry mode, and generation of siRNAs expressed as retroviruses for high transfection efficiency in host cells. It is imperative to achieve a 70% or higher transfection efficiency to effect target gene downregulation more than two fold and obtain 50% differentiation between experimental and control samples in the assay. Before optimizing the transfection protocol we were able to get on average only 20% of HeLa cells expressing the GFP marker included in the lentiviral vector pGIPZ. After the optimization, our transfection protocol resulted in 80% or higher GFP positive cells. Currently we are performing an initial genomic screen based on the cell viability assay using HeLa cells transfected with shRNAs from the Kinase Library in 96-well format and infected with *Y.enterocolitica WA0:8*.

**Analysis of *Yersinia* infection of host cells using automated confocal microscopy**

In the last year, we have been developing the capability to perform HTS to study *Yersinia* infection of host cells using automated fluorescence microscopy platform. We have acquired and installed a high sensitivity CCD camera for brightfield and UV-fluorescence excitation of samples. This system is integrated with the laser scanning confocal microscope to enable either type of light source to be sequentially used in the imaging platform, thus allowing for the use of more fluorophores and faster image acquisition, as well as providing the laser scanning system with higher spatial resolution and greater spectral selectivity. We have optimized methods of stitching together acquired images to build mosaic images with much greater field of view for each objective, without sacrificing resolution. We have developed protocols to stain filamentous and monomeric actin in host cells to use as an assay for changes in actin cytoskeleton in response to *Yersinia* infection. Finally, to employ this type of acquisition across hundreds of sample conditions requires high throughput data processing and machine learning techniques. We have acquired software for quantitatively evaluating the morphology of these cells to identify the most interesting samples for further study. This type of technique is similar to those used for the remote sensing and satellite image analysis fields, but in this case applied to microscopic samples.

## Future Work

In the second year of this project, we will continue with some of the tasks from the first year of the proposal, including completion of generating plasmid DNA from the druggable target library and construction of a siRNA library derived from human lymphocyte cDNA. We will perform HTS screens to identify host genes targeted by *Y. enterocolitica* and *Y. pestis* during infection. We plan to use the kinase and druggable target libraries in 96 well format to screen for siRNAs that block *Y. enterocolitica* or *Y. pestis* infection of human epithelial or macrophage cell lines. We will use a number of immune response assays, such as apoptosis, changes in the actin cytoskeleton, and cytokine release, as the measure of host infection. We will also use confocal microscopy to visualize changes in *Y. pestis*-infected host cells upon expression of defined siRNAs. We have purchased retroviral siRNA screening library pools (Open Biosystems) that contain inhibitory sequences against practically all human genes, in a non-renewable format, and will develop these siRNA pools for high-throughput screening assays such as by flow cytometry cell sorting or plate screening methods. Candidate genes will then be sequenced and further validated using a variety of molecular biology assays in Year 3.

## Conclusion

This project will contribute significantly to the study of host-pathogen interactions, a key strategic research capability that supports the LANL mission of biothreat reduction and protection of national security. Yersinia pestis, a potential agent of bioterrorism, is a CDC Category A pathogen, signifying great potential risk for adverse impact on public health. The proposed research will seek to identify host proteins targeted by Y. pestis during infection. New strategies to counteract Y. pestis infection, based on increased fundamental understanding of Y pestis virulence, can greatly impact our ability to contain potential outbreaks of plague in the population.

## References


1. Cornelis, G. R.. Yersinia type III secretion: send in the effectors. 2002. *Journal of Cell Biology.* **158**: 401.

2. Hannon, G. J., and J. J. Rossi. Unlocking the potential of the human genome with RNA interference. 2004. *Nature.* **431**: 371.

3. Zauberman, A., S. Cohen, E. Mamroud, Y. Flashner, A. Tidhar, R. Ber, E. Elhanany, A. Shafferman, and B. Velan. Interaction of Yersinia pestis with macrophages: limitations in YopJ independent apoptosis. 2006. *Infection and Immunity.* **74**: 3239.


## Publications


Micheva-Viteva, S., K. Rector, and E. Hong-Geller. Functional gene discovery in Y. pestis infection using RNAi-based gene silencing. To appear in *2009 Chemical and Biological Defense Science and Technology Conference.* (Dallas, TX, 16-20 Nov. 2009).

# A Visionary New Approach to Assess Regional Climate Impacts on Vegetation Survival and Mortality

*Nathan G. Mcdowell*
20090305ER

## Introduction

Models of climate change and its impacts on ecological systems must be accurate at regional scales for predictions to be of use to policy-makers. By regional scale, we mean at the level of individual states and smaller. We propose to dramatically improve climate change and climate impacts modeling at the regional scale through a two component, integrated project. Our first component will test cutting edge theory of plant survival and mortality with both empirical and modeling efforts to develop the first mechanistic model of vegetation dynamics in response to climate. Our second component will improve downscaled predictions of climate over the 50 year timespan. By downscaled we mean taking climate predictions made at the global level and scaling them to the scale of individual states and smaller. We will integrate these two facets into an improved model of regional climate change and ecological impacts.

## Benefit to National Security Missions

This project supports the Office of Science mission to understand and predict climate change and its ecological impacts.

## Progress

Our progress to date has exceeded our expectations. We have hired two top-notch postdocs, Rosie Fisher and Sara Rauscher. They have incredibly strong backgrounds in dynamic vegetation modeling and regional climate modeling, respectively. They began at LANL in March 2009. Both postdocs have successfully conducted initial runs of our goal model CLM (Common Land Model). Fisher has successfully tested our hybrid to CLM, which is SPA (soil plant atmosphere model) against vegetation and ecosystem carbon cycle observations made over 15 years at TA-51. Her analyses have resulted in novel understanding of the controls over surface energy exchange after vegetation mortality, and are already providing publication quality figures. A manuscript is in preparation. In addition, Fisher and McDowell have assessed the impact of ecological parameters not typically included in CLM, such as seed dispersal, on model output. The striking results are the basis for a manuscript which is now in review. Rauscher has successfully run the regional climate model that is part of CLM, WRF (Weather Research and Forecast) using a 50 km mesh over the US with an embedded 4 km cloud-resolving mesh over the Southwest USA. Her comparisons of predicted verses observed climate are very encouraging, and suggest that future precipitation declines in southwestern USA may be drastic. Both postdocs have attended meetings with NCAR (National Center for Atmospheric Research), the primary owner of CLM and WRF. Fisher is currently (Fall 2009) working at NCAR to complete the integration of CLM with her models developed at LANL. Both PI's (Ringler and McDowell) are also heavily engaged in developing the relationship with NCAR and the other major players developing CLM for port into CCSM, the Community Climate System Model. CCSM is the primary American model for IPCC climate predictions. Together we have given five invited presentations regarding this project, and McDowell presented testimony to Congress regarding the need for this type of research. Additionally, McDowell has one published paper, two in press, and a fourth in review (not including the one that Fisher lead), all of which cite LDRD ER support. Rauscher is preparing two manuscripts under LDRD ER support, one of which will be submitted to PNAS. We have made numerous presentations citing this LDRD support, and have already begun the process of obtaining follow-on funding.

Rauscher and Ringler hosted a three-day workshop in July that brought together national leaders in regional climate modeling. While the workshop was sponsored by IAS, the workshop would not have been possible without the LDRD funding necessary to hire Rauscher. The LDRD ER support was cited in the meeting summary that has been accepted to EOS.

## Future Work

Our current overall focus is to couple the improved downscaled atmosphere climate simulations (Rauscher and Ringler) to the improved land-surface model

simulations (Fisher and McDowell). This is the major objective for the next 12 months. Sub-objectives to help us along this path are many. On the terrestrial side, Fisher and McDowell are focused on conducting final tests of the accuracy of the land surface model at the plot to region scale. This includes testing if we get the right results for the right reasons (getting the mechanisms correct). On the climate side we will be focused on comparing our simulations to observations to gain confidence in our ability to model the present-day climate of the Southwest USA.

Second, models currently run at large grid scales that do not capture the heterogeneity of climate drivers that exist within regions, leading to "average" climate simulations that may not be representative of smaller areas. To overcome these problems, we will test cutting edge theory of plant survival and mortality with both empirical and modeling efforts to develop the first mechanistic model of vegetation dynamics in response to climate.

Rauscher and Ringler will be working toward a better understanding of the regional hydrological cycle through the analysis of both observational data and model simulation data. With an understanding of the "baseline" hydrological budget for the Southwest USA, we will be able to better understand the consequences of further changes to the hydrological cycle driven by greenhouse gas emissions.

## Conclusion

This project is developing fundamental understanding of climate change and of ecological impacts. We are developing a tool that can be used to make regional scale predictions of climate change and its impacts. Improved understanding will allow this tool to be more accurate, greatly enhancing our ability to inform policy makers of coming changes within their regions.

# Membrane Micro-chromatography: A Novel Approach to Preparative Nucleic Acid Sample Processing

*Goutam Gupta*
20090363ER

## Introduction

The original project was conceived by Dr. R. Bruce Cary. The current formulation of the Specific Aims and Deliverables retain the original scope of the project although minor adjustments have been made to ensure the success of the project with the in-house expertise. The work plan also leaves room for collaboration with Dr. Cary without compromising his entrepreneurial effort outside LANL.

The project focuses on developing the lateral flow microarray (LFM) platform that allows detection of specific signatures from a pathogen as well as host biomarkers that report different stages of pathogen-induced infection. The LFM is ideally suited for the detection of nucleic acid signatures from the pathogen and host. The LFM platform design involves four key steps:

1. Discovery and validation of pathogen and host signatures for a particular type of human, animal, or plant infection.
2. Design and immobilization of an LFM platform with capture probes.
3. Extraction of nucleic acid from the infection sample and isothermal amplification.
4. Colorimetric detection of nucleic acid signatures with the aid of detection probes.

Figure 1 schematically describes the steps 1 through 4. Figure 2 shows how the LFM platform allows detection of two different pathogens based upon different sets of host markers.

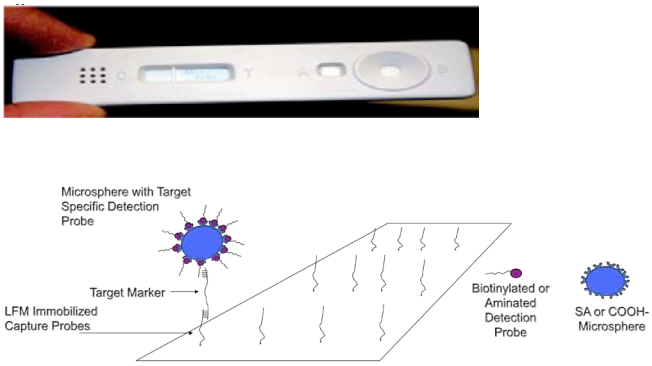


*Figure 1. LFM platform and detection principle*

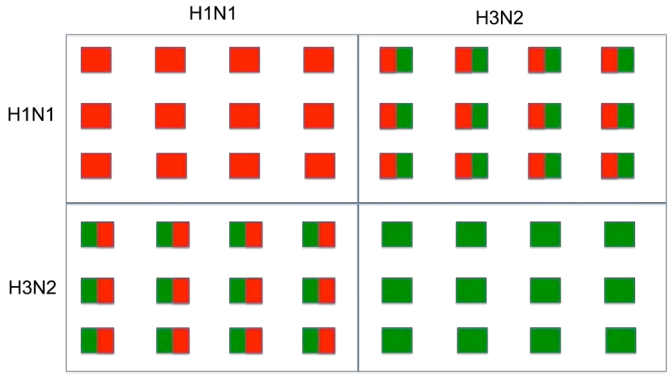


*Figure 2. Desirable set of host markers for detection on the LFM platform. This illustrates how common and specific markers for infection by two different influenza strains (e.g. H1N1 in red and H3N2 in green) may be interpreted on this platform.*

## Benefit to National Security Missions

This project will support DOE missions in threat reduction and non-proliferation by providing a previously unavailable capacity to reliably detect DNA signatures and biological threats under field conditions. Additionally, the technology supports missions in homeland security by providing the capability to detect, identify and respond to a biological threat.

## Progress

For the first year (FY09), we focused on designing an LFM platform with two specific objectives:

1. To detect host gene markers that appear early during influenza A infection

2. To distinguish early infections by strains of influenza A with high and low pathogenicity

With the flu threat looming large, it is timely and appropriate that we develop a platform for detecting influenza A infection during the early stages to facilitate better disease management. As shown in Figure 3, the influenza A lifecycle consists of multiple steps. First, the virus attaches to the cell surface and then enters the host via a process called endocytosis. Upon entry, the influenza A virus utilizes the host machinery to complete the rest of the steps in viral lifecycle that include replication, transcription, and translation of viral RNA, packaging and assembly of viral RNA and proteins, and finally formation of viral envelop and release of mature virus particles. The host-virus interactions trigger two competing responses: one in which the host immune defense system attempts to clear the virus and the other in which the viral machinery tries to hijack the host cellular systems to propagate its growth and establish infection. Viral attachment/entry and replication/transcription/translation occur during the first 24 hours of influenza A infection. Two sets of host markers are induced. One is classified as the set of anti-viral genes implicated in the suppression of viral lifecycle whereas the other is classified as the pro-viral genes involved in promoting viral lifecycle. The host pro-viral genes are expected to dominate influenza A infection with high pathogenicity strains whereas host anti-viral genes are expected to dominate influenza A infection with low-pathogenicity strains. Indeed, that was the trend of host gene expression that we observed for the high-pathogenicity H1N1 and H3N2 low-pathogenicity strains. As shown in Figure 2, the LFM detection platform should typically contain host markers unique to H1N1 and H3N2 and common to both of them; these genes are induced relative to the negative control.

We, in collaboration with LANL (PI: Ruy Ribeiro, T-6) and external groups (Lovelace, UC, Univ. Florida, USDA), have been developing host-pathogen interaction studies to discover and validate host response markers during the early stages of human and plant infections using gene and protein expression analysis [1-2]. For H1N1 and H3N2, we relied on the whole genome microarray data showing altered (up or down) expression of genes due to the infection of the human respiratory tract from studies conducted by various laboratories including ours at LANL [3-7]. We selected a set of host genes specific for influenza A infection and validated them by real-time Polymerase Chain Reaction (PCR) by designing appropriate primers for the test genes. Figure 3 shows the host markers (about 200 in all validated by real-time PCR) for H1N1 and H3N2 infection (both common and specific ones as described in Figure 2). Our primary focus is on the host genes that belong to the innate immune pathways and are induced 0-24 hours-- i.e. during viral attachment, entry, replication, transcription, and translation. We identified the 16 most informative genes for the LFM platform belonging to 4 classes (4 in each class) representing: (i) negative controls not induced by H1N1 and H3N2 infections, (ii) genes unique to H1N1, (iii) genes unique to H3N2, and (iv) genes common to both of them. We are currently designing capture and target probes (see Figure 1) for designing an LFM platform for the detection of H1N1 and H3N2 infection.

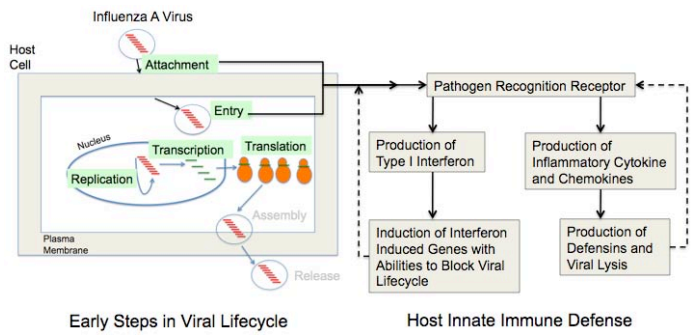


| Pathway | Relevance | Representative Genes |
|---|---|---|
| a. Inflammatory Cytokine/Chemokine | Overstimulation is correlated with disease symptoms | TNF-α, IL1β, IL6, CXCL9-11, SOCS1,3* ; *block inflammation |
| b. Anti-viral Type I Interferon | Can block viral lifecycle but can be suppressed by pathogenic strains | IFN-α/β, MXA/B, OAS, IFITs, GBP |
| c. Anti-microbial Defensin | Can lyse the virus but can be blocked by pathogenic strains | hβD-2, hαD-5 |
| d. Pathogen Recognition Receptor | Can induce pathways b & c but can be blocked by pathogenic strains | TLR2/3, TRIMs, NOD2/27 |
| e. Solute Carrier | Modified during virus attachment and entry can be toxic to the host | SLC26, SLC2, SLC15 |

*Figure 3. Schematic representation of the host innate immune genes (highlighted in green) that are induced in the early stages of viral infection. Note the presence of feedback loops (broken arrows between gene groups) results in amplified levels of innate immune genes. The table shows the putative host markers for H1N1 and H3N2 specifically in relation to gene and pathway relevance in early immune response to flu virus.*

We have also obtained samples from Lovelace to analyze H5N1 (both high and low-pathogenic) infections. Note that H5N1 represents influenza strains that jumped from birds to humans whereas H1N1 and H3N2 strains can circulate in both human and swine populations. In addition, we are preparing to perform experimental analysis of host micro-RNA using Solexa sequencing. This involves isolation of micro-RNA (small in size) and training to operate the Solexa sequence experiment. Note that micro-RNAs are specifically induced during influenza A infection. Each micro-RNA targets a specific gene and control the level of the protein produced by the gene. Thus, in addition to gene expression (i.e., level of messenger RNA as described in Figure 3), specific micro-RNAs can also be informative host signatures of influenza A infection.

(*Work presented in refs. 1-2 was partially supported by this (20090363ER) project.)*

## Future Work

Specifically, we propose to accomplish the following aims.

**Specific Aim 1: LFM fabrication**
DNA oligonucleotide probes complementary to the target signature sequences will be deposited onto the lateral flow nitrocellulose surface via UV cross-linking. Multiple probes targeting multiple pathogen signatures and/or host biomarkers will be deposited on the LFM surface.

**Specific Aim 2: Sample preparation**
Host or pathogen cells from biological sample will be isolated by immuno-capture using surface specific antibodies. Nucleic acids will then be isolated and purified from the pathogen and/or host cells by using in-house methodology developed Paige Pardington.

**Specific Aim 3: Target Amplification**
The target sequences will first be amplified by conventional PCR with thermocycling and selected PCR products will further be tested by real-time PCR for quality control. After establishing quality control, isothermal Nucleic Acid Specific Based Amplification (NASBA) ' will be performed on the target sequences.

**Specific Aim 4: Detection on LFM**
The amplified targets (from pathogen and host) will be detected on the LFM by a sandwich assay. In addition to the probes on the LFM surface (mentioned above), the detection scheme utilizes complementary nucleic acid sequences on the color beads that are added in the flow. The sequence on the color bead is designed to hybridize with the same target sequence that is complementary to the probe on the LFM. The simultaneous binding of the probes on the bead and LFM surface is detected by colorometric change.

## Conclusion

Assessment of early stages of infection is a crucial need for effective surveillance and management of human, animal, and plant diseases caused by natural, emerging, and engineered pathogens. In this regard, a set of host (human/animal/plant) genes that are specifically altered during the early phase of infection can be sensitive as well as serve as informative markers for such assessment and possibly for pre-symptomatic diagnosis. A significant advance in the surveillance and management of infectious diseases requires *accurate identification of these markers for a particular infection* and *rapid, sensitive,* and *efficient detection of these markers on a platform amenable to laboratory and field use*.

This project builds a LANL capability in:

1. Identification and validation of nucleic acid signatures for pathogen-specific infection (markers for both the pathogen and the host).
2. Design of lateral flow microarray that detects the host and pathogen markers of infection using RNA from infected cells.

## References

1. Dandekar, Abhaya M., F. Martinelli, C. Davis, A. Bhushan, W. Zhao, O. Fiehn, K. Skogerson, G. Wohlgemuth, R. D'Souza, S. Roy, R. L. Reagan, D. Lin, R. B. Cary, P. Pardington, and G. Gupta. Analysis of early host responses for asymptomatic disease detection and management of specialty crops. To appear in *Critical Reviews in Immunology.*

2. Zeytun, A., A. Chaudhary, P. Pardington, R. B. Cary, and G. Gupta. Induction of cytokines and chemokines by toll-like receptor signaling: strategies for control of inflammation. To appear in *Critical Reviews in Immunology.*

3. Baskin, C. R., H. Bielefeldt-Ohmann , T. M. Tumpey, P. J. Sabourin, J. P. Long, A. García-Sastre , A. E. Tolnay, R. Albrecht , J. A. Pyles, P. H. Olson, L. D. Aicher, E. R. Rosenzweig, K. Murali-Krishna , E. A. Clark, M. S. Kotur, J. L. Fornek, S. Proll , R. E. Palermo, C. L. Sabourin, and M. G. Katze. 3. Early and sustained innate immune response defines pathology and death in nonhuman primates infected by highly pathogenic influenza virus. 2009. *Proceedings of the National Academy of Sciences U S A.* **106** (9): 3455.

4. Baskin, C. R., A. García-Sastre , T. M. Tumpey, H. Bielefeldt-Ohmann , V. S. Carter, E. Nistal-Villán , and M. G. Katze. Integration of clinical data, pathology, and cDNA microarrays in influenza virus-infected pigtailed macaques (Macaca nemestrina). 2004. *The Journal of Virology.* **78** (19): 10420.

5. Kash, J. C., C. F. Basler, A. García-Sastre , V. Carter, R. Billharz, D. E. Swayne, R. M. Przygodzki, J. K. Taubenberger, M. G. Katze, and T. M. Tumpey. Global host immune response: pathogenesis and transcriptional profiling of type A influenza viruses expressing the hemagglutinin and neuraminidase genes from the 1918 pandemic virus. 2004. *The Journal of Virology.* **78** (17): 9499.

6. Zeytun, A., J. Foster-Harris, H. Cai, P. Pardington, R. B. Cary, R. Ribeiro, K. Harrod, and G. Gupta. Early responses to influenza virus exposure. Presented at *American Society for Microbiology Proceedings of the 6th International Innate Immunity Conference.* (Crete, Greece, 21-26 June 2009).

7. Kobasa, D., S. M. Jones, K. Shinya, J. C. Kash, J. Copps, H. Ebihara, Y. Hatta, J. H. Kim, P. Halfmann, M. Hatta, F. Feldmann, J. B. Alimonti, L. Fernando, Y. Li, M. G. Katze, and Y. Kawaoka. Aberrant innate immune response in lethal infection of macaques with 1918 influenza virus. 2007. *Nature.* **445**: 319.

# Isotopic Tracer for Climate Relevant Secondary Organic Aerosol

*Thomas A. Rahn*
20090425ER

## Introduction

Aerosols by definition are simply fine solid particulates or liquid droplets suspended in a gas. In Earth's atmosphere these can take many forms - from fine dust particles to clusters of inorganic molecular species to amalgams of complex organics and as a whole, they have a profound influence on Earth's radiation budget, cloud and precipitation distribution and climate. The least understood of the atmospheric aerosols are the Secondary Organic Aerosols (SOA), those aerosols that result from the oxidation and coalescence of volatile organic gaseous compounds. In this proposed work, we will begin to unravel some of the intricacies of the formation and evolution of these SOA by applying state of the art isotopic and ultrahigh resolution mass spectrometry techniques, as well as chemometric techniques. In particular, we will develop novel triple oxygen isotope analytical techniques (oxygen having three stable isotopes of atomic masses 16, 17 and 18) that will elucidate pathways of oxidation and details of structure that have heretofore been elusive. These techniques will be applied to SOA generated in a series of controlled experiments in our laboratory at LANL. In addition we will utilize the National High Magnetic Field Laboratory to analyze the SOA by ultrahigh resolution mass spectrometry thus providing precise empirical formulas for SOA produced in these experiments. We will then begin the process of comparing these laboratory results to actual atmospheric samples collected in a few select environments to determine how the origin of volatiles and subsequent processing and environmental exposure control the evolution of these complex compounds.

## Benefit to National Security Missions

By identifying the production pathways of secondary organic aerosol formation, this project will support DOE's Office of Science Atmospheric Science Program's stated mission "to develop a comprehensive understanding of the atmospheric processes that control the transport, transformation, and fate of energy related chemicals and particulate matter" and in particular the focus of "characterization of aerosol properties, and transformations."

## Progress

As stated in our proposal, our year one milestones are to:

1. Acquire M&S required to develop the triple oxygen isotope technique as well as ozone generator and SOA chamber.
2. Begin initial photochemical chamber experiments for SOA generation by ozonolysis of alpha-pinene
3. Begin oxygen isotope analysis of lab generated ozone.
4. Lab generated ozone will be analyzed for confirmation of the $^{17}O$ anomaly controlled by temperature and pressure.
5. Develop and refine pyrolysis and gas conversion for oxygen analysis of SOA.
6. Demonstrate errors of analysis of standard laboratory materials, and report findings in analytical methods paper.

As of October 2009, we have designed and had manufactured a 1.5 cubic meter Teflon aerosol chamber and have installed it in our laboratory space. We have also acquired the requisite ozone generator as well as monitors for both inside the chamber and in the laboratory (with alarm for lab safety). An Integrated Work Document (IWD) has been prepared and approved ensuring safe operation protocols for safe generation of organic aerosols.

With the IWD in hand, we are beginning generation of SOA in the laboratory in our aerosol chamber. Initial production of aerosols has proven difficult to quantify however since the quantities produced are small and gravimetric results are within the error of the balance currently at our disposal. We are negotiating with a colleague internal to LANL who has at their disposal a Scanning Mobility Particle Sizer for counting and characterization of aerosol particles. Once SOA production has been shown to be quantifiable and

reproducible, we will begin filter collection for chemical and isotopic analyses.

Isotopic analysis of ozone ($O_3$) requires first converting the $O_3$ to molecular oxygen ($O_2$) with subsequent isotopic analysis of $O_2$. Therefore, before performing $O_3$ isotopic analysis (pending approval of our IWD covering $O_3$ generation in the lab) we have concentrated on optimizing and determining the precision of the isotopic analysis of $O_2$. Since the aerosol samples that we will generate in our chamber will be in microgram quantities and will be eventually converted to O2 for analysis, it is imperative

that we determine the detection limits and optimize the mass spectrometer tuning in order to achieve as good precision as possible. We have established a procedure for analyzing $O_2$ aliquots as small as 100 nanomoles with precisions for $^{18}O$ of 0.2 per mil and $^{18}O$ of 0.8 per mil (Figure 1).

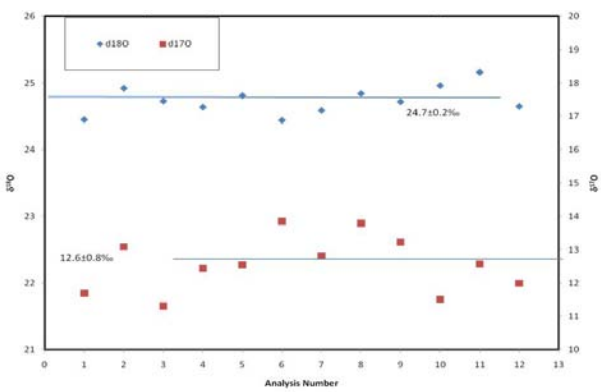


*Figure 1. Demonstration of reproducibility and precision of the isotopic content of repeat analyses of 100 nanomol size samples of atmospheric $O_2$.*

The required apparatus for the separation of $O_3$ from an air sample stream has been constructed in our Isotope Laboratory and as of this writing, is being tested for its collection efficiency and the production of oxygen isotope anomalies under various temperature and pressure conditions.

Prior to performing isotopic analyses on laboratory generated SOA, we have been experimenting with analyses of oxygen bearing organic acids in order to optimize conditions of pyrolysis and to determine detection limits and reproducibility. For direct pyrolysis of a suite of 7 organic acids to carbon monoxide (CO) we have shown precision for $^{18}O$ analysis of microgram size samples ranging from 0.04 to 1.36 per mil. It was also our hope that by fine-tuning the parameters of the pyrolysis procedure that we would be able to erase the carbon isotope signature of the original organic material in the glassy carbon pyrolysis chamber, thus allowing direct measurement of $^{17}O$ by differencing pyrolysis and combustion samples. Our results have shown however, that samples pyrolyzed in the presence of glassy carbon retain at least a fraction of their original carbon thus negating a potential breakthrough in methodology (Figure 2). We are therefore proceeding as originally set forth in our proposal with the development of fluorination techniques to extract molecular oxygen from our surrogate organic acids and eventually from lab produced SOA.

As described above, we have developed techniques for analysis of both $O_2$ and surrogate organic acids and once we have developed an extraction technique for oxygen from organic acids and SOA, we will begin preparation of our first manuscript.

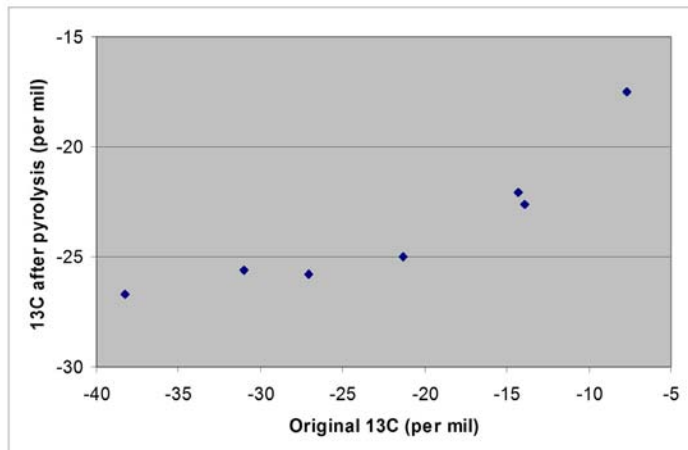


*Figure 2. Plot demonstrating the dependence of samples pyrolyzed in the presence of glassy carbon on the isotopic content of the original material.*

## Future Work

Secondary Organic Aerosols (SOA) comprise as much 70 percent of the global carbonaceous aerosol burden by mass. Because aerosols have multiple feedback mechanisms to Earth's radiation budget, a complete understanding of the formation and fate of aerosols is imperative for understanding their influence on global climate. SOA in particular are poorly understood due to the multitude of precursors responsible for their formation and because they are a complex, heterogeneous mixture of organic species. Because the atmosphere is, in general, an oxidizing environment, the evolution from precursor organic gas species to aerosol results from reaction of biogenic and anthropogenic organic gases with various oxidizing species. The oxygen atoms that are found in SOA are derived, for the most part, from reactive oxygen species that have been shown to carry a mass independent signature in the stable isotopes of oxygen. The $^{17}O$ anomaly from reactive oxygen species that is transferred to the secondary organic compound reaction products can thus serve as a quantitative signature of the pathways of SOA generation. Our goals are to develop an optimized methodology for sensitive $^{17}O$ measurement of mixed carbonaceous species generated by controlled ozonolysis of biogenic volatile organic compounds (a first) and

then to extend this measurement technique to ambient atmospheric SOA samples collected in biogenic dominated regions. This project will investigate the processes by which secondary organic aerosols are formed and how they “age” under varying atmospheric conditions.

## Conclusion

This project will yield the first ever oxygen isotope analyses of Secondary Organic Aerosols thus yielding new insight into the pathways of their formation and elucidating how they “age” under varying atmospheric conditions.

# Evolving a Thermostable Cellulase by Internal Destabilization and Evolution

*Andrew M. Bradbury*
20090443ER

## Introduction

Cellulose is the "backbone" of all plant material, and the predominant material in all plant matter. Biofuel generation has largely focused on the sugar/starch containing plant matter, which is the foundation of the global food market. Increases in food prices have been attributed to greater use of foodstocks for biofuel production. Cellulose materials are largely the "waste" from food production, and as a result their use for biofuel is not expected to influence food prices and supply in the same way. The main research goal of this proposal is to create a highly thermostable version of a widely used cellulase, for which thermostability has been a long desired goal. This could be used in the generation of bioethanol, or other biofuels, and would facilitate the use of cellulose, rather than maize, as feedstock, so permitting the use of otherwise marginal land. By carrying out this goal, we will also have carried out an important secondary goal: the demonstration of the universality of a new protein thermostabilization method we recently developed, by its application to an important industrial enzyme. We expect success in this project to position LANL well to exploit future funding in bioenergy for which enzyme and protein thermostabilization are required.

## Benefit to National Security Missions

By developing a new method to stabilize cellulases, this project will support the DOE mission in energy security. Cellulases are enzymes that breakdown cellulose to sugars suitable for fermentation. However, commercial cellulases tend not to be sufficiently thermostable for industrial processes, a problem we hope to solve.

## Progress

The year 1 goals for this project included:

- Synthesize cellulase gene with E. coli / yeast codons
- Establish cellulase expression in E. coli or yeast
- Establish cellulase screening assay

At the start of this project we had no experience whatsoever in cellulase expression or assays, and this represented a new direction for the laboratory. All three goals for the first year have been completed. In particular, we have synthesized a T. reesei cellulase gene for expression in E. coli, and three forms of this gene have been expressed in the cytoplasmic compartment of E. coli. Two of these were functional, one was not. In addition, two forms of this gene have been functionally expressed in E. coli in the periplasmic space. Plate based assays for cellulase screening has been established that allow direct selection of E. coli colonies expressing functional cellulase (Figure 1). Within the context of the creation of these screening assays, the following variables were examined and optimized: Bacteria: BL21 (different vectors); Induction temperature: 18°C; Induction time: 24-48 hours ; IPTG concentration: 1mM; Assay temperature: 50°C; Assay time: 1 hour; Assay pH: 5; Thickness of CMC layer: 4ml in petri dish.

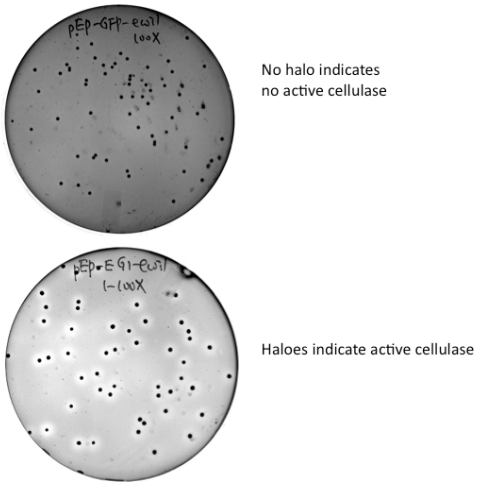


*Figure 1. The top figure shows bacterial (E. coli) colonies not expressing cellulase. As can be seen there is no halo around any colony (the black dots). In contrast in the lower figure, each colony is surrounded by a halo, indicating production and release of cellulase. This assay will be used to identify bacterial mutants expressing active cellulases.*

It is important to emphasize that the most problematic aspects of this proposal have been successfully addressed. T. reesei cellulase is a protein normally expressed in fungi, and expression of functional protein in a heterologous host, such as E. coli can be very problematic. Although there are other forms of the enzyme we will still express and test, even if these other forms were not functional we would be able to use the information already available now to continue to the next phase.

## Future Work

The aim of this proposal is first to develop a thermostable cellulase enzyme that can be used in bio-ethanol production from cellulose and second to validate a new method to thermostabilize proteins we have developed. The development of more thermostable cellulases has been a long desired goal in the biofuel field where success to date has been modest. We recently developed a novel method (Insertional Destabilization Evolution And Synthesis - IDEAS) to thermostabilize proteins that we successfully applied to a fluorescent protein. We believe this method is applicable to any other protein, providing 1) a crystal structure; 2) an assay for the protein function which can be used in high throughput; and 3) a recombinant expression system, are available. The protein we plan to evolve, the Trichoderma reesei endoglucanase I fulfills all three requirements and is the most widely used industrial cellulase. Based on the crystal structure, six insertion sites far from the active site in exposed surface loops have been identified. Mutants containing inserts at three of these sites have already been generated, and will be evolved using IDEAS and the CMC plate assay to monitor activity. We are working to produce mutants with inserts at the remaining sites. Throughout the mutation and selection procedure, positive clones will be sequenced to obtain information on which mutations are selected. In common with the fluorescent protein, we will synthesize genes corresponding to the proteins without inserts after evolution has restored activity. Each newly synthesized gene will be expressed, purified and fully characterized for enzyme activity, refolding kinetics and stability. By the end of this project, we expect to have demonstrated that internal destabilization and evolution can be applied to proteins other than fluorescent proteins, and also to have developed a thermostable endoglucanase, with the potential to be directly usable in those bioethanol production plants in which Trichoderma reseei endoglucanase is presently used.

## Conclusion

Cellulose is the most abundant potential biofuel raw material. The first step in the conversion of cellulose into ethanol, or other fuels, is to break it down into simple sugars. This is a process carried out by enzymes called cellulases. Presently used cellulases are derived from natural sources and poorly suited for industrial processes in which high temperatures are used. In this proposal we anticipate we will derive a thermostable cellulase that will facilitate the breakdown of cellulose containing plant matter for biofuels. The American taxpayer should care, because eventually this will help reduce the cost of transportation fuel.

# Functional Proteomics Studies of Bacillus Anthracis

*Ryszard Michalczyk*
20060437ER

## Abstract

The project addresses a central challenge in pathogen biology: understanding the role of the uncharacterized majority of proteins in bacterial pathogens. In *Bacillus anthracis*, as in most bacteria, the function of majority of the genes is completely unknown. Characterizing protein structure and changes in cellular physiology that result from removing proteins (by gene inactivation) provide vital insights to their general role and specific function. We targeted 6 genes encoding *B. anthracis* proteins of unknown function that are implicated in pathogenesis, with the goal to express the proteins in *E. coli*, characterize their three-dimensional solution structure and compare their structural homology with known proteins to identify functional relationships. In parallel, we undertook preparation of gene knock-out mutants.

To this end we have developed new tools for generation of *Bacillus anthracis* mutants, which yield promising preliminary results. We have also cloned and expressed five proteins in various expression vectors and purified two proteins to homogeneity. NMR studies of the two purified proteins are in progress. Furthermore, we have performed biochemical characterization of one of these proteins, PagR, and characterized DNA binding properties of this repressor. The results show that the protein does not discriminate between promoters for three genes regulated by PagR and binds them with affinities ranging from 19 to 43 nM. Salt dependence of DNA binding indicates that DNA binding results in release of two ions from DNA phosphate groups.

The results obtained in the project will serve as basis for subsequent in depth studies of function of the targeted proteins with the possibility of developing specific anti-anthrax agents.

## Background and Research Objectives

The research undertaken in this project addresses a central challenge in pathogen biology: understanding the role of the uncharacterized majority of proteins in bacterial pathogens. In *Bacillus anthracis*, as in most bacteria, the function of majority of the 3025 genes is completely unknown. Characterizing protein structure and changes in cellular physiology that result from removing proteins (by gene inactivation) provide vital insights to their general role and specific function.

Infection with Bacillus anthracis, a Gram-positive spore-forming soil bacterium, can result in cutaneous disease, readily treatable with antibiotics, or systemic disease, which is often fatal. The continuing natural incidence of anthrax and potential use of *B. anthracis* as a biological weapon warrant continued investigation of this organism, its virulence mechanism, routes of possible therapeutic intervention and new vaccine development. In this regard, regulatory proteins and protein products of unknown function present important targets of investigation as potential new therapeutic targets. Particularly interesting are the proteins unique to *B. anthracis*, without known homologs, since targeting these genes would allow for elimination of the pathogen with potentially very low side effects to the human host.

Bacillus anthracis produces a three protein toxin system consisting of edema factor, lethal toxin and protective antigen [1]. This system is of outmost interest for prevention/therapeutic intervention. In addition, other potential targets are located on pathogenicity island of pXO1 plasmid. These include the protective antigen repressor, PagR, implicated in regulation of protective antigen levels and hence virulence and six genes of unknown function [2]. At least three of these genes are expressed in *B. anthracis* and one of them is upregulated by the major anthrax regulatory protein, AtxA [3]. The proteins have not been studied before and their biochemical characteristics, structure and function are unknown. They show no homology to any known proteins, which makes prediction of their structure and function impossible without additional

experimental evidence. These proteins are expressed under growth conditions required for virulence and are attractive potential anti-anthrax targets. Thus, if they play important roles in virulence of the bacterium, targeting these proteins could potentially be achieved with low toxicity and cross-reactivity with other bacteria. The proteins investigated in this project are proteins of unknown function not investigated anywhere else, to our knowledge. These proteins are not targets of Structural Genomics Centers – the only targets of interest listed for *B. anthracis* are protein products of chromosomal genes. This research is therefore unique. The proteins of interest are shown on the genetic map of pXO1 plasmid in Figure 1.

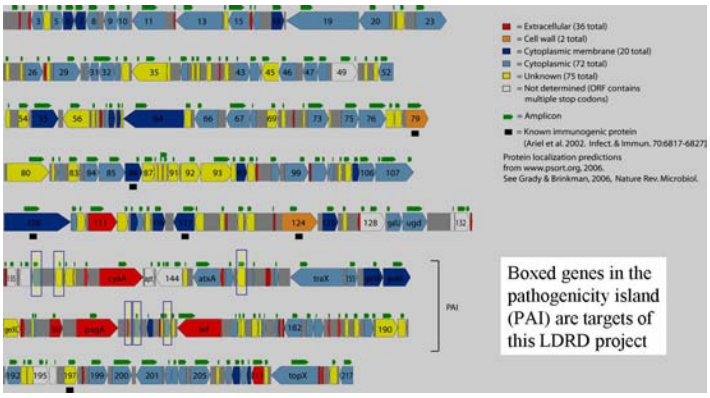


*Figure 1. Genomic map of pXO1 plasmid of Bacillus anthracis. Pathogenicity island is bracketed and the target genes are marked by boxes.*

Insight into the function of proteins of interest and their role in bacteria may be gained through the use of gene knock-outs. The creation of genetically modified *B. anthracis* strains lacking individual genes of interest enables comparison of wild-type and modified bacteria. Creation of knock-out strains of *B. anthracis* has proven very difficult. Changes in the viability and infectivity of *B. anthracis* as well as changes in protein expression patterns due to the lack of the gene of interest can be identified and interpreted in terms of the specific biochemical pathways affected. In addition to gene deletions, structural information can provide new insights into biology by establishing relatedness to proteins of known function that have little sequence homology, and by identifying binding motifs and catalytic centers, even for proteins of unknown function.

The overall goal of this project is to characterize the structure and assess functions of putative *B. anthracis* proteins encoded on the virulence plasmid pXO1. Objectives for achieving this goal are the following:

1. Express the *B. anthracis* proteins in *E. coli*, and evaluate as candidates for structure determination.
2. Characterize the three-dimensional structures of the expressed and folded proteins.
3. Perform a structural homology search to assess structural similarity to known proteins and establish functional relationships between proteins.
4. Prepare deletion mutants of *B. anthracis* lacking genes of interest.
5. Assess effects of gene deletions on bacterial growth and patterns of protein expression.

We have also set out to characterize structure and DNA binding properties of the protective antigen repressor, PagR, an important regulatory protein in *B. anthracis* [4, 5]. While it is known that PagR binds DNA, the consensus DNA sequence and the details of the interaction are uncertain [5]. Biochemical characterization of PagR is also lacking.

## Scientific Approach and Accomplishments

**Generation of knock-out mutants.**
*Bacillus anthracis* is known to be recalcitrant for molecular biology manipulations and generation of mutants is difficult. Initially we attempted to use a standard knock-out vector, in which an antibiotic resistance gene is flanked by DNA sequences from the target gene. The vector is introduced into the bacterium and replaces the target gene through double recombination, thus inactivating it. In principle, only bacteria with inactivated gene survive antibiotic selection. We attempted to generate five mutants using this approach. Approximately 200 clones were screened for each mutant. We found the selection process to be ineffective, since all clones were single recombinants and therefore false positives.

To alleviate the problems, we have constructed a vector containing a suicide gene in addition to mutagenesis cassette (Figure 2A). In single recombinants, the suicide gene becomes active upon nutrient depletion and kills the host, while the desired double recombinants lose the suicide gene and survive selection. We attempted creating two mutants using this process and screened 200 colonies/mutant. Only false positives were detected. Subsequently, we attempted to insert additional temperature sensitivity into the mutagenesis vector to render it more unstable (Figure 2B). Several attempts failed and we were unable to insert a suicide gene into temperature sensitive mutant.

Our final approach involved introducing a gene encoding endonuclease into the mutagenesis vector (Figure 2C). Induction of endonuclease gene upon nutrient depletion kills single recombinants and also destroys the vector,

eliminating false positives. So far, the use of this vector resulted in dramatic decrease of number of colonies created. We are currently screening three clones (~200 colonies/clone) using this approach.

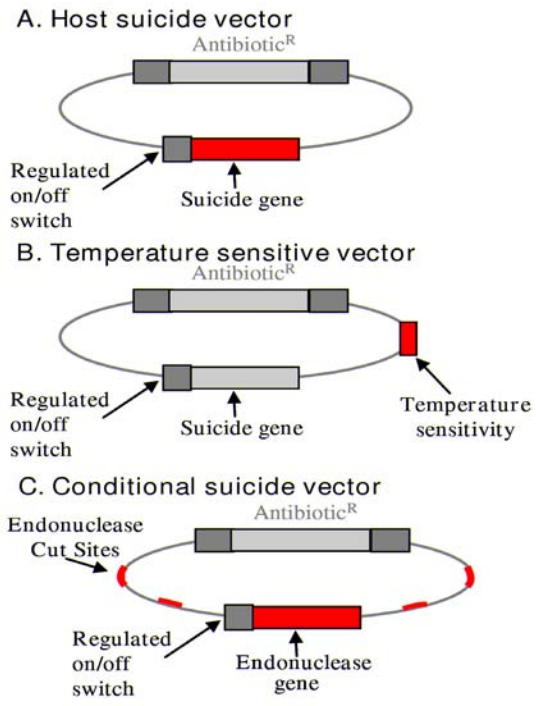


*Figure 2. Cloning vectors designed for generation of knock-out mutants in Bacillus anthracis.*

**Protein expression and purification**

All proteins that are subject of this study are small (<125 amino acids) and therefore it is important for structural and functional studies to produce them with minimal additional residues as a result of cloning. Initially we cloned all proteins into pET9a vector for expression of native sequence only. This approach resulted in successful expression of pXO1-166 (PagR) protein, while the other proteins yielded insoluble products or no products at all. Subsequently, we cloned the proteins into pGSK vector, in which they are expressed as a fusion with GST protein. In many cases GST tag enhances protein expression and solubility. The fusion can be cleaved with thrombin to yield native protein sequence with addition of one N-terminal amino acid. This approach yielded soluble expression for pXO1-137. The remaining proteins were then cloned into pET-SUMO vector for expression as SUMO-tagged proteins. The SUMO tag is specifically recognized by a protease and cleaved following expression. In this system, we have successfully expressed pXO1-138 and pXO1-173. Cloning and expression of pXO1-190and pXO1-167 in all of the above vectors suffered setbacks. Initially, all obtained clones contained mutations and after resolving that problem, the proteins were not induced and expressed in cells, regardless of the vector tried. Suspecting that the proteins may be toxic to E. coli, we have generated primers and created templates for these two genes for commercially available cell-free expression system. So far, the untagged versions of these proteins failed to yield soluble products. We are preparing histidine-tagged and TEV-protease tagged templates for these two genes in hopes to improve solubility and simplify purification.

Proteins pXO1-137 and pXO1-166 have been purified to homogeneity and also expressed in 13C, 15N-labeled media for NMR studies. pXO1-137 was expressed as GST-tagged version, purified on GST-agarose and the tag cleaved with thrombin. The NMR experiments and resonance assignments on labeled protein are in progress. In the nearest future we will acquire 3D NMR experiments necessary for structure determination. This work will result in 1-2 publications.

pXO1-166 was expressed and purified as an untagged protein containing only native structure. The protein was purified using standard chromatographic methods on two ion exchange columns and its biochemical characterization has been performed. We have also produced the protein stable isotope labeled and collected NMR data for resonance assignments, which are in progress.

**Biochemical characterization of pXO1-166 (PagR)**

It has previously been discovered that pXO1-166 gene encodes the protective antigen repressor, PagR, and that the protein binds to promoter sequences of three *B. anthracis* genes [5]. The structure of the protein, its biochemical characteristics and DNA binding properties remained uncharacterized. Following purification, we have performed biochemical characterization of the protein. PagR exists in solution as a dimer (molecular weight 23kDa), similarly to many other DNA-binding proteins. The protein is very basic, with isoelectric point of 9.6. Secondary structure analysis using circular dichroism (CD) shows the protein to be ~50% alpha-helical and 10% beta-sheet with significant amounts of loops and extended structure. NMR experiments indicate presence of well defined tertiary structure. The protein is also very stable in buffer containing >150 mM salt, with melting point of 71$^o$C determined from CD data.

To characterize DNA binding properties of PagR we have used Surface Plasmon Resonance (SPR) method (Figure 3A). The DNA molecules corresponding to previously identified promoters for pagA, sap and eag genes were used in the study. PagR was found to bind all three promoters with similar affinity, with binding constants ranging from 19 to 43 nM. We were also able to narrow down the binding site for PagR. Initial studies indicated

that the DNA sequences for PagR binding range from 48 to 81 base pairs. For the protein as small as PagR this is unusual. We have used the previously identified sequences as starting point for exploration of minimal binding site and found that reducing the size of DNA to 34 base pairs does not significantly reduce binding affinity (Figure 4). This size of DNA corresponds closely to sequences bound by ArsR family receptors to which PagR exhibits some homology. Despite identifying shorter cognate sequences, comparison of sequences from pagA, sap and eag genes shows very limited similarity and does not allow for deducing the consensus binding sequence. It is quite likely that PagR recognizes structure of the DNA promoter fragments rather than their sequence, similarly to another *B. anthracis* regulatory protein, AtxA [6].

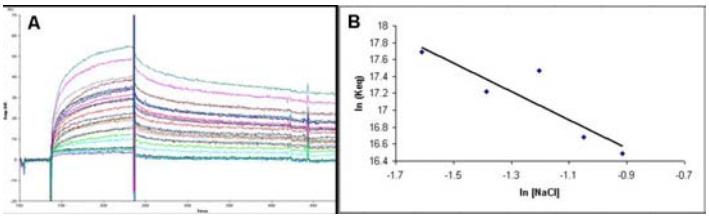


*Figure 3. A. SPR data showing 9 concentrations of PagR binding to pagA-81. Association time was 100s, dissociation lasted 180s. Concentrations of PagR used were 10, 50, 100, 200, 300, 400, 500, 600 and 700 nM. B. Salt dependence of PagR affinity. The logarithm of the equilibrium binding constant determined for PagR binding versus the logarithm of NaCl concentration. Gray line represents linear fit of the data with a slope of 1.69 ± 0.29.*

| DNA | $k_a$[1] | $k_d$[2] | $K_D$[3] |
|---|---|---|---|
| pagA-81 | $7.4 \pm 4.9 \cdot 10^4$ | $1.39 \pm 0.19 \cdot 10^{-3}$ | $1.9 \pm 1.5 \cdot 10^{-8}$ |
| pagA-49 | $9.4 \pm 6.7 \cdot 10^4$ | $1.27 \pm 0.12 \cdot 10^{-3}$ | $1.4 \pm 1.1 \cdot 10^{-8}$ |
| pagA-34 | $8.0 \pm 6.2 \cdot 10^4$ | $1.36 \pm 0.08 \cdot 10^{-3}$ | $1.7 \pm 1.4 \cdot 10^{-8}$ |
| eag-62 | $4.3 \pm 2.2 \cdot 10^4$ | $1.35 \pm 0.33 \cdot 10^{-3}$ | $3.2 \pm 2.4 \cdot 10^{-8}$ |
| eag-44 | $7.6 \pm 5.0 \cdot 10^4$ | $1.57 \pm 0.41 \cdot 10^{-3}$ | $2.1 \pm 1.9 \cdot 10^{-8}$ |
| sap-48 | $5.2 \pm 3.3 \cdot 10^4$ | $2.24 \pm 0.33 \cdot 10^{-3}$ | $4.3 \pm 3.4 \cdot 10^{-8}$ |
| sap-34_1 | $5.9 \pm 4.0 \cdot 10^4$ | $2.17 \pm 0.34 \cdot 10^{-3}$ | $3.7 \pm 3.1 \cdot 10^{-8}$ |
| sap-34_2 | $4.0 \pm 3.5 \cdot 10^4$ | $2.13 \pm 0.25 \cdot 10^{-3}$ | $5.3 \pm 5.1 \cdot 10^{-8}$ |
| NS-40 | $1.7 \pm 1.4 \cdot 10^4$ | $3.7 \pm 2.0 \cdot 10^{-3}$ | $2.2 \pm 2.9 \cdot 10^{-7}$ |

1. Association rate constants are in $M^{-1}s^{-1}$
2. Dissociation rate constants are in $s^{-1}$
3. Dissociation constants are in M

*Figure 4. Association and dissociation rate constants and thermodynamic dissociation constants for PagR binding to DNA constructs.*

We have also performed binding studies for PagR as a function of salt concentration (Figure 3B). When the protein binds DNA, the positive ions in solution condensed on negative DNA phosphate backbone are displaced. When binding constants are measured as a function of salt concentration the number of displaced ions, and therefore the number of phosphate groups directly contacted by the protein, can be deduced. For PagR the binding data indicate displacement of two ions, indicating that each protein monomer contacts directly one DNA phosphate group.

The results of PagR studies have been submitted for publication in Zeitschrift fűr Naturforschung C.

## Impact on National Missions

The research in this project complements LANL efforts in biothreat reduction and proteomics. It is directly related to DOE's biothreat reduction initiatives as part of national security mission. The project is also related to the goals of the DOE's Genomes to Life programs.

The project contributes directly to B-division's maturing programs in pathogen biology, biothreat reduction and proteomics. There is a growing core of researchers in B division focused on *B.anthracis* pathogenesis. Our work will contribute to establishing a *B.anthracis* center of excellence. This will also enable us to establish a track record in *B.anthracis* research, so that we can transition to NIH/DHS funding for future studies on a broader array of uncharacterized proteins in *B.anthracis* and other pathogens. The research also leverages the Stable Isotope Resource within the Bioscience Division, since isotope labeling is crucial to NMR structural studies.

The project resulted in evaluation and development of new genetic tools for molecular manipulations of bacterial genomes. It has also resulted in developing conditions for expression of *B. anthracis* proteins, which will lead to availability of these proteins for further biochemical studies. So far, the project generated one publication submitted and two additional in preparatory stages. Results generated in the progress of this project will be used in application for funding from NIH and DOE in 2010.

The funding from this project supported a graduate research assistant and partially a postdoctoral research associate. The graduate student obtained his PhD degree from University of New Mexico School of Medicine during the course of the project and is now a postdoc at the Air Force Research Laboratory.

## References

1. Welkos, S. L., N. J. Vietri, and P. H. Gibbs. Non-toxigenic derivatives of the Ames strain of Bacillus anthracis are fully virulent for mice: role of plasmid pX02 and chromosome in strain-dependent virulence. 1993. *Microbial Pathogenesis.* **14**: 381.

2. Okinaka, R. T., K. Cloud, O. Hampton, A. R. Hoffmaster, K. K. Hill, P. Keim, T. M. Koehler, G. Lamke, S. Kumano,

J. Mahillon, D. Manter, Y. Martinez, D. Ricke, R. Svensson, and P. J. Jackson. Sequence and organization of pXO1, the large Bacillus anthracis plasmid harboring the anthrax toxin genes. 1999. *Journal of Bacteriology.* **181**: 6509.

3. Bourgogne, A., M. Drysdale, S. G. Hilsenbeck, S. N. Peterson, and T. M. Koehler. Global effects of virulence gene regulators in a Bacillus anthracis strain with both virulence plasmids. 2003. *Infection and Immunity.* **71**: 2736.

4. Hoffmaster, A. R., and T. M. Koehler. Autogenous regulation of the Bacillus anthracis pag operon. 1999. *Journal of Bacteriology.* **181**: 4485.

5. Mignot, T., M. Mock, and A. Fouet. A plasmid-encoded regulator couples the synthesis of toxins and surface structures in Bacillus anthracis. 2003. *Molecular Microbiology.* **47**: 917.

6. Hadjifrangiskou, M., and T. M. Koehler. Intrinsic curvature associated with the coordinately regulated anthrax toxin gene promoters. 2008. *Microbiology.* **154**: 2501.

## Publications

Shiflett, P. R., S. Iyer, and R. Michalczyk. DNA binding properties of PagR, the protective antigen repressor from Bacillus anthracis. *Zeitschrift fur Naturforschung.*

# Drug Binding and Catayltic Mechanism in DHFR

*Paul A. Langan*
20070131ER

## Abstract

Dihydrofolate reductase (DHFR) is an important housekeeping enzyme which is conserved across most species, including humans. It catalyzes a chemical reaction (a reduction) which converts the molecule dihydrofolate (DHF, also called the substrate) to another called tetrahydrofolote (THF). This chemical reaction is required for DNA and protein synthesis. Because of DHFR's vital role in biosynthesis it is an important drug target. DHFR is targeted against cancer (with the drug called Methotrexate or MTX), and for anti-microbial agents (with the drug called trimethoprim). With the emergence of anthrax as a bio-terrorism threat, DHFR is also being considered as a valid drug target for anthrax. The main goals of this proposal were two-fold. First, we were to develop crystallization and perdeuteration (replacing hydrogen by deuterium) capabilities for DHFR in order to allow us to use neutron crystallography to unravel exactly how it changes DHF to THF i.e. its catalytic mechanism. The second goal was to determine the X-ray structure of anthrax DHFR. During the last three years we have successfully accomplished both goals. Initially, we developed a recombinant molecular biology system with the bacterium *E. coli*, for producing large quantities of DHFR (100 mg/L of *E. coli* culture). Then a way of perdeuterating DHFR was optimized using algae to provide large amounts of perdeuterated DHFR for neutron diffraction studies. The perdeuterated protein was used to produce crystals together with the drug MTX and another molecule called NADPH which is also required for the reaction (called the cofactor). The crystals have been subjected to neutron diffraction studies at the Protein Crystallography Station (PCS) at the Los Alamos Neutron Scattering Center (LANSCE). The crystals diffract to 2.4 Å resolution. We have also determined the X-ray structure of the anthrax DHFR bound to MTX and another bound to MTX-NADPH. These structures were used to develop dual-site inhibitors against anthrax.

## Background and Research Objectives

Dihydrofolate reductase (DHFR) is an important housekeeping enzyme which catalyzes the chemical conversion of the molecule dihydrofolate (DHF, which is called the substrate) to another called tetrahydrofolote (THF, the active form of the vitamin folic acid) [1]. THF is used in living cells in the chemical synthesis of certain amino acids, the small molecule building blocks of proteins, and also purines and pyrimidines, the small molecule building blocks of DNA. Inhibiting (or preventing it from working) DHFR interrupts DNA synthesis and leads to cell death. DHFR is therefore a target for anti-cancer therapy (with the drug called methotrexate or MTX) and for anti-microbial agents (with the drug called trimethoprim).

DHFR has been widely studied by NMR [2,3] and X-ray crystallography [4-6]. These studies show that its structure consists of certain motifs. There is a central 8-stranded β-sheet which can be thought of as two domains. An upper domain of 4 sheets where the cofactor binds and a lower domain of 4 sheets where the substrate binds (Figure 1). Substrate and cofactor bind in a cleft at the interface of the upper and lower domains. The conformation or shape of the Met20 regulatory loop (amino acid residues 9-24) fluctuates from closed to occluded as the reaction proceeds.

Catalysis consists of proton and hydride transfer across a double chemical bond on the pteridine ring of the DHF substrate. A number of catalytic mechanisms have been proposed that differ in the protonation states of the ligand and a key active site residue (called Asp27), as well as the exact pathway of proton transfer to DHF. X-ray crystallography has not been able to demonstrate any of these proposals because although it can be used to determine the carbon, oxygen and nitrogen (C, O and N) atom positions that make up the skeleton of DHFR, it seldom provides the positions of the more mobile hydrogen (H) atoms that transfer between enzyme and

substrate during catalysis (X-rays are scattered by atomic electron clouds and with just one electron an H atom is almost invisible; in fact, a proton is completely invisible).

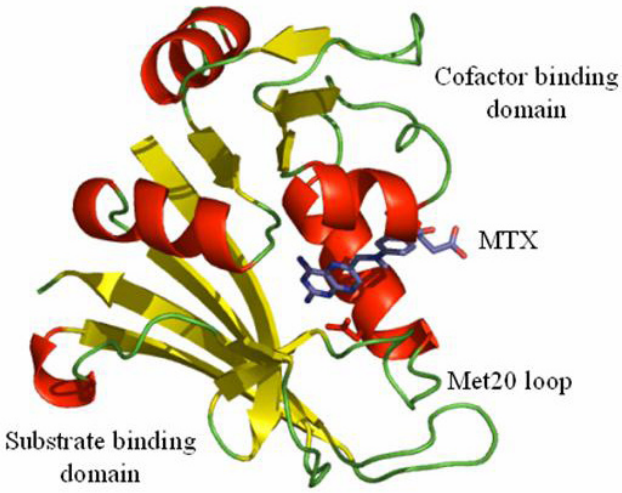


*Figure 1. The X-ray structure of DHFR from E. coli.*

Neutron crystallography is a powerful method for locating H atoms in enzymes (H, and in particular its isotope D, interacts with neutrons very efficiently), although its use has been limited by the availability of relatively weak neutron beams, requiring large sample sizes [7]. The Protein Crystallography Station (PCS) at Los Alamos Neutron Scattering Center (LANSCE), built by Bioscience division and funded by the Office of Biological and Environmental Research of the US Department of Energy, allows neutron data to be collected very efficiently with high signal-to-noise ratios by employing time-of-flight data collection methods [8]. In work completed before this project, we used the PCS to locate H positions in DHFR from the bacterium called *E. coli* (ecDHFR), complexed with the chemotherapeutic MTX, from a crystal around 0.25mm$^3$ in volume that had been soaked in $D_2O$ (replacing H by D increases the scattering efficiency and soaking replaces labile accessible H atoms bound to O and N) [9]. We demonstrated that the N1 atom of MTX is protonated when bound to ecDHFR while the catalytic Asp27 is negatively charged (Figure 2), providing unique information that will be exploited to enhance target-drug interactions, the primary motive behind therapeutic discovery regimes. We also tried to collect neutron data from a ecDHFR-NADPH-DHF ternary complex in order to address the enzyme's mechanism, but with crystal volumes of ~0.1mm$^3$ the diffraction was too weak. To circumvent this problem in this project we have developed protocols for making large crystals of perdeuterated DHFR. In perdeuterated DHFR all H, even when covalently bound to C, has been replaced by D. Perdeuterated DHFR crystals make it possible to collect neutron crystallographic data from smaller crystals as the incoherent scattering from H atoms (which adds to scattering background and reduces signal-to-noise levels) is significantly reduced, and D has a stronger coherent scattering contribution (which increase the signal-to-noise level). The perdeuteration protocols that we have developed are now used to perdeuterated large quanitities of several different proteins in a new deuteration capability.

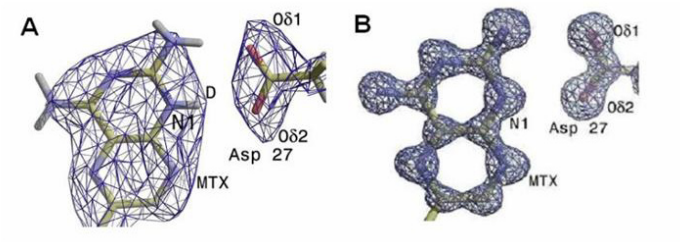


*Figure 2. (A) Shown in blue is neutron scattering density and (B) X-ray scattering density. In the neutron structure a D atom is found bound to the N1 atom of MTX.*

On a second front, in this project we conducted studies on DHFR from *B. anthracis*, an organism of therapeutic importance. Spores of *Bacillus anthracis*, the infectious agent that causes anthrax, are a known weapon of bioterrorists. Current antibiotic treatments are not optimal due to resistance and patient age restrictions; thus, additional targets for therapeutic intervention must be evaluated. One possible candidate is dihydrofolate reductase (DHFR) because it is necessary for anthrax pathogenicity. *B. anthracis* and human DHFR have considerable (amino acid) sequence differences, and those differences suggest that there is potential for the development of anti-Anthrax drugs. Even though their primary sequences are ~31% identical (~52% similar), there exist major differences between Anthrax and human DHFR at the regulatory loop regions near the active site, a consequence that may be exploited in species-specific drug design. In fact, there seems to be a minor insertion (2-3 amino acid residues) at the N-terminus of human DHFR which is not present in *B. anthracis* DHFR (baDHFR). Our plan was to use crystallography, of baDHFR structures to provide information on the protonation states of the catalytic groups, proton positions of crucial solvent molecules that can be mimicked to enhance selectivity and potency using the rational approach as used in designing HIV I protease inhibitors.

## Scientific Approach and Accomplishments

**Perdeuteration of *E. coli* DHFR**

We designed and synthesized a plasmid of DNA called a Sumo-ecDHFR construct to produce large amounts of

DHFR using recombinant molecular biology techniques with the bacterium *E. coli.* The Sumo-ecDHFR construct was transformed (introduced) into *E. coli* and we then grew the bacterium in a $D_2O$ (heavy water) solution that also contained deuterated chemicals, so that the ecDHFR synthesized by *E. coli* from those chemicals would also be perdeuterated. We obtained the deuterated chemicals for this process by growing algae in $D_2O$ and then hydrolyzing it with acid. We explored several different strains of algae using normal incubators and generated different bacterial growth media from the hydrolysates. We found that there were differences in the amounts of protein expression with different hydrogenous hydrolysates. One of the best performers was chlorella. We have now been able to grow chlorella routinely on 90% and above $D_2O$ so we can perdeuterate large quantities of protein for crystallization trials. Another good performer was botryococcus braunii which we can grow in almost 100% $D_2O$.

We tested using a Protein Production robot for *E. coli* fermentation with $D_2O$ and algae hydrolysate but we found (with a number of different proteins; DHFR, HIV protease and MSOX) that there was no real gain in using the robot rather than a regular incubator. Although the robot gave us much greater (x5-8) final bacterial cell densities, the amount of actual DHFR expressed was not significantly higher. We carried out mass spectrometry analysis of the various perdeuterated proteins that we have produced from our hydrolyzate to ensure full perdeuteration. With our sumo-ecDHFR construct and optimized algae hydrolyzate we were able to get expression levels of 100 mg of perdeuterated protein per 1 Liter of labeled media (Figure 3). The perdeuteration capabilities that were established through this research have been highlighted in three recent publications [7, 13, 14]. The protein was subjected to co-crystallization trials using a special deep well crystallization protocol developed in this project, in order to determine the neutron structure of the MTX-NADPH ternary complex. We have obtained crystals that have dimensions of 1x1x0.5 $mm^3$ and we have collected initial neutron crystallographic data to 2.4 Å resolution spots (Figure 4). Data processing and structure determination is currently underway.

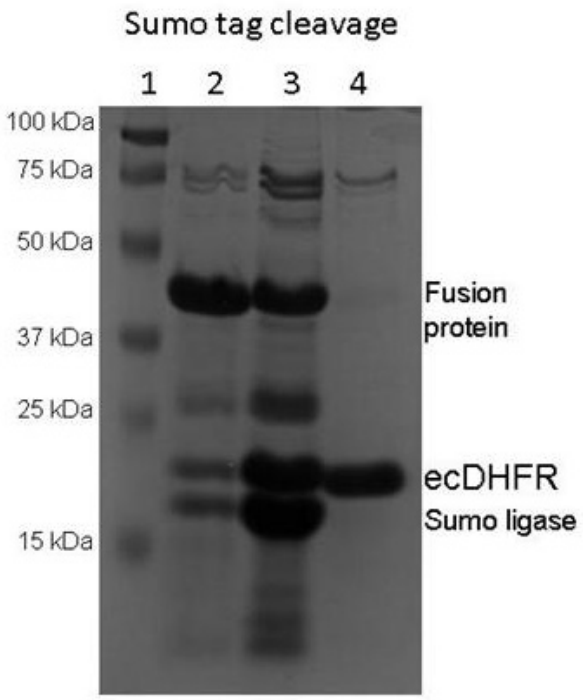


*Figure 3. Perdeuterated ecDHFR. .Lane 1: molecular eight standards; Lane 2: 1 minute cleavage with sumo protease; Lane3: 2 hour cleavage with sumo protease; Lane 4 pure perdeuterated ecDHFR after Ni-NTA purification.*

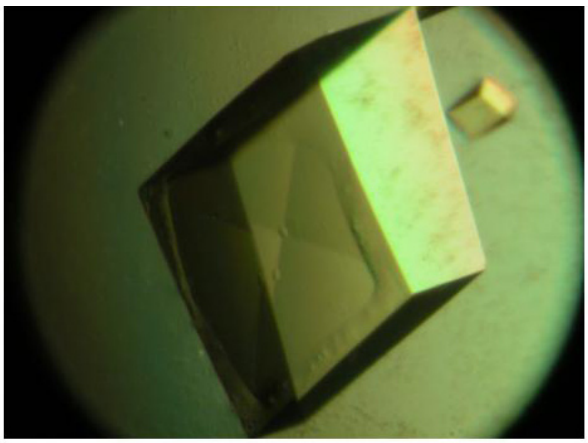

*Figure 4. New perdeuterated DHFR in complex with MTX-NADPH*

**Factors that influence HDX in a crystal**

The hydrogen-deuterium exchange (HDX) method, coupled with neutron crystallography, is a powerful method for investigating molecular dynamics. Investigating the HDX exchange method is extremely important for interpreting neutron structures. Recently, we conducted a comparison of all the available neutron diffraction structures for determining the factors that influence H/D exchange. In our study the general determinants of HDX based on 12 deposited neutron protein structures were proposed. The parameters that correlate best with HDX are depth within the protein structure of the amide nitrogen and secondary

structure type. Both the atomic displacement (*B*) factor of the amide nitrogen and the ratio of *B*/<*B*> correlate moderately. However, solvent accessibility only correlates strongly with one molecule and hydrogen bonding distance correlates with two molecules with respect to amide HDX. A global analysis of HDX was performed to overcome some of these obstacles, damping the effects of outliers and the extreme variation of the data sets due to resolution limitations. From this, amide depth and hydrogen bonding distance to the amide (a measure of interaction strength) show strong global correlation with HDX. For some structures, we could identify what may constitute the hydrophobic protein core based on contiguous regions that are resistant to exchange and have significant depth. These may, in fact, constitute minimal folding domains [10].

**Drugs against anthrax.** We have determined the three-dimensional X-ray structure of anthrax DHFR in complex with MTX [11]. Structure comparison between anthrax and human DHFR shows significant differences at the substrate binding pocket that can be exploited for designing highly selective anti-anthrax inhibitors. Recently, we have also solved the structure of the anthrax DHFR-MTX-NADPH ternary complex (Figure. 5). This structure was used for conducting *in silico* virtual screening experiments against a National Cancer Institute (NCI) small molecule library (using UNITY) to obtain dual-site inhibitor leads with potential clinical significance. A subset of 212 hits was obtained and then subjected to further screens using Surflex-Dock. 30 compounds were chosen as best candidates and we were able to obtain 15 of those compounds from the NCI. Two such molecules (1357 and 373265) inhibited baDHFR with IC50 values in the µM range [12]. Both of these compounds are derivatives of traditional antifolates and therefore they may represent the first leads of two new classes of DHFR inhibitors. We have published three manuscripts in peer review journals describing our findings. Based on the success of this project we are currently preparing a proposal for submission to NIH.

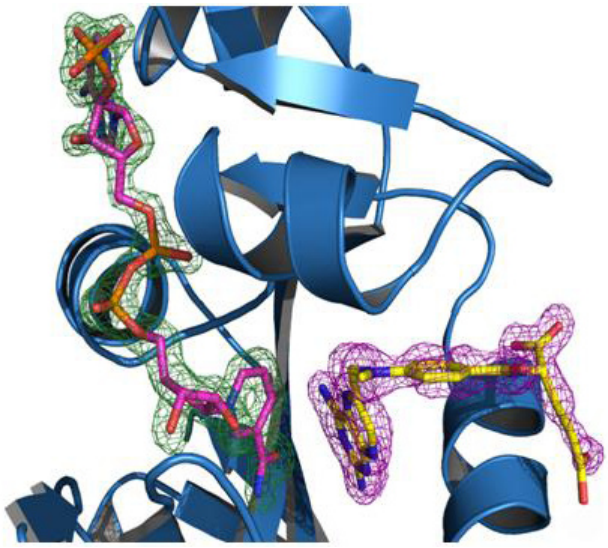

*Figure 5. The structure of anthrax DHFR (blue) in complex with MTX (yellow)-NADPH (magenta). The 2Fo-Fc Fourier electron density map drawn around the ligands are contoured at 1σ.*

## Impact on National Missions

Anthrax has emerged as an agent for bioterrorism that has to be dealt with immediately due to our current threat levels. This project supports the national security mission of biothreat reduction important to DOE, DHS, and other government agencies. Furthermore, by developing an understanding of catalytic mechanisms and how we might custom design drugs, we will impact the health and welfare of our nation. In this project we have successfully used x-ray and neutron crystallography in combination with *in silico* virtual screening experiments to identify dual-site inhibitors against anthrax, with direct relevance to Laboratory and national missions in biosecurity. This preliminary success is being used to develop a large proposal that is a direct follow on from this work. Our hope is that the follow on proposal on drug design using neutron crystallography will bring new work to the Laboratory. Furthermore, as a result of this project, a cutting edge perdeuteration facility has been developed at LANSCE, which is now routinely used to produce large quantities of deuterated proteins. The establishment of this capability was a key component in the recent success of a proposal for UCOP funds to study the cellular mechanism of the family of proteins called kinases which will be funded at a level of about $300K for the next three years. Finally, a post-doctoral fellow, Andrey Kovalevsky, was initially hired in order to work partly on this project. Shortly after his arrival, Andrey was successful in obtaining a Director's fellowship and now works on his own project. However, this project played a key role in bringing him to the Laboratory.

## References


1. Schnell, J. R., H. J. Dyson, and P. E. Wright. Structure, dynamics, and catalytic function of DHFR. 2004. *ANNU REV BIOPHYS BIOMOL STRUCT.* **33**: 119.

2. Osborne, M., J. R. Schnell, S. J. Benkovic, H. J. Dyson, and P. E. Wright. backbone dynamics in DHFR complexes: role of loop flexibility in the catalytic mechanism. 2001. *BIOCHEMISTRY.* **40**: 9846.

3. McElheny, D., J. R. Schnell, J. Lansing, H. J. Dyson, and P. E. Wright. Defining the role of active-site loop fluctuations in DHFR catalysis. 2005. *PNAS USA.* **102**: 5032.

4. Sawaya, M. R., and J. Kraut. Loop and subdomain movements in the mechanism of E. coli DHFR: Crystallographic evidence. 1997. *BIOCHEMISTRY.* **36**: 586.

5. Lee, H., V. M. Reyes, and J. Kraut. Crystal structures of E. coli DHFR complexed with folinic acid in two space groups: evidence for enolization of pteridine O4. 1996. *BIOCHEMISTRY.* **35**: 7012.

6. Davies, J. F., and e. t. al. Crystal structures of recombinant human DHFR complexed with folate and 5-deazafolate. 1990. *BIOCHEMISTRY.* **29**: 9467.

7. Blakeley, M., P. Langan, N. Nobuo, and A. Podjarny. Neutron crystallography: opportunities, challenges, and limitations. 2008. *CURRENT OPINIONS IN STRUCTURAL BIOLOGY.* **18**: 593.

8. LANGAN, P., G. GREENE, and B. P. SCHOENBORN. PROTEIN CRYSTALLOGRAPHY WITH SPALLATION NEUTRONS. 2004. *JOURNAL OF APPLIED CRYSTALLOGRAPHY.* **37**: 24.

9. BENNETT, B., P. LANGAN, L. COATES, M. MUSTYAKIMOV, B. P. SCHOENBORN, E. HOWELL, and C. DEALWIS. NEUTRON DIFFRACTION STUDIES OF E. COLI DHFR COMPLEXED WITH METHOTREXATE. 2006. *PNAS USA.* **103**: 18493.

10. BENNETT, B., A. S. GARDBERG, M. D. BLAIR, and C. DEALWIS. ON THE DETERMINANTS OF AMIDE BACKBONE EXCHANGE IN PROTEINS: A NEUTRON COMPARATIVE STUDY. 2008. *ACTA CRYSTALLOGRAPHICA .* **D64**: 764.

11. BENNETT, B., H. XU, R. F. SIMMERMAN, and R. E. LEE. CRYSTAL STRUCTURE OF THE ANTHRAX DRUG TARGET, BACILLUS ANTHRACIS DHFR. 2007. *JOURNAL OF MEDICAL CHEMISTRY.* **50**: 4374.

12. BENNETT, B., Q. WAN, M. F. AHMAD, P. LANGAN, and C. DEALWIS. X-RAY STRUCTURE OF THE TERNARY MTX.NADPH COMPLEX OF THE ANTHRAX DHFR; A PHARMACORE FOR DUAL-SITE INHIBITOR DESIGN. 2009. *JOURNAL OF STRUCTURAL BIOLOGY.* **166**: 162.

13. Blakeley, M.. Neutron Macromolecular Crystallography. 2009. *Crystallography reviews.* **15**: 157.

14. Teixeira, S., G. Zaccai, J. Ankner, M. Bellissent, R. Bewley, M. Blakeley, P. Callow, E. T. Al, and P. Langan. New Sources and instrumentation for neutrons in biology. 2008. *CHEMICAL PHYSICS.* **345**: 133.


## Publications


Bennett, B., A. Gardberg, M. Blair, and C. Dealwis. On the determinants of amide backbone exchange in proteins: a neutron crystallographic comparative study. 2008. *Acta Crystallographica .* **D64**: 764.

Bennett, B., H. Xu, R. Simmerman, R. Lee, and C. Dealwis. Crystal structure of the anthrax drug target, bacillus anthracis dihydrofolate reductase . 2007. *Journal of Medicinal Chemistry.* **50** (18): 4374.

Bennett, B., Q. Wan, M. F. Ahmad, P. Langan, and C. Dealwis. X-ray structure of the ternary MTX.NADPH complex of the anthrax DHFR: a pharmacophore for dual site inhibitor design. 2009. *JOURNAL OF STRUCTURAL BIOLOGY.* **166**: 162.

Blakeley, M., P. Langan, N. Niimura, and A. Podjarny. Neutron Protein Crystallography: Opportunities, challenges and limitations. 2008. *Current Opinion in Structural Biology .* **18**: 593.

Langan, P., M. Mustyakimov, Z. Fisher, A. Kovalevskyi, A. Valone, M. J. Waltman, P. Adams, P. Afonine, B. Bennett, C. Dealwis, C. Unkefer, and B. P. Schoenborn. Protein structures by spallation neutron crystallography. 2008. *Journal of synchrotron radiation.* **25**: 215.

Liu, X., L. Hanson, P. Langan, and R. Viola. The Effect of Deuteration on Protein Structure: A High Resolution Comparison of Hydrogenated and Perdeuterated Haloalkane Dehalogenase. 2007. *Acta Crystallographica.* **D63**: 1000.

Teixeira, S., e. t. al, and P. Langan. New sources and instrumentation for neutrons in biology. 2008. *CHEMICAL PHYSICS.* **345**: 133.

# Substrates for the Detection and Differentiation of Influenza Viridae

*David B. Kimball*
20070148ER

## Abstract

Influenza viridae are a continual worldwide health threat that is ever changing with newly emerging strains. The recent emergence of Avian and Swine flu, as well as the increasing occurrence of anti viral drug resistance, exemplifies the need for new and rapid detection methods. We have synthesized a panel of substrates for an enzyme present on the Influenza viral coat that are able to distinguish different viral strains by mass spectrometry. Stable isotope labels ($^{13}C$) were incorporated into the substrates in various patterns in order to encode mass signatures. This encoding allows the use of these biomarkers in the presence of a natural background and provides a rapid means to determine the viral subtype as well as any emergence of antiviral drug resistance. This panel of substrates therefore allows large scale Influenza detection and evaluation on real world samples in a rapid, automated fashion. In collaboration with the NCEH at the CDC, our substrates will also be used on a wide range of samples for validation of vaccines and antiviral drug efficacy.

## Background and Research Objectives

Human respiratory viruses, such as influenza A, B and C, respiratory syncytial virus (RSV) and human rhinovirus (HRV) accounted for an estimated 100 million infections in 2000 [1] in the US and the CDC reports that respiratory illnesses were the 5$^{th}$ leading cause of death in the US in 2002 [2]. Although novel antiviral drugs for the treatment of influenza, e.g. neuraminidase inhibitors, became available recently, their efficiency depends on an early diagnosis (within the first 2 days of infection). The avian flu strain H5N1 has caused more than 140 human cases from human – bird contact and human to human transmission have been reported by the World Health Organization since January 2006. The virulence of H5N1 across species and the possibility of mutations that allow the spread from human to human is particular alarming in light of high mortality rates among those infected (up to 50%). New strains of Influenza are a recurring problem, as demonstrated by the recent outbreak of Swine Flu (H1N1). The CDC reports, as of September 27-October 3, that Swine Flu is active in 37 states and that reports of flu like symptoms as well as hospitalizations are increasing faster than expected.

The common protein based receptor motifs found on Influenza viridae are hemagglutinin (*HA*) (16 subtypes) and neuraminidase (*NA*) (9 subtypes), the combination of which identifies the influenza strain. Previous pandemic influenza outbreaks were associated with H1N1 (1918), H2N2 (Asian 1957) and H3N2 (Hong Kong 1968) antigenic determinants of influenza A [1].

There are an estimated 50 copies of tetrameric *NA* and in excess of 100 copies of trimeric *HA* on the surface of an influenza viral particle [3] (Figure 1) that recognize specific complex sugar motifs (neuraminic acid, *Neu*) on the surface of the host cell for binding, aggregation and entry into the cell. As cornerstones of the infection process, the recognition elements for cell surface adhesion are highly conserved and specific for a viral strain.

The abundance of these receptors poses an ideal target for the detection of the phenotype information encoded in these proteins. Recognition molecules for influenza viruses A, B, C and avian are N-acetylneuraminic acid residues located at the carbohydrate termini of various cell surface glycoproteins [12]. Minute structural differences in the N-acetyl-neuraminic acid residues (*N-Ac-Neu*) are employed by these variants to achieve high selectivity and affinity for their receptor sites. These preferences in binding to cell surface sugars are denoted in the chemical classification of the branching sites. For example a 2-6 linkage describes the attachment of neuraminic acid at the 2 position to a sugar scaffold at its 6 position. These differences in presentation are used in this work to distinguish avian (binds 2-3) over human (binds to 2-6) influenza.

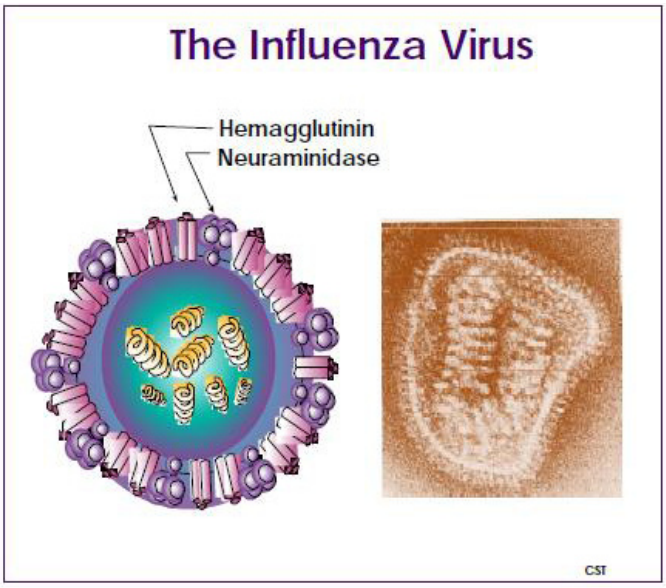


*Figure 1. Surface features on an Influenza virus.*

Another specific receptor, 5,9-$Ac_2$Neu is required for the binding of influenza C. This bisacetyl derivative serves as a high affinity receptor determinant to bind and infect human erythrocytes. This receptor is, however, not present in the human upper respiratory tract, which makes influenza C less likely to cause an infection. Influenza A and B do not recognize 9-O-acetyl-*N-Ac*-Neu [13,14] and recognition element structures of influenza A and B are more subtly distinguished. In addition to the sialyl moiety, the composition, structure and orientation of other carbohydrates in a sialyloligosaccharide have significant contributions to selective binding interactions between the influenza variants. Influenza A viruses are differentiated in the type of their *NA*, with many mutational variants. Influenza A is further divided into H1N1 and H1N3 types [4,5,6], while the current emerging avian flu variant is of the H5N1 type.

It was also found that subtle differences at the 2 position of the lactose/lactoseamine make important contributions to the binding affinities: Avian influenza recognizes 2'-3' linked sialic acids in preference over 2'-6' linked sialic acids, the natural target of human strains. HA binds three $GM_3$ [15], in addition to binding AcNeu5, which allows the discrimination of HA in the presence of NA activity. **As all *NAs* and *HAs* have minute, but distinct, binding preferences to sialic acid sites we exploit these differences in the identification of influenza [7] in multi – substrate panel assays that maximize the differential substrate cleavage rates.**

A single mutation, detectable by MS, from Ser 205 to Tyr was indicated in the switch of the binding preference for 2-6' bound *Neu* in influenza *HA* to 2-3' conformers [10] in analogy to the switch seen from human to avian influenza. A substitution R292K has been reported as the source of the emergence of *NA* inhibitor resistance [11]. Our substrate based enzyme assay directly interrrogates the enzyme and, therefore, identifies both phenotypic drift as well as the emergence of resistance to neuraminidase inhibitors. **In addition, this type of assay also aids in vaccine and antiviral drug validation, since enzyme activity could be directly monitored after treatment with a vaccine or in the presence of an antiviral drug**.

Although influenza strains have different substrate preferences, all substrates will be cleaved to some extend by all *NAs and HAs*. We therefore synthesized a panel of substrates that is optimized to show differential cleavage rates among the sugars. Figure 2 shows two substrates, one preferentially cleaved by Influenza A/B the other by H1 and N5 of avian influenza. The neuraminic acid cleaved by the enzyme is grafted onto a lactose scaffold to provide the stereochemical orientation to induce a preference. This provides selective panels of substrates for the mass spectrometric quantitation and differentiation of influenza in any biological sample. A mass spectrometry (MS) based method combines the accuracy and depth of information of MS detection, with automation and high sample trough-put capability of this platform to allow the accurate detection, differentiation of influenza viradae, monitoring of their phenotypic drift or the emergence of *NA* inhibitor resistance.

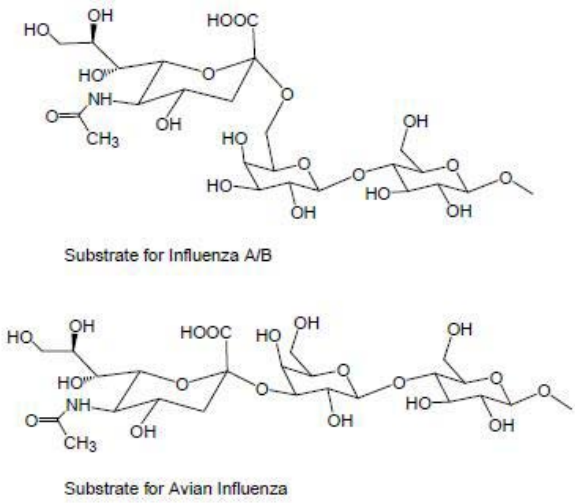


*Figure 2. Substrates for Influenza A/B and Avian Influenza*

The combination of stable isotope labeling ($^{13}C$ for our purposes) with MS allows us to discriminate between our panel of substrates and enzyme targets present in native samples.

## Scientific Approach and Accomplishments

The research approach therefore was designed to solve our research objectives in two phases: synthesis of substrates and MS validation of enzyme based cleavage. The syntheses of substrates followed previously developed routes. In contrast to reported procedures stable isotope precursors are expensive and a significant time was spent to optimize reactions and explore alternative routes to maximize yields that allow the use of stable isotopes. The majority of the synthetic steps are the introduction of protection groups that prepare commercially available Neu for the coupling to a sugar scaffold. The synthesis is designed to accommodate variation of the stereochemistry at the 2'-3' and 2'-6' linkage that provides the basis of enzyme discrimination. Acylations and alkylations at 4 and 7 positions of the lactose scaffold are easily incorporated for the synthesis of variants resistant to bacterial neuraminidases. The panel of substrate targets was chosen to incorporate maximum diversity in binding preferences and is shown in Figure 3.

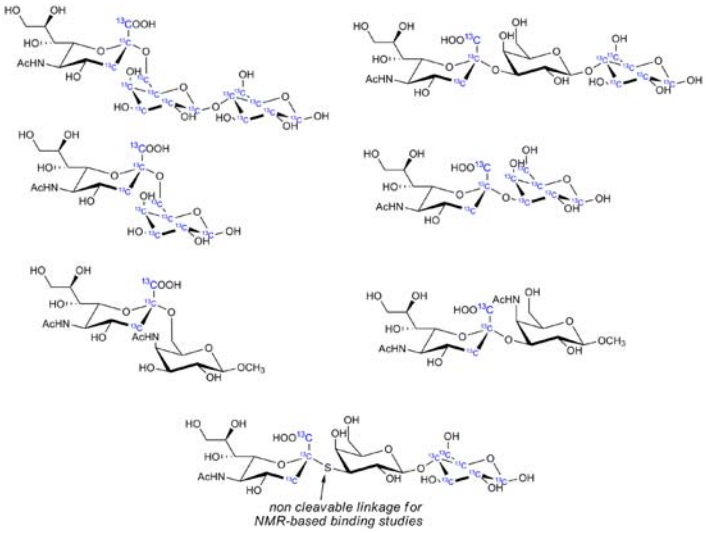


*Figure 3. Panel of stable isotope encoded substrates.*

The major challenge in sugar chemistry is to distinguish among six hydroxyl groups on the carbohydrate. Our initial synthetic efforts therefore focused on the use of acetyl based protection groups as these protection groups are easily installed and removed in generally high yield. All of our synthetic efforts were explored with natural abundance precursors, which are less costly and more readily available, in order to determine the efficiency, success, and final yield of synthetic routes.

Natural abundance lactose and *N*-acetylneuraminic acid were used for our initial evaluation. We found that for *N*-acetylneuraminic acid protection of the carboxylic acid as a methyl ester, masking every hydroxyl with an acetyl group, and conversion of the 2-O-acetyl to a 2-S-phenyl could be accomplished in high yield (>80% for 4 steps) and gave a precursor ready for glycosylation at the 2-position. Lactose suitable to couple at either the 3'-position or the 6'-position was also prepared and successfully coupled to the 2-SPh reactive sialic acid. Thus, the development of routes that lead to scaffolds of two substrate targets, 2-3 and 2-6 sialyl lactose, were accomplished in natural abundance forms.

Although these efforts validated our initial synthetic approach, especially with regard to installing the critical 2-3 and 2-6 sialyl lactose connections, there were several shortcomings in the reaction schemes. Most importantly, both the 2-3 and 2-6 couplings between the sialic acid and the lactose moieties proceeded in unacceptably low yields (<10%). These low yields were at the end of multiple step syntheses, a serious limitation for a reasonable use of early introduced isotopes. Further, low yields in selective deprotections at either the 6' or 3'-positions reduced the amount of material available for subsequent 2-3 and 2-6 couplings.

We determined that the use of the acetyl protection group while useful in the initial stages of synthesis was incompatible with reaction conditions present in later stages. Thus, we reevaluated our approach and decided to use the benzyl group to protect all hydroxyls except those predetermined for selective protection. This resulted in immediate improvements in both overall yields and ease of purification of intermediates. As an example, 2-6 coupling of sialic acid to the benzyl protected lactose was accomplished in >50% yield.

Having evaluated the best approach we began the synthesis of $^{13}C_6$ and $^{13}C_{12}$ lactose moieties suitable for coupling at the 3' and 6'-positions, respectively. Concurrently, we also began preparing $^{13}C_6$ galactose for coupling in the same manner. Both lactose moieties required individual preparation of both their glucose and galactose portions. Synthesis of the lactose scaffold was accomplished, in either selectively protected at the 3' or 6'-position, in >60% yield. This synthetic yield is impressive for 8 steps starting from glucose representing > 93% yield for every synthesis step. For the $^{13}C_6$ lactose, $^{13}C_6$ galactose required only two high yielding steps before coupling to the natural abundance glucose precursor was possible, thereby reducing the amount of valuable labeled compound potentially lost during synthesis.

Selective deprotection of the 3' and 6'-positions of the $^{13}C_6$ and $^{13}C_{12}$ lactose moieties, respectively, and the 3 and 6-positions of the $^{13}C_6$ galactose moieties was accomplished in high yield and all were successfully coupled to protected $^{13}C_3$ *N*-acetylneuraminic acid in

acceptable yields (up to 60%) to give the scaffolds of four substrate targets. Global deprotection of the remaining hydroxyls was accomplished in three steps to give 30-150 mg of each target. Although we are currently scaling up our syntheses to produce gram quantities of each substrate, we note that due to the high sensitivity of MS experiments only microgram quantities are necessary for enzyme analysis

In order to validate our MS based method of Influenza detection, we developed a protocol using sialidase enzymes and MS. There are several commercially available enzymes capable of mimicking the cleavage activity of the Influenza virus in addition to inactivated intact virus available to us. Enzyme reactions are highly dependent on buffers used, and most of the salts in buffers are not compatible with mass spectrometry instruments. Several buffer combinations were tried and we found that an ammonium formate system (pH 5) was effective in maintaining the performance of the enzyme while allowing substrate and product peaks to be detected by MS. Neuraminidase from *Clostridium perfringes* was initially used as surrogate for these experiments due to the slow cleavage rate of this enzyme for 2-6 sialyl lactose linkages compared to 2-3 linkages. We found that under the conditions used, the substrate was completely cleaved within 20 minutes. We are currently modifying our conditions to optimize the rate of cleavage in order to follow the characteristic time profiles for our panel of stable isotope labeled substrates. In parallel tests on real world influenza samples have been initiated at the CDC to validate the utility of our substrates in emerging public health monitoring needs.

## Impact on National Missions

This project augments basic science progress in the detection of pathogens and contributes to our portfolio of focused measurements and analysis of biological systems. The technology will allow monitoring of emerging threats by infectious agents, in particular influenza, and therefore supports biothreat reduction missions of DOE, DHS, and other agencies. The final result of this project was appreciable quantities of the desired modified compounds to be used in a multi-substrate panel assay capable of detecting, quantifying, and differentiating between influenza strains. Large scale sample testing will show *geographic* viral phenotype drift and the emergence of antiviral drug resistance. Thus, this project is in line with DOE objectives and mission in that it will enable novel detection techniques for an emerging health threat, specifically avian flu and swine flu. This project will not only further *Basic Science* progress in the area of carbohydrate based detection for pathogens, but contribute to our portfolio of tools for *Biothreat* monitoring and is therefore aligned with institutional efforts in *Threat Reduction*.

## References


1. Hughes, J. M., and J. W. LeDuc. Morbidity and Mortality weekly report( MMWR). 2000. *Recommendations and reports, CDC.*

2. Bridges, C. B., F. Kieji, T. M. Uyeki, N. J. Cox, and J. A. Singleton. Morbidity and Mortality weekly report (MMWR). 2002. *Recommendations and reports.CDC.*

3. Murti, K. G., and R. G. Webster. Distribution of hemagglutinin and neuraminidase on influenza virions as revealed by immunoelectron microscopy. 1986. *Virology.* **149**: 36.

4. Kobasa, D.. Amino acid residues contributing to the substrate specificity of the influenza A virus neuraminidase. 1999. *Journal of Virology.* **73** (8): 6743.

5. Sato, K.. Specificity of the N1 and N2 sialidase subtypes of human influenza A virus for natural and synthetic gangliosides. 1998. *Glycobiology.* **8** (6): 527.

6. Paulson, J. C.. Interaction of animal viruses with cell surface receptors. 1985. In *The Receptors.* Edited by Conn, P. M.. , p. 131. Orlando, Florida: Academic Press.

7. Aymard, M.. Neuraminidase assays. 2003. *Developments in Biologicals.* **115**: 75.

8. Schultze, D., Y. Thomas, and W. Wunderli. Evaluation of an Optical Immunoassay for the Rapid Detection of Influenza A and B Viral Antigens. 2001. *European Journal of Clinical Microbiology and Infectious Diseases.* **20** (4): 280.

9. Suzuki, Y.. Host mediated variation and receptor binding specificity of influenza viruses. 2001. *Advances in Experimental Medicine and Biology.* **491**: 445.

10. Varghese, J. N.. Drug design against a shifting target: a structural basis for resistance to inhibitors in a variant of influenza virus neuraminidase. 1998. *Structure.* **6** (6): 735.

11. Suzuki, Y., T. Ito, T. Suzuki, R. E. Holland, T. M. Chambers, M. Kiso, H. Ishida, and Y. Kawaoka. Sialic Acid Species as a determinant of the host range of Influenza A viruses. 2000. *Journal of Virology.* **74** (24): 11825.

12. Zimmer, G., G. Reuter, and R. Schauer. Use of influenza C virus for detection of 9-O-acetylated sialic acids on

immobilized glycoconjugates by esterase activity. 1992. *European Journal of Biochemistry.* **204** (1): 209.

13. Matrosovich, M. N., A. S. Gambaryan, A. B. Tuzikov, N. E. Byramova, L. V. Mochalova, A. A. Golbraikh, M. D. Shenderovich, J. Finne, and N. V. Bovin. Probing of the receptor binding sites of the H1 and H3 influenza A and influenza B virus hemagglutinins by synthetic and natural sialosides. 1993. *Virology.* **196**: 111.

14. Sato, T.. Binding affinity of GM3 lactone for influenza virus. 1999. *Glycoconjugate Journal.* **16** (3): 223.

15. Saito, M., and R. K. Yu. Biochemistry and function of sialidases. 1995. *Biology of the Sialic Acids.* : 261.

16. Unverzagt, C., S. Kelm, and J. C. Paulson. Chemical and enzymic synthesis of multivalent sialoglycopeptides. 1994. *Carbohydrate Research.* **251**: 285.

17. Iyer, S. S., R. M. Vermillion, and R. R. Kale. Synthetic multivalent sialic acids for the detection and differentiation of Influenza virus. *230th ACS National Meeting.* (Washington, DC, Aug. 28-Sept. 1, 2005).

18. Reuter, J. D.. Inhibition of Viral Adhesion and Infection by Sialic-Acid-Conjugated Dendritic Polymers. 1999. *Bioconjugate Chemistry.* **10** (2): 271.

19. Mochalova, L. V.. Fluorescent assay for studying the substrate specificity of neuraminidase. 2005. *Analytical Biochemistry.* **341** (1): 190.

20. Srivastava, O., G. Srivastava, M. Du, O. Hingsgaul, and D. R. Bundle. Syntheses of 4-alkyl chromogenic glycosides and 7-alkyl chromogenic glycosides of N-acetylneuraminic acids for detection of inluenza viruses. 2002. *Patent US 6420552 B1 20020716.*

## Publications

Kimball, D. B., R. Michalczyk, J. Schmidt, R. Kale, and S. Iyer. Functional carbohydrate substrates for Influenza detection. Presented at *237th ACS National Meeting.* (Salt Lake City, UT, 22-26 Mar, 2009).

# Magnetic Turbulence and Kinetic Dissipation in Solar Wind and Solar Corona Plasmas

*Hui Li*
20070170ER

## Abstract

The proposed work was to carry out the first-ever particle-in-cell (PIC) simulations that self-consistently capture both the nonlinear cascade and the kinetic dissipation of magnetic turbulence in collisionless plasmas. We in fact executed, analyzed, and published our results from the first PIC simulations of whistler turbulence and fast mode wave turbulence, and provided an interpretation of our results in terms of a variety of systems, including the spacecraft observations in the solar wind and laboratory plasma measurements such as reversed-field pinch experiments. We also carried out a series of PIC simulations that show how suprathermal solar wind electrons are scattered by various types of fluctuations, and we have done theoretical calculations providing a foundation for future PIC simulations of turbulence in electron-positron plasmas. Some of the main conclusions include: the magnetic turbulence in the kinetic regime is often anisotropic and this has important consequences on particle energization. Furthermore, fully kinetic PIC simulation is now proven to be the most direct way of capturing both cascade and dissipation in one system. This new approach could prove useful for many high-energy phenomena in space and astrophysics.

## Background and Research Objectives

In the solar wind, decades of spacecraft measurements of magnetic fluctuations suggest that this medium is turbulent. Similarly, most astrophysical environments are believed to be turbulent, as revealed by observations across the whole electromagnetic wavelengths. In laboratory plasma experiments, direct field and particle measurements have also recorded turbulent magnetic field and particle distributions. When our proposal was written in 2007, most observational and computational studies had addressed low-frequency, long-wavelength turbulence (often called the fluid limit), but there had been very little attention given to higher frequency, shorter wavelength fluctuations in the solar wind. It has generally thought that it is too difficult to study the cascade and kinetic dissipation simultaneously, thus there have not been any first principle, self-consistent studies on magnetic turbulence including all these processes. Our fundamental proposition was to use particle-in-cell (PIC) simulations to study for the first time the turbulent cascade of magnetic fluctuation energy to relatively short wavelengths, that is, wavelengths shorter than the ion inertial scale length, and to compare our results against observations of such turbulence. Our primary research objectives were to be the first to carry out short-wavelength PIC simulation of turbulence, to analyze the results in terms of the properties of both the fluctuation spectra and the associated plasma signatures, and to compare our results against solar wind observations of short-wavelength turbulence and laboratory plasma experiments. Each of these primary objectives was met.

## Scientific Approach and Accomplishments

The primary technical approach was to use particle-in-cell simulations to study homogeneous turbulence in collisionless plasmas. Although we carried out several different types of PIC simulations to address a variety of issues in plasma turbulence, one important achievement was the first-ever PIC simulation of cascading whistler turbulence. We introduced a nearly isotropic distribution of relatively long-wavelength whistler modes into a homogeneous plasma, and allowed turbulence to develop in time [1,2]. The primary results were (1) the turbulence showed a forward cascade (i.e. transfer of fluctuation energy to shorter wavelengths) with a relatively steep power spectrum, consistent with both solar wind observations and fluid models of whistler turbulence, (2) the turbulence developed a strong anisotropy with preferential propagation of fluctuations to directions relatively perpendicular to the background magnetic field, consistent with fluid models, (3) the turbulence became more anisotropic with increasing fluctuation energy [Figure 1], and (4)

the electrons were heated in directions both parallel and perpendicular to the background magnetic field. Results (3) and (4) are new predictions which should be subject to test both via observations and other models.

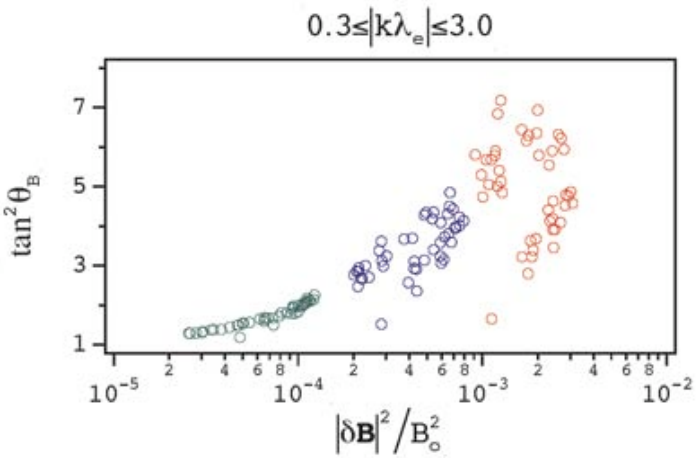


*Figure 1. Spectral anisotropy of whistler turbulence from three PIC simulations (corresponding to three different colors) as a function of the instantaneous fluctuating magnetic energy density.*

Another important achievement was the first-ever PIC simulation of cascading fast mode wave turbulence [3]. We demonstrated that a spectrum of fast wave modes with different total energies and different wave numbers will cascade to smaller scales and exhibit strong anisotropy (having more turbulent energy in the direction perpendicular to the background magnetic field). These features are demonstrated in Figure 2. The shape of the cascade is established after a few ion cyclotron periods and most of the energy in the cascade stays in the fast wave oscillations. Electrons eventually absorb most of the turbulent energy. These conclusions are being compared with solar wind and laboratory plasma experiment results.

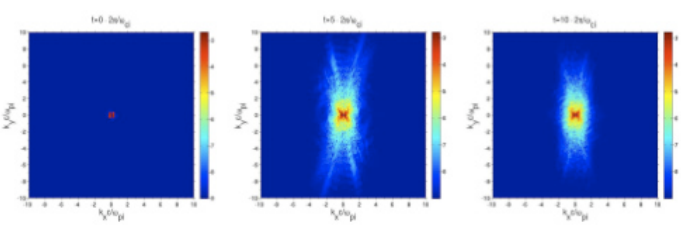

*Figure 2. Magnetic energy spectrum (the turbulent magnetic energy) as represented in the two-dimensional wavenumber space at different times. Initially, the wave spectrum is injected at small wavenumbers (left). As cascade in the wavenumber space proceeds, it develops an anisotropic spectrum, as indicated by the broad distribution in the perpendicular direction (middle). At later times, the turbulence is absorbed by electrons, so the overall spectrum "shrinks."*

## Impact on National Missions

In the three years since this LDRD project has been funded, there has been a dramatic increase in observational interest in short-wavelength turbulence in the solar wind. High-resolution magnetometer data has been used to provide the first analyses of short-wavelength turbulence in the solar wind that spans two or more decades in frequency; there have been three Physical Review Letters published on this topic since June 2009, two of which mention our simulation research. At present there is a debate in the space plasma research community as to whether whistlers or kinetic Alfven waves are the more important constituent of the short-wavelength turbulence observed in the solar wind; our LDRD-supported research will be an important benchmark in this debate. Research supported by this LDRD project was helpful in LANL winning a $450k, four-year grant from NASA for further studies of solar wind turbulence.

## References


1. Gary, S. P., S. Saito, and H. Li. Cascade of Whistler Turbulence: Particle-in-Cell Simulations. 2008. *Geophysical Research Letters.* **35**: L02104.

2. Saito, S., S. P. Gary, H. Li, and Y. Narita. Whistler turbulence: Particle-in-cell simulations . 2008. *Physics of Plasmas .* **15**: 102305.

3. Svidzinski, V. A., H. Li, H. A. Rose, B. J. Albright, and K. J. Bowers. Particle in cell simulations of wave turbulence in solar wind plasma in ion cyclotron frequency range. *Physics of Plasmas.*


## Publications


Borovsky, J. E., and S. P. Gary. On shear viscosity and the Reynolds number of magnetohydrodynamic turbulence in collisionless magnetized plasmas: Coulomb collisions, Landau damping, and Bohm diffusion. 2009. *Physics of Plasmas.* **16**: 082307.

Gary, S. P., H. Karimabadi, and V. Roytershteyn. Dissipation wavenumbers for turbulence in electron-positron plasmas. 2009. *Astrophysical Journal.* **701**: 1695.

Gary, S. P., S. Saito, and H. Li. Cascade of Whistler Turbulence: Particle-in-Cell Simulations. 2008. *Geophysical Research Letters.* **35**: L02104.

Gary, S. P., and C. W. Smith. Short-wavelength turbulence in the solar wind: Linear theory of whistler and kinetic Alfven fluctuations. *Journal of Geophysical Research.*

Gary, S. P., and H. Karimabadi. Fluctuations in electron-positron plasmas: Linear theory and implications for

turbulence. 2009. *Physics of Plasmas.* **16**: 042104.

Gary, S. P., and J. E. Borovsky. Damping of long-wavelength kinetic Alfven fluctuations: Linear theory. 2008. *Journal of Geophysical Research.* **113** (A12): A12104.

Gary, S. P., and S. Saito. Broadening of solar wind strahl pitch-angles by the electron/electron instabilities: particle-in-cell simulations. 2007. *Geophysical Research Letters.* **34**: L14111.

Saito, S., S. P. Gary, H. Li, and Y. Narita. Whistler turbulence: Particle-in-cell simulations . 2008. *Physics of Plasmas .* **15**: 102305.

Saito, S., and S. P. Gary. Whistler scattering of suprathermal electrons in the solar wind: particle-in-cell simulations. 2007. *J. Geophysical Research.* **112**: A06116.

Saito, S., and S. P. Gary. All whistlers are not created equally: scattering of strahl electrons in the solar wind via particle-in-cell simulations. 2007. *Geophysical Research Letters.* **34**: L01102.

Saito, S., and S. P. Gary. Perpendicular scattering for electron beams by the electron/electron instability in solar electron bursts. 2008. *Journal of Geophysical Research.* **113** (A4): A04S90.

Svidzinski, V. A., H. Li, H. A. Rose, B. J. Albright, and K. J. Bowers. Particle in cell simulations of wave turbulence in solar wind plasma in ion cyclotron frequency range. *Physics of Plasmas.*

Svidzinski, V. A., and H. Li. Calculation of resistive MHD and two fluid tearing modes by example of RFP-like plasma. 2008. *Physics of Plasmas.* **15**: 052106.

Svidzinski, V., H. Li, and B. Albright. Particle in cell simulations of tearing modes in reversed-field-pinch-like plasma. 2009. *Physics of Plasmas .* **16** (2): 022504.

Svidzinski, V., V. Mirnov, and H. Li. m=1 ideal kink modes in a line-tied screw pinch with finite plasma pressure . 2008. *Physics of Plasmas .* **15**: 092106.

# Understanding a Killer: A Predictive Model of Tumor Development

*Yi Jiang*
20070180ER

## Abstract

Cancer remains the leading cause of disease death for Americans. Moreover the overall effectiveness of therapeutic treatments is only approximately 50%. Therefore the development of prognostic tools could have immediate impact on the lives of millions of cancer patients. With the support of this LDRD, we have developed a multiscale, modeling framework that will help to generate predictive tools of tumor development. The multiscale framework is cell-based, and integrated three levels of cell dynamics, including a cellular model for cell dynamics, an intracellular protein regulatory network for cell cycle control and a signaling network for cell decision-making, and extracellular reaction-diffusion chemical dynamics. We have applied this modeling framework study tumor development in three aspects. First we have produced an avascular tumor growth model that could grow tumor from a single cell into a solid tumor, with growth dynamics that agree with tumor spheroid experiments. Second, we have developed a tumor angiogenesis model that can generate realistic vessel sprout patterns and test hypotheses about the biochemical and biophysical mechanisms of vasculature formation in tumor-induced angiogenesis. Third, we have also shown a vascular tumor growth model with chemotherapies, demonstrating potential for investigating chemotherapeutic strategies for tumor. This project has also lead to several publications and NIH proposals, some of which have been funded. Given the biological flexibility of the model, we believe that it can facilitate a deeper understanding of the cellular and molecular interactions associated with cancer progression and treatment, and potentially guide experimental design and interpretation.

## Background and Research Objectives

Tumor development is complex and dynamic. The microenvironment inside a tumor, which determines tumor dynamics, involves spatial and temporal variations in nutrient and waste gradients, cellular physiology and viability, energy and macromolecule metabolism, the expression patterns of genes and proteins, as well as the progression of the malignant process. The daunting complexity of a tumor in vivo has resulted in the development of simpler in vitro experimental models of the tumor microenvironment; the primary example has been the multicellular tumor spheroid (MTS) system. The MTS has the advantage of precisely controlling the external environment while maintaining the cells in a microenvironment that mimics the environment within a solid tumor [1]. This stage of tumor growth, or avascular tumor growth can only reach a few millimeters in diameter. Angiogenesis, formation of new blood vessels from existing blood vessels, is necessary for subsequent tumor expansion. Tumor cells generate angiogenic growth factors in response to their stressful microenvironment. These factors activate the vascular endothelial cells of nearby pre-existing blood vessels, and start the new vasculature development. With the new supply system, the tumor will have renewed growth beyond the avascular saturation size. Furthermore, the cells can invade the surrounding tissue, and metastasize to other parts of the body and establish secondary tumors. The interplay amongst all of these elements defines the response of a particular tumor to treatment from surgery to the newest drug.

Mathematical models based on the underlying tumor growth mechanisms can help understand and predict the tumor development in different environments and evaluate the effectiveness of different approaches for controlling the disease. When we started the project, there was no mathematical model of tumor growth that can start from a single cell and undergo the whole process of tumor development. Existing models fell in three disconnected regions: avascular tumor growth, angiogenesis, and chemotherapy for tumors with well-established vasculature, and were focused on mostly the biochemical aspect of the problem. In response to the lack

of more biophysics-based models, our objective was to develop a comprehensive tumor growth model that takes into account not only biochemical interactions, but also the biophysical environment and biomechanical effects, integrating information from molecular level to tissue level. The result is a multiscale modeling framework that can be applicable to many other problems involving multicellular dynamics. Our additional objects were to apply such modeling framework to new problems of both scientific and LANL interest. We have achieved all our objectives.

## Scientific Approach and Accomplishments

We have develop a comprehensive, multiscale, mathematical model based on experiments, to study tumor development, produce experimentally testable hypothesis, and finally predict the effects of chemotherapy on tumor development. The multiscale model includes three levels: at the intracellular level, a regulatory network of proteins for controlling cell dynamics; at the intercellular level cellular model describes cell physiology and dynamics; and the extracellular chemical environment.

We have developed a multiscale cellular model of tumor growth. Figure 1 shows a simulated spheroid with layered structure. The comparison between the growth curves of simulation and experiment under the same external chemical conditions shows excellent agreement [2]. This was the first cell-based multiscale model of tumor growth. Published in one of the top journals of the field, Biophysical Journal, it has received about 80 citations. We have parallelized this code using a novel hybrid parallelization scheme [3]. We applied this parallelized code to systematically study the mechanisms underlying the tumor growth saturation. We have discovered that without cell shedding (or equivalently, cell invasion to surrounding tissue), tumor spheroids cannot reach growth saturation. These new results have been the impetus for the grant application to NIH on tumor dormancy and a manuscript in preparation by Jiang and Freyer.

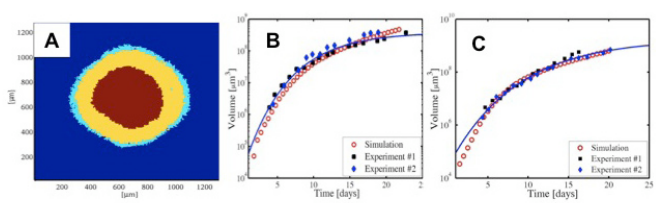


*Figure 1. Our model simulates the tumor growth from one single tumor cell into a spheroid with layered structure: a necrotic core, a thin proliferating surface layer, and the quiescent layer in between (A). Comparison of tumor growth dynamics between simulation and spheroid experiments: (B) using data from one experimental condition to fit for model parameters. (C) the model reproduces tumor growth curve with a different set of experimental conditions.*

We further developed the first cell-based model of tumor angiogenesis [4]. Published in Biophysical Journal it has received over 50 citations in less than 2 years. This model was able to produce, with cellular level details, realistic vascular sprout patterns, but also more sophisticated sprout branching and looping morphologies, that occur during tumor induced angiogenesis (Figure 2). This model also tested several important hypotheses regarding the vascular growth factor and sprout growth regions; the results were consistent with experiments. These results were featured in the Ask-the-Expert forum of NIH's CViT (Center for Virtual Integrative Tumor, www.cvit.org) for two months in 2007.

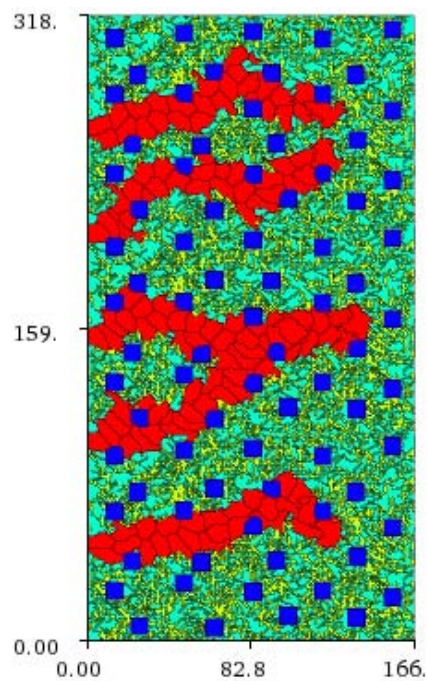


*Figure 2. Simulation of tumor induced angiogenesis: new blood vessel sprouts consist of endothelial cells that proliferate, migrate and organize into complex vessel patterns.*

We have applied the model to study the effects of biophysical properties of the tumor microenvironment, namely, the topography of the extracellular matrix, on the vasculature development in tumor angiogenesis [5]. This study, published in the PLoS Computational Biology, was the first of its kind to focus on the effects of the biophysical environment. The model predicts e.g. specific ranges of matrix fiber densities that maximize sprout extension speed, induce branching, or that interrupt normal angiogenesis, which are independently confirmed by experiment. Our results are discussed in the context of ECM targeted pro- and anti-angiogenic therapies that can be tested empirically.

We have also developed the first cell-signaling network for tumor-induced angiogenesis [6]. This paper, in press

with Journal of Theoretical Biology, is the first to propose a signal transduction model highlighting the cross-talk between key receptors involved in angiogenesis. From experimental data, we construct a stochastic network model of receptor cross-talk and analyze its dynamics. We identify relationships between receptor activation combinations and cellular function, and show that cross-talk is crucial to phenotype determination. The network converges to a unique set of known cell phenotypes. Finally, we use the model to study protein inhibition and to suggest molecular targets for anti-angiogenic therapies. This model constitutes the intracellular component of the multiscale model for tumor angiogenesis that was part of Bauer's Ph.D. thesis at University of Michigan.

To model vascular tumor growth, our first order approximation was to embed a set of simplified blood vessels into the avascular tumor. We applied this simple vascular tumor model to show that such a model could eventually be used as a predictive tool to compare the effects of different dosage and dosing schedules, toward individualized therapeutic strategies. In addition, we have developed a dynamic, realistic tumor vasculature model, which considers tumor vessel structures, blood flow in the vascular channels, and transport of oxygen, glucose and other chemical species between the vascular network and the surrounding tumor tissue. Three tasks have been completed: 1) Upgrade rheology model of blood flow to more accurately capture nonlinear dynamics. We rely on previous work [7] that described an accurate blood rheology model in which pressure drops and viscosity are functions both of vessel radius and also of hematocrit. In our vascular model, pressure and flow rate are computed in each vessel segment. Further, we have implemented the complete blood flow model, which is based on a series of experiments that elucidate the most relevant dynamics of blood flow in capillary networks [8-9]. 2) Diffusion of reactive species and feedback on vessel walls. Our model solves coupled differential equations for flow and transport in blood vessels, while in the tissue external to blood vessels it converts to reactive particles to transport oxygen and glucose and messenger molecules. Additionally, our model includes a unique property of the tumor vasculature network, leakage of the vessels. 3) Capture geometry and impact of vascular network architecture. Blood vessels in tumors are characterized by randomness, and tortuous paths, with shunts and dead-ends, as well as considerable variability in the vessel wall permeability. We have established collaboration with Prof. Secomb (U. of Arizona), who is the leading expert in the experimental studies and mathematical descriptions of blood flow. We have examples of blood vessel geometry and connectivity from reconstructions obtained from rat tumor as well as other structures (Figure 3). We are using such reconstructions directly in our numerical simulations, allowing us to increase the realism of our modeling.

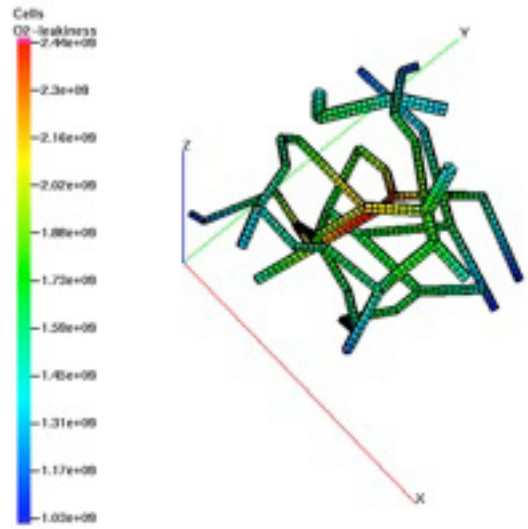


*Figure 3. Model for blood flow with a reconstruction of tumor blood vessel network from a mouse.*

On the experimental side, in order to provide more comprehensive data for model development, we have conducted a comprehensive series of spheroid growth experiments using a set of four mouse fibroblast cell lines. We have completed measurements and initial analysis of the spheroid growth curves under standard culture conditions. The spheroids demonstrated a typical growth curve with initially exponential growth rate that decreased with time until a saturation size was obtained. Interestingly, there was no significant difference in growth rates or saturation sizes for any of the cell lines, suggesting that neither HIF1-a expression nor tumorigenic status has any effect on spheroid development. Figure 4 shows there were also no significant differences in the proliferative status or the extent of necrosis for these cell lines under standard culture conditions. We have also made preliminary measurements of the rate of cell shedding from the spheroids during growth. For three independent measurements on spheroids from 2.5 to 4.4 mm in diameter, the untransformed cells had mean shedding rates of 905 and 1141 cells/mm$^2$-hour for the wild-type and null cell lines, respectively. The malignant cells had nearly two-fold higher cell shedding rates (1703 and 2030 cells/mm$^2$-hour for the wildtype and mutant cell lines, respectively). These cell shedding data demonstrate that even at growth saturation, there is still cellular proliferation at the spheroid surface. We will use the datasets described above to refine the model and to derive critical concentrations for oxygen and glucose induction of necrosis. We have completed growth curves in

five-fold increased glucose: these data show the expected increase in spheroid saturation size, to nearly a five-fold higher spheroid volume than was obtained under the lower glucose concentration. Interestingly, there was still no significant difference in the growth parameters for the wildtype and mutant cell lines of either the normal or tumorigenic cell lines. We have recently received a set of histology samples for these spheroids that are currently being analyzed, so we do not yet know if the increased glucose concentration resulted in an increased thickness of the viable cell rim. When we complete the analysis of these sections we will have generated a complete set of spheroid growth curves for four different cell lines under two different growth conditions. These data will provide a valuable source of data for future refinement of the tumor growth model.

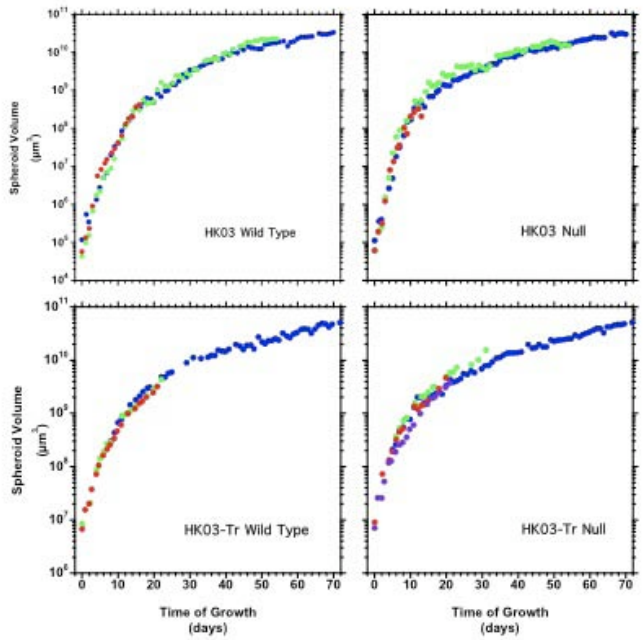


*Figure 4. Complete experimental tumor spheroid growth data for four cell lines.*

In addition to several follow-on projects, we have applied this multiscale modeling to another important problem, bacteria swarming. Many bacteria can rapidly traverse surfaces from which they are extracting nutrient for growth. They generate flat, spreading colonies, called swarms because they resemble swarms of insects. We seek to understand how members of any dense swarm spread efficiently while being able to perceive and interfere minimally with the motion of others. We investigate swarms of the myxobacterium. The understanding gained from this particular species can shed light in the spread of more malignant ones, e.g. pathogens in human airways. This study has generated a series of publications in high profile journals [10-11].

These publications have lead to many honors to Jiang, who has been invited to deliver over 45 colloquia, seminars and invited talks and lectures on this subject, including twice as Plenary Speakers and once as Topical Speaker to international conferences.

## Impact on National Missions

This project integrated simulation, theory and experiments to predict a complex biological system -- dynamics of tumor development – it fits the goal of Science based prediction perfectly. It is also an excellent example of Complex Systems Grand Challenge for LANL. We have developed state of the art capabilities in multiscale modeling, in particular in complex biological problems across multiple scales. It will be applicable to many other problems, such as problem that is important to national security – biothreat – host-pathogen interaction, progression of disease through tissue. It is a key component of a new LDRD-DR project (Transformative Capability for Bioassessment of Engineered Nanomaterials).

This project has also recruited many talented students to LANL:

Amy Bauer, GRA, spent about three years with Yi Jiang on modeling tumor angiogenesis. Yi Jiang was her co-supervisor. She is currently a postdoc associate at T6.

Kejing He, GRA, spent 6 months with Yi Jiang, developing a hybrid parallelization method to parallelize the multiscale model. This work was part of his Ph.D. thesis. Yi Jiang was his co-supervisor.

Kevin Flores, GRA, spent two summers working with Yi Jiang. He incorporated mutations into the tumor model and studied selective growth of tumor.

Yilin Wu, GRA, spent three summers with Yi Jiang. He applied the multiscale modeling framework to study the swarming behavior of myxobacteria, which was his Ph.D. thesis project and Yi Jiang was his co-supervisor.

Zhiying Sun, GRA, spent one summer with Yi Jiang on using simplified continuous equations to study the avascular and vascular tumor growth.

Gautam Muralidhar, GRA, spent one summer with Yi Jiang modeling cancer invasion.

Siri (Emma) Ader, UGA, spent one summer with Yi Jiang analyzing brain tumor images.

Christine Suss, UGA, spent one summer with Yi Jiang, modeling pathogen spread in human lung tissue.

Kristin White, UGA, spent one summer with Yi Jiang, modeling pathogen spread in human lung tissue.

Antoinette Trujillo, GRA, spent 20% time per year helping James Freyer with spheroid growth experiments.

## References


1. Freyer, J., and R. Sutherland. Regulation of growth saturation and development of necrosis in EMT6/Ro multicellular spheroids by the glucose and oxygen supply. 1986. *Cancer Research.* **46** (7): 3504.

2. Jiang, Y., J. Pjesivac-Grbovic, C. Cantrell, and J. Freyer. A multiscale model for avascular tumor growth. 2005. *Biophysical Journal.* **89** (6): 3884.

3. He, K., Y. Jiang, and S. Dong. A hybrid parallel framework for the Cellular Potts Model simulations. To appear in *The Fifteenth International Conference on Parallel and Distributed Systems (ICPADS'09).* (Shenzhen, China, 8-11 Dec. 2009).

4. Bauer, A., T. Jackson, and Y. Jiang. A cell-based model exhibiting branching and anastomosis during tumor-induced angiogenesis. 2007. *Biophysical Journal.* **92** (9): 3105.

5. Bauer, A., T. Jackson, and Y. Jiang. Topography of extracellular matrix mediates vascular morphogenesis and migration speeds in angiogenesis. 2009. *PLoS Computational Biology.* **5** (7): e1000445.

6. Bauer, A., T. Jackson, Y. Jiang, and T. Rohlf. Stochastic network model of receptor cross-talk predicts anti-angiogenic effects. To appear in *Journal of Theoretical Biology.*

7. Alarcon, T., H. Byrne, and P. Maini. A design principle for vascular beds: the effects of complex blood rheology. 2005. *Microvascular Research.* **69**: 156.

8. Pries, A. R., T. W. Secomb, P. Gaehtgens, and J. F. Gross. Blood flow in microvascular networks. Experiments and simulation. 1990. *Circulation Research.* **67** (4): 826.

9. Pries, A. R., and T. W. Secomb. Control of blood vessel structure: insights from theoretical models. 2005. *American Journal of Physiology Heart Circulation Physiology.* **288** (3): H1010.

10. Wu, Y., Y. Jiang, D. Kaiser, and M. Alber. Type IV pili facilitate the collective motion of bacteria: modeling Myxobacterial swarming. 2007. *PLoS Computational Biology.* **3** (12): e253.

11. Wu, Y., D. Kaiser, Y. Jiang, and M. Alber. Periodic reversal of direction allows Myxobacteria to swarm. 2009. *Proceedings of National Academy of Sciences, U S A.* **106** (4): 1222.


## Publications


Bauer, A. L., T. L. Jackson, and Y. Jiang. A cell-based model exhibiting branching and anastomosis during tumor-induced angiogenesis. 2007. *Biophysical Journal.* **92**: 3105.

Bauer, A. L., T. L. Jackson, and Y. Jiang. Topography of Extracel lular Matrix Mediates Vascular Morphogenesis and Migration Speeds. 2009. *PLoS Computational Biology.* **5** (7): e1000445.

Bauer, A., T. Jackson, Y. Jiang, and T. Rohlf. Stochastic network model of receptor cross-talk predicts anti-angiogenic effects. . To appear in *Journal of Theoretical Biology. .*

He, K., Y. Jiang, and S. Dong. A hybrid parallel framework for the Cellular Potts Model simulations. . To appear in *The Fifteenth International Conference on Parallel and Distributed Systems (ICPADS'09).* . ((Shenzhen, China, 8-11 Dec. 2009). ).

Jiang, Y.. A multiscale, cell-based framework for modeling cancer development. 2007. In *Lecture Notes in Computer Science.* Edited by Shi, Y., G. v. Albada, J. Dongarra, and P. Sloot. Vol. 4487, p. 770. Springer: Springer.

Jiang, Y.. Understanding a killer: a predictive model for tumor development. 2006. *Contemporary Mathematics.* **410**: 173.

Wu, Y., D. Kaiser, Y. Jiang, and M. Alber. Periodic reversal of direction allows Myxobacteria to swarm. 2009. *Proceedings of National Academy of Sciences, U S A.* . **106** (4): 1222 .

Wu, Y., Y. Jiang, D. Kaiser, and M. Alber. Type IV pili facilitate the collective motion of bacteria: modeling Myxobacterial swarming. 2007. *PLoS Computational Biology.* **3** (12): e253.

# An Experimental and Theoretical Framework for Reactive Micromixing

*Amr I. Abdel-Fattah*
20070267ER

## Abstract

Coupled small-scale mixing and chemical and/or biological reactions (i.e., reactive micromixing) is an important process underpinning many seemingly different applications. This project aimed at providing improved quantitative understanding of reactive micromixing and potential techniques for enhancing micromixing in systems devoid of turbulence (low-Reynolds number), such as microfluidics. Experimental and theoretical studies were performed in parallel in ideal low-Reynolds number (Re) systems representative of natural porous media. Micromixing between two aqueous fluids in the presence and absence of chemical reaction processes, i.e., reactive and nonreactive micromixing respectively, at the microscopic scale was studied through a series systematic laboratory experiments in well-characterized systems (micromodels). The Lattice Boltzmann Method (LBM) was utilized to simulate the experiments under similar conditions. The results of both experiments and simulations showed reasonable agreement and pointed out to key parameters controlling the micromixing process, which were utilized to develop a technique for enhancing micromixing. The experiments confirmed the applicability of the LB simulations. In addition to capturing the overall diffusive behavior in the micromodel, the LB simulations accurately reproduced the pore-scale shear phenomena of encroaching fingers and trailing streaks. We also investigated a micromixing enhancing technique based on alternating the flow rates of the two fluids. Our results showed significant enhancement in the rate and extent of micromixing and that this enhancement depends on both the frequency and amplitude of alternation. Cycling the injection flow rates of the water and dye streams 180 degrees out of phase created concentration gradients parallel to the direction of flow. These parallel gradients produced substantial enhancement of micromixing. Our results demonstrated that enhancement of micromixing is most likely to occur in the subsurface if transient concentration gradients parallel to the direction of flow exist, as might be expected during injection or flooding operations.

## Background and Research Objectives

Many natural and industrial processes that are significantly different in length scales (micrometer to kilometer) involve micromixing phenomenon, either as an underlying mechanism or as a means to promote simultaneous chemical or biological reactions and transport of molecules, macromolecules, particulates or cells through sub-millimeter or micron-size channels. The details of the fluid motion in these small channels, coupled with various reactions and interactions with the surface-dominated physics of the channels create complex phenomena, which can be difficult to predict even with the most sophisticated numerical techniques. Two extreme examples can be mentioned: (1) transport and manipulation of different species in miniature systems (microfluidic devices) in biomedical and sensor (e.g., lab on a chip) applications and flow and transport of contaminants in subsurface heterogeneous media in waste management and remediation applications.

Significant insight on mixing phenomena at the microscale was only possible from fluid mixing experiments (with or without reaction) using microfluidic devices (see reviews by Darhuber and Troian [1], Ottino and Wiggins [2] and the special issue edited by Abdel-Fattah, [3]). Microfluidics is essentially a field dedicated to miniaturized plumbing and fluidic manipulation, which offers a great possibility of solving outstanding system integration issues for the automation of numerous biological and chemical processes, to a similar extent to the revolutionary integrated circuits. In most microfluidic devices, mixing two fluids or distributing chemical species and macromolecules in microchannels is a major challenge facing microfluidics. These miniature systems can quickly reach length scales where the fundamental fluid

physics changes dramatically. One major consequence of this is the significant reduction in inertial effects stimulating the nonlinearity responsible for numerous instabilities and turbulence, thus leaving molecular diffusion as the main mass transport mechanism (i.e., low Reynolds numbers). In many situations, pure molecular diffusion is too slow to achieve adequate mixing required for the target applications. Therefore, means are desired for enhancing mixing in microfluidic devices to promote the desired chemical and/or biological interactions. In microfluidic systems of well characterized geometries, analytical solutions usually can be derived to describe their behavior [4] and the extent of mixing and interaction among different species can be reasonably predicted. However, the presence of a complex pore-grain network as well as physical and/or chemical heterogeneities, inherent to natural systems or essential for a microfluidic device to achieve its desired functionality, precludes adequate predictions of the device's performance.

In large-scale heterogeneous systems such as subsurface media and groundwater aquifers, stochastic approaches borrowed from statistical physics (e.g. Percolation theory, Monte Carlo approaches, Pore Networks etc., [5] could be useful. Available porous continuum reactive transport codes are deficient in this respect, in that they do not consider the role of small-scale mixing on chemical reaction. Modeling such systems requires writing balance equations that reflect conservation of heat, mass, and momentum, which are solved numerically. Numerical models designed to simulate natural processes abound: codes solving transport in porous media and migration of reacting chemicals in the atmosphere are two common examples. The chemical reaction term, added to the conservation of mass equations for species traveling in a fluid (groundwater, air, etc.), is generally assumed to be accessible via measurements either at the laboratory scale or in the field. The equilibrium or kinetic rate laws and their parameters, determined from such measurements, are then plugged into the transport model as is.

The ultimate goals of this project are: 1) develop a mechanistic approach for studying and quantifying micromixing phenomena in porous media, 2) provide improved quantitative understanding of the micromixing phenomena that can be used to describe reactive transport in multi-scale systems, 3) capture the transition of micromixing towards the steady state condition, and 4) use the results to develop a technique for enhancing micromixing in systems of low-Reynolds number.

## Scientific Approach and Accomplishments

Our approach involved well-controlled visualization experiments in conjunction with LBM simulations. The experiments used advanced microscopic and imaging techniques to visualize and quantify the spread of one species in another as both flow side-by-sides in a microfluidic cell comprised of well-defined pore-grain networks. In the nonreactive micromixing experiments, ultrafiltered deionized water was used as one species and a solution of Sodium fluorescein (or uranine) dissolved in ultrafiltered deionized water as the second species. In the reactive micromixing experiments, two reacting solutions – one with free Ca+ ions and the other is a calcium ion indicator (Oregon 5N BAPTA), were introduced parallel to each other into the micromodel at a very low flow rate (4 microlters/hr). The calcium indicator reacted with the free Ca+ ions in a 1:1 molar ratio and correspondingly its fluorescent intensity was increased approximately by 6 times. The molecular diffusion coefficient of the (OG5N) indicator is about 2.2 times less than that of the calcium ions. Two sets of reactive experiments were performed - one with equimolar concentration of the two species ([Ca], [OG5N] = 30 microM) and the other to have a concentration gradient ([Ca] - 100 microM, [OG5N] - 50 microM).

The microfluidic cells used in the experiments were constructed by etching a predefined pore-grain network design (overall dimensions of 1cm×2cm×40microns) into a silicon wafer using standard photolithographic techniques. A number of different designs were used in the experiments (Figure 1). The porous micromodel was housed in a custom-made stainless steel manifold and connections are made using 1/16" diameter Teflon tubing and appropriate connectors. A picture of the assembly is shown in Figure 1.

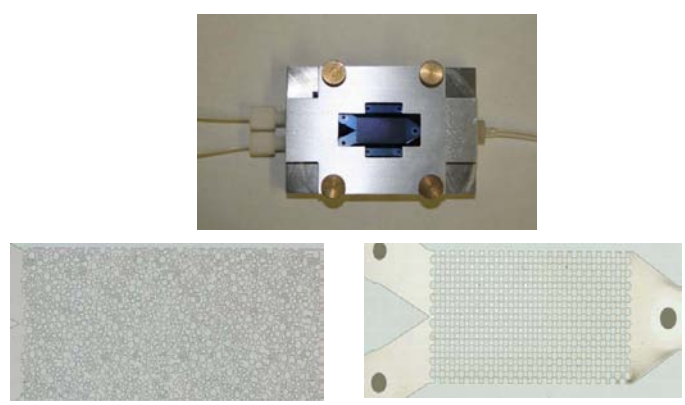

*Figure 1. Micromodel housing manifold (top) and two examples of micromodels of different pore-grain networks (bottom left and right).*

The Automated Video Microscopic Imaging and Data Acquisition System (AVMIDAS; US Patent No. 6,836,559) enabled high-resolution visualization and imaging of the entire area of the micromodel (under steady state conditions) by precisely controlling the movement of the

microscope's stage to take multiple high magnification images and stitch them together. The experiments were conducted by injecting the two fluid streams through a precision low-flow syringe pump and 100 μL syringes. Special in-line pulse dampeners were used to achieve stable flow conditions. The light intensity from the fluorophore in the transverse and longitudinal directions provided the concentration distributions of Uranine at different times, thus the extent of mixing in both directions.

In the alternating flow rate experiments, the injection flow rate of the deionized ultrafiltered water and dye solution streams was cycled alternatively between 0 and 100 μL/hr every 10 seconds. This procedure was automated by interfacing the syringe pump with a PC and programming the input flow parameters. The oscillatory flow was achieved by executing a Fortran 77 code. The experiments and simulations looked at both simultaneous (both streams injected into the flow cell at the same rate) and oscillatory (only one or the other stream injected into the flow cell at a given time) injection conditions. To ensure that the contributions of convective mass transport were distinguishable from those of diffusive mass transport, the experiments and simulations were performed under relatively high flow rates.

The experiments provided improved data pertaining to micromixing under low Peclet (Pe) number conditions. Transient behavior of micromixing, which is lacking in the reported literature, was adequately captured and quantified. Our results represent the first comprehensive data set on transitional micromixing, before and after reaching steady state. Examples of results obtained for both reactive and nonreactive micromixing experiments are shown in Figures 2 and 3.

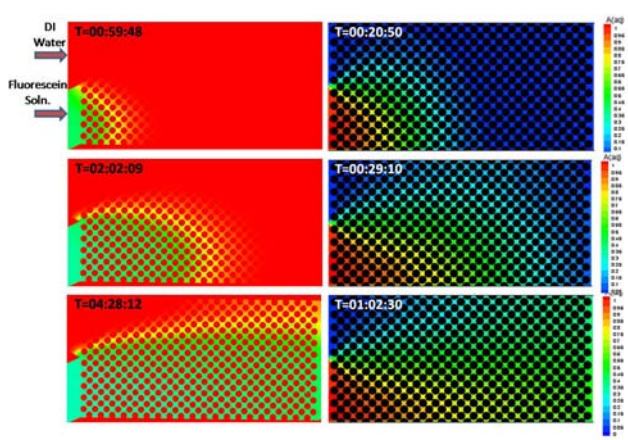


*Figure 2. Experimental (left) and LBM simulation (right) results of a non-reactive micromixing experiment employing de-ionized water and fluorescein solution at Pe ~ 2. Micromodel used: staggered array of cylindrical grains of diameter 600-μm, height 35-μm, porosity = 0.38.*

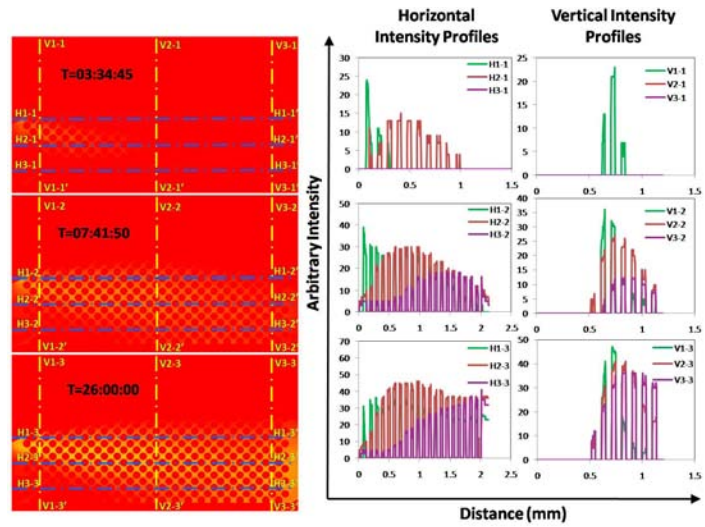


*Figure 3. Experimental results of a reactive micromixing run using a 100 microM Ca+ ions solution and a 50 microM OG5N calcium ion indicator at Pe ~ 2. Micromodel used: staggered array of cylindrical grains of diameter 600-μm, height 35-μm, porosity = 0.38.*

In this project, we further enhanced the previously developed Lattice Boltzmann methods for multi-component reactive transport. Particularly, we implemented in our code the recent development in the LBM to simulate incompressible flows, and hence eliminated the compressible error in the conventional LBM, which may be significant for flow in porous media with realistic porosity values. We also improved the boundary treatment enabling the code to handle larger Damkohler and Peclet numbers. Using the improved code, we have simulated the micromodel experiments for non-reactive mixing and reactive mixing and obtained qualitative agreement (Figure 2 and 4). In addition, we have applied the code to model the injection of a CO2-saturated brine into various porous media structures at temperatures T=25 and 80°C. In the various cases considered the porous medium consists initially of calcite with varying grain size and shape. A chemical system consisting of Na+, Ca2+, Mg2+, H+, Cl-, and CO2(aq) is considered. Flow and transport by advection and diffusion of aqueous species, combined with homogeneous reactions occurring in the bulk fluid, as well as the dissolution of calcite and precipitation of dolomite are simulated at the pore scale. The effects of the structure of the porous media on reactive transport are investigated. The results are compared with a continuum-scale model and the discrepancies between the pore- and continuum-scale models are discussed. This study sheds some light on the fundamental physics occurring at the pore scale for reactive transport involved in geologic $CO_2$ sequestration.

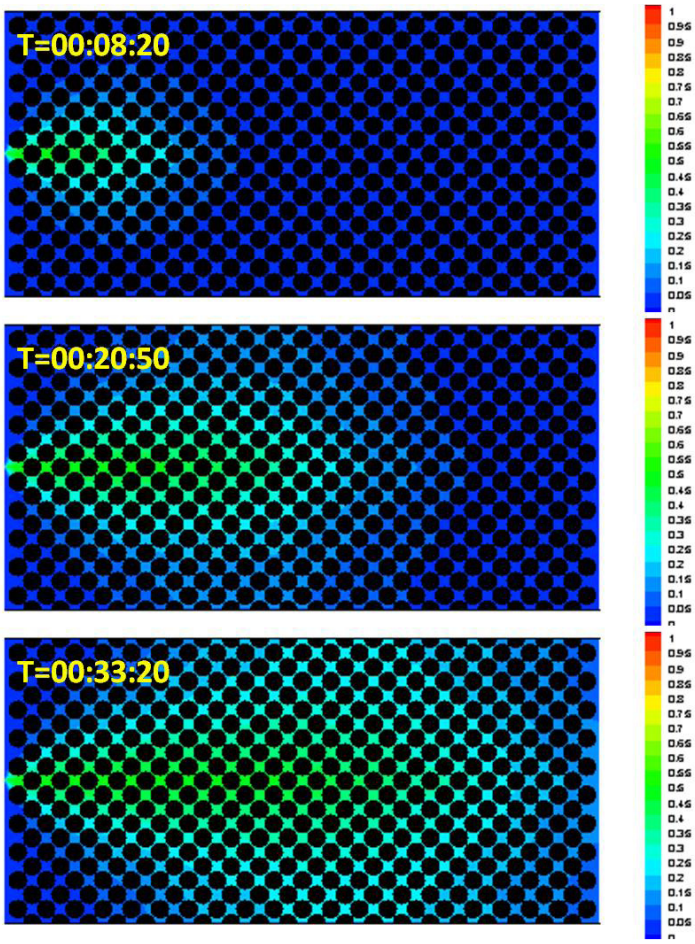


*Figure 4. LBM simulation results for the experimental run presented in Figure 2 of reactive micromixing using a 100 microM Ca+ ions solution and a 50 microM OG5N calcium ion indicator at Pe ~ 2. Micromodel used: staggered array of cylindrical grains of diameter 600-µm, height 35-µm, porosity = 0.38.*

In this project, we also developed an LBM for simulating coupled fluid flow and finite-sized particle transport and applied the method to the peristaltic transport of a macroscopic particle in two- and three- dimensional channels. We systematically investigate the effect of variation of the relevant dimensionless parameters of the system on the particle transport. We find, among other results, a case where an increase of Reynolds number can actually lead to a slight increase in particle transport, and a case where, as the wall deformation increases, the motion of the particle becomes non-negative only. We examine the particle behavior when the system exhibits the peculiar phenomenon of fluid trapping. Under these circumstances, the particle may itself become trapped where it is subsequently transported at the wave speed, which is the maximum possible transport in the absence of a favorable pressure gradient. Finally, we analyze how the particle presence affects stress, pressure, and dissipation in the fluid in hopes of determining preferred working conditions for peristaltic transport of shear-sensitive particles. We find that the levels of shear stress are most hazardous near the throat of the channel. We advise that shear-sensitive particles should be transported under conditions where trapping occurs as the particle is typically situated in a region of innocuous shear stress levels.

In the convective transport dominated regime (high flow rates), it was not practical to simulate the fluid flow and dye concentration fields simultaneously. Rather, the fluid velocity field was calculated first using an incompressible LBM algorithm, and then the behavior of the dye was simulated using the LBM algorithm for passive diffusion and the previously calculated velocity field. Constant flux inlet and outlet boundary conditions were used in the velocity field simulations. This approach allowed for a prescribed flow rate from one or both of the inlets to be achieved in the simulations. Constant concentration boundary conditions at the inlet and outlet were used during the concentration field simulations.

Successful LBM simulations of the alternating flow rate conditions required the determination of two difference velocity fields – each with constant volumetric flux from one of the two inlets and no flux from the other. The concentration field simulation then cycled between the two velocity fields at prescribed times to replicate the effects of oscillatory injection rates. Examples of the results under the alternating flow rate conditions are shown in Figure 5.

Our results showed that the presence of porous media did not significantly enhance micromixing beyond that of diffusion alone when the two fluid streams were injected into the media at equal rates, resulting in a concentration gradient perpendicular to the direction of flow. Simulations using non-diffusing particles demonstrated that the porous media shear failed to induce convective mixing perpendicular to the direction of flow, but produced significant convective mixing parallel to the direction of flow. Our experimental data and simulations showed that the mixing parallel to the flow resulted in encroaching dye fingering and trailing dye streaking of parallel concentration gradients, which in turn increased the area of contact between dye and water, thus enhanced the micromixing of the two injection streams. Interestingly, we find that the design of the inlet where the two injected streams meet plays a decisive role in the nature of the parallel concentration gradients established by alternating the two inlet flow rates.

Finally, as one of the accomplishments of this project, Kevin Connington successfully defended his dissertation on August 31, 2009 and will be conferred a PhD by the

Department of Mechanical Engineering, The Johns Hopkins University. A significant part of his thesis work was done at LANL as a visiting student supported by this LDRD project.

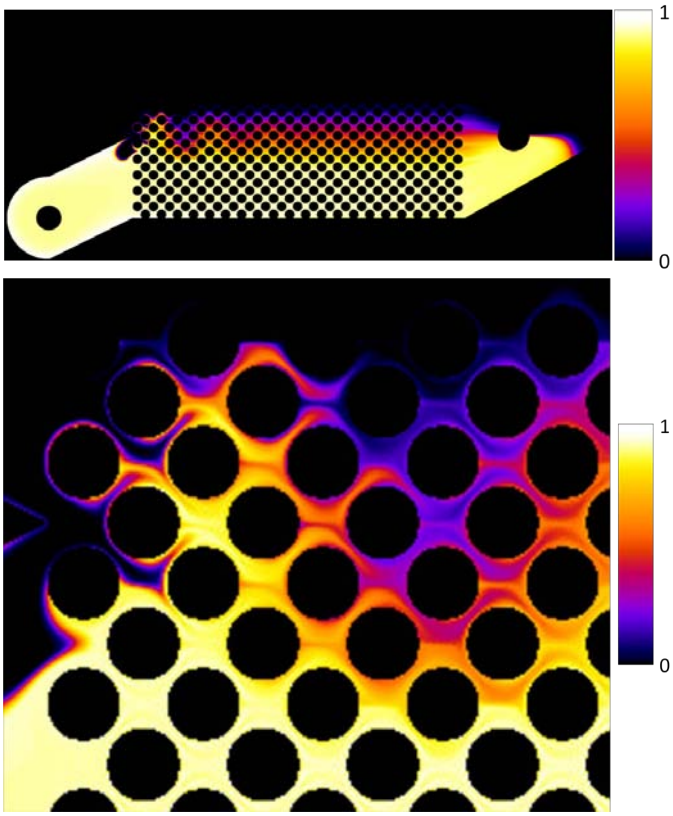


*Figure 5. (Top) LBM Simulated dye concentration field for alternating injection flow rate of 100 microliter/hr total (10 seconds per inlet), normalized to the maximum concentration. Alternating the injection of the flow cell between the dye- and non-dye-bearing inlets creates a radial wave pattern at the interface between the dye and non-dye streams. It is evident that the now posts dramatically enhance micromixing between the two streams by inducing encroaching dye fingers and trailing dye streaks. (Bottom) Close-up view detailing the simulated encroaching dye fingers and trailing dye streaks created by the posts in the micromodel.*

## Impact on National Missions

This project supports Threat Reduction and Energy Security and Science missions by improving our quantitative understanding of reactive-micromixing and its integration into larger-scale systems for environmental and energy sciences and applications. In microscopic systems such as microfluidics, this improved understanding is essential for the design and validity of chem-bio sensors. Other applications include: biological and chemical sensors and microreactors; oil recovery and fuel cells; subsurface remediation and contaminant transport. Many different important applications can benefit from this study. Examples include: a) *industrial*, such as organic synthesis, combustion, polymerisation, precipitation and fermentation; b) environmental, such as the fate of transport of contaminants in, and remediation of, subsurface media and groundwater aquifers; c) medical, biomedical and pharmaceutical, such as the design, development and use of microfluidic devices for patient diagnosis, patient monitoring, blood analysis, drug delivery, drug discovery, and microscale flow cytometers for cancer cell detection; d) homeland security and threat reduction, such as the design and use of chemical, nuclear and biological sensors; e) engineering and technological, such as chemical and nuclear reactors, MEMS, micromixers, micron-scale supersonic nozzles, ink-jets, micro-machined electrophoretic channels for DNA fractionation and polymerase chain reaction (PCR) chambers for DNA amplification, and the membraneless H-filters that separate and filter particles by size without a membrane; and f) domestic applications such as surface cleaning, fabric care, cosmetics, and painting.

## References

1. Darhuber, A. A., and S. M. Troian. Principles of microfluidic actuation by modulation of surface stresses. 2005. *Annual Review of Fluid Mechanics.* **37**: 425.

2. Ottino, J. M., and S. Wiggins. Introduction: mixing in microfluidics. 2004. *Philosophical Transactions of the Royal Society of London Series a-Mathematical Physical and Engineering Sciences.* **362** (1818): 923.

3. Abdel-Fattah, A. I.. Recent advances in electrokinetics: A collection of papers presented at the 7th International Electrokinetic Phenomena Conference (ELKIN 2004), Pittsburgh, USA, June 2004 - Preface. 2005. *Colloids and Surfaces A-Physicochemical and Engineering Aspects.* **267** (1-3): 1.

4. Stroock, A. D., S. K. Dertinger, A. Ajdari, I. Mezic, H. A. Stone, and G. M. Whitesides. Chaotic mixer for microchannels. 2002. *Science.* **295** (5555): 647.

5. Tsimpanogiannis, I. N., Y. C. Yortsos, S. Poulou, N. Kanellopoulos, and A. K. Stubos. Scaling theory of drying in porous media. 1999. *Physical Review E.* **59** (4): 4353.

## Publications

Beckham, R., S. Tarimala, P. Roberts, and A. Abdel-Fattah. Enhanced micromixing in porous media, Lattice-Boltzmann modeling and microfluidic experimental Results . Presented at *American Geophysical Union, Annual Fall Meeting 2009.* (San Francisco, 14-18 December, 2009).

Beckham, R., S. Tarimala, and A. Abdel-Fattah. Enhancing

micromixing through cycling injection between two inlets. *To be submitted to Lab on a Chip (2009).*

Connington, K., Q. Kang, H. Viswanathan, A. Abdel-Fattah, and S. Chen. Lattice Boltzmann simulation of peristaltic particle transport in a three dimensional channel. *To be submitted, Physics of Fluids (2009).*

Connington, K., Q. Kang, H. Viswanathan, A. I. Abdel-Fattah, and S. Chen. Peristaltic particle transport using the Lattice Boltzmann method. 2009. *Physics of Fluids.* **21** (5): 053301, pp16.

Connington, K., Q. Kang, H. Viswanathan, S. Chen, and A. Abdel-Fattah. Lattice Boltzmann Simulations of Peristaltic Particle Transport. Presented at *61st Annual Meeting of the APS Division of Fluid Dynamics.* (San Antonio, Texas, 23–25 November, 2008).

Connington, K., Z. Xia, S. Chen, and Q. Kang. Lattice Boltzmann Simulation of the Sedimentation of Elliptic Particles. *60th Annual Meeting of the Division of Fluid Dynamics.* (Salt Lake City, Utah, 18–20 November, 2007).

Kang, Q., P. Lichtner, H. Viswanathan, and A. Abdel-Fattah. Pore scale modeling of reactive transport involved in geologic CO2 sequestration. 2009. *Transport in Porous Media.* : DOI 10.1007/s11242.

Tarimala, S., A. Abdel-Fattah, Q. Kang, H. Viswanathan, and K. Connington. Non-reactive and reactive micromixing at low Peclet number conditions . Presented at *American Geophysical Union, Annual Fall Meeting 2008.* (San Francisco, CA, 14-19 December, 2008).

Wang, M., Q. Kang, and H. Viswanathan. Numerical modeling of electrokinetic transport and mixing enhancement in heterogeneously charged microchannels. Presented at *The 2nd ASME International Conference of Micro/Nanoscale Heat and Mass Transfer.* (Shanghai, 18-21 December 2009).

# Subsurface Transport Parameter Estimation with Multiscale, Multiobjective Optimization

*Andrew V. Wolfsberg*
20070441ER

## Abstract

Predicting contaminant migration in groundwater requires the use of computer models with parameters that describe the structure and chemistry of the rocks through which water flows. However, changes in rock properties between locations are a source of parameter scale dependence in subsurface solute transport models. Results to date indicate that model parameters estimated from centimeter-scale experiments can not be directly used for field-scale simulation. However, using parameter values measured in the laboratory along with knowledge of how other material properties change in the field leads to mathematical formulations for estimating effective parameter values at increasing scales. Key parameters affecting solute migration in fractured rock systems include the matrix diffusion coefficient, the fracture width (aperture), rock pore structure (matrix tortuosity), and reactivity of the rock (retardation factor or sorption coefficient). We have scaled each of these parameters with the multi-scale transition probability theory developed in this project. The effective field-scale transport parameters are related to statistics describing how they change between locations (the mean, variance, integral scale and the domain size along pathways through a three-dimensional flow field). Simulations conducted with upscaled effective parameters compared very well with high resolution Monte Carlo simulations capturing detailed parameter spatial variations. The scientific results from this study provide a theoretical link between controlled experimental results obtained at the laboratory bench scale and the field scale at which risk assessment and contaminant remediation are actually conducted.

## Background and Research Objectives

A significant challenge in contaminant transport modeling is to understand how model parameters change with scale, considering the influence of variations in physical and chemical properties at different scales. Although millions of dollars are spent each year for regulatory-driven investigations to characterize risk associated with contamination in groundwater, there remains no practical theory to integrate laboratory-scale data in field-scale predictions for resource analysis, risk assessment, or remedial design. The objectives of this research project are to integrate components of multiobjective optimization theory, multimode spatial statistics and upscaling algorithms, and hierarchical transition probability models to identify and then account for complex physical and chemical processes at increasing scales for subsurface flow and contaminant transport simulation.

This project develops an upscaling methodology to provide a theoretical and practical link between controlled experimental results at scales increasing from the laboratory bench to the multi-kilometer field scale at which resource assessment and remediation is actually conducted. We develop and test the upscaling algorithms for prescribing appropriately scaled parameters in numerical models of fluid flow and contaminant migration in saturated fractured media (Figure 1). In the Scientific Accomplishments section, we outline the evolution of the capability developed and its application to problems of scaling transport processes in heterogeneous media.

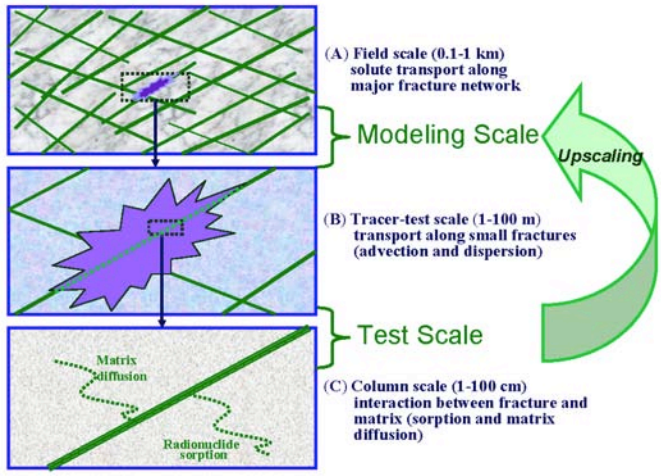


*Figure 1. Spatial hierarchical scales of fractured rock to show the gap between the test scale and the modeling scale [1].*

## Scientific Approach and Accomplishments

Scientific approach and accomplishments of the project have been made in nine primary areas, which are described below:

1. Development of fracture networks with a multi-scale transition probability model: To test concepts of parameter scaling from single fractured-rock column experiments to fracture network characterization, we have developed a multi-scale transition probability model to simulate the geometry of fracture network systems, while at the same time upscaling the fracture apertures and fracture block proportions (Figure 2). Flow and reactive solute transport in the upscaled fracture networks are simulated with a novel generalized dual-porosity model, which enables highly efficient and accurate simulations of diffusive concentration fronts moving between fractures and matrix material. The developed methodologies will have broad applications for modeling flow and reactive solute transport in the fractured rocks.

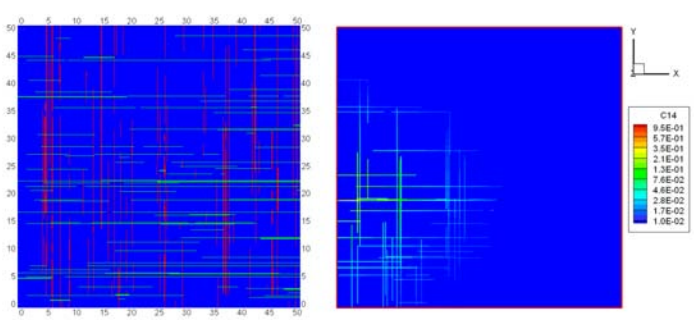


*Figure 2. A fracture network system created with multiscale transition probability models (left) and the simulated contaminant distribution in the fracture network (right).*

2. Development and testing of simultaneous inverse models for characterizing single fracture laboratory experimental parameters: Working with a novel data set developed at LANL for a series of laboratory column transport experiments, we have developed a simultaneous inversion methodology for parameter estimation from multiple experiments. Two inverse methods were developed, compared, and contrasted; one a global search algorithm and the other a local gradient-based search algorithm. Our results demonstrate that the global search method provides greater accuracy and quantification of the estimation uncertainty, but at a higher computational cost. Two papers have been prepared on this subject (first and second). Professional talks on this subject have been given at The American Geophysical Union meeting and at the Geological Society of America meeting.

3. Development and testing of mathematical upscaling formulations: Following the parameters estimated from the laboratory scale studies, we have developed a multi-modal spatial random function that upscales the critical transport parameters for fracture aperture, matrix diffusion, and solute sorption coefficient (in the matrix) for field-scale simulation (Figure 3). The effective field-scale parameters are related to their geometric mean, variance, integral scale and domain size. Their values increase with their integral scales and are larger than their geometric means. This has led to a publication in geophysical Research Letters [3,4].

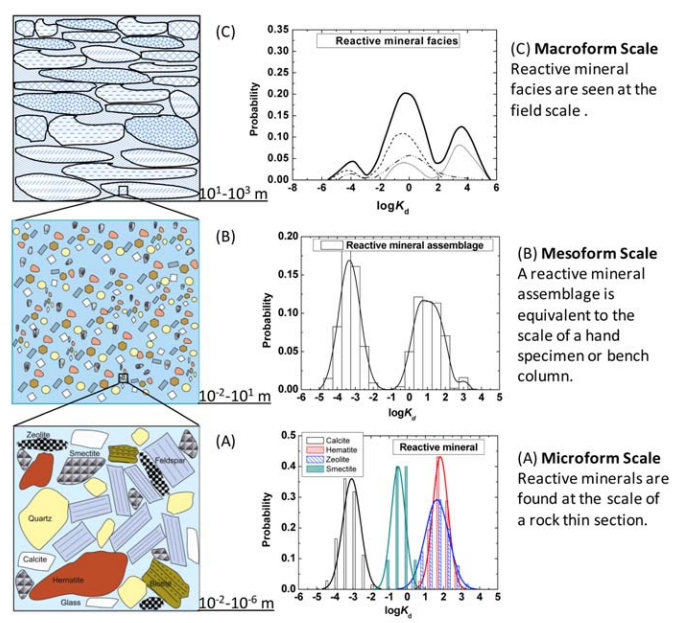


*Figure 3. Hierarchical structures of reactive mineral facies and the distributions of uranium matrix sorption coefficients in reactive minerals.*

4. Development of a stochastic inverse methodology for identifying subsurface material structure with limited hydrologic and geologic data: Upscaling laboratory parameters to the field scale requires knowledge of subsurface material structure. Therefore, using a field-scale groundwater model and associated head observations and geologic information from boreholes, we solve the inverse problem for the stochastic parameters in the transition probability model and generate the material distribution necessary for upscaling transport parameters. These results provide insight regarding material proportions, mean lengths of features, and their roles in controlling fluid flow. This aspect of the project is published in our fourth paper [5,6].

5. Development of numerical models for upscaling processes and parameters for networks of connected discrete fractures: At the field scale, predictive models are resolved at scales much larger than that of a single fracture. Thus, any grid block in a model is characterized by multiple interacting fractures. Therefore, we have developed a discrete fracture network modeling system for the purpose of estimating effective fracture parameters for any grid block in a field-scale model. Our first result has been to estimate the effective fracture aperture for a sub-grid-block system of parallel, but not identical, fractures. With this methodology, the upscaled single, effective fracture aperture reproduces the same flow dynamics as the group of smaller fractures. We also use this network model to investigate interference between fractures via diffusion in the matrix material separating them. New models using inverse Laplace Transform solutions for transport in fractured media and superposition concepts are being invoked to solve, via inversion, fracture interaction parameters applicable at larger scales.

6. Development of analytical solutions for upscaling sorption coefficients in saturated fractured rock system: We developed a methodology to upscale matrix sorption coefficients for fractured-rock systems by characterizing both the tortuosity field (physical heterogeneity) and the retardation factor field (chemical heterogeneity) in the rock matrix. We compute the effective tortuosity with a conservative tracer. Then, using a sorbing tracer, we derive the equations for upscaling the sorption coefficients in a saturated, fractured rock system (Figure 4). The derived upscaling equations for the sorption coefficients are verified with Monte Carlo simulations, which are based on a generalized dual-porosity model to enable highly efficient and accurate numerical simulations of diffusive concentration fronts moving between the fractures and matrix material [7]. One paper is in press and another is in review from this area of the study [8, 9].

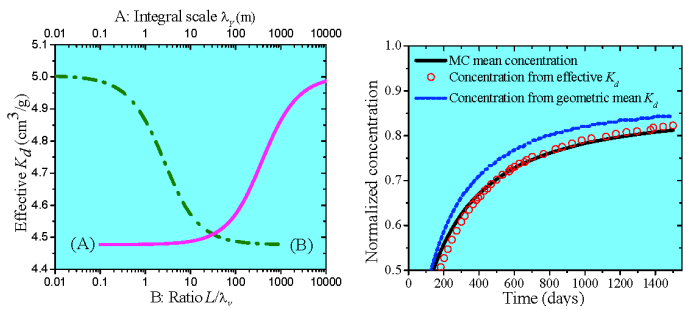


*Figure 4. Effective sorption coefficient (left) and the comparison of the concentration breakthrough curves computed from the effective sorption coefficients, geometric mean, and the Monte Carlo simulations (right).*

7. A conceptual model of reactive mineral facies in hierarchical heterogeneous porous media was developed for reactive transport in physically and chemically heterogeneous material. With this conceptual model, the following attributes are derived for a hypothetical, three-dimensional unbounded aquifer system: covariance of hydraulic conductivity, sorption coefficient, flow velocity, retardation factor, and cross-covariance between flow velocity and retardation factor. Then, with a Lagrangian approach, the scale-dependent analytical expressions are developed to describe the change trend of the effective retardation factors in temporal and spatial domains. When time and space scales become large enough, the effective retardation factors approximate their composite arithmetic mean. Correlation between the hydraulic conductivity and the sorption coefficient can seriously affect the values of the effective retardation factor in temporal and spatial domains. When temporal and spatial scales are relatively small in a reactive transport simulation, the variations of the effective retardation factors are relatively large. The results from this study provide a methodology to develop effective transport parameters for field-scale modeling of contaminant transport in heterogeneous porous media [9, 10, 11, 12].

8. Identification of chemical reaction processes in subsurface environments is a key issue for reactive transport modeling because simulating different processes at different scales requires developing different chemical-mathematical models. Two

sorption process models (equilibrium and kinetics) for laboratory-bench scales were developed for simulating neptunium and uranium sorption in fractured rock. Based on different conceptualizations of the sorption process occurring in fracture and/or matrix media, seven dual-porosity, multi-component reactive transport models were developed. The sorption processes are identified with a stepwise strategy by using multi-tracer concentration data obtained from a series of transport experiments. In the first step, breakthrough data of a conservative tracer (tritium) obtained from four experiments are used to estimate the flow and non-reactive transport parameters (i.e., mean fluid residence time in fracture, fracture aperture, and matrix tortuosity) common to all the reactive transport models. In the second and third steps, by fixing the common non-reactive flow and transport parameters, the sorption parameters (retardation factor, sorption coefficient, and kinetic rate constant) of each model are estimated using the breakthrough data of reactive tracers, neptunium and uranium, respectively. Using the inverse modeling results, the seven sorption-process models are discriminated using four model selection (or discrimination) criteria, Akaike information criterion (AIC), modified Akaike information criterion (AICc), Bayesian information criterion (BIC) and Kashyap information criterion (KIC). These criteria suggest the kinetic sorption process for modeling reactive transport of neptunium and uranium transport in both fracture and matrix at the bench scale. This conclusion is confirmed by two chemical criteria, the half reaction time and Damköhler number criterion [2,13].

9. The creative ideas and approaches developed from this project benefited two GRA students (Dylan Harp and Hailin Deng) working towards their PhD dissertations. Dylan extends our multi-scale transition probability approach to identify aquifer heterogeneous structure with stochastic inversion and Hailin works on upscaling transport parameters for contaminant transport in fractured and porous heterogeneous media. Both of them will defend their dissertations in October, 2009.

## Impact on National Missions

This project supports the DOE/NNSA missions in environment, energy, and science by enhancing our understanding of subsurface fluid and contaminant migration processes and subsurface property structures. High performance computing, new mathematical theories, and DOE/NNSA site data sets enable development of these methods to improve accuracy in important resource assessments. The new theories developed in this project will guide and utilize multi-scale data collection to better understand the structure and responses of the hydrologic systems of concern in DOE contaminant sites. We anticipate applications of the theories to DOE/NNSA sites such as the Los Alamos site, the Nevada Test Site, and the Hanford Site, as well as in emerging alternative hydrocarbon extraction investigations such as those associated with oil shale extraction from induced fractured media. Although programs at these sites cannot always develop new theories, they often employ the most recent developments in computational subsurface science, thus enabling applied programmatic growth. For example, the new FY10 DOE-EM Advanced Scientific Computing for Environmental Management initiative (ASCEM) that LANL leads in will utilize methods developed in this LDRD project. LANL's role in this new multi-lab initiative will be approximately $5M/year for three years. The impact of this initiative will be to standardize and modernize subsurface simulation for DOE-EM. The GRAs who worked on this LDRD-ER will likely stay as post docs and participate in ASCEM.

## References


1. Wolfsberg, A., Z. Dai, J. Vrugt, and P. Reimus. Inverse modeling of colloid-facilitated plutonium transport in fractured tuffaceous rock. *Journal of Contaminant Hydrology.*

2. Dai, Z., A. Wolfsberg, H. Deng, P. Reimus, M. Ding, D. Ware, and M. Ye. Identification of sorption processes and parameters for radionuclide transport in fractured rock. *Journal of Stochastic Environmental Research and Risk Assessment.*

3. Dai, Z., A. Wolfsberg, Z. Lu, and R. Ritzi. Representing aquifer architecture in macrodispersivity models with an analytical solution of the transition probability matrix. 2007. *Geophysical Research Letters.* **34** (20): L20406.1.

4. Dai, Z., A. Wolfsberg, A. Lu, and P. Reimus. Upscaling matrix diffusion coefficients for heterogeneous fractured rocks. 2007. *Geophysical Research Letters.* **34** (7): 408.1.

5. Harp, D., Z. Dai, A. Wolfsberg, J. Vrugt, B. Robinson, and V. Vesselinov. Aquifer structure identification using stochastic inversion. 2008. *Geophys. Res. Lett..* **35** (L08404): 1.

6. Dai, Z., E. Keating, C. Gable, D. Levitt, J. Heikoop, and A. Simmons. Stepwise inversion of a groundwater flow model with multi-scale observation data. To appear in *Hydrogeology Journal.*

7. Dai, Z., A. Wolfsberg, Z. Lu, and H. Deng. Scale dependence of sorption coefficients for contaminant transport in saturated fractured rock. 2009. *Geophysical Research Letters.* **36** (1): L01403.1.

8. Deng, H., Z. Dai, A. Wolfsberg, Z. Lu, and M. Ye. Upscaling Sorption Coefficients for Multimodal Mineral Phases in Fractured Rock. To appear in *Water Resources Research.*

9. Deng, H., Z. Dai, A. Wolfsberg, M. Ye, and Z. Lu. Upscaling sorption coefficients for porous media with hierarchical structure. *Geophysical Research Letters.*

10. Lu, Z., H. Deng, Z. Dai, A. Wolfsberg, and P. Reimus. Quantifying uncertainty of effective transport parameters. *Geophysical Research Letters.*

11. Lu, Z., A. Wolfsberg, Z. Dai, and C. Zheng. Characteristics and controlling factors of dispersion in bounded, randomly heterogeneous porous media. *Water Resources Research.*

12. Huang, C., and Z. Dai. Modeling groundwater in multimodal porous media withlocalized decompositions. 2008. *Mathematical Geosciences.* **40**: 689.

13. Dai, Z., J. Samper, A. Wolfsberg, and D. Levitt. Identification of relative conductivity models for water flow and solute transport in unsaturated compacted bentonite. 2008. *Physics and Chemistry of the Earth.* **33**: 177.

## Publications

Dai, Z., A. Wolfsberg, A. Lu, and P. Reimus. Upscaling matrix diffusion coefficients for heterogeneous fractured rocks. 2007. *Geophysical Research Letters.* **34** (7): 408.1.

Dai, Z., A. Wolfsberg, H. Deng, P. Reimus, M. Ding, D. Ware, and M. Ye. Identification of sorption processes and parameters for radionuclide transport in fractured rock. *Journal of Stochastic Environmental Research and Risk Assessment.*

Dai, Z., A. Wolfsberg, Z. Lu, and H. Deng. Scale dependence of sorption coefficients for contaminant transport in saturated fractured rock. 2009. *Geophysical Research Letters.* **36** (1): L01403.1.

Dai, Z., A. Wolfsberg, Z. Lu, and R. Ritzi. Representing aquifer architecture in macrodispersivity models with an analytical solution of the transition probability matrix. 2007. *Geophysical Research Letters.* **34** (20): L20406.1.

Dai, Z., E. Keating, C. Gable, D. Levitt, J. Heikoop, and A. Simmons. Stepwise inversion of a groundwater flow model with multi-scale observation data. To appear in *Hydrogeology Journal.*

Dai, Z., J. Samper, A. Wolfsberg, and D. Levitt. Identification of relative conductivity models for water flow and solute transport in unsaturated compacted bentonite. 2008. *Physics and Chemistry of the Earth.* **33**: 177.

Deng, H., Z. Dai, A. Wolfsberg, M. Ye, and Z. Lu. Upscaling sorption coefficients for porous media with hierarchical structure. *Geophysical Research Letters.*

Deng, H., Z. Dai, A. Wolfsberg, Z. Lu, and M. Ye. Upscaling Sorption Coefficients for Multimodal Mineral Phases in Fractured Rock. To appear in *Water Resources Research.*

Harp, D., Z. Dai, A. Wolfsberg, J. Vrugt, B. Robinson, and V. Vesselinov. Aquifer structure identification using stochastic inversion. 2008. *Geophys. Res. Lett..* **35** (L08404): 1.

Huang, C., and Z. Dai. Modeling groundwater in multimodal porous media withlocalized decompositions. 2008. *Mathematical Geosciences.* **40**: 689.

Lu, Z., A. Wolfsberg, Z. Dai, and C. Zheng. Characteristics and controlling factors of dispersion in bounded, randomly heterogeneous porous media. *Water Resources Research.*

Lu, Z., H. Deng, Z. Dai, A. Wolfsberg, and P. Reimus. Quantifying uncertainty of effective transport parameters. *Geophysical Research Letters.*

Wolfsberg, A., Z. Dai, J. Vrugt, and P. Reimus. Inverse modeling of colloid-facilitated plutonium transport in fractured tuffaceous rock. *Journal of Contaminant Hydrology.*

# New Frontiers in Viral Phylogenetics

*Tanmoy Bhattacharya*
20080733ER

## Abstract

The rapid advances in sequencing methodology now gives us access to unprecedented amounts of data capable of answering qualitatively new kinds of questions. However, the analytical tools are finding it difficult to keep up with the demands. For example, in the field of research on the Human Immunodeficiency Virus (HIV) that causes Acquired Immunodeficiency Syndrome (AIDS), a phylogenetic analysis of a few thousand sequences is the surest way to reveal features of evolution of the virus during acute infection, important for informing a vaccine against it. Similarly, deep sequences from individual patients are now capable of directly tracking the development of drug mutations and of escape from the immune system. The available state-of-the-art maximum likelihood phylogenetic tools, previously developed by us, are able to handle a set of few hundred sequences, which does not provide sufficient statistical power to answer these questions; both extensions in methodology and utilization of novel resources are likely to be needed to address them. This is a proposal to map this maximum likelihood problem on to Roadrunner, optimize the core computational routines, and apply it to data comparing chronic and acute sequences available through our CHAVI collaboration agreement. These core routines will also allow us, in future, to develop a Bayesian framework for phylogenetic analysis that will provide statistically valid credibility intervals on all these results.

## Background and Research Objectives

The genetic sequence of any organism is a blueprint for its development and of its strategies for survival and combat: the knowledge of the Ribonucleic Acid (RNA) sequence of rapidly mutating viruses like HIV therefore gives us enormous insights into how the virus manages to spread and evade both the immune system and medical interventions against it. The problem is, of course, the backdrop of vast amount of variation that is of little functional significance against which the interesting patterns need to be discriminated statistically. This background variation is, moreover, not random; since the strains of the virus are related by common descent, there are genealogical patterns imprinted on them too. It has become clear in recent work that a successful deciphering of the genetic correlates of viral escape strategies need us to be able to first reconstruct the phylogenetic history of the viral strains being studied (Figure 1).

For hundreds of strains of viruses, we had solved this problem before by parallelizing the maximum likelihood algorithms; and that had allowed us to answer questions about the population biology of the viruses. But such a number of sequences has too little statistical power to answer the questions we are asking today, questions about virus adaptation in individual hosts that are essential for intervention in the disease course. In these problems, we need a large number of patients to find the patterns of HIV adaptation common in all humans, as well as a large number of sequences to capture the diversity within each patient. Before the advent of the modern era of petaflop computing, it was considered impossible to do a proper analysis with the thousands of sequences that are, therefore, needed. The fundamental problem is that the set of evolutionary histories to search over is a huge discrete space, increasing faster than exponentially in the number of sequences, and the evaluation of the likelihood of the history is expensive. Even a parallel implementation guided by excellent heuristics ultimately runs across fundamental compute power limitations, requiring a impressionistic search of the space that, in the past, have been seen to lead to biased results.

In this project we planned to take that crucial enabling step of implementing the required algorithms on the highly heterogeneous computers that currently provide the largest available computational power, and that are likely to become more common in the future. If

successful, we reasoned, this would open up huge vistas, and would already be applicable to a systematic quest for the events that underlie the invasion of a HIV-naive body by the viruses; a field where experimentalists are accumulating vast amounts of data in search of useable patterns. In addition, the next major step in phylogenetic methodology is to be able to perform these calculations with a proper accounting for the statistical uncertainty. Such a development requires further advances in algorithms, but the core of the calculation still involves the likelihood calculations we hoped to develop in this project.

## Scientific Approach and Accomplishments

In this two-year project, we were successful in our goal: we implemented our existing algorithm on the Roadrunner supercomputer. Running this code for about 430,000 CPU hours on accelerated cell nodes, we were able to generate the phylogenetic history of 10,442 distinct HIV sequences, each 3,873 nucleotides long (Figure 2). We used this tree to analyze the properties of early viruses that are responsible for productive HIV infection. This analysis found that two subtypes of the HIV virus—the B subtype that dominates the US epidemic, and the C subtype that is most common in the world—differ in the characteristics of these early viruses. This result is important both in understanding how the virus manages to defeat the body's defenses, and in designing vaccines that will have worldwide coverage.

To achieve this task, we used our first year to benchmark the tasks that were necessary to adapt the maximum likelihood (ML) phylogenetics code of Bhattacharya, Olsen, and Felsenstein, to efficiently use the Roadrunner supercomputer at Los Alamos. This existing ML program developed by our group had in the past been implemented on the messaging passing interface (MPI) designed for a possibly heterogeneous collection of compute nodes. This was used to distribute the task of evaluating the likelihood of candidate histories (family trees) to the different nodes, each of which evaluated the likelihood using a serial procedure.

This basic element of the computation calculates the probability of observing the sequences if the history and assumptions about the way sequences change were correct. It proceeds by examining sequences at the lowest level ('leaves') of the tree that are descended from a recent common ancestor ('sisters') and assigns probabilities for various sequences this ancestor could have had. It then looks at the sister of this ancestor and propagates the probabilities to a more remote ancestor. This flow of information from the observed sequences to the inferred ancestors finally reconstructs a common ancestor for all observed strains, and the probabilities can then be turned into a likelihood for the entire history. The goal of the procedure is to rearrange the sequences and choose the time to the ancestors to produce the most likely tree.

The Roadrunner supercomputer, although vastly more powerful than these previous computers, has a very different architecture with nodes that themselves should be viewed as parallel compute platforms. In essence, each node consists of slow 'Opteron' processors that connect to the other nodes and to the Power Processor Element (PPE). The PPE is well suited to control tasks and sits on a data bus with the Synergistic Processor Element (SPE) that can perform fast arithmetic operations on streams ('vectors') of data. This hierarchical structure of the architecture required us to exploit parallelism also at a smaller scale in order to realize its full potential. We found that we needed to adapt the code to consider individuals, and their parents, and their grandparents, etc., one at a time using the Cell synergistic processor, rather than considering this processor as the 'node' in the previous code that evaluated entire histories at once.

This meant taking apart the program in a detailed way and putting it back together into a multi-level parallel algorithm that maps on to this machine and other anticipated parallel-within-parallel machines. The primary bottleneck that we eliminated in this process was the slowdown in the propagation of probability information through a candidate history. We now use the on-chip direct memory access (DMA) features of Roadrunner's Cell processor to move the data between `workers' that map on to on-chip processes in the current architecture. Since these tasks form the inner core, and almost the entirety of the floating-point load, of the calculation, we further hand-coded these workers to use the Cell's fast vectorization instructions.

The restructured the ML code now performs five separate 'core' numerical functions on the Cell synergistic processor units, combined by the control logic on the PPE into the likelihood evaluation. All of these operations involve intensive transfer of data, and push the Cell memory flow controller to its limit. Nonetheless, the most expensive calculation keeps the SPE processors doing useful work 90% of the time. Currently, the full code, involving the other four less compute-intensive parts don't scale as well, but we still see 40% utilization for typical data sets.

In the second year, we solved the major remaining bottleneck in the code that accepts the candidate history and does the final calculations needed to score it. This required a simple restructuring and involved the Opterons in the communications between the PPEs. The code was

then adapted to run under Data Communication and Synchronization (DaCS) library that control the Cell blades and provide the overall control logic of user interaction. Along the way, we participated in the use of improved instrumentation techniques to help optimize the single-processor -parallelized code. Our final code still uses the old heuristics for tree proposal, but is sufficiently optimized to let us achieve our immediate phylogenetic goals.

We then applied our code to data sets of HIV sequences that have been generated by our colleagues in the Center for HIV/AIDS Vaccine Immunology (CHAVI) collaboration. The fundamental question we targeted was whether there are sequence features that occur repeatedly when HIV establishes infection in a new patient: such features are likely to be indicative of adaptations that the virus needs to survive and multiply, and are worthy targets of vaccines and therapeutics. Of particular interest was the question whether the different subtypes of HIV are under similar selective pressures. Previous work had raised the possibility that a particular locus in the so-called signal peptide was less variable in the HIV sequences from early B-subtype infection. Since the infection worldwide is, however, dominated by C-subtype, we needed to both verify this claim with proper phylogenetic correction, and to test whether the result extends to the C-subtype.

For this, our colleagues put together a set of 275 B-subtype and 141 C-subtype infected patients, some acutely infected (with a couple of months of infection) and some chronic cases (infected for a couple of years). They then sequenced a total of 10,442 fragments, each 3,873-nucleotide long, from these patients covering the region of interest. This was the set we curated and analyzed. The analysis verified that the B-subtype signature could not be explained as a phylogenetic artifact, but the C-subtype sequences do *not* show the signature.

The code that we developed will be used in the future to further our understanding of HIV biology. We are part of several collaborations that study this and other viruses with an aim to design vaccines against them. In particular, rapidly advancing sequencing technology are rapidly generating data informing on many questions of interest to these projects, and with this code we now have developed the analytical tools to exploit the data beyond what was envisaged or thought possible in those projects. This, then, ideally positions the laboratory to compete for further projects in this arena.

## Impact on National Missions

Emerging pathogens and ways to deal with them is a central mission for the DOE Office of Science, and is an underpinning to biothreat reduction (DHS). Other federal agencies like NIH are also interested in the problem, and this proposal builds a capability that can help bridge the interests of NIH and DHS. It also contributes to understanding how to map interesting problems on to the new and emerging computer architectures that can translate to other projects.

# Cellulosomes in Action: Peta-Scale Atomistic Bioenergy Simulations

*Kevin Y. Sanbonmatsu*
20080755ER

## Abstract

Cellulosic ethanol has the potential to satisfy 30% of our transportation fuel demand, unlike corn-based ethanol, which is expected to be insufficient. A key step in the production of ethanol is the degradation of cellulose, the tough material in plant cell walls that exists in the form of two-dimensional crystalline sheets. Bacteria have evolved an efficient mechanism to degrade cellulose, employing a suite of nanomachines called cellulosomes. These are essentially designed to degrade of the two-dimensional crystalline sheets of cellulose; however, they must also work in the midst of the degradation products when the sheets have disintegrated into more amorphous structures. Once degradation has commenced, the changes in the morphology of the cellulose interfere with effective degradation. A major goal of this 18-month project was to adapt biomolecular simulation computer programs to use the Roadrunner architecture. This proved to be a difficult task that exhausted the 18-months of the project. Experts on Roadrunner architecture from IBM and LANL were involved at fundamental levels on the project. We achieved the first biomolecular simulation code to run on a hybrid advanced architecture supercomputer. Simulations of the cellulosome interacting with cellulose were performed, allowing us to address the central question, what parts of the cellulosome machine interact with what parts of cellulose?

## Background and Research Objectives

### Scientific Context

Cellulose, the fibrous material in plant cell walls, must first be broken down into its structural sugars before conversion to ethanol. The cellulose material is extremely tough, resisting treatment by acid and steam. Cellulose degradation is a key rate-limiting step in the production of cellulosic ethanol [1]. An enormous molecular machine capable of degrading cellulose via hydrolysis has evolved in bacteria. These fiber-eating bacteria actually use nanomachines called cellulosomes that degrade sheets of cellulose in a manner analogous to a molecular paper shredder. For optimal ethanol production, the entire cellulose sheet must be degraded. The mechanism of degradation of cellulose by cellulosomes is poorly understood at the molecular level [2-4]. We focused on designer cellulosomes, which have recently been studied experimentally to optimize the process of cellulose degradation [5].

While this molecular shredder may be designed for sheets of cellulose, it may not be optimal for partially shredded material, where molecular paper jams may occur. Cellulose exists in the form of stacked layers of two-dimension crystalline sheets. Each sheet consists of long polysaccharide chains connected in a lattice by hydrogen bonds [6]. However, a pre-treatment step is necessary to make the cellulose susceptible to breakdown by the cellulosome. In this step, the crystalline sheets are broken in random places and subject to water uptake, creating a more amorphous structure [3]. After degradation has commenced, the cellulose surface topology changes dramatically. Cellulosomes bind to a certain region of the sheet, chew away for some time, dissociate, and rebind in another random location on the sheet [7]. Midway through degradation of the entire sheet, the sheet loses its structure, resulting in a collection of cellulose fragments. The two dimensional nature of the sheets transform into a three-dimensional collection of fragments, followed by a corresponding transition from 2-D to 3-D movement of the cellulosome within the cellulose [8; 9]. Once degradation has commenced, the change in substrate surface may dramatically affect the rate of degradation. Using computer simulations, one can study the dynamics of this system in atomic detail. Such simulations have the potential to expand our understanding of one of the key bottlenecks in cellulosic ethanol production. In particular, the main goal is to understand how the cellulosome interacts with cellulose during cellulose processing.

**Computational Context**
Biomolecular dynamics simulations have a large number of important applications, including bioremediation, drug design, and bioenergy. In a biomolecular simulation, the system is simulated atom-for-atom. Equations of motion are used to evolve the system in the presence of thermal fluctuations. The enormous complexity of biomolecules, in comparison systems studied in fluid dynamics or materials science, makes the computer simulations much more difficult than traditional computational physics science applications. Because of the specific nature of each amino acid in a protein, thousands of unique atom data structures must be used. This increases the demands of memory and communication on the supercomputer. Furthermore, in the case of charged molecules, long-range interactions must be included. These interactions dramatically increase the number of calculations required for each integration of the equations of motion. They also place a large demand on the communication network. The main goal in terms of computer science was to adapt a biomolecular simulation code to the advanced architecture hybrid Roadrunner machine.

## Scientific Approach and Accomplishments

**Computational Approach and Accomplishments**
The Roadrunner architecture consists of SONY Playstation 3 processors connected to Advanced Micro Devices (AMD) processors. These are arranged groups called nodes. Each node has both SONY playstation processors ("Cell engines") and AMD processors. Nodes are connected via high speed fiber optics ("Infiniband"). Speed-ups using the SONY Playstation alone were previously achieved using the Gromacs code (~ 8x speed-up). Because Gromacs was at least 5x faster than other existing biology codes, Gromacs was chosen as the optimal code for these simulations. Because 90% of the calculation in biomolecular simulation is typically water interactions, we focused on first adapting the water interaction part of Gromacs to the Roadrunner advanced architecture. We successfully adapted Gromacs to run on the Roadrunner.

Gromacs is a versatile package to perform molecular dynamics, i.e. to simulate the Newtonian equations of motion for systems with hundreds to millions of particles. It is primarily designed for biochemical molecules like proteins and lipids that have a lot of complicated bonded interactions. One use of Gromacs within LANL is to simulate the process of cellulosome migration through partially processed cellulose, shedding light on one of the key bottlenecks in cellulosic ethanol production. Gromacs also has a wide variety of applications ranging from polymer systems to drug design.

The two main challenges involved (1) implementing the Roadrunner communication scheme that allows communication between SONY Playstation processors and AMD processors, as well as communication between nodes, and (2) changing data structures throughout the code to allow efficient communication between SONY Playstation processors and AMD processors and to optimize memory use. The first half of the project was dedicated to re-tooling the Gromacs code to include the Playstation communication language. This required us to use Data Communication and Synchronization library (DACS) code through Gromacs. The second half of the project was dedicated to re-organizing the data structures to optimize communication and memory usage. This involved many direct memory access (DMA) implementations and optimizations. For example, threads were implemented for the SONY Playstation processor units. The size of arrays were changed to exactly match the memory size useful for DMA commands. Data was accumulated and then passed in aggregate rather than piecemeal. Memory cache was used extensively. The order of operations was altered and the loop structures were modified. We are currently planning a joint project with Kevin Bowers to improve performance and to prepare for next generation advanced architecture hybrid supercomputers.

**Science Approach and Accomplishments**
The cellulosome consists of multiple identical subunits. Each subunit contains an enzyme (cellulase) that degrades the cellulose, a linking protein (cohesin) that connects subunits to each other, and a structural protein (dockerin) that connects the linking protein to the enzyme. The enzyme itself includes a cellulose binding domain, responsible for attaching the cellulosome to the cellulose, and a catalytic domain, responsible for hydrolyzing the cellulose into smaller polysaccharides. We have developed structural models of the necessary components for our system, including an example of degraded cellulose, a designer cellulosome (Figure 1) and a two-dimensional crystalline sheet of cellulose (Figure 1).

We were able to simulate the movement of strands of cellulose through the cellulosome. This process is known as translocation. Here, we used a steered simulation approach, where the end of the cleaved cellulose strand was fixed in place. The cellulase enzyme subunits were moved forward, forcing the cellulose strand to movement through the cellulosome. We interrogated the specific interactions between the cellulose and the cellulosome. We found that, depending on the parameters used, a competition exists between the interactions stabilizing the cellulose sheet and the movement of cellulose through the

cellulosome. In particular, amino acids near the entrance site of the cellulase enzyme subunit play a key role. These interact directly with the cellulose and determine the rate of "pealing" of a cellulose strand off the 2D cellulose sheet. This is the first study of its kind. In the future we will perform equilibrium simulations to determine how the uptake mechanism functions.

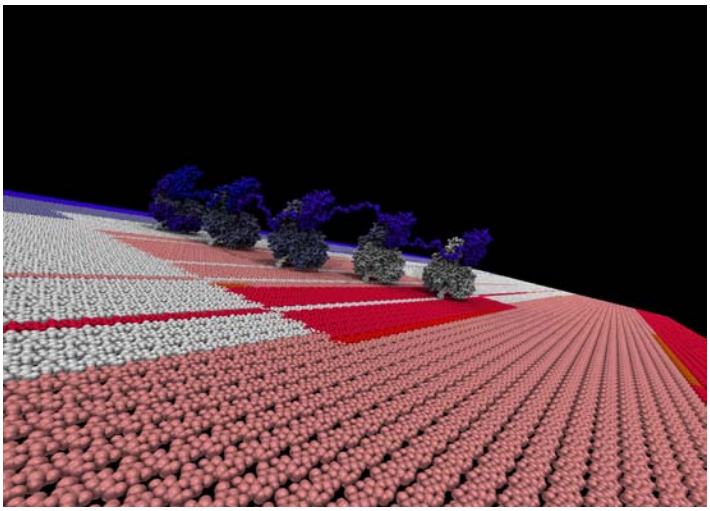

*Figure 1. Translocation of cellulosome across cellulose sheet. Grey, cellulase enzyme units. Blue/purple, connecting proteins. White, cellulose strands passing through cellulosome. Pink/red, cellulose sheet.*

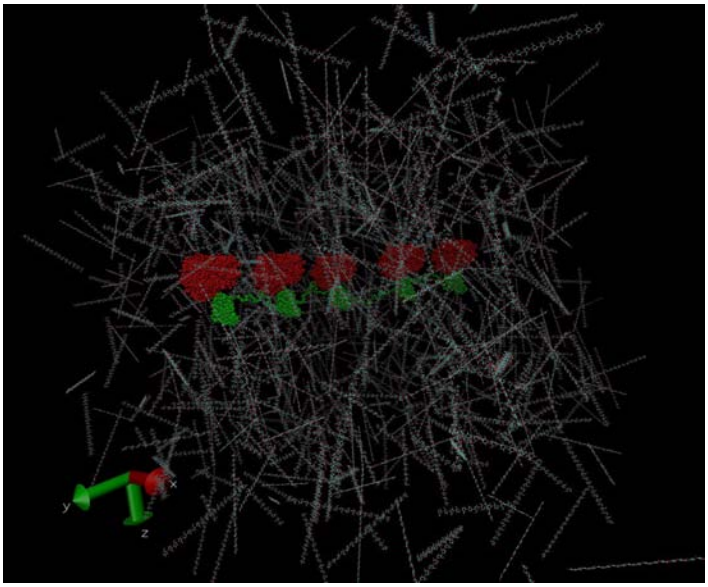

*Figure 2. Simulating cellulose processing. The three-dimensional structure of a synthetic nanosome diffuses through degraded cellulose. Cellulase enzyme units, red. Connecting protein, green. Degraded cellulose strands, cyan.*

We have also modeled the cellulosome in the context of partially degraded cellulose (Figure 2). Random cleavages were made in along polysaccharide chains to achieve a power law distribution of lengths to approximate a random degradation process. Each cellulose fragment was be displaced slightly, translated and rotated using random perturbations according to a Gaussian distribution. We used enough fragments to generate a simulation environment large enough for the cellulosome to move through. This is the first time the cellulosome has been modeled in the context of degraded or partially degraded cellulose. We find that the cellulose degradation products may easily impede the motion of the cellulosome. This may be an important correction for estimating cellulosome diffusion rates – a value used to estimate cellulose degradation inhibition.

## Impact on National Missions

**Impact on supercomputing and the DOE complex**
Our simulation is the first biomolecular simulation using an advanced architecture hybrid supercomputer, to our knowledge. We have shown that it is possible to use such a computer for biology application, despite many complexities of intricate biomolecular complexes and long-range electrostatic interactions.

**Impact on cellulosome research**
While individual cellulase enzymes have been studied extensively, both biochemically and structurally, the intact cellulosome molecular machine is poorly understood with few structural studies. Very little is known about the operational principles of the cellulosome. This study is the first simulation of the cellulosome, giving us the first glimpse into its inner workings.

**Impact on Department of Energy mission**
Our simulation is directly relevant to the mission of the DOE Bioenergy Research Program and the DOE mission to identify steps towards solutions to the challenge of producing renewable carbon neutral energy. In particular, understanding and optimizing the mechanism of the cellulosome is directly related to the "major focus... on understanding how to reengineer biological processes to develop new, more efficient methods for converting the cellulose in plant material into ethanol" (http://genomicsgtl.energy.gov/centers/).

**Impact on well being of society**
Biofuels have enormous potential to strengthen our energy security. Corn based ethanol has made a significant contribution as an alternative energy source; however, corn ethanol is not expected to be sufficient and could cause food price increases. In contrast, cellulosic ethanol has the capability to satisfy 30% of our transportation fuel demand, while reducing greenhouse gases by 88% (15). Cellulosic ethanol is made from cellulose (the tough

material in plant cell walls) as opposed to corn ethanol, which is produced directly from simple sugars. Cellulose is found in all plants and must be must first be enzymatically degraded before its component sugars can be converted into ethanol. This is a difficult task, even for the most competent bacteria. With regard to cost-efficient biofuels, this step requires significant improvement. While recent improvements in enzyme design have reduced the cost of enzymes to 20-30 cents per gallon of ethanol, the cost must be further to reduced to 3-4 cents per gallon [1].

## References


1. Stephanopoulos, G.. Challenges in engineering microbes for biofuels production. . 2007. *Science.* **315** (0): 801.

2. Bayer, E. A., L. J. Shoham, and R. Lamed. Cellulosomes-structure and ultrastructure. . 1998. *Journal of Structural Biology.* **124** (0): 221.

3. Madkour, M., and F. Mayer. Structural organization of the intact bacterial cellulosome as revealed by electron microscopy. 2003. *Cell Biol Int.* **27** (0): 831.

4. Gilbert, H. J.. Cellulosomes: microbial nanomachines that display plasticity in quaternary structure. 2007. *Molecular Microbiology.* **63** (0): 1568.

5. Perret, S., A. Belaich, H. P. Fierobe, J. P. Belaich, and C. Tardif. Towards designer cellulosomes in Clostridia: mannanase enrichment of the cellulosomes produced by Clostridium cellulolyticum. . 2004. *Journal of Bacteriology.* **186** (0): 6544.

6. Nishiyama, Y., J. Sugiyama, H. Chanzy, and P. Langan. Crystal structure and hydrogen bonding system in cellulose I(alpha) from synchrotron X-ray and neutron fiber diffraction. 2003. *Journal of the American Chemical Society.* **125** (0): 14300.

7. Helbert, W., H. Chanzy, T. L. Husum, and S. Ernst. Fluorescent cellulose microfibrils as substrate for the detection of cellulase activity. 2003. *Biomacromolecules.* **4** (0): 481.

8. Sassi, J. F., and H. Chanzy. Ultrastructural aspects of the acetylation of cellulose. . 1995. *Cellulose.* **2** (0): 111.

9. Valjamae, P., G. Pettersson, and G. Johansson. Mechanism of substrate inhibition in cellulose synergistic degradation. 2001. *European Journal of Biochemistry.* **268** (0): 4520.


## Publications


Sanbonmatsu, K. Y.. Large-scale biomolecular simulations: biomedical and bioenergy applications. 2009. In *Salishan Conference on High Speed Computing.* (Salishan, Oregon, 27-30 Apr. 2009). Vol. 0, 0 Edition, p. 0. Unpublished: unpublished.

Sanbonmatsu, K. Y., D. Modl, P. Weber, S. Swaminarayan, C. S. Tung, M. Vernon, M. Sheats, and J. Berendzen. Cellulosomes in Action: Petascale Atomistic Bioenergy Simulations. 2008. In *SuperComputing 2008.* (Austin, Texas, 15-21 Nov. 2008). Vol. 0, 0 Edition, p. 0. unpublished: unpublished.

# The Dynamics of Change in Global Energy Systems

*Rajan Gupta*
20090481ER

## Abstract

The world's energy infrastructure stands on the brink of a major revolution. The explosive economic growth in developing nations such as China and India is driving the construction of several new conventional power plants every week, leading to sharp increases in pollutants and $CO_2$ emissions. Concurrently, the risks of climate change and unprecedented high prices for oil and natural gas are transforming the economic and ethical incentives for alternative energy sources, leading to growth of nuclear and renewables, including solar, wind, biofuels and geothermal technologies. The transition from today's energy systems, based on fossil fuels, to a future carbon-neutral infrastructure is a problem of global dimensions, but one for which there is no accepted solution, at international, national, or regional levels. The National Labs are well positioned in mission and capability to provide the analysis capability for this highly complex dynamical system to accelerate the transition to sustainable, affordable and clean energy for the global population. Such a capability will require integrating multiple systems at multiple scales, include information on current systems, emerging technologies, resource constraints, policies and changes in behaviors regarding how we generate and use fuels and electric power. This report describes the progress made in developing a web based tool called Global Energy Observatory that will allow us to understand the dynamics of change in global energy systems and how they evolve under international regulations and environmental treaties in response to the threat of global warming and climate change.

## Background and Research Objectives

Predictive capability for a complex dynamical/adaptive system, such as the energy-climate challenge, requires parallel developments in collecting high quality data, building credible models and analyses, and implementing a sound process of validation through observation and modeling. The LDRD reserve funds targeted the first part – building the IS&T framework for creating and maintaining a detailed database of global energy systems.

We are creating a global real-time observatory, called Global Energy Observatory (GEO), for mapping energy infrastructure, generation, consumption, and associated emissions. Equally important, it also incorporatse (through collaborations) drivers such as demand, price, risk, environmental concerns, resource opportunities, social behavior, etc. This requires a transformative Information Science and Technology (IS&T) solution that increasingly automates collecting, editing, validating and verifying information, and facilitates a public participatory "open" data repository.

Our goal is to develop the Global Energy Observatory into an innovative one-stop site (open web tool) for understanding and quantifying the dynamics of change in energy systems and emissions from them. Energy and environmental data collection and analysis tools needed to perform a comprehensive and defensible analysis of demand growth and emissions at various spatial and temporal scales continues to grow in scale, diversity, and complexity. Unfortunately, the collected data is very incomplete and not easily available to consumers, scientists, and decision makers. The abundant yet fragmented, incomplete and heterogeneous data and data sources have created increasing demands on, and opportunities for, information technologies. Even if data exist, today we are asking new questions that were unanticipated even a few years ago. This is requiring repurposing, transforming, and integrating multiple, uncoordinated, and sometimes variously restricted or proprietary data sources. Having a comprehensive framework and database such as GEO will significantly enhance our ability to analyze the Energy-Climate challenge and provide a real time global inventory necessary for monitoring and validation of international environmental treaties, which is a LANL priority.

Through the participation of both experts and the public,

the observatory will establish and update geo-spatially and temporally referenced records and analyses of the historical, current, and evolving global energy systems, the energy end-use of individuals, and their associated environmental impacts. Such a database will allow the identification of changes in energy production, use, and infrastructure and consequently modeling of their dependence on the above mentioned drivers.

## Scientific Approach and Accomplishments

Version alpha of GEO has been developed using a traditional web-based LAMP (Linux, Apache, MySQL and PHP [1, 2]) infrastructure [3]. This work was done in collaboration with 2-3 master's students at UNM and is available at . GEO currently consists of a framework for adding, editing, querying and downloading data from four linked databases that house global information on:

1. GEOpower (Power plants): Coal, gas, geothermal, hydro, nuclear, oil, solar PV, solar thermal, waste, and wind power plants. To capture all generation capacity, we impose no cut-offs on the size of plants included. Different sizes can be resolved easily by appropriately written queries.

2. GEOresources (Fuels and resources): Gas and oil fields, coal and uranium mines, crude oil refineries, solar and wind potential, and biomass (agricultural) resource.

3. GEOtransmission (Transmission of energy): Gas and oil pipelines, coal, LNG and oil ports, rail and road links, shipping lanes and electric transmission grid. (The framework for this database is being developed and will be completed by mid July 2009.)

4. Reducing Our $CO_2$ Footprint: Carbon footprint of individual end-users, their understanding of the Energy-Climate challenge and installations of distributed generation (solar, wind, heat pumps) and storage systems for individual homes, commercial buildings, institutions and communities.

Based on the feedback from users on the alpha version, a beta-version is under development. The beta version is 80% complete, modular and much more flexible to provide a higher level of integration and interoperability. It will become the default version by end of 2009.

The project consists of five interrelated parts that will facilitate the real time collection, collation, management and analysis of global energy systems at multiple scales.

1. Development of the framework for data collection management and analysis through a web based global collaboration. Version alpha of this framework has been built over the last year and described below. The next step is to enhance this framework to host meta-data and build analysis tools.

2. Harvesting data from public websites of regulatory agencies such as EIA and EPA in the US. We regard providing multi-sector and multi-scale data in one cohesive framework as the attractor for participation by scholars, area experts, journalists and advocacy groups. About 50% of the global capacity has already been identified and most of it is already available from GEO. The goal for FY2010 is to enlarge the coverage to 75% and fill in performance and emissions details.

3. Semi-automation of tools to complete incomplete data by continuously probing for missing information, developing appropriate queries for web searches, and filters to extract desired nuggets.

4. Semi-automation of tools for moderation and validation of information provided by the public.

5. Perform, in a transparency manner, multi-scale integrated analysis to build trust in the system.

In addition to the development of GEO, we carried out two analyses: (i) global energy systems and resource constraints and (ii) Energy options and constraints for India. This work lead to four invited talks at international meetings [4, 5, 6, 7], and seminars at UC Santa Barbara, University of Washington and Utah.

## Impact on National Missions

This project is now part of the following continuing LANL efforts that, in turn, are part of the national energy-climate and Information Science and Technology initiatives:

Data fusion: The goal is to understand how to collect, collate and manage heterogeneous data and fuse it for integrated analysis.

Regional Climate Impacts: To understand how energy is generated and used and the regional impact of the emissions and pollution.

Monitoring, Measuring and Verification of emissions from energy systems for developing international environmental treaties in order to reduce the emissions of green house gases.

Harihar Shankar successfully defended his master's thesis *Automating the Moderation Process in GEO using Trust Metrics* based on the GEO project [8]. This project resulted in the recruiting of Harihar Shankar to work with Herbert Van der Sompal in the LANL Research Library.

## References


1. Berners-Lee, T.. Linked Data. 2009. *World Wide Web Consortium.*

2. MySQL and PHP Manual. 2009. *World Wide Web Consortium.*

3. Standley, J.. LAMP Infrastructure. *World Wide Web Consortium.*

4. Gupta, R., H. Shankar, and A. Venkata. Global Energy Observatory (GEO): A One-stop Site for Information on Energy Systems, Infrastructure and Emissions. Presented at *EPA 18th International Emission Inventory Conference - "Comprehensive Inventories - Leveraging Technology and Resources.* (Baltimore, 13-17 April 2009).

5. Gupta, R.. Global Energy Observatory: a One-stop Site for Information on Energy Systems. Presented at *29th Annual CNLS Conference ``Energy for the 21st Century''.* (Santa Fe, 18-22 May 2009).

6. Gupta, R.. GEO: An Open Database to Understand, Visualize, and Analyze Global Energy System. Presented at *International School of Scientific Journalism and Communication, 6-9 July 2009, Ettore Majorana Foundation and Center for Scientific Culture Erice, Sicily, Italy..* (Erice, Sicily, Italy, 6-9 July 2009).

7. Gupta, R.. Promoting India's Development -- energy security and climate security are convergent goals. Presented at *International Conference on "Sustainable Development & Climate Change" organized by The Observer Research Foundation (ORF), New Delhi, and Rosa Luxumbourg Foundation, Berlin.* (New Delhi, India, 2009).

8. Shankar, H.. Automating the Moderation Process in GEO using Trust Metrics. 2009. *Masters Thesis, Electrical and Computer Engineering Department, University of New Mexico.*

# Transformative Capability for Bioassessment of Engineered Nanomaterials

*Rashi S. Iyer*
20090484ER

## Abstract

Engineered nanomaterials (ENMs) represent a fascinating new category of 'chemical agent' due to their unprecedented complexity in properties and potential for size-dependent biological interactions. Critically, the potential for bio-impact cannot be assessed by simply knowing the ENM 'chemical formula,' as is essentially the case for traditional chemical threats. Individual particle-by-particle testing using conventional approaches (cell®animal®human) for assessing the bio-impact of chemical agents are grossly inadequate to address the extent of the ENM problem. The overarching goal of our larger proposed effort was to enable predictive and high-throughput screening of the bio-impact of ENMs. However, within the context of a one-year Director's Reserve Funded project, we proposed to limit scope and focus on two key experimental tasks: (1) demonstrate the utility a 3-D human skin-tissue bio-platform for a system-level assessment of ENMs, and (2) assess and compare the toxicity of ENMs as a function of ENM geometry. These preliminary experiments facilitated the validation of our proposed experimental approach, providing a key 'proof-of-principle.' Importantly, demonstrating the use of a 3-D tissue bio-platform for the rapid assessment of ENMs would immediately establish a new state-of-the-art capability for the toxicological analyses of nanomaterials. In the current study, we evaluated the biochemical and molecular level responses of an *in vitro* reconstructed 3-D skin tissue on exposure to semiconductor nanomaterials. Since shape of a particle is considered to play a determinant role in the response of biological systems to particle exposure we compared the effects of quantum dots versus quantum wires. In addition, we also performed a comparative analysis of the biological responses elicited by differentially functionalized fullerenes.

## Background and Research Objectives

Currently, the intense interest in engineered nanomaterials is fueling a $1B industry that is expected to reach $35B by 2020. Beyond commercial considerations, ENMs provide the potential to address such national and global issues as energy security and weapons of mass destruction through realized and potential applications in energy harvesting, efficient lighting, biomedical science, catalysis, and sensor technologies. This rapid pace of ENM development is outpacing our ability to understand their biological impact. Currently, the 'informed' design of new ENMs is function and application-driven with generally little attention given to the impact of the ENM on biological systems. To fully realize the potential of ENMs, future development will ideally be informed both by function/application *and* health considerations, where the latter will ultimately determine the feasibility of use as production scales are increased and new government regulations are introduced. Due to the increased or modified chemical/biological activity, photoactivity and physical dispersibility of ENMs, it is not possible to directly translate what is understood about bulk materials to the nanoscale. This non-trivial problem is compounded by its multifactorial nature – each ENM composition can be synthesized in a variety of geometries, surface chemistries, and reactivities that can act singly or in unison to elicit biological responses from multiple-level bio-systems (gene, protein, cellular, tissue and microenvironment). This problem cannot be adequately addressed on a particle-by-particle basis, nor by using conventional bio-assessment protocol (cell®animal®human). A potential solution would synergize experimental and computational approaches to provide for a rapid and pertinent analysis of the biological impact of ENMs and enable *comprehensive* intelligent design of new ENMs, keeping LANL and the US at the forefront of this important emerging industry.

Engineered ENMs encompass a broad range of materials classes, including metal nanoparticles (e.g., gold), carbon nanoparticles (e.g., carbon nanotubes), super-paramagnetic nanoparticles (e.g., $Fe_3O_4$), and semiconductor nanoparticles (e.g., CdSe quantum dots—QDs). Each ENM type has to some degree been the subject of toxicological investigations, and each

has been shown capable of eliciting adverse biological responses at the cellular or the animal level. The toxicological studies have recently been comprehensively reviewed.[3] When viewed collectively, it becomes apparent that ENMs elicit particular bio-responses based on their physicochemical properties. Unfortunately, the extent to which ENM properties are correlated and act collectively or individually in causing a particular bio-impact (e.g., cell death) is generally absent from existing nanotoxicological data. Further, studies typically rely upon commercially provided ENMs, limiting the ability of these reports to *systematically* address the properties-impact correlation. Until this correlation is more precisely understood, the ability to control and assess ENM properties should be fundamental to any analysis of biological impact, as the potential 'Modes of Interaction' are complex.

The second major shortcoming in bio-impact assessment relates to the inadequacy of current bio-assessment platforms and research strategies used for ENM evaluation. Alternatives to human exposures come with their attendant drawbacks. Monolayer cell cultures lack the structural integrity and complexity of an organ-tissue, limiting their ability to predict the biological responses of a real organism, explant cultures (organ cultures) and volunteer organ biopsies are 'hard to obtain' and show high variability making it difficult to interpret the data. And finally, though animal studies are still the 'gold standard', their use in biological studies has come under scrutiny due to several reasons: questionable validity of animal models in correlative studies due to marked species dissimilarities (for example, rat Vs. pig: Which species more closely 'mimics' human physiology?), relatively protracted experiments, high costs, and, finally, the associated ethical issues. A solution is available in the form of *in vitro* reconstructed human tissue equivalents, typically referred to as 3-dimensional tissue cultures or organotypic raft cultures. These tissue cultures closely represent the complexity and structural integrity of an actual organ tissue system (much akin to a tissue biopsy sample) and correspond anatomically, physiologically and functionally far more closely to human biology than animal models.

In this project our primary task was to develop and establish the use of an '*in vitro' tissue construct* to accurately assess exposures to ENMs in multiplexed fashion (Figure 1). Considering the limited scope of this study, we focused on a skin tissue system representing the highly relevant dermal exposure route. Assays and experimental protocols developed using this 'organ-tissue' model will be broadly applicable to other organ-tissues of choice, including but not limited to lung (inhalation), oral (ingestion) and liver (metabolism of toxicants).

Moreover, we hypothesized that ENMs will impact biological systems through 4 'Modes of Interaction': (1) Metals toxicity, (2) ENM geometry—size and shape effects, (3) ENM surface chemistry effects, and/or (4) ENM redox activity dependent. For this study, we focused on only one mode of interaction: ENM geometry-dependent effects. Here, we will answer two specific questions: (1) Do ENM size and shape influence their *ability to penetrate* a 3-D skin tissue? and (2) Do ENM size and shape extremes lead to *enhanced toxic response*?

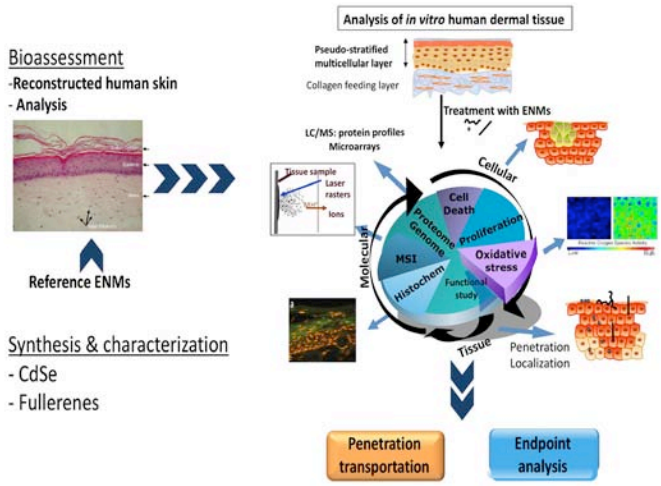


*Figure 1. Properties-dependent assessment of the bioimpact of ENMs using a human reconstructed skin tissue.*

As our model ENM system, we synthesized semiconductor nanomaterials – nanocrystal quantum dots (NQDs) and nanowires. These comprise a technologically important class of ENM for which the physicochemical properties can be precisely controlled using the synthesis and characterization capabilities available in our laboratories (LANL Center for Integrated Nanotechnologies, CINT). The ability to control and knowledgeably characterize the ENM of interest is critical to any systematic study of properties-bioimpact correlations. Not surprisingly, to date, many NQD toxicity studies have relied upon commercially available materials and largely on a single composition, CdSe. Such commercial materials are effectively a "black box" to the nanotoxicologist, where NQD composition, substructure (e.g., core/shell nature of the NQD), and exact surface chemistry are unknown, jeopardizing accurate data interpretation. *Thus, by judicious choice of ENM composition and explicit control over ENM properties, we will be able to for the first time understand the specific effects of geometry extremes on nano-bio interactions, with the 3-D human tissue bio-platform providing a unique and highly relevant biological 'test bed.'*

## Scientific Approach and Accomplishments

### Establish a 3-D skin-tissue bioassesment platform enabling multiplex analyses

A major shortcoming in toxicological assessments relates to the inadequacy of current bio-assessment platforms and research strategies used for ENM evaluation. Relevant high-throughput bio-assessment platforms that accurately mimic human responses are now a critical need. The 3-D tissue cultures developed in this task correspond more stringently to human biology (anatomically, physiologically and functionally) than animal models and closely mimic human responses to environmental insults. In addition, a unique advantage offered by the tissue model is the ability to rapidly screen multiple ENMs simultaneously using a multi-well format. We performed a concurrent and replicate analysis of parameters such as penetration depth, cytotoxicity and proliferative function. A combination of fluorescence microscopy and well-established high throughput biochemical assays were employed to evaluate the responses of quantum dots vs wires.

Our results indicate that negatively charged NQDs induce significant skin tissue damage compared to neutral NQDs. In addition, though neutral NQDs can penetrate several cell layers they do not appear to cause any structural damage to the tissue. When the skin tissue was exposed to nano wires we observed significant tissue damage, more so than NQDs. In regards to composition, we observed that nano shell (CdSe core-ZnS shell) may be relatively less toxic than the nano core (CdSe). In conclusion, preliminary results suggest that shape may potentially determine the severity of response observed (Figure 2).

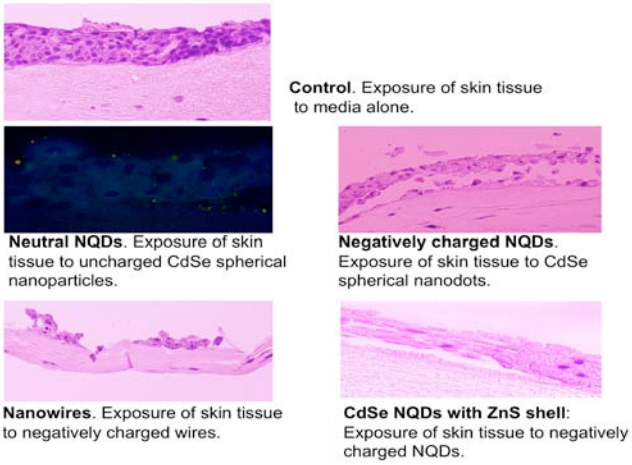


*Figure 2. Treatment of human skin tissue with nano quantum dots and wires.*

Further, we also investigated the response of our skin tissue to functionalized fullerenes. We analyzed the cytotoxic and proliferative bioactivity of functionalized fullerenes. In the present study, we compared the bioimpact of two chemically modified fullerene derivatives, hexa carboxyl fullerene adduct (Hexa-C60) and tris carboxyl fullerene adduct (tris-C60) to pristine fullerene C60 encapsulated with gamma (γ)-cyclodextrin C60 (CD-C60). In these experiments, we noted that pristine C60 and hexa-carboxylated C60 induce necrotic cell death in the skin tissue, while tris-carboxylated C60 is relatively non-cytotoxic (Figure 3A). To further determine the effect of fullerenes on cell proliferation and tissue growth we employed the MTT cell proliferation assay. At the higher dose of 200 µg/ml all three fullerenes induced cell proliferation whereas, at the lower dose of 100 µg/ml no significant changes were observed compared to untreated tissue (Figure 3B).

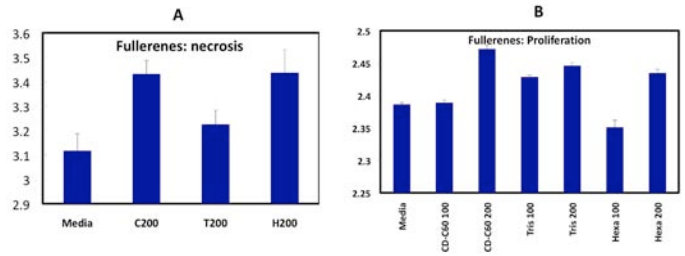


*Figure 3. Cytotoxicity and proliferation in fullerene treated skin tissue.*

### Test bioimpact as a function of ENM geometry and composition

For this initial exploratory effort, ENMs were synthesized in two stages in an attempt to answer two distinct questions: (1) Do nanocrystal quantum dots (NQDs) of small size (<10 nm) penetrate skin tissue? and (2) Is there a difference in toxic response as a function of ENM size and shape? To evaluate (1), strongly emitting and reasonably robust (core)shell (CdSe)2CdS2ZnS NQDs were prepared using a successive ionic layer adsorption and reaction (SILAR) approach (i.e., 2 monolayers of CdS were grown monolayer-by-monolayer onto CdSe NQD cores followed by 2 monolayers of ZnS). In general, NQD cores were synthesized using colloidal synthesis involving reaction of metalorganic precursors at elevated temperatures in the presence of coordinating/passivating molecules (a.k.a., ligands). These NQDs were subsequently transferred into water using a ligand exchange approach whereby the original "growth" ligands are replaced by charged ligands (in this case negatively charged) that render the NQDs water-soluble. The choice of strongly emitting NQDs allowed us to use fluorescence to monitor whether the NQDs penetrated the tissue. Here, we compared charged and uncharged (original ligand layer left intact; NQDs dispersed in oleic acid) 7 nm (measured by TEM) (CdSe)2CdS2ZnS NQDs. Monitoring fluorescence in the media collected below the tissue, we observed that both neutral and negatively charged NQDs can penetrate the skin tissue model. We found a semi-quantitative result for neutral NQDs: i.e., PL intensity for a 1:20 dilution was ~1/2

PL for a 1:40 dilution. We observed no significant oxidative degradation of the NQDs in resulting from exposure to the tissue environment, as no PL blue-shifting was seen. Finally, no significant NQD aggregation in media was observed, as no PL red-shifting occurred (Figure 4).

| ENM | Surface charge (zeta potential) | Solvent | ENM diameter | Hydrodynamic diameter |
|---|---|---|---|---|
| CdSe/2CdS/2ZnS NQD | Neutral | Decanol (toxic) ($3.21 \times 10^{-6}$M) | 7 nm | -- |
| CdSe/2CdS/2ZnS NQD (see PL data below) | Neutral | Oleic acid ($9.15 \times 10^{-6}$ M) | 7 nm | -- |
| CdSe/2CdS/2ZnS NQD (see PL data below) | Negative (by MUA) (-40.9 mV) | Water ($1.24 \times 10^{-6}$M) | 7 nm | ~10 nm and some 100 nm clusters |
| CdSe/2CdS/2ZnS NQD | Positive (by cysteamine) (+78 mV) | Water ($2.8 \times 10^{-6}$M) | 7 nm | ~10 nm and some 100 nm clusters |
| CdSe NWs | Negative (by MUA) | Water | 10-15 nm x 1-5 micron | -- |
| New: Large and small CdSe NQDs | Negative (by MUA) | Water | 16 nm and 4 nm | Not-yet-available |

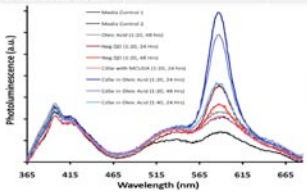


**Conclusions from photoluminescence (PL) data for neutral and negatively charged NQDs collected in media below tissue:**

- Both neutral and negatively charged NQDs can penetrate skin tissue model
- Semi-quantitative result for neutral NQDs: PL for 1:20 dilution ~1/2 PL for 1:40 dilution
- No significant oxidative degradation of the NQDs in the tissue environment (no PL blue-shifting)
- No significant NQD aggregation in media (no PL red-shifting)

*Figure 4. Synthesis and characterization of quantum dots and wires*

To evaluate (2), we synthesized CdSe NQD cores of two sizes (4 and 16 nm), as well as CdSe nanowires (10-15 nm in diameter x 1-5 microns in length). Similar to the NQDs, the nanowires were synthesized using a solution-based approach that yields well-dispersed ENMs comprising the semiconductor "core" along with a surface ligand layer, but the exact method is particular to NWs, namely, it is a solution-liquid-solid (SLS) growth process. The NWs were also rendered water-soluble using a ligand-exchange approach. None of these ENMs were sufficiently fluorescent to allow detection by this optical method. TEM of tissue slices or the underlying media will be required to assess ENM penetration in this regard. Nevertheless, critical to question (2), bioresponse data was generated as a function of ENM size and shape.

In addition, we synthesized water-soluble carboxyfullerenes substituted with a total of 12 and 6 carboxyl groups, respectively. The carboxyl groups were affixed as hexa- and tris-substituted malonic acid adducts, and for convenience we refer to the 12-carboxylate species as hexa-C60 (C60[C(CO2H)2]6) and the 6-carboxylate species as tris-C60 (C60[C(CO2H)2]3). We also prepared a cyclodextrin-C60 fullerene complex (referred to as CD-C60), which is not a modification of the fullerene itself. However, encapsulation by cyclodextrin renders the otherwise hydrophobic C60 into a water-soluble fullerene, making it a better control particle than native C60.

Results from our studies demonstrate the utility of a contemporary 3-dimensional human organ-tissue bioassessment platform as a valid alternative to animal and human testing. Instead of the conventional particle-by-particle evaluation, our approach of understanding 'properties-dependent' bioimpact of ENMs will provide for a rapid and pertinent analysis of the biological impact of ENMs. In addition, our controlled synthesis and extensive physicochemical characterization of ENMs enables a 'properties-dependent' correlation of the biological impact of ENMs on human health. Synergizing our biological and materials expertise, our approach provides guiding principles for the design and synthesis of high-function and low-bioimpact nanomaterials

## Impact on National Missions

ENMs provide the potential to address such mission-critical national and global issues as energy security and weapons of mass destruction through realized and potential applications in energy harvesting, efficient lighting, biomedical science, catalysis, and sensor technologies. Recently, NSF/EPA invested $25M in setting up a center focused on environmental toxicology of ENMs. While this represents an unprecedented effort to address toxicological issues of ENMs in a more holistic manner, it focuses on environmental effects and does not address the related—but independent—health effects of ENMs. Following suit, funding agencies such as NIH and NIOSH, are becoming increasingly concerned about the potential health impact of ENMs and have recognized that a paradigm shift is required for the reliable assessment of ENMs (*ICON NanoEHS Research Needs Assessment. Toward Nanomaterial Classes. NIH Workshop 1 Report.* **2007**). These agencies have further emphasized the as-yet unmet need to employ more relevant bio-platforms coupled with predictive science capabilities. Our larger proposed strategy will meet this need by capitalizing on the exceptional combination of LANL strengths in particle toxicology, nanomaterial chemistry and characterization, and high-performance computing.

During this year, we have actively pursued further collaborative efforts with key decision-makers from NIH, National Institute of Occupational Safety and Health, EPA, UNM and Lovelace Respiratory Research Institute to establish LANL as a center for the assessment of the bio-impact of ENMs. Additional potential for follow-on work resides outside the specific area of ENM bioassessment. Specifically, members of the team have initiated dialogue with interested agencies, such as DTRA and DHS, to seek funding to perform feasibility studies using our tissue-based bioassessment platform for chem-bio threat agents and advance the development of *in vivo* sensor technologies.

# Inferring Functional Determinants of Microbe Pathogenicity by Computational Pathogen Characterization

*H H. Cui*
20090485ER

## Abstract

Predicting whether an unknown microorganism is a human pathogen or not is critical for early medical diagnosis and treatment. However, rapid and accurate pathogen detection remains a major challenge for both public health and national security. The lack of sufficient knowledge of the fundamental differential factors between pathogens and non-pathogens has restrained our pathogen detection and characterization capability. Tremendous volumes of biological data are being generated, beyond the capabilities of existing technologies to analyze effectively. However, computational power and information science have also been advancing tremendously, providing new and powerful algorithms for analyzing this flood of data.

Our research aims to develop a new computational method to identify the causal factors embedded in the genetic code of bacteria, allowing for rapid and accurate pathogen identification. To advance pathogen detection science and technology, we combine our knowledge of infectious diseases and advanced computational machine learning techniques to search for the genetic fingerprints of bacterial pathogens.

Applying the feature selection and classification algorithms that we developed, we approach 95% overall classification accuracy when separating human pathogens from other bacteria by using genome sequence data. Our progress towards high accuracy has also resulted a series of performance benchmarks that can be used to evaluate future improvements in algorithms. While further studies are necessary to expand feature space to improve the prediction accuracy and to eliminate classification errors resulted from sampling bias, this study demonstrated the feasibility of applying computational approach to microbial classification. The success of this project will provide a computational foundation for the next generation of rapid pathogen detection technologies. The resulting technology can also aid the classification of other microbes with differential phenotypic presentations.

## Background and Research Objectives

In 1995, the complete genome sequence of *Haemophilus influenzae*, a bacterium that can cause meningitis and pneumonia was published. This was the first ever free-living organism to have its complete genetic codes fully revealed, and it signified a start of new era in microbiology. Since that time, close to a thousand bacterial genomes have been completely sequenced, and nearly two thousand are in progress of being completed. Because of the tremendous advancement in sequencing technology, the number of bacterial genomes being completely sequenced is growing rapidly (Figure 1), and this number will continue to grow exponentially in the foreseeable future. We anticipate that it will soon be possible to obtain a complete bacterial genome sequence within hours by a highly automated facility, and that sequencing will become a routine research and clinical laboratory practice.

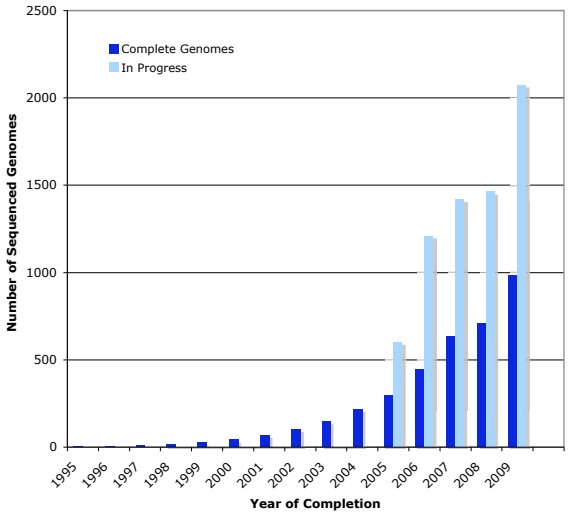


*Figure 1. The exponential increase of sequenced bacterial genomes. The figure is composed from the data source in the National Center for Biotechnology Information (NCBI) public database.*

Infectious diseases are serious concern for human health, agriculture, economy, and national security. Rapid and accurate identification and characterization of the microorganisms that cause these diseases is essential for making timely diagnoses and determining the treatment strategies. The tremendous volume of available genomic sequence data is presenting new opportunities for scientists all over the world to gain fundamental understanding of the genetic make-up of microbes and their pathogenic mechanisms. Among various pathogen markers, nucleotide sequence is an easily accessible entry point for detection. Therefore it has been the primary interest for many of the detection technology development efforts. Traditional pathogen detection involves both clinical and research laboratories. It can take weeks or months to identify new organisms capable of causing disease. Current technologies are still a far cry from the Tricorder device of Star Trek fame, but we expect that advances in genome sequencing technologies will soon (a few years) allow near real-time sequencing of bacteria and viruses. The resulting growth of genome sequence data has created both unprecedented opportunities and critical needs to develop technologies that can effectively organize and efficiently analyze these data. Developing a computational framework for using genome sequence data for pathogen detection and characterization has become a critical task.

The objective for this study is to address this challenge, explore and discover new computational methods to accelerate the pathogen characterization process. We intend to combine high performance computing and advanced machine learning algorithms to discover informative patterns in the bacterial genomes that will enable predicting the phenotype of a previously unclassified bacterial genome. Human pathogens pose the most significant concerns in public health, and therefore, we chose to tackle the difficult problem of classifying human pathogens vs. other bacterial microorganisms, as a study case for the methodology development. The identification of a set human pathogen features using a highly parallel comparison of complete bacterial genome sequences will allow for automated, rapid classification of a newly discovered bacterium.

## Scientific Approach and Accomplishments

It is a long-standing challenge in biology to correlate genetic features with functional traits. In the early stages of the genome sequencing, the primary objective was to target the bacteria that cause human or animal diseases. In the past decade, the scientific community has realized the importance of studying the "near neighbors" (the bacteria that are closely related to the pathogens but do not pose threats to humans) to increase our understanding of the mechanisms of pathogenicity. There is an enormous potential for understanding pathogenesis by comparing genomes of pathogens and non-pathogens because many bacterial species can appear very similar but behave differently. With the availability of large numbers of fully sequenced microbial genomes, we now have a unique opportunity to answer the question of "what makes a microbe a pathogen", by way of identifying the most reliable genetic signatures that distinguish a pathogenic organism (e.g., *E. coli, S. pneumonia*) from its non-pathogenic relatives. We took the following approaches towards identifying a small set of well-conserved proteins whose patterns of presence and absence together can accurately predict bacterial pathogenicity.

*We constructed the sequence similarity scores as the building block of a feature vector.* The input data were all 585 completed bacterial genome sequences publicly available from GenBank at the time when this project began. The GenBank is the official national sequence repository site. We annotated each genome as either a "human pathogen" (e.g., *B. anthracis*) or "not a human pathogen" (e.g., *X. fastidiosa*) using our expert knowledge. This includes literature searches and manual analyses of database entries. The BLAST (Basic Local Alignment Search Tool) program was used to quantify the degree of sequence similarity between every possible pair of proteins in all the genomes. Among the 2.2 million protein sequences existing in all the bacteria, the all-against-all sequence comparisons resulted in about 4.8 trillion similarity scores. This computation was performed on Los Alamos National Laboratory's high performance computing resource, Turquoise Linux Cluster.

*We then analyzed the sequence similarity score using a two-stage pathogen feature selection model that we have developed.* Feature selection is a process to identify most informative variables that can be used by a classification algorithm to separate two populations, in this study case, the human pathogens vs. other bacteria. We expanded the feature selection process into a two-stage model to further improve the classification accuracy. First, we developed the Minimum Entropy Search Algorithm (MESA) to select the well-performing 500 features out of 2.2 million all possible protein sequences, and second, we applied the forward selection method to refine the selection of the top- performing final features.

The MESA algorithm minimizes overall randomness of the similarity scores for each protein between human pathogens and others. Intuitively, this selection process is to find a protein that is well conserved in the human pathogens, and with little or no presence in the not-

human pathogens, and vice versa. Applying the concept of "entropy" from physics, we used raw similarity scores (between 0 and 1) and sorting algorithms to solve this problem. This feature selection method can handle a large number of variables, for example, 2.2 million protein sequences. It differs from the recently reported work, where a few dozen genes used to identify the genetic determinants for certain particular microbial behavior (e.g., motility) [1]. In addition, our selection algorithm minimizes the global, not just local, randomness among the similarity scores, and can handle the problem of "zero" inputs in the logarithmic function that occur with information entropy-based distance measures.

The features selected by MESA are informative but could possibly include redundant sequences. The forward selection method was therefore designed to down-select the final features with unique and complementary information. A forward selection process applies only one variable at a time to separate (or classify) the two populations. After each and every one of all the potential variables (500 in this study) was tested by the selection, the variable that yields the best accurate classification accuracy is kept as the "seed" feature. The process will then be repeated to select the best two features and so on, until the classification accuracy cannot be improved by adding more features.

We didn't find (and we didn't expect to find) a single protein that presents exclusively in either human pathogens or other bacteria. If existed, such an "evil" gene could be used to separate the two populations with 100% accuracy. Our classification algorithm, or "classifier" in short, optimizes the separation between the two groups by using multiple selected features. Support Vector Machine (SVM) is one of the machine learning techniques that has shown its strength in treating large-scale data for non-linear separation [2, 3], which can be very useful to complex classification, such as pathogens vs. non-pathogens (Figure 2). Applying the SVM technique, LANL has developed and patented a computer tool that allows the machine to identify the common features of computer viruses, and apply the selected features to further identify those suspicious malicious computer viruses in a reliable and optimal way [4, 5].

After the features were being selected, we used a 5-fold cross-validation strategy to evaluate the feature selection algorithm and the classification accuracy. The entire data set was divided into two subsets, the training data (~80% of the total data) set and the testing set (the remaining 20%). The training data was used to optimize the classifier parameters, and the reported classification accuracy was calculated based on the performance of the classifier on the testing set. The 80-20 split repeated five times with a different mix, and the performance was averaged from on the 5-fold validation.

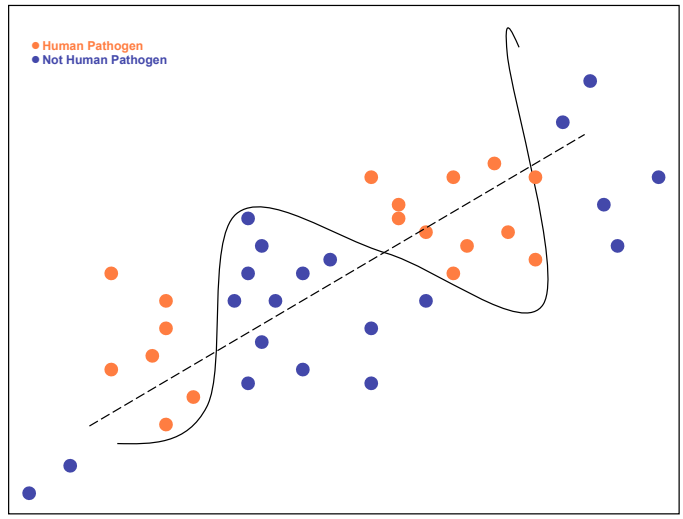


*Figure 2. Machine learning for finding the pathogen feature vector: Machine learning is a powerful technique that identifies patterns from large data sets, which may not be possible to find by the "eye." It provides the capabilities to identify the bacterial or viral genetic sequence features that are associated with pathogenicity. These features can be used to separate human pathogens and not-human pathogens in this particular study. It uses non-linear approaches, and these features may not otherwise be identified by linear separation.*

We had initially used the MESA algorithm to only choose the features without eliminating those potentially overlapping variables. The overall pathogen classification accuracy was ~ 86% with the top 50 features. By introducing the two-stage feature selection process, we have improved the classification accuracy, reaching ~ 95% overall accuracy. We compared two different cases of the two-stage cross validation. First, the full data set was used for the MESA feature selection. After the top 500 variables were selected, the SVM classifier further selected top-performing 50 features from the 500 variables. The ROC (Receiver Operating Characteristic) shows the overall classification accuracy approaching 95% when the best 50 features were used (Figure 3). The error bars show the standard deviation varies in a narrow range. Secondly, we tested the classification under a more stringent condition, where the testing data was kept separate from the MESA selection process. The two-stage feature selection was completed blindly to the testing data. The classification accuracy, under this more stringent condition, is about 93%.

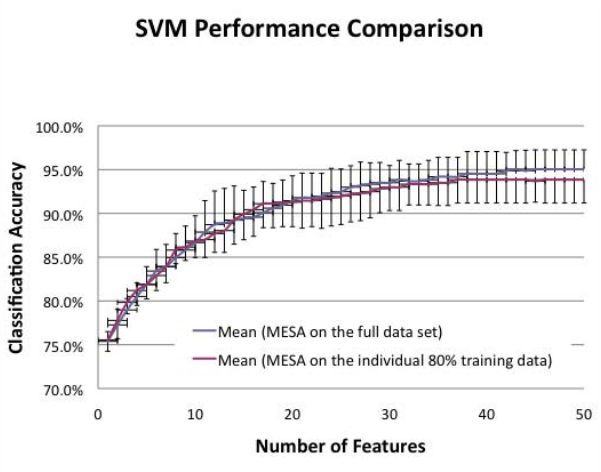


*Figure 3. SVM classification in the two case studies: In the first case, the MESA algorithm selects the top 500 features on the full data set, and then the forward selection method is applied to select the 50 unique features using SVMs. The ROC curve (blue) presents the quantified classification accuracy as a function of the number of features. In the second case, the test data was kept from the MESA selection. This is a more stringent condition that eliminates a potential for biased feature selection. The test data is blind to the two-stage feature selection process. The resulting performance accuracy is slightly lower than that resulted from using full data set (red). With 50 features, both methods reach a well-performing 93-95% classification accuracy.*

*We have also examined pathogen classification with highly stringent condition, with only a single representative allowed from each bacterial species.* The SVM is one of the machine learning techniques that has shown its strength in treating large-scale data for non-linear separation. We have also compared different machine learning algorithms, including Fisher's Linear Discriminant (FLD), phylogenetic trees, and the nearest neighbor method. We compared all methods using protein features generated by forward selection and of non-redundant bacteria. This set of bacteria was obtained by selecting a single representative from each bacterial species in both the human pathogen and not human pathogen categories. If applied correctly, this non-redundant set should allow for more accurate classification, avoiding bias resulted from replicated genome sequences in the test and training sets due to sampling bias (medically relevant bacterial species may have multiple, minor variants sequenced).

Using a highly stringent non-redundant set of genomes for classification is a harder problem to solve than using the complete set of genomes. But this approach may allow us to model the classification performance when confronted with a truly new genome (i.e., not closely related to any previously sequenced genome). As shown in Figure 4, a modest improvement (compared to the baseline accuracy of always guessing "not a human pathogen", since this category makes up 80% of the input genomes) is obtained for the ARB phylogenetic tree classifier. These results indicate that not only must the presence or absence of particular genes be considered, but also factors such as gene expression levels and subtle changes in the amino acid sequence of the proteins these genes encode can contribute to overall disease phenotype of the pathogen. We need to consider the approach to include them in the feature space.

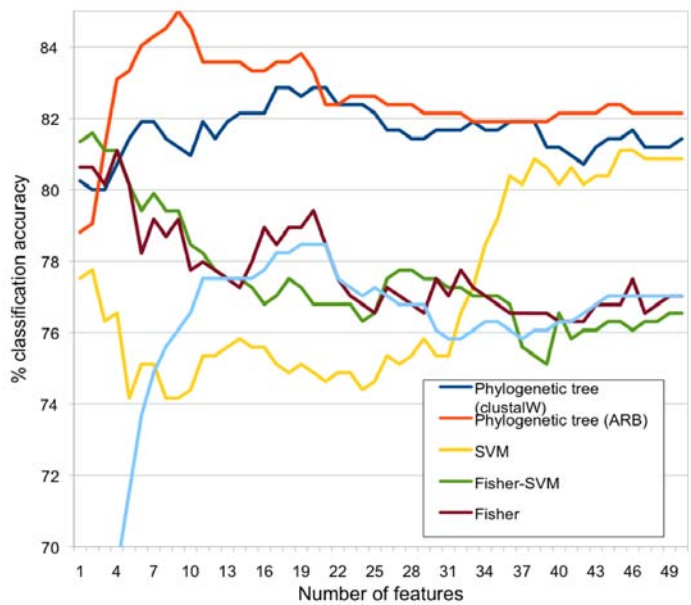


*Figure 4. A comparison of classification algorithms using a non-redundant set of bacterial genomes. All features are chosen using forward selection. ClustalW and ARB are two different algorithms for computing phylogenetic trees from bacterial 16s sequences. SVM refers to a support vector machine. Fisher-SVM uses Fisher's linear discriminant to select a set of features (by forward selection) that are then fed to a support vector machine for classification. Fisher is Fisher's linear discriminant. Near-neighbor classifies by assigning the classification label (i.e. "human pathogen" or "not a human pathogen") of the closest bacteria in the training set (as measured by a distance computed in the selected feature space).*

This study applies mature statistical and computer machine learning techniques to develop rapid and accurate computational classification of microorganisms. We developed the MESA algorithm, a feature selection algorithm, to discover the protein sequence feature set that can be used to separate human pathogens from other bacterial organisms. To the best of our knowledge, this is a first attempt of using machine learning technique for pathogen classification utilizing the full bacterial genome sequences. The resulting classification accuracy is very encouraging. A more comprehensive feature space, in theory, will further increase the classification accuracy, and will allow for mechanistic understanding of

the pathogenicity. Our study also resulted in a series of performance benchmarks that can be used to evaluate future improvements in algorithms. We will continue our efforts to consider more complex situation and expand feature space. When our objective is fully achieved, the classification of an unknown microorganism can be accomplished within the matter of minutes, automatically processed by computer in a highly reliable and optimal manner.

## Impact on National Missions

Rapid and accurate identification and characterization of an unknown microorganism is a major challenge we must address to effectively protect our Nation from health and security threats. Our research aims to advance the computational approach to identify key informative features for understanding the causal factors for microbial pathogenicity, to establish a new computational framework for next generation sequencing-based biothreat detection platforms. It supports the national health security mission. The scientific approach also contributes intellectually to the computational biology and infectious disease research communities.

The research is still in its developing stage. However, the current results have shown its promising future, as well as the areas we need to further invest our efforts for improvement. Because of the innovative scientific approach, the encouraging outcome, and the potential to address a major biodefense challenge, this research has been selected to present at various technical and mission related conferences and discussions. While additional work is necessary to reach our ultimate objective, this study demonstrates that automatic classification of microbial pathogens is indeed feasible and can be used as a foundation for next-generation biothreat detection assays. The technology can also be applied to identify microorganisms by other specified criteria, such as to separate the bacteria that are involved in carbon sequestration from other bacteria.

## References


1. Slonim, N., O. Elemento , and S. Tavazoie. Ab initio genotype-phenotype association reveals intrinsic modularity in genetic networks. 2006. *Molecular Systems Biology.* **2** (1): 1.

2. Cortes, C., and V. Vapnik. Support vector network. 1995. *Machine Learning.* **20** (3): 273.

3. Advances in Kernel Methods-Support Vector Learning . 1998.

4. Cai, D. M., M. B. Gokhale, and J. Theiler. Comparison of feature selection and classification algorithms in identifying malicious executables. 2007. *Computational Statistics & Data Analysis.* **51** (6): 3156.

5. Cai, D. M., and M. B. Gokhale. Detection of malicious computer executables. 2009. *US Patent, awarded on April 14, 2009. Patent ID: US7519998.*

# Large-Scale, Carbon-Sequestration Flows—Laboratory Measurement and Simulation

*Scott N. Backhaus*
20090487ER

## Abstract

Carbon-based fuels, especially coal, have been an inexpensive, stable, and secure source of energy for the U.S. for many decades. However, the emitted $CO_2$ can lead to climate change that threatens U.S. national security and global stability. A promising approach for managing atmospheric carbon is capturing $CO_2$ from exhaust streams and other emissions sources and sequestering the $CO_2$ in the subsurface, e.g. in depleted oil reservoirs and deep saline aquifers. [1] As long as the $CO_2$ remains a separate phase from the native brine, it is buoyant and exerts a fluid pressure on the overlying, low-permeability cap rock and attempts to escape back to the atmosphere and defeat our sequestration efforts. However, $CO_2$ is slightly soluble in brine, and the slightly denser $CO_2$-saturated brine will sink. If molecular diffusion was the only mixing process, a typical $CO_2$ plume would remain a separate, buoyant phase for tens of thousands years creating long-term risks and liabilities. However, gravity and diffusion-driven convection instabilities have been hypothesized that would generate enhanced $CO_2$-brine mixing promoting dissolution of $CO_2$ into the brine on time scale of a hundred years. These processes have been the explored with analytical calculations and numerical simulations [2,3,4], but experimental validation of the results is lacking. Direct verification in field experiments is not likely due to the long time scales, high cost of industrial-scale $CO_2$ injection, and poor resolution of seismic imaging. Instead, we have developed an experimental technique that will allow us to collect benchmark data to validate both the analytical calculations and numerical simulations increasing confidence in our ability to predict the final fate of sequestered $CO_2$. Instead of $CO_2$ and brine, our technique utilizes water and propylene glycol which have similar ratio of viscosities and density increase upon mixing. To date, the collection of data has been limited due to the experimental challenge of bringing the water and propylene glycol into contact without disturbing the interface and creating a mixed layer comparable in thickness to the diffusion-driven mixing at the onset of the gravitational instability.

## Background and Research Objectives

Carbon capture and sequestration has been identified as a promising approach for managing atmospheric carbon. In this approach, $CO_2$ is captured from exhaust streams and other emissions sources and sequestered by pumping it deep below the Earth's surface, e.g. in depleted oil reservoirs and deep saline aquifers (1000-3000 m deep). [1] When injected near the bottom of a permeable rock formation, gravity will drive the buoyant $CO_2$ upwards through the formation until it reaches a relatively impermeable cap rock, where it will then spread out in a thin layer. To gain a sense of scale, twenty years of $CO_2$ emissions from a 1-GW coal-fired power plant would spread out in a layer that, if it were 3 km in diameter, would be roughly 35 m thick.

As long as the $CO_2$ remains in this unstable, non-equilibrium arrangement, buoyancy will attempt to drive it through the cap rock to the surface and back into the atmosphere. As long as the threat persists, the $CO_2$ sequestration site will have to be monitored. Molecular diffusion ultimately mixes the $CO_2$ and brine, and $CO_2$-saturated brine is slightly denser than pure brine causing it to sink removing the threat. If the diffusion took place only at the relatively flat bottom of the $CO_2$ plume, a 35-m-thick layer would survive tens of thousands of years suggesting prohibitive monitoring costs. However, gravity and diffusion-driven convection instabilities have been hypothesized [2,3] that generate enhanced $CO_2$-brine mixing promoting dissolution of $CO_2$ into the brine on time scale of a hundred years.

At the bottom of the plume where $CO_2$ dissolves into the underlying brine, a diffusion layer of $CO_2$-rich brine forms. Depending on the conditions of the reservoir (i.e. depth and temperature), this layer is one to a few percent denser than the underlying brine. Gravitational

forces on the dense layer try to pull it down deeper into the reservoir, but conservation of mass would force a reservoir-scale circulation that is strongly suppressed by the viscosity of the brine and the permeability of the reservoir. Over time the diffusion layer grows thicker and the gravitational force builds. At a critical thickness, the diffusive layer becomes unstable and begins to sink with a finger-like structure. The onset of the instability [2,3] is determined by a competition between three physical processes: 1) the downward gravitational pull ($g$) on slightly denser ($\Delta\rho$) nascent fingers whose vertical thickness is roughly the critical layer thickness ($\delta$); 2) the resistance to finger motion due to the permeability of the porous medium ($K$) and the brine's viscosity ($\mu$); and 3) horizontal diffusion ($D$) that tries to spread the fingers out and restore a laterally uniform density. The dimensionless group $\mu D/\delta K g \Delta\rho$ expresses this competition also allows us to connect laboratory-scale measurements to the kilometer-scale plumes that will be generated by industrial-scale $CO_2$ injections.

Once the instability is generated, gravity pulls the fingers of dense $CO_2$-brine mixture further down into the brine space drawing off the dense mixture from the diffusion layer. In essence, the fingering instability short circuits the one-dimensional diffusion process occurring at the $CO_2$-brine interface. The falling fingers draw the dense fluid mixture away from the interface and increase the contact area between it and the underlying pure brine speeding the dissolution of the dense mixture and the brine. The removal of the dense mixture creates a steeper concentration gradient between the $CO_2$ and brine increasing the rate of diffusion of the $CO_2$ into the brine.

These flows involve a class of hydrodynamic problems that are notoriously difficult to simulate; the simultaneous flow of multiple fluids ($CO_2$ and brine) in inhomogeneous porous media (rock or sediment). Using simplified models, this instability has been investigated analytically and numerically. One numerical simulation [2] is shown in Figure 1. However, there has been no experimental verification of these important results. The hope for direct experimental confirmation of simulations is dim due to the difficulty of obtaining high resolution data from the subsurface and the high pressures (~100 bar), long length scales (~100 meters), and long time scales (~100 years) that are characteristic of these flows. However, by using similitude scaling based on the dimensionless number discussed above, flow visualization, and modern image processing, we seek to provide crucial measurements of these physical processes in a laboratory setting, providing data to benchmark simulation techniques and enhance their predictive power. For this initial LDRD Reserve work, we study this instability in a two-dimensional analog of a homogenous, isotropic porous medium, and our objectives are to verify analytical predictions of the onset of the instability, i.e. the time it takes for the diffusion layer to become unstable after initial fluid-fluid contact and initial finger spacing or wavelength.

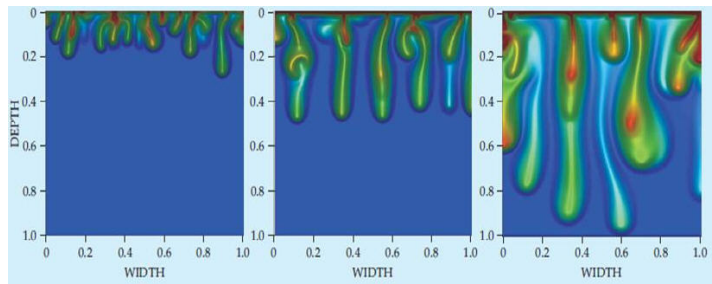


*Figure 1. Direct numerical simulation of $CO_2$ dissolving into brine in a porous medium resulting in a fingering instability. Adapted from Reference [1].*

## Scientific Approach and Accomplishments

We use a Hele-Shaw flow geometry, i.e. the flow of fluid in a narrow gap between two glass plates. Similar to flow in a porous rock, the fluid equations of motion in this geometry can be simplified to pressure gradient and gravitational driving terms balanced by the viscous flow resistance where all inertial effects can be ignored. The Hele-Shaw geometry is an analog of a two-dimensional, homogeneous, isotropic porous rock. In future work, the fluid gap can be partially filled with glass beads or other granular material to introduce inhomogeneity, and the material can oriented to produce preferred directions of flow. However, in this initial work, we will use the simple Hele-Shaw geometry to allow to direct connection to analytical calculations.

To perform the experiments with $CO_2$ and brine would require pressures above the critical point of $CO_2$, i.e. above 7.4 MPa. Such high pressures would make the experimental setup cumbersome and direct imaging of the fluid flow quite difficult. Instead, we have discovered a pair of fluids, propylene glycol (PPG) and water that imitate the relevant behavior of brine and $CO_2$. Pure PPG has a specific gravity of 1.035, and a fluid configuration with water (specific gravity of 1) overlying PPG is initially gravitationally stable. After initial contact, the water diffuses into the PPG increasing the mixture specific gravity up to a maximum of 1.044 for a mixture of 70% PPG and 30% water. The approximately 1% increase in density upon mixing is very similar to the $CO_2$-water system, however the dimensionless group $\mu D/\delta K g \Delta\rho$ controls the onset time and wavelength. [2,3] The permeability $K$ of the Hele-Shaw cell is proportional to the square of plate spacing $b$, and by varying $b$, we can confirm the dependence of the instability onset time and finger spacing/wavelength on the dimensionless number.

A schematic drawing of the experimental setup is shown

in Figure 2. Pure PPG is injected at the bottom of the Hele-Shaw cell partially filling the cell. Water is added to the top half of the cell, and the two fluids begin to mix via diffusion. (It is important that the filling technique not inadvertently mix the two fluids significantly compared to diffusion. The diffusion layer at onset is typically only a fraction of a millimeter, which has made meeting this criterion quite difficult. We discuss the filling technique below.) The index of refraction *n* of the mixture varies monotonically with the concentration of water. The spatial variations in *n* refract the incident collimated light creating an image with light and dark regions that are captured every second with a digital camera (not shown in Figure 2).

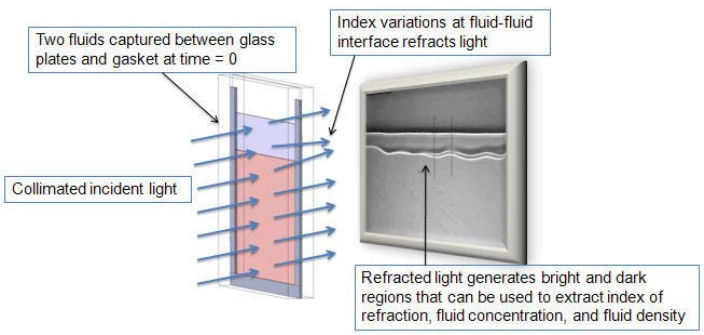


*Figure 2. Schematic drawing of the experimental apparatus.*

Figure 3 shows images at three different times for a run with plate spacing of 560 microns. At zero seconds, the PPG and water have just been brought into contact and the only features visible in the image are residual perturbations left over from merging the PPG and water. Fifty seconds later, the image shows a significant diffusion layer (approximately 0.5 mm thick), but no indication of a fingering instability. The structure in this image has the same spatial frequency as at earlier times which we interpret to be due to the initial perturbations. At a later time (110 seconds after merging), the image clearly shows growth of the fingering instability. To determine the spatial frequencies in the images, we extract curves of constant intensity, which trace the outline of the patterns in the image, and take the Fourier transform of these curves. As the instability develops, we find that the amplitude at a spatial frequency corresponding to 2.1 mm/finger grows rapidly. In Figure 4, we plot this amplitude as a function of time for three different runs in the same cell. All three runs show an onset time of approximately 60 seconds and a wavelength of 2.1 mm/finger. Analytical predictions [2] of the onset time are in rough agreement with a range from 40 to 70 seconds with the range due to the uncertainty in the density increase of the mixture and in the Hele-Shaw plate spacing. However, predictions of the spatial wavelength range from 1.2 to 1.5 mm/finger. A possible reason for the discrepancy is that the details of the concentration profile in the diffusion layer are different for the PPG-water system because the PPG and water are fully miscible while $CO_2$ is only partially miscible in brine.

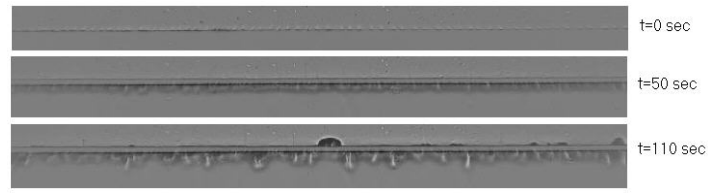


*Figure 3. Three images showing the water and PPG system just after the fluids have merged (t=0 secs), just before the fingering instability emerges (t=50 secs), and well after the instability onset (t=110 secs).*

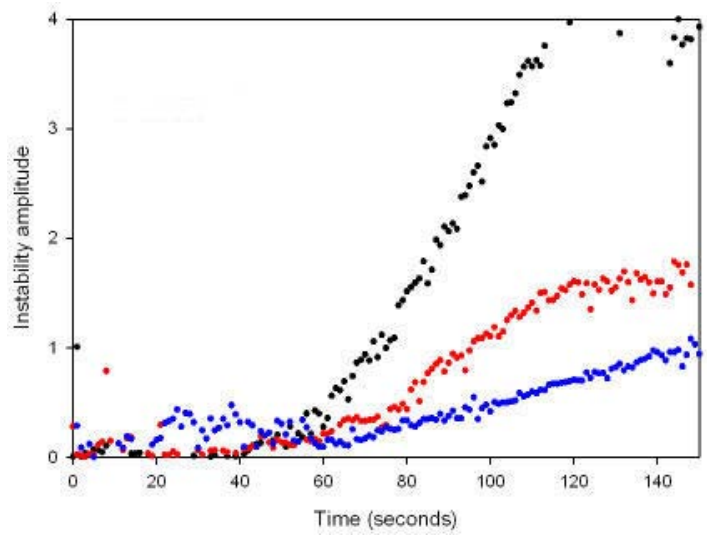


*Figure 4. Time evolution of the Fourier amplitude of the pattern in Figure 3 at a spatial wavelength of 2.1 mm/finger for three separate experimental runs.*

As seen in Figure 3, the initial perturbations due to the filling and merging of the two fluids can persist and modify the experimental results. We have tried many different techniques, and the best found so far (and used in Figure 3) is to partition the cell into upper and lower portions using a water soluble plastic membrane. The lower cell is filled its top edge, the membrane placed on top of the cell, the upper cell placed on top of the lower cell and aligned with pins, and finally the upper cell filled quickly with water. The membrane keeps any perturbations due to the filling from mixing the PPG and water. After about 20 seconds, the membrane slightly dissolves into the water and weakens to a gel-like consistency. Finally, surface tension causes the weakened membrane to form small half spheres of gel on the side of the cell. The periodicity of these spheres is visible in the top two images in Figure 3. For the plate spacing in those images (560 microns) the effect of this perturbation is not too significant. However, for a smaller spacing of 250 microns, the effect is quite dramatic. The perturbations due to the membrane remnants generate pre-instability-onset fingers that persist for a long time that cause mixing of the PPG and water that is much larger than the one-dimensional diffusion expected before onset. We continue to work to find filling and fluid-fluid merging techniques to resolve this issue.

## Impact on National Missions

Carbon-based fuels form the backbone of the world economy and have enabled nearly all of the technological innovations of the past 100 years. The U.S. and other developed countries have abundant and inexpensive domestic coal reserves that are often viewed a providing a secure energy future. In addition, as developing countries with large populations strive to attain higher standards of living, their emphasis will be on the utilization of even more of these inexpensive and abundant fossil fuels (e.g., China is currently completing construction of more than one coal plant *per week*). These trends create significant challenges due to the recognition that the environment cannot sustain the $CO_2$ released from oil, gas, and coal resources and that $CO_2$-driven climate change could pose a significant threat to U.S. national security.

For the U.S. and the world to continue to use these inexpensive fossil fuel resources while bypassing the implications, we must develop methods to avoid emitting the $CO_2$ to the atmosphere. A promising approach is to move towards a more carbon-neutral economy by capturing and sequestering the $CO_2$ in the subsurface, e.g. in depleted oil reservoirs and deep saline aquifers where overlying, low-permeability cap rocks contain the buoyant $CO_2$. [1] However, as long as the $CO_2$ remains buoyant, it remains a threat— the fluid pressure will try to drive it back though the cap rock and back into the atmosphere defeating our sequestration efforts and contributing to climate change. The $CO_2$ and brine are predicted to undergo a diffusion-driven gravitational instability that promotes the dissolution of the $CO_2$ into the brine. [2,3,4] The resulting $CO_2$-rich brine is denser than the pure brine and will sink, resulting in secure $CO_2$ sequestration. However, predictions of the evolution of multi-component fluid flows in geologic media are notoriously difficult. In our work, we seek to provide benchmark data to guide the development and validate numerical codes that can then be used to predict the flow and lifetime of injected $CO_2$ plumes—reducing the risks associated with fossil fuel consumption and helping to provide a secure energy future.

## References


1. Pacala, S., and R. Socolow. Stabilization wedges: Solving the climate problem for the next 50 years with current technologies. 2004. *Science.* **305**: 968.

2. Riaz, A., M. Hesse, H. A. Tchelepi, and F. M. Orr. Onset of convection in a gravitationally unstable diffusive boundary layer in porous media. 2006. *Journal of Fluid Mechanics .* **548**: 87.

3. Ennis-King, J., I. Preston, and L. Paterson. Onset of convection in anisotropic porous media subject to a rapid change in boundary conditions. 2005. *Physics of Fluids.* **17**: 084107.

4. Rapaka, S., S. Chen, R. J. Pawar, and P. H. Stauffer. Direct Numerical Simulation of the onset of density-driven convection in anisotropic porous media. Presented at *59th Annual meeting of the APS Division of Fluid Dynamics.* (Tampa Bay, November 19–21, 2006).

# Feasibility of GHG Monitoring from Space: Verification of Los Angeles Emissions

*Manvendra K. Dubey*
20090488ER

## Abstract

Industrial emits greenhouse gases (GHGs) that are altering our climate, in particular carbon dioxide ($CO_2$) from fossil energy and land use. To protect us from growing threats of climate change, the world is poised to negotiate a climate treaty in Copenhagen in December 2009. The verifiability of reported GHG national emissions is a critical component that requires technical means that LANL is uniquely positioned to develop. We have analyzed observations from a ground based high-resolution solar tracking Fourier Transform Spectrometer (FTS) in the Los Angeles area in March 2008 to assess the viability of column $CO_2$ measurements for space based verification of $CO_2$ emissions. The high-resolution FTS solar spectra, when degraded to lower resolutions typical of space-borne sensors and analyzed, revealed that 1 ppm accuracy in column $CO_2$ with a 380 ppm background is feasible under ideal conditions. A new retrieval method that uses the ratios of the maximum to minimum absorption for few selected $CO_2$ spectral lines was found to be less susceptible to interferences from aerosols, clouds and surface reflectance variability. Column $CO_2$ concentrations over Los Angeles were measured to fluctuate by 5-7 ppm/day by the ground FTS. There is substantial day-to-day variability in the $CO_2$ increase due to changing weather patterns. We use the Weather Research Forecast model with emissions to simulate the $CO_2$ above the Los Angeles. Our simulations reproduce the gross features of the observations, thus supporting their utility for verification. Our research shows that, with further research, space based observations can be combined with atmospheric model simulations to verify GHG emissions from large urbanized areas.

## Background and Research Objectives

A promising methodology for verification is the use of satellites to monitor GHGs. Such data are just beginning to be gathered by the Japanese Greenhouse gases Observing SATellite (GOSAT) satellite launched in January 2009. A Fourier Transform spectrometer (FTS) on the satellite measures the spectrally resolved backscattered sunlight from the earth's surface after it has traversed through the atmospheric column. These spectra are used to fingerprint and quantify the abundance of GHGs inluding $CO_2$. However, the resolution of the GOSAT Fourier FTS is coarse (0.3 $cm^{-1}$) and there is potential for interferences from other atmospheric constituents (water, clouds and aerosols) and the variations in surface reflectance. Our project has goals are:

- Develop robust retrieval algorithms by analyzing data from a ground based solar tracking Fourier Transform Spectrometer (FTS) with utra-high spectral resolution (~0.015 $cm^{-1}$).
- Measure increases in columnar $CO_2$ above a large urban region like Los Angeles using the FTS and develop a methodology to utilize them to verify emissions.

## Scientific Approach and Accomplishments

The first goal of our project was to determine whether accurate and robust retrievals of $CO_2$ from space are feasible. To achieve this we acquired high spectral resolution solar FTS spectra of the South Bay Basin (Los Angeles) from Jet Propulsion Laboratory and Caltech with a time resolution of few minutes in March 2008. To fit the spectra and retrieve column $CO_2$ we extended LANL's unique spectral chemical fingerprinting code to the near infrared region where $CO_2$absorbs sunlight. We specifically focused on the $CO_2$ spectral features near 1.6 micron, which fits the high resolution (0.015 $cm^{-1}$) spectra for a column concentration of 389 ppm as shown in Figure 1. The FTS spectra were then synthetically degraded in resolution to those relevant to satellites (0.3 $cm^{-1}$) and the fits repeated. The results indicate that under ideal conditions the accuracy of the retrieved columnar $CO_2$ decreases from about 0.05

ppm for the ground FTS to about 0.7 ppm for the coarse satellite resolutions. Next we developed a more robust and simpler retrieval method that focuses on the ratio of absorbance (max/min) for selected $CO_2$ lines that do not have any interference from other species. The fits of these lines scales linearly with $CO_2$ and indicate that a sensitivity of 0.5 ppm $CO_2$ is achievable if line ratios are measured with 0.1% accuracy. We systematically explored the effects of potential interferences from aerosols, clouds, water and reflectance variations. For example, Figure 2 shows that the effects of increasing aerosol depth (AOD) on the $CO_2$ spectral lines at the coarse spectral resolution. The broad aerosol features that appears on the baseline cancel when the ratio method is applied, resulting in very small errors in $CO_2$ retrievals (0.4 ppm).

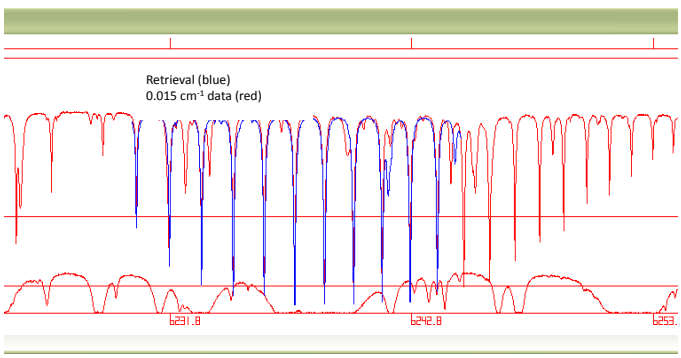


*Figure 1. Observed (red) and fitted spectra used to fingerprint and retrieve column $CO_2$ at high resolution in the 6230 to 6250 cm-1 region.*

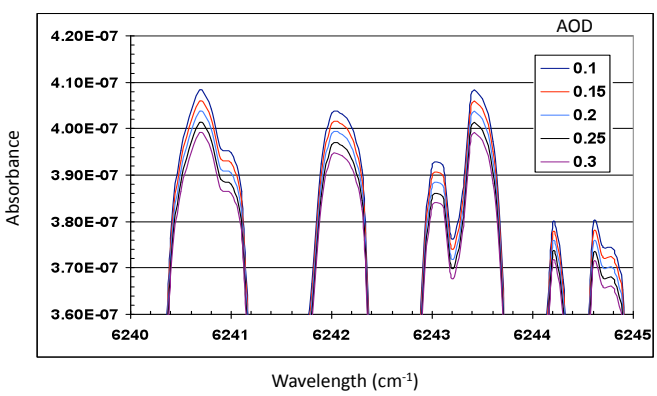


*Figure 2. Spectral fitting of the $CO_2$ bands at various Aerosol Optical Depths.*

The second goal of the project was to assess the viability of remote column $CO_2$ observations in verifying reported emissions over a large urban area. For this we utilized the FTS observations of column $CO_2$ observations made in the Los Angeles area in March 2008 [Wunch et al 2009]. The time dependence of $CO_2$, other greenhouse gases and carbon monoxide (CO), a co-emitted pollutant from combustion, for a selected week where the emissions were primarily from fossil energy sources is shown in Figure 3. The profiles are obtained by fitting the FTS spectra taken every few minutes and are available during daytime. Increases of $CO_2$ of about 5-7 ppm over a background of 380 ppm from morning to late afternoon are clearly resolved by the FTS. The topography of the Los Angeles basin, with mountains on three sides, isolates the air shed creating favorable conditions for accumulation of $CO_2$ and CO. The increase in $CO_2$ and CO begins early in the morning when traffic and industries begin emitting pollutants in the shallow boundary layer above the South Bay area. The increase continues during the day despite the expansion of the boundary layer due to the increase in emissions and their accumulation. In the late afternoon, the boundary layer grows above the mountains allowing the polluted $CO_2$ rich air mass to mix with clean air with lower $CO_2$ levels northwest of the mountains. The temporal behavior of $CO_2$, $CH_4$ and CO is virtually the same due to the same dynamical effects on relatively homogenized emissions. The variability in the increase results from the variability in dynamics, assuming that weekday emissions are relatively constant. We also note that on March 27 there is very little accumulation of $CO_2$ due to strong Santa Ana winds dispersing the emitted $CO_2$ over wide areas of the ocean.

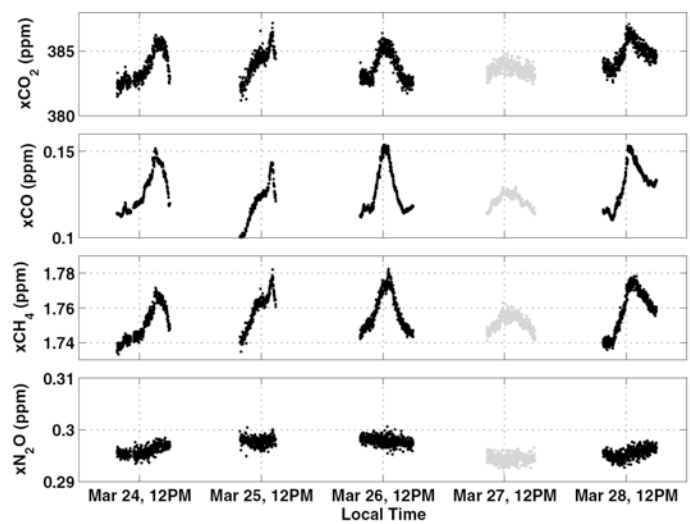


*Figure 3. Increases in $CO_2$, CO, $CH_4$ and $N_2O$ observed by the FTS at JPL/Caltech during March 24-26 2008.*

To use the column $CO_2$ observations to verify emissions we need to simulate the atmospheric dynamics over the South Bay region accurately. For this we used the Weather Research Forecast numerical model that was customized for this South Bay region. The model is run in a nested grid configuration that covers the entire western US at 54 km resolution and zooms into the Los Angeles area with 6 km resolution. This framework allows the model to capture the large-scale climatology to predict the local meteorology. We constructed a homogenized

emissions inventory for $CO_2$ from the statewide CARB inventory scaling it with the population of the South Bay region, which amounted to 55 tones/hour for each 6 km grid point. The emissions were turned on at 6 am and updated every hour in WRF, which then transported them into the atmosphere using realistic dynamics. Increases in surface $CO_2$ levels above the background (~380ppm) simulated by WRF every few hours on March 21 are shown in Figure 4. The accumulation and dispersion of the plume is evident, with increases in $CO_2$ concentrations of as much as 50ppm at the surface. The vertical evolution of $CO_2$ along a transect in Figure 5 shows $CO_2$ rich plumes rising along the mountain. In the late afternoon the boundary layer rises above the mountains allowing the mixing with cleaner air resulting in a drop in $CO_2$. We also increased the emissions by 50 %, which resulted in an increase in surface by about 20 ppm (about 50%) indicating a linear response. Furthermore, the WRF correctly simulates the Santa Ana flows on March 27 2008, with a low $CO_2$increases above Los Angeles since the emissions are transported to the ocean by the winds. Our WRF model simulations reproduce the gross dynamic features of the FTS observations. We have performed simulations with a new spatio-temporally gridded $CO_2$ emission inventory from the VULCAN project. Preliminary results indicate that the Vulcan emissions are systematically too low. We are analyzing the outputs, which will be presented as special session on Greenhouse gas information system at the fall meeting of the American Geophysical Union in December 2009.

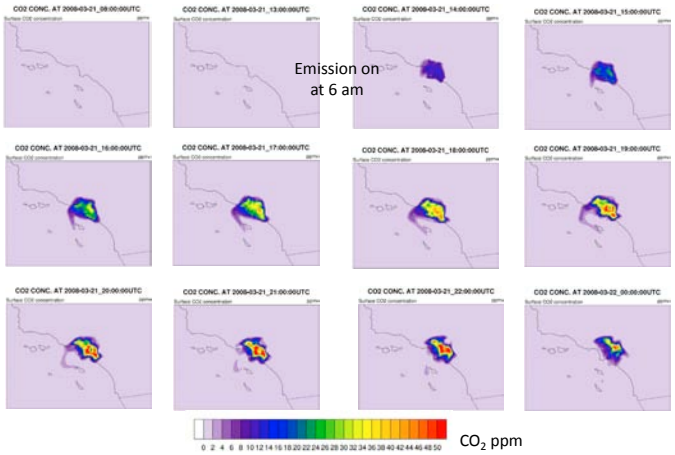


*Figure 4. Snapshots of surface $CO_2$ concentration increases (above the 380 ppm background) in the Los Angeles area with WRF using constructed emissions every few hours. The emissions are turned on at 6 am after which the increase is clearly observed.*

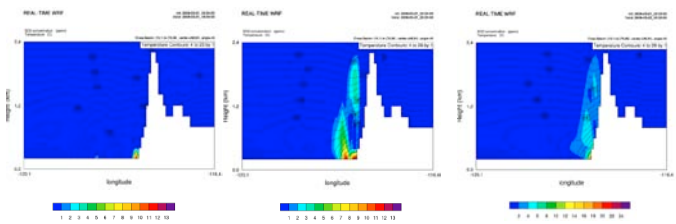

*Figure 5. Time evolution of the vertical distribution of $CO_2$ predicted by the WRF model along a transect that intersects the mountains.*

## Impact on National Missions

Our project has demonstrated that ground based remote sensing has the potential to verify urban emissions. Space based instruments like GOSAT will need higher spatial and spectral resolution perform verification. NASA's proposed Orbiting Carbon Observatory replacement is a step in the right direction. The science developed in this projected has contributed to LANL acquiring its own solar FTS (~$500K), which in addition to GHGs will also monitor signature pollutant species like $NO_2$ that makes urban smog. We will propose to deploy it in the Farmington Four Corners power plants region that has the largest NOx and $CO_2$ emissions and demonstrate the verification potential of remote sensing methods. Our LANL-team has been selected to become part of the first GOSAT data application team by the Japanese space agency. LANL is leading the charge on climate treaty verification R&D by leveraging its 50-year leadership in nuclear test ban and nonproliferation treaty monitoring.

## References

1. Wunch, D., P. O. Wennberg, G. C. Toon, and G. Keppel-Aleks. Emissions of greenhouse gases from a North American megacity. 2009. *Geophysical Research Letters.* **36** (L15810): 10.1029/2009GL039825.

## Publications

Costigan, K., and M. K. Dubey. Simulation of atmospheric CO2 concentrations in California's South Coast Basin. To appear in *American Geophysical Union Fall Meeting.* (San Francisco, 14-18 Dec. 2009).

Dubey, M., K. Costigan, P. Chylek, W. S. Smith, D. Wunch, and P. O. Wennberg. WRF Simulations of Los Angeles region Carbon-dioxide emissions: Comparisons with column observations. To appear in *American Geophysical Union Fall Meeting.* (San Francisco, 14-18 Dec. 2009).

# Simulating Vegetation Impacts on River Basin Water Balance

*Everett P. Springer*
20090529ER

## Abstract

Computer simulations models of river basins can provide data to make decisions about water resources. This study had two goals. The first goal applied the high performance computing capability at Los Alamos National Laboratory (LANL) to simulate large river basin in a timely manner. The second goal was to use the simulation model on a river basin, the Rio Ojo Caliente in New Mexico to study the effects of vegetation change on the basin's water resources. The watershed model was adapted to the parallel computers at LANL improving performance by five times. LANL also provided additional computer programs to allow rapid mesh building, which is needed for large river basins and to plot results. The division of a watershed into streams and upland areas was examined for its impact on the simulations. Three different approaches to divide the watershed were used on a large watershed represented by approximately 900,000 nodes. Results showed a speed-up of 57 times over the single processor base case for one of the partition approaches. All of the approaches had increase in speed over the base case. The simulation of the Rio Ojo Caliente required collecting data to drive the model. These data included weather, vegetation, soils, and geology. In the early 2000's, pine trees were killed in the lower part of the Rio Ojo Caliente basins. We hoped to study the impacts of this die-off on the streamflow, groundwater, and soil water. The vegetation change was developed from satellite data obtained on approximately two-week intervals. Initial simulations showed that further adjustment on watershed model parameters were needed for better results. The model parameter that distinguishes rain from snow needs to be altered for more snow accumulation. This project supports LANL's Energy Security mission focusing on the environmental impacts of climate change.

## Background and Research Objectives

The use of water resources is an issue many regions of the United States. Computer simulation models of river basins support decisions and assess impacts on water resources. There were two objectives for this project. The first objective was to modify and test the hydrologic simulation model. The second objective was to perform simulations that demonstrate the capabilities of this model. There are many other researchers doing computer simulations of river basins. The unique contribution of LANL is its computer capabilities that allow simulations of large river basins. These simulations will be faster on the LANL computers too.

The computer code that was selected is the parallel version of the TIN-based Real-Time Integrated Basin Simulator (tRIBS) [1]. The parallel tRIBS provides continuous hydrologic simulation of surface and subsurface processes. The TIN or triangulated irregular network uses triangles to represent the hills and valleys of a watershed. The TIN allows important landscape features to be included and is cost-effective for computer applications.

We were able to adapt the tRIBS code to the LANL computers. A big increase in computer speed was shown when we used several processors rather than one. Further improvement in computer speed was found when the basin was divided so that the work on the processors was more balanced with the basin geometry.

The river basin for simulation was the Rio Ojo Caliente in northern New Mexico. This basin had a large vegetation change in the early 2000's. We wanted to look for changes in water due to the vegetation change using tRIBS. Initial simulations showed the need for more model adjustments. The amount of snow that was simulated was less than the amount needed to maintain streamflow. The reasons for the low accumulation of snow were most likely due to the temperature data used in the simulation.

## Scientific Approach and Accomplishments

Parallel tRIBS provides continuous hydrologic simulation using a multiple resolution representation of complex terrain based on a TIN using domain decomposition to distribute sub-basins of a watershed across multiple processors. The stream reach graph based on the channel network structure is used to determine each sub-basin and its connectivity. Routed streamflow from each sub-basin forms the major hydrologic data exchange along the stream reach graph. Individual sub-basins also share subsurface hydrologic fluxes across adjacent boundaries. A timesaving capability, known as MeshBuilder, was developed to allow the unstructured mesh and stream flow network to be created only once, where multiple runs are required. Previously, tRIBS had to build the mesh for each run. A tRIBSReader Visualizer, which is a plugin library to be used with the ParaView visualization package, provided model debugging and results presentation. The tRIBS code had been shown to run on small and medium-sized basins [1]. This project has focused on large basin model preparation and running, requiring enhancements to parallel tRIBS, MeshBuilder, tRIBS visualizer, and the basin partitioning capability. Performance and partitioning experiments were run using the high-resolution Baron Fork basin (~900K nodes).

Computer time for this project was obtained on the Institutional Computing Resource, Coyote, per the "Sub-basin Based Parallel Hydrological Models for Semi-Arid Regions – Large Basin Studies" proposal. Two basins, Baron Fork and the Rio Ojo Caliente, were studied in this part of the project.

**Parallel tRIBS, MeshBuilder, and tRIBS Visualizer**

Running larger basins and using the digital elevation model (DEM) and dynamic vegetation tRIBS capabilities required code improvements. Blocking sends and non-blocking receives are now used for all communications to eliminate deadlock situations. A barrier has been added prior to time-consuming DEM data processing to synchronize and reduce time across all processors. Resampling of DEM data was modified to use node relative indices whether running serial or parallel. Rain and weather files are now composed of all the hourly files for a year. And dynamic vegetation files are read as needed. The restart mechanism has been modified to include handling of the position in the dynamic vegetation data.

MeshBuilder and the tRIBS Visualizer were used for debugging the high-resolution Baron Fork and Rio Ojo Caliente files. A "too sparse" distribution of stream nodes was identified using the Visualizer when MeshBuilder was not able to construct the stream network. In the case of Rio Ojo Caliente, a flood plain addition was required.

**Performance and Partitioning Experiments**

An efficient partitioning balances the computational load and minimizes message passing between processors. The number of nodes per stream reach contributes to the computational load. Connections between reaches in the steam network and subsurface flux network contribute to the messaging. Four partitionings were compared. The *default* partitioning is just a slicing up of the initial reach order creation by tRIBS. Three other partitionings, *flow*, *flow-flux*, and *flow-flux-upstream*, were produced using the Metis multi-constraint graph partitioning program. The *flow* partitioning balances the number of computer nodes (computational load) and stream reach network connectivity. The *flow-flux* partitioning additionally considers the subsurface flux connectivity. And the *flow-flux-upstream* partitioning also balances the number of reaches without upstream reaches.

**Baron Fork Basin**

The high-resolution Baron Fork basin of Oklahoma is composed of approximately 900,000 nodes, 5 million edges, and 5707 reaches. The goal was to improve performance on a 1-year run with reasonable storm activity from November 1997 to December 1998. MeshBuilder was run to create the mesh and stream flow network. Running on 1 processor for 15 hours produced only about 10 days of simulation requiring 92.479 min/simulated day. This shows that multiple processors are required to improve run times. Runs for the different sub-basin partitionings were made on 32, 64, 128, and 256 processors for November 1997 to determine the best partitioning and number of processors to be used for the 1-year run.

The *default* partitioning appears to be a random distribution of reaches across processors as seen in Figure 1 for 32 processors. The best result is 24.94 min/simulated day on 128 processors as seen in Figure 2. This partitioning balances the number of reaches across processors, but does not balance the number of nodes or computational load. Also each processor exchanges subsurface flux with all other processors requiring a lot of messaging.

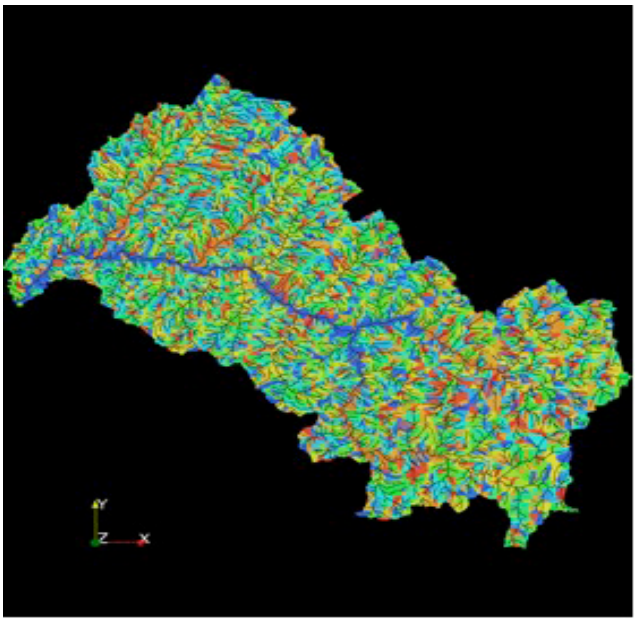

*Figure 1. ParaView visualization of the default partitioning and stream flow network for the Baron Fork basin.*

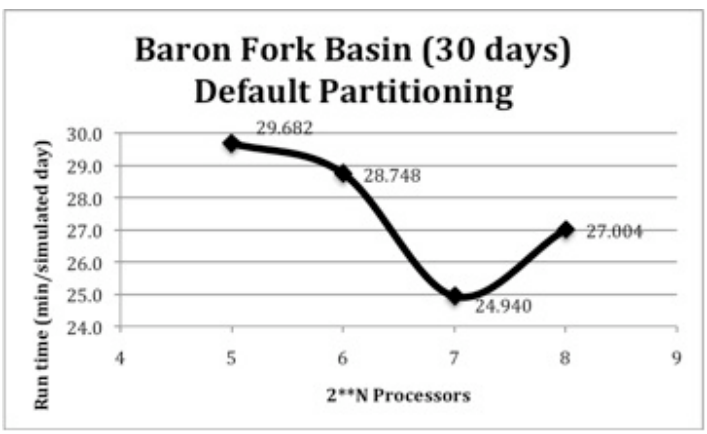


*Figure 2. Performance for default partitioning over a 30-day run on Baron Fork Basin.*

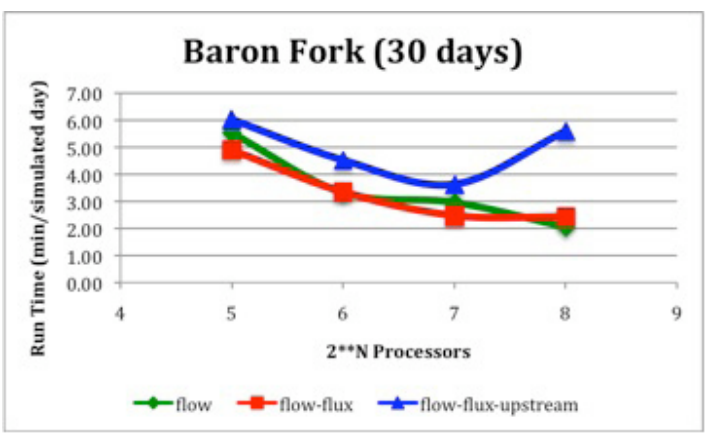


*Figure 3. Performance for flow, flow-flux, and flow-flux-upstream partitionings over a 30-day run on Baron Fork Basin.*

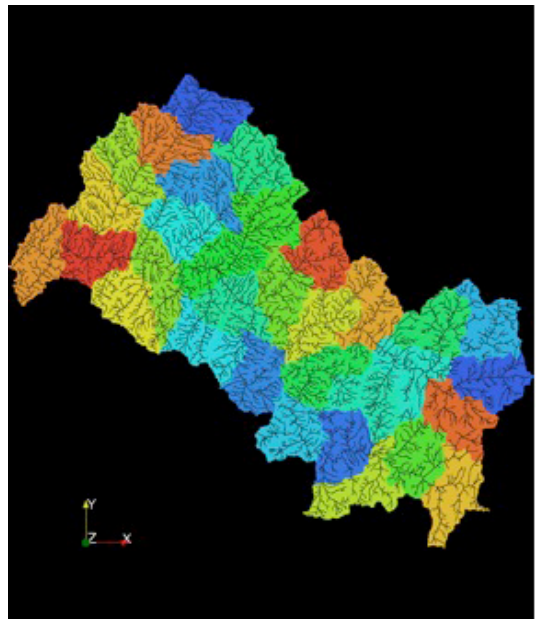

*Figure 4. ParaView visualization of the flow-flux partitioning and stream flow network for the Baron Fork basin.*

The *flow* partitioning produces a more geographic distribution of sub-basins based on the flow network. It greatly improves run time over the *default* partitioning. While 2.947 min/simulated day on 128 processors is good, 2.038 min/simulated day on 256 processors is better as seen in Figure 3. This partitioning does a good job of balancing the nodes across processors and provides the best minimization of flow exchanges between processors.

The *flow-flux* partitioning produces a geographic distribution of sub-basins based on the flow and subsurface flux networks as seen in Figure 4. It again improves run time. The best result is seen on 128 processors of 2.475 min/simulated day in Figure 3, with minimal improvement on 256 processors. This partitioning does the best job of balancing the nodes across processors and provides the best minimization of subsurface flux exchanges between processors.

Reaches without any incoming upstream reaches can be processed without waiting in each iteration. This has the potential of speeding up the run times even more. The *flow-flux-upstream* partitioning addresses this, but produces a more fragmented geographic distribution of sub-basins. This fragmentation causes more waiting and increased run time. The best run time is 3.628 min/simulated day on 128 processors as seen in Figure 3. This partitioning does a good job of balancing nodes across processors, but does not minimize flow and flux exchanges as well as other partitionings due to the fragmentation.

The *flow-flux* partitioning provides the best run time on

the least number of processors, while the *flow* partitioning provides the best overall run time. One year runs (November 1997 – December 1998) were performed using the *flow*, *flow-flux*, and *flow-flux-upstream* partitionings on 128 and 256 processors. As seen on the shorter 30-day test runs, *flow-flux* results in the best run time on 128 processors of 2.186 min/simulated day (Table 1). This is a speedup of 42 times over 1 processor with 33% efficiency. The *flow* partitioning produces the best run time on 256 processors of 1.623 min/simulated day. This is a speedup of 57 times over 1 processor with 22% efficiency.

| Partitioning | Total Run Time (hr) | Run Time (min/simulated day) | Speedup | Efficiency |
|---|---|---|---|---|
| Flow | > 15.0 | 2.504 | 36.932 | 0.289 |
| **Flow-Flux** | **13.3** | **2.186** | **42.305** | **0.331** |
| Flow-Flux-Upstream | > 15.0 | 3.400 | 27.200 | 0.212 |

*Table 1. Performance on 128 processors for partitionings over a 1-year (November 1997-December 1998) run of Baron Fork Basin. Note that Flow-Flux (bold) provides the best results.*

**Rio Ojo Caliente Basin**

The same partitioning methodology was applied to low-resolution and high-resolution versions of the Rio Ojo Caliente basin of New Mexico as part of a vegetation impacts study. The low-resolution Rio Ojo Caliente basin is composed of approximately 100,000 nodes, 600,000 edges, and 689 reaches. The high-resolution Rio Ojo Caliente basin is composed of approximately 665,000 nodes, 4 million edges, and 2,344 reaches. 100-day runs were made with the *flow-flux* partitioning to determine the best number of processors to run on. Low-resolution Rio Ojo Caliente runs best on 32 processors while the high-resolution version runs best on 64.

The low-resolution Rio Ojo Caliente with the *flow-flux* partitioning was used for a vegetation impacts study for the period 1995-2004. Up to four years were simulated per 15 hour run.

**Rio Ojo Caliente Simulation**

The goal of this task was to simulate the Rio Ojo Caliente for the years 1995 – 2004. This period included the pine tree die-off that occurred in the early 2000's. The simulation needed the following data, weather, vegetation, soils, and geology.

The weather data were obtained from the simulations of the southwestern United States [2]. In preparing the data, gaps were found, and we requested additional data from the authors [2], and they supplied the data. The weather data were formatted for tRIBS.

A new feature of tRIBS is the ability to use vegetation data that changes over time. The vegetation cover was derived from remotely sensed images that were available approximately every two weeks. The next step is to relate the vegetation to different land cover types, for example grasses, forest, woodland. Each vegetation type has certain key plants that are used in the simulation. For example, the woodland is composed of pine tress, junipers, and grasses. The tRIBS parameters for these plant types were taken from the literature or derived from data collected at the LANL Pinyon-Juniper experimental site [3]. These input parameters were constant for the different plant types over the simulation. The number of plants within the Rio Ojo Caliente watershed changed over the time period.

We were not able to complete the Rio Ojo Caliente simulation for the period to show the vegetation change impacts on water. The primary reason was that there was not enough time for such a project. The lack of time affected our ability to address initial conditions effects on the simulation. These types of computer codes need to be run for a period of time so that the initial values of variables do not have a large effect. An example of this is shown in Figure 5. The red line in Figure 5 is the simulated streamflow. Draining of the soil layers causes the large blip at the beginning. Further simulations would adjust the amount of water in the soil and the soil properties that control the flow of water to bring the flow in better agreement with the observed streamflow.

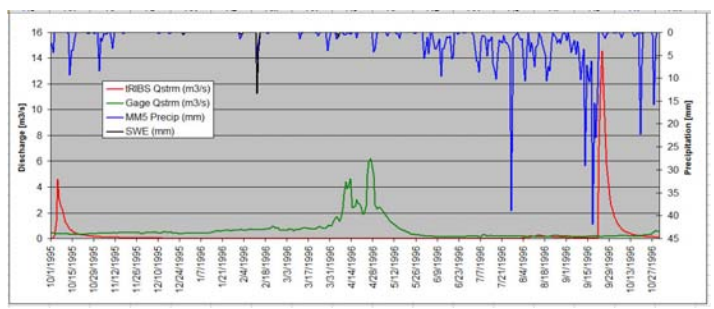


*Figure 5. Simulated Rio Ojo Caliente streamflow using parallel version of tRIBS (red line) for 1995. The green line is the observed streamflow. The precipitation is the blue line, and the amount of water in the snow or snow water equivalent (SWE) is the black line.*

The snow is another factor that needs adjustment based on Figure 5. Snow is the major part of the water balance in the Rio Ojo Caliente. From Figure 5, it can be seen that there was little snow generated for that year. The result is that no streamflow was generated at the right time of year. The need to adjust the parameters of the snow model is necessary based on the results in Figure 5. A sensitive parameter is one that causes a large change in output for a small change of the input. In the snow model in tRIBS,

the temperature that distinguishes between rain and snow is a sensitive parameter. Again, the adjustment of that temperature is needed to produce a better simulation.

The basis for the simulation for the water resources of the Rio Ojo Caliente has been completed. To complete the simulation, adjustments to the model parameters and properties are needed.

## Impact on National Missions

This project supports the LANL mission in energy security through understanding the environmental impacts of energy use and climate change. The application of LANL's high performance computing capabilities to environmental assessments will allow more rapid decisions. This project addressed the philosophy of applying models to environmental problems.

This project suppored a post-doctoral candidate at LANL.

## References


1. Ivanov, V. Y., E. R. Vivoni, R. L. Bras, and D. Entekhabi. Preserving high-resolution surface and rainfall data in operational-scale basin hydrology: a fully-distributed, physically-based approach. 2004. *Journal of Hydrology.* **298**: 80.

2. Li, J., X. Gao, and S. Sorooshian. Modeling and analysis of the variability of the water cycle in the upper Rio Grande basin at high resolution. 2007. *Journal of Hydrometeorology.* **8**: 805.

3. Breshears, D. D., N. G. McDowell, K. L. Goddard, K. E. Dayem, S. N. Martens, C. W. Meyer, and K. M. Brown. Foliar absorption of intercepted rainfall improves woody plant water status most during drought . 2008. *Ecology.* **89** (1): 41.


## Publications


Mniszewski, S., P. Fasel, E. Vivoni, A. White, and E. Springer. Increased efficiency for high-resolution Baron Fork simulations using basin structure characteristics. 2009. *Los Alamos National Laboratory Report LA-UR-09-06025.*

# Creating a Mathematical Foundation for High-Dimensional Search and Optimization Algorithms to Solve Complex Nonlinear Models

*Bruce A. Robinson*
20070560PRD1

## Introduction

Numerical simulation models, along with theory and experiments, have become fundamental tools for understanding complex nonlinear systems. However, successful application of complex models is not straightforward: many of the parameters and internal states in these models require calibration/updating before meaningful predictions and uncertainty estimates can be made. Global optimization algorithms based on evolutionary search are increasingly being used for estimating parameters and states in these models. Many recent studies have demonstrated that hybrid and adaptive methods that extract information from the sampling history to continuously update the proposal distribution during the search are dramatically more efficient than more traditional static methods. However, the field of optimization relies on heuristic approaches to test for efficiency, rather than more formal theoretical approaches. This calls into question the validity of hybrid and adaptive search and optimization methods for solving high-dimensional state and parameter estimation problems. A sound mathematical foundation, combined with testing on canonical search problems and real-world applications, is essential for advancing the field of optimization beyond its current state, and for solving emerging mission-relevant problems.

In this project, we are: 1) developing formal convergence proofs of hybrid and adaptive search methods for the solution of nonlinear single and multi-objective optimization problems, 2) continuing the development of hybrid and genetically adaptive search methods, and 3) applying these methods to environmental and other modeling problems of strategic importance to the Laboratory. This research is enabled by the opportunity to collaborate with world-class theoretical and numerical analysts and physical scientists at LANL, a large selection of mission-relevant models and emerging problems to choose from, and the excellent parallel computing facilities at LANL.

## Benefit to National Security Missions

The methods developed are integral to the advancement of the science and development of next-generation environmental models in many programs tied to the DOE energy security mission, including groundwater resource, contaminant transport, oil and gas, nuclear waste disposal, and carbon sequestration applications.

## Progress

In the past year, we have developed a novel concept of genetically adaptive multimethod search that significantly enhances the efficiency of single and multiobjective evolutionary optimization, and have developed the mathematical foundation and numerical implementation of a novel Markov Chain Monte Carlo algorithm (Differential evolution adaptive Metropolis, or DREAM) for computationally efficient posterior inference in a Bayesian framework. The algorithmic advances have been accepted / published in applied mathematical journals, and the usefulness and applicability of these methods has been demonstrated by application to various sampling and inverse problems in different fields of studies. We are currently extending the mathematical and numerical advances developed within this project to particle filtering approaches for combined parameter and state estimation.

In the area of applications, the project's advances in parameter estimation and uncertainty estimation have led to significant contributions in hydrologic modeling and hydrologic laboratory and field methods. For instance, in one study, we demonstrated that only a very limited number of discharge observations is needed to appropriately calibrate streamflow forecasting models, that data of throughfall contain insufficient information to parameterize canopy interception models appropriately, that water uptake by plant roots is difficult to estimate in the presence of significant uncertainty associated with the hydraulic properties of the soil, and that most of the uncertainty in streamflow forecasting is due to uncertainty with the observed rainfall data. The project has also placed LANL at the center of the current debate on the most appropriate methods for uncertainty estimation in hydrology. Particularly, there is strong disagreement whether an uncertainty framework

should have its roots within a proper statistical (Bayesian) context, or whether such a framework should be based on a different philosophy and implement informal measures and weaker inference to summarize parameter and predictive distributions.

On one study, we compared a formal Bayesian approach with a more common, but less formal approach for assessing uncertainty in conceptual watershed modeling. Our results demonstrated that formal and informal Bayesian approaches have more common ground than the hydrologic literature and ongoing debate might suggest. The main advantage of formal approaches is, however, that they attempt to disentangle the effect of forcing, parameter and model structural error on total predictive uncertainty. This is key to improving hydrologic theory and to better understand and predict the flow of water through catchments. Another study considered application of MCMC simulation to parameter inference in the extensively used Sacramento Soil Moisture Accounting (SAC-SMA) model, a lumped conceptual watershed model that describes the transformation from rainfall into basin runoff using six state variable reservoirs. Inputs to the model include mean areal precipitation (MAP) and potential evapotranspiration (PET) while the outputs are estimated evapotranspiration and channel inflow. This real-world study poses an interesting challenge for MCMC samplers due to the complexity of the model's response surface. We found that that DREAM exhibits superior performance in terms of the number of iterations required to reach the global optimum. In addition, our algorithm achieves a significantly lower root mean squared error than its counterpart derived with the state-of-the-art SCE-UA algorithm. Thus, the algorithms available to date converge prematurely to a sub-optimal region in the parameter space, contradicting many published studies in the literature that have shown that SCE-UA is a reliable and efficient optimizer of nonlinear watershed models. These results suggest that DREAM enhances the efficiency of MCMC simulation, and simultaneously estimates values of the SAC-SMA model parameters that improve the reliability of flood forecasts.

## Future Work

The work conducted in numerical simulation models, along with theory and experiments, have become fundamental tools for the understanding complex nonlinear systems and science based decision making. However, the usefulness and applicability of numerical system models is increasingly being held back by problems with parameter and state estimation. A sound mathematical foundation, combined with testing on canonical search problems and real-world applications, is essential for advancing the field of optimization beyond its current state, and solve emerging mission-relevant problems.

This project is coming to a close early in FY10. The project has been extremely productive: the Postdoctoral PI has organized 7 topical sessions at various (inter) national conferences, and has given 10 invited talks and seminars. In addition, 31 papers have been published or are in press, and 9 others are submitted and in review. Accomplishments on this project have set the stage for advancements in a number of areas, outlined below.

1. Extension of the work to very high dimensional problems using dimensionality reduction: Despite the exceptional progress made, the very nature of high-performance computing model applications are that they consist of an extraordinary number of degrees of freedom, or unknown parameters that can, in principle, be adjusted to optimize the model. This situation calls for a new approach to systematically reduce the dimensionality of these large-scale simulation models. By merging dimensionality reduction methods with our new optimization algorithms, we anticipate being able to expand the applicability of our research to a much broader range of models.

2. Improving computational efficiency: Our MCMC method can be improved by incorporating new ideas that enable us to reduce the number of Markov chains that are initiated, and by modifying the algorithm to enhance its performance in high-performance computing platforms.

3. Applications: Work will continue to apply the methods to environmental and other modeling problems of strategic importance to the Laboratory. Applications of interest to LANL and other scientists include those in the fields of climate science, ecology, hydrology (vadose zone and aquifer), hydrogeophysics and soil physics.

This work is methodological in nature, designed to advance the field of optimization, and will allow us to solve currently intractable nonlinear parameter and state estimation problems. This research is enabled by the opportunity to collaborate with world-class theoretical and numerical analysts and physical scientists at LANL, a large selection of mission-relevant models and emerging problems to choose from, and the excellent parallel computing facilities at LANL.

## Conclusion

This work is answering general, methodological questions on the science of optimization and mathematical model development. The methods developed in this project are being applied to natural systems models to provide insights about scientific questions of environmental interest. In each of these applications, we are collaborating with LANL scientists acquiring large, spatially distributed data sets and developing complex computer models of these natural systems. Thus, by acting as a catalyst to push the frontiers of science in these ongoing projects, we are contributing

to the Laboratory's efforts in energy security and complex natural systems.

## Publications


Behrangi, A., B. Khakbaz, J. A. Vrugt, Q. Duan, and S. Sorooshian. Comment on: Dynamically dimensioned search algorithm for computationally efficient watershed model calibration' by Bryan A. Tolson and Christine A. Shoemaker. 2008. *Water Resources Research.* **43**: W01413.

Blasch, K. W., T. P. A. Ferre, and J. A. Vrugt. Environmental controls on drainage behavior of an ephemeral stream: An example of the limitations of simple correlative data analyses. To appear in *Stochastic Environmental Research and Risk Assessment.*

Blasone, R. S., J. A. Vrugt, H. Madsen, D. Rosbjerg, G. A. Zyvoloski, and B. A. Robinson. Generalized likelihood uncertainty estimation (GLUE) using adaptive Markov Chain Monte Carlo sampling. 2008. *Advances in Water Resources.* **31**: 630.

Clark, M. P., A. G. Slater, D. E. Rupp, R. A. Woods, J. A. Vrugt, H. Gupta, T. Wagener, and L. Hay. Framework for understanding structural errors (FUSE): a modular framework to diagnose differences between hydrological models. 2008. *Water Resources Research.* **44**: W00B02.

Dane, J. H., J. A. Vrugt, and E. Unsal. Soil Hydraulic Functions from Simple Measurements of Air Permeability, Capillary Modeling and High-Dimensional AMALGAM Parameter Estimation. To appear in *European Journal of Soil Sciences.*

Dekker, S. C., R. Elkington, and J. A. Vrugt. Significant Variation in Vegetation Characteristics and Dynamics from Ecohydrologic Optimality of Net Carbon Profit. To appear in *Plant, Cell & Environment.*

F.terBraak, C. J., and J. A. Vrugt. Differential evolution Markov chain with snooker updater and fewer chains. 2008. *Statistics and Computing.* **18** (4): 435.

Feyen, L., J. A. Vrugt, B. Nuallin, J. van der Kniff, and A. de Roo. Parameter optimization and uncertainty assessment for large-scale stream flow forecasting. 2007. *Journal of Hydrology.* **332**: 276.

Feyen, L., M. Khalas, and J. A. Vrugt. Semi-distributed parameter optimization and uncertainty assessment for large-scale streamflow simulation using global optimization. 2008. *Hydrological Sciences Journal.* **53** (2): 293.

H.Diks, C. G., and J. A. Vrugt. Comparison of point forecast accuracy of model averaging methods in hydrologic applications. To appear in *Stochastic Environmental Research and Risk Assessment.*

Harp, D. R., Z. Dai, A. V. Wolfsberg, J. A. Vrugt, B. A. Robinson, and V. V. Vesselinov. Aquifer structure identification using stochastic inversion. 2008. *Geophysical Research Letters.* **35**: L08404.

Hinnell, A. W., T. P. A. Ferre, J. A. Vrugt, S. Moysey, J. A. Huisman, and M. B. Kowalsky. Improved extraction of hydrologic information from geophysical data through coupled hydrogeophysical inversion. To appear in *Water Resources Research.*

Koller, J., Y. Chen, G. D. Reeves, R. H. W. Friedel, T. E. Cayton, and J. A. Vrugt. Identifying the Radiation Belt Source Region by Data Assimilation. 2007. *Journal of Geophysical Research - Space Physics.* **112**: A06244.

Laloy, E., C. L. Bielders, J. A. Vrugt, M. Vanclooster, C. Roisin, and M. Javaux. Inverse modeling of preferential flow models using multistep outflow experiments. To appear in *Journal of Hydrology.*

Scharnagl, B., J. A. Vrugt, H. Vereecken, and M. Herbst. Information content of incubation experiments for inverse modeling of carbon pools in the Rothamsted model: a Bayesian approach. To appear in *Biogeosciences.*

Stauffer, P. H., J. A. Vrugt, H. J. Turin, C. W. Gable, and W. E. Soll. Untangling diffusion from advection in unsaturated porous media: experimental data, modeling and parameter uncertainty assessment. 2009. *Vadose Zone Journal.* **8** (2): 510.

Tittonell, P., M. T. van Wijk, M. C. Runo, J. A. Vrugt, and K. E. Giller. Analyzing trade-offs in resource and labor allocation by smallholder African farmers using inverse modeling techniques. 2007. *Agricultural Systems.* **95**: 76.

Vereecken, H., J. A. Huisman, H. Bogena, J. Vanderborght, J. A. Vrugt, and J. W. Hopmans. On the value of soil moisture measurements in vadose zone hydrology: a review. 2008. *Water Resources Research.* **44**: W00D06.

Vrugt, J. A.. Comment on: How effective and effcient are multiobjective evolutionary algorithms at hydrologic model calibration?. 2007. *Hydrology and Earth System Sciences.* **11**: 1435.

Vrugt, J. A., B. A. Robinson, and J. M. Hyman. Self-adaptive multimethod search for global optimization in real parameter spaces. 2009. *IEEE Transactions on Evolutionary Computation.* **13** (2): 243.

Vrugt, J. A., C. G. H. Diks, and M. P. Clark. Ensemble Bayesian model averaging using Markov chain Monte Carlo sampling. 2008. *Environmental Fluid Mechanics.* **8** (5-6): 579.

Vrugt, J. A., C. J. F. ter Braak, C. G. H. Diks, D. Higdon, B. A. Robinson, and J. M. Hyman. Accelerating Markov chain Monte Carlo simulation from self adaptive differential evolution with randomized subspace sampling. 2009. *International Journal of Nonlinear Sciences and Numerical Simulation.* **10** (3): 273.

Vrugt, J. A., C. J. F. ter Braak, H. V. Gupta, and B. A. Robinson. Equifinality of formal (DREAM) and informal (GLUE) Bayesian approaches in hydrologic modeling?. 2009. *Stochastic Environmental Research and Risk Assessment.* **23** (7): 1011.

Vrugt, J. A., C. J. F. ter Braak, H. V. Gupta, and B. A. Robinson. Reply to comment by Keith Beven on equifinality of formal (DREAM) and informal (GLUE) Bayesian approaches in hydrologic modeling?. 2009. *Stochastic Environmental Research and Risk Assessment.* **23** (7): 1061.

Vrugt, J. A., C. J. F. ter Braak, M. P. Clark, J. M. Hyman, and B. A. Robinson. Treatment of uncertainty in hydrologic modeling: doing hydrology backwards with Markov chain Monte Carlo simulation. 2008. *Water Resources Research.* **44**: 2007WR006720.

Vrugt, J. A., J. van Belle, and W. Bouten. Pareto front analysis of flight time and energy use in long distance bird migration. 2007. *Journal of Avian Biology.* **38**: 432.

Vrugt, J. A., P. H. Stauffer, T. Wohling, B. A. Robinson, and V. V. Vesselinov. Inverse modeling of subsurface flow and transport properties using recent advances in global optimization, parallel computing, and sequential data assimilation. 2008. *Vadose Zone Journal.* **7** (2): W00B02.

Vrugt, J. A., and B. A. Robinson. Treatment of uncertainty using ensemble methods: Comparison of sequential data assimilation and Bayesian model averaging. 2007. *Water Resources Research.* **43**: W01411.

Vrugt, J. A., and B. A. Robinson. Improved evolutionary optimization from genetically adaptive multimethod search. 2007. *Proceedings of the National Academy of Sciences of the United States of America.* **104**: 708.

Wohling, T., J. A. Vrugt, and G. F. Barkle. Comparison of three multiobjective optimization algorithms for inverse modeling of vadose zone hydraulic properties. 2008. *Soil Science Society of America Journal.* **72**: 305.

Wohling, T., and J. A. Vrugt. Combining multi-objective optimization and Bayesian modeling averaging to calibrate forecast ensembles of soil hydraulic models. 2008. *Water Resources Research.* **44**: 2008WR007154.

# The Role of NS1 in Disrupting Immune Responses During Influenza Infection: A Modeling and Experimental Approach

*Alan S. Perelson*
20070645PRD2

## Introduction

Seasonal influenza kills 36,000 people each year in the U.S. alone. While the current H1N1 pandemic has so far been relatively mild, the world faces the threat of a severe pandemic from an avian strain known as highly pathogenic H5N1. This strain has infected more than 440 humans to date, with a case fatality rate of 60%.

One question of importance in an influenza epidemic is how best to use antiviral medications, in order to minimize the size of an epidemic and the development of drug resistance. Combination therapy, which is not used for influenza, is a strategy that should be considered. This topic has been only partially examined, using epidemiological modeling.

Much also needs to be understood about the biology of influenza virus infection. The body responds immediately upon encountering the virus with an innate immune response. The production of a protein, called cathelicidin, that forms part of the innate immune response is greatly stimulated by vitamin D; cathelicidin has been shown to be extremely important in preventing tuberculosis infection. Yet no study has examined whether there is any effect of vitamin D on influenza virus infection.

Another part of the innate immune response involves signaling through cell surface receptors called TLRs. H5N1 influenza causes severe disease in part by signaling through one of these receptors, called TLR4. In response to H5N1 infection, production of proteins called serum amyloid A (SAA) is increased; SAA is hypothesized to signal through TLR4 and thus could enhance TLR4 signaling in H5N1 infection and worsen disease. In addition, it is possible that H5N1 virus particles could fragment large molecules called hyaluronic acid molecules, which can signal through TLR4, triggering severe disease. The role of SAA in highly pathogenic influenza infections has not been studied, and no influenza virus has been shown to cleave hyaluronic acid.

Little is known about these interactions between influenza and the immune system. We propose to redress these gaps in knowledge in a quantitative way, and then based on experimental findings to develop mathematical models to describe each system. The experiments for this study will be conducted using lung cells in culture infected with contemporary strains of human seasonal influenza.

The ultimate goal of this work is to understand how influenza subverts the immune response in order to generate a successful infection. If these mechanisms can be quantitatively elucidated, then new treatments might be designed. Further, we may be able to better understand why strains such as 1918 flu and highly pathogenic H5N1 are so deadly.

## Benefit to National Security Missions

This project will support the DOE mission in reducing biological threats - influenza is on the list of identified threat agents. It will also support the missions of DHS and NIH in responding to biological threats.

## Progress

This project involves both experimental and theoretical components. In order to carry out experiments a variety of training requirements have had to be met. All LANL-wide and work-specific has been completed.

Experiments are conducted in the lab space of Ahmet Zeytun, under an Institutional Biosafety Committee (IBC) protocol of Anu Chaudhary and Ahmet Zeytun. This required writing a new protocol, which allows new BSL-2 work with influenza. This protocol has been approved, and subsequently, we have also achieved approval of a new BSL-2 room for influenza work and an IWD for the work as well.

Initial experiments have been done to set up and validate an assay system for an enzymatic activity called hyaluronidase activity. Hyaluronidases cut hyaluronic acid molecules into smaller fragments, and we hypothesize that small fragments of hyaluronic acid may be triggering some of the severe symptoms caused by highly pathogenic influenza viruses such as highly

pathogenic H5N1. Our goal is to test whether influenza viruses themselves possess hyaluronidase activity, i.e., whether the virus particles can cut hyaluronic acid molecules. In collaboration with Scott Hennelly, PhD, of LANL, and Robert Stern, MD, Prof. Emeritus, UCSF, we have almost completed the assay validation process.

On the theoretical side, we have developed an epidemiological model of influenza infection, with which we can examine the effects of antiviral therapy for both prevention and treatment, using any combination of three drugs, such as oseltamivir and zanamivir, neuraminidase inhibitors, and amantadine, an M2 channel blocker. For both amantadine and, increasingly, oseltamivir, antiviral resistance has appeared; resistance to zanamivir, which is much less commonly used, has yet to develop on a significant scale. Thus, there is considerable interest in whether combination therapy consisting of both amantadine and oseltamivir could still be effective, and whether more widespread use of zanamivir could slow down the development of resistance to any or all of these drugs. The model allows the emergence of flu strains resistant to any of the drugs alone or in combination. The model also follows the spread of resistant virus through the population. The surprising result, thus far, is that combination therapy, depending on the circumstances, may or may not be expected to reduce the size or delay the progression of an influenza epidemic. In addition, combination therapy may also lead to the rapid emergence of strains resistant to any two drugs used for treatment. The model has been explored for predictions of which combinations of drugs used for prevention and treatment will minimize both the numbers of cases and the development of drug resistance, over the short and long terms. This work should be completed and submitted for publication soon.

## Future Work

In the experimental component, lung cells in culture will be infected with a strain of seasonal influenza, and the kinetics of the production and activities of these host and influenza molecules will be measured, using techniques such as quantitative RT-PCR. In addition, viral proteins will be tested for hyaluronidase activity. Based on the data, mathematical models will be developed to describe the kinetics of vitamin D levels, cathelicidin production, and infection, and of SAA production, potentially virus HA cleavage activity, and other host cell responses correlated with disease severity, at the multicellular level. Fitting the models to data will allow estimation of model parameters.

The ultimate goal of this work is to understand how influenza subverts the immune response in order to generate a successful infection. If these mechanisms can be quantitatively elucidated, then new treatments might be designed. Further, we may be able to better understand why strains such as 1918 flu and H5N1 are so deadly.

## Conclusion

Influenza infection has caused tens of millions of deaths. There is a chance that bird flu (H5N1) may start a new and severe global pandemic, and other strains of influenza, such as the present pandemic strain, are also capable of causing severe disease. This work will elucidate some of the basic mechanisms used by influenza to defeat the host immune defenses. If we can better understand how influenza proteins interact with host proteins to manipulate host cell defenses we may be able to develop new drugs that will be able to better protect us against influenza infection.

# Pore-Scale Modeling of Multiphase Flow and Reaction in Charged Porous Media

*Qinjun Kang*
20070760PRD4

## Introduction

Multiphase flow and reaction in porous media are ubiquitous in energy and environmental sciences research and pose a formidable challenge. In the present scenario of a global concern over energy security and environmental issues, the physics of transport and reaction encompassing multiple length scales prevalent in natural and synthetic porous media is poised to play a key role. Two critical research needs of prominent national and global importance within the broad spectrum of energy and environmental issues include sequestration of carbon dioxide ($CO_2$), a greenhouse gas, and clean energy harvesting via a sustainable hydrogen energy economy. $CO_2$ sequestration involves transport and reaction physics in geologic porous media, while hydrogen energy involves complex, electrochemical reaction coupled multi-physical transport phenomena in fuel cells comprising of varied synthetic porous media. However, the inherently complex morphology of such porous media coupled with multi-physical (physico-electro-chemical), reactive (chemical/electrochemical) transport and interfacial processes catering over multiple length scales (nano/micro/meso/macro) makes this problem notoriously difficult and consequently poses several open questions of fundamental and scientific interest. In this project, it is intended to develop for the first time a comprehensive pore-scale modeling framework involving multiphase (air/water), reactive (chemical/electrochemical) transport and interfacial processes in the presence of electrical charge in the sub-micron and micron length scales in porous media. The overriding objective of this project is to develop a science-based approach toward fundamental understanding of the underlying transport and reaction in charged porous media and answer some of long-standing questions in the broad spectrum of energy and environmental research, including subsurface contaminant migration, geological $CO_2$ sequestration, and fuel cell technology.

## Benefit to National Security Missions

This project will support the DOE/NNSA missions in Energy Security, Environmental Quality, and the missions of the Office of Science by enhancing our understanding of underlying multiphase flow and reaction in porous media at the pore scale in the presence of charged surfaces.

## Progress

Partha P. Mukherjee has been instrumental in applying the pore-scale modeling formalism in the fields of fuel cell research, which involves transport and reaction in disparate porous structures. Additionally, he has initiated the modeling capabilities of reaction in charged porous media to the investigation of novel electrode architectures with lithium-Ion chemistry in electrochemical energy storage systems, which represent a key clean energy research area for powering hybrid electric vehicles and portable appliances. Partha has been very active in developing project proposals involving multi-scale reactive transport phenomena with particular emphasis in energy research. He has also established a strong research collaboration with MPA-11 and the Engineering Research Institute within LANL and also with the Department of Mechanical Engineering, UC Irvine. His research accomplishments in terms of peer reviewed journal papers, invited book chapters, conference presentations, and proposal development are part of his successes.

## Future Work

Multiphase flow and reaction in porous media is among the most important and challenging problems in energy and environmental sciences. Although pore-scale interfacial phenomena govern the key processes of fluid mobility, chemical transport, adsorption, and reaction, spatial heterogeneity at the pore scale is unresolved in the continuum reactive transport models involving averaging over length scales much larger than typical grain sizes. In addition, current continuum models of surface complexation reactions ignore a fundamental property of physical systems, namely conservation of charge. Therefore, to quantitatively investigate the effects of pore scale heterogeneity on the emergent behavior at the field scale, it is necessary to understand multiphase flow, transport, and reaction processes at

the pore scale.

In this project, we will develop a comprehensive pore-scale modeling framework for investigating transport in the presence of charged mineral surface in porous media based on the Lattice Boltzmann (LB) method, a powerful numerical tool developed at Los Alamos. Due to its kinetic nature, the LB method is particularly suitable for applications involving nonequilbrium dynamics and complex geometries. Specifically, this project will involve: 1) the development of an innovative model to account for electric double layer effects on transport in single aqueous phase, multicomponent systems; and 2) the extension of the model to multiphase systems with high density and viscosity contrast. The proposed research will be based on our existing expertise in both electrochemistry and thermal-fluid sciences and experience with the LB method.

Upon accomplishment of the project, a computer code on LB simulation of multiphase multi-component reactive transport in charged porous media will be developed. At least two papers for each task outlined above will be published in leading journals. The project will have direct implications in a broad spectrum of environmental and energy research, including subsurface contaminant migration, geological $CO_2$ sequestration, and fuel cell technology.

## Conclusion

Accounting for electrochemical processes in multiphase flow and reaction is critical to understanding colloid facilitated transport of radionuclides. This project will enable a science-based approach toward fundamental understanding of the underlying transport and reaction mechanisms for the migration of radionuclides involving heterogeneous surface reactions with minerals. A computer code subject will be developed to model these processes and research results will be published in leading journals. This project will have direct implications in a broad spectrum of environmental and energy research, including subsurface contaminant migration, $CO_2$ sequestration in geologic formations, and fuel cell technology.

## Publications


Mukherjee, P. P., C. Wang, and Q. Kang. Mesoscopic modeling of two-phase behavior and flooding phenomena in polymer electrolyte fuel cells. 2009. *Electrochimica Acta.* **54** (27): 6861.

Mukherjee, P. P., M. Wang, Q. Kang, and P. C. Lichtner. Pore-scale modeling of transport in charged porous media. Presented at *Computational Methods in Water Resources XVII International Conference.* (San Francisco, CA, 6-10, July 2008).

Mukherjee, P. P., M. Wang, Q. Kang, and P. C. Lichtner. Modeling of transport in charged porous media. Presented at *5th Annual Meeting of Center of Environmental Kinetics Analysis (CEKA).* (Pennsylvania State University, 22-24 Oct. 2008).

Mukherjee, P. P., Q. Kang, R. Mukundan, and R. L. Borup. Two-Phase Transport and Flooding Behavior in PEFCs: Pore-Scale Modeling and in situ Visualization. 2009.

Mukherjee, P. P., Q. Kang, V. P. Schulz, J. Becker, A. Wiegmann, and C. Wang. Pore-Scale Modeling of Flooding Dynamics in the PEFC Gas Diffusion Layer. 2009. *Journal of the Electrochemical Society.* **to be submitted**.

Mukherjee, P. P., Q. Kang, and C. Wang. Pore-Scale Modeling of Two-Phase Transport in Polymer Electrolyte Fuel Cells - Recent Progress and Perspective. 2009. *Energy & Environmental Science Journal.* **to be submitted**.

Mukherjee, P. P., V. P. Schulz, Q. Kang, J. Becker, and A. Wiegmann. Two-Phase Behavior and Effect of Compression in the Polymer Electrolyte Fuel Cell Gas Diffusion Medium. Presented at *Electrochemical Society Meeting.* (Vienna, Austria).

Mukherjee, P. P., and Q. Kang. Micro-scale Transport in the Electrode of Electrochemical Energy Conversion Systems. 2009.

Teixidor, G. T., B. Y. Park, P. P. Mukherjee, Q. Kang, and M. J. Madou. Modeling fractal electrodes for Li-ion batteries. 2009. *Electrochimica Acta.* **54** (24): 5928

# Modeling Fast Basal Sliding of Ice Sheets for Climate and Sea Level Prediction

*William H. Lipscomb*
20070765PRD4

## Introduction

Recent observations show that outlet glaciers and ice streams in Greenland and West Antarctica have accelerated and thinned dramatically, with atmospheric and oceanic warming the likely cause. Given the potential catastrophic impacts of rapid sea level rise, it is critical to predict how ice sheets will respond to future climate warming. This is not yet possible because fundamental physical processes are not represented in ice-sheet models and are only beginning to be understood. The goal of this project is to improve ice sheet models by including realistic treatments of 1) subglacial hydrology that can evolve in response to changes in the overlying ice sheet, and 2) basal sliding in regions underlain by deformable subglacial "till." These processes are crucial for predicting the evolution of ice streams and outlet glaciers, which can flow 10 to 100 times faster than ice that is frozen to the bed. The new process models will be implemented in a state-of-the-art ice-sheet model (GLIMMER), the ice-sheet component of the Community Climate System Model (CCSM). This model will be used by glaciologists and climate modelers worldwide for regional studies and global climate projections. In particular, model results from GLIMMER and CCSM will be incorporated in the reports of the Intergovernmental Panel for Climate Change (IPCC). The most recent IPCC assessment report specifically noted the need for better ice sheet models.

## Benefit to National Security Missions

This project supports the DOE mission of the Office of Science by enhancing our understanding of physical processes that control the response of ice sheets to climate change. The project also supports NASA's mission to understand the changing climate; NASA satellite data is being used to develop and validate improved models of basal sliding of ice sheets.

## Progress

The postdoc Stephen Price has continued his work on (1) general development of an ice sheet dynamics model and (2) model development specific to his LANL project.

General model development has included the following:

1. The addition of multiple stable ice-thickness evolution solvers (for predicting the change in ice sheet geometry over time). These include a scheme based on LANL-developed "incremental remapping" (IR) and a scheme based on piecewise-parabolic-matching.

2. The addition of the ability to simulate regions of floating ice (e.g. ice shelves or ice tongues), which are fully coupled to land-bound, grounded ice. As of September 2009, this scheme has been benchmarked against, and compares well with, (1) other ice shelf models and (2) observations from the Ross Ice Shelf in West Antarctica.

3. The addition of a freely moving grounding line (the point of transition/coupling between grounded and floating ice). Work is underway to verify that grounding line migration in the model (known to be highly susceptible to grid resolution and numerical artifacts) is consistent with a series of benchmarking experiments, specifically designed to validate grounding line behavior in numerical models.

4. Work to modify the current "higher-order" omentum balance solver so that it compiles and runs within the GLIMMER/CISM ice sheet model. As of fall 2009, the output from this solver has been compared with results from another higher-order solver in CISM and, for several test cases spanning the end-member flow regimes for an ice sheet (internal deformation with no sliding versus all sliding with no internal deformation), the two solvers compare well with one another and against the benchmarks.

5. Construction of an ice-shelf / ocean coupler, based on a widely applied boundary-layer theory, in which heat and salt fluxes between the ocean and an overlying ice shelf are used to couple the boundary conditions for ice shelf and ocean circulation models in a consistent manner.

Model development specific to the goals of simulating regions of fast sliding in ice sheets includes the following:

1. The addition of a simple iteration to approximate glacier sliding over a "plastic bed." (That is, below some yield stress, no sliding occurs, and at the yield stress, sliding occurs such that basal shear stress remains at the yield stress.) Initial tests suggest that this iteration may be adequate for capturing the large-scale behavior of Antarctic ice streams.

2. Work with colleagues at the University of Cambridge on incorporating a basal-processes model into the code. The basal processes model takes information on basal hydrology (e.g., how wet the bed is) and known subglacial-interface properties (e.g. is the interface bedrock or soft, moldable till) and provides the larger model with an estimate for the required yield stress (which is implemented as the basal boundary condition for the dynamics model). Ongoing work involves updating the basal processes model to allow for interaction with an explicit, non-local, subglacial hydrology model, and applying the coupled model to explore the influence of hydrology and basal processes on evolution of the West Antarctic ice sheet. Preliminary results were presented at the 2009 West Antarctic Ice Sheet (WAIS) meeting and will also be presented at the 2009 fall AGU meeting.

3. Development and application of a straightforward and quantifiably robust method for the tuning of basal sliding parameters. This is a necessary step in obtaining a reasonable initial condition for simulations of future ice sheet mass balance. As a proof of concept, this tuning procedure has been applied to the Greenland ice sheet. The tuned model state will be used to initialize perturbation experiments exploring the response (e.g., sea level rise) of the Greenland ice sheet to environmental forcing over the next century. Results from these ongoing experiments were presented at the annual Community Climate System Model (CCSM) meeting in June 2009, and will be presented at the 2009 fall AGU meeting.

Price has presented his work to the Climate, Ocean and Sea Ice Modeling (COSIM) group and Group T-3 at LANL. In April 2009, he presented results from his work at the DOE Climate Change Prediction Program meeting in Bethesda, MD. At the June 2009 CCSM workshop, he presented an update on model experiments of the Greenland ice sheet, estimating the potential dynamic contribution to sea-level rise from several key outlet glaciers. In August 2009, he was an invited instructor at an international summer school on ice sheet modeling (http://websrv.cs.umt.edu/isis/index.php/Summer_Modeling_School) at Portland State University. In September 2009, he was co-author on an oral presentation given at the WAIS meeting and was an invited participant and speaker at the Univ. of Chicago *Collaborations in Mathematics and Geosciences Workshop on Automatic differentiation and Ice Sheet Modeling*. During fall 2009 he contributed to two NASA Venture-Class proposals that, if successful, will provide funding for two separate LANL postdocs working on ice sheet modeling and partial funding for a LANL scientist (1/6 FTE for a duration of five years). In December 2009, he will present results from various aspects of his research at the fall AGU meeting, where he is the lead author on one oral presentation, a co-author on one oral presentation and two poster presentations, and a co-chair of the Cryosphere session *Constraining and Improving Models of Glacier Dynamics Using Observations*.

## Future Work

Ice sheets will likely be primary contributors to 21st century sea level rise, but estimates of these contributions are poorly constrained because essential physical processes that control ice sheet outflow on yearly to decadal time scales are missing from predictive ice sheet models. The goal of this project is to develop improved models of subglacial hydrology and basal sliding for ice sheet and climate studies. Remaining work includes (1) the use of modern-day maps of subglacial properties (e.g., basal traction and basal water-layer thickness) to define empirical relationships linking sliding parameters with the subglacial water system, and (2) testing of a subglacial water model in GLIMMER, in which the evolution of subglacial water is linked to the evolution of sliding parameters. The improved model will be applied to outlet glaciers in Greenland and to ice streams in the Amundsen and Ross Sea embayments of West Antarctica in order to better understand the cause and future course of changes in those regions. This research will result in an ice sheet model with more accurate and realistic basal boundary conditions, which are necessary for predicting the response of the Greenland and Antarctic ice sheets to climate changes. The model will be incorporated in the U.S. Community Climate System Model and will be used by glaciologists and climate modelers worldwide for regional studies and global climate projections.

## Conclusion

The desired outcome of this effort is a next-generation ice sheet model that can be used to predict the rate of sea level rise associated with the potentially rapid retreat of the Greenland and West Antarctic ice sheets. As underscored by the recent assessment report of the Intergovernmental Panel for Climate Change, current ice sheet models are too crude to simulate rapid dynamic changes in ice outflow. Since rapid sea level rise could have huge socioeconomic impacts, improved ice sheet models are essential for evaluating risks associated with climate change.

## Publications

Catania, G. A., T. A. Neumann, and S. F. Price. Characterizing englacial drainage in the ablation zone of the Greenland ice sheet. 2008. *Journal of Glaciology.* **54** (187): 567.

Dukowicz, J. K., S. F. Price, and W. H. Lipscomb. Consistent approximations for ice sheet dynamics from a principle of least action. *Journal of Glaciology.*

Price, S. F.. From the front. 2009. *Nature Geoscience.* **2** (1): 93.

# Spectroscopic Studies and Photonic Applications of "Giant" Nanocrystal Quantum Dots

*Victor I. Klimov*
20080703PRD1

## Introduction

Nanocrystal quantum dots (NQDs) are nanosized (smaller than a millionth of an inch) semiconductor crystals that are very efficient emitters of visible light by a process of luminescence in which photons are absorbed and later re-emitted at a lower energy. The color that they emit can be tuned by adjusting the size of the dot, due to an effect called quantum-confinement. Because of these properties, nanocrystals are attractive materials for applications such as optical amplification and lasing. However, practical applications of nanocrystals in lasing are complicated by their low stability at high excitation intensities required to obtain the optical-gain regime, and fast carrier nonradiative losses resulting from multiexciton Auger recombination.

Recently, we have developed a new type of composite that comprises a small core of CdSe coated with a very thick shell (up to 20 monolayers) of a wider gap material such as CdS [1]. The overall size of these composite particles is quite large (10 – 20 nm), therefore, they have been dubbed "giant" quantum dots (g-NQDs). Compared to traditional dots, g-NQDs show greatly increased absorption and emission efficiencies, and improved stability to the environmental light and chemical agents. More surprisingly, g-NQDs inhibit a process common to colloidal quantum dots known as "blinking", where dots emit intermittently. Our initial studies also indicate that they exhibit reduced rates of Auger recombination, a process that greatly hinders the useful output of standard NQDs. All of these properties are beneficial for photonic applications, especially, in lasing technologies. The goal of this project is to evaluate the potential of g-NQDs in optical amplification and lasing through comprehensive studies of their electronic and optical properties conducted in conjunction with microstructural characterization and theoretical modeling.

## Benefit to National Security Missions

This work can potentially enable novel type of compact, tunable lasers, providing thus a contribution to several technologically important areas such as optical amplification, fiber optics, telecommunication, and remote sensing. All of these areas are of significant interest to the DOE Office of Basic Energy Sciences.

## Progress

### Theoretical modeling of g-NQDs

When a NQD absorbs a photon, an electron moves across a band gap leaving a hole in the valence band. This electron-hole pair is known as an exciton. When the electron and hole recombine (the electron returns to the lower energy state), a photon is emitted. In core-shell NQDs, such as the ones we study here, the materials used, the core size and shell thickness will determine the electronic structure, and therefore, the optical behavior of the quantum dot. In the case of CdSe cores and CdS shells, our calculations show that as the shell thickness increases, the hole remains bound to the core material while the electron leaks into the CdS shell (Figure 1). This separation of charge has very important effects such as increasing the photoluminescence lifetime (time before the exciton recombines and a photon is emitted) and the color of the light emitted. Both of these predicted effects were observed experimentally.

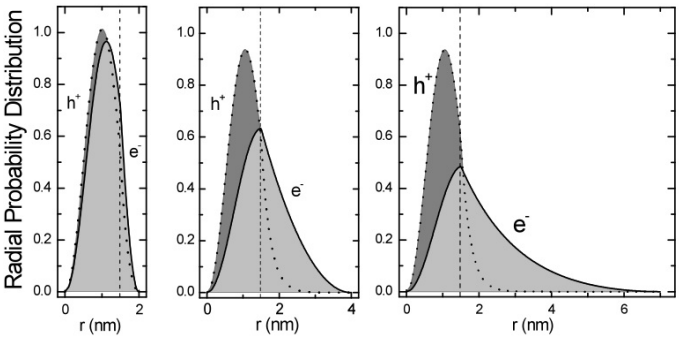


*Figure 1. The probability of finding the hole in the core remains constant as the shell thickness is increased (from left to right). The electron however leaks into the shell and both charges become spatially separated. This makes the electron-hole recombination event less likely as the shell thickness increases.*

**Experimental measurements of Auger recombination rates**

As explained before, a photon absorbed by a NQD creates a single exciton. If the NQD is illuminated at higher intensities (excitation fluence), it may simultaneously absorb two or more photons and generate multiple excitons. This is known as a multiexcitonic regime and is it is necessary to obtain stimulated emission which is the basis of optical gain in lasing devices.

In NQDs, multiexcitons have very short lifetimes due to a process known as Auger recombination. In this process, the energy of one of the excitons is transferred to a hole or electron and no photon is emitted (Auger decay is a nonradiative process). Although emission of photons from the recombination of multiexcitons is still possible, the Auger process is much faster and dominates carrier dynamics. This effect is clearly observed in Figure 2a. The emission intensity falls with time as NQDs relax. As the pump intensity (fluence) is increased, the emission of multiexcitons can be observed at short times. It can be seen their contribution is very short-lived. If the same experiment is repeated with g-NQDs (Figure 2b), multiexciton emission is observable for much longer times. Indeed, multiexcitons live about a hundred times longer than in the case of standard NQDs. This means g-NQDs are better emitters thanks to the inhibition of the Auger recombination process.

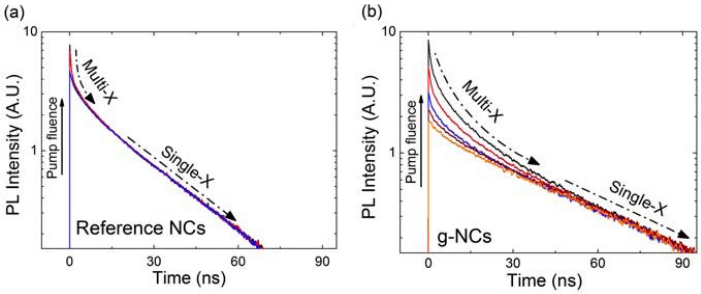


*Figure 2. (a) A commercial sample of CdS/ZnS NQDs is excited with a very narrow pulse of light (~150 fs) and the photoluminescence emission is time-resolved. At high excitation intensities the contribution from multiexcitons can be observed at very early times. (b) The same experiment on g-NQDs shows that multiexcitons contribute to emission for much longer times.*

Our demonstration of suppression of Auger recombination is a very important milestone in the NQD field since it opens many new opportunities for applications of these materials in technologies such as lasing and light-emitting diodes.

**Experimental characterization of optical gain**

Films of g-NQDs were prepared and excited with narrow pulses of light. Amplified spontaneous emission (ASE) was observed at record-low excitation thresholds when compared to results obtained with standard NQDs. ASE is a necessary requirement to develop a lasing device and is typically identified as an emission line narrows and quickly increases in intensity as the pump fluence is increased. Although this result is important by itself the most impressive observation is that up to three ASE bands were observed simultaneously at different emission energies at higher pump fluences (Figure 3). This demonstrates that g-NQDs posses a very large optical gain bandwidth. In fact, such a bandwidth (>500 meV) is the widest among condensed matter lasing media.

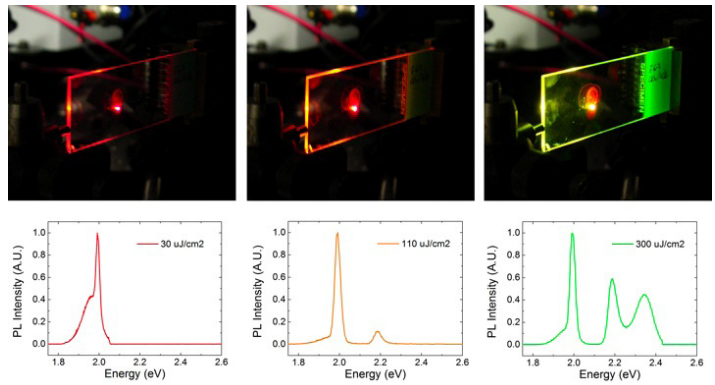


*Figure 3. Emission spectra from a g-NQD film as the pump intensity is increased (from left to right).*

## Future Work

Although we have identified a number of reasons that could lead to unusual electronic and optical properties of g-NQDs, we still have to pinpoint the main cause for a very significant inhibition of Auger recombination. Understanding the mechanisms for suppression of Auger decay is going to be the main thrust of this project in FY2010. To accomplish this goal, we will conduct the following experiments: (1) temperature-dependent studies of multiexciton recombination to understand the role and radiative and nonradiative recombination pathways, (2) single-NQD studies in the single- and multiexciton regimes to obtain information on electronic spectra not obscured by effects of ensemble averaging, and finally (3) Raman spectroscopy studies to understand the internal composition of the NQD; the latter method will allow us to detect the formation of interfacial alloys.

## Conclusion

This research is expected to lead to understanding of the electronic structure and carrier relaxation behaviors in a recently developed, new type of nanocrystal materials, giant NQDs. One specific anticipated result is understanding the role of Auger processes in recombination of multiexciton states. Since stimulated emission from multiexcitons dominates optical-gain properties of nanocrystals, this work will help us to evaluate the potential of g-NQDs in lasing technologies. An expected practical outcome of this project is the demonstration of highly efficient, color-tunable lasing structures based on these new materials.

## References

1. Chen, Y. F., J. Vela, H. Htoon, J. L. Casson, D. J. Werder, D. A. Bussian, V. I. Klimov, and H. A. Hollingsworth. Giant multishell CdSe nanocrystal quantum dots with suppressed blinking . 2008. *Journal of American Chemical Society.* **130**: 5026.

## Publications

GariciaSantamaria, F., Y. Chen, J. Vela, R. D. Schaller, J. A. Hollingsworth, and V. I. Klimov. Suppressed Auger recombination in giant nanocrystals boosts optical gain performance. 2009. *Nano Letters.* **9** (10): 3482.

# Modeling Control of Viruses by Immune Responses

*Alan S. Perelson*
20080726PRD2

## Introduction

Humans during their lifetime encounter many pathogenic microorganisms, and the adaptive immune system is responsible for clearance of many of the encountered pathogens from the host. Clearance of intracellular pathogens (such as viruses) is mainly achieved by a special type of immune cells, CD8 T cells, which are able to kill pathogen-infected cells. For several viral infections, the importance of CD8 T cells in clearance of the pathogen from the host has been clearly established. However, many quantitative properties of pathogen dynamics in the host, including the possible pathogen clearance by the CD8 T cell response, are lacking for most infections of higher mammals such as monkeys and humans. For example, there is still a hot debate about whether the limited availability of host cells susceptible to infection (target cells) or the host's CD8 T cell response control HIV early in infection. The efficacy at which CD8 T cells clear virus-infected cells is generally unknown for most infections. Without a solid framework for estimating the efficacy of T cell responses in vivo, we are not be able to predict which qualities of T cells correlate best with protection against virus infection. Thus, the main goals of our research have been 1) to develop quantitative methods for estimation of the in vivo killing efficacy CD8 T cells during acute and chronic viral infections; 2) to estimate the killing efficacy of HIV-specific CD8 T cells during the acute phase of the infection.

## Benefit to National Security Missions

This research will directly and specifically impact LANL/DOE missions and goals. One of the strategic grand challenges of LANL is to understand and harness "Complex Biological Systems," including exploring implications for national security and health. This LANL objective falls within the framework of DOE's strategic plan's priority of "Harness the Power of Our Living World". One of the unresolved challenges in immunology is how to predict the efficacy of T cell based vaccines. Work done in this project addresses this challenge

## Progress

We have used data from a set of experiments to quantify the killing efficacy of CD8 T cells, specific to several epitopes of lymphocytic choriomeningitis virus (LCMV) infection [1]. For that virus we have formulated a mathematical model that describes recruitment of targets from the blood to the spleen and killing of targets in the spleen by the virus-specific CD8 T cells [2]. The model was fitted to the experimental data and estimates of the model parameters were obtained. Analysis revealed that killing of target cells in the mouse spleen followed the law of mass-action [4]. According to this law the death rate of target cells due to T cell mediated killing is simply proportional to the total number of virus-specific CD8 T cells in the spleen (Figure 1). This has important implications for the development of T cell based vaccines since it suggests that increasing the number of memory CD8 T cells by vaccination should proportionally increase the rate of killing of virus-infected cells by the T cells response, and as a result lead to a faster clearance of the infection. We have also found that memory T cells are less efficient killers in vivo than are effector T cells. This suggests that the level of memory T cells needed for protection should exceed that generated following live infection. Overall, these results suggest practical guidelines for calculating the level of memory CD8 T cells that will be needed to be induced by vaccination to provide sterilizing immunity.

Failure of antibody-based vaccines to prevent infection of humans with HIV has shifted the focus of vaccine development towards CD8 T cells. Many of the current HIV vaccine candidates are aimed at developing large numbers of memory CD8 T cells that are thought to be able to control virus replication. In particular, CD8 T cells have been shown to be important in the control of

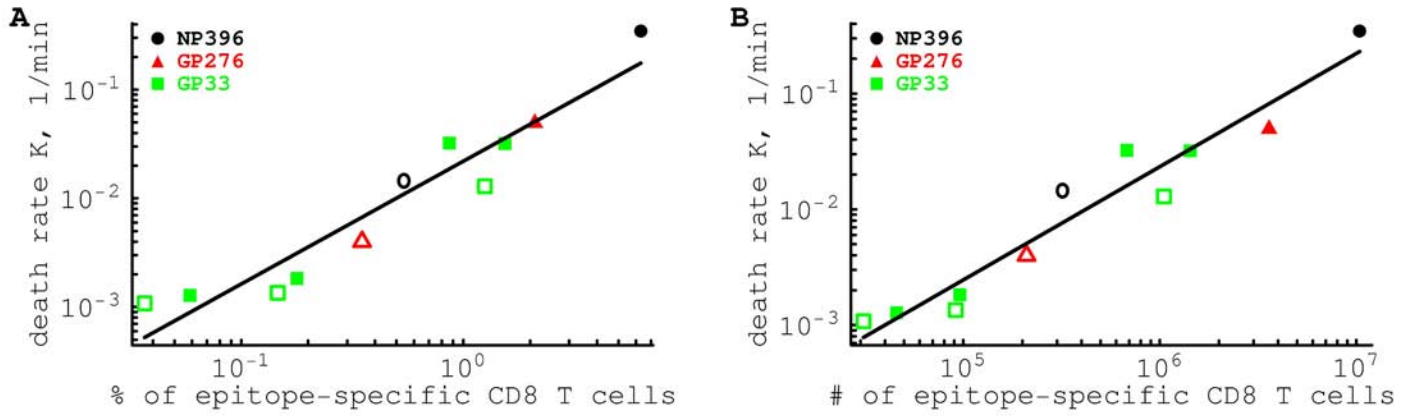


*Figure 1. The estimated death rate of peptide-pulsed targets due to killing by epitope-specific CD8 T cells is proportional to the average percent (panel A) or average number (panel B) of epitope-specific CD8 T cells in the spleen [2]. Estimates are given for targets pulsed with NP396, GP276, or GP33 peptides from lymphocytic choriomeningitis virus (LCMV). Filled symbols are for killing by effector CD8 T cells, and open symbols are for killing by memory CD8 T cells. Lines show the linear regression for the log-log transformed estimates of the death rate and density of CD8 T cells. Slopes for the regressions are not statistically different from one (panel A: slope=1.13, p=0.30; panel B: slope=0.98, p=0.80).*

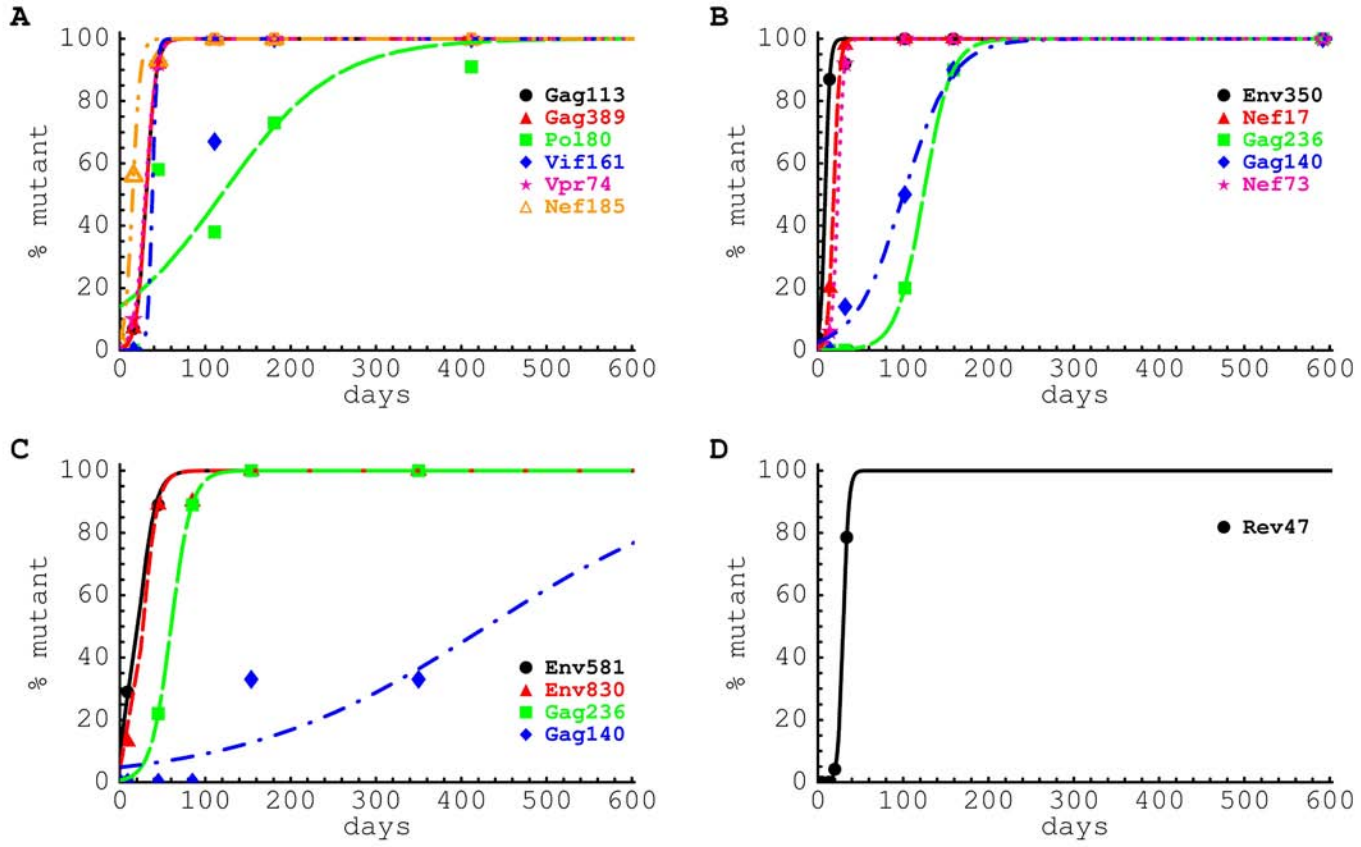


*Figure 2. Experimentally measured changes in the frequency of escape mutations in the virus population and the prediction of the mathematical model fitted to data from patients CH40 (panel A), CH77 (panel B), CH58 (panel C), and SUMA0874 (panel D). There is heterogeneity in rates at which virus escapes recognition by the CD8 T cell response in different CTL epitopes. For example, in patient CH77 (panel B), there is rapid fixation of mutations in Nef and Env. Escape mutations in Gag (epitope TW10) occur later in the infection and occur at a much slower rate. Given that a large TW10-specific CD8 T cell response is detected in this patient, a slow rate of escape implies a high fitness cost of the escape mutation [3,4].*

replication of simian immunodeficiency virus (SIV) during the chronic stages of the infection [3]. However, it is still unknown whether CD8 T cells have any influence on HIV during the acute phase of the infection. Many researchers have thought that depletion of viral target cells was the major reason for the decline of the virus after peak viremia was reached. To address this issue, we have analyzed data on the dynamics of HIV and the escape of the virus from the CD8 T cell response during the acute phase of the infection. Viruses can escape T cell responses by mutating (i.e., changing) the parts of the virus recognized by T cells. We extended our previous mathematical model [5,6], which allowed us to estimate the rate at which CD8 T cells specific to a single viral epitope kill cells infected with HIV (Figure 2), to allow for T cells to recognize multiple epitopes. We found that at the peak of viral load, HIV-specific CD8 T cells, specific to a single viral epitope, contribute to 10-40% of the death of infected cells. Since virus-infected cells generally express 2-10 epitopes, our results suggest that CD8 T cells make a major contribution to the control of HIV growth during acute infection, forming the basis for the development of T cell based vaccines against HIV.

## Future Work

Current thoughts are that vaccines will need to induce both an antibody and T cell response. The methods we have developed for modeling the ability of HIV to escape a T cell response will be modified to allow us to quantitatively assess for the first time the rate at which HIV can escape antibody responses.

Conclusion

Vaccination is one of the most successful medical achievements of the last century. Due to our limited understanding of the correlates of protection, most vaccines have been developed by a trial and error approach and we have failed to deliver vaccines for important diseases like AIDS or malaria. It is generally believed that most of the currently used vaccines provide protection by inducing high titers of pathogen-neutralizing antibodies [7]. The new vaccines that are currently being developed for devastating chronic infections, such as human immunodeficiency virus (HIV), are designed to stimulate T cell responses. Which properties of T cell responses correlate best with protection are not yet well understood. Our research has been aimed at developing quantitative tools to access the quality of T cell responses generated by vaccines or live infections. We have developed novel mathematical models to quantify the efficacy at which T cells induced after infection with viruses kill virus-infected cells. Using these models, we have shown that killing of targets by T cells follows the law of mass-action, which states that the death rate of targets is simply proportional to the magnitude of the T cell response. This result forms the basis for a prediction of the level of memory T cells needed to provide protection following infection with a virus. We have also shown that CD8 T cells play an important role in regulating replication of HIV during the acute phase of the infection by selecting variants that are not recognized by the T cell response. This work provides a compelling argument for the development of T-cell based vaccines again HIV infection.

## References


1. Barber, D., E. Wherry, and R. Ahmed. Cutting edge: rapid in vivo killing by memory CD8 T cells. 2008. *Journal of Immunology.* **171** (1): 27.

2. Ganusov, V., and R. J. De Boer. Estimating in vivo death rates of targets due to CD8 T-cell-mediated killing. 2008. *Journal of Virology.* **82** (23): 11749.

3. Jin, X., S. E. Tuttleton, S. Lewin, A. Gettie, J. Blanchard , C. E. Irwin, J. T. Safrit, J. Mittler, L. Weinberger, L. G. Kostrikis, L. Zhang, A. S. Perelson, and D. D. Ho. Dramatic rise in plasma viremia after CD8(+) T cell depletion in simian immunodeficiency virus-infected macaques. 1999. *Journal of Experimental Medicine .* **189** (6): 991.

4. Ganusov, V. V., D. L. Barber, and R. J. De Boer. Killing of targets by effector CD8 T cells in the mouse spleen follows the law of mass-action. 2009. *In preparation.*

5. Ganusov, V., and R. De Boer. Estimating Costs and Benefits of CTL Escape Mutations in SIV/HIV Infection. 2006. *Journal of Public Library of Science Computational Biology.* **2** (3): 24.

6. Goonetilleke, N., M. K. Liu, J. F. Salazar-Gonzalez, G. Ferrari, E. Giorgi, V. V. Ganusov, B. F. Kelle, G. H. Learn, E. L. Turnbull, M. G. Salazar, K. J. Weinhold, S. Moore, N. Letvin, B. F. Haynes, M. S. Cohen, P. Hraber, T. Bhattacharya, P. Borrow, A. S. Perelson, B. H. Hahn, G. M. Shaw, B. T Korber, and A. J. McMichael . The first T cell response to transmitted/founder virus contributes to the control of acute viremia in HIV-1 infection. 2009. *Journal of Experimental Medicine.* **206** (6): 1253.

7. Plotkin, S. A.. Vaccines: correlates of vaccine-induced immunity. 2008. *Clinical Infectious Diseases.* **47** (3): 401.

## Publications

Asquith, B., J. M. A. Borghans, V. Ganusov, and D. Macallan. Lymphocyte kinetics in health and disease Trends. 2009. *Journal of Immunology .* **30** (4): 182.

Ganusov, V.. Estimating in vivo death rates of targets due to CD8 T cell-mediated killing . 2008. *Journal of Virology .* **82** (23): 11749.

Ganusov, V., J. M. A. Borghans, and R. J. De Boer. Explicit kinetic heterogeneity: a new method for interpreting data from stable isotope labeling experiments. To appear in *Public Library of Science .*

Ganusov, V., and R. J Boer. Tissue distribution of lymphocytes and plasma cells and the role of the gut: response to Pabst et al. 2008. *Journal of Trends Immunology .* **29** (5): 209.

Goonetilleke, N., M. K. P Liu, J. F. Salazar-Gonzalez, G. Ferrari, V. Ganusov, E. L. Turnbull, M. G. Salazar, B. F. Keele, K. J. Weinhold, S. Moore, N. Letvin, B. F. Haynes, M. S. Cohen, P. Borrow, A. S. Perelson, B. T. Korber, B. H. Hahn, G. M. Shaw, and A. J. McMichael. The first T cells of acute HIV infection: Transient responses contribute to control of viremia. 2009. *Journal of Experimental Medicine .* **206** (6): 1253.

Lyadova, I. V., M. A. Kapina, G. S. Sepelkova, V. V. Sosunov, K. B. Majorov, T. V. Radaeva, H. J. van den Ham, V. Ganusov, R. J. de Boer, R. Racine, and G. M. Winslos. Tuberculosis progression is promoted by genetically-determined inflammatory responses rather than by the inability of the host to restrict mycobacterial growth. *Public Library of Science .*

Zilman, A., V. V. Ganusov, and A. S. Perelson. Stochastic models of cell proliferation and death. *Public Library of Science .*

# Multi-scale Analysis of Multi-physical Transport Processes of Electroosmosis in Porous Media

*Qinjun Kang*
20080727PRD2

## Introduction

Electrokinetic phenomena, such as electrophoresis and electroosmosis, were discovered nearly 200 years ago, and have had a wide range of applications in many fields since then. However, simulation and analysis of these phenomena is a great challenge because of the multi-physics nature of the problem. This problem will be further complicated if chemical reactions occur in the bulk fluid or at the fluid-solid interface. In this project, we will develop a comprehensive numerical framework to investigate electrokinetic flow coupled with reactive transport in porous media. We will approach this problem in three stages by:

1. Developing an innovative model for coupled electrokinetic flow and reactive transport in porous media, accounting for multi-physical transport processes, including fluid flow, electric potential distribution, ion convection and diffusion, as well as chemical reaction;

2. Performing nano to micro upscaling analysis of these multi-physical transport processes; and

3. Validating the numerical model through theoretical analysis and available experimental data.

The successful accomplishment of the proposed research will provide 1) an improved understanding of the multi-physical electrokinetic transport phenomena coupled with chemical reaction in micro/nanofluidic devices, 2) innovative techniques to bridge atomistic modeling based on first principals with mesoscale modeling based on statistical-analysis, and 3) a better understanding of the effect of nanoscale structures on the microscale devices.

This research will have direct implications in a broad spectrum of research highly relevant to LANL missions, including new energy exploitation (fuel cells and biofuels), fossil energy prospecting (oil and gas), environmental protection (decontamination of radionuclides in solids), biological applications (enzymatic analysis, DNA analysis, and proteomics), and biomedical applications (clinical pathology and bio-smoke alarm).

## Benefit to National Security Missions

This project will support the DOE/NNSA missions in Energy Security, Environmental Quality, and the missions of the Office of Science by enhancing our understanding of multi-physical (hydro-, thermo-, and electro-dynamic) transport processes of electroosmosis in natural porous media.

## Progress

In the past year, we have been working on developing numerical frameworks for simulating electrokinetic transport in microfluidic and nanofluidic channels.

**A multi-LBM framework to solve the highly coupled nonlinear partial differential equations**

At the pore scale (from microns to centimeters), the Poisson-Boltzmann model can be used to describe electrokinetic transports within the electric double layer (EDL) for most slow flows. However, when the scale goes down to submicrons or even to nanometers, the Boltzmann distribution assumption may break down due to the overlap of EDLs. The applicability of the Poisson-Boltzmann model is not only a fundamental problem in physics but also of significant importance for engineering applications. To investigate this problem, we have introduced a more fundamental model, the Poisson-Nernst-Planck model, without any ion distribution hypothesis. In this model, the fluid flow, electric transport, ion diffusion and convection, chemical regulation and energy transports are highly coupled together. This model brings big challenges to numerical solutions, especially at micro- and nanoscales and for complex geometries. We have developed a coupled LBM framework to solve the problem. The governing equation for each transport process is solved by a LBM and the entire process is simulated through an iteration procedure. After validation, this method is used to study the applicability of the Poisson-Boltzmann model for electrokinetic flows in microchannels. We have not only clarified some ambiguities in the applicability of the

Poisson-Boltzmann model, but also for the first time, have revealed some interesting phenomena in electrokinetic transport in microchannels. A paper on this work will appear in the Journal of Computational Physics.

**Electrokinetic transport in rough microchannels**
Since almost all solid surfaces have certain degree of roughness, either incurred during fabrication process or due to the adsorption/adhesion of other species such as macromolecules, it is imperative to better analyze and model electrokinetic transport in rough microchannels. However, there does not exist an effective way to do so because of the complexity of the problem, especially when the surface roughness is random. We have developed a numerical framework to model electrokinetic transport in microchannels with random roughness. The three-dimensional microstructure of the rough channel is generated by a random generation-growth method based on statistical macroscopic parameters and a highly efficient lattice Poisson-Boltzmann method in complex geometries solves the governing equations for the electrokinetic transport. The effects from the geometric characteristics of roughness on the electrokinetic transport in microchannels are modeled and analyzed. This work has been published on Analytical Chemistry in April, 2009.

**Electrokinetic Transport in Nanofluidic Channels**
Nanofluidics is an emerging field of interest because of its potential applications in controlling and manipulating fluids and inclusions (particles and ions) exquisitely, and in biochemomedical analysis and energy conversion systems. We have performed theoretical and numerical modeling of ionic distribution and transport in silica nanochannels based on a new counter-ion enrichment model. Our results have revealed some very interesting phenomena in electrokinetic transport in nanofluidic channels for the first time. This work has been submitted to Langmuir.

**Optimization of electrochemicomechanical energy conversion in nanofluidic channels**
When an electrolyte solution flows in a channel, the channel wall surfaces will be charged because of the physical and chemical interactions between ions and surfaces. A pressure-driven flow through a narrow channel therefore carries a net electrical charge with it, inducing both a current and a potential. These so-called streaming currents and streaming potentials can drive an external load and therefore represent a means of converting hydrostatic energy into electrical power. Such an electrokinetic effect in energy conversion devices has received much attention in the context of microfluidic and nanofluidic devices because of its potential attractive conversion efficiency and clean process of power generation. Physical modeling of electrokinetic energy conversion is needed to guide the design and optimization of these properties. Our work in this area is focusing on 1) analyzing the multiphysicochemical transport mechanisms in the microfludic and nanofluidic energy conversion using theoretical and numerical tools; 2) predicting the energy conversion efficiency and identify the key factors that limit the efficiency; 3) proposing new design and optimization schemes to improve the energy conversion efficiency. This work is to be submitted to the Journal of Power Sources.

## Future Work

Electroosmosis is the motion of polar liquid through a porous material or a biological membrane under the influence of an applied electric field. Since its discovery, this phenomenon has had a wide range of applications in many fields. Therefore, a better understanding of multi-physical (hydro-, thermo-, and electro-dynamic) transport processes of electroosmosis in porous media is critical to a wide range of fields. However, this problem is notoriously difficult and none of the existing (macroscopic, mesoscopic, or microscopic) methods can individually solve this multi-scale multi-physical transport phenomena accurately with present-day computers. Therefore it is critical to develop multi-scale modeling and analysis tools to capture the effects of microscale geometry on the macroscale multi-physical transport processes of electroosmosis in porous media.

This project will involve 1) developing innovative models for reproducing the multi-scale random microstructures of porous media through new numerical models to reflect the macroscale statistical information obtained from measurements; 2) performing micro->meso->macro upscaling analysis of multi-physical transport processes of electroosmosis in the porous structures, including fluid flow, electric potential distribution, ion convection and diffusion; and 3) developing a novel hybrid model to integrate the models for different scales so that the important information at the small scale can be captured without resolving the small scale in the entire computational domain.

The successful accomplishment of the proposed research will provide 1) an improved understanding of multi-physical transport phenomena of electroosmosis through multi-scale structures of porous media, and 2) innovative techniques to bridge atomistic modeling with mesoscale modeling based on statistical-analysis and continuum modeling. This approach will have direct implications in a broad spectrum of energy and environmental research, including new energy exploitation (fuel cells and biofuels), fossil energy prospecting (oil and gas), environmental protection (decontamination of radionuclides in solids), biomedical engineering applications, and novel materials design.

## Conclusion

This project will enable a science-based understanding of electroosmosis, a phenomenon discovered 200 years ago, and having had a wide range of applications in many fields since then. However, a better understanding of it is still lacking. In this project, an advanced numerical

method will be developed and research results will be published in leading journals. This approach will have direct applications in a broad spectrum of energy and environmental research, including new energy exploitation (fuel cells and biofuels), fossil energy prospecting (oil and gas), environmental protection (decontamination of radionuclides in solids), biomedical engineering applications, and novel materials design.

## Publications


Kang, Q., M. Wang, P. P. Mukherjee, and P. C. Lichtner. Mesoscopic Modeling of Multi-Physicochemical Transport Phenomena in Porous Media. 2009. *Advances in Mechanical Engineering.* **in review**.

Mukherjee, Partha P., M. Wang, Q. Kang, and P. C. Lichtner. Pore-Scale modeling of transport in charged porous media. Presented at *Computational Methods in Water Resources XVII International Conference.* (San Francisco, CA, 6-10, July 2008).

Wang, M. R., and Q. J. Kang. Electrokinetic Transport in Microchannels with Random Roughness. 2009. *Analytical Chemistry.* **81** (8): 2953.

Wang, M., Q. Chen, Q. Kang, N. Pan, and E. Ben-Naim. Nonlinear effective properties of unsaturated porous materials. To appear in *International Journal of Non-linear Science and Numerical Simulations.*

Wang, M., Q. J. Kang, and N. Pan. Thermal conductivity enhancement of carbon fiber composites. 2009. *Applied Thermal Engineering.* **29** (2-3): 418.

Wang, M., Q. Kang, and H. Viswanathan. Electroosmosis of dilute electrolyte solutions in microporous media. Presented at *The 2nd ASME International Conference of Micro/Nanoscale Heat and Mass Transfer.* (Shanghai, China).

Wang, M., and Q. Kang. Modeling electrokinetic flows in microchannels using coupled lattice Boltzmann methods. To appear in *Journal of Computational Physics.*

Wang, M., and Q. Kang. Electrokinetic transport in nanofluidic channels. 2009. *Langmuir.* **in review**.

# Fluvial Geomorphic Response to Permafrost Thawing: Implications for the Global Carbon Budget and Arctic Hydrology

*Cathy J. Wilson*
20080788PRD3

## Introduction

This project aims to determine how arctic river channel processes will be impacted by climate change and permafrost melting of floodplain sediments, and how changes in the rate of arctic floodplain erosion and sedimentation will enhance or reduce $CO_2$ and methane fluxes into the atmosphere as permafrost melts. Rapid scour8hg of unfrozen arctic floodplains could release large amounts of nutrients into the pacific and arctic oceans, dramatically changing the global ocean oxygen levels and biogeochemistry. Freshwater inputs to these oceans will also be altered.

## Benefit to National Security Missions

The DOE office of Science Climate Change program seeks to provide fundamental understanding of the processes driving global carbon budgets. This project directly impacts a core program of the DOE Office of Science. In addition, outcomes from this project can be used to assess transportation infrastructure vulnerabilities in the arctic, will result in new tools for feature extraction from remote sensing data sets, and new models for planetary hydrology.

## Progress

In 2009 the research has had two primary focuses: 1) the detection of changes in river position over time using remotely sensed data, and 2) the development/adaptation of a numerical model to quantify the influence of groundwater and surface water interactions on the thawing of permafrost. The remote sensing analysis has relied heavily on the application of LANL's GeniePro software to extract river channel locations from remote sensing data collected over several decades. Changes in channel location between image time periods has been perform and both the total change and the rates of change have been analyzed in detail for one primary study area (the Yukon River in central Alaska) and preliminary analysis of other arctic rivers has begun. Although this work has relied principally on the use of remote sensing datasets it also included a field reconnaissance in Alaska in June and July of 2009. The primary study area for the remote sensing and the location of the field reconnaissance has been the Yukon Flats portion of the Yukon River. Additional study areas include: the lower Yukon River, the McKenzie River in Canada, the Kolyma, Lena and Indigirka Rivers in Siberia. Results from this work have been presented at the CCSM Polar Climate and Land Model working group meetings; European Geosciences Union, and the Arctic Watershed Evolution Workshop at the International Arctic Research Center at the University of Alaska, Fairbanks. A manuscript is currently under preparation focusing on the Yukon River work and the work will be presented in a talk at the Fall meeting of the AGU.

On the modeling front, the primary effort has been on the adaptation and testing the Bryan Travis' MAGHNUM code to permafrost settings. Initial runs indicate that incorporation of groundwater flow into predictions of arctic lake thawing accelerates the rate of thawing by an order of magnitude compared to purely conductive heat transport. Ongoing model development includes incorporation of topography and predicting thermal erosion of river banks.

Based on our research efforts in this past year, we have submitted three proposals for funding to expand the scope of research to larger Arctic hydrological responses to climate change. This work has involved both internal (Bryan Travis, EES-16, Steven Brumby, ISR-2, and Paul Pope, ISR-2) and external collaborations (US Fish and Wildlife Service Fairbanks, AK and the International Arctic Research Center, UAF).

## Future Work

### Scientific Issue

In many river systems flowing through permafrost much of the bank stability is derived in part from frozen banks. As permafrost warms and the upper few meters of arctic floodplains begin to thaw, bank erosion rates are likely to increase significantly, resulting in more rapid channel migration rates and altering river morphologies. Increased river mobility will erode and mobilize carbon presently trapped in floodplains and potentially

accelerate the thawing of deeper permafrost below the active river channels. In addition, changes in permafrost will drive changes in fluxes of water to rivers, changing the timing and magnitude of fresh water fluxes to cold oceans.

**Future work includes**

1. Perform hydrograph analysis on Yukon River Basin to quantify change in timing and amount of water inputs into the river system due to changes in permafrost.
2. Run subsurface permafrost flow and heat transport model to predict changes in river hydrographs expected from permafrost thawing.
3. Apply SDSU HRR river runoff and routing model to a large basin with permafrost thawing algorithm and predict flood volume and timing and river mobility for large basin.

## Conclusion

This project will result in new models that will enable predictions of the rate of $CO_2$ release from arctic regions due to geomorphic processes that are set in motion by increased arctic temperatures. It will also result in models to predict the fluxes of nutrients into oceans in arctic regions. These models will help us to better understand the complex interrelationship between the many components that impact our global climate.

## References


1. Rowland, J. C., W. E. Dietrich, G. Day, and G. Parker. Formation and maintenance of single-thread tie channels entering floodplain lakes: Observations from three diverse river systems. . 2008. *Journal of Geophysical Research.* **114** (F02013): 1.

2. Manga, M., and J. C. Rowland. Response of Alum Rock springs to the October 30, 2007 Alum Rock earthquake and implications for the origin of increased discharge after earthquakes. 2009. *Geofluids.* **9** (3): 237.

3. Rowland, J. C., M. T. Stacey, and W. E. Dietrich. Turbulent characteristics of a shallow wall-bounded plane jet: experimental implications for river mouth hydrodynamics. 2009. *Journal of Fluid Mechanics.* **627**: 423.

4. Rowland, J. C., G. E. Hilley, and A. Fildani. A test of submarine leveed channel initiation by deposition alone. *Journal of Sedimentary Research.*

5. Day, G., W. E. Dietrich, J. C. Rowland, and A. Marshall. The rapid spread of mine-derived sediment across the Middle Fly River floodplain. 2009. In *The Fly River Papua New Guinea: Environmental Studies in an Impacted Tropical River System.* Edited by Bolton, B.. , p. 113 – 152. Asterdam; Boston: Elsevier.

# Determinaing the Mechanisms of Enzymes Xylose Isomerase and HIV Protease using Neutron Crystallography

*Paul A. Langan*
20080789PRD3

## Introduction

Understanding the structure of proteins and how they work is central to designing new drugs. Most modern-day medicines are small organic molecules that block the activity of a specific enzyme that is essential for the infectious agent's proliferation. These medicines bind to a site in the enzyme that blocks the molecule involved in the infectious process from binding, or that prevents the reaction from proceeding. X-ray crystallography provides information on structure for drug design but less on the reaction mechanism. Most mechanisms involve the transfer of hydrogen (H), but mobile H atoms are invisible to X-rays. Neutrons can be used to determine the location and movement of H during a reaction. I propose to develop neutron crystallography techniques to derive the mechanisms of the enzyme D-xylose isomerase (XI) and apply those techniques to determine the mechanism and design more effective drugs for HIV-1 protease PR. I expect to established strategies for using this information in drug design. Modern-day drug design relies on a collection of different tools and the impact of generating a new tool and new ideas for structure-assisted drug design efforts would undoubtedly by great.

## Benefit to National Security Missions

The enzymes involved in this project are important for bioenergy and energy security. Rational drug design is important for biothreat reduction. Understanding enzyme mechanism is an important fundamental science mission.

## Progress

The first major goal of determining the catalytic mechanism of XI has been achieved with the help of determining five neutron structures of XI representing stages along the enzyme's catalyzed reaction and a number of X-ray structures [1,2]. The following neutron structures were obtained:

*apo*-XI containing no metal cations or a substrate; XI complexed with two $Co^{2+}$ co-factors; XI complexed with two $Ni^{2+}$ co-factors and cyclic deuterated glucose; XI complexed with two $Cd^{2+}$ co-factors and linear deuterated glucose; XI complexed with two $Mg^{2+}$ co-factors and linear deuterated xylulose product.

A series of X-ray crystallographic data sets have been collected from crystals grown in both $D_2O$ and $H_2O$, and the putative movement of H during the reaction has been mapped out. The X-ray and neutron structures have been solved, and a new reaction mechanism has been proposed. Because such a large number of neutron data sets were required we had to collect data not only at the PCS at LANL, but also at the ILL in France. A crystallization robot and the deuteration laboratory in B division were used to optimize crystal size for neutron crystallography. The X-ray data sets were collected through collaborations with Toledo University. A paper describing the results has been submitted to journal Structure and Andrey Kovalevsky has presented his results at the Annual Meeting of the American Crystallographic Association held in Toronto in July, 2009, and at the International Conference on Neutrons in Biology in Santa Fe in October 2009. For the first time neutron protein crystallography has been used to look at the stages of an enzyme-catalyzed reaction with the ability of directly determining the positions of H atoms. We expect that the results of this work will be seen as highly significant. XI is an important enzyme for increasing the efficiency of xylose conversion to biofuels and we expect to use our results for improving its performance through protein engineering efforts. We have also started quantum chemical calculations to provide theoretical evidence for the proposed mechanism. Slower but constant progress has been made toward our second goal of determining the positions of H atoms in the active site of PR. We have deuterated PR and obtained initial crystals. Our focus for the remainder of this project will now turn to obtaining large enough crystals of PR for neutron studies. We fully anticipate achieving this over the next year.

## Future Work

XI catalyzes a reversible conversion of aldo-sugars D-xylose or D-glucose to the keto-sugars D-xylulose

and D-fructose, respectively, by using two divalent metal co-factors, such as $Mg^{2+}$, $Mn^{2+}$ or $Co^{2+}$. The reaction proceeds through several H transfer stages that we already mapped by using neutron structures. I plan to build on my current results and to obtain evidence for the proposed mechanism by performing site-directed mutagenesis in the XI active site, utilizing quantum chemical calculations, and determining X-ray and neutron structures of XI in complex with inhibitors, such as D-sorbitol which is a derivative of D-glucose. A key strategy in making XI a better protein for biofuels production is making mutant libraries and choosing a mutant with altered substrate selectivity, non-sensitivity to changes in ambient solution acidity and faster turn-over rate. The positions of H atoms in the active site of PR are believed to be crucial for its mechanism and drug binding. My goal is to exploit the strategies developed above to deuterate PR, obtain crystals and determine neutron structures for a) ligand-free (native) PR; b) PR complexed with an engineered substrate that could be trapped as a reaction intermediate; c) PR complexed with clinical drugs. I already have considerable experience with PR and drug design. I will express, purify and crystallize wild-type and mutant enzyme in the native and substrate- or inhibitor-complexed forms, collect neutron diffraction data at PCS, refine and analyze structures. I will then develop a strategy for exploiting this new information on mechanism and H location in drug design.

## Conclusion

I have obtained detailed information on the mechanism of XI and expect to do the same for PR within the next year – a leap forward in our understanding of how enzymes work on the molecular level. I also expect to established strategies for using this information in drug design. Contemporary drug design relies on a collection of different tools and the impact of generating a new tool and new ideas for structure-assisted drug design efforts would undoubtedly be great.

## References

Kovalevsky, A., A. Katz, H. Carrell, L. Hanson, M. Mustyakimov, S. Fisher, L. Coates, B. Schoenborn, G. Bunick, J. Glusker, and P. Langan. Hydrogen location in stages of an enzyme catalyzed reaction: time-of-flight neutron structure of D-xylose isomerase with bound D-xylulose. 2008. *Biochemistry.* **47**: 7595.

Kovalevsky, A., L. Hanson, S. Fisher, M. Mustyakimov, S. Mason, T. Forsyth, M. Blakeley, D. Keen, T. wagner, H. Carrell, A. Katz, J. Glusker, and P. Langan. Metal cation role and the movement of hydrogen during the reaction catalyzed by D-xylose isomerase. *Structure.*

## Publications

Kovalevsky, A., A. Katz, H. Carrell, L. Hanson, M. Mustyakimov, S. Fisher, L. Coates, B. Schoenborn, G. Bunick, J. Glusker, and P. Langan. Hydrogen location in stages of an enzyme-catalyzed reaction: time-of-flight neutron structure of D-xylose isomerase with bound D-xylulose.. 2008. *Biochemistry.* **47**: 7595.

# Analysis of Protein Structure-Function Relations in Antibiotic Biosynthesis and Signal Transducing Receptors

*Louis A. Silks III*
20090524PRD2

## Introduction

The proposal originally submitted by Dr. Koglin to apply for a Director's postdoctoral fellowship at the Los Alamos National Laboratory describes the synthesis of specifically $^{13}C$ isotopic enriched, selectively perdeuterated amino acids and metabolic amino acid precursors for *in vitro* transcription/translation (cell-free protein biosynthesis) and bacterial overexpression of selectively labeled proteins. His research interests are mainly focused on development of biophysical methods to investigate structures of biological molecules and dynamic interaction events in the molecular communication between these molecules this will allow studies of highly complex systems. Examples of these complex biological systems are (1) proteins involved in the biosynthesis of natural products, so called secondary metabolites like non-ribosomal peptide bond-forming condensation domains (C-domains), proteins that are essential for the biosynthesis of antibiotics (erythromycin, vancomycin, daptomycin and penicillin), fungal and bacterial toxins and virulence factors (aflatoxin, vibriobactin, enterobactin, mycolic acid in *M. tuberculosis*), chemotherapeutics, antiviral and antifungal compounds in Non-ribosomal Peptide Synthetases (NRPSs; Figure 1); (2) membrane proteins responsible for the export of these secondary metabolites, that show a very high peptide sequence homology to proteins responsible for the import of carbohydrates, but with inversed transport direction and (3) G-protein coupled receptors (GPCRs), membrane proteins responsible for signal transduction in mammalian cells and their malfunction plays a major role in diabetes type II, Alzheimer disease and Multiple Sclerosis. The challenge for studying protein structures, their complexes and the structural dynamic of these proteins by Nuclear Magnetic Resonance (NMR) spectroscopy is the protein size-dependent relaxation behavior of the NMR signal. With an increasing size of the proteins, not only the signal overlap increases, also the signal intensity and the line-width of a signal decrease. To solve or at least reduce this problem, other relaxation effects, like the exchange with NMR active nuclei of the solvent, can be prevented by perdeuteration. The number of NMR signals can be reduced by amino acid type specific perdeuteration and $^{13}C$-depletion or vice versa the specific $^{13}C$ and $^{1}H$ enrichment of a limited number of spins systems in an otherwise fully perdeuterated and $^{13}C$ depleted protein.

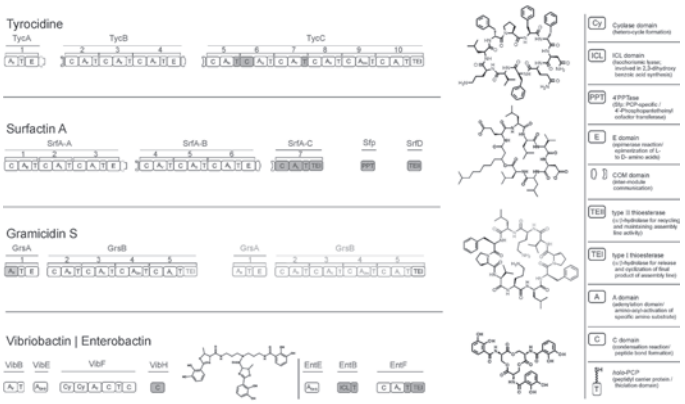


*Figure 1. Natural Product Biosynthetic Clusters*

Dr. Koglin has solved in collaboration with Prof. Gerhard Wagner and Prof. Christopher T Walsh of Harvard University, the Francis Bitter Magnet Lab of Harvard and MIT and the European excellence center for High-field NMR spectroscopy at Goethe University, Frankfurt, Germany the largest single solution protein structure of a protein essential for the maturation of a virulent iron chelator by NMR spectroscopy using advanced NMR technologies he helped to develop. This record achievement has held for several years and resulted in publications demonstrating slow-motion two-state dynamic of proteins essential for their biosynthetic function and showing the capabilities of *in vitro* translation/transcription for cell-free protein biosynthesis of very large and toxic proteins in sufficient amounts for structural studies. Dr. Koglin is applying novel methods in structural biology by combining selectively stable isotopes enriched proteins and new pulse sequences and strategies in NMR spectroscopy at LANL to further push the current technology to enable larger biological macromolecular assemblies to surrender their structures and the significance of their structural dynamic to his new methods. The successful result of this project will be used, in collaboration with Harvard Medical School, to play a key role in a center for membrane proteins, structure and

function funded by NIH.

## Benefit to National Security Missions

This project will support the DOE mission in biology by enhancing our understanding of how cellular processes work in general, how the formation of large protein assemblies is initiated, how the substrate-protein recognition is affecting the basic structural dynamic of proteins, and in tandem to form and manipulate the biosynthesis of natural products with high biomedical value.

## Progress

Dr. Koglin has been here just over six months and has made good progress toward completing phase one. Phase one involves the chemical synthesis of selectively stable isotope enriched amino acids. There are four amino acids constructed so far. Dr. Koglin has completed three of the four. The remaining amino acid involves the use of a commercially available starting substance which is expensive. The standard chemical routines to convert available and prior synthesized starting material to amino acids were developed on the other three amino acids. With support of his mentor L.A. 'Pete' Silks new synthetic routines have been developed to increase the yield of the fourth amino acid. He incorporated already the synthesized amino acids into a relatively large didomainal protein. He validated the incorporation of the amino acids into the protein for future work and used those specific labels to develop and adapt new pulse programs and resonance assignment strategies for very large proteins. The development of new pulse sequences and assignment strategies is in collaboration with Dr. Dominique Frueh and Prof. Gerhard Wagner at Harvard Medical School. The novel NMR resonance assignment strategies and pulse sequences are specifically adopted for very large and membrane proteins with selectively labeled amino acids. Dr. Koglin could already proof his concept and advances studying the structure and structural dynamic of very large proteins and protein complexes with selectively stable isotope enriched amino acids and new NMR methods. This new concept developed by collaboration with Dominique Frueh, Gerhard Wagner and L.A. 'Pete' Silks opens new avenues for size limitation for 3-dimensional protein structure and structural dynamic determination by NMR spectroscopy. This work is already published in two manuscripts in the peer-review journals JBNMR (Journal of biomolecular NMR) and JACS (Journal of the American Chemical Society) (Figure 2). The approximate time usually spent to record necessary data and to assign all significant backbone resonances of a 35 kDa is around four months. Applying the newly developed technique the entire backbone of this protein could be assigned in less than one week. This enabled us to finish the work and prepare a planned back-to-back publication describing the selectivity substrate recognition and protein-protein interactions in non-ribosomal peptide synthetases. It further allows us to pursue the structure elucidation of an enzymatic active protein complex of 74 kDa, a functional condensation domain (C domain) of an NRPS system with its two adjacent carrier proteins (T domain). Dr. Koglin was further able to clone all three permeases in expression systems for the protein over production in *E. coli* strains (Figure 3). The genetic construct needed to be alternated since tag, essential for the protein purification was interfering with the micelle formation. Detergent micelles are commonly used to mimic a membrane environment *in vitro*. The new construct includes a TEV (tobacco virus envelope protein) protease cleavage site. He is able to over produce all three membrane-inserted permeases, isolate them from the *E. coli* bacterial membrane and transfer them into micelles. The first NMR spectra are already recorded.

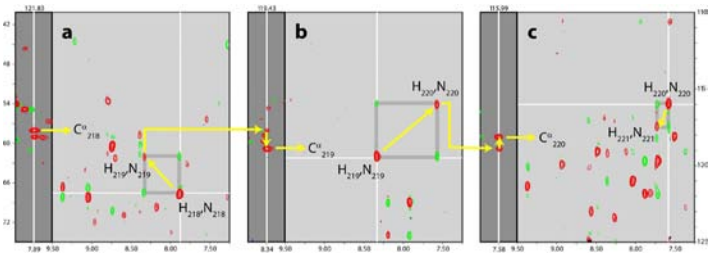


*Figure 2. Schematic Presentation of NMR Pulse Sequence and Assignment Strategy for Very Large Proteins*

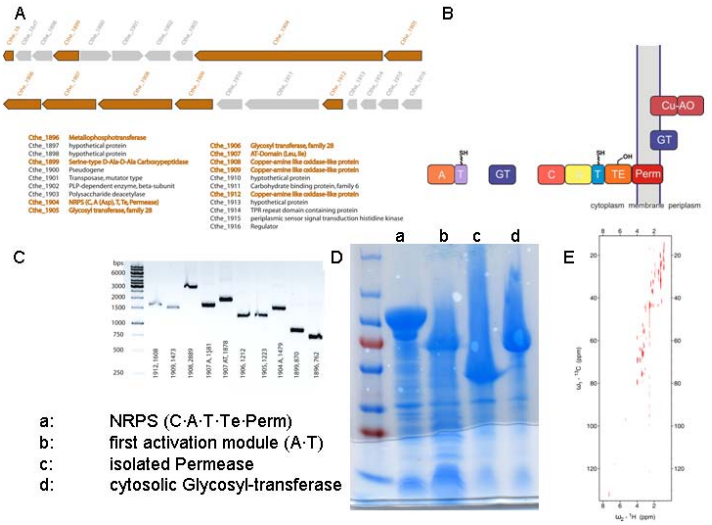


*Figure 3. A Membrane Inserted Transport Protein for NMR Solution Structure Determination: Genetic Organization, Localization in the Cell, and Purification of the Permease and Associated Proteins.*

## Future Work

The development of methods for the elucidation of protein structures, to study their interactions with ligands and other proteins, to analyze complex inter-domain communications, is accelerating. As a result, research that employs biophysical methods to investigate biological molecules and dynamic interaction events has dramatically evolved and allows studies of highly complex systems. These are biological systems like (1) non-ribosomal peptide bond-forming condensation domains (C-domains), proteins that are essential for the biosynthesis of antibiotics

(erythromycin, vancomycin, daptomycin and penicillin), fungal and bacterial toxins and virulence factors (aflatoxin, vibriobactin, enterobactin, mycolic acid in M. tuberculosis), chemotherapeutics, antiviral and antifungal compounds; (2) membrane proteins responsible for the export of these secondary metabolites, that show a high homology to proteins responsible for the import of carbohydrates and (3) G-protein coupled receptors (GPCRs), membrane proteins responsible for signal transduction in mammalian cells. The challenge for studying protein structures, their complexes and the structural dynamic of these proteins by Nuclear Magnetic Resonance (NMR) spectroscopy is the protein size-dependent relaxation behavior of the NMR signal. With an increasing size of the proteins, not only the signal overlap increases, also the signal intensity and the line-width of a signal decrease. To solve this problem, other relaxation effects, like the exchange with NMR active nuclei of the solvent, can be prevented by perdeuteration. The number of NMR signals can be reduced by amino acid type specific perdeuteration and 13C-depletion or vice versa the specific 13C and 1H enrichment of a limited number of spins systems in an otherwise fully perdeuterated and 13C depleted protein. In collaboration with L. A "Pete" Silks (B8) and Ryszard Michalczyk (B8) specifically isotopic enriched amino acids and amino acid precursor for the cell-free and bacterial expression of selectively labeled proteins and perdeuterated detergents for NMR spectroscopic analysis of membrane proteins will be synthesized.

## Conclusion

Dr. Koglin will accomplish (1) obtain the structure of the C-domain by NMR spectroscopy. This is important to gain insight into the biosynthetic processes this structure performs and this directly wimpacts the ability to design and effective antibiotics. In addition, it should possible to block the biosynthesis of bacterial and fungal toxins, (2) to understand a family of proteins in the development of antibiotic resistance, (3) and to understand the drug niacin and its binding to a membrane inserted receptor belonging to the group of G-protein coupled receptors (GPCRs). This could give rise to alternative treatment of type II diabetes. Since the general knowledge about GPCRs is very limited, every new aspect of knowledge about their fold and function will give rise to knowledge to understand diseases like Alzheimer and Multiple Sclerosis.

## Publications


Frueh, D. P., A. Leed, H. Arthanari, A. Koglin, C. T. Walsh, and G. Wagner. Time-shared HSQC-NOESY for accurate distance constraints measured at high-field in N-15-C-13-ILV methyl labeled proteins . 2009. *JOURNAL OF BIOMOLECULAR NMR* . **45** (3): 311.

Koglin, A.. Structural insights into nonrobosomal peptide enzymatic assembly lines. 2009. *Natural Products Reports.* **26** (8): 987.

Koglin, A., C. T. Walsh, D. P. Frueh, H. Arthanari, and G. Wagner. A Double TROSY hNCAnH Experiment for Efficient Assignment of Large and Challenging Proteins . 2009. *JOURNAL OF THE AMERICAN CHEMICAL SOCIETY.* **131** (36): 12880.

Koglin, A., E. R. Strieter, Z. D. Aron, and C. T. Walsh. Cascade Reactions during Coronafacic Acid Biosynthesis: Elongation, Cyclization, and Functionalization during Cfa7-Catalyzed Condensation . 2009. *Journal of the American Chemical Society.* **131** (6): 2113.

# Carbon and Oxygen Isotopic Variability in Succulent Plants and Their Spines: A New Tool for Climate and Ecosystem Studies in Desert Regions

*Claudia Mora*
20090526PRD2

## Introduction

Nearly one-third of the world's total land area is arid or semi-arid and ecosystems in these regions are among the most vulnerable to changes in precipitation, temperature, human and natural disturbance as a consequence of global climate change. Such changes may impact ecosystem structure and viability, as well as regional carbon storage, hydrological partitioning and water resources. High resolution paleoclimate records are useful to understand environmental and ecosystem response to climate change, however, arid regions lack the usual biological and geological proxy archives of climate, such as tree rings, bog or lake sediments, and speleothems (cave deposits). A new proxy, sensitive to environmental variability in arid and semi-arid regions, would represent a breakthrough in our understanding of past and future climate trends in these vulnerable regions of the world. The stable carbon and oxygen isotope variations in spines grown by long-lived cactus species may provide a novel and valuable archive of climate in arid regions. Succulent cactuses and euphorbs are vital to the functioning of their ecosystems by providing reliable sources of water, nutrients and energy in times of drought. Stable isotope variations in their spines record time-series evidence of changing climate and environment over a range of timescales (days to decades). These spines are retained for decades to centuries, grown in series along the stems of long-lived cactuses, and potentially provide the highest resolution proxy record of past environmental variability in arid regions. Little is known, however, about the relative importance of different environmental parameters in controlling isotopic compositions in cactus spines. The principal goal of this study is to understand the influence of important environmental parameters (e.g., light, temperature, relative humidity) on controlling stable isotope variability in cactus spines. Growth experiments under controlled conditions will provide a quantitative understanding of how to interpret isotope variations preserved in spines. The project will make use of two cutting-edge technologies available at LANL for high temporal (tunable diode laser) and spatial (laser volatilization IRMS) resolution stable isotope analysis of cactus response to environmental parameters.

## Benefit to National Security Missions

This project will support the DOE Office of Science mission in Biological and Environmental Research (BER) to understand relationships between climate change and Earth' ecosystems. New arid region climate proxies will improve the scientific basis for assessing the potential impacts of future changes in temperature, precipitation and pest infestations on arid ecosystems and the mortality of Western US forests.

## Progress

The post-doc, Dr. Nathan English, has assembled a preparation laboratory for processing wood and other plant materials to alpha- cellulose and for preparing, processing and storing other geologic or biologic materials (minerals, feathers, etc.) useful in climate proxy studies. These changes allow us to carry out cellulose extraction using a less hazardous and wasteful process (the modified-Brendel process) than we previously utilized. Stable carbon and oxygen isotope ratios in spines of South American altiplano species of cactus were analyzed to evaluate the portability of the cactus spine proxy to new environments and species. We observe that isotopic variability in these spines respond to environmental controls similarly to spines in North American saguaros, suggesting more widespread development of cactus spine proxies for studies of terrestrial climate change is possible. Tropical South America is one of three main centers of the Walker cell (tropospheric, equatorial and zonal circulation of the atmosphere) and is therefore extremely sensitive to changes in global climate systems. Very high resolution paleoclimate data, such as preserved in cactus spine records, will provide a novel and valuable measure of changes in this circulation over the past three centuries. We were assisted in this project by a summer student, Samantha Stutz, who Dr. English trained and mentored and who is now pursuing related research at the University of Wyoming. A collaborative study with the University of Wyoming was initiated to address the impact of light, temperature and relative humidity

on stable isotope values of cactus and other succulent plants. Dustin Bronson at University of Wyoming has completed a rudimentary gas exchange chamber for cactus that can be connected to the tunable diode laser IRMS (TDL-IRMS) at LANL. Growth experiments are scheduled to begin December of 2009. As the capabilities of the lab have expanded, we have expanded our exploration of stable isotope ratios to wood from semi-arid Western US forests that exhibit higher than normal mortality. We are evaluating stable carbon and oxygen isotope ratios of living and dead wood, to test the hypothesis that microorganisms (fungi) translocate material in wood after tree death, confounding the significance of isotope variations in these materials. A better understanding and diagnosis of tree death will be useful in managing US forests as well as modeling their carbon budgets.

## Future Work

A deeper understanding of environmental parameters controlling isotopic variability in cactus spines and rare, woody species in arid to semi-arid regions will allow us to better predict how future climate change or human disturbance may affect these foundation species and their ecosystems. To develop a quantitative basis for interpretation of stable isotope variations in these species, we will intensively monitor and sample columnar cactuses and spiny succulents euphorbs grown in environmentally controlled greenhouse and growth chambers. We will:

1. Evaluate the impact of different parameters (e.g., light, relative humidity and temperature) on the isotopic variability of succulent water and stem tissue using (a) established IRMS analytical methodologies and (b) by developing new laser volatilization techniques for higher resolution, in situ, analysis of spine material;

2. Use gas exchange measurements and online isotope analysis of respired $CO_2$ and $H_2O$ using the TDL-IRMS to examine real-time response by cacti to drought or rainfall; and

3. Develop a robust numeric model to (a) reconstruct past environmental variables based on stable isotopes in cactus spines and to (b) quantify the uncertainty associated with these reconstructions.

We will continue to examine the portability of the cactus spine proxy to new species and field locations. To extend our work to Western US forests, we will employ multiple isotope studies (C,O) of trees experiencing high rates of mortality. Studies of the “last gasps” of dying trees may reveal the proximal causes of their demise and help to define how future temperature, precipitation and pest infestation will alter forest mortality. This work will include:

1. A comparison of isotopic systematic in live and dead wood from arid forest trees;

2. Retrospective isotopic studies of forests and trees that have experienced higher than normal mortality within the context of recent climatic changes and pest infestations; and

3. Development of isotopic tools for the diagnosis, modeling and carbon budgeting of imminent tree/forest mortality as it relates to drought, pest invasion and future changes in temperature and precipitation.

## Conclusion

Arid and semi-arid lands represent almost 45% of global land area and are vulnerable to changes in global climate and attendant human and natural disturbance. This project will develop a new climate proxy utilizing stable isotope ratios in cactus spines as chemical records of past environments and climate change. Such a tool would allow us to quantify past changes in arid climate and ecosystem response, and therefore to better predict future impacts of climate change on arid ecosystems.

## Publications

English, N. B., D. L. Dettman, D. R. Sandquist, and D. G. Williams. An easy path from precipitation amount to d18O values in the spines of columnar cactuses, Carnegiea gigantea. Presented at *Geological Society of America Annual Meeting.* (Portland, OR, 18-21 Oct. 2009).

# Probing Molecular Physics of Biological Nano-channels: from Viruses to Biosensors

*Benjamin H. Mcmahon*
20090527PRD2

## Introduction

Functioning of living cells requires selective transport of molecules into and out of the cell nucleus. This transport is also important in the replication of certain viruses, such as influenza, that replicate in the nucleus. Transport occurs through channels that are able to selectively move only certain molecular species while effectively filtering out others, even very similar ones. Moreover, such channels can selectively transport their specific molecules in the presence of vast amounts of non-specific competitors. In many biological channels, efficient and selective transport occurs without direct input of metabolic energy and without transitions from an 'open' to a 'closed' state during the transport event. Examples include selective permeability of porins and transport through the nuclear pore complex in eukaryotes. Mechanisms of selectivity operational in such channels hold a great potential for applications in nano-technology and nano-medicine, which recently has lead to design artificial selective nano-channels, which mimic the selective biological channels and are built on the principles operational in those. Another subject of high practical and fundamental interest is the mechanism of entry of viruses into to the cell nucleus. Survival of the virus depends on its ability to deliver its genetic material to the cell nucleus and replicate before the infected cell is destroyed by the immune system. This process is inherently stochastic, as it depends on the transport of a single protein-DNA complex into the nucleus and the computational modeling is crucial for further progress.

## Benefit to National Security Missions

This project will support the DOE mission in Promoting Science by enhancing our understanding of basics biophysics involved in the nuclear-cytoplasmic particle exchange. The work also provides the foundational understanding of cell processes that enable development of strategies to combat both natural disease and bio-WMDs. In this way, this work supports missions of Threat Reduction by understanding the mechanisms of host -- viral pathogens interactions.

## Progress

Precise mechanisms and conditions of selective transport through such nano-channels are still unknown. I have been developing a theoretical model to explain the mechanisms of selectivity of transport through nano-channels, which contains only two essential ingredients: - i) transient trapping of the cargoes inside the channel (e.g. due to transient binding to moieties inside the channel) ii) competition between the transported molecules for the limited space inside the channel [2] - Figure 1. Parts of the work have been done in a close collaboration with the experimental colleagues at Rockefeller University who have been working on implementation of the concepts in a real nano-molecular filter [1,3].

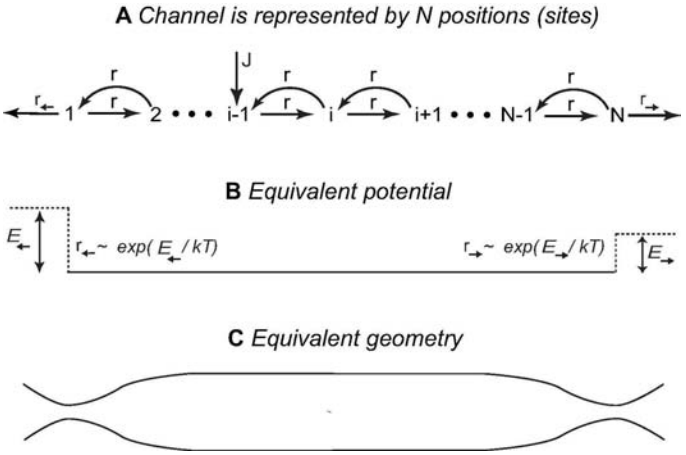


*Figure 1. Representation of the transport through a channel in terms of random hopping with exclusion.*

The theory provides a mechanism for selectivity based on the differences in the kinetics of transport through the channel between different molecules. The theory explains how the specific molecules are able to

efficiently filter out the non-specific competitors – and proposes a mechanism for sharp molecular discrimination. The theory also provides a blueprint for future creation of ever more selective artificial nano-channels. The theoretical predictions explain well previous experimental results when only single species of transported molecules are present (Figure 2) and have led to the creation of artificial nano-channel that mimics the NPC function [1] - Figure 3.

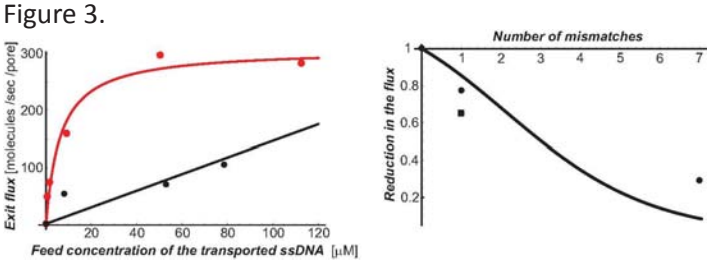


*Figure 2. Comparison of the theoretical predictions with the experimental data in the single species case. Dots - experimental results on the flux of single stranded DNA through nano-channels functionalized with DNA hairpins (Kohli et al. Science, 2004). Lines - theoretical prediction.*

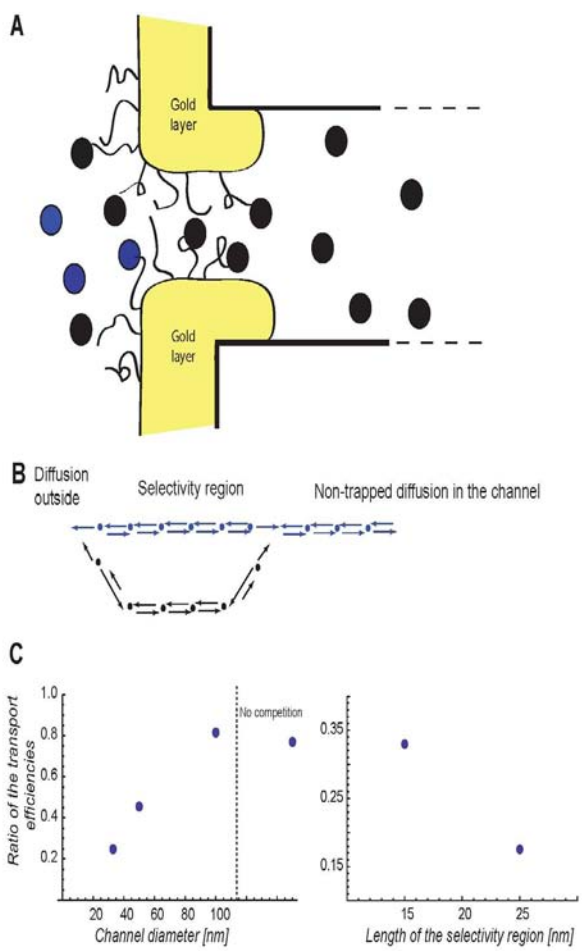


*Figure 3. Comparison with the experimental results in the multi-species case. Panel A: schematic illustration of the experimental setup of [1]. The filamentous proteins (FG nups) naturally lining the NPC are grafted to the gold layer at the channel opening, thus creating a trapping region, where the specific (NTF2-GST) and non-specific (BSA) molecules compete for space. Approximate diameter of the channel is 33 nm or 50 nm or 100 nm in different experimenst, the radius of the molecules of both species is ~3 nm. The length of the trapping region is either ~15 or ~25 nm. Panel B: schematic mapping of the actual channel onto a theoretical model. Panel C: Brief summary of the experimental findings of [1]. This panel shows the ratio of the transport efficiency of the non-binding control protein (BSA) to the transport efficiency of the tranpsort factor NTF2 (that bind the FG nup filaments) for different widths and lengths of the trapping region (normalized by their flux through a non-fucntinoalized channel). In accord with the theoretical predictions, the presence of the specific transport factor inhibits the transport of the non-specific protein and the magnitude of this inhibition decreases with the channel width and increases with the length of the trapping region.*

## Future Work

In a nutshell, one may view the NPC as a tube of ~35 nm in diameter whose walls are composed of essentially fixed structural proteins. The tube is lined by unstructured unfolded polypeptide filaments that are grafted to the walls and protrude to the tube lumen. Small molecules (<6-7 nm) in size can diffuse freely through the NPC. Larger molecules have to be shuttled through by special transport proteins. The major challenge is to understand how the basic kinetic mechanisms of stochastic transport describe above interplay with other effects, related to the filament conformation and dynamics. Accumulating experimental evidence shows that the conformation of the filament layer and its dynamic transitions during the particle passage play an important role in the transport mechanism.

### Conformation of the filaments

The current thrust of the research is to develop coarse-grained physical models of the filament conformation of the NPC (the current molecular dynamics simulations are still years away from being able to model the NPC in full atomistic details). The approach involves methods polymer physics and Brownian dynamics simulations that model the FG nups on a coarse-grained level as unstructured polymers with functional residues that can cross-link different chain and bind the transport factors. Parts of the work are performed by a GRA, Mr. Michael Opferman, who is working towards his Ph. D. at Pittsburgh University.

### Single molecule level

Eventually, transport through the NPC has to be understood on a single molecule level. Novel fluorescence microscopy techniques allow following movement of single particle inside the channel and show that it is highly stochastic. These experiments contain a wealth of information about the transport mechanism. We are working on extending

the existing techniques to include crowding in order to understand single molecule experiments [3].

## Conclusion

We expect to understand the biophysics of a selectivity of nuclear-cytoplasmic exchange through the nuclear pore and, as a result, some important aspects of the dynamics of a viral entry into a nucleus of a eukaryotic cell. It is expected that, in the future, this understanding may lead the way for a design of potent anti-viral vaccines and therapies.

## Publications

Jovanovic-Talisman, T., J. Tetenbaum-Novatt, A. S. McKenney, A. Zilman, R. Peters, M. P. Rout, and B. T. Chait. Artificial nanopores that mimic the transport selectivity of the nuclear pore complex. 2009. *Nature.* : 457.

Zilman, A.. Effects of multiple occupancy and inter-particle interactions on selective transport through narrow channels: theory versus experiment . 2009. *Biophysical Journal.* **96**: 1235.

Zilman, A., J. Pearson, and G. Bel. Effects of jamming on non-equilibrium transport times through nano-channels . 2009. *Physical Review Letters.* **103**: 128103.

Zilman, A., S. Di Talia, T. Jovanovic-Talisman, B. T. Chait, and M. P. Rout. Enhancement of transport selectivity through narrow channels by non-specific competition: a novel kinetic mechanism . To appear in *PLoS Computational Biology.*

# Photodegradation of Leaf Litter in Water-Limited Ecosystems

*Thomas A. Rahn*
20070688PRD3

## Abstract

A better understanding of influenza's potential for human-to-human transmission and severity of disease is crucial. Such knowledge will allow better preparation and deployment of countermeasures during epidemics or pandemics. Unfortunately, the knowledge to make these predictions based on robust experimental assays does not exist. We addressed this deficiency by innovatively combining experimental analyses of molecular markers with new computational tools. Our objective was to ascertain the differences in virulence among diverse types of influenza ("strains").

We developed a full program of study of influenza infection, comparing the host (human) response to infection with many different strains. We used both seasonal and high pathogenic avian influenza strains. We found that there are important differences in the response against these diverse strains. These responses should allow the prediction of differences in pathogenesis. We developed both experiments and theoretical analyses with the objective of extracting a small set of robust features that will allow the development of an assay for virulence prediction. This research was possible through the collaborative work of a multidisciplinary team of scientists. This novel approach also afforded important biological insights into influenza virulence and evolution.

This project implemented the capabilities for a new area of study at the Laboratory, in the field of viral respiratory infections. These new capabilities open the doors for opportunities of external funding. The investment made was also crucial in attracting new funding for the Laboratory and one of the project's postdoctoral researchers was converted to technical staff member. LANL now has a team of interdisciplinary scientists committed to influenza research.

## Background and Research Objectives

As the recent outbreak of novel H1N1 influenza has shown, we are not well prepared to quickly identify and characterize new influenza viruses that enter the population. In addition, there are still ongoing cases of avian (H5N1) influenza with high mortality. Thus, we need to understand influenza's potential for human-to-human transmission and severity of disease [1]. Unfortunately, the knowledge to make these predictions based on robust experimental assays does not exist. We address this gap by innovatively combining experimental analyses of molecular markers with new computational tools ("the functional profile"). Our objective is to ascertain the basis of differences in virulence among diverse influenza strains.

Many research groups are trying to address similar issues by focusing on individual virulence factors or animal experiments with limited numbers of strains [2, 3]. Our approach, studying multiple influenza strains, is innovative because we are combining theoretical and experimental tools to the problem of predicting, in a complex system, the outcome of infection. We have worked on an in vitro assay to identify predictive host responses. The potential to develop the knowledge and tools necessary to predict the pandemic potential of any influenza virus is a crucial scientific objective. Moreover, our results have significant implications for understanding genomic-virulence relationships [2].

## Scientific Approach and Accomplishments

Our objective was to find out what differentiates highly pathogenic strains (those that cause severe disease in humans) from less pathogenic ones (typically, strains responsible for yearly seasonal influenza epidemics). We used select avian H5N1 strains as prototypes of highly pathogenic strains, and select H3N2 and H1N1 seasonal strains as prototypes of less pathogenic strains. We also availed ourselves of a specific H5N1 avian strain with demonstrated low virulence in humans. We then

infected in vitro normal human lung epithelial (NHBE) cells or a lung epithelial cell line (A459 cells) with those strains. We measured the response of the cells to infection using two methodologies:

- Full genome microarrays, i.e., we measured qualitatively the response to infection of every gene in the human genome.
- Quantitative real-time polymerase chain reaction (qRT-PCR), i.e., we measured quantitatively the gene expression of a select number of genes during response to infection.

The objective was to analyze by computational tools the massive amounts of data generated to distinguish the responses to high and low pathogenic infection. The assay thus developed could be used to analyze and characterize future outbreaks of influenza with unknown strains. Thus, in the last two months of the project, we started characterizing the novel H1N1 flu strain, responsible for the current pandemic [4].

The experimental plan involved preparing >400 flu-treated airway cell samples for real-time and microarray analyses, at LANL. These samples encompass airway cell lines (A549) treated with four different low- and medium-virulence influenza strains at eight different time points, with two different multiplicities of infection and three controls. The response to infection has been analyzed by real-time PCR of 28 different genes. This produced >33,000 data points for analysis of cellular response to different strains. In addition, H5N1 infections were done by our collaborators at Lovelace Respiratory Research Institute, under bio-safety level 3 conditions. These experiments generated an additional 160 flu-treated airway cell samples. These samples encompass airway cell lines treated with three different high and low H5N1 strains at eight different time points, with two different multiplicities of infection and three controls. We then extracted and prepared the RNA for real-time PCR and microarray analyses, at LANL. This produced >13,000 data points for analysis of cellular response to H5N1. On the other hand, from the microarray measurements in NHBE cells, we obtained 54 sets of full human genome expression data. These experiments measure the level of "activation" of each of the >30,000 human genes at 0, 8h and 24h post-infection. Thus, in this project we generated massive amounts of data, detailing the human cellular response to flu infection.

Representation and analysis of such large datasets are a challenge. How to distill the data into important results that can be understood and further analyzed? Instead of approaching this as an arbitrary clustering problem, we sought to take advantage of the time course aspect of the data. We did this by applying techniques of molecular phylogeny (a.k.a. evolutionary trees) reconstruction under an appropriate model. Since the dimensionality of the space is large (30,000+) and noise and random changes are significant, trajectories in time can be described as a diffusion process. Dimensions (*i.e.*, genes) dominated by biological processes, rather than random drift or noise, are expected to reveal their relationships in the tree. Figure 1 shows a tree generated from the expression data for virus infected and mock infected cells. There are several features of Figure 1 that should be noted: most replicates (e.g., 1-3) of the same experiment are grouped; 24-hour experiments appear to diverge from the 8 hour experiments, particularly for seasonal strains (Sydney and Beijing samples); seasonal flu and the associated mock infections cluster separately from H5N1 strains.

*Figure 1. Photo of experimental setup showing solar simulator and quartz chamber.*

We can now focus the analysis on specific branches in the tree. Experiments in the neighborhood of branches of interest can be averaged. Subtracting those averages reveals the major changes between the branches. The genes are then sorted based on magnitude of change relative to noise. Complete lists of genes significantly up or down regulated as determined by these analyses are available on the internal wiki website set-up for this project. As a summary, we can indicate that this and other analyses suggest the following genes as putative markers for early and high pathogenic H5N1-specific infection: genes induced by interferons, which are molecules involved in the immune response (e.g., IFI, G1P, MX, OAS); chemokine genes (e.g., CXCL, CCL); inflammatory cytokines (e.g., IL1$\alpha/\beta$, IL6); and anti-viral serum amyloid proteins (e.g., SAA1-4). To better understand the biology of high pathogenic infection, we mapped the cellular pathways

involving genes identified by our analyses. For example, Figure 2 shows a comparison of the activation of the interferon pathway 24h after infection. Dissecting the steps in the cellular response where the differences are most pronounced will improve the reliability of our markers and also lead to better understanding of this response.

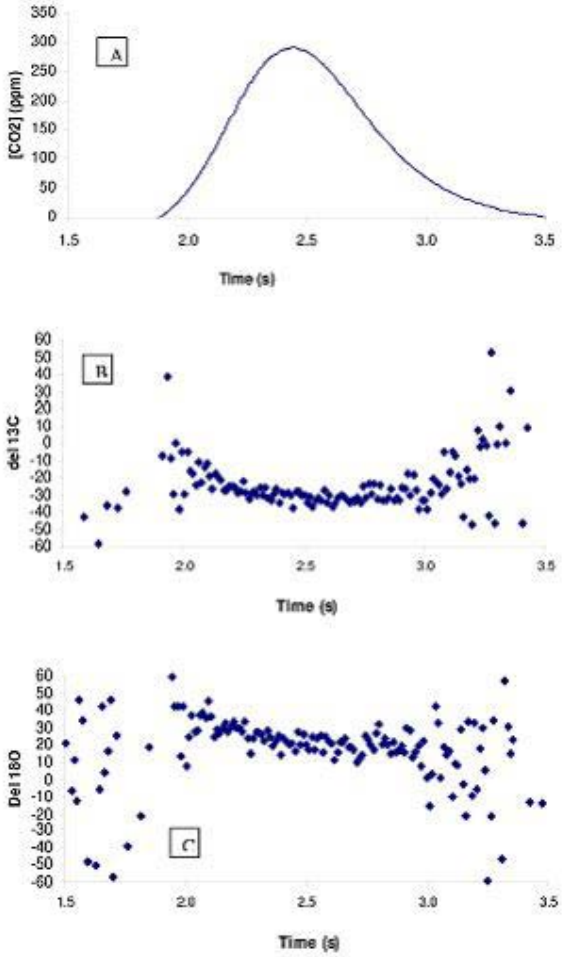


*Figure 2. Iin panel A, the peak in $CO_2$ at ~2.5 seconds is accompanied by an increase in the precision of both the 13C (panel B) and 18O (panel C) precision.*

We have also taken a complementary approach to identify and validate markers of virulence. Gene expression measured using RT-PCR was performed for different flu strains infecting a robust cell line (A549). The analysis goals were to (*i*) identify clusters in the data, i.e. similarly responding genes and similar viruses as seen by changes in gene expression, and (*ii*) seek gene expression characteristics that distinguish low and high virulence strains. Gene expression data were collected at multiple time points post-infection. An initial clustering analysis shows that the gene expression at all time points of the highly pathogenic strain clusters with the early time points of the low virulence strains (Figure 3). Does a signal exists in the gene expression data that discriminates low pathogenic from high pathogenic strains? We are employing a "decision tree" methodology to address this issue. Preliminary analyses found that decisions based on the genes FasR, IL-18 and IL-8 predicted virulence with some statistical support. FasR is involved in the apoptosis pathway, while IL-18 and IL-8 are involved in the inflammation pathway.

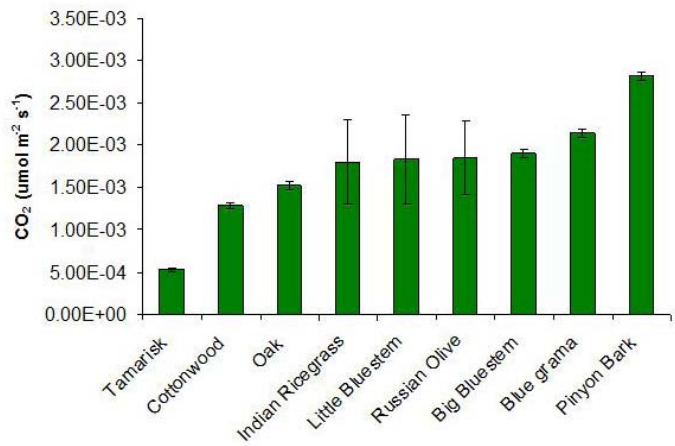


*Figure 3. The $CO_2$ production rates for the various species analyzed.*

We are interested in developing an assay that will predict virulence. Thus, we also need to understand the function of identified proteins and to look for proteins with similar function. We, therefore, developed a collection of software tools and database resources, called BIOGRAM (BIOlogical GRaph Metrics). BIOGRAM uses the mathematical structure underlying the Gene Ontology (GO) to measure protein/gene similarity based upon annotations assigned to nodes of the GO [5]. The method is "fuzzy" in nature, accounting for near misses and more distant relationships within the ontology. In addition to generating hierarchical comparison metrics for the annotation sets of pairs of proteins, BIOGRAM produces a detailed "explanation" of the similarities and differences between them. BIOGRAM has been designed as a tool to help guide the expert in an exploration of functional similarity.

Most of our work was focused on understanding the host (*i.e.*, human) response to infection. However, we also developed research to understand viral properties responsible for virulence. In this area, we developed several successful studies:

- We expanded earlier bioinformatics methods to study the evolution of highly pathogenic avian influenza A virus (HPAIV). Thus, we analyzed the evolution of HPAIV by the dual processes of re-assortment and point mutation [6]. Re-assortment allows the HPAIV to make long jumps in sequence space creating

discontinuous evolution. Point mutation operates on a finer scale, occurs more frequently, and leads to relatively smooth evolution. Surprisingly, we found that the early evolution of HPAIV was dominated by re-assortment, while more recent evolution has been largely in the absence of re-assortment. We also found that recent HPAIV have diverged into three different sub-lineages by point mutation and selection. Analyzing evolution on these two different scales allowed the identification of specific molecular signatures of the three sub-lineages. Some changes are extremely rare in the viral population as a whole, and yet are maintained within the respective HPAIV sub-lineages. By evaluating the prevalence of each signature change, we have identified 5 amino acid changes that we hypothesize are essential for the fitness of the virus. These will be tested experimentally by collaborators at the University of Wisconsin (since they have animal laboratories with the appropriate bio-safety level).

- We also studied the humanization of a well-characterized mouse antibody. This antibody recognizes domains of the viral M2 protein. M2 is a conserved protein crucial in the viral lifecycle. The antibody has shown protective activity in mouse models of influenza infection. Antibody humanization involved making the antibody sequence more human, an approach that has been used before. For therapeutics this is important as human antibodies elicit immune responses far weaker than mouse antibodies, making them far more effective. Our humanized antibody showed the same reactivity profile as the original antibody. And it was also able to reduce viral spread in an *in vitro* model [7]. The antibody recognized different forms of M2. Further work has been funded recently by the NIH.

- We studied the viral NS1 protein, which is crucial for viral replication and for preventing the host antiviral responses. Thus, NS1 is considered an important virulence factor for influenza. We developed models of this protein's structure and interactions with host molecules. Among others, as an example, we show in Figure 4 our predictions for the way NS1 may activate the human protein PI3K. This human protein is involved in regulating signaling cascades that control diverse cellular processes: cell survival, metabolism, proliferation, and inflammation/ immunity. Models of the interactions between NS1 and PI3K can lead to a better understanding of virulence (*i.e.*, how virus can defeat host immunity).

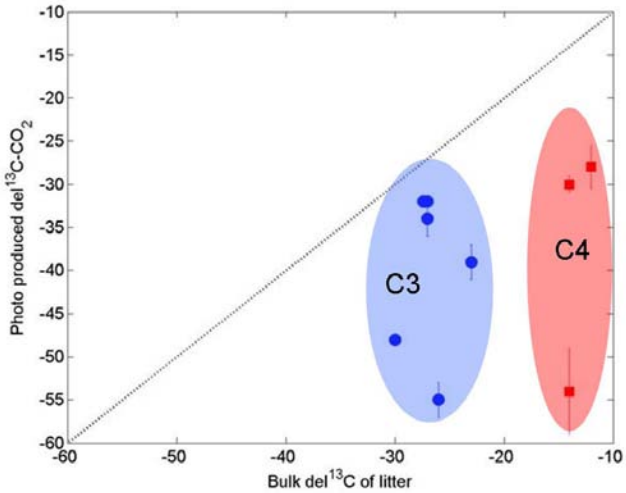


*Figure 4. Carbon 13 results of UV exposure as discussed in the text.*

- One of our objectives was to develop mathematical models of infection, which help in analyzing the results and in biological prediction. We worked on models [8] describing both the *in vitro* and *in vivo* (with mouse model data from our collaborators at St. Jude's Children's Hospital) progression of infection (Figure 5). These models allowed us to estimate critical parameters of infection, such as viral clearance and infected cell loss rates. We also used these models to analyze *in vitro* drug treatment data. In the future, they should help evaluate the effect of different therapies.

The project already generated 15 (published or about to be submitted) papers with 4 more in preparation and lead to 9 external collaborations. Our work was instrumental in successful competition for >$3,900,000 in external funding from spin-off projects. Team members have also made presentations (>10) of the results at international meetings and at invited talk at multiple institutions (USA, Austria, Canada, Australia). Finally, to engage the community, the principal investigator has given several lectures for the public.

## Impact on National Missions

From a general perspective, this project supports the DOE mission in Threat Reduction and also the mission of Harnessing the Power of the Living World, by defining and predicting what makes (influenza) viruses pathogenic. In terms of actual near-term impact, with important strategic implications for the Laboratory, we created new experimental and theoretical capabilities in influenza research. At the start of this project, there were no scientists or laboratories at LANL capable of studying viral respiratory infections. We developed the necessary

institutional bio-safety board authorizations, experimental protocols, and technical skills to carry this influenza work. These new capabilities open novel opportunities of external funding from many sponsoring agencies in important national security missions. The investment made was also crucial in attracting new funding for the Laboratory. Importantly, one of the project's postdoctoral researchers was converted to technical staff member. LANL now has a team of interdisciplinary scientists committed to influenza research from multiple, complementary approaches.

# Modeling the Immune Response to Pathogens

*Alan S. Perelson*
20070781PRD4

## Abstract

During the immune response to intracellular pathogens, the cells of the immune system (lymphocytes) undergo dramatic changes in their population size. Quantitative understanding of the kinetics of lymphocyte proliferation and death in response to infection is crucial for elucidating factors determining the magnitude, duration and efficiency of the immune response. Recent advances in quantitative experimental techniques, in particular intracellular labeling and multi-channel flow cytometry, allow one to measure the population structure of proliferating and dying lymphocytes for several generations with high precision. These new experimental techniques require novel quantitative methods of analysis. In collaboration with experimental colleagues, we have developed new mathematical tools and quantitative experimental protocols in order to quantitatively assess the kinetics of lymphocyte populations during the immune response to pathogens in experimental animals.

## Background and Research Objectives

The immune system protects higher organisms from infection by pathogenic microorganisms. For intracellular pathogens, such as viruses and certain types of bacteria, cytotoxic T lymphocytes (CTL), which kill infected cells, are the primary means of defense. The defense relies on T encountering 'antigen', e.g., a cell that appears to be infected because it is carrying non-self molecules, like the dendritic cell in Figure 1. Next, naive T cells become activated, proliferate at a rapid rate (undergo expansion) and differentiate into CTL which then kill infected cells. Normally, several days to weeks after initial infection the number of activated T cells reaches a maximum, then undergoes a reduction (called a contraction), in which most of the T cells rapidly die. The T cells that survive become `memory' cells that rapidly respond to subsequent infections by the same pathogen, as illustrated in Figure 1 [1, 2].

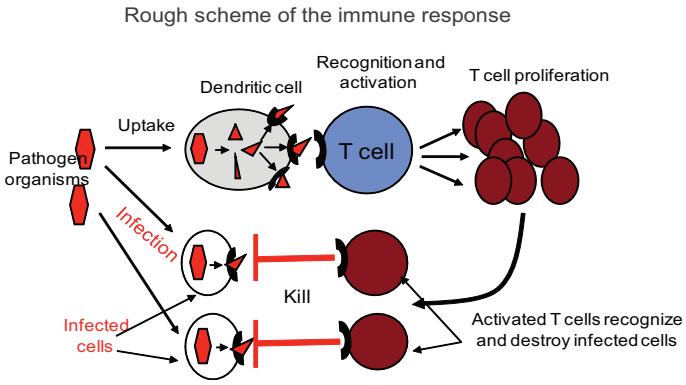


*Figure 1. Schematic illustration of the T cell immune response. Dendritic cells take up antigen, degrade it and present peptide fragments to T cells. The T cells respond by proliferating and differentiating into cytotoxic (killer) T lymphocytes (CTL) that can then kill infected cells.*

The kinetics of lymphocyte expansion and contraction affect the speed of antigen clearance and the clinical course of disease. At present, only some of the factors that regulate the differentiation, expansion and contraction of populations of activated T cells are known, and the picture of the dynamics of their proliferation and death is incomplete. In particular, recent experiments suggest that both the expansion and the contraction of antigen-specific T cells depend neither on the number of infected cells nor on their rate of clearance [1]. This has suggested that the T cell response is "programmed" and once started continues unabated irrespective of the antigen level. This makes some sense as a strategy: if the immune system constantly monitored the level of antigen and shut off expansion when it sensed that antigen was eliminated, it could make mistakes since it may be impossible to find a few infected cells in a trillion uninfected ones in some reasonable time [1, 3]. On the other hand, other experiments suggest that T cell response is not 'fully programmed' but is partially regulated by molecules (cytokines) that the T cells themselves and other immune system cells secrete during the immune

response [3, 4].

Understanding the mechanisms of regulation of the T cell response requires a quantitative approach both on the theoretical and experimental fronts. Validating or rejecting hypotheses necessitates development of quantitative mathematical models. Many prior models describe T cell dynamics in terms of ordinary differential equations [5, 6]. The predictions of such models do not agree well with existing experimental data in many circumstances [7]. One reason for this discrepancy is that the immune response is highly variable on the cellular level. In particular, the length of time a cell needs to divide as well as to die, is stochastic and change from one cell to another, from one division to the next, and with the time elapsed from the moment of infection [8]. More recent works put more realistic details into models. However, so far, the application to experimental data has been only involved *in vitro* (that is in isolated cell populations outside the animal) data and the mathematical approach has not been systematic [5-13].

Our goals were:

- Systematically develop a new generation of models of programmed and partially programmed responses that take into account the cell-to-cell and temporal variability of the immune response. Systematize and order existing empirical models within one rigorous framework.
- To develop quantitative experimental assays to measure *in vivo* various characteristics of the kinetics of the T cell populations. These include the division and death times as well as their dependence on the factors involved in regulation of lymphocyte kinetics, e.g. the precursor cell frequency, the availability of antigen, the rate of antigen presentation, and its affinity for the T cell receptor.
- Leverage the results of goals 1 and 2 in order to validate or reject hypotheses regarding the mechanisms of the regulation of the T cell response by comparing the model predictions with data, and determine to what extent immune responses are programmed and to what extent the program can be manipulated.

## Scientific Approach and Accomplishments

**Goal 1**

In order to compare the estimates obtained using different models and make meaningful inference, it is important to understand the differences and similarities in the mathematical structures of different models. It is also important to understand how the estimates obtained using different models are sensitive to the choice of model characteristics, such as the shape of the inter-division time distribution. All current models are similar in the sense that they describe the potentially complicated underlying biological processes of cellular proliferation and death in terms of effective birth and death parameters. However, at the first glance, such models are substantially different in some aspects. While many types of models have been used to describe lymphocyte proliferation and death and to estimate the birth and death rates, it still remains unclear to what extent the models are inter-changeable. Also, it is unclear to what extent the estimates of parameters depend on the choice of a specific model and on the choice of the inter-division and death distributions.

We have developed a general model based on the theory of age- and generation-structured branching processes. We have shown that other formulations are mathematically identical to it. A unique feature of our model is that in many cases it allows one to obtain an analytical description of the population behavior. An advantage of such an analytical description is that it greatly reduces the computational cost of estimating the parameters from the experimental data. Currently used approaches rely on the use of either simple models with analytical solutions (e.g., ODE models) or numerical solutions or simulations of more complex models. By contrast, we obtain analytical solutions for the number of cells that have undergone a given number of divisions for different distributions of inter-division times, such as the gamma distribution. Once the analytical solution has been obtained, there is no need of further numerical solutions or simulations in order to analyze each particular set of experimental data. This results in large savings of computational time, and higher precision of the estimates. The brief description of the model development is illustrated in Figure 2. Based on the general theory, we have developed an agent-based simulation describing the proliferation and death of lymphocyte populations. The simulation can be used in the regime where the analytical theory cannot be extended and also serves as a tool in planning experiments.

Further, we systematically explored the computational feasibility and numerical accuracy of our approach for estimation of model parameters and compared the estimates obtained using different models. When dealing with experimental data, three important questions arise. First, what distribution of inter-division times to choose? Second, how do estimates of the parameters of the cell division and death depend on the chosen distribution of inter-division times? Third, to what extent different models can be distinguished from the fit to the experimental data?

To test the feasibility of our approach, we first examined these questions in well controlled conditions, using simulated data generated by our agent based simulation. We then used our model to estimate the known parameters. As a further validation step, after calibration of the parameter estimation tools on simulated data, we applied the model to existing *in vitro* data that has been previously analyzed using other models.

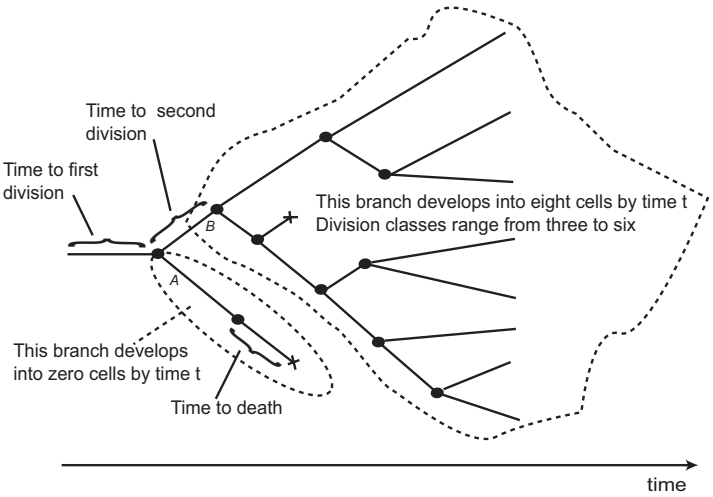


*Figure 2. Schematic illustration of the dynamics of a population of proliferating and dying cells, represented as a branching process. Each node represents a division, and each branch represents a cell lifetime - see text for details.*

The major conclusion was that the analytical solutions we developed during this project fit artificial and experimental data with reasonable quality providing a parameter estimation tool complementary to existing ones.

**Goal 2**

The main rationale for developing the methods described above was to estimate the kinetic parameters of lymphocyte dynamics under real conditions, for real infections in live animals. Ultimately, the usefulness of the approach can only be effectively tested in animal experiments.

In collaboration with the group of Dr. Eric Pamer at the Sloan-Kettering Cancer Center, NY we performed pilot experiments to test the feasibility of our approach. Recent advances in experimental techniques allowed us to follow the dynamics of lymphocyte populations during an immune response with much higher precision than before [1-3, 14]. A commonly used tool is cell labeling with carboxyfluorescein succinimidyl ester (CFSE). CSFE is an intracellular fluorescent dye that dilutes approximately two-fold each time a cell divides. By measuring the CSFE content of cells one can quantitatively follow the proliferation and death of large numbers of T cells over 6—8 divisions [6, 15].

In collaboration with Dr. Alena Gallegos in Pamer's group, we performed the following experiments. We obtained naïve T cells from a donor transgenic mouse whose T cells are all specific to one particular foreign peptide called ESAT. The extracted T cells were then labeled with CFSE and transferred into several different host mice. The host mouse was then infected with the intracellular bacterium *Listeria monocytogenes.* These bacteria were engineered to express the foreign peptide, ESAT, which the transferred T cells recognize. At successive times after the infection, the mice were sacrificed. T cells were extracted from the mice and their CSFE content measured. From this we could deduce the number of divisions each cell had undergone. The experimental procedure is illustrated in Figure 3 and Figure 4.

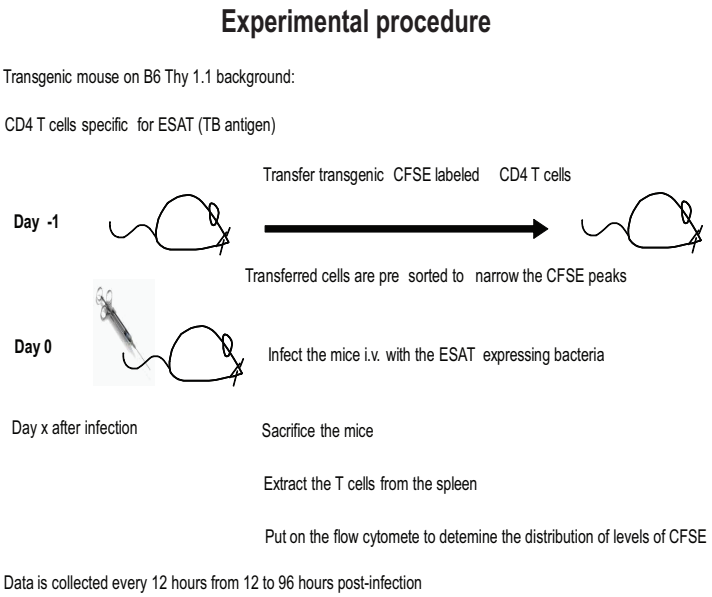


*Figure 3. Experimental design.*

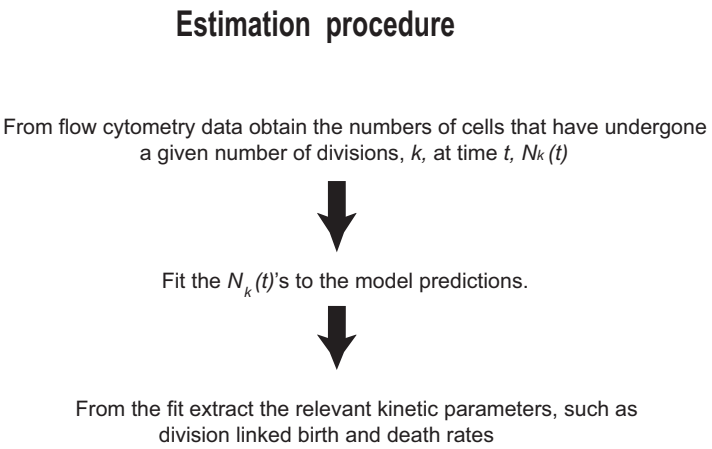


*Figure 4. Diagram of the algorithm used in the estimation of parameters from the experimental data.*

Interpreting the results from CFSE labeling experiments poses a number of conceptual and methodological challenges, which were addressed in this project. To interpret the data one needs models and computational tools for extracting the parameters that characterize the rates of cell activation, proliferation and death. One particular problem with the *in vivo* data is that it is noisy compared to *in vitro* data. Thus it is crucial to have a model that incorporates variability of inter-division and death times. It is also important to incorporate the effects of variation and noise.

Using the agent based simulations we determined that the main factor in generating the high noise levels in the *in vivo* CFSE data was the initial wide distribution in the amount of CFSE within the transferred cells. We were able to correct for this factor by sorting the cells based on the amount of CFSE they contained and only transferring cells that had a similar amount of CSFE. Finally, we used the methods developed on the artificial datasets to fit the measured number of cells that had undergone a given number of divisions by a given time after infection. We thus obtained estimates of the birth and death times of the proliferating T cells. To the best of our knowledge, this is the first time that such quantitative analysis of CFSE experiments *in vivo* has been performed. The results are summarized in Figure 5.

Experimental results

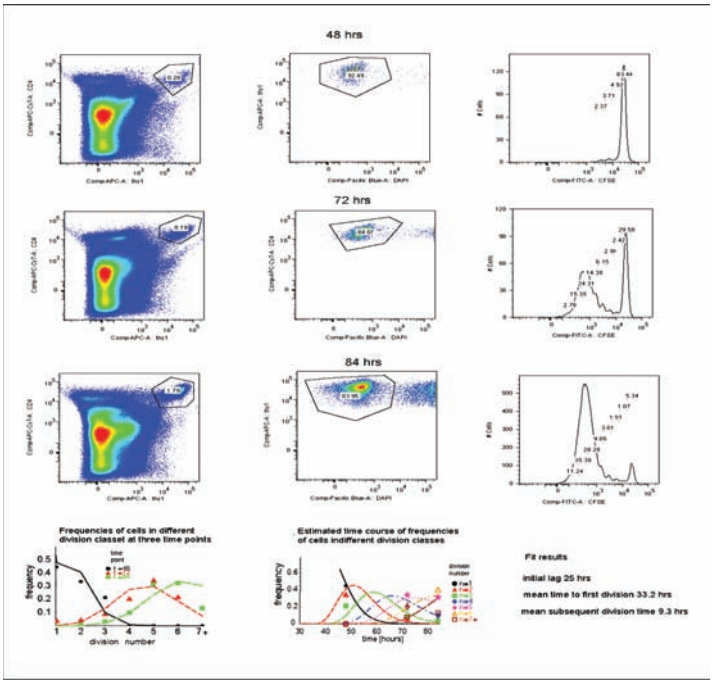


*Figure 5. Summary of the experimental results. Each row of figures shows the flow cytometry data for different times post-infection – 48, 72 and 84 hours. The last column in each row is the resulting distribution of CFSE levels in the activated and proliferating transferred T cells. The last row shows the fit of the data to the mathematical model and the estimated parameter values.*

**Goal 3**

For this in vivo data set we found that the T cell response was consistent with a model of a fully programmed response. We found that after T cells were stimulated it took a surprisingly long time until they began dividing. On average, the time to the first division was 33.2 hours. After this first division, cells divided much more rapidly with an average division time of 9.3 hours. If these results hold true for other pathogens they have important health related implications. First, the results suggest that the T cell response is initially very slow. This gives a pathogen time to grow and establish itself before the immune response gets going. Thus, antibiotics and antiviral drugs might be very important in helping to slow pathogen growth early after infection. This is consistent with the current recommendation of taking antivirals, such as Tamiflu, for influenza infection within the first 48 hours of infection. Second, it suggests that vaccines based solely on generating T cell responses might not be able to protect a person from initial infection. So far this has been true of the various experimental T cell vaccines developed and tested to fight HIV/AIDS. The T cell response that develops after vaccination has been characterized as “too little too late”, and in animal models as well as human trials, such as Merck STEP trial, protection from infection has not been established. Third, the results suggest that once the T cell response does get going, T cells can expand rapidly and potentially provide protection from ongoing disease. Our experiments and theory do not address this later stage of the immune response. Follow-up work will be needed to explore this important aspect.

In summary, we have developed a handy, robust and useful computational tool for analysis of experimental data on lymphocyte dynamics. We are working on a user-friendly software implementation of the tool that will be distributed to experimental colleagues in a pilot release. The results of this project are reported in [16].

## Impact on the Laboratory/DOE

This project supports the DOE mission in threat reduction by enhancing our understanding of the body’s ability to fight natural and engineered pathogens. It has also resulted in the establishment of important collaborations with experimental colleagues. It is important to support other missions of the Laboratory as well (e.g., Homeland Security), but not to the exclusion of the DOE/NNSA missions.

## References


1. Murphy, K. M., P. Travers, and M. Walport. Janeway's Immunobiology, 7th ed.. 2007.

2. Wong, P., and E. Pamer. CD8 T cell responses to infectious pathogens. 2002. *Annual Reviews of Immunology.* **21**: 29.

3. Ahmed, R., and R. Antia. Quantifying cell turnover using CSFE data. 2005. *Journal of Immunological Methods.* **298**: 183.

4. Badovinac, V., J. S. Haring, and J. Harty. Initial T cell receptor transgenic cell precursor frequency dictates critical aspects of the CD8(+) T cell response to infection. 2007. *Immunity .* **26**: 827.

5. DeBoer, R. J., D. Homann, and A. S. Perelson. Different dynamics of CD4+ and CD8+ T cell responses during and after acute lymphocytic choriomeningitis virus infection. 2003. *Journal of Immunology.* **171**: 3928.

6. Gett, A., and P. Hodgkin. Cell division regulates the T cell cytokine repertoire, revealing a mechanism underlying immune class regulation. 1998. *Proceedings of the National Academy of Sciences USA.* **95**: 9488.

7. DeBoer, R. J., and A. S. Perelson. Estimating division and death rates from CFSE data. 2005. *Journal of Computational and Applied Mathematics.* **184**: 140.

8. Callard, R., and P. Hodgkin. Modeling T- and B-cell growth and differentiation. 2007. *Immunological Reviews.* **216**: 119.

9. DeBoer, R. J., V. V. Ganusov, D. Milutinovic, P. D. Hodgkin, and A. S. Perelson. Estimating lymphocyte division and death rates from CFSE data. 2006. *Bulletin of Mathematical Biology.* **68**: 1011.

10. Deenick, E., A. Gett, and P. D. Hodgkin. Stochastic model of T cell proliferation: a calculus revealing IL-2 regulation of precursor frequencies, cell cycle time, and survival. 2003. *Journal of Immunology.* **170**: 4963.

11. Gett, A. V., and P. D. Hodgkin. A cellular calculus for signal integration by T cells. 2000. *Nature Immunology.* **1**: 239.

12. Hawkins, E., M. L. Turner, M. R. Dowling, C. van Gend, and P. D. Hodgkin. A model of immune regulation as a consequence of randomized lymphocyte division and death times. 2007. *Proceedings of the National Academy of Sciences USA.* **104**: 5032.

13. Lee, H. Y., and A. S. Perelson. Modeling T cell proliferation and death in vitro based on labeling data: generalizations of the Smith-Martin cell cycle model. 2008. *Bulletin of Mathematical Biology.* **70**: 21.

14. Blattman, J. N., R. Antia, D. J. Sourdive, X. Wang, K. Murali-Krishna, J. D. Altman, and R. Ahmed. Estimating the precursor frequency of naive antigen-specific CD8 T cells. 202. *Journal of Experimental Medicine.* **195**: 657.

15. Lyons, A.. Analysing cell division in vivo and in vitro using flow cytometric measurement of CFSE dye dilution. 2000. *Journal of Immunological Methods.* **243**: 147.

16. Zilman, A., V. V. Ganusov, and A. S. Perelson. Stochastic models of lymphocyte proliferation and death. *Public Library of Science One.*


## Publications


Jovanovic-Talisman, T., J. Tetenbaum-Novatt, A. S. McKenney, A. Zilman, R. Peters, M. P. Rout, and B. T. Chait. Artificial nanopores that mimic the transport selectivity of the nuclear pore complex. 2009. *Nature.* **457**: 1023.

Zilman, A.. Effects of multiple occupany and inter-particle interactions on selective transport through narrow channels: theory versus experiment. 2009. *Biophysical Journal.* **96**: 1235.

Zilman, A., J. Pearson, and G. Bel. Effects of jamming on nonequilibrium transport times in nanochannels. 2009. *Physicval Review Letters.* **103** (12): 128103.

Zilman, A., S. Di Talia, B. T. Chait, M. P. Rout, and M. O. Magnasco. Efficiency, selectivity and robustness of nucleo-cytoplasmic transport.. 2007. *PLoS Computational Biology.* : e125.

Zilman, A., S. Di Talia, T. Jovanovic-Talisman, B. T. Chait, M. P. Rout, and M. Magnasco. Enhancement of transport selectivity through narrow channels by non-specific competition: a novel kinetic mechanism . To appear in *Public Library of Science Computational Biology.*

Zilman, A., V. V. Ganusov, and A. S. Perelson. Stochastic models of lymphocyte proliferation and death. *Public Library of Science One.*

# 3-Dimensional Tracking of Single Quantum Dots: The Case for 2-Photon Excitation

*James H. Werner*
20080798PRD4

## Abstract

We are building instrumentation to follow individual molecular motion in three dimensions inside living cells. Cellular, tissue, and neural disease are often caused by a miss-communication in cellular signaling networks or protein interaction networks. Our efforts to directly follow individual signaling molecules are geared, ultimately, to better understanding the molecular basis of certain diseases, such as cancer and anaphylactic shock. To better understand these diseases, we have built and have refined methods for following individual molecules moving in 3 dimensions at biologically relevant transport rates.

## Background and Research Objectives

It has become possible to follow the motion of individual molecules in live cells. Such studies have revealed details about cellular membrane structure and motor protein kinetics that would otherwise be hidden in ensemble-averaged measurements. While powerful, these single molecule tracking methods and techniques have been confined and constrained to examining two dimensional dynamics. Our laboratory has been developing methods to observe individual molecular transport over an entire 3 dimensional cell. Our primary research objective in the current proposal was to demonstrate 3D molecular tracking was possible with a potentially more benign means of laser excitation: two photon excitation, where two photons of near infrared light are used for molecular excitation rather than a single visible laser beam.

## Scientific Approach and Accomplishments

Our approach consisted of equipping our 3D tracking microscope with the right components for two-photon microscopy (e.g. lasers, filters, detectors) and testing the tracking ability under two-photon excitation conditions. We also tested various fluorescent indicators and probes that might be useful for two-photon molecular tracking, including semiconductor nanocrystals (quantum dots), green fluorescent proteins, and organic dye molecules. Our accomplishments were a demonstration of 3D tracking of individual quantum dot labeled signaling molecules in live cells, a demonstration of 2-photon 3D tracking of quantum dots, and a demonstration of 3D tracking of individual GFPs. Our work on cellular tracking was presented at a Photonics Conference (Photonics West, in San Jose) and published in the Proceedings of the SPIE. The citation information for this manuscript is : *Wells, N.P., Lessard G.A., Phipps M.E., Goodwin P.M., Lidke D.S., Wilson B.S., Werner J.H., "Going beyond 2D: Following membrane diffusion and topography in the IgE–Fc[epsilon]RI system using 3-dimensional tracking microscopy," Proceedings of the SPIE v.7185* ***2009*** *7185-1 to 7185-13.* This paper was awarded a 1/3 share of the best paper award for the single molecule session of Photonics West.

## Impact on National Missions

This work has substantial impact on missions important for our laboratory and our nation, with a particular emphasis on biosecurity. This work advances the state of the art in molecular imaging and could be used to better understand emerging diseases of a natural or man-made origin. This work keeps our laboratory at the forefront of ultra-sensitive bioanalytical methods and single molecule detection.

## References

1. Wells, N., G. Lessard, M. Phipps, P. Goodwin, D. Lidke, B. Wilson, and J. Werner. Going beyond 2D: Following membrane diffusion and topography in the IgE–Fc[epsilon]RI system using 3-dimensional tracking microscopy . 2009. *Proceedings of the SPIE (Society of Photonic Instrument Engineers).* **7185**: 7185.

## Publications

Wells, N., G. Lessard, M. Phipps, P. Goodwin, D. Lidke, B. Wilson, and J. Werner. Going beyond 2D: Following

membrane diffusion and topography in the IgE–Fc[epsilon] RI system using 3-dimensional tracking microscopy. . 2009. In *Photonics West 2009* . (San Jose, CA, 24-29 Jan. 2009). Vol. 7185, p. 7185. Bellingham, WA: SPIE .

# Information Science & Technology

*LABORATORY DIRECTED RESEARCH AND DEVELOPMENT*

# Automated Change Detection in Remote Sensing Imagery

*James P. Theiler*
20080040DR

## Introduction

The aim of this project is to identify meaningful changes in multiple images. The images are taken of the same scene but at different times, possibly with different instruments, and inevitably under different conditions. As well as recording actual changes on the ground, the imagery will include uninteresting differences caused, for instance, by variations in illumination, calibration, or atmospheric distortion. The central effort in this project is to develop tools for distinguishing these pervasive but incidental differences from the more interesting actual changes in the scene.

The programmatic motivation for anomalous change detection (ACD) is the overwhelming quantity of image data, and the growing variety of image modalities, available for both remote sensing and intelligence applications. These data potentially contain important nuggets of useful information, but those nuggets are hidden among the terabytes of background clutter. Our approach is to combine recent advances in machine learning, particularly in anomaly detection [1], with ongoing efforts in remote sensing image analysis. We had previously proposed a machine-learning framework for anomalous change detection [2], and applied it to both Gaussian and non-Gaussian distributions; we also showed how existing algorithms could be generalized within this framework [3].

## Benefit to National Security Missions

This project will support the DOE missions in nonproliferation and national security by developing the technology to enhance an analyst's ability to identify new and/or altered sites from broad area imagery. Furthermore, our techniques rely on innovative statistical estimation tools, and this supports DOE's broader scientific mission.

## Progress

Progress on this project has been documented in articles that are already published [4-23], are in press [24-30], have been submitted [31-33], or are in preparation [34-37]. A broad overview of that work follows:

### Validation of algorithms

The ultimate test of any detection algorithm is how well it detects what is really interesting in real imagery. Anomaly detection, however, is problematic on two counts: one, what is "really interesting" is in the eye of the beholder; and two, anomalies are by definition rare. This makes it difficult to find enough of them to do statistical comparisons of algorithms, and that makes it is easy to be misdirected by anecdotal results. With a keen appreciation for the caveats and limitations of simulated data, we have been developing a simulation scheme that addresses some of these problems with anomalous change. This scheme draws a distinction between pervasive differences, which occur throughout the images, and anomalous changes which occur in only a few pixels. It is these anomalous changes that we want, in our operational scenarios, to draw to the attention of the analyst.

We initially developed a simulation framework for evaluating purely spectral ACD algorithms [4], and then extended this to both subpixel [7] and spatially extended [19] anomalous changes. We remark that none of these are "pure" *ab initio* simulations, but always start with real imagery so that the basic statistical properties of real imagery are incorporated into the simulations. Both as a starting point for our simulations, and as an ultimate sanity check in their own right, this project maintains a database of real imagery that (in some cases) includes markup identifying the "real" anomalies. This includes in-house hyperspectral longwave infrared (LWIR) data from the ORCAS sensor [6], some ground-based LWIR data from a previous project, a collection of AVIRIS datasets [38], and a larger archive of Landsat data, with triples of images, taken many years apart. We also have some in-house RGB data from an ordinary digital camera, and we obtained some hyperspectral data from Eismann and Meola [39], that include images taken hours, days, and months apart, and which further includes real anomalous changes in the form of folded-up tarps that were placed in the scene from time to time.

### Purely spectral ACD algorithms

The framework initially developed in Ref. [2] essentially treated the image as a distribution of independent pixels, each one with a specific color or (for hyperspectral images) spectrum. The framework enables one to "plug in" different distributions for the data. For Gaussian distributions, the resulting algorithms are quadratic and depend on the covariance matrix of the data. Existing algorithms, such as the "chronochrome" [40], "multivariate alteration detection" [41], and "covariance equalization" [42] are also quadratic, but are based on finding linear fits of the two images to each other, and then identifying as anomalous changes those pixels with the largest after-fit residuals. A survey of these algorithms is provided in Ref. [4], but we have recently started to investigate a detector based on a "total least squares" fit of the two images [34]. Since all of these algorithms require accurate estimates of covariance matrices, we are also investigating better ways to estimate covariances from limited data [29].

The distribution-based framework invites the use of non-Gaussian distributions, and we have had success using elliptically contoured (EC) distributions [12,24]. Like Gaussians, these distributions are characterized by covariance matrices (and have elliptical contours), but unlike Gaussians and more like real data, they can have much fatter tails. It is relatively easy to use EC distributions for target detection [9], but we discovered that the anomalous change detection problem imposed further constraints and required the development of a consistent family of EC distributions. As a kind of spin-off, the properties of these consistent families were recognized as important for understanding a larger class of kernels in support vector machines [36].

In fact, because our framework effectively recasts change detection as a binary classification problem, we can employ support vector machines more directly [22,28,31,32], to produce new anomalous change detectors. To do this effectively, in the ACD setting, we have made some improvements to the basic support vector machine technology. This was driven by the need to work in a regime of very low false alarm rates and relatively large number of data samples.

Although the notion of change detection is most easily understood when there are two images, the extension to multi-image change detection has also been explored [17].

### Spatio-spectral ACD algorithms

Although we continue to develop algorithms that look for *pixels* that have changed in interesting ways, we ultimately want to find what *objects* have appeared or disappeared or changed in a scene. Since segmentation of imagery into actual discrete objects is a difficult and open-ended task, we have taken two approaches. One is to stick with the pixel-based representation of the imagery, but to use spatial operators (smooth, dilate, erode, etc.) as part of the change detection scheme [19]. The other is to explicitly partition the image into discrete patches and either treat these patches as if they were pixels in the change detection algorithms [20], or else use them as a starting point for hierarchical image segmentation [13-15,33], which is potentially valuable when the scale of the anomaly is not known beforehand. The efficiency of this segmentation depends on the quality of detected edges. To improve edge detection, we have investigated schemes for grouping oriented segments in highly cluttered images, and developed an iterative, multiscale tensor voting approach [16,18].

While purely spectral approaches are well suited for hyperspectral imagery, spatio-spectral methodology is an important part of our research into the utility of change detection in persistent surveillance with panchromatic video imagery [11,21].

### Co-registration

Image misregistration is probably the greatest confound to accurate change detection. Corresponding pixels in a pair of images must correspond to the same point on the ground. To enforce this in an automated way requires a fast detector of corresponding interest points [26], and calibrating camera distortion [27] is an important part of that. More accurate co-registration will produce better change detection, but there will always be some residual misregistration. Thus, it is important to characterize (and optimize) the robustness of our algorithms to this inevitable misregistration [10]. Eventually, we seek a tighter "loop" between the co-registration and the change detection steps. To this end, we have recently been investigating a more pro-active way to make our algorithms robust to residual errors in registration by making local ad hoc registration adjustments and using those to improve the change detection [30,37].

## Future Work

Refs. [34-37] represent ongoing work that has not been completed, and one of the medium-term goals of this project is to complete that work. In general, however, the final year of this project will emphasize adapting the theory to applications, communicating the concept to program managers, and pursuing funding for further research. Because change detection is of broad interest in the remote sensing and intelligence communities, we have positioned this project so that follow-on research may be funded from outside the Laboratory.

## Conclusion

This project emphasizes the development of practical tools to implement innovative algorithms for detecting small but real changes in a scene, based on differences observed in remote sensing images taken of the scene. These algorithms are designed to be insensitive to pervasive differences -- such as scene illumination or calibration

(brightness, focus, contrast) -- that do not correspond to actual or interesting changes in the scene. What automated change detection can ultimately provide is a way to cull through a massive quantity of streaming or archival imagery, and chip out a small number of the most anomalous changes. A professional analyst can then decide which changes provide actionable information and/or merit further investigation.

## References


1. Steinwart, I., D. Hush, and C. Scovel. A classification framework for anomaly detection. 2005. *J. Machine Learning Research.* **6**: 211.

2. Theiler, J., and S. Perkins. Proposed framework for anomalous change detection. 2006. (Pittsburgh, PA, 29 June 2006). p. 7. Pittsburgh, PA: ICML.

3. Theiler, J., and S. Perkins. Resampling approach for anomalous change detection. 2007. *Proc. SPIE.* **6565**: 65651U.

4. Theiler, J.. Quantitative comparison of quadratic covariance-based anomalous change detectors. 2008. *Applied Optics.* **47**: F12.

5. Foy, B. R., J. Theiler, and A. M. Fraser. Hyperspectral target detection using machine learning in a reduced dimensional space. 2008. *Proc. MSS (Military Sensing Symposia) Passive Sensors Conference.* : 1.

6. Love, S. P., T. C. Hale, L. J. Jolin, J. E. Barefield, W. H. Atkins, and J. J. Tiee. The ORCAS long-wave infrared hyperspectral sensor. (Orlando, FL, Feb 2008).

7. Theiler, J.. Subpixel anomalous change detection in remote sensing imagery. 2008. (Santa Fe, 24-26 March 2008). p. 165. New York: IEEE.

8. Eads, D., and E. Rosten. Experiences using SciPy for computer vision research. 2009. *Proc. 7th Python in Science Conference.* : 22.

9. Theiler, J., and B. R. Foy. EC-GLRT: Detecting weak plumes in non-Gaussian hyperspectral clutter using an elliptically-contoured generalized likelihood ratio test. 2009. (Boston, MA, 6-11 July 2008). p. I. Boston: IEEE.

10. Theiler, J.. Sensitivity of anomalous change-detection to small misregistration errors . 2008. *Proc. SPIE.* **6966**: 69660X.

11. Porter, R., A. Fraser, R. Loveland, and E. Rosten. A recurrent velocity filter for detecting large numbers of moving objects. 2008. *Proc. SPIE.* **6969**: 69690C.

12. Theiler, J., and C. Scovel. Uncorrelated versus independent elliptically-correlated distributions for anomalous change detection in hyperspectral imagery. 2009. *Proc. SPIE.* **7246**: 7246OT.

13. Prasad, L., and S. Swaminarayan. Hierarchical image segmentation by polygon grouping. 2008.

14. Skurikhin, A. N., and P. L. Volegov. Object-oriented hierarchical image vectorization. (Calgary, Canada, 6-7 August 2008).

15. Skurikhin, A. N.. Proximity graphs based multi-scale image segmentation. (Las Vegas, NV, 1-3 December 2008).

16. Loss, L. A., G. Bebis, M. Nicolescu, and A. Skurikhin. Investigating how and when perceptual organization cues improve boundary detection in natural images. 2008.

17. Theiler, J., and S. Adler-Golden. Detection of ephemeral changes in sequences of images. 2009. *37th Applied Imagery Pattern Recognition Workshop (AIPR '08): Multiple Image Information Extraction.* : 1.

18. Loss, L., G. Bebis, M. Nicolescu, and A. N. Skurikhin. An iterative multi-scale tensor voting scheme for perceptual grouping of natural shapes in cluttered backgrounds. 2009. *Computer Vision and Image Understanding.* **113**: 126.

19. Theiler, J., N. R. Harvey, R. Porter, and B. Wohlberg. Simulation framework for spatio-spectral anomalous change detection. 2009. *Proc. SPIE.* **7334**: 73340P.

20. Prasad, L., and J. Theiler. A structural framework for anomalous change detection and characterization. 2009. *Proc. SPIE.* **7341**: 73410N.

21. Porter, R. B., N. R. Harvey, and J. Theiler. A change detection approach to moving object detection in low frame rate video. 2009. *Proc. SPIE.* **7341**: 73410S.

22. Steinwart, I., and A. Christmann. Sparsity of SVMs that use the epsilon-insensitive loss. 2009. *Neural Information Processing Systems.* **21**: 1569.

23. Foy, B., J. Theiler, and A. Fraser. Decision boundaries in two dimensions for target detection. 2009. *Optics Express.* **17**: 17391.

24. Theiler, J., C. Scovel, B. Wohlberg, and B. R. Foy. Elliptically contoured distributions for anomalous change detection in hyperspectral imagery. To appear in *IEEE Geoscience and Remote Sensing Imagery.*

25. Foy, B. R., J. Theiler, and C. R. Quick. Band selection for multispectral target detection using hyperspectral data. (Orlando, FL, Feb 2009).

26. Rosten, E., R. Porter, and T. Drummond. Faster and Better: a machine learning approach to corner detection. 2009. *IEEE Transactions on Pattern Analysis and Machine Intelligence (PAMI).* : (online).

27. Rosten, E., and R. Loveland. Camera distortion self-calibration using the plumb-line constraint and minimal Hough entropy. 2009. *Machine Vision and Applications.* : (online).

28. Steinwart, I.. Two oracle inequalities for regularized boosting classifiers. 2009. *Statistics and its Interface.* **2**: 217.

29. Cao, G., C. A. Bouman, and J. Theiler. Weak signal detection in hyperspectral imagery using sparse matrix transform (SMT) covariance estimation. (Grenoble, France, 26-28 Aug 2009).

30. Wohlberg, B., and J. Theiler. Improved change detection with local co-registration adjustments. (Grenoble, France, 26-28 Aug 2009).

31. Steinwart, I., D. Hush, and C. Scovel. Training SVMs without offset. *J. Machine Learning Research.*

32. Steinwart, I., and A. Christmann. Estimating conditional quantiles with the help of the pinball loss. *Bernoulli.*

33. Matsekh, A., A. Skurikhin, and E. Rosten. Numerical aspects of spectral image segmentation in Krylov subspaces. *Linear Algebra and Its Applications .*

34. Theiler, J., and A. M. Matsekh. Total least squares for anomalous change detection. 2009. *In preparation.*

35. Matsekh, A. M., and J. Theiler. Spectral properties of anomalous change detectors in block-diagonal form. 2009. *In preparation.*

36. Scovel, C., D. Hush, I. Steinwart, and J. Theiler. Radial kernels and their reproducing kernel Hilbert spaces. 2009. *In preparation.*

37. Wohlberg, B., and J. Theiler. Symmetrized local co-registration optimization for anomalous change detection. 2009. *In preparation.*

38. Airborne Visible/Infrared Imaging Spectrometer (AVIRIS). 2009. *Jet Propulsion Laboratory (JPL), National Aeronautics and Space Administration (NASA).*

39. Eismann, M. T., J. Meola, and R. C. Hardie. Hyperspectral change detection in the presence of diurnal and seasonal variations. 2008. *IEEE Transactions on Geoscience and Remote Sensing.* **46**: 237.

40. Schaum, A., and A. Stocker. Long-interval chronochrome target detection. 1998. *Proc. ISSSR (International Symposium on Spectral Sensing Research).* : 0.

41. Nielsen, A. A., K. Conradsen, and J. J. Simpson. Multivariate alteration detection (MAD) and MAF post-processing in multispectral bi-temporal image data: new approaches to change detection studies. 1998. *Remote Sensing of the Environment.* **64**: 1.

42. Schaum, A., and A. Stocker. Hyperspectral change detection and supervised matched filtering based on covariance equalization. 2004. *Proc. SPIE.* **5425**: 77.

## Publications

Cao, G., C. A. Bouman, and J. Theiler. Weak signal detection in hyperspectral imagery using sparse matrix transform (SMT) covariance estimation. To appear in *IEEE Workshop on Hyperspectral Image and Signal Processing: Evolution in Remote Sensing.* (Grenoble, France, 26-28 Aug 2009).

Eads, D., and E. Rosten. Experiences using SciPy for computer vision research. 2009. *Proc. 7th Python in Science Conference.* : 22.

Foy, B. R., J. Theiler, and A. M. Fraser. Hyperspectral target detection using machine learning in a reduced dimensional space. 2008. *Proc. MSS (Military Sensing Symposia) Passive Sensors Conference.* : 1.

Foy, B. R., J. Theiler, and C. R. Quick. Band selection for multispectral target detection using hyperspectral data. To appear in *Proc. MSS (Military Sensing Symposia) Conference on Battlefield Survivability and Discrimination.* (Orlando, FL, Feb 2009).

Foy, B., J. Theiler, and A. Fraser. Decision boundaries in two dimensions for target detection. 2009. *Optics Express.* **17**: 17391.

Loss, L. A., G. Bebis, M. Nicolescu, and A. Skurikhin. Investigating how and when perceptual organization cues improve boundary detection in natural images. 2008. In *2008 IEEE Computer Society Conference on Computer Vision and Pattern Recognition Workshops (CVPR Workshops) ; 23-28 June 2008 ; Anchorage, AK, USA.*

Loss, L., G. Bebis, M. Nicolescu, and A. N. Skurikhin. An

iterative multi-scale tensor voting scheme for perceptual grouping of natural shapes in cluttered backgrounds. 2009. *Computer Vision and Image Understanding.* **113**: 126.

Love, S. P., T. C. Hale, L. J. Jolin, J. E. Barefield, W. H. Atkins, and J. J. Tiee. The ORCAS long-wave infrared hyperspectral sensor. To appear in *Military Sensing Symposium (MSS).* (Orlando, FL, Feb 2008).

Matsekh, A. M., and J. Theiler. Spectral properties of anomalous change detectors in block-diagonal form. 2009. *In preparation.*

Matsekh, A., A. Skurikhin, and E. Rosten. Numerical aspects of spectral image segmentation in Krylov subspaces. *Linear Algebra and Its Applications .*

Porter, R. B., N. R. Harvey, and J. Theiler. A change detection approach to moving object detection in low frame rate video. 2009. *Proc. SPIE.* **7341**: 73410S.

Porter, R., A. Fraser, R. Loveland, and E. Rosten. A recurrent velocity filter for detecting large numbers of moving objects. 2008. *Proc. SPIE.* **6969**: 69690C.

Prasad, L., and J. Theiler. A structural framework for anomalous change detection and characterization. 2009. *Proc. SPIE.* **7341**: 73410N.

Prasad, L., and S. Swaminarayan. Hierarchical image segmentation by polygon grouping. 2008. In *2008 IEEE Computer Society Conference on Computer Vision and Pattern Recognition Workshops (CVPR Workshops) ; 23-28 June 2008 ; Anchorage, AK, USA.*

Rosten, E., R. Porter, and T. Drummond. Faster and Better: a machine learning approach to corner detection. 2009. *IEEE Transactions on Pattern Analysis and Machine Intelligence (PAMI).* : (online).

Rosten, E., and R. Loveland. Camera distortion self-calibration using the plumb-line constraint and minimal Hough entropy. 2009. *Machine Vision and Applications.* : (online).

Scovel, C., D. Hush, I. Steinwart, and J. Theiler. Radial kernels and their reproducing kernel Hilbert spaces. 2009. *In preparation.*

Skurikhin, A. N.. Proximity graphs based multi-scale image segmentation. Presented at *International Symposium on Visual Computing.* (Las Vegas, NV, 1-3 December 2008).

Skurikhin, A. N., and P. L. Volegov. Object-oriented hierarchical image vectorization. To appear in *International Conference on Geographic Object Based Image Analysis (GEOBIA).* (Calgary, Canada, 6-7 August 2008).

Steinwart, I.. Two oracle inequalities for regularized boosting classifiers. 2009. *Statistics and its Interface.* **2**: 217.

Steinwart, I., D. Hush, and C. Scovel. Training SVMs without offset. *J. Machine Learning Research.*

Steinwart, I., D. Hush, and C. Scovel. Optimal rates for regularized least squares regression. 2009. *Proc. 22nd Annual Conference on Learning Theory.* : 79.

Steinwart, I., and A. Christmann. Sparsity of SVMs that use the epsilon-insensitive loss. 2009. *Neural Information Processing Systems.* **21**: 1569.

Steinwart, I., and A. Christmann. Estimating conditional quantiles with the help of the pinball loss. *Bernoulli.*

Theiler, J.. Quantitative comparison of quadratic covariance-based anomalous change detectors. 2008. *Applied Optics.* **47**: F12.

Theiler, J.. Sensitivity of anomalous change-detection to small misregistration errors . 2008. *Proc. SPIE.* **6966**: 69660X.

Theiler, J.. Subpixel anomalous change detection in remote sensing imagery. 2008. In *IEEE Southwest Sympsoium on Image Analysis and Interpretation.* (Santa Fe, 24-26 March 2008). , p. 165. New York: IEEE.

Theiler, J., C. Scovel, B. Wohlberg, and B. R. Foy. Elliptically contoured distributions for anomalous change detection in hyperspectral imagery. To appear in *IEEE Geoscience and Remote Sensing Imagery.*

Theiler, J., N. R. Harvey, R. Porter, and B. Wohlberg. Simulation framework for spatio-spectral anomalous change detection. 2009. *Proc. SPIE.* **7334**: 73340P.

Theiler, J., and A. M. Matsekh. Total least squares for anomalous change detection. Presented at *to be submitted to: Proc. SPIE.* (Orlando, FL, 2010).

Theiler, J., and A. M. Matsekh. Total least squares for anomalous change detection. 2009. *In preparation.*

Theiler, J., and B. R. Foy. EC-GLRT: Detecting weak plumes in non-Gaussian hyperspectral clutter using an elliptically-contoured generalized likelihood ratio test. 2009. In *International Geoscience and Remote Sensing Symposium (IGARSS).* (Boston, MA, 6-11 July 2008). , p. I. Boston: IEEE.

Theiler, J., and C. Scovel. Uncorrelated versus independent

elliptically-correlated distributions for anomalous change detection in hyperspectral imagery. 2009. *Proc. SPIE.* **7246**: 7246OT.

Theiler, J., and S. Adler-Golden. Detection of ephemeral changes in sequences of images. 2009. *37th Applied Imagery Pattern Recognition Workshop (AIPR '08): Multiple Image Information Extraction.* : 1.

Wohlberg, B., and J. Theiler. Improved change detection with local co-registration adjustments. To appear in *IEEE Workshop on Hyperspectral Image and Signal Processing: Evolution in Remote Sensing.* (Grenoble, France, 26-28 Aug 2009).

Wohlberg, B., and J. Theiler. Symmetrized local co-registration optimization for anomalous change detection. 2009. *In preparation.*

# Information Science and Technology: Metagenomics

*Nicolas W. Hengartner*
20080662DR

## Introduction

Metagenomics is the science of sequencing and analyzing the DNA sequences from environmental samples consisting mostly of microbial communities. Traditional methods of genomic sequence analysis developed over the past twenty years analyze the DNA from a single organism focus on assembling the sequenced DNA fragments (reads) and annotating the genes. These methods fail for metagenomic samples because (1) many genes are not sequenced, (2) there are ambiguities in grouping the reads according to species, and (3) there are likely yet unknown species in the sample. This project seeks to develop information sciences tools to enable the analysis of metagenomic data.

Our effort is divided into two: the first efforts build upon twenty years of experience analyzing genomic data. We extend existing tools and algorithms to compare, classify and organize reads and assembled contigs. Specifically, (1) we seek to develop and implement algorithms to assign a phylogeny (genus, family, order, or phylum) to unknown 16S rRNA; and more generally (2) develop and implement algorithms for assigning phylogeny of reads. In either case, we wish to develop a secondary analysis pipeline to quantify the bio-diversity of a community and the sequencing coverage of that community.

The second approach seeks to develop *de novo* information sciences tools to seek to extract relevant information directly from unassembled reads by attributing phylogeny and function to each read. To do this, we posit that functional pressure produces short sequences within genes that are highly conserved across the tree of life. An analysis of shared short sequences between phylogenetically distant species has the potential to uncover these sequences that must be associated to fundamental functions of the bacteria. Shared sequences between more closely related species provide insight into signatures that can potentially characterize phylum and species of bacteria. We propose to develop information science and technology tools based on these shared sequences. This involves (1) developing fast algorithms to identify all such sequences using the 690+ fully sequences bacterial and archeal genomes, (2) developing algorithms to separate the shared sequences into paragenomic sequences (that characterize phylogeny) and orthogenomic sequences (that characterize function) and to organize the orthogenomic sequences according to known phylogeny to derive signatures, (3) developing fast algorithms to find signatures in short sequence reads, possibly through a combination of both software and hardware developments; (4) developing statistical analyses to ascertain the uncertainty of the attribution, (5) developing statistical analysis tools of the signatures to perform comparative metagenomic analysis.

To manage the complexity of the tasks, our methods will first be developed for Prokaryotic metagenomic data. Future efforts will seek to extend our approaches to Eukaryotes, as such extensions are both challenging and necessary to make these tools relevant to various DOE missions.

## Benefit to National Security Mission

Developing metagenomic analysis tools for shotgun sequencing, and in particular k-mer based signatures of broadly preserved functions within the bacterial kingdom makes possible the analysis of the DNA potential of microbial communities. It enables :

1. Monitoring of bacterial communities recovering from environmental insults for (1.a) environmental remediation and (1.b) understand the fate of released biological agents.

2. Phylogenetic signatures provide a novel tool to trace the origin/provenance of objects and individuals based on the genetic profiles of accompanying microbes.

3. Designing community-specific DNA hybridization tags based on observed functions tags to monitor the dynamic of communities associated with (3.a) bio-fuels, (3.b) health status of individuals, (3.c) pathogen detection/characterization.

## Progress

**Fragment recruitment**

It is possible to organize metagenomic reads and (partially) assembled contigs from shotgun sequencers by comparing them to all existing fully sequenced reference genomes. Such comparison, commonly called fragment recruiting, needs to take into account the possibility of small alterations in the DNA between individuals belonging to the same species, or genus, or order, or phylum. The classical approach is to use BLAST, as sequence comparison tool developed in the late 70's by two Los Alamos researchers that account for insertions, deletions and point mutation. Our *in silico* experiments have revealed that this method gives good results provided that the origin of the DNA is essentially from the same species as the reference genomes. To demonstrate the usefulness of fragment recruiting, Liu *et al.* [1] have used this tool to finish a genome of a bacteria commonly found in the ocean with metagenomic reads.

**Naïve Bayes classifier for 16S rRNA**

Biodiversity, both in terms of abundance and compositional profiles, and in terms of species inventory, is an important parameter of a microbial community. Traditionally species composition has been assessed via targeted sequencing and classification of 16S rRNA. The challenge with 16S rRNA surveys is that not all the species present in the survey have been inventoried, that is, it is likely that some of the sequences belong to novel species. For those new sequences, we wish to determine to what genus, family, order, and phylum they belong. The RDP classifier from the Center for Microbial Ecology at the Michigan State University is the current state-of-the-art 16S rRNA classifier. Our team has developed an improved classifier that takes advantage of the an improved model for the long range dependence of nucleotide frequencies in rRNA. Figure 1 shows that our method consistently outperforms the classification of provided by the RDP classifier. Preliminary work for that methodology was published in Liu *et al.* [2] and presented in a poster session at [3]. We are capitalizing on this success and have started a collaboration with the Center for Microbial Ecology at the Michigan State University, with the eventual goal of replacing their current algorithm with ours.

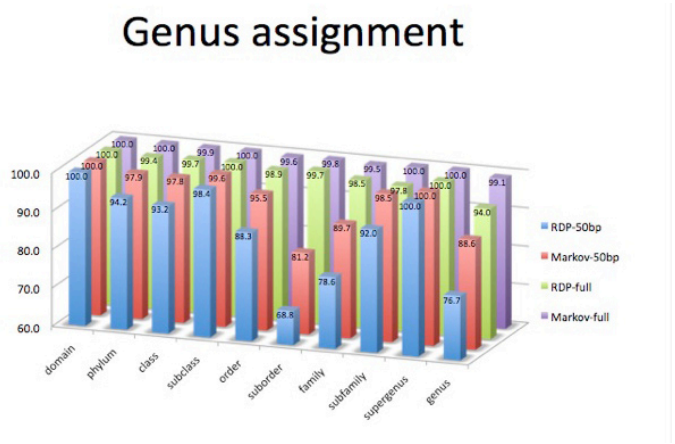


*Figure 1. Relative performance of Markov Naive Bayes classifier and state-of-the-art RDP classifier for bacterial 16S rRNA. Observe that the Markov classifier dominates the RDP classifier at all levels of aggregation.*

**K-mer based signatures**

Functional pressure and the need of proteins to bind to small molecules posits the existence of short sequences of peptides that are shared by distantly related species of bacteria that can not be explained by chance alone. It is known that a few genes, such as RNA polymeriase, are highly conserved across the bacterial kingdom. The surprising fact is that up to a third of all genes contained at least one shared 10-mer, indicative of functional conservation. Empirical evidences, such as the length distribution of shared solid patterns displayed in Figure 2, confirms the existence end prevalence of shared solid k-mers between distant species. Ideally, we want to couple known phylogeny of organisms with the k-mer they share to disambiguate between k-mers that are shared as a result of inheritance, and those that are shared because of functional pressure. Our first approach to control for phylogeny was to focus on representative sets of organisms that are approximately equidistant in evolutionary distance. We call these sets of organism isoperigenomic, and have constructed sets of representative isoperigenomic organisms for the bacterial kindom, proteo-bacteria phylum and gamma proteo-bacteria order. We have searched the Global Ocean Survey (GOS) datasets of Craig Ventner and found that roughly 35% -- 40% of all the reads contained one of our signature tags. Figure 3 shows the recruitment fraction for the various GOS datasets. This number is comparable with the fraction of recruited reads using traditional methods, such as blast. However, our approach lends itself to quantifiable uncertainty analysis, and we expect that optimization of our algorithm can potentially double the fraction of identified reads.

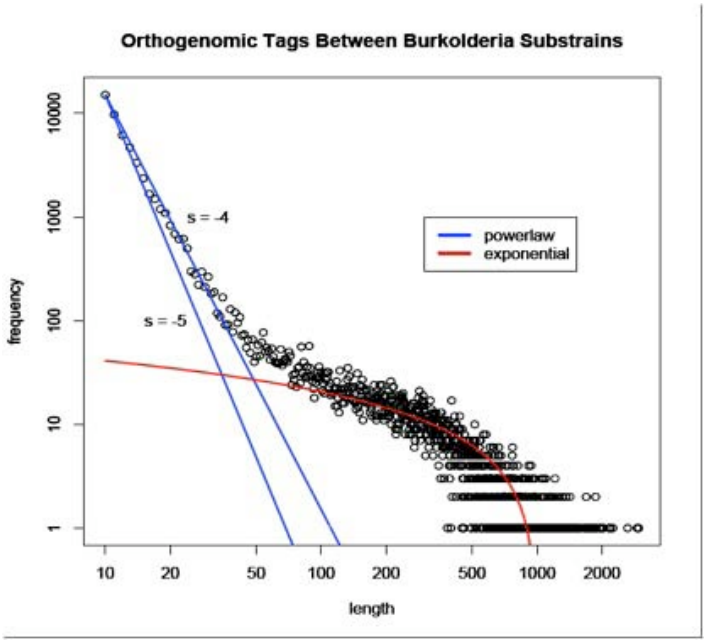


*Figure 2. Distribution of length of shared k-mers between Burkolderia strains. The distribution is a mixture of an exponential and a powerlaw. The first is associated with random mutations while the second is associated with conserved regions. The size of the "excess" from the exponential for small k is an indication of the prevalence and importance of the conserved regions.*

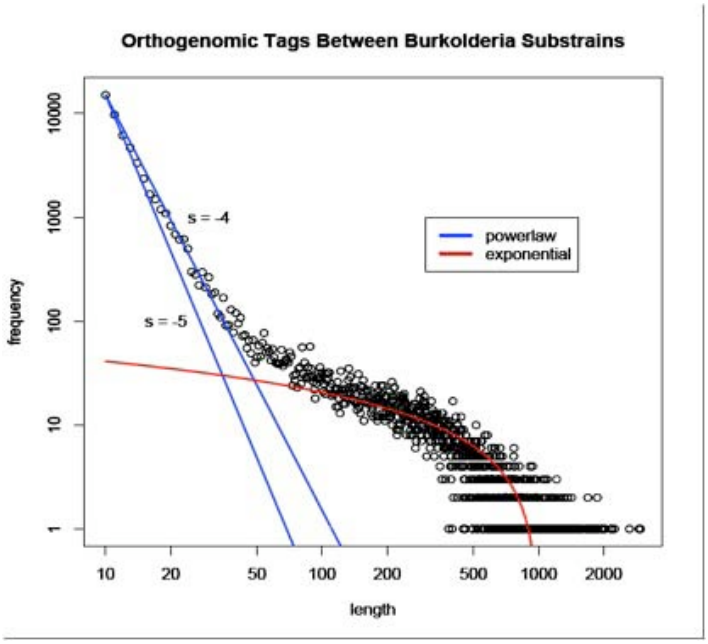


*Figure 3. Fraction of reads from the Global Ocean Survey that contained at least one curated shared k-mer. The fraction, 35% is comparable with the fraction of reads recruited by BLAST. But our method allows for optimization that may double the reported fraction, and lends itself to formal uncertainty quantification.*

A more refined approach places each shared k-mer within a known phylogenetic tree. This results in functionalizing each k-mer depending on its assigned node in the tree: k-mers that are placed near the leaves are indicative of phylogeny, whereas k-mers that occur farther away from the leaf are though to be associated with common functions. This approach allows us to use all the known genomes simultaneously without the need for us to construct an a priori isoperigenomic set of genomes.

In practice, searching a data sets for shared k-mers is fast because (1) shared are rare --- only about 1% of all 10-mers of amino acid are shared beyond an order, (2) we use indexing and map-reduce to organize and split the search, (3) we can use specialized hardware to speed up the memory intensive algorithms. In our numerical experiments, we have improved the search time of GOS by five orders of magnitude – a factor of 100,000 – over the classical BLAST type searches.

## Future Work

In metagenomics, DNA is sequenced from environmental samples containing communities of interdependent organisms. The fundamental question is to identify what signal the sequencing data contains, and how to extract it. The information science challenge is on how to organize and structure the metagenomics data to enable us to leverage past knowledge on sequenced genomes and other metagenomics data. The information technology challenge is to make our endeavor computationally efficient, so that analysis can be run on a desktop instead of a supercomputer. Task 1: Develop a data management and organization tool for generating shared k-mers from all the fully sequenced genomes that is computationally tractable. Task 2: Validate information content of shared k-mers by comparing classification of genes/ organisms based on shared k-mers with classical bio-informatics methods such as Blast and COG. Use results to quantify uncertainty. Task 3: Develop analysis tools for understanding genome organization and evolution based on shared k-mers using notions of paragenomic and orthogenomic sequence tags and position of joint occurrences of tags within multiple genomes. Task 4: Develop statistical methods and visualization tool to support scientific discoveries. Task 5: Develop binning tools that can be integrated with the JGI metagenomics toolbox.

## Conclusion

We will develop methods for extracting information and knowledge from massive amounts of data from sources that directly impact the mission of the DOE. We aim to develop a new paradigm for the analysis of metagenomic data that focus information extraction of unassembled DNA reads. To do so, we will develop data management and organization tools based that centers around short DNA sequence indexing, and develop statistical methods for information extraction and to support scientific discoveries and inferencing.

## References

1. Woyke, T., and e. all. Assembling the marine metagenome, one cell at a time. 2009. *Public Library of Science.* **4** (4): e5299.

2. Liu, K., T. Wong, G. Xie, and N. Hengartner. Improving naïve Bayesian classifier for metagenomic reads assignment. To appear in *The 2009 International Conference on Bioinformatics & Computational Biology.* (Las Vegas, July 13-16, 2009).

## Publications

Liu, K., T. Wong, G. Xie, and N. Hengartner. Improving naïve Bayesian classifier for metagenomic reads assignment. To appear in *The 2009 International Conference on Bioinformatics & Computational Biology.* (Las Vegas, July 13-16, 2009).

Woyke, T., G. Xie, A. Copeland, J. M. Gonzalez, C. Han, H. Kiss, J. Saw, P. Senin, C. Yang, S. Chatterji, J. Cheng, J. Eisen, M. Sieracki, and R. Stepanauskas. Assembling the marine metagenome, one cell at a time. 2009. *Public Library of Science.* **4** (4): e5299.

# Statistical Physics of Networks, Information and Complex Systems

*Robert E. Ecke*
20080671DR

## Introduction

We solve information science problems with techniques and insights from statistical physics. Statistical aspects, such as random, stochastic influences, correlation effects, constrained variation and large number limits play a role of increasing importance in today's information infrastructure and its management. Descriptions of phase transitions, random distributions of connections and spin glass analogies find powerful applications in cyber security challenges, power grid models, social modeling and optimization.

Driven by security concerns in communication, some of national importance, by new computing capabilities and by the availability of unprecedented data sets, the field of information science has witnessed a rapid growth spurt in the past decade with breakthroughs in graph and network theory. Large scale computing and data processing requires new techniques for data management and searches.

Responding to these pressures, we capitalize on the scientific opportunities offered by the similarity of concepts between statistical physics and computer science. We develop a powerful multi-disciplinary approach that draws strength from cross-fertilization and multiple interactions of postdocs, visitors and staff members with different backgrounds. The work on this project takes advantage of the newly appreciated connection between computer science and statistics and addresses important problems in data storage, decoding, optimization, the information processing properties of the brain, the interface between quantum and classical information science, the verification of large software programs, modeling of complex systems including disease epidemiology, resource distribution issues, and the nature of highly fluctuating complex systems. The project emphasizes and connects themes such as (i) neural computation, (ii) network theory and its applications, and (iii) a statistical physics approach to information theory. These efforts are responsible for fruitful collaborations and the nucleation of science efforts that span multiple divisions such as EES, CCS, D, T, ISR and P.

## Benefit to National Security Missions

This project will support the DOE mission in Energy Security and Nuclear Non-Proliferation by developing novel information science tools for communication, sensing, and interacting complex networks such as the internet or energy distribution systems. It will also support programs in Threat Reduction and Homeland Security such as pathomics or situational awareness.

## Progress

We apply mathematical methods and concepts of statistical physics to information science. Based on the similarities of the mathematical structures that underpin the descriptions and the deep, conceptual connections that can be revealed by a proper formulation of the underlying questions, we address overarching information science issues that bridge a variety of disciplines such as quantum physics, data transmission and storage, computer science, and neural computation. Statistics and the descriptions of correlations, phase transitions and randomness provide a unifying thread and an organizational structure.

Optimal strategies for search algorithms, for biological responses, for computer data management and for quantum communication can be described from the perspective of correlations: the influence of one unit on other units with which it communicates. CNLS postdocs Vadas Gintautas, Peter Loxley, Marko Rodriguez, Spyridon Machalakis and Jon Yard have exploited correlation aspects. Even when connections between the units are probabilistic (distributed according to specified probability distributions), quantitative and mathematically exact statements can be made about the average of the large system behavior. Depending on the parameters of the units and the distributions of the connections, the predictions for the large system averages can change abruptly, possibly varying discontinuously as parameters are altered by a tiny amount: the system undergoes a phase transition. Postdoc Lenka Zdeborova has explored phase transition behavior and the formulation of general optimization problems in terms of computing a partition function.

The behavior of a large number of units that influence each other through probabilistically distributed connections is at the core of many applications and is well described by network theory. Postdocs Jason Johnson and Milan Bradonjic developed underlying theoretical frameworks. They established the mathematical descriptions of random graphs and of the problem of 'inference' as summations over random walks and loops in such networks. Below we describe a representative sample of research results.

**Correlations**

Marko Rodriguez developed an algebra for mapping multi-relationship (relationship representing, for instance, friendship", "kinship", or "collaboration") networks into networks with single-relationship edge labels for which most of the analysis methods have been developed. It is not sufficient to execute a single-relational network analysis algorithm on a multi-relational network simply by ignoring edge labels [1]. Marko has also proposed novel methods to optimize the use of the web of data, the recently introduced set of standards and technologies for representing, querying, and manipulating globally distributed data structures. The Resource Description framework (RDF) used to interrelate data would be more generally useful if it can support other models of computing. To realize the Web of Data as a general-purpose medium for storing and processing the world's data, Marko pointed out it would be necessary to separate RDF from its logic language legacy and frame it as a data model [2].

Quantum architectures provide a new environment to realize information protocols. How robust quantum communication methods can be against fluctuation errors and how efficiency can be quantified are questions that necessitate a generalization of information theory to accommodate the laws of quantum physics. Jon Yard has proven the existence of an optimal quantum protocol for performing quantum data compression when the sender and receiver each have quantum information. Entanglement, the inability of a quantum state to be represented as a product state, is associated with a specific kind of correlations, and can, under the proper conditions be used to perform quantum computations. Postdoc Spyridon (Spiros) Michalakis has developed novel, non-local descriptions of highly entangled states in a 'gapped' quantum spin system (a system that requires a finite energy to excite the lowest energy excitation) [3].

Social computation, whether in the form of searches performed by swarms of agents or collective predictions of markets can supply remarkably good solutions to complex problems. Individuals trying to solve a problem can locally aggregate their information and work together to arrive at a superior global solution. This suggests that there may be general principles of information aggregation and coordination that can transcend particular applications. Vadas Gintautas (T-5/CNLS) has shown that the general structure of this strategy can be cast in terms of information theory and he has derived mathematical conditions that lead to optimal multi-agent searches. He illustrated the opportunities in terms of local search algorithms for autonomous agents looking for the spatial location of a stochastic source [4,5]. Cooperating nodes may also be at the heart of our unusually fast ability to discover salient features of images. Exploring the idea that this ability may be hard-wired in the visual cortex, postdocs Vadas Gintautas, Mike Ham, Marko Rodriguez have revealed a density-dependence in neural network data that indicates such cooperation mechanism [6]. Postdoc Peter Loxley is developing a neural network description in which nearby neurons share the relevant information to identify saliency features.

**Phase Transitions**

Network theory and spin glass physics provide a powerful framework to attack combinatorial problems in information science. Lenka Zdeborova showed that structural phase transitions, and the easy/hard/easy pattern in the average computational complexity persist in the 'planted' random ensembles. She also discussed the finite temperature phase diagram, finding a close connection with the liquid/glass/solid phenomenology [7,8].

**Random Graphs**

In random graphs, nodes are distributed randomly on a grid and possibly assigned different statistical weights. The edges connecting the nodes are established according to specific rules. Such systems can model real-world networks such as the wireless network and the internet. Postdoc Milan Bradonjic has revealed the timescales and efficiency with which information can be broadcast in networks of this type [9,10]. Postdoc Jason Johnson has developed a new method for calculating the partition function by randomly selecting and computing walks and loops, including methods to avoid double counting and backtracking [11,12].

## Future Work

We capitalize on similarities of statistical physics and computer science challenges. This project takes advantage of the newly-appreciated connections to address key problems in data transmission and storage, decoding, optimization, information-processing of the brain, the interface between quantum and classical information, verification of large software programs, modeling of complex systems including disease epidemiology, resource distribution issues, and the nature of highly fluctuating complex systems.

We develop theoretical and computational methods to address important problems of national interest:

Develop systematic approaches to finding computationally efficient methods that optimize the performance of classes of problems such as data transmission. We optimize the efficiency of data transmission, requiring reliability and minimal energy cost for a network of generalized transmitter/receiver units with information processing at each node.

1. Explore concepts of classical information theory applied to the coupling of quantum information systems.

2. Investigate optimal methods for relating images, either because neural connections can reveal salient features at the early stages of visual cortex signal processing, or because the images possess common features, e.g., showing groups of particles such as in fluid tracking methods or in feature recognition systems.

3. Coordinate workshops and working groups on connections between data acquisition, processing, analysis and prediction applied to complex systems.

4. Investigate network concepts applied to problems in social behavior, population dynamics, image recognition, optimization problems and power grid problems.

## Conclusion

The ability to organize, manipulate and optimize the transmission, reception and processing of information underpins much of the national infrastructure, the information-based economy and many features of national security. Our research efforts address problems in the organization and processing of information applied to efficient communication under constraints of error tolerance, bandwidth, or power consumption (as in distributed sensor systems and power grid problems). Our research also reveals how the brain processes visual stimuli to do sophisticated image processing and recognition.

## References


1. Rodriguez, M. A., and J. Shinavier. Exposing multi-relational networks to single-relational network analysis algorithms. To appear in *Journal of Informetrics.*

2. Rodriguez, M. A.. A Reflection on the Structure and Process of the Web of Data. To appear in *Bulletin of the American Society for Information Science and Technology, American Society for Information Science and Technology.*

3. Hamza, E., S. Michalakis, B. Nachtergaele, and R. Sims. Approximating the ground state of gapped quantum spin states. 2009. *Journal of Mathematical Physics.* **50** (9): 95213.

4. Gintautas, V., A. Hagberg, and L. M. A. Bettencourt. When is social computation better than the sum of its parts?. To appear in *Social Computing, Behavior Modeling, and Prediction,.* Edited by Liu, H., and J. J. Salerno.

5. A.Bettencourt, L. M., V. Gintautas, and M. I. Ham. Identification of functional information subgraphs in complex networks. 2008. *Physical Review Letters.* **100**: 238701.

6. Ham, M. I., V. Gintautas, M. A. Rodriguez, R. A. Bennett, C. L. Santa Maria, and L. M. A. Bettencourt. Density-dependence of functional development in spiking cortical networks grown in vitro. *Biological Cybernetics.*

7. Krzakala, F., and L. Zdeborova. Hiding quiet solutions in random constraint satisfaction problems. 2009. *Physical Review Letters.* **102**: 238701 .

8. Zdeborova, L., and F. Krzakala. Quiet planting in the locked constraint satisfaction problems. *SIAM Journal of Discrete Mathematics.*

9. Bradonjic, M., A. Hagberg, and A. G. Percus. The structure of geographical treshhold graphs. To appear in *Special issue of Internet Mathematics.* **5**.

10. Bradonjic, M., T. Muller, and A. G. Percus. Coloring geographical treshold graphs. To appear in *Discrete Mathematics and Theoretical Computer Science.*

11. Johnson, J., V. Chernyak, and M. Chertkov. Orbit-product representation and correction of Gaussian belief propagation. To appear in *International Conference on Machine Learning.* (Montreal, March).

12. Johnson, J., D. Bickson, and D. Dolev. Fixing convergence of gaussian belief propagation. To appear in *International Symposium on Information Theory.* (Seoul, South Korea, April 2009).


## Publications


A.Bettencourt, L. M., V. Gintautas, and M. I. Ham. Identification of functional information subgraphs in complex networks. 2008. *Physical Review Letters.* **100**: 238701.

Bettencourt, L. M., V. Gintautas, and M. I. Ham.

Identification of functional information subgraphs in complex networks. 2008. *PHYSICAL REVIEW LETTERS.* **100** (23): 238701.

Bianconi, G., N. Gulbahce, and A. E. Motter. Local structure of directed networks. 2008. *PHYSICAL REVIEW LETTERS.* **100** (11): 118701.

Bianconi, G., and N. Gulbahce. Algorithm for counting large directed loops. 2008. *JOURNAL OF PHYSICS A-MATHEMATICAL AND THEORETICAL.* **41** (22): 224003.

Bradonjic, M., A. Hagberg, and A. G. Percus. The structure of geographical treshhold graphs. To appear in *Special issue of Internet Mathematic.*

Bradonjic, M., T. Muller, and A. Percus. Coloring geographical treshold graphs. To appear in *Discrete Mathematics and Theoretical Computer Science.*

Burr, T. L., and G. Chowell. Signatures of non-homogeneous mixing in disease outbreaks. 2008. *MATHEMATICAL AND COMPUTER MODELLING.* **48** (1-2): 122.

Chertkov, M., V. Chernyak, and R. Teodorescu. Belief Propagation and Loop Series on Planar Graphs . 2008. *Journal of Statistical Mechanics.* : P05003.

Chertkov, M., and M. G. Stepanov. An efficient pseudocodeword search algorithm for linear programming decoding of LDPC codes. 2008. *IEEE TRANSACTIONS ON INFORMATION THEORY.* **54** (4): 1514.

Chowell, G., L. M. Bettencourt, N. Johnson, W. J. Alonso, and C. Viboud. The 1918-1919 influenza pandemic in England and Wales: spatial patterns in transmissibility and mortality impact. 2008. *PROCEEDINGS OF THE ROYAL SOCIETY B-BIOLOGICAL SCIENCES.* **275** (1634): 501.

Devetak, I., and J. Yard. Exact cost of redistributing multipartite quantum states. 2008. *PHYSICAL REVIEW LETTERS.* **100** (23): 230501.

Gintautas, V., A. Hagberg, and L. M. A. Bettencourt. When is social computation better than the sum of its parts?. To appear in *Social Computing, Behavior Modeling, and Prediction.* Edited by Liu, H., J. J. Salerno, and M. J. Young.

Ham, M. I., V. Gintautas, M. A. Rodriguez, R. A. Bennett, C. L. Santa Maria, and L. M. A. Bettencourt. Density-dependence of functional development in spiking cortical networks grown in vitro. *Biological Cybernetics.*

Hamza, E., S. Michalakis, B. Nachtergaele, and R. Sims. Approximating the ground state of gapped quantum spin states. 2009. *Journal of Mathematical Physics.* **50** (9): 95213.

Hayden, P., M. Horodecki, A. Winter, and J. Yard. A decoupling approach to the quantum capacity. 2008. *Information Dynamics and Open Systems.* **15** (1): 7.

Johnson, J., D. Bickson, and D. Dolev. Fixing convergence of gaussian belief propagation. To appear in *International Symposium on Information Theory.* (Seoul, South Korea, April 2009).

Johnson, J., V. Chernyak, and M. Chertkov. Orbit-product representation and correction of gaussian belief propagation. To appear in *International Conference on Machine Learning.* (Montreal, Canada, March).

Krzakala, F., and L. Zdeborova. Hiding quiet solutions in random constraint satisfaction problems. 2009. *Physical Review Letters.* **102**: 238701.

Lopez, E., R. Parshani, R. Cohen, S. Carmi, and S. Havlin. Limited path percolation in complex networks. 2007. *PHYSICAL REVIEW LETTERS.* **99** (18): 188701.

Miller, J. C., and J. M. Hyman. Effective vaccination strategies for realistic social networks. 2007. *PHYSICA A-STATISTICAL MECHANICS AND ITS APPLICATIONS.* **386** (2): 780.

Mineev, M., M. Putinar, and R. Teodorescu. Random matrix theory in 2D, Laplacian growth, and operator theory . 2008. *Topical Review, Journal of Physics A: Mathematical Theory.* **41**: 263001.

Motter, A. E., N. Gulbahce, E. Almaas, and A. Barabasi. Predicting synthetic rescues in metabolic networks. 2008. *MOLECULAR SYSTEMS BIOLOGY.* **4**: 168.

Nuno, M., T. A. Reichert, G. Chowell, and A. B. Gumel. Protecting residential care facilities from pandemic influenza. 2008. *PROCEEDINGS OF THE NATIONAL ACADEMY OF SCIENCES OF THE UNITED STATES OF AMERICA.* **105** (30): 10625.

Rodriguez, M. A.. Grammar-Based Random Walkers in Semantic Networks. 2008. *Knowledge-Based Systems.* **21** (7): 727.

Rodriguez, M. A.. A reflection on the structure and process of the Web of Data. To appear in *Bulletin of the American Society for Information Science and Technology.*

Rodriguez, M. A.. Interpretations of the Web of Data", data management in the semantic Web . *Complexity Digest.*

Rodriguez, M. A., V. Gintautas, and A. Pepe. The

relationship between concert and listening behavior. 1. *First Monday.* **14** (1): 2009.

Rodriguez, M. A., and J. Shinavier. Exposing multi-relational networks to single-relational network analysis algorithms. To appear in *Journal of Informetrics.*

Rohlf, T., N. Gulbahce, and C. Teuscher. Damage spreading and criticality in finite random dynamical networks. 2007. *PHYSICAL REVIEW LETTERS.* **99** (24): 248701.

Santhi, N.. On Algebraic Decoding of q-ary Reed-Muller and Product Reed Solomon Codes . 2007. *IEEE Transactions on Information Theory.* **1**: 1351.

Smith, G., and J. Yard. Quantum communication with zero-capacity channels. 2008. *SCIENCE.* **321** (5897): 1812.

Srinivasan, R., R. Pepe, and M. A. rodrigues. A clustering-based semi-automated techniques for cultural ontologies. 2009. *Journal of American Society for Information Science and Technology .* **60** (3): 608.

Wocjan, P., and J. Yard. The Jones polynomial: quantum algorithms and applications to quantum complexity theory. 2008. *Quantum Information and Computation.* **8**: 0147.

Yard, J., I. Devetak, and P. Hayden. Capacity theorems for quantum multiple access channels: classical-quantum and quantum-quantum capacity regions. 2008. *IEEE transactions on Information Theory.* **54** (7): 3091.

Zdeborova, L., S. Backhaus, and M. Chertkov. Message passing for Integrating and assessing renewable generation in a redundant power grid. To appear in *Hawaii International Conference on System Science - 43.* (Koloa, Kauai, Hawaii, January 5 - 10, 2010).

Zdeborova, L., and F. Krzakala. Quiet planting in the locked constraint satisfaction problems. *SIAM Journal of Discrete Mathematics.*

Zdeborova, L., and M. Chertkov. Message passing for optimization and control of power grid: toy model of distribution with ancillary lines. *Physical Review E.*

# Information Science and Technology: Streaming Data

*Sarah E. Michalak*
20080729DR

## Introduction

A key challenge in Information Science and Technology (IS&T) is extracting information from massive streams of data that are arriving in real-time. This project's contribution is to perform the research necessary to enable visualization, analysis, and storage solutions for massive streaming data.

To that end, we are developing: (1) methods for using emerging microparallelism, e.g. Cell processors and GPUs, for real-time and near-real-time pipelining and processing; (2) statistical and signal processing methods for real-time or near-real-time baselining, anomaly detection and signal detection of high-dimensional data; and (3) novel file system architectures for real-time data ingest and writing out of data identified to be of interest. The overarching research challenge presented by this work is the combination of the amount and intricacy of the data that must be processed with the complexity of the algorithms required for processing it. In many cases, a further challenge is that of data fusion: multiple streams of data must be acted on simultaneously in real-time in order to accomplish the necessary processing.

While this work is motivated by the astronomical problem of real-time detection of radio transients, the methods are general and more broadly applicable.

## Benefit to National Security Missions

The general problem of real-time detection of anomalous events has broad applicability including to cyber security, threat reduction, data from sensor networks, and systems data (biological or otherwise) in which a vector of data is recorded at every time step. In addition, much laboratory work involves streaming data. Many, if not most, emerging programs at the laboratory include some aspect of streaming data. In short, the proliferation of inexpensive sensors of all kinds makes streaming data capability one of the most important capabilities for the laboratory in the next decade.

## Progress

Significant progress has been made in four areas:

1. Processing (Correlation) of Incoming Data: This work is motivated by the Long Wavelength Array (LWA), which could be enhanced by a data streaming capability that uses the measurements from 256 antennas to search the visible sky in real-time to detect transient events. Accomplishing this requires real-time calculations on the measurements from all of the 32,640 different antenna pairs that derive from the 256 antennas. At full scale and with antenna signal bandwidths of ~67 MHz, the problem requires ~70 Tflops of continuous processing and 256 GB/s of sustained bandwidth. Methods for achieving this real-time processing rate via standard processors (Opterons) and Cell processors were investigated. A major research challenge was efficiently exploiting the spatial and temporal locality of the data to generate an effective algorithm given Cell's architecture. In a performance study, a Cell-based solution outperforms a dual-core Opteron by ~21X and outperforms a quad-socket, dual-core Opteron node by ~6X. Moreover, the Cell-based solution requires ~1/19 of the power and ~1/5 of the space of the Opteron solution. Power and space are important considerations in radio astronomy since the available power and space are frequently limited for compute equipment that must be kept in the field. These results have been detailed in a technical report [1], and a proposal has been developed and hardware procured to use this work as the basis for a Prototype All-Sky Imager at the LWA site.

2. Ring Buffer with Write-Out Capability for Temporary Storage of Incoming Data: Two complementary and novel approaches that use a ring buffer model in order to capture data continuously, but normally only retain it for brief periods (minutes to hours, since the large majority of data is not needed for analysis) are being developed. (A ring buffer offers temporary storage for data in which by default the oldest data are overwritten once the ring buffer's capacity is filled.) Our first approach is a hardware-based system. Specifically, we have designed and implemented a ring buffer system prototype that is capable of maintaining data capture speeds

near the limit of the underlying hardware, and yet still transfer "important" data to other storage without compromising the accumulation of incoming data. These quality-of-service guarantees ensure that the system can maintain steady operation up to the endurance of the hardware while reliability mechanisms protect against data loss in the event of hardware failure. Results have been submitted for publication [2]. Second, an easy-to-implement FUSE Ring Buffer File System based on File System in User Space (FUSE) is under development. While this system lacks hard quality-of-service guarantees, it can be architected to the specifications of a scientific application of interest and quickly implemented.

3. RFI Mitigation and Transient Detection: Working jointly with researchers at UC-Berkeley, we are investigating methods of mitigating radio-frequency interference (RFI) from data collected by the Allen Telescope Array. We have applied a statistical approach to mitigate the effects of outliers, 60 Hz signals and wandering power levels on the detection of chirps. These mitigations, combined with estimation of antenna sensitivities and subsequent antenna weighting, produced an event stream that was much better at differentiating signal from noise than the methods previously used. Giant pulses from the Crab pulsar were detected with stronger signal-to-noise ratios even as the false alarm rate was reduced by a factor of 26. Furthermore, signal-to-noise ratios reported in the event stream were well-calibrated to a reference Gaussian distribution demonstrating that the false alarm rate was being well-managed, even in the face of multiple types of interference. A simulation study to further explore these methods when known signals are embedded into a noisy background has been undertaken.

4. Visualization of Images of the Sky: Acceleration of the CLEAN algorithm via GPUs has been investigated. The CLEAN algorithm has two parts: a sort and a series of convolutions via FFTs. The FFTs were easily implemented and fast on the GPU, as there is now CUDA support for this. The sort was a greater research challenge, due to the small shared memory on the GPU. A full sort is not truly required, but instead only an unsorted top-N point algorithm. We implemented this by doing a partial histogram, binning points into buckets and using random sampling to select pivot points giving balance to the "histogram." We achieved a 10x speedup from the partial sort we had implemented, and the sort now takes time commensurate to the FFT.

## Future Work

We are performing the research necessary to develop key pieces of a real-time radio-transient detection system that includes: 1) processing of the incoming data; 2) temporary storage of the data that permits writing of the data identified to be of interest to long-term storage; 3) novel algorithms for excision of radio-frequency interference (RFI) and identification of signals of interest; and 4) creation of images of the sky.

Real-time and near-real-time data pipelining, data processing, and image processing are being facilitated by the use of emerging micro-parallelism, specifically GPUs and Cell processors. A key research challenge in gaining maximum performance from GPUs and Cell processors is that of efficiently exploiting the spatial and temporal locality of the data. Cell processors have been applied to the challenge of processing the incoming data, referred to as "correlation", while GPUs are being used to increase the rate of image processing using the CLEAN algorithm.

Two complementary ring buffer file systems are being developed to permit real-time data ingest with some processing of the data, which could include writing of the data identified to be of interest to long-term storage. Research challenges include architecting ring buffers to the specifications of the scientific application of interest, i.e. its rate of data inflow, frequency with which interesting chunks of data arrive, and the sizes of the interesting chunks of data that should be saved for later analysis.

Finally, statistical and signal processing methods for RFI mitigation and transient detection are being investigated. These methods aim to reduce RFI so that false positive detection rates are decreased and true positive detection rates are increased.

The remainder of the project will be devoted to completing the key research required to enable real-time detection of radio transients. First, the RFI excision and transient detection algorithms under development are being tested to ensure that they remove interfering signals while still permitting signals of interest to be detected, with the results to be submitted for publication. Next a subset of these algorithms will be ported to appropriate hardware for investigation and publication of their real-time characteristics. Use of IBM's InfoSphere Streams for this work is also under exploration. Second, the CLEAN work, which is nearing completion, will be submitted for publication. Finally, we anticipate that a protoype FUSE ring buffer system will be completed by the end of November 2009. Following additional work, we anticipate publication of related results. The hardware-based ring buffer work will continue as part of thesis research at UCSC and possibly at LANL during summer 2010, with publication of additional results forthcoming.

## Conclusion

We are developing methods for extracting information from massive amounts of data, specifically novel methods designed for real-time and near-real-time visualization and analysis of massive streaming data. The capabilities

developed will have application across LANL's threat reduction and global security mission. Many important threat detection problems, from those in cyber security domains to near-space object tracking, can be greatly facilitated by our research. These new techniques can drastically decrease the amount of time require to identify anomalies within massive streams of data, with an ultimate goal of enabling real-time detection.

## References


1. DuBois, A., C. Connor, S. Michalak, G. Taylor, and D. DuBois. Application of the IBM Cell processor to real-time cross-correlation of a large antenna array radio telescope. 2009. *Los Alamos National Laboratory Technical Report LA-UR-09-03483.*
2. Bigelow, D., S. Brandt, J. Bent, and H. B. Chen. Managing high-bandwidth real-time data storage. 2009. *Los Alamos National Laboratory Technical Report LA-UR-09-06133.*


## Publications


Bigelow, D., S. Brandt, J. Bent, and H. B. Chen. Managing high-bandwidth real-time data storage. 2009. *Los Alamos National Laboratory Technical Report LA-UR-09-06133.*

DuBois, A., C. Connor, S. Michalak, G. Taylor, and D. DuBois. Application of the IBM Cell processor to real-time cross-correlation of a large antenna array radio telescope. 2009. *Los Alamos National Laboratory Technical Report LA-UR-09-03483.*

# Synthetic Cognition through Peta-Scale Models of the Primate Visual Cortex

*Luis Bettencourt*
20090006DR

## Introduction

Understanding how the human brain performs computation, especially how it interprets the world around us through our senses remains one of the most exciting open scientific problems. Synthetic systems that can exploit some of the brains cognitive abilities would also revolutionize many aspects of technology central to the US Department of Energy's missions.

This project seeks to understand and implement the computational principles that enable high-level sensory processing and other forms of cognition in the human brain. Though the basic principles of neurons and synapses (their connections) have been known for some time, very little is understood about how they work in large networks to produce effective computation (of 10-100 billion cells in the human brain). To address these issues we are creating synthetic cognition systems (models and simulations) that emulate the functional architecture of the primate visual cortex, the best understood part of the brain. A quick calculation reveals that the human visual cortex is a petaflop computer, performing about a quadrillion operations per second. This computational scale has just been reached by a new generation of supercomputers at US Department of Energy Laboratories (Los Alamos and Oak Ridge). In this sense understanding the brain as a computational network is starting to shift from a problem that was technically unfeasible to one of determining the fundamental organization and dynamics that enable the extraordinary cognitive capabilities of the human brain.

In this project, by using petascale computational resources, combined with our growing knowledge of the structure and function of biological neural systems, we will match, for the first time, the size and functional complexity necessary to reproduce the information processing capabilities of cortical circuits. Several major scientific and technological breakthroughs are anticipated. First, the hypothesis pervading much of Artificial Intelligence for the last 50 years, that synthetic cognition approaching human levels of performance can be achieved simply by matching the scale of the human brain, can finally be tested. Second, more complex neural processing mechanisms, such as spiking dynamics, synaptic plasticity (learning), and lateral and feedback connections between cortical neurons, will be assessed quantitatively with respect to the resulting performance gains in real time cognitive tasks.

## Benefit to National Security Missions

The project supports the Department of Energy Office of Science by creating a new generation of powerful petascale computational systems that approach human visual cognition. It supports applied science missions by providing state of the art synthetic visual cognition for remote sensing, battlefield awareness, nuclear threat detection, while addressing one of the deepest questions of fundamental science.

## Progress

The project is divided into four objectives. We briefly describe progress towards each:

### 1. Test limits of feed forward models

We have now built mathematical models and their computational implementations that demonstrate state of the art performance (or slightly above it) in visual cognition, in classical problems of object identification, for example the presence of an animal (or not) in a natural scene. We have also determined the conditions under which the systems will be scaled up with more supervised and unsupervised learning. This involves two main strategies which we have now developed and are implementing: 1) the learning of visual representations and invariances in the connectivity of simple and complex cells in each layer of the model. This is achieved via exposing the system to large image data sets and video and using learning rules to update cells' representations over their receptive field [1,2], Figure 1. The learning is unsupervised so that the system needs not know which objects are present in visual scenes. To learn to discriminate objects the system must be taught via 2) large scale supervised learning. This consists of labeled image sets that expose the system to the same object in a variety of points of view and conditions. This

allows the system to build invariant representations of classes of objects and situations. We have collected most labeled datasets available in computer vision and have now also started to create our own, via large photographic collections and 3D image rendering [2]. Figure 2 shows the result of combining both unsupervised and supervised learning. The system shows systematic improvement with greater visual experience. This also exposes the fact that much larger image collections are necessary, commensurate with human visual experience (about $10^{12}$ Pixel/day, or several $10^{15}$ pixels – petapixels – in a lifetime). We are currently taking steps to scaling up training of the system via large collections of images and video, and to understand resulting representations via principles of information and computational theory.

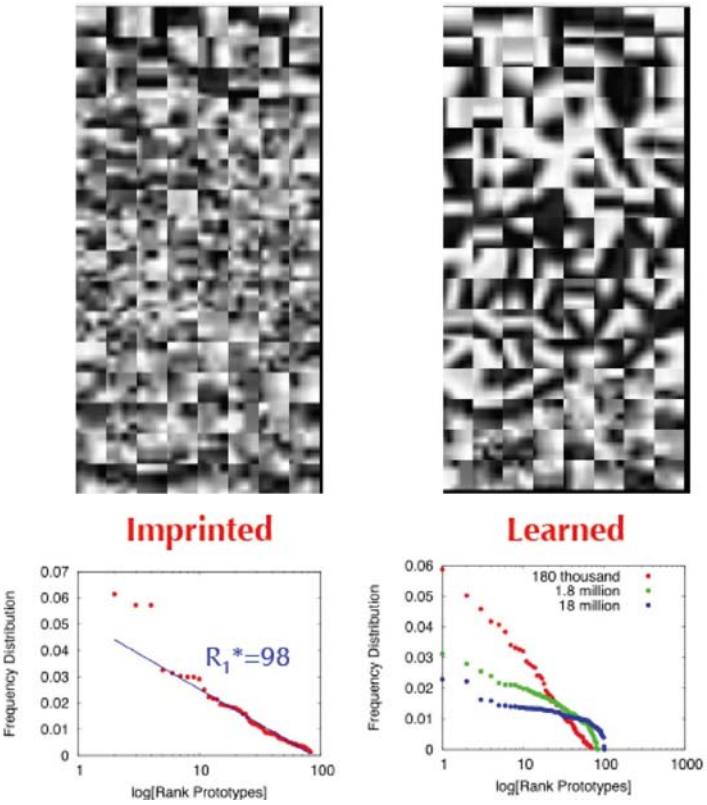


*Figure 1. Results of unsupervised learning of simple V1 cells. The left panel shows neuron receptive fields obtained via imprinting (the simplest form of learning, where the first image patch seen is retained). The right panel shows the resulting receptive fields after Hebbian learning with 18 million 5x5 pixel image patches. These show receptive fields that are compatible with sampling in vivo via electrophysiology. The lower left graph show the frequency of activation of prototypes, while the figure on lower right shows how learning creates higher entropy distributions, which are associated with optimal representation.*

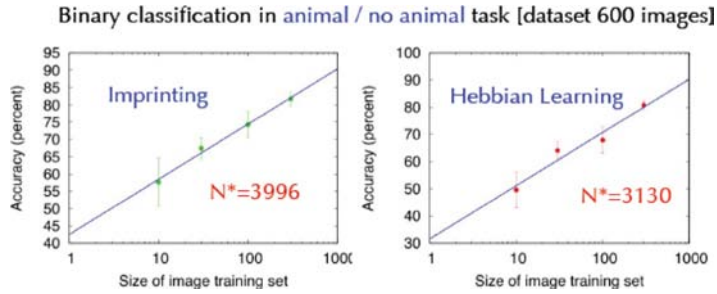


*Figure 2. Scaling of classification performance (animal/ no animal in natural scenes) with the size of the supervised training set. Left panel show the results with imprinted features and the right as the result of Hebbian learning. The extrapolation to perfect accuracy would require training sets of size 3000-4000 and suggests an advantage to learned features.*

## 2. Identify and Incorporate functional physiological elements

We have build detailed spiking neuron and mean field models of primary visual cortex and used these to explore the hypothesis that lateral (within layer) excitatory and inhibitory connection can enhance the ability to find large, topologically non-trivial objects amidst the confusion of visual clutter. We have results that show that this happens through the firing rate and persistence time of the activity of neural populations that are tuned to larger objects. These dynamical within-layer properties are not included in the original architecture of objective one. However when included they contribute performance gains in object recognition tasks. We are also studying the role of different learning rules in creating invariant representations of visual scenes.

## 3. Experimental Validation and Performance Evaluation

We have acquired permission from LANL's human subjects commission to perform experiments on human visual performance and brain imaging (EEG, MEG), We have performed several psychophysics experiments Figure 3, testing human performance in object categorization tasks - that is, testing human subjects the same way we are testing computers in objectives one and two. We are also studying the effects of masking (exposure to a second image after the original image) in degrading that performance. The original image is shown for only a tiny fraction of a second, and our ability to understand this image changes dramatically, depending on the masking image that is shown next. We measured the change in performance by varying the object and mask images [3], Figure 3. In this way we are elaborating a theory of optimal masking. This theory points to the importance of feature occlusion but also on a set of similarity transformations in image properties that may result in effective masking - that is, what it is that makes two images "similar" to our brain. We will continue to explore these hypotheses with a variety of rendered image and have started writing results up for publication.

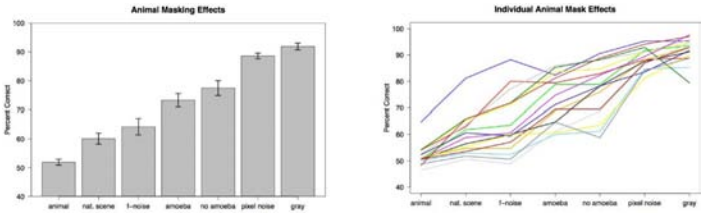


*Figure 3. Human visual performance in object recognition tasks (presence or absence of an animal in a visual scene) as a function of masking images. The left panel shows that natural scene masks are effective at decreasing human visual performance whereas pixel maps and gray screens are not. The right panel show individual subjects performance. We are currently determining which elements of the mask make it effective, via more detailed experiments that include electro-encephalograms and eye tracking.*

**4. Experimental Validation and Performance Evaluation**

We have now written object oriented versions of the codes developed under objective 1) and 2) and ported them to Bambino at the Center for Non-Linear Science, a small cell architecture machine similar to Cerrillos and Roadrunner.

We have also benchmarked our codes on different image sizes with the objective of building a system that can process High Definition video (which has a similar resolution as the human visual system) in real time. We anticipate having such a system running over the next few months, as we also continue to experiment with other computational platforms such as GPU (graphical processing units).

## Future Work

Having set up the basic architecture of visual cortex in model and computer codes and established several key features of human visual cognition through psychophysics experiments the project is now entering a crucial stage. First we will expose the model to an unprecedented quantity of visual imagery in order to create simple and complex features that represent the visual world accurately. We expect to establish stationary representations in primary visual cortex, where our current indications Figure 1, are that some optimality principles are at play, ensuring an efficient coding of information. We will then investigate whether representations with similar properties arise further up the visual cortical hierarchy. We will also study the role of supervised learning over large sets of labeled images in creating high-level representations of categories of objects and events. Our objective over the next year is to built a mathematical model and computational implementation that processes streaming visual experience (High Definition video) continuously, and that uses it to improve its internal representation of the visual world via learning. Such a system will integrate theory, computation and objective measures of visual performance in real time and provides a standard for further improvements via connectivity patterns that include lateral connections and feedback for example. In this respect we are also pursuing statistical model that make explicit the role of feedback connections in reducing object recognition uncertainty, via subjecting incoming sensory information to expectations in the for of Bayesian priors, We are also in the process of improving our visual cognition experiments via Electro-Encephalogram (EEG) recordings and eye tracking, which we expect will greatly reduce uncertainty in the observations of human subjects and help establish the role and locus of feedback in visual cognitive processes.

## Conclusion

Our objective is to deliver new synthetic cognition systems that match or surpass human visual performance in real-time object identification tasks. The project comprises four tasks: 1) to scale up hierarchical feed-forward networks to match the number of elements, connectivity and diversity of the visual cortex; 2) to include physiological elements such as spiking dynamics, lateral and feedback interactions, and time-dependent synaptic plasticity; 3) to measure brain activity, at both the single cell and systems levels, along with behavioral performance, on visual detection tasks; and 4) to develop full-scale real time models of the visual cortex. We are currently implementing such a system and in the process of unveiling the essential principles that allow the brain its extraordinary visual cognitive powers.

## References

1. Brumby, S. P., G. Kenyon, W. Landecker, C. Rasmussen, S. Swaminarayan, and L. M. A. Bettencourt. Large-Scale Functional Models of Visual Cortex for Remote Sensing. To appear in *Applied Imagery Pattern Recognition (AIPR 2009): Visions: Human, Animal, and Machines.* (Washington, DC, 13-15 Oct 2009).

2. A.Bettencourt, L. M., S. Brumby, V. Gintautas, M. I. Ham, S. Barr, P. Loxley, K. Sanbonmatsu, S. Swaminayaran, J. George, G. Kenyon, and I. Nemenman. Image categorization through hierarchical models of the primate visual system . Presented at *Neuroscience 2009 (Society for Neuroscience Annual Meeting).* (Chicago, 17-21 Oct 2009).

3. George, J. S., S. Barr, M. Ham, C. Renaudo, J. Hammond, V. Gintautas, S. Brumby, K. Sanbonmatsu, I. Nemenman, L. Bettencourt, and G. Kenyon. Not so Fast: Optimized masks increase processing time for object detection on speed-of-sight tasks . Presented at *Neuroscience 2009 (Society for Neuroscience Annual Meeting) .* (Chicago, 17-21 Oct 2009).

## Publications

Barr, S., V. Gintautas, J. L. Hammon, M. Ham, S. Brumby,

G. T. Kenyon, and L. M. A. Bettencourt. Preliminary Results from the Comparison of Human Visual Performance to Biologically Inspired Computer Object Categorization. Presented at *Decade of the Mind.* (Albuquerque, 13-15 Jan 2009).

Bettencourt, L. M.. The Rules of Information Aggregation and Emergence of Collective Intelligent Behavior . 2009. *topics in Cognitive Scienc .* **1** (4): 598 .

Bettencourt, L. M., S. Brumby, V. Gintautas, M. I. Ham, S. Barr, P. Loxley, K. Sanbonmatsu, S. Swaminayaran, J. George, G. Kenyon, and I. Nemenman. Image Categorization through Hierarchical Models of the Primate Visual System. Presented at *Neuroscience 09 .* (Chicago, 17-21 Oct 2009).

Brumby, S. P., G. Kenyon, W. Landecker, C. Rasmussen, S. Swaminarayan, and L. M. A. Bettencourt. Large-Scale Functional Models of Visual Cortex for Remote Sensing. To appear in *Applied Imagery Pattern Recognition (AIPR 2009): Visions: Human, Animal, and Machines.* (Washington DC, 13-15 Oct 2009).

George, J. S.. Casting Light on Neural Function: A Subjective History. To appear in *Imaging the Brain with Optical Methods .* Edited by Roe, A..

George, J. S., G. T. Kenyon, M. I. Ham, I. Nemenman, and L. M. Bettencourt. Modeling Consequences of Microscopic Eye Movements on Visual Spatial Perceptio. Presented at *Organization for Human Brain Mapping.* (San Francisco, 18-23 June 2009).

George, J. S., S. Barr, M. Ham, C. Renaudo, J. Hammond, V. Gintautas, S. Brumby, K. Sanbonmatsu, I. Nemenman, L. Bettencourt, and G. Kenyon. Not so Fast: Optimized Masks Increase Processing Time for Object Detection on Speed-of-Sight Tasks . Presented at *Neuroscience 09.* (Chicaho, 17-21 Oct 2009).

Kenyon, G. T.. Extreme Synergy:: Spatiotemporal Correlations Enable Rapid Image Reconstruction from Computer Generated Spike Trains . To appear in *Journal of Vision.*

# RADIUS: Rapid Automated Decomposition of Images for Ubiquitous Sensing

*Lakshman Prasad*
20090104DR

## Introduction

Today's explosive growth in the quality and quantity of satellite imagery calls for the automation of tedious and time-consuming image analysis tasks for timely Intelligence gathering. Image Intelligence analysts are overwhelmed with this flood of data. This has often resulted in lapses and delays in intelligence assessment. Automated tools that can detect and identify objects in these images reliably and at a rate faster than human experts are nonexistent. Today's computer-based image analysis largely relies on classifying image pixels based on color (spectral information) into features. This is a time-consuming operation as each satellite image typically contains hundreds of millions of pixels. Further, uniformity of color alone is not sufficient for identifying complex features on the ground. Our project addresses this limitation by taking a radically new approach to image analysis that is both efficient as well as perceptually meaningful. Rather than look at all pixels in an image, we focus only on those image pixels that lie on boundaries between image features. These edge pixels provide valuable shape information about objects and features. The main scientific goal of our project is to model human visual perception by computer programs in order to obtain meaningful completions of edges by 'joining the dots (edge pixels)'. Doing so will outline shapes in images, enabling their detection and recognition. Computing with a small subset of image pixels will result in rapid analysis, while the use of boundary pixels assures meaningful feature extraction. To ensure very high throughput, the project will realize these methods on multiprocessor computers. This high-risk scientific undertaking of computationally mimicking human visual perception has the high payoff of developing much-needed fast and powerful tools that speed up image analysis to assist Intelligence gathering for national security and defense applications.

## Benefit to National Security Missions

This project addresses the DOE mission of Threat Reduction by developing a critical capability of timely and reliable information extraction from imagery for national security applications. Additionally it supports the DOE Office of Science mission by addressing the computational modeling and simulation of human visual perception for advancing information science and technology. The generality of the problem addressed, namely image feature extraction, also supports other mission applications including environmental monitoring for remediation and restoration and space and materials image data analysis.

## Progress

In the first year of the project we developed a highly efficient and flexible computational architecture to facilitate rapid development of image analysis algorithms. The anatomy of this software architecture consists of a C program that efficiently performs computationally intensive tasks on images based on directions from algorithms written in the rapid prototype environment of Matlab. This architecture is designed to reflect and support the two overarching goals of the project, namely, 1) the development of advanced algorithms that extract meaningful information from images towards their understanding, and 2) the rapid processing of large image datasets to facilitate the timely utility of the steady stream of imagery from today's sensors. The purpose of this architecture is to enable simultaneous progress on both these fronts, namely algorithm innovation and acceleration.

It is critical that our approach to image analysis scales efficiently to utilize the available processing power to accommodate large images. We have designed efficient algorithms whose processing time is proportional to the number of pixels in an image. To ensure similar scalability with processors, we have developed parallel-processing versions of these algorithms, wherein a large image is divided up among multiple processors and all of the processors compute results for their individual allocations simultaneously. Key to achieving efficient scalability is ensuring that the individual processors' results are integrated with minimal overhead. Using a message-passing interface (MPI) to communicate between processors, we have been able to achieve processing rates of eighteen million pixels per second

(~1.5 terapixels/day) on a sixteen-core desktop computer. This early benchmark has already put us within reach of our target rate of 8 terapixels/day on a few such machines for coping with typical dataflow from modern satellites.

Our project exploits structural (e.g., shape) and spectral (e.g., color) cues in imagery to delineate features of interest. Contours in images form a starting set of feature primitives. An initial set of polygons is constructed from these contours. These polygons are then hierarchically grouped into larger polygons that result in objects and features at multiple scales. To obtain polygons faithful to image features, we have formulated several new criteria that characterize elementary perceptual rules. These are based on individual feature characteristics such as contour saliency and polygon shape, as well as ensemble properties that measure the distribution of color, texture, granularity, anomaly, etc of image polygons at each stage of the hierarchy. Further, using these criteria, we have developed polygon grouping rules that have yielded useful segmentations of images into features. This is a first and major step towards search and identification of features with a generic quality, such as man-made features, textures, etc., and also of specific features such as roads, rivers, buildings, forestry, etc. This is key to making robust categorical judgments to assist the image Intelligence analyst.

Three potential sponsors were briefed on the project showcasing the potential of the ongoing work to their areas of application/interest:

1. The National Geospatial-Intelligence Agency (NGA) was briefed on the project's goals and value to the Intelligence Community.

2. Digital Globe Inc., the worlds leading satellite-imaging company, was briefed on our use of high performance computing in large-scale image analysis. This has resulted in a new Cooperative Research and Development Agreement (CRADA) partnership for studying underwater terrain (optical bathymetry).

3. Collaborators on an ongoing NOAA environmental monitoring project NEBO (http://nebo.whoi.edu/ ) were briefed to showcase the significant improvements over what NEBO has been using for image analysis of the ocean floor. As an outcome of this briefing, NOAA will seek follow-on funding for leveraging LANL's capabilities for oceanic environmental impact studies.

4. A proposal to DOE NA-42, titled "Stabilization Radiography Tool", using methods developed in the project to analyze radiographic imagery for application to stabilization of clandestine nuclear devices was submitted. This proposal was funded to start in FY 2010.

5. A patent application was filed based on algorithms developed so far in the project.

## Future Work

In the subsequent year of the project we will develop to detect and identify specific features obtained from our hierarchical decomposition of images into features. In particular, we will develop methods that can compare two features in terms of their shape and color characteristics and decide if they are similar enough. This will give us a method of searching for objects with known/desired characteristics in images. We will then develop methods to relate objects and features in their vicinity to form contextual feature scenarios. This will help identify complex targets such as a nuclear power plant, an urban locality, or a storage facility.

In the final year, we develop methods for assigning confidence measures to detections and identifications of targets in images. This will enable the matching and recognition of complex feature scenarios and multiple related targets. We will test the methods developed in the project against commercial satellite imagery and make improvements to performance efficacy and efficiency.

## Conclusion

Scientifically, the project will provide computational insights into human-centric image understanding. Technologically, the project will develop a capability to rapidly extract and assess information from satellite and aerial imagery. Specifically, the project will deliver efficient computer algorithms and software that will scale in performance on single processor and multiprocessor platforms. This will enable the extraction of manmade and natural features and contextually relate them to identify complex and composite scenarios such as urban infrastructure, nuclear facilities and lines of communication. These identifications will be responses to analyst queries for features of interest, thus facilitating and expediting Intelligence assessment. The project will result in novel computer codes that can be used by US Defense, Intelligence and other government agencies for timely image exploitation.

## Publications

Prasad, L., and J. Theiler. A structural framework for anomalous change detection and characterization. 2009. In *SPIE Defense and Security Symposium.* (Orlando, FL, April, 2009). , p. 7341. Bellingham, WA: SPIE.

Prasad, L., and L. Latecki. Object Detection by Perceptual Edge Filtering and Chamfer Edge Matching . To appear in *Pattern Recognition.*

Prasad, L., and S. Swaminarayan. A Framework for Perceptual Image Analysis. To appear in *43rd Asilomar Conference on Signals, Systems, and Computers.* (Pacific Grove, CA, 1-4 Nov. 2009).

# The Physics of Algorithms

*Michael Chertkov*
20070063DR

## Abstract

Many problems in information processing that are important for Los Alamos are computationally complex at a fundamental level. Algorithms guaranteed to find the best solution to these problems require an exponentially large amount of time, making them completely impractical. We have applied methods from statistical physics to develop efficient *heuristic* methods that rapidly find good approximate solutions. By providing a solid theoretical basis for these heuristics, statistical physics allows us to mathematically quantify the performance of these algorithms for high-reliability applications, and to systematically design improvements. Key tasks have included solving complex statistical inference problems such as motion tracking in videos, designing distributed network algorithms for routing and community detection, and developing multi-objective optimization schemes to minimize path length and energy consumed. Many of these algorithmic problems are central to a wide array of data-intensive challenges, including understanding the spread of epidemics and identifying adversary social networks.

The broader and more ambitious objective of our project was to develop a new interdisciplinary field that has been emerging over the past five years in the international scientific arena, and to establish a long-term capability at LANL in this area. Our research contributions, supporting DOE missions in threat reduction, nuclear weapons, and renewable energy, have helped the Laboratory merge information theory, statistical physics and computer science while building an internationally-recognized community of experts in a new branch of Information Science and Technology.

## Background and Research Objectives

Current and future national security applications at Los Alamos National Laboratory depend on a fundamental set of computer science problems, involving manipulation of large collections of interacting components and analysis of large data sets. Solving these requires effective algorithms that can operate in reasonable time spans. Additionally, many of the applications, such as organizing a communication network among distributed sensors, have constraints such as physical size, energy consumption, and the specific type of information that can be processed; we need efficient algorithms to optimize the systems under such constraints. Due to the scale of the data sets and the importance of the results, proposed methods must meet higher standards than those required in most industrial and commercial settings.

Faced with the need for better algorithms for large-scale discrete computational problems, scientists have increasingly turned to techniques from statistical physics, used to analyze large-scale complex systems and produce system-level predictions. Error probabilities in efficient, nearly optimal, error-correcting codes have been quantified by a mapping to studies of disordered magnets. Predictive models for computational tractability in constraint satisfaction problems draw upon the phase transition between order and disorder. These connections have led to novel techniques, such as message-passing algorithms, that vastly outperform previously suggested methods.

Our project aimed at developing a broad capability at LANL in the physics of algorithms, applicable to modern challenges in information technology. We proposed to use a unified set of approaches, drawn from statistical physics, information theory and computer science, to develop general algorithms benefit LANL applications ranging from network monitoring to data reconstruction to logistical problems. Furthermore, the algorithmic problems studied, such as community detection, are essential to a wide array of challenges in network science, including biological networks and adversary social networks.

## Scientific Approach and Accomplishments

Broadly speaking, our research approach consisted of three key steps: (a) State the problem in terms of optimization and/or inference and/or learning, (b) Develop and extend a heuristic algorithm, and (c) Analyze the algorithm. This approach was applied to problems ranging from community detection, to spread of epidemics, to tracking of particles in turbulent fluids. Some of our main accomplishments are outlined below.

**Statistical inference**

A substantial part of our scientific contributions concerned *message-passing algorithms*, a powerful technique in probabilistic inference that has become the focus of intense study in the past few years. One of the most well-studied algorithms of this kind, *belief propagation*, is extremely successful on problems where variables can be modeled as nodes on a graph or network, and the graph contains few or no cycles.

We developed a general framework, called Loop Calculus, for expressing exact statistical inference problems using a specific form of the belief propagation algorithm that is computationally tractable, i.e., whose running time grows linearly in the number of variables in the problem, or at worst as some low power of the number of variables. A significant result was the discovery of a new class of graphical models that, in spite of containing many loops, are nevertheless solved exactly by an algorithm of the Belief Propagation type. This approach was then adapted to count solutions in graphical models, including in a number of combinatorial optimization problems where finding the optimum is already considered computationally hard (and counting optimal solutions is considerably harder).

Among the many applications of belief propagation, we considered the problems of community detection and clustering. We developed a novel algorithm that, in practice, runs in nearly linear time on graphs with the *small-world* structure characteristic of social and technological networks. In the standard "four groups" accuracy test for community detection methods, it outperformed all other polynomial-time algorithms and its performance is in many cases comparable to the best exponential-time algorithm tested there.

We also used belief propagation to track moving objects in a video sequence. We developed algorithms that input a video of stochastic particle motion, such as in a turbulent fluid, and efficiently track small identical particles in it. This is an enormous computational challenge, as it requires finding the most likely matches within a graphical model with billions of variables (corresponding to gigabyte-size video frames). An extension of the algorithm also allows efficient learning of the environment (diffusivity) and the flow (local velocity gradient).

Additional contributions included the development of a ranking algorithm that allows inference based on data that can contain systematic errors, such as upsets that occur in competitions. Statistical physics methods including scaling techniques, random-walk analysis, and Monte Carlo simulations were used to establish the algorithm and test its performance. The algorithm, which uses a gradual elimination schedule, has a running time that is polynomial in the number of ranked elements.

Finally, we developed a generalized hybrid Monte Carlo (GHMC) algorithm that solves the problem of reconstructing a contaminant release history, in both a fast and statistically optimal way. The approach is applicable in general to large-scale, strongly nonlinear systems with parametric uncertainties and data corrupted by measurement errors.

**Network problems**

We studied numerous algorithmic problems whose natural definitions involve networks, and can be described mathematically using the language of graph theory.

We developed routing algorithms for effective information diffusion in ad hoc networks and sensor networks, where communication between nodes is determined locally (and often though "selfish" decisions by each node) rather than through any centralized authority. These algorithms included a class of probabilistic, locally congestion-aware routing protocols. We developed a protocol called the Locally Minimum Cost Forwarding method where one finds, through the study of game-theoretic equilibria, that in practice the solution costs are within a constant factor of the optimum. We studied the problem of placing additional nodes owned by a single profit-maximizing entity into an existing network of nodes that pay each other according to standard mechanism design rules for forwarding each other's traffic. A number of polynomial-time heuristic algorithms were proposed for finding acceptable approximate solutions. Finally, we developed an end-to-end routing metric, ETOP, that accurately captures the expected number of link layer transmissions in wireless mesh networks, and we tested our network routing schemes against standard testbed cases.

We studied a number of structural properties of networks under addition and deletion of nodes. Using kinetic theory, we obtained analytical solutions for properties

that include the number of dangling nodes and the network diameter. We also developed and studied a set of graph reduction algorithms that took network data and generated an ensemble of smaller graphs that were statistically similar. Applied to real historical data on internet connections at the router level, this approach produced networks with features closely resembling snapshots of the (smaller) internet from several years earlier. Furthermore, we studied how synchronization of a network of identical oscillators is affected when adding, removing, and moving single edges in the network. This suggested specific strategic rewiring schemes.

For the problem of *multi-objective* optimization on different classes of networks with randomly assigned edge weights, we considered the growth in the number of pareto-optimal paths. We found the distribution of the number of paths to be independent of the distribution of weights under certain conditions, and we established new scaling properties.

Finally, merging our work on network analysis and probabilistic inference, we used additional data on the Swedish Transmission Network of HIV virus, together with an analysis based on coalescent theory, to improve our understanding of the connection between phylogenetic trees and transmission networks. We found that the coalescent theory made very definite predictions as to when the transmission network could or could not be reconstructed, and that these predictions were consistent with both the original and more recent data.

**Theoretical and mathematical underpinnings**
A number of more basic theoretical discoveries enabled many of our algorithmic results.

We developed a novel approach, called *quantum belief propagation*, for performing calculations in quantum systems and in classical systems in continuous time. In particular, this led to a new algorithmic technique for implementing belief propagation with high accuracy in systems with time dependence.

We recast the framework of Gaussian belief propagation (GaBP) based on a representation of a matrix's determinant as a product over orbits of a graph. This new perspective resulted in a new algorithm that evaluates determinants of sparse matrices in time scaling linearly with the system size.

We investigated the graph bisection problem, where a network must be cut into two pieces of equal size while minimizing the number of cut edges. A study of the physical "phase structure" of this problem on random graphs revealed a surprising clustering phase transition in the problem's solution space, and an associated algorithm that optimizes typical instances of the problem much more rapidly than was previously believed possible. A further study on a different (geometric) random model revealed a novel methodology for applying belief propagation to optimization problems with global constraints. This methodology in turn suggests efficient approximation algorithms for a large range of optimization problems with global constraints, including the notorious traveling salesman problem.

## Impact on National Missions

The aim of this project was to develop a Laboratory-wide capability in a new interdisciplinary field that impacts both science and security. An understanding of the behavior of large-scale computational algorithms is becoming central to data-intensive challenges. This challenge encompasses problems as diverse as community detection in adversary social networks and particle tracking in fluid mechanics experiments. Our results highlighted above, together with the longer-term capabilities we have developed, support Laboratory missions in Threat Reduction and Nuclear Weapons. Specific programs benefiting from these new capabilities include the Laboratory's Information Science & Technology Center, the National Infrastructure Simulation and Analysis Center (NISAC) and initiatives in interdiction analysis and power grid modeling. New work brought to the Laboratory includes a DOE/ASCR-funded project on "Algorithms for Large-Scale Network Interdiction Problems" and an NSF-funded project (through the New Mexico Consortium) on "Harnessing Statistical Physics in Computing and Communications." Additional external funding attracted by our project includes an NSF Focused Research Group grant on "Quantum Spin Systems" and a Marie Curie Reintegration grant from the European Union on "Phase Transitions in Combinatorial Optimization."

Furthermore, our project's scientific contributions have helped attract new staff of an extraordinary high caliber, helped the Laboratory build a recognized algorithmic strength in research on the DOE priority area of renewable energy, and established at Los Alamos an internationally-recognized community of experts on the Physics of Algorithms. We recruited six postdocs, including one Oppenheimer Fellow (Konstantin Turitsyn) and two Director-Funded Fellows (Lenka Zdeborova and Jason Johnson), and more than 10 graduate students worked on the project. Our work has led to an LDRD/DR new start in "Optimization and Control Theory for Smart Grids" and an LDRD/ER project on "Network Interdiction." The DR project will bring our novel tools to a national

challenge: the Smart Electrical Grid, capable of ingesting intermittent renewable sources. Our research within the broader context of the international scientific community has been anchored by a large number of productive collaborations, with institutions including MIT, Claremont Graduate University, the Institute Pasteur, Université Paris-Sud and CNRS in France, and the Landau Institute in Moscow. The first two of these have given rise to large-scale collaborations: a significant fraction of our recruited students and postdocs have come from the MIT Laboratory for Information and Decision Systems; the Claremont collaboration offers numerous future opportunities for student recruitment through the joint Mathematics Clinic that we have just initiated with the Claremont Colleges. Finally, these collaborations and our scientific recognition have been solidified by three workshops we have organized, in May 2007, March 2008 and September 2009, each attracting 40-60 participants including some of the most distinguished scientists worldwide in information theory, statistical physics and computer science.

## Publications


Antal, T., D. ben-Avraham, E. Ben-Naim, and P. L. Krapivsky. Front Propagation in Flipping Processes. 2008. *Journal of Physics A.* **41**: 465002.

Bardonjic, M., A. Hagberg, and A. G. Percus. Combinatorial Analysis of Geographical Threshold Graphs. Presented at *The 8th Latin American Theoretical Informatics Symposium, 2007 .* ( , 2008).

Ben-Naim, E., M. Hastings, and D. Israelevitz. Statistics of partial minima. 2007. *Journal of Physics A: Mathematical and Theoretical.* **40** (47): F1021.

Ben-Naim, E., and N. W. Hengartner. Efficiency of Competitions. 2007. *Phys. Rev. E.* **76**: 026106.

Ben-Naim, E., and P. L. Krapivsky. Addition-Deletion Networks. 2007. *J. Phys. A.* **40**: 8607.

Ben-Naim, E., and P. L. Krapivsky. Condensates in Driven Aggregation Processes . 2007. *Phys. Rev. E.* **75**: 011103.

Ben-Naim, E., and P. L. Krapivsky. Phase Transition with Non-Thermodynamic States in Reversible . 2008. *Phys. Rev. E .* **77**: 061132.

Boettcher, S., B. Goncalves, and H. Guclu. Hierarchical Regular Small-World Networks. 2008. *Journal of Physics A.* **41**: 252001.

Bokolamulla, D., T. Aulin, and A. Hansson. Low-complexity iterative detection based on limited bi-directional search. 2006. *IEEE Proceedings -- Communications.* **153**: 933.

Bradonjic, M., A. G. Percus, and V. P. Roychowdhury. Topology Control with Geographical Threshold Graphs. 2007. *LAUR pending.*

Bradonjic, M., T. Mueller, and A. G. Percus. Coloring geographical threshold graphs. 2008. *LA-UR08-5098.*

Chernyak, V., and M. Chertkov. Loop Calculus and Belief Propagation for $q$-ary Alphabet: Loop Tower. 2007. In *IEEE ISIT 2007, arXiv:cs.IT/0701086.* (Nice, June 20-26, 2007). , p. 1. Nice: IEEE.

Chernyak, V., and M. Chertkov. Fermions and Loops on Graphs. I. Loop Calculus for Determinant. 2008. *JSTAT.* : P12011.

Chernyak, V., and M. Chertkov. Fermions and Loops on Graphs. II. Monomer-Dimer Model as Series of Determinants. 2008. *JSTAT.* : P12012.

Chertkov, M.. Exactness of Belief Propagation for some Graphical Models with Loops. 2008. *JSTAT.* **P**: 10016.

Chertkov, M., L. Kroc, F. Krzakala, M. Vergasolla, and L. Zdebarova. Tracking particles by passing messages between images. *Proceedings of National Academy of Sciences.*

Chertkov, M., L. Kroc, and M. Vergassola. Belief Propagation and Beyond for Particle Tracking. 2008. *LA-UR-08-3645.*

Chertkov, M., V. Chernyak, and R. Teodorescu. Belief Propagation and Loop Series on Planar Graphs. 2008. *JSTAT.* **P**: 05003.

Chertkov, M., V. Gomez, and H. J. Kappen. Approximate inference on planar graphs using Loop Calculus and Belief Propagation. *Journal of Machine Learning Research.*

Eidenbenz, S., and S. Kakumanu. Local heuristics for multi-radio networks. 2007. *LAUR pending.*

Ercal-Ozkaya, G., S. Eidenbenz, A. Meyerson, and A. Percus. On a Locally Minimum Cost Forwarding Game. 2007. *LA-UR-07-6304.*

Goncalves, B., G. Istrate, A. G. Percus, and S. Boettcher. The core peeling algorithm for graph bisection: an experimental evaluation. 2006. *LA-UR 06-6863.*

Guclu, H., and M. Yuksel. Limited Scale-Free Overlay Topologies for Unstructured Peer-to-Peer Networks. 2009. *IEEE Transactions on Parallel and Distributed Systems .* **20** (5): 667.

Gutfraind, A., A. Hagberg, D. Israelevitz, and F. Pan. Interdiction of a Markovian Evader. Presented at *ALENEX09.* (ALENEX09, 2009).

Hagberg, A., D. Shult, and P. J. Swart. Exploring network structure, dynamics, and function using NetworkX. 2008. In *SciPy2008.* (Pasadena, Aug 2008). , p. 11. Pasadena: Pyton.

Hagberg, A., and D. A. Shult. Network Resistance to Synchronization. 2007. *LA-UR Pending.*

Hagberg, A., and D. Shult. Rewiring networks for synchronization. 2008. *Chaos.* **18**: 037105.

Hastings, M.. Quantum Belief Propagation. 2007. *Phys. Rev.B.* **76**: 201102.

Hastings, M.. Inference from Matrix Products: A Heuristic Spin Glass Algorithm. 2008. *Physical Review Letters.* **101**: 167206.

Hastings, M., E. Ben-Naim, and D. Izraelevitz. Statistics of Partial Minima. 2007. *Journal of Physics A.* **40**: F1021.

Istrate, G., S. Kasiviswanathan, and A. G. Percus. The cluster structure of minimum bisections of sparse random graphs. 2007. *LA-UR 06-6566.*

Istrate, G., S. Kasiviswanathan, and A. G. Percus. The cluster structure of minimum bisections of sparse random graphs. 2006. *LA-UR 06-6566.*

Jonson, J., V. Chernyak, and M. Chertkov. Orbit-Product Representation and Correction of Gaussian Belief Propagation. To appear in *International Conference on Machine Learning (ICL) '09.* (Toronto, July 2009).

Krishnamurthy, V., M. Faloutsos, M. Chrobak, J. H. Cui, L. Lao, and A. G. Percus. Sampling large internet topologies for simulation purposes. 2007. *Computer Networks.* **51**: 4284.

Percus, A. G.. The traveling salesman problem and kth-nearest neighbors. 2006. *LA-UR 06-6896.*

Percus, A. G., G. Istrate, S. Kasiviswanathan, S. Boettcher, N. Hengartner, and B. Goncalves. Belief propagation for graph bisection. 2006. *LA-UR 06-6868.*

Ramaswamy, V., A. Hansson, and S. Eidenbenz. COBRA: A multi-path adaptive local load sensing routing protocol for wireless sensor networks. 2007. *Technical Report LA-UR-07-2905.*

Rani, D., H. Guclu, and M. Yuksel. Ad Hoc Limited Scale-Free Models for Unstructured Peer-to-Peer Networks. 2008. In *IEI P2P.* (Aahen, Germany, 2008). , p. 160. Aahen, Germany : IEEE.

Wang, C., J. D. Hyman, A. G. Percus, and R. Caflisch. Parallel tempering for the traveling salesman problem. 2008. *LA-UR 08-5100.*

Yanmaz, E., and H. Guclu. Improving Event Coverage in Wireless Sensor Networks. Presented at *Infocom 2009.* (Rio de Jeneiro, Brazil , April 2009)

# Nonconvex Compressed Sensing

*Rick Chartrand*
20080128ER

## Introduction

The project will develop techniques that allow images or other signals to be reconstructed from much fewer data than are currently regarded as necessary. Whenever measurements are expensive, dangerous, or simply unavailable in large quantities, what would seem to be an impossible reconstruction task can become completely feasible. Examples being developed include image reconstruction from limited radar assets, imaging from sonar data where transmission or processing is difficult, replacing X-ray CT with a handful of X-rays that can be collected more quickly and with less dose, and rendering the much safer MRI scan more feasible by shortening scan time and increasing hospital throughput. The success of the project depends on fundamental advances in mathematics, in particular relating to difficult optimization problems that are widely regarded as intractable, yet this project has shown to be solvable using simple and highly efficient algorithms. The theoretical developments will provide insights into how to more efficiently process the information content of data, and not the data itself, which is becoming increasingly important as data sets become increasingly unwieldy.

## Benefit to National Security Missions

The ability to decrease data sizes while preserving information addresses a key challenge of DOE/SC. The ability to reconstruct satellite images from extremely limited ground-based radar measurements can have major intelligence impact. Remote sensing and sonar measurements can have operational bottlenecks removed by decreasing the amount of data that needs to be collected. Neural activity can be reconstructed from EEG measurements in a novel way, permitting neuroscience advances. These are just some of the benefits that arise from having algorithms that can successfully and efficiently reconstruct images and other signals from very few data.

## Progress

The key to the accomplishments of this project is the nonconvexity of the underlying optimization problems. This is what allows the reconstruction of images and signals from so few data. However, this flies in the face of typical optimization practice, where one often strives to make a problem convex, and thereby gain access to the many efficient algorithms available. Efficiency is crucial for many applications, where the size of a typical problem may make many algorithms intolerably slow. Consequently, a crucial development this past year has been the development, in an important special case, of an algorithm that performs extremely efficiently for nonconvex compressive sensing, competitive with the fastest state-of-the-art convex algorithms [1]. Importantly, the scaling of the algorithm to larger problems is also desirable, having the O( N log N ) computational complexity of the fast Fourier transform. Additionally, the algorithm is inherently parallelizable, allowing even larger problems to be solved when many processors are available.

An additional development has been a family of techniques that allow the above algorithm approach to be very flexible, and applied to many different computational problems. For example, one may wish to enforce a data constraint exactly when the measurements are of high quality. If the data are noisy or the model inexact, a softer, inequality constraint will give better results. One may also wish to impose other constraints, such as inequalities that dictate that the solution values cannot be negative, or exceed some maximum value. Each of these cases corresponds to a different optimization problem, which ordinarily would be solved using a different approach. However, the “operator splitting” approach used in this project decomposes the problem into simpler components, with the component corresponding to the constraints being one-dimensional (applied independently to each coordinate), and therefore very simple to adapt. This

greatly increases the applicability of the approach.

## Future Work

Our project addresses the issue of reconstructing signals (including images, network states, signals of any other form) from severely under-determined linear systems. The method is to exploit the sparsity or compressibility of essentially all useful signals. This is currently done in the recent body of work known as "compressive sensing." This project explores the use of a nonconvex variant of these methods, which appears to allow successful reconstruction using even fewer measurements than the methods in the literature.

We will develop algorithms that allow the techniques to be useful for various important applications. For many imaging examples, the algorithms must be efficient enough to be feasible on high-resolution 3-D images. This requires cutting-edge optimization methods for maximizing efficiency and scalability, as well as allowing parallelization. This is much more challenging when the optimization problems are nonconvex, as is required to obtain the benefits of reconstruction from the fewest possible measurements. Other applications will require customizing algorithm performance, such as allowing noise tolerance to vary according to heterogeneous properties of the measurements. Theoretical work will be needed to establish convergence properties of the algorithms.

## Conclusion

The algorithms being developed will allow threats to be detected in contexts where traditional methods would have insufficient data. CT scans can be made less hazardous by decreasing X-ray exposure. MRI scans are often an alternative to CT that is completely safe, but under-utilized due to the high hospital cost that results from the long scan time required. The methods being developed in this project can cut the scan time by as much as 80%, drastically increasing the feasibility of the procedure.

## References


1. Chartrand, R.. Fast algorithms for nonconvex compressive sensing: MRI reconstruction from very few data. 2009. In *IEEE International Symposium on Biomedical Imaging.* (Boston, June 28 -- July 1, 2009). , p. 262. Piscataway: IEEE.


## Publications


Chartrand, R.. Nonconvex compressive sensing and reconstruction of gradient-sparse images: random vs. tomographic Fourier sampling. 2008. In *IEEE International Conference on Image Processing.* (San Diego, 12-15 Oct. 2008). , p. 1. Piscataway: IEEE.

Chartrand, R.. Exact reconstructions of sparse signals via nonconvex minimization. 2007. *IEEE Signal Processing Letters.* **14**: 707.

Chartrand, R., W. Yin, and IEEE. Iteratively reweighted algorithms for compressive sensing. 2008. In *33rd IEEE International Conference on Acoustics, Speech and Signal Processing ; 20080330 - 20080404 ; Las Vegas, NV.* , p. 3869.

Chartrand, R., and V. Staneva. Restricted isometry properties and nonconvex compressive sensing. 2008. *INVERSE PROBLEMS.* **24** (3).

Saab, R., R. Chartrand, O. Yilmaz, and IEEE. Stable sparse approximations via nonconvex optimization. 2008. In *33rd IEEE International Conference on Acoustics, Speech and Signal Processing ; 20080330 - 20080404 ; Las Vegas, NV.* , p. 3885.

Sidky, E. Y., I. Reiser, R. M. Nishikawa, Xiaochuan Pan, R. Chartrand, D. B. Kopans, and R. H. Moore. Practical iterative image reconstruction in digital breast tomosynthesis by non-convex TpV optimization. 2008. In *Medical Imaging 2008: Physics of Medical Imaging ; 18-21 Feb.* ( 2008 ; San Diego, CA, USA). Vol. 6913, p. 691328

# Foundations for Practical Pattern Recognition Systems

*Reid B. Porter*
20080182ER

## Introduction

This project aims to provide a deeper understanding and better control of pattern recognition systems as they are used in practical environments. In practical environments the pattern recognition system is rarely used in isolation. Most of the time a human user is intimately involved in the data preparation, interpretation and validation. In recent years a firm theoretical base has been developed for large classes of pattern recognition systems. However, the main results have been for the standalone black-box type systems, and the main objective has been to remove the user from the design and validation as much as possible. This project will develop the theoretical base for the practical environment by focusing on the end-user. The first objective is to provide a theoretical foundation for a transparent pattern recognition approach, which will allow users to inspect and understand how the system makes its predictions. The second objective is to provide user-in-the-loop solutions to specific applications, and demonstrate complete pattern recognition systems, where the user and the computer work in partnership to solve complex data analysis problems.

## Benefit to National Security Missions

This project will support the NNSA mission in Nonproliferation by increasing our understanding and improving performance of mission critical pattern recognition systems used, for example, in the detection and classification of electromagnetic pulses from space, and in the identification and classification of proliferation signatures in satellite imagery and video. It also supports DHS/DNDO needs in nuclear foreinsics, for example, by providing computational tools to assist knowledge capture and knowledge management of the nuclear fuel cycle.

## Progress

The project initially focused on learning discrete classifiers for two-class classification with independent and identically distributed (IID) examples. Our first accomplishment was to investigate and develop new algorithms for optimal dyadic decision trees (DDT). Dyadic decision trees provide a solution method that exactly minimizes complexity-penalized misclassification loss. This loss can be linked to estimation error, which means the approach is consistent (with infinite samples the method approaches optimal) and provides better visibility and control than many other approaches. This project developed solutions that yield faster run times, use less memory, and simplify the user interface compared to existing methods. Specifically we have transformed the traditional bottom-up (dynamic programming) algorithm into a top-down (memorized) algorithm which allowed us to add a" look-ahead pruning" heuristic that significantly improved the run time and memory usage. We also replaced the typical "dynamic dictionary" data structure with a "universal hash table" which further improved the run time. Finally, we developed an efficient and automated algorithm for selecting the tuning parameters, which lead to a simpler user interface and low error rates. An article describing this work has been submitted to the Journal of Machine Learning Research.

Dyadic decision trees control representation, estimation, and computational errors through an efficient optimization of complexity penalized misclassification loss. While this appears to work well on general purpose computers for problem sizes up to fifteen to twenty dimensions, it does not explain the performance of other pattern classification tools which use a convex surrogate for misclassification loss and scale to much higher dimensions. Our second main accomplishment was to develop a framework for decision tree type classifiers that may address some of these questions. The approach is based on the Stack Filter model class from nonlinear signal processing. This model class commutes with thresholding and can be generalized to include all discrete mappings, e.g., the class of decision

trees. These properties provide a way to understand how a wide range of loss functions affect representation, estimation and computation errors for decision trees. We call this framework, Ordered Hypothesis Machines (OHM). We have developed a representation for the framework that increases the size of the model class (leading to arbitrarily low representation error) but does not increase the size of the optimization problem used in training (reduced computational error). We have applied OHM to several synthetic and benchmark datasets and have obtained promising results in reasonable time, e.g., comparable performance to the dyadic decision tree approach. An article describing this work was presented at the International Symposium on Mathematical Morphology.

Our third main accomplishment has been to develop the application domains for our work. These included:

Content-based search of images: we have shown that many instances of the 'query by example' problem can be cast as a particular two-class classification problem. This approach provides a new similarity measure, which quantifies the relative concentration of the query image distribution to the input image distribution, and allows us to employ our previously developed computationally efficient solution methods. Figure 1 shows an example of this approach applied to image segmentation. This work was presented an the Asilomar Conference on Signals, Systems & Computers.

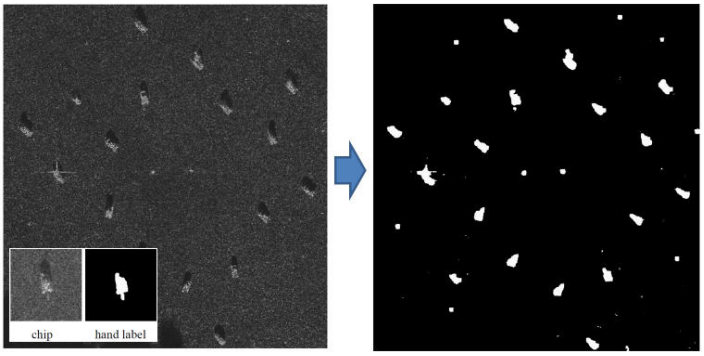


*Figure 1. Left) An input image and (insert) an example of a query image, Right) Predicted segmentation produced by the two-class classification approach.*

User modeling: we are developing a novel experimental environment for capturing human-computer interactions relevant to image and video understanding. This interactive environment is shown in Figure 2, and it forces users to solve an image recognition problem in a way that exposes their sequential decision making process. Our objective is to build discrete classifiers using these observations, and thereby captures the user's domain knowledge in a user-model, which can then be used to simulate and predict the user's interactions. There are a large number of potential applications for this novel use of pattern recognition. Our initial work contributed to several successful proposals where this approach is being developed for specific application domains e.g. nuclear forensics and geo-spatial situational awareness.

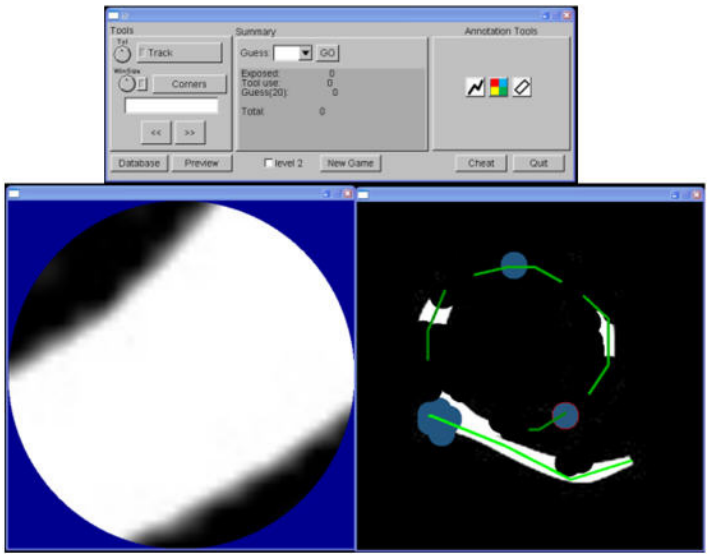


*Figure 2. An experimental environment for developing and demonstrating user-models. The user is forced to solve a sequential decision making process, which is captured by the environment, and then pattern recognition methods are used to model this process.*

## Future Work

Our main focus in the final year of the project is to expand and define how pattern recognition systems can be most effectively used within practical user environments. We will continue to develop new forms of interaction such as query by example, as well as active learning scenarios. We will continue to develop our user modeling environment with the aim of demonstrating a unique capability in what we believe is an emerging area. In addition to these new directions, we will also be finishing up theoretical work and submitting additional publications on our Dyadic Decision Tree and Ordered Hypothesis Machine research.

## Conclusion

Advancing the state-of-the-art in pattern recognition will provide an ability to digest and analyze orders of magnitude more data than we currently can, and vastly reduce data storage and exploitation costs. This project uniquely obtains these performance improvements by increasing the productivity of users in practical data analysis environments. By equipping users with pattern recognition tools they can understand and apply with confidence to tedious and labor intensive tasks, this project provides users with more time to concentrate on the more subtle and difficult data interpretation tasks.

## Publications

Hush, D., and R. Porter. Algorithms for Optimal Dyadic Decision Trees. *Machine Learning Research.*

Hush, D., and R. Porter. Density-Based Similarity Measures for Content Based Search. To appear in *Asilomar Conference on Signals, Systems, and Computers* . (Pacific Grive, CA, 1-4 Nov).

Porter, R., B. G. Zimmer, and D. Hush. Stack Filter Classifiers. 2009. In *International Symposium on Mathematical Morphology.* (Groningen, The Netherlands, 24-27 August). , p. 282. Berlin: Springer.

Porter, R., B. G. Zimmer, and D. Hush. Ordered Hypothesis Machines. 2009. *Internal Technical Report.*

Porter, R., C. Ruggiero, and J. D. Morrison. A Framework for Activity Detection in Wide-Area Motion Imagery. 2009. In *Visual Information Processing XVIII, Proceedings of the SPIE.* (Orlando, Florida, 10 March). , p. 73410O. Orlando: SPIE.

# Multilevel Adaptive Sampling for Multiscale Inverse Problems

*John D. Moulton*
20080300ER

## Introduction

Statistical inference, through the Bayesian framework, provides a powerful approach to characterizing the solution of inverse problems. The canonical inverse problem that we focus on is electrical impedance tomography (EIT). The goal of EIT is to recover the spatially varying electrical conductivity of an object from measurements of the voltage and current on its boundary. The mathematical model that maps the state (e.g., conductivity) to the measured data (e.g., voltage and current) is called the forward model. The multiscale nature of the diffusion process described by this forward model makes advances here relevant to a wide variety of applications. In the Bayesian framework, solving the inverse problem corresponds to quantifying statistics about the posterior distribution of the state (e.g., conductivities) conditioned on the measurements. Although this method is very flexible, the calculation of statistics over the posterior distribution is typically done through Monte Carlo sampling. This sampling is a computational burden for complex multiscale forward models. To avoid this burden applications often restrict their analysis to simplified forward models, in turn limiting the utility of their analysis.

The multiscale nature of the forward model in EIT has been addressed in robust multilevel solvers. However, the potential synergy of multilevel solvers with Monte Carlo sampling has been overlooked. These solvers achieve optimal algorithmic scaling by combining coarse-scale corrections with a simple smoothing iteration. The accuracy of the coarse-scale models is critical to this optimal scaling. The best coarse-scale models are derived with general multiscale concepts, such as variational coarsening. We will build on these multiscale concepts to drive the development of new efficient multilevel sampling algorithms.

## Benefit to National Security Missions

For decision making a description of the uncertainty of the system state (e.g., contaminant plume boundary) is required, as opposed to a single “best estimate”, because decisions must account for a realistic range of plausible states. Although methods in statistical inference provide a solid foundation for this analysis, they are too slow for large systems. This research will greatly advance the efficiency of these methods, making them a viable tool. The areas of impact include the calculation of weather patterns, describing the subsurface environment, and medical imaging. This work is relevant to missions in DOE and other government agencies, such as nuclear weapons diagnostics and climate modeling.

## Progress

In this work we consider steady-state EIT as a canonical inverse problem in which the forward map is multiscale diffusion. Here, the problem is to recover the spatially-dependent conductivity inside an object given data on its boundary. The data is the voltage that is measured on the boundary for a prescribed pattern of boundary currents. In the Bayesian framework the solution is described by the statistics of the posterior distribution. We draw samples from the posterior using a Markov chain Monte Carlo (MCMC) procedure. Then we calculate statistics over the posterior with these samples. This indirect approach only requires the simulation of the forward map. However, due to the high cost of the forward model many practitioners do not consider the full Bayes formulation. Instead their analysis is limited to computing the maximum a posterior (MAP) estimate, or they consider a linearized forward model. The goal of this research is to design adaptive multilevel sampling techniques that facilitate the efficient analysis of the full forward model. These techniques will impact the broad class of problems with complex multiscale forward models.

We consider a stylized EIT problem on a two-dimensional square domain. We use an orthogonal grid to discretize the forward map with bilinear finite elements. A binary conductivity representing the true state is discretized on the same grid. To establish a baseline for comparison with more complex MCMC methods, we use a single-site Metropolis MCMC sampler. A gray-scale proposal distribution is used. With this well known method

we computed a set of samples drawn from the high-dimensional multimodal posterior distribution. Also, we computed various measures of efficiency. Next we explored techniques that use components of a multilevel solver (e.g., multigrid) in the sampler. Specifically, we focused on two modified sampling strategies that support the use of approximations in the forward model. These were the delayed acceptance Metropolis-Hastings [1,2] and an augmented posterior sampler [3]. In both cases, the forward map was approximated by limiting the number of V-cycles in the black box multigrid (BoxMG) solver [4], and significantly reduced the computational cost of the solution.

However, in these advanced methods sampling and approximation are still driven at the finest scale. This design leads to a fixed speedup, and not the algorithmic scalability needed for large three-dimensional inverse problems. To obtain the scalability we need to integrate key concepts from multilevel solvers (e.g., multigrid) directly into an adaptive multilevel sampler. A key challenge in this integration is that at coarser scales the conductivity may be anisotropic. Hence, the solution at coarser scales may be unique only up to a coordinate transformation. Fortunately, the discrete representation of the forward map is unique. To explore the potential of sampling this discrete form, we used BoxMG to coarsen the set of forward maps that we created earlier. At the fine-scale this set is described by the multi-modal posterior distribution. With BoxMG we generated probability distributions for both the stencil weights and the anisotropic conductivities at coarser scales. These distributions showed a rapid decrease in multi-modality, becoming uni-modal at coarser scales. Thus, we are developing a sampling strategy that will work directly with the weights of the discrete forward model. This approach will build the posterior up from coarser scales to provide the scalability needed by three-dimensional inverse problems.

Significant progress on adaptive techniques for MCMC sampling has been made as well. This aspect of sampling is key to the efficiency at each level of the multilevel sampler, as well as its overall efficiency. In recent work we showed that the efficiency of MCMC sampling could be improved using a self-adaptive Differential Evolution learning strategy within a population based evolutionary framework. This scheme is dubbed DiffeRential Evolution Adaptive Metropolis or DREAM. For global exploration it runs multiple different chains at the same time. Also, DREAM automatically tunes the scale and orientation of the proposal distribution during the search. We have proved the ergodicity of DREAM [5]. Using tests with nonlinearity and multi-modality we showed that DREAM is generally better than other adaptive MCMC sampling approaches. However, DREAM requires the number of chains to be greater than half the number of parameters. This trait is undesirable for high-dimensional problems, as each chain must evolve to the target distribution (burn in). Recent research has led to a modification of DREAM that reduces the required number of chains to three [6]. Thus, increasing its flexibility and practical applicability.

## Future Work

The partial integration of multigrid components with the MCMC sampling in EIT improves the overall computational efficiency. However, at present sampling and approximation have only been driven at the finest scale. This design limits gains in overall efficiency. Now we are working on a multilevel sampling method that builds posterior distributions from the coarse scale to the finest scale. In this research we are designing proposal distributions for the forward map on the coarsest scale. Specifically, we are comparing the efficacy of either using the weights of the discrete forward map, or using the parameters of a generalized anisotropic forward map. We have the key advantage that at this scale, the posterior is uni-modal. Note that both samplers admit the most general model to ensure that the information we obtain may be interpreted at finer scales. To refine this solution we will use a hierarchical view of the forward map that is motivated by the coarsening in the BoxMG multigrid method. Repeating the refinement and sampling process will lead to a scalable algorithm. In addition, we will study the efficiency of the new adaptive single-scale samplers in this multilevel setting.

## Conclusion

The overarching goal of this research is to deliver a new level of efficiency and scalability to the Bayesian framework. We focus on using this framework for solving inverse problems. However, these advances will greatly impact uncertainty quantification in general. Thus far, we have used a robust variational multigrid solver with two advanced MCMC samplers to solve a stylized EIT problem. Both of these samplers can use approximations of the forward map. The first sampler is based on delayed acceptance, while the second used a multi-resolution augmented posterior. This partial integration of multigrid components with MCMC sampling has improved the performance of Bayesian inference for this class of high-dimensional problems. In addition, we further advanced the theory supporting the DREAM sampling scheme. A new variation of DREAM was developed that uses a smaller number of chains, making it even more flexible for parallel machines.

## References


1. Christen, J. A., and C. Fox. Markov chain Monte Carlo using an approximation. 2005. *Journal of Computational and Graphical Statistics.* **14**: 795.

2. Moulton, J. D., C. Fox, and D. Svyatskiy. Multilevel approximations in sample-based inversion of the Dirichlet-to-Neumann map. 2008. *Journal of Physics:*

*Conference Series.* **124**: 012035.

3. Higdon, D., C. S. Reese, J. D. Moulton, J. A. Vrugt, and C. Fox. Posterior exploration for computationally intensive forward models. To appear in *The Handbook of Markov Chain Monte Carlo.* Edited by Meng, X. L., A. Gelman, and G. Jones.

4. Dendy, J. E.. Black Box Multigrid. 1982. *Journal of Computational Physics.* **48**: 366.

5. Vrugt, J. A., C. J. F. terBraak, C. G. H. Diks, D. Higdon, B. A. Robinson, and J. M. Hyman. Accelerating Markov chain Monte Carlo simulation from self adaptive differential evolution with randomized subspace sampling. 2009. *International Journal of Nonlinear Sciences and Numerical Simulation.* **10** (3): 273.

6. terBraak, C. J., and J. A. Vrugt. Differential evolution Markov chain with snooker updater and fewer chains. 2008. *Statistics and Computing.* **18** (4): 435.

## Publications

Higdon, D., C. S. Reese, J. D. Moulton, J. A. Vrugt, and C. Fox. Posterior exploration for computationally intensive forward models. To appear in *The Handbook of Markov Chain Monte Carlo.* Edited by Meng, X. L., A. Gelman, and G. Jones.

Moulton, J. D., C. Fox, and D. Svyatskiy. Multilevel approximations in sample-based inversion of the Dirichlet-to-Neumann map. 2008. *Journal of Physics: Conference Series.* **124**: 012035.

Vrugt, J. A., C. J. F. terBraak, C. G. H. Diks, D. Higdon, B. A. Robinson, and J. M. Hyman. Accelerating Markov chain Monte Carlo simulation from self adaptive differential evolution with randomized subspace sampling. 2009. *International Journal of Nonlinear Sciences and Numerical Simulation.* **10** (3): 273.

terBraak, C. J., and J. A. Vrugt. Differential evolution Markov chain with snooker updater and fewer chains. 2008. *Statistics and Computing.* **18** (4): 435.

# Adaptive Algorithms for Inverse Problems in Imaging

*Brendt E. Wohlberg*
20080341ER

## Introduction

Image data are ubiquitous, occurring in such diverse fields as experimental physics, biology, geosciences, non-proliferation surveillance, and medical diagnosis. The family of problems including denoising, blur removal, resolution enhancement, and inpainting represent an important part of the analysis of such data. Solving such problems effectively requires some form of model of the data so that it can be distinguished from the degradation to be removed. These models are usually simplified representations designed by mathematical analysis, and cannot accurately represent all of the properties of complex data, such as images of natural scenes, radiological images, etc. In this project, in contrast, we learn appropriate data models from large sets of examples of the problem domain data, promising more accurate reconstructions and also the ability to adapt to new types of data (e.g. from a specialized scientific instrument), with unusual properties that are not compatible with the assumptions made by standard approaches for these kinds of problem. The general approach is motivated by a geometric view of the problem, distinguishing between the full space of all data that can possibly be represented, and the much smaller space of uncorrupted example data. Within this view, the desired reconstruction is achieved by finding a representation, which is close both to the measured data and the space of uncorrupted data.

## Benefit to National Security Missions

Image and related data play an important role of a number of DOE missions, including Nuclear Weapons (e.g., proton radiography of dynamics experiments) and Threat Reduction (e.g. satellite and airborne imagery). Such data also plays an important role in surveillance and reconnaissance, space science (e.g. astronomical imagery), medical and bioscience (e.g. diagnostic imagery), and has potential applications in numerous other fields. Advances in the analysis, including restoration and other inverse problems, of such data clearly advance the ability to extract useful information.

## Progress

Research effort has been concentrated on the following main areas:

### Manifold Geometry

One of the significant goals of this project is to obtain an understanding of theoretical issues related to the geometry of the space of image blocks, which we assume, for some purposes, can be considered to be a *manifold* (a non-linear space with specific mathematical properties). A particularly important question is how to estimate the local properties of this manifold given only a (possibly small) set of samples on the manifold. Considerable progress has been made from an empirical approach, based on numerical experiments, but we still have a disappointingly small number of analytical results, which can be attributed to (i) the difficulty of the problem, and (ii) the unexpected departure from LANL of a postdoc with the specialized mathematical background required for addressing this problem. A staff member with an appropriate background has recently joined the project, promising renewed progress on these theoretical issues.

### Non-Local Means

This is a recent denoising algorithm, which achieves state-of-the-art performance. This algorithm is particularly interesting since it makes use of exemplar image blocks, but it is not based on the explicit geometric view of the space of images underlying this project. We are working (in collaboration with Selim Esedoglu at the University of Michigan) on improving the performance of this algorithm, and also on building a theoretical connection between the choice of distance measure between image blocks used in this algorithm, and manifold curvature in the image space model. This work is ongoing, and has not yet delivered sufficient results to warrant publication.

**Sparse Representations**
In contrast to the well-known signal or image decompositions computed via a linear transform, sparse representations are a non-linear transform computed via an optimization algorithm. While the decomposition is non-linear, the representation is a linear combination of a set of basis vectors selected from the *dictionary*. We have found that this type of representation provides a very effective method for estimating projections into the manifold of image blocks, which is necessary to apply the geometric model of the space of image blocks to practical imaging inverse problems. While exploring this use of sparse representations, we have discovered an interesting new approach to the use of "adaptive dictionaries"; while the standard approach is to use available training data to construct a problem-specific dictionary via an expensive optimization algorithm, we have found, motivated by the geometric model of the space of image blocks, that significantly improved performance can be achieved by simply searching the large data set for nearest neighbors to the vector of interest. A paper describing this results is currently in preparation.

**Inpainting**
This is the process of estimating image content, which is missing due to sensor defects, transmission errors, or other factors. While the application area is primarily to consumer imaging, it is a very difficult inverse problem, and represents and excellent test case for the image modeling concepts explored in this project. We have developed new inpainting algorithm, based on sparse representations of image blocks on overlapping grids, which outperforms the competing algorithms with which we have been able to compare it. This work has presented at a major international conference in April 2009. Since then, significant progress has been made, with the algorithm being extended to multi-band images, and improved to handle large regions of missing content. A paper describing these new results (Figure 1) is currently in preparation.

**Variational Methods**
While the primary focus of this project is the approach to inverse problems via the geometric view, some work has been done on the more well established variational methods such as Total Variation regularization. This work has led to a full-length journal paper and two conference papers.

**Software**
One of the stated deliverables of this project was the release of an open-source code distribution. Approval for this release (requiring significant effort) has been received, and code demonstrating published work is now publicly available.

(a) Test image

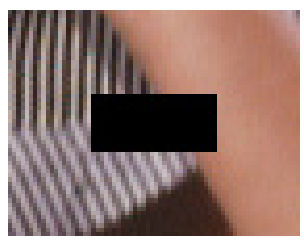

(b) Test image crop

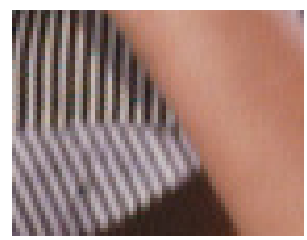

(c) Original image crop

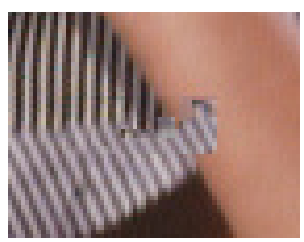

(d) Inpainted (prior) image crop

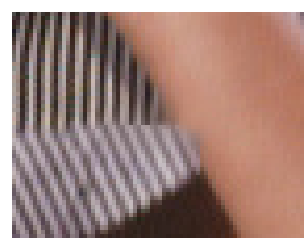

(e) Inpainted (new) image crop

*Figure 1. Inpainting example. (a) Standard test image with region removed. (b) Crop of removed region in test image (c) Crop of original content removed in test image (d) Missing region inpainted by method of Criminisi et al. [1] (e) Missing region inpainted using method developed at LANL.*

## Future Work
Research during the final year of the project will concentrate on the following issues:

**Theory**
Continuation of current work on theoretical aspects of the manifold model of image blocks, with emphasis on discovery of optimal methods for estimating local manifold properties given a set of samples on the manifold.

Particular attention will be given to understanding the geometric implications of the NL-Means algorithm, in determining how the optimal estimate of the projection of a vector into the manifold should depend on the local manifold curvature, and on the promising results in sparse representation theory, described above.

**Applications**
Continuation of development of the new inpainting algorithm. Revisit the denoising problem, using insight gained over the course of the project. If time permits, consider the problem of image resolution enhancement.

**Software**
Update the released version of the research software to reflect new published results, and ensure that it is a stable and useful release at the end of the project.

**Future Funding**
Discover applications of these ideas to problems (imaging problems to which the research can be directly applied, as well as those involving different types of data, to which the underlying abstract concepts can be applied) at LANL and externally, and explore corresponding funding opportunities for continuation of this research beyond the end of the three year term of the project.

## Conclusion
This proposal promises to advance the state of the art in solving a wide variety of problems in the analysis of image and other data. First, by learning the models instead of constructing approximations by mathematical analysis, the increased accuracy of the models is expected to deliver better performance when applied to the removal of noise, blur, etc. Second, the availability of an automated procedure for deriving a data model provides flexibility in addressing new types of data, making it possible to rapidly address such problems in the context of niche data, which have not received much research attention. Progress after the first two years of this project, together with the rapid growth of related ideas in the external research community, provide evidence for the great potential of these methods.

## References

1. Criminisi, A., P. Patrick, and T. Kentaro. Region filling and object removal by exemplar-based image inpainting. 2004. *IEEE Transactions on Image Processing.* **13** (9): 1200.


## Publications

Lin, Y., and B. Wohlberg. Application of the UPRE method to optimal parameter selection for large scale regularization problems. 2008. In *IEEE Southwest Symposium on Image Analysis and Interpretation.* (Santa Fe, NM, 24 - 26 Mar. 2008). , p. 89. New York: IEEE.

Rodriguez, P., and B. Wohlberg. Efficient Minimization Method for a Generalized Total Variation Functional. 2009. *IEEE Transactions on Image Processing.* **18** (2): 322.

Rodriguez, P., and B. Wohlberg. A Generalized Vector-Valued Total Variation Algorithm. Presented at *IEEE International Conference on Image Processing.* (Cairo, Egypt, 7 - 10 Nov. 2009).

Rodriguez, P., and B. Wohlberg. An Efficient Algorithm for Sparse Representations with lp Data Fidelity Term. Presented at *Proceedings of 4th IEEE Andean Technical Conference (ANDESCON).* (Cusco, Peru, 15-17 Oct. 2008).

Wohlberg, B.. Inpainting with sparse linear combinations of exemplars. 2009. In *International Conference on Acoustics, Speech, and Signal Processing.* (Taipei, Taiwan, 19 - 24 Apr. 2009). , p. 689. Piscataway, NJ: IEEE.

Wohlberg, B., and P. Rodriguez. An l1-TV algorithm for deconvolution with salt and pepper noise. 2009. In *International Conference on Acoustics, Speech, and Signal Processing.* (Taipei, Taiwan, 19 - 24 Apr. 2009). , p. 1257. Piscataway, NJ: IEEE.

# Designing Communication Methods for Bottom-Up Self-Assembled Nanowire Networks of Emerging Computer Architectures

*Hsing-Lin Wang*
20080380ER

## Introduction

The exponential growth of computational power experienced over the past few decades is leveling out. Physical space and temporal limitations will ultimately prevent technology from simply adding transistor density or increasing clock speed. Molecular self-assembly is often mentioned as the holy grail of nanotechnology, that could allow to easily and cheaply build systems of enormous complexity. The challenge is to use this functional and structural complexity for performing efficient communication and computations. If successful, we could expect a quantum leap in performance compared to today's traditional computing machines.

Our goal is to engineer novel computer architectures based on self-assembled nano-components and through an integrated experimental, simulation-based, and theoretical approach. The bottom-up design approach is more fabrication-friendly, cheaper, and would eventually scale up to more complex systems compared to today's top-down designs. We adopt a network and system-on-chip-based approach and focus on the interconnect challenge because interconnects have become more important than the transistors as a limiting factor of performance on modern chips. We will (1) master the technology of self-assembling conductive silver nanowires that densely interconnect traditional silicon components, and (2) develop schemes of reliable communication in such an irregular, heterogeneous, and unreliable network. The research is guided by: (1) What connectivity graphs can we obtain, and what are the control parameters for the self-assembly process? (2) How can we reliably and efficiently communicate in such irregular networks?

Bottom-up self-assembled nano-electronics is the holy grail of molecular electronics, but to exploit the computational complexity that such a technology shift offers, novel transport, computing and programming paradigms are required. We will build realistic network-on-chip interconnect models and leverage recent advances in sequential dynamical systems (SDS) to develop adaptive and robust communication schemes for such irregularly assembled, unreliable networks.

## Benefit to National Security Missions

This project will develop science to support new computational paradigms and network communication. This science supports missions in high-performance computing that benefits the entire mission space of DOE. Network science also impacts a broad mission space including threat reduction, communication, and data mining relevant for DOE and other government agencies.

## Progress

We have made significant progresses, experimental as well as theoretical, during last year. The results can be summarized as follows:

1. Demonstrate the growth of Ag nanowires (AgNWs) with a wide range of morphologies and characterize the electrical properties of the wires. We have demonstrated the fabrication of AgNWs with a wide range of structure, size, and morphologies. Our results show that the structure of these nanowires is dominated by the growth kinetics which is also associated with experimental parameters such as concentration and temperature. We have also characterized their electrical properties and found that they are morphology dependent. The electrical properties of AgNWs were measured by displacing nanowire onto an interdigitated gold electrodes supported on high-resistivity silicon substrate. A perfect linear relationship between the current and voltage was found for all AgNWs as we measure the I-V responses between a low voltage range (-0.05 to 0.05 V) as shown in Figure 1. The electrical conductivity of a smooth AgNW with a diameter of 120 nm was 2.81 x $10^6$ S/m, and that of a coarse AgNW with cubic cross-section was 1. 34 x $10^6$ S/m, slightly lower than that of bulk silver (6.25 x $10^7$ S/m). The electrical properties of these nanowires are crucial in defining underlying parameters of the random nanowire network.

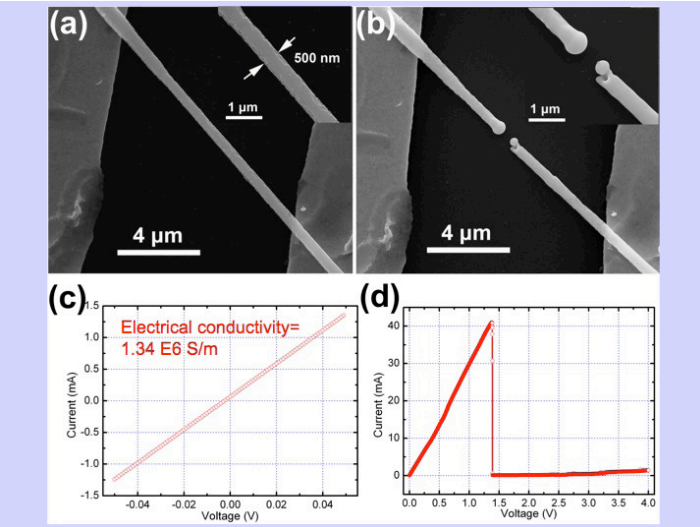


*Figure 1. SEM micrographs reveal Ag nanowires sit between two Au electrodes (a) and the break points after electrical properties measurements (b). The I-V characteristic of an Ag nanowire measured between 0.05 V to -0.05 V (c) and a sudden drop of electric current corresponds to the melting of the nanowire on a defect site to form a break point (d).*

2. Fabrication of Au electrode on various substrates and polyaniline patterns. A whole variety of interdigitated electrodes on glass and silicon surfaces have been prepared with different spacings between two electrodes. Of particular importance is to develop a unique procedure to fabricate interdigitated polyaniline pattern using deep reactive ion etching (RIE) method as shown in Figure 2. To the best of our knowledge, this is the first time it was demonstrated that micrometer sized polyaniline patterns were prepared via RIE method. These polyaniline patterns allows us to control growth of AgNWs and induce anisotroby between two specific polyaniline structures.

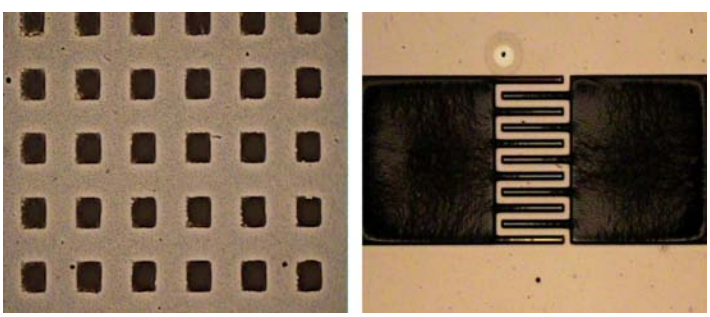

*Figure 2. The fabrication of PANI patterns from PANI films pre-deposited on silicon or glass substrates. These patterns are necessary for inserting input, output, and control nodes in random networks, or for the voltage controlled growth of self-assembled nanowires. This figure shows PANI patterns after an all-dry-process used to etch the PANI film. Left panel: an array of squares with spacing distance a few microns. Right panel: PANI inter-digitated fingers for testing the guided growth when applying a voltage bias.*

3. Using dimensional reduction techniques we have shown that the effective input-output function implemented by the network (the output node voltage as a function of the voltages applied to the input nodes) depends only on a number of reduced matrices that describe the effective interactions between input, output, and control nodes. This analysis has enabled us to estimate how the complexity of the input-output function class implemented by the network depends on the number and location of its control nodes. Moreover, we have designed and analyzed pattern classification algorithms in these random networks. Assuming a given location for the control nodes, we have first analyzed an off-line learning algorithm that determines the optimal voltages that should be applied to the control nodes in order to minimize the generalization error of the network in a binary classification task. Second, we have designed a simple on-line supervised learning algorithm that uses a teacher node in order to adaptively change the control node voltages as training input-output voltage patterns are applied to the input and teacher nodes. We have shown that this algorithm approaches the optimal control node voltages as the number of training patterns increases.

4. Study the effect of short-circuits among wires on the network, and develop network growth models.

Motivated by the fact that our nanwires will create short-circuits, we have investigated such networks in simulation and have shown that possible short-circuits in the nanowire network does not need to be a drawback, on the contrary. Short-circuits establish shortcuts in the network connectivity graph, and therefore allow to propagate the information more efficiently. This can be exploited for an improved information processing capability.

## Future Work

With the success of fabricating patterned polyaniline, we plan to demonstrate the growth of silver wire between speci c patterns. Of particular interest will be to determine how the spacing between polyaniline pattern and various experimental parameters impact the growth of silver nanowires. We plan to demonstrated guided growth of silver nanowire on a prefabricated polyaniline surface. The PANI surface has physical protrusions, which allow the Ag growth along specific directions. The above two methods are rely on self-assembly without exerting electric field.

To achieve a precise control of the nanowire growth, we plan to demonstrate the growth of silver nanowires assisted by external electric field. The idea is to demonstrate the growth between specific patterns. This precise control in Ag nanowires growth can be used to validate our simulation results (prove of principle) that our

idea is feasible. Using the already developed fabrication methodology, we will be able to prepared a much more complicated patterns depends on the structure of the proposed network.

Our research approach is unique and tries to turn the tremendous efforts in nanomaterials into useful computing architectures that can be built cheaply and easily by using self-assembling processes. By addressing the interconnect problem only, we solve a major part of the grand challenge to go beyond Moore's law, while at the same time keeping the research task realistic. We will use a combined experimental and theoretical approach to answer our research questions. What connectivity graphs can we obtain? What are the fabrication parameters? What is the distribution of wire-lengths? We will seek to obtain mostly local, but also long(er)-distance connections with a lower probability since this represents an ideal trade-off. What densities can we obtain while minimizing electrical contacts and crosstalk among the wires? What are the electrical properties? We will use the statistical connectivity data obtained from our experiments to build realistic graph classes for detailed simulations, where the processing and switch blocks will be simulated in detail as well.

## Conclusion

The expected results are a combined experimental and theoretical framework. On the theoretical side, a set of communication and routing algorithms that are efficient and robust will be developed. The experimental part will be supported and guided by realistic computer models and simulations. On the practical side, we will produce prototypes of self-assembled nanowire assemblies and measure their properties (interconnect graphs, electrical, etc.). The experimental results, on the other hand, will be used in the simulations and the theoretical framework to make them more realistic.

## Publications


Christof, C., and A. A. Hansson. Non-traditional irregular interconnects for massive scale SoC . 2008. *Proceedings - IEEE International Symposium on Circuits and Systems.* : 2785.

Rolhf, T., N. Gulbache, and C. Teuscher. Damage spreading and criticality in finite random dynamical networks. 2007. *PHYSICAL REVIEW LETTERS.* **99** (24): 248701.

Teuscher, C.. Exploring logic artificial chemistries: An illogical attempt? . 2007. *Proceedings of the 2007 IEEE Symposium on Artificial Life, CI-ALife.* : 61.

Teuscher, C., F. J. Alexander, and I. Nemenman. Novel computing paradigms: Quo vadis? . 2008. *PHYSICA D-NONLINEAR PHENOMENA.* **237** (9): 5.

Teuscher, C., H. L. Wang, A. A. Hansson, and E. Akhadov. Future and Emerging Computing Paradigms and Machines.. 2008. *ADTSC Science Highlights.*

Teuscher, C., N. Gulbahce, and T. Rohlf. Assessing random dynamical network architectures for nanoelectronics. 2008. *2008 IEEE/ACM International Symposium on Nanoscale Architectures, NANOARCH.* : 16.

Teuscher, C., T. Rohlf, and N. Gulbahce. Correlations Matter---Response of Dynamical Networks to Small Perturbations. To appear in *5th International Workshop on Computational Systems Biology..* (Leipzig, June 11-13, 2008).

Teuscher, C., and J. Triesch. To each his own: The caregiver's role in a computational model of gaze following . 2007. *Neurocomputing.* **70**: 2166.

Xu, P., S. H. Jeon, H. Chen, H. Luo, G. Zou, Q. X. Jia, J. Won, M. Anghel, C. Teuscher, D. Williams, X. Han, and H. L. Wang. Facile synthesis and characterization of silver nanowires through an electrodeless deposition routes using polyaniline . *ACS Nano.*

Xu, P., S. H. Jeon, N. H. Mack, S. K. Doorn, D. Williams , X. Han, and H. L. Wang. Field-assisted synthesis of functional metal nanoparticles using conducting polymers. *Journal of Materials Chemistry.*

# Stochastic Transport on Networks: Efficient Modeling And Applications to Epidemiology

*Nicolas W. Hengartner*
20080391ER

## Introduction

A variety of problems of relevance to biosecurity, public health, and basic science research can be viewed as special cases of a general problem of studying stochastic transport on networks. Examples include: (a) epidemilogy, where diseases spread by random interaction events among humans and/or animals tied into social and/or agricultural networks, (b) basic biochemical processes, relevant for cancer and other molecular diseases, where the response of an organism to external stimuli, such as pathogen invasions, are governed by complex stochastic dynamics on cellular regulatory and metabolic networks, and (c) many others. Detailed computational study of such stochastic processes on networks is notoriously difficult. The best algorithms involve simulation of the underlying processes event by event, which becomes computationally prohibitive when the number of possible events is astronomically large, as it is for contacts among people in a general population, or for biochemical transformations. This project is designed to create novel algorithms, based on disparate tools from physics, computer science, and information theory, to simulate these stochastic interaction events fast and rigorously. The general idea being pursued revolves around coarse-graining stochastic events, so that entire spread of an epidemics or multiple chemical reactions can be modeled as a series of complex, macroscopic steps.

## Benefits to National Security

This project will support DOE and DHS missions in bio-security by developing advanced tools for understanding of progression of epidemics, as well as early (stochastic) events in the interactions of a host and a pathogen. Furthermore, the project will support the DOE Energy security mission by enhancing the understanding of biochemical networks, an essential component for biofuels development.

## Progress

The second year of the project added a new player to the team, Dr. Golan Bel, who joined us from UCSB as a Postdoctoral Associate. The new extended, more diverse team has made substantial progress towards completion of the goals of the project. We have continued publishing a series of articles on characterization of signal processing properties of coarse-grained stochastic biochemical networks, having submitted the following article: A Mugler, E Ziv, I Nemenman, C Wiggins. Quantifying evolvability in small biological networks. IET Syst. Biol, 2009, in press. Methods for coarse-graining of small stochastic networks, and using mesoscopic experimental data to infer the microscopic structure of the network were put forward in: W de Ronde, B Daniels, A Mugler, N Sinitsyn, and I Nemenman. Statistical properties of multistep enzyme-mediated reactions. IET Syst. Biol, 2009, in press. Very importantly, a large step towards the completion of the project's final goals (namely, developing of coarse-grained numerical simulations algorithms) was taken with: A Sinitsyn, N Hengartner and I Nemenman. Adiabatic coarse-graining and simulations of stochastic biochemical networks. Proc. Natl. Acad. Sci. (USA), 2009, 106 (24). A publication in PNAS is a very uncommon result for a purely theoretical work and is a high point of the current research. A similar level of impact is expected for G Bel, B Munsky, and I Nemenman. Common complex biochemical processes exhibit simple completion time distributions. Submitted, PLoS Comp. Biol., 2009; which has been submitted to the highest impact journal in the field of computational biology. Importantly, this article opened an entirely new direction in the field of coarse-grained analysis of stochastic transport networks by noticing that the properties of the said transport for large networks may be independent of the network's details and, therefore, simplify substantially, allowing detailed theoretical analysis. Similar results were achieved in: G Bel and I Nemenman. Anomalous diffusion and scaling in

coupled stochastic processes. Submitted to New J. Phys, 2009; where we argued that naive coarse-graining tools, employed by majority of researchers in the field, are bound to fail, and new methods are needed. This work was also the first one to discover ergodicity breaking in coupled stochastic processes, a result that, undoubtedly, will have a large impact. Addition of Dr. Bel to the team has brought even more expertise in the theory of stochastic single molecule kinetics, which underlies this project, resulting in publications: A. Zilman, J. Pearson and G. Bel, "Effects of jamming on transport times in nanochannels". Submitted to Phys. Rev. Lett., (2009); G. Bel, F. L. H. Brown, "Theory for wavelength-resolved photon emission statistics in single-molecule florescence spectroscopy". Phys. Rev. Lett., 102, 018303 (2009). Finally, Dr. Sinitsyn, another Postdoctoral Associate on the project, has continued his work on deriving exact, topological results about stochastic transport on networks: V. Y. Chernyak, and N. A. Sinitsyn, "Pumping-Restriction Theorem for stochastic networks", Phys. Rev. Lett. 101, 160601, 2008; N. A. Sinitsyn, and Avadh Saxena, "Geometric phase for non-Hermitian Hamiltonian evolution as anholonomy of a parallel transport along a curve", J. Phys. A: Math. Theor. 41, 392002, 2008; and N. A. Sinitsyn, "Stochastic pump effect and geometric phases in dissipative and stochastic systems", invited review, J. Phys. A: Math.

## Future Work

Modeling transport effects on networks is an essential part of biochemistry, epidemiology, and other diverse sciences. Unfortunately, no algorithm yet exists that can model the transport effectively (that is, correctly and in a manageable time for networks of realistic sizes), taking into the account stochastic properties of the transport and heterogeneity of kinetic parameters. Based on our recent work on stochastic properties of biochemical networks, we propose to bring tools from statistical field theory and adiabatic methods from quantum mechanics to analysis of stochastic network transport, specifically in the context of epidemiology, where transport leads to spreading infections. The goal of the proposed modeling is to perform physics-inspired "coarse-graining," such that the properties of many of the microscopic nodes in a network are "integrated out," and only large-scale observable dynamics is modeled. This will be achieved by relying on three properties of complex transport networks: time scale separation (adiabaticity), existence of standard building blocks (motifs), and modular and hierarchical architecture. Using these properties, we propose to derive stochastic corrections to deterministic dynamics for common network transport models using a variety of statistical field-theoretic techniques, implement them in terms of efficient computer simulation algorithms, and to apply them to Influenza epidemics, using the developed tools for efficient modeling of the disease.

## Conclusion

This project will develop advanced tools for understanding, computer simulations, and prediction of transport phenomena in complex network. These networks include biochemical networks (relevant for bioengineering and biomedicine), social networks (relevant for epidemiology), and infrastructure networks (relevant for Homeland Security applications). All of these fields are of critical importance to the nation. For example, understanding the spread of flu, to be specifically studied in the project by means of computer simulations, has been identified as a critical need during the recent bird flu outbreaks.

## Publications


Dreisigmeyer, D., J. Stajic, I. Nemenman, W. Hlavacek, and M. Wall. Determinants of bistability in induction of Escherichia coli lac operon. 2008. *IET Systems Biology.* **2**.

Edwards, J., J. Faeder, W. Hlavacek, Y. Jiang, I. Nemenman, and M. Wall. q-bio 2007: a watershed moment in modern biology. 2007. *Mol. Syst. Biol..* **3**: 148.

Mugler, A., E. Ziv, I. Nemenman, and C. Wiggins. Serially-regulated biological networks fully realize a constrained set of functions. 2008. *IET Systems Biology.* **2**.

Munsk, B., I. Nemenman, and N. Sinitsin. Common complex biochemical processes exhibit simple completion time distributions. *Physical Biology.*

Nemenman, I., W. Hlavacek, J. Edwards, J. Faeder, Y. Jiang, and M. Wall. Editorial: Selected papers fromthe First q-bio Conference on Cellular Information Processing. 2008. *IET Systems Biology.* **2**.

Sinitsin, N., and I. Nemenman. Anomalous diffusion in coupled stochastic processes. 2009. *New Journal of Physics.* **11**: 083099.

Sinitsyn, N., N. Hengartner, and I. Nemenman. Coarse-graining stochastic biochemical networks: quasi-stationary approximation and fast simulations using a stochastic path integral technique. 2009. *Proc. Natl. Acad. Sci. (USA).* **106**: 10546.

Sinitsyn, N., and I. Nemenman. Universal geometric theory of mesoscopic stochastic pumps and reversible ratchets. 2007. *Phys. Rev. Lett.* **99**: 220408.

Teuscher, C., I. Nemenman, and F. Alexander. Novel computing paradigms: Quo vadis?. 2008. *Physica D.* **237**: v.

# Critical and Crossover Behaviors at Jamming Transitions

*Charles Reichhardt*
20080448ER

## Introduction

In this project we will develop a fundamental understanding of the jamming process in granular materials. These seemingly simple materials, such as dry sand and powders, exhibit flow behavior far different from ordinary solids, liquids, and gases. Understanding the peculiar behavior of granular materials is vital for predicting and controlling them under a variety of industrial, civil engineering and scientific conditions. Jamming plays an important role in determining the behavior of a granular medium. When the grains are widely separated or slowly moving, they can flow in a manner similar to a fluid, but when the grain separation decreases or the grain speed increases, the grains suddenly jam and resist further motion in an abrupt transition to a solid state. The fluid to solid transition associated with jamming is extremely poorly understood but is essential for any application of granular materials. For example, granular media forming a levy is normally in a solid state, but it can unjam in a catastrophic transition to a fluid state and cause the levy to fail. In contrast, when granular media is flowing, such as when a mold for a highly-filled polymer-based explosive is filled, a sudden transition into the solid state can interfere with the filling process. We are studying the jamming process and the transition between fluid and solid states and working to apply powerful concepts from statistical physics which have been successful in describing ordinary solids and liquids. If we can identify universal behaviors associated with the jamming transition, this will permit us to control the failure of materials and will also enhance our understanding of how and when complex materials fail. This would have a profound impact on the materials science, industrial, infrastructure, and national security needs of the nation.

## Benefit to National Security Missions

Jamming underlies numerous physical problems including oil exploration, aging, material failure, pollutant propagation in porous media, solid waste transportation and storage, weapons manufacturing, plastic-based-explosives, and characterization of materials out of equilibrium. DOE missions relevant to this research include energy and environmental research, weapons physics, materials science, modeling and simulation. If an underlying theoretical framework can be developed for all systems that exhibit jamming, it will provide a better understanding of how to control jamming and predict when it may occur. This is important to ensuring undisrupted flow in infrastructure and information flow networks, both of which are crucial to national security. The flow and jamming of materials is relevant to the geological stability of rock formations and the flow of toxic materials through porous media, both of which are important issues involved in designing future nuclear waste repositories.

## Progress

We are performing both a computational and an experimental study of jamming, and have focused on the paradigmatic jamming system of a collection of grains. Due to the complexity of granular systems, we are first studying the simplest granular models that exhibit jamming and are building towards more complex models. A simple model that exhibits jamming is a two-dimensional assembly of disordered disks. We have previously proposed perturbing the granular packing with a single probe particle to study the jamming transition. Below the jamming density, the probe particle can easily move within the packing, while as the jamming density is approached the probe moves with increasing difficulty. We have used simulations to show that the nature of the probe particle fluctuations change as the jamming transition is approached and that the distributions of the fluctuations assume a power law form, which is a signature of criticality. This indicates that close to jamming, even the smallest perturbation becomes relevant and spreads throughout the entire system. Away from the jamming transition, the system is more robust and the perturbation remains localized. Our results support the picture that the jamming transition in this system is a true phase transition similar to that observed at the transition from a liquid to a solid state. These results have been confirmed in recent experiments by external groups. In experiments here at LANL, we have found a tantalizing

possible connection between the behavior at jamming and earthquake dynamics. It may be that the moving faults responsible for earthquakes exhibit critical behavior, and from our results we can speculate that the criticality of the earthquake faults may fall into the same class as the criticality found at jamming. We have begun to study the next level of complexity in our model by adding friction, which makes the grains slightly sticky. Our simulations and our experiments both indicate that the jamming transition becomes fragile in the presence of friction and that the single jamming transition observed in frictionless systems breaks into two separate jamming transition. The new second jamming transition appears to be a percolation transition related to the frictional contacts in the system, and is a weaker transition than the true jamming transition found in both the frictional and frictionless systems. In addition, we have begun to study jamming in a novel system of granular chains which model certain aspects of the behavior of polymers. (See Figure 1.) Our simulations are in excellent agreement with recent experiments on this system. We have found evidence that jamming in the chain system is distinct from the jamming of disks, suggesting that there are multiple types of jamming transitions rather than a single universal jamming transition. The criticality that we observed in the jamming of the disks is lost in the chain system, and the behavior instead resembles that of a glassy system.

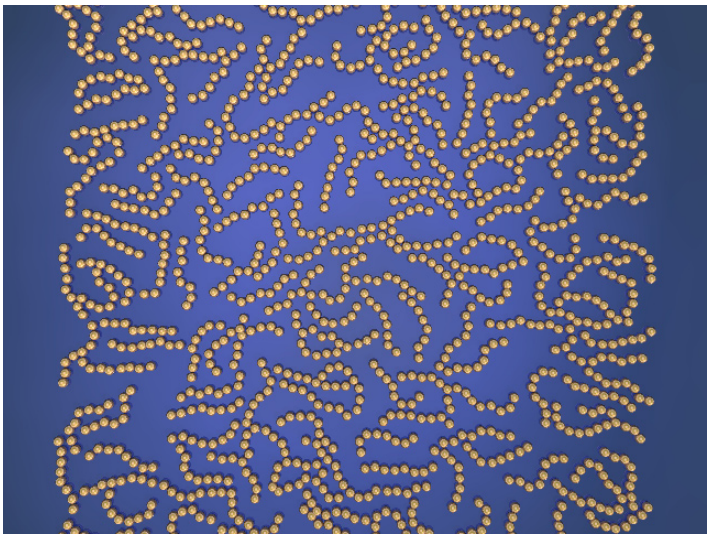

*Figure 1. Image from a two-dimensional simulation of granular chains that are each eight monomers long.*

## Future Work

We will perform further studies with the frictional grain system to more fully characterize the second weak jamming transition that we have identified. We will scale up the granular polymer simulations to consider much larger packings of grains in order to check for signs of criticality at this unique jamming transition. It is possible that the larger systems will show behavior that is even more glasslike, further supporting the idea that there is more than one jamming transition, or it is also possible that the behavior of the large system will more closely resemble jamming in the disk system, suggesting that the two jamming transitions are not unique. We will use both simulations and experiments to explore more fully the idea that earthquake behavior may be related to a jamming transition.

## Conclusion

Using experiments and simulations, we have accumulated strong evidence that jamming of frictionless disks is a true phase transition and shows critical behavior similar to that found at a thermodynamic phase transitions. Some of the ideas developed in the study of the frictionless system carry over into more complex systems, such as in the jamming of frictional disks; however, we also find that for a frictional system, a second fragile jamming transition can also occur. For models of extended granular chains, termed granular polymers, we again find a jamming behavior, but the critical properties of the jamming transition are lost and the system exhibits features similar to those found in molecular glasses. We are continuing to apply our results to the resolution of the question of whether certain signatures of the glass transition are similar to features found in jamming transitions.

## Publications


Bandi, M. M., M. K. Rivera, F. Krzakala, and R. E. Ecke. Fragile granular jamming. *Physical Review Letters.*

Libal, A., C. Reichhardt, and C. J. Olson Reichhardt. Enhancing mixing and diffusion with plastic flow. 2008. *Physical Review E.* **78** (3): 031401.

Mangan, N., C. Olson Reichhardt, and C. Reichhardt. Reversible to irreversible flow transitions in periodically driven vortices. 2008. *Physical Review Letters.* **100** (18): 187002.

OlsonReichhardt, C. J., and C. Reichhardt. Fluctuations, jamming, and yielding for a driven probe particle in disordered disk assemblies. *Physical Review E.*

OlsonReichhardt, C. J., and L. M. Lopatina. A ball-and-chain polymer model. 2009. *Science.* **326**: 374.

Reichhardt, C.. High-temperature superconductors: Vortices wiggled and dragged. 2009. *Nature Physics.* **5**: 15.

Reichhardt, C., and C. J. Olson Reichhardt. Disordering transitions and peak effect in polydisperse particle systems. 2008. *Physical Review E.* **77** (4): 041401.

Reichhardt, C., and C. J. Olson Reichhardt. Moving vortex phases, dynamical symmetry breaking, and jamming for vortices in honeycomb pinning arrays. 2008. *Physical*

*Review B.* **78**: 224511.

Reichhardt, C., and C. J. Olson Reichhardt. Random organization and plastic depinning. 2009. *Physical Review Letters.* **103**: 168301.

Reichhardt, C., and C. J. Olson Reichhardt. Switching and jamming transistor effect for vortex matter in honeycomb pinning arrays with ac drives. *Physical Review B.*

Wan, M. B., C. J. Olson Reichhardt, Z. Nussinov, and C. Reichhardt. Rectification of swimming bacteria and self-driven particle systems by arrays of asymmetric barriers. 2008. *Physical Review Letters.* **101** (1): 018102.

# Time-reversible Born-Oppenheimer Molecular Dynamics

*Anders M. Niklasson*
20080562ER

## Introduction

Quantum mechanics was developed during a few years in the mid 1920's. It can briefly be summarized by the Schrodinger equation with its special forms for Fermions and Bosons combined with a few recipes for obtaining measurable physical observables. Essentially all problems in chemistry, materials science, and biology should be possible to predict and understand directly from quantum mechanics if the constituent particles of the systems are known. Unfortunately, the computational complexity for solving even very small problems is enormous. Only by applying a hierarchy of approximations is it possible to make calculations of any realistic materials systems. Possibly one of the most important and well-tested simplifications includes the separation of the nuclear and electronic degrees of freedom in the Born-Oppenheimer approximation, where the fast electrons are assumed to be in a relaxed equilibrium around approximately stationary nuclei. Solving the Schrodinger equation and calculating the forces acting on the nuclei, within the Born-Oppenheimer approximation, the dynamics of a system can be analyzed. In this way we can study, for example, chemical reactions, phase transitions, evolving protein structures, and elastic properties of condensed matter, even at temperatures and pressures that cannot be reached within normal laboratory conditions. Born-Oppenheimer molecular dynamics has emerged as one of the most important theoretical tools in computational materials science and can be viewed as the gold standard of molecular dynamics simulations. However, challenges in nanoscience, biofuels and molecular biology, for example, require significant algorithmic improvements to allow simulations of much larger size and complexity than previously possible.

In this project we explore and develop general ab initio molecular dynamics technologies based on the new opportunities provided by the time-reversible loss-less integration approach to Born-Oppenheimer molecular dynamics that recently was invented at Los Alamos National Laboratory (LANL) by the proposal authors [1]. The time-reversible Born-Oppenheimer technique was originally only an invention to overcome some fundamental problems with long-term energy stability and accuracy of molecular dynamics simulations. Because of a required non-linear optimization or equilibrium relaxation of the electronic degrees of freedom for each new molecular configuration, the reversibility present in a true dynamical system was broken in Born-Oppenheimer simulations. The irreversibility leads to a systematic drift of the energy, i.e. the system is unintentionally heated or cooled down, which leads to uncontrollable errors and uncertainties. This serious shortcoming was considered an unsolvable problem that only partly could be avoided by a substantial increase of the computational effort. The time-reversible Born-Oppenheimer technique solved this problem and opened the door to a new generation of ab initio molecular dynamics simulation methods with unprecedented accuracy and speed. Figure 1 illustrates the ability of time-reversible Born-Oppenheimer molecular dynamics. The purpose of this project was to pursue this goal and explore and developed efficient Born-Oppenheimer molecular dynamics techniques enabled by the new time-reversible approach. Our findings may form the basis for high-performance ab initio molecular dynamics schemes that are significantly better suited to tackle present and future challenges in computational materials science, chemistry and biology. This research is at the very forefront of a highly competitive field of research that is expected to have a significant impact over a broad area of scientific disciplines.

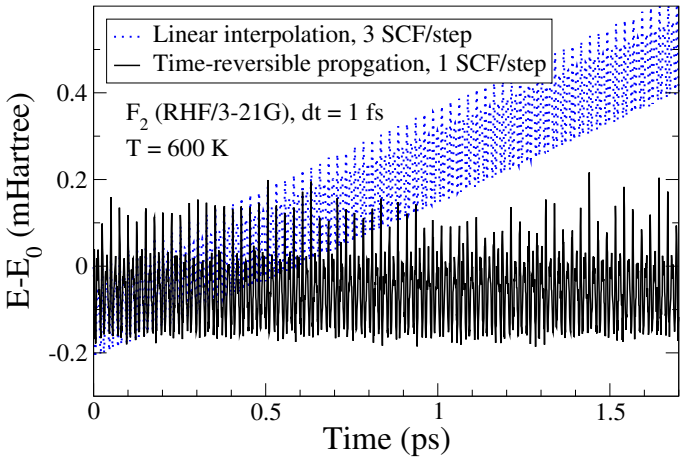


*Figure 1. Conventional Born-Oppenheimer molecular dynamics with an electronic propagation based on a linear interpolation between time steps vs. a time-reversible propagation. The time-reversible dynamics requires only 1/3 of the computational cost, as measured by the number of optimization iterations per step (SCF/step), and it has no unphysical systematic drift in the total energy.*

## Benefit to National Security Missions

The direct or indirect applications of Born-Oppenheimer molecular dynamics range from the problem of high-temperature stabilization of δ-Pu to the folding structures of protein molecules in human cells, all issues with close ties to the DOE missions in Nuclear Weapons, Threat Reduction, and Office of Science, which will benefit from enhancing our fundamental understanding of materials. Our work will provide molecular dynamics simulation tools that overcome some significant shortcomings of current ab initio molecular dynamics. These problems include a high computational cost, numerical instabilities, and a systematic drift in the total energy. We hope our work will evolve to a new generation of high-performance molecular dynamics simulation methods based on the first principles of quantum physics.

## Progress

The first two years of this project have been highly successful. The key initial discovery was an extended Lagrangian generalization of time-reversible Born-Oppenheimer molecular dynamics [2]. This generalization gave our original time-reversibility invention a rigorous theoretical framework that allows not only a deeper physical understanding of the dynamics, but also enables extensions beyond the original concept. In particular, with the new formulation we can apply higher-order symplectic or geometric integration schemes that are stable and energy conserving even under approximately converged forces acting on the atoms [2,3]. A systematic study and optimization of a large class of geometric integration schemes was performed in collaboration with the Royal Institute of Technology in Stockholm. We were able to demonstrate how the accuracy in simulations can be improved by orders of magnitude compared to previous formulations at the same level of computational cost. Figure 2 shows how the accuracy is improved with the new geometric integration schemes, as measured by the amplitude of the energy oscillations, without any additional cost in the calculation.

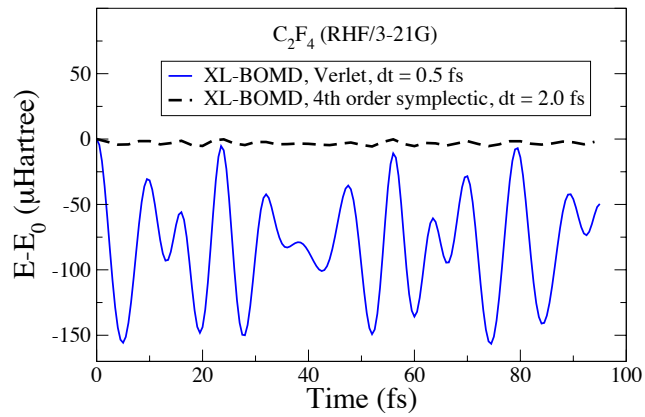


*Figure 2. The accuracy, as measured by the amplitude of the total energy oscillations for a small molecule. The extended Lagrangian Born-Oppenheimer molecular dynamics scheme (XL-BOMD) allows for higher order symplectic integration of the equations of motion that can improve the accuracy by orders of magnitude to no extra cost. This is of great importance when small energy differences have to be resolved.*

During the second year of this project the new theoretical framework of Born-Oppenheimer molecular dynamics has been further explored. A free-energy molecular dynamics was developed, which allows for simulations at elevated electronic temperatures [4,5]. This is not only of importance for studies of materials at very high temperatures, but also enables simulations of metals under normal conditions at room temperature. Figure 3 illustrates the new dynamics and the conservation of the free energy, which includes the electronic entropy (TS).

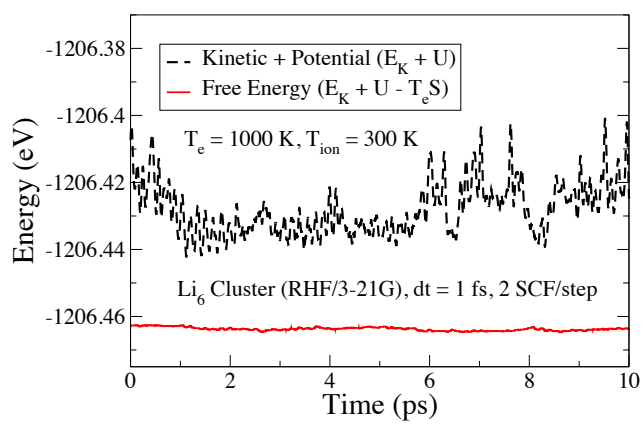


*Figure 3. Demonstration of the conservation of the free energy v.s. the total energy in extended Lagrangian free energy molecular dynamics for a simulation of a small Li cluster at an electronic temperature of 1000K.*

Because of the loss-less nature of a time-reversible dynamics, any numerical error will also propagate and never disappear. Small numerical errors that are always present in numerical computer calculations may therefore eventually accumulate to large fluctuations that destroy the simulation. An important challenge during the first two years was to overcome this obstacle. By introducing small fictitious forces acting on the electronic degrees of freedom, the error accumulation can be removed through dissipation. The key problem we managed to solve was to achieve an efficient dissipation without introducing any instabilities or significant modifications of the dynamics [6]. Our new Born-Oppenheimer molecular dynamics with dissipation is of particular importance in reduced complexity calculations. Normally the computational cost of a Born-Oppenheimer simulation scales with the cube, $O(N^3)$, of the number of atoms, $N$. Conventional simulations based directly on quantum mechanics have therefore largely failed to utilize the rapid improvement of fast computing. Even if the processing power grows by a factor of 1000, the available system size that could be studied would only increase by a factor of 10. Because of this fundamental shortcoming a new computational paradigm has evolved in electronic structure theory, where no part of a calculation is allowed to increase more than linearly with system size. Linear scaling electronic structure theory allows us to take full advantage of increased computer power. An important problem with the numerical approximations in reduced complexity schemes is that they are typically less accurate. The numerical noise is therefore more significant in linear scaling Born-Oppenheimer molecular dynamics simulations. Our new dynamics with dissipation is able to deal with this problem, though some minor problems still remain.

If wavefunctions are used to represent the propagation of the electronic degrees of freedom an arbitrary phase occurs, since the energy is invariant under rotations of the wavefunctions. We have managed to generalize the extended Lagrangian dynamics to overcome this problem. This enables implementation for a very broad class of electronic structure methods based on plane-wave or wavelet representations as well as methods based on some highly efficient direct energy minimization techniques with Wannier functions. The wavefunction propagation is still not fully developed and some practical problems, at first unnoticed, still remain.

In a generalization to a non-orthogonal representation for the electronic degrees of freedom we discovered a new form of fictitious ``Pulay force'' that is driven by the change in the basis set that follows the evolution of the nuclear degrees of freedom. Instead of being caused by the gradient with respect to position of the basis set, as in the original Pulay force, the new force arises from the second-order time derivative of the non-orthogonal electron representation.

Several implementations of our new extended Lagrangian Born-Oppenheimer molecular dynamics have been performed LANL and elsewhere, such as VASP, FreeON, Quickstep, LATTE, DFT-TB, and Quantum-Espresso. We have also been able to analyze and compare our extended Lagrangian Born-Oppenheimer molecular dynamics scheme to the famous and highly popular Car-Parrinello molecular dynamics method. Car-Parrinello molecular dynamics was invented over 20 years ago and as one of the first practical methods for performing molecular dynamics simulations based directly on the first principles of quantum mechanics it has had an enormous impact. The advantage with Car-Parrinello molecular dynamics compared to conventional Born-Oppenheimer molecular dynamics is a highly reduced computational cost but with the disadvantage of a less accurate dynamics, which is determined by the choice of certain fictitious electron mass parameters. Conventional Born-Oppenheimer has the disadvantage of a high computational cost, but the advantage of a high reliability without any adjustable fitting parameters. The new extended Lagrangian Born-Oppenheimer molecular dynamics formulation combines many of the best features of Car-Parrinello and conventional Born-Oppenheimer molecular dynamics, but without any of their most serious shortcomings.

During the last year we have tried to combine time-reversible Born-Oppenheimer molecular dynamics with a hybrid Monte-Carlo scheme, for the calculation of thermodynamic properties of materials. Apart from simple model systems, this approach does not seem very fruitful.

Beyond the original extended Lagrangian generalization of time-reversible Born-Oppenheimer molecular dynamics we have been able to find new possibilities that may further improve the efficiency of the dynamics, including adaptive reversible time stepping, and a variety of potentials used in the extension of the original Born-Oppenheimer description of the dynamics.

## Future Work

We are currently performing several implementations of our recent findings in state-of-the-art electronic structure codes that are used at LANL. These codes include FreeON, Quickstep (part of CP2K), VASP, Quantum Espresso, Latte and DFT-TB. Without a detailed in-house knowledge it has turned out to be very difficult to perform some of the implementations. Too many unknown unknowns seem to appear and cause trouble. However, with our in-house codes developed at LANL, i.e. FreeON and Latte, we have been able to achieve great results. During the final year of this project we will focus on some of the remaining issues on the propagation of the phase in plane-wave pseudo potential codes, dissipation in higher-order geometric integration schemes, as well as further analysis and dissemination of our new extended Lagrangian Born-Oppenheimer molecular dynamics theory, which we hope will form the basis for the next generation of high-

performance atomistic simulations.

## Conclusion

We have made several important discoveries and developments for a new generation of high-performance Born-Oppenheimer molecular dynamics simulations that may become a standard tool for atomistic simulations based directly on the first principles of quantum mechanics.

## References


1. N.Niklasson, A. M., C. J. Tymczak, and M. Challacombe. Time-reversible Born-Oppenheimer molecular dynamics. 2006. *Phys. Rev. Lett.* **97**: 123001.

2. N.Niklasson, A. M.. Extended Born-Oppenheimer molecular dynamics. 2008. *Phys. Rev. Lett..* **100**: 123004.

3. Odell, A., A. Delin, B. Johansson, N. Bock, M. Challacombe, and A. M. N. Niklasson. Higher-order symplectic integration in Born-Oppenheimer molecular dynamics. 2009. *LA-UR 09-03581.*

4. N.Niklasson, A. M.. A note on the Pulay force at finite electronic temperatures. 2008. *J. Chem. Phys..* **129**: 244107.

5. N.Niklasson, A. M.. Extended Lagrangian free energy molecular dynamics. 2009. *in manuscript.*

6. N.Niklasson, A. M., P. Steneteg, A. Odell, N. Bock, M. Challacombe, C. J. Tymczak, E. Holmstrom, G. Zheng, and V. Weber. Extended Lagrangian Born-Oppenheimer molecular dynamics with dissipation. 2009. *J. Chem. Phys..* **130**: 214109.


## Publications


N.Niklasson, A. M.. Extended Born-Oppenheimer molecular dynamics. 2008. *Physical Review Letters.* **100** (12): 123004.

N.Niklasson, A. M.. A note on the Pulay force at finite electronic temperatures. 2008. *J. Chem. Phys..* **129**: 244107.

N.Niklasson, A. M., P. Steneteg, A. Odell, N. Bock, M. Challacombe, C. J. Tymczak, E. Holmstrom, G. Zheng, and V. Weber. Extended Lagrangian Born-Oppenheimer molecular dynamics with dissipation. 2009. *J. Chem. Phys..* **130**: 214109.

N.Niklasson, A. M., and N. Bock. Extended Lagrangian free energy molecular dynamics. 2009. *In Manuscript.*

Odell, A., A. Delin, B. Johansson, N. Bock, M. Challacombe, and A. M. N. Niklasson. Higher-order symplectic integration in Born-Oppenheimer molecular dynamics. *J. Chem. Phys..*

# Developing Adaptive High-Order Divergence-Free Methods for Magneto-Hydrodynamics Turbulence Simulations

*Shengtai Li*
20090210ER

## Introduction

Turbulence is a common phenomenon in plasmas, which are ubiquitous from Galaxy and star formation, solar wind and space weather forecast, to the electron-magnetic field in our daily life. It is convenient to treat such turbulent plasmas in magneto-hydrodynamic (MHD) framework. MHD studies the dynamics of electrically conducting fluids. The idea of MHD is that magnetic fields can induce currents in a moving conductive fluid, which create forces on the fluid, and also change the magnetic field itself. The magnetic fields have a nice property called divergence-free condition, which means the divergence of the magnetic fields is always zero, to ensure the conservation of magnetic flux.

The MHD turbulence simulations demand methods with both high-order accuracy and divergence-free preserving property. The order of accuracy, which is also called the rate of convergence of simulation results to the true solutions, is one of main factors of the efficiency of the method. The low order method demands a much finer grid resolution than the high-order method to achieve the same accuracy. Numerical experiments show that the eighth-order scheme can save by a factor of 85 in CPU time and a factor of 64 in data storage over the second-order scheme to achieve a comparable effect in turbulence simulations. The numerical methods that preserve the divergence-free condition are also essential for MHD simulations to produce the correct dynamics. Due to the lack of highly accurate simulation software, the research and development on compressible MHD turbulence is still in its infancy. We are aware no higher than second order divergence-free method thus far in MHD simulations.

The goal of this project is to develop efficient, accurate, and robust high-order methods and software for unsteady MHD simulations, and use the software and simulations to study compressible MHD turbulence. The traditional numerical simulations use only one grid to cover the whole physical domain. The magnetic field at the cell boundaries can numerically become discontinuous due to the numerical interpolation. The unphysical discontinuity of the magnetic field can trigger numerical instability [1] and crash the simulation.

We propose a new methodology to develop numerical methods. Rather than using only one grid, we generate an overlapping dual grid from the primal grid. By solving the MHD equations on both the primal and dual grids, the cell boundaries of one grid naturally fall within the dual grid and the magnetic fields become continuous in the dual grid, and the flux is easy to calculate by using the dual grid information. The accuracy order of the method is equal to the order of the reconstruction on a cell, which can be of any high. The divergence-free condition can also be easily achieved by developing high-order divergence-free reconstruction over a cell.

With this highly accurate, divergence-free preserving numerical tool, we can study the MHD turbulence in various applications: star formation, molecular cloud in the inter-stellar medium, accretion disk, solar wind, and space weather forecast, etc. While most of available MHD turbulence research focuses on the spectrum properties of the energy cascade, we are more interested in how the energy is converted and transferred from one wave mode to another during the turbulence forming stage, which is an important issue in compressible MHD turbulence regime but none has done that yet due to the lack of proper numerical tools. We will also apply the software for other MHD simulations, such as magnetic jet, magnetic reconnection in the solar atmosphere, and disruptive processes in Tokamaks.

## Benefit to National Security Missions

This project will enhance broadly important computational methods that will impact a wide variety of mission areas including computing, fusion energy, high energy physics, and the NNSA weapons mission by addressing several needs in the new NNSA Astrophysics Initiative. These are important mission areas for DOE and other government agencies.

## Progress

We first developed a third-order divergence-free

method for ideal magneto-hydrodynamics (MHD) in two-dimension. We have found a drawback in schemes currently used by numerical MHD community. With the help of a dual grid, which is generated from the primal grid, we get rid of the cell-centered magnetic field and the spatial averaging, which is needed by conventional method. We can compute the magnetic field with any high-order accuracy. Using the overlapping dual grid, we have constructed a compact third-order divergence-free scheme for MHD simulations [2]. To our knowledge, this is the first verified higher than second-order scheme with divergence-free property for MHD simulations.

We have tested our third-order method using a suite of challenging examples. Our proposed methods show super low dissipation (10 times smaller) comparing with the conventional second-order method. We have verified the order of the accuracy using the examples with exact solutions and our method indeed achieves both the third-order accuracy and divergence-free of the magnetic field. We have developed a test suite for 2D magneto-hydrodynamics (MHD) simulations.

For MHD flows that contain shock and contact discontinuity, we proposed an essentially non-oscillatory reconstruction to preserve the monotonicity of the fluid variables. This limited reconstruction uses only adjacent nearest neighbor via a hierarchical procedure to keep a compact stencil. For multi-dimensional problem with strong shock, we have developed a new multi-dimensional limiter to preserve the monotonicity of the solutions near the shock.

For hypersonic flows and/or low-beta plasmas, where energy is dominated by either kinetic or magnetic energy, the internal energy can easily become negative as the difference of two large numbers. We have implemented an efficient dual-energy formulation to track the low-pressure more accurately [3]. This dual formulation uses available information and increases the computational cost by only a few percent.

We have also developed a 4$^{th}$-order method using the same framework as the 3$^{rd}$-order method [4]. The 4$^{th}$-order divergence-free reconstruction requires an additional constraint from the dual overlapping grid. Numerical verification using the test-suite shows that our method achieves both 4$^{th}$-order accuracy and divergence-free for the magnetic fields. We have found that the 4$^{th}$-order method costs twice as much as the 3$^{rd}$-order method. However, to achieve the same accuracy, the 4$^{th}$-order method is roughly 32 times more efficient than the 3$^{rd}$-order method for 2D problems. Figure 1 shows the 4$^{th}$-order method has much lower numerical dissipation than the 3$^{rd}$-order method.

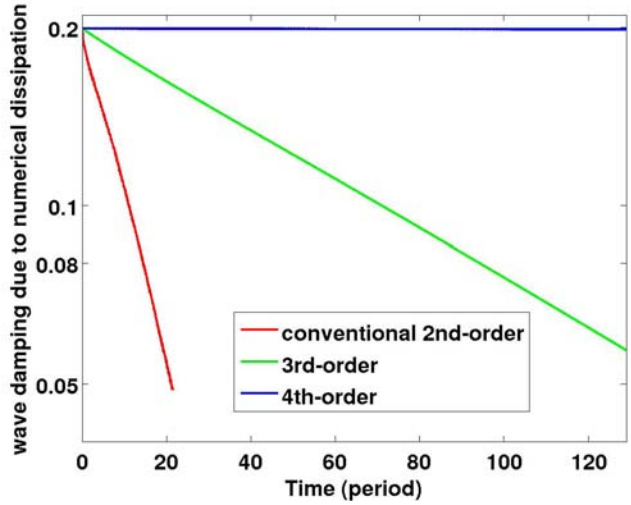


*Figure 1. Our high-order method has super lower numerical dissipation than the conventional second-order Godunov method.*

We have extended our 2D 3$^{rd}$ and 4$^{th}$-order methods to 3D. The extension is not trivial and has been documented in our paper [5]. Numerical verifications shows that we have achieved expected order of accuracy for both divergence-free and non-divergence-free method. Comparing the efficiency and accuracy of the 3$^{rd}$ and 4$^{th}$-order methods for 3D, we have found that the 4$^{th}$-order method is 64 times more efficient than the 3$^{rd}$-order method to achieve the same accuracy for 3D problems.

We have improved the performance of our code by at least a factor of 2 using a different reconstruction method and optimized memory usage. All the code (3$^{rd}$- and 4$^{th}$-order in 2D and 3D) is parallelized using message-passing interface (MPI). The parallel efficiency is 90%. We have removed code dependence on open-source software and make it self-containable. We have implemented an efficient check-pointing technique to save the current status for future restarting. We have found that data output is very expensive for distributing parallel machine. We have developed a patch-based output to allow each processor to write to the disk independently. This approach sharply reduces the disk output time.

In our numerical verification, we have found that the accuracy of the initial condition is crucial for the method to achieve the expected order of accuracy.

Our 2D software has been used to study the decaying MHD turbulence. We have found we can achieve a much longer inertial range than the available published results. The energy spectral properties at later stage before the dissipation range is very similar to the published results. We have also studied the energy conversion between different wave modes and obtained many interesting results [6].

We have published two papers related to this project. Two more papers are submitted for peer-reviewed journal. We have made three presentations related to the project in both university seminar and conferences.

## Future Work

The method we have developed is only for uniform grid now. We will extend this method to adaptive mesh refinement (AMR) grid to improve the computational efficiency. The AMR framework for a single grid (Li &Li 2005) has to be changed to accommodate both the primal grid and the dual overlapping grid.

We have found the non-oscillatory hierarchical reconstruction (Liu, 2007) does not work very well for the $4^{th}$-order method. It does not preserve the high-order accuracy for a smooth extreme either. We will investigate a different non-oscillatory reconstruction scheme.

The current method is implemented for finite-volume framework. Going to the higher order is very complicated. We will investigate the possibility to apply our method to discontinuous Galerkin regime, which is easier for developing higher-order method.

We will perform 3D large-scale simulations of both forced and decaying MHD turbulence to study the spectrum property of different wave modes. We will also study the mode conversion in 3D simulations.

## Conclusion

Our novel numerical methodology enables us to construct high-order property-preserving methods for MHD simulations. Numerical verification shows that our method has super-low numerical dissipations and dispersions, and preserves the divergence-error to machine-round-off level.

Our software package will be an ideal tool for simulations not only for MHD turbulence but also for other applications involving magnetic field. Using simulation and data analysis, we will gain new understanding on MHD turbulence. Our project will address a critical need in current MHD simulations and will have immediate impact in astrophysics and plasma physics. A number of publications on high-quality journal will be produced.

## References


Barth, T. J.. On the role of involutions in the discontinuous Galerkin discretization of Maxwell and magneto-hydrodynamics systems. . 2007. In *Compatible spatial discretization.* (Minneapolis, NM, May 11-15, 2004). Vol. 142, p. 69. New York: Springer-Verlag.

Li, S.. High order central scheme on overlapping cells for magneto-hydrodynamic flows with and without constrained transport method. 2008. *Journal of Computational Physics.* **227**: 7368.

Li, S.. A simple dual implementation to track pressure accurately. 2008. In *2nd International Conference on Numerical Modeling of Space Plasmas Flows, ASTRONUM-2007.* (Paris, France, June 10-15, 2007). Vol. 385, p. 273. San Francisco: Astronomical Society of the Pacific.

Li, S.. The Fourth-Order Divergence-Free Methods for MHD Simulations. 2009. *Submitted for publication in Journal of Computational Physics.*

Li, S., and M. J. Buoni. High-Order Divergence-Free Method for MHD flows in Three Dimensions. 2009. *will be submitted to Journal of Computational Physics.*

Buoni, M. J., S. Li, and H. Li. Wave Conversions in 2D Compressible Low-beta Turbulent MHD Flows. 2009. *will be submitted to Physical Review Letters.*


## Publications


Li, S.. High-order central scheme on overlapping cells for magneto-hydrodynamic flows with and without constrained transport method. 2008. *Journal of Computational Physics.* **227**: 7368.

Li, S.. Comparison of refinement criteria for structured adaptive mesh refinement. To appear in *Journal of Computational and Applied Mathematics.*

Li, S.. The fourth-order divergence-free method for magneto-hydrodynamic simulations. *Journal of Computational Physics.*

Li, S., and M. J. Buoni. High-order divergence-free method for MHD in three dimensions. 2009. *to be submitted.*

Xu, H., H. Li, D. Collins, S. Li, and M. Norman. Turbulence and dynamo in galaxy cluster media: implication on the origin of cluster magnetic fields. 2008. *Astrophysical Journal Letters.* : L14.

# Efficient Interdiction

*Feng Pan*
20090250ER

## Introduction

The goal of this research project is to develop efficient algorithms and models for the problem of network interdiction. In the interdiction mission an interdictor seeks to minimize the ability of an adversary to achieve high consequence activities. Conversely, the evader seeks to maximize the likelihood of success and impact of successful execution. Such a min-max problem can be posed mathematically in terms of graph analysis: the interdictor seeks to identify a set of vital arcs on an activity network whose removal minimize the maximum reliable path from a source to a destination node, while the evader seeks to find and traverse the best unimpeded path. The activity graph may represent a transportation network, but more generally may correspond to resource allocation in an activity network.

The interdiction problem has applications in many areas within threat reduction such as identifying key border control points, disrupting nuclear smuggling efforts or suicide bomber logistical support, and analysis of vulnerabilities in critical infrastructures. LANL has several programs that address the interdiction problem, but they concentrate on analysis instead of research on new capabilities. In fact, one may argue that threat reduction in toto, a major thrust within LANL, is essentially the problem of interdiction. In addition to our focus on efficient interdiction our project results may impact other research areas where combinatorial optimization problems appear such as resource allocation in operations research or coding theory in statistical physics.

## Benefit to National Security Missions

This project will support multiple national security missions by providing basic science for threat reduction through modeling and decision support capabilities of interdiction problems. The network interdiction problem has mission relevance to DOE, DHS, and other government agencies.

## Progress

In the classical max-min interdiction model, an evader is assumed to travel on an optimal (shortest distance or least cost) path, and an interdictor selects a fixed number of edges to thwart the evader's movement by increase the costs of these edges. The assumption of the evader's optimal behavior can be restrictive for certain scenarios. We developed the Markovian evader model to include the uncertainty of the evader's movements in a transportation network. In this model, instead of always following an optimal path, the evader moves on a guided random walk from the current location to the next in a probabilistic fashion according to the distance between the next location and the destination.

We investigated two variants of the guided random walk interdiction model. In the nonreactive version, the evader is not aware of interdiction actions (or doesn't have enough time to respond to them) and does not change the probability of selecting a path in post-interdiction network. In the second version, a reactive evader adjusts the transition probability after an interdiction.

Both problem variants were proven to be computationally hard (NP-complete). We developed efficient approximation algorithms based the submodular property of the nonreactive model. The performance of these algorithms is theoretically guaranteed to be within a constant factor of the optimal solution, and the algorithms are polynomial time. In the reactive model, we explored the relation between graph centrality measures and the evader's movements, and then developed polynomial time heuristic algorithms based on these centrality measures.

There can be multiple methods to quantify the uncertainty of the evader's movements. The guided random walk considers localized uncertainty. Alternatively a path-based stochastic model captures the probabilistic nature of selecting a path with the global knowledge on paths, and perception-based model includes path selection based on evader perceptions of the network. We are investigating the relation

among these three models and have established certain equivalence between the guided random walk and the path-based stochastic model.

With many different ways of quantifying uncertainties of the evader's movements, it is clearly important to develop an interdiction model, which is robust against the various evaders' strategies. Along this direction, we developed a tri-level optimization model. This model aims to increase the probability of detecting an evader on at least one edge (bottleneck edge) on every possible path (robust against uncertain evasion movements), and the worst path is a path in which the detection probability of its bottleneck edge is the smallest. The goal is to maximize the detection probability of the worst path. Since all paths are considered, this model is invariant to how an evader selects a path. In the continuous version of this tri-level model, the detection probability can be continuously improved, and we developed an efficient and exact solution method by transforming the problem into a sequence of the minimum cut problems. In general the discrete version of this class of problems is NP-complete. A surprising result is that for this tri-level model the discrete version in which we assume two states of detection probability (with and without improvement) has efficient algorithms and can be solved by polynomial algorithms. We are currently working on a stochastic version where the detection probability is probabilistic.

We also investigated distributed heuristic algorithms for classical network interdiction models. To understand the performance of such algorithms, we started with a bipartite network interdiction model. This model is NP-complete but with simpler graph structure that is important in the area of border security. We developed a message-passing algorithm based on a max-product algorithm for the bipartite network interdiction model. This message-algorithm has polynomial running time (efficient), and the preliminary computational results show that the heuristic solutions are close to optimal solutions. The theoretical understanding of the performance of this algorithm is an ongoing project goal.

Another extension of the classical interdiction model is in the area of contingency analysis for power grids. We developed an interdiction model to understand the worst-case scenario of power outage in the case of line damage. As the result of this development we are currently building an interdiction-based model as a control mechanism of the smart grid for reducing the power line overloads which can start a wide-area blackout.

## Future Work

Combinatorial optimization problems appear in various research areas and the computational complexity of these problems is a critical barrier to theoretical research and application development. This difficulty is amplified because of the uncertainties in real-world applications. The goal of this research is to develop such efficient algorithms for computationally hard combinatorial problems and provide fundamental understanding these problems when uncertainties presents, in particular the problem of network interdiction.

We will develop heuristic algorithms along several novel approaches. Recent research showed the success of belief propagation (BP) algorithms in solving inference problems (e.g., statistical physics, error-correcting coding theory.). Research on social networks has introduced the concept of centrality measures that identifies those arcs that are critical to connectivity within a network. These two areas are in close vicinity of combinatorial optimization. However, it is original to directly apply them in developing algorithms and robust models of incomplete information for general optimization problems. Our research will take the challenge to explore optimization algorithms and uncertainty modeling along these new dimensions.

We start with deterministic networks with special structures: planar road/rail networks, and the bipartite interdiction model. The development focuses on dynamic centrality measures of these networks and graphical models/loop calculus in BP. In year two, extending the results to general networks, we will develop centrality measures on stochastic networks to capture the dynamic of evader's movements and apply them to interdiction models. We will investigate variations of BP algorithms (e.g., generalized BP and survey propagation) for general network interdiction problems. In year three, we will investigate the fundamental properties of solution quality, computational efficiency, and problem structure dependency among these methods. Throughout this research, the theoretical development will be tested in simulated network and networks in an existing comprehensive global transportation network database.

## Conclusion

The object of this research is to remove the critical barriers of computational difficulty and uncertainty modeling in combinatorial optimization problems. The success of this research will impact the areas in counter-proliferation and homeland security. The development of efficient algorithms will support strategies of global sensor deployment and tactics of real-time interdiction missions. The development of uncertainty modeling will provide predictable capabilities of understanding threat behavior and movements in transportation networks with incomplete information.

## Publications

Dimitrov, N. B., D. P. Michalopoulos, D. P. Morton, M. V. Nehme, F. Pan, E. Popova, E. A. Schneider, and G. G. Thoreson. Network deployment of radiation detectors with physics-based detection probability calculations. To appear in *Annals of Operations Research.*

Gomez, V., and M. Chertkov. Approximate inference on planar graphs using loop calculus and belief propagation. *Journal of Machine Learning Research.*

Gutfraind, A., A. Hagberg, and F. Pan. Optimal interdiction of unreactive Markovian evaders. 2009. In *Lecture notes in computer science (CPAIOR 2009).* Edited by Hooker, J., and W. J. van Hoeve. , p. 102. Berlin / Heidelberg: Springer.

Hagberg, A.. Structure and dynamics of cybersecurity networks. Presented at *2009 Siam Annual Meeting.* (Denver, Co, 6 - 10 July 2009).

Pan, F., N. Santhi, and M. Chertkov. Message-passing algorithms for solving bipartite network interdiction. Presented at *2009 INFORMS Computing Society Conference.* (Chareston, SC, 11-13 Jan. 2009).

Pan, F., N. Santhi, and M. Chertkov. Network interdiction by securing edges. Presented at *The 20th International Symposium of Mathematical Programming .* (Chicago, Illinois, 23 - 28 Aug. 2009).

Santhi, N., and F. Pan. A heuristic for restricted rank semi-definite programming with combinatorial applications. Presented at *The 20th International Symposium of Mathematical Programming.* (Chicago, Illinois, 23 - 28 Aug. 2009

# A Hybrid Transport-Diffusion Method for Radiation Hydrodynamics

*Jeffery D. Densmore*
20090420ER

## Introduction

Radiation-hydrodynamics calculations involve the coupled modeling of x-ray regime radiation transport and hydrodynamic material motion. Typically, simulating radiation transport comprises the bulk of the computational effort in these types of problems. One technique for modeling radiation transport is Monte Carlo simulation. This method is very accurate, but can also be prohibitively expensive in optically thick regions, i.e., where the mean distance between photon collisions is much smaller than the size of the region. An alternative to Monte Carlo is the diffusion approximation, which is computationally inexpensive but only valid in optically thick regions. Thus, in realistic problems that contain both optically thick and optically thin regions, entirely replacing a Monte Carlo calculation with the diffusion approximation is impractical if one desires accurate solutions.

In this project, we will develop a hybrid transport-diffusion method for simulating radiation transport as part of a radiation-hydrodynamics calculation. This hybrid technique will combine the diffusion approximation and Monte Carlo to yield efficient simulations without sacrificing accuracy. Specifically, our hybrid method will employ the diffusion approximation in optically thick regions, where Monte Carlo is expensive and this approximate theory is accurate, and resort to Monte Carlo in optically thin regions, where an accurate radiation-transport solution is required.

## Benefit to National Security Missions

This project supports the DOE/NNSA mission in Nuclear Weapons by enhancing the basic science that underlies our ability to perform massive simulations. In addition, basic science studies related to astrophysics, inertial confinement fusion, and high energy density physics will also benefit.

## Progress

We have made steady and significant progress on our research and development of the Discrete Diffusion Monte Carlo (DDMC) method for thermal radiation transport in the production Implicit Monte Carlo (IMC) software from the Jayenne Project. We have made progress despite heavy Roadrunner (IBM Cell architecture) Project demands early in the year and despite less overall time available for this project.

First, the DDMC method was derived for spherical geometry and documented [1]. Our research and development of DDMC are targeted toward the production software in the Jayenne Project, which approximates curvilinear geometry with 3-D Cartesian meshes. For spherical geometry, a full radially symmetric sphere of radius R is represented exactly as a cone of height R with radiatively reflecting sides, and then that cone is represented approximately by a pyramid, which, when spatially discretized, produces cells that approximate a frustum with a longitudinal chunk of pyramid (square ends and flat, sloped sides). The discretized diffusion equation was derived for these cells and manipulated to find probabilities for a source particle to be transmitted out either longitudinal end or for being absorbed within the cell. Also derived were the equations and corresponding probability functions for when particles move between DDMC cells and IMC cells.

The DDMC method is being implemented into the production Jayenne IMC Project software, which contain the Milagro radiation-only code and the Wedgehog package that couples to hydrodynamics codes to produce a radiation-hydrodynamics capability. The underlying capabilities have been developed, tested, and committed to the software repository. These underlying capabilities are to flag which spatial cells should be treated with regular IMC transport and which should be treated with the DDMC approximation; to determine the probabilities of leakage from a DDMC cell; a DDMC particle class as a subordinate to the existing IMC particle class; methods for switching a particle from being a DDMC particle to a regular IMC particle and back; and software classes that transport the DDMC particles over multiple DDMC cells. Refactoring of the existing code was necessary to enable a more seamless introduction of DDMC to the IMC software.

These classes have been developed in accordance with the standard procedures of the Jayenne Project. For each capability, a unit test is constructed. These unit tests are software that live in the repository alongside the capability software and that are run during development and during nightly automatic regression tests. The capability developed so far consists of four major classes (DDMC_Transport, DDMC_Builder, DDMC_SubTally, and DDMC_Particle) constituting about 700 lines of code, software to enable integration with other classes at the same level, and tests numbering about 1000 lines of code.

For this fiscal year, we have completed implementing a grey (frequency-independent) spherical-geometry capability into Milagro. Next fiscal year we will extend this existing capability to cylindrical geometry, which has a similar 3-D Cartesian representation in the Jayenne Project software; research and develop a method for automatically selecting where to use DDMC; and begin researching how to perform DDMC and hybrid DDMC-IMC in frequency-dependent problems, the latter being a very challenging endeavor.

## References

1. Densmore, J. D.. Discrete Diffusion Monte Carlo for the Sphyramid mesh. 2009. *CCS-2:09-04(U).*

## Publications

Densmore, J. D.. Discrete Diffusion Monte Carlo for the Sphyramid Mesh. 2009. *CCS-2:09-04(U).*

# Robust 3D Moving Mesh Adaptation Based on Monge-Kantorovich Optimization

*John M. Finn*
20090424ER

## Introduction

Mesh or grid generation is at the heart of many numerical simulations of physics problems. The grids provide points or boundaries at which the numerical simulation is performed. This project involves optimal grid generation for the numerical solution of nonlinear partial differential equations, e. g. the equations of hydrodynamics or the equations of magnetohydrodynamics (MHD). The grid adaptation is optimal in two senses. First, it assures that the estimated grid error is distributed equally on grid cells (equidistribution), leading to the minimization of the total grid error. Second, for time stepping, this assures that the grid move a minimal amount relative to the grid at the previous time step. This latter property appears to lead to an untangled grid. Grid tangling is a serious problem for example in Lagrangian codes.

We plan to extend our preliminary work in a simple two dimensional (2D) physical region (the unit square) to more complex regions in 2D. Examples include regions with missing areas (non-simply connected regions) and regions with curved boundaries. We will then extend the work to three dimensions (3D), also involving complex physical regions. We plan to use this grid adaptation strategy in moving mesh hydrodynamics and MHD codes in 2D and 3D. We will use well developed error estimators for which our method will provide equidistribution of error. We will then apply these adaptive grid codes to several challenging problems. These include: 1) propagation of shocks, 2) Rayleigh Taylor instability, 3) Kelvin Helmholtz instability, and 4) magnetic reconnection. We will compare with commonly used methods to assess the efficiency and accuracy of our methods.

## Benefit to National Security Missions

This project endeavors to enhance simulation codes involving, for example, hydrodynamics, radiation hydrodynamics, magnetohydrodynamics, and particle-in-cell (plasma kinetic theory) codes that are immediately relevant to the DOE/NNSA nuclear weapons mission. Such computational tools should also impact astrophysics, high energy-density physics, fusion energy, space plasma physics, and other basic science mission areas.

## Progress

We have completed work on the fundamentals of Monge-Kantorovich optimization for grid generation and adaptation. In this work we formulated the equations in L_2 and compared with existing methods. We published the paper "An optimal robust equidistribution method for two-dimensional grid adaptation based on Monge-Kantorovich optimization", Delzanno, G.L., Chacon, L., Finn, J.M., Chung, Y., Lapenta, G., Journal of Computational Physics (1 Dec. 2008) vol.227, no.23, p.9841-64.

We completed work on generalization of the L_2 Monge-Kantorovich grid generation to a large class of domains in 2D and to three dimensions. PI John Finn presented an invited talk "Grid Generation and Adaptation by Monge-Kantorovich Optimization in Two and Three Dimensions" at the 17th International Meshing Roundtable in October 2008. We published a paper "Grid Generation and Adaptation by Monge-Kantorovich Optimization in Two and Three Dimensions" Finn, JM, Delzanno, GL, Chacon, L, PROCEEDINGS OF THE 17TH INTERNATIONAL MESHING ROUNDTABLE (2008) p.551-568.

We completed work on generalizing Monge-Kantorovich grid generation from the L_2 norm to the L_p norm. We formulated a generalized form of the Monge-Ampere equation (which we called the L_p Monge-Ampere equation), developed an efficient method of solving it, and compared the results with our earlier theory in L_2. The results showed that the optimal value for p is very close to p=2. We submitted the manuscript "Generalized Monge-Kantorovich optimization for grid generation and adaptation in L_p", G. L. Delzanno and J. M. Finn, submitted to SIAM Journal of Scientific Computing, Feb. 2009.

We completed work on formulating Monge-Kantorovich grid generation with the L_p norm in a fluid dynamics context. We formulated a method of solving the

resulting fluid equations efficiently. We showed that the results are identical to those obtained using the L_p Monge-Ampere equation discussed above. The advantage of the fluid dynamics formulation is that it can provide a smooth variation of the grid, and can be used in image analysis. We submitted the manuscript "The fluid-dynamic approach to equidistribution methods for grid generation and adaptation", G. L. Delzanno and J. M. Finn, submitted to SIAM Journal of Scientific Computing, Mar. 2009.

We have completed work on the use of Monge-Kantorovich grid adaptation in a time-stepping context. In this work we compared two distinct methods of performing the grid adaptation, sequential and direct. Numerical results using several challenging examples showed that the direct method provides a less distorted grid which is much less prone to tangling. Luis Chacon, Gian Luca, and John Finn are in the process of writing a paper to submit to Journal of Computational Physics.

We have organized a CNLS workshop entitled "Monge-Kantorovich optimal transport: theory and applications", held in Santa Fe October 19-21. CNLS, LDRD and IGPP each contributed 10K for conference expenses. The conference included 19 invited talks and 8 poster presentations.

## Future Work

This project involves optimal grid generation for the numerical solution of nonlinear partial differential equations, e. g. the equations of hydrodynamics, radiation hydrodynamics, or

magnetohydrodynamics (MHD). The grid adaptation scheme we will investigate is optimal in two senses. First, it assures that the estimated grid error is distributed equally on grid cells (equidistribution). This is known to lead to the minimization of the total grid error. Second, for time stepping, this assures that the L2 norm of the grid displacement (relative to the grid at the previous time step) be minimized. Grid tangling is a serious problem in, for example, Lagrangian codes, and the displacement minimization property has the potential to deliver untangled grids.

We plan to extend our preliminary work in a simple two dimensional (2D) physical region (the unit square) to more complex regions in 2D. Examples of such physical regions include non-simply connected regions (regions with holes) and regions with curved boundaries. We will then extend the work to three dimensions (3D), also involving

complex physical regions. We plan to use this grid adaptation strategy in moving mesh hydrodynamics and MHD codes in 2D and 3D. We will use well developed error estimators for which our method will provide equidistribution of error. We will then apply these adaptive grid codes to several challenging problems of importance to DOE/NNSA programs. These include: 1) propagation of shocks, 2) Nonlinear Rayleigh-Taylor instability, 3) Nonlinear Kelvin-Helmholtz instability, and 4) magnetic reconnection. We will compare our results with those obtained with commonly used methods to assess the efficiency and accuracy of our methods.

## Conclusion

Grid adaptation (GA) in numerical codes uses a fine grid in areas with large numerical errors and a coarse grid elsewhere. Adaptive griding allows more efficient computer time and memory than uniform grids. There are two issues: GA methods are often ad-hoc, suboptimal and hard to quantify; GA methods are prone to tangling, and the code must be restarted with ad-hoc modifications to mitigate the tangling. Our work is based on optimization theory, equidistributing and minimizing grid error. Our work so far indicates strongly that these methods are effective in preventing grid tangling.

## References


1. Delzanno, G. L., L. Chacon, J. M. Finn, Y. Chung, and G. Lapenta. An optimal robust equidistribution method for two-dimensional grid adaptation based on Monge-Kantorovich optimization. 2008. *Journal of Computational Physics.* **227** (23): 9841.

2. Finn, J. M., G. L. Delzanno, and L. Chacon. Grid generation and adaptation by Monge-Kantorovich optimization in two and three dimensions. 2008. In *17th International Meshing Roundtable.* (Pittsburgh, 12-15 Oct. 2008). , p. 551. Berlin: Springer-Verlag.

3. Delzanno, G. L., and J. M. Finn. Generalized Monge-Kantorovich optimization for grid generation and adaptation in L_p. *SIAM Journal of Scientific Computing.*

4. Delzanno, G. L., and J. M. Finn. The fluid dynamic approach to equidistribution methods for grid generation and adaptation. *SIAM Journal of Scientific Computing.*

5. Chacon, L., G. L. Delzanno, and J. M. Finn. Robust, multidimensional mesh motion based on Monge-Kantorovich equidistribution. *Journal of Computational Physics.*


## Publications


Chacon, L., G. L. Delzanno, and J. M. Finn. Robust, multidimensional mesh motion based on Monge-Kantorovich equidistribution. *Journal of Computational Physics.*

Delzanno, G. L., L. Chacon, J. M. Finn, Y. Chung, and G.

Lapenta. An optimal robust equidistribution method for two-dimensional grid generation based on Monge-Kantorovich optimization. 2009. *Journal of Computational Physics.* **227** (23): 9841.

Delzanno, G. L., and J. M. Finn. Generalized Monge-Kantorovich optimization for grid generation and adaptation in Lp. *SIAM Journal of Scientific Computing.*

Delzanno, G. L., and J. M. Finn. The fluid dynamic approach to equidistribution methods for grid generation and adaptation. *SIAM Journal of Scientific Computing.*

Finn, J. M., G. L. Delzanno, and L. Chacon. Grid generation and adaptation by Monge-Kantorovich optimization in two and three dimensions. 2009. In *Proceedings of the 17th international meshing roundtable.* Edited by Garimella, R. V.. , p. 551. Berlin: Springer Verlag.

# New Approach to Bayesian Inference Under Modeling Uncertainty

*Nicolas W. Hengartner*
20070172ER

## Abstract

The Bayes network (or net) methodology is a powerful and popular approach to modeling relationships between experimental variables, consisting of two key components: a topology that encodes a set of conditional independence conditions; and a set of functions that assigns conditional probabilities between directly related variables. Such models can then be used to propagate uncertainties and make statistical inferences. Although the topology in a Bayes model can often be derived from physical arguments, the conditional probabilities populating this model are usually derived experimentally, from historical data, or from expert introspection; both approaches are noisy and unreliable. A more representative model, based on second-order probabilities or "probability of probabilities", includes information about the uncertainty in these statistical relationships. These uncertainties can then be propagated through the Bayes net, resulting in "error bars" on the posteriori probability of a hypothesis. The resulting uncertainties on posterior probabilities provide insight into the *value of information* of future observations, which we use to develop efficient data acquisition strategies.

In our view, good data enables one to make good decisions confidently, and we determine the value of obtaining a particular set of data by a quantitative measure of how much that data can improve a decision. We developed two ways of analyzing data marshaling that we call cost based and asymptotic. The resulting data marshaling strategies are of immediate relevance to the Integrated Knowledge Engine (IKE) developed at the Los Alamos National Laboratory.

Finally, we consider a complementary approach to data marshalling for improving predictions. We show that it is possible to estimate the bias of nonparametric smoothers and use these estimates to get better predictions. Iterating the bias correction scheme can produce smoother that have superior performance in high dimensions. The methods we have developed are useful to improve radioisotope identification from energy spectrum data.

## Background and Research Objectives

### First Order Probabilities

As an illustration of a Bayes network, consider the following simple model that can be used to diagnose a hypothetical disease. This disease has two possible symptoms, fever and coughing. There is a certain a priori probability that a patient has the disease, as illustrated (right). Moreover, there is a certain conditional probability structure that encodes how frequently a patient will exhibit a fever given that she either has or does not have the disease, while a similar conditional probability encodes how frequently the patient will exhibit coughing given that either she has or does not have the disease. Once we have specified the topology and conditional probabilities, we can reason about the relationships between the random variables if we know the value of certain nodes (such as symptoms). This is known as statistical inference.

### Second Order Probabilities

While the relationships encoded in the Bayes net topology often have some physical justification, for example due to causal relationships, in many, if not most applications, the conditional probability relationships are not derivable from general principles and must instead be estimated from sample data or assessed qualitatively by subject matter experts. When these probabilities are explicitly modeled as uncertain, they themselves in turn become random variables, and we enter the realm of second-order probabilities. In addition, second-order probabilities can be used to encode the inherent quality of the evidence presented to the Bayes net. For example, sensor detection and false alarm statistical behavior can be encoded as second-order probabilities

on evidential nodes.

Current approaches to second order probabilities: There are several approaches developed in the literature for encoding uncertainty about conditional probabilities. The most common and flexible approach is to use stochastic simulations. Essentially, we instantiate many different models, each having slightly different modeling parameters, i.e., conditional probabilities, and we collect the results of reasoning using each of these different instantiated models. We can then compute numerical estimates of the statistics of the model output. A more formal approach consists of modeling the distribution of each conditional probability explicitly and analytically propagating this distribution through the model. Walley and others have studied the use of probability intervals and their propagation extensively. A more recent approach uses Beta or Dirichlet distributions to model the underlying second order probability using mean and variance.

**Need for an Analytical Approach**

None of the approaches so far developed in the literature address the problem adequately. For example, stochastic simulations are computationally expensive. The use of probability intervals is problematic because probability intervals tend to broaden, leaving little insight into the uncertainty structure. The use of Beta distributions is also inadequate since it is easy to show that the Beta distribution property is not preserved under any probability propagation function. Moreover, the Beta distribution is not flexible enough to represent some second order probability distributions of interest, such as multi-modal distributions. We propose definition of a more general analytical inference method where constants in a probabilistic inference such as P(A), P(B|A), etc. become random variable themselves and are treated as such.

**Why study uncertainty?**

We take the ansatz that a good observation enables us to make a good predictions confidently. This means that both the bias and the uncertainty of our predictor need to be small. Since the uncertainty is tied to the observations, we can compare the "after we observe" uncertainty of various data collection schemes to help compare and select useful data acquisition schemes. When balancing the reduction in uncertainty from data obtained from various individual data sources with the cost of acquiring the data, we can find cost effective learning schemes that we call data marshaling. Whereas notions of "most valuable observations" have permeated the statistics literature, the compromise between information, costs for acquiring the data, and the computational complexity (or computational costs) has not been previously addresses. But balancing these three aspects is central to the development and implementation of the Integrated Knowledge Engine (IKE) tool.

**Bias reduction**

The other factor involved in making good predictions in the bias, or systematic error, in the estimate. Reducing the bias may be an attractive alternative to reducing the uncertainty, if the former does not increase the variance too much. In classical examples related to nonparametric smoothing, a modern statistical prediction tool, we know that smaller bias is always associated with larger variance. Nevertheless, some substantial reductions in bias may sometimes only increase a little bit the variance. It then becomes interested to attempt to seek the maximal bias reduction possible before the uncertainty becomes to dominate. We have developed and applied our bias reduction techniques in the context of estimating the energy spectrum of various radio-isotope to help their identification.

## Scientific Approach and Accomplishments

**Generalization to Dirichlet mixture**

The application of second order probability to the problems of interest requires the end user to specify specification uncertainty to multinomial probabilities constrained by experts knowledge about the means and variances of all the vector of probabilities. While the Dirichlet distribution, the classical model for quantifying uncertainty for multinomial, is not flexible enough to accommodate the specified moments, we have shown that suitable mixtures of Dirichlet can accommodate the preset moments and associated uncertainties. The practical importance of this model is that it leads computationally tractable estimates of the uncertainty of the hypothesis. This allows us to scale the size and complexity of the models while keeping the computation time to a minimum. These methods have been implemented in the Integrated Knowledge Engine (IKE) have been extensively used in various projects. Figure 1 shows the interface GUI for the IKE tool. The colored bars in the right-hand panels represent the uncertainty associated with the inputs and various hypotheses.

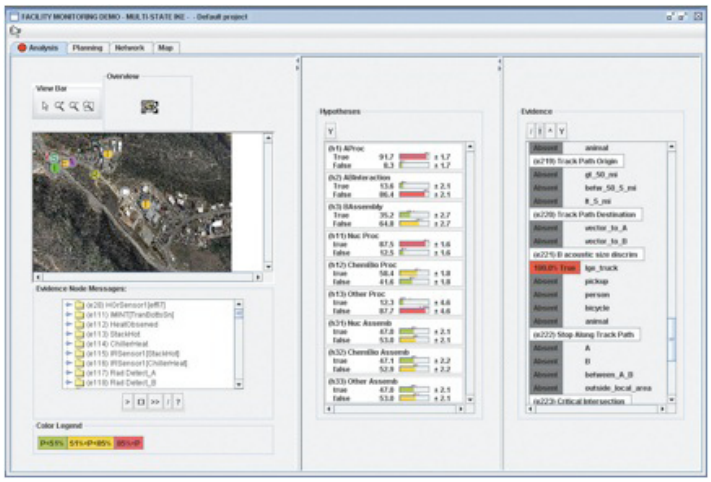

*Figure 1. Example of the implementation of second order probability uncertainty calculations within the Integrated Knowledge Engine framework. The figure shows how various sources of information about a facility of interest impact our knowledge and the uncertainty about that knowledge.*

**Approximate likelihood**

A study of the impact on the posterior probability of a hypothesis of distribution of second order probability reveals that the exp-gamma distribution is a natural model because it allows for explicit calculations under special circumstances. To our knowledge, this is the first example of an explicit solution to this problem, which allows for dramatic improvements in computational times over the classical brut force simulation approach. Further refinements of our analysis approximate the likelihood to get approximate analytic solutions. The surprise is how good such approximations are in the real cases we have considered. In particular, the intrinsic variability (or uncertainty) dominates the approximation error in the examples we have considered. Thus we now have explicit expressions (either exact or approximate) for the uncertainty implied by the second order probabilities.

**Data Marshalling**

We aimed to develop a theoretical basis for choosing amongst options for obtaining data. In our view, good data enables one to make good decisions confidently, balanced by the cost of acquiring that observation and the computational burden to evaluate the decision rule. The answers to that compromise depend on whether we get to select a measuring instrument (or data stream) that provides a possibly unlimited stream of data, or an individual datum. We refer these to cases as the asymptotic and cost based analysis. We have drawn on our experience with cosmic ray muon radiography to develop the asymptotic based analysis, and present a toy model for the cost based analysis.

*Asymptotic based analysis*

Suppose that a buyer must choose between two instruments each of which could make one measurement per second over long time intervals. If the 1st kind of instrument is more expensive but makes more discriminating measurements, an asymptotic analysis will provide guidance to the buyer. The analysis provides the ratio between the times required by the two instruments to achieve a specified quality of discrimination. As an example, we consider the task of using natural cosmic ray muons to distinguish between human flesh and cellulose nitrate (an explosive). We consider two instrument options, one that measures the scattering angle of rays that pass through material and another that measures the energy lost by such rays. The simulated distributions of energy loss for samples of both flesh and cellulose nitrate appear in Figure 2. Our analysis shows that to get both the probability of false alarm and the probability of missing a detection less than 1/1000000, one must measure either the energy lost by about 17 muons or the angle of scatter of about 510 muons. Thus the energy loss instrument can do the job about 30 times faster. Asymptotic analysis calculates the limit of such a ratio as the required probability of error goes to zero.

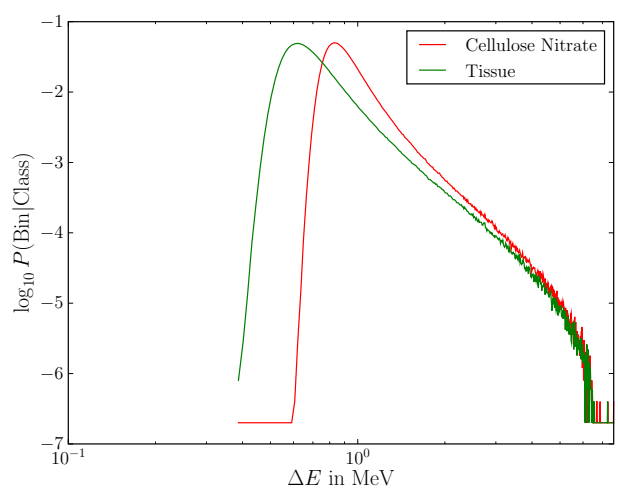


*Figure 2. The information in data about a hypothesis can be extracted from their probability density functions. It is by exploiting the differences between the probability densities under the various hypothesis that the truth about the hypothesis is revealed. The figure shows the probability density of the energy loss in human flesh and an explosive. The observed differences implies that it is possible to distinguish flesh from explosive from energy loss measurements.*

*Cost based analysis*

Suppose that we must decide whether or not to align the front wheels of a car. Before making a decision, we can do one of the following two experiments: "Look for uneven

tire wear" or "Check for hands-free straight driving". We suppose that the probability of a false indication from tire wear is 20% whether an alignment is actually required or not, while the driving test will mislead with a probability of 30% if an alignment is actually required but only 10% if not. Thus costs can determine the value of evidence and for different cost values different measurements are preferred. The determination of which experiment is more cost effective depends on the expense for replacing the tires and the cost of rotating them. Under special circumstances, it is possible for the optimal solution not to depend on the cost. These situations are rare, but provide a good starting point for further analysis.

**Bias reduction**

We have developed numerous strategies for bias reduction in nonparametric regression. Developed in the context of energy spectrum estimation, we have devised a multiplicative bias reduction scheme that preserved the positivity of the estimate, enhances the peaks and valley, while leaving the other regions of the spectrum essentially unchanged. The most important feature of new smoother is that its asymptotic bias is zero while its asymptotic variance remains unchanged. That is, we have an "asymptotic" free lunch. Both in practice and in simulations, we see that our method enjoys its asymptotic qualities even for modest sample sizes. Figure 3 shows the improvement obtained by the proposed bias reduction procedure. The top panel shows the raw counts and a reasonable spline smoothers (red) and the bias corrected smoother in green. The bottom panel shows the relative error of the spline smoother and an estimate of that error to correct the pilot smoother.

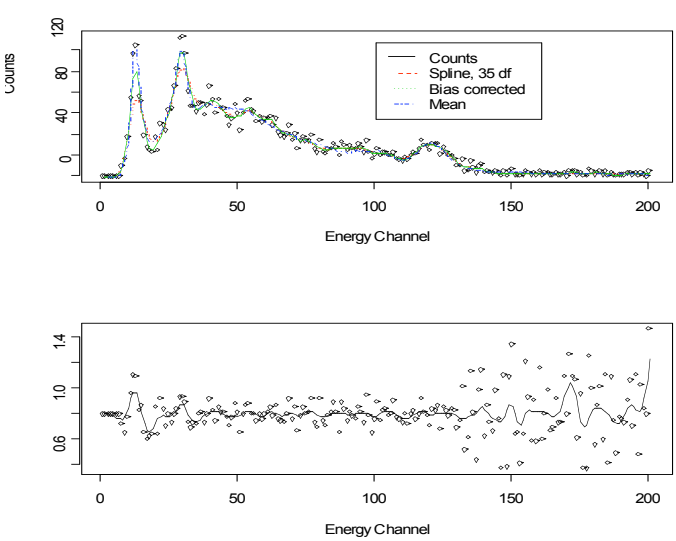


*Figure 3. Example of bias corrected energy spectrum smoother. The top panel shows a histogram of the raw counts together with various smoothers for the energy spectrum, including the bias corrected smoother. Note how the corrected smoother more aptly estimates the energy peaks and valleys, yet does not appear to be more variable than the other smoothers. The bottom panel shows the ratio between the pilot smoother and a noisy estimate of the truth, together with a smoother for that ratio. Estimating that ratio enables us to propose a multiplicative bias correction scheme.*

The bias corrected smoother remains biased, and thus further bias correction steps may be beneficial for finite samples. We have shown that an iterative bias correction scheme is related to the celebrated boosting algorithm of machine learning. But this new interpretation of boosting helps explain the qualitative behavior of the sequence of bias corrected smoothers. To our surprise, these iterated bias corrected smoothers have exceptional performance in high dimensions. We can explain this by the ability of these smoothers to adapt (in the statistical sense) to smoothness of the underlying regression function. While it has been common practice to use structurally constrained smoothers in high dimensions, such as additive or multiplicative models, we find that optimally exploiting the smoothness often leads to better predictors. We have compared our method with the state-of-the-art smoothers on a few classical open source data sets, and found that we reduced the out-of-sample prediction error by at as much as 30%. To help the divulgation of our method, we have released an R add-on package to the statistical community.

## Impact on National Missions

We have been utilizing Bayesian Networks within our IKE (Integrated Knowledge Engine) methods and tools to support Los Alamos National Laboratory's mission in Threat Reduction. Specifically, IKE supports monitoring and surveillance of WMD threats by modeling these threats using Bayesian networks where variables represent indications of threats and their relations to those threats. Threats can include probability of an IED (improvised explosive device) attack, probability of a mobile missile attack, etc. As a result of the success we have achieved to date in our LDRD-ER, we have implemented the multi-state Dirichlet mixture based numerical simulation method and are now using that for second order probability representation and inference in several customer projects. This allows us to model uncertainty on our priors, conditional probabilities and evidence. Below we show screen shots of a system supporting quantified detection of activities at a WMD processing facility and its subsequent relation to a WMD assembly facility.

The theoretical work on data marshalling lies at the hart of the modeling work that is needed by several nonproliferation agencies. We have obtained follow-up funding to expand that aspect of this LDRD-ER and port

and expose our ideas in a white paper for a sponsor.

The work on bias reduction has had an immediate impact on the energy spectrum estimation that is required for radio-isotope identification. The preliminary results are encouraging and we will continue to explore their utility within the Remote Portal Monitoring Project (RPMP) project.

Finally, the theoretical work on the iterative bias correction scheme is of general interest and broad applicability. Indeed, the problem of making predictions is a ubiquitous problem in science, and we foresee that our software will be useful to many project. To make our tool even better for making predictions in high dimensions, we are currently seeking to develop a variable selection capability within the bias reduction framework.

## Publications


Burr, T., N. Hengartner, E. Matzner-Lober, and L. Rouviere. Bias reduction in action. 2009. In *Joint Statistical Association Meeting.* (Denvers, July 28 - Aug 5, 2008). , p. 1129. Alexandria, VA.: American Statistical Association.

Burr, T., N. Hengartner, E. Matzner-Lober, and L. Rouviere. Smoothing low resolution spectral data. To appear in *IEEE Transaction on Nuclear Sciences.*

Cornillon, P. A., N. Hengartner, and E. Matzner-Lober. IBR: An R package for multidimensional smoothing. 2009. *CRAN: R comprehensive Archive.*

Cornilon, P. A., N. Hengartner, and E. Matzner-Lober. Recursive bias estimation for high dimensional regression smoothers. *Journal of the Scandinavian Statistical Association.*

Fraser, A. L.. Hidden Markov models and dynamical systems. 2008.

Hengartner, N., E. Matzner-Lober, T. Burr, and L. Rouviere. Multiplicative bias corrected nonparametric smoothers with application to nuclear energy spectrum estimation. *Journal of the Canadian Statistical Society.*

Hengartner, N., and E. Matzner-Lober. Unbiased density estimation. 2009. *ESAIM.* **13** (1): 1.

Izraelevitz, D., H. Martz, D. Leishman, and W. Gibson. On representing second-order uncertainty in multi-state systems via moments of mixtures of Dirichlet distributions. 2009. *Journal of Statistical computing and simulations.* **79** (7): 869.

Sinitsin, N., N. Hengartner, and I. Nemenman. Adiabatic coarse-graining and simulations of stochastic biochemical networks. 2009. *Proceedings on the National Academies of Scoences (PNAS).* **106**: 10546.

# Sharp Characterization of Minimizers (typically) Involving Interfaces in Images

*Pieter J. Swart*
20070187ER

## Abstract

The need to understand image and video data for a wide range of applications has exploded in the last few years. Imaging data in the medical, scientific, intelligence, and industrial communities have grown out of the ubiquity of exponentially increasing streams of image and video data.

As a consequence, there is an ongoing interest and need for improving our understanding of effective image processing algorithms of new datasets on new hardware. Typical problems we face include:

- the challenge of dealing with noise at different resolutions
- in-painting of missing regions, contaminated by excessive noise
- change detection in the presence of noise

The noise can be due to a wide variety of sources; to instrument or device error, poor resolution, blurring due to rapid motion, transmission noise, and even active interference by foreign governments. The study and removal of noise has become an important field of scientific study (as a subfield of Information Science) and is integral to successfully uncovering and understanding of the real signal.

Our research is aimed at creating new abilities to understand precisely how important new image processing methods work, what we can know from the output of those methods, and also what we can prove about these methods. We used methods from Geometric Measure Theory to study some of the new and successful methods that are poorly understood. We are also generating new algorithms that expand the information we extract from the images. While this work demands deep insights from intricate mathematical areas, it has already begun delivering concrete, practical results that improve our ability to analyze images and extract information in the presence of noise.

## Background and Research Objectives

There is a great need to extract information from an unprecedented increase of imaging data in the medical, scientific, intelligence, and industrial communities. Multi-billion dollar scientific applications such as the Hubble Space Telescope and the Large Hadron Collider demand the best algorithms to extract information from expensive but incomplete, indirect and noisy data. In these applications the resolution is so important that image analysis and de-noising is performed on state-of-the-art supercomputers. Medical applications range from radiography, MRI, Tomography and Ultrasound Imaging. As a national security laboratory, at LANL there are several important projects that rely on the careful analysis of streaming satellite or airborne images to assist in monitoring adherence to treaties or allow US military forces to better understand threats in foreign urban environments. These algorithms often need to run in real-time and on small, robust supercomputers. Another booming market for image processing is the ongoing revolution in consumer-driven digital photography, and the marriage of digital cameras with PDAs and cell-phones. One of the most influential technologies has been the growth of computer generated imaging in the entertainment (gaming and movie) industry.

Historically, image processing evolved as a subfield of signal processing, and therefore the traditional approaches to image de-noising has its mathematical roots in Fourier and other spectral methods. Over the past two decades exciting new discoveries in mathematics have had a substantial impact on the field. Conversely, image analysis has had an exciting impact on mathematics.

The discovery of *wavelets* in the late 1980's brought

an unexpected renaissance of deep mathematics applied to image processing. These discoveries have now penetrated the international standards used in satellite communication and image formats (notably JPEG) used by digital cameras and cell phones. Underlying this power is the speed of the *wavelet lifting scheme* (discovered in 1990 by Wim Sweldens), a novel algorithm that has now entered the top-10 list of most important algorithms.

A very different approach to noise removal is the use of various dynamical algorithms to morph an image in a fashion that sharpens boundaries while removing noise. Note that it is easy to remove noise (e.g. the noise in under-exposed photos) by blurring, i.e. replacing each pixel with some local average. Unfortunately this will also blur all sharp edges. A more sophisticated approach exploits *nonlinear dynamics*. This is a rich subfield of modern mathematics and physics that has seen years of research in applications such as pattern formation during chemical reactions, fluid dynamics applied to planetary weather and climate prediction, wave propagation down optical fibers, and robotics, to name but a few. This approach allowed insights obtained from years of studying and simulating a wide range of nonlinear dynamics problems, and also utilized deep results from the mathematical field of Partial Differential Equations. With time it became clear that another way of understanding these methods, and their effectiveness at de-noising images, is that they should really be viewed as a dynamical approach to solving an optimization problem. The following is a layman's description of this optimization problem. The image can be considered as some ideal image $f$ plus a noise component $g$. Here we can represent the image $f$ as a grayscale intensity field, with a value at each pixel in the image. The problem of de-noising is then posed as finding a new image $f'$ that minimizes $|f\text{-}f'|_X + \lambda|f'|_Y$. The first term represents the magnitude of morphing allowed. The second term measures the amount of "variation" in the new image. Imagine the value of $\lambda$ as a knob that can tune from $\lambda$=0 (where all smoothing is switched off) to some small $\lambda$ (where there is a balance between morphing and some allowed noise.) There are many ways to measure the amount of morphing and the "variation" or amount of noise.

The minimization in the above problem is performed not over all possible images, but over some much smaller subset of realistic images. Their study led to the field of *natural images*. Natural images are quite different from, say, cartoons or scanned images from texts. Imagine a smooth lake surrounded by trees. In fall the leaves form overlapping structures in between open clear areas that reflect a fractal and self-similar reflection of the surrounding forest. Any method designed to analyze and de-noise a high-resolution digital rendition of such a scene must be able to remove noise without destroying the self-similar, fractal, and overlapping mosaic of textures. Choosing the right form of the second term in the above formula is essential to making this possible. A key development came in 1992, when Rudin, Stan Osher, and Fatemi suggested using the so-called total variation (TV) measure for the latter when de-noising images. This approach revolutionized the field of image de-noising, infusing the field with many new ideas from variational analysis and nonlinear analysis as well as new algorithms. The suggestion and its success (10000 journal publications in the field) also connected image processing with the new field of Geometric Measure Theory. The resulting Rudin-Osher-Fatemi TV regularized de-noising algorithm is now well-established and has been used in many interesting the classic approach for achieving this. Compared to other methods, this approach to de-noising by finding a minimizer to an optimization problem is powerful, but poorly understood by the image processing community (given that it relies on rather deep theoretical and is very expensive to compute in practice.) The precise nature of the minimizers is an intricate mathematical. In this project our goal was the generation of new insights into the nature of de-noised images when using this approach and especially in the development of new fast algorithms.

## Scientific Approach and Accomplishments

The natural framework for our approach uses the mathematics of Geometric Measure Theory (GMT) to develop new algorithms and in quantifying their performance. GMT is an extension and generalization of the study of smooth surfaces in higher dimensions. It removes the requirement of smoothness, allow for fractal boundaries and noisy deviations that live on lower-dimensional spaces. For example, the classic theory of differential geometry provides the natural framework for 3D figures such as a smoothly morphed torus. At every point on the surface we can construct a tangent plane and thereby perform local analysis that allow the application of all the tools of classic calculus. When this 3D surface is now polluted by, say, white noise, all these tools become useless. In addition, if instead of a smooth 3D surface we are confronted by the multi-fractal surfaces observed in natural images, then the proper mathematical framework requires tools from Geometric Measure Theory. The power of being able to deal with non-smooth and fractal structures comes with a price. The mathematics required to deal with such exotic structure is considered to be one of the deeper branches of mathematics, and largely unexplored by applied scientists. As a consequence the computational application of this field to image analysis is but in its infancy. This was what this

proposal set out to remedy.

In the first year of the project, we made an exciting new discovery connecting the so-called "flat norm" from GMT to the L1TV functional form used in image analysis. This discovery is now being rapidly leveraged to provide us with new methods to describe and understand shape and image data, explore the statistics of shapes, and greatly generalize the L1TV functional to data previously beyond its domain. By the second year of this project we have gained significant understanding into this new approach and has developed numerical implementations to test this. The underlying mathematics of our approach is rather novel, and therefore does not have a long history of algorithm development. In the third year of this project we worked with external collaborators to design new algorithms based on graph theory to calculate these minimizers, and this required testing and careful testing and comparison with other methods, and with comparisons on more challenging data sets than classic benchmarks. We also explored applications, especially to medical datasets. This work has been submitted for publication and was done in collaboration with Kevin Vixie and collaborators at Washington State University and Wotau Yin at Rice University.

This approach is not limited to 2D images, but can be extended to regularize higher dimensional data sets, such as 3D geometric shapes or structures in hyperspectral datasets. This analysis is being explored in recent work by our collaborators Eseduglo and Elsey at the University of Michigan.

The multi-scale signature that immediately resulted from the discovery by Vixie and Morgan is also being applied to shape recognition and other related shape tasks.

## Impact on National Missions

The analysis of image and video data for "value" is a critical component to rapid data assessment and analysis. Numerous missions related to threat reduction, weapons data analysis, nonproliferation, and basic science is directly impacted by our projects on new algorithms for image analysis. Our work on this project brought new capabilities in Geometric Analysis of image and video data, added two young scientists in this field, and established enduring collaborations with some of the leaders in this field. It has added important and novel tools to the arsenal that we can rely on to understand future data sets. An unexpected application was in the medical field, where this method is currently further developed in collaboration with Dr. Yi Jiang of LANL to analyze experimental datasets in her studies on the dynamics of cellular dynamics during tumor growth.

## Publications


Allard, W. K.. Total variation regularization for image denoising I: Geometric theory. 2007. *SIAM Journal on Mathematical Analysis.* **39** (4): 1150.

Allard, W. K.. Total variation regularization for image denoising III: Examples. 2009. *SIAM Journal Imaging Sciences.* **2**: 532.

Allard, W. K.. Total variation regularization for image denoising II: Examples. . 2008. *SIAM Journal Imaging Sciences.* **1**: 400.

Morgan, S. P., and K. R. Vixie. L1TV computes the flat norm for boundaries. 2007. *Abstract and Applied Analysis.* **2007**: Article ID 45153.

Vixie, K. R.. Some properties of minimizers for the Chan-Esedoglu L1TV functional. 2007. *http://arxiv.org/abs/0710.3980.*

Vixie, K. R., K. Clawson, T. J. Asaki, G. Sandine, S. P. Morgan, and B. Price. Multiscale Flat Norm Signatures for Shapes and Images. To appear in *Applied Mathematical Sciences.*

# Instabilities Driven Turbulence and Mixing in Convergent Geometries

*Daniel Livescu*
20070195ER

## Abstract

Many of the flows of interest for the Laboratory involve species with different molecular masses and occur in the presence of a constant or time varying acceleration. The acceleration generates differential body forces, leading to instabilities which grow in time so that the resulting flow ultimately becomes turbulent. In many situations such flows occur in convergent geometries (e.g. cylindrical or spherical). Examples include Inertial Confinement Fusion targets, laser induced launching of a flyer plate, stellar pulsations, or supernova explosions. Fundamental turbulence studies and high resolution simulations of these flows in Cartesian geometry only recently have started to be performed and there is no such study in convergent geometries. Moreover, even in Cartesian geometry studies addressing the variable density (corresponding to large density differences) or compressible cases are scarce and not much is known about turbulent mixing under these conditions. In addition, early time analytical studies are almost entirely confined to immiscible fluids and incompressible flows with very few studies addressing the case of variable density or compressible flows and none the miscible case.

We have pursued a multi-pronged, multi-investigator research program to improve the computational and modeling capabilities for instability-driven flows in Cartesian and convergent geometries and advance the understanding of the mathematics and physics characterizing turbulence generated in such conditions. In the 22 publication resulted from this work, our study has provided analytical results for early time (linear and non-linear) growth, new tools for mixing description, fundamental turbulence and turbulent mixing studies showing new and unexpected physics, a turbulence modeling methodology, and Direct Numerical Simulations data.

## Background and Research Objectives

Molecular mixing as a consequence of stirring by turbulence is an important process in many practical applications. If the microscopic densities of the fluids participating in the mixing are very different, we refer to such flows as variable density (VD) flows in contrast to the Boussinesq approximation in which the densities are commensurate. In such flows, due to the tight coupling between the density and velocity fields, in addition to the quadratic non-linearities of the incompressible Navier-Stokes equations, new cubic nonlinearities arise. Many of these flows are driven by acceleration (e.g. gravity in geophysical and astrophysical flows) which, because the density is not uniform, leads to large differential fluid accelerations. If the acceleration is constant and the fluid configuration is unstable (i.e. density gradient points opposite to the body force), a fluid instability is generated in which small perturbations of the initial interface between the two fluids grow, interact nonlinearly, and lead to turbulence. This instability is known as the Rayleigh-Taylor instability (RTI).

RTI and its impulsive counterpart, the Richtmyer – Meshkov instability, are of fundamental importance in a multitude of applications ranging from the turbulent mixing in inertial confinement fusion (ICF), to combustion, and to astrophysical phenomena. For example, it is known that RTI generated turbulence leads to severe degradation of target performance in ICF capsules. A better understanding and control of turbulence in these conditions could help achieve controlled ignition. Another example from astrophysics is the flame propagation in type Ia supernovae. Thus, RTI is the dominant acceleration mechanism for the flame. When this occurs, it is the fluid motion mixing the fuel with hot ashes that controls the burning, rather than thermal conduction. The flows in many of the applications in which Rayleigh-Taylor and Richtmyer-Meshkov instabilities are encountered occur in

convergent geometries (spherical or cylindrical) as is the case with the two examples above.

In general, RTI driven flows begin from laminar or weakly chaotic state and the initial perturbations start interacting nonlinearly as they grow. Thus smaller and larger scales are generated, ultimately leading to turbulence. Therefore the problem is both an instability growth and mixing problem and also a turbulence problem. There are many studies of the early stages instability growth, in various configurations, however most assume incompressible fluids. Variable density or compressibility effects, although important, are usually not included in the analysis due to difficulties added to the analytical treatment. Less analytical or theoretical work has been performed including these effects for the weakly or fully nonlinear regimes and published studies become scarce for the turbulent stage.

Turbulence in itself is a ubiquitous phenomenon important for both science and engineering. Important progress has been made in recent years in our understanding of turbulence, although a complete quantification, description, prediction, simulation, and control still eludes us. Most of the fundamental turbulence studies have been concentrated on several canonical flows with periodic boundaries or simple jets, wakes, or boundary layers. Rayleigh-Taylor turbulence at non vanishing density differences has been studied only recently in Cartesian geometry [1] and this work fills several gaps in our understanding of mixing and turbulence properties at moderate to large Atwood numbers [2-15]. Some attempts to study turbulence in converging geometries have been made, but mostly in the context of moment closures. This project provides the first analytical study of instability growth in cylindrical geometry. The study addressed both the incompressible and compressible cases [16-18].

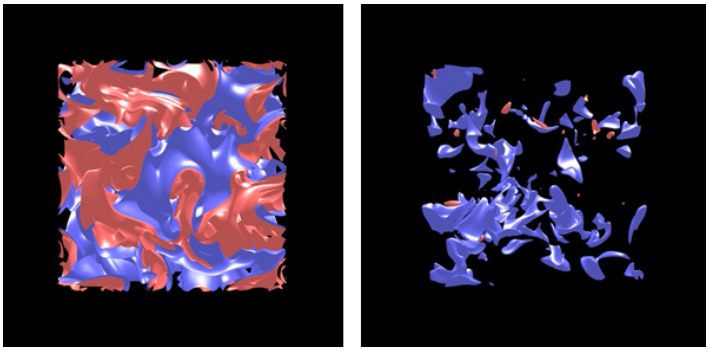

*Figure 1. Mixing between two fluids with different densities. Initially there are equal amounts of the fluids (a). As the mixing proceeds, there is a clear asymmetry between the amount of pure light fluid (red) and the pure heavy fluid (blue) left in the flow (b). From Refs. [7, 12].*

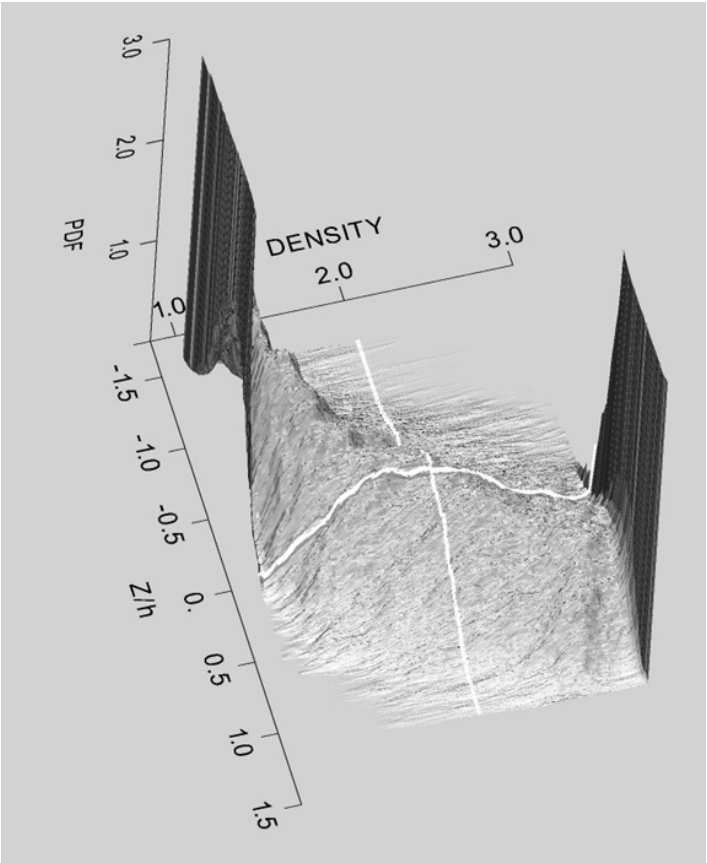


*igure 2. Density probability density function (PDF) across the variable density RTI showing the mixing asymmetry between the pure light and heavy fluids. From Ref. [12].*

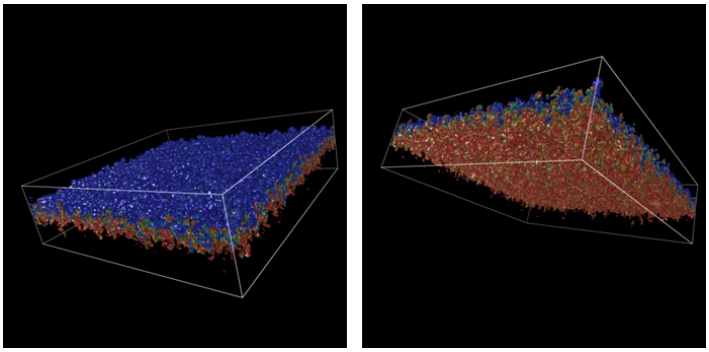

*Figure 3. Rayleigh-Taylor layer edges show signficant asymmetry at high Atwood numbers between a) bubble side and b) spike side. From Ref. [15].*

If “ideal” turbulence is in a homogeneous, isotropic Kolmogorov steady state, then “non-ideal” turbulence can occur due to time-dependence, anisotropy, inhomogeneity, or coupling with active scalars. Unlike kinetic theory, where significant departure from a weakly perturbed local Maxwelian is exceptional, the analogous state of non-ideal turbulence is what is typical, yet the only successful turbulence theory so far is the Kolmogorov’s 1941 theory. Numerous modeling strategies have been proposed, and, while there is no universally “best” strategy, each of

the approaches has its own advantages and domains of applicability. Among them, we note the so-called analytical closures (e.g. Kraichnan's Direct Interaction Approximation [19]) which offer vastly more information than the single point, engineering models in use today, or Large Eddy Simulations strategies. Analytical closures are well suited for studying the interactions between scales and to help deriving improved engineering models. Unfortunately, the only tractable analytical theories proposed to date require periodic boundaries; current extensions to inhomogeneous turbulence are computationally intractable. But the difficulties are also conceptual: whereas triad interactions provide a simple key to the physical meaning of analytical closure in the homogeneous case, nothing comparable exists for inhomogeneity. We have recently proposed the use of representation theory to define inhomogeneity as a perturbation about homogeneous turbulence, as a key for deriving a tractable analytical description of in-homogeneous turbulence [20-21]. In cylindrical and spherical geometries there is at least one periodic direction, which simplifies even more our closure approach.

Turbulence theory and the subsequent model development rely on experimental or high resolution Direct Numerical Simulations (DNS) data for development and verification and validation. The DNS technique seeks ``exact'' solutions of the governing equations, so that all relevant scales are accurately solved, using high resolution numerical simulations based on high order accurate discretization algorithms. DNS are conducted without resort to subgrid modeling or the introduction of ``artificial'' numerical dissipation or other algorithm stabilizing schemes. With the recent advances in supercomputing technology and algorithms, it is now possible to perform simulations at Reynolds numbers comparable or even larger than those obtained in large laboratory experiments. As petascale computing becomes available, the situation is further improving and fundamental turbulence studies for more complex flows are becoming feasible. As part of this project, we have also developed a high performance DNS code for instability driven flows [2] which was successfully used on some of today's largest supercomputer platforms (e.g. on the 147,456 processors LLNL Dawn computer [15]). The code was also ported to the heterogeneous Roadrunner architecture in a spin-off project (LDRD 200800747ER) with some of the key concepts developed within the present project [22]. The project also pursued an alternate methodology for Direct Numerical Simulations of compressible Rayleigh-Taylor instability, based on the wavelet transform, through an external collaboration with the University of Colorado [23-24]. As part of this collaboration, the PI became co-advisor (with Prof. O. Vasilyev) for Ph.D. student S. Reckinger. The methodology, though not yet suitable for supercomputer calculations, has emerged lately as a promising approach for turbulence simulations [25].

Since DNS generate large amounts of "raw" data, efficient visualization becomes challenging and standard techniques may be exceedingly slow or even inappropriate. As part of the project, we started collaboration with P. McCormick (CCS-1), by co-mentoring a Ph. D. student (S. Martin) to use heterogeneous computing architectures for visualization of large data sets [15].

In summary, our study has provided for instability driven turbulence:

- new tools for mixing description,
- fundamental turbulence studies,
- analytical results for early time (linear and non-linear) convergent geometry growth,
- novel turbulence modeling and computational methodologies, and
- Direct Numerical Simulations data.

## Scientific Approach and Accomplishments

The flows under investigation occur in the continuum limit so that they are described by the Navier-Stokes equations. Both the classical RTI and an idealized triply periodic RTI configuration (hereafter named HRTI) were investigated in order to better isolate the physics of mixing and turbulence properties. The two configurations are described below:

**RT I**

The two fluids are initially segregated in an unstable configuration. For the curved geometries there are two different arrangements: convergent (gravity acting inward) and divergent (gravity acting outward). The horizontal, for the Cartesian geometry, or tangential, for curved geometries, directions are periodic and the statistics are calculated as planar (or surface) averages. The interface is perturbed by a small amplitude single- or multi-mode perturbation which grows, interacts non-linearly, and eventually leads to turbulence.

**HRTI**

The two fluids are initialized as random blobs of pure fluids in a triply periodic domain. The kinetic energy grows initially as the fluids are accelerated by the body force, then decays as viscous forces overcome the buoyancy forces reduced by molecular mixing. During the growth

stage the flow corresponds to the interior of the turbulent RT layer. The statistics are calculated as averages over the whole volume and ensemble of realizations.

The code employed for this project is the CFDNS code, developed by the PI and collaborators within the CCS-2 group over the last 5 years. For the cylindrical and spherical configurations, the numerical singularities at the origin are avoided by appropriate coordinate transformations. In this approach, there is no loss of accuracy near the origin and no regularization condition is needed. Thus, the code allows flow and non-zero gradients at the origin. The code has been employed on numerous standard computing architectures and recently used to perform the largest turbulence simulation to date, Rayleigh-Taylor instability at A=0.75 (a 7 to 1 density ratio), on LLNL Dawn computer.

Below, the main results for the several thrusts of the project are briefly described:

**Turbulence and mixing in variable density (large density ratio), instability-driven turbulence [2-15]**

*Results highlights:*

- Unlike the Boussinesq, low density difference case, in variable density turbulence the mixing process is *asymmetric*, with the pure light fluid mixing faster than the pure heavy fluid (Figure 1). This asymmetry also leads to higher penetration distances of the pure heavy fluid in RTI (Figure 2) and explains the bubble-spike anomaly (higher velocities of the spike front compared to the bubble front and significant shape differences between the two sides, Figure 3) which was observed experimentally but never explained. None of the mixing metrics usually used by models can capture the asymmetry and thus new metrics have been proposed.
- Bounds on the fluid composition based on low order moments of the density probability density function (PDF) have been analytically derived. These bounds can be used as realizability conditions or to describe the mixing state in low dimensional modeling.
- There is a persistent anisotropy of the smallest scales of motion due to buoyancy, despite the intermediate scales becoming nearly isotropic. This is contrary to the usual universality assumption on the decoupling and independence of the small scales of motion from the large scales and has important consequences on the popular Large Eddy Simulations turbulence modeling approaches.

**Variable density, Rayleigh-Taylor turbulence [6, 9, 10, 13, 14, 15]**

*Results highlights:*

- The large scale quantities, layer width, kinetic energy, mass flux, mean density, reach a self-similar behavior, however, turbulence length-scale does not. This is due to the finite energy cascade time to small scales and is conjectured to occur in all non-equilibrium (or rapidly changing) flows.
- Due to the lack of self-similarity of the turbulence length-scale, the usual closures for the moment equations using this length-scale and gradient transport hypothesis for turbulence transport or similarity arguments for the dissipation fail in Rayleigh-Taylor turbulence. A new modeling approach has been proposed.

**Early time instability development in cylindrical geometry [16-18]**

*Results highlights:*

- The non-uniqueness of the compressible to incompressible limit,
- Large differences between explosion (gravity acting outward) and implosion (gravity acting inward) compared to the Cartesian geometry, and
- Qualitative differences between the 2-dimensional circular case compared to the 3-dimensional case.

**Analytical models for inhomogeneous turbulence (as occurring in RTI) [20-21]**

*Results highlights:*

- A new analytical approach has been proposed for inhomogeneous turbulence, which may overcome the computational intractability which rendered ineffective the previous attempts.
- The model has also provided useful in explaining the nature of anisotropy in inhomogeneous turbulence.

**Accurate adaptive, wavelet-based computations of compressible instability-driven turbulence [23-24]**

*Results highlights:*

- Proof of concept for using adaptive mesh calculations

for DNS of turbulent flows.

- Role of compressibility on late time RTI growth.

**Direct Numerical Simulations data**

*Results highlights:*

- The simulations performed within this project represent the largest so far for the respective configurations. In particular, the high Atwood number Rayleigh-Taylor simulation performed on LLNL Dawn [15] is the largest turbulence simulation ever performed, with a resolution of 2304x4096^2. The simulation will be continued in a future study on up to 4608x4096^2 mesh size on Roadrunner.

- As part of the project, the largest Rayleigh-Taylor simulation [1] before the LLNL Dawn calculation has been analyzed through a successful LANL-LLNL collaboration [14].

## Impact on National Missions

The project has supported the DOE mission in Nuclear Weapons and Office of Science missions in Fusion Energy Sciences and Advanced Scientific Computing Research by advancing our understanding of the instability-generated turbulence in Cartesian and convergent geometries using theory and large scale, high performance computational tools.

The CFDNS code employed by the project has been integrated within the programmatic efforts at the Lab (Campaign 4) and future funding has been secured to apply the modeling strategies suggested by the project to programmatic efforts. In addition, in order to help foster the new generation of researchers joining the Lab, funds from this project were used to support two Ph.D. students and a postdoc.

## References


1. Cabot, W. H., and A. W. Cook. Reynolds number effects on the Rayleigh-Taylor instability with possible implications for type Ia supernovae. 2006. *Nature Physics.* **2**: 562.

2. Livescu, D., and J. R. Ristorcelli. Buoyancy-driven variable-density turbulence. 2007. *Journal of Fluid Mechanics.* **581**: 43.

3. Livescu, D., and J. R. Ristorcelli. Variable density mixing in buoyancy driven turbulence. 2007. (Salt Lake City, 19-21 Nov. 2007). Vol. 5217 Editionp. 253. Salt Lake City: APS.

4. Livescu, D., and J. R. Ristorcelli. Mixing characteristics in buoyancy driven turbulence. 2007. In *Advances in Turbulence XI.* Edited by Palma, J. M., and S. Lopez. Vol. 117p. 544. Oporto, Portugal: Springer.

5. Livescu, D., and J. R. Ristorcelli. Molecular mixing and the mix parameter in variable density buoyancy driven turbulence. (Santa Fe, 14-18 July 2008).

6. Livescu, D., J. R. Ristorcelli, and R. A. Gore. High-Reynolds number Rayleigh-Taylor turbulence. (Santa Fe, 14-18 July 2008).

7. Livescu, D., and J. R. Ristorcelli. Variable density mixing in buoyancy driven turbulence. 2008. *Journal of Fluid Mechanics.* **605**: 145.

8. Livescu, D.. Comment on 'Compressibility effects on the Rayleigh-Taylor instability of three layers' [Phys. Fluids 19, 096103 (2007)]. 2008. *Physics of Fluids.* **20** (2): 029103.

9. Livescu, D., J. R. Ristorcelli, R. A. Gore, and S. H. Dean. High Reynolds number Rayleigh-Taylor turbulence. 2008. (San Antonio, 23-25 Nov. 2008). Vol. 5315 Editionp. 182. San Antonio: APS.

10. Livescu, D., J. R. Ristorcelli, and R. A. Gore. Variable density Rayleigh-Taylor turbulence. (Trieste, Italy, 26 July - 7 Aug. 2009).

11. Livescu, D., and J. R. Ristorcelli. Mixing asymmetry in variable-density turbulence. (Marburg, Germany, 7-10 Sept. 2009).

12. Livescu, D., and J. R. Ristorcelli. Mixing asymmetry in variable density turbulence. To appear in *Advances in Turbulence XII.* Edited by Eckhardt, B..

13. Livescu, D., J. R. Ristorcelli, and R. A. Gore. Variable density Rayleigh-Taylor turbulence. To appear in *Physica Scripta.*

14. Livescu, D., J. R. Ristorcelli, R. A. Gore, S. H. Dean, W. H. Cabot, and A. W. Cook. High Reynolds number Rayleigh-Taylor turbulence. 2009. *Journal of Turbulence.* **10** (13): 1.

15. Livescu, D., M. R. Petersen, S. Martin, and P. McCormick. Spikes and bubbles in turbulence mixing: High Atwood number Rayleigh-Taylor instability. (Minneapolis, 21-23 Nov. 2009).

16. Yu, H., and D. Livescu. Compressible Rayleigh-Taylor

instability in cylindrical geometry. 2007. (Salt Lake City, 19-21 Nov. 2007). Vol. 5217 Editionp. 287. Salt Lake City: APS.

17. Yu, H., and D. Livescu. Compressible Rayleigh-Taylor instability in cylindrical geometry. (Santa Fe, 14-18 July 2008).

18. Yu, H., and D. Livescu. Rayleigh-Taylor instability in cylindrical geometry with compressible fluids. 2008. *Physics of Fluids.* **20** (10): 104103.

19. Kraichnan, R. H.. Physics of Fluids. 1964. *Direct-Interaction Approximation for shear and thermally driven turbulence.* **7**: 1048.

20. Rubinstein, R., W. R. T. Bos, D. Livescu, and S. L. Woodruff. Closure models for inhomogeneous turbulence. (Marburg, Germany, 7-10 Sept. 2009).

21. Rubinstein, R., W. R. T. Bos, D. Livescu, and S. L. Woodruff . Closure models for inhomogeneous turbulence. To appear in *Advances in Turbulence XII.* Edited by Eckhardt, B..

22. Mohd-Yusof, J., and D. Livescu. Turbulence direct numerical simulations on RoadRunner. (Reno, 10-16 Nov. 2007).

23. Reckinger, S., D. Livescu, and O. Vasilyev. Compressibility effects on the single mode Rayleigh-Taylor instability. (Trieste, Italy, 26 July - 7 Aug. 2009).

24. Reckinger, S., D. Livescu, and O. Vasilyev. Compressibility effects on single mode Rayleigh-Taylor instability using a wavelet-based method. To appear in *Physica Scripta.*

25. Schneider, K., and O. Vasilyev. Wavelet techniques to solve Navier-Stokes equations. 2010. *Annual Review of Fluid Mechanics.* **42**: 473.

## Publications

Livescu, D.. Comment on 'Compressibility effects on the Rayleigh-Taylor instability of three layers' [Phys. Fluids 19, 096103 (2007)]. 2008. *Physics of Fluids.* **20** (2): 029103.

Livescu, D., J. R. Ristorcelli, R. A. Gore, S. H. Dean, W. H. Cabot, and A. W. Cook. High Reynolds number Rayleigh-Taylor turbulence. 2009. *Journal of Turbulence.* **10** (13): 1.

Livescu, D., J. R. Ristorcelli, R. A. Gore, and S. H. Dean. High Reynolds number Rayleigh-Taylor turbulence. 2008. In *APS DFD08.* (San Antonio, 23-25 Nov. 2008). Vol. 53, 15 Edition, p. 182. San Antonio: APS.

Livescu, D., J. R. Ristorcelli, and R. A. Gore. High-Reynolds number Rayleigh-Taylor turbulence. Presented at *11th International Workshop on the Physics of Compressible Turbulent Mixing.* (Santa Fe, 14-18 July 2008).

Livescu, D., J. R. Ristorcelli, and R. A. Gore. Variable density Rayleigh-Taylor turbulence. To appear in *Physica Scripta.*

Livescu, D., J. R. Ristorcelli, and R. A. Gore. Variable density Rayleigh-Taylor turbulence. Presented at *2nd International Conference Turbulent Mixing and Beyond.* (Trieste, Italy, 26 July - 7 Aug. 2009).

Livescu, D., M. R. Petersen, S. Martin, and P. McCormick. Spikes and bubbles in turbulence mixing: High Atwood number Rayleigh-Taylor instability. To appear in *APS DFD09.* (Minneapolis, 21-23 Nov. 2009).

Livescu, D., and J. R. Ristorcelli. Variable density mixing in buoyancy driven turbulence. 2008. *Journal of Fluid Mechanics.* **605**: 145.

Livescu, D., and J. R. Ristorcelli. Variable density mixing in buoyancy driven turbulence. 2007. In *APS DFD07.* (Salt Lake City, 19-21 Nov. 2007). Vol. 52, 17 Edition, p. 253. Salt Lake City: APS.

Livescu, D., and J. R. Ristorcelli. Mixing characteristics in buoyancy driven turbulence. 2007. In *Advances in Turbulence XI.* Edited by Palma, J. M., and S. Lopez. Vol. 117, p. 544. Oporto, Portugal: Springer.

Livescu, D., and J. R. Ristorcelli. Molecular mixing and the mix parameter in variable density buoyancy driven turbulence. Presented at *11 International Workshop on the Physics of Compressible Turbulent Mixing.* (Santa Fe, 14-18 July 2008).

Livescu, D., and J. R. Ristorcelli. Mixing asymmetry in variable density turbulence. To appear in *Advances in Turbulence XII.* Edited by Eckhardt, B..

Livescu, D., and J. R. Ristorcelli. Mixing asymmetry in variable-density turbulence. Presented at *12th European Turbulence Conference.* (Marburg, Germany, 7-10 Sept. 2009).

Livescu, D., and J. R. Ristorcelli. Buoyancy-driven variable-density turbulence. 2007. *Journal of Fluid Mechanics.* **581**: 43.

Mohd-Yusof, J., and D. Livescu. Turbulence direct numerical simulations on RoadRunner. Presented at *Supercomputing07.* (Reno, 10-16 Nov. 2007).

Reckinger, S., D. Livescu, and O. Vasilyev. Compressibility

effects on single mode Rayleigh-Taylor instability using a wavelet-based method. To appear in *Physica Scripta.*

Reckinger, S., D. Livescu, and O. Vasilyev. Compressibility effects on the single mode Rayleigh-Taylor instability. Presented at *2nd International Conference Turbulent Mixing and Beyond.* (Trieste, Italy, 26 July - 7 Aug. 2009).

Rubinstein, R., W. R. T. Bos, D. Livescu, and S. L. Woodruff. Closure models for inhomogeneous turbulence. Presented at *12th European Turbulence Conference.* (Marburg, Germany, 7-10 Sept. 2009).

Rubinstein, R., W. R. T. Bos, D. Livescu, and S. L. Woodruff . Closure models for inhomogeneous turbulence. To appear in *Advances in Turbulence XII.* Edited by Eckhardt, B..

Yu, H., and D. Livescu. Compressible Rayleigh-Taylor instability in cylindrical geometry. 2007. In *APS DFD07.* (Salt Lake City, 19-21 Nov. 2007). Vol. 52, 17 Edition, p. 287. Salt Lake City: APS.

Yu, H., and D. Livescu. Rayleigh-Taylor instability in cylindrical geometry with compressible fluids. 2008. *Physics of Fluids.* **20** (10): 104103.

Yu, H., and D. Livescu. Compressible Rayleigh-Taylor instability in cylindrical geometry. Presented at *11th International Workshop on the Physics of Compressible Turbulent Mixing.* (Santa Fe, 14-18 July 2008).

# Moment-Based Interface Tracking for Multi-Material Flows

*Rao V. Garimella*
20070202ER

## Abstract

Accurate tracking of material interfaces is an important aspect of many multi-material flow simulations in national energy and security applications. Recently, a novel interface reconstruction method called the Moment-of-Fluid (MoF) method was invented at LANL to better track material interfaces. The MoF method is a significant development in material interface tracking after nearly two decades of incremental improvements. At the start of this project, MoF was only shown to be effective on simple geometric test cases. In this project we incorporated the MoF method into a fluid flow code in order to study its performance in complex flows. We demonstrated that the MoF method captures interfaces better than traditional Volume of Fluid (VoF) methods in flows with more than two materials or flows with filamentary structures. We also demonstrated that it performs as well as VoF methods for simpler two material flows. At the same time, the burden of using MoF is only slightly more than VoF and is offset by its ability to capture flow features at a slightly lower mesh resolution. Finally, we showed that the extra information carried by MoF can be used to adaptively refine the mesh and obtain solutions with the same accuracy with fewer elements. As proposed originally, we have demonstrated the suitability and readiness of this new method for use in the large multi-material flow simulation code projects at LANL and other national labs. We have published five peer-reviewed papers on different aspects of this work and have presented our results at international conferences.

## Background and Research Objectives

Accurate tracking of material interfaces is an important aspect of many flow simulations in national energy and security applications. For example, the National Ignition Facility at LLNL attempts to initiate fusion in a BB-sized target filled with hydrogen fuel with the help of 192 giant laser beams directed into a gold capsule (hohlraum) enclosing the fuel. This process is called Inertial Confinement Fusion or ICF. The intense heat generated by the lasers causes the outer layer of the fuel pellet to explode, generating a reactionary shock wave that drives the remaining material towards the center of the pellet. To design and understand this experiment, it is critical to simulate and understand how the different materials travel after the ablation of the external layer.

In our LDRD project, we aimed to advance multi-material gas dynamics simulations by demonstrating the feasibility of using the Moment-of-Fluid (MoF) method for tracking multi-material interfaces. Unlike the Volume-of-Fluid (VoF) method which only tracked the volumes of different materials in computational cells, the MoF method also tracks the centroids of the materials in the cells. This leads to a more accurate and more efficient tracking of material interfaces in simulations like ICF. The higher fidelity of simulations made possible by this new method is expected to better our understanding of the phenomena that occur in such applications.

The goals of our project as laid out in the proposal were:

- develop an error estimator for the MoF interface approximation
- conduct the convergence analysis for curvature estimation
- implement multi-segment interface approximation
- study automatic partitioning schemes for multi-material mixed cells
- develop a robust moment update algorithm for incompressible and compressible flows
- implement adaptive mesh refinement for the MoF method

## Scientific Approach and Accomplishments

At the start of the project, we had a preliminary algorithm for reconstructing interfaces in two material cells given the exact volume fraction and centroids of the materials. We developed this algorithm further to fashion a method for reconstructing the interfaces in cells with three or more materials. Like the VoF technique, MoF also carves materials out from a mixed cell one by one. Naturally, this leads to a strong dependence of the reconstructed interfaces on the order in which the materials are processed. However, unlike VoF, MoF has a built in error estimator to indicate how good the reconstruction is. This error estimate is based on the discrepancy of the centroid of the reconstructed material with respect to the specified centroid of the material. When we sum the discrepancies in the centroids of all the materials in the cell, we get a measure of the "goodness" of the reconstruction. By trying all possible sequences of material reconstructions, we can automatically choose the best reconstruction as the one that minimizes the discrepancies in the centroids. We can take this logic further and reconstruct more complex configurations by carving off pairs of materials at a time and then carving off the individual materials from the resulting polygons. While trying all possible combinations could be prohibitive if the number of materials is very large, we typically do not expect more than 3 or 4 materials and therefore, the computational cost is manageable. This work has been detailed in a paper published in the Journal of Computational Physics [1].

We also enhanced the initial algorithm to allow for the interface to be represented by two segments in a cell instead of just one segment. This allows for the method to capture sharp corners and also approximate curved interfaces more accurately.

The main part of our project was to incorporate VoF and MoF procedures into an incompressible flow solver, Qacina, developed by Mark Christon, a former project member.

Initially, we incorporated the VoF and MoF procedures into Qacina and implemented procedures to update the volume fraction and moment (centroid) data using the velocities obtained from the flow solver. Using this we demonstrated that MoF tracks interfaces with second-order accuracy if the velocities are second-order accurate. Demonstration of second-order accuracy is important since it allows us to cut the error in the numerical solution by four times by halving the size of the mesh cells.

Then we completed the coupling between MoF and Qacina by accounting for different material densities in mixed cells in the momentum (not moment) update equations (Variable Density Momentum Update). We also made the code multi-threaded so that we could run larger simulations.

Using this coupled code, we conducted convergence studies showing that MoF maintains a second order rate of convergence when fully coupled with a flow solver. For the study we used the vortex-in-a-box test case where an initially circular blob of four materials is deformed into a spiral using an analytical velocity (Figure 1). We also simulated a bubble of light material rising in a fluid of denser material (without surface tension effects) and compared it with VoF type methods (1st order Youngs and 2nd order Swartz methods). Finally, we simulated the collision of two bubbles of different density, one rising and one falling (Figures 2 and 3). In all these tests, we observed that MoF captures small features like thin filaments better than VoF and that MoF is clearly superior in accurately capturing interfaces in problems with three or more materials. The detailed results of this study are published in the International Journal of Numerical Methods in Fluids [2].

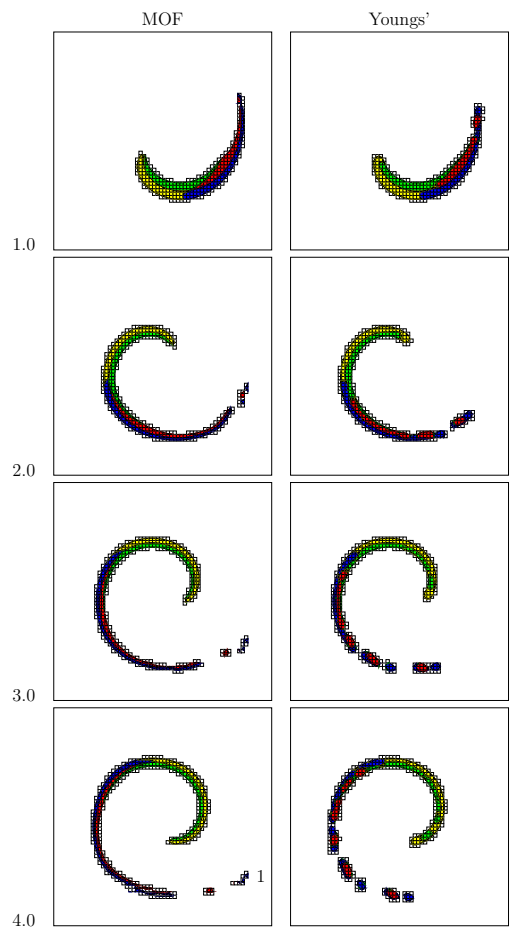


*Figure 1. Comparison of the stretching of a four material circle by the MoF and VoF methods. Note that the MoF method keeps the materials in their correct positions relative to each other and exhibits less fragmentation. These characteristics are important in capturing the interfacial physics correctly in more realistic simulations.*

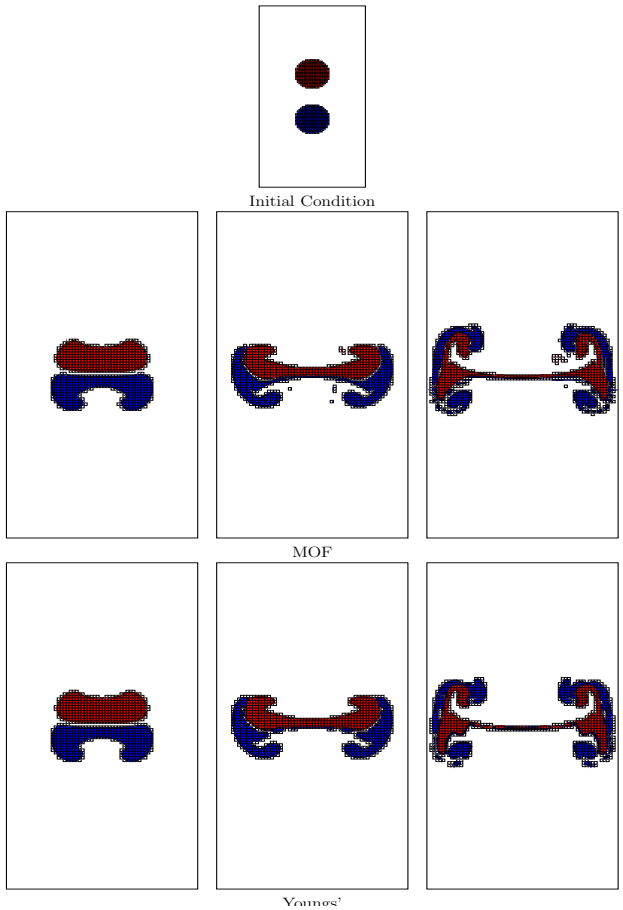


*Figure 2. Comparison of the MoF and VoF methods while simulating the collision of two bubbles. Note that the MoF method maintains the filamentary structures better than the traditional VoF method.*

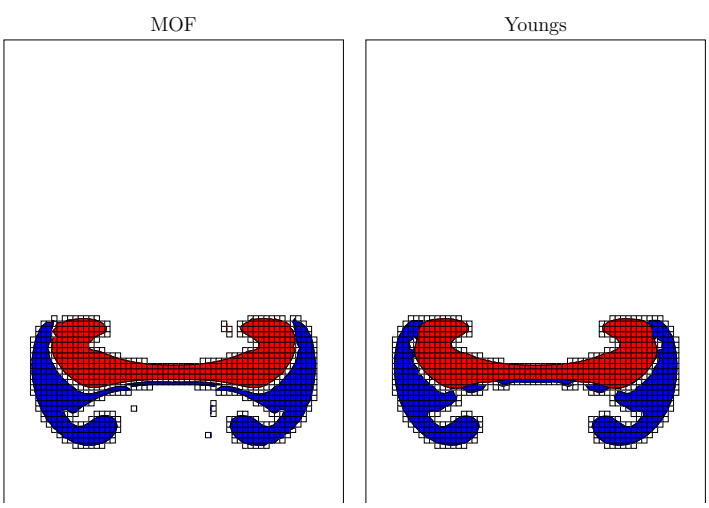


*Figure 3. Zoom in of simulation of two bubbles colliding with MoF and VoF.*

We also contributed code and expertise to a separate effort to simulate multi-material compressible flows using MoF interface reconstruction. We performed a comparative study of MoF, VoF and Power-Diagram reconstructions (another technique developed by the PI) on two high-speed gas dynamics simulations. From this study, we again concluded that MoF with automatic material ordering gives the best results for complex multi-material flows followed by VoF with the correct material order. The Power-Diagram reconstructions did an adequate job while VoF with the wrong material order performed very poorly. These results are also published in a paper in the Journal of Computational Physics [3].

Since reconstruction of a straight line interface in a cell requires only two parameters (angle w.r.t. the X-axis and the intercept on the Y-axis) while the input to MoF is three parameters (X and Y coordinates of the centroid and the volume fraction of the material), we have extra information that could be used to indicate how good an MoF reconstruction is. The error of a MoF reconstruction is defined as the discrepancy between the centroid of the reconstruction and the input centroid for the material. Since MoF can capture linear interfaces exactly, a non-zero error in the reconstruction points to the presence of a curvilinear interface.

Using the discrepancy in the input centroid and the reconstructed centroid, we have developed a method for estimating the curvature of the interface in a cell. Unfortunately, this method is non-convergent and the error in the estimated curvature blows up as the mesh size decreases. We also estimated the curvature of the interface by fitting a circle that matches the volume fraction and centroid data of the material in that cell. Unfortunately, the characteristics of the non-linear function that needs to be solved for this process are very poor and it is extremely difficult to arrive at the solution if the initial guess is even slightly far away. We also investigated the estimation of curvature using only volume fraction data from multiple cells (typical for VoF methods). Again, this system of non-linear equations is not solved easily if the initial guess is even a little far away. In all, we tried 6 methods for estimating curvature out of which we found only one method, namely the height function method) that converges at all. Unfortunately, the height function method is only applicable to structured meshes. The results of this study were presented at the SIAM Annual Meeting in San Diego in July 2008.

Since the height function method works so well, while the others fail so badly, we have spent considerable energy attempting to understand and extend the height function method for estimating curvature. As a result, we have successfully extended the height function method from uniform rectangular meshes to non-uniform rectangular meshes. The method can be used to estimate curvatures with second order accuracy for such meshes. This work has been accepted for publication in the Journal of

Computational Physics [4]. We have devised a method for extending this technique to unstructured meshes but we fear that the order of accuracy will drop to zero in this case.

We plan to use the curvature estimates based on the height function method to incorporate surface tension forces into Qacina.

We have also developed a method for conformally refining quadrilateral meshes for use in adaptive mesh refinement in Qacina. In conformal meshes, mesh cells always intersect only at mesh vertices or mesh edges. In other words, a node of one cell cannot lie on the edge of another cell. While there has been a lot of work on conformal refinement of triangles and on non-conformal refinement of quadrilaterals, few techniques have been proposed for conformally refining quadrilateral meshes. However, conformal refinement allows codes like Qacina to adapt meshes without special procedures to handle mismatched cells. Our technique for mesh refinement and coarsening produces hierarchically refined conformal meshes while maintaining high mesh quality and can be driven by an error estimate such as the one from MoF. This work will be published in the peer-reviewed proceedings of the International Meshing Rountable to be held in Salt Lake City, UT, Oct 2009 [5].

## Impact on National Missions

Accurate reconstruction of material interfaces is important for prediction of interfacial physics in hydrocodes used at national labs. Such codes are used in simulations for a wide variety of national energy and security applications, for example, inertial confinement fusion. We have demonstrated that the Moment-of-Fluid method is superior to traditional techniques in reconstructing interfaces more accurately with coarser grids. We have also developed several tools (automatic material ordering, curvature estimation, mesh refinement) that can be used with MoF to deliver superior prediction capabilities. This work prepares MoF to be easily incorporated into large software used at LANL and other national labs to simulate multi-material flows. Use of MoF in these codes will enhance the accuracy of our predictions in applications of national importance.

## References


1. Dyadechko, V., and M. Shashkov. Reconstruction of multi-material interfaces from moment data. 2008. *Journal of Computational Physics.* **227** (11): 5361.

2. Schofield, S., M. Christon, V. Dyadechko, R. Garimella, R. Lowrie, B. Swartz, and M. Shashkov. Multi-material incompressible flow simulation using the moment-of-fluid method. To appear in *International Journal of Numerical Methods in Fluids.*

3. Kucharik, M., R. Garimella, S. Schofield, and M. Shashkov. A comparative study of interface reconstruction methods for multi-material ALE simulations. To appear in *Journal of Computational Physics.*

4. Francois, M., and B. Swartz. Interface curvatures via volume fractions, heights and mean values. To appear in *Journal of Computational Physics.*

5. Garimella, R.. Conformal refinement of unstructured quadrilateral meshes. 2009. In *18th International Meshing Roundtable.* (Salt Lake City, UT, 25-28 Oct, 2009). Vol. 1, 1 Edition, p. 0. Berlin, Germany: Springer-Verlag.

6. Garimella, R., and B. K. Swartz. Curvature estimation for Multi-Material Flow SImulations. Presented at *SIAM Annual Meeting.* (San Diego, CA, July 2008).

7. Schofield, S., and R. Garimella. Interface tracking methods for multi-material flow simulations. Presented at *SIAM Conference on Computational Science and Engineering.* (Miami, FL, Mar. 2009).

8. Schofield, S., R. Garimella, M. Christon, V. Dyadechko, and M. Shashkov. Multi-material flow simulations using the moment-of-fluid method. Presented at *US National Congress on Computational Mechanics.* (Columbus, OH, July 2009).

9. Schofield, S., R. Garimella, M. Christon, B. Swartz, and M. Shashkov. Multi-material flow simulations using the moment-of-fluid method. Presented at *Numerical Methods for Multi-material Fluids and Structures (Multimat 09).* (Pavia, Italy, Sep 2009).

10. Francois, M. M., and B. Swartz. Estimating interface curvatures using volume fractions and mean values on non-uniform rectangular grids. Presented at *US National Congress on Computational Mechanics.* (Columbus, OH, July 2009).

11. Francois, M. M., and B. Swartz. Estimating Interface Curvatures using volume fractions and mean values on non-uniform rectangular grids. Presented at *Numerical Methods for Multi-Material Fluids and Structures (Multimat09).* (Pavia, Italy, Sep. 2009).


## Publications


Dyadechko, V., and M. J. Shaskov. Reconstruction of Multi-material interfaces from moment data. 2008. *Journal of*

*Computational Physics.* **227** (11): 5361.

Francois, M., and B. Swartz. Interface curvatures from volume fractions, heights and mean values. To appear in *Journal of Computational Physics.*

Garimella, R.. Conformal refinement of unstructured quadrilateral meshes. To appear in *18th International Meshing Roundtable.* (Salt Lake City, UT, 25-28 Oct, 2009).

Kucharik, M., S. Schofield, R. Garimella, and M. Shashkov. A comparative study of interface reconstruction methods for multi-material ALE simulations. To appear in *Journal of Comptational Physics.*

Schofield, S., M. Christon, V. Dyadechko, R. Garimella, B. Swartz, R. Lowrie, and M. Shashkov. Multi-material incompressible flow simulation using the moment-of-fluid method. To appear in *International Journal for Numerical Methods in Fluids.*

# Hyperbolic Polynomials Approach to Approximate Counting and Lower/Upper Bounds in Combinatorics, Statistical Physics and Computational Geometry

*Leonid Gurvits*
20070243ER

## Abstract

A wide variety of ``hard'' counting problems in physics, combinatorics and omputational geometry is equivalent to computation/approximation of the mixed partial derivative respect to all variables(MPD) of a corresponding effectively computable homogeneous polynomial(HP). This point of view was previously used only as a tool to obtain simply exponential exact algorithms. This project introduced and substantially developed a novel approach: there exists a wide class of (HP) for which it is possible to reduce approximation of (MPD) to some convex minimization problem. Most importantly, it is possible to prove lower and upper tight bounds for such convex relaxation. This novel approach opened the following two main possibilities: 1.New effective algorithms; 2. A new, potentially short and transparent, ways to prove lower bounds. The first class, studied in the project, consisted of positive hyperbolic polynomial(PHP), a notion that originated in the theory of partial differential equations (PDEs). In the course of the study, we shown that that it is easier to work with so called H-Stable polynomials(HSP) and introduced a new class of so called strongly log-concave entire functions(SLCEF). We realized with great success two above possibilities. Our main success in the algorithmic part is the first randomized poly-time algorithm approximating the mixed volume of convex sets within simply exponential factor [1]. Our main success in the theoretical part is a variety of lower bounds, as improving the previously known as well settling conjectured ones [2]. We quote from a recent exposition paper by a renown computer scientist[3]:``The proof of Falikman and Egorychev requires some nontrivial theorems, and the proof of Schrijver is combinatorially complex. It was a big surprise when Leonid Gurvits [2008] gave an amazingly short proof of the two bounds. En route, he improved Schrijver's theorem.''

## Background and Research Objectives

The three main sources of our motivation: Quantum Entanglement applications from the previous ER project (mixed discriminant and 4D Pascal's hyper-determinant), approximation of the mixed volume (the main tool in modern computational algebra that provides a tight upper bound on the number of isolated solutions of a system of nonlinear equations) and the computation of monomer-dimer entropy (a major problem in computational chemistry). These quantities are generalizations of the Matrix Permanent(M-Per) (like the Determinant quantity, but without alternating signs). We needed far reaching generalizations of two major achievements in theory of (M-Per): a solution of the Van der Waerden conjecture (VDW-Con) on the minimum of the permanent of doubly-stochastic matrices and a subsequent A. Schrijver's result of the exact asymptotic of the minimal number of perfect matchings in k-regular bipartite graphs. The previous techniques were practically non-generalizable, which explains the lack of the progress. We proved all the needed generalizations and shown how they can be turn into efficient algorithms. We still don't have a full proof of 4D analogue of the (VDW-Con), but got some important partial results in [4]. The expertise developed in the course of work, especially in determinantal polynomials, allowed solving two important problems in Control Theory [5], [6] and added to the broad Laboratory capability to address many related problems in computational physics and quantum theory.

## Scientific Approach and Accomplishments

We found a new method, much more powerful and surprisingly more transparent than previous approaches, based on the capacity of ``good'' homogeneous polynomials(HP). A wide variety of ``hard'' counting problems in physics, combinatorics and computational geometry is equivalent to computation/approximation of the mixed partial derivative respect to all variables(MPD) of a corresponding effectively computable (HP). This point of view was previously used only as a tool to obtain exact algorithms of simply

exponential complexity. We introduced and substantially developed a novel approach: there exists a wide class of (HP) for which it is possible to reduce multiplicative approximation of (MPD) to computing of so called capacity(CAP) and , in turn, (CAP) is obtained by solving some convex minimization problem. Most importantly, it is possible to prove lower and upper tight bounds for such convex relaxation, i.e. lower and upper bounds on the ratio (MPD)/(CAP). The main discoveries: 1.We proved in [2] a far reaching generalization of (VDW-Con) and the Schrijver's lower bound(SLB): essentially one theorem, which contain(and even in some cases improves) all previously known results. For instance, we extended (SLB) to general sparse matrices. The results from [2] together with additional probabilistic tricks were used in [7] to solve an important open problem in monomer-dimer theory, which essentially extended (SLB) on the minimal number of perfect matching to partial matchings of given size. This gave the most accurate estimate of the monomer-dimer entropy of 3D and 4D lattices. 2. We proved analogues of (VDW-Con) and (SLB) for the mixed volume of convex sets. Based on these bounds we introduced and analyzed the first poly-time randomized algorithm approximating the mixed volume within simply exponential factor [1]. Additional complexity-theoretic results in this direction were obtained in [8]. 3. We extended in [4] the technique from [2] to a wide class of (non-homogeneous) multivariate entire functions with non-negative coefficients: so called strongly log-concave functions. The results in [4] have far reaching applications to combinatorics, algebraic geometry and complexity theory. 4. Using the theory of determinantal polynomials and the measure theory, we proved in [6] that checking absolute switching stability in continuous time setting is NP-HARD . This result settled a major problem in the theory of hybrid systems.

The paper [2] was nominated for Fulkerson Prize in discrete mathematics and made the short list. The results of the project were published in major international peer-reviewed journals and conferences; a number of invited talks were given all over the world. The results were already given exposition in works of prominent scientists in Russia, India, France, Holland and USA. The results are being already taught at major universities, a number of exposition seminars were given (not by PI) all over the world. Importantly, the exposition

article [3] will appear in American Mathematical Monthly, which is a mathematical analogue of ``Nature."

## Impact on National Missions

It was very recently shown in that, in a sense, quantum computing can be reduced to specific additive approximation of (M-Per) of certain matrices. Those discoveries put (M-Per) in the heart of Computing Science, as from practical (RSA code can be broken by a Quantum Circuit) as well theoretical point of view. The success of this and previous ER-projects led by the PI uplifted LANL into one of the main international centers in the theory of (M-Per). A number o bright young researchers from all over the world already expressed interest to join PI team. We expect the achievements, the accumulated expertise and reputation will result in future funding and discoveries.

## References


1. Gurvits, L.. A polynomial-time algorithm to approximate the mixed volume within a simply exponential factor. 2009. *Discrete and computational geometry.* **4** (41): 533—555.

2. Gurvits, L.. Van der Waerden/Schrijver-Valiant like conjectures and stable (aka hyperbolic) homogeneous polynomials: one theorem for all. 2008. *Electronic Journal of Combinatorics.* **1** (15): 1.

3. Laurent, M., and A. Schrijver. On Leonid Gurvits' proof for permanents. To appear in *American Mathematical Monthly.*

4. Gurvits, L.. On multivariate Newton-like inequalities. 2009. In *Advances in Combinatorial Mathematics'.* Edited by Kotsireas, Ilias S., and Eugene V. Zima. Vol. 1, first Edition, p. 150. Berlin and Heidelberg: Springer.

5. Gurvits, L., O. Mason, and R. Shorten. On the Stability of Switched Positive Linear Systems. 2007. *IEEE Transaction on Automatic Control .* **52** (6): 1099.

6. Gurvits, L., and A. Olshevsky. On the NP-hardness of checking matrix polytope stability and continuous-time switching stability. 2009. *IEEE Transaction on Automatic Control.* **2** (54): 337.

7. Friedland, S., and L. Gurvits. Lower bounds for partial matchings in regular bipartite graphs and applications to the Monomer-Dimer entropy. 2008. *Combinatorics, Probability and Computing.* **3** (17): 347.

8. Gurvits, L.. On complexity of the mixed volume of parallelograms. 2009. In *25th European Workshop on Computational Geometry.* (Brussels, 16-18 Mar. 2009). Vol. 1, 1 Edition, p. 35. Brussels: ACM.

9. Gurvits, L.. A Short Proof, Based on Mixed Volumes, of Liggett's Theorem on the Convolution of Ultra-Logconcave Sequences. 2009. *The electronic journal of combinatorics.* **16** (1): R66.

## Publications

Barnum, H.. Semidefinite programming characterization and spectral adversary method for quantum complexity with noncommuting unitary queries. 2007. In *Algorithms and Complexity for Continuous Problems.* (Dagstuhl, Germany, 24-29 Sept. 2006). Vol. 06391, p. Electronic. Dagstuhl, Germany: IBFI.

Friedland, S., and L. Gurvits. Lower bounds for partial matchings in regular bipartite graphs and applications to the monomer-dimer entropy. 2008. *Combinatorics, Probability and Computing.* **17** (3): 347.

Gurvits, L.. Van der Waerden / Schrijver-Valiant-like conjectures and stable (aka hyperbolic) homogeneous polynomials: one theorem for all . 2008. *Electronic Journal of Combinatorics.* **15** (1): R66.

Gurvits, L.. Polynomial time algorithms to approximate mixed volumes within a simply exponential factor. 2007. *Electronic Colloquium on Computational Complexity.* **TR07**: 037.

Gurvits, L.. A short, based on the mixed volume, proof of Liggett's theorem on ultra-logconcave sequences. 2009. *Journal of Combinatorial Theory.* **5** (1): 5.

Gurvits, L.. A polynomial-time algorithm to approximate the mixed volume within a simply exponential factor. 2009. *Discrete and Computational Geometry.* **41** (4): 533.

Gurvits, L.. On multivariate Newton-like inequalities. 2009. In *Advances in Combinatorial Mathematics.* Edited by Kotsireas, Ilias S., and Eugene V. Zima. Vol. 1, 1 Edition, p. 50. Berlin and Heidelberg: Springer.

Gurvits, L.. On complexity of the mixed volume of parallelograms. 2009. In *25th European Workshop on Computational Geometry.* (Brussels, 16-18 Mar. 2009). Vol. 1, 1 Edition, p. 30. Brussels: ACM.

Gurvits, L., O. Mason, and R. Shorten. On the stability of switched positive linear systems. 2007. *IEEE Transaction on Automatic Control.* **52** (6): 1099.

Gurvits, L., and A. Olshevsky. Stability testing of matrix polytopes. 2007. In *European Control Conference, 2007.* (Kos, Greece, July 2007). , CD-ROM Edition, p. 3919. Saint Martin d'Heres, France: European Union Control Association.

Gurvits, L., and A. Olshevsky. On the NP-hardness of checking matrix polytope stability and continuous-time switching stability. 2009. *IEEE Transaction on Automatic Control.* **54** (2): 337.

# Excited States and Optical Response of Nanosized Molecules at Linear Scaling Numerical Cost

*Sergei Tretiak*
20070256ER

## Abstract

The project aims to develop theoretical methods and numerical algorithms allowing computation of excited state properties of large molecular systems at a reduced, linear scaling cost with respect to system size. These algorithms permit calculation of the excited state optical response directly from first principles, and have been implemented in the LANL-developed FreeON suite of quantum chemistry programs. In addition to linear scaling cost, the numerical methods appear to have achieved new breakthroughs in the rate of convergence. Increased rate of convergence, together with a reduced linear scaling cost are breakthrough achievements in electronic structure simulation that allow access to the computation of bulk excitons in systems with extended conjugation.

## Background and Research Objectives

Many nanoscale materials have already found applications or have great technological potentials for photovoltaic, light emitting devices, and bio-sensors, to name a few. Frequently, understanding their complex electronic dynamics is the main challenge for applications. Theory, modeling and simulation should match experimental advances so as to interpret the data and extract relevant information on photoexcitation, emission, transport and decay mechanisms, which is vital for designing new functional nano-materials and devices. Over the years, electronic structure calculations, such as density functional theory (DFT), transformed theoretical chemistry and materials science by creating a new capacity to describe the electronic structure and complex dynamics in molecules with hundreds of atoms. The approach based on the time-dependent DFT (TDDFT) recently became a method of choice for calculations of electronic excitations in both molecular systems and solids. Still, DFT (TDDFT) calculations require atomistic information (electrons and orbitals). Consequently, the most advanced algorithms for the first principle calculations of excited states (such as TDDFT) require cubic scaling of computational effort (i.e., O(N^3), N being the number of atoms in the molecule). Typically this limits the calculations to few excited states of molecules up to ~100 atoms in size. The proposed work overcomes these limitations by developing stable and efficient algorithmic procedures for finding a partial eigenspectrum of a tetradic (N^2xN^2) non-Hermitian, non-sparse Liouville matrix at O(N) (linear) computational cost. This will be achieved by simultaneous application of two techniques: Krylov subspace eigensolvers (producing O(N^6) to O(N^3) reduction) and sparse matrix methods (permitting an additional O(N^3) to O(N) deduction). We intend to deliver a complete set of theoretical tools for rapid calculations of excited states and optical properties in large molecular systems. These algorithms will be integrated into LANL-developed FreeON software suite. The developed tools will achieve O(N) scaling regime when computing excited state properties as a function of molecular size N. This project will strongly contribute to several fields: 1) Computational science: we will provide a first of its kind iterative algorithm combining Krylov subspace solvers and sparse matrices schemes; 2) Molecular modeling: our research will create a practical scheme for fast O(N) calculation of molecular excited states - a major breakthrough in the computational chemistry; 3) Materials science and nanotechnology: applications of our methodology will elucidate the fundamental trends governed by quantum-mechanics, which in turn dictate the electronic properties of large molecular systems. The outcome will have immediate technological implications, and, more generally, offer valuable guidance for synthesis and experiment, while providing insight into the nature and behavior of excitations in soft optical materials such as conjugated organics. These cutting edge computational capabilities will find broad applications in numerous programs at LANL as well as general scientific community.

## Scientific Approach and Accomplishments

Developing stable *inexact* Krylov-space algorithms and formulating computable criteria to bound the inexactness was the first milestone of this project. We started by testing and modifying a existing algorithms for numerical stability by simulating 'linear scaling' *inexact* conditions. First, we have created a prototype 'orbital free' code for calculating excited states incorporating a simple conjugated gradient algorithm. Our article on the benchmark results of our developed conjugated gradient algorithm in application to the model system (chain of hydrogens) have been published in the Journal of Chemical Physics [1]. Over the first year of the project we have extended our prototype 'orbital free' code for calculating excited states to real molecular systems. This code now includes four optimized algorithms, namely modified Lanczos, Arnoldi, Davidson, and Rayleigh Quotient Iterative (RQI) procedures. These procedures have been modified from their original parent techniques applicable to the Hermetian eigen-problems only, so that they are able to deal with the J-symmetric structure of the random Phase Approximation (RPA) eigen-equation. All algorithms work in the representation-independent (i.e. orbital-free) framework. Conventional orbital based algorithms for solving the time-dependent Self-Consistent Field (TD-SCF) equations restrict the solution subspace to a particle-hole and hole-particle (ph-hp) symmetry by construction. In an orbital independent formulation, we impose this ph-hp symmetry by using the occupied subspace projector, the idempotent ground state density matrix. The algorithms also utilize indefinite inner product for ortho-normalization of excitation vectors and 'Wilkinson shift' methodology for obtaining many excited states. Their convergence is ensured by application of the Thouless variational principle. These approaches are readily transferrable for a linear-scaling implementation of both Hartree-Fock and Kohn-Sham self-consistent field theories for the calculation of excitation energies and frequency-dependent molecular responses, by solving the RPA (non-Hermitian) and Tamm-Dancoff Approximation, TDA (Hermitian) eigenvalue equations in the molecular orbital-free framework. Convergence behavior and stability has been numerically benchmarked for computations of excited states of realistic molecular systems (conjugated polymers and carbon nanotubes), see Figure 1. All developed numerical approaches have been thoroughly tested with respect to the imposed numerical noise to address linear-scaling conditions, see Figure 2. We found that algorithm convergence critically depends in the quality of to the initial guess.

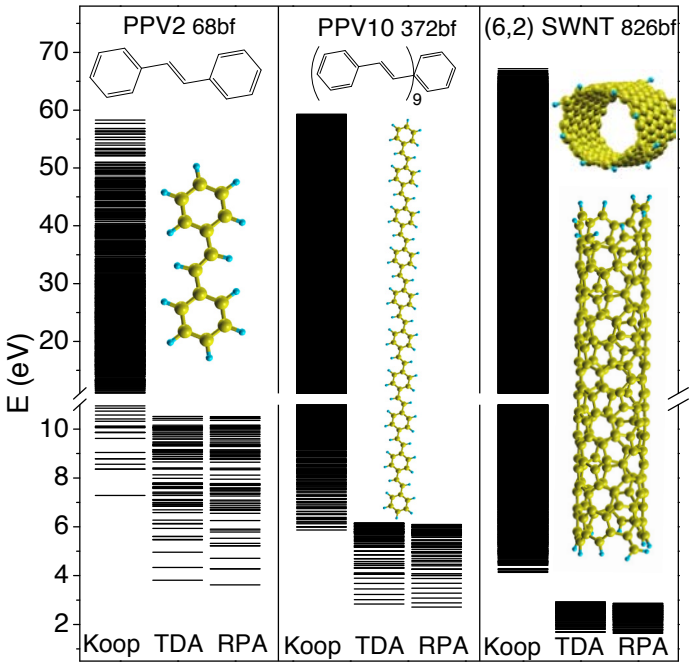


*Figure 1. Characteristic density of states in representative molecules used for numerical tests, polyphenylene-vinylene oligomers (PPV2, PPV10), and (6,2) single-walled carbon nanotube, which have increasing numbers of basis functions. The insets show the respective molecular structures.*

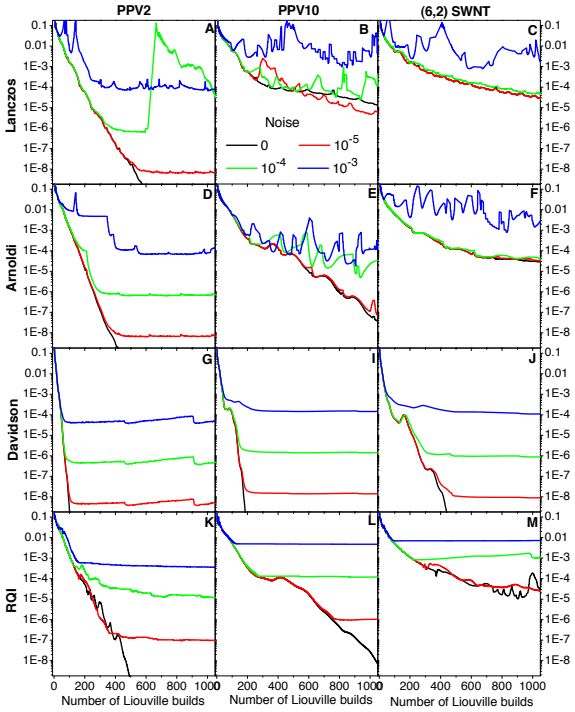


*Figure 2. Convergence rates of the first excited state in the presence of numerical noise in the tested methods. The horizontal axis (number of Liouville builds) shows the associated numerical expense. Ideally, the convergence parameter should reach a certain floor defined by the numerical noise and should stay nearly constant at this value for a number of iterations. RQI and Davidson algorithms show the best stability.*

Consequently, we have developed a ladder of improving approximations for the initial guesses and tested their performance as shown in Figure 3. Also, we explored several implementations on numerical pre-conditioners allowing accelerating algorithmic convergence. The results allow us to single out the most efficient procedure, namely modified Davidson algorithm - suitable for large-scale calculations of electronic excitations in the time-dependent perturbation theory in the linear scaling regime. Thus, during the second year we have followed the outlined milestones of the project and finalized the prototype code containing four distinct routines for 'orbital free' calculations. The second manuscript summarizing our numerical studies has been published in the Journal of Chemical Physics [2].

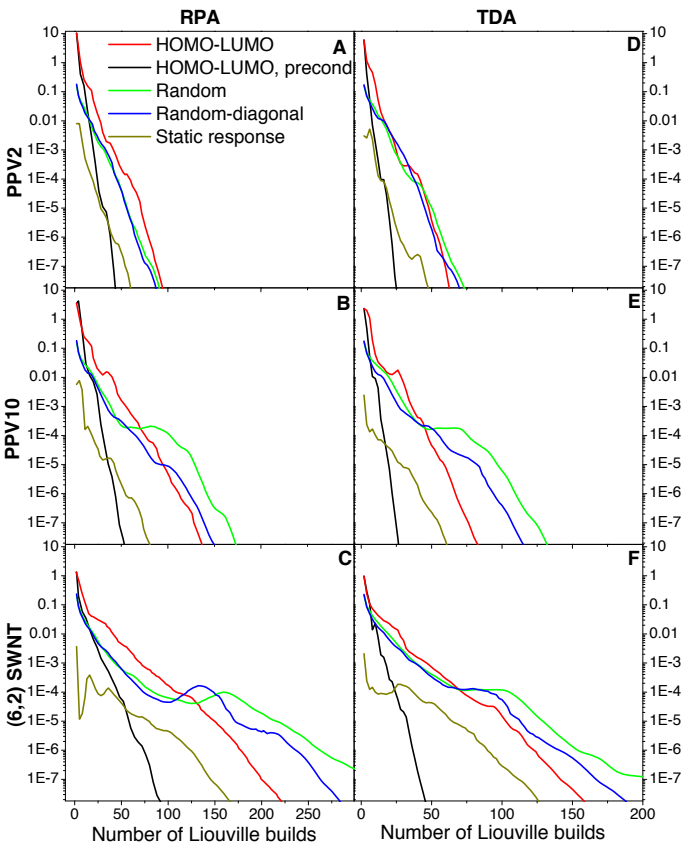


*Figure 3. Convergence rates as a function of the initial guess in Davidson's algorithm. Five different approximations for initial guesses are tested. Koopmans guess and density matrices induced in response to a static external electric field (linear response) show the best performance.*

Finally, we have built upon our experience in the first two years, and developed a completely new way to solve the time-dependent self-consistent-field equations. This new method solves the J-symmetric problem as two weakly coupled Hermetian problems, again in an orbital free representation, using a dual non-linear conjugate gradient optimization. This new scheme, called QUasi-Independent Rayleigh Quotient Iteration (QUIRQI), is variational with respect to linear scaling approximation, and also achieves rates of convergence that are equivalent to the best case solution of the corresponding Hermetian TDA problem. This new algorithm has been implemented in version Sep-18-2009 of the LANL-unique FreeON suite of linear scaling quantum chemistry programs, which is in the public domain (). FreeON/QUIRQI has been used to compute, at linear scaling cost, the limit of bulk excitons in polymers with extended conjugation, including polyphenylene vinylene (Figure 4) and (4,3) carbon nanotubes (Figure 5). This work is the first demonstration of linear scaling solution of the TD-SCF eigenproblem, and has been written up for Physical Review Letters [LAUR 09-06104]. A second paper is expected, on the application of these methods to periodic systems (one- and two-dimensional bulk materials), which is straight forward but high impact.

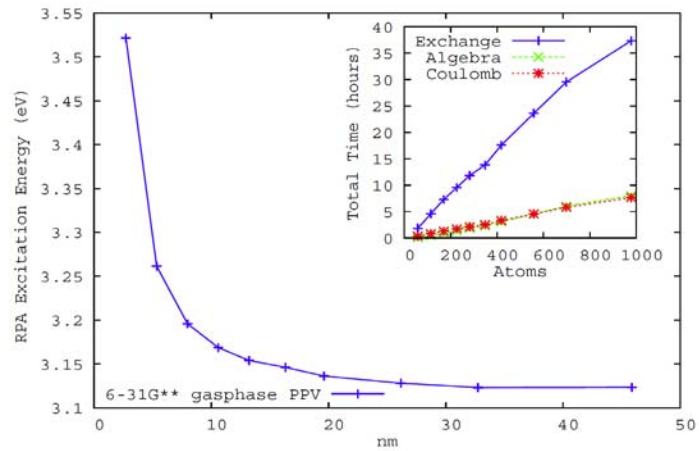


*Figure 4. Convergence to the bulk limit of the first excited state of polyphenylene vinylene (PPV) demonstrating linear scaling numerical cost. All calculations reached convergence in about 25 steps.*

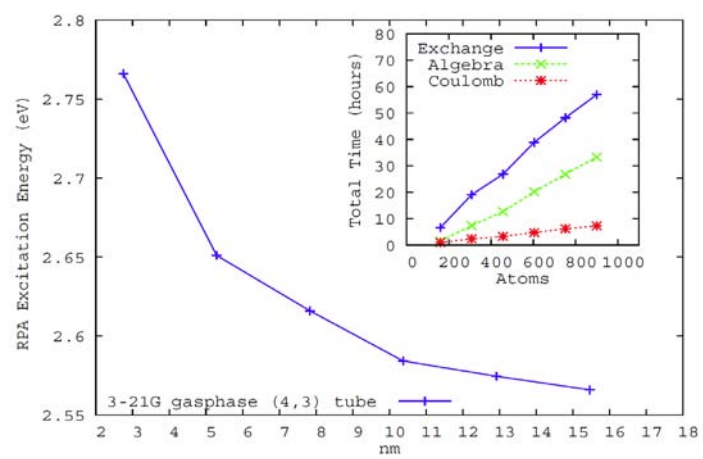


*Figure 5. Convergence to the bulk limit of the first excited state of (6,2) single-walled carbon nanotube demonstrating linear scaling numerical cost. All calculations reached convergence in about 40 steps.*

## Impact on National Missions

Successful completion of the proposed research permit a practical computational approach to optical properties and enable theoretical spectroscopy of nano-sized systems boosting computationally treatable molecules to 1000-10000 atoms range. This research has helped to develop the FreeON suite of linear scaling quantum chemistry programs, an inhouse toolset for large scale simulation of materials modeling, biological simulation and device physics. This code is a major tool for applications to various materials, and is expected to result in a fundamental understanding of electronic processes in functional matter (such as photo-sensing, photo-labeling, light harvesting and bio-functionalities), provide novel design strategies for new electronic materials, and foster integration and improvements in experimental LANL research in nanoscience. In addition, the linear scaling algorithms for solving the Time-Dependent Self-Consistent-Field problem have a direct impact on parallel computing at the capability and capacity level through reduced complexity and enhanced data locality. Relative to conventional N^3 algorithms, one can expect a 10^3 increase at the TFlop capability region, and a 10^9 increase at the exascale. The computational tools created will provide powerful predictive simulations for several classes of complex systems, including advanced optical and sensing device physics for Nuclear Weapons and Threat Reduction.

In addition to creating more powerful computational tools, the ability to achieve linear scaling for the RPA opens up the potential for new, highly accurate theories that include long range dispersion and van der Waals interactions through rigorous models based on the exact Hartree-Fock exchange and the RPA correlation energy. These models with correct long range behavior are extremely important for problems that occur in National Security Materials, including the structure and response of organic crystals, interfacial problems related to the sensing, detection and attribution of chem and bio-agents, as well as a host of related materials, chemistry and biology problems.

To sum up, the computational tools created will provide powerful predictive simulations for complex materials problems that include Nuclear Weapons and Threat Reduction activities, will benefit missions relevant to DOE, DHS, and other government agencies, and open the door for a broad class of new more accurate simulations with even greater impact.

## References


1. Lucero, M. J., A. M. Niklasson, S. Tretiak, and W. M. Challacombe. Molecular-Orbital-Free Algorithm for Excited States in Time-Dependent Perturbation Theory. 2008. *Journal of Chemical Physics.* **129**: 064114.

2. Tretiak, S., C. M. Isborn, A. M. Niklasson, and W. M. Challacombe. Representation independent algorithms for molecular response calculations in time-dependent self-consistent field theories. 2009. *Journal of Chemical Physics.* **130** (5): 054111.

3. Challacombe, M.. Linear Scaling Solution of the Time-Dependent Self-Consistent-Field Equations with Quasi-Independent Rayleigh Quotient Iteration. *Physical Review Letters.*


## Publications


Challacombe, M.. Linear Scaling Solution of the Time-Dependent Self-Consistent-Field Equations with Quasi-Independent Rayleigh Quotient Iteration. *Physical Review Letters..*

Lucero, M. J., A. M. Niklasson, S. Tretiak, and W. M. Challacombe. Molecular-Orbital-Free Algorithm for Excited States in Time-Dependent Perturbation Theory. 2008. *Journal of Chemical Physics.* **129**: 064114.

Tretiak, S., C. M. Isborn, A. M. Niklasson, and W. M. Challacombe. Representation independent algorithms for molecular response calculations in time-dependent self-consistent field theories. 2009. *Journal of Chemical Physics.* **130** (5): 054111.

# Agent-Based Modeling and Simulation of Cellular Signaling Systems

*William S. Hlavacek*
20070416ER

## Abstract

Proteins in cellular regulatory systems, because of their multicomponent composition, can interact in a combinatorial number of ways to generate myriad protein complexes, which are highly dynamic. This feature of protein-protein interactions has been called combinatorial complexity, and it is recognized as a major barrier to understanding cell biology. The problem of combinatorial complexity is alleviated by using a rule-based computational approach to model protein-protein interactions. For a review of rule-based modeling, see Faeder et al. [1]. In this approach, proteins and protein complexes are represented as structured objects (graphs) and protein-protein interactions are represented as (graph-rewriting) rules that operate on these objects to modify their properties, consistent with transformations mediated by the interactions being represented. Rules can serve as definitions of individual reactions or entire reaction classes, and they can be used as generators of reactions. The assumption underlying this modeling approach, which is consistent with the modularity of regulatory proteins, is that interactions are governed, at least to a first approximation, by local context that can be captured in simple rules (e.g., by the availability of binding sites on two binding partners). Rules can, in principle, be used to generate reaction networks that account comprehensively for the consequences of specified protein-protein interactions. However, the size of a rule-derived network can severely challenge conventional methods for simulating reaction kinetics. This project has been aimed at developing new methods for simulating rules that imply large-scale chemical reaction networks and then using these methods to gain insights into the complex systems that cells use to make decisions in response to environmental stimuli.

## Background and Research Objectives

The motivation for the project is well summarized in two recent perspective papers [2,3]. Cell signaling systems respond to multiple inputs, such as ligands of cell-surface receptors; and produce multiple outputs, such as changes in gene expression and cellular activities, including motility, proliferation, differentiation, and death. This "macroscopic" input-output behavior is generated by a web of molecular interactions that can be viewed as taking place at a lower, "microscopic" level. These interactions prominently involve posttranslational modification of proteins and the nucleation of protein complexes. Behaviors at both the micro- and macroscopic levels are complex and must be probed systematically and characterized quantitatively as a prelude to the development of a predictive understanding of a cell signaling system. We must also have a theoretical framework or a mechanics within which we can determine how macroscopic behaviors emerge from known microscopic behaviors or change with manipulations of microscopic behaviors. To connect behaviors at both levels, the mechanics of rule-based modeling is useful, in that this formalism enables one to track the site-specific details of molecular interactions in a model, such as the phosphorylation status of individual amino acid residues within a protein.

As exemplified by our understanding of the role of tyrosine phosphorylation in cell signaling, we now have a fairly clear picture of the types of molecular mechanisms that are responsible for cellular responses to environmental changes, even as the molecular-level details of particular signaling systems continue to emerge. In cell signaling systems, information processing is mediated by posttranslational modifications of proteins, which turn binding and catalytic activities on and off; and the nucleation of protein complexes, in which enzymes and substrates are colocalized to control enzyme specificity and activity. This picture is powerful enough to have contributed to the development of drugs that target specific signaling molecules that drive disease, such as inhibitors of tyrosine kinases. Current understanding of cell signaling, however, is

often insufficient to predict how mutations or potential therapeutic interventions at the molecular level will affect cellular behavior. To make further progress in the treatment of diseases caused by dysfunctional cell signaling, we are faced with the challenge of obtaining a predictive understanding of cellular decisions in terms of the underlying molecular mechanisms of cell signaling, which are exceedingly complex. This challenge is similar to the one faced by those in the 19th century who embraced the atomic theory, such as Maxwell, Boltzmann, and Gibbs, and developed statistical mechanics to explain the macroscopic properties of matter in terms of the microscopic properties of atoms and molecules. As at that time, a new mechanics is needed to bridge two levels of behavior: "macroscopic" behavior at the level of the inputs and outputs of cell signaling systems and "microscopic" behavior at the level of the molecular interactions that process the inputs and generate the outputs. Just as importantly, experimental studies are required to systematically probe and quantitatively characterize the behaviors of cell signaling systems at both the macro- and microscopic levels.

There is strong motivation to better understand the processes of cellular signaling, in which protein interactions play a central role. Indeed, we would like to make accurate predictions about the functional roles of proteins and the effects of modifying protein interactions in particular systems. Our ability to make such predictions is a measure of our basic understanding of molecular cell biology and a range of practical consequences may stem from an improved capability to rationally manipulate cellular regulatory systems on the basis of predictive mathematical models. Current models of signaling systems are far from capturing all of the relevant mechanistic details necessary to make accurate predictions, in part because it is difficult to account for the enormous number of post-translational modifications and protein complexes that can be generated by interactions among even small sets of proteins. The rule-based modeling approach overcomes this limitation in principle, but our practical ability to simulate and analyze rule-based models has been limited. The main goal of this project was to develop efficient simulation methods for rule-based models regardless of the size of the reaction networks implied by sets of rules. The methods that we have developed are capable of accurately simulating the reaction kinetics defined by rules that imply large-scale reaction networks. The development of these methods improves our capabilities to develop mechanistic models and represents a significant step toward predictive understanding of cellular regulatory systems.

## Scientific Approach and Accomplishments

The key accomplishments are reported in 10 papers or reports (see list of references). The most important accomplishments are two algorithms that enable the simulation of rule-based models that cannot otherwise be simulated [4,5]. We have also developed software called DYNSTOC that implements one of these methods [5] and we have demonstrated how the method of Yang et al. [4] can be used to study multivalent ligand-receptor interactions [6]. The DYNSTOC simulation tool can be used as a stand-alone software application or accessed via a web-based interface that we have developed called GetBonNie [7].

The first method developed [4] is an agent- or particle-based simulation method in which 1) a time increment is sampled from an exponential distribution, 2) a rule is selected from among a weighted list of rules, just as reactions are sampled in the well-known Gillespie's method, and 3) the selected rule is used to generate a reaction event (i.e., to select reactants to participate in a type of reaction defined by the selected rule). Generation of the network of reactions implied by a set of rules, which is expensive, is avoided entirely. In an application of the method, we used it to study multivalent ligand-receptor binding, obtaining results that are relevant for characterizing an experimental system that has been studied in the laboratory of our collaborator, Dr. Richard G. Posner (Translational Genomics Research Institute, Phoenix). These results suggest why a trivalent ligand is able to potently stimulate a strong cellular response to the ligand [6]. The method has been reported in *Physical Review E* [4]. The application of the method will be reported in a January 2010 issue of *Biophysical Journal* [6].

The second method developed as part of this project, also an agent- or particle-based kinetic Monte Carlo method, is a generalization of a method, implemented in software called StochSim. The generalized method can be used to model a greater variety of molecular interactions than the original and we have implemented the method in general-purpose software called DYNSTOC. A paper about the method and software was published in *Bioinformatics* [5]. This method, a null-event method with a fixed time step, is expected to be less efficient than the first method developed, but the method is easier to implement software. Software implementation of the new methods is fairly difficult because of a requirement to explicitly track all reactive sites included in a model and our desire that software be able to understand a general-purpose model-specification language that we call the BioNetGen language (BNGL) [1].

An additional method of simulation was developed that

involves no null events. In this method, every time step results in a change of system state. The method was first developed for a specific class of problems [8] and then generalized [9]. The method has been implemented in software called RuleMonkey [9]. RuleMonkey is capable of simulating any model specified in BNGL. Finally, we have developed an alternative approach to model specification using BNGL, which is perhaps a more powerful approach. This approach is based on a finite-state-machine formalism [10].

Now that appropriate methods and software tools have been developed for simulating rule-based models that embody large-scale chemical reaction networks, we have started to build such models. We are building large mechanistic models for signal-transduction events triggered by the epidermal growth factor (EGF), the cytokine TGF-beta, and co-crosslinking of CD28 and the T cell receptor (TCR). These signaling pathways play important roles in cancers and immunity. We have also started to build a model for metabolism in the bacteria *Escherichia coli* that accounts for the fates of every carbon atom of metabolites in enzyme-catalyzed reactions. In future work, we expect to be able to apply our novel simulation tools to the study of these systems to obtain insights into the molecular mechanisms of cancer and immunity and into how metabolism might be reengineered for useful purposes.

## Impact on National Missions

The results of this project have the potential to broadly impact missions of DOE and NIH related to bio-energy and bio-security, as these missions depend in part on our ability to obtain a predictive understanding of key cellular regulatory systems. The methods developed in the course of this project allow mechanistic models of cellular regulatory systems incorporating site-specific details of molecular interactions to be developed and analyzed. Predictive models of key cellular regulatory systems found in microbes, for example, may eventually enable the engineering of microbes for useful purposes, such as bio-fuel production and environmental remediation. Models of regulatory systems found in the human immune system may enable the development of novel vaccines. In terms of program development, this project laid important groundwork (the ability to simulate large-scale models for signal-transduction systems) for a successful NIH P50 grant application (approximately $15M total costs over five years), which established a national center for systems biology in New Mexico. The modeling team of this center is led by LANL.

## References


1. Faeder, J. R., M. L. Blinov, and W. S. Hlavacek. Rule-based modeling of biochemical systems with BioNetGen. 2009. *Methods in Molecular Biology.* **500**: 113.

2. Hlavacek, W. S.. How to deal with large models?. 2009. *Molecular Systems Biology.* **5**: 240.

3. Hlavacek, W. S., and J. R. Faeder. The complexity of cell signaling and the need for a new mechanics. 2009. *Science Signaling.* **2**: pe46.

4. Yang, J., M. I. Monine, J. R. Faeder, and W. S. Hlavacek. Kinetic Monte Carlo method for rule-based modeling of biochemical networks. 2008. *Physical Review E.* **78**: 031910.

5. Colvin, J., M. I. Monine, J. R. Faeder, W. S. Hlavacek, D. D. Von Hoff, and R. G. Posner. Simulation of large-scale rule-based models. 2009. *Bioinformatics.* **25**: 910.

6. Monine, M. I., R. G. Posner, P. B. Savage, J. R. Faeder, and W. S. Hlavacek. Modeling multivalent ligand-receptor interactions with steric constraints on configurations of cell-surface receptor aggregates. To appear in *Biophysical Journal.*

7. Hu, B., G. M. Fricke, J. R. Faeder, R. G. Posner, and W. S. Hlavacek. GetBonNie for building, analyzing and sharing rule-based models. 2009. *Bioinformatics.* **25**: 1457.

8. Yang, J., and W. S. Hlavacek. Rejection-free rule-based kinetic Monte Carlo simulation of multivalent ligand-receptor interactions. 2008. *Los Alamos Technical Report LA-UR-08-07624 (available at http://arxiv.org/abs/0812.4619).*

9. Colvin, J., M. I. Monine, W. S. Hlavacek, D. D. Von Hoff, and R. G. Posner. Rejection-free stochastic simulation of BNGL-encoded models. 2009. *Los Alamos Technical Report LA-UR-09-06600.*

10. Yang, J., and W. S. Hlavacek. Modeling biomolecular interactions with molecular finite state machines. 2009. *Los Alamos Technical Report LA-UR-xxxxx.*


## Publications


Colvin, J., M. I. Monine, J. R. Faeder, W. S. Hlavacek, D. D. Von Hoff, and R. G. Posner. Simulation of large-scale rule-based models. 2008. *Los Alamos Technical Report LA-UR-08-04860.*

Faeder, J. R., M. L. Blinov, and W. S. Hlavacek. Rule-based

modeling of biochemical systems. 2009. *Methods in Molecular Biology.* **500**: 113.

Hlavacek, W. S.. How to deal with large models?. 2009. *Molecular Systems Biology.* **5**: 240.

Hlavacek, W. S., and J. R. Faeder. The complexity of cell signaling and the need for a new mechanics. 2009. *Science Signaling.* **2**: pe46.

Hu, B., G. M. Fricke, J. R. Faeder, R. G. Posner, and W. S. Hlavacek. GetBonNie for building, analyzing and sharing rule-based models. 2009. *Bioinformatics.* **25**: 1457.

Monine, M. I., R. G. Posner, P. B. Savage, J. R. Faeder, and W. S. Hlavacek. Modeling multivalent ligand-receptor interactions with steric constraints on configurations of cell-surface receptor aggregates. To appear in *Biophysical Journal.*

Yang, J., M. I. Monine, J. R. Faeder, and W. S. Hlavacek. Kinetic Monte Carlo method for rule-based modeling of biochemical networks. 2008. *Physical Review E.* **78**: 031910.

Yang, J., and W. S. Hlavacek. Rejection-free rule-based kinetic Monte Carlo simulation of multivalent ligand-receptor interactions. 2009. *Los Alamos Technical Report LA-UR-08-07624.*

# Fast Approximation Algorithms for Systems of Linear Inequalities

*Donald R. Hush*
20070421ER

## Abstract

Consider the following problem: given a collection of red and blue dots scattered randomly on a flat piece of paper, position a line that best separates the red and blue dots. Formally the paper is a *two-dimensional space*, the red and blue dots are *points* in this space, and the line is a *one-dimensional plane*. We can extend this problem to three dimensions by imagining a collection of tiny red and blue balls suspended in mid-air in a room (*points* in a *three-dimensional space*), and positioning a flat sheet of paper (a *two-dimensional plane*) that best separates the red and blue balls. When this problem is extended to even higher dimensions, e.g. 10, 100 or even 1000, it becomes notoriously difficult. As it turns out this is a core problem in computer science and, although not obvious, it is also the computational bottleneck for many important applications. Examples of such applications include identifying the smallest subset of genes that exhibit a coordinated response to a particular stimuli, determining the suppliers, consumers, and middle-men in large networks of individuals or institutions that are connected by the flow of money or information, and detecting anomalies on a computer network. It is well known that the red-blue dot problem cannot always be solved, that is there is no computer algorithm that solves all cases. In fact, prior to this project, the best-known algorithms could only solve very special cases (e.g. cases where the red and blue dots are well-separated). The main contribution of this project is a new algorithm that solves the red-blue dot problem for much more general cases. A consequence of this new algorithm is that we can now compute solutions to many important applications faster and more accurately than ever before.

## Background and Research Objectives

Consider a red-blue dot problem with N dots in a D-dimensional space. The best separating plane can be found by a brute force algorithm whose run time scales like N to the power D, but this is impractical for D larger than about three. In special cases, e.g. when the red and blue dots are well separated, this problem can be solved for any D using a well-known linear programming algorithm. In practice however the red-blue dots do not conform to these special cases and the ad hoc algorithms that are commonly used produce inferior solutions, which translate into poor system performance. For example in the network anomaly detection problem this poor performance is often manifested as an unacceptably high false alarm rate.

Recent work in machine learning, by ourselves and others, has led to three important discoveries: new methods for characterizing the *learnability* of data distributions (i.e. the degree to which we can extract information about a data distribution from a collection of data points produced by the distribution); new mathematical tools that help us quantify how accurately we're extracting information from data points; and new algorithms for information extraction that are simple, practical, and possess surprisingly fast run times. This project combined and extended these discoveries to develop provably fast algorithms for the red-blue dot problem. The end product is a computer algorithm that is guaranteed to solve much more general cases of the red-blue dot problem, and also guaranteed to scale to extremely large problem sizes (i.e. large values of N and D).

## Scientific Approach and Accomplishments

The development of these algorithms was divided into the following five tasks. First we developed a rigorous understanding of the red-blue dot distributions that admit computationally efficient solution algorithms. This work revealed a larger class of distributions than previously known, verifying that it was theoretically possible to solve much more general cases of the red-blue dot problem. Second we designed a (simpler) surrogate optimization problem whose solutions are

good approximations for the red-blue dot problems determined in the first step. Third we designed a specific solution algorithm for this surrogate problem. Here we used a novel approach that decomposed the surrogate optimization problem into a nesting of two optimization problems: a large convex problem nested inside a small non-convex problem. Fourth we designed and analyzed algorithms for the nested optimization problems. Here we developed and analyzed algorithms for the large convex problem, making sure that they scaled to very large problem sizes. Then we developed algorithms for the small non-convex problem, with the goal of striking an optimal balance between the computational efficiency and the accuracy of the approximate solution. The end result is an algorithm that is now the fastest and most accurate known solver for the red-blue dot problem.

Our last task was to perform extensive testing of our algorithm on both synthetic and real data. For example we tested our algorithm with up to 1,000,000 data points (red and blue dots) in 1000 dimensions, which is several orders of magnitude larger than the problem sizes accommodated by previous algorithms. We also used these algorithms to compute a new solution for a network monitoring problem (see below), and demonstrated a false alarm rate reduction of three orders of magnitude. Similar improvements were demonstrated for portal monitoring at shipping ports, and damage detection for wind turbine blades.

We now describe the application of our algorithm to cyber security. A common challenge in cyber security is to identify particular types of activity in *encrypted* network flows (a network flow is a sequence of network packets with well-defined start and end points; network flows are the fundamental data unit processed by network analysis tools). Here we attempt to identify the flow type "CHAT", but our approach applies to other types of activity as well. When a flow is *unencrypted* it is relatively easy to determine the flow type by examining the flow packet contents. However this is useless for encrypted flows and so determining their flow type is a difficult problem.

A standard approach is to develop CHAT signatures from the high level meta-data associated with the flow, and then compare network traffic to these signatures. This approach is simple, but it is ad hoc, lacks robustness to the data distribution, is unable to adapt to the changing network statistics, and its accuracy is unknown.

In our approach we use the algorithms developed in this project to build a different CHAT detector every hour. The large volume of network data and the real time requirements would have made this approach impossible prior to the existence of our algorithm. In particular we extracted 301 pieces of information from the *packet size* and *wait time* sequences to form a D=301 dimensional red or blue dot for each flow. The blue dots corresponded to *encrypted* network flows and red dots to CHAT flows from *unencrypted* traffic. This data was collected (and processed in real time) from a busy computer network that peaked at over 1 million flows per hour. By solving multiple instances of the red-blue dot problem, where each instance placed a different emphasis on the red and blue dot errors, we were able to identify the encrypted flows most likely to be CHAT and to estimate the accuracy of our method. With the detection rate fixed at 0.9, Figure 1 shows the alarm rate (i.e. the fraction of *encrypted* flows predicted to be CHAT) of our method compared to the signature method over eight days of network traffic. The alarm rate of our method was approximately three orders of magnitude lower than the signature method, confirming the superiority of our method and the extremely high error rate of the signature method. Note also that our method gave zero alarms during most of the nighttime hours, which is consistent with our prior expectations.

In summary, the algorithms developed in this project allowed us to develop a practical solution for monitoring encrypted network traffic that is computationally efficient, robust to the data distribution, adapts to the changing network statistics, and superior to existing methods.

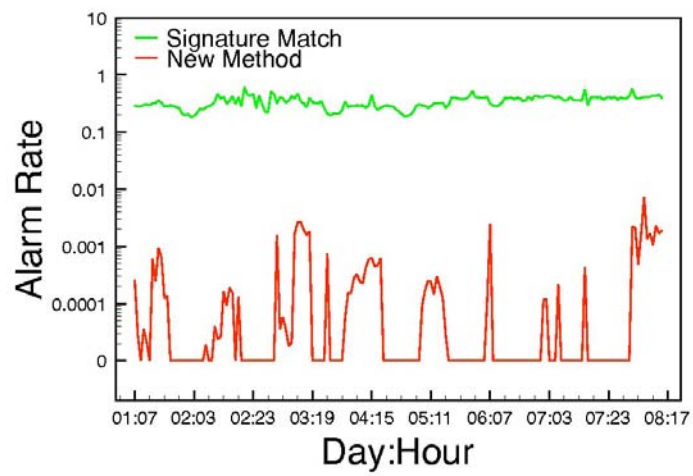


*Figure 1. Comparison of alarm rates over eight days of network traffic.*

## Impact on National Missions

We have produced a new algorithm for a core problem in computer science that appears frequently in practice, and is solved very poorly by existing algorithms. Indeed, it is the first practical algorithm to scale to very large problem sizes and guarantee optimal solutions. This substantially advances our problem solving capabilities for applications such as the development of regulatory network models

in genomics, the analysis of organizational networks (e.g. people-to-people networks) for national security, the analysis of surveillance imagery for threat reduction, network monitoring for cyber-security, high precision machining for manufacturing, and damage detection for wind turbine blades.

## References


1. Scovel, C., D. Hush, and I. Steinwart. Approximate duality. 2007. *Journal of optimization theory and applications.* **135** (3): 429.


## Publications


List, N., D. Hush, C. Scovel, and I. Steinwart. Gaps in support vector optimization. 2007. In *Lecture Notes in Computer Science.* Vol. 4539, p. 336. Berlin:Heidelberg: Springer.

Scovel, C., D. Hush, and I. Steinwart. Stability of unstable learning algorithms. 2007. *Machine Learning.* **67** (3): 197.

Scovel, C., D. Hush, and I. Steinwart. Approximate duality. 2007. *Journal of optimization theory and applications.* **135** (3): 429.

Steinwart, I., D. Hush, and C. Scovel. Learning from dependent observations. 2009. *Journal of Multivariate Analysis.* **100**: 175.

Steinwart, I., D. Hush, and C. Scovel. Optimal rates for regularized least squares regression. 2009. In *(COLT 09) The 22nd Conference on Learning Theory.* (Montreal, 18-21 June 2009). Vol. 1, p. 1. Berlin:Heidelberg: Springer.

# Minimal Description of Complex Shapes with Applications to Experiments and Validation of Large-Scale Codes

*Mark B. Mineev*
20070483ER

## Abstract

Moving unstable patterns are ubiquitous in numerous real and computational experiments. Often they pose a challenge of being complicated and even are fractals. At the same time there are numerous classes of these complex shapes, which exhibit universal behavior in a long time asymptotics (statistically), however complicated these patterns can visually be.

This Report presents background and major accomplishments of mathematical research in the actively evolving field of minimal description of complex two-dimensional shapes, which represent patterns, both in Nature and in computational modeling of unstable nonlinear processes, which take place far out of equilibrium. This research was motivated by various applications of these processes, both of commercial and strategic nature, by many puzzles, complex interfaces exhibit in Nature on fundamental levels, and by recent discoveries of rich mathematical structure lying behind many of these processes. This mathematical structure was discovered by several individuals during the last 20 years, including the PI of the project. It gave rise to many efficient analytical methods to obtain exact close form time-dependent non-trivial solutions for moving complex domains in various nonlinear processes and to identify a global geometric quantities, which are either conserved in time or slowly change. The report contains a summary of major results in various processes and geometries including the experimental work, which confirms our theory and robustness of our mathematical description. The report is concluded by a brief outline of potential impacts to major missions and grand scientific challenges for LANL.

## Background and Research Objectives

In science and engineering, it is often of great importance to find the two dimensional image of an object from indirect measurements (often the moments) of the underlying shapes to be recovered. It is not less important to characterize these images using a minimal number of parameters in order to save computational efforts. The problem of a domain recovery from its moments is very common in mathematics, has a long history and many important applications, such as signal processing, computed tomography, geophysics (magnetic and gravitational anomaly detection) just to name a few. Recovery of shapes by moments is universally accepted as a notoriously difficult inverse problem, because it is often ill-posed, non-linear and unstable. However, during last two decades, new powerful methods were developed (significant part of this development was made by participants of this project). These methods allowed the moment problem to be solved exactly in a complete closed form for so-called quadrature domains (QD) and in series of complex nonlinear two-dimensional free boundary processes, having a name of Laplacian growth ([2] and references therein). It is also remarkable that these solutions are based on techniques of numerical linear algebra, which provide very fast and stable computational algorithms and reveals a deep connection between the shape-from-moments problem and the theory of numerical quadrature over planar regions. Our research in two-dimensional interface dynamics, independently of works in quadrature domains revealed a deep mathematical structure behind these processes and helped to obtain exact closed form analytic solutions. We tried to analyze complex shapes obtained in experiments and simulations using a minimal number of parameters, which are to be found from moments - geometrical quantities, given for each particular interface.

The method is remarkably simple and stems from research of Russian mathematician A. Markov in XIX century. The idea was to recover a non-negative function $f(x)$ from a given list of integrals of this function with integer powers of $x$. A series of deep results, followed after Markov, revealed connections of this problem with continuous fractions, Gauss

quadrature formulae, theory of orthogonal polynomials, and the theory of analytical approximations (Stieltjes, Hamburger, Hausdorff, Szego, and Bergmann). However, a real challenge lied in a two dimensional version of the moments problem, where two dimensional shapes were to be recovered. As said above, impressive results obtained recently in quadrature domains and integrable free boundary problems (mostly Laplacian growth) made possible to extend these methods to more general and more complex two dimensional images, which are important for various applications, including those vital for LANL.

## Scientific Approach and Accomplishments

Because of the lack of space we will describe here only six major accomplishments. It is of particular importance to perform detailed mathematical analysis of self-similar growing patterns, often observed in various kinds of unstable growth. We have chosen the analysis of self-similar patterns in Laplacian Growth, because this process often generates universal self-similar patterns in a long-time asymptotics. Self-similarity determines the analytic structure of the main mathematical object in our theory - the so-called Schwarz function of the moving boundary. The knowledge of this analytic structure allows us to derive the integral equation for the conformal map. We showed that solutions to this integral equation obey a Schroedinger equation with the well-known integrable potential [1]. The solutions, expressed through the Gauss hyper-geometric function, characterize the geometry of self-similar patterns in a wedge. We also found the potential for the Coulomb gas representation of the self-similar Laplacian growth in a wedge and calculated the corresponding free energy.

We had also elaborated a theory of Random Matrices, a rich concept in a modern mathematical physics, and utilized this subject for complex growing two dimensional patterns [2]. Since it was first applied to the study of nuclear interactions by Wigner and Dyson, almost 60 years ago, the Random Matrix Theory has developed into a field of its own within applied mathematics, and is now essential to many parts of theoretical physics, from condensed matter to high energy. The fundamental results obtained so far rely mostly on the theory of random matrices in one dimension (the dimensionality of the spectrum, or equilibrium probability density). In a last few years this theory has been extended to the case where the spectrum is two-dimensional, or even fractal, with dimensions between 1 and 2. In this work, we presented and analyzed these recent developments (including our original results) and indicated a list of physical problems where the theory is expected to be applied.

A next significant accomplishment in the project was a substantial extension of the Laplacian growth to a so-called 'elliptic growth'. The planar elliptic extension of the Laplacian growth is, after a proper parametrization of a moving boundary, is presented in a form of a solution to the equation for area-preserving diffeomorphisms. The infinite set of conservation laws associated with the process is interpreted in terms of potential theory. The constants of integration for closed form solutions are identified as the singularities of the Schwarz function, which are located both inside and outside the moving contour. Well-posedness of the recovery of the elliptic operator governing the process from the continuum of interfaces parametrized by time were addressed, and two examples of exact solutions of elliptic growth are presented [3].

The next major advance in this project is of great importance for closed form solutions and minimal description of complex two-dimensional analytic domains [4]. Namely, we have obtained a new class of solutions to Laplacian growth (LG) with zero surface tension and showed that they contain all other known solutions as special or limiting cases. These solutions, which are time-dependent conformal maps with branch cuts inside the unit circle, are governed by a nonlinear integral equation and describe fjords of viscous liquid with non-parallel walls in fingering experiments in Hele-Shaw cells. Integrals of motion for the multi-cut LG solutions in terms of singularities of the Schwarz function were found. The subclass of these solutions with linear Cauchy densities on the cuts of the Schwarz function is of particular importance, because in this case the integral equation for the conformal map becomes linear. These solutions also are of physical importance by representing oil/air interfaces, which form oil fjords with a constant opening angle, in accordance with our recent experiments in a Hele-shaw cell.

We should also mention here our experimental work, performed in collaboration with The Center for Nonlinear Dynamics (U. of TX, Austin [5]). This work was devoted to an experimental verification of our theory of harmonic moments, which are indispensable to characterize an unstable growth of complex two-dimensional patterns. Harmonic moments are integrals of integer powers of $z = x+iy$ over a domain. Here the domain is an exterior of a bubble of air growing in an oil layer between two horizontal closely spaced plates. Harmonic moments are a natural basis for Laplacian growth phenomena because, unlike other representations, these moments linearize the zero surface tension problem (Richardson, 1972), so that all moments, except the lowest one, are conserved in

time. From our experiments we directly determined the harmonic moments and showed that for non-zero surface tension all moments (except the lowest one) decay in time rather than exhibiting the divergences typical for other representations. Further, we derived an expression that relates the derivative of an arbitrary harmonic moment to measurable quantities (surface tension, viscosity, the distance between the plates, and two line integrals over the contour encompassing the growing bubble). The laboratory observations are in good accord with the expression we derived for the rate of change of harmonic moments, which is proportional to the surface tension; thus in the zero surface tension limit, the all moments (above the lowest one) are conserved, in accord with Richardson's theory. In addition, from the measurements of the time evolution of the harmonic moments we obtained a value for the surface tension that is within 20% of the accepted value. In conclusion, our analysis and laboratory observations demonstrate that an interface dynamics description in terms of harmonic moments is physically realizable and robust.

Another major accomplishment we addressing here is a creation and development of the stochastic layer model of two-dimensional discrete growth [6]. This model embraces the classical Laplacian growth and the universal diffusion-limited aggregation as two opposite limits of a general random process, where a fixed number of small particles of equal areas accrue to a growing two-dimensional cluster after the same elementary time interval. The probability of accrual is a harmonic measure of a given segment of a cluster boundary. (For readers, who are not familiar with this mathematical terminology, a harmonic measure of a given point at the boundary of a domain under consideration is just a density of equi-potential lines near the point of interest – a direct analog of an electric field created at the metal surface by external charges.) If particle aggregates on the cluster one by one, this is a well-known universal fractal growth, a so-called 'diffusion-limited aggregation'. It possesses universal global geometric features, such as a fractal dimension, which equals 1.71 plus/minus .01, and still is a great puzzle and a long-standing challenge to understand it and to obtain it analytically. If on the other hand a number of particles which are simultaneously deposited at the growing boundary, is very large (specifically, it should be much greater than the whole length of a boundary measured in terms of a linear size of a particle to be deposited), then the process has a well-posed continuous limit and is nothing but a classical Laplacian growth, which is a mathematical fundament of this project.

We succeeded to calculating the probability of a final cluster with a given configuration, obtained during this process and thus have established a variational formulation of this general layer growth. This is a significant achievement in efforts of minimal description of complex images. Besides obtaining a new powerful tool of describing various complex shapes and assigning them a probability of a growth in a standard functional form, we opened a possibility to calculate various global geometric characteristics, such as fractal dimension of complex shapes, using a conventional statistical averaging. This work is expected to give rise of many directions and fruitful developments in a field of random complex shapes obtained as a result of various scenarios of random growth.

## Impact on National Missions

These achievements are exacted to have the following impact on several key missions of LANL and Grand Challenges, which have been formulated a few years ago by Director Anastasio. We will address briefly here the following four potential impacts: (a) LANL key mission in the field of unstable interfaces of hydrodynamic nature, (b) mission in the area of validation and verification (V & V in short) of large-scale computational codes developed for description of complex and often unstable phenomena, (c) significant data compression in data analysis when data flows are represented by quickly changing two dimensional images, and finally (d) application of the developed methods and techniques on the high-strained material dynamics far from equilibrium.

(a) The bottleneck for applications of our two-dependent conformal mapping technique to two-dimensional hydrodynamic processes, such as KH, RT, and RM, was a non-potential nature of a fluid velocity vector field which was excluded in the original description of a free boundary problem, which exhibited a powerful structure, mentioned above. After an extension of the mathematical description to processes, which allow vorticity in a bulk of fluid [3], we opened a way to treat analytically (and sometimes in a close form) these free boundary processes. While for a general case a work is yet to be done, several important cases can already be described using our method in the presence of vortices in a bulk of fluid.

(b) The extension of the Laplacian growth, described in [3] and exact solutions of the `multi-cut' nature [4] significantly widened applications to V&V approaches to existing large-scale codes. Since a list of well-known and widely applicable exact solutions in nonlinear hydrodynamics is very limited, these new class of exact solutions is expected to substantially enrich the list of applications to large codes to perform V&V testing.

(c) Remarkable properties of the Schwarz function of complex domains and quadrature domains, developed in the course of the project allowed us to minimize description of two dimensional images using a combination of powerful techniques of orthogonal polynomials and universal features of the Schwarz function. Optimal description with extraordinary quick convergence [2] can save significant computational volume of work in comparison with a standard `pixelation' of complex two dimensional images.

(d) Finally, our progress in complex nonlinear two dimensional interface dynamics has significantly enriched a mean-field description of a free boundary process (via the so-called matrix models - main details are addressed in [2]). This mean-field description of complex interface dynamics constitutes a so-called *field-phase model*, which appeared to be a particularly flexible and powerful tool in dealing with dynamics of solid materials far from equilibrium. This method, introduced by J.S. Langer in 1980s, was stemmed from unstable two-dimensional interface dynamics, and today is probably the most universal and powerful tool to study microstructure dynamics in a regime of extreme loads. This field belongs to one of LANL Grand challenges, specifically one that concerns material science. In short, our advances achieved in the project are expected to empower computational treatment of material dynamics under high strains and stresses.

In summary, the achievements made in the reported project are expected to impact several LANL programs mentioned above.

## References


1. Abanov, A., M. Mineev-Weinstein, and A. Zabrodin. Self-similarity in Laplacian Growth. 2007. *Physica D.* **235**: 62.

2. Mineev-Weinstein, M., M. Putinar, and R. Teodorescu. Random Matrices in 2D, Laplacian Growth, and Operator Theory . 2008. *Journal of Physics, A, Math. Theor. .* **41**: 263001.

3. Khavinson, D., M. Mineev-Weinstein, and M. Putinar. Planar Elliptic Growth. 2009. *Journal of Complex Variables and Operator Theory.* **3** (2): 425.

4. Abanov, A., M. Mineev-Weinstein, and A. Zabrodin. Multi-Cuts Dynamics in Laplacian Growth. 2009. *Physica D (Nonlinear Phenomena).* **238** (No. 17): 1787.

5. Leshchiner, A., M. Thrasher, M. Mineev-Weinstein, and H. L. Swinney. Dynamics of Harmonic Moments in Laplacian Growth. To appear in *To appear in Phys. Rev. E. .*

6. Mineev-Weinstein, M., D. Leshchiner, and I. Gruzberg. Stochastic Laplacian Growth. 2009. *To be submitted to Journal of Statistical Physics.*


## Publications


Abanov, A., M. Mineev-Weinstein, and A. Zabrodin. Self-similarity in Laplacian Growth. 2007. *Physica D.* **235**: 62.

Abanov, A., M. Mineev-Weinstein, and A. Zabrodin. Multi-Cuts Dynamics in Laplacian Growth. 2009. *Physica D (Nonlinear Phenomena).* **238** (No. 17): 1787.

Crowdy, D., M. Mineev-Weinstein, and M. Putinar. Preface. 2009. *Compl. Anal. Oper. Theory.* **3** (2): 331.

Leshchiner, A., M. Thrasher, M. Mineev-Weinstein, and H. L. Swinney. Dynamics of Harmonic Moments in Laplacian Growth. To appear in *Phys. Rev. E.*

Mineev-Weinstein, M., D. Khavinson, and M. Putinar. Planar Elliptic Growth. 2009. *Journal of Complex Variables and Operator Theory.* **3** (2): 425.

Mineev-Weinstein, M., I. Gruzberg, and D. Leshchiner. Stochastic Laplacian Growth. 2009. *To be submitted to Journal of Statistical Physics.*

Mineev-Weinstein, M., M. Putinar, L. Sander, and A. Zabrodin. Preface. 2007. *Physica D.* **235**: vii.

Mineev-Weinstein, M., M. Putinar, and R. Teodorescu. Random Matrices in 2D, Laplacian Growth, and Operator Theory (Review). 2008. *Journal of Physics, A, Math. Theor..* **41**: 263001.

Mineev-Weinstein, M., and A. Yu. Orlov. Harry Dym and KdV equation, contour dynamics and vector fields. 2009. *to be submitted to Communications of Mathematical Physics .*

Mineev-Weinstein, M., and A. Zabrodin. Corrections to Darcy law from the model of complex random matrices. 2009. *to be submitted to Physica D.*

Mineev-Weinstein, M., and V. Kazakov. Matrix model and laplacian growth: unsolved problems. 2009. *The Report to be published.*

# A New Architecture Revolution for Supercomputing

*Zachary K. Baker*
20090508ER

## Abstract

Achieving high performance on petascale computers is difficult without detailed knowledge of the bandwidth, data delay and low-level communication details. This difficulty occurs due to the gap between the end-goal of computer designers and the goals of end-user scientists. A scientist's time is better spent doing science, not struggling with low-level details. The "PetaFlops Router" provides the performance of highly parallel, custom hardware. As well, it allows the user to program in easy-to-use, high-level concepts. The current version provides automatic parallelization and creation of streaming signal processing applications.

## Background and Research Objectives

A scientist's time is better spent doing science, not struggling with low-level programming details. The PetaFlops Router provides the performance of highly parallel, custom hardware, while allowing the user to program in easy-to-use, high-level concepts. Achieving high performance on modern computers is difficult without detailed architectural knowledge. The goals of computer designers and end-user scientists are often at odds. A computer designer is happy to tie together a variety of high-end processors, each with its own strengths. Using these systems requires intimate knowledge of the components. This makes it difficult for anyone other than an expert to achieve maximum performance. The end-user scientist would prefer to not have to learn these system details.

The goal of this effort was to abstract away many of the highly time consuming aspects of hardware and software design. Simultaneously, it will provide improved performance through the use of custom hardware architectures and instruction sets. The combination of these goals will provide custom hardware performance to scientists while maintaining ease of use (Figure 1).

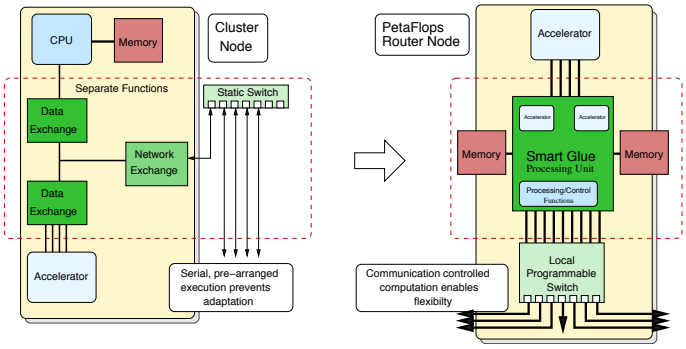


*Figure 1. Traditional cluster supercomputer approach (left) and the PetaFlops Router approach (right). Higher bandwidth network links are more closely attached to processors and memory resources, providing improved performance.*

## Scientific Approach and Accomplishments

The PetaFlops Router is based on Field Programmable Gate Arrays (FPGA), a reconfigurable integrated circuit technology that is widely used in the telecommunications industry. FPGAs provide the performance of custom chips and yet can be optimized for many different classes of applications. By using FPGAs in the system, the system can be optimized through changes of the intra-chip logic. Also, by rerouting the flow of data through the inter-chip network (Figure 2). This change represents a key innovation of the system: the entire computer system can be optimized for an application. Key components of the PetaFlops Router include:

- Field-Programmable Gate Arrays (FPGAs)
- Computation and data-routing

- SmartGlue runtime system
- Automatic extraction of parallelism

- Network crossbars
- Flexible data routing

- External computation accelerators
- Use of FPGA as fast, smart data router

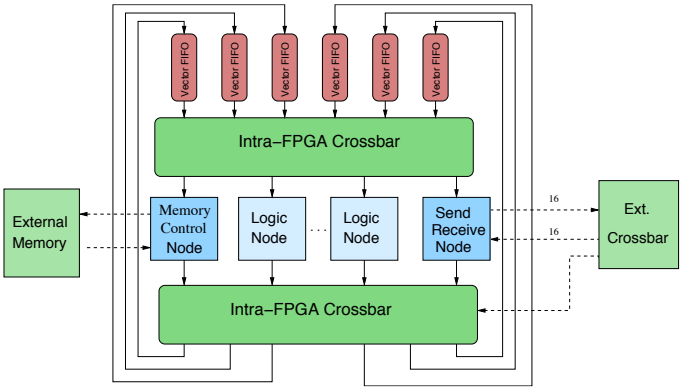


*Figure 2. SmartGlue component composed of crossbar, vector registers, and computational components.*

We have developed the basic PetaFlops Router hardware node design, based on Xilinx FPGA technology (Figure 3). This board consists of a uTCA (a telecom standard) based card with a Xilinx Virtex 5 FX130T combined with the Mindspeed M21141 72x72 crosspoint switch. The Virtex 5 includes external memory and a PCI express endpoint to connect to a coprocessor. Thirty-two fast serial connections are routed to the inputs on the card which will allow local network communication. The remaining serial connections are connected to the uTCA backplane to provide network connection to other nodes within a single chassis.

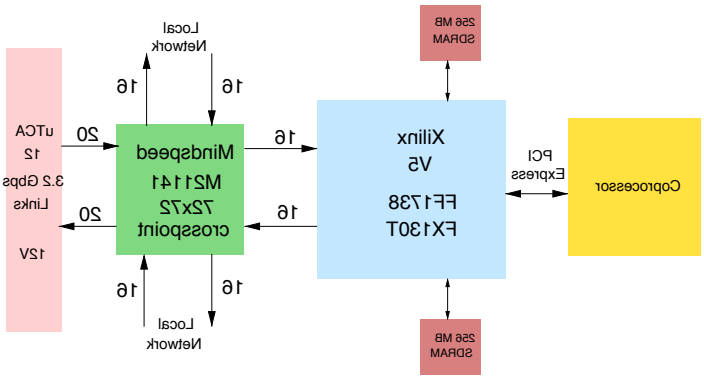


*Figure 3. Current PetaFlops Router Hardware Node Design*

We have acquired two of these nodes (Figure 4). These boards contain the Virtex-5 SmartGlue routers, together with the Mindspeed Analog Crossbar switches, and with 512 MegaBytes of local high-speed memory. The boards arrived at the lab late in the effort, so we were only able to do simple tests of the hardware. Most of our development work was done on a different FPGA system acquired for a previous program. Both FPGAs systems share identical interfaces, so connecting the two systems together should be feasible for building a larger testbed in the future.

*Figure 4. Photograph of PetaFlops Router board.*

**Modeling Effort**

We have developed the elements of a high-level model that will allow the PetaFlops Router to be simulated. Simulation of the entire system will help develop the high-level data-movement and understand the costs of computation. Scaling systems can be difficult despite bandwidth and available routing. The PetaFlops Router requires exploration of different approaches and algorithms to find the best approach with our hardware.

The current models are written in SystemC. SystemC is an open approach to hardware modeling that allows anyone to compile and simulate a design using the SystemC library. SystemC extends C++ software objects to provide different levels of hardware simulation. Standard hardware modeling languages (e.g., VHDL and Verilog) require separate simulators. SystemC is open and can be compiled with standard compilers and run on any system.

Current SystemC models include network components, compute modules and programmable control. These provide the ability to study new operators and gain knowledge about operator synergy. Further effort is needed for local and global data transfer, and memory access. These will allow larger system issues to be explored and evaluated before creating firmware for the hardware components. Models speed up the design process by easing the exploration of different ideas.

**Software Effort**

We have developed a collection of new software support packages for the PetaFlops Router system. This includes a graphical user interface (GUI) for generating a customized instruction set for the system. The GUI simultaneously creates a programming file for the FPGA, instruction set table, and map of operating units. This is a significant: a custom instruction set is provided, customized to one's application. This supports far more sophisticated instructions than a general-purpose processor.

We also produced a custom assembler that converts user programs into a sequence of instructions for the PetaFlops Router. This system is relatively simple compared to a sophisticated compiler. We chose to implement an

assembler with a primitive syntax as it was far easier to develop in the short period of funding available.

**Firmware Effort**

We have developed a single-chip version of the on-chip datarouting network and the automatically negotiated interaction of various computation kernels and vector data storage. This is a foundational part of the SmartGlue system. This is the most time-critical aspect of the system, as these interactions determine how fast data can be switched through the system. The data-switching system is managed by an embedded microcontroller, which also acts as the scheduler for the assembled program code. Significant features of the functional prototype system include:

- "SmartGlue" runtime system running on a single FPGA node, controlled by embedded processor
- Network and vector data storage
- Interprets programs generated by assembler
- Automatic pipelining of streaming operators

The current system provides automatic extraction of parallelism and generation of streaming computation templates. This is based on basic dependency analysis. However, this functionality is very exciting as it can provide better utilization of computational units that a general purpose microprocessor.

Continuing this work to a multi-chip system is a significant R&D challenge. We will then begin to integrate and develop an approach for managing communication across congested links. This is key to developing the system to scales usable for large computations.

**Accelerator Effort**

We are exploring the use of NVIDIA Graphics Processing Units, Achronix Speedster and Tilera TileExpress64 accelerators. Each technology has a particular interest to the PetaFlops Router. NVIDIA GPUs have the appeal of programming in a C-style language, which is easier for developers. However, NVIDIA has proprietary drivers that interpret programs for a particular board. This makes it easy to migrate to new boards as they are released, but makes it difficult for the Router to control directly. The Achronix board is similar to an FPGA in that it is programmed in standard hardware description language (VHDL). However, for certain programs it can run two to three times faster that an FPGA. This is much faster than the 300-400 MHz expected from an FPGA. Using this device as an accelerator is appealing because of the speed advantage and simplicity of interfacing two systems that we explicitly design. The final accelerator system we have explored is the Tilera TileExpress 64 processor, which has 64 integer CPUs that are connected by an on-chip network. Much like GPUs, the Tilera system is programmable in standard C. It supports standard parallel programming models, which means that the parallel version of the code can be run and tested on desktop computers. However, because Tilera only supports floating point via software emulation, the goal of having fast hardware acceleration for floating point kernels is not satisfied.

## Impact on National Missions

The PetaFlops Router can impact two aspects of the national mission, namely supercomputing for advanced modeling and simulation and embedded surveillance and reconnaissance applications. In the near term, smaller instantiations of the system consisting of a few nodes will provide fast development of sophisticated Radio Frequency (RF) applications. The functional demo consists of signal processing kernels similar to what is required for the RF Sensing mission (e.g. Electronics Warfare and Signals Intelligence).

RF Sensing is the national security branch of the much larger commercial field of Wireless Communications. In both of these disciplines the ability to adapt the receiver for both wide and focused area search by using multiple antennas is valuable. The term for such a function is Beamforming or Phased Array. Here, individual sensors outputs are combined much as small waves in an ocean can combine to form very large waves. Many military and commercial systems have used analog adaptive phased array antennas in order to provide enhanced performance.

The PetaFlops Router can run a digital phased array antenna system as an application. A bank of 7 or more antennas each feed separate input ports of the Beamformer application. The PetaFlops Router then processes the digitized signals. Each port must be processed with computationally expensive operations with extensive.

The PetaFlops Router will enable an accelerated integration of the elements that are required to implement the system. These include a 16K integer Fast Fourier Transform (FFT), streaming vector add and multiply units, complex arithmetic cores, and pattern recognition elements. The PetaFlops Router allows development and proofing of these elements more efficiently than a full custom hardware implementation. The Beamformer application is an excellent example of how the PetaFlops Router can be immediately used in high value Global Security missions. We hope to implement the Beamformer in the next round of funding for the PetaFlops Router.

On a longer time scale, with further technology development, the PetaFlops Router will advance supercomputing beyond current capabilities. Understanding how the system will scale to a larger system useful in an HPC context will guide our future design decisions. We expect the Router to demonstrate particularly high performance when data latency and throughput are significant. In a traditional cluster, data bandwidth and latency are computation bottlenecks, however, the PetaFlops Router system provides the following advancements for HPC applications:

- The PetaFlops Router uses FPGAs and co-processors to provide improved bandwidth and compute performance
- PetaFlops Router co-locates network and memory management for increased bandwidth, decreased latency
- High bandwidth analog inputs processed through multi-node distributed computation
- Automatic network adaptation to match application needs
- Custom instruction set optimized to fit the application
- Availability of orders of magnitude more raw compute power for highly parallel applications.

## Publications

Baker, Z. K., T. Bhattacharya, M. Dunham, P. S. Graham, R. Gupta, J. Inman, A. Klein, G. J. Kunde, A. McPherson, M. Stettler, and J. L. Tripp. The PetaFlops Router: An Architecture Revolution for Supercomputing. 2009. In *Symposium on Application Accelerators in High-Performance Computing (SAAHPC'09).* (Urbana, July 25-28, 2009). , p. n/a. Urbana: U. Illinois.

Baker, Z. K., T. Bhattacharya, M. Dunham, P. S. Graham, R. Gupta, J. Inman, A. Klein, G. J. Kunde, A. McPherson, M. Stettler, and J. L. Tripp. The PetaFlops Router: Harnessing FPGAs and Accelerators for High Performance Computing. 2009. In *High Performance Embedded Computing (HPEC 2009).* (Massachusetts, Sept 22-23, 2009). , p. n/a. Lexington: MIT.

# Towards Human Level Artificial Intelligence: A Cortically Inspired Semantic Network Approach to Information Processing and Storage

*Luis Bettencourt*
20080724PRD2

## Introduction

The research goals of this LDRD will be achieved by implementing our best understanding of neural computational primitives - the underlying mechanisms of the brain - on the fastest computers in the world. Unique to our project, all of this will be realized from a computer science/algorithmic perspective different from that of the older neural network researchers of the past. This research is cutting edge in the fact that it is focusing on developing algorithms to synthesize network (graph) structures that compute in a manner similar to natural cortical networks. This research is high risk in that many solutions been proposed in the neural network paradigm of artificial intelligence research with modest results. However, even partial success will be significant for advancing brain understanding and inspiring new application algorithms, and substantial success would be revolutionary. Methods for large-scale graph storage and querying will be developed, methods for multi-relational (semantic) network analysis will be developed, and methods for encoding computational processes within a graph structure will be developed.

## Benefit to National Security Missions

Nuclear nonproliferation and energy security are all challenged by massive volumes of heterogeneous data that overwhelm human analysis. The same is true across the DoD and homeland security missions. Success will advance the areas of complex systems, distributed sensing in natural and social environments, and information science and technology.

## Progress

Upon engaging in this project, it was assumed that the Semantic Web community (an extension of the Web of Data community) had developed the necessary infrastructure and approach to support other forms of knowledge representation and reasoning beyond first-order predicate logic. Thus, given this assumption, what was needed was to extend the assumptions of these designers to account for cortical/connectionist-based knowledge representation and reasoning [1]. Ultimately, this would lead to human-level artificial intelligence as it is known that first-order predicate logic is frail and computationally expensive for problems faced by humans. Unfortunately, the state of the Semantic Web effort has not moved beyond first-order predicate logic [2]. In order to model the process of cognition as seen from the perspective of cognitive and neurobiologist, a new reasoning system would be needed for the Web of Data [3]. This realization brought the project to invite the Non-Axiomatic Reasoning System (NARS) and Logic (NAL) group to present at Los Alamos and various venues in Santa Fe. After a significant review of the landscape and demonstrations, NARS/NAL appears to be the closest logic in existence for modeling human-level conceptual intelligence (while there are means for doing robotics-based AI with NARS/NAL, this is not the goal of the LDRD). What was realized was that NARS/NAL would be feasible to represent in the Web of Data given a parallel-computing environment to execute its simple, massively-parallel reasoning system. After much deliberation, it was realized that if a cortically-inspired model of information processing and storage at the world stage was going to occur, then a completely novel infrastructure for distributed computing on the Web of Data was needed to make the project successful [4]. Providing a distributed process infrastructure to this distributed data structure has begun. The Linked Process effort, currently involves Marko Rodriguez, Herbert Van de Sompel, Ryan Chute, and Stephan Drescher of the Digital Library Research and Prototyping Team at Los Alamos, Peter Neubauer and students of Sweeden's NeoTechnology and OPSJ, Pei Wang of Temple University, and Joshua Shinavier of Rensselaer Polytechnic Institute. The power of this idea has yielded the efforts of many with the LDRD only supporting of Marko and Josh. People involved realize the potential that this will yield not only for this LDRD, but for the future of massive-scale, distributed data management and processing.

Given the implementation of the specification being designed by the Linked Process group, it will them be possible to create a plausible NARS/NAL reasoner and thus, provide cortically-inspired human level artificial intelligence. We expect that both Linked Process and

a Web of Data version of NARS/NAL will be complete when this LDRD postdoctoral project concludes. As it is accomplished, LANL will have made a large impact in this domain.

## Future Work

In a 2001 Scientific America article, Tim Berners-Lee (the inventor of the World Wide Web) defined the Semantic Web as "an extension of the current web in which information is given well-defined meaning, better enabling computers and people to work in cooperation." However, the Semantic Web is more general than this application-specific definition as it is a general-modeling substrate that can be used to model many types of system—conceptual, physical, virtual, etc. This point was made salient in Dr. Rodriguez's doctoral thesis where he developed a new theory for embedding general-purpose computers within this distributed network substrate. Previous to this conceptual advance, the Semantic Web was solely considered a space where the structure of the world could be modeled, not its process.

One of the "hard" problems of modern neuroscience is specifying how the human neocortex computes at the various levels of abstraction (i.e. molecular, cellular, network, etc.). While seemingly a difficult problem, our hypothesis is that the cortical algorithm is not difficult to understand and, ultimately, simulate for the purpose of yielding cortical-based artificial intelligence. It is the area of "cortical computing" that Dr. Rodriguez will tackle during his Postdoctoral work at the Los Alamos National Laboratory. This research goal will be achieved through the abstraction and implementation and integration of neural computational primitives proposed in the neuroscience literature. However, given his area of expertise, all of this will be realized from a computer science/algorithmic perspective different from that of the older neural network researchers of the past or of explicit simulations of neurons and synapses. Working with others at the CNLS, experiments will be conducted with both designed and self-organized large-scale, cortically inspired networks that actively learn patterns in temporally and spatially changing signals and apply them to modern day large-scale graph substrates such as the Semantic Web.

## Conclusion

This research aims at creating a new generation of synthetic computational systems capable of open-ended artificial learning and prediction such that eventually, large-scale artificial cortical networks may match and surpass the reasoning abilities of the human brain. Other expected results include formal methods (both computational and algebraic) for analyzing and creating multi-relational (semantic) graph structures, methods for storing and querying large-scale graph structures, and methods for creating computational primitives that can be represented as a graph.

## References


1. Rumelhart, D., and J. McClelland. Parallel Distributed Processing: Explorations in the Microstructure of Cognition. 1993.

2. Fensel, D., and F. van Harmelen. Unifying reasoning and search to web scale. 2007. *IEEE Internet Computing.* **11** (2): 94.

3. Wang, P.. From inheritance relation to non-axiomatic logic. 1994. *International Journal of Approximate Reasoning.* **11**: 281–319.

4. Rodriguez, M. A.. A Reflection on the Structure and Process of the Web of Data,. 2009. *Bulletin of the American Society for Information Science and Technology.* **35** (6): 38.


## Publications


Ham, M. I., V. Gintautas, M. A. Rodriguez, R. Bennet, C. L. Santa Maria, and L. M. A. Bettencourt. Density-Dependence of Functional Spiking Networks in Vitro. To appear in *Biological Cybernetics.*

Rodrigez, M. A., A. Pepe, and J. Shinavier. The Dilated Triple. 2009. In *Emergent Web Intelligence.* Edited by Chbeir, R., A. Hassanien, A. Abraham, and Y. Badr. , p. 1. Heidelberg: Springer Verlag.

Rodriguez, M. A.. Grammar-Based Random Walkers in Semantic Networks. 2008. *Knowledge-Based Systems.* **21** (7): 727.

Rodriguez, M. A., J. Bollen, and H. Van de Sompel. Automatic Metadata Generation using Associative Networks. 2009. *ACM Transactions on Information Systems* . **27** (2): 1.

Rodriguez, M. A., and A. Pepe. On the Relationship Between the Structural and Socioacademic Communities of a Coauthorship Network. 2008. *Journal of Informetrics.* **2** (3): 195.

Rodriguez, M. A., and J. Geldart. An Evidential Path Logic for Multi-Relational Networks. 2009. *Association for the Advancement of Artificial Intelligence.* **SS-09** (09): 114.

Rodriguez, M. A., and J. Shinavier. Exposing Multi-Relational Networks to Single-Relational Network Analysis Algorithms. To appear in *Journal of Informetrics.*

Srinivasan, R., A. Pepe, and M. A. Rodrigez. A Comparison Between Ethnographic and Clustering-Based Semi-Automated Techniques for Cultural Ontologies. 2009. *Journal of the American Society for Information Science and Technology.* **60** (2): 1.

# Finite State Projection for Accurate Solution of the Master Equation

*Michael E. Wall*
20080730PRD2

## Introduction

Random events are a cornerstone of a variety of subjects, from statistical physics to control theory. They are also central to problems in biology that address cell chemistry, evolution, and studies of infectious disease. Most researchers use the master equation to study such events. Unfortunately, it is difficult to solve for all but the simplest systems.

Dr. Munsky invented a fast way of solving the master equation. He developed the Finite State Projection (FSP) algorithm, which enables one to ignore unimportant contributions to the master equation. The method is having a large impact already.

Still, a big hurdle in applying the FSP remains: many biological systems have millions of interacting components, preventing sufficient simplification of the master equation. The goal of this project is to make the FSP approach work even in these extremely complicated cases. Dr. Munsky is developing methods for further reducing the complexity of the equations by focusing only on the variables that are relevant to answering specific questions. These methods will use control theory and information theory techniques. He will also demonstrate the utility of the FSP approach by applying it to specific biological problems.

## Benefit to National Security Missions

This project will support the DOE mission in Threat Reduction. The tools developed will impact many fields in science, medicine, and industry. They can be applied to problems throughout LANL and DOE in genomics, fluid dynamics, global climate, social networks, disease spread, and material science. Understanding cellular networks is a major stated goal of DOE/OS/BER and multiple NIH institutes.

## Progress

Dr. Munsky has made progress on five tasks related to this project:

**Stochastic model validation for the Pap (pili) epigenetic switch (with Brooke Trinh, David Low, Bruce Braaten and Mustafa Khammash--UCSB)**

This ongoing task introduces a model to predict regulation of pili expression in uropathogenic E. coli. Dr. Munsky inferred model parameters using in vitro Mobility Shift Assays and in vivo Florescence Activated Cell Sorting techniques. The result is highly predictive model, which can now be extended to discover new behaviors in this and similar biological systems.

**Simplicity of Completion Time Distributions for Common Complex Biochemical Processes (With Golan Bel and Ilya Nemenman--CNLS/CCS3)**

Many cellular processes involve a large number of distinct, reversible steps. For example, in kinetic proofreading, cells use serial reactions to precisely construct large protein complexes. In this work, we study the dynamics of such systems and statistically characterize the time required to complete a process. We determined equations for the mean and the variance of the completion time for a kinetic proofreading process, and numerically analyzed more complicated systems. As the system size grows, the completion time can cease to be random or can become exponentially distributed. In other words, the full complex system starts looking like it has a simple transition from one simple behavior to another. We expect the behaviors of many complex cellular processes to simplify in a similar manner, and suggest that cellular behavior might be robust to the details of elementary reactions.

**Specificity and Completion Time Distributions of Biochemical Processes (With Golan Bel and Ilya Nemenman--CNLS/CCS3)**

In the previous task we examined a system of serial reactions. In this task we considered a branched system that leads to two possible outcomes. We determined equations not only for the completion time distribution but also for the tendency of the system to follow the desired branch. We also showed that the full system

behaves like a simple three-point process. Our model paves the way for understanding the interplay between specificity and completion times as well as testing the validity of different models for biological systems.

**Identification of Gene Regulatory Networks Based Upon Stochastic Gene Expression and Flow Cytometry Measurements (with Brooke Trinh, David Low, Mustafa Khammash--UCSB and Babetta Marrone, B9-LANL).**

We showed that randomness can be exploited to reverse engineer genetic regulatory networks. Cellular noise changes as it propagates through a molecular network, carrying with it a distinctive fingerprint with information about the structure of the network. We demonstrate that analysis of noise can enable identification of all network parameters, including those that may otherwise be difficult to measure. Our approach is general and can be used to identify other cellular networks.

**Identification of Gene Regulatory Networks Based Upon Stochastic Gene Expression and Fluorescence in Situ Hybridization (FISH) Measurements (with Gregor Neuert (MIT) Alex van Oudenaarden (MIT) and Mustafa Khammash (UCSB)).**

Investigators at MIT have used a newly developed method to count the number of mRNA molecules in individual yeast cells exposed to different environmental conditions. We are applying FSP to the data to identify a model of gene regulation for this system.

## Future Work

The Finite State Projection (FSP) algorithm was developed to enable the difficult task of analyzing noisy cellular systems. Where previous methods simulate the random behavior of an individual cell, the FSP directly describes how the statistics of a population of cells changes over time and better matches the available experimental data. Dr. Munsky will continue to extend the FSP approach to efficiently and accurately analyze noisy cellular systems that are beyond other approaches. Several publications along these lines are anticipated in the final year of his postdoc. Importantly, the FSP method is beginning to have a real impact on experimental studies of cellular systems; he will therefore focus on increasing collaboration with experimental labs and on leading his own experimental studies in collaboration with B-div. This work is the subject of a revised R21 proposal that might enable continuation of this work at LANL beyond the term of his postdoc.

## Conclusion

Dr. Munsky invented the Finite State Projection approach for analysis of noisy systems. This approach now enables analysis of systems that are too complex for other approaches. It is being applied to analyze experimental data from noisy cellular systems and is making an impact in biology.

## Publications


Bel, G., B. Munsky, and I. Nemenman. Simplicity of completion time distributions for common complex biochemical processes. To appear in *Physical Biology.*

Khammash, M., and B. Munsky. Stochastic gene expression: modeling, analysis, and identification. To appear in *The control handbook.*

Munsky, B., B. Trinh, and M. Khammash. Listening to the noise: random fluctuations reveal gene network parameters. 2009. *Molecular Systems Biology.* **5** (318): .

Munsky, B., I. Nemenman, and G. Bel. Specificity and completion time distributions of biochemical processes. To appear in *Journal of Chemical Physics.*

Munsky, B., and M. Khammash. Transient analysis of stochastic switches and trajectories with applications to gene regulatory networks. 2008. *IET Systems Biology.* **2**: 323.

Munsky, B., and M. Khammash. Using noise transmission properties to identify stochastic gene regulatory networks. 2008. In *46th IEEE Conference on Decision and Control.* (Cancun, Mexico, Dec, 2008). , p. 768. Cancun: IEEE.

# Statistical Physics of Optimization

*Michael Chertkov*
20080787PRD3

## Introduction

In many areas of science, from computer science and information theory to engineering and statistical physics, as well as in biology or social sciences, optimization problems are widespread and important. Optimization typically involves a large number of variables, e.g. particles, agents, cells or nodes, and a cost function depending on these variables, such as energy, measure of risk or expenses. In this project we address the following fundamental questions that concern general combinatorial optimization setting: How to recognize if an optimization problem is typically hard and what are main reasons for this? How to find efficiently an approximate solution of a hard problem? Answering these questions is crucial for developing new algorithms for optimization problems.

Our research combines physics-based ideas with standard optimization methods and with learning and inference methods from artificial intelligence. The common denominator in our work is the use of message passing approach, such as belief propagation, to tackle both the theoretical and algorithmic questions. In statistical physics the message passing approach translates into the cavity method that is used to study disordered systems with complex energy landscape.

## Benefit to National Security Missions

Our goal is to use statistical physics models to predict, understand and improve communication mechanisms. Our methods will enable communication protocols required to work with yet unseen amounts of data. This project will support DOE mission in National Security by enhancing understanding of new principles for Information Communication and Storage.

## Progress

In [1] and [2] we studied the planted ensemble of constraint satisfaction problems (CSPs). CSPs are benchmarks of hard optimization problems. Statistical analysis of random formulas of CSPs sheds light on the origin of the algorithmic hardness and helped understanding performance of heuristic algorithms. We studied constraint satisfaction problems on the so-called 'planted' random ensemble, where the formula is chosen in such a way that a certain predefined configuration of variables is satisfying that formula. We showed that for a certain large class of problems many of the properties of the usual random ensemble are quantitatively identical in the planted random ensemble. We described the structural phase transitions, and the easy/hard/easy pattern in the average computational complexity. The fact that the planted configuration is a equilibrium configuration may also be used to enhance numerical simulations of the random ensemble in these intrinsically hard to equilibrate systems.

Algorithmic hardness of many optimization problems is caused by their glassy nature, i.e. the cost function landscape has many local minima and many basins of attraction - states. The cavity method is a very powerful tool to describe properties of these states in random optimization problems. In [3] we generalized the cavity method to describe the separate states in more detail and follow their behavior when an external parameter (e.g. temperature) is changed. Our generalization describes analytically the behavior of slow simulated annealing and other similar algorithms. Figure 1 illustrates the study.

In [4] we suggested and validated an approach to infer parameters of the equations of motion without reconstructing individual trajectories (Figure 2). We show that the problem can be rephrased as a maximization of a partition function of a matching (linear assignment) problem. We use the belief propagation algorithm to approximate this partition function and its maximum. We illustrate the precision of the method in the regime of high densities (or low image frequency) where reconstruction of the individual trajectories is no longer possible. The method is easily generalizable to problems of non-interacting objects, where the laws of motion are known or are to be tested, but their parameters are unknown.

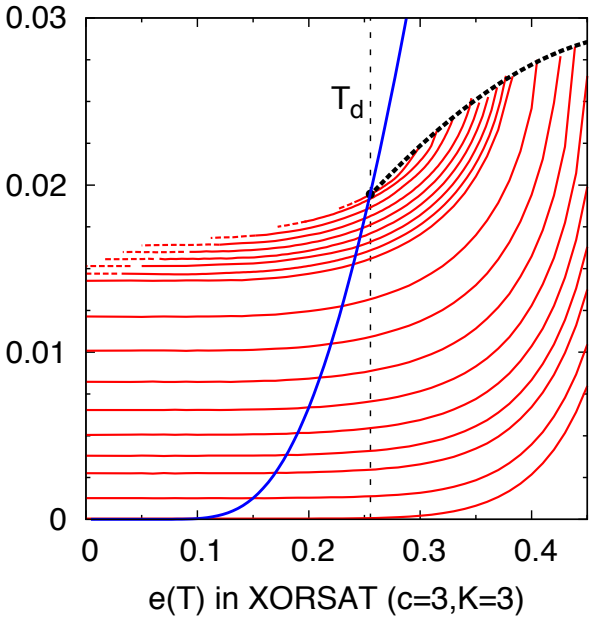


*Figure 1. Red lines depict the evolution of different basins of attraction in the landscape (states) in a mean field glassy model with Ising spins interacting via random 3-body interactions, the lattice being a random graph of coordination fixed to 3. Energy of different states is plotted as a function of the temperature. The blue line corresponds to the thermodynamic energy of the system at a given temperature and the vertical line depicts the glass phase transition in the system.*

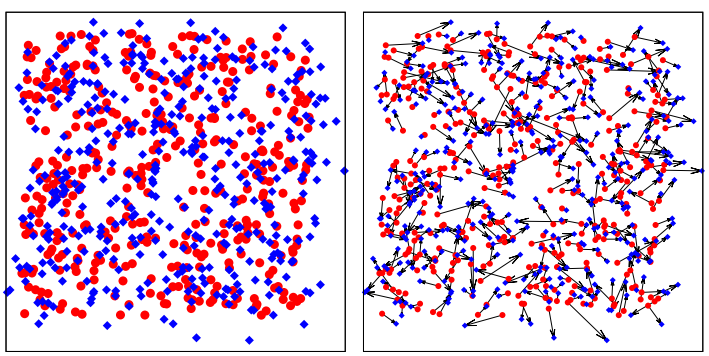

*Figure 2. An example of particle tracking, with N=400 particles moving from their original positions (red circles) to new one (blue diamonds). The particles are transported by a turbulent fluid flow. The parameters describing the local stretching, shear, vorticity and diffusivity of the flow are a*=0.28, b*=0.54, c*=0.24 and T*=1.05. The figure on the right shows the actual motion of each particle. Evidently, the simple criterion of particle proximity fails to pick the actual trajectories, and the mapping of the particles between the two images is intrinsically uncertain. Nevertheless, the inference algorithms we developed rapidly obtain excellent predictions a=0.32, b=0.55, c=0.19 and T=1.00 for the parameters of the flow.*

In [5] we developed a smart grid model with redundancy and renewables. We consider the power grid with M generators and N consumption units. Each consumer demand is drawn from a predefined distribution, thus mimicking instant uncertainty in the load. Each generator has a maximum power cap. A generator is not overloaded if the sum of loads of consumers connected to the generator does not exceed the power cap. In the standard grid each consumer is connected only to its designated generator, while we consider a more general organization of the grid when a consumer selects one generator depending on the load from a pre-defined consumer-dependent and sufficiently small set of generators which can all serve the load. We show that the redundancy allows significant expansion of the domain of parameters where the probability for a generator overload is asymptotically zero. Our results also translate into an algorithmically efficient and distributed message-passing control scheme achieving the asymptotically optimal selection of loaded links. In the same setting we also discussed the integration of fluctuating renewable generation in [6]. We explored the capacity of the renewable generation by determining the level of "firm" generation capacity that can be displaced for different levels of redundancy.

## Future Work

We plan to extend our studies of the particle tracking by including spatial inhomogeneity and bringing our algorithm to practical implementation in real particle tracking experiments. We also plan to work on other applications relevant for the future smart grid. We will extend our model with additional lines to the case when the final structure of power line is not a tree and hence Kirchhoff's laws pose additional constraints on our solution. Another smart-grid related problem we plan to address is optimization of a feeder line with high penetration of renewable generation. In the present grid the units producing renewable generation inject only real power into the network, however, future inverters will be able to inject also reactive power into the network. This additional degree of freedom can be used to enhance stability of the voltage and frequency. We plan to study this system and develop efficient control algorithms.

We also plan to extend the range of methods and problems we study. In particular, we want to use our recent understanding of static optimization problems to the analysis of more challenging dynamical problems that arise in adapting or competing environments. For this purpose we will study problems in game theory, in particular generalizations of the ideal rationality notion of Nash equilibrium on graphical games to the case of finite rationality of the agents. Another direction is to include global constraints in the methods of message passing. An example of application is the graph bisection problem, important in load balancing in parallel computing. We will develop a message-passing algorithm for the graph

partitioning problem. This approach can be used to estimate the correlation between nodes and hence used within today's best heuristic algorithms.

## Conclusion

We apply concepts from the statistical physics of disordered systems to problems of computer science, information theory and artificial intelligence. Insights coming from models and methods of statistical physics are fruitful in these domains and bring novel predictions, understanding and practical results. Our work concentrates both on development of theoretical methods and applying new methods to practical problems. The first is illustrated in our work on planted random ensemble and the study of energy landscape of hard optimization problem, the second in our work on particle tracking and the smart grid. We plan to continue this line of research, some problems we want to study in detail in the next year is feeder line optimization in a smart grid, message passing approach to the graph partitioning problem, and statistical physics approach to game theory of agents with bounded rationality.

## References


1. Krzakala, F., and L. Zdeborova. Hiding Quiet Solutions in Random Constraint Satisfaction Problems. 2009. *Physical Review Letters.* **1-2**: 238701.

2. Zdeborova, L., and F. Krzakala. Quiet Planting in the Locked Constraint Satisfaction Problems. *Physical Review Letters.*

3. Krzakala, F., and L. Zdeborova. Following Gibbs States -- The Energy Landscape of Mean Field Glassy Systems. *Physical Review.*

4. Chertkov, M., L. Kroc, F. Krzakala, L. Zdeborova, and M. Vergassola. Tracking particles by passing messages between images. *PNAS.*

5. Zdeborova, L., A. Decelle, and M. Chertkov. Message Passing for Optimization and Control of Power Grid: Toy Model of Distribution with Ancillary Lines. 2009. *Physical Review E.* **80**: 046112.

6. Zdeborova, L., S. Backhaus, and M. Chertkov. Message Passing for Integrating and Assessing Renewable Generation in a Redundant Power Grid. To appear in *HICSS 43.* (Kaui, 5-8 Jan. 2010).


## Publications


Chertkov, M., L. Kroc, F. Krzakala, M. Vergassola, and L. Zdeborova. Tracking particles by passing messages between images. *PNAS.*

Krzakala, F., and L. Zdeborova. Hiding Quiet Solutions in Random Constraint Satisfaction Problems. 2009. *Physical Review Letters.* **102**: 238701.

Krzakala, F., and L. Zdeborova. Following Gibbs States -- The Energy Landscape of Mean Field Glassy Systems. *Physical Review.*

Zdeborova, L., A. Decelle, and M. Chertkov. Message Passing for Optimization and Control of Power Grid: Toy Model of Distribution with Ancillary Lines. 2009. *Physical Review E.* **80**: 046112.

Zdeborova, L., S. Backhaus, and M. Chertkov. Message Passing for Integrating and Assessing Renewable Generation in a Redundant Power Grid. To appear in *HICSS 43.* (Kaui, 5-8 Jan. 2010).

Zdeborova, L., and F. Krzakala. Quiet Planting in the Locked Constraint Satisfaction Problems. *Physical Review Letters.*

# Multiscale Variational Approaches to Markov Random Fields

*Michael Chertkov*
20090516PRD1

## Introduction

Graphical models, also known as Bayesian networks or Markov random fields, are statistical models for complex systems of random variables represented as a graph. The nodes of this graph correspond to random variables while its edges denote statistical interactions among those variables. Graphical models have now come to play a central role in many computational fields such as image restoration, computer vision, information theory, statistical signal processing in oceanography and seismology and biological applications. However, optimal inference and estimation in these models is generally intractable for very large problems. This has driven research and development of principled yet tractable approaches to approximate inference for this rich class of models. These approaches typically involve a distributed message-passing algorithm that serves to propagate information throughout the graph. The performance of these method, however, often suffers in graphical models, which exhibit strong long-range correlations. Handling such situations is precisely the goal of multi-scale methods such as the renormalization group method of statistical physics or the multi-grid method for solving large-scale linear systems. It is the aim of this project to develop a new class of algorithms that combine modern advances in approximate inference and appropriate multi-scale algorithms inspired mainly by the renormalization group method of statistical physics. Our basic strategy is to first consider equivalent reformulation of the inference problem as a multi-scale model by defining an equivalent graphical model depended on an extended set of variables including new auxiliary variables that can be used to represent large-scale interactions of the model. Then, recently developed variational methods can be applied in this extended model where the new auxiliary variables provide additional degrees of freedom to obtain a more accurate solution.

## Benefit to National Security Missions

This project will support the DOE mission in Office of Science by enhancing our understanding of Inference and Optimization Techniques. Our multi-scale approach is relevant to long-range correlations and non-local measurements such as seismic or gravity inversion in geophysics, tomography, and radiography of all types, with several national security applications.

## Progress

Our work thus far can be split into two areas: (1) advances in understanding of the belief propagation method in Gaussian and binary graphical models and improvements/corrections to this algorithm; and (2) new variational approaches to approximate inference in graphical models inspired by approaches such as Kadanoff's "bond moving" renormalization group method in statistical mechanics. We discuss these two areas below.

### Gaussian Belief Propagation

A Gaussian graphical model is a graphical model in which the joint distribution of all variables is Gaussian. Such models are specified by a sparse information matrix, which is the inverse of the covariance matrix. Inference in this model basically reduces to computing the determinant or the inverse of this information matrix. Belief propagation may be adapted to this problem to provide a fast, distributed message-passing algorithm to approximate the determinant or certain elements of the covariance matrix (e.g. variances of each variable). We have recently developed a deeper graphical understanding of this method [1]. Specifically, we have shown that the determinant is equivalent to computing a product over all orbits (closed, cyclic walks) in the graph and that belief propagation computes a particular subset of these orbits. This is useful to characterize the accuracy of belief propagation and also to compute corrections based on the missing orbits of the graph. In particular, we developed a method to efficiently compute all orbits up to a given length in certain sparse graphs such as grids which allows one to compute the determinant to any given accuracy with computational complexity growing only linearly in the number of variables. We have also developed a method for fixing convergence of Gaussian belief propagation in graphical models where belief propagation is unstable [2]. This

involves using a modified model (in which the algorithm is stable) as a preconditioner of a simple iterative method to solve for the correct estimate in the original (unstable) problem.

**Extension to Generalized Belief Propagation**
We have extended this work to interpret generalized belief propagation in the Gaussian model [3]. Generalized belief propagation (developed by Yedidia, Freeman and Weiss) is based on a collection of larger regions of the graph. We have found that, depending on how these regions are chosen, this may lead to over-counting of orbits in the Gaussian case and can actually degrade the quality of approximation or cause the algorithm to become unstable. However, If the regions are chosen properly, so as to avoid over-counting of orbits, then generalized belief propagation can successfully capture a larger subset of orbits of the graph, and thereby leads to improved inference in the Gaussian model.

*Extension to Binary Graphical Models.* More recently, we have begun to apply many of these methods developed for Gaussian graphical models to analyze belief propagation in the context of graphical models having binary variables (e.g. where each node's variable has two states such as {0,1} to denote "bits" in information theory or {-1,+1} to denote "spins" in statistical physics). This is based on earlier works on planar graphs where several methods have been developed to reduce inference in these models to computing either a determinant (Kac, Ward; Feynman; Sherman) or a Pfaffian (Kasteleyn; Fisher), both of which can be computed using Gaussian elimination. In fact, the Kac-Ward method was shown by Feynman and Sherman to be equivalent to evaluating a signed, non-backtracking orbit-product of the graphical model. Although these methods are only valid in planar graphical models, our recent work has shown that these concepts are nonetheless relevant to analyze belief propagation in general (non-planar) binary-variable models. The key idea is to reformulate BP as inference in a planar cover of the graph (similar to the usual "computation tree" interpretation of belief propagation). By applying those earlier methods for planar graphs to this planar cover representation of binary BP, we essentially obtain a "Gaussian" representation of binary BP. We are currently exploring the implications of this new view of belief propagation in binary variable models and expect it to yield information about the convergence and error properties of binary BP.

**Variational Renormalization-Group Method**
Kadanoff introduced a method called bond- moving for theoretical analysis of critical phenomena in lattice models of statistical mechanics. This involves iteratively coarse-graining to compute upper-bounds to the free energy of the model. First, one modifies the model by moving some interactions of the lattice to parallel edges so as to produce a sparser lattice model with some interactions set to zero and others being made stronger. Kadanoff shows that this operation can only increase the free energy. Next, one performs decimation in this thinned model so as to produce a coarse-grained model on a sub-sampled lattice. One then analyzes the effect of iterating this coarse-graining operation to study critical phenomena of the model. We have shown that Kadanoff's method can be reinterpreted as an instance of the recently developed method of convex-decomposition of graphical models. This framework, pioneered by Martin Wainwright, allows approximation of the intractable model in terms of tractable models defined on sub-graphs (such as spanning trees of the graph). In our new interpretation of Kadanoff's method, one performs this relaxation to more tractable graphs in stages rather than all at once: at each stage the lattice is approximated as a convex combination of models defined on coarser lattices. This new view of Kadanoff's method actually allows us to generalize his approach to inhomogeneous lattice models, or even to general graphical models defined on other graph structures beside lattices. In the most general formulation of the method, which we call variational decimation, we allow for elimination of one variable at a time with each elimination step being following by a convex relaxation step to upper-bound the free energy. We find that this leads to a global convex optimization problem that is tractable to solve using modern methods for convex optimization.

## Future Work
We will develop a new class of approximate inference methods which blend recently developed variational-combinatorial approaches from the graphical modeling literature with a multi-scale approach inspired by renormalization group theory in statistical physics. Inference in the graphical models can be reduced to computation of the log-partition function, also known as the cumulant generating function in statistics. Hence, we will focus our efforts on developing a multi-scale variational method to approximate the log-partition function. This will combine three key elements: (1) combinatorial methods to decompose the log-partition function as a sum of interactions defined on subregions of varying size, (2) a multi-scale method to approximate complex multi-variable interactions from a coarse-scale representation of the field, and (3) variational methods to improve the quality of approximation by optimizing over all reparameterizations of the model. This approach is similar to multi-grid methods in linear algebra, but differs in that we also address non-linear models and pose a single, global optimization criterion based on "re-summing'' effects across multiple scales.

## Conclusion
It is expected that by combining the multi-scale method with modern computational heuristics for graphical models, such as belief propagation and other variational methods, we can achieve improved performance (both

better accuracy and faster convergence of distributed iterative algorithms) in those most challenging applications where current methods either fail or are inaccurate. This will then be an important advance for solving a wide range of challenging computational problems in science and engineering.

## References


1. Johnson, J., V. Chernyak, and M. Chertkov. Orbit-Product Representation and Correction of Gaussian Belief Propagation. To appear in *International Conference on Machine Learning (ICML).* (Montreal, June 2009).

2. Johnson, J., D. Bickson, and D. Dolev. Fixing Convergence of Gaussian Belief Propagation. To appear in *International Symposium on Information Theory (ISIT).* (Seoul, June 2009).

3. Johnson, J.. Orbit-Product Interpretation of (Generalized) Gaussian Belief Propagation. 2009. *Presented at the Physics of Algorithms Workshop. Santa Fe, NM, USA. September, 2009.*


## Publications


Johnson, J., D. Bickson, and D. Dalev. Fixing Convergence of Gaussian Belief Propagation. To appear in *International Symposium on Information Theory (ISIT).* (Seoul, June 2009).

Johnson, J., V. Chernyak, and M. Chertkov. Orbit-Product Representation and Correction of Gaussian Belief Propagation. To appear in *International Conference on Machine Learning (ICML).* (Montreal, June 2009).

# Quantum Information Processing: Capabilities and Limitations

*Robert E. Ecke*
20090520PRD2

## Introduction

Controlling quantum states is an exciting possibility for engineering and computer science. Because quantum systems are hard to simulate on conventional computers, computers that use quantum coherence should be more powerful than their usual counterparts. For example, fast quantum algorithms exist for factoring numbers, for algebraic and optimization problems, and for simulating physical systems. Quantum noise is an obstacle for building a quantum computer. One way to fight noise is error correction. The quantum capacity of a noisy process is the amount of quantum data that can be protected from many transmissions affected by the noise. Classical capacity is defined similarly. Calculating these capacities from a description of the noise is an open problem. Another proposal to fight noise tries to build materials with topological order, as they are believed to have noise-resistant excitations that could be used to build a quantum computer. Topological order appears in the quantum Hall effect and may play a role in other materials such as high-temperature superconductors. Jon Yard will determine the quantum and classical capacities for practical noise models and will seek better theoretical understanding of quantum capacity. He will use quantum information concepts he has developed to study physical systems with topological order and how they can be used to protect quantum information. He will find new algorithms for solving hard problems on a quantum computer and will build mathematical tools to determine the ultimate power of quantum computation.

## Benefit to National Security Missions

Understanding how quantum information processing can promote, or jeopardize, security, supports Threat Reduction. Quantum information helps understand properties of matter, such as superconductivity, bearing on materials and device design for the Energy and Office of Science missions. Long-term leadership in cutting-edge computation supports all Laboratory missions.

## Progress

Jon Yard published a paper this year in IEEE Transactions on Information Theory, with Igor Devetak from the University of Southern California, containing the mathematical details of his previous work that describes quantum correlations between many systems. He is exploring connections between this result and a known measure of topological order known as topological entropy. Together with Matt Hastings, who is formerly from Los Alamos and is now at Microsoft Research, he has identified one such connection by determining how hard it is to build a topologically ordered state with a quantum computer. He has also found another interpretation of the topological entropy as the amount of quantum information needed to move parts of a topologically ordered state between different configurations. For this, he is generalizing a certain technical tool used in information theory, so that it can apply to the sort of excitations that happen in topologically ordered systems. He also continues his research on channel capacities by building on his earlier result with Graeme Smith from IBM Research Laboratory, which was published in Science in 2008. This work showed that there are pairs of quantum channels that are too noisy to be used alone for quantum communication, but that can nevertheless be useful together (Figure 1). He gave several talks on this result during the past fiscal year at the Canadian Mathematical Society meeting, at the Young Researchers Conference (Perimeter Institute), at the Information Theory and Applications Workshop (U.C. San Diego) and at the SQuint Workshop. He will also be awarded the prestigious Pat Goldberg Memorial Best Paper Award for this work, which is given to the best scientific papers each year from within all of IBM Research. He has continued working with Smith to determine why quantum channels can be more useful together. He has found that this is because quantum noise becomes correlated when certain types of quantum data are input. Besides making this idea more precise, he is trying to use it to develop better quantum codes. Finally, with collaborators Leonid Gurvits (from Los Alamos) and Cris Moore (from the University of New Mexico and

the Santa Fe Institute), Yard has been using tools from geometry, mathematics, and the study of symmetry to determine the power of classical and quantum computers.

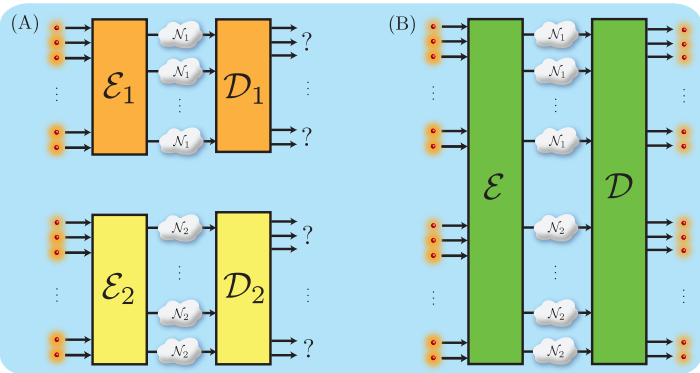


*Figure 1. Two quantum channels can be more useful together than apart.*

## Future Work

Jon Yard's Science paper showed that quantum capacity could be much larger than expected for some types of noise, and perhaps should be replaced with a more general concept. This suggests that a generalization of channel capacity describing how channels combine is needed. Yard will work toward developing such a generalization. He will also determine capacities for practical noise models. He will also continue work on relating his description of quantum correlations to the topological entropy. Yard will develop new algorithms for solving hard problems on a quantum computer. These include computing topological invariants, such as whether a knot can be untied without cutting, implementing Fourier transforms over new types of groups, and simulating physical systems. He will also find ways to efficiently perform certain measurements with a quantum computer, leading to practical coding schemes and providing key subroutines for classes of quantum algorithms.

## Conclusion

Determining the quantum capacity of quantum channels will help in developing designs for reliable quantum computers and in improving quantum methods for secret key distribution. Yard's work on classical capacity could provide methods for achieving higher data rates in existing free-space and fiber optical networks. The algorithms he will design will help us understand whether and how one might design public-key cryptographic systems (e.g. for e-commerce, banking, and authenticated digital communication) resistant to quantum code-breaking. New algorithms, and theoretical concepts form quantum information, could help understand the properties of physical systems, for example, materials properties important in energy efficiency engineering.

## Publications

Yard, J., and I. Devetak. Optimal quantum source coding with quantum side information at the encoder and decoder. 2009. *IEEE Transactions on Information Theory.* **55** (11): 5339.

# Self-Organizing Wireless Ad-Hoc and Sensor Networks with Functional Guarantees

*Stephan J. Eidenbenz*
20061624PRD4

## Abstract

In this work, we investigated the connectivity, coverage, and self-organization of wireless ad hoc and sensor networks. While a routing protocol for efficient data dissemination was also investigated, the focus was mainly on the design and impact of mobility on the topology, connectivity, security, and event detection capability of wireless sensor networks.

## Background and Research Objectives

Wireless sensor networks have found various application venues in environmental monitoring, health monitoring, target tracking in hostile situations, etc. Especially, in the case of monitoring physically inaccessible or dangerous areas for humans to enter, such as wildfire tracking, glacier or volcano monitoring, liveliness detection in emergencies or hazardous material tracking, use of wireless sensor networks is expected to increase tremendously. Due to the inaccessibility of the geographical areas in these applications, the sensor nodes either need to be dropped forming a random static network or mobile robots equipped with sensors are needed to be deployed.

## Scientific Approach and Accomplishments

First, a topology-dependent mobility model was proposed to improve the connectivity of a static wireless network overlaid by a small-size mobile network. The model took into account the degree of the nodes in the network and it is assumed that a mobile node moves toward higher degree nodes with a higher probability. The performance of the model was studied in the presence of node failures and it was shown that ingesting a few number of mobile nodes over the wireless network is very beneficial and the deployed network can continue to operate even with more than 30% node failure.

Next, the impact of mobility on the security of a hybrid (i.e., static and mobile) and pure mobile wireless sensor network was studied. With the emergence of computer worms that can spread over air interfaces, wireless ad hoc and sensor networks can be vulnerable to node compromises even if the deployed network is not connected to the backbone. Depending on the physical topology of the wireless network, even a single infected node can compromise the whole network. It is shown that the epidemic spread threshold and size depend on the physical topology of the underlying wireless network as well as the mobility model employed by the infected mobile nodes. More specifically, results showed that in a fully-connected wireless network targeted attacks are more effective, whereas for a random topology random attacks can be sufficient to compromise the whole network.

Finally, the impact of mobility on the event detection performance of wireless networks was studied. If the event to be detected by the sensor network is of time-critical nature, the coverage of the network should be sufficiently high to be able to respond to the detected event in a timely manner; such as wildfire monitoring or liveliness detection under rubble in case of an earthquake, where the emergency personnel work against the clock. In such cases, using a mobile sensor network would be highly beneficial both in terms of event detection and utilization of the available system resources. To this end, a coverage-based, cooperative mobility model was proposed to improve event coverage in wireless sensor networks without prior knowledge of the physical topology and by using only local topology information. An empirical study was conducted to test the performance of the proposed model, where a finite-duration, stationary (such as a live body under rubble) or mobile event (such as a moving target) is assumed to occur at a random location in the geographical area

to be monitored. It was shown that the coverage-based mobility model consistently results in a better performance than the other mobility models and the desired event detection probability could be achieved by the minimum number of nodes estimated by the analysis.

## Impact on National Missions

The work supports the development of smart systems of miniature deployed sensors, with applications to environmental monitoring, urban warfare, assessing the status of safeguarded nuclear facilities, and border defenses, to name just a few of the national security applications. As a result of Evsen's work, we have a better understanding of protocol behavior in sensor networks.

## Publications


Yanmaz, E.. Mobility, Failure, and Self-organization in Wireless Networks. 2007. *Los Alamos National Laboratory.*

Yanmaz, E.. Impact of Topology-dependent and independent Mobility Models on the Connectivity of Wireless Networks. To appear in *IEEE Sarnoff Symposium, 2008.* (Princeton, NJ, March 30 - April 1, 2008).

Yanmaz, E.. Impact of Mobility Pattern on Epidemic Propagation in Wireless Networks. To appear in *IEEE International Symposium on Personal, Indoor and Mobile Radio Communications (PIMRC), 2008.* (Cannes, France, 15 - 18 September 2008).

Yanmaz, E., and T. K. Karrels. A Multi-tracking Wireless Ad hoc Routing Protocol. To appear in *IEEE International Wireless Communications and Mobile Computing Conference (IWCMC), 2008.* (Crete Island, Greece, 6-8 August 20008).

Yanmaz, E., and T. Karrels. Routing Protocols in Wireless Ad hoc Networks. 2007. *Los Alamos National Laboratory.*

# Physics

LABORATORY DIRECTED RESEARCH AND DEVELOPMENT

# Development of a Magnetically Driven Target for Thermo-Nuclear Burn Studies (*U)

*Robert G. Watt*
20070518DR

## Introduction

This LDRD project is developing a magnetically driven cylindrical confinement system for the creation of a small region of material at extreme density and temperature. Using a low cost multi-MA electrical current source, an aluminum cylinder will be driven radially inward until it impacts on a series of nested, less massive gold shells whose purpose is to provide a very high velocity innermost gold shell. The velocity of this last shell will be at a level where further impact on an object in the center will produce a region in which material conditions are sufficient for many types of physics studies not currently possible in the laboratory. The system being developed in this LDRD project has a broad range of potential applications. It utilizes the fact that the final velocity of a small mass impacted by a larger mass can exceed the impact velocity by as much as a factor of two in a single collision. It is possible to use several sequential collisions to produce an object moving much faster than the original source object. In a cylindrical geometry, this process can use an aluminum shell imploding at several km/sec, using multiple cylindrical collisions, and produce a gold shell imploding at a velocity in excess of 200 km/sec. In addition to creating a high energy density platform for boost physics studies in the central region of the final gold shell, such a system provides a cylindrical configuration for the study of nuclear fusion. The conditions achieved would be similar to those created in a spherical capsule at the National Ignition Facility under the Inertial Confinement Fusion program, and could provide an inexpensive complement to the study of fusion at large laser facilities.

## Benefit to National Security Missions

The tie to the nation's energy needs lies in the application of the system to studies of ICF fusion as an alternative tool in the national grand challenge of ignition. The tie to weapons physics is classified, and is therefore in the vault

## Progress

Following a midterm review in May 2008, this LDRD project made a switch from being heavily computation- and theory- oriented studying the feasibility of magnetically driven multi-shell cylindrical implosions for stably attaining very high velocities, over to design and execution of proof of concept experiments. The resulting design of a 25-35 MA cylindrical multi-shell implosion system was first fielded in August 2009 (shot MS-0). MS-0 utilized an high explosive pulsed power (HEPP) magnetic flux compression generator (FCG) to drive 36 MA into a static load to test the current source and load delivery systems. The FCG uses a coaxial metal transmission line with inner and outer conductors through which a 3 MA seed current ($I_{seed}$) flows to establish the initial magnetic flux in the void between conductors. By explosively reducing the void volume, the magnetic flux is compressed to a much higher value. This causes the generator current to increase from $I_{seed}$ up a peak current equal to $I_{seed} * \ln((R_1-R_s)/(R_2-R_s))$, where $R_s$ is the inside radius of the outer conductor, $R_2$ is the final outer radius of the inner conductor, and $R_1$ is the initial radius of the inner conductor before the high explosive inside it causes it to expand outward. This ratio reached approximately 60 in MS-0, resulting in a current increase from 3.3 MA up to 36 MA. The 54" long, 18" diameter "Ranchero" FCG used had unique active switching. One switch isolated the load region from the FCG during the time period when the generator was being seeded with its initial magnetic flux. (A seed current circuit in parallel with the load circuit feeds this flux.) A second set of switches removed the seed current circuit at the same time the load was connected to the generator. This eliminates an energy loss that would reduce the efficiency of energy transfer to the load. The initial load isolation removes a potentially deleterious current from running through an imploding liner prematurely. Such isolation is needed to insure the best integrity of the liner at the start of the main drive current pulse and the most optimal final implosion of the liner. This first test verified the successful operation of the drive system. Figure 1 shows a cutaway model of the entire system used in MS-0. Figure 2 shows an overlay of the generator current (black curve) and the load current (red curve) which will drive the imploding liner on subsequent

shots, showing successful load switching at ~ 90 us.

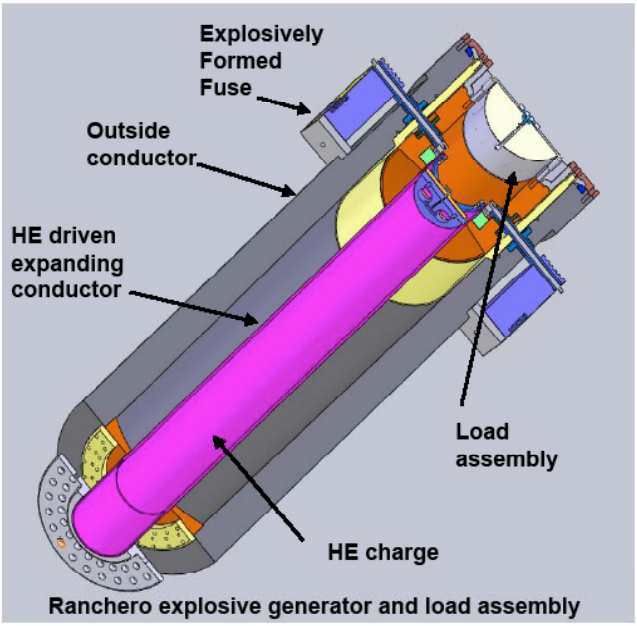


*Figure 1. Cutaway model view of the Ranchero generator and load assembly used during the MS-1 system test.*

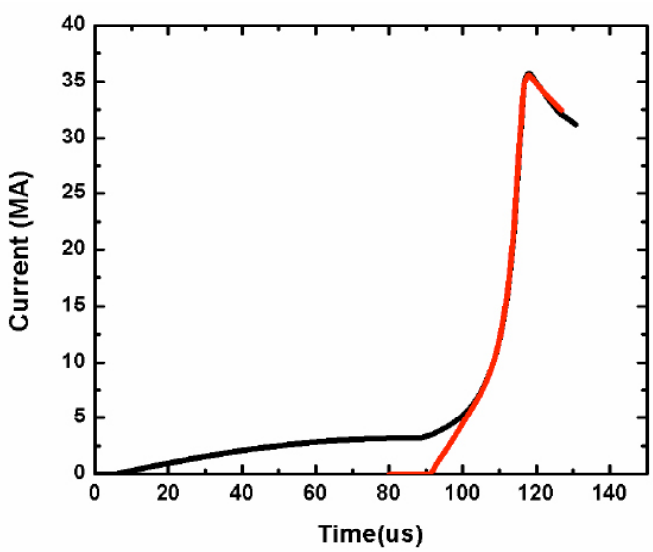


*Figure 2. Current waveforms from MS-1 showing the generator current (black) and load current (red), verifying successful load connection at ~ 90 microsec.*

Several items were successfully tested during MS-0:

1. As anticipated FCG operation resulting in a 36 MA output current to drive the load.

2. Active connection between the generator and the load, on command, to avoid deleterious early time current in the load.

3. Active removal of the parallel seed current circuit, on command, thus removing an energy loss mechanism that would reduce available load energy.

4. Design validation of two 36 MA current joints used to couple the generator current to the load region.

5. Verification of electrical breakdown free operation of all power flow components.

6. Active interrogation of the motion of metal walls in the conductors carrying current to the load, during current delivery. This is the first time such motion has been measured unambiguously. The diagnostic used will measure the imploding shell velocities on subsequent shots. The technique used allows measurement at velocities up to 20 km/sec, with extensions up to 200 km/sec after a modification of the detection system.

While MS-0 was a functional system test for the most part, it also tested the primary shell velocity diagnostic that will be used on subsequent implosion shots. The first implosion shot (MS-1) will implode two Al liners in two adjacent cavities using a common drive current from the switched FCG. One cavity will have only the Al and should attain a velocity of order 7 km/sec for the Al inside surface prior to stagnation after compressing the air inside the liner. The second cavity will have the same Al liner but add a set of three Au shells inside it, with plastic cushions between the Au shells to control kinetic energy transfer efficiency and instability growth. This liner set is expected to attain a velocity of order 13 km/sec on the inner surface of the last Au shell. The inside surface velocity in both cavities will be measured by the technique tested in MS-0. MS-1 is expected to take place in Nov. 2009.

## Future Work

The project is developing the electrical and mechanical techniques required to take energy from a high current source (30MA with 100 us duration) and utilize it to create an Al shell moving radially inward at a velocity approaching 10 km/sec. Subsequent collisions with cushioned, less massive Au shells will sequentially increase that velocity into the 100-300 km/sec range. In effect, the cylindrical system of nested shells acts as the mechanical analog of an electrical pulse compression system capable of increasing power at the expense of energy. Velocities of moving metals such as Au in that range become useful for ICF implosions in a cylindrical geometry, providing an alternative platform for fusion studies. This platform can also be useful to study other physics issues that are classified. Such physics issues are covered by descriptions in the vault.

The task to be completed is the design and demonstration of a velocity multiplier system driven by a high explosive pulsed power high current generator. The final goal is the

demonstration of current extraction from the generator into the load assembly, velocity multiplication within the load assembly, and the ability to accurately simulate the experiments with existing MHD and radiation-hydrodynamics codes available at LANL. Follow on work will then utilize those codes for design of experiments in relevant areas using the platform developed under this project, as well as perform such experiments. Those experiments will reside within the center of the last shell driven by this platform.

## Conclusion

Expected project result: proof of current driven velocity multiplication in a cylindrical geometry for applications requiring extreme pressures, densities, and temperatures.

In an Inertial Confinement Fusion context, this project will provide a current driven platform for creating a Au pusher having an inner surface velocity in the 100-300 km/sec range, comparable to that of the inner surface of a NIF ICF capsule. As in a laser driven ICF spherical capsule, DT fusion reactions can be created inside such a shell. The use of a high velocity gold pusher theoretically allows the DT to reach ignition with a lower invested energy per unit DT mass than is the case in the more common plastic or Be single shell NIF point design. This allows the system to be used for studies of alternative ignition modes in ICF.

In addition, there are classified expected results in the vault.

## Publications


Atchison, W., A. Kaul, C. L. Rousculp, and R. G. Watt. Optimization of a Ranchero driven high energy liner driver system (U) . Presented at *MegaGauss XII.* (Moscow, Russia, 13-18 July 2008).

Colgate, S., R. G. Watt, W. Atchison, and C. Rousculp. Equilibrium ignition by a cold adiabat: ICF via multi-collision velocity multiplication (U) LA-UR-08-06915. 2008. *Presentation to be given at Sandia National Laboratory, Nov. 6, 2008.*

Guzik, J., R. G. Watt, W. Atchison, and S. Colgate. An LDRD project to develop a fusion target driven by velocity multiplication using colliding shells (U) LA-CP-08-01191. 2009. In *NECDC 2008.* (Livermore, Ca., 20-24 Oct. 2008). , p. 1. Livermore, Ca.: Livermore National Laboratory.

Guzik,R.G.Watt,W.L.Atchison, J. A., S. A. Colgate, J. Goforth, D. Holtkamp, A. Kaul, R. Kirkpatrick, Hui Li, R. Menikoff, H. Oona, P. Reardon, and C. Rousculp, S. Sgro, T. Tierney. A LDRD project to develop a fusion target driven by velocity multiplication using colliding shells (U) LA-CP-08-01191 . Presented at *NECDC 2008.* (Livermore National Laboratory, Ca., Oct. 20-24, 2008).

Sgro, A. G.. Studies of a magnetically driven liner for TN burn (U) LA-CP-08-. Presented at *NECDC 2008 LA-CP-08-01230.* (Livermore, Ca., 20-24 Oct. 2008).

Sgro, T.. Magnetically driven liner - glide plane interactions. Presented at *NEDPC 2009, LA-CP-09-00666.* (Livermore, Ca., Oct. 26-30, 2009).

Watt, R. G., S. A. Colgate, W, L. Atchison, J. H. Goforth, J. Griego, J. Guzik, D. Holtkamp, G. Idzorek, R. Kirkpatrick, R. Menikoff, R. Meyer, H. Oona, P. Reardon, C. L. Rousculp, A. G. Sgro, and L. Tabaka. Status of LDRD-DR 20070518 Development of a magnetically driven arget for thermo-nuclear burn studies. (U) . 2009. *NEDPC 2009, Oct. 26-30, 2009, LLNL LA-UR-09-06620 .*

Watt, R. G., W. Atchison, and S. Colgate. LDRD 20070518-dr midterm review: a project to develop a magnetically driven target for thermo-nuclear burn studies (U) LA-CP-08-00675. 2008. *Presentation to LANL LDRD Office, May 22, 2008.*

Watt, R. G., W. Atchison, and S. Colgate. LDRD 20070518-DR Development of a Magnetically Driven Target for Thermo-nuclear Burn Studies (U) LA-CP-07-1593. Presented at *NEDPC 2007.* (Los Alamos, NM, 22-26 Oct. 2007).

Watt, R. G., W. Atchison, and S. Colgate. Development of a Magnetically Driven Target for Thermo-nuclear Burn Studies (U) . Presented at *JOWOG37 2008.* (Los Alamos, NM, 11-14 Feb. 2008).

Watt, R. G., W. L. Atchison, S. A. Colgate, J. H. Goforth, J. Griego, D. Herrera, D. Holtkamp, G. Idzorek, R. Kirkpatrick, E. Lopez, R. Menikoff, R. Meyer, H. Oona, P. Reardon, C. L. Rousculp, A. G. Sgro, L. Tabaka, and D. Torres. Postshot report for MS-0 fired August 6, 2009 (U). 2009. *LA-UR 09-06959 .*

# Prompt and Radiochemical NTS Diagnostics and New Measurements (U)

*David J. Vieira*
20080009DR

## Introduction

We are refining the analysis of existing underground test data, improving explosion code calculations, and delivering new nuclear cross section measurements. New scientific developments are needed that go beyond the currently baseline weapons physics program, in order to fully utilize the information contained within the irreplaceable archival underground test (UGT) data. Our main thrust is to combine neutron pinhole imaging and refined arsenic radiochemistry diagnostics to provide new constrains on weapons code simulations. Once delivered to the weapons program, these tools will improve our understanding of weapons performance. Advanced science from LDRD projects has contributed to the understanding radiochemistry in the past. This project takes the next step. Using the isotope production facility at Los Alamos Neutron Scattering Center (LANSCE), we will produce radioactive targets of 73As (80 day half-life) and 74As (18 day). These targets will be used to undertake first-of-their-kind neutron-induced cross section measurements that are needed to improve the interpretation accuracy of the 73As/74As radiochemistry diagnostic data. The new cross section measurements are challenging because we use radioactive targets, which complicate the detection of the actual reactions of interest. Many of the experiments will be done in collaboration with scientists from several universities that are separately supported through the NNSA Stewardship Science Academic Alliance (SSAA) Program. Finally, this work also helps in the training of new scientists and radiochemists that will benefit the stockpile stewardship program in the long run, as well as our evolving needs in threat reduction and nuclear forensics.

## Benefit to National Security Missions

This project will support the DOE / NNSA mission in nuclear weapons by enhancing our understanding of weapons performance and by improving our predictive capability on which the certification of the US nuclear stockpile is currently based. In particular, this work builds upon, enhances, and brings together several essential Laboratory core capabilities to focus on a key problem that currently limits our simulation codes from being fully predictive. This project also advances new radiochemical and nuclear science capabilities to undertake forefront nuclear measurements, which are of fundamental as well as, applied interest.

## Progress

Good progress has been made on this project during the last year. The project was favorably reviewed by a committee of scientists from Lawrence Livermore National Laboratory and Los Alamos National Laboratory who meet in early June 2009, at the mid-point of this three year project. However, the report of the committee and most of the details about this project is of a classified nature, so only the unclassified highlights of this project can be reported here. The LDRD office has a copy of the classified committee report as well as additional information about this project on file.

During the past year, three UGT events have been re-analyzed and simulated using explosion code models. The archived prompt neutron pinhole image and neutron leakage data have been re-analyzed to provide new information about these events. A special emphasis has also been placed on understanding the arsenic radiochemical data. A new nuclear reaction production and destruction library for arsenic has been prepared and used in the explosion code simulations. Progress has also been made in undertaking the measurement of three key nuclear reactions that effect the interpretation of the 73As/74As radiochemical diagnostic data. These are very challenging, first-of-a-kind measurements involving radioactive targets of 73As (80d) and 74As (18 d). During the past year these radioisotopes have been produced by irradiating a germanium target with protons at the LANSCE isotope production facility (IPF). Curie amounts of these arsenic isotopes were produced at the IPF and then chemically separated and made into experimental targets using our hot cell facilities at TA-48. In July we undertook the first measurement of the 74As(n,p) reaction using the lead slowing-down spectrometer located at the weapons research facility at LANSCE. This data is currently under analysis. Additional measurements are planned for 2010. Improved Hauser-Feshbach calculations for other reaction

channels that cannot be measured have recently been performed. This new information will be incorporated into the arsenic reaction library in the near future and additional simulations will then be performed.

In short, this project involves a multi-disciplinary effort with a wide variety of scientists from several different research Divisions at LANL. The good progress that we have made has also attracted the interests of LLNL and AWE scientists who are studying similar issues and we are forming new collaborations with them to further advance this research. We also continue to work closely with several universities supported through the NNSA / SSAA program to undertake new experimental measurements.

## Future Work

The project addresses the Laboratory's Grand Challenge "fundamental science underlying nuclear performance of our stockpile stewardship mission." The concept of the project is to advance our understanding of the key processes by constraining weapons simulations using existing UGT radiochemistry and prompt diagnostic archived data. New cross section data on arsenic radioisotopes will be measured at LANSCE and Triangle Universities Nuclear Laboratory in North Carolina. Theory will provide other cross sections that cannot be measured to improve the interpretation of radiochemical diagnostic data.

This project will advance a unique combination of arsenic radiochemistry and prompt diagnostics data to constrain and improve weapons simulations and to better understand performance. This R&D involves the non-trivial production of radioactive targets of various arsenic isotopes; the undertaking of three state-of-the-art nuclear cross-section measurements for the 73As(n,gamma), 73As(n,2n), and 74As(n,p) reactions; a reliance on nuclear theory to predict cross sections for other arsenic production and destruction network reactions that can not be measured at this time; a re-analysis of high-resolution prompt (PINEX and NUEX) diagnostics from the UGT archived database; and integrated simulations of a selected set of UGT events. Additional information is contained in the classified LDRD files.

This project involves scientists from several different Divisions at the Laboratory - C, LANSCE, P, T, and X. The cross section measurements will also be done in collaboration with scientists from Duke University, the University of North Carolina, and North Carolina State University. The cross section measurements will be published in the open literature.

## Conclusion

If successful, this project will have a high impact on our stockpile stewardship mission, significantly improving our understanding and predictive capability of performance. This project involves the non-trivial production of radioactive targets; the undertaking of three state-of-the-art nuclear cross-section measurements; a reliance on nuclear theory to predict cross sections for other reactions that can not be currently measured; a re-analysis of high-resolution prompt diagnostics and radiochemical diagnostics from our archives of underground tests; and the simulations of a selected set of UGT events using advanced simulation codes.

## Publications


DeYoung, A.. RIFs as a New Constraint on Mix Models (U). 2009. *Nuclear Explosives Design Physics Conference - NEDPC, Lawrence Livermore National Laboratory, Livermore, CA, Oct. 26-30, LA-CP-09-01284..*

Gorman, T. J.. Development of a Nuclear Testbed for Boost (U). 2008. *Weapons Science Capability Review, Los Alamos National Laboratory, Los Alamos, NM, May 5-8, 2008..*

Gorman, T. J.. Beyond Initial Conditions Non-DPE (U). 2008. *Weapons Science Capability Review, Los Alamos National Laboratory, Los Alamos, NM, May 5-8, 2008.*

Gorman, T. J., T. McKee, and D. J. Vieira. New Radiochemical Calculations of Three NTS Experiments (U). 2009. *JOWOG 32P, Los Alamos National Laboratory, Los Alamos, NM May 18-20, 2009, LA-CP-09-00552..*

Keksis, A. L.. Neutron Capture Measurements on Arsenic (U). 2008. *Radiochemistry Inter-Laboratory Working Group - ILWOG 41, AWE Aldermaston, UK, Sept. 6-15, 2008, LA-UR-08-05692..*

Obst, A. W.. Coalora TIP/TRP Orientation (U). 2008. *Los Alamos National Laboratory memo to X-Division, dated Sept. 23, 2008, LA-CP-08-01162..*

Vieira, D. J.. Prompt and Radiochemical NTS Diagnostics and New Measurements: A LDRD Project on Boost (U). 2008. *Weapons Science Capability Review, Los Alamos National Laboratory, Los Alamos, NM, May 5-8, 2008..*

Vieira, D. J.. Radiochemistry and PINEX Diagnostics Focused on Boost - A LDRD/DR Project. 2009. *Fission Workshop, Los Alamos National Laboratory, Los Alamos, NM, Feb. 5-6, 2009..*

Vieira, D. J.. Radiochemistry and PINEX Diagnositcs Focused on Boost - A LDRD/DR Project (U). 2009. *N-Division Seminar, Lawrence Livermore National Laboratory, Livermore, CA, March 30, 2009, LA-CP-09-0317..*

Vieira, D. J.. Arsenic Radiochemical Diagnostics (U). 2009. *Nuclear Explosives Design Physics Conference (NEDPC), Lawrence Livermore National Laboratory, Livermore, CA, Oct. 26-30, 2009, LA-CP-09-01478..*

Williams, M.. A Formation of Time Integrated Mix (U). 2009. *Nuclear Explosives Design Physics Conference (NEDPC), Lawrence Livermore National Laboratory, Livermore, CA, Oct. 26-30, 2009, LA-CP-09-01431..*

# Global Monitoring of the Sky with Thinking Telescopes: Finding and Interrogating Cosmic Explosions

*W T. Vestrand*
20080039DR

## Introduction

We are creating the technology for the world's first integrated global grid of persistent monitoring telescopes and rapid response follow-up telescopes in order to find and to interrogate the optical light from space objects and cosmic explosions. Our project integrates Information Science, Robotic Instrumentation, and Distributed Sensor Network technology into a full, end-to-end, globally distributed search engine for persistently monitoring the night sky. This fully autonomous robotic network will feed its observations back to real-time decision engines, pose new questions for interrogation, conduct triage, and optimize the network hardware configuration for real-time knowledge extraction. Our grid of Thinking Telescopes is designed to observe the full night sky searching for optical transients, simultaneously monitor more than 10 million persistent sources, recognize anomalous behavior, select targets for detailed interrogation, and make real-time, follow-up observations---all without human intervention. This challenging goal is only within our reach because of significant LANL achievements in robotic instrumentation, distributed networks, artificial intelligence, advanced database technology, and time-domain astrophysics. The principal focus of our scientific effort is developing an understanding of Nature's most powerful explosions, Gamma Ray Bursts (GRBs). But, the tools and methodologies developed on this project have general applicability to areas of Defense, Intelligence, and Homeland Security, and have direct applicability to specific problems in Space Situational Awareness.

## Benefit to National Security Missions

This project will support DOE missions by developing a new paradigm employing robotic, distributed, instrumentation for situational monitoring. The tools and methodologies developed will have general applicability to areas of Defense, Intelligence, and Homeland Security, and have direct applicability to specific problems in Space Situational Awareness and ubiquitous sensing. The *bulk of our effort* on this project during the last eighteen months has been devoted to the development and demonstration of technology for a modern, paradigm shifting, approach to Space Situational Awareness—an area of growing importance to the Nation and one of the Global Security Directorate's highest-priority areas. Our project is a "flagship" effort that is being successfully used to demonstrate new approaches to Space Situational Awareness (SAA).

## Progress

We completed the construction and began commissioning of RAPTOR-K (Figure 1). RAPTOR-K is a wide-field, persistent optical monitoring array with unprecedented capability. It is composed of 16 wide-field telescopes carried on a single rapidly slewing mount. Each telescope has a 2Kx2K E2V back-illuminated CCDs at the focal plane and has a 3-sigma limiting magnitude of R~16$^{th}$ magnitude in 30 seconds. Altogether the 16 telescopes have an instantaneous field-of-view of ~1,000 sq-degrees. In normal operation, the array is capable of patrolling the full visible sky above 20 degree elevation on 6-minute circuit. It is roughly 30 times more sensitive than any other full sky optical monitor capable of finding transients with durations measured in minutes. This system is a fully autonomous robot and runs without human intervention.

*Figure 1. The RAPTOR-K telescope array.*

To optimize the response for a global network of telescopes it is essential to monitor the transparency conditions for the full sky at each site. We designed, tested, and deployed a new system called RQD2 (Raptor-Q/demonstrator-2), which is fully autonomous and easily deployable to remote locations around the

World. It is a small portable robotic observatory (Figure 2) developed for the purpose of real-time sky condition monitoring that also has the capability to detect bright astronomical transients. RQD2 consists of five wide field telescopes that, altogether, simultaneously view 14,500 square degrees---approximately 90% of the sky above 12 degrees elevation. The limiting sensitivity of the RQD2 system for a 10 second exposure is R≈10$^{th}$ on a clear, moonless, night. The system normally detects about 55,000 objects in each set of exposures. Using those measurements our real-time photometry pipeline and machine learning algorithms are able assess the conditions over the full sky every 20 seconds That information can then be feed back into the network to help task observations by the narrow field telescopes at that site as plan the tasking of time critical observations throughout the global network. These RQD2 nodes, which will be deployed around the world, will provide essentially continuous monitoring of the full sky at each site and detect a variety of objects including variable stars, asteroids, and bright explosive transients. Each week a single RQD2 system takes about 18,000 images of the sky corresponding to about 0.3 TBytes. Our first RQD2 system began normal operations on March 9, 2009.

*Figure 2. The RQD2 portable sky monitoring observatory.*

We also completed the construction of a RAPTOR-T telescope and enclosure that is modified for a deployment in Northern Australia. RAPTOR-T is an array of four co-aligned 0.4-meter telescopes deployed on a rapidly slewing mount that is capable of slewing to point anywhere in the visible sky to begin imaging in less than ten seconds. Each telescope uses a CCD with a 1024x1024 back- illuminated E2V chip and images through a different (clear/VRI) filter. The cameras are synchronized to provide simultaneous multi-color measurements with a R-band sensitivity of ~19$^{th}$ magnitude in 60 seconds. The telescope array and enclosure are now complete and awaiting shipment to Australia.

Fully autonomous operation is a key feature of our system. An ability to delegate increasingly complex data analysis and decision making tasks to machines (software agents) is the key to success in this area. We have developed an approach that employs state of the art Machine Learning (ML) algorithms to dramatically simplify the problem of finding optimal decision boundaries in high dimensional feature spaces. We focused on supervised learning techniques that require training by a human analyst prior to application on new data, but generally are more mature and offer better performance. To that end, we developed a software framework that enables us to quickly extract new features from a standard set of our data products and evaluate (cross-validate) the performance of candidate ML classifiers over a range of models and parameters. Support for feature selection allows us to explore alternative feature spaces by weighting the relative importance of each dimension in the input data. Our ML tool set has been integrated into the software package that can be rapidly deployed to a new node on the network.

We also developed a mechanism for efficient search and retrieval of RAPTOR data that is distributed throughout the global network. This was challenging because the physical location of required imagery, or even knowledge of which image supports an event in question, is often unknown. We developed an approach, called RAPSTER, that leverages design patterns and lessons learned from the public internet peer to peer file sharing community. As each site node processes imagery it reports to a RAPSTER database which constructs temporal and spatial indexes of available imagery. This database is then capable of constructing a list of imagery which intersects an arbitrary region of interest across the celestial sphere, optionally filtered by time. A request is then submitted to a distributed storage mesh for each required image. The mesh decides which location holds the desired image and streams it back.

A scientific highlight was our analysis of the observations, collected by eight of our telescopes, of a spectacular cosmological transient that for a few seconds was bright enough to be visible to the “naked eye”. This bright optical flash was generated by a gamma-ray burst (GRB 080319B) at a distance of about 7.5 billion light years, making it the most luminous optical object ever detected by humankind. The comprehensive sky monitoring and multi-color optical observations collected by our telescope network enabled unpredicted observations of the development of the explosion and the afterglow in the minutes before, during, and after the stellar collapse. The unmatched dynamic range of our network allowed us to measure the evolution of the extremely bright transient over more than 12

magnitudes and measure properties that are normally not detectable.

Another key scientific accomplishment came from our study of the early afterglows from all GRBs with measured distances. We found that the temporal behavior of the early optical afterglows can be divided into four morphological classes: fast-rising with an early peak, slow-rising with a late peak, flat plateaus, and rapid decays since first measurement. We found that the fast-rising optical afterglows display correlations among peak flux, peak epoch, and post-peak power-law decay index. This can be understood if we are seeing structured outflows off-axis. We also found that the afterglows with plateaus and slow-rises show a similar correlation between peak flux and peak time. That correlation can also be explained by the same model, if the observer is farther from the event axis than for the fast-rising afterglows or with a longer lived injection of energy and/or ejecta in the blast-wave.

## Future Work

The primary focus of our final year of research will be the application of our technology to the persistent monitoring of objects in the night sky. Our goals are:

1. Deploy a Thinking Telescope node at a location more than 3,000 miles from LANL and demonstrate the ability to autonomously hand-off and maintain monitoring of an object from site to site;

2. Quantify the space object measurement accuracy and system sensitivity; and

3. Develop an independent record of the behavior of variable sources in the night sky and demonstrate the ability to trigger on important changes.

## Conclusion

We will demonstrate a new approach to dynamic monitoring of the full night sky that has important applications to Space Situational Awareness and well as basic astronomical research. Our telescopes, the world's most powerful for finding and exploring changes with durations measured in seconds, are allowing us to probe the nurseries of the first black holes as well as detect extreme stellar flares and novae, unpredicted encounters with solar system objects, and find the nearby supernovae needed to calibrate estimates of dark energy in the universe.

## Publications


Hoffman, D., T. Harrison, and J. Coughlin et al. New Beta Lyrae and Algol candidates from the Northern Sky Variability Survey. 2008. *Astronomical Journal.* **136** (3): 1067.

Kumar, P., and A. Panaitescu. What did we learn from gamma-ray burst 080319b?. 2008. *Monthly Notices of Royal Astronomical Society.* **391** (1): L19.

Panaitescu, A.. X-ray flares, plateaus and chromatic breaks of GRB afterglows from up-scattered forward-shock emission. 2008. *Monthly Notices of Royal Astronomical Society.* **383** (3): 1143.

Panaitescu, A.. An external-shock origin of the relation for gamma-ray bursts. 2009. *Monthly Notices of the Royal Astronomical Society.* **393** (3): 1010.

Panaitescu, A., and W. T. Vestrand. Taxonomy of gamma-ray burst optical light curves: identification of a salient class of early afterglows. 2008. *Monthly Notices of Royal Astronomical Society.* **387** (2): 497.

Perley, D., J. Bloom, and N. Butler et al. The troublesome broadband evolution of GRB 061126. 2008. *Astrophysical Journal.* **672** (1): 449.

Rykoffetal, E.. Looking into the fireball: ROTSE-III and Swift observations of early GRB afterglows. 2009. *Astrophysical Journal.* **702**: 489.

Vestrand, W. T., H. Davis, and J. Wren et al. Autonomous global sky surveillance with real-time robotic follow-up: night sky awareness through Thinking Telescopes technology. 2009. In *Advanced Maui Optical and Space Surveillance Technologies Conference.* (Maui, 14-16 Sept. 2008). , p. p.E71. Maui: Maui Economic Development Board.

White, R., H. Davis, W. T. Vestrand, and P. Wozniak. Distributed intelligence in an astronomical distributed sensor network. 2008. *Astronomische Nachrichten.* **329** (3): 278.

White, R., and A. Allan. An overview of the heterogeneous telescope network system: concept, scalability and operation. 2008. *Astronomische Nachrichten.* **329** (3): 232.

Wozniak, P., W. T. Vestrand, and A. Panaitescu et al. Gamma-Ray Burst at the extreme: 'the naked eye burst' GRB 080319B. 2009. *Astrophysical Journal.* **691**: 495.

Yuanetal, F.. Prompt optical observations of GRB 080330 and GRB 080413A . 2008. In *2008 Nanjing Gamma-Ray Burst conference.* (Nanjing, China, October 2008). Vol. 1065, p. 433. Melville, New York: American Institute of Physics.

# Carrier Multiplication in Nanoscale Semiconductors for High-Efficiency, Generation-III Photovoltaics

*Victor I. Klimov*
20080057DR

## Introduction

The solution to the global energy challenge requires revolutionary breakthroughs in areas such as the conversion of solar energy into electricity. One such breakthrough is high-efficiency generation of multiple electron-hole pairs (excitons) from absorption of single photons known as carrier multiplication (CM). For more than 20 years it has been recognized theoretically that such a process has the potential to significantly increase the power conversion efficiency of photovoltaic devices via an enhanced photocurrent for a fixed photovoltage. In 2004, using a novel experimental approach, we discovered that semiconductor nanocrystals (NCs), in distinction from bulk materials, undergo this process very efficiently within the range of solar photon energies. In this project, we conduct theoretical and experimental studies of the fundamental physics of CM and relevant phenomena (e.g., charge and exciton extraction from the nanocrystals) that will ultimately lead to the development of novel principles, materials, and architectures for making use of this process in practical photovoltaic technologies. Specifically, to identify the factors that control the energy onset and the efficiency of multiexciton generation, we perform detailed studies of the CM mechanism in nanoscale semiconductors. Further, we test the CM performance of elongated nanocrystals (quantum rods) and quantum wires because these two types of nanostructures have good transport properties and are readily incorporated into devices, which could simplify practical realization of photovoltaics utilizing multiexciton generation. Finally, we investigate energy- and charge-transfer processes in engineered energy-gradient structures in the context of extraction of multiple charges produced via CM from the nanocrystals.

## Benefit to National Security Missions

This project directly supports DOE mission in Energy Security, specifically, in areas of alternative energy sources and energy efficiency. The proposed studies also address several critical research areas relevant to LANL challenges in "Carbon-Neutral Energy" and "Design, Synthesis and Properties of Photoactive Nanostructures."

## Progress

During FY2009, our work in this project has focused in the following areas: (i) CM and competing process, and specifically, the role of photocharging, (ii) synthesis and spectroscopic studies of Ge NCs, (iii) the effect of three-dimensional confinement on carrier-carrier interactions in indirect-gap semiconductors, and (iv) exciton transfer in semiconductor nanowires probed by single-nanostructure spectroscopy. These studies resulted in 10 papers including 3 *Phys. Rev. Lett*., a feature article in *Acc. Chem. Res.,* 2 *J. Am. Chem. Soc.* publications, 2 *Phys. Rev. B* reports, etc.; 3 more papers have been submitted. Our studies have been presented in numerous conference talks, including 11 invited presentations at important scientific forums such as *March APS 2009 Meeting*, *Annual ACS 2009 Meeting*, *Gordon Research Conference on Nanoclusters and Nanostructures*, *Annual OSA 2009 Meeting*, *Topical OSA Meeting on Nonlinear Optics*, *Conference on Excitonic Phenomena in Semiconductors*, etc. The work conducted in this project helped in the preparation of the LANL *Energy Frontier Research Center* (EFRC) proposal. Below, we provide a highlight on our most recent studies of the CM process.

One goal of the last year studies was to understand the influence of NC photoionization on the measured apparent CM yields. Following the original 2004 report on high-efficiency CM in PbSe NCs, this effect was observed in NCs of many different compositions including PbS, PbTe, CdSe, InAs, and Si. However, eventually this process has become a subject of intense controversy because of large variations in reported CM yields. It has been commonly conjectured that these discrepancies result either from possible measurement

errors or variations in NC surface properties. However, our studies demonstrate that dramatically different apparent CM yields can be obtained even from the same sample but under slightly different experimental conditions. Specifically, the observed multiexciton can differ by a factor of more than 3 according to whether the NC solution is static or stirred. Based on our studies, we have concluded that this discrepancy arises from photoinduced charging of the NCs by high-energy photons, which leads to exaggeration of CM signatures and increased apparent CM yields in the case of static solutions. The static-stirred differences observed in our work are similar to the magnitude of variations in published reports suggesting that uncontrolled ionization of the NCs is likely the main reason for large literature discrepancies.

As the next step, we have developed a quantitative model that provides a description of apparent CM yields in a mixed ensemble of neutral and charged NCs. We use it to extract true CM efficiencies from measurements of static solutions with known degrees of photocharging. Using this model we have shown that the CM results obtained under different conditions converge to the same value after we accurately account for the effects of photocharging. The significance of these studies is that they clarify the recent controversy over CM in NCs and highlights some of the issues that must be carefully considered in spectroscopic studies of this process. The brief summary of this work is under consideration at Nature Physics while a more detailed report has been submitted to Nano Lett.

## Future Work

In FY 2010, we will focus on the following topics:

- Studies of the effect of dimensionality on CM efficiencies
- Studies of CM in the regime of intraband re-excitation
- Energy transfer as a means for exciton extraction and transport
- Studies of single- and multiexciton effects in group IV nanostructures

The research proposed for topics (i) through (iii) is described in great detail in the original LDRD proposal. Topic (iv) has emerged as a result of our recent success in the synthesis of Ge nanocrystals (NCs) (D. Lee, I. Robel, J. Pietryga, and V. I. Klimov, *J. Am. Chem. Soc*. 2009). Previously used fabrication methods resulted in Ge NCs of poor quality (highly polydisperse and non-emitting) not well suited for spectroscopic studies. Therefore, available spectroscopic data on this material are sparse and often inconsistent. Using our newly developed high-quality Ge NCs, we should be able to address many important questions concerning photophysics of these interesting nanostructures. One focus of our studies will be multiexciton phenomena such as Auger recombination and CM.

CM has been recently reported for the first time in Si NCs by NREL, showing that the phenomenon can occur in a bulk indirect gap semiconductor. However, while the bulk energy gap of Si ($E_g$ = 1.1 eV) is well-suited to traditional single-junction photovoltaics, it is too large to be of much value for applications that target carrier multiplication. Our recent detailed-balance calculations indicate that the optimal energy gap in the presence of multiplication is around 0.5 – 0.7 eV. This result indicates that Ge, whose energy gap is 0.66 eV, is more suitable for applications in multiplication-enhanced photovoltaics than Si. Furthermore, Ge NCs have an absorption cross section that is about an order of magnitude larger than that of Si through most of the solar spectrum. Therefore, less Ge material is required for use in solar cells, compensating for the higher price of Ge compared to Si, and enabling the use of thinner NC films with favorable conduction properties and lower recombination losses.

Prior to exploring CM, the spectroscopic signatures of multiple excitons need to be established. Therefore, we will perform intensity-dependent transient absorption and photoluminescence measurements to determine the exciton degeneracy of the lowest excited states as well as the spectral and dynamic signatures of biexcitons and higher order multiexcitons. Auger recombination rates will be extracted from relaxation dynamics by careful comparison with single-exciton decay rates. Once reliable signatures of multiexcitons are obtained, carrier multiplication will be investigated by analyzing the exciton multiplicity as a function of the excitation wavelength in the low-intensity regime. The goal of these experiments will be to determine whether CM is efficient in Ge NCs, and further, to establish size-dependent trends for parameters such as the CM threshold, the efficiency, and the electron-hole pair creation energy.

## Conclusion

As a result of the research conducted in this project, we expect to develop novel photoactive materials and new types of photovoltaic structures that will allow high efficiency conversion of solar energy into electricity using the CM process. Specific results expected from our work are:

- The development of reliable approaches for evaluating the CM efficiency of various nanoscale materials

- Understanding the potential influence of extraneous effects that can lead to CM-like signatures in spectroscopic data
- A proven physical model of carrier multiplication in nanostructures, which would help in the development of novel materials with enhanced CM performance, and
- The development of approaches for efficient extraction of charge carriers from the NCs on time scales competing with those of radiative and nonradiative recombination.

## Publications


Bussian, D., A. Malko, H. Htoon, Y. Chen, J. A. Hollingsworth, and V. I. Klimov. Quantum optics with nanocrystal quantum dots in solution: Quantitative study of clustering. 2009. *Journal of Physical Chemistry C.* **113** (6): 2241.

Durach, M., A. Rusina, V. I. Klimov, and M. I. Stockman. Nanoplasmonic renormalization and enhancement of Coulomb interactions. 2008. *New Journal of Physics.* **10**: 105011.

Glennon, J. J., R. Tang, W. E. Buhro, R. A. Loomis, D. A. Bussian, H. Htoon, and V. I. Klimov. Exciton localization and migration in single CdSe quantum wires at low temperatures. 2009. *Physical Review B.* **80** (8): 081303.

Htoon, H., S. A. Crooker, M. Furis, S. Jeong, Al. L. Efros, and V. I. Klimov. Anomalous circular polarization of photoluminescence spectra of individual CdSe nanocrystals in an applied magnetic field. 2009. *Physical Review Letters.* **102**: 017402.

Joo, J., J. M. Pietryga, J. A. McGuire, S. H. Jeon, D. J. Williams, H. L. Wang, and V. I. Klimov. A reduction pathway in the synthesis of PbSe nanocrystal quantum dots. 2009. *Journal of American Chemical Society.* **131** (30): 10620.

Klimov, V. I., J. A. McGuire, R. D. Schaller, and V. I. Rupasov. Scaling of multiexciton lifetimes in semiconductor nanocrystals. 2008. *Physical Review B.* **77** (19): 195324.

Lee, D. C., J. M. Pietryga, I. Robel, D. J. Werder, and R. D. Schaller. Colloidal synthesis of infrared-emitting germanium nanocrystals. 2009. *Journal of American Chemical Society.* **131**: 3436.

McGuire, J. A., J. Joo, J. M. Pietryga, R. D. Schaller, and V. I. Klimov. New aspects of carrier multiplication in semiconductor nanocrystals. 2008. *Accounts of Chemical Research.* **41**: 1810.

Pietryga, J. M., D. J. Werder, D. J. Williams, J. L. Casson, R. D. Schaller, V. I. Klimov, and J. A. Hollingsworth. Utilizing the lability of lead selenide to produce heterostructured nanocrystals with bright, stable infrared emission. 2008. *Journal of American Chemical Society.* **130** (14): 4879.

Pietryga, J. M., K. K. Zhuravlev, M. Whitehead, V. I. Klimov, and R. D. Schaller. Evidence for barrierless Auger recombination in PbSe nanocrystals: A pressure-dependent study of transient optical absorption. 2008. *Physical Review Letters.* **101**: 217401.

Robel, I., R. Gresback, U. Kortshagen, R. D. Schaller, and V. I. Klimov. Universal size-dependent trends in Auger recombination in direct- and indirect-gap semiconductor nanocrystals. 2009. *Physical Review Letters.* **102**: 177404.

Sun, B. Q., A. T. Findikoglu, M. Sykora, D. J. Werder, and V. I. Klimov. Hybrid photovoltaics based on semiconductor nanocrystals and amorphous silicon. 2009. *Nano Letters.* **9**: 1235.

Sykora, M., L. Mangolini, R. D. Schaller, U. Kortshagen, D. Jurbergs, and V. I. Klimov. Size-dependent intrinsic radiative decay rates of silicon nanocrystals at large confinement energies. 2008. *Physical Review Letters.* **100** (6): 067401.

# Probing Physics Beyond the Standard Model through Neutron Beta Decay

*Alexander Saunders*
20080116DR

## Introduction

This project explores for Physics Beyond the Standard Model by using neutron beta decay in three ways, each at the cutting edge of the field. First, it uses ultra-cold neutrons, neutrons that have such low temperature that they can be stored for hundreds of seconds in material bottles, to measure the neutron lifetime. This lifetime, with a value of about 15 minutes, is only known to about one second. Unfortunately, existing experiments disagree at the six second level. The present work is unique in using a gravito-magnetic trap (Figure 1) to store the ultra-cold neutrons while they decay, thus eliminating the leading uncertainties in previous work. Second, this project is establishing the technology that will be used for the next generation of neutron beta decay correlation experiments, which measure the correlations between the outgoing particles from neutron decay and the original polarization of the neutron. Previous experiments have detected only the outgoing beta particle, with rough energy calibration; the result of the present work will be a new generation of experiments that measure the outgoing electron and proton in coincidence, with unprecedented energy resolution. Finally, we are advancing the theory of neutron beta decay in two ways: first, by linking low energy neutron experiments to high energy kaon decay experiments that follow similar decay processes, and second, by exploring the impacts that different values of the decay correlations and neutron lifetime can have on the new physics emerging beyond the standard model.

## Benefit to National Security Missions

This project supports the DOE mission in Nuclear Physics by enhancing our understanding of physics beyond the standard model. This project will provide measurements of neutron properties, a main goal of the DOE Nuclear Physics Long Range Plan. Fundamental nuclear science underlies the weapons program and nuclear threat reduction.

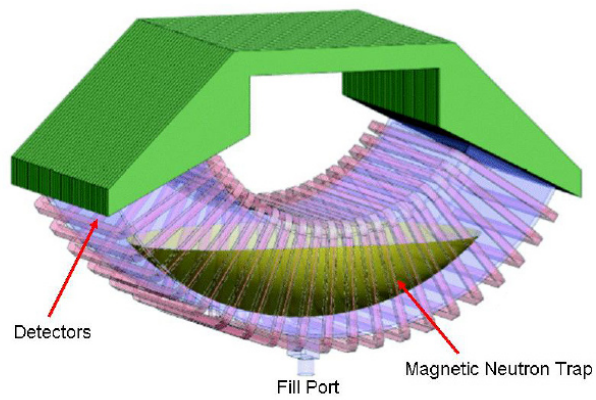


*Figure 1. The apparatus for the UCN neutron lifetime experiment. Neutrons are filled into the magnetic trap from the bottom trap door. Their decay products are detected using wire chambers at each end of the experiment.*

## Benefit to National Security Missions

This project supports the DOE mission in Nuclear Physics by enhancing our understanding of physics beyond the standard model. This project will provide measurements of neutron properties, a main goal of the DOE Nuclear Physics Long Range Plan. Fundamental nuclear science underlies the weapons program and nuclear threat reduction.

## Progress

Progress has been made on all three main goals of the project. The first goal is developing and building a prototype experiment that will measure the neutron lifetime. The ultimate goal of the full experiment is to measure the neutron lifetime to a precision better than any previous experiment (<1 s), and with entirely unique systematic uncertainties. The goal of this part of the LDRD project is to build and test a prototype, which will make a measurement of the neutron lifetime to about the 10 second level or better. The experiment is based on storing ultra-cold neutrons (UCN) in a gravito-

magnetic trap[1]; that is, a trap which is closed on the bottom and sides by an array of permanent magnets and on the top by gravity. Since UCNs rise about one meter in the earth's gravity field, the scale of the trap is about one meter high by one meter wide by two meters long.

Construction of the experiment continues. Assembly and testing of the magnetic trap continues at an offsite contractor, while the construction and assembly of all the support structures and vacuum hardware is now complete. While construction continues on the trap hardware, we have pursued our studies of the dominant systematic uncertainties of this experiment, which are the presence of long-lived quasi-bound neutron states in the trap and the variability of the efficiency of detecting the neutrons as a function of time. Either of these effects can lead to substantial systematic uncertainty in the measured lifetime of the neutron. We are developing novel solutions to these problems, by controlling the orbits of neutrons in the trap and by developing monitor detectors that have no time dependence in their efficiency.

In pursuit of the second goal of the project, to develop the next generation of neutron beta decay experiments, we have designed, and worked with the manufacturer to construct, the first large-area ion-implanted silicon detectors for neutron beta decay studies. We have expanded the thickness of working prototypes of detectors from an initial 0.5 mm, to now 1.0, 1.5, and 2.0 mm. Detectors of at least 1.5 mm thickness are required to determine the energy of all electrons from neutron beta decay. We are currently testing the critical properties of these detectors, including entrance window thickness, energy resolution, and rise time.

We have continued exploring improved measurements of neutron decay correlations using UCNs and the silicon detectors being developed in this project. The most promising appear to be the parameters b and B. b is the Fierz interference term in the neutron decay that distorts the shape of the electron spectrum, if scalar or tensor interactions due to physics beyond the Standard Model interfere with the vector or axial vector interactions in the Standard Model. B is the correlation between the neutron spin and the momentum of the anti-neutrino. There is recent interest in precision measurement of B as it has been shown to be sensitive to certain extensions to the Standard Model [2].

Adapting the existing UCNA decay magnet to electrostatically accelerate the decay protons to about 20 keV and replacing the existing detectors with silicon detectors could measure B. The silicon detectors allow detection of the (accelerated) protons in coincidence with the electrons. This allows determination of the proton asymmetry as a function of electron energy, as required to extract B. We estimate that a statistical uncertainty of approximately 10^-4 can be obtained. This is sufficient to put new limits on the supersymmetric models described above. We have published a paper outlining the concept of a UCN measurement of B [3]. A first test measurement will be attempted in December 2009, if beam time is available.

Finally, we have continued our theoretical investigations of the consequences of the next generation of neutron beta decay experiments. The theory effort in this LDRD-DR project has two main goals, aimed to assess the impact and significance of the proposed experimental effort. During the FY 2009, the theory effort in this LDRD-DR project has focused on studying the implication of precise determinations of $V_{ud}$ and $V_{us}$ on extensions of the Standard Model (SM) at the TeV scale.

We have investigated in a model-independent framework the impact of quark-lepton universality (CKM unitarity) tests on physics beyond the Standard Model. We have identified a minimal set of twenty-five weak scale effective operators describing corrections beyond the SM to precision electroweak measurements and semileptonic decays. In terms of new physics corrections at the TeV scale, we have derived the low-energy effective Lagrangians describing muon decay and beta decays. We have performed the phenomenological analysis assuming nearly flavor blind new physics interactions, under the well motivated assumption that flavor breaking at the TeV scale is suppressed by a symmetry principle or by the hierarchy $\Lambda_{flavor}$ >> TeV. We have shown that, in this limit, the extraction of $V_{ud}$ and $V_{us}$ from any decay mode should give the same result and the only significant probe of physics beyond the SM involves the quantity $\otimes_{CKM} = (|V_{ud}|^2 + |V_{us}|^2 + |V_{ub}|^2 - 1)$. We have shown that $\otimes_{CKM}$ receives contributions from four short distance operators, two of which correspond to corrections to the W-fermion-antifermion vertex, the other two parameterizing four-fermion contact interactions. This result applies to any weakly coupled extension of the Standard Model, thus allowing us to study the interplay of $\otimes_{CKM}$ with other precision measurements in a model-independent way. The main conclusions of our analysis [4] are:

The current phenomenological constraint $\otimes_{CKM} = (-1\pm6)\times10^{-4}$ [5] bounds the scale of all four effective operators contributing to quark-lepton universality violation to be Λ >11 TeV 90 \% C.L.). For three of these operators this constraint is at the same level as the Z-pole measurements, as illustrated in Figure 2. For the four-fermion operator $O_{lq}^{(3)}$ involving two left-handed quark doublet and two left-handed lepton doublets, the $\otimes_{CKM}$ constraint improves existing bounds from LEP2 cross-section measurements by one order of magnitude.

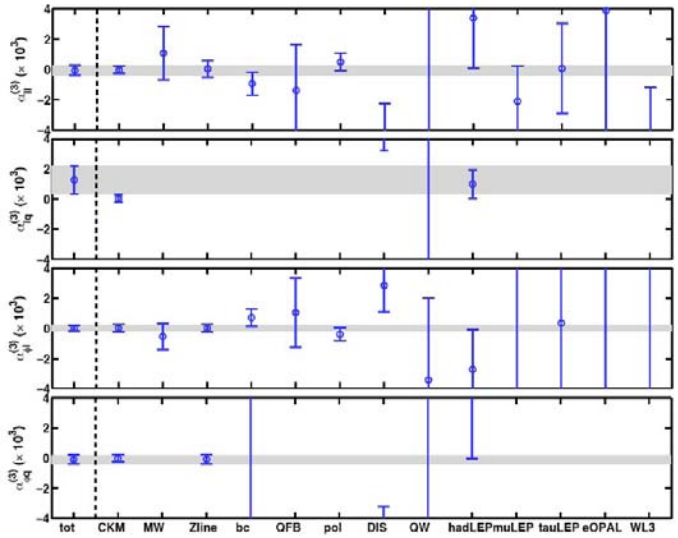


*Figure 2. The 90% C.L. allowed regions for the coefficients αn = v2/Λ2 (v=185 GeV) of the four effective operators that induce violations of Cabibbo universality. The first column displays the constraint from all precision observables except ΔCKM .The second column displays the constraint coming exclusively from ΔCKM. The remaining columns display the constraint derived from various subsets of precision measurements (both at high and low-energy). The ΔCKM constraint implies an effective scale of new physics Λ> 11 TeV (90% CL).*

- Another way to state this result is as follows: should the central values of $V_{ud}$ and $V_{us}$ move from the current values [5], precision electroweak data would leave room for sizable deviations from quark-lepton universality (roughly one order of magnitude above the current direct constraint). Essentially only the four-fermion operator $O_{lq}^{(3)}$ could be responsible for $\otimes_{CKM} \neq 0$, as the others are tightly bound from Z-pole observables.

Our conclusions imply that the study of semileptonic processes and Cabibbo universality tests provide constraints on new physics beyond the SM that currently cannot be obtained from other electroweak precision tests and collider measurements.

## Future Work

In the last year, we intend to bring to conclusion all three parts of this project. First, we will complete an initial measurement of the neutron lifetime using our revolutionary magnetic ultra-cold neutron trap. Second, we will establish the optimal approach to next-generation experiments measuring the neutron beta decay parameters, and demonstrate our silicon detectors, which will likely be used for these experiments. Finally, we will complete our investigations into the theory of neutron beta decay, including pushing down the theoretical uncertainties in the decay process and studying the impact of more precise measurements on the Standard Model of Nuclear and Particle Physics.

## Conclusion

Relying on LANL traditional capabilities and strengths, this program of neutron decay experiments and theoretical support will:

- Result in a world-class measurement of the neutron lifetime during the project and justify future programmatic funding of asymmetry measurements
- Significantly improve our knowledge of light quark (up and down) mixing induced by weak interactions, and as a consequence, put stringent constraints on or detect the presence of a fourth generation of quarks, the violation of quark-lepton universality (due to supersymmetry or extra-dimensions), or the presence of new gauge bosons.

## References

Walstrom, P. D., J. D. Bowman, S. I. Penttila, C. Morris, and A. Saunders. A magneto-gravitational trap for absolute measurement of the ultra-cold neutron lifetime. 2009. *Nuclear Instruments and Methods in Physics Research A.* **599**: 82.

Profumo, S., M. J. Ramsey-Musolf, and S. Tulin. Supersymmetric contributions to weak decay correlation coefficients. 2007. *Physical Review D.* **75** (7): 075017.

Wilburn, W. S., V. Cirigliano, A. Klein, M. F. Makela, P. L. McGaughey, C. L. Morris, J. Ramsey, A. Salas-Bacci, A. Saunders, L. J. Broussard, and A. R. Young. Measurement of the Neutrino-Spin Correlation Parameter B in Neutron Decay using Ultracold Neutrons. To appear in *Revista Mexicana de Fisica.*

Cirigliano, V., M. Gonzalez-Alonso, and J. Jenkins. Semileptonic decays of light quarks beyond the Standard Model. *Nuclear Physics B.*

Antonelli, M., and V. Cirigliano. Flavor Physics in the Quark Sector. *Physics Reports.*

## Publications

Cirigliano, V.. Precision tests of the Standard Model with leptonic and semileptonic kaon decays. 2008. *The FlaviaNet Working Group on Kaon Decays.*

Cirigliano, V., M. Giannotti, and H. Neufeld. Electromagnetic effects in Kl3 decays. 2008. *Journal of High Energy Physics.* **11**: 6.

Walstrom, P. L., J. D Bowman, S. I. Penttila, C. Morris, and A. Saunders. A magneto-gravitational trap for absolute measurement of the ultra-cold neutron lifetime . 2009. *Nuclear Instruments and Methods in Physics Research, Section A.* **599** (1): 82.

# Cosmic Explosions Probing the Extreme: X-Ray Bursts, Superbursts, and Giant Flares on Neutron Stars

*Sanjay Reddy*
20080130DR

## Introduction

Some of the most common cosmic explosions occur on neutron stars (NS). Over the past decades x-ray satellites have observed x-ray bursts, superbursts, and giant flares on NSs in great detail. These observations have provided new insights, and an excellent account of these developments can be found in [1]. Yet, a comprehensive theoretical study of these phenomena needed to interpret observations in terms of fundamental processes is lacking.

Due to the large gravity, the density in NSs increases rapidly with depth. In Figure 1 the density profile and the ground state composition are shown. In the crusts of NSs (the outermost 1-2 km of the star), the density increases from $10^6$ g/cm$^3$ at depth of 1 meter to $10^{14}$ g/cm$^3$ at the inner edge of the crust down at about 1.5 kms. Nuclei become increasing neutron-rich and strong electric forces between densely packed nuclei organize these exotic nuclei into a strongly interacting liquid at shallow depth and a dense solid deeper down. The objective of this project is to develop the theoretical and computational tools to model this extreme matter alongside an effort to model explosive phenomena that occur in accreting and magnetized NSs. In accreting NSs, matter (mostly in the form of hydrogen and helium) from a companion star falls and accumulates. The explosive burning of this material produces the commonly observed x-ray bursts and the occasional x-ray superbursts [2]. In highly magnetized NSs known as magnetars, transitions between different configurations of the magnetic field is expected to trigger magnetic reconfiguration and magnetic energy release akin to solar flares [3]. Developing physics based models for thermonuclear and magntic explosions is one of the main thrusts of this research project.

Another major thrust is modeling the spectra and light-curves for a wide range of supernova explosions. These explosions can be either driven by thermonuclear energy as in the case of Type I supernova or gravitational binding energy that drives core collapse supernova. In both these cases, the light curves, which are easily

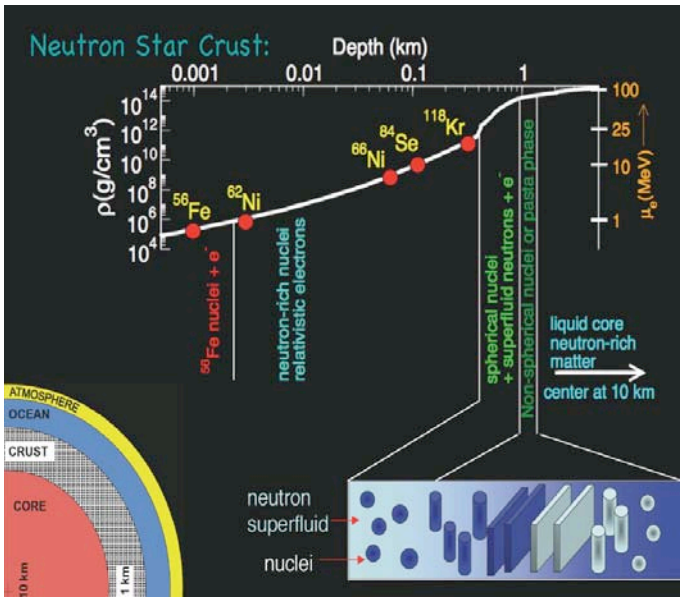


*Figure 1. Schematic of the neutron star outer regions.*

observable, provide a key diagnostic. To take full advantage of current and upcoming data (from Large Synoptic Survey Telescope LSST and x-ray missions such as the proposed Energetic X-ray Imaging Survey telescope EXIST), the theory must exist to accurately connect the observations to our understanding of these explosions. This project uses LANL expertise in supernova explosions mechanisms and progenitors, computational physics, radiation transport, and atomic physics to develop state-of-the art codes to model the emission from supernova explosions. With the codes validated on supernova explosions, we can attack a wider range of cosmic explosion emissions.

## Benefit to National Security Missions

This project involves the modeling of multi-scale (explosive) phenomena in extreme environments. The

underlying nuclear, plasma and atomic physics, and the computational techniques for radiation hydrodynamics, are relevant to Department of Energy missions, especially the nuclear weapons mission.

## Progress

The thermal state of the NS crust plays a role in igniting thermonuclear bursts. It is determined by the competition between nuclear heating, neutrino cooling and heat conduction. We made important progress in understating all three of these processes. Gupta, Moller and Kawano demonstrated that reactions involving neutron emission in the crust change the reaction pathways and results in robust heating [4]. Reddy and collaborators have discovered a new mechanism for heat transport in the inner past of the crust [6]. Here, neutrons coexist as a fluid surrounding nuclei and is superfluid like liquid helium at low temperature. The collective excitations of the neutron superfluid, called superfluid phonons, provide an efficient mode of heat transport. This mode of conduction was shown to play a role in hot accreting stars and is important in magnetars where electronic heat conduction is suppressed in direction perpendicular to the magnetic field [6]. In Figure 2, the thermal conductivity of this superfluid mode is compared to the conventional electronic heat conduction. In addition, Daligault and Gupta have reexamined the electron conduction in accreting stars using molecular dynamics simulations and find that the outer crust is amorphous with a low conductivity [5].

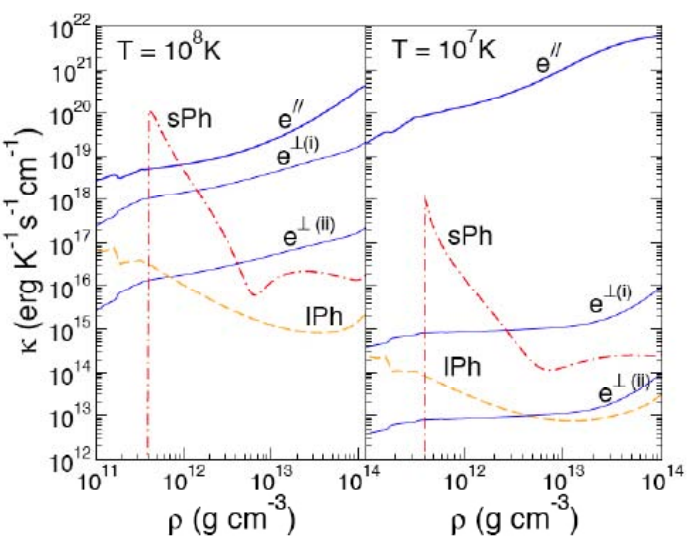


*Figure 2. Thermal conductivity in a NS crust for T =108K (left) and T = 107 K (right). The dot–dashed (red) curve shows the contribution due to sPhs. The thick (thin) solid lines show the electron conductivity in the direction longitudinal (perpendicular) to the magnetic field lines for B = 1013 G (i) and B = 1014 G (ii). The dashed lines (yellow) is the lPh contribution.*

To evaluate if superfluidity in the inner crust is robust we need to ascertain the critical temperature below which superfluid properties manifest. The critical temperature is determined by the magnitude of the pairing energy. Carlson and Gezerlis have performed Monet Carlo simulations requiring about 1 million CPU hours to determine the pairing energy. They found that the pairing energy was significantly larger than all earlier estimates [7].

Outbursts on magnetars called flares occur due to the sudden release of magnetic energy [3]. The triggers for this release are poorly understood. Epstein, Li and Price have studied thermo-resistive instability in middle-age magnetars and find that this may be a viable trigger mechanism. This instability occurs because a temperature perturbation is amplified due to an increase in ohmic resistance–a thermal perturbation could feed on itself resulting in a runaway growth.

Crust cracking can also trigger bursts [3]. Here the magnetic field stresses the solid crust until a sudden catastrophic structural failure initiates a global magnetic field rearrangement. To determine the strength of the crust and the dynamics involved in crust breaking Kadau and Horowitz have developed large-scale molecular dynamics (MD) simulations of up to $10^7$ million ions on LANL computers using LANL developed MD codes. They demonstrated that the breaking strain of the crust was large – ten times larger than previous estimates [8]. This finding marks a watershed in the field of neutron star dynamics with important implications for the production of gravity waves from neutron stars [8].

We have developed a toolset to model supernova spectra and light-curves by adapting an existing code (RAGE). This required adding a transport scheme for the gamma-ray photons emitted in the decay of radioactive nickel and as well as modifying the code to run through the extreme range of conditions required to model supernova light-curves. The initial testing phase is complete and our paper on light-curves from “failed supernovae” on the subject has been accepted for publication [9]. This paper makes direct ties to transients discovered by surveys such as the Palomar Transient Factory and provides the initial data for the Large Synoptic Survey Telescope (LSST). Fryer has been a member of LSST transient science working group for 5 years and he contributed to an LSST-sponsored book, now entering the editing processing, on transient science. These transients tie to a wide range of observations and have important implications for ultraviolet and X-ray studies and we are developing ties with the Swift supernova search teams and the proposed EXIST satellite.

As an example, the emission from an accretion-induced collapse of a white dwarf in a range of wave bands as a function of time (a.k.a. the light curve in these bands) is shown in Figure 3. The high ultraviolet (Swift W1, W2 and M2 bands) are strong signatures of an accretion-induced collapse. With this signal, we hope to distinguish observations of these explosions from other type Ia/Ib/Ic counterparts.

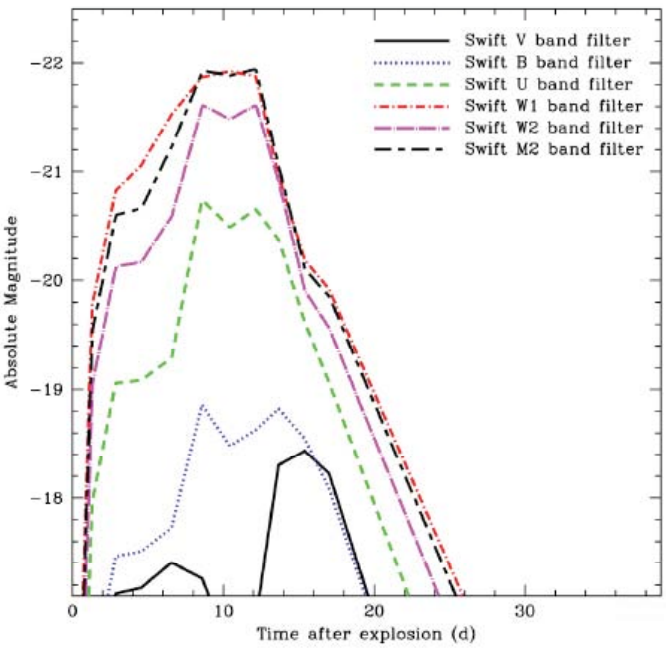


*Figure 3. Absolute Magnitude (emission) versus time in 6 different bands of an accretion-induced collapse of a white dwarf. The strong emission in the ultraviolet (Swift W1, W2, and M2 bands) are strong indicators of this type of explosion.*

The light curve effort is now focusing on a wider set of transients including all types of supernovae. In collaboration with the Chicago FLASH center, this effort was part of a successful NSF proposal. Among other things, these funds will cover a post-doc to work between the FLASH center and LANL. The first project using FLASH explosion data is in preparation and should be published by the end of the year. Here we have studied type Ia supernovae produced in the merger of two white dwarfs ("double degenerate"). We have used tools developed in this to model the merger of two white dwarfs. These merger calculations provide the initial conditions for our light-curve calculations. Using a FLASH explosion for the inner 1.4 solar masses, we then run the explosion through the density/temperature structure produced by these mergers. In this manner, we can study the light-curves produced in double degenerate merger models of type Ia supernovae.

## Future Work

During the last year we intend to confront data on x-ray bursts, superburst and giant flares to extract the neutron star properties such as mass, radius and internal temperature. We anticipate that the improved microphysics described above and our new simulation tools will mitigate any ambiguity or degeneracy in the interpretation. Our effort to predict supernova light-curves using detailed radiation hydrodynamic calculations coupled to modern atomic opacities with data will continue to focus on identifying key observable features that can help us distinguish between different supernova engines and quantify systematic uncertainties associated with using supernova as standard candles to measure cosmological distances.

## Conclusion

We have developed a realistic model for the NS crust and identified important physical processes that occur at these extreme densities. New mechanisms and improved quantitative input physics will enable us to test these models with existing data and provide a quantitative understanding of the some of the features we observe in the x-ray emission from neutron star explosions. It would provide a means to determine the neutron star mass, radius and internal temperature. Such a determination is the holy grail of neutron star research. It would help constrain the properties of matter in the core where the density is well in excess of the density within atomic nuclei.

Our current work to build a full suite of models for supernova light-curves that include the relevant physics of the underlying explosion and radiation transport with the relevant atomic opacity is well underway. This effort will quantify uncertainties associated with using supernova as standard candles.

## References


1. Bildsten, L., and T. Strohmayer. New views of neutron stars. 1999. *Physics Today.* **52**: 40.

2. Strohmayer, T., and L. Bildsten. New Views of Thermonuclear Bursts. *ArXiv Astrophysics e-prints.*

3. Thompson, C., and R. C. Duncan. The soft gamma repeaters as very strongly magnetized neutron stars - I. Radiative mechanism for outbursts. 1995. *Monthly Notices of the Royal Astronomical Society.* **275**: 255.

4. Gupta, S. S., T. Kawano, and P. Moller. Neutron Reactions in Accreting Neutron Stars: A New Pathway to Efficient Crust Heating. 2008. *Physical Review Letters.* **101**: 231101.

5. Aguilera, D., V. Cirigliano, J. Pons, S. Reddy, and R. Sharma. Superfluid Heat Conduction and the Cooling of Magnetized Neutron Stars. 2009. *Physical Review Letters.* **102**: 091101.

6. Daligault, J., and S. S. Gupta. Electron-Ion Scattering in Dense Multi-Component Plasmas: Application to the Outer Crust of an Accreting Neutron Star. 2009. *Astrophysical Journal.* **703**: 994.

7. Gezerlis, A., and J. Carlson. Strongly paired fermions: Cold atoms and neutron matter. 2008. *Physical Review C.* **77**: 032801.

8. Horowitz, C. J., and K. Kadau. Breaking strain of neutron star crust and gravitational waves. 2009. *Physical Review Letters.* **102**: 191102.

9. Fryer, C. L.. Spectra and Light Curves of Failed Supernovae. *Astrophysical Journal .*

## Publications

Aguilera, D., V. Cirigliano, J. Pons, S. Reddy, and R. Sharma. Superfluid heat conduction and the cooling of magnetized neutron stars. 2009. *Physical Review Letters.* **102**: 091101.

Daligault, J., and S. S. Gupta. Electron-Ion Scattering in Dense Multi-Component Plasmas: Application to the Outer Crust of an Accreting Neutron Star. 2009. *Astrophysical Journal.* **703**: 994.

Fryer, C. L., and S. Diehl. On the road to understanding Type Ia progenitors: Precision simulations of double degenerate mergers. 2008. In *Hydrogen-Deficient Stars ASP Conference Series.* (Eberhard Karls University, Tübingen, Germany, 17-21 September, 2007). Vol. 391, p. 335. San Francisco: Werner and Thomas Rauch. .

Fryeretal., C.. Spectra and Light Curves of Failed Supernovae . *Astrophysical Journal .*

Fryeretal., C. L.. Constraints on Type Ib/c supernovae and gamma-ray burst progenitors. 2007. *The Publications of the Astronomical Society of the Pacific.* **119** (861): 1211.

Gezerlis, A., and J. Carlson. Strongly paired fermions: Cold atoms and neutron matter. 2008. *Physical Review C.* **77**: 032801(R).

Gupta, S., T. Kawano, and P. Moller. Neutron reactions in accreting neutron stars: a new pathway to efficient crust heating. 2008. *Physical Review Letters.* **101**: 231101.

Horowitz, C. J., and K. Kadau. Breaking Strain of Neutron Star Crust and Gravitational Waves. 2009. *Physical Review Letters.* **102**: 19102.

Liu, S., Z. H. Fan, C. L. Fryer, J. M. Wang, and H. Li. Stochastic electron acceleration in shell-type supernova remnants. 2008. *Astrophysical Journal.* **683**: L163.

Steiner, A., and S. Reddy. Superfluid response and the neutrino emissivity of neutron matter. 2009. *Physical Review C.* **79**: 015802.

Young, P. A., and C. L. Fryer. The local environments of long-duration gamma-ray bursts. 2007. *Astrophysical Journal.* **670**: 584.

# Novel Signatures of Beyond the Standard Model at the Large Hadron Collider

*Rajan Gupta*
20080661DR

## Introduction

The standard model of elementary particles is very successful at describing all fundamental interactions at energy scales up to 100 times the mass of the proton: there are no significant discrepancies between theoretical predictions and experimentally measured results. Despite this success, a number of fundamental questions have been left out of the purview of the model. With the upcoming high energy physics experiments this is now an unsatisfactory situation and we need the answer to a number of questions, both to take the next logical step in theory design and in suggesting further measurements and analyses. These include questions about the nature of the Higgs sector--whether the particle is elementary or composite, the mechanism that stabilizes the electroweak scale against quantum corrections, the number of spatial dimensions at the weak scale, and whether an as yet unobserved symmetry called supersymmetry is realized by nature at the electroweak scale to both stabilize it and lead to grand unification.

This project addresses these questions by focusing on the signatures of new physics at the Large Hadron Collider experiment at CERN Geneva. The primary work (a) explores the nature of the Higgs' particle and its decay modes that could be tested at LHC and (b) studies decays of proposed supersymmetric particles in which various leptons can be used as triggers or aids in interpreting the new data. It will explore the hierarchy of these particles to understand which theoretical constructs fit observations and if they are candidates for dark matter. In addition, the effort will also identify experimental techniques that can guide in searches for novel events and in elucidating the nature of new physics.

## Benefit to National Security Missions

We support the high energy physics component of the DOE Office of Science mission by addressing four of its six long-term goals: discover the Higgs' particle, measure matter-antimatter asymmetry, probe the high energy frontier, and directly discover dark matter particles. Our instrumentation expertise will build capability for nuclear nonproliferation.

## Progress

The two members of the team (Graesser, Kitano) have produced in the past year 7 research articles that are published in peer-reviewed journals. They have given a number of invited talks at international conferences and institutions, including a plenary talk given by Graesser at the preSUSY 09 international conference. A selection of these accomplishments is discussed next.

In anticipation of the LHC, it is important to investigate novel scenarios for new physics, such as the recent class of models invented by Georgi [1,2] (dubbed ``unparticles"). What distinguishes unparticles is the existence of a continuous spectrum, which can be excited in collisions of Standard Model particles at the LHC.

Georgi, and also Grinstein, Intriligator, and Rothstein (GIR) [3] raise a number of issues about this scenario. Friedland, Giannotti and Graesser [4,5] decided to obtain a simple model in which a number of these questions can be addressed. They show that the well-known Randall-Sundrum model having a single brane, possesses all the properties of ``unparticles", while also satisfying the unitarity constraints found by GIR. Specifically: the unitarity bound on CFT vector operators is obtained by considering brane-to-brane scattering and applying the optical theorem; the mysterious phase in the two-point function is due to the production and escape of Kaluza-Klein particles through the horizon; the contact interactions and cancellations of divergences found by GIR at weak coupling are found to extend to strong coupling; these contact interactions dominate scattering amplitudes, but interactions at a finite distance are dominated by the CFT; and finally, the contact interactions are not really fundamental: at short enough distances the contact interactions are resolved. Some of these results generalize and extend the results found by GIR to strong coupling.

If supersymmetry is correct then the LHC will produce a

number of new particles. Identifying the masses, quantum numbers and interactions of these new particles will provide critical information needed to infer the underlying theory at the TeV scale.

In [6] Graesser and Shelton focus on final states involving jets, missing energy and third generation particles such as the b quark or the tau lepton. The taus or b quarks can be produced with substantial rates in the decays of gluinos or squarks to the dark matter particle and visible matter, providing for a potentially rich phenomenology and insight into the underlying theory. Invariant mass distributions formed from combinations of b-quarks and leptons, or pairs of hadronic taus, are found to be sensitive to the gauge quantum numbers of the intermediate states and on mixing parameters. Signing the charge of the b-quark using the soft muon in its semi-leptonic decay can be used to obtain further sensitivity to the quantum numbers of the sbottoms and sleptons, as well as the mixing angles. Further work on b-l distributions is in progress. Such a model-independent approach had not been done before - previous literature has focused on specific model parameter points.

Kitano has explored experimental consequences of his "sweet spot supersymmetry". Here the gravitino is the dark matter and the next-to-lightest superpartner is a stau, which is charged. Experimentally the stau appears in the detector as a heavy muon and its mass can be measured. This provides critical information, for it can then be used to reconstruct other masses and mixing parameters of the underlying Lagrangian.

In [7], Kitano studies the production of a pair of charginos or of a neutralino and a chargino. These fermions subsequently decay to staus and a tau neutrino or a tau lepton. At the LHC, Kitano finds that this final state can be completely reconstructed up to a two-fold ambiguity. Using this information, Kitano demonstrates that this system can be used to reconstruct the chargino and neutralino masses, and confirm that these particles have spin 1/2. Finally, the distribution of the energy of the lepton is found to be sensitive to the chiral coupling of the stau to the neutralino, allowing for a measurement of these interactions.

In [8], Graesser, Kitano and Director's Fellow Kurachi construct an effective field theory for supersymmetry broken close to the TeV scale. In their scenario i) susy breaking is weakly communicated to the SM particles and their superpartners. and ii) there might be additional light particles that are composites out of the sector that breaks supersymmetry. Using their formalism it is possible to write down operators coupling the Standard Model particles (+ superpartners) to the light composites, in a manifestly supersymmetric manner. This is a non-trivial result since the composite will not appear in complete susy representations, in general.

As an application, they show: i) that one Higgs boson is needed to give mass to both up and down-type quarks; ii) that a spin-2 particle can partially unitarize the goldstino-goldstino scattering channel (Figure 1); and iii) this spin-2 particle can be produced at the LHC with a large enough rate to make discovery possible (Figure 2), in a region of parameters in which the effective theory is reliable (Figure 3). The first result i) is new and explicitly disproves the standard lore that two Higgs doublets are needed if supersymmetry is realized non-linearly. In short, the experimental signatures of this scenario are novel: the LHC will discover superpartners to all the SM particles, except the Higgs boson; and here the discovery of a spin-2 resonance is interpreted as due to strong supersymmetric dynamics at the TeV scale, rather than the more conventional interpretation of it being the first resonance of an extra dimension.

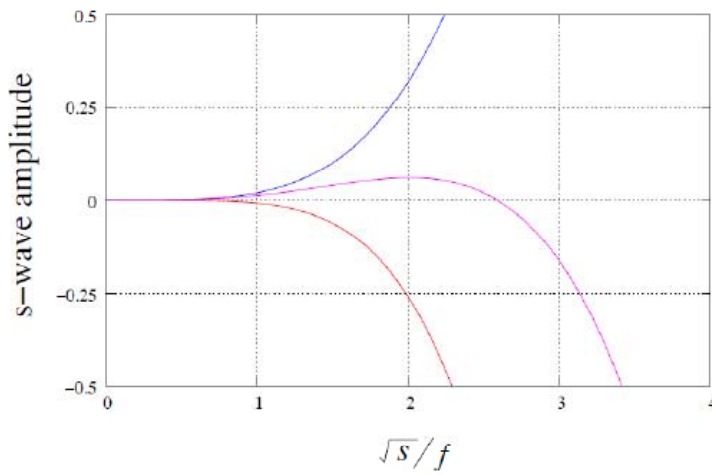


*Figure 1. S-wave amplitude for elastic goldstino-goldstino scattering. The two contributions are: Akulov-Volkov action (blue); spin-2 resonance exchange (red); their sum (pink). Note the partial improvement in the growth of the amplitude once the contribution of the spin-2 resonance is included.*

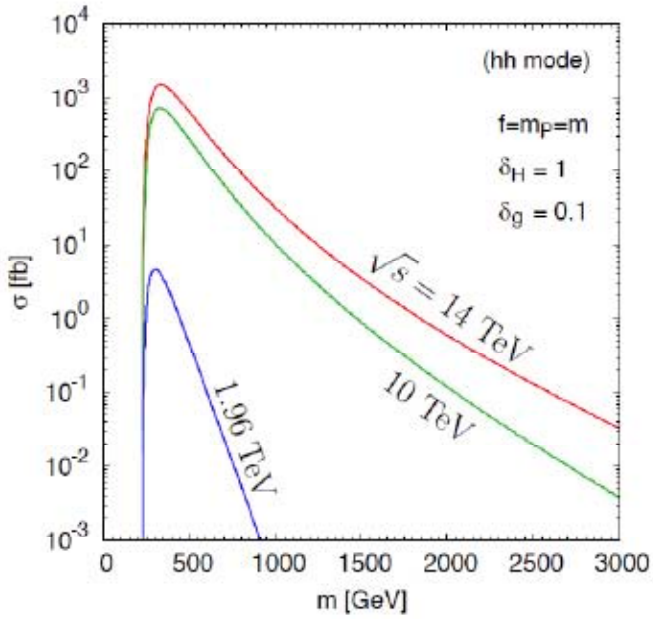


*Figure 2. The production cross-section to two Higgs bosons through the spin-2 resonance, as a function of the graviton mass, for three choices of the center of mass energy. Note that production cross-sections at the Large Hadron Collider (green,red) are sizable for sub-TeV mass, while those at the Tevatron (blue) are small enough to not be excluded.*

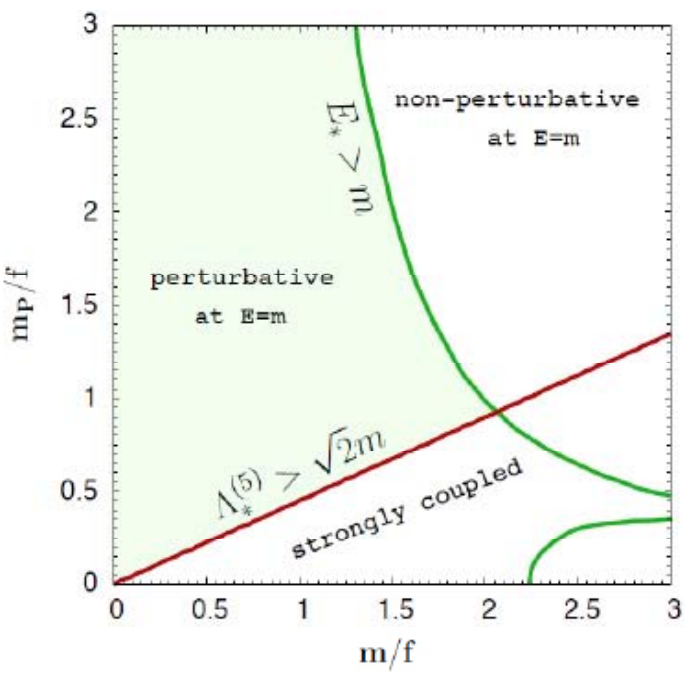


*Figure 3. Region of parameters allowed by perturbativity is to the left of the two lines (shaded).*

## Future Work

In the final year of this project several directions will be pursued:

1. Realistic collider study of using signed b-quarks in events containing leptons and missing energy to assess the potential for probing the SU(2) quantum numbers of the new particles (specifically, sbottoms, stops and sleptons).

2. What is the best strategy for discovering the composite spin-2 particle? Can the Higgs boson be discovered in the decay of the spin-2? Can the sub-jet analysis of [9] be used in this channel to discover the Higgs boson in its decay to b-bbar?

3. New physics can modify our expectations about the properties of the Higgs boson. It may have new decay channels, not occurring within the Standard Model. If so, the upcoming experiment, LHC, may be looking at the wrong place for the Higgs boson. One part of this proposal is to investigate the potential for the LHC to discover and measure these unusual Higgs boson decays.

4. A final direction includes investigating and understanding conformal field theories at the TeV scale, and its possible application to electroweak physics.

## Conclusion

This proposal is expected to answer some of the most pressing questions regarding the microscopic description of nature and the large scale structure of the universe, including:

What are the well-motivated models of physics beyond the Standard Model?

What signatures of such models will allow them to be tested by upcoming experiments?

What other experiments can provide independent tests of these models?

What new elementary particles will explain dark matter and baryon asymmetry of the Universe and what is the underlying theory that governs them?

## References

1. Georgi, H.. Unparticle Physics. 2007. *Physical Review Letters.* **98**: 221601.

2. Georgi, H.. Another Odd Thing About Unparticle Physics. 2007. *Physics Letters B.* **650**: 275.

3. Grinstein, B., K. Intriligator, and I. Rothstein. Comments on Unparticles . 2008. *Physics Letters B .* **662**: 367.

4. Friedland, A., M. Giannotti, and M. Graesser. On the RS2 realization of unparticles . 2009. *Physics Letters B.* **678**: 149.

5. Friedland, A., M. Giannotti, and M. Graesser. Vector Bosons in the Randall-Sundrum 2 and Lykken-Randall models and unparticles. 2009. *Journal of High Energy Physics .* **0909**: 033.

6. Graesser, M., and J. Shelton . Probing Supersymmetry with Third Generation Cascade Decays . 2009. *Journal of High Energy Physics.* **0906**: 039.

7. Kitano, R.. Study of Chargino-Neutralino production at hadron colliders in a long-lived slepton scenario . 2008. *Journal of High Energy Physics .* **0811**: 045

8. Graesser, M., R. Kitano, and M. Kurachi. Higgsinoless Supersymmetry and HIdden Gravity . To appear in *Journal of High Energy Physics.*

9. Butterworth, J., A. Davison, M. Rubin, and G. Salam. Jet substructure as a new Higgs search channel at the LHC . 2008. *Physical Review Letters .* **100**: 242001.

## Publications

Friedland, A., M. Giannotti, and M. Graesser. On the RS2 realization of unparticles . 2009. *Physics Letters B.* **678**: 149.

Friedland, A., M. Giannotti, and M. Graesser. Vector Bosons in the Randall-Sundrum 2 and Lykken-Randall models and unparticles . 2009. *Journal of High Energy Physics .* **0909**: 033.

Graesser, M., R. Kitano, and M. Kurachi. Higgsinoless supersymmetry and hidden gravity . To appear in *Journal of High Energy Physics .*

Graesser, M., and J. Shelton. Probing Supersymmetry with Third Generation Cascade Decays. 2009. *Journal of High Energy Physics .* **0906**: 039.

Ibe, M., and R. Kitano. Minimal direct gauge mediation . 2008. *Physical Review D.* **77**: 075003.

Ibe, M., and R. Kitano. Sweet spot supersymmetry and composite messengers . 2008. *Physics Letters B.* **663**: 242.

Kitano, R.. Study of chargino-neutralino production at hadron colliders in a long-lived slepton scenario. 2008. *Journal of High Energy Physics .* **11**: 045.

Kitano, R.. A clean slepton mixing signal at the LHC. 2008. *Journal of High Energy Physics .* **03**: 023.

Kitano, R., H. Murayama, and M. Ratz. Unified origin of baryons and dark matter . 2008. *Physics Letters B.* **669**: 145.

# High-Precision Spectroscopic Search for Variation of the Fine-Structure Constant

*Justin R. Torgerson*
20080663DR

## Introduction

Without a doubt, our current physical theories of Nature are incomplete and numerous investigations have be launched in attempts to understand some of the most obvious missing pieces in our understanding such as Dark Matter and the nonzero Cosmological Constant. Equally as perplexing, data from astrophysical sources have been analyzed to imply that the Fine Structure Constant (α), which quantifies the strength of electromagnetism, was smaller in the distant past as compared to its current value. It has long been surmised the strength of the fundamental forces, strong, weak, electromagnetism and gravity, may be space-time dependent yet our current theories cannot explain such variation. The discovery of modern space-time variation of strengths of the fundamental forces would dramatically change the way we interpret nature.

We are developing an experimental apparatus capable of searching for modern-day variation of α with unprecedented sensitivity. Our technique will use two optical frequency standards reference to ytterbium ions (laser sources locked accurately to narrow transitions in these ions) that will be compared through a femtosecond laser-based frequency comb (FLFC). Specifically, the femtosecond laser will be referenced to a transition in $Yb^+$ and some light from the FLFC will be frequency-quadrupled (using nonlinear optics techniques) and used to drive a narrow transition in trapped $Yb^{2+}$ ions. In this way, the FLFC becomes a second optical frequency reference with its stability determined by Nature through the $Yb^+$ frequency lock. Measurements of the FLFC's frequency offset and repetition rate in this "locked" state are sufficient to determine possible time variation of α at one part in $10^{18}$. In addition to possibly changing the way we view Nature, this experiment will perfect the technique of optical atomic spectroscopy with light generated directly from a FLFC. Our technique opens a new paradigm in optical spectroscopy since nonlinear optics and a FLFC can be used to generate nearly any color of light, overcoming a serious limitation for many transitions of interest in the science community.

We are also working on a collaborative experiment at UC Berkeley that uses two nearly degenerate atomic levels in dysprosium with the same goal in mind. In this experiment, the optical frequency references are replaced with a single radio-frequency (rf) reference. Atomic Dy is the only known system with opposite parity levels that are close enough in energy to allow transitions between them to be driven with a commercial rf source. The techniques and systematic effects that will ultimately limit the accuracy of these two experiments are very different from each other, but are still quite similar in many practical ways that make them complimentary.

## Benefit to National Security Missions

The primary research proposed here directly supports the Grand Challenge of "Beyond the Standard Model" and is directly relevant to DOE, Office of Science missions. Other impacts resulting from this project include better optical frequency standards and quantum state manipulation of trapped ions which can be important for national security and information security. Other immediate technology developments are advanced, highly sensitive optical detection techniques of atoms and molecules based on Nobel prize winning optical frequency comb technology, which can be important for homeland security and threat reduction. For example, we have recently developed a method to remotely detect airborne mercury emissions from as far away as 10 km and are actively seeking support to prove the technique experimentally. It also appears likely that the technique can be modified to detect other airborne signatures of interest.

## Progress

This past year, we have continued to advance towards our goal to improve our knowledge of variation of α at the level of $(d\alpha/dt)/\alpha \sim 10^{-18} yr^{-1}$. Last year our most exciting progress was trapping of isotopically pure $Yb^{2+}$ in a radio-frequency Paul trap, but we had focused on trapping of the even isotopes since they are significantly easier to trap than odd isotopes. The odd isotopes possess a nuclear magnetic moment that splits the

ground state of the $Yb^+$ ions, as shown in Figure 1, which allows a deleterious effect called "optical pumping" to occur. However, the odd isotopes are highly desirable for our work due to a far smaller response to environmental perturbations. This year we have succeeded in trapping and laser cooling isotopically-pure odd isotopes of $Yb^+$ as well. In particular, we have focused on $^{171}Yb^+$. This work required a more powerful source of 369.5 nm laser light and we designed and constructed one from first principles this past year based upon frequency doubling of a titanium-doped sapphire (Ti:Sapph) laser source.

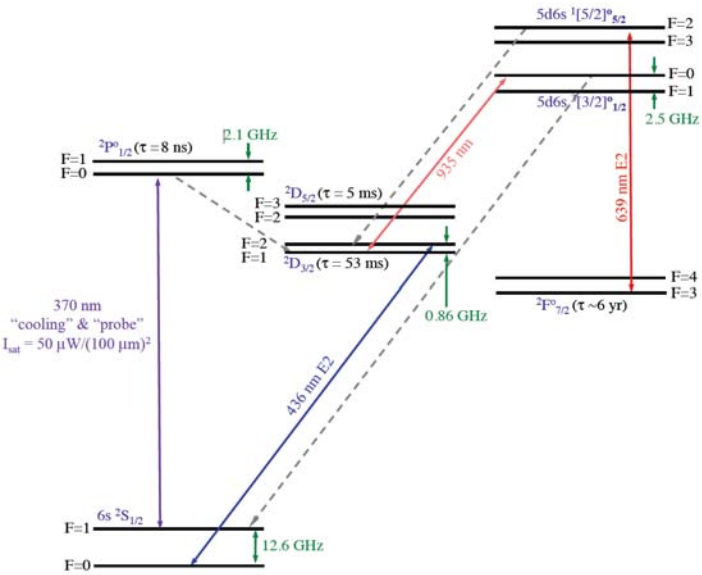


*Figure 1. Partial energy level diagram of the 171-Yb+ ion. The cooling transition is shown in violet and requires a 370 nm laser source to drive it. The "clock" transition is shown in blue and requires 436 nm laser light, but at a very low intensity due to the extremely narrow line - 3.1 Hz compared to the cooling transition linewidth of 30 MHz. The hyperfine splitting are denoted in green text. The even isotopes such as 174-Yb+, do not possess a split level structure and only half of the energy levels shown here exist in these ions.*

This new source is capable of supplying over 50 mW (as compared with 3 mW from our older source) which is enough power for locking the laser to a $Yb^+$ absorption cell for frequency stability as well as supplying power to the eliminate the loss of cooling power and fluorescence signal from the optical pumping within the ground state of $^{171}Yb^+$. We only recently succeeded in trapping and crystallizing $^{171}Yb^+$ ions in large clouds and are still working to isolate single ions of this species. Work to stabilize this new laser source to a $Yb^+$ plasma source is also underway presently.

We investigated collisional decay channels in $Yb^+$ that have not been studied previously involving the cooling and clock states and two other metastable states. We have measured the cross-sections for the two dominant collisional decay channels involving these transitions and have published the results in Physical Review [1].

We completed the development of the frequency-doubled femtosecond frequency comb for direct spectroscopy of the $Yb^+$ "clock" transition at 436 nm. The repetition rate ($f_{rep}$) and the carrier-envelope offset ($f_0$) of the FLFC are both currently locked to a Cs-beam frequency reference with a long-term stability of $5\times10^{-12}$. We have acquired all the necessary apparatus to lock a second Ti:Sapph laser to an optical resonator with a finesse ~$10^5$ through two intermediate resonators to achieve a linewidth <1 Hz. This is the first operating FLFC at LANL. The repetition rate and high peak power make this system ideal with which to perform atomic and molecular spectroscopy using light directly from the comb or with its harmonics. In particular, narrow transitions can be driven with light from the FLFC without problematic AC Stark shifts and a broad spectrum of light can be generated easily with single-pass nonlinear optics.

With single-pass nonlinear optical crystals, we have generated several mW of light at 436 nm with a bandwidth of ~2 nm for ~1 μW per spectral component. Saturation of the $^2S_{1/2}$–$^2D_{3/2}$ "clock" transition in $Yb^+$ requires less than 10 nW for our optical arrangement. This agrees with our calculations and also shows us that the same technique is more than adequate to saturate the 221 nm "clock" transition in $Yb^{2+}$ that requires a second step of frequency doubling.

We also worked closely with our collaborators at UCB on our second search for variation of α based on nearly-degenerate levels in atomic dysprosium. In 2007, we reported our first limit on variation of α, $(d\alpha/dt)/\alpha=(-2.7^+/-2.6)\times10^{-15}$/yr from this experiment. This past two years, we have designed and constructed a new, dedicated spectrometer that will reduce the influence of the systematic effects due to the background pressure, residual magnetic fields, inhomogeneities in the rf electric field, as well as other systematic effects expected to be important below the 1-Hz level. We have also recently succeeded in laser cooling the transverse dimensions of the Dy atomic beam as shown in Figure 2. This success is important for increasing the signal/noise for our measurements as well as to reduce or eliminate problematic systematic effects for our improved determinations of $(d\alpha/dt)/\alpha$.

Finding qualified scientists to support such experimental efforts such as this is always a challenge and it is worth noting here that we have hired four excellent postdocs within the past 18 months.

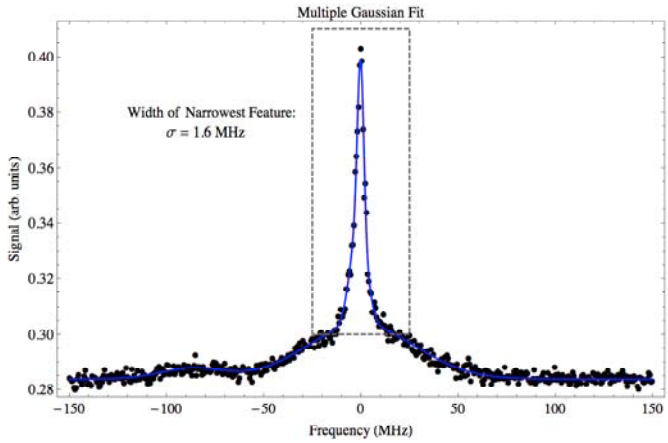


*Figure 2. Data showing the narrowed line of the atomic dysprosium beam. The natural linewidth of this transition is less than 1 MHz, but Doppler broadening of the collimated beam is still 21.2 MHz without transverse cooling.*

## Future Work

Over the next 12 months, we will perform high resolution spectroscopy on the $^2S_{1/2}$–$^2D_{3/2}$ "clock" transition in $Yb^+$ with laser light synthesized directly from our optical frequency comb. The initial goals of this spectroscopy are a resolution of $\Delta\omega/\omega=5\times10^{-14}$, or 50 times better than the current state-of-the-art comb spectroscopy.

Our work with $Yb^{2+}$ is also novel and is the first trapped-ion investigation with a doubly-charged species. This work opens a new paradigm for trapped-ion laser spectroscopy studies as well as optical frequency standards. We will also perform spectroscopy on $Yb^{2+}$ to investigate several aspects of this system which require a thorough analysis before it can be used as the reference for an optical frequency reference. These investigations include an understanding of the decay mechanisms from the excited states of the "cooling" and "clock" transitions and the magnitude of the ground and excited state magnetic moments.

We plan to continue the characterization of the newly-constructed apparatus for measurements of $(d\alpha/dt)/\alpha$ in atomic Dy and to incorporate our recent success with transverse optical cooling of Dy into the apparatus. We expect to reach a sensitivity of $\sim1\times10^{-16}$/yr within the next 12 months or shortly thereafter.

## Conclusion

Measurement of a nonzero variation of α on physics and metrology would play a crucial role in the development of a unified theory of Nature. We are making excellent progress towards our goal of measuring $(d\alpha/dt)/\alpha$ with an expected level of sensitivity of $\sim10^{-18}yr^{-1}$. LANL's work on $Yb^{2+}$ is also of interest to the National Institute for Science and Technology (NIST), since it can be the basis for a new optical frequency standard of exceptional stability. Finally, we are developing powerful frequency synthesis techniques based upon optical frequency comb technology that can be immediately applied to sensitive detection of atoms and molecules such as mercury (as mentioned above) and others.

## References

Schauer, M. M., J. R. Danielson, A. T. Nguyen, L. B. Wang, X. Zhao, and J. R. Torgerson. Collisional population transfer in trapped Yb+ ions. 2008. *Physical Review A.* **79**: 6062705.

## Publications

Leefer, N. A., A. Cingoz, D. Budker, S. J. Ferrell, V. V. Yashchuk, A. Lapierre, A. T. Nguyen, S. K. Lamoreaux, and J. R. Torgerson. A laboratory search for variation of the fine-structure constant using atomic dysprosium. 2008. *European Physical Journal.* **163**: 71.

Leefer, N. A., A. Cingoz, D. Budker, S. J. Ferrell, V. V. Yashchuk, A. Lapierre, A. T. Nguyen, S. K. Lamoreaux, and J. R. Torgerson. Variation of the Fine-Structure Constant and Laser Cooling of Atomic Dysprosium. To appear in *Symposium on Frequency Standards and Metrology .* (Pacific Grove, CA, 5-11 October, 2009).

Nguyen, A. T., L. B. Wang, M. M. Schauer, and J. R. Torgerson. Extended temperature tuning of an ultraviolet diode laser for trapping and cooling single Yb+ ions. *Revews of Scientific Instruments.*

Porsev, S. G., V. V. Flambaum, and J. R. Torgerson. Transition frequency shifts with fine-structure constant variation for Yb II. 2009. *Physical Review A.* **80**: 042503.

Rellergert, W. G., D. DeMille, E. R. Hudson, R. Greco, M. Hehlen, and J. R. Torgerson. Investigation of the optical transition in the 229Th nucleus: Solid-state optical frequency standard and fundamental constant variation. *Physical Review Letters.*

Schauer, M. M., D. Feldbaum, A. T. Nguyen, L. B. Wang, X. Zhao, and J. R. Torgerson. Trapping and spectroscopy of singly- and doubly-charged ytterbium ions. Presented at *39th Annual Meeting of the Division of Atomic, Molecular, and Optical Physics.* (State College, PA, 27-31 May, 2008).

Schauer, M. M., J. Danielson, D. Feldbaum, M. S. Rahaman, B. Sun, X. Zhao, and J. R. Torgerson. Trapping and Optical Detection of Doubly-charged Ytterbium Ions. Presented at *40th Annual Meeting of the Division of Atomic, Molecular, and Optical Physics.* (Charlottesville, VA, 19-23 May, 2009).

Schauer, M. M., J. R. Danielson, A. T. Nguyen, L. B. Wang, X. Zhao, and J. R. Torgerson. Collisional population transfer in trapped Yb+ ions. 2008. *Physical Review A.* **79**: 6062705.

# Double Beta Decay

*Steven R. Elliott*
20090053DR

## Introduction

The answer to the question: "Is the neutrino its own anti-particle?" is critical for theories of particle mass. It is also needed to help uncover the reasons matter dominates over anti-matter in our Universe. The neutrino mass will not only tell us about the energy scale at which the Standard Model breaks down, but also has implications for the large-scale structure of the Universe. Finally, lepton-number violation is significant in its own right.

Neutrinoless double-beta decay is the only practical method for investigating the particle/anti-particle question. If the neutrino is its own anti-particle, neutrinoless double-beta decay will have the best sensitivity to neutrino mass of any laboratory technique. Calculations of the nuclear matrix elements for this process have driven the advancement of nuclear shell-model codes. Our double-beta decay program will greatly influence the wider-particle physics, nuclear physics, astrophysics and cosmology endeavors.

If this nuclear decay process exists, one would observe mono-energetic beta emission originating from certain isotopes. This is in contrast to classical single beta decay, in which the beta particles (electrons) are spread over a wide range of energies. One isotope that may undergo double-beta decay is Ge-76. Germanium-diode detectors fabricated from material enriched in Ge-76 have established the best half-life limits and the most restrictive constraints on the effective Majorana mass. This material holds great promise for future advances in double-beta decay experimental techniques. Eventually, these future experiments could detect a double-beta decay lifetime as long $10^{27}$ y, which produces only about 1 event per ton per year. At this sensitivity, we can look for neutrino mass values near that indicated by the atmospheric neutrino oscillation results.

The primary goal of this proposal is to establish the experimental and theoretical technology for a "near background-free" search for neutrinoless double-beta decay in Ge-76. This proposal supports the construction of a first cryostat using detectors fabricated from natural-abundance Ge. This first cryostat will be an effective prototype for the future 2 cryostats that will be populated with detectors fabricated from enriched material.

## Benefit to National Security Missions

The Nuclear Physics Long Range Plan strongly endorses research in this area of double beta decay. The DOE Office of Nuclear Physics has defined this research as a mission need. The similarity of requirements means that this R&D will be applicable to certain environmental monitoring applications. Furthermore, this work will develop sensor technology for Threat Reduction, e.g. Nonproliferation, and for materials management in the weapons program.

## Progress

Progress has been made on several fronts during our first year. Our efforts have been divided between a better understanding of the various types of background that could make our search for double beta decay difficult, beginning the construction of the first cryostat of detectors, and theory efforts.

We have continued to do a number of experiments to investigate the background contributions for a double beta decay experiment. Much of our recent work in this area has exploited the nearby proximity of the neutron facility. We have just published a paper on neutron interactions in lead, to determine a rate for a particularly troublesome background reaction. We have made progress analyzing similar data we have for Ge and Cu. We plan to take similar data on the material cadmium zinc telluride (CZT) this summer. We have studied the production rates of troublesome isotopes that result from interactions with cosmic-ray neutrons. We have also completed taking data to understand surface alpha backgrounds, and the analysis of those data is nearing completion.

We are working closely with the designers of the Sanford Underground Laboratory (SUL) at Homestake to prepare for occupation of an underground laboratory

there. We will be one of the initial experiments to reside in that facility. Through our direction, SUL has prepared a laboratory design that will meet our requirements. There has been a bit of delay in the anticipated beneficial occupancy date of the finished lab. However, some of this schedule risk has been mitigated by a plan to install a temporary lab to begin the time critical electroforming of the low-activity shield parts. These parts must be built underground, so they are not contaminated by cosmic-ray activation. This step is very time consuming and hence it is important to get it started soon. We now anticipate having access to the full lab in mid to late 2010.

Significant progress has been made on the shield and calibration engineering. (See Figure 1 for a concept drawing.) The shield will be composed of a large mass of Cu and Pb. We have purchased the required lead and it has been delivered. We have also purchased the Cu stock required for the shield and it has been delivered and is being stored underground at SUL. Our design engineer has completed an initial conceptual design for the shield. This design is being refined and the engineering is beginning.

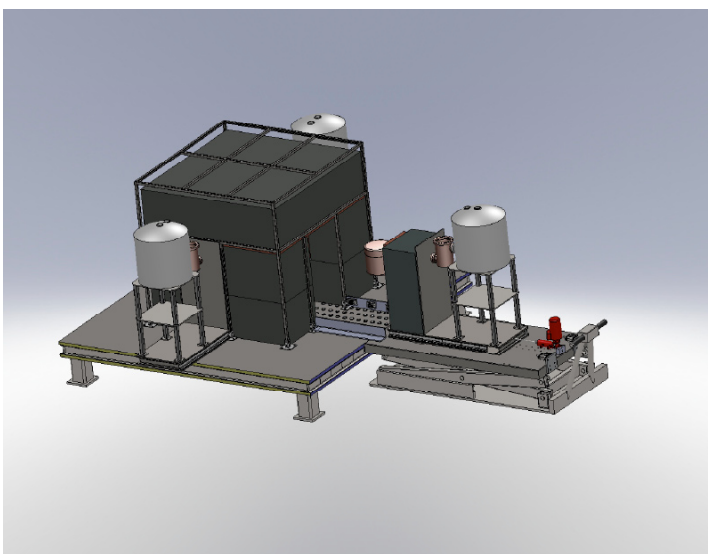

*Figure 1. A concept drawing of the shield design for the experiment.*

We ordered and received 18 Ge detectors, which will comprise about half that needed for the first cryostat. We plan to purchase an additional batch of detectors next year. We have done acceptance testing of these 18 detectors.

The theory team has investigated the nuclear matrix element of neutrinoless double beta decay. This matrix element is required to obtain the absolute mass scale of neutrinos from an experimental signal. Jonathan Engel from the University of North Carolina has collaborated with the T-division team examining short-range parts of the matrix element and setting up exact calculations in small systems where the approximations of the full calculations in real nuclei can be tested. The former work has helped to limit the uncertainties arising from the short-range correlations. The latter is just initiated, but should allow significant tests of shell model and related theories.

## Future Work

The Standard Model (SM) has been very successful in describing the fundamental forces of nature for several decades. However, the preponderance of matter over anti-matter in the Universe, the origin of mass, and the unification of the forces are key aspects of the theory that are unanswered.

The fundamental properties of the neutrino are critical to understanding these basic components of the SM. The answer to the question: “Is the neutrino its own anti-particle?,” is needed to help uncover the reasons matter dominates over anti-matter in our Universe. If the neutrino is its own anti-particle, then a natural explanation for the matter/anti-matter asymmetry arises (leptogenesis). The answer is also critical for theories of the origin of mass. Another question: “What is the neutrino mass?”, has implications for the large-scale structure of the Universe. A third question: “Is lepton number violated?”, is also a significant test of the SM - an observation of lepton violation would mean that a new model is needed. Neutrinoless double-beta decay (BB) is the only practical experimental method for investigating the neutrino particle/anti-particle question. And if the neutrino is its own anti-particle, BB will have the best sensitivity to neutrino mass of any laboratory technique.

If this nuclear-decay process exists, one would observe a mono-energetic line originating from an isotope subject to this decay mode. One such isotope that would undergo this decay is Ge-76. Germanium-diode detectors fabricated from material enriched in Ge-76 have established the best BB half-life limits and the most restrictive constraints on the effective neutrino mass. Therefore, this material holds great promise for future advances in BB techniques. The technology has now reached the point that results from BB projects will address the critical questions listed above.

We will test several technologies to determine if ton scale Ge-based BB experiments are feasible.

## Conclusion

The results from this project will demonstrate that the proposed technique is capable of reaching the sensitivity required for future double beta experiments. These experiments have the potential to elucidate the origin of the matter-antimatter asymmetry of the Universe and hence address the question of why galaxies, stars, and planets were possible.

## Publications

Burrittandothers, T. H.. Surface-alpha backgrounds for the Majorana neutrinoless double-beta decay experiment. 2008. *Journal Physics Conference Series.* **136**: 042051.

Elliott, S. R.. Double Beta Decay: Solid-State and Semiconductor Detectors. Presented at *Conference on the Intersections of Particle and Nuclear Physics.* (San Diego, CA, May 2009).

Gehman, V. M., S. R. Elliott, and D. M. Mei. Systematic Effects in Pulse Shape Analysis of HPGe Detector Signals for Neutrinoless Double-Beta Decay. To appear in *Nuclear Instruments and Methods.*

Guiseppe, V. E., M. Devlin, S. R. Elliott, N. Fotiades, A. Hime, R. O. Nelson, D. M. Mei, and D. V. Perepelitsa. Neutron inelastic scattering and reactions in natural Pb as a background in neutrinoless double-beta decay experiments. 2009. *Physics Review C.* **79**: 054604.

Guiseppeandothers, V. E.. The production of 68Ge in Ge detectors due to fast neutrons. Presented at *April Meeting of the American Physical Society.* (Denver, CO, May 2009).

Guiseppeandothers, V. E.. The MAJORANA Project. Presented at *Implications of Neutrino Flavor Oscillations.* (Santa Fe, NM, July 6-10, 2009).

Henningandothers, R.. An R&D Project Towards a Tonne-Scale Germanium Neutrinoless Double Beta Decay Search. To appear in *Conference on the Intersections of Particle and Nuclear Physics.* (San Diego, CA, May 2009).

Mei, D. M., Z. B. Yin, and S. R. Elliott. Cosmogenic Production as a Background in Searching for Rare Physics Processes. 2009. *Astroparticle Physics.* **31**: 417420.

# Turbulence By Design

*Malcolm J. Andrews*
20090058DR

## Introduction

The prediction, design and control of turbulence have challenged our ingenuity for thousands of years. Roman water systems, air flight, climate, and Inertial Confinement Fusion (ICF) highlight the range of scientific problems that involve fluid turbulence. Los Alamos National Laboratory (LANL) has led developments of high fidelity fluid flow diagnostics, and the discovery that starting conditions can influence the development of hydrodynamic turbulence and material mixing in buoyancy driven flows. These leading edge advances have come about through studies of buoyancy driven turbulence in ICF targets. This Directed Research (DR) project couples a well-balanced set of unique LANL facilities and advanced diagnostics with experts in theory and computation. This synergistic expert team is determining the role of designed starting conditions and characterizing their effect on the development of material interpenetration, mixing, and turbulence. Thus, a timely opportunity has arisen to develop a new paradigm for buoyancy driven turbulence, namely "Turbulence by Design" (TbD), with LANL fluid dynamics research at the leading edge. The central goal of this DR is to determine the extent to which certain starting conditions can be used to predict and design turbulent transport/material mixing, Figure 1. The broad impact of this research includes the ability to design ICF targets for net energy gain, determination of early-time astrophysical processes, a better understanding of climate and ocean flow dynamics and, more generally, a scientific basis for understanding the development of buoyancy driven turbulence and its prediction/design/control.

## Benefit to National Security Missions

This project will support the DOE and NNSA mission in Nuclear Weapons and Energy by determining the effect and use of initial conditions on Inertial Confinement Fusion, and code validation for Stockpile Stewardship. Additional high impact on climate, energy generation and usage, astrophysics, and any technological area that involves turbulence.

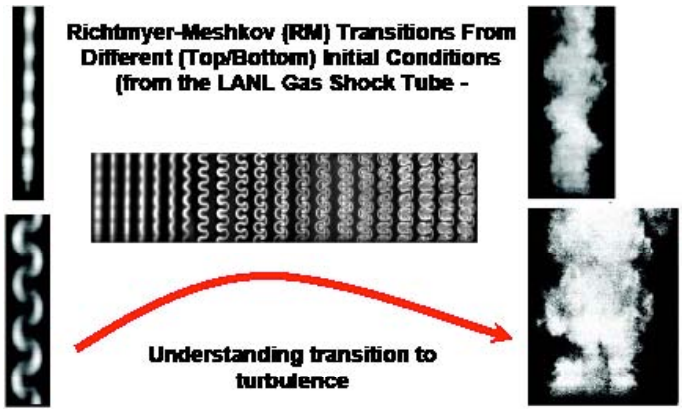


*Figure 1. Memory of initial conditions (on the left) is NOT lost during turbulence development (left to right).*

## Progress

Over this first 12 months of the project we have produced six journal publications, given eight seminars and six conference papers, and presented four conference posters (including a 1st Place at the LANL LDRD DAY, 9/15/2009). In addition we have successfully hired four post-docs and purchased approximately $150K of needed experimental equipment, materials and supplies.

Major scientific achievements for the first 12 months of the project include:

- Completion of single mode analysis using linear and non-linear analysis, with the implementation of a ordinary differential equation (ODE) solver for multiple modes that produces results comparable with 3-D transient simulations of different initial conditions (PI, co-PI: Andrews and Ristorcelli). The ODE solver will permit the development of an optimization design route for turbulence based on "best" initial conditions

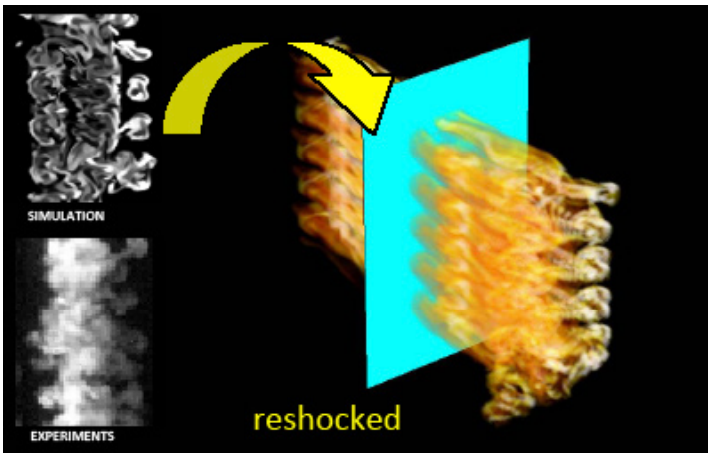


*Figure 2. Computer simulations (on the right) that use the RAGE computer code are being used to design, and then interrogate, experiments (on the left) to explore the late-time effects of initial conditions.*

- Execution of Richtmyer-Meshkov experiments and comparison with ILES simulations based on measured initial conditions - the comparison was excellent, Figure 2, and sets the scene for experimental/computational/theoretical investigations of alternative initial conditions (Co-PI's: Prestridge and Grinstein).

- Formulation of turbulence modeling parameters based on linear and non-linear stability analysis that will permit inclusion of initial conditions in simulations of transient turbulent mixing simulations. This key component of the research is central to our transition plan, and will provide a major impact across predictive science for variable density flows and turbulence. (co-PI: Ristorcelli).

- Roadrunner-executed 3-D Direct Numerical Simulations Rayleigh-Taylor mixing, with de-mixing, Figure 3. These are the first numerical simulations of turbulent mixing on Roadrunner, and will form one of our canonical datasets against which we will be testing our methodologies for "Turbulence By Design" (co-PI: Livescu).

Aside from these major scientific advances, we performed numerous other supporting analyses and experiments.

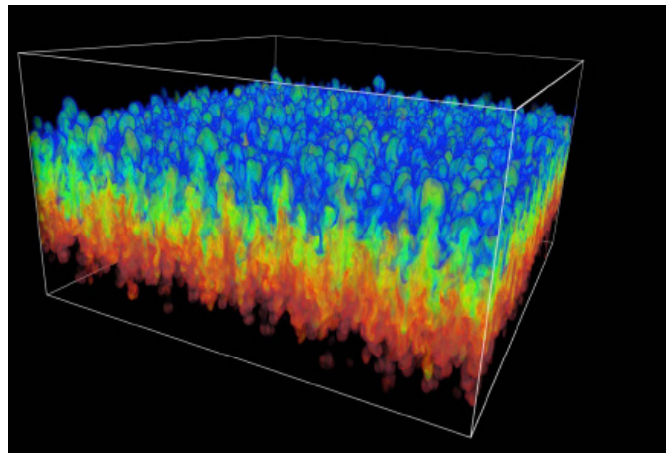

*Figure 3. Rayleigh-Taylor mixing layer, computed from a Direct Numerical Simulation (DNS) on the LANL Petascale Roadrunner computer. Such mixing conditions occur during the implosion phase of Inertial Confinement Fusion (ICF). At late times the flow structures become seemingly random, however their random properties are, in part, determined by characteristics of the initial conditions.*

## Future Work

Recent work at Los Alamos National Laboratory (LANL) has shown that buoyancy driven turbulence can be affected at late-time by initial conditions, and memory of the initial conditions is not lost. This is a remarkable discovery that suggests an important opportunity to predict and "design" late-time buoyancy driven turbulence, i.e. Turbulence by Design (TbD), with transformative impact on our understanding and prediction of Inertial Confined Fusion (ICF), free-convection, environmental and technological flows, and general fluid mixing processes. Often, and especially in turbulence research, the assumption is made that initial conditions (ICs) wash-out (loss of memory) and that the turbulence develops to a universal self-similar end state. However, there is a growing body of fundamental research that indicates only special turbulent flows are truly self-similar. Indeed, empirically-based turbulence modification is commonly used for example with golf-ball dimples. At the heart of our TbD blue-print for turbulence prediction and thus design lies the hypothesis that initially seeded small amplitude, long wavelength, perturbations can develop at late-time and be used to control turbulence transport and material mixing.

The broad impact of this hypothesis extends well beyond our interest in buoyancy and shock driven flows and incorporates the possibility of scientifically designing boundary conditions/shapes for passive turbulence control. Thus, we envision a transformative opportunity for LANL to define a new paradigm for turbulence research that leaves behind the universal "fully-developed" equilibrium concept, and embraces late-time turbulence

in ICF through prescribed ICs that enhance, suppress, or maintain turbulence intensity/structure for practical gain as related to LANL Grand Challenges. The late-time signatures of ICs also imply a better understanding of mix dominated buoyancy problems such as supernovas, solar ponds, ocean over-flows, and heat-transfer enhancement by rotating flows, and thus address a broad class of technological problems with the potential of revolutionary advances and discoveries.

## Conclusion

This fundamental research will control the development of turbulence by design of starting conditions. Our focus is Inertial Confinement Fusion, with the goal of enhanced energy gain, lower energy costs, and reduce US dependence on foreign energy sources. However, more immediate impacts will be felt since oil trapping salt domes in Texas and the Gulf are also buoyancy formed structures whose location, size, and orientation depend on how they start and thus lend their prediction to our research. Other applications include more efficient engine fuel sprays, reduction of drag, cooling technologies, and weather prediction.

## Publications


Andrews, M. J.. LDRD-DR: Turbulence by design: 1st year review. 2009. *Poster given at the HED&P&F Capability Review, LANL, May 13, 2009. LA-UR 09-02673..*

Andrews, M. J.. Turbulence by design. 2009. *Poster, LDRD Day, Los Alamos National Laboratory, September 15, 2009. LA-UR # 09-05195. .*

Andrews, M. J.. LDRD-DR: Turbulence by design: 1st year review. Presented at *LDRD-DR 1st year review.* (Los Alamos National Laboratory, 13 May 2009).

Andrews, M. J., A. Duggleby, and Y. Doron. A PDF of molecular mix measurements in high Schmidt number Rayleigh-Taylor turbulence. Presented at *Turbulent Mixing and Beyond.* (Trieste, Italy, 27 July - 7 August, 2009).

Andrews, M. J., F. F. Grinstein, D. Livescu, and K. Prestridge. LDRD-DR: Turbulence by Design. 2009. *Poster presentation, at Boost Fest, Sandia National Laboratory, April 4, 2009. LA-UR 09-02673..*

Balakumar, B. J., K. P. Prestridge, G. Orlicz, S. Balasubramanian, and C. Tomkins. High resolution experimental measurements of Richtmyer-Meshkov turbulence in fluid layers after reshock using simultaneous PIV-PLIF. To appear in *APS Shock-Compression of Condensed Matter.* (Nashville, TN, June 29 – July 3, 2009).

Banerjee, A., and M. J. Andrews. 3D Simulations to investigate initial condition effects on the growth of Rayleigh–Taylor mixing. To appear in *International Journal of Heat and Mass Transfer.*

Grinstein, F. F.. On integrating large eddy simulation and laboratory turbulent flow experiments. 2009. *Transactions of the Royal Society.* **A** (367): 2931.

Grinstein, F. F.. Verification and validation of CFD based turbulent flow experiments. To appear in *Encyclopedia of Aerospace Engineering.* By Shyy, W..

Grinstein, F. F.. On Integrating LES and Laboratory Turbulent Flow Experiments. Presented at *Discussion Meeting on "Applied Large Eddy Simulation" of the Royal Society.* (London, 27-28 October 2008).

Grinstein, F. F.. Simulating vortex dynamics, transition, and turbulent mixing in high Reynolds-number flows. Presented at *Tutorial at "Turbulent Mixing and Beyond" Conference.* (Trieste, Italy, 5 August 2009).

Grinstein, F. F., and A. Gowardhan. On the simulation of shock-driven material mixing in high Reynolds-number flows. Presented at *Turbulent Mixing and Beyond .* (Trieste, Italy, 6 August 2009).

Livescu, D.. Direct Numerical Simulations of turbulence. Presented at *High energy Density Plasmas and Fluids Capability Review.* (Los Alamos National Laboratory, 13 May 2009).

Livescu, D., H. Yu, and R. McLarren. Temperature effects on the Rayleigh-Taylor instability. *Physics of Fluids.*

Livescu, D., J. R. Ristorcelli, and R. A. Gore. Variable-density Rayleigh-Taylor turbulence. *Physica Scripta.*

Livescu, D., J. R. Ristorcelli, and R. A. Gore. Mixing asymmetry in variable density turbulence. Presented at *62nd APS Dvision of Fluid Dynamics Annual Meeting.* (Minneapolis, MN, 24 November 2009).

Livescu, D., M. J. Petersen, S. Martin, and P. McCormick. Spikes and bubbles in turbulent mixing: High Atwood number Rayleigh-Taylor instability. 2009. *Poster to be presented at the 62nd APS/DFD annual meeting, Minneapolis, 2009..*

Livescu, D., and J. R. Ristorcelli. Mixing asymmetry in variable density turbulence. 2009. In *Advances in Turbulence XII.* Edited by Eckhardt, B.. Vol. 132, p. Not known. Berlin: Springer.

Prestridge, K. P., B. J. Balakumar, C. Tomkins, and S.

Balasubramanian. Experiments for understanding shock-driven mixing and turbulence. Presented at *High Energy Density Plasmas and Fluids (HEDPF) Capability Review.* (Los Alamos National Laboratory, 13 May 2009).

Prestridge, K. P., B. J. Balakumar, G. Orlicz, C. Tomkins, C. Zoldi-Sood, and R. A. Gore. Understanding Turbulence in Richtmyer-Meshkov unstable flows. Presented at *NEDPC.* (Lawrence Livermore National Laboratory, 27 October, 2009).

Prestridge, K. P., B. J. Balakumar, G. Orlicz, and C. Tomkins. High resolution experimental measurements of Richtmyer-Meshkov turbulence in fluid layers after reshock. Presented at *APS Shock-Compression of Condensed Matter.* (Nashville, TN, 2 July 2009).

Prestridge, K. P., B. J. Balakumar, G. Orlicz, and C. Tomkins. Understanding experimental diagnostics and results for code and model validation. Presented at *Turbulent Mixing and Beyond.* (Trieste, Italy, 27 July 2009).

Reckinger, S., D. Livescu, and O. Vasilyev. Compressibility effects on single mode Rayleigh-Taylor instability. 2009. *Poster given at Turbulent Mixing and Beyond Conference, Trieste, Italy, July 27, 2009..*

Ristorcelli, J. R., and N. Helmn. Initial conditions for the turbulence moments at an unstable quiescent stochastic material interface. *Journal of Turbulence.*

Ristorcelli, R. J.. Stochastic linear stability theory: obtaining statistics for moment closure models. Presented at *Turbulent Mixing Colloquium.* (Los Alamos National Laboratory, 1 July 2009).

# New and Enhanced Capabilities in Quantum Information Processing

*Malcolm G. Boshier*
20090476DR

## Introduction

This project will search out and exploit new connections between several areas of quantum physics and information science to build new tools and technologies, which support the Laboratory mission.

1. We will develop the new field of quantum sensing, using the power of quantum mechanics to create sensors of forces and fields performing beyond the current state of the art. This requires both theory to develop optimum measurement strategies, and experiment to provide the tightly-controlled quantum systems which can implement these strategies.

2. We will explore the many interlocking aspects of many-body physics, atomic and optical physics, and quantum control essential to understanding, controlling, and predicting the properties of materials. The focus will be on understanding those materials relevant to energy, such as high Tc superconductors.

3. We will use the tools of quantum information science to gain new insights into the power and potential of quantum computers to solve otherwise intractable problems and to increase information security. In particular we hope to find new classes of algorithms for quantum computers and new techniques for increasing the range of quantum key distribution for provably secure protection of information.

## Benefit to National Security Missions

This project will support the DOE missions of the Office of Science by enhancing our understanding of basic quantum physics and of the properties of matter. It will also support the nonproliferation mission by investigating quantum sensing methods. The understanding of superconductors will benefit energy transmission technology.

## Progress

This project is finding and exploiting new connections between several areas of quantum physics and information science and building new tools and technologies, which support the Laboratory mission. In the first year of the project we have made progress in three of these areas:

**Quantum Information Theory**

Our focus here is on finding ways to use quantum technologies to increase the security and capacity of communication channels.

Patrick Rice, working with Jim Harrington and Israel Owens, has analyzed two methods for entanglement-based quantum key distribution, with a comparison of the methods' secret bit yields as a function of loss and noise. He has also carried out numerical simulations to analyze the performance of a particular topological color code under various error models. We believe that the quantum information science community will see this as groundbreaking work for understanding the utility of these codes for use in fault-tolerant quantum computation. A paper on this work [1] has been submitted for publication.

Jon Yard has completed a project with collaborator Igor Devetak (USC) that proves the existence of a optimal quantum protocol for performing quantum data compression when the sender and receiver each have quantum side information [2]. With Matt Hastings, he has made progress in relating this optimal protocol to the notion of topological entanglement entropy, which is an entropic signature of topological order in two-dimensional quantum spin systems. This is important because topological order is expected to play a role in the design of novel materials and devices, including high-Tc superconductors and quantum computers. This research illustrates the connections between quantum information science and quantum many-body physics developed in this project. Yard has also begun work with Cris Moore (UNM/SFI) and Alex Russell (UConn) on developing a new algorithm for approximating topological invariants on quantum computers, part

of our goal to develop new algorithms for quantum computers and to better understand the origin of the power of quantum computing.

**Technology for Quantum Sensing and Quantum Information Processing**

Warren Lybarger and Jon Chiaverini have increased our experimental trapped-ion quantum sensing and quantum computing capability by building a scanning transfer cavity laser-stabilization system to maintain several of the lasers at the required frequency within 1 MHz over several hours. This stability of one part in a billion has been achieved in a straightforward system that allows for changing of the individual laser frequencies while locked, a necessity for precision laser cooling, spectroscopy, and control of individual atoms. They are also exploring the use of dynamically configurable trapping array microstructures for advanced quantum processing schemes. By transforming the RF trap electrodes in real time during an experiment, qubit manipulation and transport can be greatly simplified over current methods.

Alexander Chumak and Vyacheslav Gorshkov (Nat. Acad. of Sciences, Ukraine) have been working with LANL's Gennady Berman, Boris Chernobrod, Alan Bishop and colleagues on applications of quantum technologies to communication and sensing. First, they have proposed a new free space optical communication system based on spectral encoding of a broadband laser. This novel technology gives high data rates combined with reduced sensitivity to beam wandering and atmospheric scintillation [3]. Second, they have investigated how tiny micromechanical mirrors might be used as room temperature sensors of infrared and terahertz radiation [4], a region of the spectrum where there is a pressing need for sensitive detectors, which do not require cooling.

**Quantum Many-body Physics**

David Roberts is pursuing two tasks in collaboration with Andrew Sykes (Queensland) building on their unique expertise in solving the scattering problem in a bosonic superfluid (one of the most important quantum many-body systems). First, using new solutions obtained while investigating drag forces in a quasi-1D geometry, they are calculating the lifetime of a "black soliton", which would be important for a theoretical understanding of solitons as well as their experimental realization. Second, they are also adapting methods of investigating drag forces in bosonic superfluids to systematically calculate for the first time similar effects in BCS fermionic systems that are experimentally realizable. Roberts is also working with Ashton Bradley (University of Otago) on a classical field study of the transverse force of a moving vortex in a superfluid in finite temperature BECs. This has been an outstanding problem since the 1960s with important implications for superfluids and superconductors.

Wojciech Zurek, collaborating with Jacek Dziarmaga and his graduate student Marek Rams of the Jagiellonian University in Krakow, has been investigating topological defect formation in the course of a phase transition. Very recently they have made significant progress in understanding the quantum aspects of defect formation (in particular, their decoherence). They have also studied defect formation in the Bose-Einstein condensate ring lattice that can now be realized by experimentalists at LANL. Finally, Dziarmaga, Michael Zwolak, and Zurek have developed a simple implementation of a "topological Schroedinger cat" in the quantum Ising model. The analysis is at this point only partly completed, but will likely lead to a paper that sheds novel light on symmetry breaking in phase transitions and the quantum-classical transition.

## Future Work

The main scientific issue to be addressed in this project is exploiting more fully the potential of quantum mechanical coherence and entanglement, particularly in areas, which cross boundaries between traditional scientific disciplines. In the next year our high-level plan is as follows.

Working at the intersection of information science and quantum physics, we will address the important question of identifying the origin of the power of quantum computing. Most physicists believe that entanglement is key, but much remains to be understood. The goal here is to gain additional insight and understanding of this key issue. We expect to investigate network quantum information theory, quantum conditional information, and their roles in understanding and computational modeling of complex quantum systems. Another challenge for quantum information processing is to develop quantum algorithms for problems whose computational complexity renders them insoluble on classical hardware. In this project, we will seek new quantum algorithms for an important class of problems in the mathematical theory of knots.

We will also continue to investigate the emerging field of quantum sensing. Here the goal is to find ways to build instruments with sensitivities to forces, accelerations, and electromagnetic fields which exceeds the standard limits due to shot noise, etc. Tasks include the theoretical issue of devising optimum measurement strategies, and the practical challenge of implementing those strategies on suitable quantum hardware, such as trapped ions or ultracold atoms.

Finally, we will build a coalition to work at the fertile overlap of atomic and optical physics, quantum information science, and condensed matter physics. Here one goal is to devise new techniques for computing quantum systems in the face of exponential complexity. Another is to link the very clean quantum phase transitions observed in ultracold gases to the quantum critical

behavior, which is important in many materials, such as unconventional superconductors.

## Conclusion

Our project is on track. Success will produce:

1. New quantum sensing technolgies with sensitivity far beyond the current state of the art. Applications range from surface microscopy to precise measurements of gravity and electromagnetic fields.

2. New techniques and computational tools for understanding, controlling, and predicting the properties of materials and other many-boson systems, including those relevant to energy such as high-Tc superconductors.

3. New algorithms for quantum computers to allow solutions of classes of mathematical problems which are currently intractable, and new techniques for improving the range of applicability of quantum key distribution, which enables completely secure distribution of cryptographic key material.

## References


1. Rice, P., and I. J. Owens. Comparison between continuous wave and pulsed laser EQKD Systems. 2009. *To Be Submitted.*

2. Yard, J., and I. Devetak. Optimal quantum source coding with quantum side information at the encoder and decoder. To appear in *IEEE Transactions on Information Theory.*

3. Berman, G. P., A. R. Bishop, B. M. Chernobrod, A. A. Chumak, and V. N. Gorshkov. Suppression of scintillations and beam wandering in free space gigabit rate optical communication based on spectral encoding of a partially coherent beam. To appear in *Photonics West.* (San Jose, 24-29 January, 2009).

4. Berman, G. P., B. M. Chernobrod, A. R. Bishop, and V. N. Gorshkov. Uncooled infrared and terahertz detectors based on micromechanical mirror as a radiation pressure sensor. To appear in *Photonics West.* (San Jose, 24-29 January).


## Publications


Berman, G. P., A. R. Bishop, B. M. Chernobrod, A. A. Chumak, and V. N. Gorshkov. Suppression of scintillations and beam wandering in free space gigabit rate optical communication based on spectral encoding of a partially coherent beam. To appear in *Photonics West.* (San Jose, 24-29 January).

Berman, G. P., B. M. Chernobrod, A. R. Bishop, and V. N. Gorshov. Uncooled infrared and terahertz detectors based on micromechanical mirror as a radiation pressure sensor. To appear in *Photonics West.* (San Jose, 24-29 January, 2009).

Rice, P., and I. J. Owens. Comparison between continuous wave and pulsed laser EQKD Systems. 2009. *To Be Submitted.*

Yard, J., and I. Devetak. Optimal quantum source coding with quantum side information at the encoder and decoder. To appear in *IEEE Transactions on Information Theory.*

# Revolutionary Science at the Intersection of Extreme and Transient Events, Natural Hazards, and National Security

*Gerald L. Geernaert*
20090477DR

## Introduction

The project goal is to advance the science of extreme phenomenology associated with astrophysics, space physics, geoscience, and climate change. Specific issues to be addressed include: initiation of earthquakes, seismic, and volcanic events; arctic climate change; regional climate prediction and impacts; and space plasma and astrophysical transients that require advanced modeling and simulation. Novel concepts involved are also developed, in support of the broader set of issues. This LDRD project is executed under the technical leadership of the Institute for Geophysics and Planetary Physics. While it must meet the same criteria for excellence as other LDRD projects, this project is related to the broader natural sciences mission of IGPP. In support of this project's scope and tasks, Institute of Geophysics and Planetary Physics (IGPP) uses its General and Administrative (G&A) and LDRD resources to assess science needs and opportunities, develop strategies, and support the most cutting edge basic scientific research. The tasks under this LDRD project, in turn, promote workforce development and science excellence.

## Benefit to National Security Missions

The research supports DOE missions associated with energy security, climate change, geophysical hazards, and astrophysics. Much of the research ties to capabilities associated with weapon simulation and space and/or surface based detection of nuclear activities.

## Progress

Progress during FY09 is distributed per the broad categories: astro- and space- physics; geosciences; and climate science.

In our astrophysics and space science effort, we modeled the evolution of magnetic fields in galaxy clusters. These simulations show that the mergers of mini-halos during the cluster formation lead to and sustain the intercluster turbulence. The turbulence amplifies the "seed" magnetic fields that emerge from active galactic nuclei (AGN) in the deep past at high redshifts. We found that cluster mergers and accretion can spread the AGN scale magnetic fields to the whole cluster, through both bulk motion and turbulent diffusion [3,5,6]. We also investigated neutrino flavor evolution in cosmic explosions. In the dense regions of exploding stars, neutrinos interact with matter and change their flavors (electron, muon or tau). We simulated the shock breakout epoch of a 15 solar mass core collapse supernova. We found that coherent flavor-evolving behavior is very pronounced, even though coupling to electrons is always orders of magnitudes larger. Our results to date show that coherent neutrino-neutrino scattering can affect energy deposition, nucleosynthesis, and neutrino signals from supernovae. This is because flavor oscillations can occur much deeper than through the standard mechanism and can be extraordinarily sensitive to neutrino mixing parameters to levels much smaller than any terrestrial experiment [12,13]. We have studied Sunyaev-Zel'dovich (SZ) clusters, which contain hot gas that distorts the spectrum of the microwave background [4]. We have used a combination of analytic, numerical, and statistical modeling to obtain cosmologically relevant results from both the thermal as well as kinetic SZ effects. We have created thermal and kinetic SZ images from simulations including adiabatic gas dynamics. From our simulations, we created mock SZ images for all the halos and at all redshift slices. These will be used to compare with observed survey data. We have developed advanced data analysis techniques for modern Compton gamma-ray telescopes [10]. During Compton event reconstruction, the measured positions and energies are transformed into the photon scattering sequences. We have developed enhanced methods for event reconstruction based on Bayesian and neural network methods in order to achieve improved source recognition and background. These methods will allow us to identify, and measure the spectra of gamma rays

sources in future space missions [11]. We studied the dynamics of the Saturn's magnetosphere with data from the Cassini spacecraft. We found beams of H+ and O+ that escape from Saturn's moon Enceladus and entered the magnetosphere [7,8].

Progress in geoscience research included advances in our understanding of the dynamics of rift valleys; hydrological-geological systems; and flow through porous geological media.

- To advance rift valley dynamics, a three-dimensional finite element model of the Rio Grande Rift and Bandelier Tuff were used to describe the evolution of multiple interacting rift systems, and to address rotational dynamics. The models were validated with field observations [1,2,9]. In order to explore global similarities, field data were collected during FY09 in the East African rift, including geological, structural, paleomagnetic, beryllium, and biomarker data; the data will be analyzed during the remainder of the LDRD project.
- A reactive transport code was developed and applied to the evolution of hydrological systems on small icy planetary bodies (including moons) [14,18]; the study was applied to Jupiter's moon Encelaedus and Saturn's moon Europa with excellent data validation [17].
- To advance flow through porous media, process modeling of large fractured rock systems was able to demonstrate on limestone fractures that buoyant convection is a governing process [15,16].

Progress in climate sciences focused on two tasks: one addressing a key process governing Indian Ocean – Atlantic Ocean interactions, and the other systems dynamics involving climate-infrastructure-economic interactions. For the first, we made major strides forward in explaining dynamical interactions between the Indian Ocean and Atlantic Ocean, i.e., involving the Agulhas Ocean current. Because vortex rings within the Agulhas current act as the dominant mechanism for heat and mass exchange between the two oceans, our studies of Agulhas current dynamics focused on the formation of discrete boundary current rings in the Indian Ocean that migrate around the southern tip of Africa into the southern Atlantic Ocean. These rings govern in large part the global ocean controls over the Meridional Ocean Circulation that in turn affects northern hemispheric climate during, in particular, rapid climate change episodes. We developed a theoretical description for these rings, and began numerical simulations to simulate their behavior. In the second climate task, we developed a systems dynamic tool to describe the impacts of local and regional climate change on energy, water, transport, and economic infrastructures. The systems dynamics tool is able to operate on the scale of a typical US county, and determine the matrix of infrastructure design choices that are necessary to satisfy jurisdictional goals, e.g., carbon footprint reduction, mix of renewables to be inserted into the grid, and benefits of economic instruments. The tool has been demonstrated using data test beds obtained from various US counties, and it will be extended to address a variety of instruments applicable to energy, water and transport infrastructures.

## Future Work

Research will focus on several broad themes. In the first theme (astro- and space physics), we will address cosmological modeling developments associated with gamma-ray events, neutron star physics, supernova evolution, cosmological structure formation and the plasma environment of the Earth. We will, in particular, simulate cosmological flows including gravity, plasma physics, and gas dynamics via adaptive mesh refinement. We will apply this capability to the analysis of galaxy clusters and the distribution of matter on scales from hundreds of megaparsecs down to kiloparsecs. Our work is aimed at interpreting observational data from the various cosmological surveys. In addition, we will explore plasma sheet, magnetospheric, and reconnection dynamics of the Earth's upper atmosphere, in order to explain episodic and severe phenomenology.

In the second theme focusing on geosciences, we will explore the necessary geophysics in order to better understanding crustal seismic events. We will focus on seismic "noise" and silent slip (or tremor). These recently recognized but poorly understood phenomena may be precursory phenomena to major earthquakes. We will develop better methods of recognizing slip events within the seismic records, determining the spatial distribution of slip events, and locating them within seismogenic zones. We will also use seismic data obtained from *active* sources to understand crustal deformation within a continental rift zone. Faults are indicators of the broader strain field in the crust. We are interested in the geometry of faults and their growth through time, and how faults affect the distribution of resources such as hydrocarbons and water. Finally, we will use our expertise in numerical modeling and code-development to simulate how large (decimeter- to meter-scale) voids can develop in carbonate rocks (a process called "karstification"), and how these voids affect fluid flow through rock layers containing them. All of the above efforts push the state of the art in their fields, yet have important applied and basic importance.

In the third theme of climate change, we will improve models of future climates, by addressing hydrology-ice sheet-permafrost interactions, regional climate prediction and impacts, and impacts on hurricane formation. In the third theme, we will advance our understanding of earthquake initiation, volcano-atmosphere interactions, subduction zones, and flow through porous media.

## Conclusion

The research is expected to lead to the following:

- a much finer resolution prediction of climate change, including predictions of extremes in future climate states that affect energy infrastructures and improved predictions of sea level rise;
- a better understanding of the precursors of earthquakes and the processes associated with earthquake initiation and evolution.
- a better understanding and prediction of middle atmospheric phenomena that affect the safety and security of satellite operations;
- an improved understanding of the evolution of the universe, in particular dark matter and dark energy; and
- improved models of fluid flow, transport of materials, and distribution of resources in the crust of the earth.

## References


1. Chaudhuri, A., H. Rajaram, and H. Viswanathan. Alteration of fractures by precipitation/dissolution in gradient reaction environments: computational results and stochastic analysis . 2008. *Water Resources Research.* : 23.
2. Chaudhuri, A., H. Rajaram, H. Viswanathan, G. Zyvoloski, and P. Stauffer. Buoyant convection resulting from dissolution and permeability growth in vertical limestone fractures . 2009. *Geophysical Research Letters.* : 36.
3. Carlson, J., M. White, and N. Padmanabhan. A critical look at cosmological perturbation theory techniques, . 2008. *Astrophysical Journal.* : 479.
4. Heitmann, K., M. White, C. Wagner, S. Habib, and D. Higdon. The Coyote Universe I: Precision Determination of the Nonlinear Matter Power Spectrum . To appear in *ApJ.*
5. Lui, S., C. Fryer, and H. Li. Black Hole Accretion in Low States: Electron Heating. To appear in *The Open Astronomy Journal .*
6. Martin, K., S. Liu, C. Fragile, C. Yu, and C. Fryer. Modeling emission from the supermassive black hole in the galactic center with GRMHD simulations. To appear in *Physics Journal.*
7. Jiang, W. J., S. Liu, C. Fragile, C. Yu, and C. Fryer. Cascade and damping of Alfv´en-cyclotron fluctuations: application to solar wind turbulence. To appear in *Astrophysics Journal.*
8. Hill, T. W., M. F. Thomsen, M. G. Henderson, R. L. Tokar, A. J. Coates, H. J. McAndrews, and G. R. Lewis. Plasmoids in Saturn's magnetotail. 2007. *Geophysical Journal.* : 113.
9. Hinz, E. A., J. F. Ferguson, L. Pellerin, and A. F. Ramenofsky. A geophysical investigation of subsurface structures and Quaternary geology of San Marcos Pueblo, New Mexico. 2008. *Archaeological Prospection.* : 247.
10. Zoglauer, A.. Application of Neural Networks to the Identification of the Compton Interaction Sequence in Compton Imagers. 2008. *Proceedings of SPIE.* : 70113F.
11. Zoglauer, A.. MEGAlib - Simulation and Data Analysis for Low-to-medium-energy Gamma-ray Telescopes. 2008. *Proceedings of SPIE.* : 70113F.
12. Duan, H., G. M. Fuller, and J. Carlson. Simulating nonlinear neutrino flavor evolution. 2008. *Computational Science and Discovery.* **1**: 200.
13. Duan, H., G. Fuller, J. Carlson, and Y. Z. Qian. Flavor Evolution of the Neutronization Neutrino Burst from an O-Ne-Mg Core-Collapse Supernova. 2008. *Physical Review Letters.* : 100.
14. Burt, D. M., L. P. Wohletz, and M. F. Sheridan. Surge deposit misidentification at Spor Mountain, Utah and elsewhere: A cautionary message for Mars. 2008. *Volcanology and Geothermal Research .* : 755.
15. Ogden, D. E., K. H. Wohletz, G. A. Glatzmaier, and E. E. Brodsky. Numerical simulations of volcanic jets: Importance of vent overpressure. 2008. *Geophysical Research.* : 113.
16. Ogden, D. E., S. W. Kieffer, X. Lu, g. Mcfarquhar, and K. H. Wohletz. Fluid Dynamics of High Pressure Volcanic Eruptions. To appear in *Geophysical Research.*
17. Huebner, W. F., L. N. Johnson, D. C. Boice, P. Bradley, S. Chocron, A. Ghosh, P. T. Giguere, and R. Goldstein. A

comprehensive program for countermeasures against potentially hazardous objects (PHOs). To appear in *Solar System Research.*

18. Wohletz, K. H., D. Giguere, D. Steedman, and D. Zhang. PHO mitigation simulations using computational fluid and solid mechanics,. 2008. *Los Alamos National Laboratory Report.* : 10.

## Publications

Burt, D. M., L. P. Knauth, K. H. Wohletz, and M. F. Sheridan. Surge deposit misidentification at Spor Mountain, Utah and elsewhere: A cautionary message for Mars. . 2008. *Volcanology and Geothermal Research.* : 755.

Carlson, J., M. White, and N. Padmanabhan. A critical look at cosmological perturbation theory techniques. 2008. *Astrophysical Journal.* : 479.

Chaudhuri, A., H. Rajaram, and H. Viswanathan. Alteration of fractures b precipitation/dissolution in gradient reaction environments: computational results and stochastic analysis. 2008. *Water Resources Research.* : 23.

Chaudhuri, A., H. Rajaram, and H. Viswanathan. Bouyant convection resulting from dissolution and pereability growth in vertical limestone fractures. 2009. *Geophysical Research Letters.* : 36.

Duan, H., G. Fuller, J. Carlson, and Y. Z. Qian. Flavor Evolution of the neutroni8zaiton neutrino burst from an O-Ne-Mg Core-Collapse Supernova. 2008. *Journal of Applied Physics.* : 100.

Duan, H., G. M. Fuller, and J. Carlson. Simulating nonlinear neutrino flavor evolution. 2008. *Computational Science and Discovery.* : Vol 1.

Heitmann, K., M. White, C. Wagner, S. Habib, and D. Higdon. The Coyote Universe I: Precision determination of the nonlinear matter power spectrum. 2009. *Astrophysical Journal.* : 50.

Hill, T. W., M. F. Thomsen, M. G. Henderson, R. L. Tokar, A. J. Coates, H. J. McAndrews, G. R. Lewis, D. G. Mitchell, C. M. Jackson, C. T. Russell, M. K. Dougherty, F. J. Crary, and D. T. Young. Plasmoids in Saturn's magnetotail. 2008. *Journal of Geophysical Research.* : 113.

Hinz, E. A., J. F. Ferguson, L. Pellerin, and A. F. Ramenofsky. A geophysical investigation of subsurface structures and quaternary geology of San Marcos Pueblo, NM . 2008. *Archaeological Prospection.* : 247.

Huebner, W. F., L. N. Johnson, D. C. Boice, P. Bradley, S. Chocron, A. Ghosh, P. T. Giguere, R. Goldstein, J. A. Guzik, J. J. Keady, J. Mukherjee, W. Patrick, C. Plesko, J. D. Walker, and K. Wohletz. A comprehensive program for countermeasures against potentially hazardous objects. . To appear in *Solar System Research.*

Jiang, W., S. Liu, C. Fragile, C. Yu, and C. Fryer. Cascade and damping of Alfv' en-Cyclotron fluctuations: application to solar wind turbulence. To appear in *Astrophysical Journal.*

Lui, S., C. Fryer, and H. Li. Black hole accretion in low states: electron heating. To appear in *Astronomy Journal.*

Martin, K., S. Liu, C. Fragile, C. Yu, and C. Fryer. Modeling emission from he supermassive black hole in the galactic center with GRMHD simulations. *Physics Journal.*

Ogden, D. E., K. H. Wohletz, G. A. Glatzmaier, and E. E. Brodsky. Numerical simulations of volcanic jets: Importance of vent overpressure. 2008. *Geophysical Research.* : 113.

Ogden, D. E., S. W. Kieffer, X. Lu, G. McFarquhar, and K. H. Wohletz. Fluid Dynamics of High Pressure Volcanic Eruptions. To appear in *Geophysical Research.*

Wohletz, K. H., D. Steedman, P. Giguere, and D. Zhang. PHO mitigation simulations using computational fluid and solid mechanics. 2008. *Los Alamos National Laboratory Report.* : 10.

Zoglauer, A.. Application of neural networks to the identification of the compton interaction sequence in compton igagers. 2008. *IEEE.* : 701137.

# Beyond the Neutrino Matrix

*Andrew Hime*
20070003DR

## Abstract

The discovery of solar and atmospheric neutrino oscillations opened new questions and opportunities at the intersection of nuclear and particle physics, astrophysics and cosmology. This project funded a diverse experimental program to elucidate the fundamental properties of neutrinos and to seek out the missing or "dark matter" in the universe.

A major effort involved research and development of a novel detector concept, dubbed CLEAN for Cryogenic Low Energy Astrophysics with Noble liquids, to directly search for dark matter utilizing targets of liquid argon and liquid neon operating deep beneath the earth's surface. Substantial progress was made in the engineering design and fabrication of major components for the MiniCLEAN detector. With a 500 kg target, and operating in the newly excavated SNOLAB, MiniCLEAN will provide a competitive search for dark matter and serve as prototype to a massive (10 to 100 ton) CLEAN detector capable to study dark matter and simultaneously make a precision measurement of low-energy neutrinos from the sun.

This project also supported, in part, research and development for a detector (Majorana) in search of neutrinoless double beta decay and the antineutrino phase of MiniBooNE (Booster Neutrino Experiment) at FermiLab. A theoretical component to the project provided computational support relevant to the experimental program and in interpreting the experimental data provided world wide in the context of fundamental theories within and beyond the Standard Model.

The project is summarized under the major headings below with subheadings pointing to its major components; MiniCLEAN, Majorana, MiniBooNE.

## Background and Research Objectives

**MiniCLEAN**

Neutrinos, now known to have non-zero rest masses, constitute at least as much mass as do all of the stars in the universe but they cannot provide the observed matter density or large-scale structure required of non-baryonic, cold dark matter. A compelling candidate for dark matter requires new physics in the form of Weakly Interacting Massive Particles (WIMPs), the likes of which could be directly detected as the recoil in ultra-low background detectors operating deep underground. The challenge hinges on our ability to achieve sensitivities some three orders of magnitude beyond the state-of-the-art. This requires novel detector technologies capable of scaling to very large target masses (ultimately, 1 ton and beyond) and maintaining unprecedented levels of radioactive background (ultimately, less than 1 event per ton per year).

The CLEAN program seeks to detect dark matter directly using interchangeable targets of liquid argon (LAr) or liquid neon (LNe). Unlike most other noble liquid dark matter detectors, CLEAN will operate as a liquid-only "single-phase" detector, observing only the scintillation light produced by WIMP scatters. Our approach follows that of the very successful non-accelerator neutrino program, emphasizing scale and simplicity. The basis for our background rejection is threefold: external backgrounds from radioactivity in the photomultiplier tubes (PMTs) and detector structure are reduced by self-shielding and removed by fiducial volume restriction, neutrons scattering within the volume are removed by self-shielding and a delayed-coincidence tag, and internal backgrounds from radioactivity inside the target liquid are reduced using pulse-shape discrimination. The last is made extremely effective because of the remarkable difference in the time profile of the scintillation light produced by WIMP-like nuclear recoils and electron-like backgrounds (see Figure 1), and the superior light collection achievable in a single-phase detector. As with large-scale neutrino experiments, our design approach scales well to very large masses since there are no large electric fields,

the target material cost is low, and the fast signals minimize event pileup. In many ways, the experiment becomes simpler as it becomes larger because of improved fiducialization, self-shielding, and simpler optics. For details of our approach, please see Refs.[1] and [2].

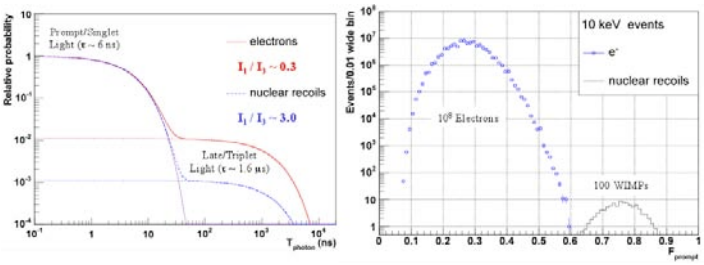


*Figure 1. The left panel shows the scintillation time distribution in LAr where the intensity of the late light relative to the prompt light is different for backgrounds (electrons and gamma rays) compared to nuclear recoil (WIMP) signals. The right panel is from an earlier simulation by Boulay & Hime (ref.[1]) based on the realization in the utility of prompt-to-total light yield as a powerful means of Pulse-Shape-Discrimination (PSD) in LAr.*

The scientific and technical objectives of the MiniCLEAN component of this project include a detailed conceptual design, guided by sophisticated Monte Carlo simulations to ensure a scientific reach competitive with other experiments planned on a similar timeline. A full engineering design made up a significant portion of the project, including the construction of dedicated apparatus in the laboratory to test all major components of the MiniCLEAN detector prior to fabrication. Equally important was the growth and development of the MiniCLEAN collaboration and a plan for detector fabrication and assembly underground.

**Majorana**

The data obtained from neutrino oscillation experiments tells us the difference between neutrino masses but not the absolute mass scale, knowledge of which determines the role that neutrinos play at subatomic to cosmological scales. Moreover, unlike their charged partners, neutrinos can be indistinguishable from their antiparticles. Neutrinoless double beta decay is the only practical means to directly explore the absolute mass scale of neutrinos and to determine whether or not the neutrino is its own antiparticle[3,4]. The objective of the Majorana experiment is to study neutrinoless double beta decay with an effective Majorana-neutrino mass sensitivity indicated by atmospheric neutrino oscillations. This exciting physics goal is technically within our grasp and best pursued using the well-established detector technology based on enriched $^{76}$Ge, augmented with recent advances in signal processing and detector design. Majorana will consist of a large mass of $^{76}$Ge in the form of high-resolution intrinsic germanium detectors located deep underground within a low-background shielding environment. Detector modules would be fabricated in a stepwise fashion, starting with a single 60 kg module that would serve to demonstrate the Majorana methodology and provide a stringent test of recent claims[5] for a positive signal.

**MiniBooNE**

The MiniBooNE experiment at FermiLab was constructed to test the evidence for neutrino oscillations found at LSND (Liquid Scintillator Neutrino Experiment). A confirmation of the LSND result would require physics beyond the standard paradigm of neutrino mixing amongst the three known generations of active neutrinos. Results from the MiniBooNE neutrino run were not consistent with the LSND data when interpreted as standard neutrino oscillations, however, an unexpected excess of events was found in the low-energy part of the neutrino spectrum. Results from the antineutrino run also show no support for the previous LSND result and, curiously, also do not reveal the low-energy excess observed in the neutrino run [6].

This LDRD project supported LANL collaborators on MiniBooNE to create new and improved techniques for analyzing the data and maximizing the scientific reach of the experiment by comparing the neutrino data to the antineutrino data. In addition, studies were performed and proposals written for potential new experiments that could shed further light on the results obtained from LSND and MiniBooNE.

## Scientific Approach and Accomplishments

**MiniCLEAN**

Our conceptual model for the MiniCLEAN detector is shown in Figure 2. The central target of liquid cryogen will be contained in a low-background stainless steel vessel (the Inner Vessel - IV). The IV contains ports to accommodate PMT optical modules that will view the inner liquid via light guides. The front faces of the light guides are coated with a wavelength shifter that shifts the extreme ultraviolet scintillation light into the blue. The light guides transport the blue light to PMTs immersed in the cryogen. With a 150 kg (500 kg) fiducial (target) mass and two years of operation, MiniCLEAN will achieve sensitivity to the WIMP-nucleon scattering cross-section of ~$2\times10^{-45}$ cm$^2$ for a 100 GeV WIMP mass, as shown in Figure 3 and based upon our simulations and constraints from measurements made with prototype detectors and test-benches operated in the laboratory. Also shown in Figure 3 are predictions in sensitivity based on scaling the clean concept to a fiducial mass of 40 tons, the minimal scale thought useful for a simultaneous study of low-energy solar neutrinos using LNe as the target material.

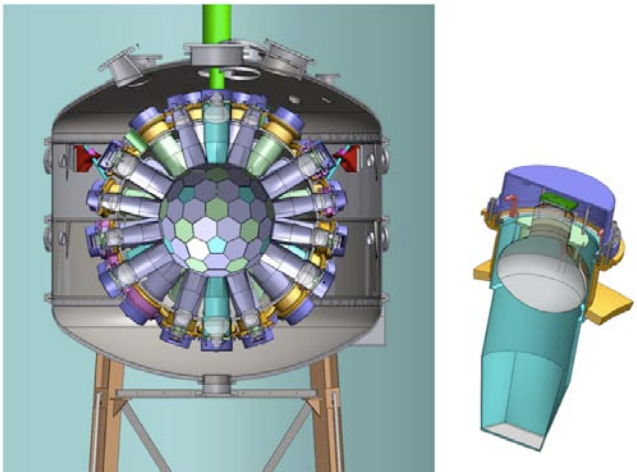

*Figure 2. The central target of liquid cryogen will be contained in a low-background (Stainless Steel) SS-vessel (the Inner Vessel - IV). The IV contains ports to accommodate optical cassettes (right) providing a "cold-seal" to the IV and viewing the inner liquid via light guides made from low-radioactivity acrylic. The front faces of these light guides provide the 4π Wave-Length-Shifting (WLS) sphere viewing the target volume and that shift the Extreme-Ultra-Violet (EUV) scintillation light into the "blue" where it can be detected by an array of photomultiplier tubes (PMTs). When coated with an optically reflective material, the acrylic light guides transport the blue light to the array of PMTs, the signals of which are read out via conventional digital electronics and hardware. The IV and optical cassette/PMT array is contained within an Outer Vacuum Vessel – OV, also fabricated from low-radioactivity SS, that provides the thermal shielding and basic containment of the central cryogen. The optical cassettes require assembly, and insertion into the IV, in a radon-free environment so as to prevent the plate-out of radon daughters onto the inner-facing WLS surfaces.*

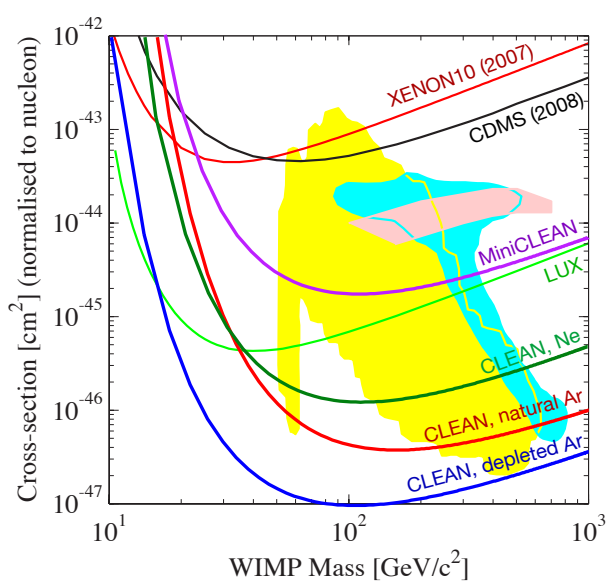


*Figure 3. The spin-independent WIMP-nucleon cross-section versus WIMP mass. Sensitivity contours are shown for the existing "state-of-the-art" experiments (CDMS and XENON10) and next generation detectors in light of the predictions of supersymmetric models (shown as the solid colored island). MiniCLEAN is designed for a 400 kg target (150 kg fiducial mass) of LAr/LNe and to be competitive with the forthcoming LUX (Large Underground Xenon) experiment. At the 40-ton scale, CLEAN can largely cover the phase space predicted by supersymmetric models and simultaneously provide a precision measurement of the low-energy (pp-fusion) neutrinos from the Sun.*

Significant accomplishments were made as it concerns the engineering design and fabrication of the MiniCLEAN detector. At this time the vacuum vessel, inner detector vessel, cryogenic systems, purification systems, electronics, initial calibration systems, and underground infrastructure at SNOLAB have been designed, with detailed engineering drawing packages available. This has lead to fabrication of major components of the detector, including the outer vacuum vessel (Figure 4) and the central sphere comprising the inner, cryogenic vessel. The inner vessel provided a significant engineering challenge and its design was modified at a relatively late point in the project to ensure that the necessary tolerances could be met at an affordable cost. The design of the inner vessel is tightly coupled to that of the optical modules that form the wavelength shifting surface, light guides and contain the PMTs. A conceptual design that fosters ease of assembly in a low-radon environment is in hand and the complete array of PMTs has been delivered. Progress was also made in the purchase of the major ancillary systems servicing the central detector, including the cryogenic and purification systems, digital electronics and data acquisition.

*Figure 4. The Outer Vacuum Vessel (OV) for MiniCLEAN is presently in fabrication from PHPK, Inc. in Ohio. It is constructed in pieces so as to facilitate its movement and assembly underground at SNOLAB.*

Significant progress has been made in the development of the MiniCLEAN collaboration which now boasts some 65 individuals (~35 FTE) from 16 institutions in the US and Canada. This includes SNOLAB who is providing the underground infrastructure for the MiniCLEAN detector and endorsement for its installation in its newly excavated Cube

Hall. The MiniCLEAN collaboration, under LANL leadership, has formulated an organizational structure for managing the project.

**Majorana**
We installed and operated a detector in a cryostat to test the mechanical, thermal, and electronic designs for Majorana. We learned that we can cool the detectors effectively by weak coupling, instead of the traditional effective conduction technique. We have also learned much about our design that has led to changes in the basic design for Majorana. Independent experiments were also performed to characterize radioactive backgrounds such as surface contamination from alpha emitters and cosmogenic production. A program was also carried out at LANSCE to measure inelastic neutron reactions on Ge, Cu, and Pb, information that was previously absent in the nuclear-data base.

**MiniBooNE**
New analysis techniques were developed for the antineutrino data. By comparing neutrino to antineutrino data it was found that many systematic uncertainties cancel, allowing a much more sensitive search for differences between neutrino and antineutrino oscillations. In this analysis a sizeable excess of low energy events is still found in the neutrino data but still none are observed in the antineutrino data. Prompted by this remaining anomaly in the neutrino data, a proposal for a new experiment, OscSNS, was written to place a MiniBooNE-like detector at the ORNL SNS Facility. In addition, a letter-of-intent (BooNE) was submitted to build a new MiniBooNE detector (or to move the existing MiniBooNE) detector at a distance of ~200m from the neutrino target at FermiLab. These experiments would determine whether or not the low-energy excess in MiniBooNE is caused by neutrino oscillations, provide unprecedented sensitivity to muon-to-electron neutrino oscillations, and allow a search for sterile neutrinos as well as signatures of CP and CPT violation.

## Impact on National Missions
The work performed under the auspices of this project is central to LANL's Grand Challenge to understand physics Beyond the Standard Model. It is also supports basic research missions of the DOE Office of Science, namely to obtain a fundamental understanding of the universe through the elucidation of neutrino properties and the identification of cosmological dark matter.

The project supported key personnel at the Laboratory, both in senior and early career positions and spanning across a diverse set of groups and divisions. The team boasts six Fellows of the American Physics Society and two Laboratory Fellows. The project recruited some of the best young students and post-doctoral research associates (PDs) from around the globe. Indeed, two of our younger PDs, Laura Stonehill and Keith Rielage, were promoted to staff members during the course of the project.

The project also seeded several new opportunities and carry-on projects. The work associated with development of Majorana led to the successful award of an FY09 LDRD-DR for "Double Beta Decay" and significant future funding is eminent from the DOE Office of Nuclear Physics. The work on CLEAN led to the successful award of an FY10 LDRD-DR proposal for the "CLEAN Detection and Identification of Dark Matter". With LANL management, doors are now opened with the DOE Office of High Energy Physics and promise for a strong dark matter program at LANL.

## References

1. Boulay, M. G., and A. Hime. Direct WIMP Detection using the Scintillation Time Distribution in Liquid Argon. 2006. *Astroparticle Physics.* **25**: 179.

2. Boulay, M. G., A. Hime, and J. Lidgard. Design Constraints for a Dark Matter and Solar Neutrino Detector using Liquid Neon. 2004. *nucl-ex/0410025.*

3. Elliott, S. R., and P. Vogel. Double Beta Decay. 2002. *Annual Review of Nuclear and Particle Physics.* **52**: 115.

4. Elliott, S. R., and J. Engel. Neutrinoless Double Beta Decay. 2004. *Journal of Physics.* **G30**: 183.

5. Klapdor-Kleingrothaus, H. V.. Evidence for Neutrinoless Double Beta Decay. 2002. *Foundations of Physics.* **32**: 1181.

6. Aguilar-Arevaloetal, A. A.. Search for Electron Antineutrino Appearance. 2009. *Physical Review Letters.* **103**: 111801.


## Publications

Aguilar-Arevaloet.al., A. A.. Search for electron neutrino appearance. 2007. *Physical Review Letters.* **98**: 231801.

Avignone, F. T., S. R. Elliott, and J. Engle. Double Beta Decay, Majorana Neutrinos and Neutrino Mass. 2008. *Reviews of Modern Physics.* **80**: 481.

Duan, H., G. M. Fuller, J. Carlson, and Y. Z. Qian. Analysis of collective neutrino flavor transformations in supernovae. 2007. *Physical Review.* **D75**: 125005.

Duan, H., G. M. Fuller, J. Carlson, and Y. Z. Qian. Flavor Evolution of the Neutronization Neutrino Burst from an O-Ne-Mg Core-Collapse Supernovae. 2008. *Physical Review Letters.* **100**: 021101.

Duan, H., G. M. Fuller, J. Carlson, and Y. Z. Qian. Neutrino Mass Hierarchy and Stepwise Spectral Swapping of Supernovae Neutrino Flavors. 2007. *Physical Review Letters.* **99**: 241802.

Gehman, V. M., and S. R. Elliott. Multiple isotope comparison for determining neutrinoless double beta decay mechanisms. 2007. *Journal of Physics.* **G34**: 667.

Goldman, T., G. J. Stephenson, and B. H. J. McKellar. Multichannel oscillations and relations between KARMEN, LSND and MiniBooNE. 2007. *Physical Review.* **D75**: 091301.

Lippincott, W. H., K. J. Coakley, D. Gastler, A. Hime, E. Kearns, D. N. McKinsey, J. A. Nikkel, and L. C. Stonehill. Scintillation Time Dependence and Pulse Shape Discrimination in Liquid Argon. 2008. *Physical Review C.* **78**: 035801.

Mei, D. M., A. Hime, Z. B. Yin, and L. C. Stonehill. A Model of Nuclear Recoil Scintillation Efficiency in Noble Liquids. 2008. *Astroparticle Physics Journal.* **30**: 12.

Mei, D. M., S. R. Elliott, A. Hime, V. M. Gehman, and K. Kazkaz. Neutron inelastic scattering processes as background for double beta decay experiments. 2008. *Physical Review C.* **77**: 054614.

# Dark Energy and the Cosmic Web

*Katrin Heitmann*
20070005DR

## Abstract

Only a decade has passed since the astonishing discovery of a mysterious agent driving an accelerated expansion of the Universe. Since confirmed by different probes, this discovery has been hailed as the harbinger of a revolution in fundamental physics and cosmology. Why is there so much excitement? Simply because no fundamental understanding exists: Cosmic acceleration demands completely new physics. It challenges basic notions of quantum theory, general relativity, and the fundamental make-up of matter. In order to understand the nature of the accelerated expansion of the Universe, we have to disentangle the expansion history of the Universe, as captured by the Hubble expansion rate, from the growth of structure as seen in the evolution of the distribution of galaxies – the cosmic web. At Los Alamos National Laboratory, we carry out some of the world's largest simulations of the evolution of the structure in the Universe to guide the interpretation of observations from the world's largest galaxy surveys. During this project we have carried out research on different large scale structure probes of dark energy, proved for the first time that simulations can reach the required accuracy to interpret future high-precision measurements of the distribution of galaxies, built a unique simulation data base, and a new statistical framework to analyze cosmological data from high-precision simulations. The project made important contributions to areas crucial for the Laboratory's mission: high-performance computing, verification and validation, and quantification of margins and uncertainties.

## Background and Research Objectives

The cause for the accelerated expansion of the Universe is a complete mystery. No compelling theoretical explanation has been proposed so far. Currently, the two most popular explanations are a dark energy, maybe driven by a scalar field, or a modification of general relativity on the largest scales. In order to make progress in either direction, we first have to characterize the underlying cause for the acceleration. Only then will we be able to distinguish different scenarios. The two major sources of information we have are (1) measurements of the expansion history of the Universe, and (2) the evolution of structure in the Universe. Structure in the Universe forms by gravity-driven amplification of primordial density fluctuations, leading to the complex distribution of mass as traced by the distribution of galaxies, the cosmic web. The intrinsic geometry of the web defined by dark matter and galaxies, and the properties and evolution of its structural components, such as galaxy clusters, are the twin information reservoir for dark energy. They provide data on the evolution history of the Universe and the growth rate of structure formation, essential for distinguishing dark energy from modified gravity. The key to optimally and robustly extracting encoded information is an integrated theory, simulation, and analysis program that puts the observational datasets to full use.

In this project we targeted three large-scale structure probes of dark energy: baryon acoustic oscillations, clusters of galaxies, and weak gravitational lensing. The complementary nature of these probes provides essential cross-checks on the results obtained. All three probes rely heavily on the ability to make precise theoretical predictions at the level of 1% accuracy. At the start of this project, predictions at the 10% level accuracy were state-of-the-art. A major aim of this project has been therefore to establish new standards and improve the state-of-the-art by an order of magnitude. Since the large-scale structure probes involve nonlinear physics, high-performance simulations are crucial to make such predictions. A major objective has been to establish for the first time ever that the theoretical predictions indeed can reach the required accuracy to interpret ongoing and future observations to characterize dark energy. Without such an effort, it would not be possible to analyze future cosmological

observations at the level required to understand the causes for dark energy. These efforts would be theory limited.

Once this high accuracy had been reached, the major second objective has been to develop a statistical framework built on a relatively small number of very costly high precision simulations that would provide accurate predictions for cosmological statistics such as the two-point correlation function or power spectrum, in a large parameter space. We have developed the very first framework in cosmology that fulfills these requirements. We carefully tested it and showed that it works to the required accuracy. A public release is under way.

These two major objectives of the project have led to many scientific insights in cosmology, including insights into the structure and evolution of clusters of galaxies, the evolution of the dark matter power spectrum (which is the essential statistic for weak lensing and baryon acoustic oscillations), new methods for code verification, leading to one of the biggest simulation data bases (the Coyote Universe) available. We elaborate on these results below.

## Scientific Approach and Accomplishments

Our project required a three-pronged approach, combining high-performance simulations with sophisticated statistics, and verification and validation, all of them integral to the Laboratory's mission. We summarize here our major results.

**Precision determination of cosmological statistics**

A first major task was to prove that it is possible to obtain results at the 1% accuracy from complex simulations. As a first step, we carried out an international code comparison and validation project. Almost all leading cosmological simulation groups world-wide participated in this project (including groups from Germany, Switzerland, Princeton, and Berkeley) leading to a comparison of 10 codes. The overall agreement over a wide dynamic range was at the 10% level, an order of magnitude shy of what is required. As part of this project, new components for ParaView have been developed (ParaView is a visualization tool that has been developed in part at Los Alamos and allow for comparative visualization) to make such a comparison easier. An invited paper on the major findings has been published [1]. Figure 1 shows an example for the comparison of a simulated cluster from four different codes. The simulations are particle based – ParaView enabled the easy and fast translation of the particle information into density information. The density information is much easier to interpret since it provides a view of the overall structure of the halo. The work has led to three follow up publications in the visualization literature [2-4] discussing new visualization techniques to easily identify differences in simulations and to streamline the comparison process. An additional paper is currently under review.

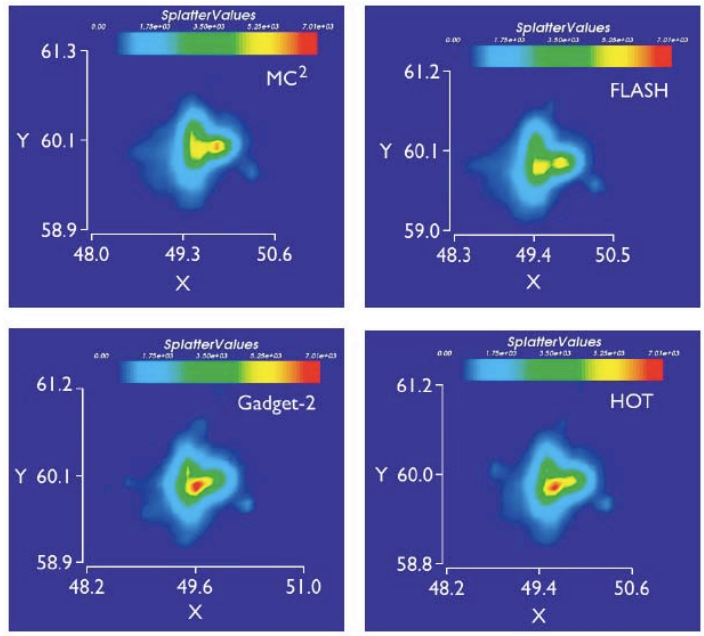


*Figure 1. Comparison of a simulated cluster from four different cosmology codes. Shown is the two dimensional density. Gadget-2 and HOT are two high resolution codes while MC2 and FLASH were run at medium resolution. The difference in the center of the cluster (the high-density red region in Gadget-2 and HOT) is clearly visible and due to the resolution difference. The analysis was carried out with ParaView.*

Since the aim was to reach accuracy at the 1% level, next two focused projects were carried out, analyzing the halo mass function (the key observable from clusters of galaxies) and the dark matter power spectrum (the key observable for weak lensing and baryon acoustic oscillations). The first project was based on a simulation database of 60 high-performance simulations and resulted in a comprehensive study of the mass function and its time evolution [5]. Convergence criteria for the required force resolution, simulation box size, halo mass range, and initial and final redshift were established. In combination with the excellent statistics from the large number of simulations, it was possible to obtain predictions at the few percent accuracy level. In addition, the project led to new insights about the universality of the mass function (its dependence on cosmology parameters and how to project this dependence onto linear quantities) and the evolution at high redshifts. In the second project it was proven that the nonlinear power spectrum can be obtained from simulations at the 1% level accuracy out to length scales relevant for current observations [6]. This project has led to the "Coyote Universe" simulation suite

that encompasses almost 1,000 simulations of varying resolution, a unique 60 TB database in the cosmological community. In this simulation suite we went beyond the currently favored cosmological constant model for dark energy and allowed for different values of the dark energy equation of state. Currently, two more projects (one on the power spectrum and one on weak lensing) are carried out by researchers at the University of Hawaii and UPenn, based on this data set. We expect the community to use the simulation suite for a large variety of different projects that researchers would not be able to carry out otherwise.

**Cosmic Calibration Framework**

In order to interpret ongoing and upcoming observations and extract useful cosmological information from them, such as the dark energy equation of state, very costly high precision, multi-physics simulations must be performed. A single high-resolution simulation at the desired accuracy requires roughly 20,000CPU hours on a modern supercomputer. Including waiting times in the submission queue, this translates to approximately a week of real run time. A statistical analysis of cosmological data based on simulations would require 10,000 – 100,000 simulations of different cosmological models, impossible to carry out currently. It is therefore essential to any effort to create a prediction capability – a so-called emulator – that can be built from a small set of simulations. The emulator then provides highly accurate predictions in the full parameter space via interpolation in parameter space covered by the simulations. We have developed such a framework based on (1) sophisticated design methods (Orthogonal Array Latin Hypercube designs) to decide at which parameter settings to run the simulations, (2) Gaussian Process models for creating the emulator itself, and (3) Markov Chain Monte Carlo methods to extract cosmological information from simulations and observations. We first demonstrated that the method works on a set of medium resolution simulations and simulated data for large-scale structure and cosmic microwave background measurements [7]. We extended the work to include covariances in Ref. [8]. Based on the Coyote Universe we built an emulator for the dark matter power spectrum accurate at the 1% level [9]. Figure 2 shows the comparison of the emulator to a high-resolution simulation result. The agreement at different cosmological epochs is at the 1% level. The emulator is ready for public release and will play a crucial role for current and future analysis of weak lensing and baryon acoustic oscillation experiments. The Cosmic Calibration Framework will be immensely important in future cosmological surveys that attempt to extract information from the nonlinear regime of structure formation, specifically for baryon acoustic oscillations and weak lensing. Without such a framework, this task is impossible. The work has led to several invited colloquia and seminars world-wide and other research groups are starting to develop tools along the same lines now.

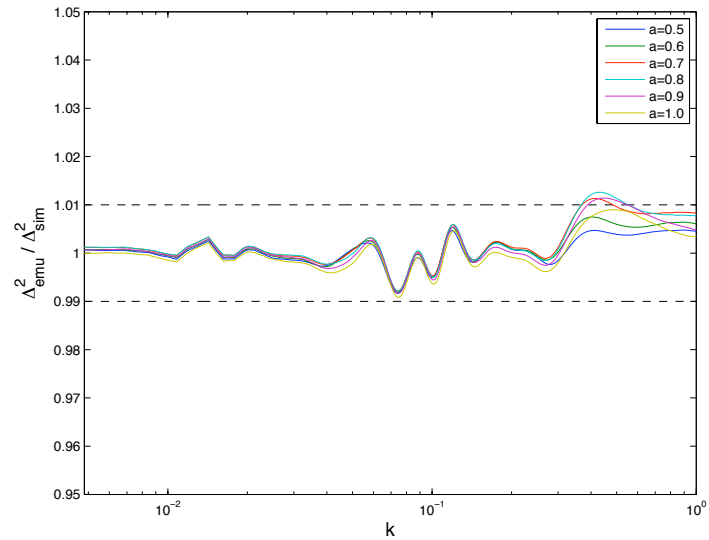


*Figure 2. Comparison of the prediction from our new emulator to a high-resolution simulation result. Shown is the ratio of the power spectrum from the emulator prediction to the simulation result for six different cosmological epochs. The precision of the emulator is at the 1% level, fullfilling the accuracy requirements for weak lensing and BAO surveys. This reult improves the current state-of-the-art by an order of magnitude.*

**Clusters of galaxies**

Clusters of galaxies and their count as a function of mass – the so-called mass function – are important probes of dark energy. We have contributed to the currently best measurement of the dark energy equation of state from clusters of galaxies [10,11]. The measurements were obtained from Chandra observations. In a second observational project, based on the same Chandra database we have investigated the properties of a special class of clusters and groups of galaxies, so-called fossil groups [12,13]. Fossil groups are groups or clusters of galaxies that are dominated by a single bright galaxy in the center and an extended X-ray halo, but they lack the typical large number of galaxies usually associated with such a system. It is important to understand the properties of such system if one wants to use clusters of galaxies as a precision probe of cosmology. We discovered several new such systems and carefully analyzed their properties. Figure 3 shows one of the systems in the X-ray and Figure 4 shows the same system in the optical waveband. We also carried out theoretical studies related to clusters of galaxies in addition to the project on the evolution of the mass function, mentioned above.

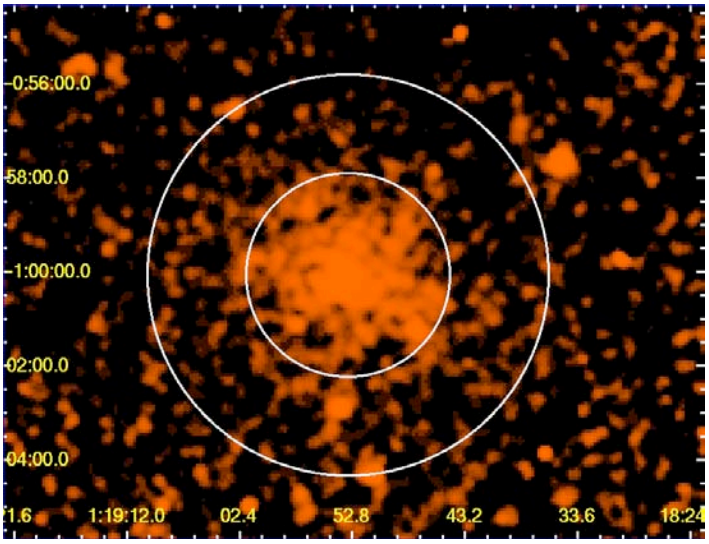


*Figure 3. X-ray image of one of the fossil groups described in Ref. [12]. The inner circle shows the area where the X-ray spectroscopy was performed. The out circle corresponds to the radius at a certain overdensity.*

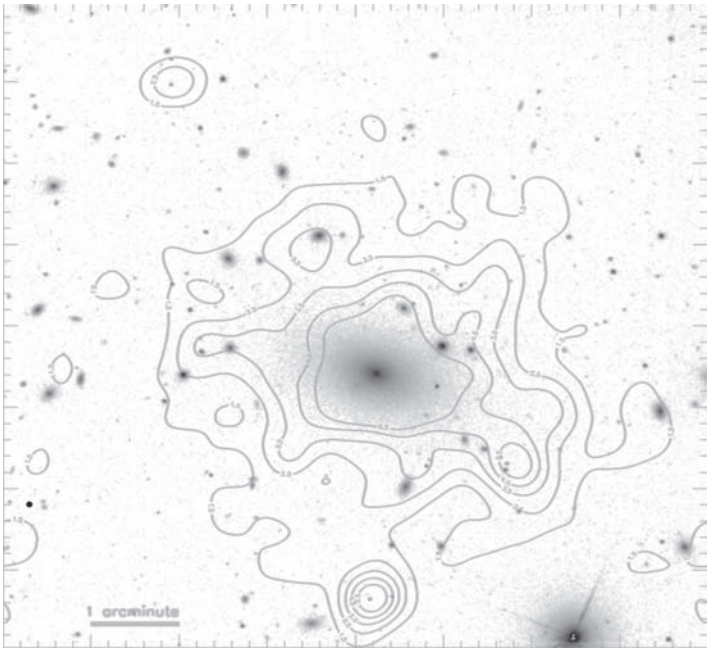


*Figure 4. X-ray contours overlayed on an optical image from SDSS data for the same fossil group shown in Figure 3. The central bright galaxy is very easy to identify. The brightness of this galaxy and the relative faintness of the other galaxies belonging to the group are the characteristic features of a fossil system.*

From simulations, we estimated the bulk virial scaling relation of halos formed in an ensemble of simulated cold dark matter cosmologies [14]. We showed that the result is insensitive to cosmological parameters, the presence of a gas component, and numerical resolution. This relation was combined with the halo mass function and it was shown that a high normalization condition is favored, in contrast to the findings from cosmic microwave background measurements at that time. In the recent past, the cosmic microwave background measurements have been improved and the results are now much closer to our theoretical predictions.

A major concern with respect to mass function measurements is the definition of a dark matter halo in a simulation. Figure 5 illustrates how different halo definitions will lead to different halo mass estimates.

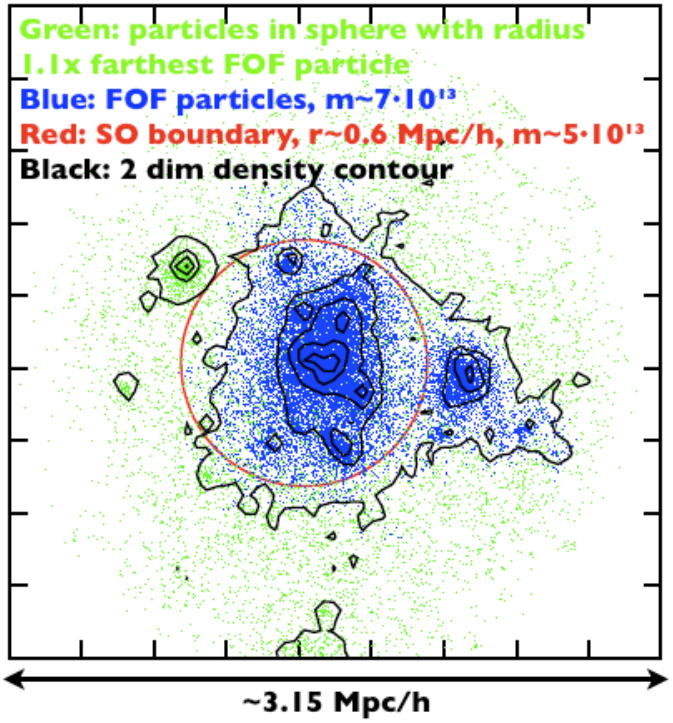


*Figure 5. Dark matter halo extracted from a cosmological simulation. Shown are different definitions of the halo, the red circle indicates the halo boundaries if it is identified by an overdensity method, the blue particles belong to the halo of it is identified with a friends-of-friends algorithm, and the black line shows the iso-density contour in this region. It is clear from this figure that different definitions of a dark matter halo will lead to different masses. This in turn will lead to different cosmological constraints. We have established connections between different definitions which allow the translation of the masses from one to the other.*

In observations, we cannot measure the dark matter mass directly, instead we measure for example the gas temperature or count the numbers of galaxies in a cluster and infer the mass from that. In simulation, we can measure the dark matter halo mass directly, but we have to be able to connect this measured mass to observables. Therefore, we have to find a definition of dark matter halos that can be easily connected to observations. In Ref. [15] we have studied this question in detail. As part of this work we developed a new approach to extract cosmological information from the number of systems that have more

than one dark matter halo component. Preliminary studies from SDSS data by a group at Princeton seem to agree well with our predictions.

**First cosmological hybrid architecture code**
During this project we initiated the development of the first cosmology code that can take advantage of new hybrid architectures, such as the Roadrunner supercomputer at Los Alamos. We showed that we could achieve speed-ups of a factor of 50-100 with such a code and outlined the principle design. Due to these very promising results, a separate project was funded to fully develop the code. This new code ran successfully on Roadrunner and led to some of the largest cosmological simulations ever performed.

Overall, the project has led to a large number of scientific publications, has been presented at more than 30 occasions (conferences and Universities), has led to new funding from DOE Office of Science High Energy Physics, NASA, and NSF (in collaboration with Universities).

## Impact on National Missions

As part of this research, we developed new, world leading simulation techniques to exploit modern supercomputing architectures. We developed new methods for validation and verification of complex computer simulations. We contributed to studies of quantification of margins and uncertainties. We developed new and innovative statistical methods to extract scientific information form a limited set of simulations combined with high-precision observations. We advanced our understanding of the Universe, its make-up, and its evolution.

The effort enabled us to attract a new Oppenheimer Fellow (Ujjaini Alam) and a new Director's Fellow (Adrian Pope).

## References


1. Heitmann, K., Z. Lukic, P. Fasel, S. Habib, M. S. Warren, M. White, J. Ahrens, L. Ankeny, R. Armstrong, B. W. O'Shea, P. M. Ricker, V. Springel, J. Stadel, and H. Trac. The cosmic code comparison project. 2008. *Computational Science and Discovery.* **1** (1): 015003.

2. Haroz, S., and K. Heitmann. Multiple uncertainties in time-variant cosmological particle data. 2008. *IEEE Computer Graphics and Applications.* **28** (5): 37.

3. Haroz, S., K. Ma, and K. Heitmann. Multiple uncertainties in time-variant cosmological particle data . 2008. (Kyoto, 4-7 March 2008). p. 207. Kyoto: Piscataway, NJ, USA : IEEE.

4. Anderson, E., C. Silva, J. Ahrens, K. Heitmann, and S. Habib. Provenance in comparative analysis: A study in cosmology . 2008. *Computing in Science and Engineering.* **10** (3): 30.

5. Lukic, Z., K. Heitmann, S. Habib, S. Bashinsky, and P. M. Ricker. The halo mass function: High redshift evolution and universality. 2007. *Astrophysical Journal.* **671**: 1160.

6. Heitmann, K., M. White, C. Wagner, S. Habib, and D. Higdon. The Coyote Universe I: Precision determination of the nonlinear matter power spectrum. To appear in *Astrophysical Journal.*

7. Habib, S., K. Heitmann, D. Higdon, C. Nakhleh, and B. Williams. Cosmic calibration: Constraints from the matter power spectrum and the cosmic microwave background. 2007. *Physical Review D.* **76**: 083503.

8. Schneider, M. D., L. Knox, S. Habib, K. Heitmann, D. Higdon, and C. Nakhleh. Simulations and cosmological inference: A statistical model for power spectra means and covariances. 2008. *Physical Review D.* **78**: 063529.

9. Heitmann, K., D. Higdon, M. White, S. Habib, B. Williams, and C. Wagner. The Coyote Universe II: Cosmological models and precision emulation of the nonlinear matter power spectrum. 2009. *Astrophysical Journal.* **705**: 156.

10. Vikhlinin, A., R. A. Burenin, H. Ebeling, W. R. Forman, A. Hornstrup, C. Jones, A. V. Kravtsov, S. S. Murray, D. Nagai, H. Quintana, and A. Voevodkin. Chandra cluster cosmology project II: samples and X-ray data reduction . 2009. *Astrophysical Journal.* **692** (2): 1033.

11. Vikhlinin, A., A. V. Kravtsov, R. A. Burenin, H. Ebeling, W. R. Forman, A. Hornstrup, C. Jones, S. S. Murray, D. Nagai, H. Quintana, and A. Voevodkin. Chandra cluster cosmology project III: Cosmological parameter constraints. 2009. *Astrophysical Journal.* **692** (2): 1060.

12. Voevodkin, A., C. Miller, K. Borozdin, K. Heitmann, S. Habib, P. Ricker, and R. Nichol. X-ray observations of optically selected giant elliptical-dominated galaxy groups. 2008. *Astrophysical Journal.* **648**: 204.

13. Voevodkin, A., K. Borozdin, K. Heitmann, S. Habib, A. Vikhlinin, A. Mescheryakov, and A. Hornstrup. Fossil systems in the 400d cluster catalog. To appear in *Astrophysical Journal.*

14. Evrard, A. E., J. Bialek, M. Busha, M. White, S. Habib, K. Heitmann, M. S. Warren, E. Rasia, G. Tormen, L. Moscardini, C. Power, A. R. Jenkins, L. Gao, C. S.

Frenk, V. Springel, S. D. M. White, and J. Diemand. Virial scaling of massive dark matter halos: Why clusters prefer a high normalization cosmology . 2008. *Astrophysical Journal.* **672**: 122.

15. Lukic, Z., D. Reed, S. Habib, and K. Heitmann. The structure of halos: implications for group and cluster cosmology. 2009. *Astrophysical Journal.* **692** (1): 217.

## Publications

Anderson, E., C. Silva, J. Ahrens, K. Heitmann, and S. Habib. Provenance in comparative analysis: A study in cosmology . 2008. *Computing in Science and Engineering.* **10** (3): 30.

Evrard, A. E., J. Bialek, M. Busha, M. White, S. Habib, K. Heitmann, M. S. Warren, E. Rasia, G. Tormen, L. Moscardini, C. Power, A. R. Jenkins, L. Gao, C. S. Frenk, V. Springel, S. D. M. White, and J. Diemand. Virial scaling of massive dark matter halos: Why clusters prefer a high normalization cosmology . 2008. *Astrophysical Journal.* **672**: 122.

Habib, S., K. Heitmann, D. Higdon, C. Nakhleh, and B. Williams. Cosmic calibration: Constraints from the matter power spectrum and the cosmic microwave background. 2007. *Physical Review D.* **76**: 083503.

Haroz, S., K. Ma, and K. Heitmann. Multiple uncertainties in time-variant cosmological particle data . 2008. In *IEEE Pacific Visualization Symposium.* (Kyoto, 4-7 March 2008). , p. 207. Kyoto: Piscataway, NJ, USA : IEEE.

Haroz, S., and K. Heitmann. Multiple uncertainties in time-variant cosmological particle data. 2008. *IEEE Computer Graphics and Applications.* **28** (5): 37.

Heitmann, K., D. Higdon, M. White, S. Habib, B. Williams, and C. Wagner. The Coyote Universe II: Cosmological models and precision emulation of the nonlinear matter power spectrum. 2009. *Astrophysical Journal.* **705**: 156.

Heitmann, K., M. White, C. Wagner, S. Habib, and D. Higdon. The Coyote Universe I: Precision determination of the nonlinear matter power spectrum. To appear in *Astrophysical Journal.*

Heitmann, K., Z. Lukic, P. Fasel, S. Habib, M. S. Warren, M. White, J. Ahrens, L. Ankeny, R. Armstrong, B. W. O'Shea, P. M. Ricker, V. Springel, J. Stadel, and H. Trac. The cosmic code comparison project. 2008. *Computational Science and Discovery.* **1** (1): 015003.

Higdon, D., K. Heitmann, C. Nakhleh, and S. Habib. Combining simulations and physical observations to estimate cosmological parameters. To appear in *The Oxford handbook of applied Bayesian analysis.* Edited by O'Hagan, A., and M. West.

Li, C., D. E. Holz, and A. Cooray. Direct reconstruction of the dark energy scalar-field potential. 2007. *Physical Review D.* **75**: 103503.

Lukic, Z., D. Reed, S. Habib, and K. Heitmann. The structure of halos: implications for group and cluster cosmology. 2009. *Astrophysical Journal.* **692** (1): 217.

Lukic, Z., K. Heitmann, S. Habib, S. Bashinsky, and P. M. Ricker. The halo mass function: High redshift evolution and universality. 2007. *Astrophysical Journal.* **671**: 1160.

Schneider, M. D., L. Knox, S. Habib, K. Heitmann, D. Higdon, and C. Nakhleh. Simulations and cosmological inference: A statistical model for power spectra means and covariances. 2008. *Physical Review D.* **78**: 063529.

Skillman, S. W., B. W. O'Shea, E. J. Hallman, J. O. Burns, and M. L. Norman. Cosmological shocks in adaptive mesh refinement simulations and the acceleration of cosmic rays. 2008. *Astrophysical Journal.* **689** (2): 1063.

Vikhlinin, A., A. V. Kravtsov, R. A. Burenin, H. Ebeling, W. R. Forman, A. Hornstrup, C. Jones, S. S. Murray, D. Nagai, H. Quintana, and A. Voevodkin. Chandra cluster cosmology project III: Cosmological parameter constraints. 2009. *Astrophysical Journal.* **692** (2): 1060.

Vikhlinin, A., R. A. Burenin, H. Ebeling, W. R. Forman, A. Hornstrup, C. Jones, A. V. Kravtsov, S. S. Murray, D. Nagai, H. Quintana, and A. Voevodkin. Chandra cluster cosmology project II: samples and X-ray data reduction . 2009. *Astrophysical Journal.* **692** (2): 1033.

Voevodkin, A., C. Miller, K. Borozdin, K. Heitmann, S. Habib, P. Ricker, and R. Nichol. X-ray observations of optically selected giant elliptical-dominated galaxy groups. 2008. *Astrophysical Journal.* **648**: 204.

Voevodkin, A., K. Borozdin, K. Heitmann, S. Habib, A. Vikhlinin, A. Mescheryakov, and A. Hornstrup. Fossil systems in the 400d cluster catalog. To appear in *Astrophysical Journal.*

# High-Current, High-Energy, Laser-Driven Ion Accelerators: An Enabling and Revolutionary Scientific Research Tool

*Juan C. Fernandez*
20070023DR

## Abstract

This project aimed at extending the scientific understanding in relativistic laser-matter interactions to develop a revolutionary class of ion beams, driven by high-energy short-pulse lasers. Specifically, we demonstrated conversion of laser energy into nearly mono-energetic ion beams at >100 MeV, and peak ion energies of >0.5 GeV. Relativistic laser-matter interactions is at the frontier of plasma physics, and more generally, high-energy density physics (HEDP), which was called "The X-games of Contemporary Science" in a recent study commissioned by the National Research Council of the National Academies of Science. This research supports and relies on scientific disciplines critical to LANL, such as atomic physics, accelerator physics, and large-scale computation of multi-scale phenomena. The research supports the development of advanced compact accelerators at LANSCE, by enabling the technology for complementary co-located capabilities lacking today, such as high-current heavy ion beams, and by providing novel paths to upgrade existing capability, such as advanced proton injectors. The development of these laser-driven beams will enable LANL to push the research frontiers significantly in important areas. We discuss below three of these applications: weapons physics research in the area of boost physics, ion-driven fast ignition of inertially-confined fusion targets, and cancer tumor therapy. Within this project we succeeded to experimentally demonstrate a new ion acceleration mechanims, Break-Out Afterburner (BOA) acceleration. This was the first such demonstration of a fundamentally new ion acceleration mechanism in 10 years and an unmatched proof of the predictive capabilities of our VPIC plasma code, which not only had predicted the existence of this mechanism but also the quantitative parameters later observed in the experiments. Using both our experimental and numerical data, we developed a reduced analytical model that also showed excellent predictive capability within its range of applicability. With respect to the envisioned applications we were able to demonstrate the three fundamental parameters for carbon-driven fast ignition individually: 500 MeV carbon ions, <20% energy spread and >10% conversion efficiency. A follow-on project funded by the Office of Fusion Energy Sciences will study the challenge of bringing them all together simultaneously. We also demonstrated 100 MeV mono-energetic carbon ions as required by the weapons/boost related uses of ignition project funded by Campaign 10. With respect to cancer therapy, Trident does not have the right parameters to demonstrate the 4 GeV required for tumor therapy, however, we could show that our models for the BOA acceleration work and are in excellent agreement with the observed experimental data, showing the principle feasibility of reaching such energies and allowing extrapolation for design of the required system.

## Background and Research Objectives

Ultrahigh-intensity lasers today routinely reach intensities of $10^{20}$ - $10^{21}$ W/cm$^2$. When interacting with matter at intensities above $10^{18}$ W/cm$^2$ the ponderomotive potential of the laser field will be on the order of the rest mass of an electron resulting in immediate acceleration of electrons to relativistic velocities within a half cycle of the laser field. To accelerate protons directly in the laser field, the ponderomotive potential would need to reach the proton rest mass energy of 1 GeV, which corresponds to intensities >$10^{24}$ W/cm$^2$ and is thus still 3 orders of magnitude from current laser capabilities. However, the accelerated electrons can in turn be used to accelerate other particles like protons and heavier ions. Since the laser-created fields are more than a million times stronger than in conventional accelerators, lasers have the potential to shrink those km long machines to room sized devices suitable for universities, industry and hospitals. However, so far the ion energy is still too low for many applications and the up to now employed acceleration mechanism seems to have hit

a threshold. This project set out to demonstrate for the first time a new acceleration mechanism called Break-Out Afterburner acceleration, that has the potential of increasing achievable ion energies by more than an order of magnitude for a given set of laser parameters. Utilizing ultrahigh pulse contrast and nm-scale targets we can thus reach energy regimes relevant to a wide array of applications ranging from fusion energy production to medicine and tumor therapy.

Prior to this project, the most promising mechanism for directed laser-driven ion acceleration was the so called TNSA (Target-Normal Sheath Acceleration) scheme [1,2], where a high-energy, high intensity short-pulse laser incident on a µm-thick foil target heats electrons to relativistic energies, which in turn creates a virtual cathode on the rear of the target that accelerates the ions (typically adsorbed protons unless the target is cleaned in situ) on the rear target surface. However, there are limitations on that process as implemented to date, which include a broad quasi-Maxwellian ion distribution which is not suitable for many applications, and energies are typically in the ~ 1- 10 MeV/nucleon range for laser intensities of $10^{19}$-$10^{20}$ W/cm$^2$, regardless of laser energy.

During the proposal stage of this project, a new acceleration mechanism for heavy ions, called the Breakout Afterburner (BOA) [3,4] was discovered at LANL in massive particle in cell (PIC) simulations using the VPIC code, the most advanced PIC code existant, running on the Lightning computer (Roadrunner prototype), the most powerful for this type of application. In this novel mechanism, a linearly-polarized ~ $10^{21}$ W/cm$^2$ laser pulse drives all the electrons under the laser spot in an ultra-thin (~ 10-100 nm) target. The target becomes transparent and the laser continues to couple to the same electrons for the duration of the pulse. Energy transfers efficiently to the ions via a kinetic Buneman instability, driven by the relative electron-ion drift [4]. The result is ~ GeV carbon ion energies. Since then, another advanced mechanism, Radiation Pressure Acceleration (RPA), has been discovered [5] and verified with VPIC. RPA relies on a circularly polarized laser at about the same intensity as BOA, to push on the electrons without heating, which couple their energy to the ions electrostatically.

The work in this LDRD Directed Research (DR) project has been aimed principally towards the experimental validation of these advanced acceleration mechanisms with heavy (non-hydrogen) ions, developing a better understanding of how to utilize these beams in key missions.

Specifically, the project as proposed had one primary goal and two secondary goals:

**Primary goal**
Experimental demonstration of Break-Out Afterburner Acceleration and significant progress in understanding the underlying physics

(From the proposal: "This project has a primary goal of developing a revolutionary ion beam technology based on the laser-plasma afterburner.")

**Secondary Goals**
Deploy a laser-accelerated ion beam (probably heavy ions such as Pd) in a demonstration integrated experiment relevant to boost.

Optimize beam performance and assess the suitability of these beams for two selected missions: to demonstrate a high-power C-ion beam in the 30-40 MeV/nucleon range, the energy suitable for FI and to demonstrate feasibility of a high-energy C-ion beam of >100 MeV/nucleon, as required for cancer therapy.

## Scientific Approach and Accomplishments

To achieve the stated goals we formulated a research program that integrates theory, modeling and experiments. We made use of a multi-disciplinary, multi-division and indeed multi-institution team to synergistically combine all relevant capabilities into a single project. Participants from P-24 and X-1 from LANL participated in this project, forming the experimental and modeling branches of project, respectively. Furthermore we were able to form a strong collaboration with the University of Munich and the Max-Planck-Institute for Quantum Optics in Garching, Germany, where the co-PI Hegelich held a Visiting Professorship for the last 2 years of the project as a co-appointment with his LANL position in P-24. This constellation allowed us to bring additional capabilities to bear that are not present at Los Alamos, e.g. the development of ultrathin, ultrarobust free standing nm Diamond-like Carbon films (DLC), access to laser systems with parameters substantially different from Trident, and theory support.

The main modeling tools were the VPIC code on the Lightning and FLASH LANL supercomputer clusters. Smaller PIC simulations were performed at MPQ with their legacy codes in the framework of a collaboration (see below). The main experimental facility was the LANL Trident laser, delivering pulses of ~50-100 J, ~500-800 fs into a 3.5µm radius spot at ultrahigh contrast, resulting in an on target intensities of 1-5 x $10^{20}$ W/cm$^2$. Additional experiments where performed within the Munich collaboration (see below) at the Ti:Sapphire laser of the Max-Born-Institute in

Berlin, Germany, delivering pulses of 0.7J, 45fs, $3x10^{19}$ W/cm$^2$ on target.

To accomplish the proposed research goals the original proposal put forth the following broad tasks:

- mitigate laser pre-pulse at Trident to the required level
- demonstrate the required hydrodynamic performance of a target with reduced prepulse;
- develop suitable ultrathin targets
- implement ex situ methods for producing the surface ultra-thin film layers required for laser targets;
- implement on Trident the in situ target conditioning required;
- perform the suite of PIC simulations necessary to understand better the enhanced TNSA and the laser-plasma afterburner regimes and, ultimately, develop reduced models to inform experimental design;
- design the targets and the experimental campaign;
- deploy the initial validation experiments of the afterburner concept;
- assuming success, evaluate the results and refine the theoretical models;
- use the refined theoretical models to demonstrate the beam parameters and beam-ion species necessary for our three identified customers: boost, FI and cancer therapy;
- deploy a demonstration integrated experiment relevant to boost;
- publicize and share our results with our collaborators in other fields (FI, etc.);
- preliminary assessment on how to integrate this accelerator technology at a major accelerator facility such as LANSCE."

Due to insights gained during the project as well as focus shifts within one of the potential customer programs (C1-Boost), some of these tasks were modified or discarded. In the following we will describe the progress achieved for each task and then summarize the results in the context of our primary goal.

**Mitigate laser pre-pulse at Trident to the required level**
The key parameter to shooting nanotargets is the so-called laser contrast, which describes how fast the pulse turns on. Due to the nature of Chirped Pulse Amplification, where a short sub-ps laser pulse is stretched in time (ns) then amplified and then recompressed to its original short duration, the short high intensity pulse sits on a ns pedestal of incompressible noise. In addition reflections in the system can also cause short prepulses before the main pulse. The laser contrast is ratio of the pedestal/prepulse intensity to the peak of the main pulse. For a typical ultrahigh intensity system that ratio is on the order of one millionth ($10^{-6}$) at ~1ns before the 500fs main pulse. If the focused main pulse intensity is ~$10^{20}$ W/cm2, the prepulse intensity will be ~$10^{14}$ W/cm$^2$, i.e. more than enough to create a plasma and to destroy the target before the main pulse can interact with it. For the BOA process to work it is imperative that the target is still overdense at the peak of the pulse. Therefore, at peak intensities above $10^{20}$ W/cm$^2$ very good contrast ratios of better than $10^{-11}$ at ~ps are required. To realize these extreme, ultrahigh contrast conditions, we developed a new cleaning system based on Short Pulse Optical Parametric Amplification (SPOPA) [6]. Using an additional compressor stretcher pair and exploiting two quadratic ($\chi^2$) nonlinearities we obtain cubic cleaning performance at great stability at modest intensity, realizing a contrast good enough to ensure main pulse interaction with an overdense target. The thus realized contrast is below the detection threshold of our optical diagnostics and therefore better than $10^{-10}$ at 10 ps before the peak of the pulse. Damage threshold measurements on the used targets put it as low as $<2x10^{-12}$ for a 1.2ns pedestal and $<5x10^{-10}$ for 0.5ps. Figure 1 shows the latest contrast measurement.

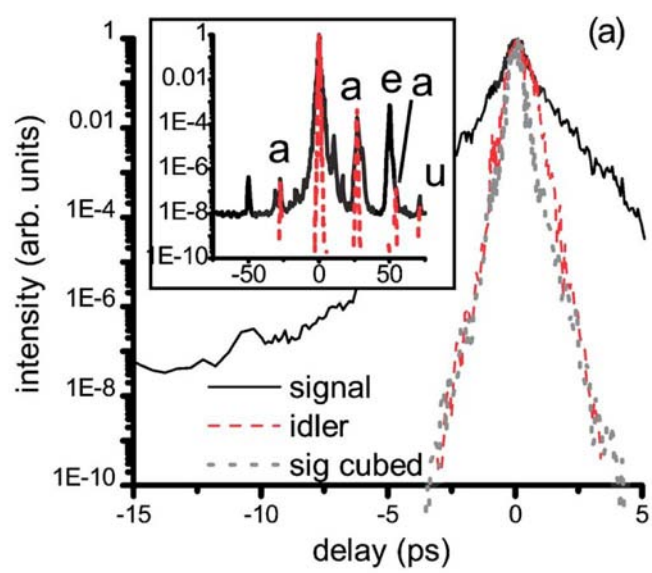


*Figure 1. Temporal contrast measurement of the Trident laser pulse before (black) and after (red) cleaning, with an overlayed calculated cube fit to the cleaned signal (grey). Inset shows a larger temporal range: a - known artifacts, e - etalon reflection. Black curve is before cleaning, red is after cleaning.*

**Demonstrate the required hydrodynamic performance of a target with reduced prepulse**
Shooting targets of various thicknesses with the old frontend and with the new ultrahigh contrast frontend we determined the hydrodynamic target performance by means of a Backscatter Imaging diagnostic [7]. This diagnostic shows if a target is still overdense at the time of the peak pulse interaction or if the prepulses/pedestals damaged it and it suffered hydrodynamic expansion to an underdense state. With the old frontend this could be observed for targets of 100nm and thinner. The new, high contrast frontend allows shooting targets as thin as 3nm in an overdense state.

**Develop suitable ultrathin targets**

- implement ex situ methods for producing the surface ultra-thin film layers required for laser targets
- implement on Trident the in situ target conditioning required

Earlier experiments used ultrathin source layers on µm sized targets to achieve an enhanced, mono-energetic TNSA. However, it became clear in the early stages of the proposal that freestanding nanotargets were required for BOA. Such targets were developed and fielded in collaboration with the University of Munich and the Kurchatov Institute in Moscow. These targets, Diamond-like Carbon (DLC) foils can be as thin as 3nm while freestanding over ~1mm$^2$. Up to 75% sp3 (diamond bonds) have been achieved, resulting in target densities of up to 2.8 g/cc.

**Perform the suite of PIC simulations necessary to understand better the enhanced TNSA and the laser-plasma afterburner regimes and, ultimately, develop reduced models to inform experimental design**
A suite of special PIC simulations in 1D, 2D and 3D has been performed over a range of different laser and target parameters, reproducing laser and target conditions as used in the experiments as closely as possible. They show excellent qualitative and quantitative agreement for both the carbon energies and the spectral shape. Based on the detailed analysis of this simulations combined with the observed experimental data, a reduced analytical model has been developed (HYT-model, Hegelich-Yan-Tajima), that describes the maximum ion energies for a given set of laser and target conditions. The model is also in excellent agreement with both the simulations and the experimental data. Figure 2 shows the maximum carbon cutoff energies as measured in experiments on Trident, predicted by VPIC simulations and by the HYT-model.

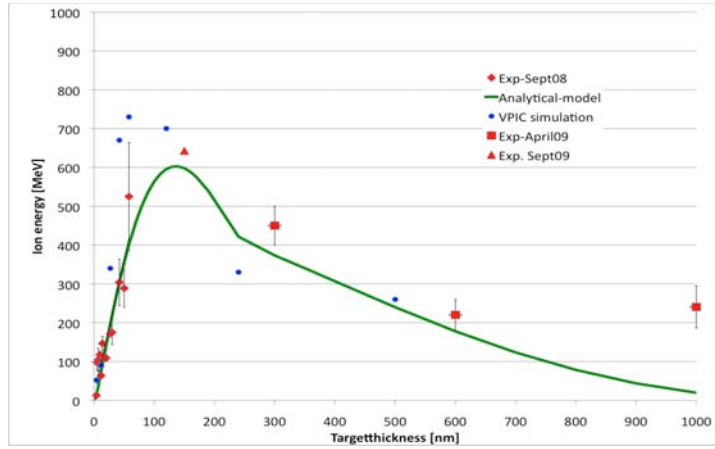


*Figure 2. Cutoff energy vs. Target thickness: Comparison of experimental data, simulations and analytical model. The squares are the measured mean (red) and maximum (black) cutoff energies for different target thicknesses, the different sized error bars are the result of different number of shots for the respective thicknesses. The blue diamonds are the equivalent cutoff energies obtained by VPIC simulations both 1D and 2D. One can observe a slight variation not in small part due to fluctuating laser parameters at different shots in the experiment while having a fixed set of parameters ("typical") for the simulation. The green line is the prediction by our analytic model, which is in excellent agreement over the validity range of the model up to ~600nm. Beyond that the model predicts much lower energies since it does not contain the physics of thick target interaction and therefore underestimates the TNSA component in this regime.*

**Design the targets and the experimental campaign**
After successful target and laser development a number of experimental campaigns were designed, starting out with a first demonstration of BOA and building onto that to investigate the details of the mechanisms and its dependence of various laser and target parameters. This resulted in four experimental campaigns, in April 2008, September 2008, April 2009 and September 2009.

**Deploy the initial validation experiments of the afterburner concept**
Initial scoping experiments were performed in April 2008, at this point however without the full contrast cleaning setup. Instead, a double plasma mirror setup was used that provided good contrast but at the cost of half the available pulse energy, thus limiting us to intensities of ~5 x $10^{19}$ W/cm$^2$, roughly one order of magnitude less than desired for first BOA demonstration. Nevertheless we could observe a first onset of a relativistic transparency regime. Results have been published in [8].

The first full BOA experiment was fielded in September 2008, now with the new ultrahigh contrast frontend. It was an immediate success, resulting in the first demonstration of BOA acceleration of carbon ions to >0.5 GeV as shown in Figure 3. The results have been reported at various

interational conferences and led to the development of a predictive reduced model. Together, with the subsequent experiments they now form a complete dataset that is in preparation for publication in Nature.

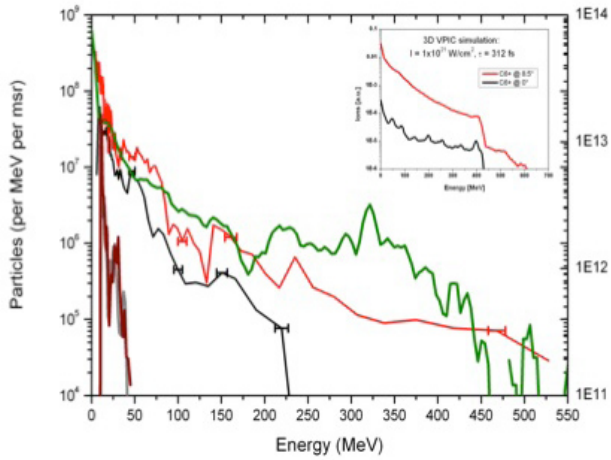


*Figure 3. Ion spectra from BOA acceleration from a 58nm DLC target, optimized for carbon acceleration under Trident conditions (this shot: 90J, 540 fs, 2x1020 W/cm², contrast <10-10 @ xx ps): The highest ion energies where observed at an 8.5° angle in the plane orthogonal to the laser polarization (red line) and agree well with a 2D VPIC simulation with the same shot parameters (green line). The energy on axis (black line) is significantly lower, as predicted in 3D BOA simulation (inset). The accelerated protons (grey, brown) obtain the same energy per nucleon, i.e. the same velocity, as predicted for the BOA regime.*

**Assuming success, evaluate the results and refine the theoretical models**

Based on the successful first beam time we conducted two more experimental campaigns. The to date developed models supplied us with predictions for target parameters (thickness) and laser parameters that had not been shot before. In the subsequent experiments we tested those predictions which and obtained excellent agreement between theory and experiment, as shown in Figure 2.

**Use the refined theoretical models to demonstrate the beam parameters and beam-ion species necessary for our three identified customers: boost, FI and cancer therapy**

Applying our models it is now possible to evaluate laser and target parameters for the abovementioned customers. For fast ignition the individual parameters have now been demonstrated: i.e. >0.5 GeV particle energies (Figure 3), >20% energy spread (Figure 4) and >10% conversion efficiency (Figure 5). However, those were not achieved simultaneously and not even on the same laser system in case of the conversion efficiency. Bringing them together will require laser capabilities beyond what Trident can deliver. Based on our models we now understand that not only the intensity and pulse duration is important but also the actual pulse shape. More precisely, the sharper the rise time of the pulse, the clearer the mono-energetic features and the higher the conversion efficiency. That means that even for an optimum pulse duration of ~100fs, which already is significantly shorter than what Trident can deliver, one would want a rise time as short as possible, on the order of ~10fs, requiring the same bandwidth as a true 10fs pulse. A way around this at least for proof-of-principle experiments was discovered during the last phase of this project: it appears to be feasible to use the nanotargets as pulseshaping mechanism, to deliver significantly steeper flanks than normally possible. A number of follow on proposals will pick up this idea to realize different laser-plasma interactions. However, for significant future advances lasers with substantially shorter pulses than Trident at the same or higher intensities will be required.

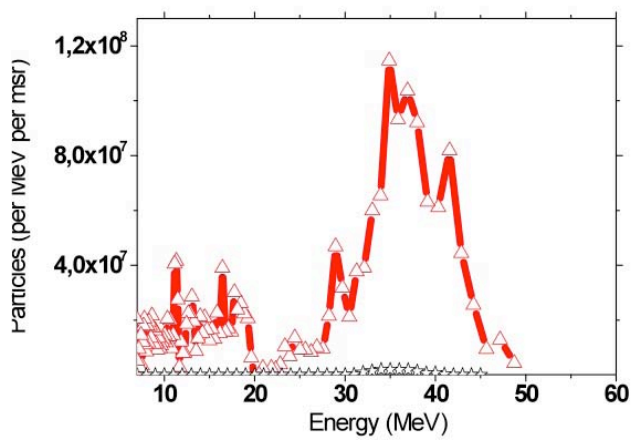


*Figure 4. Mono-energetic carbon ions from a 5nm DLC target shot at Trident. The energy spread is ~20%, at more than 100x higher particle numbers than previously best record with micron Pd-C targets (also Trident, Hegelich et al., Nature 2006).*

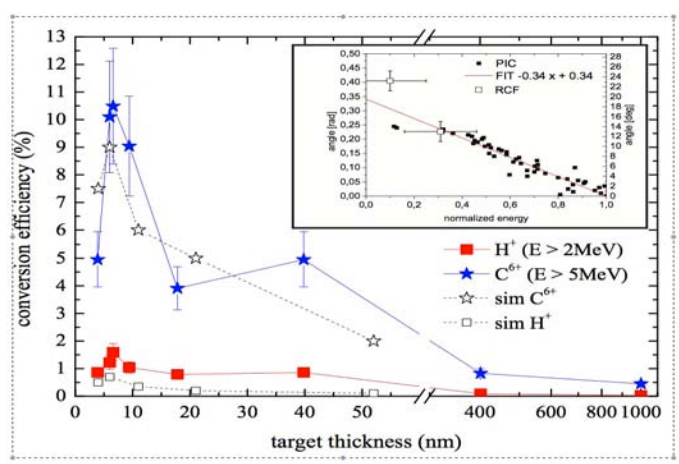


*Figure 5. Calculated conversion efficiency for protons and $C^{6+}$ ions as a function of target thickness for DLC targets shot at a 1J, 45fs laser system at MBI Berlin.*

**Deploy a demonstration integrated experiment relevant to boost**
This task was dismissed due to the lack of resources (personnel and beam time) and due to a focus shift from the potential sponsor which made it unlikely that even a success would generate follow-on funding.

**Publicize and share our results with our collaborators in other fields (FI, etc.)**
This project has already resulted in the publication of 17 papers in peer reviewed journals by us and our collaborators and 10 more are currently under preperation. It also resulted in more than 30 invited talks at international conferences, symposia and colloquia by the co-PI (Hegelich) alone plus a multitude of contributed talks and posters. We can state without exaggerating that this project established Los Alamos as the one of the top institutions in relativistic laser matter interactions in general and the world's leading institution in laser-driven ion acceleration in particular.

**Preliminary assessment on how to integrate this accelerator technology at a major accelerator facility such as LANSCE"**
In collaboration with Dr. I. Hoffmann from GSI Darmstadt we performed a preliminary assessment on how to integrate a laser driven front end into the SIS-18 synchrotron at GSI. In contrast to earlier assessments this now is a feasible endeavor given sufficient funding. We also started to investigate the opposite possibility of developing a relativistic booster amplifier for LANSCE based on the results of this project. First joined assessments with LANSCE personnel are currently beginning and will, if warranted, result in future proposals.

To summarize, we can say that prior to this project, the most promising mechanism for directed laser-ion acceleration was Target-Normal Sheath Acceleration (TNSA). The successful demonstration of Break-Out Afterburner (BOA) acceleration has lead to a paradigm shift in laser-driven ion acceleration. We are now reaching energies and efficiencies that make applications, staging and the use of smaller systems with higher repetition rate feasible.

Within this project we then studied and determined the laser parameters necessary for an experimental demonstration (12/2007) such as ultrahigh contrast laser pulses, conceived and developed optical technology to realize these parameters (3/2008) and implemented them in the Los Alamos Trident laser system (9/2008). Not only did this make Trident the highest contrast laser systems of its class by orders of magnitude in the world, giving LANL unique experimental capabilities, the successful implementation led directly to the first demonstration of BOA acceleration (10/2008) and detailed experimental studies of the mechanism. Using these results we directly validated our code VPIC in this physics regime and we were able to develop a reduced analytical model describing the basic features of the new mechanism that showed true predictive capabilities within its parameter range. Furthermore we experimentally demonstrated (individually) the required particle energy for carbon-driven fast ignition, as well as the required narrow energy spread $\Delta E/E$ and a laser-to-ion energy conversion efficiency of ~10%. This result is a huge step towards establishing the feasibility of carbon fast ignition, moving the challenge from the principal question *if* the necessary parameters can be achieved at all to the question on *how* to achieve them simultaneously, marking a transition from a fundamental science question to an engineering science question.

## Impact on National Missions

This project has strongly and demonstrably supported multiple national missions. These include both the fundamental science and the national security missions. Specifically, this project has supported three important components of the national security mission: energy security, global security and nuclear weapons physics.

This project has advanced the frontiers of fundamental scientific research in the areas of relativistic laser-plasma interactions and plasma physics, as well as the interdisciplinary subjects of advanced multi-scale supercomputer modeling, high-energy density physics, high-power high-energy laser systems, and applied materials science (through the development of self standing ultra-thin [~ nm] diamond films as laser targets). The former are important science topics stewarded by several federal funding agencies, such as NSF and DOE Office of Fusion Energy Science (OFES) through the emerging High Energy Density Laboratory Plasmas (HEDLP) joint program with NNSA. The latter multidisciplinary subjects are also important components of the scientific underpinnings of large DOE programs, such as Fusion Energy in Office of Science and the nuclear weapons science campaigns in Defense Programs.

Two broad examples can be cited for the scientific impact of this project. One example is represented by the various refereed scientific publications enabled by this LDRD project, listed in this report, with more to come. In fact, as a direct result of the LANL LDRD investment, Los Alamos is now recognized as the center of excellence for the emerging worldwide capability for laser-driven ion acceleration. Another example of impact is the fact that the ability to accelerate C ions to hundreds of MeV, as championed by this project, has enabled a novel concept

for fast-ignition fusion, based on laser-driven ion beams to ignite the target, as documented in Ref. [Fernandez2009]. That impact is further underscored by the fact that the further development of laser-driven ion beams has been funded in a four-year multi-institutional project by the joint OFES-NNSA HEDLP program.

As mentioned above, this project has impacted several aspects of the national security mission. In the area of energy security, the impact through inertial fusion energy and fast ignition has been outlined above. In the area of nuclear weapons research, some of the techniques for ion acceleration are being further developed at the Omega EP facility at the Univ. of Rochester, and being incorporated in designs of weapons physics experiments planned for the National Ignition Facility (NIF) at the Lawrence Livermore National Laboratory. Moreover, the development as part of this LDRD project of techniques to achieve ultra-high contrast laser pulses is likely to be incorporated by other major laser facilities (mostly operated by NNSA), further improving the research capability available to Defense Programs. The more novel impact is in the area of global security. The techniques for ion acceleration developed as part of this LDRD project can also be applied to develop ~ GeV proton beams. Such beams would be immensely useful as a tool for active interrogation to detect special nuclear material. In recognition of this, a research proposal was submitted to, and funded by the Domestic Nuclear Defense Office (DNDO) of the Dept. of Homeland Security. This three year proposal entails an investment of $3.8M by DNDO.

The two recently funded follow-on projects illustrate the tremendous scientific and programmatic potential of this laser-driven ion acceleration capability developed by the LDRD program. Besides the missions mentioned above, other applications include affordable ion-beam-based human therapy for cancer tumors, advanced accelerator development and rare isotope production. Indeed, this LDRD investment is likely to pay off for years to come.

## References


1. Snavely, R. A., M. H. Key, S. P. Hatchett, T. E. Cowan, M. Roth, T. W. Phillips, M. A. Stoyer, E. A. Henry, T. C. Sangster, M. S. Singh, S. C. Wilks, A. MacKinnon, A. Offenberger, D. M. Pennington, K. Yasuike, A. B. Langdon, B. F. Lasinski, J. Johnson, M. D. Perry, and E. M. Capmbell. Intense High-Energy Proton Beams from Petawatt-Laser Irradiation of Solids. 2000. *Physical Review Letters.* **85**: 2945.

2. Hatchett, S. P., C. J. Brown, T. E. Cowan, E. A. Henry, J. S. Johnson, M. H. Key, J. A. Koch, A. B. Langdon, B. F. Lasinski, R. W. Lee, A. J. MacKinnnon, D. M. Pennington, M. D. Perry, T. W. Phillips, M. Roth, T. C. Sangster, M. S. SIngh, R. A. Snavely, M. A. Stoyer, S. C. Wilks, and K. Yasuike. Electron, photon, and ion beams from the relativistic interaction of Petawatt laser pulses with solid targets. 2000. *Physics of Plasmas.* **7**: 2076.

3. Yin, L., B. J. Albright, B. M. Hegelich, K. J. Bowers, K. A. Flippo, T. J. T. Kwan, and J. C. Fernandez. Monoenergetic and GeV ion acceleration from the laser breakout afterburner using ultrathin targets (invited). 2007. *Physics of Plasmas.* **14** (5): 056706.

4. Albright, B. J., L. Yin, K. J. Bowers, B. M. Hegelich, K. A. Flippo, T. J. T. Kwan, and J. C. Fernandez. Relativistic Buneman instability in the laser breakout afterburner. 2007. *Physics of Plasmas.* **14**: 094502.

5. L.Robinson, A. P., M. Zepf, S. Kar, R. G. Evans, and C. Belle. Radiation pressure acceleration of thin foils with circularly polarized laser pulses. 2008. *New Journal of Physics.* **10**: 1.

6. Shah, R. C., R. P. Johnson, T. Shimada, K. A. Flippo, J. C. Fernandez, and B. M. Hegelich. High-temporal contrast using low-gain optical parametric amplification. 2009. *Optics Letters.* **34** (15): 2273.

7. Gautier, D. C.. A novel backscatter diagnostic for the Trident 200 TW laser. 2008. *Review of Scientific Instruments.* **79** (10): 10F547.

8. Henig, A., D. Kiefer, K. Markey, D. C. Gautier, K. A. Flippo, S. Letzring, R. P. Johnson, T. Shimada, L. Yin, B. J. Albright, K. J. Bowers, J. C. Fernandez, S. G. Rykovanov, H. - C. Wu, M. Zepf, D. Jung, V. Kh. Liechtenstein, J. Schreiber, D. Habs, and B. M. Hegelich. Enhanced Laser-Driven Ion Acceleration in the Relativistic Transparency Regime. 2009. *PHYSICAL REVIEW LETTERS.* **103**: 045002.


## Publications


Albright, B. J., L. Yin, K. J. Bowers, B. M. Hegelich, K. A. Flippo, T. J. T. Kwan, and J. C. Fernandez. Relativistic Buneman instability in the laser breakout afterburner. 2007. *Physics of Plasmas.* **14**: 094502.

Albright, B. J., M. J. Schmitt, J. C. Fernandez, G. E. Cragg, I. Tregillis, L. Yin, and B. M. Hegelich. Studies in capsule design for mid-Z ion-driven fast ignition. 2008. *Journal of Physics: Conference Series.* **112** (2): 022029 .

Bowers, K. J., B. J. Albright, L. Yin, B. Bergen, and T. J. T. Kwan. Ultrahigh performance three-dimensional electromagnetic relativistic kinetic plasma simulation (invited). 2008. *Physics of Plasmas.* **15** (5): 055703.

Fernandez, J. C., B. J. Albright, K. A. Flippo, B. M. Hegelich, T. J. Kwan, M. J. Schmitt, and L. Yin. Progress on ion based fast ignition. 2008. *Journal of Physics: Conference Series.* **112** (2): 022051.

Fernández, Juan C., J. J. Honrubia, Brian J. Albright, Kirk A. Flippo, D. Cort Gautier, Björn M. Hegelich, Mark J. Schmitt, M. Temporal, and L. Yin. Progress and prospects of ion-driven fast ignition. 2009. *Nuclear Fusion.* **49**: 1.

Flippo, K. A., E. d'Humieres, S. A. Gaillard, J. Rasuchine, M. Schollmeier, B. Albright, M. Bakeman, T. E. Cowan, D. C. Gautier, K. Harris, R. P Johnson, S. Letzring, F. Nurnberg, M. Roth, J. C. Fernandez, and B. M. Hegelich. Increased efficiency of short-pulse laser generated proton beams from novel flat-top cone targets (invited). 2008. *Physics of Plasmas.* **15** (5): 056709.

Flippo, K., B. M. Hegelich, B. J. Albright, L. Yin, D. C. Gautier, S. Letzring, M. Schollmeier, J. Schreiber, R. Schulze, and J. C. Fernandez. Laser-driven ion accelerators: spectral control, monoenergetic ions and new acceleration mechanisms. 2007. *Laser and Particle Beams.* **25** (1): 3.

Fuchs, J., Y. Sentoku, E. d'Humieres, T. E. Cowan, J. Cobble, P. Audebert, A. Kemp, A. Nikroo, P. Antici, E. Brambrink, A. Blazevic, E. M. Campbell, J. C. Fernandez, J. C. Gauthier, M. Geissel, M. Hegelich, S. Karsch, H. Popescu, N. Renard-LeGalloudec, M. Roth, J. Schreiber, R. Stephens, and H. Pepin. Comparative spectra and efficiencies of ions laser-accelerated forward from the front and rear surfaces of thin solid foils. 2007. *Physics of Plasmas.* **14**: 053105.

Gautier, D. C.. A novel backscatter diagnostic for the Trident 200 TW laser. 2008. *Review of Scientific Instruments.* **79** (10): 10F547.

Gautier, D. C., K. Flippo, J. C. Fernandez, B. M. Hegelich, and J. Fuchs. Time resolved analysis of the expansion of isochoricly heated thin foils. 2007. In *2007 IEEE Pulsed Power Plasma Science Conference.* (Albuquerque, NM, USA, 17-22 June 2007). Vol. ISBN 978-1-4244-0913-6, p. 610. Piscataway, NJ, USA: IEEE.

Habs, D., M. Hegelich, J. Schreiber, M. Gross, A. Henig, D. Kiefer, and D. Jung. Dense laser-driven electron sheets as relativistic mirrors for coherent production of brilliant X-ray and γ -ray beams. 2008. *Applied Physics B.* **93**: 349.

Harres, K., M. Schollmeier, E. Brambrink, P. Audebert, A. Blazevic, K. Flippo, D. C. Gautier, M. Geissel, B. M. Hegelich, F. Nurnberg, J. Schreiber, H. Wahl, and M. Roth. Development and calibration of a Thomson parabola with microchannel plate for the detection of laser-accelerated MeV ions. 2008. *Review of Scientific Instruments.* **79** (9): 093306.

Hegelich, B. M.. Ultra-high intensity laser acceleration of ions to MeV/nucleon energies. 2007. In *2007 IEEE PARTICLE ACCELERATOR CONFERENCE.* (Albuquerque, NM, USA, 25-29 June 2007). Vol. ISBN 978-1-4244-0916-7, p. 2512. Piscataway, NJ, USA: IEEE.

Hegelich, B. M., L. Yin, B. J. Albright, K. J. Bowers, K. A. Flippo, D. C. Gautier, A. Henig, R. P. Johnson, D. Jung, D. Kiefer, S. Letzring, V. Liechtenstein, R. Shah, T. Shimada, X. Yan, D. Habs, T. Tajima, and J. C. Fernández. Towards GeV laser-driven Ions: First demonstration of Break-Out Afterburner Acceleration. 2009. *In preparation for Nature.*

Henig, A., D. Kiefer, K. Markey, D. C. Gautier, K. A. Flippo, S. Letzring, R. P. Johnson, T. Shimada, L. Yin, B. J. Albright, K. J. Bowers, J. C. Fernandez, S. G. Rykovanov, H. - C. Wu, M. Zepf, D. Jung, V. Kh. Liechtenstein, J. Schreiber, D. Habs, and B. M. Hegelich. Enhanced Laser-Driven Ion Acceleration in the Relativistic Transparency Regime. 2009. *PHYSICAL REVIEW LETTERS.* **103**: 045002.

Kiefer, D., A. Henig, D. Jung, D. C. Gautier, K. A. Flippo, S. A. Gaillard, S. Letzring, R. C. Shah, T. Shimada, J. C. Fernandez, V. Kh. Liechtenstein, J. Schreiber, B. M. Hegelich, and D. Habs. First observation of quasi-monoenergetic electron bunches driven out of ultra-thin diamond-like carbon (DLC) foils. To appear in *THE EUROPEAN PHYSICAL JOURNAL D.*

Schollmeier, M., K. Harres, F. Nurnberg, A. Blazevic, P. Audebert, E. Brambrink, J. C. Fernandez, K. A. Flippo, D. C. Gautier, M. Geissel, B. M. Hegelich, J. Schreiber, and M. Roth. Laser beam-profile impression and target thickness impact on laser-accelerated protons. 2008. *Physics of Plasmas.* **15** (5): 053101.

Schollmeier, M., M. Roth, A. Blazevic, E. Brambrink, J. A. Cobble, J. C. Fernandez, K. A. Flippo, D. C. Gautier, D. Habs, K. Harres, B. M. Hegelich, T. Hessling, D. H. H. Hoffmann, S. Letzring, F. Nurnberg, G. Schaumann, J. Schreiber, and K. Witte. Laser ion acceleration with micro-grooved targets. 2007. *Nuclear Instruments and Methods in Physics Research A.* **577**: 186.

Schollmeier, M., S. Becker, M. Geissel, K. A. Flippo, A. Blazevic, S. A. Gaillard, D. C. Gautier, F. Gruner, K. Harres, M. Kimmel, F. Nurnberg, P. Rambo, U. Schramm, J. Schreiber, J. Schutrumpf, J. Scharwz, N. A. Tahir, B. Atherton, D. Habs, B. M. Hegelich, and M. Roth. Controlled transport and focusing of laser-accelerated protons with miniature magnetic devices . 2008. *Physical Review Letters.* **101** (5): 055004.

Shah, R. C., R. P. Johnson, T. Shimada, K. A. Flippo, J. C.

Fernandez, and B. M. Hegelich. High-temporal contrast using low-gain optical parametric amplification. 2009. *Optics Letters.* **34** (15): 2273.

Yan, X. Q., T. Tajima, M. Hegelich, L. Yin, and D. Habs. Theory of laser ion acceleration from a foil target of nm thickness. To appear in *Applied Physics B.*

Yin, L., B. J. Albright, B. M. Hegelich, K. J. Bowers, K. A. Flippo, T. J. T. Kwan, and J. C. Fernandez. Monoenergetic and GeV ion acceleration from the laser breakout afterburner using ultrathin targets (invited). 2007. *Physics of Plasmas.* **14** (5): 056706.

# Cold Atom Surface Imaging

*Eddy M. Timmermans*
20070028DR

## Abstract

We exploited the exquisite sensitivity of cold atom Bose-Einstein condensates (BECs) – the matter wave analog of lasers - and we explored the advantages offered by the quantum nature of BEC-systems to probe surface forces. We targeted one force in particular: the electro-magnetic quantum fluctuation-induced Casimir-Polder force experienced by an atom near surfaces, of interest in nanotechnology. This project also explored the laser-like coherence of cold atom Bose-Einstein condensate (BEC) systems for developing a coherent optics to image surface forces. Coherent BEC optics could give access to the ten nanometer resolution that remains a challenge in surface microscopy.

The participants focused on quantum fluctuations relevant to near-surface physics; they proposed ultra-sensitive probes and have explored their realization. They developed the tools for an optics technique with Bose-Einstein condensates (BEC's) as a novel surface microscopy. The work has been organized around three focal points: (I) near-surface quantum fluctuation physics, (II) ultra-sensitive quantum probes and (III) slow matter wave holography.

We developed novel theory-concepts and experimental, numerical and mathematical tools. We proposed an ultra-sensitive weak force probe that consists of phase separated BECs, and a Josephson-like ring BEC that can take on a macroscopic Schrodinger cat state – a linear superposition of two very distinct many-body states – that can exhibit extraordinary sensitivity to external forces. We calculated Casimir forces for corrugated surfaces and wedge-like metal surfaces and we studied highly sensitive macroscopic Schrodinger cat states in first-order quantum phase transitions. We studied the limitations on canceling interactions to reduce the phase diffusion effect in cold atom interferometers and we studied standing wave BEC-patterns to use ring-BECs as gyroscopes. We explored the use of freely expanding BECs to image external potentials holographically. The tools include a mathematical framework to describe quantum evolution in many-body systems, a numerical fast Schrodinger solver, and an experimental trap to contain BECs in a 2D-geometry with arbitrary potential.

## Background and Research Objectives

Quantum mechanics manifests itself at atomic scale lengths. Nanotechnology reaffirmed this truism in a somewhat unexpected context by struggling with the effects of electromagnetic vacuum quantum fluctuations when engineering micro and nano-scale devices: MEM's and NEM's (micro and nano electromechanical devices) such as nano-cantilevers. Cantilevers are tiny mechanical bridge-like structures sticking out of the surface that can resonate at well-defined vibrational frequencies. Such structures have been used as switches and as probes to measure weak fields such as the magnetic field of a small spin samples (important for future quantum computation architectures). Similar structures are developed to detect single virus cells in biomedical application of nanotechnology: cantilevers coated with anti-bodies can detect single virus cells as they change their vibration frequency when a single virus cell is captured. However, the engineering of ultra-small and ultra-sensitive cantilevers is hampered by vacuum fluctuations of the electromagnetic field. Generally, the Casimir force attracts the cantilevers to the surface, collapsing smaller and more fragile cantilevers onto the surface (known as the problem of stiction).

The sudden relevance of quantum fluctuations was predicted a long time ago by Feynman In his 1959 talk 'There's plenty of room at the bottom'. A simple order-of-magnitude estimate makes the point: due to its coupling to the electromagnetic field modes, a single rubidium atom located a distance of 1 micron from a flat surface, perfect conductor is attracted to that surface with an acceleration that is approximately half a 'g' (the acceleration experienced by falling objects at the surface

of the earth). At a distance of 10 micron, this acceleration is reduced by a factor of $10^5$ (at zero temperature). For general surface shapes and material compositions, Casimir forces, which are not additive, are difficult to compute. These forces are, however, important: not only do small scale geometrical shapes significantly alter the Casimir force, but different material compositions involving materials with strong magnetic response may give rise to repulsive instead of attractive forces.

The measurement of Casimir forces with specific surface geometries remains a challenge in spite of well-developed surface microscopy techniques. While scanning tunneling microscopes can image individual atoms and while atomic force microscopes are very sensitive, surface technology remains unable to image surfaces on the tens of nanometer scale relevant to nanotechnology and force components parallel to the surface remain hard to measure. The presence of a single spin has been detected but the detection process is time consuming (twelve hours) and the measurement involves a high magnetic field to orient the spin, yet several proposed architectures for solid state quantum computers explicitly rely on single spin measurements. Also quantum issues such as collapsing the spin component in the measurement process, backaction on the measured spin, and decoherence play a crucial role. A general strategy involves probes that are themselves quantum objects and that utilize many-body quantum effects to yield ultra-sensitive probes. It has been suggested, for instance, that a many-body Schrodinger cat state of N atoms in a state that is a superposition of all N atoms in one spine state and all atoms in another spin state might measure an optical frequency with a relative error that is N times smaller than the error of measuring the same frequency with one particle – the Heisenberg limit. We refer to such device as a Schrodinger cat sensor. Alternatively, new strategies have been suggested in this project: The Loschmidt echo is highly sensitive to a weak field that that breaks the time reversal so that realizing a Loschmidt echo and detecting how good the initial state can be reached after nearly complete time reversal can give a highly sensitive probe of the weak field. Other macroscopic Schrodinger cats are highly sensitive: a superconducting quantum interference device (SQUID)-like ring-BEC with a Josephson junction and quantum droplets that nucleate in a first order quantum phase transition. Cold atom interferometers are currently limited by the phase diffusion caused by inter-particle interactions and we have studied the limitations of canceling interactions with a Feshbach resonance.

## Scientific Approach and Accomplishments

**Near-Surface Quantum Fluctuation Physics**

We developed methods to calculate Casimir forces for atoms near specific geometrical surface structures – a corrugated surface [1-3] in one case and a wedge [4,5] in another. We found non-trivial effects of geometry in dispersion atom-surface forces, constructed exact analytical solutions, revealed the interplay between geometry, material properties and temperature [6]. We proposed experiments to use cold atoms, and BECs in particular, to probe quantum and thermal fluctuation forces in the presence of surface structures. We calculated the effects of corrugation and roughness of material surfaces on the normal and lateral Casimir-Polder force on a BEC. We proposed different methods to measure such interactions: the use of a “BEC cantilever” to measure lateral frequency shifts of the center-of-mass oscillation of the BEC due to Casimir forces, the use of a “BEC AFM” (BEC Atomic Force Microscope) to map the energy landscape of the Casimir potential, and the use of two-photon Bragg spectroscopy [7] to measure Casimir-induced modifications of the low-energy Bogoliubov spectrum of the BEC in proximity to a material surface.

The cold atom experimental explorations of Casimir forces focused on demonstrating a measurement of the Casimir force caused by corrugated surfaces of specific dimensions. We had the surface for this measurement fabricated in Sandia National. LANL surface experts characterized the Sandia-fabricated nanoscale patterns with atomic force microscopy to determine width, depth, and step edge angles as calibrations for BEC imaging. We developed an RF off-axis magnetron sputter deposition capability to produce $La_{0.7}Sr_{0.3}MnO_3$ films on $LaAlO_3$ substrates. This combination of film and substrate gave a lattice mismatch that induced out-of-plane tensile stress resulting in out-of-plane maze-like patterns of magnetic stripes suitable for holographic BEC imaging. We developed a deposition capability to produce magnetic oxide films with out-of-plane domain patterns for holographic imaging. We obtained a NanoMan software computer program from Veeco Instruments, Inc. to produce stripe patterns using the atomic force microscope by either scratching or electric field induced surface modification on both thin gold films and single crystal silicon surfaces. We produced and characterized surface patterns consisting of multiple striped patterns with different spacings than those from the Sandia micro-fabrication facility.

**Ultra-sensitive Quantum Probes**

The project focused on alternative probes – we showed that the tunability of trapping frequencies of trapped

phase-separated BEC's can nearly cancel the buoyancy and trapping force experienced by a phase separated bubble immersed in an immiscible, larger trapped BEC [8]. Near the cancellation point, the bubble position becomes very sensitive to an external force that is experienced differently by the atoms in the bubble than by the atoms in the larger, surrounding BEC and the displacement of the bubble is proportional to the external force. This device, which we have called a BEC-level (in analogy with the spirit-level used in construction work) yields a hypersensitive weak force detector. Estimates of the experimental accuracies suggest a sensitivity that could allow Casimir force measurements as far away from the surface as 50 or 80 micron.

Phase diffusion, the loss of the phase memory induced by inter-particle interactions, is expected to be the ultimate limitation of the accuracy of BEC-interferometers. One way around this problem is the cancellation of the interactions using a Feshbach resonance. However, while the Feshbach resonance can cancel the inter-particle interactions for a specific relative momentum vector, there is still a momentum dependence that remains. Particularly if the separated BEC blobs are contained by tight BEC-traps, the interacting pairs of BEC-atoms experience a range of relative momentum vectors. We studied Feshbach resonance interactions and we described the low relative momentum expansion of the scattering amplitude and the effective interaction near the point of vanishing scattering length [9].

We showed that the zero temperature phase separation in mixtures of fermions and bosons, which is a first-order quantum phase transition, can spontaneously create many-body Schrodinger cat states allowing oscillations between separated and non-separated states [10-12]. While such state does not lend itself to probe external forces, the experimental realization of this state would allow an important, direct observation of the rate of decoherence and the fragility of the quantum many-body state [13-17].

We proposed a quantum interference device-like device with a cold atom BEC confined to a ring-shaped potential containing a tunnel junction [18]. This system can take on metastable states carrying nonzero persistent currents, realizing a cold atom analog of the Superconducting Quantum Interference Device (SQUID) that found numerous applications, such as ultrasensitive magnetometers. We studied various properties such as transitions between different current carrying states and means of their control, and we showed that the measurements can be performed in a standard "time-of-flight" experiment.

On the subject of spin probes, we proposed the detection of critical points of quantum phase transitions with a Loschmidt echo [19-21], taking advantage of the sensitivity of the systems near criticality. The accuracy of quantum probes depends sensitively on quantum effects in its time evolution. We have developed a novel mathematical framework for treating quantum effects in the dynamics of many-body systems [22-24]. We developed a consistent dynamical theory for observables of open many body quantum nonlinear bosonic systems. We show that non-quadratic (nonlinear) terms in a Hamiltonian provide a singular ''quantum" perturbation for observables in some ''mesoscopic" region of parameters. In particular, quantum effects result in secular terms in the dynamical evolution that grow in time. We argue that even for open quantum nonlinear systems in the deep quasi-classical region, these quantum effects can survive after decoherence and relaxation processes take place. We demonstrate that these quantum effects in open quantum systems can be observed, for example, in the frequency Fourier spectrum of the dynamical observables, or in the corresponding spectral density of noise. For BEC's we show that the characteristic time of deviation of quantum from classical dynamics for observables coincides with the characteristic time-scale of the well-known quantum nonlinear effect of phase diffusion. We apply our results to the Bose–Einstein condensates in a one-dimensional toroidal geometry, and derive the estimates for the observation of the discussed effects in experiments [22].

The flow in a long, thin BEC can register exceedingly weak potential variation near a surface. How can one detect the superfluid flow? By observing the fringe positions in a long-lived standing wave BEC pattern induced by a localized attractive potential in a larger BEC, one could measure small potential differences. We have studied the formation of such standing wave patterns and their dynamical stability. As the potential depth is increased, the time-independent Gross-Pitaevskii equation describing the BEC develops solutions where the BEC wavefunction has nodes. We subject the solutions to a linear stability analysis to clarify when they are stable. One of the interesting results is that the system can exhibit reentrant stability, whereby a nodal BEC state can go from being stable to unstable to stable again whilst the depth of the potential is increased [25].

**Cold Atom Holography**

Another focus was 'slow matter wave holography': a cold atom BEC scatters off a surface potential and interferes with the directly emitted wave to give holographic fringes in the recorded density pattern. The BEC wave is 'launched' by switching off the trapping potential of the BEC that has been transported close to the surface. To avoid integrating out the fringes, the atomic density should be measured within a thin slice of space in three

dimensions. The experimental effort of this project aims at a proof-of-principle demonstration. We developed a sophisticated computer-controlled deflection system that allows us to create completely arbitrary 2D potentials (Figure 1). Rather than work in 3D and image just a slice of the interference pattern, we decided to use a cylindrically-focused red-detuned laser beam to form a light sheet trap which confines all of the atoms to a horizontal plane. Superimposed on the sheet is a tightly-focused red-detuned beam which propagates vertically, forming an "optical tweezer" within the light sheet. The tweezer beam is controlled by our deflection system, so it can be rapidly switched from a single beam trap to painting a complex potential. The system can now also paint a blue-detuned beam to create repulsive potentials, or indeed combinations of attractive and repulsive. The experiments are guided by numerical simulations of the scattering process using the full 3D time-dependent Gross-Pitaevskii equation. This system was intended to simply provide the scattering object in the holography demonstration, but the technique has turned out to be much more powerful than expected, opening up new possibilities in the final year of the project. Our publication [26] describing how this technique can be used to produce Bose-Einstein condensates in arbitrary shapes (Figure 2) and evolve them with arbitrary dynamics was picked up and highlighted by both *Nature* and *Optics and Photonics Focus*.

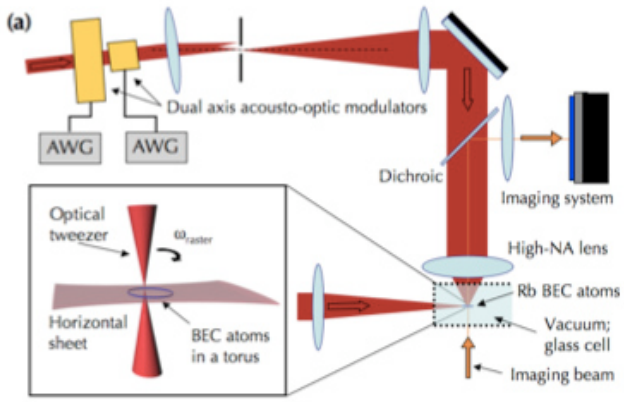


*Figure 1. Schematic of the set-up to trap 2D-BEC and subject them to arbitrary, dynamic potentials.*

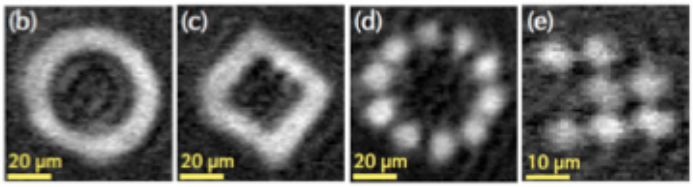


*Figure 2. Measured Density Patterns of BECs contained in the 2D-trap.*

## Impact on National Missions

This project supports the DOE mission in basic science by developing cold atom systems, of fundamental interest, into practical sensing and microscopy technologies, which can probe condensed matter surfaces on novel length scales. The results can enhance the LANL capabilities in material science and quantum information. Advances in quantum information bring potential benefits to the laboratory mission on information science and technology, the advances in sensing can benefit the security missions.

## References


1. R.Dalvit, D. A., P. A. Maia Neto, A. Lambrecht, and S. Reynaud. Probing quantum vacuum geometrical effects with cold atoms. 2008. *Physical Review Letters.* **100**: 040405.

2. R.Dalvit, D. A., P. A. Maia Neto, A. Lambrecht, and S. Reynaud. Lateral Casimir-Polder force with corrugated surfaces. 2008. *Journal of Physics A: Mathematical and Theoretical.* **41**: 164028.

3. Messina, R., D. A. R. Dalvit, P. A. Maia Neto, A. Lambrecht, and S. Reynaud. Dispersive interactions between atoms and non-planar surfaces. 2009. *Physical Review A.* **80**: 022119.

4. C.N.Mendes, T., F. S.S. Rosa, A. Tenorio, and C. Farina. Dispersion forces between an atom and a perfectly conducting wedge. 2008. *Journal of Physics A.* **41**: 164029.

5. S.S.Rosa, F., T. N.C. Mendes, and C. Farina. Spontaneous emission of an atom near a wedge. 2008. *Journal of Physics A.* **78**: 012105.

6. S.Rosa, F. S.. On the possibility of Casimir repulsion using metamaterials. 2009. *Journal of Physics Conference Series.* **161**: 012039.

7. Moreno, G., D. A. R. Dalvit, and E. Calzetta. Bragg spectroscopy for measuring Casimir-Polder interactions with Bose-Einstein condensates. *Physical Review A.*

8. Bhongale, S., and E. Timmermans. BEC-level for measuring small forces. 2008. *Physical Review Letters.* **100**: 185301.

9. Kalas, R., and E. Timmermans. Simplified description of narrow Feshbach resonances. To appear in *Physical Review A.*

10. Mozyrsky, D., I. Martin, and E. Timmermans. Coherent macroscopic tunneling in boson-fermion mixtures. 2007. *Physical Review A.* **76**: 051601.

11. Solenov, D., and D. Mozyrsky. Quantum nucleation and macroscopic quantum tunneling in cold atom boson-fermion mixtures. 2008. *Physical Review A.* **78**: 053611.

12. Solenov, D., and D. Mozyrsky. Kinetics of the phase separation transition in cold-atom boson-fermion mixtures. 2008. *Physical Review Letters.* **100**: 150402.

13. Gurvitz, S. A., and D. Mozyrsky. Quantum mechanical approach to decoherence and relaxation generated by fluctuating environment. 2008. *Physical Review B.* **77**: 075325.

14. Merkli, M., I. M. Sigal, and G. P. Berman. Decoherence and thermalization. 2007. *Physical Review Letters.* **98**: 130401.

15. Merkli, M., I. M. Sigal, and G. P. Berman. Resonance theory of decoherence and thermalization. 2008. *Annals of Physics.* **323**: 373.

16. Celardo, G. L., F. M. Izrailev, V. G. Zevelinsky, and G. P. Berman. Open system of interacting fermions: statistical properties of cross-sections and fluctuations. 2007. *Physical Review E.* **76**: 031119.

17. Berman, G. P., G. L. Celardo, F. M. Izraelev, and V. G. Zelevinsky. Transition from isolated to overlapping resonances in the open system of interacting fermions. 2008. *Physics Letters B.* **659**: 170.

18. Solenov, D., and D. Mozyrsky. Metastable states and macroscopic quantum tunneling in a cold atom Josephson ring. *Physical Review Letters.*

19. Zhang, J., F. M. Cucchietti, C. M. Chandrashekar, M. Laforest, C. A. Ryan, M. Ditty, A. Hubbard, J. K. Gamble, and R. Laflamme. Direct observation of quantum criticality in Ising spin chains. 2009. *Physical review A.* **79**: 012305.

20. Quan, H., and F. M. Cucchietti. Quantum fidelity and thermal phase transitions. 2009. *Physical review E.* **79**: 031101.

21. Zurek, W. H., F. M. Cucchietti, and J. P. Paz. Gaussian decoherence and Gaussian echo from spin environments. 2007. *Acta Physica Polonica B.* **38** (5): 1685.

22. Berman, G. P., D. A.R. Dalvit, G. V. Schlyapnikov, N. Tarkhanov, and E. M. Timmermans. On the stability of a Bose-Einstein condensate trapped in a one-dimensional toroidal geometry. 2008. *International Journal of Theoretical Physics.* **47**: 2393.

23. Berman, G. P., D. A. R. Dalvit, and F. Borgonovi. Quantum dynamical effects as a singular perturbation for observables in open quasi-classical nonlinear mesoscopic systems. 2009. *Chaos, Solitons and Fractals.* **41**: 919.

24. Merkli, M., G. P. Berman, and I. M. Sigal. Resonant perturbation theory of decoherence and relaxation of quantum bits. *Advances in Mathematical Physics.*

25. Kalas, R., D. Solenov, and E. Timmermans. Reentrant Stability of standing wave BEC patterns. *Physical Review A.*

26. Henderson, K., C. Ryu, C. MacCormick, and M. G. Boshier. Experimental demonstration of painting arbitrary and dynamics potentials for Bose-Einstein condensates. 2009. *New Journal of Physics.* **11**: 043030.

## Publications

A.R.Dalvit, D., P. A. Maia Neto, A. Lambrecht, and S. Reynaud. Probing quantum vacuum geometrical effects with cold atoms. 2008. *Physical Review Letters.* **100**: 040405.

Berman, G. P., D. A. R. Dalvit, and F. Borgonovi. Quantum dynamical effects as a singular perturbation for observables in open quasi-classical nonlinear mesoscopic systems. 2009. *Chaos, Solitons and Fractals.* **41**: 919.

Berman, G. P., D. A.R. Dalvit, G. V. Schlyapnikov, N. Tarkhanov, and E. M. Timmermans. On the stability of a Bose-Einstein condensate trapped in a one-dimensional toroidal geometry. 2008. *International Journal of Theoretical Physics.* **47**: 2393.

Berman, G. P., G. L. Celardo, F. M. Izraelev, and V. G. Zelevinsky. Transition from isolated to overlapping resonances in the open system of interacting fermions. 2008. *Physics Letters B.* **659**: 170.

Berman, G. P., and N. Tarkhanov. Quantum dynamics in the Fermi-Pasta-Ulam problem. 2006. *International Journal of Theoretical Physics.* **45**: 1865.

Bhongale, S., and E. Timmermans. BEC-level for measuring small forces. 2008. *Physical Review Letters.* **100**: 185301.

C.N.Mendes, T., F. S.S. Rosa, A. Tenorio, and C. Farina. Dispersion forces between an atom and a perfectly conducting wedge. 2008. *Journal of Physics A.* **41**: 164029.

Celardo, G. L., F. M. Izrailev, V. G. Zevelinsky, and G. P. Berman. Open system of interacting fermions: statistical

properties of cross-sections and fluctuations. 2007. *Physical Review E.* **76**: 031119.

Gurvitz, S. A., and D. Mozyrsky. Quantum mechanical approach to decoherence and relaxation generated by fluctuating environment. 2008. *Physical Review B.* **77**: 075325.

Henderson, K., C. Ryu, C. MacCormick, and M. G. Boshier. Experimental demonstration of painting arbitrary and dynamical potentials for Bose-Einstein condensates. 2009. *New Journal of Physics.* **11**: 043030.

Kalas, R., D. Solenov, and E. Timmermans. Reentrant stability of standing wave BEC patterns. To appear in *Physical Review A.*

Kalas, R., and E. Timmermans. Simplified description of narrow Feshbach resonances. To appear in *Physical Review A.*

Merkli, M., G. P. Berman, and I. M. Sigal. Resonant perturbation theory of decoherence and relaxation of quantum bits. *Advances in Mathematical Physics.*

Merkli, M., I. M. Sigal, and G. P. Berman. Decoherence and thermalization. 2007. *Physical Review Letters.* **98**: 130401.

Merkli, M., I. M. Sigal, and G. P. Berman. Resonance theory of decoherence and thermalization. 2008. *Annals of Physics.* **323**: 373.

Messina, R., D. A. R. Dalvit, P. A. Maia Neto, A. Lambrecht, and S. Reynaud. Dispersive interactions between atoms and non-planar surfaces. 2009. *Physical Review A.* **80**: 022119.

Moreno, G., D. A. R. Dalvit, and E. Calzetta. Bragg spectroscopy for measuring small forces. *Physical Review A.*

Mozyrsky, D., I. Martin, and E. Timmermans. Coherent macroscopic tunneling in boson-fermion mixtures. 2007. *Physical Review A.* **76**: 051601.

Quan, H., and F. M. Cucchietti. Quantum fidelity and thermal phase transitions. 2009. *Physical Review E.* **79**: 031101.

R.Dalvit, D. A., P. A. Maia, A. Lambrecht, and S. Reynaud. Lateral Casimir-Polder force with corrugated surfaces. 2008. *Journal of Physics A: Mathematical and Theoretical.* **41**: 164028.

S.Rosa, F. S.. On the possibility of Casimir repulsion using metamaterials. 2009. *Journal of Physics Conference Series.* **161**: 012039.

S.S.Rosa, F., T. N.C. Mendes, and C. Farina. Spontaneous emission of an atom near a wedge. 2008. *Journal of Physics A.* **78**: 012105.

Solenov, D., and D. Mozyrsky. Kinetics of the phase separation transition in cold-atom boson-fermion mixtures. 2008. *Physical Review Letters.* **100**: 150402.

Solenov, D., and D. Mozyrsky. Quantum nucleation and macroscopic quantum tunneling in cold atom boson-fermion mixtures. 2008. *Physical Review A.* **78**: 053611.

Solenov, D., and D. Mozyrsky. Metastable states and macroscopic quantum tunneling in a cold atom Josephson ring. *Physical Review Letters.*

Zhang, J., F. M. Cucchietti, C. M. Chandrashekar, M. Laforest, C. A. Ryan, M. Ditty, A. Hubbard, J. K. Gamble, and R. Laflamme. Direct observation of quantum criticality in in Ising spin chains. 2009. *Physical Review A.* **79**: 012305.

Zurek, W. H., F. M. Cucchietti, and J. P. Paz. Gaussian decoherence and Gaussian echo from spin environments. 2007. *Acta Physica Polonica B.* **38** (5): 1685.

# Multiscale Modeling of Strongly Interacting Systems

*Robert E. Ecke*
20070505DR

## Abstract

The most challenging and, arguably, relevant class of many-body systems are intractable by brute force-methods, because their physics depends crucially on the role of interactions and correlations and/or on the interplay of multiple length and/or time scales. The list of problems that fall within this category -- turbulence in fluids, disordered systems, classical and quantum phase transitions, conventional and high-temperature superconductivity -- illustrate their ubiquity in nature, their relevance, and the central role they have played in the development of science. The complexity that follows from the intertwining of scales and the nonlinearity that results from the inclusion of inter-particle interactions and correlations places the description of this physics among the most challenging focal points of science. We have focused on fluid turbulence and instability, on elastic-plastic deformation in solids, on collective effectives in cold atoms, superconductors and superfluids, and on materials properties at the nano-scale. In addition to focusing on fundamental, frontier physics, this project impacts practical engineering areas and contributes to core missions of the Laboratory.

## Background and Research Objectives

The nature of multi-scale systems has varying degrees of difficulty and challenge. Perhaps the most straightforward is the problem of fluid turbulence where the physics of energy transfer is almost the same at every scale and the challenge is to solve this strongly coupled nonlinear problem using a number of approaches, because no one method has been discovered to deal with the whole problem. There is strong coupling of turbulence with both fundamental mathematics and important physical applications such as the mixing of different fluid components. Our research goal in this area is to use experiment, theory and simulation in a combined attack on important problems in turbulence.

Another challenging multi-scale system involves the coupling of the dynamics of discrete, atomic-scale defects such as dislocations with continuum elastic fields at large scales. Merging dislocations with such continuum descriptions is beyond the capabilities of molecular dynamics approaches and requires other methods. Of particular utility is the concept introduced by Landau in which the state of the system is determined by minimizing a free energy function. We incorporate dislocation descriptions into the energy function theory to give an improved quantitative tool for understanding complex materials such a martensites.

Soft condensed matter systems such as granular materials or colloids are also of great current research interest because of their inherent non-equilibrium aspects and because of the ability to directly compute or experimentally measure detailed properties arising from the discrete nature of the particles. We use these systems to understand granular kinetic energy distributions, to determine the underlying constitutive relations coupling discrete grain motion and macroscopic flows, and to explore states with co-existing phases such as fluid-solid behavior in avalanching flow.

Superconducting materials and cold atom systems comprise an important frontier of materials science. In these systems many components, e.g., electrons, atoms, etc., strongly interact to display unexpected cooperative effects. Further, nano-scale materials such as carbon nano-tubes exhibit novel effects arising from their small spatial scale, scales where quantum effects are extremely important. We study a broad range of such systems to better understand and model the many-body interactions that lead to unique macroscopic materials properties.

## Scientific Approach and Accomplishments

Our scientific approach is based on an interdisciplinary attack on challenging problems involving systems

with interacting degrees of freedom over a wide range of spatial and temporal time scales. In the past year, our project has spawned a number of new insights by exploring intriguing prospects of new technologies (such as cold atom physics and nanotechnology), by employing non-equilibrium transport approaches to quantum problems, by applying Ginzburg-Landau free-energy approaches to the description of plasticity in martensitic phase transformations, by transferring techniques across fields (such as between nonlinear physics and many-body quantum physics) and by exploiting the power of novel numerical techniques coupled to precision experiments (turbulence). This multi-disciplinary approach provides a powerful strategy to bring fundamental advances and provides different angles of attack to the description of multi-scale systems.

A very active part of this project involved systems where a fluid is driven to a turbulent state through the application of an external applied force. One interesting aspect of such turbulent systems is the resultant mixing that occurs to species (temperature, concentration, reactive chemicals, etc.) immersed in the turbulent flow. We showed how one can use dynamical systems concepts of stable and unstable manifolds and Lyapunov exponents to characterize the mixing rates and associated spatial structures driving the mixing in a two-dimensional experimental flow [1]. Figure 1 shows the "stretching fields" (stable and unstable manifolds) for several different realizations of the turbulent flow. In related theoretical and numerical work, we convincingly elucidated the physical mechanisms for the inverse energy cascade of 2D turbulence [2] by using an analysis approach of decomposing the velocity field into large-scale and small-scale components and calculating the flux of energy between the two parts. We used this approach to show how the process of an inverse cascade of vorticity could be applied usefully to 3D turbulence in pipe flow [3] and to model sub-grid (the small-scale part) flux of a passive scalar [4]. We also demonstrated [5] that for a stratified shear flow, vertical mixing can be described very efficiently by a Prandtl mixing length model, with implications for easy parameterization of mixing in outflows of marginal seas and river flows into lakes. These results may help provide better understanding of turbulence and mixing in the ocean and may be useful in producing more efficient and accurate global ocean models. Further, we explored mixing that occurs in the Rayleigh-Taylor instability [6] with accompanying chemical reactions [7], an important process in, for example, supernova events. Figure 2 illustrates how the Rayleigh-Taylor instability is affected by the inclusion of chemical reactions: mixing becomes more localized to isolated patches when the dynamical evolution time becomes larger than the characteristic reaction time. Finally, we showed numerically how turbulence arises in complex fluids with an elastic component such as a polymer additive [8]. This "elastic turbulence" provides a mechanism for mixing in micro-fluidics which are usually highly laminar and resistant to mixing.

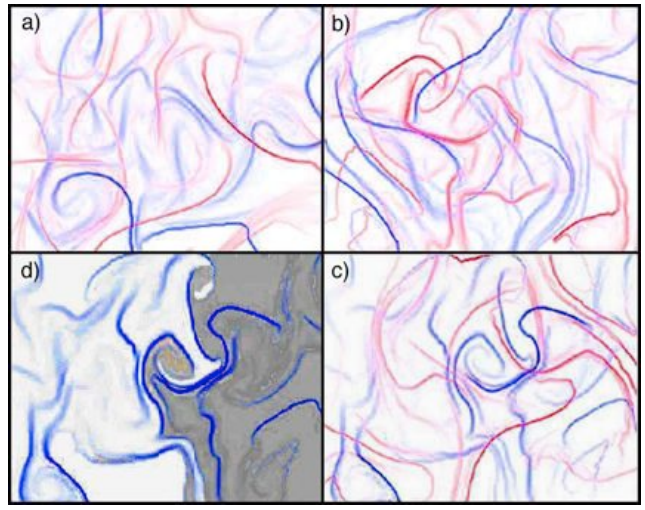


*Figure 1. Stretching fields of periodically-forced 2D turbulence with red (blue) indicating forward (backward) in time fields: a) periodic flow for Reynolds number Re = 8, b) turbulent flow Re = 108), c) same as in b) but one period later, d) reverse stretching fields for field shown in b) with virtual dye placed in the flow and advected by the velocity fields to demonstrate how lines of large stretching affect mixing of the fluid.*

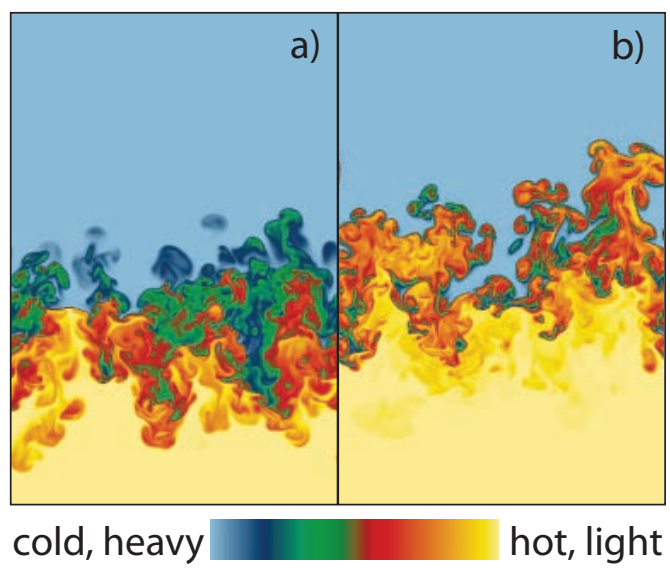


*Figure 2. Comparison of Rayleigh-Taylor growth for different ratios of evolution time to characteristic inter-species chemical reaction time: a) 12.5 and b) 0.5. The color map for density/temperature is shown below. In a) the growth and structure of the instability is almost unaffected by the reaction but in b) one starts to see that the reaction rate affects the growth, leading to more unreacted fluid.*

In other work on fluids, we tested aspects of non-equilibrium fluctuations in experimental [9] and numerical [10-11] realizations of turbulent flows, demonstrated a power-law dispersion of clusters of slowly falling particles [12], and described how hyperviscosity - often used in numerical simulations – can produce a "bottle-neck" effect in the energy spectrum [13]. Further, we investigated how the process of wave breaking is related to singularities of nonlinear hyperbolic equations [14] and elucidated the role of hydrodynamic boundary conditions in superflow [15]. We also used a novel computation approach, the lattice-Boltzmann method, to study the stability of laminar rectangular jets [16], to compute mass transfer in thermally-driven cavity flows [17], and to demonstrate that turbulent-like heat transport scaling could be obtained in a laminar natural convection state [18].

Granular materials can take on states that are very similar to familiar gas, fluid and solid states of matter. We showed how singular energy distributions arise in driven and undriven granular media [19]. We performed a detailed analysis of experiments on avalanche dynamics of thin granular layers on an inclined plane where we distinguished between rather gentle avalanches that formed smooth shock-like fronts and more violent avalanches where the front breaks and grains are propelled faster than the avalanche front speed [20]. In work related to our fluids efforts on turbulence, we showed how power-law scaling for cluster size distribution arise from simple properties such as desorption and fragmentation [21]. Colloidal systems, which have many features in common with granular materials, are of both fundamental and applied interest. We studied the properties of colloid layers using novel computational approaches [22] and showed how multi-layer structures form on surfaces [23]. Other related work on soft condensed matter systems includes enhanced mixing and diffusion with plastic flow [24] and a surprising transition from reversible to irreversible flow in periodically-driven vortices [25].

Many multi-scale problems involve difficult mathematical challenges. In this area, we have had considerable success. In particular, we have built on work first performed in CNLS over a decade ago on the formulation of complex Hamiltonians in quantum mechanics. This work led to the entire field of so-called PT (parity-time) symmetric Hamiltonians that have a non-Hermitian character. We elucidated the nature of such Hamiltonians in a review article [26], pointed out spontaneous breaking of PT symmetry in classical systems [27], described the interaction of different types of Hamiltonians, and used the complex plane representation to build a nonlinear construction of orthogonal polynomials [28]. We also developed efficient methods for diffusive relaxation [29] and developed closures for characterizing degenerate density states [30]. Finally, the discovery that certain classes of nonlinearly coupled oscillators spontaneously synchronize has found many applications to natural systems and to technology. We discovered that the Kuramoto model of nonlinearly coupled oscillators, which has been used to illustrate synchronization, can be reformulated as a linear coupling problem, which allows the exact solution of classes of Kuramoto models that were previously not soluble and which gives novel insight into the dynamics of the synchronization transition [31].

One of the most challenging of multi-scale systems is the problem of elastic-plastic deformation in materials: the structures giving rise to plastic deformation are atomic scale defects such as dislocations whereas elastic continuum field descriptions are necessarily macroscopic in nature. We demonstrate [32] that the presence of the incompatibility of elastic strain with microscopic dislocations gives rise to an additional long-range contribution in the inhomogeneous part of the Landau free energy and to the corresponding stress fields describing martensitic materials. Competition among the local and long-range interactions results in frustration in the evolving order parameter (elastic) texture. Figure 3 shows a comparison of domains with and without the dislocation structures that can be accommodated using our energy functional approach. We also demonstrate how a generalized self-consistent field theory for polymer melts that includes elastic stress and strain fields can be applied to the study of copolymers melts [33]. By obtaining the stress distributions for volume conserving strain loadings where lamellar and hexagonal structures are stable, we show that the local stress is reduced at the domain interface but slightly enhanced in the immediate vicinity of the interface. Other work in describing the structural properties of materials include the construction of a potential from simulations of extended defects in tungsten [34], an elucidation of the discrepancy between the theoretical and measured yield stress in body-centered cubic metals [35], and applying ideas from spin glass theory to martensitic shape-memory alloys [36].

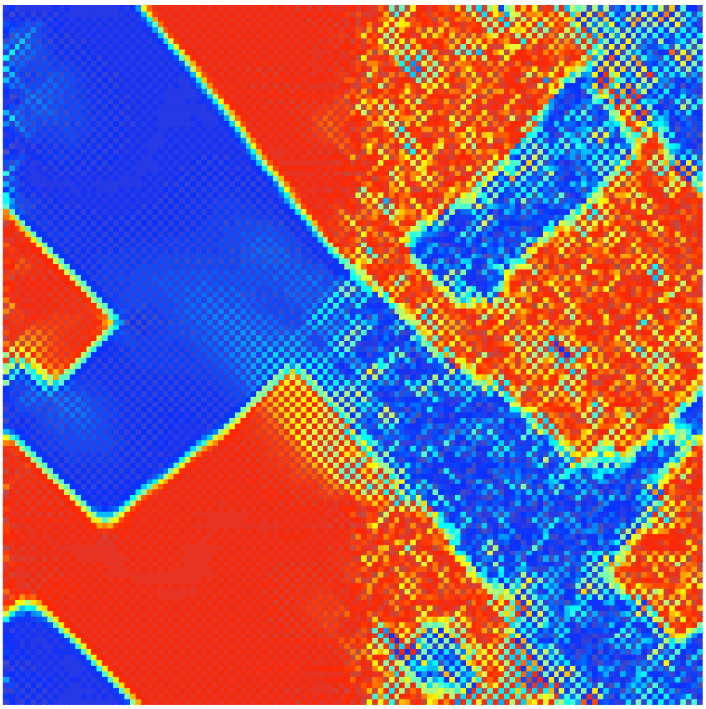

*Figure 3. Distribution of an elastic order parameter that minimizes the Landau-Ginzburg free energy functional for the martensite, low-temperature phase of a shape memory alloy. The texture is entirely due to the nonlocal part of the free energy functional. In the left half of the domain one has a perfect crystal with no dislocations or vacancies, interstitials, etc., whereas in the right half of the domain each mesoscopic cell contains a coarse-grained dislocation.*

Multi-scale systems often have a strong nonlinear component, giving rise to coherent structures such as solitons. Such structures have emerged as important signatures of nonlinear interactions in cold atom Bose-Einstein condensates (BEC). In one study [37], we consider solitons in sine-Gordon systems with additive inhomogeneities and show, by means of a collective coordinate approach, that the soliton moves like a particle – a "soliton rachet" in an effective potential that is the result of the inhomogeneities. In other work we explored localized structures on discrete lattices [38-40] and demonstrated the soliton-like structures – static and dynamic phyllotaxis – that arise in both natural and artificial "magnetic" cacti [41]. In Figure 4, we illustrate a comparison of these natural and artificial cacti.

The description of promising applications in nanotechnology and cold atom physics and of important classes of materials such as strongly correlated electron systems and high-temperature super-fluids combine the demands of addressing multi-scale complexity with the challenges of understanding inherent, macroscopic quantum behavior. In cold atom physics, we have shown the emergence of long-range diagonal order (crystal order) in mixtures of Bose-Einstein condensates (BEC's) [42]. This system displays a super-solid-like response to small rotations. We have shown the existence and dynamical stability (in specific regimes) of standing wave patterns in the BEC-wave function subject to a localized potential well.

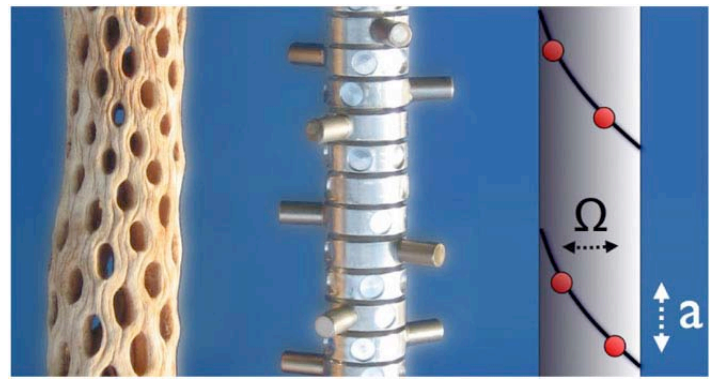


*Figure 4. A specimen of Mammillaria elongata displaying a helical morphology ubiquitous to nature, a magnetic cactus of dipoles on stacked bearings, and a schematic of a wrapped Bravais lattice showing the angular offset Omega (screw angle) and the axial separation a between particles.*

We have suggested and studied the prospect of observing odd-pairing superfluidity in fermion-BEC mixtures close to the line of mechanical instability with respect to phase separation (the spinodal decomposition line) [43]. This exotic form of fermion super-fluidity can compete successfully with p-wave pairing and is characterized by a double time super-fluid order parameter that is odd with respect to exchanging the time variables. We have shown that cold atom ring-BEC's with a constriction that acts as Josephson junction can undergo macroscopic quantum tunneling and can be brought into a macroscopic Schrodinger cat state.

In materials studies we have developed improved time dependent density functional theory (TDDFT) descriptions [44-45]. Specifically, we have worked out methods for calculating exchange interaction energies exactly in certain limits. We have applied TDDFT to investigate optical response and phonon induced dynamics in CdSe and PbSe quantum dots, to study excitons in semiconductor carbon nano-tubes [46], to model complex molecules using an exciton scattering approach [47], and to understand the self-assembling mechanisms of semiconductor carbon nano-tubes functionalized by DNA [48]. In nanotechnology, we have developed optimal methods for designing optical properties of nano-scale quantum systems. We found that optimal design may lead to an improvement of specific optical properties (such as electric field intensity in the nanostructure at specified frequency) by more than three orders of magnitude [49]. Our approach has been applied to the design of extra sensitive

single molecule detectors, and for the design of nano-capacitors with high energy density.

## Impact on National Missions

Modeling multi-scale systems underpins many aspects of LANL missions. Much of our work is aimed at fundamental capabilities in these areas including the turbulence work that impacts climate modeling and the Rayleigh-Taylor instability studies that are important in astrophysics and in ICF programs. Materials science efforts on elastic-plastic deformation are closely related to theoretical support for the LANL MaRIE initiative. Granular materials and colloids represent soft condensed matter systems that couple traditional statistical and solid-state physics with emergent properties in biological systems. These opportunities are bearing fruit under the auspices of the DOE-funded Center for Integrated Nanotechnology. Much of the research on computational chemistry is also having strong impact on related CINT efforts in carbon nanotubes and other nano-scale photonic structures.

## References


1. Twardos, M. J., P. E. Arratia, M. K. Rivera, G. A. Voth, J. P. Gollub, and R. E. Ecke. Stretching fields and mixing near the transition to nonperiodic two-dimensional flow. 2008. *PHYSICAL REVIEW E.* **77** (5): 056315.

2. Xiao, Z., M. Wan, S. Chen, and G. L. Eyink. Physical mechanism of the inverse energy cascade of two-dimensional turbulence: a numerical investigation. 2009. *Journal of Fluid Mechanics.* **619**: 1.

3. Eyink, G. L.. Turbulent flow in pipes and channels as cross-stream “inverse cascades” of vorticity. 2008. *Physics of Fluids.* **20** (12): 125101.

4. Chumakov, S. G.. A priori study of subgrid-scale flux of a passive scalar in isotropic homogeneous turbulence. 2008. *Physical Review E.* **78** (3): 036313.

5. Odier, P., J. Chen, M. K. Rivera, and R. E. Ecke. Fluid Mixing in Stratified Gravity Currents: The Prandtl Mixing Length. 2009. *Physical Review Letters.* **102** (13): 134504.

6. Vladimirova, N., and M. Chertkov. Self-similarity and universality in Rayleigh-Taylor, Boussinesq turbulence. 2009. *Physics of Fluids.* **21** (1): 014110.

7. Chertkov, M., V. Lebedev, and N. Vladimirova. Reactive Rayleigh-Taylor turbulence. 2009. *Journal of Fluid Mechanics.* **633**: 1.

8. Berti, S., A. Bistagnino, G. Boffetta, A. Celani, and S. Musacchio. Two-dimensional elastic turbulence. 2008. *PHYSICAL REVIEW E.* **77** (5): 055306.

9. Bandi, M. M., J. R. Cressman, and W. I. Goldburg. Test of the fluctuation relation in Lagrangian turbulence on a free surface. 2008. *JOURNAL OF STATISTICAL PHYSICS.* **130** (1): 27.

10. Bandi, M. M., and C. Connaughton. Craig XY distribution and the statistics of Lagrangian power in two-dimensional turbulence. 2008. *PHYSICAL REVIEW E.* **77** (3): 036318.

11. Bandi, M. M., S. G. Chumakov, and C. Connaughton. Probability distribution of power fluctuations in turbulence. 2009. *Physical Review E.* **79** (1): 016309.

12. Daniel, W. B., R. E. Ecke, G. Subramanian, and D. L. Koch. Clusters of sedimenting high-Reynolds-number particles. 2009. *Journal of Fluid Mechanics.* **625**: 371.

13. Frisch, U., S. Kurien, R. Pandit, W. Pauls, S. S. Ray, A. Wirth, and J. -Z. Zhu. Hyperviscosity, galerkin truncation, and bottlenecks in turbulence. 2008. *Physical Review Letters.* **101** (14): 144501.

14. Pomeau, Y., M. Le Berre, P. Guyenne, and S. Grilli. Wave-breaking and generic singularities of nonlinear hyperbolic equations. 2008. *NONLINEARITY.* **21** (5): T61.

15. Pomeau, Y., and D. Roberts. On the hydrodynamic boundary condition for superfluid flow. 2008. *Physical Review B.* **77**: 144508.

16. Yu, H., and S. S. Girimaji. Study of axis-switching and stability of laminar rectangular jets using lattice Boltzmann method. 2008. *COMPUTERS & MATHEMATICS WITH APPLICATIONS.* **55** (7): 1611.

17. Yu, H., J. Zhang, and N. Li. Lattice Boltzmann simulation of mass transfer in thermally driven cavity flows. 2008. *PROGRESS IN COMPUTATIONAL FLUID DYNAMICS.* **8** (1-4): 206.

18. Yu, H., N. Li, and R. E. Ecke. Scaling in laminar natural convection in laterally heated cavities: Is turbulence essential in the classical scaling of heat transfer?. 2007. *Physical Review E.* **76** (2): 026303.

19. Ben-Naim, E., and A. Zippelius. Singular energy distributions in driven and undriven granular media. 2007. *JOURNAL OF STATISTICAL PHYSICS.* **129** (4): 677.

20. Borzsonyi, T., T. C. Halsey, and R. E. Ecke. Avalanche dynamics on a rough inclined plane. 2008. *PHYSICAL REVIEW E.* **78** (1): 011306.

21. Connaughton, C., R. Rajesh, and O. Zaboronski. Constant flux relation for aggregation models with desorption and fragmentation. 2007. *PHYSICA A-STATISTICAL MECHANICS AND ITS APPLICATIONS.* **384** (1): 108.

22. Weronski, P., and M. Elimelech. Novel numerical method for calculating initial flux of colloid particle adsorption through an energy barrier. 2008. *Journal of Colloid and Interface Science.* **319** (2): 406.

23. Adamczyk, Z., P. Weronski, and J. Barbasz. Formation of multilayered structures in the layer by layer deposition of colloid particles. 2008. *Journal of Colloid and Interface Science.* **317** (1): 1.

24. Libal, A., C. Reichhardt, and C. J. Reichhardt. Enhancing mixing and diffusion with plastic flow. 2008. *Physical Review E.* **78** (3): 031401.

25. Mangan, N., C. Reichhardt, and C. J. Reichhardt. Reversible to irreversible flow transition in periodically driven vortices. 2008. *PHYSICAL REVIEW LETTERS.* **100** (18): 187002.

26. Bender, C. M.. Making sense of non-Hermitian Hamiltonians. 2007. *Rpts. Prog. Phys..* **70** (6): 947.

27. Bender, C. M., and D. W. Darg. Spontaneous breaking of classical PT symmetry. 2007. *Journal of Mathematical Physics.* **48** (4): 042703.

28. Bender, C. M., and E. Ben-Naim. Nonlinear-Integral-Equation Construction of Orthogonal Polynomials. 2008. *Journal of Nonlinear Mathematical Physics.* **15** (3): 73.

29. Haack, J. R., and C. D. Hauck. OSCILLATORY BEHAVIOR OF ASYMPTOTIC-PRESERVING SPLITTING METHODS FOR A LINEAR MODEL OF DIFFUSIVE RELAXATION. 2008. *Kinetic and Related Models.* **1** (4): 573.

30. Hauck, C. D., C. D. Levermore, and A. L. Tits. Convex duality and entropy-based moment closures: Characterizing degenerate densities. 2008. *SIAM JOURNAL ON CONTROL AND OPTIMIZATION.* **47** (4): 1977.

31. Roberts, D., and R. Teodorescu. A linear path toward synchronization: Anomalous scaling in a new class of exactly solvable Kuramoto models. 2008. *European Physical Journal.* **165**: 103.

32. Groger, R., T. Lookman, and A. Saxena. Defect-induced incompatibility of elastic strains: Dislocations within the Landau theory of martensitic phase transformations. 2008. *Physical Review B.* **78** (18): 184101.

33. Maniadis, P., T. Lookman, E. M. Kober, and K. O. Rasmussen. Stress distributions in diblock copolymers. 2007. *Physical Review Letters.* **99** (4): 048302.

34. Mrovec, M., R. Groger, A. Bailey, D. Nguyen-Manh, C. Elsasser, and V. Vitek. Bond-order potential for simulations of extended defects in tungsten. 2007. *Physical Review B.* **75**: 104119.

35. Groger, R., and V. Vitek. Explanation of the discrepancy between the theoretical and measured yield stresses in body-centered cubic metals. 2007. *Philosophical Magazine Letters.* **87**: 113.

36. Sherrington, D.. A simple spin glass perspective on martensitic shape-memory alloys. 2008. *JOURNAL OF PHYSICS-CONDENSED MATTER.* **20** (30): 304213.

37. Stehr, V., P. Muller, F. G. Mertens, and A. Bishop. Soliton ratchets in sine-Gordon systems with additive inhomogeneities. 2009. *Physical Review E.* **79** (3): 046210.

38. Law, K. J., P. G. Kevrekidis, D. J. Frantzeskakis, and A. R. Bishop. Emergence of unstable modes in an expanding domain for energy-conserving wave equations. 2008. *PHYSICS LETTERS A.* **372** (5): 658.

39. Law, K. J., P. G. Kevrekidis, V. Koukouloyannis, I. Kourakis, D. J. Frantzeskakis, and A. R. Bishop. Discrete solitons and vortices in hexagonal and honeycomb lattices: Existence, stability, and dynamics. 2008. *Physical Review E.* **78** (6): 066610.

40. Law, K. J., A. Saxena, P. G. Kevrekidis, and A. R. Bishop. Localized structures in kagome lattices. 2009. *Physical Review A.* **79** (5): 025801.

41. Nisoli, C.. Static and Dynamical Phyllotaxis in a Magnetic Cactus. 2009. *Physical Review E.* **80**: 026110.

42. Roberts, D. C., and S. Rica. Impurity crystal in a Bose-Einstein condensate. 2009. *Physical Review Letters.* **102**: 025301.

43. Kalas, R. M., A. V. Balatsky, and D. Mozyrsky. Odd-frequency pairing in a fermion-boson cold atom mixture. 2008. *Physical Review B.* **78**: 184513.

44. Tao, J., G. Vignale, and I. V. Tokatly. Quantum stress focusing in descriptive chemistry. 2008. *PHYSICAL REVIEW LETTERS.* **100** (20): 075325.

45. Tao, J., J. P. Perdew, L. M. Almeida, C. Fiolhais, and S. Kummel. Nonempirical density functionals investigated for jellium: Spin-polarized surfaces, spherical clusters, and bulk linear response. 2008. *PHYSICAL REVIEW B.* **77** (24): 245107.

46. Kilina, S., and S. Tretiak. Excitonic and vibrational properties of single-walled semiconducting carbon nanotubes. 2007. *ADVANCED FUNCTIONAL MATERIALS.* **17** (17): 3405.

47. Wu, C., S. V. Malinin, S. Tretiak, and V. Y. Chernyak. Multiscale modeling of electronic excitations in branched conjugated molecules using an exciton scattering approach. 2008. *PHYSICAL REVIEW LETTERS.* **1** (5): 057405.

48. Kilina, S., S. Tretiak, D. A. Yarotski, J. X. Zhu, N. Modine, A. Taylor, and A. V. Balatsky. Electronic properties of DNA base molecules adsorbed on a metallic surface. 2007. *Journal of Physical Chemistry C.* **111** (39): 14541.

49. Grigorenko, I., and H. Rabitz. Optimal control of the local electromagnetic response of nanostructured materials: Optimal detectors and quantum disguises. 2009. *Applied Physics Letters.* **94** (25): 253107.

## Publications

Adamczyk, Z., P. Weronski, and J. Barbasz. Formation of multilayered structures in the layer by layer deposition of colloid particles. 2008. *Journal of Colloid and Interface Science.* **317** (1): 1.

Bandi, M. M., J. R. Cressman, and W. I. Goldburg. Test of the fluctuation relation in Lagrangian turbulence on a free surface. 2008. *JOURNAL OF STATISTICAL PHYSICS.* **130** (1): 27.

Bandi, M. M., S. G. Chumakov, and C. Connaughton. Probability distribution of power fluctuations in turbulence. 2009. *Physical Review E.* **79** (1): 016309.

Bandi, M. M., and C. Connaughton. Craig XY distribution and the statistics of Lagrangian power in two-dimensional turbulence. 2008. *PHYSICAL REVIEW E.* **77** (3): 036318.

Ben-Naim, E., and A. Zippelius. Singular energy distributions in driven and undriven granular media. 2007. *JOURNAL OF STATISTICAL PHYSICS.* **129** (4): 677.

Bender, C. M.. Making sense of non-Hermitian Hamiltonians. 2007. *Rpts. Prog. Phys..* **70** (6): 947.

Bender, C. M., and D. W. Darg. Spontaneous breaking of classical PT symmetry. 2007. *Journal of Mathematical Physics.* **48** (4): 042703.

Bender, C. M., and E. Ben-Naim. Nonlinear-Integral-Equation Construction of Orthogonal Polynomials. 2008. *Journal of Nonlinear Mathematical Physics.* **15** (3): 73.

Bender, C. M., and H. F. Jones. Interactions of Hermitian and non-Hermitian Hamiltonians. 2008. *JOURNAL OF PHYSICS A-MATHEMATICAL AND THEORETICAL.* **41** (24).

Bender, C. M., and J. Feinberg. Does the complex deformation of the Riemann equation exhibit shocks?. 2008. *JOURNAL OF PHYSICS A-MATHEMATICAL AND THEORETICAL.* **41** (24).

Berti, S., A. Bistagnino, G. Boffetta, A. Celani, and S. Musacchio. Two-dimensional elastic turbulence. 2008. *PHYSICAL REVIEW E.* **77** (5): 055306.

Borzsonyi, T., T. C. Halsey, and R. E. Ecke. Avalanche dynamics on a rough inclined plane. 2008. *PHYSICAL REVIEW E.* **78** (1): 011306.

Cassidy, A., I. Grigorenko, and S. Haas. Formation of collective excitations in quasi-one-dimensional metallic nanostructures: Size and density dependence. 2008. *PHYSICAL REVIEW B.* **77** (24): 245404.

Chertkov, M., V. Lebedev, and N. Vladimirova. Reactive Rayleigh-Taylor turbulence. 2009. *Journal of Fluid Mechanics.* **633**: 1.

Chumakov, S. G.. A priori study of subgrid-scale flux of a passive scalar in isotropic homogeneous turbulence. 2008. *Physical Review E.* **78** (3): 036313.

Connaughton, C., R. Rajesh, and O. Zaboronski. Constant flux relation for aggregation models with desorption and fragmentation. 2007. *PHYSICA A-STATISTICAL MECHANICS AND ITS APPLICATIONS.* **384** (1): 108.

Daniel, W. B., R. E. Ecke, G. Subramanian, and D. L. Koch. Clusters of sedimenting high-Reynolds-number particles. 2009. *Journal of Fluid Mechanics.* **625**: 371.

Demsar, K., J. Stare, and J. Mavri. Structure and vibrational dynamics of hydrogen bond in hydrogenbissulfate anion in the gas phase and in the solid state: A computational study. 2007. *JOURNAL OF MOLECULAR STRUCTURE.* **844**: 215.

Eyink, G. L.. Turbulent flow in pipes and channels as cross-stream “inverse cascades” of vorticity. 2008. *Physics of Fluids.* **20** (12): 125101.

Fransson, J.. Detection of exchange interaction in STM

measurements through Fano-like interference effects. 2007. *Physical Review B.* **76** (4): 045416.

Fransson, J.. Subnanosecond switching of local spin-exchange coupled to ferromagnets. 2008. *PHYSICAL REVIEW B.* **77** (20): 205316.

Fransson, J., and J. Zhu. Spin dynamics in a tunnel junction between ferromagnets. 2008. *NEW JOURNAL OF PHYSICS.* **10**: 013017.

Frisch, U., S. Kurien, R. Pandit, W. Pauls, S. S. Ray, A. Wirth, and J. -Z. Zhu. Hyperviscosity, galerkin truncation, and bottlenecks in turbulence. 2008. *Physical Review Letters.* **101** (14): 144501.

Grigorenko, I.. Analytical solution for optimal squeezing of wave packet of a trapped quantum particle. 2008. *JOURNAL OF CHEMICAL PHYSICS.* **128** (10): 104109.

Grigorenko, I.. Analytical solution for optimal squeezing of wave packet of a trapped quantum particle. 2008. *Journal of Chemical Physics.* **128** (10): 104109.

Grigorenko, I., S. Haas, A. Balatsky, and A. F. Levi. Optimal control of electromagnetic field using metallic nanoclusters. 2008. *NEW JOURNAL OF PHYSICS.* **10**: 043017.

Grigorenko, I., and H. Rabitz. Optimal control of the local electromagnetic response of nanostructured materials: Optimal detectors and quantum disguises. 2009. *Applied Physics Letters.* **94** (25): 253107.

Groger, R., T. Lookman, and A. Saxena. Defect-induced incompatibility of elastic strains: Dislocations within the Landau theory of martensitic phase transformations. 2008. *Physical Review B.* **78** (18): 184101.

Groger, R., and V. Vitek. Explanation of the discrepancy between the theoretical and measured yield stresses in body-centered cubic metals. 2007. *Philosophical Magazine Letters.* **87**: 113.

Gurvitz, S. A.. Quantum mechanical approach to decoherence and relaxation generated by fluctuating environment. 2008. *PHYSICAL REVIEW B.* **77** (7): 075325.

Haack, J. R., and C. D. Hauck. OSCILLATORY BEHAVIOR OF ASYMPTOTIC-PRESERVING SPLITTING METHODS FOR A LINEAR MODEL OF DIFFUSIVE RELAXATION. 2008. *Kinetic and Related Models.* **1** (4): 573.

Hauck, C. D., C. D. Levermore, and A. L. Tits. Convex duality and entropy-based moment closures: Characterizing degenerate densities. 2008. *SIAM JOURNAL ON CONTROL AND OPTIMIZATION.* **47** (4): 1977.

Kalas, R. M., A. V. Balatsky, and D. Mozyrsky. Odd-frequency pairing in a fermion-boson cold atom mixture. 2008. *Physical Review B.* **78**: 184513.

Kilina, S., E. R. Batista, P. Yang, S. Tretiak, A. Saxena, R. L. Martin, and D. L. Smith. Electronic structure of self-assembled amorphous polyfluorenes. 2008. *ACS NANO.* **2** (7): 1381.

Kilina, S., S. Tretiak, D. A. Yarotski, J. X. Zhu, N. Modine, A. Taylor, and A. V. Balatsky. Electronic properties of DNA base molecules adsorbed on a metallic surface. 2007. *Journal of Physical Chemistry C.* **111** (39): 14541.

Kilina, S., and S. Tretiak. Excitonic and vibrational properties of single-walled semiconducting carbon nanotubes. 2007. *ADVANCED FUNCTIONAL MATERIALS.* **17** (17): 3405.

Klein, W., H. Gould, N. Gulbahce, J. B. Rundle, and K. Tiampo. Structure of fluctuations near mean-field critical points and spinodals and its implication for physical processes. 2007. *Physical Review E.* **75** (3): 031114.

Lakshmanan, M., and A. Saxena. Dynamic and static excitations of a classical discrete anisotropic Heisenberg ferromagnetic spin chain. 2008. *PHYSICA D-NONLINEAR PHENOMENA.* **237** (7): 885.

Law, K. J., A. Saxena, P. G. Kevrekidis, and A. R. Bishop. Localized structures in kagome lattices. 2009. *Physical Review A.* **79** (5): 025801.

Law, K. J., P. G. Kevrekidis, D. J. Frantzeskakis, and A. R. Bishop. Emergence of unstable modes in an expanding domain for energy-conserving wave equations. 2008. *PHYSICS LETTERS A.* **372** (5): 658.

Law, K. J., P. G. Kevrekidis, V. Koukouloyannis, I. Kourakis, D. J. Frantzeskakis, and A. R. Bishop. Discrete solitons and vortices in hexagonal and honeycomb lattices: Existence, stability, and dynamics. 2008. *Physical Review E.* **78** (6): 066610.

Libal, A., C. Reichhardt, and C. J. Reichhardt. Enhancing mixing and diffusion with plastic flow. 2008. *Physical Review E.* **78** (3): 031401.

Mangan, N., C. Reichhardt, and C. J. Reichhardt. Reversible to irreversible flow transition in periodically driven vortices. 2008. *PHYSICAL REVIEW LETTERS.* **100** (18): 187002.

Maniadis, P., T. Lookman, E. M. Kober, and K. O.

Rasmussen. Stress distributions in diblock copolymers. 2007. *Physical Review Letters.* **99** (4): 048302.

Mrovec, M., R. Groger, A. Bailey, D. Nguyen-Manh, C. Elsasser, and V. Vitek. Bond-order potential for simulations of extended defects in tungsten. 2007. *Physical Review B.* **75**: 104119.

Muniz, R. A., S. Haas, A. F. Levi, and I. Grigorenko. Plasmonic excitations in tight-binding nanostructures. 2009. *Physical Review B.* **80** (4): 045413.

Nisoli, C.. Static and Dynamical Phyllotaxis in a Magnetic Cactus. 2009. *Physical Review E.* **80**: 026110.

Nisoli, C., D. Abraham, T. Lookman, and A. Saxena. Thermal Stability of Strained Nanowires. 2009. *Physical Review Letters.* **102** (24): 245504.

Odier, P., J. Chen, M. K. Rivera, and R. E. Ecke. Fluid Mixing in Stratified Gravity Currents: The Prandtl Mixing Length. 2009. *Physical Review Letters.* **102** (13): 134504.

Pomeau, Y., M. Le Berre, P. Guyenne, and S. Grilli. Wave-breaking and generic singularities of nonlinear hyperbolic equations. 2008. *NONLINEARITY.* **21** (5): T61.

Pomeau, Y., and D. Roberts. On the hydrodynamic boundary condition for superfluid flow. 2008. *Physical Review B.* **77**: 144508.

Pryadko, L. P., and P. Sengupta. Second-order shaped pulses for solid-state quantum computation. 2008. *Physical Review A.* **78**: 032336.

Roberts, D. C., and S. Rica. Impurity crystal in a Bose-Einstein condensate. 2009. *Physical Review Letters.* **102**: 025301.

Roberts, D., and R. Teodorescu. A linear path toward synchronization: Anomalous scaling in a new class of exactly solvable Kuramoto models. 2008. *European Physical Journal.* **165**: 103.

Schmidt, P., I. Grigorenko, and A. F. Levi. Design of resonators using materials with negative refractive index. 2007. *JOURNAL OF THE OPTICAL SOCIETY OF AMERICA B-OPTICAL PHYSICS.* **24** (11): 2791.

Sengupta, P., A. Raghavan, and S. Haas. Disorder-enhanced phase coherence in trapped bosons on optical lattices. 2007. *New Journal of Physics.* **9** (4): 103.

Sengupta, P., and L. Pryadko. Quantum degenerate Bose-Fermi mixtures on 1-D optical lattices. 2007. *Physical Review B.* **75**: 132507.

Sengupta, P., and S. Haas. Quantum glass phases in the disordered Bose-Hubbard model. 2007. *Physical Review Letters.* **99** (5): 050403.

Sherrington, D.. A simple spin glass perspective on martensitic shape-memory alloys. 2008. *JOURNAL OF PHYSICS-CONDENSED MATTER.* **20** (30): 304213.

Stare, J., J. Panek, J. Eckert, J. Grdadolnik, J. Mavri, and D. Hadzi. Proton dynamics in the strong chelate hydrogen bond of crystalline picolinic acid N-oxide. A new computational approach and infrared, Raman and INS study. 2008. *JOURNAL OF PHYSICAL CHEMISTRY A.* **112** (7): 1576.

Stehr, V., P. Muller, F. G. Mertens, and A. Bishop. Soliton ratchets in sine-Gordon systems with additive inhomogeneities. 2009. *Physical Review E.* **79** (3): 046210.

Tao, J., G. Vignale, and I. V. Tokatly. Quantum stress focusing in descriptive chemistry. 2008. *PHYSICAL REVIEW LETTERS.* **100** (20): 075325.

Tao, J., J. P. Perdew, L. M. Almeida, C. Fiolhais, and S. Kummel. Nonempirical density functionals investigated for jellium: Spin-polarized surfaces, spherical clusters, and bulk linear response. 2008. *PHYSICAL REVIEW B.* **77** (24): 245107.

Tao, J., V. N. Staroverov, G. E. Scuseria, and J. P. Perdew. Exact-exchange energy density in the gauge of a semilocal density-functional approximation. 2008. *PHYSICAL REVIEW A.* **77** (1): 012509.

Twardos, M. J., P. E. Arratia, M. K. Rivera, G. A. Voth, J. P. Gollub, and R. E. Ecke. Stretching fields and mixing near the transition to nonperiodic two-dimensional flow. 2008. *PHYSICAL REVIEW E.* **77** (5): 056315.

Velizhanin, K. A., S. Kilina, T. D. Sewell, and A. Piryatinski. First-Principles-Based Calculations of Vibrational Normal Modes in Polyatomic Materials with Translational Symmetry: Application to PETN Molecular Crystal. 2008. *Journal of Physical Chemistry.* **112** (42): 13252.

Vladimirova, N., and M. Chertkov. Self-similarity and universality in Rayleigh-Taylor, Boussinesq turbulence. 2009. *Physics of Fluids.* **21** (1): 014110.

Weronski, P., and M. Elimelech. Novel numerical method for calculating initial flux of colloid particle adsorption through an energy barrier. 2008. *Journal of Colloid and Interface Science.* **319** (2): 406.

Wu, C., S. V. Malinin, S. Tretiak, and V. Y. Chernyak. Multiscale modeling of electronic excitations in branched

conjugated molecules using an exciton scattering approach. 2008. *PHYSICAL REVIEW LETTERS.* **1** (5): 057405.

Xiao, Z., M. Wan, S. Chen, and G. L. Eyink. Physical mechanism of the inverse energy cascade of two-dimensional turbulence: a numerical investigation. 2009. *Journal of Fluid Mechanics.* **619**: 1.

Yu, H., J. Zhang, and N. Li. Lattice Boltzmann simulation of mass transfer in thermally driven cavity flows. 2008. *PROGRESS IN COMPUTATIONAL FLUID DYNAMICS.* **8** (1-4): 206.

Yu, H., N. Li, and R. E. Ecke. Scaling in laminar natural convection in laterally heated cavities: Is turbulence essential in the classical scaling of heat transfer?. 2007. *Physical Review E.* **76** (2): 026303.

Yu, H., and S. S. Girimaji. Study of axis-switching and stability of laminar rectangular jets using lattice Boltzmann method. 2008. *COMPUTERS & MATHEMATICS WITH APPLICATIONS.* **55** (7): 1611.

# Understanding Dynamical Diversity of Extrasolar Planets

*Hui Li*
20070171ER

## Introduction

The discovery of 170 extrasolar planets in the past decade has stimulated an explosive growth in studying the basic processes that regulate planet-system evolution. At least two fundamental mysteries have emerged. One is that proto-planet embryos that are formed farther out in protoplanetary disks could migrate towards their central stars through tidal interactions with their nascent gaseous disks. This seriously limits the time available for these embryos to grow into giant planets, contrary to the discoveries of many giant planets both in our Solar system and many extra-solar planet systems. Another mystery is how the orbital evolution of protoplanets/embryos produces the observed large diversity in semi-major axis and eccentricity distributions, which are completely different from solar system planets. Our models, run on supercomputers, will address these mysteries.

## Benefit to National Security Missions

The proposed research will push the limits of supercomputing and help to establish the Laboratory as a leading institution in computational protoplanetary research. Protoplanetary science is becoming a major research area in astronomy. We can make an immediate impact in this field and enhance the DOE mission in basic science.

## Progress

We have completed a major study on understanding the influence of disk viscosity on the migration of protoplanets. We discovered that, when the disk viscosity becomes small, the gas density in the disk around the planet shows systematic changes so that the net torque on the planet motion is greatly reduced. This is because the density evolution is determined by the damping of density waves driven by the planet. So, when the viscosity is low, this feedback process is quite efficient so the torque on the planet is greatly reduced. This causes the migration of planets to slow down drastically and, in some cases, the migration is completely halted. We have carefully examined the dependence of important feedback process on the disk viscosity, planet mass, and disk sound speeds. This result has important implications on the migration rate of planets and on the crucial question whether small mass planet can survive in the protoplanetary disks or not. We find that planets will be able to survive if the disk viscosity is small. This work is published in the Astrophysical Journal Letters. In addition, we have completed a systematic study on the migration of low mass planets over long-term (> 100,000 years). We find that there exists a wide range of disk viscosity in which migration is halted and the disk condition is favorable for giant planet formation. This result has been submitted to the Astrophysical Journal for publication.

We have also completed a linear theory analysis of the Rossby vortex instability (RVI) in the presence of magnetic field. We discovered the RVI a few years ago and we have shown that it plays an important role in determining the flow dynamics in the co-orbital region of a planet. Our new work elucidated the influence of magnetic fields on this instability. We find that, when the magnetic field becomes stronger, the RVI is gradually stabilized by the magnetic fields. We attribute this stabilizing effect to the tension of the fields. This work will have implications for understanding both the linear and nonlinear outcome of the RVI when disk magnetic fields are present. This work has been published in the Astrophysical Journal.

Further important improvements were made to our numerical simulation package. In addition to already high resolution and highly efficient implementation of the disk-planet interaction schemes, our newly developed fully two-dimensional disk self-gravity solver has been proven to be extremely efficient and accurate. Furthermore, we have developed the adaptive mesh refinement schemes to enable very high resolution near the planet so that the gas flow around the planet can be accurately followed and studied. Thus far, we have been able to make simulation runs that are of the highest resolution and the longest evolution time when compared to other groups in the community. Adequate

computing resources from LANL's Institutional Computing machines have made this possible. A full description of our advanced simulation package is being written up for journal publication.

## Future Work

We will continue the study of planet migration in low viscosity disks and in disks with strong self-gravity. We will concentrate on the eccentricity evolution of planets. The scenario we will explore is the fact that the massive disks can both drive and damp the planet's eccentricity during the planet's orbital evolution. We will examine these processes in detail and perform a series of hydrodynamic simulations to see if eccentricity can be excited. In addition, we will also continue the study on the migration and dynamics of multiple protoplanets or embryos in disks.

## Conclusion

We propose a comprehensive theoretical and computational study of the orbital evolution of both single and multiple protoplanets/embryos in gaseous protoplanetary disks. We will investigate our newly discovered instability, associated with the disk's potential vorticity profile, affects protoplanetary evolution. This instability produces vortices that cause the torques on the protoplanet/embryo to experience large changes. We will also examine the effects of disk self-gravity and the effect of having more than one protoplanet, neither of which have been well studied. Our simulations will push the limits of supercomputing.

## Publications

Li, H., S. Lubow, S. Li, and D. Lin. Type I Planet Migration in Nearly Laminar Disks. 2009. *Astrophysical Journal Letters.* **690**: 52.

Li, S., M. J. Buoni, and H. Li. A Fast Potential and Self-Gravity Solver for Nonaxisymmetric Disks. 2009. *Astrophysical Journal Supplements.* **181**: 244.

Li, S., and H. Li. Verification of Runaway Migration in a Massive Disk. *Astrophysical Journal.*

Li, S., and H. Li. A fast parallel Simulation Code for studying the Interaction between Proto-Planetary Disk and Embedded Proto-Planets. *Astrophysical Journal Supplements.*

Yu, C., H. Li, S. Li, S. Lubow, and D. Lin. Type I Planet Migration in Nearly Laminar Disks - Long Term Behavior. *Astrophysical Journal.*

Yu, C., and H. Li. Nonaxisymmetric Rossby Vortex Instability with Toroidal Magnetic Fields in Radially Structured Disks. 2009. *Astrophysical Journal.* **702**: 75.

# Precision Cosmology and the Neutrino Sector

*Salman Habib*
20080031ER

## Introduction

The Standard Model of particle and nuclear physics is now known to provide only a very partial description of the fundamental constituents of the Universe. Solid -- now overwhelming -- evidence for Beyond Standard Model (BSM) physics first came from cosmological observations and terrestrial neutrino experiments. Significantly, precision cosmology and the neutrino sector are intimately related and each provides complementary information about the other. Cosmology provides the best known limits on the sum of all neutrino species, currently very difficult to constrain with terrestrial experiments. In addition, cosmological observations can probe new directions in neutrino physics such as the existence of sterile neutrinos, which have no Standard Model interactions. In this project, we conduct an integrated research program that connects state-of-the-art experiments, observations, and theory, to shed light on the neutrino mass, the effective number of neutrinos, and the sterile neutrino sector. We target robust constraints on the neutrino mass to an accuracy of 0.05 eV, a fractional error on the number of neutrino species of 0.2, and to confirm or exclude the sterile neutrino as a viable warm dark matter candidate. This collaboration will have access to the latest and upcoming cosmological observations and leading cosmological theory and simulation capabilities. Our results will help motivate the design of future neutrino oscillation experiments.

## Benefit to National Security Missions

This project will support the DOE Office of Science (HEP/NP) mission by enhancing our understanding of the neutrino sector using ground-based and satellite observations. The high-performance computing and verification and validation pieces of the proposal tie in to aspects of NNSA threat reduction and stockpile stewardship programs. The neutrino sector is a key aspect of the LANL NPAC portfolio.

## Progress

In the past year, the project work has focused in two directions. The first is the understanding of how velocity dispersion in the dark matter affects structure formation. This is important to understand two different physics problems: (i) the effect of neutrino free-streaming and nonlinear influence on structure formation for conventional low-mass (less than 1eV) neutrinos, (ii) constraints on properties of warm dark matter such as sterile neutrinos. Along with extending our own code, we have also been working to develop a new code using the IPPL framework developed at PSI, led by Andreas Adelmann. Code tests are now underway. Yves Ineichen, Dr. Adelmann's student, will visit in Nov/Dec 2009 to add a new initializer to the IPPL code for neutrino simulations. The second major direction is the construction of an emulator for the cosmic microwave background and the density fluctuation power spectrum with neutrino properties taken into account. This methodology is very useful to analyze data soon to be taken by Planck -- we have been invited to help the Planck analysis team at JPL/LBNL with their work.

To understand the velocity dispersion problem, we have included multiple particle species in our cosmology simulation code. We have also run warm (all the way to hot) dark matter simulations in comparative runs against cold dark matter simulations with the same phases in the initial conditions. With this method, we can directly compare the difference between the predictions in a way independent of statistical variance. This method will allow the halo mass function to be fine-tuned as a probe of warm dark matter and of specific properties of sterile neutrinos. (For sterile neutrinos it is important to have realistic and accurate transfer functions for putting in the appropriate initial conditions for sterile neutrino applications, these have been generated by Kev Abazajian at the University of Maryland and incorporated into our code.) In addition to halo properties, halo assembly over time is also affected by having warm dark matter. In order to investigate this, we have written a code to analyze the halo merger statistics over time (the "merger tree"). Analysis of the merger trees has been carried out. A paper describing our results is now being completed.

The analysis of precision cosmological simulations can only be performed by Markov Chain Monte Carlo methods. These require very large numbers of simulations, typically in the tens of thousands to hundreds of thousands. We have recently applied sophisticated statistical methods to reduce the number of required simulations to only of order hundreds, using high-dimensional interpolation to construct “look-up” emulators as a replacement for brute force simulation. We are now building emulators for the cosmic microwave background temperature anisotropies that include neutrino properties as an input. These emulators have 10 degrees of freedom and cover a dynamic range more or less consistent with that of Planck, the latest cosmic microwave background satellite mission, launched last month. The aim is to produce emulators with errors at the sub-percent level, a very challenging requirement for a system with so many degrees of freedom. Recently, we have realized that aside from the principal components we were using to represent the data, axis rescalings help considerably in reducing the difficulty of data representations. The new cosmic background anisotropy emulator will be ready for release in December 2009.

## Future Work

Precision cosmology provides key observational probes of the neutrino sector. Cosmological observations can be very sensitive to the neutrino mass and less so to mass splittings and mixing angles, while terrestrial experiments strongly constrain the mass differences, but provide less stringent constraints on the absolute mass. Cosmology also provides constraints on the total neutrino energy density, including the existence of possible additional sterile neutrino degrees of freedom (a sterile neutrino does not possess any Standard Model interactions).

Because control of systematic errors is essential in cosmology, this project takes an integrated approach to addressing three problems we believe to be the most promising scientifically as well as timely in terms of upcoming observations and experimental results. These are the total neutrino mass, the number of neutrino species, and constraints on the sterile sector. The analysis requires significant advances in theoretical predictions for the effects of neutrinos on the microwave background (high-resolution data from Planck and polarization results from ground-based observation) and large scale structure (results from galaxy surveys, weak gravitational lensing, and analysis of the quasar Lyman-alpha forest), and in combining observational and experimental data with results from large-scale simulations to yield the required constraints with robust error bounds. As a consequence of some recent work at Los Alamos, we are in an excellent position to achieve mass limits of order .05 eV, constrain the number of neutrino species within +/- .2, and to confirm or exclude sterile neutrinos as a warm dark matter candidate.

## Conclusion

The Standard Model (SM) of particle and nuclear physics is one of the crowning scientific achievements of the last century. Despite its successes, the SM is incomplete. The dominant components of the Universe -- dark energy and dark matter -- are not included in the SM. Nonzero neutrino masses also provide compelling evidence for physics beyond it. Significantly, cosmology and neutrino physics are themselves inextricably connected. We expect to attain significantly improved constraints on the sum of neutrino masses, the number of neutrinos, and how structure formation in the Universe is influenced by the neutrino sector.

# Finding the First Cosmic Explosions

*Daniel Holz*
20080080ER

## Introduction

The very first stars in the universe end their lives in the most powerful thermonuclear explosions in all of nature. Although these events are intrinsically extraordinarily bright, we have yet to directly observe them. These stars, a critical underpinning of our cosmological model, only exist on paper and in large computer simulations. In this proposal, we outline an approach to directly observe these events, thereby either confirming a pillar of cosmology, or revolutionizing our understanding of stellar formation. We combine state-of-the-art modeling of the explosions with advanced techniques to estimate gravitational lensing. The former tells us what we are looking for, and the latter tells us whether we can hope to actually see them. We will model the lightcurves (the spectrum of emitted light) of the explosions, determining how bright they are, and how often they happen. We will also model the cosmic magnification, which causes very distant objects to be significantly brightened due to the gravitational effects of intervening matter. We are breaking new ground on both of these aspects, leading the theoretical effort in estimating the source brightnesses, and well as establishing the very first gravitational lensing results for sources at the edge of the Universe. By combining both of these advances, we will definitely answer whether or not it will be possible to directly observe the very first cosmic explosions.

## Benefit to National Security Missions

Large-scale computer simulations will be used to study the basic science of stellar evolution. Current hydrodynamic codes will be used and tested in astrophysical environments, contributing to the verification and validation effort. Techniques developed to simulate and predict observational data may contribute to threat reduction missions.

## Progress

This project has been tremendously productive over the past year. On the Population III side, we have made major progress on the topic of Mixing in Zero and Solar Metallicity Supernovae, and well as establishing a Cosmological Radiative Transfer Comparison Project, with a focus on  Radiation-Hydrodynamic Tests. On the lensing side, we have explored the impact of lensing on dark energy, finding that corrections need to be incorporated into current lensing approaches.

In an unanticipated spinoff, we have also done work on the detectability and origin of recent, very exciting observations of high-redshift gamma-ray bursts has also been written. We explored population synthesis models of GRBs, focusing on the very earliest populations. GRB 080913, discovered by SWIFT, was the most distant gamma-ray burst (GRB) known to-date, with a spectroscopically determined redshift of z=6.7 (although it has since been surpassed; more on this below). The detection of a burst at such an early epoch of the Universe significantly constrains the nature of GRBs and their progenitors. To evaluate these constraints, we perform population synthesis studies of the formation and evolution of early stars and calculate the resulting formation rates of short- and long-duration GRBs at high redshift. The peak of the GRB rate from Population II stars occurs at z=7 for a model with efficient/fast mixing of metals, while it is found at z=3 for an inefficient/slow metallicity evolution model. We show that for at z=6.7 essentially all GRBs originate from Population II stars, independent of the adopted metallicity evolution model. At this epoch Population III (metal free) stars, representing the very first generation of stars, most likely have already completed their evolution, and Population I stars (representing the present population) have just begun forming. We argue that Population II stars (having small, but non-zero metallicity) are the most likely progenitors of both long GRBs (collapsars) and short GRBs (NS-NS or BH-NS mergers) in the redshift range $6<z<10$. Since the predicted rates, after correction for modeling and observational biases, are very similar at these epochs we cannot definitively conclude which of these two progenitor scenarios is more likely in the case of GRB 080913. Further information about these high-z events, such as their spectral energy distribution and host galaxy properties, will be needed for a much larger sample to consolidate the progenitor models considered here.

These results are, of course, crucially related to the ear-

liest generation of stars, and thus are directly related to key elements of this proposal. It is a major observational advance that GRBs are being directly observed at redshifts greater than eight (!!). This is our earliest observational clue to the nature of the first generation of stars, and thus is a fundamental development in this proposal. Our latest paper considers sources at redshift z=6, and we are hard at work extending these results to the latest observations, in an attempt to further elucidate the nature of these earliest objects.

## Future Work

Current cosmological simulations for the first stars to form in the universe, so called Population III stars, as well as theoretical models for the cooling of primordial gas and gravitational instabilities indicate that these stars have been much more massive than stars forming today. If made of primordial compositions, such stars will retain most of their initial mass until they finally collapse. Stars with an initial mass of more than hundred solar masses may undergo the electron-positron capture instability after they depleted central carbon burning. This leads to rapid collapse and a powerful explosions similar to the supernovae we see in stars today, but possibly even more powerful by up to one hundred times. In some cases even repeated supernova-like eruptions can occur and lead to very bright optical display. One part of this project is to understand the evolution and explosions from these stars which has not been explored in detail to date. We will simulate their explosions in multiple dimensions using modern hydrodynamical codes. However, these supernovae may still not be bright enough to be seen directly, even with the best telescopes. Gravitational lensing occurs more frequently for distant objects - and this proposal looks at the most distant cosmic explosions. Some small fraction of the sky can be highly magnified and it is highly probable that some of these supernovae are affected by the lensing. This provides a unique tool to find and see them. Hence a second goal of this project is to determine, based on modern cosmological simulations as well as analytic theory, how often such events are magnified, and by how much. This provides valuable information and theoretical background for upcoming hundred-million dollar telescopes and astronomical surveys in the United States and internationally.

## Conclusion

The fundamental goal of this project is basic science. Computer codes developed at LANL and with US university collaborators will be used and compared to observational data. This project will perform large-scale computer simulations to study the explosions of the first supernovae in the universe. Our results and predictions are important for upcoming telescopes and astronomical survey projects. We will provide an independent test of current cosmological models of the beginning and the early evolution of the universe.

## References


1. Joggerst, C. C., S. Woosley, and A. Heger. Mixing in Zero- and Solar-metallicity supernovae. 2009. *Astrophysical Journal.* **693**: 1780.

2. Iliev, I., and D. Whalen. Cosmological radiative transfer comparison project - II. The radiation-hydrodynamic tests. 2009. *Monthly Notices of the Royal Astronomical Society.* **400**: 1283.

3. Whalen, D., B. van Veelen, B. O'Shea, and M. Norman. The destruction of cosmological minihalos by primordial supernovae. 2008. *Astrophysical Journal.* **682**: 49.

4. Joudaki, S., A. Cooray, and D. Holz. Weak lensing and dark energy: The impact of dark energy on nonlinear dark matter clustering. 2009. *Physical Review D.* **80**: 023003.

5. Belczynski, K., D. Holz, C. Fryer, E. Berger, D. Hartmann, and B. O'Shea. On the Origin of the Highest Redshift Gamma-Ray Bursts. 2010. *Astrophysical Journal.* **708**: 117.


## Publications


Belczynski, C., D. Holz, C. Fryer, E. Berger, D. Hartmann, and B. O'Shea. On The Origin Of The Highest Redshift Gamma-Ray Bursts. To appear in *Astrophysical Journal.*

Heger, A., S. Woosley, and C. Joggerst. Mixing in Zero- and Solar-Metallicity Supernovae. 2009. *Astrophysical Journal.* **693** (2): 1780.

Hu, W., D. Holz, and C. Vale. CMB cluster lensing: cosmography with the longest lever arm. 2007. *Physical Review D (Rapid Communications).* **76** (12): 127301.

Iliev, I., and D. Whalen. Cosmological radiative transfer comparison project - II. The radiation-hydrodynamic tests. To appear in *Monthly Notices of the Royal Astronomical Society.*

Joudaki, S., D. Holz, and A. Cooray. Weak lensing and dark energy: The impact of dark energy on nonlinear dark matter clustering. 2009. *Physical Review D.* **80** (2): 023003.

Lai, D., M. Bolte, J. Johnson, S. Lucatello, A. Heger, and S. Woosley. Detailed Abundances for 28 Metal-poor Stars: Stellar Relics in the Milky Way. 1524. *Astrophysical Journal.* **681**: 2008.

Sarkar, D., A. Amblard, D. Holz, and A. Cooray. Lensing and supernovae: quantifying the bias on the dark energy equation of state. 2008. *Astrophysical Journal.* **678**: 1.

Tinker, J., A. Kravtsov, A. Klypin, K. Abazajian, M. Warren, G. Yepes, S. Gottlober, and D. Holz. Toward a halo mass function for precision cosmology. 2008. *Astrophysical Journal.* **688** (2): 709.

Woosley, S. E., S. Blinnikov, and A. Heger. Pulsational pair instability as an explanation for the most luminous supernovae. 2007. *Nature.* **450**: 390.

# Materials and Device Optimization towards Room Temperature Spin-Transport through Single-Walled Carbon Nanotubes

*Stephen K. Doorn*
20080164ER

## Introduction

Our purpose is to develop integrated structures based on carbon nanotubes that will allow the manipulation of electron spin for electronics and computing applications (spintronics). The ultimate goal is to produce a carbon-nanotube structure capable of transmitting, manipulating, and preserving information carried in electron spin orientation at room temperature. Adding the extra dimension of spin control to computation will enable tremendous leaps in computing speed and in device and memory density. We will combine new advances in synthesis of defect-free carbon nanotubes with novel ferromagnetic thin films to approach this goal. This goal will be reached through approaches that maximize injection of spin-information while minimizing its loss within the nanotube-based devices. Our approach will be to:

- Maximize spin-polarization of our electrode materials through improvements in their domain structure via advances in epitaxial materials synthesis.
- Maximize spin injection into the nanotubes through engineering of the electrode/nanotube interfacial composition and interaction
- Minimize spin loss through minimizing spin scattering in the nanotube by use of suspended CVD-grown single-walled structures that eliminate defect scattering sites.

This first-time demonstration of spin transport through single-walled nanotubes (SWNTs) will allow us to approach the room-temperature barrier through simultaneous optimization of the magnetic and carbon-based materials involved. The results will be a fundamental understanding of spin-loss mechanisms in these integrated materials. Significant advances in new magnetic interface materials and the development and exploration of the integrated functionality of these novel nanoscale devices will also result.

## Benefit to National Security Missions

This research supports the development of advanced functional nanomaterials in support of threat reduction, energy security and basic science missions in DOE and other government agencies. Developing SWNT spintronics materials provides understanding and control of fundamental properties at the nanoscale to enable energy-efficient next-generation computing in support of advanced materials modeling.

## Progress

Initial efforts used SWNT samples generated at Duke University for incorporation into our first-generation devices. Sixteen prototype SWNT device chips with four devices per chip were fabricated at Sandia National Laboratory with gold and vanadium electrodes (a substitute for the LSMO films). These were characterized using both AFM and SEM microscopy. The results revealed significant materials compatibility and device engineering issues in our approach that required us to redefine our strategy for generating our electronic devices. The initial lithographic techniques used to pattern the required ferromagnetic electrodes were inadequate. They did not provide the proper alignment of the several overlapping features we envisioned and damaged the nanotube components. Additionally, we envisioned depositing our high-temperature ferromagnetic films ($La_{0.7}Sr_{0.3}MnO_3$, or LSMO) over our nanotubes. Alternatively, the nanotubes might be grown over initially deposited films. However, we found the reducing environment of the nanotube growth would destroy the films. Conversely, the oxidizing environment of the film deposition would destroy the nanotubes. Our current strategy is to directly pattern our entire device structure from a large-scale LSMO film. Pre-grown nanotubes will then be incorporated into the devices by using a direct transfer technique. Thus, all three problems can be solved.

To accomplish this new strategy, the thrust of the work

for FY09 was directed toward making significant progress in four critical areas:

1. Develop a LANL capability to fabricate dense arrays of parallel SWNTs.
2. Develop an approach to directly transfer the SWNT arrays from their growth substrate to the electronic device structures.
3. Develop and evaluate multiple approaches to synthesis of LSMO films.
4. Design and pattern new LSMO device structures to integrate with the SWNT arrays.

These accomplishments are detailed below:

**Synthesis of Nanotubes**

We developed a new capability at LANL for growth of arrays of long (mm to cm) SWNTs. The approach is to grow SWNTs in a tube furnace using chemical vapor deposition with ethanol as the carbon source. We have successfully developed techniques to grow well-aligned (highly parallel) arrays. These are produced on both single crystal quartz and SiO2 coated silicon substrates. The resulting arrays grow in the plane of the substrate. This is necessary for incorporating them into spintronics devices. Example arrays are shown in Figure 1.

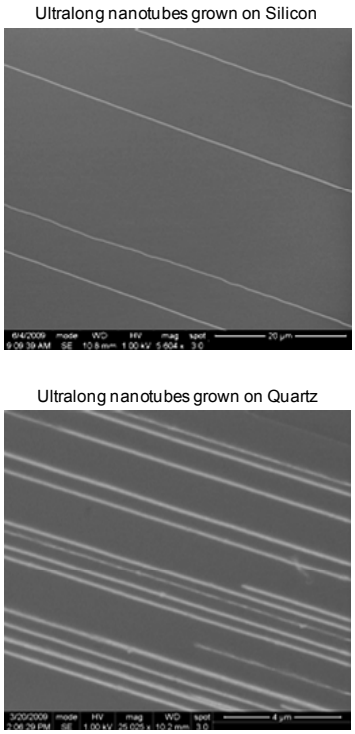


*Figure 1. Scanning electron micrographs of example arrays of SWNTs grown on silicon (top) and on quartz (bottom).*

**Development of Nanotube Transfer Technique**

We worked with collaborators at Duke University to develop the technology for transferring SWNT arrays from the growth substrate onto pre-patterned microchips. A polymer coated substrate is used to effectively lift off an existing SWNT array from its growth substrate. A polymer layer is first deposited on the SWNT array to be transferred. The layer is then peeled from the substrate. The assembly is then pressed onto the destination substrate (device structure). The polymer is subsequently removed with an acetone wash, leaving behind pristine SWNTs in well-defined locations. The technique can now be applied reproducibly with the required accuracy in final SWNT location.

**Synthesis of Ferromagnetic LSMO Films**

We have developed two approaches to deposition of LSMO thin films. LSMO is of interest for our electrode materials because it exhibits ferromagnetism at relatively high temperatures. We are using our newly developed radio-frequency (RF) off-axis sputtering deposition capability for growing high-quality LSMO thin film electrode materials. Properties were optimized by growing the films at 800°C and an Argon (60%) to O2 (40%) mix at a chamber pressure of 50 mTorr. We have also evaluated methods to improve the magnetic properties of these thin film materials through post-deposition annealing procedures. Annealing of the films in oxygen at 975°C for 3 hrs is found to improve the domain structure of the films. Films were also grown on silicon, $LaAlO_3$, and MgO substrates. The highest quality results were obtained on $LaAlO_3$. Currently optimized films are illustrated in Figure 2. We have also explored using a pulsed laser deposition (PLD) technique for LSMO growth. The quality of the resulting films is not as high as with the RF approach. However, the films can be generated more quickly and will provide a suitable source of material to establish our electrode etching approach for final device fabrication (see below).

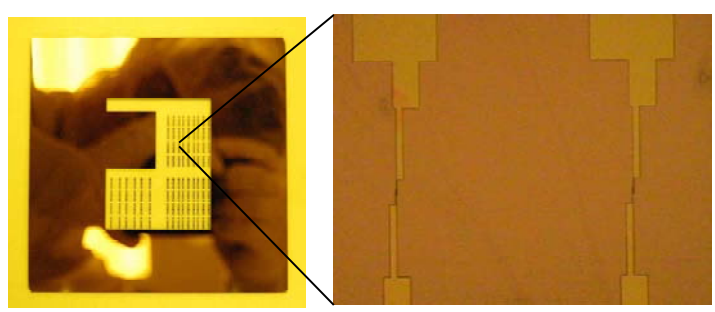

*Figure 2. Image of mask plate for patterning of LSMO device structures.*

**Device Patterning and Development**

Our new strategy for device fabrication is to now directly pattern electrode structures from LSMO films via an etching or ion milling process. Nanotubes will be deposited on the final structures as described in point 2 above. We have now designed a prototype electrode structure and the protocol for fabricating this structure. Mask plates for patterning of photoresist have been completed (Figure 3). To date we have deposited the necessary masks on LSMO test films. Etching of the patterns has been tested using both wet and dry etching procedures. We have found that the robustness of the LSMO films makes such reactive etching unsuitable. We are switching to an ion-milling approach as an alternative. This will be tested early in FY10 when the capability comes back online at CINT. We have also fabricated silicon microchips with trench structures, over which SWNT arrays have been directly grown. We anticipate depositing test structures of Co electrodes over these arrays for pursuing fundamental transport measurements that do not require the LSMO films.

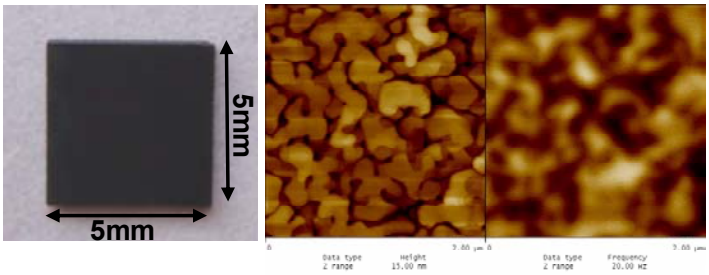


*Figure 3. Optical image of example LSMO thin film (left). Atomic force (center) and magnetic force (right) micrographs of annealed LSMO film domain structure.*

**Materials Characterization**

We have used a combination of advanced atomic force microscopy (AFM) and magnetic force (MFM) techniques and scanning electron microscopy (SEM) to characterize the properties of the LSMO films and the SWNTs. Measurements of magnetization versus temperature for the LSMO films were used to demonstrate that post annealing improves the film characteristics. This result correlates well with the improvement in domain structure observed via MFM. Raman, SEM, and AFM, measurements of the SWNT arrays have shown the SWNTs to be of high quality and suitable for incorporation into our device structures.

## Future Work

All the components required for generating a functional spintronics device are now in place. We are also poised to generate devices that will allow us to directly probe the fundamental spin-scattering mechanisms inherent to nanotube spin channels. Our final year's effort will focus on the following goals:

We will complete the fabrication of LSMO electrode structures and integrate them with nanotubes using our transfer process. We will measure spin transport in these devices as a function of temperature. This will demonstrate the goal of a high-temperature spin-transport device. In parallel we will continue to improve the LSMO film characteristics to improve spin injection and transport. We will also correlate spin transport properties with nanotube defect density and surface interactions. This will initially be done using the Co electrode structures discussed above. Active incorporation of defects into initially pristine structures will be accomplished with electron-beam irradiation. Defect density will be probed using Raman spectroscopy.

## Conclusion

We have made significant progress in the past year at putting into place and demonstrating the capability to generate all components that are required for fabricating our nanotube-based spintronics devices. In our final year we are now well-positioned to accomplish the primary goals of this project. We will demonstrate spin transport through single walled carbon nanotubes. The use of the LSMO electrodes will allow us to push the upper bound of temperature for transport. We will also generate a greater understanding of spin scattering phenomena in these complex integrated materials.

# The First Precise Determination of Quark Energy Loss in Nuclei

*Ivan M. Vitev*
20080201ER

## Introduction

Precise theoretical and experimental determination of the stopping power of materials for electrons was one of the great early successes of the classical and quantum theories of electro-magnetic interactions. Today, its practical applications range from medical imaging to national security applications, such as proton and muon radiography. In contrast, very little is known about the stopping power of nuclear matter for strongly interacting particles, such as quarks. It is widely recognized in the nuclear and particle physics communities that progress in this area is urgently needed. It will have immediate impact on our understanding of the fundamental forces in nature and the interpretation of the data coming from the current and future heavy ion experiments (areas of basic research where the US has made large strategic investments) [1]. This project embraces the unique opportunity to make the first precise determination of quark energy loss in large nuclei using as a platform upcoming experiments at the Fermilab and JPARC facilities in the US and Japan, respectively. It is based on a synergy of novel theoretical techniques (first ever calculation of initial-state energy loss), improvements in detector technology (design and deployment of readout electronics) and development of software simulation packages (optimization of the experimental setup for the breakthrough measurements). We expect that the successful completion of this project will lead to the determination of the shortest radiation length (a fundamental characteristic of the strength of particle-matter interactions) ever measured in nature.

## Benefit to National Security Missions

This project will support DOE's mission in Science by enhancing understanding of "Nuclear Matter in Extremis", a primary goal of the Office of Science and LANL's Beyond the Standard Model capability. Technology developed will support National Security areas of Threat of Weapons of Mass Destruction and Detection of Nuclear Materials.

## Progress

### Theory

To calculate the energy loss of strongly interacting particles in nuclear matter we combined field-theoretic techniques with an algebraic recurrence relation approach to multiple quark and gluon (parton) scattering. We found the complete solution to the problem of medium-induced gluon emission from partons propagating through large nuclei [2]. The differential bremsstrahlung spectrum, where quantum mechanical interference effects known as Landau-Pomeranchuk-Migdal suppression are fully accounted for, was calculated for three different cases:

1. A generalization of the results by Bertsch and Gunion for jets that are asymptotically on-shell (i.e. they do not undergo hard scattering in the nucleus);

2. Initial-state energy loss of incoming jets that undergo hard scattering (relevant to the production of weakly interacting final-state particles, such as electrons and muons that we plan to study experimentally);

3. Final-state energy loss of jets that emerge out of a hard scatter (relevant to strongly interacting final-state particles, for example in reactions known as semi-inclusive deeply inelastic scattering).

We are the first team to calculate the stopping power of matter for the Drell-Yan production process off of nuclei. We demonstrated that, contrary to the naive assumption, energy loss in cold nuclear matter could be large. These new results have significant implications for heavy ion phenomenology in both p+A and A+A reactions. Our theoretical findings have been implemented in projects that address direct photon production [3] and heavy flavor production [4] at the Relativistic Heavy Ion Collider (RHIC). They have

has received considerable attention form the physics community that works at the Department of Energy (DOE) nuclear and high energy physics facilities.

We also completed the development and implementation of a next-to-leading order code for the calculation of di-lepton production in elementary nucleon-nucleon collisions. Here, next-to-leading order stands for a more refined simulation with dramatically reduced theoretical uncertainties when compared to leading order results. We have checked that this code gives a very good theoretical description of existing Drell-Yan data. An example of the accuracy that we can achieve in describing the experimental measurements is given in Figure 1. We have also generated the baseline cross sections at the center of mass energies applicable to the E906 and the future JPARC experiments and are in the process in incorporating nuclear effects into the code.

**Hardware (muon ID)**

The proportional tubes that will be used to identify muons were successfully tested at LANL and shipped to Fermilab at the end of May [5]. Each tube was checked for broken sense wires and functioning readout electronics. They are now located at the Experimental Hall (KTeV Hall) staging area waiting for installation. After arrival, we confirmed that all 50 muon detector modules (800 proportional tubes) are in good mechanical and electrical condition, and thus ready for operation. The gas leakage rates were checked and found to be well under the required safety limit. The detectors are shown being tested in Figure 2. Later this summer we set up a cosmic test station and checked the response of several modules to cosmic rays, confirming that they are in working condition [6]. We are in the process of designing mechanical supports to mount the detectors once the experimental area is cleaned up for installation.

**Simulation**

We have adapted a simulation package from high-energy physics (GEANT) to study the physics observables of E906. With the help of an undergraduate student from South Carolina State University, we successfully implemented this newly developed GEANT full detector simulation code on a LANL Linux workstation. We are in the process of tuning and optimizing the geometry and detector materials inside the simulation code [7]. After that is completed, we will perform a large number of simulation jobs to study the Drell-Yan signal and background rates. A preliminary result for the background rates at Station 4 is shown in Figure 3.

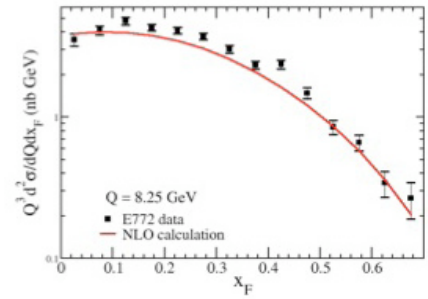


*Figure 1. Comparison of our next-to-leading order code to existing E772 Drell-Yan cross section data versus Feynman x.*

*Figure 2. Testing the muon modules at the Fermilab E906 experimental hall. 50 detector modules were delivered from LANL to Fermilab.*

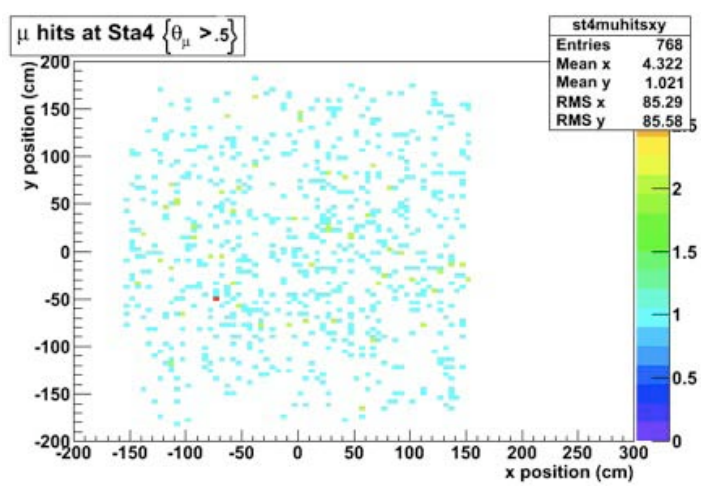


*Figure 3. Full Monte Carlo GEANT4 simulation of the muon hit position distribution in the X-Y plane of the Station-4 muon chamber. The entries correspond to one million proton-proton collisions.*

**Impact**

Theoretical progress related to this project is documented in the published manuscript "Non-Abelian energy loss in cold nuclear matter," I. Vitev, Phys. Rev. C75 :064906, 2007. It has been presented as a part of an invited plenary talk at "Quark Matter 2008", the biggest conference in the field of heavy ion physics ("Theoretical developments in heavy and light flavor energy loss", I. Vitev, J. Phys. G35 :104011, 2008.). With Dr. B. Zhang joining this project, we have been able to expand our studies of the phenomenological implications of the stopping power of cold nuclear matter to new physics channels, such as direct photons: "A Systematic study of direct photon production in heavy ion collisions", I. Vitev, B.W. Zhang, Phys. Lett. B669: 337-344, 2008. The advancements in the development and deployment of new readout electronics, as a part of our hardware project, P. McGaughey, and the development of software simulation packages, M. Liu, have been presented in talks at the E906 collaboration meetings, the Division of Nuclear Physics of the American Physical Society 2009 meeting, and in a poster at the Quark Matter 2009 conference. Work related to this project, LDRD 20080201ER has been presented at invited seminars at Kent State U., Wayne State U., the U. of Texas at Austin and LBNL by I. Vitev, B. Zhang, R. Sharma and M. Liu. Benwei Zhang has received a full professorship position in Central China Normal University and Ivan Vitev has received a 2009 Presidential Early Career Award for Scientists and Engineers.

## Future Work

The biggest gap in our knowledge of nuclear reactions in extremis is the stopping power of cold nuclei for quarks and gluons. In the coming year we will complete the joint theoretical and experimental project to provide the basis for the first precise determination of the stopping power of cold nuclear matter for the strongly interacting particles. The collaboration between theory and experiment that we have here fostered will extend beyond the end of this project to provide interpretation of the experimental results and the actual extraction of the shortest radiation length in nature.

The theoretical task that remains is to calculate the effect of energy loss, together with other nuclear effects, on the di-lepton (Drell-Yan) production cross section in proton-nucleus (p+A) collisions. The experimental task of this project is to develop the simulation tools and construct the muon identifier hardware suitable for Drell-Yan measurements at fixed target p+A experiments (such as E906 at Fermilab). Some minor problems with the detector modules, likely due to the presence of humidity and dust in the experimental hall, remain to be fixed. These issues will be addressed in the design of the mechanical support structure, which will now include a special cage to protect the readout end from moisture and dust. We are also working with engineers from ANL to design the mechanical and service framework for the muon detectors. We expect to finish the structure design and construction in the next few months. Simulations of detector response (based on the software packages that we have developed and implemented) are in progress.

Based on the approval/timescales of the experiment E906 at Fermilab, the actual experimental measurement and their interpretation (based on the techniques and technology developed in this project) may extend beyond three years. These will be made possible by our work in this project.

## Conclusion

We have performed the first consistent theoretical derivation of the stopping power of nuclear matter for strongly interacting particles. We are in the process of predicting signature observables that can be used to experimentally determine the energy loss of these particles in nuclear matter. We have adapted instrumentation developed for homeland security to instrument an experiment at Fermilab (E906) to carry out the pivotal measurements of energy loss. Simulation software developed for this project will be useful for future heavy-ion research. This work will enhance our understanding of nuclear matter under extreme conditions, such as in the early universe.

## References


1. Vitev, I.. Theoretical developments in heavy and light flavor energy loss. 2008. (Jaipur, India, 4-10 February). Vol. 35p. 104011. Journal of Physics G: IOP.

2. Vitev, I.. Non-Abelian energy loss in cold nuclear matter. 2007. *Physical Review C.* **75**: 064906.

3. Vitev, I., and B. Zhang. A Systematic study of direct photon production in heavy ion collisions. 2008. *Physics Letters B.* **669**: 337.

4. Sharma, R., I. Vitev, and B. Zhang. A light-cone wavefunction approach to open heavy flavor dynamics in QCD matter. To appear in *Physical Review C.*

5. McGaughey, P.. E906 muon identifier status. (Batavia, IL, 20-21 June 2008).

6. Liu, M.. A study of quark energy loss in p+A collisions. (Knoxville, 29 Mar. - 3 Apr. 2009).

7. Liu, M.. Precision determination of high energy

quark energy loss in the Fermilab E906 experiment. (Waikoloa, Oct. 13-17).

## Publications

Liu, M.. Future high energy dimuon experiments at Fermilab and JPARC. Invited presentation at *LBL seminar.* (Berkeley, CA, 2007).

Liu, M.. A study of quark energy loss in p+A collisions. Presented at *Quark Matter 2009.* (Knoxville, 29 Mar. - 3 Apr. 2009).

Liu, M.. Precision determination of high energy quark energy loss in the Fermilab E906 experiment. Presented at *Fall meeting of the DNP of the APS.* (Waikoloa, Oct. 13-17).

McGaughey, P.. E906 muon identifier status. Invited presentation at *E906 Collaboration Meeting at Fermilab.* (Batavia, IL, 20-21 June 2008).

Sharma, R., I. Vitev, and B. Zhang. A light-cone wavefunction approach to open heavy flavor dynamics in QCD matter. To appear in *Physical Review C.*

Vitev, I.. Non-Abelian energy loss in cold nuclear matter. 2007. *Physical Review C.* **75**: 064906.

Vitev, I.. Theoretical developments in heavy and light flavor energy loss. 2008. In *Quark Matter 2008 .* (Jaipur, India, 4-10 February). Vol. 35, p. 104011. Journal of Physics G: IOP.

Vitev, I.. The first precise determination of quark energy loss in nuclei. Invited presentation at *E906 Collaboration Meeting at Fermilab.* (Batavia, IL, 20-21 June 2008).

Vitev, I., and B. Zhang. A Systematic study of direct photon production in heavy ion collisions. 2008. *Physics Letters B.* **669**: 337.

Zhang, B., and I. Vitev. Direct photon production in d+A and A+A collisions at RHIC. 2009. In *Hot Quarks 2008.* (Estes Park, CO, 17-23 Aug. 2008 ). Vol. 24, 33 Edition, p. 2649. Modern Physics Letters A: World Scientific.

# Entanglement in Quantum Ground States

*Michael Chertkov*
20080342ER

## Introduction

This project studies the nature of ground states in quantum systems from the point of view of quantum entanglement, a concept that generates stronger than classically possible correlations between particles, is behind the rapidly developing fields of quantum computing and quantum key distribution. Such quantum computers may be able to perform computations that are not tractable on a classical computer, while processing and transmitting information at the quantum level guarantees provably secure communication. Within the field of quantum computing, this study involves looking at very carefully engineered states, which are created by carefully controlling the system. On the other hand, this project looks at the kind of quantum entanglement that is present in naturally occurring systems. We consider correlations in ground states of local quantum systems. This offers two possible rewards. First, certain naturally occurring ground states, like those in the quantum Hall effect, have nontrivial entanglement that can be used to do quantum computation, without requiring the careful control required by other approaches. This approach, called topological quantum computation, is possible and potentially a very robust approach to quantum computation. Second, many other naturally occurring ground states have fairly simple entanglement, and can well be described classically. Then, it should be possible to develop novel algorithms to model the ground state and dynamics of these systems using existing classical computers. This can lead to new advances in materials.

## Benefit to National Security Missions

This project supports the DOE Office of Science Mission in Basic Energy Sciences by enhancing our understanding of ground state properties of quantum systems such as in materials science and quantum chemistry, and by enhancing our understanding of which systems are useful for building a quantum computer.

## Progress

We made progress in the following five areas:

1. The Quantum Hall Effect Revisited. For T = L x L, a finite subset of the two dimensional lattice with periodic boundary conditions, let us denote by H the matrix (known as the Hamiltonian of the system) encoding the energy profile of interactions between particles. We assume that the interactions have finite range, finite strength and a unique ground state with a non-vanishing spectral gap (the gap between the lowest and second lowest energy level) persists as the linear length, L, of the system increases. Using a tight-binding model of fermionic interactions, we showed that the celebrated Quantum Hall Conductance is quantized in integer multiples of e^2/h. Our main tools involve Lieb-Robinson bounds (estimates for the speed with which interactions spread on the lattice) for approximations to the adiabatic evolution of the ground state (the state with the lowest energy.) Our proof of quantization removes the long-standing assumptions of persistent spectral gap throughout the adiabatic evolution of the ground state, as well as any averaging of the conductance over flux space. Instead, we prove quantization up to corrections that decay as a stretched exponential in the linear length L of the system. Finally, our result settles one of the top open problems in mathematical physics, as listed on Michael Aizenman's website at Princeton University and has been submitted for publication at the prestigious Annals of Mathematics.

2. Approximating the ground state of gapped quantum spin systems. We consider quantum spin systems defined on finite sets V equipped with a metric. In typical examples, V is a large, but finite subset of Z^d. For finite range Hamiltonians with uniformly bounded interaction terms and a unique, gapped ground state, we demonstrated a locality property of the corresponding ground state projector. In such systems, this ground state projector can be approximated by the product of three operators with quantifiable supports (i.e. regions on which the operators act non-trivially.) In fact, given any subset, X, of the volume V the ground state projector can be

approximated by the product of two projections, one supported on X and one supported on the complement of X, and a bounded observable supported on a boundary region between X and its complement, in such a way that as the boundary region increases, the approximation becomes better. Such an approximation was useful in proving that the entanglement between different blocks of particles on a one-dimensional chain is bounded by a constant, independent of the length of the chain. This result corresponds to a multi-dimensional analogue and has direct applications to the study of 2-dimensional materials whose ground state properties are useful for reliable quantum computation.

3. Matrix Product States for dynamical simulation of infinite chains. We proposed a new method for computing the ground state properties and the time evolution of infinite chains of particles based on a transverse contraction of the tensor network - a network of bonds between real and virtual particles. The method does not require finite size extrapolation and avoids explicit truncation of the bond dimension along the evolution. By folding the network in the time direction prior to contraction, time dependent expectation values and dynamic correlation functions can be computed after much longer evolution time than with any previous method. Moreover, our algorithm can be used for the study of some non-invariant infinite chains, including impurity models.

4. Light Cone Matrix Product. We show how to combine the light-cone and matrix product algorithms to simulate quantum systems far from equilibrium for long times. For the case of the XXZ spin chain at Delta=0.5, we simulate to a time of approx 22.5. While part of the long simulation time is due to the use of the light-cone method, we also described a modification of the iTEBD algorithm with improved numerical stability, and we described how to incorporate symmetry into this algorithm. While statistical sampling error means that we are not yet able to make a definite statement, the behavior of the simulation at long times indicates the appearance of either “revivals” in the order parameter as predicted previously or of a distinct shoulder in the decay of the order parameter.

5. Fermions and Loops on Graphs. This research is the first in the series devoted to evaluation of the partition function in statistical models on graphs with loops in terms of the Berezin/fermion integrals. We focus on a representation of the determinant of a square matrix in terms of a finite series, where each term corresponds to a loop on the graph. The representation is based on a fermion version of the Loop Calculus, previously introduced by the authors for graphical models with finite alphabets. Our construction contains two levels. First, we represent the determinant in terms of an integral over anti-commuting Grassman variables, with some reparametrization/gauge freedom hidden in the formulation. Second, we show that a special choice of the gauge, called BP (Bethe-Peierls or Belief Propagation) gauge, yields the desired loop representation. The set of gauge-fixing BP conditions is equivalent to the Gaussian BP equations, discussed in the past as efficient (linear scaling) heuristics for estimating the covariance of a sparse positive matrix.

## Future Work

We will study ground states in quantum systems, with applications to topological quantum computing. The locality of interactions in physical quantum systems means in many cases that correlations are short-ranged. This enables us to accurately represent the ground state by matrix product states. Topological quantum computation is a concept for building a quantum computer using certain systems which are topologically ordered, having degenerate ground states which are protected against decoherence due to topological (macroscopic) properties. Computation is performed by operations such as moving particles around each other. We have the following major objectives: (1) characterize ground states of local quantum Hamiltonians, using matrix product states and determine which of these states are useful for topological quantum computation (2) determine the robustness of these phases against perturbations such as disorder found in real-world systems. We will perform the following tasks: (1) determine bounds on ground state entropy, compare to area laws; (2) compute explicit matrix product operator representations for quantum Hall states and other related systems; (3) using locality properties of the Hamiltonian, determine robustness of the ground state against external perturbations and determine change in matrix product state representations; (4) determine ability to represent the ground state of an arbitrary local Hamiltonian using matrix product state; and (5) compute topological properties of entropy in matrix product states and use to study topological order in the ground state, characterizing the usefulness for topological quantum computation. Obtaining these goals will lead to new ways of building quantum computers and will advance our understanding of the fundamental nature of materials, especially strongly correlated materials and non-Fermi liquid materials.

## Conclusion

Topological quantum computing is a proposed method for doing quantum computation that avoids problems with decoherence that currently are preventing other approaches from working in a reliable and scalable fasion. We will characterize which physical systems, such as quantum Hall systems, are useful for topological quantum computing. This work will be based on a representation

of the ground state using a class of states called "matrix product states." We will determine how accurately matrix product states represent physical ground states, in particular in systems with disorder. This work will also benefit our fundamental understanding of materials and simulation of quantum systems.

## Publications


Chertkov, M., R. Teodorescu, and V. Chernyak. Belief propagation and loop series on planar graphs. 2008. *Journal of Statistical Mechanics.* (P05): 003.

Chertkov, M., and V. Chernyak. Fermions and loops on graphs. I. loop calculus for determinant. 2008. *arXiv:0809.3479.*

Chertkov, M., and V. Chernyak. Fermions and loops on graphs. II. monomer-dimer model as series of determinants. 2008. *arXiv:0809.3481.*

Hastings, M. B.. Topology and phases in fermionic systems. 2008. *JSTAT.* **01**: L001.

Hastings, M. B.. Observations outside the light-cone: algorithms for non-equilibrium and thermal states. 2008. *Physical Review B.* **77**: 144302.

Hastings, M. B.. A counterexample to additivity of minimum output entropy. 2009. *Nature Physics.* **5** (4): 237.

Wolf, M. M., F. Verstraete, M. B. Hastings, and J. I. Cirac. Area laws in quantum systems: mutual information and correlations. 2008. *Physical Review Letters.* **100**: 070502.

# CP-violating Moments of Atoms and Nuclei

*Anna C. Hayes-Sterbenz*
20080424ER

## Introduction

The "Standard Model" is a widely accepted theory that describes our understanding of matter and radiation. The existence of and precise magnitude of the electric dipole moment (EDM) is a test of some of the most basic underpinnings of the Standard Model. If a measurable EDM is found, it signifies the existence of physics "beyond the Standard Model," providing a new breakthrough in our understanding of the Universe.

A permanent electric dipole moment (EDM) of a physical system requires time-reversal (T) and parity (P) violation, as described by the Standard Model. Experimental programs are currently pushing the limits on the search for EDMs in atoms, nuclei, and the neutron to regimes of fundamental theoretical interest. The Standard Model (SM) predicts values for the EDMs in these systems that are too small to be detected in the foreseeable future, and hence a measured nonzero EDM is an unambiguous signal for a new source of CP violation and for physics beyond the SM. In this project we are calculating the magnitude of PT-violating EMDs in light and heavy nuclei and determining the expected sensitivity of such a measurement to the underlying PT-violating iteractions. We are examining the complementarity of measurements in nuclei to those for the neutron in terms of their sensitivity to different components of the PT-violating interaction.

## Benefit to National Security Missions

This project will contribute to our basic understanding of forces and processes in the universe governed by the "Standard Model." It directly addresses issues in the LANL "Beyond the Standard Model" Grand Challenge and impacts basic understanding of physics that underlies nuclear weapons, a key DOE mission.

## Progress

### The Schiff moment of 3He

3He is used as a co-magnetometer in LANL's neutron EDM experiment, which means that it is used to monitor any fluctuations in the magnetic field. However, in principle, 3He could have an EDM of its own, which could be a serious but unknown background for the experiment. The main source of an atomic EDM for 3He is expected to arise from a screened nuclear EDM of 3He (the Schiff moment), which could couple to the electric field and ruin the experiment. To address this issue, we calculated the Schiff moment of 3He in the no-core nuclear shell model. The no-core shell model is the state-of-the-art model of nuclear structure for excited states of light nuclei. There are two main sources of a Schiff moment in any nucleus, (1)an EDM of the individual nucleons in the nucleus and (2) a PT-violating interaction between the nucleons. We have calculated both of these.

We carried out a no-core shell model calculation for 3He. This calculation included 40 major oscillator shells, which is the largest shell model calculation ever attempted. We found that the 3He Schiff moment was extremely small compared to the neutron and thus that it represents a negligible background to LANL's neutron EDM experiment. These calculations are essential to LANL's EDM experiment. The work is summarized in a technical memo that we sent to the PI (Martin Cooper) of the EDM experiment LA-UR-09-02424.

### The anomalous magnetic moment of 3He

In addition to the atomic EDM arising through the electron-Schiff interaction, there is also relativistic interaction between the electrons and the nuclear magnetic moment of 3He. This moment is known as the Breit moment. Unlike the Schiff moment, this magnet interaction is not screened, and could be large. The external electric field applied in EDM experiments causes the atomic electron cloud to become non-spherical. This in turn allows the nuclear magnetic moment to interact with the magnetic field created by the orbiting electrons, which would result in an atomic EDM for 3He.

Using the no-core shell model, we showed that the ratio of this EDM contribution to that of the neutron is about 5x10^(-7), which is sufficiently small that it can be neglected. Thus, the LANL neutron EDM

collaboration does not have to worry about the 3He co-magnetometer causing significant backgrounds in their measurements. This work is summarized in the technical memo LA-UR-09-02424, and is presently being written up for publication.

**Electric Dipole Polarizability of Hydrogen and Helium Isotopes**

It was important for us to use another experimental observable to test the validity of our calculations of the EDM of 3He. The electric polarizability of a nucleus, which can be determined from the electric dipole photoabsorption cross section, provides a strong test of models use to determine atomic EDMs. In addition, the polarizabilities are interesting in themselves from an atomic physics point of view. This is because they are necessary in order to correct measured atomic transitions in one- and two-electron atoms before comparisons can be made with atomic theory calculations. The corrections arise from nuclear phenomena, known as nuclear-polarization corrections.

We used the same techniques of no-core shell model to get the nuclear energies and wave functions that determine the electric polarizability. The results are in excellent agreement with electric polarizabilities determined from electric dipole photoabsorption measurements. This gives us confidence that our EDM calculations are accurate. These results have been published in Physical Review C.

## Future Work

In this project we will quantify the magnitude of CP-violating moments of those atoms and nuclei of experimental relevance and relate these to the elecri dipole moment (EDM) of the neutron. A new experimental scheme for measuring EDMs of nuclei (stripped of their atomic electrons) in a magnetic storage ring suggests that the EDM of the deuteron and of 3He could be measured to an accuracy of better that 10^-27 e cm, which is an order of magnitude better that the present limit on the neutron EDM. The LANL neutron EDM experiment, aimed at measuring d_n to an accuracy of $10^-28 e cm, requires that the measurement be made with respect to the atomic EDM of 3He. The 3He acts as a polarizer in the experiment and thus a rigorous theoretical verification that the EDM of 3He is not a significant (unknown) systematic background to the measurement is crucial. We will calculate the first fully quantum-mechanical atomic and nuclear CP-violating moments of 3He, 225Ra, and 199Hg. These calculations will allow new measurements in atoms, nuclei, and the neutron to provide stringent limits and tests of non-Standard Model theories of the origin of CP-violation.

In the first year we will determine the nuclear CP-violating moments of 3He. This will allow us to quantify the contribution of 3He as a background to LANL's EDM measurement. In the second year we will determine the expected signal for a magnetic storage ring measurement of the EDM of 3He, and compare it with that expected for the proton and the deuteron. In the third year we will carry out detailed shell model and Nilsson model calculations for CP-violation in heavy atoms. We will quantify the relative merits of measuring atomic EDMs in deformed nuclei as opposed to spherical nuclei.

## Conclusion

This project will determine the magnitude of the cp-violating moments of both atoms and nuclei and the relative merits of present and proposed experimental programs to search for these moments. These results will provide crucial input and support for the national experimental program to search for electric dipole moments in fundamental systems.

## Publications


Hayes, A. C., J. L. Friar, and P. Moller. Splitting sensitivity of the ground state and the 7.6 eV isomeric states of 229Th. 2008. *Physical Review C.* **78** (02): 024311.

Hayes, A. C., and J. L. Friar. Sensitivity of nuclear transition frequencies to temporal variation of the fine structure constant ot the strong interaction. 2007. *Physics Letter B.* **650**: 229.

Stetcu, I., C. P. Liu, J. L. Friar, A. C. Hayes, and P. Navratil. Nuclear Electric Dipole Moment of 3He. 2008. *Physics Letters B.* **665**: 168.

Stetcu, I., C. P. Liu, J. L. Friar, A. C. Hayes, and P. Navratil. Nuclear electric dipole moment of 3He. 2008. In *Capture Gamma-Ray Spectroscopy and Related Topics. 13th International Symposium* . (Cologne, Germany, 25-29 Aug. 2008 ). Vol. 1090, p. 273. USA: AIP Conferenc Proceedings.

Stetcu, I., S. Quaglioni, J. L. Friar, A. C. Hayes, and P. Navratil. Electric dipole polarizabilities of hydrogen and helium isotopes. 2009. *Physical Review C.* **79** (6): 064001.

# Ultrafast Nanoplasmonics for Photonics and Quantum Control at the Nanoscale

*Anatoly V. Efimov*
20080473ER

## Introduction

Fundamental optical diffraction laws prohibit localization of light on spatial scales much smaller than the wavelength (~1 micrometer). This fact limits the resolution of optical microscopes, precludes addressing individual molecules, nanoparticles or other quantum systems and restricts the miniaturization of photonic circuits. Nevertheless, the diffraction limit can be overcome by using light, which is bound to metallic surfaces and nanostructures – so called Surface Plasmons – local fields, which are not subject to the laws of free-space optics. The area of research that studies Surface Plasmons – Plasmonics – is a rapidly growing field that promises practical solutions in optical nanotechnology, sensing, energy, chemistry and materials science.

This project addresses fundamental scientific aspects of generating, manipulating, controlling and using Surface Plasmons on the sub-wavelength scale and their interaction with quantum systems. Our specific challenge is to learn how to manipulate these fields, not only spatially, but also, and more importantly, temporally. The temporal aspect in field design is extremely important for ultrafast processes in nature and technology, such as controlling molecular dynamics, steering chemical reactions, selective sensing, signal processing and communication. In order to better understand such processes, we use ultrashort femtosecond optical pulses in our experiments to excite and measure the ultrafast dynamics of the localized fields. It is important to realize that femtosecond time scales are characteristic to many processes in nature, such as fundamental vibrations in molecules and crystals, isomerization reactions responsible for vision and energy transfer between mesosystems. The focus of this project on controlled excitation and manipulation of broadband and ultrafast Surface Plasmons is a new direction in Plasmonics research.

## Benefit to National Security Missions

This project supports the DOE missions of the Office of Science and contribute to Threat Reduction and Energy Security missions by enhancing our understanding of the fundamental behavior of electromagnetic fields (light) localized to the nanoscale as well as their interactions with quantum systems for sensing, energy, materials science, signal processing and communications applications.

## Progress

### Theoretical

Plasmonic (metallic) structures for subwavelength light confinement either in waveguiding or localized modality are infinitely more rich as compared to previously studied dielectric structures. Thus, theoretical analysis and numerical modeling are of primary importance to correct and timely design of most effective geometries. Our theoretical investigation is focused on design and characterization of (i) efficient plasmonic antennas for increased coupling of electromagnetic fields to quantum objects; (ii) improved plasmon-polariton waveguides with increased mode confinement and propagation lengths; (iii) coupled plasmonic nanonatennas and waveguides for discovery of novel functionality and behavior.

1. Shaping optical antenna's resonant spectrum: We devised a scheme to shape and actively tune the resonant spectrum of optical antennas and to increase their quality factor, an important characteristic of any resonant structure, Figure 1. By shaping the optical antennas' response spectrum, we can control the absorption, emission and scatter spectra (as well as the corresponding rates) of quantum objects coupled to the antenna. The control mechanism is based on interaction of optical antennas with the substrate above which the antennas are located. The substrate can be a layer of metal or properly designed dielectric multilayer stack, depending properties sought. The operation of this structure is based on the delayed response of the antenna to the radiation reflected off of the substrate and interference between the radiation from the antenna and its image. This enables shaping the resonant spectrum by controlling the substrate's reflection phase and amplitude as a function of frequency. Full-wave numerical simulations indeed show that optical antenna's

local field distribution, far-field radiation, and quality factor can be controlled in a wide range.

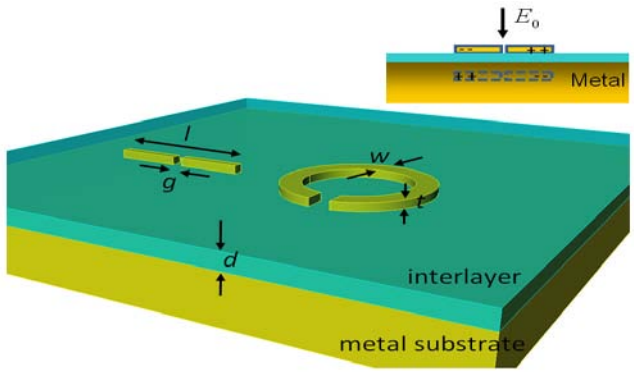


*Figure 1. Schematic illustration of a metallic dipole (left) and loop (right) antennas interacting with a substrate, which alters the overall response of the system. Inset: an image of the dipole antenna induced in the metallic substrate.*

2. Coupling in plasmonic lattices: We demonstrated [1] novel optical propagation regimes in low-dimensional plasmonic lattices – periodic structures made of different materials – in which, introduction of metallic regions enriches behavior and alters previously established paradigms. One example is a one-dimensional optical lattice with normal-anomalous alternating couplings. We investigated the resulting optical band structure and its evolution as a function of asymmetry parameter, such as bandgap closing and band crossing. When the strengths of the normal and the anomalous coupling are the same, the bandgap closes and a singularity in k-space appears. Numerical demonstrations of light propagation near the diabolic point demonstrated strong diffraction anomaly: A normally incident Gaussian beam splits into two almost non-diffracting beams, propagating at large angles with respect to the original direction, Figure 2. Similar behavior is found to occur in a more complex three-band system. These results could open a new direction in light manipulation on the nanoscale.

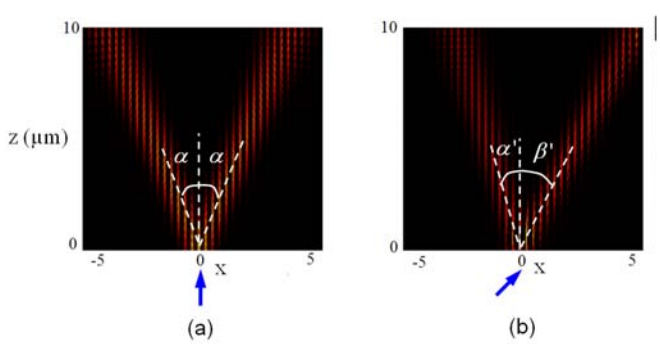


*Figure 2. Anomalous diffraction of a Gaussian beam near the diabolic point in a plasmonic array. Normal incidence, (a), and 45-degree incidence, (b) are shown. The blue arrows indicate the launching directions.*

3. Temporal control of local Surface Plasmons: We studied [2] control of the temporal profile of the local electric field in the vicinity of a small doped semiconductor or metal nanostructure/antenna, Figure 3. Unlike in the case of control in a gas or liquid phase, the collective response of electrons in the nanostructure may significantly enhance different frequency components of the field due to the excitation of local (plasmonic) resonances. This enhancement strongly depends on the geometry of the nanostructure and can substantially modify the temporal profile of the local field. We solved the direct problem of finding complex local field given the external field, as well as the inverse problem of finding the external field to generate an arbitrary target temporal profile of the local field. For a given geometry it is found that the nanostructure acts as a phase-amplitude filter and the inverse problem is solved in the first approximation by dividing the target local field by this filter function of the nanostructure.

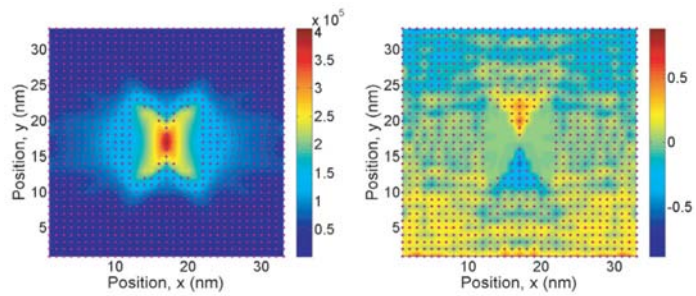


*Figure 3. Left: normalized local field intensity on the nanostructure with a bow-tie-shaped hole, at the plasmon resonance frequency. Strong field enhancement near the sharp edges at the center of the nanostructure is clearly observed. Right: induced electron density distribution at the same excitation frequency.*

4. Sub-wavelength plasmonic terahertz waveguides: We designed [3] a novel subwavelength hybrid photonic-plasmonic THz waveguide based on metal-dielectric multilayer structure. Terahertz waveguiding properties such as mode confinement, propagation length, and dispersion were analyzed numerically. Compared to metallic microstrip terahertz waveguides, the hybrid waveguides offer one order of magnitude longer (!) propagation length still maintaining subwavelength mode confinement. The investigated waveguide structure could be used as a basic building block for terahertz integrated circuits where generation, detection, and modulation components are all integrated on a single chip. This structure is also promising for efficient terahertz generation via optical rectification of guided modes.

**Experimental**

Our experimental efforts develop in parallel to the theoretical advancements, summarized above

1. Surface Plasmon-Polaritons on metallic waveguides:

Two sets of plasmonic waveguide samples, supporting a single plasmonic mode were prepared: (i) slot waveguide of metal-insulator-metal (MIM) type, gold on GaAs substrate; (ii) strip waveguide of insulator-metal-insulator (IMI) type, gold film embedded in polymer matrix. Two separate experimental setups are built to investigate in-reflection samples of type (i) and in-transmission samples, of type (ii). The MIM waveguide of type (i) is experimentally tested. Coupling of ~200 nm wide supercontinuum around 1500 nm wavelength is demonstrated. Overall non-optimized in-out efficiency of 1e-4 is demonstrated. Broadband dispersion measurements are ongoing using broadband spectral interferometry. The second experimental setup is being tested on silicon waveguides and waveguide arrays using similar supercontinuum and separately using high-intensity 100 fs laser for investigation of any nonlinear effects. Preliminary results show formation of temporal solitons and spatio-temporal solitons in waveguide arrays.

2. Plasmonic nanoantennas: We are developing a laser-coupled inverted microscope system for studying optical responses of engineered metallic antennas and nanostructures. Dipole antenna samples were prepared. Overlaying these with selected analyses, such as fluorescent dye molecules or a rare-earth ion oxide layer using Pulsed Laser Deposition (PLD) is ongoing. In the experiment we will seek to robustly observe the emssion spectrum from an ensemble of identical nanostructures and study its properties with respect to the nanostructure geometrical parameters.

## Future Work

Our planned future work will proceed along three distinct paths as briefly outlined below.

Hybrid photonic-plasmonic structures: Practical applications in Plasmonics will require interfacing with macro-world using either free-space optics or dielectric waveguide interconnects. Thus, it is essential to study such interfaces and optimize their performance. Here we will investigate hybrid structures for waveguiding and various photonic-plasmonic couplings. This direction is envisioned to result in practical recepies for simple and efficient interfacing solutions for nanoplasmonic devices.

Coupling optical nanoantennas to quantum systems: The goal here is to enhance coupling between the light and the quantum system via a resonant optical antenna as an intermediary for energy transfer. We will study absorption, fluorescent and scattering properties of the compound system. We hope to find antanna parameters and coupling strategies which will enhance desired energy transfer. This will result in increased interaction cross-sections and possibly lead to applications in controlled chemistry, selective sensing, optical communication and signal processing.

Nonlinear interactions: The goal hear is to take advantage of local field enhancement to increase the efficiency of nonlinear-optical processes, such as wavelength conversion and phase modulation, which usually require much larger devices and higher optical powers. Potential outcomes include wavelength-scale signal-processing circuits and novel sensing paradigms.

## Conclusion

This project attempts to advance the field of Plasmonics by developing the science and technology for excitation, control and detection of broadband plasmonic fields bound to metallic nanostructures. Our goal is to take advantage of the properties of Surface Plasmons for the purpose of developing novel nanophotonic devices and for manipulating the behavior of individual quantum systems and their interactions. Nanoscale plasmonics is an expanding area of study because of its importance in a broad range of applications, as well as from the fundamental point of view. This work will advance the current state of the art by focusing on the temporal aspect of the plasmonic fields and may lead to novel technologies and devices beyond sensors and towards control of nanoscale quantum systems.

## References


1. Nam, S. H., A. J. Taylor, and A. Efimov. Band Crossing & Diffraction Anomaly in Periodic Plasmonic Nanostructures. *Optics Express.*

2. Grigorenko, I., and A. Efimov. Control of the temporal profile of the localelectromagnetic field near metallic nanostructures. 2009. *New Journal of Physics.* **11**: 105042.

3. Nam, S. H., A. J. Taylor, and A. Efimov. Subwavelength Hybrid Terahertz Waveguides. To appear in *Optics Express.*


## Publications


Grigorenko, I., and A. Efimov. Control of the temporal profile of the local electromagnetic field near metallic nanostructures. 2009. *New Journal of Physics.* **11**: 105042.

# Probing physics beyond the Standard Model with Supernovae

*Alexander Friedland*
20080636ER

## Introduction

The current theoretical understanding of matter is encoded in the so-called Standard Model (SM), which describes a large body of experimental data from atomic energy scales up to the current energy frontier of a few hundreds of GeV. Despite its successes, the SM is known to be incomplete. Neutrino physics has been at the forefront of probing physics "beyond the standard model." In fact, it has given us the first and to date only direct observation of new physics beyond the SM, in the form of neutrino masses.

The goal of this project is to investigate the sensitivity of core-collapse supernova explosions and related astrophysical systems to novel neutrino properties. New physics effects at the terrascale can give rise to new interactions that change neutrino flavor. Additionally, in a large class of models the neutrino masses come together with neutrino interactions with a novel light scalar field. Both types of new physics should change supernova explosions, however, in what way is presently unknown. Other types of physics beyond the standard model can also impact the evolution of astrophysical systems. Examples are provided by the hypothetical axion particles, as well as theories with extra spacetime dimensions.

We are exploring the effect of this new physics on the evolution of supernova progenitors, and on the dynamics of the supernova explosions. We have been working on a model of a cooling protoneutron star that incorporates the mentioned new physics effects. One of our goals is to understand whether the addition of these new effects hinders or helps the explosion. In the first case, they can be excluded, in the second case perhaps we could find a mechanism responsible for the robustness of the explosion. In either case, we could gain a window into physics at the multi-TeV energy scale. Another focus area is the impact of the new physics on the neutrino signal expected from a future galactic supernova, with the application to the Deep Underground Science and Engineering Laboratory (DUSEL).

In our model, we incorporate the best-known information on neutrino cross-sections, nuclear equation of state and other ingredients. We aim to create a code that can give not only limits on new physics, but also useful predictions for the neutrino signal from a supernova within the Standard Model scenario.

## Benefit to National Security Missions

This project contributes to our basic understanding of matter and processes in the universe. It directly addresses the LANL "Beyond the Standard Model" Grand Challenge and impacts basic understanding of physics that underlies nuclear weapons (a key NNSA mission), and high-energy physics (a DOE/SC mission).

## Progress

Earlier in this project, we investigated bounds on a beyond-the-standard-model scenario, in which the photon can escape into extra dimensions. We have computed the cooling rate this hypothetical process would have on supernova, as well as on red giant stars. We found that supernovae and stars provide extremely stringent bounds on this scenario, orders of magnitude stronger than what can be feasibly achieved in the laboratory. Our results are published in Physical Review Letters [1].

The insights gained in the course of this project allowed us to tackle another active topic in modern particle physics. It has been recently proposed by Howard Georgi of Harvard University that there may exist a new, "hidden" sector of fields that is in a conformal regime and couples to the SM fields only weakly. This scenario, termed "unparticle physics", has attracted a great deal of attention, in connection with the upcoming measurements at the Large Hadron Collider (LHC). The scenario, however, proved rather subtle, with many pitfalls that were not originally appreciated. We realized that the model of the photon escape we had studied earlier provided an excellent platform for understanding most of these subtleties. We developed the connection further and published our results earlier this year in Physics Letters B [2] and JHEP [3].

We also pursued studies of the sensitivity of massive stars to the additional cooling that would arise from particle physics beyond the SM. We completed the investigation of the effect of the neutrino magnetic moment. We found that the additional cooling in this case would alter the evolution of the cores of these stars, resulting in different stellar fates. These findings were contrary to the "standard lore" in the field. Our results are graphically illustrated in Figure 1. Perhaps the most striking effect of the extra cooling is the possibility to have an explosion of the degenerate carbon core inside the massive star (marked "C/O Det." in the Figure). The details of the analysis and the resulting bounds on the neutrino magnetic moment are published in the Astrophysical Journal [4].

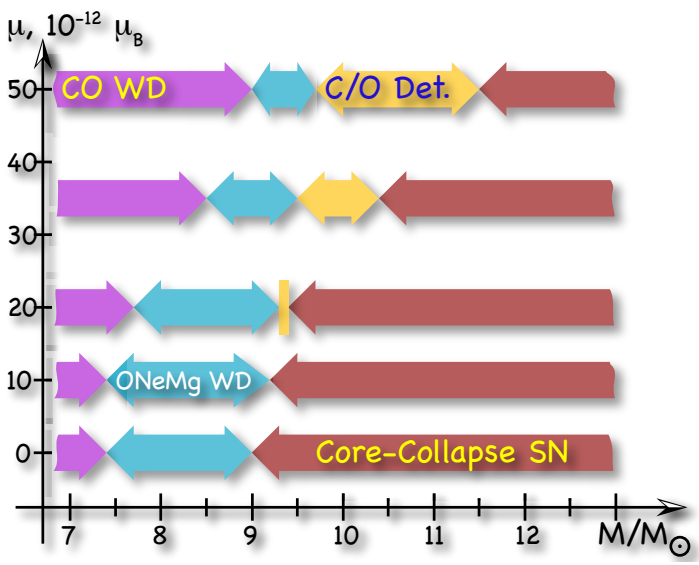


*Figure 1. Neutrino magnetic moment increases the rate with which energy is lost from the central regions of the star. The resulting evolution changes. As shown in the plot, the stars with masses 9-12 times the mass of the Suyn that normally explode as core-collapse supernovae will instead end their lives as white dwarfs. Additionally, a new type of supernova -- a type Ia exploding inside a massive star -- would appear.*

As a continuation of this work, we are presently investigating the sensitivity of massive stars to emission of axions. In Figure 2 (taken from paper in preparation), we show the effect of the axion on the duration of the Helium burning stage for stars of different masses. We discovered that this speed-up of the evolution is described by a universal function that applies to a broad range of stellar masses, from 6 times the mass of the Sun, to 40 times. This result is unexpected, and we are working to uncover the underlying physical mechanism behind it. We also found that the axion has an effect on the peak luminosity of the red giant branch. The size of the effect was also somewhat surprising and arises because of the axion cooling off-center. Further investigations are in progress.

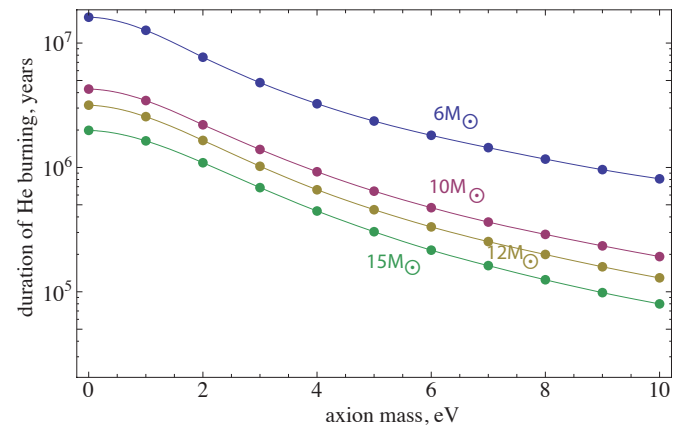


*Figure 2. Additional cooling due to axion emission shortens the duration of the Helium burning phase of the stellar evolution. The results of our calculations of this effect for stars of different masses are presented.*

In parallel, we also continued developing a quantitative model of supernova cooling, incorporating both standard and new physics effects.

We have a working a code modeling the cooling of the protoneutron star by neutrino emission. The code is a one-dimensional and treats neutrino transport in the diffusion approximation. The decoupling is treated with simple flux limited diffusion. Recent improvements to the code include state-of-the-art neutrino cross sections (diffusion coefficients).

The above model treats the decoupling of neutrinos at the neutrinosphere using the diffusion flux-limiter approximation. This is sufficient for predicting the time-scales of the evolution, but for predicting the neutrino signal we need a more accurate model. Correspondingly, we built an additional numerical model that simulates neutrino decoupling with a Monte-Carlo method. Crucially, it incorporates nuclear recoil effects and other physics that was recently shown to be very important. This will have many benefits and uses for the rest of the project (and beyond). Most immediately, we can get accurate spectra for the neutrinos streaming out of the neutrino-sphere and the angular distribution of neutrinos above the neutrino-sphere (crucial for computing the neutrino-neutrino coherent effects, see later). It is also worth mentioning that we have been working to incorporate possible convection effects in our 1-d diffusion code. This work was pursued out by Luke Roberts, a summer student from UC Santa Cruz, under the supervision of Sanjay Reddy.

Additionally, we have been investigating coherent neutrino flavor transformations in the envelop of the star ([5] and [6]). Neutrino-neutrino interaction has recently been shown to lead to large flavor transformations ("spectral swaps") close to the neutrino-sphere. It turns out that the effect, which was previously computed with two neutrino flavors, needs to be treated in the full three-

flavor framework. An example of this is depicted in Figure 3, where we compare the outcomes of the 2-flavor and 3-flavor calculations. The 2-flavor calculation incorrectly predicts the absence of the high-energy tail of the neutrino spectrum, as well as makes the high-energy tail of the antineutrino spectrum colder than it actually should be. These findings have important implications for the predictions of the supernova signal in a DUSEL detector, the r-process nucleosynthesis, and predictions of the diffuse supernova neutrino background.

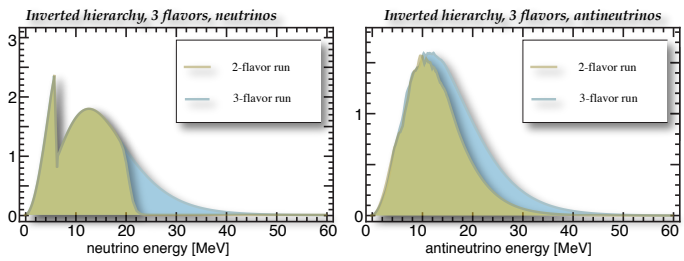


*Figure 3. Neutrino-neutrino interactions cause a complicated pattern of flavor transformations in a supernova. We have shown that previous attempts of computing this effect with only two neutrino flavors miss important physics. Shown in the Figure is the comparison of a 2-flavor and 3-flavor calculations.*

## Future Work

In connection with our findings on the 3-flavor coherent flavor transformations of supernova neutrinos, we will explore the implications for the r-process in a supernova. We are planning to do this work in collaboration with two r-process experts, G. McLaughlin (NCSU) and R. Surman (Union C.)

In connection with the prediction of the supernova neutrino signal at DUSEL, we are planning to couple three of the codes we developed: the diffusion code, the Monte-Carlo, decoupling code, and the neutrino oscillation code. The former will be used to give the energy and the lepton number flux as a function of time. These will be fed as boundary conditions in the Monte-Carlo code. Finally, the emitted spectra will be processed with the oscillation code.

We have also recently discovered that the neutrino collective oscillations, in connection with the mu-tau resonance may lead to an imprint of the shock propagation during the critical first second of the explosion. We plan to put this on the quantitative footing and make detailed predictions of this effect for the DUSEL detector.

We will also investigate the possibility of extracting a decoupling prescription to add to our diffusion code and/or the possibility of combining the diffusion code with the Monte Carlo code for the spectra formation. We will also explore adding the nonstandard flavor changing interactions to the Monte-Carlo code.

## Conclusion

The investment of effort made during the first two years of this project is starting to pay off handsomely. We now have a variety of tools for computing various aspects of supernova neutrino emission. This collection of codes represents a unique tool in the world and will greatly benefit us in the final year of the project, as we apply them to a broad spectrum of concrete physics calculations. Beyond that, they should provide an important long-term advantage to the nuclear and particle astrophysics effort at LANL.

## References


1. Friedland, A., and M. Giannotti. Astrophysical bounds on photons escaping into extra dimensions. 2008. *Physical Review Letters.* **100**: 031602.

2. Friedland, A., M. Giannotti, and M. Graesser. On the RS2 realization of unparticles. 2009. *Physics Letters B.* **678**: 149.

3. Friedland, A., M. Giannotti, and M. Graesser. Vector Bosons in the Randall-Sundrum 2 and Lykken-Randall models and unparticles. 2009. *Journal of High Energy Physics.* **0909**: 033.

4. Heger, A., A. Friedland, M. Giannotti, and V. Cirigliano. The impact of neutrino magnetic moment on the evolution of massive stars. 2009. *Astrophysical Journal.* **696**: 608.

5. Friedland, A.. Supernova neutrinos: imprints of the explosion. Presented at *Supernova physics and DUSEL.* (Los Angeles, Sept. 16-17).

6. Friedland, A.. Observing the development of supernova explosion in neutrinos: an overview. Presented at *2009 Meeting of the Division of Particles and Fields of the American Physical Society.* (Detroit, 26-31 July, 2009).

7. Friedland, A.. Effects of neutrino self-refraction in supernova at late times: a three-flavor analysis. 2009. *Submitted for LAUR; to be submitted to Physics Letters B.*


## Publications


Friedland, A., M. Giannotti, and M. Graesser. On the RS2 realization of unparticles. 2009. *Physics Letters B.* **678**: 149.

Friedland, A., M. Giannotti, and M. Graesser. Vector Bosons in the Randall-Sundrum 2 and Lykken-Randall models and unparticles. 2009. *Journal of High Energy Physics.* **0909**: 033.

Friedland, A., and M. Giannotti. Astrophysical bounds on

photons escaping into extra dimensions. 2008. *Physical Review Letters.* **100**: 031602.

Heger, A., A. Friedland, M. Giannotti, and V. Cirigliano. The Impact of Neutrino Magnetic Moments on the Evolution of Massive Stars. 2009. *Astrophysical Journal.* **696**: 608.

# Understanding the Feedback of Active Galaxies in Galaxy Clusters

*Hui Li*
20090174ER

## Introduction

Clusters of galaxies are the largest gravitationally bound objects in the Universe. They are made up by dark matter (the dominant component) and the ordinary matter (called baryons). Interestingly, because the ordinary matter can dissipate by shocks and other physical processes, there is currently a lack of detailed understanding of the baryonic component in galaxy clusters. This has seriously hindered the application of galaxy clusters as reliable probes for cosmology. We propose to investigate the feedback of Active Galaxies in galaxy clusters to address this lack of understanding, building upon the distinctive capabilities at Los Alamos. Our new cosmological magnetohydrodynamics will allow us to model accurately the evolution of magnetic energy in the clusters for the first time.

## Benefit to National Security Missions

This project will support the DOE mission in Office of Science by enhancing our understanding of how galaxy clusters evolve when important physical processes are included. Our effort will strengthen Laboratory's competencies in Basic Sciences, especially in large-scale computer modeling.

## Progress

We have completed an initial study on magnetic feedback from active galaxies (AGN) in galaxy cluster to attack the "cool flowing" problem. We performed simulations of magnetic field injection from AGN into the cores of galaxy clusters with additional cooling and heating processes to study how the intra-cluster medium (ICM) is heated by AGN feedback. These simulations form X-rays cavities and shock fronts seen in observations. We saw that large amount of the injected magnetic energy is converted into thermal, kinetic and potential energy by driving shocks and forming and lifting bubbles, then the shocks and bubbles bring injected energy away from the injection region and finally heat the ICM. We observed the heating in the centers of clusters through observations of increase of temperature as well as cooling time. We also saw the decline of the mass accretion rate (cooling flow) near the cluster center. This indicates that AGN may offset the cooling flow at least for several hundred Myr. We reported our major findings in the 2009 APS April meeting. We have also performed a study on understanding the origin of cluster magnetic fields using cosmological magnetohydrodynamic (MHD) simulations with adaptive mesh refinement. We injected magnetic fields into the ICM at high redshift (e.g. z=3) using the magnetic jet/lobe model we have developed previously. Our simulations followed the formation of galaxy cluster and the evolution of magnetic fields till the current epoch.

The injected magnetic energy is about 2e60 ergs, which is comparable to an energetic AGN outburst. We found these initial magnetic fields are spread rapidly throughout the whole cluster by the processes of cluster mergers and the ICM turbulence. The bulk flows in the ICM amplify the magnetic fields at large scales and the ICM turbulence, which is generated by the cluster mergers and the accretion shocks, amplifies the magnetic fields at small scales. The total magnetic energy increases ~25 times when the simulation ends. At low redshifts, we found the spherically averaged radial profile of magnetic field strength has a few micro G at the cluster center and drops slowly outward to just below 1 micro Gauss at about half the virial radius of the cluster. This radial profile is similar to the results from observations. We also obtained Faraday rotation measure (FRM) from our simulation data. FRM map from our simulation is close to the observations in the peak values and their spatial distributions. Our study shows that the magnetic fields from AGN possibly provide enough initial magnetic fields for the dynamo processes to magnetize the ICM to the observed level and provides a strong support to the idea that the cluster magnetic fields are originally from AGNs. These results are published in the Astrophysical Journal Letters. More data

analyses are needed to understand the ICM turbulence and the magnetic field amplification process. Additional simulations to gain a more detailed understanding of magnetic fields in the ICM by AGN magnetic feedback with different injection parameters are underway.

## Future Work

We will continue our large-scale simulations of AGN feedback in galaxy clusters. We will assemble available observations on radio galaxies in clusters so that we can conduct detailed comparisons between our simulation results and the observed galaxies and intra-cluster medium. We will also implement advanced numerical scheme so that we can perform simulations with higher resolution of dark matter particles. This is important when we need to model the galaxy dynamics more precisely.

We will also implement generation of active galaxies throughout the formation history of the cluster so that the feedback of these active galaxies can be studied in a cosmological context.

## Conclusion

The proposed research addresses an important problem in modern astrophysics and cosmology. Clusters are being used as one of the important probes of fundamental cosmological parameters. Since clusters are made by both the dark matter and ordinary matter (baryons) components, our research will provide the physics underpinning for understanding the cluster baryon dynamics. This will become important over the next decade with a flood of new cluster observations by the latest generation of X-ray observatories, large optical surveys, and measurements of cluster-induced distortions in the spectrum of the cosmic microwave background.

## Publications

Collins, D., H. Xu, M. Norman, H. Li, and S. Li. Cosmological AMR MHD with Enzo. To appear in *Astrophysical Journal Supplements.*

Xu, H., H. Li, D. Collins, S. Li, and M. Norman. Turbulence and Dynamo in Galaxy Cluster Medium: Implications on the Origin of Cluster magnetic fields. 2009. *Astrophysical Journal Letters.* **698**: L14.

Xu, H., H. Li, and M. Norman. Magnetizing the ICM by Magnetic fields from AGNs. *Astrophysical Journal.*

# The First Characterization of Large Interstellar Dust

*Sigrid Close*
20090176ER

## Introduction

Our solar system is traveling at 26 km/s through the Local Interstellar Cloud (LIC), which is a partially ionized cloud within 3 parsecs (pc, about 3 light years or 31 trillion kilometers) of the sun that is warmer and less dense than regions around it. Our limited understanding of the LIC has been gained through measurements of the spectral attenuation of star light, neutral atoms that flow to the inner Solar System, and interstellar dust (ISD), but is still largely unknown. ISDs are particularly difficult to measure due to their size and paucity; hence only a few sparse data sets exist. These data include in situ impact detections with space experiments, which have poorly determined velocity and mass measurements, and ground-based measurements of the plasma that is created when an ISD enters Earth's atmosphere (i.e. a "meteor'). An important subset of ISD is the large grains. Large grains are relatively unaffected by Lorentz forces in the interstellar medium, thus we can use large ISD to accurately determine their original provenance and allow direct measurement of debris generated during the disk formation stage of nearby stellar systems.

The current effort is directed at probing the LIC to unprecedented depth using ground-based, high-sensitivity radars.

## Benefit to National Security Missions

This project will support the missions of the Office of Science by enhancing our understanding of interstellar dust and its impact on Earth's atmosphere. In addition, we will be able to characterize the flux of particles and their potential impact on Earth orbiting satellites, including nuclear detection sensors.

## Progress

We have processed and analyzed 20 minutes (of approximately 30 hours) of High-Power, Large-Aperture (HPLA) radar data collected with the ALTAIR (Kwajelein) radar. These data include dual frequency detections of meteoroid plasma signatures, known as head echoes. Using our existing electrostatic scattering model, we have computed masses, radii and densities as well as velocities of our particles. These detections include approximately 800 meteoroids collected at VHF. Of these 800, approximately 1% have been identified as being of extra-solar origin. These particles travel with velocities greater than 72.8 km/s, which is a sum of the Earth's orbital velocity and the Sun's escape velocity. Two of these interstellar meteoroids have velocities greater than 100 km/s. The masses of these particles are at the limit of our detection - approximately 10^-7 grams. These particles appear to ablate high in the atmosphere with densities that are low (< 1 g/cm^3). We have presented these results to NASA, Marshall Space Flight Center during a visit here.

This year has also seen the development of a number of new data analysis techniques along with the declassification processing of the massive data set collected at ALTAIR. In particular, we have developed new fitting procedures which allow us to determine the accuracy with which both the velocity and the deceleration can be determined.

We have developed a new meteor deceleration model which is parameterized by the meteor density and the energy required to induce ablation, both unknowns for a given dust population. By a precise measurement of the meteor velocity, mass and deceleration, it is possible to deduce these physical parameters by fitting the data. As noted in Figure 1, the extraction of the deceleration parameters requires a sufficiently long streak because it depends on the *curvature* of the streak. Propagation of the statistical range errors to this parameter produces the error bars shown. Moreover, we have an explicit means of filtering the data to find the best experimental values. This is the first time that such a precise measurement of these parameters has been carried out.

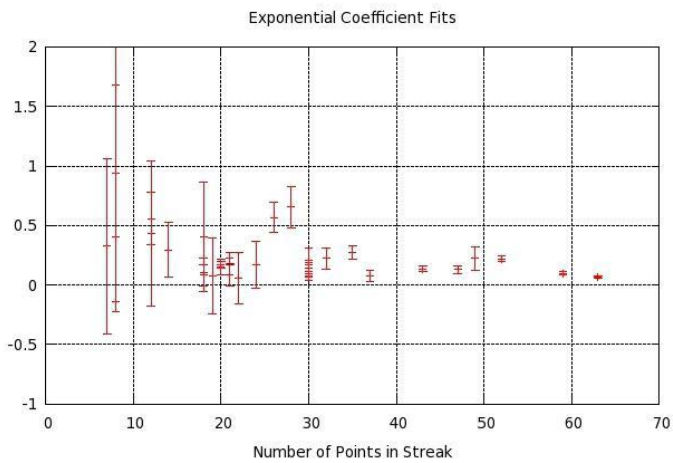


*Figure 1. Fit to the exponential term in the deceleration model which is related to the ablation coefficient and meteor density. This data shows that only the longest streaks contain sufficient points to find this coefficient with adequate accuracy. This is a result of the fact that this coefficient depends on the curvature of the range data, hence requiring the longest streaks. Error bars are based on propagation of the statistical errors from the range-vs.-time fits.*

To improve on the accuracy of the fitting, we have also developed a new approach which is based on the phase of the radar return, not just its timing (range). The phase of the return relative to a fixed reference signal can be readily found and can be shown to be related to the Doppler shift of the reflected signal. This is a direct measurement of the velocity which requires no differentiation and should lead to a much more accurate measurement. A typical result is shown in Figure 2. The total phase variation over a streak then describes the velocity variation directly. We note that due to a large number of phase wraps between the object and the radar, there is imbedded ambiguity regarding the Doppler shift. However, by comparing the results to the velocity difference from the range data, essentially a timing measurement, it is possible to remove this ambiguity completely, as shown in Figure 2. This method promises to give much greater accuracy for velocity and deceleration than previous methods.

We would also like to note the development of a new streak-finding algorithm which makes it possible to identify meteor streaks automatically in the large body of data we have assimilated. Such an algorithm is essential to be able to process the massive amount of data that has been collected. The algorithm is based on the use of web methods to determine the occurrence of a set of contiguously-spaced points indicative of a meteor. This algorithm has been shown to work well on the ALTAIR data set, and is now being further tested. A typical result is shown in Figure 3.

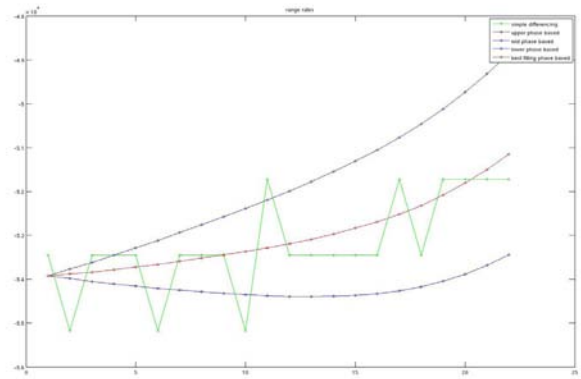

*Figure 2. Red curve represents the best fit of the phase variation to the differenced range data, producing an accurate measurement of the velocity evolution. The ambiguity caused by the distance from radar to scatterer is removed in this manner*

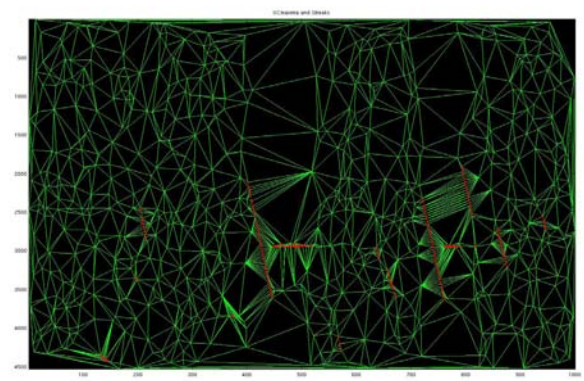

*Figure 3. Streak-finding algorithm applied to a typical data file. The vertical axis is the range and the horizontal axis is the time of the radar return. The method correctly identifies several meteor streaks which are represented by a line that traverses upper left to lower right. We note the presence of a few spurious horizontal lines of unknown origin which must be culled from the data.*

## Future Work

Using the above described data set we hope to provide the first characterization of large interstellar dust grains (ISD) using ground-based, high-power radar. Our results will include the first full characterization of ISD, including orbits, velocities, masses, densities, radii and compositions. We will then be able, for the first time, to answer the following key science questions:

- What is the bulk density of large ISD particles (which is crucial for understanding the interstellar)?
- How much has the LIC been processed?
- What do the properties of ISD tell us about the formation and dynamics of asymptotic giant branch (AGB) stars, young stellar objects and debris disks around main sequence stars?

Our approach will include both data analysis and modeling. We will calculate orbital parameters, and develop and refine elliptical scattering and ablation models and apply these to our data. We will then refine our heliospheric transport model for large ISD and validate our scattering model using multi-frequency radar and satellite data. We will then be able to derive fundamental ISD parameters, including mass, radius and density. Finally, we will derive composition and metallicity for a subset of our data that have associated trails. This will allow us to interpret results in the context of models of solar system and stellar formation and evolution.

## Conclusion

We are currently poised to analyze all the recent data collected from ALTAIR. We expect to find best fits to the deceleration parameters, which will yield the mass, meteoroid density and the three-dimensional velocity. This data will represent the primary experimental findings of this program.

Our research will then produce the first characterization of large interstellar dust grains and show the relationship between velocity, direction, mass, radius and density. Furthermore, we will be able to characterize the local interstellar cloud and potentially tie these grains to a source to determine how many interstellar particles reach Earth's atmosphere and what effect these particles have had on our ionosphere.

## Publications

Close, S., L. Cox, M. Kelley, P. Colestock, D. Suszcynsky, J. Zinn, and R. Petrin. Electromagnetic Pulses Generated by Meteoroid Impacts on Spacecraft. *Journal of geophysical research.*

Close, S., T. Hamlin, M. Oppenheim, L. Cox, and P. Colestock. Dependence of radar signal strength on frequency and aspect angle of nonspecular meteor trails. 2008. *Hournal of Geophysical Research.* **113** (A06203): 1.

Colestock, P., S. Close, and J. Zinn. A Numerical Model for Plasma Production and Scattering from Meteoroids. To appear in *American Geophysical Union Fall Meeting.* (San Francisco, Dec. 14-18, 2009).

# Soild Helium-4: A Supersolid or Quantum Glass?

*Matthias J. Graf*
20090217ER

## Introduction

The discovery of the putative supersolid state in solid Helium-4 in 2004 [1,2] ignited a race for new measurements and theories to prove the existence of this exotic state of matter. This enigmatic state is the crystalline analog of superfluidity and superconductivity. Essentially, the supersolid phase is the last remaining quantum phase that can exhibit persistent particle current of vacancies or interstitials with no dissipation. It is the analog to zero viscosity in a superfluid or zero resistance in a superconductor. If it does exist, it would mean that a supersolid could be squeezed through the tiniest orifices without resistance, just like a superfluid. Hence, the discovery and investigation of this phase is of fundamental importance to quantum physics and has created a stir far beyond the quantum solid and quantum fluid communities.

We propose to theoretically and experimentally explore the nature of the low-temperature phase in Helium-4, where a possible supersolid is reported. So far experiments involving torsion oscillators, ultrasound and shear mode probes, and specific heat measurements have recorded anomalous behavior in the temperature range of interest. The extremely low-temperature and high-pressure part of the Helium-4 phase diagram is the subject of our investigations. Complementary to our theoretical efforts, we are using neutron scattering to provide important information about possible disorder, vacancies and dislocation networks in crystalline Helium-4. Such structural information is much needed for any attempt to understand the underlying physics of the strange behavior of a quantum solid. Theory will explore the consequences of disorder and contrast a supersolid scenario with a possible quantum glass state for neutron scattering, torsional oscillator, thermal conductivity, and elastic shear modulus and specific heat experiments.

## Benefit to National Security Missions

This proposal answers to the missions of the Office of Science and LANL's Grand Challenge "Fundamental Understanding of Materials" by advancing the state-of-the-art quantum state modeling and experimentation in condensed matter physics at ultralow temperatures and high pressures, with ramifications to the Grand Challenge "High Temperature Superconductivity and Actinides."

A better understanding of supersolid or quantum glass behavior may lead to better control and predictive capabilities for thermodynamic and mechanical materials properties for a large class of materials. Modeling and characterization of dislocation quantum glasses may lead to stronger materials or new high-precision instrumentation.

## Progress

Supersolidity is the last undiscovered state of matter where the same atoms form a rigid solid lattice and yet demonstrate ability to move through the crystal without friction, i.e. exhibit superflow properties like superfluid Helium-4. It is established that supersolid behavior can occur in the presence of defects in a solid. The major question in the field is addressing what kind of defects might facilitate supersolidity and what is the exact nature of the ground state of solid Helium-4 in the presence of defects.

Our theoretical work focuses largely on the possible glassy state due to dislocations that might be responsible for the unusual behavior of solid Helium-4 at ultralow temperatures [3]. We expanded our phenomenological glass model to account for general glass relaxation processes as known from dielectric or structural glasses [4]. An extension to these results was published in the proceedings of the 25$^{th}$ International Conference on Low Temperature Physics (LT-25) held in Amsterdam, August 2008 [5]. We were invited to present our studies at LT-25

and the satellite conference for ultralow temperatures ULT, followed immediately thereafter in London. An extension of our glassy scenario to more general distributions of relaxation times has led to better agreement with experiments, Figure 1. Consequently, we were invited to present these results at the international conference QFS 2009 at Northwestern University, Evanston, in August 2009 [6].

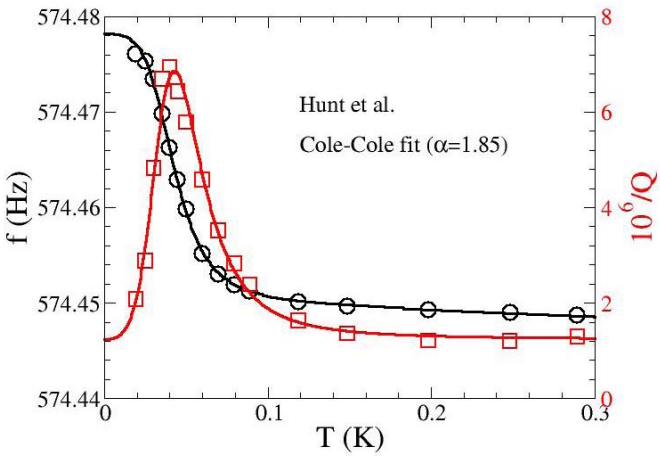


*Figure 1. The resonant frequency (black, left axis) and the dissipation (red, right axis) vs. temperature of a high-precision torsion oscillator. The glass model (solid lines) results in excellent agreement with the experimental data by B. Hunt et al. [7] when using a Cole-Cole distribution for relaxation times. The Cole-Cole exponent alpha=1.85 deviates from unity, indicating glassiness.*

Our hypothesis of a glassy component responsible for the anomalous behavior is also supported by the new torsional oscillator measurements of our external collaborators headed by Prof. J. C. Davis at Cornell University and published in the journal of Science [7]. They found, using a new generation of ultrahigh precision torsional oscillators that solid Helium-4 does exhibit very long relaxation times (sometimes lasting up to days) in the period shift and damping of the Helium-4 samples. These results clearly point to the presence of uncrystallized glassy components down to 10 mK. So far the lowest temperatures measured in this quantum solid. Their data analysis in terms of linear response functions was strongly motivated by our theoretical predictions and subsequent interactions with the group of J. C. Davis resulted in the classification of their results in terms of a superglass. That means the coexistence of supersolid and glassy phases. A possible scenario for the ground state of solid Helium-4 that requires further modeling and measurements.

In parallel to our modeling of the thermodynamics of Helium-4 and the mechanics of torsional oscillators with a glassy backaction term, we have developed a theory for describing the effects of various defects, as well as supersolidity on thermal transport measurements. With our external collaborators Prof. Ilya Vekhter and his graduate student Josh Thibodaux from Louisiana State University, we developed heat transport equations for phonons and vacancies scattering off various zero and one-dimensional defects. Based on realistic fits to existing measurements by Burns and Goodkind (1993), we derived predictions for the signatures of the onset of a possible supersolid phase transition. We have begun to interact with the experimental group by Prof. Robert Hill at the University of Waterloo, who will test these predictions and see if they validate the glass or supersolid scenario.

Finally, we have started collaborations with Prof. John M. Goodkind at the University of California at San Diego with respect to neutron scattering measurements and the development of quantum glass theories in solid Helium-4.

In addition, we have hired the postdoc Jung-Jung Su, who has been working part-time on this project since the end of July 2009.

## Future Work

We will address the fundamental quantum physics question of a possible supersolid or quantum glass state in solid He-4 by means of a combined theoretical and experimental approach. Currently, it is hotly debated whether it is a supersolid or a dislocation (quantum) glass or a conventional dislocation network. So this research will emphasize the disordered crystal state that still can exhibit supersolid behavior, because of the high mobility of vacancies. Hence, an important step is the precise characterization of the quality of solid He-4 crystals. We will use neutron scattering experiments as a direct probe of sample quality of this novel quantum matter in strong collaboration with Prof. Goodkind.

Our research has the central theoretical and experimental goals:

- Develop a theory of a (quantum) glass state of He-4. Combined with the structural properties of the bulk as determined by neutron scattering, our predictions for specific heat, thermal conductivity and shear modulus will provide important insights and guidance for new measurements and the interpretation of the putative supersolid state.

- Neutron scattering will provide the missing microscopic input for a large number of theories that rely on the effects of disorder, dislocations and vacancies. We will provide a basic characterization of solid He-4 at very low temperatures and high pressures.

We already have two approved neutron scattering

proposals at the Lujan LANSCE facility at Los Alamos. Our neutron scattering experiments are pending until technical details with providing the new dilution refrigerator environment has been resolved.

NOTE: The scope of work has changed with respect to the amount of neutron scattering experiments that will be performed. Since the departure of Wei Bao from the Laboratory, we have begun to collaborate externally with neutron scatterers and theorists on quantum glasses. This of course requires a reduction in planned neutron scattering experiments and an increase in the theoretical component on glassy dislocation networks. We expect that our collaboration with Goodkind at the University of California at San Diego and Vekhter at Louisiana State University will more than compensate for this loss of expertise.

## Conclusion

In a nutshell, the supersolid phase is the last remaining quantum phase that can exhibit persistent particle current of vacancies or interstitials with no dissipation, similar to superfluidity or superconductivity.

The outcome of this research will either confirm the putative supersolid state by identifying the fundamental quantum excitations with neutron scattering experiments or provide an alternative explanation, namely, that of a quantum glass or dislocation network and its effects on mechanical, elastic and thermal properties. Either way the results will impact the way we think about supersolidity and its hallmark signatures.

## References


1. Kim, E., and M. H. W. Chan. Probable observation of a supersolid helium phase. 2004. *Nature.* **427**: 225.

2. Kim, E., and M. H. W. Chan. Observation of superflow in solid Helium. 2004. *Science.* **305** (5692): 1941.

3. Balatsky, A. V., M. J. Graf, Z. Nussinov, and S. A. Trugman. Entropy of solid Helium-4: the possible role of a dislocation glass. 2007. *Phys. Rev. B.* **75**: 094201.

4. Nussinov, Z., A. V. Balatsky, M. J. Graf, and S. A. Trugman. On the origin of the decrease in the torsional oscillator period of solid Helium-4. 2007. *Phys. Rev. B.* **76**: 014530.

5. Graf, M. J., A. V. Balatsky, Z. Nussinov, I. Grigorenko, and S. A. Trugman. Torsional oscillators and the entropy dilemma of putative supersolid Helium-4. 2009. *J. Phys.: Conf. Ser..* **150**: 032025.

6. Graf, M. J., Z. Nussinov, and A. V. Balatsky. The glassy response of solid Helium-4 to torsional oscillations. To appear in *J. Low Temp. Phys..*

7. Hunt, B., E. Pratt, V. Gadagkar, M. Yamashita, A. V. Balatsky, and J. C. Davis. Evidence for a superglass state in solid Helium-4. 2009. *Science.* **324** (5927): 632.


## Publications


Graf, M. J., A. V. Balatsky, Z. Nussinov, I. Grigorenko, and S. A. Trugman. Torsional oscillators and the entropy dilemma of putative supersolid Helium-4. 2009. *J. Phys.: Conf. Ser..* **150**: 032025.

Graf, M. J., Z. Nussinov, and A. V. Balatsky. The glassy response of solid Helium-4 to torsional oscillations. To appear in *J. Low Temp. Phys..*

Hunt, B., E. Pratt, V. Gadagkar, M. Yamashita, A. V. Balatsky, and J. C. Davis. Evidence for a superglass state in solid Helium-4. 2009. *Science.* **324** (5927): 632.

# A Novel Millimeter-Wave Traveling-Wave Tube Based on an Omniguide Structure

*Evgenya I. Smirnova*
20090265ER

## Introduction

Millimiter (mm)-wave devices are proving to have many important applications from imaging to communication. Among the greatest impediments to exploiting this regime of the electromagnetic spectrum are the difficulties in building sources with sufficient power suitable for practical applications. This project's goal is to construct a novel traveling-wave tube (TWT) amplifier at mm-waves (100 GHz), that employs a dielectric photonic band gap (PBG) structure. A TWT is a vacuum electronics tube amplifier, operating with a purpose of delivering high microwave power across a wide frequency bandwidth. Present state-of-the-art millimeter wave TWT development has reached fundamental limitations in both frequency and bandwidth that can be overcome with a use of a periodic electromagnetic structure (so called "PBG structure"), that is at the cutting edge of the electrical engineering technology applied to a real world problem. An extremely broadband TWT based on the PBG concept would enable new applications in mm-wave communications, radar receivers, radio astronomy, and remote mm-wave spectroscopy. A cylindrically symmetric version of a PBG structure, called an "omniguide", is attractive for a proof-of-principle demonstration [1]. Omniguide TWT structures have great potential for generating high average power (up to 1 kW) with simultaneously large bandwidth (greater than 20 per cent) and linear dispersion. In addition, being cheap to fabricate, omniguides enhance the commercial transferability of the W-band TWT technology. Because of new national security spectroscopy missions that would be enabled by this technology, this research directly addresses specific needs of the laboratory grand challenge "Detection of nuclear materials (Ubiquitous sensing)."

## Benefit to National Security Missions

This project, through the development of new mm-wave sources, will impact a broad range of technical problems including imaging, sensing, and communiation. These technical areas are crucial for supporting threat reduction, nuclear material detection, and other missions important to DOE (NN), DHS (DNDO), DOD (DARPA) and other government agencies.

## Progress

The project has made significant progress up to date in three areas.

A significant level of effort was devoted to fabrication in the first year. First, three new omniguide structures were fabricated in the machine shop and prepared for tests with the electron beam (Figure 1). The structures were tested with low power rf, the transmission properties were found to be in agreement with the design.

Second, the pencil beam TWT test stand (Figure 2) was brought back to service. We checked the proper operation of all the components, including the vacuum system, the modulator, the electron gun, and steering and focusing magnets. Some new components had to be purchased to replace the old and problematic equipment. Next, the test stand was aligned first with a collimator and then with a dummy metallic structure to ensure the reliable electron beam transmission. The safety of the test stand was re-evaluated and improved during the ISR-division shut down in May, 2009. The omniguide structure is currently being installed on the test stand. The first electron beam transmission and power generation results are expected in December, 2009 [2].

Third, we conducted theoretical computations of amplification gain in the omniguide taking into account the realistic electron beam spot size and energy dispersion. It was concluded that a 10 cm long structure was required to obtain 30 dB power gain. The bandwidth of the amplifier was found to be 10 per cent (90 to 100 GHz) (Figure 3), which is better than in any currently existing mm-wave TWT. We believe that bigger 20 per cent bandwidth can be achieved by slightly altering dimensions of the omniguide tubes in the second year of the project.

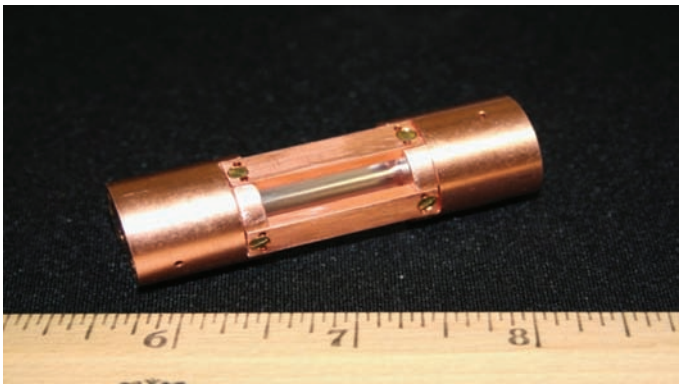

*Figure 1. Omniguide TWT structure.*

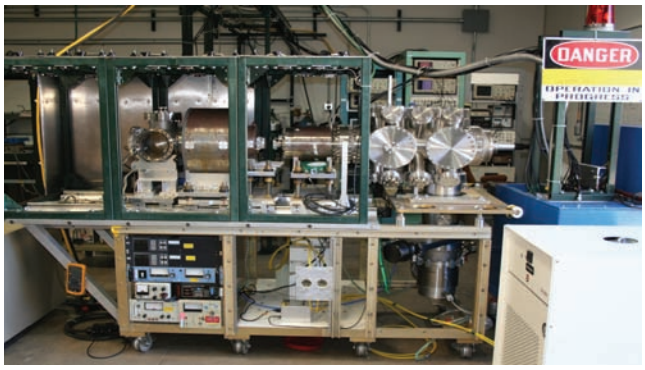


*Figure 2. The mm-wave TWT beam line opened for maintenance.*

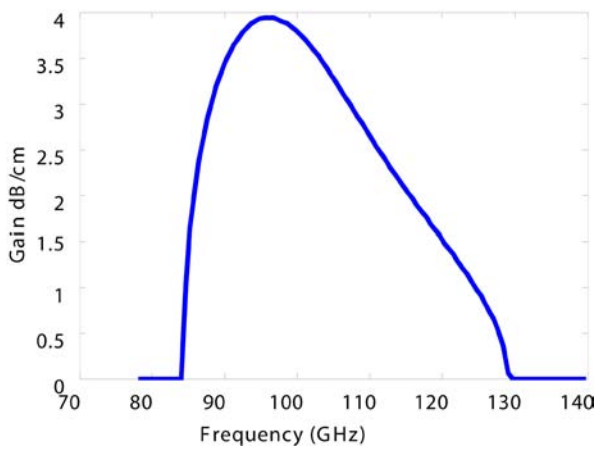


*Figure 3. The numerical calculations of the TWT net gain including the effects of the finite beam diameter and the beam energy spread.*

## Future Work

The successful completion of this project will yield a new mm-wave power-generating device, which is very compact, high power, high bandwidth and cheap to fabricate. The work can be divided into three areas as follows: initial testing of the current design of the 100 GHz omniguide traveling-wave tube structure with an electron beam; working to increase the bandwidth of the omniguide traveling-wave tube; and working to increase the peak output power of the tube. Specifically we will:

- Test the current design of the 100 GHz omniguide TWT (year 2). We will install an omniguide TWT on the pencil beam test stand. We will condition the tube and demonstrate generation of 100 W of average power with 10 per cent bandwidth.

- Increase the bandwidth for the omniguide traveling-wave tube to 20 per cent and the peak power to 200 W (year 2). We will redesign the tube's output coupler, to increase its bandwidth from 10 per cent to 20 per cent. We will also work on improving the beam steering into the tube. This should increase the peak power to 200 W.

- Increase the peak output power to 1 kW (year 3). In year 3 we will work on further increasing the average output power up to 1 kW. This will require fine-tuning of our beam steering and focusing system, so that more current enters the TWT structure. In addition we will have to continue our design work for the coupler. Although silica cylinders, which form the tube, are capable of withstanding high gradients, the current design for the output coupler has metallic parts, which may be vulnerable to breakdown. We will use CST Microwave Studio to design a novel quasioptical coupler with reduced electromagnetic fields around the metallic components.

## Conclusion

At the end of this project there will exist a new mm-wave power-generating device, that is very compact, high power, high bandwidth and cheap to fabricate. The new device will allow improved nuclear material detection and also can be used by our military forces in radars and secure communications.

## References

1. Smirnova, E. I., L. M. Earley, and B. E. Carlsten. Fabrication and low-power tests of a W-band omniguide traveling-wave tube structure. 2008. *IEEE Transactions on Plasma Science.* **36** (3): 763.

2. Smirnova, E. I., L. M. Earley, W. B. Haynes, R. M. Renneke, and D. Yu. Shchegolkov. Omniguide traveling-wave tube structure testing with a 120 keV electron beam. Presented at *36th International Conference on Plasma Science.* (San Diego, CA, 31 May - 5 June, 2009).

## Publications

Smirnova, E. I., L. M. Earley, W. B. Haynes, R. M. Renneke, and D. Yu. Shchegolkov. Omniguide traveling-wave tube structure testing with a 120 keV electron beam. Presented at *36th International Conference on Plasma Science.* (San Diego, CA, 31 May - 5 June, 2009).

# Development of a Muon to Electron Conversion Experiment at LANSCE/MaRIE: Search for Physics beyond the Standard Model

*Takeyasu Ito*
20090269ER

## Introduction

The ultimate goal of this research is to perform an experiment to search for a process in which a muon is converted to an electron without the emission of neutrinos. The muon is a particle that has very similar properties to those of the electron, except that the muon is much heavier than the electron. This process is highly suppressed in the Standard Model, a widely accepted theory that describes the ultimate constituents of matter and radiation as we understand them. However, this theory is at best incomplete and the above mentioned process is predicted by many extension of the Standard Model. Therefore, if found, this process unambiguously signifies the existence of physics beyond the Standard Model, providing a new breakthrough in our understanding of the Universe.

The LANSCE accelerator at LANL turns out to be the best facility at which to perform such an experiment. The goal of this ER project is to further develop the physics basis for the experiment to a point where it is possible for us to seek an external funding to construct the experiment.

We will perform a series of simulations to evaluate the ultimate performance of the experiment. At the same time, we will come up with a technical solution to some special beam delivery challenges that will allow us to build such an experiment at LANSCE without interfering substantially with other existing and planned activities at LANSCE. Such technical solution requires development of some new technologies.

There are competitions in other labs, namely the Mu2e project at Fermilab and the COMET project at J-Parc in Japan. If for some reason it becomes more likely that one of these two competing projects is more likely to be funded than ours, we will consider joining it so that we can contribute to the science.

## Benefit to National Security Missions

This project will contribute to our basic understanding of forces and processes in the universe governed by the "Standard Model." It directly addresses issues in the LANL "Beyond the Standard Model" Grand Challenge and impacts basic understanding of physics that underlies nuclear weapons, a key DOE mission.

## Progress

We have made the following progress toward our first-year project goals:

1. Studied various beam operation mode and evaluated the advantage and disadvantage of each mode. The goal of this study was to find a beam operation mode that would allow us to run a muon-electron conversion experiment without interfering with other operations at LANSCE.

2. Performed an experiment to measure the "extinction" of the LANSCE accelerator. The muon-electron experiment requires a beam pulse structure where the beam is on for short period of time (~ 200 ns) followed by a ~2μs or so of beam off period. The extinction is defined to be the amount of residual beam current when there is not supposed to be any beam, normalized to the amount of beam when the beam is on. For the muon-electron experiment, it is important to have an extinction of $10^{-9}$ or so. Measuring the base line extinction that the LANSCE accelerator can achieve with the front-end chopper alone is an important first step that would tell us how far we will have to push to achieve the necessary extinction.

3. We were invited to participate in an experiment to measure the reaction products of muon capture on aluminum, a major physics background process for muon-electron conversion experiment. This experiment is a joint effort by the FNAL Mu2e collaboration, the J-PARC COMET collaboration, and us from LANL (contact person: Peter Kammel, University of Illinois). The experiment is scheduled to take place at Paul Scherrer Institute in Switzerland in early July. We are in charge of measuring the

neutron energy spectrum from the muon capture in aluminum. We have purchased necessary equipment for this experiment (photomultipler tube and liquid scintillator). A test experiment was performed in May at WNR to compare the performance of different neutron-gamma discrimination method.

We have decided to join the FNAL mu2e project. This was motivated by the following two reasons:

1. Since the approval of this ER project, the political wind has shifted greatly in favor of the Mu2e project. This is seen in the fact that Mu2e is mentioned in the President's budget. Also the future of LANSCE-R is rather unclear. LANSCE-R is a necessary condition for muon-electron conversion experiment to happen at LANSCE.

2. Under the circumstances, we have come to realize that a muon-electron conversion experiment will not happen at LANSCE unless DOE decides not to fund the FNAL Mu2e. Therefore it is important for us to be part of the Mu2e collaboration at this point: if the Mu2e project goes forward, we can still contribute to the science. If the Mu2e does not go forward for some reason, we can bring the entire collaboration to LANCE.

On 1) above, we have identified a beam operation mode that would allow us to run a mu-e conversion experiment with necessary beam power and suitable beam structure in such a way that it will not interfere with current and planned operations at LANSCE. This is to use the $H^+$ beam in the macropulse in which the $H^-$ beam goes to the Lujan center.

On 2), we performed a measurement of the beam intensity at the switch yard of the LANSCE accelerator using image plates. We calibrated the response of image plates by sending a known amount of beam through the accelerator and then measured the beam intensity when the beam is blocked by the front-end chopper. We measured an extinction of $3x10^{-8}$ when the chopper was set to the normal position. When the chopper high voltage was increased, the extinction was improved by two orders of magnitude. We also measured the effect of using the ground level deflector, which is nominally used to "turn the beam off" but can be used in a manner to supplement the front-end chopper. When the ground level deflector was on, no measurable beam was observed. These results were very encouraging, indicating that we will not need to develop a high duty cycle fast speed kicker as we originally considered. The results were reported at the 2009 LANSCE Users Group Meeting in October in Santa Fe.

## Future Work

After our extinction measurement mentioned in 2) above, we realized that if we use the $H^+$ beam in the same macropulse in which the $H^-$ beam goes to Lujan center, there can be another source of background that can contribute to degrading the extinction. Namely, the $H^-$ beam leaking into the $H^+$ beam line. We plan to perform a measurement to evaluate the size of this effect on the extinction. We have a scheduled beam time at the end of December.

Our role in the mu2e project is to optimize the muon stopping target. The target material has to be choisen both physics considerations and engineering considerations taken into account. We will perform necessary calculations and simulations.

## Conclusion

We have conducted the initial phase of the planned research activities for this ER project successfully. In particular, the extinction measurement was very successful and the results are very encouraging.

## Publications

Ito, T.. Possibility of a muon electron conversion experiment at LANSCE: search for physics beyond the standard model. Presented at *LANSCE users' group meeting.* (Santa Fe, NM, 30 Sep - 1 Oct, 2009).

# Unconventional Methods for Quantum-enhanced Metrology

*Malcolm G. Boshier*
20090284ER

## Introduction

Precision measurement is crucial to many areas of national security and industrial technology, and basic science, for characterization and control of complex systems. The act of performing any physical experiment is, in fact, a measurement, and therefore metrological techniques are central to all we know about the world. There are obviously many practical applications as well; sensing of all types is rapidly becoming paramount for more complete knowledge of what is built, stored, or moved across borders, behind barriers, or underground. Reduction of the time or total energy in sensing can make the process harder for an adversary to detect. Hence reducing the resources required to make measurements to a given precision, or increasing the precision attainable with given resources, is a critical task for scientific, technological, and national security applications.

Toward these ends, we are developing quantum-informational techniques that we expect will lead to new devices capable of measuring many physical quantities to what may be extraordinary precision while requiring significantly fewer resources than devices based on traditional measurement protocols. In particular, we will use single trapped atoms and employ them for quantum enhanced measurements of externally applied fields and forces of interest, surpassing the shot-noise "limit" to measurement. Theoretically, we will explore nonlinear quantum metrology and its application to such devices. Through multi-atom couplings produced during a measurement, enhanced sensitivity may be achieved.

## Benefit to National Security Missions

This project will support the DOE mission in Threat reduction and the "ubiquitous sensing" Laboratory Grand Challenge by enhancing our understanding of how sensing can be improved beyond standard limits using quantum technology. It also supports the mission of the Office of Science for better understanding of fundamental quantum behavior, including that of complex materials.

## Progress

The experimental part of the project has made significant progress in establishing the quantum coherent control of the states of an individual trapped ion required for quantum enhanced measurement applications. For our first proof-of-principle measurements for development of quantum-enhanced metrology techniques, we will be using two of the internal electronic levels of the ion as a spin-1/2 quantum system. Quantum manipulations of this spin, controlled couplings of the spin to its environment, and coherent rotations applied depending on previous measurements should allow for estimation of external fields at precisions beyond the shot noise limit, i.e. beyond the 1/sqrt(N) scaling for resources N. This will require long-lived coherence of the ion spin. Toward this end, we have demonstrated coherence times with a two-pulse Ramsey-interferometry measurement of the quantum spin (qubit) of approximately 450 microseconds, seemingly limited by inhomogeneous broadening due to laser phase and environmental magnetic field fluctuations. This has recently been extended to coherence times of more than 2 milliseconds by interspersing spin-echo control pulses at the proper times to refocus the spin, removing some of the inhomogeneous broadening due to the slower fluctuations. This coherence time should be compared to the 10 microsecond quantum operation (applied spin rotation) times we have shown in our system, leading to a ratio of more than 200; this will enable long precession measurement times to get more precise measurements of quantities of interest. This experiment also demonstrates the required phase and state manipulation of a qubit required for many quantum information processing tasks, establishing a very useful capability in our ion lab.

The bit-by-bit parameter estimation protocol we will be using is based on an adaptive quantum measurement algorithm, and we have also recently determined the appropriate implementation of this algorithm for our ion system; we will be employing this algorithm in the near future to measure the electric field amplitude

of a probe laser approaching the Heisenberg limit. Remaining preliminary tasks include characterization and improvement of the resolved-sideband cooling procedure used to prepare the ion near the ground state of motion in its harmonic trapping well---this is currently underway and we believe it should be completed in a month or so.

We have also completed work on a scanning transfer cavity laser-stabilization system to maintain several of the ion control and cooling lasers at the required frequency within 1 MHz over several hours. This is a stability of one part in a billion, and it has been achieved in a straightforward home-built system that allows for changing of the individual laser frequencies (to within approximately a few hundred megahertz) while locked, a necessity for precision laser cooling, spectroscopy, and control of individual atoms. A manuscript describing this system is currently in preparation for submission for publication.

The theoretical part is concentrating on nonlinear quantum metrology, which holds the promise of improving over the 1/ N Heisenberg limit. Different possible implementations have been proposed in the literature, including a two-component Bose- Einstein condensate and ions trapped in nonlinear potentials. We have started studies of the effects of decoherence and noise in nonlinear quantum metrology. In particular, we have considered a nonlinear interferometer setup aimed at measuring phase shifts, and modeled the system-bath interaction via a generalized nonlinear quantum optics master equation. We have obtained exact, analytical solutions for different initial entangled and unentangled states of the quantum probe, and analyzed how metrological limits are degraded by the effects of noise and decoherence.

## Future Work

The long-term goals of our program for quantum-enhanced measurement include the development of methods for measurement far beyond the capabilities of present probes of electromagnetic fields and forces. The near-term goals involve proof-of-principle demonstrations of such methods (with modest initial enhancements beyond standard classically-enabled technologies) and theoretical investigation of novel protocols that may be derived from quantum information processing algorithms and information-theoretic principles.

We expect that precision measurement beyond the standard quantum limit (also known as the “shot noise” limit), approaching the Heisenberg limit, can be implemented in our trapped-ion quantum information processing system. In particular, we plan (i) to make determinations of parameters such as frequency, magnetic field, and force (via displacement or rotation) to a given precision using fewer resources than standard methods (such as Ramsey spectroscopy or standard displacement measurement); or (ii) to make these determinations to a higher precision using similar resources to standard methods. A quadratic, or greater, reduction in resources or increase in precision, respectively, should be possible with these methods. We plan to demonstrate such gains in the lab when measuring real parameters through a direct comparison of the proposed and standard methods. We are also starting to think about implementing quantum metrology strategies in Bose-Einstein condensates of ultracold atomic gases.

Concurrent explorations of unconventional nonlinear quantum methods for metrology will provide guidance for the experiments and establish the capability of possible future experimental methods. These will focus on many-body coherent interactions during the measurement process. Such interactions can lead to drastic minimization of the resources required for measurements made using experimental probes amenable to large-scale entanglement, such as atomic ensembles or collections of interacting quantum bits. A nonlinear scaling of the parameter estimation precision, inversely proportional to the number of particles raised to the power of the degree of interactions, may be attainable, leading to significant gains in measurement speed and precision.

## Conclusion

We hope to be able to develop, and in some cases demonstrate, proof-of-principle techniques that will allow for enhanced measurement of physical quantities whose determination is required for threat reduction and basic environmental measurement. Techniques derived from quantum algorithms will allow far more precise measurement of many parameters of interest using reduced resources, possibly enabling sensing of adversaries without detection or reductions in energy requirements for portable sensing technologies.

# First Unambiguous Measurement of Jet Fragmentation and Energy Loss in the Quark Gluon Plasma

*Gerd J. Kunde*
20090303ER

## Introduction

We are working on  the Compact Muon Solenoid (CMS) experiment at the Large Hadron collider with the goal to measure properties of the quark-gluon plasma via a new probe, the modification of particle production form the decay of the fundamental but unstable constituents of matter. We call this effect 'modification of the fragmentation functions'.

Collisions of lead nuclei at the highest energies ever created in a laboratory will lead to the production of a plasma of elementary particles, such as quarks and gluons. While detected previously the properties of this new state of matter are not know. The first collisions are scheduled for FY10.

We propose an integrated approach of physics analysis, theory development, software infrastructure and highly integrated state-of-the-art ultra-high speed data and signal processing electronics. We will study the strongly interacting quark-gluon plasma by tagging strongly interacting particles traversing the plasma with a non-interacting electromagnetic probe. Comparison of the plasma measurement with a vacuum measurement will lead to a quantitative measurement of the density and temperature of the plasma.

## Benefit to National Security Missions

Our work on developing a high speed readout system is also benefitting Threat Reduction . The Data Acquisitionneeds in space based satellites are comparable to the requirements of CMS at CERN. Indeed , some of the technology developed at LANL for CERN is also used in the next generation  satellite systems.

## Progress

Detailed studies were performed to determine the CMS machine performance in detecting andreconstructing high-transverse momentum Z0 bosons. Though the goal was to do these studies for the case of high-multiplicity environment expected in Pb+Pb collisions at the LHC, in orderto have a comparison baseline, all studies were carried out in parallel also for the case of p+pcollisions.

These studies helped reveal several inconsistencies in the official CMSSW software and were the first to propose a more straight-forward algorithm for muon reconstruction in heavy-ion environment in CMS. The results are collected in a document that addresses the physicsmotivation and the reconstruction capabilities for analyzing the Z0+jet channel in Pb+Pbcollisions at the LHC with the CMS detector.

CMS has the capability of detecting muonswith high resolution up to high transverse momentum, accessing signals like Jpsi or Upsilons and for the first time in heavy ion collisions even higher masses like Z0[TDR]. Muons are detected using a combination of 3 detectors: the Cathode Strip Chambers (CSC) in the forward pseudo-rapidity region (end caps), Drift Tubes (DT) in the central pseudo-rapidity region (barrel), and Reaction Plane Chambers (RPC), which alternate with the others.  In addition, a Si barrel pixel detector in the innermost region of CMS is used for track and vertex reconstruction. The response of this detector has been extensively simulated for p-p events and show to perform within its design parameters, only recently have simulations been done for Heavy Ion runs. After the first simulations with Heavy Ions collisions, it has become clear that there are some significantshortcomings in the Front End Electonics (FED), which could hamper severely the readout and therefore the experiment.  At LANL we have taken over the responsibility to quantify this bottleneck and have written a firstsimulation program, which emulates the readout of the FED's. Already with a fairly simple model, were we able to show that the FED in their present configuration might be leading to significant deadtime. We are now working on a simulation program, which will probe these readout modules in greater detail on the hardware level.

The past months have been devoted to making sure detectors will be efficient for the first heavy ion data taking and how they will behave with high luminosity in the future nominal run. Studies show that given the acceptance of the DT, being in the barrel region and outside of the magnet and calorimeters, most of the muons are either boosted towards the endcaps, or do

not have a big enough transverse momentum to reach DT. Indeed, the occupancy per sector is as low for p+p as heavy ions, only reaching at most 4% of occupancy in central events. The DT does not show any bottle neck with these simulations.

Significant progress has been made in developing the theory of jets in heavy ion reactions.

We demonstrated for the first time that jet shape and jet cross section measurements become feasible as a new, differential and accurate test of the underlying QCD theory. We presented a first step in understanding these shapes and cross sections in heavy ion reactions at the LHC. We demonstrated that the pattern of stimulated gluon emission can be correlated with a variable quenching of the jet rates to provide an approximately model-independent approach to determining the characteristics of the medium-induced bremsstrahlung spectrum. Surprisingly, in realistic simulations of parton propagation through the QGP we find a minimal increase in the mean jet radius even for large jet attenuation.

Following this work, both the STAR and PHENIX collaborations have presented jet suppression measurements at RHIC. We have capitalized on our leading expertise in jet physics to calculate for the first time the inclusive jet cross section in high-energy nucleus-nucleus collisions at next-to-leading order. Theoretical predictions for the medium-induced jet broadening and the suppression of the jet production rate due to cold and hot nuclear matter effects in Au+Au and Cu+Cu reactions at RHIC were presented.

One of the main theoretical goals of this project is to elucidate the differences between the universal parton fragmentation functions at finite temperature and the process-dependent cross section modification due to energy loss in the quark-gluon plasma. We calculated the charm and beauty fragmentation functions in the vacuum using their operator definitions in factorized perturbative QCD and find leading corrections that arise from the structure of the final-state hadrons. In the framework of potential models we demonstrated the existence of open heavy flavor bound states in the QGP in the vicinity of the critical temperature and provided first results for the in-medium modification of the heavy quark distribution and decay probabilities in a co-moving plasma. Dr. Rishi Sharma and Dr Benwei Zhang have taken the leadership role in this calculation.

Last but not least, among the most exciting new capabilities that heavy ion physics at the LHC will open is the ability to study $Z^0$ triggered jets. We are well on our way to providing the first systematic theoretical study of the production rate of the $Z^0$+jet cross section tagged jets in relativistic heavy ion collisions at LHC energies. We have developed a lowest order perturbative QCD code to studythis physics channel and are in the process of comparing our results to existing Tevatron data. Dr. Bryon Neufeld has taken a leadership role in this project.

## Future Work

The qualitatively new experimental approach proposed here is the measurement of jets tagged by Z0s at the Large Hadron Collider (LHC). We will also concurrently develop the supporting perturbative many-body Quantum Chromo-dynamics (QCD) theory. The muon pair resulting from the Z0 decay does not interact and escapes the collision undisturbed, while the opposite side jet probes the QGP through energy loss and scattering due to the strong nuclear force. The momentum of the muon pair is equal to the original jet momentum, thus allowing for a direct measurement of the initial and final jet energies and an unambiguous identification of the jet's energy loss in the QGP.

This breakthrough approach will allow for the first time the reconstruction of the full jet fragmentation function and its in-medium modification. (Fragmentation functions describe the probability of a quark or gluon to produce a given momentum final state hadron.) These new data will severely constrain the current theoretical models of jet energy loss and thus allow for a precise determination of the plasma properties

Experimental goals:

- Write a program in VHDLfor the Si Pixel Readout system, which will create pseudo data for the FEDs . Based on these results we will propose the necessary hardware solutionand develop a prototype.
- Measure fragmentation functions from the baseline (i.e. the p-p) data set.
- Determine the modifications of the fragmentation functions form the heavy ion data set.
- Engage in service work in CMS to get access to the data and negotiate conditions with CMS, LANL and DOE to join the collaboration.
- Extract plasma properties.
- Present and publish the results.

Theoretical goals:

1) A non-universal, and consequently non-factorizable, redistribution of the jet fragments due to collisional and radiative processes in the QGP initiated by many-body jet-medium interactions; 2) The possibility of a universal modification of fragmentation distributions in the presence of a thermalized medium.

The first approach naturally extends the current studies of

leading particle suppression (2), but requires detailed new insight into bremsstrahlung processes for much higher jet energies than presently available at RHIC.

## Conclusion

The project will lead to measurements of the properties of the quark-gluon plasma (QGP) such as its temperature and density, which are currently undetermined. The quark-gluon plasma was discover at the Relativistic Heavy Ion Collider (RHIC) in near the speed of light collisions of gold nuclei. The QGP properties can now be measured quantitatively at the Large Hadron Collider (LHC). In addition to the measurement there is a large discover potential for new physics which will revolutionize our understanding of universe. Supporting the physics goals ultra-high speed data processing will be developed, which has direct applications in ubiquitous sensing.

## Publications

Kunde, G. J., C. Mironov, and H. van Hecke. Z-tagged quark jets at the large hadron collider. 2009. *European Physics Journal C61 .* : 785.

Mironov, C., R. Vogt, and G. J. Kunde. Dilepton tagged qqbar + jet events at the LHC. 2009. *Eurpean Journal of Phyiscs J. C61.* : 893.

Sharma, R., I. Vitev, and B. W. Zhang. A light-front wave function approach to heavy quark fragmentation in the QGP. *arXiv:0904.0032 [hep-ph] .*

Vitev, I., S. Wicks, and B. W. Zhang. A theory of jet shapes and cross sections: from hadrons to nuclei. 209. *Journal of High Energy Physics 0811.* : 093.

# Breakthroughs in Magnetic Reconnection Enabled by Petaflop Scale Computing

*Lin Yin*
20090306ER

## Introduction

Magnetic reconnection is a basic process that occurs in high temperature plasmas in which magnetic field energy is rapidly converted into kinetic energy. This process is thought to play a central role in a variety of space, laboratory and astrophysical phenomena with a variety of real and potential applications. This research will lead to new advances in this field by employing Roadrunner, the world's fastest supercomputer, to perform unprecedented three-dimensional simulations of this process. The primary focus is to better understand the specific mechanisms that lead to the sudden onset of reconnection and the complex three-dimensional dynamics that control the structure and time-dependence of magnetic reconnection.

The research will involve a combination of basic theory and large-scale kinetic simulations that describe the high temperature plasma at the most fundamental level. The project will utilize the plasma simulation code VPIC, which has been carefully optimized to take full advantage of the unique hybrid computing architecture on the Roadrunner supercomputer. In order to intelligently setup and interpret these simulations, a basic theoretical approach will also be utilized for predicting the stability of these systems. Used in conjunction, these powerful new tools should lead to some definitive answers regarding the onset and nonlinear evolution of magnetic reconnection.

## Benefit to National Security Missions

This project will support the DOE mission in Nuclear Weapons by enhancing our understanding of high temperature plasmas and by pushing the limits of large-scale simulations using the new hybrid computing technology on the Roadrunner supercomputer.

## Progress

2D and 3D VPIC simulations have been performed on the heterogeneous multi-core supercomputer, Roadrunner. These simulations are leading to new scientific insight into the influence of plasma instability on the 3D evolution of reconnection layers, the primary science goal of this project. Our simulations employ open boundary conditions to model reconnection in large open systems for application to space and astrophysical plasmas. We have identified some new physics results, including two types of plasma instabilities within the electron region of the reconnection layer and the complex 3D interaction of flux ropes.

Simulations also show the formation of interacting flux ropes with guide field reconnection (Figure 1) for parameter regimes relevant to astrophysical systems and the magnetosphere. These results are consistent with predictions from linear theory, which is also part of our effort supported by this funding.

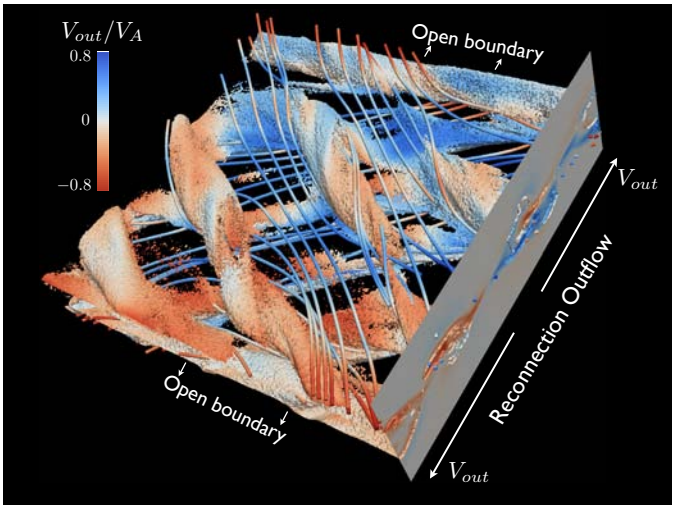

*Figure 1. Open boundary kinetic simulation of magnetic reconnection in a large-scale electron-positron plasma with a guide field equal to the reconnecting field. Shown are density isosurfaces colored by the reconnection outflow velcocity. Magnetic islands develop at resonant surfaces across the layer leading to complex interactions of flux ropes over a range of different angles and spatial scales.*

In addition, higher mass ratio simulations using open boundary conditions show strong lower hybrid drift instability at early time on the edge of the elongated electron diffusion layer (Figure 2), and then a kinking type instability within the elongated electron layer (Figure 3). These results are similar to our earlier work [1] for reconnection in pair plasmas.

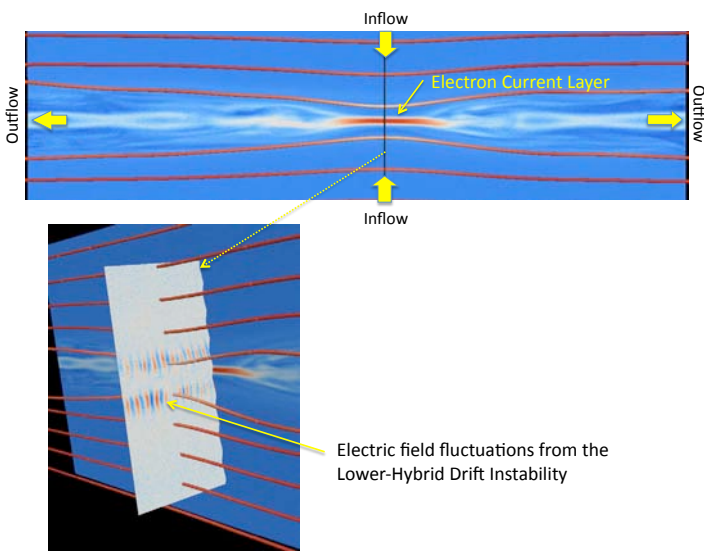


*Figure 2. Three-dimensional kinetic simulation of magnetic reconnection at high mass ratio (mi/me=200) showing the development of the lower-hybrid drift instability upstream of the electron current layer. The observed wavelength (ky*rho_e~0.6) is consistent with longstanding theoretical predictions. Since this instability remains localized on the edge of the layer, it probably does not directly influence the reconnection process.*

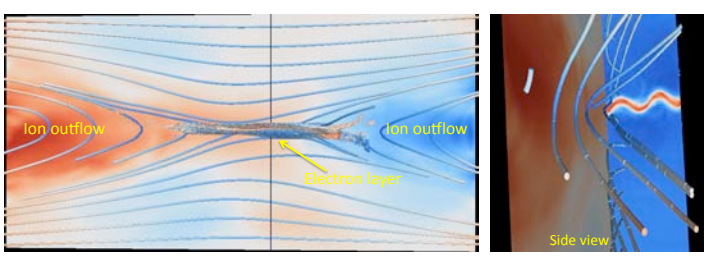


*Figure 3. Over longer time scales, the simulation in Figure 2 develops an instability within the electron layer that leads to a "kinking" or undulation of the current sheet. The wavelength and frequency of this unstable wave is roughly consistent with theoretical predictions [2]. Since this instability occurs in the central portion of the layer, it may potentially influence the reconnection process.*

In order to better understand the simulations of relativistic pair plasmas, we hired an undergraduate student (Peter Montag) to work with us on a theoretical description of the underlying plasma instabilities. This work involved extending previous theoretical treatments [2] for non-relativistic plasmas into the very high temperature regime where the plasma is fully relativistic. From these efforts, we were able to make detailed theoretical predictions regarding the growth rates and unstable wavelengths of both tearing and kink instabilities. These predictions have since been confirmed with VPIC simulations in the relativistic limit. In addition to providing a nice verification check, these theoretical calculations are expected to be useful in scoping out and guiding future simulation studies.

The pair plasma reconnection in the non-relativistic regime has been extended to highly relativistic regime for astrophysical applications. In the new regime, we found that the dynamics are very similar to those in the non-relativistic limit [1]. The diffusion becomes unstable to secondary kinking and formation of ``plasmoid-rope'' structures. The interplay among these secondary instabilities plays a key role in controlling the time dependent reconnection rate in large-scale systems. Work in this area has been carried out by postdoc Wei Liu. Wei has received invitation to give a invited talk on this work.

This project supports the effort of two postdocs, Vadim Roytershteyn of T-5 and Wei Liu of T-2. Vadim and Wei have been mentored to perform VPIC simulations and analyses for the work on this project.

## Future Work

By combining several innovative new approaches, this research effort will lead to dramatic advances in the understanding of collisionless magnetic reconnection – one of the most challenging and far-reaching problems in plasma physics. Although there are a large number of potential applications for these results, this project will focus on parameter regimes relevant to the Earth's geomagnetic tail and relativistic electron-positron plasmas for astrophysical settings. For these applications, this project will address the following two major questions:

**What is the basic structure and stability of a reconnection layer?**
There is presently a wide range of viewpoints in the published literature. Recent 2D kinetic simulations have demonstrated that both the structure and stability of a reconnection layer are vastly different than previous expectations based on simplified fluid theory. There are good reasons to believe that plasma instabilities in 3D will further modify this understanding. The availability of a petaflop scale computer will permit this project to perform first-principles 3D kinetic simulations and finally answer these long standing questions. The specific research tasks will involve performing the large-scale 3D simulations for a variety of initial conditions and geometries and analyzing the reconnection rate, structure and time-dependence of the results.

**How does reconnection get started?**
Using a combination of non-local linear Vlasov theory along with large-scale 3D kinetic simulations, this project will examine the influence of plasma instabilities on the onset of reconnection. The specific research task will include performing the linear Vlasov theory for range of different current sheet equilibria and then testing the results directly against the large-scale kinetic simulations.

## Conclusion
Scientists believe that magnetic reconnection plays a central role in a wide variety of applications such as geomagnetic substorms, solar flares and laboratory fusion machines. The ability to predict the complex nonlinear behavior of high temperature plasma is of great practical importance for these applications. For example, the results of this project may have direct application to modeling the plasma environment surrounding the Earth where communication satellites play a crucial role in modern society..

## References

1. Yin, L., W. Daughton, H. Karimabadi, B. J. Albright, Kevin J. Bowers, and J. Margulies. Three-dimensional dynamics of collisionless magnetic reconnection in large-scale pair plasmas. 1008. *Physical Review Letters.* **101**: 125001.

2. Daughton, W.. Electromagnetic properties of the lower-hybrid drift instability in a thin current sheet. 2003. *Physics of Plasmas.* **10**: 3103.


## Publications

Bowers, K. J., B. J. Albright, L. Yin, W. Daughton, V. Roytershteyn, B. Bergen, and T. J. T. Kwan. Advances in petascale kinetic plasma simulation with VPIC and Roadrunner. 2009. *Journal of Physics: Conference Series.* **180**: 012055.

Egedal, J., W. Daughton, J. F. Drake, N. Katz, and A. Lê. Formation of a localized acceleration potential during magnetic reconnection with a guide field. 2009. *Physics of Plasmas.* **16**: 050701.

Le, A., J. Egedal, W. Daughton, W. Fox, and N. Katz. Equations of State for Collisionless Guide-Field Reconnection. 2009. *Physics of Plasmas.* **102**: 085001.

Le, A., J. Egedal, and W. Daughton. Temperature Anisotropy and the Hall Magnetic Fields in Anti-parallel Reconnection. *Physical Review Letters.*

# Disentangling Quantum Entaglement

*Wojciech H. Zurek*
20090312ER

## Introduction

We will explore basic concepts of how information about a system can be extracted from its environment. This technique is known as either "environment as a witness" or "Quantum Darwinism". It is a natural extension of decoherence, which is one of the key themes of the project. It is motivated by very fundamental questions in quantum mechanics, and promises application to quantum detection as well as many body physics.

We shall use the newly established understanding of entanglement in quantum systems to study properties of many-body systems. In particular, we will develop codes that can simulate them efficiently. The efficiency of the simulation technique is based on the realization that entanglement - while still pervasive - has a limited reach for the states of interest in applications (i.e., ground states and low-lying excitations of many body systems relevant to, e.g., high-temperature superconductivity and other applications). This makes it possible to find (in the, e.g., 2^N dimensional state space of N spins) the basis of states that reduces the required memory from exponential to polynomial in the system size.

In addition to the above entanglement-based strategy, our plan is to also study and to take advantage of decoherence. Decoherence is present when the system is interacting with its environment: Even modestly sized quantum systems are next to impossible to isolate. This proposal will investigate decoherence, and whether it can help simulate open quantum systems. We expect a simplification because decoherence suppresses quantum entanglement responsible for the computational expense of representing a quantum state on a classical computer (e.g., which requires 2^N complex numbers for the state of N spins). This leads one to expect that states of the system plus environment have precisely the sort of structure that makes them amenable to efficient simulation.

## Benefit to National Security Missions

Our studies should allow us to investigate large class of many-body quantum systems of interest to advancing nanoscience, condensed matter physics, and materials science. This will impact variety of fields in which the fundamental role of quantum phenomena is now being recognized by numerous sponsors including DOE.

## Progress

For part of this project we studied how a system gets entanglement with its environment while undergoing a decoherence process [1,6]. The underlying idea is that if a system is sufficiently entangled with its environment, its state decoheres and thus it behaves classically and this limits the amount of classical resources necessary to describe the "quantumness" of the system. More specifically, we studied how this classicality arises under different initial conditions of the environment. We found that for a spin-1/2 system interacting with a qubit environment, that initially mixed environment states, e.g., states in thermal equilibrium, decohere the system just as well as initially pure environment states, but acquire less information about the system. For very mixed initial states, the amount of information acquired by a component of the environment is lowered by 1-h per qubit of the environment. Further, we proved that, under certain conditions and for all but the shortest times, this information is classical information. Only for short time dynamics does the environment carry significant quantum correlations with the system (i.e., is entangled in a complex manner). Thus, in addition to demonstrating an aspect of how our classical world arises from the ultimately quantum substrate, we have also demonstrated that there are different dynamical regimes of a quantum system interacting with an environment: one where quantum entanglement with the environment is important and one where the system, although entangled, behaves as a classical system and thus should require significantly less classical resources to simulate.

We have also studied dynamics of formation of the coherent condensate state in the presence of an incoherent environment made of uncorrelated thermal atoms [2,3]. We have found that the condensation process, induced by lowering of the temperature of the cold atom cloud, leads to production of topological defects

(solitons, i.e., some special density notches). These structures have been recently seen in an experiment done in the Engels' group at Washington State University. We have devised a general theory of non-equilibrium condensation utilizing universal properties of the system (critical exponents), as well as performed numerical simulations of the model reproducing qualitatively experimental outcomes.

We have also studied extensively decoherence of a central spin surrounded by a chain of spins undergoing a quantum phase transition: see [4] and Figure 1. A quantum phase transition is a process that leads to dramatic change of the properties of a quantum system. We have shown that non-equilibrium dynamics of the environment can completely destroy the coherence of the central spin. The rate of the decay of coherence involves both the critical exponents and the quench rate of the environment. We have also discovered several quasi-periodic features of decoherence that can be used for experimental determination of the central spin – environment coupling. Our findings are based on a remarkably accurate analytical expression derived in this project.

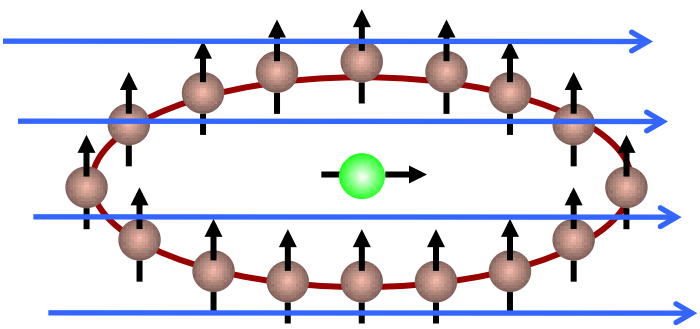

*Figure 1. Illustration of our model: a central spin-1/2 is surrounded by an Ising chain of spins placed in a magnetic field. The Ising chain serves as an environment and leads to decoherence of the central spin.*

Finally, we have studied quantum phase transition in space in the spin-1 Bose-Einstein condensate [5]. We have shown how the inhomogeneous magnetic field imposed on the cloud drives the system from magnetized to unmagnetized phase. We have fully characterized the crossover region between the two phases and discovered that an important property of the system (critical exponent characterizing divergence of the system reaction length to perturbations) can be deduced from the size of crossover region. This shall be of significant experimental interest.

## Future Work

The role of entanglement in determining complexity of quantum simulations was elucidated few years ago. The research focus was, so far, primarily on algorithms, rather than on "doing physics," which is our ultimate aim. The range of approaches that have been proposed to date is broad, although based on the same unifying recognition of the role of entanglement. The simplest ones are based on so-called Jordan-Wigner transformations. They allow one to reduce a specific (but interesting) class of spin models from exponential to O(N) computational complexity by a time-independent transformation. Broader class of models can be studied using Vidal's time-dependent approach of adjusting computational basis to suite the entangled state the specific Hamiltonian. These models have been by now generalized to more than 1-D "in principle" (but, to date, only rarely "in practice"). Finally, there are proposed approaches (Vidal's "MERA") that attempt to capitalize on the renormalization group-like approach to entanglement, and treat infinite systems.

The original motivation for studying many-body systems was condensed matter, but with recent advances of atomic physics it appears that the closest experimental connection will be in the trapped atom / optical lattice experiments. Our proposal is motivated by the need to "keep up" with them. In many of these systems (Bose-Einstein condensates) Hubbard model is a reasonable representation, and there is a long-standing suspicion that it may also play a role in (high-TC) superconductivity. Last not least, there are specific high-impact projects involving e.g. DNA, nanotech, etc. The idea of taking advantage of decoherence is central to our proposal. Dealing with decoherence involves, by now, a set of well understood procedures, some of which we have originated. We therefore expect to be successful in devising efficient codes and applying them to problems of interest.

## Conclusion

We will model open quantum systems, taking into account the role of the environment. Further, we will investigate the extent to which the suppression of entanglement in the system (due to decoherence by the environment) can be utilized to understand behavior of many body systems. These two achievements will allow us to both streamline the task of simulating open quantum systems and extend the boundaries of systems efficiently simulated on a classical computer. Overall, this proposal will enable the development of novel and robust computational tools and also an in-depth understanding of open quantum systems.

## References


1. Zwolak, M., H. T. Quan, and W. H. Zurek. Quantum Darwinism in a Mixed Environment. 2009. *Physical Review Letters.* **103**: 110402.

2. Zurek, W. H.. Causality in Condensates: Gray Solitons as Relics of BEC Formation. 2009. *Physical Review Letters.* **102**: 105702.

3. Damski, B., and W. H. Zurek. Soliton creation during a Bose-Einstein condensation. 2009. *arXiv:0909.0761*

*and LA-UR 09-05090, submitted to Physical Review Letters.*

4. Damski, B., H. T. Quan, and W. H. Zurek. Critical dynamics and decoherence. 2009. *LA-UR 09-06655, to be submitted to arXiv eprint server and Nature Physics.*

5. Damski, B., and W. H. Zurek. Quantum phase transition in space in a ferromagnetic spin-1 Bose-Einstein condensate. 2009. *New Journal of Physics.* **11**: 063014.

6. Zurek, W. H.. Quantum Darwinism. 2009. *Nature Physics.* **5**: 181.

## Publications

Damski, B., H. T. Quan, and W. H. Zurek. Critical dynamics and decoherence. 2009. *LA-UR 09-06655, to be submitted to arXiv eprint server and Nature Physics.*

Damski, B., and W. H. Zurek. Soliton creation during a Bose-Einstein condensation. 2009. *arXiv:0909.0761 and LA-UR 09-05090, submitted to Physical Review Letters.*

Damski, B., and W. H. Zurek. Quantum phase transition in space in a ferromagnetic spin-1 Bose-Einstein condensate. 2009. *New Journal of Physics.* **11**: 063014.

Wootters, W. K., and W. H. Zurek. The no-cloning theorem. 2009. *Physics Today.* : 76.

Zurek, W. H.. Causality in Condensates: Gray Solitons as Relics of BEC Formation. 2009. *Physical Review Letters.* **102**: 105702.

Zurek, W. H.. Quantum Darwinism. 2009. *Nature Physics.* **5**: 181.

Zwolak, M., H. T. Quan, and W. H. Zurek. Quantum Darwinism in a Mixed Environment. 2009. *Physical Review Letters.* **103**: 110402.

# Backward Stimulated Raman and Brillouin Scattering of Laser in the Collisional Regime

*Lin Yin*
20090394ER

## Introduction

The objective is to develop a validated predictive capability for laser-plasma interaction (LPI) that will enable more successful experimental designs in inertial confinement fusion (ICF) experiments that may, one day, impact our ability to derive energy from fusion. Furthermore, this work will impact our understanding for laser-driven ion acceleration, which has potential applications from fusion to medical accelerators. This project aims to develop the world's first truly first-principles model of LPI in laser-driven hohlraums. The proposed work uses the Roadrunner petaflop supercomputer and applies the state-of-the-art VPIC kinetic plasma simulation code, recently adapted to run efficiently on Roadrunner.

Success of this project will have several prospective payoffs: First, it directly supports the achievement of fusion ignition on the National Ignition Facility, which has manifold tie-ins into high-profile, exciting science, including carbon-neutral energy production, high energy density physics, laboratory astrophysics, and weapons science.

Moreover, by learning to control LPI, we can guide the search for new, high gain, high efficiency operating regimes for NIF ignition (including fast ignition) that simply cannot be attempted now because our understanding of the basic nonlinear physics of LPI is incomplete and parameter space is simply too large to sample experimentally in an economical way.

Finally, a high-risk/high-reward application of LPI is in novel plasma gain media (so-called Raman amplifiers) to generate extremely high power, short pulse lasers. If demonstrated experimentally, these new amplifiers could enable short pulse laser intensities and energy densities inaccessible today without going to very large, expensive facilities. Potential applications include fast ignition inertial confinement fusion, novel high fluence ion beams for nuclear physics studies, and hadrontherapy of tumors.

## Benefit to National Security Missions

This project supports the nuclear weapons mission in two ways:

1. Laser Plasma Interaction science underpins high energy density and boost physics experiments at the National Ignition Facility.
2. Improved verification and validation of the VPIC plasma code on Roadrunner supercomputer will improve modeling of processes in nuclear weapons.

## Progress

VPIC has been migrated to Roadrunner. Extensive testing and analysis was performed on Roadrunner during the stabilization phase. This work has led to advances in the stability and usability of the platform for a host of applications beyond LPI.

We have identified the key physics involving collisions and LPI:

Effects of binary particle collisions on the onset of backward stimulated Raman scattering of laser have been examined in the trapping regime using 1D and 2D VPIC simulations. The collision model implemented in VPIC allows us to study the effects of like-particle (i.e, electron-electron and ion-ion) and electron-ion collisions separately. Collisional effects on SRS are isolated from the effects of stimulated Brillouin scattering (SBS) by increasing the ion mass to suppress ion acoustic wave growth. We found that collisional de-trapping of electrons reduces nonlinear frequency shift (Figure 1). Under conditions relevant to short-pulse, single-speckle experiments at Trident, the SRS reflectivity measured as a function of the speckle intensity shows a sharp onset at a threshold intensity and a saturated level at higher intensity, consistent with the experimental

results. In the presence of both like-particle and electron-ion collisions, an increase in the SRS onset threshold intensity is observed, along with a reduction in the saturated reflectivity (Figure 2). Regimes of weak and strong collisionality are identified and collisional results are compared with those obtained in the collisionless limit.

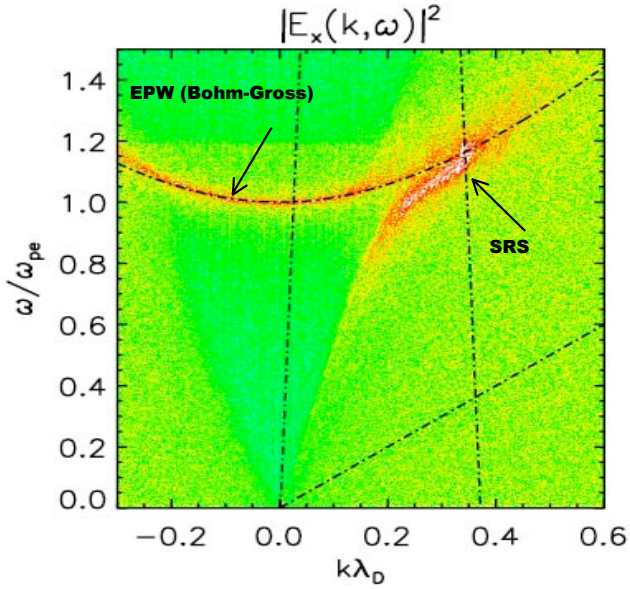


*Figure 1. Computer simulations including like-particle (electron-electron and ion-ion) collisions show that collisional electron de-trapping reduces nonlinear frequency shift.*

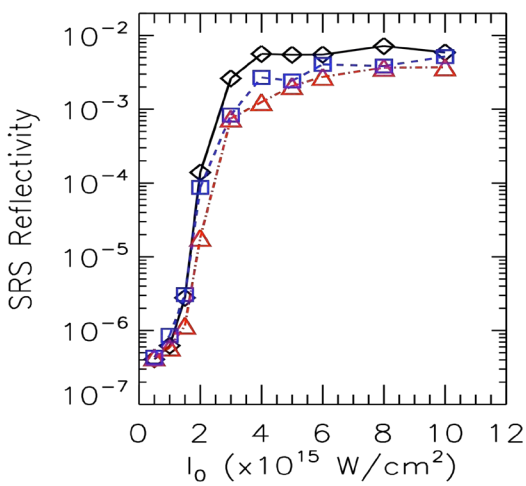


*Figure 2. Under conditions relevant to short-pulse, single-speckle experiments at Trident, the SRS reflectivity measured as a function of the speckle intensity shows a sharp onset at a threshold intensity and a saturated level at higher intensity, consistent with the experimental results. In the presence of both like-particle and electron-ion collisions, an increase in the SRS onset threshold intensity is observed, along with a reduction in the saturated reflectivity (collisional frequency increases from black to red curves).*

A suite of 2D VPIC simulations of SRS in Trident plasma has been performed on the heterogeneous multi-core supercomputer, Roadrunner. The physics governing nonlinear saturation of SRS in a laser speckle in the collisional regime is consistent with the hypothesis proposed: In addition to trapped electron nonlinear frequency shift (which has a negative value) that leads to wavefront bowing and self-focusing of electron plasma waves, we find for the first time that electron heating due to collisions gives rise to a positive frequency change (Figure 3), reduces the wavefront bowing, affects the SRS saturation, and quantitatively determines how much back-scatter can occur from a laser speckle. Moreover, collisional heating raises the electron-to-ion temperature ratio and determines crucially the onset of SBS instability.

We have hired postdoc Sean Finnegan, a U.S. citizen, into X-1-PTA; Sean has been mentored to work on this proposal. He has learned to use VPIC and to interface with P-24 experimental staff.

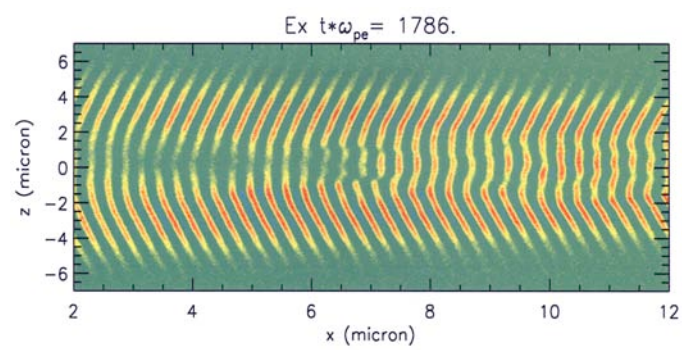


*Figure 3. Using 2D collisional VPIC simulations, we found for the first time that electron heating due to collisions gives rise to a positive frequency change, reduces the wavefront bending, affects the SRS saturation, and quantitatively determines how much back-scatter can occur from a laser speckle.*

## Future Work

VPIC is a state-of-the-art, fully relativistic, explicit, charge-conserving, electromagnetic, particle-in-cell kinetic plasma modeling code developed at LANL. VPIC has been converted to run on the hybrid Roadrunner architecture and served as one of the key codes during the Roadrunner Phase 3 acceptance. In FY10, we will continue to model laser-plasma interaction (LPI) in collisional and collisionless regimes to study nonlinear kinetics of stimulated Raman and stimulated Brillouin scattering. These calculations are important from a basic physics standpoint and are relevant to upcoming fusion ignition experiments on the National Ignition Facility.

LDRD funding support will be used for:

- further VPIC diagnostic development,
- 2D and 3D simulations and analysis on quadq on Redtail, Roadrunner, and Cerillos,
- studies of LPI in the collisional regime with large-scale 3D simulations on Roadrunner.

Part of the work in the next FY will involve Cell accelerating the collision model so that it is economical to run on Roadrunner platforms. We will carefully validate the accelerated Coulomb collision model and compare results with the unaccelerated model (which has been verified and validated as part of the initial work in this LDRD). Work will be documented in scientific journals and presentations at scientific meetings and workshops.

## Conclusion

We expect two key things to result from this study. The first is to illuminate the underlying nonlinear physics of laser-plasma instabilities (LPI), a problem of critical importance to the success of fusion ignition on the National Ignition Facility, paying special attention to the role of binary collisions in the physics. The second is to use this understanding to identify plasma parameter regimes, which are relatively safe from LPI, and to pose possible mitigation strategies to avoid their effects. This is an important basic science study directly related to mitigation of risk on a multi-billion dollar experiment.

## Publications

Bowers, K. J., B. J. Albright, B. Bergen, L. Yin, K. J. Barker, and D. J. Kerbyson. 0.374 Pflop/s Trillion-Particle Kinetic Modeling of Laser Plasma Interaction on Roadrunner. 2008. *Proceedings of the 2008 ACM/IEEE conference on Supercomputing, SC'08, Austin, Texas, IEEE Press, Piscataway, NJ, USA* . : 1.

Bowers, K. J., B. J. Albright, L. Yin, W. Daughton, V. Roytershteyn, B. Bergen, and T. Kwan. Advances in petascale kinetic plasma simulation with VPIC and Roadrunner. 2009. *Journal of Physics: Conference Series.* **180**: 012055.

Kline, J. L., D. S. Montgomery, C. Rousseaux, S. D. Baton, V. Tassin, R. A. Hardin, K. A. Flippo, R. P. Johnson, T. Shimada, L. Yin, B. J. Albright, H. A. Rose, and F. Amiranoff. Investigation of stimulated Raman scattering using short-pulse diffraction limited Laser beam near the instability threshold. 2009. *Lasers and Particle Beams.* **27**: 185.

Rose, H. A., L. Yin, and A. B. Langdon. Intensity dependent waiting time for strong electron trapping events in the onset regime of speckle stimulated Raman scatter. *Physics of Plasmas.*

# Transport in Magnetized Dense Plasmas for Magneto-Inertial Fusion

*Xianzhu Tang*
20090410ER

## Introduction

Controlled fusion is an attractive carbon-neutral energy source. Fusion has been achieved in the laboratory by imploding a fuel pellet (the so-called inertial confinement fusion or ICF) or magnetically confining a 100 million degree temperature plasma (the so-called magnetic confinement fusion or MCF). Both ICF and MCF require huge capitol investment for their development, the first to build powerful laser systems, and the second to build magnetics and sustain a large body of plasma. A hybrid approach, the so-called magneto-inertial fusion (MIF), combines the strength of ICF and MCF by imploding a magnetized plasma target with slow pushers, and offers a path towards fusion energy with orders of magnitude lower developmental cost.

This project develops the physics basis underlying the transport of particle, heat, and radiation in the MIF magnetized dense plasma target. A computational model of these transport phenomena is critical for the selection and optimization of MIF plasma target and predicting the behavior. Computational exploration of physics phenomena is an exceptionally cost effective approach to initial investigations of new systems and will provide guidance for the eventual fabrication of the experimental system and early experiments.

## Benefit to National Security Missions

This project will support the DOE mission in energy security by enhancing our understanding of the transport physics in magnetized dense plasma for magneto-inertial fusion energy development. In addition, transport phenomena are extremely important for nuclear weapons design, hence this project will also support the NNSA weapons mission.

## Progress

Progress has been made in two separate areas. The first one is to understand the 3D magnetic field in a laboratory-formed compact toroid target such as the spheromak and the spherical tokamak with a plasma center column. Normally the compact toroid targets are idealized to be axisymmetric, but 3D magnetic field component can become unavoidable in laboratory formation experiments using driven-relaxation, for example, due to the plasma amplification of intrinsic error field. Specifically, we come up with a general theory on how 3D equilibrium is determined for relaxed compact toroid plasma, and formulate a mathematical formalism to computing such 3D equilibrium states. The physics of how driven-relaxed plasma amplifies the 3D error fields produced by the external coils are now understood. A manuscript was submitted to Journal of Computational Physics on computing the 3D relaxed eigenmodes, necessary for the physics understanding and quantitative evaluation. A new equilibrium solver is being numerically implemented, which will provide the basis for computational studies on how error field determines the intrinsic helical field in an experimentally accessible compact toroid equilibrium.

The second area is to understand the physics of the magnetized plasma sheath through which the plasma interacts with the wall. This turned out to be an area of great immediate interest, so we have devoted considerable amount of resource to this problem. It is critical to the overall transport physics of magneto-inertial fusion (MIF), because of the potentially large enhancement of radiation loss by the impurities generated by wall materials sputtering. The sheath physics for MIF is rather unique that the mega-gauss magnetic field is mostly parallel to the wall. Contrary to the conventional sheath theory where electrons negatively charge the wall, MIF plasma positively charges the wall due the larger ion gyro-orbit. We have performed a systematic simulation studies of MIF sheath using the state of the art VPIC code. The following issues have been addressed in the simplified 1D collisionless plasma case with a number of interesting discoveries: (1) sheath width and the sheath potential scale with

plasma parameters; (2) force-balance in MIF sheath where pressure anisotrpy plays a prominent role; (3) details on distribution functions and the plasma oscillations. These results have been presented at the Sherwood fusion theory conference in April, 2009, and more recently as an invited talk at the American Physics Society Division of Plasma Physics annual meeting. Two manuscripts are being prepared for publication in peer-reviewed journals. The first is an invited paper in Physics of Plasmas on parallel-to-the-wall magnetic sheath, the second is a Physical Review Letters manuscript on high temperature low density plasma sheath. These 1D in space (3D in velocity) simulation studies pave the path for 2D and 3D simulations of sheath turbulence in future years.

## Future Work

This project addresses critical scientific issues underlying the performance and potential of magneto-inertial fusion (MIF), an innovative approach to fusion energy that combines attractive features of both magnetic and inertial confinement fusion. There have been many proposed ideas to achieve MIF, but a leading approach is to use an imploding metal or plasma "liner" to compress a magnetized "target" plasma to thermonuclear temperatures. If this is successful, MIF will permit fusion energy development without billion-dollar facilities, thus circumventing one of the most serious obstacles for conventional fusion development. MIF is a key area of investment for the new joint NNSA/SC program in High Energy Density Laboratory Plasmas (HEDLP). Two critical open scientific issues underlying our ability to assess, design, and optimize MIF systems are (1) the physics of transport in HED plasmas with ultra-high magnetic fields and (2) the identification of the most promising high density pre-compression target plasma. For issue (1), we propose to use state-of-the art computational tools to understand the roles of magnetic geometry, topology, and plasma microturbulence on thermal and radiation transport in the previously unexplored regime of magnetized HEDLP. The magnetic sheath transport will be resolved to understand the impact of impurity generation and transport, and to assess the enhanced radiation losses. For issue (2), we will take advantage of recent theoretical innovations in compact toroid plasmas developed at LANL to assess the relative merits of three MIF target plasma options: the field reversed configuration (FRC), the high performance spheromak, and the spherical tokamak with a plasma center column. Insights into these issues are needed to determine both the feasibility of MIF (i.e., can ignition temperatures ~10 keV be reached?) and the efficiency and maximum energy gain (i.e., how much driver power and energy are needed?).

## Conclusion

We expect both a qualitative and quantitative assessment of particle, heat, and radiation transport in magnetized dense plasma targets such as a spherical tokamak with a plasma center column, a spheromak, and a field reversed configuration. The transport rate would determine whether the magneto-inertial fusion concept can reach fusion ignition temperature and would guide target selection and optimization. If successful, it contributes to the ultimate goal of achieving controlled fusion energy and help safeguard our nation's energy security.

## References


1. Tang, X. Z.. Numerical computation of helical Chandrasehkhar-Kendall modes. *Journal of Computational Physics.*

2. Krasheninnenikova, N., and X. Z. Tang. Scaling of plasma sheath in parallel to the wall magnetic field. *Physics of Plasmas.*


## Publications


Krasheninneikova, N., and X. Z. Tang. Scaling of a plasma sheath in parallel to the wall magnetic field. *Physics of Plasmas.*

Tang, X. Z.. Numerical Computation of helical Chandrasekhar-Kendall modes. *Journal of Computational Physics.*

# Novel Cone Targets for Efficient Energetic Ion Acceleration for Light Ion-Driven Fast Ignition Fusion

*Kirk A. Flippo*
20090466ER

## Introduction

Intense particle beams are an important part of a host of applications, including fast ignition inertial confinement fusion, high energy density physics, warm dense matter, novel nuclear physics studies, and medical therapies. However, understanding the mechanisms behind these intense particle beams is in its infancy, yet this understanding is crucial for designing and optimizing systems.

The goal of this project is to understand the basic physics of ion beams produced from some unique flat-top cone targets and to improve their performance. These cone-targets enhance the conversion efficiency and ion energies, which could lead to the realization of Ion Fast Ignition (IFI) fusion energy using light ions [1], a concept recently championed by LANL [2]. The project aims at understanding, specifically, the hot electron behavior in the targets, which affect how these ion beams behave. Understanding and controlling these beams would not only make IFI fusion and energy independence closer to reality, but would also affect any potential application that would benefit from such beams. These include ion (hadron) cancer therapy [3], medical isotope production [4], radioactive waste transmutation, proton radiography [5], active interrogation, probing warm dense matter and laboratory astrophysics [6].

## Benefit to National Security Missions

This project will enhance our understanding of laser-based ion acceleration relevant for ion Fast Ignition Fusion by enabling compact directed energetic particle and x-ray sources. Laser-based accelerator technology can also impact nuclear wastes transmutation, active interrogation of special nuclear material, proton radiography and stockpile stewardship via warm dense matter studies - missions of interest to DOE, DHS, and other government agencies. This work also underpins the goal of producing compact ions sources for medical isotope production and cancer therapies of interest to the DHHS/NIH.

## Progress

As of October 2009 this project has currently completed its first full 3 week experimental run using the Trident laser with a new batch of copper micro-cone targets from the company Nanolabz. During this run we produced the world's record in proton energies from laser-accelerated ions. The cone targets have yielded protons with a maximum energy of 67.5 MeV (37% the speed of light), which is a nearly 20% energy increase. This project has not only succeeded in producing the highest energy protons observed to date, but also in reducing the amount of laser energy needed by a factor of 5 (from 400 J to 80J). Also the amount of proton energy per joule of laser energy was increased 6.5 times! Previously [7] we found that flat-top cones with a top-to-neck ratio of 4, produced ion beams with twice the energy and 5 times the efficiency of a flat foil target. This experiment was performed at 20 J of laser energy in 900 fs at Trident's intrinsic laser contrast (the ratio of amplified spontaneous emission to the main compressed laser pulse) of $10^{-8}$. In more recent experiments we also found that at 80 J at the intrinsic contrast the cones did not perform as well as expected due to pre-plasma filling in the cone from inadequate contrast [8]. Thus we use the new Enhanced Trident, capable of 80 J pulses at 500 fs with an ultra clean pulse, $>10^{-10}$ contrast, which is a unique capability in the world of high-power, high-intensity laser systems. This new laser regime is being probed and the cones have been imaged using copper K-alpha x-rays to understand the laser interaction and transport of hot-electrons in the cones. This has lead to a new understanding of this interaction, as the cones performing the best, have shown asymmetric interactions. This is understood as the laser grazing one of the cone side-walls. An electron spectrometer was used to measure the escaped hot electrons. Simulations show that this grazing interaction leads to greater hot electron generation in the target, as

well as a shift in the electron spectrum. These two effects, coupled with efficient electron transport to the cone flat-top leads to an increase in sheath density and thus proton energies. These results have been part of press releases in Germany (with our collaborators), from LANL, and from the American Physical Society as part of the 51st Division of Plasma Physics. The latter took place in Atlanta, GA in November of 2009, where these results were reported. The data and matching simulations are currently being prepared for a Nature Physics article and other supporting journal articles.

Figure 1 shows the recent experimental results of the copper K-alpha x-ray imager with the asymmetric interaction. However, the beams from these cone targets are round and follow a Maxwellian profile. Figure 2 shows a frame from a simulation movie at 1060 fs after the laser hits the cone target from the left hand side. Clearly seen is the accelerating hot electron sheath (in white) as a bulge on the rear of the flat-top cone, a white arrow is pointing to the sheath. The full movie can be seen at . Other simulations show that when the laser hits the side wall just a bit, the electron temperature increases. This explains the increase in proton energy gained in the hotter sheath.

The project currently is mentoring and training two postdocs, and four graduate students. One University of Missouri graduate student is paid directly from the LDRD, and three are paid from collaborating institutions (one student from the University of Nevada, Reno and two sponsored by the Forschungszentrum Dresden-Rossendorf in Germany). In addition one postdoc is paid from LANL and one postdoc from Sandia National Lab. These students and postdocs are getting hands on experimental training and are helping with the data analysis. They will receive co-authorship (or first authorship in two cases) of premier journal articles (Nature Physics and Physical Rev. Letters) in addition to others.

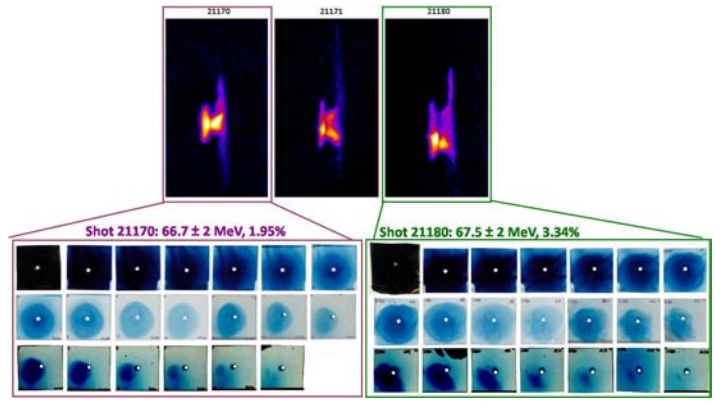


*Figure 1. The copper K-alpha x-ray self-emission from three "best performer" flat-top cone targets. Laser enters cone from the left. Each cone emission image is asymmetric if mirrored in the horizontal plane. The resulting proton beam in shown from radiochromic film stack images. The last row of each is contrast enhanced to show the end of the beam more clearly.*

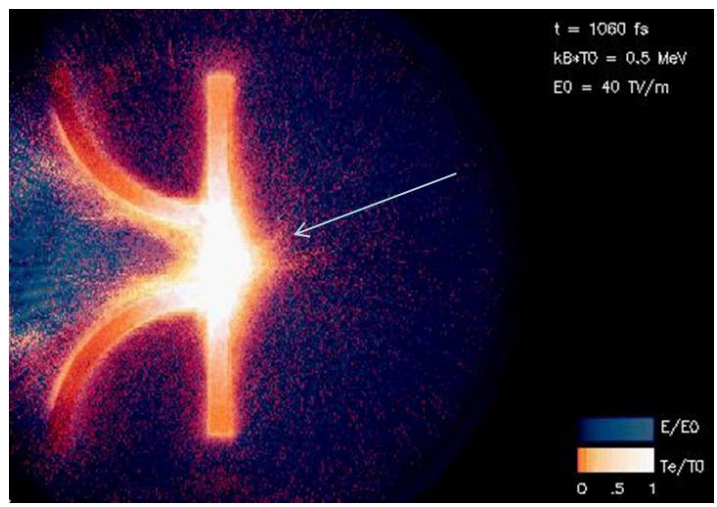


*Figure 2. A snap shot of the target at 1060 femtoseconds after the laser hits the target. Taken from a movie of the Particle in Cell (PIC) simulation. The red to white scale is normalized electron temperature. The hottest electrons are forming the accelerating sheath The blue color scale shows the laser and electron generated electric field.*

## Future Work

Work will continue on the flat-top cones using structured surfaces and alloy materials for greater x-ray self-emission diagnostics. We will study the laser-to-ion energy conversion efficiency of these Target Normal Sheath Accelerated (TNSA) protons and test some new target geometries to take advantage of the new results and simulations. With improved efficiency the door to Fast Ignition (FI) fusion using light or medium Z ions should be opened much wider. The project's continuing aim is at understanding, the hot electron transport using K-alpha x-ray imaging, which affects the characteristics of these ion beams.

We intend to:

- Use K-alpha x-ray crystal imaging and spectroscopy of alloy cones (Mo, Ni, Cu) to determine the hot electron generation localization and transport. Then we can correlate the ion beam acceleration with the electrons. We will also study new geometries to test the grazing incidence results and simulations.
- Modify the batch of cones with structured targets to make them more sinusoidal for better proton beam imprinting. This will allow us to determination the source size and emittance measurement of the beam.
- Compare these targets with others known as reduced mass targets (RMTs) which are about 100-300 microns in diameter. RMTs show hotter electron temperatures, but not good beam quality. We propose to find the reason for this difference.
- Understand through simulations the unique monoenergetic proton beam features observed in several beams so far.
- Continue the development with our partners (Nanolabz) of Pd or Pt FTCs which, when heated, should lead to a catalytic reaction producing nano-layers of carbon. This will allow us to accelerate mono-energetic carbon beams. Alternatively, targets with deposited layers of carbon on them will be made for the same purpose.
- Measure the energy and efficiency of any mono-energetic carbon beams produced.
- Further model the cones using 2D and 3D PIC simulations using PICLs from UNR and VPIC on the LANL Roadrunner supercomputer. This will help us understand the physics of the cone laser interaction and hot electron generation along with possible methods for better control.

## Conclusion

The project has yielded the world's record in proton energies for lasers, and has yielded ion beams with efficiencies on the order of 3%. We have also observed mono-energentic ion structures from the cone targets, and are working toward improving these characteristics to open many new application in compact forms, including hadron cancer therapy, isotope production, radioactive waste transmutation, proton radiography, active interrogation, fast ignition, probing warm dense matter, and laboratory astrophysics. These applications will benefit the US public in a multitude of ways becoming a new base of technological development and economic growth.

## References


1. Roth, M., T. E. Cowan, M. H. Key, S. P. Hatchett, C. Brown, W. Fountain, J. Johnson, D. M. Pennington, R. A. Snavely, S. C. Wilks, K. Yasuike, H. Ruhl, F. Pegoraro, S. V. Bulanov, E. M. Campbell, M. D. Perry, and H. Powell. Fast ignition by intense laser-accelerated proton beams. 2001. *Physical Review Letters.* **86** (3): 436.

2. Fernandez, J. C., J. J. Honrubia, B. J. Albright, K. A. Flippo, D. C. Gautier, B. M. Hegelich, M. J. Schmitt, M. Temporal, and Y. Lin. Progress and prospects of ion-driven fast ignition. 2009. *Nuclear Fusion.* **49** (6): 065004.

3. Fourkal, E., J. S. Li, M. Ding, T. Tajima, and C. M. Ma. Particle selection for laser-accelerated proton therapy feasibility study. 2003. *Medical Physics.* **30** (7): 1660.

4. Nemoto, K., A. Maksimchuk, S. Banerjee, K. Flippo, G. Mourou, D. Umstadter, and V. Y. Bychenkov. Laser-triggered ion acceleration and table top isotope production. 2001. *Applied Physics Letters.* **78** (5): 595.

5. Cobble, J. A., R. P. Johnson, T. E. Cowan, N. R. Galloudec, and M. Allen. High Resolution Laser-Driven Proton Radiography. 2002. **92** (4): 1775.

6. Kar, S., M. Borghesi, S. V. Bulanov, M. H. Key, T. V. Liseykina, A. Macchi, A. J. Mackinnon, P. K. Patel, L. Romagnani, A. Schiavi, and O. Willi. Plasma jets driven by ultraintense-laser interaction with thin foils. 2008. *Physical Review Letters.* **100** (22).

7. Flippo, K. A., E. d psila Humieres, S. A. Gaillard, J. Rassuchine, D. C. Gautier, M. Schollmeier, F. Nurnberg, J. L. Kline, J. Adams, B. Albright, M. Bakeman, K. Harres, R. P. Johnson, G. Korgan, S. Letzring, S. Malekos, N. Renard-LeGalloudec, Y. Sentoku, T. Shimada, M. Roth, T. E. Cowan, J. C. Fernandez, and B. M. Hegelich. Increased efficiency of short-pulse laser-generated proton beams from novel flat-top cone targets. 2008. *Physics of Plasmas.* **15** (5): 056709.

8. Gaillard, S. A., K. A. Flippo, M. Lowenstern, E. Mucino, J. Rassuchine, D. C. Gauthier, J. Workman, and T. E. Cowan. Proton Acceleration From High-Intensity Short-pulse Laser Interactions iwth Various Cu Micro-cone Targets at Relatively Low-Contrast (10^8). *J. of Phys.: Conf. Series.*


## Publications

Flippo, K. A., E. d psila Humieres, S. A. Gaillard, J. Rassuchine, D. C. Gautier, M. Schollmeier, F. Nurnberg, J.

L. Kline, J. Adams, B. Albright, M. Bakeman, K. Harres, R. P. Johnson, G. Korgan, S. Letzring, S. Malekos, N. Renard-LeGalloudec, Y. Sentoku, T. Shimada, M. Roth, T. E. Cowan, J. C. Fernandez, and B. M. Hegelich. Increased efficiency of short-pulse laser-generated proton beams from novel flat-top cone targets. 2008. *Physics of Plasmas.* **15**: 056709.

Gaillard, S. A., K. A. Flippo, M. Lowenstern, E. Mucino, J. Rassuchine, D. C. Gauthier, J. Workman, and T. E. Cowan. Proton Acceleration From High-Intensity Short-pulse Laser Interactions iwth Various Cu Micro-cone Targets at Relatively Low-Contrast (10^8). *J. of Phys.: Conf. Series.*

Kluge, T., M. Bussmann, S. A. Gaillard, K. Flippo, D. C. Gautier, B. Gall, B. Lockard, Y. Sentoku, K. Zeil, S. Kraft, U. Schramm, T. E. Cowan, and R. Sauerbrey. Wakefield Accelerated Electron Beams from Ultra-Thin Solid Foils. *AIP Conference Proceedings.*

# General Relativity as a Probe of Cosmology

*Daniel Holz*
20090518ER

## Introduction

We are in the midst of a revolution in astrophysics and cosmology. There has been an explosion of observational data, leading to a radical transformation in our understanding of our universe on the largest scales. The field of general relativity, with the advent of gravitational wave observatories, is also poised for major advances in the coming years. While the first direct detection of gravitational waves will be much celebrated, it is the ensuing astrophysical and cosmological observations that will have the greater scientific impact. Research in general relativity, and astrophysics and cosmology, is phenomenally vibrant and dynamic. The interplay of these fields offers particular promise, and it is here that we are focusing our work.

This proposal centers on gravitational waves and gravitational lensing: two uniquely powerful cosmological probes furnished by general relativity. The next generation of observational surveys can be expected to revolutionize the study of statistical lensing, and gravitational lensing is expected to become one of the most powerful probes of dark energy. In addition, as "first sound" for LIGO (and, hopefully, LISA) arrives, the birth of the age of gravitational-waves is imminent. We propose two complementary research directions, both of which can be expected to lead to elucidation of the nature of dark energy and dark matter.

## Benefit to National Security Missions

This project will support the DOE mission by directly addressing dark matter and dark energy, which form the heart of the unknowns in cosmology, and thus play a major role in research at the DOE Office of Science.

## Progress

Although this project has only been funded for a few months, there has already been tremendous progress. Along with collaborators, I recently submitted a paper titled "Exploring short gamma-ray bursts as gravitational-wave standard sirens" to the Astrophysical Journal [1]. This paper explores short/hard gamma-ray bursts as standard sirens, and develops the infrastructure necessary to calculate their cosmological reach (e.g., how well the might determine the Hubble constant). Recent observations support the hypothesis that a large fraction of "short-hard" gamma-ray bursts (SHBs) are associated with compact binary inspiral. Since gravitational-wave (GW) measurements of well-localized inspiraling binaries can measure absolute source distances, simultaneous observation of a binary's GWs and SHB would allow us to independently determine both its luminosity distance and redshift. Such a "standard siren" (the GW analog of a standard candle) would provide an excellent probe of the relatively nearby universe's expansion, complementing other standard candles. In this paper, we examine binary measurement using a Markov Chain Monte Carlo technique to build the probability distributions describing measured parameters. We assume that each SHB observation gives both sky position and the time of coalescence, and we take both binary neutron stars and black hole-neutron star coalescences as plausible SHB progenitors. We examine how well parameters (particularly luminosity distance) can be measured from GW observations of these sources by a range of ground-based detector networks. We find that earlier estimates overstate how well distances can be measured, even at fairly large signal-to-noise ratio. The fundamental limitation to determining distance to these sources is the gravitational waveform's degeneracy between luminosity distance and source inclination. Despite this, we find that excellent results can be achieved by measuring a large number of coalescing binaries, especially if the worldwide network consists of many widely separated detectors. Advanced GW detectors will be able to determine the absolute luminosity distance to an accuracy of 10-30% for NS-NS (out to 600 Mpc) and NS-BH binaries (out to 1400 Mpc).

I have also just completed a paper on utilizing the Big Bang Observer as an ultra-precision probe of cosmology [2]. This paper shows that gravitational-wave observations offer the possibility of the most precise probe of cosmology ever envisioned, comparable to all proposed future dark energy missions **combined**. This paper may dramatically change the focus and direction of a proposed, multi-billion dollar NASA mission. Figure 1 shows the precision with which the luminosity distance–redshift curve can be measured using binary neutron star standard sirens detected by BBO.

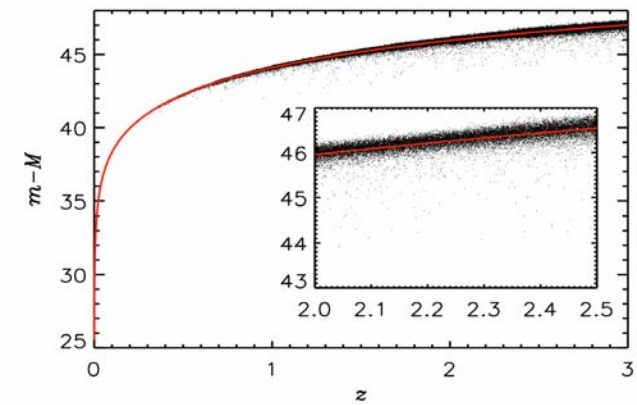


*Figure 1. Precision measurement of cosmology using binary neutron-star standard sirens detected by the Big Bang Observer. The luminosity distance-redshift is plotted. Distance is shown as distance modulus, and includes both BBO errors and gravitational lensing. The red curve is the true luminosity distance--redshift relation. Notice that lensing causes a small number of binaries to become tremendously magnified (to lower distance modulus), but there is a lower limit to the amount of de-magnification.*

In addition, I was also a senior author on a white paper for the 2010 Astrophysics Decadal Review, focusing on coordinated observations of the gravitational wave and electromagnetic skies (arXiv:0902.15270), titled "Astro2010 Decadal Survey Whitepaper: Coordinated Science in the Gravitational and Electromagnetic Skies". It is widely expected that the coming decade will witness the first direct detection of gravitational waves (GWs). The ground-based LIGO and Virgo GW observatories are being upgraded to advanced sensitivity, and are expected to observe a significant binary merger rate. The launch of The Laser Interferometer Space Antenna (LISA) would extend the GW window to low frequencies, opening new vistas on dynamical processes involving massive (M >~ 10^5 M_Sun) black holes. GW events are likely to be accompanied by electromagnetic (EM) counterparts and, since information carried electromagnetically is complementary to that carried gravitationally, a great deal can be learned about an event and its environment if it becomes possible to measure both forms of radiation in concert. Measurements of this kind will mark the dawn of trans-spectral astrophysics, bridging two distinct spectral bands of information. The aim of this white paper is to articulate future directions in both theory and observation that are likely to impact broad astrophysical inquiries of general interest. What will EM observations reflect on the nature and diversity of GW sources? Can GW sources be exploited as complementary probes of cosmology? What cross-facility coordination will expand the science returns of gravitational and electromagnetic observations?

Thus in a few short months I have already made major contributions to the science of gravitational-wave standard sirens.

## Future Work

This proposal centers on gravitational waves and gravitational lensing: two uniquely powerful cosmological probes furnished by general relativity. The next generation of observational surveys can be expected to revolutionize the study of statistical lensing, and gravitational lensing is expected to become one of the most powerful probes of dark energy. In addition, as "first sound" for LIGO (and, hopefully, LISA) arrives, the birth of the age of gravitational-waves is imminent. We propose two complementary research directions, both of which can be expected to lead to elucidation of the nature of dark energy and dark matter.

We have been actively developing a completely independent standard candle: the gravitational-wave driven inspiral of binary compact objects. These standard sirens are the gravitational-wave analogs of standard candles. The radiation emitted during the inspiral phase is well described using the post-Newtonian expansion of general relativity for the compact-object binary. Because these binary systems are relatively simple and well modeled, the gravitational waves they generate determine the source's luminosity distance with high accuracy. The goal of this proposal is to explore how well LIGO will be able to constrain cosmology, utilizing short/hard gamma-ray burst events as standard candles. We are analyzing the precision with which the Hubble Constant can be determined, and then will utilize this to constrain the dark energy equation-of-state. We will also further explore gravitational lensing at high-redshift, in an attempt to characterize and understand the effects of lensing on supermassive binary black holes sources of gravitational waves. This can have ramifications for cosmological constraints from LISA, a proposed space-borne gravitational-wave observatory.

## Conclusion

The main results of this project will be tools which will further our understanding of dark matter and dark energy. We will thus make progress in understanding some of the most profound questions: how old is the Universe? what is the Universe made out of? what is the ultimate fate of the Universe?

## References


1. Nissanke, S., S. Hughes, D. Holz, N. Dalal, and J. Sievers. Exploring short gamma-ray bursts as gravitational-wave standard sirens. To appear in *Astrophysical Journal.*

2. Cutler, C., and D. Holz. Ultra-high precision cosmology from gravitational waves. To appear in *Physical Review D.*


## Publications


Bloom, J., D. Holz, S. Hughes, and K. Menou. Coordinated Science in the Gravitational and Electromagnetic Skies. 2009. *Astro2010: The Astronomy and Astrophysics Decadal Survey, Science White Papers, no. 20.*

Cutler, C., and D. Holz. Ultra-high precision cosmology from gravitational waves. To appear in *Physical Review D.*

Nissanke, S., S. Hughes, D. Holz, N. Dalal, and J. Sievers. Exploring short gamma-ray bursts as gravitational-wave standard sirens. To appear in *Astrophysical Journal.*

# Experimental Study of Driven Magnetic Relaxation in a Laboratory Plasma

*Scott C. Hsu*
20061435ER

## Abstract
This work was aimed at exploring innovative formation methods for a magnetic fusion plasma configuration called the spheromak. The project was motivated by recent theoretical developments which led to new ideas about how to maximize the formation efficiency of the spheromak (i.e., the ratio of input energy to magnetic field strength of the spheromak). The project was successful in converting an existing LANL experimental facility into the required setup to carry out this work, including the addition of a new plasma gun source. The converted facility, called the Driven Relaxation Experiment (DRX), is now fully operational. However, due to many unforeseen (non-technical) delays beyond our control, the first experimental data-set was obtained only late in the final year of funding, and data analysis is now continuing (unfunded). The DRX facility is suitable for important follow-on spheromak research with the DOE Office of Fusion Energy Sciences as a potential sponsor. The facility may also be useful for other areas of interest for LANL and the proposed signature facility MaRIE.

## Background and Research Objectives
Fusion energy is a scientific holy grail. However, the development cost still needed for a demonstration fusion reactor, based on the leading tokamak [1] concept, is in the many tens of billions of dollars, making this a several-decades undertaking given the present political and economic climate. There are less-developed, more risky alternatives to the tokamak that might alleviate many of the tokamak's technical complexities, allowing for less expensive fusion reactors. Thus, many fusion scientists believe that a small investment in these alternatives is justified for the potential they offer. One alternative is the spheromak [2], also a toroidal plasma configuration but without the expensive and complicated magnets required by the tokamak. As noted in the recent Office of Fusion Energy Sciences (FES) Research Needs Workshop (ReNeW) final report [3], more efficient spheromak formation is one of the two most urgent research needs for development of the spheromak fusion concept. The formation problem is the primary motivation for this LDRD project.

A goal for efficient spheromak formation is to maximize the magnetic field strength for a given input energy and applied magnetic field from the plasma gun source. Spheromak plasma equilibria under sustained energy input from the plasma gun are approximated by the same mathematical equations as a nonlinear oscillator. Recent theoretical research has predicted [4] that these sustained equilibria have resonances, i.e., the total magnetic field energy in the spheromak peaks for certain values of the electrical current divided by the applied magnetic field from the plasma gun, a value known as $\lambda$ in spheromak research. However, these resonances are predicted to occur only for certain spatial current distributions within the spheromak [5]. The DRX experiment was designed to determine whether these resonances exist by varying $\lambda$ and then directly measuring the magnetic field configuration in the spheromak, and comparing the experimental data with theoretical predictions.

## Scientific Approach and Accomplishments
Our approach required converting an existing laboratory plasma facility (with existing vacuum chamber and pumps and other infrastructure) at LANL into one in which spheromaks with the desired currents, applied magnetic fields, and geometry could be formed and studied. The two main requirements were the additions of a new plasma gun source for forming the spheromak and a diagnostic for measuring the internal magnetic field of the spheromak once it was formed.

***Plasma gun source***: This consists of a (i) coaxial electrode set, (ii) an external magnetic field coil set for applying an initial magnetic field, and (iii) custom gas valves for injecting the working gas which is then ionized by the gun into a plasma, and finally power supplies for all three sub-systems. Theoretical calculations informed us of the required range of electrical current (~150 kA), its duration (~500 μs), and the applied magnetic flux (a few mWb). The main power supply for the gun was a capacitor bank with 3 stages (1 formation and 2 sustain banks) with a total of 8.5 mF capacitance and 10 kV peak voltage for the formation and 5 kV peak voltage for the sustain banks. The external magnetic field coils required

a 48 mF capacitor bank capable of delivering several hundred A of current to generate the required magnetic field patter. Finally, the 3 custom gas valves needed to inject ~$10^{20}$ $H_2$ molecules in a few tens of μs, and this required a ~1 kV, ~100 A capacitor bank for each valve to drive current in a solenoid that would displace a small metal disk to allow a quick burst of gas to flow into the vacuum chamber. Figure 1 shows a photograph of the outside of the plasma source mounted on the vacuum chamber.

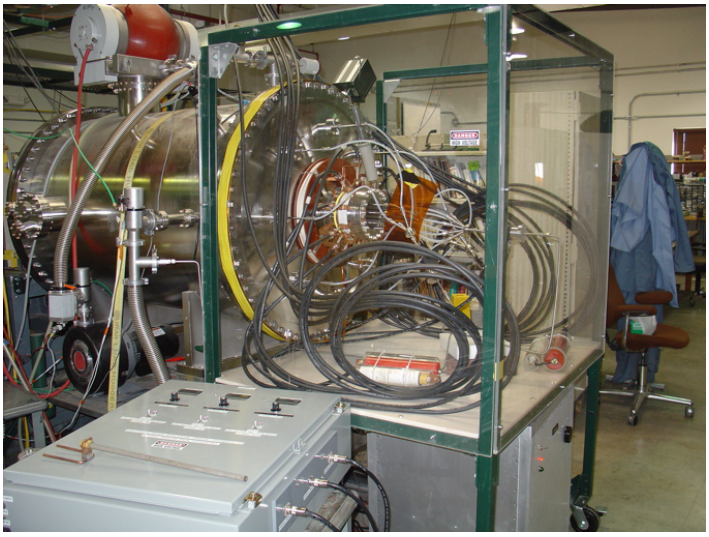

*Figure 1. Photograph of the Driven Relaxation Experiment, and in particular the exterior of the installed coaxial plasma gun source with external magnet and transmission lines for delivering current from a pulsed capacitor bank (not shown).*

**Magnetic probe diagnostic**

This is a custom two-dimensional array of small magnetic pickup coils to measure all 3 vector components of the time-varying magnetic field at 16 spatial positions, for a total of 48 channels. The probe was designed to slide radially within the vacuum chamber, so that an entire map of the magnetic field could be obtained over multiple (reproducible) plasma discharges. The voltage signal from the probe is numerically integrated to give a magnetic field strength as a function of time. Figure 2 shows a photograph of the magnetic probe array before it was installed onto the vacuum chamber.

**Accomplishments**

The new plasma source with the new magnetic probe diagnostic became fully operational in the third and final year of the project. There were many delays beyond our control that pushed back our original proposed schedule of being operational by the start of the second year. We have obtained one set of experimental data and are in the process of analyzing the data. In this dataset, we varied the plasma gun voltage and the externally applied magnetic field to change the ratio λ of gun current to bias field. The best way to compare the experimental measurements with the theory is to plot the magnetic field lines in a given *R-Z* plane (treating the interior of the vacuum chamber with cylindrical coordinates). From this data, one can also calculate the total magnetic flux (magnetic field integrated over an area) contained inside the spheromak. The eventual goal is to plot the magnetic flux versus λ for several operating conditions, and to see whether there is a peak in the flux at resonant values of λ. This analysis is proceeding slowly as it is now unfunded. If we can show this, this would validate the theory [4] that inspired these experiments. If not, it would be necessary to characterize the internal current profile of the spheromak more carefully and determine whether it matches the condition needed for the resonances to persist [5]. If the condition required is not met, then the next step would be to propose a way to modify the internal current profile, which would require perhaps launching external waves into the spheromak to drive current in localized regions.

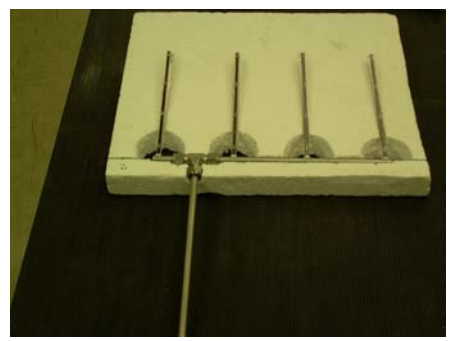

*Figure 2. Photograph of the 48 channel magnetic probe array custom built for this project.*

## Impact on National Missions

This work is relevant to the Laboratory's DOE Office of Science mission. As mentioned in the Background section, spheromak formation is an important research issue as recognized in the recent FES ReNeW final report [3]. The experimental capability enabled by this LDRD project puts LANL in a reasonably strong position to respond to expected new research solicitations from FES in FY10 and FY11. However, because LANL has chosen to focus on high energy density plasma physics (which is more closely related to its main NNSA mission) instead of magnetic fusion plasma physics, there is not a strong justification to continue work in this area at LANL. It should be noted that here is the possibility of re-directing work on this facility toward fusion materials oriented research, which would be strongly aligned with MaRIE.

## References


1. Wesson, J.. Tokamaks. 2004.
2. Bellan, P. M.. Spheromaks. 2000.
3. Research Needs for Magnetic Fusion Energy Sciences. 2009. *Report of the Research Needs Workshop, Bethesda, MD.*

4. Tang, X. Z., and A. H. Boozer. Force-Free Magnetic Relaxation in Driven Plasmas. 2005. *Physical Review Letters.* **94**: 225004.

5. Tang, X. Z.. Driven Resonance in Partially Relaxed Plasmas. 2007. *Physical Review Letters.* **98**: 175001.

## Publications

Hsu, S. C., and X. Z. Tang. A proposed experiment to study relaxation formation of a spherical torus with a plasma center column. 2007. *Journal of Fusion Energy.* **26** (1/2): 85.

# Beta Decay of Polarized Radioactive Atoms in an Optical Tweezer

*Xinxin Zhao*
20070160ER

## Abstract

The rapid advancement in laser cooling and trapping atoms has enabled many exciting breakthrough in atomic, molecular and optical physics such as the creation of Bose-Einstein condensates and superfluidity. At Los Alamos, we have developed a unique set of capabilities in radioactive atom trapping and its application in studying fundamental nuclear physics and ultra-sensitive detection of radioactive isotopes for nuclear nonproliferation and treaty verification. Radioactive atoms confined in an optical dipole trap have many intrinsic advantages for fundamental symmetry experiments, providing a highly polarized, point-like sample with minimal perturbation from the environment, which can be well characterized. Under this project, we have demonstrated the trapping of radioactive Rb-82 atoms (half-life = 75 s) in an optical dipole trap for the first time with good trapping efficiency and long trapping lifetime for a beta asymmetry measurement. We also studied the polarization of Rb atoms using both Faraday rotation polarimetry and resolved Zeeman spectroscopy techniques. These advancements are important steps toward a new generation of precision measurement with polarized trapped atoms that are important in testing the Standard Model.

## Background and Research Objectives

The "Standard Model" is a widely accepted theory that describes our understanding of matter and radiation. The Standard Model quantitatively predicts a vast array of observables by which the model can be tested. If observables are different from those predicted by the Standard Model, it signifies the existence of physics "beyond the Standard Model," providing a new breakthrough in our understanding of the Universe.

Parity violation was first suggested by Lee and Yang, and subsequently discovered in 1957 by Wu *et al.*, in the beta decay of Co-60. Today, parity violation is encompassed by the standard model (V-A) interaction between leptons and quarks. Nonetheless, the nature of these helicity couplings is derived from empirical measurements and the standard model offers no fundamental understanding of the origin of these symmetries and how they become broken at the energy scales probed by modern experiments. Low energy physics experiments that exploit nuclear beta decay continue to offer a means to probe the fundamental origin of parity violation and, more generally, the helicity structure of the weak interaction. With advantages already mentioned above, we believe that optical tweezer approach will enable a state-of-the-art beta-asymmetry measurement and provide an important test of the SM in the semi-leptonic sector.

It is well known that pure Gamov-Teller (GT) transitions offer the most direct route to study parity violation in nuclear beta decay. Historically, however, studies of pure GT transitions have been limited by the lack of good candidates, namely radioisotopes with appropriate half-life for study and with pure GT transitions that are not hindered. It is now possible to envision a new generation of GT experiments with the potential to reach the 0.1% level of precision by exploiting optical traps for radioactive atoms.

In an earlier project, we have already demonstrated a proof-of-principle experiment of parity violating beta-asymmetry of radioactive Rb-82 atoms in a magnetic time orbiting potential (TOP) trap. Rb-82 was chosen because it is easy to laser cool and trap, it decays through pure Gamow-Teller transitions and we have reliable supply because it is a key biomedical radioisotope produced at LANL. But systematic effects related to the inhomogeneous magnetic field (required for magnetic traps) and $\beta$ background from unpolarized Rb-82 lost to the walls of our chamber hampered the effort for a precision measurement. Recently, we successfully integrated an optical dipole trap

(tweezer) to our radioactive atom trapping facility. The optical tweezer eliminates the systematic effects of the magnetic trap; it is therefore an ideal approach for such a measurement. The challenges yet to be overcome are to trap a sufficient number of atoms with a long trapping lifetime and to precisely measure the sample polarization.

## Scientific Approach and Accomplishments

The LANL radioactive atom trapping team in Chemistry Division has the setup and expertise in trapping radioactive Rb isotopes in a magneto-optical trap (MOT). Briefly, to perform these experiments, $^{82}$Sr ($t_{1/2}$=25 days) samples are produced at LANSCE isotope production facility, extracted and prepared in the TA-48 hot cell and loaded into a mass-separator. The Rb-82 ion beam is mass separated, implanted into a Zr foil located inside a specially dryfilm coated trapping cell and subsequently released as neutral atoms upon heating. The atoms are trapped in the cell by a magneto-optical trap (MOT) with a temperature of ~200 microK.

Under this project, we have demonstrated loading radioactive Rb-82 from the MOT into the optical dipole for the first time and achieved good trapping efficiency (14 %) and long lifetime (55 second). This work was published in Physical Review A Rapid communication [1]. Following on the success of trapping radioactive atoms in the dipole trap, the challenges remains to polarize the atoms and precisely measure the overall polarization of the ensemble of trapped atoms. In a far-off-resonant dipole trap there are three main factors that determine the polarization of the trapped atoms. They are: (1) how well one can optically pump the atoms to the desired initial state, (2) how collisions affect the sample polarization, and (3) the spin-relaxation rate due to the light scattering from the trapping laser. To this end, we have studied polarized Rb atoms in an optical dipole trap using both resolved Zeeman spectroscopy and Faraday rotation polarimetry techniques.

To optimize the polarization, we have setup and demonstrated optical pumping of atoms in the dipole trap. We use a circularly polarized light for the optical pumping beam and align the optical pumping beam in the direction of the magnetic field. We improved the polarization of the optical pumping laser beam to better than 99%. To have better control of B field, we need to minimize the residue magnetic field. We have setup a Faraday rotation experiment to measure the magnetic field in situ. A typical Faraday rotation signal of the cold atoms in a YAG laser dipole trap is shown in Figure 1. The Faraday rotation signal provides a powerful tool for in situ measurement of the magnetic field inside the vacuum chamber. The "frequency of oscillation" is a precise measure of the residue magnetic field, while the amplitude is related to the sample polarization. This allows us to minimize the residue field with compensation coils while monitoring the oscillating Faraday signal. This reduces the uncertainty of the optical pumping B field to less than 1%. Because the amplitude of the Faraday signal is related to the polarization of the sample, Faraday rotation measurements also provides a powerful tool to study the dynamics of decoherence and the evolution of the sample polarization in the dipole trap. We have studied the time evolution of polarized atoms in the YAG trap, and found that the spin relaxation is suppressed by over an order of magnitude over the rate set by the far-off resonance scattering. We also found that the spin polarization is further enhanced and reinforced when the two-body collision loss rate of the mixed spin states is greater than the one body trap loss as shown in Figure 2. These advancements are an important step towards a new generation of precision beta decay correlation measurements with polarized atoms. This work was published in a paper titled "Polarized atoms in an optical dipole trap" [2].

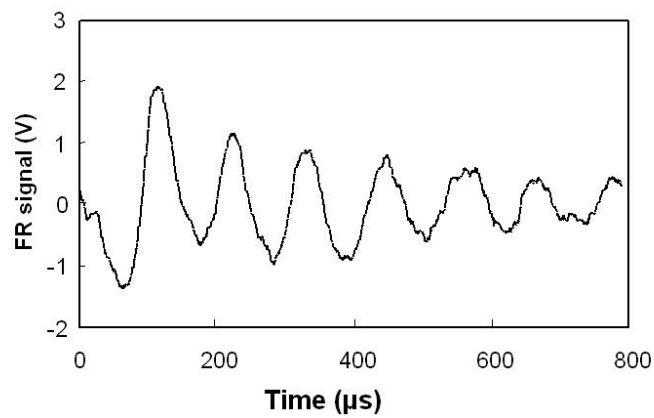


*Figure 1. A single shot Faraday rotation signal of 31,000 polarized atoms in the dipole trap. The Faraday oscillation frequency is 9.3 kHz which corresponds to 20 mG residual B field.*

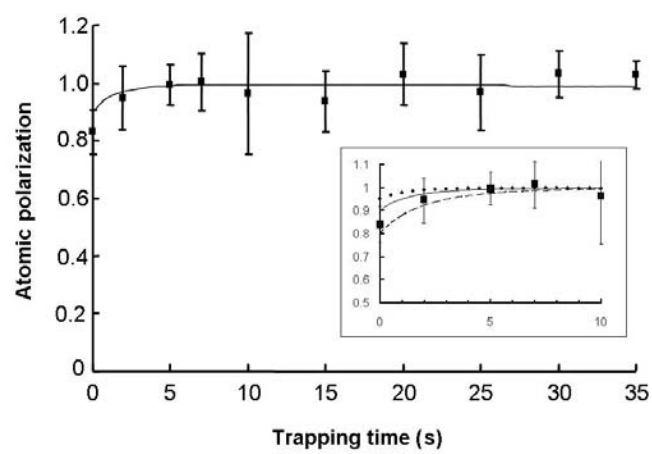


*Figure 2. The polarization evolution of Rb atoms in the FORT. Polarization rises initially and then levels off to stay in nearly fully polarized level. The inset shows the calculated 10 s evolution of samples with 95%, 90%, and 80% initial polarizations.*

Over the last few months, we have been working on improving the precision of the polarization measurement. We have improved the shot to shot stability of the Faraday rotation measurement. We also synchronized the absorption imaging with the rotating bias field. This allows us to make the rotating bias field more uniform. Demonstration of precision measurement of Rb-82 polarization in an optical dipole trap could result in a third paper.

In summary, we have trapped radioactive Rb-82 isotope with good trapping efficiency and long trapping lifetime, prepared highly polarized atoms and studied the time evolution of their polarization in a YAG dipole trap. The polarization evolution in a YAG laer optical dipole trap is determined by two mechanisms, one is the far-off-resonant photon scattering that occurs with the trap laser, the other is the two-body collision loss rate. We observed that the spin relaxation is highly suppressed relative to the far-off-resonant scattering in the YAG dipole trap. The spin polarization is further purified and maintained by the two-body collision dynamics when the two-body collision loss rate of the mixed spin state ensemble is greater than the one-body trap loss due to collisions with background gas. These are important steps toward undertaking a beta-asymmetry measurement in an optical dipole trap.

## Impact on National Missions

This project demonstrated that laser cooled and trapped radioactive atoms would open a new frontier for fundamental symmetry research. These new generation experiments can open a new window in the search for physics beyond the Standard Model and impacts basic understanding of physics, a key DOE mission. The technical spin-offs support the NNSA mission of thread reduction in ultra-sensitive detection of radioactive isotopes.

## References


1. Feldbaum, D., H. Wang, J. Weinstein, D. J. Vieira, and X. Zhao. Trapping radioactive 82Rb ion an optical dipole trap and evidence of spontaneous spin polarization. 2007. *Physical Review A Rapid Communication.* **76**: 051402(R).

2. Fang, F., H. Wang, D. Feldbaum, D. J. Vieira, and X. Zhao. Polarized atoms in a far-off-resonance yttrium-aluminum-garnet-laser optical dipole trap. 2009. *Physical Review A.* **79** (4): 043406.


## Publications


Fang, F., H. Wang, D. Feldbaum, D. J. Vieira, and X. Zhao. Polarized atoms in a far-off-resonance yttrium-aluminum-garnet-laser optical dipole trap. 2009. *Physical Review A.* **79** (4): 043406.

Feldbaum, D., H. Wang, J. Weinstein, D. J. Vieira, and X. Zhao. Trapping radioactive 82Rb ion an optical dipole trap and evidence of spontaneous spin polarization. 2007. *Physical Review A Rapid Communication.* **76**: 051402(R).

# Nano-Engineered Casimir Forces

*Diego A. Dalvit*
20070163ER

## Abstract
In the realm of the very small, weird quantum mechanical effects take place. Light can turn on and off out of nothing, like "quantum ghosts", and when these reflect from nanomachines they can produce attractive forces, the so-called Casimir force. They present opportunities and challenges to nanotechnology. Understanding these forces is important to the nation, since it can advance technology and science in different areas.

## Background and Research Objectives
How can the Casimir effect just appear out of nowhere? The answer is that it doesn't – at least not quite. According to quantum mechanics, the electromagnetic vacuum is actually foaming with particles of light (photons) that pop into existence for the briefest of moments. However, during their short lives, these photons can bounce off nearby surfaces, exerting pressure on them. When two plates are separated by less than about 5 micrometers, there appears an attractive Casimir force. Intuitively, the reason is that the separation between the plates limits the possible colors of fluctuating photons that can appear between them, but there's no such restriction on photons that appear behind the plates. There are therefore more quantum photons pressing on the plates than pushing them outwards, the net effect of which is an attractive force between the two plates (see Figure 1).

Casimir forces present opportunities and challenges for nanotechnology. On the one hand, they could lead to frictionless force transmission in the so-called "Casimir rack and pinion" (see Figure 2). On the other hand, researchers believe that the attractive Casimir force is responsible for the gumming up our ever-smaller gadgets. Nanomachines could run more smoothly, and with less or no stiction at all, if one could manipulate the Casimir force. Although escaping the Casimir force is not possible, we are on the verge of taming it by engineering the geometry and materials of the nanomachines with the goal of neutralizing the force, even making it repulsive.

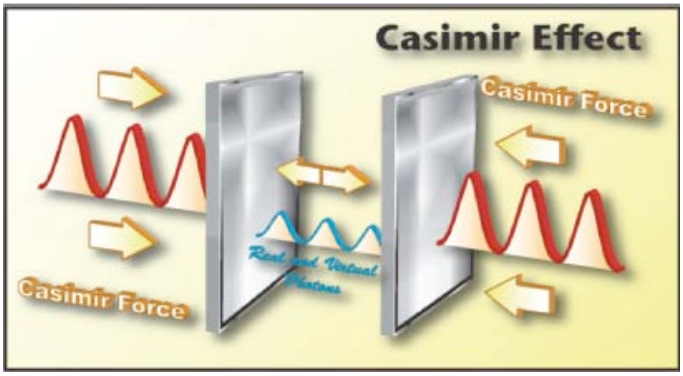


*Figure 1. Photons appear and disappear in the quantum vacuum, and cause forces between nano-objects.*

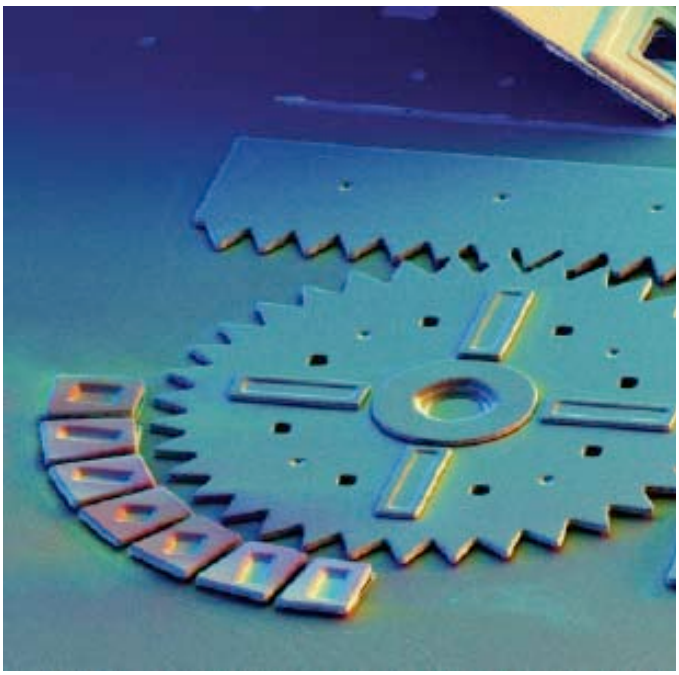

*Figure 2. A rack and pinion nanomachine.*

## Scientific Approach and Accomplishments

We formed a multidisciplinary team aimed at understanding theoretically ways to tailor the Casimir force with different material structures, which we then fabricate and use to measure the Casimir force experimentally.

It is actually quite complicated to compute the force taking into account the specific geometry and material structure of the nanomachines. We use a combination of analytical and numerical tools to do this. The basic idea is to calculate the energy of interaction between the plates in the presence of the quantum foam of photons. We use fundamental principles of Quantum Mechanics that tell us how the energy of the vacuum photons depends on the geometrical boundaries, and this in turn helps us calculate the Casimir force [1, 2].

We tailor the force in two ways: a) by using materials that exist in Nature, such as conductors [3, 4, 5, 6] (that give a strong attractive Casimir force) and semiconductors (that give a weaker attractive Casimir force); b) by engineering special materials, the so-called metamaterials (MM), that are man-made. These have designer electromagnetic properties that cannot be found in naturally occurring substances. Of particular importance to us is that they have magnetic properties, such as standard magnets, but contrary to them, metamaterials can maintain their magnetic properties in a wide range of frequencies (that is, for all colors of the Casimir "ghost" photons).

We have developed all the modeling and simulation tools to understand how to tailor the Casimir force in different material structures [8, 9]. We have fabricated some of these structures and measured Casimir forces [7] (see Figure 3).

*Figure 3. Example of a metamaterial: micrometer–sized metallic split ring resonators are assembled on a substrate. Because of their peculiar geometry, they behave as a medium with an effective non-trivial electric and magnetic response. Scaling up or down the size of each unit cell allows to engineer how the Casimir photons interact with the metamaterial.*

Casimir forces can be tailored by modifying the conductivity properties of the plates. In this example we show the Casimir energy as a function of separation between semiconductor materials, like pure germanium and silicon. The Casimir force can be expressed as a sum over individual contributions from all photons in the "vacuum foam," that is, a sum over their polatization, frequency, and momentum parallel to the Casimir plates [10, 11].

We have measured, for the first time, the Casimir force between Ge plates in a sphere-plane configuration using an ultrasensitive torsion pendulum [12], (see Figure 4). The basic idea is that when the sphere approaches the plane, the pendulum rotates due to the action of the attractive Casimir force, and one measures this rotation by detecting changes in capacitance between the two plates kept at different voltages. The upper plot shows the experimental data for the total force and the contribution due to residual electrostatic patches on the plates (dashed line). The lower plot shows their difference, which fits very well the prediction of Casimir force for different conductivity models of the Ge plates.

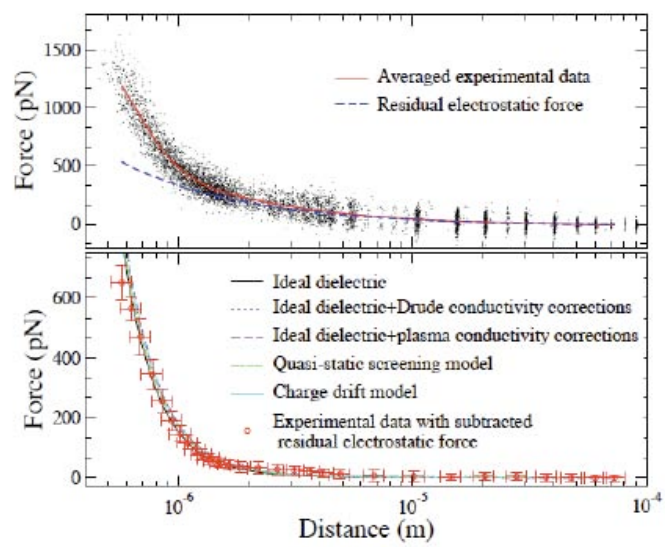


*Figure 4. Casimir force measurement between semiconductor plates.*

In summary, the key discoveries of this project were:

- Possible mechanisms to reduce Casimir attraction with magnetic metamaterials.
- The first measurement of Casimir fores with germanium plates.
- New metamaterials were fabricated with designed electromagnetic properties.

We have published several papers that are list in the References section. Our work was also highlighted in the media, including the American Physical Society Physics online journal for spotting exceptional research, the IEEE Spectrum magazine, the New Scientist magazine, and the LANL 1663 magazine. The PI of this project has given 2 invited plenary talks at international conferences, and several other invited talks at academia and national labs. It is worth emphasizing that thanks to this LDRD investment LANL is becoming a world leader in the field of Casimir force engineering, with state-of-the-art theoretical and experimental capabilities.

## Impact on National Missions

Understanding and controlling quantum forces, such as Casimir interactions, can advance technology and science in different areas:

- Neutralizing Casimir forces can have tremendous impact in nanotechnology because it will allow to solve the problem of stiction between movable parts of nanomachines. Although we don't usually see them, these tiny machines are becoming part of our everyday life: air-bags, handhelds such as iPhones, and video-game controllers, all get motion or orientation information from tiny motion sensors whose even tinier parts rotate or bend freely when the device is spun or accelerated. Casimir forces pose a risk to all these devices.

- Fundamental science also benefits from this work, as it allows basic understanding of the interaction between light and novel metamaterials. This has implications not only for Casimir forces in nanomachines, but also in the physics of atom-surface interactions. This is important for precision measurements involving atoms in close proximity to surfaces, such as in processing of quantum information in atom chips.

- Our work has transitioned to external funding via DARPA under the "Casimir Effect Enhancement" program, attesting to the importance of our work for the nation.

## References


1. Dalvitetal, D.. Exact Casimir interaction between eccentric cylinders. 2006. *Phys. Rev. A.* **74**: 010101.

2. Spagnoloetal, S.. van der Waals interactions in a magnetodielectric medium. 2007. *Phys. Rev. A.* **74**: 052117.

3. Kimetal, W.. Status report on the measurement of the Casimir force in a cylinder-plane configuration. 2007. *Proceedings of the XLII Rencontres de Moriond.* : 291.

4. Kimetal, W.. Anomalies in electrostatic calibrations for the measurement of the Casimir force in a sphere-plane geometry. 2008. *Phys. Rev. A.* **78**: 020101.

5. Kimetal, W.. On electrostatic and Casimir force measurements between conducting surfaces in a sphere-plane configuration. 2009. *J. Phys.:Conference Series.* **161**: 012004.

6. Rodriguezetal, A.. Stable suspension and dispersion-induced transitions from repulsive Casimir force between fluid-separated eccentric cylinders. 2008. *Phys. Rev. Lett..* **101**: 190404.

7. Tayloretal, A.. Complementary planar terahertz metamaterials. 2007. *Optics Express .* **15**: 1084.

8. Rosaetal, F.. Casimir-Lifshitz theory and metamaterials. 2008. *Phys. Rev. Lett..* **100**: 183602.

9. Rosaetal, F.. Casimir interactions for anisotropic magnetodielectric metamaterials. 2008. *Phys. Rev. A.* **78**: 032117.

10. Dalvitetal, D.. Contribution of drifting carriers to the Casimir-Lifshitz and Casimir-Polder interactions with semiconductor materials. 2008. *Phys. Rev. Lett..* **101**: 163203.

11. Dalvitetal, D.. Computation of Casimir forces for dielectrics or intrinsic semiconductors based on the Boltzmann transport equation. 2009. *J. Phys.:Conference Series.* **161**: 012009.

12. Kimetal, W.. Measurement of the Casimir force between Germanium plates using a torsion balance. 2009. *Phys. Rev. Lett..* **103**: 060401.


## Publications


Brown-Hayes, M., J. H. Brownell, D. A. R. Dalvit, W. J. Kim, A. Lambrecht, F. C. Lombardo, F. D. Mazzitelli, S. M. Middleman, V. V. Nesvizhevsky, R. Onofrio, and S. Reynaud. Thermal and dissipative effects in Casimir physics. 2006. *Journal of Physics A.* **39**: 6195.

Chen, H. T., J. F. O'Hara, A. J. Taylor, R. D. Averitt, C. Highstrete, M. Lee, and W. J. Padilla. Complementary planar terahertz metamaterials. 2007. *Optics Express.* **15** (3): 1084.

Dalvitetal, D.. Contribution of drifting carriers to the Casimir-Lifshitz and Casimir-Polder interactions with semiconductor materials. 2008. *Phys. Rev. Lett..* **101**: 163203.

Dalvitetal, D.. Computation of Casimir forces for dielectrics or intrinsic semiconductors based on the Boltzmann transport equation,. 2009. *J. Phys.:Conference Series.* **161**: 012009.

Kim, W. J., M. Brown-Hayes, D. A. R. Dalvit, J. H. Brownell, and R. Onofrio. Anomalies in electrostatic calibrations for the measurement of the Casimir force in a sphere-plane geometry. 2008. *Physical Review A, Rapid Communications.* **78**: 020101.

Kim, W. J., M. Brown-Hayes, D. A. R. Dalvit, and R. Onofrio. Status report on the measurement of the Casimir force in a cylinder-plane geometry. 2007. In *Recontres de Moriond.* (La Thuile, Italy, 11-18 March, 2007). , p. 291. Moriond: Moriond.

Kimetal, W.. Measurement of the Casimir force between Germanium plates using a torsion balance. 2009. *Phys. Rev. Lett..* **103**: 060401.

Kimetal, W.. On electrostatic and Casimir force measurements between conducting surfaces in a sphere-plane configuration. 2009. *J. Phys.:Conference Series.* **161**: 012004.

Mazzitelli, F. D., D. A. R. Dalvit, and F. C. Lombardo. Exact zero-point interaction between cylinders. 2006. *New Journal of Physics.* **8**: 240.

O'Hara, J. F., A. K. Azaf, H. T. Chen, A. J. Taylor, and E. Smirnova. Effects of Microstructure Variations on Macroscopic Terahertz Metafilm Properties. 2007. *Active and Passive Electronic Components.* **2007**: 49691.

R.Dalvit, D. A., and S. K. Lamoreaux. Contribution of drifting carriers to the Casimir-Lifshitz and Casimir-Polder interactions with semiconductor materials. 2008. *Physical Review Letters.* **101**: 163203.

Rodriguez, A. W., J. N. Munday, J. D. Joannopoulos, F. Capasso, D. A. R. Dalvit, and S. G. Johnson. Stable Suspension and Dispersion-Induced Transitions from Repulsive Casimir Froce between fluid-separated Eccentric Cylinders. 2008. *Physical Review Letters.* **101**: 190404.

S.Rosa, F. S., D. A. R. Dalvit, and P. W. Milonni. Casimir-Lifshitz theory and metamaterials. 2008. *Physical Review Letters.* **100**: 183602.

S.Rosa, F. S., and D. A. R. Dalvit. Casimir interactions for anisotropic magnetodielectric metamaterials. 2008. *Physical Review A.* **78**: 032117.

Singh, R., E. Smirnova, A. J. Taylor, J. F. O'Hara, and W. Zhang. Optically Thin Terahertz Metamaterials. 2008. *Optics Express.* **16**: 6537.

Spagnolo, S., D. A. R. Dalvit, and P. W. Milonni. Van der Waals interactions in a magneto-dielectric medium. 2007. *Physical Review A.* **75**: 052117.

# Probing Correlated Electron Behavior via Direct Uranium-235 Nuclear Magnetic Resonance

*Eric D. Bauer*
20070188ER

## Abstract

The fundamental understanding of the emergent behavior resulting from strong correlations between electrons that are responsible novel forms of matter such as magnetism and superconductivity is one of the grand challenges in modern condensed matter physics today. Actinide compounds are prototypical examples of such materials, and these systems often exhibit exotic forms of magnetic and superconducting order at low temperatures. By using Nuclear Magnetic Resonance (NMR) techniques, we will detect the resonance of uranium of compounds enriched with U-235. This work will offer new microscopic insight into the behavior of the correlated electrons in the exotic ordered states. While the focus of the project is on uranium-based materials, our work on these compounds will provide guidance for observing the plutonium resonance in the plutonium compounds with the isotope Pu-239. This project will support the DOE and LANL missions in the fundamental understanding of materials at the atomic scale and of exotic superconductivity, by enhancing our understanding of the complex interactions between electrons in uranium-based compounds. This project will also support the mission of threat reduction by developing new techniques for detecting illicit enriched uranium and plutonium.

## Background and Research Objectives

Understanding the behavior of interacting electrons in materials that give rise to unusual properties is one of the grand challenges of modern condensed matter physics. Just as our exquisite understanding of silicon and germanium has resulted in the invention of the personal computer, understanding these complex electronic materials is the first step towards finding energy technologies that will help solve the Nation's looming energy crisis. One important class of materials with strongly correlated electrons is the set of actinide heavy-fermion compounds with exotic order, such as coexisting superconductivity and magnetism that may be integral to future technologies. In order to probe these unusual ground states, a suite of experimental techniques can be applied to investigate the bulk thermodynamic, magnetic and electronic responses of these systems. However, there are few techniques that can probe the physics of these systems at the microscopic scale. We have developed and implemented a new method, direct Nuclear Magnetic Resonance (NMR) of the uranium-235 nuclei, which has enabled, for the first time, direct study of the nature of the 5f electrons that are responsible for the heavy-fermion state and the unusual states of matter that evolve from it. NMR provides detailed microscopic information about the static and dynamic magnetic and electronic degrees of freedom at a particular site in the unit cell. Since the naturally occurring isotope of uranium, U-238, is NMR-inactive, such information has not been previously available. Measuring the NMR directly at the uranium site using U-235 has enabled us to learn about not only the degree of hybridization of the 5f electrons across a broad class of correlated f-electron materials, but also to probe the dynamics of magnetism and superconductivity and other exotic states at the microscopic level. Our research on these uranium compounds has provided valuable information for searching for a similar direct measurement of the plutonium-239 signal in the plutonium superconductor, discovered here at Los Alamos, PuCoGa5.

## Scientific Approach and Accomplishments

Heavy-fermion systems have traditionally been investigated experimentally by applying a suite of thermodynamic and spectroscopic techniques that probe both magnetic and electronic degrees of freedom. NMR is particularly useful for probing magnetic order, however not all nuclei within a material of interest are NMR-active. For the vast majority of correlated electron systems (based on cerium or uranium), the nuclei at the magnetic site are NMR-inactive. Consequently, all of the NMR work on these systems has been done

on ligand (neighboring atoms) sites, such as Si-29 NMR in URu2Si2, or Pt-195 NMR in UPt3. In a heavy-fermion system or a superconductor, in which the spectrum of excitations of these conduction electrons is renormalized or gapped, this can strongly modify and obscure the relevant interactions of interest. Consequently there is often a lack of information about the behavior of the f-electron moments in the ordered state. An ideal probe of the behavior of the U moments is direct NMR of the U nucleus itself. U-235 has nuclear spin $I = 7/2$, with a nuclear moment of 0.43 magnetons, and a large nuclear quadrupolar moment; therefore, it is sensitive not only to the magnetic moment of the U electrons, but to their charge distribution as well. NMR of actinide (or lanthanide) nuclei is challenging in condensed matter systems because the onsite hyperfine coupling is typically on the order of hundreds of Tesla, which gives rise to fast nuclear spin relaxation that are most often too fast for detection. If, however, the magnetic moments of the 5f electrons become *static* in a magnetic state, or are (critically) slowed down in a superconductor, then the relaxation time of the U-235 or Pu-239 nuclei can be long enough to detect the NMR signal.

We have developed the necessary encapsulation to properly handle these radioactive compounds and fabricated an experimental apparatus to investigate the properties of the U-235 and Pu-239 nuclei themselves at the microscopic level. With the development of this technique, we have studied the unusual ordered state in URu2Si2, which has been a mystery since its discovery nearly 30 year ago, the spin dynamics of the U nuclei in the antiferromagnet USb2, and recently began searching for the Pu-239 signal in the plutonium superconductor PuCoGa5. Additionally, we have synthesized and characterized a number of uranium compounds with depleted uranium (minimal U-235 enrichment) to understand the underlying physics in a number of materials in order to further investigate them at the microscopic level with U-235 NMR. We outline our progress and success to date below:

The compound USb2 is an itinerant magnet, in which the magnetism results from partial filling and overlap of the energy bands with primarily f- and d-character, rather than arising from the interaction of localized uranium magnetic moments tightly bound to their atomic cores. We have investigated this compound using both U-235 and Sb-121 NMR. We have succeeded in observing the U-235 NMR signal (*a first for Los Alamos National Lab, and the first observation of the U-235 signal in the United States*) due to the large internal magnetic field of 277 Tesla in the antiferromagnetic state, which is shown in Figure 1 [1,2].

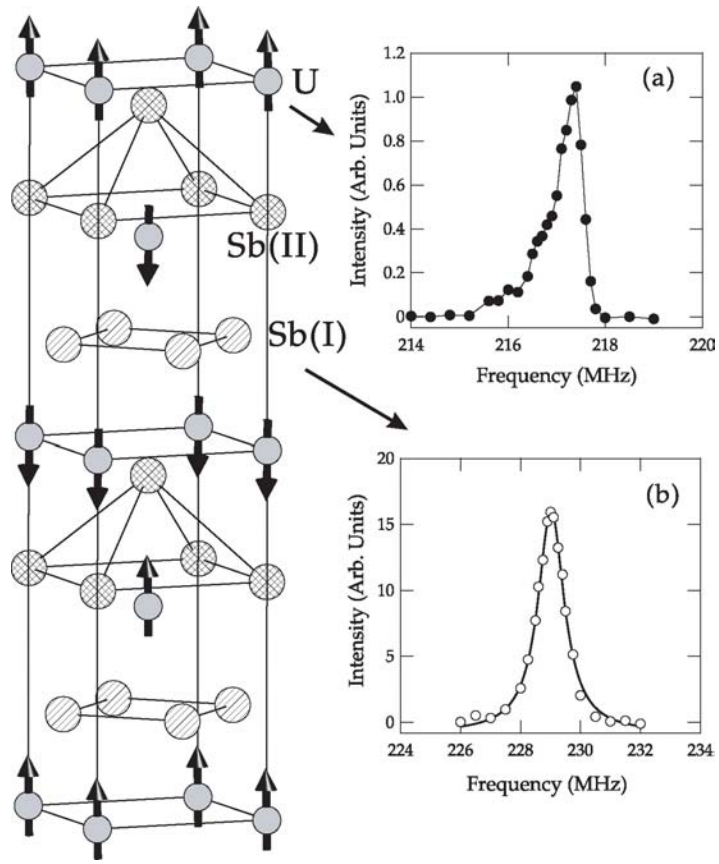


*Figure 1. The crystallographic and magnetic structure of the uranium antiferromagnet USb2. (a) U-235 NMR spectrum (b) Sb-121 spectrum in zero field.*

We successfully obtained the U-235 nuclear relaxation rates of this itinerant antiferromagnet — *the first ever direct information about the nuclear relaxation processes in a uranium intermetallic compound.* Comparison of these U-235 results to the detailed temperature dependence of the Sb-121 NMR is shown in Figure 2. We found nuclear relaxation rates for both $^{235}$U and $^{121}$Sb are governed by the same relaxation mechanism but reveal an anomaly at 5 K (see Figure 2). We attribute the anomaly to the change of the anisotropic hyperfine coupling constant at the Sb site. The origin of the change of this coupling constant is not clear at the moment but one possibility is the formation of an energy gap in the magnetic excitation spectrum, which may modify the channel of the transferred hyperfine coupling mechanism between U and Sb, resulting in the strong temperature dependence of the coupling constant (Figure 2).

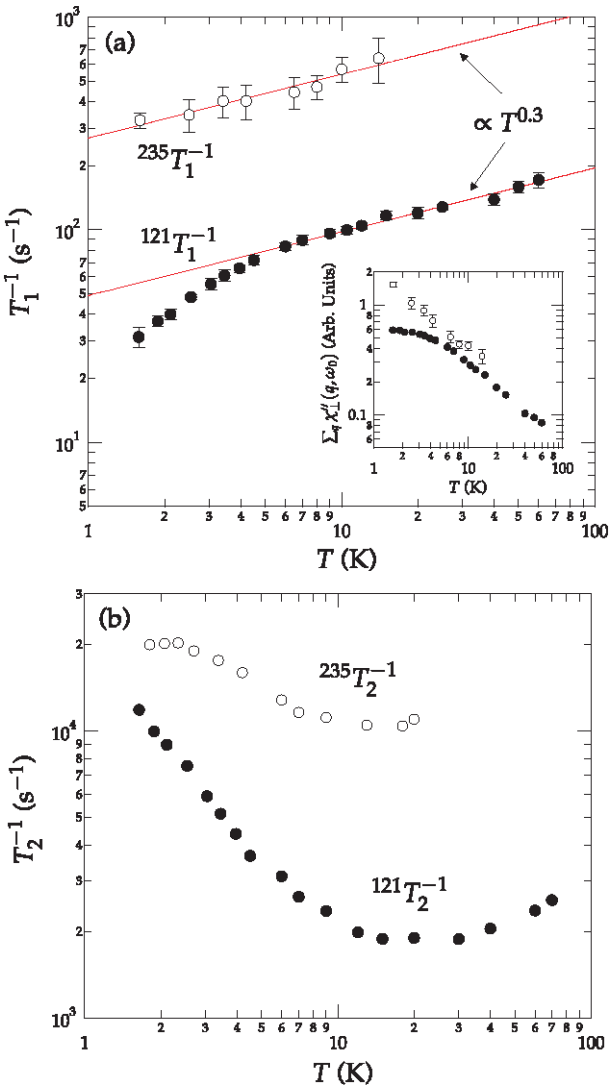


*Figure 2. Nuclear relaxation rates for both U-235 and Sb-121. (a) Spin-lattice relaxation rate 1/T1 as a function of T. An anomaly at 5 K is clearly indicated. (b) Spin relaxation $1/T_2$ also shows a similar deviation near 5 K.*

The URu2Si2 system is one of the most interesting and challenging correlated electron system as it exhibits a highly unusual ordered state at low temperature, with a yet-unidentified order parameter despite a quarter-century of intense research. By doping the pure compound with a few percent of Rh, it has been found that a new large-moment phase is stabilized in which antiferromagnetism with a large ordered moment coexists with the hidden order parameter. In an initial attempt to find the U-235 signal, we learned that the U-235 signal in a 2%-Rh doped URu2Si2 sample is too weak to be observed directly, and instead have focused our attention on a series of samples of $U(Ru1\text{-}xRhx)_2Si_2$ with U-238 to determine the nature of the hidden order phase. Our results [3] indicate that this large moment antiferromagnetic phase is not a true thermodynamic phase that competes with the hidden order phase, but rather an artifact of the intrinsic inhomogeneity that develops as a result of doping. Our Si-29 NMR spectra clearly reveal (Figure 3) an inhomogeneous coexistence between the hidden order component and the large moment antiferromagnetism. These results contrast with recent neutron scattering data, which suggested a new thermodynamic phase. In collaboration with A. Balatsky (T-11), we hypothesize that the Rh dopants locally suppress the hidden order parameter, and that the antiferromagnetism arises as a secondary effect in regions where the hidden order is suppressed.

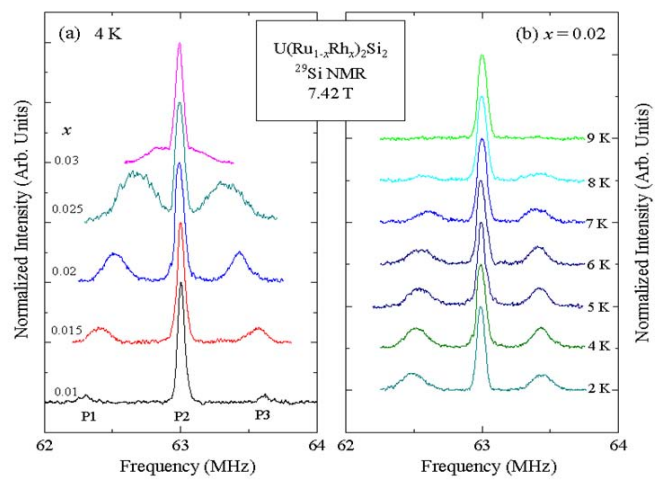


*Figure 3. a) Si-29 spectra of $U(Ru_{1-x}Rhx)_2Si_2$ as a function of Rh concentration x at 4 K. The spectra are consistent with commensurate AFM ordering with moments aligned to the c-direction. b) Temperature dependence of the spectra for x = 0.02. The AFM signature disappears gradually near 9 K without change of the ordered moment. These measurements clearly indicate the coexistence of the "hidden" order and antiferromagnetism.*

Motivated by our discovery of a new compound $U_3Bi_4Ni_3$, in which the physical properties are reminiscent, though not entirely conclusive, of Kondo insulating behavior, we performed Bi-209 NMR measurements to determine if the insulating behavior arises from hybridization of local 5*f* electrons and conduction electrons (Kondo insulator), or if it is a simple band effect. The presence of temperature independent energy gap deduced from these NMR experiments [4] of approximately 50 meV, consistent with recent photoemission measurements and electrical resistivity, together with the temperature dependence of Knight shift, provides strong evidence for Kondo insulating behavior in $U_3Bi_4Ni_3$ arising from strong correlations between the conduction electrons and the uranium local moments.

Investigating a number of different strongly correlated uranium materials with a variety of distinct ground states

has not only yielded valuable information about the microscopic behavior of uranium, but has also stretched the limits of this new and powerful technique. We have attempted to observe the U-235 signal in a superconductor U6Fe, since the nuclei will be critically slowed down in the superconducting state, making it possible for us to find the U-235 signal, in order to provide insight into whether the glue that binds superconducting electron pairs is comprised of tiny lattice vibrations (or phonons), or is made up of tiny jiggling of the uranium spins (fluctuations) associated with nearby magnetic order. Measurements designed to search for the direct U-235 signal gave a hint of a peak, which was later determined in a series of subsequent measurements with UFe2 enriched with U-235 to be due to $UFe_2$ impurities.

Motivated by our successes in investigating uranium compounds with this powerful technique, we recently started similar NMR measurements to find the Pu-239 signal in the plutonium superconductor $PuCoGa_5$. Direct microscopic information about the plutonium nuclei has never been obtained before by NMR in a metallic compound, especially one which is so closely related to the technologically important cubic phase of elemental plutonium used in nuclear weapons. A successful demonstration of this NMR technique applied to plutonium may lead to both a fundamentally new understanding of this most complex of elements and a simple but effective means to detect illicit nuclear material. As shown in Figure 4, we have performed NMR measurements on the Co-59 and Ga-69 nuclei to provide the necessary information of where to look for the Pu-239 signal, after demonstrating that this plutonium material is indeed superconducting (inset of figure 4). Our preliminary measurements of the spin-lattice relaxation rate $1/T_1$ , i.e., how long it takes the nuclei to relax back to their unperturbed state, which provides information about the various relaxation processes in the material, of Co-59 NMR in $PuCoGa_5$ for the field along the c-axis of the tetragonal crystal. The data follow a powerlaw temperature dependence, which indicates the presence of antiferromagnetic spin fluctuations (tiny jiggling of the plutonium spins) that may be responsible for the superconductivity. Further measurements [5] of the relaxation along the a-axis indicate that these fluctuations may be strongest within the basal plane of the tetragonal crystal suggest that the best place to detect the Pu-239 signal is within this plane.

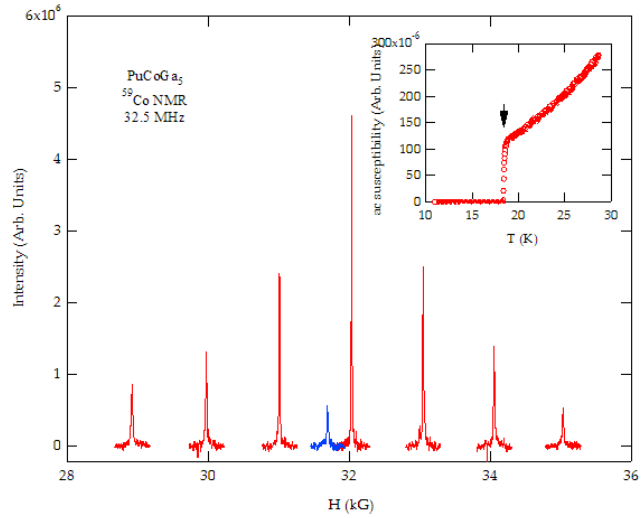


*Figure 4. Co-59 NMR spectra in $PuCoGa_5$ that consist of seven lines associated with the Co nuclear spin 7/2 transitions. For comparison, blue line is the central transition of Ga-69. Inset: Magnetic susceptibility showing the superconducting transition (arrow denotes Tc = 18.8 K).*

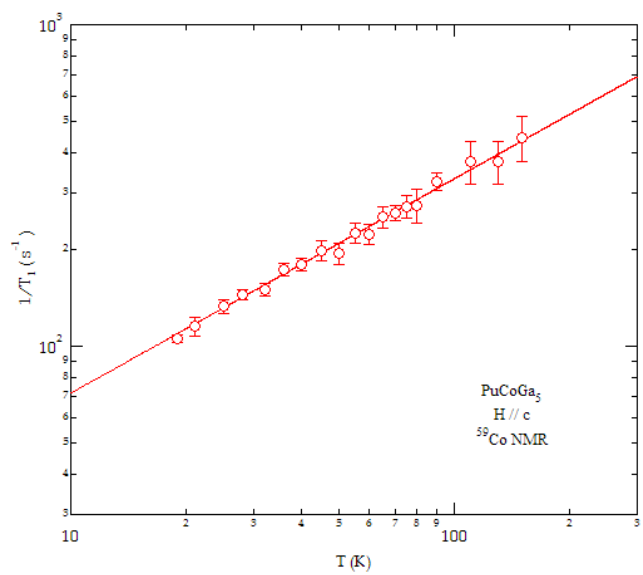


*Figure 5. Spin-lattice relaxation rate 1/T1 of Co-59 NMR in PuCoGa5 for the field along the c-axis of the tetragonal crystal. The data follow a powerlaw temperature dependence which indicates the presence of antiferromagnetic spin fluctuations (tiny jiggling of the spins) that may be responsible for the superconductivity. Additional measurements of the spin-lattice relaxation along the a-axis indicate that these fluctuations may be strongest suggest that the best place to detect the Pu-239 signal is in this direction.*

## Impact on National Missions

This project will support the DOE mission of the Office of Science, basic energy sciences, by enhancing our understanding of the complex interactions between electrons in uranium based compounds. This project will also support the mission of threat reduction by developing new tech-

niques for detecting enriched uranium and plutonium.

## References


1. Baek, S. H., N. J. Curro, E. D. Bauer, J. C. Cooley, and J. L. Smith. 235U and 121Sb NMR investigation of an itinerant antiferromagnet, USb2,. 2008. *Physica B.* **403**: 850.

2. Baek, S. H., N. J. Curro, H. Sakai, E. D. Bauer, J. C. Cooley, and J. L. Smith. 235U nuclear relaxation rates in an itinerant antiferromagnet USb2. *Physical Review B.*

3. Baek, S. H., M. J. Graf, A. V. Balatsky, E. D. Bauer, J. C. Cooley, J. L. Smith, and N. J. Curro. Uncovering the hidden Order in URu2Si2 by impurity doping. *Physical Review Letters.*

4. Baek, S. H., N. J. Curro, T. Klimczuk, H. Sakai, E. D. Bauer, F. Ronning, and J. D. Thompson. Hybridization-driven gap in U3Bi4Ni3: A 209Bi NMR/NQR study. 2009. *Physical Review B.* **79**: 195120.


## Publications


Baek, S. H., N. J. Curro, E. D. Bauer, J. L. Smith, and J. Cooley. 235Uand 121Sb NMR Investigation of an itinerant antiferromagnet, USb2. 2008. *Physica B.* **403**: 850.

Baek, S.-H., M.J. Graf, A. V. Balatsky, E. D. Bauer, J. C. Cooley, J. L. Smith, and N. J. Curro. Uncovering the Hidden Order in URu2Si2 by Impurity Doping. 2009. *Physical Review Letters.* : (submitted).

Baek, S.-H., N. J. Curro, H. Sakai, E. D. Bauer, J. C. Cooley, and J. L. Smith. 235U nuclear relaxation rates in an itinerant antiferromagnet USb2. 2009. *Physical Review B.* : (submitted).

Baek, S.-H., N. J. Curro, T. Klimczuk, H. Sakai, E. D. Bauer, F. Ronning, and J. D. Thompson. Hybridization-driven gap in U[sub 3]Bi[sub 4]Ni[sub 3]: A [sup 209]Bi NMR/NQR study. 2009. *Physical Review B (Condensed Matter and Materials Physics).* **79** (19): 195120.

# Cold Atom Quantum Liquid Mixtures

*Eddy M. Timmermans*
20070234ER

## Abstract

The cold atom technology that traps and manipulates neutral atoms at ultra-low temperatures (tens of thousands of times lower than the lowest temperatures reached previously) provides an unprecedented window on quantum many-body physics. Cold atom laboratories are then poised to explore quantum phase transitions – the zero-temperature analogues of ordinary phase transitions that play a crucial role in strongly correlated electrons and high $T_c$ superconductivity – and to realize novel atom optics techniques to measure weak fields (magnetic and gravitation) with unprecedented resolution. In this theory project, we have opened up avenues for cold atom explorations of many-body physics and for the creation of non-interferometric high-sensitivity force measurements, capitalizing on cold atom gas mixtures of different species of atoms.

We have shown that cold atom gas mixtures can realize odd-frequency pairing [1], an exotic form of superconductivity-like behavior. The PI had shown how an impurity atom embedded in a Bose-Einstein condensate (BEC) -- the matter analogue of a laser -- can self-localize into a polaron like state [2]. We have calculated the polaron size in a Feynman path integral study [3], and we have revealed how the acceleration of localized objects through the BEC gives rise to phonon Bremstrahlung. We have studied how the impurity-boson interactions can be finite-ranged using narrow Feshbach resonances [4], and how a BEC-embedded object can induce a standing wave BEC-pattern [5]. Following up on collective excitation studies of mediated interactions that revealed the importance of retardation effects [6], [7], we have studied mediated interactions in the equation of state of fermion-BEC mixtures [8]. We have shown that mediated interactions cause the divergence of the compressibility and cause phase separation. We have shown that the fermion-BEC phase separation, a first-order quantum phase transition [9], nucleates into isolated droplets of pure BEC [10], [11] and that the nucleation process can take place as the macroscopic quantum tunneling process [12] predicted in helium fluids but never observed experimentally [13]. We have shown how controlling potential and/or interaction parameters in a phase separated BEC-mixture can yield an ultra-sensitive measurement of external forces by nearly canceling the forces that act on a droplet of separated BEC [14].

## Background and Research Objectives

Mimicry or the ability to emulate other systems of nature has been at the heart of the success of cold atom physics. The cold atom systems, created in carefully controlled ultra-high vacuum conditions, are dilute: their density is typically one thousand to ten thousand times lower than the density of air. Nevertheless, because of the extremely low temperatures reached by laser cooling, the dilute, cold atom gases exhibit superfluid properties. The term “superfluidity” refers to a series of counter-intuitive phenomena that are associated with macroscopic quantum behavior: e.g. dissipationless flow, interference fringes (regular wiggle patterns) that are consistent with the atoms moving in perfect, laser-like lock-step coherence, and quantized vortices (swirling patterns) in which each atom has exactly the same angular momentum corresponding to Panck’s constant. Unlike traditional superfluids, the relevant length and time scales are nearly macroscopic – tens to hundreds of thousands of times larger than in traditional, condensed matter superfluids. As a consequence, cold atom superfluids exhibit unprecedented experimental accessibility and control. The richness of the experiments was greatly enhanced when the cold atom traps were able to trap multiple spin components and even multiple species of atoms. Cold atom technology can exert different forces on the different kinds of atoms and image them separately. By applying a homogeneous magnetic field, tuned near specific field strengths, the experimentalists can control the interaction strength between any pair of particle types (although one can

only tune one pair of interactions at the time).

This project pursued the new basic science prospects offered by the superfluid nature of the systems, the unprecedented access and control and the ultra-low temperatures to explore fundamental many-body quantum properties. We have focused on prospects that have not been accessible to traditional low temperature physics such as those implied by multi-spin manipulation and inter-particle interaction control. On the applied science side, the project explored new measurement strategies, strategies that rely on the cold atom capability of trapping cold atom mixtures and that differ from the interferometry schemes.

## Scientific Approach and Accomplishments

The general approach of this project combined a thorough knowledge of the experimental capabilities with a multi-disciplinary theory-approach to many-body problems. Specifically, the polaron, superfluidity, mediated interaction and quantum phase transition descriptions were borrowed from condensed matter; the macroscopic tunneling descriptions combine condensed matter and quantum optics expertise; the phonon Bremstrahlung description relied on a mixture of hydrodynamic and field theory methods; the finite range effective interaction studies were conducted with the separable potential model of nuclear physics and used a scattering description; the stability of the standing wave BEC-patterns was investigated by the tool of linear stability analysis of nonlinear physics, and the BEC-level measurement device was described as phase separated, compressible fluids. Such mixing of expertise is typical of today's cold atom physics: the cold atom prospects cover a wide range of many-body phenomena of interest to several areas of physics. Below, we describe the main achievements.

**Odd-pairing fermion superfluidity in cold atom mixtures**

We have studied a novel "odd frequency" pairing mechanism in a cold gas mixture of a single species of fermions with bosons [1]. A pure fermion gas composed of a single hyperfine species, i.e., a "spin-polarized" Fermi gas, acts as a non-interacting ideal Fermi gas because the Pauli exclusion principle forbids direct s-wave scattering, and p-wave scattering can be neglected at the relevant ultra-cold temperatures. If one mixes a BEC into this spin-polarized Fermi gas, however, longer-range effective interactions can occur. In addition to the direct boson-fermion interaction, the mixture will also have mediated interactions, i.e., the fermions, which were non-interacting on their own, will have boson-mediated interactions due to the phonon field of the bosons. The phonon field can lead to pairing of the fermions, but since the fermion system is spin-polarized, only triplet pairing states are possible. Due to symmetry arguments, one would then normally expect the dominant pairing mechanism to be in the p-wave channel, similar to the p-wave triplet pairing that occurs in $^3$He. However, it turns out that an exotic pairing mechanism known as "odd-frequency" pairing could occur in the s-wave triplet channel. This odd-frequency pairing was first proposed for $^3$He and later for high-$T_C$ superconductors, but has never been observed. We have shown that, in certain regimes, the s-wave odd-frequency phase might become dominant over the standard p-wave mechanism in cold gas mixtures, and have suggested signatures of this novel superfluid state of matter.

**BEC-polarons**

As a superfluid, the BEC and the superfluid fermion system, the neutral particle analogue of a superconductor, support low lying collective excitations that are phonon-modes (i.e. Goldstone modes with a linear dispersion in the long wavelength limit). The coupling of an impurity atom with the phonon modes reduces the description of the impurity atom in the BEC to a polaron description. As was pointed out by the Principle Investigator [2], a sufficiently strong impurity-boson interaction leads to self-localization in a mechanism that is similar to the self-localization of an electron in an ionic crystal – the traditional polaron problem. Unlike traditional polarons, the interactions between the polaron particle and the bosons can be continuously varied. The BEC-impurity system could then be used to address some of the unanswered questions of polaron physics: for instance, does the derivative of the effective polaron mass vary discontinuously with increasing polaron-boson interaction when the polaron self-localizes [15]. Interestingly, a recent calculation by the Principle Investigator with Jacques Tempere [3], who visited LANL with support from this project, shows a non-monotonic variation of the polaron size with increasing fermion-boson interaction strength. Is this counter-intuitive variation a signature of 'self-localization'?

**Finite range effective inter-particle interactions in cold atom systems**

As mentioned above, the ability to emulate interesting many-body quantum systems has provided a prime motivation for cold atom physics. However, the range and details of the inter-particle interactions has played an important, sometimes decisive role in many of the many-body systems of fundamental interest. Cold atom physics, in contrast, has only been able to explore short-range contact interactions so far. The restriction to short-range interactions has been a severe limitation in the cold atom's capacity for many-body emulation.

Our recent studies [4] of narrow Feshbach resonances,

however, show that effective finite-range cold atom inter-particle interactions can be accessed with existing technology: narrow Feshbach resonances with magnetic field widths that can be resolved with today's technology give rise to effective finite-range interactions. Moreover, we have shown that the corresponding binary-atom interactions take on a particularly simple form, at least in the narrow limit. In the impurity-BEC systems, the narrow resonance can energetically favor non-vanishing BEC-impurity velocities.

**Standing Wave Patterns in BEC's**

A localized object embedded in a BEC such as a self-localized impurity BEC polaron, a tightly trapped distinguishable atom or ion, or a localized, external potential well modifies the density of the surrounding BEC. Can the BEC, in response to such localized attraction take on a standing wave pattern with a density that vanishes at the surfaces on which the BEC wavefunction changes sign? If such patterns can be supported by the BEC as long-lived structures, their behavior or motion could be used to detect a flow of the BEC and observe, for instance, the rotation of a rang-BEC which could act as a gyroscope. We have studied the standing wave patterns and their stability [5].

We elucidate the nature of the different standing wave BEC-patterns and study their dynamical stability in two dimensions. Our analysis reveals general trends, valid in two and three dimensions, independent of the symmetry of the localized potential well, and suggestive of the behavior in general, short- and large-range potentials. One set of nodal BEC-wavefunctions resemble the single particle n-node bound state wavefunction of the potential well, the other wavefunctions resemble the n-1 node bound-state wavefunction with a kink state pinned by the potential. The second state, though corresponding to the lower free energy value of the pair of n-node BEC-states, is always unstable, whereas the first can be dynamically stable in intervals of the potential well depth, implying that the standing wave BEC can evolve from a dynamically unstable to stable, and back to unstable status as the potential well is adiabatically deepened, a phenomenon that we refer to as ``reentrant dynamical stability''.

**Mediated interactions in fermion-BEC mixtures**

The participants of this project have discovered [8] how and why mean-field descriptions of quantum degenerate fermion-boson gas mixtures fail near the first order quantum phase transition that causes the mixture to phase separate. In addition to providing a significant correction to the densities at which the phase separation takes place, the studies also show the culprit to be fermion-mediated interactions that counteract the short distance boson-boson repulsions and cause an overall attraction which tends to break up the BEC. On the mixed phase side, the mediated interactions become longer and longer ranged near the phase separation point and they also cause the compressibility of the boson gas to diverge. Exactly how the range and the compressibility diverge remains a challenging question. The scaling coefficients, which could be measured experimentally, could provide the first measurement of quantum critical scaling. We have studied the equation of state of the mixed phase and pointed out the qualitative differences of its predictions for the density profile in inhomogeneous traps with the predictions of mean-field theory.

The mediated interactions studied in this project also cause the phase separation of the traditional condensed low temperature $^3$He and $^4$He. Unlike the situation in traditional superfluids, the inter-species interactions can be varied in cold atom systems and, perhaps, used for gate operations in quantum information experiments. The self-localization induced by increasing the interaction of a single impurity atom with the boson atoms of a Bose-Einstein condensate (BEC) can finally allow cold atom experimentalists to localize and transport atoms inside a BEC, suggesting new studies of superfluidity, light localization and, perhaps, the creation of a quantum register of movable cold atom qu-bits.

**Quantum nucleation in fermion-BEC mixtures**

The phase separation can set in at densities below the values at which the system becomes mechanically unstable. The mechanical instability causes the phases to separate into chunks of roughly the same size and is known from finite temperature (ordinary) phase separation transitions as 'spinodal decomposion' [10], [11]. Below the line of spinodal decomposition, the phase separation can happen as the result of a process that overcomes the free energy barrier that separates the two minima of the transition. At finite temperature, this process is thermal activation - local collision processes push the system over the barrier - but at sufficiently low temperatures, the system has to quantum tunnel through the barrier. The nucleation process that causes the phases to separate in ultra-low temperature fermion-boson mixture is a many-body macroscopic tunneling process, which suggests that such cold atom mixtures could give the first clean observations of macroscopic quantum tunneling [12]. We have explored the prospect of studying this type of macroscopic quantum tunneling in cold atom systems.

**Phonon radiation emitted by the motion of localized objects through a BEC**

We have studied the near-equilibrium dynamics of a BEC with moving impurity atoms. The description we

developed of the BEC-response (involving the creation and annihilation of phonon modes) emphasizes the analogy with electromagnetism. This description reveals the reason for why accelerating impurities cause phonons to radiate. The underpinning mechanism is closely analogous to that causing accelerating charges to emit light (a process known as Bremstrahlung). The BEC-study allows us to qualitatively predict the energy loss of cold atoms that are being cooled at velocities below the critical velocity for BEC-superfluidity (subsonic cooling. We have shown how effective subsonic cooling can be if the experimentalists insert an optical potential in the cold atom trap in an effort to cool impurity atoms down to lower temperatures than currently reached with sympathetic cooling. This treatment also reveals the finite system limitations of cold atom physics in studying fundamental superfluid phenomena such as the predicted Casimir-like drag and the study of self-localized BEC polarons.

## Impact on National Missions

This project supports the DOE mission of basic science and explores the prospect of ultra-high resolution sensors. This project has explored many-body physics that plays a role in low temperature material and actinide science, and it has investigated prospects for quantum information experiments. The sensors measure weak external forces, which could be helpful in the security mission of the laboratory.

## References


1. Kalas, R. M., A. V. Balatsky, and D. Mozyrsky. Odd-frequency pairing in a binary mixture of bosonic and fermionic cold atoms. 2008. *Physical Review B.* **78**: 184513.

2. Cucchietti, F., and E. Timmermans. Strong coupling polarons in dilute Bose-Einstein condensates. 2006. *Physical Review Letters.* **96**: 210401.

3. Tempere, J., W. Casteels, M. K. Oberthaler, and E. Timmermans. Feynman path-integral treatment of the BEC-impurity polaron. To appear in *Physical Review A.*

4. Kalas, R., and E. Timmermans. Simplified description of narrow Feshbach resonances. *Physical Review A.*

5. Kalas, R., D. Solenov, and E. Timmermans. Reentrant stability of standing wave BEC-patterns. To appear in *Physical Review A.*

6. Santamore, D. H., S. Gaudio, and E. Timmermans. Zero sound in a mixture of a zero-sound fermion gas and a Bose-Einstein condensate. 2004. *Physical Review Letters.* **93**: 250402.

7. Santamore, D. H., and E. Timmermans. Collective oscillations of low-density fermion-boson quantum liquid mixtures. 2005. *Physical Review A.* : 53601.

8. Santamore, D. H., and E. Timmermans. Fermion-mediated interactions in a dilute Bose-Einstein condensate. 2008. *Physical review A.* **78**: 013619.

9. Viverit, L., and C. J. Pethick. Zero temperature phase diagram of binary boson-fermion mixtures. 2000. *Physical Review A.* **61**: 053065.

10. Solenov, D., and D. Mozyrsky. Quantum Nucleation and Macroscopic Quantum Tunneling in Cold-Atom Boson-Fermion Mixtures. 2008. *Physical Review A.* **78**: 053611.

11. Solenov, D., and D. Mozyrsky. Kinetics of phase separation transition in cold-atom boson-fermion mixtures. 2008. *Physical Review Letters.* **100**: 150402.

12. Mozyrsky, D., I. Martin, and E. Timmermans. Coherent macroscopic quantum tunneling in boson-fermion mixtures. 2007. *Physical Review A.* **76**: 051601.

13. Takagi, S.. Some candidate systems for macroscopic quantum tunneling. 2005. In *Macroscopic quantum tunneling.* By Takagi, S.. , Second Edition, p. 41. Cambridge: Cambridge University Press.

14. Bhongale, S., and E. Timmermans. Phase separated BEC for high-sensitivity measurement. 2008. *Physical Review Letters.* **100**: 185301.

15. Larsen, D. M.. Polaron energy levels in magnetic and Coulomb fields. 1972. In *Polarons in ionic crystals and polar semiconductors.* Edited by Devreese, J. T.. , p. 237. Amsterdam: North-Holland Publishing Company.


## Publications


Bhongale, S., and E. Timmermans. Phase separated BEC for high-sensitivity measurement. 2008. *Physical Review Letters.* **100**: 185301.

Cucchietti, F. M., B. Damski, J. Dziarmaga, and W. H. Zurek. Dynamics of the Bose-Hubbard Model: Transition from Mott insulator to Superfluid. 2007. *Physical Review A.* **75**: 023603.

Cucchietti, F. M., S. Fernandez-Vidal, and J. P. Paz. Universal Decoherence induced by an Environmental Phase Transition. 2007. *Physical Review A.* **75**: 032337.

Kalas, R., A. Balatsky, and D. Mozyrsky. Odd-frequency pairing in binary boson-fermion cold atom mixtures. 2008.

*Physical Review A.* **78**: 184513.

Kalas, R., D. Solenov, and E. Timmermans. Reentrant stability of standing wave BEC-patterns. To appear in *Physical Review A.*

Kalas, R., and E. Timmermans. Simplified description of narrow Feshbach resonances. *Physical Review A.*

Mozyrsky, D., I. Martin, and E. Timmermans. Coherent Mesoscopic tunneling in Boson Fermion Mixtures. 2007. *Physical Review A.* **76** (5): 051601(R).

Santamore, D., and E. Timmermans. Fermion mediated interactions in a dilute Bose-Einstein Condensate. 2008. *Physical Review A.* **78**: 013619.

Solenov, D., and D. Mozyrsky. Quantum Nucleation and Macroscopic Quantum Tunneling in Cold-Atom Boson-Fermion Mixtures. 2008. *Physical Review A.* **78**: 053611.

Solenov, D., and D. Mozyrsky. Kinetics of phase separation transition in cold-atom boson-fermion mixtures. 2008. *Physical Review Letters.* **100**: 150402.

Tempere, J., W. Casteels, M. K. Oberthaler, and E. Timmermans. Feynman path-integral treatment of the BEC-impurity polaron. To appear in *Physical Review A.*

# Investigation of Energetic Ion Generation and Transport in Ultra-Intense Laser-Matter Interaction

*Brian J. Albright*
20070235ER

## Abstract

Intense, short-pulse lasers interact with thin (<10s of micron) foils to make ion beams with remarkable properties. These beams promise to revolutionize several areas of Laboratory interest in areas such as energy, exotic matter, medicine, active interrogation, and national security. Laser-generated ion beams beat conventional accelerators in many key areas. They have tiny beam emittance, huge electric fields, and sub-ps beam duration. Prior to this work, advances have been driven empirically, as theory and modeling lagged experiments. Not so, any more. Now, with the application of VPIC, our kinetic plasma modeling, we have modeled these experiments at realistic laser and plasma conditions. This work, the first of its kind, has born fruit with the invention of a *new* acceleration mechanism that improves conventional beams by an order of magnitude in beam energy and efficiency. VPIC is many times faster than conventional codes of its type, and allows simulations to be done with rapid turn-around time. VPIC is also one of the few codes that runs efficiently on Roadrunner, presently the world's most powerful supercomputer. The unique combination of computing, theory, experiments, and targeted R&D investment have hoisted LANL to world leadership in this important field.

## Background and Research Objectives

As described in the Abstract, laser-generated ion beams are a subject of intense interest at the Laboratory and the Complex for their potential to impact a host of applications. The proposed work was to study the laser-ion acceleration mechanism in ultra-intense-laser thin-foil irradiation experiments and to examine the propagation of these intense beams into high density matter (solid and beyond). Dependence of ion acceleration on target parameters (thickness, composition, conductivity) and laser parameters (intensity, temporal and spatial profiles, spot size, pre-pulse properties) was to be established. This work built upon (1) investigator expertise in the simulation and theory of ultra-intense laser-matter interaction (2) a unique simulation capability that is ideal for the study of these problems, and (3) Institutional Computing resources (1.05 million hours allocated, starting 3QFY06) available for this work.

The broad goal of the project was to advance our understanding of relativistic laser-matter interactions. The specific goal is to validate theoretical models of energetic ion production and transport and to provide a predictive capability for the design of experiments and optimization of compact high-energy high-quality ion beams for a host of follow-on applications. We met these goals.

We refined our understanding of novel mechanism for ion acceleration, the Break-Out Afterburner (BOA). This mechanism has the promise to deliver table-top GeV ion beams for several applications. We uncovered the physics underlying the enhanced ion acceleration in the BOA. We developed a predictive capability for laser absorption in ultrathin media, which includes self-similar target expansion at the sound speed. This inspired experiments which led to world-record ion beam production on the Trident laser. We contributed to the first-ever demonstration of relativistic transparency. We investigated ion beam propagation into dense plasma targets, such as those used in ion driven fast ignition and we were able to set beam criteria for success of such experiments.

The two figures show highlights of our work. Figure 1 is a comparison of VPIC simulations, analytic theory, and Trident experiments of laser-ion acceleration in the BOA from our recent paper containing the first ever demonstration of laser-induced relativistic transparency [1]. Relativistic transparency happens when electrons in a plasma become very hot—hundreds of billions to as high as trillions of Kevlin. When the plasma becomes

so hot, the electrons become relativistically heavy and are unable to oscillate in the laser field fast enough to short out the oscillating electric field of the laser. This causes the matter to "bleach" in the laser field. It turns out that the act of turning transparent is key to the BOA; the details relating to how were discovered and explored in the proposed work. Figure 2 shows integrated LASNEX simulations of an ion-driven fast ignition target [2]. This was the first ever demonstration of the feasibility of ion driven fast ignition and shows that indeed laser-driven ion beams can penetrate into a compressed inertial confinement fusion target and ignite the plasma. This demonstration has generated much excitement in the field (as well as several follow-on publications) and has led to the funding of a new DOE Office of Science, Office of Fusion Energy Sciences project in ion-driven fast ignition, led by LANL researchers.

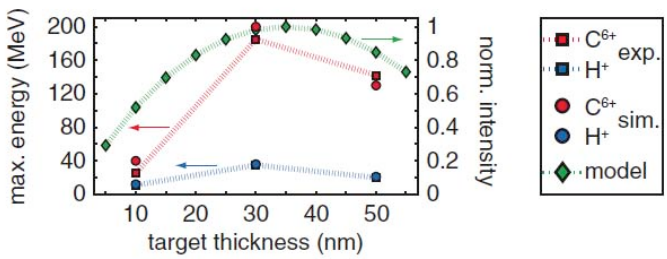


*Figure 1. Normalized laser intensity (diamonds) at burn-through time in 30 nm diamond-like carbon foil at the Trident laser based on model developed in this project. Also shown is a comparison of Trident experimental data and VPIC modeling of this experiment. Details of this work are reported in Ref. [1].*

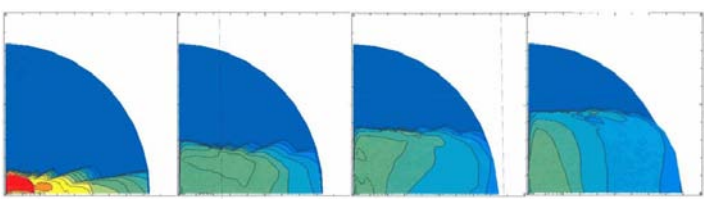

*Figure 2. Thermonuclear burn rate from integrated radiation hydrodynamics simulations of a laser-driven inertial confinement fusion capsule subject to a pair of counter-directed ion beams of 500 MeV (+/- 50 MeV) fully-ionized carbon ions. If these beams have of order 10 kJ of total beam energy, fusion ignition ensues [2].*

## Scientific Approach and Accomplishments

We refined our understanding of novel mechanism for ion acceleration, the Break-Out Afterburner (BOA). This mechanism has the promise to deliver table-top GeV ion beams for many applications. We uncovered the physics underlying the enhanced ion acceleration in the BOA. We developed a predictive capability for laser absorption in ultrathin media, which includes self-similar target expansion at the sound speed. This inspired experiments which led to world record ion beam production on Trident laser. We contributed to the first-ever demonstration of relativistic transparency. We investigated ion beam propagation into dense plasma targets, such as those used in ion driven fast ignition and we were able to set beam criteria for success of such experiments.

Papers, Invited Talks, Awards and Honors: Published 19 peer-reviewed papers, including two Physical Review Letters. We have a Nature article in preparation (to be submitted soon) and three papers in preparation. Presented 18 invited and plenary talks. Team member won the 2008 Katherin E. Weimer Award for Women in Plasma Science, an APS Div. of Plasma Physics Career Award. Two LANL Distinguished Performance awards (1 large team, 1 small team). Two DOE/NNSA Defense Programs Awards of Excellence. PI named to Congressional Record in Senate Resolution S7974. Three LANL Spot Awards won—one for postdoc mentoring, two for X Div. Review Committee. Selected to present project to LANS Mission Committee. Selected to present project to High Energy Density Physics and Fluids Capability Review. Contributed to LDRD Day presentation, which won Poster of Exceptional Merit award. Recruited a postdoc who won a prestigious Director's Fellowship.

## Impact on National Missions

This work has accomplished the goals of the project. It has resulted in a significantly improved understanding of ultra-intense laser-plasma interaction. Motivated by VPIC simulation results, the Trident short-pulse laser has been redesigned to both deliver higher power and much improved laser contrast. This gives LANL a unique capability unmatched by others and has contributed to the refactoring of Trident into a User Facility. This capability has also been used to do short-pulse laser-plasma-interaction studies relevant to conventional inertial confinement fusion research as well as fast-ignition.

Several follow-on projects were enabled by this work. This includes an LDRD ER project (PI: Flippo) and a PRD project (PI: Albright). The Investigators secured funding from outside the Laboratory from DNDO and NNSA/DOE Office of Science. This project led to several improvements in the VPIC code, particularly in hybrid (fluid electron, particle ion) and collision modeling. Improvements to VPIC led to two special LDRD projects on science using Roadrunner as well as improved capability in laser-plasma interaction for the Science Campaigns (particularly C10) as well as ASC Physics and Engineering Models.

Over the course of this project we hired three postdocs, including one Director's Postdoctoral Fellow. One of the postdocs on this project has since gone on to a staff position at the Naval Research Laboratories.

## References


1. Henig, A., D. Kiefer, C. Gautier, K. Flippo, S. Letzring, R. P. Johnson, T. Shimada, L. Yin, B. J. Albright, K. J. Bowers, J. C. Fernandez, S. G. Rykovanov, H. C. Wu, M. Zepf, V. Kh. Liechtenstein, J. Schreiber, D. Habs, and B. M. Hegelich. Enhanced laser-driven ion acceleration in the relativistic transparency regime. 2009. *Physical Review Letters.* **103**: 045002.

2. Albright, B. J., M. J. Schmitt, J. C. Fernandez, G. E. Cragg, I. Tregillis, L. Yin, and B. M. Hegelich. Studies in capsule design for mid-Z ion-driven fast ignition. 2008. *Journal of Physics Conference Series.* **112**: 022029.


## Publications


Albright, B. J., L. Yin, B. M. Hegelich, K. J. Bowers, C. Huang, A. Henig, J. C. Fernandez, K. A. Flippo, S. Gaillard, T. J. T. Kwan, X. Q. Yan, T. Tajima, and D. Habs. Ultraintense laser interaction with nanoscale targets: a simple model for layer expansion and ion acceleration. To appear in *Journal of Physics Conference Series.*

Albright, B. J., L. Yin, Kevin J. Bowers, B. M. Hegelich, K. A. Flippo, T. J. T. Kwan, and J. C. Fernandez. Relativistic Buneman instability in the laser break-out afterburner. 2007. *Physics of Plasmas .* **14**: 094502.

Albright, B. J., L. Yin, Kevin J. Bowers, B. M. Hegelich, K. A. Flippo, T. J. T. Kwan, and J. C. Fernandez. Relativistic Buneman instability in the laser break-out afterburner. 2007. *Virtual Journal of Ultrafast Science.* **6**: 10.

Albright, B. J., M. J. Schmitt, J. C. Fernandez, G. E. Cragg, I. Tregillis, L. Yin, and B. M. Hegelich. Studies in capsule design for mid-Z ion-driven fast ignition. 2008. *Journal of Physics Conference Series.* **112**: 022029.

Bowers, K. J., B. J. Albright, B. Bergen, L. Yin, K. J. Barker, and D. J. Kerbyson. 0.374 Pflop/s trillion-particle kinetic modeling of laser plasma interaction on Roadrunner. To appear in *2008 Association of Computing Machinery/ Institute for Electrical and Electronic Engineers Conference on Supercomputing.* (Austin, Texas, USA, 17-22 Nov., 2008).

Bowers, K. J., B. J. Albright, L. Yin, W. Daughton, V. Roytershteyn, B. Bergen, and T. J. T. Kwan. Advances in petascale kinetic plasma simulation with VPIC and Roadrunner. To appear in *2009 Scientific Discovery through Advanced Computing (SciDAC) Conference.* (San Diego, California, 14-18 June, 2009).

Bowers, Kevin J., B. J. Albright, L. Yin, B. Bergen, and T. J. T. Kwan. Ultra high performance three-dimensional electromagnetic relativistic particle-in-cell simulation. 2008. *Physics of Plasmas .* **15**: 055703.

Cragg, G. E., and A. K. Kerman. Coherent decay of Bose-Einstein condensates. 2007. *Physical Review Letters.* **98**: 080405.

Cragg, G. E., and A. K. Kerman. Independent pair approximation for attractive Bose condensates. 2007. *Physics Letters A.* **371**: 7.

Fernandez, J. C., Brian J. Albright, Kirk A. Flippo, Bjorn M. Hegelich, Thomas J. T. Kwan, Mark J. Schmitt, and L. Yin. Progress on ion based fast ignition. 2008. *Journal of Physics Conference Series.* **112**: 022051.

Fernandez, J. C., J. J. Honrubia, B. J. Albright, K. A. Flippo, D. Cort Gautier, B. J. Hegelich, M. J. Schmitt, M. Temporal, and L. Yin. Progress and prospects of ion driven fast ignition. 2009. *Nuclear Fusion.* **49**: 069004.

Flippo, K., B. M. Hegelich, B. J. Albright, L. Yin, D. C. Gautier, S. Letzring, M. Schollmeier, J. Schreiber, R. Schulze, and J. C. Fernandez. Laser-driven ion acceleators: spectral control, monoenergetic ions and new acceleration mechanisms . 2007. *Laser and Particle Beams.* **25** (1): 3.

Flippo, K., E. d'Humieres, S. A. Gaillard, J. Rassuchine, M. Schollmeier, F. Nurberg, J. Adams, B. Albright, M. Bakeman, D. C. Gautier, N. R.-L. Galloudec, K. Harris, R. P. Johnson, J. L. Kline, G. Korgan, S. Letzring, S. Makelos, T. Shimada, M. Roth, T. E. Cowan, J. C. Fernandez, and B. M. Hegelich. Increased efficiency of short-pulse laser generated proton beams from novel flat-top cone targets. 2008. *Physics of Plasmas .* **15**: 056709.

Henig, A., D. Kiefer, C. Gautier, K. Flippo, S. Letzring, R. Johnson, T. Shimada, L. Yin, B. J. Albright, J. Fernandez, K. Markey, M. Zepf, V. Kh. Liechtenstein, S. G. Rykovanov, H. C. Wu, J. Shreiber, D. Habs, and B. M. Hegelich. Enhanced laser-driven ion acceleration in the relativistic transparency regime. 2009. *Physical Review Letters.* **103**: 045002.

Kline, J. L., D. S. Montgomery, R. A. Hardin, K. A. Flippo, T. Shamada, R. P. Johnson, L. Yin, H. A. Rose, and B. J. Albright. Investigation of laser plasma instabilities using picoseconds laser pulses. 2008. *Journal of Physics Conference Series .* **112**: 022042.

Lemons, D. S., B. J. Albright, D. Winske, Kevin J. Bowers, and W. Daughton. Collision models for plasma simulation codes (U). 2008. In *Proceedings of the Nuclear Explosives Design Physics Conference.* (Los Alamos, NM, 22-26 Oct. 2007). , p. 1. Livermore, California: LLNL.

Lemons, D. S., W. Daughton, D. Winske, and B. J. Albright.

Small-angle Coulomb collision model for PIC codes. 2009. *Journal of Computational Physics.* **228**: 1391.

Yan, X. Q., T. Tajima, B. M. Hegelich, L. Yin , and D. Habs. Theory of laser ion acceleration from a foil target of nanometer thickness. To appear in *Applied Physics B, Lasers and Optics.*

Yin, L., B. J. Albright, Kevin J. Bowers, B. M. Hegelich, K. A. Flippo, T. J. T. Kwan, and J. C. Fernandez. Monoenergetic and GeV laser ion acceleration from the laser break-ouit afterburner using ultrathin targets. 2007. *Physics of Plasmas .* **14**: 056706.

# New States of Matter in Stars, Nuclei and Cold Atoms

*Sanjay Reddy*
20070276ER

## Abstract

We have studied strongly interacting many-fermion systems that exhibit superfluid properties. Using both computational and analytic methods we demonstrate that these systems show universal behavior. A fermion system of $^6$Li atoms cooled to nano-Kelvin temperatures in the laboratory shares several similarities with ultra-dense neutron matter in neutron stars. Both these systems exhibit strong pairing between particles through cooperative phenomena essential for superfluid behavior in Fermi systems. The strength of this pairing is fundamental property of these systems and is characterized by a quantity called the pairing gap. Our theoretical work predicted the strength of this pairing gap and related properties. We showed that a simple and robust experimental measurement of density profiles in cold-atom experiments would be sufficient to determine the gap. The gap extracted in this way was in excellent agreement with our theoretical prediction. In addition to symmetrical Fermi systems where the densities and masses of the pairing partners are equal, we have studied asymmetrical systems composed of different number densities and masses. In asymmetrical systems we find that multiple phases with varying degrees of local asymmetry can coexist in cold atom experiments. We identify the general conditions for phase coexistence between normal and superfluid phases. These conditions are likely to provide new insights on phase transitions in very dense fermionic matter expected to exist inside neutron stars where asymmetrical Fermi systems occur naturally.

## Background and Research Objectives

Cold and dense matter containing fermions is ubiquitous in nature. Electrons in terrestrial solids and compact astrophysical objects called white dwarfs, nucleons in nuclei, nucleons and perhaps de-confined quark matter inside neutron stars are well-studied examples. Since the pioneering work of Bardeen, Cooper and Schrieffer (BCS) over 50 years ago [1] it has been realized that these many-fermion systems with attractive interactions will exhibit novel properties such as superfluidity and superconductivity. Their work provided a microscopic theory that explained superconductivity in some metals as arising from strong pairing between spin-up and spin-down electrons due to an attractive interaction induced by the vibrations of the solid. Decades earlier in 1925 Wolfgang Pauli had postulated the now celebrated "Pauli Principle" that stated that no two identical fermions could occupy the same state [2]. A natural consequence of this exclusion principle is that a dense gas of identical fermions would occupy a continuum of momentum states. Further the number of states with different momentum vectors but very similar energies would grow rapidly with density. This feature is called degeneracy since there exists a large number of particles with the largest momentum (pointing in different directions) but with similar energies. This characteristic large momentum is called the Fermi momentum and the corresponding energy is called the Fermi energy. BCS theory provided a major breakthrough in our understanding of these degenerate systems by providing a theoretical framework that demonstrated that even small attractive interactions in degenerate systems leads to cooperative phenomena where fermions form pairs. This leads to radically different behavior from that expected in non-interacting fermion systems. Unlike normal non-interacting Fermi systems, where it costs an infinitesimal energy to excite a fermion from an occupied to an unoccupied state, the energy cost to create such an excitation in a system with attractive interactions where pairing is inevitable is finite. This finite excitation energy is called the energy gap or simply the gap of is a fundamental property of the superfluid or superconducting state [1].

These basic notions regarding fermions with attractive interactions have been around for many years, yet, surprisingly, it has taken physicists more than 50 years to develop the experimental and theoretical methods

necessary to measure the gap and related properties in systems where the fundamental interaction strength can be tuned. This is critical if we are to establish a relationship between the strength of the fundamental interaction and the size of the pairing gap. When the strength of the interaction is small, theoretical methods to calculate the gap based on perturbation theory are well developed and there is consensus that they should apply to weakly interacting Fermi systems. However, the regime of its validity has never been experimentally tested.

In the past decade breakthroughs in experimental atomic physics have made it possible to realize a superfluid state of fermion matter where the fundamental interaction can be both measured and tuned. In the laboratory alkali metal atoms (atoms with one electron in the outermost orbit) of either $^{6}$Li or $^{40}$K atoms are trapped and cooled to nano-Kelvin temperature and are shown to exhibit superfluid behavior [4,5,6]. In these systems, the strength of the interaction between atoms in different hyperfine states can be tuned by an external magnetic field. Loosely speaking, and to evoke an analogy with electron superconductors, we can think of the two hyperfine states of interacting atoms as spin-up and spin-down states of the atom. The interaction has a range that is much smaller than the inter-particle distance and is therefore always negligible between identical atoms - as one would infer from Pauli's exclusion principle. On the other hand since spin-up and spin-down atoms can get arbitrarily close to each other their interactions would be important. This interaction could be tuned by applying an external magnetic field through a process known as the Feschback resonance. We will not discuss the details of this process in this brief report but it will suffice to mention that it allows the experimentalist to adjust the interaction from weak attraction where the interaction is not strong enough to bind the two atoms together, to very strong attraction that can tightly bind atoms together into a molecule. A quantity called the scattering length is measure of this short-range interaction strength is typically denoted by "a." When the interaction is weak and attractive the scattering length is small and negative and when the interaction is strong enough to tightly bind it is positive. Somewhere in between, the scattering length changes sign as it becomes infinitely large. This point, where the scattering length is infinite is called the unitary regime. It separates the regions with and without bound states for the two-atom system. In the many-particle system, these two regimes are called the BCS (attractive interactions but no two particle bound state) regime and the BEC regime (strong attractive interactions with a two-body bound state). This is illustrated in Figure 1, where loosely bound overlapping pairs (the analogue of electron Cooper pairs in BCS theory) with spatial extent much larger than the inter-particle distance are shown in the right lower corner (labeled BCS). Tightly bound molecules form bosons when the interaction is very strong and here the size of the boson is much smaller than the inter-particle distance (labeled BEC for Bose-Einstein condensate regime).

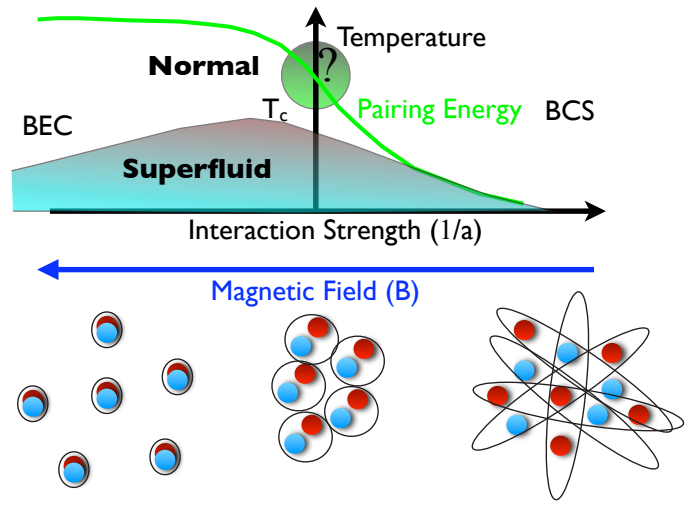


*Figure 1. Schematic figure showing the strong and weak coupling regions being explored in cold atom experiments. The unitary regime separates the BCS and BEC regions (see text for an explanation).*

The unitary regime where the scattering length is infinite presents a unique many-particle system. It is strongly interacting and yet there is no dimensional measure of this strength. All properties of the system can be expressed as a function of the particle density - as in the case of a non-interacting gas of fermions. For example, the energy per particle at near zero-temperature will have the form $E = \xi E_{FG}$ where $E_{FG}$ is the energy per particle of a non-interacting Fermi gas. $\xi$~0.4 is a universal constant that had predicted by theoretical work and confirmed experimentally in cold atom experiments. Similarly, the energy gap of the superfluid state at unitarity is given by $\Delta = \delta E_F$ where $\delta$ is a universal constant. Developing theoretical methods to predict the value of $\delta$ from a microscopic theory and devising a strategy to measure this directly in an experiment has been a major goal in this area of research. In the subsequent section we shall describe how our research helped address both of these issues.

While cold atom experiments have now firmly established that symmetric Fermi systems with attractive interactions show superfluid behavior at low temperature, the phase structure and properties of asymmetric systems is largely unknown. The asymmetry can be caused either by trapping different numbers of spin-up and spin-down fermions, or by trapping atoms with different masses (a mixture of $^{6}$Li or $^{40}$K atoms), or both. For the case of equal masses but

different densities, theoretical predictions span a wide range of possibilities. They include: (i) phase separation into symmetric (unpolarized) superfluid state that coexists with macroscopic regions of normal state with a high degree of polarization (polarization here implies an excess of one species); (ii) A uniform superfluid state with a finite polarization in the bulk (this phase is also called a gapless superfluid because the excess species behaves like a normal Fermi system);(iii) inhomogeneous superfluid state where the energy gap varies periodically in space. Inhomogeneous states were proposed earlier by Ferrel and Fulde [8] and by Larkin and Ovchennikov in the context of polarized electronic systems [9]. Finding unambiguous signatures of these novel asymmetric phases has however been elusive in electronic systems and cold atom systems where we have more control on the interactions and asymmetry may provide a better environment to discover them. In the subsequent section we describe our work on asymmetric Fermi systems and identify specific conditions under which we expect novel phases to appear in the cold atom experiments.

## Scientific Approach and Accomplishments

Strongly interacting matter is difficult to study using analytic methods developed to treat quantum mechanics and statistical physics. These methods are based on perturbation theory and typically apply only in regimes where the interaction energy is small compared to the kinetic energy. The exact energy of the system can in principle be written in the form a many dimensional integral. However, this integral cannot in general be obtained using analytic methods and computational methods to evaluate this integral rely in the Monte Carlo method where repeated random sampling of the integrand is used to obtain a statistical measure of the integral. This computational method called Quantum Monte Carlo (QMC) has been applied extensively to study problems in quantum chemistry and nuclear physics. In nuclear physics the interactions are strong and of short-range – analogous to the cold atom systems being studied in recent experiments. Carlson and collaborators developed over the past decade various approaches to study strongly interacting nucleons and we have applied these same methods to cold atom system where controlled experiments are now being performed as described earlier. In earlier work, Carlson and collaborators had predicted the energy per particle of symmetric Fermi gas in the unitary regime [10]. Our main goal was to apply these same techniques to determine the superfluid properties and investigate the possibility of realizing novel states in asymmetric Fermi systems.

During the course of this work Carlson and Reddy performed QMC simulations to extract the value of the energy gap of the superfluid state in the unitary regime [11]. We simulated a symmetric system with one excess fermion and calculated the energy cost associated with this extra particle. Further, by varying the momentum of the extra particle we were able to obtain a curve that described how the energy of the extra particle changed with its momentum. This relation between the energy of the extra particle, which is called a quasi-particle because in the medium its interactions modify its properties, is called the quasi-particle dispersion relation. The minimum of this dispersion curve corresponds to the energy gap [1]. Our next task was to determine how this gap could be measured experimentally. We realized that to measure this we would have to find a situation in which the system would preferentially favor the excitation of only one of the two species involved in the pair present in the symmetric state. Asymmetric systems where there was an excess of one hyperfine species of atoms in the trap naturally provided such an environment. Here measurements of the density profiles of the both species in the trap were already available from experiments done at MIT [12]. These experiments showed that decreasing temperature the trapped Fermi gas phase separated into a cloud of nearly symmetric (unpolarized) superfluid state in the center and a highly polarized normal state in the outer regions. This transition grew increasing sharp with decreasing temperature. A schematic illustration in Figure 2 shows the density profiles in the trap with an excess of spin-up atoms.

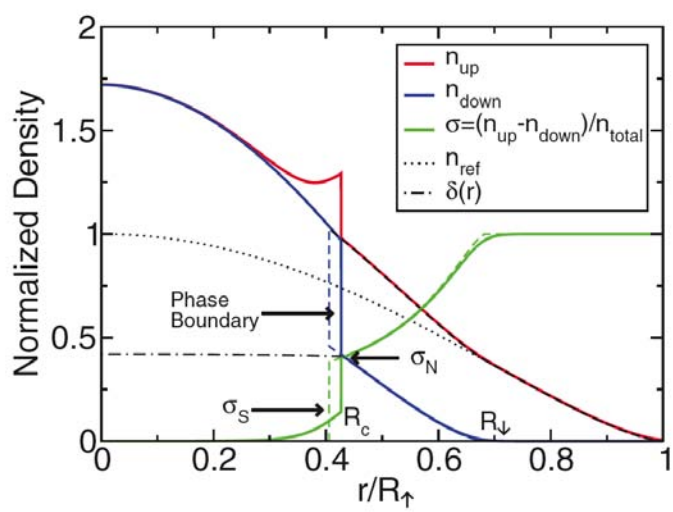


*Figure 2. Superfluid and normal regions inside a cold atom trap. Thermally excited particles exists near the superfluid-normal interface.*

Upon careful examination we discovered that the region close to transition boundary was especially susceptible to generating a polarization because the system favored

exciting the majority species. We used theoretical arguments to show how this polarization in the boundary region within the superfluid state was extremely sensitive to the energy gap and to the temperature and found a means of extracting both of these quantities from the experimentally observed density profiles. We found that the gap $\Delta = (0.45 \pm 0.05)\ E_F$ where $E_F$ is the Fermi energy. This was the largest gap (relative to the Fermi energy) that has been experimentally measured and was in excellent agreement with our QMC prediction [11].

Carlson and Gezerlis then adapted their method to study simultaneously neutron matter at the large densities relevant inside the crusts of neutron stars and cold atoms [13]. They demonstrated the energy per particle and the superfluid gaps showed similar behavior. Further since the method was validated by comparisons to cold atom experiments for both the energy and energy gap, their predictions for neutron matter were significantly more reliable than earlier estimates. In particular, they found that the energy gap was significantly larger than those obtained using approximate many-body methods. This increase in the energy gap is likely to have important implications for modeling thermal evolution of neutron stars where superfluidity of neutron matter is known to affect both the heat capacity and the modes of heat transport in the neutron star [14].

To identify experimental configurations in the cold atom context where novel asymmetrical phases of superfluid matter would occur we explored two different approaches. In the first approach, Sharma and Reddy employed analytic methods, study the conditions under which the homogenous system become unstable to small perturbations that produce gradients in the superfluid density [15]. These methods are quantitatively reliable only when the interactions are weak but often provide qualitative guidance even in the strong coupling region. Our results suggested several parameters that experimentalists can tune to discover these gradient instabilities that are precursors to inhomogeneous supefluidity. In the second approach, Gezrelis, Gandolfi, Schmidt and Carlson studied a system of fermion with different masses - mixtures of $^{6}$Li and $^{40}$K atoms [16]. They find interesting patterns of phase separation in these systems that could be experimentally realized and tested. At unitarity, they predict that such a system would contain three regions as depicted in Figure 3. Here a superfluid is sandwiched between two highly asymmetric normal phase.

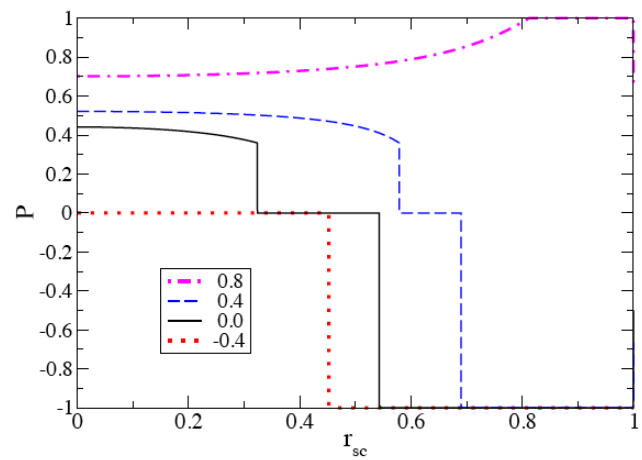


*Figure 3. The superfluid and normal phases in a cold atom trap containing heavy and light species of fermions.*

## Impact on National Missions

Devising and testing theoretical methods to describe strongly coupled fermion systems has a broad range of applications and will help address important questions in nuclear physics, astrophysics and condensed matter physics. We anticipate that our work will impact DOE office of science missions in nuclear physics and nuclear astrophysics since they bridge the gap between terrestrial experiments in nuclear physics such as the planned Facility for Rare Isotopes (FRIB) at Michigan State University and its implications for nuclear astrophysics observations.

## References


1. Bardeen, J., L. N. Cooper, and J. R. Schrieffer. Theory of Superconductivity. 1957. *PHYSICAL REVIEW.* **108**: 1175B.

2. Pauli, W.. On the Cconnexion between the completion of electron groups in an atom with the complex structure of spectra. 1925. *Z. PHYSIK.* **31**: 765.

3. Bohr, A., B. R. Mottelson, and D. Pines. Possible analogy between the excitation spectra of nuclei and those of the superconducting metallic state. 1958. *PHYSICAL REVIEW.* **100**: 936.

4. Regal, C. A.. Observation of resonance condensation of fermionic atom pairs. 2004. *PHYSICAL REVIEW LETTERS.* **92**: 040403.

5. Kinast, J.. Evidence for Superfluidity in a Resonantly Interacting Fermi Gas . 2004. *PHYSICAL REVIEW LETTERS.* **92**: 150402.

6. Bartenstein, M.. Collective excitations of a degenerate gas at the BEC-BCS crossover. 2004. *Physical Review Letters.* **92**: 203201.

7. Holland, M.. Resonance superfluidity in a quantum degenerate fermi gas. 2001. *PHYSICAL REVIEW LETTERS.* **87**: 120406.

8. Fulde, P., and R. A. Ferrel. Superconductivity in a strong spin-exchange field . 1964. *PHYSICAL REVIEW.* **135**: A550.

9. Larkin, A. I., and Y. N. Ovchinnikov. Inhomogeneous superconductivity. 1965. *JOURNAL OF EXPERIMENTAL AND THEORETICAL PHYSICS.* **20**: 762.

10. Carlson, J., S. Y. Chang, V. R. Pandharipande, and K. E. Schmidt. Superfluid fermi gases with large scattering length. 2003. *PHYSICAL REVIEW LETTERS.* **91**: 050401.

11. Carlson, J., and S. Reddy. Superfluid Pairing Gap in Strong Coupling. 2008. *Physical Review Letters.* **100**: 150403.

12. Shin, Y., C. H. Schnuck, A. Schirotzek, and W. Ketterle. Tomographic rf Spectroscopy of a Trapped Fermi Gas at Unitarity. 2007. *PHYSICAL REVIEW LETTERS.* **99**: 090403.

13. Gezerlis, A., and J. Carlson. Strongly paired fermions: Cold atoms and neutron matter . 2008. *PHYSICAL REVIEW C.* **77**: 032801.

14. Brown, E. F., and A. Cumming. Mapping crustal heating with the cooling light curves of quasi-persistent transients. 2009. *ASTROPHYSICAL JOURNAL.* **698**: 1020.

15. Gezerlis, A., S. Gandolfi, K. E. Schmidt, and J. Carlson. Heavy-light fermion mixtures at unitarity . 2009. *PHYSICAL REVIEW LETTERS.* **103**: 060403.

16. Sharma, R., and S. Reddy. A mean field analysis of pairing in asymmetric fermi systems at finite temperature. 2008. *PHYSICAL REVIEW A.* **78**: 063609.

## Publications

Alford, M. G., M. Braby, S. Reddy, and T. Schafer. Bulk Viscosity due to Kaons in Color-Flavor-Locked Quark Matter. 2007. *PHYSICAL REVIEW C.* **75**: 055209.

Carlson, J., and S. Reddy. The superfluid gap in strong coupling . 2008. *PHYSICAL REVIEW LETTERS.* **100**: 150403.

Gezerlis, A., S. Gandolfi, K. E. Schmidt , and J. Carlson. Heavy-Light fermion mixtures at unitarity. 2009. *Physical Review Letters.* **103** (6): 060403.

Gezerlis, A., and J. Carlson. Strongly-Paired Fermions: Cold Atoms and Neutron Matter. 2008. *Physical Review C.* **77** (3): 032801(R).

Sharma, R., and S. Reddy. A mean field analysis of pairing in asymmetric Fermi systems at finite temperature. 2008. *PHYSICAL REVIEW C.* **78**: 063609.

# Ultra-Low Field Resonant Absorption Magnetic Resonance Imaging of Neural Activity

*Petr L. Volegov*
20070349ER

## Abstract

The prospect of creating an accurate functional mapping of the brain by directly imaging neural activity through magnetic resonance methods has captured the interest of the neuroscience community due to its potential revolutionary impact and far-reaching consequences, both for better diagnosing neurological disorders and for better understanding how the brain works in general. Although much work has already been done in this area, a conclusive in-vivo demonstration of direct neural imaging (DNI) has yet to be seen. The purpose of this project was to demonstrate, with computational modeling and physical experimentation, the feasibility of using the mechanism of resonant absorption to directly image neural activity in the human brain using magnetic resonance imaging (MRI) techniques at ultra-low field (ULF). This project has direct application to NNSA and DHS missions. It directly contributes to laboratory mission areas in complex biological systems, engineering, and health security.

## Background and Research Objectives

The importance of understanding how the brain works has been recognized by the entire scientific community. The brain is one of the most complicated systems known to science, and although much is known about the structure and architecture of this system, very little is understood about how exactly this system works to manifest human cognition.

In order to understand this, researchers must be able to "see the brain in action". The prospect of creating an accurate functional mapping of the brain by directly imaging neural activity through magnetic resonance methods has captured the interest of the neuroscience community due to its potential revolutionary impact and far-reaching consequences, both for better diagnosing neurological disorders and for better understanding how the brain works in general.

In terms of functional neuroimaging, there are currently two techniques that are considered the state-of-the-art. The first is functional magnetic resonance imaging (fMRI) [1]. This technique is based on the assumption that the neural activity in the brain will be associated with local hemodynamic changes (increases in blood flow, blood oxygenation, and blood volume). fMRI detects changes in the MRI signal that are induced by these hemodynamic changes.

There are a few issues surrounding the use of fMRI to create accurate functional maps of the brain. First, while it has excellent spatial resolution (<mm), it has poor temporal resolution (2-5 sec, where the neural activity occurs on the order of ms) [2]. This is due to the natural physiological delay of the hemodynamic response, which therefore presents a fundamental limitation to this technique. Second, it is really only an indirect measure of neural activity, since it is actually measuring energy consumption of the neural tissue. Because of this, the fMRI signal is not necessarily co-located with the actual neural activity, and its magnitude is not necessarily linearly correlated with the strength of the neural response [3].

The second technique is electro-/magneto-encephalography (EEG/MEG) [4]. This technique utilizes the fact that the neural currents associated with neural activity in the brain will produce electric and magnetic fields. These fields can be detected just outside the head, and the spatial distributions of the fields can be used to back calculate where the fields originated, thus localizing the neural activity. Unfortunately, many possible solutions exist for a single field distribution (ill-posed electromagnetic inverse problem), and therefore, prior knowledge of brain activity must be used in order

to narrow down the solutions [5].

It has been proposed that magnetic resonance imaging (MRI) may actually be able to directly detect neuronal activity [6]. The basic premise is that the magnetic fields produced by the neuronal currents associated with neural activity will perturb the proton spin dynamics, thus altering the MRI signal directly. The tissues in the body are primarily composed of water, and the protons of the water molecules each have a net nuclear spin. In general, these spins are oriented in random directions, but when an external magnetic field is applied, they can become aligned to the direction of that field. Once aligned, the spins are then "tipped" to be perpendicular to the direction of the field, after which, they precess around the direction of the field at a frequency called the Larmor frequency. Eventually, the spins dephase and relax back to the direction of the applied field. The proton spin dynamics (frequency and dephasing time) are affected by the local strength of the magnetic field. Thus, a perturbing field introduced by activated neurons would alter the precession locally, and change the MRI signal.

In the past 10 years, several research groups have conducted studies aimed at directly imaging neural activity using magnetic resonance techniques [7-9]. Among these have been a significant number of reports of in-vivo detection [7], where evoked neuronal responses have been imaged using conventional high field (HF) MRI instruments. However, to date, none of these in-vivo claims have been reproduced [9]. The primary confounding factor in each of these studies was the presence of the much larger blood oxygenation level dependent (BOLD) signal, where the MRI signal is altered by the increase in blood flow and blood oxygenation near the area of the neural activity [10]. It has been proposed [11] that the large BOLD effect on the MRI signal may become insignificant at ultra-low fields (ULF), where the magnetic field used to induce the proton spin precession (which gives rise to the MRI signal) is ten thousand times less than HF MRI magnetic fields[12].

Our group [12], together with two other groups [13,14], has experimentally demonstrated ULF-MRI. While the NMR signals underlying MRI, known as the free induction decay (FID), are dramatically weaker at ULF than HF, we acquired high signal-to-noise measurements of FIDs at ULF using superconducting quantum interference device (SQUID) technology. The recognition that BOLD artifacts are virtually nonexistent at ULF led us to attempt to measure the effect of electrophysiological activity on NMR signals [11] with marginal success. The effect our team measured was a faster dephasing ($T_2$*) in the ULF-MRI signal from a 'stressed' muscle as compared to a 'relaxed' muscle. The marginal statistics we obtained demonstrate the difficulty of such a measurement, even for a strong bioelectric source such as a muscle. Confounding the problem even further are systematic effects such as cell elongation, muscle motion, etc. that can not be readily decoupled from the desired electrophysiology.

However, while very careful optimization of our ULF system, described in Reference [15], might still enable us to detect a correlation between $T_2$* and neural activity in the brain, there exists another benefit to attempting DNI at ULF that is potentially much more significant than simply removing the BOLD artifact. Specifically, there is an additional enhancement of the DNI signal that is only possible at ULF. This enhancement arises when the Larmor precession frequency of the proton spins overlaps with the frequency content of the neural activity. The Larmor precession frequency is set by the magnitude of the external magnetic field used in the MRI protocol. Thus, at HF conditions, this can be several hundred MHz; but for ULF conditions, the Larmor frequency can be brought down to a few hundred Hz. Because the frequency content of neural activity is limited to <1000Hz, ULF is necessary to achieve this overlap and the corresponding signal enhancement. Thus, the DNI signal will be further enhanced under ULF conditions (only) by a resonant coupling between the spin precession dynamics and the frequency content of the neural activity.

We had several research objectives aimed at testing our hypothesis that the NMR signal resulting from a population of protons with a given spin alignment will decay more quickly as a consequence of spin relaxation caused by resonant absorption when the proton Larmor frequency overlaps with frequency bands of cortical activity containing significant energy.

Our first objective was to experimentally test this hypothesis with simple phantoms consisting of a current source in a bolus of saline solution. These experiments were successful in demonstrating that the signal from the current can be enhanced significantly under resonant absorption conditions.

Our second objective was to use a neural model developed at LANL [15] in conjunction with an interaction Hamiltonian for nuclear spin states to predict the effect of resonant absorption on spin relaxation. Again, these efforts were successful in allowing us to create an accurate neuronal model and simulation toolset to predict both the magnitude and the phase of the DNI signal, taking into account any resonant absorption effects.

Our third and fourth objectives were to experimentally demonstrate a statistically significant reduction of proton

$T_2$* with cortical activation using well known stimuli protocols, and to use gradient-encoding to spatially localize the DNI activity using ULF-MRI techniques [12,16]. Although we were not able to successfully demonstrate DNI in-vivo, we were able to use the insight gained from the successful completion of the previous two objectives to determine the best course of action to achieve these goals. This knowledge is being used to design improved experiments for demonstrating DNI in-vivo under other grants.

## Scientific Approach and Accomplishments

With respect to the first objective, we have explored our hypothesis with several first-principal demonstration experiments. As reported previously [17], we performed several current phantom experiments to determine the correct measurement field for detecting currents in the range of neurally-generated currents. The current phantoms consisted of 1% NaCl + 0.5g/l CuSO4. We applied three different waveforms: a DC current, a modulated sinc pulse, and a pseudo-random waveform (designed to mimic the typical neuronal response). Using these current waveforms, we detected a current of approximately 10 µA which generated a field of 20 pT in a voxel of 3 mm x 3 mm x 2mm. This current value was chosen to be physiologically realistic, based on previous estimates of neuronal current strengths. In addition, these studies revealed that DNI signal enhancement did indeed occur – and that this enhancement was measureable – when the Larmor frequency overlapped with the frequency content of the current waveform. However, we were not able to conclusively determine the spatial location of the enhanced signal.

We have developed a multiple echo protocol for generating magnetic resonance images at ultra-low fields. These MRI techniques are the prerequisites for refining the protocols to elicit the direct neuronal images. The details of the techniques are included in [18-20].

Using this protocol, we have performed some additional phantom experiments. We detected a phase change in the MRI signal that was localized to the position of the current in the phantom.

For the second objective, we have constructed a library of neurons consisting of the major cell types found in the cerebral cortex. To ensure that the neurons are as realistic as possible, we investigated the effects of changing the distribution and composition of these conductances on the firing patterns of the neurons and adjusted them to match experimental data. Using anatomical and electrophysiological data, we connected these neurons in such a way as to produce neurons with functional receptive fields. This network of neurons was given realistic input to produce firing patterns that were consistent with experimental data.

Furthermore, we derived the theoretical time evolution behavior of the proton spin in the presence of a generalized time-varying perturbing magnetic field. This has revealed the additional resonant absorption effect that we hypothesized. The perturbing magnetic field will not only change the MRI signal phase and amplitude (which are the effects utilized in high field MRI studies), but it will *enhance* the change in the MRI signal amplitude if it has time-harmonic components that overlap with the Larmor frequency from the applied measurement field. Because the frequency content of neural activity is limited to <1000Hz, ULF is necessary to achieve this overlap and the corresponding signal enhancement. Thus, we have found that the DNI signal can be substantial if this condition is met and the power spectral density of the neuronal activity shows significant power present at the overlap frequency.

We have used this derivation to write a 3D Finite Difference Time Domain code that is capable of calculating the MRI signal from arbitrary time-varying current waveforms throughout time. We have found that this resonant absorption effect could cause significant changes in the MRI signal. A characteristic resonance curve is observed when the frequency of the sine wave passes through the "on-resonance" condition. For the third and fourth objectives, we have used the successes and insight gained from the first two objectives to refine our imaging protocols and determine the best possible experimental conditions for observing DNI in-vivo. We have designed and build several SQUID-based ULF NMR/MRI systems: a one-channel ULF NMR system to study relaxation properties of materials at ULF, field-of-view (FOV) Ø5×5cm; a 7-channel ULF MRI system for human brain imaging, FOV Ø20×5cm; a 7-channel ULF-MRI system for liquid classification, Ø30×10cm (DHS-funded MagViz project).

Based on our calculations and experimental results, the best possibility of conclusively demonstrating DNI is through imaging an epileptic brain using ULF MRI. First, because the neural currents associated with epileptic activity are 1-2 orders of magnitude larger than typical evoked response activity in the brain [21], the DNI signal from this activity is expected to be much larger. Second, the DNI signal will be further enhanced under ULF conditions by a resonant coupling between the spin precession dynamics and the frequency content of the epileptic activity[17]. The higher frequency content of epileptic activity will allow us to use a higher measurement field to achieve resonance and to achieve a better signal-

to-noise ratio. Third, the DNI signal will be easier to detect due to the large spatial extent of the epileptic activity in the brain [22]. Fourth, attempting DNI at ULF rather than HF eliminates the need to extract the small DNI signal from the much larger BOLD signal, as mentioned above. Thus, we believe that the accomplishments we have obtained in this grant has laid the foundation for the final successful demonstration of DNI in-vivo through carefully controlled experiments that are designed to explore a "best case scenario" condition.

## Impact on National Missions

The technique of ultra-low field MRI developed here, because of the ability to detect and differentiate a vast array of materials, has direct application to NNSA and DHS missions, including Threat Reduction, by developing technologies to detect nuclear materials and/or other threat materials. Specifically, our work in this area has fed into a new program under DHS to detect the presence of threat substances at airport screening portals (the MagViz project).

"Understanding the human brain" has been identified as one of the main focus areas within the Complex Biological Systems Grand Challenge, this work directly addresses this challenge. Future work can build off of our accomplishments here for advancing neuroscience research, building new imaging and diagnostic tools, and developing novel methods for disease identification, thus contributing to laboratory mission areas in complex biological systems, engineering, and health security. This work directly feeds into the lab missions of reducing global threats and solving other emerging national security challenges.

## References


1. Ogawa, S., and T. M. Lee. Brain magnetic resonance imaging with contrast dependent on blood oxygenation. 1990. *Proc. Natl. Acad. Sci. USA* . **87**: 9868.

2. Kim, S. G., and W. Richter. Limitations of temporal resolution in functional MRI. 1997. *magn. Reson. Med..* **37**: 631.

3. Birn, R. M., and Z. S. Saad. Spatial heterogeneity of the non-linear dynamics in the fMRI BOLD response. 2001. *NeuroImage.* **14**: 817.

4. Hamalainen, M., and R. Hari. Magnetoencephalography - theory, instrumentation, and applications to noninvasive studies of the working human brain. 1993. *Rev. Mod. Phys..* **65**: 413.

5. George, J. S., and C. J. Aine. Mapping function in the human brain with magnetoencephalography, anatomical magnetic resonance imaging, and functional magnetic resonance imaging. 1995. *J. Clin. Neuroph.* **12**: 406.

6. Bodurka, J., and P. A. Bandettini . Toward direct mapping of neuronal activity: MRI detection of ultraweak, transient magnetic field changes. 2002. *Magn Reson Med* . **47** (6): 1052.

7. Xiong, J., and P. T. Fox. Directly mapping magnetic field effects of neuronal activity by magnetic resonance imaging. 2003. *Hum Brain Mapp* . **20** (1): 41.

8. Cassara, A. M., and G. E. Hagberg. Realistic simulations of neuronal activity: a contribution to the debate on direct detection of neuronal currents by MRI. 2008. *NeuroImage.* **39** (1): 87.

9. Parkes, L. M., and F. P. de Lange. Inability to Directly Detect Magenteic Field Changes Associated With Neuronal Activity. 2007. *Magnetic Resonance in Medicine* . **57**: 411.

10. Logothetis, N. K.. The neural basis of the blood-oxygen-level-dependent functional magnetic resonance imaging signal. 2002. *Philos Trans R Soc Lond B Biol Sci.* . **357**: 1003.

11. Espy, M. A.. SQUID-based Simultaneous Detection of NMR and Biomagnetic Signals at Ultra-low Magnetic Fields. 2005. *IEEE Trans Appl. Superconductivity* . **15**: 635.

12. Matlashov, A. N., and P. L. Volegov. SQUID detected NMR in microtesla magnetic fields. 2004. *J. Magn. Reson.* **170**: 1.

13. McDermott, R., N. Kelso, and S. K. Lee. SQUID-detected magnetic resonance imaging in microtesla magnetic fields. 2004. *J. Low Temp. Phys.* **135**: 793.

14. Burghoff, M., and S. Hartwig. Nuclear magnetic resonance in the nanoTesla range. 2005. *Appl. Phys. Lett.* . **87**: 054103.

15. Travis, B. J.. A computational model of one pathway in the cat subcortical auditory system,. 1995. *Mathematics and Computers in Simulation* . **40**: 81.

16. Volegov, P. L., and J. C. Mosher. On concomitant gradients in low-field MRI. 2005. *J. Magn. Resn.* **175**: 103.

17. KrausJr., R. H., P. Volegov, A. Matlashov, and M. Espy.

Towards direct neural current imaging by resonant mechanisms at ultra-low field. 2008. *NeuroImage* . **39**: 310.

18. Zotev, V. S., and A. N. Matlashov. Microtesla MRI of the human brain combined with MEG. 2008. *Journal of Magnetic Resonance* . **194**: 115.

19. Zotev, V. S., and P. L. Volegov. Parallel MRI at microtesla fields. 2008. *Journal of Magnetic Resonance* . **192**: 197.

20. Zotev, V. S., and A. N. Matlashov. SQUID-based instrumentation for ultralow-field MRI. 2007. *Superconductor Science and Technology* . **20**: 367.

21. Akaike, K., and S. Tanaka. Kainic acid-induced dorsal and ventral hippocampal seizures in rats. 2001. *Brain Res* . **900** (1): 65.

22. Gupta, D., and C. J. James. Narrowband vs. broadband phase synchronization analysis applied to independent components of ictal and interictal EEG. 2007. In *Conf Proc IEEE Eng Med Biol Soc* . (Lyon, France, August 23-26, 2007). , p. 3864. Quincy, FL : The Printing House, Inc..

## Publications

Espy, M., M. Flynn, J. Gomez, C. Hansen, R. Kraus, P. Magnelind, K. Maskaly, A. Matlashov, S. Newman, M. Peters, H. Sandin, I. Savukov, L. Schultz, A. Urbaitis, P. Volegov, and V. Zotev. Applications of ultra-low field magnetic resonance for imaging and materials studies. 2009. *IEEE Trans. Appl. Supercond.* **19** (3): 835 .

Flynn, M. C., P. Volegov, J. Mosher, A. Matlashov, M. Espy, and R. H. Kraus, Jr.. Simulation of magnetic fields for direct neuronal imaging. Presented at *Society for Neuroscience.* (San Diego, CA, 2-7 Nov. 2007).

Heller, L., B. Barrowes, and J. George. Modeling Direct Effects of Neural Current on MRI. 2009. *Human Brain Mapping.* **30** (1): 1.

Kraus,Jr., R. H., P. Volegov, A. N. Matlachov, and M. Espy. Toward direct neuronal current imaging by resonance mechanisms at ultra-low field. 2008. *NeuroImage.* **39** (1): 310.

KrausJr, R. H., M. A. Espy, P. L. Volegov, and A. M. Matlachov. Toward SQUID-Based Direct Measurement of Neural Currents by Nuclear Magnetic Resonance. 2007. *IEEE Trans on Appl Superconductivity.* **17** (2): 854 .

Maskaly, K. R., M. A. Espy, M. C. Flynn, J. J. Gomez, R. H. Kraus Jr, A. N. Matlashov, J. C. Mosher, S. G. Newman, T. Owens, M. V. Peters, J. H. Sandin, L. J. Schultz, A. V. Urbaitis, P. L. Volegov, and V. S. Zotev . Direct Neural Imaging using Ultra-Low Field Magnetic Resonance. To appear in *The American Physical Society March Meeting, 2009.* (Pittsburgh, Pennsylvania, March 16–20, 2009).

Volegov, P., H. Sandin, V. Zotev, M. Flynn, K. Maskaly, A. Matlashov, J. Mosher, M. Espy, and R. Kraus Jr. Direct Neuronal Imaging by Ultra Low Field MRI. Invited presentation at *the 14th Annual Meeting of The Organization for Human Brain Mapping.* (Melbourne, Australia, 15-19 June 2008).

Volegov, P., V. Zotev, M. Espy, M. Flynn, J. Gomez, C. Hansen, R. Kraus Jr, P. Magnelind, K. Maskaly, A. Matlashov, S. Newman, M. Peters, H. Sandin, I. Savukov, L. Schultz, and A. Urbaitis. Concurrent Ultra Low Field MRI and Brain Function Measurements. Invited presentation at *16th International Conference on Biomagnetism.* (Sapporo, Japan, 25-29 Aug. 2008).

Zotev, V. S., A. N. Matlashov, I. M. Savukov, T. Owens, P. L. Volegov, J. J. Gomez, and M. A. Espy. SQUID-Based Microtesla MRI for In Vivo Relaxometry of the Human Brain . 2009. *IEEE Transactions on Applied Superconductivity.* **19** (3): 835 .

Zotev, V., A. Matlashov, P. Volegov, I. Savukov, M. Espy, J. Mosher, J. Gomez, and R. Kraus Jr. Microtesla MRI of the human brain combined with MEG. 2008. *Journal of Magnetic Resonance* . **194**: 115.

Zotev, V., P. Volegov, A. Matlashov, M. Espy, J. Mosher, and R. Kraus Jr. Parallel MRI at microtesla fields. 2008. *Journal of Magnetic Resonance* . **192**: 197.

# Unique Observations of Nature's Largest Explosions

*W T. Vestrand*
20070382ER

## Abstract

This program constructed the world's fastest robotic telescopes and used them to make unprecedented color cosmic cinematography of explosive phenomena in the Universe. Key technical achievements were: (1) the deployment of robotic systems capable of collecting simultaneous multi-color observations of the optical light from gamma-ray bursts within 10 seconds of the notification of the explosion and (2) the fielding of a new technology camera that is capable of imaging fast optical flashes with much greater temporal resolution than is possible with conventional astronomical cameras. Using these assets we were able to study the brief flashes of light emitted when some of the very first stars born in the universe collapsed to form black holes. By studying these gamma-ray burst explosions through its flash of visible light and the afterglow generated by the interaction of the explosive ejecta with the surrounding material, we obtained important new clues about nature's largest explosions and the early universe in the era before our solar system was formed.

## Background and Research Objectives

Since their discovery by scientists at LANL in the early 1970's [1] the study of gamma ray bursts (GRBs) has been one of the most intriguing areas of research in astrophysics. These fleeting flashes of gamma-ray emission occur at random positions in the sky, typically last less than a minute, and are usually the brightest object in the gamma-ray sky. Further, for the gamma-rays to escape the intense internal radiation fields in these explosions, the emitting material must be accelerated to speeds that are 99.99% of the speed of light.

In recent years, substantial progress has made in understanding these cosmic explosions because satellite gamma-ray detectors have gained the capability to localize quickly the GRB positions with sufficient accuracy to allow timely follow-up observations at lower energies. The result has been the discovery of fading radio, optical, and X-ray afterglows at the locations of the GRBs respectively. Optical spectroscopy of those afterglows taught us that gamma-ray bursts are more amazing than almost everyone had dared to speculate—they are the largest explosions since the Big Bang, the most distant objects known in the Universe, and provide an avenue to observe the environment and the birth of the very first black holes in the Universe. The current distance record holder, GRB 090423 at a distance of 13 billion light years, occurred only 630 million years after the Big Bang—less than one-twentieth of its current age.

Optical afterglow observations taken many hours after the GRB have provided burst distances, identified host galaxies, and determined the long-term temporal behavior of the burst afterglows. Based on those observations, it is now believed that approximately 2/3 of GRBs are rare cataclysmic endpoints of stellar evolution where a massive star collapses to form a black hole and another 1/3, so-called short/hard GRBs, are probably generated by neutron star- neutron star or neutron star-black hole mergers. But observations of afterglows taken hours later tell us nothing about the details of these cataclysmic events. The extreme ultra-relativistic nature of the outflow also means that the complex history of interactions and deceleration of the flow, which occurs on the timescale of a day in the frame of the moving gas, is carried by emission that arrives at Earth within the span of minutes.

The goal of our project was to build the world's fastest robotic telescope and to use it to make unprecedented cinematography of the GRBs during the critical first few minutes of the explosions. This record of the fast variability of the flash of visible light from the explosion will help us unravel the nature of explosive itself as well as the interaction of the fragments with the surroundings. But, since these flashes of light typically last less than a minute, we needed to solve the technical

challenge of deploying the cameras on ultra-fast slewing telescopes that can point to any direction in the sky and begin the cinematography in less than ten seconds.

To understand fully the nature of the explosion and the physics of the radiation mechanism, this cinematography must be color cinematography or, as it is called in astronomy, simultaneous multi-color imaging photometry. Normally multi-color imaging photometry is obtained using a color filter wheel to rotate filters into the optical path, one at a time, to construct a color image. But this will not work for studying GRB explosions because the brightness variations and likely intrinsic color variations are too fast for the slow filter wheel approach. Further, there is also observational evidence [2] that many GRBs are associated with dusty star formation regions that are blocking much of the initial flash and theoretical calculations [3] that indicate that the ultraviolet light from the explosion is sufficient to destroy the dust during the first minutes after the burst---producing strongly variable obscuration. Clearly, in order to study the intrinsic spectral and temporal evolution during the first minutes, the effects of a variable dust screen have to be measured and removed from consideration. Simultaneous multi-color observations in three filters, when coupled with standard assumptions about the dust extinction law, allow one to separate the contributions from each effect. Two of our key objectives were therefore: (1) to construct an instrument capable of truly simultaneous multicolor photometry starting within 10 seconds of the burst onset and (2) measuring the color evolution during the explosive and early afterglow phase of those GRBs located by NASA's Swift satellite.

These instrumental/observational goals were complemented by a theoretical modeling effort aimed at understanding the radiation mechanism, or mechanisms, responsible for generating the flash, or so-called prompt, emission generated by GRBs. In particular, our goal was to study the viability of the Synchrotron Self-Compton (SSC) mechanism—where the synchrotron photons generated by energetic electrons embedded in a magnetic field are scattered to higher energies by Compton scattering with the same parent population of energetic electrons.

## Scientific Approach and Accomplishments

We carefully considered several approaches for building instrumentation to explore the expected fast spectral (i.e. color) variations in GRBs. Since the real time positions of the GRBs provided by the Swift BAT (Burst Alert Telescope) typically have an uncertainty of a couple of arc-minutes, one cannot use conventional slit spectroscopy. Other options include an integral field spectrograph (too expensive) or slit-less spectroscopy employing an objective prism (adds too much to the telescope moment of inertia), a grism, or a transmission grating. The later techniques disperse light and re-image it onto the CCD (charge-coupled device) camera so the spectrum is recorded as spatial brightness variations. A serious disadvantage of this approach is that the integrated sky background over the entire wavelength range falls into the pixels that carry source signal from a narrow wavelength range. Such sky background issues are particularly problematic for fast focal ratio telescopes because, for a given sky brightness, the sky background photons per pixel scale as (pixel size/focal ratio)$^2$ independent of the telescope aperture. We concluded that the dramatic reduction in sensitivity and the spectral confusion problems make grating techniques a poor choice for relativity small telescopes that aim to study spectral variations during the first minutes of a GRB.

We found that the optimal approach for measuring rapid spectral variations in the first minutes after a GRB trigger is direct imaging photometry through broad-band filters. The idea is to simultaneously image the GRB location either through multiple co-aligned telescopes with different filters or a single telescope with dichroic splitters and a multi-color camera system. To maximize the signal-to-noise ratio (SNR) one should opt for the highest focal ratio possible. For a given CCD chip size, the maximum focal length of the telescope is constrained by the required field-of-view (FOV). The requirement of a FOV at least 10 arc-minutes across, placed by the BAT GRB location uncertainties, limits the focal length to less than 4.8 meters for a 14mm chip. For a 0.4-meter telescope this corresponds to a focal ratio of *f*/12 and yields, given the same pixel size, 36 times fewer sky background photons per pixel than a fast telescope with focal ratio *f*/2. The best photometric sensitivity is achieved by direct CCD imaging, with a slow focal ratio telescope through a broad-band filter, employing a back illuminated chip with a pixel size that gives Nyquist sampling of the point spread function and has a fast readout scheme with minimal read noise.

This project supported the completion of our RAPTOR-T(echnicolor) telescope that employs an array of telescopes to conduct simultaneous imaging through broad-band filters. The telescope is composed of four high-end COTS (commercial off-the-shelf) optical tube assemblies that are co-aligned and co-located on a single rapidly slewing mount (Figure 1). Each of the four tube assemblies is a 0.41-meter f/10 cassegrain telescope. To make simultaneous multicolor observations of the prompt and early optical afterglow emission from GRBs, each RAPTOR-T optical tube images the same field but through a different broad-band (clear-VRI) filter. A limiting magnitude of R~18.5 in 10 seconds is achieved at our

Fenton Hill observatory site using a camera at the focal plane that employs a 1Kx1K Marconi back-illuminated CCD chip. All four cameras are synchronized in order to perform simultaneous multi-color imaging.

*Figure 1. The RAPTOR-T rapid response telescope that is capable of simultaneous multi-color imaging anywhere in the visible sky in less than 10 seconds.*

An advantage of this approach, beyond speed of development and lower cost, is the much more compact size of the telescope for a given focal ratio. This in turn translates into a lower moment of inertia and makes it much easier to achieve the extremely rapid slewing speeds needed to begin observations of GRB optical emission in less than 10 seconds after a GRB trigger. The RAPTOR-T servo motors and drive system has been significantly scaled up to achieve the same slewing speed and settling specifications as the previous generation of our mounts—able to be on a burst location and begin observations in as little as six seconds after the GRB trigger. No other telescope with an effective aperture as large as RAPTOR-T is capable of observing prompt optical emission from GRBs within ten seconds of the GRB trigger.

This RAPTOR-T telescope array provided interesting information on the color evolution of the optical emission during the critical first minutes after the start of a GRB explosion. For example, we collected important measurements of GRB080319a—the most luminous object ever detected by mankind. It was so bright that it saturated all the cameras on RAPTOR-T during the intense prompt flash. But, as the flash faded, we measured color evolution (Figure 2) consistent with a rapidly decaying red component followed by emergence of a blue afterglow. Straightforward interpretation of the observations suggests that the rapidly decaying red component is the detection, for the first time, of large angle prompt optical emission [4]. The blue component that emerged later is best understood as afterglow generated by forward shock interaction with the surrounding environment.

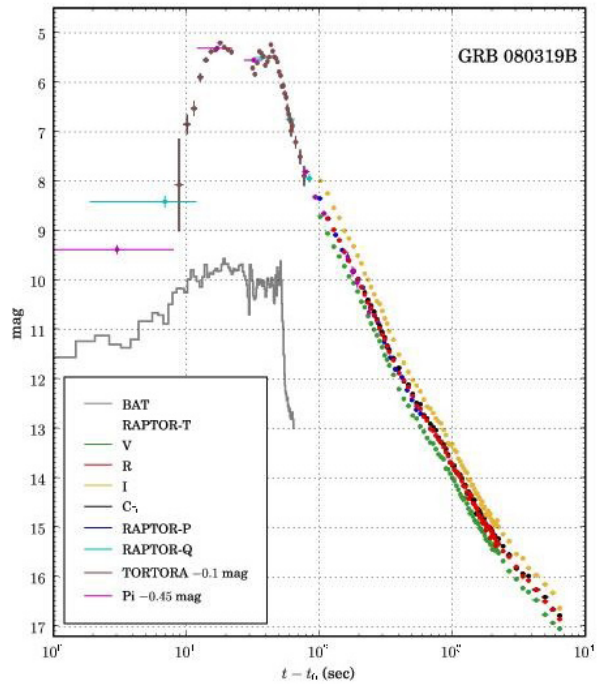


*Figure 2. The optical light curve for GRB 080319b---the "naked eye" burst---collected by our RAPTOR network. The transient was independently detected and followed over an unprecedented dynamic range by four fully autonomous instruments in the RAPTOR telescope network: a rapid response, simultaneous multi-color, imaging array, RAPTOR-T; a wide-field survey array RAPTOR-P; and an all-sky monitor RAPTOR-Q. Our rapid response telescopes were saturated during the bright prompt emission at (t-to)<60 seconds, but the RAPTOR-Q full-sky monitor measurements agree well with the data collected by other small monitors reporting detections: TORTORA and Pi-of-the-sky. Our RAPTOR-Q measurements for ~30 minutes before the GRB rule out significant optical precursor emission.*

We also combined our early time RAPTOR optical measurements with multi-wavelength measurements made by other groups to pose interesting questions about the nature of the broad-band afterglow in GRBs and show that the physics is still not fully understood. For example, we detected a very bright early afterglow from GRB

061126 that, when combined with observations by the Berkeley Group, showed an optical to infrared spectrum that is an excellent fit to a power law, but exhibits red-to-blue color evolution at about 500 s after the burst. Like GRB 080319a, this color change is contemporaneous with a switch from a relatively fast decay to slower decay. This rapidly decaying early afterglow is consistent with synchrotron emission from a reverse shock, but the bright forward-shock emission predicted—in the standard afterglow picture---by the X-ray observations was not observed. Further, the flat the optical-to-X-ray spectral shape observed at late times would qualify this burst as a "dark burst" despite its remarkable early-time brightness. However the observations showed no evidence for host galaxy extinction, requiring either large quantities of gray dust in the host system or separate physical origins for the X-ray and optical afterglows [5].

Another key technical achievement of our program was the deployment of the first Electron Multiplication CCD (EMCCD) for gamma-ray burst research. EMCCDs are similar to conventional CCDs except an additional gain register is placed between the readout register and the output amplifier. That gain register is composed of a large number of impact ionization stages. In each stage, the number of electrons is only increased by a percent (or less). But the number of stages is large (~500-1000) so that individual signal photons can generate thousands of output electrons. This dramatically improves the signal-to-noise ratio and allows sensitive high-cadence imaging with a relatively high quantum efficiency (~80%) chip. During the final phase of the project, we deployed a EMCCD on our new RAPTOR-Z (0.5-meter, f/7, Ritchey-Chretien) telescope which is the fastest slewing mount ever constructed for astronomical research. The RAPTOR-Z telescope (Figure 3) is capable of pointing to any direction in the sky and starting imaging in less than 5 seconds. This new technology gives us a capability--- unmatched anywhere in the world--- to explore the sub-second optical variability of GRB explosions.

The theory component of our program also had several significant accomplishments. For example, Alin Panaitescu, a postdoctoral student working on the project, completed numerical modeling of broadband (radio, optical, and X-ray) afterglow emission from GRBs. In particular, he expanded the standard fireball model to include outflows with angular structure, energy injection in the blast wave, and a more complete picture of reverse shock emission. This work was applied to the interpretation of the new classes of afterglow behavior that were identified for the first time in our paper [6]. It has also given us the capability to constrain, when used in conjunction with our RAPTOR observations, the fundamental parameters of the relativistic outflow.

These tools were applied to an analysis of the synchrotron self-Compton (SSC) model for the prompt optical and MeV gamma-ray emission from GRB 080319B. We were to determine to the GRB source location, Lorentz factor, and magnetic field strength. The Compton parameter inferred from our observations, led to the conclusion that, if the SSC model is correct, GRBs should be capable of generating bright, very high-energy (GeV) emission, whose properties (flux, spectrum) can be measured by NASA's recently launched Fermi observatory.

*Figure 3. The RAPTOR-Z telescope is a 0.5-meter Ritchey-Chretien that has been modified to withstand very high accelerations. This robust telescope assembly and high speed mount allow the telescope to begin ultra-high cadence light curve measurements for a source anywhere in the visible sky in less than 5 seconds after receipt of an event trigger. The deployment of a new technology electron multiplication imager on this telescope gives us an capability that is unmatched, worldwide, for the study of the flash of prompt optical emission from gamma-ray burst explosions.*

## Impact on National Missions

This work developed important new capabilities that can be applied to Space Situational Awareness and the study of rapid astrophysical transients. The capability we developed to make rapid response observations with high cadence EMCCD imagers, for example, led to a new four year NASA-funded research program to study the optical emission from gamma-ray bursts localized by NASA's Swift mission. Our work also received significant favorable attention in the popular press. For example we were featured prominently in an article on the future of astronomy in Astronomy magazine entitled "Invasion of the Robotic

Telescopes" and the National Geographic Television program entitled "Monster Black Holes."

## References


1. Klebesadel, R. W., I. B. Strong, and R. A. Olson. Observations of gamma-ray bursts of cosmic origin. 1973. *Astrophysical Journal.* **182**: L85.

2. Paczynski, B.. Are Gamma-Ray Bursts in Star-Forming Regions?. 1998. *Astrophysical Journal.* **494**: L45.

3. Waxman, E., and B. T. Draine. Dust sublimation by gamma-ray bursts and Its implications. 2000. *Astrophysical Journal.* **494**: 796.

4. Wozniak, P. R., W. T. Vestrand, A. Panaitescu, J. Wren, H. Davis, and R. White. Gamma-Ray Burst at the extreme: "The Naked-Eye Burst" GRB 080319B. 2009. *Astrophysical Journal.* **691**: 495.

5. Perleyetal, D. A.. The troublesome broadband evolution of GRB 061126: Does a gray burst Imply gray dust?. 2008. *Astrophysical Journal.* **672**: 449.

6. Panaitescu, A., and W. T. Vestrand. Taxonomy of gamma-ray burst optical light curves: identification of a salient class of early afterglows. 2008. *Monthly Notices of Royal Astronomical Society.* **387** (2): 497.


## Publications


Panaitescu, A., and P. Kumar. A unified model for the gamma-ray and prompt optical emissions of GRB 990123. 2007. *Monthly Notices of Royal Astronomical Society.* **376**: 1065.

Panaitescu, A., and W. T. Vestrand. Taxonomy of gamma-ray burst optical light curves: identification of a salient class of early afterglows. 2008. *Monthly Notices of Royal Astronomical Society.* **387** (2): 497.

Perleyetal, D. A.. The troublesome broadband evolution of GRB 061126: Does a grey burst imply grey dust?. 2008. *Astrophysical Journal.* **672** (1): 449.

Ruiz-Velascoetal., A. E.. Detection of GRB 060927 at z = 5.47: Implications for the use of gamma-ray bursts as probes of the end of the dark ages. 2007. *Astrophysical Journal.* **669** (1): 1.

White, R. R., W. T. Vestrand, J. Wren, and P. R. Wozniak. Using distributed sensor network architecture to link heterogeneous astronomical assets. 2008. *Astronomische Nachrichten.* **329** (3): 278.

White, R. R., and A. Allen. An overview of the heterogeneous telescope network concept, scalability and operations capability and distributed architecture. 2008. *Astronomische Nachrichten.* **329** (3): 232.

Wozniak, P., W. T. Vestrand, A. Panaitescu, J. Wren, H. Davis, and R. White. Gamma-Ray Burst at the extreme: "The Naked-Eye Burst" GRB 080319B. 2009. *Astrophysical Journal.* **691**: 495.

Yostetal, S.. Exploring broadband GRB behavior during gamma-ray emission. 2007. *Astrophysical Journal.* **657** (2): 925.

Yostetal, S. A.. The dark side of ROTSE-III prompt GRB observations. 2007. *Astrophysical Journal.* **669** (2): 1107.

# Electron-Neutrino Correlation in Neutron Beta Decay

*Wesley S. Wilburn*
20070488ER

## Abstract
We have developed techniques required for a series of precision neutron decay experiments at ORNL. We have demonstrated that all significant sources of systematic errors can be controlled to the required level, with the exception of precision neutron polarimetry. In the latter case we have collected a set of high-quality neutron data at LANSCE, that we believe will be sufficient to demonstrate neutron polarimetry at the 0.1% level. Analysis of this data will be completed in the near future by our external collaborators. A proposal has been written and submitted for future experiments to test the Standard Model using the cold neutron beam at ORNL.

## Background and Research Objectives
Precision studies of neutron properties are important ways to look for new physics and test new theories. The current Standard Model of nuclear and particle physics provides a framework for all of nuclear and particle physics and includes very precise predictions for how the neutron decays through emission of an electron and a neutrino (beta decay). These predictions, for example the probability that the electron or neutrino is emitted in the same direction as the neutron spin, or the probability that the electron and neutrino are emitted in the same direction, can be tested by precise experiments. Differences between the predicted and measured results would indicate the discovery of new, “Beyond the Standard Model” physics. For these reasons, the neutron acts as an important laboratory for nuclear and particle physics. To measure these decay parameters with the required precision, sufficient neutrons must be available to provide adequate statistics. The Spallation Neutron Source, currently being commissioned in Oak Ridge Tennessee, will provide an intense beam of neutrons suitable for such experiments. In addition, false effects (systematic errors) must be reduced to very low levels. One such effect is imperfect knowledge of the neutron polarization. This project studied the feasibility of reducing all such systematic errors to the required level of precision to demonstrate that a precision neutron decay experiment can be conducted that is an order of magnitude more precise than previous experiments [1].

## Scientific Approach and Accomplishments
The project has made major project on three fronts: demonstration of a new precision neutron polarization technique, further analysis of systematic errors, and conceptual design of the experiment.

Precision neutron polarization at the 0.1% level is a key requirement for precision neutron decay experiments. Our design relies upon the unique interaction of neutrons with polarized helium-3 gas. Circularly polarized laser light produces atomically polarized rubidium, which spin-exchanges with helium-3 to produce nuclear-polarized helium-3. Cold neutrons passing through the polarized helium-3 are absorbed with high probability if their spins are opposite to the helium-3, and with much lower probability if theirs spins are the same as the helium-3. This produces a high neutron polarization, and gives a powerful method of measuring the neutron polarization, since the interaction between the neutrons and helium-3 is understood to a few parts in 10^5. In principle, the neutron polarization can be determined with this technique with a precision of less than the required 0.1%. What limits the actual precision of this technique are neutron backgrounds, electronic noise, and other practical matters.

We constructed an experiment at LANSCE to test this technique consisting of a polarized helium-3 cell with neutron transmission monitors, plus a neutron polarization analyzer, a spin flipper, and an additional transmission monitor to check the polarization with an independent technique (Figure 1). The first of three planned runs was conducted during the 2007 LANSCE run cycle and resulting in a statistically and

systematically limited precision of 0.7%. The main systematic was due to noise in the beam monitors. Because the data is still be analyzed by external collaborators, the resulting precision is not yet known. However, the monitor noise was reduced significantly, and we believe a 0.1% precision is possible from this data. Figure 2 shows a preliminary analysis of a subset of this data. In addition we definitively answered a question from previous experiments about the mechanism for depolarization of helium-3 by intense neutron beams. This result has been published in the journal Physical Review Letters.

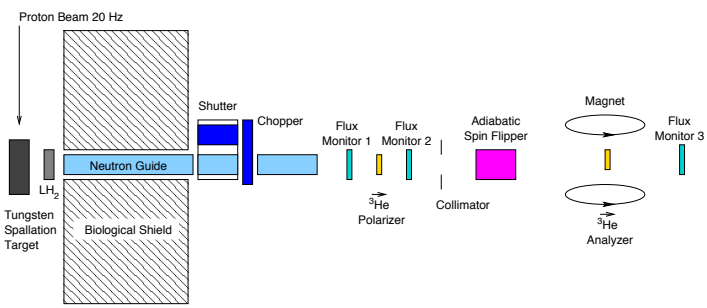


*Figure 1. Schematic drawing of the precision neutron polarimetry apparatus used for the experiments at LANSCE.*

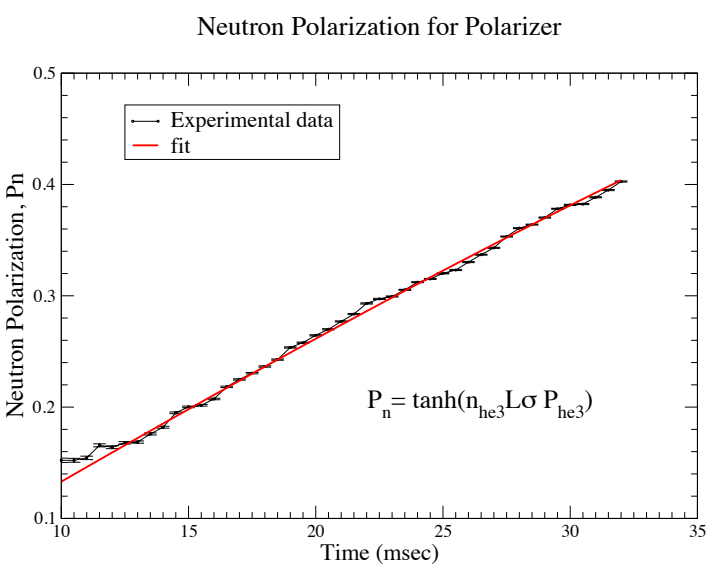


*Figure 2. Preliminary determination of neutron polarization as a function of neutron time-of-flight.*

An experiment at the 0.1% precision level requires careful control of systematic effects that can result in an incorrect measurement. We have carefully investigated several such effects and presented the findings in a 98-page beam time proposal to the Spallation Neutron Source (SNS) Fundamental Neutron Physics Beamline (FnPB) Physics Review and Advisory Committee (PRAC). Systematic effects that have now been analyzed include: neutron depolarization effects, electric and magnetic field inhomogenieties, electron and proton backscattering from detector surfaces, detector timing and energy resolution, proton scattering from residual gas, and electron trapping by Penning traps. In total, 18 separate potential systematic effects are analyzed in this document. As an example, proton scattering from residual gas is analyzed to show that the 10^-8 mbar vacuum planned for the spectrometer will be sufficient to meet the goals of the experiment.

The conceptual design of the experiment has advanced in several aspects. The spectrometer magnet, originally conceived to be a monolithic superconducting magnet, is now envisioned as a modular device, consisting of separate coil sections. This arrangement will allow the configuration to be optimized for the different neutron decay parameters. We are working with an engineer at SNS to fully develop the concept for the magnet. A second example is a load-lock system that will allow the detectors to be installed and removed from the cryogenic spectrometer without warming the spectrometer to room temperature. A LANL engineer has generated the conceptual design for this mechanism and as a preliminary cost estimate.

DOE Office of Nuclear Physics has asked ORNL for a detailed cost estimate for a first phase of this experiment, called Nab, that will measure the unpolarized correlation coefficients *a* and *b* from neutron decay. This experiment has approval from ORNL to begin installation in 2013, contingent upon DOE funding. ORNL has also asked for an update on the precision neutron polarization work performed in this project, to reach a decision on approving the full experiment, call abBA, that will measure four correlation parameters in neutron decay.

## Impact on National Missions

Testing a model that describes the most basic properties of matter is a core DOE mission. Furthering our understanding of these properties of matter also impacts other mission areas including nuclear weapons and fusion research. Finally, particle detectors developed here will impact the threat reduction missions of DOE and DHS.

## References

1. Alarcon, R., S. Balascuta, S. Baessler, E. Frlez, D. Pocanic, L. Barron-Palos, J. D. Bowman, T. V. Cianciolo, S. I. Penttila, K. P. Rykaczewski, G. R. Young, J. R. Calarco, F. W. Hersmann, V. Cirigliano, A. Danagoulian, T. Ito, A. Klein, J. Ramsey, W. S. Wilburn, T. E. Chupp, M. Sharma, C. Crawford, T. R. Gentile, M. Gericke, A. Micherdzinska, S. Page, G. L. Greene, and R. K. Grzywacz. Precise measurement of neutron decay parameters. 2007. *Beam Time Request to SNS FNPB*

*Proposal Review Advisory Committee (and references therein) http://nab.phys.virginia.edu/ABBA_proposal_2007.pdf.*

## Publications

Alarcon, R., S. Balascuta, S. Baessler, E. Frlez, D. Pocanic, L. Barron-Palos, J. D. Bowman, T. V. Cianciolo, S. I. Penttila, K. P. Rykaczewski, G. R. Young, J. R. Calarco, F. W. Hersmann, V. Cirigliano, A. Danagoulian, T. Ito, A. Klein, J. Ramsey, W. S. Wilburn, T. E. Chup, M. Sharma, C. Crawford, T. R. Gentile, M. Gericke, A. Micherdzinska, S. Page, G. L. Greene, and R. K. Grzywacz. Precise measurement of neutron decay parameters - The abBA experiment. 2008. *Beam Time Request to SNS FNPB Proposal Review Advisory Committee.*

Sharma, M., E. Babcock, K. H. Andersen, L. Barron-Palos, M. Becker, S. Boag, W. C. Chen, T. E. Chupp, A. Danagoulian, T. R. Gentile, A. Klein, S. Penttila, A. Petoukhov, T. Soldner, E. R. Tardiff, T. G. Walker, and W. S. Wilburn. Neutron beam effects on spin-exchange-polarized 3He.. 2008. *Physical Review Letters.* **101** (8): 083002.

# Experimental and Computational Studies of Magnetic Bubble Expansion as a Model for Extra-galactic Radio Lobes

*Scott C. Hsu*
20070506ER

## Abstract

Magnetized "bubble" plasmas are ubiquitous in both astrophysical environments and in laboratory fusion experiments, and they are thought to be governed by very similar physics. Examples include extra-galactic radio lobes, which persist for a Hubble time ($10^{10}$ years) and laboratory "compact toroids" (CTs) which have many applications in magnetic fusion energy research. This LDRD has focused on the theory and numerical modeling of the injection of magnetized bubble plasmas into a lower density background plasma, with both astrophysical and fusion applications in mind. A key astrophysically-relevant result of this work is the demonstration of how a magnetic field allows the persistence of a radio lobe for a Hubble time, and an important fusion-relevant result is the identification of a parameter regime where CT injection into a reactor-grade tokamak plasma could potentially be used for re-fuelling, as needed on the International Thermonuclear Experimental Reactor (ITER).

## Background and Research Objectives

Magnetized "bubbles" are very common in the Universe. Observations in the X-ray spectra show "cavities" with diameters of tens of thousands of light-years [1]. It is thought that these X-ray cavities were formed by radio-emitting lobes emanating from galaxies. Recent observations show that the radio lobe plasmas have appreciable magnetic fields [2]. This has led to new theoretical models [3], in which radio lobes are thought to be gigantic plasmas with twisted magnetic fields. The details of how radio lobe plasmas evolve and interact with the intergalactic media are not well understood. They depend on underlying plasma physics phenomena that are the subjects of this research. In order to develop further insights into extragalactic radio lobes, a laboratory plasma experiment called the Plasma Bubble Expansion Experiment (PBEX) [4] has been built to study some of the underlying plasma physics issues upon which leading radio lobe models are based. The experiment is to study the related model problem of a magnetized plasma "bubble" expanding into lower pressure background plasma. The first significant task of this project has been to perform three-dimensional numerical simulations of this experiment.

Magnetized bubbles are also very important in magnetic fusion plasma research. It is important to deliver new fuel into the core of a tokamak fusion plasma to maintain its steady-state operation. One proposed way to do so is to inject a magnetized bubble plasma called a compact toroid (CT) into the tokamak. CT fuelling is considered to be the most promising method because the injection speed via this method is far higher than those of competing methods, and the fuel can be delivered into the core of the tokamak. Although extensive worldwide efforts have been devoted to studying CT fuelling [5], the dynamics of core CT fuelling of large devices such as ITER [6] is not well understood, and thus this was the second significant focus of this LDRD project.

## Scientific Approach and Accomplishments

For the numerical study of PBEX, a high density magnetized rotating bubble plasma is injected radially into a cylindrical plasma volume confined by a weak axial magnetic field. The numerical simulations were done with a new three-dimensional (3D) ideal magnetohydrodynamic (MHD) code [7]. The simulations mimic PBEX and use experimentally measured or inferred parameters. The numerical modeling helped guide the experiments and data interpretation. These simulations predict several key features of the bubble evolution. First, the direction of bubble expansion depends on the ratio of the bubble azimuthal to non-azimuthal magnetic fields, with a higher ratio leading to expansion predominantly in the direction of propagation and a lower ratio leading to expansion predominantly normal to the direction of propagation. Second, a

shock is formed ahead of the bubble as it propagates into the background plasma (Figure 1). Third, the bubble expansion and propagation develop asymmetries about its propagation axis due to the asymmetric way in which the bubble magnetic field interacts with the background field. These results were published in a *Physics of Plasmas* [8] peer-reviewed article.

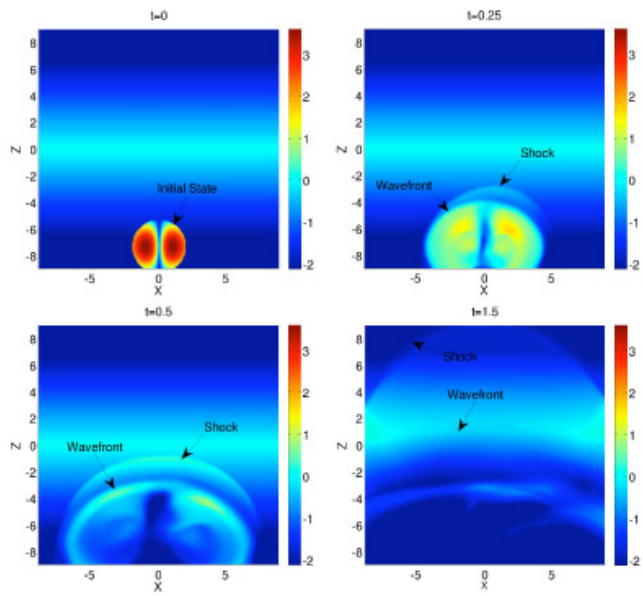


*Figure 1. Density plot (logarithmic color scale) of plasma bubble propagating into a background plasma, where Z is the propagation direction, from ideal MHD simulations. Ahead of the bubble we identify a leading shock and a trailing wavefront. The bubble evolution develops asymmetry about the propgation axis due to the asymmetric background magnetic field.*

For the study of CT fueling, we employed a simple idealized model of CT propagating into a uniform slab plasma with a uniform magnetic field perpendicular to the CT injection direction, mimicking CT fuelling into a large tokamak. This model helped us identify different regimes of operation in terms of CT injection speed, density, and magnetic field strength, as well as understand the essential physics occurring during CT injection. Compared with past work on CT injection numerical simulations, we investigated new regimes especially in terms of higher injection velocity and a more ITER-relevant ratio of CT-to-background magnetic field. Simulations with higher injection velocity were made possible by the shock-handling capability of our three dimensional MHD code [7]. The lower CT-to-background magnetic field ratios, compared with past work, was enabled by the higher resolution of our code, which allowed the boundary layer between the CT and background plasma to be properly resolved. Key discoveries are as follows. A regime is identified in terms of CT injection speed and CT-to-background magnetic field ratio that appears promising for precise core fuelling. Shock-dominated regimes, which are probably unfavorable for tokamak fuelling, are also identified. For the favored regime, the entire CT evolution can be divided into three stages: (1) initial penetration, (2) compression in the direction of propagation, and (3) coming to rest and spreading in the direction perpendicular to injection (Figure 2). The CT forms a line-shaped structure almost parallel to the background magnetic field (Figure 2). We have also studied how the penetration depth is determined and have found empirical rela1tionships between the penetration depth versus the initial injection speed and CT plasma density, *i.e.*, the CT penetration depth is proportional to the CT injection speed and density (Figure 3). A core fuelling system is all that a burning plasma may have to alter core plasma conditions and for burn control. If a CT injection system is within the ITER relevant, no-shock/wavefront regime we identified, then precise core deposition with minimal background equilibrium perturbation may be possible. These results appear in a *Nuclear Fusion* [9] peer-reviewed article.

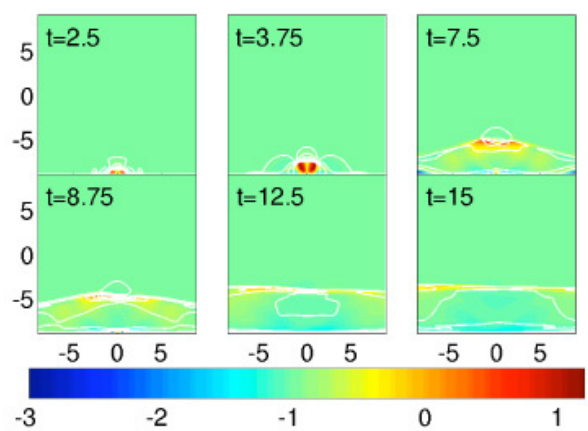


*Figure 2. Density (logarithmic color scale) in the X-Z plane at Y=0 as function of time. White lines are contours of constant magnetic pressure. The evolution can be divided into 3 stages: initial penetration, contraction and interaction of bubble and background magnetic fields, and finally the bubble coming to rest and spreading in the X direction.*

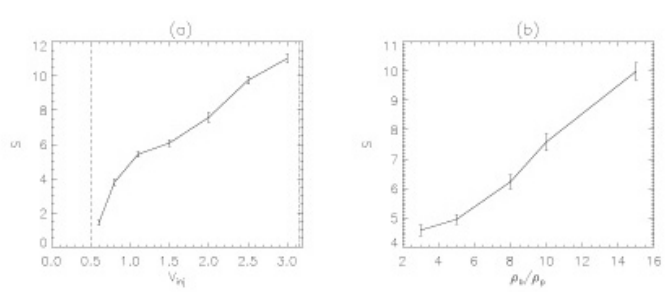


*Figure 3. CT penetration depth versus (a) injection speed and (b) density. The penetration depth is proportional to injection speed and initial CT density. The line spread is around small compared to the system size, implying good localized deposition.*

## Impact on National Missions

This work supported fundamental plasma physics and plasma astrophysics research at LANL, and it brought a postdoc (Wei Liu) to the Theoretical Astrophysics Group in T-Division. The CT-injection work supports DOE Office of Science (SC) work in Fusion Energy Sciences (FES), which is part of LANL's research portfolio in SC programs. Because of this work, LANL is in a good position to propose and lead future research programs in the area of tokamak fueling.

## References


1. Bizan, L., D. A. Rafferty, B. R. McNamara, M. W. Wise, and P. Nulsen. A systematic study of radio-induced X-ray cavities in clusters, groups, and galaxies . 2004. *Astrophysical Journal.* **607**: 800.

2. Kronberg, P. P., Q. W. Dufton, H. Li, and S. A. Colgate. Magnetic energy of the intergalactic medium from galactic black holes . 2001. *Astrophysical Journal.* **560**: 178.

3. Li, H., G. Lapenta, J. M. Finn, S. Li, and S. A. Colgate. Modeling the large-scale structures of astrophysical jets in the magnetically dominated limit . 2006. *Astrophysical Journal.* **643**: 92.

4. Lynn, A. G., Y. Zhang, S. C. Hsu, H. Li, W. Liu, M. Gilmore, and C. Watts. Experimental and Numerical Studies of Magnetic Bubble Expansion a a Model for Extra-Galactic Radio Lobes. 2007. In *American Physical Society Division of Plasma Physics.* (Orlando, FL, 12-16 Nov. 2007). , p. 53. College Park: APS.

5. Parks, P. B.. Refueling of tokamaks by injection of compact toroids. 1988. *Physical Review Letters.* **61**: 1364.

6. ITER Technical Basis 2001. 2001. *International Atomic Energy Agency.*

7. Li, S., H. Li, and R. Cen. CosmoMHD: a cosmological magnetohydrodynamics code . 2008. *Astrophysical Journal Supplement Series.* **174**: 1.

8. Liu, W., S. C. Hsu, H. Li, and A. G. Lynn. Ideal magnetohydrodynamic simulation of magnetic bubble expansion as a model for extragalactic radio lobes. 2008. *Physics of Plasmas.* **15**: 072905.

9. Liu, W., S. C. Hsu, and H. Li. Ideal magnetohydrodynamic simulations of low beta compact toroid injection into a hot strongly magnetized plasma. 2009. *Nuclear Fusion.* **49**: 095008.


## Publications


Liu, W., H. Li, S. Li, and S. C. Hsu. Long-term evolution of magnetized bubbles in galaxy clusters. 2008. *Astrophysical Journal Letters.* **684**: L57.

Liu, W., S. C. Hsu, H. Li, S. Li, and A. G. Lynn. Ideal magnetohydrodynamic simulation of magnetic bubble expansion as a model for extragalactic radio lobes. 2008. *Physics of Plasmas.* **15**: 072905.

Liu, W., S. C. Hsu, and H. Li. Ideal magnetohydrodynamic simulations of low beta compact toroid injection into a hot strongly magnetized plasma. 2009. *Nuclear Fusion.* **49**: 095008.

# Three-Dimensional Dynamics of Magnetic Reconnection in Space and Laboratory Plasmas

*William S. Daughton*
20080735ER

## Abstract

Magnetic reconnection is a fundamental process that occurs within hot ionized gases known as plasmas. The motion of electrons and ions in the plasma are strongly influenced by the presence of magnetic fields. In many types of plasma, the magnetic fields can store a large amount of energy. Under certain circumstances, the process of magnetic reconnection causes a rapid conversion of energy stored within the magnetic fields into kinetic energy of the charged particles. This process is thought to play an important role in a range of applications including solar eruptions, the Earth's magnetosphere, magnetic fusion machines, and a wide variety of astrophysical problems. Despite a great deal of effort, scientists are still working to understand a range of basic questions regarding the physics of this process. In particular, one of the most outstanding issues is the role of plasma instabilities in controlling the evolution. The goal of this project was to address this question using numerical simulations that describe the physics at the most basic level. This was accomplished by using the plasma simulation code VPIC, which was optimized to run on the new Roadrunner supercomputer. These simulations were setup to study the magnetic reconnection process for both space and laboratory plasmas. During the Roadrunner open science campaign, a series of simulations were performed of unprecedented scale and complexity. These new results demonstrate that the three-dimensional evolution of magnetic reconnection is highly complicated due to a spectrum of plasma instabilities. Some of these new results are remarkably similar to observations from recent laboratory experiments. During the fall of 2009, Los Alamos researchers will be working to compare these results with the laboratory experiment and to write-up the results for publication.

## Background and Research Objectives

In the study of magnetic reconnection, many of the scientific challenges arise from the large separation between the microscopic motion of the charged particles and the large problem sizes. High temperature plasmas are very good conductors of electricity. Normally this constrains the magnetic field lines to move together with the plasma motion. For magnetic reconnection to proceed, it is necessary to break this constraint within so-called *diffusion regions*. These diffusion regions are quite small in comparison to the larger problems of interest, but play a critical role in the evolution. Thus researchers are working to understand the basic physics of these regions, as well as the coupling to the larger problems of interest. Due to the complicated nonlinear physics, computer simulations have played an important role in the scientific progress. Most previous simulation studies have focused on simplified two-dimensional (2D) models. With increasing computer power, these 2D simulations have progressed to larger problems and have raised a number of new questions. In particular, recent 2D simulations have demonstrated that diffusion regions often develop very long current sheets that are potentially unstable to a variety of different instabilities that may dramatically alter the energy conversion process. The main scientific goal of this project was to better understand the three-dimensional (3D) evolution of these layers. This is a formidable challenge that clearly requires large scale computing.

## Scientific Approach and Accomplishments

The equations necessary to describe magnetic reconnection can change depending on the temperature and density of plasma. For certain applications, it is very important to properly treat the individual interactions (or collisions) between the charged particles in the plasma. However, for higher temperatures, these collisions can be neglected and the plasma is referred to as *collisionless*. The scientific goal of this project was to better understand the influence of these plasma instabilities in both collisional and collisionless plasmas. In order to properly describe the physics, this

project employed a rigorous treatment of the collisions within the VPIC code [1,2]. These types of computer calculations describe the plasma at the most basic level, and are commonly referred to as *kinetic* simulations. After first carefully benchmarking the method [3], a series of 2D simulations were performed to examine how the physics changes with the plasma temperature [3,4]. This is the first time this transition has ever been examined with a kinetic simulation and the results have already attracted significant interest. These results demonstrate that magnetic reconnection tends to form highly elongated current sheets for a wide range of density and temperature. Furthermore, these elongated layers are unstable to a plasma instability that gives rise to the formation of magnetic islands as illustrated in Figures 1 and 2. While the existence of these islands was known previously for the collisional regime, these new results demonstrate this instability can play an important role in causing the rate of energy release to explosively increase under certain conditions [4]. In addition to these new science results, the 2D simulations paved the way for performing 3D simulations on the Roadrunner machine.

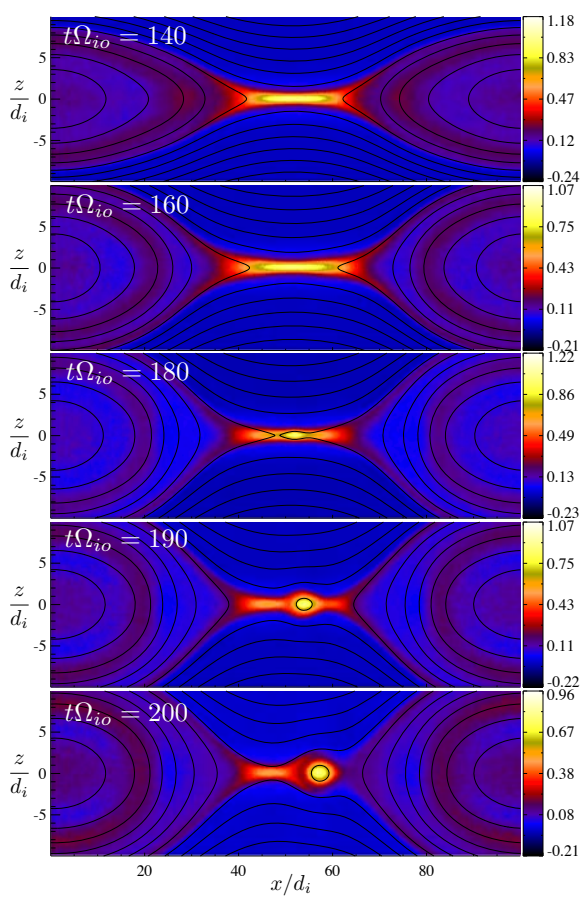


*Figure 1. Weakly collisional electron scale layers are unstable to plasmoid formation in two-dimensional simulations as discussed in Ref. [3].*

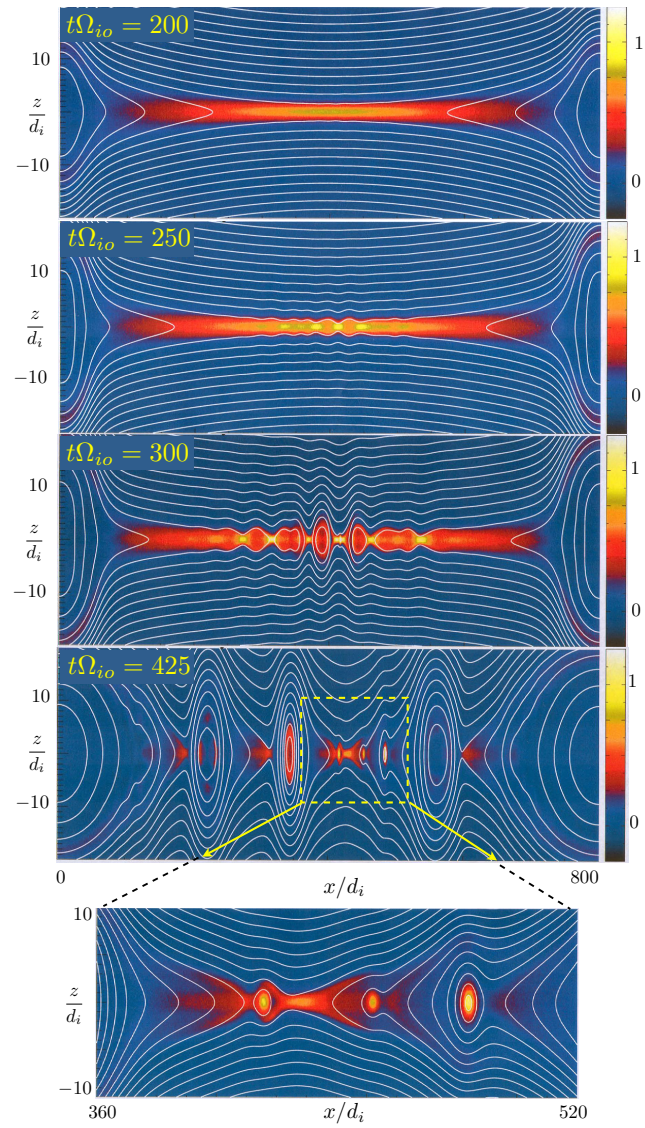


*Figure 2. Formation of secondary magnetic islands may play a central role in causing reconnection layers to transition between collisional and kinetic regimes as described in Ref. [4].*

Kinetic simulations of magnetic reconnection must resolve all of the microscopic physical scales in the plasma, including both the electron and ion motions. However, in space and astrophysical plasmas, the reconnection process occurs for problem sizes that are much larger than these small-scale motions. In order to fit the problem on a computer, it is necessary to carefully choose the simulation setup in a number of ways. First, it is necessary to reduce the separation between the ion and electron motions by employing artificial ion to electron mass ratios in the range ~100-300. Furthermore, it is important to focus on the most interesting regions for the development of magnetic reconnection. These preferred sites are thin current sheets, where the intense current density gives rise to a rapid rotation in the magnetic field. As reconnection develops, a flow pattern is setup that brings new plasma

and magnetic flux towards a reconnection site and expels the reconnected plasma as a high-speed jet tangent to the initial layer. It is possible to accommodate these flows and effectively mimic a larger system by allowing the plasma to cross the simulation boundaries [5]. This approach was employed to study several types of initial conditions on Roadrunner, resulting in a wealth of interesting new results.

Several of these simulations focused on a particular type of setup, where the magnetic field rotates by 180 degrees across the initial current layer. After the initial evolution, the simulations feature elongated electron current layers that are unstable to several distinct instabilities. As illustrated in Figure 3, one of these instabilities causes the electron layer to undergo flapping (or kink) type motions. This unstable wave has a number of properties that are consistent with predictions from recent theory [6]. The other instability in Figure 3 gives rise to the formation of *flux ropes*, in which the magnetic field lines wrap into rope-like structures. This instability is the 3D extension of magnetic island formation that has been previously reported in 2D simulations [5]. Similar instabilities have been previously observed in recent kinetic simulations of electron-positron plasmas [7], but this is the first time they have been observed for high mass ratio plasmas that are now feasible with Roadrunner. While researchers are still exploring the implications of these results, they are potentially of great interest from several perspectives. First, the kink instability may allow the electrons and ions to exchange momentum, which can then produce an effective resistivity within the layer. This issue has been of longstanding theoretical interest in reconnection physics, but has never been conclusively demonstrated. In addition, the formation of a flux rope effectively breaks the electron layer into two shorter layers and thus provides a mechanism to control the length. Since the length of these layers can influence the energy conversion rate, researchers are very interested to understand the various processes that can control the layer length.

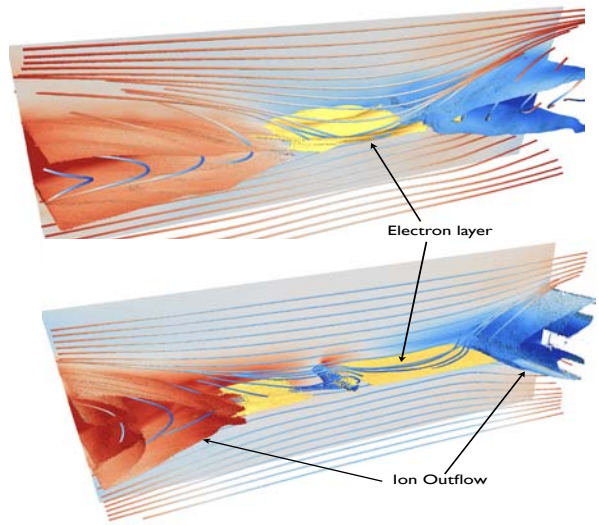


*Figure 3. Open boundary simulations for neutral sheet geometry feature two types of secondary instabilities within the electron layer: an electromagnetic kink wave (top) and flux rope formation (bottom). The boundary conditions permit inflow of new plasma (the top and bottom) and outflow of reconnected plasma (left and right). The outflow jets are visualized with a particle density isosurface colored by ion outflow velocity while the central electron current sheet (yellow) corresponds to an isosurface of electron current density. Sample magnetic field lines are colored by the magnitude of the magnetic field. Simulation was performed with mass ratio mi/me=300, using 4096 ranks, 245 million cells and 147 billion particles*

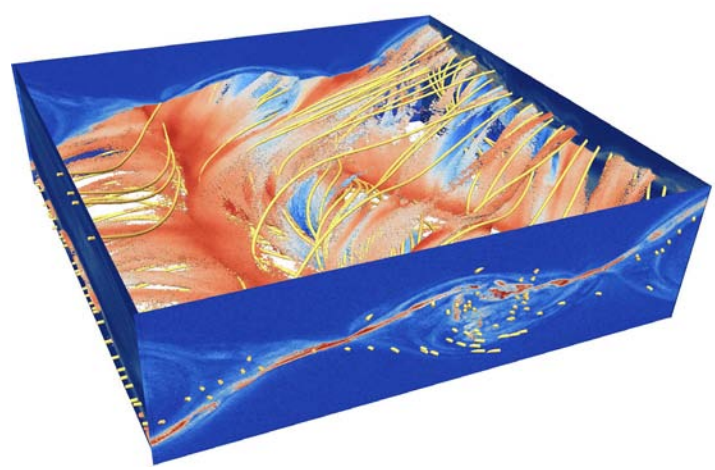

*Figure 4. Open boundary simulations for guide field geometry feature highly elongated electron current layers that are unstable to flux rope formation over a wide range of angles. These plasma instabilities cause the sheets to break into filaments as illustrated by an isosurface of the current density colored by the plasma density. Some sample magnetic field lines are shown in yellow and cutting planes along the perimeter also show current density. This simulation was performed with a guide field equal to 50% of the reconnecting field, mass ratio mi/me=64, 2048 ranks, 360 million cells and 72 billion particles.*

The formation of flux ropes is more complicated for other types of initial conditions as illustrated in Figure 4. In this example, the magnetic field rotates across the layer but always remains finite. This type of initial condition is unstable to flux rope formation at oblique angles across the initial ion scale layer. This results in the formation of new electron current sheets that are unstable to flux ropes over a wider range of oblique angles. As illustrated in Figure 4, the current density forms intense filaments leading to complicated magnetic field structures. The resulting 3D evolution is dramatically different than would occur in simplified 2D models, and is raising many new questions. Los Alamos scientists are presently working to understand how certain features in this complex evolution compares with predictions from theory. Future efforts will be focused on understanding the role flux rope interactions may play in the acceleration of highly energetic particles.

The physics of magnetic reconnection is also of great interest in laboratory experiments. Here it is possible to study the structure and dynamics in a controlled setting. While researchers expect the physics to be similar in laboratory experiments, the plasma conditions are quite different than in space. Three-dimensional kinetic simulations can play a valuable role in helping scientists extrapolate ideas that have been tested in the laboratory to regimes of relevance to space and astrophysical plasmas. The Magnetic Reconnection eXperiment (MRX) at the Princeton Plasma Physics Laboratory (PPPL) is one leading experiment that has reported measurements of magnetic reconnection. In particular, these results include detailed measurements of the electron current sheet that develops during reconnection [8]. In the experiment, reducing the current within two doughnut shaped coils called flux-cores drives the reconnection process. In order to capture this physical geometry, the simulations performed with VPIC used a realistic treatment of the experimental setup [9]. For the density and temperature in this experiment, it was also important to properly model collisions between the ions and electrons in the plasma [3]. On Roadrunner, a series of simulations were performed to examine the influence of both collisionality and plasma instabilities on the structure of the reconnection layer. The results clearly demonstrate that both effects play an important role in understanding this experiment. The example 3D simulation shown in Figure 5 illustrates a plasma instability within the electron current sheet. This instability has certain similarities with the kink wave discussed in Figure 3. It leads to the broadening of the layer and may potentially play a role in facilitating momentum exchange between electrons and ions. Researchers at LANL are working with the scientists at PPPL to perform detailed comparisons with these new simulation results. These validations efforts will include the characteristic thickness and length of the electron layer and properties of the observed waves. Together with ongoing theoretical work, these efforts are expected to shed new light on the influence of plasma instabilities on magnetic reconnection.

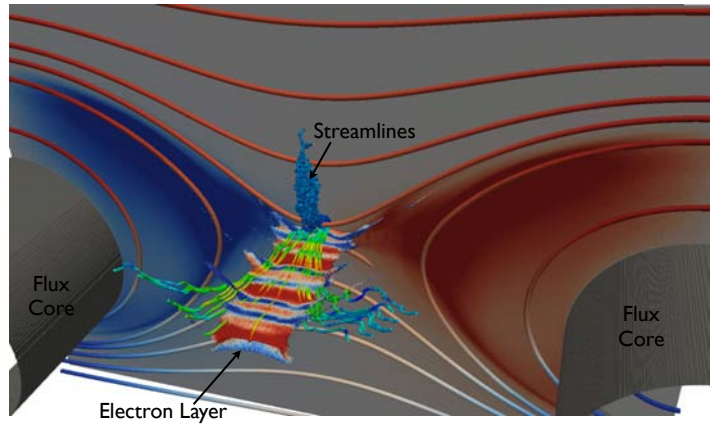


*Figure 5. Simulations were performed on Roadrunner with geometry and boundary conditions relevant to the MRX experiment including the influence of weak Coulomb collisions. The reconnection process is driven by reducing the currents inside the flux cores (grey cylinders) which pulls magnetic flux inward towards the cores. The resulting ion flow velocity is illustrated on the back cutting plane along with characteristic magnetic field lines. The central electron current sheet is illustrated with an isosurface of the current density, colored by vertical component of the current density to show the plasma instability within the electron layer. Sample electron streamlines illustrate the electron flow from the upstream region through electron layer into the downstream region. This simulation was performed with mass ratio mi/me=300 using 2880 ranks, 720 million cells and 158 billion particles.*

## Impact on National Missions

This project supported the DOE mission in Nuclear Weapons by enhancing our understanding of high temperature plasmas and exploiting the new hybrid computing technology on Roadrunner. The project supported the energy mission by advancing our understanding of magnetic reconnection, which is an important dynamical process in magnetic fusion machines. This research may indirectly benefit the nonproliferation mission since magnetic reconnection is also important in modeling the near-Earth space environment to better understand and mitigate the risks to satellites from extreme space weather events. The new simulation tools and theoretical expertise resulting from this project has attracted external support from the NASA Heliophysics Theory Program (3 year $1.2M). This new project will examine some detailed aspects of magnetic reconnection that occurs at the Earth's magnetopause, in support of ongoing and future NASA missions. The LDRD project also

recruited and trained a new postdoc (Vadim Roytershteyn from MIT) who is now highly capable in performing and analyzing these large plasma simulations for a variety of new applications.

## References


1. Bowers, K. J., B. J. Albright, L. Yin, B. Bergen, and T. J. T. Kwan. Ultrahigh performance three-dimensional electromagnetic relativistic kinetic plasma simulation. 2008. *Physics of Plasmas.* **15**: 055703.

2. Bowers, K. J., B. J. Albright, B. Bergen, L. Yin, K. J. Barker, and D. J. Kerbyson. 0.374 Pflop/s trillion-particle kinetic modeling of laser plasma interaction on Roadrunner. 2008. In *Proceedings of the 2008 ACM/IEEE conference on Supercomputin.* (Austin, Texas). , p. 1. Piscataway, NJ: IEEE Press.

3. Daughton, W., V. Roytershteyn, B. J. Albright, H. Karimabadi, L. Yin, and K. J. Bowers. Influence of Coulomb collisions on the structure of reconnection layers. 2009. *Physics of Plasmas.* **16**: 072117.

4. Daughton, W., V. Roytershteyn, B. J. Albright, H. Karimabadi, L. Yin, and K. J. Bowers. Transition from collisional to kinetic regimes in large-scale reconnection layers. 2009. *Physical Review Letters.* **103**: 065004.

5. Daughton, W., J. Scudder, and H. Karimabadi. Fully kinetic simulations of undriven magnetic reconnection with open boundary conditions. 2006. *Physics of Plasmas.* **13**: 072101.

6. Daughton, W.. Electromagnetic properties of the lower-hybrid drift instability in a thin current sheet. 2003. *Physics of Plasmas.* **10**: 3103.

7. Yin, L., W. Daughton, H. Karimabadi, B. J. Albright, K. J. Bowers, and J. Margulies. Three-dimensional dynamics of collisionless magnetic reconnection in large-scale pair plasmas . 2008. *Physical Review Letters.* **101**: 125001.

8. Ren, Y., M. Yamada, H. Ji, S. Dorfman, S. P. Gerhardt, and R. Kulsrud. Experimental study of the Hall effect and electron diffusion region during magnetic reconnection in a laboratory plasma . 2008. *Physics of Plasmas.* **15**: 082113.

9. Dorfman, S., W. Daughton, V. Roytershteyn, H. Ji, Y. Ren, and M. Yamada. Two-dimensional fully kinetic simulations of driven magnetic reconnection with boundary conditions relevant to the Magnetic Reconnection Experiment. 2008. *Physics of Plasmas.* **15**: 102107.


## Publications


Bowers, K. J., B. J. Albright, L. Yin, W. Daughton, V. Roytershteyn, B. Bergen, and T. J. T. Kwan. Advances in petascale kinetic plasma simulation with VPIC and Roadrunner. 2009. *Journal of Physics: Conference Series.* **180** (2009): 012055.

Daughton, W., V. Roytershteyn, B. Albright, H. Karimabadi, L. Yin, and K. J. Bowers. Influence of Coulomb collisions on the structure of reconnection layers. 2009. *Physics of Plasmas.* **16** (7): 072117.

Daughton, W., V. Roytershteyn, B. J. Albright, H. Karimabadi, L. Yin, and K. J. Bowers. Transition from collisional to kinetic regimes in large-scale reconnection layers. 2009. *Physical Review Letters.* **103**: 065004.

Dorfman, S., W. Daughton, V. Roytershteyn, H. Ji, Y. Ren, and M. Yamada. Two-dimensional fully kinetic simulations of driven magnetic reconnection with boundary conditions relevant to the Magnetic Reconnection Experiment. 2008. *Physics of Plasmas.* **15**: 102107.

Yin, L., B. J. Albright, Kevin J. Bowers, W. Daughton, T. J. T. Kwan, J. Margulies, E. M. Nelson, and H. Karimabadi. New insights into collisionless magnetic reconnection enabled by ultra-high performance three-dimensional kinetic simulations. 2008. *IEEE Transactions on Plasmas Science.* **36** (4): 1110.

Yin, L., W. Daughton, H. Karimabadi, B. J. Albright, Kevin J. Bowers, and J. Margulies. Three-dimensional dynamics of collisionless magnetic reconnection in large-scale pair plasmas. 2008. *Physical Review Letters.* **101**: 125001.

# The Roadrunner Universe

*Salman Habib*
20080743ER

## Abstract

The Roadrunner Universe project was aimed at designing, building, and running a next-generation cosmological structure formation code on the hybrid supercomputer Roadrunner (and its open counterpart Cerrillos), the world's first petaflop platform. Roadrunner's architecture presents opportunities and difficulties characteristic of next-generation supercomputing. Our new code is designed to optimize performance and scalability by explicitly matching the underlying algorithms to the machine architecture, and by using the physics of the problem as an essential aid in this process. While applications will differ in specific exploits, such a design process will become an essential aspect of high performance computing as we proceed from the petascale to the exascale. Cosmological simulations handle physics on the largest of scales: structure on scales greater than several Mpc (megaparsec; 1 parsec=3.26 light-years) is determined primarily by gravity. On smaller scales (Mpc and smaller), complex baryonic physics requires modeling of (magneto) hydrodynamic, thermal, chemical, and radiative processes. Because dark matter outweighs baryons by a factor of five, gravity-only N-body simulations provide the bedrock on which all other techniques rest. For next-generation sky surveys, simulation requirements include box-sizes as large as the entire visible universe and particle counts ranging from the hundreds of billions to trillions, all with force resolution sufficient to resolve individual galaxies. These requirements are about one to two orders of magnitude beyond the current state of the art and set the framework for the project. The development of codes for next-generation machines all the way out to exascale computing is recognized as a national high performance computing imperative. The work in this project will serve as a pathfinder for scientific computing not just in astrophysics and cosmology, but many other applications.

## Background and Research Objectives

Over the last three decades observational cosmology has made extraordinary progress in determining the make-up of the Universe and its expansion history. The first precision observations were obtained from the cosmic microwave background (CMB), beginning with the all-sky temperature anisotropy measurements from COBE that provided the first detailed confirmations of current theories of the early Universe and the formation of large scale structure. Follow-up measurements from the ground, balloons, and space have resulted in constraints on the main cosmological parameters at better than the 10 percent level of accuracy, and the recently launched Planck satellite CMB mission promises even further improvement. But CMB measurements are not the only observational source for precision cosmology. Structure formation probes such as large-scale surveys of the galaxy distribution, and weak lensing and cluster surveys, are aiming to reach similar levels of statistical and systematic control, as are supernova observations. These newer techniques, exemplified by contemporary surveys such as the Sloan Digital Sky Survey (SDSS) and those of the future, such as observational campaigns at the Large Synoptic Survey Telescope (LSST) and the Joint Dark Energy Mission (JDEM), provide complementary data to the CMB to help determine the large-scale description of the Universe.

Precision measurements from several different cosmological probes have revealed a highly unexpected result: roughly 70 percent of the Universe is made up of a mysterious dark energy causing an accelerated expansion of the Universe. Understanding the nature of dark energy is the foremost challenge in cosmology today. Ground-based telescopes and satellite missions have been proposed or are under development to measure the equation of state parameter of dark energy, w, at the one percent level, and its time derivative to 10 percent.

To date, the four most promising lines of investigation are: (i) Supernovae Type Ia, as standard candles to measure the expansion history of the Universe, (ii) clusters of galaxies, whose mass and number distribution measure both the expansion history and growth of structure, (iii) baryon acoustic oscillations, spatial features in the galaxy distribution that measure the expansion history, and (iv) gravitational weak lensing, the statistically measured distortion of the shapes of background galaxies by the foreground mass distribution used to measure the expansion history and the growth of structure. All three structure formation-based probes require the understanding of nonlinear physics at different length scales. At small scales, in addition to gravity, gas physics plays an important role, significantly complicating the modeling task. The last two probes, baryon acoustic oscillations and weak lensing, rely the most strongly on precise predictions of nonlinear matter clustering. Numerical simulations are essential for carrying out this task, not only to provide predictions for survey observables, but also to provide the underlying skeleton of cosmological structure from which object (e.g., galaxies, clusters, etc.) catalogs can be built. The resulting mock catalogs have many uses: to design and test observational strategies, to understand possible systematic errors therein, and to confront theoretical predictions with observations.

The computational requirements set by the observational demands are very strict. Aside from sheer size, the time to completion for a single run is a significant factor. Current state of the art simulations can take months to complete. Such long times are quite unacceptable if simulations are to play an important role in the inverse analysis of observational data, as they must for next-generation surveys. Parameter estimation require tens of thousands to hundreds of thousands of simulation runs. Although, as shown by us recently, sophisticated statistical techniques can be used to lower this requirement by two to three orders of magnitude [1], one still desires an individual run to take a few days at most, i.e., an order of magnitude faster than present practice. Therefore, in terms of overall throughput, the current N-body simulation capability needs to be enhanced by two to three orders of magnitude. This is the first petascale computing challenge for precision cosmology that our work is designed to meet.

## Scientific Approach and Accomplishments

The Roadrunner Universe project code, MC3 (Mesh-based Cosmology Code on the Cell), uses grid and direct particle methods to balance the capabilities of Roadrunner's conventional cluster (Opteron) and accelerator (Cell BE) layers. The long-range force-solver is grid-based and functions entirely at the Opteron layer. The short-range force solver is particle-based and all particle information stays at the Cell layer. During time-stepping, only grid information is exchanged between the two layers solving the communication bottleneck problem that exists between the cluster and accelerator layers.

The code uses sophisticated digital (spectral) filtering techniques to smoothly match the long and short range forces; significantly, this method removes the need for possibly complex particle-grid interaction templates. The last point is particularly important since it allows for efficient code implementation at the Cell layer.

Another key feature is the use of a mirrored particle cache at every Cell node. The cache sacrifices memory for communication with the advantage that no particle communication is needed across computational nodes. As a result, the scaling properties of the code become entirely decoupled from possible limitations of the inter-layer communication; scaling tests on medium resolution MC3 runs show perfect weak scaling all the way from hundreds of nodes to the full machine. This is demonstrated in Figure 1.

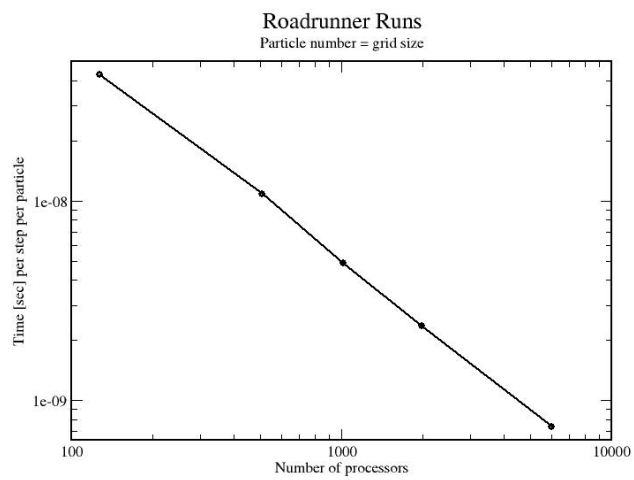


*Figure 1. Perfect weak scaling of the (medium resolution) MC3 code on Roadrunner. As the problem size is increased, commensurate with the number of processors, the time-step per particle reduces as expected, all the way out to the full machine size.*

Finally, because very large amounts of data can be generated during code runs (petabytes), which are then very difficult to store and analyze, our code incorporates very fast analysis routines that are run along with the main code in an "on the fly" mode. This design significantly reduces the data storage and post-processing loads, greatly simplifying the task of extracting scientific results from the simulations. A detailed description of the code is given in Reference [2].

During the Open Science phase, our code was run on Roadrunner for a few months, during the shakedown period for the machine. In this period, as the machine was being stabilized, several machine issues were unearthed by our code and other simulation codes. This led to modifications in the machine's system software, significantly improving its usability. The main simulations we ran on Roadrunner were large medium resolution runs for baryon acoustic oscillation science for the SDSS-III Baryon Oscillation Spectroscopic Survey (BOSS). These simulations were run with a 4000 cubed grid and 64 billion particles, some of the largest cosmology simulations ever performed. The results from these simulations are now being analyzed and a paper is under preparation.

## Impact on National Missions

The impact on national missions of this work is twofold. The first is directed at the science of interest, impact on the design of cosmological surveys and interpretation of the associated observational data. This is only possible with next-generation codes such as MC3. The second impact is related to the development of next-generation hybrid computing platforms and how scientific codes should be written for them. Because these architectures are non-traditional the code must be matched to the architecture – this aspect is termed "codesign" in current parlance. MC3 represents one of the very few examples of a successful codesign exercise and serves as a pathfinder for many large-scale applications that are now being redesigned for next-generation supercomputers.

## References


1. Habib, S., K. Heitmann, D. Higdon, C. Nakhleh, and B. Williams. Cosmic calibration: constraints from the matter power Spectrum and the cosmic microwave background. 2007. *Physical Review D .* **76**: 083503.

2. Habibetal., S.. Hybrid petacomputing meets cosmology: The Roadrunner Universe project. 2009. *Journal of Physics: Conference Series.* **180** (1): 012019.


## Publications


Habibetal., S.. Hybrid petacomputing meets cosmology: The Roadrunner Universe project. 2009. *Journal of Physics: Conference Series.* **180** (1): 012019.

# Implicit Monte Carlo Calculations of Supernova Light-Curves

*Aimee L. Hungerford*
20080744ER

## Abstract
Models of supernova explosions in two dimensions using Implicit Monte Carlo radiation transport were completed on the Roadrunner machine. Code capability that was added, and obstacles that were overcome to progress on these simulations is discussed.

## Background and Research Objectives
Supernovae play an important role across a wide range of fields in physics and astronomy: they mark the endpoint in the life of stars but are an important source of energy to galaxies and play a role in the formation of new stars; they are produced in the formation of stellar-massed compact objects and, possibly, the seeds of the most massive black holes in the universe; they produce the bulk of the heavy elements in the universe and are the foundations of nuclear astrophysics; and, finally, they require many of the same broad numerical and physics expertise in which laboratory scientists have excelled, placing Los Alamos National Lab (LANL) in an ideal position to model these objects.

The importance of supernovae has become even more critical with the realization that type Ia supernovae can be used as distance estimators based on the fact that their peak luminosity can be calibrated and determined from the time-dependent behavior of these supernovae, allowing the discovery of dark energy. This discovery has marked one of the major scientific discoveries of the past decade and has galvanized the scientific community to use supernovae to do more than discover, but to characterize dark energy using supernovae. Many new supernova search projects have grown out of this exciting result, immensely increasing the data we have on supernovae. Both the National Science Foundation (Large Synoptic Survey Telescope - LSST) and NASA/ DOE (Joint Dark Energy Mission - JDEM) are sponsoring major missions to study supernovae, representing a multi-billion dollar U.S. scientific effort.

The expertise at LANL in numerical hydrodynamics, radiation transport, atomic opacities and nuclear physics (both physics and experiment) provides an ideal opportunity for LANL to make major contributions to the study of supernovae. In this project, we also take advantage of LANL's excellence in high performance computing through use of LANL's Roadrunner machine. Roadrunner's heterogeneous architecture uses a cell processor to accelerate computation on the base Opteron processors. A series of advanced algorithms were developed by LANL computer scientists to best take advantage of the cell processor acceleration. A basic version of the Wedgehog implicit Monte Carlo (IMC) radiation transport code was one of the resulting codes from these efforts (we shall call this initial base version RRIMC). Our project's goal was to make the necessary alterations to this initial RRIMC code so that it could be brought to bear on the radiation-hydrodynamic problem of supernova light curves.

## Scientific Approach and Accomplishments
There were a variety of capabilities required to turn the base RRIMC code produced by the Advanced Algorithm's team into a tool capable of attempting this supernova light curve problem. First, the stand-alone RRIMC radiation package needed to be recast as a subroutine to be called by a hydrodynamics host code. This was accomplished by implementing interface routines into both RRIMC and the RAGE (Radiation Adaptive Grid Eulerian) hydrodynamics code to enable calls from RAGE to the RRIMC code package for the radiation part of the simulation timestep. This new code package, created by merging these two numerical packages, is called CASSIO.

Next, a set of physics capabilities, necessary for the supernova regime, were added to CASSIO. Electron scattering dominates the opacity in the ejecta from the supernova explosion. The original RRIMC code did not include electron scattering physics; our team implemented the electron scattering treatment present

in the production Wedgehog IMC code into the RRIMC version. In addition to adding a treatment for electron scattering physics, the specific supernova regime required some algorithm performance enhancements to make the treatment of electron scattering efficient enough for the simulation to complete in a reasonable time. A random walk treatment used in the production Wedgehog IMC was mildly altered and implemented in the CASSIO code to address this issue. Finally, velocities in the supernova regime are quite large and the flow of radiation in optically thick regimes are dominated by radiation carried along with the hydrodynamic material flows. A material advection treatment was also implemented into the CASSIO code from the standard treatment present in the main line Wedgehog IMC code.

Early on, our team had concerns about possibly exceeding the computer memory for domain replicated parallelism in our 2-dimensional simulations of supernova ejecta. To ameliorate this situation, two options were made available for the RRIMC package in CASSIO.

1. Non-reproducible random number generator: parallel reproducibility (i.e. getting the same numerical answer regardless of number of processors) is an important feature during code development phases. However, the extra information stored to track the random number generator state in order to achieve exact reproducibility (as opposed to merely getting the same answer to within our statistical accuracy) is a significant memory cost. By linking to a non-reproducible version of our random number generator routine, we cut the memory cost of each particle by 65%.

2. Spatial Domain Decomposition: it is a high memory cost to replicate the entire spatial mesh on every processor. The memory footprint on each processor can be reduced by breaking the mesh into pieces and spreading the pieces out over the available processors. The penalty for doing this is that the Monte Carlo particles are then tied to their spatial mesh piece and this is frequently not the best way to decompose the particle work in the problem. However, as the number of cells in the problem grows this is often the only way to avoid running out of memory on the available processors. Without previous knowledge of how the supernova problem would evolve in memory usage, spatial domain decomposition was implemented into CASSIO as protection against a scenario where domain replication was not possible.

As the project progressed to actually running supernova simulations on Roadrunner, we identified several issues with the heterogeneous RRIMC package and with its integration into CASSIO. Because these runs required large numbers of mesh cells and IMC particles, the supernova simulations exposed problems that had not appeared during earlier small-scale testing. Some of the issues involved intrinsically parallel portions of the code; other issues were rare single-node, single-timestep problems that appeared during the supernova simulations because of the large number of nodes used and timesteps taken.

Parallel scalability issues are almost guaranteed when running any code at untested problem sizes. On Roadrunner, the supernova problem experienced a small variety of failures during some message-passing operations. The largest of these issues occurred in large domain-decomposed problems, when the IMC package's communication pattern could overwhelm the MPI library's ability to buffer messages; switching to a synchronous send mode implemented a natural throttling mechanism with no impact on performance.

The rare single-node issues were often more difficult to isolate, but they usually resulted from failure to consider the asynchronous nature of data movement among the various address spaces on a hybrid Roadrunner node (Opteron main memory, Cell main memory, and synergistic processing element-SPE local store), and they were usually found first in large supernova simulations. In one case, an SPE could receive invalid instructions for processing a set of particles because the SPE received a "retrieve new instructions from this address" command from the PPE, and retrieved the contents of that address from Cell main memory, before those new instructions had actually been written to main memory from PPE cache. In another case, a DMA from main memory to an SPE could trigger a segmentation fault in a particular rare arrangement of the contents of the heap.

The supernova problem also highlighted several implementation issues and optimization opportunities in the IMC package and the interface to Cassio. The most significant issue was a mismatch between actual and expected contents of an array used to calculated momentum deposited by radiation, which showed up first in the supernova problem (Figure 1) but was eventually isolated and corrected in much smaller test problems. The "random walk" capability, taken from the Wedgehog IMC package, was also improved by extending the sizes of random-walk spheres all the way to the nearest edge of the enclosing cell; this helped with performance in the extremely optically which interior of the supernova ejecta.

Despite these challenges, we did have some success at advancing a pair of supernova explosion simulations through a partial phase of the evolution where

the explosion shock is first emerging from the star. Observations of this phase can help astrophysicists determine precise values for stellar radii or stellar wind densities, thereby placing constraints on our theories for the evolution of stars. Figures 2 and 3 show snapshots of the internal energy from our two explosion simulations. Figure 2 is an explosion with an imposed bi-polar asymmetry and Figure 3 is the symmetric explosion as mapped from a 1-dimensional core-collapse code.

Post-processing of these radiation-hydrodynamic calculations is needed to determine the spectral response of the shock break-out phase in these models. This work will be forthcoming.

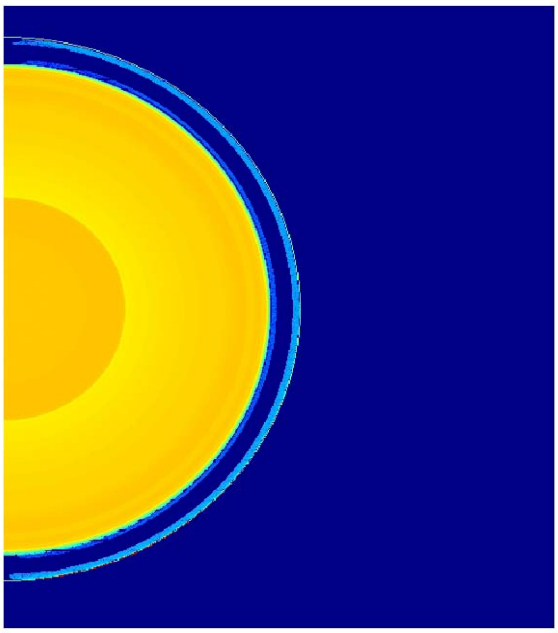

*Figure 1. Momentum array was sized incorrectly in the code interface leading to incorrect momentum deposition in the radiation hydrodynamics calculation. This plot shows the ejecta speed; the incorrect momentum deposition is evident from the striping near the poles of the explosion.*

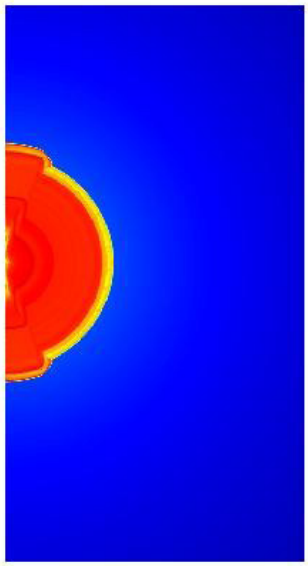

*Figure 2. Plot of supernova ejecta internal energy for an asymmetric explosion during the shock breakout phase. The asymmetry was imposed to mimic magnitude of asymmetries thought to exist from the core-collapse explosion engine.*

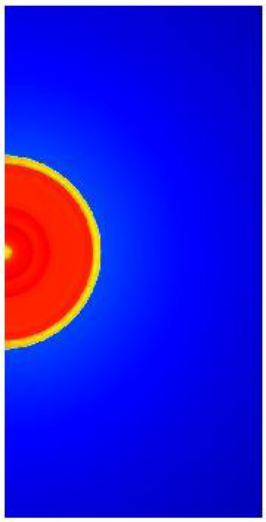

*Figure 3. Plot of supernova ejecta internal energy for a symmetric explosion during the shock breakout phase.*

## Impact on National Missions

This was a first attempt to place a complex coupled multiphysics code (radiation transport coupled to hydrodynamics) on the hybrid architecture of Roadrunner. Many of the laboratory's National missions involve the use of computational multiphysics tools. As we move to routine petascale and exascale computing, the viability of our work depends on our success at using these hybrid computers for our multiphysics problems. The obstacles overcome in our project are lessons learned for the future of our computational expertise here at LANL.

# Instabilities Driven Reacting Compressible Turbulence

*Daniel Livescu*
20080747ER

## Abstract

This was a short LDRD-ER project (16 months) with the primary goal of participating in the Roadrunner "open science runs." Thus, the main thrust of the project was to port the compressible turbulence Direct Numerical Simulations (DNS) code, CFDNS, to the hybrid architecture of Roadrunner and add the new necessary components required by the science runs. The purpose of the simulations is to advance our understanding of turbulence and turbulent mixing beyond the "standard" configurations, by performing Direct Numerical Simulations (such that all scales of motion are accurately solved) of reacting compressible turbulence with different configurations of fuel : ``well-stirred'' and two-component, corresponding to premixed and non-premixed burning. The parameters for the reacting simulations were chosen to be relevant to burning in Type Ia supernovae and type I X-ray bursts and allow to determine ``effective'' flame propagation speeds. The turbulent flame speed is the main uncertainty in the large scale supernova models and accurate estimates would allow improved precision in the determination of distances in the universe.

In order to take advantage of the hybrid architecture, the CFDNS code has been completely re-written for the Roadrunner version. The new version achieved excellent performance (up to 50x serial and 20x parallel speed-up compared to standard architecture). The overall effort required to adapt the CFDNS code to the Roadrunner hybrid architecture was considerable, but the benefits in terms of performance improvements are likewise significant. The changes made to the underlying data structures and algorithms will likely be beneficial on most future architectures and accelerators, due to the trend towards more vector processors (e.g. Cell, GPU, SSE). This commonality means that the changes made to the CFDNS code will lead to improved code performance on many emerging architectures for the foreseeable future.

## Background and Research Objectives

The conditions characterizing turbulent (nuclear) combustion in energetic astrophysical events such as supernovae and type I X-Ray bursts are novel and have no direct analogue on earth. This makes such conditions interesting for testing new physics, but it also means that our terrestrial intuition regarding flames can be misleading. For example, it is thought that laboratory flames in the Ka >> 1 regime, where Ka is the Karlovitz number, simply go out because they are unable to maintain their heat in the presence of so much turbulence. But the flame in a supernova can never "go out" until the star comes apart and, in terms of local flame variables, that takes a very long time. The relevant time scale is the hydrodynamic time scale for the whole star, ~1 s, not the shorter local turbulent time scale. Also, the star is very large, > $10^8$ laminar flame thicknesses and 100 integral scales. Rare events have many opportunities for realization.

Although several mechanisms for detonation have been proposed, the debate around deflagration/detonation models is still not settled. However, there are no DNS of reacting turbulence under these conditions; the only moderately high resolution simulations performed to date are in the low Mach number approximation, and do not capture the wave propagation. Very high resolution DNS of compressible reacting flow could elucidate the deflagration-to-detonation transition and help understand the Type Ia supernova explosion [1]. Similar transitions may also occur in the Type I X-ray bursts or in late helium flashes in AGB stars. In these cases, the dominant reaction is two-component and there are no high resolution simulations reported in the literature.

Turbulence theory and the subsequent model development rely on experimental or high resolution DNS data for development and verification and validation. The DNS technique seeks "exact" solutions to the governing equations, so that all relevant scales

are accurately solved, using high resolution numerical simulations based on high order accurate discretization algorithms. DNS are conducted without resort to subgrid modeling or the introduction of "artificial" numerical dissipation or other algorithm stabilizing schemes. The DNS generated database can be used to examine the physics of turbulence, test modeling ideas as well as a benchmark for verification of other (non-DNS) codes. Rigorous modeling techniques for the unclosed or sub-grid terms are essential to facilitate the use of these low resolution calculations in science-based prediction. Large scale simulations of canonical incompressible turbulent flows have been performed and advanced our understanding of the turbulence phenomena. As a result, several modeling approaches now work reasonably well for coarse mesh simulations of these simple flows, even though a complete parameterization of turbulence still eludes us. In many important applications, however, fluid turbulence is accompanied by complicating physics: compressibility, exothermic reactions, and differential accelerations. Fundamental turbulence studies and high resolution simulations of these flows have not been performed and the appropriate modeling paradigms are not known.

Thus, the goals of the simulations are:

1. Determine accurate turbulent flame propagation speeds under conditions present in Type I X-ray bursts and Type Ia supernovae.

2. Elucidation of the compressibility role on the flame development and detonation initiation.

3. Burning characteristics in the distributed regime.

4. Testing of the existing turbulence modeling paradigms and the appropriate approaches, which could be used in the coarse mesh (astro)physics codes. The DNS results can constitute a database for verification of such codes.

5. Testing of the turbulence theories at Reynolds numbers much higher than previously achieved in computations and beyond the "standard" (canonical flows) configurations.

At the time of the report, although the "open science runs" ended, the simulations are still ongoing. The project funding did not include all the actual simulations or the analysis of the results and these are continued with other funds. Nevertheless, the simulations performed as part of the "open science runs" demonstrated the ability of the code to perform as designed, both in terms of the performance achieved and capturing all the physics intended. The simulations completed thus far represent the largest non-reacting and reacting compressible turbulence simulations to date.

The status of the simulations at the time of the report is:

1. 3-D isotropic turbulence runs to generate the inlet conditions for the reacting runs and probe the differences between ideal gas turbulence and turbulence under supernova conditions have been performed and are currently under analysis.

2. 1-D reacting flow runs to generate the initial conditions for the reacting runs and measure the laminar flame speed have been performed at larger parameter ranges than previously done and are currently under analysis.

3. Fully coupled 3-D reacting simulations to study the nuclear flame propagation and measure the turbulent flame are under progress.

The simulations are performed at different values of the dilatational to solenoidal energy ratio and cover a range of Damkholer and Karlovitz numbers larger than previously achieved, in a regime close to the conditions thought to lead to the detonation initiation. The isotropic turbulence simulations have already showed new physics related to the dilatational motions and spectra [2].

From the computational science point of view, the doubly heterogeneous computing environment of the Roadrunner system introduces new complexity into the programming model. The bulk of Roadrunner's compute power lies in the Cells, with only ~50 Tflops attributed to the Opterons. This introduces significant challenges for efficient algorithmic development for applications which are memory limited as is the case with fluid flow simulations. Nevertheless, the changes to underlying data structures and algorithms induced by Roadrunner are advantageous to all of the current high-performance hybrid and conventional acceleration frameworks (Cell, GPU, SSE) and are therefore fundamentally necessary to leverage future architectures. From this perspective, Roadrunner is a conservative machine, a bridge between yesterday's homogeneous clusters and tomorrow's heterogeneous hardware. In addition, one of the roadblocks to further increases in supercomputer power is the dramatic increase in energy consumption. While Roadrunner is #1 on the June and November, 2008 Top500 lists, it is also #7 on the November, 2008 Green500 list, the first #1 Top500 machine to place in the top 10 for efficiency. Roadrunner is cited for "extraordinary energy efficiency." This is a strong indication for the pertinence of the algorithms developed for this work, beyond their general relevance, for the future supercomputer platforms.

The goals of the Roadrunner implementation are:

- Design new algorithms, underlying data structure, and memory access patterns for a highly efficient version of the CFDNS code on the Roadrunner architecture.
- Demonstrate that large hydrodynamics codes can be efficiently implemented on hybrid architectures.

The project successfully met both of these objectives. Thus porting the CFDNS code represents the first implementation of a large hydrodynamics code to the Roadrunner architecture and the performance of the new version of the code is impressive.

## Scientific Approach and Accomplishments

The flows under investigation occur in the continuum limit so that they are described by the compressible Navier-Stokes equations, continuity, energy, and species mass fractions transport equations. Two reacting flow configurations are considered:

1. "Well-stirred" single component burning, $^{12}C(^{12}C,\gamma)^{24}Mg$, relevant to Type Ia supernovae. The flame advances into the cold fuel (12C) in a C-O mixture and leaves behind hot product (24Mg). Inflow/outflow boundary conditions are imposed in the vertical direction so that the moving flame remains inside the domain.
2. Two component, $^{12}C(p,\gamma)^{13}N$, burning, relevant to Type I X-Ray bursts.
3. The physical transport properties are appropriate for the astrophysical situations investigated and are calculated within new modules added to the code. Thus, the thermal transport includes both radiative and electron transport (accounting for degenerate regimes) contributions. The equation of state considers radiative, ion, and electron contributions. To reduce the computational effort, pre-calculated tables for the transport properties, EOS, and nuclear energy rates are used.

The simulations are performed in three stages (Figure 1):

1. Generate the isotropic background turbulence,
2. Generate 1-D profiles of the flow and thermodynamic variables through the flame, and
3. Perform fully coupled 3-D reacting flow simulations, initialized with the 1-D profiles with the isotropic turbulence introduced through the inflow boundary.

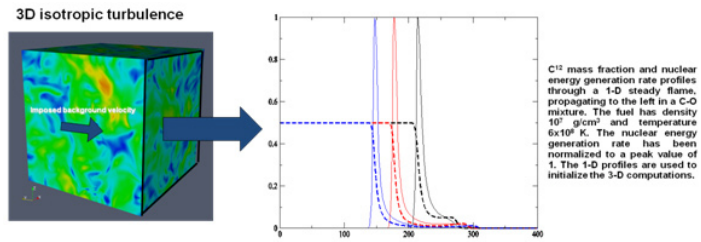


*Figure 1. The three stages for performing fully coupled, turbulent flames simulations.*

All simulations are performed with the same code. One interesting by-product of this approach is to also examine the turbulence properties for flows involving non-ideal fluids, which is not known.

The code employed for this project is the CFDNS code, developed by the PI and collaborators within the CCS-2 group over the last 6 years. ***This is the first implementation of a large structured fluid dynamics code on the Cell architecture*** [3-6]. In contrast to other applications that have been ported to the Cell, codes of this type are typically limited by memory bandwidth. The resulting imbalance between inter-node communication and compute speed required refactoring of several key sections of the code. In addition, the dual memory spaces of the hybrid architecture are leveraged to maximize performance and available memory, enabling the largest compressible turbulence simulations to date.

The serial implementation showed significant speedups of 30x ($128^3$ local mesh) to 50x ($64^3$ local mesh) [3], primarily due to the Cells ability to independently access main memory, allowing an effective memory access rate of ~12 GB/s (50% of theoretical peak). This serial speedup necessitated development of a novel implementation of the finite difference scheme used for spatial derivatives.

The excellent serial speedup resulted in an imbalance between compute and communication times compared to an un-accelerated cluster. This required a re-examination of the original communication patterns to absolutely minimize latency and data movement. This lead to a new distributed tri-diagonal solver algorithm [4-6]; the new form requires twice as much local computation, but significantly less data movement, and allows significantly better performance of the parallel solver. The overall speedup for the parallel solver is in the range 15-20x compared to the Opteron only version.

The table lookup for the equation of state (EOS) computation and transport properties evaluations are the least amenable to acceleration as these parts are very memory intensive, with reduced computational

intensity. Again, the algorithms were completely redesign to vectorize the calculations and minimize the memory access time, in order to take full advantage of the Cell architecture, even when this lead to repeating some of the local operations. The overall algorithm showed, again, excellent performance [6].

## Impact on National Missions

By demonstrating that hybrid architectures can be used for accurate calculations of reacting turbulence flows, the project has shown a path forward for mission sensitive predictive science, and as such has shown leadership through what was a foggy future. The project supports the current mission of the laboratory (with implications for Campaign 1, Campaign 4, and the ASC program) with its port of a complex hydrodynamics code and scientific results, and also future missions and capabilities associated with the national security mission of the laboratory.

Both the new Roadrunner code and the original CFDNS code have already been integrated within the programmatic efforts at the Lab (Campaign 4) and reacting simulations exploring various parameters and conditions are ongoing. In addition, individual algorithms developed for the CFDNS code (e.g. table look-up) are being used to improve the performance of other codes within several programs at the Lab.

## References


1. Petersen, M. R., and D. Livescu. Forcing schemes for statistically stationary compressible turbulence. *Physics of Fluids.*

2. Livescu, D.. Plans for Unstable Flame Calculations on Roadrunner. (Stanford, 7-9 April 2008).

3. Mohd-Yusof, J., D. Nehal, and D. Livescu. Roadrunner: Compressible Turbulence Simulation. (Reno, 10-17 November 2007).

4. Mohd-Yusof, J., D. Livescu, T. Kelley, M. Petersen, and N. Desai. Roadrunner application: Simulation of compressible turbulence. (Austin, 10-17 November 2008).

5. Mohd-Yusof, J., D. Livescu, T. Kelley, M. R. Petersen, and N. Desai. Fluid flow simulations on Roadrunner. (Miami, FL, 2-6 March 2009).

6. Mohd-Yusof, J., D. Livescu, and T. Kelley. Adapting the CFDNS compressible Navier-Stokes solver to the Roadrunner architecture. (Moffett Field, CA, 18-22 May 2009).


## Publications


Livescu, D.. Plans for Unstable Flame Calculations on Roadrunner. Presented at *ASC Computational Astrophysics Consortium Meeting.* (Stanford, 7-9 April 2008).

Mohd-Yusof, J., D. Livescu, T. Kelley, M. Petersen, and N. Desai. Roadrunner application: Simulation of compressible turbulence. Presented at *International Conference for High Performance Computing, Network, Storage, and Analysis.* (Austin, 10-17 November 2008).

Mohd-Yusof, J., D. Livescu, T. Kelley, M. R. Petersen, and N. Desai. Fluid flow simulations on Roadrunner. To appear in *Proceedings of the SIAM Conference on Computational Science and Engineering (CSE09).* (Miami, FL, 2-6 March 2009).

Mohd-Yusof, J., D. Livescu, and T. Kelley. Adapting the CFDNS compressible Navier-Stokes solver to the Roadrunner architecture. To appear in *Proceedings of the 21st International Conference on Parallel Computational Fluid Dynamics (ParCFD2009).* (Moffett Field, CA, 18-22 May 2009).

Mohd-Yusof, J., D. Nehal, and D. Livescu. Roadrunner: Compressible Turbulence Simulation. Presented at *International Conference for High Performance Computing, Network, Storage, and Analysis.* (Reno, 10-17 November 2007).

Petersen, M. R., and D. Livescu. Forcing schemes for statistically stationary compressible turbulence. *Physics of Fluids.*

# Saturation of Backward Stimulated Scattering of Laser In The Collisional Regime

*Lin Yin*
20080761ER

## Abstract

The VPIC code has been converted to run on the Roadrunner supercomputer and served as one of the key codes during the Roadrunner Phase 3 acceptance and open science stabilization phase. Access was granted to 6.7M hours on the full Roadrunner system during this stabilization phase for state-of-the-art VPIC kinetic plasma modeling of laser-plasma interaction (LPI) to study the nonlinear kinetics of stimulated Raman scattering in the collisional regime. These calculations are important from a basic physics standpoint and are relevant to upcoming fusion ignition experiments on the National Ignition Facility. LDRD funding support is was provided for: (1) VPIC diagnostic development, (2) relevant, smaller-scale two-dimensional (2D) simulations on Cerrillos to isolate key collisional physics and gain confidence in vital subsystems such as MPI and I/O, (3) prepare relevant scientific calculations for a LANL Gordon Bell Prize submission in late Spring, 2008, and (4) verification and validation of LPI nonlinear physics with large-scale 3D simulations on Roadrunner.

## Background and Research Objectives

In 2010, inertial confinement fusion (ICF) experiments begin at the National Ignition Facility (NIF), where over a Megajoule of laser energy will be focused within a gas-filled hohlraum. The hohlraum walls absorb the laser energy and re-radiate it as x-rays, which absorb in a spherical capsule at the center. This causes the capsule to compress, bringing deuterium-tritium fuel to the temperatures and pressures required for thermonuclear fusion. To prevent the hohlraum walls from ablating during the ~$10^{-8}$-second laser drive, a fill gas of hydrogen or helium is used. As the laser propagates through the fill gas, laser-plasma instabilities may arise, which scatter laser light out of the hohlraum, degrade capsule implosion symmetry, and pre-heat the fuel with hot electrons, making compression harder to achieve.

Stimulated Raman scattering (SRS), the resonant amplification of electron density fluctuations by a laser, is one of the LPI of concern for ICF. In ICF experiments, nearly uniform laser intensity is maintained across the beam by use of random phase plates that break the beam into an ensemble of laser speckles. For the success of fusion experiments on the NIF, we must first understand the physics of onset and saturation of SRS in a single laser speckle, which acts as a fundamental building block of a NIF laser beam. In a laser speckle, SRS manifests as the amplification of a forward directed electron plasma wave (EPW) and the backward scattering of laser light. Unlike the linear growth of SRS, the nonlinear physics was not well understood until recently [1,2]. Roadrunner has been used to assess the impact of nonlinear SRS physics on laser penetration and energy deposition in fusion experiments, as well as verify and validate key collisional LPI physics.

## Scientific Approach and Accomplishments

Until recently it has not been possible to simulate the comparatively large 3D plasma volumes of laser speckles. However, on Roadrunner, fully kinetic plasma simulations employing the VPIC particle-in-cell code [3-5] have been performed in large plasma volumes in 3D at unprecedented range of time and space scales. In particular, simulations of LPI have been done using 4096 Cell chips at a range of laser intensity values (Figure 1). These simulations [6] showed that SRS reflectivity within a solitary speckle exhibits a sharp increase in reflectivity at a threshold intensity, whereby reflectivity increases abruptly to a level orders of magnitude higher than linear theory predicts over a small range of intensity, and a saturation in SRS reflectivity at higher laser intensity. This generic behavior matches that measured in single speckle experiments at the LANL Trident Laser facility [7] with physics that cannot be captured by linear gain models of SRS growth within the speckle.

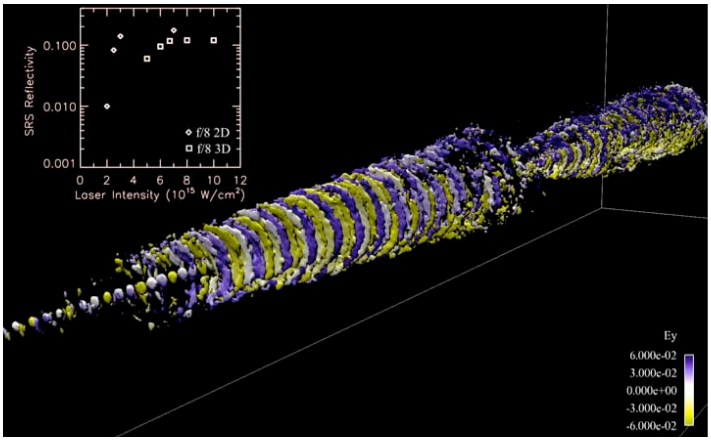


*Figure 1. Single-speckle LPI calculations using 16 CU of Roadrunner (11,520 ranks), nearly the full system; this calculation employed a record 0.4 trillion particles, >2 billion cells, and ran for nearly 58,160 time steps (~1019 floating point operations), long enough for two bursts of stimulated Raman scattering to grow from noise to significant amplitude at a laser intensity near the SRS onset. The inset shows the scaling of SRS reflectivity vs. laser intensity for 2D and 3D VPIC calculations; in 3D, the onset threshold is higher, owing to increased side loss of hot electrons from laser speckles.*

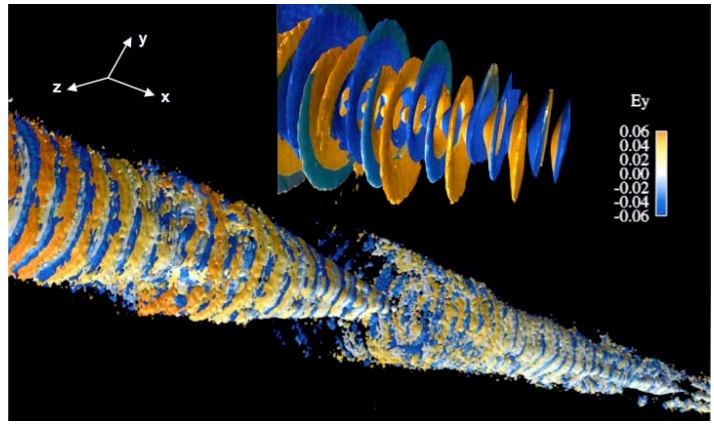


*Figure 2. (Top) A snapshot taken from a 3D VPIC LPI simulation at SRS pulse saturation of a f/4 laser beam, showing bending of iso-surfaces of EPW electric field across the speckle. The iso-surfaces are colored by the laser electric field intensity, graphically showing the source for SRS backscatter has become incoherent. (Bottom) Self-focusing and filamentation in two bursts of SRS, a snapshot taken from a 3D VPIC LPI simulation of a f/8 laser beam. The speckle volume is 16x larger than the f/4 simulation, permitting more transverse self-focusing modes to develop. This leads to chaotic EPW phase variation across the speckle. This further reduces SRS source coherence and increases wave damping, quenching the SRS pulse.*

As a highlight of the unique simulations afforded by Roadrunner, the largest of these calculations was run on 16 CUs using 11,520 ranks, nearly the full Roadrunner system, and employed a record 0.4 trillion particles, over 2 billion computational cells, and ran for nearly 58,160 time steps (~$10^{19}$ floating point operations), long enough for two bursts of stimulated Raman scattering to grow from noise to significant amplitude at a laser intensity near the SRS onset. Figure 1 shows isosurfaces of electrostatic field associated with these bursts; the wave fronts exhibit bending or "bowing," arising from nonlinear electron trapping, as well as self-focusing, which breaks up the phase fronts.

As a result of this effort, the essential nonlinear physics governing SRS saturation has now been identified: The scattering manifests as a series of pulses, each of which passes through 4 distinct phases: (1) SRS grows linearly from density fluctuations. (2) Electrons trapped by the EPW reduce the wave frequency and phase velocity by an amount that scales with EPW amplitude. (3) Near the speckle center, where the amplitude is highest, the EPW phase velocity is lower than at the speckle's edge; EPW phase front bending ensues as shown by the top image in Figure 2. (4) The EPW wave amplitude exceeds the electron trapped particle modulation instability (TPMI) threshold [8,9]. TPMI generates waves off-axis from the laser direction and leads to EPW filamentation, self-focusing and phase front breakup, shown by the bottom image in Figure 2. Self-focusing increases transverse loss of trapped electrons and increases EPW damping.

In order to gain confidence in our understanding, theory and simulation results must be validated by laboratory experiments. A suite of single-speckle experiments [10,11] performed at the Trident laser facility reduced the laser pulse length from 200 ps [7] to 3 ps. Such a reduction made it possible to model the duration of a laser pulse with a single VPIC simulation. While qualitative agreement exists between results from 2D simulations and experimental data from Trident [10,12], the absence of collisional physics in the simulations has made direct comparisons problematic until now. A binary particle collision model [13] has been implemented in VPIC allowing for the effects of collisions to be isolated and studied independently.

A series of 1D and 2D VPIC simulations have been performed on the Cerrillos machine, a Cell-based supercomputer like Roadrunner, to study the effects of particle collisions on trapped-particle nonlinearities involved in SRS. The laser and plasma parameters have been chosen to match conditions in the Trident short-pulse experiments [10,11]. Simulations were performed using two different temporal profiles for input laser intensity. For quantitative comparison with experimental data, a Gaussian temporal profile with a pulse duration of 3 pico-seconds at full-width-half-maximum (FWHM) was used to mimic Trident experimental conditions. In addition, a constant laser profile, with a short rise time, was used to eliminate any temporal dependencies caused by a time-

dependent laser intensity. To isolate collisional effects on SRS from the ion dynamics, ion density fluctuations were suppressed by increasing the mass of the plasma ion species.

Single-speckle Trident experiments showed a sharp onset of SRS reflectivity at a threshold laser intensity followed by saturation at higher intensities [10]. Collisionless VPIC simulations showed the same qualitative behavior, yet predict a value for the onset threshold laser intensity smaller than the experimentally observed value. When like-particle collisions (e.g., electron-electron) were included, we found that collisional particle detrapping reduces the SRS backscatter for all laser intensities, as shown in Figure 3a. This reduction in SRS reflectivity results in an increase in the predicted value for SRS onset threshold, closer to experimentally observed values. In addition, we found a delay in the onset and a reduction in the saturated amplitude of the first peak in instantaneous SRS reflectivity, (Figure 3b). The observed delay in the development of the first SRS peak results from a collisional reduction in the convective gain-rate for SRS.

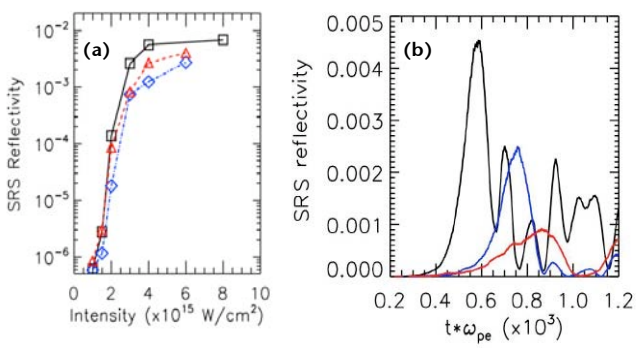


*Figure 3. (a) Time-integrated SRS reflectivity scaling with laser intensity (calculated from 1D VPIC simulations having a Gaussian temporal laser profile as in Trident) is plotted for three values of electron collisionality (from black to blue, the collisionality increases). (b) First temporal pulse of SRS backscattered light (calculated from 1D VPIC simulations with constant laser profile) for three values of electron collisionality which increases from black to red.*

In addition, Trident experiments show that the spectral width of SRS backscattered light increases with increasing laser intensity [11]. This same behavior was observed in VPIC simulations, as shown in Figure 4. In both collisional and collisionless simulations we observe an initial linear increase in the spectral width of SRS with increasing laser intensity, and saturation in spectral width at higher intensities (Figure 4b). Collisionless simulations overestimate the SRS spectral width compared with values observed experimentally. When experimentally relevant values of electron collisionality are included, however, the predictions for the SRS spectral width are much closer to experimental measurements. Furthermore, it is shown in Figure 4c that the observed broadening in the SRS spectral width is the direct result of trapped electrons nonlinearly shifting the EPW frequency. The dashed curve in Figure 4c is the theoretically predicted value for the SRS spectral width as a function of the nonlinear frequency shift, based on frequency and wavenumber matching conditions for parametric three-wave coupling. The agreement between theory and simulation (black diamonds: 1D collisionless VPIC, red triangles: 1D collisional VPIC, blue squares: 2D collisional VPIC) as well as between simulation and experiment leads to the conclusion that recent Trident measurements of broadening in the SRS spectral width constitute one of the first measurements of a nonlinear frequency shift due to electron trapping in SRS.

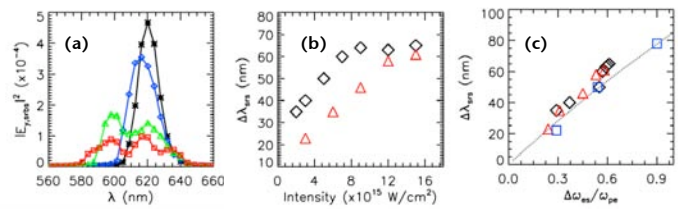


*Figure 4. (a) SRS spectra for a range of laser intensities, 2x1015 w/cm2 (black), 3x1015 w/cm2 (blue), 5x1015 w/cm2 (green), and 9x1015 w/cm2 (red) (calculated from 1d VPIC simulations with constant temporal laser profile). (b) SRS spectral width scaling with laser intensity for collisionless (black diamonds) and collisional (red triangles) cases (calculated from 1d VPIC simulations with constant temporal laser profile). (c) SRS spectral width scaling with nonlinear frequency shift of EPW for the 1d collisionless VPIC simulations (black diamond) and 1d collisional VPIC simulations (red diamond) in (b), as well as 2D collisional VPIC simulations (blue squares). Theoretical prediction depicted by dashed line.*

Invited talks

- LANL Supercomputing Conference, Plenary Talk – Albright
- LANL Supercomputing Conference, Invited Talk – Albright
- Plenary talk, High Energy Density Physics Workshop – Albright
- APS DPP invited talk – Albright
- SciDAC Invited Talk – Bowers
- International Conference on Numerical Simulation of Plasmas Invite Talk – Bowers
- APS DPP career award (Katherine Weimer award) and APS invited talk – Yin

- IBM/LANL Quarterly Review for Roadrunner Project – Yin

Presentations were given on this work to LANL external review committees, including talks to the LANS/LLNS Mission Committee and HEDP Capability review.

We have hired postdoc Sean Finnegan, a U.S. Citizen, into X-1-PTA, who has advanced the understanding of collisional LPI physics.

## Impact on National Missions

To Laboratory missions; actual impact on programs including both (a) changes to direction of existing programs and (b) new work brought to the Laboratory; new capabilities that the project brought to the Laboratory, particularly new staff.

This work has had significant impact on inertial fusion activities at LANL, across the DOE complex, and has changed the complexion of LPI research worldwide.

## Impact to DOE/LANL missions:

- Advances fundamental science and contributes to the success of inertial fusion experiments on NIF that commence in 2010
- Boost and Carbon-Neutral Energy Sources
- High performance computing for predicting complex systems
- Tools & expertise common to many other HEDP applications

From these basic science simulations, researchers are now able to understand better the essential nature of LPI nonlinear onset and saturation. Current research focuses on determining whether neighboring speckles can interact via exchange of hot electrons or waves to produce higher backscatter than they would individually, the kind of study only possible on Roadrunner, where “at scale” kinetic simulations of laser-plasma interaction in 3D at realistic laser speckle and multi-speckle scales can be prosecuted at unprecedented size, speed, and fidelity.

This work is widely considered the leading work in the world in the area of nonlinear laser plasma interaction science, as evinced by the large number of invited talks and awards. As a consequence of this effort, the VPIC code is known worldwide as a unique, best-in-class kinetic plasma modeling capability.

## References


1. Yin, L., B. J. Albright, K. J. Bowers, W. Daughton, and H. A. Rose. Saturation of backward stimulated scattering of laser in kinetic regime. 2007. *Physical Review Lettters.* **99**: 265004.
2. Yin, L., B. J. Albright, K. J. Bowers, W. Daughton, and H. A. Rose. Saturation of backward stimulated scattering of laser in kinetic regime: Wavefront bowing, trapped particle modulational instability and trapped particle self-focusing of plasma waves. 2008. *Physics of Plasmas.* **15**: 013109.
3. Bowers, K. J., B. J. Albright, L. Yin, B. Bergen, and T. J. T. Kwan. High performance 3d electromagnetic relativistic kinetic plasma simulation. 2008. *Physics of Plasmas.* **15**: 055703.
4. Bowers, K. J., B. J. Albright, B. Bergen, L. Yin, K. J. Barker, and D. J. Kerbyson. 0.374 pflop/s trillion-particle kinetic modeling of laser plasma interaction on Roadrunner . 2008. In *The ACM/IEEE Conference on Supercomputing.* (Austin, 16-20 Nov. 2006). , p. 1. Piscataway, NJ, USA: IEEE Press.
5. Bowers, K. J., B. J. Albright, L. Yin, W. Daughton, V. Roytershteyn, B. Bergen, and T. J. T. Kwan. Advances in petascale kinetic plasma simulation with VPIC and Roadrunner. 2009. *Journal of Physics: Conference Series.* **180**: 012055.
6. Yin, L., B. J. Albright, H. A. Rose, K. J. Bowers, B. Bergen, D. S. Montgomery, J. L. Kline, and J. C. Fernandez. Onset and saturation of backward stimulated Raman scattering of laser in trapping regime in three spatial dimensions. To appear in *Physics of Plasmas.*
7. Montgomery, D. S., J. A. Cobble, J. C. Fernandez, R. J. Focia, R. P. Johnson, N. Renard-LeGalloudec, H. A. Rose, and D. A. Russell. Recent Trident single hot spot experiments: Evidence for kinetic effects, and observation of Langmuir decay instability cascade. 2002. *Physics of Plasmas.* **9**: 2311.
8. Rose, H. A.. Langmuir wave self-focusing versus decay instability. 2005. *Physics of Plasmas.* **12**: 012318.
9. Rose, H. A., and L. Yin. Langmuir wave filamentation instability. 2008. *Physics of Plasmas.* **15**: 042311.
10. Kline, J. L., D. S. Montgomery, L. Yin, R. A. Hardin, K. A. Flippo, T. Shimada, and R. P. Johnson. Investigation of laser plasma instabilities using picoseconds laser pulses. 2008. *Journal of Physics: Conference Series.* **112**: 022042.

11. Kline, J. L., D. S. Montgomery, C. Rousseaux, S. D. Baton, V. Tassin, R. A. Hardin, K. A. Flippo, R. P. Johnson, T. Shimada, L. Yin, B. J. Albright, H. A. Rose, and F. Amiranoff. Investigation of stimulated Raman scattering using short-pulse diffraction limited laser beam near the instability threshold. 2009. *Lasers and Particle Beams.* **27**: 185.

12. Yin, L., B. J. Albright, K. J. Bowers, J. L. Kline, D. S. Montgomery, K. A. Flippo, and H. A. Rose. Kinetic simulations of stimulated Raman and Brillouin scattering of Trident short-pulse laser in a single-hot-spot . 2008. *Journal of Physics: Conference Series.* **112**: 022033.

13. Takizuka, T., and H. Abe. A binary collision model for plasma simulation with a particle code. 1977. *Journal of Computational Physics.* **25**: 205.

## Publications

Bowers, K. J., B. J. Albright, B. Bergen, L. Yin, K. J. Barker, and D. J. Kerbyson. 0.374 pflop/s trillion-particle kinetimodeling of laser plasma interaction on Roadrunner. 2008. In *0CM/IEEE Conference on Supercomputing.* (Austin, 16-20 Nov 2006). , p. 1. Piscataway, NJ, USA: IEEE Press.

Bowers, K. J., B. J. Albright, L. Yin, W. Daughton, V. Roytershteyn, B. Bergen, and T. J. T. Kwan. Advances in petascale kinetic plasma simulation with VPIC and Roadrunner. 2009. *Journal of Physics: Conference Series.* **180**: 012055.

Kline, J. L., D. S. Montgomery, C. Rousseaux, S. D. Baton, V. Tassin, R. A. Hardin, K. A. Flippo, R. P. Johnson, T. Shimada, L. Yin, B. J. Albright, H. A. Rose, and F. Amiranoff. Investigation of stimulated Raman scattering using short-pulse diffraction limited laser beam near the instability threshold. 2009. *Lasers and Particle Beams.* **27**: 185.

Rose, H. A.. Intensity dependent waiting time for strong electron trapping events in the onset regime of speckle stimulated Raman scatter. *Physics of Plasmas.*

# Lagrangian Approach to Capturing Interactions Between Wind-Energy Turbines and Atmosphere

*Rodman R. Linn*
20090489ER

## Abstract

Wind is the fastest developing renewable energy resource today. The U.S. Department of Energy (DOE) has set the goal of supplying 20% of the national energy demand with wind power by 2030. Achieving this goal requires significant advances in science and technology, which will in turn contribute to this nation's energy security. To successfully develop wind power resources, an improved ability to account for turbine interactions with complex wind events and adapt wind-turbine technology to these events is required. Turbine lifespan, reliability, and performance are significantly affected by their interaction with the often site-specific and evolving wind conditions to which they are exposed, including those driven by topography, daytime/nighttime transitions of the atmosphere, drainage flows, and low-level jets. Developing viable wind farms is dependent on the ability to account for the two-way interaction between numerous turbines and the resulting complex winds. Los Alamos National Laboratory (LANL) has developed and demonstrated a new technique for characterizing the turbine/wind interaction at length scales ranging from blade-scale (meters) to turbine-array-scales (kilometers). This achievement has been made by leveraging a combination of unique expertise and R&D100 winning numerical tools. Implementation of this technique in LANL's high-resolution atmospheric dynamics model, HIGRAD, has provided critical capability that will benefit government labs and commercial firms striving to improve wind-energy technologies. The functionality that was added to HIGRAD is referred to as WindBlade.

## Background and Research Objectives

The primary objective of this work was to further develop, initiate implementation, and begin demonstration of a new technique for simulating the two-way interaction between operating wind turbines and three-dimensional unsteady/spatially-variable wind fields over turbine-array-scale domains. This project was intended to position LANL to lead the investigation of critical wind-energy science questions and develop key partnerships to address others.

This work was focused on developing ways to address critical needs identified by both the wind turbine industry and recent DOE-facilitated wind energy assessments. The two-way interaction between wind-turbines and their environment dictates the viability of wind-power generation, and more specifically affects the performance, predictability, reliability, and maintenance/lifetime of turbines and turbine arrays. This interaction is complicated by numerous environmental phenomena that alter atmospheric turbulence and the nature of the vertical and directional shear of incoming winds. In turbine arrays, upwind turbines further modify the magnitude, turbulence, vorticity, and shear of the wind fields that reach the downwind turbines. The variability of the wind environments, which normally have a minimum turbine-hub-height speed of around 10 m/s, is affected by the vegetation structure, topography, diurnal cycle, and atmospheric stability as well as the turbines themselves. Some of the most troublesome turbine/wind interactions involve wind structures with length scales on the order of tens of meters. This project was focused on capturing the turbine/wind interactions at scales as small as a few meters, while retaining the ability to simulate the evolution of wind structures over multiple kilometers. With this range of scales in mind, the net influences of turbines on each other in turbine arrays can also be captured. The development and initial implementation and testing of WindBlade have been accomplished by combining LANL's R&D100 winning atmospheric hydrodynamics model, HIGRAD/FIRETEC, with novel uses of Lagrangian techniques.

The need for new techniques for capturing essential turbine/wind interactions is driven by the developing need to resolve:

1. A critical range of length scales including blade-cord-

scale structures (meters) to those that suddenly engulf entire turbines (100s of meters) such as those resulting from Kelvin-Helmholtz billows in slightly stable conditions to the evolution of atmospheric structures moving through numerous rows of turbines in wind farms (kilometers).

2. Three-dimensional atmospheric responses to blade segments that move between 50 m/s and 90 m/s relative to the surrounding air near the blade tips, and the resulting forces and bending moments on the blades.

3. Interactions between flow structures induced directly by the turbine blades, like streamwise vorticies or even tip vorticies, and larger atmospheric structures such as directional shears or low-level jets. These atmospheric couplings strongly affect the influence of one turbine on another through the turbine-induced mixing of the air from one height to another.

4. Winds in rugged terrain with turbine yaw angles that are not constrained to being in alignment with the grid directions (turbines need to be capable of adjusting to wind directions).

Prior to this project, no existing tool captured this set of critical features. In this project, LANL took advantage of the fact that it is ideally positioned to provide a working prototype of this model.

## Scientific Approach and Accomplishments

The foundation for the implementation of the turbine/wind interaction model, WindBlade, was the LANL-developed HIGRAD/FIRETEC code, which has been developed for the investigation of a variety of atmospheric phenomena ranging from explosive and passive dispersion to cloud physics. HIGRAD is the underpinning computational fluid dynamics (CFD) base for LANL's hurricane modeling research and R&D100 winning wildfire-modeling work, FIRETEC. Through the development of HIGRAD for these various applications, it has been validated for numerous scenarios that illustrate its ability to accurately capture the interaction between the atmosphere, vegetation, infrastructure, heat sources, and other disturbances at length scales similar to those of importance for wind energy production. This tool is well adapted for resolving multi-meter scale processes on multi-kilometer scale domains, and had a proven track record of efficient use of LANL's state-of-the-art Institutional Computing platforms. HIGRAD includes multi-phase representation of flows through tree canopies, sub-grid modeling for shear layers near structures, and a multi-scale turbulence model.

The development of WindBlade added to the functionality of HIGRAD through the use of Lagrangian techniques that allow forces to be exchanged between the atmosphere and turbine as it rotates. Wind turbines are divided into pieces or segments. The turbine blade segments are modeled as Lagrangian elements with known shapes, positions, and orientations that travel through the Eulerian finite difference mesh in a constrained path. This path is currently following the simple rotation of the blade around the hub, but could incorporate dynamic flexing of the blade in future projects. The dynamics of the wind flow are computed on the Eulerian HIGRAD terrain-following or generalize-coordinate system with a resolution expected to be between 1 and 5 m. Resolved winds are modified by the forces placed on the air by the blade segments. These forces are calculated based on the location and relative orientations and velocities of the Lagrangian blade segments with respect to ambient winds. Using this information and the local velocities, the drag and lift forces for specific blade cross sections are calculated based on relative attack angle and velocity of the moving blade relative to the winds at that location. These forces, which are nonunifom along the length of the blade, also drive changes in the angular momentum of the blade and cause the stresses, torques, and bending moment on the blades and turbine hub. The feedback of those forces on the wind flow forms turbine wakes, which affect other turbines in a wind turbine array.

The Eulerian grids can be constructed independently of the wind turbine geometry, so any kind of grid structure is possible. Coordinate systems such as terrain-following grids are advantageous for this type of simulation, since the effects of the terrain can be accounted for most accurately. The turbine elements are not bound to the Eulerian grid structure, so the secondary motion of the wind turbine can be captured.

During FY09, WindBlade was implemented and initial validation and testing was performed.

## Impact on National Missions

This project has started the development of a capability, WindBlade, which would help LANL to move into a position to provide science-based explanations for critical events that currently compromise performance and reliability of turbines, increase maintenance costs, reduce turbine life times, and prevent accurate prediction of wind generation viability. This work will hopefully eventually help link the atmospheric science and turbine/blade design communities by enabling the study of critical feedbacks between the aerodynamics of the blades and the larger flow fields surrounding the turbines as well as a better

characterization of the turbine-influenced flow fields that the blades operate in. This is especially important since wind turbines are increasing in size – they are expected to approach 120 m in blade span diameter - in order to achieve greater energy production and reach the 2030 goal. Larger blades increase the exposure and sensitivity to the spatial complexity and variability of incoming winds, which in turn complicates the design process for turbines and turbine arrays.

This new technique, which was submitted for a patent in FY09, will provide both a basis for collaborative research ventures with other research laboratories and partnerships with commercial entities. Private companies such as Clipper Windpower, Inc have voiced strong interest in LANL's development of this technique and within the past month larger wind energy companies have suggested interest. LANL's technology transfer experts are currently working on the marketing of this HIGRAD wind turbine tool, WindBlade.

Key collaborations have been initiated in FY09 with National Renewable Energy Laboratory (NREL) regarding this developing capability and Sandia National Laboratory (SNL) has voiced interest. NREL and SNL have longstanding programs in wind energy engineering and technology.

Based on the developments of this project, a DOE EERE proposal was submitted and has been positively reviewed, however funding decisions are awaiting congressional budgets. Also, WindBlade is a key component of the newly funded LDRD DR "Intelligent Wind Turbines", which will combine WindBlade with structural models.

# High Altitude Water Cherenkov Observatory

*Brenda L. Dingus*
20090515ER

## Abstract
HAWC is a proposed wide field of view gamma-ray observatory with over 10 times the sensitivity of similar existing detectors. With this LDRD funding, we investigated the scientific capabilities of HAWC by studying data from its predecessor, the Milagro gamma-ray observatory at LANL, and from the new lower energy Fermi gamma ray observatory. These studies were incorporated into a proposal to NSF and DOE High Energy Physics for HAWC and the results were published in peer reviewed journals, such as Science and Astrophysical Journal.

## Background and Research Objectives
Astrophysical sources accelerate particles to energies millions of times higher than possible with man-made accelerators. These particles, called cosmic rays, wander through the Universe being deflected by magnetic fields. Cosmic rays are continuously bombarding Earth from all directions.

Some of the cosmic rays interact near their sources and transfer their energy to photons. These energetic photons, called gamma rays, travel straight to Earth allowing us to determine the location of the sources and to study the cosmic accelerators.

Cosmic accelerators are extreme astrophysical sources with intense magnetic and gravitational fields. They are not normal stars, but typically involve black holes or neutron stars.

Very-high-energy (VHE) gamma rays (those with energies above 100 GeV) probe the most extreme astrophysical environments in the universe and can explore fundamental physics in regions not easily accessible with traditional techniques. Outstanding astrophysical questions addressed include the origin of the cosmic radiation and understanding particle acceleration in the cosmos.

The exciting science being done by the current generation of VHE gamma-ray instruments and the large number of new VHE sources naturally raises the question of what could be done in the future with more sensitive instruments. The Division of Astrophysics of the American Physical Society commissioned a white paper that concludes that there is a very compelling case for the construction of an all-sky monitor, extensive air shower array with sensitivity an order of magnitude better than the present best instrument, Milagro.

LANL pioneered the water Cherenkov technique with the Milagro observatory and that has lead to a plethora of discoveries with this wide-field instrument. With Milagro we discovered VHE emission from the Galactic plane, new extended sources of VHE gamma rays, unexpected anisotropies in the VHE cosmic radiation (an indication of a nearby cosmic-ray accelerator), the highest energy gamma rays from any source (up to 100 TeV), and the longest continuous light curve of variable VHE emission from a supermassive black hole.

With a previous LDRD ER grant we developed the detector design for a future experiment, the HAWC (High Altitude Water Cherenkov) Observatory. This instrument will have 10x the sensitivity of Milagro. With HAWC we will discover more than 10 times as many sources and have the ability to detect transients in 1/100 the time. This LDRD Reserve Project allowed us to improve on the scientific justification for HAWC by (1) finishing Milagro analysis which points to new sources and new capabilities for HAWC and (2) analyzing data from the Fermi Gamma-Ray Observatory which launched in 2008 and is a wide field observatory similar to HAWC but observes lower energy gamma rays.

## Scientific Approach and Accomplishments
This LDRD project investigated the data from the Milagro Gamma-ray Observatory and the Fermi Gamma Ray Space Telescope to learn more about the astrophysical

accelerators associated with black holes and neutron stars. First, a correlation was found between the lower energy Fermi data and the higher energy Milagro data (Figure 1), which proves that spinning neutron stars, called pulsars, are the most prevalent cosmic accelerators in our Galaxy. Second, the Fermi observations of gamma ray bursts indicates that the emission continues up to the highest energies detectable by Fermi as seen in Figure 2, requiring even higher energy particles are accelerated by these putative black holes.

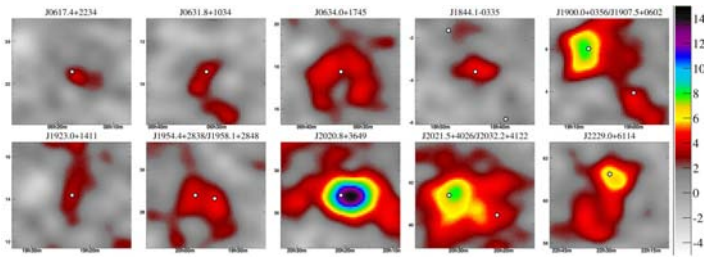

*Figure 1. Milagro observations (color) coincide with Fermi sources (dots), yet the physical mechanisms producing the pulsed Fermi emission differ from those producing the angularly extended Milagro emission. The lower energy Fermi emission is produced near the surface of the neutron star and is pulsed with the sub-second rotation period of the neutron star. The higher energy Milagro emission is due to a wind of particles flowing away from the neutron star and interacting with the ambient light to produce gamma rays.*

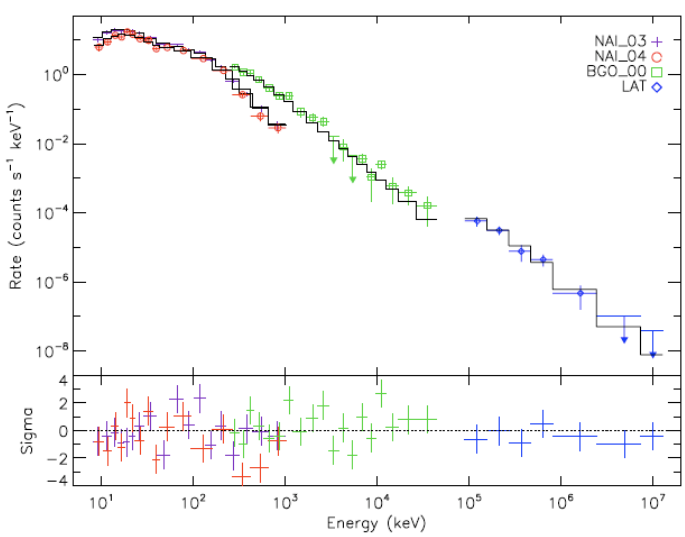


*Figure 2. Fermi observations of gamma-ray bursts show emission extending to energies high enough to be detectable by the HAWC observatory. Such emission requires that these sources (which are likely black holes) eject particles with unprecedented velocities. Such high energy emission also tests fundamental physics postulates, such as Lorentz invariance.*

Both of these results imply interesting scientific opportunities for HAWC. For example, the weakest sources seen in Figure 1 will be strongly detected by HAWC allowing the measurement of the energy spectrum of the gamma rays to extend to high enough energies to determine whether these sources are the producers of the galactic cosmic rays. Also, the Fermi observation of Figure 2 implies that HAWC will have the sensitivity to constrain the emission to even higher energies, such as would be required if these sources accelerate the extragalactic cosmic rays.

These results also attracted much attention in the field of particle astrophysics and beyond, leading to the following invited talks by Brenda Dingus.

- "Cosmic Ray Anisotropies Observed by Milagro", Snowbird Particle Astrophysics and Cosmology Symposium, Utah, Feb 2009
- "Gamma-Ray Astrophysics", Multi-Messenger Relativistic Astrophysics Inaugural Conference, Center for Relativistic Astrophysics, Georgia Tech University, May 2009
- "Gamma Rays to Probe the Origin of Galactic Cosmic Rays", University of Heidelberg Astronomy Colloquium, June 2009
- "Unexplained TeV Cosmic Ray Anisotropies", University of New Hampshire Physics Department Seminar, July 2009
- "HAWC (High Altitude Water Cherenkov) Observatory Surveying the TeV Sky", TeV Particle Astrophysics Symposium, Stanford Linear Accelerator, July 2009
- "Gamma Ray Astrophysics with Milagro and Fermi", Nuclear Physics Gordon Conference, July 2009
- "Milagro and HAWC Surveying the TeV Sky", University of New Mexico Physics Department Colloquium, September 2009

## Impact on National Missions

Gamma-ray Astrophysics is a forefront area of research as evidenced by multiple National Academy studies and investments by NASA, NSF, and DOE in GLAST, VERITAS, Milagro, and now HAWC observatories. This field addresses LANL's Grand Challenge to study physics beyond the standard model. LANL led the Milagro collaboration and LANL staff member Brenda Dingus is the co-spokesperson for HAWC and the project manager.

With Milagro and the development of HAWC, LANL has clearly established itself as a leader in the field of VHE astrophysics. With project we helped ensure that HAWC will be in an excellent position for future NSF and/or DOE

funding. The National Science Foundation has established a $1M MRI (Major Research Initiative) to perform the R&D required to eliminate the technical risk associated with the HAWC detector concept and to establish a small test array at the HAWC site (Sierra Negra, Mexico). They have also established a path forward for determining which set of projects they will fund in this area of research. The NSF and DOE convened a Particle Astrophysics Science Advisory Group (PASAG) in the Spring/Summer of 2009. Brenda Dingus gave a presentation to the PASAG in Washington DC in June 2009. The PASAG will review and rank the projects in the field. While the HAWC NSF proposal received excellent reviews, the full HAWC funding, ~$10M, will require approval of the PASAG. One of the strongest arguments for building HAWC are the scientific results of Milagro and GLAST that were accomplished with this LDRD Reserve Project.

## References


1. Buckley, J., K. Byrum, B. L. Dingus, A. Falcone, P. Kaaret, H. Krawzcynski, M. Pohl, V. Vassiliev, and D. A. Williams. The status and future of ground-based TeV gamma-ray astronomy. . 2008. *A White Paper prepared for the Division of Astrophysics of the American Physical Society.*


## Publications


Abdo, A.. Fermi Observations of High-Energy Gamma-Ray Emission from GRB 080916C. 2009. *Science.* : 1169101.

Abdo, A.. Milagro Observations of multi-TeV Emission from Galactic sources in the Fermi bright source list. 2009. *Astrophysical Journal Letters.* **700**: 127.

Abdo, A.. Fermi Gamma-Ray Burst GRB090510 observations limit variation of speed of light with energy. To appear in *Nature* . : 08574.

Band, D. L.. Prospects for GRB science with the Fermi Large Area Telescope. 2009. *Astrophysical Journal.* **701**: 1673.

# Gamma-Ray Bursts and Gravitational Waves from Compact Mergers

*Christopher L. Fryer*
20070574PRD1

## Introduction

The two main thrusts of this project are to study the progenitors of gamma-ray bursts and supernovae, and to study sources of gravitational wave emission.

The primary progenitors of both gamma-ray bursts and type Ia supernovae are binary star systems. In this project, we are modeling the populations of these systems to determine their formation throughout the history of the universe. By comparing these results to observations, we can probe the early universe and help devise better experiments to study dark energy. We are using a Monte-Carlo population synthesis code on LANL and New Mexico (Encanto) computers to run these calculations.

We are also modeling the sources of gravitational wave emission as part of our work as a Laser Interferometric Gravitational-Wave Observatory (LIGO) member. This work leads much of the general relativity work done at the laboratory into a focus that is closer to that of mainstream science.

## Benefit to National Security Missions

This project takes full advantage of the computational and physics expertise developed at the national laboratories as part of their mission in nuclear weapons. It has direct relevance to DOE Office of Science missions such as SNAP (Supernova/Acceleration Probe) and may impact LANL's "Beyond the Standard Model" Grand Challenge.

## Progress

Chris Belczynski has continued to focus on developing stronger ties with LANL scientists and LANL science while pushing forward the fields of binary star evolution. He has submitted 12 papers in the past year to refereed journals on a broad range of binary star topics: type Ia supernovae, gravitational wave sources, compact object distributions and gamma-ray bursts.

With his student (at NMSU) and Fryer at LANL, Belczynski studied the rates of type Ia supernovae. The population synthesis models of these type Ia supernova progenitors are now being used in light-curve studies as part of a DR on cosmic explosions. In this way, Belczynski's efforts are providing direct input into simulations run with the ASC code RAGE (Fryer has been running the simulations working with Belczynski to determine the input). In this way, this work ties to DOE/NNSA projects.

Type Ia supernovae may be produced in the merger of two white dwarfs. These objects are also sources of gravitational wave emission that might be detected by the NASA Laser Interferometer Space Antennae (part of NASA's long-term beyond Einstein satellite plan). Belczynski has worked on a paper discussing the gravity wave signal from these objects. In addition, he has studied gravitational wave sources for ground-based gravitational wave detectors. This work ties to both NASA and NSF missions.

One of the gravitational wave sources also happens to be the progenitor of short-duration gamma-ray bursts. Working with Fryer and Holz at LANL, Belczynski has studied gamma-ray burst progenitors at high redshift. With NASA's Swift satellite discovering higher and higher redshift gamma-ray bursts, his results inform the analysis of data from this major NASA mission.

Belczynski has worked on a number of projects studying the formation of compact objects: neutron stars and black holes. Tying to work by Fryer on core-collapse supernova engines, he has produced a set of papers studying the remnant left by collapsing massive stars. This will ultimately lead to a new standard for compact object mass distribution. This brings together LANL's expertise in supernova modeling to tie it to a broader scientific field.

Finally, he has continued his work studying specific

pulsar and X-ray binary systems, publishing a number of papers on these systems with collaborators across the country.

All of this work has led to a number of invitations as speaker at meetings across the world and Belczynski has traveled extensively to spread the science he has done at LANL. He has attended meetings organized by NASA and NSF programs on gravitational waves, NASA's EXIST mission (he has now become a member of this mission) as well as more general meetings on astrophysics, gravitational wave physics, and particle physics. His summer of 2009 was particular busy with meetings and collaboration visits.

Finally, Belczynski's student, Ashley Ruiter, successfully defended her thesis. This is Belczynski's first student to graduate and a major achievement for any post-doc. As adjunct faculty at NMSU, he presided over her defense and worked hard to ensure that her thesis was high quality. Fryer has worked directly with Ashley and ascertained that she agrees that Belczynski provided her excellent training. She has accepted a post-doctoral position at the Max-Planck-Institute for Astrophysics in Garching, Germany. This is a very prestigious position and will serve her well in a full scientific career. We have already begun a series of collaborations with her in her new role.

## Future Work

The primary issue with gamma-ray burst progenitors for short-duration bursts is the evolution of binaries. This also dominates many of the uncertainties in determining the signals from these binaries with respect to gravitational waves. Our project will focus on this binary evolution. The goal of this project is to first revamp our binary population synthesis code by developing better physics codes to determine the parameters in this code: advanced stellar evolution models developed at LANL taking advantage of detailed models of mixing, binary merger calculations using the LANL-developed Smooth Particle Hydrodynamics (SNSPH) code, using the latest developments in nuclear physics to revamp our understanding of neutron stars. After developing the tools and running them to revamp the binary evolution code, we will then begin an intensive study of these binaries focusing on the observational implications of such physics-based calculations including both gamma-ray bursts and gravitational wave detections.

These goals are summarized as follows:

**Revamp the Code**

1. Revamp code using advanced stellar evolution models:

- determine what is currently available and begin simulations for what pieces are missing
- incorporate these results into binary evolution code similar steps can be used for other physics

2. Merger calculations

3. Nuclear physics estimates

4. Insert remaining critical physics

**Simulations and comparison to observations**

1. Compare to gamma-ray burst data. Explain the current discrepancies in the data and work to make future predictions. This should have implications back on the physics so we should be able to use this to constrain current physics models and update (even validate) our codes.

2. Use tested codes to make predictions for gravitational wave observations.

We have completed the first studies of these mergers and these papers are almost through the refereeing process.

## Conclusion

This project will rule out many of the proposed gamma-ray burst progenitors allowing theorists to focus on the few remaining progenitors for detailed numerical study. These massive explosions play such an important role in our understanding of the universe from large-scale cosmology (these bursts are so powerful that they can be observed in the early universe and hence can be used as standard candles) to our understanding of the earth (it has been proposed that a GRB, not an asteroid, caused the extinction of the dinosaurs). By understanding their progenitors, we make all of these broader studies tractable.

## Publications

Fragos, T., V. Kalogera, K. Belczynski, G. Fabbiano, N. J. Brassington, D. W. Kim, L. Angelini, L. R. Davies, J. S. Gallagher, A. R. King, S. Pellegrini, G. Trinchieri, S. Zepf, and A. Zezas. Transient Low-mass X-ray Binary Populations in Elliptical Galaxies NGC 3379 and NGC 4278. 2009. *Astrophysical Journal.* **702**: L143.

Linden, T., J. F. Sepinsky, V. Kalogera, and K. Belczynski. Probing Electron-Capture Supernovae: X-ray Binaries in Starbursts. 2009. *Astrophysical Journal.* **699** (2): 1573.

Ruiter, A. J., K. Belczynski, and C. L. Fryer. Rates and Delay Times of Type Ia Supernovae. 2009. *Astrophysical Journal.* **699** (2): 2026.

# Detecting Dark Matter with Cryogenic Liquids

*Andrew Hime*
20070751PRD4

## Introduction

Stan Seibert's primary research objectives focus on two major experiments: the Sudbury Neutrino Observatory (SNO) and the MiniCLEAN dark matter experiment. SNO is a heavy water Cherenkov detector whose primary goal is to measure solar neutrinos in order to better understand fundamental neutrino properties and fusion processes in the sun. SNO finished data collection in November 2006 and LANL continues to play a lead role in the final analyses of this unique data set. Stan has led the SNO collaboration's effort to dramatically reduce the uncertainties in the measurement by including lower energy events in the data sample. This Low Energy Threshold Analysis (LETA) is particularly challenging due to the high level of precision required and the large amount of radioactive background present at low energies.

The MiniCLEAN dark matter experiment is presently under construction and designed to search for Weakly Interacting Massive Particles (WIMPs) that are hypothesized to constitute the dark matter in the universe. MiniCLEAN is a spherical detector with ~150kg of liquid argon or neon target imaged by an array of 91 photomultiplier tubes. Stan leads the simulation and analysis effort for the project and was this year elected by the collaboration to serve as Analysis Coordinator.

The LETA analysis for SNO was completed and a paper submitted for publication in Physical Review C. The preprint has been well received by the scientific community. As MiniCLEAN Analysis Coordinator, Stan coordinated the collaboration's efforts to develop a complete Monte Carlo simulation code for the experiment and organized a very successful workshop at the University of Pennsylvania in June to coordinate various simulation and analysis activities.

## Benefit to National Security Missions

This project supports DOE Office of Science missions in basic research to elucidate the fundamental properties of neutrinos using the sun as a unique astrophysical source and in the development of novel detector technologies for low-energy solar neutrinos and cosmological dark matter. The development of such technologies can potentially contribute to capabilities for nuclear threat reduction.

## Progress

The 53-page Physical Review C paper describing the LETA results from SNO was finished in October. The result boasts the lowest energy threshold ever achieved in a water Cherenkov detector and significant improvement in the measurement of Boron-8 neutrinos from the sun (Figure 1). The results improve our understanding of how different neutrino flavors transform into one another as well as contributing to the ongoing astrophysical debate regarding the chemical composition of the sun. Every aspect of the LETA analysis was carefully scrutinized by members of the SNO collaboration. Given the complexity of this precision experiment, the review required nearly a year to complete and was paramount to establishing the robustness and veracity of our signal extraction techniques.

Concurrent with the successful LETA program, Stan also completed the development of a novel method for obtaining the probability of an electron neutrino not transforming into another neutrino, called the "electron neutrino survival probability." Knowledge of how this survival probability varies as a function of neutrino energy is extremely useful as it shows how neutrinos interact with the matter in the sun. The SNO collaboration has never been able to report the electron neutrino survival probability function for solar neutrinos because we have not had a good way to extract it directly from our data. Thanks to the massive computing power available from standard, commercially available

3D graphics cards, Stan demonstrated a technique for obtaining this information and applied it to the LETA data in time to be included in the final publication.

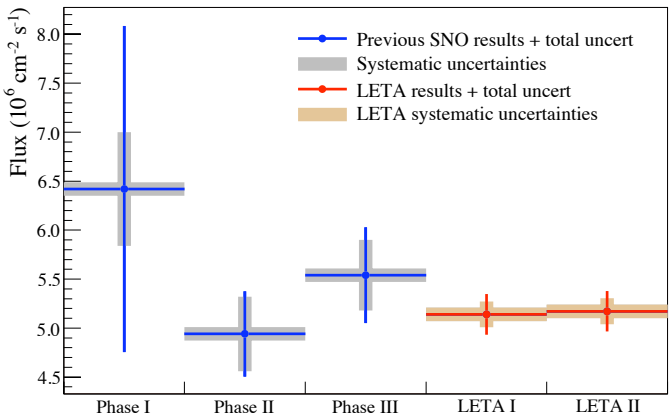


*Figure 1. The total Boron-8 neutrino flux measured in SNO in previous papers (Phase-I, Phase-II, and Phase-III) compared to the new low-energy threshold results (LETA-I and LETA-II). LETA-I and LETA-II refer to two independent analyses of the same data that were performed to verify the results.*

Since we anticipate commissioning the MiniCLEAN detector underground at SNOLAB in about 1 year's time, it is critical to organize and distribute simulation and analysis tasks effectively across the collaboration. Elected as the MiniCLEAN's Analysis coordinator, Stan brought together collaborators from 8 institutions at a very successful analysis workshop. Great progress was made in improving the microphysics input and accuracy of the MiniCLEAN simulation code, which has been critical to understanding our calibration needs, and in refining our methods to reject radioactive backgrounds in the experiment. This work has also allowed Stan to continue to leverage his experience in high performance computing and the use of commercial 3D graphics cards as numerical coprocessors.

Stan, in addition, mentored two undergraduate summer students on a project to measure the fluorescence efficiency of the wavelength-shifting fluor chosen for the MiniCLEAN experiment. The students were chosen to present their work this past Fall at the American Physical Society Division of Nuclear Physics meeting. Thanks to the LDRD contribution to this project, the scope of this measurement was expanded and we plan to draft and publish a paper describing this work in 2010. The results from this effort will be of great interest the scientific community in general where it concerns use and knowledge of these fluors.

## Future Work

With the LETA analysis for SNO complete and published, our efforts on SNO are ramping down although Stan will continue to serve as an advisor and reviewer for the SNO collaboration's effort to perform a full and final analysis encompassing all three phases of data collected from the experiment. Future efforts will be heavily focused on the MiniCLEAN experiment and, specifically upon full implementation of the analysis and simulation software that will be crucial as the detector becomes commissioned and we obtain initial calibration data.

## Conclusion

In conclusion, Stan Seibert has had a remarkably productive year in seeing the SNO LETA analysis to fruition along with its highly visible publication in Physical Review C. Stan's leadership as Analysis Coordinator for MiniCLEAN has led to the critical progress needed for the experiment to become a reality and this will continue to be the area of focus during the second year of this project.

## Publications

O.Collaboration, S. N.. Low Energy Threshold Analysis of the Phase I and Phase II Data Sets of the Sudbury Neutrino Observatory. To appear in *Physical review C.*

Sebert, S.. The Low Energy Threshold Analysis of the First Two Phases of the Sudbury Neutrino Observatory. Presented at *INFO09.* (Santa Fe, NM, July 6, 2009).

# Dynamics of Quantum First Order Phase Transitions

*Dima V. Mozyrsky*
20080689PRD1

## Introduction

We investigate the kinetics (i.e. dynamics) of the first-order quantum phase transitions in cold atom mixtures. These phase transitions - the quantum equivalent of water freezing to ice - are the subject of active research. They are relevant to many areas of theoretical physics, ranging from the evolution of the universe at its early stages to cluster dynamics in magnetic systems. At the same time, not many experimental observations have been confirmed. One of the first but not very conclusive results came from experiments on He-isotope liquids. This question has stimulated large experimental and theoretical efforts in the field. The dynamics of a system undergoing a first order phase transition is typically characterized by the process of nucleation. In nucleation, one component forms a droplet (nuclei) separating itself from the other. Unlike numerous commonly-found temperature-driven transitions, low temperature nucleation relies solely on quantum fluctuations and has not yet been consistently observed. Another type of process that closely resembles physics of quantum nucleation is so-called “phase-slip” process. It occurs when the phase of macroscopic quantum system is altered at some microscopic region (usually inside some potential barrier). As the result of a phase-slip the system, usually of cycle geometry, can support stable currents. The decay of these currents at low temperatures takes place via macroscopic quantum tunneling – the process, when all the involved particles undergo transition in exactly the same fashion (as in quantum nucleation). Cold atom systems provide an excellent opportunity to measure these phenomena. We investigate boson-fermion cold atom mixtures and ultra-cold boson systems to provide theoretical and numerical guidance for experiment. The investigation will provide advancements in understanding, observation, and measurement of quantum phase separation as well as macroscopic quantum effects associated with quantum nucleation. We also expect this investigation to shed some light onto unconventional mechanisms of high-temperature superconductivity, which appear to be related to quantum phase transitions of this sort.

## Benefit to National Security Missions

The project will support the DOE mission by enhancing our understanding of fundamental properties of complex systems. These areas of research constitute two major grand challenges pursued by the Los Alamos National Laboratory. Quantum systems may lead to new means of sensing and computing for missions such as Threat Reduction.

## Progress

Our investigation has taken several directions. We have demonstrated that quantum nucleation transition in cold atom mixtures is significantly suppressed by the dissipative processes. As the result, measurement of the nucleation rate need to be carried out in mixtures with certain ratio between masses of the atomic species, where dissipation is minimal. On the other hand, macroscopic quantum tunneling phenomena associated with phase separation is more accessible. Moreover, its rate is controlled by the density rather then the total number of particles, and therefore it can be easily controlled and measured. We proposed to measure the dissipative transition in the nucleation regime by analyzing expansion of an externally initiated droplet. We also investigated possible stable superfluid configurations in the system near the phase separation transition point. Finally, we explored possibilities to observe macroscopic quantum tunneling between current states in a single species boson system. In the following we address all these points in a greater detail.

In the first stage of our project we have investigated the possibility of observing quantum nucleation [1]. We studied kinetics of phase separation transition in boson-fermion cold atom mixtures. Starting from a macroscopic description of a boson-fermion mixture, we derived an effective action that describes the system

in terms of the boson density representing an order parameter. We analyzed the characteristic length scale and identified three different regimes of phase separation. The first regime corresponds to nucleation. The droplet of fermion fraction formed during the transition has distinctive boundaries. It forms when the densities of the two species are close to the critical density of the mixture. We obtained the asymptotic behavior for the droplet's size dynamics and demonstrated that the nucleation is significantly suppressed by dissipation when the fermion particle mass is greater or equal to that of a boson. Therefore, we concluded that experimental observation of quantum nucleation is feasible only in the mixtures with light fermion and heavy boson atoms. In addition, measurable rates (the number of created droplets per unit of time) require highly interacting mixtures. While such mixtures are experimentally possible, they are not easy to prepare and require state-of-the-art trapping and cooling techniques. We, therefore, propose an alternative scheme to probe dissipative dynamics associated with the nucleation. It is based on the analysis of expansion of an externally initiated droplet of fermions. Measurable changes associated with the dissipative transition take place for moderate interactions. As a result, the measurement can be done for relatively dilute easy-to-prepare systems.

Critical dynamics near the absolute instability of the mixture is fundamentally different. Here, the characteristic length scale diverges and the droplet boundary is not well defined. This regime is suitable for observing macroscopic quantum tunneling phenomena. The potential barrier separating mixed and phase separated situations is small. The system quantum-mechanically tunnels through this barrier creating an excess of fermion species in relatively large volume of the mixture. We calculated the tunneling exponents as a function of the system parameters, such as density and interaction strengths. We demonstrated that macroscopic quantum tunneling phenomenon can be observed in experimentally well-accessible dilute mixtures. In addition, due to the modification of boson-mediated interaction near the absolute instability, this regime presents an opportunity to test novel unconventional superconductivity mechanisms within the boson-fermion framework. In particular we have shown [2] that a thermodynamically stable superconducting phase can exist in a odd-frequency channel. Further work has to be done to develop microscopic interpretation of this unconventional phase.

Finally, we have investigated metastable macroscopic quantum states in a singe species boson system in Bose-Einstein condensation regime [3,4]. In particular, we have analyzed transitions between macroscopic current-carrying states in a ring-shaped Bose-Einstein condensate. Estimates for geometric parameters have been obtained [4] to support experimental observation of macroscopic quantum transitions in this system. The possibility to create well-controlled Bose-Einstein condensate of ring geometry has been recently confirmed by LANL experimental group within novel "painted potential" trapping technique. Our result indicates that, for experimentally feasible geometries, coherent macroscopic quantum tunneling phenomena should be accessible, see Figure 1, at temperatures of about tenth of a nano-Kelvin. While such temperatures are certainly achievable, we advise to begin with the thermal transition in currently available higher-temperature systems. This should allow performing fine tuning of the geometrical parameters. We have also demonstrated that as soon as the coherent quantum tunneling is achieved the system can be tuned [5] to quantum two-state regime. This regime provides a unique opportunity to explore a well controlled quantum system of two macroscopically distinct states (almost visible to a naked eye upon measurement).

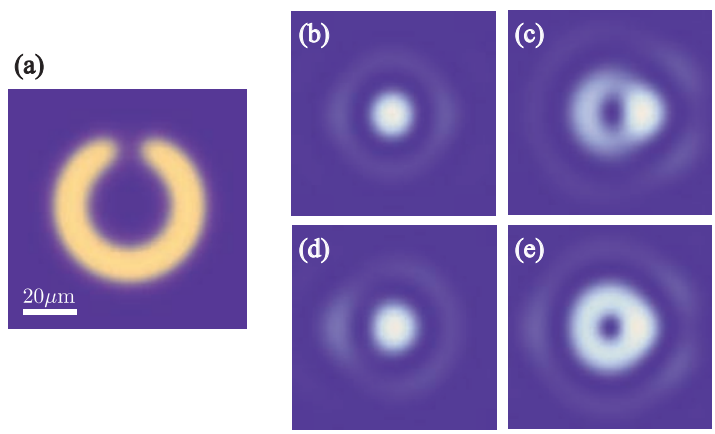


*Figure 1. Kinetics of single species cold atom Bose-Einstein Condensate of ring geometry. (a) The shape of typical condensate cloud. The system has rich structure or current-carrying state visible upon measurement (b,c,d,e). Macroscopic tunneling from the current state should be clearly visible in free expansion measurement (calculated): (b) the free expansion cloud in the case when tunneling took place, (c) expansion cloud indicating that the tunneling did not happen. Similarly for the tunneling from the zero current state (d,e). In both cases absence of density in the center of the expansion cloud hints the presence of non-zero current state.*

## Future Work

The project will study the kinetics of quantum first order phase transitions in cold atom traps. Extremely low temperatures achieved in the traps allow one to deal with an unusual state of matter—quantum condensates—on a macroscopic scale. Quantum dynamical effects associated

with quantum nucleation become potentially measurable. We should outline the major goals a follows: 1) We will investigate the phase separation transition in the system of trapped atomic mixtures of bosons and fermions (e.g. atoms with overall spin zero and one-half). 2) The investigation of dissipation in connection to the phase transitions in the above mentioned systems is necessary and will be conducted. 3) We will also investigate macroscopic quantum transitions in single species boson systems. In particular, the prospects and application of macroscopic two-state quantum system will be analyzed. 4) Investigation of noise levels in macroscopic cold-atom current-carrying systems will be performed to support the search for applications for the macroscopic two-state quantum system. 5) Phase diagram of unconventional odd-frequency superconductor in an unbalanced two species fermion system will be analyzed. In particular, novel quantum phase transition between different odd-frequency phases is expected to appear when the relative number of fermions (between the species) is modified. In all these directions we also aim at understanding the macroscopic collective quantum phenomena beyond particular cold atom setup. At the same time, we expect that the work will guide experimental efforts in cold atom systems in Los Alamos National Laboratory and worldwide. In particular, we will focus on supporting efforts to observe non-classical effects, such as quantum tunneling, on macroscopic scale. Macroscopic quantum tunneling phenomena is important in many physical processes associated with the first order quantum phase transitions, from cosmology to dynamics of nano-size magnetic systems, as mentioned above. This stimulates large on-going experimental and theoretical efforts in the field. At the same time, not many experimental observations have been confirmed (one of the first results came from experiments on 3He, 4He systems). The outlined project will also affect research in closely related topics such as, for instance, superconductivity and quantum computing.

## Conclusion

Understanding of the dynamics of quantum phase transitions may answer a number of fundamental questions. These questions range from the evolution of the universe at its early stages to the problems of cluster dynamics in magnetic systems. Contemporary cold atom systems, such as atoms or molecules confined in a magnetic trap, provide a perfect setup where such phase transitions can be observed and controlled with a desired accuracy. The work will set up the theoretical framework for the description of the dynamics of the first order phase transitions in these systems and will guide experimental efforts.

## References


1. Solenov, D., and D. Mozyrsky. Quantum nucleation and macroscopic quantum tunneling in cold-atom boson-fermion mixtures . 2008. *Physical Review A.* **78**: 053611.

2. Solenov, D., I. Martin, and D. Mozyrsky. Thermodynamical stability of odd-frequency superconducting state. 2009. *Physical Review B.* **79**: 132502.

3. Solenov, D., and D. Mozyrsky. Metastable states and macroscopic quantum tunneling in a cold atom Josephson ring. *Physical Review Letters.*

4. Kalas, R. M., D. Solenov , and E. Timmermans. Reentrant stability of BEC standing wave patterns. *Physical Review A.*

5. Solenov, D., and D. Mozyrsky. Macroscopic two-state system with cold atoms: towards BEC flux qubit. *Physical Review Letters.*


## Publications


Kalas, R. M., D. Solenov , and E. Timmermans. Reentrant stability of BEC standing wave patterns. *Physical Review A.*

Solenov, D., I. Martin, and D. Mozyrsky. Thermodynamical stability of odd-frequency superconducting state. 2009. *Physical Review B.* **79**: 132502.

Solenov, D., and D. Mozyrsky. Kinetics of the phase separation transition on cold-atom boson-fermion mixtures. 2008. *Physical Review Letters.* **100**: 150402.

Solenov, D., and D. Mozyrsky. Quantum nucleation and macroscopic quantum tunneling in cold-atom boson-fermion mixtures . 2008. *Physical Review A.* **78**: 053611.

Solenov, D., and D. Mozyrsky. Metastable states and macroscopic quantum tunneling in a cold atom Josephson ring. *Physical Review Letters.*

Solenov, D., and D. Mozyrsky. Macroscopic two-state system with cold atoms: towards BEC flux qubit. *Physical Review Letters.*

# Nonequilibrium Quantum Phase Transitions

*Eli Ben-Naim*
20080723PRD2

## Introduction

Nonequilibrium quantum phase transitions are poorly understood. The overall goal of the present project is to develop a firm theoretical foundation for quantum phase transitions. As applications of nanotechnological devices controlled by quantum behavior multiply and diversify, this understanding is increasingly important.

This project comprises two complementary subjects. The first is developing an understanding of quantum synchronization, in which different regions of a material spontaneously lock into the same quantum phase. Not only will this be of fundamental interest in itself, but, more importantly, it will have strong implications for decoherence, the mechanism which connects the quantum and classical worlds, and will help to bridge the gap between the classical and quantum physics. Moreover, a fleshed-out theory of quantum synchronization may have direct practical applications such as interpreting and understanding the spectrum of molecules such as polyethylene, disordered superconductor films, and the quantum behavior observed in collective atomic recoil lasing.

The second subject is quantum drag, which will give us new fundamental understanding of superfluidity. The phenomenon of superfluidity is one that we have known of for over half a century, yet it remains enigmatic in many respects. As the key to numerous applications, both current and future, such as atom lasers, precision clocks, and gyroscopes, it is of great importance that we move towards a more precise grasp of the physics underlying superfluidity.

## Benefit to National Security Missions

This work supports the energy security mission as it leads to better fundamental understanding of superconductors, materials that have zero resistance. These materials' energy applications include efficient electric power transmission and power storage devices, and sensors for threat reduction. This also supports LANL's competencies in quantum science and nanotechnology.

## Progress

Using analytical and numerical means, we showed that one should be able to construct a solid out of superfluid components, specifically by overlapping distinct dilute Bose-Einstein condensates (BECs) to form a mixture. Unlike previous research efforts that propose supersolid order in configurations of BECs, our work does not externally impose any length scale in order to achieve solid order. Our findings are an important step towards understanding the nature of supersolids, a new form of matter whose existence has generated much controversy within the low-temperature community.

We also calculated the drag experienced by an impurity of any strength moving through a quasi one-dimensional BEC. We derived new analytical solutions of the equations governing these systems, which allowed us to calculate the drag solutions exactly. We showed, for the first time, that such a force exists in this geometry, and have also been able to calculate the force's dependence on velocity and impurity strength. These results are crucial for demonstrating the presence of this effect in ultracold dilute atomic gases.

In addition, we have also published a review paper summarizing the results of this Casimir-drag force analysis. We have also helped organize a successful conference on Casimir physics in Santa Fe that was attended by leading international experts in the field.

We have extended our previous results on the linear reformulation of the canonical model of synchronization. Part of the extension addresses the issue of anomalous scaling that was found to occur in this new class of exactly solvable models.

## Future Work

Future work in superfluids includes exploring the Casimir-drag effect numerically through the truncated Wigner approach, an approximation from quantum optics that has been applied successfully towards the simulation of quantum noise effects in BECs.

We will also study the problem of Casimir drag in superfluids in the context of a fermionic system. Our hypothesis is that the scattering of quantum fluctuations within a flow of superfluid fermions gives rise to a drag force. Positive demonstration of this effect would constitute the first evidence of such a drag force existing in fermonic systems.

Finally, we will study whether the controversial transverse acoustic force, the Iordanskii force, exists in superfluids. We are using a new numerical technique for simulating dilute Bose-Einstein condensates (Projected Gross-Pitaevskii technique). This has been a long-standing open question.

Other projects include the investigation of the finite-time collapse of self-trapped electronic states in nanowires and applying spectral theory to generalize our linear reformulation of Kuramoto synchronization to much larger classes of coupled systems.

## Conclusion

This project constructs a theoretical framework of nonequilibrium Quantum Phase Transitions. This research has potential for science and technology because such phase transitions involve significant quantum-level events that have a direct macroscopic effect and, as such, lend themselves to myriad applications in the rapidly expanding field of nanotechnology.

This project also builds an understanding of superfluidity that has the accuracy needed to turn the new dilute ultracold atom systems into applications such as atom lasers, precision clocks, and gyroscopes as well as prompt a review of our fundamental notions about areas of science related to superfluidity.

## Publications


Herrera, M., D. C. Roberts, and N. Gulbahce. Mapping the evolution of scientific ideas. *PLoS ONE.*

Pomeau, Y., and D. C. Roberts. On the hydrodynamic boundary condition for superfluid flow. 2008. *Phys. Rev. B.* **77**: 144508.

Rica, S., and D. C. Roberts. Induced interaction and crystallization of self-localized impurity fields in a Bose-Einstein condensate. 2009. *Physical Review A.* **80**: 013609.

Roberts, D. C.. Solving the Kuramoto model of a self-synchronizing, finite population of glob ally coupled oscillators. 2008. *Phys. Rev. E.* **77**: 03114.

Roberts, D. C.. When superfluids are a drag. 2009. *Contemporary Physics.* **50**: 453.

Roberts, D. C., and R. Teodorescu. A linear path toward synchronization: Anomalous scaling in a new class of exactly solvable Kuramoto models. 2008. *European Physical Journal.* **165**: 103.

Roberts, D. C., and R. Teodorescu. A linear path towards self-synchronization: Analysis of the fully locked transition of the Kuramoto model. 2008. In *First International Workshop on Nonlinear Dynamics and Synchronization INDS'08.* (Klagenfurt, Austria, 18-19 July, 2008). , p. 184. Germany: Shaker Verlag.

Roberts, D. C., and S. Rica. Impurity crystal in a Bose-Einstein condensate. 2009. *Physical Review Letters.* **102**: 025301.

Ruderfer, D. M., D. C. Roberts, E. O. Perlstein, S. L. Schreiber, and L. Kruglyak. Predicting individual drug response in a panel of 104 genotyped and expression-profiled yeast strains. . 2009. *PLoS ONE.* **4** (9): e6907.

Sykes, A. G., M. J. Davis, and D. C. Roberts. Drag force on an impurity below the superfluid critical velocity in a quasi-one-dimensional Bose-Einstein condensate. 2009. *Physical Review Letters.* **103**: 085302 .

# Dissipation and Decoherence in Complex Many-Body Systems

*Wojciech H. Zurek*
20080728PRD2

## Introduction

We are investigating the dynamics and decoherence of quantum phase transitions in open many-body systems. In general, quantum information processing, including emulating quantum many-body systems, requires quantum hardware for its implementation. However, it was recently realized (by looking at quantum systems from the point of view inspired by quantum information processing ideas) that a large and interesting category of quantum evolutions can be simulated on a classical computer with resources that are only polynomial (rather than exponential) in the size of the system. We are applying this and related methods to simulate the time-dependent evolution of quantum systems. Our immediate goal is to study the dynamics of quantum phase transitions that are beginning to be investigated experimentally in, e.g. Bose-Einstein condensates (BEC's). However, in the process we expect to improve and generalize this novel method so that it can be applied much more broadly to study the exact quantum time evolutions of systems with approximately 100-10,000 independent components (which will include sixth generation quantum computers, but potentially also other systems such as molecules, nuclei, etc.).

## Benefit to National Security Missions

This project will support the missions of the Office of Science by enhancing our understanding of materials and comprehension of complex natural systems. This work will also support the Threat Reduction mission of the Laboratory by bringing the encryption breaking power of quantum computing one step closer to reality.

## Progress

Simulation techniques for decohering/dissipating quantum systems: A recent work of ours examined how different portions of the environment influence the dynamics of a system of interest and used this knowledge to create a novel representation of the environment that significantly reduced the computational cost for simulating certain environments. Since then, we have examined how information about the system of interest is distributed into environments that create decoherence. We demonstrated that noisy environments can effectively acquire and communicate certain classical information about the system, but at a reduced rate compared to "clean" environments. However, quantum information about coherence in the system is distributed globally into the environment, regardless of its noise level, and is therefore effectively lost. In the process, we developed a simulation technique that can simulate symmetric qubit environments with a polynomial computational cost (and thus, we have gone up to 200 qubits, i.e., a state space of 2^200, which is far out of the reach of direct diagonalization). This work supports the LANL mission of gaining a fundamental understanding of materials and of complex natural systems. This work has recently appeared in the prestigious journal Physical Review Letters and also one paper in preparation.

Nanoscale electronic sensors: We investigated two issues in the behavior of nonequilibrium nanoscale systems: (i) the effect of noise on the ability to detect biomolecules with electronic sensors and (ii) how ionic transport occurs through nanopores. For (i), we examined decoherence (also known as dephasing) and inelastic scattering effects on rapid DNA sequencing using transverse electronic transport measurements and nanopores. We found that the efficient distinguishability of the bases is not influenced by white noise unless it is unrealistically strong, thus reaffirming that electronic transport might serve as a process for rapid DNA sequencing. For (ii), we studied how ions move from bulk into a nanopore to create an ionic current. This is process that occurs in natural (biological ion channels) as well as artificial systems (synthetic nanopores, e.g., made for sequencing and molecular detection). We showed that there should be a precipitous drop in ionic current when the radius of the nanopore is shrunk

below the radius of the first hydration layer of the ions. This research will help the development of nanopore-based electronic sensors that will create new possibilities for ubiquitous sensors, and thus this work addresses the LANL mission of Threat Reduction. As well, such sensors open up new avenues for investigation into the complex interface between solids, liquids, and biomolecules, and increase our understanding of how materials behave at the nanoscale. The work has resulted in two recent articles, both in prestigious journals: one in Physical Review Letters and one in Biophysical Journal.

Quantum phase transitions and decoherence: We are studying the dynamics of quantum phase transitions in the presence of decoherence. In particular, in the absence of decoherence, topological defects are generated – i.e., these are features of the quantum state that can not be changed with local perturbations to the state of the system and are therefore "protected" from local decoherence (a feature that is necessary in quantum computing). However, when driving the system, superpositions of defects are also created. We find that these superpositions are actually extraordinarily sensitive to local noise and will collapse essentially instantaneously from a coherent quantum state to an incoherent mixture of states with a single topological defect that remains protected. We have developed a proposal that will allow for the direct observation of this instability. This finding sheds light on a fundamental issue in the dynamics of quantum phase transitions and also on what types of states might be useful for quantum computing. This work supports the LANL mission of gaining a fundamental understanding of materials and of complex natural systems. We are currently finishing an article describing this work.

## Future Work

Nonequilibrium physics is at the heart of some of the most beautiful and spectacular phenomena in nature, from pattern formation in biological systems to phase transitions in exotic superconductors. Furthermore, the nonequilibrium characteristics of many physical systems form the basis of their projected technological use, yet, in most cases, they remain poorly understood. In particular, a general category of nonequilibrium systems is composed of quantum systems out of equilibrium with their environment, which gives rise to the processes of dissipation and decoherence (D&D). The dynamics of quantum systems, though, are notoriously hard to simulate classically due to the presence of a unique quantum correlation called entanglement. We are carrying out a two-step research program revolving around D&D: 1) Building on our past research on the efficient representation of partially entangled states, we are developing an innovative computational method that can simulate the dynamical behavior of thousands of atoms or particles as it interacts with the outside world. 2) Using this method along with analytical techniques, we are investigating several distinct but interrelated issues involving D&D in complex many-body systems. For all these issues, our current understanding is hampered by the lack of accurate methods to study D&D. In particular, we will (i) calculate the physical characteristics of dissipative materials relevant to superconductivity and evaluate the possibility of engineering a dissipative transition to create a room-temperature superconductor; (ii) simulate the precise behavior of decoherence in (solid-state) architectures for quantum computing and delineate approaches for suppressing and correcting for decoherence; and (iii) simulate electronic transport across molecules in the presence of strong D&D in order to assess the effect of the aqueous environment on practical application of nanoscale electronic sensors, and more generally to study open scientific issues and challenges at the interface between solids, liquids, and biomolecules.

## Conclusion

The research will result in the development of novel simulation techniques for driven, nonequilibrium, and dissipative quantum and nanoscale systems. In addition, the research will result in a greater understanding of quantum computing. Further, the research will result in setting the underlying theoretical basis of nanoscale, biological/single-molecule sensors. The realization of our stretch goals could revolutionize computing and medical treatments, giving us increased security and health.

## Publications

Krems, M., M. Zwolak, Y. V. Pershin, and M. Di Ventra. Effect of Noise on DNA Sequencing via Transverse Electronic Transport. 2009. *Biophysical Journal.* **97**: 1990.

Zwolak, M., H. T. Quan, and W. H. Zurek. Quantum Darwinism in a mixed environment. 2009. *Physical Review Letters.* **103**: 110402.

Zwolak, M., J. Lagerqvist, and M. Di Ventra. Quantized ionic conductance in nanopores. 2009. *Physical Review Letters.* **103**: 128102.

# Strongly Coupled Fermion Systems: From Atomic Gases to Dark Matter

*Sanjay Reddy*
20080731PRD2

## Introduction

Our research attempts to better understand the fundamental nature of matter. Although the Standard Model can in principle predict the properties of all matter, in practice, even approximately computing the properties of a few particles - such as a proton comprising only three quarks - is a Herculean computational challenge. Our innovative approach is to develop an accurate model that combines computer simulations (Monte-Carlo), experiments, and analytic properties to understand systems of many fermions. Universality in the underlying theory allows this model to be applied to many systems, from cold atoms and superconductors, to nuclear matter, stellar matter, and possibly even the elusive dark-matter that hold galaxies together. Some of these systems can be studied in the lab, allowing for the model to be tested and then applied with confidence to those systems outside of experimental control.

## Benefit to National Security Missions

This research on strongly interacting Fermi systems ties in well with Office of Science missions relating to nuclear physics, astrophysics and condensed matter physics. The results of this work will enhance our basic understanding of materials through an ability to model superfluid and superconducting matter in both the terrestrial and astrophysical context.

## Progress

Much or our research energy has been directed toward the continued development and improvement of the Density Functional Theory (DFT) code. The updated improvements in the code include:

- Better control on truncation errors with the core Discrete Variable Representation (DVR) method used to solve for the wavefunctions.
- Ability to calculate more complicated geometries such as elliptical traps, allowing for direct comparison with experiments.
- Allow the code to be run on multiple processors so the larger bases required to study more complicated geometries can be efficiently run on clusters.
- Improved solver technology for better convergence. In particular, a generalized Broyden method has been implemented to maximize the efficiency of the solvers when used with expensive function evaluations.
- Development of geometric multigrid linear equation solvers for computing classical approximations of the DFT's.
- Alternative boundary conditions for studying vortex properties and surface tension effects.

These modification are in the process of being tested and will be applied to the problems of: a) unequal masses, b) surface tension and finite size transition effects and c) finite sized system effects.

One important use of the DFT is to provide approximate wavefunctions as input for fixed-node Green's function Monte Carlo (GFMC) techniques. The GFMC techniques developed here at LANL are among the most accurate calculational tools available for many-body systems, but are plagued by an infamous "Fermion sign problem" that amounts to the requirement of adding up exponentially many contributions of opposite sign that cancel. In order to obtain a signal from out of these cancellations would require an exponential amount of time, making the naive implementation useless.

To overcome this difficulty, a "fixed-node" approximation is used that restricts the MC averaging to components of a single sign, thereby averting the sign problem. The catch is that the nodal structure needs to provide a

good characterization of the ground state. For the most symmetric systems, this approach has produced state of the art numerical calculations of the universal parameters governing dilute fermion systems.

Our goal is to use the same techniques for calculating properties of asymmetric systems. To this end, we are developing techniques for using the wavefunction provided by our DFT approach to fix the nodal structure of the starting wavefunctions for the more accurate GFMC calculation. In this way, we hope to provide quantitative evidence for new states of matter predicted by the DFT -- in particular, the crystalline supersolid Larkin-Ovchinnikov--Fulde-Ferrell (LOFF) state. Progress is underway testing this approach for the known symmetric systems.

Our work has been presented to the cold Fermion labs at MIT and at the Institute of Quantum Optics and Information (IOQOI) in Innsbruck, and in an invited talk at the Conference on Research Frontiers in Ultra-Cold Atoms in Trieste to convince members of the cold atom community of the potential of the DFT. In collaboration with the experimentalists we identified several key ideas for measuring properties of these systems predicted by the DFT, including the presence of a new supersolid (LOFF) phase as well as surface and finite size effects at phase boundaries (especially looking at the decay of collective oscillations in harmonically trapped clouds).

We made a successful proposal for a three-month program at the Institute for Nuclear Theory (INT) in Seattle. The program "Fermions from Cold Atoms to Neutron Stars: Benchmarking the Many-Body Problem" will take place in the spring of 2011 and has the support of some of the leading theorists and experimentalists in the field.

**Neutron Stars**

Closely related to the DFT work on cold atoms, we are currently investigating the structure and properties of ionic lattices in dilute nuclear matter. In particular, we aim to calculate properties such as the compressibility and shear moduli for these lattices. What is novel about our calculation is that we allow for the nuclei to deform -- previous estimates treat the nuclei as fixed shape objects. These results are of physical importance in neutron star crusts: in particular, for investigation vibrational modes (phonons) in the crust that can transport energy and momentum, affecting the cooling behavior of the stars.

This project is quite technically challenging as a large-scale non-linear indefinite Helmholtz-like problem must be solved. This has required the development of the geometric multigrid technique discussed above and substantial improvements in the non-linear Broyden solver. We presently have solutions for one-dimensional lattice structures and are presently scaling this up to two and three-dimensional structures.

**Dark Matter**

A second major project is investigating a potential dark matter candidate in the form of quark antimatter nuggets. This potentially solves two of the major outstanding problems in cosmology: 1) Baryogenesis or where is all the antimatter? and 2) What is the nature of the hitherto unobserved dark matter that holds our universe together? Our proposal hides the antimatter in macroscopic "nuclei" formed at the QCD phase transition, thus solving both problems.

What is intriguing about this proposal is that, not only is it consistent with present constraints, but it predicts that the dark matter should be directly observable. The idea is that regular matter in our galaxy (hydrogen for example) will annihilate on these antimatter nuggets releasing observable radiation. Our model makes definite predictions about both 511 keV radiation resulting from electron-positron annihilation as well as diffuse radiations in the 10 keV, 10 MeV and mircro-wave bands.

All of these emissions have observational constraints, and our preliminary analysis found that -- with a few reasonable phenomenological parameters -- our model is not only consistent with the observations, but could provide a compelling explanation. In our resent paper [LA-UR 09-06331], we have used semi-classical DFT approximation to determine the density profile of the electrosphere of these quark nuggets. This allowed us to directly compute some of these phenomenological parameters from unambiguous microscopic physics. We found that the phenomenological values required to explain the observations emerged naturally from the microscopic calculation, providing another piece of strong evidence for our proposal. The comparison of our results with the observations is shown in Figure 1.

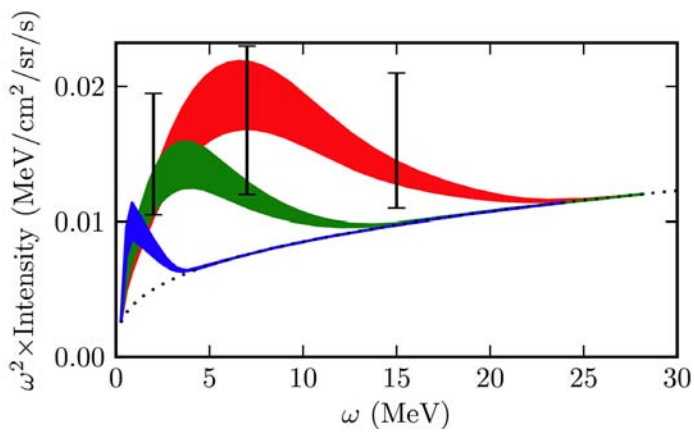


*Figure 1. Spectral density (scaled by w^2 to compare with [40] of photons emitted by an electron annihilating on antiquark nuggets with incoming velocities v = 0.01c (red), v = 0.005c (green) and v = 0.001c (blue) from right to left respectively, including the cosmic ray background determined in [40] (dotted line). The thickness of the bands includes a ±10% variation in the positronium annihilation rate (12). The overall normalization is fixed to the observationally unrelated 511 keV line as discussed below (21). The three error bars are the Comptel data points. The observed spectrum will be an average of these, exhibiting a dependence on the distributions of velocities v along the line of sight to the core of the galaxy.*

## Future Work

The main goal is to combine experiment, numerical, and analytic results to develop a density functional theory (DFT) that quantitatively describes two-component cold-atom gases. Once this DFT is verified with cold-atom systems, it can be applied to other systems such as nuclear matter and quark matter.

A subset of the following tasks will establish this theory: 1) Validate that the DFT can describe finite systems using Monte-Carlo (MC) simulations. 2) Investigate the importance of gradient corrections to the DFT using MC simulations of deformed traps. 3) Apply the DFT to calculate properties of inhomogeneous systems including 4) Crystalline LOFF states, 5) Surface tensions of phase boundaries, and 6) other finite size effects. 7) Extend the model to capture the effects of temperature on the gap and pseudo-gap. 8) Apply these models to nuclear and astrophysical systems.

The second goal is to confirm or rule out our proposal that dark matter consists of quark anti-matter nuggets. This includes 1) improving the quantitative accuracy of the emission calculations to provide detailed predictions with which to better test the theory. 2) Working with other astrophysicists to compile tests of our current proposal from existing data. 3) Search for additional observational evidence to confirm or rule out the proposal. 4) Solidify the formation mechanism. 5) Investigate how the phenomenology of these objects might constrain the many-body properties of quark matter. 6) Investigate alternative explanations for some of the anomalous emissions we presently attribute to dark matter. Finally, a related task is to investigate additional astrophysical phenomena to determine additional signatures for pairing and exotic many-body physics from astrophysical objects.

## Conclusion

We will continue to develop many-body techniques to accurately compute the basic properties of matter relevant to cold atom experiments, nuclei, and dense nuclear matter. This is a prerequisite to identifying potential applications of new materials, and for calculating the properties of exotic nuclei and nuclear matter that cannot easily be studied in experiments. We will use these methods to predict properties of astrophysical matter (neutron stars), shedding light on some great mysteries of our universe, including the nature of the mysterious dark-matter that forms most of the mass of the universe, but which has yet to be directly observed.

## References

1. Forbes, M. M., K. Lawson, and A. R. Zhitnitsky. The Electrosphere of Macroscopic “Quark Nuclei”: A Source for Diffuse MeV Emissions from Dark Matter. *Physical Review D.*

## Publications

Forbes, M. M., K. Lawson, and A. R. Zhitnitsky. The Electrosphere of Macroscopic “Quark Nuclei”: A Source for Diffuse MeV Emissions from Dark Matter. *PHYSICAL REVIEW D .*

# Matter and Light

*Katrin Heitmann*
20080786PRD3

## Introduction

Cosmology relies on melding diverse measurements to understand the composition and evolution of the Universe. Microwave background observations showed that the Universe is flat, but studies of the clustering of matter found only one-third of the matter required. Famously, supernovae observations then showed that dark energy provided the missing energy density, bringing all measurements into concordance. This project is aimed at future surveys that will measure the distribution of galaxies in the Universe with very high accuracy. From these measurements, new cosmological constraints will be derived and these will advance our understanding of the fundamental constituents of our Universe: dark matter and dark energy.

Current and near-future galaxy surveys probe such huge volumes and such a large range of distance scales that it is a computational "grand challenge'' to compare our theoretical understanding of galaxy clustering with the surveys. It is vital to develop efficient statistical and numerical techniques that can enable the making of such comparisons.

## Benefit to National Security Missions

The project targets two of the top priorities of the DOE mission: understanding the nature of dark energy and high-performance computing. In addition, the project is relevant for the threat reduction arena in providing new techniques to extract information from diverse and very large data sets.

## Progress

The major focus of the project is to connect theoretical predictions with observational data to derive new cosmological constraints. One of the major tools on the theoretical side is N-body simulation. The size of such simulations has to be enormous in order to cover the observational surveys adequately.

While the final goal of the project is the development of new statistical tools that will help to keep the number of necessary simulations at a minimum, the use of simulations cannot be avoided. Dr. Pope concentrated therefore during the start of the project on developing extremely efficient simulation and analysis tools. Dr. Pope made very impressive progress with this difficult task. A code version that allows for medium resolution simulation has been finished, tested and successfully ran on Roadrunner to produce some of the world's largest simulations. Figure 1 shows a zoom-in to a snapshot from one of these simulations. The excellent mass resolution allowed us to resolve structures in great detail. A high-resolution extension of the code is almost completed. All major analysis tools have been developed and implemented in the code infrastructure. These tools will enable the second step in the project. Dr. Pope gave an invited talk at UIUC on his work and published invited proceedings for the SciDAC conference 2009 together with Salman Habib (LANL) [1]. A second invited paper to Computing in Science and Engineering is almost completed, Dr. Pope is the lead author on this publication.

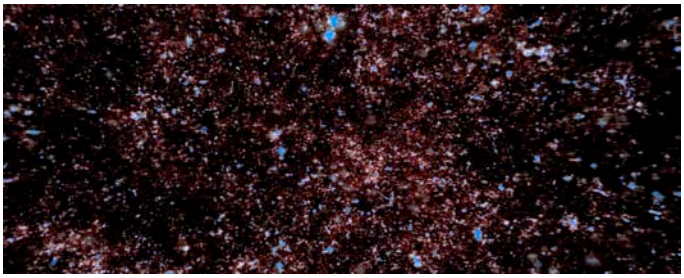

*Figure 1. Zoom-in to a snap-shot from one of the Roadrunner simulations. Shown is the halo density field colored with respect to mass variation. The figure demonstrates the high mass resolution of the simulation, many halos are resolved.*

The Roadrunner simulation suite was used to explore the imprints of baryon acoustic oscillations in the matter distribution of the universe. The baryon acoustic

oscillations leave their imprint at a certain scale in the matter distribution. The imprint manifests itself in the correlation function as a distinct peak. The position, height, and shape of the peak hold clues about the origin of dark energy. It was recently proposed that this observation can be obtained from Lyman-alpha forest observations, a major target of the ongoing Sloan Digital Sky Survey III. In order to detect the peak in the Lyman-alpha forest, very large simulations have to be carried out. The baryon acoustic oscillation signal in the Lyman alpha forest was successfully extracted from the Roadrunner simulations (Figure 2). New clues for observing and analysis strategies have been found. The results are currently being written up for a publication in the Astrophysical Journal.

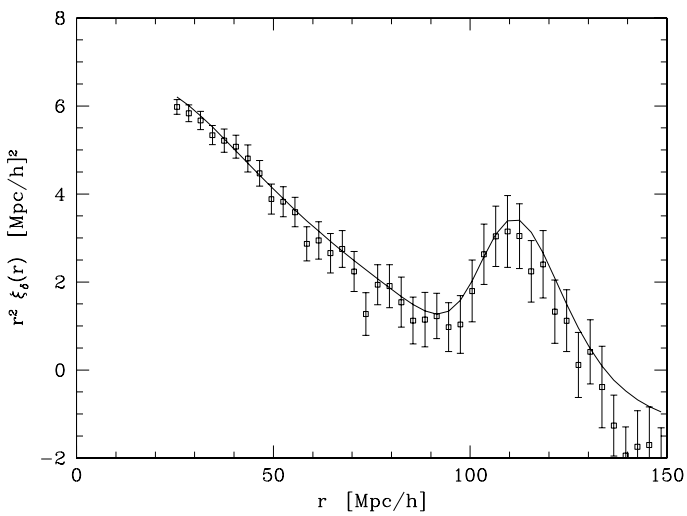


*Figure 2. Correlation function from the Roadrunner simulations. The baryon acoustic oscillation peak is clearly resolved.*

## Future Work

Our measurements of large-scale structure statistics from large-volume cosmological surveys are becoming so good that a new generation of matching theoretical tools must be developed. In principle, N-body simulations provide detailed views of the clustering of dark matter, but the volumes and resolution necessary to mimic large surveys make it prohibitive to produce a large suite of N-body simulations covering a range of different cosmological parameters. The cosmic calibration project initiated at Los Alamos National Laboratory by Habib, Heitmann, and Higdon is an important step in using a limited number of large-scale simulations to predict large-scale structure statistics with high precision. During this project the framework will be extended and developed in an important new direction: modeling the effects of galaxies as biased tracers of matter when predicting the shape of the galaxy correlation function and other large-scale structure statistics.

After completing the high-resolution N-body code, the next step will be to populate the simulations with galaxies. The necessary tools for this have been developed. This will lead to mock catalogs, mimicking the distribution of galaxies in large-scale surveys such as the Sloan Digital Sky Survey III and the Large Synoptic Survey Telescope. Dr. Pope will use these mock catalogs to analyze currently available data and to provide predictions and new insights for future observations.

## Conclusion

Our current understanding of the Universe relies heavily on measurements of its large-scale structure as probed by the clustering of galaxies. These studies are complicated by the fact that the luminous baryonic matter in galaxies (stars, gas) is only a tracer for the dark matter, whereas theoretical models directly predict the clustering properties of dark matter. This project focuses on understanding the connection between light and matter. Dr. Pope is successfully developing new simulation and prediction capabilities to facilitate this understanding. This will be a crucial step for interpreting new cosmological observations and obtaining constraints on dark energy. Important new results on constraining dark energy from baryon acoustic oscillations in the Lyman-alpha forest have been derived. The project will lead to new insights about the evolution and content of the Universe.

## References

1. Habib, S., A. Pope, Z. Lukic, D. Daniel, P. Fasel, N. Desai, K. Heitmann, C. Hsu, L. Ankeny, G. Mark, S. Bhattacharya, and J. Ahrens. Hybrid petacomputing meets cosmology: the Roadrunner Universe project. 2009. (San Diego, 14 - 18 June, 2009 ). Vol. 180p. 012019. Journal of Physics: Conference Series: IOP.

## Publications

Habib, S., A. Pope, Z. Lukic, D. Daniel, P. Fasel, N. Desai, K. Heitmann, C. Hsu, L. Ankeny, G. Mark, S. Bhattacharya, and J. Ahrens. Hybrid petacomputing meets cosmology: the Roadrunner Universe project. 2009. In *SciDAC 2009.* (San Diego, 14 - 18 June, 2009 ). Vol. 180, p. 012019. Journal of Physics: Conference Series: IOP.

# Unconventional Superconductivity in Heavy Fermion Materials

*Cristian D. Batista*
20090491PRD1

## Introduction

Our goal is to model unconventional superconductivity of f-electron materials. Some materials can conduct electricity without dissipating energy, i.e., with no energy losses in the form of heat. These materials are known as superconductors, and their unique properties lead to several technological applications. Unfortunately, the known materials that exhibit this property are superconductors only at low temperatures. One of the challenges for future technologies is to find materials that can superconduct at room temperature. To find guiding principles for designing such materials we need to understand the microscopic origin of superconductivity. This is the main purpose of this project. In particular, the project will be focused on f-electron materials that are at the center of the experimental effort of LANL (MPA-10 group).

## Benefit to National Security Missions

This project supports DOE, Office of Science missions by enhancing our understanding of unconventional superconductivity, which is needed for future energy transmission and storage applications, and addresses the Laboratory's mission in superconductivity from 5f electrons.

## Progress

During the past year we made significant progress on two problems. In first place, we demonstrated that dominating superconducting fluctuations appear in a correlated Kondo Lattice Chain whenever the antiferromagnetic correlation length is long enough. This workhas been published in Physical Review B. We are currently expanding these results to the case of a ladder geometry to demonstrated that the superconducting mechanism survives in dimension higher than one. Our preliminary results clearly indicate that this is indeed the case. This result is very relevant for understanding the physical principles that lead to unconventional superconductivity in f-electron compounds.

The second problem that we addressed during the past year is a description of the transition between the localized and mixed valence regimes of the Periodic Anderson model (minimal model for describing f-electron compounds). Our results demonstrate conclusively that there is a mixed valence state that has not been even considered in the most traditional approaches. The new state has characteristics that are very similar to a doped Mott insulator, i.e., the f-electrons behave as a single correlated band, which is virtually decoupled from the broad conduction band of s, p or d-electrons. This discovery is crucial for bridging the physics of the f-electron unconventional superconductors with the high temperature superconductors (cuprates) that were discovered by Bernordz and Muller in 1987. This is so because the physics of the cuprates is effectively described by a single correlated band (doped Mott insulator). We are currently writing a long article about our results in this area.

## Future Work

This work will be oriented to modeling unconventional superconductivity of f-electron materials. To carry out our study, the postdoc will use both numerical and analytical techniques. The numerical techniques consist of algorithms for solving models of interacting electrons. These techniques are the Density Matrix Renormalization Group (DMRG) and Quantum Monte Carlo (QMC). The results of the numerical simulations will compared with the experimental data collected at the MPA-10 group. To model the superconducting order with QMC, we will develop a new algorithm for computing pair-pair correlation functions. In addition to its importance to the current project, this improvement will be a breakthrough for QMC simulations of fermionic systems.

## Conclusion

The discovery nearly 20 years ago of high temperature superconductivity in complex copper oxide materials held great promise for revolutionizing electrical power transmission and storage. The promise of this discovery has not been realized fully, in part because we still do not understand how electrons interact strongly to produce unconventional superconductivity in these and related f-electron materials. This project focuses on providing basic understanding of the interacting electrons and how these electrons affect the utility of unconven-

tional superconductors for energy applications. We expect to provide theoretical phase diagrams that can be directly compared against the experimental data.

## Publications

Al-Hassanieh, K. A., C. D. Batista, G. Ortiz, and L. N. Bulaevskii. Field-induced orbital antiferromagnetism in Mott insulators. To appear in *Physical Review Letters.*

Al-Hassanieh, K. A., C. D. Batista, P. Sengupta, and A. E. Feiguin. Robust pairing mechanism from repulsive interactions. 2009. *Physical Review B.* **80**: 115116.

Paduan-Filho, A., K. A. Al-Hassanieh, P. Sengupta, and M. Jaime. Critical Properties at the Field-Induced Bose-Einstein Condensation in NiCl2-4SC(NH2)2. 2009. *Physical Review Letters.* **102**: 077204.

Samulon, E. C., Y. Kohama, R. D. McDonald, M. C. Shapiro, K. A. Al-Hassanieh, C. D. Batista, M. Jaime, and I. R. Fisher. Asymmetric Quintuplet Condensation in the Frustrated S=1 Spin Dimer Compound Ba3Mn2O8. 2009. *Physical Review Letters.* **103**: 047202.

# Disorder in Frustrated Systems

*Avadh B. Saxena*
20090493PRD1

## Introduction

Dr. Nisoli's multifaceted research style allowed him to work on a variety of subjects before and after starting his position at Los Alamos National Laboratory, within the general topic of disorder in frustrated systems and mostly in the field of Statistical Mechanics, Complex Systems, Nonlinear Physics and Condensed Matter. In the field of Statistical Mechanics, in collaboration with Prof. Douglas Abraham (Oxford University) and researchers at the Lab, he has employed different theoretical methods to shed light on thermal stability of quasi-one-dimensional systems of tremendous and timely technological importance, such as nanowires, nanotubes, or DNA filaments. Again, in statistical mechanics he has worked with collaborators at Penn State University to further the study of artificial spin ice, a novel magnetic meta-material. In the field of Nonlinear Physics and Complex Systems, with collaborators at Cornell University and Penn State, he has shown that the beautiful patterns typical of botany of plants can be reproduced in many physical systems, especially when novel nonlinear dynamics can emerge. In the field of Condensed Matter, Dr. Nisoli has advanced theoretically the study of the electro-dynamical effects in carbon nanostructurs, such as graphene or carbon nanotubes, all objects of intense current interest. These diverse research fields and collaborations have resulted in seven papers of which Dr. Nisoli is the first author (four of which have been published already, while three are under review) and three other papers in which he is a coauthor (one published, two under review), all in high profile journals, since he came to the Laboratory fifteen months ago. Below I succinctly elaborate on a few of his different projects.

## Benefit to National Security Missions

Work on nanostructures, electromechanics of carbon nanotubes, nanowires are very important to national security because of the many applications. So is his work on magnetic recording devices.

## Progress

### Artificial spin ice

When a number of interactions compete within a system they cannot all prevail, so the resolution of 'frustrated' forces is an important determinant of the overall behavior of a system. In particular, geometrical frustration among spins in magnetic systems can lead to exotic effects such as 'spin ice', a state where atomic magnetic moments mimic the frustration of hydrogen ion positions in water ice. With collaborators at Penn State University we had created artificial spin ice using lithographically fabricated arrays of nanoscale magnets [Nature 439, 303 - 306 (2006)]. Magnetic moments in the lattice follow the two pointing-in/ two-out 'ice rule' typical of spin ice. With this model it is possible to study frustration in great detail; this is relevant to magnetic recording, where ferromagnetic elements are being pushed to ever-higher densities.

### Mathematical regularities in plant structures and physics: dynamical phyllotaxis

Phyllotaxis, the study of mathematical regularities in plants, challenged Kepler and Leonardo da Vinci, inspired the Bravais lattice of crystallography, and may have motivated humanity's first mathematical inquiries. With collaborators from Pennsylvania State University and Cornell University he has experimentally obtained for the first time the fascinating patterns of botany, and then explored the intriguing collective excitations of the phyllotactic geometry: multiple classical excitations called rotons and a huge family of interconverting topological solitons. We constructed a magnetic cactus consisting of 50 outward pointing, dipolar permanent magnets (spines) mounted on stacked coaxial bearings free to rotate about a vertical axis (stem), shown in Figure 1. We annealed the system into a lower-energy state by mechanical agitation. The spines on the magnetic cactus, analogous to those of the plant, form a helix around the cylindrical stem by growing around

these particular angles. We made the first investigations of dynamic linear and nonlinear phyllotaxis. A simple geometrical mismatch underpins both static and dynamic phyllotaxis phenomena.

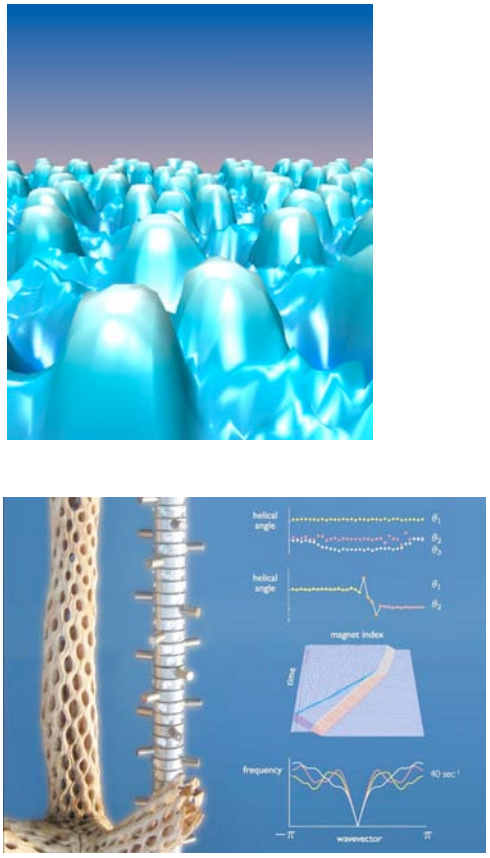


*Figure 1. (top) Magnetic-forec microscope image showing the magnetic moments of artificial ice. (bottom) Phyllotaxis: magnetic cactus.*

**Thermal stability of nanowires formation**

The investigation of the formation of two dimensional nanostructures during epitaxial growth not only has provided a fundamental understanding of surface physics, but is also of pivotal technological importance. In fact it can lead to self assembly of nanostructures of size much lower than what can be achieved with lithographic ablation. In particular it is known that under certain circumstances, the accumulated strain in the epitaxial layer leads to self assembly of long nanowires. In collaboration with Prof. Douglas Abraham (CNLS and Oxford University), Avadh Saxena and Turab Lookman (T-4) he has studied theoreticaly the stability of these nanowires under thermal fluctuations. Via statistical mechanics, Dr. Nisoli found that above a critical temperature the wire does indeed become unstable, and nanoislands form in their place. He related this critical temperature with the threshold of the plastic relaxation of the film. Moreover, he found that the wires become unstable even as the deposition continues, at constant temperature. Finally, Dr. Nisoli found that the transition can be more or less sharp depending on the average length of the wires, and is preceded by regions of coexistence of wires and islands. Within this framework he could produce a phase diagram in temperature and deposition and explain recent experimental results obtained by Prof. Q. Cai's group at Fudan University. This experimental group had obtained phase transitions from nanowires to nanoislands, both when increasing post-annealing temperatures at fixed coverage and when increasing coverage (and thus the height of nanostructures) at fixed post-annealing temperatures, and witnessed the predicted region of coexistence.

## Future Work

In the future Dr. Nisoli plans to continue his collaborations on the study of frustrated materials, their effective thermodynamics, and relationship with granular materials. Also he plans to further explore the novel dynamical phenomena of physical phyllotaxis, in particular those associated with transport properties in nanosystems. He will continue collaborating with Prof. D. Abraham of Oxford University on the Statistical Mechanics of quasi-one-dimensional nanostructures. He also plans to apply his two-field formalism to study piezoelectricity at the nanoscale, e.g. in boron nitride.

## Conclusion

Dr. Nisoli has worked on many different subject of timely technological and theoretical importance collaborating with many researchers in the Laboratory and outside and producing a large number of high profile publications.

## References

1. Wang,C.Nisolietal.,, R.. Artificial 'spin ice' in a geometricallly frustrated lattice of nanoscale ferromagnetic islands. 2006. *Nature.* **439**: 303.

2. Nisoli,R.Wang,W.McConville,etal., C.. Ground state lost but degeneracy found: the effective thermodynamics of artificial spin ice. . 2007. *Physical Review Letters.* **98**: 217203/1.

# Measurement of Transverse Single-Spin Asymmetries of Neutral Pion and Eta Meson Production in Polarized p+p Collisions Using the PHENIX Detector at RHIC

*Melynda L. Brooks*
20090498PRD2

## Introduction

Dr. Aidala performs data analysis on data collected by the PHENIX detector at the Relativistic Heavy Ion Collider (RHIC) at Brookhaven National Laboratory for polarized proton-proton collisions. The purpose of her data analysis is to try to shed light on how the proton's spin - a fundamental property of the proton - is formed. It was originally thought that the three constituent quarks' spin (up, up and down) would completely determine the spin of the proton. However, data collected to date have shown that the constituent quarks can only account for approximately 20-30% of the proton's spin. The remaining portion is assumed to come from the sea of quarks and gluons, which bind the quarks together, or from an intrinisic angular momentum carried by the proton. By colliding polarized protons on polarized protons and carefully measuring any asymmetry in particles produced, the contributions of the sea quarks and gluons can be extracted. To this end, Dr. Aidala is looking at pion and eta production in the forward direction (near the direction of the colliding particles) and looking at asymmetries that are produced when the protons are polarized transversely with respect to the beam direction. These asymmetries can be related back to the quark and gluon contributions to the proton spin, and can also potentially be related back to the angular momentum. Since quark contributions have already been measured, the gluon contributions can then be extracted. With this new data, important new constraints are expected to be placed on the proton spin contributions and with this fundamental new information about how the basic building blocks of nature are formed by their constituents.

## Benefit to National Security Missions

This project will support the DOE missions of the Office of Science by enhancing our understanding of the origin of the proton's spin, and adding detector capabilities to the RHIC PHENIX detector, which will also gather data to study the Quark Gluon Plasma.

## Progress

A PHENIX Collaboration paper entitled "Double Helicity Dependence of Jet Properties from Dihadrons in Longitudinally Polarized p+p Collisions at sqrt(s) = 200 GeV" has been submitted to Physical Review D. The paper describes a novel, exploratory measurement attempting to access the orbital angular momenta of quarks and gluons inside the proton and their contributions to the proton's spin. Dr. Aidala took responsibility for the physics description and discussion of results in the paper. While no significant net difference in the quark and gluon transverse motion was found for colliding protons with the same versus opposite helicity states, further data taken by PHENIX will be able to improve the sensitivity of the measurement, and publication of the current result will likely stimulate discussion in the field of how to best make use of this novel class of measurements. A preprint of the manuscript is available as arXiv:0910.1029.

A second PHENIX manuscript intended for publication in Physical Review D, entitled "Measurement of Transverse Single-Spin Asymmetries for J/Psi Production in Polarized p+p Collisions at sqrt(s) = 200 GeV," is currently undergoing internal review within the collaboration. The transverse single-spin asymmetry for J/Psi production was proposed in 2008 as a new observable sensitive to the J/Psi production mechanism, a long-standing question in QCD. A significant portion of the data analysis for the paper was done by Han Liu, a postdoc toral research associate in the P-25 group. Again, Dr. Aidala took responsibility for the physics description and discussion of results in the paper.

Dr. Aidala has continued her work with UC Riverside graduate student David Kleinjan on analysis of the transverse single-spin asymmetry in forward eta meson production using the Muon Piston Calorimeter (MPC) in PHENIX, the first such measurement in PHENIX.

Preliminary results from the STAR experiment at RHIC indicate that the single transverse-spin asymmetry of eta production may be larger than that of neutral pion production, providing evidence that the large transverse single-spin asymmetries observed for pions are not a valence quark effect as previously believed. Further measurements of eta asymmetries will be important to shed light on the observed effects. Significant progress has been made in understanding backgrounds, and preliminary results for the single-spin asymmetry are expected to be released in February.

Dr. Aidala is also working to publish a PHENIX paper with results on eta meson production at central rather than forward rapidities. As part of this effort, she has coauthored an internal PHENIX Analysis Note entitled, "BBC Efficiency for Neutral Pions and Etas in the Central Arm in Run-06 p+p at sqrt(s)=200 GeV." The paper will include the double-longitudinal spin asymmetry in eta production, the eta production cross section, and the production ratio of eta mesons to neutral pions. The spin asymmetry can provide sensitivity to $\Delta G$, the gluon spin contribution to the spin of the proton, if a parameterization for the fragmentation of quarks and gluons into eta mesons becomes available.

In support of her work on analysis of eta meson production at PHENIX, Dr. Aidala has been collaborating with two individuals outside the PHENIX collaboration, Marco Stratmann of the Universities of Regensburg and Wuerzburg and Joseph Seele of MIT, to parameterize the eta fragmentation functions, thus far unavailable in the published literature. The fragmentation functions will allow perturbative QCD calculations of eta production to be performed, permitting interpretation of RHIC data from both PHENIX and STAR as well as predictions for measurements at other facilities, for example for hadronization studies in cold nuclear matter at a future Electron-Ion Collider. It has been agreed with PHENIX Management that the eta cross section measurement from the 2006 data will be incorporated into the fragmentation function parameterization, and the PHENIX manuscript will be submitted simultaneously with the fragmentation function manuscript to Physical Review D.

As a leader on transverse spin physics and transverse-momentum-dependent distribution and fragmentation functions within PHENIX, Dr. Aidala has been serving as a member of the PHENIX Transverse Spin Task Force, formed in December 2008 with the charge of developing a coherent PHENIX transverse spin program and assisting efforts to upgrade PHENIX to make transverse spin physics accessible. Within this group, she has focused on investigating potential heavy flavor probes of proton transverse spin structure, as well as helped to develop the transverse spin physics case for a planned forward calorimeter upgrade to PHENIX, the FOCAL. A formal proposal for the FOCAL is expected to be submitted within the next months.

In addition to her work on the eta meson, transverse spin physics, and transverse-momentum-dependent distributions, she has been working closely with a graduate student from UMass Amherst, Amaresh Datta, to analyze PHENIX data on midrapidity charged hadron production in proton-proton collisions at sqrt(s)=62.4 GeV. The double-longitudinal asymmetry analysis, sensitive to the gluon spin contribution to the proton spin, is complete, and her current work in this area is focused on measurement of the invariant cross section. She has coauthored an internal PHENIX Analysis Note entitled, "Cross section of Inclusive Charged Hadron Production in p+p Collisions at sqrt(s)=62.4 GeV," and the analysis is expected to be finalized by December, at which point a paper draft for Phys. Rev. D will be started. The cross section will be published together with the asymmetry measurement, and it will provide important information regarding which theoretical tools of perturbative QCD can best be used to interpret the asymmetry data at this moderate center-of-mass energy.

## Future Work

Dr. Aidala will perform work to measure the cross sections and transverse single-spin asymmetries of neutral pion and eta meson production in the RHIC PHENIX proton-proton data sets, via their decay to two photons. The asymmetry measurements extend previous work on the transverse spin structure of the proton and transverse-momentum-dependent distributions, which are sensitive to the intrinsic motion of quarks and gluons, and will provide essential data to continue fueling the rapid advance of the study of the origin of the proton's spin. The proton-proton cross sections will also serve as critical baseline measurements to compare to the deuteron-gold results in search for gluon saturation effects in heavy nuclei.

## Conclusion

Dr. Aidala is expected to publish results that will constrain the contribution that the gluon makes to the proton spin. The origin of the proton's spin is a basic scientific question, which has yet to be understood based on data collected to date, and answering this will improve our understanding of one of the most fundamental building blocks of nature.

## Publications

Adare, A., and E. Tal. Double helicity dependence of jet properties from dihadrons in longitudinally polarized p+p collisions at sqrt(s) = 200 GeV. *Physical Review D.*

# Exploring the Expanding Universe and the Nature of Dark Energy

*Katrin Heitmann*
20090521PRD2

## Introduction

In 1998, two independent teams measuring the light from distant supernovae made an extraordinary discovery: the expansion of the Universe is accelerated. In the last 10 years, this discovery has been confirmed by completely different measurements of the large-scale distribution of galaxies in the Universe, of the cosmic microwave background radiation, and by measuring the abundance of clusters of galaxies in the Universe. The cause of the accelerating expansion is completely unknown and understanding this cause is the major field of research in cosmology. The aim of the current project is to characterize the nature of dark energy with special emphasis on the dark energy equation of state. Currently, a cosmological constant is consistent with all measurements, but its size is in contradiction with the Standard Model of particle physics by ~100 orders of magnitude. In order to exclude a cosmological constant, the dark energy equation of state would be a dynamical quantity. In this project, three major research directions are investigated: (i) How can we extract a time variation in the dark energy equation of state from current and upcoming data in a model-independent way? (ii) What would be the observational signatures of an early dark energy scenario, which would point to different physics than a cosmological constant? (iii) How can we distinguish dark energy from a modification of gravity on the largest scales? The project will make use of sophisticated statistical methods, simulations, and publicly available data.

## Benefit to National Security Missions

This project will support the DOE mission of the Office of Science and NASA, which have made unraveling the secrets of dark energy one of their top priorities. In addition, as part of this project new statistical methods will be developed which will be important for our national security mission in general.

## Progress

The project has made significant progress in two of the three target areas outlined above: (i) the reconstruction of the dark energy equation of state from current data; (ii) identifying observable signatures of early dark energy scenarios.

In order to reconstruct the dark energy equation of state in a non-parametric way, we have developed a new approach based on Gaussian process modeling. In order to test the stability and reliability with which the new approach can capture complex time variations in the equation of state of dark energy, we have generated three simulated supernova data sets, mimicking the data quality we expect from future dark energy missions in space. The underlying equations of state for these data sets vary from very simple (constant) to more complex. The method worked exceptionally well on all simulated data sets. One of the results is shown in Figure 1. This equation of state is based on a scenario where the origin of the dark energy is due to a scalar field. We showed that other commonly used methods based on parametric reconstruction approaches completely failed to capture the time evolution of w. A paper on the results and a description of the method is in preparation and will be submitted to Physical Review D. Encouraged by these results we applied our new method to currently available measured supernova data. We reconstructed for the first time reliably the continuous history of the dark energy equation of state out to redshift z=1.5. The result is shown in Figure 2. This work constitutes a major breakthrough in determining the origin of the accelerated expansion of the Universe. A paper is currently prepared and will be submitted to Physical Review Letters. The next step is to include different dark energy probes. We will focus on baryon acoustic oscillation measurements and cosmic microwave background measurements. First, promising results have been obtained.

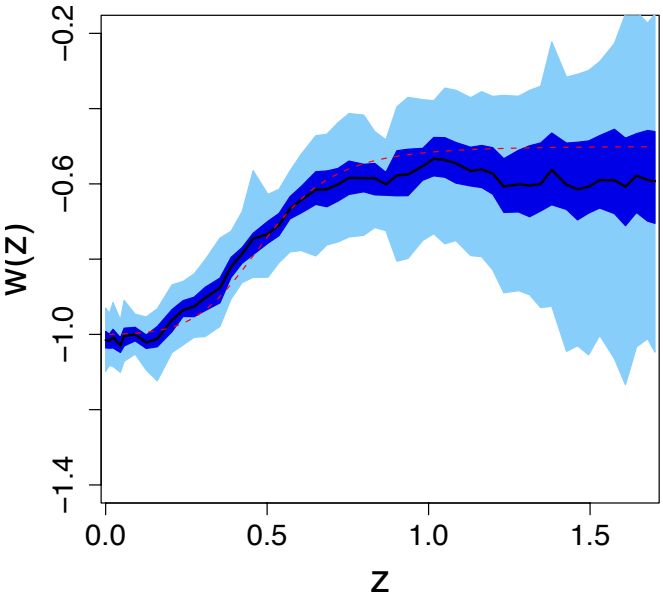


*Figure 1. Reconstructed dark energy equation of state (black line) from simulated supernova data. The red line is the input model from which one realization of supernova data was derived. The dark blue and light blue regions show the 68% and 95% confidence limits, respectively.*

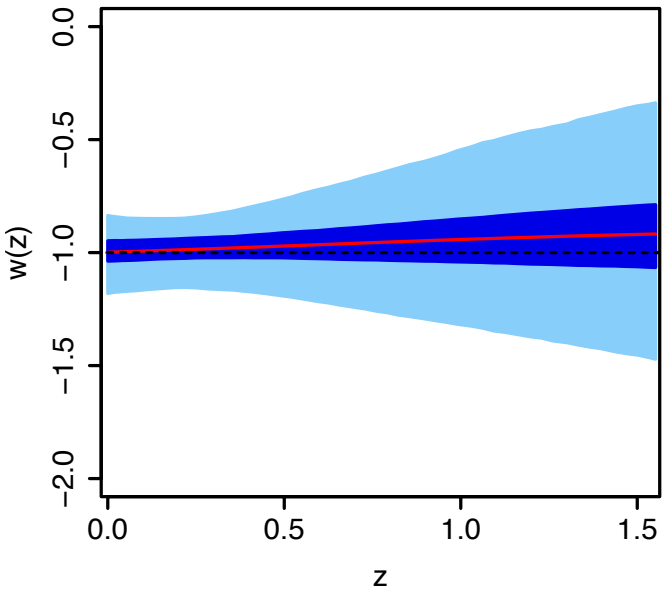


*Figure 2. Reconstruction of the dark energy equation of state as a function of redshift from current supernova data.*

In order to investigate the imprints of dynamical dark energy models on observations, the first step is to derive a self-consistent theory for dark energy perturbations. The next step is to implement the resulting equations into numerical codes that lead to predictions for cosmological observables. We have successfully set up the necessary theoretical framework and implemented dark energy perturbation into CAMB (Code for Anisotropies in the Microwave Background), a publicly available Boltzmann code. CAMB allows us to explore the effects on cosmic microwave background measurements and to get first estimates for the effects on large-scale structure probes. We found that in fact the peak height and position of the first peak in the temperature power spectrum of the cosmic microwave background is sensitive to different early dark energy models (Figure 3). We currently perform a statistical analysis of current data to obtain new constraints on dynamical dark energy models. We have also started investigating the effect of early dark energy on the mass function of clusters of galaxies. First results indicate that the mass function at high redshift is indeed sensitive. More detailed studies on this finding are underway.

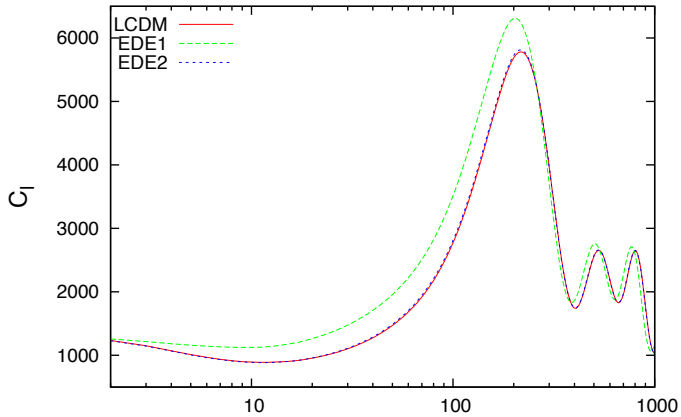


*Figure 3. Temperature anisotropy power spectrum predictions for two dynamical dark energy models (green and blue) and a cosmological constant model (red). The models can be clearly distinguished.*

## Future Work

This project targets the characterization of dark energy. Currently, the accelerated expansion of the Universe can be explained by introducing a cosmological constant into Einstein's theory of general relativity. A cosmological constant has several theoretical problems: the origin is unclear and the prediction for such a term from the Standard Model of particle physics is ~100 orders of magnitudes different from what we observe. In order to disprove a cosmological constant, the first step is to find a time-dependence in the dark energy equation of state. We have reached the first major aim of this project and develop a new way to constrain such a time dependence in a non-parametric way. The next step is to include different dark energy probes. This will allow us to tighten our constraints on the time variation of the dark energy equation of state. In addition, new supernova measurements are becoming available which will be included into our analysis. The second major aim of the project concerns the investigation of early dark energy models and their imprints on current and future

cosmological observations. Since have completed the set-up to investigate the imprints of early dark energy we can now carry out a comprehensive analysis of currently available data and extend our investigations from the cosmic microwave background to include large scale structure probes of dark energy. The third major part of this project concerns the question of how to distinguish a dark energy from modification of general relativity on largest scales. If this turns out to be the reason for the accelerated expansion of the Universe, it would disprove the existence of a cosmological constant.

## Conclusion

During the first few months of the project we have made considerable progress in two of our three major aims. We successfully developed a non-parametric reconstruction method for characterizing the dark energy equation of state. The method has been proven to work on simulated data and has been applied to currently available supernova measurements. Two publications on this work are almost completed. These results are very exciting – this is the first continuous reconstruction of the dark energy equation of state as a function of redshift. Our early dark energy investigations have let to the first very promising results. This line of research will allow us to obtain new constraints on a possible dynamical origin of dark energy.

This project will advance our understanding of the nature of dark energy, which makes up 70% of the content of the Universe and is one of the biggest puzzles in science today. Large billion dollar national and international programs are devoted to understanding the origin of dark energy.

# Neutrino Physics and Its Applications

*Joseph A. Carlson*
20090522PRD2

## Introduction

This project involves large-scale simulations of neutrinos interacting in astrophysical environments like supernovae. Neutrinos are nearly massless particles. Different types (flavors) of neutrinos oscillate into each other during their propagation in space and in matter. We find that these oscillations are qualitatively different when neutrinos are dense enough to scatter off each other. We will investigate this behavior in different types of supernovae and under different scenarios for the properties of neutrinos, attempting to understand what we can learn from neutrino observations of supernovae. This project requires large-scale simulation capabilities which will be advanced through this project, in particular the solution of strongly-coupled non-linear differential equations. This understanding is critical for extracting the most valuable information from many DOE and NSF funded projects including neutrino oscillation experiments at Fermilab and future neutrino observations at the underground lab.

## Benefit to National Security Missions

This work is very important to the DOE/SC program (nuclear and high energy physics) in neutrino physics. DOE/SC has funds large scale experiments that will be able to detect neutrinos from supernovae, this work will allow these experiments to successfully interpret complex signals yielding fundamental properties of the neutrino.

## Progress

Huaiyu Duan has only arrived part way through September. We have set up initial codes and doing comparisons for new work to publish results of full 3-flavor neutrino evolution with full angular dependence. The comparisons between various codes agree, and we are beginning to study several different scenarios.

## Future Work

This project will provide more realistic calculations of neutrino propagation in supernovae environments. Realistic calculations must include neutrino-neutrino interactions and the additional oscillations they induce. Previous calculations have either not included the full 3x3 flavor (electron, mu, and tau) structure of neutrinos or they have used simplified geometries for the relevant astrophysical environment. We will work to improve calculations in both these areas.

During the first part of the project we will concentrate on doing a full 3x3 flavor calculation with all angles of neutrino propagation. At this stage the underlying geometry will still be spherical. These results will allow us to check previous calculations which employed highly simplified scenarios. We will also be able to study neutrino propagations with different assumptions about the neutrino properties. For example, we can assume the electron neutrino is lighter or heavier than the mu and tau neutrinos. We can also check the dependence on the mixing angle between electron and tau neutrinos. This mixing angle is not yet known from experiments, only an upper bound is available.

During the next period of the project (after the first year) we will explore more complicated geometries and the dependence of the signatures on astrophysical properties of the environment. In particular we will study how turbulence in the underlying supernovae can affect the neutrino evolution. We will also explore different geometries related to supernovae (spherical), collapsars (disk geometry), etc. This will allow us to reliably predict neutrino signals from astrophysical sites and their dependence upon the particle physics properties of the neutrino.

## Conclusion

We will attempt to obtain a clear signature for different possible scenarios for neutrino properties, includ-

ing whether they have normal or inverted hierarchies and the mixings of different types of neutrinos. We will also attempt to better understand neutrino interactions with matter, which is important for many DOE experiments in neutrino physics.

# Non-equilibrium Phenomena in Physics, Biology and Computer Science

*Michael Chertkov*
20090525PRD2

## Introduction

The main theme of our research is non-equilibrium phenomena arising in various disciplines: physics, computer science, electrical engineering and biology. Specifically we are interested in the following broad range of problems:

1. Dynamics of microscopic soft objects (i.e. polymer macromolecules, vesicles) in external flow of fluid.
2. Generic models of transport networks with strong fluctuations, for instance queuing networks.
3. Various stochastic and dynamical problems related to the electric power grids with strong penetration of renewable generators and smart controllers.
4. Stochastic algorithms like Markov Chain Monte Carlo (MCMC) that are based on statistically irreversible dynamics.

Our main goals include but are not limited to proposing new analytical techniques to describe the statistics of fluctuations, developing fast modeling algorithms, analyzing various control and inference techniques, adapted to the specifics of the above systems.

## Benefit to National Security Missions

This project will support the DOE mission in Basic Science by enhancing our understanding of the dynamics of biological membranes, vesicles and polymers, and developing modeling approach aimed at discovering which microscopic features can be inferred from the experimental measurements. Resulting algorithms and inference/control techniques will extend LANL capabilities in modeling and designing power grids.

## Progress

During the last half year we have finished or significantly progressed the following tasks:

1. Statistics of heat dissipation of flow driven polymer molecule. Explicit analytical expressions were derived for the large deviation function of heat dissipation. The resulting expressions were confirmed by numerical simulations. (in collaboration with M. Vucelja, M. Chertkov)
2. Nonequilibrium compressibility of the membrane induced by thermal fluctuations. A novel low-dimensional dynamical model of vesicle was developed, that accounts for compressibility of the membrane. The resulting framework is necessary for explaining recent experimental results from Prof. Steinberg group in Weizmann Institute. (in collaboration with S. Vergeles and V. Lebedev)
3. Statistics of currents in queuing networks. Previously developed large deviation techniques were applied to queuing networks with arbitrary number of servers. Universal expressions were derived for the large deviation function (in collaboration with D. Goldberg, M. Chertkov, V. Chernyak)
4. Control of losses and consumption in power grids. New models were introduced for studying control techniques of total power consumption with smart controllers. (In collaboration with S. Backhaus, M. Chertkov, P. Sulc)
5. Disconnection of Air Bubble. Manuscript published in Physical Review Letters. (in collaboration with L. Lipeng, W. Zhang)

## Future Work

The main goals for the next months are:

1. Preparation of publication manuscripts on the recently finished projects (## 1,2,3 from progress section).
2. Analytical and numerical studies of the proposed power grid models. Specifically, we will focus on

the performance assessment of various control techniques. We will compare decentralized control schemes that require limited or none communication of the smart devices with the global optimization techniques. We will also explore applications of game theory for modeling of human behavior in power systems and for design of learning algorithms of artificial agents, like smart inverters.

3. The irreversible MCMC will be applied to various real physical systems, including spin systems, lattice models of polymers.

4. We will start developing the numerical code for modeling multiphase systems (like droplets, vesicles) in low Reynolds number flows. Novel algorithms will be based on spectral approach, and will incorporate thermal fluctuations.

## Conclusion

The results will improve our understanding of the nonequilibrium processes in wide range of natural and artificial system. Our studies of control techniques in power grids will result in specific proposals for power engineers working on the smart grid. The numerical codes developed for simulation of membranes can be later integrated into large scale simulations. Understanding the statistical properties of noise in non-equilibrium systems should be useful for developing new micro-rheological experimental techniques. Finally, the irreversible modifications of MCMC algorithms could be incorporated into existing codes to accelerate simulations of proteins and macromolecules, biological and artificial networks, and other condensed and soft matter systems.

# Theoretical/Computational Research on Particle Acceleration by Intense Laser Pulse

*Brian J. Albright*
20090528PRD2

## Introduction

Generation and acceleration of charged particles are of importance to many fields of activities, such as tumor treatment with proton/ion beams in medical physics, “fast ignition” of fuel capsule with electron/proton beams for inertial fusion energy and radiation sources from electron beams for chemistry, biology and material science.

Conventional technologies to produce and accelerate charged particles are costly, however recently a class of novel particle sources and efficient acceleration methods has emerged following the development of high-power-lasers. When these lasers are tightly focused onto gas jets or solid targets, reaching ultrahigh-intensities of above 10^18 W/cm^2, acceleration fields as high as 10s of TV/m can be produced from the intense laser plasma interactions, surpassing those in conventional accelerators by six orders of magnitude. Electrons or ions in the targets can be accelerated promptly, forming unprecedented beams with low-emittance, short-duration and high-brightness. At LANL, the Trident facility with 250TW, 500fs laser beam is well suited for the study of laser-ion acceleration. A proposed Extreme Light Infrastructure in Europe or a similar facility being considered at LANL as part of MaRIE would enable the laser matter interaction in ultra-relativistic regime (I >10^23 W/cm2) opening doors to energetic particles and radiation beams of femtosecond to attosecond duration.

We plan to explore new concepts such as staging of ion acceleration with double foils to improve beam quality and develop theoretical understanding of such processes with the help of large-scale Particle-In-Cell (PIC) computer simulations on Lobo, Coyote, and the open Roadrunner supercomputers. The proposed work will interface and collaborate with the Trident short pulse experimental team from LANL P-24 in designing and interpreting experiments for laser ion acceleration.

## Benefit to National Security Missions

This project will support the DOE mission in Nuclear Weapons by enhancing our understanding of laser-particle sources related to boost and ICF physics; it is important to support other missions of the Laboratory as well (e.g., Homeland Security), but not to the exclusion of the DOE/NNSA missions.

## Progress

In the very short time between hire-on date and the FY end, the postdoc became acquainted with the particle-in-cell simulation tool that will be used in this project and he developed a suite of custom simulation diagnostics that he is employing on the problem of ultra-intense laser-matter interaction. Moreover, he apprised himself with the literature representing the present state of the art in the field.

## Future Work

Many applications (e.g. fast ignition, hadron therapy) require 200MeV-1GeV quasi-monoenergetic beams. However current laser ion acceleration schemes, such as the Target Normal Sheet Acceleration, the Break-Out Afterburner and the Radiation Pressure Acceleration could not easily achieve these goals. We plan to explore new concepts (such as staging of ion acceleration with double foils) to improve beam quality and develop theoretical understanding of such processes with the help of large scale Particle-In-Cell (PIC) computer simulations on Lobo, Coyote, and the open Roadrunner supercomputers. The VPIC code has reached peak performance of 374 TFlops on Roadrunner, which will dramatically improve the capability to conduct high fidelity simulation of laser particle acceleration. For the most stringent simulation needs for modeling high energy electron beams from laser acceleration, a multi-scale PIC code such as QuickPIC can be utilized. The proposed work will interface and collaborate with the Trident short pulse experimental team from LANL P-24

in designing and interpreting experiments for laser ion acceleration.

Metrics for this work include publications in refereed journals, participation in scientific meetings, and presentation of results at high level technical conferences and workshops.

## Conclusion

The proposed work will answer the fundamental questions regarding the possibility of using high intensity laser for particle acceleration and the methodology of experimental design and optimization for practical usages. It will explore new regimes of operation. These unique particles sources with ultra-short duration, excellent collimation and high-intensity will lead to a host of emerging technologies, e.g., ion driven fast ignition, hadron therapy of tumors, radiography, preparation and probing of warm dense matter, compact electron accelerator and ultra-short high-brightness X-ray sources.

# Single-Nanocrystal Photon-Correlation Studies of Carrier Multiplication

*Victor I. Klimov*
20090532PRD3

## Introduction

Carrier multiplication (CM) is the process by which a single absorbed photon produces more than one electron-hole pair (commonly referred to as an exiton) in a semiconductor. This process offers the potential of increased power conversion efficiency in low-cost single-junction photovoltaics. With carrier multiplication, the extra energy in a blue solar photon is not wasted. To date, transient absorption, the change in absorption spectral features owing to photon absorption, has been the tool of choice for detecting CM and quantifying its efficiency. This method is based on a significant difference in the recombination dynamics of multiexcitons, which decay via fast non-radiative Auger recombination, and single excitons, which decay via a slow radiative process. However, this technique is not applicable to nanomaterials in which Auger recombination is not pronounced, such as colloidal quantum rods or epitaxial quantum dots. Furthermore, transient absorption requires that measurements are performed on ensembles of particles, which reveal only an average response that may smear out the response of individual particles based upon nanoparticle size, shape, surface passivation, etc.

Here, we will demonstrate a principally new method for studying CM via the analysis of statistics of photons emitted by individual nanocrystals. In comparison to traditional "dynamical" ensemble methods, this new technique offers several advantages including (1) single-nanoparticle sensitivity, (2) elimination of complications associated with ensemble heterogeneities and (3) applicability to structures that do not exhibit resolvable Auger decay. This new technique will be based upon photon anti-bunching, which is a phenomenon of individual chromophores (light emitters) that results from a wait time between successive photon emission events. Nanoparticles containing more than one electron-hole pair exhibit a photon bunching signal that arises from the occurrence of emission of two photons (one for each electron-hole pair contained in the particle).

## Benefit to National Security Missions

This work aims to understand the process of carrier multiplication (production of more than one electron-hole pair per absorbed photon of sufficient energy). Carrier multiplication can potentially increase the efficiency of photovoltaics and photocatalytics, which is of relevance to societal energy security, remote power sources, and catalytic chem/bio threat neutralization.

## Progress

Richard Sandberg was hired on June 8th, 2009. The report on his efforts and progress toward studying CM in nanocrystals through photon anti-bunching involve severals aspects. These aspects will be described in the following sections: finding a suitable fast infrared (IR) detector, testing a superconducting nanowire single photon detector (SSPD), and possible alternative studies such as studying anti-bunching in lead sulfide nanocrystals and developing a new technique for studying CM in ensemble colloidal samples.

After completing the relevant safety training, Sandberg began learning the experimental systems relevant to study CM in single nanocrystals through photon anti-bunching. The main system relevant to this project is a confocal microscope system for studying photoluminescence, the process by which exitons in nanocrystals recombine and give up their energy by photon emission. Since this system is a crucial element of the anti-bunching experiment, a basic understanding is important in order to appreciate efforts and goals of this project.

This system, hereafter called the microPL system at CINT-LANL, enables the confocal illumination and observation through an inverted microscope of single colloidal nanocrystals that have been deposited on

a transparent substrate. Additionally, the sample can be placed in a liquid helium flow cryostat to enable cryogenic sample temperatures. For optical wavelengths (400-700 nm) to the near IR (up to about 1000 nm), the microPL system has both a silicon charged-coupled device (CCD) camera mounted on a monochromator for measuring photoluminescence (PL) spectra or two fast silicon avalanche photodiodes (APD) for measuring dynamical PL emission with 150 ps resolution. The two silicon APD's are the detectors that are used for optical photon anti-bunching experiments, however, these detectors will not be useful for anti-bunching in lead-selenide (PbSe) nanocrystals since their emission is typically at wavelengths longer than 1000 nm. Since PbSe nanocrystals are the best candidate for higher efficiency nanocrystal-based photovoltaics currently, finding a suitable fast (ideally sub-100 ps), IR (> 1000 nm), single photon counting detector for anti-bunching studies has been one of the top priorities of this project.

Beginning early in his appointment and throughout this project, Sandberg has conducted literature searches to find a fast, IR single-photon detector. Such a reliable detector with sub-100 ps resolution is not currently commercially available, however, several demonstrations of prototype systems were found in the literature. One of the most attractive systems is a superconducting nanowire single-photon detector (SSPD). Sandberg along with his mentor, Han Htoon, contacted the group of Sae Woo Nam at the Boulder, Colorado campus of the National Institute of Standards and Technology (NIST). The NIST-Boulder SSPD system involves a portable setup that can have up to 50 ps resolution with decent detector efficiencies (1-10 %) throughout the 1000 - 2000 nm range. Sandberg and Htoon agreed upon a week in September when they could travel to Boulder to test the system. Throughout this time, Sandberg studied cadmium based nanocrystals that emit in the optical range and carbon nanotubes on the CINT-LANL microPL system both as a way of learning the experiment but also to find suitable samples to take to NIST-Boulder as trial samples. These studies may also lead to publishable results in the near future.

Sandberg and Htoon traveled to NIST-Boulder the week of September 21st and tested the NIST-Boulder's SSPD coupled to a confocal microscope and cryostat on samples of carbon nanotubes and ensemble PbSe nanocrystals. They learned a lot about the detector system and realized that the optical coupling losses into the SSPD were higher than they had expected and will make anti-bunching experiments on single PbSe nanocrystals difficult. However, they also realized that the NIST-Boulder confocal microscope setup may not have as high a collection efficiency as Htoon's confocal microscope at CINT-LANL.

Currently, Sandberg is continuing efforts to measure the collection efficiency of the CINT confocal microscope using single carbon nanotubes as a comparison metric since they are brighter than single PbSe nanocrystals. Also, they are discussing times with the NIST-Boulder team when they can bring their SSPD system to Los Alamos for further characterization experiments and hopefully conduction photon anti-bunching experiments on single PbSe nanocrystals. Additionally, Sandberg is looking at other possible fast IR single photon detectors such as novel carbon nanotube or graphene based detectors that have been reported in the literature in the last weeks. Additionally, efforts in the team have begun on developing a fast IR single photon detector based on colloidal nanocrystals. Sandberg reported his efforts and visit to NIST-Boulder at a recent Softmatter Nanotechnology Team meeting on October 20th, 2009.

In addition to finding a detector for photon anti-bunching studies with PbSe nanocrystals in the IR range, Sandberg has also been working on other alternatives for studying carrier multiplication. A possible alternative to PbSe for studying CM in a single nanocrystal is small lead-sulfide (PbS). Very recently, Bhola Nath Pal, a chemistry post doc in our group, has synthesized small colloidal PbS samples that emit at about 900 nm making them suitable for photon anti-bunching studies with the current microPL system and silicon APD's. Also, Sandberg has been developing a method to measure CM in ensemble PbSe nanocrystal samples by measuring the PL signal of nanocrystals by re-exciting previously excited exitons by time-delayed ultrafast IR pulses.

## Future Work

Transient absorption, the change in absorption spectral features owing to photoexcitation, has been the tool of choice for detecting CM and quantifying its efficiency. This method is based on dynamical differences in the recombination dynamics of multiexcitons, which decay via fast non-radiative Auger recombination, and single excitons, which decay via a slow radiative process. However, this technique is not applicable to nanomaterials in which Auger recombination is not pronounced, such as colloidal quantum rods or epitaxial quantum dots. Furthermore, transient absorption requires that measurements are performed on particle ensembles, which reveal only an average response that may smear out the individual particles effects based on nanoparticle size, shape, surface passivation, etc.

We will develop a new method for studying CM via the analysis of statistics of photons emitted by individual

nanocrystals. In comparison to traditional “dynamical” ensemble methods, this new technique offers several advantages including single-nanoparticle sensitivity, elimination of complications associated with ensemble heterogeneities and applicability to structures that do not exhibit resolvable Auger decay. This new technique will be based upon photon anti-bunching, which is a phenomenon of individual chromophores that results from a wait time between successive photon emission events. Nanoparticles containing more than one electron-hole pair exhibit a photon bunching signal that arises from the occurrence of emission of two photons (one for each electron-hole pair contained in the particle).

Photon bunching intensities will be measured and related to CM efficiencies for several photon energies in individual particles. These studies may reveal resonant CM phenomena, which quantum mechanical mechanisms predict, or continuous energy effects, which incoherent scattering models predict. Either finding will inform and constrain theoretical models of CM. It is generally agreed that the mechanism of CM in nanoparticles is the key to producing optimally efficient CM materials for possible higher efficiency photovoltaics.

## Conclusion

Photon bunching intensities will be measured and related to CM efficiencies for several photon energies in individual particles and may reveal resonant CM phenomena or continuous energy effects. Either type of finding will inform and constrain theoretical models of CM. It is generally agreed that understanding the mechanism of CM in nanoparticles is the key to producing optimally efficient CM materials, for applications in photovoltaics and elsewhere.

# Ultrafast Phenomena: Short-Pulse laser Interactions with Atoms and Molecules

*Lee A. Collins*
20061600PRD4

## Abstract

The project has focused on two areas of theoretical and computational research: 1) the construction of sophisticated techniques to examine the interaction of ultrafast laser pulses with atoms and molecules and 2) the development of large-scale quantum molecular dynamics simulation techniques to model fluid mixtures in the warm, dense matter (WDM) regime. The former draws upon the exciting new experimental findings encountered with pulses of the same duration as the basic atomic time scale and the ability to actually follow and control very intricate atomic, molecular, and nano-material properties. The latter provides a diverse set of tools to study a regime very difficult to probe experimentally and for which the validity of simple existing models remains uncertain. A particular area of concern rests with rules that govern the mixing of individual atomic species to form composite materials.

## Background and Research Objectives

The project aims at the theoretical and computational study of the interaction of ultrashort laser pulses with atoms and molecules as well as the behavior of composite materials under extreme conditions. With the duration of electromagnetic pulses reaching the fundamental time period of electron motion, we have attained a critical threshold for probing, manipulating, and understanding the basic interactions and processes that govern matter at the atomic scale. For example, experiments have recently observed in "real" time (~attoseconds, $10^{-18}$s) the migration of electrons in solids from conduction bands to the surface and the jumping of electrons from different sites within a molecule. Such ultrafast exchanges hold substantial promise for assembling new nano-materials and altering fundamental electronic mechanisms that govern the outcome of intricate quantum mechanical events. A thorough knowledge of the simplest of these mechanisms is required in order to piece together more complicated systems. Therefore, we began our studies with simple systems in order to explicate the basic mechanics. This study in turn required the development of sophisticated computational techniques to solve the basic underlying quantum mechanical equations. In addition, we performed a complementary study on more extended systems such as mixtures of atoms in the warm, dense matter regime, typical of planetary interiors and inertial confinement fusion capsules. Our goal again concentrated on the understanding of basic quantum mechanical interactions as a means of extracting certain prescriptions for determining the properties of the composite from the pure atomic constituents. Such rules have extensive application in the modeling of macroscopic phenomena and play vital roles in the construction of microscopic property tables that underlie many large-scale simulation projects such as in radiation hydrodynamics.

## Scientific Approach and Accomplishments

### Ultrafast Dynamics

Several areas in regards to the interaction of atoms and molecules with intense and ultrashort laser fields have received particular attention including the double photoionization of Helium and the Hydrogen molecule. The first investigations have focused on small two-electron systems since they provide an effective testbed for more complicated targets, for cleanly resolving basic interactions and mechanisms, and for comparisons with experiments. They also provide the simplest systems for the study of correlation, which arises solely through quantum mechanical effects, and can dramatically alter certain processes from a classical or perturbative picture. For Helium, our studies have disentangled very complicated cross sections in terms of sequential and nonsequential processes in regards to whether the system absorbs two photons simultaneously or one after the other. The knowledge of such fundamental internal processes is essential to understanding the means

of manipulating and controlling atoms, molecules, and nanosystems by external electric and magnetic fields. In addition, the formalism has been expanded to determine not only the distribution of the electrons but also of the recoiling ion. This full characterization of the kinetic and spatial distributions of the final states of the particles can be directly compared to elaborate experimental results from sophisticated detectors, giving a complete view of the photoionization process that allows separation of the various competing mechanisms. This ability to separate mechanisms has lead to the resolution of several long-standing controversies on the importance of certain processes during the ionization of multi-electron systems. By combining both time-independent and time-dependent simulations, we have shown that perturbative approaches and explanations of these mechanisms have definite shortcomings and that the full correlation correctly represented in our approaches is essential to a detailed understanding.

All these intricate comparisons arise from our ability to solve the time-dependent Schrodinger equation that describes the quantum mechanical nature of these systems. To this end, we have improved our finite-element discrete variable representation program by extensions to massively-parallel constructions and more accurate temporal propagators. The program scales linearly on parallel platforms of over hundreds of processors.

A related set of calculations focuses on the Hydrogen molecule. An interesting speculation has arisen in these ultrashort interactions as to whether the ejected electron in passing between the nuclear centers can undergo interference much as in the famous double-slit experiment by Young with light. The electrons under these conditions display quantum mechanical behavior, acting like matter waves breaking on the two nuclei, which serve as the "slits." Our theoretical results have placed distinct limits on this mechanism and questioned this interpretation of recent experiments at low photon energies. We have also devised elaborate visual display packages that permit a clear examination of the complicated spatial probability distributions that describe the exiting particles. We depict in Figure 1 an example of the election distribution of the fast electron after the double photoionization of the hydrogen molecule.

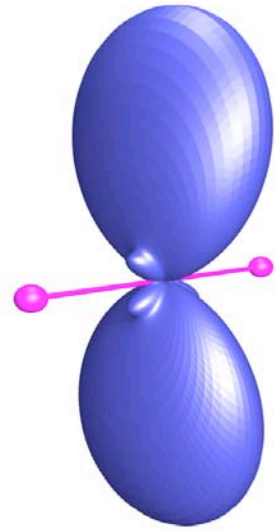

*Figure 1. Photo-electron distribution following ionization of a hydrogen molecule.*

**Mixtures**

A second component of the project focuses on mixtures of various elements in the regime of Warm, Dense Matter (WDM). This regime, which encompasses temperatures from hundreds to millions of degrees Kelvin and densities from hundredths (1/100) to hundreds of times solid, consists of a very complex material environment that exists in such locales as planetary interiors, White Dwarf surfaces, inertial confinement fusion (ICF) capsules, and high energy density physics (HEDP) devices such as Z-pinch machines. The internal structure consists of a rapidly-changing "soup" of atoms, ions, free electrons, and molecules. The nature of WDM requires a quantum mechanical treatment based on the explicit interactions of a significant number of atoms, which until recently lay beyond practical implementation. With the advent of density functional theory (DFT) and the concomitant rise of fast distributed-memory parallel computers, the sophisticated treatment of WDM through quantum molecular dynamics (QMD) has become a reality. This method permits the collective treatment of large samples of atoms and incorporates quantum mechanical effects such as exchange and correlation, essential to the accurate representation of such extended systems. Transient processes such as ionization, recombination, dissociation, binding, and collisions naturally arise from the DFT and molecular dynamics formulations. In Figure 2, we display a snapshot at a representative time during the evolution of a dense mixture of lithium and hydrogen that plots the probability density for the electrons around and between the nuclear centers marked by the red and blue balls.

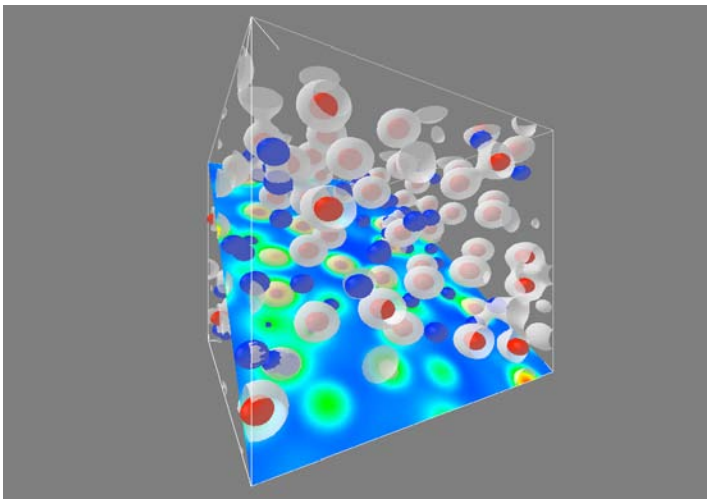

*Figure 2. Electron probability density for electrons in a LiH mixture.*

The basic QMD approach consists of performing a DFT calculation on a fixed sample of atoms in order to extract a state wave function that contains the global properties for all the electrons. From this state function and from the Columbic interactions among the nuclear charges, we extract a force acting on the nuclei. Simple Newtonian mechanics then predict the next position of the nuclei. The DFT is run on this new configuration, yielding a force, and the process continues to evolve the system in time until various properties converge. The procedure produces a consistent set of static (equation-of-state), dynamical (diffusion/viscosity), and optical (opacities/reflectivities/conductivities), a great advantage in assessing the validity of other models. Many macroscopic modeling programs take these properties from different formulations, thus making an assessment of the relative effects on inter-related components difficult. The integrated nature of QMD overcomes this problem.

Mixtures provide a particularly important area in which such an integrated approach could have significant impact. Since the approaches that can treat all the intra- and inter- species interactions in the form of QMD have only recently matured, the properties of mixtures had basically been determined by combining single-species properties by particular, many times arbitrary, rules. Some of these prescriptions were drawn from ideal gas or on solid-solid interfaces pictures. Neither of these conditions describes properly the WDM regime so that the validity of these *ad hoc* rules remained in substantial doubt. Unfortunately, experiments are very difficult to mount and interpret in this transient state of dense matter. Therefore, one effective means of obtaining a comprehensive representation of such a system was through QMD, which given the sophistication of the treatment of the electrons and nuclei, could serve as an effective "computational experiment" to validate various mixing rules.

To this end, we have applied density functional theory approaches to atomic mixtures such as Lithium Hydride (LiH) in the warm, dense matter regime. These large-scale quantum simulation techniques stringently test various mixing rules devised to combine pure atomic properties to form those of the composite. To effect a consistent control, we first performed QMD calculations on the individual species and determined the resulting mixture properties for several standard mixing schemes. These results could then be compared with QMD simulations of the fully-mixed system. This approach provided a best-case scenario for judging the efficacy of the mixing rules since the test had internal consistency in all the components. We explored two popular mixing rules, one based on combining the atomic components based on an ideal gas, and the other based on equating pressures. We found in general that the ideal gas rule functions best for low densities and temperatures while the pressure rule shows promise at the other extreme. For equation of state, the atomic mixing rules gave errors by as much as 40% when compared with the QMD simulation for the full mixture. For opacities, a measure of the ability of a material to absorb light, larger disparities arose, especially in particular frequency regimes. These finding have profound ramifications for the basic tables used in many radiation-hydrodynamic programs which model complicated macroscopic systems from stars to nuclear weapons.

While the DFT provides a highly accurate and predictive representation of the WDM regime, the technique requires massive computational resources that limit the range of its effectiveness. As the temperature rises, the method demands the generation of larger sets of eigensolutions from the diagonalization of huge matrices. This basically limits the range of temperatures to a few tens of electron volts (~200,000 K). To explore deeper into the WDM region requires a modified approach. Generally as the temperature rises, the need to represent electronic interactions in detail wanes since most of the ions have become significantly ionized and molecular processes have ceased. The electrons, while still having interactions with the ionic centers, form a fairly uniform collective fluid. This implies that less sophisticated methods such as Thomas-Fermi (TF) theory might function at a reasonable accuracy with vast savings in computational time. The savings arise from the ability to formulate TF in terms of a probability density on a grid instead of employing orbitals as in full (Kohn-Sham) DFT. We have in collaboration with a group at the French Atomic Energy Commission (CEA) developed a TF or orbital-free (OF) molecular dynamics program based

on the TF and some its flavor to bridge the gap between the DFT-MD and simple thermodynamical models, which become applicable at very high temperatures. Initial tests show great promise in examining temperatures between ten and hundreds of electron volts. Larger-scale simulations on LiH show a smooth transition from QMD to OFMD around 5 electron volts (~ 50,000K) for such properties as pressures and diffusion coefficients. Due to the time-savings engendered by the TF formation, much larger samples can be treated by OFMD. This capability should have important consequences for modeling impurity effects within mixtures, an important problem for example in understanding the equation-of-state for extrasolar planets, which in addition to their predominantly hydrogen-helium composition contain different smatterings of various impurity elements or more prosaicly dirt. These impurities can have profound effects on the structure and evolution of these objects.

## Impact on National Missions

The ability to probe material properties on the time scale of atomic motion promises better understanding of basic materials from the solid to the plasma state. These probes will greatly improve our fundamental knowledge of important materials, impacting DOE missions from materials for energy to sensors for threat reduction. Examples include the assembly of new materials, the *in vacuo* imaging of larger biological molecules, remote sensing, and control of basic molecular processes. The dense matter component provides an accurate benchmark for validating various models and mixing rules that abound in many macroscopic modeling programs at the Laboratory that treat composite materials environments under extreme conditions.

## Publications


Horner, D. A., C. W. McCurdy, and T. N. Rescigno. Triple differential cross sections and nuclear recolil in two-photon double ionization of helium. To appear in *Physical Review A.*

Horner, D. A., J. D. Kress, and L. A. Collins. Quantum molecular dynamics simulations of warm dense lithium hydride: examination of mixing rules. 2008. *Physical Review B.* **77**: 064102.

Horner, D. A., S. Myabe, T. N. Rescigno, C. W. McCurdy, F. Morales, and F. Martin. Classical two-slit interference effects in two-photon double ionization of molecular hydrogen at high energies. To appear in *Physical Review Letters.*

Horner, D. A., T. N. Rescigno, and C. W. McCurdy. Decoding sequential versus non-sequential two-photon double ionization of Helium using nuclear recoil. 2008. *Physical Review A.* **77**: 030703(R).

Horner, D., F. Morales, T. Rescigno, F. Martin, and C. McCurdy. Two-photon double ionization of helium above and below the threshold for sequential ionization. 2007. *Physical Review A.* **76**: 030701.

Horner, D., W. Vanroose, T. Rescigno, F. Martin, and C. McCurdy. Role of nuclear motion in double ionization of molecular hydrogen. 2007. *Physical Review Letters.* **98**: 073001.

Kress, J., L. Collins, S. Mazevet, and D. Horner. Quantum molecular dynamics simulations of optical reflectivity of shock-compressed Tin. 2007. *American Institute of Physics Proceedings.* **995**: 1433.

Vanroose, W., D. Horner, F. Martin, T. Rescigno, and C. McCurdy. Double photoionization of aligned molecular hydrogen. 2006. *Physical Review A.* **74**: 052702.

Yip, F., D. Horner, C. McCurdy, and T. Rescigno. Singlr and triple differential cross sections for double ionization of H-. 2007. *Physical Review A.* **75**: 042715.

# Theoretical and Experimental Investigation of Relaxation Mechanisms in Ultra-low Field NMR for Magnetic Resonance Imaging

*Michelle A. Espy*
20070626PRD2

## Abstract

The work is a theoretical and experimental investigation of NMR relaxation mechanisms in ultra-low magnetic fields (ULF, microtesla magnetic fields) for magnetic resonance imaging (MRI). In addition we have extended our sensor capabilities into atomic magnetometry. Progress on this work includes construction of the first atomic magnetometer at Los Alamos. With this device we have recorded the first MRI with an atomic magnetometer (which has enormous scientific and technological implications). We have also completed magnetic contrast agent measurements at ULF, which have significant promise for the medical development of ultra-low field MRI. We have also investigated the theoretical aspects of relaxation (in the presence of contrast agents) and made predictions about how to optimize contrast agent properties for the best signal. Our recent efforts are towards the first ever images of human anatomy via ULF MRI with an atomic magnetometer.

## Background and Research Objectives

The primary focus of the work was an investigation of NMR relaxation mechanisms in ultra-low (micro-Tesla) magnetic fields for applications in ultra-low-field (ULF) MRI and spectroscopy. The differences in relaxation times at ULF may enable new methods for imaging and material differentiation that cannot be realized at high fields (~Tesla). For example, the difference in relaxation time (T1 or T2 "contrast") is a powerful tool in clinical (high field) MRI. It has been reported that while some tissue types have little, if any relaxation time contrast at fields >1T, significant contrast is observed at ULF. Currently, it is a baffling mystery why closely related materials (e.g. healthy and tumor tissue) have significantly different relaxation times. Relaxation times and mechanisms at ULF have not been investigated as measurements in this regime have only recently become feasible. Due to absence of large superconducting magnets, ULF MRI also brings advantages such as lower cost, portability, safety, and supplements conventional high-field MRI in situations where it cannot be used due to strong-field restrictions. The challenge of this research is that the signal is much smaller than in conventional NMR, so the most sensitive magnetic detectors and shielding have to be used.

The objectives of the work was to 1) develop the instrumentation required for ULF MRI, 2) apply ULF MRI instrumentation to measurements of relaxation times for various substances of scientifically interesting chemical composition (biological tissue, liquid explosives) as a function of magnetic field and analyzed relaxation mechanisms to extract the relevant parameters 3) implemented an anatomic magnetometer of similar sensitivity to existing SQUID (superconducting quantum interference device) sensor technology.

## Scientific Approach and Accomplishments

Our first objective was to develop the instrumentation required for ULF MRI. We have used a combination of ULF MRI instrumentation based on the superconducting quantum interference device (SQUID) as well as built a new laser-based atomic magnetometer. We applied this instrumentation to address a variety of scientific questions.

One such application was to a measurement of ULF NMR of $^3$He to analyze the expected signal strength and relaxation dynamics. This work was in support of a collaboration headed by LANL to measure the neutron electric dipole moment (nEDM). In addition, an analysis of the shielding required for the nEDM experiment was performed. The work on $^3$He has been published in the Journal of Magnetic Resonance Imaging [1].

Another accomplishment was the successful demonstration of the world's first in-situ MRI with an atomic magnetometer. The major technical problem to applying an atomic magnetometer to such

measurements is their sensitivity to the applied magnetic fields required for MRI. This problem was solved by the development of a novel flux transformer scheme as shown in Figure 1, and has resulted in the first MRI with an atomic magnetometer. The image is shown in Figure 2, the upper image was attained with a SQUID and the lower with our atomic magnetometer. The work has been accepted for publication in the Journal of Magnetic Resonance [2]. The MRI hardware has been described elsewhere [3]. Application of an atomic magnetometer to ULF MRI is an important step towards commercialization, since atomic magnetometers do not require liquid cryogens as SQUIDs do. This is being filed by LANL for a patent, LAD 2008-076/S-112.

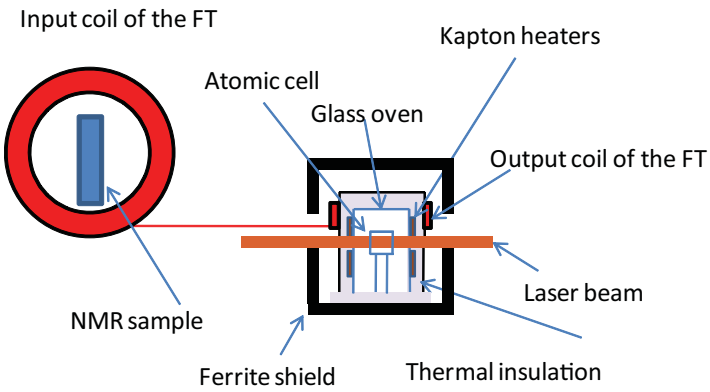


*Figure 1. A schematic diagram of the atomic magnetometer developed for magnetic resonance imaging. The flux transformer (FT) couples the NMR sample, a small cylinder of water, to the atomic magnetometer located ~ 1 m away.*

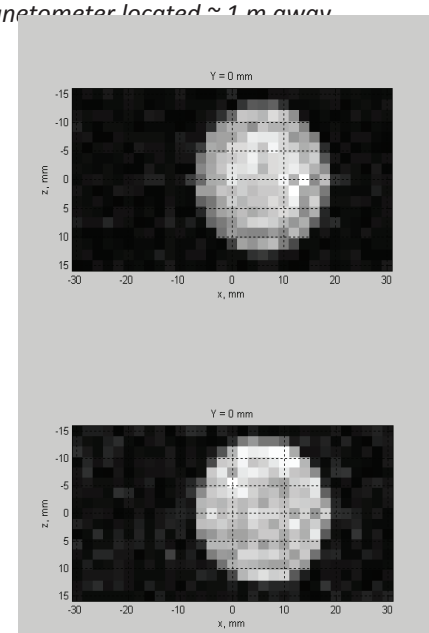


*Figure 2. Ultra-low field MRI at 3.2 kHz. The upper image was taken with a SQUID system. The lower image was taken with our newly developed atomic magnetometer. The sample was a small cylinder of water ~ 2cm in diameter and 3 cm deep.*

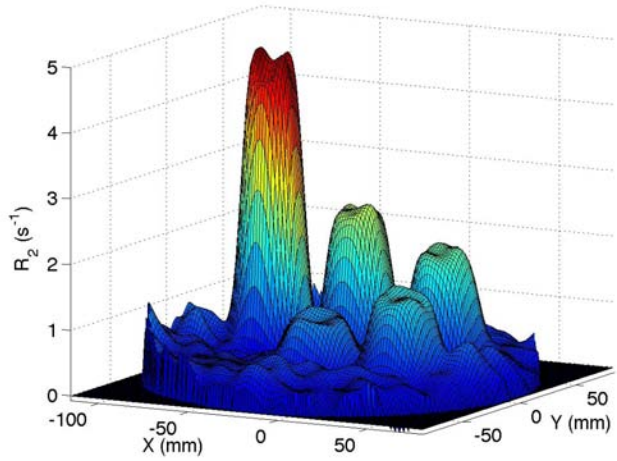


*Figure 3. Map of the transvers relaxivity (R2) of samples with the height/color indicating the R2 values. The MRI showed contrast induced by various concentrations of 20 nm nanoparticles dissolved in water. The samples contain 30 ml and are surrounded by water. The image shows the 4th echo at ~420 ms. The imaging sequence consisted of: pre-polarization field 35 mT, measurement field 3000 Hz, read-out gradient 2.53 Hz/mm, and phase-encoding gradient 2.14 Hz/mm.*

We were also able to study, via ULF MRI, relaxation times for various substances of scientifically interesting chemical composition (biological tissue, liquid explosives) as a function of magnetic field. In conjunction with the experimental work, we applied current theories of relaxation time to formulate an understanding of the relationship between relaxation times vs. applied magnetic field strength with a particular interest in understanding the theoretical basis of the observed difference in relaxation times for biological tissue and contrast agents [4]. Figure 3 presents a contrast agent enhanced image obtained via ULF MRI, with contrast provided by various concentrations of 20 nm nanoparticles. The results of this work indicate that contrast agents can be used to provide T1 contrast greatly exceeding that available at high fields.

## Impact on National Missions

LANL has developed a world-class capability in ultra-low field MRI that has been applied to problems in Threat Reduction, DOD, DHS, and Office of Science. The technology is immediately relevant to applications in portable and low-cost imaging for clinical and combat medicine. The overlap of the Larmor frequency with "slow" (10 µs to 100 ms) molecular dynamic processes such as diffusion, molecular motion, chemical reactions, and biological processes, can be exploited for studies of plant function for applications in energy and environment. In security and nonproliferation applications, ULF MR methods are being developed for detection of the

products of Uranium processing. Ultra-low field magnetic resonance imaging has already demonstrated successful application of basic science to needs in national security. The LANL capability in ULF MRI anatomical brain imaging was directly leveraged by the MagViz project, funded by DHS, to detect liquid explosives. This work is addressing a critical security need for the Nation, and has resulted in positive publicity for LANL as well as a multi-year research effort into detection and characterization of material properties of liquids.

The work here has advanced our understanding and abilities in ULR MRI by providing a more complete understanding of the underlying contrast mechanisms at ULF MRI, and presenting several novel applications of the approach to problems in medical imaging.

## References


1. Savukov, I., A. Matlashov, P. Volegov, M. Espy, and M. Cooper. Detection of 3He spins with ultra-low field nuclear-magnetic resonance employing SQUIDs for application to a neutron electric dipole moment experiment. 2008. *Journal of Magnetic Resonance.* **195**: 129.

2. Savukov, I. M., V. S. Zotev, P. L. Volegov, M. A. Espy, A. N. Matlashov, J. Gomez, and R. H. Kraus, Jr.. In situ MRI with an atomic magnetometer. To appear in *Journal of Magnetic Resonance.*

3. Zotev, V. S., A. N. Matlashov, P. L. Volegov, I. M. Savukov, M. A. Espy, J. C. Mosher, J. J. Gomez, and R. H. Kraus, Jr.. Microtesla MRI of the human brain combined with MEG. 2008. *Journal of Magnetic Resonance.* **194** (1): 115.

4. Magnelind, P., I. Savukov, Y. Araya, A. Matlashov, P. Nath, P. Volegov, V. Zotev, and M. Espy. Superparamagnetic nanoparticle contrast agents for ultra-low field MRI. Presented at *50th Experimental NMR Conference.* (Pacific Grove, California, March 29 - April 3, 2009).


## Publications


Savukov, I.. Atomic Magnetometers. To appear in *Multi-disciplinary University Research Initiative.* (Boulder, CO, July 18-20).

Savukov, I.. Applications of atomic magnetometers to MEG and NMR. To appear in *International Brain Mapping Intraoperative Surgical Planning Society.* (Washington, DC, Sept 6-8, 2007).

Savukov, I. M., V. S. Zotev, P. L. Volegov, M. A. Espy, A. N. Matlashov, J. Gomez, and R. H. Kraus, Jr.. In situ MRI with an atomic magnetometer. To appear in *Journal of Magnetic Resonance Imaging.*

Savukov, I., A. Matlashov, P. Volegov, M. Espy, and M. Cooper. Detection of 3He spins with ultra-low field nuclear-magnetic resonance employing SQUID's for application to a neutron electric dipole moment experiment. 2008. *Journal of Magnetic Resonance.* **195**: 129.

Zotev, V. S., A. N. Matlashov, P. L. Volegov, I. M. Savukov, M. A. Espy, J. C. Mosher, and R. H. Kraus, Jr.. Microtesla MRI of the human brain combined with MEG. 2008. *Journal of Magnetic Resonance.* **194**: 115.

Zotev, V. S., P. L. Volegov, A. N. Matlashov, I. M. Savukov, T. Owens, and M. A. Espy. SQUID-based microtesla MRI for in vivo relaxometry of the human brain. To appear in *IEEE Transactions on Applied Superconductivity.*

# Noise in Biochemical Networks: Rigorous Analysis with Field-Theoretic Tools

*Ilya M. Nemenman*
20070649PRD2

## Abstract

This project analyzed a variety of small biochemical reaction networks, which form basic building blocks of all concerted interactions among molecules in a cell. Effects of the noise coming from the small number of molecules on the ability of these networks to function reliably were analyzed, efficient simulation software was developed, and the geometric phase, a staple of quantum mechanics never before observed in classical stochastic systems, processes was discovered. This project served as an essential first step for understanding and manipulating many biochemical signaling networks, involved, for example, in energy production and diseases, such as cancer, and may eventually lead to breakthroughs on both of these fronts. Emerging understanding can help us design better molecular machines, such as chemical batteries.

## Background and Research Objectives

Various problems in diverse fields, from statistical physics to cellular regulatory networks, involve analysis of stochastic properties in transport phenomena on a variety of networks. This analysis is usually very difficult due to the intrinsic stochastic nature of the processes, which necessitates their computational modeling in a computationally prohibitive event-by-event fashion.

In this project, Nikolai has developed ways to transplant the tools that have proven to be effective in mesoscopic condensed matter physics into the realm of stochastic processes on networks. If successful, many decades of successful work in one field will come to bear fruits in another, allowing fast and efficient simulations and analysis of the processes, and impacting a variety of fields, from basic biomedical sciences, to biosecurity and energy security.

A critical notion in the work is the geometric phase, a common property of quantum and mesoscopic systems, but previously unseen in the stochastic domain. In the course of the project, Nikolai has discovered the phase in certain biochemical processes, and it is expected that similar results will hold in a wide class of systems. The phase has been the main conduit for connections between mesoscopic quantum systems and the stochastic transport on networks.

## Scientific Approach and Accomplishments

This project has discovered the geometric phase in classical stochastic systems. More specifically, suppose that, in a stochastic system, one changes certain kinetic rates with time. This happens, for example, in cells due to the natural time of day variations, and in epidemiological networks due to the variation of the infection rates in the course of the year. It turns out that the stochastic nature of the processes results in the contribution to the transported amounts in these networks, which would not be expected from a pure deterministic treatment. This contribution, as we have discovered, is a precise analogue of the Berry (or geometric) phase in quantum mechanics, but this is the first time such an effect has been found in a non-quantum system. The finding is quite remarkable: in particular, it has been believed that, to find details of a macroscopic structure of a network, one should be able to conduct experiments that are able to track all of the aspects of its stochastic dynamics. In contrary, we have found that much of this information is available through the geometric phase observation in a bulk, mean-value experiment, provided the experiment traces responses to temporal perturbations. These results are expected to be used to uncover properties of ion channels in neurons in a collaboration with the NIH group of Dr. Sergey Bezrukov; a recent trip to NIH has started the collaboration. Similarly, these results seem to be important for a burgeoning field of nonequlibrium statistical physics, such as applications of the theory of stochastic ratchets to molecular motors, etc. A collaboration with Chris Jarzynski (University of Maryland) has been initiated.

Since the start of the project, the funding has been used in the following research projects.

The upcoming *PNAS* article (Sinitsyn et al., 2009) is the culmination of the research, resulting in a practical algorithm for simulation of noisy biochemical processes, which beats most other competitive approaches by orders of magnitude.

Refs (Sinitsyn and Nemenman, 2007 and Sinitsyn and Nemenman, 2007a) were the original works where the geometric phase in stochastic kinetics has been noted, and the tools developed in the context of the quantum-mechanical Berry phase were used to solve a variety of problems in chemical kinetics, nonequilibrium statistical physics, and mathematical epidemiology.

In (Sinitsyn and Ohkubo, 2008; Sinitsyn, Dobrovitski, et al., 2008; Sinitsyn, 2007; Sinitsyn and Saxena, 2008; de Ronde et al., 2009) Nikolai SIntsyn further developed the theory of the geometric phase in statistical physics problems, and related the phenomenon to geometric phases in classical and quantum mechanics, using the latter two to help with solutions of important applied problems, such as the motion of magnetic domain walls.

Refs (Sinitsyn, 2008; Nunner et al, 2007; Borunda et al, 2007) have studied, in particular, geometric effects in traditional condensed-matter problems of relevance to nanotechnology.

Applications of the geometric phase to nonequlibroum statistical physics problems have revealed an important question: under which conditions does a small, periodic perturbation of a system result in an nonzero current through it? This question was answered fully in (Chernyak and Sinitsyn, 2008).

Additional publications (see the full publication list) have dealt with related problems on the interface of condensed matter physics and stochastic processes theory, and provided extensive reviews of the obtained results. Notably, (Sinitsyn, 2008) review article has been called one of the Top Articles in J Phys by its editors for 2008. A more recent review (Sinitsyn, 2009), summarizes the geometric effects theory in stochastic systems.

Finally, a new practical application has emerged as a result of this project, and appropriate grant applications have been submitted. Namely, existence of the geometric phase and the ability to evaluate it analytically and numerically allows for creation of control theory for stochastic systems, where small molecular copy number fluctuations are not avoidable. Dr. Sinitsyn has suggested that this can be used for optimal design of biochemical batteries, where periodic perturbations of the system, such as F1ATPase, can be used to design a high efficiency, optimized devicetransforming electrical energy into a chemical storage, and vice versa. This possibility needs to be explored in detail due to its obvious importance for the Nation.

## Impact on National Missions

The project has developed predictive capabilities applicable to the biosciences mission of DOE, specifically for bioenergy research; it has advanced the scientific understanding of basic biochemical processes of interest to DOE bioenergy mission and will be useful for threat reduction applications in the context of host-pathogen interactions, supporting DOE and DHS missions.

## References


1. Sinitsyn, N., N. Hengartner, and I. Nemenman. Coarse-grained stochastic biochemical networks: quasi-stationary approximation and fast simulations using stochastic path integral technique. To appear in *PNAS.*

2. Sinitsyn, N., and I. Nemenman. The Berry phase and the pump flux in stochastic chemical kinetics. 2007. *EPL.* **77**: 58001.

3. Sinitsyn, N., and I. Nemenman. Universal geometric theory of stochastic pumps and reversible ratchets. 2007. *PRL.* **99**: 220408.

4. Sinitsyn, N., and J. Ohkubo. Hannay angle and geometric phase shifts under dissipative evolutions. 2008. *J. Phys A.* **41**: 262002.

5. Sinitsyn, N., V. Dobrovitsky, S. uradzhin, and A. Saxena. Geometric control over the motion of magnetic domain walls. 2008. *Phys. Rev. B.* **77**: 212405.

6. Sinitsyn, N.. Reversible stochastic pump currents in interacting nanoscale conductors. 2007. *Phys. Rev. B.* **76**: 153314.

7. Sinitsyn, N., and A. Saxena. Geometric phase for non-Hermitian Hamiltonian evolution as anholonomy of a parallel transport along a curve. 2008. *J. Phys. A: Math, Theor..* **41**: 392002.

8. deRonde, W., B. Daniels, A. Mugler, N. Sinitsyn, and I. Nemenman. Statistical properties of multistep enzyme-mediated reactions. To appear in *IET Syst. Biol..*

9. Nunner, T., N. Sinitsyn, M. Borunda, A. Abanov, C. tim, T. Jungwirth, J. Inoue, V. Dugaev, A. MacDonald, and J. Sinova. Anomalous Hall effect in two-dimensional electron gas. 2007. *Phys. Rev. B.* **76**: 235312.

10. Borunda, M., T. Nunner, T. Luck, N. Sinitsyn, C. Timm,

J. Wunderlich, T. Jungwirth, A. MacDonald, and J. Sinova. Absence of skew scattering mechanism in two dimensional systems: a test of anomalous Hall effect theory. 2007. *Phys. Rev. Lett..* **99**: 066604.

11. Sinitsyn, N., and V. Chernyak. Pumping restriction theorem for stochastic networks. 2008. *Phys. Rev. Lett..* **101**: 160601.

12. Sinitsyn, N.. Semiclassical theories of the anomalous Hall effect. 2008. *J. Phys.: Cond. Matt..* **20**: 023201.

13. Sinitsyn, N.. Stochastic pump effect and geometric phases in dissipative and stochastic systems. 2009. *J. Phys. A: Math, Theor..* **42**: 193002.

## Publications

Borunda, M., T. Nunner, T. Luck, N. Sinitsyn, C. Timm, J. Wunderlich, T. Jungwirth, A. MacDonald, and J. Sinova. Absence of skew scattering mechanism in two dimentional systems: a test of anomalous Hall effect theory. 2007. *Phys. Rev. Lett..* **99**: 066604.

Chernyak, V., and N. Sinitsyn. Pumping-Restriction Theorem for stochastic networks. 2008. *Phys. Rev. Lett..* **101**: 160601.

Dahal, H., Z. Hu, N. Sinitsyn, K. Yang, and A. Balatsky. Edge states in a honeycomb lattice: effects of anisotropic hopping in mixed edges. To appear in *Phys. Rev. B.*

Nunner, T., N. Sinitsyn, M. Borunda, A. Abanov, C. Timm, T. Jungwirth, J. Inoue, V. Dugaev, A. MacDonald, and J. Sinova. Anomalous Hall effect in two-dimensional electron gas. 2007. *Phys. Rev. B.* **76**: 235312.

Sinitsyn, N.. Semiclassical theories of the anomalous Hall effect. 2008. *J. Phys.: Cond. Matt..* **20**: 023201.

Sinitsyn, N.. Reversible stochastic pump currents in interacting nanoscale conductors. 2007. *Phys. Rev. B.* **76**: 153314.

Sinitsyn, N.. Stochastic pump effect and geometric phases in dissipative and stochastic systems. 2009. *J. Phys. A: Math, Theor..* **43**: 193001.

Sinitsyn, N., A. MacDonald, T. Jungwirth, V. Dugaev, and J. Sinova. Anomalous Hall effect in 2D Dirac band: link between Kubo-Streda formula and semiclassical Boltzmann equation approach. 2007. *Phys. Rev. B.* **75**: 045315.

Sinitsyn, N., N. Hengartner, and I. Nemenman. Coarse-graining stochastic biochemical networks: quasi-stationary approximation and fast simulations using a stochastic path integral technique. To appear in *Proc. Natl. Acad. Sci. (USA).*

Sinitsyn, N., V. Dobrovitski, S. Urazhdin, and A. Saxena. Geometric control over the motion of magnetic domain walls. 2008. *Phys. Rev. B.* **77**: 212405.

Sinitsyn, N., and A. Saxena. Geometric phase for non-Hermitian Hamiltonian evolution as anholonomy of a parallel transport along a curve. 2008. *J. Phys. A: Math. Theor..* **41**: 392002.

Sinitsyn, N., and I. Nemenman. Universal geometric theory of mesoscopic stochastic pumps and reversible ratchets. 2007. *Phys. Rev. Lett.* **99**: 220408.

Sinitsyn, N., and I. Nemenman. The Berry phase and the pump flux in stochastic chemical kinetics. 2007. *EPL.* **77**: 58001.

Sinitsyn, N., and J. Ohkubo. Hannay angle and geometric phase shifts under dissipative evolution. 2008. *J. Phys. A: Math. Theor..* **41**: 262002.

deRonde, W., B. Daniels, A. Mugler, N. Sinitsyn, and I. Nemenman. Mesoscopic statistical properties of multistep enzyme-mediated reactions. To appear in *IET Syst. Biol..*

# Entanglement and Correlations in Complex Physical Systems

*Wojciech H. Zurek*
20070653PRD2

## Abstract

During the past year Dr. Zwolak researched several interrelated topics involving entanglement and classical correlations in physical systems that have direct implications for many areas of physics, system modeling, and biological/single-molecule sensors. Much of this work has been on understanding how a quantum mechanical system gets correlated with its environment, i.e., what parts of the environment correlate strongly with the system and how are these parts of the environment influencing the systems behavior. These questions underlie many physical and technologically important issues, including how to understand and model decoherence in solid-state architectures for Quantum Computing and how one can construct efficient methods for simulating many-body quantum systems (such as strongly correlated systems in the presence of dissipation or electronic transport in nanoscale systems). In addition to these central questions regarding quantum systems embedded in their environment, Dr. Zwolak also worked on biophysical problems relating to DNA sequencing and ionic transport.

## Background and Research Objectives

The possibility of quantum computing (QC) holds our imagination captive and its successful implementation would have far-reaching consequences. On the one hand, it would enable an enormous speedup in certain types of computation. The most outstanding current example is the exponential speedup in factoring large numbers, with which one could break some modern encryption techniques. On the other hand, another potential use of QC would be, paradoxically, to simulate quantum systems themselves, which would facilitate the discovery and understanding of quantum phenomena. This latter application, as a way to overcome the exponential slowdown of a classical computer, was the motivation for Feynman's proposal of a quantum computer in the early 80's. What makes a quantum computer powerful, and correspondingly what makes quantum systems so hard to simulate classically, is the presence of a purely quantum mechanical correlation called entanglement. The primary objectives of my research over the past year were to (i) obtain a fundamental understanding of how quantum mechanical systems become entangled with their environment and (ii) develop efficient computational techniques to capture the influence of the environment on a system's behavior (with the long term goal of being able to simulate dissipation and decoherence in superconducting systems and also systems relevant to quantum computing).

Dr. Zwolak also maintained a long-standing interest in issues related to DNA sequencing and ionic transport. Core among them is a proposal to sequence DNA using nanopore-based electronic transport measurements. This is a novel single-molecule approach that has the potential to greatly reduce the time and cost of sequencing (and also, more generally, give a new approach to molecular detection). The successful implementation of this technique would have enormous implications for medicine and biology. His research in this area over the past year has mainly focused on investigating ionic transport in nanopores. A longer-term project is on using the techniques above (on the influence of the environment) to simulate electronic transport in the presence of the strongly fluctuating environment of the type present in nanopore experiments.

## Scientific Approach and Accomplishments

### DNA Sequencing and Molecular Detection

One of the first research milestones Dr. Zwolak achieved was the completion of a review article entitled "Physical approaches to DNA sequencing and detection." This article, published in the prestigious journal Reviews of Modern Physics in January 2008, is a seminal contribution to the areas of nanopores and DNA sequencing. It makes accessible to a wide audience, including graduate students, the recent progress in the field and also critically evaluates different proposals for a rapid and low-cost DNA sequencing device and, more generally, molecular detection device. Such a technology will create new possibilities for ubiquitous sensors, and thus addresses the LANL mission of Threat Reduction. As well, such sensors open up new avenues

for investigation into the complex interface between solids, liquids, and biomolecules, and increase our understanding of how materials behave at the nanoscale. The impact of this work is already being felt, as demonstrated by a recent (July) Nature Physics article "The law of accelerating returns" (Nature Physics 4, 507 (2008)) detailing our contribution to the field and its prospects.

**Computational Algorithms for Open Systems**
Dr. Zwolak 's long-term goals are to develop efficient simulation techniques for "open" quantum systems, e.g., nanoscale systems interacting with external probes and their environment, or quantum systems dissipating energy into the environment. In this direction, he was the first to examine how different portions of the environment influence the dynamics of a system and he used this knowledge to create a novel representation of the environment for numerical simulations. The latter significantly reduces the computational cost necessary to accurately simulate the dynamics of quantum systems in contact with certain environments. In particular, the computational cost was reduced from $N^3$ to $N^2$ to achieve a given simulation accuracy. This means that if one needs 100 degrees of freedom, N, to simulate the effect of the environment, that the computational time of the simulation is reduced by a factor of 100 if one uses his method. This work has culminated in an article "Finite representations of continuum environments," that recently appeared in the high-impact Journal of Chemical Physics. The influence of this work is wide-ranging: it increases our ability to simulate quantum systems in realistic situations and thus enhances our ability to make predictions about physical systems, potentially as different as high-temperature superconductivity (how the environment impacts the transition temperature, for instance) and DNA sequencing with nanoscale electrodes (see above). This work thus supports the strategic thrust of science-based prediction, as well as provides a computational basis for further investigation into threat reduction, complex systems, and materials.

**Dynamics and Decoherence of Open Quantum Systems**
Working with Laboratory Fellow Wojciech Zurek and fellow postdoctoral scholar Haitao Quan, Zwolak investigated how the environment acquires information about a quantum system. This is related to the project described above on simulating open systems, but approaches the issue from a very different perspective. They derived a number analytic results regarding how information spreads into an environment, as well as developed an efficient numerical technique to exactly simulate the dynamics of 100's of spin-1/2 qubits, i.e., it is a technique that drops the exponential cost of simulating a quantum system down to a polynomial cost in the number of spins for systems symmetrically coupled to their environment. They are currently completing this research. This work is increasing our understanding of how complex materials behave at the nanoscale and is relevant to our ability to control quantum systems. It thus supports the LANL mission of gaining a fundamental understanding of materials.

This LDRD project ended after eleven months when Dr. Zwolak was named to a Feynman Fellow position, which will be a new LDRD project.

## Impact on National Missions
Dr. Zwolak's research is very important to obtaining a fundamental understanding of the behavior of complex physical systems. In particular, it addresses how quantum systems evolve when in the presence of their environment, which is a situation that has to be accounted for in order to understand virtually any material or device. In addition to obtaining a theoretical understanding of this behavior, it also addresses how to construct efficient simulation techniques to tackle very complex physical systems where many interacting components of a physical system are also interacting or being driven by their environment. More specific examples are given below under accomplishments.

My work in the biophysical arena is helping us comprehend how nanoscale devices detect molecules and physical processes. The successful fabrication and implementation of the sensors I study will revolutionize how we approach sensing at the nanoscale, e.g., in threat detection, and bring novel technologies into the medical/biological communities.

Further, this project has supported the DOE mission in Scientific Discovery & Innovation and Energy Security by enhancing our understanding of nanoscale electronics, molecular detection, and using simulations for science-based prediction. It is important to other missions of the Laboratory as well, e.g., Homeland Security and Threat Reduction.

## References

1. Zwolak, M.. Finite representations of continuum environments. 2008. *Journal of Chemical Physics.* **129**: 101101.

2. Zwolak, M., and M. Di Ventra. Colloquium: Physical approaches to DNA sequencing and detection. 2008. *Reviews of Modern Physics.* **80**: 141.


## Publications

Zwolak, M.. Finite representations of continuum environments. 2008. *Journal of Chemical Physics.* **129**: 101101.

Zwolak, M., and M. Di Ventra. Colloquium: Physical approaches to DNA sequencing and detection. 2008. *Reviews of Modern Physics.* **80**: 141.

# Detecting the Highest Energy Gamma-Rays and Neutrinos to Determine the Origin of Cosmic Rays

*Brenda L. Dingus*
20070658PRD2

## Abstract
Milagro was a LANL-led experiment to provide a view of the most energetic processes in the universe: the acceleration of cosmic radiation. Milagro observed cosmic rays and gamma rays from all across the universe and this project contributed to three significant results. First, we identified new sources of high-energy gamma rays. Second, we measured diffuse emission from the Galactic plane. Finally, we discovered two unexpected regions of excess cosmic rays, which defy explanation and could point to the source of cosmic radiation.

## Background and Research Objectives
This project aimed to address the question of what the source of cosmic rays is. This is an old question dating back almost 100 years when cosmic radiation was first discovered. Cosmic rays are energetic particles (protons, helium and other nuclei) that we observe at Earth. Since these particles are charged, they bend and twist in magnetic fields and when they finally arrive at Earth from their sources, they no longer point back to their origin.

When these cosmic rays finally reach Earth, they interact high in the atmosphere and produce a cascade of secondary particles. The original cosmic ray will produce a few high-energy particles that will themselves produce more high-energy particles. This process continues until all the energy is used up but by then we have millions of particles. We call this cascade of particles an extensive air shower (EAS). These particles eventually reach the ground and that is where our experiment comes in. Our experiment, Milagro, can detect an EAS by looking for high-energy particles reaching the ground all at the same time. When that happens we can use the time of each particle arrival and determine where the original particle came from.

Milagro detects these high-energy cosmic rays but, because they are randomized in the Galactic magnetic field, we cannot assume that the direction they come from is the direction of their source. However, in addition to the cosmic rays that Milagro sees, we also see gamma-rays. These particles produce an EAS when they reach earth, but they are much more rare. Gamma-rays are important, though, because they are neutral. Being neutral, they are unaffected by the magnetic fields in our galaxy and when they reach us we can identify astrophysical objects that they come from. Even though we want to identify the source of cosmic rays, it is often more useful to look for gamma-rays since we can tell where they come from and since we expect a source of high-energy cosmic rays to also be a source for high-energy gamma rays.

The objectives of this LDRD project were to identify the best potential sources for cosmic radiation by searching through the full Milagro dataset for gamma-ray sources. Milagro is unique because it observes the entire overhead sky every day and it is the perfect instrument to discover new sources. We focused on the algorithms to distinguish gamma rays from cosmic rays as well as algorithms and techniques to determine how high in energy the gamma ray emission extends.

## Scientific Approach and Accomplishments
This work utilizes the Milagro extensive air shower array. Milagro consists of a water pond about the size of a football field. This water pond contains more than 700 detectors, called photomultiplier tubes or PMTs, capable of measuring single photons of light. By carefully determining the time each of these PMTs sees light, we can determine where EASs are coming from. Some of the PMTs are located deep in the water in order to assist in determining whether a particular EAS was caused by a gamma ray or a cosmic ray. An EAS due to a cosmic ray tends to produce larger signals in these deep PMTs and we look for these large signals to identify cosmic ray events.

This LDRD project includes three major scientific accomplishments, each published in peer-reviewed journals and each of which contributes to the question of the origin of cosmic rays.

The first result is our identification of new gamma-ray sources. The way this works is that for each EAS that Milagro detects, we determine where it was coming

from, what time the event occurred, how many PMTs were hit and how hard the deep PMTs were hit. We take this information and trace back to see what was in the sky at that location at that time. After doing our best to determine whether the event was likely a gamma ray or a cosmic ray, we make a make a map of the sky showing all the gamma-ray events. Figure 1 shows this map along the plane of the Galaxy. The colored areas show regions where we detect gamma rays more significantly. The figure includes purple dots overlaid at the location of known lower-energy sources detected by the Fermi Large Area Telescope. By comparing the list of known sources to the Milagro data we can identify which sources are likely to be producing the gamma rays that we are seeing. In this way we have identified 14 sources which each produce a significant number of gamma-rays in Milagro. Of these 14 sources, 9 had never before been detected at our energies. It is possible that these sources are not cosmic-ray sources but they are good candidates and are being followed up by other instruments.

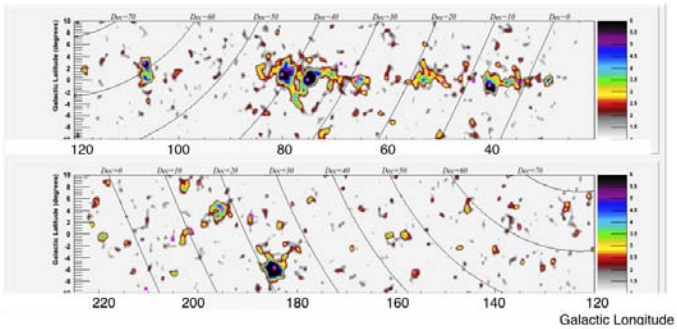


*Figure 1. This figure shows the Milagro view of the sky along the Galactic plane. The colors indicate how significantly the regions are detected in high-energy gamma rays. The purple points indicate the location of lower-energy sources detected by the Fermi Large Area Telescope. In addition to the discrete sources, a haze of diffuse emission can be seen along the whole plane.*

The second result can also be seen in Figure 1. Besides the isolated, discrete sources of gamma rays, there is a 'haze' of emission from the Galactic plane. This is the first time that this diffuse emission has been observed by an experiment at Milagro energies. This diffuse emission is due to two main sources. First, there are sources that we have not yet identified, but are dim. If there are enough of these such sources they can add up and look like a diffuse cloud of emission. Second, when a cosmic ray – by random chance – doesn't make it to Earth but happens to interact elsewhere in the Galaxy, we can observe gamma rays at Earth produced in this interaction. Since it is random where these gamma-rays interact we just see a cloud of excess gamma-rays along the Galactic plane. Determining how much of the diffuse emission that Milagro observes is due to these two mechanisms is a task for later experiments, but the measurements that we have serve as an important probe of how much cosmic radiation there is elsewhere in the Galaxy.

The first two results are made by looking for gamma rays and trying to exclude cosmic rays. The third result is shown in Figure 2 and is a map of the sky where we turn the analysis on its head and look for regions of cosmic radiation. Doing so, we isolated two well-localized regions of cosmic radiation, near the Orion constellation. Up to this point, scientists believed the cosmic rays to be arriving at Earth very uniformly without small-scale structure, but these results prove differently. Since these results are new and unexpected, there are not yet any compelling explanations. The most tantalizing suggestion is that Milagro is seeing cosmic rays from a nearby cosmic ray source. Until recently, we have believed that even a nearby cosmic ray source would not produce this data, so we have called into question our understanding of how cosmic rays propagate through the magnetic field of the Galaxy.

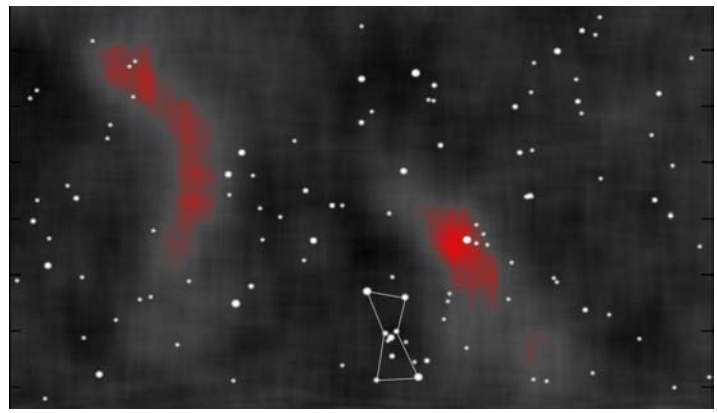

*Figure 2. This figure shows two regions of excess cosmic rays measured by Milagro. The red color indicates the regions that are observed. For reference, the nearby stars are shown in white with the constellation Orion indicated.*

## Impact on National Missions

Gamma-ray Astrophysics is a forefront area of research as evidenced by multiple National Academy studies and investments by NASA, NSF, and DOE in GLAST, VERITAS, Milagro, and now HAWC observatories. This field addresses LANL's Grand Challenge to study physics beyond the standard model. LANL led the Milagro collaboration and LANL staff member Brenda Dingus is the co-spokesperson for HAWC and the project manager.

With Milagro, LANL has clearly established itself as a leader in the field of VHE astrophysics. The work on Milagro has led to the development of the High Altitude Water Cherenkov experiment, HAWC, and LANL is in an excellent position for future NSF and/or DOE funding. The National Science Foundation has established a $1M MRI (Major Research Initiative) to perform the R&D required to eliminate the technical risk associated with the HAWC detector concept and to establish a small test array at the HAWC site (Sierra Negra, Mexico).

## Publications

Abdo, A.. Discovery of localized regions of excess 10-TeV cosmic rays. 2008. *Physical Review Letters.* **101** (22): 221101.

Abdo, A.. Milagro Observations of Multi-TeV Emission from Galactic Sources in the Fermi Bright Source List. 2009. *Astrophysical Journal Letters.* **700**: 127.

Abdo, A.. A Measurement of the Spatial Distribution of Diffuse TeV Gamma-Ray Emission from the Galactic Plane with Milagro. 2008. *Astrophysical Journal.* **6888**: 1078.

# Anti-Neutrino Oscillation and Cross Section Measurements at MiniBooNE

*Geoffrey B. Mills*
20070701PRD3

## Abstract

Sam Zeller has made significant accomplishments during her two year appointment as a LANL Director's-funded Postdoctoral Fellow. As the MiniBooNE analysis coordinator and the leader of the MiniBooNE Cross Section Group, Sam oversaw the publication of eleven papers, including seven in Physical Review Letters, two in Physical Review, one in Physics Letters, and one in Nuclear Instruments and Methods. Thanks to her efforts, MiniBooNE has made the world's best neutrino and antineutrino cross section measurements at the 1 GeV energy scale and the world's best neutrino and antineutrino oscillation searches at the 1 $eV^2$ mass scale. MiniBooNE has also observed an unexplained excess of electron-like events at low energies but, so far, has not observed any low-energy excess in antineutrino mode. These results may be due to CP or CPT-violating neutrino oscillations involving sterile neutrinos. This work is of great importance to future long-baseline neutrino oscillation experiments, which will search for a difference between neutrino and antineutrino oscillations.

## Background and Research Objectives

The MiniBooNE experiment at Fermilab was designed to test the evidence for neutrino oscillations coming from the LSND experiment at Los Alamos. After several years of running in neutrino mode, MiniBooNE observed an unexplained excess of low-energy events that could be due either to an unexpected neutral-current background process or to neutrino oscillations involving sterile neutrinos. In order to check whether there are antineutrino oscillations (as observed by LSND), MiniBooNE switched to antineutrino running approximately three years ago. The objectives of the antineutrino data taking were to measure antineutrino cross sections, search for antineutrino oscillations, and search for a difference between neutrino and antineutrino oscillations. A difference between neutrino and antineutrino oscillations would be especially interesting because it would imply either CP or CPT violation, where C is charge conjugation, P is parity inversion, and T is time reversal. New sources of either CP or CPT violation could possibly help explain the baryon asymmetry of the universe.

## Scientific Approach and Accomplishments

Sam Zeller devoted her Director's-funded postdoctoral Fellowship to measuring neutrino and antineutrino cross sections, searching for neutrino and antineutrino oscillations, and searching for a difference between neutrino and antineutrino oscillations. As the MiniBooNE analysis coordinator and the leader of the MiniBooNE Cross Section Group, Sam oversaw the publication of eleven MiniBooNE papers, including seven in Physical Review Letters, two in Physical Review, one in Physics Letters, and one in Nuclear Instruments and Methods. (Note that she is not one of the first authors because the MiniBooNE authors are listed in alphabetical order.) Thanks to her efforts, MiniBooNE has made the world's best neutrino and antineutrino cross section measurements at the 1 GeV energy scale and the world's best neutrino and antineutrino oscillation searches at the 1 $eV^2$ mass scale. MiniBooNE has also observed an unexplained excess of electron-like events at low energies but, so far, has not observed any low-energy excess in antineutrino mode. In addition, at present, the antineutrino oscillation results are consistent with what is expected from the LSND oscillation signal. These results may possibly be due to CP or CPT-violating neutrino oscillations involving sterile neutrinos.

## Impact on National Missions

This project has great relevance to the Laboratory's missions in Nuclear Physics and High Energy Physics research and, in particular, to future long-baseline neutrino oscillation experiments, which will search for electron-neutrino and antielectron-neutrino appearance and a difference between neutrino and antineutrino

oscillations. Due partly to this project, LANL has begun working on the near detector complex of the Long Baseline Neutrino Experiment (LBNE), which involves building a neutrino beam at Fermilab that will point to an underground detector over 1000 km away.

## Publications


Adamsonetal., P. D.. Measurement of numu and nue events in an off-axis horn-focused neutrino beam. 2009. *Physical Review Letters.* **102**: 211801.

Aguilar-Arevaloetal., A. A.. Search for electron antineutrino appearance at the delta m**2 ~ 1 eV**2 scale. 2009. *Physical Review Letters.* **103**: 11180.

Aguilar-Arevaloetal., A. A.. Measurement of the ratio of the numu charged-current single-pion production to quasielastic scattering with a 0.8 GeV neutrino beam on mineral oil. 2009. *Physical Review Letters.* **103**: 081801.

Aguilar-Arevaloetal., A. A.. Search for muon neutrino and antineutrino disappearance with MiniBooNE. 2009. *Physical Review Letters.* **103**: 061802.

Aguilar-Arevaloetal., A. A.. Neutrino flux prediction at MiniBooNE. 2009. *Physical Review D.* **79**: 072002.

Aguilar-Arevaloetal., A. A.. Unexplained excess of electronlike events from a 1-GeV neutrino beam. 2009. *Physical Review Letters.* **102**: 101802.

Aguilar-Arevaloetal., A. A.. The MiniBooNE Detector. 2009. *Nuclear Instruments and Methods A.* **559**: 28.

Aguilar-Arevaloetal., A. A.. Compatibility of high-delta m**2 nue and nuebar neutrino oscillation searches. 2008. *Physical Review D.* **78**: 012007.

Aguilar-Arevaloetal., A. A.. First observation of coherent pi0 production in neutrino nucleus interactions with neutrino energy <2 GeV. 2008. *Physics Letters B.* **664**: 41.

Aguilar-Arevaloetal., A. A.. Measurement of muon neutrino quasi-elastic scattering on carbon. 2008. *Physical Review Letters.* **100**: 032301.

Aguilar-Arevaloetal., A. A.. Search for electron neutrino appearance at the delta m**2 ~ 1 eV**2 scale. 2007. *Physical Review Letters.* **98**: 231801.

# Phase Transitions in Quantum Systems and Quantum Information

*Wojciech H. Zurek*
20070705PRD3

## Abstract

The development of quantum information science has fertilized modern statistical and condensed matter physics. In this project, by using techniques from quantum information processing, we made contributions to the theoretical understanding of quantum phase transitions in various complex systems, ranging from quantum magnetic materials to unconventional superconductors. We also studied the non-equilibrium dynamics of quantum phase transitions and their important applications in quantum information processing, such as the control of decoherence and the optimization of operation time in quantum computing. In addition, we studied the quantum-classical transition from the perspective of information transfer. These studies are not only of fundamental interests to basic science, but also of great importance to the LANL and DOE missions.

## Background and Research Objectives

Quantum phase transitions [1] happen at a temperature of absolute zero and are triggered by a change in parameters of the system's Hamiltonian. An experimentally observed case is the superfluid-insulator phase transition of ultra-cold atoms in optical lattices – laser induced egg carton-like traps [2]. Different from the usual phase transitions triggered by a change of the temperature, such as the melting of the ice, a quantum phase transition can occur without symmetry breaking. Thus the Landau theory, which deals with the second order classical phase transitions by making use of the local order parameter and symmetry breaking [3], does not apply. Therefore, the search of a comprehensive characterization of quantum phase transitions in various systems has become one of the most challenging issues in physics. In this project, one of our main objectives was to develop novel approaches to quantum phase transitions by borrowing new techniques developed by progresses in quantum information technology. Two concepts in particular – fidelity [4] and decoherence [5]– can be utilized to characterize quantum critical phenomena with "intrinsic" and "external" dynamics, respectively. Our first main goal was to understand and characterize the phase transitions in quantum systems from the perspective of quantum information.

Another interesting recent research direction is the dynamics of quantum phase transitions. When a quantum system is driven through a quantum critical point (quenching), non-equilibrium effects will arise. This non-equilibrium transition can lead to the creation of topological defects [6], an analog of the domain walls generation after quenching a high-temperature metal. This spectacular phenomenon is closely related to implementing a non-standard quantum computation algorithm, known as adiabatic quantum computation [7]. By utilizing the quantum superposition principle, quantum computers are expected much more powerful than the current electronic or classical computer. When we implement these theoretical quantum computing algorithms into real physical systems (the hardware), we face many problems, such as the influence of the noise of the environment and the stability of the operation. How to evaluate various implementations and strategies of adiabatic quantum computing [8] by utilizing the results from the studies of dynamics of quantum phase transitions? This was the second main objective of this project. In addition, our research objectives also included understanding how the classical world emerges from the ultimate quantum substrate from the perspective of information transfer.

## Scientific Approach and Accomplishments

In the past two years, Dr. Quan has worked on the following topics, which center around the above research objectives, and has produced several papers.

**Decoherence, quench dynamics, and adiabatic quantum computation**

Quantum decoherence (or loss of quantum coherence of a quantum system) is the key to how the classical world emerges from underlining quantum mechanics (i.e., the quantum-to-classical transition) [5]. Thus, its understanding is essential for creation of devices that require long-time quantum coherence (e.g., quantum computers). We studied the dynamics of decoherence of a system under a new environment – when its environment is driven across a quantum phase transition. The quantum Ising model in the transverse field serves as the environment and the central spin represents the decoherencing system. We found that as the environment is driven through the critical point, the decoherence factor of a single spin undergoes rapid decay. The rate of decay is related to the critical exponent of a phase transition that encodes critical exponents. In addition to the numerical effort, we also derived a simple analytical expression that describes the post-transition decoherence. This research connected the theory of decoherence with quantum phase transitions and non-equilibrium dynamics, and brought important insights to the control of decoherence.

A related problem was about the quench dynamics in a complex system and the adiabatic quantum computation. To implement this kind of quantum computation algorithm, it is essential that the system maintain in their lowest energy state when it evolves. However, there is no effective method to ensure that the system remains in its ground state. We proposed an echo quench method to solve this problem. We studied the implementing of the adiabatic quantum computing [8] algorithm, and evaluate various implementations and strategies of adiabatic quantum computing by utilizing the results from the studies of dynamics of quantum phase transitions. We obtained the exact relation between the upper limit of the operation speed and the size of the quantum computer. Our numerical simulation results agreed with the analytical results. This study promised important application in future implementation of quantum computers.

**Quantum-classical transition from the perspective of information transfer**

Quantum mechanics is extremely successful in all practical applications, but this theory cannot be reconciled with our everyday experience about the physical world. This is the so-called “quantum-to-classical” transition problem [5]. We developed a novel approach to understand how the classical world emerges from quantum mechanics. We studied this famous old problem from the perspective of information transfer between quantum systems. In this approach, the information about the system was selectively proliferated into its environment. As a result, the classical world emerges from the quantum substrate through a selection mechanism similar to the Darwinism (survival of the fittest) in biology. In our study [9], we performed large-scale numerical simulations. Different analytical approaches were developed and numerically verified. From the numerical result, we found that the environment, such as the sun light, acts as a communication channel. Even a hazy environment, which is a noisy communication channel, supports this quantum Darwinism mechanism. This study not only shed new light on the understanding of the fundamental aspects of quantum mechanics, i.e., the way in which classical reality of our everyday experience arises within our quantum universe, but also brought important insights to the comprehension of the deep and intrinsic relation between information and physics.

**A novel quantum-information-theoretical approach to quantum phase transitions**

Quantum fidelity is a tool used in quantum information science to evaluate errors of quantum computing. It has a geometric nature. Dr. Quan and his collaborators borrowed this tool and used it to study quantum phase transitions in different materials [4]. In the last two years, Dr. Quan and his collaborators further generalized fidelity approach to study the thermal phase transition, which is induced by a change of the temperature such as the melting of the ice [10]. As examples, they studied phase transitions in both magnetic materials and composite systems of strong radiation-atom interaction. Both the analytical and numerical results verified the validity of fidelity as a useful tool to characterize both quantum and thermal phase transitions. They further established the connection between the fidelity and traditional criteria for thermal phase transitions, such as susceptibility and specific heat. This exploration connected disparate fields: information theory and statistical mechanics, hence has profound impact to our understanding of the nature of phase transitions and the quantum to classical transition of the system.

Another problem [11] that Dr. Quan worked on is about footprints of quantum phase transitions at finite temperature. Since absolute zero can never be achieved experimentally, to understand the quantum critical conundrum, it is essential to study the consequences or footprints of a quantum phase transition at finite temperature. Motivated by the theory of quantum-classical mapping in statistical mechanics, Dr. Quan found a finite-temperature scaling behavior of magnetic susceptibility of 1D quantum Ising chain. Both the analytical and the numerical results confirmed this

scaling behavior. He also revealed the relation between the magnetic susceptibility and geometric phase factor, a genuine quantum observable. This study revealed the profound influences of quantum phase transitions to the properties of the system at nonzero temperature and opened the possibility of observing the quantum criticality experimentally.

**Novel quantum phases and quantum phase transitions in superconducting material**

One of the most fascinating aspects of the quantum-many-body system is the superconducting state of metals or compounds under extreme conditions, such as the extreme low temperature or the extreme high pressure. In these materials electric current can flow without resistance. In the family of superconductors, there is an inhomogeneous state, called Fulde-Ferrell state [12], which was first theoretically predicted more than forty years ago, but has never been observed in experiments convincingly. Probably its instability is due to its stringent conditions for such a state to exist stably. With his collaborator Dr. Quan studied this problem from the first principles [13]. In order to realize a stable Fulde-Ferrell state, they designed theoretically a metal material with different geometries, and imposed them into extreme conditions, such as strong magnetic fields. By solving numerically the microscopic theoretical model, they obtained different phases and the phase boundaries of such materials. The intriguing point is that they found a stable Fulde-Ferrell phase in the ring geometry in the presence of an external magnetic flux. The predicted stable Fulde-Ferrell phase could be observed in experiments of cold atoms. They also studied the magnetic flux periodicity in a hollow unconventional (d-wave) superconducting cylinder [14]. Their analytical calculations and numerical simulations revealed that the flux periodicity in the supercurrent is sensitive to the detailed electronic band structure and electron density, which successfully explained a recent experiment. These studies not only promoted our understanding of the properties of the nonconventional superconducting state, but also brought important insights to the adaptive design of other advanced materials.

## Impact on National Missions

The novel approaches to quantum phase transitions from quantum information will provide conventional statistical physics and condensed matter theory with deep insights into fundamental problems, and shed new light on developing advanced material, which is definitely critical to DOE missions. Understanding the dynamics of quantum phase transitions is of fundamental interest; applications range from low temperature and condensed matter physics to cosmology. Most importantly for LANL's strategic priorities, a thorough understanding of dynamics of quantum phase transitions is necessary for making quantum computers.

## References


Sachdev, S.. Quantum Phase Transition. 1999.

Greiner, M., O. Mandel, T. Esslinger, T. W. Hansch, and I. Bloch. Quantum phase transition from a superfluid to a Mott-insulator in a gas of ultracold atoms. 2002. *Nature.* **415**: 39.

Landau, L. D., and E. M. Lifshitz. Statistical Physics. 1980.

Zanardi, P., H. T. Quan, X. G. Wang, and C. P. Sun. Mixed-state fidelity and quantum criticality at finite temperature. 2007. *Physical Review A.* **75**: 032109.

Zurek, W. H.. Decoherence and the Transition from the Quantum to the Classical. 1991. *Physics Today.* **44** (10): 36.

Zurek, W. H., U. Dorner, and P. Zoller. Dynamics of a quantum phase transition. 2005. *Physical Review Lettetters.* **95** (10): 105701.

Nielsen, M. A., and I. L. Chuang. Quantum Computation and Quantum Information. 2000.

Farhi, E., J. Goldstone, S. Gutmann, J. Lapan, A. Lundgren, and D. Preda. A quantum adiabatic evolution algorithm applied to random instances of an NP- complete problem. 2001. *Science.* **292**: 472.

Zwolak, M., H. T. Quan, and W. H. Zurek. Quantum Darwinism in a mixed environment. 2009. *Physical Review Lettetters.* **103** (11): 110402.

Quan, H. T., and F. M. Cucchietti. Quantum fidelity and thermal phase transitions. 2009. *Physical Review E.* **79** (3): 031101.

Quan, H. T.. Finite-temperature scaling of magnetic susceptibility and the geometric phase in the XY spin chain. 2009. *Journal of Physics A: Mathematical and Theoretical.* **42**: 395002.

Fulde, P., and A. Ferrell. Superconductivity in a strong spin-exchange field. 1964. *Physical Reivew.* **135**: A550.

Quan, H. T., and J. X. Zhu. Interplay between the Fulde-Ferrell phase and Larkin-Ovchinnikov phase in the superconducting ring pierced by an Aharonov-Bohm flux. To appear in *Physical Review B.*

Zhu, J. X., and H. T. Quan. Magnetic flux periodicity in a hollow d-wave superconducting cylinder. *Physical Review B.*

## Publications

Quan, H. T.. Finite-temperature scaling of magnetic susceptibility in XY spin chain. 2009. *Journal of Physics A: Mathematical and Theoretical.* **42**: 395002.

Quan, H. T.. Quantum thermodynamic cycles and quantum heat engines (II). 2009. *Physical Review E.* **79**: 041129.

Quan, H. T., S. Yang, and C. P. Sun. Microscopic work distribution of small system in quantum isothermal process. 2008. *Physical Review E.* **78**: 021116.

Quan, H. T., and F. M. Cucchietti. Quantum fidelity and thermal phase transition. 2009. *Physical Review E.* **79**: 031101.

Quan, H. T., and J. X. Zhu. Interplay between the Fulde-Ferrell phase and Larkin-Ovchinnikov phase in the superconducting ring pierced by an Aharonov-Bohm flux. *Physical Review B.*

Zhu, J. X., and H. T. Quan. Magnetic flux periodicity in a hollow d-wave superconducting cylinder. *Physical Review B.*

Zwolak, M., H. T. Quan, and W. H. Zurek. Quantum Darwinism in a mixed environment. 2009. *Physical Review Letters.* **103**: 110402.

# The Dynamics of Dark Energy

*Katrin Heitmann*
20070775PRD4

## Abstract

Dark energy is one of the central topics of research in cosmology today. Type Ia supernovae provided the first evidence for its existence: In the late nineties it was found that distant supernovae appear fainter than expected, implying that the expansion of the universe is accelerated. In a matter-dominated universe, objects attempt to gravitate towards each other, and the expansion rate decreases with time. Thus the observations imply that some sort of energy other than matter is dominant at present – this is the "dark energy."

Only now is reliable data on the total energy density of the universe (obtained from the ages of clusters of galaxies) becoming available. Combined with probes of the matter density, this can directly constrain the dark energy density – potentially more powerful than supernovae, which measure only the integration of the energy density. Probes of the mass distribution such as baryon acoustic oscillations provide another effective data dimension, which has been exploited in this project.

This one-year project covered some specific aspects of the theory and observations of dark energy. It focused on the reconstruction of cosmological matter perturbations from diverse cosmological probes. Such a reconstruction program enables the distinction between different models of dark energy. Both currently available data and simulated data have been investigated in this project.

## Background and Research Objectives

Over the last decade, observations of Type Ia supernovae have shown that the expansion of the universe is currently accelerating. This remarkable discovery has led cosmologists to hypothesize the presence of dark energy, a negative pressure energy component that dominates the energy content of the universe at present. Many theories have been propounded to explain this phenomenon, the simplest of which is the cosmological constant, with a constant energy density and the equation of state w=-1. Although the cosmological constant appears to explain all current observations satisfactorily, to do so its value must necessarily be very small. So, it represents a new small constant of nature in addition to those known from elementary particle physics, many of them very small if expressed in the Planck units. However, since it is not known at present how to derive the cosmological constant from these small constants and it is also unclear if dark energy is in fact time independent, other phenomenological explanations for cosmic acceleration have been suggested. These are based either on the introduction of new physical fields (quintessence models, Chaplygin gas, etc.), or on modifying the laws of gravity and therefore the geometry of the universe (scalar-tensor gravity, f(R) gravity, higher dimensional `Braneworld' models, etc). The plethora of competing dark energy models has led to the development of parametric and non-parametric methods as a means of obtaining model independent information about the nature of dark energy directly from observations.

The next decade will see the emergence of many new cosmological probes. A large number of these are likely to make important contributions to the field of dark energy. The Sloan Digital Sky Survey began its stage III observations in 2008, and its Baryon Oscillation Spectroscopic Survey (BOSS) is expected to map the spatial distribution of luminous galaxies and quasars and detect the characteristic scale imprinted by baryon acoustic oscillations in the early universe. The Joint Dark Energy Mission (JDEM) is expected to discover a large number of supernovae, and also provide important data on weak lensing and baryon acoustic oscillations. The Square Kilometer Array (SKA) will map out over a billion galaxies to redshift of about 1.5, and is expected to determine the power spectrum of dark matter fluctuations as well as its growth as a function of cosmic

epoch. Important clues to the growth of structure will also come from current and future weak lensing surveys, galaxy redshift-space distortions as well as galaxy cluster mass functions at different redshifts. With the wealth of data expected to arrive over the next several years, it is important to explore different methods of analyzing these datasets in order to extract the optimum amount of information from them.

The objective of this project was to develop a new method that would enable the distinction between different dark energy models. Such a method has to be tested on simulated data and its sensitivity to different dark energy models has to be explored. Once it is confirmed that the new approach is working, it has to be applied to real data. The objectives in the project have been successfully completed.

## Scientific Approach and Accomplishments

In this project, a new method has been developed to reconstruct cosmological matter perturbations and therefore to distinguish imprints of different dark energy models. More specifically, the method is based on reconstructing the linearized growth of density perturbations in the non-relativistic matter that makes up galaxies and clusters of galaxies.

In the case of physical dark energy, the effective gravitational constant appearing in the equation for linear density perturbations in this matter coincides with the Newton gravitational constant measured in the laboratory and using Solar system tests. If, additionally, there is no direct non-gravitational interaction between dark energy and dark matter, the density contrast reconstructed in this manner should match that determined directly from observations of large scale structure. In this case the methods developed in this project will provide an important consistency check on dark energy models. On the other hand, geometrical models of dark energy (braneworlds, scalar-tensor gravity, etc.) usually predict a different growth rate from that in general relativity. Models where dark energy has a direct non-gravitational interaction with dark matter, or where dark energy and dark matter are unified, have a similar property even in the framework of GR. In this case, a reconstruction of the linearized density contrast from observations will not match with the density contrast determined directly from large-scale structure probes. Therefore, the method developed during this project will help address important issues concerning the nature of dark energy and gravity. The new method is model independent and unbiased.

The project proceeded in three steps:

1. Development of the reconstruction method for cosmological matter perturbations; technical details on this can be found in Ref. [1].

2. Application to simulated data to verify the correct implementation of the method and to gauge how well the method will work on high-quality data expected from future surveys.

3. Apply the new methodology to currently available data.

Figure 1 shows the results for the reconstruction of the growth rate for a modified gravity model. Here, data of JDEM quality has been simulated. The black dotted line shows the results from the reconstruction based on probes that measure the expansion history of the universe (such as supernovae), the green dashed line shows results for the reconstruction from gravitational clustering (such as weak lensing). For a cosmological constant model, both lines would have fallen on top of each other. The new method developed in this project therefore provides a successful new method to distinguish between different models for the accelerated expansion of the universe.

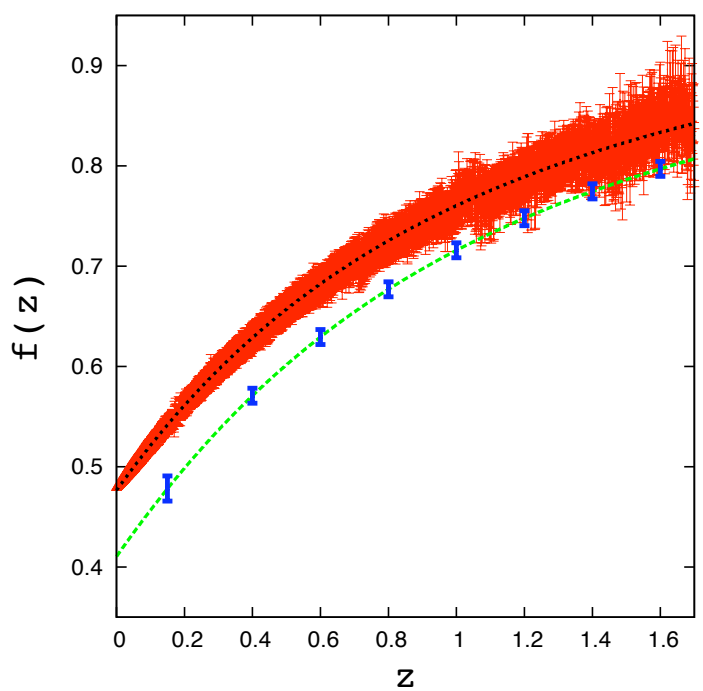


*Figure 1. Reconstructed growth rate for a JDEM-like dataset using a modified gravity model. The thick black dotted line represents the result expected from just the expansion history, while the green dashed line represents the result expected from gravitational clustering. The discrepancy between the two would act as a signal for modified gravity.*

Figure 2 shows the reconstructed growth rate for currently available supernova data and large-scale

structure measurements. Currently, the error bars in these measurements are too large to distinguish between different explanations for the accelerated expansion and the results are consistent with the simplest model, a cosmological constant.

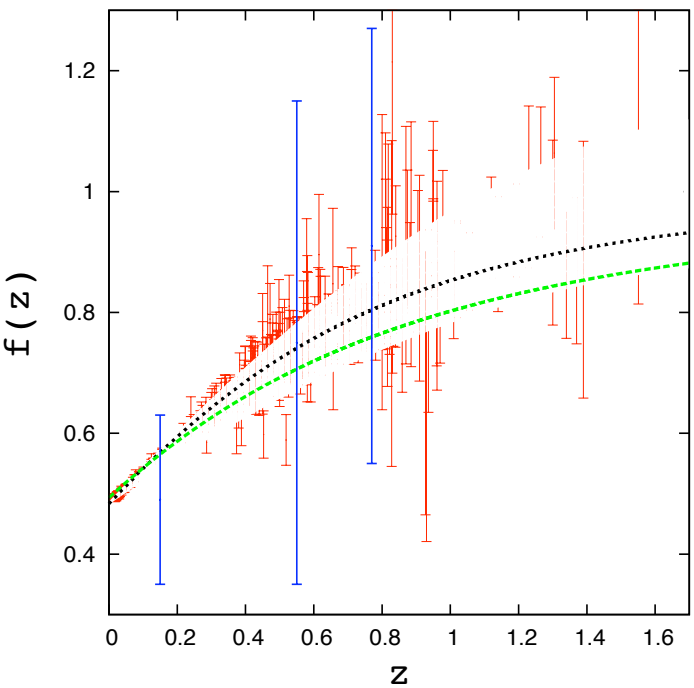


*Figure 2. Reconstructed growth rate for a current set of supernova data. The red solid lines show the 1 sigma limits for reconstructed growth parameter using the integral reconstruction method, while the green dashed shaded area shows the 1 sigma limits for the parameter using a smoothing scheme for the integral reconstruction method. The black dotted line shows the growth rate for a cosmological constant model, the green dashed line shows the growth rate for a model with variable dark energy equation of state. The three vertical blue lines show the current measurements of the growth rate from current large-scale structure probes.*

## Impact on National Missions

The project targets one of the top DOE priorities, understanding the nature of dark energy. New methods to extract information from complex data sets have been developed and reconstruction methods. Such methods have general applicability to a large variety of different data sets.

## References


1. Alam, U., V. Sahni, and A. Starobinsky. Reconstructing cosmological matter perturbations using standard candles and rulers. 2009. *The Astrophysical Journal.* **704**: 1086.


## Publications


Alam, U., S. Sahni, and S. Starobinsky. Reconstructing cosmological matter perturbations using standard candles and rulers. 2009. *The Astrophysical Journal.* **704**: 1086.

# Strong Dynamics in Physics Beyond the Standard Model

*Rajan Gupta*
20080698PRD1

## Abstract
The Standard Model of elementary particles is extremely successful experimentally, but we still do not have any experimental confirmation of the Higgs boson. Moreover, there are theoretical reasons for expecting that the Higgs boson of the Standard Model is incomplete; that is, that they are new degrees of freedom at the TeV scale that will complete the theory of Nature into a more complete and compelling form.

## Background and Research Objectives
A strong theoretical motivation for the Higgs boson comes from considering the scattering amplitude of WW gauge bosons. In the Standard Model without the Higgs boson, this amplitude grows with energy and eventually becomes non-perturbative. With the Higgs boson, or its supersymmetric incarnations, added to the theory, the scattering amplitude does not grow uncontrollably, and perturbative unitarity is maintained. There are however, competing theories for the Higgs boson, in addition to supersymmetry. These are Higgsless models [1,2], or models in which the Higgs boson is composite [3].

This project explored the phenomenological implications of these, and other scenarios in which new composite degrees of freedom occur at the TeV scale. What are some of their phenomenological signatures? What are examples of non-supersymmetric, conformal theories? For the latter question, the only tool that we have to use is the lattice.

## Scientific Approach and Accomplishments
In [3], Kurachi, with LANL scientists Graesser and Kitano, construct an effective field theory for supersymmetry broken close to the TeV scale under the following additional working assumptions: i) the effective theory has supersymmetry realized non-linearly; ii) the particles of the Standard Model – quarks, leptons and gauge bosons – are weakly coupled to the sector that breaks supersymmetry; and iii) there might be additional light particles that are composites out of the sector that breaks supersymmetry.

They show that by using their formalism it is possible to write down operators coupling the Standard Model particles (+ superpartners) to the light composites, in a manifestly supersymmetric manner. This is a non-trivial result since the composites will not appear in complete susy representations, in general.

The authors then discuss two scenarios for the light composites: i) the Higgs boson is composite; and ii) both the Higgs boson and a spin-2 particle (massive "graviton") are composite.

They show: i) that only one Higgs boson is needed to give mass to both up and down-type quarks; ii) that a spin-2 particle can partially unitarize the goldstino-goldstino scattering channel; and iii) this spin-2 particle can be produced at the LHC with a large enough rate to make discovery possible. The first result i) is new and explicitly disproves the standard lore that two Higgs doublets are needed if supersymmetry is realized non-linearly. In short, the experimental signatures of this scenario are novel: the LHC will discover superpartners to all the SM particles, except the Higgs boson; the Higgs boson is composite, as in [4]; and here the discovery of a spin-2 resonance is interpreted as due to strong supersymmetric dynamics at the TeV scale, rather than the more conventional interpretation of it being the first resonance of an extra dimension.

In [5], Kurachi and external collaborators propose a new nonperturbative scheme for the running coupling on the lattice using Wilson loops. They performed a successful test of their proposal against known theoretical calculations. In [6], Kurachi and his collaborators present a non-perturbative study of the running coupling constant in the Twisted Polyakov Loop scheme. They investigate how the systematic and statistical errors can be controlled via a feasibility study in SU(3) pure Yang-

Mills theory. In addition, they show that their method reproduces the perturbative determination of the running coupling in the UV. They also present preliminary results for $N_f$=12 flavor QCD, where an IR fixed point may be present.

Finally, in [7], Kurachi and collaborators continue their phenomenological studies of the three-site model, which has been offered as a benchmark for studying the collider phenomenology of Higgsless models [1]. In this paper they analyze how well the three-site model performs as a general exemplar of Higgsless models in describing $W_L$ $W_L$ scattering, and which modifications can make it more representative. They demonstrate that $W_L$ $W_L$ scattering in the "ring model" can very closely approximate scattering in the continuum models, provided that the hidden local symmetry parameter `a' is chosen to mimic rho-meson dominance of pion-pion scattering in QCD. The hadron and lepton collider phenomenology of they extended models is briefly discussed, with a focus on the complementary information to be gained from precision measurements of the Z' line shape and ZWW coupling at a high-energy lepton collider.

## Impact on National Missions

We support the high energy physics component of the DOE Office of Science mission by addressing two of its six long-term goals: discover the Higgs' particle, and probe the high energy frontier.

## References


1. Csaki, C., C. Grojean, H. Murayama, L. Pilo, and J. Terning. Gauge theories on an interval: Unitarity without a Higgs. 2004. *Physical Review D.* **D69** (055006): 1.

2. Csaki, C., C. Grojean, L. Pilo, and J. Terning. Towards a realistic model of Higgsless electroweak symmetry breaking. 2004. *Physical review Letters.* **92** (101802): 1.

3. Giudice, G. F., C. Grojean, A. Pomarol, and R. Rattazzi. The Strongly-Interacting Light Higgs. 2007. *Journal of High Energy Physics .* **0706** (045): 1.

4. Graesser, M., R. Kitano, and M. Kurachi. Higgsinoless Supersymmetry and Hidden Gravity. 2009. *arXiv.org.*

5. Bilgici, E.. A New scheme for the running coupling constant in gauge theories using Wilson loops. 2009. *Physical Review D.* **80** (034507): 1.

6. Bilgici, E.. Search for the IR fixed point in the twisted Polyakov loop scheme. 2009. *arXiv.org.*

7. Belyaev, A.. W(L) W(L) Scattering in Higgsless Models: Identifying Better Effective Theories. 2009. *Physical Review D.* **80** (055022): 1.


## Publications


Belyaev, A., R. Chivukula, N. Christensen, H. He, M. Kurachi, E. Simmons, and M. Tanabashi. W(L) W(L) Scattering in Higgsless Models: Identifying Better Effective Theories. 2009. *Physical Review D.* **80** (055022): 1.

Bilgici, E., A. Flachi, E. Itou, M. Kurachi, C. Lin, H. Matsufuru, H. Ohki, T. Onogi, and T. Yamazaki. A New scheme for the running coupling constant in gauge theories using Wilson loops. 2009. *Physical Review D.* **80** (034507): 1.

Bilgici, E., A. Flachi, E. Itou, M. Kurachi, C. Lin, H. Matsufuru, H. Ohki, T. Onagi, E. Shintani, and T. Yamazaki. Search for the IR fixed point in the twisted Polyakov loop scheme. 2009. *arXiv.org.*

Graesser, M., R. Kitano, and M. Kurachi. Higgsinoless Supersymmetry and Hidden Gravity. 2009. *arXiv.org.*

# Richtmyer-Meshkov Instability Studies

*Katherine P. Prestridge*
20080792PRD4

## Abstract
This LDRD was Director's Funding for Devesh Ranjan, a postdoctoral researcher working on the gas shock tube project. Devesh began his postdoc in January 2008, supported by another project. Director's funding began in December 2008. Devesh subsequently left the Laboratory at the beginning of January 2009 for an Assistant Professor position at Texas A&M University. Consequently, the project was prematurely terminated after less than one month.

## Background and Research Objectives
The purpose of this research was to study the temporal dependence of the shock impact timing on Richtmyer-Meshkov instabilities and mixing. In this flow, a heavy gas curtain is struck by a Mach 1.2 shock wave. A hydrodynamic instability develops, and the curtain grows and mixes. In these experiments, the instability was then reshocked with a reflected wave. By varying the reshock timing, we hoped to understand how the mixing characteristics of the layer changed.

## Scientific Approach and Accomplishments
Preliminary experimental results were presented at the APS Division of Fluid Dynamics Meeting in November 2008. During December 2008, when the postdoc charged to the LDRD project, he analyzed the data. The experimental results have not yet been published.

## Impact on National Missions
This work is not yet completed, and it will likely be completed in the future under programmatic deliverables, if possible. The experimental data directly impact code validation and modeling efforts for the weapons program.

## References
1. Ranjan, D., B. J. Balakumar, G. Orlicz, K. Prestridge, and C. Tomkins. Experimental analysis of a reshocked gas curtain. Presented at *American Physical Society Division of Fluid Dynamics Annual Meeting 2008.* (Texas, 23-25 Nov. 2008).

# Technology

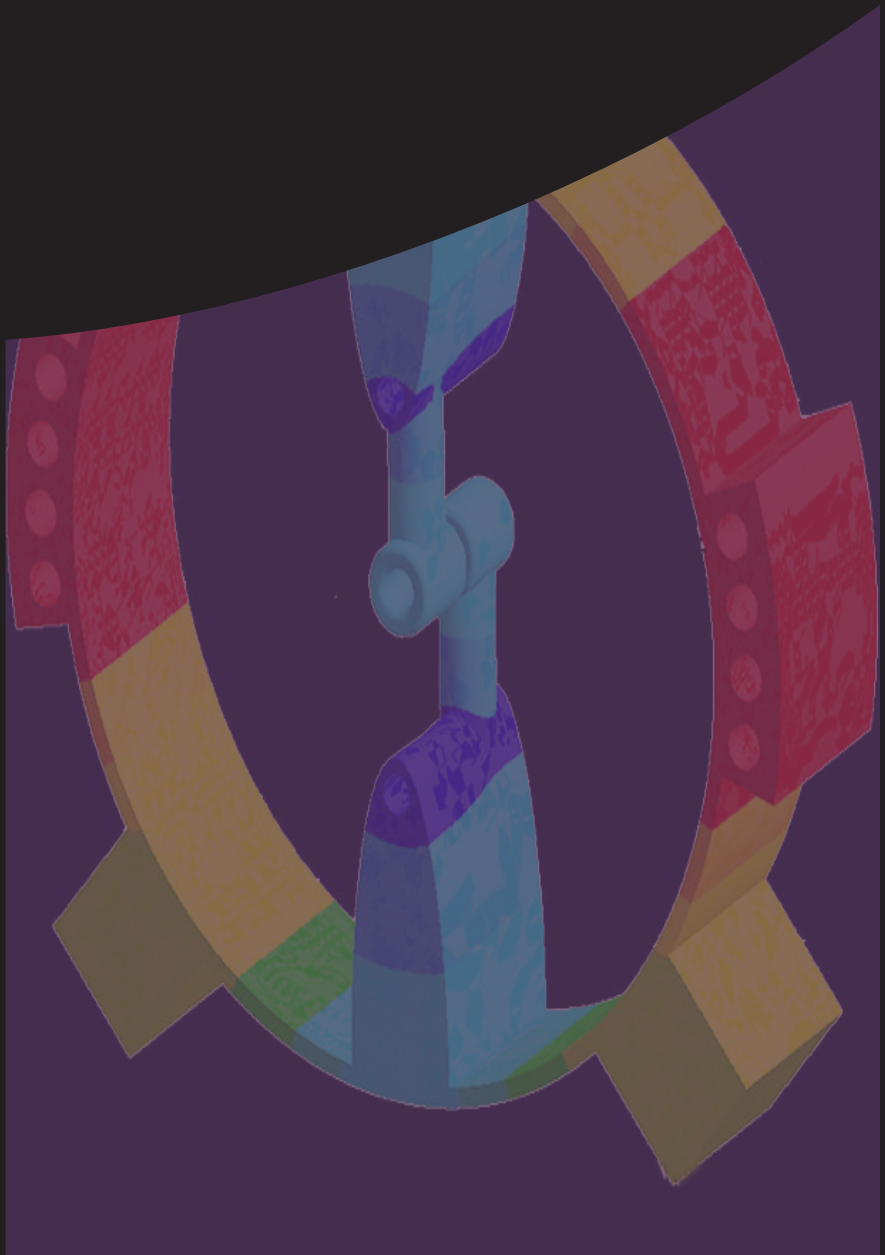

LABORATORY DIRECTED RESEARCH AND DEVELOPMENT

# Construction and Use of Superluminal Emission Technology Demonstrators with Applications in Radar, Astrophysics, and Secure Communications

*John Singleton*
20080085DR

## Introduction

The project demonstrates that sources of electromagnetic radiation, such as radio waves, can be made to be superluminal, that is travel faster than the speed of light. Although this may sound like science fiction, no laws of physics are in fact being broken; the source consists of a wave-like disturbance in a special antenna made of alumina, and it obeys the principles of Relativity and Electromagnetism. Most people will be familiar with the idea of a sonic boom, an intense burst of sound encountered some distance from a high-performance airplane that accelerates through the sound barrier. This occurs because the airplane overtakes the sound waves that it has emitted, pushing them together to make the "boom". In the same way, our superluminal source overtakes its own radio waves (which travel at the speed of light), producing an "electromagnetic boom"; a region of very tightly-focused and powerful radio waves [1-3]. This effect has many potential applications, including medicine (focusing beams to kill tumors), radar, long-range communications (e.g. with distant space probes) and security (e.g. disabling stolen cars without harming people in and around them). In addition to building three superluminal technology demonstrators, the current project looks at the very difficult mathematics of the electromagnetic boom (e.g. how to predict and control it) [1-3] and ties superluminal emission to astronomical phenomena [3-5]. We have recently shown that pulsars, neutron stars that emit pulses of radiation seen by astronomers on Earth, are natural superluminal sources; using our mathematical models, we are able to predict all of the properties of their radiation [3-5]. The models are now being turned to other space phenomena such as gamma-ray bursts [6] and Quasars.

## Benefit to National Security Missions

This project supports the DOE mission in nonproliferation by providing secure, low-power surveillance and monitoring technologies. Superluminal sources are also relevant to secure communications, radar and directed-energy applications. They provide insights into the basic principles that govern the Universe, supporting Office of Science missions.

## Progress

This project covers three major areas: development of practical superluminal sources, or technology demonstrators; mathematical and numerical modeling of superluminal sources and the search for astronomical objects that behave like superluminal sources. We shall deal with each area in turn.

The detailed electromagnetic modeling, component testing and circuit board design of the project's first year have borne fruit, in that two practical superluminal sources have been completed, an 8-element proof-of-principle machine and Technology Demonstrator 1 (TD1), a full-circle 72-element machine of 125 mm radius (Figure 1). In addition, Technology Demonstrator 2 (TD2), a linear accelerator, has been designed in full and the control electronics built. One of the antenna elements of TD2 is illustrated in Figure 2; as this report is being written (November 2009), these components are under construction. It is planned that the machine can be assembled at the end of 2009 for testing in early 2010.

The 8-element proof-of-principal source was used to test all of the control electronics and antenna elements of the subsequent larger machines (TD1 and TD2). In experiments carried out in the anechoic chamber at ISR-6, it was shown that the source speed can be controlled very precisely, with speeds as large as six times the speed of light in vacuo being reached. The proof-of-principle machine was also used to debug the software that controls the source speed and experimental data acquisition. Experiments entail rotating the antenna assembly (Figure 1), moving a detector aerial, distinguishing between different

emitted frequencies from the source and recording the emitted power at each frequency; all were successfully demonstrated. Finally, the 8-element machine showed that the antenna elements are efficient, as predicted by electromagnetic modeling in the first year of the project. As all of the antenna elements and electronic components are built on modular principles, the results were immediately extendable to TD1 and TD2. Consequently, TD1 is already in use prior to being moved to a larger anechoic chamber at Kirtland Air Force Base in Fall 2009 for radar demonstrations, fundamental physics experiments and simulations of astronomical objects.

Turning to the mathematical and numerical work, it should be remembered that the solution of Maxwell's Equations for a source traveling faster than the speed of light is nontrivial [1-3]. Multiple retarded times must be considered, and there are divergences in the fields [1,2]. The modeling of the technology demonstrators and astronomical objects such as pulsars [3-6] therefore demands a considerable amount of mathematical and numerical groundwork; sources that move faster than their own waves have been little considered thus far, and the field is at an early stage of development. Hence, members of the project have been developing the mathematical framework necessary to understand superluminal sources, and publishing papers and technical reports that are the foundations of this new area of electromagnetism; a summary of progress and project publications is given in [2,3]. In addition to the papers listed under Performance Data, one of the students on the project is writing a Master's thesis on her contribution to this mathematical work.

The astronomical part of the project has had some notable successes (Figure 3) [3-6]. First, we have demonstrated using a statistical model that the emission from pulsars that reaches Earth falls off in intensity as 1/distance, rather than the familiar inverse square law; this is a fundamental property of rotating superluminal sources (Figure 3 (a)) [4]. Second, we have shown that a simple superluminal source model can explain the emission spectra of nine pulsars over 16 orders of magnitude of frequency using essentially only one or two adjustable parameters (Figure 3(b) [3,5]. Given that previous models struggled to explain very small fractions of an individual pulsar's emission spectrum, this is a considerable breakthrough [5]. Finally, two other papers (one in preparation, one submitted [6]) compare superluminal models with gamma ray bursts. Observations of gamma-ray bursts with fast time-resolution equipment are being carried out to further strengthen the case for superluminal emission mechanisms.

Efforts to develop applications and communicate developments to future sponsors in US industry and government continue, in full consultation with LANL Technology Transfer Division. In this context, part of the intellectual property surrounding superluminal sources was protected by the filing of a patent. A US Government agency has indicated willingness to support studies of secure communications using superluminal sources; the exact amount and form of support is under current discussion. A local NM company is interested in licensing superluminal technology for medical applications. To protect LANL intellectual property should this go ahead, the architecture of TD-1 is being copyrighted.

## Future Work

Superluminal sources are exceptional in that the radiation received from them can contain contributions from more than one retarded time. Moreover, when a superluminal source accelerates, contributions from an extended period of source time can arrive simultaneously at an observer.

The technology demonstrators (TD1-3) explore these issues and study communication, radar, astrophysics and directed-energy applications of superluminal sources. TD1 animates a polarization current around a circular dielectric and is a 72-element device with a radius of 125 mm operating at 2.4 GHz (Figure 1). It modulates the emitted signal at the rates required for communication and radar applications. Its compactness, also demonstrating the scalability of the technology to future industrial sponsors, means that experiments are performed in the LANL RF anechoic chamber and, shortly, will be carried out in larger chambers at AFRL, Kirtland Air Force Base. This is invaluable for verifying the numerical models of superluminal emission that form an important part of the project.

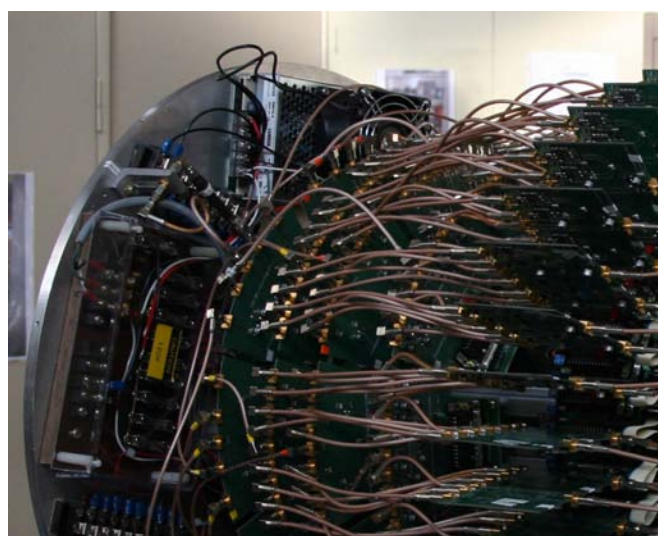

*Figure 1. The 72-element circular superluminal source known as Technology Demonstrator 1 (TD1), under commissioning tests. The 72-element dielectric antenna can be seen at the right-hand end. The electronic boards for controlling and*

*measuring the speed of the source are situated to the left of the circular aluminum plate carrying the antenna. The unique cylindrical architecture of the device ensures accurate speed control and interchangeability of components in the field. The device is mounted on a turntable for angular mapping of the emitted radiation. TD-1 is being used to prototype radar and communications applications of superluminal sources, and as a ground-based astronomy experiment (simulated pulsar).*

For directed energy applications, a linear acceleration of the polarization current is more fruitful, as it will produce energy concentration at a point; elsewhere, energy concentration will be small, reducing collateral damage. TD2 (Figure 2) is therefore a low-power linear accelerator, using the same modules as TD1; it is under construction and will be used to study energy concentration in the anechoic chamber. Later, the feasibility of constructing a high-power device (TD3) employing kV electronics will be assessed.

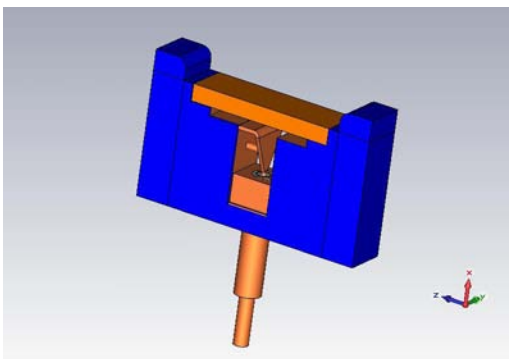

*Figure 2. Diagram of one of the 32 antenna elements for the linear accelerator source Technology Demonstrator 2 (TD-2), presently under construction. The supporting frame, made of G-10, is shown in blue. The light orange slab at the top is the alumina where the polarization current is created. The triangular transition that matches the 50 Ohm cylindrical coaxial line (below) to linear polarization in the alumina is visible in the center of the structure.*

The wave fronts emitted by sources that travel faster than light are unlike the radiation generated by any other known emission mechanism [1-3,5]. Our results suggest that superluminal emission is an important process in the observable universe, occurring, for example, in pulsars and nuclear explosions [3-6]. In addition to simulating communications and radar applications of superluminal sources, numerical computations [1,2] continue to model the electromagnetic radiation from astrophysical objects such as pulsars [3-6]. By comparing these to observational data it is becoming possible to deduce the internal structure of pulsars [3-5]. This work is continuing and being extended to other astronomical objects [6].

## Conclusion

The new method for generating radio waves, superluminal emission, is an almost completely unexplored technological field. It has potential applications in secure communication, radar, electronic countermeasures, electronic weapons and long-range, low-power transmission. To develop these applications, three prototype transmitters, each designed to exploit a particular property of superluminal emission, are being constructed and used at LANL. These compact machines serve as technology demonstrators for radar, communications and directed-energy, and verify the computer models of superluminal emission. They are also being used to explore possible spin-off technologies in areas such as medical diagnostics and therapy.

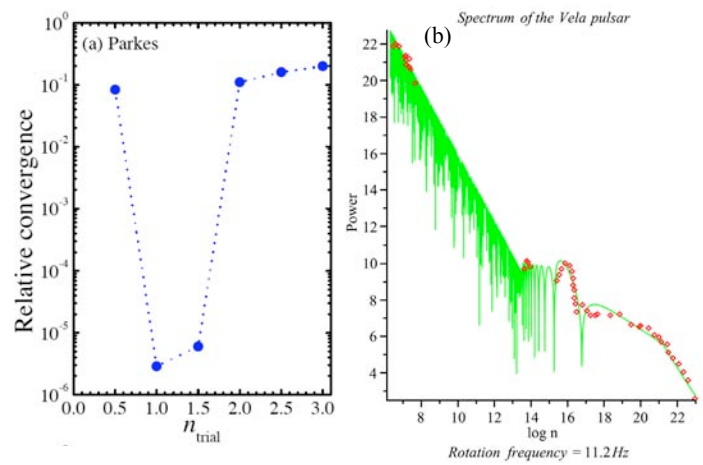


*Figure 3. Successful modeling of astronomical observations using the superluminal emission model. (a) A Maximum Likelihood Model (MLM) fit of intensities and distances of 980 pulsars. The intensity and distance data are taken from the Parkes Multibeam Survey, a catalog of pulsar observations. The MLM tests how the intensity varies with distance by attempting to fit the data to a distance power law (intensity varies as 1/distance to the power n). A small relative convergence error for a particular value of n shows a good fit of the data. The deep minimum at n = 1 (notice the logarithmic scale) shows that the intensity diminishes as 1/distance, in accord with the superluminal model. A conventional source of radiation would obey the inverse square law, i.e. the intensity would diminish as 1/distance squared, leading to a minimum at n = 2. (b) Fit of the superluminal model (green curve) to observations of the Vela pulsar (red points), plotted as power versus radiation frequency, where the radiation frequency is given in terms of the rotational frequency, 11.2 Hz. There are essentially only two adjustable parameters in the model, and yet it is able to fit the observations very precisely over 16 orders of magnitude of frequency. Similar fits have been carried out for 8 other pulsars, forming the subject of a paper currently in press.*

## References


1. Ardavan, H., A. Ardavan, J. Singleton, J. Fasel, and A. Schmidt. Fundamental role of the retarded potential in the electrodynamics of superluminal sources. 2009. *Journal of the Optical Society of America A- Optics Image Science and Vision.* **26** (10): 2109.

2. Ardavan, H., A. Ardavan, J. Singleton, J. H. Fasel, and A. Schmidt. Inadequacies in the conventional treatment of the radiation field of moving sources . 2009. *Journal of Mathematical Physics.* **50**: 103510.

3. Ardavan, A., H. Ardavan, J. Fasel, J. Middleditch, M. R. Perez, A. Schmidt, and J. Singleton. A new mechanism for generating broadband pulsar-like polarization. 2009. (Rome, 16-17 Oct. 2008). Vol. Proceedings of Sciencep. 016. Rome: SISSA.

4. Singleton, J., P. Sengupta, J. Middleditch, T. L. Graves, M. R. Perez, H. Ardavan, and A. Ardavan. Violation of the inverse square law by the observed flux-distance relationship for pulsars. *Nature.*

5. Ardavan, H., A. Ardavan, J. Singleton, J. Fasel, W. Junor, J. Middleditch, M. R. Perez, A. Schmidt, P. Sengupta, and P. Volegov. Comparison of multiwavelength observations of 9 broad-band pulsars with the spectrum of the emission from an extended current with a superluminally rotating distribution pattern. *Astrophysical Journal.*

6. Middleditch, J.. Pulsed Gamma-Ray-Burst Afterglows . *Astronomy and Astrophysics.*


## Publications


Aradavan, H., A. Aradavan, J. Singleton, and M. R. Perez. Mechanism of generation of the emission bands in the dynamic spectrum of the Crab pulsar. 2008. *Monthly Notices of the Royal Astronomical Society.* **388** (2): 873.

Ardavan, A., H. Ardavan, J. Fasel, J. Middleditch, M. R. Perez, A. Schmidt, and J. Singleton. A new mechanism for generating broadband pulsar-like polarization. 2009. In *Proceedings of Polarimetry Days in Rome: Crab Status, Theory and Prospects.* (Rome, 16-17 Oct. 2008). Vol. Proceedings of Science, p. 016. Rome: SISSA.

Ardavan, H., A. Ardavan, J. Singleton, J. Fasel, W. Junor, J. Middleditch, M. R. Perez, A. Schmidt, P. Sengupta, and P. Volegov. Comparison of multiwavelength observations of 9 broad-band pulsars with the spectrum of the emission from an extended current with a superluminally rotating distribution pattern. *Astrophysical Journal.*

Ardavan, H., A. Ardavan, J. Singleton, J. Fasel, and A. Schmidt. Fundamental role of the retarded potential in the electrodynamics of superluminal sources. 2008. *Journal of the Optical Society of America A (Optics, Image Science and Vision) .* **25** (3): 543.

Ardavan, H., A. Ardavan, J. Singleton, J. Fasel, and A. Schmidt. Spectral properties of the nonspherically decaying radiation generated by a rotating superluminal source. 2008. *Journal of the Optical Society of America A (Optics, Image Science and Vision) .* **25** (3): 780.

Ardavan, H., A. Ardavan, J. Singleton, J. Fasel, and A. Schmidt. Morphology of the nonspherically decaying radiation generated by a rotating superluminal source: reply to comment. 2008. *Journal of the Optical Society of America A (Optics, Image Science and Vision) .* **25** (9): 2167.

Ardavan, H., A. Ardavan, J. Singleton, J. Fasel, and A. Schmidt. Response to comment on method of handling the divergences in the radiation theory of sources that move faster than their own waves. 2008. *http://xxx.lanl.gov/.* : 1.

Ardavan, H., A. Ardavan, J. Singleton, J. Fasel, and A. Schmidt. Fundamental role of the retarded potential in the electrodynamics of superluminal sources. 2009. *Journal of the Optical Society of America A- Optics Image Science and Vision.* **26** (10): 2109.

Ardavan, H., A. Ardavan, J. Singleton, J. H. Fasel, and A. Schmidt. Inadequacies in the conventional treatment of the radiation field of moving sources . 2009. *Journal of Mathematical Physics.* **50**: 103510.

Middleditch, J.. Pulsars, cosmology and science with giant telescopes. Invited presentation at *Science with giant telescopes.* (Chicago, 15-18 June 2008).

Middleditch, J.. Pulsed Gamma-Ray-Burst Afterglows . *Astronomy and Astrophysics.*

Middleditch, J., and M. R. Perez. The Kinematics of the SN 1987A Beam/Jet(s). 2008. *Bulletin of the American Astronomical Society .* **40** (2): 206.

Middleditch, J., and M. R. Perez. The SN 1987A Beam/Jet and Its Associated Mystery Spot. 2008. *Bulletin of the American Astronomical Society .* **39** (4): 742.

Perez, M. R., B. McCollum, M. E. van den Ancker, and M. D. Joner. The enigmatic young object: Walker 90/V590 Monocerotis. 2008. *Astrnomy and Astrophysics.* **486** (2): 533.

Schmidt, A., H. Ardavan, J. Fasel, M. Perez, and J. Singleton. Superluminal emission processes as a key to understanding pulsar radiation. 2008. *Bulletin of the American*

*Astronomical Society .* **39** (4): 917.

Singleton, J.. Lawbreakers? Superluminal sources in the laboratory and as a model for pulsars. Invited presentation at *23rd Annual New Mexico Symposium.* (Socorro, October 2007).

Singleton, J., A. Schmidt, J. Fasel, H. Ardavan, A. Ardavan, and M. R. Perez. Polarization currents that travel faster than the speed of light in vacuo: laboratory demonstrations and a model for pulsar observational data. 2008. *Bulletin of the American Astronomical Society .* **39** (4): 950.

Singleton, J., P. Sengupta, J. Middleditch, T. L. Graves, M. R. Perez, H. Ardavan, and A. Ardavan. Violation of the inverse square law by the observed flux-distance relationship for pulsars. *Nature.*

# Image Reconstruction with Time-Reversal Mirrors

*Paul A. Johnson*
20060046DR

## Abstract

Conventional imaging relies on determining time delays and amplitude changes from one or more sources to one or more receivers, and then inverting for the velocity or attenuation structure. Normally, just the compressional (P) wave is used, but occasionally the shear (S) wave is used as well. Remarkably, all of the remaining wave energy rattling around the system, known as the "coda" in seismology and acoustics, is thrown away in conventional imaging, yet the coda contains almost all of the wave source and scattering-source information! If that information in the waveform could be used, we could obtain the complete transfer function between the sources and the receivers, as well as characterize individual sources.

Our work is focused on applying *elastic-wave time reversal* to imaging real and virtual sources (wave scatterers). The work is revolutionizing imaging itself while simultaneously developing the means to learn about the characteristics of a complex source like an earthquake or a virtual source (scatterer) like a disbond in a part.

We have the means to image "around corners" for instance, because we use all of the waveform. The idea proposed here has never before been conceived of nor attempted. The approach we have taken is to use the concept of the Time Reverse Mirror. The Time Reverse Mirror is a simple and ingenious way to recreate from measured signals a virtual source (e.g., a scatterer like a pit anomaly) or a real source (e.g., an earthquake). The Time Reverse Mirror can be understood as follows: imagine filming a pebble dropped into a pond of water. Ripples emanate outward from the pebble, a "real" wave source. A rock protruding from the pond, a "virtual" source scatters the waves. Stop the movie some time after the scattering took place, and run it backwards to the time when waves intersect the reed; then to the time when the pebble impacts the surface. We can "reconstruct" each of the two sources by freezing the movie at different times. This analogy describes the idea behind the time reversal mirror technique. Time reversal works because the wave equation does not depend on whether the wave propagates forward or backwards in time. This is called reciprocity. We are advancing the Time-Reversal Mirror method to develop a universal high-resolution image reconstruction approach, and integrate it with sophisticated image analysis.

Of note is that the method we are developing may be the only means to reliably locate recently discovered earthquakes known as "non-volcanic tremor", that have produce long, rumbling seismic signals. The implications of locating tremor in regards to earthquake prediction may be significant. Other seismic sources that are impossible to locate by other means include Earth "hum", the source of which remains elusive. Similar sources of interest to DOE that are challenging to locate include buried structures or tunnels that emanate machine noise. Our work has a direct impact on their location.

## Background and Research Objectives

The 2004 Indian Ocean earthquake occurred at 07:58:53 local time on December 26, 2004, generating a tsunami that was among the deadliest disasters in modern history, killing well over 200,000 people. At a magnitude of 9.0, it was the largest earthquake since the 9.2 magnitude Good Friday Earthquake off Alaska in 1964, and tied for fourth largest since 1900. The earthquake originated in the Indian Ocean off the western coast of northern Sumatra, Indonesia. The hypocenter of the main earthquake was 160 km west of Sumatra, at a depth of 30 km below mean sea level (initially reported as 10 km). This is at the extreme western end of the Ring of Fire, an earthquake belt that accounts for 81% of the world's largest earthquakes. The earthquake was unusually large in geographical extent. An estimated

1200 km of faultline slipped about 15 m along the zone where the India Plate subducts beneath the Burma Plate. The slip did not happen instantaneously but took place in at least two phases over several minutes. Seismographic data indicate that the first phase was composed of a rupture about 400 km long and 100 km wide, located 30 km beneath the sea bed. The rupture proceeded at a speed of about 2 km/s, beginning off the coast of Aceh and proceeding north-westerly over about 100 s. A pause of about another 100 s took place before the rupture continued northwards towards the Andaman and Nicobar Islands. The details of this earthquake illustrate important aspects in our knowledge (and lack thereof) regarding how earthquakes work. Although much is known, the particulars of how the fault slipped, including the true rupture length and the details of the successive slip comprising the earthquake, are still being studied.

This earthquake illustrates the research objectives of our work, to revolutionize imaging and characterization of (1) *real* seismic or ultrasonic sources (the pebble striking the pond) and (2) *virtual* sources (the reed in the pond). For example, isolating defects such as delaminations or small cracks in weapons or industrial components is often very difficult. Computed Tomography (CT) has limited resolution for objects of interest to Los Alamos due to low X-ray transparency. Acoustic methods are useful in thin plates, but are nearly useless when geometries are complex. The methods we have developed images virtual sources such as interfaces, cracks, delaminations and voids in materials and has had a major impact on defect identification and increasing the limits of imaging spatial resolution by at least another order of magnitude.

## Scientific Approach and Accomplishments

The basic concept behind the TRM is that the wave equation is symmetric with respect to time as the pond-ripple analogy described in the Summary illustrates. This means the wave equation may be run forward (the ripples run forward in time) or backward in time (reverse the movie and the ripples run backwards); the physics is the same. Suppose a source of acoustic energy is excited at some time and location, and the resulting wave field is captured and recorded on some closed surface surrounding the source (Figure 1). If the recorded wave field is reversed in time and emitted from the surface back into the medium then the wave equation guarantees that the acoustic energy will propagate back to and collapse at the original source point.

In fully elastic imaging problems with multiple sources, the complexity of mode conversion of waves adds enormous difficulty. Therefore it has been necessary to address a sequence of problems of increasing complexity, each building on the previous. The first problem was (a) imaging and characterizing a real source (the pebble). The next order of complexity was to (b) add a virtual source (the reed) and solve the combined problem. The next order of complexity was to (c) image multiple virtual sources in heterogeneous acoustic media (P-waves only). The last was (d) imaging and characterizing multiple virtual sources in fully elastic media (P- and S-waves).

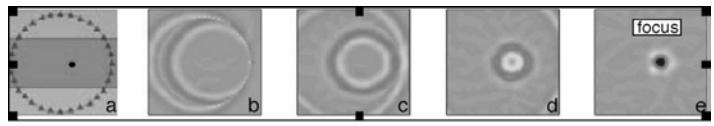


*Figure 1. A two-dimensional, elastic model (P- and S-waves [see text]) of TRM imaging exhibiting the necessary steps to image a sound (real) source. In (a), a computer model of a layered structure is shown; each layer has a different velocity. A sound source, indicated by the dot, is surrounded by 32 detectors indicated by the triangles. A wave is propagated in the model from the source to the receivers as shown in the snapshot in (b), like the waves emanating from the pebble in the pond. The detected sound-signals are time-reversed at the wave positions shown in (b)—they are literally reversed about the time axis— and sent backwards. (c-e) show snapshots of the waves, simulating the backward, time reversed propagation of the wave to the original source location (like the ripples described above, running backwards in a movie). In (e) we see the focus of the back-propagated field to the source location. The focused signal contains all of the source characteristics. The figure shows how time reversal works and the ingredients required to locate a sound source: a model to propagate waves, a known velocity "structure" (in reality obtained from standard acoustical imaging) and time reversal. All that is missing are the lab or earth wave data.*

The specific applications we chose were leveraged for additional scientific results at each step. They were, (a) determining the spatial-temporal characteristics of a single, real earthquake source; (b) characterizing earthquake depth with a single, virtual source (surface reflection); and (c) 3-D, high-resolution imaging of defects in fully elastic, multiple virtual sources in inhomogeneous and geometrically complicated weapons and industrial components. Solving each problem has been significant in itself, leading to high-visibility publications and high programmatic and societal impact.

Our accomplishments have been many, and there have been a number of spin-off projects as a result of this work. Demonstration of our accomplishments is supported by the large number of papers published (see our publication list) and the new projects created. The following lists our major accomplishments. We note that all results listed are new and no other research group has attained such

accomplishments.

**Earth**

- We made a careful study of what wave phases may be most important in locating a large earthquake applying seismometers located all over the globe. We find the surface waves are dominant in locating and probing earthquakes at this scale. A paper is in progress describing this result.

- We conducted a study of artifacts created in the earth time reversal problem. The paper noted above describes these important results.

- We conducted regional seismic studies using seismometers located near the earthquake. We studied the 2004 Parkfield California earthquake for this purpose. We found that the earthquake could be easily located and the source mechanism could be accurately extracted.

- We realized half way into the project that nonclassical earthquake sources could be located. These include a rumbling of the earth, know as tremor, as well as other similar sources such as earth hum. A first paper describing progress is in currently in press. These sources are impossible to locate using standard seismic techniques. In addition, there and many problems of interest to DOE that are similar. These include locating of underground structures that emanate cultural noise, tunnels and other buried structures. A follow-on proposal to continue this work was recently funded by Institutional Support.

- Spin off applications to characterize and image oil reservoirs have been in progress for more than a year. The work is being jointly conducted, and funded, by a major oil company. One patent is in progress resulting from this work and another will follow.

- In collaboration with MIT we are developing a method to determine the depth of seismic events. This is the single most important and most difficult problem in discerning an explosion from an earthquake (earthquakes are deep; explosions are near the Earth's surface.). This work is now been funded by NN-20.

**Laboratory**

- We demonstrated that mode conversion of different types of waves had no detrimental influence on the time reversal process. This was one of our original questions.

- We combined time reversal and material elastic nonlinearity (nonlinearity is extremely sensitive to damage) in order to image surficial cracks and other damage in a variety of specimens. This work has led to a number of publications as well as spin off work into the weapons program at LANL.

- We extended the method to image hidden (buried) cracks in objects. This work is currently under review in a journal. This was a major goal of our work.

- We combined laboratory time reversal experiments with modeling in order to image solids.

- We extended the laboratory plus modeling imaging to discern the difference between cracks and other features such as voids, by combing time reversal imaging with nonlinearity. A number of publications resulted from this work and the general technique will be used in the weapons program at LANL.

- We began to develop methods of importance to Rendersafe, and that work continues under funds from NN-20.

- We worked on discerning multiple acoustic sources that were more-or-less close to each other, in support of the earthquake problem Earthquakes are comprised of complex slip events in succession that each produce seismic waves. We succeeded in determining resolution limits based on laboratory studies. This work has been published.

- We worked on developing innovative new methods by which to image sources that are based on wave characteristics such as wave direction. These are a major advance in location of sources of the original wave and wave scattering sources. This work is in press.

- We developed a three component time-reversal-based imaging apparatus known as the Displacement Vector Microscope, which is a fabulous research tool for understanding the interaction the dynamics of waves with cracks. It will have important impact in understanding the interaction of seismic waves with faults for instance, as well as be a probe of the basic physics of cracks—their frictional aspects in particular.

- A non-contact time reversal source has been developed that is currently being patented. No effective non-contact sources currently exist although there is much need.

Moreover, we have become the recognized leaders in studies and applications of time reversal in the Earth and in solids in laboratory studies, and the combination of

nonlinearity with time reversal. We have developed and currently sustain collaborations with many institutes in the US and Europe. These collaborations have helped speed progress considerable. We have sponsored yearly scientific meetings on this topic as well.

## Impact on National Missions

Our work has had broad impact on missions. These include basic science where we have made tremendous progress in defining and advancing this domain of research and development. In addition, we have had significant spin off work into a number of areas: oil and gas reservoir imaging; new diagnostics and imaging of weapons components; and Ground Based Nuclear Explosion Monitoring in regards to determining a seismic source depth.

## Publications


Anderson, B., M. Griffa, C. Larmat, T. J. Ulrich, and P. Johnson. Time reversal. 2008. *Acoustics Today.* **4**: 5.

Anderson, B., M. Griffa, T. J. Ulrich, P. A. Johnson, and R. A. Guyer. Improving spatial resolution of a time-reversed focus using frequency-domain signal processing. 2007. *Journal of the Acoustical Society of America.* **122**: 3072.

Anderson, B., M. Scalerandi, A. Gliozzi, M. Griffa, T. J. Ulrich, and P. Johnson. Selective source reduction to identify masked smaller sources using time reversed acoustics (TRA). 2008. In *Review of Quantitative Nondestructive Evaluation.* (Golden, CO, 22-27July 2007). Vol. 27, p. 978. US: AIP.

Anderson, B., R. Guyer, T. J. Ulrich, P. Y. Le Bas, C. Larmat, M. Griffa, and P. A. Johnson. Energy current imaging condition for time reversal in elastic media. 2009. *Applied Physics Letters.* **95** (2): 021907.

Anderson, B., R. Guyer, T. J. Ulrich, and P. A. Johnson. Energy current imaging condition for time reversal in elastic media. 2009. *Applied Physics Letters.* **94**: 111908.

Anderson, B., T. J. Ulrich, M. Griffa, P. Y. Le Bas, M. Scalerandi, A. S. Gliozzi, and P. A. Johnson. Experimental identification of masked sources using the Selective Source Reduction (SSR) method. 2009. *Journal of Applied Physics.* **105**: 083506.

Griffa, M., R. Guyer, T. J. Ulrich, B. Anderson, and P. Johnson. Investigation of the robustness of Time Reversal Acoustics in solid media through the reconstruction of temporally symmetric sources. 2008. *J. Physics D: Applied Physics.* **41**: 5.

Griffa, M., R. Guyer, T. J. Ulrich, B. Anderson, and P. Johnson. Investigation of the robustness of Time Reversal Acoustics in solid media through the reconstruction of temporally symmetric sources. 2008. *Journal of Physics D.* **41**: 85415.

Guyer, R. A., and P. A. Johnson. . 2009. In *Nonlinear Mesocopic Elasticity* . , First Edition, p. 350. Berlin: Wiley-VCH.

Guyer, R., and P. Johnson. Nonlinear Mesoscopic Elasticity: The Complex Behaviour of Rocks, Soil, Concrete. 2009. In . , First Edition, p. 410. Berlin: Wiley-VCH.

Johnson, P. A.. Imaging Mechanical Defects: Time Reversal Nonlinear Elastic Wave Spectroscopy (TR NEWS) and Time Reversal Imaging Methods,. 2009. In *McGraw Hill 2009 Yearbook of Science & Technology.* By Blumel, D., S. Malmoli, and J. Netting. , First Edition, p. 174. USA: McGraw-Hill.

Larmat, C., J. P. Montagner, M. Fink, and J. Tromp. Time reversal location of glacial earthquakes. 2008. *Journal of Geophysical Research.* **113**: B09314.

Muller, M., D. Mitton, M. Talmant, P. Laugier, and P. Johnson. Nonlinear ultrasound can detect accumulated damage in human bone. 2008. *Journal of Biomechanics.* **41**: 1062.

Muller, M., J. TenCate, T. Darling, A. Sutin, R. Guyer, M. Talmant, P. Laugier, and P. Johnson. Nonlinear Resonant Ultrasound Spectroscopy (NRUS) applied to damage assessment in bone. 2006. In *International SYmposium on Nonlinear Acoustics.* (State College, PA, 18-22 July 2005). , p. 71. US: AIP.

Muller, M., T. J. Ulrich, M. Talmant, P. Laugier, and P. Johnson. Assessment of damage in cortical bone using nonlinear acoustic techniques, in, Biomedical applications of vibration and acoustics for imaging, characterization and diagnostics. 2008. In *Bone.* Edited by Al-Jumaily, A.. , p. 253. USA: ASME Press.

Muller, M., T. J. Ulrich, M. Talmant, P. Laugier, and P. Johnson. Assessment of damage in cortical bone using nonlinear acoustic techniques. 2008. In *in Biomedical applications of vibration and acoustics in imaging and characterizations.* Edited by Al-Jumaily, A.. , p. 253. US: ASME.

Scalerandi, M., A. Gliozzi, B. Anderson, M. Griffa, P. Johnson, and T. J. Ulrich. Selective source reduction to identify masked weaker sources using time reversal acoustics. 2008. *Journal of Physics D.* **41**: 155504.

Scalerandi, M., A. Gliozzi, B. Anderson, M. Griffa, P. Johnson, and T. J. Ulrich. Selective source reduction to identify masked weaker sources using time reversal acoustics. 2008. *Journal of Physics D.* **41**: 155504.

Ulrich, T. J., A. Sutin, R. Guyer, and P. Johnson. Time reversal and nonlinear elastic wave spectroscopy TR NEWS techniques. 2008. *International Journal of Nonlinear Mechanics.* **43**: 209.

Ulrich, T. J., A. Sutin, T. Claytor, P. Pappin, P. Y. LeBas, and J. TenCate. The time reversed elastic nonlinearity diagnostic applied to evaluation of diffusion bonds. 2008. *Applied Physics Letters.* **93**: 151914.

Ulrich, T. J., A. Sutin, and P. Johnson. Imaging nonlinear scatterers applying the time reversal mirror. 2006. *Journal of the Acoustical Society of America.* **119**: 1514.

Ulrich, T. J., B. Anderson, P. Johnson, A. Sutin, and R. Guyer. Nonlinear dynamics and time reversed acoustic imaging in damaged solids. 2007. *Journal of the Acoustical Society of America.* **121**: 3164.

Ulrich, T. J., M. Griffa, and B. Anderson. Symmetry-based imaging condition in time reversed acoustics. 2008. *Journal of Applied Physics.* **104**: 064192.

Ulrich, T. J., P. A. Johnson, and R. A. Guyer. Investigating Interaction Dynamics of Elastic Waves with a Complex Nonlinear Scatterer Applying the Time Reversal Mirror. 2007. *Physical Review Letters.* **98**: 10430.

Ulrich, T. J., P. Johnson, M. Muller, D. Mitton, M. Talmant, and P. Laugier. Application of nonlinear dynamics to progressive fatigue damage in human cortical bone. 2007. *Applied Physics Letters.* **91**: 213901.

Ulrich, T. J., P. Johnson, and A. Sutin. Imaging and characterizing damage using time reversed acoustics. 2007. In *Quantitative Nondestructive Evaluation* . (Golden, CO, 22-27 July). , p. 650. US: AIP.

# Terahertz Generation Harnessing the Two-Stream Instability

*Kip A. Bishofberger*
20080210ER

## Introduction

The terahertz regime of the electromagnetic spectrum is situated between traditional high-frequency microwave and extremely far-infrared light. Both producing and detecting terahertz waves has been both difficult and the focus of significant efforts world-wide. Because of the very specific absorption and transmission properties of terahertz radiation, there are potentially many high-impact applications including medical imaging, secure or covert communication, and cloaking.

High-power sub-millimeter and terahertz-frequency sources have remained an elusive target of physicists and engineers over the past many years. While lasers and microwave circuitry have conquered higher and lower frequencies, this missing band has a vast range of scientific, commercial, and military applications. A group at LANL has shown that a particular instability in a particle beam, a phenomenon well-known and strongly avoided by most accelerator laboratories, can actually be harnessed, controlled, and utilized to produce high-power terahertz radiation. Simulations predict that this experiment could break open the barrier to this band of frequencies, opening the door to future applications.

## Benefit to National Security Missions

This project has the potential to impact a broad range of missions including threat reduction (e.g. imaging and communication technologies), supporting the INTEL communicty (secure or covert communication, covert imaging, etc.), to improving human health (DOE/SC, NIH) through enabling new medical imaging technologies.

## Progress

We are excited to report the latest simulation and experimental developments of our LDRD-funded research. The first phases of our research has been completed and not only are we striving to complete our last phase, but simulations of the physics have yielded new and unexpected facets of the project.

This project has centered around simulating and constructing a sub-millimeter radiative device that utilizes a well-known phenomenon called the two-stream instability. This technique allows us to develop a simple, robust source of sub-millimeter radiation, through the terahertz range, while dispensing with complicated metallic structures and difficult tolerances.

The following is a list of our achievements so far:

1. Simulations have yielded a wealth of information about the gain of the device. Before getting funding, we had a simplistic, one-dimensional model of the effect. With two-dimension and three-dimension simulations, we can see that the gain of the device does not degrade significantly. In fact, within certain specific parameter spaces, the perceived gain is actually higher in the simulations than what the simplistic model predicts. This result is very exciting, as it shows that a realistic device may actually perform better than our first predictions.

2. Of course, the simulations have proven that a number of parameters have certain effects on the growth of the radiative modes. Without these crucial tests, it would have proved improbable that the experimental device would perform as expected. Additionally, other effects, such as how the beam propagates through a beampipe, determines which mode (which frequency) has the highest gain. Again, these results have directly influenced the specifics of the experiment.

3. Other results show that the bandwidth of the device is exceedingly large. This is great news for development of wideband communications and feedback-driven oscillators. It implies that by seeding the beam at the “frequency of interest,” we can amplify that frequency without having to tailor the beam parameters.

4. The experiment has been partially constructed; all of the hardware is in place. Due to the simulation results, we refined the demonstration to a significantly smaller space than originally planned (one optical table, including all power supplies, vacuum equipment, etc).

5. Initial results were marginal, but after using the experimental data to influence the simulations, we realized we had made some faulty assumptions in construction of the device. We are currently redesigning the experiment, and we feel confident that, once under operation again, we will generate results that concur with that of the simulations. Of course, publishing the results and trying to push toward a more deployable-like design will be our final goals of this project.

6. The last difficulty to overcome is how to turn a "beam mode" into a "radiative mode:" essentially converting the energy into a beam that can be harnessed for applications. From a small gathering of prominent physicists, two of them are writing a code to simulate Coherent Synchotron Radiation (CSR). This deleterious effect has been a thorn in many accelerator research projects world-wide. This simulation code is crucial to the success of our LDRD research, but it will be applicable (and publishable) for general CSR development as well.

7. The above achievements are all based on the simulations that have been occurring over the past two years (especially the lasts six months, after we learned the dimensions that function the best). As testimony to this research, we have:

   - a Ph.D. thesis that is currently being written,
   - several peer-review articles being written or submitted,
   - numerous presentations at conferences in the past two years,
   - a software code being developed for general CSR calculations.

We are grateful for the opportunity that the LDRD program has provided to work on this exciting and significant physics research.

## Future Work

We plan to model/test a new concept to generate high-power sub-millimeter and terahertz-frequency radiation. Such a source has been a challenging goal in recent history, while the applications of such a device continue to grow. This device will use the Two-Stream Instability, a well-known phenomenon that can easily occur in accelerator-physics laboratories around the world. Previously avoided in accelerator-based experiments, we have successfully simulated the instability and shown that it can be utilized to generate and amplify sub-millimeter and terahertz-frequency radiation in a reliable and efficient manner.

It is important to note that such research can be immediately utilized in a variety of scientific, commercial, and military applications. In particular, Threat Reduction has desired efficient, adaptable devices in this frequency range for remote sensing, communications, and imaging applications. Terahertz radiation is seen as a vital tool: it combines the penetrating power of microwaves with the high resolution of IR and visible imaging. We look forward to developing such a device for such applications.

Our project can be split into three main tasks:

1) Dvelopment of the concept at approximately 100 GHz.

2) Nonlinear analysis and numerical simulations of the interaction at higher frequencies, to 1 THz.

3) Construction of a prototype at these high frequencies.

We foresee the first two goals occurring somewhat simultaneously, as each will foster progress in the other. By the end of the experiment, we predict that we will have a working prototype of a sub-millimeter source utilizing a new physics technique and directly applicable to a variety of applications.

## Conclusion

This project focuses on modeling and constructing a sub-millimeter radiative source using a well-known physics phenomenon. This compact device, loosely similar to a laser, is predicted to produce a beam of this radiation which is applicable to numerous scientific, commercial, and security-based military applications. For example, this frequency range can be used for extremely high-bandwidth communications or image the contents of shipping containers arriving daily at American ports. It is capable of detecting specific environmental hazards. Like lasers today, terahertz sources would be ubiquitous in countless future applications once these sources exist.

# Nano-Fission-Material based Neutron Detectors

*Ernst I. Esch*
20080221ER

## Introduction

Fission chambers are ionization chambers containing one or more foils thinly coated with uranium. They are commonly used to measure neutron flux for nuclear physics experiments, such as those performed at the Los Alamos Neutron Science Center (LANSCE). These detectors are easy to operate, are not damaged by radiation, and have an acceptable efficiency for many beam-line applications. The fission chamber detector works by first capturing op the neutron by the U atom. Neutron capture is a kind of nuclear reaction in which an atomic nucleus collides with one or more neutrons and they merge to form a heavier nucleus. Many times, the heavier nucleus will be unstable and fission into two nuclei, called daughter products. The daughter products escape the foil and ultimately deposit their energy into the surrounding gas. This process involves ionizing the gas atoms to produce a cascade of electrons, which are collected as an electrical current. The magnitude of the current is proportional to the energy deposited in the gas, directly analogous to a Geiger counter. However, these detectors typically have rise times of several hundred nanoseconds, making them prone to pulse pile-up. In addition, in order to allow the fission fragments to escape the foils, their uranium coatings must be very thin, resulting in low neutron detection efficiency. Thus long measurement times are needed in low-flux environments. Fission chambers are also bulky, fragile, pose a contamination hazard if punctured, and require frequent maintenance.

We propose to address these issues by developing a nanocomposite fission detector, consisting of nanoparticles of fissionable material dispersed in a scintillating matrix. This will produce a detector that can be loaded with up to two orders of magnitude more uranium and has a pulse rise time that is two orders of magnitude faster. In addition, the use of a plastic matrix would make the detector far more robust than current fission chambers.

Our team includes members of C, LANSCE, MPA, MST, and N divisions and brings to the project several years' experience in fabricating and characterizing nanoparticles. We have successfully fabricated $CeF_3$ nanoparticles, suspended them in liquid matrices, and extensively characterized their structural, optical, and radiation detection properties, including comparing their performance in the beam at LANSE with commonly used detector modules.

## Benefit to National Security Missions

The main goal of this project is to improve upon some of the neutron detection capabilities at LANSCE. Maintaining expertise and growing knowledge in neutron nuclear science and neutron technology is a central activity for LANSCE. Using protons and neutrons, LANSCE provides the NNSA with an efficient, cost effective, and timely means to meet its Stockpile Stewardship mission. Projects that could benefit from enhanced neutron detection capability also address the growing concern of nuclear proliferation, nuclear forensics and the development of a new class of safer, cleaner, and more proliferation-resistant fuels—fuels the nation needs to provide energy security and independence, protect the environment, and impede nuclear terrorism.

## Progress

We began by synthesizing fissionable molecules, rather than nanoparticles, as a first proof of principle. The first molecule synthesized was $UO_2(NO_3)_2(TBP)_2$, using $^{238}U$. Depleted uranium (DU) was selected, despite having a lower fission cross-section than $^{235}U$ or $^{236}U$, because it was more readily available and calculations indicated that sufficient loading could be achieved to compensate for the smaller cross-section. The molecule was mixed with a liquid scintillator made from toluene and two wavelength-shifting dyes, 2,5diphenyloxazole **(**PPO) and *p*-phenylenbis(5-phenyl-2-oxazol) (POPOP). Typical loadings of the fissionable molecules were between 1-5

weight percent.

The optical and radiation properties of the solutions were thoroughly characterized and difference between the radioluminescence (RL) of the depleted uranium/liquid scintillator solution and that of liquid scintillator alone were observed. Liquid scintillator consists of toluene with a primary wavelength shifter and a secondary wavelength shifter. The primary shifters absorption band overlaps the toluene emission band and the secondary shifters absorption band overlaps the primary shifters emission band. The peak RL emission of the $^{238}U$ (DU) solution occurs at a slightly higher wavelength than the RL of the unloaded liquid scintillator, and has several additional peaks. This most likely results from luminescence by the $UO_2^{2+}$, whose absorption band overlaps the emission band of PPO, the primary wavelength shifter used in the liquid scintillator [1]. Unfortunately, the RL of the DU solution is also much less intense, indicating quenching of the liquid scintillator by the DU complex. The weak luminescence of the DU solution, as well as the solution's yellow color, which absorbs some of the blue scintillation light, resulted in pulse height spectra, using $^{60}Co$ and $^{137}Cs$ sources that were indistinguishable from background. Although originally it had been hoped that the uranium luminescence would allow us to eliminate the need for wavelength-shifting dyes, the RL and gamma response indicated that the liquid scintillator would need to be reformulated to avoid energy transfer to the uranium molecules.

We explored this possibility by replacing POPOP, the secondary wavelength shifter, with 3-hydroxyflavone (3HF). This would shift the emission from about 420 nm to about 530 nm, which should reduce the energy transfer between the $UO_2^{2+}$ and the secondary shifter. However, this has no effect on the energy transfer due to the overlap of the primary shifter emission with the $UO_2^{2+}$ absorption. The RL of the DU-loaded liquid scintillator consisting of toluene and PPO was much more intense than the RL of the same solution with the addition of 3HF, indicating that the energy transfer predominately takes place between the primary shifter and the $UO_2^{2+}$. This was further confirmed by the observation of 3HF luminescence, though the total number of counts was much smaller, indicating that the energy transfer process is inefficient.

Based on these results, we decided to switch to a molecular form of thorium, $Th(NO_3)_2(TBP)_2$, which has a lower fission cross-section and threshold neutron energy but is colorless and does not luminesce in the uv-vis region. As shown in Figure 1, the addition of $^{232}Th$ to the liquid scintillator increases the RL intensity slightly, likely due to the higher effective Z increasing the x-ray absorption. More importantly, this does not shift the wavelength of the emission, indicating there is no quenching of the liquid scintillator by the thorium compound. This result indicated that the solution's response to neutron irradiation was worthy of investigation at LANSCE.

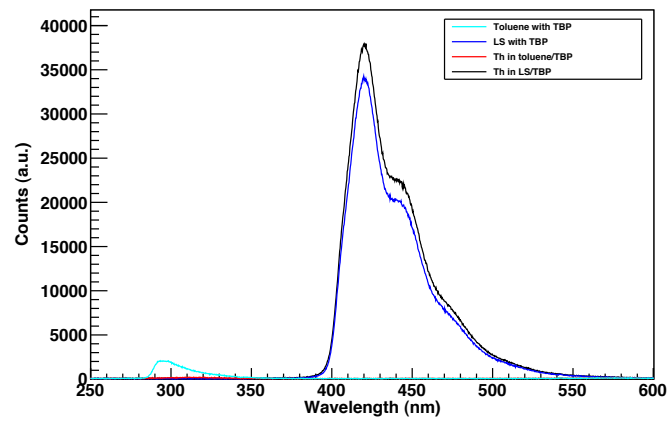


*Figure 1. Radioluminescence of liquid scintillator with and without thorium compound.*

A 100 mL liquid scintillator solution loaded with thorium was prepared and placed in the neutron beam at LANSCE. A region of the resulting pulse height distribution is shown in Figure 2. The peak visible near -0.3 V is the result of fission events. Subsequent analysis of the pulse-area distribution illustrates the potential to identify different events in the detector based on the area of the resulting pulses.

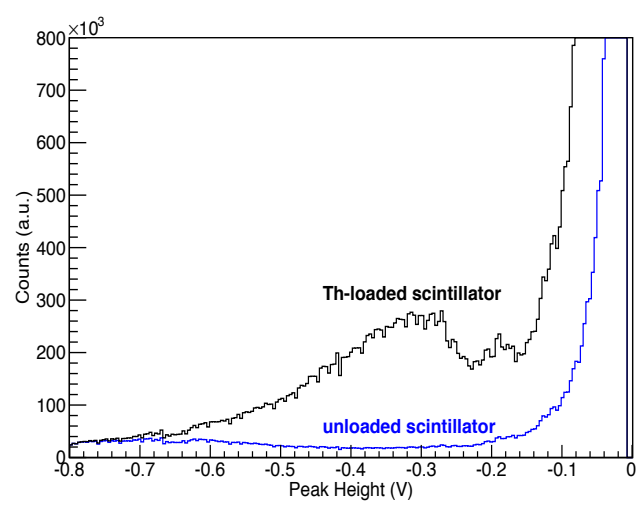


*Figure 2. Pulse height distribution from Thorium-loaded liquid scintillator.*

## Future Work

Future research focuses on the synthesis of fissionable nanoparticles. As shown in Figure 3, $^{232}Th$ has a neutron energy threshold for fission, so a thorium-based detector

will be unable to detect neutrons with energies less than a few keV. Using nanoparticles of $^{235}U$, $^{238}U$, or $^{237}Np$ may enable us to minimize the coloring and luminescence effects that made the uranium molecular solutions unsuitable. The first stage of this research involves the synthesis of $^{232}Th$ nanoparticles, to determine how the response of a nanocomposite scintillator differs from that of a molecular scintillator.

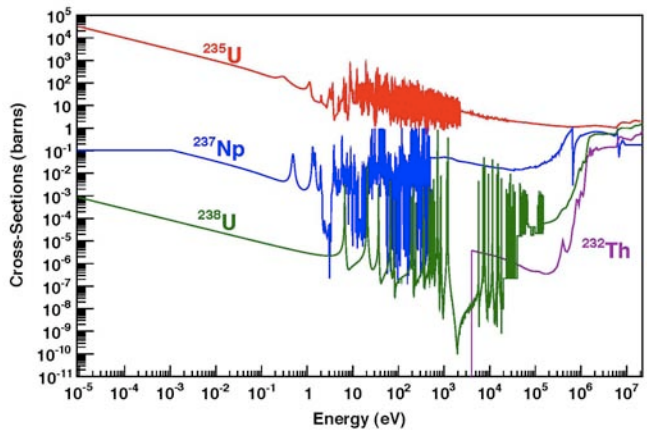


*Figure 3. Total fission cross-sections of isotopes of interest for nano-fission detectors.*

It was determined that synthesizing the nanoparticles originally proposed for Year 1 ($^{209}Bi$, $^{197}Au$, and $^{181}Ta$) would not produce useful information on synthesizing actinide nanoparticles, the eventual goal of this project. Loading a fully-optimized liquid scintillator with fissionable molecular material instead fulfilled the proof-of-principle goal. We are still on track to produce actinide nanoparticles during the period of this project, and have recently added an actinide chemist to our team to head this effort.

## Conclusion

We have optimized the liquid scintillator and measured its optical and gamma-ray detection properties, both with and without the addition of fissionable material. We have manufactured four detector elements suitable for fission flux monitors, with volumes of 100, 200, and 350 mL. We have loaded these detector modules with a solution of liquid scintillator and thorium and characterized their responses in the LANSCE beamline, partially fulfilling a Year 3 milestone and providing us with data acquisition and experiment setup experience that will allow us to streamline additional beamline tests. We have reached most of the milestones listed in our proposal for Year 1 and Year 2, and are on track for Year 3.

## References


1. Blasse, G., and A. Bril. Investigation of some Ce3+ activated phosphors. 1967. *J. Chem. Phys.*. **47**: 5139.


## Publications


Esch, E., S. Stange, A. J. Couture, R. E. Del Sesto, L. Jacobsohn, T. M. McCleskey, E. A. McKigney, R. E. Muenchausen, D. Ortiz-Acosta, R. Reifarth, F. L. Taw, and F. Tovesson. Nano-composite based radiation detectors for beam experiments. Presented at *CAARI 08.* (Ft. Worth, TX, August 08).

Esch, E., S. Stange, R. E. Del Sesto, R. E. Muenchausen, D. Ortiz-Acosta, and F. K. Tovesson. Research status on new fission based solid-state neutron detectors. To appear in *IEEE 08.* (Dresden, Germany, October 2008).

Stange, S., E. I. Esch, R. E. Muenchausen, R. E. Del Sesto, F. L. Taw, F. Tovesson, and E. Burget. Nano-fission detector program at LANL. To appear in *IEEE NSS 09.* (ORlando, FL, Octoberr 09).

# Efficient Structures for Low-Energy Acceleration of Light Ions

*Sergey S. Kurennoy*
20080228ER

## Introduction

Compact particle accelerators are important and enabling technologies for a variety of applications from medical therapy to imaging to active interrogation. Our project aims to develop novel compact and efficient accelerator structures for low-energy charged particles. The H-mode resonator cavities are about ten times more efficient at the beam velocities around a few percent of the speed of light compared to the usual drift-tube linear accelerator (DTL). The H-mode accelerators also have transverse dimensions a few times smaller than those of the DTLs. However, keeping the beam transverse size small to avoid losses is inherently difficult in H-cavities compared to the DTL where the beam focusing is achieved with electromagnetic quadrupole magnets placed inside its large drift tubes. We suggested inserting permanent-magnet quadrupoles (PMQs) inside the H-cavity small drift tubes to solve the focusing problem without any reduction of the accelerating efficiency [1]. The high efficiency of the H-PMQ accelerator gives a new option of using small inexpensive radio-frequency (RF) generators as its power source instead of usual large and expensive RF klystrons. The high-efficiency H-mode accelerator structures with PMQ beam focusing for low-energy light ions have multiple applications, either in stand-alone accelerators or as a part of the front end in ion linear accelerators.

Designing such an accelerator for considerable ion-beam currents requires a careful balance of beam-physics and engineering considerations. We plan to achieve this balance by combining electromagnetic 3-D modeling with beam dynamics simulations and engineering thermal-stress analysis.

## Benefit to National Security Missions

This project will support the DOE missions of Treat Reduction, Non-Proliferation, Homeland Security, and the Office of Science research missions, by providing high-efficiency accelerators of light ions. For example, a compact 4-MeV deuteron accelerator can drive a mobile intense neutron and gamma source for interrogation of special nuclear materials.

## Progress

Significant progress has been made in developing room-temperature H-mode accelerator structures with PMQ beam focusing for low-energy ions. The focus for the FY09 was to design a complete inter-digital H-mode (IH) tank using combined electromagnetic (EM) and beam-dynamics (BD) modeling, and engineering thermal-stress analysis (EA). Our previous efforts focused on analyzing just one or a few periods of the H-mode structures [1-5]. An IH tank includes many periods and two end cells where the magnetic flux turns to make a loop; the end-cell design is complicated but very important since it influences the field profile in the tank. We chose to design a short IH tank, 2-3 feet long, since it is easier to manufacture here at LANL. On the other hand, its design incorporates all details of the full-length IH tank. The aluminum model of such a tank will serve as a cold model that we will test at low RF power in FY10.

We designed two different short IH tanks. The first IH tank (IH1) [6] can be the first stage, after a short radio-frequency-quadrupole (RFQ) accelerator, in a 1-4 MeV IH-PMQ 201.25-MHz deuteron accelerator with 50-mA beam current, for interrogation of SNM in cargo. The tank includes 20 drift tubes (DT) containing PMQs and covers the beam velocity range from 3.3 to 5 percent of the speed of light, corresponding to the deuteron beam energies from 1 to 2.25 MeV, with the accelerating gradient of 2.5 MV/m. Its total length is 63 cm; the cavity inner radius is 11.5 cm. For the nominal duty factor of 10%, the power dissipated in the tank walls is 1.34 kW, which is significantly smaller than the power put into the beam, 6.25 kW. Beam-dynamics simulations for IH1 in an axisymmetric approximation with the Parmila code showed that the 50-mA beam fills a significant part of the aperture that can lead to particle losses.

Based on these results, we increased the beam-injection energy from 1 to 1.5 MeV, where the space-charge forces are lower and beam size is smaller. Using the developed iterative procedure, the second short IH tank (IH1L) was designed much faster, in a few days. It covers the beam velocity range from 4 to 5.5 percent of the speed of light (deuteron beam energies from 1.5 to 2.8 MeV), with 2.5 MV/m gradient. The tank IH1L is longer, with the total length of 73.5 cm; the cavity inner radius is 11.9 cm, Figure 1. At the nominal duty factor of 10%, the power dissipated in the tank walls is 1.91 kW, while the power put into the beam is 6.5 kW. The RF power input for such power values can be provided with a simple loop on the tank wall.

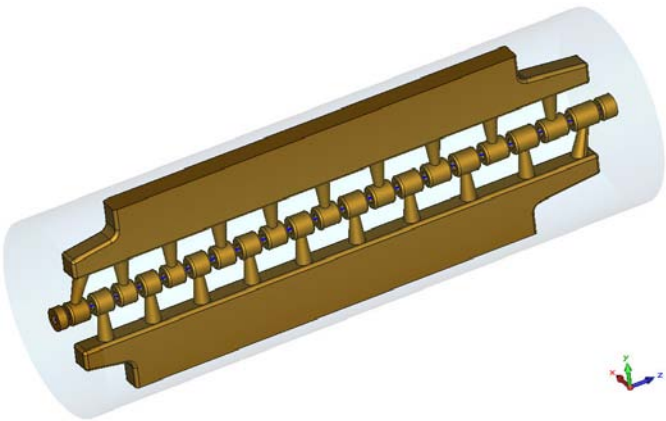

*Figure 1. MWS model of a short IH-tank (73.5 cm) with gradually increasing cell lengths. The drift tubes are supported by stems attached alternatively to two vanes. The outer cavity wall is removed to show the end-cell design.*

EM and BD iterations have been performed to adjust the electric field profile along the tank to be consistent with the PMQ focusing for a 50-mA deuteron beam. We have developed a simple algorithm similar to that in the Parmila linac design code that allows performing quick design iterations based on the on-axis electric field computed by our 3-D electromagnetic (EM) code, MicroWave Studio (MWS). For multi-particle BD simulations we made modifications of the Parmila simulation code and used the input from the MWS. In the IH1 tank the electric field profile was tuned to be flat [6]. For the tank IH1L we made the electric field gradually increasing along the tank at the same rate as the cell length increases, so that the average accelerating gradient per cell is constant. We also adjusted the locations of the accelerating gaps to correspond to the required RF-phase ramp along the structure. All these modifications lead to a better beam dynamics. The results of the Parmila multi-particle simulation prove that the tank can accelerate a 50-mA deuteron beam with the realistic emittance without losses using only two families of the PMQs.

Following our research plan, we have developed an interface for transferring data between the 3-D EM code, MWS, and engineering codes, COSMOS and ANSYS. We performed iterative EM-engineering analysis of the IH tank and demonstrated the effectiveness of its water cooling with cooling channels located only in the vanes supporting the structure drift tubes [4-6]. The temperatures of PMQ in the tank DTs, as well as the structure stress, remain well within the acceptable range. For the IH1 tank with water cooling in vanes, the highest temperature was below 35° C for 10% duty operation [6], Figure 2. This confirms feasibility of room-temperature H-PMQ accelerator concept since in effective H-mode structures there can be no cooling channels inside DTs while the PMQ temperatures must be kept below 150-200° C.

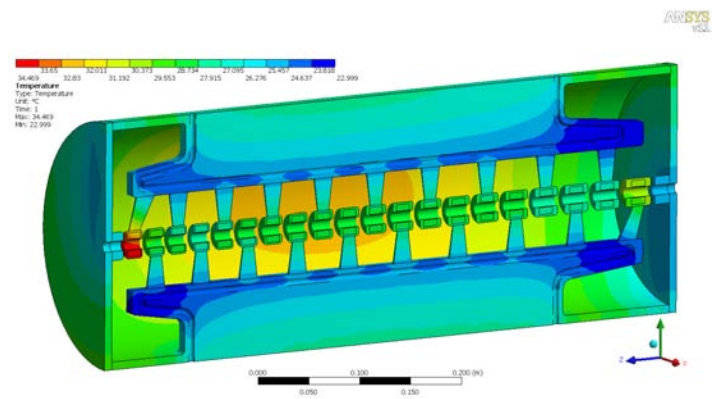

*Figure 2. Temperature distribution in the IH tank with two cooling channels in the vanes and two simple cooling loops in the end walls at the nominal 10% duty.*

We explored the frequency and field sensitivity of the working mode in the IH tank to tank dimension variations using 3-D EM MWS modeling. A simple scheme with slug tuners for frequency and field-tilt tuning of the tank was developed; it will be implemented in the cold model. The cold-model design was finalized, and the drawings were completed in Sep. 2009.

We made a good progress in developing a procedure for transferring 3-D EM fields in H-mode structures computed by the MicroWave Studio to the multi-particle tracking codes, like Parmela and TRACK. This procedure now allows us to perform detailed multi-particle beam-dynamics simulations using realistic fields from 3-D EM analysis, both RF fields from MWS and the magnetic fields of 16-segment PMQs computed by the CST Electromagnetic (EM) Studio. We have just completed a first full 3-D multi-particle analysis of the IH1L tank with the Parmela code, and the results indicate no particle losses at the level of $5{\cdot}10^{-5}$, Figure 3. Such simulations will help explore the structure sensitivity to manufacturing errors and establish the manufacturing tolerances for the accelerator.

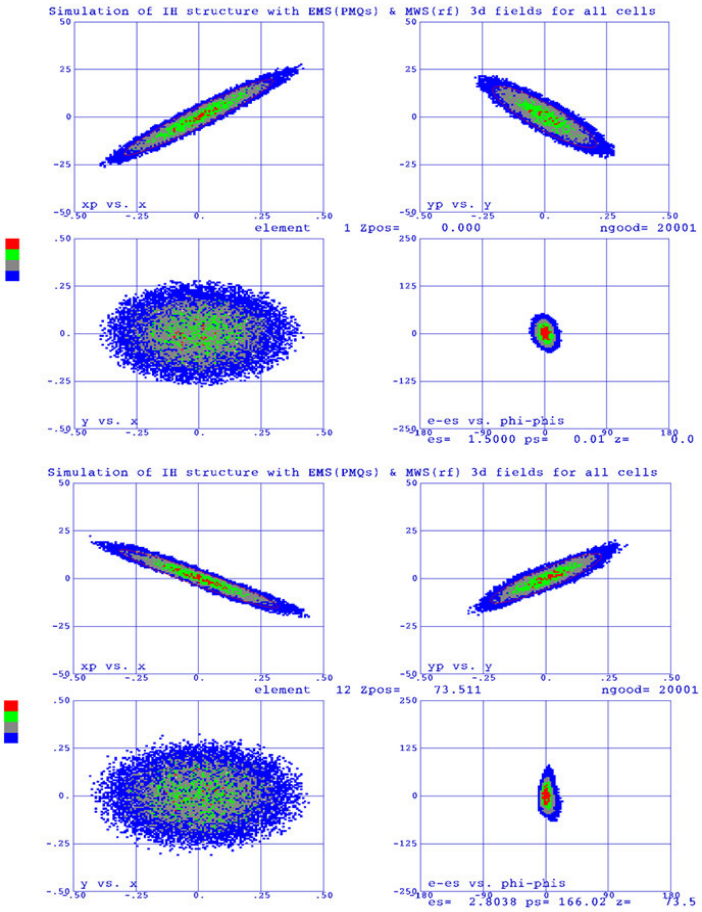


*Figure 3. Results of Parmela multi-particle beam dynamics simulation of the IH-PMQ structure in Fig. 1 with 50-mA deuteron beam: top - matched input beam at 1.5 MeV; bottom - output beam at 2.8 MeV. Computed 3D RF and magnetic (PMQ) fields were employed in simulation.*

Our project to date resulted in three invited talks, five conference publications, and four technical notes. There is a significant interest to the IH-PMQ accelerator technology from industry and medical-accelerator projects. We had discussions on possible CRADA agreements with two industrial companies. In particular, AccSys Technology Inc (Pleasanton, CA) is interested in acquiring our H-mode linac technology for medical applications. The company included funds for a CRADA with us in their budget for CY09; unfortunately, the final decision to proceed with the CRADA was postponed due to their uncertain financial situation.

## Future Work

We are developing novel room-temperature accelerator structures for low-energy protons or deuterons by combining H-mode resonator cavities and a strong transverse beam focusing using permanent-magnet quadrupoles (PMQ). Achieving a balance of the structure efficiency, beam quality, and thermal management requires multiple iterations of electromagnetic modeling (EM), beam dynamics (BD), and engineering thermal-stress analysis (EA). We have developed the efficient interface between the available EM, BD, and EA codes for this process.

The project milestones for the FY10 are:

- IH-tank cold model manufactured and tested.
- Full 3-D multi-particle analysis of the beam propagation through the IH tank completed.

## Conclusion

We expect that our research will produce the following results:

1. Conceptual design of novel high-efficiency room-temperature accelerating structures for light ions in the low-beam-velocity range, based on H-mode cavities with a strong transverse beam focusing by permanent-magnet quadrupoles, which can be used in multiple applications;
2. Effective interface between the codes for a combined Electromagnetic-Beam-dynamics-Engineering analysis that will also be useful for various accelerator projects at LANL or other labs;
3. Cold model (full-size aluminum model tested at low RF power) of H-mode accelerating structure that confirms the design and fabrication concept.

Among many possible applications of room-temperature H-mode structures, two deserve our special attention. One is a compact 4-MeV deuteron accelerator for homeland defense (an intense neutron and gamma source for interrogation of special nuclear materials). Another application could be a cost-effective replacement of the aging DTL in the LANSCE linear accelerator.

## References

1. Kurennoy, S. S., L. J. Rybarcyk, and T. P. Wangler. Efficient accelerating structures for low-energy light ions. 2007. (Albuquerque, NM, USA, 25-29 June 2007). p. 3824. New York, NY: IEEE.
2. Kurennoy, S. S., S. Konecni, J. F. O'Hara, and L. J. Rybarcyk. IH accelerating structures with PMQ focusing for low-energy light ions. 2008. (Genoa, Italy, 23-27 June 2008). p. 3428. Geneva, Switzerland: European Physical Society .
3. Kurennoy, S. S.. IH accelerating structures with PMQ focusing. 2008. *Los Alamos National Laboratory Report*

*LA-UR-08-03795.*

4. Kurennoy, S. S., J. F. O'Hara, and L. J. Rybarcyk. Compact linac for deuterons. 2008. (Nashville, TN, USA, 25-29 Aug. 2008). p. 428. Nashville, Tennessee, USA : ORNL.

5. Kurennoy, S. S., J. F. O'Hara, E. R. Olivas, and L. J. Rybarcyk. Efficient low-beta H-mode accelerating structures with PMQ focusing. 2008. (Victoria, BC, Canada, 29 Sep. - 3 Oct. 2008). p. 954. Victoria, BC, Canada: TRIUMF.

6. Kurennoy, S. S., J. F. O'Hara, E. R. Olivas, and L. J. Rybarcyk. Development of IH accelerating structures with PMQ focusing for low-beta ion beams. To appear in *Particle Accelerator Conference 2009 (PAC2009).* (Vancouver, BC, Canada, 4-8 May 2009).

## Publications

Kurennoy, S. S.. IH accelerating structures with PMQ focusing. 2008. *Los Alamos National Laboratory Report LA-UR-08-03795.*

Kurennoy, S. S., J. F. O'Hara, E. R. Olivas, and L. J. Rybarcyk. Efficient low-beta H-mode accelerating structures with PMQ focusing. 2008. In *XXIV Linear Accelerator Conference (Linac08).* (Victoria, BC, Canada, 29 Sep. - 3 Oct. 2008). , p. 954. Victoria, BC, Canada: TRIUMF.

Kurennoy, S. S., J. F. O'Hara, E. R. Olivas, and L. J. Rybarcyk. Development of IH accelerating structures with PMQ focusing for low-beta ion beams. To appear in *Particle Accelerator Conference 2009.* (Vancouver, BC, Canada, 4-8 May 2009).

Kurennoy, S. S., J. F. O'Hara, and L. J. Rybarcyk. Compact linac for deuterons. 2008. In *42nd ICFA Advanced Beam Dynamics Workshop on High-Intensity High-Brightness Hadron Beams.* (Nashville, TN, USA, 25-29 Aug. 2008). , p. 428. Nashville, TN, USA: ORNL.

Kurennoy, S. S., L. J. Rybarcyk, and T. P. Wangler. Efficient accelerating structures for low-energy light ions. 2007. In *Proceedings of Particle Accelerator Conference 2007.* (Albuquerque, NM, USA, 25-29 June 2007). , p. 3824. New York, NY: IEEE.

Kurennoy, S. S., S. Konecni, J. F. O'Hara, and L. J. Rybarcyk. IH accelerating structures with PMQ focusing for low-energy light ions. 2008. In *Proceedings of European Particle Accelerator Conference 2008.* (Genoa, Italy, 23-27 June 2008). , p. 3428. Geneva, Switzerland: European Physical Society.

# Compact Millimeter Wave Spectrometer Based on a Channel Drop Filter

*Lawrence M. Earley*
20080409ER

## Introduction

Terahertz and millimiter-wave devices are proving to have many important applications from sensing and imaging to communication. Among the greatest impediments to exploiting this regime of the electromagnetic spectrum are the difficulties in building sources with sufficient power and sensors with the necessary sensitivity suitable for practical applications.

In this project, we have designed and are constructing a novel passive mm-wave spectrometer based on a Photonic Band Gap (PBG) channel-drop filter (CDF). There is a need for a compact wide-band versatile and configurable mm-wave spectrometer for applications in mm-wave communications, radio astronomy, and radar receivers for remote sensing and nonproliferation. We have designed different CDF spectrometers working in the frequency range from 90 to 300 GHz. The spectrometer operating at 250 GHz can be employed in remote sensing missions for detection of methyl chloride. The primary objective of the research is to develop a fabrication technique for PBG CDF spectrometers at mm-waves, and test proof-of-principle spectrometers. We consider the Micro-Electro-Mechanical Systems (MEMS) technology for fabrication, which involves dry-etching the PBG structure on a 6-inch silicon wafer and then bonding it in between the metallic plates. Fabrication of a mm-wave PBG CDF is at the cutting-edge of MEMS technology, in particular, it pushes the limits of the dry-etching process. However, MEMS is the very high potential technology for fabrication of the devices at mm-waves to fill the so-called "terrahertz gap," where the conventional fabrication techniques are not applicable. Therefore, exploring and advancing the limits of MEMS technology is of the great importance. Creation of a novel ultra-compact, wide-band, configurable, and easy to operate under all weather conditions mm-wave spectrometer would enable Laboratory missions in both national security and basic research and directly addresses the laboratory grand challenge "Detection of nuclear materials (Ubiquitous sensing)."

## Benefit to National Security Missions

This project, through the development of a new mm-wave spectrometer, will impact a broad range of technical problems including imaging, sensing, and communication. These technical areas are crucial for supporting threat reduction, nuclear material detection, and other missions important to DOE (NN), DHS (DNDO), DOD(DARPA) and other government agencies.

## Progress

The project has made significant progress up to date. Several configurations of the Photonic Band Gap (PBG) Channel-Drop Filters (CDFs) were designed and experimentally evaluated.

In the first year, we have studied fabrication of a 98 GHz version of the PBG CDF with a MEMS process. The MEMS fabrication process for the channel-drop filter consists of four stages. First stage is fabrication of the high-resistivity (resistivity of 100 Ohm*cm) silicon wafers. Second stage is the creation of the thermal oxide mask on top of the wafer. Third stage is the dry-etching of the wafers to create the PBG structures. And the final stage is the gold-plating of the PBG structure and bonding with the metallic plates. The first two fabrication stages were very successful. The dry-etching process, however, was found to push the limits of the existing technologies. Fabrication of the proof-of-principle filter at the frequency of 98 GHz required etching PBG rods, which are 1000 micro-meters high. However we have discovered that etching beyond 650 micro-meters caused degrading of the thermal-oxide mask. Even when it was decided to limit height of the PBG rods to 500 um, the PBG structure suffered from significant undercuts, which resulted in poor performance and additional losses. The gold-plating and bonding processes also proved to be successful. We have learned however that

at higher frequencies, in particular at the frequencies around 250 GHz, which are important for detection of methyl chloride and other chemicals, the third step of the fabrication process will be successful due to smaller dimensions of the structure.

Based on the outcome of the first year, the second year progressed as follows. The laboratory equipment was upgraded with the new testing heads that would allow us to conduct mm-wave measurements in the 220-325 GHz frequency range. The CDF was re-designed to operate at the frequency of 235 GHz (Figure 1). The fabrication procedure was re-evaluated and the fabrication of the higher frequency filter was started. New high-resistivity silicon wafers were purchased with the resistivity of 5000 Ohm*cm, which is 50 times higher than in the first year. This should significantly decrease Ohmic losses in the structure. New mask designs were developed to reduce the undercuts during the etching process. These new designs incorporated retaining walls of different shapes that were supposed to confine plasma and make undercuts smaller. The results of the etching were perfect with the undercuts less than 1.5 degrees (Figure 2). The undercuts were the smallest for the designs with retaining walls. The structures were successfully diced from the wafers and bonded to gold plates on top and bottom and cleaned. The detailed fabrication process was thoroughly documented. Several of the produced devices (Figure 3) were tested in a mm-wave laboratory. All samples produced similar results. Measured transmission characteristics were in excellent agreement with computations. In our best sample, we have observed the frequency of 240 GHz being transmitted into the sampling channel.

In the second experiment, we have redesigned the W-band CDF to be fabricated with metal rods. We employed the conventional machine shop to fabricate the metal filter. However, it was predicted, that the standard machining tolerance would be insufficient for the proper operation of the filter, and therefore some tuning would be required in the experiment. The metal filter was tested in the laboratory and tuning was performed. At the frequency of 106 GHz a strong peak in transmission was observed, which perfectly agreed with the design. However, the design was not mechanically robust due to metal rods sliding in an out of the filter. To solve the problem, we decided to manufacture the metal filter in a different way. The filter is now being electroformed as a single copper crystal with no separate parts. We are currently studying different tuning concepts for the electroformed device.

The results of this work were reported at the 34th International Conference on Infrared, Millimeter, and Terahertz Waves in Busan, Korea [1] and a paper was submitted to Applied Physics Letters [2].

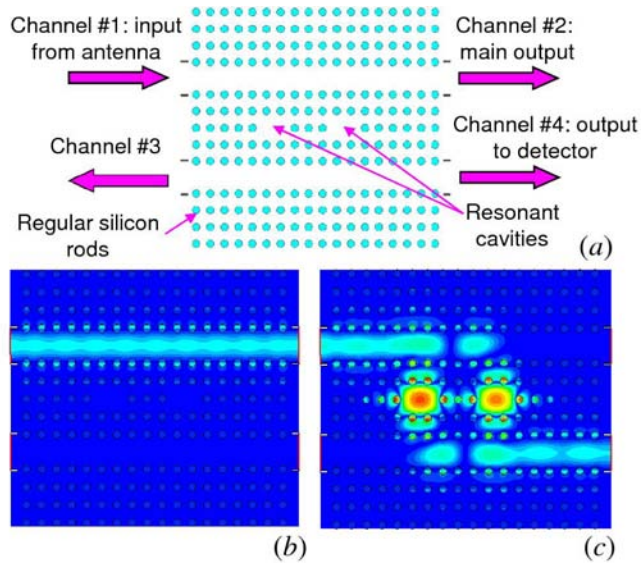


*Figure 1. Schematic of a channel-drop filter (a). Electric field energy density for non-resonant frequency (b) and for the resonant frequency (c). Power transmits straight into channel 2 for all frequencies, except for the resonance, when it transmits into channel 4 through the resonant cavities.*

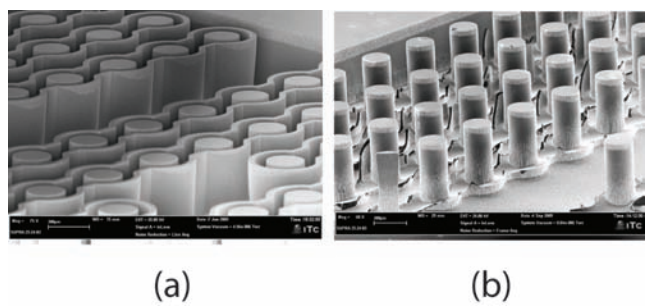


*Figure 2. Microscope image of the silicon rods of the channel-drop filter with sacrificial structures still in place (a), and following mechanical removal of sacrificial walls (b).*

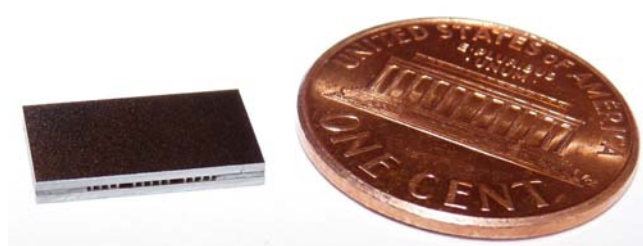

*Figure 3. Photograph of the channel-drop filter and scale.*

## Future Work

Based on the progress up to date the work plan for the FY 2010 was modified as follows:

- We will fabricate, test and tune a single-channel metal filter operating at the frequency of 100GHz.

- We will design and fabricate the silicon CDF spectrometer for detection of the methyl chloride lines of 237 GHz, 262 GHz, and 288 GHz. We will measure the characteristics of the constructed filter and measure the methyl chloride spectra.

## Conclusion

At the end of this project there will exist a new electronic device that will be capable of enhancing several national security missions. This new device will be a small and lightweight spectrometer that can be used for detection of nuclear material and be used by our military forces in radar and secure communications. The new device will allow improved nuclear material detection and make our military systems more secure with better performance.

## References


1. Yu.Shchegolkov, D., C. E. Heath , L. M. Earley, and E. I. Smirnova. Design and Testing of Photonic Band Gap Channel-Drop-Filters. To appear in *34th International Conference on Infrared, Millimeter, and Terahertz Waves.* (Busan, Korea, 21-25 September, 2009).

2. Smirnova, E. I., L. M. Earley, C. E. Heath, D. Yu. Shchegolkov, and B. D. Schultz. FIRST EXPERIMENTAL DEMONSTRATION OF A PHOTONIC BAND GAP CHANNEL DROP FILTER AT 240 GHZ. *Applied Physics Letters.*


## Publications


Smirnova, E. I., L. M. Earley, C. E. Heath, D. Yu. Shchegolkov, and B. D. Shchultz. First experimental demonstration of a photonic band gap channel drop filter at 240 GHz. *Applied Physics Letters.*

Smirnova, E. I., L. M. Earley, C. E. Heath, and D. Yu. Shchegolkov. Design and fabrication of a 100 GHz channel-drop filter. 2008. In *33rd International Conference on Infrared, Millimeter, and Terahertz Waves.* (Pasadena, CA, 15-19 Sept. 2008). , p. 1175. Online: IEEE.

YuShchegolkov, D., L. M. Earley, C. E. Heath, and E. I. Smirnova. Design and testing of photonic band gap channel-drop-filters. To appear in *The 34th International Conference on Infrared, Millimeter and Terahertz Waves.* (Busan, Korea, 21-25 September, 2009).

# Novel High Performance Terahertz Metamaterial Photonic Devices

*John F. O'Hara*
20080414ER

## Introduction

The control of electromagnetic (EM) waves influences nearly every aspect of our lives, from communications with cell phones, radios, and fiber optics to simply capturing a photograph with a camera. Technological advances have made it possible to control EM waves of nearly every type including radio waves, microwaves, infrared, visible, and ultraviolet light, and x-rays. There is one notable exception: terahertz (THz) waves. Terahertz science has been pursued heavily since the early 1990's in an effort to overcome this hurdle. Still, practical devices suitable for controlling THz waves simply do not exist and THz technology has consequently failed to graduate into real-world usability. Despite this, THz science remains an important pursuit because there are many promising THz applications including: covert identification of chemical and biological agents, security screening where THz is used to see inside of closed packages, ultra-broadband communications, and even environmental and quality control. The problem is that known natural materials are suitable to control almost all EM waves except THz. Our project is to create new materials that control THz waves very well; these are called metamaterials. Metamaterials are engineered materials that allow designers to control EM waves in numerous ways. We combine natural materials (e.g. metals, insulators, and semiconductors) to create metamaterials that are specifically tuned for THz control. Furthermore, they can be manipulated in real-time to actively adjust this control, something very few natural materials can do. This cutting-edge approach offers unprecedented levels of functional versatility. In short, metamaterials provide a method of controlling THz in ways not previously possible. This represents a major impact to THz science, engineering, and technology, but it also offers fundamentally new science opportunities.

## Benefit to National Security Missions

This project serves as a benefit to national security in several ways. It enhances our fundamental understanding of materials, creates new capabilities in sensing, and opens the door for new threat reduction technologies by improving our ability to use this unique (and largely unused) portion of the electromagnetic spectrum. Due to the fundamental but applied nature of this work, it broadly supports numerous important mission areas for DOE, DOD, DHS, and other government agencies. In fact, the work has already led to further financial support from external government agencies in the form of related, but more applied, projects.

## Progress

There has been excellent progress so far on this project, mainly in modulation of freely propagating THz waves. Briefly, modulation is the altering of a wave frequency, phase, or amplitude for the purpose of imprinting information on that wave. Modulation of freely propagating waves is the backbone of myriad important technologies, such as radar and wireless communications. Since methods to modulate THz waves are so immature, any such technology enabler is a very important step forward. We have now demonstrated numerous state-of-the-art THz modulators.

To begin, we demonstrated fast amplitude modulation of freely propagating THz waves with modulation depths up to ~50% (previous comparable technologies reached only ~3% modulation depth) and at speeds up to 2 MHz. This work has transitioned into actual device research where we have demonstrated a new form of spatial light modulator, a device useful for THz imaging applications. We have also successfully demonstrated frequency-modulating metamaterials. Frequency modulation is one of the core concepts in modern technology, but has never before been demonstrated in THz waves. In this work, metamaterials were designed with special semiconductor inclusions. The semiconductors act like miniature switches that, when illuminated by laser light, change the electronic structure of the metamaterial. Essentially the semiconductors act like weights added to

a clock's pendulum. When weight is added to a pendulum it swings more slowly, or equivalently its resonance frequency is lowered. Similarly, when our semiconductors are illuminated, they lower the metamaterial's resonance frequency, thus modulating the frequency at which the material and THz waves interact. These important results were published in the prestigious Nature Photonics journal.

In the last year we have had numerous important breakthroughs. For one, we have that our modulating devices may operate over a wide frequency range despite the fact that they are tuned to operate at a single frequency. This fortunate but unexpected result stems from the fact that metamaterials manipulate THz waves simultaneously in many ways, a fact we can exploit for improving THz technology. We have also found a technique that uses metamaterials to control the polarization of THz waves. We can use this metamaterial with a THz generator that emits two separate THz waves, each one having a different polarization and each one controlled by a user-provided electronic signal. Polarization-sensitive metamaterials convert these two waves into a single modulated wave that can carry the information provided by the user. The method effectively converts a polarization-modulated THz wave, which can be created relatively easily, into a frequency-modulated wave, which is very difficult to create. We believe this may enable a new form of secure, giga-bit per second wireless communications. We have already published results on our polarization-controlling metamaterials, but are still developing the full modulator system.

Our metamaterial modulator work has also transitioned into a related technology in which THz waves may be modulated with sub-wavelength hole arrays. These are thin sheets of metal fabricated on semiconductors and perforated with periodic arrays of holes. Their purpose is to create surface plasmons, which are EM waves that travel along the metal/semiconductor interface. Their effect is like metamaterial resonators in that they modulate the amount of wave energy that can travel through the device. With this structure we have demonstrated yet another form of ultrafast THz wave modulation at room temperature using photonic (laser) control.

Also, we are nearly completing the development of an electronically controlled frequency modulator. Until now, we have only accomplished frequency modulation by means of photonic control. Electronic control is far more convenient from an applications perspective and also relieves certain loss problems associated with photonic metamaterial control. We have now designed and are fabricating a THz frequency modulator that is electronically controlled by combining metamaterials with a nonlinear semiconductor device, known as a varactor. We anticipate measured results on the performance of this device within a couple of months.

Finally, we have begun fabricating a special THz lenses suitable for focusing freely propagating THz waves. Based on numerous studies, we have determined that very thin metamaterials can be used to achieve the same focusing behavior as a traditional thick lens. Such an approach has the benefit of producing extremely lightweight and compact lens designs. In addition metamaterials enable even greater performance gains. For example, metamaterial lenses can be modified so that they cannot reflect any THz waves and therefore do not waste any THz energy in doing their job. This is all comparable to making eyeglasses in which the lenses are paper-thin, flat, and invisible but still correct the wearer's vision. We have just submitted a paper for publication demonstrating this anti-reflection behavior.

## Future Work

Our future tasks will be to complete the several ongoing studies involving THz modulation, high-speed communication via polarization-sensitive metamaterials, creating the metamaterial THz lenses, and the electronic frequency modulator. This should bring us nearly to the end of this LDRD project, however, the research is proving to be very fruitful and we expect numerous additional developments as we continue. Already the work has drawn small follow-on funding from external sponsors eager to utilize our science in new applications.

## Conclusion

We have developed new devices for manipulating freely propagating terahertz waves. These devices include frequency and amplitude modulators, high-speed communication components, and focusing devices, all of which did not previously exist or were extremely immature THz technologies. Most of our work has been experimentally demonstrated and the remaining is in development. Our new devices all utilize metamaterials concepts to overcome the weaknesses inherent in natural materials with respect to controlling THz waves. Most of our devices also utilize novel concepts that permit a user to actively control the performance of the device. This work represents fundamentally new advances in manipulating terahertz waves. This is increasingly interesting for myriad homeland security and/or defense related missions as it represents a unique and untapped technology.

## Publications


Azad, A. K., H. T. Chen, S. R. Kasarla, A. J. Taylor, Z. Tian, X. Lu, W. Zhang, H. Lu, A. C. Gossard, and J. F. O'Hara. Ultrafast Optical Control of Terahertz Surface Plasmons in Subwavelength Hole Arrays at Room Temperature. 2009. *Applied Physics Letters.* **95**: 011105.

Azad, A. K., Z. Tian, H. T. Chen, X. Lu, S. R. Kasarla, W. Zhang, A. J. Taylor, and J. F. O'Hara. Ultrafast Optical Control of Terahertz Surface Plasmon Polariton in Subwavelength Hole-Arrays at Room Temperature. 2009. In *Conference on Lasers and Electro-Optics.* (Baltimore, May 31 - June 5, 2009). , p. CWG4. New Jersey: Piscataway.

Azad, A., H. Chen, E. Akhadov, N. Weisse-Bernstein, A. Taylor, and J. O'Hara. Multi-layer planar terahertz electric metamaterials on flexible substrates. 2008. In *Conference on Quantum Electronics and Laser Science Conference on Lasers and Electro-Optics, CLEO/QELS 2008 ; May 4-9 2008 ; San Jose, CA, United States.*

Chan, W. L., H. T. Chen, A. J. Taylor, I. Brener, M. J. Cich, and D. Mittleman. A Spatial Light Modulator For Terahertz Beams. 2009. *Applied Physics Letters.* **94**: 213511.

Chen, H. T., W. J. Padilla, M. J. Cich, A. K. Azad, R. D. Averitt, and A. J. Taylor. A Metamaterial Solid-State Terahertz Phase Modulator. 2009. *Nature Photonics.* **3**: 148.

Chen, H. T., W. J. Padilla, M. J. Cich, A. K. Azad, R. D. Averitt, and A. J. Taylor. A Broadband Terahertz Metamaterial Electrical Modulator. 2009. In *Conference on Lasers and Electro-Optics (CLEO).* (Baltimore, May 31-June 5, 2009). , p. CThX1. New Jersey: Piscataway.

Chen, H., A. Azad, D. Shrekenhamer, W. Padilla, R. Averitt, A. Taylor, and J. O'Hara. Frequency tunable terahertz metamaterials. 2008. In *Conference on and Quantum Electronics and Laser Science Conference Lasers and Electro-Optics, QELS 2008 ; May 4-9 2008 ; San Jose, CA, United States.*

Chen, H., J. O'Hara, A. Azad, A. Taylor, R. Averitt, D. Shrekenhamer, and W. Padilla. Experimental demonstration of frequency-agile terahertz metamaterials. 2008. *NATURE PHOTONICS.* **2** (5): 295.

Chen, H., S. Palit, T. Tyler, C. Bingham, J. O. Zide, J. O'Hara, D. Smith, A. Gossard, R. Averitt, W. Padilla, N. Jokerst, and A. Taylor. Hybrid metamaterials enable fast electrical modulation of freely propagating terahertz waves. 2008. *APPLIED PHYSICS LETTERS.* **93** (9): 091117.

O'Hara, J., E. Smirnova, A. Azad, H. Chen, and A. Taylor. A circuit model for terahertz metafilms and effective medium implications. 2008. In *Conference on Quantum Electronics and Laser Science Conference on Lasers and Electro-Optics, CLEO/QELS 2008 ; May 4-9 2008 ; San Jose, CA, United States.*

Padilla, W. J., Hou-Tong Chen, J. F. O'Hara, A. J. Taylor, and R. D. Averitt. Opto-electronic control of terahertz metamaterials. 2007. In *Photonics: Design, Technology, and Packaging III ; 5 Dec.* ( 2007 ; Canberra, ACT, Australia). Vol. 6801, p. 68010H.

Peralta, X. G., E. I. Smirnova, A. K. Azad, H. T. Chen, A. J. Taylor, I. Brener, and J. F. O'Hara. Metamaterials for THz Polarimetric Devices. 2009. *Optics Express.* **17** (2): 773.

Peralta, X. G., I. Brener, A. K. Azad, H. T. Chen, E. Smirnova, A. J. Taylor, and J. F. O'Hara. THz Polarimetric Components Based on Metamaterials. 2009. In *Conference on Lasers and Electro-Optics (CLEO).* (Baltimore, May 31 - June 5, 2009). , p. CThFF. New Jersey: Piscataway.

# Efficient and Selective Photon Detection

*Michael D. Di Rosa*
20090189ER

## Introduction

Nearly all light-detection technologies to date involve a compromise between quantum efficiency and spectral selectivity. Quantum efficiency refers to the conversion of photons to measurable signal. Spectral selectivity refers to the slice of the broad electro-magnetic spectrum that the detector "sees". Techniques that narrow the spectral window through which a detector sees ordinarily reduce the overall quantum efficiency of the detector, sometimes drastically. Further, the spectral selectivity afforded by common methods often lets through a broader spectral slice than ideally wanted. Applications in light detection are sometimes abandoned in the wake of these limitations or untenable sacrifices in performance. However, those applications might be reconsidered if a new technology surmounted this age-old compromise between sensitivity and selectivity.

Our goal is to demonstrate a new photon-detection technology that promises a unique combination of near-perfect quantum efficiency and high spectral discrimination. The novel aspect involves an unconventional light amplifier. The amplifier draws on a quantum-coherent process known as amplification without inversion (AWI), a phenomenon of recent study that has not been analyzed in the context of light detection. The archetypal system of our study involves an atomic vapor and the detection of visible wavelengths. The spectral selectivity of amplification is a very narrow 10 one-millionths of a nanometer. Considering the breadth of the visible spectrum, this selectivity is the equivalent of choosing a particular one-inch segment from a 600-mile expanse. Other important characteristics include suitability for imaging applications, temporal gating, and a remarkably low noise of amplification. In practical use, this light amplifier would be the front-end to a common detector or detector array. The overall system would inherit the special properties of the amplifier. Because AWI, in principle, can be generated in many systems—atoms, molecules, and semiconductor materials—we believe our concept to be generally adaptable to different media and tunable to work at various wavelengths.

## Benefit to National Security Missions

Research on light detection, especially of faint signals and single photons, has numerous important applications including detecting chemical/biological agents, low-light imaging, and weapons activities. A new weak-light detection method is consistent with many missions including threat reduction, human health, and basic science of interest to DOE, DHS, and other government agencies.

## Progress

We made good progress this past year in the three aspects of theory, simulation, and experiment that compose our research. Our experimental work made particularly important strides toward our main research objective. As covered in the research proposal, we found a good match to our theoretical template for amplifying faint light signals through coherent, laser-driven process in the energy diagram of atomic mercury. Besides being a good match to theoretical constructs, atomic mercury (Hg) has other attributes, such as a high vapor pressure at room temperature and isotopes with zero nuclear spin, that favor its use in an initial study of these particular coherent processes.

While mercury had not been used before in studies of laser-driven coherent processes, the abundant literature on the spectroscopy of mercury confirmed its appropriateness and advantages in such studies. Our hurdle, and perhaps the hesitation of others to undertake similar studies with Hg, lay with the experimental manipulation of Hg into excited internal-energy states that gain entry into all the advantages that Hg appears to afford in studies of coherent processes. These states also had to be generated—continuously, steadily, and ideally easily—in order to adjust and

"lock" laser frequencies to particular transitions of Hg that partake in the coherent processes. This past year, and as described below, we made and tested a simple plasma discharge that excites mercury atoms into the needed levels. At the very least, the source is sufficient to serve as a reference for locking laser frequencies. Moreover, to our pleasant surprise, we found the excitation efficiency to be also high enough for us to use this source for initial experiments into the relevant coherent processes.

A low-pressure plasma discharge of Hg vapor can produce excited states of Hg. These discharges are commonly available as light sources for atomic-absorption spectrometers. We bought several Hg lamps and found all to be unsatisfactory for our needs. We then designed and made our own low-pressure discharge, a photograph of which in operation appears in Figure 1. Among its features is a so-called see-through cylindrical hollow cathode, 2 cm long, through which one or more laser beams can pass axially. Design emphasis was placed on discharge stability, longevity, and uniformity. Our design also minimized an unwanted phenomenon called "self-absorption" that displayed significantly in all discharges we tested. Radiating mercury atoms cause the bluish to violet glow seen in Figure 1.

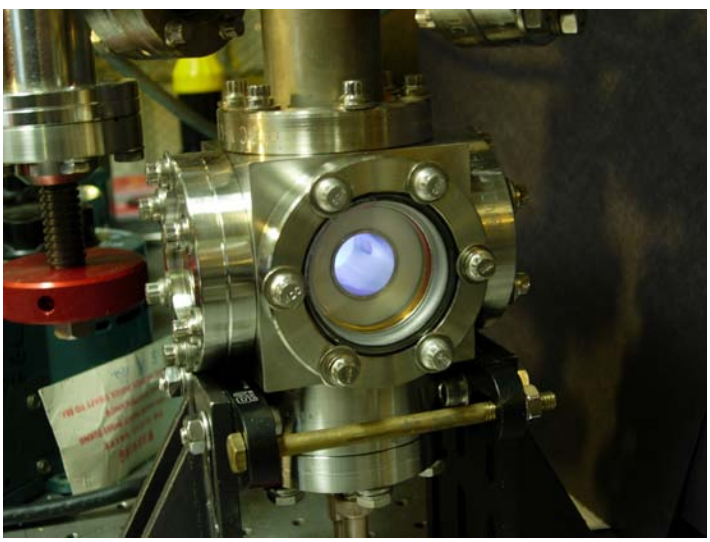

*Figure 1. Our low-pressure, hollow-cathode dc-discharge of mercury vapor, shown in operation with a background gas of 30 kPa Argon. The discharge is housed within a stainless-steel conflat cube of 7.0 cm per side.*

By our design emphases, we expected to concede efficiency. Excited-state populations might be steady but weakly present, and we prepared to detect these excited states indirectly through a technique known as optogalvanic spectroscopy. On testing our discharge, we indeed found the excited-state populations to be steady. We also found that the transitions of interest absorbed a traversing laser beam by a remarkable 10%, indicating an efficient transfer of population from the ground state of Hg to its excited states. The optogalvanic method was happily unnecessary; we could measure the transitions directly in absorption. The unexpectedly high amount of absorption will ultimately allow us to (1) lock laser frequencies with a high feedback bandwidth (as needed) and (2) study aspects of the coherent processes that lead to light amplification. We also made custom, low-noise detectors that will aid both laser-frequency locking and the initial coherent-processes study. Figure 2 shows an absorption spectrum of mercury's "green line" (at 546.1 nm) in our discharge with isotopic resolution. The divots atop each peak are Lamb dips produced by a counterpropagating beam that saturates the transition and better resolves the isotopic components.

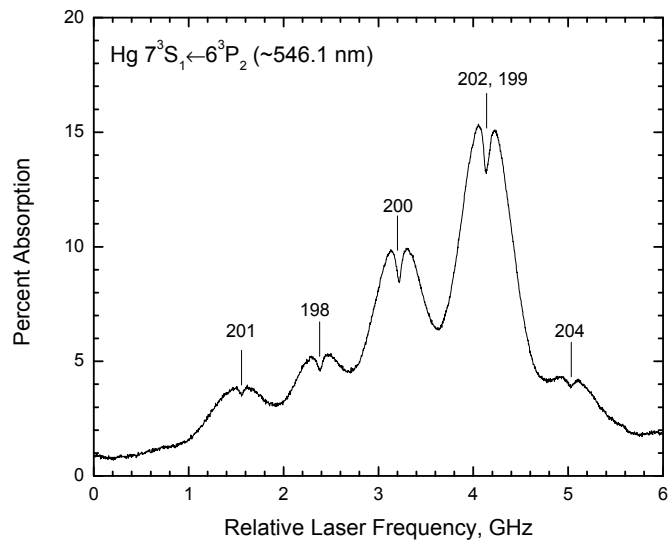


*Figure 2. Saturated absorption spectrum of the mercury green line (546.1 nm) obtained from our dc discharge. Absorption peaks and associated Lamb dips are labeled by isotopic component.*

We presented our work, including preliminary results from the Hg discharge, at the March 2009 meeting of the American Physical Society [1]. The overall concept was well received and acknowledged by peers as a creative yet feasible adaptation of quantum coherence for a new light-detection technology, with likely spinoffs into the quantum-information sciences. A publication on the discharge and associated spectra is forthcoming, and we anticipate publishing results on coherent processes in the discharge afterwards.

Our theoretical models are gaining the sophistication needed to interpret and guide real experiments. Both modeling and experiments will see continued development this year toward our goal of faint-light detection through

quantum-coherent processes. Along with aiding the experiments, we expect our theory will be robust enough to answer new questions, including whether coherent processes can improve upon traditional laser-based approaches for discerning isotopes.

The research has also inspired us to investigate the interaction of light with strongly dispersive media—a feature induced by the quantum-coherent interaction we use in our research—in thought provoking ways. Theoretical work along these lines will appear in *Optics Communications* [2]. Two more papers on dispersive media are in preparation for *Physical Review A*. In connection with these theoretical developments, we can foresee many applications of strongly-dispersive media in specialized devices.

## Future Work

With many of the rudimentary experimental and modeling needs now in place, we are in position to test our light-detection concept by year's end. Included in those tests will be measurements of quantum efficiency, spectral bandwidth, and noise, for comparison with theoretical expectations. With success, our experiments will introduce a detector with a presently unknown coincidence of high detection efficiency and resolving power. Applications and variations of this unique potential would likely follow from the broader community.

## Conclusion

Research on light detection, especially of faint signals and single photons, is expected to grow in importance given the current military and civilian interest in improved surveillance and the detection of chemical and biological agents. For spectroscopic applications in particular, the needed spectral selectivity often incurs a troubling loss of quantum efficiency. This tradeoff commonly occurs when spectral filters are placed in front of photodetectors. Here, we challenge this usual compromise between sensitivity and spectral selectivity by exploiting a quantum-coherent technique that promises to amplify faint light over a very narrow range of wavelength with little noise. Quantum efficiency is, theoretically, nearly 100%, and the expected spectral resolving power is ten million. Either characteristic for a detector would be unique; their combination would be unprecedented. Our theoretical work has served as a template for building an experimental test of this concept, which is the focus of our project. In brief, our aim is to apply the quantum-coherent phenomenon called amplification without inversion in the context of low-light detection and imaging. Through conferences, professional peers have evaluated our approach and considered it creative yet feasible. Our goal by project's end is to demonstrate and test a working archetype of this radically different approach to faint-light detection.

## References


1. Mertes, K. M., and M. D. Di Rosa. Efficient and selective photon detection using amplification without inversion. Presented at *2009 American Physical Society March Meeting.* (Pittsburgh, PA, 16-20 March 2009).

2. Bradshaw, D. H., Z. Shi, R. W. Boyd, and P. W. Milonni. Electromagnetic momenta and forces in dispersive dielectric media . To appear in *Optics Communications.*


## Publications


Bradshaw, D. H., Z. Shi, R. W. Boyd, and P. W. Milonni. Electromagnetic momenta and forces in dispersive dielectric media . To appear in *Optics Communications.*

Mertes, K. M., and M. D. Di Rosa. Efficient and selective photon detection using amplification without inversion. Presented at *2009 American Physical Society March Meeting.* (Pittsburgh, PA, 16-20 March 2009).

# Compact Solid State Tunable THz Source

*Nathan A. Moody*
20090321ER

## Introduction

Terahertz and millimiter-wave devices are proving to have many important applications from biological imaging to chemical detection and covert communication [1-6]. Among the greatest impediments to exploiting this regime of the electromagnetic spectrum are the difficulties in building sources with sufficient power and sensors with the needed specificity that are suitable for practical applications [3,4,7]. We are working toward a new THz source technology using a novel application of superconductive Josephson junctions that directly addresses many of the critical barriers for practical utilization of the THz spectrum. The pioneering approach we pursue has already generated interest in follow-on development of other THz devices. These include filters, mixers, oscillators, amplifiers, modulators, and receivers. Such development would completely revolutionize the field by providing a much-needed suite of compatible components with which to build entire THz systems. Our group has designed and has begun initial fabrication steps required to use Josephson junctions as THz emitters [2,8], and perhaps even the building blocks of other functional elements to detect and control such radiation. Our goal in this project is to transition our source design into a working prototype using LANL's unique fabrication capabilities, experience in millimeter-wave systems, and superconductivity expertise.

## Benefit to National Security Missions

This project will impact a broad range of technical problems including imaging, sensing, and communication. Enhancing our understanding of THz radiation particularly suited to spectroscopy applications for detection of chemical, nuclear, and biological threats, supporting threat reduction and other missions important to DOE, DHS, and other government agencies.

## Progress

This has been a successful first year toward the development of an Intrinsic Josephson Junction (IJJ) based THz source. The accomplishments align with our goals for the year and can be divided into five tasks, which are either fully completed or nearly so.

### Methods for calculating line-width and other parameters

Understanding the fundamental IJJ oscillation was our starting point in the first year of this research program. We selected a Bismuth-based high temperature superconducting material, termed BSCCO, as the host crystal and began developing analytical methods for evaluating emission line-width, stability of the radiative state, tolerances for crystalline purity, and anticipated heat load. These crucial parameters obtained in the first year guide the experimental steps in the second year as we begin testing of the first devices. We have shown, based on analytical methods developed during the first several months of this program, that line-width of emission for a junction stack consisting of >20,000 junctions is better than 1 MHz when the center frequency is several THz (i.e., df /f < 1E-9). This is a very encouraging result because, combined with frequency tunability, it confirms that this source is indeed appropriate for sensitive spectroscopy applications (one of the justifications for funding this project). The anticipated heat load is calculated to be less than 100mW, which can be managed routinely using a micro-cooler, which will be bought next year. The calculated tolerance for crystalline purity, expressed in % deviation of the c-axis resistivity, is predicted to be about 10%. This is another encouraging first year result because it demonstrates that typical defect densities can be tolerated (especially since their effects are shown to be averaged across an entire cuprate plane) while still achieving self-synchronization among the IJJ oscillators. We have obtained several conventionally grown samples and are modifying them to the extent possible using

focused ion beam milling as laser cutting to the dimensions specified in our design.

**Development of experimental processes to grow BSCCO with an in-plane c-axis orientation**
As called out in the listed goals, we have outlined an experimental process for high purity BSCCO growth that enables the desired crystalline expression (i.e., c-axis parallel to the substrate plane). This process may be explored this year (second year) in a limited fashion as devices are being tested, if funding permits. Four different compounds, all insulators, have sufficiently identical lattice parameters as BSCCO. These include SrLaAlO, $NdCaAlO_4$, $NdGaO_3$, and $LaO_3$. By using pulsed laser deposition to grow BSCCO on these ceramic sub-layers (or buffer layers) we can ideally take control of crystal orientation. This process is above and beyond the mainline approach of modifying pre-grown crystalline samples in the form of whiskers. We have requested reserve funding to explore the buffered layer growth process further and feel it is a promising and necessary technology for larger follow-on programs. The fact that the buffers are insulators guarantees that they will not interfere with the radiative process or electrical characteristics of the junctions.
In previous growth processes, with substrates such as sapphire, the natural orientation was a-b planar growth. Additionally, we have demonstrated the ability to wire bond to delicate thin film BSCCO structures.

**Obtained high purity BSCCO crystals (5 samples)**
Through collaborations with T-division, we have obtained five high purity samples of BSCCO enabling us to baseline our growth processes (with modified crystal orientation) against that of high purity growth in the standard orientation. It also enables us to use focused ion beam milling to create IJJ stacks whose current-voltage (IV) curves and emission characteristics can be immediately explored. Such baseline tests were part of our first-year goals and we have nearly completed preparations of the probe station where these will be tested and so far taken one IV measurement. We found we needed to upgrade to higher sensitivity meters and recently installed this equipment in preparation for additional measurements early this coming year.

**Purchase of standardized bolometer test station for detecting THz radiation up to 70 THz**
Developed the technical specifications for a hot electron bolometer, which will be used during the second year for calibrated measurements of THz output power and spectral content. The chosen device, from Insight Products, will have an operating frequency from 0.1 – 30 THz and a response time of 1 ns, with a 100 MHz bandwidth. This purchase was initiated in July 2009 and we have since worked with the vendor to ensure a timely delivery and integration into our probe station during February 2010.

**Began working with Tech Transfer to secure IP associated with the project**
To protect the current and future intellectual property generated from this project, the PI has worked with Tech Transfer and Legal Counsel toward the completion of patent application #116259. It was submitted to legal counsel and approved for filing before the end of the FY.

## Future Work

The "THz gap" refers to the portion of the electromagnetic spectrum from approximately 0.3 to 5 THz in which there are few practical sources of radiation. This same spectral region, because of its unique propagation characteristics and interaction with matter, corresponds to some of the most exciting applications to date for national security. The well-established emission techniques for the neighboring microwave and optical regions of the spectrum have proven ineffective for the THz band, despite over a decade of intense effort. In contrast, the Josephson junction interaction is naturally suited to operate in the THz band, as it naturally converts a dc voltage (1 mV corresponds to 0.483 THz) into millimeter wave radiation via a quantum mechanical tunneling resonance called the Josephson effect. The potential for future work is significant. Our immediate focus in on the future work in this program, as outlined below, but we maintain that these early successes pave the way for follow-on efforts that address THz component development on a much larger scale.

Our approach in this project consists of three major tasks, all driven by simulation studies: 1.) develop a BSCCO design and potential fabrication processes to produce high quality crystals of the desired orientation; 2.) demonstrate that IJJs can be used as a scalable, compact source of THz radiation; and 3.) validate and expand our radiation model to predict other types of IJJ interactions at THz frequencies.

Each goal roughly corresponds to each of the three years of this research program. In year 1, we began to modify our facility to grow and modify BSCCO and completed device modeling. In year 2, we will characterize pre-grown samples and systematically modify their size and geometry to accommodate any constraints encountered in fabrication, and mount & wire bond samples without degradation. In year 3, we will transition the source design into a working prototype, demonstrating emitted power at 1 THz and demonstrate the ability to sink the associated heat load using a commercially available cryo-cooler.

## Conclusion

This work will extend our knowledge of and provide raw materials for a new, portable mechanism for creating non-ionizing THz radiation, which is ideal for determining certain properties of materials that are not apparent when using other types of radiation (such as microwave, light, or x-rays). THz radiation can be used to actively interrogate a variety of environments, including human subjects, in search of dangerous materials to protect both soldiers and civilians. Our work could also lead to tissue-safe low cost THz imaging, which could be used to supplement and/or replace harmful x-ray doses typical in medical imaging.

## References


1. Bulaevskii, L., and A. Koshelev. Radiation from Flux Flow in Josephson Junction Structures. 2006. *Journal of Superconductivity Research.* **19** (3): 349.

2. Bulaevskii, L. N.. Detection of electromagnetic waves by use of Josephson oscillations in layered superconductors. *Physical Review Letters.* **Submitted for publication**.

3. DeLucia, F. C., D. T. Petkie, R. K. Shelton, S. L. Westcott, and B. N. Strecker. THz + 'X': A search for new approaches to significant problems. 2005. In *Terahertz for Military and Security Applications.* (Orlando, FL, 28 March 2005). Vol. 5790, p. 219. Orlando: SPIE.

4. Federici, J., B. Schulkin, F. Huang, D. Gary, R. Barat, F. Oliveira, and D. Zimdars. THz imaging and sensing for security applications, explosives, weapons and drugs. 2005. *Semiconductor Science and Technology.* **20** (7): S266.

5. Tonouchi, M.. Cutting-edge terahertz technology. 2007. *Nature Photonics.* **1** (2): 97.

6. Zhou, T., H. Yating, Z. Shengnan, and A. S. Shaolin Yan. THz radiation sensing and emission: The phase-locking properties of Josphson junction arrays coupled with THz frequency Fabry-Perot resonators. Presented at *Nano/Micro Engineered and Molecular Systems, 2008. NEMS 2008. 3rd IEEE International Conference on.*

7. Fitch, M., and R. Osiander. Terahertz Waves for Communications and Sensing. 2004. *APL Technical Digest.* **25** (4): 348.

8. Bulaevskii, L. N., A. E. Koshelev, and M. Tachiki. Shapiro steps and stimulated radiation of electromagnetic waves due to Josephson oscillations in layered superconductors. 2008. *Physical Review B (Condensed Matter and Materials Physics).* **78** (22): 224519.


## Publications


Bulaevskii, L. N.. Detection of electromagnetic waves by use of Josephson oscillations in layered superconductors. 2009. *PRL.* Submitted for publication.

Bulaevskii, L. N., A. E. Koshelev, and M. Tachiki. Shapiro steps and stimulated radiation of electromagnetic waves due to Josephson oscillations in layered superconductors. 2008. *Physical Review B (Condensed Matter and Materials Physics).* 78 (22): 224519.

Bulaevskii, L. N., and N. A. Moody. Stability and linewidth of Josephson radiation from layered Superconductors. To appear in *Applied Physics Letters.*

Koshelev, A. E., and L. N. Bulaevskii. Resonant electromagnetic emission from intrinsic Josephson-junction stacks with laterally modulated Josephson critical current. 2008. *Physical Review B (Condensed Matter and Materials Physics).* 77 (1): 014530.

# Cerium-Doped Glass Scintillators

*Markus P. Hehlen*
20070134ER

## Abstract

The primary goal of this project was to explore and develop cerium-doped sulfide glasses as potential low-cost high-performance gamma-ray scintillators. The screening of a wide range of sulfide glass compositions identified gallium-sodium-sulfide (GNS) glass as the most attractive candidate material because of its large band-gap energy compared to the cerium 5d excited state. We have shown that doping GNS glass with cesium chloride (CsCl) further increased the band gap energy to 3.32 eV, a record for any sulfide glass reported to date. Cerium ($Ce^{3+}$) doped into GNS:CsCl provided the first-ever observation of bright $Ce^{3+}$ luminescence in a sulfide glass. This was enabled by the high band-gap energy of the host which diminished quenching of the $Ce^{3+}$ excited state via non-radiative energy transfer into the conduction band. The $Ce^{3+}$ luminescence in the blue-green (500 nm) is favorably matched with the sensitivity of charge-coupled detectors (CCD). However, quenching of the $Ce^{3+}$ excited state was found to still be important at room temperature, even for the highest band gap material GNS:20%CsCl. Furthermore, the scintillation yield was measured to be only about one-thousanth of that of BC408 plastic scintillator, indicating that defect formation and excitation trapping in the glass network dominate all other loss channels. The results of this comprehensive study of $Ce^{3+}$-doped sulfide glasses are presented in two peer-reviewed publications and one LANL invention disclosure. The project also afforded mentoring of a graduate student in the field of glass chemistry and resulted in a LANL Student Distinguished Performance Award. During the study of GNS glasses we discovered that metal halide nanocrystals can be precipitated in this glass during a thermal post-processing step, yielding translucent nano-structured glass ceramics. This result opens the prospects of creating large-volume scintillators via inexpensive glass-ceramic processing. Respective program development efforts and preliminary experiments are currently underway.

## Background and Research Objectives

High-throughput radiation screening of vehicles and cargo at ports of entry poses a particularly challenging national security and non-proliferation problem of urgent importance. Gamma-ray radiation emanating from an illicit object has to be detected and identified in a short period of time and in the presence of a wide variety of naturally radioactive benign goods such as tile, granite, bananas, potatoes, fertilizer, and kitty litter. Additional shielding around a threat object adds yet another level of complexity. These sources can be identified, in principle, by high-performance scintillators that can not only detect the presence of a radioactive source but also provide the gamma-ray spectrum of the source, which is a fingerprint of the isotopic composition of the source. Such gamma-ray spectrometers require scintillators with both high efficiency and good energy resolution. For room-temperature operation, the best gamma-ray scintillators available today are single crystals of metal halides, such as cerium-doped lanthanum bromide ($LaBr_3:Ce^{3+}$) [1] and europium-doped strontium iodide ($SrI_2:Eu^{2+}$) [2]. These materials absorb and thermalize gamma energy to excite chromophores (e.g. cerium or europium), which subsequently emit visible light that can be measured by a photodetector such as a photomultiplier tube. $LaBr_3:Ce^{3+}$ and $SrI_2:Eu^{2+}$ offer state-of-the-art scintillation performance in efficiency and energy resolution. But their crystalline nature and extreme moisture-sensitivity critically limits their size and makes them prohibitively expensive to grow in large sample volumes and quantities. High-throughput spectroscopic portal monitors that can detect and identify gamma-ray sources are therefore still beyond current capabilities. What is urgently needed is a gamma-ray scintillator that not only has high efficiency and energy resolution but also can be fabricated in large sizes at reasonable cost. Such a material does not exist today.

The main goal of this Laboratory Directed Research and Development (LDRD) Exploratory Research (ER) project

20070134ER was to explore a novel class of materials that may enable low-cost large-volume gamma-ray scintillators. Specifically, the project focused on cerium ($Ce^{3+}$) doped sulfide glasses with the objective of combining the attractive scintillation properties of the $Ce^{3+}$ chromophore with low-cost large-volume glass fabrication processes. Scintillation properties of many common oxide and fluoride glasses doped with cerium had been studied in the past (e.g. Refs [3,4]), and their low efficiency had failed to meet the needs of gamma-ray spectroscopy. The main reason for their low efficiency was proposed to be radiation damage, i.e. the formation of shallow traps and permanent defects during the thermalization of the absorbed gamma energy. These early observations provided the main motivation for the present work. While the chemical bonding in oxide and fluoride glasses is primarily ionic, the chemical bonding in sulfide glasses is primarily covalent. Our hypothesis was that such covalent metal-sulfur bonds would be more resilient against defect formation and would, therefore, enable a more efficient scintillation process. The high covalency in the metal-sulfur bond however was also expected to lower the band gap energy and thus to enhance the quenching of the excited $Ce^{3+}$ chromophore via non-radiative de-excitation into the conduction band [5]. The main question to be answered was if the increased quenching of the chromophore by the low-lying conduction band is outweighed by a higher efficiency of exciting the chromophore though the covalent sulfur glass network.

## Scientific Approach and Accomplishments

The project was structured into four phases: (1) screen for possible candidate sulfide glass hosts, (2) establish the synthesis methods and optical properties of the sulfide glasses, (3) study the spectroscopic properties of the cerium chromophore, and (4) measure the gamma-ray scintillation properties of the final material.

New processes for the synthesis of sulfide glasses were developed for this project, and the resulting samples underwent comprehensive characterization by a broad suite of techniques. Several new state-of-the-art capabilities were created, including fabrication of large sulfide glass samples under tightly controlled inert atmosphere, ultrafast XUV spectroscopy (in collaboration with the University of New Mexico), and refractive-index dispersion measurement by white-light frequency-domain interferometry. Other characterization techniques included densitometry, energy-dispersive x-ray spectroscopy, scanning electron microscopy, x-ray diffraction, optical spectroscopy (absorption, photoluminescence, and photoluminescence excitation), pulsed laser spectroscopy, radioluminescence spectroscopy, and gamma-ray spectroscopy.

The early screening of a variety of sulfide glasses found quenching of the $Ce^{3+}$ excited state via the conduction band to be important. Glasses such as $Ga_2S_3$-SrS, $Ga_2S_3$-CaS, $Ga_2S_3$-SrS-CaS, $Ga_2$-SrS-$SrCl_2$, $Ga_2S_3$-SrS-$BaCl_2$ were excluded from further study because their band gap energy was too low relative to the 5d excited state of $Ce^{3+}$. In contrast, $Ga_2S_3$-$Na_2S$ (GNS) and $Ga_2S_3$-$Na_2S$-CsCl glasses showed favorably large band gap energies and were chosen for detailed further study. The results of this project are described in detail in two publications. The first publication, submitted to Optical Materials [6], presents the synthesis methods and optical properties of the sulfide glasses developed in this project. A second publication, pending submission to the Journal of Luminescence, presents the spectroscopic and scintillation properties of $Ce^{3+}$ in these glasses. Furthermore, a LANL Invention Disclosure [7] describes the key processes needed to grow sulfide glasses of correct and tightly controlled composition.

The most significant accomplishments and discoveries are summarized below:

- The band gap energy ($E_g$) in GNS glass can be tuned by the addition of CsCl. In particular, the band gap energy increases from of 2.97 eV in GNS glass to 3.32 eV in GNS glass doped with 20 mol% CsCl. Figure 1 shows this 12% increase in $E_g$ and established the highest band gap energy ever observed in a sulfide glass. Tuning $E_g$ is significant because the $Ce^{3+}$ excited state in sulfide glasses is around 2.9 eV, and it can quench via non-radiative energy transfer to the conduction band if the latter has similar or lower energy. The high band-gap energy found in GNS:20%CsCl played a key role in diminishing this quenching process and enabling $Ce^{3+}$ luminescence.

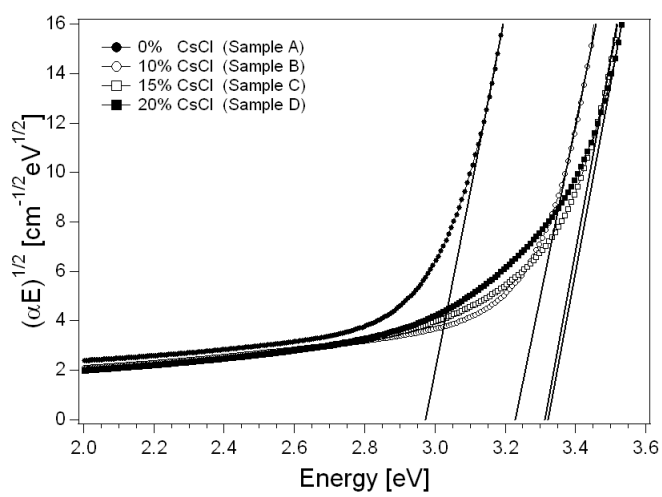


*Figure 1. Tauc plot of √αE versus E for several CsCl-doped GNS samples, where α and E are the absorption coefficient and energy, respectively. The Tauc band gap energies E_T are derived from the E-axis intercepts of linear fits (solid lines) to the linear regime of the √αE versus E curves.*

- Early attempts of fabricating CsCl-doped GNS glasses found a significant loss of CsCl by evaporation during the melting of the glass due to the high vapor pressure of CsCl. Energy dispersive x-ray spectroscopy was carried out at the Center for Integrated Nanotechnologies (CINT) to determine the actual Cs elemental concentration in a series of glasses. These measurements enabled calibration and correction of the glass preparation process and resulted in the synthesis of CsCl-doped GNS glasses with the correct final composition. This is illustrated in Figure 2, which illustrates the high accuracy of the final glass composition achieved by proper glass fabrication. This process development was critical as many of the material properties were found to be sensitive to the CsCl concentration. An example is shown in Figure 3, which compares the glass transition temperatures ($T_g$) of samples prepared with and without control of CsCl evaporation.

- Cerium was doped into a series of GNS:CsCl glasses and produced the first-ever bright luminescence form a $Ce^{3+}$-doped sulfide glass. Figure 4 shows representative luminescence spectra at room temperature along with a picture of the bright green cerium luminescence excited by a blue (435 nm) light-emitting diode. The cerium emission is centered in the blue/green around 500 nm, i.e. it occurs at a significantly longer wavelength than in traditional $Ce^{3+}$-doped scintillator crystals such as $LaBr_3$:$Ce^{3+}$ (380 nm). This longer emission wavelength in GNS glasses is advantageous as it is well matched to the sensitivity of charge-coupled detectors (CCD) that would enable a lower-cost compact detection compared to the traditional scintillation light detection with photomultiplier tubes.

- The primary quenching mechanism of the $Ce^{3+}$ 5d excited state was found to be non-radiative relaxation via the conduction band. Figure 5 shows cerium excited-state lifetimes measured by pulsed laser spectroscopy at different temperatures for various cerium-doped GNS:CsCl glasses. The lifetime shortens (and thus the quantum efficiency decreases) by 20-25% from 77 K to room temperature. This is direct evidence for quenching of $Ce^{3+}$ excitation via the conduction band by a thermally-activated energy-transfer process.

- Finally, the room temperature scintillation light yield of GNS:Cs,Ce glass was measured by comparing its radioluminescence (RL) intensity to a calibrated reference sample (BC408 plastic scintillator). The glasses achieved a light yield of only about one-thousands of the light yield of BC408 plastic scintillator, which produces 8,000-10,000 photons/MeV. Quenching of the $Ce^{3+}$ excited state via the conduction band alone cannot account for this low scintillation light yield. We therefore conclude that most of the gamma energy is lost non-radiatively during the thermalization processes following gamma-ray absorption. It appears that the covalent nature of the metal-sulfur glass-network bonds did not provide the anticipated stability against the formation of defect centers.

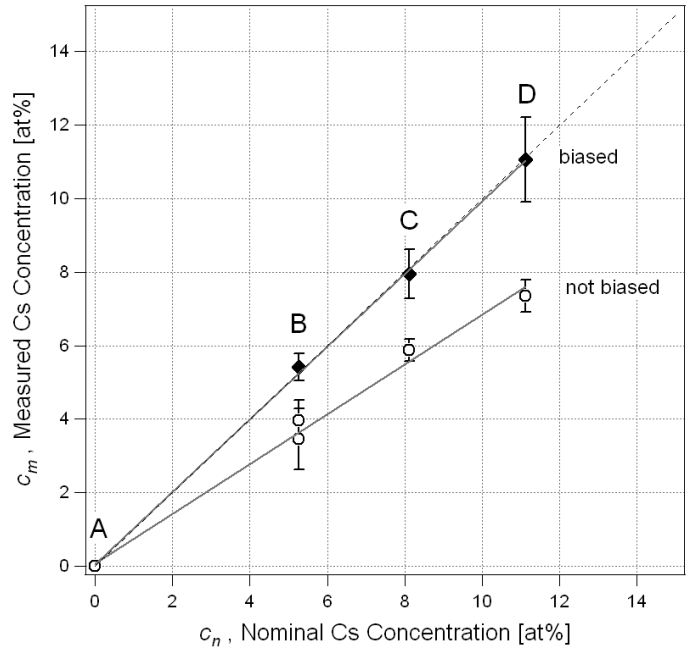


*Figure 2. Cesium (Cs) concentration (in at% relative to the total metal concentration) measured by EDX for several GNS:CsCl samples along with respective linear fits (solid lines). Samples prepared from nominal batches (open circles) suffer from substantial CsCl evaporative loss while samples prepared from initial batches with 1.47-fold CsCl concentration biasing (diamonds) produce the correct final stoichiometry (dashed line).*

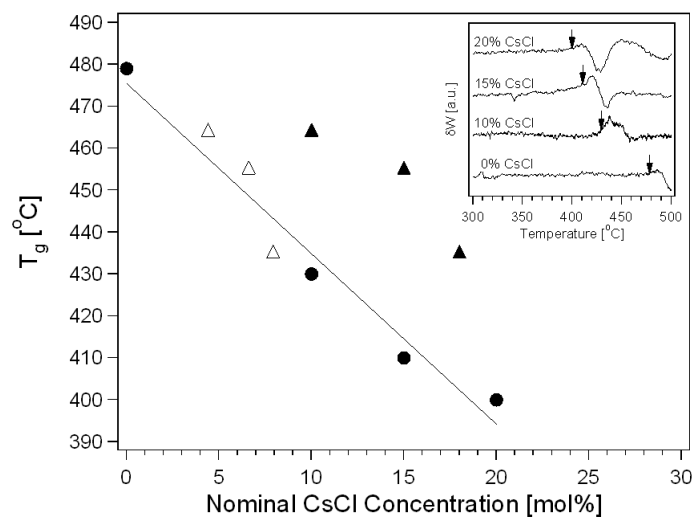


*Figure 3. Glass transition temperature (Tg) of several GNS:CsCl samples (solid circles). The insert shows the differential heat flow (δW) as a function of temperature from the DSC measurement with the arrows indicating Tg. Glass transition temperatures of CsCl-doped GNS glasses reported by Barbosa et al (solid triangles) best match the linear fit of the present data when the CsCl concentration is scaled by a factor of 0.44 (open triangles), indicating substantial CsCl evaporative losses in the uncontrolled samples.*

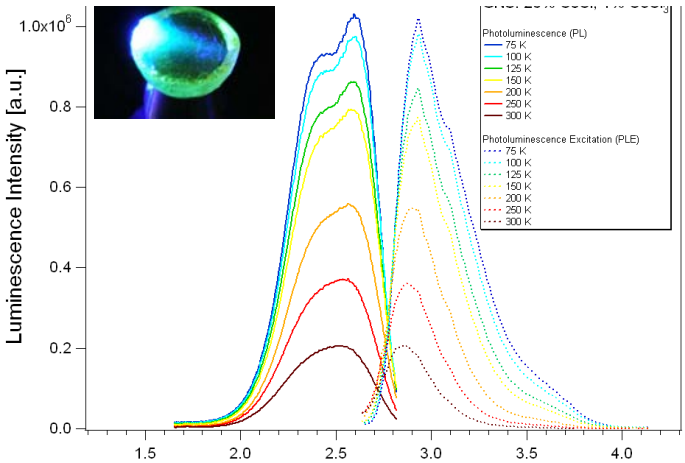


*Figure 4. Photoluminescence (PL) and photoluminescence excitation (PLE) spectra of GNS glass doped with 20% CsCl and 1% CeCl3 at different temperatures. The photoluminescence peak is centered around 2.5 eV (500 nm). The inset shows a picture of the bright green luminescence obtained upon exciting the sample with a blue (435 nm) light emitting diode at 300 K.*

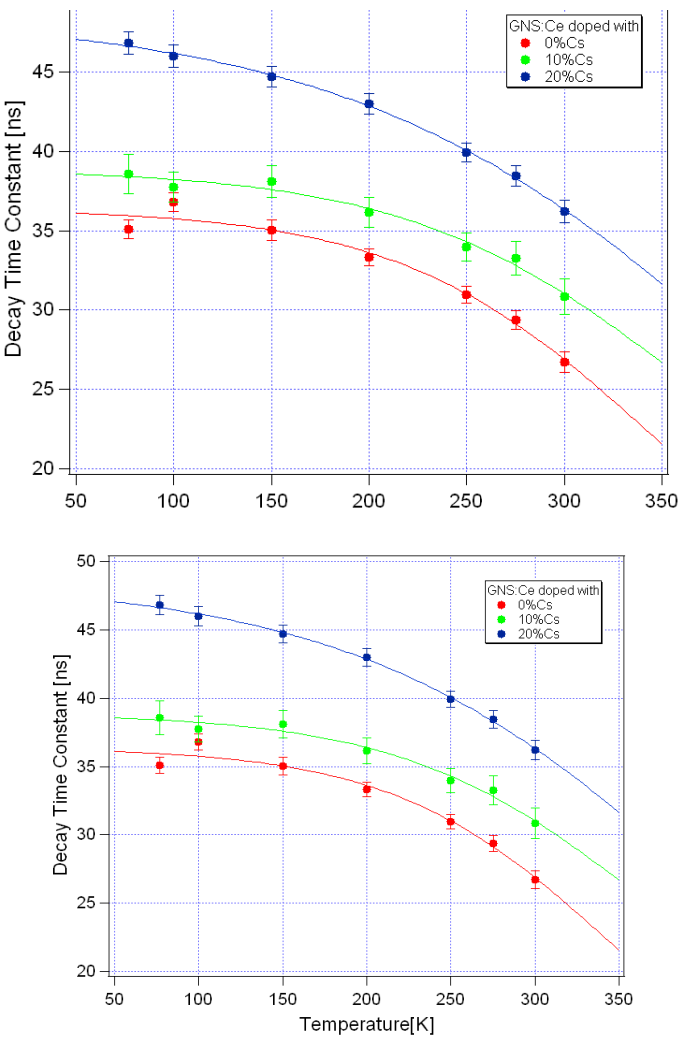


*Figure 5. Cerium 5d excited state lifetimes for three CsCl-doped GNS glasses doped with 1% $CeCl_3$ at different temperatures. The lifetime decreases by 20-25% from 77 K to room temperature.*

From our extensive studies of $Ce^{3+}$-doped sulfide glasses we therefore conclude that (1) defect formation in the sulfide glass network was not substantially suppressed by covalent bonding and (2) the $Ce^{3+}$ excited states are partially quenched at room temperature via the conduction band. As a result, these materials were found to not exceed the performance of earlier cerium-doped oxide and fluoride glasses. While the detailed study has disproven our initial hypothesis, this project has achieved several scientific successes that have opened up new avenues for research and funding. Specifically:

- We have found that doping the sulfide glass with metal halides can lead to the precipitation of nanocrystals in the glass matrix during a thermal post-processing step, thus forming a transparent/translucent nano-structured glass ceramic. This observation has led to the discovery of other glass ceramics, such as YAG:Ce and LaF3:Ce that may have application as scintillators. Such nano-structured glass ceramics are amenable to low-cost production of large translucent shapes containing a high density of highly efficient scintillating nanocrystals. As part of out collaboration with the University of New Mexico, we have recently proposed further development of such materials to DTRA. In addition, a small follow-on grant was secured from the LANL Institute of Geophysics and Planetary Physics (IGPP) to further explore the formation of nano-structured glass-ceramics and to study their gamma scintillation properties. First experiments on cerium-fluoride ($CeF_3$) glass ceramic scintillators are also currently underway as a NPDF User Experiment at the Los Alamos Neutron Science Center (LANSCE).

- We have discovered that the band gap energy in sulfide glasses can be tuned via the glass composition and proper melting conditions. This new knowledge has resulted in a sulfide glass having the highest band gap energy ever reported (3.32 eV). This property, combined with the low phonon energy in sulfides, makes this glass an attractive host material for a variety of luminescent centers such as $Er^{3+}$, $Tm^{3+}$, and $Yb^{3+}$. Potential applications include upconversion lasers, optical amplifiers, and optical refrigerators [8].

## Impact on National Missions

The urgent need for a low-cost large-volume efficient gamma-ray scintillator still exists, and many research groups worldwide continue to work on this area. However, no groundbreaking material has emerged anywhere during the past three years. While the specific cerium-doped GNS glasses investigated by this project did not offer the initially anticipated scintillation performance, the work has

laid the foundation for several ongoing efforts in the area of next-generation scintillator materials. First, the project has developed unique inert-atmosphere glass melting as well as material characterization capabilities. Beginning in FY10, this infrastructure is supporting a DNDO-funded program at LANL on nanophosohor scintillators by performing synthesis of high-purity starting materials, crystal growth, and optical characterization. Second, the preliminary results achieved by the project in the area of nano-structured glass-ceramic scintillators have attracted the interest of DNDO and NA-22. Respective program development efforts are currently underway, in part in collaboration with the University of New Mexico (UNM). Third, this project has provided training opportunities for Ms. Wendy Patterson, a UNM graduate student, who has been awarded the LANL Distinguished Student Performance Award for her work on halide glasses performed at LANL under the mentorship of Dr. Markus Hehlen.

## References


1. D.vanLoef, E. V., P. Dorenbos, C. W. E. van Eijk, K. Kramer, and H. U. Gudel. High-energy-resolution scintillator: Ce3+ activated LaBr3 . 2001. *Applied Physics Letters.* **79** (10): 1573.

2. D.vanLoef, E. V., C. M. Wilson, N. J. Cherepy, G. Hull, and S. A. Payne. Crystal Growth and Scintillation Properties of Strontium Iodide Scintillators . 2009. *IEEE Transactions on Nuclear Science.* **56** (3): 869.

3. Jiang, C., Q. Zeng, and F. Gan. Scintillation properties of cerium-doped germanate glass. 2000. *Proc. SPIE.* **4141**: 309.

4. Jiang, J., G. Zhang, and M. Poulain. Cerium-containing glasses for fast scintillators. 1998. *Journal of Alloys and Compounds.* **275-277**: 733.

5. Quimby, R. S., and B. G. Aitken. Anomalous temperature quenching of fluorescence in Pr3+ doped sulfide glass. 1997. *Journal of Applied Physics.* **82** (8): 3992.

6. Hehlen, M. P., B. L. Bennett, A. Castro, D. J. Williams, S. C. Tornga, and R. E. Muenchausen. Synthesis and optical properties of CsCl-doped gallium-sodium-sulfide glasses . *Optical Materials.*

7. Hehlen, M. P.. Cerium-doped sulfide glass scintillator. 2008. *LANL Idea-08-220.*

8. Hehlen, M. P.. Design and fabrication of rare-earth-doped laser cooling materials. 2009. In *Optical refrigeration - Science and applications of laser cooling of solids.* Edited by Epstein, R. I., and M. Sheik-Bahae. , p. 33. Weinheim: Wiley.


## Publications


Hehlen, M. P.. Cerium-doped sulfide glass scintillator. 2008. *LANL Idea-08-220.*

Hehlen, M. P., B. L. Bennett, A. Castro, D. J. Williams, S. C. Tornga, and R. E. Muenchausen. Synthesis and optical properties of CsCl-doped gallium-sodium-sulfide glasses. *Optical Materials.*

# Nano-Structured Foams for Hydrogen Storage

*Erik P. Luther*
20070173ER

## Abstract

Hydrogen is a candidate energy carrier for applications such as zero emission vehicles. One of the main barriers to using hydrogen in automotive applications is safe storage. This project investigated a novel material, nanostructured foams, to store hydrogen. Fabrication of monolithic metallic nanoporous foams is difficult using conventional methods. We have developed a relatively simple method of synthesizing monolithic, ultralow density, nanostructured metal foams utilizing self-propagating combustion synthesis of metal precursors. We have produced metal foams via this method including titanium, iron, cobalt, nickel, zirconium, copper, palladium, silver, hafnium, platinum and gold and characterized them. We have measured the hydrogen absorption properties of several foams and developed a model for the sorption rates of hydrogen in the foams. This project supports U.S. energy security and supports basic understanding of materials, both of which are key DOE missions.

## Background and Research Objectives

Climate change science warns of a potential environmental catastrophe due to the runaway accumulation of carbon dioxide in the world's atmosphere. In recognition of this fact and to decouple our energy future from unstable political climates, our nation has proclaimed a desire for energy independence, which has made the development of an alternative, carbon neutral energy source imperative. Hydrogen has been proposed as an energy carrier to replace carbon based fuels. In many ways, hydrogen is an ideal fuel because it is abundant and is easily oxidized to produce energy with a "waste product" of pure water. One elegant method of generating electricity from hydrogen, fuel cell technology, is a relatively mature field that is ironically limited in use by the seemingly mundane challenges in generating and storing hydrogen.

As a candidate fuel for zero emission vehicles, safe storage of hydrogen, the lightest and lowest density element, is a huge barrier. Storage techniques such as pressurized cylinders have made significant progress. Current cylinders are capable of 10,000 psi. Honda is marketing a vehicle with two 5,000 psi cylinders that store approximately 150 L (3.75 kg) of hydrogen allowing a driving range of perhaps 250 miles. However, pressurized storage is intrinsically unsafe. Alternatives such as cryogenic storage of liquid hydrogen consume large amounts of energy to refrigerate and insulation to prevent loss is bulky. Several solid storage approaches have been investigated among them, interstitial storage of hydrogen in metals.

Interstitial hydrogen storage materials can store hydrogen without pressurization concerns or extreme temperatures. However, in order for an interstitial hydrogen storage material to store a similar amount of hydrogen and weigh on the order of 10 gallons of gas (~28 kg), materials with ~13 wt% capacity are needed. (FreedomCar goals are more moderate at 6 wt% by 2010 and 9 wt% by 2015.)

Unfortunately, despite decades of research, current hydrogen storage materials based on metal hydrides have a capacity of less than 2 wt% hydrogen under conditions suitable for passenger vehicles. [1] Despite this fact, metal hydrides are currently used for hydrogen storage in certain applications. Improvements in a well-studied material such as $LaNi_5$ could be made by improving the kinetics of hydrogen storage. However, to achieve realistic needs, new classes of materials must be investigated. Metal nitrides are a promising, new class of ceramic hydrogen storage materials. For instance, lithium nitride has been shown to reversibly store over 6 wt% hydrogen and can theoretically store over 10 wt%. [2] Nitride materials such as this produced into foams with high surface area would result in high capacity hydrogen storage materials with rapid hydrogen

adsorption/desorption kinetics.

The goal of this project was to investigate novel materials, i.e., nanostructured foams, to store hydrogen. The foam must store large amounts of hydrogen quickly and repeatedly and release them in a controlled manner. The foams were expected to adsorb and desorb hydrogen quickly due to the tremendous amount of surface exposed to the hydrogen gas.

The process developed for synthesizing metal foams has no parallel. There are very few methods of making nanomaterials in bulk form. This method not only produces a foam with nanometer size pores, it does so extremely rapidly by burning a precursor material. There is no obvious limit to the size or shape of the foam that can be created in this manner. As a rapid, large scale production method for making nanomaterials, there is no equal. Beyond storing hydrogen, this research sought to understand and control the foam making process such that it could be used for the intended application.

As described below, tremendous progress was made on the synthesis of nanostructured foams. A wide variety of precursor materials were synthesized and characterized. The thermodynamic properties of the precursors were measured and their burn behavior characterized. Nanostructured foams were analyzed physically and chemically. An in depth understanding of the pore structure and chemical makeup has been gained.

Synthesis of palladium foams was demonstrated to adsorb hydrogen as expected. The purity of the foam limited the quantity of hydrogen adsorbed. One of the main goals of the program, synthesis of lithium based metal foams proved elusive. Numerous lithium precursors were made but all proved to be relatively inert. Attempts to make known hydrogen storage alloys also proved to be difficult. Precursor mixtures were produced to attempt to alloy metals. Even highly miscible metals were found in discrete areas when the precursor materials were intimately mixed and burned to form a foam.

Modeling of the kinetics of hydrogen adsorption in palladium foams and powders proved to be more complex than originally expected. Simple Fickian diffusion was insufficient to explain the behavior and further studies are continuing.

## Scientific Approach and Accomplishments

One of the main goals of this project is to produce novel ceramic nitride foams that would be capable of rapid uptake of hydrogen. Lithium nitride has been reported as a candidate storage material with high hydrogen storage capacity. By producing lithium nitride in foam form, improved sorption kinetics were anticipated due to high surface area, nanosized grains and pores and fast heat conduction.

Numerous metal foams, some with high nitrogen content, have been produced including iron, cobalt, nickel, titanium, copper, silver, gold, platinum, palladium, and zirconium all produced by burning metal bi(tetrazolo) amine (BTA) precursors. [3,4] The BTA metal complexes were synthesized in an aqueous solution by reaction of the monohydrated bi(tetrazolato)amine, or ammonium bi(tetrazolo)amine and a metal salt as described in detail elsewhere. [5,6] The metal BTA precursor is dried to a powder and pressed into a pellet. The pellet is placed in an inert atmosphere under pressure and ignited by laser or a heated wire. Combustion of the pellet eliminates non-metallic elements and produces large quantities of gas that expand the remaining metal elements resulting in a foam. Figure 1 shows a scanning electron microscopy (SEM) image of palladium foam, which shows prototypical foam like microstructure. Unfortunately, using the same approach for lithium was unsuccessful. LiBTA (lithium bi(tetrazolo)amine) was produced with the goal of the combustion synthesis of lithium nitride foam. This precursor and all of the lithium compounds synthesized to date, lithium bitetrazole (BT), bi(tetrazolo)amine (BTA), and bistetrazolylaminotetrazine (BTATz), have failed to support combustion, likely due to the low inherent energy content of such salts.

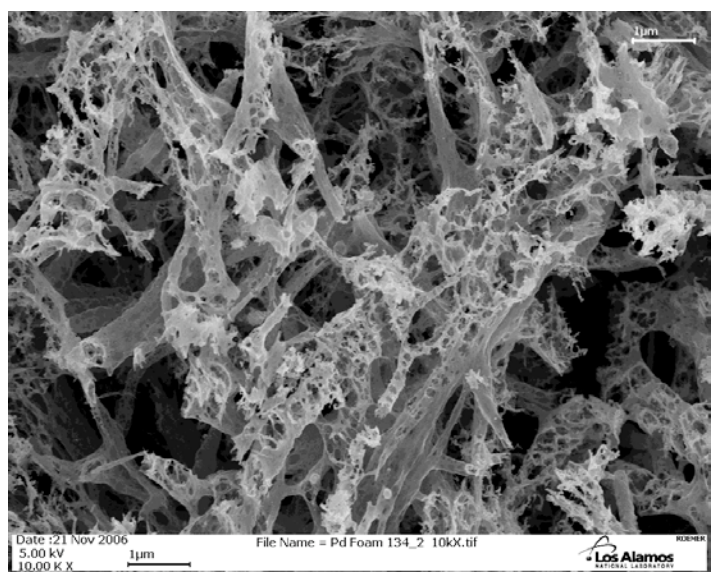


*Figure 1. Scanning electron microscopy image of a nanostructured palladium foam.*

Various synthesis techniques for lithium compounds have been attempted, and these materials all showed almost no response to ignition at atmospheric or elevated

pressures, which was suspected to be in part because of chemically bound "waters of hydration". The materials were meticulously dried under vacuum; however, and yet no change was observed in the combustion properties, so it was determined that the water of hydration was too tightly bound, and three new synthesis routes were attempted, two of them non-aqueous. Recently, however a new high-temperature dehydration procedure was produced, and the LiBTA was most certainly dehydrated, but still did not exhibit combustion properties sufficient for self-propagating combustion synthesis.

It is believed that MgN foams and/or lithium containing MgN foams will also have interesting hydrogen storage properties. Because of this, a MgBTA salt was produced, and based on Mg high affinity for nitrogen, it was expected that in the combustion of this material the MgN would be formed. Like many of the BTA salts, it was discovered that the MgBTA is hydrated, having approximately 1.5 $H_2O$ per MgBTA. This hydrate suffers from the same combustion problems as the hydrate as the LiBTA, however unlike the LiBTA, once dehydrated burns quite well. MgBTA (combined with a small amount of elemental magnesium needed to support combustion) was pressed into pellets. The pellet burned well and the resulting monolith was studied by SEM. Figure 2 shows an SEM image of the resulting material. Although the material is porous, it is not "foam-like" as seen in the palladium foam. Surprisingly, the magnesium did not bond with abundant nitrogen in the combustion chamber as expected from thermodynamic calculations.

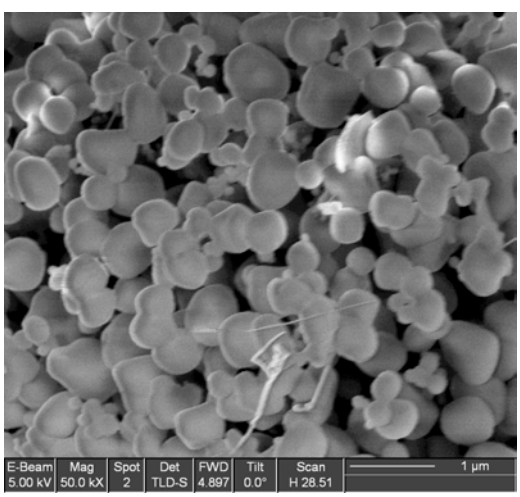


*Figure 2. Scanning electron microscopy image of a magnesium foam.*

$LaNi_5$ is a well-known, well-characterized hydrogen storage material. Attempts to synthesize this alloy in order to compare the kinetics of hydrogen uptake of bulk versus foam material were made. Lanthanum bi(tetrazaolo) amine was synthesized as a component for the metal hydride $LaNi_5$ and was subjected to the drying procedure. Unexpectedly, the complex was stable after loss of all water, confirmed by weight loss and in differential scanning calorimetry. As the anhydrous complex, the La retains two BTA ligands and one $NH_4^+$ counter ion. The combustion properties of this $La(BTA)_2(NH_4)$ were much improved as evident by small-scale screening, but not optimal.

Two complexes of NiBTA have been synthesized, one that is the $NiBTA(NH_3)_5$ complex, and one that is $Ni(BTA)_2(NH_4)_2$, the former having no useful combustion properties, and the latter with poor, but usable combustion properties. It was discovered that the $Ni(BTA)_2(NH_4)_2$, also contains two waters of hydration, and after dehydration, the combustion properties are much improved.

Appropriate mixtures of LaBTA and NiBTA were formulated to achieve appropriate stoichiometry of a $LaNi_5$ hydrogen storage alloy. The precursors were dissolved and co-precipitated in order to intimately mix the precursors. The dried powder was pressed into a pellet and burned following established procedures. As seen in Figure 3, a metal foam was generated; however, energy dispersive spectroscope (EDS) indicated that the normally miscible lanthanum and nickel had not alloyed as desired but formed separate regions in the foam structure.

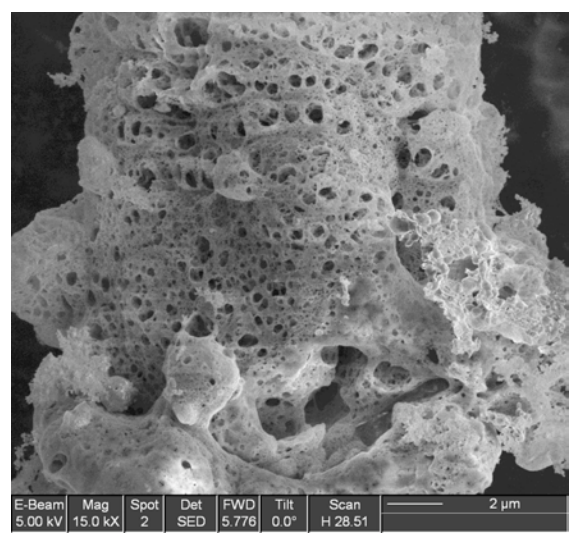


*Figure 3. Scanning electron microscopy image of a lanthanum and nickel containing foam.*

Attempts to synthesize $Fe_xTi_y$, another hydrogen storage alloy, were also made. $Ti(BTA)_2$ was synthesized and formulations of TiBTA/FeBTA were produced at various ratios to produce $Fe_xTi_y$ foams. These formulations produced very low-density foam that was flaky and not a single monolith. Similar to the $LaNi_5$, EDS characterization indicated that contrary to expectations, the iron and

titanium has segregated as opposed to alloying.

**Hydrogen Adsorption**

The hydrogen sorption properties of palladium nanofoams were evaluated by heating the samples to a fixed temperature (isotherm) and introducing pressurized hydrogen (1000 mbar). Identical isotherms were performed on palladium foam, powder (~0.5 µm diameter) and sheet (~0.1 mm thick). Figure 4 shows a representative isotherm at 50˚C for the foam compared with palladium powder. As seen in the figure, the rate of adsorption for both the powder and foam are quite fast; however, there is a significant difference in the curve profiles. The modeling described below is hoped to explain this difference. As expected the rate of hydrogen uptake in palladium sheet is significantly longer.

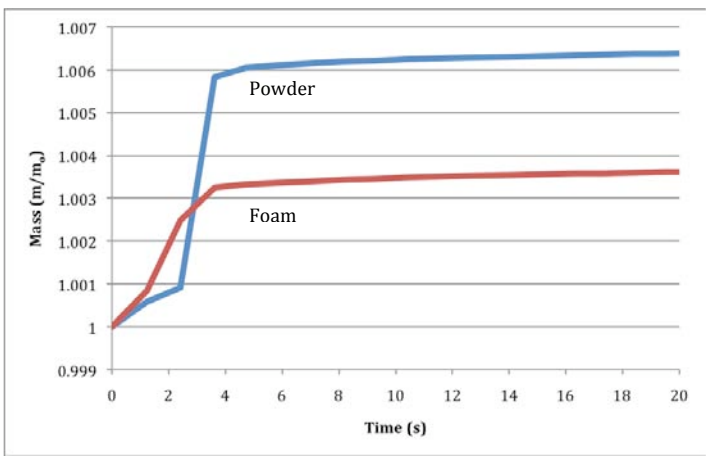


*Figure 4. Hydrogen isotherm to 1000 mbar at 50˚C.*

The amount of hydrogen absorbed by the nanofoam was found to be only about half that of powder or sheet. A decrease in hydrogen capacity was somewhat expected due to the lower purity of the palladium produced by the combustion process. The combustion process leaves residual carbon and nitrogen that could not be fully removed. Even after many cycles of absorption and desorption of hydrogen, no obvious physical degradation of the foam took place and no decrease in hydrogen storage occurred. These are extremely important practical aspects for a material to be reliable in service.

Despite the fact that the MgN, $LaNi_5$ and TiFe foams did not alloy as expected, hydrogen adsorption studies similar to those above but up to higher temperatures (100 ˚C) and pressures (15 bar) were attempted. In all cases, no measurable hydrogen absorption was recorded.

**Modeling**

In order to numerically model the hydrogen absorption in palladium foams we built on our previous work regarding the kinetics of oxygen removal from ceria. [7] We developed a computer implementation of a chemical diffusivity model that takes into account the composition dependence of the diffusion coefficient and activation energy.

Simulations for a variety of geometries and boundary conditions are being performed. To understand the hydrogen diffusion in palladium, we used an idealized model representation of the system as a collection of identical spherical aggregates (particles) as discussed in detail elsewhere [8].

## Impact on National Missions

U.S. energy security is an important, evolving national mission. This project sought to develop, understand and utilize a novel, advanced material system, nanostructured foam, for enabling renewable energy sources. The process yields metal foams of the lowest density and highest surface area known to the authors. With the extremely high surface areas and flexibility in materials that can be accessed by this technique, a truly unique material has been researched. Numerous applications are suggested by the favorable combinations of materials properties offered by metal foams. The high surface area combined with the inherent high electrical conductivity of metals is attractive for electrode applications in batteries, fuel cells and supercapacitors. The high surface area and nanoporosity suggests applications in catalysis. Other areas of interest include high temperature insulation and energy absorption.

In pursuit of the research goals: A) A variety of new nanostructured metal foams was produced. B) Additional understanding of the chemistry of precursor materials synthesis was gained. C) A better understanding of how the foams are formed was gained. D) Hydrogen storage properties of foams were measured. E) Thermodynamic properties of the precursors were measured. F) Modeling of the kinetics of hydrogen sorption/desorption was performed.

## References

1. Ritter, J., A. Ebner, J. Wang , and R. Zidan. Implementing a Hydrogen Economy. 2003. *Materials Today.* **6**: 18.

2. Chen, P., Z. Xiong , J. Luo , J. Lin , and K. Tan. Interaction of Hydrogen with Metal Nitrides and Imides. 2002. *Nature.* **420**: 302.

3. Tappan, B., S. Steiner, and E. Luther. A New Frontier in High-Surface-Area Solids: Nanoporous Metal Foams. To appear in *Angewandte Chemie.*

4. Tappan, B., S. Steiner, A. Mueller, S. Mandal, A. Sen, M. Dirmyer, B. Scott, and E. Luther. Combustion Synthesis of Ultralow-Density Nanoporous Gold Foams. *ACS Nano.*

5. Tappan, B., M. Huynh, M. Hiskey, D. Chavez, S. Son, D. Oschwald, and D. Naud. Preparation of nanoporous metal foam from high nitrogen transition metal. 2006. *US Patent 7141675.*

6. Tappan, B., M. Huynh, M. Hiskey, D. Chavez, E. Luther, J. Mang, and S. Son. Ultra-low Density Nanostructured Metal Foams: Combustion Synthesis, Morphology, and Composition. 2006. *Journal of the American Chemical Society.* **128**: 6589.

7. Stan, M.. Kinetics of Oxygen Removal from Ceria. 2004. *Journal of Applied Physics.* **95**: 3358.

8. Luther, E., B. Tappan, A. Mueller, B. Mihaila, H. Volz, P. Papin, J. Veauthier, and M. Stan. Nanostructured Metal Foams: Synthesis and Applications. 2009. In *Advances in Powder Metallurgy and Particulate Materials - 2009.* (Las Vegas, 28 July 2009). Vol. II, part 9, p. 129. Las Vegas: Metal Powder Industries Foundation.

## Publications

Luther, E., B. Tappan, A. Mueller, B. Mihaila, P. Papin, H. Volz, J. Veauthier, and M. Stan. Nanostructured Metal Foams: Synthesis and Applications. 2009. In *Advances in Powder Metallurgy and Particulate Materials - 2009.* (Las Vegas, July 28). Vol. II, part 9, p. 129. Las Vegas: Powder Metal Industry Foundation.

Tappan, B., S. Steiner, A. Mueller, S. Mandal, A. Sen, M. Dirmyer, B. Scott, and E. Luther. Combustion Synthesis of Ultralow-Density Nanoporous Gold Foams. *ACS Nano.*

Tappan, B., S. Steiner, and E. Luther. A New Frontier in High-Surface-Area Solids: Nanoporous Metal Foams. To appear in *Angewandte Chemie.*

# Nano-Composite Scintillator for Neutron Capture Measurements

*Ernst I. Esch*
20070176ER

## Abstract

We have investigated the feasibility of nanocomposite materials for detecting gamma-rays produced by neutron capture experiments. Several areas of nuclear science require the measurement of neutron capture rates for isotopes with short half-lives. Examples span the design of more proliferation-resistant reactors to research into the creation of matter in the early universe, These measurements require detection systems that can handle high count rates and have fast recovery times. Presently available detectors that meet these requirements cannot be produced in the necessary sizes and quantities. In this project we have investigated embedding tiny particles of a scintillating material in a matrix made of low-cost material. Scintillation is the process by which the energy deposited within a material by ionizing radiation is converted into flashes of light. The goal is to develop an inexpensive fabrication method for gamma-ray detectors for use in a neutron environment. Los Alamos National Laboratory has recently developed techniques to produce $LaF_3$:Ce nanoparticles. Our project furthered this approach to synthesize nanoparticles of $CeF_3$. We have successfully fabricated cerium fluoride (CeF3) nanoparticles and dispersed them in both hydrogen-containing and non-hydrogenous liquid matrices. Additionally, their optical, physical and nuclear properties were characterized. These include the optical transmission, radio- and photo-luminescence, nanoparticle crystallinity and size, and detector energy resolution, pulse width, scintillation decay constant, and neutron sensitivity. The performance of prototype detectors used to measure gamma responses in high neutron-flux environments is also reported.

## Background and Research Objectives

At experiments such as n-TOF (the Neutron Time-Of-Flight Facility at CERN) and DANCE (the Detector for Advanced Neutron Capture Experiments at Los Alamos National Laboratory), neutron capture cross-sections are measured using the time-of-flight method. In the time-of-flight method, neutrons are captured on a target. This results in an excited target nuclei that emits gamma rays when they de-excite. In the de-excitation process, multiple gamma rays are emitted. Although many combinations of gamma-ray energies are possible, the total de-excitation energy, or Q-value, is fixed for a given isotope. Time-of-flight experiments work by detecting these gamma-rays and using them to identify neutron capture events. Once a neutron capture event has been identified, the neutron time-of-flight can be determined. This can subsequently be used to calculate the neutron energy. Detection of all of the neutron capture gamma-rays is essential to accurately measure the Q-value. Thus, modern neutron capture experiments use spherical arrays of detectors, such as that shown in the diagram of DANCE in Figure 1. The importance of detecting all the neutron capture gamma-rays also means that the detectors must have high gamma-ray efficiency and a fast signal decay time. In addition, the detectors must have low neutron sensitivity, since neutron capture events in the detector will cause errors in measuring the Q-value. The current standard detectors for neutron capture experiments are barium fluoride ($BaF_2$) scintillators. $BaF_2$ has a low neutron sensitivity and a high gamma-ray efficiency. Unfortunately, it also has a two-component signal with a fast decay time of 0.3 nanoseconds (one billionth of a second) and a slow decay time of 630 ns. The long signal decay time of the slow component, which contains 80% of the scintillation energy, limits $BaF_2$ detector arrays to measuring the cross-sections of isotopes with half-lives greater than a few hundred days. Shorter-lived isotopes produce a high event rate in the detectors, the result of two phenomena. First, radiation produced by the rapidly decaying sample itself is detected. Second, in the process of producing the high neutron flux needed to measure the cross-section of a short-lived isotope, a large number of gamma-rays are also generated. These

gamma-rays, called the gamma flash, arrive at the target before the neutrons, since they travel at the speed of light. They also deposit energy into the detector via Compton scattering. The gamma flash saturates the detectors and causes pile-up in the data acquisition system. This limits the detection of neutron capture gamma-rays. Also, until the detectors have recovered from the gamma flash, it is impossible to definitively identify a neutron capture gamma-ray.

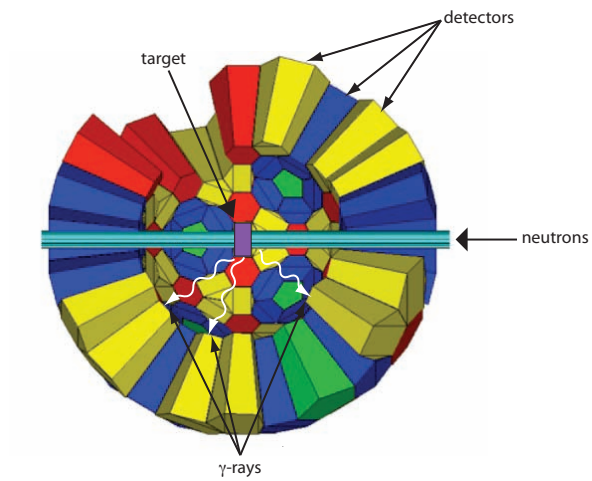


*Figure 1. Schematic setup of the DANCE detector.*

Cerium fluoride ($CeF_3$) is a possible substitute for $BaF_2$. $CeF_3$ has low neutron sensitivity and high gamma-ray sensitivity. Like $BaF_2$, $CeF_3$ has a two-component decay; however, the decay times of its two components are 3 ns and 27 ns. The shorter decay time of its long component, compared with $BaF_2$, allows a $CeF_3$ detector to recover more quickly from the gamma flash. $CeF_3$ was first identified as a scintillator in 1989, but crystals are not currently produced in large enough sizes or quantities to make a spherical detector array. However, the faster decay time of $CeF_3$ makes it suitable for neutron capture cross-section measurements. Thus we chose it as a good candidate for a nanocomposite scintillator replacement for $BaF_2$. Nanocomposite scintillators consist of nanoscale (< 10 nm diameter) particles of a scintillator suspended in a matrix material. [3] Due to their size being much less than the wavelength of light, nanoparticles should scatter light more efficiently in the "forward" direction the direction of travel of the incoming ray). This results in a longer optical scattering length and greater optical transparency.

## Scientific Approach and Accomplishments

The work will be summarized in terms of the parallel effort of materials fabrication, materials characterization, gamma-ray response, and performance in beam physics experiments:

**Materials Fabrication**

The $CeF_3$ nanoparticles are fabricated by combining sodium fluoride (NaF) and cerium nitrate ($Ce(NO_3)_3$) in a heated mixture of water and ethanol. This results in the reaction, $3NaF + Ce(NO_3)_3$ goes to $CeF_3 + 3NaNO_3$ This reaction occurs spontaneously, and if it is allowed to proceed unabated, the CeF3 molecules assemble in their most stable state, a crystalline precipitate. We ensure that the crystals remain nanoscale by stirring the mixture constantly to inhibit agglomeration and through the addition of a capping agent, which attaches to on the $CeF_3$ nanocrystals to retard their growth into the precipitate. Following the reaction, the nanoparticles are washed to remove the solvents and the excess capping agent. For characterization purposes, the nanoparticles are dispersed in solution. The solution typically used is a liquid scintillator consisting of toluene and two wavelength-shifting dyes at approximately 1.0 % and 0.1 % weight concentrations.

**Materials Characterization**

The response of the CeF3/liquid scintillator solutions to optical and x-ray excitation is characterized using photoluminescence (PL) and radioluminescence (RL) spectroscopy, respectively. The RL spectrum of a $CeF_3$/ liquid scintillator solution, compared with the spectrum of liquid scintillator alone, is identical except for an increase in overall intensity that can be attributed to an increase in the x-ray energy deposition into the sample. This is an atomic property that rapidly increases with increasing atomic number (Z); for example, for every x-ray that deposits its energy on a carbon atom, more than five hundred will deposit their energy on a Ce atom. Thus, even a 1% addition of $CeF_3$ will cause a measurable increase in the RL intensity.

Since a transparent nanocomposite requires a sufficiently small nanoparticle for Rayleigh scattering to dominate, the size of the $CeF_3$ nanoparticles is an important parameter. We used a number of optical and structural characterization techniques to determine the particle size, including transmission electron microscopy (TEM), x-ray diffraction (XRD), light scattering measurements, and measurement of the ultraviolet and visible light transmission. These techniques are complementary, providing slightly different information about the particle structure and size. For example, XRD provides a measurement of the average nanoparticle size, while TEM allows us to view individual nanoparticles. In TEM, a beam of electrons from an emission source passes through a sample. The transmitted electrons are collected, forming an image of the sample from which the particle sizes can be measured. A TEM image is shown in Figure 2. The left side of the figure shows a number of $CeF_3$ nanoparticles,

all with diameters of about 10 nm. The poor contrast of this image is typical of TEM of high-Z nanoparticles. The right side of the figure shows a single $CeF_3$ nanoparticle at higher magnification. The diagonal lines running across the nanoparticle are the planes of atoms, whose spacing and orientation depend on the crystal structure. The ability to distinguish the crystalline planes enables us to verify that this is a single crystal, rather than an agglomerate.

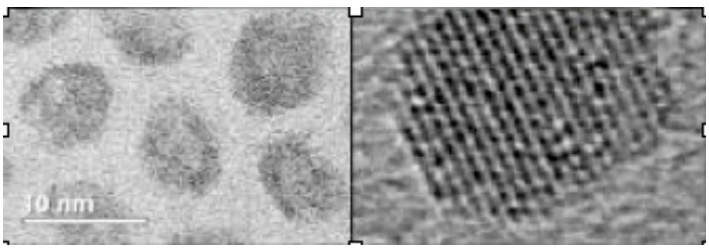


*Figure 2. TEM results on nano-particles.*

In XRD, a beam of monoenergetic x-rays is diffracted by the atoms of a crystalline sample. This produces constructive and destructive interference. Since the x-rays are diffracted by multiple planes of atoms, the net effect is destructive interference except at scattering angles that are integer multiples of L/d, where L is the x-ray wavelength and d is the distance between crystal planes. A x-ray diffractogram is a plot of the scattering intensity as a function of the scattering angle. It shows a peak when the scattering condition for constructive interference, or Bragg condition, is satisfied. The locations and relative intensities of the observed diffractogram for the $CeF_3$ nanoparticles match very well with the known crystal structure. However, the width of the diffractogram peaks is much broader for the nanoparticles. This effect can be analyzed to provide an estimate for the particle size, assuming that all particles are identical spheres. This Debye-Scherrer analysis yields an estimated particle diameter of less than 10 nm, in excellent agreement with the TEM results.

**Gamma-ray response**

In order to characterize the radiation response of the $CeF_3$ nanoparticles, small volumes were subjected to radiation from a $^{137}Cs$ sealed source. A typical spectrum for a solution containing 20% $CeF_3$ nanoparticles suspended in liquid scintillator is shown in Figure 3. The spectrum shows features typical of two types of gamma-ray interactions, a Compton continuum below 477 keV resulting from Compton scattering by both the liquid scintillator and the $CeF_3$ and a photopeak at 662 keV resulting from the photoelectric effect on $CeF_3$. Since the cross-section of the photoelectric effect goes roughly like $Z^{4.5}$, the low-Z liquid scintillator was not expected to display a significant photopeak, and indeed, liquid scintillator-only detectors of this volume showed only a Compton continuum. We rely on detecting the full energy of each neutron capture gamma-ray to identify a neutron capture event. Thus the photopeak, which results from the deposition of a gamma-ray's entire energy, is a necessary characteristic for a useful detector.

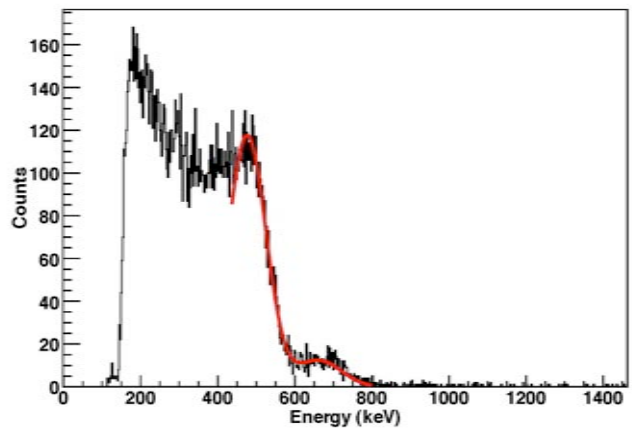


*Figure 3. A typical spectrum for a solution containing 20% $CeF_3$ nanoparticles suspended in liquid scintillator.*

**Performance in beam experiments**

Several weeks of beam time has been allocated at the Los Alamos Neutron Science Center (LANSCE), over the course of two years, for testing of prototype nanocomposite gamma-detectors. In the first test, two 70 mL $CeF_3$/liquid scintillator detectors were placed near the neutron beam at LANSCE. We characterized their response to neutrons and neutron capture gamma-rays. The detectors were placed on either side of the neutron beam, with a target suspended between them in the center of the beam. Tantalum, carbon, cobalt, and gold targets were used. All of these materials have well-characterized neutron capture cross sections. In addition, carbon has a very low neutron capture cross-section and a high neutron scattering cross-section, so it provided a good measurement of the background. A $BaF_2$ detector module from DANCE was also placed near the beam, in order to compare its response with that of the $CeF_3$ detectors. The responses of a $CeF_3$ detector and the $BaF_2$ detector, as compared with the neutron capture cross-section for tantalum from the Evaluated Nuclear Data File (ENDF) database, are shown in Figure 4. The neutron capture resonances for energies below 40 eV are identifiable in both the $CeF_3$ and the $BaF_2$ responses. However, no signal is seen in the $BaF_2$ detector from neutrons with energies higher than 40 eV. This is the result of the long signal decay time of $BaF_2$ during the arrival of higher-energy neutrons. As explained previously the detector is still recovering from the gamma flash. In the response from the $CeF_3$ detector, on the other hand, it is possible to discern several neutron capture resonances well above 40 eV.

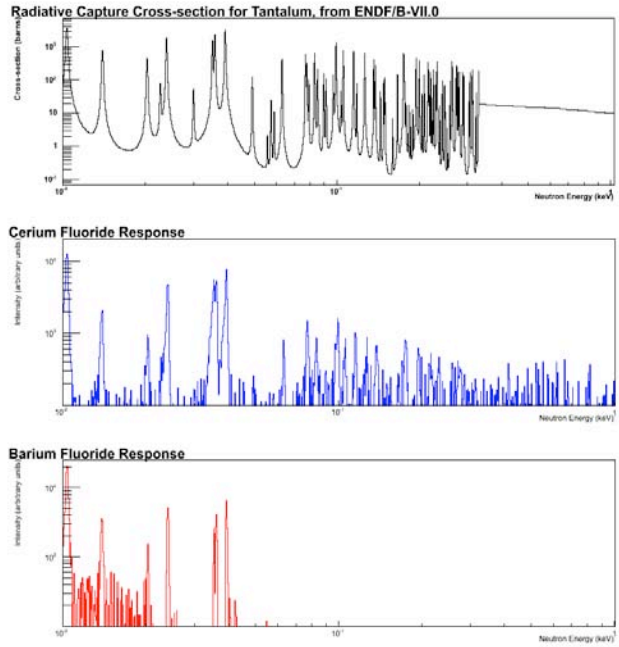


*Figure 4. The responses of a $CeF_3$ detector and the $BaF_2$ detector, as compared with the neutron capture cross-section for tantalum from the Evaluated Nuclear Data File (ENDF) database.*

However these data also indicate a problem with this first $CeF_3$ nanocomposite prototype detector. Detector response past 400 eV cannot be due to neutron capture events. Theory must be due to neutron interaction within the detector. These come about because there is efficient energy transfer between neutrons and the hydrogen atoms within the liquid scintillator matrix. The primary component used to formulate a liquid scintillator is an aromatic hydrocarbon, such as toluene. The scintillation properties of aromatic compounds arise from electronic excitations between their pi-orbitals. It is the subsequent de-excitation to the ground state that leads to the observation of scintillation. It is possible to synthesize a liquid scintillator using aromatic organic compounds whose hydrogen molecules have been replaced by higher-Z atoms, such as fluorine. This will significantly inhibit the proton recoil mechanism, ideally making the matrix material neutron insensitive to much higher neutron energies, while still scintillating in response to gamma-rays.

## Impact on National Missions

Measurement of the neutron capture cross-sections of a number of short-lived isotopes is needed to advance both pure and applied scientific research. Neutron capture data support the calculation of criticality and waste production estimates for important DOE programs such as the Advanced Fuel Cycle Initiative and the analysis of data from nuclear weapons tests. But of more fundamental significance, they also impact our understanding of nucleosynthesis, the process by which matter was created in the early universe. Currently, measurement of these cross-sections requires a scintillation detector with a faster signal decay time than currently in use. Crystals of faster detector materials are not available in sufficient sizes and quantities to supply these large-scale accelerator experiments.

Our development of nanocomposite detectors directly addressed this research need. A tangible outcome of this research will be to refine the design criteria for the DANCE II detector. If the $CeF_3$/fluorinated scintillator shows the expected performance, this would have far-reaching effects for all neutron capture cross-section measurements.

Perhaps less tangible but also worth mentioning is that this project allowed for the continued refinement of fluoride nanoparticles synthesis and characterization. This has already lead to another PD opportunity with ISR to develop $^6$LiF nanocomposite fibers for neutron detection. Success with this pilot project would directly address the replacement of $^3$He neutron detectors and thus grow into a full proposal to NA-22.

## Publications

Esch, E. I., A. J. Couture, R. E. Del Sesto, R. D. Gilbertson, and R. E. Muenchausen. Nano-composite based radiation detectors for beam experiments. *CAARI.* (Ft. Worrth, TX, Aug. 2008).

Stange, S., E. I. esch, L. O. Brown, A. J. Couture, R. E. Del Sesto, R. D. Gilbertson, T. M. McCleskey, E. A. McKigney, R. E. Munchausen, and R. Reifarth. Characterization of cerium fluoride nanocomposite scintillators. To appear in *INMM annual meeting.* (Tucson, AZ, July, 2009).

# From Novel Principles to Novel Device Structures for High-Efficiency Generation of Solar Electricity

*Victor I. Klimov*
20070338ER

## Introduction

Semiconductor nanocrystals (NCs) are promising materials for the realization of low-cost, high-efficiency photovoltaics (PV) [1]. They can be synthesized and processed via solution-based techniques readily applicable to the fabrication of large-area devices including solar cells. NCs also exhibit a number of unique physical properties that can benefit PV applications. For example, the NC-size-controlled energy gap can be used to tailor the absorption spectrum for the best match to the solar radiation spectrum. Further, one can boost power conversion efficiency via NC-specific processes such as generation of multiple charges by single photons (carrier multiplication) [2] and/or hot-electron extraction in the presence of a "phonon bottleneck" in intraband relaxation. The first practical step toward utilization of the unique properties of NCs in the PV technologies could be through their integration into traditional semiconductor thin-film devices. The goal of this project was the development of a new type of hybrid solar cells that combine colloidal NCs and semiconductor charge-extraction layers. In our initial proof-of-principle studies, we focused on devices comprising CdSe NCs and amorphous silicon (a-Si). We showed that in these structures, NCs and silicon are electronically coupled, and the regime of this coupling can be tuned by altering the alignment of NC states with regard to silicon band edges. We also demonstrated that in these devices, a photoresponse is exclusively due to the NCs. As the next step, we extended our work to NCs of narrow-gap, infrared-active PbS. In these next-generation structures, both the NCs and silicon contribute to photocurrent, which results in the PV response extending from the visible to the near infrared [3]. The work conducted in this project demonstrates the feasibility of hybrid PV devices that combine advantages of mature silicon fabrication technologies with the unique electronic properties of semiconductor NCs.

## Background and Research Objectives

A significant challenge in practical applications of NCs in devices such as PV cells and light-emitting diodes (LEDs) is the development of methods for efficient charge extraction/injection and carrier transport. Most of the reported NC-based PV cells and LEDs utilize blends or multilayers of organic molecules (often conducting polymers) and NCs, wherein charge carriers are delivered to or from the electrodes through percolated networks formed by the NCs and the organic molecules [4,5]. Such structures, however, suffer from low carrier mobilities and poor environmental and photo-stability, primarily because of the involvement of the organic component. To mitigate these problems, in our earlier work [6] we applied a hybrid LED architecture, in which colloidal NCs were encapsulated in a *p-n* junction formed by inorganic GaN injection layers. This strategy took advantage of well-established GaN thin-film growth techniques and allowed for efficient injection of electrical charges into NCs with the added benefit of greatly improved stability of the devices.

In this project, we explore a similar strategy – integration of NCs into traditional thin-film structures – but in application to PV devices. At present, the PV market is dominated by crystalline silicon (c-Si) cells. However, cost considerations have lead to rapid expansion of the PV market segment utilizing amorphous silicon. In addition to reduced fabrication cost, a-Si provides the advantage of increased light absorptivity, which allows one to reduce the thickness of a solar cell, and hence material consumption, and the device weight. The efficiencies of a-Si solar cells are still lower than those of devices made of c-Si (~9% versus ~25%).

The purpose of this project was to develop practical approaches for improving the performance of a-Si devices via infrared sensitization with narrow-gap colloidal NCs. Specific goals of our work were the demonstration of successful incorporation of the NCs

into thin-film a-Si solar cells as well as understanding of electronic interactions at the NC/a-SI interfaces. We expected that Inclusion of the NCs would enhance the performance of a-Si PV structures through added flexibility in tailoring the device absorption spectrum, application of tandem architectures, and perhaps, increased conversion efficiency in the ultraviolet through carrier multiplication [2,7].

## Scientific Approach and Accomplishments

### Device fabrication

In this project, we studied devices comprising either wide-gap CdSe NCs or narrow-gap PbS NCs. CdSe NCs capped with trioctylphosphine oxide (TOPO) and trioctylphosphine (TOP) were fabricated using a modified procedure developed by Murray *et al.* [8] while PbS NCs were synthesized according to a modified literature route [9].The NCs were spin-coated onto indium tin oxide (ITO) electrodes. Amorphous Si films were grown at room temperature in a vacuum chamber using either electron-beam (e-beam) evaporation or radio-frequency (rf) magnetron sputtering. For the first method, the growth rate was ~0.1 nm per second with a chamber background pressure of $1x10^{-6}$ Torr. The film thickness was monitored by a quartz crystal monitor and then verified by a cross-sectional analysis using transmission electron microscopy (TEM). The stray electrons from the source beam were shielded by an aluminum foil to prevent potential damage to the NCs. For magnetron sputtering, argon was used as a carrier gas (4.5 mTorr pressure and 20 sccm flow rate). The sputtering power was 250 W, which provided a growth rate of 0.08 nm per second. To complete the device, aluminum electrodes were evaporated through a shadow mask giving a contact active area of 1 - 3 $mm^2$.

### Control of PV performance by the quantum-size effect in CdSe NC/a-Si devices

A PV structure made of a-Si and CdSe NCs is schematically depicted in Figure 1a. It comprises a layer (90 to 150 nm thickness) of pyridine-capped CdSe NCs sandwiched between ITO and a-Si layers (see the TEM image in Figure 1b). Both e-beam evaporation and rf magnetron sputtering allow deposition of a-Si on top of NCs without adversely affecting their physical properties. Direct deposition of Si onto the NC layer was essential for obtaining electronic coupling at the Si/NC interface. Test structures fabricated by an alternative procedure - spin-coating NCs onto pre-fabricated Si films - did not show any photocurrent.

The higher-resolution TEM images in Figures 1c and 1d show resolvable lattice fringes of CdSe NCs, which indicates that the NC integrity is preserved during silicon film growth. The latter is also confirmed by spectroscopic studies. Specifically, optical absorption measurements show that the lowest-energy, 1S absorption feature of the NCs is preserved in the final device structure (compare Figures 1e and 1f). Further, NC photoluminescence (not shown), although quenched, is still observable following silicon deposition.

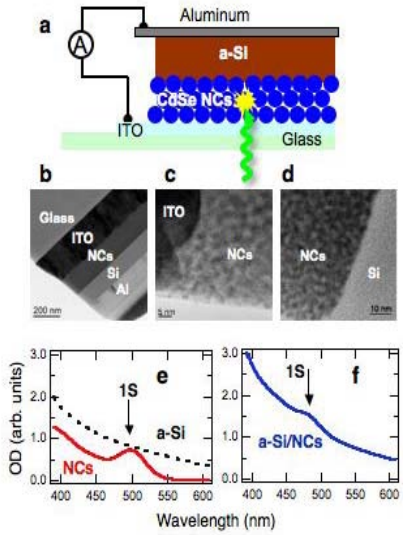


*Figure 1. Hybrid a-Si/NC PV structures: TEM and spectroscopic characterization. (a) Schematic of the PV device. (b) A cross-sectional TEM image of the PV structure. (c) and (d) High-resolution TEM images of the ITO/NC and the NC/a-Si interfaces, respectively. (e) The absorption spectra (in terms of optical density, OD) of the NC and a-Si films separately deposited on glass slides. (f) The absorption spectrum of the hybrid a-Si/NC structure.*

To understand the performance of the fabricated devices, one needs to take into consideration the alignment of CdSe NC electronic states with respect to those of a-Si. In Figure 2a, we show the energies of the conduction and the valence band edges (denoted CB and VB, respectively) of a-Si together with NC-size-dependent positions of the lowest-energy electron ($1S_e$) and hole ($1S_h$) levels plotted as a function of NC energy gap, $E_g$. In the case of a CdSe-NC/Si interface the tunability range provided by the quantum-size effect is sufficient to shift the $1S_e$ level from below to above the a-Si conduction-band edge (Figure 2a). The latter should dramatically modify the regime of electronic interactions at the NC/Si interface if NCs and Si are in direct electrical contact. Specifically, NCs of larger sizes with $E_g$ below $E_{g,c}$ = 2.3 eV should act as acceptors of electrons from the conduction band of Si, while smaller NCs ($E_g > E_{g,c}$) should efficiently inject photogenerated electrons into Si (Figure 2a).

To study electronic interactions at NC/Si interface, we analyze the PV response of devices fabricated using NCs of two different sizes (energy gaps 2.5 and 2.1 eV) that

according to the diagram in Figure 2a correspond to two different injection regimes. Since these structures are composed of thin layers of undoped materials, we expect that their operation is similar to that of, for example, thin-film polymer PV cells and can be described by the metal-insulator-metal (MIM) model. If such devices are under the short-circuit condition, the Fermi levels in the electrode materials come to equilibrium, which results in the buildup of an internal electric field, *E*. In the case of ITO and Al, this field provides a driving force that directs electrons toward the Al electrode, while holes are directed to the ITO contact as illustrated in Figure 2b. Under the open-circuit condition, a difference in electrode's work functions defines an output voltage ($V_{oc}$).

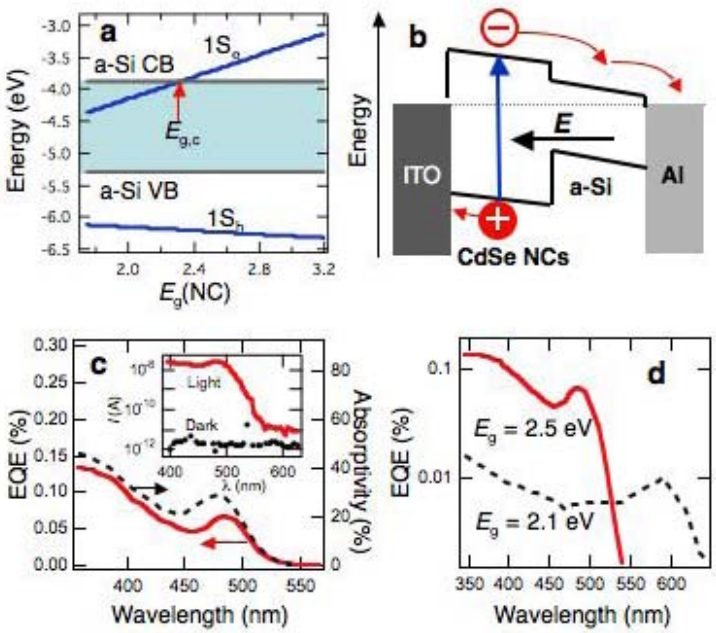


*Figure 2. The effect of NC size on the PV performance of a-Si/NC structures. (a) The size-dependent energies of the NC 1S electron and hole levels (blue lines) plotted as a function of the NC energy gap in comparison to the band-edge positions of a-Si (grey lines); all energies are measured versus vacuum. Eg,c is the critical NC gap; sufficiently small NCs with Eg > Eg,c can inject a photoexcited electron into a-Si. (b) Schematics of energy structures in a PV device operating under short-circuit conditions; the horizontal arrow shows the direction of the internal electric field, E. (c) The EQE spectrum (solid red line) of the PV device fabricated using NCs with energy gap of 2.5 eV in comparison to the NC absorption spectrum measured in terms of percentage of absorbed photons (dashed black line). Inset: The spectral dependence of the photocurrent (solid red line) and the dark current (black circles). (d) Comparison of PV performance (in terms of EQE on a log scale) of the devices fabricated using NCs with energy gaps of 2.5 eV (solid red line) and 2.1 eV (dashed black line).*

Given the alignment of the valence-band states at the Si/NC interface and the direction of the internal field, the PV response of the fabricated structures should be exclusively due to the NCs, because holes generated in silicon are blocked from the ITO contact by a large potential barrier. On the other hand, holes generated in the NCs can be efficiently collected by the ITO electrode for all NC sizes. The situation, however, is different for photogenerated electrons. For larger NCs, in which the 1S$_e$ level is below the a-Si conduction-band edge, the electrons are blocked from the Al electrode by a potential barrier. On the other hand, NCs of sufficiently small size with $E_g > E_{g,c}$ can inject electrons into Si, which should result in a photocurrent.

Experimental data indeed indicate a strong dependence of a photoresponse of the fabricated structures on NC size. For the device that comprises NCs with $E_g$ = 2.5 eV, the spectrum of external quantum efficiency (EQE – the number of electrons extracted from a device per single incident photon) mimics the NC absorption spectrum (Figure 2c; compare solid red and dashed black lines). The leakage current measured under "dark" conditions is very small, on the order of 1 picoamp per mm$^2$ (inset in Figure 2c), as expected for these structures made of undoped materials. The EQE values are greatly reduced in the device made of the NCs with $E_g$ = 2.1 eV (compare dashed black and solid red lines in Figure 2d), because for this NC size, the 1S$_e$ level is below the a-Si conduction band edge, which inhibits electron injection into the silicon layer. These results indicate the possibility of obtaining good electronic coupling between NCs and Si, and also demonstrate our ability to control the charge flow at the NC/Si interface through the quantum-size effect.

**Demonstration of an enhanced infrared PV response in PbS NC/a-Si devices**

In the structures comprising CdSe NCs, the PV response is entirely due to the NCs, while photons absorbed in the a-Si film do not contribute to photocurrent. One might expect that the overall PV performance can be improved using structures, in which PV response is due to charge carriers generated in both the NCs and the a-Si layer. To realize this type of performance, we combine a-Si deposited via rf-magnetron sputtering with infrared absorbing PbS NCs. According to the diagram in Figure 3a, electrons photogenerated in PbS NCs can be transferred into amorphous silicon and then collected at the Al electrode. Further, the alignment of the valence-band states at the PbS NC/a-Si interface favors hole transfer from silicon into NCs followed by collection at the ITO electrode. Thus, this structure is expected to show photocurrent due to both a-Si and the NCs.

The PbS NC-based devices show PV performance, which is considerably improved compared to that of structures comprising CdSe NCs. One factor contributing to this improvement is increased spectral coverage. Specifically, the use of narrow-gap NCs allows us to extend the device operational range into the infrared region, and thus, efficiently harvest low-energy photons. For example, for the structure in Figure 3a, the 1100 nm photons are converted into electrical charges with EQE of ~7% (Figure 3b). Further, these devices also show high quantum efficiencies in the visible (EQE is up to ~50% in the green-blue region of the optical spectrum), which is a result of both a steep increase in absorbtivity of PbS NCs at shorter wavelengths and increasing contribution from carriers generated in the a-Si layer (Figure 3b; the main panel and the inset).

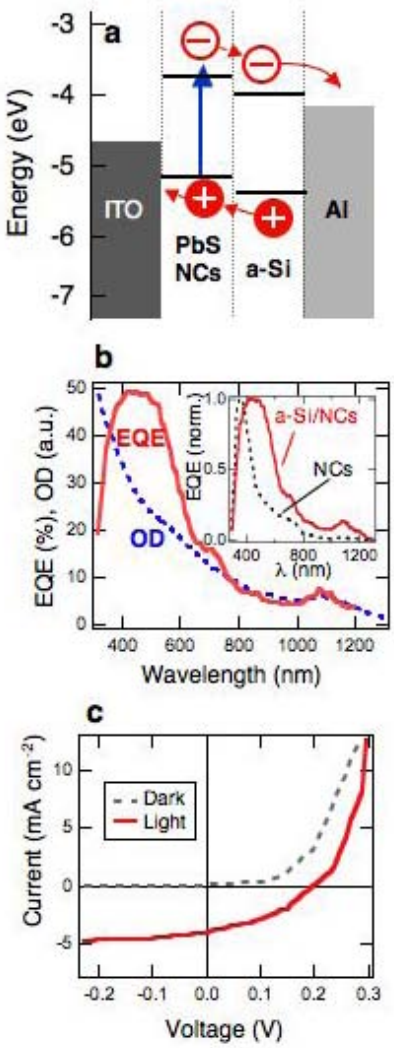


*Figure 3. Hybrid a-Si/PbS NC PV structures: Schematics and characterization of PV performance. (a) An approximate diagram of energy states (shown vs. vacuum) in a PbS NC/a-Si device under the open circuit condition; filling of defect states at the NC/a-Si interface may lead to band bending (not shown) due to formation of a Schottky junction. (b) Comparison of the EQE spectrum of the hybrid PV structure comprising PbS NCs (solid red line) with the absorption spectrum of the NCs (dashed blue line); the NC lowest absorption peak is at 1100 nm. Inset: Comparison of the normalized EQE spectra of the hybrid a-Si/NC device (solid red line) and the all-NC PV structure made without the a-Si layer (dashed black line). (c) The I-V characteristic of the devices comprising PbS NCs and a-Si (layer thicknesses are 200 nm and 50 nm, respectively) in dark (dashed gray line) and under illumination (solid red line).*

To further characterize our PbS-NC based devices, we study their I-V characteristics in dark (dashed gray line in Figure 3c) and under white light illumination (unfiltered light from a xenon lamp) at 36.5 mW cm$^{-2}$ (solid red line in Figure 3c). These measurements indicate the open circuit voltage of 0.2 eV, the short-circuit current ($I_{sc}$) of 4.13 mA cm$^{-2}$, and the fill factor of 0.39, which corresponds to a power conversion efficiency of 0.9%.

## Impact on National Missions

In this project, we have demonstrated functional PV structures that combine colloidal NCs with amorphous silicon. The PV response of these devices can be controlled by varying energies of electronics states in NCs by either changing the NC size or the composition. As expected based on energy offsets at the a-Si/NC interface, the structures comprising nanoparticles of CdSe show a PV response, which is exclusively due to the NC device component. Further, by changing the NC size, we can control the efficiency of charge transfer across the a-Si/NC interface, and hence, the generated photocurrent. By replacing CdSe NCs with infrared active NCs of PbS, we obtain a photoresponse that has contributions from both NCs and a-Si, again in agreement with the alignment of energy states at the a-Si/PbS NC interface. The PbS NC-based devices show a strong PV response extended into the near infrared with EQEs of ~7% at 1100 nm and up to ~50% in the visible. These results represent the first successful demonstration of near-infrared sensitization of a-Si solar cells, which points toward a practical approach for solving the important problem of low infrared absorbtivity of thin-film silicon PV. An encouraging practical aspect of this work is that magnetron sputtering, which is a common industrial fabrication technique, is apparently compatible with colloidal NCs, which should facilitate practical applications of these newly developed hybrid PV devices.

The work conducted in this project is relevant to LANL and DOE interests in both world-class fundamental science and strategic applications. Successful implementation of new strategies to "hybrid" PV developed in the project will yield solar-energy-conversion technologies relevant to DOE and LANL missions in *Energy Security*. At the 2005 DOE workshop on *Basic Research Needs for Solar Energy*

*Utilization*, it was recognized that while solar PV is an important clean energy source, the practical large-scale applications of solar cells would require new concepts and novel materials for solar energy conversion. A novel concept of hybrid NC/a-Si PV explored in this project can potentially lead to such breakthrough technologies that combine low fabrication costs with high power conversion efficiencies.

The work conducted in this project has been also important in the area of program development. Our results on NC-size-control of PV performance of hybrid solar cells were included in the successful LANL Energy Frontier Research Center (EFRC) proposal, where they were used to illustrate a large potential of nanoscale semiconductors in practical PV technologies. This project has also lead to the development of a new LANL capability in the area of new types of hybrid solar cells that combine colloidal nanoparticles with traditional thin film semiconductors.

## References


1. Gur, I., N. A. Former, M. L. Geier, and A. P. Alivisatos. Air stable all-inorganic nanocrystal solar cells processed from solution . 2005. *Science.* **310** (5747): 462.

2. Schaller, R. D., and V. I. Klimov. High efficiency carrier multiplication in PbSe nanocrystals: Implications for solar energy conversion. 2004. *Phys. Rev. Lett..* **92** (18): 186601.

3. Sun, B., A. Findikoglu, M. Sykora, D. Werder, and V. I. Klimov. Hybrid photovoltaics based on semiconductor nanocrystals and amorphous silicon . 2009. *Nano Lett,.* **9** (3): 1235.

4. Greenham, N., X. G. Peng, and A. P. Alivisatos. Charge separation and transport in conjugated-polymer/semiconductor-nanocrystal composites studied by photoluminescence quenching and photoconductivity . 1996. *Phys. Rev. B.* **54** (24): 17628.

5. Jiang, X., R. D. Schaller, S. B. Lee, J. M. Pietryga, V. I. Klimov, and A. A. Zakhidov. PbSe nanocrystal/conducting polymer solar cell with an infrared response to 2 micron. 2007. *J. Mat. Res..* **22** (7): 2204.

6. Mueller, A. H., M. A. Petruska, M. Achermann, D. Werder, E. A. Akhadov, D. D. Koleske, M. A. Hoffbauer, and V. I. Klimov. Multicolor light-emitting diodes based on semiconductor nanocrystals encapsulated in GaN charge injection layers. 2005. *Nano Lett..* **5** (6): 1039.

7. Klimov, V. I.. Detailed-balance power conversion limits of nanocrystal-quantum-dot solar cells in the presence of carrier multiplication. 2006. *Appl. Phys. Lett..* **89** (12): 123118.

8. Murray, C. B., D. J. Norris, and M. G. Bawendi. Synthesis and characterization of nearly monodisperse CDE (E = S, SE, TE) semiconductor nanocrystallites. 1993. *J. Am. Chem. Soc..* **115** (19): 8706.

9. Hines, M. A., and G. D. Scholes. Colloidal PbS nanocrystals with size-tunable near-infrared emission: Observation of post-synthesis self-narrowing of the particle size distribution . 2003. *Adv. Mater..* **15** (21): 1844.


## Publications


Jiang, X. M., R. D. Schaller, S. B. Lee, J. M. Pietryga, V. I. Klimov, and A. A. Zakhidov. PbSe nanocrystal/conducting polymer solar cells with an infrared response to 2 micron. 2007. *J. Mater. Res..* **22** (8): 2204.

Klimov, V. I.. Detailed-balance power conversion limits of nanocrystal-quantum-dot solar cells in the presence of carrier multiplication . 2006. *Appl. Phys. Lett..* **89** (12): 123118.

Klimov, V. I.. Spectral and dynamical properties of multiexcitons in semiconductor nanocrystals . 2007. *Annu. Rev. Phys. Chem.* **58**: 635.

McGuire, J. A., J. Joo, J. M. Pietryga, R. D. Schaller, and V. I. Klimov. New aspects of carrier multiplication in semiconductor nanocrystals. 2008. *Acc. Chem. Res..* **41** (12): 1810.

Sun, B., A. T. Findikoglu, M. Sykora, D. J. Werder, and V. I. Klimov. Hybrid photovoltaic devices based on semiconductor nanocrystals and amorphous silicon . 2009. *Nano Lett..* **9** (3): 1235.

# X, Gamma, Alpha : Ultra-High Resolution Spectroscopy

*Michael W. Rabin*
20070367ER

## Abstract

We have developed and improved extremely sensitive cryogenic detectors for X-ray, gamma-ray, and alpha-particle spectrometry. In each case the unsurpassed energy resolution of microcalorimeter detectors reveals previously invisible spectral features of nuclear materials. These dramatic improvements in detector performance, material identification, and quantitative analysis are applicable to problems in international nuclear safeguards, treaty verification, and nuclear forensics. Our research focus on cryogenic detector innovation and novel applications has lead to several results, including:

- **Increased gamma ray energy range**—detector, fabrication, and materials improvements have doubled the energy range without decrease in resolution or speed.
- **High-resolution alpha spectrometry**—First demonstration of alpha particle energy spectrometry with a cryogenic detector suitable for plutonium isotopic analysis.
- **Mixed actinide analysis**—First analysis of an actinide mixture fully resolving crucial nuclear-forensics peaks.
- **Advanced Monte-Carlo simulation**—Demonstration of both spectral fidelity and correct absolute efficiency.

Significant work will be required to fully understand the ultimate performance limits, these results have allowed lead to two follow-on projects directed toward advanced instrumentation (DOE) and nuclear forensics (DHS).

## Background and Research Objectives

Over the past decade, cryogenic photon detectors based on superconducting devices have emerged as cutting-edge tools for science and security applications. The fundamental advantage of cryogenic sensors to detect X-rays and gammas is ultra-low noise due to low operating temperature, typically 0.1 to 10 K, which can be used for extremely high-precision measurement of particle energy, interaction time, or incident power [1,2]. Early on, progress in scientific applications preceded and outpaced that for security applications, with emphasis on astrophysics, cosmology, dark matter search, neutrino mass measurement, biopolymer mass spectrometry, quantum information, and X-ray materials analysis (especially on the nanoscale). This broad range of scientific problems spurred intense creativity in the field and the invention of several new classes of cryogenic devices, including superconducting nanowire single photon detectors, kinetic inductance bolometers, micro-serpentine time-of-flight particle (ion) detectors, nonequilibrium phonon sensors, and the voltage-biased transition-edge sensor (TES). Fundamentally, a TES is a very precise thermometer operated on the superconducting-to-normal transition (the edge). Imaging arrays of TES bolometers are now in use world wide for astronomy and TES calorimeters are under development for X-ray space telescopes. The microfabrication of arrays, implementation of specialized array-readout circuitry and advanced cryogenic systems were essential for progress, establishing the technological basis for the field.

Roughly speaking, these science instruments can be categorized as event detectors, spectrometers, imaging arrays, or combinations, such as spectral imagers for X-ray astrophysics with high spatial and spectral resolution. Frequently, cryogenic detectors are at the back end of an experiment or sophisticated instrument: cameras, telescopes, dispersive (grating) spectrometers, spectral filters, polarizers, antennae, feed horns, electron microscopes, mass spectrometers, fiber-optic communication networks, accelerator beam lines, or (perhaps) more complex “filters” (Fourier-transform spectrometers, Hadamard masks, coded apertures, spatial phase modulators). Given the possible

instrument configurations and signatures, it is reasonable to anticipate a broad range of national and international security applications of ultrasensitive cryogenic detectors. As with the science applications, the advantages of ultra-low noise, high-confidence of detection, and measurement precision must be compared to the performance features, lower cost, and user-community acceptance of conventional technology, e.g. CCD cameras, microchannel plates for ion detection, and high-purity germanium (HPGe) gamma-ray spectrometers. Strong contenders for security applications where the benefits of cryogenic detectors are likely to outweigh the associated costs and difficulties have been identified, including fiber quantum cryptographic key distribution, detection and imaging of concealed weapons or explosives, and nuclear materials analysis.

So far, the principal goal of nuclear materials analysis research with cryogenic detectors has been obtaining high-resolution energy spectra resolving peak overlaps that cannot be resolved using conventional detectors. Important materials to characterize include the actinides, their decay daughters, fission products, neutron activation products, and mixtures of these. In particular, plutonium is the canonical example of a material with a complex spectrum of many overlapping X- and gamma-ray peaks (Figure 1); resolving and analyzing these peaks is a major motivation in this small research field. By themselves, high-resolution spectra can allow peak identification by eye, and in some cases definitively distinguish between constituent radioactive materials (Figure 2). Such spectra also have the potential for a major improvement in quantitative analysis of material composition, i.e. elemental and isotopic ratios with significantly reduced uncertainties. Experimental work has focused on ionizing radiation (photons, neutrons, alpha particles) emitted as a consequence of spontaneous nuclear decay; the peaks in the energy spectra for these particles correspond to characteristic nuclear or atomic transitions. In all schemes considered to date, the ultra-low noise at low temperature allows the detector to measure the energy of individual particles of radiation with high precision, in turn allowing us to obtain high-resolution spectra. Modern cryogenic sensors for nuclear materials analysis were initially advocated for gamma-ray spectroscopy. Successful demonstration of ultra-high energy resolution required development of the compound TES microcalorimeter. Subsequent sensor design improvements lead to the first published spectra clearly resolving the complex X-gamma overlap region of plutonium (~100 keV) [3]. New applications such as neutron spectroscopy, the non-destructive assay (NDA) of spent nuclear fuel [4,5], and nuclear forensic alpha spectrometry [6] have emerged only recently. Multiplexed microcalorimeter gamma-ray detector arrays (Figure 3) are now in use, and have revealed unprecedented spectral detail of special nuclear material (SNM). As shown in Figure 2, a TES-microcalorimeter gamma-ray array has been used to discriminate between the primary signature peak of highly enriched uranium and the ubiquitous background isotope Ra-226 found in many common materials. The overlap between these peaks in conventional spectra is the most common source of false alarms for operational nuclear detection programs in The basic research objective of this project was to develop TES microcalorimeter detectors for X-ray, gamma-ray, and alpha-particle energy spectrometry. Prior to the start of this project, preliminary results indicated that TES microcalorimeters could produce high-resolution X- and gamma-ray spectra for energies up to ~100 keV, but these early devices had significant limitations, e.g. unacceptably high membrane stress, excess noise, need for an external magnetic field to increase dynamic range, and gain instabilities. High precision measurement of alpha particle energy with modern superconducting devices for actinide analysis had never been attempted, and it was unclear if the chemical methods for alpha sample preparation would provide actinide samples of sufficient quality to exploit the theoretical detector resolution. Furthermore, advanced Monte-Carlo simulation of particle-by-particle transport had not been fully applied to problems in cryogenic detector development. Specific goals of this project included addressing each of these issues. We have been successful at achieving these objectives. transportation, commerce, and border-crossings.

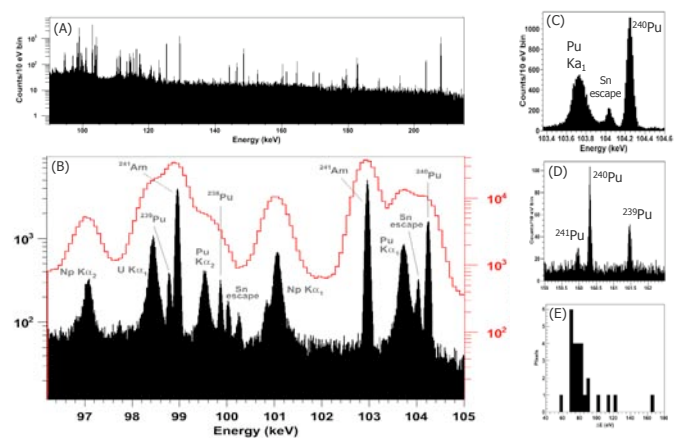


*Figure 1. X- and gamma ray spectrum of Pu taken using 14 of the 66 pixels on the chip shown in Figure 3. (A) Wide region spectrum showing dynamic range of ~200 keV; logarithmic vertical axis. (B) Direct comparison HPGe (red) and microcalorimeter spectra in the 96 to 105 keV region; logarithmic vertical axis. In the microcalorimeter spectrum, X-rays of Np, U, and Pu are easily identified and isotope specific gamma rays of Pu-238, -239, & -240 are resolved. (C) Zoom view on linear scale of Pu-Kα1 and Pu-240 gamma ray with Sn X-ray escape peak in between. This Pu-240 gamma ray is crucial to isotopic analysis. (D) Zoom view near 160 keV, showing three Pu gamma rays. (E) Histogram of FWHM energy resolution, with most pixels ~75 ev.*

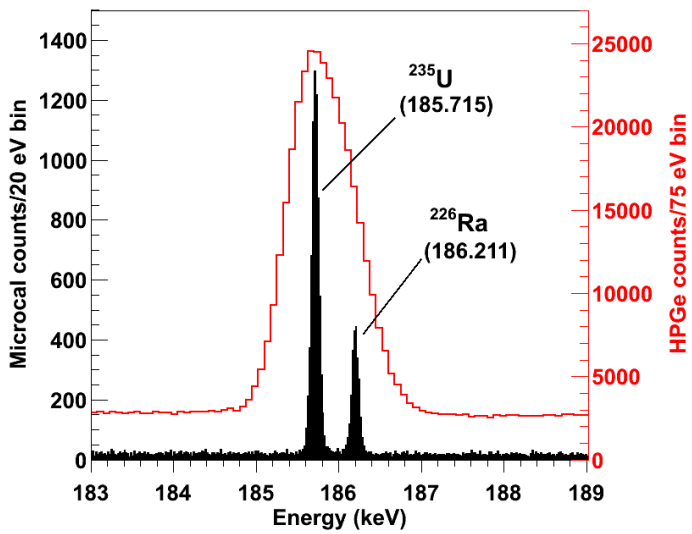


*Figure 2. Microcalorimeter array spectrum (black) clearly resolving the primary signature peak of highly enriched uranium from the common background material Ra-226. HPGe (red) cannot do this.*

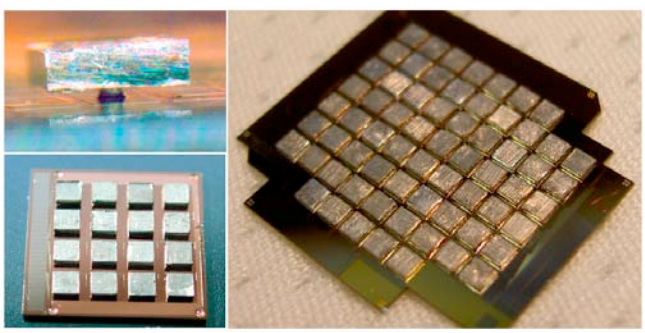

*Figure 3. Progression of gamma-ray detector array size. CCW from top left: single pixel prototype (2005), 16-pixel array (2006), 66-pixel array (2008).*

## Scientific Approach and Accomplishments

Our core detector technology for consists of a thin-film superconducting TES coupled to a bulk absorber for photon stopping efficiency. At the most basic level, the detector is a very precise thermometer. The TES is a thin-film Mo/Cu bilayer with a superconducting transition temperature near 100 mK. When operated in the normal-to-superconducting transition region, the resistance of the TES is a strong function of its temperature. A photon interacting with the bulk absorber will deposit energy that raises the temperature and increases the resistance of the TES. The TES serves as a variable resistor in a circuit that also includes a series inductance, such that changing current in the circuit produces a magnetic field that is subsequently detected by a superconducting quantum interference device (SQUID). A coherent series-array of SQUIDs is used to amplify the signal. The dynamic energy range of a sensor can be adjusted by modifying the heat capacity of the TES. For these sensors the energy resolution is proportional to the square root of heat capacity, so increasing the dynamic range comes with a tradeoff of reduced resolution. For each detected event, a pulse record is stored for subsequent analysis. Data processing occurs offline using an optimal filter technique. For each channel, an average pulse and frequency-space weighting function are computed. Each pulse is processed using an optimal (for a linear system with stationary noise) pulse height estimator, and the amplitude of the time-domain filtered pulse is recorded. Pile-up pulses are rejected. Data from each channel is energy-calibrated and corrected for drift of detector gain over time. Finally, data from all channels are summed to produce the final spectrum.

Several design, fabrication, and materials improvements have been implemented. Our single-pixel and small-scale array detectors (left-hand panels in Figure 3) used a single epoxy post for attaching the tin absorber directly to the TES thermometer. This approach, unfortunately, introduced poorly controlled strain in the Mo/Cu bilayer thermometer. Insufficient heat capacity in early devices also required us to apply an external magnetic field to increase dynamic range by broadening the superconducting to normal transition width. The strain, magnetic field, and idiosyncrasies of flux trapping within individual tin absorbers (type I superconductors) lead to substantial detector-to-detector variations including kinks and high noise points in the transition curve. A multi-post attachment method to a normal-conducting metal layer that in turn makes a thermal connection to the TES thermometer has allowed us to tune the heat capacity and simultaneously prevent attachment-induced strain in the Mo/Cu bilayer. This approach was first tested for an alpha-particle detector using a copper layer, and has subsequently implemented in our X/gamma detectors. In conjunction with improved magnetic shielding, the newer detectors have significantly improved gain stability. Still, an individual microcalorimeter pixel is a complex object described by at least five independent parameters. When microcalorimeters are integrated into close-packed arrays, additional parameters that determine the electrical and thermal interactions between pixels become relevant.

A principle objective of international nuclear safeguards is the accurate and precise NDA of plutonium-bearing materials. For decades the state-of-the-art technology of choice for this mission has been high-purity germanium (HPGe). HPGe detectors provide reasonable collection efficiency and good energy resolution compared to other commonly available technologies. However, the photopeaks in multi-isotope plutonium spectra are

numerous and often have energy spacing less than what can be completely resolved with HPGe resolution. As a result, the limiting factor in NDA measurements with HPGe is systematic error associated with peak fitting and de-convolution, rather than statistical error. Improvements to Pu NDA measurements must therefore make use of improved detector technology to overcome current limitations. Peak de-convolution can be particularly difficult in situations where low-intensity peaks are very near much higher intensity peaks. Microcalorimeter detectors, providing an order of magnitude improvement in energy resolution over HPGe, can fully resolve plutonium spectra and dramatically reduce systematic errors. Figure 1 shows a multi-isotope plutonium spectrum in the 100 keV region as measured by an HPGe detector and a microcalorimeter array (simultaneous operation of 14 pixels from the 66-pixel chip like that shown in Figure 3). The HPGe resolution is insufficient to completely resolve the numerous closely spaced peaks, while the resolving power of the microcalorimeter data is obvious. A particularly impressive demonstration of the microcalorimeter resolution is found by noting the completely resolved $^{239}$Pu peak at 98.81 keV, which is separated by only 190 eV from a $^{241}$Am peak that is nearly an order of magnitude more intense. The superior energy resolution of microcalorimeter technology can provide a significant advance in the area of plutonium NDA.

Microcalorimeters can dramatically streamline nuclear forensic analysis by eliminating the need for elemental separation of mixed actinide samples while simultaneously providing isotopic information that presently is determined by mass spectrometry. The relative amounts of $^{240}$Pu and $^{239}$Pu reveal the history and intended purpose of a Pu sample and the reactor in which it was manufactured. Hence, the $^{240}$Pu/$^{239}$Pu ratio in plutonium can be used to verify the stated purpose and indicate the operating history of a reactor. However, the strongest alpha peaks of $^{240}$Pu and $^{239}$Pu are separated by only 11.6 keV and cannot by resolved by Si detectors. To demonstrate this point, we have used a microcalorimeter to unambiguously measure the $^{239}$Pu and $^{240}$Pu isotopic fractions in a mixed-isotope Pu sample. The spectrum from a mixed isotope Pu source taken with a state-of-the-art silicon detector is shown in Figure 4A. The silicon detector is unable to separate the $^{240}$Pu and $^{239}$Pu peaks because of a combination of finite resolution and straggling. A measurement of the same mixed Pu source by the microcalorimeter is shown in Figure 4B. The most intense peaks from $^{240}$Pu and $^{239}$Pu at 5168 keV and 5157 keV, respectively, are now well separated. The forensic measurement and discrimination of $^{238}$Pu and $^{241}$Am is also important in revealing the history and intended purpose of nuclear material, e.g. the $^{238}$Pu/$^{239}$Pu ratio is indicative of the irradiation neutron energy spectrum. However, the alpha particle energies of these isotopes are nearly indistinguishable by traditional Si detectors. Typically, a time-consuming and laborious radiochemical separation of these isotopes is required prior to analysis by alpha spectrometry. As shown in Figure 4, our microcalorimeters are able to resolve the alpha particle emissions from a mixed $^{238}$Pu and $^{241}$Am source to the point where all major emissions are clearly distinct and quantifiable. By eliminating the need for radiochemical separation, microcalorimeters improve the speed and effectiveness of determining the $^{238}$Pu/$^{241}$Am ratio. It is also conceivable that other isotopes that currently require radiochemical separations to facilitate their analysis may also be simultaneously quantified by microcalorimeters. Further, a whole suite of actinides may eventually be analyzed simultaneously with simplified separation chemistry, saving precious hours in both routine and emergency situations.

There are several important applications for simulations, including assessment of the technology for specific measurement scenarios, guidance in the design of the detectors and cryostat, and interpretation of measured data. We have recently demonstrated the applicability of the GEANT4 modeling and simulation code to microcalorimeter detectors. The measured and simulated spectra from $^{153}$Gd are shown in Figure 5. The two strong photopeaks are shown on the right, while the more complex lower energy region is shown at left. This region contains tin X-ray escape peaks, weak gamma-rays at 69.67 and 75.42 keV, and gold fluorescence X-rays at 66.99 and 68.8 keV from a coating on one of the cryostat components. The ability of the simulation to reproduce measured spectral features is impressive.

## Impact on National Missions

The extraordinary sensitivity of cryogenic sensors enables high-confidence detection and high-precision measurement even of the faintest signals. Science applications (e.g. cosmology, dark matter search, neutrino mass measurement) are more mature, but several national and international security applications have been identified where cryogenic detectors have high potential payoff. International safeguards and nuclear forensics are areas needing new technology and methods to boost speed, sensitivity, precision and accuracy. Successfully applied, improved nuclear materials analysis will help constrain nuclear materials diversion pathways and contribute to treaty verification. Specifically, our technical success has lead to follow-on projects with the DOE's Office of Nonproliferation Research and Verification and DHS' National Technical Nuclear Forensics Center. These

projects are focused on continuing to solve outstanding scientific problems for cryogenic detectors, advanced instrumentation, chemical methods for nuclear forensic analysis, and international nuclear safeguards.

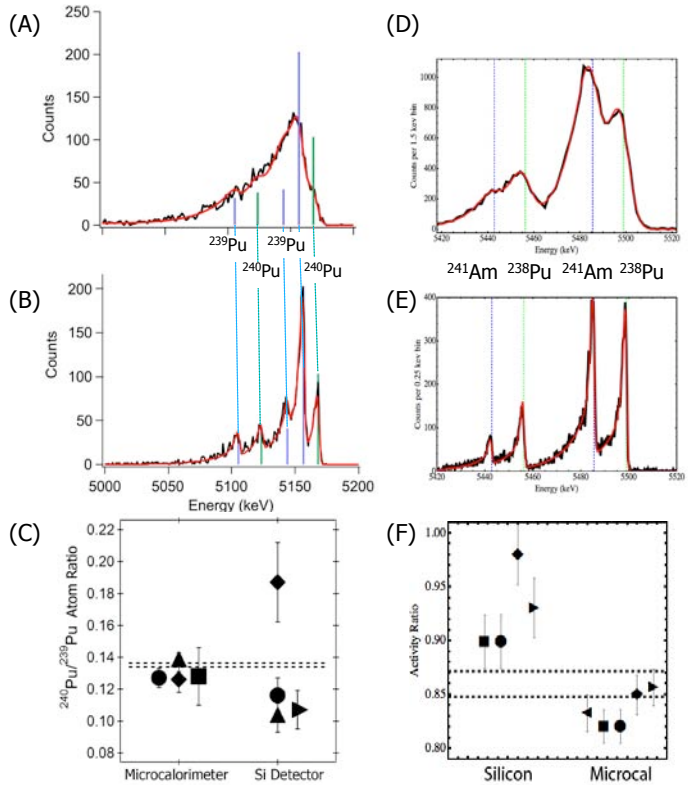


*Figure 4. Analysis of isotopic and elemental mixtures by alpha particle energy spectrometry. Panels (A)-(C) show the isotopic analysis of Pu-239 and Pu-240; panels (D)-(F) show the analysis of a mixed actinide sample containing Pu-238 and Am-241. The improved resolution and reduced straggling of the microcalorimeter greatly clarify the 240Pu/ 239Pu ratio. (A) Pu spectrum taken with a state-of-the-art Si detector. (B) Pu spectrum taken with microcalorimeter detector. Both spectra are of the same source with the same integration time. (C) Determination of isotopic ratio from fitting Si and microcalorimeter data with the multiple peak-shape models [6]. (D) Spectrum from a mixture of Pu-238 and Am-241 taken with Si detector. (E) Spectrum from a mixture of Pu-238 and Am-241 taken with microcalorimeter detector. Both spectra are of the same source with the same integration time. (F) Determination of activity ratio from mixed actinide spectra. For panels (C) & (F), all included fits have a reduced chi-squared value close to one. Vertical error bars show 1 σ statistical error for each model. The known ratio is shown by two dotted lines that represent the 1 σ error window. Red curves in (A) and (B) are fits with the peak-shape model of Bortels [6].*

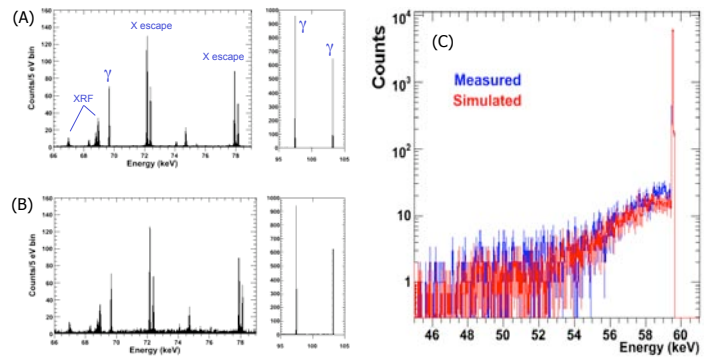


*Figure 5. The upper left plot (A) shows a measured Gd-153 spectra. The two photopeaks occur at 97.43 and 103.18 keV. At left is the more complex region from 66 to 79 keV. This region of the spectrum contains a collection of Gd-153 gamma-rays (69.67 and 75.42 keV), gold fluorescent X-rays (66.99 and 68.8 keV), and tin escape X-rays (all others). (B) The simulation does an excellent job of reproducing the observed data. (C) Some incident photons will scatter in one of the thin cryostat entrance windows before depositing energy in the detector. This plot shows the region just below the 241Am photopeak where these scattered events appear in the energy spectrum. Measured data (points) are overlayed on the simulated data (histogram). The bin width used is wider than would normally be appropriate for the detector resolution in order to improve bin statistics for this region, which is more than two orders of magnitude below the photopeak.*

## References


1. Irwin, K. D.. Seeing with superconductors. 2006. *Scientific American.* **295** (5): 86.

2. Topics in Applied Physics Cryogenic Particle Detection. 2005.

3. Ullometal, J. N.. Development of large arrays of microcalorimeters for precision gamma-ray spectroscopy. 2006. In *Nuclear Science Symposium.* (Puerto Rico, 21-18 Oct 2005). , p. 1154. New York: IEEE.

4. Hooveretal, A. S.. Application of GEANT4 to simulation of high energy-resolution microcalorimeter detectors. 2009. *IEEE Transactions on Nuclear Science.* **56** (4): 2294.

5. Hooveretal, A. S.. Measurement of plutonium in spent nuclear fuel by self-induced X-ray fluorescnce. To appear in *Institute for Nuclear Materials Management.* (Tuscon, AZ, 12-19 July 2009).

6. Horanskyetal, R. D.. Superconducting calorimetric alpha particle sensors for nuclear nonproliferation applications. 2008. *Applied Physics Letters.* **93**: 123504.

## Publications


Bacrania,etal, M. K.. Large-area microcalorimeter detectors for ultra-high-resolution x-ray and gamma-ray spectroscopy. 2009. *IEEE Transaction on Nuclear Science.* **56** (4): 2299.

Croce,etal, M. P.. Cryogenic Microcalorimeter System for Ultra-High Resolution Alpha-Particle Spectrometry. To appear in *Proceedings of the 13th International Workshop On Low Temperature Detectors (LTD-13) (American Institute of Physics).* (Stanford, CA, 20-24 July 2009).

Doriese, W. B.. Large arrays of multiplexed gamma-ray microcalorimeters for nuclear-materials analysis. 2008. *Journal of Low Temperature Physics.* **151**: 754.

Doriese, W. B., J. N. Ullom, J. A. Beall, W. D. Duncan, L. Ferreira, G. C. Hilton, R. D. Horansky, K. D. Irwin, J. A. B. Mates, C. D. Reintsema, L. R. Vale, Y. Xu, B. L. Zink, M. W. Rabin, A. S. Hoover, C. R. Rudy, and D. T. Vo. 14-pixel, multiplexed array of gamma-ray microcalorimeters with 47 eV energy resolution at 103 keV. 2007. *Applied Physics Letters.* **90**: 191910.

Hoover,etal, A. S.. Simulating the response of ultra-high energy resolution X- and Gamma-ray microcalorimeter detectors. 2007. In *IEEE Nuclear Science Symposium.* (San Diego, CA, Oct 2006). , p. 847. New York: IEEE.

Hoover,etal, A. S.. Monte Carlo studies of high resolution microcalorimeter detectors. 2007. In *IEEE Nuclear Science Symposium.* (San Diego, CA, Oct 2006). , p. 1268. New York: IEEE.

Hoover,etal, A. S.. Application of GEANT4 to the Simulation of High Energy-Resolution Microcalorimeter Detectors. 2009. *IEEE Transactions on Nuclear Science.* **56**: 2294.

Hoover,etal, A. S.. Microcalorimeter arrays for ultra-high energy resolution X- and gamma-ray detection. *J Radioanal Nucl Chem, DOI 10.1007/s10967-009-0223-3..*

Hoover,etal, A. S.. Measurement of Plutonium in Spent Nuclear Fuel by Self-Induced X-ray Fluorescence. To appear in *50th Annual Meeting of the Institute for Nuclear Materials Management.* (Tuscon, AZ, July 2009).

Horansky,etal, R. D.. Superconducting absorbers for use in ultra-high resolution gamma-ray spectrometers based on low temperature microcalorimeter arrays. 2007. *Nuclear Instruments & Methods In Physics Research Section A.* **579**: 169.

Horansky,etal, R. D.. Superconducting calorimetric alpha particle sensors for nuclear nonproliferation applications. 2008. *Applied Physics Letters.* **93**: 123504.

Horansky,etal, R. D.. Analysis of nuclear material by alpha spectroscopy with a transition-edge microcalorimeter. 2008. *Journal of Low Temperature Physics.* **151**: 1067.

Jethava,etal, N.. Improved isotopic analysis with large arrays of gamma-ray microcalorimeters. 2009. *IEEE Transactions on Applied Superconductivity.* **19**: 536.

Karpius, P. J.. A First Application of the FRAM Isotopic Analysis Code to High-Resolution Microcalorimetry Gamma-ray Spectra. 2009. *IEEE Transactions on Nuclear Science.* **151**: 2284.

Rabin, M. W.. National and international security applications of cryogenic detectors -- mostly nuclear safeguards. To appear in *Proceedings of the 13th International Workshop On Low Temperature Detectors (LTD-13) (American Institute of Physics) .* (Stanford, CA, 20-24 July 2009).

Rabin, M. W., A. S. Hoover, C. R. Rudy, S. P. Lamont, D. M. Tournear, D. T. Vo, J. A. Beall, W. B. Doriese, W. D. Duncan, L. Ferreira, G. C. Hilton, R. D. Horansky, K. D. Irwin, G. C. O'Neil, C. D. Reintsema, J. N. Ullom, L. R. Vale, K. Chesson, and B. L. Zink. Microcalorimeter Nuclear Spectrometers. 2006. In *IEEE Nuclear Science Symposium 2006.* (San Diego, CA, Oct 2006). Vol. 1, p. 544. New York: Nuclear Science Symposium Conference Record, 2006.

Tan,etal, H.. High rate pulse processing algorithms for microcalorimeters. To appear in *Proceedings of the 13th International Workshop On Low Temperature Detectors (LTD-13) (American Institute of Physics) .* (Stanford, CA, 20-24 July 2009).

Ullom, J. N.. Materials analysis with cryogenic sensors. 2008. *Journal of Low Temperature Physics .* **151**: 746.

Ullom,etal, J. N.. Multiplexed microcalorimeter arrays for precision measurements from microwave to gamma-ray wavelengths. 2008. *Nuclear Instruments and Methods in Physics Research A .* **579**: 161.

Vo, D. T.. Plutonium isotopic analysis of microcalorimeter gamma-ray spectra. 2008. In *Transactions of the American Nuclear Society.* (Anaheim, CA, June 2008). Vol. 98, p. 403. Washington, DC: American Nuclear Society.

Zink, B. L.. Array-compatible transition-edge sensor microcalorimeter gamma-ray detector with 42 eV energy resolution at 103 keV. 2006. *Applied Physics Le*

# A Novel Approach to Manufacturing Ultra-Tall Carbon Nanotube Forests

*Quanxi Jia*
20070368ER

## Abstract

Carbon nanotubes (CNTs) are the strongest materials ever discovered by mankind, and have the potential to revolutionize many technologies in the area of aerospace, space exploration, energy, and body armor as well as sport equipments. However, to realize these potential applications, it is critical to grow long and spinnable CNT forests, to spin high-strength CNT fibers, and to make CNT composites with superior properties. In this project, we have synthesized the long CNT forests, the strongest CNT fibers, novel CNT composites, as well as various other CNT products. These results have been published in many prestigious journals, one of which was reported as a "fast-breaking" paper by Science Watch. In addition, our work has won a Nano50 award and a LANL "Best Idea" award. Our work in this project has brought recognitions to LANL. In addition, our patents have been licensed by a startup company for commercialization.

## Background and Research Objectives

Individual carbon nanotubes (CNTs), with tensile strengths as high as 150 GPa, are at least one order of magnitude stronger than any other known materials [1]. To put this in perspective, Kevlar fibers for bullet-proof vests have strengths of 3 GPa, and graphite fibers in aerospace structures have strengths of just 2-5 GPa. The extremely high strength and stiffness of CNTs make them ideal for many applications. However, to fully utilize their superb mechanical properties, it is essential to first produce ultra-tall carbon nanotube forests (arrays) in which individual nanotubes are very long. This is because 1) only long nanotubes can effectively carry loads in structural components; 2) the good alignment of nanotubes in such a forest is another critical requirement for making strong nanotube structures such as fibers and composite components.

Previous carbon nanotubes are either too short to make effective use of their strength or in an aggregate form that cannot be used for structural applications. Recently, we have made 40-mm long *individual* carbon nanotubes on Si substrates [2]. However, although such long nanotubes are perfect for electronics and sensors, they cannot be used to make any meaningful structural components because their quantity is too little and they cannot be removed from the substrate. The tallest carbon nanotube forests reported previously in the literature are only 2.5 mm [3]. In addition, such CNT forests are not conducive to spinning high strength fibers.

The objective of this project is 1) to synthesize long CNT forests and 2) to synthesize the longest spinnable forests for fabricating high-strength carbon nanotubes fibers and composites. We have synthesized CNT forests with lengths > 4.5 mm, and reported the results in the prestigious journal of *Advanced Materials*, which was later recognize as a "Fast Breaking" paper by Science Watch (). In addition, we have also synthesized the longest spinnable CNT forests, from which we have fabricated CNT fibers with the highest strength per weight (specific strength). This paper has also been published in the *Advanced Materials*. Furthermore, we have also synthesized various other CNT forests and fabricated CNT composites. These results have been published/accepted for publication in various prestigious scientific journals (see the publication list).

## Scientific Approach and Accomplishments

### CNT forests

Long CNT arrays were synthesized in a 1 inch diameter (1 inch = 2.54 cm) quartz tube furnace. Forming gas (argon with 6% hydrogen) was used as the carrier gas, and pure ethylene as the carbon source. To study the effect of water vapor on the CNT growth, some CNT arrays were grown with water vapor, which was introduced into the furnace by passing a small fraction of argon gas through a bubbler. The catalysts used in this study were alumina (10 nm)/iron (0.3–1.0 nm) on silicon wafers with a 1

mm $SiO_2$ layer. The iron and alumina films were deposited by sputtering and ion beam assisted deposition (IBAD) techniques, respectively. Typically, CNT growth was carried out at 750 °C with flowing ethylene and forming gas.

Figure 1 shows the scanning electron micrographs of the longest CNT array (4.5 mm) grown at 750°C for 2 hours with the assistance of water vapor. To our knowledge, this was the longest CNT array grown on a catalyst film without feeding any other catalyst into the furnace. A close examination of the array (Figure 1b) reveals that the CNTs are well aligned. Transmission electron microscopy (TEM) revealed that the CNTs are multi-walled with an average diameter of ~10 nm. Interestingly, without water vapor, our CNT arrays grew 3 mm long in 2 hours (not shown here), which are still longer than the previous record. In addition, our process requires low total flow rate of gases (100 sccm ethylene and 100 sccm forming gas with 6% $H_2$), which makes the process safer and cheaper for industrial productions.

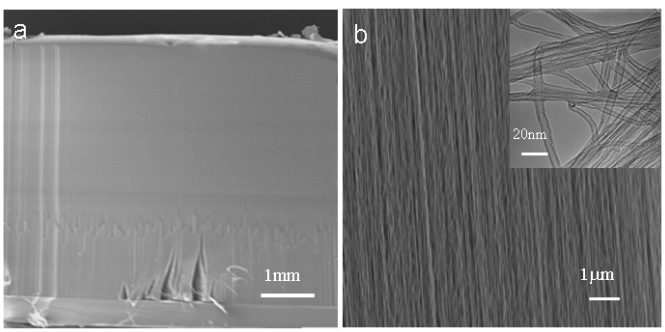


*Figure 1. (a) 4.5 mm long CNT arrays grown on the catalyst SiO2/ $Al_2O_3$(10 nm)/Fe(1 nm) with the assistance of water vapor; (b) Enlarged SEM image showing well-aligned CNTs, the inset is a typical TEM image of CNTs.*

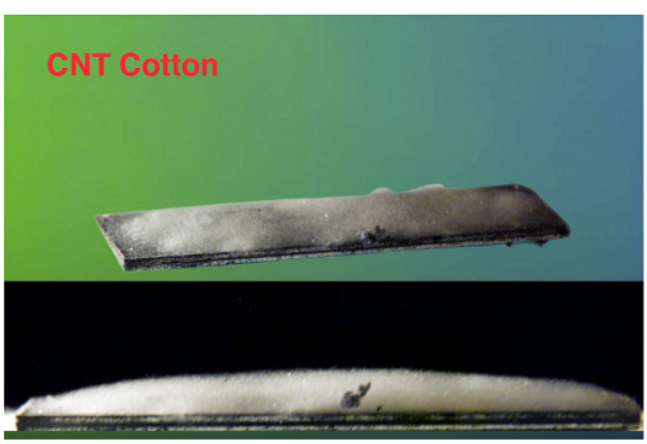


*Figure 2. CNT cotton synthesized in this project, where CNT collectively show the morphology of white cotton.*

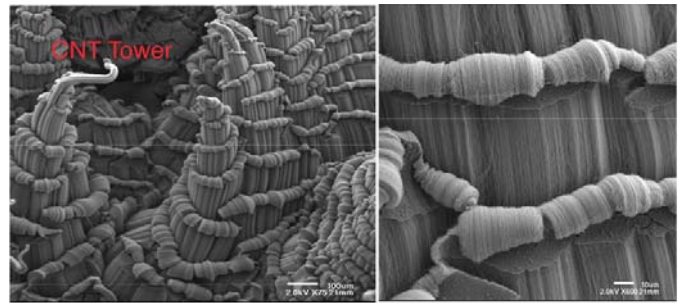


*Figure 3. CNT tower synthesized in this project.*

**CNT fibers**

For a wide variety of envisioned applications in space explorations, energy-efficient aircraft and armor, materials will be required to be significantly stronger, stiffer, and lighter than what is currently available. In this project, we have made carbon nanotube (CNT) fibers that are many times stronger and stiffer per weight than the best existing engineering fibers and over twenty times better than other reported CNT fibers. Additionally, our CNT fibers are non-brittle and tough, making them far superior to existing materials for preventing catastrophic failure. These new CNT fibers will not only make tens of thousands of products stronger, lighter, safer and more energy efficient, but also will make it possible for many envisioned technologies that have been so far unfeasible due to material restrictions.

CNT fibers were spun from a CNT array described above using a spindle made of a microprobe. The microprobe spindle was mounted on a motor with adjustable rotation speed. The spinning process was monitored under optical microscope. The tip of the microprobe was deposited with 2 μm silicon nitride particles in order to increase its roughness, which is needed to initiate the spinning. CNT fibers were spun with a rotation speed in the range of 1500 to 2500 rpm and a drawing speed of about 5 cm/min. At first, a CNT ribbon was pulled off the array. Then the rotating microprobe was moved to touch and entangle the CNT ribbon, after which the spindle moved away from the array at a constant linear speed, rotation rate and desired angle with respect to the array.

Our CNT fibers have specific strength and specific stiffness that are much higher than those of any current engineering fibers as well as previously reported CNT fibers. As shown in Figure 4, the specific strength of our strongest CNT fiber is 5.3 times that of the strongest commercial fiber (T1000), and the specific stiffness of our CNT fiber is 4.3 times that of the commercial fiber (M70J). Furthermore, the specific strength and specific stiffness of our CNT fiber are more than 23 times and 35 times higher, respectively, than those of CNT fibers reported previously.

The key to the superior properties of our CNT fibers is the *ultra-long (1mm) and ultra-light* individual CNTs in arrays used for spinning the fibers. Scanning electron microscopy (SEM) images of an as-spun CNT fiber are shown in Figures 5a and 5b. Figures 5c and 5d show the images of a CNT fiber holding a 0.1 mm diameter Ni wire and the enlarged image of the two-ply CNT fibers twisted together. These images clearly demonstrate the high quality of our CNT fibers.

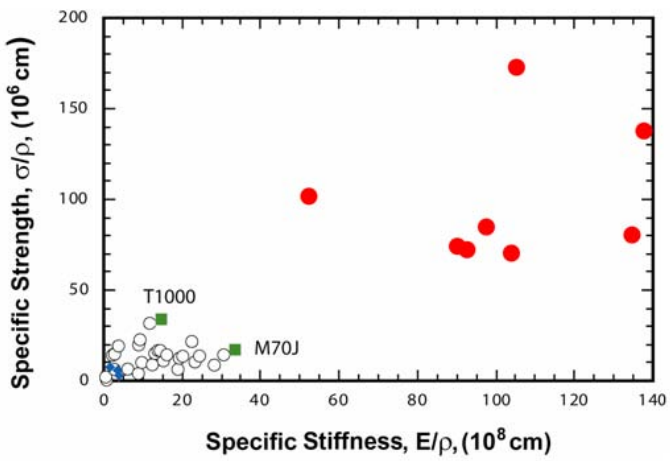


*Figure 4. Comparison of the specific strengths and specific stiffness (stiffness is defined as Young's modulus) of our CNT fibers (solid circles) with other existing engineering fibers (unfilled circles), the strongest and stiffest carbon fibers (solid squares), and CNT fibers reported previously (solid diamonds).*

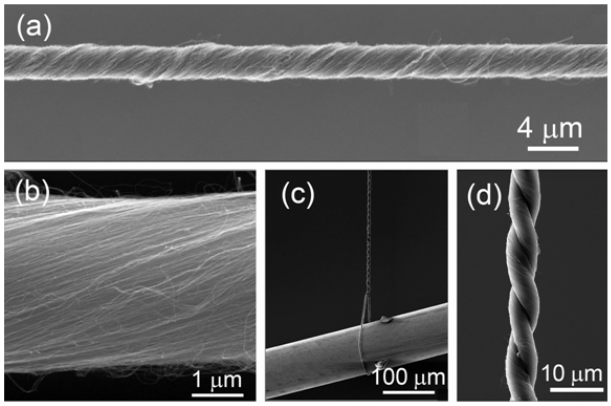


*Figure 5. SEM images of CNT fibers. (a) CNT fiber at low magnification. (b) CNT fiber at high magnification. (c) CNT fiber forming a loop around a Ni wire and then twisted. (d) Twisted two-ply section of the fiber in (c).*

**CNT Composites**

We have also recently made a breakthrough in fabricating CNT composites with super aligned long nanotubes. The composite showed high strength and is also expected to show good conductivity. The results are to be published in prestigious scientific journals.

## Impact on National Missions

This project supports DOE Office of Science missions in nanotechnology. Carbon nanotubes are currently at the frontier of materials science. Our work in this project has brought recognitions to LANL, as attested by the papers published in prestigious journals as well as awards. In addition, our patents have been licensed by a startup company for commercialization.

## References


1. Demczyk, B. G., Y. M. Wang, J. Curnings, M. Hetman, W. Han, A. Zettl, and R. O. A. Ritchle. Direct mechanical measurement of the tensile strength and elastic modulus of multiwalled carbon nanotubes. 2002. *Materials Science & Engineering.* **A334** (1-2): 173.

2. Zheng, L. X., M. J. O'Connel, X. Z. Liao, Y. H. Zhao, E. A. Akhadov, S. K. Doorn, B. J. Roop, Q. X. Jia, M. A. Hoffbauer, R. C. Dye, D. E. Peterson, Y. M. Huang, J. Lu, and Y. T. Zhu. Ultralong single-wall carbon nanotubes . 2004. *Nature Materials.* **3** (10): 673.

3. Hata, K., D. N. Futaba, K. Mizuno, T. Namai, M. Yumura, and S. Iijima. Water-assisted highly efficient synthesis of impurity-free single-waited carbon nanotubes . 2004. *Science.* **306** (5700): 1362.


## Publications


Li, Q. W., Y. Li, X. F. Zhang, S. B. Chikkannanavar, Y. H. Zhao, A. M. Dangelewicz, L. X. Zheng, S. K. Doorn, Q. X. Jia, D. E. Peterson, P. N. Arendt, and Y. T. Zhu. Structure-Dependent Electronic Properties of Carbon Nanotube Fibers. 2007. *Adv. Mater .* **19**: 3358.

Usov, I. O., Y. Q. Wang, Q. W. Li, Y. T. Zhu, R. F. DePaula, and P. N. Arent. Impurity Elements Study of Carbon Nanotubes Fabricated by Chemical Vapor Deposition. 2007. *Nuclear Inst. And Methods in Physics Research.* **261**: 574.

Wang, Z. L., D. W. Tang, X. B. Li, X. H. Zheng, W. G. Zhang, L. X. Zheng, and Y. T. Zhu. Length-Depedent Thermal Conductivity of an Individual Single-Wall Carbon Nanotube on Substrate. 2007. *Appl. Phys. Lett..* **91**: 123119.

Wang, Z. L., D. W. Tang, X. Zheng, W. Zhang, and Y. T. Zhu. Length-dependent Thermal Conductivity of Single-wall Carbon Nanotube: Prediction and Measurements. 2007. *Nanotechnology.* **18**: 475714.

Yao, Y. G., Q. W. Li, J. Zhang, L. Y. Jiao, Y. T. Zhu, and Z. F. Liu. Temperature Mediated Growth of Single-Wall Carbon Nanotube Intramolecular Junctions. 2007. *Nat. Mater..* **6**: 283.

Zhang, X. F., Q. W. Li, T. G. Holesinger, P. A. Arendt, J. Y. Huang, T. G. Clapp, R. F. Depaula, X. Z. Liao, Y. H. Zhao, L. X. Zheng, D. E. Peterson, and Y. T. Zhu. Ultrastrong, Stiff, and Lightweight Carbon Nanotube Fibers. 4198. *Adv. Mater.* **19**: 2007.

Zhang, X. F., Q. W. Li, Y. Tu, Y. Li, Y. H. Zhao, L. X. Zheng, Q. X. Jia, D. E. Peterson, and Y. T. Zhu. Multifunctional Carbon Nanotube Fiber with Excellent Mechanical Properties. 2007. *Small.* **3**: 244.

Zhang, Y. Y., L. Stan, P. Xu, H. L. Wang, S. K. Doorn, H. Htoon, Y. T. Zhu, and Q. X. Jia. A Double-layered Carbon Nanotube Array with Super-hydrophobicity. To appear in *Carbon.*

Zheng, L. X., X. F. Zhang, Q. W. Li, S. B. Chikkannan, Y. Li, Y. H. Zhao, X. Z. Liao, Q. X. Jia, S. K. Doorn, D. E. Peterson, and Y. T. Zhu. Carbon-Nanotube Cotton for Large-Scale Fibres. 2007. *Adv. Mater..* **19**: 2567.

# Optical, Electronic, and Magnetic Doping of ENABLE Grown Semiconducting Films

*Mark A. Hoffbauer*
20070436ER

## Abstract

The goal of this project was to utilize a unique LANL growth technique, Energetic Neutral Atom Beam Lithography & Epitaxy (ENABLE), to grow and dope new, novel materials based on the InGaN ternary semiconductor alloy system. A path for creating high-quality, doped In-rich InGaN materials is highly sought after because these materials are important for future photovoltaic (PV) and solid-state lighting (SSL) applications. ENABLE is a thin film growth technique that uses highly reactive, energetic nitrogen atoms allowing for reduced substrate temperatures during film growth. This feature of ENABLE is important for growing In-rich InGaN materials and doping them. We have successfully demonstrated growing and doping of device-quality GaN films making them p-type semiconductors. Building on this success, we grew In-rich InGaN materials spanning the entire Ga/In alloy compositional range, with particular focus on alloy compositions yielding materials relevant to PV and SSL applications. We also have shown evidence for p-type doping in In-rich InGaN films. In addition to fixed composition InGaN films, we have also demonstrated isothermal growth of fully compositionally graded InGaN films. These films have potentially exciting applications for efficient PV and SSL devices. Overall, this project has been successful beyond our initial expectations, fostering related work involving industrial partnerships and considerable follow on funding opportunities.

## Background and Research Objectives

The discovery and development of a wide range of semiconductor materials has made a huge impact on our lives, including powerful computers and high-speed communications. A number of emerging areas important for energy production and use await advances in new materials with properties that can be tuned for specific needs. As a result of numerous scientific and engineering efforts over the last two decades, GaN-based thin film materials have emerged as the most important class of semiconductor materials since silicon. For example, GaN-based materials are now routinely used in efficient UV and blue light emitting diode (LED) applications, providing more than seven times the energy efficiency of incandescent lighting and up to five times the energy efficiency of fluorescent lighting [1].

In addition to the exceptional developments that have taken place for GaN-based materials, it was recently discovered that indium nitride (InN) has a bandgap of ~0.7 eV.[2] When alloyed with GaN (bandgap of 3.4 eV) it is possible to produce $In_{1-x}Ga_xN$ thin films ($0 \leq x \leq 1$) with bandgaps tunable from 0.7eV to 3.4 eV—a near perfect match to the terrestrial solar spectrum as shown in Figure 1. This wide bandgap tunability makes InGaN materials ideal candidates for efficient photovoltaic (PV) devices, solid-state lighting (SSL), and many other applications. Fortunately, all compositions of $In_{1-x}Ga_xN$ are direct bandgap semiconductors giving them large light absorption cross sections for PV applications and for efficient light emission when electrically pumped. In fact, the InGaN film thickness required for complete absorption of incoming solar photons is <1 micron, more than 200 times thinner that that required for Si-based PV cells. In addition, InGaN-based PV devices using multi-junction PV cell designs made by stacking $In_{1-x}Ga_xN$ layers of different bandgaps have theoretical efficiencies exceeding 70% with solar concentration. Clearly, the development and widespread utilization of these tunable bandgap materials for PV applications alone could significantly impact our Nation's energy security.

To fabricate optoelectronic devices from semiconducting GaN-based materials their growth must be carefully controlled to achieve uniform materials that can be doped for controlling their electrical properties. In spite of InGaN's clear technical advantages, there are still significant challenges related to producing high-quality, uniform alloys of InGaN-related materials suitable for optoelectronic devices. Forming uniform alloys of

InGaN materials containing substantial amounts of In (In > 25%) is a difficult challenge, limiting the potential uses of these materials for PV and SSL applications. Of equal technological importance is achieving high-quality p-type doping of In-rich InGaN-based semiconducting films. In addition, doping GaN-based materials with unconventional materials such as magnetic atoms, nanocrystals, and other species is particularly difficult.

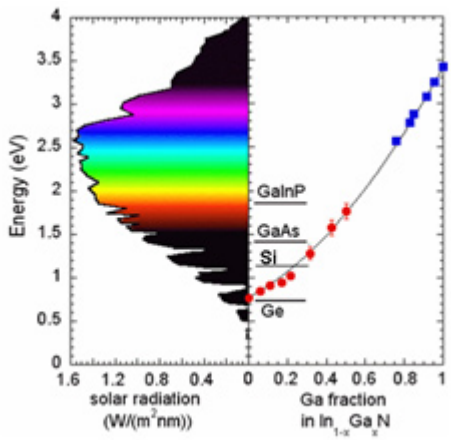


*Figure 1. Terrestrial solar radiation spectral distribution (left) and common semiconductor bandgaps (right). The tunable bandgap range for the InGaN alloy system is also shown (right).*

The lack of control of InGaN film uniformity and the dopant's lattice position and chemical environment often require thermal processing steps that limit the alloy composition and/or dopant materials to those that are thermally stable. For example, the desire to exploit InGaN for widely tunable PV and LED applications is severely hampered by clustering of In at concentrations greater than about 20%, preventing the formation of uniform alloys of In-rich InGaN [3]. While doping of GaN by Mg is known to produce device quality p-type materials, the percentage of active/usable Mg in the films is limited by their high temperature growth conditions. These high temperature process conditions likely prevent successful p-type doping of In-rich InGaN and InN films. Similarly, the clustering of magnetic dopant atoms (e.g. Co, Mn, and Cr) has severely hindered the development of GaN-based high-temperature dilute magnetic semiconductor materials for spintronic applications. This difficulty **inhibits** the development of an entire new field of spin-based devices for a host of applications including quantum computing.

Common techniques for incorporating high concentrations of In atoms, Mg atoms as dopants, and other species into GaN thin films during growth have proved to be extremely difficult. This project's main goal was to develop novel solutions to these problems by combining energetic neutral atom beam lithography & epitaxy (ENABLE, a novel low-temperature film growth technology recently developed at and unique to LANL) with novel film growth and doping schemes. We have successfully grown high-quality In-rich InGaN materials over the full range of compositions (from GaN to $In_{0.5}Ga_{0.5}N$ to pure InN) and have demonstrated p-type Mg doping of GaN and InGaN thin films. Our results have produced unique InGaN-based optoelectronic materials with novel electronic, optical, and structural properties for energy security applications ranging from high-efficiency, full-spectrum PV devices to efficient SSL applications.

## Scientific Approach and Accomplishments

To achieve our goals of growing In-rich InGaN materials and doping them, we have focused on utilizing ENABLE for low temperature growth of thin film materials. ENABLE utilizes an energetic beam of neutral N atoms (kinetic energies from 1 to 5 eV), eliminating the need for high substrate temperatures to overcome reaction barriers. The high kinetic energy and high reactivity of N atoms allow low-temperature growth of device quality GaN-related films by simultaneously exposing substrates to energetic N atoms and an evaporated Ga and In metal flux (growth rates are >3 micron/hr over an ~30cm$^2$ area).

The ability to reduce film growth temperatures using ENABLE is important since most efforts to create In-rich $In_xGa_{1-x}N$ and doping of these materials are hindered by the high substrate temperatures required for conventional growth techniques such as metal-organic chemical vapor deposition (MOCVD) and molecular beam epitaxy (MBE). Our growth efforts were supported by extensive thin film characterization efforts including x-ray diffraction (XRD), photoluminescence (PL) measurements, and carrier transport measurements. Results demonstrate that ENABLE-based film growth eliminates phase segregation and clustering in InGaN films, allows better control of film composition over a broad range, and improves electronic doping of the materials by enhancing dopant activation.

In this project, considerable initial effort focused on improving the quality of GaN films to the level needed for optoelectronic device fabrication. GaN films grown using ENABLE now have characteristics equivalent to materials grown by MOCVD and MBE techniques, but they are grown at much lower temperatures (typically 400 to 750˚C *vs*. ~1050˚C). A number of high-quality GaN samples were grown by ENABLE, with results indicating that elevated substrate temperatures improve the film crystal structure by enhancing surface diffusion. Preliminary data also indicate that higher N-atom kinetic energies provide additional improvement to the film crystallinity.

An example of high-quality GaN grown on sapphire is

shown in Figure 2. Our GaN films show excellent quality measured by XRD with rocking curves peak widths of <400 arcsec. The films also show bright band edge PL at room temperature (inset of Figure 2). These results are indicative of high-quality GaN films. Carrier mobility measurements of GaN films show mobilities of ~300 $cm^2/Vs$ with carrier concentrations below $2x10^{17}/cm^3$. We have also demonstrated growth of high quality InN showing similar XRD metrics. Our InN films show excellent crystalline quality and the expected low band gap of ~0.70 eV as measured by PL with mobilities of ~1400 $cm^2/Vs$ and carrier concentrations below $2x10^{18}/cm^3$. These mobilities are among the highest ever reported for InN. For our GaN and InN films, most of the metrics are suitable for making prototype devices.

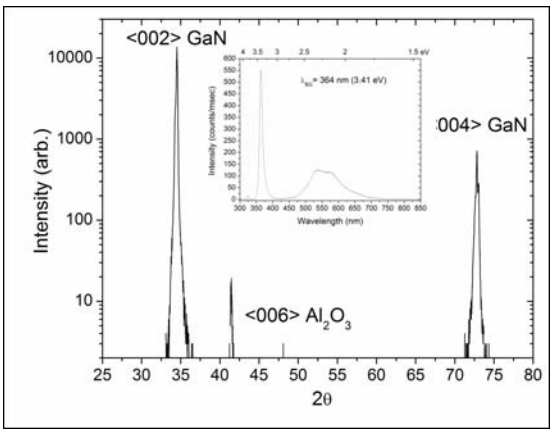


*Figure 2. ϑ-2ϑ XRD scan showing high quality GaN. PL spectra of GaN film showing large intensity and good bandgap to defect band ratio (inset).*

Our next objective was to demonstrate ENABLE-based growth of In-rich $In_{1-x}Ga_xN$ films of various fixed and graded compositions. We grew $In_xGa_{1-x}N$ films with bandgaps spanning the entire visible range. The XRD peaks shown in Figure 3 confirm that our mixed-alloy $In_xGa_{1-x}N$ films have excellent crystallinity and are single-phase uniform alloys. Bright band-edge PL intensity plots vs. wavelength and electroluminescence (EL) intensity vs. energy are shown in Figure 4 colored according to their peak emission wavelength. As the indium content increases, the PL peak wavelengths shift from 513 to 596 nm or from green to orange-red wavelengths (~2.35 eV to 1.9 eV). EL data in Figure 4 (right) confirm successful p-type doping of InGaN grown by ENABLE. These are very important results since p-type doping of In-rich InGaN is considered technologically very difficult. Electrical measurements show carrier mobilities of 20 to >100 $cm^2/Vs$ (donor conc. in the low $10^{17}/cm^3$ range). The carrier mobilities far exceed those of other growth techniques known to encounter serious problems with compositional uniformity of $In_{1-x}Ga_xN$ films with higher than ~20% In content.

Achieving these results was an important aspect of this project since the ability to create $In_xGa_{1-x}N$ of any particular composition is critically important for taking these results to the stage of making materials for efficient PV and SSL devices. We note that no other thin film growth technique is able to successfully create high-quality $In_xGa_{1-x}N$ over the entire compositional range comparable to the quality produced by ENABLE. These results are summarized in a recent publication [4] and resulted in a LANL patent disclosure.

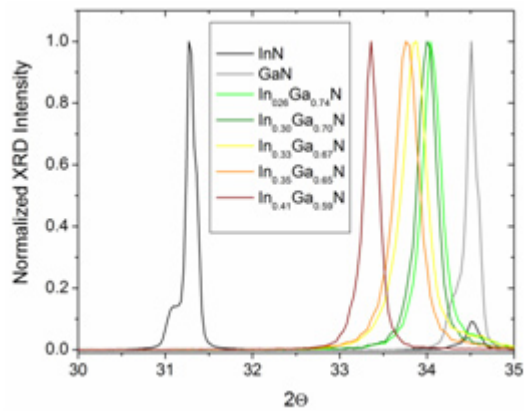


*Figure 3. XRD 2ϑscans of ENABLE grown InN, InGaN alloys, and GaN films showing uniform compositions and single phase material with no appreciable segregation. The peaks are color coded according to their peak photoluminescence.*

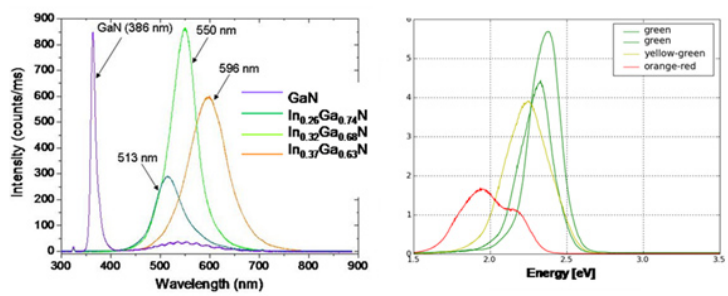


*Figure 4. Photoluminescence intensity vs. wavelength (left) for three InGaN films grown using ENABLE at 750 °C. The absolute PL intensities are plotted along with ENABLE grown GaN. The films were all ~800 nm thick. (Right) Electroluminescence of p-type InGaN films grown using ENABLE at 600 °C.*

Additional experiments have focused on growing compositionally graded $In_xGa_{1-x}N$ films where the In composition was graded starting with pure GaN and grading to InN and starting with pure InN and grading to GaN (e.g x=0 to x=1 and for x=1 to x=0). In both cases, isothermal growth at 500°C made possible using ENABLE resulted in graded InGaN films showing physical and optical characteristics consistent with good film quality, uniform and smooth grading of the film composition, and interesting optical properties as reported in a recent

publication [5]. We do not observe any evidence of phase segregation in ENABLE-grown, compositionally graded $In_xGa_{1-x}N$. PL spectra taken from compositionally graded InGaN films show that the most dominant PL is coming from an energy level closest to InN, even though the film was uniformly graded over the entire compositional range. The same dominant peak is observed with photo excitation from the In-rich side or the Ga-rich side of the film, indicating that photogenerated carriers in higher bandgap regions of the film travel to the lower bandgap regions before recombining. This evidence confirms that we are able to create graded $In_xGa_{1-x}N$ films that could be critical for making efficient PV devices with simplified designs that are the subject of a patent application.

Another important accomplishment of this project has been to successfully demonstrate electronic doping of GaN and InGaN materials. Our efforts focused on p-type doping using Mg as the dopant material that was evaporated onto the actively growing nitride material. Results to date show definitive evidence of successful Mg incorporation into the GaN films as shown in Figure 5. The optical signatures show quenching of the GaN band edge PL peak and the appearance of lower energy peaks assigned to Mg acceptors. The location of these peaks is consistent with published results. Interestingly, the measured concentration of Mg indicates and unusually high fraction of active Mg dopant atoms in the films approaching ~10%, significantly higher than that obtained by conventional growth techniques. These encouraging results are likely indicative of the absence of hydrogen during growth and emphasize the important role of low growth temperatures that are characteristics of ENABLE. Electrical characterization of Mg-doped GaN films show successful p-type doping, with carrier concentrations exceeding $2x10^{18}/cm^3$, levels necessary for fabricating prototype PV devices. Preliminary experiments mentioned above related to Figure 4 (right) indicate successful p-type doping of In-rich InGaN films and set the stage for doping GaN, InGaN, and InN materials with a host of other species. This development is made possible by exploiting the low-temperature film growth capability of ENABLE as a means of incorporating thermally sensitive and/or fragile materials into semiconducting films.

Taken as a whole, the successful growth of In-rich InGaN and p-type doping of GaN and InGaN demonstrate that we have exceeded the original goals of this project. These results have built a solid platform for expanding this LDRD exploratory research effort into a much bigger project to develop new tunable bandgap PV and SSL materials and device architectures. The resulting materials are expected to have improved optical and electronic properties, leading to novel devices important for PV electrical power production and for efficient SSL devices for reducing energy usage.

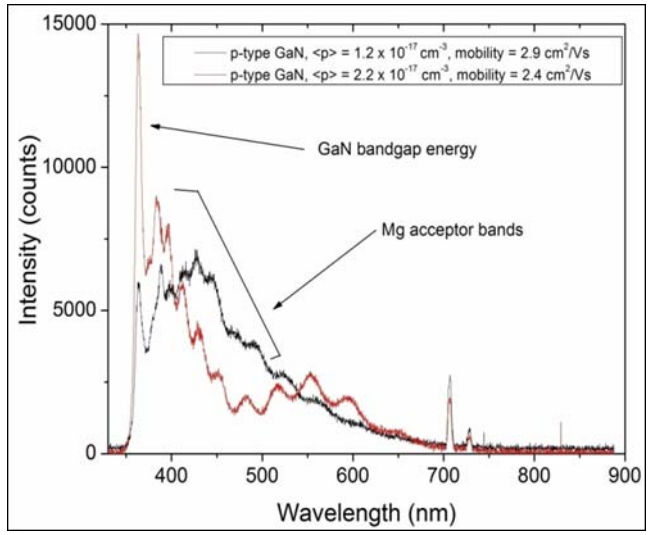


*Figure 5. Strong photoluminescence spectral signatures for p-type doing of GaN using Mg as the dopant. The electrical properties are summarized in the figure inset.*

## Impact on National Missions

Electronic and photonic materials directly support the national energy security and threat reduction missions of LANL and DOE. This project has significantly improved the quality and properties of InGaN-related semiconducting materials for a wide range of applications. Our results show that alternative techniques can yield a wide range of InGaN compositions and electronically-active doped materials.

This research directly supports DOE's core mission by developing an entirely new material system for PV and SSL applications offering unprecedented efficiency and lower costs. The results of this project have positioned us to compete for follow-on funding from DOE (e.g. DOE/BES, ARPA-E, NETL, and EERE initiatives) to expand this effort into a much larger program in both high-efficiency PV and SSL devices. There is growing DoD program interests in this area (satellite power, battlefield systems, etc.) including DARPA (proposal submitted). Given the potential of the InGaN materials system, our results will be valuable in realizing the full potential of the InGaN materials system for making practical, high-efficiency PVs and SSL widely available.

Additionally, this work layed the foundation for bringing funding to LANL from a CRADA partner interested in developing and commercializing high-efficiency PVs based on InGaN and the ENABLE technology. Another spinoff of this project saw the development of methods for growing

thin superconducting niobium nitride (NbN) films that are the basis for a new LDRD project starting in FY10 to turn superconducting NbN films into high-speed single photon detectors with broad applications to LANL and DOE national security missions in the area of nonproliferation. We were also very fortunate to have recently converted a postdoctoral associate who worked on this program, Todd Williamson, to a new technical staff position at LANL.

## References


1. Basic Research Needs for Solid-State Lighting. 2006. *Report of the Basic Energy Sciences Workshop on Solid-State Lighting.*

2. Wu, J., W. Walukiewicz, K. M. Yu, J. W. Ager III, E. E. Haller, H. Lu, J. Schaff, Y. Saito, and Y. Nanishi. Unusual properties of the fundamental band gap of InN. 2002. *Applied Physics Letters.* **80**: 3967.

3. Walukiewicz, W., J. W. Ager III, K. M. Yu, Z. Liliental-Weber, J. Wu, S. X. Li, R. E. Jones, and J. D. Denlinger. Structure and electronic properties of InN and In-rich group III-nitride alloys. 2006. *Journal of Physics D: Applied Physics.* **39**: R83.

4. Williamson, T. L., M. A. Hoffbauer, K. M. Yu, L. A. Reichertz, M. E. Hawkridge, R. E. Jones, N. Miller, J. W. Ager III, Z. Liliental-Weber, and W. Walukiewicz. Highly luminescent InGaN thin films grown over the entire composition range by energetic neutral atom beam lithography & epitaxy (ENABLE). 2009. *Physica Status Solidi C.* **6** (S409): S409.

5. Miller, N., R. E. Jones, K. M. Yu, J. W. Ager, Z. Lilental-Weber, E. E. Haller, W. Walukiewicz, T. L. Williamson, and M. A. Hoffbauer. Low-temperature grown compositionally graded InGaN films. 2008. *Physica Status Solidi c.* **5**: 1866.


## Publications


AgerIII, J. W., L. A. Reichertz, K. M. Yu, W. J. Schaff, T. l. Williamson, M. A. Hoffbauer, N. M. Haegel, and W. Walukiewicz. InGaN/Si Heterojunction Tandem Solar Cells. 2008. In *33rd IEEE Photovoltaic Specialists Conference.* (San Diego, CA, May 11-16, 2008). Vol. , Edition, p. 1. : .

Miller, N., R. E. Jones, K. M. Yu, J. W. Ager, Z. Lilental-Weber, E. E. Haller, W. Walukiewicz, T. L. Williamson, and M. A. Hoffbauer. Low-temperature grown compositionally graded InGaN films. 2008. *Physica Status Solidi c.* **5**: 1866.

Reichertz, Lothar A., Kin M. Yu, Y. Cui, Michael E. Hawkridge, Jeffrey W. Beeman, Z. Liliental-Weber, Joel W. Ager III, W. Walukiewicz, William J. Schaff, Todd L. Williamson, and Mark A. Hoffbauer. InGaN Thin Films Grown by ENABLE and MBE Techniques on Silicon Substrate. 2008. *Materials Research Society Symposium Proceedings.* **1068**: C06.

Williamson, T. L., M. A. Hoffbauer, K. M. Yu, L. A. Reichertz, M. E. Hawkridge, R. E. Jones, N. Miller, J. W. Ager III, Z. Liliental-Weber, and W. Walukiewicz. Highly luminescent InGaN thin films grown over the entire composition range by energetic neutral atom beam lithography & epitaxy (ENABLE). 2009. *Physica Status Solidi C.* **6** (S409): S409.

# Accuracy of Laser-Induced Breakdown Spectroscopy for Trace Detection

*Roger C. Wiens*
20080718ER

## Abstract

We are developing new data processing methods to improve the sensitivity and accuracy of a laser sensing technique called laser-induced breakdown spectroscopy (LIBS). The LIBS technique detects nearly all elements in solid, liquid, or gaseous form with no sample preparation. The data processing methods fall into the broad category of multivariate analysis (MVA). Some of the MVA methods involve advanced classification using data "training sets", that is, standards of known composition that mimic the samples of interest. Other methods are focused on obtaining more accurate elemental compositions of the samples. While the traditional method of determining elemental composition required calibrating a single optical emission line for its intensity as a function of elemental abundance, some of the new MVA methods use the entire spectrum to calibrate a given element abundance. The methods can thereby take into account "interferences" from other elements or physical properties, which might lead to a poor calibration if ignored. Applications include threat-reduction for explosives, chem.-bio, and nuclear, as well as mining and industry applications. Additionally, LANL is sending a LIBS instrument on NASA's next Mars mission and is actively exploring LIBS for future Moon and Venus missions.

## Background and Research Objectives

Laser-induced breakdown spectroscopy (LIBS) is a technique that is used to determine elemental compositions of samples at some distance (up to tens of meters) with no sample preparation. Laser pulses focused on the target produce plasma "sparks" composed of material ablated from the target (Figure 1). Each element present in the sample produces light at unique wavelengths. By measuring the optical spectrum of the emitted light (the color) from the sparks, the elemental composition can be determined. However, looking at just one emission peak for a given element turns out not to be very accurate. This project explores the application of data analysis techniques that use all wavelengths for each element, allowing many peaks to be interrogated simultaneously. In effect, we go from one data point per element, to 6,000 channels per element, using a group of techniques classified as multivariate analysis (MVA).

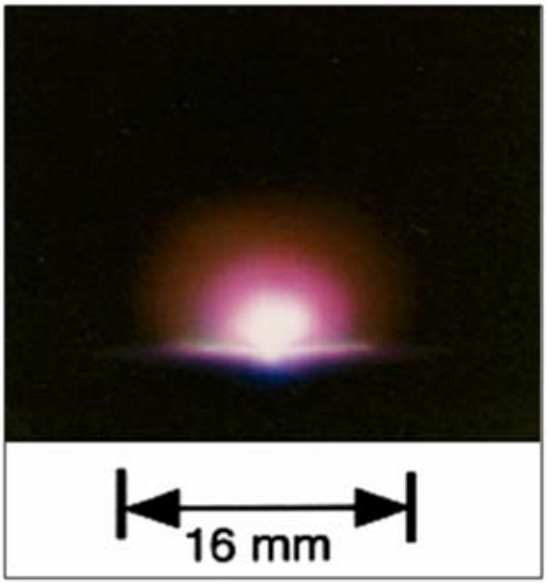


*Figure 1. Light emitted when an invisible laser beam strikes a solid surface. This is a "LIBS plasma emission". (Photo from D. Cremers).*

We have started with two types of MVA. One, called principal components analysis (PCA), simply groups samples by spectral characteristics, starting with the strongest correlation (principal component), second strongest, third strongest, etc. We can use this analysis to determine if a new sample is similar to previous samples, or has significant differences.

A second and more powerful MVA technique is partial least squares (PLS). As used here, PLS quantitatively determines the compositions of samples analyzed by

LIBS. It does this by being given the elemental composition of a "training set" of standards similar to the unknowns. It determines the correlations among all 6000 channels and uses that information to determine the composition of the unknown sample.

Preliminary results indicate that these MVA techniques will significantly increase the accuracy of the LIBS technique, but there are a lot of details that need to be understood. Key aspects are how to correct for the effects of sample-to-instrument distance, how many standards are needed for this type of analysis, and how close the standards need to match the sample in composition.

## Scientific Approach and Accomplishments

### Scientific approach

Geologic samples represent an elementally diverse and hazard-free data set that is relatively challenging for classification and quantification techniques. Soil and rock samples are also the background against which measurements are often made when searching for pathogens and/or explosive residues. Because of this, we used geologic samples as the medium to which we applied the data analysis techniques.

Approximately sixty geologic standards were selected and obtained. These include samples from all three classes of rocks, focusing on both igneous and sedimentary samples. The standards include a number of different basalts and olivine-rich standards, several gypsum standards, and a number of stream sediments. These are mostly in the form of powders, but we are also using a few glasses and several ceramics. In contrast to mineralogical methods such as x-ray diffraction, LIBS does best with mineralic mixtures, as are encountered by the LIBS laser beam in remote LIBS experiments.

The standards were run at 1.5, 3.5, and 5.5 meters from a stand-off LIBS instrument. The complete set of standards was used in the 3.5 meter set-up, while the 1.5 and 5.5 meter arrangements used a subset of thirty standards. Each standard was analyzed in five separate spots, each spot being a collection of fifty laser shots and spectra. Background spectra (50 each) were taken to correspond with each standard. In total, we collected some 37,000 spectra.

### Classification

The data taken at each distance were processed through a principal component analysis (PCA) software package to understand its power in classifying samples. Figure 2 shows an example of the type of plot that can be generated for classification purposes. What is not shown is that the result is many-dimensional, so that samples which appear indistinguishable in the first two principal components, shown in Figure 2, can be distinguished in succeeding principal components. Because geological samples contain many different elements above the LIBS detection limits, many principal components can be used effectively. In addition, we are finding that different plasma conditions can at times distinguish different minerals which have the same chemical composition, so that PCA helps LIBS to effectively become much more than a chemical assay tool.

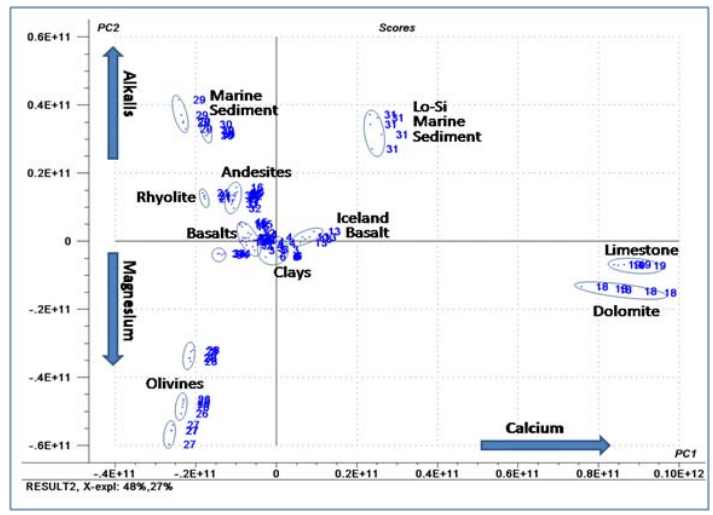


*Figure 2. Sample classification plot produced by principal components analysis (PCA).*

### Quantitative elemental compositions

Previously LIBS was only considered to be a semi-quantitative analysis tool because of the fact that it suffered from chemical matrix effects. Chemical matrix effects are defined as some chemical or physical property of the material that affects the relationship between abundance and emission line intensity for a given element. Figure 3 illustrates one type of chemical matrix effect. It shows that the barium emission line intensity in an obsidian sample does not follow the expected relationship between abundance and emission line intensity. Most of the other rock samples fall along a linear trend. Obsidian is a much more glassy rock than the other samples shown on the plot. The glassy nature of the rock may be responsible for this chemical matrix effect. The error induced by this difference is on the order of several hundred percent, which is huge.

A calibration plot produced by PLS is shown in Figure 4. Using the training set approach, PLS is able to account for chemical matrix effects. The data points in Figure 4 represent many different rock types and yet they all fall very close to the line. Some of our work involved understanding how many standards are needed in the training set in order to produce an accurate calibration

curve, how much difference between the training set and the unknowns is allowable, and whether replicate analyses of the same samples are helpful for the training set.

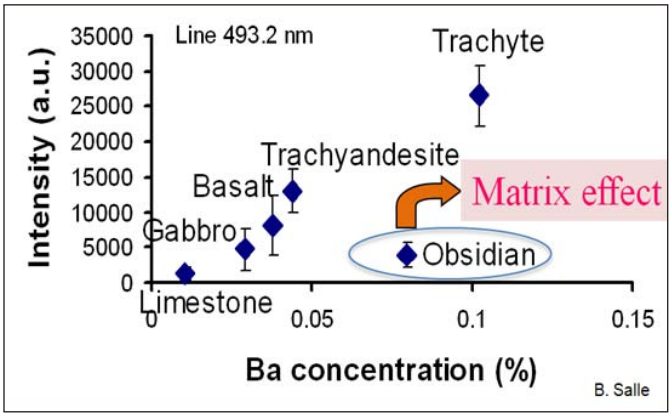


*Figure 3. Calibration plot for barium in various volcanic rocks, the data for which were produced by observing a single optical emission line at a wavelength of 493.2 nanometers. The data should fall along a straight line. The very large error for the obsidian sample is the result of a chemical matrix effect.*

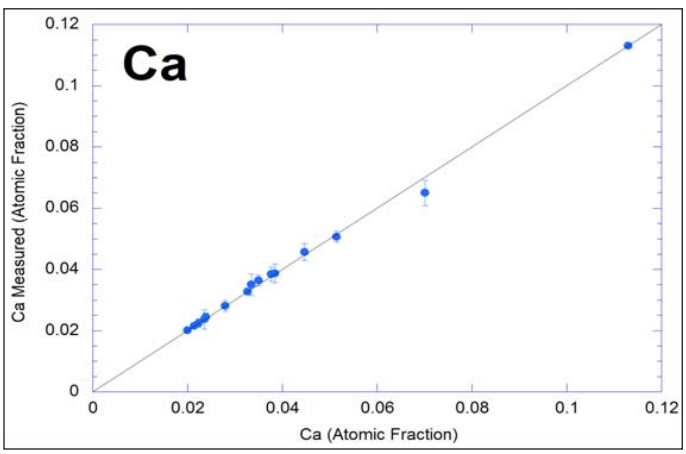


*Figure 4. Example of a calcium calibration line produced by partial least squares analysis (PLS) which takes into account the chemical matrix effects when producing the calibration.*

**Calibrating at different distances**

One key issue is the effect of varying the distance to samples and standards. Can one analyze a set of standards at one distance and apply the data correctly to an unknown sample at another distance? How does this degrade the accuracy, and are there ways to correct for it? For this initial study we used data taken on nine different standards at three different distances. Five replicate analyses were made on each standard at each distance. The results were normalized, so that the primary distance effect, that of overall intensity, would be removed. The results were analyzed by the Unscrambler PCA program. The first two principal components had relatively little distance effect, successfully grouping the five replicate analyses from each standard into respective tight clusters independent of distance. However, if one zoomed in on the individual clusters, one could still see a distance effect which appeared to incorrectly assign higher silicon abundances to measurements taken at greater distances. Higher principal components all had strong distance effects. Wavelength channels that had a strong weighting in the higher PCs were identified.

The PCA analysis was then performed with distance as one of the components. The first principal component now corresponded to the instrument-to-sample distance. The correlations of each wavelength channel with distance are shown in Figure 5. The original spectra were then corrected by adding or subtracting a factor obtained by multiplying the distance by each channel's distance correlation coefficient (Figure 5). The result was then fed back into the PCA program with the distance coefficient as a cross-check. The distance correlation had indeed been removed. The results were then used in the PLS program to see if quantitative uncertainties were reduced by the distance correction. The results clearly needed further correction, which we believe is the result of the baseline, described in the next paragraph.

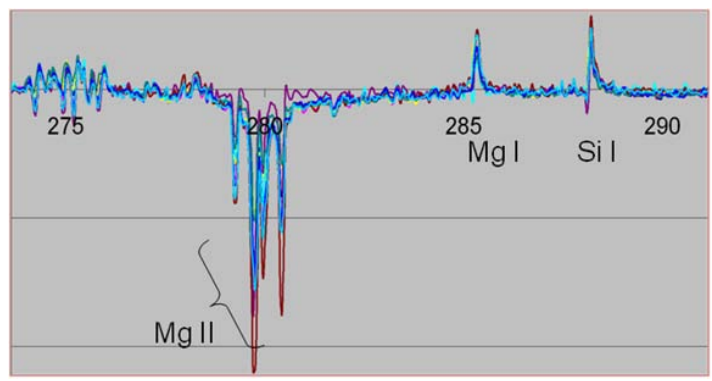


*Figure 5. Distance correlations for a small part of the LIBS spectrum between 275 and 295 nanometers wavelength. The neutral emission lines of magnesium and silicon on the right side of the plot have much less drop-off with distance than the once-ionized lines of magnesium in the middle-left of the plot. Since the data were normalized, the emission lines with little distance effect appear positive while the emission lines with large distance effects appear negative.*

Background subtractions for LIBS spectra generally involve taking spectrometer exposures of identical duration to the LIBS exposures, only without the laser. However, in addition to emission peaks, LIBS produces a broad light continuum that the typical background subtraction does not remove. This can be removed by flattening the baseline. It was noted from PCA plots that much of the distance correlation was the result of differing broad light continua. We therefore produced a routine to flatten the

baseline after background subtraction and before entering the data into the multivariate routines.

## Impact on National Missions

The LIBS technique shows increasing promise in many areas important to our mission:

1. During the time of this LDRD, the International Atomic Energy Agency (IAEA) has contracted the LIBS group at LANL to begin building portable instruments capable of determining the isotopic ratio of uranium in field tests. The results are instant and accurate.

2. We have on-going environmental work quantifying carbon sequestration in soils which benefits from applying multivariate analysis. Previously soil analyses had to use three different calibration curves taking into account the nature of the soil (i.e., loamy, sandy, etc.). By using MVA, only a single calibration curve is now required, and the results are significantly more accurate.

3. We are partnering with industry to produce better analytical products. During 2008 we discussed developing a CRADA with several mining companies. We partnered with the Energy Research Corporation (ERCo) on an SBIR proposal to further develop hydrogen analytical capabilities with LIBS. We are currently talking with LabStart about technology spin-offs.

4. Interest in using LIBS for planetary exploration has increased. We participated in a proposal to develop a Venus lander incorporating a combined LIBS and Raman spectrometer as the centerpiece of the landed science investigation. LANL would build the LIBS/Raman instrument for approximately $20M. The US has never successfully conducted science from the surface of Venus, which is shrouded in a 93 bar atmosphere at a temperature of 500 degrees C. The proposal is currently being evaluated by NASA. We anticipate in the next six months submitting a proposal for a combined LIBS/Raman instrument to prospect for water in permanently shaded craters at the south pole of the Moon. We also participated in several additional NASA proposals: one involving performing LIBS investigations of Mars-analog sites in the US and Canada, one investigating the identification and classification of organic materials with LIBS, and a successful proposal to involve LIBS to investigate the Haughton impact structure in northern Canada.

## References


1. Clegg, S. M., R. C. Wiens, J. E. Barefield, E. Sklute, and M. D. Dyar. Quantitative remote laser induced breakdown spectroscopy by mutivariate analysis. 2009. *Spectrochimica Acta B.* **68**: 1036.


## Publications


Clegg, S. M., R. C. Wiens, J. E. Barefield, E. Sklute, and M. D. Dyar. Quantitative remote laser induced breakdown spectroscopy by mutivariate analysis. 2009. *Spectrochimica Acta B.* **68**: 1036.

Forni, O., S. Clegg, R. C. Wiens, S. Maurice, and O. Gasnault. Multivariate analyses of ChemCam first calibration samples. 2009. In *Lunar and Planetary Science Conference XL.* (The Woodlands, Texas, 23-27 Mar. 2009). Vol. XL, p. 1523. Houston: The Lunar and Planetary Institute.

Lanza, N. L., S. M. Clegg, A. M. Ollila, J. E. Barefield, H. E. Newsom, and R. C. Wiens. Calibrating the ChemCam LIBS for carbonate minerals on Mars. *Applied Optics.*

# Assimilation and Prediction of Low Earth Orbit (LEO) Environment for Space Situational Awareness

*Geoffrey D. Reeves*
20090486ER

## Abstract

Since the launch of the first Vela Hotel satellite in 1963, the US Department of Energy (DOE) has had a diverse and ongoing set of satellite-based national security programs. As part of those programs, DOE has flown a variety of instruments to measure the space environment. This experience, in turn, led to the development of broad capability and expertise in understanding the changes in the space environment and the effects of that environment on space systems – causes and effects now collectively referred to as Space Weather. Space Weather can affect satellites and space instruments in a variety of ways ranging from backgrounds that reduce sensor performance - to anomalous (i.e. faulty) operation of space systems - to the catastrophic failure of entire satellites. As our society increases its reliance on technology we increase our reliance on space-based infrastructure.

The (formerly LDRD-sponsored) Dynamic Radiation Environment Assimilation Model (DREAM) uses sophisticated physics-based models and data assimilation techniques to specify the structure of the Earth's radiation belts and their dynamic changes in response to solar activity (Figure 1). DREAM has been shown a ten-fold improvement in specification (or "nowcasting") of the high altitude space radiation environment. One major weakness in DREAM, however, is its inability to specify or predict the conditions in Low Earth Orbit (LEO). Prediction of the Low Earth Orbit environment is difficult because LEO satellites orbit just above the tenuous upper edge of the Earth's atmosphere. LEO is the most populated class of orbits because of the distance to the Earth's surface and relatively low launch costs. Examples of LEO satellites include the Iridium constellation, communications satellites, imagers, radars, weather satellites, and the International Space Station.

Charged particles (electrons and ions) that are trapped on the Earth's magnetic field lines scatter off the tenuous neutral atmosphere and are quickly absorbed. This leads to a very steep "loss cone" at Low Earth Orbit where radiation intensities can drop many orders of magnitude over a few tens of kilometers (a very small distance compared to the many thousands of kilometers that a magnetic field line can fill between the North and South poles). Further complicating the picture, the rate of decrease of radiation intensity with altitude can also vary by orders of magnitude so that both the intensity and the gradient of the intensity vary wildly.

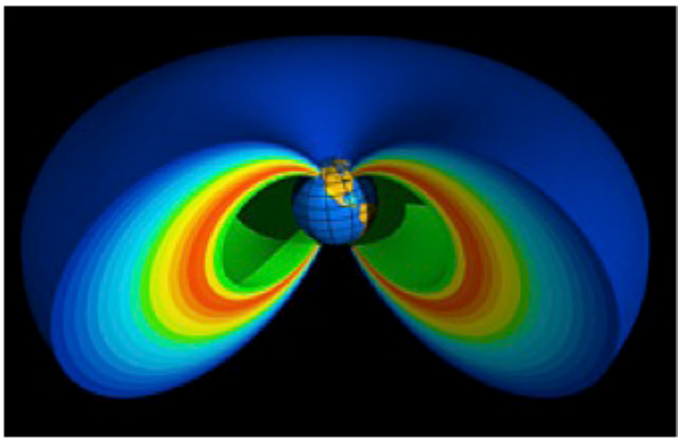

*Figure 1. Fluxes of natural radiation belt electrons shown in a cut-away view based on observations from NASA's POLAR satellite. This figure assumes that the flux (intensity) of electrons remains constant along a magnetic field line regardless of how close it is to the atmosphere. Observations from other satellites show that the fluxes actually decrease by many orders of magnitude as electrons scatter off the tenuous upper edge of the Earth's atmosphere.*

Our challenge was to construct a model of the variation in radiation belt electron flux (intensity) that takes into account the dynamics of the radiation belts due to solar and geomagnetic activity in order to quantitatively understand the relationship between the space environment at Low Earth Orbit and the space environment at higher altitudes.

## Background and Research Objectives

The United States has several long-running satellite programs that include instruments for monitoring the space environment (or Space Weather). Those include civilian and military systems at geosynchronous orbit (GEO), the 24-satellite Global Positioning System (GPS), and other civilian and military systems at Low Earth Orbit (LEO). Recently the National Oceanic and Atmospheric Administration (NOAA) and the US Air Force were instructed by congress to combine their LEO programs into an integrated National Polar Orbiting Environmental Satellite System (NPOESS). However, due to budget over-runs and the Nunn-McCurdy provision, many of the space environment systems were removed from the system. This has increased the need to *predict* the LEO space environment based on measurements at the higher-altitude GEO and GPS systems.

At the same time, there is increasing national concern over the threat posed by High Altitude Nuclear Explosions (HANE). High Altitude Nuclear Explosions produce artificial radiation belts that can be hundreds of times more intense than the Earth's natural belts. This occurred, for example, in the Starfish nuclear test which produced an artificial belt that lasted tens of years. While HANE poses a very different threat to satellites than the natural radiation belts, the physical processes that control the dynamics of the artificial belt are identical. Therefore our work can simultaneously focus on the connection high- and low-altitude environments in either case.

## Scientific Approach and Accomplishments

We have approached the challenges of connecting the low-altitude and high-altitude space environments using detailed comparison of low-altitude fluxes and high-altitude fluxes for specific case studies and through development of a first-of-its-kind statistical model of the low-altitude space environment

If the Earth's space environment did not change with time in response to solar activity then the connection between the low- and high-altitude space environments would be simple to model and simple to understand. Charged particles that are trapped in the Earth's magnetic field bounce back and forth along the field between the Northern and Southern hemisphere. As they move from the magnetic equator toward the Earth's surface along magnetic field lines the strength of the magnetic field increases. Particles moving exactly parallel to the magnetic field will travel along the field and eventually hit the atmosphere where they are absorbed and lost from the radiation belts. Particles that don't move exactly parallel to the field will "mirror" at some point along the field where the magnetic field strength, B, becomes large enough. The "mirror point" is determined by a the angle between B and the particle's velocity, an angle known as the "pitch angle" (Figure 2), which is normally referenced to it's value at the magnetic equator. Particles with 0° or 180° pitch angles move exactly along the field. Particles with pitch angles near 90° mirror near the magnetic equator and particles with intermediate pitch angles mirror at various points along the field. If a particle's mirror point is in the atmosphere it will be absorbed and lost from the radiation belts. The range of pitch angles with mirror points in the atmosphere is known as the "loss cone."

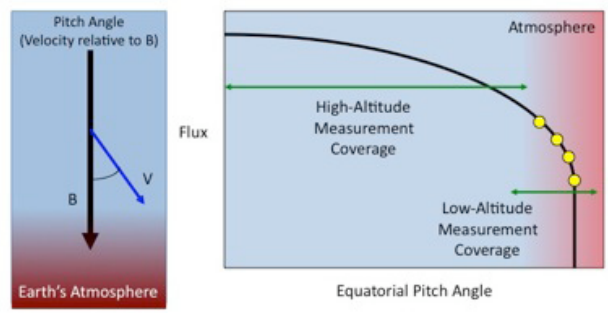


*Figure 2. A schematic showing the definition of pitch angle with the Earth's atmosphere shown with red shading. The right-and panel shows electron flux as a function of pitch angle going from 90° down to 0°. Low-altitude measurements only cover pitch angles near 0° but the ratio between 0° and 90° fluxes changes in response to geomagnetic activity.*

The pitch angle of electrons and ions in the radiation belts is not fixed. Processes such as the interaction between electrons (or ions) and plasma waves can scatter particles and change their pitch angles. Therefore pitch angle scattering plays a critical role in determining the lifetime of particles in the space environment and in determining the relationship between the low- and high-altitude space environments. The amount of pitch angle scattering depends on the location in space and the level of geomagnetic storm activity – which, in turn, is controlled by solar activity. High levels of geomagnetic activity generally lead to high levels of pitch angle scattering. High levels of scattering lead to populations with "flat" pitch angle distributions – i.e. the flux of particles is roughly independent of pitch angle. In those conditions the number (or flux) of particles with pitch angles near 0° (i.e. near the loss cone) are nearly equal to the number of particles with pitch angles near 90° and the ratio between them is nearly 1. Since particles with near 90° pitch angle mirror near the magnetic equator they never reach Low Earth Orbiting satellites. But if the ratio of 0° and 90° particles is nearly 1 then the measurements of the high altitude space environment almost perfectly predict what

should be seen at Low Earth Orbit.

When the rates of pitch angle scattering are low, though, particles with near 0° pitch angles are more likely to be scattered into the atmosphere and be lost than particles with near 90° pitch angles. In that case, gradually the number of particles near 0° will decrease while the number near 90° remain constant and the ratio between low- and high-altitude fluxes will decrease. As we show in Figure 3, the ratio between those fluxes varies by orders of magnitude. During high activity the low- and high-altitude fluxes are nearly equal but as activity (and pitch angle scattering) decrease the ratio becomes smaller and smaller. Such a period is shown from day 170 to 200 where the absolute value of the fluxes and the ratio of fluxes both decrease dramatically.

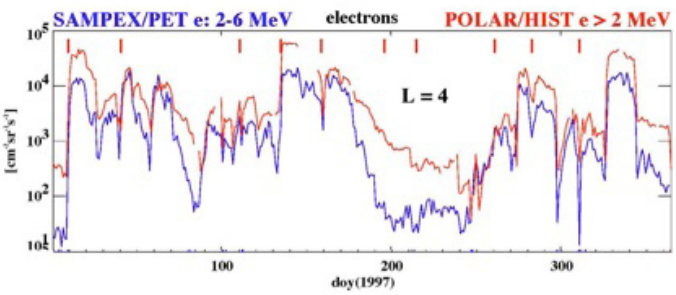


*Figure 3. High-altitude electron flux from the POLAR satellite and low-altitude flux measured by the Low Earth Orbiting satellite SAMPEX.*

In our statistical work we developed a new empirical model of the radiation-belt electrons in the low-Earth-Orbit region using upon long-term in-situ observations from several Low Earth Orbit satellites. This model provides the electron environment conditions needed to predict the LEO space environment and to connect it to the environment at higher altitudes. This model presents electron flux values for five energy ranges (0.03 – 1.1MeV, 0.1 – 1.1MeV, 0.3 – 1.1MeV, 1.5 - 6MeV, and 2.5 - 14MeV) within the space with the altitude <~600km.

In Figures 4 and 5 we show results from our statistical study compared to the standard model of electron fluxes used for spacecraft design and operations, known as AE-8. The plots show dipole magnetic field lines and contours of constant equatorial pitch angle (Figure 4). Following standard nomenclature we identify a given field line using the parameter, L, which is the radial distance at which the field line crosses the equator (in units of Earth Radii, $R_E$). For each bin in L and pitch angle we calculate the statistical distribution of electron fluxes. These statistics, which we have calculated for the first time, provide not only averages but also probabilities that enable prediction of low, medium, high, or extreme space radiation hazard. Comparing to the de-facto standard empirical model of AE-8 shows that, in addition to providing the first compilation of statistical probabilities, our model has better coverage in L and pitch angle. (We note that the coverage in altitude is limited by the available satellite observations and cuts off at an altitude of 600 km. The L and pitch angle for 600 km altitude varies with latitude and longitude.)

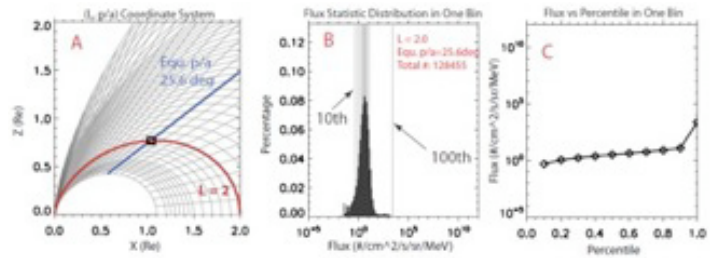


*Figure 4. The technique used to produce our statistical model. We bin data according to magnetic field lines (identified by L) and equatorial pitch angle. Within each bin we calculate the statistical distribution and percentiles of that distribution. "Maps" of the LEO space environment are represented by color coding fluxes in each bin using criteria such as energy and percentile.*

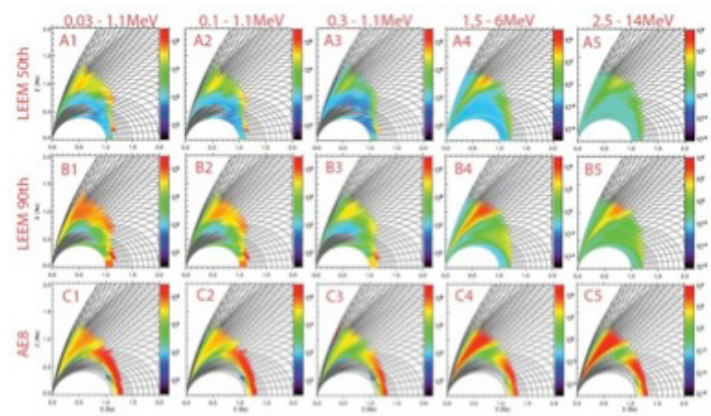


*Figure 5. Results from our statistical study of Low Earth Orbit electron fluxes. The AE8 model -the standard engineering model used for the design and operation of commercial and military satellites – is shown in the lowest row (C). Results from our statistical study are shown in the top row for the 50th percentile and in the middle row for the 90th percentile. Each column represents a different energy range.*

Several features are new and noteworthy. In both models the two-zone structure of the inner and outer electron radiation belts are evident but the AE-8 model implies that the inner belt is more intense than the outer belt and cuts off abruptly at a lower altitude boundary. Those "features" are artifacts of contamination of the electron channels by protons and from limitations on the statistical compilation method. Notice how, in the inner belt, on field

lines that extend out to approximately 2 $R_E$, fluxes go from red to yellow to zero. Our model shows much smoother transitions (particularly at lower energies), more realistic gradients and no artificial cut-offs. Fluxes at low altitude do still go to near zero values but do so smoothly through low flux values as shown by green and blue colors.

The refined pitch angle structure of our new model is one of its most important results. The improvement is best seen in the highest energy channels (1.5-6 MeV) as shown in plots A4, B4, and C4. Following a given magnetic field line (Figure 4) fluxes pitch angles appear color-coded with smaller pitch angles closer to the Earth (lower altitude mirror points) and larger pitch angles further from Earth. As we show schematically in Figure 2 and quantitatively in Figure 3, The fluxes should decrease with pitch angle and the decrease should be smooth but not linear. All those features are captured in our model. Furthermore, our model shows subtle but important refinements based on the statistical distribution of fluxes. Note that the flux maps represented by the 50$^{th}$ percentile (median) of the distribution look notably different than those showing the 90$^{th}$ percentile of the distribution.

These results are important for more accurately quantifying the risk to Low Earth Orbit satellites due to the low-altitude portion of the Earth's radiation belts. They can be used for improving design, optimizing performance/ risk trade-offs, and for ensuring more reliable operation of LEO satellites. The results are also important for improving physical understanding of the pitch angle scattering processes that connect low-altitude and high-altitude populations – processes that are also responsible for determining the lifetime of electrons in the Earth's radiation belts. Full answers to those questions are beyond the scope of this 1-year project. They are, in fact, a primary objective of the NASA Radiation Belt Storm Probes (RBSP) mission in which LANL plays a leading role. This work provides important stand-alone results as well as providing a key missing piece of the foundation needed for that more complete understanding.

## Impact on National Missions

We have provided the first ever statistical model of the low-altitude edges of the Earth's radiation belts. The majority of US satellites operate in Low Earth Orbit (LEO) where they encounter the low-altitude radiation belts. LEO satellites include Irridium, communications satellites, reconnaissance satellites, weather satellites, the International Space Station, and others.

The model provides key information for understanding the connection between environments measured at Low Earth Orbit (LEO) and those measured at higher altitude orbits such as Medium Earth Orbits (MEO) such as GPS, High Earth Orbits (HEO), or geosynchronous orbit (GEO). Each class of orbit has critical civilian and military space applications and each experiences a distinctly different portion of the space environment. Understanding the physical and statistical relationship of the environments measured in those different orbits gives us the tools necessary to

- design more reliable LEO satellite systems for the future
- optimize the tradeoff between satellite instrument performance and risk
- ensure more reliable operation of LEO satellites
- recover more quickly from LEO satellite anomalies, and
- mitigate the impacts on US Space Weather capabilities due to rescope of the National Polar Orbiting Environmental Satellite System (NPOESS).

# Designing Intelligence into the Next Generation Wind Turbine

*Francois M. Hemez*
20090499ER

## Abstract

Wind energy in the United States is the fastest growing source of clean, renewable domestic energy. A recent DOE technical report proposed the potential for meeting 20% of the nation's energy needs through wind power. As manufacturers strive to increase power and efficiency, the trend is toward more complex wind turbines with longer and heavier rotor blades. There has been minimal research, however, focused on developing techniques for real-time monitoring and control of turbines under true wind loading. There is a great need, therefore, to develop the concept of "intelligent wind turbines," which will enhance performance, increase reliability, and reduce life-cycle costs (Figure 1).

*Figure 1. Seven-foot diameter turbine acquired for aero-dynamics and structural testing.*

In this project, we propose a multi-disciplinary research that will develop physics-based predictive models, advanced sensing technologies, novel data interrogation techniques, active performance control, and reliability-based decision making algorithms [1]. We will then merge these technologies to provide a revolutionary capability to develop future generations of wind turbines with increased energy conversion efficiencies and dramatically reduced lifecycle costs. We are planning to develop i) multi-physics modeling capabilities to assess and control the effect of coupled aerodynamic and structural conditions on power output and blade health; ii) sensing technologies to measure wind turbine response on multiple time-scales and length-scales for state awareness, control, and damage detection; and iii) active turbine and blade control to improve efficiency and compensate for structural damage. We envision that these components will be coupled with novel data interrogation [2] and uncertainty quantification techniques [3] to produce the hardware and software tools necessary to realize a system state awareness, control, and prognostic capability for wind turbines. Our team is unique in that we can combine these complimentary tasks into a single coordinated effort that will significantly impact the practice of harvesting wind energy and position LANL to bring innovative technology to this rapidly growing alternative energy area.

## Background and Research Objectives

Turbine/wind interactions that lead to turbine failures are not well understood. Design criteria, largely based on the European wind industry, do not reflect the more severe dynamic shear environments that occur in the U.S. wind corridor. Modern wind turbines typically fail 2.6 times per year during their first 10 years. Our hypothesis is that these turbulent wind interactions translate to severe blade loading that are transmitted to the turbine hub and gearbox, eventually leading to compromised rotor integrity and failure (Figures 2, 3).

The concept of "intelligent" wind turbines develops prognostics solutions that understand, monitor and simulate how blades interact aero-dynamically and structurally with atmospheric wind conditions.

Intelligent wind turbines are capable of adapting to their environment and structural condition to optimize reliability and power output.

*Figure 2. Upper left: two-bladed scaled-model wind turbine rotor used for prototyping the laser velocimetry measurements. Right: 1.2 m by 1.3 m low speed wind tunnel at NMSU.*

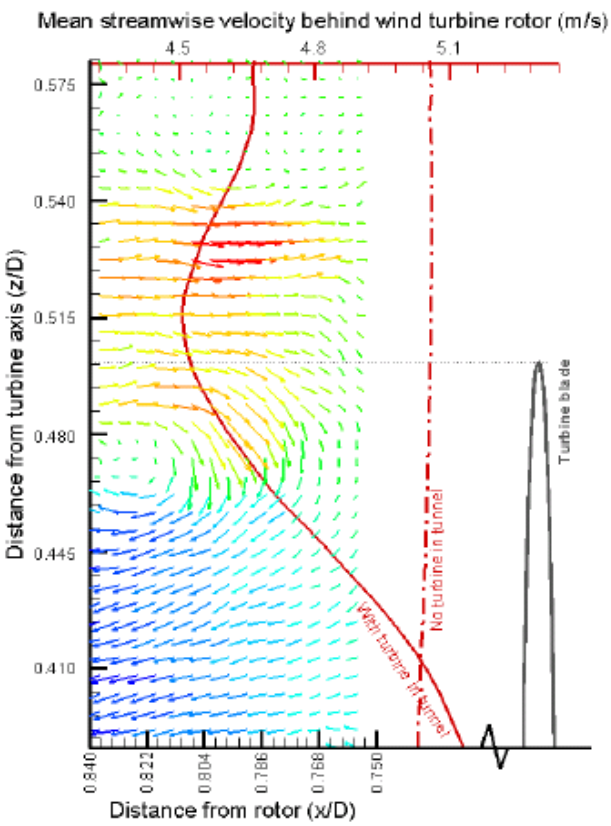


*Figure 3. Near wake velocity field measured behind the scaled-model wind turbine (using settings Re = 74000 and tip-speed ratio = 7).*

## Scientific Approach and Accomplishments

Our approach is to design and demonstrate the deployment of a prognostics solution that integrates advanced sensing, statistical signal processing, and predictive modeling and simulation. Until recent successful developments at LANL, there has been no method for modeling the interaction between landscape-scale wind events and spinning wind turbines (Figure 4). We propose to develop a modeling capability, that currently does not exist, for simulating two-way interactions between realistic wind fields, deforming blades, and the resulting stresses imparted on the blades, hub and gearbox (Figures 4, 5).

Los Alamos is also a World-class leader in the design and deployment of advanced sensing modules for structural health monitoring and damage prognostics [4, 5]. Finally, we will leverage years of experience developing methods to verify the performance of numerical algorithms, validate models, and assess measurement and prediction uncertainty to analyze the reliability of wind turbines.

First and foremost, we have learned that designing and successfully deploying a prognostics capability is a multi-disciplinary effort. Expertise from AET Division, EES Division, X Division and the Engineering Institute is being integrated to solve this problem. Our one-year feasibility study has indicated that we currently have working solutions for the sensing [6], power requirements [7], modeling of atmospheric conditions [8], and modeling of structural response [9]. We need to demonstrate how these technologies can be integrated to understand, identify, and manage turbine rotor damage.

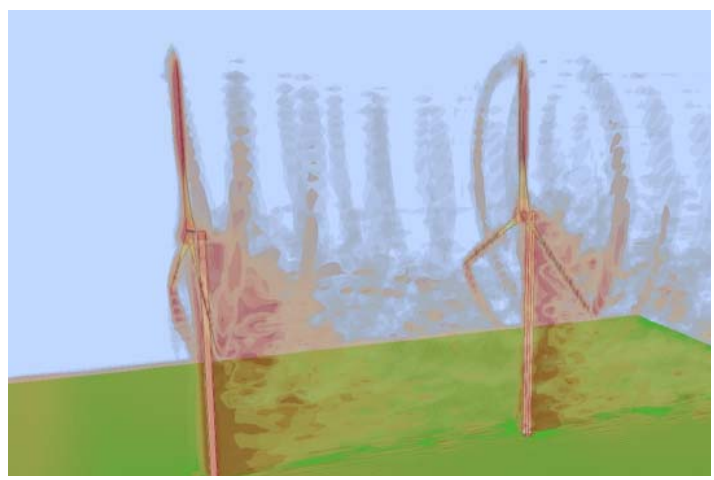

*Figure 4. Atmospheric simulation of wind loading using WindBlade (computational fluid dynamics).*

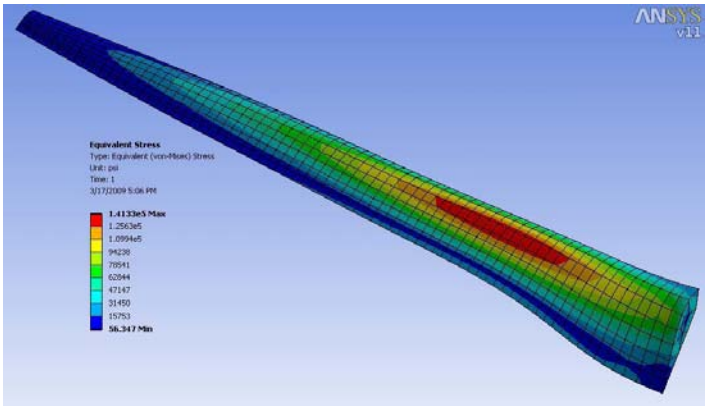


*Figure 5. Simulation of structural response with ANSYS (computational solid mechanics).*

## Impact on National Missions

The U.S. Department of Energy proposes to meet 20% of the nation's energy needs with wind power by the year 2030 to address both energy security and carbon footprint concerns. Achieving this target will increase the installed wind capacity by more than ten-fold, from 25 GW to 305 GW. Current reliability challenges of the wind turbine technology, if not resolved, risk derailing this ambitious goal.

One of the biggest obstacles to a viable, unsubsidized U.S. wind industry is cost, currently at $35-to-60 per MW-hour. Operation and maintenance costs, however, climb steadily as wind plants age, starting out at $5 per MW-hour in the first year, and increasing to $15-to-20 per MW-hour by year 20. Deploying "intelligent" wind turbines offers the potential of reducing these maintenance costs by half.

## References

1. Hemez, F.. Fiscal year 2009 final report of the engineering grand challenge feasibility study on "intelligent wind turbines". 2009. *Technical Report LA-UR-0907722 of the Fiscal Year 2009 Feasibility Study "Intelligent Wind Turbines," Los Alamos National Laboratory, Los Alamos, New Mexico.*

2. Raby, E.. Wind turbine sensor node development. 2009. *Technical Report of the Fiscal Year 2009 Feasibility Study "Intelligent Wind Turbines," Los Alamos National Laboratory, Los Alamos, New Mexico.*

3. Hush, D.. Damage detection for wind turbine blades. 2009. *Technical Report of the Fiscal Year 2009 Feasibility Study "Intelligent Wind Turbines," Los Alamos National Laboratory, Los Alamos, New Mexico.*

4. Figueiredo, E., G. Park, K. Farinholt, and C. Farrar. Time series analysis of piezoelectric active-sensing for structural health monitoring applications. *Journal of Sound and Vibration.*

5. Sobin, A., A. Light-Marquez, K. Farinholt, and G. Park. Structural damage identification in wind turbine blades using piezoelectric active sensing. To appear in *28th SEM International Modal Analysis Conference (IMAC-XXVIII).* (Jacksonville, Florida, February 1-4, 2010).

6. Taylor, S., K. Farinholt, G. Park, M. Todd, and C. Farrar. Application of a wireless sensor node to health monitoring of operational wind turbine blades. To appear in *28th SEM International Modal Analysis Conference (IMAC-XXVIII).* (Jacksonville, Florida, February 1-4, 2010).

7. Carlson, C., A. Schlichting, S. Ouellette, K. Farinholt, and G. Park. Energy harvesting to power sensing hardware onboard wind turbine blade. To appear in *28th SEM International Modal Analysis Conference (IMAC-XXVIII).* (Jacksonville, Florida, February 1-4, 2010).

8. Balakumar, B. J., and R. C. Alarcon. Velocity field measurements of a model wind turbine. *AIAA Journal.*

9. Haynes, C., N. Konchuba, K. Farinholt, and G. Park. Modeling, estimation, and monitoring of force transmission in wind turbines. To appear in *28th SEM International Modal Analysis Conference (IMAC-XXVIII).* (Jacksonville, Florida, February 1-4, 2010).

## Publications

Balakumar, B. J., and R. C. Alarcon. Velocity field measurements of a model wind turbine. *AIAA Journal.*

Carlson, C., A. Schlichting, S. Ouellette, K. Farinholt, and G. Park. Energy harvesting to power sensing hardware onboard wind turbine blade. To appear in *28th SEM International Modal Analysis Conference (IMAC-XXVIII).* (Jacksonville, Florida, February 1-4, 2010).

Figueiredo, E., G. Park, K. Farinholt, and C. Farrar. Time series analysis of piezoelectric active-sensing for structural health monitoring applications. *Journal of Sound and Vibration.*

Haynes, C., N. Konchuba, K. Farinholt, and G. Park. Modeling, estimation, and monitoring of force transmission in wind turbines. To appear in *28th SEM International Modal Analysis Conference (IMAC-XXVIII).* (Jacksonville, Florida, February 1-4, 2010).

Hemez, F.. Fiscal year 2009 final report of the engineering grand challenge feasibility study on "intelligent wind turbines". 2009. *Technical Report LA-UR-0907722 of*

*the Fiscal Year 2009 Feasibility Study "Intelligent Wind Turbines," Los Alamos National Laboratory, Los Alamos, New Mexico.*

Hush, D.. Damage detection for wind turbine blades. 2009. *Technical Report of the Fiscal Year 2009 Feasibility Study "Intelligent Wind Turbines," Los Alamos National Laboratory, Los Alamos, New Mexico.*

Raby, E.. Wind turbine sensor node development. 2009. *Technical Report of the Fiscal Year 2009 Feasibility Study "Intelligent Wind Turbines," Los Alamos National Laboratory, Los Alamos, New Mexico.*

Sobin, A., A. Light-Marquez, K. Farinholt, and G. Park. Structural damage identification in wind turbine blades using piezoelectric active sensing. To appear in *28th SEM International Modal Analysis Conference (IMAC-XXVIII).* (Jacksonville, Florida, February 1-4, 2010).

Taylor, S., K. Farinholt, G. Park, M. Todd, and C. Farrar. Application of a wireless sensor node to health monitoring of operational wind turbine blades. To appear in *28th SEM International Modal Analysis Conference (IMAC-XXVIII).* (Jacksonville, Florida, February 1-4, 2010).

# Chiral Metamaterials for Terahertz Frequencies

*John F. O'Hara*
20080796PRD4

## Introduction

Many materials in nature are made from molecules that share a chemical composition, but are mirror images of each other. They are often called left and right-handed materials, in reference to this "handedness" property. The technical term describing this nature is chirality. Chirality has attracted much interest since it was first discovered in the 1840's because biological processes often utilize only one of the two forms of a species. For example, the widely used antibiotic penicillin can inhibit bacterial growth in its right-handed form, but is completely inactive in its left-handed form. Clearly it is important to be able to control and measure chirality in materials.

Chirality can be measured using polarized light. As electromagnetic (EM) waves propagate through a chiral medium their polarization, or the direction in which the electric field points, rotates in an amount that is determined by simple optical instruments. This effect, known as optical activity, is well understood as the continual and mutual exchange of energy between the incident wave's electric and magnetic components. Natural materials usually have very weak chirality, so their optical activity is very limited. However, in certain technological applications, it may be very beneficial to create materials having strong optical activity.

Recently proposed chiral metamaterials are specially engineered materials suitable for creating extremely strong optical activity and have been researched for polarization control applications at microwave and optical frequencies. Chiral metamaterials are made of sub-wavelength resonators that lack certain internal symmetry [1-3]; these are analogous to the chiral molecules in natural materials. Importantly, the optical activity of chiral metamaterials can be five orders of magnitude stronger than that of natural chiral media, e.g. a quartz crystal [2]. At the last International Workshop on Electromagnetic Metamaterials we even showed that chiral metamaterials lead to negative refractive index for circularly polarized waves due to their extremely large optical activity [4,5]. Terahertz metamaterials clearly represent a convenient and tunable platform for studying the fundamental interactions of light and chiral materials. Our project is to create THz metamaterials that exhibit giant optical activity. But we also wish to show that these materials can be made to have dynamically tunable optical activity, which adds a level of control not available in any known natural material.

## Benefit to National Security Missions

This project will enhance our fundamental understanding of materials, capabilities in ubiquitous sensing, and threat reduction by enhancing our ability to efficiently manipulate THz and optical waves. Specifically, the ability to improve the performance of optical materials and also to manipulate THz waves efficiently will enable new forms of covert communications, data exfiltration, spectroscopy, remote sensing, and non-invasive imaging (particularly life-sciences imaging), relevant to important mission areas for particularly for Intel agencies, DOE, DOD, and DHS. In addition this work supports fundamental understanding of engineered electromagnetic materials, certain to be part of future technology generations.

## Progress

Excellent progress has been made in this project, mainly in the design of tunable chiral metamaterials at THz frequencies. By integrating semiconductors [6] into the chiral metamaterial design, we are able to create materials whose optical activity is dynamically controllable. Microscopically, the optical activity originates in the deliberate creation of magnetic effects that are excited by the electric wave components, and vice versa. In this work, specially designed semiconductor components are fabricated into the chiral metamaterial designs. When the semiconductors

are illuminated with infrared light, the magnetic response changes according to the illumination intensity. By varying the infrared illumination intensity, we are able to control the THz optical activity of the chiral metamaterials. Our numerical simulations show that active chiral metamaterials can tune the optical activity induced on a linearly polarized wave over a large range (Figure 1). Our active chiral metamaterial design enables applications such as polarization controllers and ultra-thin circular polarizers for optoelectronic, life science microscopy and display applications.

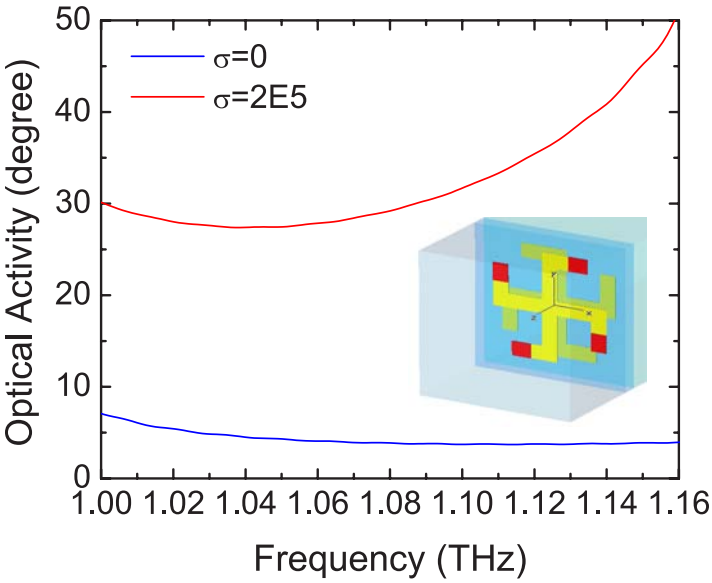


*Figure 1. Simulated tunable optical activity in a chiral metamaterial. As the semiconductors (shown as red patches on the structure) are illuminated they become more conductive and the metamaterial optical activity changes dramatically (from blue to red curve).*

Utilizing progress from our previous research, we are also designing a dynamic THz metamaterial that should be tunable by means of electronic signals, instead of infrared illumination. It is based on an array of metamaterial resonators that have integrated varactors (Figure 2). A varactor is a semiconductor device with voltage-controlled capacitance. The varactor consists of five semiconductor layers grown on a gallium arsenide substrate via molecular beam epitaxy. When a DC electrical bias is applied to the varactor, charges within the layers effectively distance themselves from each other, changing the device's overall capacitance. Since the resonance frequency of a metamaterial is a function of this capacitance, we are able to tune the bulk metamaterial with the DC bias. Unlike our tunable metamaterial realized through infrared-excited semiconductors [6], the voltage-controlled tunable metamaterial features low loss, continuous tunability and a larger tunable range. Based on our numerical simulations, we should realize continuously tunable resonances over a 40% range in frequency. Currently, we have finished the design of this new type of metamaterial and are preparing the first sample. This approach is very general, and should represent a significant step forward in numerous THz technology applications. And importantly, it can also be applied to chiral metamaterials. Upon completion of our experimental characterization, we will integrate the concept with chiral metamaterial to produce electronically tunable chiral materials. An important step in this research is tailoring this method of tunabilty to our chiral metamaterials. We expect to observe a significant benefit in this method (over infrared control) since it eliminates severe loss mechanisms, which we now know play a large role in chiral metamaterials.

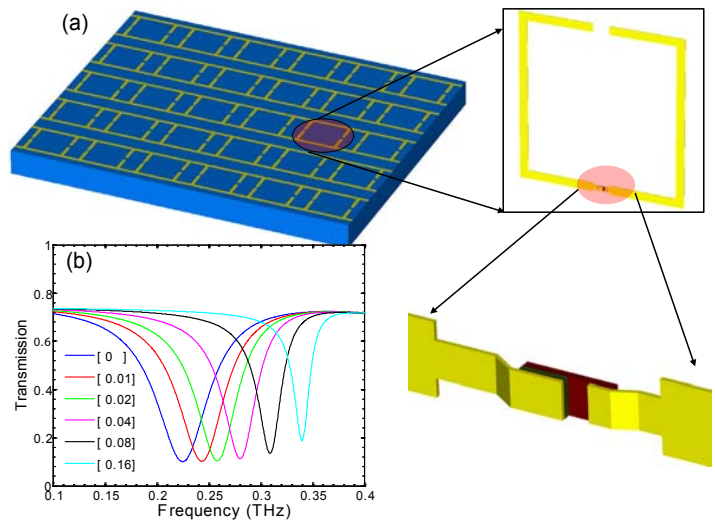


*Figure 2. Electronically controlled tunable metamaterial. (a) Schematic of metamaterial and its constituent resonator particle including the varactor inclusion. (b) Plot of THz transmission through metamaterial versus frequency. Different curves show the frequency-shifting response as a DC voltage is applied to the varactor.*

We have also investigated the application of our chiral metamaterials to the field of Casmir force tuning [7]. The Casimir force is a physical force that occurs between two very closely spaced objects, such as might be found in micro- or nano-technology. The Casmir force is nearly always attractive, and often degrades or prohibits the operation of microelectromechanical systems (MEMS) due to the introduction of stiction and friction. Therefore, the study of the Casimir force has both fundamental and applied importance. We have shown that metamaterials with large chirality may be able to reverse the Casimir force [8]. These important results were published in Physical Review Letters, a prestigious journal in physics. We continue to develop a greater understanding of chiral metamaterials and how they might be optimized for reducing or reversing Casimir forces.

## Future Work

Our future tasks will be to complete the fabrication and characterization of the electronically tunable metamaterials so that we may begin to study their integration into tunable chirality designs. We also continue to investigate chiral metamaterial designs that optimize optical activity while suffering minimally from loss. As we progress, we will seek to demonstrate novel THz technology (polarization rotators, reversers, etc.) that utilizes our chiral metamaterials. We will also continue our ongoing collaboration with numerous research groups nationwide with rapidly growing interest in Casimir force tuning. Our increasing expertise in chiral metamaterials, and a similar but broader category of bi-anisotropic metamaterials, should prove very fruitful in these collaborations.

## Conclusion

We are developing novel chiral metamaterials for generating giant optical activity in the THz frequency regime with the aim of creating novel technology such as dynamic, ultra-thin, and low-loss polarization rotators. Importantly, the concepts developed here will scale to higher frequencies, thus possibly enabling new polarization control devices for optical imaging in the life-sciences. Part of our recent work has been to design electronically tunable metamaterials using varactor-loaded metamaterial resonators. This approach should minimize losses and improve the dynamic range of metamaterial tunability, both of which are important steps forward in chiral materials research. Finally, our work has proven useful in efforts to tune the quantum Casimir force, which may have very important implications in improving micro- and nano-technology devices. Every one of our related research directions represents a fundamental advance in manipulating electromagnetic waves to the benefit of technological applications.

## References


1. Pendry, J. B.. A Chiral Route to Negative Refraction. 2004. *Science.* **306** (5700): 1353.

2. Rogacheva, A. V., V. A. Fedotov, A. S. Schwanecke, and N. I. Zheludev. Giant Gyrotropy Due to Electromagnetic-Field Coupling in a Bilayered Chiral Structure. 2006. *Physical Review Letters.* **97** (17): 177401.

3. Plum, E., V. A. Fedotov, A. S. Schwanecke, N. I. Zheludev, and Y. Chen. Giant Optical Gyrotropy Due to Electromagnetic Coupling. 2007. *Applied Physics Letters.* **90** (22): 223113.

4. Plum, E., J. Zhou, J. Dong, V. A. Fedotov, T. Koschny, C. M. Soukoulis, and N. I. Zheludev. Metamaterial with Negative Index Due to Chirality. 2009. *Physical Review B.* **79**: 035407.

5. Zhang, S., Y. S. Park, J. Li, X. Lu, W. Zhang, and X. Zhang. Negative Refractive Index in Chiral Metamaterials. 2009. *Physical Review Letters.* **102**: 023901.

6. Chen, H. T., J. F. O'Hara, A. K. Azad, A. J. Taylor, R. D. Averitt, D. B. Shrekenhamer, and W. J. Padilla. Experimental Demonstration of Frequency-Agile Terahertz Metamaterials. 2008. *Nature Photonics.* **2**: 295.

7. Casimir, H.. On the Attraction Between Two Perfectly Conducting Plates. 1948. *Proceedings of the Royal Netherlands Academy of Arts and Sciences.* **51**: 793.

8. Zhao, R., J. Zhou, T. Koschny, E. N. Economou, and C. M. Soukoulis. Repulsive Casimir Force in Chiral Metamaterials. 2009. *Physical Review Letters.* **103**: 103602.


## Publications


Zhao, R., J. Zhou, T. Koschny, E. N. Economou, and C. M. Soukoulis. Repulsive Casimir Force in Chiral Metamaterials. 2009. *Physical Review Letters.* **103**: 103602.

Zhou, J., B. Wang, E. Plum, T. Koschny, V. Fedotov, H. T. Chen, A. J. Taylor, J. F. O'Hara, N. Zheludev, and C. Soukoulis. Chiral Metamaterials with Negative Refractive Index. Presented at *International Workshop on Electromagnetic Metamaterials III: Toward Real World Applications.* (Los Alamos, NM, 18-19 May, 2009).

Laboratory Directed Research & Development
Los Alamos National Laboratory
PO Box 1663, MS M708
Los Alamos, NM  87545
505-667-1235 (phone)